PROCEEDING

The 11th International Conference on QiR (Quality in Research)

QiR

Organized by:




Faculty of Engineering
University of Indonesia

3 - 6 August 2009,
Faculty of Engineering
University of Indonesia
http://qir.eng.ui.ac.id

ISSN 114-1284

Faculty of Engineering
University of Indonesia

Bachelor Degree Program

Regular Class Bachelor Degree, Extention Program Bachelor Degree,
International Class Bachelor Degree

Master Degree Program

Doctor Degree Program

Study Programs

Civil Engineering, Mechanical Engineering, Electrical Engineering,
Metallurgy & Material Engineering, Architecture, Chemical Engineering, Industrial Engineering

For further information on the program,
Please contact:
Gedung Pusat Administrasi Fakultas (PAF)
Kampus Baru UI, Depok 16424
Tel. 021 78888 430, 7888 7861
Fax. 021 78888 076, 786 3507

www.eng.ui.ac.id

PROCEEDING

The 11th International Conference on QiR (Quality in Research)

QiR

Organized by:




Faculty of Engineering
University of Indonesia

3 - 6 August 2009,
Faculty of Engineering
University of Indonesia
http://qir.eng.ui.ac.id

ISSN 114-1284

Conference Organizations

Advisor
Prof. Dr. Ir. Bambang Sugiarto M. Eng
Dean of Faculty of Engineering, UI

Dr. Ir. Dedi Priadi, DEA
Vice Dean of Faculty of Engineering, UI

Dr. Ir. Sigit Pranowo Hadiwardoyo, DEA
Faculty Secretary of Faculty of Engineering, UI

Chairman
Dr. Ir. Bondan T. Sofyan, M.Si.

Vice Chairman
Dr. Mohammed A. Berawi, M.Eng

Technical Committee
Dr.-Ing. Eko Adhi Setiawan
Toha Saleh, ST., M.Sc
Ir. Warjito, M.Sc., Ph.D
Dr. Ir. Badrul Munir, ST., M.Sc.Eng
Yulia Nurliani Lukito, ST., M.Des.S
Arian Dhini, ST., MT
Farizal, Ph.D

Secretariate
Ayomi Dita Rarasati, ST., MT
Herra Astasusmini, SE
Lanny Delima Bastari
Nuruli Exsiarni

Treasurer
Evi Supriningsih, S.Pd, MM

Program & Protocol
Dr. Ir. Anondho Wijanarko, M.Eng
Dwinanti Rika Marthanthy, ST., MT

Publication & Documentation
Dr. Abdul Halim
Tikka Anggraeni, S.Sos
Pijar Suciati, S.Sos
Aryadi

Web & System Information
Arief Udhiarto, ST., MT
Dr. Abdul Muis, ST., M.Eng
Dedi Triyanto, ST
I Gde Dharma N., ST., M.T
Elmansyah, ST

Sponsors & Exhibition
Armand Omar Moeis, ST., M.Sc
Deni Ferdian, ST., M.Sc

Venue
Dr.-Ing. Ir. Nandy Setiadi Djaja Putra
Teguh Iman Santoso, ST
Jumiardi

Catering
M.G. Sri Redjeki

Conference Organizing Committee :
Faculty of Engineering, University of Indonesia
Dekanat Building 3rd Floor
Kampus UI, Depok 16424, Indonesia

Phone : +62 – 21 - 9114 5988/ 786 3503
Fax : +62 - 21 – 7270050
Email : qir@eng.ui.ac.id, qir.ftui@gmail.com
www.eng.ui.ac.id

Welcome from the Rector of University of Indonesia

I am honoured to have the opportunity to officially welcome you to the 11th International Conference on QiR (Quality in Research) 2009. The conference provides an excellent forum for engineering professionals, business executives, industry practitioners, and academicians to exchange ideas and to share their experience, knowledge and expertise with each other. I believe the participants will also learn about the latest trends in the development of new tools, knowledge and skills in various engineering design and technology.

As we agree that engineering products or projects bring together resources, skills, technology and ideas to achieve business objectives and deliver business benefits and it comes in all shapes and sizes from the simple and straight-forward to the large and unmentionably complex, thus we need an application of knowledge, skills, tools, and techniques necessary to develop and successfully execute the products or projects plan so it will meet or exceed our customer and stakeholder needs and expectations.

The ultimate concern of engineering product or project is three-fold: the product/project meeting its targets and purposes, the product/project on schedule, and the product/project cost within budget. As the Indonesian economy is growing, local enterprises are obliged to upgrade their skills in innovation and product design. There are also increasingly aware of the importance of professionalism in various engineering areas for industries needs and many professionals are keen to upgrade their capability.

Having said that, I hope this conference can be a kick-off for strengthened our action and partnerships on creating a platform for us; national and international thinkers, academics, government officials, business executives and practitioners, to present and discuss the pivotal role of engineers in the achievement of excellence organizations.

I am sure you will find the 11th International Conference on QiR (Quality in Research) 2009 both informative and stimulating. I would like to thank the Faculty of Engineering, University of Indonesia for organizing this meaningful and timely event, and the supporting organizations for their participation and contributions. With this, I wish you all a fruitful conference. Thank you.

Prof. Dr. der. Soz. Gumilar Rusliwa Somantri
Rector of University of Indonesia
University of Indonesia

Welcome from Dean of Engineering University of Indonesia

On behalf of the Faculty of Engineering, University of Indonesia, it is my greatest pleasure to extend our warmest welcome to all of you to the 11th International Conference on QiR (Quality in Research) 2009. As we know that this conference is conducted to cover a wide range of engineering design and technology issues. I hope these four days of the conference will be spent in interesting discussion and exchange of ideas. I also hope this conference would be able to provide a state-of-the-art information and knowledge in the challenging world of engineering design and technology. The growing success of our institutions and expertise should urge us to develop our competitive capabilities, especially as we face certain challenges which would be overcome with more hard work and working together hand by hand. We will work together to develop a common path and collaboration opportunities for future action and research on multi disciplinary engineering areas.

I am delighted that you have accepted our invitation to this conference in such large numbers as indicated that we will have many international keynote speakers' lectures and papers from various countries to be presented and discussed during these two days conference. We will explore various engineering techniques and tools in various industries that can be used to build better stakeholder performance and relationships, to enable us to create wealth through innovation, to promote productivity through technology, and to foster our collaboration.

I would like to thank you to our sponsors, supported bodies and various contributors for their generous support of this conference. I would also like to thank our distinguished speakers for agreeing to share their insights with us. To our friends from overseas and other provinces of Indonesia, I would also like to extend a warm welcome to you and wish you an enjoyable stay in Jakarta. Last but not least, I would invite you to join me in thanking the committed staff that made this conference happen and to make it a success.

I wish you a very pleasant stay here in Jakarta and a successful and productive discussion at the conference. Thank you.

Prof. Dr. Bambang Sugiarto
Dean of Engineering University of Indonesia

Welcome from the QiR 2009 Organizing Committee

On behalf of the Organizing Committee, it is my greatest pleasure to extend our warmest welcome to all of you to the 11th International Conference on QiR (Quality in Research) 2009.

I am sure that you will all find this conference stimulating and rewarding. As we are aware of, the impact of globalization has resulted in a very competitive business environment that makes the fulfillment of customer/clients' ever-sophisticated project or product or service needs most challenging. Without any doubt, a good engineering design and technology is powerful in helping our industries to enhance their productivity and competitiveness. Thus, it is our aim and hope that the conference would be able to provide an international forum for exchange knowledge and research expertise as well as to create prospective collaboration and networking on various fields of engineering and architecture.

With its continuous presence in the last 11 years, QiR has become an icon of Faculty of Engineering University of Indonesia in serving the objectives to provide engineering excellence for both national and international needs. The QiR 2009 consists of 2 special issues and 4 symposia covering almost all aspect in engineering, design and architecture. I am delighted to inform you that we have such large numbers of participants today as indicated that we will have 7 keynote speakers' presentation and more than 240 papers from various countries to be presented and discussed during these two days conference. We are fortunate to have a lot of good quality of papers that belongs to:

70 papers on Radio Frequency Identification (RFID) as a Bridge between Computing and Telecommunication
36 papers on Green Infrastructure for Sustainable Development and Tropical Eco-Urbanism.
56 papers on Industrial Engineering Approach for Productivity Improvement
56 papers on Advanced Materials and Processing
30 papers on Energy Conservation through Efficiency in Design and Manufacturing

I would like to thank you to various contributors, speakers and participants for your generous support of this conference. It is my pleasant duty to thank all the members of Organizing Committee and the International Board of Reviewers for their advices and help. We are grateful to all the Sponsors, Supporters and Exhibitors for their spontaneous response and encouragement by way of committing funds and extending help in kind.

I would like to sincerely thank the Dean of Engineering, for fully supporting the Committee and providing all supports to make this conference happen and to make it a success.

I wish you a very pleasant stay here in Jakarta and finally, let me wish all of you a meaningful and fruitful conference. Thank you and hope to see you again in QiR 2011.

Dr. Bondan T. Sofyan
Organizing Chairperson of QiR 2009

International Board of Reviewers :

- Prof Dr James Holm-Kennedy, *University of Hawaii*, USA
- Prof. Dr.-Ing. Axel Hunger, *University of Duisburg*, Germany
- Dr. Monto H Kumagai, *XtremeSignPost.Inc*, Davis, California, USA
- Prof. Chit Chiow Andy T, PhD, BSc (Eng), FIEAust, Peng, *Queensland University of Technology*, Australia
- Prof. Josaphat Tetuko Sri Sumantyo, PhD, *Chiba University*, Japan
- Prof. C.F. Leung, *National University of Singapore*
- Prof. Dr. Low Shui Pheng, *National University of Singapore*
- Prof. Dr. Ghassan Aouad, *University of Salford*, United Kingdom
- Dr. Roy Woodhead, *EDS Consulting Service*, United Kingdom
- Prof. Dr. Hamzah Abdul Rahman, *University of Malaya*, Malaysia
- Prof. Tae Jo Ko, *Yeungnam University*, South Korea
- Prof. Dr. Freddy Boey, *Nanyang Technological University,* Singapore
- Prof. Dr. M. Misbahul Amin, *University Malaysia Perlis*
- A/Prof. Iis Sopyan, *International Islamic University Malaysia*
- Prof. Ir. Gunawan Tjahjono, M.Arch., Ph.D, *University of Indonesia*
- Prof. Abidin Kusno, *British Columbia University*, Canada
- Prof. Lai Chee Kian, *National University of Singapore*
- Prof. Efstratios Nikolaidis, PhD, *University of Toledo*, USA
- Prof. Katsuhiko Takahashi, *Hiroshima University*, Japan

National Board of Reviewers :

- Prof. Dr. Ir. Djoko Hartanto, M.Sc, *University of Indonesia*
- Prof. Dr. Ir. Tommy Ilyas, M.Eng, *University of Indonesia*
- Dr. Ir. R. Danardono A. Sumarsono DEA. PE, *University of Indonesia*
- Dr –Ing. Ir. Bambang Suharno, *University of Indonesia*
- Prof. Dr. Ir. Djamasri, *Gadjah Mada University*, Indonesia
- Ir. Isti Surjandari, Ph. D, *University of Indonesia*
- Prof. Dr. Ir. Mohammad Nasikin, M. Eng, *University of Indonesia*

QiR Proceeding 2009
3 – 6 August 2009
ISSN 114-1284

Editorial Board

Editor- in-Chief
Dr.-Ing. Eko Adhi Setiawan, Universitas Indonesia

Managing Editor
Dr. Ir. Badrul Munir, ST. M.Eng.Sc., Universitas Indonesia

Editorial Members :
A/Prof. Iis Sopyan, International Islamic University Malaysia
Arian Dhini, ST., MT., Universitas Indonesia
Ayomi Dita Rarasati, ST., MT., Universitas Indonesia
Prof. Abidin Kusno, British Columbia University, Canada
Dr. Ir. Anondho Wijanarko, M.Eng., Universitas Indonesia
Prof. Dr.-Ing.Axel Hunger, University of Duisburg, Germany
Dr.-Ing. Ir. Bambang Suharno, Universitas Indonesia
Dr. Ir. Bondan T. Sofyan, M.Si, Universitas Indonesia
Prof. C. F. Leung, National University of Singapore
Prof. Chit Chiow Andy T., Ph.D, Chiba University, Japan
Prof. Dr. Ir. Djamasri, Gadjah Mada University, Indonesia
Prof. Dr. Ir. Djoko Hartanto, M.Sc., Universitas Indonesia
Prof. Efstratios Nikolaidis, Ph.D., University of Toledo, USA
Farizal Ph.D, Universitas Indonesia
Dr. Ir. Feri Yusivar, Universitas Indonesia
Prof. Dr. Freddy Boey, Nanyang Technological University, Singapore
Prof. Dr. Ghassan Aouad, University of Salford, United Kingdom
Prof. Ir. Gunawan Tjahjono, M.Arch., Ph.D, Universitas Indonesia
Prof. Dr. Hamzah Abdul Rahman, University of Malaya, Malaysia
Dr. Heri Hermansyah, ST., M.Eng., Universitas Indonesia
Ir. Isti Surjandari, Ph.D., Universitas Indonesia
Prof. Dr. James Hol-Kennedy, University of Hawaii, USA
Prof. Josaphat Tetuko Sri Sumantyo, Ph.D, Chiba University, Japan
Prof. Katsuhiko Takahashi, Hiroshima University, Japan
Prof. Lai Chee Kian, National University of Singapore
Prof. Dr. Low Shui Pheng, National University of Singapore
Dr. M. A. Berawi, Universitas Indonesia
Prof. Dr. M. Misbahul Amin, University Malaysia Perlis
Prof. Dr. Ir. Mohammad Nasikin, M.Eng, Universitas Indonesia
Dr. Monto H. Kumagai, XtremeSignPost.Inc., Davis, California, USA
Dr.-Ing. Ir. Nandy Setiadi Djaja Putra, Universitas Indonesia
Dr. Ir. R. Danardono A. Sumarsono, DEA.PE., Universitas Indonesia
Dr. Roy Woodhead, EDS Consulting Service, United Kingdom
Prof. Tae Jo o, Yeungnam University, South Korea
Prof. Dr. Ir. Tommy Ilyas, M.Eng., Universitas Indonesia
Toha Saleh, ST., M.Sc., Universitas Indonesia
Ir. Warjito, M.Sc., Ph.D., Universitas Indonesia
Yulia Nurliani Lukito, ST., Universitas Indonesia

TABLE OF CONTENTS

PREFACE

SYMPOSIUM PAPER

A. SPECIAL ISSUES ON RFID

B. SPECIAL ISSUES ON GREEN INFRASTRUCTURE FOR SUSTAINABLE DEVELOPMENT

C. SYMPOSIUM ON TROPICAL ECO-URBANISM

D. SYMPOSIUM IN ENERGY CONSERVATION TROUGH EFFICIENCY IN DESIGN AND MANUFACTURING

E. SYMPOSIUM ON ADVANCED MATERIALS AND PROCESSING

F. SYMPOSIUM ON INDUSTRIAL ENGINEERING APPROACH FOR PRODUCTIVITY

Special Issues on Radio Frequencies Identification (RFID)
as a Bridge Between Computing and Telecommunication

Symposium A

SPACE TECHNOLOGY

MECHANICAL, ELECTRICAL, ENGINEERING & MANUFACTURING

Vision

"To become competitive engineering and manufacture company that prioritize service and products with supports from strong resources"

Mission

"Creating value for customers through management based on esteem for human dignity"

JL. Damar Delta Silicon II Blok F1-03, Lippo Cikarang, Cibatu
Cikarang Selatan – Bekasi - Indonesia
Telp : (021) 89902215 (Hunting), Fax: (021) 89902223
http://spacetech.co.id

Electrical Characterizations of Electroosmosis in Prototypes of Straight Microchannels

A. Kusumadjaja[1], G.O.F. Parikesit[2], H.P. Uranus[1,3]

[1]*Department of Electrical Engineering,*
Universitas Pelita Harapan, Lippo Karawaci,
Tangerang 15811, Indonesia.
email: arts_works@yahoo.com

[2]*Laboratory for Aero and Hydrodynamics,*
Delft University of Technology, Leeghwaterstraat
21 - 2628 CA, Delft, The Netherlands.
email: G.O.F.Parikesit@tudelft.nl

[3]*Graduate Program in Electrical Engineering,*
Universitas Pelita Harapan, Wisma Slipi,
Jl. Let. Jend. S. Parman Kav. 12, Jakarta 11480, Indonesia.
e-mail: h.p.uranus@alumnus.utwente.nl

ABSTRACT

The development in the field of health care has been a major concern nowadays. Lab-on-a-chip (LOC) is one form of realization of the progress. LOC has most of the ability that a laboratory actually can do, and packaged in a smaller scale. Such size gives a number of advantages and challenges. With changes of scale, factors such as characteristics of the fluid flow are also changed. This paper reports experimental study on one of phenomena in LOC systems, namely electro-osmosis (i.e. electrically-driven fluid transport) in micro-scale straight channels. The electrical characterization of this phenomenon is performed by measuring the electrical current (which is proportional to the speed of electro-osmotic flow, EOF) of various electrolyte concentrations and length of channels of microfluidic prototype chips. The chips are customarily made by using plates of PMMA that sandwich a layer of double-sided sticky tape (with layer thickness in the order of ~100 microns), which thickness determines the micro-scale channel depth. Several parameters that we investigated in order to find the relevance with the EOF velocity in the channel are electrolyte concentration, channel length, and source's voltage.

Keywords

electrical characterization, electro-osmosis, straight microchannel, microfluidics, pulsed dc source

1. INTRODUCTION

Research on process in micrometer and nanometer scale are still new and growing. This area is very prospective because there is a big chance to have innovative breakthroughs. On this scale, technology allows increased flexibility and capability beyond the macro scale, and when combined with science, will bear a new breakthrough in fields like health care. One example is Lab-on-a-chip (LOC), which is in the areas of micro-and nano-fluidic, with applications in the field of biomedical.

LOC is a technology of the future, as it combines an actual ability of a laboratory with the portability and a quick analysis features. As in a laboratory on general macro scale, LOC is designed to analyze the liquid, ion, and other particles. The only difference lies on the scale that the analysis is conducted where the portability feature can be employed.

In its development, LOC incorporates many disciplines. To learn its nature, characteristics, and how fluid works in micro-channels or even nano-scale, a physicists are needed. When it involves substances or a mixture of chemistries needed in the analysis, it is a biologist or chemist area of expertise. Manufacturing techniques of chips with micro or nano-channels, are area of expertise of micro-technology engineer. Sensor design and supporting instrumentation requires an electrical engineer's expertise.

This complexity makes LOC interesting to be studied. Therefore, study on the basic principles of controlling nanoliter liquid flow is indispensable. One way of controlling fluid flow in microchannels is using electronic methods through the electro-osmosis phenomenon.

2. ELECTROOSMOSIS

In LOC, there are two types commonly used actuator, namely hydrodynamics which utilizes pressure in controlling flow of fluids, and electrokinetics that utilizes the difference in voltage to control the flow of fluids. In this paper, we are experimenting on one of the electrokinetic phenomena known as the electro-osmosis [4].

Electro-osmosis is the flow of fluids, relative to the stationary surface, influenced by the electric field. There are two factors that influencing the electro-osmosis: (1) electric

double layer or EDL, and (2) external electric field applied across the channel.

2.1 Electric double layer

EDL is composed of two parts, namely a fixed layer of counter-ion (Stern layer) and a moveable layer (Gouy-Chapman layer). These layers contribute to the flow when combined with external electric field applied on the channel because of the attract and repel situation between ions. The EDL is illustrated in Fig. 1.

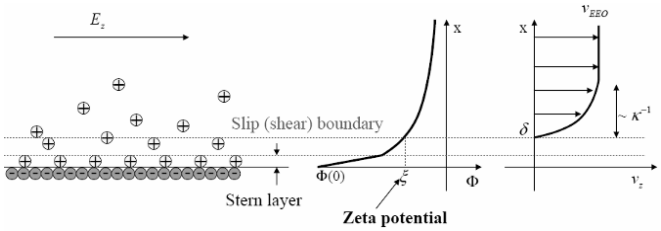

Figure 1. Electric Double Layer (EDL) [1].

2.2 Zeta potential

In order to find electro-osmosis speed of flow, we need to find potential differences between its fixed layer of counter-ion (Stern layer) and moveable layer (Gouy-Chapman layer). The electrical potential on the shear plane also called zeta potential (ζ).

For most applications of electro-osmosis, scale of ζ that can work well for various type of concentration is ζ ~ pC or equal to ζ ~ - log C, where C is the concentration of the substrate [2]. The relationship between zeta potential with the substrate concentration for composition relevant to our experiment can be represented by following equation [2],

$$\zeta = 15\,(-\log(C)). \qquad (1)$$

which is illustrated in Fig. 2.

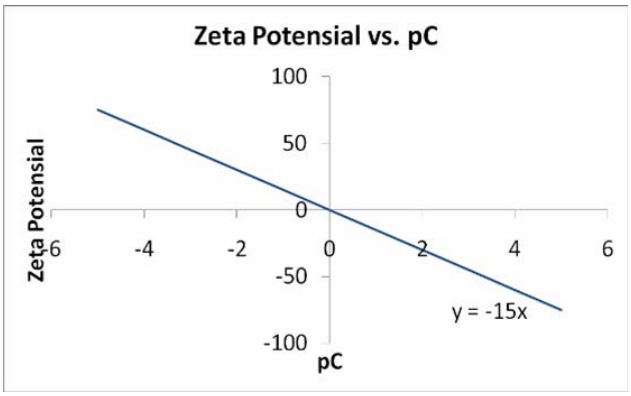

Figure 2. A plot of equation 1, which is describe the relationship between Zeta potential vs pC [2].

2.3 Flow speed

The electro-osmosis flow speed can be found by using [3]:

$$\mathbf{v}_{EO}(x,y,z) = (\varepsilon\varepsilon_0 / \mu)\,(\psi(z) - \zeta)\,\mathbf{E} \qquad (2)$$

with,

$$\partial^2\psi(z) / \partial z^2 = (2n_\infty Ze) / (\varepsilon\varepsilon_0)\,\sinh\,(Ze\,\psi(z) / k_bT) \qquad (3)$$

where **E** is the electrical field, induced by the electric voltage difference between the ends of the channel.

In special cases, where the width of the EDL is much less than the channel width, the value of the average flow speed in every point on the channel can be expressed with the Helmholtz-Smoluchowski formula below.

$$\mathbf{v}_{EO}(x,y) = (\varepsilon\varepsilon_0 / \mu)\,(-\zeta)\,\mathbf{E}(x,y) \qquad (4)$$

3. DESIGN & CIRCUITS

Our work consists of 3 parts, i.e. (1) fabrication of the prototype chips (2) the DC characterization circuit design, and (3) the pulsating circuit design.

3.1 Chip fabrication

The fabrication of these chips does not require sophisticated technology. It can be done with simple tools. Selected materials, which are required in the fabrication of the chips, are also easily obtained and inexpensive. They are commercial PMMA board, known as acrylic, and commercial double-sided sticky tape that can be found in any bookstore.

PMMA works as the foundation and cover for the channel. The wall of the channel is made of double-sided sticky tape. The double-sided tape does not have to have any special specification, except the width of the tape should be adjusted to the width of acrylic. In this experiment, we were using 1" wide double-sided sticky tape with thickness about 0.01 cm and a 4 cm x 6 cm x 0.2 cm PMMA board. Fig 3 shows the schematic cross-section of the chips. Fig. 4 shows the fabricated chips.

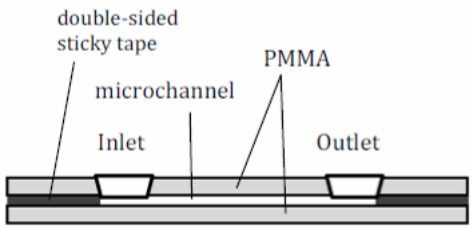

Figure 3. The customarily microfluidic chip made by using double-sided sticky tape sandwiched between two chips of PMMA fabricated in this work. The dimension of the channel inside the chip is 5 mm wide and has varied length from 10-20mm. Channel thickness is identical with the thickness of the double-sided sticky tape (±100 μm).

Figure 4. Photographs of the customarily microfluidic chips made by using double-sided sticky tape that are used in this experiment.

3.2 DC circuit

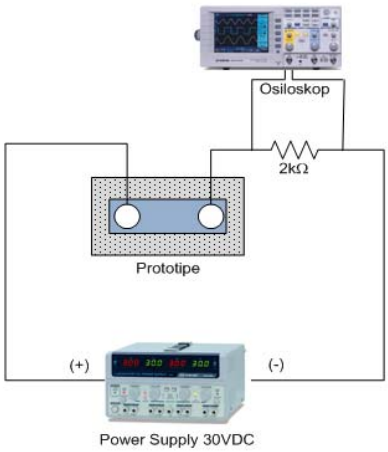

Figure 5. The diagram of the measurement setup used for electrical characterization of the prototype microfluidic chip. The chip and the 2 kΩ resistor are placed in series.

With NaCl solutions in the channel, the electro-osmotic flow reading is done by measuring the voltage on a resistor which can be converted into current flow by dividing its value with resistor's value (2000 Ohm). Such current flow is proportional to the speed of the electro-osmosis flow. Fig. 5 shows the measurement setup diagram while Table 1 shows the parameters for DC excitation experiments.

Table 1. DC excitation setup

Voltage source	30 VDC
NaCl Concentration	1M, 1.5M, 2M, 2.5M
Channel	Lenght 1cm, 1.2cm, 1.5cm, 1.8cm, 2cm Wide 0.5cm Height 0.005cm - 0.01cm

3.3 Pulsating circuit

Table 2. Pulsating excitation setup

Voltage source	Series of 30 VDC pulse
NaCl Concentration	1M, 1.5M, 2M, 2.5M
Channel	Lenght 1cm, 1.2cm, 1.5cm, 1.8cm, 2cm Wide 0.5cm Height 0.005cm - 0.01cm

In order to generate one second of on and off pulse width, we use electronic switch controlled by a microcontroller. The uses of microcontroller ease any modification which might be required for future experiments. We also use opto-couplers for the circuit to separate electrically between low voltage part and high voltage part of the circuit. Fig. 6 shows the schematic diagram of the pulsating circuit.

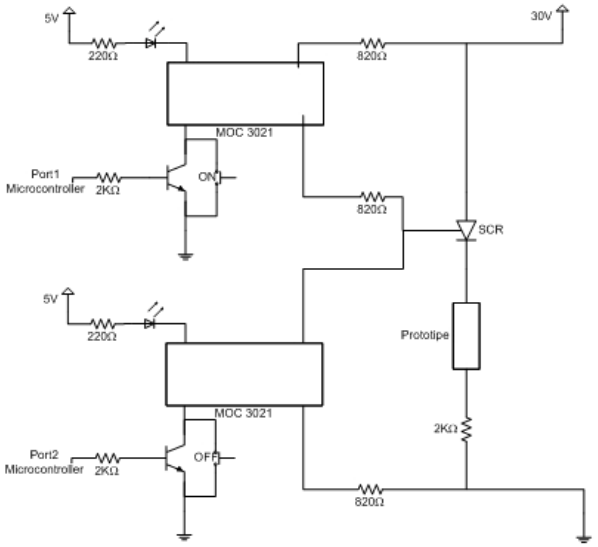

Figure 6. The electronic switch used for pulse excitation.

4. EXPERIMENTAL RESULT

4.1 Effect of Electrolyte Concentration

Using equation (4), we computed theoretical U_{EOF} to be expected in the channel. According to the concentration for each channel length, we grouped each section and computed theirs average. The results are shown in Table 3.

Table 3. U_{EOF} vs Concentration

	1M	1.5M	2M	2.5M
1.0cm	0	6.31113E-06	1.07935E-05	1.42718E-05
1.2cm	0	5.25928E-06	8.99456E-06	1.18931E-05
1.5cm	0	4.20742E-06	7.19565E-06	9.51451E-06
1.8cm	0	3.50618E-06	5.99637E-06	7.92876E-06
2.0cm	0	3.15557E-06	5.39673E-06	7.13588E-06
Average	**0**	**4.48792E-06**	**7.67536E-06**	**1.01488E-05**

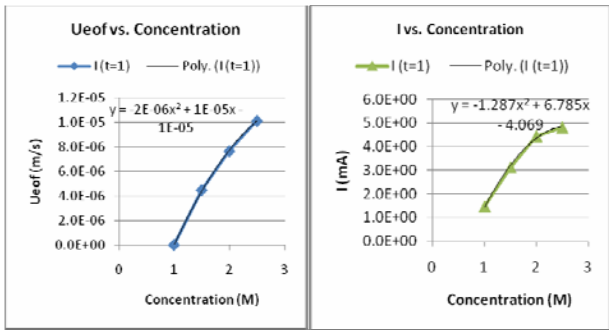

Figure 7. Theoretically computed graph of U_{EOF} vs. concentration (left) and graph of electrical current vs.

concentration derived from the experimental result (right) showing agreement in characteristic and trend.

Then, by plotting out the data, we can see that the trends of the theoretical and measured results agree well as shown in Fig. 7.

4.2 Effect of Channel length

Using the previously computed U_{EOF} data, we can plot another graph by grouping data into series of concentration which current is changing for variety of lengths. Figure 8 shows that channel length contributes to the shifting in the value of electrical field either in the experimental result or theoretical prediction.

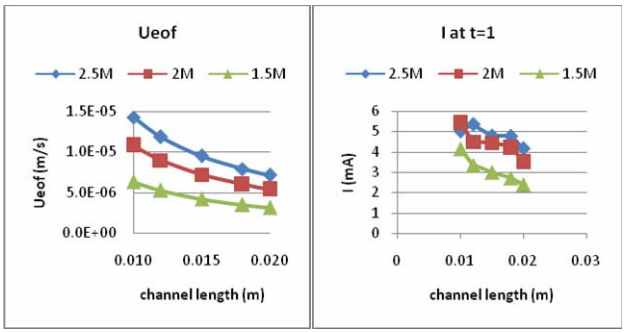

Figure 8. Theoretically computed graph of U_{EOF} vs. concentration (left) and graph of electrical current vs. concentration derived from the experimental result (right) showing agreement in characteristic and trend.

4.3 Voltage source

In this section, we observed the effect of using different kind of voltage source, by pulsating the 30VDC with 0.5 Hz frequency.

Using a digital oscilloscope, reading of voltage drop at the 2 kΩ resistor is noted every minute or when any changes occurred on the curve. When changes occur in the same minute, we compute average value of the data by summarizing the data from each screen capture.

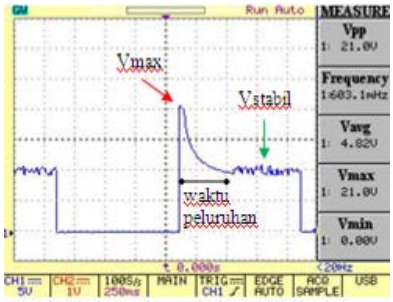

Figure 9. The 34th screen capture of experiment with 1.5M NaCl on a 10 mm channel length. Vmax is the peak value of the graph and Vstable is the value when the curve slope ~ 0.

When compared with the results of the DC excitation, different trend occurred. On DC experiment, we have velocity of the electro-osmosis flow being proportional to the concentration. On pulsating voltage source, there is slight difference, i.e. for concentration more than 2M, the velocity of the electro-osmosis flow is no longer proportional with the NaCl concentration.

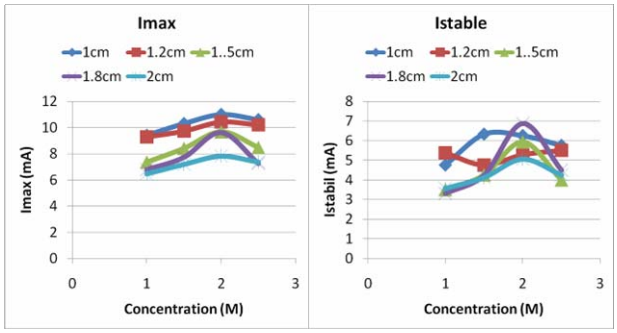

Figure 10. Graph of Imax vs. concentration (left) and Istable vs. concentration, showing anomalies on Imax ≥2M and random curve on Istable caused by pulsating voltage source.

The pulse experiments reveal unusual dynamic behavior of electrolyte flow, which still need further studies to understand it.

4.4 Concentration and saturation time

We also measured how much time is needed to reach stable condition from a peak. The results on various concentration show that all resemble a parabolic curve that looked like a "U"-shape. Higher concentration makes the minimum point of the parabolic curve shifted away from the y-axis, and the distance between peaks are getting farther apart, making it a larger curve as shown in Fig. 11.

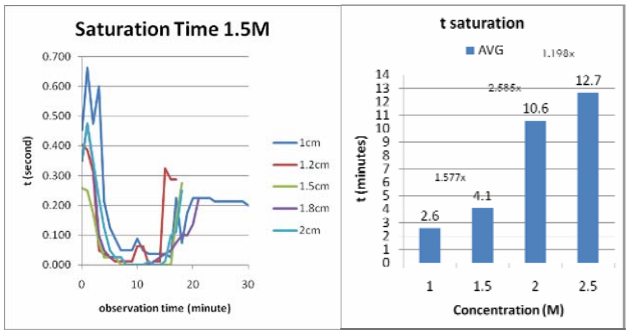

Figure 11. Track of time needed for 1.5M NaCl to became saturated (left) and average saturation time needed for each concentration (right) which are computed by averaging all value of the same concentrate.

4.5 Direction of electro-osmosis flow

During the experiment, observations on the electro-osmosis velocity are limited to visual observations. The direction of the electro-osmosis flow can be seen by observing a yellow color that appears in the inlet and outlet.

The color always occurs in every experiment. In the first minute, the yellow color appears on the negative electrode. It slowly moves toward the positive electrode and turns into green when comes near at the positive electrode.

ISSN 114-1284

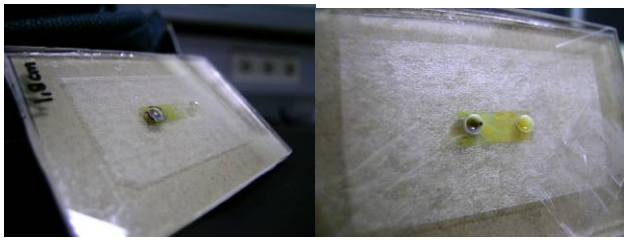

Figure 12. Photograph of the unexpectedly appeared yellow color inside the channel. The yellow color moves from cathode to anode.

This movement of the yellow color can be explained using equation 4 where the direction of flow is influenced by the values of the zeta potential and the electric field. In general, the direction of electro-osmosis flow is on the same direction of the electric field applied. Flow direction changed if the value of zeta potential is not negative. By using substance with concentration greater than 1M, the direction of electro-osmosis flow is contrary to the electric field. The relationship between zeta potential and the concentration being used can be found in equation 1. In this way, the electro-osmosis flow will be reversed, where fluids move from negative to positive electrodes.

5. CONCLUSION

From this work, we conclude that:

1. I (=Ueof) are proportional to the electrolyte concentration.
2. The use of pulsed voltage source affects the current reading. Observations through monitoring I_{max} and I_{stable}, show differences in trends.
3. Increased concentration also affects the time the current needed to reach saturation conditions.
4. In pulse excitation, the increased of concentration produces shifting of peak of the curve away from y-axis. This means that the time required to reach saturation for higher concentration will be longer than before.
5. Electro-osmosis velocity occured in the channel, marked with trace of yellow solution from the negative electrode to the positive.

ACKNOWLEDGMENT

This work is supported by Universitas Pelita Harapan through project P-003-FTI/IV/2009.

REFERENCES

[1] Han, Jongyoon. *Lecture #8 : Today's outline*. [pdf] 2007.
[2] Kirby, Brian J. Zeta potential of microfluidic substrates: Part 2. *Electrophoresis.* Livermore : s.n., 2004, hal. 203-213.
[3] Parikesit, Gea Oswah Fatah. *Nanofluidic electrokinetics.* Enschede : Gildeprint Drukkerijen B.V., 2008.
[4] Devasenathipathy, S. dan Santiago, J.G. *Electrokinetic Flow Diagnostics.* Stanford : Stanford University, 2003.

Dielectric Loaded Cylindrical Cavity Resonator

Aditya Inzani W, Muhamad Tajudin, Fitri Yuli Zulkifli, Eko Tjipto Rahardjo

Antenna Propagation and Microwave Research Group (AMRG)
Center for Information and Communication Engineering Research (CICER)
Electrical Engineering Department
Faculty of Engineering
University of Indonesia, Depok 16424
Tel: (021) 7270011 ext 51. Fax: (021) 7270077

ABSTRACT

In this paper, cavity filter is discussed due to advantages such as narrow bandwidth, better slope, and can be used for high power consumption application without changing or modifying the existing circuit. To decrease the size of the cavity filter, cylindrical design for the cavity & type of dielectric materials plays an important role. Meanwhile, in designing the cavity filter, the performance of the filter depends on several parameters. In this paper only dielectric constant and the dimension of the dielectric material inside the cavity will be discussed.

The cavity filter is designed by using Ansoft HFSS v.11 which uses the finite element computational method. The simulation results show that the dielectric constant and dimension of the dielectric material inside the cavity influence the resonant frequency in the cylindrical cavity filter.

Keywords
cylindrical cavity filter, dielectric material, resonant frequency

1. INTRODUCTION

Wireless communication is widely used in Indonesia due to its high mobility, can be easily accessed by everyone and without geography limitation. However, there is one major disadvantage which occurs to wireless communication namely interference.

Interference is caused by nearby frequencies from another system, which interferes with the resonant frequency of the used system. To overcome this interference, filter is used.

Microwave resonators are used in a variety of applications, including filters, oscillators, frequency meters, and tuned amplifiers. Resonators can also be constructed from closed sections of waveguide, which should not be surprising since waveguide are a type of transmission lines. Electric and magnetic energy is stored within the cavity, and power can be dissipated in the metallic walls of the cavity as well as in the dielectric filling the cavity [1].

Dielectric resonator is a term used by Richmeyer, who showed that a dielectric ring could confine high frequency electromagnetic waves and thus form a resonator [2]. In general a dielectric resonator is a disk of ceramic material with dielectric constant sufficiently high to contain an electromagnetic standing wave. A dielectric of this geometry will support many resonant modes. The most commonly used mode is the $TE_{01\delta}$ because it is a fundamental mode and has the highest unloaded Q [3]. Such dielectric resonators are similar in principal to the rectangular or cylindrical cavities. High dielectric constant of the resonator ensures that most of the fields are contained within the dielectric but unlike metallic cavities, there are some field fringing or leakage from the sides and ends of the dielectric resonator, such a resonator is generally smaller in size, and weight than an equivalent metallic cavity, and can very easily be incorporated into microwave integrated circuit and coupled to planar transmission lines [4].

This paper discusses the effect of the dimension and the dielectric constant (ε_r) from several dielectric materials inside cylindrical cavity resonator compared to the resonant frequency of the cylindrical cavity resonator with dielectric inside.

2. RESONATOR DESIGN

Figure 1 shows the geometry of a cylindrical cavity.

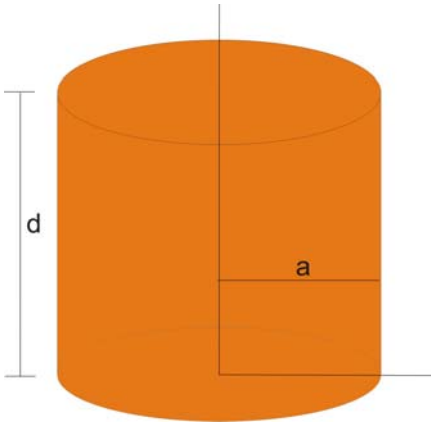

Figure 1: Cylindrical Cavity

The transverse electric fields (E_ρ, E_Φ) of the TE_{nm} or TM_{nm} circular waveguide mode can be written as

$$\bar{E}_t(\rho,\Phi,z) = \bar{e}(\rho,\Phi)\left[A^+ e^{-j\beta_{nm}z} + A^- e^{j\beta_{nm}z}\right] \quad (1)$$

where $\bar{e}(\rho,\Phi)$ represents the transverse variation of the mode, and A^+ and A^- are the arbitrary amplitudes of the forward and backward traveling waves, and the resonant frequency of the TE_{nml} mode is,

$$f_{nml} = \frac{c}{2\pi\sqrt{\mu_r\varepsilon_r}}\sqrt{\left(\frac{p'_{nm}}{a}\right)^2 + \left(\frac{l\pi}{d}\right)^2} \quad (2)$$

where
l = waveguide length
c = light velocity
ε_r = relative permittivity
μ_r = relative permeability
P'_{nm} = root from derivatives of Bessel function

Circular cylindrical dielectric resonators have been widely used because of their simple geometry, commercial availability, and easier to analyze. The geometry of the cylindrical dielectric resonator is shown in Fig. 2. The dielectric resonator is considered as a short length, d, and diameter of r, of dielectric waveguide open at both ends.

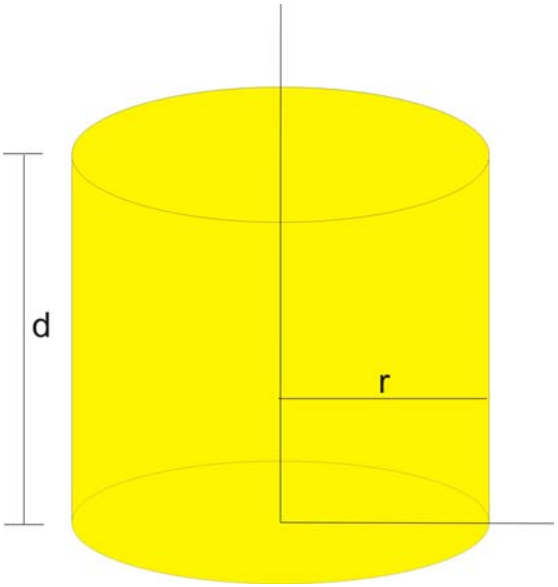

Figure 2: Dielectric Resonator

Because of the high permittivity of the resonator, the propagation along z-axis can occur inside the dielectric at the resonant frequency, but the fields will be cut off (evanescent) in the air region around the dielectric. Thus, the equivalent circuit of the resonator looks like a length of transmission lines terminated in pure reactive loads at both ends [4].

2.1 Cylindrical Cavity Resonator Design with Ansoft HFSS 11

From equations (2), with a and d respectively 50mm and 100mm, as shown in Fig. 3, the resonant frequency is obtained at 2.326 GHz using HFSSv.11 with Eigenmode solutions[5]. Eigenmodes are the resonances of the structure. The eigenmode solver finds the resonant frequencies of the structure and the fields at those resonant frequencies as from equation (3):

$$[S]x + k_o^2[T]x = b \quad (3)$$

Where S and T are matrices that depend on the geometry and the mesh, $\boldsymbol{x}$ is the electric field solution, k_o is the free-space wave number and b is the value of the source defined for the problem.

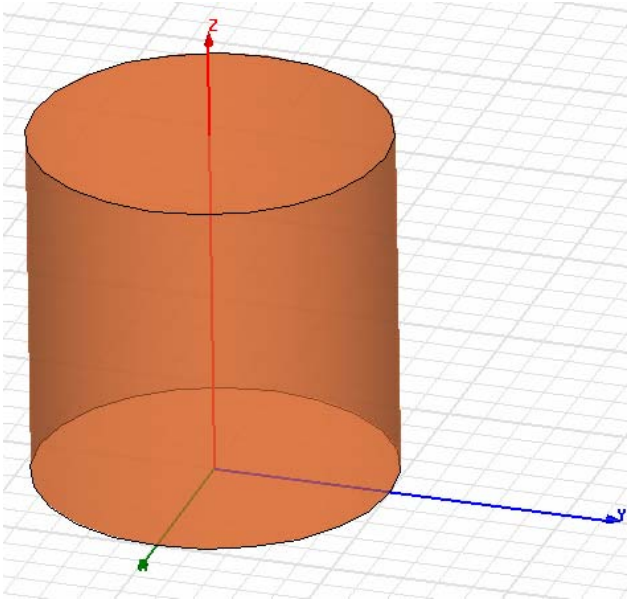

Figure 3: Cavity Resonator Design using HFSSv.11

However, in order to find the resonances of the structure, the eigenmode solver sets b to zero, and solves the equation as in equation (4):

$$[S]x + k_o^2[T]x = 0 \quad (4)$$

For the sets of (k_o,$\boldsymbol{x}$), there are one ko for every $\boldsymbol{x}$. The variable x is still the electric field solution, and k_o is the free space wave number corresponding to that mode. The wave number ko is related to the frequency of the resonant modes through the following equation (5):

$$f = \frac{k_o c}{2\pi} \quad (5)$$

This cylindrical cavity resonator design will be used for the next design of cavity resonator with dielectric material inside.

2.2 Cylindrical Cavity Resonator with Dielectric Material Inside Design with Ansoft HFSS 11

With the cylindrical cavity resonator shown in Fig. 3, the dielectric material design is placed inside the cavity, as shown in Fig. 4.

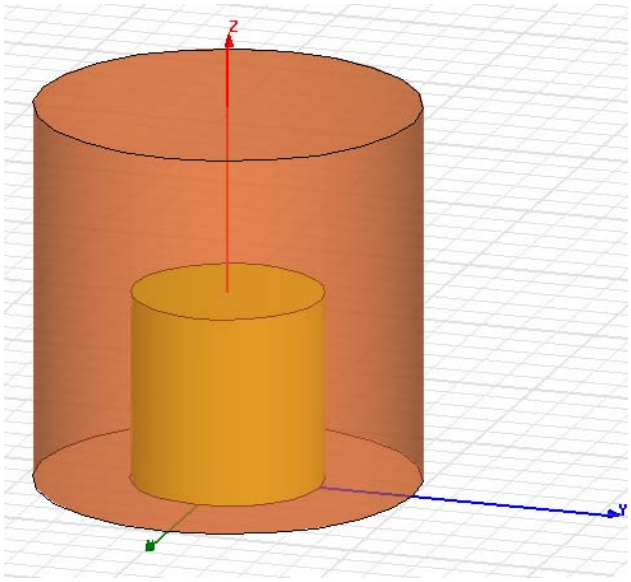

Figure 4: Dielectric placed inside the cavity

The dielectric material which is placed inside the cavity has the radius of r =25mm. In this paper, variation of height and dielectric materials are varied to see the impact towards the dimension of the resonator.

3. RESULT AND DISCUSSION

Simulation results were obtained from the variation of height (d) from 10mm to 100mm, and also from different kinds of dielectric materials. The dielectric materials chosen were Teflon (ε_r = 2.1), porcelain (ε_r = 5.7), Taconic CER-10 (ε_r = 10), and diamond (ε_r =16.5).

Figure 5 shows the influence of using the dielectric material Teflon to the resonator. The resonant frequency of the cavity resonator after placing dielectric material Teflon (εr = 2.1) inside, tends to decrease as the height increases. With the height 10 mm, the resonant frequency shows at 2.26 GHz

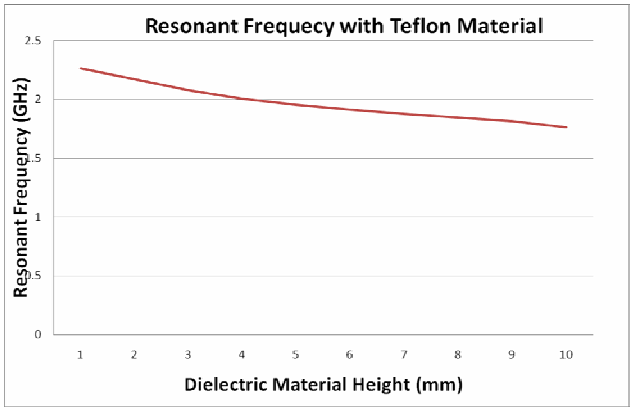

Figure 5: Graphic of Resonant frequency with Teflon material

The next simulation result is placing a higher dielectric material than Teflon, which is porcelain. The simulation result is shown in Figure 6 and shows a lower resonant frequency for the same height compare to Teflon. For the height d = 10 mm, the resonant frequency is 2.17 GHz.

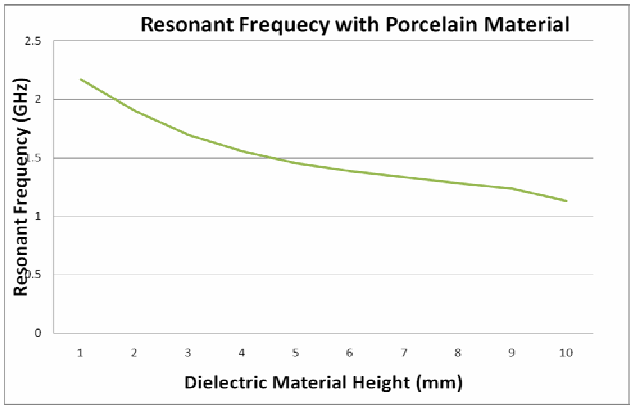

Figure 6: Graphic of Resonant frequency with porcelain material

The next dielectric material used is Taconic CER-10 with ε_r = 10 as the dielectric material. The simulation result depicted in Fig.7 shows that the resonant frequency of the cavity resonator became to 2.12117 GHz at d = 10 mm and shows a lower resonant frequency compared to Teflon and porcelain.

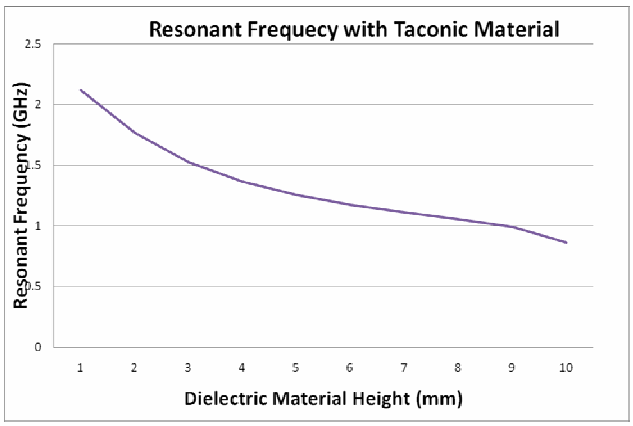

Figure 7: Graphic of Resonant frequency with Taconic material

The last material compared is diamond. Diamond (ε_r =16.5) has higher dielectric constant compared to the other materials. The simulation result as in Fig. 8 shows that the resonant frequency is lower than the other dielectric material which has smaller dielectric constant. The diamond shows at height 10 mm has a resonant frequency at 2.05 GHz.

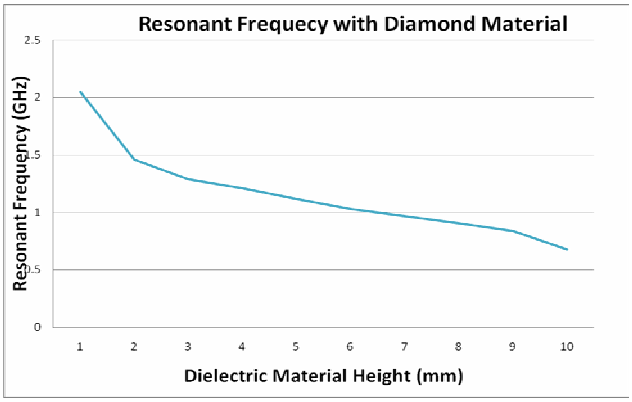

Figure 9: Resonant frequency with Diamond material

The simulation is than varied from height 10 mm to 100 mm and the result is shown in Table 1 and in Fig. 8. Before the dielectric is placed inside the cavity, the resonant frequency is 2.326 GHz. After placing the dielectric, the resonant frequency tends to decrease.

Table 1: Simulation result

d (mm)	*Teflon (GHz)*	*Porcelain (GHz)*	*Taconic CER-10 (GHz)*	*Diamond (GHz)*
10	2.26641	2.17048	2.12117	2.05045
20	2.17355	1.90001	1.76722	1.45818
30	2.08127	1.69362	1.52436	1.28741
40	2.01008	1.55578	1.36726	1.20981
50	1.95784	1.45319	1.25765	1.12059
60	1.91470	1.38467	1.17384	1.02978
70	1.88010	1.33057	1.11158	0.966764
80	1.84810	1.28305	1.05542	0.904497
90	1.81465	1.23217	0.996501	0.838119
100	1.76470	1.13055	0.864752	0.677936

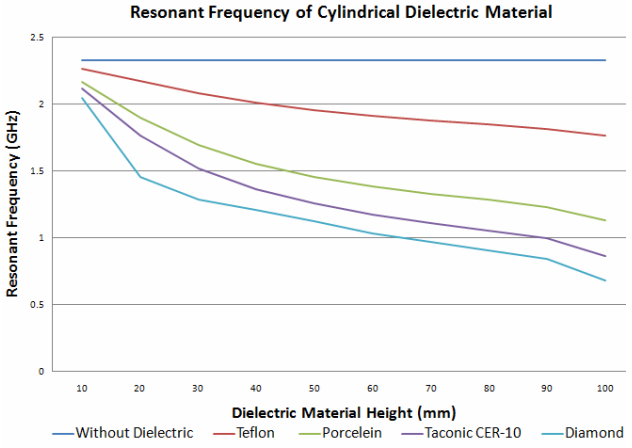

Figure 8: Resonant frequency of Cylindrical Resonator Cavity

The decrease of resonant frequency caused of different dielectric materials, also occurs for other dielectric materials. The higher the dielectric constant (εr) is, than the lower the resonant frequency decreases.

As shown in Table 1, using Diamond for the height of 100 mm results to a resonant frequency of 0.67 GHz compared to Teflon, Porcelain and Taconic CER-10 of 1.76 GHz, 1.13 GHz and 0.86 GHz, respectively.

This result confirms with the equation (2), which shows that high dielectric constant is very important for miniaturization of the resonator's size. The resonator is reduced by a factor of $\sqrt{\varepsilon_r}$. The dielectric constant must be sufficiently high for the operating frequency to provide enough miniaturization.

4. CONCLUSION

To design microwave resonator with low resonant frequency, dielectric material must be added inside it, to miniaturize the cavity resonator.

Simulation results show, that the use of dielectric material can decrease resonant frequency. Higher dielectric constant and dimension will influence greatly to the decrease of the resonant frequency.

REFERENCES

[1] Pozar , David M, *Microwave Engineering*, John Wiley & Sons, 1998, ch. 6, pp. 313.
[2] Richmyer, R.D., *Dielectric Resonator*, J. Appl. Phys., Vol. 10,pp.391-398, June 1939.
[3] Handbook of low and high dielectric constant materials and their application volume 2, edited by H.S.Nalwa , Academic Press, 1999. Chapter 10 pp. 524
[4] Pozar , David M, *Microwave Engineering*, John Wiley & Sons, 1998, ch. 6, pp. 323-324.
[5] Lioubtchenko ,Dmitri, *Mili-Meter Waveguide*. KLUWER ACADEMIC PUBLISHERS, 2003, pp. 30-35.

Estimation Analysis of Measurement Error in Power System

Adyson Utina

Lecturer,Electrical Engineering Dept,Engineering Fac.,University of Haluoleo
Ali Malaka Street 10,Anduonohu,Kendari,Southeast Sulawesi,Indonesia
Tel: +62 021 32845648 Mobile: +62 81341507884/ +62 85880509225 .
email: ady.utina@gmail.com

ABSTRACT

Many problems are encountered in monitoring of power system. These problems come primarily from the nature of the measurement devices and from communications problems in transmitting the measured values back to operation control center. These like problems will be subject to errors. Further more, the errors can cause misinterpretation by those reading the measured values. For these reasons that power systems state estimation techniques have been developed. This paper shows an analysis of state estimation in power system to minimize small random errors in measurement.

Keywords:
analysis,measurement,estimation,power, system

1. INTRODUCTION

State estimation (SE)[2][3] is the process of assigning a value to an unknown system state variable based on measurement from that system or SE can be defined as a statistical procedure for deriving, from a set of system measurements, a "*best*" estimate of the system state[2][3]. In the field of power system, the objective is to provide a reliable and consistent data base for security monitoring, contingency analysis and system control. To meet the above objectives, SE is required to :

- Produce a "best" estimate of the state variable
- Detect, identify and suppress gross measurement errors
- Produce an estimate of non-metered or lost data points

A major factor in the success of producing a good estimate of the system state is the ability to handle errors that exist in the input to the estimation process[1][4][5]. Such errors may be classified as :

- Measurement noise
- Gross measurement errors
- Topological errors
- Model parameter errors

Measurement noise is handled inherently by the filtering process of the estimation algorithm itself. Gross measurement errors are detected and identified through suitable hypothesis testing on the measurement residuals. The identified gross errors are then suppressed from the estimation procedure. The models of the power system components used are taken as static with their reliability and accuracy usually established by extensive analysis prior to their use.

2.STATE ESTIMATION IN POWER SYSTEM

Centralized automatic control of power system dispatch requires knowledge of the steady-state performance of the system[1][2][3]. This performance must be inferred from system measurements communicated to the control center. If enough measurements could be obtained continuously, accurately, and reliably, this would provide all the information needed for control. However, a perfect data acquisition system is often technically and economically infeasible so that the control center must depend on measurements that are incomplete, delayed, inaccurate, and unreliable. The function of state estimator is to process whatever information is available and to produce the best possible estimate of the true state of the system.

2.1 Weighted Least Square Estimation (WLS)[2][3][5]

The development of the notions of state estimation may proceed along several lines, depending on statistical criterion selected. Of the many criteria that have been examined and used in various applications, WLS criterion is perhaps the most commonly used.

In WLS, the objective is to minimize the sum of the squares of the weighted deviations of the estimated measurements from the actual measurements.
The measurement state is related to the true state of the system by the equation

$$z^{meas} = f(x) + e$$

where :

z^{meas} = measurement vector
$f(x)$ = network model relating the state variable to the measurement set
x = state variable vector
e = measurement error vector

The WLS estimation procedure is then the minimization of the function

$$J(x) = \left[z^{meas} - f(x)\right]^T \left[R^{-1}\right] \left[z^{meas} - f(x)\right]$$

where :

$$[R] = \begin{bmatrix} \sigma_1^2 & & & \\ & \sigma_2^2 & & \\ & & \ddots & \\ & & & \sigma_{Nm}^2 \end{bmatrix}$$

= the diagonal matrix of measurement

$J(x)$ = measurement residual

Table Estimation Formula

Case	Description	Solution
Ns < Nm	over determined	$x^{est} = [[H]^T[R^{-1}][H]]^{-1}$
Ns = Nm	completely determined	$x^{est} = [H]^{-1} z^{meas}$
Ns > Nm	under determined	$x^{est} = [H]^T[[H][H]^T]^{-1} z^{meas}$

2.2 Bad Data Detection and Identification[1][4][5]

The detection of bad data is posed as a statistical testing problem of the following form :
H0 : For the given confidence level, no bad exists
H1 : Reject H0. For the given confidence level, error exist.

Chi-Squared Distribution
H0 : The overall estimate is good
H1 : The overall estimate is not good
Accept H0 if $J(x) < \chi^2(K)\ or\ J(x) < t_j$, reject otherwise

K = degrees of freedom of chi-squared distribution
K = Nm - Ns
where :
Nm = number of measurement
Ns = number of states = (2n-1)
n = number of buses in the network

Residual Test
H0 : a data point is good
H1 : a data point is not good
Accept H0 if
$y_i / \sigma_{y_i} < y_i^{norm}\ or\ (z - f)/\sigma_{y_i} < y_i^{norm}$
Reject H0 (Accept H1) otherwise

The form of the residual test above is referred to as the Weighted Residual test. A different form is the Normalized Residual test which has more discriminating properties in identifying bad data for low redundancy systems.

For a given estimate, the above tests are performed. The J(x) test evaluates the overall estimate for consistency. The residual test is used to identify individual data points which are likely to be in error. Those found to be most likely in error are suppressed and a new estimate is obtained. The process is repeated until a good estimate of the voltage magnitudes and angles of the network is produced. Present estimators stop at this point and use the estimated voltage magnitudes and angles to derive an estimate of the bus injections and branch flows in the system without regard to the possibility of topological errors. To the system operator, the only inkling to the presence of such configuration errors is suppression of measurements which appear to be good by human intuition. The effects could be disastrous, however, if the process proceeds and the estimates are used for controlling the system and performing contingency analysis.

3.DISCUSSION

An Example WLS State Estimation[2][3][4][5]

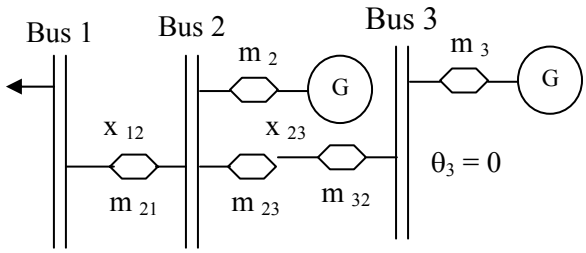

Figure 1 [2][3][4][5]

The network of example was solved using DC power flow with reactance (on 100 MVA base) as follows : x_{12} = 0,10 pu and x_{23} = 0,25 pu.
Some meter readings located as shown in Figure 1. Now investigate the case where all the meter readings have slight errors (σ = 0,01 pu). Suppose the reading obtained are :

m_3 = 102 MW
m_{32} = 98 MW
m_{23} = -135 MW
m_2 = 49 MW
m_{21} = 148 MW

The results :

$$H = \begin{bmatrix} 0 & -4 \\ 0 & 4 \\ -10 & 10 \\ -10 & 14 \\ 0 & -4 \end{bmatrix},$$

$$R = \begin{bmatrix} 10^{-4} & & & & \\ & 10^{-4} & & & \\ & & 10^{-4} & & \\ & & & 10^{-4} & \\ & & & & 10^{-4} \end{bmatrix},$$

$$z^{meas} = \begin{bmatrix} 0{,}98 \\ -1{,}35 \\ 1{,}48 \\ 0{,}49 \\ 1{,}02 \end{bmatrix}$$

$$x^{est} = \left[[H]^T [R]^{-1} [H] \right]^{-1} \left[[H]^T [R]^{-1} z^{meas} \right]$$

$$x^{est} = \begin{bmatrix} \theta_1^{est} \\ \theta_2^{est} \end{bmatrix} = \begin{bmatrix} -0{,}428071 \\ -0{,}274643 \end{bmatrix}$$

$$J(x) = \sum_{i=1}^{Nm} \frac{\left[z_i^{meas} - f_i(x) \right]^2}{\sigma_i^2} = 893{,}428571$$

(i.e., α = 0,01) will be found t_j = 11,345. Therefore, it seems reasonable to assume that there is "bad" measurement present.

Using y_i and σ_{y_i} normalized residual for each measurement can be calculated. Measurements having the largest absolute normalized residual are labeled as prime suspect. These prime suspects are removed from the state estimator calculation one at a time, starting with the measurement having the largest normalized residual. After a measurement has been removed, the state estimation calculation is rerun. The measurement with the largest absolute y_i^{norm} is the again removed and the entire procedure repeated successively until J(x) is less than t_j.[2][3][4][5]

4. CONCLUSIONS

The ability to detect and identify bad measurement is extremely valuable to a power system's operation department. Measurement devices may have been wired incorrectly or the measurement device itself may be malfunctioning so that it simply no longer gives accurate readings. The statistical theory required to understand and analyze bad measurement detection and identification is straightforward but lengthy.

The ability to detect (using the chi-squared statistic) and identify (using normalized residuals) are extremely useful features of a state estimator. Without the state estimator calculation using the system measurement data, those measurement whose values are not obviously wrong have little chance of being detected and identified. With the state estimator, the operations personnel have a greater assurance that quantities being display are not grossly in error.

REFERENCES

1. Wood, A. J.,Wollenberg, B. F., Power Generation, Operation and Control, John Wiley & Sons, Inc.,2003.
2. Larson, R. E., Tinney, W. F., Peschon, J., "State Estimation in Power System : Theory and Feasibility", IEEE Transactions on Power Apparatus and Systems, Vol.PAS-189, March 2006, 348-352.
3. Lugtu, R. L., Hackett, D. F., Liu, K. C., Might, D. D., "Power System State Estimation : Detection of Topological Errors", IEEE Transactions on Power Apparatus and Systems, Vol.PAS-99, Nov/Dec 2008.
4. Sianipar, G., "Pemantauan dan Keamanan Sistem Tenaga Listrik", ITB-Bandung, 5th June 2002.
5. Utina, Adyson, "An Approach Model Optimalization Instrument of Energy Meter on Power System",QMUL Science TechMgz London, no.pub May 2003.

=========aaauuu========

IMPACT OF RFID TO RETAIL SUPPLY CHAIN COLLABORATION

Agus Purnomo
Industrial Engineering Department
Engineering Faculty – Pasundan University Bandung 40153
e-mail : nrpsga@yahoo.com ; aguspurnomo@unpas.ac.id

ABSTRACT

The retail industry is experiencing problems in the supply chain because there is no formal collaboration between the retailer and supplier. Retailers need innovative ways to differentiate themselves in highly saturated and cluttered markets. Demand uncertainty in the supply chain, known as the "bullwhip effect," results in excess inventory and inefficiencies in the supply chain. Demand forecasts and orders are often distorted unless they are developed jointly by the partners. These factors create a need for supply-chain integration and a way to provide supporting collaborative forecasting and replenishing processes, with the goal of increasing sales and reducing inventory investments and cycle time. Collaboration can reduce waste in the supply chain, but it can also increase market responsiveness, customer satisfaction, and competitiveness among all of the members of the partnership. Radio Frequency Identification (RFID) provides a major advantage to supply chain management. Implementing supply chain collaboration along with RFID can enable retailers to achieve the best level of business performance. Retailers can expect extensive inventory and labor-cost savings. RFID has the most potential to offer in streamlining the value-chain management, but handling the amount of data by RFID in the retail industry limits the potential of RFID benefits. In this paper, we explore RFID and propose a research agenda to address a series of broad research questions related to how RFID technology: 1) is developed, adopted, and implemented by retail; 2) is used, supported, and evolved within organizations and alliances; and 3) impacts individuals, business processes, organizations, and markets.

Keywords : business value, supply chain collaboration, diffusion of innovations, radio frequency identification, technology adoption.

1. INTRODUCTION

The traditional retail supply chain consists of all the parties involved directly or indirectly in fulfilling a customer request, including manufacturers, suppliers, transporters, warehouses, retailers, and the customers themselves [9]. Each retail supply-chain entity includes functions like product development, marketing, operations, distribution, finance, and customer service. The only information that is available to the supplier is the purchase order issued by the retailer. Because there is no overall picture of the external demand that is placed by customers, inventory can increase at every level of the supply chain. The main goal of each member of the supply chain is to reduce unwanted inventory levels and increase ROI [13].

Since the early 1990s, there has been a growing understanding that supply chain management should be built around the integration of trading partners [6], the sharing of information and benefits [15] and the collaboration of organizations [16]. Supply chain collaboration as understood today has begun to take form since the mid-1990s, when the forms of collaboration multiplied [17] and new forms of information sharing extended their focus to include not only a passive exchange of information between partners, but also a more proactive approach through common planning and synchronisation of activities and business processes [21], taking advantage of innovative technologies. Anthony [3] suggests that supply chain collaboration occurs when two or more companies share the responsibility of exchanging common planning, management, execution, and performance measurement information. Bowersox et al. [8] state that firms collaborate in the sense of leveraging benefits to achieve common goals.

Supply chain collaboration in retailing and Fast Moving Consumer Goods industry (FMCG) has mainly been expressed in the form of practices such as Vendor Managed Inventory (VMI), Continuous Replenishment Program (CRP), and Collaborative Planning, Forecasting and Replenishment (CPFR). VMI is probably the first trust-based business link between suppliers and customers [6], whereby the manufacturer (supplier) has the sole responsibility for managing the customer's inventory policy, including the replenishment process, based on the variation of stock level in the customer's main warehouse or distribution center [11]. CRP moves one step ahead of VMI and handles the inventory policy not only with the variations of inventory levels at the customers' main stock-holding facility but also with sales forecasting, based on point-of-sales (POS) data from the retailer's stores [1]. Collaborative Planning, Forecasting and Replenishment (CPFR) can be seen as an evolution from VMI and CRP, addressing not only replenishment but also joint demand forecasting and promotions planning, focusing on promotions and special-line items [12]. CPFR is based on extended information sharing between retailer and supplier, including POS data, forecasts and promotion plans. Pramatari et al. [18] further suggest a new form of CPFR, named Process of Collaborative Store Ordering (PCSO), addressing the daily store replenishment process. This process is supported by special IT infrastructure (a web collaborative platform) allowing: the daily online sharing of store-level information (e.g. POS data, store assortments, stock level in the store, promotion activities, out-of-shelf alerts, etc), the sales forecasting and order generation, the online collaboration of the trading partners,

and finally the order exchange and order status tracking. Based on these short descriptions, VMI and CRP are more about efficient replenishment and supply, whereas CPFR puts more emphasis on the demand side.

There is a clear evolution path in the capabilities and sophistication of the Information Technology (IT) infrastructure supporting all these collaboration practices, in the amount of information exchanged between the trading partners and in the process(es) enabled by this information sharing supporting former versus later forms of collaboration. Compared to the traditional ordering process, VMI/CRP and CPFR highly increase the total volume of information transmitted between retailers and suppliers on a daily basis. The volume of information exchanged and the intensity of interaction are expected to further increase dramatically when the advanced data capture capabilities of Radio Frequency Identification (RFID) technology coupled with unique product identification and real-time information gathering are employed. The emergence of RFID is expected to revolutionize many of the supply chain processes, especially those involving collaborating partners (Prater et al., 2005). Figure 1 [17] below summarizes the evolving path of supply chain collaboration practices in retail and the underlying information technologies that have enabled this collaboration over time.

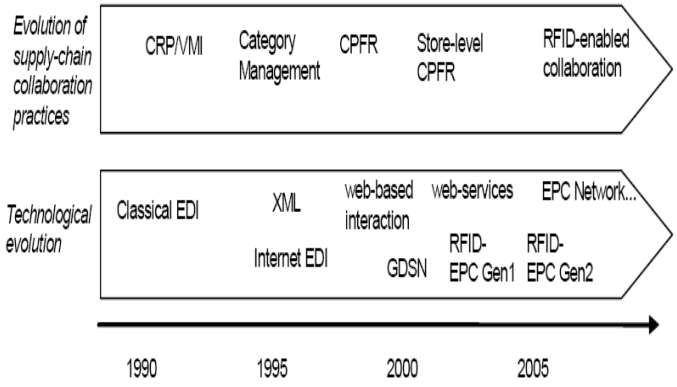

Figure 1: Evolution of supply chain collaboration practices and enabling technologies in retail industry

In this context, this paper proposes eight RFID-enabled supply chain collaboration services (e.g. dynamic pricing, smart recall, in-store promotion management, outof-shelf response) in a networked retail business environment. The services are characterized, on a high-level, by the information shared between retailers and suppliers, the level of tagging (pallet/case/item level) and the location of the tag readers. However, this paper presents the first findings of a research-in-progress with the ultimate purpose to assess and categorize the RFID-enabled supply chain collaboration scenarios according to four dimensions: the extent of collaboration required between retailers and suppliers, the RFID technology requirements, the transformation of existing (or the introduction of new) processes and the business performance impact of the RFID-enabled collaborative service.

2. SUPPLY CHAIN COLLABORATION

Collaboration is defined as two or more companies sharing the responsibility of exchanging common planning, management, execution, and performance-measurement information [3]. The critical step that many companies have not been able to take so far is to incorporate customer-demand information into their production and inventory-control processes. Companies that collaborate typically exchange information on a high level, but the production planning process remains unchanged, which eliminates the opportunity for a radical improvement of the dynamics in the supply chain. In our view, the critical feature is not only to exchange information, but to alter the replenishment and planning decision structure. The demand at the retailer drives the combined inventory and production control process, together with feedback on complete supply-chain inventory, rather than at individual tiers in the supply chain [13].

Manufacturers must secure and emulate the cooperation and dedication of relevant supply-chain partners to adapt in the most cost-effective way. Effective adaptation requires nearly real-time access to reliable, dispersed information to make quick, accurate, proactive decisions that can dramatically improve supplychain performance. True collaboration goes far beyond sharing forecasts and automating the purchase order (PO) process. It requires sharing data regarding sales orders, manufacturing runs, inventory levels, and purchasing activities, see figure 2 [13]. One solution for this particular task is called the Collaborative Planning, Forecasting, and Replenishment (CPFR) process. CPFR is defined as “an initiative among all participants in the supply chain intended to improve the relationship among them through jointly managed planning processes and shared information” [12].

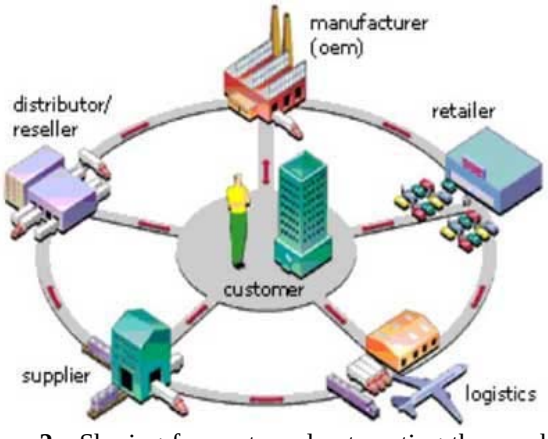

Figure 2 : Sharing forecasts and automating the purchase order (PO) process

The Strategy & Planning cycle establishes the ground rules for the collaborative relationship, determines product mix and placement, and develops event plans for the period (Figure 3). The Demand & Supply Management cycle projects consumer (point-of-sale) demand, as well as

order and shipment requirements over the planning horizon. The Execution cycle places orders, prepares and delivers shipments, receives and stocks products on retail shelves, records sales transactions, and makes payments. The Analysis phase monitors planning and execution activities for exception conditions, aggregates results, calculates key performance metrics, shares insights, and adjusts plans for continuously improved results. While these collaboration activities are presented in logical order, most companies are involved in all of them at any moment in time.

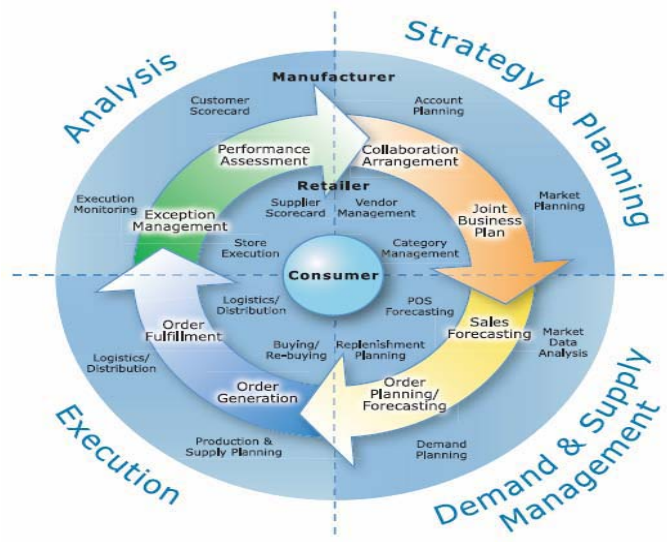

Figure 3 : The Strategy & Planning cycle establishes the ground rules for the collaborative relationship

There is no predefined sequence of steps. Execution issues can impact strategy, and analysis can lead to adjustments in forecasts. This clearly illustrates that CPFR complies with the supply-chain collaboration principles, yet there are issues that hinder the development of true supply-chain collaboration. There is a gap between the true customer demand and the inventory at any time. There is still no visibility of the product through the supply chain; the retailer still experiences out-of-stock conditions; and customers are unsatisfied [22].

3. ADOPTING RFID IN SUPPLY CHAIN

Radio Frequency Identification (RFID) is a generic technology concept that refers to the use of radio waves to identify objects (Auto-ID Center, 2002). The core of RFID technology is the RFID transponder (tag) – a tiny computer chip with an antenna. Consumer good suppliers attach these tags to logistic units (palettes, cases, cartons and hanger-good shipments) and, in some cases, to individual items. Logistic units and individual items are identified by the Electronic Product Code (EPC). An RFID reader is used to identify the EPC stored on the RFID tag (Loebbecke, 2007). The antenna enables the microchip to transmit the object information to the reader, which transforms it to a format understandable by computers (Angelles, 2005). Finkenzeller (1999) provides a general overview of RFID technology while Sarma (2002) describes the specific technology for supply chain management.

Nowadays, many in the retail sector are already looking to the business case of RFID as the "next generation of barcode" through its capabilities to uniquely identify, track and trace consumer products along the entire supply chain requiring neither direct human contact nor line of sight, to store much more information and to enable a broad spectrum of supply chain applications ranging from upstream warehouse and distribution management down to retail-outlet operations, including efficient inventory management, shelf management, promotions management and innovative consumer services, as well as applications spanning the whole supply chain, such as product traceability (Sarma et al., 2002, Loebbecke, 2007). Although RFID technology is still emerging, RFID adoption is pushed by major retailers (RFID journal, 2003) which are already executing a number of pilot applications.

The benefits of RFID adoption in various application areas can be sought across the following axes (Pramatari, 2006): 1) the automation of existing processes, leading to time/cost savings and more efficient operations; 2) the enablement of new or transformed business processes and innovative consumer services, such as monitoring of product shelf availability or consumer self check-out; 3) the improvement of different dimensions of information quality, such as integrity, accuracy, timeliness etc. (Ballou et al., 1998) and 4) the formation of new types of information, leading to a more precise representation of the physical environment, e.g. a product's exact position in the store, a specific product's sales history etc. For the full benefits to be ripped, the information needs to be shared among the supply chain partners in a complex network of relationships and decision making. The internal exploitation of RFID technology by a network leader-retailer looking solely at its own benefits is expected to have a negative impact on RFID market acceptance and adoption rates since suppliers will confront RFID as another unfortunate strategic necessity (Barua et al., 1997).

4. RFID-ENABLED SUPPLY CHAIN COLLABORATION SERVICES

The proposed system, categorized as a distributed Web-based decision support system, with participating user companies being European grocery retailers and suppliers from the fast-moving consumer goods sector [23]. Companies in the sector already have a more-than-ten-years collaboration history and some collaboration processes havebecome standard business practice across Europe, such as CRP/VMI employed in retail warehouse replenishment or Category Management dealing with the marketing aspects of managing product categories in the store [17].

The proposed architecture is a generic distributed architecture that can potentially support various supply chain collaboration and decision support scenarios, whether these are enabled by RFID technology or not [23] :

1) Backroom Visibility
In this scenario, both retailer and suppliers have a clear picture of the products' stock level in the store, as well as of the products' sales and collaborate on order placement for store replenishment. The store personnel receive from the system real time information about the backroom inventory level of each product. If a product is out-of-shelf, but there is available stock in the backroom, the store personnel is informed to refill the shelf; otherwise, if there is no stock (out-ofstock), a new store order is placed and sent to the distribution center. The salesmen of direct-store-delivery suppliers have also direct access to this information through their PDAs. The system updates the backroom inventory records automatically and sends the information to the PDA of the suppliers' salesmen. The salesmen inform the store staff to refill the shelf, but if there is no backroom stock, they prepare an order based on the inventory information provided by the system. At the retailer's headquarters, they can monitor the orders that the suppliers' salesmen have placed. The salesmen leave the store satisfied, since they succeeded in moving their products to the shelves and they also took efficient ordering decisions to avoid out-of-stock & out-of-shelf. The tags are applied on case and item level. The tag readers are fixed on the backroom entrance and the backroom to sales floor entrance.
2) Out-of-shelf Response
The last 50 yard problem of product shortages on the shelf is a crucial issue in retail operations, both for the supplier and the retailer. On one hand the retailer should be aware of the time to move items from the backroom to the shelf, and on the other hand the supplier should be able to monitor the level of out-of-shelf in the stores, in order to identify problems and take corrective actions about the service level of new products to the end customer. The system monitors the stock in the backroom and on the shelves and when there are out-of-shelf cases it generates an out-of-shelf alert and sends specific instructions on the PDA of backroom personnel about which goods to move from the backroom to the shelf. This collaborative scenario enables the store personnel to better manage the shelf replenishment process, which is currently one of the major causes behind the outof-shelf problem.
3) Remote Shelf management
Retailers and suppliers are provided with real time information about the actual shelf layout and have the opportunity to collaboratively manage the shelves allocation and appearance. RFID readers "scan" and "read" the shelves and provide their "digital image", including information about the size, specific products' position and layout, as well as information about the shelves' performance. By using the system, the suppliers are now able to check if the products get the room they deserve on the shelf and are neatly positioned according to the store's planogram. If the suppliers notice that some of the products have fewer facings on the shelf, than what has been agreed with the retailer, or that some shelf space has been left empty, they informs the retailer, as well as the merchandiser to visit the store and take care of the shelf.
4) Dynamic Pricing
Retailers and suppliers have the opportunity to identify products that are close to their expiration date, or are standing still on the shelves for a long time. For these reasons they can dynamically reduce the products' price, in order to boost consumer demand and reduce waste. This collaborative service is very useful for fresh products, such as dairy products, bread, meat, etc. When consumers visit the store with their shopping list, they usually purchase products with the longest expiration date, since they cost the same. Thus, in order to avoid big on-hand stock of expired products, the system does periodic checks of on-hand stock to identify products approaching expiration date and then informs the suppliers. The suppliers, based on the system's recommendations, suggest to the retailer to decrease the price of these products. The retailer approves the suppliers' proposal for price change. In this case, the customers face a dilemma, if they should sacrifice the longest expiration date for a better price. But there are economic difficulties, so they usually choose the cheaper one. As a result, the customers leave the store happy that they managed to save money and both the retailer and the supplier are also satisfied because they managed to sell products that would otherwise be trashed. The tags are applied on case and item level. The tag readers are fixed on the shelves, on the backroom entrance, and on the backroom to the sales floor entrance.
5) In-store Promotion management and Promotion evaluation
Customers get direct information about special offers and promotions relevant to the product they just picked up from the shelf. When the consumer picks up the product, the fixed tag reader scans it and the customer gets a promotion message on a special information screen or even its mobile phone. The system distinguishes between shelf sales and promotion stands sales. The suppliers use the system to monitor the sales of products in every store and get assistance in the design of new in-store promotion events. The system even provides them with statistics, evaluation reports, recommendations and specific locations in the store to use, based on their performance and cost. The tags are applied on item level. The tag readers are fixed on the shelves, on the promotion stands and near the special information screens.
6) Demand management
According to this scenario, retailers and suppliers are capable of monitoring the inventory and the sales of products in every store and relocate them, if needed, (e.g. in case of a special promotion event) in order to eliminate lost sales opportunities. Using the system, they receive, on real time, from every retail outlet the on-hand inventory level in the backroom, on the shelves, and even on the promotion stands. They also get sales data from the Point-Of-Sales system. For example, if the supplier runs a promotion campaign for product A and notices that product A is almost out-of-stock in store Y, where it has high sale rates, but in store X there is a lot of product inventory that is not sold then he issues an order "Move product A from store X to store Y". The tags are applied

on case and item level. The tag readers are fixed on the backroom entrance, on the backroom entrance to the sales entrance, on the shelves and on the promotion stands.

7) Traceability information

According to this scenario, the consumer at the end-point-of-sales (retail store) has a clear view of the products' history and origin. When the consumer reaches the shelf, he cannot be sure for the product's quality and safety. So, he picks up the product, the fixed tag reader scans it and, by special information screens, the customer gets details about production date and origin, expiration dates and other unique product's information that can ensure product authenticity and safety. The tags are applied on item level. The tag readers are fixed near the special information screens. The traceability information that belongs to the suppliers is shared with the retailers, in order to enable this collaboration service.

8) Smart Recall

Retailers and suppliers have the capability to identify the location of products with specific characteristics and recall them fast and at minimum cost from the market, e.g. in case there is a risk with consumer safety. When a crisis happens and the products of a specific production lot are found defective, the suppliers' quality managers issue an order "Recall the defective production lot from the market". The system identifies the products and provides with all the locations in the retailer's stores where the products of the specific production lot have been sent. The store personnel is informed to withdraw the products from the specific shelves, promotion stands and the backroom and prepare them to be sent back to the suppliers. As a result, the retailer has avoided the customers' dissatisfaction and for the suppliers it was not necessary to recall all the products of the kind. The tags are applied on case and item level. The tag readers are fixed on the backroom entrance and shelves, on the backroom to the sales floor entrance, on the shelves and on the promotion stands.

Table 1 summarizes the above RFID-enabled supply chain collaboration services. Each scenario is presented according to the information shared between the collaborating retailers and suppliers, the tag readers location, and the tagging level.

Table 1: Characteristics of the eight RFID-enabled Supply Chain Collaboration Services

RFID-enabled Collaboration service	Information shared	Tag Readers Location	Tagging Level
Backroom visibility	Backroom on-hand stock Orders POS data	Backroom entrance Backroom to sales floor entrance	Case, Item
Out-of-shelf response	Backroom on-hand stock Shelves on-hand stock Out-of-shelf alerts	Backroom entrance Backroom to sales floor entrance Sales floor shelves	Case, Item
Remote shelf management	Number of products' facings Products' position Shelf layout Shelf sales	Sales floor shelves	Item
Dynamic Pricing	Products expiration date Backroom on-hand stock Shelves on-hand stock	Backroom entrance Backroom to sales floor entrance Sales floor shelves	Case, Item
In-store Promotion management and Promotion evaluation	Shelf sales Promotion stands sales POS data	Sales floor shelves Promotion stands near the special information screens	Item
Demand management	POS data Backroom on-hand stock Shelves on-hand stock Promotion stands on-hand stock	Backroom entrance Backroom to sales floor entrance Sales floor shelves Promotion stands	Case, Item
Traceability information	Product traceability information (production date and origin, expiration date, product history, etc.)	near the special information screens	Item
Smart Recall	Product information Product location information	Backroom entrance Backroom to sales floor entrance Backroom shelves Sales floor shelves Promotion stands	Case, Item

5. CONCLUSIONS

Supply chain collaboration in retailing and Fast Moving Consumer Goods industry (FMCG) has mainly been

expressed in the form of practices such as Vendor Managed Inventory (VMI), Continuous Replenishment Program (CRP), and Collaborative Planning, Forecasting and Replenishment (CPFR). The emergence of RFID is expected to revolutionize many of the collaborative supply chain processes and to empower new collaboration scenarios, such as anticounterfeiting, product recall and reverse logistics, collaborative in-store promotion management and total inventory management. This paper proposes eight RFID-enabled supply chain collaboration services (e.g. dynamic pricing, smart recall, in-store promotion management, out-of-shelf response) in a networked retail business environment. The services are characterized, on a high-level, by the information shared between retailers and suppliers, the level of tagging (pallet/case/item level) and the location of the tag readers. However, these RFID-enabled supply chain collaboration scenarios will be further assessed according to four dimensions : the extent of collaboration required between retailers and suppliers; the RFID technology requirements the transformation of existing (or the introduction of new) processes and the business case contribution of the service.

REFERENCES

[1]. Andraski, J.C. : Foundations for successful continuous replenishment programs, *International Journal of Logistics Management*, Vol. 5, No. 1, 1994, pp. 1-8.

[2]. Angelles R.: RFID Technologies: Supply Chain Applications and Implementation Issues, *Information Systems Management*, 2005, pp. 51-65.

[3]. Anthony, T.: Supply chain collaboration: success in the new Internet economy. Achieving Supply Chain Excellence Through Technology, *Montgomery Research Inc.*, 2000, pp. 241-44.

[4]. Auto-ID Center: Technology Guide, Auto-ID Center White Paper, 2002.

[5]. Ballou, D., Wang, R., Pazer, H., and Tayi, G.: Modeling information manufacturing systems to determine information product quality, *Management Science*, Vol. 44, No. 4, 1998, pp. 462.

[6]. Barratt, M. and Oliveira, A.: Exploring the experience of collaborative planning initiatives, *International Journal of Physical Distribution and Logistics Management*, Vol. 31, No. 4, 2001, pp. 266-289.

[7]. Barua, A., and Lee, B.: An Economic Analysis of the Introduction of an Electronic Data Interchange System, *Information Systems Research*, Vol. 8, No. 4, 1997, pp. 398-422.

[8]. Bowersox, D.J., Closs, D.J. & Stank, T.P.: Ten mega-trends that will revolutionize supply chain logistics, *Journal of Business Logistics*, Vol. 21, No. 2, 2000, pp. 1-16.

[9]. Chopra, Sunil, and Peter Meindl. *Supply Chain Management*. Upper Saddle River, NJ: Prentice Hall, 2004.

[10]. Finkenzeller K.,: "RFID Handbook: Fundamentals and Applications in Contact-less Smart cards and Identification,"John Wiley & Sons, 1999.

[11]. Frantz, M.,: CPFR pace picks up, Consumer Goods. Available at: www.consumergoods.com/archive/ Mar 09, 1999.

[12]. Hölmstrom, J., Framling, K., Kaipia, R. and Saranen, J.: Collaborative planning forecasting and replenishment: new solutions needed for mass collaboration, *Supply Chain Management: An International Journal*, Vol. 7, No. 3, , 2002, pp. 136-145.

[13]. Holweg, Matthias, Stephen Disney, Jan Holmström, and Johanna Småros : Supply Chain Collaboration: Making Sense of the Strategy Continuum. *European Management Journal*, Vol. 23, No. 2. 2005.

[14]. Loebbecke, C.: Piloting RFID Along the Supply Chain: A Case Analysis, *Electronic Markets*, Vol. 17, No. 1, 2007, pp. 29-37.

[15]. Mclaren, T., Head, M. and M., Y. Y.: Supply chain collaboration alternatives: Understanding the expected costs and benefits, Internet research: *Electronic networking applications and policy*, Vol. 4, 2002, pp. 348-364.

[16]. Patrakosol, B. and Olson, D.: How interfirm collaboration benefits it innovation, *Information & Management*, Vol. 44, No. 1, 2007, pp. 53-62.

[17]. Pramatari, K.: Collaborative Supply Chain Practices and Evolving Technological Approaches, *Supply chain management: an International Journal (Forthcoming)*, 2006.

[18]. _____ et al.: New forms of CPFR, *The ECR Journal-International Business Review*, Vol. 2, No. 2, 2002, pp. 38-43.

[19]. Prater, E., Frazier, G.V. and Reyes, P.M.: Future impacts of RFID on supply chains in grocery retailing, *Supply chain management: An International Journal*, Vol. 10, No. 2, 2005, pp. 134-142.

[20]. Sarma, S.,Weis, S. and Engels, D.: Low cost RFID and the electronic product code, *In the Workshop on Cryptographic Hardware and Embedded Systems*, LNCS, 2002, pp. 6, Berlin.

[21]. Skjoett-Larsen, T., Thernøe, C. and Andresen, C.: Supply chain collaboration theoretical perspectives and empirical evidence, *International Journal of Physical Distribution and Logistics Management*, Vol 33, No. 6, 2003, pp. 531-549.

[22]. VICS CPFR Advisory Team: Collaborative Planning, Forecasting, and Replenishment (CPFR®), Voluntary Interindustry Commerce Standards (VICS), 2004.

[23]. Zhang, S., and Goddard, S.: A software architecture and framework for Web-based distributed Decision Support Systems, *Decision Support Systems*, Vol. 40, 2005.

Study of Reliability and Continuity Supply of Micro Wind Power at Sebesi Island, South Lampung

Agus R. Utomo, Chairul Hudaya, Herlina Wahab

Electric Power and Energy Studies
Department of Electrical Engineering Faculty of Engineering
University of Indonesia, Depok 16424
http://www.ee.ui.ac.id/epes
E-mail : arutomo@eng.ui.ac.id or c.hudaya@nuklir.info

ABSTRACT

Micro Wind Turbine (MWT) is a small scale wind turbine of Micro Wind Power (MWP) with major application for buildings. The power range is varied, however, it's defined that MWP has power until 1,000 W. According to its axis, MWP can be divided into 2 parts; horizontal axis WT and vertical axis WT.

Sebesi island is located at 5o 55' 37,43" - 5o 58'44,48" SL and 105o 27' 30,50" - 105o 30' 47,54" WL, at Lampung gulf, close to Krakatau archipelagos. The island has area of 2,620 ha and is inhabited by approximately 2,500 people. Main occupation of the people is fishing and farming. Loads at Sibesi Island are supplied by 2 diesel power plants with existing capacities of 40 kW and 50 kW. The fuel used is high speed diesel (HSD). Due to economical reason, everyday the power plant can only operate for 8 hours taking at 4.00 pm to 12.00 am of which the peak load usually happens at 8.00 pm as much as 49 kW.

This study is aimed for conducting simulation if the current power supply is integrated or even eliminated with the application of MWP. We demonstrated the reliability and continuity supply of that integration so that the power can be delivered along day. Pessimistic scenario we used in simulation resulted in the application of MWT may save energy for about 21.02 – 840.96 kWh per year.

Keywords : *Micro Wind Power (MWP), Wind Turbine, Reliability and Continuity Supply, Sibesi Island*

1. INTRODUCTION

Wind is air flowing from which higher pressure to lower pressure. Due to this movement, kinetic energy can be driven, and it depends on mass and velocity. Equation 1 expresses the kinetic energy formula :

$$E = \tfrac{1}{2} m V^2 \quad (1)$$

If $m = A.V.q$ and thus

$$P = \tfrac{1}{2} q A V^3 \quad (2)$$

Betz describes Wind Turbine (WT) can only convert wind kinetic energy not more than 59.3 %. This boundary is then called Betz limit which is 0.592593. According to this limit, the power resulted by WT can be obtained by equation 3 below :

$$P = 0.592593 \left(\tfrac{1}{2} q A V^3\right) \quad (3)$$

Notes :
m = mass of air block [kg],
A= surface area of air block [m2],
q = air density [kg/m3]
V = air velocity [m/sec],
E=energy [Joule],
P=power[Watt].

The wind velocity depends on at what height the measurement is conducted. Besides, it also depends on roughness of earth surface which is represented by equation 4 below :

$$\frac{V}{V_r} = \left[\frac{H}{H_r}\right]^{\alpha} \quad (4)$$

Where $\alpha = \dfrac{0.37 - 0.088 \ln(V_r)}{1 - 0.088 \ln\left[\dfrac{H}{10}\right]}$

The graph below represents α :

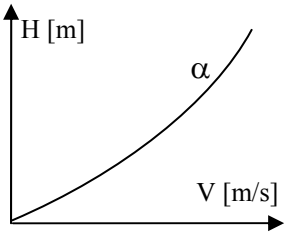

Figure 1. Friction coefficient of earth surface

Notes :

V = wind velocity at height H [m/sec],
Vr = wind velocity at referenced height Hr [m/sec],
H = height at which measurement conducted [m],
Hr = referenced height [m]
α = Earth surface friction coefficient

2. THEORETICAL OVERVIEW

Micro wind power (MWP) is the systems of wind power having micro power. The power range is varied, however, it's defined that MWP has the power until 1,000 W. According to its axis, MWP can be divided into 2 parts; horizontal axis WT and vertical axis WT. Figure 2 and 3 describe those kinds of WT.

Figure 2. Wind Turbine with Horizontal Axis

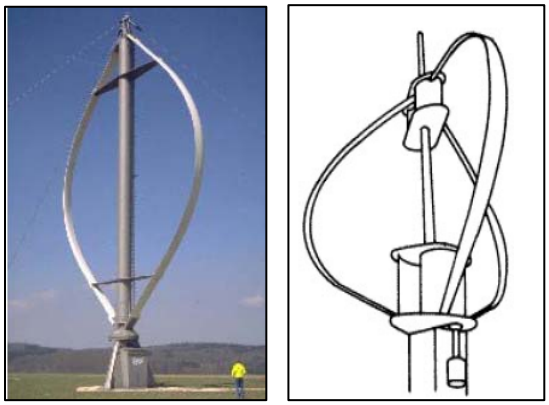

Figure 3. Wind Turbine with Vertical Axis

Micro horizontal axis WT is usually used on the roof building or beside the building. Figure 4 shows the application of horizontal axis WT.

Figure 4. Application of Horizontal Axis Wind Turbine

For the areas with low wind velocity, the MWP is equipped with batteries and electronic control equipment. Figure 5 shows the application of vertical axis wind turbine.

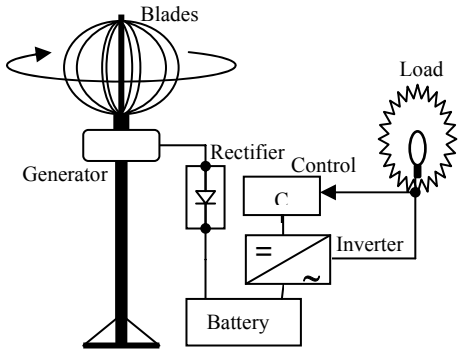

Figure 5. Wind Power Systems

Nowadays some of WT are using permanent magnet induction generator as for electricity generation. The rotor is composed by strong-permanent magnet made by Neodymium (NdFeB). The flux resulted by this material can achieve 10 times higher than that of conventional magnet (Ferrite). Besides, the rotor and stator have also simple shapes, in the plate-form. Figure 6 shows the rotor and stator of MWT.

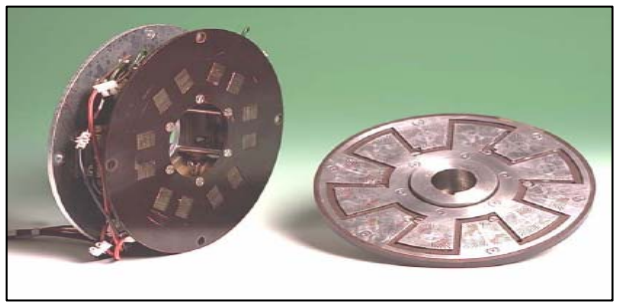

Figure 6. Stator and Rotor of Micro Wind Turbine

3. METHODOLOGY

3.1 Study Area

Sebesi island is located at 5o 55' 37,43" - 5o 58'44,48" SL and 105o 27' 30,50" - 105o 30' 47,54" WL, at Lampung province gulf, close to Krakatau archipelagos. The island has area of 2,620 ha and is inhabited by approximately 2,500 people. Main occupation of the people is fishing and farming. Figure 7 shows the location of Sibesi Island captured by Google Earth Map :

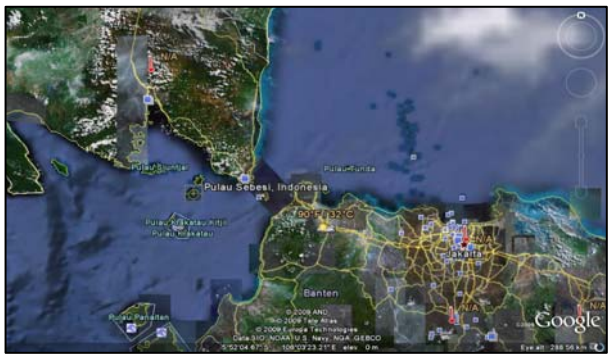

Figure 7. Location of Sibesi Island

3.2 Data Gathering

In this simulation, we did not measure the wind velocity at the proposed area. We are utilizing the data obtained from the website of www.weatherbase.com. The website informs that the average wind velocity in Sibesi Island measured at height of 10 m is 4.17 m/s. The annual wind velocity of Sibesi Island can be seen at Figure 8 below :

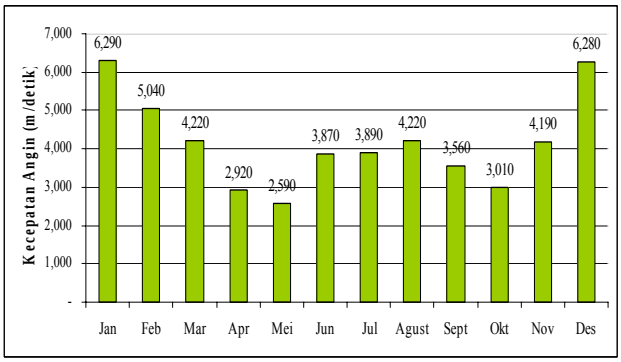

Figure 8. Average Wind Velocity in Sibesi Island

According to Apriansyah, reporting daily load for Sibesi Island to PT. PLN (Persero) branch Lampung in 2009, the loads are supplied by 2 diesel power plants with existing capacities of 40 kW and 50 kW. The fuel used is high speed diesel (HSD). Due to economical reason, everyday the power plant can only operate for 8 hours taking at 4.00 pm to 12.00 am. The peak load usually happens at 8.00 pm as much as 49 kW. The daily curve load of Sibesi Island may be seen in Figure 9 below.

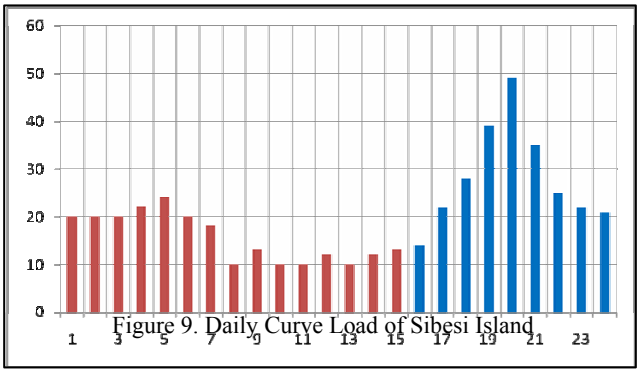

Figure 9. Daily Curve Load of Sibesi Island

Notes :
The blue bar shows the real load. The red bar presents the daily curve load if the load's supplied by full 24 hours a day.

4. RESULT AND ANALYSIS

The study is then conducted be assessing the systems if the loads are supplied by a continued power, 24 hours a day. For this case, we apply the HOMER software, a micropower optimization software developed by National Renewable Energy Laboratory USA. The result shows the daily loads profile of Sibesi Island as can be seen in Figure 10.

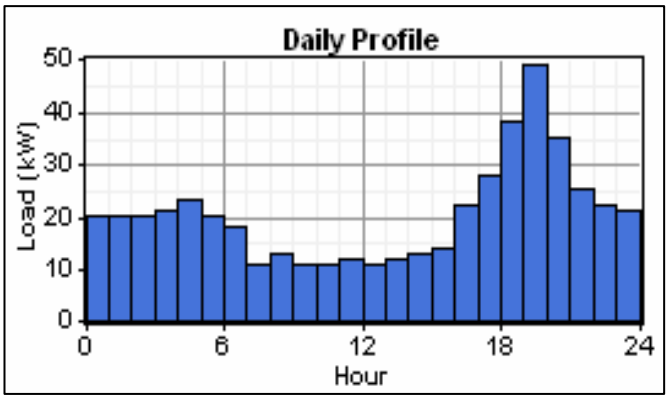

Figure 10. Daily Curve Load of Sibesi Island with Continued Supply (Simulated by HOMER software)

The simulation used pessimistic scenario, suited with the location. We assumed the loads are buildings at Sibesi Island. The number of user and usage period can be predicted as below :

- Number of User : 0.8 x 1/5 building/people x 2000 people = 400 users.
  The value of 0.8 is the user factor.
- Usage time for 1 year : 0.6 x 8760 jam = 5260 jam
- WT height is approximated 4 m.

The MWT used in this simulation is with capacity of 400 W. Wind velocity is ranged at 2.8 – 6.29 m/s. The simulation resulted in the annual energy production of MWT as table 1 below :

Table 1. Annual energy production of MWT

% User	Energy [MWh]			
	25%	50%	75%	100%
10	21.02	42.05	63.07	84.10
20	42.05	84.10	126.14	168.19
30	63.07	126.14	189.22	252.29
40	84.10	168.19	252.29	336.38
50	105.12	210.24	315.36	420.48
60	126.14	252.29	378.43	504.58
70	147.17	294.34	441.50	588.67
80	168.19	336.38	504.58	672.77
90	189.22	378.43	567.65	756.86
100	210.24	420.48	630.72	840.96

Or it's more convinience by showing it through Figure 11 below :

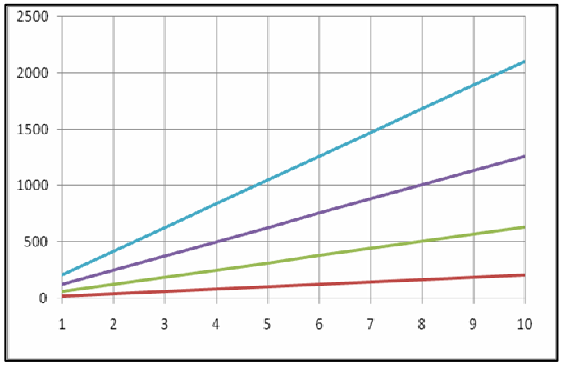

Figure 11. Annual energy production of MWT

The above table informs by using the lowest wind velocity and the less users, the MWT may save the energy as much as 21.02 kWh per year. Meanwhile, by using highest approach, the MWT may produce energy as much as 840.96 kWh. The pessimistic scenario was taken sonce the power purchse of the people living at Sibesi Island is still low. By applying MWT, the peak load not only will be suppled by diesel power plant, but also by MWT. As the matter of fact, the system will more reliable and the dependance to fossil fuel can be decreased, even may be eliminated from the grids.

5. CONCLUSION

The investigation of continuity and reliability supply of MWT at Sibesi Island has been studied. The simulation shows the application of MWT results in the higher reliable of the systems. Consequently, the use of high speed diesel as the fuel can be decreased. Pessimistic scenario delivers the application of MWT may save energy for about 21.02 – 840.96 kWh per year.

REFERENCES

[1]. Abdul Kadir, "*Energi : Sumber Daya, Inovasi, Tenaga LIstrik dan Potensi Ekonomi*.", Published by Universitas Indonesia (UI Press), Jakarta, 1995.

[2]. Fingersh, Lee Jay., "*An Introduction to Wind Turbine Electrical Systems*", National Renewable Energy Laboratory (NREL), 2008.

[3]. De Marco, Patricia., "*Wind For The Future*", Rachel Carson Homestead Association, www.rachelcarsonhomstead.org, 2007.

[4]. Conlon, Michael, "*Development of Wind Energy : Resource, Turbine controls, Configuration of Generators, and Integration into Supply Network*", School of Control Systems and Electrical Engineering, DIT, Dublin.

[5]. "*Betz Limit : Understand the Betz Limit and how it affects wind turbines*", Renewable Energy Website, reuk.co.uk, 2007

[6]. "*Roof Mounting of Wind Turbines*", Renewable Energy Website, reuk.co.uk, 2007

[7]. Gipe, Paul., "*Rooftop turbine: Rooftop Mounting and Building Integration of Wind Turbines*", www.wind-works.org, 2005.

[8]. "*Neodymimium Magnetic*", Renewable Energy Website, reuk.co.uk, 2007

[9]. Peters, E., "*Different 600 kw Designs of an Axial Flux Permanent Magnet Machines For Wind Turbine*", 2nd IASME/WSEAS International Conference On Energy And Environment, Portorose, Slovenia, 2007.

[10]. Wahab, Herlina., "*Studi Implementasi Pembangkit LIstrik Hibrida di Pulau Sebesi, Lampung Selatan*", Thesis, Master Program, Department of Electrical Engineering, University of Indonesia, Depok, July 2009.

ISSN 114-1284

Improvement of SIMPLE-O: Increased Computational Performance for Automatic Essay Grading Assessment using JAMA

Anak Agung Putri Ratna[a], Natalia Evianti[b]

[a]*Electrical Engineering Department, Faculty of Engineering*
University of Indonesia, Depok 16424
Tel: (021) 7270078 ext 101. Fax: (021) 7270077
E-mai : ratna@@eng.ui.ac.id
[b]*E-mail: natalia.evianti@gmail.com*

ABSTRACT

Web based automated essay grading system using Latent Semantic Analysis (LSA) method for Indonesian language has been developed in Electrical Engineering Department, University of Indonesia. The system which is called SIMPLE-O is developed using PHP and MATLAB for essay grading process. SIMPLE-O has some weaknesses based on previous research. First: consumed maximum of processor time (resource) to process essay grading; second: does not support multisession.

Improvement of SIMPLE-O is designed by replacing MATLAB with Java Matrix (JAMA). JAMA is a basic linear algebra package for Java and compatible with PHP language. Performance analysis is executed by benchmarking and perflogs tools. Benchmarking result shows the summary of throughput and percentage of running system while perflogs tools show the percentage of processor time.

The analysis results of implementation SIMPLE-O with JAMA have shows an improvement on its performance which is enhancement in time of request approximately two times faster for single user and also for multiple user. An improvement on processor performance is shown by its efficient and effective time to handle single and multiple users. The testing result shows that request failure is decrease compare to the SIMPLE-O before the implementation of improvement design.

Keywords

LSA, JAMA, optimization, benchmarking, performance

1. INTRODUCTION

Assessment is very important component in every education system to evaluate student understanding of the whole study materials. There are two main forms of assessment questions [1]: objective form and essay form. Objective type of question is multiple choices with several answers available to choose. While essay form, do not provide answers. Student must answers the question with their own thought, therefore answers will vary.

Assessment with essay form is more preferable for lecturer to evaluate student's ability because it provides an opportunity for student to demonstrate wide range of skill and knowledge including higher-order thinking skills such as synthesis and analysis [2]. Although assessing student's writing is the most expensive and time consuming, and also hard to give objective judgment.

On e-learning concept, assessment made online start from answer the question until grading with numbers. This evaluation system uses computers to give faster and accurate grading and also handle large scale of assessment.

Next problem is how to make effective grading process in the system. The idea of automated essay grading is based on this problem. Several automated essay grading methods on computer based system already being developed. Each method has its own grading system.

One of the developed automated essays grading method is Latent Semantic Analysis (LSA). In its grading process, LSA method only considers the word contexts does and does not appear without consider its linguistic characteristic [3]. This method is based on linier algebra computation, Singular Value Decomposition (SVD), which is a mathematical matrix decomposition technique. Matrix is representation of the text, where each row stands for a unique word and each column stands for a text passage. In SVD, a rectangular matrix is decomposed into the product of three other matrices. These matrices are reconstructed after one of the matrix, which is diagonal matrix containing scaling value being simplified. Reconstructed matrix has shown strong correlation between topic and text. This method is relatively simple but quiet accurate compare to human raters. Because of it simplicity and accurate, this method is interesting to be developed as essay grading on web-based distance learning system.

Doctoral research at Electrical Engineering Department, University of Indonesia, has developed an automated essay grading using LSA [4]. This system was originally given the name SIMPLE, and then become SIMPLE-O (SIsteM PeniLaian Esei Otomatic) which can be accessed from the intranet/internet through a web browser. This system process students' answers with LSA method to calculate the final mark. This web-based system developed with PHP programming language and MATLAB as a computing device to perform the SVD on the matrix of LSA.

The results of performance analysis [5], SIMPLE-O has some weaknesses, namely:

1. SIMPLE-O using the processor (resource) to 100% for the process essay grading.

2. SIMPLE-O does not support multisession. There was some process failure in the entire request that not successfully perform.

On this paper, the weaknesses above are fixed to improve the system performance, where it can be more effective and efficient. Therefore, the improvement of SIMPLE-O is designed by replacing MATLAB with other applications that are expected to process the SVD calculation faster and do not burdensome processor work, which is JAMA (Java Matrix). Code optimization is also need to carry out by using ZEND compiler and afterward convert the PHP 4 into PHP 5.

2. AUTOMATED ESSAY GRADING

Conventional essay grading is generally done by human raters. Now, many automated essay grading has been developed. Automatic in this context means that the essay grading is done by the tool, which is computer.

Some methods of automatic essays grading by computers have been developed which are *Project Essay Grade* (PEG), *Intelligent Essay Assessor* (IEA), *Electronic Essay Rater* (E-Rater), *Conceptual Rater* (C-Rater), *Bayesian Essay Test Scoring System* (BETSY), and *Automark, Scema Extrack Analyse Report* (SEAR) [6]. Every method has its own way to grade. One of the automated essays grading that being developed on Bahasa Indonesia based exam is SIMPLE-O.

2.1 SIMPLE-O

SIMPLE-O using the Latent Semantic Analysis (LSA) method to evaluate the students' essay exam answers. Basically, an LSA compare a text with the words chosen as a reference. LSA represents the words in a text in a semantics matrix. A relationship between each word is obtained by matrix algebra technique known as singular Value Decomposition (SVD).

2.1.1 Latent Semantic Analysis (LSA)

LSA is a technique to extract and represent sentences with mathematical or statistical calculation. The strength of the LSA technique lies in the syntax structure insensitive, thus the words processed are words from a bag of words ignoring the sequence of the sentences. LSA express the ideas about the meaning of the word, where words are occupying a position in semantic space and the meaning is the relationship between one sentences to another [7].

Assumptions that underlie LSA are that the similarities and differences in the meaning of words can be influenced by the similarities and differences in the overall context in which the word is there or not. Conversely, in the meaning of the sentence can be verbal outline of the combination (in the form of mathematics) from the words within it. This assumption implies that usually the dominant verbal meaning is based on the selection and combination of words in the speech. And for various purposes, the order in a text can be ignored in the sense to estimate similarity with only slight loss of accuracy. Thus the assessment of any text with the LSA more emphasis on the words contained in any text without notice a linguistic characteristics, such as grammar, how to write, and order of words in a sentence, therefore a sentence does not require a good rhetoric.

To apply to the basic assumption in computing systems will require a model where the word is a representation of mathematics function as a set of the observed linguistic context, and representation of linguistic context is a mathematical function of the words that are in it. In LSA, the linier function between word and meaning of text and linier factorization are used to construct text into the form of high dimension vectors. In LSA, the text is a combination of the vectors containing the words, and words are the meaning of the vectors from the observed text. Computation form that is used in the LSA is an algebra method of Singular Value Decomposition (SVD) matrix, continued with the dimensional reduction.

2.1.2 Singular Value Decomposition

Singular Value Decomposition (SVD) is a mathematical matrix decomposition technique. Matrix formed from whether there is or there isn't a specific word appears in a text (usually already defined as keywords). This matrix by Singular Value Decomposition divided into 3 (three) matrices [3]. In reconstructed matrix from decomposed matrix using SVD will be seen strong correlation between topics or sentences joined in a specific group.

After the 3 matrices are obtained, the next process is reducing matrix dimension by reducing the second matrix dimension, a diagonal matrix. Reducing the dimension of a diagonal matrix is performed by setting all diagonal values of the second matrix into zero (0) except for certain chosen dimension. And if the three matrices components are multiplied, it will produce other reconstruction matrix for desired correlation value purpose.

Mathematically, a matrix can be well decomposed if it has small factor value compared to smallest dimension of the original matrix. Thus, the best matrix reconstruction will be obtained when the factor value is smaller than the sum of factor used

2.1.3 JAMA: JAVA MATRIX

JAMA: Java Matrix is a basic linear algebra package for Java [8]. It provides user-level classes for constructing and manipulating real, dense matrices. JAMA is comprised of six Java classes: *Matrix, CholeskyDecomposition, LUDecomposition, QRDecomposition, Singular Value Decomposition* and *Eigenvalue Decomposition.*

The Matrix class provides the fundamental operations of numerical linear algebra. Five fundamental matrix decompositions, which consist of pairs or triples of matrices, permutation vectors, and the like, produce results in five decomposition classes. These decompositions are accessed by the Matrix class to compute solutions of simultaneous linear equations, determinants, inverses and other matrix functions. The five decompositions are

1. Cholesky Decomposition of symmetric, positive definite matrices
2. LU Decomposition (Gaussian elimination) of rectangular matrices
3. QR Decomposition of rectangular matrices
4. Eigenvalue Decomposition of both symmetric and nonsymmetric square matrices
5. Singular Value Decomposition of rectangular matrices

Currently, there are six classes JAMA on the programming language PHP. Class has been converted into the PHP language that can be used on systems with the function call.

2.1.4 Benchmarking

In computing, a benchmark is the act of running a computer program, a set of programs, or other operations, in order to assess the relative performance of an object, normally by running a number of standard tests and trials against it.

An effective way to test and design a system to detect the bottleneck is with the benchmarking of traffic simulation [14]. Benchmarking is a method to measure the ability and speed of a computer program. Tools that can be used to perform benchmarking is Apache Bench.

One of the benchmarking tools is ab, Apache benchmarking. This tool is one package with Apache web server and is usually already installed on systems that run Apache. Ab's working concept is by sending a number of client requests to simulate a web server with a certain delay to access the same URL.

3. DESIGN OF IMPROVED SIMPLE-O

3.1 System Specification:

- Software: PHP 5.3.11, MySQL 5.0.45, Apache 2.0.49, JAMA 1.0.1 and Windows XP
- Hardware: minimum requirements are Pentium 4 with 2 GHz and Memory 512

3.2 Architecture

Figure 1 below shows the architecture of Automated Essay Grading by using LSA method (SIMPLE-O) with JAMA. The block component of JAMA has replaced MATLAB.

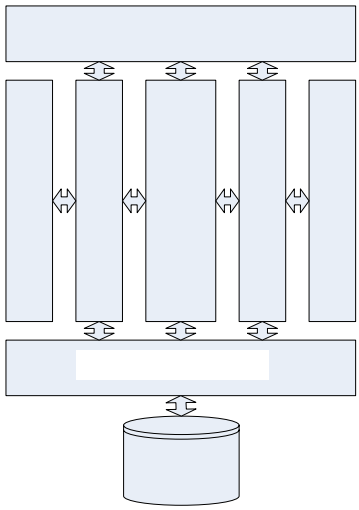

Figure 1 Architecture of improved SIMPLE-O

At the server side, web server program is installed with MySQL and JAMA. MySQL has a function as structure process while JAMA program has a function as a center of grading computation, where the singular value decomposition function on JAMA is utilized to do the computation based on Latent Semantic Analysis system. Library of singular value decomposition function on JAMA being connected or called from PHP program on client web browser.

JAMA used in this architecture is JAMA API that has been ported or compile into PHP. Thus the evaluation process on essay exams is expected to be faster.

3.3 Optimize Code

Code optimization to improve performance of SIMPLE-O is done using the software Zend Studio. With Zend Studio, scripting SIMPLE-O, who was originally using PHP 4, converted to PHP 5. This is done because there are some limitations on PHP 4. A limitation in the PHP 4 is located on the object oriented model, where

List Ujian

No	Kode	Mata kuliah	Pilih
1	EKP310022E	Algoritma dan Pemrograman	Lihat soal
2	EKP32006E	Org. dan Arsitektur Komputer	Lihat soal
3	EKP41007E	Rekayasa Perangkat Lunak	Lihat soal
4	EKP31001E	Jaringan Komputer	Lihat soal
5	EKP41009E	Pengolahan Citra	Lihat soal
6	EKP42010E	Advance Computer Network	Lihat soal
7	EKP42011E	Aplikasi E-Learning	Lihat soal
8	EKP42012E	Jaringan Komputer Lanjut B2	Lihat soal
9	EKP42013E	Teknologi Informasi B	Lihat soal
10	EKP42014E	Teknologi Informasi C	Lihat soal
11	EKP42015E	Teknologi Informasi C2	Lihat soal
12	EKP42015A	Jaringan Komputer Lanjut B1	Lihat soal
13	EKP42016A	Teknologi Informasi D1	Lihat soal
14	EKP42016B	Teknologi Informasi D2	Lihat soal
15	EKP42018A	Teknologi Informasi A1	Lihat soal
16	EKP43001A	Informasi dan Tenaga Listrik	Lihat soal
17	EKP44001A	Informasi Lst A1	Lihat soal

duplication of a semantic object type as its native. This is clearly visible at the time to send a variable (that point to another variable), then a copy of the object will be created. Developers assume that the two variables refer to the same object, although in reality the two variables are different duplicate objects. Changes in the value of an object will not change the value of the duplicates object. These limitations

affect performance even trigger the emergence of strange bugs.

4. IMPLEMENTATION AND TESTING OF IMPROVED SIMPLE-O

The performance improvement design of SIMPLE-O is implemented in a notebook computer that functions as a client while the server software with the support that has been previously installed.

Implementation on optimization is done by changing the method in the iteration algorithm of the search word in the database with the method of internal searching in PHP, which is array_search. This method is the method dichotomy search, the search process so much faster than the search method sequential. In addition, this method is a method of internal PHP functions that speed up the process of search and iteration.

JAMA on the implementation of the SIMPLE-O is done by placing the folder containing the six classes JAMA on same the folder with SIMPLE-O. If not placed in the same folder then needed include ¬ _path in php.ini file, so that PHP can call JAMA.

To analyze the performance of SIMPLE-O, testing is made with 2 types. Trial conducted with the purpose to know the performance of SIMPLE-O with the number of:

1. Only one user (single user).
2. Many users (multiple users).

4.1 Single user testing

Testing is done when user's type a URL in a browser to access SIMPLE-O http://localhost/bobotsama. After that the login page will appear before login to the system, where the user must enter userid and password. Userid and password has been registered before by the administrator. Userid used for the testing has a role as student that can only access 'Pilih Ujian' (take exam) and 'Lihat Nilai' (grade/mark). When student clicks the 'Pilih Ujian', the page will looks as seen in Figure 2.

Figure 2 List of Exam

After student clicks the 'Submit' button, the SIMPLE-O will process student's answers with LSA method. Processes are

1. Form answers matrix where there are:
   - the separation of each word in the student answers
   - the process of keyword searches and similar word of each word answers from students
2. compare the reference matrix and the answers matrix
   - computing the matrix SVD
   - Frobenius normalization and alpha Cosinus

To get the test data as much as 10 times, testing is done by using the ApacheBench to simulate the functioning of sequential communication. This method is used to see the performance of SVD in to calculate a LSA method.

4.2 Multiple user testing

Testing aims to analyze the performance of SIMPLE-O at the same time accessed by many users. With only one computer, then the testing is done using the ApacheBench which is able to simulate the user traffic. To test this, ApacheBench configured with 50 concurrent users and client as 5. So SIMPLE-O runs through ApacheBench send a request to calculate the simulated value of 50 students from the user, where the calculation is done for 5 users at one time simultaneously.

5. ANALYSIS OF TESTING RESULT

5.1 Result of single user testing

At this testing, the one of tools in Administrative Tools, the Performance Logs and Alerts being used to capture *%Processor Time* on the Apache and MySQL. *% Processor Time* is percentage of time that is used by the processor to execute a thread. *Counter* is the main indicator of processor activity and displays average percentage of processor work. The results is shown in Table 1 below

Table 1: Single user testing result (% Processor Time)

Time	Apache %	MySQL%
7:44:23 PM	21	0
7:44:24 PM	99	0
7:44:25 PM	98	0
7:44:26 PM	100	0
7:44:27 PM	99	0
7:44:28 PM	99	0
7:44:29 PM	96	0
7:44:30 PM	99	0
7:44:31 PM	100	0
7:44:32 PM	97	0
7:44:33 PM	98	0
7:44:34 PM	99	0
7:44:35 PM	100	0
7:44:36 PM	99	0
7:44:37 PM	99	0
7:44:38 PM	99	0
7:44:39 PM	99	0
7:44:40 PM	99	0
7:44:41 PM	37	0
Average	**90.28571**	**0**
Max	**100**	**0**
Min	**37**	**0**
Std Deviation	**23.49975**	**0**

Figure 3 shows the results of SIMPLE-O simulation with JAMA for 10 alternate user with the Concurrency Level = 1. The average time per request was 1.761 seconds. Data in Figure 3 also shows the throughput of requests per second = 0.57 and time per request = 1.761533 seconds. Percentage indicates the end of that time to the maximum of a request is 1.812 seconds.

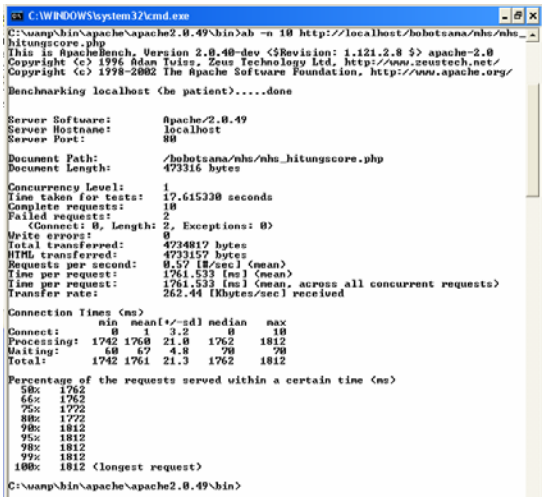

Figure 3 Simulation result of SIMPLE-O with JAMA from *ApacheBench* with 10 requests.

Figure 3 also shows 2 requests fails from 10 requests that run through the simulation ApacheBench, the SIMPLE-O with JAMA and the B-Tree indexing the failure of 20%.

Compare to previous research [5], the average time per request is 78, 854 seconds. The throughput of requests per second = 0.01 and time per request = 78.854 seconds. The last percentage indicates the maximum time of a request is 82.949 seconds. 10 request from the 2 runs that have failed the request. Thus SIMPLE-O experienced failures of 20%.

5.2 Result of multiple user testing

Table 2 is the result of the testing with 50 users of the Performance Logs and Alerts tool. ApacheBench run for 50 users and 5 Concurrent clients by using the option-n and-c.

Table 2: Multiple user testing result (% Processor Time)

Time	Apache	MySQL%
Average	98.18852	0
Max	100	0
Min	53	0
Std Deviation	4.41884	0

Figure 4 Simulation result of SIMPLE-O with JAMA from *ApacheBench* with 50 requests and 5 concurrent clients.

Figure 4 is summary result of SIMPLE-O with JAMA for 50 users with 5 concurrent clients. The results showed the failure of a request is 4 out of 50 requests. The percentage request failure has reach 8%. The average time per request was 2.431 seconds, where the average is taken of the overall concurrent request. Data in Figure 4 also shows the throughput of requests per second = 0.41 and time per request = 12.1575 seconds. The last percentage indicates the maximum time of a request is 23.163 seconds.

The result of a simulation SIMPLE-O with 50 users on the previous research [5] is the average time per request is 114, 671 seconds. This simulation test results shows 8 request fail out of 50 requests. Number of concurrent, which should be processed, is 5 requests. This means that each group of 5 Concurrent with any request that fails to request 0.8 Percentage with 16%. The result also shows the throughput of requests per second = 0.01 and time per request = 215.121 seconds. The last percentage indicates the maximum time of a request is 781.083 seconds.

5.3 Analysis of testing

5.3.1. Analysis of single user testing

The monitor results in Table 1 further analyzed with emphasis on the distribution of the appearance of significant numbers shows improvement of SIMPLE-O. Data processed with the frequency of all numbers that also appear to use the normal distribution function for the distribution of data. A result of processing data as a graph is shown in Figure 5 for % processor time. This result will be compared with the results of previous research, where the SIMPLE-O is still using MATLAB. Figure 6 shows the result graph of previous research.

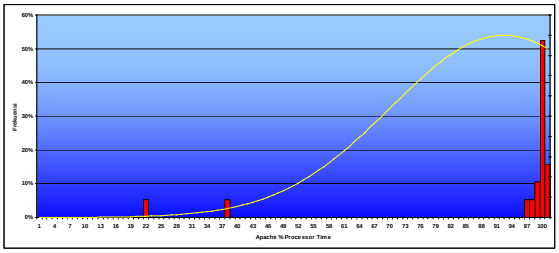

Figure 5 the graph of percentage distribution of the processor Apache on SIMPLE-O with JAMA

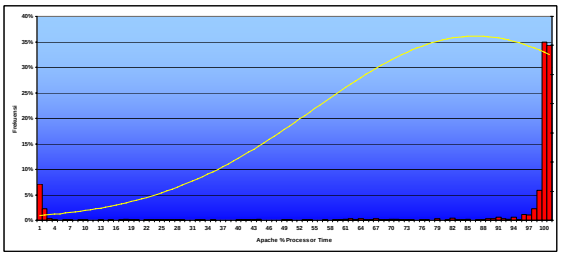

Figure 6 the graph of percentage distribution of the processor Apache on SIMPLE-O

From the graph in Figure 5 shows that the performance of processor becomes more efficient in processing system, with less idle time compare to the previous research. The idle time on the SIMPLE-O system is due to waiting on the results of computing MATLAB.

In Figure 3, the average request was 1.761 seconds. Compared to the results of previous research that reaches the time 78.854 seconds. Thus, SIMPLE-O with JAMA has speed up the process of assessment of the essay grading 44 times faster.

5.3.2. Analysis of multiple user testing

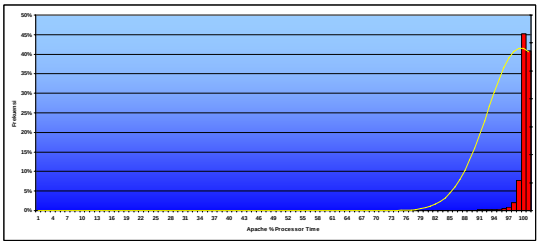

Figure 7 the graph of percentage distribution of the processor Apache on SIMPLE-O

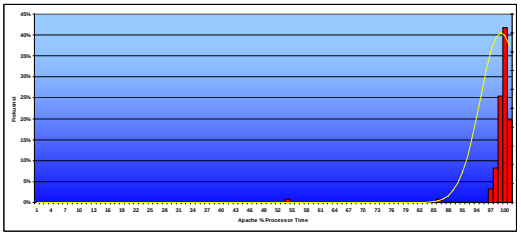

Figure 8 the graph of percentage distribution of processor Apache on SIMPLE-O with JAMA

From the graphs in Figure 7 and Figure 9, visible changes in the chart with wide differences in the distribution of standard deviation from the previous 6.848932 SIMPLE-O 4.41884 on a SIMPLE-O with JAMA and the B-Tree indexing. This change is in line with expectations from previous research that is SIMPLE-O after the improvements will have a standard deviation that is smaller and the distribution of the graph becomes smaller.

In Figure 4, the average request was 2.431 seconds. Compared to the results of previous research that reaches the 114.671 seconds, thus SIMPLE-O JAMA has speed up the process of essay grading into 47 times faster. And also the percentage request failure has reach 8%, decrease by 8% compare to previous research.

6. CONCLUSION

Implementation and analysis of system's testing result on a SIMPLE-O with JAMA have produced the following conclusions:

1. Multisession, reduce the request failure into 8% for multiple users
2. Improvement algorithm is become efficient as evidenced from the time of the request (time to process a request), which increased 44 times faster for single user and 47 times faster for multiple users

REFERENCES

[1] Asmawi Zainul, Noebi Nasution, "Penilaian Hasil Belajar", PAU untuk peningkatan dan Pengembangan Aktivitas Instruksional Direktorat Jendral Pendidikan Tinggi Departemen Pendidikan Nasional, Jakarta, 2001.

[2] Lawrence M Rudner, Tahung Liang, "Automated Essay Scoring Using Bayes Theorem", The Journal of Technology, Learning and Assessment, 1(2), Juni 2002.

[3] Thomas K. Landauer, Peter W. Foltz, Darrel Laham, "Introduction to Latent Semantic Analysis", Discourse Processes, 25 (1998).

[4] Anak Agung Putri Ratna. "SIMPLE: Penilaian Esei Otomatis Berbasis Latent Semantic Analysis Dengan Menggunakan Bahasa Indonesia." Disertasi, Program Pasca Sarjana Bidang Ilmu Teknik UI, Depok, 2006, hal.112.

[5] Anak Agung Putri Ratna, Natalia Evianti, "Analisa Unjuk Kerja Dan Rancangan Perbaikan Unjuk Kerja Sistem Penilaian Esei Otomatis (Simple-O)", Seminar, Program Pasca Sarjana Bidang Ilmu Teknik UI, Depok, 2008..

[6] Salvatore Valenti, Francesca Neri, Alessandro Cucchiarelli, "An Overview of Current Research on Automated Essay Grading", Jurnal of Information Technology Education, II (2003).

[7] Thomas K. Landauer, Joseph Psotka, "Simulating text understanding for educational application with Latent Semantic Analysis: Introduction to LSA", University of Colorado at Boulder, US Army Research Institute, 2001

[8] JAMA: A Java Matrix Package (National Institute of Standards and Technology, 2005). http://math.nist.gov/javanumerics/jama/

[9] Andi Gutmans, Stig Saether Bakken, Derrick Rethans, PHP 5 Power Programming (Prentice Hall PTR, 2004)

Optimization of Renewable Energy Penetration for Electrical Supply at Base Transceiver Station (BTS) in Pecatu Bali

Angga Rizky. P[a], Eko Adhi Setiawan[b]
[a] *Faculty of Engineering*
University of Indonesia, Depok 16424
Tel : (021) 7270011 ext 51. Fax : (021) 7270077
E-mail : angga_rizky85@yahoo.com

[b] *Faculty of Engineering*
University of Indonesia, Depok 16424
Tel : (021) 7270011 ext 51. Fax : (021) 7270077
E-mail : eko@daad-alumni.de

ABSTRACT

Providing uninterrupted power to a remote telecommunication site has been a problem for industry for many years This paper discussed about the way to design the aspects of a hybrid power system that will target for Base Transceiver Station (BTS) in Pecatu Bali. The main power system is emphasizes on the photovoltaic panels, wind turbine and combine generator as backup units to obtain a reliable autonomous system with the optimization of the component sizes and the improvement of the capital cost. The optimization software used for this paper is Hybrid Optimization Model for Energy Renewable (HOMER). HOMER is a design models that determines the optimal architecture and control strategy of the hybrid system. It can also determine the sensitivity of the outputs to changes in the inputs. It performs an hourly time series analysis on each of different configurations. The results of HOMER simulation for electrical BTS shows that annual production consists of Photovoltaic (12,330 kWh/yr), wind turbine (9,423 kWh/yr), and generator (6,032 kWh/yr), AC primary load consumption 14,308 kWh/yr, and DC primary load 11,480kWh/yr. Besides the results shows unmet load (electrical load that the power system is unable to serve) in system 0.07% or 17.5kWh, it is indicates that the power system from hybrid energy is reliable within supply BTS power load.

Keyword
Hybrid energy, BTS(Base Transceiver System), Telecommunication, Photovoltaic, Wind Turbine, Generator.

1. INTRODUCTION

The fuel price in Indonesia country always changed overtime, the effect of fuel price makes the inflation rate going into fluctuation. This uncertainty condition influenced telecommunication sector which is the cost of network load system increased expensively. For example, to generate electrical power BTS (Base Transceiver Station) in remote area can not reliable only from Government, so we can used renewable energy and generator to back up power and can support the available electricity energy system and provide the continuity of supply demand for whole year.

Renewable energy designs depending on the nature resources in that area [1]. This paper is concern about the configuration of hybrid power system planning for BTS in Pecatu Bali. Pecatu located in South of Bali Island, with the coordinate 8° 49' 50" South and 115° 07' 37" East. Pecatu have global solar radiation 4,82kWh/m2/d [2] and annual wind speed 4,37 m/s [3]. BTS needs power load AC 39kWh/d and power load DC 31kWh/d [4]. With utilize aught natural resources, therefore renewable energy concept that is utilized namely combine the sun energy and the wind energy, and diesel generator for meeting energy requisition while system experiences trouble, so network will make a abode stable. Acquired gain of BTS renewable energy among those is increase electricity, more electric reserve long-lasting, penny wise its preserve, and doesn't result perilous waste. The electricity of wind turbine and solar cell will keep in battery. On normal condition, battery will meet the need electricity. In designs of BTS alternative energy, can be helped by named software Homer. Homer, the micro optimization model, simplifies the task of evaluating designs of both off-grid and grid-connected power system for a variety of applications [5].

2. RENEWABLE RESOURCE DATA

2.1 Wind Resources Information

The preliminary study was done using data obtained from Kuta wind report (www.windfinder.com). The report data observations taken between 12/2002 - 2/2009 daily from 7am to 7pm local time with annual wind speed average 4.37 m/s. Based on the available data, the average wind speed at 10m height for each month in Pecatu is plotted in fig. 1.

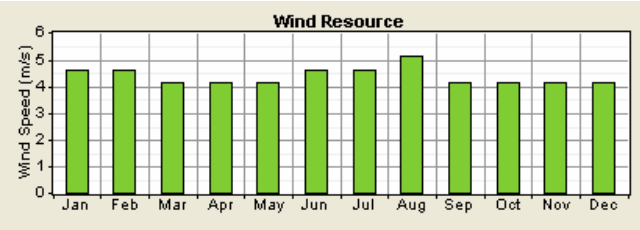

Figure 1. Pecatu average monthly wind speed

2.2 Solar Resources Information

The solar resources for this study are obtained from NREL and NASA data. The monthly average solar irradiance is summarized in Figure 2.

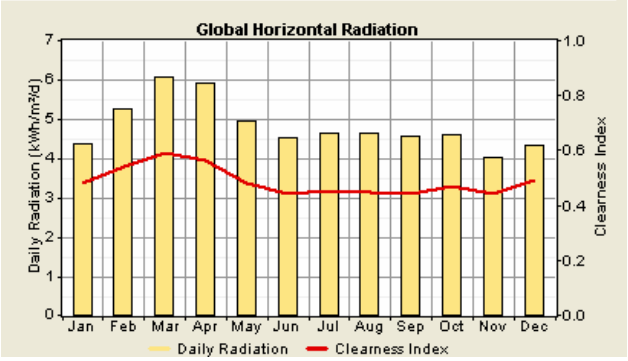

Figure 2. Pecatu average monthly solar irradiance

3. ELECTRICAL LOAD DATA

Pecatu load data collected over three days (March 1-3 2008) which represents weekday and weekend load. Based on Indosat telecommunication operator, the BTS load consists of AC and DC load. The daily AC load power consumed 39kWh/d, and DC power load consumed 31kWh/d. Minimum load occurring betweens midnight until 6 am, due to the reduction of telephone calls during this period. Figure 3, and figure 4 is an annual graph of the site loading as produced by HOMER software.

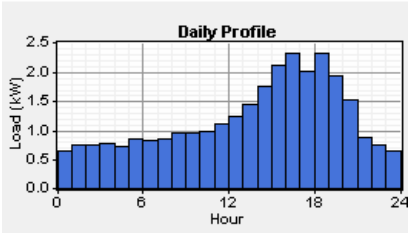

Figure 3. The annual DC Power load

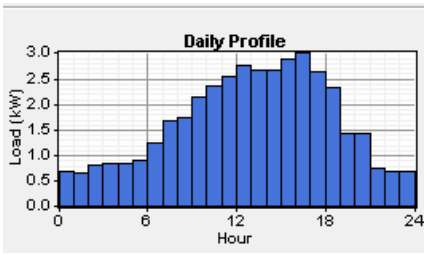

Figure 4. The annual AC Power load

4. HYBRID SYSTEM COMPONENT

The main components of an isolated grid connected PV-Wind-diesel hybrid system are solar cell, wind turbines, and diesel generator. A typical PV-Wind-diesel system used in HOMER software is shown in Figure 5. The system consists of solar cell, wind turbine, diesel generator, converter, battery bank, AC-DC bus and primary load. The cost of each component, the number of units used in simulation, the economical and control parameters required by software are discussed in the forthcoming paragraphs.

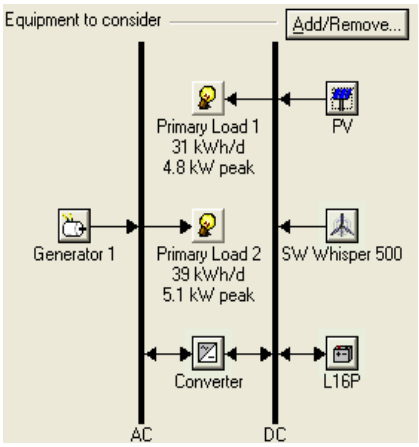

Figure 5. PV-Wind-Diesel system

4.1 Photovoltaic

Solar cell panel utilized MA100. One solar cell panel gets capacity 100W at the price $875.00. That cost included ordering cost via online, shipping, installation charge. In a general way, solar cell module marketed by capacity 100 peak's Watts (Wp) and its multiple. Solar unit Watt peak is power unit (Watt) one that gets to be generates by photovoltaic module in Standard Test Condition (STC) [6]. In one system, this solar panel can be arranged and is strung up as many panels, according to energy which is needed. This solar panel have excess which is film coat structure photovoltaic that weatherproof, stable regular under tall temperature up to summer. Lifetime of the modules has been taken as 25 years.

4.2 Wind Turbine

HOMER models a wind turbine as device that converts the kinetic energy of the wind into AC or DC electricity. Wind turbine type used SW Whisper 500, between another wind turbine data one provided by HOMER, this turbine has best performance for wind speed quality average 4m/s. Wind turbine have energy of 3kW at the price $6,300, and warranty up to 5 years [7].

4.3 Generator

Generator consumes fuel to produce electricity, and possibly heat as a by-product. Generator is designed not for supply peak load entirely, because largely load charges serviced by solar and wind energy. The capital costs of the diesel generator are set to $2110, replacement costs $2110, and operation & maintenance costs $0.2/hr [8].

4.4 Converter

Converter is device that converts electric power from AC to DC in a process called rectification, and from DC to AC in a

process called inversion. HOMER can model the two common types of converters: solid state and rotary. The converter type that is used in this system is Xantrex 4kW 12V 50A Inverter Charger [9]. The converter supporting component consists of inverter and rectifier. Converters have efficiency of 95.9% and 95.9%. Cost for converter buy as big as $3130, warranty up to 15 years.

4.5 Battery Bank

HOMER uses the kinetic battery model and represents batteries as a "two tank" system. One tank provides immediately available capacity while the second can only be discharged at a limited rate. Trojan L16P 2x6V nominal capacity 420Ah was chosen because they are a popular and inexpensive option [10]. HOMER considered up to 50 of these batteries.

5. SUPPORTING FACTOR SYSTEM

Fuel Price

In this system uses diesel as a fuel of generator. Fuel price data gets based on Pertamina corporation, diesel price per liter as big as 6,000 IDR [11] or $0.6 (1USD = 10.000 IDR, June 2009).

Economical parameters

Annual interest rate is the discount rate used to convert between one-time costs and annualized costs. The project lifetime was taken as 20 years and the annual real interest rate as 7% [12].

System Control

The system control input define, how HOMER models the operation of battery bank and generators. The dispatch strategy determines how systems charge the battery. This system used dispatch strategy load following, the load following strategy is a dispatch strategy whereby whenever a generator operates, it produces only enough power to meet the primary load. Lower-priority objectives such as charging the battery bank or serving the deferrable load are left to the renewable power sources.

Emissions Inputs

Issue penalty factor is fine one be put on to firm, to draw the line resulting issue systems if exceed specified bounds. Base Energy Information Administration's data (EIA), done by CO2 issue penalty of $100 / ton, NO_2 of $5000/t and SO_2 of $2000/t [13].

System Constraints

Constraints are conditions which systems must satisfy. HOMER discards systems that do not satisfy the specified constraints, so they do not appear in the optimization results or sensitivity results. Maximum annual capacity shortage is the maximum allowable value of the capacity shortage fraction, which is the total capacity shortage divided by the total annual electric load, assumed by its point of 0.5 %. Minimum renewable fraction is he minimum allowable value of the annual renewable fraction, on renewable fraction was done to sensitivity analysis of 75%, 80%, 90%.

HOMER adds this percentage of the hourly average primary load (AC and DC separately) to the required operating reserve for each hour. A value of 10% means that the system must keep enough spare capacity operating to serve a sudden 10% increase in the load.

6. RESULT AND DISCUSSION

6.1 Optimization Result

The simulation software provides the results in terms of optimal systems and the sensitivity analysis. In this software the optimized results are presented categorically for a particular set of sensitivity parameters like wind speed, solar radiation, and fuel price.

Homer groups 5 systems configurations that variably to each component. The results of optimization for wind speed of 4.37 m/s, solar radiation of 4.82kWh/m^2/d, and diesel price of $0.6.

In this BTS case gotten by system configurations as, 8 kW PV panel, 2 wind turbines (6kW), 5kW generator, 50 battery bank, 4kW converter. This configuration is chosen on row first Figure 9, based on the lowest total Net Present Cost (NPC) of $265,317, with Initial Capital Cost of $122,960, and Cost of Energy (COE) of $0.883/kWh. Homer got 78.3% for simulation renewable fraction results. During project lifetime, generator working up to 2,421 hours, with fueled consumption as much 2,476 Liters.

HOMER calculates all of total electrical energy production from hybrid energy and total electrical energy consumption that consists of AC primary load (14.308kWh/yr) and DC primary load (11.490kWh/yr). In this system, PV array generates 12.330kWh/yr, wind turbine of 9.423 kWh/yr, and generator of 6.032kWh/yr. The unmet load of the system is 0.07% or 17.5kWh/yr, capacity shortage is 43.6 kWh/yr, and excess electricity as big 562 kWh/yr. The electrical simulation result is shown in Figure 11. The equation of total production PV and wind turbine shows in below.

Total Production PV = Mean output x 8760 h
= 1.41 kW x 8760 h
= 12,330kWh/yr

Total Production Wind = Mean output x 8760 h
= 1.08 x 8760h
= 9,423kWh/yr

Figure 6 shows the daily contribution of PV, wind turbine, Generator, Batteries on March 1st.

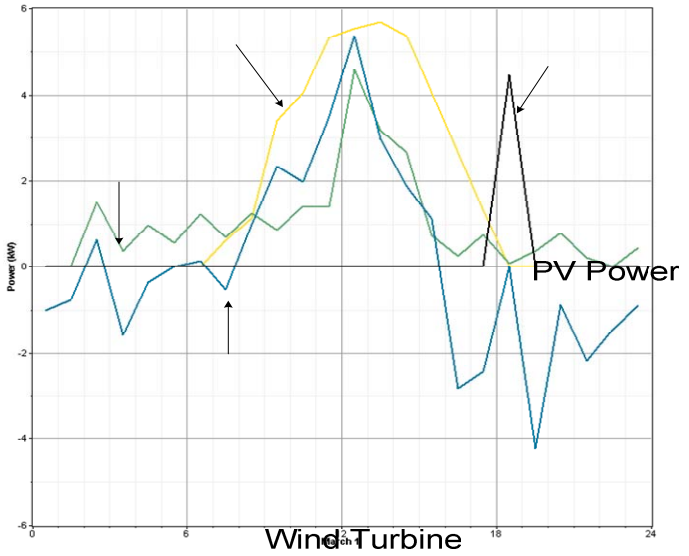

Figure 6. Daily simulation results: contribution of PV/Wind turbine/Generator/Battery on March 1st.

Renewable fraction designed of 75%, it because of wants to maximize energy resource potencies that exist at that region, after simulates, HOMER results renewable fraction of 78%. It means that system was supplied by energy of PV array and wind turbine of 78%, and diesel generator generates energy of 22% to service during a year. The function of generator is only for back up energy when energy from solar cell and wind turbine decrease. Figure 6 shows monthly average electric production by diesel generator, PV, wind turbine, with 78% renewable fraction.

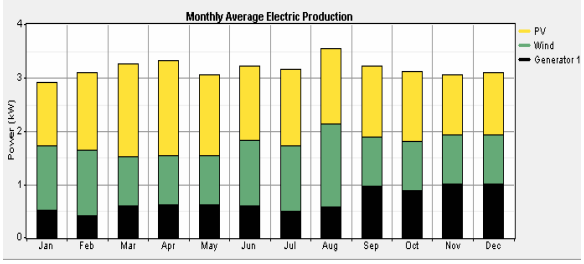

Figure 7. Monthly average electric production with 78% renewable fraction

Renewable fraction influence total NPC and COE. The greater renewable fraction, makes total NPC and COE will greater too (Table 3). It is caused because more system used a lot of hybrid energy where purchasing wind turbine and solar cell more expensive if as compared to generator.

The equation of COE is shown in below :

$$\text{COE 75\%} = \frac{\text{total annualized cost}}{\text{Total consumption energy}} = \frac{\$22{,}767}{25{,}788\text{kWh/yr}} = 0.883$$

$$\text{COE 80\%} = \frac{\text{total annualized cost}}{\text{Total consumption energy}} = \frac{\$22{,}912}{25{,}787\text{kWh/yr}} = 0.888$$

$$\text{COE 90\%} = \frac{\text{total annualized cost}}{\text{Total consumption energy}} = \frac{\$25{,}162}{25{,}797\text{kWh/yr}} = 0.975$$

Table1. Comparison of renewable fraction to output parameter

Renewable fraction (%)	Initial Capital ($)	NPC ($)	COE ($/kWh)	Excess Electricity (%)	Emmision (kg/yr)
78	**122,960**	**265,317**	**0.883**	**2.02**	**6,521**
80	144,525	267,003	0.888	3.55	5,591
90	159,525	293,222	0.975	10.7	5,968

When renewable fraction of 78%, excess electricity that resulting system is seen very small as compared to renewable fraction of 80 and 90%. Excess electricity is surplus electrical energy that must be dumped because it cannot be used to serve a load or charge the batteries. Total excess electricity can be reduced by adds total battery bank, because battery bank function as DC energy storage, but if battery bank increases, it will make systems expensively and changed system configuration entirely. Hybrid power systems have disadvantages in cost sector. To build BTS hybrid energy power system needs fund approximately $122,960**.**

The advantages of BTS hybrid energy systems is increases electricity, durable electrical reserve, economical maintenance, can reduce pollution, and do not depends on government.

6.2 Sensitivity Analysis

Each category was done sensitivity analysis to anticipate uncertainty condition if the value changed on some years, and each changing will determine configurations of systems. Renewable energy system for this BTS will be done for 3 categories sensitivity analysis which is wind speed (3, 4.37, 5, 6m/s), solar radiation (4.82, 5, 6kwh/m2/d), and diesel fuel price (0.3, 0.45, 0.6, 0.8 $/L). So as a whole configuration result is 120 possible configuration systems of 48 sensitivity cases, with simulated time up to 58 minute 32 seconds. The result of sensitivity analysis shows with OST Graph (Optimal System Type).

6.2.1 Condition 1 (Fuel price $0.6/L and $0.8/L)

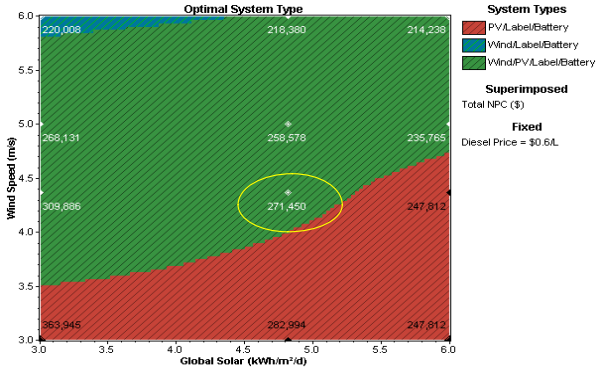

Figure 8. OST graph wind speed and solar radiation: Diesel price $0.6/L

The large of wind speed and solar radiation influenced the result of optimization systems, meanwhile diesel price does not influenced the configuration. It is caused because system utilize hybrid energy of 78%, and generator only 22%, so the system does not consumed a lot of diesel fuel. The most optimal results configurations are PV/Wind/Generator /Battery, with PV and wind turbine as main electrical source. Total NPC and COE cost rise up when the diesel fuel price increase become $0.6/L to $0.8/L.

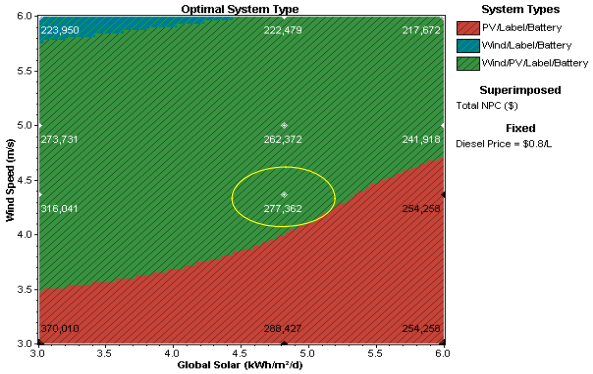

Figure 9. OST graph wind speed and solar radiation: Diesel price $0.8/L

Figure 13 shows graph diesel price $0.6/L, and Figure 14 shows graph diesel price $0.8/L. The different of both figures indicates that total NPC cost changed from $271,450 to $277,362, and total COE changed from $0.903 to $0.923.

6.2.2 Condition 2 (Solar radiation 3 kWh/m^2/d and 6 kWh/m2/d)

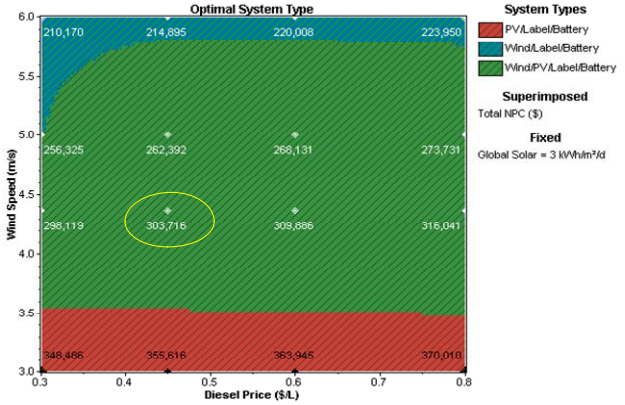

Figure 10. OST graph wind speed and diesel price: Solar radiation 3 kWh/m^2/d

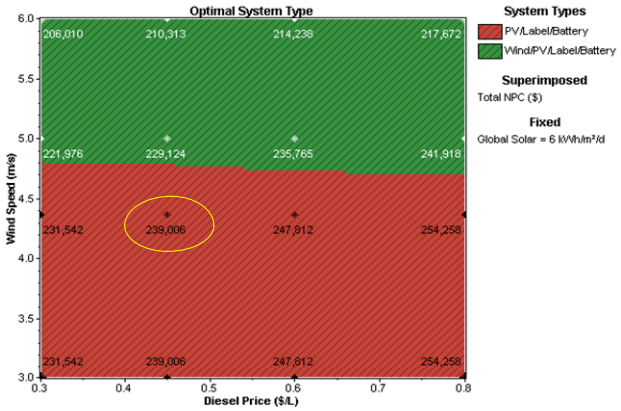

Figure 11. OST graph wind speed and diesel price: Solar radiation 6 kWh/m^2/d

Figure 15 and Figure 16 shows that solar radiation changed from 3kWh/m^2/d to 6 kWh/m^2/d. Alternating solar radiation, influence system configuration and total cost production system. If solar radiation is bigger, hence the configuration system will more rely on solar cell as main hybrid source. Total NPC changes from $300,716 to $233,009.

6.2.3 Condition 3 (Wind Speed 3 m/s and 6 m/s)

HOMER optimization results produce configurations system when the wind speed of 3m/s, consists of PV 16kW, 50 Battery bank, 4kW converter, 5kW Generator. Total NPC system NPC of $275,055, and total COE of $0.915/kWh. Figure 17 shows OST graph when wind speed of 3m/s.

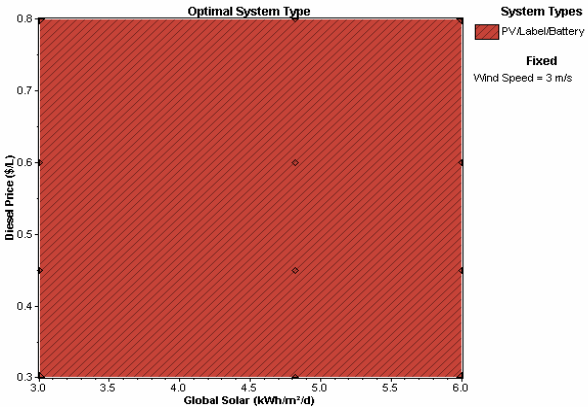

Figure 12. OST graph and diesel price and solar radiation: Wind speed 3m/s

When wind speed increase become 6m/s, configuration system does not change, but total cost production system decrease, total NPC of $213,920, total COE of $0.712/kWh, Initial Capital $87,960.

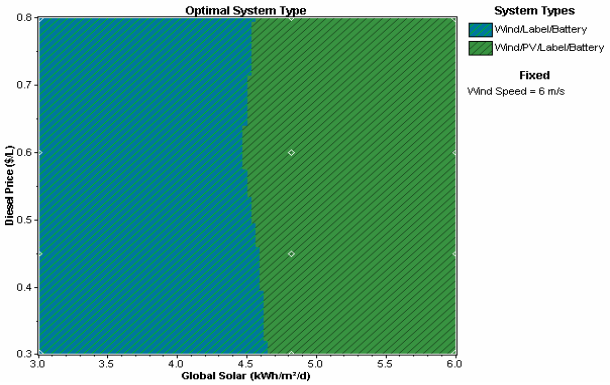

Figure 13. OST graph and diesel price and solar radiation: Wind speed 6m/s

7. CONCLUSION

Providing uninterruptible power for a BTS remote telecommunication in Pecatu Bali is possible using hybrid renewable energy. Pecatu Bali have good annual wind speed (4.37m/s), and solar radiation (4.82kWh/m^2/d). HOMER optimization result has shown configuration system most optimal as 8kW PV array, 6kW wind turbine, 5kW diesel generator, 50 battery bank of 108kWh, and 4kW converter. Total NPC system of $265,317, and COE system of $ 0.883.

Total COE system very expensively, it is caused by renewable fraction system BTS of 78%. However, the greater renewable fraction makes generator carbon issue can be reduced. If wants to economize fuel, reducing pollution, preventing global instillation, and creating environmental clearly, and do not depend on government, and then renewable energy solar cell and wind turbine can be considered, but with expensive cost consequence.

8. ACKNOWLEDGEMENTS

The author would like to thank the support of Indosat corporation for site load data, National Renewable Energy Laboratory (www.nrel.gov) for the use of HOMER optimization software.

9. REFERENCES

[1] M. Marwan Mahmoud and H.Imad Ibrik, Techno-economic feasibility of energy supply of remote villages in Palestine by PV-system, diesel generators and electric grid. “Renewable and Sustainable Energy Reviews”. 2006;10: 128-138.
[2] NASA Surface Meteorology and Solar Energy, http://eosweb.larc.nasa.gov
[3] Kuta Bali wind report, http://windfinder.com
[4] Network Monitoring System Indosat. Jakarta 2008
[5] Givler,T and Liliental P. Using HOMER Software, NREL Micropower Optimization Model, “Micropower System Modelling With Homer”, Mistaya Engineering. NREL: USA.2006
[6] Mitsubishi Photovoltaic Panel Models, http://energymatters.com.au/mitsubishi-solar-panel-100w-20%brochure.pdf
[7] Wind turbin SW Whisper 500 Catalogue, http://windenergy.com
[8] Mitsubishi Diesel Generator MGE400 Models, http://bigskypower.com/Mitsubishi/generators/html
[9] Xantrex Converter 12V 50A Inverter Charger, http://xantrex.com
[10] Trojan L16P Battery Bank, http://trojanbattery.com
[11] Indonesia Fuel Price, http://bphmigas.go.id/
[12] Indonesia Interest Rate BI on June, http://BI.com
[13] Energy Information Administration Penalty, http://eia.com

ISSN 114-1284

Performance Analysis of Spatial Multiplexing MIMO OFDM With SVD Chanel Model for Mobile WiMAX

Asvial, M.*, and Sengki, IGP*

** Electrical Engineering Department, Faculty of Engineering, Universitas Indonesia*
Kampus Ui Depok, 16424
Telp: 021-7270078, Fax: 021-7270077
E-mail: asvial@ee.ui.ac.id

ABSTRACT

MIMO OFDM technology have ability to minimizing BER, increasing channel capacity and efficiently of bandwidth used. In this paper, simulation and analysis of spatial multiplexing MIMO OFDM technique with SVD channel model for Mobile WiMAX is proposed. Channel modeling that used in this simulation based on Singular Value Decomposition (SVD). The evaluation of system performance is proposed to Bit Error Rate (BER), Channel Capacity and Throughput parameter toward Eb/No value. System performances are simulated with three type of modulation, they are QPSK, 16-QAM and 64-QAM. In addition, three type of Error Control Coding is used in this simulation with different code-rate value. Beside that, there are two user condition in this simulation, that are idle user (v = 0 m/s) and mobile user (v = 10 m/s). The simulation results show that the system performance with high Eb/No value is most better. This condition is shown for BER, channel capacity, throughput and signal space graph. In addition, we can see the performance with code rate 1/3 is also better than other code rate values.

Keywords
MIMO, OFDM, Spatial multiplexing, SVD, Mobile WiMAX

1. INTRODUCTION

The development of wireless telecommunication technology leads to fulfilled high capacity needs, using efficiently of bandwidth and ability to protect data from noise and minimizing error.

OFDM is multicarrier modulation that have ability to work in multipath fading condition and give a solution of real time high speed access needs[1]. Combination of MIMO OFDM have ability to support high speed communication access, reliable, flexible and also using efficiently of bandwidth[2]-[5], but the complexity of the system with conventional channel modelling is high with poor performance.

In this paper, simulation and analysis of spatial multiplexing MIMO OFDM technique with SVD channel model for Mobile WiMAX is proposed. Channel modeling that used in this simulation based on Singular Value Decomposition (SVD). The evaluation of system performance is proposed to Bit Error Rate (BER), Channel Capacity and Throughput parameter toward Eb/No value. System performances are simulated with three type of modulation, they are QPSK, 16-QAM and 64-QAM. In addition, three type of Error Control Coding is used in this simulation with different code-rate value. Beside that, there are two user condition in this simulation, that are idle user (v = 0 m/s) and mobile user (v = 10 m/s). The simulation results show that the system performance with high Eb/No value is most better. This condition is shown for BER, channel capacity, throughput and signal space graph. In addition, we can see the performance with code rate 1/3 is also better than other code rate values.

2. MIMO and OFDM SYSTEM

2.1. Multiple Input Multiple Output (MIMO)

Multiple Input Multiple Output (MIMO) antenna system consist of some transmitter and receiver antenna. MIMO system use multipath condition to create some equivalent channel as though separate one to others, that in normal condition, multipath will introduce fading that affect data transmission. There are two type MIMO technique that used in mobile wireless communication, that are spatial multiplexing and spatial diversity. Spatial multiplexing technique transmits different parallel data and coded for each transmitter antenna. The purpose of using this technique is to gain high channel capacity with dividing high stream data into low stream parallel data depends on number of transmitter antenna. Low stream datas are flow over certain matrices that this matrices have function to combine signals from all parallel stream datas with certain combination. This proses is multiplex that happen in spatial dimension because each combination of parallel data guided to one of transmitter antenna. Singular value decomposition (SVD) matrices operation used here to diagonalizing channel matrices and get eigen value from that matrices in purpose to estimate channel matrices response. Channel matrices respon result is shown as follow:

$$H = U_H \Sigma_H V_H^* \quad \text{.....(1.1)}$$

Channel capacity of MIMO system is calculated based on Shannon formula:

$$C_{1x1} = E\left[\log_2\left(1+\frac{P|h_{11}|^2}{\sigma_n^2}\right)\right] \; bps/Hz \quad \text{…(1.2)}$$

With SVD operation, Shannon capacity channel representated by:

$$C_{RxT} = E\left[\log_2\left(\det\left(I_{R_o}+\frac{P}{T\sigma_n^2}HH^h\right)\right)\right]$$

$$= E\left[\sum_{i=1}^{rank(H)}\log_2\left(1+\frac{P}{T\sigma_n^2}\delta_i^2\right)\right] \; bps/Hz \quad (1.3)$$

With C is channel capacity in bps/Hz, E is expectation of all channel realisation, P is avarage power that transmited in channel, H is gain of random complex channel, σ_n^2 is noise variant, I_{R_o} is identity matrices with *rank(H)* dimension depends on number receive antenna, T is number spatial channel, H^h is hermitian matrices, *rank(H)* $\leq$ min{R,T}, δ_i^2 is singular value square that related with power from each channel decomposition matrices HH^h results, and P/σ_n^2 is *signal-to-noise* (SNR) average ratio in each receiver side.[4]

2.2 OFDM

OFDM is multicarrier transmition scheme that combine modulation technique and multiplexing. The basic idea from OFDM is separation data transmition into an amount subcarriers and modulated with low rate . In the other word, a OFDM signal consist of a number *narrowband carrier* that transmitted from same source and different frequency.
Each subcarriers are orthogonal. Orthogonality introduce overlapping spectral between subcarriers, that spectrum from each subcarriers have null value on center frequency other subcarriers with the result interference between subcarrier will not happen. This is the point of differences between OFDM and FDM, where channel separation in FDM only based on frequency with guard interval between channel to avoid interference. From this point, clearly show that OFDM more efficient in using bandwidth compared with FDM.

3. SYSTEM MODELLING

Transmiter scheme is shown in figure 4.1.

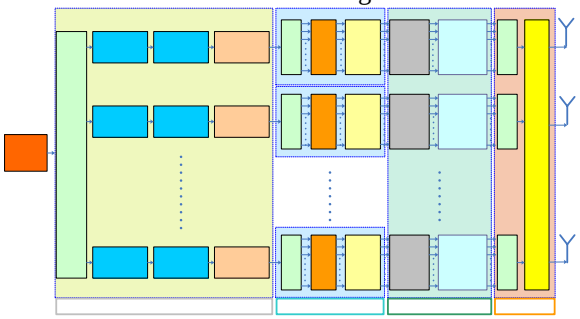

Figure 1 *Transmitter*

Data is to be transmited are generated by data generator. With serial to parallel algortihm, data divided into some data stream (depends on number transmit antenna), where in this simulation, data divided into 2 stream data. Convolutional encoder used here as channel encoder to minimizing error rate while transmit data. Coderate values that used for convolutional encoder in this simulation are 2/3, ½, 1/3. To minimizing burst error in transimition data, interleaver is used. Next, mapping data into complex symbol through data modulator, that three type of modulation used here, that are QPSK, 16-QAM and 64-QAM.
IFFT and also FFT in receiver side, are main component in OFDM system. OFDM subchannel parameter using ULTRA WIDEBAND COMMNICATION SYSTEM parameter. Width of each bandwidth channel is 10 MHz. 256 subcarrier will become subchannel with carrier frequency between 3400-3600 MHz or lecated in band frequency 3.5 GHz. Every subchannel modulated by IFFT, in order to representate data in time domain. Then, OFDM symbol complex resulted from IFFT combined into serial data and added cyclic prefix to avoid ISI and ICI. Next, upsampling data with factor 4 and upconversion data into passband to facilitate transmision of complex signal.

Before transmission signal, matrices V that have function as prefilter, multiply with signal in purpose to get symbols that will transitted from transmit antenna. The using of prefilter with matrices V because of Singular Value Decomposition that used in MIMO channel.

In receiver side, process that happen to signal are inverse from process in the transmitter side, as shown in figure 4.2. Because of using SVD operation in matrices channel, symbol that received by receive antenna multiply with demultiplex matrices U^h, that act as postfilter. Then, signal will process with downconversion, downsample, cyclic prefix removal, FFT, Demodulator, Deinterleaver and Channel decoder.

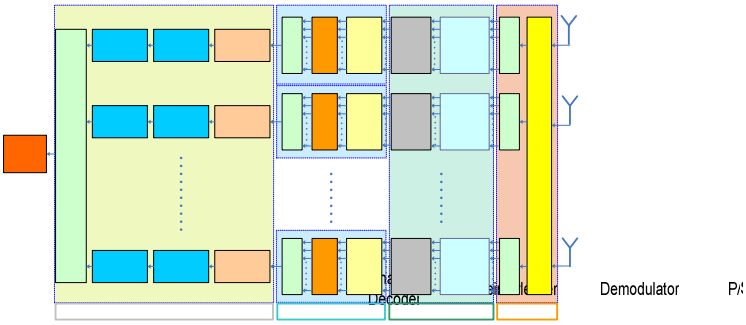

Figure 2 *Receiver*

4. SIMULATION RESULTS

Generally, the results of the simulation can be divided into 2 part, that are system performance graph, consists of BER, channel capacity , throughput toward EbNo and signal space graph. System performance, analyzed with system without ECC and system with ECC. Beside that, there are two other condition that used in this simulatioan to see system performance, that are idle user (v = 0 m/s) and mobile user (v = 10 m/s).

The analysis of throughput parameter, same with other parameter, as shown in Figure 3, where high throuhput is reach with system that using ECC. This thing caused of BER value affect throughput system. Maximum throughput is reached when BER = 0. Thus, because of system with ECC reach BER = 0 at EbNo value that smaller than system without ECC, then maksimum throughput for system with ECC also reached faster.

System performance for mobile and idel user aer shown in Figure 4, 5, and 6. Generally, BER for idle user have smaller value compared with mobile user. BER value for QPSK and 16-QAM modulation type, are close and reach zero value at EbNo = 5 dB and 9 dB for QPSK and 16 QAM sequently. For 64 QAM modulation, zero value of BER for idle user is reached at EbNo = 17 db (higher than other modulation type), and for mobile user, high BER value still exist.

Channel capacity performance shown in figure 4. From figure 4 we ca see that the channel capacity for both idle and mobile user doesn't have sigificant difference. Next figure shows throughput performance. From graph 5 we ca see that the maksimum throughput for both system condition are close / same. Throughput system affected by BER value. So, when BER value is zero, throughput system will reach maximum state. As seen at figure 5, for idle user and 16-QAM modulation, reach

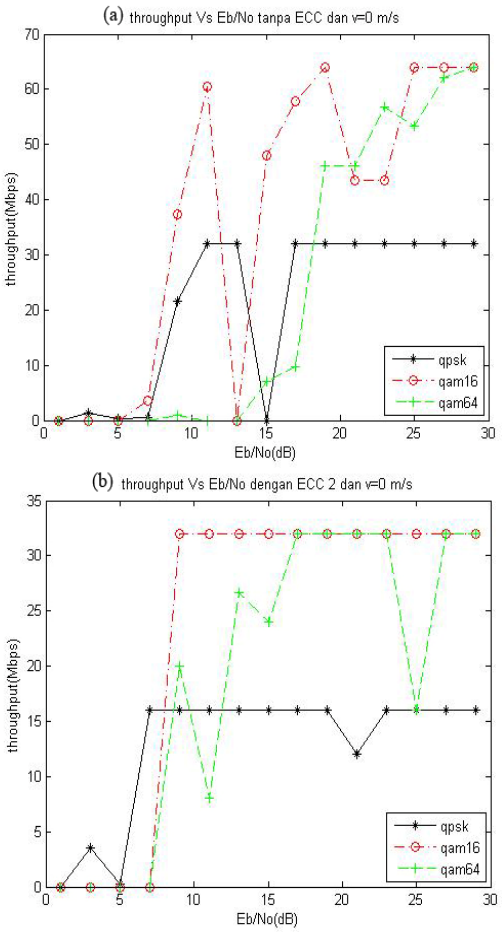

Figure 3 Throughput vs Eb/No V = 0 m/s

maximum state at EbNo = 9 dB, and also occur for mobile user with same modulation type. In the end, generally system performance between idle user and mobile user in this simulation doesn't have significant difference. But, for whole parameter, system performance with idle user a little better than system with mobile user.

Channel capacity performance are shown in figure 4. From figure 6 seen channel capacity for both idle and mobile user doesn't have sigificant difference. Next figure shows throughput performance. From graph 7we can see that maksimum throughput for both system condition are close / same. Throughput system affected by BER value. So, when BER value is zero, throughput system will reach maximum state. As shown in Figure 5, for idle user and 16-QAM modulation, reach maximum state at EbNo = 9 dB, and also occur for mobile user with same modulation type. In the end, generally system performance between idle user and mobile user in this simulation doesn't have significant difference.

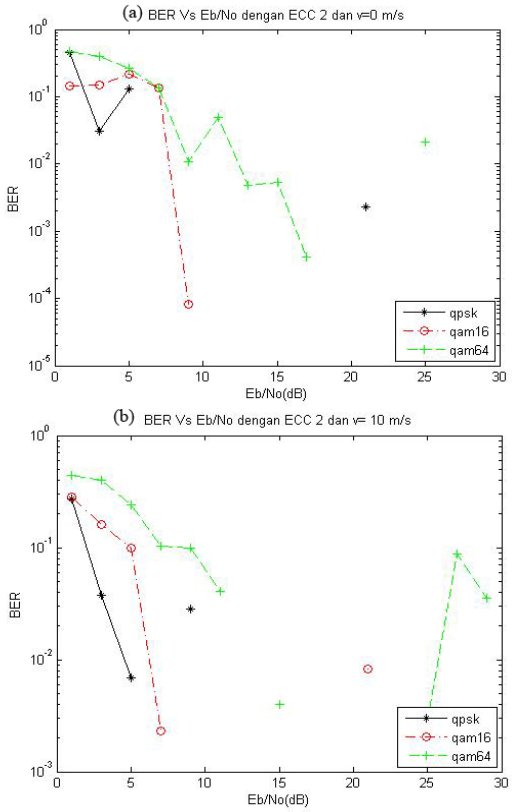

Figure 4 BER vs Eb/No ECC = 2

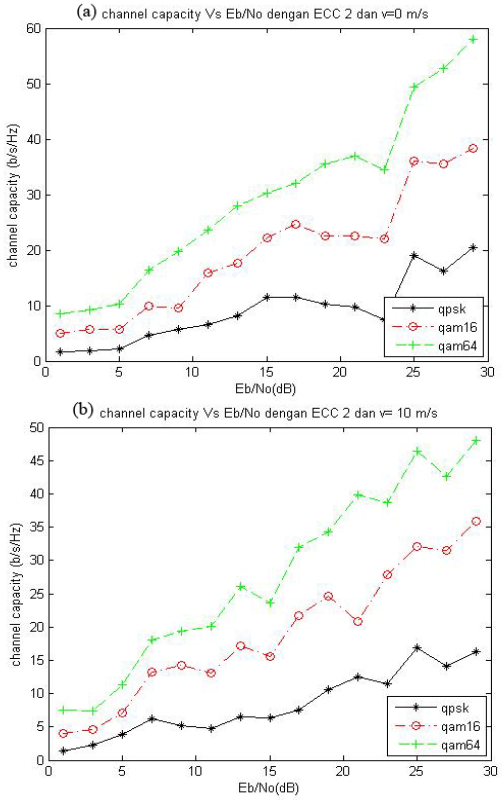

Figure 5. Channel capacity vs Eb/No ECC = 2

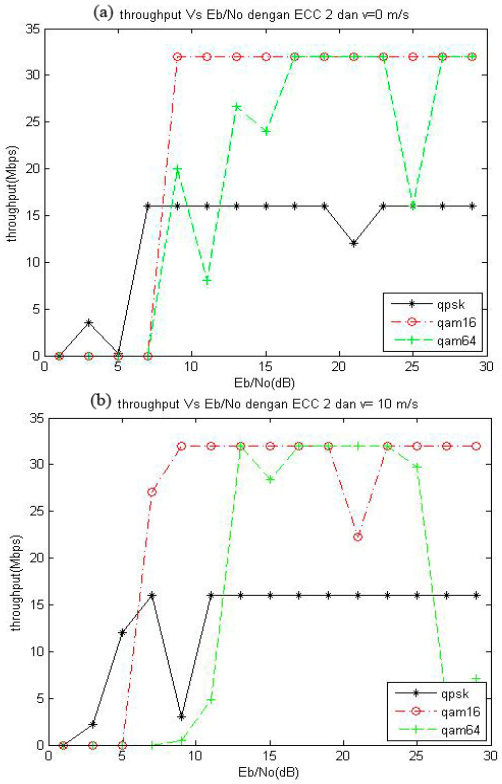

Figure 6. *Throughput* vs Eb/No ECC = 2

5. CONCLUSION

From spatial multiplexing MIMO OFDM based on SVD simulation, can be concluded in following sentences.

1. MIMO OFDM systems with spatial multiplexing technique have advantage at high speed data transfer side.
2. Performance for system with ECC is better than system without ECC, that is shown from BER, channel capacity and throughput graph.
3. Performance of system with idle user is better than system with mobile user, eventough in this simulation, the differences is not significant.
4. The better perforamnce can be achieved in channel coding with high code rate.

REFERENCES

[1] _____, *"Orthogonal Frequency Division Multiplexing(OFDM)"*,Aplication for Wireless Communication with Coding

[2] Michael Steer, "*Beyond 3G,*" IEEE Microwave Magazine No.1 (Februari,2007).

[3] Jaehak Chung, Yungsoo Kim, Eungsun Kim, "*Multiple Antenna System for 802.16 Systems"*, IEEE 802.16 Broadband Wireless Access Working Group.2001

[4] Abdullah Mandan. “Pemodelan Kanal MIMO OFDM Sistem Komunikasi UWB Menggunakan Singular Value Decomposition”. Skripsi, Program Pasca Sarjana Fakultas Teknik UI,Depok, 2008.
[5] Philippe Duplessis, "*Exploiting OFDM and MIMO to take UMTS beyond HSDPA / HSUPA*", Nortel Technical Journal, Issue 2, Nortel, Kanada
[6] Allert van Zelst, “MIMO-OFDM For Wireless LAN,” Disertasi Ph.D, Technisce Universiteit of Eindhoven, Eindhoven, 2004.
[7] Kamal Hamzah. “Sistem Komunikasi Nirkabel Dan Bergerak Dengan Menggunakan Teknik MIMO OFDM”. Seminar, Program Sarjana Fakultas Teknik UI, Depok,2008.
[8] _____, "*Mengenal Teknologi Frequency Division Multiplexing (OFDM) pada Komunikasi Wireless*".Diakses 7 mei 2008 dari elektro Indonesia. www.elektroindonesia.com
[9] Wang, Yin, et al. “*MIMO with MUMS*”. Project course in signal processing and Digital Communication. KTH, Swedia. 2004
[10] Wahyu Mahendra. “Simulasi Sistem MIMO-STBC dengan Smart Antenna Algoritma Referensi Temporal ”. Skripsi, Program Sarjana Fakultas Teknik UI, Depok,2008.
[11] K Sam Shanmugam, “Digital and Analog Communication Systems” (New York: John Wiley & Sons, 1979).
[12] Gunawan Hendro. “Simulasi WCDMA dan WiMAX”. Skripsi, Program Sarjana Fakultas Teknik UI, Depok,2006
[13] Tim C W Schenk, Guido Dolmans, Isabella Modonesi. "*Throughput of a MIMO OFDM based WLAN System*". Proc. Syposium IEEE Benelux Chapter on Communications and vehicular Technology, Belgium. 2004

ISSN 114-1284

Network Modeling for Broadband PLC

Basuki Rahmat[1]; Rinaldy Dalimi[2] ; Kalamullah Ramli[2]

[1]*Electrical Engineering Department*
Institut Teknologi Telkom
Jl. Telekomunikasi. No.1. Ters. Buah Batu, Bandung 40257
Tel : (022) 7564108 Ext 2303. Fax : (022) 7565933
E-mail : bas@ittelkom.ac.id; basuki.rahmat71@ui.edu

[2]*Department of Eletrical Engineering, Faculty of Engineering*
Universitas Indonesia, Depok 16424
Tel : (021) 7270011 ext 51. Fax : (021) 7270077
E-mail : rinaldy@eng.ui.ac.id; k.ramli@ee.ui.ac.id

ABSTRACT

Broadband Power Line Communication (PLC) network is more possible to be implementation at low voltage powerline network. However, utilization of electric powerline as access network is still very limited, in spite of a currently some of the approaches are Multi-Carrier Modulation, Multi-Carrier Spread Spectrum, OFDM-FDMA, MC-CDMA, and some coding method is already applied at physical layer. Those coding techniques are supposed to handle bandwidth limited and error data transmission due to disturbance of noise problem in a shared transmission medium[2].
Normally, users are connected into broadband PLC network in form of a bus topology. Base stations as a central network has responsibility to manage of communication link for inter- subscribers and subscribers to telecommunication backbone network. At the transmission media, in addition to information traffic, impulse noise which appear in broadband PLC network. This additional noise will there fore decrease the performance of broadband PLC from a satisfying QoS requirement and hence must be compensated. In this paper, we propose a state equation to describe a dynamic model of broadband PLC network. This model is used to expose of broadband PLC network behavior, included the impacts of environment condition to the system. Knowing the behavior of broadband PLC network, we can turn in the performance of the system to an expected level.

Keywords: *Broadband PLC, dynamic model, QoS, state equation, .*

1. INTRODUCTION

At the beginning, powerline is designed only for electricity power distribution in interval of frequency (50-60) Hz. Theoretically, electricity power transmision possible to pass frequency signal over 60 Hz until order of 100 MHz (In practical point of view, current technology can support frequency up to 30 MHz). PLC's technology has been used in electrical power system for long time ago in (125 Hz-1500 kHz) frequency using medium and high voltage for electricity power system management.
During 1990 decade, researchers and developers started to realize the possibility of broadband PLC using powerline. This possibility, thus, can provide broadband communication to rural area or residence area which has less or no telecommunication infrastructure. In fact, powerline network has wider coverage area than PTSN network in most countries, include Indonesia[1,2].
Main problem in broadband data communication using powerline network is impulse noise from internal network. This impulse noise, for examples, originates from the electrical load and electricity power system itself. Somes technical approach have been applied, e.g Multi Carrier Spread Spectrum Modultion scheme, Orthogonal Frequency Division Multiplexing (OFDM), and CDMA in transmission PLC system. These modulation schemes are aimed to produce efficient and wider bandwith capacity. In addition, these modulation schemes can also increase the robustness of broadband PLC network against impulse noise interference[2,5].
Researches on PLC network at physical layer (such as modulation, coding, etc) had done extensively. However, research on network level and higher level of implementation, unfortunately, is very less. Thus, despite of promising future, mayority of powerline network capacity are still useless, as depicted in Figure. 1. below.

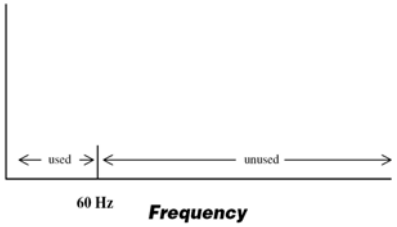

Figure 1. Frequency occupancy area of *powerline* [7]

ISSN 114-1284

At Network Layer, for example, mostly MAC protocol layer that apply for PLC broadband, such as CSMA/CA and TDMA, are coming from IEEE 802.11 which originally used for wireless technology. Since wire and wireless technology certainly have difference characteristics and environments, therefore applying wireless protocol for wire communication is not appropriate.

Technically, to increases the performance of broadband PLC network one should choose an appropriate medium access control (MAC) protocol layer. This MAC protocol should take in to account the condition of Physical Layer, the Dynamic characteristic of Network, and the QoS of the Network. For that reason, we need to model these three aspects into broadband PLC network modeling. The development for access control mechanism in MAC protocol layer then will be based on this model. In this paper we propose a state equation to describe a dynamic model for broadband PLC network.

2. BROADBAND POWERLINE COMMUNICATION (PLC) NETWORK

Broadband PLC is a wide band communication technology through the electricity power transmission channel in frequency over 1 MHz. Interfacing between communication systems to electricity power using a coupling. Broadband PLC network is built on the powerline distribution network at low voltage which is inherently forms of bus network topology. For this topology, one line bus is shared as transmission medium for all users. Therefore, it is an obligation, in such situation, to introduce a fair access control mechanism for all users. Therefore, OFDM-FDMA scheme have been applied to handle multiple access control.

2.1. Powerline network

Electrical powerline network consists of three levels:

- level : 110-380 kV, from generator to huge user area (distance up to 100 km).
- level : 10-30 kV, wide area powerline network (city, industries or commercial users, distance up to 10 km).
- level : 230-400 V or 110 V, is a powerline network to user, individual user (distance within several meters).

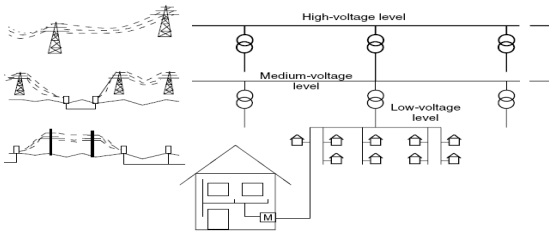

Figure 2. Power electric network level

2.2. Broadband PLC channel model

Broadband PLC channel is described using two approaches. *First*, physical channel approach. In this approach, the main focuses are *attenuation* and *transmission in frequency domain*. In physical view, impulse response of channel causes echo signal. This echo is mainly due to the variation of impedance of Broadband PLC channel within frequency in orde (1-1000) Ohm. Wire impedance characteristic, network topology and electric load all accumulate to produce echo at receiver side. Network multipath has caused discontinued-impedance that causing reflection and multipath signal transmission, as Figure 3.

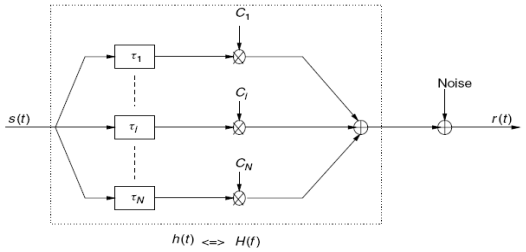

Figure. 3. Multipath channel model[2]

In Figure 3, echo from multipath channel powerline model is describes as transmitted in PLC channel will break through several N branches. Each i branch has delay (τ_i) and attenuation factor (C_i). PLC channel in frequency domain[2,5] therefore can be expressed as:

$$H(f) = \sum_{i=1}^{N} g_i . e^{(a_0 + a_1 . f^k) l_i} . e^{-j2\pi f \tau_i} \quad \ldots(2.1)$$

Second, logically model approach. A number transmission channel is used by a number subscribers which have dynamic behavior with four probability conditions: (1) busy, (2) idle, free (3) error, dan (4) reserve. Figure 4, describes these conditions and the possible change of each condition.

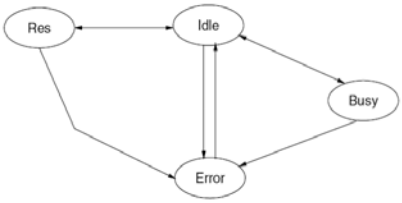

Figure.4. Diagram model state channel [3]

2.3 Noise in broadband PLC network.

As previous explained that in broadband PLC channel, besides Additive White Gaussian Noise (AWGN) also appear some impulse noise disturbance with power greater than AWGN power. The whole of disturbances are classified into five types based on four categories: disturbances based on duration, spectrum, occupancy, and intensity, as depicted in Figure 5.

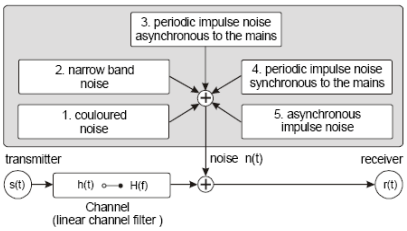

Figure 5 : *noises* in PLC[6],

Broadband PLC noise environment is a superposition of background noise with some narrowband noise interference.

$$n_{imp}(t) = \sum_{i=-\infty}^{\infty} A_i . p(\frac{t - t_{a.i}}{t_{w.i}}) \text{ .....(2.2)}$$

Impulsive noise is formed from synchronous and asynchronous periodic impulse noise within electrical power frequency itself. Impulse is modeled with *train pulse* (wide: t_w, amplitude : A; inter-arrival time : t_a), *function pulse* $p(t/t_w)$, where *i* random variable.

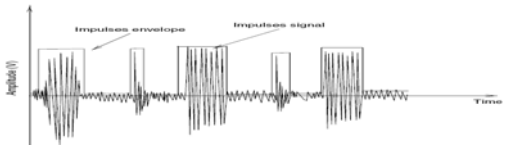

Figure 6 : *Impulse noise* in time domain [3]

2.4. Broadband PLC Access Network.

Broadband PLC access network is realized in low voltage distribution network, as depicted in Figure 7, below.

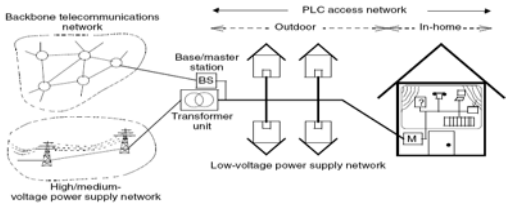

Figure 7: Access network *PLC*[2]

As previously explained that broadband PLC is a bus topology network. Base station as central network acts as communication interface from users to WAN, and from user to user in centralized network structure.

Figure 8 : Logical bus structure PLC network [2] ;

3. DYNAMIC MODEL BROADBAND PLC NETWORK

Mathematical model is used to show network dynamic in accordance to *traffic information, noise,* and *channel characteristics* of electricity power system.

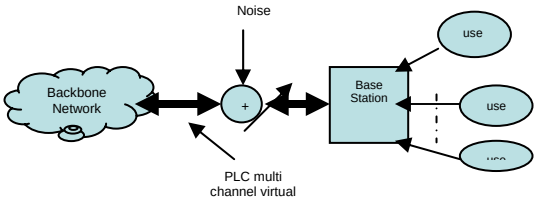

Figure 9: Broadband PLC's network environment

Mechanism processes that take place in broadband PLC access network, is described in Figure 10.

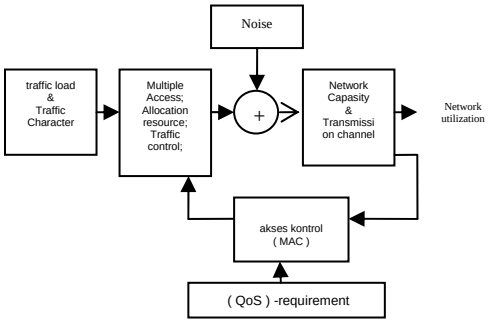

Figure. 10. Block Diagram of dynamic network process

Diagram above can be explained as follows, broadband PLC network, especially the Base Station node and link toward backbone network, will change every time due to traffic load and noise disturbance from the electricity system. These changes will influence the network utilization indicator. MAC protocol as an agent in regulating access control, actively regulate and manage resources in accessing the shared transmission channel, MAC protocol is responsible in accessing the number of free available channels. Every resources or users, who are currently accessing the shared media, utilized the multiplexing techniques based on OFDMA. This multiplexing technique also responsibles in suppressing the transmission error due to impulse noise.

Since the traffic and noise are stochastic process, then changes of network state is also a dynamic process. Dynamic transition of network is modeled as a state equation which mathematically expressed in (3.1)

$Q(t+1) = Q(t) + AQ(t) + BU(t)$ .....…...(3.1)

where :

Q(t+1): Vector of network next state

Q(t) : Vector of network current state

A : Matrix of network state

B : Matrix of control

U(t) : Vector of control

4. CONCLUSION

Equation (3.1) describes the probability of broadband PLC's network state transition from *Q(t)* to *Q(t +1)* state as function of *information traffic*, *impulse noise* from the electricity power network, and *control process by MAC protocol* layer scheme.
How probability of state transition occurs, that to be works in our future research.

REFERENCES

[1] T. Chiras1, P. Koutsakis2 and M. Paterakis1;" A New MAC Protocol for Broadband Powerline Communications Networks", IEEE GLOBECOM 2006 proc.
[2] H. Hrasnica, A. Haidine and R. Lehnert, "Broadband Powerline Communications: Network Design", John Wiley & Sons, 2004.
[3]. H.Hrasnica, A. Haidine :" Modeling MAC Layer for Powerline Communications Networks ",Dresden University of Technology 01062, Germany
[4] Y.-J. Lin, H. A. Latchman, J. C. L. Liu and R. Newman, "Periodic Contention-Free Multiple Access for Broadband Multimedia Powerline Communication Networks", in Proc. Of the 9th International Symposium on Power Line Communications and its Applications (ISPLC), Vancouver, Canada, 2005.
[5].P. Amirshahi , S.M. Navidpour and M. Kavehrad : "Fountain Codes for Impulsive Noise Correction In Low-Voltage Indoor Power-line Broadband Communications**" ;** The Pensylvania State University, Department of Electrical Engineering, Center for InfoCom Technology Research (CICTR) ;University Park, PA 16802;(C) IEEE 2006;
[7]. H. Gilbert, : " Understanding broadband over power line / Gilbert Held", Published in 2006 by Auerbach Publications-Taylor & Francis Group-6000 Broken Sound Parkway .
[8]. P.Topfer; Jacqui Bridge ; Anthony Seipolt : " TECHNOLOGY REVIEW OF POWERLINE COMMUNICATIONS (PLC) TECHNOLOGIES AND THEIR USE IN AUSTRALIA **Final Report** Prepared for The Department of Communications, Information Technology and the Arts ; 7 October 2003.
[9]. C. Gomez : " An Introduction to Broadband Power Line (BPL) Technology" DS2 – VP Technology & Strategic Partnerships IEEE Consumer Electronics Society SCV Meeting Cupertino - Nov 29th,2005.
[10]. G. Jeong, D. Koh, and Jongsu Lee :" Analysis of the Competitiveness of Broadband over Power Line Communication in Korea" . ETRI Journal, Volume 30, Number 3, June 2008.
[11]. L. Rock,AR :" *BPL – A Broadband Solution for Rural Amerika*" pada MARC 2005 Conference.
[12]. T. Mastrangelo:" Ensuring ESA Capabilities during Network Transformation", An Aztek Networks™ White Paper ; *The Windsor Oaks Group LLC 2007.*
[13].www.centerdigitalgov.com :" Arizona Broadband Initiative Framework Analysis and Report ", Center for Digital Government.2007.
[14]. www.upaplc.org :" Universal Powerline Association Ships 4.5 Million Chips while Championing Interoperability, Universal Functionality and Standardization of all Powerline Communications . Juli 2008.
[15]. JM. Kang, CK. Park, EH Kim JWK Hong, Y.Lim, S. Ju, M Choi, B Lee & D Hyun :" Design and Implementation of Network Management System for Power Line Communcation Network", POSTECH, Pohang, KOREA; IEEE International Symposium on Power Line Communications and its Applications (ISPLC 2007).
[16]. *K.Tripathi*, *JD. Lee, H. Latchman, J. McNair* & *S. Katar :"* Contention Window based Parameter Selection to Improve Powerline MAC Efficiency for Large Number of Users ",University of Florida Gainesville, Florida, USA 2005.
[17]. MS Kim, DM Son, YB Ko & YH Kim :" A Simulation Study of the PLC-MAC Performance using Network Simulator-2", Graduate School of Information & Communication, Ajou University, LS Industrial System, Korea. ITA-2008.
[18]. D.D Barr,JR & Amato : " TECHNICAL INFORMATION BULLETIN 07-1 Broadband over Power Lines" ; NATIONAL COMMUNICATIONS SYSTEM Technology and Programs Division, Arlington, Virginia January 2007.
[19].The "CIAC Year in Review 2006" document notes.
[20]. K Rudd, S Conroy, and L Tanner :" A Broadband Future for Australia – Building a National Broadband Network", ALP Marc 2007.
[21]. P. Ramjee.: " OFDM for wireless communications systems ",Artech House, Inc. Boston • London www.artechhouse.com ; **2004.**
[22]. A.R.S.Bahai and B.R.Saltzberg : "Multi-Carrier Digital Communications: Theory and Applications of OFDM", ©2002 Kluwer Academic Publishers - New York,
[23]. V.P. Ivatov : " Spread spectrum and CDMA Principle Application"; John Wiley & Sons, Ltd @ 2005.
[24]. S.Meyn :" Control Techniques for Complex Network", Cambridge University Press

ISSN 114-1284

The Study of Single-Tuned Filter Design as a Solution for Harmonic Problem of 1300 VA Household Loads

Budi Sudiarto, Chairul Hudaya, Iwa Garniwa, Aris Pramnanto

Electric Power and Energy Studies
Department of Electrical Engineering Faculty of Engineering
University of Indonesia, Depok 16424
http://www.ee.ui.ac.id/epes
E-mail : budi@ee.ui.ac.id or c.hudaya@nuklir.info

ABSTRACT

The increasing of non-linear loads causes the increasing of harmonic distortion level on the electric grids. Harmonic distortion is the change of waveform of both current and voltage from the ideal sinusoidal waveform. This phenomena result in several disadvantages to the power quality such as increasing losses on the transmission, derating of transformers and other stuffs.

The household loads are the main cause for harmonic phenomena. This is because the household loads are generally using non-linear loads such as refrigerator, air conditioner, water pump, electronic ballast lamp, and computer. The study investigate the design of harmonic filter to reduce harmonic level to be applied for those kinds of loads for household with power of 1300 VA. The surveys of electricity equipments broadly used in the household are then conducted and the data are simulated to view the load characteristics. The harmonic filter developed in this study is the single-tuned filter which has harmonic distortion of current and voltage of order 3. The result shows that the filter plays important role in decreasing the harmonic distortion level, lowering the active power consumed by equipments, and increasing power factor which will in turn upgrade the power quality of the grids.
.

Keywords : *single-tuned filter, non-linear loads, harmonic distortion, power quality.*

1. INTRODUCTION

Power quality has 3 main parameter : voltage, current, and frequency. The deviation of the three-parameters will degrade the quality of power supplied for the loads. The degrading in power quality will cause failure or wrong in operation at the consumer side. The stated-owned electric company (PLN) is still trying to overcome the problems arising due to this issue started on transmission and distribution systems until the costumers receive the power. However, the power quality problems are also coming from the load side which will in turn affect the systems.

One of power quality related problems coming from load side are harmonic distortion. Harmonic distortion is the change of waveform of both current and voltage from the ideal sinusoidal waveform. This phenomena result in several disadvantages to the power quality such as increasing losses on the transmission, derating of transformers and other stuffs.

Indonesia is the fast-growth populated country which is demanding huge electric energy needs especially household loads. In line with the huge household loads, the harmonic distortion may also be huge when it's accumulated. Thus, The study investigate the design of harmonic filter to reduce harmonic level to be applied for those kinds of loads for household with power of 1300 VA

2. THEORETICAL OVERVIEW

Harmonic is the phenomena of sinusoidal wave forming in which the new frequency is the multiply of rational number with its base frequency. If there is superposition between base frequency and harmonic frequency, it therefore will form distorted sinusoidal wave, meaning the wave is not sinusoidal anymore. The phenomena is then called as harmonic distortion.

The sum of non-sinusoidal wave can be analyzed by using Fourier series as below :

$$Y(t) = Y_0 + \sum_{n=1}^{n=\infty} Y_n \sqrt{2} \sin(n 2\pi f t - \varphi_n) \qquad (1)$$

Notes :

- Y_0 amplitude of DC components in distribution systems , usually zero valued.
- Y_n: root mean square (rms) value of harmonic component -n
- f base frequency (50 *Hz*)
- φ_n Phase angle od harmonic component -n

The equation (1) represented the distorted sinusoidal wave. It may be seen at Figure 1 as below :

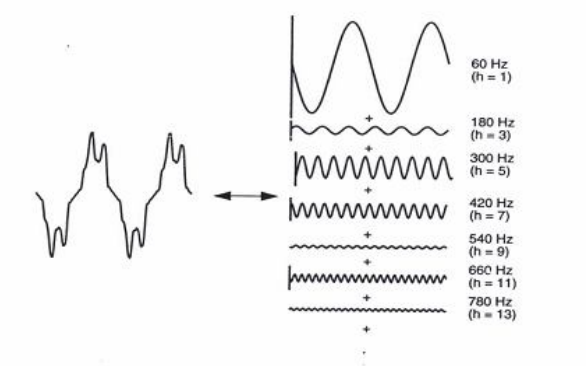

Figure 1. Fourier Series of Distorted Sinusoidal Wave

Total Harmonic Distortion (THD) express the amount of distortion arised by all harmonic components which can be stated as :

$$THD = \frac{\sqrt{\sum_{n=2}^{n=\infty} M_n^2}}{M_1} \quad (2)$$

Notes:
THD Total Harmonic Distortion
M_n RMS of harmonic current and voltage –n
M_1 RMS of base current and voltage

THD may also represent as a potential heating as the result of relative harmonic against its base frequency.

Harmonic current and voltage can cause the different effects to the electric stuffs, depending on its load characteristics. However, generally the effect may be divided into three main parts :

1) RMS value of current and voltage will be higher
2) Peak value of voltage and current will rise
3) The frequency systems will decrease

Each element in electrical load systems generates specific distortion. The higher RMS value may cause heating in the conductor. The current and voltage which are higher than the peak value will cause the failure in measurement. And the increase of frequency will affect the conductor impedance. If the conductor often receives the peak value of voltage, it will result in high of drop voltage. The resonance phenomena will appear at certain frequency which cause the increasing current.

3. METHODOLOGY

The methodology of this study is divided into 3 main works :

1) Identification of general electric equipments widely used by households with power of 1,300 VA
2) Measurement of harmonic loads
3) Designing of harmonic single-tuned filter

3.1 Identification of general electric equipments

According to survey we conducted, the general household electric equipments with power of 1,300 VA are as follow :

Table 1. Specification of Measured Loads

No.	Electric Stuffs	Unit	Power (W)	Voltage (V)	Frequency (Hz)
1	LHE				
	A	4	8	170-250	50/60
	B	4	14	170-250	50/60
	C	4	18	170-250	50/60
2	Television	1	65	180-270	50/60
3	AC	1	1150	220	50/60
4	Computer				
	CPU	1	350	110/220	50/60
	Monitor	1	240	100-240	50/60
	Speaker	1	10	220	50
5	Refrigerator	1	77	220	50/60
6	Dispenser	1	300	220	50

Notes :
LHE : *Lampu Hemat Energi* (Energy-Saved Light)

3.2 Measurement of Harmonic Loads

After considering the general electric stuffs widely used by households, we then conducted the measurement of each harmonic loads by using power quality analyzer. The results are shown in Table 2.

3.3 Designing of Harmonic Single-Tuned Filter

In order to design the filter, it is necessary to obtain the highest voltage harmonic (THD V) and current harmonic (THD I) in the loads systems. The data may be seen in table 2 and 3. The highest THD V is used for determining at what order the current harmonic will be filtered.

According to the experiment, we found the highest THD V is on the third order. This leaves the passive filter will be designed on the order 3.

After determining the filter's order, the next step is to fix the reactive power should be supplied to the systems. This effort is aimed at improving the power factor of the systems. For this reason, we calculated the total power of the systems which can be seen in Table 4.

Table 4. Power Loads Characteristic in Household

Power	Average	Maximum	Minimum
P (W)	1444	1702.5	1297.3
Q (VAR)	72.1	97.6	43.2
S (VA)	1541.7	1777.8	1404

Table 2. Harmonic Voltage of Each Loads

Order	THD V (%)							
	LHE 18W	LHE 14W	LHE 8W	TV	PC	AC	Refrigerator	Dispenser
2	0.20	0.17	0.18	0.20	0.24	0.67	0.27	0.23
3	2.67	2.25	2.34	1.95	2.38	1.23	1.39	1.60
4	0.06	0.06	0.06	0.08	0.10	0.19	0.06	0.05
5	1.50	1.31	1.40	1.52	1.39	1.19	1.30	1.45
6	0.07	0.05	0.05	0.05	0.07	0.13	0.07	0.05
7	1.01	1.03	1.06	1.05	1.00	0.93	1.12	1.11
8	0.04	0.06	0.04	0.06	0.07	0.10	0.05	0.05
9	0.41	0.61	0.53	0.51	0.67	0.69	0.59	0.57
10	0.06	0.04	0.05	0.05	0.07	0.08	0.05	0.07
11	0.40	0.30	0.33	0.33	0.46	0.26	0.26	0.27
12	0.03	0.03	0.04	0.04	0.05	0.07	0.05	0.03
13	0.26	0.21	0.20	0.16	0.29	0.18	0.17	0.20
14	0.03	0.04	0.04	0.04	0.08	0.06	0.06	0.04
15	0.40	0.50	0.42	0.44	0.38	0.49	0.59	0.56
16	0.03	0.04	0.04	0.03	0.05	0.03	0.04	0.03
17	0.20	0.26	0.27	0.20	0.34	0.18	0.29	0.35
18	0.04	0.04	0.03	0.03	0.04	0.03	0.04	0.04
19	0.24	0.22	0.18	0.22	0.11	0.13	0.14	0.15
20	0.03	0.04	0.03	0.02	0.04	0.03	0.04	0.05
21	0.33	0.31	0.35	0.18	0.25	0.28	0.21	0.27
22	0.04	0.04	0.04	0.03	0.03	0.03	0.04	0.06
23	0.17	0.18	0.15	0.15	0.22	0.11	0.22	0.19
24	0.04	0.05	0.05	0.03	0.05	0.04	0.04	0.04
25	0.22	0.16	0.18	0.12	0.14	0.17	0.13	0.10
26	0.06	0.04	0.04	0.03	0.04	0.03	0.04	0.03
27	0.22	0.25	0.26	0.14	0.19	0.17	0.19	0.14
28	0.05	0.06	0.05	0.04	0.05	0.04	0.04	0.05
29	0.15	0.14	0.13	0.11	0.13	0.07	0.20	0.16
30	0.05	0.04	0.05	0.03	0.05	0.04	0.04	0.05

Tabel 3. Harmonik Arus Pada Beban Total

Order	THD I (%)	Order	THD I (%)	Order	THD I(%)
1	100	11	1.28	21	1.41
2	8.29	12	5.30	22	0.47
3	12.92	13	1.73	23	0.52
4	3.34	14	0.89	24	0.49
5	3.17	15	2.84	25	0.71
6	1.93	16	0.58	26	0.43
7	4.72	17	1.71	27	0.45
8	1.71	18	0.56	28	0.41
9	5.06	19	0.80	29	0.86
10	1.34	20	0.51	30	0.37

The power factor may be found by applying the equation 2 below :

$$PF = \frac{P}{S} \quad (2)$$

From the above equation, maximum power factor are obtained as much as 0.9576. The maximum approach was taken to anticipate reactive power in the systems. If the filter is designed for improving power factor until 0.98, the reactive power needed can be calculated by using equation 3 as below :

$$Q_{VAR} = \sqrt{\left[\frac{P_1}{PF_0}\right]^2 - P_1^2} - \sqrt{\left[\frac{P_1}{PF}\right]^2 - P_1^2} \quad (3)$$

The calculation shows that the reactive power as much as 166.5 VAR should be injected to the systems in order to improve power factor from 0.9576 to 0.98. Reactive power obtained through equation 3 are then used to determine capacitor impedance by applying the equation below :

$$X_C = \frac{kV_{rated}^2}{M\ \mathrm{var}_{rated}} \quad (4)$$

With rating voltage of 220 V and rating VAR of 166.5 VAR, it is obtained that the capacitor impedance as much as 290.7 Ω. The capacitor capacitance is then calculated by equation 5 below :

$$C = \frac{1}{2\pi f X_C} \quad (5)$$

The calculation result in capacitor capacitance as much as 11 µF. After that, we quantify the filter impedance by applying the equation 6 as below :

$$X_L = \frac{X_C}{n^2} \quad (6)$$

Note : n = voltage harmonic order after filtered

In this experiment we decrease the order a little bit into 2.9. This is as tolerance of filter component to prevent resonance in the systems. The calculation gives the filter impedance would be 34.57 Ω. The inductance of inductor can be obtained by applying equation 7 below:

$$L = \frac{X_L}{2\pi f} \quad (7)$$

From the calculation we got inductance as much as 110 mH.

To evaluate the designed systems, we then assessed the systems by implementing the other system (model) which was quite different with the proposed system. The specification of the proposed systems and the model may be seen in the Table 5 below :

Table 5. Filter inductance and capacitance

	Desain	Model
L	110 mH	100 mH
X_L	34.5	31.4
C	11 µF	12 µF
X_C	289.5	265.4

4. RESULT AND ANALYSIS

The result shows that the filter works efficiently when the systems are on full loads mode. This is because the filter compensate the reactive power and reduce filter when all loads are operated. However, because in the experiment we couldnot operate the full loads, therefore, the manual calculation were conducted by considering all currents, both fundamental and harmonic, taking into account its phases. Figure 2 is the graph of current harmonic at full loads :

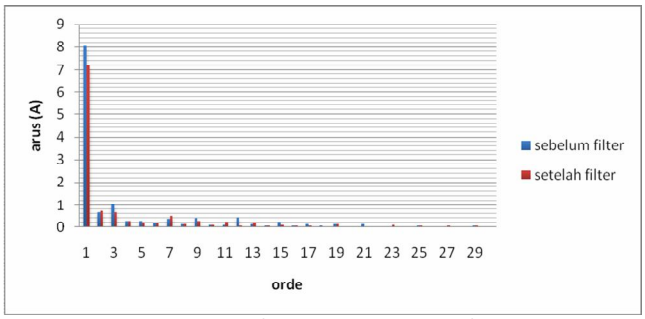

Figure 2 Graph of current harmonic at full loads

Before the filter was applied, the amount of THD I was 19.07 % with RMS current was 8.1913 A. After it's applied, the THD I decreased into 17.79 % with RMS current of 7.3120 A. Table 6 shows the comparison of RMS current between the systems prior filtered and after filtered below:

Table 6. RMS current of each load

Loads	Before Filtered	After Filtered
LHE 18 W	0.4985	1.2569
LHE 14 W	0.3761	1.1697
LHE 8 W	0.2156	1.1086
TV	0.5202	1.1229
PC	1.2903	1.5067
AC	4.2626	4.4361
Refrigerator	0.6762	0.6215
Dispenser	1.8556	0.7422
Total	**8.1913**	**7.3120**

The above comparison shows the filter can reduce the current harmonic on the total loads and compensate the reactive power to the systems. The total load currents

which are inductive are then injected to the filter loads which are capacitive. This, if it's added can weaken each other. As the result, the fundamental and harmonic current will decrease.

The experiment also shows most of odd-order of harmonic currents decrease. Contrary, the even-order of harmonic currents rises. Though the odd-order harmonic current affect THD, it is not significant enough to change the wave produced by the systems. The Fourier transformation informs that the even-order of harmonic current has mutual disappear each other, so that this order may be neglected.

The filter design qualifies to reduce harmonic current at order 3. At this order, the harmonic current decreases from 12.95 % at 1.0397 A into 9.45 % at 0.68 A.

5. CONCLUSION

The study to design the single-tuned filter has been conducted. The conclusion of this study are :

1) For each household load, the highest THD V can be found at the order 3 with varied percentages compared to base voltage ranging from 1.23 % to 2.67 % . This gives the filter's designed at the order 3 to reduce the harmonic current.
2) To prevent resonance of frequency, the single-tuned filter is set to be work at order 2.9 or at frequency of 145 Hz.
3) Inductive and capacitive impedance are synchronized so that it's obtained the minimum impedance at order 2.9.
4) The designed filter has RMS current of 1.4 A, peak voltage of 341.5 V, RMS voltage of 265.9 and total VAR of 372.3 VAR.
5) The maximum active power decreases from 1,702.5 W into 1,390.9 W after the systems apply the filter.

REFERENCES

[1]. Roger C. Dugan, et al., "*Electrical Power systems Quality*" (New York: McGraw Hill, 2002), hal. 233-252
[2]. Rifky Cahyadi. "*Upaya Penghematan Energi Listrik Dengan Cara Mereduksi Distorsi Harmonik Menggunakan Single Tunned Notch Filter*." Bachelor Thesis, Department of Electrical Engineering, Depok
[3]. Adrianto. "*Optimalisasi Penempatan Filter Pasif Untuk Mereduksi Rugi-Rugi daya Akibat Arus Harmonik Pada Industri Baja*." Bachelor Thesis, Department of Electrical Engineering, Depok

Design of Interface System RISC Processor with RTC based on Advanced Microcontroller Bus Architecture (AMBA)

Catherine Olivia Sereati

Faculty of Engineering
Atma Jaya Catholic University of Indonesia
Jl.Jendral Sudirman 51, Jakarta 12930
Tel.+6221 5708826 fax. +6221 57900573
email: catherine.olivia@atmajaya.ac.id

Abstract

Nowadays, RISC (Reduced Instruction Set Computer) architecture processor is used rapidly in multimedia, telecommunication, and household application. In order to support those application, RISC processor have to be integrated as system-on-chip (SoC) with some peripherals. This level of design requires bus systems which have high performance and low power consumption. In order to solve that problem, AMBA (Advanced Microcontroller Bus Architecture) is used to support interface system between processor and another component or peripheral in SoC level design.
The objective of this research is to design an interfacing system based on AMBA and to design RTC as peripheral which support RISC Processor. Proposed design used SIEGE32 processor which is based on RISC Architecture which is integrated with RTC (Real Time Clock) as peripheral for this processor. The design process started by designing AHB system, Bridge system, and APB system. After that the design continued by RTC (Real Time Clock).
This system is design and simulated using ModelSim 6.0, The simulation result show that this system is work at 180MHz and enable to operate in single transfer mode, where one cycle of AHB or APB could only acces one data packet of one address.

Keywords
SoC, RISC, SIEGE32, RTC, ModelSim

1. INTRODUCTION

Within the development of *System-On-Chip* technology, processor with RISC (*Reduced Instruction Set Computer*) architecture is used commonly in multimedia, telecommunication, and household appliance. To support those applications, RISC processor has to be integrated as system-on-chip (SoC) with some peripherals. This level of design requires bus systems which have high performance and low power consumption. In order to solve that problem, AMBA (*Advanced Microcontroller Bus Architecture)* is used to support interface system between processor and another component or peripheral in SoC level design transfer, which both of them have different specification.

This paper will describe how to design an interfacing system based on AMBA and peripherals which support RISC Processor. SIEGE32 is a processor that based on RISC architecture. In this research, SIEGE32 will be connected with RTC (*Real Time Clock*) as peripheral for SIEGE32 Processor.

2. BASIC THEORY

Host processor on system *on-chip* need bus interface system that optimize to connect processor with other modules which have different specification in bandwidth, power consumption and architecture complexity. Making specification boundary when design that interface system will inhibits the reuse of peripheral macro cells. To solve that problem, AMBA (*Advanced Microcontroller Bus Architecture*) can be used to solve that interface connection problem . Three buses are defined within the AMBA specification [2]:

- AHB (*Advanced High performance Bus*)
- ASB (*Advanced System Bus*)
- APB (*Advanced Peripheral Bus*)

Figure 1 shows a typical AMBA system:

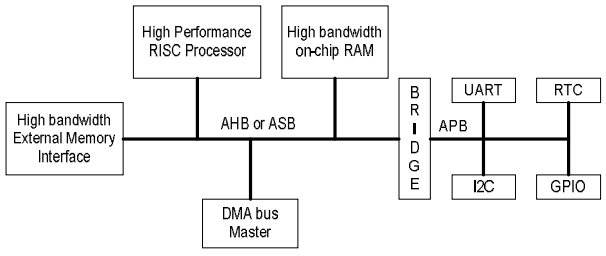

Figure.1. A typical AMBA-Based System, consist of AHB/ASB, Bridge and APB [8]

The AHB dan ASB is used to connect high performance system modules (ex. CPU, *on-chip* memory, and DMA (*Direct Memory Acces*)), APB is used for low performance peripheral, optimized for lower power consumption and to support interface system with low bandwidth. Bridge system is used to connect AHB and APB to support the compatibility of AHB to APB.

2.1. AHB (*Advanced High performance Bus*)

AHB is a part of AMBA bus which is intended to address the requirements of high-performance synthesizable designs. It is a high-performance system bus that supports multiple bus masters and provides high-bandwidth operation. AMBA AHB implements the features required for high-performance, high clock frequency systems including:

• burst transfers
• split transactions
• single-cycle bus master handover
• single-clock edge operation
• non-tristate implementation
• wider data bus configurations (64/128 bits).

An AMBA AHB design may contain one or more bus masters, typically a system would contain at least the processor. Bus Master is a system bus that initiated transfer operated, including read and write process. The external memory interface, APB Bridge and any internal memory are the most common AHB slaves.

2.2. APB (*Advanced Peripheral Bus*)

The APB is part of the AMBA hierarchy of buses and is optimized for minimal power consumption and reduced interface complexity. The AMBA APB appears as a local secondary bus that is encapsulated as a single AHB slave device. The AMBA APB should be used to interface to any peripherals which are low bandwidth and do not require the high performance of a pipelined bus interface.

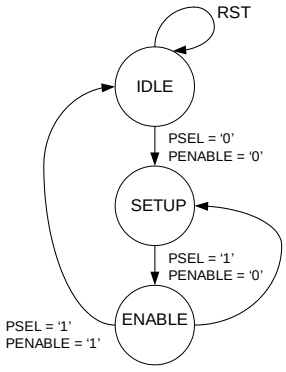

Figure .2. APB *State Diagram* [8]

Operation of the state machine is through the three states described below:

- IDLE: APB default state.
- SETUP: When a transfer is required the bus moves into the SETUP state, where the appropriate select signal, **PSELx**, is asserted. The bus only remains in the SETUP state for one clock cycle and will always move to the ENABLE state on the next rising edge of the clock
- ENABLE: In the ENABLE state the enable signal, **PENABLE** is asserted. The address, write and select signals all remain stable during the transition from the SETUP to ENABLE state. The ENABLE state also only lasts for a single clock cycle and after this state the bus will return to the IDLE state if no further transfers are required. Alternatively, if another transfer is to follow then the bus will move directly to the SETUP state. It is acceptable for the address, write and select signals to glitch during a transition from the ENABLE to SETUP states.

2.3. Bridge AHB-APB

The APB Bridge is the only bus master on the AMBA APB. In addition, the APB Bridge is also a slave on the higher-level system bus. The bridge unit converts system bus transfers into APB transfers and performs the following functions:

- Latches the address and holds it valid throughout the transfer.
- Decodes the address and generates a peripheral select, **PSELx**. Only one select signal can be active during a transfer.
- Drives the data onto the APB for a write transfer.
- Drives the APB data onto the system bus for a read transfer.
- Generates a timing strobe, **PENABLE**, for the transfer.

Bridge consist of:

- AHB Interface
- APB Interface
- Control Block
- Address Decoder

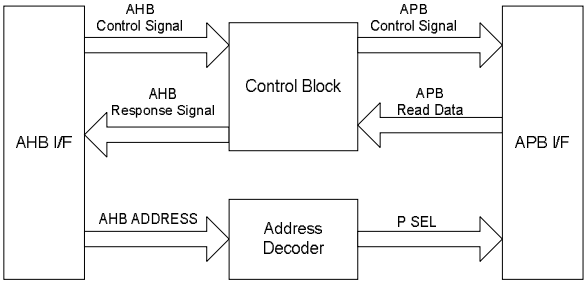

Fig 3. Architecture Bridge AHB-APB.

AHB Control Signal: HWRITE, HTRANS, HSIZE, HBURST

APB Control Signal: PWRITE
AHB Response Signal: HREADY, HRESP

Communication between AHB master and APB slave could be done by select the appropriate slave and drive the address, data and control information to selected slave and then show all the receiving data in AHB data bus

2.4. AHB Master and Slave

AHB *Maste*r is a bus system which initiated read and write process by giving appropriate address and control signal information. In this design SIEGE 32 processor [5] acts as AHB Master. *Bridge* AHB-APB is AHB Slave, which respond read or write operation that giving by AHB master.

2.5. RTC (*Real Time Clock*)

Real Time Clock (RTC) is a *peripheral* in AMBA bus system which use as timer, basic alarm, and long time base counter. In AMBA bus system, RTC is connected to APB as peripheral for RISC processor. Interface connection between AMBA APB with RTC is shown figure bellow.

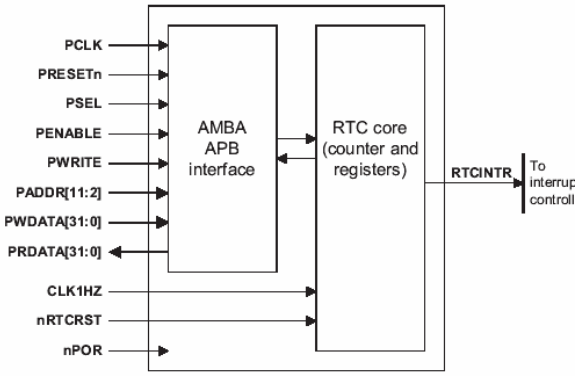

Figure. 4 Interface connection AMBA APB to RTC [8]

Parts of RTC are :

- AMBA APB *Interface* : produce read and write information for RTC
- Register Block : register to store data being read or write via AMBA APB
- Control Block : to control interrupt of RTC. If the value of counter match with the value of . RTC Match Register (RTCMR) inside, interrupt will generated (RTCINTR = '1')
- Counter Block : 32 bit up counter that work base on RTC clock.

Pin configuration of RTC is show in figure 5 below

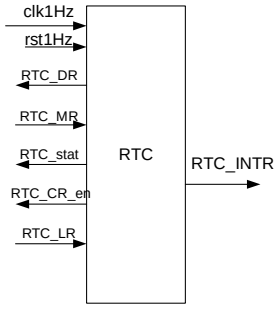

Figure 5. RTC Pin Configuration.

Function of each pins is explained in table 1.

Table 1. Pin Configuration of RTC.

Port	I/O	Wide (bit)	Function	Synch
clk1Hz	I	1	system Clock RTC	-
rst1Hz	I	1	system Reset RTC	
RTC_DR	O	32	RTC *Data* Register.	Clk 1Hz
RTC_MR	I	32	*Match Register*,	Clk 1 Hz
RTC_Stat	O	32	RTC *Status* Register,	Clk 1hz
RTC_CR _en	O	1	RTC *Clear Enable*.	Clk 1 Hz
RTC_LR	I	32	RTC *Load Register*.	Clk 1 Hz
RTCINT R	O	1	Interrupt Condition	Clk 1 Hz

Counter 32 bit is incremented in rising edge of clock RTC. Counting in one second interval is achieved by use of a 1Hz clock input in RTC. The counter is loaded with a start value by writing to load register RTCLR(RTC *Load Register*). If counter has reached the maksimum value 0Xffffffff, it wraps to 0X00000000 and continues incrementing. The value of incrementing can be read anytime via register RTCDR (RTC *Data Register*).

Interrupt signal is produced by comparing the value from register RTCMR (RTC *Match Compare Register*) and the value from counter incrementing. If the value is same, the interrupt signal will be generated. RTC Timing Diagram can be shown in Figure 6 :

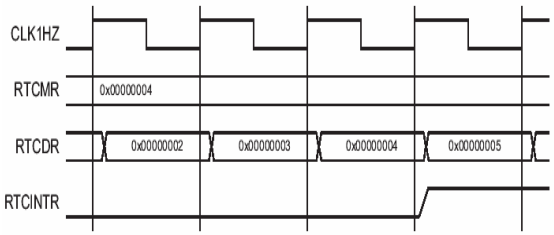

Figure.6 RTC Timing Diagaram.

Masking interrupt is controlled by register RTCCR (RTC *Control Register*. Interrupt status can be read vai register RTCstat.

2.6. Clock Divider

Each components on this system have different frequency value. SIEGE32 processor work at 27 MHz, meanwhile RTC work at 1 Hz. Figure 7 show the clock divider diagram block.

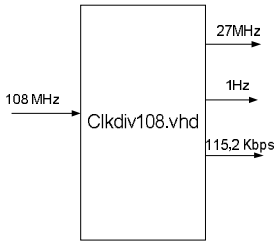

Figure. 7 Clock Divider Block Diagram

Frequency input for clock divider is 108Mhz, and then divide to produce 27MH and 1Hz frequency value.

3. SYSTEM DESIGN

This section will discussed steps of designing interface system of RTC as peripheral for SIEGR32 with AMBA bus system as interface protocol.

3.1. AHB Master dan Slave Design

AHB *Master* is a bus system which initiated read and write process by giving appropriate address and control signal information. In this design SIEGE 32 processor act as AHB Master. *Bridge* AHB-APB is AHB Slave, which respond read or write operation that giving by AHB master. Figure 8 show the connection of SIEGE32 processor to AHB as bus master to Bridge system.

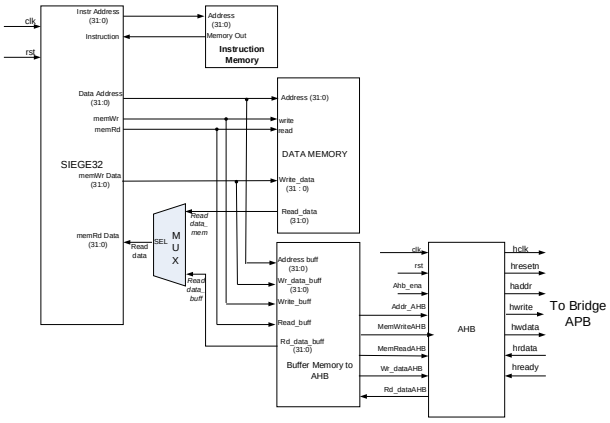

Figure 8. System Connection SIEGE32 processor to AHB bus system [5]

When operated as AHB Master, addressing system must be used to connect processor with peripheral as a slave module. In this design address 0x2F0 – 0x300 is used to RTC access.

Modificiation in instruction memory module must be doing support transfer between processor and bus system. The example of modification in HDL programming is :

```
architecture behave of inst_memory is
  begin
  inst_out <=
  --put your program here--

X"E3B0000A" when address = conv_std_logic_vector
(0,32) else -- move(MOV) data 0Ah to register R0

X"E58E02F4" when address = conv_std_logic_vector
(4,32) else -- store (STR) data from register R0 to
address 2F4

       X"E59E42F0"       when       address       =
conv_std_logic_vector (40,32) else --  load (LDR)
data from address  2F0 and store it to register 3
```

3.2. RTC design and integration with AMBA bus

RTC is designed to have 32 bit data wide, and have 1second time reference. Diagram block of interfacing system RTC with AMBA bus is shown in figure 9.

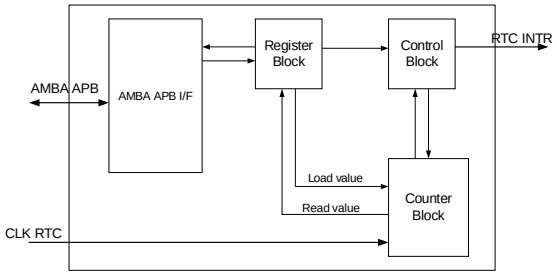

Figure 9. RTC Functional Diagram Block [8]

Parts of RTC are :

- Register Block : including RTCDR (RTC *Data register*) and RTCLR (RTC *Load Register*). RTCDR is a register which store the incremental value from *Counter Block*, RTCLR is a register which load by the first value of incremental value.
- Control Block : including RTCMR (RTC Match Register), which the output of RTCINTR will be '1' if he value of counter is same as the value of RTCMR (see the state diagram of RTC in figure 10) RTCINTR will disable if RTCCR (RTC Clear Register) is '1' . The condition of RTC interrupt can be read in register RTCstat (RTC status)

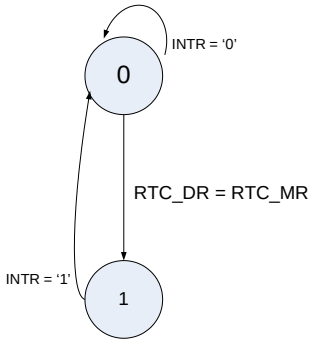

Figure. 10. State diagram RTC

- Counter Block : is a 32 bit counter increments by one of rising edge of RTC clock.

Connection of AMBA bus with RTC can be shown in figure 11.

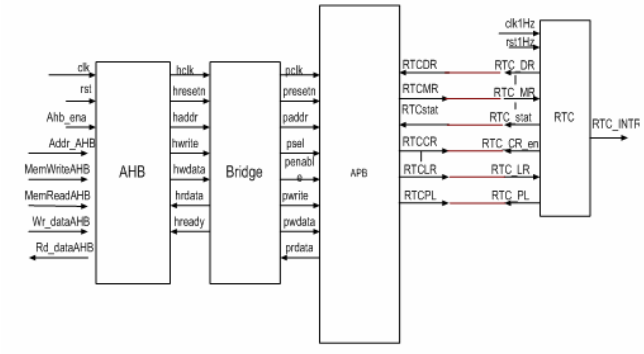

Figure.11 Connection of AMBA bus with RTC

Interface connection in figure 8 can be described in HDL programming below.

```
entity apb_periph is
port(

    -- APB Port --
    ------------ RTC REG'S BLOCK -----
RTCDR : in std_logic_vector (31 downto 0);
RTCMR : out std_logic_vector (31 downto 0);
RTCSTAT: in  std_logic_vector (31 downto 0);
RTCLR  : out std_logic_vector (31 downto 0);
RTCCR  : out std_logic_vector (31 downto 0);
req_RTC   : out std_logic;
busy_RTC  : in std_logic;
```

If APB bus wants to read RTC data, it will send request signal (req_rtc) to RTC. First the condition of write enable (write_en) is set to '0'.

```
req_rtc <= '1' when write_en = '0' else '0';
```

Meanwhile, to transfer data from APB bus to RTC can be described in HDL programming below :

```
if (paddr = X"000002f0" ) then
  if (write_en ='1') then
   case state is
     when IDLE_st =>
       data_buff <= (others => 'Z');
     when SETUP_st =>
       data_buff <= (others => 'Z');
     when ENABLE_st =>
       data_buff <= pwdata;
     when others =>
       data_buff <= (others => 'Z');
     end case;
     elsif (read_en = '1')then --

    case state is
      when IDLE_st =>
       if (busy_RTC = '1') then
         prdata <= (others => 'Z');
       else
         prdata <= (others => 'Z');
        end if;
      when SETUP_st =>
         if (busy_RTC = '1') then
          prdata <= (others => 'Z');
         else
          prdata <= (others => 'Z');
         end if;
      when ENABLE_st =>
         if (busy_RTC = '1') then
           prdata <= (others => 'Z');
         else
           prdata <= RTCDR;
         end if;
      when others =>
           prdata <= (others => 'Z');
      end case;
      end if;
      end if;
    if (paddr = X"000002f4" ) then  -- RTCMR
     if (write_en ='1') then
```

```
      case state is
       when IDLE_st =>
         RTCMR <= (others => 'Z');
       when SETUP_st =>
         RTCMR <= (others => 'Z');
       when ENABLE_st =>
         RTCMR <= pwdata;
       when others =>
         RTCMR <= (others => 'Z');
       end case;

elsif (read_en = '1') then
  case state is
    when IDLE_st =>
      prdata <= (others => 'Z');
    when SETUP_st =>
      prdata <= (others => 'Z');
    when ENABLE_st =>
      prdata <= (others => 'Z');
    when others =>
      prdata <= (others => 'Z');
    end case;
  end if;
end if;
          -- etc
```

RTC addressing system is :

- Address 0x2F0 : read data from RTCDR
- Address 0x2F4 : send data for RTCMR
- Address 0x2F8 : read RTCSTAT condition
- Address 0x2FC : send data for RTCLR
- Address 0x300 : send RTCCR condition

VHDL Coding above show assignment port for register blok RTC in every state condition (IDLE, SETUP, and ENABLE) and in every address for each port (0x2F0 – 0x300). On write process (write_en = '1') data from pwdata will be send to register RTCMR and RTCLR as 32 bit data , , and to RTCCR as 1 bit data . On read process (read_en = '1'), APB bus will read data which send by RTC on ENABLE state, and if busy condition of RTC (busy_rtc) = '0' which means RTC is ready to send data trough APB bus.

4. EXPERIMENTAL RESULT

Testing is doing by using *ModelSim* Simulation. First, each modules is tested by stand alone system, and then tested as integrated system with AMBA bus. Result of ModelSim Simulation for the integrated system is shown in figure below.

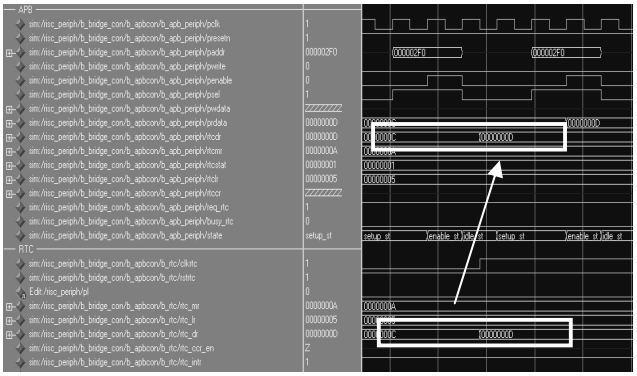

Figure 12. Read data RTC to APB bus

Figure 12, shown one example of the transfer data process from RTC to APB. In this simulation RTC is doing data counting which value is store in RTCMR (0Ah). RTCDR count the data and the incrementing counter value from RTCDR is read by APB bus through register prdata, when pwrite = '0'. APB read data on address 2F0 (read data from RTCDR), and using the instruction :

```
X"E59E42F0"       when       address       =
conv_std_logic_vector (40,32) else -- LDR
2F0
```

Figure 13 show when the value of RTCDR is same as RTCMR (0Ah). The interrupt condition is high (RTCINTR ='1'), and RTCstat = '1'. This condition is read by APB as 01h.

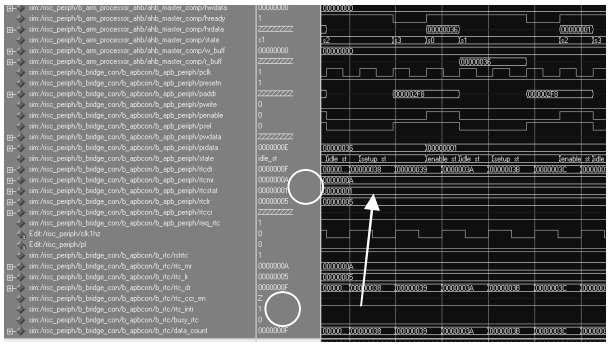

Figure 13. Read data RTCINTR to APB

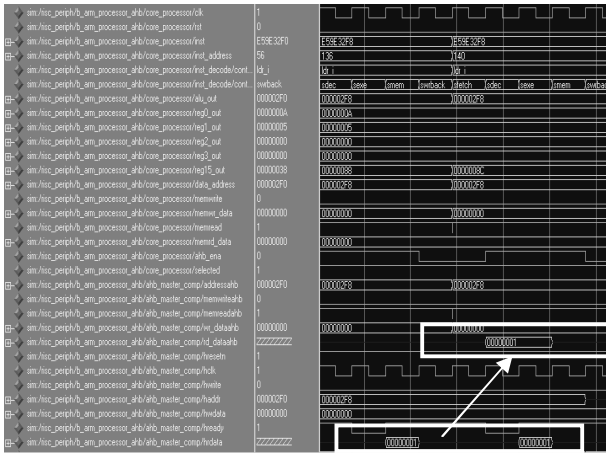

Figure 14. Read data RTC_DR to AHB

After read by APB, the interrupt value of RTC (01h) is read in register hrdata of AHB when there is LDR instruction and address show 2f8 (figure 14). This condition will make the data is sent to processor and can be read in register rd_dataahb of processor.

5. CONCLUSIONS

The result of simulation and synthesis show that system works at 180MHz and able to operate in single transfer mode, where one cycle of AHB or APB could only acces one data packet of one address.

Each bus AHB and APB capable to work in their specification, and *Bridge* is used to converts system transfer AHB to APB by controling state machine condition for each bus.

Data transfer process from processor to RTC can work properly. RTC able to do it function as counter and timer in processor SIEGE32 system.

REFERENCES

[1] Arnold, Ken, “Embedded Controller Hardware Design” , LLH Technology Publishing, USA, 2000.
[2] Furber, Steve., “ARM-system on-chip architecture” , Pearson education Limited ,Addison-Wesley, Great Britain, 2000.
[3] Hwang, Enoch.O, “Microprocessor Design VHDL”, Brooks/Cole, 2004.
[4] Keating, Michael and Pierre Bricaud, “Reuse Methodology Manual For System On Chip Designs”, Kluwer Academic Publisher, 1999.
[5] Sutisna, Nana, “Desain dan Implementasi RISC Processor 32 bit SIEGE32”, ITB, Bandung, 2005.
[6] Pelgrims, Patrick,Tom Tierens and Dries Driessens, “Overview AMBA, AVALON, CORECONECT, WISHBONE, “DeNayer Instituite 2003.
[7] www.arm.com.
[8] www.synopsys.com/designware.

Near Field to Far Field Transformation Using FFT Method for Antenna Measurement

Catur Apriono[1], Fitri Yuli Zulkifli[2], A. A. Lestari[3] and Eko Tjipto Rahardjo[4]

[1,2,4] *Antenna Propagation and Microwave Research Group (AMRG)*
Center for Information and Communication Engineering Research (CICER)
Electrical Engineering Department
Faculty of Engineering
University of Indonesia, Depok 16424
Tel: (021) 7270011 ext 51. Fax: (021) 7270077
E-mail: [1]apriono_catur@yahoo.co.id, [2]yuli@ee.ui.ac.id, [4]eko@ee.ui.ac.id

[3]*International Research Centre for Telecommunication and Radar – Indonesion Branch (IRCTR-IB)*
STEI-ITB, Jln. Ganesha 10 Bandung 40132, Indonesia
E-mail: alestari@irctr.tudelft.nl

ABSTRACT

To measure the performance of an antenna, the measurement system which is usually used is the far field method. However, if the antenna has a large size, a problem occurs concerning the large distance needed for the far field method to measure the radiation pattern of the antenna. For an antenna measurement conducted in an anechoic chamber with limited space, this cannot be achieved.
One solution to overcome this problem is to use near field method. There are three near field methods known which are the planar, cylindrical and spherical surfaces. In this paper, the design of the near field method with planar surface is proposed due to the advantages of the formula and computation process simplicity compared with the other near field surface methods.
The data is transformed from near field to far field data using the fast Fourier transform (FFT) method. This FFT method is more efficient for the computer process compared to other method. The transformed data can show the far field radiation pattern of the antenna.

Keywords: *near field, planar, radiation pattern*

1. INTRODUCTION

Antenna measurement is needed to ensure that the design of an antenna in accordance with the expected performance. Measurement antenna is usually done using the far field method. In the far field method, when the antenna has a large size, a problem occurs concerning the large distance needed for the far field method to measure the radiation pattern of the antenna [1]. However, the measurement of the antenna can only be done with near field method [1].

There are three near field methods known which are: the planar, cylindrical and spherical surfaces [1]-[3]. The design of the near field method with planar surface is proposed due to the advantages of the formula and computation process simplicity compared with the other near field surface methods. Although this planar surface method is not an accurate method, this planar surface method can be used well to predict measurement of the antenna's radiation pattern.
In this paper, the measurement design is developed to transform near field data to far field data. It uses the fast Fourier Transform (FFT) method for the computation process. This FFT method is more efficient for the computer process compared to other method.

2. THE PLANAR NEAR FIELD MEASUREMENT SYSTEM

The design of the near field measurement system will provide significant flexibility to increase the measurement capability. Figure 1 shows the planar nearfield measurement system. The design of this system can be divided into 3 parts; they are the scanner with the scanning area, measuring equipment and management system [4].

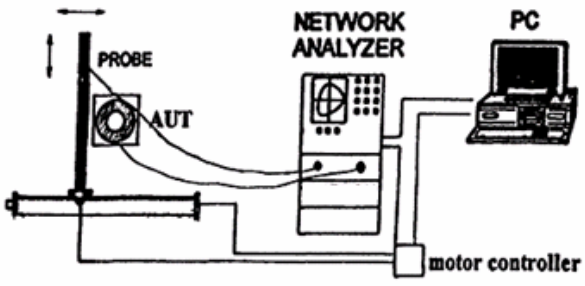

Figure 1: Planar Near Field Measurement System [4]

The scanner has a probe antenna that moves in certain points of the planar surface. The scanning area is designed

to cover the planar surface in the near field region of the antenna under test (AUT). Furthermore, the probe also can be rotated to get the variable component in the vertical and horizontal polarization. This design will be very appropriate to be placed in an anechoic chamber with limited dimension.

The scanner has a pair of stepper motor which is controlled by a computer to determine the probe position on the planar surface scanning area. It is also needed to change the polarization of the probe.

The scanning area was designed to 2 x 2 meters that consist of 128 x 128 data, the distance between the sampling points of measurement is 15.62 mm. The distance of the sampling point must be correctly calculated because it concerns with the accuracy in the evaluation of the Fourier integral. The Fourier integral requires grid spacing Δy and Δz on the measurement surface to be less than or equal to $\lambda/2$ [7].

Figure 2 shows the distribution of the measurement locations on the surface of the planar scanning area[1]. Therefore the distance between the AUT and probe antenna is 38 cm. For the planar surface method, if the distance between AUT and scanning area is defined for 0.38 meter, the measurement system designed can reach the point of θ in the range of 20.80^o to 158.89^o and φ in the range of -69.19^o to 68.89^o.

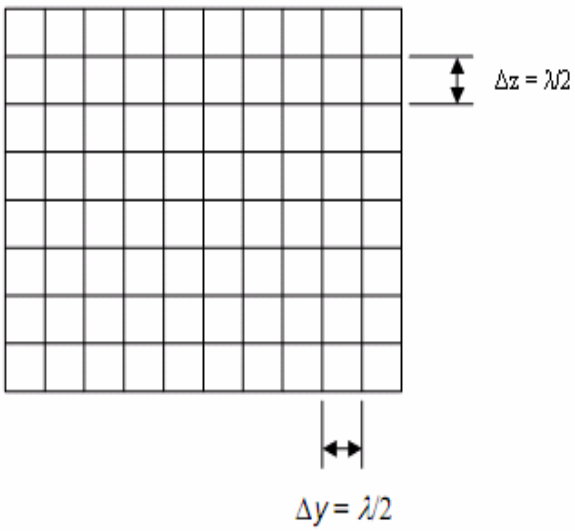

Figure 2: The Sample of Scanning Surface [7]

The measurement equipment is the Vector Network Analyzer (VNA), provided in the anechoic chamber, Electrical Engineering Department, Faculty of Engineering, University of Indonesia. At the same time, a computer as management and communication system is used to control the movement of the stepper motor. This is to obtain data from the VNA and the data transferred from the VNA to the computer. This computer will than calculate near field to far field transformation.

The probe movement in the planar measurements is described in Figure 3. From the measurement data pattern of each measurement point, it will appear as the data is on a line with few points. Furthermore, the measured data will be obtained only in the form of (m x n, 1) matrix data, with m and n respectively are the amount of sampling points in each vertical and horizontal line. The dimensional measurement data will be arranged to the matrix of (m x n), and there has to be a procedure to convert the early data measured. The design of the system can be developed into the cylindrical measurement system by adding the rotating feature on the AUT [4].

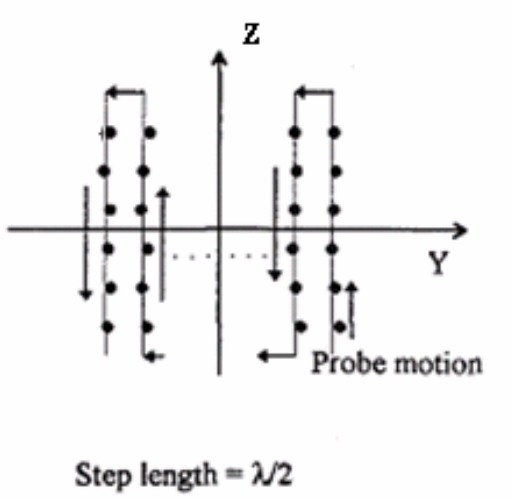

Figure 3: The pattern of the Probe Motion [4]

After the design of planar near field measurement is completed as implemented in Fig. 1, the process of planar near field measurement can be carried out. The processes are generally divided into two parts, consists of data acquisition and data transformation. At the first stage, the process takes place on the hardware system. The main objective is to obtain data from the near field antenna under test that consists of several phases which are [5]:

1. The computer will determine the measurement position on the measurement area
2. The probe moves into the position which was determined
3. The measurement is done in that position and than save the measurement result
4. Repeat step 1 until all position measured for both polarizations: horizontal and vertical.

Data transformation is used to process the near field measured data which is obtained from the previous process. The near field data is used for transformation into far field data to see the antenna performance. These processes can be divided into two steps, they are the transformations of near field measurements to far field data and plot the results of the transformation [5].

3. Near Field to Far Field Transformation

Following is the general far field equation, where θ is the elevation angle while φ is the azimuth angle from the point of the far field observation [2].

$$E(\theta,\varphi) = E_\theta(\theta,\varphi)\hat{\theta} + E_\varphi(\theta,\varphi)\hat{\varphi} \quad (1)$$

$$H(\theta,\varphi) = \frac{1}{\eta}[E_\theta(\theta,\varphi)\hat{\theta} - E_\varphi(\theta,\varphi)\hat{\varphi}] \quad (2)$$

The above mentioned equation can be obtained from the near field data. To transform the near field to far field data, the E-field from the probe antenna has to be determined. The determined E-field from the probe antenna is used to define the determinant of the system (Δ(θ, φ)), as follow [2]:

$$E_\theta(\theta,\varphi) = \frac{\sin\theta\cos\varphi}{\Delta(\theta,\varphi)}[I_H(\theta,\varphi)E_\varphi{}^V(\pi-\theta,\varphi) - I_V(\theta,\varphi)E_\varphi{}^H(\pi-\theta,\varphi)] \quad (3)$$

$$E_\varphi(\theta,\varphi) = \frac{\sin\theta\cos\varphi}{\Delta(\theta,\varphi)}[I_H(\theta,\varphi)E_\theta{}^v(\pi-\theta,\varphi) - I_V(\theta,\varphi)E_\theta{}^H(\pi-\theta,\varphi)] \quad (4)$$

Where,

$$\Delta(\theta,\varphi) = E_\theta{}^H(\pi-\theta,\varphi)E_\varphi{}^V(\pi-\theta,\varphi) - E_\theta{}^V(\pi-\theta,\varphi)E_\varphi{}^H(\pi-\theta,\varphi) \quad (5)$$

From the determinat of the system and from the probe response (I_v and I_H), the far field of the AUT can be obtained.The probe response is obtained from the complex voltage of AUT [2].

$$I_V(k_y,k_z) = \exp(jk_x x_0). \int_{-\infty}^{\infty}\int_{-\infty}^{\infty} v_V(x_0,y,z)\exp(jk_y.y + jk_z.z)dydz \quad (6)$$

$$I_H(k_y,k_z) = \exp(jk_x x_0) \int_{-\infty}^{\infty}\int_{-\infty}^{\infty} v_H(x_0,y,z)\exp(jk_y.y + jk_z.z)dydz \quad (7)$$

where $k = \frac{2\pi}{\lambda}$, $k_y = k\sin\theta\sin\varphi$, $k_z = k\cos\theta$ and $k_x = k\sin\theta\cos\varphi$

The equation (6) and (7) can be solved using FFT, while $v_H(x_o,y,z)$ and $v_v(x_o,y,z)$ are the near field complex voltages of the AUT.

From all of the equations above, it can be organized into a flow chart that describes the measurement process such as depicted in Figure 4.

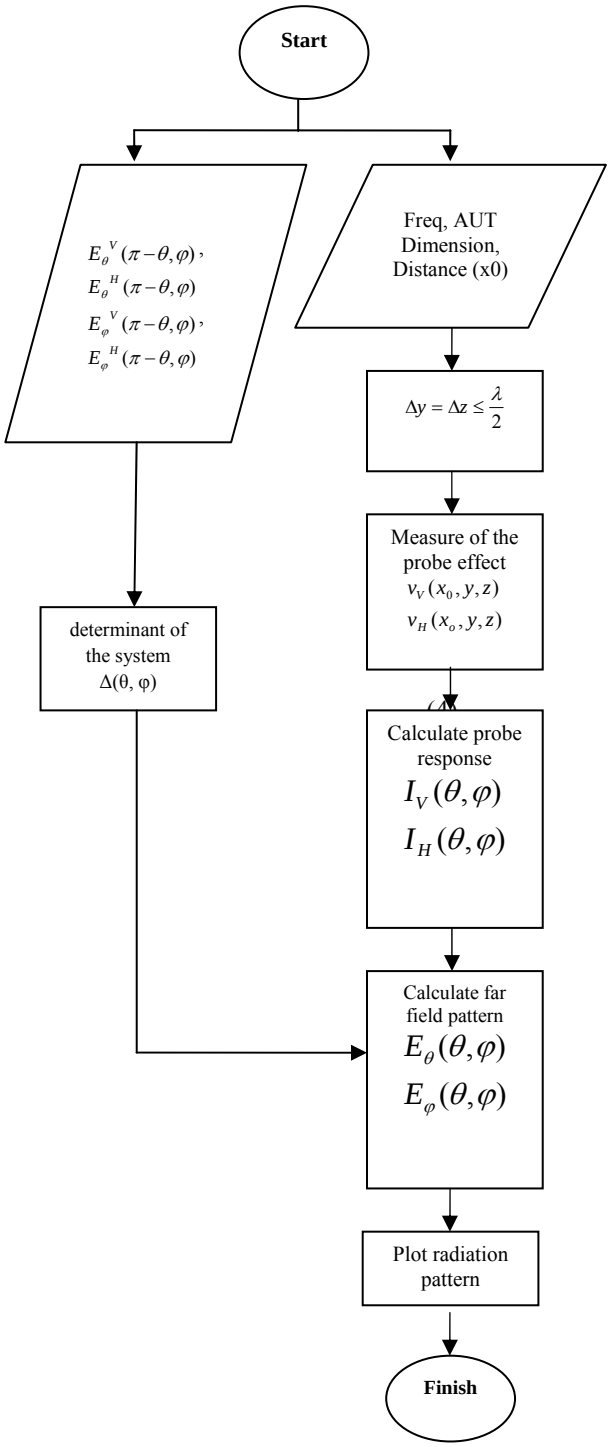

Figure 4: Flow Chart Measurement and Transformation

The measurement and visualization can be easily defined by assuming the position of the data which is taken from the sampling points. The sampling points show the position to be measured and this is the component of the matrix data as described in Figure 5. In Fig. 5 shows 9x11 data but the actual data is extended to 128 x 128 data as aforementioned in previous chapter.

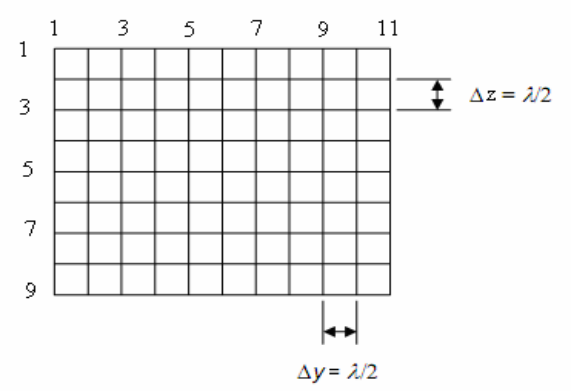

Figure 5: the position of data

Future development of this work is to implement the simulation program into the hardware of the near field measurement system.

4. Conclusions

By knowing the steps of the data transformation from planar near field to far field data, the program can be designed to obtain the process of transformation. The result of the transformation process may represent the far field performance of the antenna.

Acknowledgement

This work is supported by Universitas Indonesia under National Research Strategic grant contract no. 407C/DRPM-UI/A/N1.4/2009.

References

[1] A. D. Yaghjian, "An overview of near-field antenna measurements", IEEE Trans. Antennas Propagat. , Vol. AP-34, no. 1, pp. 30-45, January 1986

[2] E. B. Joy, W. M Leach, and G. P. Rodrigue, "Applications of probe-compensated near-field measurements", IEEE Trans. Antennas Propagat., Vol. AP-26, no. 3, pp. 379-389, May 1978

[3] D. T. Paris, W. M. Leach, and E. B. Joy, "Basic theory of probe-compensated near-field measurements", IEEE Trans. Antennas Propagat., Vol. AP-26, no. 3, pp. 373-379, May 1978

[4] B. Yan, S. A. Saoudy, B. P. Sinha, "A low cost *planar* near-field/far-field antenna measurement system", C CORE, Memorial University of Newfoundland, IEEE, 1997

[5] D. Slater, G. Hindman, "A low cost portable near-field", Near field System Incorporated, October 9-13, 1989

[6] M.S. Narasimhan and M.Karthikeyan, "Evaluation of fourier transform integrals using FFT with improved accuracy and its applications", IEEE Trans. Antennas Propagat., vol. AP-32, no.4, pp. 404-408, April 1984

[7] I. R. Tkadlec, "Near-Field Antenna Measurements", Dept. of Radio Electronics FEEC BUT

ISSN 114-1284

Performance Analysis of Delta-zigzag (Dz) Connection Transformer With Secondary symmetrical Cross-winding Minimized Harmonics Based on the Rating of Volt-Ampere Output Power

Chairul Gagarin Irianto
[1]Electrical Engineering Departement, FTI – Trisakti University, Jakarta
Email: chairul_irianto@trisakti.ac.id

ABSTRACT

An investigative and comparative test of the performance of secondary Dz connection transformer with 2 windings and secondary Dz with Symmetrical 3 Cross-winding on symmetrical and non-symmetrical load operations due to the harmonics distortion of the non-linear load, executed through mathematical modelling and laboratory testing approaches. The wave-form approaching the pure sinusoidal form without any non-sinusoidal wave distortions is the ideal description of the characteristics of transformer loading with attention to the influence of load imbalance. Mathematic modelling and operational testing of imbalanced phase-3 loading showed that the THD current value of secondary Dz with 2 windings and secondary Dz with Symmetrical 3 Cross-winding are different, even though they are loaded with the same amount of Volt-Ampere output power. Because the connection scheme of the secondary Dz with 2 windings has an imbalanced structure, the imbalance limiting performance of the phase-3 is worse than that of the 3-windings secondary zigzag delta connection scheme, the latter which is expected to be able to change the 3-phase-3 power into 2-phase and 1-phase power more effectively.

This paper is explaining to reduce the harmonics, especially 3rd order of harmonics and its multiplication, using transformer technology. In this paper, Dz transformer with 3 coils on the secondary part is used to reduce harmonic pollution. This paper also explaining about how the transformer handles unbalanced load because of the 3rd order (and its multiplication) of harmonics distortion that are produced by non linear loads in distribution system. This paper proposes solution to reduce harmonics problems direct from their source. Based on mathematics analysis and experiment on its parameter, the transformer is engineered to have: (1) Configuration of primary and secondary coil design, (2) Separation of interconnection in secondary coil part, (3) Magnetized coupling within secondary coil part, (4) Magnetized coupling between primary and secondary coil part, (5) Coupling between coil and core, and (6) Series connection with polarity sequence in secondary coil part.

The Dz transformer with crossed connection in its secondary part is purposed to isolating and reducing harmonics distortion in distribution system. The Dz transformer damps harmonic distortion load current. The transformer would damps high frequency band effectively. The principal of Dz transformer is resists the phase by doubling the series inductance in secondary part. The phase is resisted by dividing the secondary coil part by 3 symmetrically, which each part is connected to 3 different phase. By arranging series connection on each 1/3 part of coil in one phase, the MMF induction polarity can be enforcing or the opposite. So, there is one coil part in the same phase which has opposite phase angle until 180o. Therefore because of the 180 o opposition, the MMF induction in 2 groups of coil will resist each other, so the crossing of harmonic frequency signal would never happen. The transformer acts as low frequency filter. Hopefully, the specially designed transformer connection wild reduce harmonics distortion 1.3 – 1.4 times as compared to the conventional one therefore the transformer will be able to increase the system power capacity up to 10 %. The calculation results of the simulations show that the form of the current waveforms on the primary or source side is became near pure sinusoidal form because the THD current value is reduced.

Keywords: total harmonics distortion, non linear loads, unbalanced loads, 3rd order harmonics current, delta zigzag transformer.

1. Introduction

The problem of harmonics distortion is an important issue in the efforts to supply electrical power, in line with the higher attention the people is giving to the issue of the quality of electrical power. Harmonics distortion is the deviation of the power or current wave from the ideal sinusoidal wave. The problems of harmonics distortion is getting more difficult, because there is increasing use of power electronic-based devices that give additional benefits due to their efficiency and effectiveness. According to Prabhakara [1], in 2020 more than 50% of the electrical power capacity generated serves phase-1 non-linear loads, which have imbalanced distribution and

thus even bigger power rating. This means that the impact of current harmonics and load that it causes to the distribution system of the electrical power and to the load becomes more serious. Some of the negative impacts of harmonics distortion are overheating of transformers and motors, operational malfunctions of electronic components, excessive currents in neutral areas, operational problems on computer and telecommunications equipments, etc.

The latest technological developments have given many solutions for electrical power quality problems caused by harmonics distortion due to the imbalanced loading of one-phase linear load. Examples of these are filters, K-rated transformers, Dy transformers, zigzag transformer and phase-shifter combos, Scott transformers, Le Blanc transformer and filter combos, etc. Limiting the impacts of imbalanced loading of one-phase non-linear loading requires special connection transformers. The research done by Cheng-Ping Huang et al. [2] on the Vee/vee, Scott and Le Blanc models for resolving load imbalance on the performance of special connection transformers has not given maximum results.

The analysis results state that the Vee/vee connection scheme causes a more serious imbalance disturbance on three-phase sources than the Scott and Le Blanc connection scheme [2]. The Scott connection does not provide delta windings for circulating 3rd harmonic currents, so the triplene harmonic currents remain on the primary and secondary circuits of the transformer. With the delta connection of the primary side of the three-phase Le Blanc connection, the excess of the connection in these windings are able to limit the triplene harmonic voltages. However, if the secondary windings of a Le Blanc transformer are given a large capacity load between the phase lines to the neutral, then the loading becomes imbalanced.

For that purpose, tertiary delta-connected windings or a filter on the secondary side is needed [4]. From the above explanation of transformer technology, we know that the primary delta winding design is not yet optimum for resisting the currents of distorted harmonics from the secondary side caused by imbalanced load. So the first thing to do is to reduce the level of load imbalance by balancing the resultant mmf induced by load currents. This is done by balancing the resultant mmf induction of load currents by distributing mmf induction symmetrically to the three core legs. In this way, the resultant mmf induction of the load harmonics component does not become excessive, and it can be limited by circulating the harmonics currents through the primary delta windings. Limiting the circulation of harmonic currents will reduce the lost heat of transformer windings, as well as reduce the current of the electromagnetic field current to the supply line side.

This text discusses symmetrical cross-winding secondary Dz special connection transformers as a solution to the harmonics distortion problem caused by non-linear load on balanced and imbalanced loading conditions based on three principles: first is the principle of minimising the quantity and balancing the induction of mmf load currents on the secondary side. The second is the principle of phase-resisting method, which is resisting the electromagnetic energy caused by harmonics currents from the secondary side to the primary side by increasing the leak inductance in secondary windings. Last is the isolator principle, which is isolating the remnants of induction mmf of load currents by circulating them in the connection circuit of the primary delta.

The first principle is executed by dividing each number of secondary phase winding coils into three symmetrical parts, then place each 1/3, *n* part of these windings on three different legs. The second principle serially connects each *n* part of the windings between the three core legs in a symmetrical cross that forms one phase winding. The third principle is executed by connecting the primary windings in the delta to eliminate the 3rd harmonics current induction by circulating the triplene harmonics induction currents generated by non-linear load on the secondary side of the transformer.

The 2nd part of this text presents the ideas for the methods and the study of the mathematical models of the Dz special connection transformer. The 3rd part investigates the minimising of harmonics in balanced and imbalanced loading conditions of the phase-1 non-linear loads. Part 4 represents the results of the investigation and discussion. Part 5 contains the conclusion of this research.

2. Dz Connection Transformer with Symmetrical Secondary Cross-windings in order to Minimise Harmonics Distortion

   a. *Symmetrical Secondary Two Cross-windings Dz Special Connection Transformer*

      On the secondary side of each number low-voltage phase winding, N_2 is divided into two equal parts: $n = N_2/2$. Each n of the phase winding part is placed in a symmetrical cross on three different core legs, as shown in Figure 1 (b). The two n parts of the winding are serially placed to form one phase winding. The result is that the resultant magnetic motive force (*mmf*) of the phase winding is √3 x n, or each half part of the mmf.

      The advantage of this configuration is that it is able to limit the triplene harmonics current between the lines of the load and neutral phases by counter-positioning the phase of each n voltage in the serial winding part.

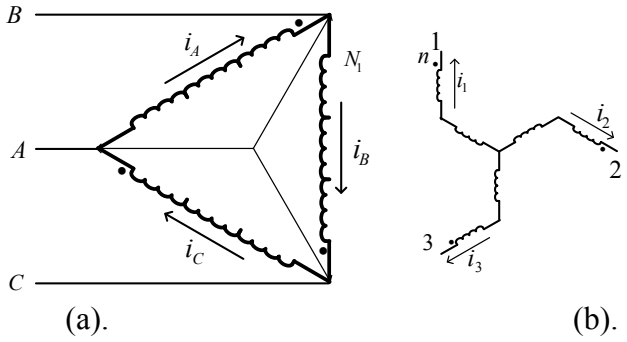

Figure 1 The Secondary 2-winding Dz Transformer Connection

As we can see in Figure 2, the diagram shows that the Dz transformer scheme supplies equal non-linear one-phase loads. Each non-linear one-phase load generates equal 3rd harmonic currents I_3 in each phase conductor. From the diagram, we know that the ampere-winding mmf on the same core leg on the secondary side cancel out (eliminate) each other. This results in the lack of 3rd harmonic currents circulating in the primary delta side.

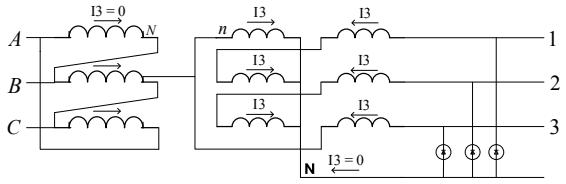

Figure 2 3rd Harmonics Current on Secondary 2-winding Dz Transformer

However, in practice, the 3rd harmonic current components are not always equal on the phase currents, so the resultant mmf ampere-winding on the same leg on the secondary side do

not minimise each other totally [14]. As a result, 3rd harmonic currents remain circulating in the primary winding and in the power supply line.

b. Symmetrical Secondary Three Cross-windings Dz Special Connection Transformer

The idea of the zigzag three winding connection on the secondary side is based on the transpositional theory of phase-3 power transmission line wires for resolving non-symmetry due to the geometrical position of the zigzag windings [11]. On the secondary winding side of each low-voltage phase winding number, N_2 is divided into three equal parts: $n = N_2/3$. Each n of the winding part of the phase is placed cross-symmetrically on three different core legs. The three parts of the n windings are then placed serially to compose one phase winding (see Figure 3). The resultant mmf phase winding is ½ for each n, or 1/3 of the mmf part.

The advantage of this configuration is that it is able to limit the harmonics triplene current between the load and neutral phase lines by counter-positioning the phase of each n voltage of the serial winding. With this zigzag secondary side configuration, the impedance of the secondary 3-winding Dz transformer is bigger than that of standard transformers.

The diagram of the Symmetrical Cross-winding Secondary Dz transformer is as follows:

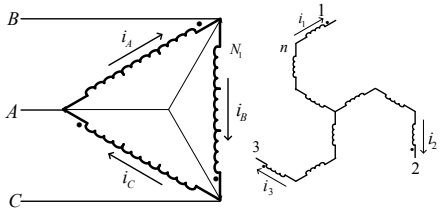

Figure 3 The Secondary 3-winding Dz Transformer Connection

Because the above mmf vector connection of secondary phase windings is formed of zigzag winding connections, then the currents at the zigzag windings minimised at the delta windings are:

$$i_A = (n/N_1)(-i_1 - i_2 + i_3) \quad (1)$$

$$i_B = (n/N_1)(i_1 - i_2 + i_3) \quad (2)$$

$$i_C = (n/N_1)(i_1 + i_2 - i_3) \quad (3)$$

Three parts of secondary windings build up the magnetic flux in the transformer's core, where the phase angle has a 180 electrical degree difference. This way, the magnetic flux from the three winding parts reduces each other and the signals of harmonic frequencies are eliminated. Afterwards, there is no electromagnetic energy transfer from the core to secondary windings. This means that the currents of the transformer's primary delta winding phases are expected to contain little 3rd harmonic component, as this component is expected not to show in the source line currents.

c. Comparison of the Inductance Values of Dz Special Connection Transformers

As stated in sections *a* and *b*, the mmf (ampere-winding) requirements for generating V_2 effective output value of equal size between two divisions of windings per phase and three divisions of windings per phase are different (see **Figure 4**).

ISSN 114-1284

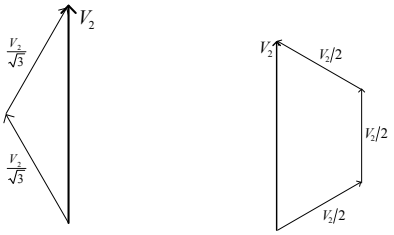

(a). **(b).**

Figure 4 Scheme of Effective Output Voltage Phasor of the Secondary Side
(a) Zigzag with 2 winding parts (b) Zigzag with 3 winding parts

From **Figure 4** we see that the total mmf amount for generating equal effective secondary output voltages on 2 parts and 3 parts winding per phase are respectively $2V_2/\sqrt{3}$ and $3V_2/2$. So the ratio of mmf requirement between 3-winding and 2-winding secondary Dz transformer is:

$$\frac{E_{z3}}{E_{z2}} = \frac{3V_2/2}{2V_2/\sqrt{3}} = 1{,}3 \quad (4)$$

Based on the fact that the 3-winding parts secondary Dz transformer requires 1.3 times mmf than the 2-winding parts secondary Dz transformer to create the same effective voltage output. The same phase winding current means that the number of *N* winding in the secondary 3-winding parts is 1.3 times bigger than the 2-winding parts, as we can see in equation (4). For the same winding conductor cross-section, the number of the secondary 3-part zigzag winding is bigger and longer. This results in a larger resistive impedance value in the 3-part secondary zigzag winding coil than the resistive impedance value of 2-part secondary zigzag winding coil, as we can see in equation (5),

$$R = \rho \frac{l}{A} \quad (5)$$

Where R = the value of resistive impedance [Ohm], ρ = the conductive capability of the material, l = the length of the conductor [m], and A = the cross-section size of the conductor [m^2].

Large L inductive impedance when the harmonic frequency is increased is expected to be able to resist 3rd harmonic currents and triplene harmonics on the secondary windings of the transformer. This resistance can prevent the flow of electromagnetic energy distorted 3rd harmonic current from circulating in the primary windings. The performance of the transformer becomes more efficient, and energy can be saved because the lost electric power is reduced and because obstructing 3rd harmonics can improve the impacts of secondary voltage distortion. These filter-capability transformers are expected to generate cleaner, more economical power quality.

3. Testing Scheme

Laboratory testing on the 380/220V 4-wire phase-3 electrical power distribution system was connected to non-linear loads. The loads were comprised of fluorescent lamps with electronic return. AC sources from the laboratory were used as distribution points. A 1250 VA, 380 V/6 x 55 V, 50 Hz symmetrical cross-winding secondary Dz transformer was used as the mitigation/obstruction harmonic distortion device, and 3 x 40 electronic return fluorescent lamps of 10 Watts each were the non-linear phase-1 harmonic generator loads. For balancing the load of Dz transformers, each secondary phase voltage output terminal supplied a 450 Volt-Ampere power. Imbalanced loading of Dz transformers uses secondary phase voltage output terminals which supplied 360, 270, and 270 Volt-Amperes. The scheme of the simulation was as shown in Figure 4:

ISSN 114-1284

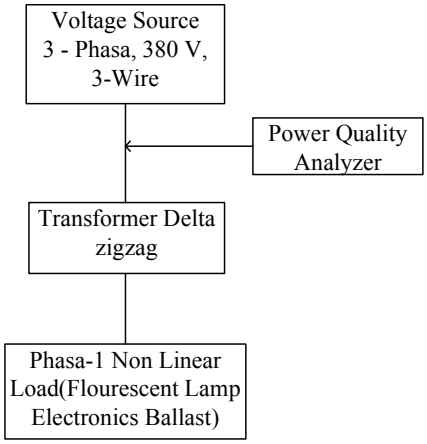

Figure 4 Measurement Test Flow chart

Measurements were taken under the following conditions:

a. Balanced and imbalanced direct connection to panel points of distribution through a Symmetrical Two Cross-winding Secondary Dz Transformer.
b. Balanced and imbalanced direct connection to panel points of distribution through a Symmetrical Three Cross-winding Secondary Dz Transformer.

4. Results and Discussion

Table 1 and Table 2 show harmonics reading when the load is connected to the source panel through a Symmetrical 2 Cross-winding Secondary Dz Transformer. As expected, the non-linear phase-1 load of LHE lamps with half-wave director creates 3rd, 5th, 7th, and triplene harmonic frequencies that can be lowered 40%-44% using the Symmetrical 2 Cross-winding Secondary Dz Transformer, both on balanced and imbalanced load conditions.

Table 1
Harmonic Reading on Symmetrical Load Condition throughSymmetrical 2 Cross-winding Secondary Dz Transformer

Current	Phase		
	L1	L2	L3
S (VA)	450	450	450
P (Watt)	300.49	305.24	305.09
Q (VAr)	334.88	331.05	330.71
I_{Total}	2.028	2.102	1.833
THD (%)	38.24	39.6	39.72
1	1.912	1.978	1.750
3	0.166	0.086	0.080
5	0.606	0.699	0.617
7	0.365	0.320	0.279
9	0.049	0.049	0.022
11	0.046	0.091	0.095
13	0.030	0.045	0.082
15	0.012	0.012	0.011
17	0.023	0.020	0.030
19	0.010	0.001	0.005
21	0.008	0.012	0.006

Table 2
Harmonic Reading on Symmetrical Load Condition through
Symmetrical 2 Cross-winding Secondary Dz Transformer

Current	Phase		
	L1	L2	L3
S (VA)	360	270	270
P (Watt)	239.47	182.94	179.67
Q (VAr)	268.75	198.57	201.58
I_{Total}	1.295	1.580	1.220
THD (%)	43.78	44.28	44.2
1	1.211	1.446	1.124
3	0.231	0.221	0.025
5	0.375	0.524	0.433
7	0.280	0.276	0.219
9	0.042	0.053	0.010
11	0.075	0.076	0.091
13	0.018	0.022	0.015
15	0.005	0.009	0.008
17	0.014	0.005	0.009
19	0.018	0.013	0.014
21	0.008	0.011	0.008

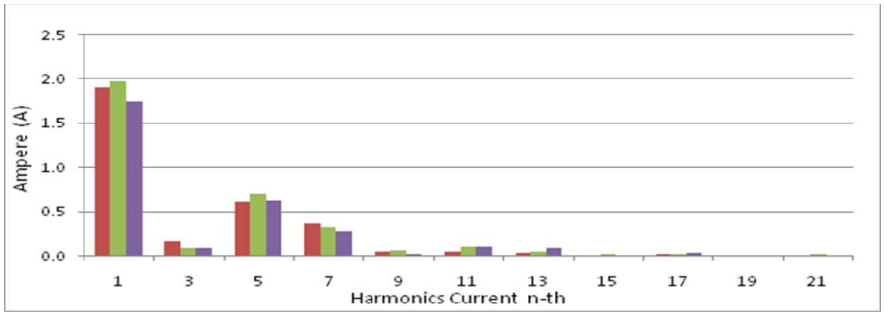

(a).

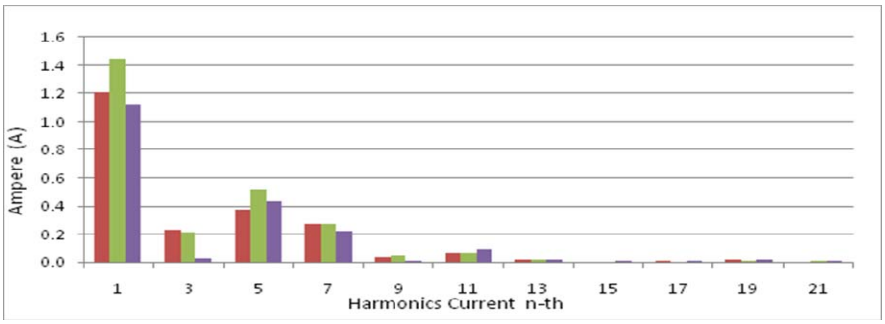

(b).

Figure 4 Spectrum of Harmonic Current Frequency on Connection Configuration through Symmetrical 2 Cross-winding Secondary Dz Transformer to:

ISSN 114-1284

(a) Balanced Loads, and (b) Imbalanced Loads

Figures 4 (a) and 4 (b) show the spectrum of harmonic currents on balanced and imbalanced loads. Harmonic currents are the largest part of the current flowing through the conductor.

Tables 3 and 4 show the influence of special connection Dz transformers on electrical systems. We can see in Tables 3 and 4 that a special connection Dz transformer placed between the load and the source panel of a phase-3 voltage highly influences the harmonic content. Using transformers with large inductive impedance values will make the transformer able to filter and eliminate triplene harmonics, and reduce other sequential harmonic contents. Current THD is reduced from 39% to 28% in balanced load conditions, and from 44% to 34% in imbalanced condition. This means a 10% increase in the power capacity of the system.

Table 3 Harmonic Reading on Balanced Load through Symmetrical 3 Cross-winding Secondary Dz Transformer

Current	Phase		
	L1	L2	L3
S (VA)	451.7	446	465
P (Watt)	314.2	305	324
Q (VAr)	324.5	326	333
I_{Total}	1.791	1.84	1.72
THD_I (%)	24.58	28.95	31.18
1	1.73	1.757	1.624
3	0.089	0.026	0.072
5	0.395	0.492	0.482
7	0.115	0.092	0.108
9	0.024	0.036	0.011
11	0.018	0.066	0.058
13	0.044	0.032	0.052
15	0.009	0.012	0.008
17	0.015	0.011	0.02
19	0.015	0.007	0.018
21	0.007	0.003	0.007

Table 4 Harmonic Reading on Imbalanced Load through Symmetrical 3 Cross-winding Secondary Dz Transformer

Current	Phase		
	L1	L2	L3
S (VA)	375	297.5	289
P (Watt)	258	201.1	198
Q (Var)	272	219.2	211
I_{Total}	1.248	1.355	1.037
THD_I (%)	33.53	30.48	39.17
1	1.179	1.297	0.943
3	0.134	0.109	0.078
5	0.318	0.354	0.342
7	0.128	0.098	0.095
9	0.024	0.037	0.013
11	0.073	0.081	0.051
13	0.033	0.027	0.023
15	0.012	0.015	0.007
17	0.005	0.014	0.021
19	0.01	0.009	0.011
21	0.007	0.009	0.005

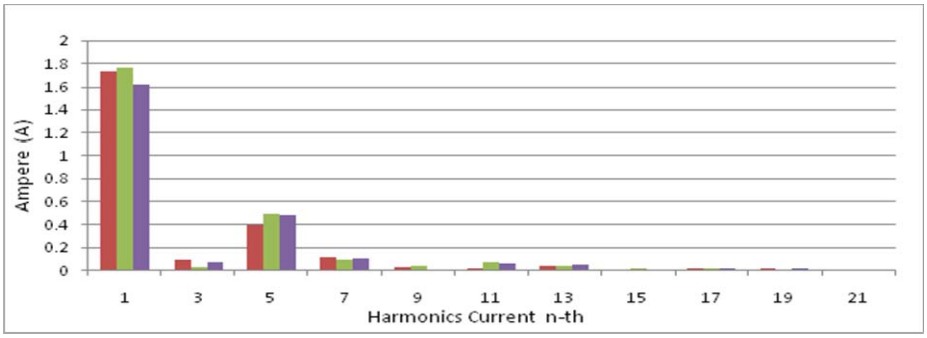

(a)

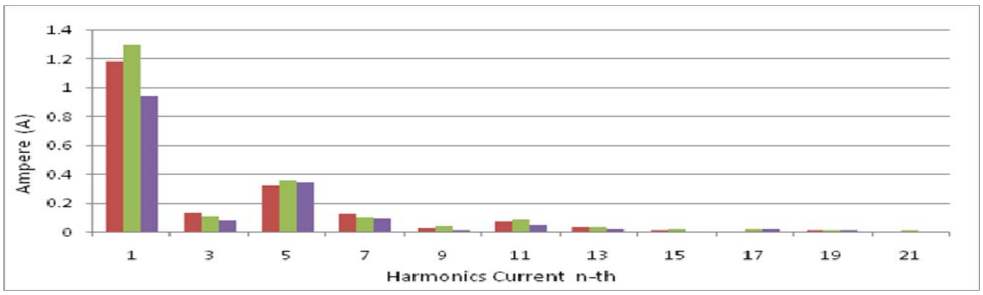

(b)

Figure 5 Spectrum of Harmonic Current Frequency on Connection Configuration through Symmetrical 3 Cross-winding Secondary Dz Transformer to:
(a) Balanced Loads, and (b) Imbalanced Loads

(b) Figures 5 (a) and 5 (b) show the spectrum of harmonised currents for balanced and imbalanced loading connected to Dz transformers, where the graph shows the reduction of triplene harmonics.

5. Conclusion

Laboratory tests show that symmetrical cross-winding secondary Dz transformers can limit harmonics in the phase-3 electrical power distribution system. Symmetrical 3 cross-winding secondary special connection Dz transformers are able to limit the harmonic distortion of currents in the utility side better than the symmetrical 2 cross-winding secondary Dz in balanced loading condition. The level of harmonic distortion in the utility side is reduced more when using the symmetrical 3 cross-winding secondary special connection Dz transformer than when using the symmetrical 2 cross-winding secondary Dz. Placing a number of small-capacity Dz transformers on the distribution panel may improve the overall performance of the system and reduce power quality problems due to harmonics.

6. Acknowledgements

The author thanks the Faculty of Industrial Technology of Trisakti University for financing this research through the Research Budget of the 2008/2009 Academic Year until the time this paper can be published.

7. Reference

1. Bin-Kwie Chen, Bin-Song Guo, Three Phase Models Of Specially Connected Transformers, IEEE Transaction On Power Delivery, Vol.11. no. 1, January 1996.
2. Cheng-Ping Huang, Chi-Jui Wu, Yung-Sung Chuang, Shih-Kai Peng, Jung-Liang Yen, and Ming-Hong Han, "Loading Characteristics Analysis of Specially connected Transformers Using Various Power Factor Definitions", IEEE Transaction On Power Delivery, Vol.21. no. 3, July 2006.
3. Thomas M. Gruza, A Studi of Neutral Currents in Three-Phase Computer Power Systems, IEEE Transactions On Power Delivery, Vol. 26, N0. 4, July 1990.

4. Sy-Ruen Huang, Bing-Nan Chen, Harmonic Study of Le Blanc Transformer for Taiwan Railway's Electrification System, IEEE Transactions on Power Delivery, Vol.17 No.2 April 2002.
5. W. Mingli, X. Chengshan, Y. Fan and T.Q.Zheng, "Performance and mathematical Model of three-phase three-winding transformer used in 2 x 25 kV electric railway", IEE Proc. Electr. Power Appl. Vol.153. no. 2. March 2006.
6. H. K. Høidalen, R. Sporild, Using Zigzag Transformers with Phase-shift to reduce Harmonics in AC-DC Systems, Presented at the International Conference on Power Systems Transients (IPST'05) in Montreal, Canada on June 19-23, 2005 Paper No. IPST05 – 44.
7. Julius Sentosa Setiadji, Tabrani Machmudsyah, Yanuar Isnanto, "Pengaruh Ketidakseimbangan Beban Terhadap Arus Netral dan Losses Pada Transformator Distribusi", Jurnal Teknik Elektro, Universitas Kristen Petra, Vol. 7, No. 2, Hlm. 68-73, Surabaya, September 2007, ISSN 1411-870X.
8. J. Desmet, I.Sweertvaegher G. Vanalme, K. Stockman, R. Belmans, "Analysis of the neutral conductor current in a three phase supplied network with non-linear single phase loads", IEMDC/IEEE Conf. MIT, Cambridge, Massachusetts, USA, 17-21 June, electronic proc, hal. 2.
9. Rudy Setiabudy, Iwa Garniwa, Analisis Rugi-Rugi Pada Saluran Udara Tegangan Rendah Akibat Pengaruh Harmonik Pada Lampu Hemat Energi Yang Menggunakan Balas Elektronik, Jurnal Teknologi, Fakultas Teknik – Universitas Indonesia, Edisi No. 2, Tahun XIX, Juni 2005, 133-139, ISSN: 0215-1685.
10. Syafrudin Masri1, Che Mat "Suatu Survei Kualitas Daya Sistem Distribusi Tenaga Listrik Pada Pusat Komputer", Electric, Control, Communication & Information Seminar 2004 Seminar Nasional Bidang Energi, Elektronika, Kendali, Telekomunikasi dan Sistem Informasi, Gedung Widyaloka, Universitas Brawijaya Malang, 25-26 Mei 2004, hal. 2.
11. Chairul Gagarin Irianto dan Rudy Setiabudy, et al, Membatasi Pengaruh Distorsi/ Harmonisa Tegangan Dan Arus Dari Peralatan Nonlinier Pada Sistem Distribusi Daya Listrik, ISBN:978-979-18265-1-8 Prosiding Seminar Nasional Penelitian Teknologi Industri, Fakultas Teknologi Industri – Universitas Trisakti, Jakarta 28 Januari 2008.
12. Cadence Design Systems, Inc, PSpice® User's Guideincludes PSpice A/D, PSpice A/D Basics, and PSpiceProduct Version 15.7July 2006.
13. Leon M. Tolbert, Harold D. Hollis, Peyton S. Hale, Jr."Evaluation Of Harmonic Suppresion Devices" IEEE IAS Annual Meeting, Oct. 6-10, 1996, San Diego, CA, pp. 2340-2346.

Prototype Design of Broadcast AM Radio Communication System with Frequency Hopping

Damar Widjaja

Electrical Engineering Department,
University of Sanata Dharma, Yogyakarta 55282
Tel: (0274) 883037. Fax: (0274) 886529
Email: damar@staff.usd.ac.id

ABSTRACT

Frequency Hopping (FH) technique is one of data transmission method in the telecommunication system. FH can help system to resolve transmission problems, i.e. jamming, noise, interference, and multipath fading. The goal or this research is developing AM broadcast radio communication system with frequency hopping. Transmitter and receiver are not synchronized.

System that has been designed is using PLL (Phase Lock Loop) as a carrier signal oscillator. There are two carrier signal oscillators to be set to perform FH technique, which are at frequency of 1000 kHz and 1050 kHz. The change in frequency is controlled by programmable divider.

This research produces AM broadcast radio communication system with frequency hopping. After some tests were performed, it turns out that the prototype can work well. Information signal that was transmitted by AM transmitter can be well received at the receiver. Frequency hopping has been well performed with hopping period of one carrier signal is 0.5 second. The system can be further developed by adding the number of carrier frequency for hopping technique and synchronization between transmitter and receiver.

Keywords
Frequency hopping, AM broadcast, radio communication

1. INTRODUCTION

Information signal should be put on the radio signal that has higher frequency as a carrier. The method to add the two signals is called modulation [1]. Modulate means change the parameter of carrier signal that has higher frequency with information signal that has lower frequency.

Analog signal modulation that is used in this research is amplitude modulation (AM). The amplitude of carrier signal is changed according to the change of information signal amplitude.

Information signal often suffer from distortion during transmission due to fading, delay, attenuation, interference, jamming, and noise. Information signal will be corrupted and the received signal quality will be decreased [2]. Jamming is a transmission of interferer signal deliberately in the same channel and disturbs the existing service channel [3].

Interference and jamming will appear as the number of transmitter increase in a fix allocation of frequency spectra. If the transmitter operates in moderate quality factor, then the bandwidth will disturb other transmitter on the adjacent channel.

Above mention problem does not occur in the AM radio frequency spectrum due to the number of broadcast AM radio transmitter that is getting smaller. Jakarta has only 13 transmitters [4–6], whereas the frequency allocation for AM radio transmitter is very wide. This trend happens because there is much interference experienced inherently by information signal that is transmitted with AM technique. Nowadays, most of AM radio broadcast transmitters settled into FM technique. FM technique is more interesting due to the ability to suppress interference problem [1].

One of the techniques to solve this problem is spread spectrum that has antijam capability, interference suppression, ability to combat multipath fading, and security features [7]. One of the well-known spread spectrum techniques is Frequency Hopping Spread Spectrum (FHSS). The use of random channel can resolve jamming problem, especially when jamming target is only a particular frequency. FHSS can suppress interference, especially when interference hits a particular frequency. FHSS can also combat multipath fading, especially frequency selective fading. This technique will increase the channel capacity, so that more transmitters can use the same frequency spectrum with different hopping sequence [8].

This research produces AM broadcast radio communication system with frequency hopping. The equipment that has been designed is laboratory scale system prototypes that can be develop as commercial equipment. The system consists of AM radio transmitter and receiver with two carrier frequencies, 1000 kHz and 1050 kHz that hopped every 0.5 second. Transmitter and receiver are independent, not synchronize, and will be tested separately.

The result of this research can be considered as a starting point and reference of further development of the application of FH in broadcast communication system. Proper development will increase the quality of communication service and efficiency of spectrum utilization. The number of broadcast AM radio transmitter will rapidly increase without worrying about service quality decrement. AM radio spectrum potentially become an interesting alternative for

broadcast radio transmitter to grow like the old time.

2. THEORETICAL BACKGROUND

2.1. Amplitude Modulation

Amplitude modulation (AM) is a modulation process that changes the carrier signal amplitude according to the amplitude of information signal with fix carrier frequency. The instantaneous carrier frequency can be expressed as [1]

$$e_c(t) = E_{c\max}\cos(\omega_c t + \phi_c) \quad (1)$$

where $E_{c\max}$ is carrier signal amplitude, ω_c is carrier angle frequency, and ϕ_c is carrier phase. The wave shape of carrier signal is depicted in Figure 1.

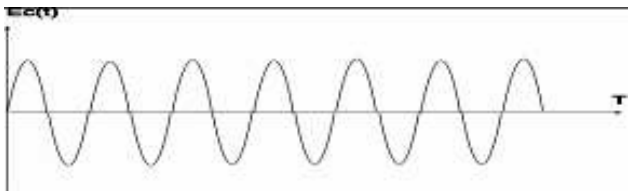

Figure 1: Carrier wave shape [1]

Modulating signal can be expressed as [1]

$$e_m(t) = E_{m\max}\cos(\omega_m t + \phi_m) \quad (2)$$

where $E_{m\max}$ is modulating signal amplitude, ω_m is modulating signal angle frequency, dan ϕ_m is modulating signal phase. The wave shape of modulating signal is depicted in Figure 2.

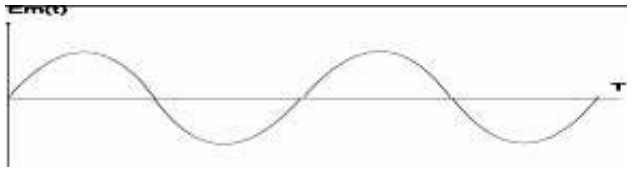

Figure 2. Modulating wave shape [1]

Modulation process produce modulated signal, which can be expressed as [1]

$$e(t) = [E_{c\max} + e_m(t)]\cos(\omega t + \phi) \quad (3)$$

The wave shape of modulated signal is depicted in Figure 3.

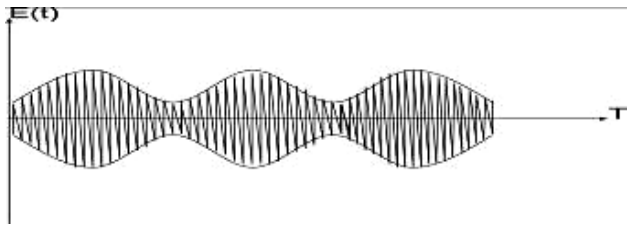

Figure 3. Modulated wave shape [1]

2.2. Frequency Hopping

Frequency hopping (FH) is a change of carrier frequency periodically that is controlled by certain algorithm [8]. The particular frequency will carry the information signal in a certain period and then the carrier frequency will change to other frequency as it is depicted in Figure 4.

The bended arrow in Figure 4 shows the hopping sequence that is from $f_1 \rightarrow f_3 \rightarrow f_7 \rightarrow f_2 \rightarrow f_5 \rightarrow f_4 \rightarrow f_6$, and repeated continuously. The change of carrier frequency can be done hundreds times per second. The receiver should be able to tune the change of frequency, so that the information can be well received.

FH is one of the spread spectrum technique and the bandwidth is wider than minimum bandwidth that is needed for sending the same information if using single carrier. System that use spread spectrum technique will have advantages such as antijam ability, interference suppression, combat multipath fading, low probability of intercept, secure communication, and increase spectral efficiency [7]

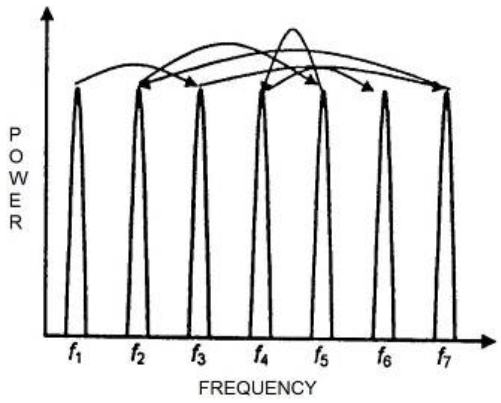

Figure 4: FH technique [8]

The hop process, from one frequency to another, is usually controlled sequentially or randomly using pseudorandom code. If interference appear and disturb one of the channels, e.g. f_2, then this frequency will always suffer the disturbance, but only when its turn to carry the information signal. This mechanism is shown in Figure 5.

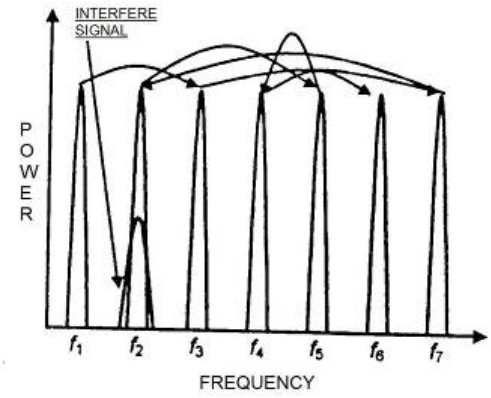

Figure 5: Interference on FH transmission [8]

3. RESEARCH METHODOLOGY

3.1. System Model

System model can be depicted in Figure 6 (transmitter) and Figure 7 (receiver). Two carrier signals with different frequency (f_1 and f_2) will work consecutively. Carrier signal changes was done by switching device. Oscillator was designed using PLL (Phase Locked Loop) with programmable counter to generate two frequencies. Modulated signal will be amplified prior to trasmitting from antenna.

In the receiver side, radio signal will be amplified prior to demodulation process. In the AM demodulator, modulated signal will be combined with signal from local oscillator that was designed using PLL. This PLL has the same configuration with the one in the transmitter.

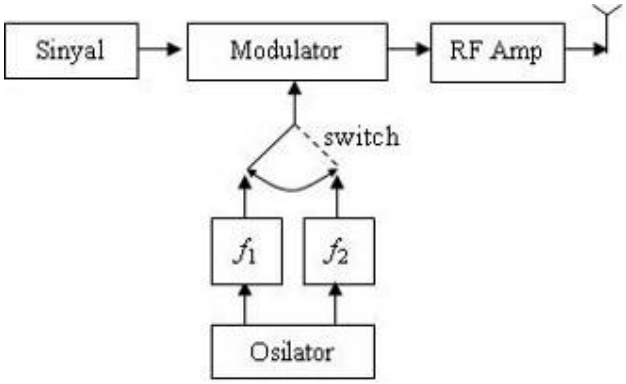

Figure 6: Transmitter model

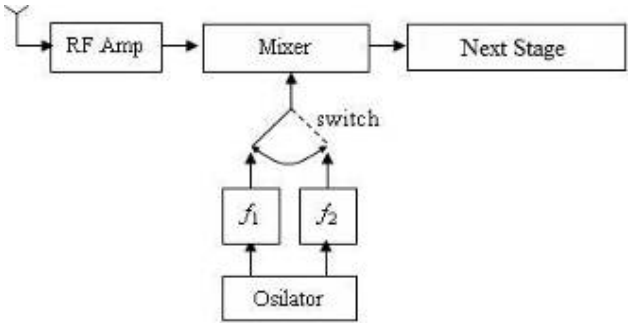

Figure 7: Receiver model

3.2. System Design

Figure 8 shows the block diagram of AM transmitter with FH. ORF is a reference oscillator, PD is a phase detector, LPF is a Low Phase Filter, VCO is a Voltage Controlled Oscillator, and PT is programmable divider. PLL operation is established by PD, LPF, and VCO.

Programmable divider is controlled by electronic switch. The output of programmable divider will be compared with reference frequency in the phase detector. The phase detector will produce DC voltage level to control the VCO and generate the carrier frequency.

The circuit of AM receiver with FH is depicted in Figure 9. Figure 9 shows that radio signals come from the antenna and will be driven to RF amplifier. Signal is then passed through the mixer, mixed with signal from local oscillator as a reference signal, so that generate an Intermediate Frequency (IF). Signal amplitude is amplified in IF amplifier and then passed through the detector for information and carrier signal separation. After separation, signal is processed in the LPF to suppressed the noise prior to be processed in volume control and speaker. The function of mixer, IF amplifier and detector is replaced by IC ZN414.

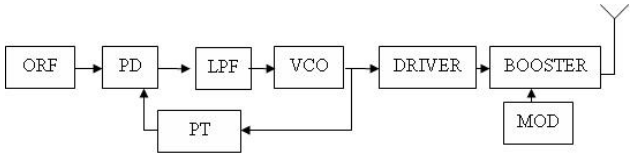

Figure 8. Block diagram of AM transmitter with FH

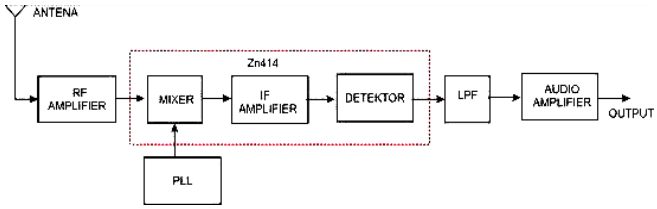

Figure 9. Block diagram of AM receiver with FH

4. DISCUSSION

4.1. AM Transmitter with FH

4.1.1. Transmitter Transmission Testing

The test was performed using system model that is illustrated in Figure 10. Transmitter block sends information signal using two carrier frequencies, i.e. 1000 kHz and 1050 kHz. Signal that is sent from the transmitter is received by two AM receivers, each of them are tuned at 1000 kHz and 1050 kHz.

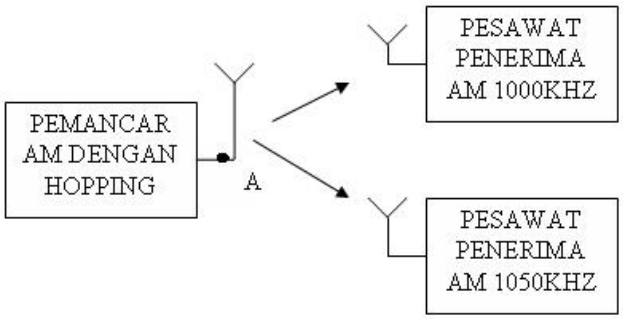

Figure 10. System model for transmitter transmission testing

Figure 11 shows the display of frequency spectrum of transmitter that was taken in point A of Figure 10. It is shown that transmitter has a good and stable carrier frequency at 1000 kHz and 1050 kHz.

ISSN 114-1284

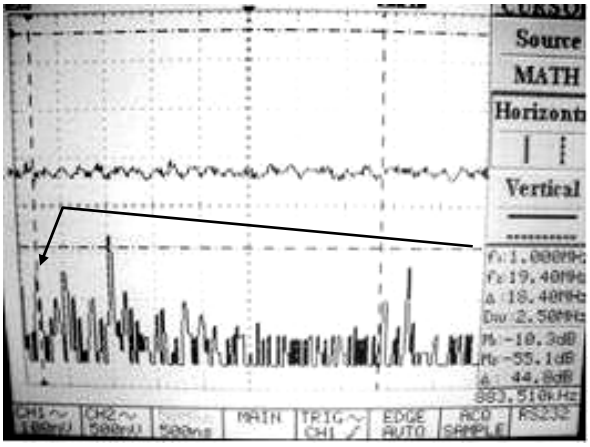

(a)

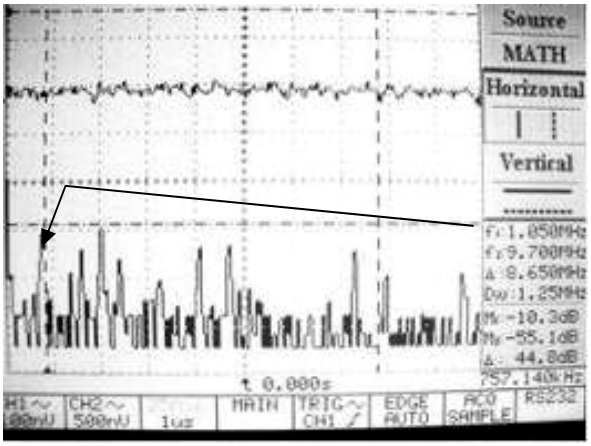

(b)

Figure 11. Carrier frequency spectrum of transmitter at (a) 1000 kHz (b) 1050 kHz

Transmitter is also tested to prove that it works on AM technique. Sinusoidal information signal with frequency 4 kHz is sent with both carriers. The wave shape of the modulated signal as the result of modulation process is shown in Figure 12. Figure 12 shows that the transmitter works on AM technique.

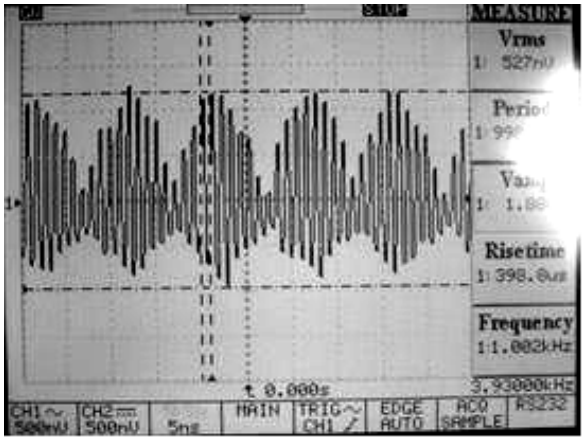

(a)

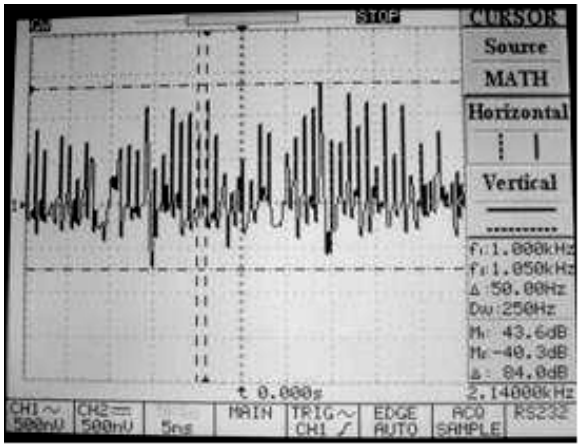

(b)

Figure 12. AM technique with carrier frequency (a) 1000 kHz (b) 1050 kHz

Figure 12. (cont'd) AM technique with carrier frequency (a) 1000 kHz (b) 1050 kHz

Observation is also done by listen the tone sound quality at AM receiver speaker. The higher the information signal frequency, the higher the tone sound. Figure 13 shows the frequency spectrum of audio signal from the speaker in the AM receiver. The spectrum at the receiver has the same fundamental frequency with the signal transmitted.

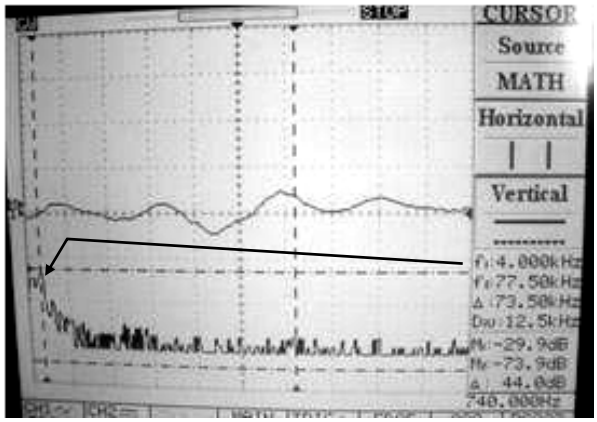

(a)

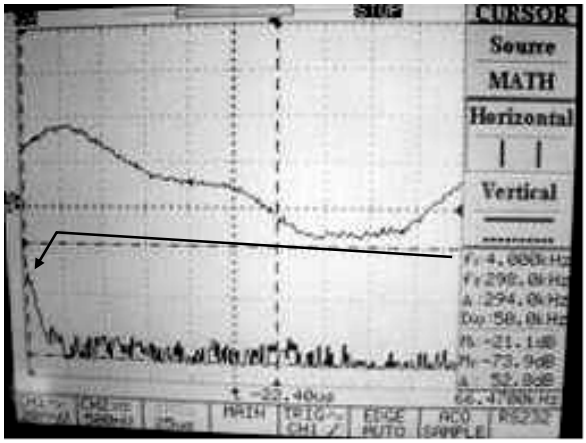

(b)

Figure 13. Audio frequency spectrum at the AM receiver with carrier frequency (a) 1000 kHz. (b) 1050 kHz

4.1.2. Carrier Frequency Stability Testing when Hopping

The test was performed using system model that is illustrated in Figure 14. Output signal of transmitter block is measured using frequency counter for 300 seconds. Table 1 shows the data when hopping. Data were taken every 50 seconds.

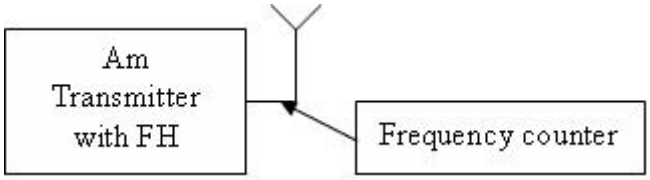

Figure 14. Transmitter stability testing when hopping

Table 1. Data of transmitter stability testing when hopping

Time (s)	Carrier Frequency 1 (KHz)	Carrier Frequency 2 (KHz)
50	1000,0	1050,0
100	1000,2	1050,6
150	1000,4	1050,2
200	1000,0	1050,1
250	1000,0	1050,3
300	1000,1	1050,8
Average	1000,1	1050,3
Error (%)	0,01	0,28

Table 1 show that average error percentage of carrier frequency is very small, that is 0.01 % for carrier frequency 1000 MHz and 0.28 % for carrier frequency 1050 MHz. The error percentage shows that transmitter has stable carrier frequency when hopping.

4.2. AM Receiver with FH

The test was performed using system model that is illustrated in Figure 15 at point 1 and point 2. RF Generator send 50% modulated signal over carrier signal with frequency 1000 kHz and 1050 kHz.

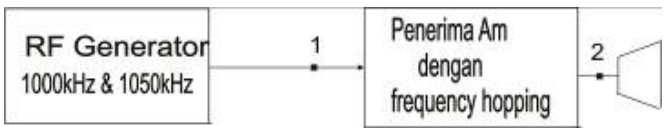

Figure 15. AM receiver testing

Figure 16 (a) shows the input signal of AM receiver that was observed at point 1. Calculation of carrier frequency refers to Figure 16 (b) that is the enlarge version of Figure 16 (a) with time/division on the oscilloscope is set at $T = 2x0{,}5x10^{-6} = 1x10^{-6}\,s$. So that carrier frequency received by receiver can be defined as

$$f = \frac{1}{T} = \frac{1}{1x10^{-6}} = 1000kHz \qquad (4)$$

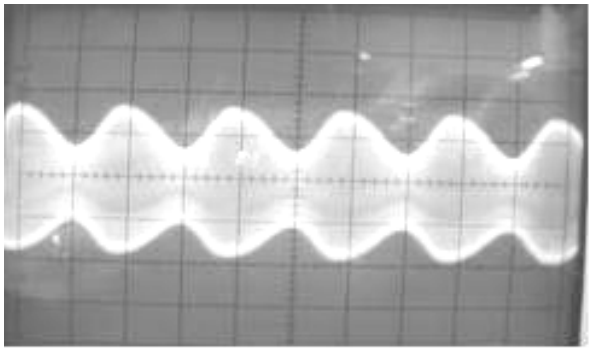

(a)

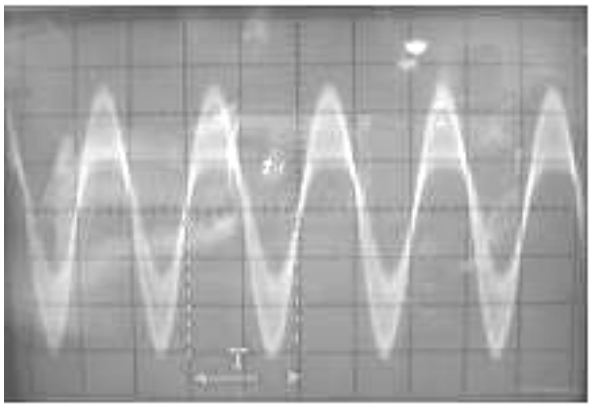

(b)

Figure 16. (a) Input signal of AM receiver at 1000 kHz
(b) Enlarge version of (a)

Figure 17 (a) shows the input signal of AM receiver that was observed at point 1. Calculation of carrier frequency refers to Figure 17 (b) that is the enlarge version of Figure 17 (a) with time/division on the oscilloscope is set at $T = 1{,}9x0{,}5x10^{-6} = 9{,}5x10^{-7}\,s$. So that carrier frequency received by receiver can be defined as

$$f = \frac{1}{T} = \frac{1}{9{,}5x10^{-7}} = 1052kHz \qquad (5)$$

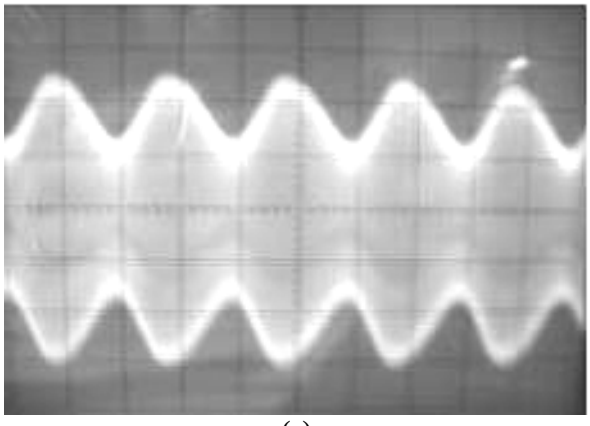

(a)

Figure 17. (a) Input signal of AM receiver at 1050 kHz (b) Enlarge version of (a)

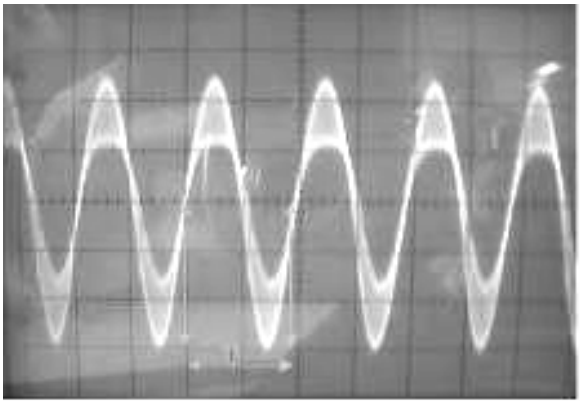

(b)

Figure 17. (cont'd) (a) Input signal of AM receiver at 1050 kHz (b) Enlarge version of (a)

Figure 16 and Figure 17 shows that AM receiver can receive signal correctly. Frequency spectrum also shows that frequency transmitted is correct. Carrier frequency spectrum at 1000 kHz and 1050 kHz is depicted in Figure 18.

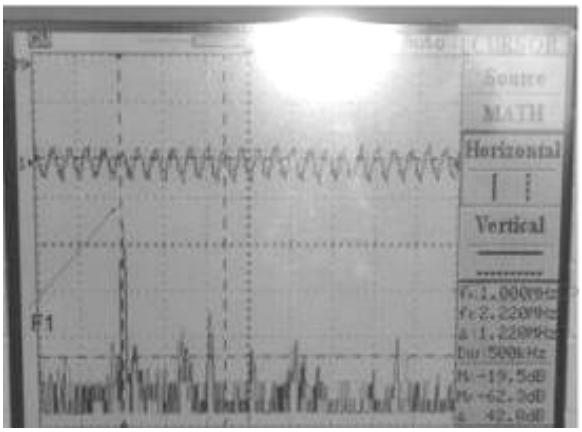

(a)

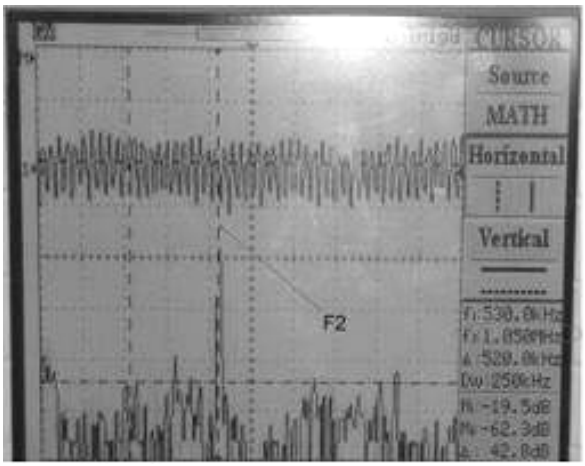

(b)

Figure 18. Carrier frequency spectrum (a) 1000 kHz, (b) 1050 kHz

F1 in Figure 18 (a) shows the highest signal peak at 1000 kHz. F1 in Figure 18 (b) shows the highest signal peak at 1050 kHz. Test was performed for each carrier frequency consecutively. For each carrier frequency, only one tone with particular frequency can be listened.

Test for defining the audio frequency that is produced by AM receiver is done at point 1 and point 2 simultaneously. Modulated signal carries audio signal with frequency 1 kHz. When point 1 receives carrier frequency of 1000 kHz, point 2 is measured and the result is depicted in Figure 19 (a). When point 1 receives carrier frequency of 1050 kHz, point 2 is measured and the result is depicted in Figure 19 (b).

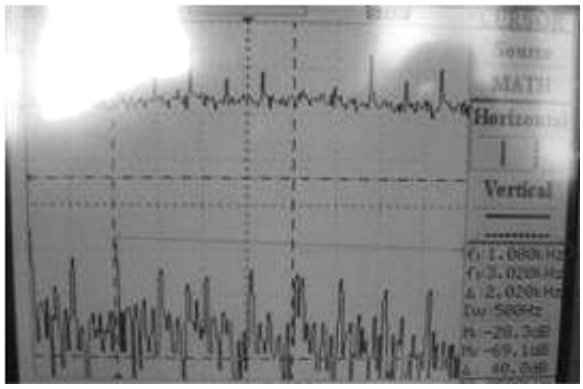

(a)

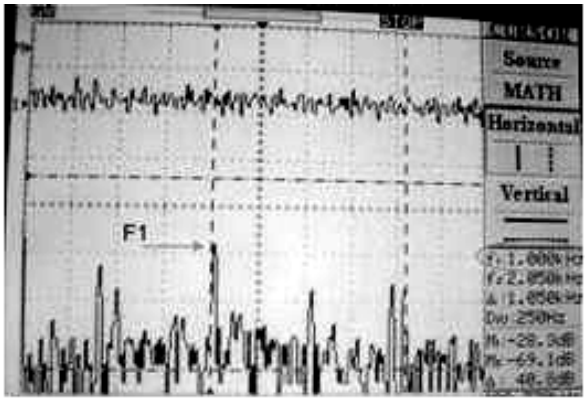

(b)

Figure 19. Audio signal with frequency 1kHz on carrier frequency (a) 1000kHz (b) 1050kHz

F1 shows the fundamental frequency with many harmonics. The harmonics signal does not affect system performance. It seems that fundamental frequency shows the difference between frequency received and frequency transmitted. Pointer can not be placed in the middle of the signal peak, so that the measurement that is shown in Figure 19 is the best measurement that can be taken. However, the performance of AM receiver is already met the design specification.

Frequency hopping process can not be clearly observed as the time domain of the output of timer is too tight comparing the output of VCO as PLL output. Figure 20 shows the hopping process when carrier frequency 1000 kHz change to 1050

kHz. Measurement is done at timer output and VCO output simultaneously.

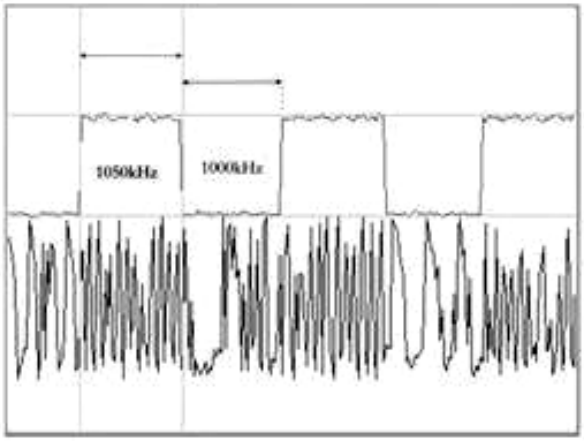

Figure 20. Hopping process of two carrier frequencies.

Carrier signal with frequency 1050 kHz looks tighter than carrier signal with frequency 1000 kHz. When timer is ON, it generates carrier frequency 1050 kHz. When timer is OFF, it generates carrier frequency 1000 kHz. The test result shows that hopping process is agreeing with the design.

5. CONCLUSION AND SUGGESTION

5.1. Conclusion

a. The prototype that has been made can work well according to the design.
b. AM receiver can tune the signal from transmitter with carrier frequency 1000 kHz and 1050 kHz consecutively.
c. Hopping period for one carrier frequency is 0.5 seconds.

5.2. Suggestion

a. The system can still be developed with synchronization mechanism for transmitter and receiver.
b. The number of carrier frequency can be improved for better FH technique.

6. REFERENCE

[1]. D. Roddy and J. Coolen, *"Electronics Communication"*, *Komunikasi Elektronik*. Jakarta: PT. Prenhallindo. 2001.
[2]. W. Hioki, *"Telecommunication, 3rd edition"*. New Jersey: Prentice Hall. 1998.
[3]. R.S. Roberts. *"Audio, Radio, and Video Dictionary"*, *Kamus Audio, Radio dan Video*. Jakarta: PT. Elek Media Komputindo. 1994.
[4]. http://en.wikipedia.org/wiki/Lists_of_radio_stations_in_ Jakarta,_Indonesia (accessed March 2007)
[5]. http://en.wikipedia.org/wiki/Lists_of_radio_stations_in_ Surabaya,_Indonesia (access March 2007)
[6]. http://id.wikipedia.org/wiki/I-Radio_Jogjakarta (accessed March 2007)
[7]. Rustamaji and D. Elan, *"Spread Spectrum Frequency Hopping Transmitter for Information Signal Security"*, Pemancar Frequency Hopping Spread Spectrum untuk Pengamanan Sinyal Informasi. IT Journal. 2002. http://www.informatika.lipi.go.id/pemancar-frequency-hopping-spread-spectrum-untuk-pengamanan-sinyal-informasi (accessed August 2007).
[8]. D. Wijaya, "The increment of system capacity and signal quality in the GSM network using frequency hopping", Peningkatan Kapasitas Sistem dan Kualitas Sinyal Pada Jaringan GSM dengan Frekuensi Hopping. *Majalah SIGMA*, vol 5. No 2, pp. 171-183. July 2002.
[9]. Kennedy, George. *"Electronic Communication System"*, 3rd edition, New York: McGraw Hill. 1984.

ISSN 114-1284

Prototype Design of Broadcast FM Radio Communication System with Frequency Hopping

Damar Widjaja

Electrical Engineering Department,
University of Sanata Dharma, Yogyakarta 55282
Tel: (0274) 883037. Fax: (0274) 886529
Email: damar@staff.usd.ac.id

ABSTRACT

Frequency Hopping (FH) technique is one of data transmission method in the telecommunication system. FH can help system to resolve transmission problems, i.e. jamming, noise, interference, and multipath fading. The goal or this research is developing FM broadcast radio communication system with frequency hopping. Transmitter and receiver are not synchronized.

System that has been designed is using PLL (*Phase Lock Loop*) as a carrier signal oscillator. There are two carrier signal oscillators to be set to perform FH technique, which are at frequency of 90 MHz and 100 MHz. The change in frequency is controlled by programmable divider.

This research produces FM broadcast radio communication system with frequency hopping. After some tests were performed, it turns out that the prototype can work well. Information signal that was transmitted by FM transmitter can be well received at the receiver. FM receiver can tunes two carrier frequencies, 90 MHZ and 100 MHz. Hopping period of one carrier signal is 0.5 second. The system can be further developed by adding the number of carrier frequency for hopping technique and synchronization between transmitter and receiver.

Keywords
Frequency hopping, FM broadcast, radio communication

1. INTRODUCTION

Information signal should be put on the radio signal that has higher frequency as a carrier. The method to add the two signals is called modulation [1]. Modulate means change the parameter of carrier signal that has higher frequency with information signal that has lower frequency.

Analog signal modulation that is used in this research is frequency modulation (FM). The frequency of carrier signal is changed according to the change of information signal amplitude.

Information signal often suffer from distortion during transmission due to fading, delay, attenuation, interference, jamming, and noise. Information signal will be corrupted and the received signal quality will be decreased [2]. Jamming is a transmission of interferer signal deliberately in the same channel and disturbs the existing service channel [3].

Interference and jamming will appear as the number of transmitter increase in a fix allocation of frequency spectra. If the transmitter operates in moderate quality factor, then the bandwidth will disturb other transmitter on the adjacent channel.

For example, there are 47 broadcast FM radio transmitters in Jakarta with allocation of frequency spectra between 87.6 MHz up to 107.8 MHz [4]. Surabaya has 37 transmitters [5] and Yogyakarta has 43 transmitters [6]. The frequency band for each transmitter is about 300 kHz, so Jakarta is already saturated. If there were an additional transmitter operated, there will be interference and jamming occurs among transmitters. Surabaya and Yogyakarta still can be expanded in limited number. One day, the spectrum will full up and there is no space to expand.

One of the techniques to solve this problem is spread spectrum that has antijam capability, interference suppression, ability to combat multipath fading, and security features [7]. One of the well-known spread spectrum techniques is Frequency Hopping Spread Spectrum (FHSS). The use of random channel can resolve jamming problem, especially when jamming target is only a particular frequency. FHSS can suppress interference, especially when interference hits a particular frequency. FHSS can also combat multipath fading, especially frequency selective fading. This technique will increase the channel capacity, so that more transmitters can use the same frequency spectrum with different hopping sequence [8].

This research produces FM broadcast radio communication system with frequency hopping. The equipment that has been designed is a laboratory scale system prototype that can be develop as commercial equipment. The system consists of FM radio transmitter and receiver with two carrier frequencies, 90 MHz and 100 MHz that hopped every 0.5 second. Transmitter and receiver are independent, not synchronize, and will be tested separately.

The result of this research can be considered as a starting point and reference of further development of the application of FH in broadcast communication system. Proper development will increase the quality of communication service and efficiency of spectrum utilization. The number of broadcast radio transmitter will rapidly increase without worrying about service quality decrement.

2. THEORETICAL BACKGROUND

2.1. Frequency Modulation

Frequency modulation (FM) is a modulation process that changes the carrier frequency according to the amplitude of information signal with fix carrier amplitude [9]. Figure 1 shows that when information signal amplitude is positive, carrier frequency is deviated by Δf and become f_1. When information signal amplitude is negative, carrier frequency is deviated by Δf and become $-f_1$. As information signal amplitude increase, the frequency deviation is also increase and potentially capable of disturbing other transmitter [1]. The instantaneous carrier frequency can be expressed as

$$f_i(t) = f_c(t) + ke_m(t) \quad (1)$$

Information signal as modulating signal, e_m, is used to change the carrier frequency. The change in frequency is ke_m, with k is a frequency deviation constant, and f_c is an unmodulated carrier frequency.

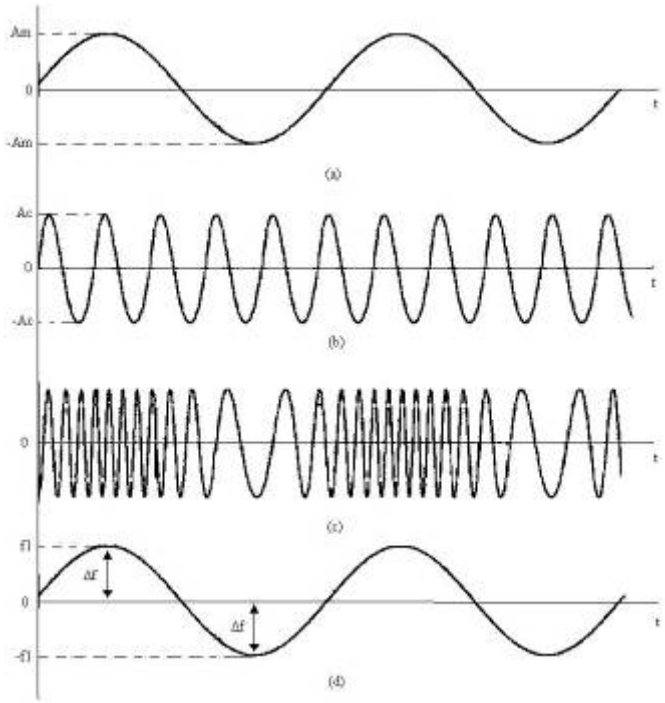

Figure 1: FM [9] (a) Information signal (b) *Carrier* signal. (c) Amplitude vs. time (d) Frequency vs. time

2.2. Frequency Hopping

Frequency hopping (FH) is a change of carrier frequency periodically that is controlled by certain algorithm [8]. The particular frequency will carry the information signal in a certain period and then the carrier frequency will change to other frequency as it is depicted in Figure 2.

The bended arrow in Figure 2 shows the hopping sequence that is from $f_1 \rightarrow f_3 \rightarrow f_7 \rightarrow f_2 \rightarrow f_5 \rightarrow f_4 \rightarrow f_6$, and repeated continuously. The change of carrier frequency can be done hundreds times per second. The receiver should be able to tune the change of frequency, so that the information can be well received.

FH is one of the spread spectrum technique and the bandwidth is wider than minimum bandwidth that is needed for sending the same information if using single carrier. System that use spread spectrum technique will have advantages such as antijam ability, interference suppression, combat multipath fading, low probability of intercept, secure communication, and increase spectral efficiency [7]

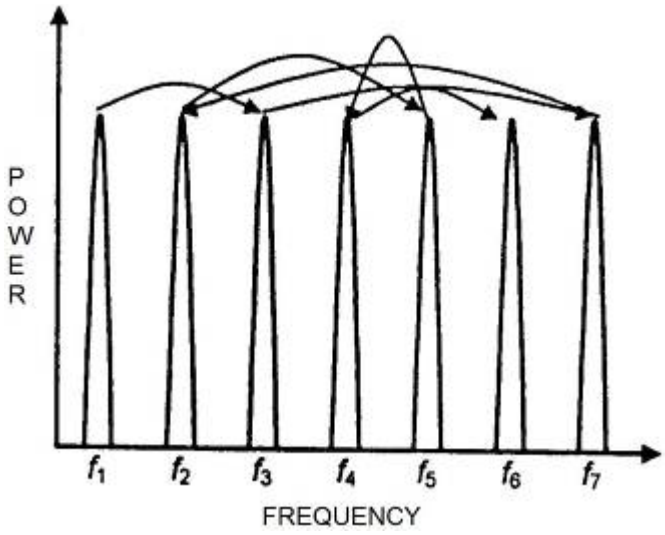

Figure 2: FH technique [8]

The hop process, from one frequency to another, is usually controlled sequentially or randomly using pseudorandom code. If interference appear and disturb one of the channels, e.g. f_2, then this frequency will always suffer the disturbance, but only when its turn to carry the information signal. This mechanism is shown in Figure 3.

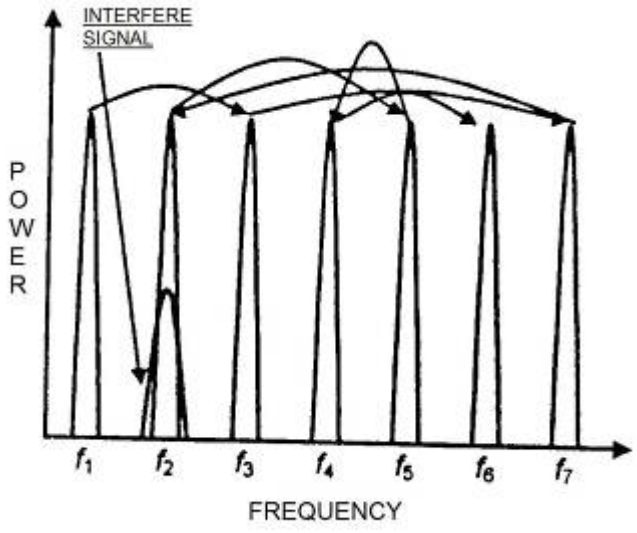

Figure 3: Interference on FH transmission [8]

3. RESEARCH METHODOLOGY

3.1. System Model

System model can be depicted in Figure 4 (transmitter) and Figure 5 (receiver). Two carrier signals with different frequency (f_1 and f_2) will work consecutively. Carrier signal changes was done by switching device. Oscillator was designed using PLL (Phase Locked Loop) with programmable counter to generate two frequencies. Modulated signal will be amplified prior to trasmitting from antenna.

In the receiver side, radio signal will be amplified prior to demodulation process. In the FM demodulator, modulated signal will be combined with signal from local oscillator that was designed using PLL. This PLL has the same configuration with the one in the transmitter.

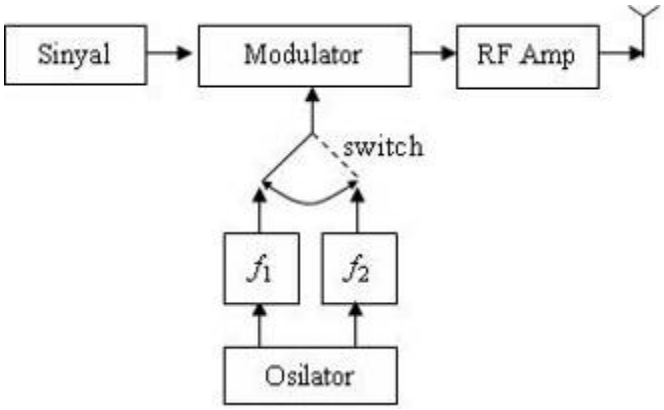

Figure 4: Transmitter model

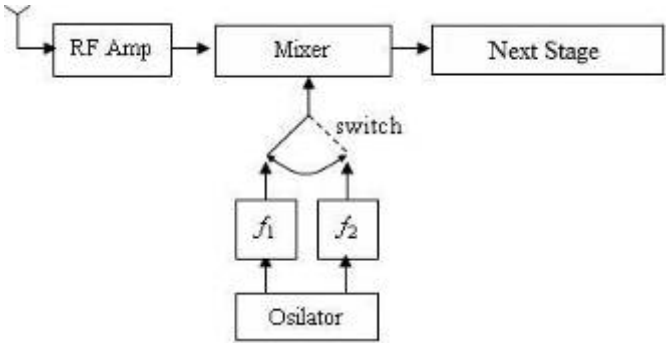

Figure 5: Receiver model

3.2. System Design

Figure 6 shows the block diagram of FM transmitter with FH. The function of prescaler block is as preliminary divider for output signal frequency of VCO (Voltage Controlled Oscillator) block, because this frequency is still too high to be divided in the programmable divider.

Programmable divider is controlled by electronic switch (switch 1 and switch 2). The output of programmable divider will be compared with reference frequency in the phase detector. The phase detector will produce DC voltage level to control the VCO and generate the carrier frequency.

The circuit of FM receiver with FH is depicted in Figure 7. The circuit consists of nine parts. These nine parts is classified in two main groups. The first groups is radio signal processing group that consist of RF (Radio Frequency) amplifier, mixer, IF (Intermediate Frequency) amplifier, Q.D. (Quadrature Detector), AF (Audio Frequency) amplifier. The second group is FH controlling group that consist of crystal oscillator, PLL, VCO and programmable counter/divider.

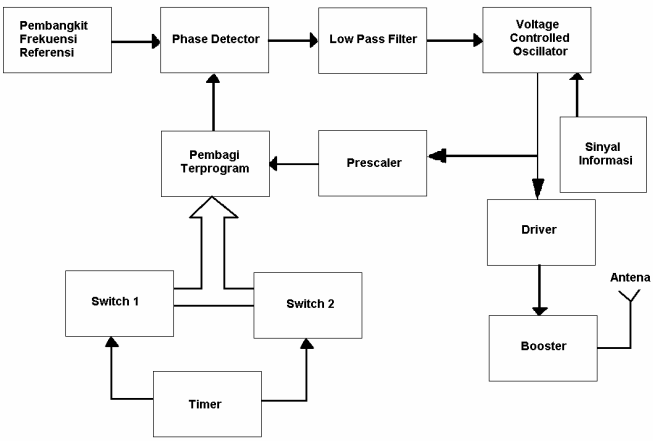

Figure 6. Block diagram of FM transmitter with FH

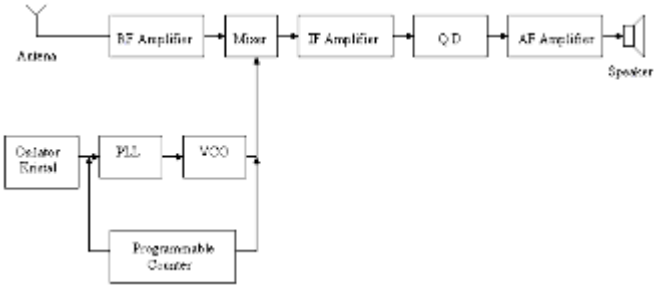

Figure 7. Block diagram of FM receiver with FH

Antenna receives all radio signals that exist. RF amplifier together with mixer will select a particular FM signal and amplify it. FM signal will be combined with local oscillator signal. Local oscillator is built from PLL and VCO circuit that has been set by programmable counter in the mixer. The output of mixer is an IF signal. IF signal will be amplified by IF amplifier. QD is used to separate audio signal from carrier signal. The audio signal will be amplified so that the power of the signal can drive the speaker.

4. DISCUSSION

4.1. FM Transmitter with FH

4.1.1. Transmitter Transmission Testing

The test was performed using system model that is illustrated in Figure 8. Transmitter block sends information signal using two carrier frequencies, i.e. 90 MHz and 100 MHz. Signal that is sent from the transmitter is received by two FM

receivers, each of them are tuned at 90 MHz and 100 MHz.

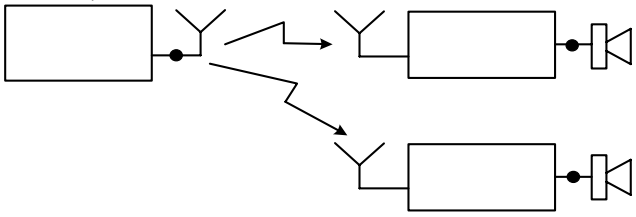

Figure 8. System model for transmitter transmission testing

Figure 9 shows the display of frequency spectrum of transmitter that was taken in point a of Figure 8. It is shown that transmitter has a good and stable carrier frequency at 90 MHz and 100 MHz.

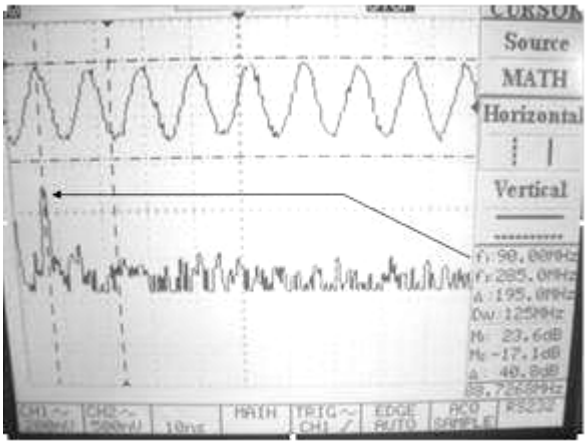

(a)

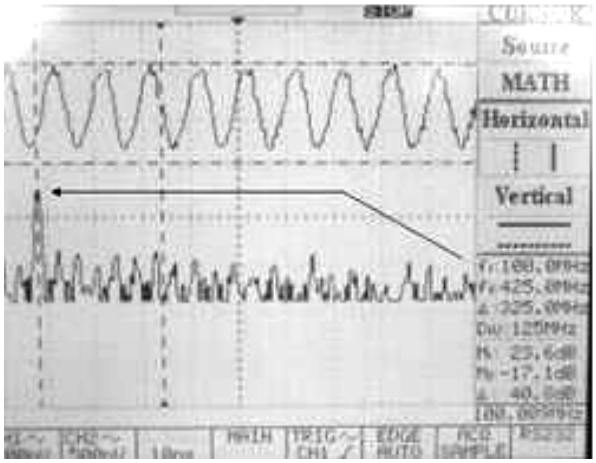

(b)

Figure 9. Carrier frequency spectrum of transmitter at (a) 90 MHz (b) 100 MHz

Transmitter is also tested to prove that it works on FM technique. Sinusoidal information signal with frequency 4 kHz 10 Vpp is sent with both carriers. The wave shape of the modulated signal as the result of modulation process is shown in Figure 10. Figure 10 shows that the transmitter works on FM technique.

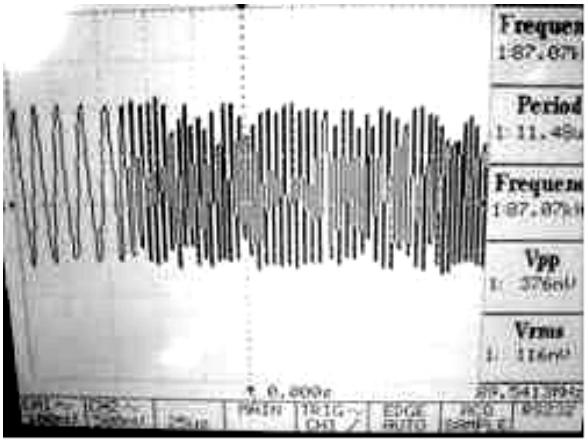

(a)

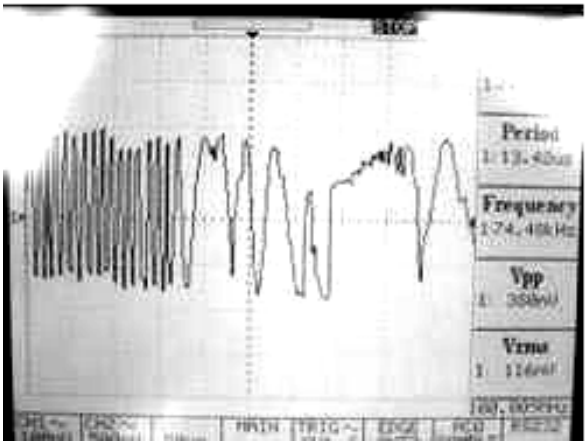

(b)

Figure 10. FM technique with carrier frequency (a) 90 MHz (b) 100 MHz

Point b and point c in Figure 8 is testing points of information signal that is received by FM receiver. Figure 11 shows the frequency spectrum of audio signal from the speaker in the FM receiver. It shows that the received signal is the same of the transmitted signal. The spectrum at the receiver has the same fundamental frequency with the signal transmitted.

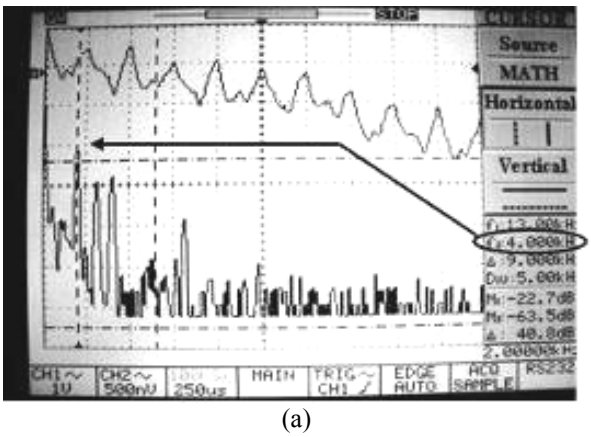

(a)

Figure 11. Audio frequency spectrum at the FM receiver with carrier frequency (a) 100 MHz. (b) 90 MHz

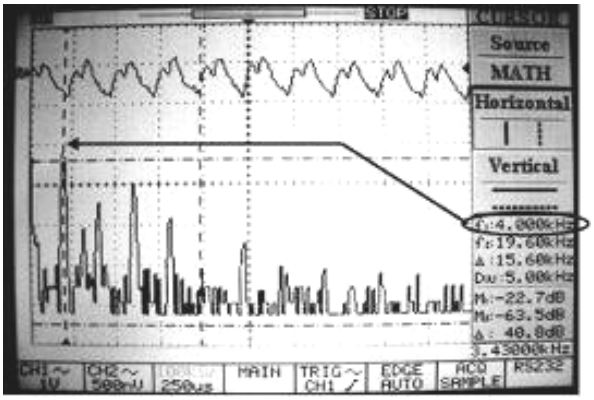

(b)

Figure 11. (cont'd) Audio frequency spectrum at the FM receiver with carrier frequency (a) 100 MHz. (b) 90 MHz

4.1.2. Carrier Frequency Stability Testing when Hopping

The test was performed using system model that is illustrated in Figure 12. Output signal of transmitter block is measured using frequency counter for 500 seconds. Table 1 shows the data when hopping. Data were taken every 50 seconds.

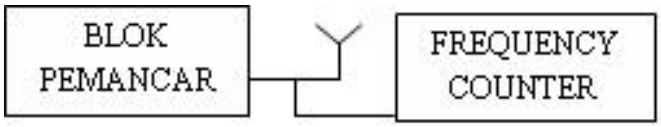

Figure 12. Transmitter stability testing when hopping

Table 1. Data of transmitter stability testing when hopping

Time (s)	Frequency *Carrier* 1 (MHz)	Frequency *Carrier* 2 (MHz)
50	90,0	99,8
100	89,9	99,9
150	89,8	99,9
200	90,0	100,0
250	89,9	100,0
300	90,0	99,9
350	90,0	100,0
400	90,0	99,9
450	90,0	100,0
500	89,9	99,9
Average($\overline{X}$)	89,95	99,93
Persen *error* (%)	0,001	0,0007

Table 1 show that average error percentage of carrier frequency is very small, that is 0.001 % for *carrier* frequency 90 MHz and 0.0007 % for *carrier* frequency 100 MHz. The error percentage shows that transmitter has stable carrier frequency when hopping.

4.2. FM Receiver with FH

4.2.1. Receiving Quality Testing

The test was performed using system model that is illustrated in Figure 13. Two of FM transmitter blocks are set to send carrier signal with frequency 90 MHz and 100 MHz. Signal is received by FM receiver with FH.

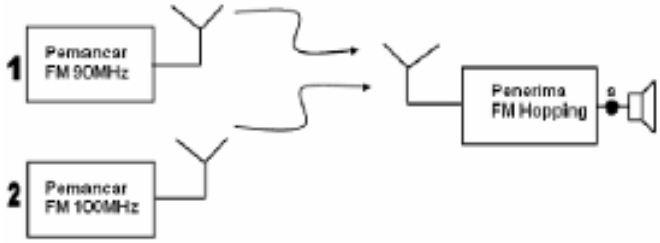

Figure 13. Receiving Quality Testing

The RF output testing was performed when transmitter sends modulated signal with frequency of information signal is 2 kHz and amplitude 2.5V. It is proven that RF amplifier can tune frequency 90 MHz and 100 MHz as it is shown in Figure 13.

Figure 13 also shows that received signal at RF amplifier is FM signal. Figure 13 (a) is received signal shape when 90 MHz transmitter is activated and Figure 13 (b) is the signal spectrum. Figure 14 (a) is received signal shape when 100 MHz transmitter is activated and Figure 14 (b) is the signal spectrum.

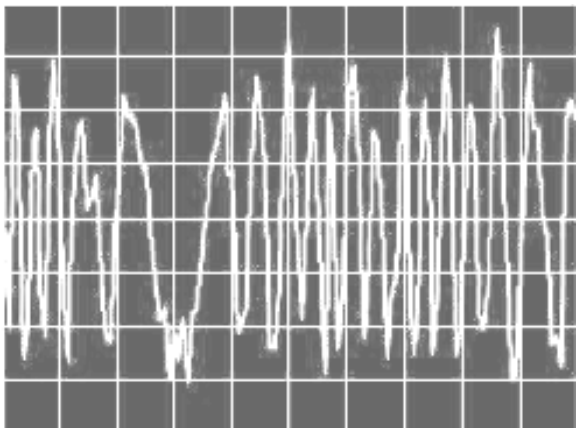

(a)

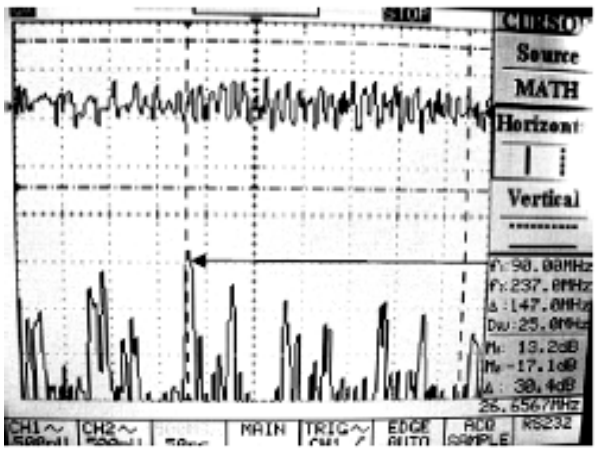

(b)

Figure 13. RF amplifier output signal at frequency 90 MHz
(a) RF amplifier output signal
(b) RF amplifier output spectrum

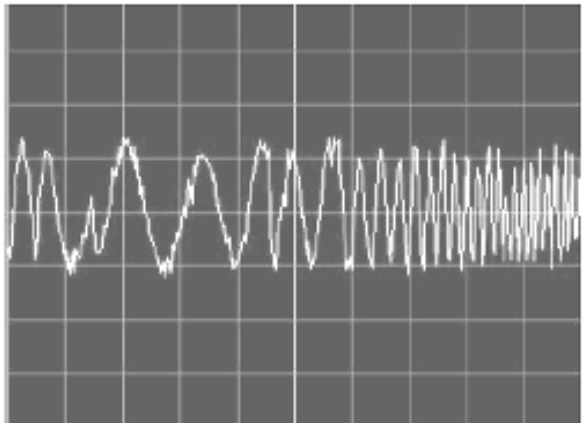

(a)

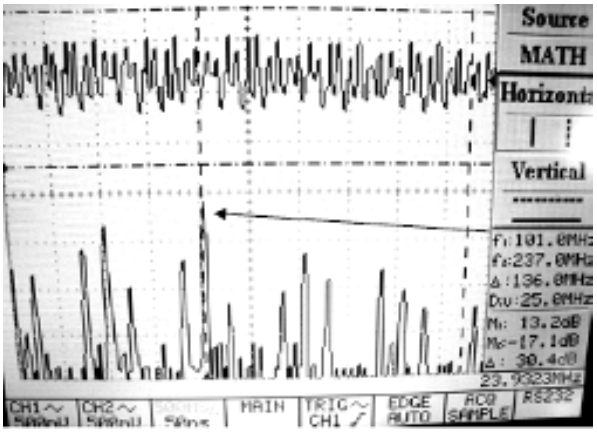

(b)

Figure 14. RF amplifier output signal at frequency 100 MHz
(a) RF amplifier output signal
(b) RF amplifier output spectrum

After some test at RF amplifier, it is also known that the gain of the amplifier is very small. However, overall performance is not so affected and system still can work well according to design. Output signal amplitude of RF amplifier at frequency 90 MHz is 616 mVpp. Measured transmit signal amplitude at the antenna is 8 Vpp, for frequency 90 MHz and 100 Mhz. Therefore, the gain of RF amplifier is 0,077 for frequency 90 MHz and 0,074 for frequency 100 MHz. Although, the test result can not be compared with the design, but it is obvious that the gain of RF amplifier is very small.

Test was also performed by observing and listening the information signal quality that has been received by receiver. Figure 15 shows transmitted information signal that is sinusoidal signal form AFG (*Audio Function Generator*). Information signal is a tone that has 5 Vpp amplitude and frequency 2 kHz. Point a in Figure 13 is a test point of received information signal at FM receiver.

Figure 16 shows the audio output spectrum at FM receiver. It is also shown that frequency spectrum of audio signal from the speaker in the FM receiver is the same of the transmitted signal. The spectrum at the receiver has the same fundamental frequency with the signal transmitted.

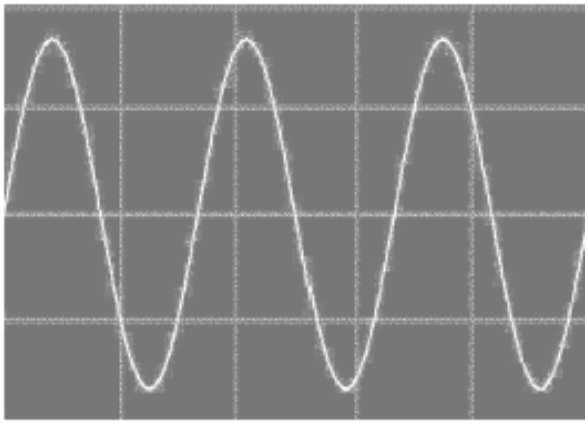

Figure 15. Information signal with frequency 2 kHz.

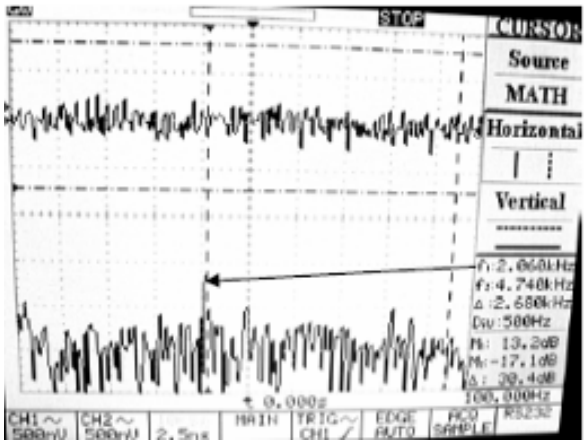

(a)

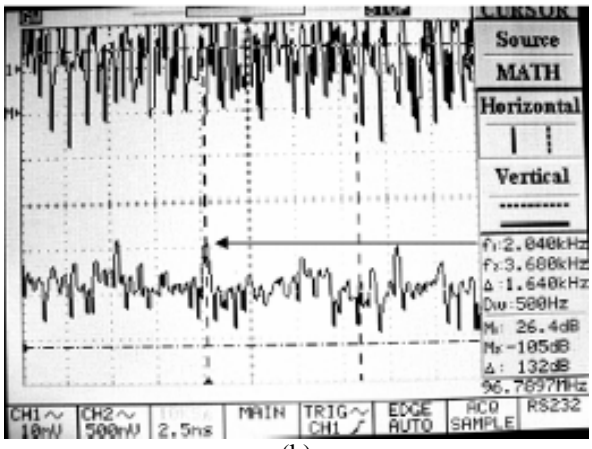

(b)

Figure 16. Audio frequency spectrum at FM receiver and carrier frequency (a). 90 MHz. (b) 100 MHz.

5. CONCLUSION AND SUGGESTION

5.1. Conclusion

a. The prototype that has been made can work well according to the design.
b. FM receiver can tune the signal from transmitter with carrier frequency 90 MHz and 100 MHz consecutively.
c. Hopping period for one carrier frequency is 0.5 seconds.

5.2. Suggestion

a. The system can still be developed with synchronization mechanism for transmitter and receiver.
b. The number of carrier frequency can be improved for better FH technique.
c. Clock should be set accurately so that the change in carrier frequency more stable.

6. REFERENCE

[1]. Roddy, Dennis and Coolen, John. *Komunikasi Elektronik*. Jakarta: PT. Prenhallindo. 2001.
[2]. Hioki, Warren. *Telecommunication, 3rd edition*. New Jersey: Prentice Hall. 1998.
[3]. Roberts, R.S. *Kamus Audio, Radio dan Video*. Jakarta: PT. Elek Media Komputindo. 1994.
[4]. http://en.wikipedia.org/wiki/Lists_of_radio_stations_in_Jakarta,_Indonesia (access March 2007)
[5]. http://en.wikipedia.org/wiki/Lists_of_radio_stations_in_Surabaya,_Indonesia (access March 2007)
[6]. http://id.wikipedia.org/wiki/I-Radio_Jogjakarta (access March 2007)
[7]. Rustamaji and Elan, Djaelani. Pemancar Frequency Hooping Spread Spectrum untuk Pengamanan Sinyal Informasi. IT Journal. 2002. http://www.informatika.lipi.go.id/pemancar-frequency-hopping-spread-spectrum-untuk-pengamanan-sinyal-informasi (access August 2007).
[8]. Wijaya, Damar. Peningkatan Kapasitas Sistem dan Kualitas Sinyal Pada Jaringan GSM dengan Frekuensi Hopping. *Majalah SIGMA*, vol 5. No 2, hal. 171-183. Juli 2002.
[9]. Kennedy, George. *Electronic Communication System*, 3rd edition, New York: McGraw Hill. 1984.

Observation and Analysis of Negative Group Delay in Electronic Circuits

Dede A. Budiman[1], H. P. Uranus[2], and Ihan Martoyo[3]

[1]*Dept. of Electrical Engineering,*
Universitas Pelita Harapan, Lippo Karawaci, Tangerang 15811, Indonesia
e-mail: dd_3173@hotmail.com

[2]*Dept. of Electrical Engineering,*
Universitas Pelita Harapan, Lippo Karawaci ,Tangerang 15811, Indonesia
Graduate Program in Electrical Engineering, Universitas Pelita Harapan,
Jl. Let. Jend. S. Parman Kav. 12, Jakarta 11480, Indonesia
e-mail: h.p.uranus@alumnus.utwente.nl

[3]*Dept. of Electrical Engineering,*
Universitas Pelita Harapan, Lippo Karawaci, Tangerang 15811, Indonesia
e-mail: ihan_martoyo@uph.edu

ABSTRACT

Delay has been a problem in electronic system that can't be removed completely. Many efforts has been done in order to compensate for delay occured in a system, e.g. in PID control system, the derivative element is used to increase its dynamic response performance by predicting the system behavior. Negative delay is thought to be one of the ways to compensate for delay. The main purpose of this work is to get a better insight about negative delay occurred in electronic circuit. The circuit which we observed, comprised of 3 main parts, i.e. a pulse generator, a 4th - order low-pass filter, and a negative delay circuit. In this work, we observed the input and output signals of the negative delay circuit using an oscilloscope. The waveform obtained by the oscilloscope is captured and analyzed using own-made MATLAB code. There are several parameters that we investigated in relevance with the negative delay, such as delay length, signal correlation, and delay circuit's resistor R value. The result shows that increasing value of R will increase the length of the negative delay but in the same time decrease the correlation between input and output signal.

Keywords

Negative delay, low-pass filter, correlation

1. INTRODUCTION

Negative delay is already implemented in various application implicitly, e.g in a hot-wire anemometer, the signals from the slow sensors are compensated using a differentiator. In PID control system, the derivative element is used to predict the system behaviour and to improve its dynamic response. A feedback loop with a derivative element is needed, when a capacitive load connected to the output of an op-amp, which is known as the lead compensations. All these efforts are performed to compensate delays in a system [1]. Negative delay in electronic circuit is also helpful in gaining a better insight about superluminal group velocity [2]. Superluminal group velocity has been proved experimentally in various systems [3], but there are still some question left unanswered. Hopefully, by observing the negative delay in electronic circuit, some of those questions can be answered. Negative delay experiment using electronic cicruit is far simpler and easier to do than in other system, while the insight gained can help to understand negative delay in a more complicated system.

2. NEGATIVE DELAY

A band-limited input signal $E_{in}(t)$ can be expressed as a product of the carrier $\exp(i\omega_0 t)$ and the envelope $\varepsilon_{in}(t)$: $E_{in}(t) = \varepsilon_{in}(t)e^{i\omega 0t} + c.c$, where $c.c$ represent the complex conjugate. By expanding in terms of Fourier component $\tilde{\varepsilon}_{in}(u)$ of the envelope $\varepsilon_{in}(t)$, the signal becomes

$$E_{in}(t) = \int_{-\Omega/2}^{\Omega/2} du\tilde{\varepsilon}_{in}(u)e^{i(\omega_0+u)t} + c.c \qquad (1)$$

where Ω is the bandwidth and u is the offset frequency from ω_0. The transfer function $H(\omega)$ is defined for each frequency $\omega=\omega_0+u$, and the output can be written as

$$E_{out}(t) = \int_{-\Omega/2}^{\Omega/2} du\tilde{\varepsilon}_{in}(u)H(\omega)e^{i(\omega_0+u)t} + c.c$$

$$E_{out}(t) = \int_{-\Omega/2}^{\Omega/2} du\tilde{\varepsilon}_{in}(u)A(\omega)e^{i(\omega_0+u)t}e^{i\phi(\omega)} + c.c \qquad (2)$$

We assumed that within the bandwith $(|u|<\Omega/2)$, the amplitude $A(\omega)$ is nearly unity and the phase $\phi(\omega)$ can be approximated by a linear function that is,

$$A(\omega) \sim 1, \qquad \Phi(\omega) \sim \Phi(\omega_0) - u.t_d. \tag{3}$$

The group delay t_d is defined as

$$t_d = -\left.\frac{d\phi}{d\omega}\right|_{\omega_0}. \tag{4}$$

The envelope of the output is obtained from (2) and (3) as

$$\varepsilon_{out}(t)=\varepsilon_{in}(t-t_d)e^{i\Phi(\omega 0)}. \tag{5}$$

From Eq. (5), we can say that the envelope of the output is shifted by the group delay t_d, while maintaining its shape. Negative delay happens for $t_d < 0$ so that the output precedes the input [1], [4].

3. THE CIRCUITS

The circuit that will be tested comprised of three parts, i.e pulse generator, low-pass filter, and negative delay circuits. The system's schematic is shown in Figure 1. The system was made based on the work of Nakanishi *et al* [1], [4].

3.1 Pulse Generator

For generating pulse, we are using a monostable multivibrator circuit utilizing the 555 timer IC. This circuit will create a pulse when triggered as seen in Figure 2.

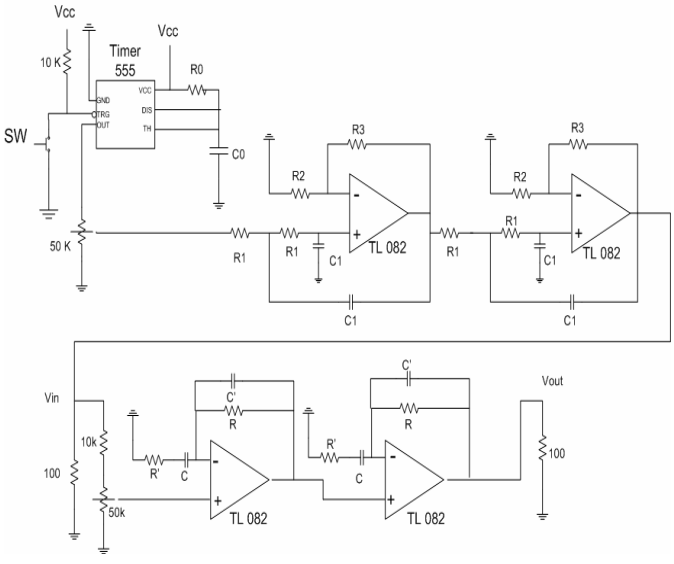

Figure 1. Schematics of the tested system

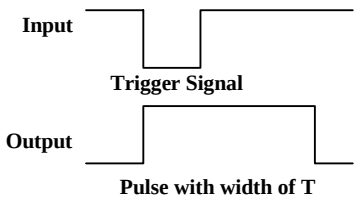

Figure 2. Monostable Multivibrator timing diagram

The width of the pulse depends on the value of the resistor R and capacitor C employed in the circuit. For this work, we used a 6.8 MΩ resistor and a 0.22 μF capacitor. The pulse width produced by the circuit is 1.5 s.

3.2 Low-Pass Filter

To prepare a band-limited pulse we introduce low-pass filters. The rectangular pulse produced by the pulse generator has high-frequency components. Because of these components, the negative delay circuit does not work properly [4]. We must eliminate the high frequency components with low-pass filters. As seen in Figure 1, we used a two-stage low-pass filter. We used Bessel filter for this system, since it has a smoother response and small overshoot for rectangular waves. The transfer function for Bessel filter is

$$H_B^{(m)}(\omega) = \frac{y_m(0)}{y_m(i\omega\alpha_m T_L)} \tag{6}$$

where $y_m(x)$ is m^{th} order of Bessel Polynomial, T_L is the inverse of cut-off frequency, and α_m is a parameter chosen such that

$$H_B^{(m)}(T_L^{-1}) = 1/\sqrt{2}\,. \tag{7}$$

The total order of the filter being used is $m = 4$, where each filter is a 2^{nd} order filter with transfer function

$$H_B^{(2)} = \frac{1}{1 + i\omega\alpha_2 T_L + \frac{(i\omega\alpha_2 T_L)^2}{3}} \tag{8}$$

where $T_L = 1.272R_1C_1$, and $\alpha_2 = 1+R_3/R_2 = 1.268$. All these parameters are chosen so that

$$\omega_c = \frac{0.35}{T} \tag{9}$$

Where $T = RC$ is the time constant of the negative delay circuit [1], [4]. With Eq. (9) satisfied, the $A(\omega)$ and $\Phi(\omega)$ can be assumed to be constant and linear.

3.3 Negative Delay Circuit

The negative delay circuit is basically a non-inverting differentiator as shown in Figure 3. The transfer function for this circuit is

$$H(\omega)=A(\omega)e^{i\Phi(\omega)}=1+i\omega T \tag{10}$$

where $T=RC$. In time domain, the corresponding input and output relation is

$$v_{out}(t)=\left(1+T\frac{d}{dt}\right)v_{in}(t)=v_{in}(t)+T\frac{dv_{in}(t)}{dt} \quad (11)$$

From Eq. (11) we can say that for the rising edge, which has a positive slope, the two terms interfere constructively, while for the falling edge, which has a negative slope, the two terms interfere destructively such that the pulse peak advance [1], [4].

$H(\omega)$, in the low frequency region $(|\omega|<<1/T)$, can be approximated by

$$A(\omega)=1+O(\omega^2T^2) \quad (12)$$

$$\Phi(\omega)=\omega T+O(\omega^3T^3) \quad (13)$$

From (12) and (13), we can say that the amplitude is nearly constant and the phase increases linearly with the frequency. The group delay also becomes negative

$$t_d=-\left.\frac{d\phi}{d\omega}\right|_{\omega_0}=-T<0 \quad (14)$$

The higher order terms in Eqs. (12) and (13) induce distortion of the waveform of the output [1], [4].

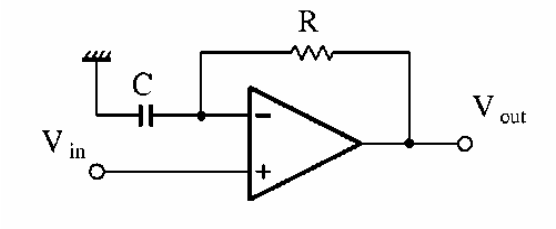

Figure 3. The negative delay circuit

The actual negative delay circuit in Figure 1 differs from that shown in Figure 3. In the actual the resistor R' and capacitor C' are added to suppress high-frequency noises. The parameters are chosen to satisfy $R'C$, $C'R << T$. Thus, the phase $\Phi(\omega)$ for $|\omega|T<1$ is not affected.

4. EXPERIMENTAL RESULT

4.1 Negative Delay

Figure 4 shows the observation result of the system shown in Figure 1. As seen in Figure 4 the peak of the output signal precedes the peak of the input signal as consequence of the resulted negative group delay. The waveform in Figure 4 is obtained using an oscilloscope and then extracted using an own-made MATLAB code. The extracted curve were then fitted to a 4th order Gaussian curve using MATLAB. The result is as shown in Figure 4. The time difference between the input and output peak in Figure 4 is 0.41 s. This delay quantitatively agrees with the expected negative delay derived using Eq. (14). The expected negative delay is $2T$ = 0.44 s. The delay is multiply by 2 because we connected two circuits in series for larger effect. The pulse width also increases from 1.5 s to about 6 s. It is because of the delay caused by the low-pass filter. The steep edge of the rectangular pulse, is smoothened by the low-pass filter which results in the pulse widening

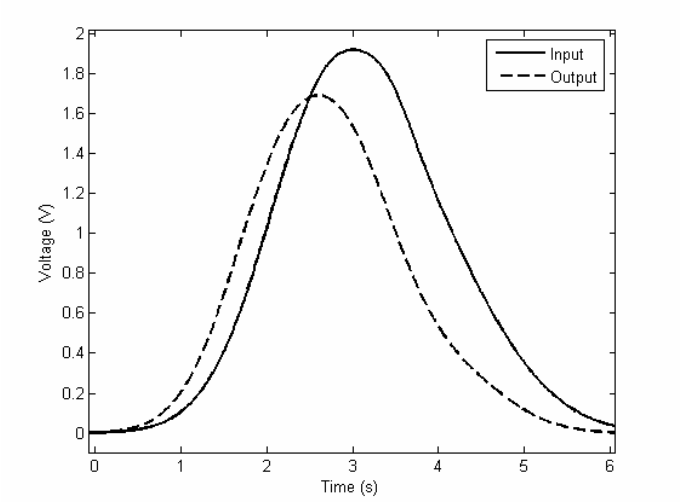

Figure 4. Negative delay circuit observation result

4.2 The Effect of Increasing the Value of Resistor R to the Negative Delay

In this stage of experiment, we observed the effect of increasing the value of resistor R to the negative delay. The increase in R will increase the time constant T so that the length of the negative delay will increase as well according to Eq. (14). In this experiment, the resistor value range from 1 MΩ to 2 MΩ with increment of 0.1 MΩ for each observation. Figure 5 shows the input and output signal for all resistor value, while Table 2 shows the delay produced by each resistor value.

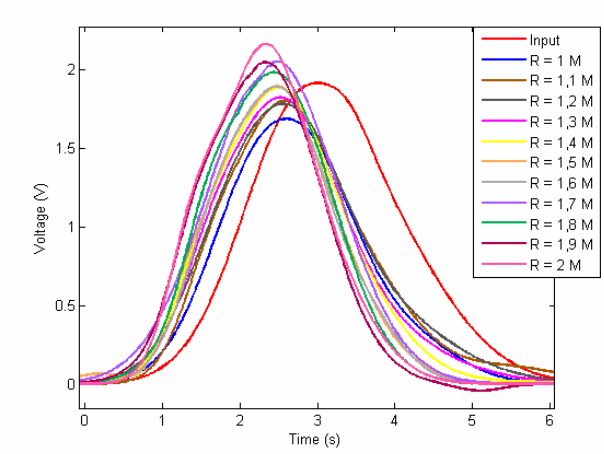

Figure 5. Input and output signals for all resistor value.

There are several things that we can learn from Figure 5 and Table 2. First, generally the increase in resistor value, resulting in increasing the length of the negative delay. However, the increment is different from the expectation based on Eq. (14). As shown in Table 2, for several resistor values, the negative delay produced is the same. We assumed that it is because Eq. (14) is based on approximation. Besides, the curve extraction and delay measurement were performed manually.

Table 2. Observation result for various R values.

R Value (MΩ)	Delay Observed (s)	Delay Expected (s)	Difference (%)
1	0.41	0.440	6.82
1.1	0.43	0.484	11.16
1.2	0.45	0.528	14.77
1.3	0.52	0.572	9.09
1.4	0.52	0.616	15.58
1.5	0.53	0.660	19.70
1.6	0.53	0.704	24.72
1.7	0.53	0.748	29.14
1.8	0.57	0.792	28.03
1.9	0.66	0.836	21.05
2	0.66	0.880	25.00

4.3 The Effect of Increasing the Value of Resistor R to the Correlation Between The Input and Output Signals.

Using the data obtained from previous measurement, we calculated the correlation between the input and output signals. The correlation is computed using MATLAB. There are two method, in the first method, before calculating the correlation, we shift the data so that the peak of both input and output signals coincide. Then, we calculate the correlation. The result is shown in Table 3 and Figure 6. In the second method, we use the cross-correlation function. The cross-correlation method will produce an x,y pair, where x is the shift in x axis and y is the intersection between the curve. The highest y value shows the time when the intersection area between the two curve is the biggest, it represents the highest correlation between the curve and the corresponding x value shows the shift need to be made to produce such result. We assumed that the highest y value will be produced when the x value equal to the negative delay, and this y value will equal to the correlation calculated with the first method. Table 4 shows the cross correlation result. The delay and correlation calculated using the cross correlation are different from the one calculated before. Despite the difference, Table 3, Table 4, and Figure 6 show a decreasing trend of the correlation for increasing R value. However, there are some inaccuracy. We speculate that it happens because of error due manual extraction of the data. But the decreasing trend tells us that with increasing R value, which implies increasing length of the negative delay, the correlation decreases, which mean more information are lost. This lost is a consequence of causality. Also, as discussed in Section 3, the higher order terms in Eqs. (12) and (13) induce distortion of the wave form of the output [1], [4]. These terms are dependent to the time constant $T = RC$, so that increasing R value will cause the distortion to increase as well.

Table 3. Correlation between input and shifted output signals for various R values

R Value (MΩ)	Delay (s)	Correlation
1	0.41	0.9894
1.1	0.43	0.9982
1.2	0.45	0.9983
1.3	0.52	0.9938
1.4	0.52	0.9941
1.5	0.53	0.9888
1.6	0.53	0.9796
1.7	0.53	0.9897
1.8	0.57	0.9792
1.9	0.66	0.9792
2	0.66	0.9755

Tabel 4. Cross correlation between input and output signals.

R Value (MΩ)	Delay (s)	Correlation
1	0.42	0.9959
1.1	0.42	0.9984
1.2	0.54	0.9999
1.3	0.54	0.9952
1.4	0.6	0.9955
1.5	0.66	0.9910
1.6	0.66	0.9873
1.7	0.72	0.9917
1.8	0.78	0.9844
1.9	0.78	0.9884
2	0.78	0.9834

We assumed that the difference in delay and correlation is caused by the difference in determining the reference point to calculate the negative delay. The negative delay calculated in Section 4.1 uses the peak of the signal as the reference point, while the cross-correlation method is uses the highest correlation as the reference point. It means that the highest correlation doesn't always happen when the signal's peaks coincide. The reference point being used to determine the negative delay, depends on the application of the negative delay. In application that only needs a small portion of the signal, e.g the peak for triggering, we use the signal's peak as the reference point. Otherwise, in application that needs the whole information contained in the signal, we use the highest correlation as the reference point.

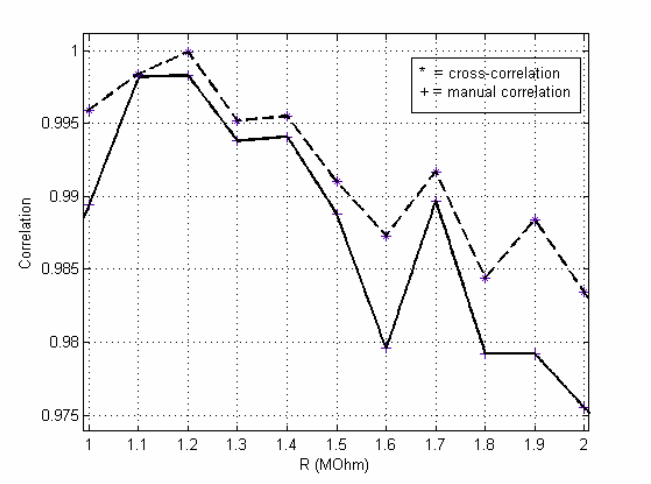

Figure 6. Correlation vs R value

5. CONCLUSION

From the observations and experiments of the negative delay circuit, we conclude that:

1. The system under study can create a negative delay.
2. The negative delay circuit works by increasing the slope of the rising and falling edges of input signal so that the pulse peak is advanced.
3. The increment in resistor R value results in the increment of the negative delay length. However, this increment is different from the expected increment due to distortion that depends to the time constant T and frequency ω.
4. The increment in resistor R value also results in the decrement of the correlation between input and output signal. It means that the longer the negative delay, more information is lost.
5. In calculating the negative delay, there are two reference points that can be used i.e, the signal's peak and the correlation between the signal. The reference point depends on the application of the negative delay.

REFERENCES

[1] M.Kitano, T.Nakanishi, K.Sugiyama, "Negative Group Delay and Superluminal Propagation: An Electronic Circuit Approach," *IEEE Journal of selected topic in quantum electronics, Vol. 9, No. 1, January/February 2003, pp. 43-51.*

[2] H.P. Uranus and H.J.W.M. Hoekstra, "Modeling of loss-induced Superluminal and Negative Group Velocity in Two-port Ring-resonator-circuits," *IEEE J. Lightwave Technology, Vol. 25, No. 9, Sept. 2007, pp. 2376-2384.*

[3] H.P. Uranus, L. Zhuang, C.G.H. Roeloffzen, and H.J.W.M. Hoekstra,"Pulse Advancement and Delay in An Integrated Optical Two-port Ring-resonator Circuits," *Optics Letter, Vol. 32, No. 17, Sept. 2007, pp. 2620-2622.*

[4] M.Kitano, T.Nakanishi, K.Sugiyama, "Demonstration of negative group delays in a simple electronic circuit," *Am. J. Phys., Vol. 70, No. 11, November 2002*, pp. 1117-1121.

[5] S.Haykin, B. Van Veen, *Signals and Systems 2nd Edition*, New York: John Wiley and sons, 2003.

[6] R.Gayakwad, *Op-Amps and Linear Integrated Circuit 4th Edition*, N.J.: Prentice Hall, 2000.

ISSN 114-1284

The effectiveness E' Government services either using mobile phone Technologies (SMS) or Computer (Internet)

Dinar Mutiara K N, MInfoTech(Comp)

Faculty of Engineering
Semarang University,Tlogosari, Semarang
Tel : (024)6702757. Fax : (024) 6702272
E-mail : dinar.mutiara@gmail.comu

ABSTRACT

The paper "The effectiveness E' Government either using mobile phone Technologies (SMS) or computer (Internet), seeks to find the best technology for narrowing the digital gap, and to develop a model for implementing e-government. The main reason for this is to ascertain the appropriate services that will maximise access for the citizen. In most developing countries the technology that can be most easily afforded by the society is mobile phone technology. So, it is important to look at the e-government and m-government benefits and disadvantages, and at the models and services available in developed countries and to see what developing countries can learn from that.

Keywords

e-government, m-government, digital divide, SMS, internet

1. INTRODUCTION

Electronic government or e-government can be defined as office automation and internal management and expert systems, as well as client-facing web sites and the use of Information and Communication Technology (ICT) to promote efficient, convenient, and cost-effective government services. In the beginning the e-Government project involves using information technologies, particularly web-based Internet applications. However, these functions are now spreading with the use of mobile and wireless technologies and creating a new direction: mobile government (m-government). As a result, it can be seen that m-government and e-government are not in fact two separate entities. M-government extends e-government availability to those confined to the use of mobile technologies such as mobile phones. The benefits for the governments are things such as, a reduction in response time, a reduction in paper work and the provision of new and improved services to the customer. For citizens, E-government offers a huge range of information and services, including information for research, the provision of government forms and other services, public policy information, employment and business opportunities, voting, tax filing, license registration or renewal, payment of fines and submission of comments to government officials. Moreover, the users of governmental information services will be benefited by the fact that many services previously available only during explicit office hours can now be accessed twenty-four hours a day, seven days a week.

The paper, "The Effectiveness E' Government services by mobile phone Technologies (SMS) and computer (Internet), seeks to find the best technology for narrowing the digital gap, and to develop a model for implementing e-government. The main reason for this is to ascertain the appropriate services that will maximise access for the citizen. In most developing countries the technology that can be most easily afforded by the society is mobile phone technology. So, it is important to look at the e-government and m-government benefits and disadvantages, and at the models and services available in developed countries and to see what developing countries can learn from that.

2. E- GOVERNMENT AND M- GOVERNMENT

The meaning of the term, e-government, is quite nebulous in that it means different things to different users. E-government is sometimes defined to included office automation and internal management and expert systems, as well as client-facing web sites and using ICT to promote efficient, convenient, and cost-effective government services. Such internal factors are seen as critical to the provision of greater public access to information and to make government more accessible to citizens [25]. Furthermore the OECD (2006) defines e-government as a tool to achieve better government services by using information and communication technologies

2.1 The e- government relationships

E-government relationships are categorized as government to citizen (G2C), government to employee (G2E), government to business (G2B) and government to government (G2G) [17].

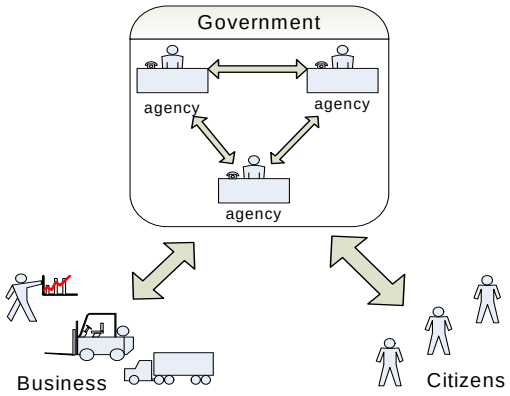

Figure 1: E-Government relationship[17]

2.1.1 The benefit and disadvantages of e-government

From the citizens' point of view, e- government can give many benefits, such as:

- More and easier access to services.

It is obvious that people do not like having to wait in a line for an hour or more to access a service that takes only five minutes at a counter to transact. In addition, they do not want to have to take time off from their work or business in order to conduct a transaction with the government that is only provided during their work hours. This becomes a problem because usually the "government hours" are the same as the general business and working hours of the society [16]. E-government is a good solution for these problems. Using e-government gives citizens 24-hour access to government information and services. For example, citizens will know that they can use the Internet to find out about such things as contact and service availability.

- Citizens can find their own information.

Citizens often need help with routine transactions and often ask similar questions about them, therefore e-government sites can use facilities such as Frequently Asked Questions pages (FAQs) to avoid wasting time answering common questions that have standard answers. This means that more time can be spent dealing with those issues that are specific to a particular client or situation and require responses that are difficult to standardise. This can make service delivery much faster and smoother for citizens as well as for the government agency providing the service. These standardised procedure pages can provide information dealing with quite complex policies and can provide up-to-date news and information, and even standardised responses to common situations via automatic emails [17].

- Transparency of government service (to reduce the scope for corruption).

For instance, there was a case in Gujarat in India, which adopted an e- government service for controlling border checks. The result was a reduction in corruption and a significant increase in Gujarat State's tax base. The new e-government system gave a three-fold increase in tax revenue in two years; increasing from $12m to $35m and subsequently repaying the cost for implementing the e-government system, $4m, in just six months [15].

- Better communication with rural and remote communities

For countries that have a widely dispersed population, an e-government service allows the citizens who live in remote areas to have an equal opportunity to access services as those citizens who live in cities. In developed countries Canada is an example of a country with a widely dispersed population; Canada has ranked first in the Accenture's global e-government survey for the past five years [68]. Canadian GOL (Government On-line) provides 30 percent of government transactions in Canada. Wireless infrastructure improves the possibility for regional and rural communities to have the same levels of access to information and government transactions, and their service expectations are aligned with the enhanced capability of the technology.

- Reduce the cost of operations.

Using e- government can reduce the operational cost of providing services and information. Because, it changes a paper based system to an electronic system, e-Government allows the service process to be handled by fewer employees. It is important to note that it is not only individuals who need to interact with the government; businesses and government agencies also need to do so. There is interaction between different sections of one department, or between different government agencies. These types of intergovernmental transactions have been investigated by the Australian government Department of Finance and Administration, and they found that the use of e-government is achieving cost reductions through a combination of direct savings, lower cost of delivery, and improved internal or business processes. The report also suggested that "participating agencies were expecting reductions in costs of about $100 million from 24 e-government programs" [66].

2.1.2 The weaknesses of E-government

Despite the many facts that show that e-government can provide many benefits not only for the society but also for the government itself, e- government still has disadvantages for some citizens, such as:

- Not everyone can access e-government.

Many countries are made up of economically, educationally and ethically diverse populations. Therefore introducing a service that relies on Internet technology creates an inherent problem. In order to use the service a person must firstly have a computer with connection to the Internet and secondly the user must have adequate technical knowledge to use the

facilities provided on e-government service web pages. This means that e-government services are only be available to the citizens within a country that are of a certain financial and educational standing. Consequently, implementing an e-government service can potentially isolate large numbers of citizens who have no, or only limited access to the online service.

- E-government segmenting the society

Many countries are made up of various ethnic groups. Therefore consideration has to be given to the selection of languages provided within the e-government service. For example, in Canada, the country is dived into French and English speaking regions, and this fact has to be dealt with by making on-line services available in both French and English [68].

- E-government creates ways in which government officials could use technology to avoid taking responsibility for their duties.

As anything available on an e-government site can be taken down or altered with little evidence that corrections or changes have been made, it is possible that there may be a reduced effort by government officials to perform duties correctly. Furthermore, the technology of e-government has the potential to become a standard excuse for government officials as an explanation for all problems regardless of their true nature [46].

- With technology-based services it is often too easy to avoid real issues by make an excuse that problems with the service provided are because of the technology.

It is often a lot easier to ignore an email than to ignore a person or to make the excuse that a person's account was not updated because of a 'server going down' and rather than because of an employee not doing their job properly [46].

For the concept of e-government to be true to its meaning, it has to be implemented in such a way that meets the following ideals: the majority of citizens have easy access to ICT at an affordable price; every citizen owns the technologies required for access; and everybody knows how to use those technologies.

2.2 M- Government

The efficiency and effectiveness of e-government using current information technologies, especially in the web based Internet is effectively proven. However, with the growth of mobiles technologies, the concept of e-government is spreading into this field. The use of mobile technologies for e-government drives it in a new direction, causing it to become m-government (mobile government). Eventually m-government may lead to even more intensive and wide spread government services than is possible using e-government forms, further evolving the relationship between government and citizens.

2.2.1 Definition of m-government

M-government is a strategy and an implementation that involves the utilization of mobile technology [40]. It includes services, applications and devices for improving and extending the benefits supplied by the use of e-government. A key task of government is supplying information to its citizens, and in many countries this is often not an easy job. Both e-government and m-government offer the potential for improving the delivery of information delivery to the public, but the mobile form would seem to offer greater benefits overall.

2.2.2 What is the reason for using m-government?

It is simply a fact that there are more people who can afford to cell phone or other similar wireless devices as compared to those who have access to PCs. This is supported by data from ITU (2006) that compares the rates of the usage in Information and Mobile Communication Technologies. Moreover this ITU data shows that the use of mobile phones is increasing rapidly, as can be seen in the figure below:

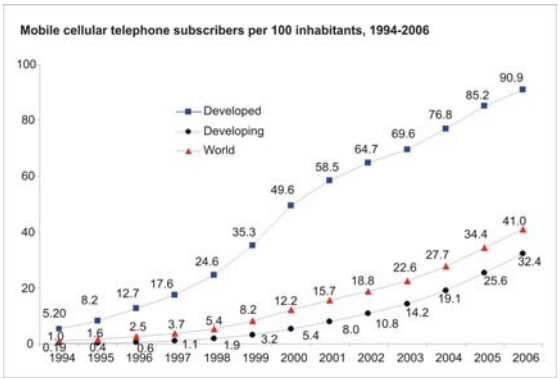

Figure 2: Mobile cellular telephone subscribers per 100 inhabitants, 1994-2006

In addition, since 2000, Internet penetration has grown at a slower rate than the usage of mobile phones. This can be seen from the following figure.

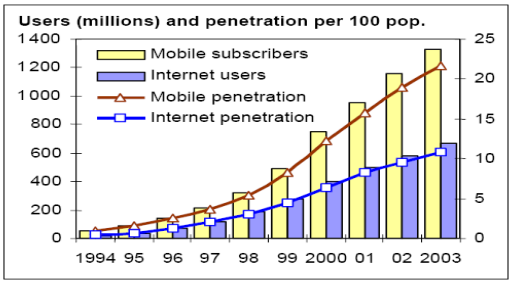

Source: ITU World Telecommunication Indicators Database.

Figure 3: Graph of Internet penetration and Mobile Penetration

3. THE DIGITAL DIVIDES

A widely accessible and affordable communications infrastructure is one of the critical success factors for the delivery of government services online. However, the world can be divided into the information rich and the information poor. Therefore, ICT access and e-Government must be closely linked. Many of the most successful e-Government initiatives include, or are launched in combination with measures that are designed to expand access to more of the community. In addition, the availability of e-Government services that can save citizens and businesses time and money will, in turn, tend to drive demand for ICT access, further boosting infrastructure development and driving down the cost of access.

The digital divide exists not only between countries and regions but also within a country's borders, most commonly between rich and poor, between men and women, and between urban and rural areas. Urban areas tend to receive a disproportionately large share of public and private ICT investment in relation to the rest of the country. Usually, urban areas have at least a basic communications infrastructure and therefore are able to take advantage of ICTs, while rural areas tend to lack the infrastructure. Often ICT service providers do not have an incentive to invest in rural areas. The digital divide may correlate not only with income but also with cultural attitudes towards technology. Given the centrality of ICTs to both education and economic opportunity, those without access to ICTs are likely to fall further behind in a process that becomes a sort of vicious circle.

3.1 The major digital divide between develop and developing country

- The major reasons why the digital gap occurs between developed and developing countries are: The developing countries do not produce the technology, but they use the technology
- The major barrier limiting Internet access in both developed and developing counties is income level.
- Using a computer and the Internet is more complicated than sending a text messages by mobile phone or dialling a telephone. Meaningful use of the Internet requires computer, and cognitive skills for such things as seeking information, developing community networks, or participating in political activities.

4. ICT'S INFRASTRUCTURE APPROACHES FOR E-GOVERNMENT

There are five technologies that the government should consider for public access to e-government services. The importance of these approaches have been summarised in the table 1 below

Table 1: ICT's infrastructure approaches for e-government

User	Technology	Access	Hardware	Location	Accessibility
1st	Dial Up	Home Access	• Reliable electricity • Personal Computer • Modem dial up • Phone line	• Residential Access	• Pay their need for internet access.
2nd	Fixed Hot Spots	Easy access for commuter	• PDA • Laptop • Smart Mobile Phone • Wireless connections	• Post Office • Shopping centre • Community centre • University	• Free for accessing the internet, but they using their own work station for accessing the internet.
3rd	Kiosk	For public who want to access e-government and communication with email	• Reliable electricity • Share PC • Internet access (Dial up) • Share PC	• Post Office • Shopping centre • Community centre • Government office	• Access government web site • Open and reply email
4th	Mobile Kiosk	Rural and remote are society	• Share PC • Storage • Satellite • Vehicle (bus, boat or etc)	• Mobile library • Mobile Post office	• Mobile Kiosk which go to the rural area • access government web site • open and reply email
5th	SMS	Access for public who has a mobile phone	• Mobile Phone • Infrastructure for mobile phone	• Movable with the citizens	• Small text due to the limitation of the mobile phone screen

In the first approach, it is assumed that the phone line infrastructure exits in the area. Consequently, with the phone line, the user can access the Internet using a dial up modem and their PCs. The majority of these users are citizens that live in cities and urban areas. Therefore, there are no problems for this section of society in accessing government services through web sites.

The second alternative is for the consumers who have their own portable workstations such as PDAs, laptops or smart phones, but do not have internet access at home. They can use fixed wireless hot spots for accessing the Internet. This enables them to access government web sites in certain

places, for instance, post offices, public libraries, internet cafes and shopping centres.

The third alternative is for those members of the society who do not have Internet access or a portable work station. This section of the public can use shared PCs provided in kiosks only for accessing government web sites. So, the purpose of the kiosk is only to provide the means for the public to access government websites and email services.

The fourth alternative is for the government to use buses that provide shared PCs (bus kiosk). This facility is for people who live in the remote areas. The public can use shared PCs in the bus kiosk only for accessing government web sites and email services. The main purpose of this approach is that the kiosk goes to the rural area.

The fifth approach is using SMS services for delivering e-government. This approach would seem to provide the greatest scope for implementing e-government services quickly and widely, as most people in developing country already own mobile phones and the infrastructure to support this means of service delivery already exists in most places, as discussed in the previous sections. By providing e-government via the SMS service, the government can bypass many of the problems caused by limited access to infrastructure that are inherent in other technologies.

As for the use of mobile phones, it seems that SMS or mobile messaging is the most favoured of e-government activities in society. This can be seen from the number of e-government activities that are done by mobile messaging. Best practises from other countries are:

- Mobile Parking in Austria.

The M-parking system allows users to pay for parking via their mobile handsets. By day 7 of its inauguration in October 2003, a total of 20,604 m-parking applications had been received, a milestone which had not been expected to be reached until April 2004 [13].

- Malta launches "M-government" education initiative.

The government of Malta has launched an "M-government" initiative and is providing examination results by SMS. Other applications include notifications of court deferrals to clients and their lawyers, and sending renewal notifications for trade licences [53].

- More are paying bus fares in Finland by SMS.

During the summer months of 2002, sales of SMS tickets for Helsinki's public transport system (Finland) increased dramatically, by 30 percent SMS Tickets can be ordered by sending a text message and the user is billed through his or her regular mobile phone bill. The public transport ticket is also delivered to the commuter by SMS [9].

- Text messaging tests China's freedom.

Mobile users in China, the world's largest mobile market, can now send SMS to the 2,987 deputies of the National People's Congress. The new service lets people test the bounds of a new freedom of expression in China, where politically charged jokes have begun to spread like wildfire from the Internet onto cell phones [37].

- Hungarian SMS Elections.

In March 2002, two of the leading Hungarian portal operators invited Hungarian mobile subscribers to vote via SMS three weeks before the real parliamentary elections [44].

5. SMS proposed model for e-government

In order to make the use of SMS for e-government widespread , much strategic planning in developing SMS e-government services is required. The SMS applications can be classified with different methodologies, according to the parties involved, for example Government to Citizens (G2C), and according to the coverage (national or local).
In this research, both classifications will be used.

- Local Coverage

The local applications presented have significance in terms of their natural advantages. These applications are usually Government-to-Citizen applications that have a high chance of usage penetration in the near future. These applications are highly influenced by the high mobile penetration in Indonesia, the ease of use of mobile phones, and the mobile platform's ability to reach people anywhere/anytime. The penetration of these applications would increase the usage of the online governmental services they complement significantly; a factor that is of crucial importance. Also the anywhere/anytime nature of these services increase the convenience and the satisfaction levels of citizens extensively, with an incremental investment that is relatively low compared to other forms of e-Government investments.

- National Coverage

The national applications present general information for a national coverage. These applications are usually Government to Citizen applications that have a high chance of increasing citizens' participation in the Government's activities such as national elections etc.

Following is a set of recommendations or model based on our previous study of SMS applications in several countries:

- Stage 1: Alert information or an Announcement

In this stage of e-government SMS, the government is able to notify citizens about important public information. The information tends to be an alert or emergency notification. These services work when the public applies for this service.

- Stage 2: Pull information

This stage primarily involves the digitalising of available information and making it available and up-to-date. In this stage, the government provides two-way communications, where the citizen is able to access public or personal information by sending a request message and the citizen will get a feedback message from the government server or database. In this level, the type of SMS request must be in a certain format, so the SMS server recognises the keywords and can give an automatic response.

- Stage 3: Communicative Information (SMS based television or radio)

In the second stage, many interactions and services with a large of number of citizens are possible. This communicative information level provides the public with an opportunity to contribute and become apart of e-government services. The public can be involved in discussions or SMS voting systems in government shows on television or radio.

By giving public control over something meaningful, in government television or radio programs, SMS is a simple and pervasive technology for interactive e-government services. In this level, the SMS system is only designed for the sender to send a question or give input messages or participate in government' television or radio show. The replies for the public are by watching or listening to the radio or television show. In this stage the government could use Television or Radio networks that are already widespread in Indonesia for communicative information.

- Stage 4: Transactional presence

In the fourth stage, a wide variety of government transactions can be conducted by using SMS. These can include payment for donations, licences, fines, fees, bills and taxes. In addition, more sophisticated functions including passwords and encryption are also provided.

In this SMS model there is no dependency or correlation between each stage.

6. CONCLUSION

It is undeniable that there is a digital gap between the developed countries and the developing countries that has caused many of the implementations of e-government in developing countries to fail. One of the main factors in these failures is the fact that the services were imported without regard to local conditions. The digital gap takes many forms, it can be at the economic level, skill levels in English and IT proficiencies, and at the basic infrastructure level. In addition, the digital gap not only occurs between countries, but it also happens inside a country, such as the gap between the ICT facilities available in cities, compared to those in villages and remote areas. This gap also creates a different kind of user of ICT. There are users that use internet and mobile phone application (SMS).

Using SMS messages in mobile phone technologies can help to narrow the gap for people who want to use e-government services but who can't access the Internet. Moreover, the mobile phone network has developed surprisingly fast and it is one of the e-government tools applied in almost all of society. More precisely, using SMS messages from mobile phones for e-government applications is widespread in developed and developing countries. The use of SMS can be a significant factor in e-government in increasing the effectiveness of e-government relations between Governments and Citizens.

In order to make the use of SMS for e-government widespread, there needs to be a strategic plan involving a staged introduction of services. These stages can be loosely classified according to the parties involved, Government to Citizens (G2C), and according to the coverage (national or local).

REFERENCES

[1] 3GNewsroom.com, n.d, What is 3G?, viewed 18 October 2008, available: <http://www.3gnewsroom.com/html/what_is_3g/>
[2] Amine, B & Yosra, K 2005, M- Government : The Convergence e-government and wireless technology, viewed 20 March 2008, available: <http://medforist.grenoble-em.com/Contenus/Conference%20Tunisia%20IEBC%202005/papers/June25/12.pdf>
[3] Antovski, L & Gusev,M 2005, M-Government Framework, viewed 20 April 2008, available: <http://www.mgovernment.org/resurces/euromgov2005/PDF/5_R368AL.pdf>
[4] Badan Pusat Statistik (BPS), viewed 8 November 2008, available: <http://www.bps.go.id/ >
[5] Bhatnagar, S 2004, e-government From Vision to Implementation A practical Guide with Case Studies, SAGE publications, London
[6] Boostup.org 2007, SMSs to Surpass 2 Trillion Messages in Major Markets in 2008, viewed 11 march 2008, available: < http://www.cellular-news.com/story/28126.php?source=rss>
[7] CIA. Gov, n.d, The World Factbook: Indonesia , viewed 2 September 2008, available:< https://www.cia.gov/library/publications/the-world-factbook/print/id.html>
[8] City of Melbourne 2006, 'Send a hero message by iHub', City of Melbourne Council, viewed 23 March 2008, available: <http://www.melbourne.vic.gov.au/info.cfm?top=228&pg=715&st=584,>
[9] CIVITAS 2008,Public transport company in Odense introduces SMS-ticket, CIVITAS. Org, viewed 20 August 2008, available: < http://www.civitas-initiative.org/news.phtml?id=433&lan=en&read_more=1 >
[10] Directorate General Of Post dan telecommunications The Republic of Indonesia 2007, Internet Development in Indonesia, viewed 1 November 2008, available:

<http://www.itu.int/asean2001/documents/pdf/Document-21.pdf>

[11] Directorate General Of Post dan telecommunications The Republic of Indonesia 2007, viewed 1 November 2008, available: < http://www.postel.go.id >

[12] Drishtee Development And Communication ltd, 2008, Dristhee activity, viewed 17 August 2008, available: <http://www.drishtee.com/>

[13] eGovernment News 2004, AT: 'M-Parking' increasingly popular in Austrian cities, European Communities 2008, viewed 1 June 2008, available: <http://www.epractice.eu/document/1269>

[14] EUROTECHNOLOGY, n.d, 4G mobile communications in Japan, viewed 15 October 2008, available:<http://www.eurotechnology.com/market_reports/4G/ >

[15] Falahi, M 2007, The Obstacle and Guidelines of Establishing E-Government in Iran, Master thesis, Lulea University of Technology, Sweden

[16] Fang, 2002, E-Government in Digital Era:Concept, Practice, and Development, International Journal of The Computer, The Internet and Management, Vol. 10, No.2, 2002, p 1-22, viewed 1 September 2008, available : <http://www.journal.au.edu/ijcim/2002/may02/article1.pdf>

[17] FedEE, 2005, Untangling the myths of working time, viewed 10 May 2008, available: <http://www.fedee.com/workinghours.shtml>

[18] Gatner Group 2000, Gartner's Four Phases of E-Government Model, viewed 3 March 2008, available: <http://www.gartner.com/DisplayDocument?id=317292>

[19] Gordon, V n.d, SDNP Jamaica Information Technology Comes to Community Centers, UNDP.org, viewed 18 August 2008, available:<http://www.sdnp.undp.org/stories/jamaica.html >

[20] Guerin, B 2003, Indonesian telecoms boom lures neighbours, Asiatimes Online, viewed 20 August 2008, available:<http://www.atimes.com/atimes/Southeast_Asia/EE07Ae03.html>

[21] Guerin, B 2005, Mobile boom in Indonesia, AsiaTimes Online, viewed 28 Septemebr 2008, available: <http://www.atimes.com/atimes/Southeast_Asia/GG28Ae02.html>

[22] Gupta, M.P & Kumar P, 2006, e-Governance impacts Gujarat : Corruption reduced, tax revenues increase at interstate border checkposts, viewed 11 may 2008, available : <http://www.egovonline.net/articles/article-details.asp?Title=e-Governance-impacts-Gujarat&ArticalID=507&Type=IN%20PRACTICE>

[23] Haryono,T & Widiwardono, Y. K 2006,Current Status and Issues of E-Government in Indonesia, ASEAN, viewed 17 November 2008, available:< http://www.aseansec.org/13757.htm >

[24] Heeks, R. and Lallana, E. 2004, M-government benefits and challenges, viewed 20 March 2008, Available :<http://www.e-devexchange.org/eGov/mgovprocon.htm

[25] Heeks. R 2006, Implementing and Managing e-Government. SAGE Publications, Chennai, India

[26] IBRD, 2008, viewed 12 June 2008, available :< http://egov.sonasi.com/>

[27] ICRS project 2004, E-government in Hongkong, viewed 4 September 2008, available:< http://www.info.gov.hk/digital21/e-gov/eng/index.htm>

[28] IDABC 2005 'Impressive e-government take up in Canada'; e-government news 08/04/05, viewed 10 May 2008, available <http://europa.eu.int/idabc/en/document/4083/5800>

[29] International Data Center (IDC) 2006, viewed 11 November 2008, available:< http://www.idc.com/home.jhtml >

[30] International Telecommunication Union (ITU) 2002, ITU report : Indonesia Case Study, viewed 2 March 2008, available:http://www.itu.int/itudoc/gs/promo/bdt/cast_int/79476.html

[31] International Telecommunication Union(ITU) 2003, Mobile Overtakes Fixed : Implications for Policy and Regulation, viewed 10 March 2008, available:< http://www.itu.int/osg/spu/ni/mobileovertakes/Resources/Mobileovertakes_Paper.pdf>

[32] International Telecommunication Union(ITU) 2004, ITU Internet report 2004: "the Portable Internet", viewed 10 march 2008, available :< http://www.itu.int/osg/spu/publications/portableinternet/>

[33] International Telecommunication Union (ITU) 2007, World Telecommunication/ICT Indicators Database, viewed 12 April 2008, available:<http://www.itu.int/ITU-D/ict/publications/world/world.html>

[34] ITU 2006, ITU internet report 2006: Digital Life, viewed 27 February 2008, available:<http://www.itu.int/osg/spu/publications/digitalife/docs/digital-life-web.pdf>

[35] Jaeger P & Thompson K, 2003, Government Information Quaterly 20 (2003) 389–394, 'E-government around the world, Lessons, Challenges and Future Directions';

[36] Kardoyo, H 2008, Generation "Y" will challenge the business world traditions, The Jakarta Post, viewed 18 September 2008, available:< http://www.thejakartapost.com/news/2008/10/03/generation-%E2%80%9Cy%E2%80%9D-will-challenge-business-world-traditions.html>

[37] Kiss, J 2007, China cracks down on SMS, journalism.co.uk, viewed 25 August 2008, available:< http://www.journalism.co.uk/2/articles/5970.php >

[38] Kurose, J.F & Ross W.K 2005, Computer networking: a top-down approach featuring the internet, 3rd edn, Pearson Education, New York.

[39] Kushchu, I & Halid Kuscu, M 2004, From E-government to M-government: Facing the Inevitable, MGov-Lab. Org, viewed 15 March 2008, Available: <http://mgovernment.alfabes.com/resurces/mgovlab_ikhk.pdf>

[40] Kushchu, I. and Borucki, C. (2003) "A Mobility Response Model for Government" in the proceeding of European conference on E-Governemnt (ECEG 2003), Trinity College, Dublin

[41] Kushchu, I. and Kuscu, H (2003) "From E-government to M-government: Facing the Inevitable" in the proceeding of European conference on E-government (ECEG 2003), Trinity College, Dublin.

[42] Lallana, E 2004, eGovernment for Development, M-government Definitions and Models, viewed 20 March 2008, available: <http://www.egov4dev.org/mgovdefn.htm>

[43] Lallana, E 2004, SMS and Democratic Governance in the Philippines, viewed 20 March 2008, available: <http://www.apdip.net/projects/e-government/capblg/casestudies/Philippines-Lallana.pdf>

[44] Marty 2005, SMS in Hungarian Elections 2002, MobileAcyive.org, viewed 26 August 2008, available:< http://mobileactive.org/sms-hungarian-elections-2002 >
[45] Media- Culture 2007, Modernity and the Mobile Phone, viewed 28 September 2008, available : <http://journal.media-culture.org.au/0703/06-humphreys-barker.php>
[46] Minges, M 2001, Mobile internet for developing countries, viewed 20 March 2008, available <http://www.isoc.org/inet2001/CD_proceedings/G53/mobilepaper2.htm>
[47] Mobilecomms-technology.com 2008, SMS (Short Message System) Mobile Technology, International, SPG Media, viewed 30 September 2008, available: < http://www.mobilecomms-technology.com/projects/sms/>
[48] MobileInfo.com n.d, 4G - Beyond 2.5G and 3G Wireless Networks, viewed 10 October 2008, available:< http://www.mobileinfo.com/3G/4GVision&Technologies.htm>
[49] Nair, V.V 2005, Ericsson bets on 3G for Indian mobile phone market growth, Business Line, viewed 12 January 2008, available: <http://www.thehindubusinessline.com/2005/03/08/stories/2005030800980500.htm>
[50] Nyamai, C n.d, Harnessing ICTs for community health - The AfriAfya initiative, AfriAfya.org, viewed 18 August 2008, available: <http://unpan1.un.org/intradoc/groups/public/documents/other/unpan022126.pdf>
[51] OECD 2006, OECD e-Government studies: The e-Government Imperative, OECD@oecd.org
[52] Ozeki Messages Server 2008, SMS API for Database developers (SQL), viewed 29 September 2008, available: <http://www.ozeki.hu/SMS-SQL-tutorial/index.php?ow_page_number=425>
[53] Pavlichev, A & Garson, G.D 2004, Digital Government: Principles and Best Practices, IDEA Group Publishing, USA
[54] Radio Republik Indonesia(RRI), n.d, viewed 17 November 2008, available:< www.rri-online.com>
[55] Rannu, R & Semevsky, M 2005, Mobile services in Tartu, Mobi Solutions, viewed 30 August 2008, available :< http://www.ega.ee/files/Mobile%20services%20in%20Tartu%20FINAL1.pdf>
[56] Rinne, J 2001, Citizen Service Centers in Bahia, Brazil, The World Bank Group 2008,viewed 17 August 2008, available: <http://web.worldbank.org/WBSITE/EXTERNAL/TOPICS/EXTINFORMATIONANDCOMMUNICATIONANDTECHNOLOGIES/EXTEGOVERNMENT/0,,contentMDK:20486008~isCURL:Y~menuPK:1767268~pagePK:210058~piPK:210062~theSitePK:702586,00.html>
[57] Rynecki, S 2007, DOT-COM Activity: Kyrgyzstan eCenter Project, ICT@USAID, 2008, viewed 17 August 2008, available: <http://www.dot-com-alliance.org/activities/activitydetails.php?activity_id=110>
[58] Salahuddin, M & Rusli, A Information Systems Planning for e-government in Indonesia, The Second International Conference on Innovations in Information Technology (IIT'05), viewed 18 August 2008, available:< http://www.it-innovations.ae/iit005/proceedings/articles/G_7_IIT05_Salahuddin.pdf>
[59] Sandy & Millan,Mc 2005 ,A Success Factors model for m-Government, viewed 2 September 2008, available:<http://www.mgovernment.org/resurces/euromgov2005/PDF/36_R348SG.pdf>
[60] Shepler, J 2005, 1G, 2G, 3G, 4G, TechTarget 2008, viewed 10 Octber 2008, available: <http://searchmobilecomputing.techtarget.com/generic/0,295582,sid40_gci1078079,00.html>
[61] Sunario, T n.d, Indonesia's Young Consumers are Mobile and Up To Date, Ministry of Culture and Tourism, Republic of Indonesia, viewed 20 September 2008, available:< http://www.budpar.go.id/page.php?id=2013&ic=611>
[62] Supangkat, S.H 2007, CIO Innovation and Leadership in Indonesia, viewed 11 November 2008
[63] Susanto, D.T & Goodwin, R 2006, Opportunity and Overview of SMS-based e-Government in developing Countries, WIT Transactions on Information and Communication Technologies, vol 36, viewed 14 March 2008,available:<www.witpress.com>
[64] Susanto, T. D & Goodwin, R 2007, Content Presentation and SMS-based e-Government, Proceedings of the International Conference on Electrical Engineering and Informatics Institut Teknologi Bandung, Indonesia June 17-19, 2007, viewed 10 January 2008, available;< http://tonydwisusanto.files.wordpress.com/2007/12/content.pdf >
[65] Televisi Republik Indonesia (TVRI), n.d, viewed 17 November 2008, available:< http://www.tvri.co.id/>
[66] The National Office for the information economy Australia 2003, e-government benefit study, viewed 9 may 2008, available: <http://www.agimo.gov.au/__data/assets/file/0012/16032/benefits.pdf> [5]
[67] Trimi & Sheng 2008, Emerging trends in e-government, ACM digital libray, viewed 1 September 2008, available: <http://delivery.acm.org.ezproxy.flinders.edu.au/10.1145/1350000/1342338/p53-http://www.agimo.gov.au/__data/assets/file/0012/16032/benefits.pdftrimi.pdf?key1=1342338&key2=8483630221&coll=portal&dl=ACM&CFID=1390901&CFTOKEN=92462022 >
[68] UNA-Canada, n.d, Information Technology for Development Case Study: Internet Access: A Citizen`s Right and Cornerstone to Liberty in Estonia, UNA-Canada, viewed 17 August 2008, available:< http://www.unac.org/en/link_learn/monitoring/susdev_undp_techcase.asp>
[69] UNDP 2007, Human Development reports 2007/2008: Indonesia, viewed 21 October 2008, available:< http://hdrstats.undp.org/countries/data_sheets/cty_ds_IDN.html >
[70] World Health Organization 2006, Mortality Country Fact Sheet 2006, viewed 18 November 2008, available : <http://www.who.int/whosis/mort/profiles/mort_searo_idn_indonesia.pdf>

Automatic Vehicle Identification and Inventory System using RFID Technology

Dodi Sudiana[1)], Arief Udhiarto[1)], Aji Nur Widyanto[1)]

[1)]Optics and Remote Sensing (OPRES) Research Group, Department of Electrical Engineering,
Faculty of Engineering Universitas Indonesia,
Kampus Baru UI Depok 16424, Indonesia
E-mail: dodi@ee.ui.ac.id

Abstract

*We developed an automatic vehicle identification and inventory system using RFID technology. RFID is a new identification technology which needs no direct contact between the object and the identifier. It is consisted of a transponder (tag) and a reader. The proposed system consists of automatic RFID reading, inventory, database, microcontroller and gate actuator subsystems for vehicles. According to the Ministry of Communication and Information, the reader works at 923-925 MHz frequency range. Middleware software has been developed using Borland Delphi 7. The experiment has been conducted to test the functionality and reliability of the system which consisted of vehicle identification, validation, inventory, opening/closing gates, and data recapitula*tion for reporting.

Keywords: RFID, tag, reader, vehicle identification, vehicle inventory, Delphi

1. Introduction

Universitas Indonesia as a big university has been flocked by cars and motorcycles every day and the number of vehicles entering and leaving the campus is increasing from time to time. Those vehicles (especially cars) are verified manually at the gate and if there is no license, the driver has to pay to the officer. To pay, and take an entrance card at the gate, each car has to spend about 10 seconds. In peak hours (morning), vehicles have to wait in a very long queue before entering the campus as shown in Fig. 1. Since there is no authorization for each vehicle in the campus vicinity, so the security risk is very high. When leaving the university exit gate, the driver just gave the entry card back to the officer. There is no record on vehicle identity such as license plate number, vehicle type, color, owner's name, address, etc. Therefore an automatic vehicle identification and inventory which could work fast with high accuracy urgently needed.

Fig. 1. Vehicles queueing in the UI entrance

In this research, we developed an automatic vehicle identification and inventory system based on Radio Frequency Identification (RFID) technology. RFID is a new identification technology which needs no direct contact between the tag attached to an object and the reader. The technology could automatically detect and identify an object, track and store the information of an object or part of it electronically.

RFID technology consists of tag, reader and collection, distribution and data management system which usually interfaced by a middleware as shown in Fig. 2. In practice, RFID tags could be implemented as labels, key chains, stickers, cards, coins, rings, or other forms. These tags could receive radio wave transmitted from the reader, convert it as an electric energy, feed the memory circuit inside it and transmit the ID content back to the reader.The distance between the tag and the reader, depends on the reader power and working frequency could range from several centimeters to tenth meters.

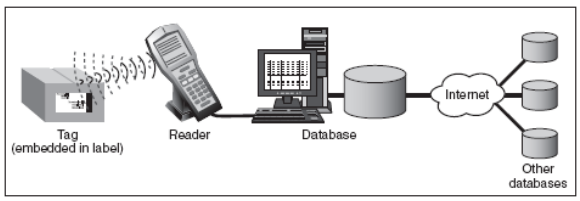

Fig. 2. RFID system and its components

The advantages of RFID are: needs no line-of-sight connection, dynamic information carrier, larger memory size, anti-collision (several tags could be read simultaneously), reliable and weather proof, affordable for long time investment, needs no human intervention

and maintenance-free. Therefore the system could be implemented to increase the effectivity and efficiency in parking and vehicle management system in the Universitas Indonesia.

1. Methods

Automatic vehicle identification and inventory system using RFID is implemented in the Universitas Indonesia. The system consists of tags and a reader which works at 923-925 MHz frequency range as recommended by the Ministry of Communication and Informatics. The reader is installed at the gate IN and OUT of the parking area. To control the gate opening and closing, a microcontroller is used as an interface between the PC and the gates. LED indicators are Fig. 2 showed the proposed system.

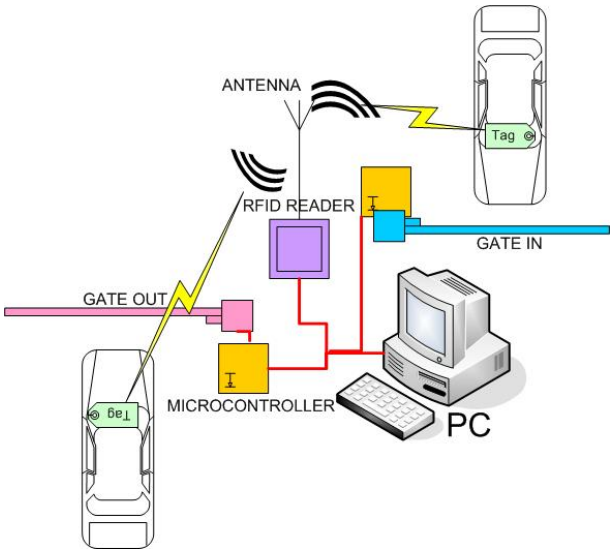

Fig. 3. Proposed vehicle identification and inventory system

As is generally the vehicle entrance gate, then there will be two routes, namely the entrance and exit. In design, this system uses only one RFID tag reader to detect the vehicles through this paths. Single RFID reader system itself can not distinguish directly enter the vehicle or the outside, but with the help of software. The software will run an algorithm to distinguish vehicles that enter or exit.

Vehicle that can go through the door of access into the parking area in the campus must have a tag that is registered on the database system. If the vehicle is detected by RFID reader, the software will match if the vehicle is registered in the database system or not. When the data obtained on the vehicle may not pass the gate access in the main program the software will provide information to the mikrokontroller action to set what should be done on the vehicle. If the data in the database have a vehicle then mikrokontroller will be ordered the doors to open access doors, if not then the door remains closed.

In general, the automatic parking system architecture consists of several parts. The first section is comprised of a RFID reader and tag. The second part is middleware or in the form of a computer system which contains the program and database. The third is microcontroller a function to set the exit and entrance gate, access entrance gate will be made by using the Servo motor. Figure 3 shows the system architecture of automatic vehicle inventory developed.

Read the data stored in the database system that is on the PC. Information read from the RFID reader to have a database on a PC using the software. The software used in the automatic parking system will be created using Delphi 7.

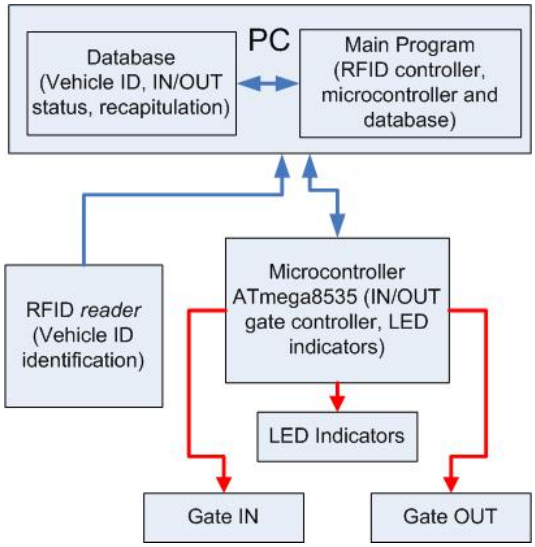

Fig. 4. System block diagram

Data communication between the RFID and the main program on the PC lasted only one direction, namely from RFID to the PC via RS232 serial port. And data communication between mikrokontroller with the main program on the PC also take direction from one PC to mikrokontroller through RS232 serial port. Communication from the PC to be used to run mikrokontroller Servo motor that serves as a parking lot gate. Servo Motor that will be used in this system amounted to 2 which functions as the entrance gate and gate to gate.

3.1. Flowchart Automatic Parking System

This flowchart describes the system-based automatic vehicle inventory RFID work, begining from RFID to be detected until stored in the database. Flowchart shown in Figure 4 with the following explanation:

1. System will continue detect by using RFID technology, if there are vehicles that pass the gate of access to parking or not.
2. If you have a vehicle that comes in, the system will detect whether the vehicle has entered the

appropriate code tags with the database system or not.

3. If it is not appropriate, the system will send commands to mikrokontroller to close the gate.
4. If the code tag in accordance with the database, the system will determine whether the vehicle entrance or exit by using the algorithms that run in the main program on the PC.
5. After that, information about the code tag will be entered into the database. Information is entered in the database, namely the identity of vehicles and their owners. In addition, the entry and exit times of vehicles will also be recorded on the database. Time of entry and exit this will be used to accumulate the cost of parking the vehicle owner listed in the database.
6. Then, the software will command the entrance or exit is opened or closed.
7. After the close the gate open, the system will return to the detection process vehicles as they are. This detection continues until the system is turned off manually.

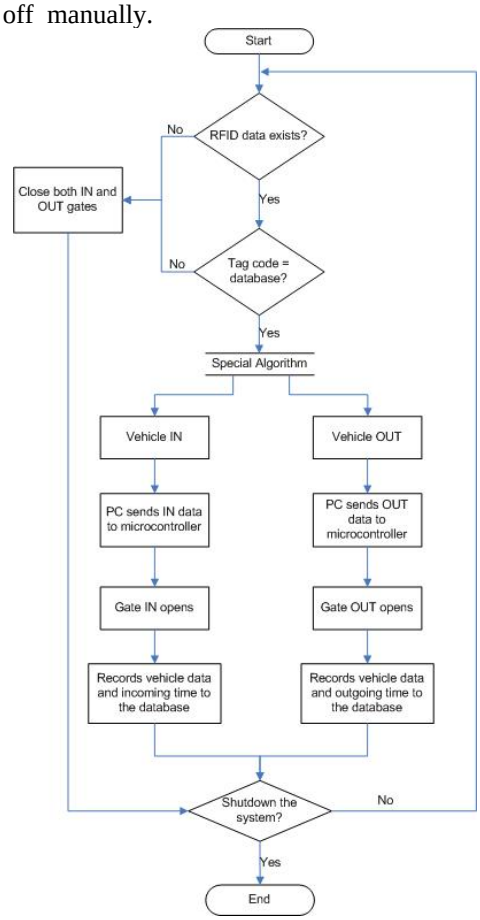

Fig. 5. Flow chart of the system

3.2. Automatic Vehicles Inventory System

In development, this system is gradually becoming some subsystem. In general, subsystems are responsible for certain functions, namely:

1. Subsystem with the vehicle identification RFID
2. Subsystem open-close gate
3. Subsystem software (the main program)
4. Subsystem database
5. Subsystem interfacing software with hardware

a. Vehicles Identification with RFID

The process of identification of vehicles with RFID is to place RFID tags on the vehicle and the RFID reader in a certain place in the parking lot near the gate. So if the vehicle through the gate of the identity of the vehicle will be directly recognized. This identification process will be based on the ability of the RFID reader is used.

Communication between the RFID reader with the PC itself can use some kind of communication, namely communication among parallel and serial communication. RFID communication depends on this component of the output is provided by the RFID reader is used. RFID tag data format is read by the reader as ASCII data with the following formats:

STX – MT – RT – 4 digits card number – 2 digits project number- EXT – LRC1 – LRC2 – CR – LF

Description:
STX = data prefix; MT = data type; RT = type RFID reader; 4 digits card number = 4-digit card number RFID tags in ASCII code; 2 digits project number = 2-digit project number in the RFID tag code ASCII; EXT = End of data; LCR1= first byte checksum; LCR2 = second byte checksum; CR = Carriage return (0x0D); LR = Line feed (0x0A)

b. Open – Close Parking Gate

In designing the system, opening and closing the gate using a Servo motor equipped with a latch. Latch to be used of the two: one for the entrance gate and one gate for exit.

The motor will be done by microcontroller that receive instructions from a computer to open or close the parking gate.

c. Software(Main Program)

Inventory control system for automatic vehicle uses software Delphi. Delphi itself is high-level language programming used in object-oriented Programs.

Software functions to the system and run the algorithm also connects with the database system so that the system is running well. To connect the database with Delphi components, are used in the Delphi ADO (Active Data Object).

In addition, this software also serves to connect the (interfacing) between the computer hardware that will be connected later as microcontroller and RFID. In communicating with the hardware, using a Delphi component called Com-Port.

d. Database

To save data vehicles in detail, required the database. MS Access is used in developing this system because it is a Microsoft Office database program so that easier for management. Database filled with data that are required such as RFID tag number, vehicle owner name, address, vehicle plate number, type and color of vehicle.

MS Access database will be accessible by the main program (in this case Delphi) using components found in the ADO (Active Data Object). With ADO, the distribution of the program only requires a program file (. Exe) and database (*. mdb) only. Database that are connected with the Delphi program shown in Figure 5.

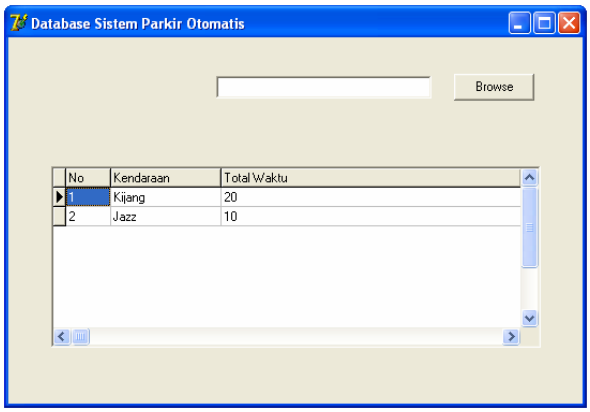

Fig. 5. Connection between DELPHI and *database*

e. Interfacing Software and Hardware

Inventory system has an automatic vehicle software and hardware devices which communicate with each other. Communication between software and hardware uses two communications, the serial communication and parallel communication.

But on this system later will use the serial communication as a means of communication between the hardware and software. In Delphi software itself is actually already available with the communication component of the hardware that is ComPort. ComPort akan disetting in accordance with the characteristics of the hardware. Figure 6 shows a description of the components ComPort is in Delphi.

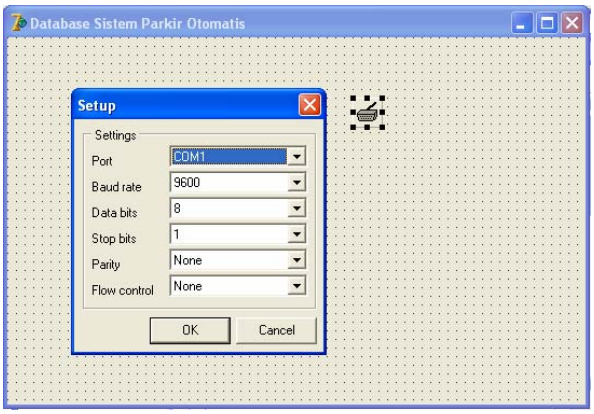

Fig. 6. The components ComPort in Delphi

Each of the hardware that is connected in the system will be configured first, starting from the port number to the parity is not used. Disettingnya with the hardware, the system will run properly and in accordance with the design.

2. Results and Discussion

The system was tested to verify the hardware and software functionalities of the system.

a. Hardware functionalities
b. Software functionalities
c. Overall system functionalities
d. Real-time functionalities

2.1. Hardware functionalities

The RFID reader (model DL910) has the reading distance capability up to 15 meters. The direction of readings are set as shown in Fig. 7.

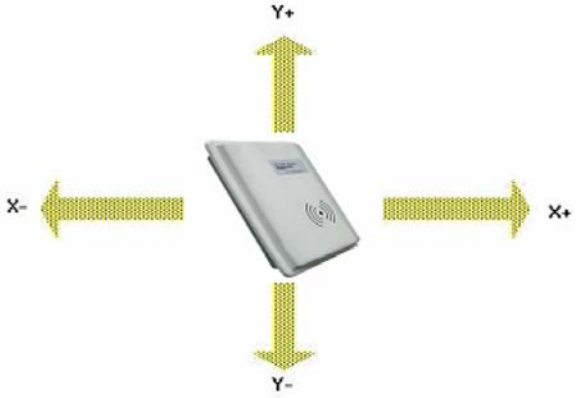

Fig. 7. The directionality of reading

Reading capability (in % of output power) of the reader in 4 directions (no angle, -30°, +30 and) are shown in Fig. 8, 9, and 10, respectively. The data was taken for 10 times for each direction. The results showed a relative strong reading capability for distance less than

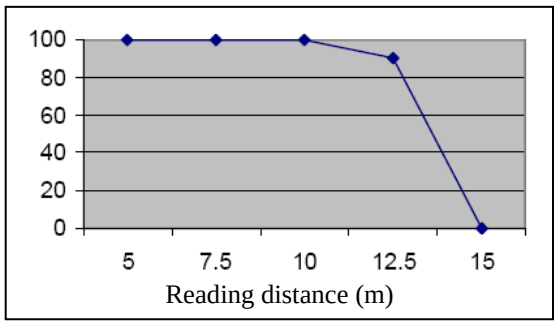

10 meters.

Fig. 8. Reading capability (in %) for -30° of X+ direction

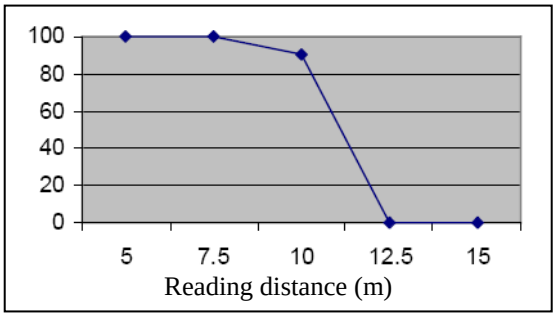

Fig. 9. Reading capability (in %) for +30° of X+ direction

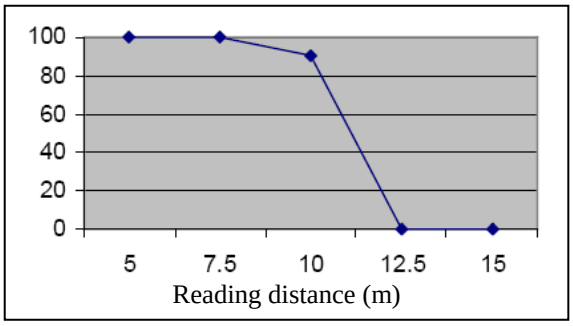

Fig. 10. Reading capability (in %) for -30° of X+ direction

2.2. Software functionalities

To test the software functionality, we checked the system durability for about 8 hours continously. The sample vehicles (for total 5 cars) with tag attached on its windshield are moved in and out and the test results showed a perfect recognition without any errors. The durability test of 5 tags is shown in Table 1.

Table 1. Durability of 5 tags for full performance

Tag distance	Tag1	Tag2	Tag3	Tag4	Tag5
5 m	×	×	×	×	×
4 m	×	×	×	×	×
3 m	✓	✓	✓	✓	✓
2 m	✓	✓	✓	✓	✓
1 m	✓	✓	✓	✓	✓

As shown in Table 1, the system could not recognize the tags attached in the cars for distance more than 3 meters. Therefore the system could be applied in real condition since there are only limited space near the parking gate.

4. Conclusion

Automatic parking system using RFID is designed and perform well for real application. Ideally the DL-910 could read up to 12.5 meters, but in real condition, the reading capability was decreased only to 3 meters. The durability of 5 tags tested was quite good for distance less than 3 meters.

Acknowledgment

We would like to thank the Directorate of Research and Public Service Universitas Indonesia for supporting this research in Riset Unggulan UI scheme 2008.

References

[1] A White Paper on: *The RFID Business Planning Service, Venture Development Corporation Automatic Identification and Data Collection Practice*, May 2005.
[2] Xingxin (Grace), Gao. *An Approach To Security And Privacy of RFID System For Supply Chain.* IEEE, 2004.
[3] K. Klaus, *RFID Handbook*, Chapter 3, John Wiley & Sons Inc, 2003.
[4] Juels, Ari, *RFID Security and Privacy: A Research Survey*. RSA Laboratories, 2005.
[5] Karygiannis, Tom, et al. *Guidelines for Securing Radio Frequency Identification* (*RFID*) *Systems*. USA: National Institute of Standards and Technology, 2007.
[6] ITAA, *Radio Frequency Identification*. USA: Information Technology Association of America, 2004.
[7] GAO. *Informaton Security Radio Frequency Identification Technology in the Federal Government*. USA: Government Accountability Office, 2005.
[8] Molnar, David and David Wagner, *Privacy and Security in Library RFID Issues, Practices, and Architectures*. USA: Berkeley, 2004.
[9] Lan, Zhang and Friends, *An Improved Approach to Security and Privacy of RFID Application System.* IEEE, 2005.
[10] Bolotnyy, Leonid and Gabriel Robins. *Randomized Pseudo-Random Function Tree Walking Algorithm for Secure Radio-Frequency Identification.* University of Virginia.

ISSN 114-1284

DISCRETE WAVELET TRANSFORM – k-NEAREST NEIGHBORS METHOD FOR SPEAKER RECOGNITION

Endra[1], Donny[2], Bima Putra[3], Rico Then[4]

Department of Computer Engineering, University of Bina Nusantara
Jl K.H. Syahdan No.9 Kemanggisan / Palmerah, 11480, Jakarta, Indonesia
endraoey@binus.edu[1], abet_donny@yahoo.com[2], shichinintai_87@yahoo.com[3], rico_then@yahoo.com[4]

ABSTRACT

A Speaker recognition system was created in this research by using discrete wavelet transform (DWT) and *k-Nearest Neighbor (k-NN). Evaluation of this research is using 45 data training database which represents 9 types of sound identity (3 speaker identities and 3 text identities). In summary, this system works by using the data sample of sound through the cutting stage, DWT, Dynamic Time Wrapping (DTW), and k-NN algorithm. The average success of this system in recognizing the sample of this speaker and text identity sound in the database is 98.33% with the average time recognition is 59.03 seconds. This result is achieved through level-2 wavelet decomposition and the usage of approximation coefficients (cA) along with detail coefficients (cD). The average success of this system in recognizing the sample of sound which the speaker and text identity is not available in the database is 72.33%.*

Keywords

Speaker Recognition, Discrete Wavelet Transform, k-Nearest Neighbors

1. INTRODUCTION

Speaker recognition was a digital signal processing technique for recognize, identification or speaker verification (speaker). Function of speaker recognition was classic example of problem in pattern recognition, which in general is useful to found kind of pattern from data got by the censor. Training process is needed for all of pattern recognition problem. For example in s*peaker authentication system*, user voice need to register. During that process, the system is "learn" the user voice that want to recognize. Speaker recognition can be text dependent or text independent. The word "text" in this context is a words is spoken by user [1]. In "*Speech Recognition for Controlling Movement of the Wheelchair*" using *Linear Predictive Coding* (*LPC*) and *Euclidean Squared Distance*, the maximum sucessful percentage that can be achieved is 78.57 % [2]. In this paper a speaker recognition system is developed by using Discrete Wavelet Transform (DWT) and k-Nearest Neighbors (k-NN). Evaluation of this system is using 45 data training database which represents 9 types of sound identity (3 speaker identities and 3 text identities).

2. THEORY

2.1 Discrete Wavelet Transform

Discrete Wavelet Transform (DWT) work by doing wavelet transform in discrete signal. The basic principle of *discrete wavelet transform* is how to get the representation of time and scale from a signal that using digital filter technique and sub-sampling operation or down-sampling operation. The signal first must be process in high pass filter and low pass filter, and then half of the output signal will be taken as sample with down-sampling operation. This process called the decomposition process one degree. The output from low-pass filter will be used as the input of the next decomposition process. This process will be repeated until the decomposition level that desire. Union of the signal output from high-pass filter and one output from the last low-pass filter is called wavelet coefficient, which contain the signal information in the form compressed signal. The explantion of two that process can be explain at Figure 1. Couple of *high-pass filter* and *low-pass filter* that used must be in the form *quadrature mirror filter* (QMF), which fulfill this equation:

$$h[n] = (-1)^n g[L+1-n] \qquad (1)$$

with $h[n]$ is *high-pass filter*, $g[n]$ is *low-pass filter* and L is length of *filter* [3].

2.2 Dynamic Time Warping

Dynamic Time Warping (DTW) is a method that used to calculate the distance between 2 data coefficient that may different in time and speed. The distance will represent how much the similiarity between that 2 data coefficient. As example, in the first recording process, the user speak with more fast, meanwhile in the second recording process, the user speak more slowly than the first recording process. Both the recording process, the user say same words with different in the speed, will produce the different length of distance. By using DTW method, the distance (similiarity) of between the two recording process can be known. This is the main advantage of DTW method. In general, *DTW* is a method that make a computer calculate the most optimal distance (similiarity) between the 2 coefficients given. The coefficients will be "warp" in non-linear in time domain to calculate the distance (similiarity) of the 2 coefficients [4].
Coefficient-coefficient can be arrange distance on the sides grid like at Figure 3. Figure 3 above is describe data coeffcient that want to identify (bottom side grid) and data coefficient reference that save in database (left side grid). Two data coefficient is begin from left side grid. Distance result is representative by blue grid. After that line had found will be get nearest distance between input data coefficient with data coefficient reference database. DTW algorithm is all distance in the grid. Because of that data coefficient will be result probability distance too much. DTW method will be result comparison process between 2 data coefficient.

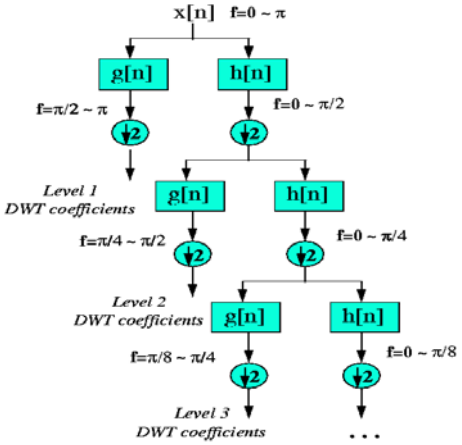

Figure 1: Decomposition Process in *Discrete Wavelet Transform*

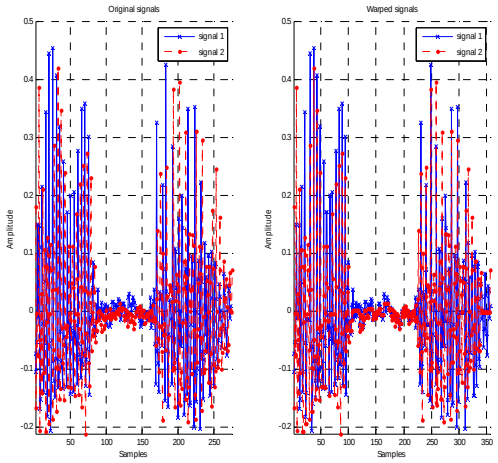

Figure 2 : Signal before (left) and after (right) *Dynamic Time Warping*

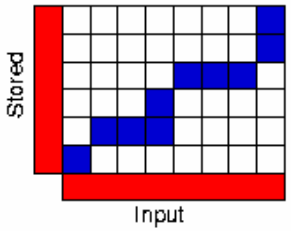

Figure 3 : *Dynamic Time Warping Grid*

2.3 k-Nearest Neighbors

k-Nearest Neighbors (k-NN) Method is method to do classification object by data that have nearest distance with object. Data will be projection to many dimension space, severally dimension representation feature from the data. That space consist many parts based on data learning. One point in the space will be sign c if c class have classification that the most in the k neraset neighbors [5]. Close or far neighbor usually computation based on euclidean distance that equation like: For $P = (p_1, p_2, ..., p_n)$ and $Q = (q_1, q_2, ..., q_n)$,then $\text{Distance} = \sqrt{\sum_{i=1}^{n} (p_i - q_i)^2}$ (2)
Figure 4 below explain about classification on k-NN method. Small green circle on the centre is a sample, the box symbols (blue) show the first class or speaker 1 and the triangle symbols (red) show the second class or speaker 2. If resolution value used is 3, then the result of k-NN algorithm will be second class classification or speaker 2 because there are 2 triangle symbols and only 1 box symbol in the resolution circle on Figure 4 below. And if the resolution

value changed be 5, this method will produce first class decision or speaker 1 because there are 3 box symbols and only 2 triangle symbols in the resolution circle on Figure 4 below.

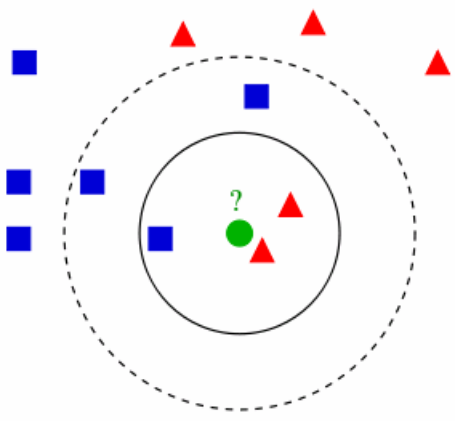

Figure 4 : Example of classification with *k-Nearest Neighbor* method

3. IMPLEMENTATION

1. System recognition mode.
2. Recording process.
   On recording process, user say the words which it's identify has saved in database.
3. System run.
4. Program show the outputs.
   The output are sound signal on speaker and decision logic result showed on user interface display.
5. Fill the result experiment as table data.

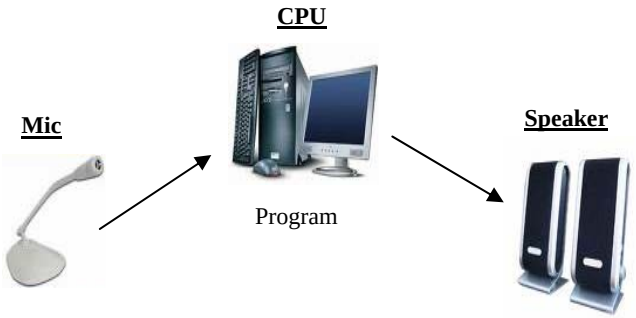

Figure 5 : System Block Diagram System

4. EVALUATION

Based on experiment data, the optimal result (success percentage or recognition time) got on experiment with sampling frequency 11,025 Hz, wavelet decomposition level-3, wavelet filter "db10", using Approximation Coefficients (cA) and Detail Coefficients (cD). By using that parameter configuration, the result sucessful percentage of the system is 91.11 % and average recognition time 20.64 second. Here's some results of the system with parameter above :

1. Speaker + Text : Bima + Open
   Sucessful percentage : 77.5 %
   Average Recognition Time : 22.90 second
2. *Speaker* + *Text* : Donny + Open
   Sucessful percentage : 95 %
   Average Recognition Time : 20.47 second
3. *Speaker* + *Text* : Rico + Open
   Sucessful percentage : 95 %
   Average Recognition Time : 20.84 second

For evaluation using 45 data training database which represents 9 types of sound identity (3 speaker identities and 3 text identities), the average success of this system in recognizing the sample of this speaker and text identity sound in the database is 98.33% with the average time recognition is 59.03 seconds. This result is achieved through level-2 wavelet decomposition and the usage of approximation coefficients (cA) along with detail coefficients (cD). However, on the testing system with level-3 wavelet decomposition, it is achieved that the average success is 91.11% with the average time recognition is 20.64 seconds, and on the testing system with level-4 wavelet decomposition, it is achieved that the average success is 50.28% with the average time recognizition is 8.20 seconds. The average success of this system in recognizing the sample of sound which the speaker and text identity is not available in the database is 72.33%. The average success of this system in recognizing the sample of the sound which the identity (Speaker and Text) is in the database with sampling frequency 44,100 Hz is 100% with the average time recognizition is 313.75 seconds. The research data shows a conclusion that the optimum result (both in the percentage of success and the time recognition) is achieved through testing with the sampling frequency 11,025 Hz, level-3 wavelet decomposition, type of wavelet filter "db 10", and the usage of approximation coefficients (cA) along with detail coefficients (cD).

5. CONCLUSION

From data implementation and evaluation system , got a conclusions like: first a success speaker recognition and

speaker recognition time turned comparison with level decomposition wavelet that use. Second a success speaker recognition straight comparison with speaker recognition time. Third, had got data result from optimal research (a success percentation and recogition time) got from system experiment with sampling frequency 11,025 Hz, decomposition *wavelet* level-3, *wavelet* filter 'db10' and *approximation coefficients* (cA) with *detail coefficients*.

REFERENCES

[1] Heinz, Heirtlein. 2008. Definitions. *The Speaker Recognition Homepage*, (Online), (http://speaker-recognition.org, accessed on December 26, 2008).

[2] Thiang. 2007. *Speech Recognition for Controlling Movement of the Wheelchair*. International Conference on Optics and Laser Applications. 2nd. Dept.of Electrical Engineering, University of Indonesia, Depok.

[3] Mallat, Stephane. 1999. *A Wavelet Tour of SignalProcessing, 2nd ed.*, San Diego : Academic Press.

[4] Berndt, D.J., Clifford, J., 1996. *Finding Patterns in Time Series : A Dynamic Programming Approach, Advances in Knowledge Discovery and Data Mining*. Menlo Park : American Association for Artificial Intelligence.

[5] Dasarathy, Belur V. 1991. *Nearest Neighbor (NN) Norms : Nn Pattern Classification Techniques*. Massachusetts : IEEE Computer Society Press.

The Effects of Vertical Scaling to the SiGe HBT with Different Lateral Dimension

Engelin Shintadewi Julian

Electrical Engineering Department Faculty of Industrial Technology
Trisakti University, Jakarta 11440
Tel : (021) 5663232 ext 8433. Fax : (021) 5605841
E-mail : eshintadewij@yahoo.com

ABSTRACT

In this paper, the effects of vertical scaling to the SiGe HBT with different lateral dimension are reported. The research methodology is as follows. First, the reference device structure is defined. And then physics parameters model and simulator control parameters are determined. The simulations were done with the help of Bipole3 devices simulator. The next step was lateral scaling. In this step the emitter finger width was scaled consistent to the minimum feature size lithographic developments i.e. from 0.25μm to 0.18μm, 0.12μm and 0.09μm. The last step was vertical scaling. In this step the base width of SiGe HBTs with different lateral dimension was reduced from 39nm to 32nm and their effects to the transistor performances were observed. The results show that vertical scaling has stronger effect to the SiGe HBT with larger lateral dimension than devices with smaller lateral dimension.

Keywords
SiGe, HBT, vertical scaling

1. INTRODUCTION

The concept of the HBT was patented by Shockley in 1951 [1] and the HBT theory was published by Kroemer in 1957 [2]. In 1987, the first SiGe HBT is reported [3] but world wide attention became focused on SiGe technology at 1990 with demonstration of SiGe HBT with peak cutoff frequency f_t of 75GHz [4]. Until about 1998, peak cutoff frequency remained in the 50 – 75GHz range. In this time period most research were focused on the vertical scaling and Ge profile optimization of the SiGe HBT [5-8]. Vertical scaling is the most efficient way to enhanced the cutoff frequency of SiGe HBT.

Since 2001 the SiGe HBTs frequency performances have been continue to increase and SiGe HBT with 350Ghz peak cutoff frequency was recorded in 2002 [9] while SiGe HBT with 350GHz peak maximum frequency of oscillation f_{max} was recorded in 2004 [10]. Higher frequency performances were achieved from SiGe HBT with smaller lateral dimension [11]. The ability to produce SiGe HBT with smaller lateral dimension depend on the minimum feature size of lithography technology. Reduction on feature size lithographic allows us to laterally scale down the SiGe HBT to enhance device performance.

In this paper, the effects of vertical scaling to the SiGe HBT with different lateral dimension are reported. The research methodology is as follows. First, the reference device structure is defined. Next, the physics parameters model and simulator control parameters are determined. The simulations were done with the help of Bipole3 devices simulator. The next step was lateral scaling. In this step the emitter finger width was scaled consistent to the minimum feature size lithographic developments i.e. from 0.25μm to 0.18μm, 0.12μm and 0.09μm. The last step was vertical scaling. In this step the base width of SiGe HBTs with different lateral dimension was reduced from 39nm to 32nm and their effects to the transistor performance were observed.

2. REFERENCE DEVICES

The lateral dimension of the reference device is shown in Fig. 1. The reference device has single emitter finger, two base contacts and single collector contact. The emitter finger area A_E = 0.25 μm × 10 μm. Each base contact has the same area as the emitter finger area. The collector contact area A_C = 0.50 μm × 12 μm.

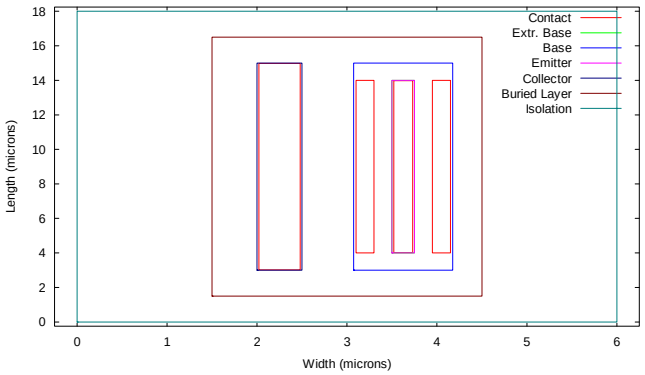

Figure 1: Lateral dimension of the reference device

The emitter, base and collector widths, doping profiles and Ge profile in the vertical direction are shown in Fig. 2. The emitter width W_E = 12 nm, base width W_B = 39 nm and collector width W_C = 650 nm. The Ge profile is rectangular with 5% Ge concentration. Peak doping concentrations in the emitter, base and collector are 10^{20} cm^{-3}, 10^{19} cm^{-3}, and 2×10^{18} cm^{-3}. The collector has selective implant collector (SIC) profiles.

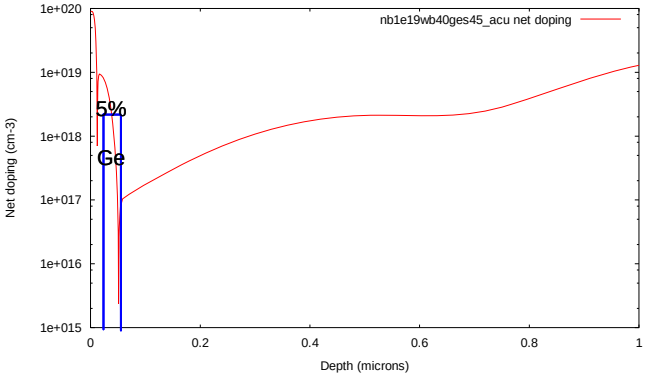

Figure 2: Vertical profile and dimension of the reference device

3. RESULTS AND DISCUSSIONS

3.1 Lateral Scaling

The lateral scaling process is divided into two steps. First, the emitter finger width of the reference SiGe HBT is scaled down from 0.25 µm to 0.18 µm, 0.12 µm and 0.09 µm. The simulation results shows that all SiGe HBTs have collector emitter breakdown voltage BV_{CEO} 2.8 V. The effects of emitter finger width to the SiGe HBT performances for collector base voltage V_{CB} = 0 V are shown in Table 1. The results show that scaling down the emitter finger width enhances the maximum frequency of oscillation significantly while its effect to the cutoff frequency is very small. Scaling down emitter finger width from 0.25 µm to 0.18 µm and from 0.18 µm to 0.12 µm enhances the peak f_{max} 16 GHz, while scaling down emitter finger width from 0.12 µm to 0.09 µm only enhances peak f_{max} 11 GHz. All of SiGe HBTs have peak cutoff frequency about 60 Ghz while the peak current gain vary from 160 to 150.

Tabel 1: The effects of emitter finger width to the SiGe HBT performances

A_E (µm x µm)	Peak f_t (GHz)	Peak f_{max} (GHz)	Peak β_{dc}
0.25 × 10	59	120	162
0.18 × 10	62	136	169
0.12 × 10	62	152	159
0.09 × 10	63	163	153

After the emitter finger width is scaled down, the total area in the lateral direction of each SiGe HBT is scaled down by reducing base and collector contact width, space between emitter and base contact, space between base diffusion and collector, and the device length. In this work, the emitter finger length is scaled down from 10 µm to 5 µm. The simulation results are shown in Fig. 3. An example of SiGe HBT with 0.09 µm emitter finger width before and after the lateral area is scaled down is shown in Fig. 4.

Simulation results in Fig. 3 show that after the emitter finger width scaling, further scaling the lateral area doesn't affect the peak f_t and f_{max} values, however wider devices have peak f_t and f_{max} at higher collector current I_C. Lateral scaling does not affect the collector emitter breakdown voltage BV_{CEO}.

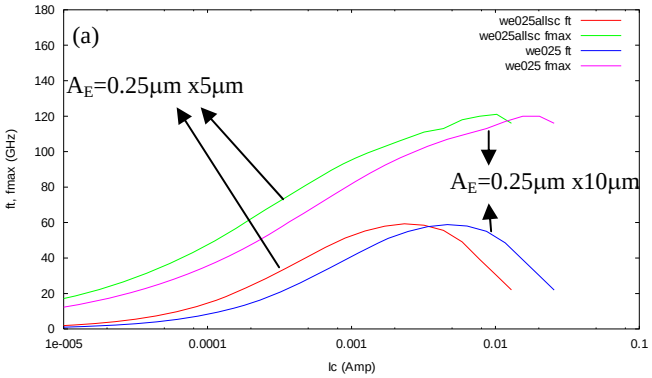

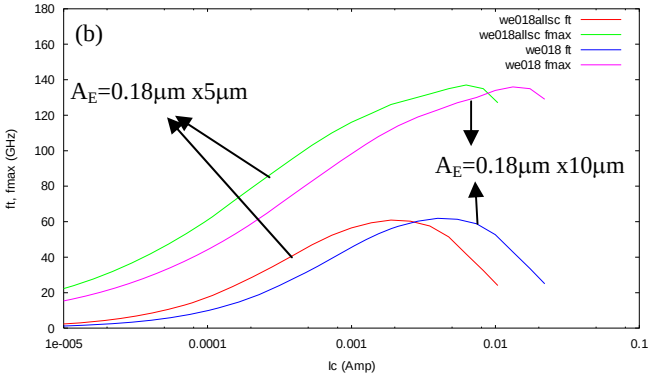

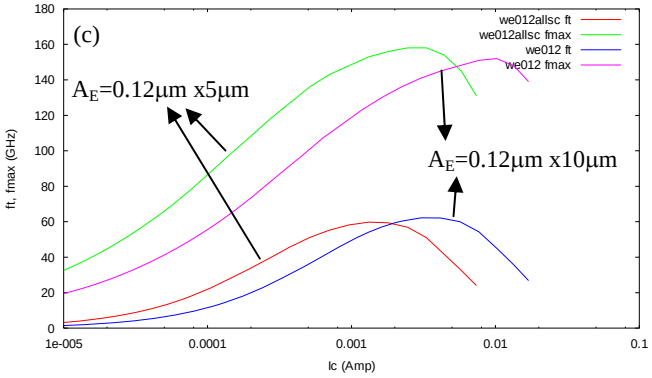

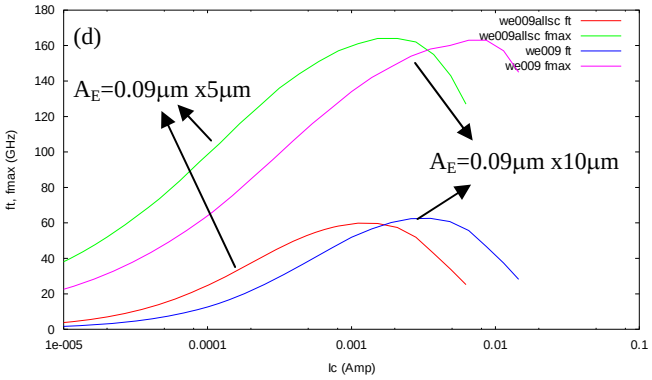

Figure 3: The f_t and f_{max} vs I_C curve of SiGe HBT with different lateral dimension

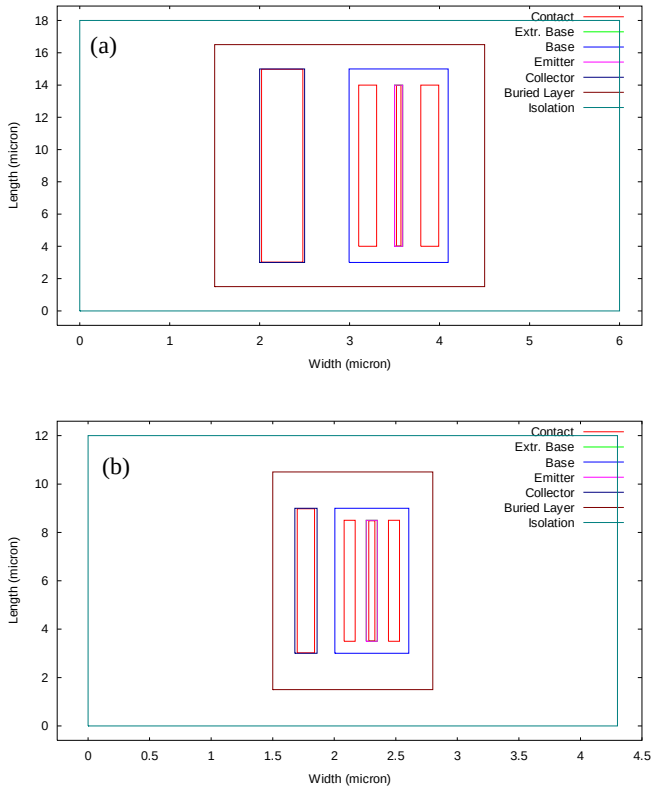

Figure 4: SiGe HBT with 0.09 μm emitter finger width (a) before and (b) after area scaling

3.2 Vertical Scaling

In this work, the vertical scaling is limited to the base width scaling because the base delay is the most dominant delay time in the reference device. As shown in Fig. 5, at the minimum total delay, the base delay component (TBASE) is about twice TRE (delay time due to $r_e \times (C_{je}+C_{jc})$ time constant) or TSCL (delay time due to collector space charge layer transit time). In this work, the base is scaled down from 39 nm to 32 nm which is about 80% from the original base width.

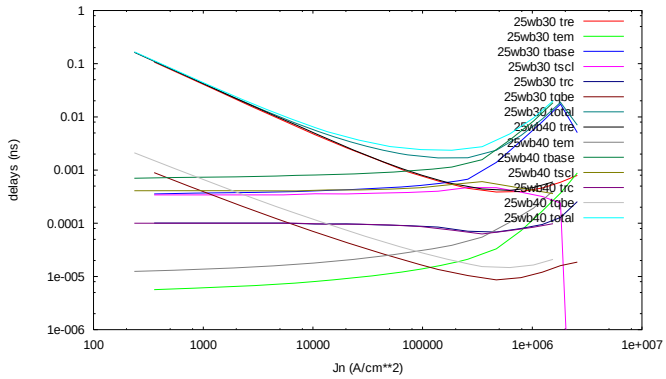

Figure 5: Delay time of SiGe HBTs with base width 39nm and 32nm, A_E=0.25 μm ×10μm.

For SiGe HBT with emitter area A_E = 0.25 μm × 10 μm, reducing base width from 39 nm to 32 nm decreases base delay from 0.76 ps to 0.39 ps and lowered the total delay about 0.6 ps. Simulation results for SiGe HBT with A_E = 0.18 μm × 10 μm, 0.25 μm × 10 μm and 0.25 μm × 10 μm are similar to the SiGe HBT with A_E = 0.25 μm × 10 μm because all of SiGe HBTs have the same the vertical profiles and dimensions. Devices with 32 nm base width have lower total delay time which mean higher cutoff frequencies. Relationship between total delay with cutoff frequency is:

$$f_t = \frac{1}{2\pi\tau_{ec}} \quad (1)$$

where τ_{ec} is the total delay.

The effects of base width scaling to SiGe HBTs performances are summarized in Table 2. All of SiGe HBTs with 32 nm base width have collector emitter breakdown voltage 2.5 V, lower than devices with 39 nm base width. This is happen because when the base width is reduced, the collector doping profile in the base-collector junction is affected.

SiGe HBTs with thinner base have higher current gain because they have higher collector current. This is consistent with the theory:

$$J_C = -\frac{qD_{nB}n_i^2}{N_B W_B}\left\{\exp\left(\frac{qV_{BE}}{kT}\right)-1\right\} \quad (2)$$

where q is the electron charge, D_{nB} is electron diffusion cofficient in the base, ni is intrinsic carrier concentration, N_B is base doping concentration, W_B is base width, V_{BE} is base emitter voltage, k is Boltzmann constant and T is temperature.

For SiGe HBTs with 0.25 μm and 0.18 μm emitter finger width, reducing base width enhance f_{max} about 10 GHz each but has no effect to SiGe HBTs with 0.12 μm and 0.09 μm emitter finger width. For all SiGe HBTs, reducing base width enhance f_t significantly. From Table 2 it is clear that the base width scaling affect wider SiGe HBT more than the narrower devices.

Tabel 2: The effects of base width scaling to SiGe HBTs performances

W_B (nm)	A_E (μm×μm)	Peak f_t (GHz) @ I_C (mA)	Peak f_{max} (GHz) @ I_C (mA)	Peak β_{dc}	BV_{ceo} (V)
39	0.25 × 10	59 @ 4,6	120 @ 15	162	2.8
32	0.25 × 10	80 @ 4.6	130 @ 20	234	2.5
39	0.18 × 10	62 @ 4	136 @ 13	169	2.8
32	0.18 × 10	80 @ 2.6	147 @ 8	217	2.5
39	0.12 × 10	62 @ 3	152 @ 10	159	2.8
32	0.12 × 10	72 @ 3.5	152 @ 10	179	2.5
39	0.09 × 10	63 @ 3.5	163 @ 6.5	153	2.8
32	0.09 × 10	70 @ 2.8	161 @ 6.7	163	2.5

4. CONCLUSIONS

The effects of vertical scaling to the SiGe HBTs with different lateral dimension are reported. The simulation results with Bipole3 show that scaling down the base width yields enhancement in f_t, f_{max} and β_{dc}. Base width scaling has stronger effect to the wider device compared to narrower SiGe HBT.

ACKNOWLEDGMENT

The author likes to thank DP2M Dikti Depdiknas for their sponsorship and Prof. Djoko Hartanto for his support for this work.

REFERENCES

[1] W. Shockley, U.S. Patent 2,569,347, issued 1951.
[2] H. Kroemer, "Theory of a wide-gap emitter for transistors," *Proc. IRE*, vol. 45, pp. 1535-1537, 1957.
[3] S.S. Iyer et al., "Silicon-germanium base heterojunction bipolar transistors by molecular beam epitaxy," *Tech. Dig. IEEE Int. Elect. Dev. Meeting*, pp. 874-876, 1987.
[4] G.L. Patton et al., "75 GHz *fT* SiGe base heterojunction bipolar transistors," *IEEE Elect. Dev. Lett.*, vol. 11, pp. 171-173, 1990.
[5] R.J.E. Hueting, *Charge Carrier Transport in Silicon Germanium Heterojunction Bipolar Transistors*, Ph.D. Thesis, Netherland:Delft University of Technology, 1997.
[6] D. M. Richey, J. D. Cressler, and A. J. Joseph, "Scaling Issues and Ge Profile Optimization in Advanced UHV/CVD SiGe HBT's," *IEEE Trans on Electron Dev.* Vol. 44, No. 3, pp. 431 – 439, 1997.
[7] J. D. Cressler, J. H. Comfort, E. F. Crabbe, G. L. Patton, J. M. C. Stork, Y.-C. Sun and B.S. Meyerson. "On The Profile Design and Optimization of Epitaxial Si- and SiGe-Base Bipolar Technology for 77 K Applications- Part I: Transistor DC Design Considerations," *IEEE Trans on Electron Dev.* Vol. 40 No. 3, pp. 525 – 540, 1993.
[8] E. F. Crabbe, B.S. Meyerson, J.M.C. Stork, and D. L. Harame, "Vertical Profile Optimization of Very High Frequency Epitaxial Si- and SiGe-Base Bipolar Transistors," *IEDM*, pp. 83-86, 1993.
[9] J.-S. Rieh, B. Jagannathan, H. Chen, K. Schonenberg, D. Angell, A. Chinthakindi, J. Florkey, F. Golan, D. Greenberg, S. –J. Jeng, M. Khater, F. Pagette, C. Schnabel, P. Smith, A. Stricker, K. Vaed, R. Volant, D. Ahlgren, G. Freeman, K. Stein, and S. Subbana, "SiGe HBTs with cut-off frequency of 350GHz," *IEDM Tech. Dig.*, pp. 771-774, 2002.
[10] M. Khater, J.-S. Rieh, T. Adam, A. Chinthakindi, J. Johnson, R. Krishnasamy, M. Meghelli, , F. Pagette, D. Sanderson, C. Schnabel, K. Schonenberg, P. Smith, K. Stein, A. Stricker, S. – J. Jeng, D. Ahlgren, and G. Freeman, "SiGe HBT technology with fMAX/fT=350/300 GHz and gate delay below 3.3 ps," *IEDM Tech. Dig.*, pp. 247-250, 2004.
[11] S. Zhang, G. Niu, J. D. Cressler, A.J. Joseph, G. Freeman, and D. L. Harame, "The Effects of Geometrical Scaling on the Frequency Response and Noise Performance of SiGe HBTs," *IEEE Trans on Elect. Dev.* Vol 48 No. 3, pp. 429-435, 2002.

Performance Comparison of rtPS QoS Class on mSIR and WRR Scheduling Algorithms for WiMAX Environment

Fanny Fauzi, Ida Nurhaida, Taryudi, Riri Fitri Sari

Faculty of Engineering
University of Indonesia, Depok 16424
E-mail: fanny.fauzi@ui.ac.id, idariyan@yahoo.com, taryud@yahoo.com, riri@ui.ac.id

ABSTRACT

In the last few years WiMAX technology has become the main topic of discussion between vendor and world telecommunications operator. WiMAX have more capabilities compared with BWA (Broadband Wireless Access) technology and becomes one of challenger of the 3G (third generation cellular system) to fulfill the requirement high-speed access. WiMAX is a very promising technology. The main promises are the high throughput and the large coverage. It is necessary to provide Quality of Service (QoS) guaranteed with different characteristics, quite challenging, however, for Broadband Wireless Access (BWA) networks. Therefore, an effective scheduling is critical for the WiMAX system. Many traffic scheduling algorithms are available for wireless networks, e.g. Weighted Round Robin (WRR) and maximum Signal-to-Interference Ratio (mSIR). Among these conventional schemes, some cannot differentiate services, while some can fulfill the service differentiation with a high-complexity implementation. The focus of this paper is to compare the performance between those two scheduling algorithm, Weighted Round Robin (WRR) and maximum Signal-to-Interference Ratio (mSIR) on the real-time Polling Service (rtPS) QoS Class. WRR scheduling, is an extension of the RR scheduler, is designed to better handle servers with different processing capacities, based on static weights. mSIR is a new scheduler based on the allocation of radio resources to get efficient utilization. rtPS is designed to support real-time service flows that generate variable size of data packets on a periodic basis.

For all new technologies, performance studies are required. The network simulation is considered as a solution to test the performance of technologies and especially the wireless networks. Network Simulator 2 (NS-2) is a widely used tool to simulate wireless networks. To analyze the behavior both of WRR and mSIR scheduling algorithm, we use WiMAX module that run on NS-2. The simulations result in our scenario has figured the hypothesis that mSIR throughput is better than WRR. Some case might have different results, depend on the number of UGS, rtPS and BE users, traffic type and traffic load. Our scenario use propagation model of Two Ray Ground, Omni antenna model, transmits power of 0.025 and frame duration of 0,02s. The number of node is 14 which consists of 1 sink node, 1 Base Station, 9 UGS nodes, 9 rtPS nodes and 2 BE nodes. UDP traffic is used by UGS and rtPS. TCP traffic is used by BE. Performance metrics evaluated in this work is the number of delivered data packets compared with traffic load. Our work shows that using the same traffic load, the mSIR enables more data packets delivered compared with WRR.

Keywords

WiMAX Scheduler, mSIR, WRR, rtPS QoS Class

1. INTRODUCTION

World Interoperability for Microwave Access (WiMAX) is intended to reduce the barriers to widespread broadband access deployment with standards-compliant wireless solutions engineered to deliver ubiquitous fixed and mobile services such as Voice over IP (VoIP), messaging, video, streaming media, and other IP traffic. WiMAX enables delivery of last-mile broadband access without the need for direct Line Of Sight (LOS). It's ease of installation, wide coverage, and flexibility make it suitable for a range of deployment over long-distance and regional networks, in addition to rural or underdeveloped areas where wired and other wireless solutions are not easily deployed and LOS coverage is not possible.

As a complement to the existing Wi-Fi installation base, WiMAX is expected to dramatically increase the availability of wireless connectivity by helping to fill in the broadband gaps between more than 127

million public hotspots and 223 million home-based Wi-Fi networks worldwide. Due to the increasing number of notebook computers, handhelds, and consumer electronics devices combined with WiMAX and Wi-Fi modules, customers will expect more seamless connectivity as they travel in and out of hotspots. Wi-Fi has become nearly a default feature in notebooks, with over 97 percent shipping with integrated Wi-Fi, and an increasing number of handhelds and consumer electronics devices adding Wi-Fi capabilities as well. WiMAX is designed to blanket large metropolitan, suburban, or rural areas with multimegabit per second mobile broadband Internet access. Although the wide-area Internet connectivity offered by 2.5G and 3G cellular data services has been mobile, these services do not provide the broadband speeds to which users have become accustomed to which can be delivered by WiMAX. Theoretically, the coverage range can reach 30 miles and the throughput can achieve 75 Mbit/s. Yet, in practice the maximum coverage range observed is about 20 km and the data throughput can reach 9 Mbit/s using User Datagram Protocol (UDP) and 5 Mbit/s using File Transfer
Protocol (FTP) over Transmission Control Protocol (TCP). The theoretical values do not always reflect the reality.

The WiMAX Forum Applications Working Group (AWG) has determined five initial application classes, listed in Tabel 1. Initial WiMax Forum Certified systems are capable of supporting these five classes simultaneously. The following is the classes:

- **Unsolicited Grant Service** (**UGS**) is used for real-time services like T1 and E1 lines, and for VOIP services with fixed packet sizes.
- **Real Time Polling Service (rtPS)** is used for real-time services such as streaming video. This offers a variable bit rate, but with a guaranteed minimum rate and guaranteed delay. Another example where this could be used is in enterprise access services. It is quite popular for fixed wireless operators (or WISPs) to guarantee E1/ T1-type data rates with wireline-equivalent SLAs, but to allow customers to burst higher if and when there is extra capacity on the network. This is quite a successful strategy for wireless operators competing against incumbent wireline providers.
- **Enhanced Real-Time Polling Service (erTPS)** is specified in 802.16e, and will be used for VOIP services with variable packet sizes as opposed to fixed packet sizes – typically, where silence sup- pression is used. This will include applications such as Skype – and partly explains why 802.16e equipment is not as good at supporting VOIP without vendor-specific tweaks to the standard MAC

Tabel 1. 802.16 QoS Classes [5]

Class	Description	Minimum rate	Maximum rate	Latency	Jitter	Priority
Unsolicited Grant Service	VOIP, E1; Fixed-size packets on periodic basis		x	x	x	
Real-Time Polling Sevice	Streaming audio/video	x	x	x		x
Enhanced Real Time Polling Service	VOIP with activity detection	x	x	x	x	x
Non-Real-Time Polling Service	FTP	x	x			x
Best-Effort	Data transfer, Web browsing, etc		x			x
X = QoS specified						

- **Non-Real-Time Polling Service (nrtPS)** is for services where a guaranteed bit rate is required, but guaranteed delay is not. This might be used for file transfer, for example.
- **Best-Effort** (**BE**) is the old standby for email and browsing and so forth, and is largely what people have on a DSL line at home today.

The objective of this paper is to provide differentiated services according to their QoS requirements, especially rtPS QoS class. Our extensive simulation showns that the proposed scheduling algorithm to enhance the throughput, and distinguishes the services in terms of the average delay. Therefore, we implemented the proposed scheduling used for rtPS QoS class by showing the simulation results.

2. THE WiMAX SCHEDULING ALGORITHMS

Scheduling algorithms serve as an important component in any communication network to satisfy the QoS requirements. The design is especially challenged by the limited capacity and dynamic channel status that are inherent in wireless communication systems. To design MAC layer protocol which can optimize the system performance, the following features and criteria should be concerned.

- Bandwidth utilization
  Efficient bandwidth utilization is the most important in the algorithm design. The algorithm must utilize the channel efficiently.
- QoS requirements

The proposed algorithm should support different applications to exploit better QoS. To support delay-sensitive applications, the algorithm provides the delay bound provisioning. The long-term throughput should be guaranteed for all connections when the sufficient bandwidth is provided.

- Fairness
  The algorithm should assign available resource fairly across connections. The fairness should be provided for both short term and long term.
- Implementation complexity
  In a high-speed network, the scheduling decision in making process must be completed very rapidly, and the reconfiguration process in response to any network state variation. Therefore, the amount of time available to the scheduler is limited. A low-complexity algorithm is necessary.
- Scalability
  The algorithm should operate efficiently as the number of connections or users sharing the channel increases.

In downlink operation, packets arrive from the network at the base station are placed in downlink user traffic queues. The scheduler decides which user traffic to map into a frame from the queues, and the appropriate burst is generated, together with the appropriate MAP information element. Users are scheduled according to their service classes (UGS, rtPS, ertPS, nrtPS, and BE). MAPs contain information on transmission to/from all users for each frame, including modulation and coding type, and size and position of allocation. The description of WRR scheduling and mSIR scheduling techniques that we use in this simulation is presented in the following.

2.1. Weighted Round Robin

Round-robin (RR) is one of the simplest scheduling algorithms for processes in an operating system, which assigns time slices to each process in equal portions and in circular order, handling all processes without priority. Round-robin scheduling is both simple and easy to implement, and starvation-free. Round-robin scheduling can also be applied to other scheduling problems, such as data packet scheduling in computer networks.

The **Weighted Round-robin** (WRR) scheduling, as an extension of the RR scheduler, is designed to better handle servers with different processing capacities. Each server can be assigned a weight, and an integer value that indicates the processing capacity. Servers with higher weights receive new connections before those with less weight, and servers with higher weights get more connections than those with less weights and servers with equal weights get equal connections. The weighted round-robin scheduling is better than the round-robin scheduling, when the processing capacity of real servers are different. However, dynamic load imbalance among the real servers if the loads of the requests vary highly. In short, there is the possibility that a majority of requests requiring large responses may be directed to the same real server. Actually, the round-robin scheduling is a special instance of the weighted round-robin scheduling, in which all the weights are equal.

2.2. Maximum Signal-to-Interference Ratio (mSIR)

A cellular network divides a region into cells (or zones) to process calls. Each cell has an antenna to receive and answer your call. The antenna is often on a pole with other communication equipment called a base station. The network determines which cell a mobile user is in, assigns a communication channel, and monitors the strength of the signal using the cell base station. When a user approach the boundary of the cell, the neighboring cell's base station, which has also been monitoring the signal, will switch the channel to one in that cell. This is sometimes called "handing off" the call. There are two base station antennas that are transmitting a signal of equal power to the phone; the primary base station of the cell in which the car is moving and a secondary base station in the neighboring cell the car is approaching. The signal from the secondary station causes interference with the signal from the primary station resulting a degradation of the cell phones capabilities. Thus the power of the signal received by the cell phone varies as the car moves along.

An uplink signal-to-interference ratio for each of multiple mobile radio terminal connections supported in a cell in a cellular communications system is estimated. A signal-to-interference ratio error is determined for selected ones of the estimated uplink signal-to-interference ratio. The **signal-to-interference ratio** (SIR) is the quotient between the average received modulated carrier power *S* or *C* and the average received co-channel interference power *I*, i.e. cross-talk, from other transmitters than the useful signal. From the explanation above we can make a definition :

 (1)

Where,
Pr = Power of the received signal
L = Distance from the phone
This formula applies to both the primary base station as well as the secondary base station.

$$SIR = \frac{Pr1}{Pr2} \quad (2)$$

Where,

SIR = Signal to interference ratio
Pr1 = Power of received signal from primary station
Pr1 = Power of received signal from primary station

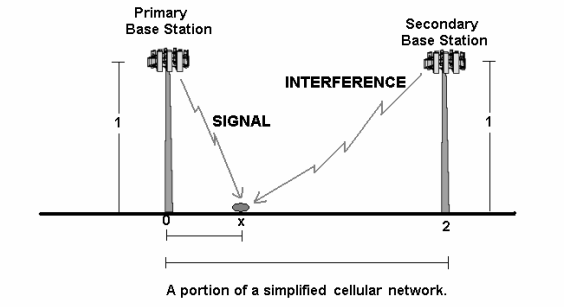

Figure 2. The simplified model for illustration [6]

The height of the antennas and the distance between base stations, both the power of the received signals and hence the signal-to-interference ratio can be computed. The goal is to determine the location x of the cell phone so that the signal-to-noise ratio is maximized.

In this project, we use the maximum Signal-to-Interface Ratio (mSIR) scheduler. This method work on radio allocation resources to subscriber stations which have the highest Signal-to-Interference Ratio (SIR). This scheduler also allows the highly efficient utilization of radio resources.

3. DESIGN AND IMPLEMENTATION SCHEDULING ALGORITHMS

In our work, we have compiled implemented WiMAX module *patch-QoS-WiMAX_prerelease-10-27-2008* and *QoS-includedWiMAX_27.10.2008.tar.gz* on NS-2 version 2.29 running on Linux Kernel 2.6. The module represents the scheduling algorithm that compared between WRR and mSIR. The mSIR scheduler is implemented the following scenario; one Sinknode via the BS sorts the SS according to their received SIR. The traffic that has the best SIR will be served first, until all the symbols are allocated.

WRR algorithm is implemented on a scenario on which according to the weights of the different SSs, the BS determines the SS that will be served. If there are still remaining symbols, the BS serves the next SS until all the symbols are allocated.

For the rtPS connections, the BS allocates periodic unicast request opportunities and then, according to these requests, the symbols needed for the rtPS connections. If the BS allocates unicast request opportunities and resource grants for rtPS connections in the same frame, the BS cannot immediately take into account the new length of the uplink data connection of the subscriber. The reason is that the BS allocates symbols for rtPS connections before receiving the latest unicast bandwidth request.

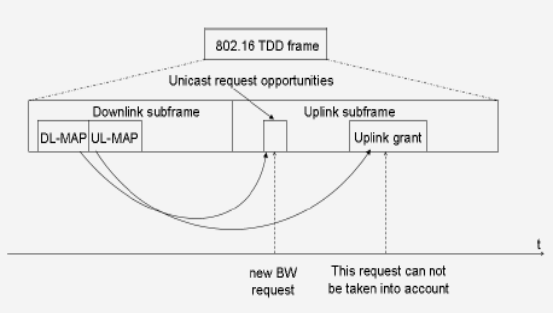

Figure 3.Allocation of symbol for rtPS connection [7]

Moreover, the mSIR scheduler serves those subscribers having the highest SIR at each frame. Therefore, subscribers with a slightly smaller SIR may not be served and then the mean delay to deliver data increases. The patch-QoS-WiMAX_prerelease-10-27-2008 module is modified the mSIR scheduler in order to decrease the mean time of sojourn. The mean sojourn time is the average time a data packet spends from its generation to its delivery at destination.

4. SIMULATION RESULT

4.1. Simulation Overview

As with many digital modulation schemes, the constellation diagram is a useful representation. In QAM, the constellation points are usually arranged in a square grid with equal vertical and horizontal spacing, although other configurations are possible (e.g. Cross-QAM). Since in digital telecommunications the data are usually binary, the number of points in the grid is usually a power of 2 (2, 4, 8 ...). Since QAM is usually square, some of these are rare—the most common forms are 16-QAM, 64-QAM, 128-QAM and 256-QAM. By moving to a higher-order constellation, it is possible to transmit more bits per symbol. However, if the

mean energy of the constellation is to remain the same (by way of making a fair comparison), the points must be closer together and are thus more susceptible to noise and other corruption; this results in a higher bit error rate and so higher-order QAM can deliver more data less reliably than lower-order QAM, for constant mean constellation energy.

64-QAM and 256-QAM are often used in digital cable television and cable modem applications. In the US, 64-QAM and 256-QAM are the mandated modulation schemes for digital cable (see QAM tuner) as standardized by the SCTE

Tabel 2. Main parameters of the simulation model [8]

Parameter	Values
Frame duration	20 ms
Propagation Model	Two Ray Ground
Antenna Model	Omni antenna
Antenna height	1.5 m
Transmit power	0.025
Receive power threshold	$2025e^{-12}$
Carrier sense power threshold	0.9*Receive power threshold

(Society of Cable Telecommunication Engineer) in the standard ANSI/SCTE 07 2000. It is also known as QAM-64 and QAM-256. In the UK, 16- QAM and 64-QAM are currently used for digital terrestrial television (Freeview and Top Up TV).

Communication systems designed to achieve very high levels of spectral efficiency usually employ very dense QAM constellations. One example is the ITU-T standard for networking over existing home wiring (coaxial cable, phone lines and power lines), which employs constellations up to 4096-QAM (12 bits/symbol).

For simulation purposes, we integrate not only both WRR and mSIR scheduler into NS-2 module but also QoS Parameter and rtPS services classes. The main parameter are given in Tabel 2. In our simulation, there are nine UGS, two BE, and nine
rtPS connections using 16QAM3/4. Since the mSIR scheduler provides high throughput with a good SIR then we assume that the rtPS connection can use 16QAM3/4.

4.2. Simulation NS-2

As mention in simulation overview, our scenario consists of 9 UGS nodes, 9 rtPS nodes and 2 BE nodes. The reason of simulating QAM is because according to the WiMAX module, mSIR scheduler provides high throughput, lot of nodes (create-god 22) only can be run in QAM modulation, not in QPSK. Based on that condition we choose 16QAM3/4 as option in our scenario. The Network Animator (NAM) shown in Figure 4.

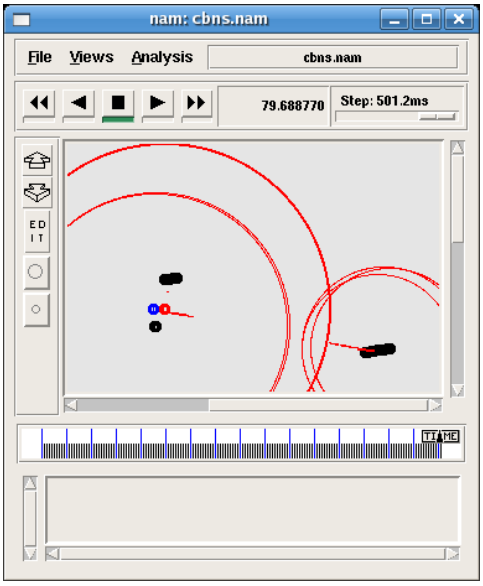

Figure 4. Network Animator (NAM) consists of nine UGS nodes, nine rtPS nodes and two BE nodes, one SinkNode and one Base Station

Tabel 3. Description of approach in NS-2 (WiMAX module) based on table 2

Characteristic	Values
Frame duration Mac/802_16 set frame_duration_ 0.020	20 ms
Propagation Model set opt(prop) Propagation/TwoRayGround ;# radio-propagation model	Two Ray Ground
Antenna Model set opt(ant) Antenna/OmniAntenna ;# antenna model	Omni antenna
Transmit power Phy/WirelessPhy set Pt_ 0.025 ;#transmit power	0.025
Receive power threshold Phy/WirelessPhy set RXThresh_ 2.025e-12 ;#500m radius	$2025e^{-12}$
Carrier sense power threshold Phy/WirelessPhy set CSThresh_ [expr 0.9*[Phy/WirelessPhy set RXThresh_]]	0.9*Receive power threshold

Throughout this simulation's throughput is computed as follows:

$$\text{Throughput} = \sum_{i=r_n}^{i=r_{n-1}} \text{Packet Size}; 0 \leq n \leq t \quad (3)$$

Throughput Graph Result (QAM Modulation, 9 UGS nodes, 9 rtPS nodes and 2 BE nodes) between mSIR – WRR can be seen in Figure 5.

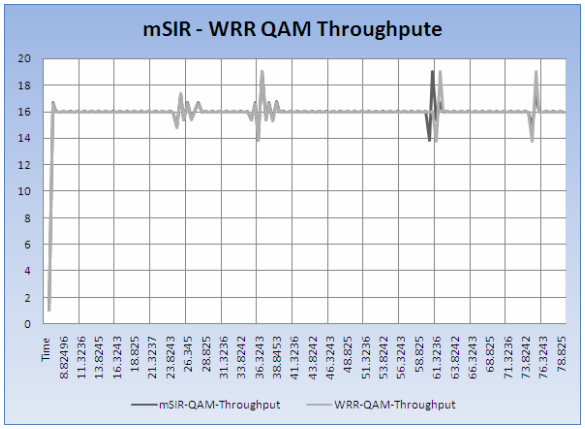

Figure 5. Throughput mSIR – WRR in XGraph

Jitter2 vs Received Time Graph Result mSIR-WRR can be seen in Figure 6.

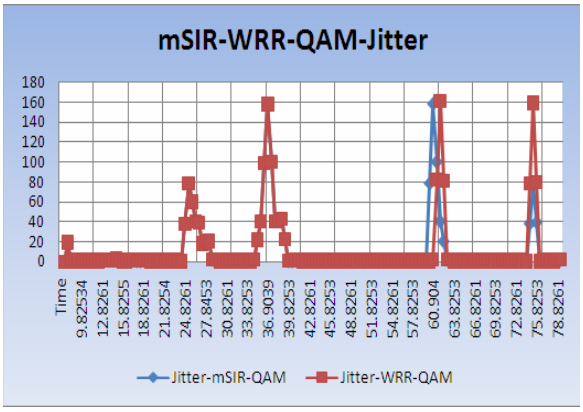

Figure 6. Jitter vs Received Time mSIR – WRR in XGraph

The graph shown in Figure 5 (according to our scenario, QAM Modulation, 9 UGS nodes, 8 rtPS nodes and 2 BE nodes) shows that (based on current time) mSIR deliver packets faster than WRR.

Throughput Graph Result (QPSK Modulation, 2 UGS nodes, 2 rtPS nodes and 2 BE nodes) between mSIR – WRR can be seen in Figure 7.

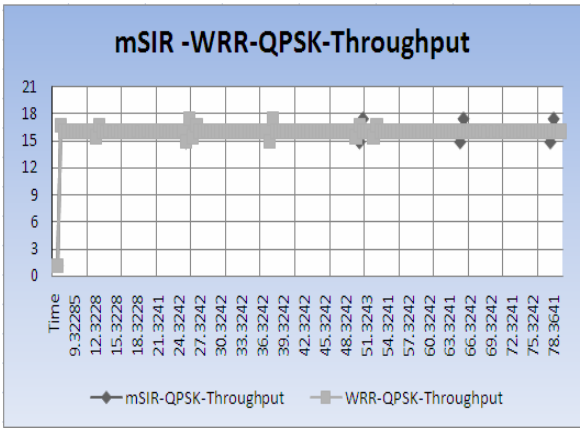

Figure 7. Throughput mSIR – WRR in XGraph

Jitter2 vs Received Time Graph Result mSIR-WRR can be seen in Figure 8.

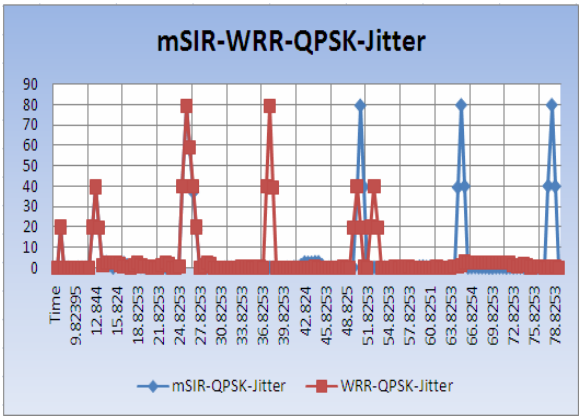

Figure 8. Jitter vs Received Time mSIR – WRR in XGraph

The graph shown in Figure 7 (according to our scenario, QPSK Modulation, 2 UGS nodes, 2 rtPS nodes and 2 BE nodes) shows that (based on current time) WRR deliver packets faster than WRR.

5. CONCLUSION

In this paper, we presented the behavior of WiMAX scheduling algorithms in rtPS schedulers. We based our work on the network simulation and implemented WiMAX module such as WRR and mSIR

scheduling, taking into account the QoS classes and its requirements. Algorithms compared are from different approaches so that all available approaches can be covered which can be useful guide for further research in this field. We have tabulated the different parameters on which QoS algorithms can be compared, which will be useful for developing new QoS algorithms. Our future work will be to implement an algorithm and suggestion for improving its performance in term of delay, throughput and other QoS.

According to throughput and jitter that we have from the simulation, to define what scheduler appropriate in certain case, we have to look amount of nodes, and some case depend on traffic load and traffic type.

REFERENCES

[1] Belghith Aymen, Nuaymi Loutfi, "Comparison of WiMAX scheduling algorithms and proposals for the rtPS QoS class",14th European Wireless 2008, EW2008, pages 1-6, Prague, Czech Republic, 22-25 June 2008

[2] Belghith Aymen, Nuaymi Loutfi, and Maille Patrick,"Pricing of differentiated-QoS services WiMAX Networks", IEEE Global Communication Conference, IEEE GLOBECOM 2008, Pages 1-6. New Orleans, LA, USA 30 November – 4 December 2008

[3] Belghith Aymen, Nuaymi Loutfi, "Design and Implementation of a QoS-included WiMAX Module for NS-2 Simulator",, *SIMUTools* 2008, March 3-7, 2008, Marseille, France Copyright 200X ACM 978-963-9799-20-2.

[4] The Design and Implementation of WiMAX module for ns-2 Simulator: http://ndsl.csie.cgu.edu.tw/wimax ns2.php

[5] http://www.friendspartners.org/utsumi/Global_ University/Global%20University%20System/Southwest%20Asia/Palestine_Gaza%20Strip_&_West%20Bank/Infrastructure/WiMAX__FINAL_REPORT_Dr%5B1%5D._Harazeen%20copy.pdf (last access: june 01 2009)

[6] http://mathdemos.gcsu.edu/mathdemos/ cellsir/cellsir.html (Last access: june 01 2009)

[7] Belghith Aymen, Nuaymi Loutfi, "Comparison of WiMAX scheduling algorithms and proposals for the rtPS QoS class"

[8] Comparison of WiMAX scheduling algorithms and proposals for the rtPS QoS class Aymen Belghith, Loutfi Nuaymi

ISSN 114-1284

Economic Analysis of Mobile Mining Fleet Replacement Using Mean Time Between Failure A Framework

Farizal

Faculty of Engineering
University of Indonesia, Depok 16424
Tel : (021) 7270011 ext 51. Fax : (021) 7270077
E-mail : farizal@ie.ui.ac.id

ABSTRACT

Mining companies rely heavily on their fleets for their operation (production). However, unfortunately, many time they are facing difficult decisions whether to continue to use their old equipments or replace them with the new ones. Fleets in mining work at dynamic environment that changing with time. Several approaches have been used to determine the replacement age for the mining fleets. On this paper, we propose to utilize mean time between failure, MTBF. We argue that this measure is a good approach to represent the utilization of the fleets and the site. Thus, it will give a more realistic replacement age.

Keywords
replacement analysis, MTBF, mining, fleet

1. INTRODUCTION

There are basically two models of replacement analysis in industry. The first one is defender-challenger model. This model involves determining whether to continue to use the old asset (usually called as the defender) or to replace the existing asset with the new one (called as the challenger). This type of studies happen on situation when a company wants to install new facilities due to new technology advancement, or makes new products that require using new machines, or increases production lines which can be achieved by using bigger capacity equipments. The second model of replacement analysis involves determining in advance the economic life of an asset. This type of studies happens when setting up a new venture (with new facilities) or on a situation where there is no significant advancement of technology; meaning that there is no challenger on the analysis. Fleet replacement in mining industry belongs to this second line of study.

Mining is a kind of industry that requires high intensive capital. The industry uses many kinds of heavy equipments such as draglines, excavators, bulldozers, dump trucks, and so on to exploit the ore. Productivity of a miner depends on these assets.

Fleets in mining work at dynamic environment that changing with time. Not like their counterpart, non mining fleet which is utilized in almost similar environment during their useful life time, fleet in mining facing a more challenging environment as the time elapses. As the time goes by the workload increases (the environment changing; the mine getting deeper) till the miners move to a new place. At this point the work load is started normal and the pattern is repeated. The workload as a function of time resembles ripple pattern (Figure 1). This factor should be taken into consideration when analyzing replacing the fleet.

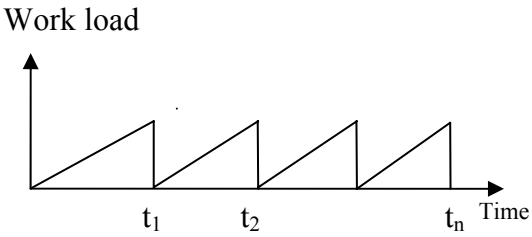

Figure 1: Work load vs time

The complex nature of the machineries and the environment where they are operated makes the management and maintenance of these assets a difficult task. In addition, the costs associated with running and maintaining these trackless fleets are substantial. However, effective management of the assets have not been fully understood or addressed by the miners. For instance the costs increases from older machines are not well understood (or quantified) thus accumulated to a big portion of hidden and/or known costs.

In this study, we proposed a new approach that uses mean time between failures as a measure to represent the pattern. We argue that this method is much better than using old one. The logic is as the work load increases the number of failures increases. As well the machines getting older the number of failures increases. Before we describe the approach, this paper will explain the methods that used in mining fleet replacement followed by the

challenge/difficulties surrounding the issue. The paper is closed by citing conclusions.

2. METHOD TO DETERMINE FLEET ECONOMIC OF LIFE

Several methods are utilized, four most common one are elaborated here:

1. Theory of Depreciation

Depreciation is the decrease in value of (physical) assets with the passage of time. Depending on the method of depreciation used the life of the assets is determined at the end of depreciation; meaning that replacement occurs when the book value of the asset is zero. This replacement method is easy, thus becomes a favorite one to be used albeit it has no solid ground and the replacement point can be unlimited. Depreciation is actually an accounting concept that mainly used to determine income tax instead of determining productive life of an asset.

2. Theory of vehicle replacement.

This method is basically based on the trade-off between decreasing capital cost and increasing running costs. As the age of the equipments increases the capital cost per unit time decreases. Considering only the capital cost, one will use the equipment as long as possible to minimize the capital cost. However, the older the machines the higher its running costs. The optimal time to replace the equipment, is then the point where the total cost is minimum.

3. Cost per ton trends

This approach uses the total machine costs divided by the number of tons a machine produces. It is based on the principle that as a machine ages, the running costs increase and as the availability of the machine decreases, the tons are reduced, hence increasing the cost per ton. The minimum cost per ton is the optimal replacement point. In a sense, this method uses a similar methodology of a cost-benefit or payback analysis. Cost per ton trends is very appropriate to use since the purpose of the machine is to produce tons, thereby, using this measure as a financial indicator. However information about the tons produced is required and often not available

4. Equivalent annuity Cost (EAC)

EAC methodology is commonly applied to replacement problems. This method looks at the cash flows associated with the machine and the times in which they are incurred. It uses the time value of money concept to compare different timing alternatives. This method is very powerful and is an accepted asset appraisal method, although it is commonly not easily understood and hence accepted

Theoretically, in any given year, total EAC has two components, i.e. EAC of capital and the EAC of operations and maintenance. The relationship is expressed as $EAC_t = EAC_{Cap,t} + EAC_{O\&M,t}$

$EAC_{Cap,t}$ is the component of cost associated with the capital in year t. The amount is based on the initial investment and subsequent depreciation of the asset, yielding a residual value at the end of year t. The $EAC_{Cap,t}$ curve is downward sloping, producing a lower value over time. In some instances, the curve decreases to a level which indicates that the salvage value of the underlying asset is equal to its scrap value.

$EAC_{O\&M,t}$ is the cost of operating and maintaining the vehicle in year t. Operational costs include labor, fuel, lubricants, electricity, supervision, insurance and so forth. Maintenance costs typically consist of labor, spares and costs associated with third parties – for example, subcontracted maintenance crews and service companies. Maintenance and operating costs can be divided into three parts: direct costs, indirect costs and administrative costs. As mentioned previously, the cost of operating and maintaining a vehicle tends to increase as it gets older.

The correct derivation EAC, which ultimately calculates the economic life of equipment, relies on the inclusion of all costs related to its replacement. However, the calculation should only include those costs which are related to the use of a particular machine or vehicle. Overhead costs such as administrative costs are irrelevant as they do not bear a direct or indirect correlation to the age of the vehicle.

The EAC methodology is a straightforward decision principle which is based on the shape of the total EAC curve: replace the equipment or machine whenever EAC_t reaches its minimum point. Figure 2 illustrates the likely shape of the $EAC_{Cap,t}$ and $EAC_{O\&M,t}$ curves as well as the resultant EAC_t

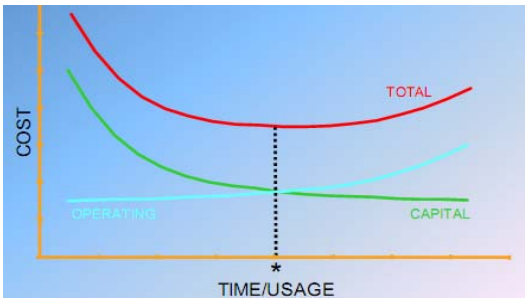

Figure 2: EAC against equipment life.

A policy which anticipates or delays equipment replacement decisions so that it diverges from the minimum value of the EAC_t curve is necessarily suboptimal and leads to a loss of value. In practice, of course, the decision is not often quite as direct. There are cases where the curvature of the EAC_t schedule rests only briefly at its minimum and other cases where the minimum point occurs over an interval. Here, the EAC decision principle is subject to an indifference zone; that is, the replacement of one vehicle for another can take place at any point during this interval. Where the decision to replace equipment is unclear, management may consider practical limitations such as budget restrictions to establish the optimal replacement time within this period of indifference.

3. THE CHALLENGE ON THE FIELD

Number of factors exist on the field that need to be included in the replacement decision. Some of which are relatively simple to calculate and others which prove somewhat more difficult. Some of the reasons include the fact that the parameters themselves can be difficult to quantify, over and above the lack of data, quality of these data or the format of the data available. A challenge in developing an appropriate model is to retrieve and use realistic and representative data in the absence of accurate quantitative information. The aim is to quantify the causes—factors influencing the replacement decision. This can be done by looking at the effects that are assumed to be representative of the causes, in this case the costs of running machines and the machine availability.

Another challenge with the mining replacement is difficulty to standardize the process since the operation environment is different and continuously evolved. For instance, the capacity and life-span of equipment differ significantly from those suggested by the supplier. Furthermore, it is reasonable to assume that two identical haulage trucks operating in different mines of varying characteristics have different economic lives. For instance dump trucks use at an open pit is different with dump trucks use at close pit. however, the to the equipments mobility, the number of fleets, and the environment complexity, it is almost impossible to manage such kind of asset.

The relevant indicator of economic life is not equipment availability, rather, it is equipment utilization – that is, the percentage of time in which the equipment remains operating. Idle time such as pauses, delays due to shift changes, temporary mine closure as a result of blasting and so forth, are deducted from the equipment's total available time. This reflects a clear shift from physical to economic life cycles. However, EAC theory refers to asset utilization which is not necessarily equal to calendar years.

4. PROPOSED APPROACH

Mean time between failures (MTBF) is the expected time of failure rate. The MTBF is for a repairable system. The model assumes the failed system is immediately repaired (zero elapsed time). Contrast to the mean time to failure (MTTF) which measures average time between failures with the modeling assumption that the failed system is not repaired. MTBF is calculated in term of its density function *f(t)* as:

$$MTBF = \int_0^\infty t\ f(t)\,dt \qquad (1)$$

with $$\int_0^\infty f(t)\,dt = 1 \qquad (2)$$

Assuming that all the failures have equal probability to occur, MTBF can be defined as the arithmetic mean (average) time between two consecutive failures and equation (1) can be calculated as:

$$MTBF = \sum_{i=1}^{n} \frac{(Downtime_{\ i+1} - Downtime_{\ i})}{n} \qquad (3)$$

Example: an equipment that can be repaired when there is a failure is used. The first failure (D_1) happens at 10 hours and it takes 2 hours to fix. The second failure (D_2) is at 19 hours and the repair duration is 3 hours. Then after working for 5 hours, the system fails at 27 hours (D_3). The repair lasts for 4 hours and the system is restored at 31 hours (see figure 3).

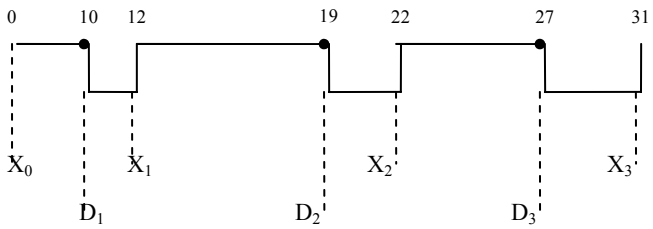

Figure 3: Failure and Repair Process for a Repairable System without Scheduled Replacements

Using equation (3), the MTBF = ½ (9 + 8) = 8.5 hours, if we use only the observations of 2 complete cycles. If we consider all the cycles, then the MTBF = ⅓ (9 + 8 + (D_1 - x_0) + (x_3 - D_3)) hours.

MTBF of a system usually depends on time, with the rate varying over the life cycle of the system. MTBF of a system, for instance an automobile, will be smaller as it grows older. MTBF in its fifth year of service may be many times smaller than its MTBF during its first year of service; one will not expect failure for a brand new automobile. This means as the equipment getting older, its operational period ($D_{i+1} - x_i$) will be shorter. On the contrary, as the equipment getting older, its repair time ($x_i - D_i$) getting longer. This condition due to more components need to be fixed as well the intensity of the failure is getting more serious resulting with more time to repair.

Reliability is defined as the probability that the product will perform its intended function, for a required period of time within a certain environment. Reliability is a function of MTBF with the relation:

$$R = 1 - F = 1 - \frac{1}{MTBF} \qquad (4)$$

Equation (4) indicates that MTBF is also environment

dependent. This property fits well to be used for mining industry since as mentioned earlier on the introduction, fleets in mining work at dynamic environment that changing with time. Figure 1 shows that as the time goes by the workload increases (the environment changing; the mine getting deeper) till the miners move to a new place.

Reliability Estimation Methods

MTBF can be estimated thru measuring the field data or using reliability information of similar equipments.

Similar Item Prediction Method

Similar item prediction method is based on historical reliability data of similar item to estimate an equipment. Its effectiveness mostly depends on how similar the new equipment is to the existing item which field data is available. Similarity should exist on the aspects of manufacturing processes, operating environments, product functions and designs. This method is especially useful for products that follow an evolutionary path, since it takes advantage of the past field experience. However, differences in new designs should be carefully investigated and accounted for in the final prediction. Since the method relies on the similarity of the two equipments, it can be used as a quick means for estimating reliability. This method is applicable on mining industry since mining fleet technology is very much the same.

Field Data Measurement Method

The field data measurement method is based on the actual field experience of products. This method, often referred to as Reliability Growth Management, is perhaps the most used method by manufacturers since it is an integral part of the manufacturers' quality control program. Because it is based on real field failures, this method accounts for failure modes that prediction methods sometimes miss. The method consists of tracking a sample population of new products and gathering the failure data. Once the data is gathered, the failure rate and MTBF are calculated. The failure rate is the percentage of a population of units that are expected to "fail" in a calendar year.

5. CONCLUSION

1. Methods have been developed for mining fleet replacement analysis do not take into consideration the ever-changing environment where the fleets are worked, even though this character is the one that differentiates mining industry with other industries. MTBF better fits for the purpose since the concept inherently includes the environment aspect.
2. One challenge in mining fleet replacement analysis is data collection. MTBF is relatively easier to use than methods explained on part 2. Data collected is simple as well the mechanism to record. Method such as similar item prediction and field data measurement can be used here.

REFERENCES

Bethuyne, G. (1998). *Optimal Replacement Under Variable Intenstity Of Utilization And Technological Progress*. The Engineering Economist, 43(2), page 85-106

Canada, J.R, W.G. Sullivan, and J.A. White, Capital Investment Analysis for Engineering and Management, 2nd ed. Prentice Hall, Inc. 1996

Dobs, Ian M. *Replacement Investment : Optimal Economic Life Under Uncertainty.* England: Department of Accounting and Finance

Farizal and E. Nikolaidis, 2007, "Assessment of Imprecise Reliability Using Efficient Probabilistic Reanalysis," SAE Special Pu blication SP-2119, paper 2007-01-0552, pp. 71-88

Galisky, Ron and Ignacio Guzmán. (2008). *Optimal Replacement Intervals for Mining Equipment: A CRU Model To Improve Mining Equipment Management.* CRU Strategies

MIL-HDBK 217F Notice 2, Reliability Prediction of Electronic Equipment, 28 February 1995

Mondro, M.J. (2002), Approximation of Mean Time Between Failure When a System Has Periodic Maintenance, *IEEE Transaction on Reliability* 51(2): 166-167

Nurock, D and Porteous, C. (2008). *Methodology to determine the optimal replacement age of mobile mining machine.* Third International Platinum Conference '*Platinum in Transformation'*. The Southern African Institute of Mining And Metallurgy

Torell, W and V. Avelar, Mean Time Between Failure: Explanation and Standards, White Paper #78, APC Legendary Reliability 2004

Xie, M, Y-S Dai, and K-L Poh, Computing System Reliability Models and Analysis, Kluwer Academic Publishers, 2004

Design of Voice Authentication System Using Mel Frequency Cepstral Coefficient (MFCC) and Hidden Markov Model (HMM)

Fetty Amelia [a)], Hestu Waskito [b)], Theresia Natalia [c)], and Surya Darma [d)]

[a] *National Crypto Institute, Bogor, Indonesia 16330*
Tel: (0251)542021. Fax: (0251)541825
E-mail : Fetty_Amelia2003@yahoo.com
[b] *National Crypto Institute, Bogor, Indonesia 16330*
Tel: (0251)542021. Fax: (0251)541825
E-mail : hestupotter@yahoo.com
[c] *National Crypto Institute, Bogor, Indonesia 16330*
Tel: (0251)542021. Fax: (0251)541825
E-mail : re_lia2005@yahoo.com
[d] *Department of Physics, FMIPA, University of Indonesia, Depok 16424*
Tel: (021)7270160 ext.258. Fax: (021)7863441
E-mail : suryadarma@ui.ac.id

ABSTRACT

The rapid expansion of science and technology has given a lot of effect in human life, including the information technology. However, it will bring some threats. One of those threats is there would be someone impersonates to get the illegal access. The authentication system can be a solution for this problem. The most popular authentication technique is the use of username and password. But that technique has a lot of weaknesses, for example, password can be forgotten, and compromised. Password chosen can also be weak so people can guess it easily. Therefore biometric can be a solution of problems related to the authentication technique using password.

Biometric authentication relies on any automatically measureable physical characteristic or personal trait that is distinctive to an individual. The biometric process consists of two features, the feature extraction and the feature matching. In this paper, the input system is a voice signal that will be processed with digital signal processing to get a real number that can represent an individual characteristic using the MFCC method. The real number is stored in the database. Someone who will try to get the access must give their voice as an input. The input will be extracted and compared with the values in database. If they are equal, then access will be granted, and if they are not, the access will be denied.

MFCC is used in feature extraction because it is the best known and most popular extraction method. MFCC is best on the known variation of the human ear's critical bandwidths with frequency. Hidden Markov Model is used in feature matching to compare the voice input and the values that have been stored in database. HMM is used so that the matching process can be optimized. The combination of both processes is expected to be the alternative solution in order to increase the quality of authentication system that using voice biometric.

Keywords

Biometric, voice authentication, MFCC, HMM.

1. INTRODUCTION

Authentication technique typically used by inputing a keyword or a password. Such a technique is very common in used because of its easy to use and process. But as many problems occurs become weakness of this technique, i.e, one can easily forget, lost or stolen the password. Other possibilities are the choosen of the passwod itself can be easily guess by other people, using the same password for diffrent systems or using the previous password which has been used before.

Speech is one of the natural forms of communication. Recent development has made it possible to use it in the security system. In speaker identification, the task is to use a speech sample to select the identity of the person that produced the speech from among a population of speakers. In speaker verification, the task is to use a speech sample to test whether a person who claims to have produced the speech has in fact done so [4].

This technique makes it possible to use the speaker's voice to verify their identity and control access to services such as voice dialing, banking by telephone, telephone shopping, database access services, information services, voice mail, security control for confidential information areas, and remote access to computers.

2. PRINCIPLES OF SPEAKER RECOGNITION

Speaker recognition methods can be divided into text-independent and text-dependent methods. In a text-independent system, speaker models capture the characteristics of somebody's speech which show up irrespective of what one is saying. In a text-dependent

system, on the other hand, the recognition of the speaker's identity is based on his or her speaking one or more specific phrases, like passwords, card numbers, PIN codes, etc. Every technology of speaker recognition, identification and verification, whether text-independent and text-dependent, each has its own advantages and disadvantages and may require different treatments and techniques. The choice of which technology to use is application-specific. At the highest level, all speaker recognition systems contain two main modules feature extraction and feature matching.

Speech processing has a wide use of its applications. Figure 1 shows part of the area and how the speaker recognition becomes part of it.

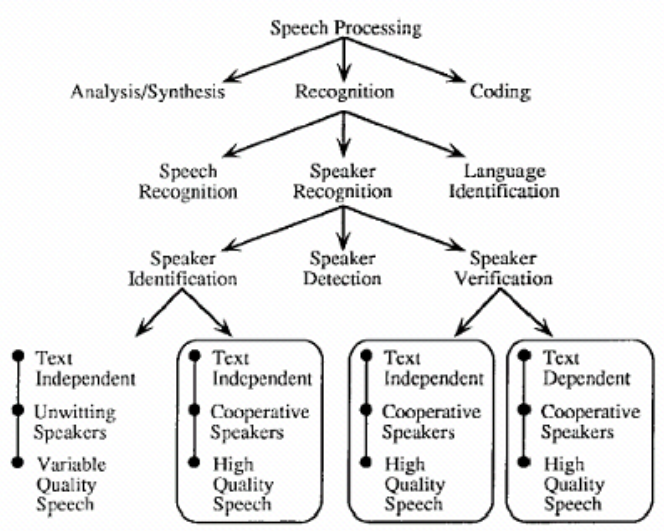

Figure 1: Signal Processing Tree to Speech Recognition

3. FEATURE EXTRACTION

The purpose of this part is to convert the speech waveform to some type of parametric representation (at a considerably lower information rate). The speech signal is a slowly time varying signal (it is called quasi-stationary). When examined over a sufficiently short period of time (between 5 and 100 ms), its characteristics are fairly stationary. However, over long periods of time (on the order of 0.2s or more) the signal characteristics change to reflect the different speech sounds being spoken. Therefore, short-time spectral analysis is the most common way to characterize the speech signal. A wide range of possibilities exist for parametrically representing the speech signal for the speaker recognition task, such as Linear Prediction Coding (LPC), Mel Frequency Cepstrum Coefficients (MFCC), and others. MFCC is perhaps the best known and most popular, and this feature has been used in this paper. MFCC's are based on the known variation of the human ear's critical bandwidths with frequency. The MFCC technique makes use of two types of filter, namely, linearly spaced filters and logarithmically spaced filters. To capture the phonetically important characteristics of speech, signal is expressed in the Mel frequency scale. Normal speech waveform may vary from time to time depending on the physical condition of speaker's vocal cord. Rather than the speech waveforms themselves, MFFCs are less susceptible to the said variations.

3.1 MFCC Processor

A block diagram of the structure of an MFCC processor is given in Figure 2. The speech input is recorded at a sampling rate of 22050Hz. This sampling frequency is chosen to minimize the effects of aliasing in the analog-to-digital conversion process. Figure 2 shows the block diagram of an MFCC processor and the sequensial process in it.

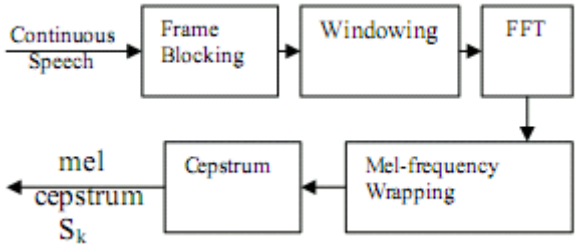

Figure 2: Block Diagram of a MFCC Processor

3.2 Mel-frequency Wrapping

The speech signal consists of tones with different frequencies. For each tone with an actual frequency, f, measured in Hz, a subjective pitch is measured on the 'Mel' scale. The Mel-frequency scale is linear frequency spacing below 1000 Hz and a logarithmic spacing above 1000 Hz. As a reference point, the pitch of a 1 kHz tone, 40 dB above the perceptual hearing threshold, is defined as 1000 mels. Therefore we can use the following formula to compute the mels for a given frequency f in Hz:

mel(f)= 2595*log10(1+f/700) …….. (1)

One approach to simulating the subjective spectrum is to use a filter bank, one filter for each desired mel-frequency component. The filter bank has a triangular bandpass frequency response, and the spacing as well as the bandwidth is determined by a constant mel-frequency interval.

3.3 Cepstrum

In the final step, the log mel spectrum has to be converted back to time. The result is called the mel frequency cepstrum coefficients (MFCCs). The cepstral representation of the speech spectrum provides a good representation of the local spectral properties of the signal for the given frame analysis. Because the mel spectrum coefficients are real numbers (and so are their logarithms), they may be converted to the time domain using the Discrete Cosine Transform (DCT). The MFCCs may be calculated using this equation [4]:

$$\tilde{c_n} = \sum_{k=1}^{K} (\log \tilde{S}_k) \left[n\left(k - \frac{1}{2}\right)\frac{\pi}{K} \right], \quad \text{where } n=1,2,\ldots K \qquad \ldots\ldots(2)$$

The number of mel cepstrum coefficients, K, is typically chosen as 20. The first component, c~0, is excluded from the DCT since it represents the mean value of the input signal which carries little speaker specific information. By applying the procedure described above, for each speech frame of about 30 ms with overlap, a set of mel-frequency cepstrum coefficients is computed. This set of coefficients is called an acoustic vector. These acoustic vectors can be used to represent and recognize the voice characteristic of the speaker. Therefore each input utterance is transformed into a sequence of acoustic vectors. The next section describes how these acoustic vectors can be used to represent and recognize the voice characteristic of a speaker.

4. FEATURE MATCHING

The state-of-the-art feature matching techniques used in speaker recognition include, Dynamic Time Warping (DTW), Hidden Markov Modeling (HMM), and Vector Quantization (VQ). HMM may be used to improve the efficiency and precision of the segmentation to deal with crosstalk, laughter and uncharacteristic speech sounds.
Deterministic approach is intuitive reason, but stochastic model has been developed recently which offer more flexibility and more probabilistic theoretically.

By stochastic model, pattern matching problem can be formulated as probabilistic of an observable event (A vector feature from unknown speaker vector) given as a speaker model. Observation means a random vector with conditional probability density functions (pdf) depend on the speaker. Conditional pdf for one speaker can be estimated from a set of training vector which then put in database as a value to compare. Estimated pdf can be a parameteric or non parametric model. From such model, for every frame of voice (or mean of frame series) probalility used to get unique information for everyone voice. Probabilistic is a match score. If using parametric model, a specific pdf can be assumed and exact parameter from pdf can be determined using the biggest probalilistic.

HMM is the most popular stochastic model. At Markov tradisional model, every state corresponds to every deterministic observable. In HMM, observation is a probabilistic function from state in the model, which is a stochastic process in double value. One value of it which is the prime value cannot be observable directly (means hidden) can only be seen through another set of stochastic process which gives an observable series. HMM is a limited state machine where a pdf (or stochastic model from feature vector) p(x|si) associated fro every state of si (base prime model). Every state connected by a transition net, where probability of transition state is aij = p(si|sj). As an example, HMM with 3 state hipotesis shown in Picture 3.

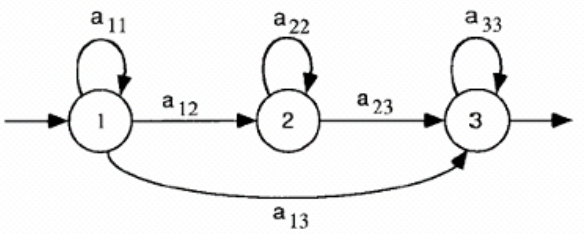

Figure 3: Example of 3 state of HMM

Probability of a frame voice series generalize by this model using Baum-Welch decoding. Probability here means score of frame L from voice input given by the model.

$$p = (x(1;L) \mid \text{model}) = \sum_{\text{semuaderetkemungkinan}} \prod_{i=1}^{L} p(x_i \mid s_i) p(s_i \mid s_{i-1}) \qquad \ldots(3)$$

5. RESULTS

The system has been implemented in Matlab 7.5.0 on windowsXP platform.The result of the study has been presented in Table 1 and Table 2. The probability database consists of 6 speakers, each person said letter "a" for 50 times. in this experiment, we obtained the probability of recognized speaker voice by the system for each spelling.

Table 1:
Probability of recognized speaker for each spelling (1-25.)

Experiment Number	Speaker					
	S*1	S*2	S*3	S*4	S*5	S*6
1	0.8125	0.575	0.575	0.5875	0.5125	0.7375
2	0.65	0.6	0.5375	0.6375	0.4625	0.775
3	0.575	0.6375	0.6125	0.4375	0.5625	0.725
4	0.4875	0.6125	0.6125	0.575	0.675	0.75
5	0.575	0.6625	0.5625	0.65	0.65	0.7
6	0.575	0.55	0.5875	0.6125	0.6625	0.625
7	0.85	0.8	0.675	0.6375	0.6875	0.475
8	0.55	0.6	0.6625	0.7375	0.575	0.7125
9	0.55	0.6125	0.6	0.8625	0.85	0.6625
10	0.475	0.6875	0.775	0.8875	0.5625	0.85
11	0.7125	0.525	0.6875	0.6375	0.5375	0.675
12	0.7	0.5375	0.6125	0.5	0.7625	0.65
13	0.8	0.7	0.475	0.6375	0.6125	0.5375
14	0.6375	0.6625	0.575	0.5	0.8625	0.6125
15	0.625	0.5375	0.5875	0.425	0.525	0.6
16	0.5125	0.6875	0.6	0.45	0.55	0.6125
17	0.525	0.55	0.4375	0.6125	0.5	0.525
18	0.55	0.6125	0.5875	0.675	0.8625	0.475
19	0.65	0.5375	0.525	0.65	0.5875	0.625
20	0.6375	0.55	0.5625	0.5	0.825	0.525
21	0.65	0.625	0.55	0.7875	0.5625	0.625
22	0.45	0.475	0.6625	0.675	0.525	0.7
23	0.65	0.6	0.5875	0.7875	0.5375	0.525
24	0.5375	0.6	0.7	0.525	0.775	0.7
25	0.5	0.6125	0.675	0.475	0.7625	0.6125

S* is Speaker (real name not for published but available through author).

Table 2:
Probability of recognized speaker for each spelling (25-50).

Experiment Number	Speaker					
	S*1	S*2	S*3	S*4	S*5	S*6
26	0.575	0.5	0.675	0.575	0.85	0.825
27	0.5375	0.7	0.55	0.675	0.5125	0.7875
28	0.55	0.5875	0.5625	0.775	0.725	0.675
29	0.6125	0.8	0.675	0.6875	0.6625	0.725
30	0.725	0.65	0.7375	0.725	0.7625	0.5625
31	0.4	0.5375	0.5	0.4625	0.5625	0.5
32	0.575	0.5625	0.5625	0.625	0.6875	0.6625
33	0.6	0.675	0.55	0.55	0.85	0.3625
34	0.4875	0.6375	0.55	0.6375	0.6375	0.7125
35	0.5625	0.6125	0.8	0.4875	0.7125	0.725
36	0.5125	0.525	0.6	0.5375	0.575	0.75
37	0.6375	0.5375	0.525	0.7125	0.6	0.675
38	0.6125	0.575	0.675	0.45	0.4375	0.775
39	0.5625	0.6875	0.6125	0.5	0.8	0.5
40	0.65	0.525	0.6625	0.6125	0.55	0.45
41	0.6	0.5875	0.575	0.3625	0.85	0.8
42	0.5375	0.5125	0.6125	0.5875	0.625	0.5875
43	0.5875	0.6	0.325	0.5625	0.85	0.4875
44	0.6	0.575	0.45	0.5875	0.375	0.8375
45	0.5125	0.5625	0.6125	0.85	0.5125	0.6125
46	0.5625	0.5875	0.8	0.6125	0.7	0.65
47	0.7125	0.7	0.75	0.5	0.575	0.7875
48	0.4875	0.45	0.6375	0.7125	0.4375	0.6625
49	0.6375	0.5	0.575	0.6625	0.75	0.6375
50	0.65	0.5	0.6	0.85	0.4875	0.575

5. ANALYSIS

By using Analysis of Variance (ANOVA), we can tested the hypotesis of average similarity from three or more population. The assumption in this ANOVA are:

1. The sample is been taken randomly and independently
2. Normal distribution of population
3. The population have variance similarity.

Next table, shows ANOVA table that must be calculate first to be able to do analysis.

Table 3 : ANOVA table for comparing means

Source	SS *(Sum of Squares, the numerator of the variance)*	DF *(the denominator)*	MS *(Mean Square, the variance)*	F
Treatment *(or Between or Model)*	$SST = \sum_{i=1}^{p} \sum_{j=1}^{n_i} (\bar{y}_i - \bar{y})^2$	$p-1$	$MST = \frac{SST}{p-1}$	$F = \frac{MST}{MSE}$
Error *(or Within)*	$SSE = \sum_{i=1}^{p} \sum_{j=1}^{n_i} (y_{ij} - \bar{y}_i)^2$	$n-p$	$MSE = \frac{SSE}{n-p}$	
Total	$TSS = \sum_{i=1}^{p} \sum_{j=1}^{n_i} (y_{ij} - \bar{y})^2$	$n-1$		

The solution using variance analysis in experimentation testing are:

- Hypothesis:

  H_o: $\mu_1 = \mu_2 = \mu_3 = \mu_4 = \mu_5 = \mu_6$

  H_1: there is an average value that is not equal
- Significancy level $\alpha = 0{,}01$
- Since df_1 = the denominator Treatment = 5 dan df_2 = the denominator Error = 294, so f(0,01; 5; 294) = 3,02)
- So, H_O rejected if F > 3,02)

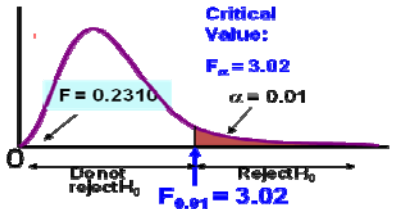

Figure 4: ANOVA Curve

Table 4: ANOVA Calculation Table

Source	DF (the denominator)	SS (Sum of Square, , the numerator of the variance	MS (Mean Square, the variance)	F
Treatment	5	0.1286	0.02572	0.2310222
Error	294	3.27314	0.11133129	
Total	299	3.40174		

Analysis :
Since F_{count}= 0.2310222 < 3,02, the H_0 approved.
So, $\mu_1 = \mu_2 = \mu_3 = \mu_4 = \mu_5 = \mu_6$ or in other words, there is similarity between mean of all person, with level of trust is *99% (α =0.01).*

From the experimentation, by using 99 % level of trust), we obtained approving profile as :

Table 5 : User acceptance profile

Acceptance Group	Range (%)	Speaker						Sum of Sampel	Acceptance (%)
		S*1	S*2	S*3	S*4	S*5	S*6		
Good Acceptance	81-100	2	0	0	4	8	3	17	5.666666667
Fair Acceptance	61-80	18	20	23	24	18	32	135	45
Loosy Acceptance	41-60	30	30	26	21	23	14	144	48
Bad Acceptance	21-40	0	0	1	1	1	1	4	1.333333333
Verry bad Acceptance	1-20	0	0	0	0	0	0	0	0
Total								300	100

6. CONCLUSION

With 99% level of trust (α=0.01), the system yields the similarity of means of each group of object. Thus, the system has a good level of accurateness. It means, MFCC and HMM is a good "method" to be implemented for voice authentication.

The Author has categorized the result into two groups, the first one is accepted group (*good dan fair acceptance*) and

the other one is unaccepted group (*loosy, bad, dan very bad*), with each presentation are 50,667% and 49,33%.

The present study is still ongoing, which may include following further works. We can reduce noise and "optimize" the feature extraction including "eliminating the zero voice (wait signal)" to increase the acceptance rate in this method.

REFERENCES

[1] Ali Mustofa. 2008. Sistem Pengenalan Penutur dengan Metode *Mel-frequency Wrapping*. In press.
[2] Arun A. Ross, Karthik Nandakumar, Anil K. Jain, 2006. *Handbook of Multibiometrics*. Springer.
[3] Ganchev, Todor et al. *Comparative Evaluation of Various MFCC Implementations on the Speaker Verification Task*. Wire Communications Laboratory, University of Patras. In press.
[4] Lawrence Rabiner and Biing-Hwang Juang, 1993. Fundamental of Speech Recognition", Prentice-Hall, Englewood Cliffs, N.J.
[5] Md. Rashidul Hasan, Mustafa Jamil, Md. Golam Rabbani Md. Saifur Rahman. "Speaker Identification Using Mel Frequency Cepstral Coefficients" in 3rd International Conference on Electrical & Computer Engineering, ICECE 2004, 28-30 December 2004, Dhaka, Bangladesh. In press.
[6] Mutohar, Amin. 2007. *Voice Recognition*. Fakultas Matematika dan Ilmu Pengetahuan Alam, Institute teknologi Bandung. In press.
[7] http://mutohar.files.wordpress.com/2007/11/voice-recognition.pdf

Design of GSM Authentication Simulation with A3 Algorithm Using Microcontroller AT89S52

Fitri Yuli Zulkifli, Arman D. Diponogoro and T. Maulana Habibi

Center for Information and Communication Engineering Research (CICER)
Electrical Engineering Department
Faculty of Engineering
University of Indonesia, Depok 16424
Tel: (021) 7270011 ext 51. Fax: (021) 7270077

ABSTRACT

This paper discusses the design of the GSM authentication simulation and the process of GSM authentication suitable for the mobile station. The design uses triplet's authentication to generate SRes using Microcontroller AT 89S52.
The result shows that the process of GSM authentication with A3 algorithm using microcontroller AT 89S52 as computation data could be displayed through LCD (Liquid Crystal Display).

Keywords
GSM Authentication, A3 Algorithm, Microcontroller

1. INTRODUCTION

Information security is a principle problem for cable or wireless communication network. Security information system includes the network security, security of information and the physical/equipments itself.

For mobile phone applications, high security system is needed because the transmission media via air can be tapped or cloned by unwanted person [1]. To counter serious information leakage the security system must be well developed.

Commonly, the security system consists of authentication, integrity of information and identification [2]. For Global System for Mobile Communication (GSM), the security among others can be in the form of the authentication SIM card GSM.

This paper proposes a design of user authentication. The user authentication design can prevent the illegal user to enter the network.

Authentication is a procedure which is used to check the validity identity of GSM subscribers to access GSM network and to use all of the facilities offered by GSM networks.

GSM Authentication uses certain algorithm [3]. The A3 Algorithm is an authentication algorithm for security and safety of GSM, functioning to generate response which is known well as SRes (Signal Response) and answer from random challenge recognized as Rand. The design uses triplet's authentication to generate SRes using Microcontroller AT 89S52.

2. GSM AUTHENTICATION

The main functions of authentication process conducted by GSM are:

1. Protection of GSM Network from accessing effort by illegal user and with no authority.
2. Protecting the privacy of customers from accessing effort by unwanted party/intruder.
3. Protecting data, this is transmitted at radio band, by sub-system radio during the pursuance of communications relation.

If the mobile subscriber (MS) will access the GSM system, the system will check the identity of the MS. The system delivers or transmits RAND (Random Number) to be accepted by the MS. The Mobile Equipment (ME) than delivers the RAND to Subscriber Identity Module (SIM) card, which will process the random number by using Authentication Key (Ki) in the SIM card so that it will result in a signal respond SRES (Signal Response) based on RAND, Ki and Algorithm A3.

The MS then delivers the SRES to the system, and the system will compare this SRES with its own calculation result (SRES from system) and if the same result occurs, this means that the authentication process succeeds. On the contrary, if the authentication process fails, than the system will stop the contact and sends indication at the MS that the authentication failed. This system is expressed in Fig.1.

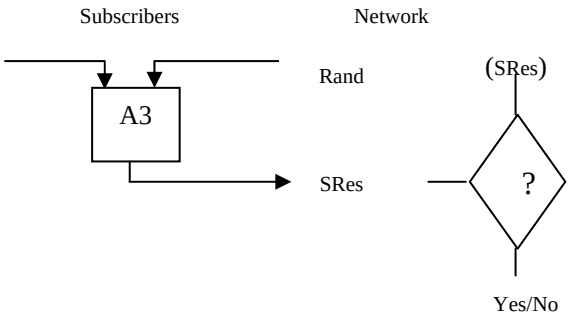

Figure 1: Elementary principle of authentication procedure at the GSM network.

During the execution of the authentication process, several procedures of signaling transfer occurs shown in Fig. 2 and explained as follow:

1. If MS accesses the GSM network by delivering signal (Request) to MSC (Mobile Service Switching Center) to be sent to VLR (Visitor Location Register), than the MS will be authenticated. The authentication process begins to be executed after the VLR accepts the MAP message from MSC.
2. If the MS is not recognized by VLR, than the VLR will ask the parameter authentication (triplets) from Home Location Register (HLR) or Authentication Center (AuC) or from previous VLR (from where the MS comes) by delivering message of authentication Information Request.
3. VLR then begins the execution of authentication procedure by delivering message authentication (Authentication Request) to MSC. This message contains the parameter of authentication RAND.

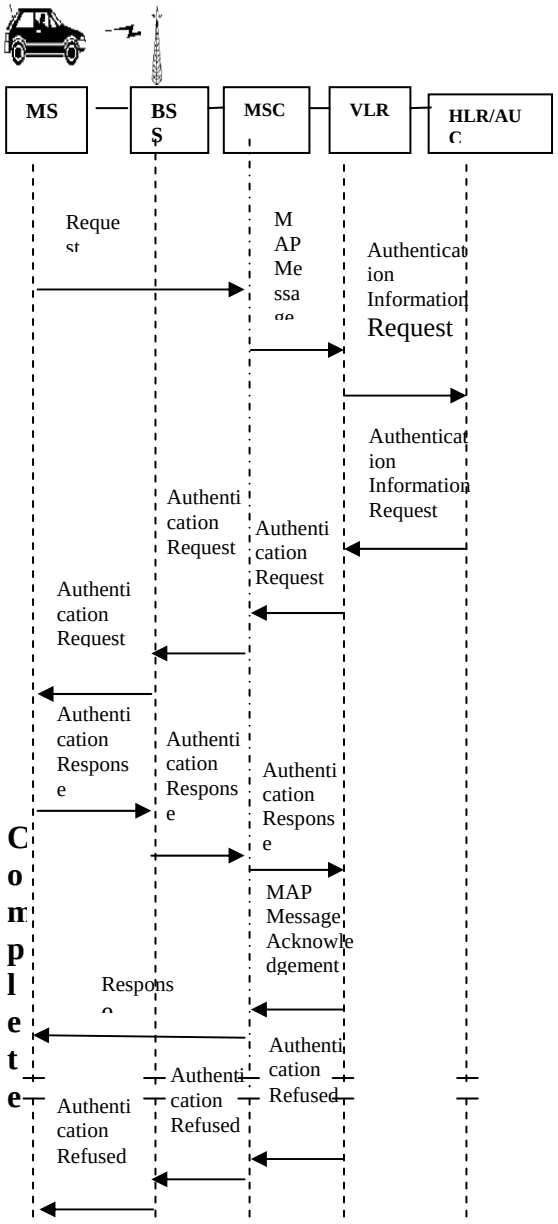

Figure 2: Signal transfer during authentication process [3]

4. The RAND authentication is sent to MS as message Authentication Request.
5. MS will respond by sending parameter SRes in the message Authentication Response. For the checking process of authentication SRes is sent to the message Authentication Response to VLR.
6. If the overall authentication process succeeds to be executed (complete), then the request (access) done by MS will be fulfilled, with the indication of the delivery signal (Response) from MSC to MS.
7. If the authentication process to MS failed to be executed, then the effort of accessing GSM network by the MS is refused/canceled (indicated with the message of Authentication Refused), followed with relation disconnection of communications

3. DESIGN OF GSM AUTHENTICATION SYSTEM

The design of GSM authentication system is shown in Fig. 3 and Fig. 4. Figure 3 represents the block diagram from the GSM authentication system.

Figure 3: Block diagram of GSM authentication system

The block diagram consists of Keypad, Power, Microcontroller and LCD. The system works as follow:

1. The power supply supplies the power for the microcontroller so that the microcontroller can operate properly. The communications between the power supply with the microcontroller is a one way communication. The microcontroller communicates with the simcard reader to take the Ki data, which will be read and computed with the rest of the data.
2. The Keypad with the microcontroller also has a one way communication relationship. The microcontroller receives instruction from the keypad such as the password and also the simulation of the data input. The Keypad also gives the command to be run by the microcontroller.
3. The LCD as the output from all of the process that happened receives all the input from the microcontroller. The LCD shows the data process processed by the microcontroller. Therefore, the communication between the LCD with microcontroller is also a one way communication.

Figure 4 shows the block diagram of the processing and transfer of data controlled by Microcontroller AT89S52.

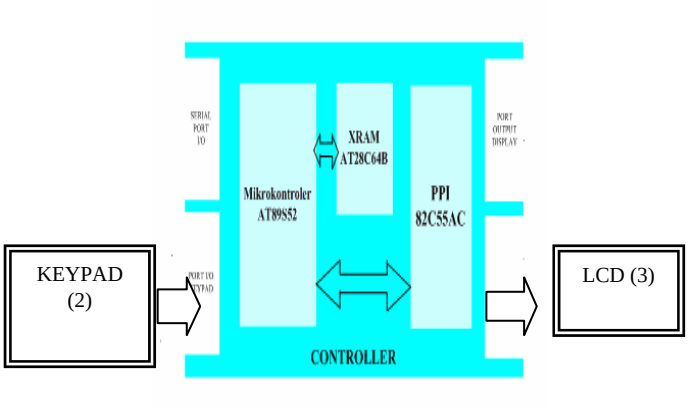

Figure 4: Block diagram system of processing and transfer of data Controlled by Microcontroller AT89S52

The block diagram works as follow:

1. The Keypad represents the part of I/O delivering signal pin to port PPI 82C55 and requires the address from the microcontroller to operate it. The PPI 82C55 address starts from 2000H to 3FFFH in the microcontroller.
2. The microcontroller delivers data to LCD as output display, and the LCD processes every input of command which is wanted to be shown from the microcontroller
3. The execution process can also be shown on the display monitor using the hyper terminal.

The main design of A3 algorithm is shown in Fig. 5. The input of the comparator is Rand which is a random number with maximal 128 bits and authentication key (Ki) which consists of maximal 128 bits. The input data will be compressed to 64 bits of Rand and 64 bits of Ki. Both input data will be XOR as a comparator function. This function is to prevent identical computational output.

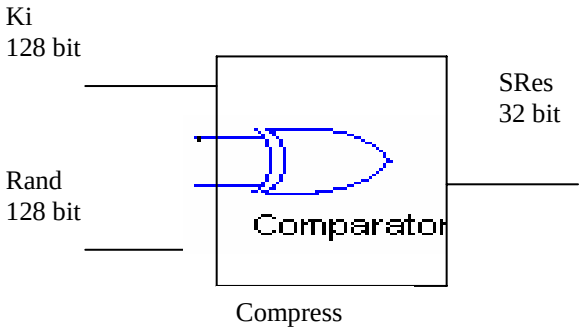

Fig 5 Design of A3 Algorithm

.

3.I Compress Data Value with Butterfly Structure

The input of the comparator which consists of 128 bits Ki and 128 bits Rand is compress using the butterfly structure. The butterfly structure is depicted in Fig.6.

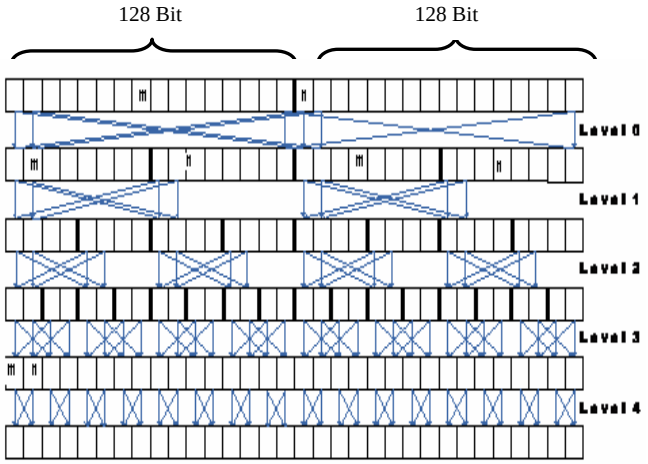

Figure 6: Compress data value using butterfly structure

The butterfly structure consists of 5 compression level. Each compression level produce bytes which is dependant of the previous input data bytes expressed as:

$$X=(Z[m]+2*Z[n])\bmod 2^{(9-j)} \quad (1)$$

$$Y=(2*Z[m]+Z[n])\bmod 2^{(9-j)} \quad (2)$$

Z [m] = T j [X] [m new result of look up table from element X]

Z [n] = T j [Y] [n new result of look up table from element Y]

Where:
Xn = Element X in level m
Yn = Element Y in level n
Z[m]/Z[n] = Matrix Z contains new value after Xm and Yn from previous computational result and substituted with the value from the authentication table.

This computational process is executed to five levels as shown in the butterfly structure.

3.2 Compress Data Capacities

The output of the data value compression process using the butterfly structure is changed into bit value per nibble. Therefore the output consists of 128 bits. The output compression data will be changed to bytes as shown in Fig. 7.

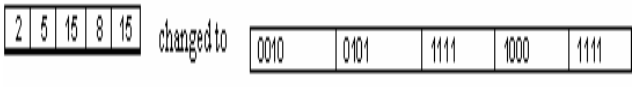

Fig. 7 Output value changed to Bytes

The butterfly which consists of 5 level compression changes bit to bytes (Data capacities compression 32 bytes becomes 8 byte) and than will form a matrix for permutation as shown in Fig.8.

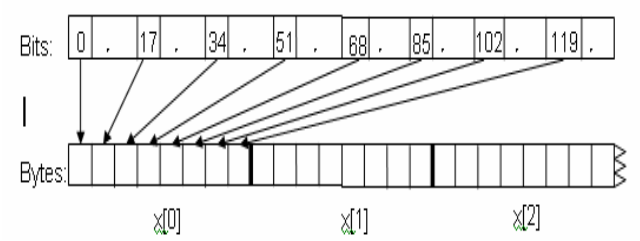

Figure 8: Change of bit to byte matrix permutation

Bits which are taken from Fig.8 goes to the final compression process (Data capacities compression 8 Byte becomes 4 Byte) with permutation process to create SRes as shown in Fig. 9.

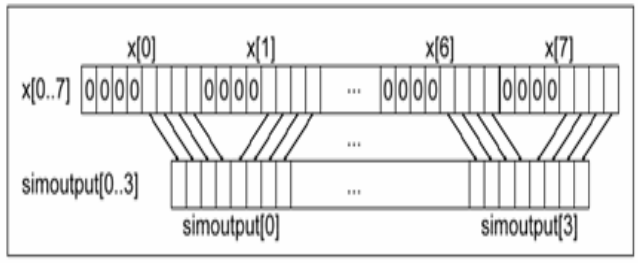

Figure 8: Change of matrix permutation to matrix value SRes

The output parameter of SRes matches the specification standard from ETSI.

4. SIMULATION RESULT AND ANALYISIS

The design of GSM authentication system is analyzed step by step in creating the SRes value.To verify the output value of SRes using A3 algorithm, the amount of SRes has to be 32 bit according to the ETSI specification standard.

Analyzing the important role of each step in the A3 algorithm to produce the SRes value of 32 bits, can be analyzed as follow:

- The data value 2^8 at the input is minimized to become 2^4 by using the butterfly structure
- The input capacities 32 bytes is compressed to become 8 byte
- The capacitiy of 8 bytes is compressed again to become 4 bytes.

The output released shows different byte values because the algorithm uses different inputs from previous level. If the output shows similar to the input that means the A3 algorithm does not work as preferred. This means that the A3 algorithm can not prevent illegal users to use the system because the authentication system does not work according to the A3 algorithm system.

Trial test was carried out to verify the design. The trial test shows if the output from customer's side is the same as the output from the network, the authentication process is achieved. In contrary, if the output from customer's side is not the same as the output from the network, then the authentication process is achieved.

5. CONCLUSION

Based on the simulation design of the authentication process, the design shows level of security and safety from the GSM authentication. The simulation design has worked based on A3 algorithm output as according to the ETSI specification standard.

REFERENCES

[1] Wang Kleiner, "GSM Cloning.ppt" accessed: 8 December 2008
[2] Ratih,"Studi dan Perbandingan simcard dan kriptografi kunci simetri dan asimetri pada telepon selular", http://www.itb.ac.id, accessed: 1 October 2008
[3] Ariadi, " Implementasi rancangan algoritma A3/A8 pada model simulasi proses autentikasi system telepon bergerak selular digital", Skripsi, FTUI, 2007

Finite-Element Simulations of Electrically-Driven Fluid Transport in Straight Channels for Lab-on-a-chip Systems

Hendrik[a], G.O.F. Parikesit[b], A. Sopaheluwakan[c], H.P. Uranus[d]

[a]*Department of Electrical Engineering*
University of Pelita Harapan, Lippo Karawaci, Tangerang 15811, Indonesia
E-mail: henz_dm@yahoo.com

[b]*Laboratory for Aero and Hydrodynamics*
Delft University of Technology, Leeghwaterstraat 21 - 2628 CA , Delft, The Netherlands
E-mail: g.o.f.parikesit@tudelft.nl

[c]*LabMath-Indonesia Research Institute, Jl. Anatomi No. 19, Bandung 40191, Indonesia*
E-mail: ardhasena@labmath-indonesia.or.id

[d]*Department of Electrical Engineering*
University of Pelita Harapan, Lippo Karawaci, Tangerang 15811, Indonesia
Graduate Program in Electrical Engineering
University of Pelita Harapan, Wisma Slipi, Jl. Let. Jend. S. Parman Kav. 12, Jakarta 11480, Indonesia
E-mail:h.p.uranus@alumnus.utwente.nl

ABSTRACT

This paper reports the computation of electro-osmotic flow (EOF) velocity using our own codes based on Matlab software by implementing finite element method (FEM) to solve the governing equations of EOF using an approach known as the Helmholtz-Smoluchowski (HS) approach. We also modify one equation of the approach so it takes into consideration the effects of electric field leakages through the channel walls using the differential form of Gauss's law and hence generalizing our method to include the cases of chips with inhomogeneous material composition. For simplicity, we only performed two-dimensional simulations with the assumption that our chip model consists of only a single and straight channel and the fluid material used to conduct the electroosmosis is salt (NaCl) solution. We then studied the relation between four physical parameters with the EOF velocity: (i) voltage difference across the channel, (ii) channel length, (iii) dielectric constant of the channel material, and (iv) salt concentration. The main conclusion of this paper is we managed to simulate the EOF using our own-built code based on Matlab software, which in this case is very cost-efficient (rather than using commercial software e.g. COMSOL).

Keywords:
Microfluidics, finite element method, electroosmosis, straight channels, simulation.

1. INTRODUCTION

Lab-on-a-chip (LOC) is new technology developed to enable the execution of the laboratory functions such as analyzing and controlling fluids, ions and other particles on a single chip of only millimeters to a few square centimeters in size.

LOC has a lot of advantages compared with the conventional laboratory:

1. Low consumption of fluid volumes, e.g. less than pico liters (10^{-12} liters).
2. Faster analysis and response times due to small volumes of the fluids and reagents required.
3. Massive parallelization due to compactness, which allows various processes to be executed simultaneously.
4. Portability of the chip, due to its size, which allows it to be carried out with ease.

Even though the LOC has many advantages, it also provides some difficulties and challenges:

1. It is a new technology and hence still need development in many areas.
2. Further study is required to investigate the physical effects in smaller scale, e.g. micro- and nano-scale, which are not the same as the physical effects in the larger scale, e.g. milli-scale.
3. As the scale of the channels becomes smaller, it becomes less practical to use hydrostatic pressure to control the flow, as it requires increasingly large pressure to control the flow in such a small scale.

This paper discusses one solution to the third problem, where electrodes (rather than pressure sources) are utilized to create electrostatic fields which are then used to direct and control the flow. The technique is called electroosmosis, while the resulting flow is named electro-osmotic flow (EOF).

In this paper, the EOF velocity is calculated by implementing a numerical technique called the finite element

method (FEM) to the governing equations of EOF using one approach known as the Helmholtz-Smoluchowski (HS) approach.

2. BASIC TERMS IN MICROFLUIDICS

Reynolds number is a dimensionless number which is used to differentiate between the laminar or turbulent flow. It is defined as *inertial forces/viscous forces* [1]. High and low Reynolds number, respectively, represent the turbulent flow and the laminar flow.

Electric double layer (EDL) is a layer formed when an electrolyte is brought in contact with a solid surface. It consists of two layers, i.e. Stern and Diffuse layers, and has a thickness defined by the so-called Debye length, λ_D. The Stern layer is a fixed layer, usually only one ion wide, whereas the diffuse layer is a mobile layer which can be set in motion upon the application of an external electric field. The Stern and diffuse layer are separated by the Shear Plane whose potential is called the ζ potential.

Electroosmosis is the movement of ionized fluid in a capillary tube or microchannel when an external electric field is applied parallel to the surface.

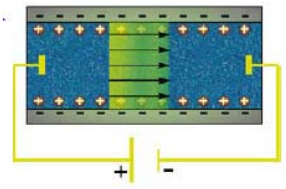

Fig. 1 The EOF in a microchannel [2]

3. THE HS APPROACH

The Helmholtz-Smoluchowski (HS) approach is an approach to calculate the EOF velocity based on the assumptions: (i) The EDLs thickness is very thin compared to the channel dimensions, e.g. channel height, and hence the EDLs do not overlap with each other, (ii) Low Reynolds number, i.e. steady flow, and (iii) no pressure gradient is applied across the channel [3].

The HS approach uses three equations, i.e. the differential form of Gauss's law (DFGL) defined by

$$\partial_x\left(\varepsilon_m\,\partial_x\phi(x,y)\right)+\partial_y\left(\varepsilon_m\,\partial_y\phi(x,y)\right)=0 \qquad (1)$$

to calculate the electric potential distribution, ϕ, and the HS equation defined by

$$\vec{u}_{eo}(x,y)=\left(-\frac{\varepsilon_S}{\mu}\zeta\right)\vec{E}(x,y)=\alpha_{eo}\vec{E}(x,y), \qquad (2)$$

to calculate the EOF velocity, $\vec{u}_{eo}$, where ε_m is the permittivity of the channel material, ε_s is the permittivity of the electrolyte solution, μ is the viscosity of the electrolyte solution, $\vec{E}$ is the electric field in the channel while the x and y coordinate, respectively, correspond to the 2-D channel geometrical coordinates. The electric field, $\vec{E}$, in Eq. (2) can be derived from the electric potential, ϕ, in Eq. (1) using the relation $\vec{E}=-\nabla\phi$, which is modified for the 2-dimensional case.

4. GEOMETRIC DESCRIPTION OF THE MICROFLUIDIC CHIP UNDER STUDY

The 2-dimensional geometry of the microfluidic chip is given below.

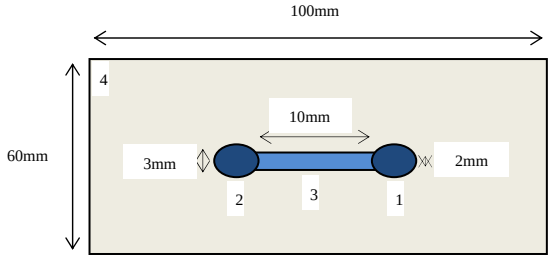

Fig. 2 The geometry of the microfluidic chip (see text for details on the number notations)

Details:

1. The chip consists of only a single and straight channel with two wells, i.e. the input and output wells, respectively, labeled as '1' and '2' in Fig. 2. Label '3' represents the channel while label '4' represents the other areas of the chip.
2. The chip is made of *polymethyl methacrylate* (PMMA), which is also known commonly as acrylic.
3. The channel is placed exactly in the middle of the chip both in the horizontal and vertical direction.

5. FEM IMPLEMENTATION OF THE DFGL

The FEM used is the Galerkin method [4], which is initiated by taking the weak formulation of the equation to be solved. The weak form of Eq. (1) is

$$\int_\Omega\left(\partial_x\left(\varepsilon_m\,\partial_x\phi\right)+\partial_y\left(\varepsilon_m\partial_y\phi\right)\right)w\,d\Omega=0, \qquad (3)$$

where Ω is the whole problem domain and w is a test function, i.e. an arbitrary chosen function whose values are not zero. As seen in Fig. 2, Ω can be divided to two sub-domains, i.e. sub-domain inside the channel, Ω_1, and sub-domain outside the channel, Ω_2, each having its own permittivity denoted respectively as ε_{m1} and ε_{m2}. The zero Neumann boundary condition (ZNBC), i.e. $\partial_n\phi=0$, is also imposed as the boundary condition for the outermost boundary in Fig. 2, i.e. all four sides of the rectangle. This means, physically, that the chip is insulated electrically, i.e.

no electric potential flux at the chip boundary [3]. Hence, Eq. (3) becomes

$$\int_{\Omega_1} \varepsilon_{m1} \left(\partial_x \phi \partial_x w + \partial_y \phi \partial_y w \right) d\Omega + \int_{\Omega_2} \varepsilon_{m2} \left(\partial_x \phi \partial_x w + \partial_y \phi \partial_y w \right) d\Omega = 0 \quad (4)$$

The next step is to replace ϕ with its two-dimensional finite elements approximation, where the three-node triangular elements are chosen. Using the derivation in [5], the discretized form of Eq. (4) is

$$[G]_{n \times n} [\phi]_{n \times 1} = [0]_{n \times 1}, \quad (5)$$

where $[G]$ is the global matrix defined as in [5], $[\phi]$ is the electric potential vector, $[0]$ is a zero vector, and n is the number of nodes in the domain discretization. The matrix system in Eq. (5) is then arranged using the method in [5], which then can be solved using the direct solver in Matlab.

6. DESCRIPTION OF THE SIMULATION PARAMETERS

There are 3 observation points in the simulation, i.e. a point near the channel's inlet, a point in the middle of the channel, and a point near the channel's outlet. The location of each point is shown in Fig. 3.

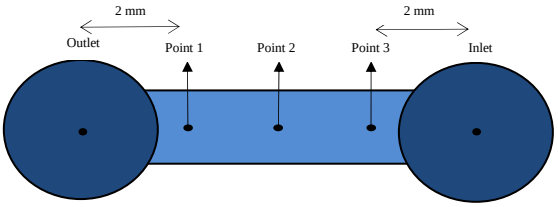

Fig. 3. Location of observation points in the channel geometry

6.1. Voltage Difference

The voltage difference across the channel is produced by the electrodes placed at the channel wells, i.e. circular-shaped electrodes with a diameter of 1mm is placed in the middle of each well. In the simulation, it is assumed that the electrode at the channel outlet connects to the electrical ground (0V) whereas the other electrode connects to positive electric potential. The variation of voltage difference ranges from 10V to 190 V with interval of 20 V.

6.2. Channel Length

The variation of channel length is as follows: 11 mm, 12 mm until 18 mm with the interval of 1.5 mm, 19 mm, and 20 mm until 95 mm with the interval of 5 mm.

6.3. Dielectric Constant

In addition to acrylic (PMMA), other polymer materials such as *poly dimethyl siloxane* (PDMS), *polycarbonate* (PC), *nylon* and *poly tetra fluoro ethylene* (PTFE or Teflon) are used in the simulation. Many of these materials are currently used for microchip fabrication [6]. The dielectric constant values for each polymer are as follows: (i) PTFE = 2.0, (ii) PDMS = 2.5, (iii) PC = 3.0, (iv) PMMA = 3.5, and (v) Nylon = 4.5.

6.4. Salt Concentration

Salt concentration, M, is a measure of the amount of NaCl molecules in water solution. In this paper, the concentration is replaced by the concentration variable defined by

$$pC = -\log M, \quad (6)$$

where M unit is in Molar. The pC serves as a useful normalization for the ζ potential on polymer substrates in contact with indifferent univalent counter-ions [6]. The relation of pC with the ζ potential can be approximately fitted to a linear relation, which can be found in [6]. The pC values from 1 until 4 with the interval of 0.5 are used in the simulation.

7. SIMULATION RESULTS

7.1 Electric Potential Distribution

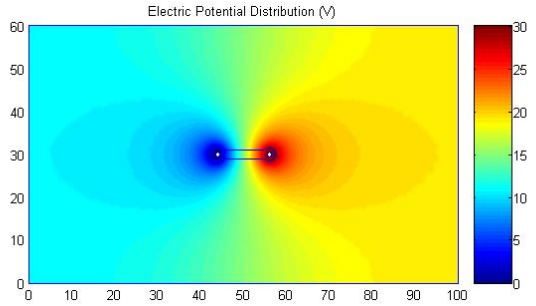

Fig. 4. Simulation result of electric potential distribution

Data for the simulation are as follows:

- Number of triangular elements = 75392
- Number of nodes = 37887
- Voltage difference = 30 V
- ε_s (NaCl solution) = 78.4 ε_0 (inside the channel)
- ε_m (PMMA) = 3.5 ε_0 (outside the channel)
- Boundary locations = 42.5 mm from the leftmost side and rightmost side of the channel and 28 mm from the uppermost side and lowermost side of the channel

Note: ε_0 is the permittivity of vacuum or free space.

In Fig. 4, it can be shown that the electric potential distribution in the chip model is symmetric vertically due to the symmetry of the chip geometry and the imposing of ZNBC.

7.2. Electric Field Distribution

Fig. 5 shows that the magnitude of electric field far away from the channel is zero. This phenomenon is a result of electric field confinement in the chip due to the imposing of ZNBC. Moreover, it can also be shown from Fig. 5 that there is electric field leakage through the channel. This electric field leakage is a result of the application of the DFGL as the governing equation for the electric potential distribution.

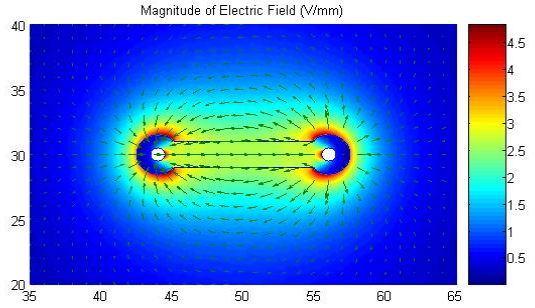

Fig. 5. Simulation result of electric field distribution

8. ANALYSIS AND DISCUSSIONS

In this section, the EOF velocity data in the simulation obtained from the points of interest mentioned previously are discussed. The EOF velocity is calculated using the parameters as follows, unless stated otherwise:

- ζ = -30 mV
- ε_0 = 8.854 × 10^{-12} kg^{-1} m^{-3} s^4 A^2
- μ = 8.9 ×10^{-4} kg m^{-1} s^{-1}

8.1. Variation of Voltage Difference

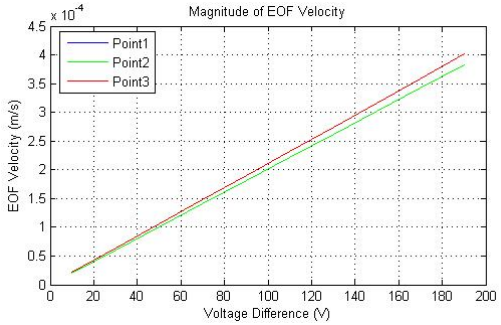

Fig. 6. Curves of magnitude of EOF velocity with variation of voltage difference

In Fig. 6, it can be shown that the magnitude of EOF velocity has a linear relationship with the variation of voltage difference. The order of EOF velocity in the figure ranges from □ 10^{-5} m/s to □ 10^{-4} m/s, which is in accordance to the order of velocity in [1]. This fact indicates that the data in the figure are quantitatively correct.

Another observation reveals that the EOF velocity at Point 1 (near the channel outlet) is equal to the velocity at Point 3 (near the channel inlet). This characteristic indicates that the distribution of magnitude of EOF velocity in the channel is symmetric horizontally due to the symmetry of the channel geometry.

Analyzing the curves quantitatively further shows that for a particular voltage difference, the magnitude of EOF velocity at Point 2 (in the middle of the channel) is a bit smaller than the velocity at Point 1 and Point 3. Thus it can be concluded that the trend of magnitude of EOF velocity observed from the channel inlet is as follows: it has the maximum value near the channel inlet and then continues to decrease until it reaches a minimum value in the middle of channel, and afterwards, it continues to increase until it reaches its maximum value again near the channel outlet.

The linear relation between the EOF velocity and the variation of voltage difference can be deduced from Eq. (2), where the magnitude of electric field can be approximated as

$$|E| \approx \frac{\Delta\phi}{\Delta d}, \qquad (7)$$

where $\Delta\phi$ is the change in the voltage difference across the channel and Δd is the change in the distance between the two electrodes in the channel.

8.2. Variation of Channel Length

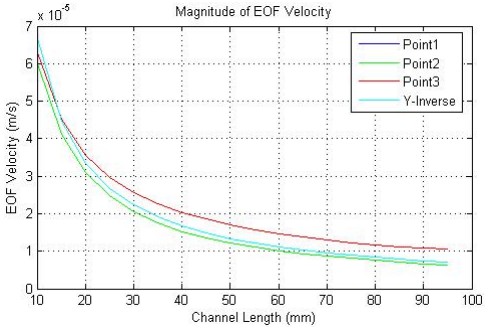

Fig. 7. Curves of magnitude of EOF velocity with variation of channel length

In Fig. 7, it can be shown that the relation of EOF velocity with the variation of channel length is not linear. From Eqs. (2) and (7), it is known that an inverse function defined by $u_{eo} = c / x_L$, should be able to fit the data. Here, u_{eo} is the EOF velocity, c is an arbitrary constant, and x_L is the channel length. Using the trial and error method, it can be known that the value of c is about 6.7×10^{-4}.

Another interesting phenomenon to be observed is that the curves move towards a saturation point, i.e. the point at which the EOF velocity does not change regardless of further extension of the channel length. It can be inferred

from Fig. 7 that the curves saturate when the channel length reaches approximately 100 mm.

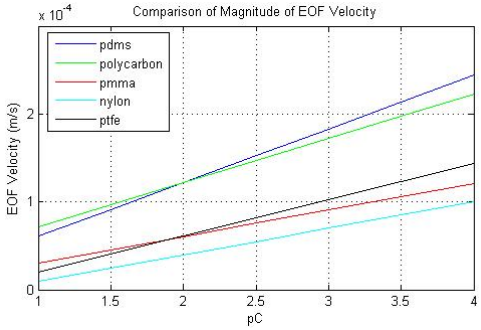

Fig. 8. Curves of magnitude of EOF velocity at Point 2 for various chip material with variation of variable concentration

8.3. Variation of Dielectric Constant and Salt Concentration

It can be shown from Fig. 8 that the relation of EOF velocity with the variation of concentration variable, pC, is linear. The relation can be derived analytically by combining Eq. (2) with the relation of ζ potential and pC in [6]. Therefore, the EOF velocity can be concluded to have linear relationship (indirectly) with pC, and due to Eq. (6), it is also proportional to the negative logarithm of the salt concentration, $-\log M$.

9. CONCLUSIONS

Based on the discussed analyses, it can be concluded that the EOF velocity is:

1. linearly proportional to the variation of voltage difference across the channel.
2. inversely proportional to the variation of channel length.
3. linearly proportional to variation of concentration variable, pC, or proportional to the variation of negative logarithm of salt concentration in the fluid, $-\log M$.

In this work, we also successfully use our own Matlab code, rather than commercial software (e.g. COMSOL) that may not always be cost efficient for research in Indonesia, to simulate the electric field leakage in the channel, which represents a practical and important phenomenon in LOC applications.

REFERENCES

[1] Parikesit, Gea Oswah Fatah, "Nanofluidic Electrokinetics in Quasi-Two-Dimensional Branched U-Turn Channels," Ph.D dissertation, Delft Univ., The Netherlands, January 2008.

[2] http://www.myfluidix.com/Materials/03_Physics_07.pdf

[3] Markesteijn, Anton P., Gea O. F. Parikesit, Yuval Garini, Jerry Westerweel, "Numerical Simulation of Electroosmotic Flow in Complex Micro- and Nanochannels," Article Barga, 25th April 2006.

[4] Kwon, Young W., Hyochoong Bang, "The Finite Element Method Using Matlab," CRC Press, Florida: 1997.

[5] Hendrik, "Finite-Element Simulations of Electroosmosis in Straight Microchannels," Bachelor thesis, Univ. Pelita Harapan, Indonesia, 2009.

[6] Kirby, Brian J., Ernest F. Hasselbrink, "Zeta Potential of Microfluidic Substrates: 2. Data for Polymer," Electrophoresis 2004, 25, 203-213.

PERFORMANCE OF TOROID CORE PERMANENT MAGNET WITH RLC LOADS

Herawati ys.[a]

[a]*Faculty of Electrical Engineering*
University of Indonesia, Depok 16424
Tel : (021) 7270011 ext 51. Fax : (021) 7270077
E-mail : siti_herawati_aminah@yahoo.com

[b] *Faculty of Electrical Engineering*
University of Indonesia, Depok 16424
Tel : (021) 7270011 ext 51. Fax : (021) 7270077
E-mail :

ABSTRACT

Part of Cuk converter Slobodan, was modified with toroid core, which was used as the controller of the ripple current and load, in watt-meter. So the watt-meter could measure the active, reactive power and power factor. And the result of measurement could be transmitted to the receiver. In order to solve this problem, the real toroid with some models of air gap, surface material must have chosen, to find a better one, and then use the approachment methods from magnetic circuit to electric circuit.

Modified Cuk converter with RLC loads and ripple current around less than 1% has a good geometry of core toroid in Cuk converter Slobodan. The twisted coil winding could be reduce the frequencies, so the ripple current become lower and increase the efficiency.

Toroid core as magnetic circuit could be calculated as approachment method applied to electric circuit where the matterial could be generate the source like air gap, and the real sources coil winding in primary and secondary. Modification conductor in coil winding in primary and scondary was fifty degrees twisted. The Twist could minimize the ripple from 3.2% become 0.21%.

Keywords

Toroid core, Cuk converter, air gap, surface of conductor, low ripple and high frequency.

1. INTRODUCTION

In nano technology era, all devices become smaller, more compact, higher efficiency, lower in ripples and automatically controlled. Cuk Slobodan converter was always used in any system such as in automotive technology, electrical measurement, sound system, home theatre, and etc., but the real of Cuk Slobodan converter has ripple around 30%. In better system, like in industrial applications, the chemical coloring only allowed the ripple current around 3%.

Special design of toroid transformer for winding, shape, material and size with higher permeability could increase the efficiency and minimize the ripple. The good material air gap with low losses could increase the potential as gyrator capacitor. The core magnetic as inductor, capacitor and resistor, as equivalent capacitor and the winding as generated magnetomotance or Gyrator which is control the variable load as variable voltage control current source VVCS or curent controlled voltage source CCVS if the load has variable R,L and C. All of them could be reduce the ripple until 0.3 % and can generate the frequencies become KHz, with paralleling the material like two port and twisted more than one conductor. The winding could increase the frecuencies about GHz. [1]

Before twisted with the radius of conductor about r = 4.10^{-4} m, 8.10^{-4} m, 16.10^{-4} m has efficiences about 3.2 %, 4.3 %, 5% and after twisted be come 81 %, 85 %, 92 %

The output rippel current of Cuk converter where the inductance are 3 μH, 2.27 μH, and 1.83 μH before modification coil winding about 2.5 %, 1.6 %, 1.2 % after modification with twisted about 2.1 %, 1.2 % and 0.98 %, with toroid core become 98 %.

Gyrator capacitor which are increase the energy, could be minimise the losses [2] could be controlled the variable load RL and C .

2. GYRATOR CAPACITOR

Gyrator [3] as generate the voltage as two port could be increase the current source as hybrid circuit like Figure 1.

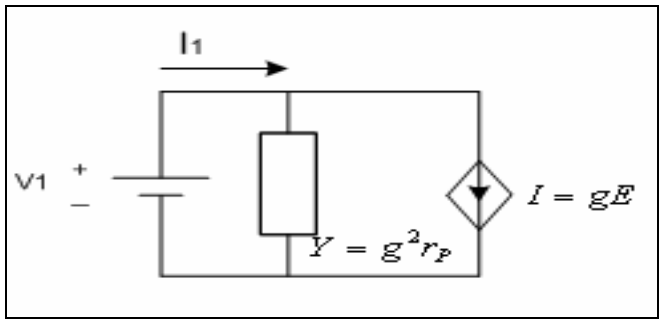

Figure 1: Gyrator as Voltage control current source.

From figure 1, the electric circuit is

$$i_a = V_s g^2 r_P + gE \quad (1)$$

And the gyrator load is

$$i_a = gV_s \quad (2)$$

Where:

r_p	:	The inner resistive.
i_a	:	Load current
i_s	:	Current source
g	:	Conductor of Gyrator.
i_{sc}	:	The short circuit current
RL	:	Resistance load

The sensitivity of current source with voltage system:

$$S_{V_S}^{i_S} \to 0$$

$$S_{E}^{i_S} \to 1$$

$$S_{g}^{i_S} \to 1 \quad (3)$$

3. CAPACITOR

The capacitor, as storage device has loading electricity, it takes from permanent magnetic air gap [4] which is depend on the material, circular mill, the long of magnet permanent, and permeability of magnetic permanent, if the force depend on reluctance it's hybrid of the electric as for hybrid parameter given by

$I_1 = g_{11}V_1 + g_{12}I_2$

$V_2 = g_{21}V_1 + g_{22}I_2 \quad (4)$

The equivalence magnetic circuit to electricity from equation 3 is showed in table 1. From the capacitance of magnetic circuit such as the twisted winding was taken from skin effect of current conductor.

4. DESIGN OF THE TOROIDAL CORE

The design for any type of air gap and the core of toroidal with the twisted conductor, in primary and scondary coil winding, with the angle of twisted, could reduce the qualities and efficiency. For the first step, the inductance of cunductor must be taken from the lentgh, radius, circular mill, resistivity the material of coil winding conductor where the data length of conductor are $l_1 = l_2 = 3$ m, for one conductor which is change with two conductor, $r_1 = r2 = 8.10^{-4}$, 4.10^{-4} , or 16.10^{-4} m, so it could calculated of the effective long l_{1e} wire gauge. The long efective coil winding in primary and scondary l_{1e} are : 1 - 2.7 m, so it could fixing some parameters [5] :

- the length of $l_e = l \cos(\beta/2)$,
- Where $\beta = 50^0$,
- $l_{1e} = 3\cos(50^0/2) = 3 \times 0.9 = 2.7$,
- resistivity of Cu, $\rho = 1.72.10^{-8}$ ohm/m,
- permeability of air $\mu_0 = 4\pi^7$ weber/amp,
- frequencies f = 25 KHz,
- conductivities $\sigma = 5.8.10^7$ Ω/m,

so the coupling could be calculated

$$k_1 = r\sqrt{\omega.\mu_0.\pi/2\rho}$$

$$k_1 = 1{,}7 \quad (5)$$

The efficiency will depend on the resistance DC of magnetic circuit toroidal from the modify coil winding

$R_{D\,1} = \rho\, l_1/(\pi\, r_) = 0.1$ Ohm,

Where the resistance DC is as resistance of Gyrator R_G.

Coupling factor in primary winding is alternating current AC resistance R_{A1}, which is depend on the coupling factor. Because of coupling factor in primary K_1 is bigger or equal than 1, the AC resistance AC RA1:

$R_{A1} = R_{D1}\,[(1/4) + k_1 + (1/64)(1/k_1^3)] = 0{,}19\ \Omega$ so

The self inductance in wire gauge primary coil winding L_{i1}:

$L_{i1} = (\mu_0.l_1/2).[(1/k_1) - (1/64)(1/k_1^3)] = 1{,}09\ \mu H$

The mutual inductance M because $l_{1e} \le l_2$,

$M = (\mu_0/2\pi).l_{1e}.\{\log[2.l_{2e}/(r_1+r_2)] - 1 = 1{,}53\ \mu H$

Inductance on in primary in AC L_1,

$L_1 = L_{i1} + (\mu_0/2\pi)l_1.\{\log[2l_1/r_1] - 1\} = 3\ \mu H$

So it cold be calculate the new efficiency

$$\eta = (R_L.M^2.w^2)/\sqrt{\left[L_1L_2w^2 - M^2w^2 - R_{A1}(R_L + R_{A2})\right]^2} + \sqrt{\left[L_1w(R_l + R_{A2} + R_{A1}L_2w\right]^2\left[(L_2w)^2 + (R_L + R_{A2})^2\right]}\cos\phi_1 \quad (6)$$

5. DISCUSSION

For the first condition where's the original Cuk konverter have big rippel like showed in Figure 2.

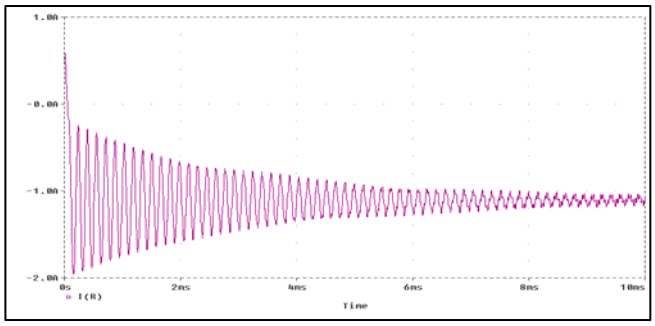

Figure 2: The Output ripple current of Cuk convertor Slobodan.

In figure 2 the output ripple current of Cuk converter Slobodan before the modification is more than 30 %.

After reduced with any component like one inductor coventional with two inductor but still the result was not

ISSN 114-1284

reduce the ripple current. After that, two Inductors changed with a special transformator torroidal design. The first is show the capacitance approachment like in Figure 3.

From the new parameter and the result of data input calculation in Pspice simulator software, it is found that the performance of toroidal capacitance is going better. So it will show any capacitance approachment in one shape toroidal.

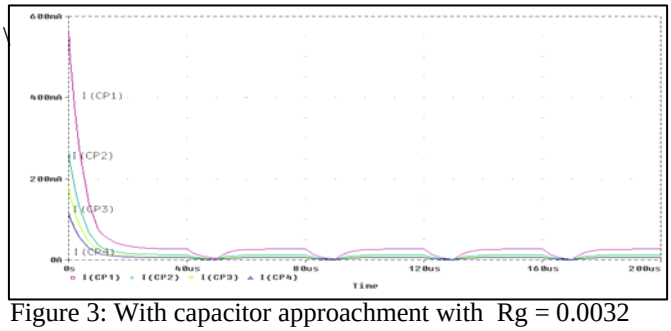

Figure 3: With capacitor approachment with Rg = 0.0032

With some variable, resistance of gyrator depend on the size of toroid shape and air gap. the smaller resistance of gyrator would make the smaller ripple current graphic as shown in figure 4.

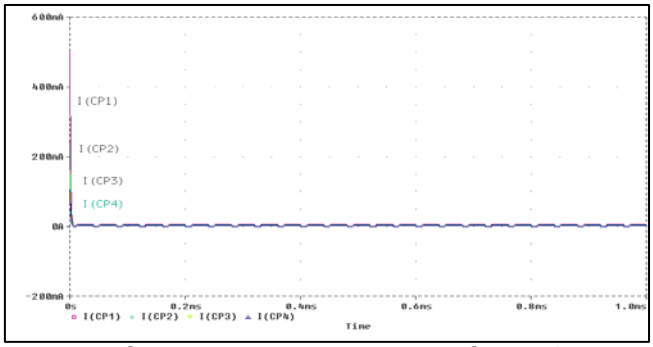

Figure 4: The current capacitance approachment (I_{CP1}, I_{CP2}, I_{CP3}, I_{CP4}) Vs Gyrator resistan R_G = 0.0064 Ohm

In figure 4 the current capacitor approachment, looks like more stable and the ripple is smaller. In condition of RL and C loading (I_{CP1}, I_{CP2}, I_{CP3}, I_{CP4}) vs. R_G =0.0012 ohm. The ripple current is shown in Figure 5.

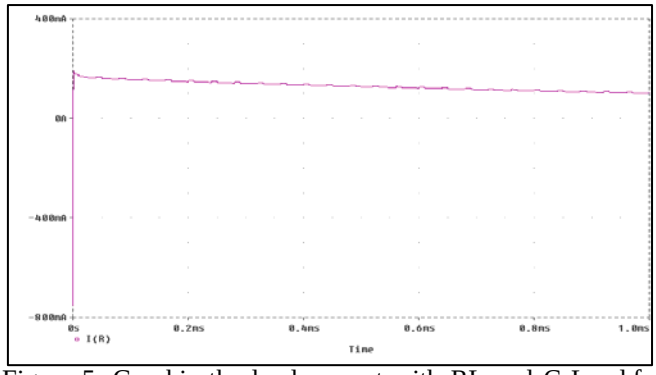

Figure 5: Graphic the load current with RL and C Load.for resistan Gyrator = 0.0012 Ohm.

The polygon curves introduce the output ripple current in twisted moment and the twisted chart is shown in figure 6.

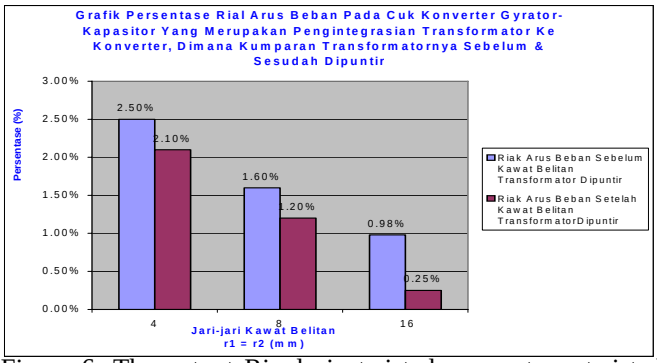

Figure 6: The output Ripple in twisted moment vs. twisted coil winding.

The polygon curve explains the current output of ripple current for the twisted is minimized the ripple current output.

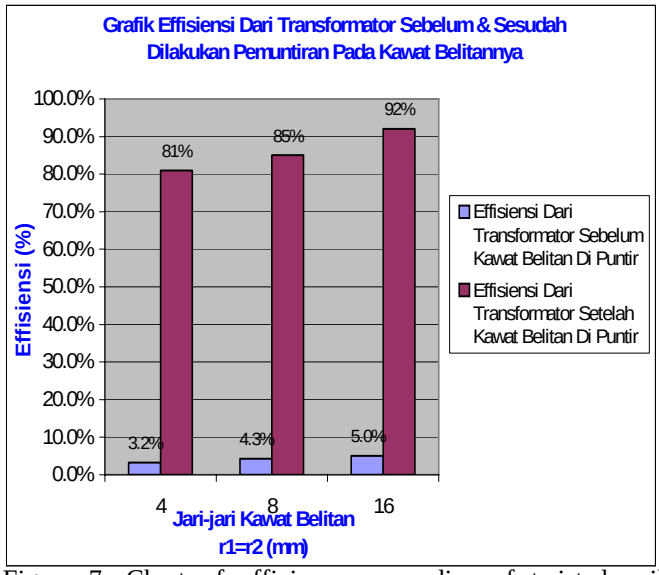

Figure 7: Chart of efficiency vs. radius of twisted coil winding.

In figure 7 the efficiency the cu coil winding after twisted and before twisted. The efficiency is higher when the twisted coil winding.

6. CONCLUSION

The size of toroid core as variable resistance of Gyrator, is causing the less of resistor Gyrator which have lower ripple current and higher efficiency.

REFERENCES

[1]. Jawad Faiz, B. Abed-Ashtiani, and M. R. Byat, *"Lumped Complete Equivalent Circuit of a Coreless High-Frequency Transformer"*, IEEE Transaction On Magnetic, Vol. 3

[2]. A. W. Lotfi, Pawel M. Gradzki and Fred C. Lee, *"Proximity effect in coil for high frekuency power application"*, IEEE Transaction on Magnetic , Vol 28, No. 5, September 1992.

[3]. David C. Hamil,*"Lumped Equivalent Circuit Of Magnetic Componen, The Gyrator – Capacitor Approach"*, IEEE Transaction On Power Electronics, Vol. 8, No. 2, April 1993.
[4]. Hj. Herawati A, Ir. MT, THesis, *"Perancangan konverter Cuk Slobodan Akumulasi Energi Dengan Metoda Pendekatan Rangkaian Magnet Gyrator – Kapasitor untuk meminimisasi Arus Riak"*.
[5]. H. M. Schlicke, Dr.-ing., *"Essentials of Dielectromagnetic Engineering"*, John Wiley & Sons, Inc, New York, London 1961.

CO_2 EMISSION AND COST OF ELECTRICITY OF A HYBRID POWER PLANT IN SEBESI ISLAND SOUTH OF LAMPUNG

Herlina[1], Uno Bintang Sudibyo[2], Eko Adhi Setiawan[3]

[1]*Faculty of Engineering*
University of Indonesia, Depok 16424
Tel : (021) 7270011 ext 51. Fax : (021) 7270077
E-mail : herlinawahab@yahoo.com

[2]*Faculty of Engineering*
University of Indonesia, Depok 16424
Tel : (021) 7270011 ext 51. Fax : (021) 7270077
E-mail : uno@eng.ui.ac.id

[3]*Faculty of Engineering*
University of Indonesia, Depok 16424 ms
Tel : (021) 7270011 ext 51. Fax : (021) 7270077
E-mail : ekoas@ee.ui.ac.id

ABSTRACT

Hybrid power plants based on diesel generator and renewable energy sources, like photovoltaic and wind energy, are an effective option to solve the power-supply problem for remote and isolated areas far from the grids

HOMER, a micropower optimization modeling software is used to analyze data for both wind speed and solar radiation in Sebesi Island. The software optimize the system configuration of the hybrid system by calculating energy balance on an hourly basis for each of the yearly 8760 hours, simulating system configurations at once and rank them according to its net present cost [1]. In this paper, configuration design optimization of the hybrid system is analyzed to fulfill the electricity demand in Sebesi Island taken into account the issue of CO_2 emission reduction due to utilization of fossil fuel during diesel generator operation.

Optimization is done with three conditions, a first condition with 2 diesel generating unit 40 kW and 50 kW each, second condition a hybrid system with 25% maximum renewable fraction and a third condition a hybrid system with more than 25% minimum renewable fraction. The result obtained for the PV - wind - diesel hybrid are with 30% renewable fraction : 25% reduced CO_2 emissions or 48 ton / year or 25% from the first condition with 2 diesel generating unit, and the cost of electricity is the highest at $ 0,786 per kWh, the net present cost of $ 1.503.710, the initial capital cost of $ 738.010 and excess power reaching 85.212 kWh or 31.4%.

Key words: *Simulation, Hybrid Power Plant, Renewable fraction, Cost of Electricity, CO_2 emission*

1. INTRODUCTION

The Sebesi island is located south of Lampung Bay with 5° 55 '37.43 "- 5° 58'44, 48" latitude and 105° 27' 30.50 "- 105° 30 '47.54" longitude , close to the Krakatau islands. Administratively, this island is located in the Tejang Village Sebesi Island, Rajabasa Subdistrict, South Lampung Regency. The region consists of 4 (four) villages : Regahan Lada, Inpres, Tejang, and Segenom. The island covers a total area of 2620 ha and is inhabited by more than 2500 people, living mostly on agricultural products and fisheries. The island with a coastlines of 19.5 km has enough resources such as mangrove, the yet, and coral reefs [2].

It is a beauty islands located close to the Krakatau islands making it a tourist destination after the Krakatau islands. Unfortunately, potential tourism island is not supported by sufficient facilities by the local government, such as electricity. Nowadays the island get electricity only at night for about eight hours from 16.00 afternoon until 00.00 at night with a peak load of 49 kW which is supplied by two diesel generators with an installed capacity of 40 kW and 50 kW each.

In this study the electrical demand of the island will be analyzed using 2 units of diesel generating sets of 40 kW and 50 kW as first condition, and comparing them with the optimized hybrid system using HOMER software. Also analyzing CO_2 emissions, cost of electricity, and excess electricity of the system.

2. THE HYBRID SYSTEM AND ITS COMPONENTS

The hybrid system consists of two diesel generators 40 kW, 50 kW each, a photovoltaic array of 60 WP, a 7,5 kW wind turbine, a battery and an inverter. Figure 1 shows the hybrid system .

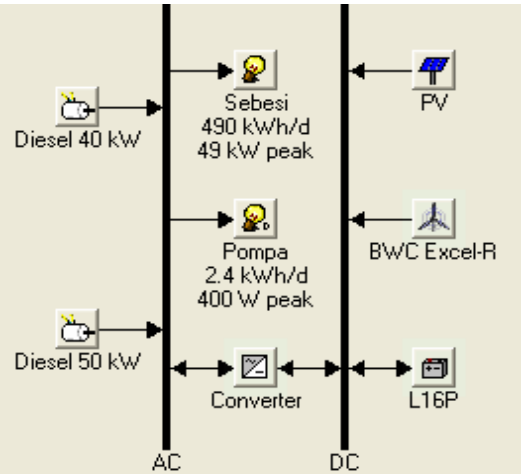

Figure 1. The Hybrid System

The hybrid system is simulated by three conditions, the first condition using 40 kW and 50 kW diesel, second condition a hybrid system with 25% maximum renewable fraction and a third condition a hybrid system with more than 25% minimum renewable fraction. All conditions are simulated with fixed load, wind speeds between 3 m/s - 7 m/s, fuel price between 0.4 – 1.0 $/l. Project lifetime of the system is 25 years, interest rate is 8%, the dispatch strategy is cycle charging and the generators are allowed to operate under the peak load.

3.1 The Load Demand

The load demand consists of 2 types, namely:

3.1.1 Primary Load

The electricity is consumpted majorly for household lighting, television and others. The daily average load on the island is about 490 kWh/day with 49 kW peak load from 19.00 till 20.00 o'clock.

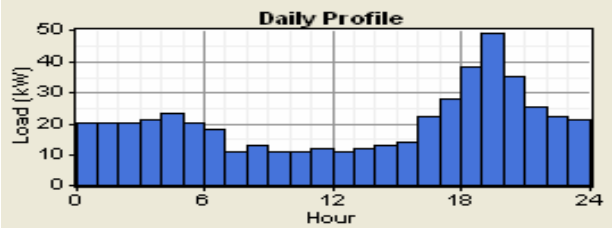

Figure 2. The Daily Load Profile of Sebesi Island [3]

3.1.2 Deferrable Load

A water pump of 400 Watts power has to be operated 6 hours per day to fill a fresh water tank designed to have a storage capacity of two days demand. So, there will be a 2.4 kWh/day average deferrable load or 4.8 kWh for two days storage. The minimum load ratio is 50%. Figure 3. shows the deferrable load of the water pump.

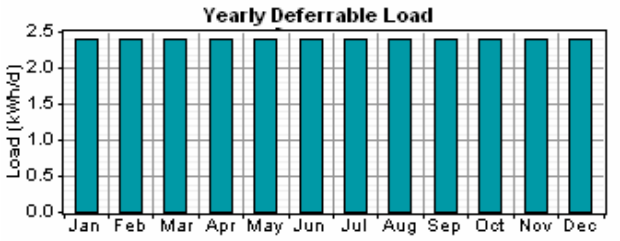

Figure 3. The yearly Deferrable Load of the Water Pump[4]

3.2 Wind turbines

The wind turbine used in this system is a 7.5 kW DC, 20 meter hub height, and a project lifetime of 15 years. Initial capital cost of the 7.5 kW wind turbine is $ 27.170, replacement cost $ 19.950, operation and maintenance cost is $ 1.000 a year

The HOMER software need the wind speed data to optimize the hybrid power plant. The following figure is the average wind speed data in Sebesi island, measured at 10 meters height.

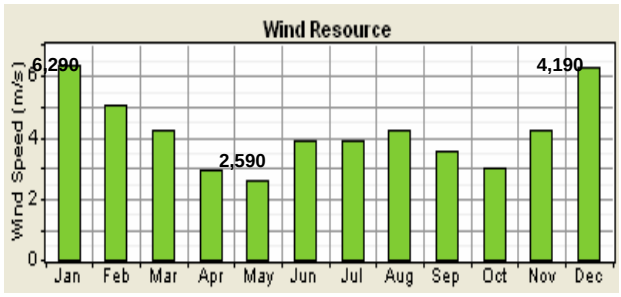

Figure 4. Wind Speeds on the Sebesi Island [5]

3.3 Photovoltaic Modules

The PV module used in this hybrid power plant has a maximum power of 60 Watt Peak (WP). The module derating factor is 90%, at a slope of 5.92 degrees, 180 degrees of azimuth, a ground reflectance of 20%, and a project lifetime of 25 years without tracking. The Initial capital cost for the 12 kW PV module is $ 66,000, replacement cost is $ 66,000 with no operating and maintenance costs.

To optimize the performance of the hybrid system, the software also needs yearly clearness index and daily radiation (kWh/m^2/day) data at the island. The yearly average clearness index is 0,477 and the daily average

radiation is 4,761 kWh/m^2/day. In figure 5 the clearness index and daily radiation data of the island is shown.

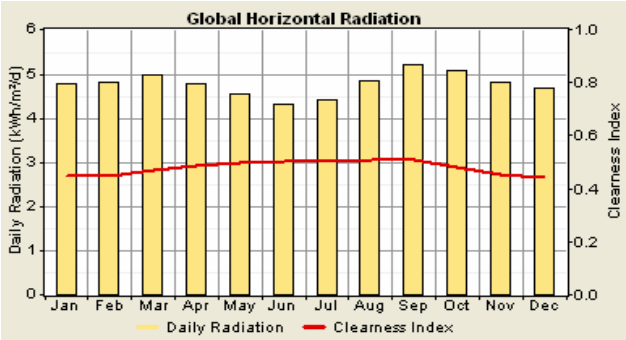

Figure 5. The yearly clearness index and daily radiation of Sebesi island [5]

3.4 The Diesel Generator

Two units of diesel generator is used in the hybrid system with an installed capacity of 40 kW and 50 kW each. The operating hour for each diesel generator is estimated to be 15,000 hours with a minimum load ratio of 30%. The 40 kW diesel generators has initial capital costs of $ 22,000, a replacement cost of $ 18,000, an daily operation and maintenance cost of $ 0.5. While the 50 kW diesel generators have an initial capital costs $ 27,000, a replacement cost $ 22,000, and an daily operation and maintenance cost of $ 0.5.

3.5 The Battery System

The hybrid system is designed to use lead acid batteries with nominal voltage of 6 V, a nominal capacity of 360 Ah, an initial capital cost of $ 620, a replacement cost of $ 620 and a 50 $ yearly operation and maintenance cost.

3.6 The Inverter

A bidirectional inverter (rectifier-inverter) is used in this hybrid system with a 90 % inverter efficiency, and a lifetime of 10 years. The rectifier has efficiency 85% relative to the inverter capacity of 100%. The 8 kW bidirectional inverter has an initial capital cost of $ 5960, replacement cost of $ 5,960 and an yearly operating and maintenance cost of $ 596.

4 CALCULATION OF THE HYBRID SYSTEM DESIGN

4.1 Calculation of the PV Array Power Output

The software uses the following equation to calculate the power output of the PV array:

$$P_{PV} = Y_{PV} f_{PV} \left[\frac{\overline{G}_T}{\overline{G}_{T,STC}} \right] \left[1 + \alpha_p \left(T_c - T_{c,STC} \right) \right]$$

where:

Y_{PV} is the rated capacity of the PV array, meaning its power output under standard test conditions [kW]

f_{PV} is the PV derating factor [%]

$\overline{G}_T$ is the solar radiation incident on the PV array in the current time step [kW/m2]

$\overline{G}_{T,STC}$ is the incident radiation at standard test conditions [1 kW/m^2]

α_p is the temperature coefficient of power [%/°C]

T_c is the PV cell temperature in the current time step [°C]

$T_{c,STC}$ is the PV cell temperature under standard test conditions [25 °C]

5. SIMULATION RESULTS

Different results of simulation and optimization are using the software in accordance to its minimum renewable fraction.

The result of simulation and optimization of the first condition using two diesel generating units of 40 kW and 50 kW are the cost of electricity (COE) of 0,510 $/kWh, an excess of electricity of 0.01% and CO_2 emission of 191 ton/year.

Figure 6 is shows the load demand supplied by two diesel generator of 40 kW and 50 kW.

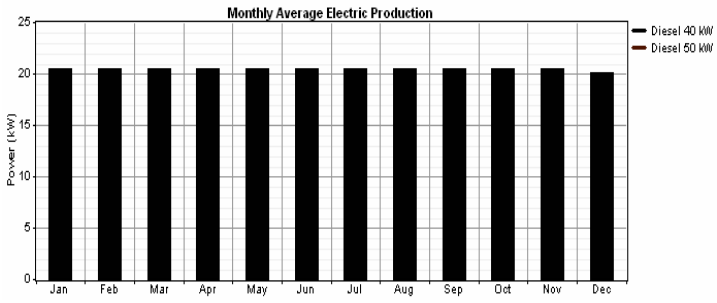

Figure 6. Supply of Load Demand by 40 kW and 50 kW diesel generators

In the second condition the minimum renewable fraction is 0%, the configuration of the hybrid system consist of 1 diesel generating unit – photovoltaic modules (PV) - wind turbines without battery. The results are as follows: for PV - diesel having 0,515 $/kWh of COE, excess electricity is 1.202 kWh/year or 0.66%, and the CO_2 emission is 188 ton/year. For wind - PV - diesel having COE 0,496 $/kWh, excess of electricity is 2.288 kWh/year or 1.24%, and the CO_2 emission is 173 ton/year.

The load demand is supplied by the hybrid system consisting of 82% by diesel generating unit, 3% by PV and 15% by wind turbine.

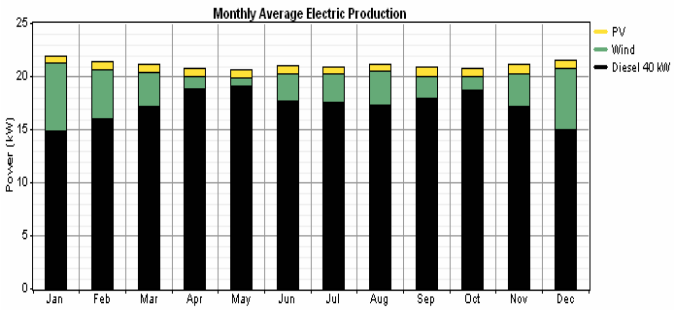

Figure 7. Supply of load demand by diesel, PV, and wind turbine with a maximum renewable fraction of 25%

When the hybrid system is simulated and optimized with 25% of maximum renewable fraction, the CO_2, SOx decrease caused by reduction of fuel consumption of the diesel generating unit. In figure 8, the blue line is the CO_2 emission and the pink line is the SOx. If the renewable fraction is 0% the CO_2 emission is 192 tons/year. CO_2 emission become 174 tons/year if the renewable fraction is 18%, a reduction of CO_2 emission as much as 18 tons/year decrease from 385 kg/year to 349 kg/year for a renewable fraction of 0% to 18%. This means a 36 kg reduction of SOx.

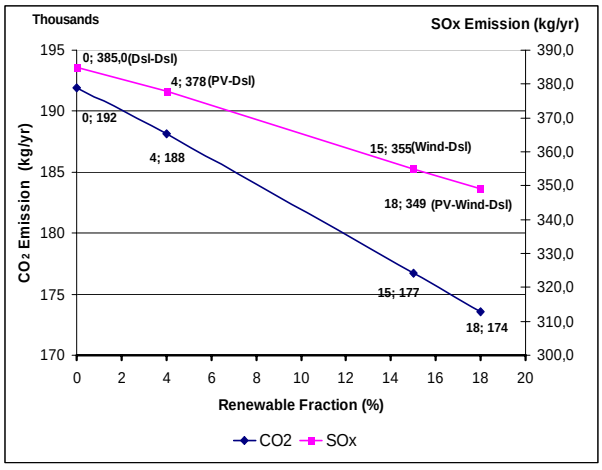

Figure 8. CO_2, SOx emissions – 25% maximum renewable fraction

In Figure 9, CO2 emissions decreased if renewable fraction increased as described above. The value of COE fluctuates with the changement of renewable fraction. When the renewable fraction is 0%, the load is supplied by 2 diesel generating units with a COE of 0,510 $/kWh, total NPC of $ 976.834. While the of renewable fraction is 4%, the hybrid system consisting of PV – diesel without battery, the COE increases to 0,515 $/kWh, NPC increases to $ 986.761. The lowest COE is 0,496 $/kWh if the renewable fraction is 15% and the hybrid system is consisting of wind-diesel with no battery, its NPC is $ 950.510. if the COE increase again to 0,510 $/kWh, the renewable fraction is 18%, the system consists of PV-wind-diesel without battery, its NPC is $ 976,801. Based on the conditions above, the author recommended a hybrid system consisting of wind-diesel.

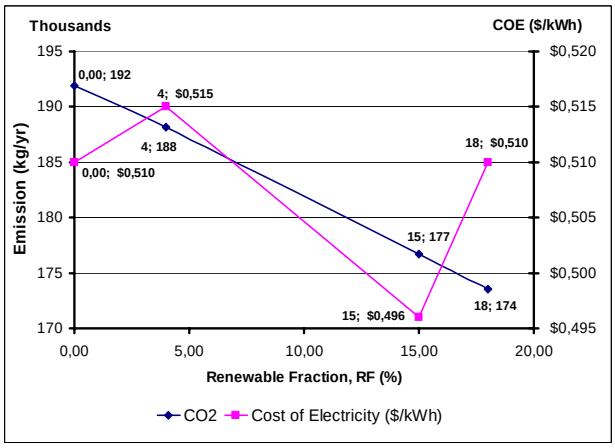

Figure 9. CO_2 emissions – cost of electricity (COE) – 25% maximum renewable fraction

In the third condition with a more than 25% renewable fraction the hybrid system consists of 1 diesel generating unit – PV – wind turbine without battery. The results for this condition are as follows: for PV – diesel, COE is 0,607 $/kWh, excess of electricity 22.464 kWh/year or 11%, and CO_2 emission is 174 ton/year. For wind - PV – diesel, COE is 0,785 $/kWh, excess of electricity 85.212 kWh/year or 31,4%, and CO_2 emission is 144 kg / year.

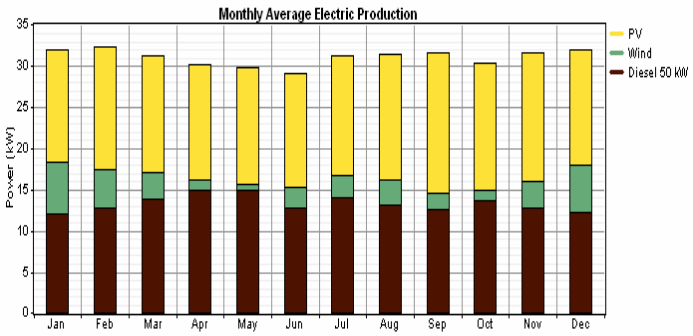

Figure 10. Supply of Load Demand by Diesel Generator, PV, Wind turbine with more than 25% renewable fraction

A Configuration of PV – wind – diesel with renewable fraction more than 25%, COE 0,510 $/kWh having the highest NPC of $ 738,010, excess electricity reaching 85,212 kWh/year or 31.4%, CO_2 emissions decreased as much as 48 ton/year or 25%. The load served by the hybrid system can be seen in figure 10 above.

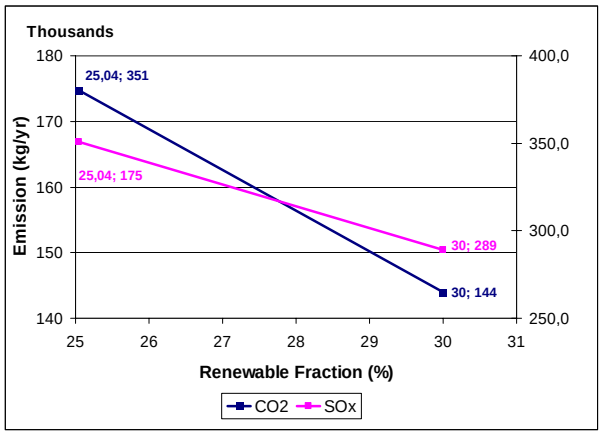

Figure 11. CO_2, SOx emission – more than 25% renewable fraction

In figure 11 above, the hybrid system is simulated and optimized with a more than 25% renewable fraction, the CO_2 and SOx emission levels decrease with decrease of the fuel consumption effect diesel generating unit. The CO_2 emission becomes 144 tons/year if renewable fraction 30% reduced as much as 48 tons/year. The SOx emissions, is reduced from 385 kg/year to 289 kg/year when renewable fraction increase from 0% to 30%. The SOx emission is reduced as much as 96 kg/year.

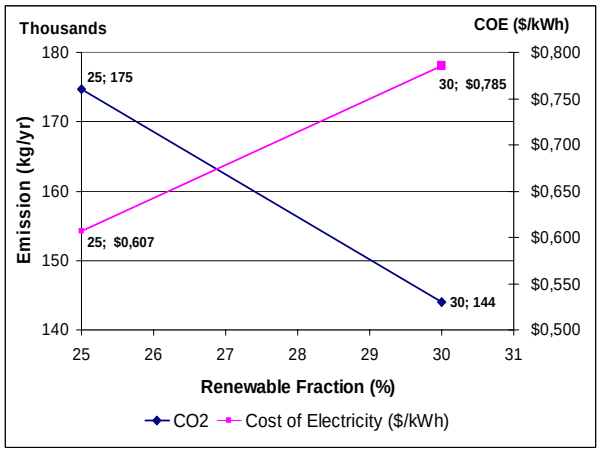

Figure 12. CO_2 emission – with a renewable fraction of 30%

In figure 12 the value of COE increased if the renewable fraction increases from 25% to 30%. If the renewable fraction is 25%, the COE is 0,607 $/kWh and the hybrid system consists of PV - diesel with no battery with 48 kW capacity of PV. Total NPC for this system is $ 1.163.327 with initial capital cost of PV is $ 264.000. If the renewable fraction is 30%, the COE is 0.785 $/kWh, the hybrid system consisting of PV - wind – diesel with no battery. Total NPC for this system is $ 1.503.710, the initial capital cost of 120 kW PV is $ 660.000. Based on results of simulation and optimization with a more than 25% renewable fraction, it is recommended to select a hybrid system consisting of PV-diesel with the lowest value of COE.

6 CONCLUSIONS

The value of COE, CO_2 and SOx emissions and excess of electricity fluctuated on different renewable fraction, it depending on total power generated and the total load served by the system. Which is the same following daily load curve of Sebesi Island? The largest excess power occurred at 30% of renewable fraction. A water pump as a deferrable load can be used to absorb this excess electricity.

The optimum hybrid system at 15% of renewable fraction, consist of wind – diesel with COE 0,496 $/kWh, NPC is $ 950.510 and the CO_2 emissions is 177 ton/year.

ACKNOWLEDGMENTS

The author would like to thank the Renewable Energy and Microgrid research group of the Department of Electrical Engineering University of Indonesia.

REFERENCES

[1] Gilman, P., Lambert, T., “Homer the micropower optimization model software started guide”, National Renewable Energy Laboratory of United States Government (2005)
[2] Wiryawan, B., Yulianto I., Susanto, A. H., “ Profil Sumberdaya Pulau Sebesi, Kecamatan Rajabasa, Lampung Selatan”, Penerbitan Khusus Proyek Pesisir, Coastal Resources Center, University of Rhode Island, Narraganset, Rhode Island, USA (2003)
[3] Apriansyah, “Laporan Data Beban Harian Pulau Sebesi”, PT. PLN (Persero) Wilayah Lampung Cabang Tanjung Karang Ranting Kalianda (Februari 2009).
[4] Gilman, P., Lambert, T., “optimization model software”, National Renewable Energy Laboratory of United States Government (2005)
[5] www.weatherbase.com, “wind speed for Sebesi Island”, 2009.
[6] http://eosweb.larc.nasa.gov, ‘”clearly index and daily radiation for sebesi island”, 2009.
[7] http://www.solarex-solar.com/pv/pvlist/pvsiemens /pvsiemens.htm, “Price and Product for Photovoltaic Module”. (2009)
[8] http://bergeywindpower.com/7.5 kW.htm, “Price and Product for Wind Turbin 7.5 kW DC”. (2009)
[9] http://www.powerscity.com/32_Deutz-diesel-engine-TD226B-4D--Stamford-alternator.html (2009).
[10] http://www.sma-america.com/en_US/products/off-grid-inverters.html. (2009)
[11] http://www.affordable solar.com/trojan.battery.l16p 390ah.htm. (2009)
[12] Nayar. C. , Tang. M,, Suponthana. W., “An AC Coupled PV/Wind/Diesel Microgrid System Implemented in A Remote Island in The Republic of Maldives”, Proceedings of the AUPEC Conference, Perth (December 2007).
[13] Milani. N.P., “Performance Optimization of A Hybrid Wind Turbine – Diesel Microgrid Power System”, Master of Science Thesis, North Carolina State University (2006).
[14] Setiawan, A.A., Nayar, C.H., ”Design of Hybrid Power System for a Remote Island in Maldives”, Department of Electrical and Computer Engineering Curtin University of Technology, Australia (2004).

Single Axis Sun Tracking Using Smart Relay

I. Daut[a], M. Sembiring[b], M. Irwanto[a], S. Hardi[a]
HS. Syafruddin[a], Indra N[a], Risnidar C[a], K. Anayet[a]

[a] *Cluster Power Electronic and Machine Design*
School of Electrical System Engineering
University Malaysia Perlis (UniMAP)
Perlis, Malaysia
E-mail : irwanto@unimap.edu.my

[b] *School of Mechatronic Engineering*
University Malaysia Perlis (UniMAP)
Perlis, Malaysia
E-mail :merdang@unimap.edu.my

ABSTRACT

Photovoltaic (PV) converts solar energy directly into direct current electric energy. The amount of electrical energy which will be obtained from the photovoltaic (PV) system is directly proportional to the intensity of the sun light which falls on the module surface. Sun tracking system is designed in a way to track the sun on single axis. The movement of PV module is controlled to follow the sun's radiation by LDR sensor using smart relay SR2 B121JD. Maximum benefit is derived from solar energy by providing that the PV module system be oriented at a right angle to the sun which will be got maximum power. Each of two 50 W of PV modules is compared, one of PV modules placed on fix position (without solar tracking) and the other with solar tracking. PV module output terminal is loaded by a lamp 12 V/5 W. Open circuit voltage (V_{oc}), load voltage (V_L), load current (I_L) and power (P) of PV module output terminal are measured every 30 minutes from 9.00 am to 5.00 pm. The result the average improvement of V_{oc} = 4.5 %, V_L = 11.43 %, I_L = 4.70 %, and P = 16.45 %.

Keywords
Photovoltaic, solar tracking, smart relay

1. INTRODUCTION

Photovoltaic system is a very important alternative energy and its efficiency been increasing by researcher. There are three method for increasing the efficiency of PV, the first is the increasing the efficiency of solar cell, the second is the energy conversion system included MPPT control algorithm and the third is the using solar tracking system [1]. The method of maximum power point is based on closed loop current control, in which the reference current is determined from the fitted function of I_{mpp} versus $P_{\max}$, points of a particular photovoltaic generator (PVG) [2]. A simplified computer model of the PVG is given and computer simulation for demonstrating the effectiveness of the proposed algorithm are presented. From the result of the simulations and experiment studies, it is concluded that that the proposed approach can be used as a robust and fast acting maximum power point tracking.

In this paper is proposed to developed PV of 50 W tracking system using smart relay SR2 B121JD. The system was designed into two parts, that are mechanical movement and electrical controller. The mechanical movement consist of dc motor and gears for moving the PV module from east to west. The electrical controller consist of a voltage and current divider circuit [3] and smart relay.

2. PHOTOVOLTAIC AND SOLAR TRACKING

2.1 Photovoltaic

Physics of the photovoltaic (PV) cell is very similar to the classical p-n junction diode (Figure 1). When light is absorbed by the junction, the energy of the absorbed photon is transferred to the electron system of the material, resulting in the creation of charge carriers that are separated at the junction.

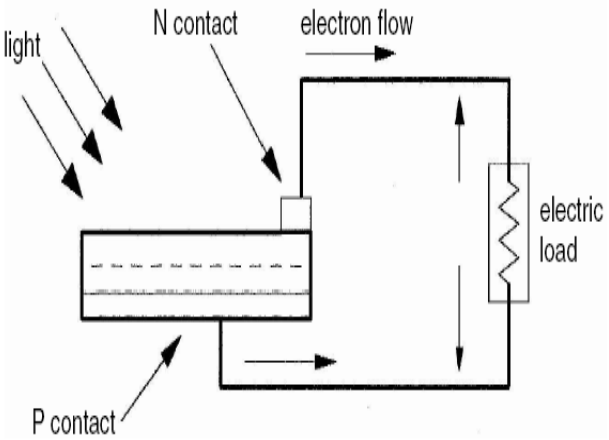

Figure 1: Photovoltaic effect converts the photon energy into voltage across the p-n junction

The charge carriers may be electron-ion pairs in an electron hole pairs in a solid semiconducting material. The charge carriers in the junction region create a potential gradient, get accelerated under the electric field and circulate as the current through an external circuit. The current squared times the resistance of the circuit is the power convert into electricity. The remaining power of the photon elevates the temperature of the cell [4].

For obtaining high power, numerous such cell are connected in series and parallel circuits on a module area of several square feet (Figure 2). The solar array or panel is defined as a group of several modules electrically connected in series and parallel combinations to generate the required current and voltage.

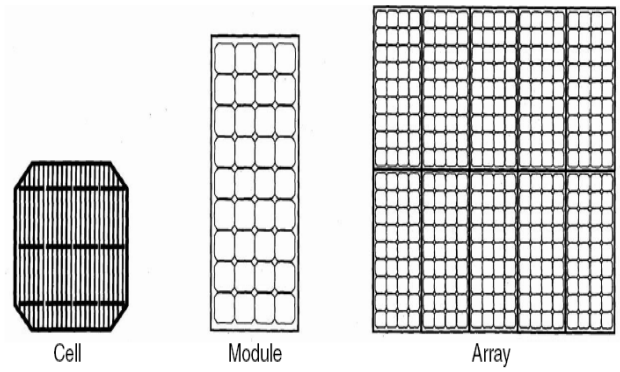

Figure 2: Several pv cells make a module and several modules make an array

Figure 3 shows the actual construction of a polycrystal silicon solar module in a frame.

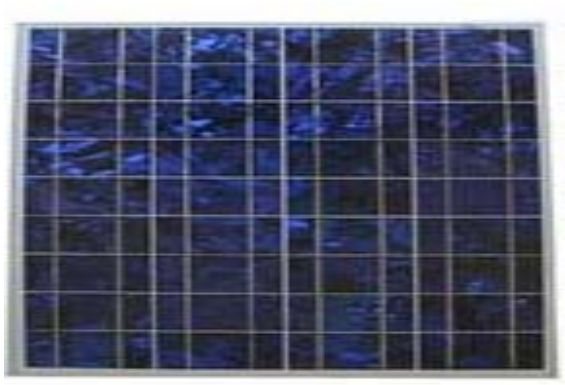

Figure 3 : A polycrystal silicon solar module in a frame

PV converts solar energy directly into direct current electric energy. The amount of electrical energy which will be obtained from the photovoltaic (PV) system is directly proportional to the intensity of the sun light which falls on the module surface. However, the change observed in sun light does not occur linearly, for this reason it is desired that the solar panel be fixed in a way that they face the sun or that they have a system which tracks the sun. Sun tracking system is designed in a way to track the sun on single axis. The movement of PV module is controlled to follow the sun's radiation by LDR sensor using smart relay SR2B121JD. Maximum benefit is derived from solar energy by providing that the PV module system be oriented at a right angle to the sun which will be got maximum power.

2.2 Solar Tracking Circuit

The solar tracking circuit is be shown in Figure 4.

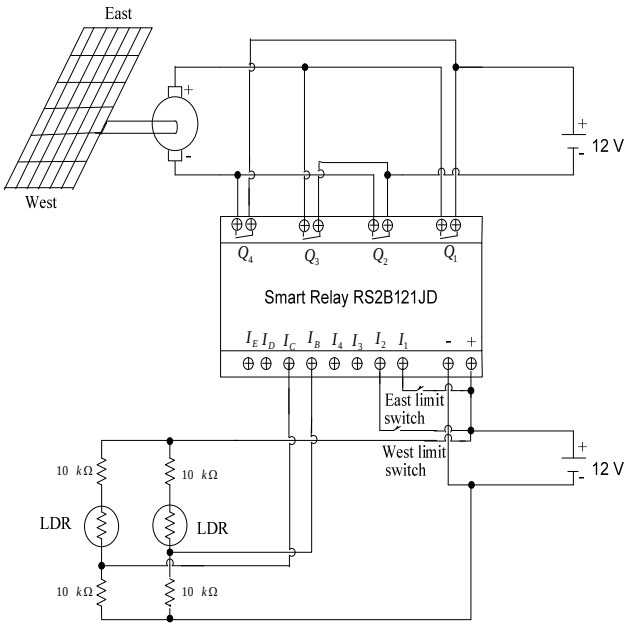

Figure 4 : Solar tracking circuit

Two LDRs are installed on east and west of PV module. If the east LDR gets intensity of the sun light is higher than west LDR, the PV module will move to east. Otherwise, if the west LDR gets higher intensity , the PV module will move to west. When the intensities of both LDRs are same, the DC motor will stop. The east and west limit switch will stop DC motor, when they are touched by PV module.

3. RESEARCH METHODOLOGY

3.1 The Used Devices in This Research

The used devices in this research consist of :

1. Hardware
   The hardware that were used in this research :
   a. Photovoltaic 50 W
   b. Direct current motor
   c. Smart relay SR2B121JD
   d. Voltage and current divider circuit

2. Software
   The used software is Zeliosoft2. This software is needed to create ladder diagram and loaded to smart relay.

3. 2 Research Procedure

The research procedure can be drawn by a flow chart in figure 5.

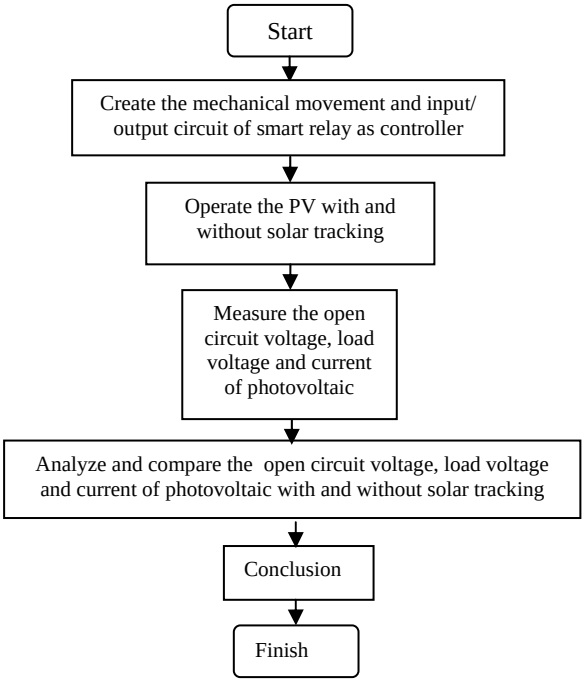

Figure 5: Flow chart of research procedure

4. RESULT AND DISCUSSION

Each two 50 W of PV modules is compared, one of PV modules placed on fix position (without solar tracking) and one other with solar tracking. PV module output terminal is loaded by a lamp 12 V/5 W. Open circuit voltage (V_{oc}), load voltage (V_L), load current (I_L) and power of PV module output terminal are measured every 30 minutes from 9.00 AM to 5.00 PM. V_{oc} - H, V_L - H, I_L -H, and P-H curve are shown in Figure 6,7, 8and 9, respectively.

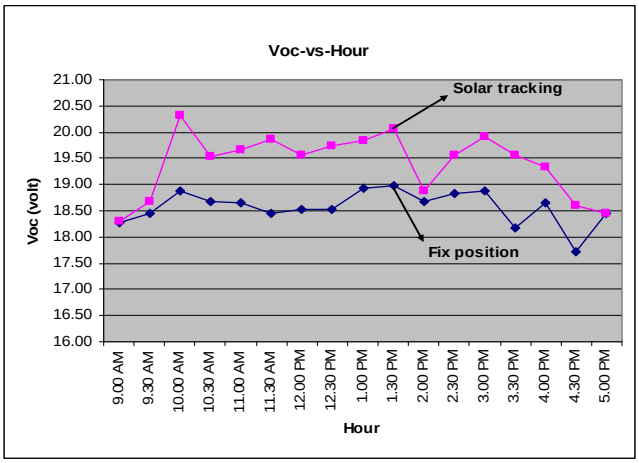

Figure 6. V_{oc} - H curve

Figure 6 shows that with solar tracking open circuit voltage V_{oc} of PV module increase compared to fix position.

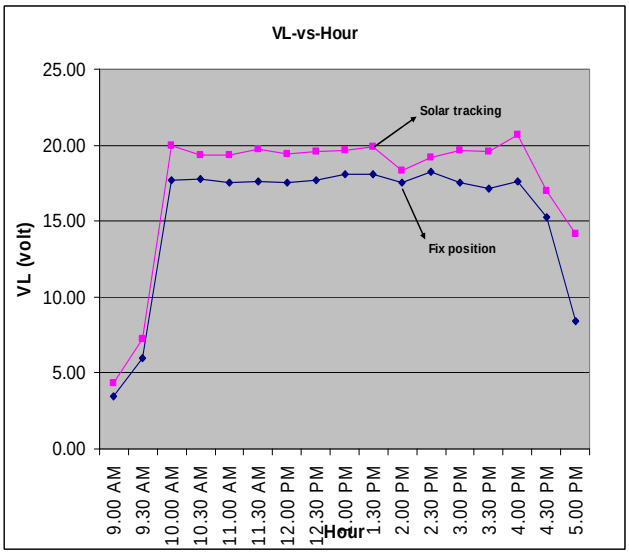

Figure 7: V_L - H curve

Figure 7 shows that with solar tracking load voltage V_L of PV module increase compared to fix position.

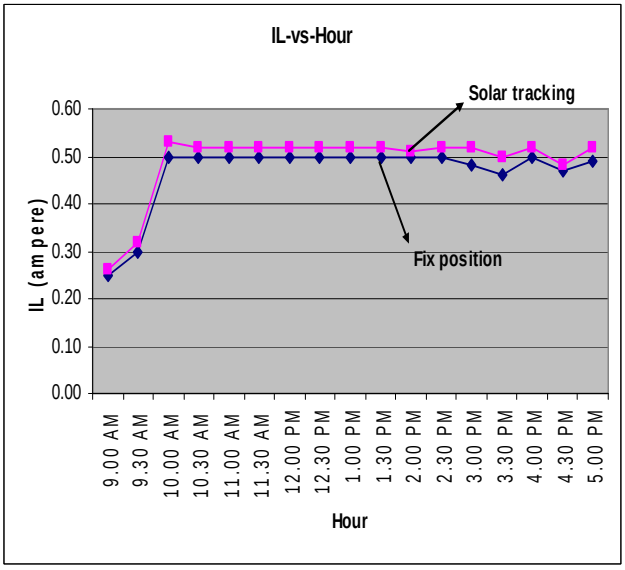

Figure 8: I_L -H curve

Figure 8 shows that with solar tracking load current I_L of PV module increase compared to fix position.

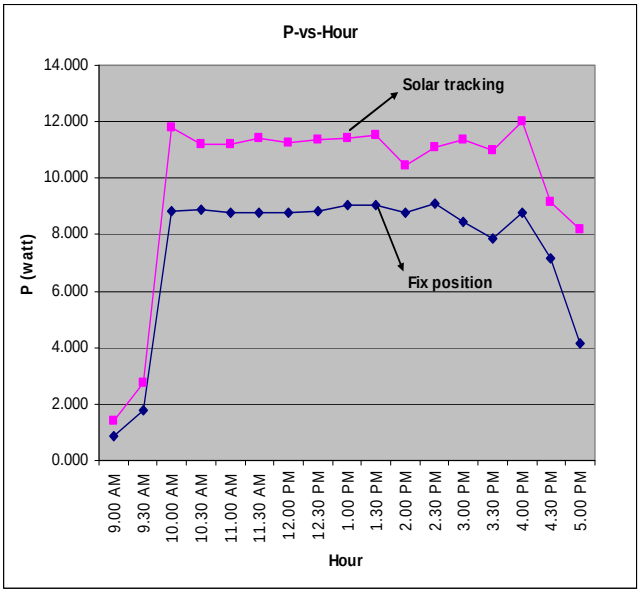

Figure 9. P-H curve

Figure 9 shows that with solar tracking power P of PV module increase compared to fix position.

From Figure 6 to 9 are seen that the PV module with solar tracking better than fix position (without solar tracking). The average improvement of open circuit voltage (V_{oc}), load voltage (V_L), load current (I_L) and power (P) are shown as below.

Table 1. Electric variable average improvement of PV module

Electric variable	V_{oc}	V_L	I_L	P
Average improvement (%)	4.50	11.43	4.70	16.45

5. CONCLUSION

According to the research result can be concluded

1. The smart relay and its input circuit (voltage and current divider circuit) can be used to track solar.
2. The performance of PV module with solar tracking is better than fix position (without solar tracking). The average improvement of Open circuit voltage (V_{oc}) is 4.5 %, load voltage (V_L) is 11.43 %, load current (I_L) is 4.70 %, and power (P) is 16.45 %.

REFERENCES

[1] Z.G. Piao, J.M. Park, J.H.Kim, G.B. Cho, H.L. Baek, " A Study on the Tracking Photovoltaic System by Program Type", ScienceDirect, Elsevier, pp. 971-973.
[2] H.T. Duru, " A maximum power Tracking Algorithm Based on $I_{mpp} = f(P_{\max})$ Function for Matching Passive and Active Loads to a Photovoltaic Generator, ScienceDirect, Elsevier, 2 August 2005, pp. 812-817.
[3] Robert, L.B, 2007, *Introductory Circuit Analysis*, Pearson Prentice Hall, United State of America.
[4] Mukund R.P, 2006, *Wind and Solar power System*, Taylor and Francis Group, New York London.

STUDY OF POWER SYSTEM HARMONIC EFFECTS ON DISTRIBUTION TRANSFORMER

[a]Indra N., [a]Ismail D., [b]Syafrudin M., [a]Surya H., [a]Risnidar C.B.

[a]Cluster of Power Electronic and Machine Design-School of Electrical Systems Engineering, University Malaysia Perlis, 01000 Kangar, Perlis, Malaysia
e-mail: indra@unimap.edu.my

[b]School of Electrical and Electronic Engineering, University Sains Malaysia, 14300 Nibong Tebal Penang, Malaysia

ABSTRACT

This paper presents the effects of harmonic distortion load current and voltages on distribution transformers. A delta-wye transformers are usually used in distribution power system with load may be either the single-phase or the three-phase. Three-phase four-wire distribution power system has been widely used for supplying low-level voltage to office buildings, commercial complexes, manufacturing facilities etc. Most of these loads have nonlinear input characteristic and high input current harmonics that will effect to the transformer losses. The primary effect of the power system harmonics on the transformers are the additional losses, heating and reduce of a transformer life. The load losses components get affected by the harmonic current are the I^2R_{dc} loss, winding eddy current loss & the other stray losses.

Keywords: *Transformer, Harmonics and Power Loss.*

1. INTRODUCTION

Harmonics current and voltage distortion in power system have been present for decades ago. However the advanced technologies in power electronics development over the past decade, the application of power electronics in commercial and industrial buildings can cause of significant increase the level of harmonics distortion in the power system networks. Many distribution transformers were designed to operate at rated frequency but their loads gradually replaced with non-linear that inject the harmonic currents to the systems. The principal effect of non-sinusoidal voltages on the transformer's performance is the generation of extra losses in the core [1]. Non-sinusoidal currents generate extra losses & heating of the conductors, enclosures, clamps, bolts etc, thus reducing the efficiency of the transformer & accelerating the loss of life of the insulation due to the additional heating of the windings. The harmonic currents will have some effects to the distribution transformer such as [1]:

- Increase temperatures of windings, cleats, leads, insulation and can reach unacceptable levels.
- Increase leakage flux density outside the active parts and can cause the additional eddy current heating in metallic parts linked by the flux.
- The combination of the main flux & the increased leakage & zero sequence flux imposes restrictions on possible core over excitation.
- As the temperature changes, the moisture & gas content in the insulation & in oil will change.
- Bushings, tap changers, cable-end connections and current transformers will also be exposed to higher stresses, which encroach upon their design & application margins.

The most important effects of power system harmonics to the transformer are winding eddy losses, stray losses in other structural parts and potential regions of excessive heating. Due to the skin effect, the electromagnetic flux may not totally penetrate the strands in the winding at high frequencies. The increased of eddy current losses produced by a non-sinusoidal load current can cause excessive winding losses and hence abnormal temperature rise. Therefore the influence of the current harmonics is more important, not only because of the assumed square of the harmonic order but also because of the relatively large harmonic currents present in the power system.

2. REVIEW OF POWER TRANSFORMER LOSSES

Traditionally, transformer losses are divided into no load losses and load losses. The total loss can be expressed as:

$$P_T = P_{NL} + P_{LL}$$

Where: P_{NL} core or no load loss (watt), P_{LL} load loss (watt), P_T is total loss in watt.

P_{NL} is the loss due to the voltage excitation of the core and P_{LL} is loss due to P_{dc} and stray losses (P_{SL}). Stray loss is caused by electromagnetic fields in the winding, core clamps, magnetic shields, enclosure or tank wall, etc [2]. The stray losses can be further divided into winding eddy losses and structural part stray losses. Winding eddy losses consist of eddy current losses and circulating current losses. Other stray losses are due to losses in structures other than windings, such as clamps, tank or enclosure walls, etc.; this can be expressed in equation form [2]:

$$P_{LL} = P_{dc} + P_{EC} + P_{OSL}$$

The total stray losses P_{SL} is:

$$P_{SL} = P_{EC} + P_{OSL} = P_{LL} - P_{dc}$$

3. EFFECT OF POWER SYSTEM HARMONICS ON TRANSFORMERS LOSSES

3.1 Effect of voltage harmonics

According to Faraday's law the transformer voltage terminal can be determines by the flux level.

$$N_1.\frac{d\phi}{dt} \cong u_1(t) \qquad (1)$$

Transfer equation (1) into the frequency domain which shows the relation between the voltage harmonics and the flux components.

$$N_1.j(h\omega).\phi_h \cong U_h \qquad h = 1,3,... \qquad (2)$$

3.2 Effect of current harmonics

a. P_{dc} Losses

The increasing of rms value of the load current caused by harmonic component, the I^2R loss will be increase accordingly.

b. Winding eddy losses

Conventionally, the eddy current losses (P_{EC}) generated by the electromagnetic flux are assumed to be proportional with the square of the rms load current and the square of the frequency (harmonic order *h*), [3]-[4]

$$P_{EC} = P_{EC-R}\sum_{h=1}^{h=\max} h^2\left(\frac{I_h}{I_R}\right)^2$$

c. Other stray losses

The other stray losses are assumed to vary with the square of the rms load current and the harmonic frequency to the power of 0.8, [3]-[4].

$$P_{OSL} = P_{OSL-R}\sum_{h=1}^{h=\max} h^{0.8}\left(\frac{I_h}{I_R}\right)^2$$

The factor of 0.8 has been verified in studies by manufacturers and others, and accepted in the standards.

3.2.1 Winding eddy-current loss factor for transformers

The winding loss at a certain spot can be calculated as:

$$P_W = P_{dc} + P_{EC} \text{ W/m}$$

The normalized winding loss with the P_{dc} losses can be expressed as:

$$\frac{P_W}{P_{dc-R}} = \frac{P_{dc}}{P_{dc-R}} + \frac{P_{EC}}{P_{dc-R}} \qquad (3)$$

The first term,

$$\frac{P_{dc}}{P_{dc-R}} = \left(\frac{I}{I_R}\right)^2 = \frac{\sum_{h=1}^{h=\max} I_h^2}{I_R^2} \qquad (4)$$

The contribution of eddy current losses caused by magnetic field is obtained:

$$P_{EC} \approx \frac{\pi^2 f^2 T^2 B^2}{3\rho}$$

The leakage magnetic field *B* is directly proportional to the load current *I*, i.e

$$B = K_B I$$

When the load current is periodic but non-sinusoidal, its rms value,

$$I = \sqrt{\sum_{h=1}^{h=\max} I_h^2}$$

Where, I_h is the rms current harmonic of order *h*,
Hence,

$$P_{EC} \cong K\sum_{h=1}^{h=\max} h^2 I_h^2 \qquad (5)$$

where, $K = \frac{\pi^2 f^2 T^2 K_B^2}{3\rho}$

f is the rated frequency.

When the transformer is loaded at rated current I_R, the corresponding rated eddy current losses are

$$P_{EC-R} = KI_R^2 \qquad (6)$$

From (5) and (6)

$$P_{EC} = P_{EC-R}\sum_{h=1}^{h=\max} h^2\left(\frac{I_h}{I_R}\right)^2 \qquad (7)$$

Hence, the eddy current losses produced by a harmonic current load can be predicted based on the eddy current losses at rated current and fundamental frequency.
Substituting (4) and (7) into (3) gives:

$$\frac{P_W}{P_{dc-R}} = \left[\frac{\sum_{h=1}^{h=\max} I_h^2}{I_R^2} + \frac{P_{EC-R}}{P_{dc-R}}\sum_{h=1}^{h=\max} h^2\left(\frac{I_h}{I_R}\right)^2\right] \qquad (8)$$

Equation (8) was derived based on the assumption that the measured applied currents are taken at the rated currents of the transformer. Since this is seldom encountered in the field, a new term is defined based on the winding eddy losses at the measured current and power frequency, which may be read directly on a meter. A harmonic loss factor is defined in the IEEE standard [4].

$$\frac{P_W}{P_{dc-R}} = \frac{\sum_{h=1}^{h=h_{\max}} I_h^2 I_h^2}{I_R^2}\left[1 + \frac{P_{EC-R}}{P_{dc-R}}\frac{\sum_{h=1}^{h=h_{\max}} h^2 I_h^2}{\sum_{h=1}^{h=h_{\max}} I_h^2}\right]$$

The harmonic loss factor can be normalized to either the fundamental or the rms current:

$$F_{HL} = \frac{\sum_{h=1}^{h=h_{\max}} h^2 I_h^2}{\sum_{h=1}^{h=h_{\max}} I_h^2} = \frac{\sum_{h=1}^{h=h_{\max}} h^2\left(\frac{I_h}{I_1}\right)^2}{\sum_{h=1}^{h=h_{\max}}\left(\frac{I_h}{I_1}\right)^2}$$

$$P_W(pu) = I^2(pu)\left[1 + P_{EC-R}(pu)F_{HL}\right]$$

Where, $I^2(pu)$ is the normalized current squared, $P_{EC\text{-}R}(pu)$ is the normalized eddy current loss under rated conditions, F_{HL} is the harmonic loss factor. The harmonic loss factor is a key indicator of the current harmonic impact on the winding eddy losses. Under rated sinusoidal current $I(pu)=1$, $F_{HL}=1$ and the hot spot specific power loss is:

$$P_W(pu) = 1 + P_{EC-R}(pu)$$

4. CORRECTED WINDING EDDY CURRENT LOSS FACTOR

The assumption of eddy current losses in a winding are proportional to the square of harmonic order is only reasonable for transformers with small conductors. For larger conductors such an assumption leads to conservative results. A more accurate winding eddy current loss factor based on the following equation published in [5].

$$P_{EC} = \frac{\pi^2 f^2 T^2 B^2}{3\rho} F(\xi)$$

Where,

$$F(\xi) = \left[\frac{3\sinh\xi - \sin\xi}{\xi\cosh\xi - \cos\xi} \right]$$

When the current is non-sinusoidal as in (5),

$$P_{EC} = K' F(\xi) h^2 I^2$$

Where,

$$K' = \frac{\pi^2 f^2 T^2 K_B^2}{3\rho}$$

f is the rated frequency.

Hence,

$$P_{EC} = K' \sum_{h=1}^{h=\max} F(\xi) h^2 I_h^2$$

Normalizing the eddy current losses produced by a harmonic current load to the eddy current losses at rated condition a corrected eddy loss factor $h^2 F(\xi_h)/F(\xi_R)$ is achieved.

$$\frac{P_{EC}}{P_{EC-R}} = \frac{\sum_{h=1}^{h=\max} F(\xi_h) h^2 I_h^2}{F(\xi_R) I_R^2} \qquad (9)$$

Substituting (4) and (9) into (3) gives:

$$\frac{P_W}{P_{dc-R}} = \left[\frac{\sum_{h=1}^{h=\max} I_h^2}{I_R^2} + \frac{P_{EC-R}}{P_{dc-R}} \frac{\sum_{h=1}^{h=\max} h^2 F(\xi_h) \left(\frac{I_h}{I_R} \right)^2}{F(\xi_R)} \right] \qquad (10)$$

The corrected eddy losses factor as a function of the harmonic order h at 75°C immersed in an alternating field with 50 Hz fundamental frequency is shown in Figure 1. Figure 2 shows the corrected loss factor which is based on equation (9). The harmonic loss factors are presented as a function of the harmonic order, for different copper conductor thicknesses at 75°C immersed in alternating fields based on 50 Hz fundamental.

It can be seen that for small conductors skin effect is insignificant and only for large conductor dimensions at high harmonics does the difference become significant. It can be said that using the assumed eddy current loss factor h^2 predicts losses accurately for small conductors and low harmonics but produces a certain degree of error for a combination of large conductors and higher frequencies.

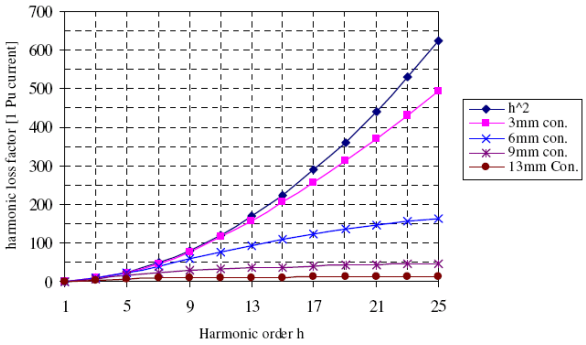

Figure1: Corrected winding eddy-current loss factor as a function of harmonic order h for different rectangular copper conductor dimensions [6]

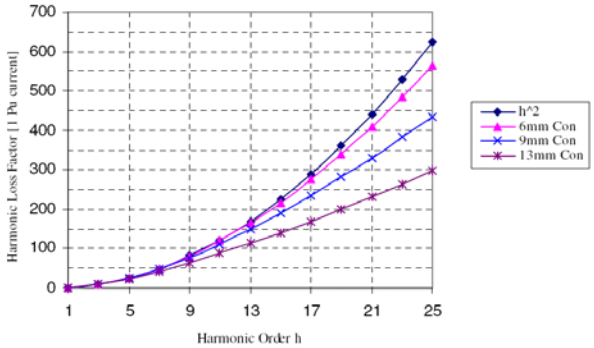

Figure 2: Corrected winding eddy-current loss factor as a function of harmonic order h for different rectangular copper conductor thickness [5]

5. COMPONENTS OF TRANSFORMER STRAY LOSS

The stray loss components can be estimated by thorough loss measurements at different frequencies or simply as recommended in [7].

$$P_h = P_{dc} + (P_{EC} x h^2) + (P_{SL} x h^{0.8})$$

$$P_1 = P_{dc} + P_{EC} + P_{SL}$$

Furthermore, Bendapudi [8] evaluated the frequency-dependent factors of winding eddy losses and other stray losses for specific transformer designs based on measurements at different frequencies. The harmonic loss factor K_h was defined as:

$$K_h = \frac{P_1 - P_o}{P_1} \left[w h^q + (1-w) h^r \right] + \frac{P_o}{P_1}$$

where, h is the harmonic order, K_h is the harmonic factor P_n/P_1, P_n is the load loss at the h^{th} harmonic, P_1 is the load loss at fundamental frequency, P_o is the loss due to the DC resistance, w are the winding eddy losses as a fraction of the total stray losses at fundamental frequency, (1-w) are the other stray losses as a fraction of the total stray losses at fundamental frequency.

The value of w is based on the calculation of the particular transformer design. Curve fitting was used to determine the best value for q and r. J. Drisen [9] suggested a

practical method to determine the winding frequency dependent factor with short circuit tests at harmonic frequencies. The loss factor was defined as:

$$K(f) = \frac{R_{AC}(f) - R_{DC}}{R_{AC}(f_1) - R_{DC}}$$

5. CONCLUSION

Harmonics effects on power system components and loads are important considerations in evaluating of harmonics impact on the distribution transformer. The main effects of harmonics on transformer are excessive winding loss and hence abnormal temperature. The excessive winding loss is due to the increasing of eddy current losses caused by harmonics.

Eddy current losses can be assumed to vary with the square of current and the square of the frequency for a small conductor. For large conductors and high frequencies, a corrected loss factor which considers the skin effect is needed. This leads to a more accurate prediction of transformer capability when subject to non-sinusoidal load currents.

6. REFERENCES

[1] R Jayasinghe, J.R Lucas, K.B.I.M. Perera, "Power System Harmonic Effects on Distribution Transformers and New Design Considerations for K Factor Transformers", *IEE Sri Lanka Annual Sessions* – September 2003.

[2] Linden W. Pierce "Transformer Design and Application Considerations for Nonsinusoidal Load Currents" *IEEE Transactions on Industry Applications* Vol.32 No. 2, PP 633-645 May/June 1996.

[3] IEC 61378-1 Standard Publication: 1997, "*Transformers for Industrial applications*".

[4] IEEE Std C57-110-1998, "*Recommended Practice for Establishing Transformer Capability when Supplying Non sinusoidal Load currents*".

[5] Elmoudi, Asaad, Lehtonen, Matti and Nordman, Hasse, "Corrected Winding Eddy Current Harmonic Loss Factor for Transformers Subject to Non-sinusoidal Load Currents" *2005 IEEE PowerTech'2005*, St. Petersburg, Russia, June, 27- 30, 2005, Paper 226, 6 p.

[6] S . N. Makarov, A. E. Emanual, "Corrected Harmonic Loss Factor For Transformers supplying Non-sinusoidal Load current" *Proc. of the 9th International conference on Harmonics and Power Quality*, vol. 1, Oct. 2000, pp.87-90.

[7] Working Group 12/14.10, "Load Loss In HVDC Converter Transformers" *Electra*, no.174 pp.53-57.

[8] S. R. Bendapudi J. C. Forrest, G. W. Swift "Effect of Harmonics on Converter Transformer Load Losses" *IEEE Trans. on Power Delivery*, vol. 6, no.1, Jan 1991, pp.153-157.

[9] J. Driesen, T. V. Craenenbroeck, B. Brouwers, K. Hameyer, R. Belmans, "Practical Method to Determine Additional Load Losses due to Harmonic Currents in Transformers with Wire and Foil Windings" *IEEE Power Engineering Society Winter Meeting*, 2000,Vol. 3, 23-27 Jan. 02 pp.2306 – 2311

Dual Band Triangular Microstrip Antenna Using Slot Feed By Electromagnetic Coupling

Indra Surjati, Yuli KN and Bramanto Seno
Electrical Engineering Department
Faculty of Industrial Technology Trisakti University
Jl. Kyai Tapa No.1 Grogol - Jakarta 11440 - Indonesia
Email : *indra@trisakti.ac.id*

ABSTRACT

Wimax is a wireless broadband technology which suitable for data communication. Modern communication system, such as satellite, radar and Wimax requires operation at two frequencies. When the system require at two frequencies too far apart, dual band patch antenna may avoid the use of two different antennas. This paper proposed a design of dual band triangular microstrip antenna using two slots feed by electromagnetic coupling. The two resonant frequencies can be generated by controlling the height and the distance between the two slots. Also adjusting the right length of the triangular and the second slot and the left length of the triangular and the first slot. Return loss of -31.90 dB with VSWR 1.05 for the first resonant frequency at 2.3 GHz and return loss of -13.49 dB with VSWR 1.49 for the second resonant frequency at 3.32 GHz. The results shown that the proposed antenna have the impedance bandwidth of 5.72% for the first frequency and 3.01% for the second frequency.
Keywords*: Dual band, triangular microstrip antenna, electromagnetic coupling*

1. INTRODUCTION

Patch antenna possesses many advantages such as low profile, light weight, small volume and compability with microwave integrated circuit (MIC) and monolithic microwave integrated circuit (MMIC). When modern communication system, such as for satellite, radar and wimax requires operation at two frequencies, dual frequency patch antennas may avoid the use of two different antennas [1]. Although rectangular and circular geometries are most commonly used, other geometries having greater size reduction find wide applications in modern communication systems, where the prime concern is compactness. The triangular patch antenna configuration is chosen because it has the advantage of occupying less metalized area on substrate than other existing configurations. Dual band operation of triangular patch microstrip antenna have been studied by many researchers using probe feed or direct coupling [2][3].

Basically, feeding system can be divided into two types such as direct coupling and electromagnetic coupling [4]. The use of electromagnetically coupled is to avoid the disadvantages of probe mechanism and can permit for improving bandwidth. In further development, the electromagnetic coupling will be identified as microstrip line and coplanar waveguide. To create dual frequency operation of triangular microstrip antenna using microstrip feed line from the top of the triangular patch antenna is already reported [5].

This paper therefore proposed a new design of dual band operation of triangular microstrip antenna using two different height slots and the feeding line is in the bottom of the triangular patch antenna. Details of the proposed antenna design and the results of the dual band performances are presented.

2. ANTENNA DESIGN

The geometry of the proposed antenna using two slot with different height for dual band operation feed by microstrip line can be shown in Figure 1a and 1b. The proposed antenna is constructed on two layers with the same dielectric substrate. On the first layer, the patch antenna is realized on FR 4 substrate having a relative permittivity (ε_r) = 4.98, substrate of thickness (***h***) = 1.53 mm and loss tangent ($\tan\delta$) = 0.09 and the microstrip feed line is realized on the second layer. Therefore the microstrip line feeding system is electromagnetically coupled to the patch.

From Figure 1a, ***a*** is the dimension of the side length of the triangular patch antenna, ***a1*** is the left length of the triangular and the first slot, ***a2*** is distance between the first slot and the second slot, ***a3*** is the right length of the triangular and the second slot. Beside that, ***x1*** and ***y1*** are the length and width of the first slot, ***x2*** and ***y2*** are the length and the width of the second slot. From Figure 1b, ***W1*** and ***L1*** are the length and width of the proposed feeding system and ***r*** is the distance from the left side of the triangular patch antenna to microstrip feed line. Table 1 shown the parameters of the proposed antenna and the microstrip feed line.

3. EXPERIMENTAL RESULTS

The dual band operation can be generated by inserting the two slots at the bottom side of the triangular patch antenna. The two resonant frequencies can be generated by controlling the two height slots while keeping the width of the slot fixed at 1 mm. By varying the distance of the two slots ***(a2),*** the input impedance matching of the feeding system can be characterized. This result is achieved by using an ordinary triangular patch antenna then is realized using this result.

Figure 2a and 2b shows the measured return loss can be achieved at ***a2*** = 5 mm. The first band frequencies from 2.238 GHz until 2.37 GHz, return loss of -31.90 dB can be obtained at the frequency 2.3 GHz with VSWR 1.05. While at the second band frequencies 3.27 GHz until 3.37 GHz, return loss of -17.27 dB can be reached at the frequency 3.3 GHz with VSWR 1.49.

Figure 3a and 3b, also Figure 4a and 4b shows the comparison between the simulation and the measurement results for the return loss and VSWR from the patch antenna. From Figure 3a and Figure 4a, the impedance bandwidth at frequency 2.3 GHz from the simulation is at 2169 MHz until 2442 MHz and the centre frequency is at 2.302 GHz with return loss -22.65 dB and VSWR 1.159. While the centre frequency from the measurement result is at 2.304 GHz with return loss -31.90 dB and VSWR 1.05 and has the impedance bandwidth from 2238 MHz until 2370 MHz or about 5.72%.

Figure 3b and Figure 4b shows that at frequency 3.3 GHz, the impedance bandwidth from the simulation is at 3155 MHz until 3449 MHz and the centre frequency is at 3.3 GHz with return loss -20.37 dB and VSWR 1.212. The impedance bandwidth from the measurement result is from 3270 MHz until 3370 MHz or about 3.01% at frequency 3.3 GHz. The centre frequency is at 3.32 GHz with return loss -13.49 dB and VSWR 1.49.

In general, the impedance bandwidth of the traditional microstrip antenna using probe feed is only a few percent. From the simulation results shown that the impedance bandwidth at frequency 2.3 GHz can be increased until 11.86% and at frequency 3.3 GHz is about 8.9%. One of the advantages using microstrip feed line is to enhance bandwidth. But from the measurement results, the impedance bandwidth is only 5.72% at the first frequency and 3.01% for the second frequency. It is shown that the impedance bandwidth for the simulation is wider than the measurement results, because the simulation is an ideal condition. Beside that, there is a movement when the patch and the feed line were combined each other. Table 2 shows the comparison parameters between the simulation and measurement results.

4. CONCLUSIONS

A novel configuration to excite dual band operation for Wimax application using slot feed by microstrip line has been experimentally studied. It is shown that the two frequencies can be easily controlled by varying the slot height and adjusting the distance between the two slots. It is observed that return loss of -31.90 dB with VSWR 1.05 can be achieved for the first frequency at 2.3 GHz and the impedance bandwidth is about 5.72%. For the second frequency at 3.32 GHz, return loss of -13.49 dB with VSWR 1.49 has the impedance bandwidth of 3.01%. Therefore the proposed antenna is applicable as a new candidate for dual band antenna microstrip for Wimax application.

REFERENCES

[1] Maci, S and Biffi Gentili, "Dual Frequency Patch Antennas", *IEEE Antennas and Propagation Magazine*, Vol.39, No.6, December 1997

[2] Fang, S.T and Kin Lu Wong, "A Dual Frequency Equilateral Triangular Microstrip Antenna With A Pair Of Narrow Slots", *Microwave And Optical Technology Letters*, Vol.23, No.2, October 1999

[3] Wong,K.L, *"Compact and Broadband Microstrip Antenna"*, John Wiley & Sons.,Inc.,NewYork, 2002

[4] Rahardjo, E.T, *"Studies On The Microstrip Antennas Fed By Electromagnetic Coupling"*, Doctoral Thesis, Saitama University, March 1996

[5] Surjati, Indra, "Dual Frequency Operation Triangular Microstrip Antenna Using A Pair Of Slit", *11th Asia Pacific Conference on Communications*, Perth, Western Australia, October 2005

Table 1 Parameters of the proposed antenna and microstrip feed line

Parameter	Length (mm)
a	24
a1	9
a2	5
a3	8
x1	10
x2	8
y1	1
y2	1
W1	2.8
L1	12,5
r	18

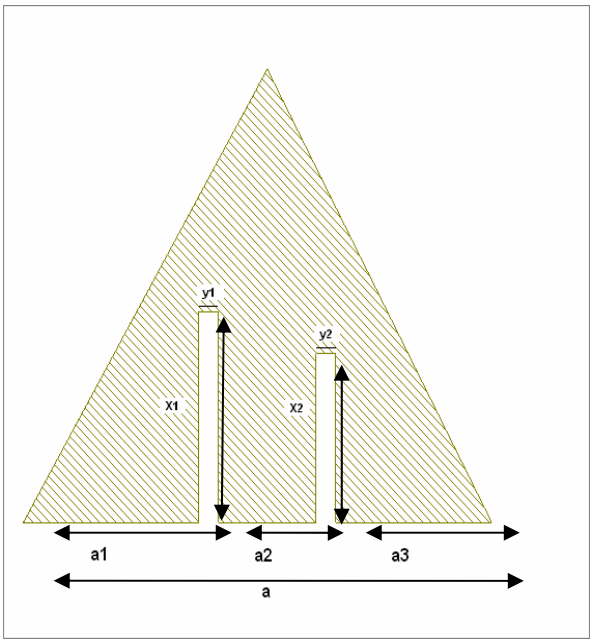

Figure 1a Geometry of the proposed antenna

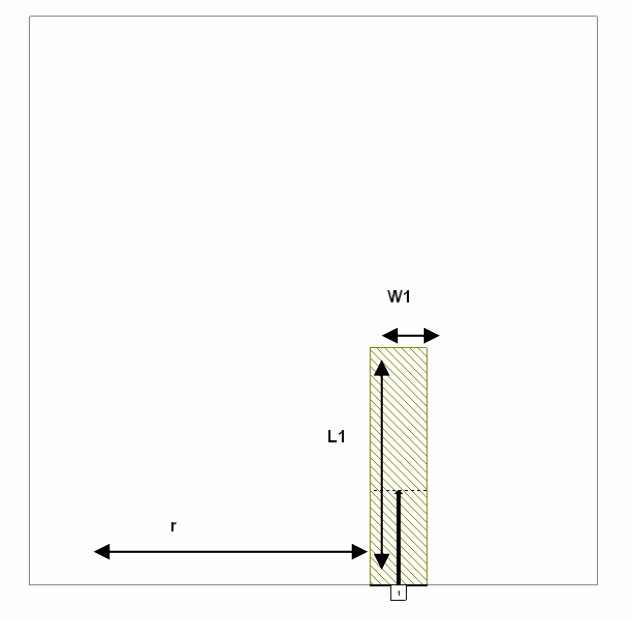

Figure 1b Geometry of the proposed microstrip feed line

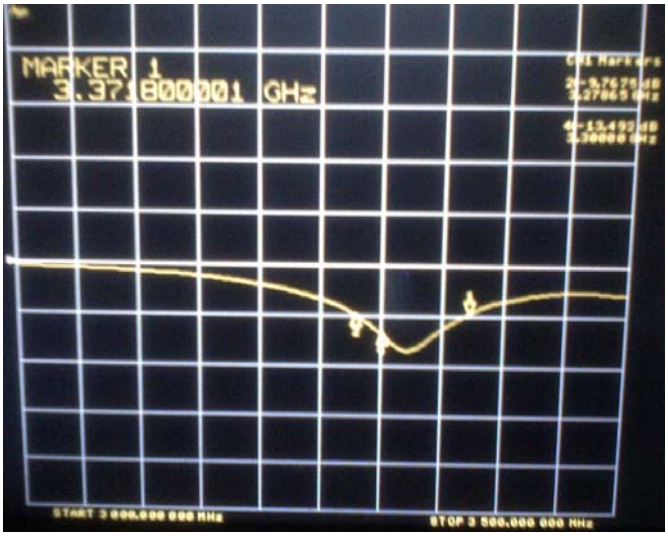

Figure 2a Measured return loss at frequency 2.3 GHz

ISSN 114-1284

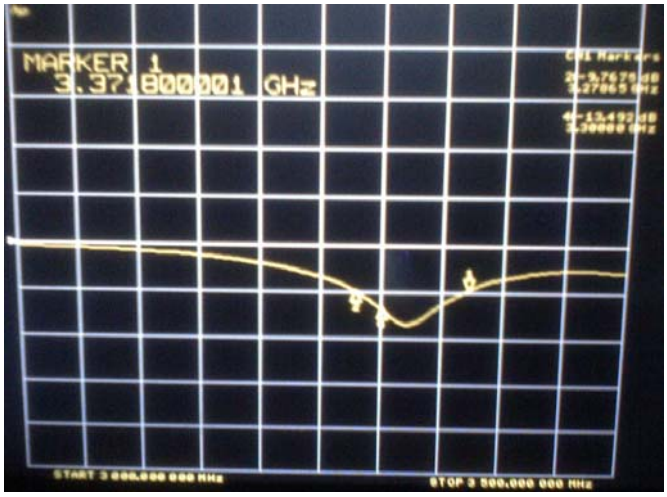

Figure 2b Measured return loss at frequency 3.3 GHz

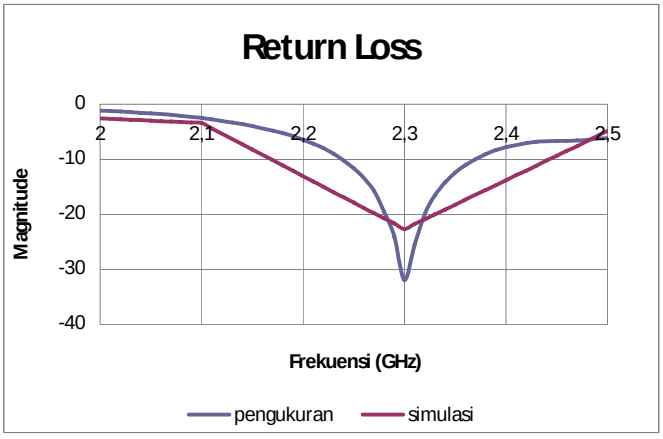

Figure 3a Comparison for return loss at frequency 2.3 GHz

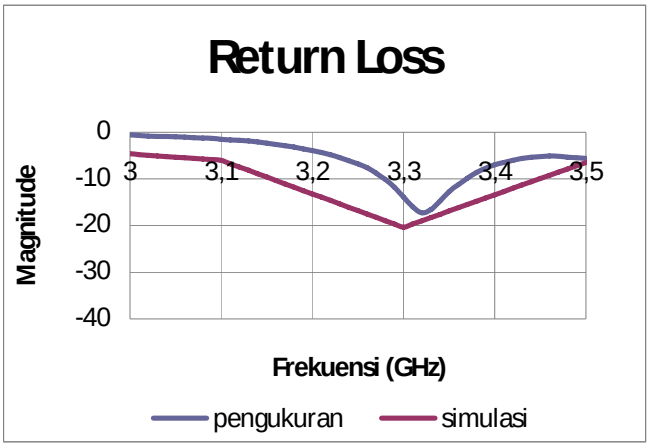

Figure 3b Comparison for return loss at frequency 3.3 GHz

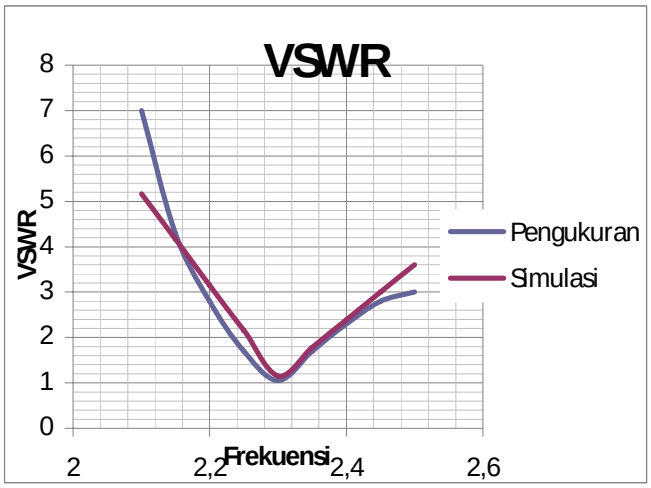

Figure 4a Comparison for VSWR at frequency 2.3 GHz

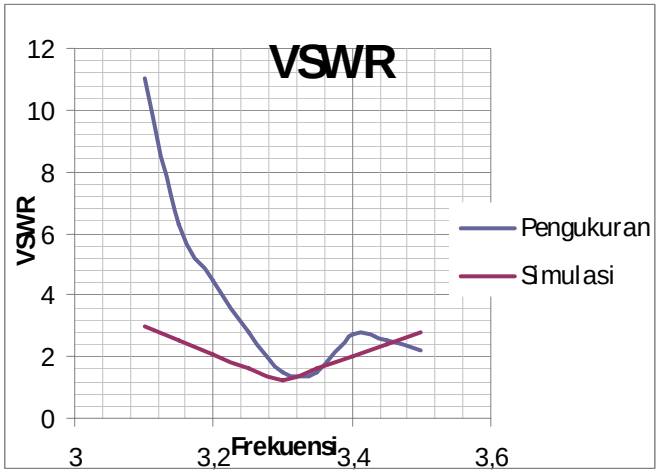

Figure 4a Comparison for VSWR at frequency 3.3 GHz

Table 2 Comparison parameters between the simulation and the measurement

Parameter	Simulation		Measurement	
Frequency	2.3 GHz	3.3 GHz	2.3 GHz	3.3 GHz
Impedance Bandwidth	2169 MHz – 2442 MHz or 11.86%	3155 MHz – 3449 MHz or 8.9%	2238 MHz – 2370 MHz or 5.72%	3270 MHz – 3370 MHz or 3.01%
Center Frequency	2.3 GHz	3.3 GHz	2.3 GHz	3.32 GHz
Return Loss	-22.65 dB	-20.37 dB	-31.9 dB	-13.49 dB
VSWR	1.159	1.212	1.05	1.49

ISSN 114-1284

In-plane Flux Distribution in 23^o T-joint of 3Phase Transformer Core with Staggered Yoke 10mm

I. Daut[a], Dina M.M. Ahmad[b], S. Zakaria[c]

[a]*School of Electrical System Engineering,*
Universiti Malaysia Perlis (UniMAP),
P.O Box 77, d/a Pejabat Pos Besar
01007 Kangar Perlis, Malaysia
Email address: ismail.daut@unimap.edu.my

[b]*School of Electrical System Engineering,*
Universiti Malaysia Perlis (UniMAP),
P.O Box 77, d/a Pejabat Pos Besar
01007 Kangar Perlis, Malaysia
Email address:dina@unimap.edu.my

[c] *School of Electrical System Engineering,*
Universiti Malaysia Perlis (UniMAP),
P.O Box 77, d/a Pejabat Pos Besar
01007 Kangar Perlis, Malaysia
Email address: shuhaimi@unimap.edu.my

ABSTRACT

This paper describes the result of measurement of in-plane flux distribution on 100kVA 3phase distribution transformer assembled with 23^o T-joint and mitred lap corner joint with stagger yoke of 10mm. The measurement involves the fundamental, third and fifth harmonic of the easy and hard direction of flux density at each location measurement. The flux distributions have been measured using no load test by arrays of search coil in M5 (CGO) grades material of transformer core laminations. The localised flux density at the outer 23^o T-joint is 0.147T and rises to be 0.206T at the inner edges of 23^o T-joint when the transformer core energized 1.5 T 50Hz. Harmonic occurs mostly in the T-joint where local regions are saturated and the flux deviates from the rolling direction.A small amount of flux deviation from the rolling direction occurs at the overlap, but no rotational flux is present in the joint.

Keywords
Grain oriented silicon iron, transformer core, in-plane flux distribution.

1. INTRODUCTION

Transformer iron loss can be reduced either by improving the quality of the steel or by using better building and design techniques. The efficiency of a transformer core is also largely dependent upon the design of the joints at the junctions of the yoke and limbs. In these regions the flux may deviate from the rolling direction of the steel or become distorted so that local areas of the high loss are produced. [1] The use of grain-oriented silicon iron has been the main beneficial factor in increasing transformer efficiency. [2]

The behaviour of this investigation is to understand the in-plane flux distribution of the transformer core built from electrical steel (M5) with 3% silicon iron assembled with 23^o T-joint and mitred lap corner joint with stagger yoke of 10mm by using arrays of search coil.

2. EXPERIMENT APPARATUS AND MEASURING TECHNIQUES

The main apparatus consist of a model cores three-phase 100kVA transformer assembled with three limbs core with T-joint cutting angle 23^o assembled from CRGO (M5 grades) 3% Si-Fe material. The core has 550 mm x 580 mm with the limbs and yokes 100 mm wide as shown in Figure 1. The experimental cores assembled with T-joint 23^o, mitred overlap corner joints with staggered yoke and overlap length is 10mm as shown in Figure 2 and assembled from 0.3 mm thick laminations of M5 grain-oriented silicon iron (CRGO). Associated instruments are used to measurement fundamental, third and fifth harmonic content of the localised flux density distribution.

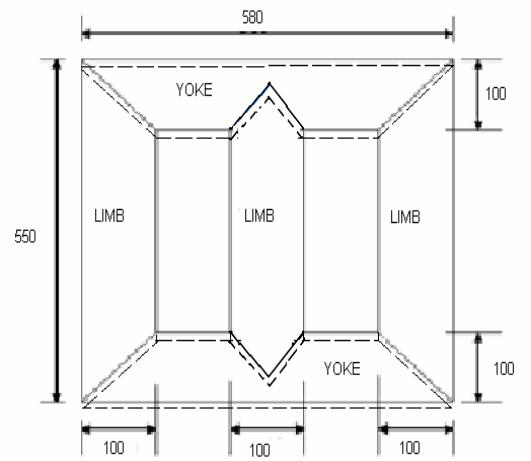

Figure 1: Dimension (mm) of 100kVA transformer model

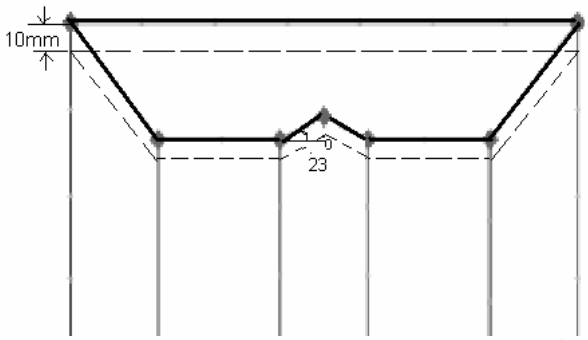

Figure 2: Transformer core type T-joint 23°

The localized flux density distribution in individual laminations is measured using search coils. The samples are drilled with an aid of drilling machine. It is constructed from 0.15 mm diameter wire treaded through 0.8 mm diameter holes 10 mm a part as shown in Figure 3. Each measuring position suitable coils are wound to measure the easy and hard direction flux density. The search coil induced voltages are analysed to find the magnitude and plane coil induced voltage of flux density by using power analyzer [PM6000] as shown in Figure 4.

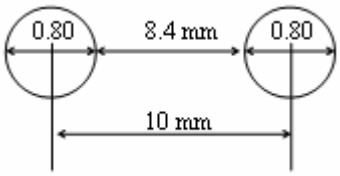

Figure 3: Dimensions [mm] of the holes drilled in the specimen

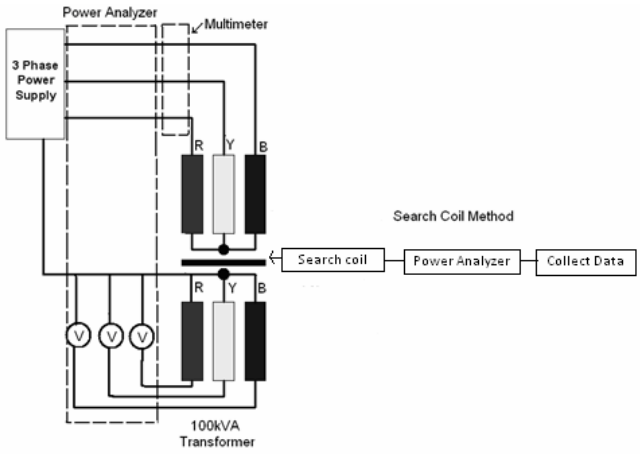

Figure 4: The diagram of the methods that used to measure the localised flux density.

The magnitude and direction with reference to the x axis of the in-plane instantaneous flux density can be written in the form [3]:

$$|b| = \frac{1}{4\,fNAn}[\bar{e}_x{}^2 + \bar{e}_y{}^2]^{1/2} \qquad (1)$$

And

$$\alpha = \tan^{-1}\left(\frac{e_y}{e_x}\right) \qquad (2)$$

Where
f = frequency supply
N = Number of transformer winding
A = Cross section area of transformer core lamination that measured
n = number of layer of transformer core lamination
e_x = maximum value of the component of induced emf in the easy direction
e_y = maximum value of the component of induced emf in the hard direction

Sample calculation as follow:
From transformer frame are obtain number of turn is 254 turns, area of lamination is 0.000003m^2 with number of layer is 15 layers and frequency supply is 50 Hz. When the supply adjusted to transformer at 1.5T so at the search coil will find the induced emf by oscilloscope measurements at easy direction is 190mV and hard direction is 180mV. By using the equation (1) will find the flux density at this point is 103mT.

The primary induced emfs in the windings of the three phase transformers core were monitored by three identical voltmeters and voltages displayed during the measurement were only allowed to vary well within ± 0.4% of the induced voltage corresponding to the required flux density.

Flux distribution in the Cold Rolled Grain Oriented (CRGO) is measured by using an array of search coils to get the

ISSN 114-1284

satisfactory result. In this investigation an array of single turn search coil is employed to measure in-plane (longitudinal and transverse) of flux density in the lamination within the transformer core as indicated in figure 5.Because the flux tends to deviate out of the longitudinal direction in some region, small 10mm search coils are used to measure localized longitudinal and transverse flux component. The locations are chosen to cover the areas where the flux is more likely to vary direction so as to find distribution of the flux behavior as shown in Figure 5.

The testing process is done by using the No-Load Test Frame. The No-Load Test Frame consisting of three windings for each three phase core are designed in order not only to avoid introducing stress to the laminations but also to keep the magnetism exactly constant in all limbs of the cores. Each winding only extends along 85% on each limb in order to enable the stagger length of the three phase core to be varied. An extra softwood base 200mm high is used to raise the overall height of the core, in order to minimize the effect of the stray flux on the localized measurements.

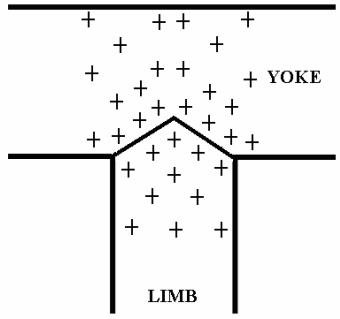

Figure 5: Location of orthogonal search coils in the three phase core.

Installation search coil takes quite a long time in completing this step which every hole needs to be inserted with search coil. Search coil is the enamel copper coated 0.1mm diameter wire. Each set of test point (4 holes) consist of easy and hard direction where the holes of easy and hard direction will be inserted search coil and the leads are twisted together. All the holes at testing point need to be repeated the same method of inserting and twisting the leads.

After the search coils are wound and the leads twisted together, the holes are filled with polyurethane varnish to give added insulation protection. The search coil leads, which are twisted to prevent any spurious pick up, are stuck to the lamination by a polyurethane varnish. The leads from all the search coils are taken to a junction box placed in the core to prevent any interference from the core or magnetising windings.

3. RESULTS AND DISCUSSION

The instantaneous magnitude and direction of flux at this instant is shown in Figure 6 on a larger scale. At this instant the total flux in the centre limb reaches its maximum and outer limb carry half their maximum flux. A small amount of flux deviation from the rolling direction occurs at the overlap.

The rotational flux produced in the T-joint region of the three-phase three limbs transformer core are due to a combined effect of alternating and rotating fields. This rotational flux illustrates the locus of the variation of the variation of the localized flux distribution throughout the magnetizing cycle. The rotational flux of the fundamental component (50Hz) of flux density in the 10mm staggered core at a core flux density of 1.5T is shown in Figure 7. A large rotational flux is present in the yoke area which near with centre limb. Rotational flux in this region is more circular. Some large rotational flux is also observed in or near the T-joint region.

Figure 8 shows the rotational flux of the third harmonic component of flux density in the T-joint of the core assembled with 23^0 at core flux density of 1.5T. The extent of rotating flux at this frequency is more widespread. As with the 50Hz component, a large amount of rotating flux is present in the T-joint region between the right yoke and centre limb in all four cores. A small rotating flux occurs also observed in the middle of centre limb region in all four cores. There is more rotational flux present in this region.

The major axes of the locus do not always follow those of the fundamental component (particularly the 23^0 T-joint of core) but tend to be parallel to butt joints over much of the core where the fundamental components also deviate from the longitudinal direction of the strip in the yoke.

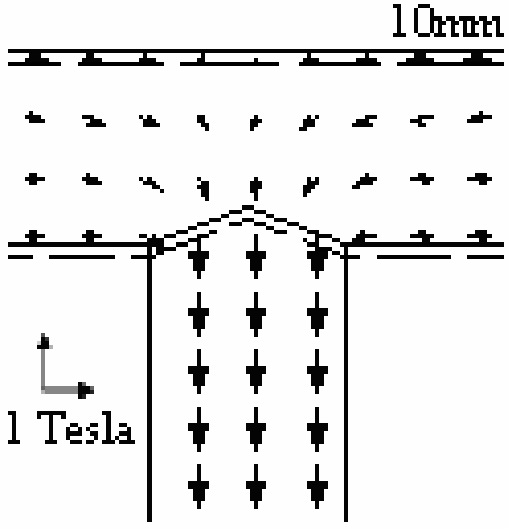

Figure 6: Distribution of localized flux density at 23^o T-joint

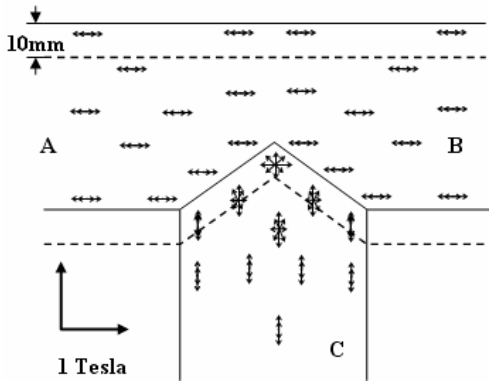

Figure 7: Locus of the fundamental component of localised flux density in 23^0 T-joint staggered core with overlap length 10 mm at 1.5T, 50Hz

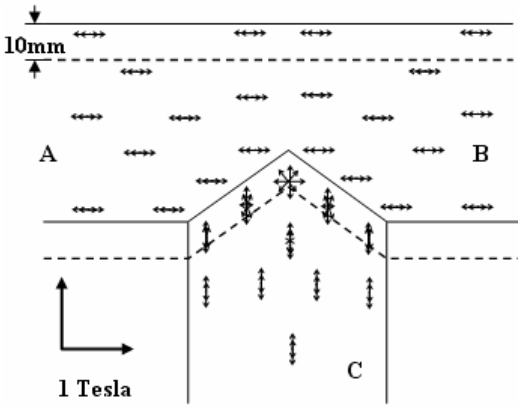

Figure 8: Locus of the third harmonic component of localised flux density in 23^0 T-joint staggered Core with overlap length 10 mm at 1.5T, 50Hz.

Figure 9 shows that the rotational flux of the fifth harmonic component of flux density in the T-joint of the core assembled with 23^0 at core flux density of 1.5T is more widespread. The magnitude of the rotational flux is small compared with that of the fundamental and third harmonic. The distribution of the fifth harmonic component is classified to a region near to and within the T-joint.

A large amount of rotating flux is present in the T-joint region between the right yoke and centre limb in the core. Rotating flux in this region is elliptical with the 23^0 T-joint of core showing the highest value. A small rotating flux occurs also observed in the middle of centre limb region in the core.

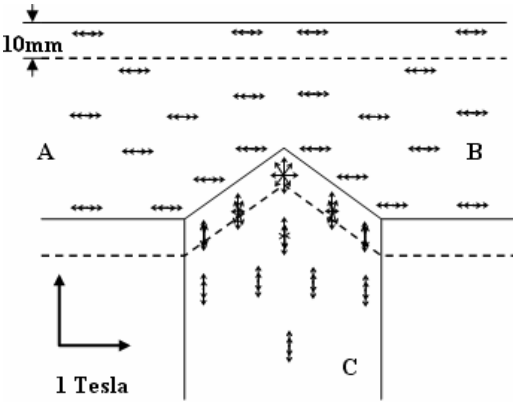

Figure 9: Locus of the fifth harmonic component of localised flux density in 23^0 T-joint staggered cores with overlap length 10 mm at 1.5T, 50Hz

Figure 10 shows the measuring point of location and localized flux densities at 23^o T-joint that are measured by using the search coil on transformer core. This result is produced by calculating localized flux density after the search coil measures the vector of the voltage in the easy and hard direction at the lamination.

The flux density in the yoke then drops rapidly as the flux distributes itself equally between the laminations. The flux density reaches a peak at the inner of 23^o T-joint; this is caused by the saturated material. The minimum flux density occurs at the outer of 23^o T-joint of transformer core lamination. The localised flux density will increase from the outer to the inner edge of the 23^o T-joint. The localised flux density at the outer 23^o T-joint is 0.190T and rises to be 0.217T at the inner edges of yoke at 23^o T-joint when the transformer core energized 1.5 T 50Hz.

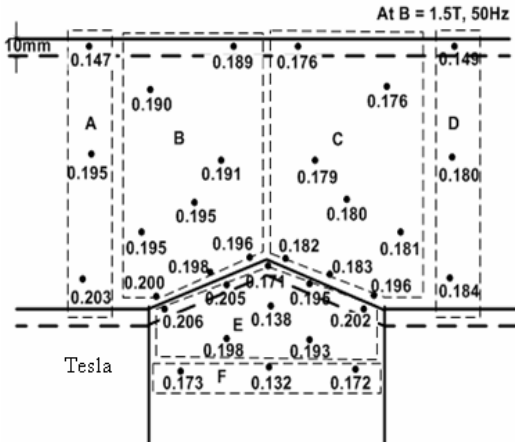

Figure 10: Local variations in the Tesla of the fundamental peak in-plane flux density of the lamination in 23^0 T-joint of three phase staggered core with overlap length 10 mm at 1.5T, 50Hz.

The local variation in magnitude of the third harmonic component of peak in-plane flux density in the 23° T-joint at a core flux density of 1.5T is shown in Figure 11. Most of the high third harmonic flux occurs in the T-joint region. The high third harmonic of peak in-plane flux occurs at the inner edge of right yoke passes over to the Butt-joint of centre limb is 23.4mT. Harmonic occurs mostly in the T-joint where local regions are saturated and the flux deviates from the rolling direction. However, it has been confirmed experimentally that harmonics circulated in individual laminations in the limbs and yokes.

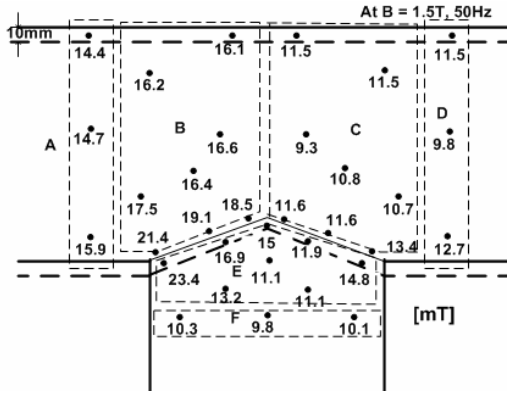

Figure 11 Local variations in the mT of the third harmonic peak flux density to the fundamental component in-plane of the lamination in 23^0 T-joint of three phase staggered core with overlap length 10 mm at 1.5T, 50Hz.

The local variation in magnitude of the fifth harmonic component of peak in-plane flux density in the 90° T-joint at a core flux density of 1.5T is shown in Figure 12 to be very small.

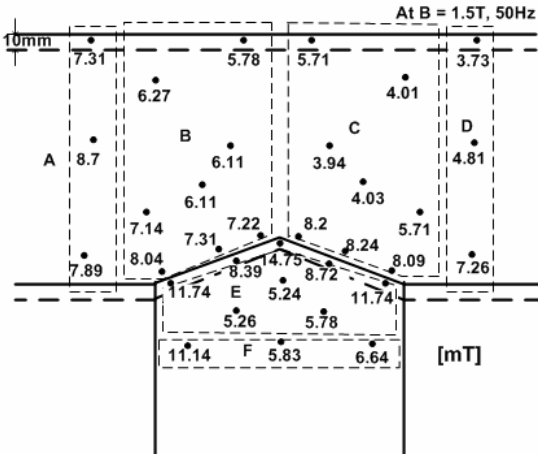

Figure 12: Local variations in mT of the fifth harmonic peak flux density to the fundamental component in-plane of the lamination in different T-joint of three phase staggered core with overlap length 10 mm at 1.5T, 50Hz.

4. CONCLUSION

The flux distribution in cores assembled with M5 material was found varies along overlap area of the stagger at the T-joint. The localised in-plane flux density will increase from the outer to the inner of the 23° T-joint. The localised flux density at the outer edges 23° T-joint is 0.147T and rises to be 0.206T at the inner edges of 23° T-joint when the transformer core energized 1.5 T 50Hz. A large rotational flux is present in the yoke area which near with centre limb. Rotational flux in this region is more circular.

The high third harmonic of peak in-plane flux occurs at the inner edge of right yoke passes over to the Butt-joint of centre limb is 22.2mT.Harmonic occurs mostly in the T-joint where local regions are saturated and the flux deviates from the rolling direction.
A small amount of flux deviation from the rolling direction occurs at the overlap, but no rotational flux is present in the joint.

The local variation in magnitude of the fifth harmonic component of peak in-plane flux density in the 23° T-joint at a core flux density of 1.5T is to be very small

ACKNOWLEDGMENT

The authors would like to express their gratitude to the Malaysian Transformer Manufacturing (MTM) for the supply of transformer core material.

REFERENCES

[1] Jones, A. J., Moses, A. J., Comparison of the Localized Power Loss and Flux Distribution in the Butt and Lap and Mitred Overlap Corner Configurations, *IEEE Tans. ON MAG.*, VOL. MAG-10, No. 2, june 1974.
[2] Mansel A Jones and Antony J. Moses, Comparison of the Localized Power Loss and Flux Distribution in the Butt and Lap and Mitre Overlap Corner Configurations, *IEEE Trans. On Mag.*, Vol, MAG-10, No.2, June 1974
[3] Daut, I and Moses, A.J., Some Effects Of Core Building On Localised Losses And Flux Distribution In A Three-Phase Transformer Core Assembled From Powercore Strip, *IEEE Trans. On Mag.*, Vol. MAG-26, No 5, pp. 2002, Sept 1990
[4] Daut, I.,"*Investigation of Flux and Loss Distribution in Transformer Cores Assembled From Amorphous Powercore Material"*, 1992, PhD Thesis University of Wales
[5] Beckley P., *Electrical Steels for rotating machines*, The Institution of Electrical Engineers, 2002.

[6] Indrajit Dasgupta, *Design of Transformers Handbook*, Tata Mc-Graw Hill, India, 2002.
[7] James H. Harlow, *Electric Power Transformer Engineering*, CRC Press LLC, 2004.
[8] Daut I., Dina M.M. Ahmad and S. Taib, *Measurement of flux distribution on 100kVA 3phase distribution transformer assembled with 60^o T-joint and mitred lap corner joint with stagger yoke by using search coil*, MUCET2008 8th-10th March 2008, Hotel Putra Palace, Perlis, Malaysia.
[9] Daut, Dina M.M. Ahmad, and S. Taib , *Measurement of Flux Distribution on 100kVA 3phase Distribution Transformer Assembled With 45^o T-Joint And Mitred Lap Corner Joint With Stagger Yoke By Using Search Coil*, IASTED AsiaPES2008, 2nd-4th April 2008, Meritus Pelangi Beach Resort Hotel, Langkawi, Malaysia, ISBN CD: 978-088986-732-1
[10] Daut, Dina M.M. Ahmad, and S. Taib , *Comparison Between The Localized Power Loss and Flux Distribution in a Three Phase Distribution Transformer 100 kVA Assembled From Various Type of T-Joint Geometry with Staggered Yoke*, IASTED AsiaPES2008, 2nd-4th April 2008, Meritus Pelangi Beach Resort Hotel, Langkawi, Malaysia, ISBN CD: 978-088986-732-1,
[11] Dina M.M. Ahmad, Ismail Daut, *Measurement of Flux Distribution on 100kVA 3phase Distribution Transformer Assembled With 23^o T-Joint and Mitred Lap Corner Joint with Stagger Yoke by Using Search Coil*, The 2ndInternational Power Engineering and Optimization Conference (PEOCO2008), Shah Alam, Selangor, MALAYSIA. 4-5 June 2008.

Proceeding of the 11th International Conference on QiR (Quality in Research)
Faculty of Engineering, University of Indonesia, Depok, Indonesia, 3-6 August 2009
ISSN 114-1284

The Localized Loss on 100kVA 3-Phase Distribution Transformer assembled with 23° T-joint

I. Daut[a], Dina M.M. Ahmad[b], Z.Mat Isa[c], S. Zakaria[d]

[a]*School of Electrical System Engineering,*
Universiti Malaysia Perlis (UniMAP),
P.O Box 77, d/a Pejabat Pos Besar
01007 Kangar Perlis, Malaysia
Email address: ismail.daut@unimap.edu.my

[b]*School of Electrical System Engineering,*
Universiti Malaysia Perlis (UniMAP),
P.O Box 77, d/a Pejabat Pos Besar
01007 Kangar Perlis, Malaysia
Email address:dina@unimap.edu.my

[c]*School of Electrical System Engineering,*
Universiti Malaysia Perlis (UniMAP),
P.O Box 77, d/a Pejabat Pos Besar
01007 Kangar Perlis, Malaysia
Email address: zainuddin @unimap.edu.my

[d]*School of Electrical System Engineering,*
Universiti Malaysia Perlis (UniMAP),
P.O Box 77, d/a Pejabat Pos Besar
01007 Kangar Perlis, Malaysia
Email address: shuhaimi@unimap.edu.my

ABSTRACT

This paper describes the result of measurement of localized loss distribution on 100kVA 3phase distribution transformer assembled with 23° T-joint and mitred lap corner joint with staggered yoke. The measurement involves the variation of temperature rise. The localized loss have been measured using no load test by arrays of thermistor on the surface of M5 (CGO) grades material of transformer core laminations. The localised loss at the outer 23° T-joint is 1.05 W/kg and rises to be 1.26 W/kg at the inner 23° T-joint when the transformer core energized 1.5 T 50Hz. The several harmful effects can occur because the flux flows out of the rolling direction.

Keywords
Grain oriented silicon iron, transformer core ,temperature rise, power loss..

1. INTRODUCTION

An important factor in the design of the T-joint in three limbs, three-phase power transformers is the localized loss variation within the joint. Not only is the overall loss of the core affected by the T-joint, but high localized losses can generate hot spots in the core. The power-loss distribution depends upon the localized flux density variation, which in turn depends on the design of the joint. A particular joint configuration might produce rotational flux, normal flux between layers of laminations, or alternating flux directed away from the rolling direction of the laminations, all of which tend to increase the core loss. [1]

The objective of this investigation is to obtain the localised loss distribution of the transformer core built from electrical steel (M5) with 3% silicon iron assembled with 23° T-joint and mitred lap corner joint with stagger yoke by using thermistor.

2. EXPERIMENT APPARATUS AND MEASURING TECHNIQUES

A 3-phase,3 limb stacked cores are assembled with 23° T-joint and mitred lap corner joints as indicated in Figure 1.The core is 550 mm x 580 mm with the limbs and yokes 100 mm wide. The core is assembled from 0.3 mm thick laminations of M5 grain-oriented silicon iron (CGO) as indicated in Figure 2 and the core comprises of 15 layers has staggered yoke of core with overlap length of 5 mm from other adjacent lamination. Staggering alternate layers of laminations in the

yoke direction as indicated in figure 2 is known to reduce the losses of core assembled from silicon iron [2]

Localised loss on the Cold Rolled Grain Oriented (CRGO) is measured by using an array of thermistor to get the satisfactory result. The locations chosen must cover the areas where the loss is more likely to vary direction so as to find distribution of the flux behavior as shown in Figure 3.

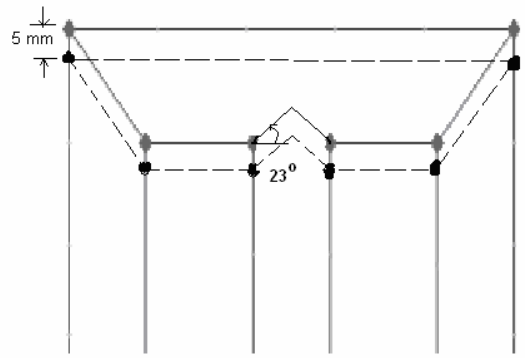

Figure 1: Transformer core type with T-joint 23°

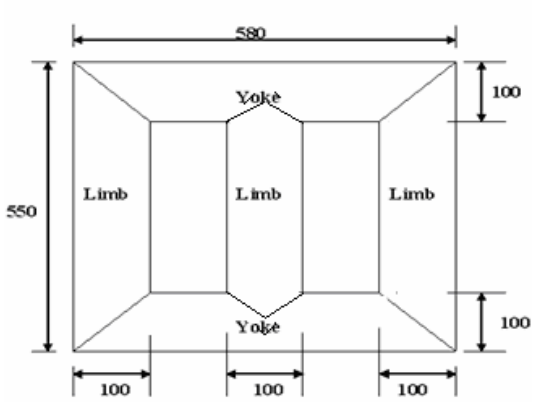

Figure 2: Dimension (mm) of 100kVA transformer model

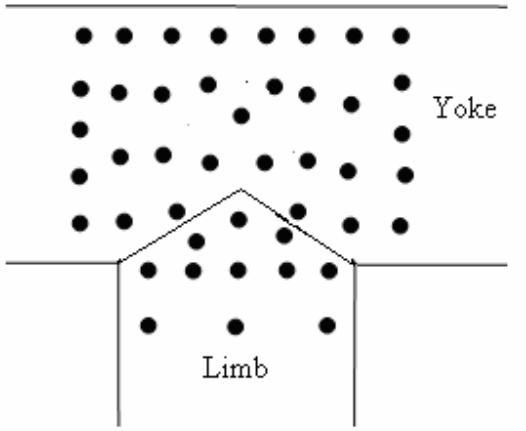

Figure 3: The thermistor position on the T-joint of transformer core

The testing process is done by using the No-Load Test Frame. The No-Load Test Frame consisting of three windings for each three phase core are designed in order not only to avoid introducing stress to the laminations but also to keep the magnetism exactly constant in all limbs of the cores as indicated in figure 4. The core could be energized to 1.5 T (50Hz)

Loss will be obtained by calculating the multiple of gradient temperature on the lamination to relationship constant of gradient temperature and power loss reference. The power loss reference is obtained by using Epstein Test measurement with comparison temperature rise in the the middle of the limb of core lamination and nominal loss at adjusted 1.5T, 50Hz.

The relationship between loss and temperature rise will be found from the equation as follows:

$$P_{loss} = C \, dT/dt \qquad (1)$$

where C is the relationship constant that is C = 14 [W-minutes/kg-°C]

dT/dt is temperature rise from measurement

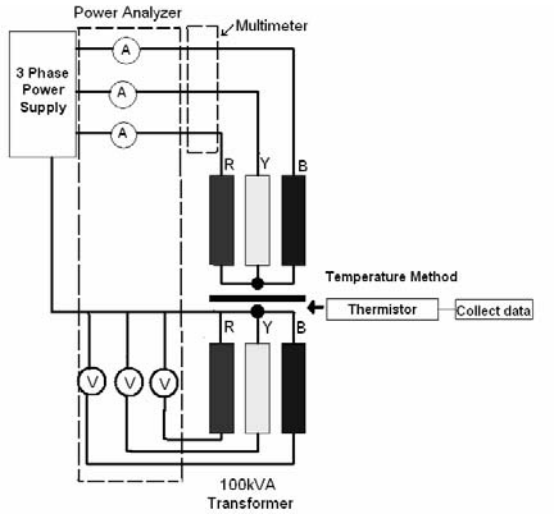

Figure 4: The diagram of the methods that is used to measure the localised temperature rise

3. RESULTS AND DISCUSSION

Figure 5 shows the mesh graph of the localised loss measured by using the thermistor at the 23° T-joint of transformer core lamination. This mesh graph is drawn by using the Matlab software based on the result of this investigation. The power loss at 23° T-joint shows that the power loss reaches a peak at the inner edge of 23° T-joint and the minimum power loss occurs at the outer edge of 23° T-joint of transformer core lamination. The localised power loss will increase from the outer edge to the inner edge of the 23° T-joint. The localised

power loss at the outer edge of 23° T-joint is 1.05 W/kg and rise to be 1.26 W/kg at the inner edge of 23° T-joint when the transformer core energized 1.5 T 50Hz. The major regions where the flux deviates from the rolling direction are at the 23° T-joint where the flux passes from the yoke to the limbs. Here several harmful effects can occur because the flux flows out of the rolling direction.

Figure 6 shows the measuring point of location and localised power loss that are measured by using thermistor at 23° T-joint. This result is produced by calculating the multiple of temperature rise on the lamination to relationship constant of temperature rise and power loss reference.

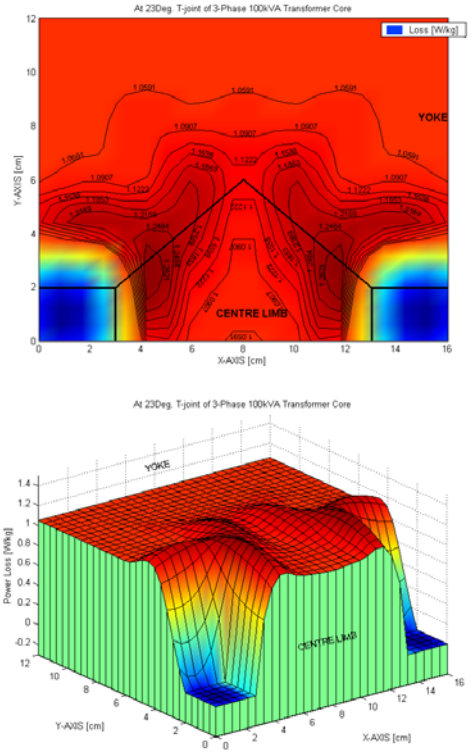

Figure 5: The mesh graph of the localised loss measured by the temperature method at the 23° T-joint.

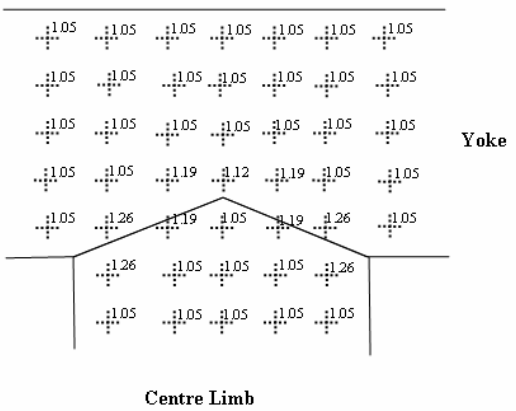

Figure 6: The average localized power loss at 23° T-joint (the values are expressed in W/kg) is measured by using temperature method.

4. CONCLUSION

The localised loss distribution on cores assembled with M5 materials varies along overlap length of 23° T-joint of core laminations. The localised power loss will increase from the outer edge to the inner edge of the 23° T-joint. The localised power loss at the outer edge of 23° T-joint is 1.05 W/kg and rise to be 1.26 W/kg at the inner edge of 23° T-joint when the transformer core energized 1.5 T 50Hz. The T-joint of core lamination occur several harmful effects caused by the flux flows out of the rolling direction.

ACKNOWLEDGMENT

The authors would like to express their gratitude to the Malaysian Transformer Manufacturing (MTM) for the supply of transformer core material.

REFERENCES

[1] Anthony j. Moses and bleddeyn Thomas, The Spatial Variation of Localized Power Loss in Two Practical Transformer T-Joints, *IEEE Trans. On Mag., VOL. MAG*-9, no. 4, december 1973

[2] Daut, I and Moses, A.J., Some Effects Of Core Building On Localised Losses And Flux Distribution In A Three-Phase Transformer Core Assembled From Powercore Strip, *IEEE Trans. On Mag., Vol. MAG-26*, No 5, pp. 2002, Sept 1990

[3] Daut, I.,"*Investigation of Flux and Loss Distribution in Transformer Cores Assembled From Amorphous Powercore Material*", 1992, PhD Thesis University of Wales

[4] Beckley P., *Electrical Steels for rotating machines*, The Institution of Electrical Engineers, 2002.

[5] Indrajit Dasgupta, *Design of Transformers Handbook*, Tata Mc-Graw Hill, India, 2002.

[6] James H. Harlow, *Electric Power Transformer Engineering*, CRC Press LLC, 2004.

ISSN 114-1284

Simulation of Flux Distribution and Loss Calculation at Three-Phase Three Limbs of Transformer Core with 23° T-Joint

I. Daut[a], Dina M.M. Ahmad[b], Izzat Rosli[c]

[a]*School of Electrical System Engineering,*
Universiti Malaysia Perlis (UniMAP),
P.O Box 77, d/a Pejabat Pos Besar
01007 Kangar Perlis, Malaysia
Email address: ismail.daut@unimap.edu.my

[b]*School of Electrical System Engineering,*
Universiti Malaysia Perlis (UniMAP),
P.O Box 77, d/a Pejabat Pos Besar
01007 Kangar Perlis, Malaysia
Email address:dina@unimap.edu.my

[c]*School of Electrical System Engineering,*
Universiti Malaysia Perlis (UniMAP),
P.O Box 77, d/a Pejabat Pos Besar
01007 Kangar Perlis, Malaysia
Email address: izzat_rosli @unimap.edu.my

ABSTRACT

This paper describes the result of simulation of flux distribution on 100kVA 3phase distribution transformer assembled with 23° T-joint and mitred lap corner joint with stagger yoke and limb for one lamination. The simulation involves the variation of flux. The flux distributions have been simulated using 2DFEM by Quickfield Software built from M5 (CGO) grades material of transformer core laminations. The flux density is 1.78 T maximum at the centre limb of transformer core and the loss calculation is 1.274 W/kg.

Keywords
Grain oriented silicon iron, transformer core, 2DFEM, power loss calculation.

1. INTRODUCTION

The electrical transformer was invented by an American electrical engineer, William Stanley, in 1885 and was used in the first ac lighting installation at Great Barrington, Massachusetts. The first transformer was used to step up the power from 500 to 3000 V and transmitted for a distance of 1219 m (4000 ft). At the receiving end the voltage was stepped down to 500 V to street power and office lighting. By comparison, present transformers are designed to transmit hundreds of megawatts of power at voltages of 700 kV and beyond for distances of several hundred miles. [1]
Loss evaluation has become important because of high energy cost. Therefore, it is necessary to know in detail the behaviours of flux in transformer in order to develop cores with higher efficiency.

The efficient operation of power transformer cores depends to a large extent on the design of the joints between their limbs and yokes. In the three-phase, three limb core the most complex joints are the T-joints at the intersection the centre limb and yokes.[5]

The quantitative analysis of localized flux and loss distributions has become easier through the remarkable progress of numerical field calculations such as the finite element method. The numerical simulation is more effective and economical than experimental method. Moreover, useful suggestions for improving transformer can be obtained from the calculated flux and loss distribution

The objective of this simulation is to know the flux distribution and calculate the losses occur on the transformer core with 23° T-joint built from M5 grade material using 2D FEM.

2. METHODOLOGY

Methodology that is used to complete this investigation had been divided into three major tasks:

1. Drawing transformer core assemble with 23° T-Joint and M5 grade material
2. Simulation of the transformer core drawing
3. Loss calculation for the transformer core material

Drawing the transformer core configuration is the first step before doing the simulation. In this simulation, this drawing had been done using Quickfield v5.2 software. QuickField is an interactive environment for electromagnetic, thermal and stress analysis. In QuickField, it works with several types of documents: problems, geometry models, material libraries and others. QuickField can perform linear and nonlinear magnetostatic analysis for 2-D and asymmetric models. The program is based on a vector potential formulation.
Dimension of the 100kVA transformer core model are as figure 1. The configuration of T-Joint is drawing in Figure 2.

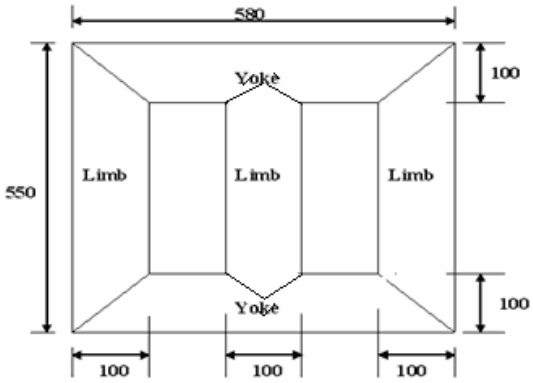

Figure 1: Dimension (mm) of 100kVA transformer core model

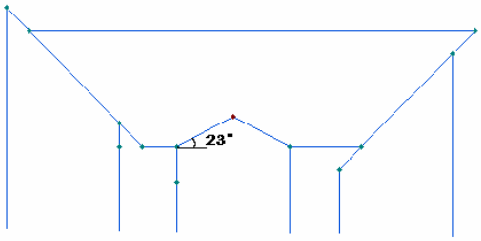

Figure 2 : Transformer core type 23° T-joint

To identify the material, B-H curve reading need to be tuck at the data column for each of the limb. The values for material can be obtained from the B-H curve. The data should be tucking as indicated in table 1.

Table 1: B-H curve data from the exciting force

Flux Density [T]	M5 grades H (Am/g)
0.5	-130
0.6	-129.4
0.7	-129.2
1	-120
1.1	-116.5
1.3	-110.5
1.4	-96
1.5	-80
1.6	0
1.7	310
1.8	1870
1.9	9370

B-H curve data can be took from the hysteresis loop magnetizing curve of the material. Magnetizing curve for M5 grade material is obtained from the technical details of the CRGO material. Each of the limb and yokes block label need to be entering with the data such as coercive force of magnet, field source and others.

Directions of the coercive force of magnet are set to same to both of right and left limb. Only the centre limb are set different direction pole from the both right and left limb. In this drawing, the pole were set to be 90˚ for the right and left limb and the centre limb will be set to -90˚. This will make sure flux from left and right limb will flow through the centre limb. Meanwhile for the upper yoke and lower yoke the direction were set to zero degree for both upper and lower yokes. [2]

After entering the related data for each of the block label properties, data label for edge also need to be set also. In this drawing, only air type and steel type need to be set for the edge label property. In the edge properties, for every edge of the steel need to be assign to tangential field and for the air edge, it need to be assign to magnetic potential

Before any simulation took place, the drawing should be check either mesh can produce all over the drawing or not. There is button build mesh on top of the drawing toolbar. When building mesh is finish, the drawing will be cover with green line all over the drawing.

Simulation only can be executed after mesh had been built off. To execute the simulation, there is executing button on the toolbar icon. If the simulation success without having any error on the drawing a result with flux line flow through the core will come out. Value of flux density can be obtained from the field picture by right clicking on the result drawing. To check the local value, click on local value button and just pointing mouse at any space of the simulation result to get the result value.

3. ANALYSIS

Flux Density formula:

$$B = \mu H \quad (1)$$

$$\mu = \mu_o \mu_r \quad (2)$$

where μ = material permeability
H = material intensity from the table

The flux density is assumed to lie in the plane of model (xy or zr), while the vector of electric current density **j** and the vector potential **A** are orthogonal to it. Only j_z and A_z in planar or j_θ and A_θ in axisymmetric case are not equal to zero. We will denote them simply j and A. Finally, the equation for planar case is

$$\frac{\partial}{\partial_y}\left(\frac{1}{\mu_y}\frac{\partial A}{\partial y}\right)+\frac{\partial}{\partial y}\left(\frac{1}{\mu_x}\frac{\partial A}{\partial y}\right)=-j+\left(\frac{\partial H_{cy}}{\partial x}-\frac{\partial H_{cx}}{\partial y}\right) \quad (3)$$

and for axisymmetric case is

$$\frac{\partial}{\partial_r}\left(\frac{1}{r\mu_z}\frac{\partial (rA)}{\partial y}\right)+\frac{\partial}{\partial z}\left(\frac{1}{\mu_y}\frac{\partial A}{\partial z}\right)=-j+\left(\frac{\partial H_{cy}}{\partial z}-\frac{\partial H_{cz}}{\partial r}\right) \quad (4)$$

where components of magnetic permeability tensor μ_x and μ_y (μ_z and μ_r), components of coercive force vector H_{cx} and H_{cy} (H_{cz} and H_{cr}), and current density j are constants within each block of the model.

In order to find the loss of energy per cycle or magnetization of transformer core lamination as follow;
Let l = mean of iron bar
A = its area of cross section
N = No of turns of wire of the solenoid.
with relate the B-H curve of core material shown in figure 3.

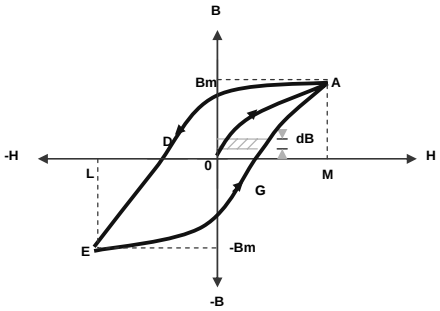

Figure 3: Hysteresis curve

If B is the flux density at any instant, then $\Phi = BA$ when current through solenoid changes, then flux also changes and so produces and induced e.m.f whose value is

$$e = N\frac{d\Phi}{dt} volt \quad (5)$$

$$e = N\frac{d(BA)}{dt} = NA\frac{dB}{dt} volt \quad (6)$$

Now, $H = NI/l$ or $I = Hl/N$ (7)

The power of rate of expenditure of energy is maintaining the current 'I' against induced e.m.f 'e' is

$$= eI.watt = \frac{H.l}{N}\times N.A\frac{dB}{dt} = A.l.H\frac{dB}{dt} \text{ Watt} \quad (8)$$

Energy spent in time 'dt

$$A.l.H\frac{dB}{dt}\times dt = A.l.H.dB \text{ Joule}$$

Total network done for one cycle of magnetization is

$$W = A.l.\oint H.dB \text{ Joule} \quad (9)$$

Hence $\oint H.dB$ = area of the loop, i.e the area between B-H curve and the B-axis.
So, *work done, cycle = A.l x (area of the loop)* Joule
Now *A.l = volume of material*
So *net work done/cycle/m^3 = (loop area)* Joule
Or W = (area of B-H loop) joule/m^3/cycle

4. RESULT AND DISCUSSION

As an overview flux will flow through the core limb in various patterns. From figure 4 it shows that flux flow through centre limb from each left and right limb. Simulation using Quickfield software showing the flux lines flow through the limb and yoke of transformer core.

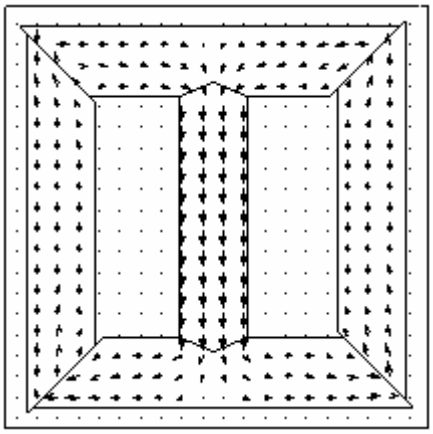

Figure 4: Flux lines flow through transformer core

The flux density value from simulation is 1.78 T as indicated in figure 5. Flux density that is flow through the transformer core is not uniform. The maximum flux density is found in the centre limb of transformer core. Because the flux density that is flow from the left and right limb of the transformer core is enter toward the centre limb of transformer core.

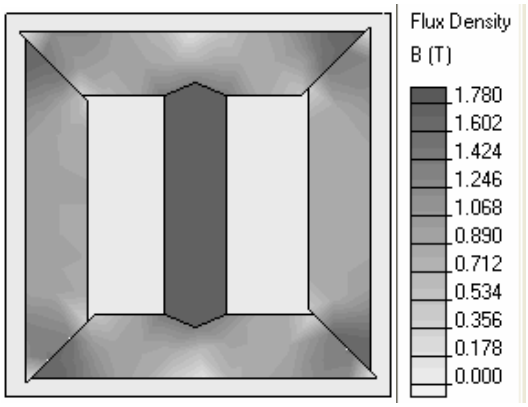

Figure 5: The flux density occur in the transformer core lamination

An energy density value is recorded in unit J/m³. For M5 grade material of the transformer core has the value of energy density is 195 J/m³. Energy density obtained from the simulation result is shown in figure 6. In this figure shows the energy density occurs at the left and right limb of transformer core.

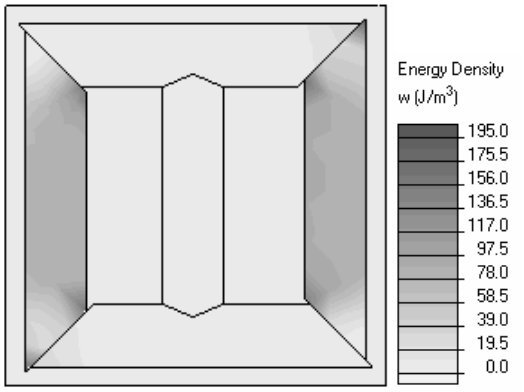

Figure 6: Energy density simulations on transformer core

From the simulation result, some data can be obtained such as;
Energy Density, ωH = 195 J/m^3
Density = 7.65kg/dm^3 (from the B-H curve)

In order to find frequency, the equation is;

$$f = \frac{1}{t} = \frac{1}{t\,\text{sec}} = 50Hz \;;\; t = \frac{1}{50}\text{sec} = 0.02\,\text{sec}$$

From simulation result data, power loss per kg can be calculated using;

$$Power.Loss/kg = \frac{195J/m^3}{7.65kg/dm} = \frac{195J/m^3}{7.65\times10^3 kg/m^3}$$

$$= \frac{195}{7.65\times10^3} J/kg = \frac{195\times50}{7.65\times10^3} J/\text{sec}/kg \quad \mathbf{= 1.274 Watt/kg}$$

5. CONCLUSION

Loss evaluation has become important because of high energy cost. Therefore, it is necessary to know in detail the behaviours of flux in transformer in order to develop cores with higher efficiency.The values for material can be obtained from the B-H curve

From the result of simulation found the flux density is 1.78 T and the loss calculation is 1.274 W/kg. Flux density that is flow through the transformer core is not uniform. The maximum flux density is found in the centre limb of the transformer core.

REFERENCES

[1] Nakata, T., Numwrical Analysis of flux and loss distribution in Electrical Machinery (invited), *IEEE Trans. On Mag., Vol. MAG-20, no. 5* Sept. 1984.
[2] Richard C. Dorf , *The Electrical Engineering Handbook*, 2nd Edition,CRC Press, pp: 32-35 1997.
[3] I. Daut, Dina M.M. Ahmad, S. Zakaria, S. Uthman and S. Taib, Comparison of Losses and Flux Distribution in 3 phase 100kVA Distribution Transformer Assemble from Various Type of T-Joint Geometry, *American Journal of Applied Science* 3 (9):1990-1992, 2006
[4] Gunther F. Mechler, Ramsis S.Girgis Magnetic Flux Distribution in Transformer Core Joints, *IEEE Transaction on Power Delivery Vol. 15,No 1*, Jan. 2000
[5] Ismail Daut, Dina Maizana,Electrical Engineering Principle, Kolej Universiti Kejuruteraan Utara Malaysia (KUKUM) 2005.
[6] Anthony J. Moses, Bleddyn Thomas, and John E. Thomson, Power Loss and Flux Density Distributions in the T-Joint of a Three Phase Transformer Core, *IEEE Trans. On Mag., Vol. MAG-8, no. 4* Dec 1972.

INVESTIGATION OF HARMONIC EFFECT IN LABORATORY DUE TO NONLINEAR LOADS

**I.Daut, Risnidar. Chan, S. Hardi, Norhaidar H,
I.Nisja, Syafruddin HS, M.Irwanto**

Electrical Engineering Department University Malaysia Perlis (UniMAP) Pusat Pengajian Kejuruteraan Sistem Elektrik
Kompleks Pusat Pengajian UniMAP, Tkt I Blok A, jalan Satu, Taman Seberang jaya 3, 02000,
Tel. 04-9851636, Fac: 04-9851431, Kuala Perlis, Perlis, Malaysia
email: ismaildaut@unimap.edu.my, risnidar@unimap.edu.my, surya@unimap.edu.my, norhaidar@unimap.edu.my, indra@unimap.edu.my, syafruddin@unimap.edu.my, irwanto@unimap.edu.my

ABSTRACT

In this research, we focus to the customer side of the meter, which is the effect of harmonic on a laboratory in Electrical System Engineering School at K.Wai Perlis due to nonlinear loads. Harmonic currents in equipments can cause them to experience overheating and increased losses, while harmonic voltage produces magnetic fields rotating at a speed corresponding to the harmonic frequency. This also results in equipments heating, mechanical vibrations and noise, reduced efficiency, reduced life, and voltage stress on insulation of equipment windings.

With the operation of varying nonlinear loads, the injected harmonic current magnitudes and phase angles vary in a random way. In order to attack the problem of power quality, this study will also focus on the development of a computer program to detect and compensate any effects of harmonic distortions. Models are developed to represent the main electrical devices

This research offers the advantage of providing the utility a wealth of information on the effects of harmonics in their equipments. This will subsequently makes them aware of the causes of increased cost and reduced efficiency that may be experienced by using the equipments. In this paper described the investigation cost of harmonic effect as THD, and harmonic energy losses cost

Keyword: *nonlinear loads, Energy losses cost, harmonic, THD.*

1. INTRODUCTION

Because electrical devices that act as nonlinear loads draw current non linearity, they are responsible for injecting harmonic currents into the electricity network. Harmonic is a more important issue for the industry, commerce and the home consumer now than it was a few decades ago. The equipments in laboratory are motor, transformer instrumentations, generator, lamps, Adjustable Speed Drives (ASD), and a variety of load, cable etc, where all of them can be similarly as medium scale industry. There are many causes of harmonics on a power system. In distribution system, transformers are capable of producing harmonics due to magnetic core saturation [1-4]. The effects of harmonics on equipment are: cause additional heating and higher dielectric stress on the capacitors, interruption capability of circuit breakers, the skin effect of the conductors, reduce lamp life, measurement errors in instrument like wattmeter, voltmeter etc, overheating, pulsating torque and noise on rotating machines, etc [5]. The cost to end users comes when the harmonic currents add to the normal load and increase losses and loading on their distribution systems. The increased losses reduce the capacity of the system, including conductors, transformers and motors. The increased loading generates heat and accelerates the aging of power equipment, like transformers and motors [5-6].

2. LITERATURE REVIEW

Harmonic distortion is not new and it constitutes at present one of the main concerns for engineers in the several stages of energy utilization within the power industry. In the past, harmonics represented less of a problem due to the conservative design of power equipment and to the common use of delta-grounded wye connections in distribution transformer. But, the increasing use of nonlinear loads in industry, is keeping harmonic distortion in distribution networks on the rise. Before analyze the harmonic effect, we define the characteristic and model of equipment as below.

2.1 Characteristics and Modeling of Equipment

One important step in harmonic analysis is to characterize and to model harmonic source and all components in system. As we know, the equipments in laboratory are motors, transformers instrumentations, generators, lamps, Adjustable Speed Drives (ASD), and a variety of load, cable etc, where all of them can be similarly as medium scale industry. So, the each equipment can be model as follow:

2.1.1 Personal Computer

Personal computer has significant contribute of harmonics problem to low voltage distribution system

2.1.2. Fluorescent Lamp

The fluorescent lamp was the first major advance to be a commercial success in small-scale lighting since the tungsten incandescent bulb. Fluorescent lamps are about 2 to 4 times as efficient as incandescent lamps at producing light at the wavelengths that are useful to useful to humans [3]. Due to heavy use of non-linearity gas discharge lamp, the fluorescent lamps that employ magnetic or electronics ballast are considered as a significant contributor to

2.1.3. Current source

Each current source data consist of the bus number at which the current source is provided. This followed by injected current at the bus for harmonic orders.

2.1.4. Loads

The three-phase group is used mainly in industry applications and in the power system. For example: Adjustable speed drive, Large UPS's, Arc furnaces, HVDC-links, SVC's [3]. The load is modeled as: a) loads are not considered in the power flow at harmonic frequency, b) parallel combination of resistance and inductive reactance, c) reactance is assumed to be frequency dependent while parallel resistance is kept constant, d) derived by measurements on medium voltage load using audio frequency ripple control generators, e) the load impedance calculated at 50 Hz remains constant for all frequencies and f) series combination of resistance and inductive reactance. In this paper the load model as parallel combination of resistance and reactance.

2.1.5. Series Capacitors

Series capacitors can be modeled as series element consisting of resistance (usually zero or negligible value) in series with reactance

2.1.6. Transmission Line

The series impedance of a line section *l* is represented by z=r+jx as a 3x 3 matrix r, x, and the susceptance too [1]

2.2 Harmonic Indices

The most common harmonic index, which related to the voltage waveform, is the THD, as the root mean square (rms) of the harmonics expressed as a percentage of the fundamental component. It can for voltage and current as follow:

$$THD = \frac{\sqrt{\sum_{h=2}^{\infty} V_h^2}}{V_1} \quad (1)$$

And the power losses due to harmonic:

Active Power:

$$P = \frac{1}{T}\int_0^T p(t)dt = \sum_{h=1}^{\infty} V_h I_h \cos(\theta_h - \delta_h) = \sum_{h=1}^{\infty} P_h \quad (2)$$

Reactive Power:

$$Q = \frac{1}{T}\int_0^T q(t)dt = \sum_{h=1}^{\infty} V_h I_h \sin(\theta_h - \delta_h) = \sum_{h=1}^{\infty} Q_h \quad (3)$$

Apparent Power:

$$S^2 = P^2 + \sum_{i=1}^{n} V_i I_i \sin(\varphi_i) + D^2 \quad (4)$$

And for three phase systems, the per phase (*k*) vector apparent power S_v:[3]

$$S_v = \sqrt{\left(\left(\sum_k P_k\right)^2 + \left(\sum_k Q_{bk}\right)^2 + \left(\sum_k D_k\right)^2\right)} \quad (7)$$

2.3. Standardization of harmonic levels

The rms value of a voltage waveform, considering the distortion produced by harmonic current, IEEE-519 defines the limits as a function of the ratio between the short circuit current at the PCC (I_{sc}) and the average current corresponding to the maximum demand during a period of 12 months (I_L).

3. METHODOLOGY

The methodology in this research as Figure 1 below:

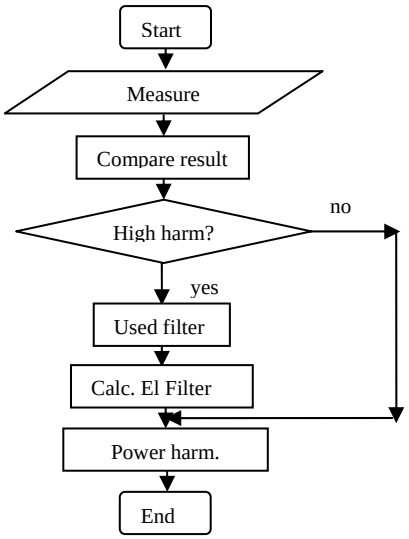

Figure 1 Flow Chart research

4. DATA AND RESULT

The research was measured with PM300 as Figure 2.

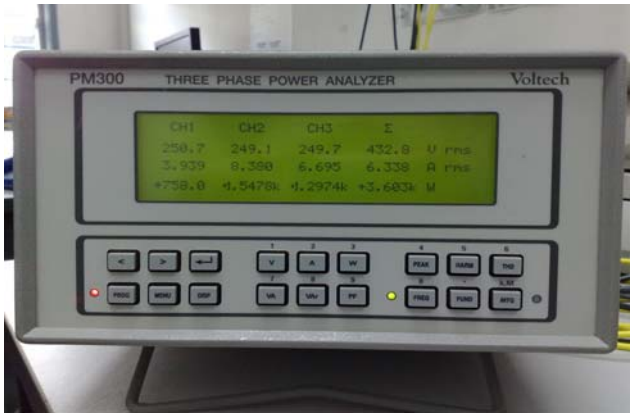

Figure 2.Three phase power analyzer (PM300)

The data at the laboratory is as follow:

Fundamental Results

File Tools

	CH1	CH2	CH3	SUM	NEUT.
Watts.f=	630.3	1.3142K	1.4354K	3.380 K	
VA.f=	633.2	1.3152K	1.4361K	3.385 K	
VAr.f=	60.56	52.15	45.18	157.89	
Volts.f=	243.8	241.0	242.8	420.1	
Amps.f=	2.597	5.458	5.914	4.656	3.264
cos phi=	-0.995	-0.999	-0.999	-0.999	
Resis=	93.44	44.12	41.04		
React=	8.978	1.7508	1.2918		

RMS Results

File Tools

	CH1	CH2	CH3	SUM	NEUT.
Watts=	629.5	1.3106K	1.4339K	3.374 K	
VA=	790.6	1.6393K	1.6791K	4.109 K	
VAr=	478.2	984.6	873.8	2.345 K	
Volts=	243.8	241.1	242.9	420.2	
Amps=	3.242	6.801	6.913	5.652	9.904
P.F.=	0.796	0.799	0.854	0.821	
V. Peak=	333.8	330.4	331.5		
A. Peak=	6.194	-15.267	14.043		-16.461
V.C.F.=	1.3690	1.3709	1.3647		
A.C.F.=	1.9106	-2.245	2.031		-1.6621
V. THD=	1.9169%	1.8125%	1.9580%		
A. THD=	71.38%	72.72%	59.46%		280.9%
Freq.=	49.92	49.92	49.92		
Imp.=	75.22	35.45	35.13		

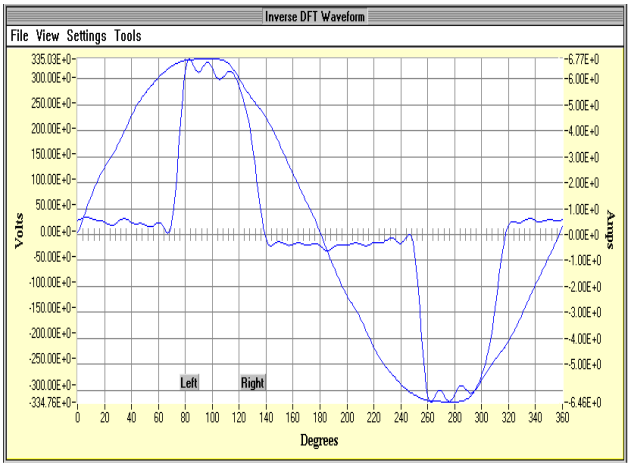

Figure 3 Waveform for CH1:

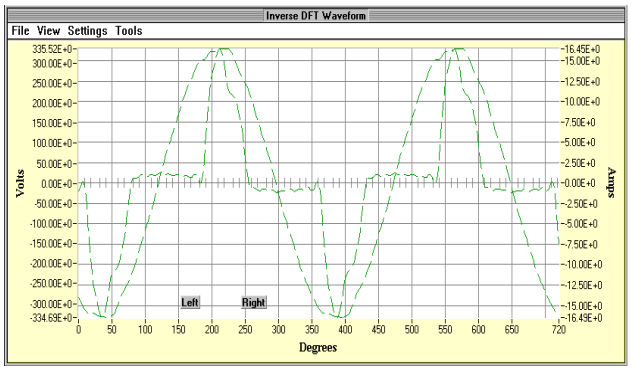

Figure 4 Waveform for CH2:

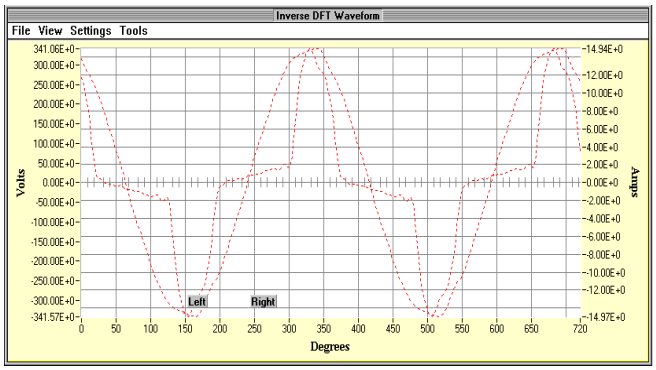

Figure 5 Waveform for CH3:

5. ANALYSIS

From the data and results, we find that the system has unbalanced nonlinear loads, where in fundamental condition Ch1, CH2 and CH3 have 2.597 A, 5.458 A, and 5.914 A. And voltage at CH1, CH2, and CH3 are: 243.8V, 241.0V and 242.8V. Also, it can be shown from Figure 3 to 5.

Powers for each channel in fundamental condition are: 630.3W, 1.3142KW, and 1.4152KW, while for RMS result are: 629.5W, 1.310KW, and 1.4339KW. This due to the each harmonic powers maybe plus or minus sign. So, the power at fundamental is bigger then RMS result. The total power losses due to harmonic for channel CH1, CH2 and CH3 are: -0.368W, -3.209W and -1.46W. For Apparent power (VA) at channel CH1, CH2 and CH3 in fundamental condition are: 633.2VA, 1.3152KVA and 1.4361KVA, while in RMS are: 790.6VA, 1.6393KVA, and 1.6791KVA. This is due to harmonic orders. For reactive power (VAR) at channel CH1, CH2 and CH3 in fundamental condition are: 60.5VAR, 52.15VAR and 45.18VAR, while in RMS are: 478.2VAR, 984.6VAR and 873.8VAR. This is due to harmonic too.

The voltage THD for CH1, CH2 and CH3 are: 1.92%, 1.81% and 1.96%. And from calculation are: 2.12%, 2.12% and 2.2%. The current THD for channel CH1, CH2 and CH3 are: 71.38%, 72.72% and 59.46%, while from calculation are: 72.5%, 74.8% and 60.2%.

In fundamental condition, the cosφ at channel CH1, CH2 and CH3 are: -0.995, -0.999 and 0.999, while in RMS, p.f. at channel CH1, CH2 and CH3 are: 0.796, 0.799 and 0.854. This is due to cosφ is ratio between load power and apparent power of fundamental component, while p.f. is ratio between load power and total apparent power (including harmonics).

6. CONCLUSION

From result and analysis we conclude as follow:

1 Loads are unbalanced and nonlinear.
2 THD for voltage in each channel are smaller than standardization level IEEE519, where 2.12%, 2.12% and 2.2%. are smaller than 5% in system <6.9KV.
3 THD for current in each channel are smaller than standardization level IEEE519, where 71.38%, 72.72% and 59.46% are smaller than 115%,
4 So, the system do not required filter.

7 AKNOWLEDGEMENTS

The authors would like to express their gratitude to the Fundamental Research Grant Scheme (FRGS), School of Electrical System Engineering of Universiti Malaysia Perlis (UniMAP) and Power Electronics and Electrical Machine Design Research Cluster for the supply of research facility respectively.

8 REFERENCES

[I] J.Arrilaga, N.R. Watson, “Power System Harmonics”, John.Wiley, 2nd edition, Chennai, India, 2003, page 66, 172.
[II] C. Sankaran, “Power Quality”, CRC PRESS, Boca Raton, 2002Francisco, page 92
[III] F. C. De La Rosa, “Harmonics and Power Systems”, Taylor & Frencis, CRC, Boca Raton, 2006, page 6, 36-37,
[IV] Prof Mack Grady, “Understanding Power System Harmonics”, Dept of Electrical & Computer Engineering, University of Texa at Austin, June 2006
[V] E. Wagner, et al, “Effects of Harmonics on Equipment”, Report of IEEE Task Force on the Effects of Harmonics Equipment, IEEE transactions on Power Delivery, Vol 8, No. 2, April 1993, pp 672-680.
[VI] Barry W. Kennedy, Power Quality Primer, McGraw-Hill, Singapore, 2000.

No-Load Current Harmonic of a Single-Phase Transformer with Low Frequency Supply

Ismail Daut[1], Syafruddin Hasan[2], Soib Taib[3], M.Irwanto[4], Risnidar Chan[5], I.Nisja[6], M. Irwan[7]

[1,2,3,4,5,6,7]*School of Electrical Systems Engineering*
Universiti Malaysia Perlis (UniMAP)
02000 Kuala Perlis, Malaysia
I.daut@unimap.edu.my, *syafruddin@unimap.edu.my*

ABSTRACT

Power transformers are an integral part of almost all electrical transmission and distribution networks. Their reliable service is of the utmost importance in modern society which is dependent on a constant electricity supply. There are a range of factors that can hinder the operation of power transformer. The harmonic components of the no-load current of the transformer are influenced by many factors, such as the frequency of voltage supply, the flux density, the degree of saturation and the core stacking technique. The affect of high frequency supply (i.e. lower than 50 Hz) to the no-load current harmonic in term of volt ampere reactive (VAR) power consumption is discussed in this paper. The total harmonic distortion percentage (THD) and crest factor (CF) as the harmonic contents are evaluated also. The transformer is connected to variable voltage variable frequency (VVVF) source and the investigation is done on the same flux density. The result has been compared with normal frequency supply (50 Hz). It was found that the harmonic content of no-load current with high frequency were slightly higher than normal one

Key words: *VAR power, single phase transformer, no- load current harmonic, low frequency, VVVF*

1. INTRODUCTION

The no-load loss of a power transformer is the active power loss in the power transformer when it is energized but not supplying a load. Primarily, it consists of a core loss, which is a function of the magnitude, frequency and wave shape of the excitation voltage. It is also varies with temperature, and it is particularly sensitive to distortion of the supply voltage waveform. The no-load loss is very small part of power rating of a power transformer, usually less than 1%. For a constant operating voltage and frequency, it is essentially constant and does not vary with load. However, it can represent a significant operating expense for a utility, especially if its energy costs are high. Accurate measurement of these losses are essential for the correct evaluation of power transformer since the no-load losses are often a determining factor when electrical utilities select a supplier for their power transformer purchases [1][2].

No-load losses are usually reported based on a sinusoidal voltage excitation and normal (50 or 60 Hz) frequency. However, even with a sinusoidal source voltage, the nonlinear relation between the flux density and the magnetic field strength in the transformer core will introduce significant harmonics into the excitation current. The harmonic components of the no-load current of the transformer are influenced by many factors, such as the frequency of voltage supply, the flux density, the degree of saturation and the core stacking technique [3].

The measurements of the transformer no-load current is addressed in IEC Standard 76-1 under clause 10.6 “Measurement of the harmonics of no-load current”[4]

An effect which can also stem from core saturation is increased volt ampere reactive (VAR) power consumption, leading to voltage-control problems, generating significant harmonic currents, and cause heating of the internal components of transformer itself, leading to gas relay alarm/operation as well as possible damage [2]. The VAR absorption can be explained by realizing that core saturation result in magnetizing current which is basically an inductive current. If saturation is severe the VAR absorption will increase and become noticeable, along with an associated in displacement power factor.

Real power

$$P = V I \cos\varphi \quad (1)$$

Reactive power

$$Q = V I \sin\varphi = P \tan\varphi \quad (2)$$

Where: P = real power (watt)
Q = reactive power (VAR)
V = input voltage (volt)
I = input current (Ampere)
$\cos\varphi$ = input power factor

ISSN 114-1284

2. TRANSFORMER OPERATION WITH LOW FREQUENCY SUPPLY

The general form of emf induced in primary and secondary windings of a single-phase transformer is

$$E = 4.44\ N\ f\ B_{max}.A \qquad (3)$$

where N is number of windings, f is supply frequency (Hertz), B_{max} is magnetic flux density in core (Tesla) and A is effective core area (m^2). Because of A is constant (can be calculated from core configuration), and by assuming, that the input voltage equal to primary emf induced, the magnetic flux density can be varied by varying the input voltage, meanwhile the frequency is maintained constant.

There are three methods of estimating harmonic load content: the Crest-factor (CF), Harmonic Factor or Percent Total Harmonic Distortion (%THD) and "K-Factor". In this paper we focuses on the very simple harmonic estimation technique is the Crest Factor. Crest Factor is a measure of the peak value of the waveform compared to the true rms value. The mathematical definition, of the crest factor is the ratio of the peak value of the waveform divided by the rms value of the waveform:

$$CF = \frac{Peak\ of\ waveform}{rms\ of\ waveform} \qquad (4)$$

By definition, a perfect sine wave current or voltage will have a crest factor of the square root of 2 or 1.414 and any deviation of this value represents a distorted waveform. Note that the crest factor can also be lower than 1.414. A square wave, for example, would have a CF of 1 [6].

The percent total harmonic distortion (%THD) can be defined in two different ways, as a percentage of the fundamental component (the IEEE definition of THD) or as a percentage of the rms (used by the Canadian Standards Association and the IEC) [6]. In this paper we uses the later one.

$$THD = \frac{\sqrt{\sum_{h=2}^{\infty} V_{h,rms}^2}}{V_{rms}} x100\% \qquad (5)$$

where $V_{h,rms}$ is the amplitude of the harmonic component of order h (i.e., the *h*th harmonic) and V_{rms} is the rms values of all the harmonics) that can be represented as

$$V_{rms} = \sqrt{\sum_{h=1}^{\infty} V_{h,rms}^2} \qquad (6)$$

The total power factor is called distortion power and results from the harmonic component of the current:

$$PF = \frac{1}{\sqrt{1+\left(\frac{THD}{100\%}\right)^2}} \qquad (7)$$

3. MODEL

The transformer test (handheld based) has the specification as: single-phase transformer, core type with primary winding of 220 turns and secondary of 220 turns respectively. The lamination of core material is M5, 3 millimeter thickness and 10 cm width. It consists of 12 layers with 10 cm corner overlap length configuration.

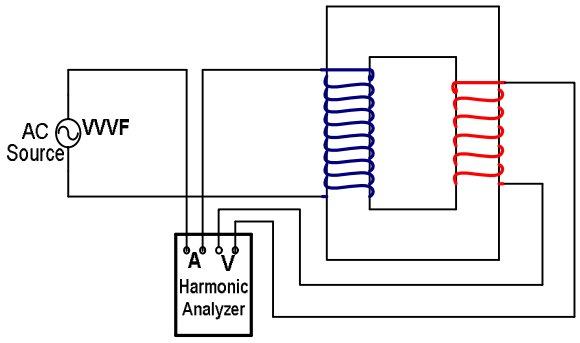

Figure 1 Arrangement of experimental set-up

The arrangement of equipment set-up which used in this research work is as shown in Figure 1. The input current to harmonic analyzer (PM 300) is connected to ac variable voltage variable frequency supply and its voltage is come from the secondary side of transformer test. The experiment was conducted with different flux density by varying the input voltage and frequency.

Example of voltage supply calculation:
Core Area, A = 17 x 0.1 x 0.0003 = 0.00051 m^2
for N = 220
f = 40 Hz
B = 1.5 T
Voltage, V = 4.44 x 220 x 40 x 1.5 x 0.00051
V = 19.93 V
The same procedures is used to calculate the voltage supply for the others frequency and magnetic flux density values.

4. RESULT

The examples of current and voltage waveforms and the individual harmonic distribution for the different input (primary) voltages or different magnetic flux density (1.5 T and 1.8T) with frequency 40 Hz are shown in Figure 2 to Figure 5.

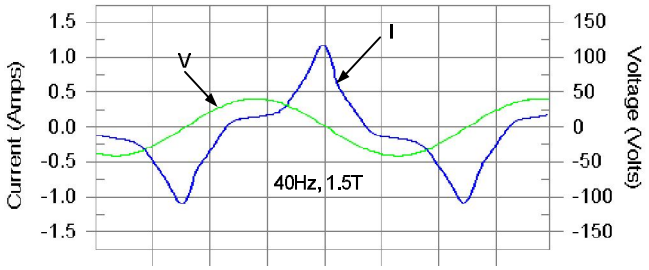

Figure 2 Current and Voltage waveforms for B = 1.5T

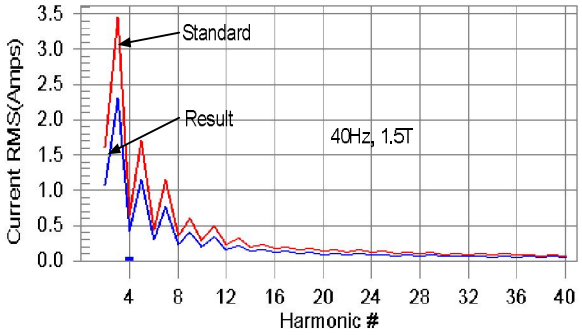

Figure 3 Individual harmonic distribution of input current for f = 40Hz, B=1.5T

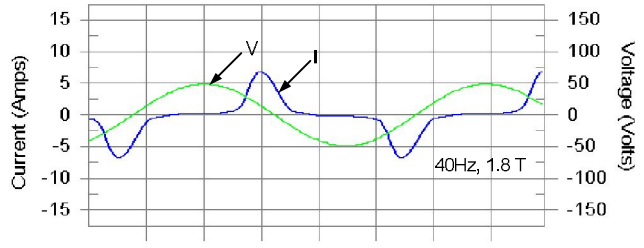

Figure 4 Current and Voltage waveforms for B = 1.8 T

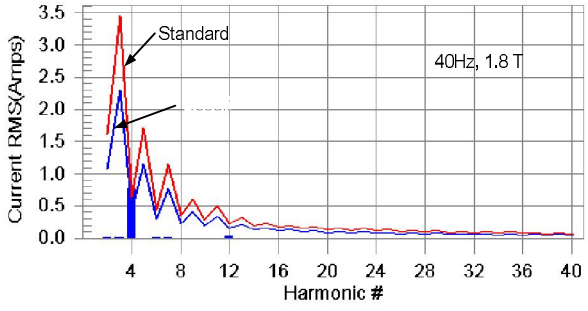

Figure 5 Individual harmonic distribution of input current for f = 40Hz, B=1.8T

5. DISCUSSION

Figure 2 shows that the input current waveform for lower magnetic flux density (B = 1.5 T) is better (more sinusoidal) than for B = 1.8 T as its shown in Figure 4. These conditions are more clearly displayed in term of individual harmonic distribution in Figure 3 and Figure 5. The distortion pattern displayed in Figure 5 is a result of waveform for f = 40Hz, B=1.8T. As the magnetic core tends to saturate, some of individual harmonic has reach out of limit (Standard). This situation can be used as the reason why the transformer is always suggested to operate at magnetic flux density below the saturation condition.

The characteristics of volt ampere reactive (VAR) power consumption to variable magnetic flux density is shown in Figure 6. The graphs of the percentage of input current total harmonic distortion and crest factor to magnetic flux density are displayed in Figure 7 and Figure 8. With respect to Figure 7, the VAR absorption for higher frequency (in this investigation is 50 Hz) supply is slightly higher. The changes of harmonic contents are not so significant. These conditions are shown in Figure 7 and 8. One of the important thing is changes (increment) of VAR, %THD and CF are very significant when the magnetic flux density is increased from 1.5 T to 1.8 T. This phenomena can be used as saturated measured interm of VAR power consumption and harmonic contents.

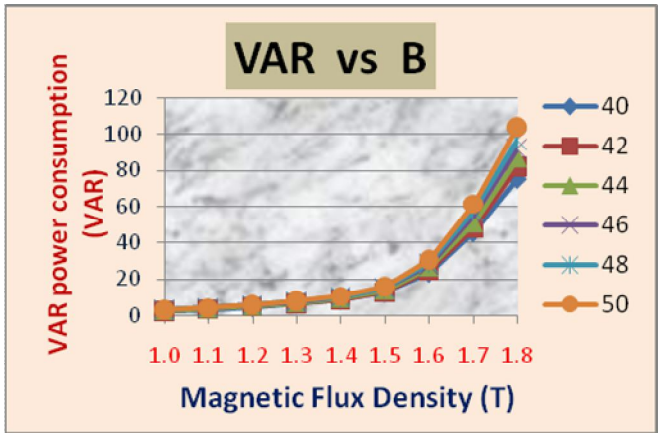

Figure 6 VAR vs Magnetic flux density(B)

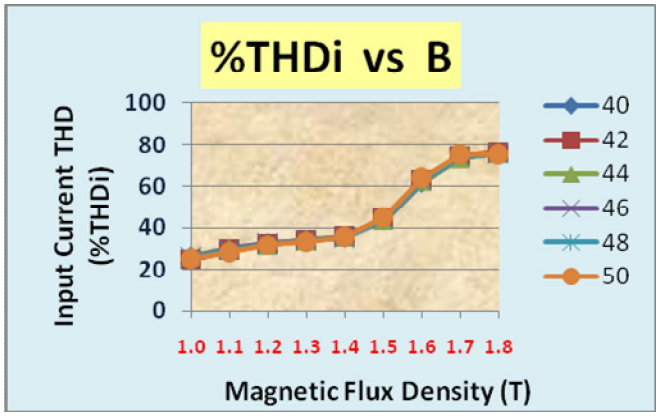

Figure 7 %THD vs Magnetic flux density(B)

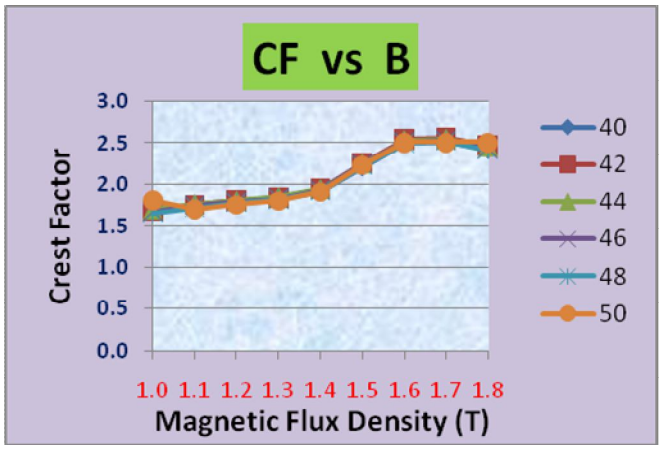

Figure 8 Crest Factor vs Magnetic flux density(B)

6. CONCLUSION

A number of investigations were conducted to determine the volt ampere reactive power consumption and harmonic performance of a single phase transformer operating under various low frequencies supply (i.e., 40 to 50 Hz) and at different magnetic flux density. The result shows that the VAR power consumption is lower when primary winding subjected to low frequency supply.

The harmonic content of the input currents are not so differ, however, the increasing of VAR and harmonic content are quite significant when the magnetik flux density increas from 1.5 to 1.8 T.

ACKNOWLEDGMENT

The authors wish to thank to the Power Electronic and Electrical Machine Design Cluster, and R&D Universiti Malaysia Perlis (uniMAP) for the technical and financial support as well.

REFERENCES

[1]. Eddy So, Rejean Arseneau, and Ernst Hanique, "No-Load loss Measurements of Power Transformers under Distorted Supply Voltage waveform Conditions", IEEE Transaction on Instrumentation and Measurement, Vol. 52, No. 2, pp. 429-432, April 2003

[2]. Rejean Arseneau, Eddy So, and Ernst Hanique, "Measurements and Correction of No-Load Losses of Power Transformers", IEEE Transaction on Instrumentation and Measurement, Vol. 54, No. 2, pp. 503-506, April 2005

[3]. Aiman Hassan Al-Haj and Ibrahim El-Amin, "Factors that Influence Transformer No-Load Current Harmonics", IEEE Transaction on Power Delivery, Vol. 15, No. 1, pp. 163-166, January 2000

[4]. International Electrotechnical Commission Standards, IEC 76, part one, Power Transformers, 2nd ed., 1993

[5]. Price, PR, "Geomagnetically Induced Current Effects on Transformers," IEEE Transaction on Power Delivery, vol.17, October, no.4, 2002, pp. 257–265.

[6] Skavarenina L.Timothy, DeWitt E.William, *Electric Power and Controls*, Pearson-Prentice Hall, New Jersey, United States of America, 2004.

Normal Flux Distribution in 23° T-joint of Three Phase Transformer Core with Staggered Yoke 10mm

I. Daut [a], Dina M.M. Ahmad [b], S. Taib [c]

[a]*School of Electrical System Engineering,*
Universiti Malaysia Perlis (UniMAP),
P.O Box 77, d/a Pejabat Pos Besar
01007 Kangar Perlis,
Malaysia Email address: ismail.daut@unimap.edu.my

[b]School of Electrical System Engineering,
Universiti Malaysia Perlis (UniMAP),
P.O Box 77, d/a Pejabat Pos Besar
01007 Kangar Perlis, Malaysia
Email address:dina@unimap.edu.my

[c]School Of Electrical & Electronic Engineering
USM, Engineering Campus
14300 Nibong Tebal
Penang, Malaysia
Tel: +604 - 5995810 Ext.6012. Fax: +604 – 5941023
Email address: soibtaib@eng.usm.my

ABSTRACT

This paper describes the result of an investigation in 3-phase 100kVA transformer core assembled with staggered yoke of 10mmoverlap length. The investigation involves the variation of normal flux distribution in the core lamination. The normal flux distribution has been measured at T-joint core model of 15 layers of lamination by arrays of search coil. The highest normal flux distribution occurs at the upper edge of the middle limb that is 0.170T and lowest at upper edge of yoke that is 0.1T. The average value of normal flux distribution is high at flux transfer region of the lamination. The flux transfer mechanism shows that two separate path flowing horizontally in the yoke before leaving the lamination to vertically adjacent layer and combine with the flux in that layer. The Fluxs will drops in the T-joint are approached as flux diverts to adjacent laminations above and below to avoid the high reluctance air gap.

Keywords: Grain oriented silicon iron, transformer core, normal flux distribution, fundamental flux.

1. INTRODUCTION

Power transformers are usually employed in electric power stations, high voltage transmission lines and large utilities. On the other hand, distribution transformers can be found in small and midsize industries, hotels, hospitals, schools, entertainment centers, residential areas and etc [1]. Transformers are ubiquitous in all part of the power system, between all voltage levels, and exist in many different sizes, types and connections [2]. Grain-oriented 3% silicon-iron is used for transformer cores where high efficiency and low weight are often paramount [3]. The efficient operations of power transformer cores depend on a large extend on the design of the joints between their limbs and yokes. The most complex joint in three limb cores are the T-joints at the intersection of the centre limb and yokes. Under ideal conditions the total flux in the limbs of a transformer core has a sinusoidal waveform, but in the corners of the core the flux is far from sinusoidal. The additional loss caused by the flux distortion can lead to localized heating within the joints [4]. The objective of this research is to measure normal flux distribution on the lamination of transformer core that built from the electrical steel (M5 grade material) 3% silicon-iron assembled with 23o T-joint mitred lap corner joint with staggered yoke by using array of search coils.

2. EXPERIMENT APPARATUS AND MEASURING TECHNIQUES

Three phase 100kVA distribution transformers are assembled with 23° T-joint, mitred overlap corner joints length of 10mm as indicated in figure 1. Each core is 550 mm x 580 mm with the limbs and yokes 100 mm wide as indicated in figure 2. The main apparatus consisted of three phase cores, two yoke cores and three limbed cores and the cores are assembled from 0.3 mm thick laminations of M5 grain oriented silicon iron (CRGO) [7]. Each core comprises of 15 layers. The system for measuring normal flux density is shown in Figure 3.

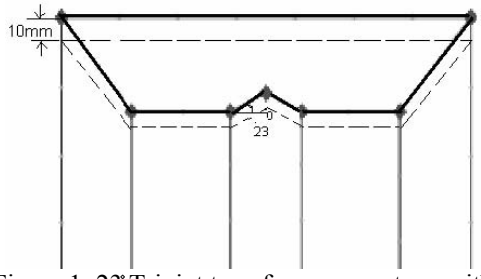

Figure 1: 23° T-joint transformer core type with staggered yoke 10mm

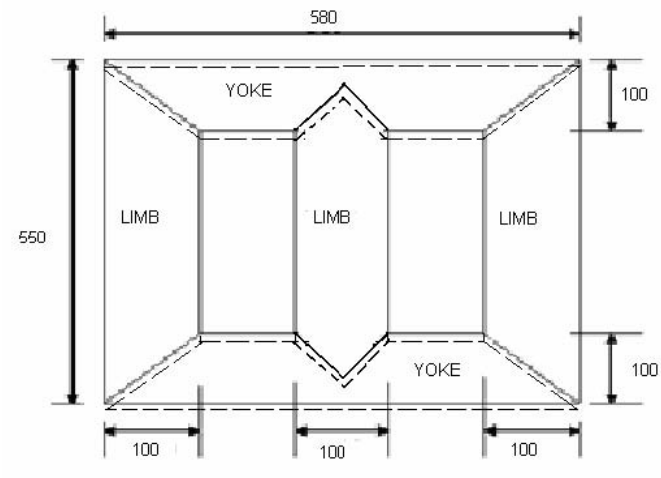

Figure 2: Dimension (mm) of 23° T-joint 100kVA transformer model

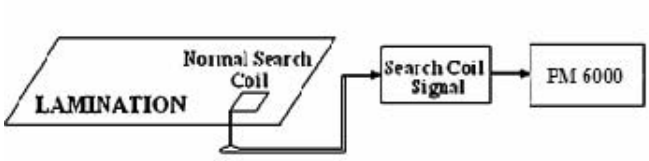

Figure 3: Associated system for measuring normal flux density.

In order to study the normal flux density variation, normal search coil arrays are used to measure normal flux density variation along and across the lamination. The squares of 10mm x 10mm normal search coils are placed on a layer of lamination at the T-joint of the transformer core. The locations chosen must cover the areas where the flux is more likely to vary direction so as to find the mechanism distribution of the flux behavior. The location of the investigation for the transformer core is shown in figure 4.

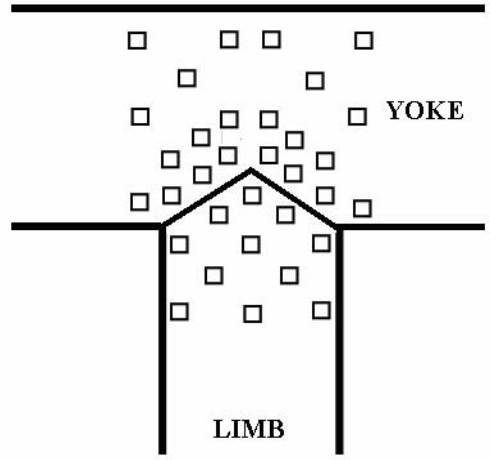

Figure 4: The normal search coils position in the T-joint of transformer core

3. RESULTS AND DISCUSSION

Fundamental normal flux density at T-joint flowing in a direction normal to the plane of the lamination in the staggered yoke 10mm 1.5T, 50Hz is shown in figure 5.

The magnitude of the normal flux density is high at and close to an intersection between two adjacent laminations. The highest normal flux occurs at the corner edges of centre limb that is 0.170T at flux density 1.5T, 50Hz. The average magnitude of normal flux density is largest at the overlap region and smallest at the upper edge of the right yoke. The fundamental normal flux density increases as it approaches the T-joint and gradually decrease as it travels further away from the joint. The magnitude of fundamental normal flux density traveling between joints reaches minimum at the mid point of centre limb. This alteration in the fundamental normal flux density is due to increase and decrease of flux density that has been energized.

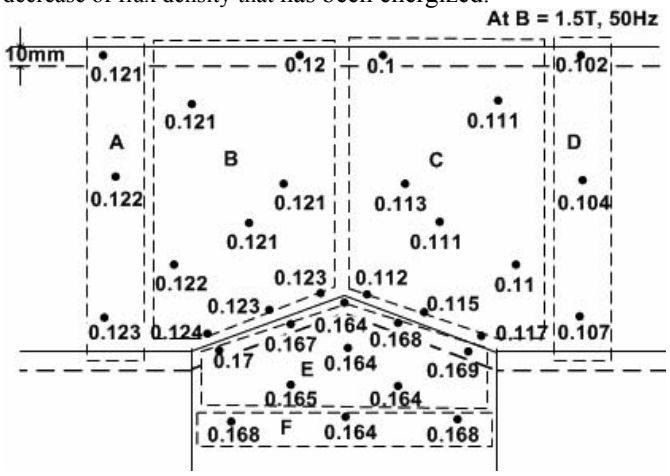

Figure 5: Distribution of the normal direction of fundamental flux density at T-joint with overlap length of 10mm during 1.5 at 50Hz.

The instantaneous magnitude and direction of flux at this instant is shown in figure 6 at this instant the total flux in the centre limb reaches its maximum and both right and left yoke carry half their maximum flux.
Since the yokes carry only half the maximum value of the total flux, the majority of the flux from the outer of right and left yoke is carried through the inner half of junction of middle limb and the largest flux concentration is found in the upper edges of middle limb.

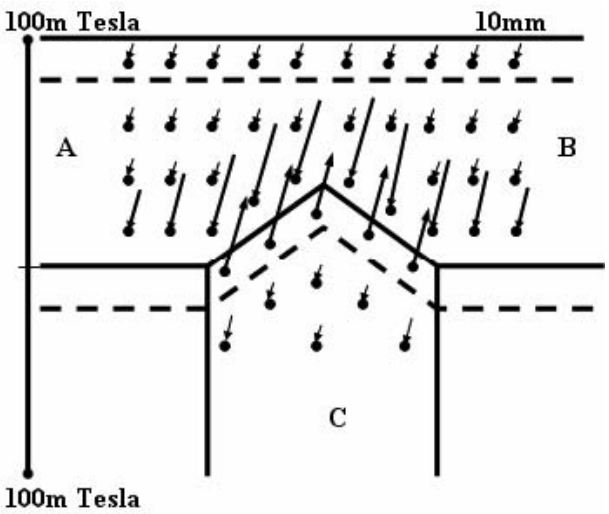

Figure 6: Distribution of the fundamental component of localised normal flux density in the 23° T-joint of three phase core built at different instant in time when ωt=60°.

Flux path and flux transfer mechanism between laminations at the T-joint has been illustrated as figure 7 for staggered yoke arrangement. The diagram shows that the flux transfer mechanism between yoke and limb in the T-joint may occur simultaneously at the same instant in time. This can be seen for example at the A and B region where two separate path flowing horizontally before leaving the lamination to vertically adjacent layer of D and F respectively and combines with the flux in that layer. Consequently, the core material in this region approaches saturation. At the same time, this existing flux will transfer back to the C region and extend to the whole length of the middle limb. It has been noticed that the magnitude of normal flux density high at the inner edges of yoke at junction between yoke and middle limb and decrease as the distance away from the joint.

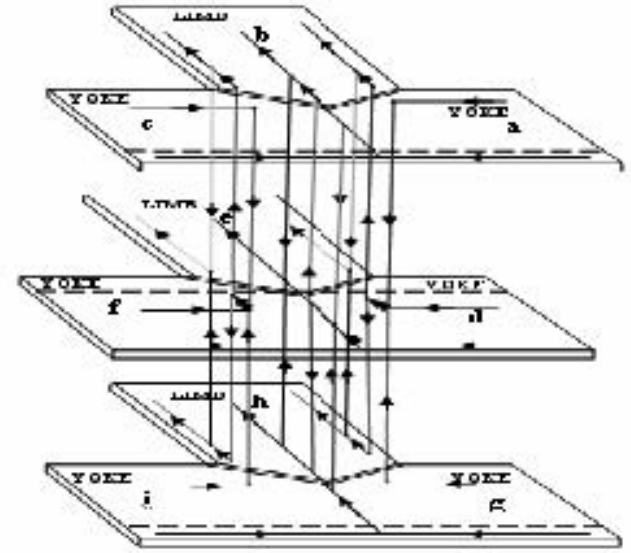

Fig. 7: Flux transfer between laminations of staggered yoke limb arrangement at the T-joint.

4. CONCLUSION

From the result of this investigation, the normal flux distribution in the cores assembled with 23° T-joint was found varies along overlap area of the staggered at the T-joint. High normal flux distributions occur in the corner edge of the centre limb that is 0.170T and gradually decrease as it travels far away from the joint area.
The flux transfer mechanism between yoke and limb in the T-joint may occur simultaneously at the same instant in time. The flux transfer mechanism most occur at T-joint of the transformer core compared to the other places. The magnitude of normal flux density is high at nearest of the junction of T-joint and decrease as the distance away from the joint.

ACKNOWLEDGEMENTS

The authors would like to express their gratitude to the Malaysian Transformer Manufacturing (MTM) for the supply of transformer core material.

REFERENCES

[1] C. Hernandez, M.A. Arjona, and Shi-Hai Dong, "Object-Oriented Knowledge-Based System for Transformer Design," *IEEE Transactions On Magnetics*, vol. Mag-44, No. 10, October 2008.
[2] O.A. Mohammed, Fellow, IEEE, N.Y. Abed and S. Liu, "Investigation of the Harmonic Behavior of Three Phase Transformer Under Nonsinusoidal Operation Using Finite Element and Wavelet Packets,"
[3] J. Moses, T. Meydan, and H. F. Lau, "Domain Structures in Silicon-Iron in the Stress Transition Stage," *IEEE Transactions On Magnetics*, vol. 31, No. 6, November 1995
[4] Moses,A. J., B. Thomas, and J. E.Thompson, "Power Loss and Flux Density Distributions in the T-Joint of a Three Phase Transformer Core," *IEEE Transactions On Magnetics*, vol. Mag-8, No. 4, December 1972.
[5] Jones, A. J., Moses, A. J., Comparison of the Localized Power Loss and Flux Distribution in the Butt and Lap and Mitred Overlap Corner Configurations, *IEEE Tans. ON MAG., VOL. MAG-10*, No. 2, june 1974.
[6] Mansel A Jones and Antony J. Moses, Comparison of the Localized Power Loss and Flux Distribution in the Butt and Lap and Mitre Overlap Corner Configurations, *IEEE Trans. On Mag., Vol, MAG-10,* No.2, June 1974
[7] Daut, I and Moses, A.J., Some Effects Of Core Building On Localised Losses And Flux Distribution In A Three-Phase Transformer Core Assembled From Powercore Strip, *IEEE Trans. On Mag., Vol. MAG-26*, No 5, pp. 2002, Sept 1990
[8] Daut, I.,"*Investigation of Flux and Loss Distribution in Transformer Cores Assembled From Amorphous Powercore Material*", 1992, PhD Thesis University of Wales
[9] Beckley P., *Electrical Steels for rotating machines*, The Institution of Electrical Engineers, 2002.
[10] Indrajit Dasgupta, *Design of Transformers Handbook*, Tata Mc- Graw Hill, India, 2002.
[11] James H. Harlow, *Electric Power Transformer Engineering,* CRC Press LLC, 2004.

[12] Daut I., Dina M.M. Ahmad and S. Taib, *Measurement of flux distribution on 100kVA 3phase distribution transformer assembled with 60^{o} T-joint and mitred lap corner joint with stagger yoke by using search coil*, MUCET2008 8th-10th March 2008, Hotel Putra Palace, Perlis, Malaysia.

[13] Daut, Dina M.M. Ahmad, and S. Taib , *Measurement of Flux Distribution on 100kVA 3phase Distribution Transformer Assembled With 45^{o} T-Joint And Mitred Lap Corner Joint With Stagger Yoke By Using Search Coil*, IASTED AsiaPES2008, 2nd-4th April 2008, Meritus Pelangi Beach Resort Hotel, Langkawi, Malaysia, ISBN CD: 978-088986-732-1

Proceeding of the 11th International Conference on QiR (Quality in Research)
Faculty of Engineering, University of Indonesia, Depok, Indonesia, 3-6 August 2009
ISSN 114-1284

The Operating Method of a Stand-Alone Wind/Diesel/Battery Hybrid Power System

Ismail Yusuf

Faculty of Engineering
University of Tanjungpura, Pontianak 78124
Tel: (0561) 740186
E-mail : isyusfar2@yahoo.com

ABSTRACT

A new method for operating a stand-alone wind/diesel/battery system is presented in this paper. The diesel generator is controlled so that the state of charge (SOC) of the battery may be maintained at a certain specified charge level in daily time. The battery is discharged when the SOC is higher than the specified charge level and charged when lower. A simulation is carried out over one year using the hourly data of electric load, wind speed, and atmospheric temperature on Kamishima Island, Japan in 2006. This method is compared with other operating methods: a conventional operating method maintaining the battery charge level at the full level (FCL), and dynamic programming (DP) operating method. The results show that for diesel generator fuel consumption, this method is better than FCL, although not to the DP.

Keywords

Hybrid system, fuel consumption, simulation, battery charge level.

1. INTRODUCTION

Many stand-alone wind/diesel/battery systems have been installed on remote islands. These systems are operated so that the fuel consumption of the diesel generator (DG) is minimized without causing any blackouts. In such operation, the battery has the role of storing surplus energy or of assisting a wind turbine generator. The operation method of the battery differs with the purpose for which it is controlled. For example, if the battery is used as an energy sink, it is desirable to hold the state of charge at a limited low level. On the other hand, if it is used as an energy source, it is desirable to hold the state of charge at a limited high level. In this study, the purpose is to reduce the yearly fuel consumption of DG as low as possible. For that purpose, the wind energy is stored temporarily in the battery when wind turbine generator (WTG) output is higher than electric load, and used effectively when WTG output is lower than electric load. To do this, the state of charge must be held at an intermediate level between the limited high and low levels. For this reason, the Specified Charge Level operating method (SCL) is proposed. A simulation was performed for over one year using the hourly data of electric load and wind speed on Kamishima Island, Japan in 2006. The most suitable battery charge level was sought, i.e., the level at which fuel consumption is lowest. The SCL method is compared with other methods from the viewpoints of annual fuel consumption and excess energy.

2. ENERGY FLOWS

Energy flows in the wind/diesel/battery power system are shown in figure 1, in which $P_W(t_i)$ is the output of the wind generator, $P_d(t_i)$ is the output of diesel generator, $P_l(t_i)$ is the electric load, $P_{dl}(t_i)$ is the excess energy dumped to dummy load, and $P_b(t_i)$ is the charge or discharge energy of the battery. $P_b(t_i)$ is positive when the battery is discharged, otherwise is negative. t_i is the hourly time. These flows must satisfy the equation (1).

$$P_w(t_i) + P_d(t_i) + P_b(t_i) = P_l(t_i) + P_{dl}(t_i) \qquad (1)$$

The operation of the system is divided into three scenarios depending on the electric load, $P_l(t_i)$, the output of WTG, $P_w(t_i)$, and the battery charge level, $X(t_i)$, as follow:

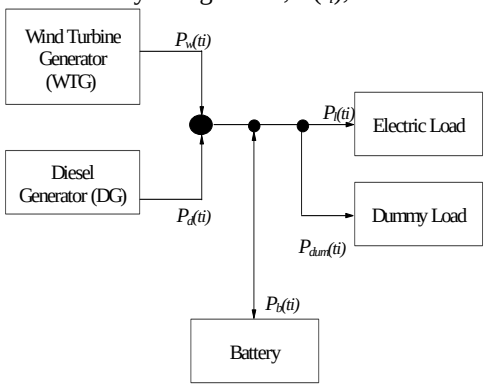

Figure 1: Energy flows in wind/diesel/battery system

ISSN 114-1284

Scenario 1: $P_l(t_i) > P_w(t_i) + P_{dr}$
Scenario 2: $P_l(t_i) \le P_w(t_i) + P_{dr}$ and $X(t_i) \le X_s$
Scenario 3: $P_l(t_i) \le P_w(t_i) + P_{dr}$ and $X(t_i) > X_s$
Where, P_{dr} : the rated output of DG
X_s : a specified charge level of battery

3. ELECTRIC LOAD AND WIND ENERGY

The monthly variations of electric load and wind turbine generator output at Kamishima Island are shown in figure 2. The electric load is high in July and August. Since the yearly electric load energy is 1,538 MWh and the peak load is 393 kW, so the load factor is 46%. The average daily electric load is 4,336 kWh.

Matching the power-wind speed characteristics of a commercial wind turbine generator with hourly wind speed data from over one year makes the wind energy calculations. The characteristics of the wind turbine generator are described by an equation (2). The calculation result is for a case in which the rated output of WTG is 250 kW. The wind energy is high in January, February, March, November and December.

4. OUTPUT CHARACTERISTIC OF SYSTEM COMPONENTS

4.1 Characteristic of Wind Turbine Generator

Output - wind speed characteristics (P_w - v characteristics) of WTG is shown in Figure 3. It is formulated as equation (2):

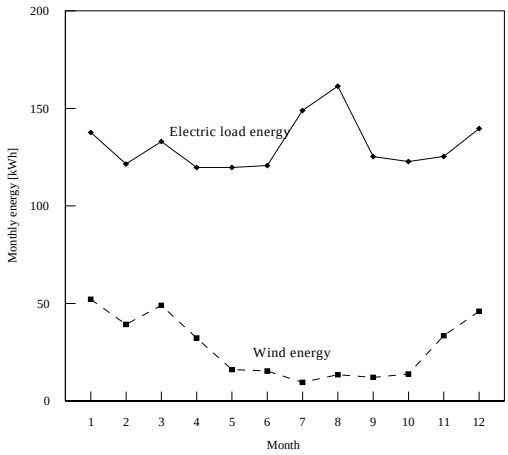

Figure 2: Monthly variations in electric load and wind energy.

$$P_w(t_i) = \begin{cases} 0 & (v(t_i) < v_c,\ v_o \leqq v(t_i)) \\ P_{wr} \times (v(t_i) - v_c)/(v_r - v_c) & (v_c \leqq v(t_i) < v_r) \\ P_{wr} & (v_r \leqq v(t_i) < v_o) \end{cases} \quad (2)$$

Where P_{wr} is the rated output of WTG, v_c is the cut-in wind speed, v_r is the rated wind speed and v_o is the cut-out wind speed. Here, P_{wr} = 250 kW, v_c = 3 m/s, v_r = 12 m/s, v_o = 25 m/s.

4.2 Characteristic of Diesel Generator

The fuel consumption of the diesel generator is calculated using the following equation:

$$F_d = a \cdot P_d^{\,2} + b \cdot P_d + c \quad (3)$$

Where F_d is the fuel consumption and P_d is the output. The coefficients a, b, and c are determined by fitting the equation (3) to the characteristic of a commercial DG. The DG output is controlled between 20% and 100% of the rated power. In this study, the rated outputs are taken as parameters: 250, 300, 350, and 400 kW.

4.3 Characteristic of Battery

At present, a lead battery is exclusively used as the energy storage. In the near future, however, a sodium sulfur (NaS) battery will be commercially available. NaS battery's performance is higher than the lead battery. The characteristic of NaS battery is utilized in this study.

The battery capacity is taken as a parameter and expressed in percentages. The capacity of 100% is equivalent to an average daily electric load (4,336 kWh). Charging and discharging efficiencies are 85% and 100% respectively. Battery hourly charge rates are limited to 10% and 20% of the battery capacity when charging and discharging, respectively.

5. THE OPERATING METHOD

The integrated wind/diesel/battery system must meet the daily and annual energy demand as well as the peak load at any time. In that condition, it is technically desirable to reduce fuel consumption and excess energy to as low a level as possible. The fuel is consumed in DG. In the event that the output from WTG exceeds the electric load and the battery charge level is maximum, then the excess energy is drained away to the dummy load that is installed parallel to the electric load. Therefore, the battery and the DG have to be so operated that the system may meet these requirements. Here the WTG is assumed to be uncontrollable. In this study, a new operating method that we call the Specified Charge Level method (SCL) is proposed. In this method, the system is so operated that the battery charge is kept at a specified level as long as possible. That level is between 20 and 100 % of battery capacity. When the charge is lower than the specified level, the output of DG has to be increased to charge the battery, but when the charge is higher than the specified level, the output of DG has to be decreased to discharge the battery. Should the charge drop to less than a 20 % level, a shortage supply would occur. On the other hand, when the charge rises to around the 100 % level, excess energy generated by the WTG must be dissipated. Therefore the specified charge level has to be selected appropriately.

The operation of the system is divided into three scenarios depending on the electric load, $P_l(t_i)$, the output of WTG, $P_w(t_i)$, and the battery charge level, $X(t_i)$.

A Flow chart of the SCL method is shown in figure 3. First, data of the electric load, wind speed, and system parameters are read. After reading the specified charge level of the battery, X_s, the initial charge level $X(0)$ is set as same as X_s. Then the output of WTG is calculated, and the diesel generator and the battery are operated comparing $X(ti)$ with X_s such as in scenarios 1, 2, and 3. The calculation is repeated hourly, and finally the annual fuel consumption is obtained.

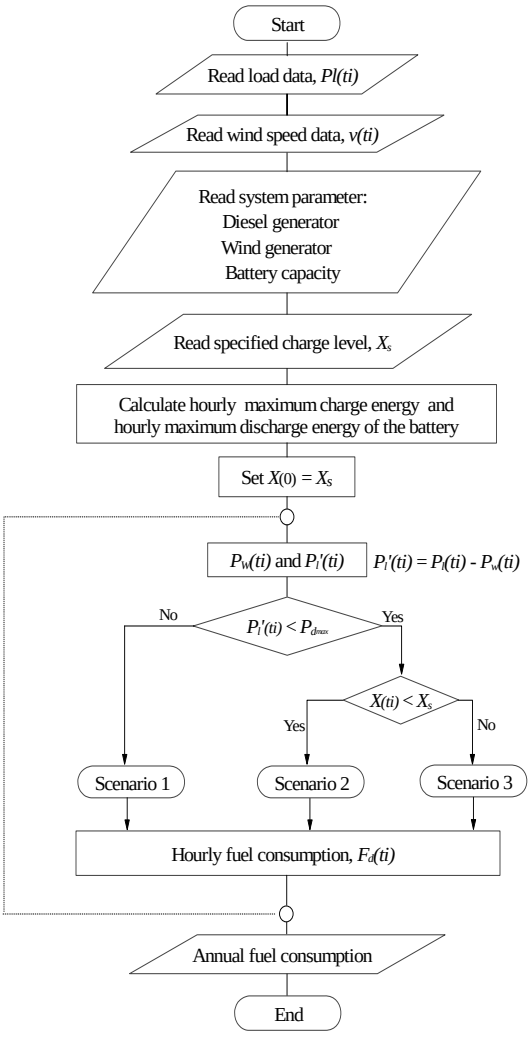

Figure 3: Flowchart of SCL operating method.

6. RESULTS AND DISCUSSION

6.1 Fuel Consumption and Minimum Specified Charge Level

Figure 4 shows annual fuel consumption as functions of the battery specified charge level for different rated outputs of DG, the battery capacity is 100 %. Fuel consumption is almost constant at specified levels from 20 % to 90 % and increases as the specified level rises from 90 % to 100 %. It also increases as the rated power of DG increases.

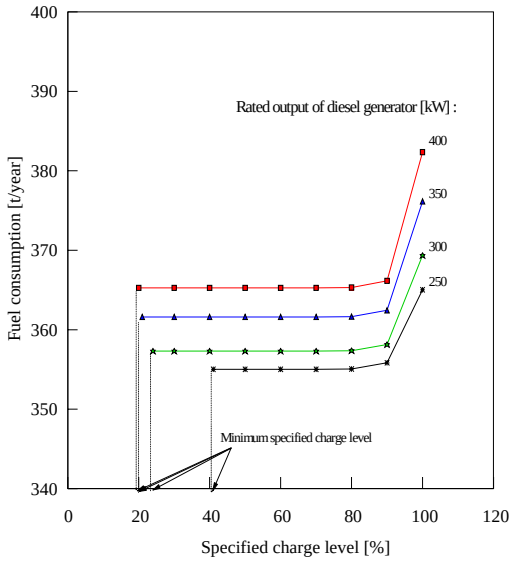

Figure 4: Annual fuel consumption vs. specified charge level.

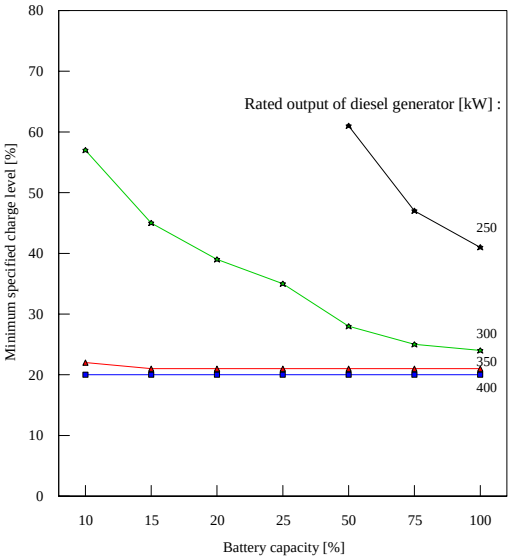

Figure 5: Minimum specified charge level vs. battery capacity for various diesel generator sizes.

Figure 5 shows the minimum specified charge level as a function of battery capacity for different rated outputs of DG. When the rated output of DG is 400 kW, the minimum specified charge level remains at 20 %, and rises to 21 % if the rated output of DG is 350 kW. However, when the rated output of DG is 300 or 250 kW, the minimum specified level would increase at the same battery capacity.

6.2 Comparison to Other Operating Methods

In order to estimate the SCL operating method, it has to be compared to other operating methods. Here, two methods are adopted: The full charge level (FCL) operating method and the dynamic programming (DP) operating method.

6.2.1 FCL Operating Method

As mentioned above, the stand-alone wind/ diesel/battery power system has to avoid the shortage of power supply to the electric load. Hence, it is favorable to maintain the battery charge at a full level, i.e., 100%. The FCL operating method is the common operating method and corresponds to the SCL operating method in which the specified charge level is set to 100%.

6.2.2 DP Operating Method

If the hourly data on electric load, and wind speed are known for one full year, the dynamic programming (DP) method could be available as the system operating method. In the DP method, the estimated value is the annual fuel consumption, the control variable is the DG output, and the state variable is the battery charge level. The DP operating method theoretically gives the lowest fuel consumption.

6.2.3 Comparison Results

Figure 6 shows the annual fuel consumption as functions of battery capacity for different operation methods, FCL, MSCL (SCL at minimum charge level), and DP. It is evident that the fuel consumption of the MSCL method is lower than that of the FCL method by 12 t (3 %), although higher than that of the DP method by 14 t (4 %). It is concluded that the MSCL method is superior to the FCL method although inferior to the DP method.

7. CONCLUSION

An operating method, SCL operating method, applicable to a stand-alone wind/diesel/battery power system is introduced in this paper. The output of diesel generator is controlled not only to meet the electric load but also to maintain the battery charge at certain specified charge level. A simulation is performed over one year using the hourly data of electric load and wind speed of Kamishima Island, Japan in 2006.

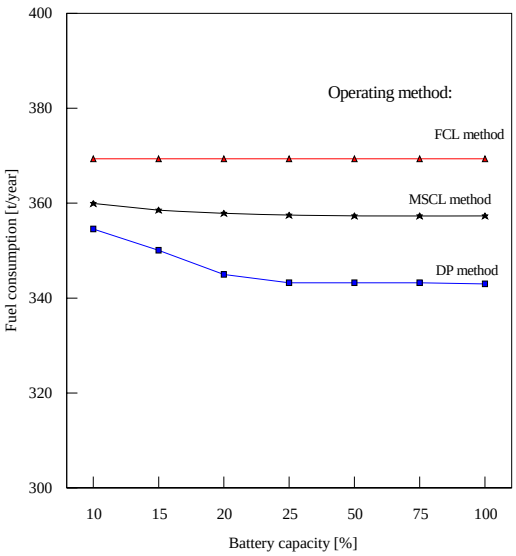

Figure 5: Fuel Consumption of Various Methods.

The SCL operating method is compared with others, i.e., the FCL operating method and the DP operating method. By the simulation results, the fuel consumption of the SCL operating method is lower than that of the FCL operating method but not than the DP.

REFERENCES

[1] Mosgrove, A.R. deL., "The Optimization of Hybrid Energy Conversion Systems Using the Dynamic Programming", International Journal of Energy Research, 1988, Vol.12, p.p. 447-457.

[2] T. Kawamoto and T. Sakakibara, "Design and Operation on Supplementary Wind Generator System for Community Uses", 1983, Transaction IEE of Japan, Vol. 103-B, p.p. 742-750.

[3] Y. Kemmoku, K. Ishikawa, S. Nakagawa, T. Kawamoto, and T. Sakakibara, "Life Cycle CO_2 Emissions of a Photovoltaic/Wind/Diesel Generating System", Transaction IEE of Japan, 2000, Vol. 120-B, No.7, p.p. 923-930.

[4] P.C. Bandopadhayay, "Economic Evaluation of Wind Energy Application for Remote Location Power Supply", Wind Engineering, Vol. 7, 1983, p.p. 67-78.

[5] W. D. Kellogg, M. H. Nehrir, G. Venkataramanan, and V. Gerez, "Generation Unit Sizing and Cost Analysis for Stand-Alone Wind, Photovoltaic, and Hybrid Wind/PV System", IEEE Transaction on Energy Conversion, 1998, Vol. 13, p.p. 70-75.

[6] J.G.F. Holland and G. Cramer, "Rathin Island Wind/Diesel/Battery System", Renewal Energy, Conference Publication, 385, 1993, p.p. 183-189.

Algorithm for RFID-Based Red Light Violation Detection

Iswanjono[a], Bagio Budiarjo[b], Kalamullah Ramli[b]

[a]*Doctorate Student of Dept. of Electrical Engineering*
Faculty of Engineering
University of Indonesia, Depok 16424
E-mail : iswan.id@staff.usd.ac.id

[b]*Dept. of Electrical Engineering*
Faculty of Engineering
University of Indonesia, Depok 16424
Tel : (021) 7270011 ext 51. Fax : (021) 7270077
E-mail : bbudi@ee.ui.ac.id; kalamullahr@gmail.com

ABSTRACT

This paper proposes an algorithm for RFID-based red light violation detection. Previous works of red light violation detection were developed using by the camera or the video and the combination digital camera-sensor of magnetic flux systems. We propose a red light violation detection algorithm using by combine of the RFID technology and the sensor of magnetic flux. Two algorithms is used, the first algorithm uses the ID track from one RFID Reader to another to detect vehicle movement. The second algorithm measures timing between the RFID Reader and the RFID Flux sensor and tags detection.

We hope our proposed system is better than previous system using the camera or the video and the combination of camera-RFID systems. Our design opens the possibility of detecting the violating vehicle in more accurate manner in terms of: able to detect dynamic vehicle speed, independent of lighting condition and more numbers of vehicles detection on a capture time.

Keywords:
Red Light Violation, Tracking Algorithms, RFID tags, RFID Reader, flux sensor, Traffic Light Controller (TLC)

1. INTRODUCTION

RFID (radio frequency identification) is a flexible technology that is convenient, easy to use, and well-suited for automatic operation. It combines advantages not available with other identification technologies. RFID can be supplied as read-only or read/write, does not require contact or line-of-sight to operate, can function under a variety of environmental conditions, and provides a high level of data integrity. In addition, because the technology is difficult to counterfeit, RFID provides a high level of security.

The term RFID describes the use of radio frequency signals to provide automatic identification of items. RFID is used in applications such as:

- Electronic toll collection (ETC)
- Railway car identification and tracking
- Intermodal container identification
- Asset identification and tracking
- Item management for retail, health care, and logistics applications
- Access control
- Animal identification
- Fuel dispensing loyalty programs
- Automobile immobilizing (security)

Radio frequency (RF) refers to electromagnetic waves that have a wavelength suited for use in radio communication. Radio waves are classified by their frequencies, which are expressed in kilohertz, megahertz, or gigahertz. Radio frequencies range from very low frequency (VLF), which has a range of 10 to 30 kHz, to extremely high frequency (EHF), which has a range of 30 to 300 GHz [1],[2]. RFID components are RFID tag, RFID reader and RFID database.

In this paper, we propose on the rfid application issues with red light violation detection. The previous papers [3],[4] have explained the red light violation detection by using a video or a camera and combine a digital camera and a sensor of magnetic flux . By video or camera is resulted video detect up to 50% of the capturing rate on day time and up to 45% of the capturing rate on night time. By combine a digital camera and a magnetic flux is resulted coil detect fewer than 95% of the capturing rate on day time and fewer than 90% of the capturing rate on night day [4]. We propose the red light detection violation using by combine the RFID technology and the sensor of magnetic flux.

Automatic license plate recognition plays an importance role in numerous applications and a number of techniques have been proposed. The former characterized by fuzzy disciplines attempts to extract license plates from an input image, while the latter conceptualized in terms of neural subjects aims to identify the number present in a license plate [5]. A high-resolution image of the number plate is obtained by fusing the information derived from multiple, subpixel shifted, and noisy low-resolution observations. The image to be superresolved is modeled as a Markov random field and is estimated from the observations by a graduated nonconvexity optimization procedure. A discontinuity adaptive regularizer is used to preserve the edges in the reconstructed number plate for improved readability [6].

In the proposal method, a tracking algorithm is presented to monitor a vehicle movement. A vehicle with RFID tag moves inside RFID network that is placed at a road cross-section. The RFID tag fills a license number information of the vehicle. For simplicity we assume a quarter of road cross-

section. The RFID reader is placed on a left side of road corner of each section. A radiation area of antenna of RFID reader is adjacent each others, there are not overlapping.

This paper is organized as follows. In section 2, the tracking method is discussed. In section 3, we propose a tracking algorithm for red light violation detection. Section 4 presents the performance evaluation by computer simulations. Finally we conclude this paper in section 5.

2. TRACKING METHOD FOR OBJECT MOVEMENT

2.1 Principle of VRT Algorithm [7]

The theoretical basis of virtual route tracking (VRT) algorithm is that the interrogation range of RFID system is very short compared to the distance between readers. Instead of powering the RFID tag directly by battery, it gets power through magnetic, electric and electromagnetic coupling with RFID readers. RFID tags are grouped into two categories: Passive and Active. All power supply of Passive tag is induced from RFID readers in contactless method. For Active tag, one or more batteries are embedded. However, the embedded battery only provides power to run chips, and data are transferred from transponder to reader by modulating on reflected electromagnetic waves emitted by RFID reader, like the ways of Radars. Consequently, the achievable range of RFID system is very small, varied from a few millimeters to several meters.

On the contrast, the range of wireless technology used to connect RFID readers is large. It can connect two readers within 10 meters, and Bluetooth or Wi-Fi is effective at the distance of 100 meters. Therefore, when a tag is sensed by a reader, i.e., the tag is located in the interrogation zone of this reader; the real distance between reader and tag is less than the range of the RFID system. So we use the position of the corresponding reader to stand for the current position of tag. When the scale of the RFID Reader Network is large enough and the distance of deployed readers is relatively long, VRT algorithm is very accurate.

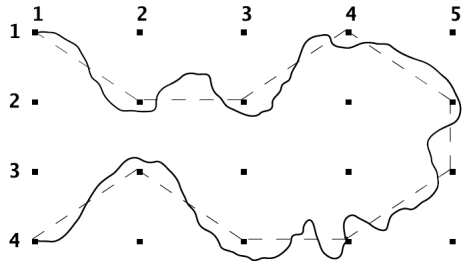

Figure 1: Principle of VRT algorithm

In Figure 1, the black point stands for a RFID reader and the matrix is a RFID Reader Network. As Figure 1 depicted, when a transponder moves from reader (1, 1) to reader (2, 2), the straight line between them is regarded as the track of the transponder by us. Therefore, when moving along the thick curve in the figure, which denotes the real path of a person or object in the RFID Network, the transponder is interrogated by readers along the path. And the virtual line (coined Virtual Route) is defined as the track of the transponder. So the track in Figure 1 is:

Track = *Virtual Route* = (1,1)→(2,2)→(2,3)→(1,4)→(2,5)
→(3,5)→(4,4)→(4,3)→(3,2)→(4,1)

It is noted that, when a reader interrogates one transponder, the next reader interrogating it along the track MUST be adjacent to the previous reader. In Figure 1, it is obvious that the transponder at (2, 3) cannot jump to (2, 5) directly without activating reader (1, 4), (2, 4) or (3, 4). Hence, the next reader of (2, 3) along the track MUST be one of following readers:

$\{(1,2), (1,3), (1,4), (2,2), (2,4), (3,2), (3,3), (3,4)\}$

Therefore, VRT algorithm MUST choose adjacent readers along the track. If two successive readers along the track are not adjacent to each other, special mechanism will be executed to guarantee that each reader along the track is contiguous to its last and next reader in real-word position. The virtual line connecting readers in Fig. 1 looks like a Route transferring data packets along the nodes. Due to this route is not real we name it "Virtual Route". In VRT algorithm, we use "Virtual Route" to stand for track of transponder in the RFID Reader Network. And that is why this algorithm is coined Virtual Route Tracking (VRT).

Of course, real-world RFID Reader Network is impossible to place readers so regular (exactly like a Matrix), and Figure 1 here only depicts fundamental of this algorithm theoretically.

2.2 Definition of Tracking Vector

More important, the concept of Tracking Vector (TV) is proposed here. Tracking vector plays a key role in collecting tracking information and calculating the track. We define the combination of the transponder identity, the interrogation time and the identifier of reader as Tracking Vector. The structure of TV is:

$$<T_i, t_j, R_k> = < Tag\ i, timestamp\ j, Reader\ k >$$

Here, the tag identity is a global unique number stored in the electronic chip of each tag and interrogated by reader. VRT algorithm can simultaneously track tens, even hundreds of tags tagged on objects or persons within a single network by classifying different tags according to the unique identity in each Tracking Vector.

Timestamp is the interrogation time of RFID reader when the tag entering its interrogation zone. We assume that all RFID readers in RFID Reader Network are synchronous. And only one tracking vector is generated no matter how long a tag stays within the interrogation zone of one reader.

The third parameter in tracking vector is the identifier of the reader. VRT algorithm uses the position of readers to track tags. It is noted that successive selected readers are all adjacent to each other and therefore can form a Virtual Route, therefore, reader identifiers of two successive Tracking vectors MUST stand for two contiguous readers in real network.

2.3 Two Special Conditions

As Figure 2 shows, when one tag moves along path *a*, three tracking vectors containing the same reader identifier are generated by reader R_1. At this time, VRT algorithm only chooses the first vector and deletes others.

$$\left.\begin{matrix} <T_x,t_1,R_1> & <T_x,t_2,R_1> \\ <T_x,t_3,R_1> & \end{matrix}\right\} \Rightarrow \{<T_x,t_1,R_1>\}, (t_1 < t_2 < t_3)$$

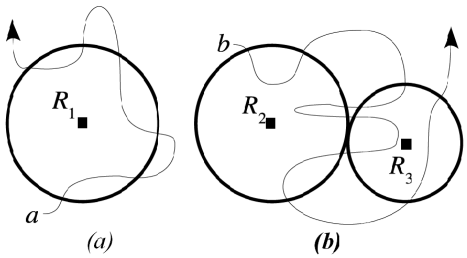

Figure 2: Two special paths

Suppose the tag alternates between two readers, e.g., R_2 and R_3 in Figure 2, only the first two or three tracking vectors should be remained. The method is specified as follows.

$$\begin{cases} R_2 & \Rightarrow R_2 \\ R_2 \to R_3 & \Rightarrow R_2 \to R_3 \\ R_2 \to R_3 \to R_2 & \Rightarrow R_2 \to R_3 \to R_2 \\ R_2 \to R_3 \to R_2 \to R_3 & \Rightarrow R_2 \to R_3 \\ R_2 \to R_3 \to R_2 \to R_3 \to R_2 & \Rightarrow R_2 \to R_3 \to R_2 \\ R_2 \to R_3 \to R_2 \to R_3 \to R_2 \to R_3 & \Rightarrow R_2 \to R_3 \\ R_2 \to R_3 \to R_2 \to \cdots\cdots\cdots \to R_2 & \Rightarrow R_2 \to R_3 \to R_2 \\ R_2 \to R_3 \to R_2 \to \cdots\cdots\cdots \to R_3 & \Rightarrow R_2 \to R_3 \end{cases}$$

For example, according to the above method, the tracking vectors of path *b* in Figure 2 are processed as:

$$\begin{Bmatrix} <T_x,t_1,R_2> & <T_x,t_2,R_3> & <T_x,t_3,R_2> \\ <T_x,t_4,R_3> & <T_x,t_5,R_2> & <T_x,t_6,R_3> \end{Bmatrix} \Rightarrow \begin{Bmatrix} <T_x,t_1,R_2> \\ <T_x,t_2,R_3> \end{Bmatrix}$$

$$(t_1 < t_2 < t_3 < t_4 < t_5 < t_6)$$

3. RESEARCH METHOD

3.1 Research Design

Figure 3 is shown diagram block of the research design. The system constrains traffic light controller (TLC), microcontroller for control management system, RFID readers, RFID tags, personal computer (PC) for database system and sensors of magnetic flux.

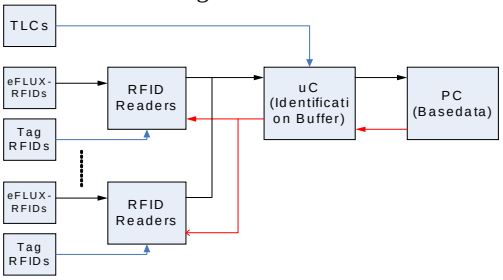

Figure 3: Block diagram of the research design.

The architecture of the research method of the RFID-based red light violation detection is shown at Figure 4. The crossroad is quarter section. The RFID readers make an adjacent network at the each left corner of the crossroad to monitor rfid tags movement. We assume that the range of antenna radiation of the RFID Reader. Three sensors of magnetic flux place at three lines of road branch, respectively. First sensor detect turn left of vehicle, second sensor detect straight destination and third sensor is turn right detection. We assume that Indonesia traffic is turn left go ahead.

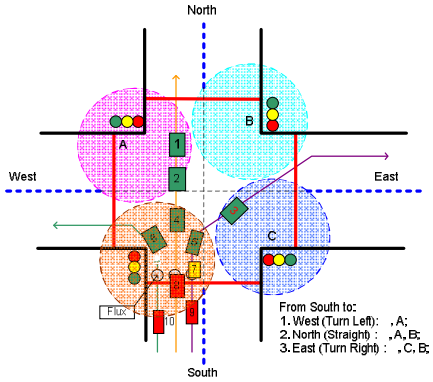

Figure 4: The architecture of the RFID-based red light violation detection

3.2 Algorithm Detail

The previous papers have been proposed in development of algorithm, for examples are Design of Traffic Light Control Systems Using Statecharts [8], Road Data Input System using Digital Map in Roadtraffic Simulation [9] and The Vehicle Junction Model and its Verification in Traffic Simulation [10] The speed of vehicle pass on crossroad is low until medium speed. In this algorithm, we take the vehicle speed up to 60 km/h or 0.0167 m/ms. If a range of antenna radiation of RFID readers are 10 meters and the time of sampling per RFID reader is 120 ms, so we result 5 samplings.

$$v = 0.0167 m/ms$$

$$x = 10m$$

$$t = \frac{x}{v} = \frac{10}{0.0167} = 600ms$$

$$T_s = 120ms$$

$$S = \frac{t}{T_s} = \frac{600}{120} = 5times$$

Where, v = vehicle speed (*meter/millisecond, m/ms*)
x = range of antenna radiation (*meter, m*)
t = time to pass antenna radiation (*millisecond, ms*)
T_s = Time of sampling (*ms*)
S = number of sampling (*time*)

The time of sampling is important to determine accuracy of violation detection.

The procedure algorithm is below:

1. Set Structure of Vector Tag ID
2. Choose direction road to check its status lamp
3. Note time-checking
4. If status lamp is green or yellow read ID tags from RFID Reader. Flux status is neglected.
5. Save time-checking, code of RFID Reader and ID tags into temporary memory address.
6. Monitor and track the ID tags, if there are IDs moves to another RFID Reader, delete the IDs from temporary memory address.
7. If status lamp is red, then check flux status. If flux status is not active, do step 5th.

8. If flux status is active/enable, read ID tags from RFID Reader and save time-checking, RFID Reader code and ID tags into temporary address of violator candidate.
9. Monitor and track the ID tags in temporary address of violator candidate to known its movements. If there are IDs moves to another RFID Reader, so the IDs are violator. Save the violator into violator memory address.

Figure 5 is shown the flow-chart of this algorithm.
From this algorithm, we hope to result some informations of the ID such as: (1) red light violator; (2) speed prediction of vehicle; and (3) number of vehicle on a capturing.

The vehicle is indicated as violator if on a capturing it is read by Reader as time as sensor of magnetic flux detection. The microcontroller system tracks its ID to monitor movement. If the vehicle ID have not read this Reader and/or read other Reader, so the vehicle is violator.

By assuming that the time of sampling is 120*ms* and the range of the antenna radiation of Readers is 10 meters, we can prediction speed of vehicle in Table 1. As comparing we take only if the time of sampling is 100*ms* in Table 2. As Table 1, we see that the time sampling will determine number of sampling. However, smaller number of sampling is very influence in determine speed of vehicle. So we assume that the maximum speed of vehicle passed crossroad is 60*km/h*.

Table 1: Speed prediction. (a) T_s = 120ms; (b) T_s = 100ms

(a)

Number of Sampling	Time	Speed	
	(*ms*)	(*m/ms*)	(*km/h*)
1	120	0.08333	300.00
2	240	0.04167	150.00
3	360	0.02778	100.00
4	480	0.02083	75.00
5	600	0.01667	60.00
6	720	0.01389	50.00
7	840	0.01190	42.86
8	960	0.01042	37.50
9	1080	0.00926	33.33
10	1200	0.00833	30.00
12	1440	0.00694	25.00
14	1680	0.00595	21.43
16	1920	0.00521	18.75
18	2160	0.00463	16.67
20	2400	0.00417	15.00
25	3000	0.00333	12.00
30	3600	0.00278	10.00
35	4200	0.00238	8.57
40	4800	0.00208	7.50
45	5400	0.00185	6.67
50	6000	0.00167	6.00
55	6600	0.00152	5.45
60	7200	0.00139	5.00

(b)

Number of Sampling	Time	Speed	
	(*ms*)	(*m/ms*)	(*km/h*)
1	100	0.10000	360.00
2	200	0.05000	180.00
3	300	0.03333	120.00
4	400	0.02500	90.00
5	500	0.02000	72.00
6	600	0.01667	60.00
7	700	0.01429	51.43
8	800	0.01250	45.00
9	900	0.01111	40.00
10	1000	0.01000	36.00
12	1200	0.00833	30.00
14	1400	0.00714	25.71
16	1600	0.00625	22.50
18	1800	0.00556	20.00
20	2000	0.00500	18.00
25	2500	0.00400	14.40
30	3000	0.00333	12.00
35	3500	0.00286	10.29
40	4000	0.00250	9.00
45	4500	0.00222	8.00
50	5000	0.00200	7.20
55	5500	0.00182	6.55
60	6000	0.00167	6.00

By referring the range of radiation of the Reader antenna is 10 meters and a minimum length of vehicle is 3.5 meters, so we can count the number of vehicle on a capturing. Figure 6 is shown a vehicle situation on a capture time. The maximum number of vehicle is 13 by a capture time. If the time of sampling, T_s, is 100*ms*, so the maximum number of vehicle is 130 per second.

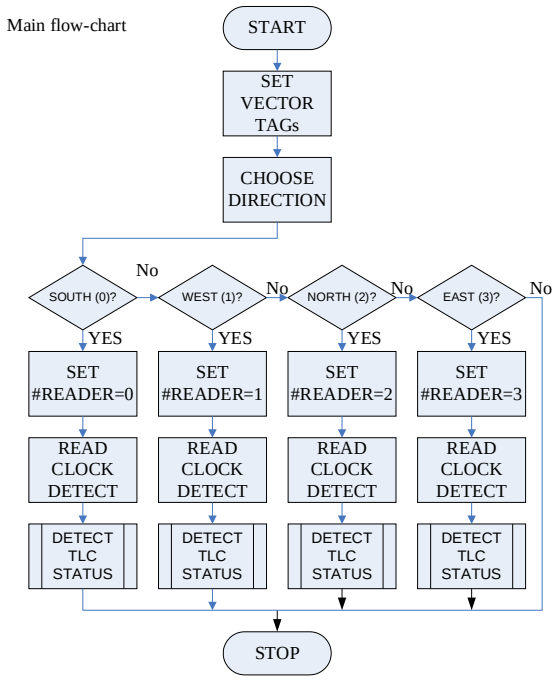

Figure 5: The flow-chart of the algorithm for RFID-based red light violation detection

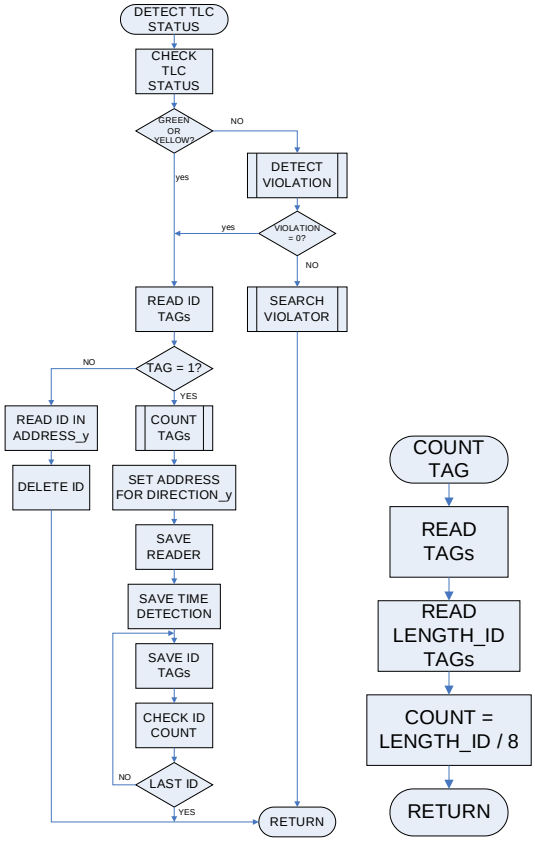

Continuation of Figure 5

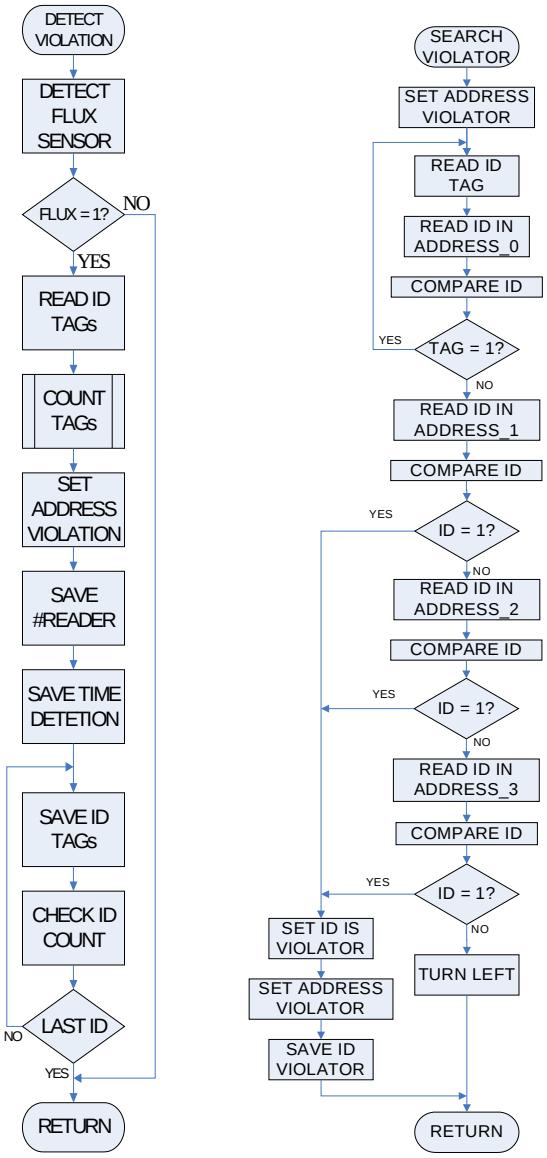

Continuation of Figure 5

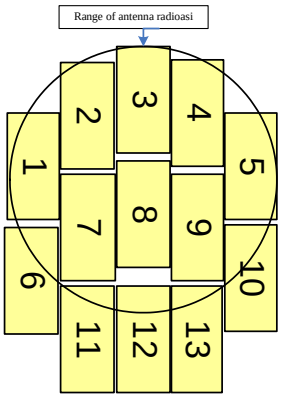

Figure 6: Prediction of vehicle number on a capturing

4. DISCUSSION

In this paper, we propose a tracking algorithm for RFID-based red light violation detection. We will do to simulate this use MadLab/Simulink. The database generator is built with the Visual Query Builder (VQB) or Microsoft Office Access.

5. CONCLUSION

By scenario in this proposal, we can take some in formations: (1) vehicle violator; (2) scalability on prediction system; (3) detection system of object on dynamic speed; (4) visibility of system is independent by solar.

REFERENCES

[1] Http://www.intermec.com, "RFID Overview: Introduction to Radio Frequency Identification", access date November, 18 2008.

[2] Http://www.paxar.com/, "RFID Basics", access date November, 18 2008.

[3] George E. Frangos G.E., "Digital-Based Red Light Running Detection A Building Block Technology for ITS", http://www.roadtrafffic-technology.com/ contrator/detection/noptel/noptel.pdf, access date Dec, 11 2008.

[4] Http://www.superrfid.net/english/index/, "Automatic vehicle identification (AVI) and city traffic management system", access date May, 23 2008.

[5] Chang S.L., Chen L.S., Chung Y.C., Chen S.W., "Automatic License Plate Recognition", IEEE Transaction on Intelligent Transportation Systems, Vol. 5, No. 1, March 2004, IEEE, 2004.

[6] Suresh K.V., Kumar G.M., Rajagopalan A.N., "Superresolution of License Plates in Real Traffic Videos", IEEE Transaction on Intelligent Tranportation Systems, Vol. 8, No. 2, June 2007., IEEE, 2007.

[7] Jiang W., Yu D., Ma Y., "A Tracking Algorithm in RFID Reader Network", Proceeding of the Japan-China Joint Workshop on Frontier of Computer Science and Technology (FCST'06), IEEE, 2006.

[8] Huang Y.S., "Design of Traffic Light Control Systems Using Statecharts", The Computer Journal, Vol. 49 No. 6, 2006, Published by Oxford University Press on behalf of The British Computer Society, 2006.

[9] Namekawa M., Aoyagi N., Ueda Y. and Satoh A., "Road Data Input System using Digital Map in Roadtraffic Simulation", http://mssanz.org.au/ modsim07/papers/55_s53/RoadDatas53_Namekawa.pdf, tanggal akses 20 Mei 2009.

[10] Namekawa M., Ueda F., Hioki Y., Ueda Y. and Satoh A., "The Vehicle Junction Model and its Verification in Traffic

Simulation", Proceedings of 2nd International Conference on Asian Simulation and Modeling 2007, (*ASIMMOD2007)*, Chiang Mai, Thailand.

COPYRIGHT

All papers submitted must be original, unpublished work not under consideration for publication elsewhere. Authors are responsible to obtain all necessary permission for the reproduction of tables, figures and images and must be appropriately acknowledged. The paper is not defamatory; and the paper does not infringe any other rights of any third party.

The authors agree that the Technical Committee's decision on whether to publish the paper in the Conference's proceedings shall be final. The authors should not treat any communication from the Technical Committee members who reviewed their work as an undertaking to publish the paper.

Prior to final acceptance of the paper, authors are required to confirm in writing that they hold all necessary copyright for their paper and to assign this copyright to the Conference Organizer.

Test of 0.5 HP AC Induction Motor Based on DC Resistance and Block Rotor Test

K. Anayet[1], I. Daut[2], N. Gomesh[3], M. Muzhar[4], M. Asri[5], Syatirah[6]

[1,2,3,4,5,6]*Power Electronics and Electrical Machine Design Research Cluster*
School of Electrical Systems Engineering
Universiti Malaysia Perlis (UniMAP), Malaysia
Email: anayet@unimap.edu.my, gomz_84@yahoo.com

ABSTRACT

This paper presents the way to investigate 0.5 hp three phase induction motor parameters by performing the DC resistance and the block rotor test. The data is produced based on lab tests and the relevant formula is used to investigate the parameters. The parameters obtained in this paper from stator and rotor of the induction motor. Several parameters such as R_1, R_2, I_2, X_1, X_2 and Z_2 are presented here.

Keywords
DC resistance, Block rotor, Induction motor test etc

1. INTRODUCTION

For many years the blocked-rotor test has been the accepted procedure for determining the AC winding resistances and the leakage reactance of three phase induction motors. Therefore, it has been necessary to lock the rotor of the machine in a fixed position (a carefully-selected position in the case of wound-rotor motors) with the stator windings energized with full-load current. Further, a reduced-frequency, reduced-voltage power source has been needed to provide that rated current for all but the smallest machines. The very-detailed procedure for the testing of induction machines is contained in IEEE Standard 112-1984 [l]. Squirrel cage induction rotors can be one of the toughest things to analyze. Rotor Defects were estimated to be responsible for approximately 10% of motor failures based on a 1980's research effort on squirrel cage induction motors sponsored by EPRI and performed by General Electric. Things have certainly changed since the 1980's. Not only in rotor design, but more importantly, in the analysis equipment available to detect rotor defects. Equipment like the MCE has increased the ability for the technician to identify rotor defects long before they become catastrophic. [9]

The squirrel cage induction rotor comes in many different varieties. These various types of rotor designs may affect the severity of a rotor defect. The first thing that usually comes to mind when discussing a squirrel cage induction rotor design is whether the rotor bars are comprised of copper or aluminum. These bars are either cast or pressed into the rotor slots then shorted together at either end of the rotor using copper or aluminum "shorting" rings. Shorting rings are commonly referred to as end rings. The rotor bars are welded, brazed, or bolted to the end rings. If it is a cast aluminum rotor the shorting ring and the rotor bars are cast at the same time and no connecting joints exist. Both aluminum and copper have advantages and disadvantages. Aluminum is more likely to have porosity, while copper is more likely to develop high resistance connections at the end rings. There is a test for stator coil R_1 independent of R_2, X_1, and X_2 .This test is called the DC resistance test. There is another test that can be performed on an induction motor to determine its rotor circuit parameters is called the block rotor test or sometimes called the locked rotor test [9].

2. DC RESISTANCE TEST

Basically, a DC voltage is applied to the stator windings of an induction motor, because the current is DC; there is no induced voltage in the rotor circuit and no resulting rotor current flow. Also, the reactance of the motor is zero at direct current. Therefore, the only quantity limiting current flow in the motor is the stator resistance and that resistance can be determined .The basic circuit is shown in Figure 3 .This figure shows the DC power supply connected to two of three terminals of a star connected induction motor. To perform the test, based on Figure 1, the current in the stator windings is adjusted to the rated value, and the voltage between the terminals of a star connected induction motor is measured. The current in the stator windings is adjusted to the rated value in an attempt to heat the windings to the same temperature they would have during normal operation (remember, winding resistance is a function of temperature) the current in Figure 3 flows through two of the windings, so the total resistance in the current path is $2R_1$.
Therefore,

$$R_1 = \frac{V_{DC}}{2I_{DC}} \qquad (1)$$

With the value of R_1 the stator copper loss at no load may be determined, and the rotational losses maybe found as the difference between the input power at no load and the stator

copper losses. This test is verifying the winding balanced resistance at ambient temperature. The standards accept a deviation (dispersion) of 5% from the average value. However, it has been demonstrated that such a deviation could lead to a wrong assessment of the winding connection brazing points. At the brazing point small discharges (sparks) may occur between the unconnected wire and the brazed point generating a "hot connection". The heat will be transferred in the neighborhood causing long term degeneration of inter turns or a short circuit of interconnections [1] [7].

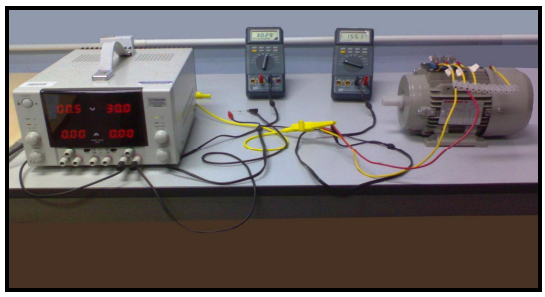

Figure 1: DC Resistance Lab Setup.

3. BLOCK ROTOR TEST

This test is used to determine the series parameters of circuit model of an induction motor. The circuit is similar to that of a transformer short circuit test. Short circuiting the load resistance in the circuit model corresponding to making the slip= 1 so that $R_2^{'}\frac{1}{s-1}=0$. This means that the rotor must be stationary during this test, which requires that it be blocked mechanically from rotating while the stator is excited with appropriate reduce voltage [2]. The resulting voltage, current, and power are measured. Figure 2 shows the test setup for the block rotor test. Figure 5 shows the connections for the blocked rotor test.

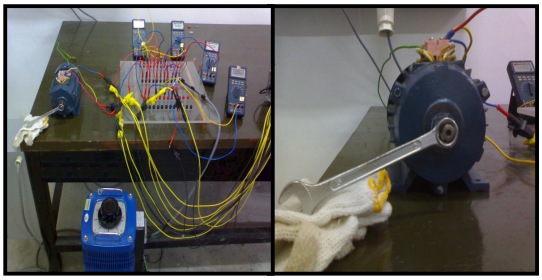

Figure 2: Block rotor lab test setup.

To perform the blocked rotor test, an AC voltage is applied to the stator, and the current flow is adjusted to be approximately full-load value. When the current is full load value, the voltage, current, and power flowing into the motor are measured. The equivalent circuit for this test is shown in Figure 5. Notice that since the rotor is not moving, the slip=1, and so the rotor resistance R_2 / s is just equal to R_2 (quite a small value),Since R_2 and X_2 are so small, almost all the input current will flow through them, instead of through the much larger magnetizing reactance X_m. Therefore, the circuits under these condition looks like a series combination of X_1, R_1, X_2 and R_2 as in Figure 6.

After a test voltage and frequency have been setup, the current flow in the motor is quickly adjusted to about the rated value, and the input power, voltage, and current are measured before the rotor can heat up too much. Unfortunately, there is no simple way to separate the contributions of the stator and rotor reactance from each other. Over the years, experience has shown that motors of certain design types have certain proportion between rotor and stator reactance [5] [6].

4. DC RESISTANCE TEST ANALYSIS

Based on Figure 3 the circuit shows the test circuit for a DC resistance test that is assembled.Table 1 shows the test data after the experiment is conducted.

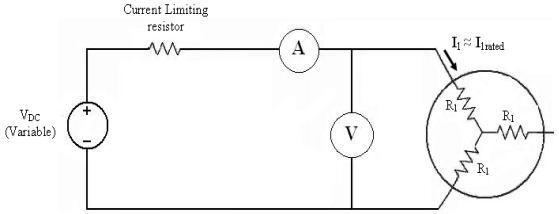

Figure 3: Test Circuit for DC Resistance Test.

Since the 0.5 Hp induction motor has a rated current of 1.07 A, the motor is tested at rated current and Table 1 shows the data.

Table 1: DC Resistance Test Data

Supply Voltage (V)	V_{dc}	I_{dc}	Coil resistance (R1)
10	54.7	1.07	25.6

Based on equation (1), it gives the stator coil resistances as:

$$R_1 = \frac{54.7V}{2\times 1.07A} = 25.6\Omega$$

So with this we know the value of stator resistor is 25.6Ω and this will be easy in obtaining the value of rotor resistance.

ISSN 114-1284

5. BLOCK ROTOR TEST ANALYSIS

The block rotor is assembled as shown in Figure 4

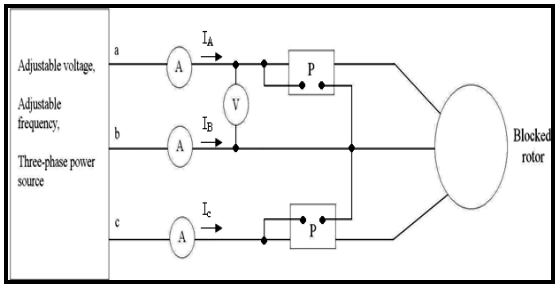

Figure 4: Blocked rotor test circuit for AC induction motor.

Based on the test analysis, Table 2 is obtained for further analysis.

Table 2: Blocked Rotor Test Measurement Data

Voltage line-line (V_{L-L}/V_{BR})	Phase Voltage (V_{Phase})	Input power (P_{in})	Input Current (I_{in})	Power Factor
210.1	121.32	149.59	1.0598	0.386

Since in the blocked rotor condition the value of n_r is 0 (the shaft of the induction motor is clamped to avoid rotation) so the slip will be,

$$s = \frac{n_{slip}}{n_s} = \frac{1500-0}{1500} \times 100\%$$
$$= 1$$

The slip is equals to 1 and so the rotor resistance R_2/s is just equal to R_2 (quite a small value).

$$\text{At} V_{BR} = 210.1V \quad I_{BR} = 1.0598A \ (I_{rated} = 1.07A)$$
$$P_{BR} = \sqrt{3} V_{BR} I_{BR} Cos\theta$$

$$\text{Angle}, \theta = \cos^{-1} 0.386 = 62.29°$$

Block rotor impedance:

$$|Z_{BR}| = \frac{V_{BR}}{\sqrt{3} I_{BR}} = \frac{210.1V}{\sqrt{3}1.0598} = 114.46\Omega$$

$$R_{BR} = Z_{BR} Cos\theta = 114.46 \times 0.386 = 44.182\Omega$$
$$R_{BR} = R_1 + R_2$$

From DC Resistance Test: R_1 =25.6 Ω

Then rotor resistance

$$R_2 = R_{BR} - R_1 = 44.18 - 25.6 = 18.58\Omega$$

Block rotor reactance

$$X'_{BR} = |Z_{Br}| Sin\theta_{BR} = |114.46| \times 0.9225 = 105.6\Omega$$

For normal motors of less than 20 hp rating, the effects of frequency are negligible and the blocked rotor test can be performed directly at the rated frequency [6]. But if it is above 20hp rating of any motor, must be reduced the frequency to 50% of the rated frequency.

(At 50 Hz, the block-rotor power factor angle is typically around 50^0)

$$X_{BR} = \frac{f_B}{f_t} \times X'_{BR} = \frac{50}{50} \times 105.6 = 105.6\Omega$$

$$x_1 = x_2 = \frac{1}{2} X_{BR} = \frac{105.6}{2} = 52.8\Omega$$

f_t = Frequency of the blocked-rotor test voltage

f_B = Rated frequency

The rotor current is given by;

$$I_2 = \frac{V_p}{(R_2/s) + jX_2} = = 0.3232A\angle -8°$$

The rotor loss is given by

$$P_{RCL} = 3I_r^2 R_r = 3I_2^2 R_2$$
$$= 3 \times (0.3232)^2 \times (18.58) = 5.82W$$

Through both the DC resistance and block rotor analysis, Table 3 can be summarized for 0.5Hp induction motor.

Table 3: Induction Motor Parameters

0.5 HP Induction Motor Parameters	Value
Line-Line Voltage(V_{L-L})	210.1V
Power Factor (pf)	0.386
Slip At Block Rotor	1
Rotor Current (I_2)	0.3232A
Stator Resistance (R_1)	25.6Ω
Rotor Resistance (R_2)	18.58Ω
Block Rotor Input Power (P_{br})	149.59W
Block Rotor Impedance (Z_{br})	114.46Ω
Block Rotor Reactance(X_{br})	105.6Ω
Leakage Reactance (X_1 & X_2)	52.8Ω
Rotor Copper Loss (P_{RCL})	62.61W

6. DRAWBACKS OF BLOCK ROTOR TEST

There is one problem with this test, however. In normal operation, the stator frequency is line frequency of power system i.e. 50 or 60Hz. At starting conditions, the rotor is also line frequency .However, at normal operating conditions, the slip of most motors is only 2 to 4 percent, and the resulting rotor frequency is in the range of 1-3 Hz. This creates a problem in that the line frequency does not represent the normal operating conditions of the rotor. Since effective rotor resistance is a strong function of frequency for design class B and C motors, the incorrect rotor frequency can lead to misleading results in this test. A typical compromise is to use a frequency 25-50 percent less of the rated frequency. While this approach is acceptable for essential constant resistance rotors (design class A and D), it leaves a lot to be desired when one is trying to find the normal rotor resistance of a variable-resistance rotor. Because of these and similar problems, a great deal of care must be exercised in taking measurements for these tests [6].

7. DISCUSSION

In the conventional squirrel-cage motor at full load, the slip and the current are low but the power factor and the efficiency are high. However, at start, the torque and power factor are low but the current is high. If the load requires a high starting torque, the motor will accelerate slowly. This will make a large current flow for a longer time, thereby creating a heating problem. The resistances in the rotor circuit greatly influence the performance of an induction motor. A low rotor resistance is required for normal operation, when running, so that the slip is low and the efficiency is high. However a higher rotor resistance is required for starting so that the starting torque and power factor are high and the starting current is low. An induction motor with fixed rotor circuit resistance therefore requires a compromise design of the rotor for starting and running conditions.

The block rotor test on an induction motor, like the short circuit test on the transformer, gives information about block rotor impedances (Z_{BR}) [4]. In this test the rotor is blocked so that the motor cannot rotate, and balanced poly phase voltages are applied to the stator terminals. The blocked rotor test should be performed under the same condition of the rotor current and frequency that will prevail in the normal operating conditions. For example, if the performance characteristics in the normal running condition (i.e. low-slip region) are required, the blocked rotor test should be reduced frequency (corresponding to lower values of slip).When an induction motor is operating normally, the slip is so small that the frequency of the magnetic reversal in the rotor core is only of the order of one or two per sec, therefore iron losses occurring in the rotor are very small and can be neglected, hence output of stator becomes the input of rotor and the input of rotor is the output of rotor plus with copper loss in rotor.

The slip for the blocked rotor test is unity since the rotor is stationary. The resulting speed-dependent equivalent resistance $\frac{R_2}{s}(1-s)$ goes to zero and the resistance of the rotor branch of the equivalent circuit becomes very small. Thus, the rotor current is much larger than current in the excitation branch of the circuit.

7. CONCLUSION

The purpose of this paper is to evaluate the performance characteristics 0.5 hp three phase induction motor parameters by performing the DC resistance and the block rotor test.

During starting moment of block rotor condition, the induction motor speed is zero (S = 1), but the electromagnetic torque is positive so when three-phase fed, the induction motor tends to start (rotate); to prevent this, the rotor has to be stalled. Thorough testing of induction motor at zero speed generally completed up to rated current. Consequently, lower voltages are required, thus avoiding machine overheating. A quick test at rated voltage is done on prototypes or random induction motors from, production line to measure the peak starting current and the starting torque. This is a must for heavy starting applications (nuclear power plant cooling pump-motors, for example) as both skin effect and leakage saturation notably modifies the motor starting parameters.

ACKNOWLEDGMENT

The authors wish to thank School of Electrical Systems Engineering, Universiti Malaysia Perlis (UniMAP) for the technical and financial support.

REFERENCES

[1] IEEE standard 112-1984, "*IEEE Standard Test Procedure for Polyphase Induction Motors and Generators"*, IEEE, New York, NY, 1984
[2] G. McPherson, "*An Introduction to Electrical Machines and Transformers"*, J Wiley, New York, NY 1981, Fig 4-15, pp 291- 300
[3] V. Del Toro, "*Basic Electric Machines"*, Inglewood, N.J., 1990, Fig 4-7f), pp 182-188
[4] N. Balabanian, "*Fundamentals of Circuit Theory"*, Allen & Bacon, Boston, Mass. 1961, pp 307-317
[5] Sinisa Jurkovic**, "***Induction Motor Parameters Extraction*".
[6] P. C. Sen, "*Principles of Electric Machines & Power Electronics"*, Wiley 1999

[7] Stephan J. Chapman, "*Electric Machinery Fundamentals*", 4/E McGraw-Hill, New York (2005).
[8] Kent Davey, "*Predicting Induction Motor Circuit Parameters*", IEEE Transaction On Magnetics, Vol. 38, No. 4, July 2002.
[9] Donald L. Skaar , "*Circumventing The Blocked Rotor Test When Evaluating Model Elements Of Three Phase Induction Motors*", IEEE Transactions on Energy Conversion, Vol. 9, No. 2, June 1994

RISC Processor NICCOLO32 Design dan Implementation

Karel Octavianus Bachri
Atma Jaya University Jakarta
karel.bachri@atmajaya.ac.id

Abstract-Reduced Instruction Set Computer (RISC) is a computer architecture that reduces chip complexity by executing only simple instructions, which allows high speed operation. NICCOLO32 is a RISC processor with SPARC V8 architecture.

RISC processor NICCOLO32 is verified to ensure system functionality. Verification is done using modelsim. NICCOLO32 is then implemented as chip layout using Astro from Synopsys with CMOS 0.18 µm standard cell. Implementation gives maximum clock speed of 31.46 MHz and core area of 0.512 mm^2.

Keywords : *RISC, SPARC, processor*

I. INTRODUCTION

Microprocessors are divided into two groups, complex instruction set computer (CISC) and reduced instruction set computer (RISC). CISC is designed using as few instructions as possible to execute a task. While in RISC, to execute the same task CISC perform, more instruction required to achieve one instruction per cycle.

RISC is designed to reduce instruction complexity to allow high speed operation. Several technique used in RISC design are one instruction per cycle, fixed instruction length, only load / store access memory, simplified addressing mode, fewer and simpler operations, and let the compiler do it. Using these technique, smaller memory is required and access time can be reduced.

The objective of this research is to design RISC processor NICCOLO32 and implement it as chip layout with CMOS standard cell 0.18 µm.

II. DESIGN METHOD

NICCOLO32 design is divided into several steps

Step 1 : chose instructions NICCOLO32 can perform.

Step 2 : design register transfer notation (RTN) for each instruction chosen. RTN is a notation which describe inter register data transfer in the system designed.

Step 3 : design datapath that supports all instructions chosen. Datapath is a diagram describing data transfer in the system.

Step 4 : design control unit. Control unit is a unit controlling data transfer in a system.

Step 5 : integrate datapath and control unit.

Step 6 : verification to ensure system functionality. System is verified by feeding test vector into the system. Instruction is chosen to be the test vector to show system functionality.

Step 7 : implement RISC processor NICCOLO32 into chip layout with CMOS 0.18 µm standard cell technology using Astro CAD tool from Synopsys.

III. NICCOLO32 INSTRUCTION

NICCOLO32 is a RISC processor with SPARC V8 architecture. To design RISC processor NICCOLO32, instruction and register must compatible with SPARC V8 architecture.

Instructions are divided into three categories, load / store, arithmetic / logic / shift / sethi, and control transfer.

- Load / store : the only instructions access memory. **Load** instruction gets data from memory and store it in registers, while **store** instruction **store** data from registers to memory.
- Arithmetic / shift / logic / sethi : this type of instructions computate two operands and store the result in register.
- Control transfer : this type of instructions change program counter (PC).

Table 1. Instruction to be Implemented

No.	Mnemonic	Operation
1.	**ADD**	Rd = Rs1 + Rs2/simm13
2.	**ADDCC**	Rd = Rs1 + Rs2/simm13
3.	**SUB**	Rd = Rs1 - Rs2/simm13
4.	**SUBCC**	Rd = Rs1 - Rs2/simm13
5.	**UMUL**	Rd = Rs1 **x** Rs2/simm13
6.	**UMULCC**	Rd = Rs1 **x** Rs2/simm13
7.	**AND**	Rd = Rs1 **AND** Rs2/simm13
8.	**ANDCC**	Rd = Rs1 **AND** Rs2/simm13
9.	**ANDN**	Rd = Rs1 **ANDN** Rs2/simm13
10.	**ANDNCC**	Rd = Rs1 **ANDN** Rs2/simm13
11.	**OR**	Rd = Rs1 **OR** Rs2/simm13
12.	**ORCC**	Rd = Rs1 **OR** Rs2/simm13
13.	**ORN**	Rd = Rs1 **ORN** Rs2/simm13
14.	**ORNCC**	Rd = Rs1 **ORN** Rs2/simm13
15.	**XOR**	Rd = Rs1 **XOR** Rs2/simm13
16.	**XORCC**	Rd = Rs1 **XOR** Rs2/simm13
17.	**XNOR**	Rd = Rs1 **XNOR** Rs2/simm13
18.	**XNORCC**	Rd = Rs1 **XNOR** Rs2/simm13
19.	**SLL**	temp:=(IR<13>=0→R[IR<4..0>]<4..0>:IR<13>≠0→IR<4..0>); Rd = Rs1<(31-temp)..0>#0@temp
20.	**SRL**	temp := (IR<13>=0→R[IR<4..0>]<4..0>:IR<13>≠0→IR<4..0>); Rd = 0@temp#Rs1<31..temp>
21.	**SRA**	temp := (IR<13>=0→R[IR<4..0>]<4..0>:IR<13>≠0→IR<4..0>); Rd←Rs1<31>@temp#Rs1<31..temp>

Fig 1 shows SPARC V8 instruction format.

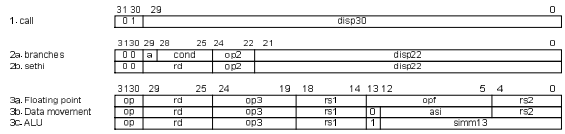

Fig.1. SPARC V8 instruction format.

Load / Store instructions need 5 clock cycle, arithmetic / shift / logic instructions need 3 clock cycle, while control transfer instructions need 4 clock cycle.

Table 1 shows instructions to be implemented by RISC processor NICCOLO32.

IV. SYSTEM SPECIFICATION AND DESIGN

System specifications are:

- Use load-store architecture, only load and store access memory. Data transfer can be done from register to register, from register to memory, and from memory to register, but not from memory to memory in one instruction.
- 32-bit data format.
- Fixed length 32-bit instruction
- External and separated data and instruction memory.
- Multicycle with no pipeline, each instruction has its own cycle, instruction must be completely performed before another instruction is fetched.
- 32 registers, with no register window mechanism.
- Three buses used, bus a is for operand 1, bus b is for operand 2, and bus c for the result.
- 32 bit linear memory address.
- Two addressing modes, register-register and register-immediate.
- Triadic register addresses, most instructions compute two operands and store the result in the third operand.

V. REGISTER TRANSFER NOTATION DESIGN

Register Transfer Notation (RTN) is a notation describing data transfer in a system. Data is transferred between registers. It is uniquely designed for each instruction each clock cycle.

RISC processor NICCOLO32 registers are divided into two groups, special purpose registers and general purpose registers. Special purpose registers are registers with certain function, it can not be used for other purposes. General purpose registers are used to store instruction result.

Special purpose registers are processor status register (PSR), program counter (PC), next program counter (nPC), memory data register (MDR), memory address register (MAR), instruction register (IR) and Y register.

General purpose registers are 32 registers in register bank and named r0, r1, r2, …, r30, and r31. These registers store the operation results and can be used in any order.

Table 2 shows RTN for **Add** instruction. Table 3 shows RTN for **Addcc** instruction. At cycle T0, the content of memory pointed by Program Counter (PC) is copied into instruction register (IR). At cycle T1, operands are available. The first operand is directly taken from RS1, while the second operand is multiplexed by the selector i. If i = 0, RS2 is selected as the second operand. If i = 1, signed extended 13 (simm13) is selected as the second operand. **Add** operation performed by arithmetic logic unit (ALU). At cycle T2, the result is then stored in RD. For **Addcc,** suitable condition codes are changed.

Table 2. *Register Transfer Notation*, **Add**

STEP	RTN
T0	IR ← M[PC] : PC ← PC + 4;
T1	alu_s := ((IR<13>=0)→R[rs1]+R[rs2]: (IR<13>!=0)→R[rs1]+19@IR<12>#IR<12..0>);
T2	R[rd]←alu_s;

Table 1. *Register Transfer Notation*, **Addcc**

STEP	RTN
T0	IR ← M[PC] : PC ← PC + 4;
T1	alu_s := ((IR<13>=0)→R[rs1]+R[rs2]: (IR<13>!=0)→R[rs1]+19@IR<12>#IR<12..0>);
T2	R[rd]←alu_s: alu_s=0→psr<22>←1: alu_s<31>=1→psr<23>←1: alu_s<33>≠0→psr<21..20>←"11";

Table 4 shows RTN for **Sub** instruction. Table 5 shows RTN for **Subcc** instruction. At cycle T0, the content of memory pointed by Program Counter (PC) is copied into instruction register (IR). At cycle T1, operands are available. The first operand is directly taken from RS1, while the second operand is multiplexed by the selector i. If i = 0, RS2 is selected as the second operand. If i = 1, signed extended 13 (simm13) is selected as the second operand. **Sub** operation performed by ALU.). At cycle T2, the result is then stored in RD. For **Subcc,** suitable condition codes are changed.

Table 4. *Register Transfer Notation*, **Sub**

STEP	RTN
T0	IR ← M[PC] : PC ← PC + 4;
T1	alu_s := ((IR<13>=0)→R[rs1]-R[rs2]: (IR<13>!=0)→R[rs1]-19@IR<12>#IR<12..0>);
T2	R[rd]←alu_s;

Table 5. *Register Transfer Notation*, **Subcc**

STEP	RTN
T0	IR ← M[PC] : PC ← PC + 4;
T1	alu_s := ((IR<13>=0)→R[rs1]-R[rs2]: (IR<13>!=0)→R[rs1]-19@IR<12>#IR<12..0>);
T2	R[rd]←alu_s: alu_s=0→psr<22>←1: alu_s<31>=1→psr<23>←1: alu_s<33>≠0→psr<21..20>←"11";

Table 6 shows RTN for **Umul** instruction. Table 7 shows RTN for **Umulcc** instruction. At cycle T0, the content of memory pointed by Program Counter (PC) is copied into instruction register (IR). At cycle T1, operands are available. The first operand is directly taken from RS1, while the second operand is multiplexed by the selector i.

If i = 0, RS2 is selected as the second operand. If i = 1, signed extended 13 (simm13) is selected as the second operand. **Umul** operation performed by ALU. At cycle T2, the result is then stored in RD. For **Umulcc,** suitable condition codes are changed.

Table 6. *Register Transfer Notation*, **Umul**

STEP	RTN
T0	IR ← M[PC] : PC ← PC + 4;
T1	mul_s:=((IR<13>=0)→R[rs1]*R[rs2]: (IR<13>!=0)→R[rs1]*19@IR<12>#IR<12..0>);
T2	R[rd]←mul_s<31..0>:Y←mul_s<63..32>;

Table 7. *Register Transfer Notation*, **Umulcc**

STEP	RTN
T0	IR ← M[PC] : PC ← PC + 4;
T1	mul_s:=((IR<13>=0)→R[rs1]*R[rs2]: (IR<13>!=0)→R[rs1]*19@IR<12>#IR<12..0>);
T2	R[rd]←mul_s<31..0>:%Y←mul_s<63..32>: mul_s<31..0>=0→psr<22>←1: mul_s<31>=1→psr<23>←1: psr<21..20>←"00";

Table 8 shows RTN for **And** instruction. Table 9 shows RTN for **Andcc** instruction. At cycle T0, the content of memory pointed by Program Counter (PC) is copied into instruction register (IR). At cycle T1, operands are available. The first operand is directly taken from RS1, while the second operand is multiplexed by the selector i. If i = 0, RS2 is selected as the second operand. If i = 1, signed extended 13 (simm13) is selected as the second operand. **And** operation performed by ALU. At cycle T2, the result is then stored in RD. For **Andcc,** suitable condition codes are changed.

Table 8. *Register Transfer Notation*, **And**

STEP	RTN
T0	IR ← M[PC] : PC ← PC + 4;
T1	alu_s :=((IR<13>==0)→R[rs1]^R[rs2]: (IR<13>!=0)→R[rs1]^19@IR<12>#IR<12..0>);
T2	R[rd]←alu_s;

Table 9. *Register Transfer Notation*, **Andcc**

STEP	RTN
T0	IR ← M[PC] : PC ← PC + 4;
T1	R[rd]←((IR<13>==0)→R[rs1]^R[rs2]: (IR<13>!=0)→R[rs1]^19@IR<12>#IR<12..0>);
T2	alu_s<31..0>=0→psr<22>←1: alu_s<31>=1→psr<23>←1: alu_s<63..32>≠0→psr<21>=1: psr<20>←'0';

Table 10 shows RTN for **Andn** instruction. Table 11 shows RTN for **Andncc** instruction. At cycle T0, the content of memory pointed by Program Counter (PC) is copied into instruction register (IR). At cycle T1, operands are available. The first operand is directly taken from RS1, while the second operand is multiplexed by the selector i. If i = 0, RS2 is selected as the second operand. If i = 1, signed extended 13 (simm13) is selected as the second operand. **Andn** operation performed by ALU. At cycle T2, the result is then stored in RD. For **Andncc,** suitable condition codes are changed.

Table 10. *Register Transfer Notation*, **Andn**

STEP	RTN
T0	IR ← M[PC] : PC ← PC + 4;
T1	alu_s :=((IR<13>==0)→¬(R[rs1]^R[rs2]): (IR<13>!=0)→¬(R[rs1]^19@IR<12>#IR<12..0>));
T2	R[rd]←alu_s;

Table 12 shows RTN for **Or** instruction. Table 13 shows RTN for **Orcc** instruction. At cycle T0, the content of memory pointed by Program Counter (PC) is copied into instruction register (IR). At cycle T1, operands are available. The first operand is directly taken from RS1, while the second operand is multiplexed by the selector i. If i = 0, RS2 is selected as the second operand. If i = 1, signed extended 13 (simm13) is selected as the second operand. **Or** operation performed by ALU. At cycle T2, the result is then stored in RD. For **Orcc,** suitable condition codes are changed.

Table 11. *Register Transfer Notation*, **Andncc**

STEP	RTN
T0	IR ← M[PC] : PC ← PC + 4;
T1	alu_s :=((IR<13>==0)→¬(R[rs1]^R[rs2]): (IR<13>!=0)→¬(R[rs1]^19@IR<12>#IR<12..0>));
T2	R[rd]←alu_s: alu_s<31..0>=0→psr<22>←1: alu_s<31>=1→psr<23>←1: alu_s<63..32>≠0→psr<21>=1: psr<20>←'0';

Table 12. *Register Transfer Notation*, **Or**

STEP	RTN
T0	IR ← M[PC] : PC ← PC + 4;
T1	alu_s :=((IR<13>==0)→R[rs1]vR[rs2]: (IR<13>!=0)→R[rs1]v19@IR<12>#IR<12..0>);
T2	R[rd]←alu_s;

Table 13. *Register Transfer Notation*, **Or**cc

STEP	RTN
T0	IR ← M[PC] : PC ← PC + 4;
T1	alu_s :=((IR<13>==0)→R[rs1]vR[rs2]: (IR<13>!=0)→R[rs1]v19@IR<12>#IR<12..0>);
T2	R[rd]←alu_salu_s<31..0>=0→psr<22>←1: alu_s<31>=1→psr<23>←1: alu_s<63..32>≠0→psr<21>=1: psr<20>←'0';

Table 14 shows RTN for **Orn** instruction. Table 15 shows RTN for **Orncc** instruction. At cycle T0, the content of memory pointed by Program Counter (PC) is copied into instruction register (IR). At cycle T1, operands are available. The first operand is directly taken from RS1, while the second operand is multiplexed by the selector i. If i = 0, RS2 is selected as the second operand. If i = 1, signed extended 13 (simm13) is selected as the second operand. **Orn** operation performed by ALU. At cycle T2, the result is then stored in RD. For **Orncc,** suitable condition codes are changed.

Table 14. *Register Transfer Notation*, **Or**n

STEP	RTN
T0	IR ← M[PC] : PC ← PC + 4;
T1	alu_s :=((IR<13>==0)→¬(R[rs1]vR[rs2]): (IR<13>!=0)→¬(R[rs1]v19@IR<12>#IR<12..0>));
T2	R[rd]←alu_s;

Table 15. *Register Transfer Notation*, **Or**ncc

STEP	RTN
T0	IR ← M[PC] : PC ← PC + 4;
T1	alu_s :=((IR<13>==0)→¬(R[rs1]vR[rs2]): (IR<13>!=0)→¬(R[rs1]v19@IR<12>#IR<12..0>));
T2	R[rd]←alu_s: alu_s<31..0>=0→psr<22>←1: alu_s<31>=1→psr<23>←1: alu_s<63..32>≠0→psr<21>=1: psr<20>←'0';

Table 16 shows RTN for **Xor** instruction. Table 17 shows RTN for **Xorcc** instruction. At cycle T0, the content of memory pointed by Program Counter (PC) is copied into instruction register (IR). At cycle T1, operands are available. The first operand is directly taken from RS1, while the second operand is multiplexed by the selector i. If i = 0, RS2 is selected as the second operand. If i = 1, signed extended 13 (simm13) is selected as the second operand. **Xor** operation performed by ALU. At cycle T2, the result is then stored in RD. For **Xorcc,** suitable condition codes are changed.

Table 16. *Register Transfer Notation*, **Xor**

STEP	RTN
T0	IR ← M[PC] : PC ← PC + 4;
T1	alu_s :=((IR<13>==0)→R[rs1] xor R[rs2]: (IR<13>!=0)→R[rs1] xor 19@IR<12>#IR<12..0>);
T2	R[rd]←alu_s;

Table 17. *Register Transfer Notation*, **Xor**cc

STEP	RTN
T0	IR ← M[PC] : PC ← PC + 4;
T1	alu_s :=((IR<13>==0)→R[rs1] xor R[rs2]: (IR<13>!=0)→R[rs1] xor 19@IR<12>#IR<12..0>);
T2	R[rd]←alu_s: alu_s<31..0>=0→psr<22>←1: alu_s<31>=1→psr<23>←1: alu_s<63..32>≠0→psr<21>=1: psr<20>←'0';

Table 18 shows RTN for **Xnor** instruction. Table 19 shows RTN for **Xnorcc** instruction. At cycle T0, the content of memory pointed by Program Counter (PC) is copied into instruction register (IR). At cycle T1, operands are available. The first operand is directly taken from RS1, while the second operand is multiplexed by the selector i. If i = 0, RS2 is selected as the second operand. If i = 1, signed extended 13 (simm13) is selected as the second operand. **Xnor** operation performed by ALU. At cycle T2, the result is then stored in RD. For **Xnorcc,** suitable condition codes are changed.

Table 18. *Register Transfer Notation*, **Xnor**

STEP	RTN
T0	IR ← M[PC] : PC ← PC + 4;
T1	alu_s :=((IR<13>==0)→R[rs1] xnor R[rs2]: (IR<13>!=0)→R[rs1] xnor 19@IR<12>#IR<12..0>);
T2	R[rd]←alu_s;

Table 19. *Register Transfer Notation*, **Xnor**

STEP	RTN
T0	IR ← M[PC] : PC ← PC + 4;
T1	alu_s :=((IR<13>==0)→R[rs1] xnor R[rs2]: (IR<13>!=0)→R[rs1] xnor 19@IR<12>#IR<12..0>);
T2	R[rd]←alu_s: alu_s<31..0>=0→psr<22>←1: alu_s<31>=1→psr<23>←1: alu_s<63..32>≠0→psr<21>=1: psr<20>←'0';

Table 20 shows RTN for **SRL** instruction. At cycle T0, the content of memory pointed by Program Counter (PC) is copied into instruction register (IR). At cycle T1, operands are available. The first operand, which is data to be shifted, directly taken from RS1, while the second operand, which is the shift value, is multiplexed by the selector i. If i = 0, RS2 is selected as the second operand. If i = 1, signed extended 13 (simm13) is selected as the second operand. **SRL** operation performed by ALU. At cycle T2, the result is then stored in RD.

Table 20. *Register Transfer Notation*, **SRL**

STEP	RTN
T0	IR ← M[PC] : PC ← PC + 4;
T1	temp := (IR<13>=0→R[IR<4..0>]<4..0>: IR<13>≠0→IR<4..0>);
T2	R[rd]←0@temp#R[rs1]<31..temp>;

Table 21 shows RTN for **SRA** instruction. At cycle T0, the content of memory pointed by Program Counter (PC) is copied into instruction register (IR). At cycle T1, operands are available The first operand, which is data to be shifted, directly taken from RS1, while the second operand, which is the shift value, is multiplexed by the selector i. If i = 0, RS2 is selected as the second operand. If i = 1, signed extended 13 (simm13) is selected as the second operand. **SRA** operation performed by ALU. At cycle T2, the result is then stored in RD.

Table 21. *Register Transfer Notation*, **SRA**

STEP	RTN
T0	IR ← M[PC] : PC ← PC + 4;
T1	temp := (IR<13>=0→R[IR<4..0>]<4..0>: IR<13>≠0→IR<4..0>);
T2	R[rd]←R[rs1]<31>@temp#R[rs1]<31..temp>;

Table 22. *Register Transfer Notation*, **SLL**

STEP	RTN
T0	IR ← M[PC] : PC ← PC + 4;
T1	temp:=(IR<13>=0→R[IR<4..0>]<4..0>: IR<13>≠0→IR<4..0>);
T2	R[rd]←R[rs1]<(31-temp)..0>#0@temp;

Table 22 shows RTN for **SLL** instruction. At cycle T0, the content of memory pointed by Program Counter (PC) is copied into instruction register (IR). At cycle T1, operands are available. The first operand, which is data to be shifted, directly taken from RS1, while the second operand, which is the shift value, is multiplexed by the selector i. If i = 0, RS2 is selected as the second operand. If i = 1, signed extended 13 (simm13) is selected as the second operand. **SLL** operation performed by ALU. At cycle T2, the result is then stored in RD.

Table 23 shows RTN for **Sethi** instruction. At cycle T0, the content of memory pointed by Program Counter (PC) is copied into instruction register (IR). At cycle T1, operands are available. The first operand is directly taken from RS1, while the second operand is multiplexed by the selector i. If i = 0, RS2 is selected as the second operand. If i = 1, signed extended 13 (simm13) is selected as the second operand. At cycle T2, the result is then stored in RD.

Table 23. *Register Transfer Notation*, **Sethi**

STEP	RTN
T0	IR ← M[PC] : PC ← PC + 4;
T1	alu_s ← IR<21..0>#0@10;
T2	R[rd] ← alu_s;

Table 24 shows RTN for **LD** instruction. At cycle T0, the content of memory pointed by Program Counter (PC) is copied into instruction register (IR). At cycle T1, operands are available. The first operand, which is address, directly taken from RS1, while the second operand, which is also address is multiplexed by the selector i. If i = 0, RS2 is selected as the second operand. If i = 1, signed extended 13 (simm13) is selected as the second operand. At cycle T2, the result is then stored in MAR as data address. At cycle T3, data is copied from memory pointed by MAR to MDR. At cycle T4, the data is then copied from MDR to RD.

Table 24. *Register Transfer Notation*, **LD**

STEP	RTN
T0	IR ← M[PC] : PC ← PC + 4;
T1	alu_s:=((i = 0) →rs1+ rs2 : (i != 0) → rs1+19@IR<12>#IR<12..0>));
T2	MAR←alu_s;
T3	MDR←M[MAR];
T4	R[rd] ← MDR;

Table 25 shows RTN for **ST** instruction. At cycle T0, the content of memory pointed by Program Counter (PC) is copied into instruction register (IR). At cycle T1, operands are available. The first operand, which is address, directly taken from RS1, while the second operand, which is also address, is multiplexed by the selector i. If i = 0, RS2 is selected as the second operand. If i = 1, signed extended 13 (simm13) is selected as the second operand. At cycle T1, the result is then stored in MAR as data address. At cycle T2, data is obtained from RD and stored in MDR. At cycle T4, data from MDR is stored in memory pointed by address MAR.

Table 25. *Register Transfer Notation*, **ST**

STEP	RTN
T0	IR ← M[PC] : PC ← PC + 4;
T1	alu_s:=((i = 0) →rs1+ rs2 : (i != 0) → rs1+19@IR<12>#IR<12..0>));
T2	MAR←alu_s;
T3	MDR←R[rd];
T4	M[MAR] ← MDR;

VI. DATAPATH AND CONTROL UNIT DESIGN

Based on RTN, datapath is designed. Datapath must support RTN of all instructions. Fig 2 shows RISC processor NICCOLO32 datapath.

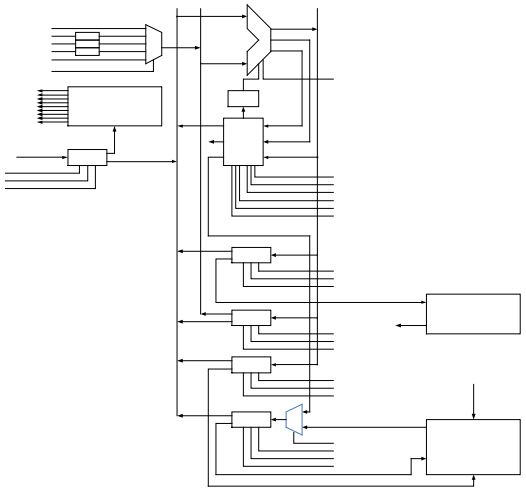

Fig.2. RISC processor NICCOLO32 datapath.

Add instruction is for an example. At cycle T0, instruction is fetched from instruction memory and stored in IR. The value of PC is increased by 4. This is where the next instruction is located. At cycle T1, operands are ready. ALU performs **Add** operation. The result is then stored in RD.

ALU performs arithmetic, logic, and shift operation. Each kind of operation consists of several specific operations. Specific arithmetic operations are **Add, Sub,** and **Umul**. Specific logic operations are **And, Andn, Or, Orn, Xor, Xnor,** and **Not**. Shift operations are **SRL, SRA,** and **SLL.** Fig 3 shows ALU block diagram.

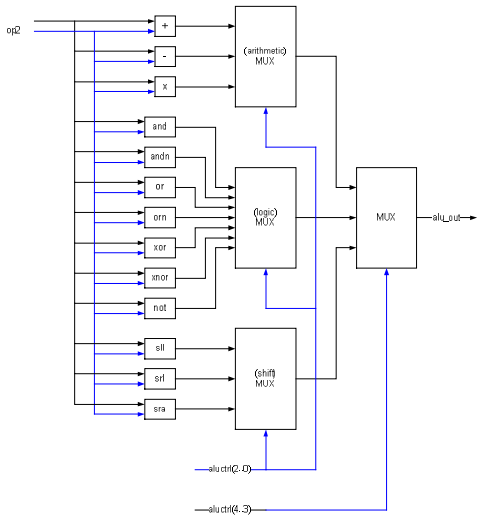

Fig 3. Arithmetic Logic Unit

ALU is controlled by 5-bit-signal "aluctrl". The first 2 bit determine the type of the operation, while the last 3 bit determine the specific operand, as seen on Table 26.

Table 26. Signal aluctrl Description

aluctrl<4..3> aluctrl<2..0>	00 arithmetic	01 logic	10 shift	11 Inc4/dec4
000	**Bypass**	**And**	**SRL**	**Inc4**
001	**Add**	**Or**	**SRA**	**Dec4**
010	**Sub**	**Xor**	**SLL**	
011	**Umul**	**Not**		
100		**Andn**		
101		**Orn**		
110		**Xnor**		

To ensure data transfer works properly, control unit is designed. Control unit is designed by finite state machine (FSM) for each type of instructions. Fig.4. shows FSM of each type of instructions. At first, the processor is in the "idle" state. When the "enable" signal is '1', it is then in the T0 state. At T0, instruction is fetched from instruction memory and stored in IR. The next state is T1. At T1, operands are ready. The next state is T2. At T2, operands are processed by ALU and the result is stored in register. If the instruction is arithmetic/shift/logic, the processor will go back to T0, which mean the next instruction will be fetched. If the instruction is not arithmetic/shift/logic, the processor will proceed to T3. If the instruction is control transfer, the processor will go back to T0 to fetch the next instruction, otherwise it will proceed to T4. At T4, for load instruction, loaded data will be stored in register, while for store instruction, data will be stored in memory.

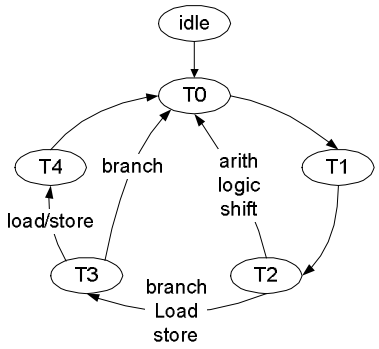

Fig.4. Instruction FSM.

VII. SYSTEM VERIFICATION

System is verified to ensure system functionality. RISC processor NICCOLO32 is verified using modelsim. To obtain the result that show system functionality, instruction is set to be the test vector. Instructions are generated by compiling C language program into SPARC assembly. NICCOLO32 core is connected to instruction memory (ROM) and data memory (RAM) as Fig.5. shows.

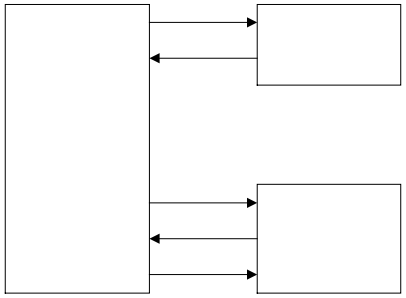

Fig..5. System verification block Diagram.

For example, Fig 6 shows **Add** and **Addcc** instruction.

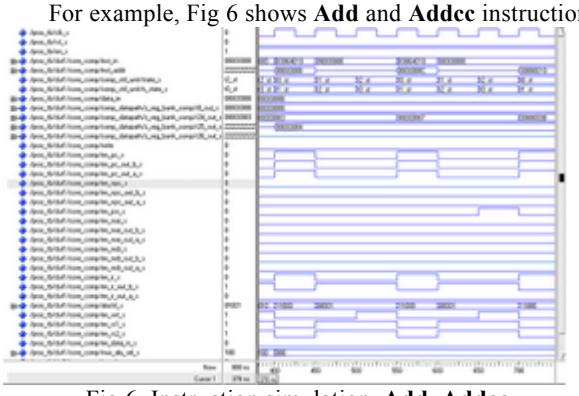

Fig 6. Instruction simulation, **Add**, **Addcc.**

VIII. NICCOLO32 IMPLEMENTATION

RISC processor NICCOLO32 is then implemented as chip layout with CMOS 0.18 µm standard cell technology. Layout processes are data preparation, floorplanning, placement and routing. Report shows 31 MHz timing constraint fulfilled. No design rule error and layout versus schematic error. Chip layout is shown in Fig 8.

```
*******************************************************
*
*  Astro Timing Report
*
*  Tool   : Astro
*  Version : V-2004.06-SP1 for IA.32 -- Sep 13, 2004
*
*******************************************************
-------------------------------------------------------------------------------
Rising edge of clock clk          35.0000   35.0000
Clock Source delay                 0.0000   35.0000
Clock Network delay                0.0000   35.0000
Clock Skew                         0.0000   35.0000
Setup time                         0.8534   34.1466
-------------------------------------------------------------------------------
Required time                               34.1466
Arrival time                                31.7838
-------------------------------------------------------------------------------
Slack                                        2.3628  (MET)
```

Fig 7. Astro timing report.

Timing report on Fig 7 shows the processor's maximum speed is 31.46 MHz.

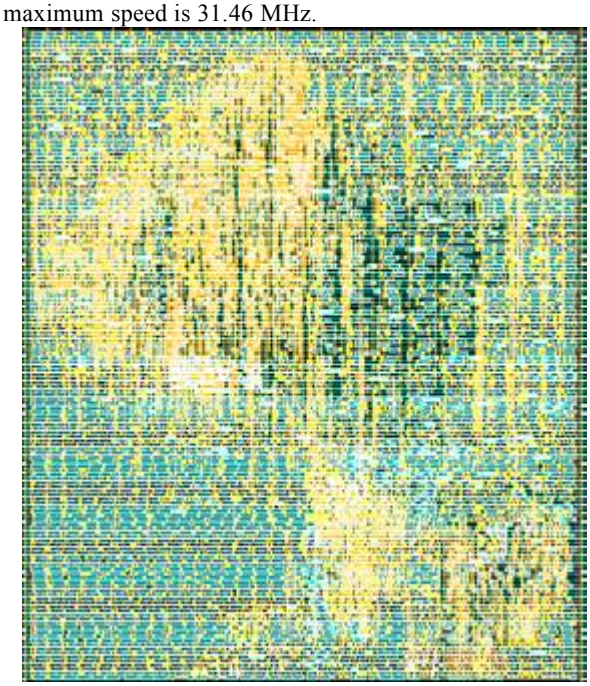

Fig 8. Chip layout.

IX. SUMMARY

RISC processor NICCOLO32 functionally works, instructions are correctly executed.

RISC processor NICCOLO32 can execute instruction generated by compiling C language program.

Multicycle instruction implemented. Each type of instructions requires various cycle.

X. REFERENCES

[1]. Brown, S. and Z Vranesic, *"Fundamental of Digital Logic Design with VHDL design"*, international ed. Singapore : McGraw-Hill companies, 2000.

[2]. Chang, K.C., *"Digital System Design with VHDL and Synthesis : an Integrated Approach"*. Los Alamos, Calif : IEEE Computer society, 1999.

[3]. Hennessy, J.L. and D. A. Patterson, "*Computer Organization and Design"*, 2nd ed. California : Morgan Kaufmann Publishers Inc., 1998.

[4]. Heuring, V.P. AND H. F. Jordan, "*Computer System Design and Architecture*". California : Addison Wesley Inc., 1997.

[5]. Pedroni, V.A., *"Circuit Design with VHDL"*, Cambridge, London : MIT Press, 2004.

[6]. Smith, D.J., *"HDL Chip Design"*, 6th ed. Madison, AL : Doone Publications., 1999.

[7]. *"SPARC Architecture Manual : Version 8"*, revision SAV080SI9308. Menlo Park, CA : SPARC International, Inc., 1992.

[8]. *"The SPARC Technical Papers"*, Mountain View, CA : Sun Microsystems, Inc., 1991.

ISSN 114-1284

Designing Process of a UAV-Rocket Boosted Separator

Larasmoyo Nugroho, M.Des [a)]
Dr. Edi Sofyan [b)]
Robertus Heru Triharjanto, M.Sc [c)]

[a]*Rocket Control Division*
LAPAN Pustekwagan, Rumpin, Bogor 16424
Tel : 0856-213 2809
E-mail : larasmoyo@gmail.com

[b]*Rocket Control Division*
LAPAN Pustekwagan, Rumpin, Bogor 16424
E-mail : edisofyan@hotmail.com

[c]*Rocket Structure Division*
LAPAN Pustekwagan, Rumpin, Bogor 16424
E-mail : rtriharjanto@yahoo.com

ABSTRACT

The take-off pattern used by LAPAN's UAV RKX-530 Sengkelat is a throwing system using rocket booster. Separator would be the element key for the UAV to detach the rocket as booster from the body fuselage which use turbojet machine as sustainer. The main aim of this designing process is to find the right configuration to separate the rocket that is efficient but also safe. The methodology of designing this separator is design totality.

Keywords :
UAV, rocket, jet, configuration, trade-off, design

1. INTRODUCTION

UAV-jet type is still not a major player in aeronautical world of Indonesia. There's still no jet-powered UAV that is used intensively by state's defense department to protect this nation's sovereignty. To answer this need, LAPAN develops a jet-powered UAV that would be used as main tool in a big surveillance system deployed in the outer border of Indonesia's territory.

RKX-530 Program is a LAPAN's most important project that is beginned from year 2008 as a framework to guard this country's sovereignty especially at the outmost borders. RKX-530 is a combination of a jet-powered UAV with rocket booster as launching device. This kind of launching mode is very useful for mobility pattern required in the military system in the air, sea and land.

Figure 1. RKX-530 Sengkelat

Main tasks in this project is to design and to build the flying vehicle prototype, to find and test its flight dynamics characteristic, to design and test the autopilot control for cruise phase and homing phase, and finally to find a launching system which would be the most suitable with the LAPAN's rocketry. The RKX-530 design which has a diameter of 530 mm, must be examined first through the making of few scaled-down model prototype with diameter of 300 mm that would be used as testbed for the launching system, rocket booster separation system, flight control stability system, and for ground testing system. These model prototypes are born from Rumpin, the fabrication is done in Bandung, while the flight tests and launch tests are done in Batujajar and Pameungpeuk. Those model prototypes are named HSFTB (high speed flying testbed), Dummy of the HSFTB, Dummy of the dummy of the HSFTB (dum-dum). The numerical simulation are done for each vehicle using Matlab dan Xplane, the parameter sought are aerodynamic characteristic, flight dynamic, flight performance, and flight control.

Figure 2. High Speed Flying Testbed (HSFTB)

Figure 3. Dummy of the HSFTB

Figure 4. Dummy of the dummy of the HSFTB (dum-dum)

Rocket used to catapult HSFTB is an RX-100 which has 100 mm of diameter, with average thrust of 1500 N or 150 kg. If we put it side by side with the vehicles's MTOW (maximum takeoff weight) at 55 kg, we will get thrust-to-weight ratio 3, quite big even for a vertical launch. After including the drag factor, this rocket could give an acceleration of 2.5 to 3G. This RX-100 have a burntime no more than 2.5second, and at burnout the vehicle will have velocity of 60 m/s or 216 km/h or 0.18 Mach. This speed is more than enough to propel the aircraft to take-off (Vto = 100km/h), therefore this method of launching using this rocket is expected to work effectively with zero-length runway.

Figure 5. Booster Roket RX-100

2. STATEMENT OF THE PROBLEM

Using rocket with such capability means that the selection of a robust separation system is going to be a delicate task. The choice of booster placement location should be taken care with extra precaution, because it will determine the failure or success of the launching phase.

The main consideration of finding the location of rocket placement are :

- Flight Performance
- Separation effectivity
- Practicability of Production
- Flight Safety

These four basic consideration are called the design requirements, which would be concluded from three rocket placement configuration.

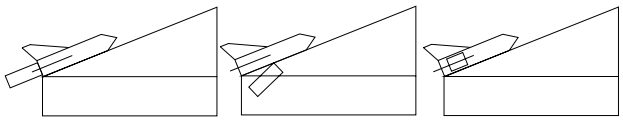

Figure 6. Three configuration of rocket placement (left: aft of fuselage, center : under belly, right : both side of fuselage)

Each rocket placement configuration has its own characteristic. Those design characteristics include:

- Position of Xcg, Zcg and Ycg
- Ballast Placing Mode
- Difficulty of measuring of Xcg, Zcg andYcg
- Elevation Angle of the rail launcher
- Complexity to install the rocket and the separator
- Reliability of Rocket Separation Mechanism

3. CONCEPTUAL SOLUTION TO SOLVE THE PROBLEM

HSFTB as a small aircraft is constructed from composite material with various degree of strength. The wing is the most heavy-duty component which would absorb all major forces including lift & weight, so its material is the strongest. The fuselage has weaker strength, due to its thinner skin, but gives weight reduction in return. The wing and fuselage are detachable, so it can be carried easily inside a pickup box. The strength of the wing structure comes from the thick spar, so that it could act as a hanger and as shock absorber when tthe belly crash occur, or any rollover tumbling. Over this consideration of strength, it is expected that the vehicle will achieve belly landing rather than nose diving. This is the main reason for placing the rocket under belly.
Main obstacle to place the rocket underbelly is the necessity to point the rocket thrustline right into the c.g. position of the vehicle. The center of gravity in the X-line (longitudinal axis) is easy to find, but not for the Z-line (directional axis) because of asymmetry of an aircraft. For the sake of easiness of finding the Z-c.g and to aim thrustline into it, that's the main reason for placing the rocket aft (behind) of the fuselage exhaust.
Main obstacle to place the rocket aft of the fuselage is the existence of the jet exhaust that has average temperature at 600 deg Celsius (http://www.jetaces8rc.com/Jetcat/jetcat_usa.htm) which can augment the heat of the rocket body and accidentally explode it. The second obstacle is the landing pattern that tends to be nose-diving and will cause fuselage breakup. But this could be avoided by commanding the airplane to pitchup.
At the same time, the third configuration is to put 2 rockets in both side of the fuselage. Its main obstacles are the rocket flame exhaust will burn the elevator, the alignment of the rocket must be symmetrically accurate, the separation mode would be twice the complexity of the underbelly configuration, and the timing of burn between right and left rocket must be uniform.

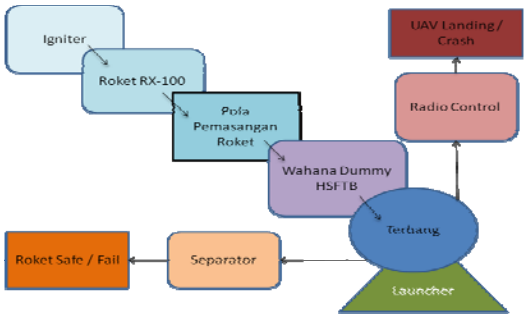

Figure 7. Diagram of interaction between subsystem and the effect results.

4. METHODOLOGY

To minimize failure and in addition to optimize the cost, this research looking for the best configuration is done in 4 steps. First, computation. Two, dummy launch to prove concept. Three, dummy launch to train piloting. Fourth, flight test using jet-powered HSFTB.

4.1. Computation

This computation phase aims for :
-To adjust the dynamic stability of the vehicle
-To predict the flight trajectory and aircraft's attitude for each configuration of rocket placement
-To find the best maneuver command to control the aircraft to achieve the best trajectory

Software used are Matlab-Simulink dan X-Plane

4.2. Dummy launch to prove concept the configuration

To reduce risk of destruction of the High Speed Flying Testbed, we make dummy HSFTB which has the same appearance with the actual vehicle just without jet and electronic control unit. But apparently, the cost is still high, so that we make another type of vehicle that is far cheaper and so simple that it just focus on the configuration of the placement of the rocket. This vehicle functions as the dummy of the dummy of the HSFTB, we call it dum-dum. The rocket used for this vehicle is also a scaled down from the real one, it has diameter of 70 mm with the thrust of 90 N and two rocket with thrust of 35 N.

4.3. Dummy launch to train pilot

Before launching the real HSFTB, the pilot must train to control the vehicle right after the burnout. Starting from the boost phase, continue to gliding phase and maintain until landing phase.
This replica of the HSFTB is so authentic that it can be used to test the structural damage pattern on the fuselage if the crash landing occur.
The rocket used is the real RX-100.

4.4. Flight Test of the Jet-powered HSFTB

In this phase, the HSFTB used turbojet engine and the launching system used the best configuration of rocket placement. The autopilot system ideally is also applicated in this phase.

5. Experimental Results

5.1. Computation

From the numerical simulation, we produce data that shows that all configuration could achieve succesful flight trajectory. The rail launch elevation is set to 20 deg. The launches are simulated in 2 mode, without control and with pitchup control.

Table 1. Uncontrolled flight results.

	Underbelly		Aft of Fuselage	
	HSFTB/ dummy	Dum-dum	HSFTB/ dummy	Dum-dum
Distance	90 m	140 m	180 m	80 m
Height	90 m	10 m	14 m	6 m

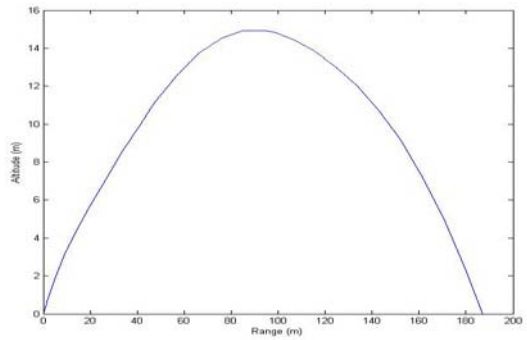

Figure 8. HSFTB Dummy's Aft of Fuselage Uncontrolled Flight Trajectory

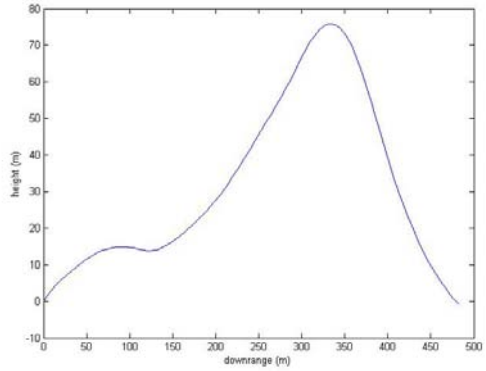

Figure 9. HSFTB Dummy with Underbelly Rocket Controlled Flight Trajectory

From table 1, it seems that dum-dum launched using underbelly configuration would have a better flight performance than from the aft of the fuselage. The reason is, the thrustline from underbelly rocket would be projected into horizontal axis and vertical axis. That is why we put the underbelly rocket configuration as our top priority to be tested.
The configuration of aft of the fuselage is considered as second priority because of its simplicity in the matter of pointing the thrustline to c.g. position.
While the third configuration (both-side of the fuselage) has the latest priority, due to its complexity of installation, c.g. pointing, and separation process.

5.2. Dummy launch to prove concept the configuration

The experiment results show that :

- The separator doesn't work unless the aircraft crash severely
- The dumdum vehicle doesn't even slide in the rail launcher, and it just directly lift-off

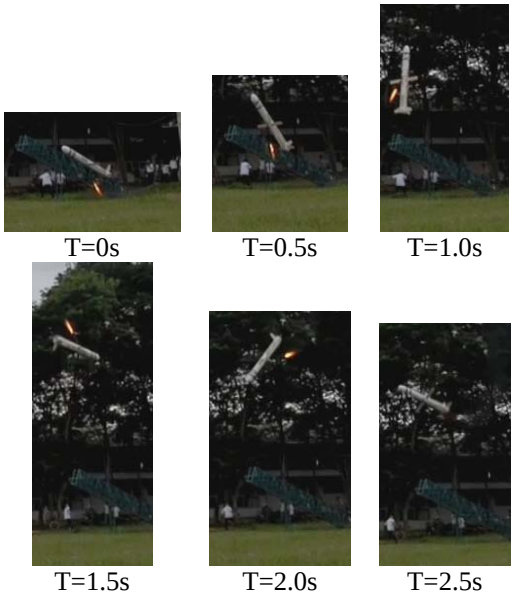

Figure 10. Chronology of Launch Test of the Dum-dum using Underbelly Rocket

- The flight vehicle pitches up easily and make a loop or two (630 deg for 2 seconds), this was caused by the existence of a GIGANTIC moment arm (25 cm) between thrustline and c.g. position

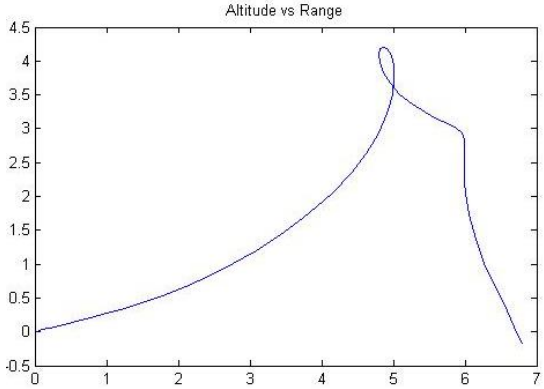

Figure 11. Flight Trajectory of Launch Test of the Dum-dum using Underbelly Rocket with moment arm 25cm

- The vehicle tends to roll or bank to its right side

5.3. Dummy launch to train pilot

On the launch test of the HSFTB dummy at Pameungpeuk, December 2008, with moment arm 2 cm, there was a torque force whose magnitude is equal to 150kg x 0.03m that produced a pitchup loop of 90 degrees in 2 seconds. This moment arm was not yet able to be minimized because the installation of the ballast was not practical then, the door access at the nose was too far behind to reach and complicate to put the ballast properly. The experiment results showed that the launch test trajectory was similar with the computational trajectory.

t= 2.5s

t= 2.0s

t=1.0s

t=0.5s

Figure 12. Chronology Pitchup Loop of the Dummy HSFTB using Underbelly Rocket

GPS Data

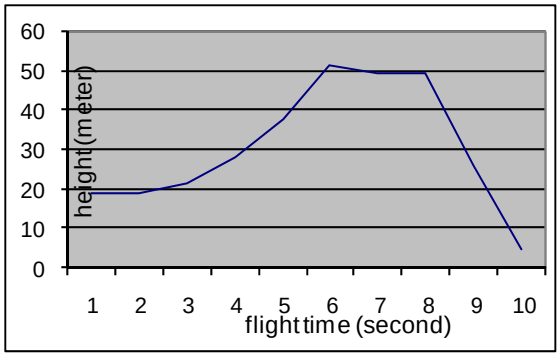

Figure 13. Flight Trajectory History from GPS data

From the first second until 2nd second the aircraft pitches up 90 deg, pilot act quickly by compensating it using pitch down maneuver using elevator, but the vehicle is still climbing with same angle until the 6th second. From 6th to 8th seconds, the altitude of the aircraft is hold on 50 meter height, where the aircraft is making an aerobatic pitchup loop with the intention is to avoid crash landing accidentally upon the spectator. From 8th to 10th the aircraft glides in 2 seconds with the Falling Speed about 45 m/s or 162 km/hour.

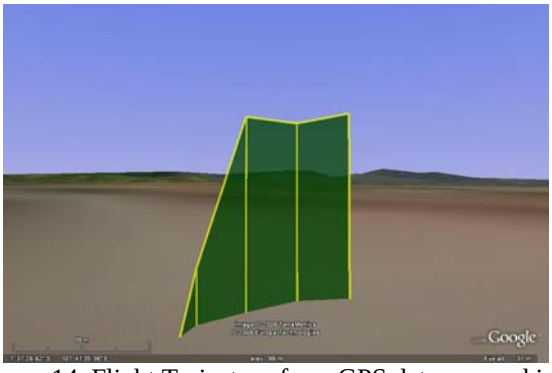

Figure 14. Flight Trajectory from GPS data mapped into Google Earth

The graphic above shows that the dummy of HSFTB's launch test make flight trajectory to the right-side, and plunge vertically from the height of 50 meter til the ground impact.

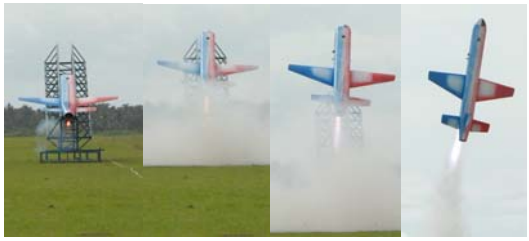

Figure 15. The dummy HSFTB tends to produce roll-yaw coupling to the right side of the fuselage

When the vehicle takes off, the maneuver happened was not just pitching up but also roll-yaw coupling. This roll movement was caused by two possibility, the elevators are not in the same deflection angle, or there must be yawing moment from the beginning of the boost. This yawing moment could be caused by rail shoes that are not really parallel, so that the longitudinal axis of the fuselage is not aligned with the longitudinal axis of the rail launcher.

Accelerometer Data

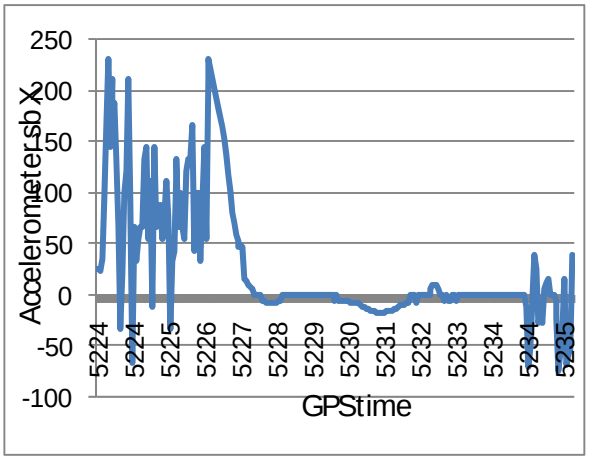

Figure 16.a. Accelerometer X-axis

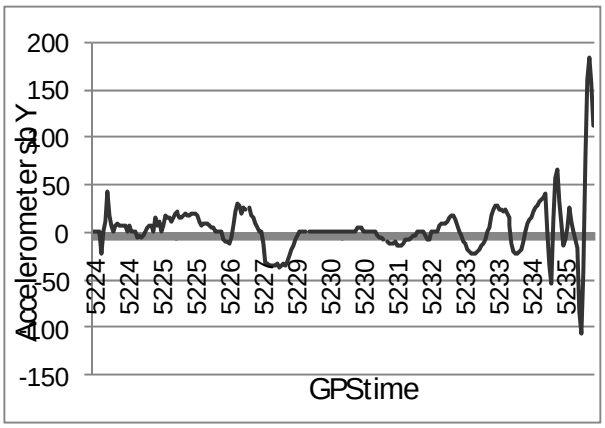

Figure 16.b. Accelerometer Y-axis

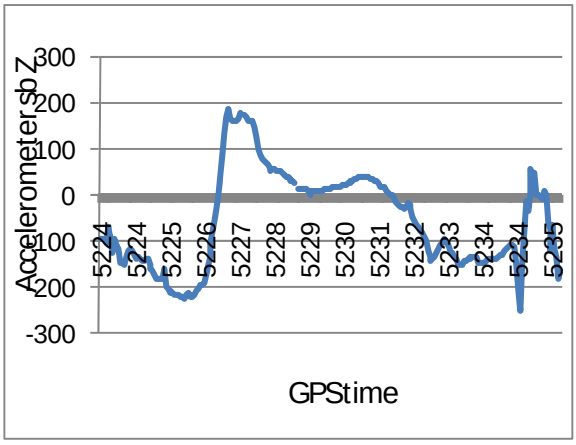

Figure 16.c. Accelerometer Z-axis

From the accelerometer data above, the booster rocket start burning at the GPS-time of 5224 and burning out at GPS-time of 5226. That means the burning time is 2 seconds.
From the perspective of flight dynamics the graphics informations are :

- The aircraft experiences a big acceleration in the longitudinal axis of the body at the boost start time, this is noticeable from the vibration at GPS-time 5224-5226. In theory, the axial acceleration happened was 2.7G (thrust*cos20 / Wbody).
- At the burnout, the X-acceleration drop to zero in one second (gliding). More interesting is to examine the acceleration in the Z-axis. From 5224-5226 the aircraft experience a negative G (average -200 units) that means pitchup with high degree (Figure 16c). While from 5226 to 5227 the aircraft experience an inversion of G (from -200 to 200) that means the aircraft is commanded to compensate the pitchup by pitching down abruptly. After that, from 5227 to 5229 the aircraft pitchup is diminishing, this was caused by looping without power (in the gliding phase).

Rate Gyroscope Data

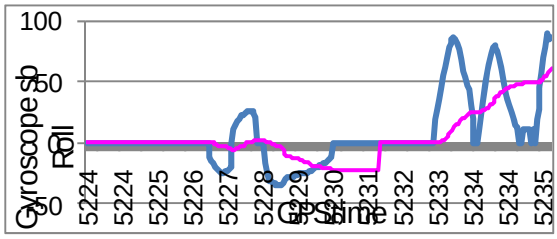

Figure 17.a. Gyroscope at Roll-axis

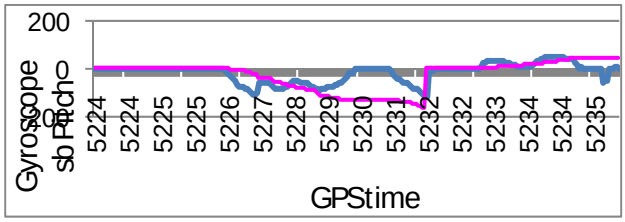

Figure 17.b. Gyroscope at Pitch-axis

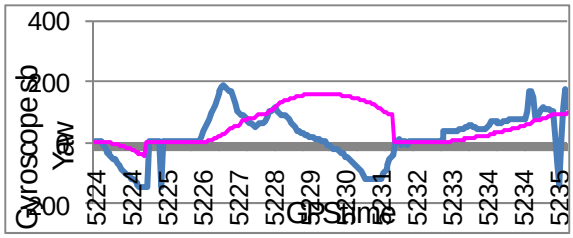

Figure 17.c. Gyroscope at Yaw-axis

From all graphics above, it could be seen (darkline-angle rate, lightline-angle) that since GPS time 5226 until 5232, the vehicle tends to make a looping constant maneuver that develops into a helix to the right side of the body.

6. Discussion

Some remarks that constructed from discussion about these experiments are :

- The underbelly rocket configuration has great potential to generate arm moment. Using delicate photometry we could reduce the magnitude of this arm moment, but the arm is still there.

Figure 18. Manual method photometry to discover the c.g location

- The vertical force generated from the underbelly rocket configuration is beneficial for extending range of the gliding phase, but very reactive to generate trouble in the boosting phase due to its big influence to form moment arm.
- There is a constant tendency for the aircraft to generate roll-yaw coupling to the right direction. More experiments needed to comprehend the moment of inertia nature of each vehicles and to control it

7. Conclusion

Conclusion that could be drawn from these experiments are :

- It is understood from the simulation that the underbelly rocket configuration has better flight performance than any other configuration. But the experiments show that it has narrow margin of success to launch the HSFTB vehicle, due to the magnitude of the vertical projection of the thrust. So the top-priority configuration now is not underbelly rocket anymore, but rocket at the aft of fuselage would be used for the fourth phase of this research.
- The existence of a pilot as human in the loop is proved to be beneficial to comprehend and apprehend the flight dynamics characteristic of the aircrafts, although the pilot will give extra precaution to the safety of the launch flight, the research could take benefit from the unpredicted maneuver done by the pilot

ACKNOWLEDGMENT

This work is supported by LAPAN, Pustekwagan, under the direction of Mr. Yus Markis, Dipl-Ing. The Rocket Control Division is headed by Mrs. Rika Andiarti, Dr. The first author would like to thank also Mrs. Wijaya Dewi Wuri Handayani from Physic Department, ITB for her generous technical support.

REFERENCES

[1] Danielle S. Soban, Dimitri N. Mavris, "*Methodology for Assessing Survivability Tradeoffs in the Preliminary Design Process*," 2000 World Aviation Conference, San Diego, CA

[2] Robert L. Geisler, Thomas L. Moore, Eric M. Rohrbaugh, Carl R. Pignoli. "*Unlocking the Mystery of the D-21B Solid Rocket Boosted Air-Launched Mach-3 UAV*," 2007, Alliant Techsystems and AIAA

[3] Manley C. Butler, Jr., Troy Loney. "*Design, Development and Testing of a Recovery System for the Predator™ UAV*," 1995, 13th AIAA Aerodynamic Decelerator Systems Technology Conference, Clearwater Beach, FL

[4] Dimitri N. Mavris, Daniel A. DeLaurentis , Danielle S. Soban "*Probabilistic Assessment of Handling Qualities Characteristics in Preliminary Aircraft Design*" Aerospace System Design Laboratory (ASDL), School of Aerospace Engineering, Georgia Institute of Technology

[5] Dr. Danielle Soban, Dr. Daniel DeLaurentis. "*An Approach to the Design of a New System: Methodology as Applied to the MAGTF Expeditionary Family of Fighting Vehicles*," 2003. Office of Naval Research Naval Surface Warfare Center

[6] Dr. Dimitri N. Mavris, Danielle S. Soban, Matthew C. Largent. "*An Application of a Technology Impact Forecasting (TIF) Method to an Uninhabited Combat Aerial Vehicle*," 1999 SAE, International and the American Institute of Aeronautics and Astronautics.

ISSN 114-1284

Modelling and Analysis of A Two-Link Flexible Robot Manipulator Incorporating Payload

M. Khairudin[a]

[a]*Dept. of Electrical Eng., Faculty of Engineering*
Yogyakarta State University,Yogyakarta 55281, Karangmalang Yogyakarta
Tel : (0274) 586161 ext 293
E-mail : moh_khairudin@uny.ac.id

ABSTRACT

This paper presents dynamic modelling of a two-link flexible manipulator system. The kinematic model is based on standard frame transformation matrices describing both rigid rotation and modal displacement, under small deflection assumption. A two-link flexible manipulator incorporating structural damping, hub inertia and payload is considered. An explicit, complete, and accurate nonlinear dynamic model of the system is developed using assumed mode method. Moreover, the effects of payload on the response of a two-link flexible manipulator are studied.

Keywords *:*
Assumed mode, modelling, two-link flexible manipulator

1. INTRODUCTION

Flexible robot manipulators exhibit many advantages over rigid robots. They require smaller actuator, consume less power, require less material, are lighter in weight, have less overall cost, are more manoeuvarable and transportable and higher payload to robot weight ratio. In order to control the two-link flexible manipulators to achieve and maintain accurate positioning is challenging. Due to the flexible nature of the system, the dynamics are significantly more complex. Moreover, flexible link causes significant technical problems. The problem increases dramatically for a two-link flexible manipulator with varying payload. In order to achieve high-speed and accurate positioning, it is necessary to control the manipulator's response in a cost effective manner. Control algorithms are required to compensate for both the vibration and the static deflection of the system.

The main goal on the modelling of a two-link flexible manipulator is to achieve an accurate model representing the actual system behaviour. Each flexible link can be modelled as distributed parameter system where the motion is described by a coupled system of ordinary and partial differential equations (PDE). Various approaches have been developed which can mainly be divided into two categories: the numerical analysis approach and the assumed mode method (AMM). The numerical analysis methods that are utilised include finite difference and finite element methods. Both approaches have been used in obtaining the dynamic characterisation of a single-link flexible manipulator system incorporating damping, hub inertia and payload [1,2]. Subudhi and Morris [3] have used a combined Euler-Lagrange formulation and AMM approach to model the planar motion of a manipulator consisting of two flexible links and joints. The conventional Lagrangian modeling of flexible link robots does not fully incorporate the bending mechanism of flexible link as it allows free link elongation in addition to link deflection. De Luca and Siciliano [4] have utilised the AMM to derive a dynamic model of multilink flexible robot arms limiting to the case of planar manipulators with no torsional effects. The equations of motion that can be arranged in a computationally efficient closed form with respect to a suitable set of constant mechanical parameters have been obtained [5].

This paper presents modelling of a two-link flexible manipulator using Lagrangian technique in conjunction with the AMM. The links are modelled as Euler-Bernoulli beams satisfying proper mass boundary conditions. A payload is added to the tip of the outer link, while hub inertias are included at the actuator joints. Simulation of the dynamic model is performed using Matlab and Simulink. Angular position and modal displacement responses of the system responses are investigated. The effects of payload on the dynamic characteristics of the system are also studied.

ISSN 114-1284

2. A TWO-LINK FLEXIBLE ROBOT MANIPULATOR

Figure 1 shows the schematic diagram of a two-link flexible manipulator system considered in this study. The links are cascaded in serial fashion and are actuated by rotors and hubs with individual motors. An inertial payload of mass M_P and inertia I_P is connected to the distal link. The proximal link is clamped and connected to the rotor with a hub. The *i*th link has length l_i and uniform mass density per unit length ρ_i. E and I represent Young modulus and area moment of inertia of both links respectively. A payload is attached at the end-point of link-2.

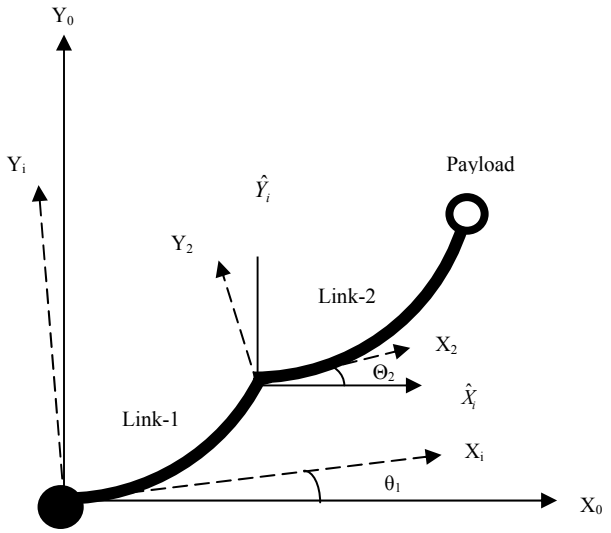

Figure 1: Schematic diagram of a two-link flexible manipulator

The first link is clamped on the rotor of the first motor. The second motor is attached to the tip of the first link. X_0 and Y_0 are the inertial coordinate frame. θ_1 and θ_2 are the angular position and $v_i(x_i,t)$ are the transverse component of the displacement vector. M_p is an inertial payload mass with inertia J_p at the end-point of second link. The description of kinematics is developed for a chain of n serially connected flexible links, revolute joints and motion of the manipulator on a two-dimensional plane, the rigid transformation matrix, A_i, from $X_{i-1}Y_{i-1}$ to $X_i Y_i$ is written as

$$A_i = \begin{bmatrix} \cos\theta_i & -\sin\theta_i \\ \sin\theta_i & \cos\theta_i \end{bmatrix} \quad (1)$$

The global transformation matrix T_i transforming co-ordinates from X_0Y_0 to X_iY_i follows a recursion as below

$$T_i = T_{i-1}E_{i-1}A_i \quad (2)$$

The dynamic equations of motion is derived for a two-link flexible manipulator, the total energy associated with the manipulator system needs to be computed using the kinematics formulations explained previously. The total kinetic energy of the manipulator (T) is given by

$$T = T_R + T_L + T_{PL} \quad (3)$$

where T_R, T_L and T_{PL} are the kinetic energies associated with the rotors, links and the hubs, respectively.

As Figure 1 show and the kinematics formulation described previously, the kinetic energy associated with the payload can be written as

$$T_{PL} = \frac{1}{2}M_p \dot{p}_{n+1}^T \dot{p}_{n+1} + \frac{1}{2}I_P(\dot{\Omega}_n + \dot{\upsilon}_n'(l_n))^2 \quad (4)$$

where $\dot{\Omega}_n = \sum_{j=1}^{n}\theta_j + \sum_{k=1}^{n-1}\dot{\upsilon}_k'(l_k)$; n being the link number, prime and dot represent the first derivatives with respect to spatial variable x and time, respectively. The potential energy of the system due to the deformation of the link i by neglecting the effects of the gravity can be written as

$$U = \sum_i^n \frac{1}{2}\int_0^{l_i}(EI)_i\left(\frac{d^2\upsilon_i(x_i)}{dx_i^2}\right)^2 dx_i \quad (5)$$

A two-link flexible manipulator motion equation is derived using the generalized modelling scheme. Consider two units of the n-link with the first one clamped and a payload attached at the tip of the second link.

Using the generalized modeling scheme described, equations with a two-link flexible manipulator links are described in this section. In this case, the effectiveness masses at the end of the individual links are set as

$$M_{L1} = m_2 + m_{h2} + M_p$$

$$J_{L1} = J_{o2} + J_{h2} + J_p + M_p l_2^2 \quad (6)$$

where

$$MD_1 = 0 \qquad M_{L2} = M_p$$

$$J_{L2} = J_p \; MD_2 = 0$$

The co-ordinate vector consists of link positions, (θ_1, θ_2) and modal displacements (q_{11}, q_{12}, q_{21}, q_{22}). The force vector is F = $\{\tau_1, \tau_2, 0, 0, 0, 0\}^T$, where τ_1 and τ_2 are the torques applied by rotor-1 and rotor-2, respectively. Therefore, the following Euler–Lagrange's equations result, with i = 1 and 2 and j = 1 and 2:

$$\frac{\partial}{\partial t}\left(\frac{\partial L}{\partial \dot{\theta}_i}\right) - \frac{\partial L}{\partial \theta_i} = \tau_i \qquad (7)$$

$$\frac{\partial}{\partial t}\left(\frac{\partial L}{\partial \dot{q}_{ij}}\right) - \frac{\partial L}{\partial q_{ij}} = 0 \qquad (8)$$

A set of dynamic equations can be written in compact form as

$$M(\theta,q)\begin{Bmatrix}\ddot{\theta}\\ \ddot{q}\end{Bmatrix} + \begin{Bmatrix}f_1(\theta,\dot{\theta})\\ f_2(\theta,\dot{\theta})\end{Bmatrix} + \begin{Bmatrix}g_1(\theta,\dot{\theta},q,\dot{q})\\ g_2(\theta,\dot{\theta},q,\dot{q})\end{Bmatrix} + \begin{Bmatrix}0\\ D\dot{q}\end{Bmatrix} + \begin{Bmatrix}0\\ Kq\end{Bmatrix} = \begin{Bmatrix}\tau\\ 0\end{Bmatrix} \qquad (9)$$

where f_1 and f_2 are the vectors containing terms due to coriolis and centrifugal forces, M is the mass matrix, and g_1 and g_2 are the vectors containing terms due to the interactions of the link angles and their rates with the modal displacements. K is the diagonal stiffness matrix which takes on the values $\omega_{ij}^2 m_i$ and D is the passive structural damping.

3. SIMULATION RESULT

Table 1 shows the physical parameter of the two-link flexible manipulator used in this simulation. M_{Li}, EI and G represent the mass of link, flexural rigidity and gear ratio respectively. J_{hi} is the inertia of the motor and hub and M_{h2} is the mass of centre rotor at the second motor.

Table 1: Parameters of The System

Symbol	Parameter	Value	Unit
M_{L1}=M_{L2}	Mass of link	0.1	kg
ρ	Mass density	0.2	kgm^{-1}
G	Gear ratio	1	-
EI	Flexural rigidity	1.0	Nm^2
J_h	Motor and hub inertia	0.02	kgm^2
M_p	Payload mass	0.4	kg
l	Length	0.5	m
I_p	Payload inertia	0.002	kgm^2
M_{h2}	Mass of the centre rotor	1	kg

A two-link flexible manipulator was excited with symmetric bang-bang torque inputs with amplitude of 0.2 Nm and 1 s width as shown in Figure. 2. For validation of the dynamic models, simulations were conducted on the manipulators with the same input trajectories. A bang-bang torque has a positive (acceleration) and negative (deceleration) period allowing the manipulator to, initially, accelerate and then decelerate and eventually stop at target location.

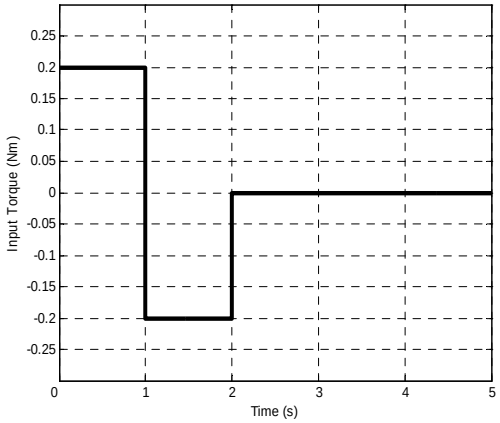

Figure 2. The Bang – bang Input Torque

Figures 3 and 4 show the angular positions, modal displacement and end-point acceleration responses of the two-link flexible manipulator without payload for both links. It is noted that a steady-state angular position levels of 54.56 degrees and -122.33 degrees were achieved within 1.8 s for link-1 and link-2 respectively. The time responses specifications of angular position for link-1 were achieved within the settling time and overshoot of 2.00 s and 1.35 % respectively. On the other hand, the settling time and overshoot for link-2 were obtained as 1.99 s and 0.35 % respectively.

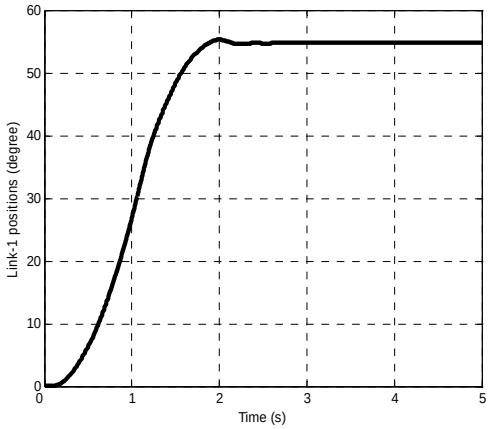

Figure 3: Angular position of link-1 the system without load.

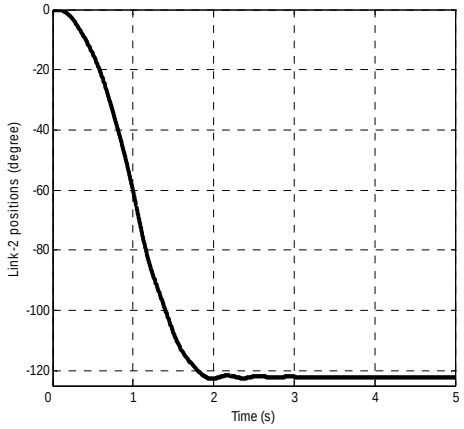

Figure 4: Angular position of link-2 the system without load.

Figures 5 and 6 show The modal displacement responses of link-1 and link-2 were found to oscillate between -6.1x10^{-3} m to 9.3x10^{-3} m and -11.2x10^{-3} m to 17.3x10^{-3} m respectively.

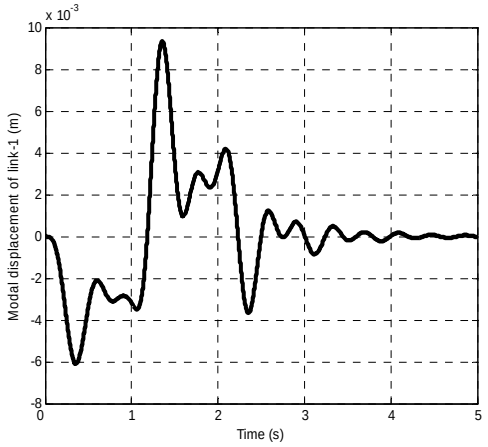

Figure 5: Modal displacement of link-1 of the system without load.

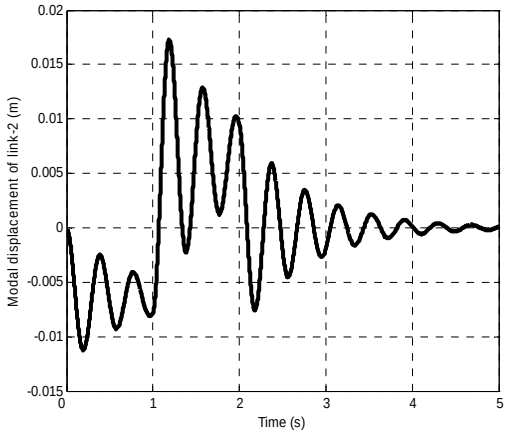

Figure 6: Modal displacement of link-2 of the system without load.

To demonstrate the effects of payload on the dynamic characteristics of the system, the payload of up to 0.4 kg was examined. Figures 7 and 8 show the system responses of the flexible manipulator with payloads of 0.4 kg for link-1 and link-2 respectively. It is noted that the angular positions for link-1 decrease towards the positive direction whereas the angular positions of link-2 decrease in the negative direction with increasing payloads. For payloads 0.4 kg, the steady-state angular position levels for link-1 were obtained as 20.36 degrees respectively whereas for link-2, these were obtained as -40.19 degrees.

The time response specifications of angular positions have shown significant changes with the variations of payloads. With increasing payload, the system exhibits higher settling times and overshoots for both links. For link-1, the response exhibits an overshoot of 7.26 % with the settling time of 4.32 s 0.4 kg respectively. For link-2, the response exhibits a percentage overshoot of 2.68 % with the settling time of 2.98 s for 0.4 kg payload.

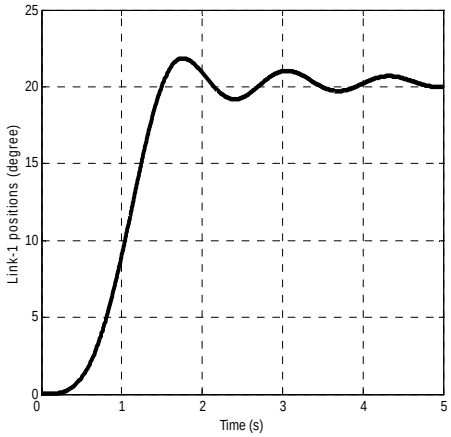

Figure 7: Angular position of link-1 the system with load 0.4 kg.

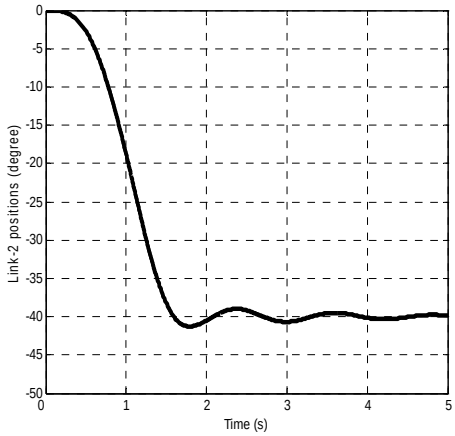

Figure 8. Angular position of link-2 the system with load 0.4 kg.

Figures 9 and 10 show modal displacements and end-point acceleration responses of the system with payloads respectively. It is noted with increasing payloads, the magnitudes of vibration of modal displacement increase for both links. In this case, the modal displacement responses of link-2 were found to oscillate between -8.73×10^{-3} m to 13.7×10^{-3} m and -53.9×10^{-3} to 74.0×10^{-3} m for payloads of 0.1 kg and 0.5 kg respectively.

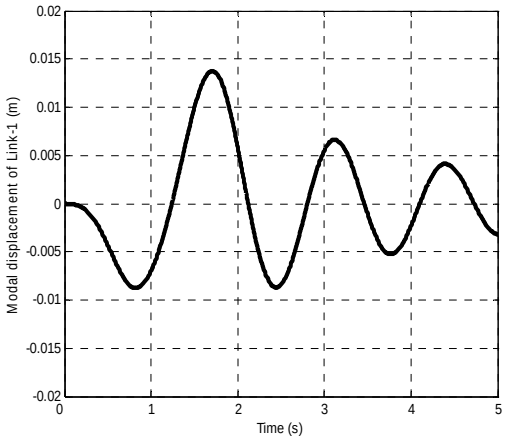

Figure 9: Modal displacement of link-1 of the system with load 0.4 kg.

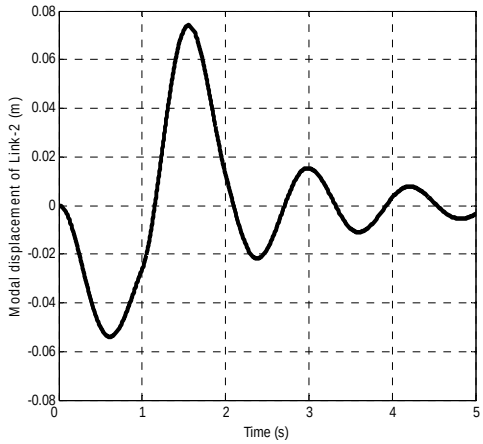

Figure 10: Modal displacement of link-2 of the system with load 0.4 kg.

Table 2 summarises the relationship between time response specifications (rise time, settling time and overshoot) and payload.

Table 2: Relation between payload and specifications of angular position

Payloads (kg)	Time responses specifications of angular positions			
	Link-1		Link-2	
	Settling time (s)	Overshoot (%)	Settling time (s)	Overshoot (%)
0	1.76	1.35	1.80	0.35
0.4	4.32	7.26	2.98	2.68

5. CONCLUSSION

The development of a dynamic model of a two-link flexible manipulator has been presented. The model has been derived using Eular-Lagrange and AMM. Simulation exercises have been conducted without and with payload to study and verify the performance of the system. The angular positions and displacements of link-1 and link-2 of the systems have been obtained and analysed.

REFERENCES

[1] Tokhi MO, Mohamed Z, Azad AKM, "Finite difference and finite element approaches to dynamic modelling of a flexible manipulator," Proceeding of IMechE-I: Journal of Systems and Control Engineering, 1997; 211:145-156.
[2] Tokhi MO, Mohamed Z, Shaheed MH, "Dynamic characterization of a flexible manipulator system," Robotica, 2001;19:571-580.
[3] Subudhi B, Morris AS., "Dynamic modelling, mimulation and control of a manipulator with flexible links and joints," Robotics and Autonomous System, 2002; 41:257-270.
[4] A. De Luca, B. Siciliano, "Closed-form dynamic model of planar multi-link lightweight robots," IEEE Transactions on Systems, Man, and Cybernetics **21** (4) .1991. 826-839.
[5] A. S. Morris, A. Madani, "Inclusion of shear deformation term to improve accuracy in flexible-link robot modelling", Mechatronics, Vol. 6, No. 6. 1996, pp. 631-647.

ISSN 114-1284

Modelling and Vibration Suppression of A Two-Link Flexible Robot Manipulator

M. Khairudin[a]

[a]*Dept. of Electrical Eng., Faculty of Engineering*
Yogyakarta State University,Yogyakarta 55281, Karangmalang Yogyakarta
Tel : (0274) 586161 ext 293
E-mail : moh_khairudin@uny.ac.id

ABSTRACT

This paper presents a dynamic modelling of a two-link flexible manipulator model. An explicit, complete, and accurate nonlinear dynamic model of the system is developed using assumed mode method. The Lagrangian approach is used to derive the dynamic model of the structure. To study the effectiveness of the controller, a PID control is developed. PID controller will implement to the system of a two-link Flexible Manipulator.

Keywords *:*
Assumed mode, modelling, PID, two-link flexible manipulator

1. INTRODUCTION

Robot manipulators are constructed very massively to make them precise and stiff. The arms of these can be considered rigid, which allows a simple control joints. The drawback of their heavy construction is, that the robots need very powerful actuators and their operating speed is strongly limited by their own inertia. Lightweight robots are developed to overcome these drawbacks and allow high speed movements with the same or even better precision. These are commonly used in space applications, because the take-off weight of space shuttles is strongly limited. In order to improve higher productivity, it is required to reduce the weight of the arms and/or to increase their speed of operation. For these purposes it is very desirable to build flexible robotic manipulators. Morever, flexible manipulators are lighter, faster and less expensive than rigid ones.

Each flexible link can be modeled as distributed parameter system where the motion is described by a coupled system of ordinary and partial differential equations (PDE). Various approaches have been developed which can mainly be divided into two categories: the numerical analysis approach and the assumed mode method (AMM). The numerical analysis methods that are utilised include finite difference (FD) and finite element (FE) methods.

The FD and FE approaches have been used in obtaining the dynamic characterisation of a single-link flexible manipulator system incorporating damping, hub inertia and payload [1,2].

Subudhi and Morries [3] have used a combined Euler-Lagrange formulation and AMM approach to model the planar motion of a manipulator consisting of two flexible links and joints. The conventional Lagrangian modeling of flexible link robots does not fully incorporate the bending mechanism of flexible link as it allows free link elongation in addition to link deflection. De Luca and Siciliano [4] have utilized the AMM to derive a dynamic model of multilink flexible robot arms limiting to the case of planar manipulators with no torsional effects. The equations of motion which can be arranged in a computationally efficient closed form that is also linear with respect to a suitable set of constant mechanical parameters have been obtained [5].

The controller strategies for flexible manipulator systems can be classified as feedforward and feedback control schemes. A number of techniques have been proposed as feedforward control schemes for control of vibration [6].

This paper presents modeling of a two-link flexible manipulator using Lagrangian technique in conjunction with the AMM. The links are modeled as Euler-Bernoulli beams satisfying proper mass boundary conditions. A payload is added to the tip of the outer link, while hub inertias are included at the actuator joints. To demonstrate the effectiveness of the controllers in reducing vibration of a two-link flexible manipulator, PID controller utilizing the hub angle and hub velocity is developed.

ISSN 114-1284

2. A TWO-LINK FLEXIBLE ROBOT MANIPULATOR

The structure of a two-link flexible manipulator system is shown in Figure 1. The links are cascaded in serial fashion and are actuated by rotors and hubs with individual motors. An inertial payload of mass M_P and inertia I_P is connected to the distal link. The proximal link is clamped and connected to the rotor with a hub.

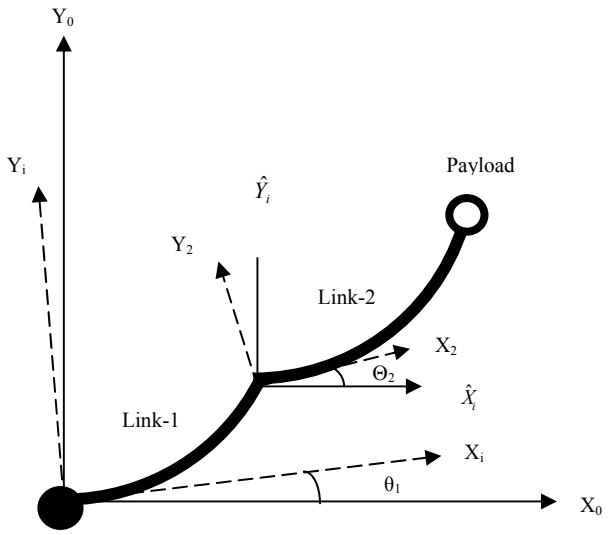

Figure 1: Schematic diagram of a two-link flexible manipulator

The *i*th link has length l_i and uniform mass density per unit length ρ_i. The first link is clamped on the rotor of the first motor. The second motor, is attached to the tip of the first link. *E* and *I* represent Young modulus and area moment of inertia of both link. A payload is attached at the end-point of link-2. X_0Y_0 is the inertial coordinate frame. θ_1 and θ_2 are the angular position and $v_i(x_i,t)$ are the transverse component of the displacement vector. M_p is an inertial payload mass with inertia J_p at the end-point of link 2.

The description of kinematics is developed for a chain of *n* serially connected flexible links, revolute joints and motion of the manipulator on a two-dimensional plane, the rigid transformation matrix, A_i, from $X_{i-1}Y_{i-1}$ to X_iY_i is written as

$$A_i = \begin{bmatrix} \cos\theta_i & -\sin\theta_i \\ \sin\theta_i & \cos\theta_i \end{bmatrix} \qquad (1)$$

The global transformation matrix T_i transforming co-ordinates from X_0Y_0 to X_iY_i follows a recursion as below

$$T_i = T_{i-1}E_{i-1}A_i \qquad (2)$$

The dynamic equations of motion is derived for a two-link flexible manipulator, the total energy associated with the manipulator system needs to be computed using the kinematics formulations explained previously. The total kinetic energy of the manipulator (*T*) is given by

$$T = T_R + T_L + T_{PL} \qquad (3)$$

where T_R, T_L and T_{PL} are the kinetic energies associated with the rotors, links and the hubs, respectively.

As Figure 1 show and the kinematics formulation described previously, the kinetic energy associated with the payload can be written as

$$T_{PL} = \frac{1}{2}M_p\dot{p}_{n+1}^T\dot{p}_{n+1} + \frac{1}{2}I_P(\dot{\Omega}_n + \dot{\upsilon}_n'(l_n))^2 \qquad (4)$$

where $\dot{\Omega}_n = \sum_{j=1}^{n}\theta_j + \sum_{k=1}^{n-1}\dot{\upsilon}_k'(l_k)$; *n* being the link number, prime and dot represent the first derivatives with respect to spatial variable *x* and time, respectively. The potential energy of the system due to the deformation of the link *i* by neglecting the effects of the gravity can be written as

$$U = \sum_i^n \frac{1}{2}\int_0^{l_i}(EI)_i\left(\frac{d^2\upsilon_i(x_i)}{dx_i^{\,2}}\right)^2 dx_i \qquad (5)$$

A two-link flexible manipulator motion equation is derived using the generalized modelling scheme. Consider two units of the *n*-link with the first one clamped and a payload attached at the tip of the second link.

Using the generalized modeling scheme described, equations with a two-link flexible manipulator links are described in this section. In this case, the effectiveness masses at the end of the individual links are set as

$$M_{L1} = m_2 + m_{h2} + M_p$$

$$J_{L1} = J_{o2} + J_{h2} + J_p + M_p l_2^2 \qquad (6)$$

where

$$MD_1 = 0 \qquad M_{L2} = M_p$$

$$J_{L2} = J_p \; MD_2 = 0$$

The co-ordinate vector consists of link positions, (θ_1, θ_2) and modal displacements (q_{11}, q_{12}, q_{21}, q_{22}). The force vector is F = $\{\tau_1, \tau_2, 0, 0, 0, 0\}^T$, where τ_1 and τ_2 are the torques applied by rotor-1 and rotor-2, respectively. Therefore, the

following Euler–Lagrange's equations result, with i = 1 and 2 and j = 1 and 2:

$$\frac{\partial}{\partial t}\left(\frac{\partial L}{\partial \dot{\theta}_i}\right)-\frac{\partial L}{\partial \theta_i}=\tau_i \qquad (7)$$

$$\frac{\partial}{\partial t}\left(\frac{\partial L}{\partial \dot{q}_{ij}}\right)-\frac{\partial L}{\partial q_{ij}}=0 \qquad (8)$$

A set of dynamic equations can be written in compact form as

$$M(\theta,q)\begin{Bmatrix}\ddot{\theta}\\ \ddot{q}\end{Bmatrix}+\begin{Bmatrix}f_1(\theta,\dot{\theta})\\ f_2(\theta,\dot{\theta})\end{Bmatrix}+\begin{Bmatrix}g_1(\theta,\dot{\theta},q,\dot{q})\\ g_2(\theta,\dot{\theta},q,\dot{q})\end{Bmatrix}+\begin{Bmatrix}0\\ D\dot{q}\end{Bmatrix}+\begin{Bmatrix}0\\ Kq\end{Bmatrix}=\begin{Bmatrix}\tau\\ 0\end{Bmatrix} \qquad (9)$$

where f_1 and f_2 are the vectors containing terms due to coriolis and centrifugal forces, M is the mass matrix, and g_1 and g_2 are the vectors containing terms due to the interactions of the link angles and their rates with the modal displacements. K is the diagonal stiffness matrix which takes on the values $\omega_{ij}{}^2 m_i$ and D is the passive structural damping.

3. SIMULATION RESULT

Table 1 shows the physical parameter of the two-link flexible manipulator used in this simulation. M_{Li}, EI and G represent the mass of link, flexural rigidity and gear ratio respectively. J_{hi} is the inertia of the motor and hub and M_{h2} is the mass of centre rotor at the second motor.

Table 1: Parameters of The System

Symbol	Parameter	Value	Unit
M_{L1}=M_{L2}	Mass of link	0.1	kg
ρ	Mass density	0.2	kgm^{-1}
G	Gear ratio	1	-
EI	Flexural rigidity	1.0	Nm^2
J_h	Motor and hub inertia	0.02	kgm^2
M_p	Payload mass	0.5	kg
l	Length	0.5	m
I_p	Payload inertia	0.0025	kgm^2
M_{h2}	Mass of the centre rotor	1	kg

A two-link flexible manipulator was excited with symmetric bang-bang torque inputs with amplitude of 0.2 Nm and 1 s width as shown in Figure. 2. For validation of the dynamic models, simulations were conducted on the manipulators with the same input trajectories. A bang-bang torque has a positive (acceleration) and negative (deceleration) period allowing the manipulator to, initially, accelerate and then decelerate and eventually stop at target location.

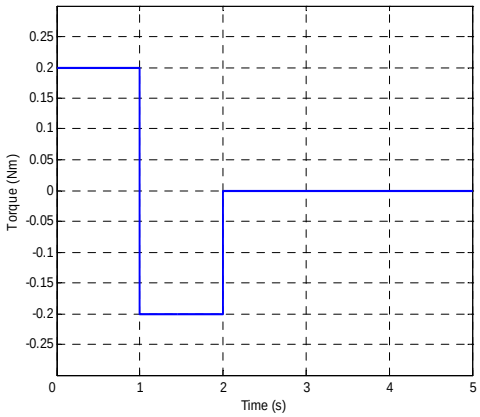

Figure 2. The Bang – bang Input Torque

Figure 3 shows the response of the angular positions of link-1 and link-2 of the system with torque amplitudes of 0.2 Nm. As expected, by increasing the payload mass, the angular position decreases. Moreover overshoot increases by increasing torque amplitude. It is also noted that the angular positions for Link-1 of 16.5 degree and Link-2 is -34 degree, respectively, were achieved within 2 s.

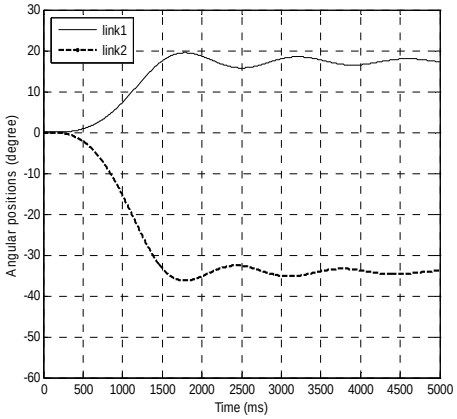

Figure 3. Angular Position of Link-1 and Link-2

Figure 4 and 5 show modal displacement of link-1 and link-2. The pattern of modal displacement of link-1 between $\pm 8.8\times10^{-3}$ m and $\pm 5.5\times10^{-3}$ m and link-2 between ± 0.08 m and $\pm 2.5\times10^{-3}$ m for the first and second modes respectively.

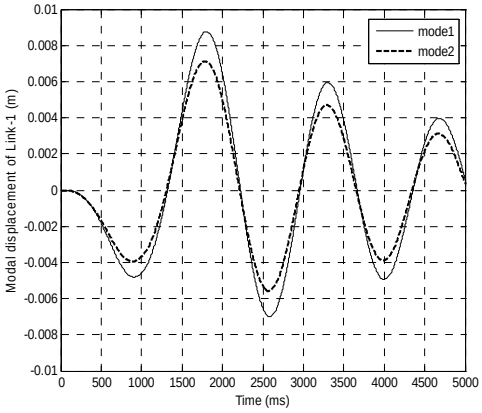

Figure 4. Modal Displacement of Link-1.

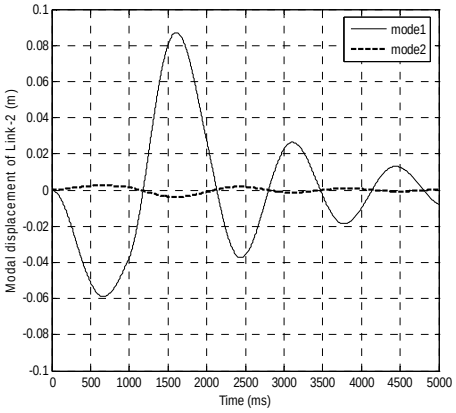

Figure 5. Modal Displacement of Link-2.

Figure 6 shows response of the end-point acceleration of link-1 and link-2. The end-point acceleration results which were found to oscillate between $\pm$ 0.23 m/sec^2 for link-1 and $\pm$ 1.30 m/sec^2.

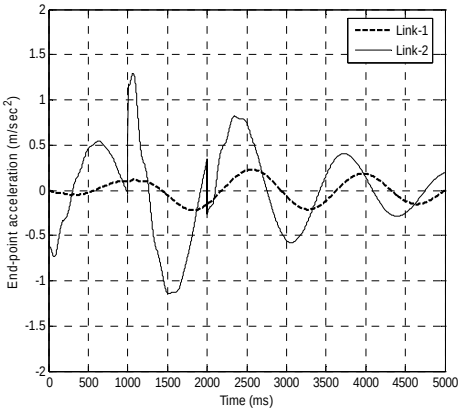

Figure 6. Response of end-point acceleration.

Figure 7 shows response of PSD of end-point acceleration of link-1 and link-2. For payload 0.5 kg, the resonance frequencies for the first two modes of vibration respectively were obtained as 1 Hz and 7 Hz for link-1 and 1 Hz and 7 Hz for link-2.

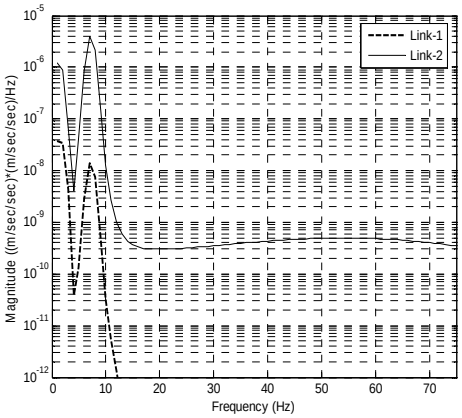

Figure 7. PSD of end-point acceleration.

4. PID CONTROL

In this study, Ziegler-Nichols closed loop method is used in designing the PID controller. The Ziegler-Nichols closed loop method is one of the more common method used to tune control loops. The closed loop method determines the gain at which a loop with proportional only control will oscillate, and then derives the controller gain, integrator, and derivative values from the gain at which the oscillation are sustained and the period of oscillation at that gain.

The closed loop method also known as ultimate cycle method tuning Kp, Ki and Kd components based on Ku and Pu. Practically, the ultimate gain (Ku) and the ultimate period (Pu) is found by setting the integral (Ki) and derivative (Kd) components of the PID controller to zero and incrementally increasing the proportional (Kp) component until oscillations begin. In other words, the trial process is repeated which increased or decreased controller gain Kp (Ki=Kd=0) until a stable oscillation is achieved.

Then, from the format of PID controller as

$$G_c = K(1 + \frac{R}{s} + T \bullet s) \qquad (10)$$

The value of Kp=0.6, Ki=0.24 and Kd=0.375 components is found and installed into the systems as figure 8.

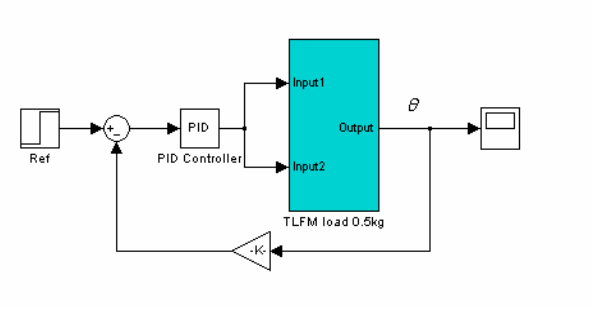

Figure 8. The PID control structure

Figure 9 shows the response of angular positions of link-1 of the system with PID controller and without controller using the step input of 1.5 degrees. As expected, by inserting the controller, the angular position enhances. Moreover overshoot decreases by inserting the PD controller. The vibration of link-1 can be reduced by inserting PID controller. The vibration of angular positions can be reduced by PID controller, for link-1 of 1.53 degrees.

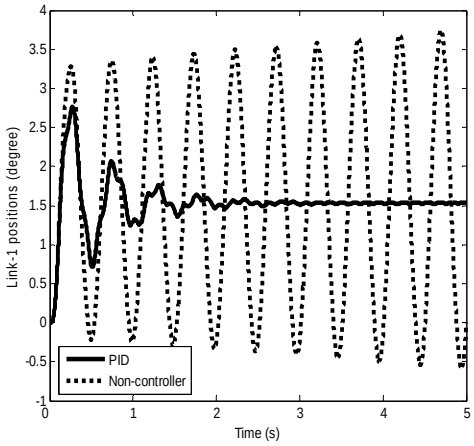

Figure 9. Angular Position of Link-1

Figure 10 shows the response of angular positions of link-2 of the system with PID controller and without controller using the step input of -3 degrees. It is noted the vibrations of link-2 reduce by inserting the PID controller. The angular positions for link-2 is -3.07 degrees.

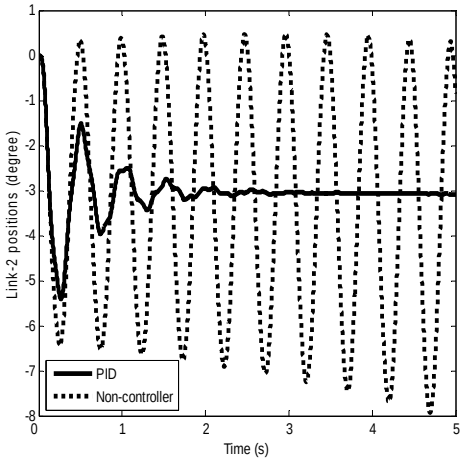

Figure 10. Angular Position of Link-2

5. CONCLUSSION

The development of dynamic model of a two-link flexible manipulator has been presented. The model has been derived using Eular-Lagrange and AMM. Simulation exercises have been conducted with various torque amplitudes to study and verify the performance of the system. A PID controller has been developed for control of a two-link flexible manipulator. It has been demonstrated that reduction in the system vibration with the PID controller.

REFERENCES

[1] Tokhi MO, Mohamed Z, Azad AKM, "Finite difference and finite element approaches to dynamic modelling of a flexible manipulator," Proceeding of IMechE-I: Journal of Systems and Control Engineering, 1997; 211:145-156.

[2] Tokhi MO, Mohamed Z, Shaheed MH, "Dynamic characterization of a flexible manipulator system," Robotica, 2001;19:571-580.

[3] Subudhi B, Morris AS., "Dynamic Modelling, Simulation and Control of a manipulator with flexible links and joints," Robotics and Autonomous System, 2002; 41:257-270.

[4] A. De Luca, B. Siciliano, "Closed-form dynamic model of planar multi-link lightweight robots," IEEE Transactions on Systems, Man, and Cybernetics **21** (4) .1991. 826-839.

[5] A. S. Morris, A. Madani, "Inclusion of Shear Deformation Term to Improve Accuracy in Flexible-Link Robot Modelling", Mechatronics, Vol. 6, No. 6. 1996, pp. 631-647.

[6] Z. Mohammed, J.M. Martins, M.O. Tokhi, J. Sa'da Costa, M.A. Botto, "Vibration control of very flexible manipulator system," Control Engineering Practise 13 (2005), 267-277.

Performance and Evaluation of Sonoelectrolyzer Cell

M.Rosyid Ridlo

Research Center for Physics-Indonesian Institute Of Sciences
Puspiptek Serpong Tangerang
Email: muha041@lipi.go.id

ABSTARCT

In a row with fast development of Fuel Cell device, hydrogen as energy carrier could replace the petrochemical fuel. The challange is to produce hydrogen at a cost competitive with current fuels and morever the hydrogen production methods must use renewable sources and environmental friendly. The last two characteristics can be fulfiled by elelectrolysis method. Furthemore,low cost production could be achieved by increasing the conversion energy efficiency of electrolysis system. At present , ultrasonics energy was used to increase the efficiency. The cell was constructed using 2 cm^2 surface area of nickel cathode/anode with diaphragm between theme, so hydrogen and oxygen gas can be separated in diffrent gasket. The rod of ultrasonics horn was put in the midle of electrodes with max power 80 watt. As electrolyte 36 cm^3 of 5M KOH was used and its temperature can be varied to 60^0 C. The electrical current was adjusted between 100 mA to 1000 mA. The data shows that the energy efficiency increases to about 3 % in comparison with cell without ultrasonics. In this paper the evaluation of ultrasonics effects on the cell performance also be discussed.

Keyword:
hydrogen,electrolysis,ultrasonics,efficiency,energy

1.INTRODUCTION

Due to usage of fossil fuel, the increament of carbon polution is difficult to avoid. In the year 2001, CO2 concentration increase from 280 ppm to be 370 ppm at the area around industries locations [1]. The experts agree the increament of CO2 as principle cause of global warming. To reduce the rate of increase of CO2 concentration, the shift to free emission fuels is necessary. Hydrogen is the excellent choice.
Hydrogen can be produced by water electrolysis method. As electrical source used to separate water molecule come from wind turbine or solar cell energy, so the H2 production system is CO2 free or environmental clean. The process also renewable because of only water is used as input materials. Therefore, this production method is to agree with hydrogen economy concept.
But the efficiency of this method is still low. Efforts have been carried out to increase the efficiency. At present, we try to use ultrasonic energy to increase the efficiency. This idea is based on cavitation fenomena in which from some research results can accelerate the chemical processes.
The preliminary study data show the over potential of cell electrolysis decrease as ultrasonic wave irradiated in electrolyte solution [2-5]. In this paper, we construct cell sono-electrolyzer i.e: the device represents of integration ultrasonic source with cell electrolysis. That cell was equipped with separated hydrogen and oxygen gas channels, so the hydrogen/oxygen production rate can be observed. From the change of hydrogen production rate data, it can be calculated the cell efficiency.

2.EXPERIMENTAL

The cell designed use two nickel electrodes dimension 2 x 1 cm and put paralel with distance 6 mm (fig 1a,b,c)

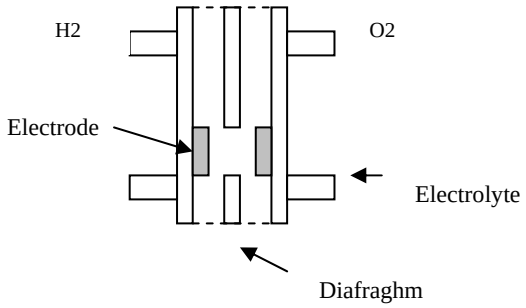

(a)

(b)

Figure :1 Sono -Electrolysis system a: cell schematic, b:photo of the system

5M KOH as electrolyte put into the cell and circulated so the KOH concentration not change during process. The electrolyte volume in the cell is about 6 x 6 x 1 cm and the themperature was kept at 60 C. Here, it could be observed the different of cell performance with or without ultrasonic wave iirradiation on electrolyte. The electrical current source was adjusted from 100 mA to 1 A.

Figure 2: The equipments to test sono electrolyzer cell.

The sono electrolyzer test system set up is pointed out at fig. 3 with ultrasonic frequency is 20 kHz and the maximum power 80 watt. The ultrasonic probe is silinder in the shape 1 cm in diameter.

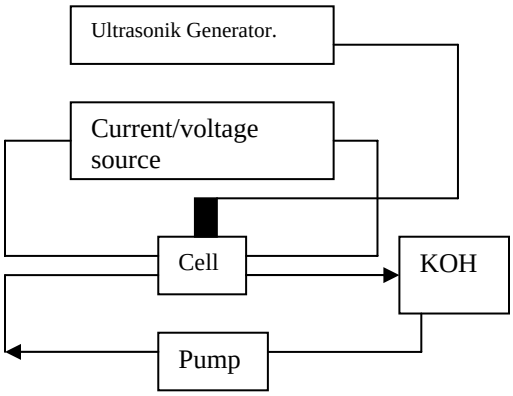

Figure3: Cell performance test model

3.DATA AND ANALYSIS

Fig.4 shows hydrogen production rate increase during ultrasonic irradiation to 0.6 Liter/h.
This fenomena clearly seem at the electrical current reach 1 Amp.

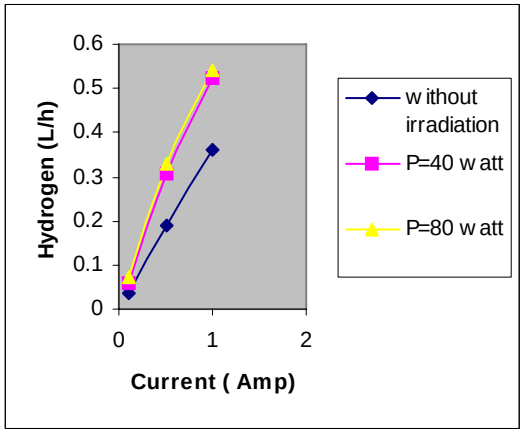

Figure 4: Hydrogen rate production with and without ultrasonic irradiation

From Faraday formula that rate equal the increase in electrical current 0.35 A (fig. 5).

Faraday formula:[6]

$Vol.H_2=R.I.T.t/(F.p.z)$ (1)

Here: R gas constant, I current,T themperature, t time, F faraday constant,p pressure and z =2 (for hydrogen)
This data confirm the preliminary study that this fenomena related existance of the surface electrode characteristic changes .

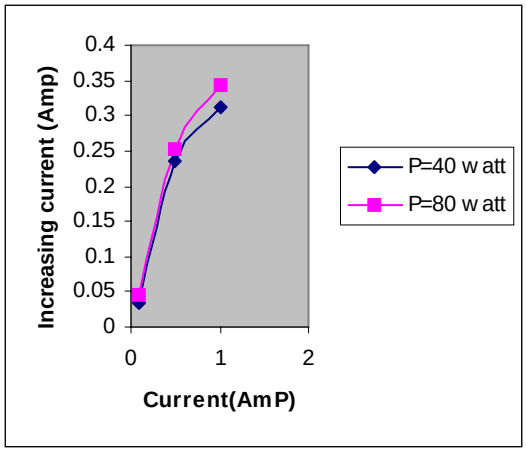

Figure5: Increasing in electrical current during irradiation

However if the ultrasonic power increased two times, but then the production rate do not increase two times too. It was supposed not all ultrasonic power can be converted to increase the current, the other part was wasted in heat form of energy. The ultrasonic energy accept capability probably depend on the electrode dimension. It needs more investigation.
The cell efficiency can be calculated from relation:[6]

$E_{ff}=1.42/celloverpotential$ (2)

More low of overpotensial more efficient of the cell. From fig. 6 it can be seen the overpotensial decrease during irradiation especially at low current.As consequencely, the cell efficiency increase bigger allmost 3% at low current . word, ultrasonic irradiation cause the increase in electrical current. The increasing value do not follow linier propotion of ultrasonik energy. At the cell sono - electrolyzer has been constructed the increase of efficiency is about 3% at low current.
As hypotetical suggestion: for energy balance investigation adding number of the cell is necessary so the ultrasonic energy can be irradiated to all the cell.

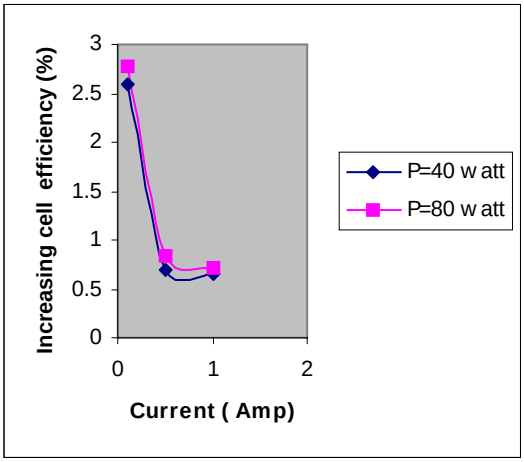

Figure 6: The change in efficiency caused by irradiation

4.Conclusions

Generally, it can be say that the use of ultrasonic energy can increase the hydrogen rate production.

REFERENCES

[1] Sigurvinsion. et all" *On the cost of production hydrogen by alkaline electrolysis*",Proc.Inter.Hydrogen conggerss and exhibition,Turkey 2005
[2] M.Rosyid Ridlo, A Subhan,A Oemry," *Effect of ultrasonic wave On the water electrolysis"*,Proc.Sem.Nas Chemestry,UI Jakarta,2007.
[3] M.Rosyid ridlo et all," *Sonication effect on electrolyte resistance of electrolysis for hydrogen production",* Proc.Nas.Conf,UGM Jogyakarta 2008
[4] M.Rosyid Ridlo et all," *The mechanism of cell overpotensial decreasing caused byultrasonic irradiation*", Proc.Nas.Conf,UPI Bandung 2008.
[5] Cory B et all," *Electroanalityc effect of ultrasound on hydrogen production reaction in KOH"*,Proc.33 rd IEEE Photovoltaic Specialist Conf,USA 2008.
[6] Robert B Dopp," *Hydrogen generation via water electrolyisusing highly efficient nanometal electrode",* www/doppstein.com

ISSN 114-1284

Security Analysis of Smart Card System in Universitas Pelita Harapan

Margaritifera J. I. Tilaar, Ihan Martoyo, Kuniwati Gandi

Electrical Engineering
Universitas Pelita Harapan, Lippo Karawaci, 15811 Tangerang, Indonesia
E-mail : tiaratilaar@yahoo.com, ihan_martoyo@uph.edu, kuniwati@uph.edu

ABSTRACT

Universitas Pelita Harapan (UPH) uses RFID (Radio Frequency Identification) system, also known as smart card, for many applications such as building access, paying fine in the library, paying for food in the Food Junction, identifying books borrowers in the library, and using the copy-machine in the library. Because of the many applications, it is necessary to know whether the smart card is secure enough for those applications. The research was done by trying to figure out the weaknesses and testing the smartcard through its weaknesses. The testing was done in two ways, technical probing and social probing. It was found that there are several flaws in the system implementation using smart card. A security level of RFID system is then proposed based on the mechanism of the access bit. Every application is grouped according to its security level. The probing revealed some data stored in the smart card and the key that is being used in some applications. According to the probing results, the flaws that have been found so far are not critical to the security of the whole system.

Keywords
RFID, security analysis, MIFARE Classic

1. INTRODUCTION

Radio-frequency identification (RFID) is an automatic identification method which can transmit and receive data using devices called RFID tags or transponders. RFID tags consist of two parts. The first is an integrated circuit for storing and processing information, modulating and demodulating RF (radio frequency) signal, and other special functions. The second part is an antenna to receive and transmit signals.

One of international standards, ISO 14443 RFID, controls the use of proximity card (smart card proximity) for identification. ISO 14443 is divided into four sections, which are [1]:

1. Physical characteristics.
2. Characteristics of radio frequency (RF).
3. Protocol for initialization and collision control.
4. Transmission protocol.

The use of RFID systems have become common and varied, ranging from building access-control until payment transaction. It is also being used as a form of identification. Universitas Pelita Harapan (UPH) is one of the institutions that take advantage of RFID systems, which are known as smart cards. Smart card applications in UPH are organized for many activities. UPH smart cards are used for identification cards, instruments for paying fine in the library and for transactions in the Food Junction, for building access, photocopying, printing, and controlling students' meal quota. It can be seen that many applications are using smart card. Therefore, an analysis is conducted to determine the security level of smart card applications in UPH.

UPH smart card is an RFID-based system of MIFARE Standard 1k card. In this work, the security of the system was tested by technical probing, using software and a Universal Reader. Another testing method was the social probing, which took a closer look at the whole operation of the smartcard system to identify its weaknesses. The aim of the work is to reveal the weaknesses in the UPH smart card system. An analysis was also performed to clarify available security levels based on the access conditions of the smart cards. Appropriate security levels for specific applications will be proposed.

2. MIFARE SMART CARD AND UPH APPLICATIONS

2.1 MIFARE Classic Logic Structure

MIFARE Classic Card is in essence a memory card with some additional functionality. The memory on the card is divided into several blocks of data each consisting of 16 bytes. Blocks of data are grouped into sectors. MIFARE Classic 1k has 16 sectors, each sector consists of 4 blocks of data. The last block of data on each sector is called the sector trailer. The schematic of the MIFARE Classic 1k memory is shown in Figure 1.

Block 0 and sector 0 contain special data. The first four bytes of data contain the unique identifier of the card (UID) followed by 1 byte bit count check (BCC). BCC is obtained as a result of applying XOR on all UID bytes. The bytes after the BCC are used to insert the manufacture data. This data block can only be read.

Sector trailer contains key A and B for the authentication process. Access condition determines the operations that can be done in the sector. Sector trailer has special access conditions. Key A can never be read, and key B can be set

to be readable. Beside the access condition (AC) and the key, there is one byte of data (U) that does not have any important meaning. The schematic of the sector trailer is shown in Figure 2.

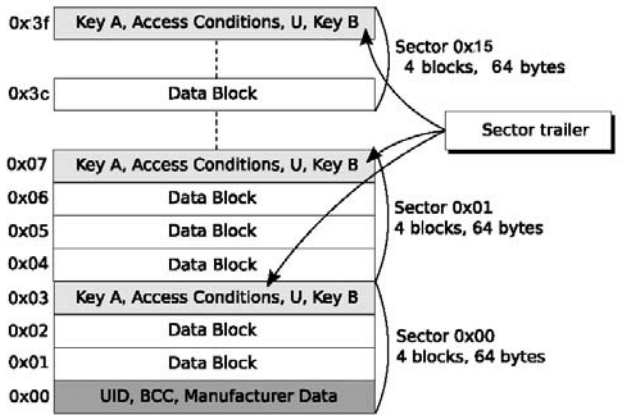

Figure 1: Schematic of MIFARE *Classic* 1k memory [2]

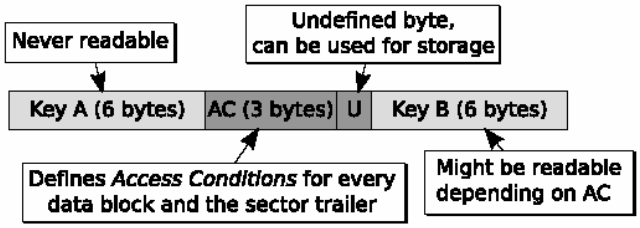

Figure 2: Sector Trailer [2]

There are several commands on the MIFARE Classic to access blocks and sectors. The access condition is always checked each time a command occurs, to determine whether the command can be executed in the requested sector. Read and write commands are for reading or writing one block of data or value blocks. The write command can format a block into a value block or just for storing data only.

The next commands are decrement, increment, restore, and transfer. All commands can only be done in the value block. Increment and decrement commands will increase or decrease the value in the value block with a particular value and save the result in the register memory. Restore command takes the value from the register memory without changing it and then move it to the same or a different block with the command transfer.

2.2. Smart Card Applications in Universitas Pelita Harapan

The first application in UPH is the building access. Here, the smart card is used for opening the door of the library or laboratory facilities such as the English Laboratory. For example, to enter the library, visitors must tap the smart card, which is an RFID tag, to the reader. The reader will check if the card holder can enter the library.

The second application is the identification for borrowing books in the library. The borrowing procedure is started by tapping the smart card to the RFID reader. The content of the smart card is displayed on the screen, and the ID number (NIM) and the name that appear on the display are checked whether they match the data listed on the smart card. Other data that can be seen are the borrowed books, the status of the student and the amount of unpaid fines. Students who are working on their final project may borrow one extra book.

The third application is using the smart card to pay for photocopies. Smart cards are placed on the balance reader of a photocopy machine. The reader checks the balance available to do photocopies. If there were sufficient balance, the photocopy process can be carried out and the balance in the smart card will be reduced according to the number of photocopies. The photocopies balance is different from the micropayment balance.

The fourth application is the fine payment in the library. The smart card is brought to the reader to see the amount of the remaining balance. If the balance is insufficient or the smart card has not been activated for micropayment, it can not be used for paying fine. If there were sufficient balance, it would be debited as much as the fine that must be paid.

The fifth application is the micropayment. Smart cards are charged with some amount of money, and then used for transactions in the Food Junction. The micropayment system is also applicable for the payment of fines in the library.

3. SECURITY ANALYSIS

3.1 Smart Card Types, Personalization and Activation Procedures

The UPH smart card is owned by every staffs and students of UPH. There are some differences between the smart card of students and staffs. The cards for students are printed with red stripes, green stripes are for lecturers and blue stripes for the non-academic staffs. The words “undergraduate”, “faculty” are also printed accordingly.

According to the status or condition of a smart card, it can be divided into:

1. impersonalized smart cards (similar condition to the newly released cards from the factory),
2. smart cards that have been personalized but not activated for micropayment,
3. smart cards that have been activated for micropayment.

The micropayment activation is required so that the smart card can be used for transactions in the Food Junction and paying fine in the library. In addition, the cash balance in the smart card can be exchanged with a number of photocopies in the library.

The physical difference, which distinguishes smart cards that has been activated for micropayment and the one that

has not, is the appearance of a virtual bank account number on the back of the card. The account number of each card is different, which is used to receive and transfer money. Through top-ups the amount of money is added onto the smart card.

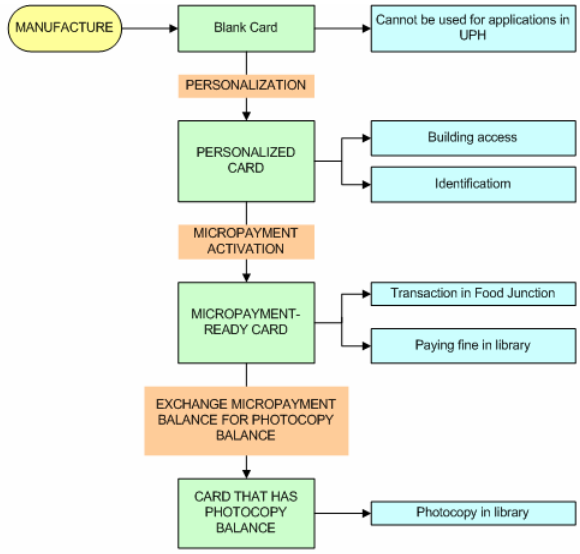

Figure 3: Smart card activation procedure

Smart cards which have not been personalized are in similar conditions to the newly released ones from the factory and contain only the UID. This type of smart cards can not be used for any application in UPH. The content of this smart card can be accessed with the key A: FFFFFFFFFFFF. In this kind of smart card the content from sector 1 until sector 15 is the same as sector 0 except for block 0. The sector 0 block 0 contains the UID, whereas block 0 in sector 1 until sector 15 are still empty, as well as the data on sector 0 block 1 and block 2. Block 3 in each sector contains the access bits that set the access configuration of that sector. Access bits for sector 0 until 15 are FF0780. The key A can not be displayed, therefore the reader indicates 0000000000000 as a result. The key B is not used and the content of the data is FFFFFFFFFFFF.

After the personalization, the smart card can be used for identification and to access the library or a specific room. The change in the card after the personalization is resulted from some new data stored through the personalization process. Additionally, all access bits are changed. The only sector that can be read using the universal key A: A0A1A2A3A4A5 is only sector 4.

Results from reading sector 4 showed that the data are in ASCII (HEX). Examples of the reading of sector 4 are shown as follows:

Block 0:
ASCII (HEX) : 303332323030343030323307E7E7E7E7E
Character : 03220040020~~~~~
Block 1:
ASCII (HEX) : 7E7E7E7E7E7E4D617267617269746966
Character : ~~~~~~Margaritif
Block 2:
ASCII (HEX) : 6572612054696C6161727E7E30303100
Character : era Tilaar~~001

From the results of the reading, block 0 contains the student number, block 1 and 2 contain the name of the student. Sector 4 in the lecturer's smart card was also read. The results show differences in the pattern of data between smart card for lecturers and students, and basically the content of sector 4 remains the same, namely the number and the name of the owner. After the personalization, the smart card can be activated for micropayment. The sector 0 on the micropayment-ready smart card can be read with the key A: A0A1A2A3A4A5.

Contents of block 0 until block 2 in the sector 0 do not change through personalization. However, the difference can be seen in block 3, which is a sector trailer. The access bits, which were initially FF0780 are changed to F78780. In addition, the byte where key B is stored, is no longer readable (the data show 0000000000000). This indicates that the key B is used to process the data exchange between tag and reader. For security reasons the key B is showed to be unreadable. Thus it can be concluded that the smart card system of UPH is using the two keys for security purposes.

.

Table 1: Comparison of smart card types in UPH

Comparison Factor	Impersonalized	Personalized	Activated for Micropayment
Key A	FFFFFFFFFFFF.	Key A is different for each sector.	Key A is different for each sector.
	Can read all sectors.	The use of key A in each sector is different, depends on the access bits.	The use of key A in each sector is different, depends on the access bits.
	Can modify all blocks in sector 0 except for block 0.		
Key B	Unused.	Key B is used, but remains unknown.	Key B is used, but remains unknown.
Access bits	Access bits for all sectors are same, FF0780.	Access bits for each sector can be different.	Access bits for each sector can be different.
Sector 0	Can be accessed using key A, FFFFFFFFFFFF.	Cannot be accessed because keys are unknown.	Can be accessed using key A, A01A2A3A4A5.
	Access bits are FF0780.	Access bits are unknown.	Access bits are F78780.
	Data block contains nothing except for block 0.	Data block contains nothing except for block 0.	Data block contains nothing except for block 0.
Sector 4	Can be accessed using key A, FFFFFFFFFFFF.	Can be accessed using key A, A01A2A3A4 A5.	Can be accessed using key A, A01A2A3A4A5.
	Block data contains nothing.	Block data contains name and ID number.	Block data contains name and ID number.
	Access bits are FF0780.	Access bits are 878787.	Access bits are 878787.
Other sectors	The condition is the same as sector 0 and 4.	Cannot be accessed because keys are unknown.	Cannot be accessed because keys are unknown.

3.2 Security Test for UPH Smart Card

The security test was done by changing the contents of the data block and the key on the card whose contents can still be modified. This includes testing the security of the smart card implementation such as:

1. building access (the library and the English language laboratory),
2. personalization test using card that has been altered,
3. identification for borrowing books in the library,
4. micropayment.

Smart card that can be used for building access is the one that has been personalized. Therefore, this application's security was tested using empty card, which could not be used for any application in UPH.

The attempts were done by:

1. changing the key of sectors 0 to 15 in the blank card,
2. changing the contents of data block in sector 4 in accordance with the contents of one of the smart card that has been personalized.

Test results indicate that the card that has not been personalized can not give access to the library even though the key was changed to another default key. Changing the contents of sector 4 gave the same result. Thus, it can be concluded that the sector 4 does not set the ability of the smart card for building access.

The next test is to find out whether we can impair (or possibly) destroy the function of the smartcard by simply changing the key or the data. The content and key of pre-personalized smart card were modified; the smart card was then handed over for personalization. As the key A was changed, the reader could not read the contents of the smart card. However, there is an option in the personalization program that can restore the initial condition of the smart card. The key A can be reset to FFFFFFFFFFFF. Thus, the threat is not very meaningful for the UPH smart card system.

The security test for identification is to determine whether the blank card can be used for identification by changing the content of sector 4, which contains the name and the ID number of the card owner. The security test was done using a smart card that has not been personalized. This proved successful because the smart card owner can display his ID in the library, although the card is not personalized. This shows the existence of a threat, in which someone can use a blank card to borrow books using the name of another person, provided he/she gets passed the library door without using a smart card.

The next test is the probing of the micropayment security using an impersonalized card. Before handed over for personalization, the blank smart card data were filled with specific patterns. Each data block is filled with specific data following a certain pattern according to the location of the data block. It was hoped that the personalization process will not reset the data to zero, thus some sectors may still contain the data. The data with the pattern were intended to reveal the micropayment sector through the pattern. However, after personalization and activation for micropayment, the balance in the smart card remains zero. With the results and the limited knowledge about the sector that stores micropayment data, it can be concluded that there is no significant threat to the security of the micropayment system.

3.3 Configurations of Sectors and Blocks

One sector has 12 access bits. These access bits are divided into four groups, each group consists of three bits. Each group set up the configuration of one block. The first three groups (C10C20C30, C11C21C31, and C12C22C32) contain data access bits, and the last group (C13C23C33) contains trailer access bits.

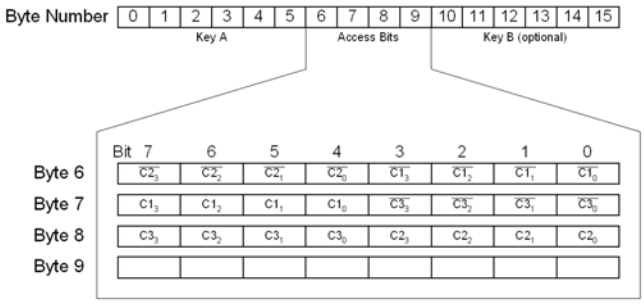

Figure 4: Access Bits [3]

The sector trailer can be set into three conditions based on the access bits. Sector trailers with the access bits 001, 011, 101 are in fluid condition, where the access bits can be replaced by knowing the correct key. Sector trailers with the access bits 000 and 100 are on restricted condition, where the access bits and the free byte can not be changed, but the key can still be changed. The last condition is frozen condition, with the access bits 010, 110, 111, where the sector trailer can not be modified anymore.

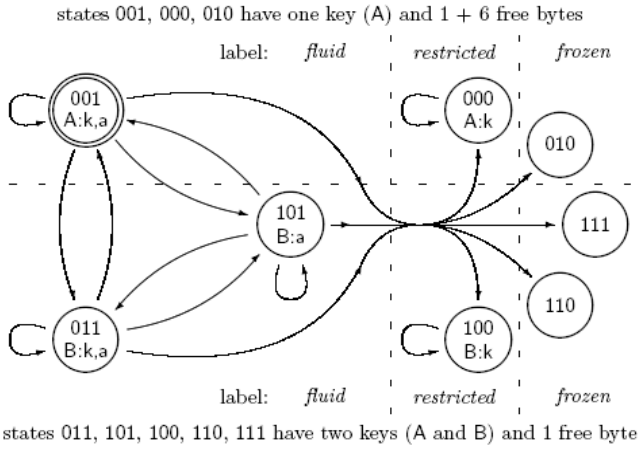

Figure 5: Diagram of state transition of trailer access bits [4]

ISSN 114-1284

The available setting for the data block is rather different from the sector trailer. The dead condition for the data block means that it can not be accessed at all. While the frozen condition means that it can only be read. Restricted condition means that the block content can be changed, but cannot be changed to all conditions. The fluid condition offers the highest freedom, which means that the block content can be changed to any conditions. All these settings for the data block are shown in Table 2.

Table 2: Data access bits [4]

$C1_3C2_3C3_3$	one-key, i.e. 000, 001*, 010		Two-key, i.e. 011, 100, 101, 110, 111		
$C1_jC2_jC3_j$	A	label	A	B	label
000*	r w d i	Fluid	r w d i	r w d i	fluid
110	r d	restricted	r d	r w d i	Fluid
100	R	frozen	r	r w	fluid
011		Dead		r w	fluid
001	r d	restricted	r d	r d	restricted
010	R	frozen	r	r	frozen
101		Dead		r	frozen
111		Dead			dead

3.4 Security Level of Smart Card

By setting the access bits configuration of data blocks and sectors, various security levels for smart card implementations can be setup. Because smart cards are used for a variety of applications where each application requires a different level of security, a general security scheme can be helpful. Such general security scheme is shown in Table 3.

Table 3: Smart card security level

Security Level	Description
A	• Access bits cannot be changed. • Keys can be changed. • Data block cannot be modified, can be read only.
B	• Access bits cannot be changed. • Key can be changed. • Block can be changed but only to certain values (read and decrement).
C	• Access bits cannot be changed. • Keys can be changed. • Data block can be changed (read dan write).
D	• Access bits cannot be changed. • Keys can be changed. • Data block can be changed (read, write, decrement, increment).
E	• Access bits can be changed, where trailer access bits and data access bits are in fluid condition. • Keys can be arranged so that can be changed or not by changing access bits.

Considering the access bits, the keys and the configuration capabilities of the blocks and sectors, there are many possible setups for a sector. However, there are several considerations that can be used as guidelines for RFID applications. First, it is not recommended to use only one key (key A). With one key configuration, there are only three available options for the trailer access bits, namely 001, 000, 010. In addition, if only key A is used, the bytes for key B becomes a data block and it is readable. This is quite dangerous especially if the access bits can be replaced. The key B can therefore be replaced, and the access bits can be modified to a state requiring the key B. Thus the reader that has been programmed to only use the key A, cannot recognize the tags that have been modified.

Another important consideration is that the trailer access bits should not be in the frozen conditions. If key leakage occurs, the key of all operating tags can still be replaced. Frozen conditions make the modification of access bits and keys impossible. Similar to that, the data access bits should not be in the dead conditions. In this case the data block is not accessible. Non-operating smart card should better be destroyed physically.

With these three considerations, the options for smart card configurations are simplified. This configuration determines the security level that can be seen in Table 3. According to this scheme, the building access application is quite safe because using the UID of the smart card makes duplication rather difficult. It requires more than tempering with the data block with a universal reader,

For the identification application, the data block should better be in the frozen condition, as the name and ID number may not change, and the trailer access bits should be set in the restricted conditions so that the access bits can not be modified. This is the security level A.

For the micropayment, access bits should be in a fluid state so it is easy to change the data block. The trailer access bits should be at 101 state so that the key can not be replaced, unless the state changes. The data block or value block state should be changeable according to the smart card condition. While smart cards are in the hands of users and are not used, the value block should be in the restricted or frozen state. When the card is used for transaction, the value block becomes restricted when previously frozen, or remains unchanged when previously restricted. When the checking of the remaining balance or the top-up transfer takes place, the value block should be changed to the fluid state, which is 000 or 110. Then the procedure continues to check the content of value block or increases the data in the value block if top-up transfer was done. Once completed, the access bits of the value block are returned to 001.

4. CONCLUSIONS

The testing of Universitas Pelita Harapan (UPH) smart card system reveals no critical security threads which can be exploited by a simple tempering of the smart cards. Each smart card application in UPH occupies a different sector in the smart card. The smart card data are stored in the form of ASCII hex. The application for identification, whose data located in sector 4, shows a weakness. One can falsify his identity in the process of borrowing books in the library. However, this weakness can be simply patched by making

sure that all distributed smart cards are personalized with the security level A.

No serious weakness was found in the building access application. The sector for the micropayment application cannot be identified through simple observation and tempering using a universal reader. It has also been discovered that the micropayment application is using both the key A and key B, thus ensuring more security of the system. Various security levels have also been proposed by analyzing the access configurations for the data and the keys.

REFERENCES

[1] "ISO 14443", International Organization for Standardization, http://www.otiglobal.com/objects/ISO%2014443%20WP%204.11.pdf, accessed on Oct 27, 2008.
[2] G. De Koning Gans, J. Hoepman, F. D. Garcia, "A Practical Attack on the MIFARE Classic", Computing Science Department, Radboud University Nijmegen, The Netherlands, 2008, http://www.sos.cs.ru.nl/applications/rfid/2008-cardis.pdf, accessed on Sept 15, 2008.
[3] "MF1 IC S50 Functional Specification", NXP Phillips, http://www.nxp.com/acrobat_download/other/identification/M001053_MF1ICS50_rev5_3.pdf, accessed on Dec 26 2008.
[4] W. Teepe, "Making the Best of Mifare Classic", Computing Science Department, Radboud University Nijmegen, The Netherlands, 2008, http://www.sos.cs.ru.nl/applications/rfid/2008-thebest-updated.pdf, accessed on Nov 19, 2008.
[5] K. Finkenzeller, *RFID Handbook: Fundamentals and Applications in Contactless Smart Cards and Identification*, Translated by R. Waddington, West Sussex: John Wiley & Sons, Inc., 2003.
[6] W. Mao, *Modern Cryptograhy: Theory and Practice*, New Jersey: Prentice-Hall, 2003.
[7] "Standing Document ", Working Group 8, ISO/IEC, http://wg8.de/sd1.html, accessed on Oct 20, 2008.
[8] J. N. Wibowo, *Analisis Keamanan Sistem RFID Berbasis MIFARE (*Security Analysis of MIFARE Based RFID System), Thesis, Karawaci: Universitas Pelita Harapan, 2008.

ISSN 114-1284

Mobile Robot with Prospective Memory for manufacturing

P.Velrajkumar[a], Dr.CK Loo[b], Dr.EK Wong[c], Dr.Srinivasan Purushothaman[d]

[a,b,c,d]*Faculty of Engineering and Technology*
Multimedia University, Melaka, Malaysia
[a]*E-mail : p.velrajkumar@mmu.edu.my*

ABSTRACT

This research work implements a robot for monitoring of production machines status in an industrial environment. The robot acts as the supervisor and switches a machine on when a task has to be done by the machine. In any case the machine is in idle status, it will be switched off by the robot. Video information of the cell path through which the robot is moving and the sounds from the turning machines have been used. The sounds acquired have been analyzed using cepstral analysis and the video information is processed with contextual clustering. An initial approach has been attempted and improvements leading to accuracy of recognition have to be done.

Keywords

Mobile robot, Prospective memory, Contextual clustering, Cepstrum analysis

1. INTRODUCTION

Mobile robots play an important role in executing herculus task that cannot be handled by human without extra protection for himself. Some of the situations like rumbled buildings, chemical handling, ore mining, underwater navigation where human cannot execute tasks by frequently sacrificing his life due to one form of natural accidents, that prevails. As such the concept of robot developed in one form or other have not really catered to human requirements without his assistance in the form of tele-control, wireless control. The robots can self navigate only in a safe environment without human assistance.

Existing robot that have been developed are mostly fixated to a place and they do repeated job in industry by rotating through an axis. Robots that have been developed for exploring purposes are not full-fledged in performing extreme tasks. They have predefined tasks. In this research work, Prospective Memory (PM) based tasks that warrant exposure to various information which must have been coded into the memory is implemented. Prospective Memory is the ability to remember and recollect to do things in the future (e.g., remembering a machining operation or loading / unloading operation at a given time on particular day, when robot is on move).

Given a sequence of manufacturing oriented tasks to the robot, it has to execute as and when required and it is not time based and it is occasion based, meaning task-1 will be executed when a situation comes across to definitely execute task-1 while performing task-2 to task-n.

An attempt is made to explore and find the possibilities of how to make a real time robot which can sense manufacturing information from machines by capturing the sound waves emanated at different frequencies. The waves emanated can be from heat, grease or oil odor from the work piece, type of machine, size of the object (surface area of the object) and many more.

In order to really implement a robot that can self navigate by understanding the environment, a combination of sensors that can do collaborative signal processing (CSP) using the different types of information received from the environment have to be implemented.

Herman et.al [1] tried to cast the phenomenon of cue-dependent prospective memory into a conceptual form, which can furthermore be cast into a mathematical description that eventually can be implemented on the computer. More specifically, the above formalism was developed in a way that allows a realization of the parallel synergetic neural network specified by Haken (1991) in synergetic computers and cognition, as well as on a serial computer whose output mimics the process of self organization. In this way, it might serve as a model of a real brain that operates by means of self-organization rather than by computer programs.

Recent recordings of place field activity in rodent hippocampus have revealed correlates of current, recent past, and imminent future events in spatial memory tasks. To analyze these properties, a brain-based device has been used. Darwin XI that incorporated a detailed model of medial temporal structures shaped by experience-dependent synaptic activity. Darwin XI was tested on a plus maze in which it approached a goal arm from different start arms. In the task, a journey corresponded to the route from a particular starting point to a particular goal. During maze navigation, the device developed place-dependent responses in its simulated hippocampus. Journey-dependent place fields, whose activity differed in different journeys through the same maze arm, were found in the recordings of simulated cortical sensory area (*CA1)* neuronal units. An approximately equal number of journey-independent place fields were found. The

journey-dependent responses were either retrospective, where activity was present in the goal arm, or prospective, where activity was present in the start arm. Detailed analysis of network dynamics of the neural simulation during behavior revealed that many different neural pathways could stimulate any single *CA1* unit. That analysis also revealed that place activity was driven more by hippocampal and entorhinal cortical influences than by sensory cortical input. Moreover, journey-dependent activity was driven more strongly by hippocampal influence than journey-independent activity. [2]

The Cellular Nonlinear Networks (CNN) wave based computation is an approach for real time robot navigation in a complex environment based on the idea of considering the environment in which the robot moves as an excitable medium. Obstacles represent the sources of auto wave generation. The waveform propagating in the CNN medium provides to the robot all the information to achieve an adaptive motion avoiding the obstacles. Arena et.al [3] implements entirely this strategy on the ACE16K CNN-chip.

Teruko et.al [4] aims at development of sensors for small size indoor mobile robots. A new sonar-ring which can measure accurate direction and distance to reflecting points rapidly for this purpose has been proposed. This new sonar ring needs to receive echo signal by multiple receivers and to detect multiple Time-of-Flights (TOFs) in received signal at each receiver simultaneously for achieving fast and accurate measurement. It is **i**mpossible to satisfy them by conventional circuit.

For the perception of spatial arrangements, Heiko Hoffman [5] demonstrates that this concept can be realized in a mobile robot. The robot first learned to predict how its visual input changes under movement commands. With this ability, two perceptual tasks could be solved: judging the distance to an obstacle in front by 'mentally' simulating a movement toward the obstacle and recognizing a dead end by simulating either an obstacle-avoidance algorithm or a recursive search for an exit. A simulated movement contained a series of prediction steps. In each step, a multilayer perceptron anticipated the next image, which, however, became increasingly noisy. To denoise an image, it was split into patches, and each patch was projected onto a manifold obtained by modeling the density of the distribution of training patches with a mixture of Gaussian functions.

Memory-based methods estimate self-location by directly comparing the input image with stored images in memory. This approach has received much attention, because the localization accuracy will increase by simply increasing the number of images to memorize. A novel self-localization method based on eigenspace analysis as one of memory-based methods has been proposed. An omni directional image sensor that can take an image of surrounding environment of the sensor at video-rate has been used. The proposed method identifies the sensor's location by evaluating the similarity between autocorrelation images which are converted from omni directional images and are invariant against the rotation of the sensor. To reduce the computational cost and memory space, autocorrelation images are projected into eigenspaces. The similarity is evaluated in eigenspaces to reduce the computational cost. The experimental results show that our method is capable of estimating the location of sensor even with low dimensional images. [6].

A new technique for vision-based robot navigation has been proposed. The basic framework is to localize the robot by comparing images taken at its current location with reference images stored in its memory. The only sensor mounted on the robot is an omni directional camera. The Fourier components of the omni directional image provide a signature for the views acquired by the robot and can be used to simplify the solution to the robot navigation problem. The proposed system can calculate the robot position with variable accuracy ("hierarchical localization") saving computational time when the robot does not need a precise localization (e.g. when it is traveling through a clear space). In addition, the system is able to self-organize its visual memory of the environment. The self-organization of visual memory is essential to realize a fully autonomous robot that is able to navigate in an unexplored environment. Experimental evidence of the robustness of this system is given in unmodified office environments. [7]

Yoshio et.al [8] applied the omni directional vision sensor to their view-based navigation method and proposes an extended model of a route called the "omni view sequence." Secondly we propose a map named the "view-sequenced map" which represents an entire corridor environment in a building. A method for the automatic acquisition of a view-sequenced map based on the exploration in a corridor using both stereo and omni directional vision is also described. Finally experimental results of the autonomous navigation and the map acquisition are presented to show the feasibility of the proposed methods.

2. SCHEMATIC DIAGRAM

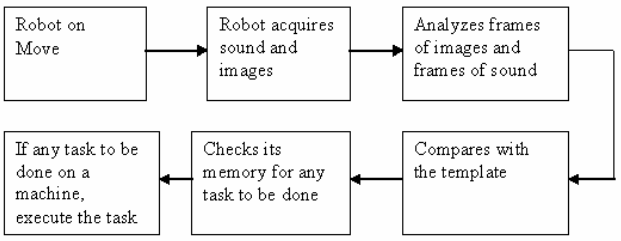

3. CEPSTRUM ANALYSIS

Cepstral analysis is an important tool for processing nonlinear sound signal. This separates high frequency

noise from low frequency information signals. In this work, cepstrum analysis is used.

Steps involved in converting sound data are given below:

1. Acquire sound data at 44 KHz.
2. Remove zeros which does not give any information.
3. Apply linear predictive analysis.
4. Apply fast Fourier transform.
5. Apply log for the output in step 4.
6. Apply inverse fast Fourier transform.
7. Apply levinson Durban equation.
8. Repeat step 3 to step 7 for every 10 samples of the data acquired from microphone and average all values to finally get only 10 values.
9. Label the 10 features of each sound wave.
10. Repeat step 9 for 4 different working conditions of the machine. The labeling of each condition will be (1 – 4).

4. CONTEXTUAL CLUSTERING

Segmentation refers to the process of partitioning a digital image into multiple regions (sets of pixels). The goal of segmentation is to simplify and/or change the representation of an image into something that is more meaningful and easier to analyze. Image segmentation is typically used to locate objects and boundaries (lines, curves, etc.) in images. The result of image segmentation is a set of regions that collectively cover the entire image, or a set of contours extracted from the image. Each of the pixels in a region are similar with respect to some characteristic or computed property, such as color, intensity, or texture. Adjacent regions are significantly different with respect to the same characteristics. Several general-purpose algorithms and techniques have been developed for image segmentation.

Contextual clustering algorithms which segments an image into background (ω_0) and object region (ω_1). The pixel intensities of the background are assumed to be drawn from standard normal distribution.

1. Define decision parameter T_{cc} (positive) and weight of neighbourhood information β (positive). Let N_n be the total number of pixels in the neighbourhood. Let Z_i be the intensity value of pixel i.
2. Initialization: classify pixel with $z_i > T_\alpha$ to ω_1 and pixels to ω_0. Store the classification to C_0 and C_1.
3. For each pixel I, count the number of pixels u_i, belonging to class ω_1 in the neighbourhood of pixel i. Assume that the pixels outside the image area belong to ω_0.
4. Classify pixels with $z_i + \frac{\beta}{T_{cc}}(u_i - \frac{N_n}{2}) > T_\alpha$ to ω_1 and other pixels to ω_0. Store the classification to variable C_2.
5. If $C_2 \neq C_1$ and $C_2 \neq C_0$, copy C_1 to C_0, C_2 to C_1 and return to step 3, otherwise stop and return to C_2.

5. EXPERIMENTAL DATA

The experimental setup includes collection of sound from the turning machine under four different conditions: Tool approaching job (Figure 1), Spindle rotates (Figure 2), Machining taking place (Figure 3), Machine starting (Figure 4). The sound were collected using PCB 130 series of Array Microphones coupled with ICP sensor powered preamps and are thus referred to as ICP microphones. The 130 series provide an extremely cost effective method for large channel count sound pressure measurements.

Similarly video taken during the movement of robot along the cell is shown in Figure 5. Only 15 frames are shown due to space availability. The video has been taken using the special digital camera meant to be used on the real time robot.

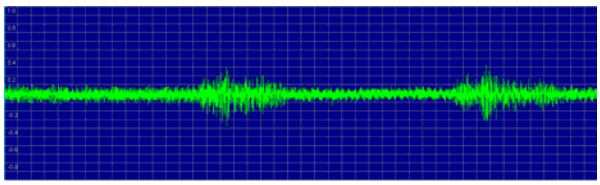

Figure 1: Tool approaching job

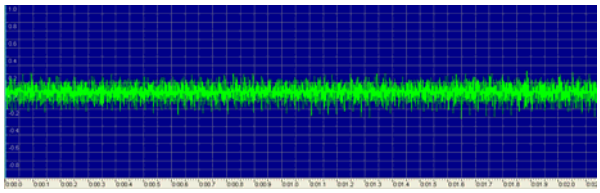

Figure 2: Spindle rotates

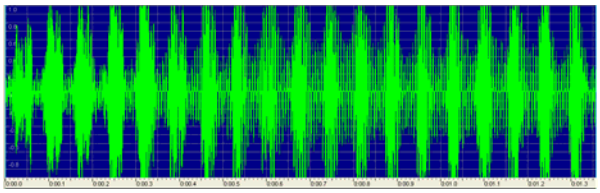

Figure 3: Machining taking place

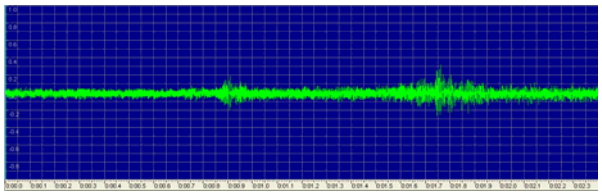

Figure 4: Machine starting

Figure 5: A portion of video shots taken along the cell path

Figure 6: Contextual clustering segmented images

6. RESULTS AND DISCUSSIONS

6.1 Cepstrum analysis

Table 1 shows 10 cepstral values for Figures (1 – 4). The cepstral vectors are different for different sound signal. The vectors will be used as template for comparison.

Table 1: Cepstral coefficients for Figures (1- 4)

Tool approaching job	1.0000,1.9944,-0.1634, -1.2007,-1.8690,0.0126, 1.8437,1.1752,-0.3709, -1.9715
Spindle rotates	1.0000,-8.8539,-7.6612, 6.9310,13.5889,0.7697, -13.2264,-8.2355,6.6355, 10.1756
Machining taking place	1.0000,-0.0028,-0.1553, 0.4935,0.6979,0.2659, 0.3036,0.2567,0.2308, 0.1333
Machine starting	1.0000,1.9142,0.3560, -8.6024,0.0607,11.5663, -0.8703,-8.7402,1.0950 2.3649

6.2 Output of Contextual clustering

The video frames segmented by contextual clustering are shown in Figure 6. The black patched outputs indicate the path through which the robot is moving.

The microphone and the video camera fitted with the robot acquires sound and images and process them for easy navigation of the robot and for the robot to recognize different sounds coming from the machine. Any task that has been preloaded into the memory of robot will be used as Prospective Memory to implement tasks during its movement.

7. CONCLUSION:

In this work, sounds and video have been acquired during the movement of robot in an industrial environment. The robot can identify its path based on information in the video and can recognize different sounds from the machines. There is lot of improvements that have to be done as part of improvements in the robot performances.

REFERENCES:

[1] Herman Haken, Juval Portugali, 2005 “A synergetic interpretation of cue-dependent prospective memory” Cogn Process (2005) 6: Pp 87 – 97.

[2] Jason G. Fleischer, Joseph A. Gally, Gerald M. Edelman, and Jeffrey l. Krichman, 2007 “Retrospective and prospective responses arising in a modeled hippocampus during maze navigation by a brain-based device”, PNAS, Vol. 104 no.9, Pp 3556 – 3561.

[3] P.Arena, L.Fortuna, M.Frasca, G.Vagliasindi, A.Basile, M.E.Yalsin, J.A.K.suykens, 2005, “CNN Wave based computation for robot navigation on ACE16K”, IEEE, pp 5818 – 5821

[4] Teruko YATA, Akihisa OHYA, Shin'ichi YUTA, 2000, “Using one bit wave memory for mobile robots' new sonar-ring sensors”, IEEE International conference on systems, Man and Cybernetics, Vol.5, Pp 3562 - 3567.

[5] Heiko Hoffmann, 2007, “Perception through Visuomotor Anticipation in a Mobile Robot” Neural Networks, Elsevier Science, Vol.20, Issue 1, Pp 22 – 33.

[6] Nobuhiro Aihara, Hidehiko Iwasa, Naokazu Yokoya, and Haruo Takemura, 1998, “Memory-Based Self-Localization Using Omni directional Images”, Proceedings, 14th International conference on pattern recognition, Vol.2, Pp 1799 – 1803.

[7] Emanuele Menegatti, Takeshi Maeda and Hiroshi Ishiguro, 2004, “Image-based memory for robot navigation using

properties of omni directional images", Elsevier Science, Vol.47, Issue 4, Pp 251 - 267.

[8] Yoshio Matsumoto, Masayuki Inaba, Hirochika Inoue, 2003, "View-based navigation using an omni view sequence in a corridor environment", Machine Vision and Applications, Volume 14 , Issue 2 , Pp 121 – 128, 2003.

Proceeding of the 11th International Conference on QiR (Quality in Research)
Faculty of Engineering, University of Indonesia, Depok, Indonesia, 3-6 August 2009
ISSN 114-1284

Discontinuous Galerkin Method for Solving Steady and Unsteady Incompressible Navier Stokes Equations

Pranowo[a,b], A. Gatot Bintoro[c], & Deendarlianto[d]

[a] [a]Ph.D. Student of the Department of Electrical Engineering, Faculty of Engineering, Gadjah Mada University, Jalan Grafika No. 2, Yogyakarta 55281, Indonesia

[b]Lecturer of the Department of Informatics Engineering, Yogyakarta Atma Jaya University, Jl. Babarsari 43, Yogyakarta 55281, Indonesia.
Email: pran@mail.uajy.ac.id

[c]Lecturer of the Department of Industrial Engineering, Yogyakarta Atma Jaya University, Jl. Babarsari 43, Yogyakarta 55281, Indonesia.

[d]Lecturer of the Department of Mechanical and Industrial Engineering, Gadjah Mada University, Jalan Grafika No. 2, Yogyakarta 55281, Indonesia

ABSTRACT

Purpose: *To develop high order discontinuous galerkin method for solving steady and unsteady incompressible flow based on artificial compressibility method.*
Design/methodology/approach: *This paper uses discontinuous galerkin finite element procedure which is based on the artificial compressibility technique in connection with a dual time stepping approach. A second order implicit discretization is applied to achieve the required accuracy in real time while an explicit low storage fourth order Runge Kutta scheme is used to march in the pseudo-time domain. A nodal high order discontinuous galerkin finite element is used for the spatial discretization.*
Findings: *Provides stable and accurate methods for solving incompressible viscous flows compared with previous numerical results and experimental results.*
Research limitations: *It is limited to two-dimensional steady and unsteady laminar viscous flow.*
Practical implications *– A very useful source of information and favorable advice for people is applied to piping system and low speed aerodynamics.*
Originality*: This works presents an extension of the previous work of [1] and [2] to time and space accurate method for solving unsteady incompressible flows.*

Keywords: *steady and unsteady flows, discontinuous galerkin, artificial compressibility.*

1. INTRODUCTION

Numerical Solutions of the incompressible Navier-Stokes equations are of interest in many engineering applications. Problems which can be addressed by incompressible Navier-Stokes equations include internal flows, hydrodynamics flows, low speed aerodynamics and external flows. There is a continuing interest in finding solution methodologies which will produce accurate results in time and space. The problem of coupling changes in the velocity field with changes in pressure field while satisfying the continuity equation is the main difficulty in obtaining solutions to the incompressible Navier-Stokes.

There are two types of method using primitive variables which have been developed to solve the equations. The first type of methods can be classified as pressure-based methods. In these methods, the pressure field is solved by combining the momentum and mass continuity equations for form a pressure or pressure-correction equation. The second type of methods employs the artificial compressibility (AC) formulation. This idea was first introduced by Chorin [3] and extensively used by other researchers since. In this method, a pseudo-temporal pressure terms is added to continuity equation to impose the incompressibility constraint. Several authors have employed this method successfully in computing unsteady problems.

The original version of the AC method is only accurate for steady-state solutions to the incompressible flows [4, 5], however there are some efforts which conducted to solve unsteady flows using dual time stepping AC method. Reference [6] used third order flux difference technique for convective terms and second-order central difference for viscous terms. The semi discrete equations are solved implicitly by using block line-relaxation scheme. Reference [1] used finite element method for spatial discretization. A second-order discretization is employed in real time while an explicit multistage Runge Kutta is used to march in pseudo time domain.

This work presents an extension of the previous work of [1, 2] to time and space accurate method for solving unsteady incompressible flows. A nodal high order discontinuous galerkin finite element is used for the spatial discretization a second order implicit discretization is applied to achieve the required accuracy in real time while an explicit low storage fourth order Runge Kutta scheme is used to march in the pseudo-time domain. The computed results show accuracy of the code by presenting the steady and unsteady flow past a 2-dimensional circular cylinder.

2. PROBLEM DESCRIPTION

Artificial compressibility method is introduced by adding a time derivative of pressure to the continuity equation. In the steady-state formulation, the equations are marched in a time-like fashion until the divergence of velocity vanishes. The time variable for this process no longer represents physical time. Therefore, in the momentum equations t is replaced with τ , which can be thought of as an artificial time or iteration parameter [7]. As a result, the governing equations can be written in the following form:

$$\frac{\partial \mathbf{U}}{\partial \tau}+\frac{\partial \mathbf{F}^j}{\partial x_j}+\frac{\partial \mathbf{G}^j}{\partial x_j}=0\ , \quad j=1,2 \tag{1}$$

Where

$$\mathbf{U}=\begin{bmatrix} p \\ u_1 \\ u_2 \end{bmatrix} \quad \mathbf{F}^j=\begin{bmatrix} \varepsilon^2 u_j \\ u_1u_j+p\delta_{1j} \\ u_2u_j+p\delta_{2j} \end{bmatrix} \quad \mathbf{G}^j=\begin{bmatrix} 0 \\ \tau_{1j} \\ \tau_{2j} \end{bmatrix} \quad \tau_{ij}=\frac{1}{\mathrm{Re}}\left(\frac{\partial u_i}{\partial x_j}+\frac{\partial u_j}{\partial x_i}\right) \tag{2}$$

In these equations, τ is the artificial time variable, u_i is the velocity in direction x_i, p is the pressure, τ_{ij} is stress tensor, ε is an artificial compressibility parameter, δ_{ij} is Kronecker delta and Re is the Reynolds number.

The extension of artificial compressibility method to unsteady flow is introduced by adding physical time derivative of velocity components to 2 momentum equations in Equations (2) [6, 1]. The obtained equations can be written as:

$$\frac{\partial \mathbf{U}}{\partial \tau}+\mathbf{I}^M\frac{\partial \mathbf{U}}{\partial t}+\frac{\partial \mathbf{F}^j}{\partial x_j}+\frac{\partial \mathbf{G}^j}{\partial x_j}=0\ , \quad j=1,2 \tag{3}$$

Where

$$\mathbf{I}^M=\begin{bmatrix} 0 & 0 & 0 \\ 0 & 1 & 0 \\ 0 & 0 & 1 \end{bmatrix}$$

3. DISCRETIZATION

The spatial derivatives are discretized by using a discontinuous galerkin method. The simplified of Eq. (3) according to Galerkin's procedure using the same basis function ϕ within each element is defined below:

$$\begin{aligned} &\left(\phi,\frac{\partial \mathbf{U}}{\partial \tau}+\mathbf{I}^M\frac{\partial \mathbf{U}}{\partial t}+\frac{\partial \mathbf{F}^j}{\partial x_j}+\frac{\partial \mathbf{G}^j}{\partial x_j}\right)=0 \\ &\Leftrightarrow\left(\phi,\frac{\partial \mathbf{U}}{\partial \tau}+\mathbf{I}^M\frac{\partial \mathbf{U}}{\partial t}\right)_\Omega+\left(\phi,n_j\mathbf{F}^j+n_j\mathbf{G}^j\right)_{\partial\Omega} \\ &-\left(\frac{\partial}{\partial x}\phi,\mathbf{F}^j\right)_\Omega-\left(\frac{\partial}{\partial x}\phi,\mathbf{G}^j\right)_\Omega=0 \end{aligned} \tag{4}$$

Integrate by parts again equation (4):

$$\begin{aligned} &\left(\phi,\frac{\partial \mathbf{U}}{\partial \tau}+\mathbf{I}^M\frac{\partial \mathbf{U}}{\partial t}+\frac{\partial \mathbf{F}^j}{\partial x_j}+\frac{\partial \mathbf{G}^j}{\partial x_j}\right)=0 \\ &\Leftrightarrow\left(\phi,\frac{\partial \mathbf{U}}{\partial \tau}+\mathbf{I}^M\frac{\partial \mathbf{U}}{\partial t}\right)_\Omega+\left(\phi,\frac{\partial}{\partial x}\mathbf{F}^j\right)_\Omega+\left(\phi,\frac{\partial}{\partial x}\mathbf{G}^j\right)_\Omega \\ &+\left(\phi,n_j\left(\hat{\mathbf{F}}^j-\mathbf{F}^{j-}\right)+n_j\left(\hat{\mathbf{G}}^j-\mathbf{G}^{j-}\right)\right)_{\partial\Omega}+=0 \end{aligned} \tag{5}$$

Where

$\hat{\mathbf{F}}^j{}_{\partial\Omega}=\hat{\mathbf{F}}^j\left(\hat{\mathbf{F}}^{j-},\hat{\mathbf{F}}^{j+}\right)\Big|_{\partial\Omega}$ and $\hat{\mathbf{G}}^j{}_{\partial\Omega}=\hat{\mathbf{G}}^j\left(\hat{\mathbf{G}}^{j-},\hat{\mathbf{G}}^{j+}\right)\Big|_{\partial\Omega}$

are the numerical fluxes.

Here $(.,.)$ represents the normal L_2 inner product and third term is flux vector. In this problem the numerical flux for convective terms is calculated by using the Lax-Friedrich flux and local discontinuous galerkin for viscous terms.

Here, we took the Kornwinder Dubiner function on straight sided triangle as the basis written in equation (5) (see figure 1 and 2):

$$\phi_{ij}(r,s)=\sqrt{\frac{2i+1}{2}}\sqrt{\frac{2i+2j+2}{2}}P_i^{0,0}\left(\frac{2(1+r)}{(1-s)}-1\right)P_j^{2i+1,0}(s) \tag{6}$$

where, $P^{\alpha,\beta}$ is orthogonal Jacobi polynomial. All straight sided triangles are the image of this triangle under the map:

$$\begin{pmatrix} x \\ y \end{pmatrix}=-\left(\frac{r+s}{2}\right)\begin{pmatrix} v_x^1 \\ v_y^1 \end{pmatrix}+\left(\frac{1+r}{2}\right)\begin{pmatrix} v_x^2 \\ v_y^2 \end{pmatrix}+\left(\frac{1+s}{2}\right)\begin{pmatrix} v_x^3 \\ v_y^3 \end{pmatrix} \tag{7}$$

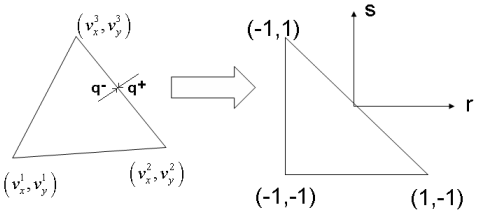

Figure 1: Coordinate transformation

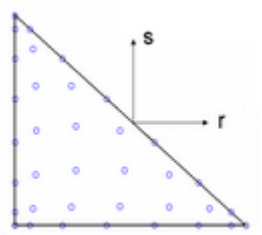

Figure 2: Seventh order Gauss Lobatto quadrature nodes ; equation (6),

$$p(r,s) = \sum_{i=0}^{N}\sum_{j=0}^{N-i}\phi_{ij}(r,s)\hat{p}_{ij} \qquad (8)$$

$$p(r_n,s_n) = \sum_{m=1}^{m=M}\mathbf{V}_{nm}\hat{p}_m \qquad (9)$$

$$\hat{p}_m = \sum_{m=1}^{m=M}\left(\mathbf{V}^{-1}\right)_{mj}p(r_j,s_j)$$

$$\frac{\partial p}{\partial r}(r,s) = \sum_{i=0}^{N}\sum_{j=0}^{N-i}\frac{\partial \phi_{ij}}{\partial r}(r,s)\hat{p}_{ij} = \hat{\mathrm{D}}^r\mathbf{V}^{-1}p(r,s)$$
$$\frac{\partial p}{\partial s}(r,s) = \sum_{i=0}^{N}\sum_{j=0}^{N-i}\frac{\partial \phi_{ij}}{\partial s}(r,s)\hat{p}_{ij} = \hat{\mathrm{D}}^s\mathbf{V}^{-1}p(r,s) \qquad (10)$$
$$\hat{\mathbf{D}}^r = \frac{\partial \phi}{\partial r}\ ;\ \hat{\mathbf{D}}^s = \frac{\partial \phi}{\partial s}$$

where $\mathbf{V}_{ij}$ and N are Vandermonde matrix and the order of Jacobi polynomial respectively.

The semi discrete of equation (5) can be written in the following form:

$$\frac{\mathrm{d}\mathbf{U}}{\mathrm{d}\tau} + \mathbf{I}^M\frac{\mathrm{d}\mathbf{U}}{\mathrm{d}t} = \mathbf{R} \qquad (11)$$

A dual time stepping approach is employed for marching equation (12) in time. The real time t is discretized using second order implicit backward difference formula. The resulting equation becomes:

$$\frac{\mathrm{d}\mathbf{U}^{n+1}}{\mathrm{d}\tau} + \mathbf{I}^M\frac{\left(3\mathbf{U}^{n+1} - 4\mathbf{U}^n + \mathbf{U}^{n-1}\right)}{2\Delta t} = \mathbf{R}^{n+1} \qquad (12)$$

where superscript n denotes the current time level t, and n-1 refers to the previous time step t-Δt, while the unknowns are calculated at time t+Δt by n+1. Equation (12) can be written in a simpler form as:

$$\frac{\mathrm{d}\mathbf{U}^{n+1}}{\mathrm{d}\tau} = \overline{\mathbf{R}}^{n+1} \qquad (13)$$

where $\overline{\mathbf{R}}$ contains the right hand side of equation (12) and the second term on left hand side of this equation. Equation (13) represents a pseudo-time evolution of flow field and has no physical meaning until the steady state in pseudo-time is reached.

The Equation (8) is integrated in pseudo-time marching by using five stage of fourth order 2N-storage Runge-Kutta scheme as developed by [8]. The final equations are found as written in Eqs. (14) and (15) :

$$\frac{\mathrm{d}\mathbf{U}}{\mathrm{d}\tau} = \overline{\mathbf{R}}(\tau,\mathbf{U}(\tau)) \qquad (14)$$

$$d\mathbf{U}_j = A_j d\mathbf{U}_{j-1} + d\tau\overline{\mathbf{R}}(\mathbf{U}_j) \quad ; \quad j = 1,5 \qquad (15)$$
$$\mathbf{U}_j = \mathbf{U}_{j-1} + B_j d\mathbf{U}_j$$

where $d\tau$ is the pseudo-time step. The vectors **A** and **B** are the coefficients that will be used to determine the properties of the scheme.

4. INITIAL AND BOUNDARY CONDITIONS

Initial and boundary conditions The governing equations (1) or (3) require initial condition to start the calculation as well as boundary conditions at every time step. In the calculations presented in this paper, the uniform free-stream values are use as initial conditions: $p = p_\infty$; $u_1 = u_{1\infty}$; $u_2 = u_{2\infty}$. For external flow applications, the far-field bound is placed far away from the solid surface. Therefore, the free-stream values are imposed at the far-field boundary except along the outflow boundary where extrapolation for velocity components in combination with $p = p_\infty$ is used. On the solid surface, the no-slip condition is imposed for velocity components: $u_1 = 0$; $u_2 = 0$. The surface pressure distribution is determined by setting the normal gradient of pressure to be zero: $\frac{\partial p}{\partial n} = 0$

5. RESULTS AND DISCUSSION

The accuracy of the proposed method is demonstrated by solving incompressible flow past 2-dimensional circular cylinder. The Reynolds number is varied from 20 to 40 for steady flow and from 100 to 200 for unsteady flow. The computational domain for steady flow is rectangle (-15, 25) × (-15, 15) and for unsteady flow is (-20, 20) × (-20, 80) wherein a circular cylinder of diameter d =1 placed at (0, 0). The mesh consists of 1228 triangles for steady flow and 5092 triangles for unsteady flow. For all the calculation, we took a

ISSN 114-1284

fixed order of polynomial N =4, Prandtl number is 0.717 and fixed artificial compressibility parameter is equal to unity.

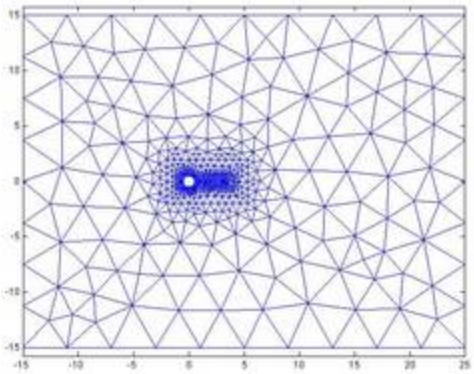

Figure 3a: Mesh for steady flow

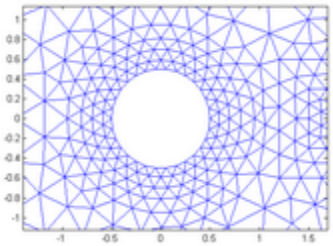

Figure 3b: Close-up mesh around cylinder for steady flow

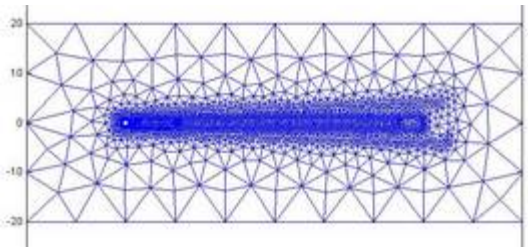

Figure 4a: Mesh for unsteady flow

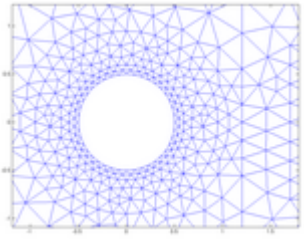

Figure 4b: Close-up mesh around cylinder for unsteady flow

Pseudo time step is $\Delta\tau = 0.0012$ for steady flow. The results can be seen in figure 5 and 6. In front of object, pressure strongly varies and a region of high pressure is formed near separation point and two regions of low pressure are developed next. From figure 5, it can be seen the development of a recirculation zone behind the object with reverse velocity. Figure 5 and 6 give the computed pressure for different values of Reynolds number (Re=20 and 40). As shown, the DG scheme gives excellent pressure stabilization, with the computed pressure contours being highly smooth and non-oscillatory.

The calculated results for steady flows are compared with the other numerical data. Table 1 compares the Drag coefficient (Cd). The agreement is quite good.

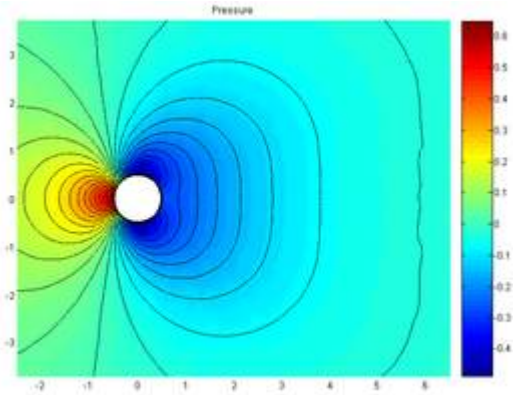

Figure 5a: Isobar of Re=20

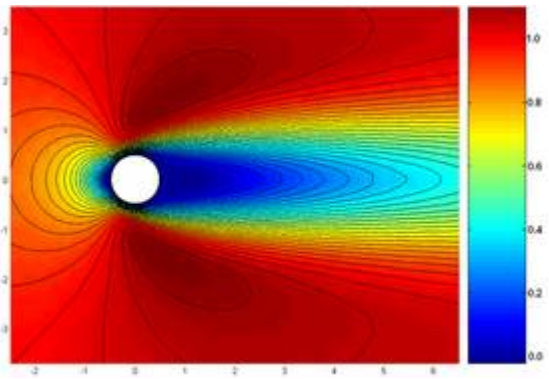

Figure 5b: Horizontal velocity of Re=20

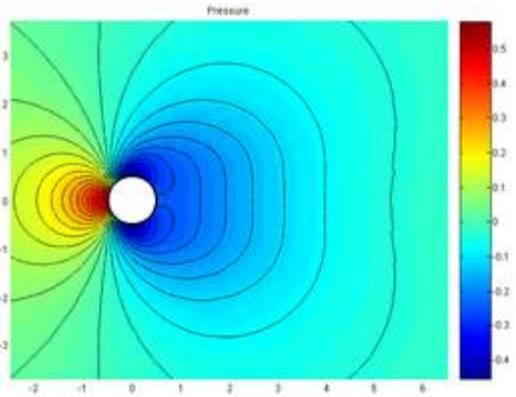

Fig. 6a. Isobar of Re=20

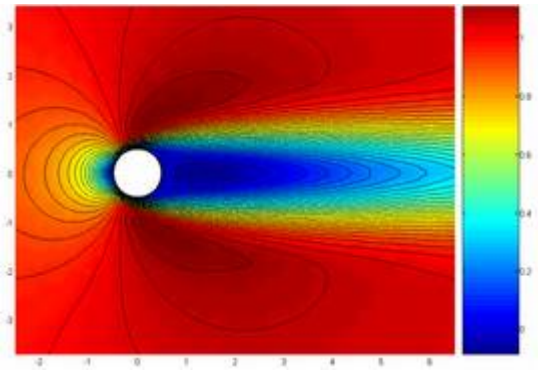

Figure 6b: Horizontal velocity of Re=20

Table 1. Drag coefficient (Cd) comparisons for steady flows

Author	Re=20	Re=40
Takami *et al.**	2.003	**1.536**
Dennis *et al.**	2.045	**1.522**
Tuann *et al.**	2.253	**1.675**
Ding *et al.**	2.180	**1.713**
Nithiarasu *et al.**	2.060	**1.564**
Thomas*	2.076	**1.603**
Present work	**2.040**	**1.527**

*: adapted from [9]

The ability of the discontinuous galerkin scheme with dual time-stepping to simulate transient flow is illustrated here by computing the vortex shedding in the wake of flow past a circular cylinder at Re = 100 and 200. This has been a popular test case for validating the transient part of numerical schemes. The problem is solved using is Δt = 0.1 and $\Delta\tau$ = 0.001 and total of 250 pseudo-time iterations. Figure 7 provides a full simulation analysis of the Cl and Cd histories for each real time step on the mesh. As can be seen, once the initial transient stage has passed, the simulation settles down to an almost periodic convergence pattern. After the initial transient, each variable develops a periodic variation. This is due to the periodic shedding of vortices from behind the cylinder. This can be seen more clearly in figure 7, 8 and 9. A quantitative analysis of the results was also conducted and is shown Table 2. Generally, all the results shown for DG scheme are in good agreement with the other results.

Table 2: Cl, Cd and St comparisons for unsteady flows

Author	Re=100		
	Cl	Cd	St
Roger & Kwak [6]	±0.358	1.376 ±0.011	**0.163**
Pontaza [10]	±0.356	1.356	**0.167**
Mittal [11]	±0.356	1.386	**0.169**
Roshko (exp) [12]	-	-	-
Bintoro & Pranowo [13]	-	-	-
Rosenfeld [12]	-	-	-
Li [14]	-	-	-
Present work	**±0.3644**	**1.3440 ±0.013**	**0.1563**

Re=200		
Cl	Cd	St
	-	
±**0.65**	1.23±0.05	**0.185**
-	-	-
-	-	-
-	-	**0.18**
±**0.552**	1.24±0.09	**0.17**
±0.674	1.329±0.044	**0.197**
±1	1.17±0.15	**0.18**
±0.645	**1.311± 0.036**	**0.176**

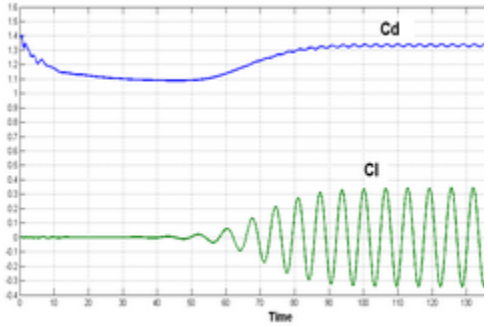

Figure 7a: Cd & Cl History for Re=100

The qualitative results are shown in figures 8 and 9. Here, the contours of pressure and vorticity are shown, for the real non-dimensional times of 100 and 120 respectively. All results are of high quality with no non-physical oscillations. The narrowing of the wake and the increase in shedding frequency, as the Reynolds number increases, is clear from these plots. We observe that at higher Reynolds numbers the vortices in the far-downstream wake coalesce and the region of coalescence moves upstream as the Reynolds number increases.

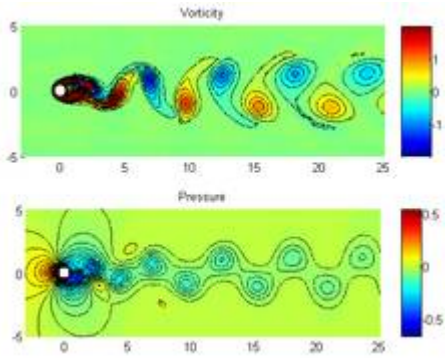

Figure 8a: Iso-vorticity and Isobar for Re=100 at t=100

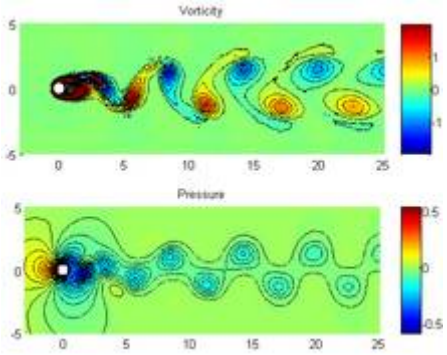

Figure 8b: Iso-vorticity and Isobar for Re=100 at t=120

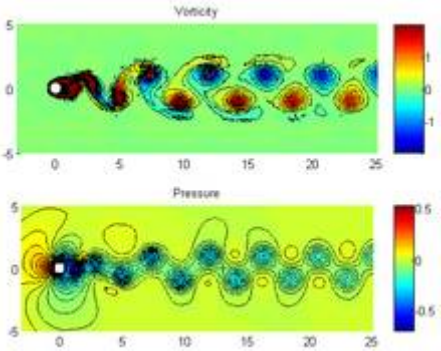

Figure 9a: Iso-vorticity and Isobar for Re=200 at t=100

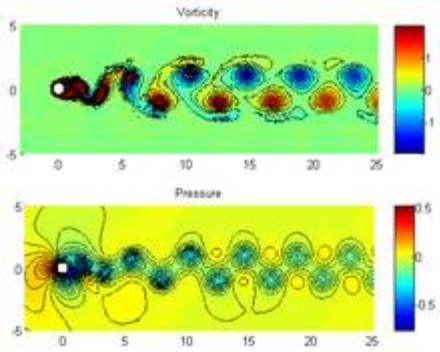

Figure 9a: Iso-vorticity and Isobar for Re=200 at t=120

It can be seen from the plots that the proposed method is stable for long time simulations. In addition, the plots show evidence that the outflow boundary condition allows for a smooth exit of the flow field and does not distort the flow upstream.

7. CONCLUSION

In this paper, we have presented a discontinuous galerkin method for steady and unsteady in artificial compressibility formulation connection with a dual time stepping approach. The method exhibits good numerical stability. The numerical results have a good agreement with the proposed experimental and numerical results reported in the previous studies.

ACKNOWLEDGMENT

We are very grateful to Prof. Hesthaven from Brown University USA for the valuable discussion and sharing his "Nudg" code.

REFERENCES

[1] M. T. Manzari, "A time-accurate finite element algorithm for incompressible flow problems", *International Journal of Numerical Methods for Heat & Fluid Flow,* Bradford: 2002. Vol.13 No.2, pp. 158-177.

[2] Pranowo and Deendarlianto, "Numerical solution of steady state free convection using unstructured discontinuous galerkin method". *Proceeding of the 3rd international conference on product design & development*, 12-13 December 2007, Jogjakarta, Indonesia

[3] A. J. Chorin, "Numerical method for solving incompressible viscous flow problem", *Journal of Computational Physics,* Vol. 2, pp. 12-26, 1967.

[4] M. T. Manzari, "An explicit finite element algorithm for convection heat transfer problems", *International Journal of Numerical Methods for Heat & Fluid Flow*, Bradford: 1999, Vol. 9-8, p. 860.

[5] F. Papa, et al., "A Numerical calculation of developing laminar flow in rotating ducts with a 180° bend", *International Journal of Numerical Methods for Heat & Fluid Flow*, Bradford: 2002, Vol.12 No.7, pp. 780-799.

[6] S. E. Rogers, and D. Kwak, "Steady and Unsteady Solutions of the incompressible Navier Stokes Equations", *AIAA Journal Part A*, Vol.29, No.4, pp. 603-610, 1991.

[7] N. T. Duc, "An implicit scheme for incompressible flow calculation with artificial compressibility method", *VNU Journal of Science, Mathematics-Physics*., T. XXI, no. 4, 2005.

[8] M. H. Carpenter and C. A. Kennedy, "Fourth-order 2N-Storage Runge-Kutta Schemes", *NASA Technical Memorandum* 109112, 1994, NASA Langley Research Center, Hampton, Virginia.

[9] C. G. Thomas, "A locally conservative Galerkin (LCG) finite element method for convection-diffusion and Navier-Stokes equations", *Ph.D. Thesis*, 2006, University of Wales Swansea.

[10] J. P. Pontaza. "A least-squares finite element formulation for unsteady incompressible flows with improved velocity-pressure coupling", *Journal of Computational Physics* 217, pp. 563-588, 2006.

[11] S. Mittal, V. Kumar, and A. Raghuvanshi, "Unsteady incompressible flows past two cylinders in tandem and staggered arrangements", *International Journal for Numerical Methods in Fluids,* 1997, 25: 1315-1344

[12] M. Rosenfeld, "Grid refinement test of time periodic flows over bluff bodies", *Int. Journal of Fluid and Computers*, Vol. 23, no. 5, 1994.

[13] A. G. Bintoro, and Pranowo, "Perhitungan numeris pembebanan hidrodinamis aliran fluida laminar viskos tak tunak melewati silinder pada bilangan Reynold rendah", *Jurnal Teknologi Industri*, Vol. VI, April 2002.

[14] J. Li et al., "Numerical study of laminar flow past one and two circular cylinders", I*nt. Journal of Fluid and Computers*, Vol. 21, no. 3, 1991.

ISSN 114-1284

Design of a Flexible Framework for a Synchronous Groupware

Prima Dewi Purnamasari[a], Axel Hunger[b], Angela Tanuatmadja[c]

[a]*Department of Electrical Engineering*
Faculty of Engineering
Universitas Indonesia, Depok 16424
E-mail :prima@ee.ui.ac.id

[b]*Institute of Computer Engineering*
Faculty of Engineering
Universität Duisburg-Essen, Germany
E-mail : axel.hunger@uni-due.de

[c]*Institute of Computer Engineering*
Faculty of Engineering
Universität Duisburg-Essen, Germany
E-mail : angela.tanuatmadja@uni-due.de

ABSTRACT

Based on the gained experiences and some limitations founded in PASSENGER, a new synchronous groupware system is under development at the institute of Computer Engineering, University of Duisburg-Essen (UDE). The new system is envisioned to overcome the boundaries of limitations, thus providing a groupware that allows a tailor-made configuration of the system prior to a session and flexible adaptations to special scenarios and situations during a session. The approach to provide flexible and tailor-made groupware is done by using component based software for the development of the groupware and hybrid collaborative architecture for the replication and communication between server and clients. Further, several mechanism—floor control, concurrency control, replication, distribution—will be investigated. To bring flexibility and tailorability, the system will attempt to offer best choice, but decision will depend on the user.

KEYWORDS

synchronous groupware, flexibility, tailorability, component based software

I. INTRODUCTION

At University Duisburg-Essen, a synchronous groupware named PASSENGER has been developed at the institute of Computer Engineering throughout the last years. This client-server based groupware application enables student teams to communicate and cooperate via Internet, even if the members are located at distributed sites. The client application is implemented in a way that it consists of a fixed set of tools to support exactly one scenario (Software Engineering education).

Apart from its good feature, there are some limitations from the system that this thesis project wants to solve. First of all, the system does not allow integrating any other tools. Fixed tools of the system—CASE-tool, text messages, video streaming, voice conference—are always available. They neither can be turned off, nor can be added with other tools. Secondly, the usage of the system is limited to a fixed arrangement of groups. There is only 4 person allowed to joined a session at maximum, and there is no way for late joiners to enter an ongoing session. Furthermore, the system is only intended to be used in Software Engineering education. Therefore, the system is not suitable to be used in other scenarios. From these illustrations, it can be seen that PASSENGER has no flexibility. User must accept all conditions available. Or refuse it all.

Based on the gained experiences and some limitations founded, a new system is under development at the institute of Computer Engineering, University of Duisburg-Essen (UDE). The new system is envisioned to overcome the boundaries of limitations, thus providing a groupware that allows a tailor-made configuration of the system prior to a session and flexible adaptations to special scenarios and situations during a session.

The main problem of this thesis work is to provide flexible adaptation and tailor-made configuration of a synchronous groupware, which in this thesis defined as:

Tailor-made configuration: includes the selection of components and tools and their configuration according to special group parameters (e.g. number of members and their possible roles, openness of group) and scenarios (e.g. brainstorming, design session, text reviewing).

Flexible adaptation: regarding the change of situations during a session (for e.g. allowing the creation of sub-groups) and behaviors of members (e.g. change of floor control policy is due to multicultural background of members). The system should be flexible enough to provide alternatives or to suggest alternatives according to group parameters or profiles of participants.

The approach to provide flexible and tailor-made groupware by using component based software for the development of the groupware and hybrid collaborative architecture for the replication and communication between server and clients. Further, several mechanism—

floor control, concurrency control, replication, distribution—will be investigated. To bring flexibility and tailorability, the system will always offer best choice, but decision will be back to the user.

II. REQUIREMENT ANALYSIS

The future enterprise groupware applications need to be able to cover the whole range of all groupware aspects in a way that is flexible and that can dynamically change [1]. Or it can be broadly summarized in two categories: (a) increased flexibility of groupware applications and (b) increased support of dynamism by groupware technology [1]. To meet this requirement of enterprise groupware, we will develop a highly flexible and tailorable framework for groupware.

The system is intended to provide synchronous communication strategy. Because the main aim of this system is to provide a synchronous collaboration work, same time different place. This is translated into the use of available different tools and application at the same time for the users who joined the same session. The variety of tools and application will be described later. But it dos not mean that the system will not use asynchronous communication, because asynchronous communication will undeniably be needed to do the management issues. Below are the requirements for a highly flexible and tailorable framework for a synchronous groupware:

The system should bring a synchronous system strategy

The system will be based on client server architecture. The idea of client server architecture is by utilizing proxies in both sides, server and client, so that the invocations of program can be done as if the program is local.

Communications between clients are based on client server architecture

To support flexibility and tailor-ability, the system is build per object component based.

The program must be separated between master and client (GUI)

The system must be separated between program, data objects and user interface objects components

System will provide a list of applications for each phases of group work

A group can choose from the list of applications, which one they want to use in the working session at runtime

Main server will hold a database of every session

The database will save automatically every 15 minutes

Before a session start, a group may continue working on the previous work stored in the database

At the end of the session, user is asked whether he/she wants to save the work locally.

Authoring is implemented by using different colors for each member in the session.

The system can flexibly operate in centralized or hybrid/semi- replicated architecture

In a hybrid/semi-replicated, partitioning in the network is needed

In 1 partition, there will be 1 replication.

The system should be able to know the condition of the network connection to and between its client

The system should be able to know the condition of resource power of each user

The system is provided with the ability to give suggestion on distribution architecture as well as optimal partitioning based on user network condition and profile

To give tailor-ability feature, the system will only give suggestion, while the decision is depend on users.

The system must be provided with all basic distribution transparency; access transparency, location transparency, replication transparency and fragmentation transparency

The system must be provided with data consistency control mechanism; vector clock will be used to synchronize a shared object

The system must be provided with concurrency control, which will be translated into locking mechanism

Update and synchronization protocol is needed

Every user must register to the system by giving the required profile

Every group must register to the system by giving the required profile

User and Group registration must be done before requesting a session

A user can be associated to one or more group

The number of users may range from 2 to 8 people

System will allow session owner to define the session openness at session registration

A group will provide the characteristics of the session; openness (allowing latecomers or not), role of each user in a group (moderator, observer, custom), floor control model, which phase is the session

The website should provide 5W&1H information of sessions and users

The system has capacity of 10 session at a time

The system has an open table showing a free slot of time that can be chosen by a group. Each slot of time is defined as 1 hour

A group may register (request) a session before the requested date and time of the session or directly before the session start as long as there are free slots

A group can ask a session for one or more slot of time

III. DISTRIBUTION ARCHITECTURE

This system will provide 2 alternative of architecture of its components, namely centralized and hybrid/semi replicated architecture. This distributed system will also allow partitioning of the network. Network partition in this case will be based on client physical locations. The network partition can also be based on the version of this groupware (light version for low resource mobile device, and full version for PC) but that will be a future work.

3.1 Network Partitioning

Based on requirements, in one partition of network, there will be one or more clients which the number of client is corresponds to the number of UI and one program replica should be provided. The example of scenario of network partitioning can be seen in Figure 1.

In this sample scenario, Main Server is located in Germany. There are 6 Clients want to join a session. The sequence of request is based on the number on the client names. Another scenario possible is the group leader registers all clients at the same time when requesting a session. Server recognizes location of the client. Then, it suggests partition of the user network by observing the location. It can be seen in Figure 1 server makes 3 partitions; Region 1, 2 and 3. Server tests the network connection to each client and chooses the best connection in each region as the replicated master. Server asks the chosen clients if they are wiling to be a replicated master. If the chosen client is not willing to be replicated master, server asks another client in the same region to be the replicated master, only if the computer specification supported. If there is none of client in one region is able to be the replicated master, all clients in that region will be clients to a replicated master in the other region (start from the nearest neighbor). It can be the main server itself.

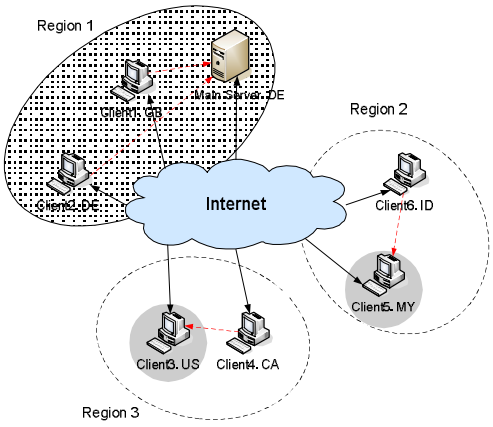

Figure 1. Network Partitioning Scenario

In this sample scenario, Main Server in Germany (DE) becomes a master for Client1 in United Kingdom (GB), and Client2 in Germany (DE). Client5 in Malaysia (MY) becomes a master for Client6 in Indonesia (ID), and Client2 in USA (US) becomes a master for Client4 in Canada (CA).

Late Joiners

When Late Joiners Mode is enabled, there are 3 possibilities of adaptability. The adaptability is based on the network connection to each user and condition of users. How server know this information will be described later. As usual, the system only suggests while the decision always at the user side. Continuing the above example, there is a late joiner, Client7 in Australia (AU) who wants to join a session. There will be 3 scenarios possible for adaptability of the system regarding this late joiner.

Late Joiner uses nearest replicated master. Because the nearest partition is Region 2, Client7 join Region 2 and become a client of Client5, as can be seen in Figure 2.

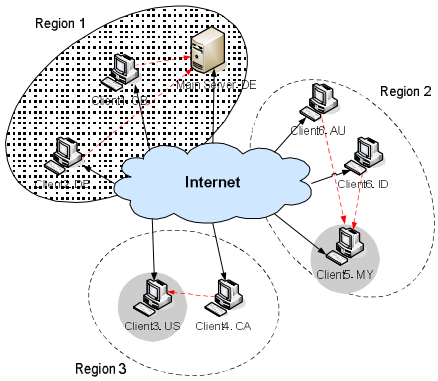

Figure 2. Late Joiner uses nearest replicated master

Late Joiner becomes a new replicated master in a new partition. The system suggests Client7 to make a new partition, because the network condition form AU to every existing replicated master is not good. The illustration can be seen in Figure 3.

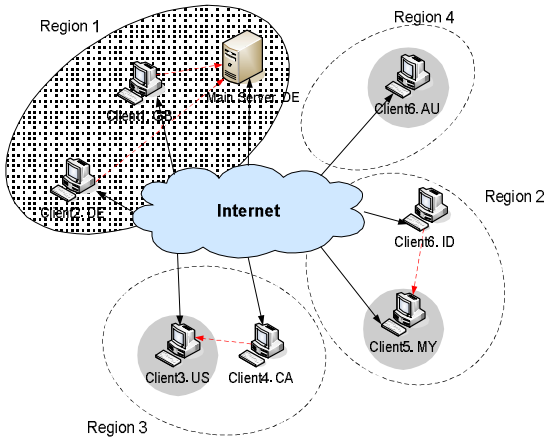

Figure 3. Late Joiner becomes new replicated master in a new partition

Late Joiner becomes a new replicated master in existing partition. The system suggest Late Joiner to become a new replicated master in existing region, because the connection of Late Joiner is better than the old replicated master in that region. Thus the network partitioning becomes like Figure 4.

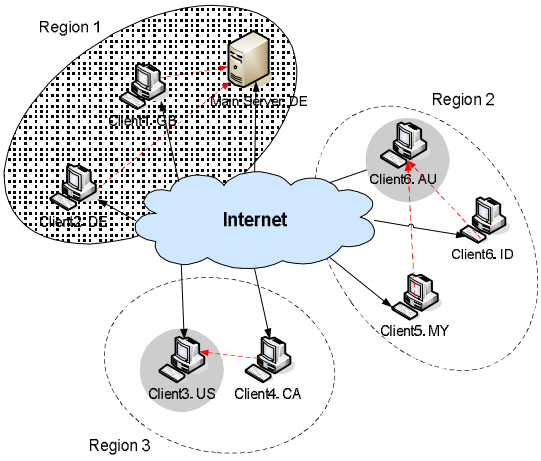

Figure 4. Late Joiner become a new replicated master in existing region

3.2 Role of User

There are 4 roles that are available in a session; moderator, member, floor handler, observer. Take into notice that moderator will have double role at the same time, which is a role as moderator and another role from 3 roles available. Class diagram of Role can be seen in 0Figure 5.

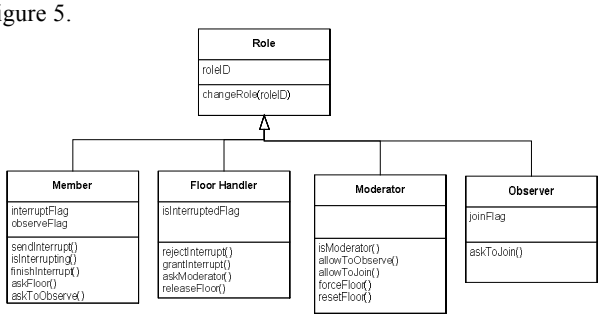

Figure 5. Role Class Diagram

The following are the roles and their corresponding privileges in a session:

Moderator

- Choose type of floor control model to be used in the session
- Force Member to leave a session (kick out)
- Reset floor list in Sequential Control Model
- Force to free the token from Floor Holder in Free Control Model
- Become the first Floor Holder in a session
- Grant or reject request to become an Observer
- Grant or reject latecomer

Member

- Ask to interrupt Floor Holder
- Ask a token before it is released by the Floor Holder
- Ask to become an Observer
- Leave a session early
- Join a session late

Floor Holder

- Can grant or reject interruption
- Can grant or reject request of token
- Release token

Observer

- Can ask to become a **Member** (rejoin a session)

In Figure 6, the state transition diagram of role transformation is illustrated.

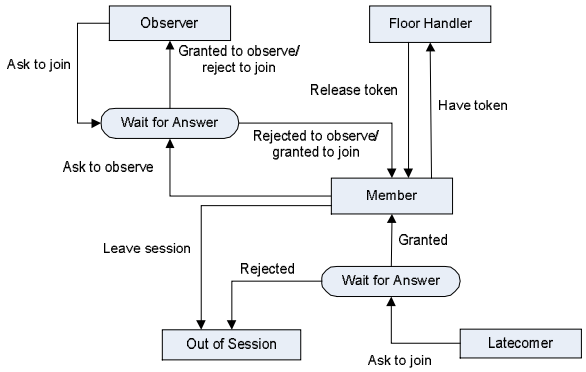

Figure 6. Role State Transition Diagram

3.3 Floor Control Model

At start up, moderator are given the right to choose between three types of floor control available from the system. To bring flexibility in more advanced way, moderator can also change the type of floor between these types anytime when the session is running as shown in Figure 7. The three type of floor control model available are Free Flow, Sequential Flow and Shared Floor Control Model.

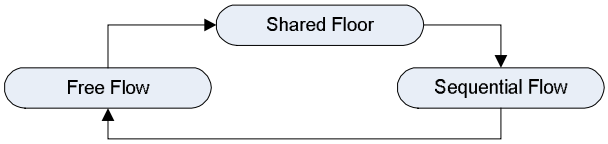

Figure 7. Control Model State Transition Diagram

Sequential Floor Control Model

In sequential flow control, user can access the system only if it is his turn according to the floor list. This floor list can also be analogically thought as token ring network. By default, a Member who is also a Moderator will be the first person in the list. The next sequence in the list is according to the sequence of Member asking for the floor, until all Members in the session is on the list. Notice that Observer will not be in the list, because he can not ask to have the floor unless he is a common Member.

To prevent the floor being possessed too long by the Floor Holder, the Moderator has the privilege to force the

Floor Holder to release the floor and allow the next Member in the list to become Floor Holder.

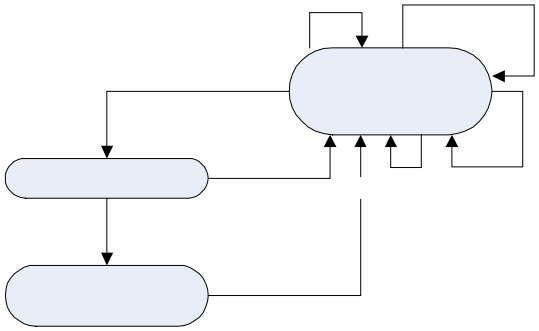

Figure 8. Sequential Flow Control Model State Transition Diagram

Member has privilege to make interruption, and possess the floor even though he is not the actual Floor Holder. But the actual Floor Holder has the right to grant or reject the request of this interruption. After this Member finish his interruption, the floor is passed to the actual Floor Holder and continue the floor possession based on floor list. 08 illustrates this model.

Whenever there is a change in the number of Member, the floor list will be updated, but not being reset. The change of number of Member in the session can be caused by early leaver, latecomer, a Member becomes Observer, or an Observer becomes a Member. The new Member should ask the floor to be updated in the floor list. If a Member leave, either he become an Observer or leave the session, his place on the list is deleted.

Whenever Moderator thinks that it is necessary, he has the privilege to reset the floor list. In this case, the list will be empty. The mechanism to fill the floor list is based on the sequence of request of the floor.

This model is best suited for all active users session, for example in brainstorming phase.

Free Flow Control Model

In this flow control, the system provides 1 token for all user on the session to possess a floor, or in other words to change his role from Member to Floor Holder.

To prevent the token being possessed too long by one Member, the Moderator has the privilege to force the Floor Holder to release the token. Member has privilege to ask the actual Floor Holder to pass the token, but Floor Holder can grant or reject his request. Figure 9 illustrates this model. Regarding the latecomer or early leaver, this flow control will not face a problem like in the previous model, since the token is independent. Update is not needed like in Sequential Flow Control Model.

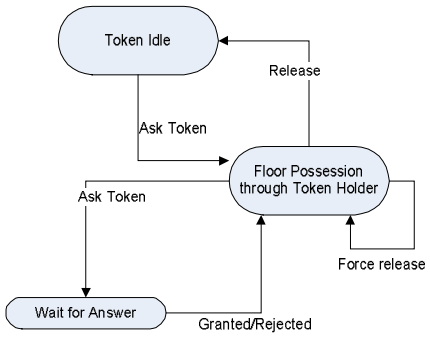

Figure 9. Free Flow Control Model State Transition Diagram

This flow control model is appropriate for presentation-like session, where only one person holds a session for a long time.

Shared Floor Control Model

In this model, there is no different role. All users are members and have the same privileges. In this flow control model, rigorous 2-phase locking [2] is applied. Shared floor control model leads to a pure distributed system. It may be suitable for some applications, but not all. One example is as example Electronic Brainstorming System (EBS).

The main idea of this floor control model is to provide comfortability to users to express their ideas in a session, without having to wait someone else to finish his work. It will also save the session time. But trade off should be taken into account, that a more complex locking and updating mechanism should be provided.

IV. COMPONENT

In component based software, applications are developed from components. These components themselves might be built up from several small components. Components might be added or removed during runtime. This solved the tailor-ability issue that we have. Since we use hybrid-replication architecture, a replication mechanism of the components, should also be determined.

4.1 Separation of Components

To support flexibility, in this system we will separate objects or components of the software based on its functionality into program, data, and user interface objects. Remember that components can be built up from other components.

Therefore, in a session there will be some clients, some program replica, and some data objects as illustrated in Figure 10.

ISSN 114-1284

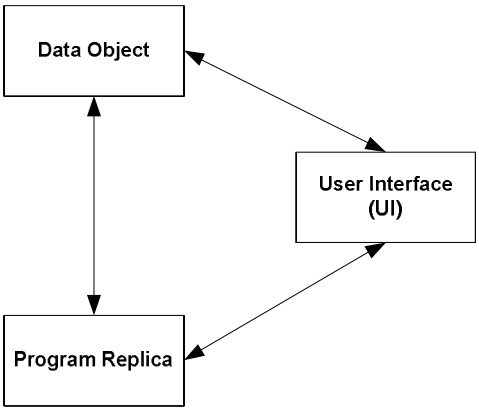

Figure 10. Separation of Components

The definitions of each object are described below:

User Interface (UI) is part of the program which provides interface to the main program. It is translated as the GUI of the program. UI is the medium for the user to interact with the program and the data object

Program replica is the copy of program, the brain, the processor with the computing and executing ability. Program replica has the ability to interact with the data object.

Data Object is part of the program where the information stored. It can be translated as a functional part of the program or as a part of the artifact.

4.2 Extensibility of Components

Components can be changed, extended or curtailed, during runtime. The changes however should not disrupt the application and it should be transparent to the user. The extensibility patterns of components proposed by Hummes and Merialdo [3] enable the extensibility to be encapsulated in one component. The extensibility pattern is intended to be used to provide a default behavior which can be changed at run time [3]. The application will only see the specific behavior of a Proxy class. The class diagram to illustrate it can be seen in Figure 11. The illustration of this pattern is slightly modified from the real one proposed by Hummes and Merialdo [3], to adopt the later design in this work.

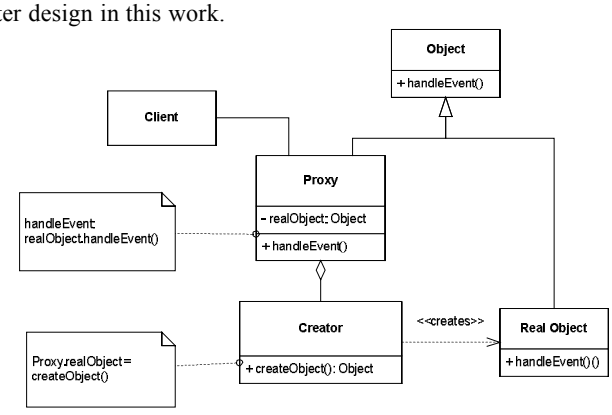

Figure 11. Class Diagram of Extensibility Patterns

According to this pattern, Proxy extends the interface of an Object, which may be inserted at run time. Inside this Proxy, exists a Creator which is responsible to create a new object of an arbitrary class Real Object corresponds with the interface Object. This pattern is combination of the Proxy and the Factory Method patterns.

The design is adapted from this pattern. Client will always communicate to the object through the Proxy. At start up, Creator will automatically instantiate an Object, a Default Object, and pass the reference of the Default Real Object to the Proxy. Any event that Proxy receives will be delegated to the Default Object. When the creator receive an event to create a new real subject, it instantiates the respective class and sets the reference in the Proxy to the newly created New Real Object. The Proxy from now, forward all subsequent events to this object, unless the Creator changes the reference to the Default Real Object again. The interaction between objects is illustrated in the sequence diagram in Figure 12.

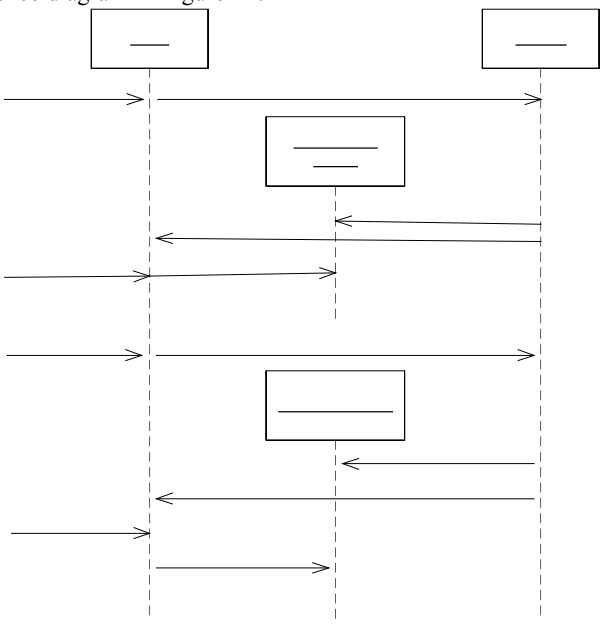

Figure 12. Sequence Diagram of Extensibility Pattern

Following the creation of a new Object, Proxy can delete the existing Real Object or simply create the new Real Object while storing the old ones. The incoming events are then forwarded to corresponding Real Objects. This variation will be best used if the newly added Real Object has a different functionality than the old ones.

V. CONCURENCY CONTROL

Concurrency control deals with the issues involved with allowing multiple people simultaneously access to shared entities, be they objects, data records, or some other representation [www1]. The goal of concurrency control is to allow several transactions to be executed simultaneously, but in such a way that the collection of data items (e.g. files or database records) being manipulated, is left to consistent state. This consistency is

achieved by giving transactions access to data items in a specific order whereby the final result is as the same as if all transactions had run sequentially.

Parallel operations on a shared data are possible to bring interference to each other. Possible problems that might occur are [www2]:

- Lost update. This problem occurs when overwrites uncommitted data.
- Inconsistency retrieval. This problem occurs when reading uncommitted data.
- Unrepeatable read. This problem occurs when reading one object twice with two different results.
- Incorrect summary problem. This problem occurs if one transaction is calculating an aggregate summary function on a number of records that are being updated at the same time by a second transaction.

To prevent those problems, in this system we will use locking and updating mechanism. Locking will be implemented for the role **Floor Holder**. While updating mechanism is implemented to all users.

5.1. Logging Mechanism

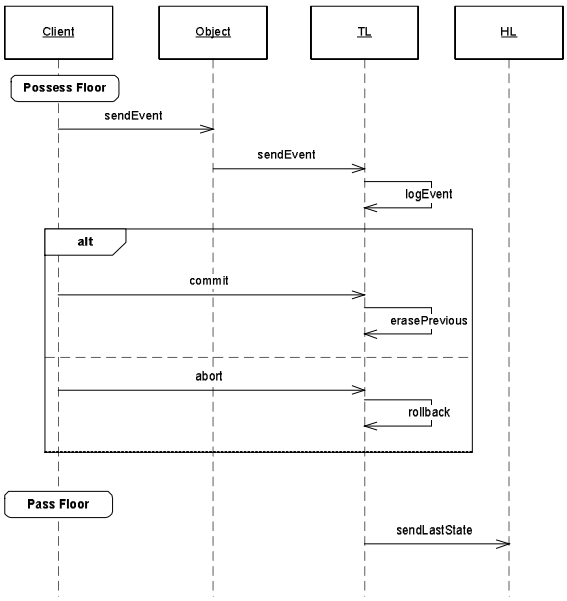

Figure 13. Sequence Diagram for Logging Mechanism

In this system we will need a dynamic replication mechanism, since this system use a hybrid-replicated architecture. The approach proposed in this thesis is by using logging mechanism. Logger and logable mechanism is based on mechanism proposed by [4]. But in our scenario, to implement logging mechanism, there will be two dedicated component which functioning as logger; History Logger (HL), and Temporary Logger (TL). The histories of all committed events are stored in the HL. While the events before a user who has the lock decided to commit or abort are stored in TL. Logger is a component that belongs to the program. Therefore it stays with the client who acts as replicated master. Synchronization and updating protocol should be implemented in the logger. Therefore, there is no need to synchronize all shared data objects, but only the logger. If all consequent states in the logger are synchronized, then the data objects will also be synchronized.

Every event will be stored temporarily in the TL until the user who holds the lock commit or abort those events. If the user decides to abort all subsequent events, then a rollback mechanism should be performed. The rollback mechanism is simply done by erasing all events in TL, and use the last state in HL. When the user decides to commit the subsequent events, the logger simply copy the last state in TL to HL and erases all events in TL.

5.2 Updating Mechanism

In this proposal, a logger is not only store the data, but also implements synchronization and updating protocol. Therefore, loggers will actively communicate with each other.

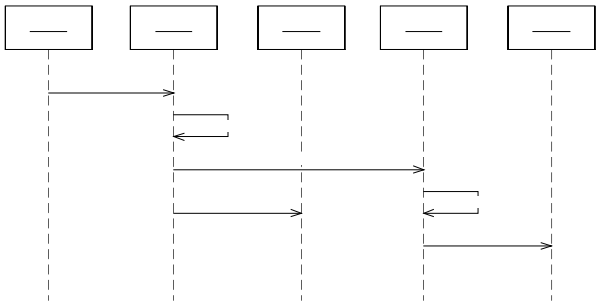

Figur 14. Sequence diagram for Updating Mechanism

This mechanism is also applied when generating components. Through a proxy, client command the proxy to generate objects, as explained in Figure 12. Local proxy will communicate to the other proxy with the same mechanism as Figure 14.

5.3 Locking Mechanism

There are 4 terms of locking mechanism used in distributed systems; lock, commit, abort, and unlock as defined in [5].

In a pure distributed system locking mechanism should be decided carefully. In a pure distributed system scenario, every task can have the same privilege to work on some shared objects at the same time. In groupware, it can be translated to the condition where every member in a session can work on the same artifact at the exactly same time. For example, in a design session by using CAD tools, every member may have his own cursor and modify the drawing at the same time as illustrated in Figure 14. Another example, in electronic Brainstorming System (EBS), every member might have possibility to write his ideas simultaneously, without having to wait the floor or token.

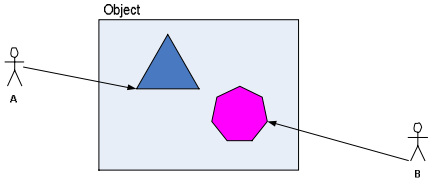

Figure 14. Pure distributed system

Thus, it leads to a situation where more than one task change an object and therefore possible problems mentioned above might be happened. To provide a pure distributed system, an expensive resource should be given.

In our scenario, when a user changes his role from Member to Floor Holder**,** automatically he will get a lock. Locking mechanism begins by the time the floor hands to him. There will be no further problem of locking in sequential and free floor control model, since there is one floor holder at a time. There is a single locking which the floor holder automatically receives. The groupware provide a commit and abort button that can be chosen by the floor holder either during his possession to the floor or at the end of his possession. System will prompt floor holder if he choose neither commit or abort at the end.

But when shared floor control model is used, locking should be applied carefully. Inside an application, there are some objects. Each user will only lock one object at a time. By the time he click an object, locking is applied, thus no one else can modified his possessed object. After he finished working on an object, he should choose either to commit or to abort. If for some period of time, he does not make any decision, the system will prompt him to make a decision.

This mechanism is only applied when there is many separated objects inside the application. Thus it can be applied to EBS, CAD tool, but not an application like Text Editor, or Presentation Display.

VII. IMPLEMENTATION TOOLS

The development of this groupware is designed to be implemented by using JavaBeans [www3], which based on Java [www4] language. As well as Java, JavaBeans implement the basic rules "Write Once, Run Anywhere™".

In our groupware, JavaBean components will be used as building blocks in composing applications. Such builder tool will be used to connect together and customize a set of JavaBean components to act as an application. But it does not necessarily that all programming are written in the shape of Beans (component). Classes, which are best written in modules, will be written in Java classes.

The communication of distributed components will be using the advantages of CORBA. Java is now supporting CORBA IDL. Thus, it is solving the problem that a basic JavaBeans could not support remote interaction in distributed applications. The other reason of choosing JavaBeans is because it supports communications to JDBC, Java RMI, as well as CORBA server.

CONCLUSION

It should be clearly enough how this paper contributes to the new highly tailorable and flexible groupware system by defining 32 main requirements for the system. The distribution architecture used in this proposal is hybrid architecture with network partitioning. Roles of user and the respective sequence in each flow controls are also explained. Concurrency control is applied by using logging, locking and updating mechanism. The system design in presented in this paper will be implemented using component based software, e.g. JavaBeans.

ACKNOWLEDGMENT

This research is conducted in University of Duisburg Essen, during final thesis in Double Degree Master Program Universitas Indonesia-Universität Duisburg-Essen. The study in Universität Duisburg-Essen is funded by the Ministry of National Education Republic of Indonesia.

REFERENCES

[1] Terzis S., Nixon P., Wade V. P., Dobson S. A., Fuller J., 2000, "The Future of Enterprise Groupware Applications," International Conference on Enterprise Information Systems, pg. 99 - 106

[2] Tanenbaum A.S., van Steen M., 2002, "Distributed Systems Principles and Paradigms," International Ed., Prentice Hall.

[3] Hummes J., Merialdo M., 2000, "Design of Extensible Component-Based Groupware," Kluwer Academic Press, Computer Supportive Cooperative Network 9: pg. 53-74.

[4] Chung G., Dewan P., 2004, "Towards Dynamic Collaboration Architectures," Proceedings of the 2004 ACM conference on Computer supported cooperative work

[5] Weis T., 2007, "Transaction and Concurrency Control," Distributed System Lecture, University of Duisburg Essen.

[www1]http://www.agiledata.org/essays/concurrencyControl.html, accessed 31 July 2008.

[www2]http://lsirwww.epfl.ch/courses/iis/2007ss/project/files/iis-summary.pdf, accessed 31 July 2008.

[www3]http://java.sun.com/javase/technologies/desktop/javabeans/index.jsp, accessed 18 August 2008.

[www4]http://java.sun.com/ accessed 18 August 2008.

Proceeding of the 11th International Conference on QiR (Quality in Research)
Faculty of Engineering, University of Indonesia, Depok, Indonesia, 3-6 August 2009
ISSN 114-1284

Development of Optical Free-Space Communication System to Improve Flexibility of RFID Microcell Network Deployment in Urban Area

Purnomo Sidi Priambodo, PhD.

Faculty of Engineering
University of Indonesia, Depok 16424
Tel : (021) 7270078 Fax : (021) 7270077
Email : pspriambodo@ee.ui.ac.id

ABSTRACT

Communication channels are one of the mandatory requirements to support RFID micro-cell network deployment in urban area. The communication channel infrastructures can be in the form of fiber-optic cable network, point-to-point microwave, RF wireless and coaxial ethernet cable network. However, in the case of dense and complex network, for instance a network which consists of many RFID mirocell, the use of fiber-optic and microwave is not flexible enough to support the communication channel requirements. The reason is because of the rigidity of the infrastructure and network topology. For those reasons, it is required to develope another new technology which is more flexible, less expensive and own large bandwidth.

To improve the flexibility of RFID Microcell Network Deployment, this paper introduces an initiative to develop optical free-space communication system. This system owns characteristics such as: wireless, point-to-point and having a capability to handle large bandwidth channel which is larger than the one microwave system does. The three main advantages of optical free-space communication system are: (1) more flexible and easy for installation; (2) own large bandwidth and (3) lower investment. However, this system has also some disadvantages, such as: non-immune to the atmospheric propagation noise and distorsion which cause high attenuation, hence it limits the distance of the channel not more than 2 kms.

The optical free-space communication system is technological engineering of the existing fiber-optic technology to obtain the new technology which is wireless, flexible, less expensive and large bandwidth. The entire components used in this optical free-space communication system are taken from the existing fiber-optics system. In this paper, the author elaborates optical free-space propagation characteristics, i.e., attenuation, polarizaton effect, Rayleigh scattering and possible fading. Further, the statistical model for spatial diversity reception is introduced to evaluate possible implementation of multi receivers. The model will be used to design the optimal optical free-space communication system.

Keywords: *free-space optical communication, RFID, microcell, atmospheric-propagation, atmospheric turbulence, spatial diversity reception*

1. INTRODUCTION

Free-space optical communications (FSOC) is a line-of-sight (LOS) technology where a modulated beam of visible or infrared light is transmitted through the atmosphere for broadband communications [1]. Similar to fiber optical communications, free-space optical communication uses a light emitting diode (LED) or laser source for data transmission [2]. The beam is collimated and transmitted through space or atmosphere rather than being guided through a fiber-optics cable. Free-space optical communications offer data rates comparable to fiber optical communications at a fraction of the deployment cost of microwave or fiber-optics links. The other advantages of this technology are flexible installation and extremely narrow laser beam widths provide no limit to the number of free-space optical links that may be installed in a given location. Thus advantages are justified and suitable to be implemented on microcell networks in urban area.

At this time, this technology can be installed license-free worldwide, can be installed in less than a day. This line-of-sight technology approach uses invisible beams of light to provide optical bandwidth connections [3]. It's capable of sending up to 1.25 Gbps of data, voice, and video communications simultaneously through the air — enabling fiber-optic connectivity without requiring physical fiber-optic cable. This optical connectivity doesn't require expensive fiber-optic cable or securing spectrum licenses for radio frequency (RF) solutions. While fiber-optic communications gained worldwide acceptance in the telecommunications industry, FSOC is still considered relatively new. This FSOC technology approach has a number of advantages:

1. Requires no RF spectrum license.
2. Easy to upgrade, and its open interfaces support equipment from a variety of vendors.
3. It is immune to radio frequency interference or saturation.
4. It can be deployed behind windows, eliminating the need for costly antenna building such as for RF technology.
5. No fiber-optic cables deployment required.

Applications:

FSOC technology can be applied for two different implementations. The first are applications for space communications between satellites, spacecrafts and deep-space between planets. The second are applications for terrestrial communications, similar to point-to-point or line-of-sight in microwave communication technology. For space communications, there are some facts that free-space optical communications will enable space missions to return 10 to 100 times more data with 1% of the antenna area of current state-of-the-art communications systems, while utilizing less mass and power. Data can also be exchanged between a more remote spacecraft and a station on /or near Earth. For example, planetary probes can generate a lot of image data, and a major challenge is to send large amount of data back to Earth. Until recently, radio links operating e.g. in the X band or Ka band were the only available technology. The basic advantage of the optical technology over radio links is that the much shorter wavelength allows for a much more directional sending and receiving of information. In technical terms, the antenna gain can be much higher. This is particularly important for bridging interplanetary distances. In the future FSOC will become the fundamental communication technology for deep-space communi-cations.

The second are applications for terrestrial communi-cations and omni-wireless, such as point-to-point communications between base-stations in cellular networks and omni Wi-Fi Local Area Networks (LANs). When the traffics increase, the cellular networks need to migrate become microcellular networks where the cell areas is about less than 1-km^2. The number of cellular base-stations (BTSs) increases in large number, the consequence is to deploy the communication channels between BTSs. Fiber-optics deployments are not flexible and very expensive for short distance between BTSs, while point-to-point microwaves do not give a good large bandwidth. The answer is FSOC, which gives us flexibility such as point-to-point microwaves, large bandwidth, easy deployment, not heavy and inexpensive investment. Applications for terrestrial are more challenging than applications for space communications, because terrestrial applications facing the effects of atmospheric turbulence.

The fundamental limitation of free-space optical communications for terrestrial links arises from the atmospheric medium through which it propagates. Free-space optical communication systems can be severely affected by fog and atmospheric turbulence [4]. Fog is vapor composed of water droplets, which are only a few hundred microns in diameter but can modify light characteristics or completely hinder the passage of light through a combination of absorption, scattering, and reflection. This can lead to a decrease in the power density of the transmitted beam, decreasing the effective distance of a free-space optical link. The atmospheric turbulence is mostly due to wind and temperature gradient, causes the index of refraction gradient by time and space. This refractive index gradient deflects and diverge the light beam, while the turbulence-wind will cause the light beam wandering.

The items that limit the FSOC performance, then listed in the following systematical parameters:

1) **Absorpsion** occurs when suspended water molecules in the terrestrial atmosphere absorb photons. This causes a decrease in the power density (attenuation) of the FSO beam and directly affects the availability of a system. Absorption occurs more readily at some wavelengths than others. However, the use of appropriate power, based on atmospheric conditions, and use of spatial diversity (multiple beams within an FSO-based unit) helps maintain the required level of network availability.
2) **Scattering** is caused when the wavelength collides with the scattering-particles. The physical size of the scattering-particles determines the type of scattering. When the particles are smaller than the wavelength, this is known as Rayleigh scattering. When the particles are of comparable size to the wavelength, this is known as Mie scattering. When the particles are much larger than the wavelength, this is known as non-selective scattering. In scattering — unlike absorption — there is no loss of energy, only a directional redistribution of energy that may have significant reduction in beam intensity for longer distances.
3) **Polarization-rotation** is caused by water molecules in the terrestrial atmosphere act like dipole-molecules with arbitrary orientation. Statistically it change the polarization of the light beam.
4) **Scintillation** is the temporaland spatial variation in light intensity caused by atmospheric turbulence. Such turbulence is caused by wind and temperature gradients that create pockets of air with rapidly varying densities and, therefore, fast-changing indices of optical reflection. These air pockets act like lenses with time-varying properties and can lead to sharp increases in the bit-error-rates of free-space optical communication systems, particularly in the presence of direct sunlight.

5) **Beam-Wandering** arises when turbulent wind current (eddies) larger than the diameter of the transmitted optical beam cause a slow, but significant, displacement of the transmitted beam. Beam wander may also be the result of seismic activity that causes a relative displacement between the position of the transmitting laser and the receiving photodetector.

Another concern in the implementation of FSOC is safety, because the technology uses lasers for transmission. The proper use and safety of lasers have been discussed since FSO devices first appeared in laboratories more than three decades ago. The two major concerns involve eye exposure to light beams and high voltages within the light systems and their power supplies. Strict international standards have been set for safety and performance, comply with the standards.

The main design challenges in FSOC are solving to overcome the effects of thus absorption, scattering, polarization rotation, scintillation and beam-wandering, which are due to the existence of fog and atmospheric turbulence. The first step prior to overcome the combination of atmospheric disadvantage parameters is by creating propagation model as explained in the next section.

Transmission Issues in Terrestrial Free Space Optical Communications

Particularly for large transmission distances, it is essential to direct the energy of the sender accurately in the form of a well-collimated coherence light beam. For long distance (5-km) applications with large bandwidth, it is suggested to use lasers that have narrower bandwidth and long coherence-length. However, for applications those require inexpensive investment with shorter distance and smaller bandwidth, it is sufficient to use collimated LED. The collimated light beam is required in order to limit the loss of power between the sender and the receiver due to beam expansion. However, the one needs large beam radius with high-quality optical front-wave to keep the receiver in line with the transmitter when beam-wandering happens. The one should use a diffraction-limited light source and a large high-quality optical telescope for collimating a large beam radius. Due to the short wavelength of light, the beam divergence of an optical transmitter can be much smaller than that of a radio or microwave source of similar size. Using a frequently used term in the area of radio transmission, the antenna gain can be much higher for optical transmitters over 100 dB even for moderate telescope diameters of e.g. 25 cm.

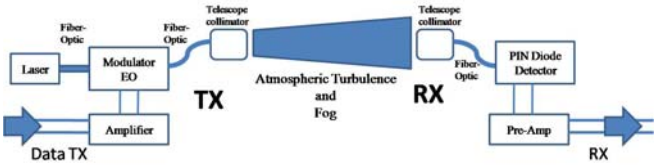

Fig. 1: Setup for a Simplex FSOC system. Although the transmitter signal is approximately collimated, part of the transmitted power may miss the detector.

It is also advantageous to have a large high-quality optical telescope on the side of the receiver. It is essential not only to collect as much of the sender's power as possible, but also to minimize disturbing influences, e.g. from background light, which introduces noise and thus reduces the data transmission capacity. Both high sensitivity and high directionality can be achieved by using a large high-quality telescope at the receiver end. High directionality also requires high precision in the alignment of the sender and receiver.

An important issue is the power budget of a free-space link, including the transmitter's power and all power losses. The remaining power at the receiver largely determines the possible data transmission rate, even though this is also influenced by the modulation format, the acceptable bit error rate, and various noise sources, in particular laser noise, pre-amplifier noise, excess noise in the receiver (e.g. an avalanche photodiode), and background light. The latter can often be efficiently suppressed with additional narrow-band optical filter and high-quality telescope, since the optical bandwidth of the signal is fairly limited, whereas background light is usually very broadb*a*nd.

Severe challenges can arise from the effects of atmospheric disturbances such as clouds, dust and fog, which can cause not only strong signal attenuation but also inter-symbol interference. To solve this problem, it is suggested to use sophisticated techniques of forward error correction embedded in the datalink layer, which allow for reliable high-capacity optical links even through thick clouds.

2. SPATIAL DIVERSITY RECEPTION MODEL TO IMPROVE PERFORMANCE

In this section, the authors will elaborate a statistical model of spatial diversity reception to overcome the effects of atmospheric turbulence. Spatial diversity reception, which has been introduced for RF applications, is a potential method to overcome the degradation due to atmospheric turbulence [5-9]. Application of spatial diversity reception in FSOC has been introduced in some researches [7-9]. The performance of spatial diversity reception on FSOC has been studied and proposed [8], Assuming that atmospheric-turbulence fading is

ISSN 114-1284

uncorrelated at each of the optical receivers. In order for this assumption reasonable, the spacing between receivers should exceed the fading correlation length in the plane of the receivers. It may be hard to satisfy this assumption in practical situation, for any reasons. Available space may not permit enough receivers spacing. In power-limited links, which employ collimated beam with large diameter, the receiver spacing required obtaining uncorrelated fading, may exceed the beam diameter.

2.1. Maximum-Likelihood (ML) Diversity Detection on Turbulence Channels

In the case of spatial diversity reception with n-receivers, the received signal is presented by *n*-component vector. Taking account of correlation between the receivers, bit-error probability equation for maximum-likelihood in [4] is modified as follows:

$$P\left(\vec{r}\,|\,Off\right)=\exp\left[-\sum_{i=1}^{n}\frac{r_i^2}{N_i}\right]\prod_{1}^{n}\frac{1}{\sqrt{\pi N_i}} \tag{1}$$

$$P\left(\vec{r}\,|\,Off\right)=\int_{\vec{X}} f_{\vec{X}}\left(\vec{X}\right)\bullet\exp\left[-\sum_{i=1}^{n}\frac{\left(r_i-\eta I_0 e^{2X_i-2E[X_i]}\right)^2}{N_i}\right]\bullet\prod_{1}^{n}\frac{dX_i}{\sqrt{\pi N_i}} \tag{2}$$

Where $N_i / 2$ is noise covariance of the *i-th* receiver and

$$f_{\vec{X}}\left(\vec{X}\right)=\frac{\exp\{-\frac{1}{2}\left[\left(X_1-E[X_1]\right)\cdots\left(X_n-E[X_n]\right)\right]C_X^{-1}\begin{bmatrix}\left(X_1-E[X_1]\right)\\ \vdots\\ \left(X_n-E[X_n]\right)\end{bmatrix}}{(2\pi)^{n/2}\,|C_X|^{1/2}} \tag{3}$$

C_X is the covariance matrix of the log-amplitude in the *n*-receivers. The likelihood function is

$$\Lambda\left(\vec{r}\right)=\frac{P\left(\vec{r}\,|\,On\right)}{P\left(\vec{r}\,|\,Off\right)}=\int_{\vec{X}} f_{\vec{X}}\left(\vec{X}\right)\bullet\exp\left[-\sum_{i=1}^{n}\frac{\left(r_i-\eta I_0 e^{2X_i-2E[X_i]}\right)^2-r_i^2}{N_i}\right]d\vec{X} \tag{4}$$

The ML detector uses the decision rule $\Lambda\left(\vec{r}\right)\underset{<Off}{>On}1$. Since the log-amplitude follows a joint log-normal distribution, calculation of the likelihood function in (4) involve multi-dimensional integration. It is emphasized that this decision rule has been derived under the assumption that the receiving side knows the fading correlation but not the instantaneous fading state.

The bit-error probability of the ML receiver is given by

$$P_b = P(Off)\ .\ P(Bit\ Error|\ Off) + P(On)\ .\ P(Bit\ Error|On) \tag{5}$$

where *P(Bit Error| Off)* and *P(Bit Error| On)* denote the bit-error probabilities when the transmitted bit is off and on, respectively. Without considering inter-symbol interference, which can be ignored when the bit rate is not high and multipath effects are not pronounced, we have:

$$P\left(Bit\ error\,|\,Off\right)=\int_{\Lambda\left(\vec{r}\right)>1} p\left(\vec{r}\,|\,Off\right)d\vec{r} \tag{6}$$

and

$$P\left(Bit\ error\,|\,On\right)=\int_{\Lambda\left(\vec{r}\right)<1} p\left(\vec{r}\,|\,On\right)d\vec{r} \tag{7}$$

To evaluate the optimal ML diversity detection scheme, we compare it with the conventional equal-gain combining (EGC) scheme [ ]. In the EGC scheme, it is assumed that the receiving side has knowledge of the marginal distribution of the channel fading, in every receiver, but has no knowledge of the fading correlation or the instantaneous fading state. For each single individual receiver output, it is able to find an optimum threshold τ_i. Then the EGC detector adds together the *n*-receivers output with equal gains and compares the sum to the threshold

$$T_{th}=\sum_{i=1}^{n}\tau_i \tag{8}$$

The error probability of EGC is

$$P_b=\int_{\vec{X}} f_{\vec{X}}\left(\vec{X}\right)P\left(Bit\ Error\,|\,\vec{X}\right)d\vec{X} \tag{9}$$

where

$$P\left(Bit\ Error|\vec{X}\right)=P(Off)\,Q\left(\frac{T_{th}}{\sqrt{2N}}\right)+P(On)\,Q\left(\frac{\eta I_0\left(e^{2X_1-2E[X_1]}+e^{2X_2-2E[X_2]}\right)-T_{th}}{\sqrt{2N}}\right) \tag{10}$$

2.2. Numerical Simulations for Multi Receivers

In this section, we intend to present numerical simulations of the performance of spatial-diversity reception/detection with multi-receivers and dual-receivers as well. However, up to this Conference submission deadline our research group has not finished the numerical simulation yet. The structure of multi-receiver link that is represented by dual-receiver is illustrated by Fig.2. As described above, the ML receiver (Fig.2a) has full knowledge of the turbulence-correlated fading matrix C_X, while the EGC receiver (Fig.2b) has knowledge only the marginal distribution of fading at the

receivers. It is assumed that $E[I_1] = E[I_2] = E[I]$ and $N_1 = N_2 = N$ and define the electrical signal-to-noise ratio $SNR = (\eta E[I]^2)/N$.

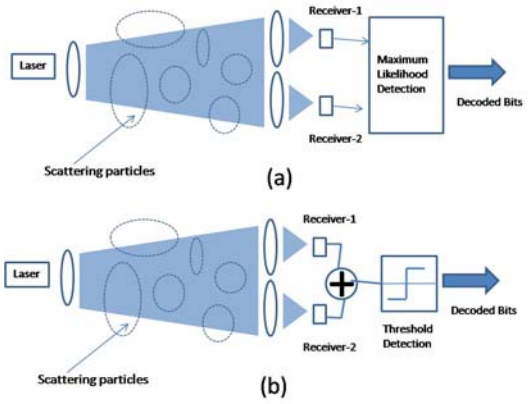

Fig. 2: Dual-receiver model on atmospheric turbulence channels with correlated turbulence fading. (a) Maximum-likelihood detection. (b) Equal-Gain combining with threshold detection.

To obtain simulation results, it is assumed that $E[X] = 0$ and $\sigma_X = 0.1$, varying the normalized correlation ρ_d from 0 to 0.9. It is also compared to set up value $\delta_X = 0.25$. We expect that turbulence correlated fading will cause a larger degradation of bit error probability when the standard deviation noise δ_X is larger. Hipothetically, with two-receivers, ML detection achieves a better performance than EGC for a given SNR. The advantage of ML over EGC method is more pronounced when the correlation ρ_d between the two receivers is high. It is more reasonable when the SNR is high, then the errors are caused mainly by turbulence-correlated fading, as opposite to the noise.

3. CONCLUSION

Free space optical communications through atmosphere is under intensive researches, where various methods have been proposed to overcome turbulence-effects communication signal fading. In this paper we introduce spatial diversity reception model for free space optical communications. This model can be use to analyze and later on to overcome the effects due to turbulence-correlated log-amplitude fluctuations.

ACKNOWLEDGMENT

This research is supported by Universitas Indonesia Research Grant called RUUI-2009, Nb.DRPM/RUUI Unggulan/2009/I/3342 .

REFERENCES

[1] V. W. S. Chan, “Optical Space Communications”, IEEE J. Sel. Top. Quantum Electron. 6 (6), 959 (2000)

[2] O. Caplan, “Laser communication transmitter and receiver design”, J. Opt. Fiber Commun. Rep. 4, 225 (2007)

[3] K. F. Büchter *et al.*, “All-optical Ti:PPLN wavelength conversion modules for free-space optical transmission links in the mid-infrared”, Opt. Lett. 34 (4), 470 (2009)

[4] Xiaoming Zhu and Joseph M. Khan, “Free Space Optical Communication Through Atmospheric Turbulence Channels,” IEEE Transactions on Communications, Vol. 50, No. 8, August 2002

[5] G. L. Stuber, *Principles ofMobile Communication.* New York: Kluwer Academic, 1996.

[6] J. G. Proakis, *Digital Communication,* 3rd ed. New York: McGraw-Hill, 1995.

[7] M. Srinivasan and V. Vilnrotter, “Avalanche photodiode arrays for optical communication receivers,”, NASA TMO Progress Rep. 42-144, 2001.

[8] M. M. Ibrahim and A. M. Ibrahim, “Performance analysis of optical receivers with space diversity reception,” *Proc. IEE—Commun.,* vol. 143, no. 6, pp. 369–372, December 1996.

[9] X. Zhu and J. M. Kahn, “Maximum-likelihood spatial-diversity reception on correlated turbulent free-space optical channels,” presented at the IEEE Conf. on Global Commun., San Francisco, CA, Nov.–Dec. 27–1, 2000.

ISSN 114-1284

Content-Based Image Retrieval (CBIR) Web-based System for Osteoporosis X-Ray Image Database: A Preliminary Result

Ratnasari N. R[a,b], Lukito E. N.[b], Th. Sri Widodo[c], Adhi Susanto.[d], Nurokhim[e]

[a]*Faculty of Engineering*
University of Muhammadiyah Surakarta
Tel : (0271) 717417 ext 223. Fax : (0271) 715 448
E-mail : rnrums@yahoo.com

[b,c,d]*Faculty of Engineering*
University of Gadjah Mada
E-mail : lukito@mti.ugm.ac.id

[e]*BATAN*
E-mail : nurokhim@batan.go.id

ABSTRACT

This paper presents design and preliminary results of research on Content-Based Image Retrieval (CBIR) web-based system for osteoporosis X-Ray images database. In client-server architecture, server provides five query image result based on user's (client) image content. System's basic concept consists of two components: features extraction and similarity measurement. Feature extraction in offline process is conduct to find appropriate feature to role as image descriptor in CBIR. In online process, feature extraction is conduct to extract user's image content (feature) and similarity measurement is conduct in retrieval process. We used statistical approach Grey level co-occurance matrix (GLCM) and wavelet transform for extracting image feature. We also used log-polar transform prior to wavelet transform to reduce rotation and scaling effect. Selection on image feature is conduct by choosing feature vector gives optimum accuracy on image classification test. Experiment on small databases shows promising result in applying CBIR web-based systems for osteoporosis database. Feature vector selected as descriptor is two-dimension vector consist of Contrast measured from GLCM and norm-1 of approximation wavelet decomposed image. Test on log-polar transforms shows that this transforms is improving accuracy on classification.

Keywords
CBIR, osteoporosis, descriptor

1. INTRODUCTION

Application computer in telemedicine has improved medical service in healthcare area. One of the applications is in applying databases on medical information such as medical record or medical image. Several researchers devoted their works in designing such database and in finding the most efficient method in image retrieve from the databases. This attempt related to the specific purposes of medical image that is one of diagnostic tools.

Recently, compare to common method textual-base image retrieval, CBIR is considered as the more appropriate choice method for image retrieval in medical image databases. This method retrieves images from database using information directly derived from the contents of image themselves, rather than from accompanying text or annotation [1]. Time-consuming process in giving annotations on each image, on the textual-bases images retrieval method, is one of the reasons for choosing this method. The specific properties of medical image, such as recognition image from its pathological value give another difficulty on applying textual-base medical image retrieval. Difficulty found in describing medical image pathological area in word, because of irregular shape of pathological area in the image. Moreover, different radiologist would give different opinion on each medical image. All those difficulties expected to overcome by applying CBIR on medical image database.

In this paper, we present preliminary results in research on CBIR web-based systems for osteoporosis X-Ray image database. In this system, user could retrieve image based on user's example image. As the result, system presented five images which has similarity feature as example image. Data in this research are Digitized X-Ray image already known the osteoporosis level based on Index Singh due to simple verification on validity.

2. CBIR ON OSTEOPORISIS X-RAY IMAGE DATABASE

This section presents design on CBIR Web-based Systems for Osteoporosis X-Ray image database. We describe here the basic concept, method for feature extraction and selection, and software implementation.

2.1 Basic Concept

System built in this research is planed to be web-based system in client-server architecture (Fig. 1). In this system, server will provide image from database for user in client side. Retrieval image method in this system is based on client's image content. Principle process in this system consists of two components (Fig.1): Feature extraction and Similarity measurement. Feature extraction conduct for images on database (offline process) and user's image (online process). In offline process (only in server side), feature extracted from each images in database (descriptor) stored in database along with the image. In online process, system extract feature vector from user's image and uses it on image retrieval purposes. Image retrieval is conducted by computing distance (i.e., similarities) between feature vector of user's image and those of images in database. As result, the system will than provide five most similar images (five closest distance images). I this research we also provide textual information for each image in database if available.

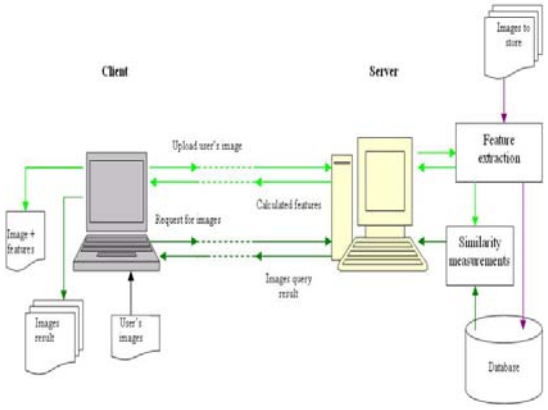

Figure 1. Web-based CBIR basic concept

2.2 Features Extraction and Selection

Osteoporosis is characterized by an absolute decrease in the amount of bone to a level below that required for mechanical support of normal activity and by the occurrence of non-traumatic skeletal fracture [2]. The observation of *trabecular* pattern change for diagnosis of osteoporosis was first proposed in the 1960s using radiographs of proximal femur. The diagnosis was known as Singh Index grading system.

In this research, we used this structure pattern as image feature. We used 4 grades of Singh indexed image (grade 3 to grade 6) from women patients between 45 – 65 years of age. Image feature extraction is done by image textural analyzing which will produce feature vector of each image. This feature vector is used as descriptor on the image retrieval systems. We used statistical approach and wavelet transform for extracting textural feature from image.

On statistical approach we use grey-level co-occurance matrix (GLCM) methods to extract feature (Fig.2). As X-Ray image represent as grey-level image, this method is considered as suitable method. From GLCM, quantities measured as feature are *Contrast* and *Uniformity*.

$$Contrast = \sum_{i=i}^{K}\sum_{j=1}^{K}(i-j)^2\, p_{ij} \qquad (1)$$

$$Uniformity = \sum_{i=1}^{K}\sum_{j=1}^{K} p_{ij}^2 \qquad (2)$$

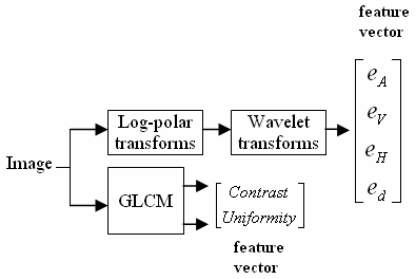

Figure 2. Feature extraction using GLMC and Wavelet transform

Wavelets transforms provide good multiresolution analytical tools for texture analysis and classification [3][4]. Experimental results show that this approach can achieve a high accuracy rate [5]. However, this approach assumes that the texture images have the same orientation and scale, which is not realistic for most practical application. A number works address the problem on rotation and scale on image. One on these works that shows promising results is using log-polar transforms on image [5][6] and combined wavelet packet transforms. Considered that image data in this research are obtained from scanning X-Ray analog image, which usually subject to certain random skew angles and scaling, we use this method prior to wavelets transforms on image texture-based feature extraction [6] (Fig. 2). Quantities calculated as features in this approach are the norm-1 *e* from all component of wavelet decomposed image (approximation, vertical, horizontal, and diagonal component).

$$e = \frac{1}{N^2}\sum_{k=1}^{N}|C_k|^2 \qquad (3)$$

Not all of the measure features above are considered as descriptor. In this paper, feature vector as descriptor is a two-dimension vector using combination of two features, one from statistical approach and another from wavelet transform. Defining which feature vector as descriptor is done by trial and error (Fig. 3).

Test on image classification is conduct on some sample data using each combination of two features. A simple minimum distance classifier method was chosen for this testing process. Feature vectors giving optimum accuracy on classification is selected. Feature vectors selected is used as descriptor for the systems and henceforth, system would only extract these features from images.

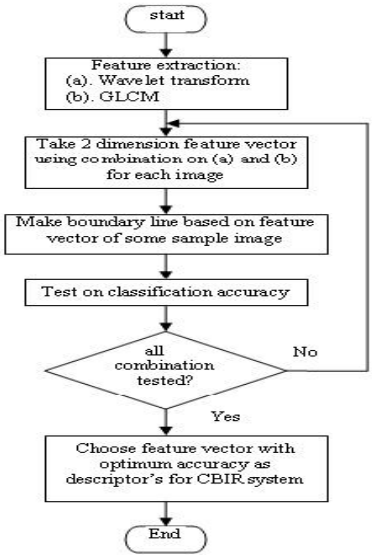

Figure 3. Flowchart on feature vector selection process

2.3 Similarity Measurements

Similarity measurement is conduct on image searching from database. The similarity of two images I_a and I_b is the distance between their descriptor $\mathbf{f}_a$ and $\mathbf{f}_b$. In this research, Euclidean distance $D(\mathbf{f}_a, \mathbf{f}_b)$ was adopted to measure the similarity between the query image and example (user's) image.

$$D(\mathbf{f}_a, \mathbf{f}_b) = \left[(\mathbf{f}_a - \mathbf{f}_b)^T(\mathbf{f}_a - \mathbf{f}_b)\right]^{\frac{1}{2}} \qquad (4)$$

The smaller distance is, the more similar the two images are. After calculating the distance, systems ranks similarity in descending order and then returns the top five images that are most similar to the user's image.

2.4 Software Implementation

Java RMI (Remote Method Invocation) is chosen in establishing systems based on Client-server architecture. We also used JAI (Java Advanced Imaging) library for image process supporting. On client side, we use Java Applet that runs in Internet browser. Important class developed in establishing this system shown in Table 1 below.

Table 1: Classes built in software implementations.

Class	Explanations
`OsteoObj`	Hold image data object.
`ImageRead`	Reading image in BMP format (grayscale), hold image in matrix forms.
`Convolusion`	Performing convolution operation, hold convoluted image in matrix form.
`Matrice`	Hold matrix data, perform operations used in this research.
`FilterRow`	Hold filter for wavelet transform.
`DBImageObjecs`	Hold all instance objects from OsteoObj.
`DBImagePane`	UI Panel to hold and display image databases
`RemoteInterface`	Remote interface for RMI Server
`ServerOsteo`	RMI Sever
`JApplletOsteo`	Java Applet for browser implementation

3. EXPERIMENTS AND PRELIMINARY RESULTS

3.1 Pre-process (Feature extraction and selection)

Experiment on feature selection shows that only four feature vectors (Table 2): $[e_A \ \textit{Contrast}]^T$, $[e_A \ \textit{Uniformity}]^T$, $[e_V \ \textit{Uniformity}]^T$, and $[e_D \ \textit{Uniformity}]^T$, that result in clustering in classification process. Among all those

combination, combination consist of *Contrast* on GLCM and Norm-1 on approximation component $[e_A \quad Contrast]^T$ is the best choice for image descriptors. Figure 4 shows classification based on this feature vector. Boundary lines are performed based on feature vectors (descriptor) of 37 images in databases.

Table 2: Classification accuracy achieved on classification process using four feature vectors

Classes	Classification acuracy using feature vectors: (%)			
	$[e_A \quad Contrast]$	$[e_A \quad Uniformity]$	$[e_V \quad Uniformity]$	$[e_D \quad Uniformity]$
Grade 3	91.67	75.00	66.67	75.00
Grade 4	70.00	80.00	60.00	30.00
Grade 5	83.33	83.33	66.67	25.00
Grade 6	100.00	100.00	100.00	100.00

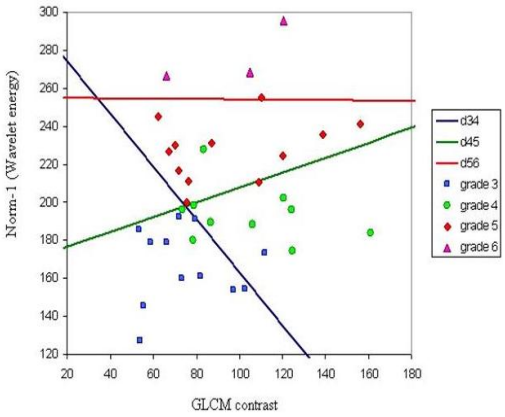

Figure 4. Decision boundary of minimum distance classifier based on $[e_A \quad Contrast]^T$.

3.2 Web-based implementation

Web-based implementation experiment shows that systems can perform image retrieval based on image contents. Previously, system presents user's example image and its features (Fig. 5). Furthermore, after conducting image searching, system present five images result from database (Fig.6). Those five images presented in Scroll Panel and accompany with some textual information (if any): feature vector, grade index, and some comment from expertise. The first order image present is the closest and the last image presented is the farthest to the user's example image.

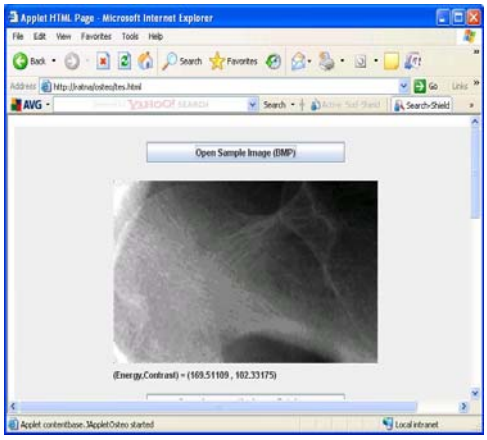

Fig.5. Presentation of user's image on user's screen.

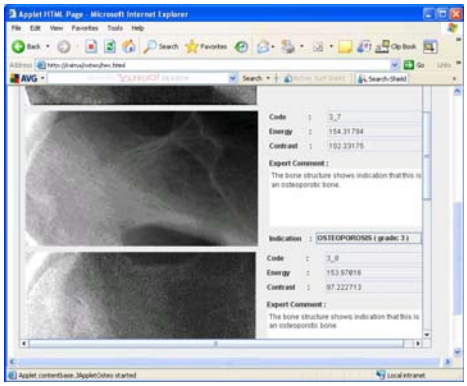

Fig.6. Presentation of retrieval image result in Scrolling Panel on user's screen.

3.3 Test on Log-polar transforms

Experiment for examine log-polar transform impact on image rotation and scaling effect shows that log-polar only reducing error in wavelet energy measured on rotated image (0.9% to 0.2%) and not on scaled image. Test conduct in classification process also shown that log-polar transform improving classification accuracy from 66.56% to 75.42 % (in average). However, on image retrieval process (on-line), although impact on image query result order, do not giving significant effect in image query result. This small impact is due not only on the use two-dimension vector, combination of wavelet energy and contrast on GLCM, but also from small images present on query results (only five images). When order is an important factor and more then five images result is to be presented, the use of log-polar transform prior to wavelet transforms is an important requirement.

4. CONCLUSION

Preliminary result in this works shows promising result in applying CBIR for osteoporosis X-Ray image databases. Combination on wavelet energy signature and contrast on GLCM as two-dimension vector descriptor, give sufficient accuracy for the CBIR purposes. Improvement in classification accuracy shown that, the use of log-polar transform prior to wavelet transform is useful in classification study. The log-polar transform is also become an important requirement if order in image query result is important and more than five image result is to be presented to the user.

However, only small database used for verification in this preliminary research, and most of data has already confirmed its index Sigh. Further works would be applying bigger database and more indistinct indicated data to the system. Moreover, feature vector dimension would need to be increased.

ACKNOWLEDGMENT

F. A. Author thanks to Mr. J. Tjandra Pramudityo for giving copy on data of osteoporosis X-Ray images used in this research.

REFERENCES

[1] El-Naqa, I., Yang, Y., Galatsanos, N. P., & Wernick, M. N., "A similarity learning approach to content-based image retrieval: Application to digital mammography", *IEEE Transaction on Medical Imaging*, vol. 23, no. 10, pp. 1233-1244, 2004.

[2] H.W. Wahner and Fogelman I., *The Evaluation of Osteoporosis: Dual Energy X-ray Absorptiometry in Clinical Practice*, Martin Dunitz Ltd., London, 1994.

[3] T. Chang, C.C. J. Kuo, "Texture Analysis and Classification with Tree-Structured Wavelet Transform", *IEEE Transaction on Image Processing*, vol.4, pp. 1549-1560, Nov. 1995.

[4] A. Laine and J. Fan, "Texture Classification by Wavelet Packet Signatures," *IEEE Transaction on Pattern Analysis and Machine Intelligent*, vol. 8, pp. 472 – 481, July 1986.

[5] Chi-Man Pun and Moon-Chuen Lee, " Log-Polar Wavelet Energy Signature for Rotation and Scale Invariant Texture Classification", *IEEE Transaction on Pattern Analysis and Machine*, 25 (5), 500 – 603, 2003.

[6] Ratnasari N. R, Lukito E. N, Thomas Sri W., Adhi Susanto, Nurokhim. "Design and Preliminary Result on Content-Based Image Retrieval (CBIR) System for Osteoporosis X-Ray Image Database.", *Proceeding of International Conference on Rural Information and Communication Technology 2009*, pp. 199–202, July 2009.

Proceeding of the 11th International Conference on QiR (Quality in Research)
Faculty of Engineering, University of Indonesia, Depok, Indonesia, 3-6 August 2009
ISSN 114-1284

The Influence of Moment Inertia to Induction Motor Rotation in Sensorless Direct Torque Control and Duty Ratio

Ridwan Gunawan[a], Muhammad Luniara Siregar[b]

[a]*Faculty of Engineering*
University of Indonesia, Depok 16424
Tel : (021) 7270011 ext 51. Fax : (021) 7270077
E-mail : ridwan@eng.ui.ac.id

[b]*Faculty of Engineering*
University of Indonesia, Depok 16424
Tel : (021) 7270011 ext 51. Fax : (021) 7270077
E-mail : m.luniara@gmail.com

ABSTRACT

The vector control has become the first alternative in control of three phase induction motor. One of the vector control method which is commonly used is a direct torque control (DTC) method. However, this system has drawback as the existence of ripples torque. The addition of duty ratio control base on fuzzy logic can give better performance when is compared to conventional DTC. By doing an examination on DTC and duty ratio using small, medium and big capacities of three phase induction motors can be shown the influence from moment inertia to rotor rotation. This paper uses MATLAB SIMULINK for the simulation study with three types of motors power, for example 1, 10 and 50 hp. It is shown that using the same parameters, a motor with a larger moment inertia gives a better performance in comparison to a motor with smaller moment inertia.

Keywords : *induction motor, direct torque control, duty ratio,fuzzy logic, moment inertia*

1. INTRODUCTION

Direct Torque Control was introduced by I. Takahashi,T. Noguchi and Depenbrock as a new strategic in induction motor control, using inverter as voltage source [1-2].This method gives direct control torque and flux motor with to chose voltage vector, it used to limit the torque and flux error, is bounded in hysteresis band and to acquire the torque response at a short time. The DTC method does not use coordinate transformation as the *Field Oriented Control* method, not necessary voltage modulation block and torque, so that it has simple computation, the weakness of this method is torque ripple.

At steady state condition and constant torque, a voltage vector is applied to motor , so that gives torque response rise until end of switching period after that null voltage vector is applied for to drop the torque to reference value until end of the switching period, this event result torque ripple. The last research [3], had done the ripple torque using to give various *hysterisis band* value in hysterisis comparator, but the torque ripple motor as same as before.

The reasearch in this paper has goal , to do control simulation with to less torque ripple using DTC method and *duty ratio* . Simulation control torque ripple is applied to three phase induction motor using different power capacity, 1, 10 and 50 hp, and how the influence moment of inertia to motor's speed.

2 MODELLING

Three phase Induction motor model equations in αβ axis with parameter stator current and rotor flux is shown as below

$$\frac{d}{dt}i_{s\alpha}=\frac{L_r}{L_sL_r-L_m^2}\left(-R_s-\frac{L_m^2R_r}{L_r^2}\right)i_{s\alpha}+\frac{L_m}{(\sigma L_sL_rT_r)}\psi_{r\alpha}+\frac{L_m\omega_r}{(\sigma L_sL_r)}\psi_{r\beta}+\frac{1}{\sigma L_s}V_{s\alpha} \quad (2.1)$$

$$\frac{d}{dt}i_{s\beta}=\frac{L_r}{L_sL_r-L_m^2}\left(-R_s-\frac{L_m^2R_r}{L_r^2}\right)i_{s\beta}-\frac{L_m\omega_r}{(\sigma L_sL_r)}\psi_{r\alpha}+\frac{L_m}{(\sigma L_sL_rT_r)}\psi_{r\beta}+\frac{1}{\sigma L_s}V_{s\beta} \quad (2.2)$$

$$\frac{d}{dt}\psi_{r\alpha}=\frac{L_m}{T_r}i_{s\alpha}-\frac{1}{T_r}\psi_{r\alpha}-\omega_r\psi_{r\beta} \quad (2.3)$$

$$\frac{d}{dt}\psi_{r\beta}=\frac{L_m}{T_r}i_{s\beta}+\omega_r\psi_{r\alpha}-\frac{1}{T_r}\psi_{r\beta} \quad (2.4)$$

where $\frac{L_r}{L_sL_r-L_m^2}=\frac{1}{\sigma L_s}$ and $T_r=\frac{L_r}{R_r}$

Torque equation :

$$T_e=N_pL_m(i_{r\alpha}i_{s\beta}-i_{r\beta}i_{s\alpha}) \quad (2.5)$$

speed and rotor position equation :

$$\frac{d}{dt}\omega_r=\frac{(T_e-T_l)}{J} \quad (2.6)$$

$$\frac{d}{dt}\theta_r = \omega_r \qquad (2.7)$$

Equations (2.1), (2.2), (2.3), and (2.4) can be written in matrix form:

$$\frac{d}{dt}\begin{bmatrix} i_{s\alpha} \\ i_{s\beta} \\ \psi_{r\alpha} \\ \psi_{r\beta} \end{bmatrix} = \begin{bmatrix} a_{11} & a_{12} & a_{13} & a_{14} \\ a_{21} & a_{22} & a_{23} & a_{24} \\ a_{31} & a_{32} & a_{33} & a_{34} \\ a_{41} & a_{42} & a_{43} & a_{44} \end{bmatrix} \begin{bmatrix} i_{s\alpha} \\ i_{s\beta} \\ \psi_{r\alpha} \\ \psi_{r\beta} \end{bmatrix} + \begin{bmatrix} b_{11} & b_{12} \\ b_{21} & b_{22} \\ b_{31} & b_{32} \\ b_{41} & ba_{42} \end{bmatrix} \begin{bmatrix} V_{s\alpha} \\ V_{s\beta} \end{bmatrix}$$

where :

$$a_{11} = a_{22} = \frac{L_r}{L_s L_r - L_m{}^2}\left(-R_s - \frac{L_m{}^2 R_r}{L_r{}^2}\right)$$

$$a_{13} = a_{24} = \frac{L_m}{(\sigma L_s L_r T_r)}$$

$$a_{12} = a_{21} = a_{32} = a_{41} = 0$$

$$a_{14} = -a_{23} = \frac{L_m \omega_r}{(\sigma L_s L_r)}$$

$$a_{31} = a_{42} = \frac{L_m}{T_r}$$

$$a_{33} = a_{44} = -\frac{1}{T_r}$$

$$a_{34} = -a_{43} = \omega_r$$

$$b_{12} = b_{21} = b_{31} = b_{41} = b_{42} = 0$$

$$b_{11} = b_{22} = \frac{1}{\sigma L_s}$$

Output vector is written

$$I_s = CX$$

$$\begin{bmatrix} i_{s\alpha} \\ i_{s\beta} \end{bmatrix} = \begin{bmatrix} 1 & 0 & 0 & 0 \\ 0 & 1 & 0 & 0 \end{bmatrix} \begin{bmatrix} i_{s\alpha} \\ i_{s\beta} \\ \psi_{r\alpha} \\ \psi_{r\beta} \end{bmatrix}$$

Induction motor parameters:

Rs, Rr = stator and rotor resistant (ohm)
Np = number of poles
Ls, Lr = stator and rotor inductance (henry)
Te = electromagnetic torque (Newton.meter)
Lm = magnetic inductance (henry)
ω_r = rotor speed (radian/second)

3. DIRECT TORQUE CONTROL

The Block diagram DTC consist of hysterisis comparator control, torque estimator, flux magnitude, stator flux position and voltage selector, are used as input voltage inverter (*Voltage Source Inverter* –VSI *)* [8].

Basic DTC block diagram can be viewed in Figure 3.1 below :

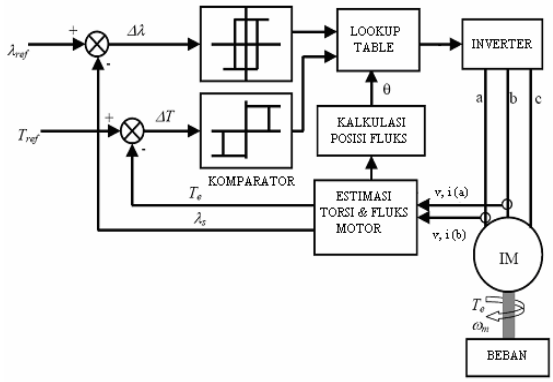

Figure 3.1 Basic DTC block diagram

Figure 3.1 describes DTC method uses hysteresis comparator, what will be compared between stator flux reference and torque with results of stator flux reference and torque motor estimate and stator flux position will be used to choose voltage vector.

3.1 Hysterisis Comparator

The torque control uses hysteresis comparator with three level torque conditions (cT_e). The value of (cT_e) is 1, if the torque must be raise, -1 if decrease and zero , if torque value is constant.

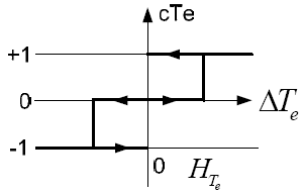

Figure 3.2 Hysteresis Comparator Torque Three Level

The flux controller uses hysteresis comparator with two level. Value of ($c\psi$) is 1, if the flux must be raise and -1 if decrease.

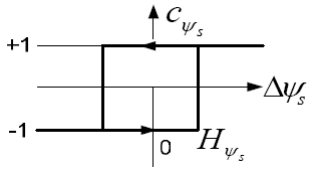

Figure 3.3 Hysteresis Comparator Flux Two Level

3.2 Choosing Voltage Vektor

The voltage vector has six sector and angle of each sector is 60º. The first sector begin -30º until 30º and second sector begin 30º – 90º, further each sector is added by interval 60º until sector 6th with angle between 270º - 30º. Figure 3.4 is chosen voltage vector at time the stator flux in first sector, the voltages V_1 and V_4 are not

used because parallel with normal line. In each sector has flux condition raise (FN) and decrease (FT), also torque condition raise (TN), constant and decrease (TT), what is seen from tangential axis (tan) and normal axis (n).

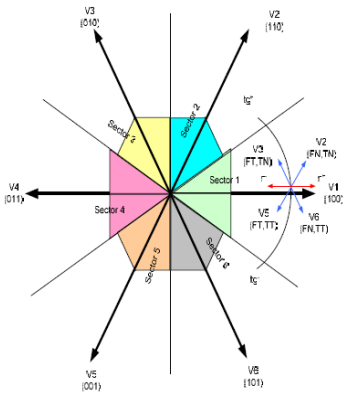

Figure 3.4 Voltage vector when flux at first sector

Voltage vector from each sector is written as switching below in table 3.1

Table3.1 The Choosing voltage vector [8]

φ	Te	Sector					
		1	2	3	4	5	6
cφ = 1	$c_T = 1$	V2	V3	V4	V5	V6	V1
	$c_T = 0$	V7	V0	V7	V0	V7	V0
	$c_T = -1$	V6	V1	V2	V3	V4	V5
cφ = -1	$c_T = 1$	V3	V4	V5	V6	V1	V2
	$c_T = 0$	V0	V7	V0	V7	V0	V7
	$c_T = -1$	V5	V6	V1	V2	V3	V4

The cφ = 1 means flux must be risen and if cφ = -1 , the flux must be decreased, and for the torque condition, c_T = 1 means torque must be risen, c_T = 0, the torque is constant and c_T = -1 the torque must be decreased

3.3 Inverter

Inverter voltage source has six switch or three couples, which each couple works to change over, means each couple of switch cannot work at the same time. If the value of Sa is 1 then the value of Sa' is 0.

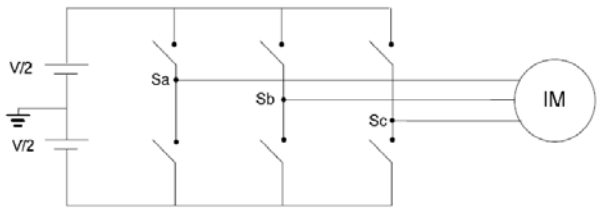

Figure 3.5 Inverter voltage source diagram

The inverter output is three phase voltage as input induction motor is written in equation:

Vn=(Sn–Sn')xVDC/2 (n=a,b,c) 3.1

Tabel 3.2 Switching base on voltage vector

	Sa	Sb	Sc
V0	0	0	0
V1	1	0	0
V2	1	1	0
V3	0	1	0
V4	0	1	1
V5	0	0	1
V6	1	0	1
V7	1	1	1

3.4 Estimate current model using *Observer*

For estimate values of stator flux, torque and stator flux position used the *observer* represents the estimate current model and rotor speed. [3].

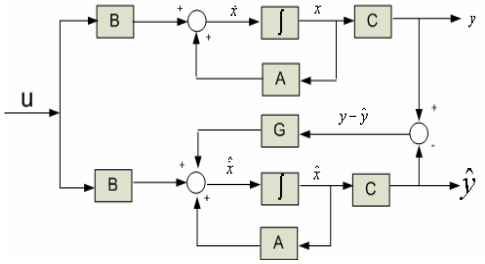

Figure 3.6 The Observer Block Diagram

3.4.1 *Full Order Observer*

The *observer* is designed base on three phase induction motor model using stator reference, stator current model and rotor flux. The *gain matrix full order observer* can be viewed as below:

$$G=\begin{bmatrix} g_1 & -g_2 \\ g_2 & g_1 \\ g_3 & -g_4 \\ g_4 & g_3 \end{bmatrix}=\begin{bmatrix} -(k-1)\left(\frac{R_s}{\sigma L_s}+\frac{R_r}{\sigma L_r}\right) & -(k-1)\hat{\omega}_r \\ (k-1)\hat{\omega}_r & -(k-1)\left(\frac{R_s}{\sigma L_s}+\frac{R_r}{\sigma L_r}\right) \\ c(k-1)\left(\frac{R_s}{\sigma L_s}+\frac{R_r}{\sigma L_r}\right) & (k-1)c\hat{\omega}_r \\ -(k-1)c\hat{\omega}_r & c(k-1)\left(\frac{R_s}{\sigma L_s}+\frac{R_r}{\sigma L_r}\right) \end{bmatrix}$$

The motor model estimate using *full order observer*, that the estimate current model is :

$$\frac{d}{dt}i_{s\alpha}=\frac{L_r}{\sigma L_s L_r-L_m^2}\left(-R_s-\frac{L_m^2 R_r}{L_r^2}\right)i_{s\alpha}+\frac{L_m}{\sigma L_s L_r}\psi_{r\alpha}+\frac{L_m\omega}{\sigma L_s L_r}\psi_{r\beta}+\frac{1}{\sigma L_s}V_{s\alpha}+g_1\left(\bar{i}_{s\alpha}-\hat{i}_{s\alpha}\right)-g_2\left(\bar{i}_{s\beta}-\hat{i}_{s\beta}\right) \quad (3.2)$$

$$\frac{d}{dt}i_{s\beta}=\frac{L_r}{\sigma L_s L_r-L_m^2}\left(-R_s-\frac{L_m^2 R_r}{L_r^2}\right)i_{s\beta}-\frac{L_m\omega}{\sigma L_s L_r}\psi_{r\alpha}+\frac{L_m}{\sigma L_s L_r}\psi_{r\beta}+\frac{1}{\sigma L_s}V_{s\beta}+g_2\left(\bar{i}_{s\alpha}-\hat{i}_{s\alpha}\right)-g_1\left(\bar{i}_{s\beta}-\hat{i}_{s\beta}\right) \quad (3.3)$$

$$\frac{d}{dt}\psi_{r\alpha}=\frac{L_m}{T_r}i_{s\alpha}-\frac{1}{T_r}\psi_{r\alpha}-\hat{\omega}_r\psi_{r\beta}+g_3\left(\bar{i}_{s\alpha}-\hat{i}_{s\alpha}\right)-g_4\left(\bar{i}_{s\beta}-\hat{i}_{s\beta}\right) \quad (3.4)$$

$$\frac{d}{dt}\psi_{r\beta}=\frac{L_m}{T_r}i_{s\beta}+\hat{\omega}_r\psi_{r\alpha}-\frac{1}{T_r}\psi_{r\beta}+g_4\left(\bar{i}_{s\alpha}-\hat{i}_{s\alpha}\right)+g_3\left(\bar{i}_{s\beta}-\hat{i}_{s\beta}\right) \quad (3.5)$$

3.4.2 Speed Estimate using Lyapunov

The speed estimate equation is written as below

$$\hat{\omega}_r=Kp\left(\hat{\psi}_{r\beta}e_{is\alpha}-\hat{\psi}_{r\alpha}e_{is\beta}\right)+Ki\int\left(\hat{\psi}_{r\beta}e_{is\alpha}-\hat{\psi}_{r\alpha}e_{is\beta}\right)dt \quad (3.6)$$

Where :

$\hat{\omega}_r$: rotor speed estimate (radian/second)

$\hat{\psi}_{ra}$: rotor flux estimate in α axis (Weber)

$\hat{\psi}_{rb}$: rotor flux estimate in β axis (Weber)

$e_{is\alpha}$: stator current error in α axis (Ampere), $e_{is\beta}$: stator current error in β axis (Ampere), Kp : proporsional contant and

Ki : integral constant

3.5 *duty ratio* controller design

The *duty ratio* controller uses two *rule base*. The first uses, when stator flux fewer than flux reference (error value is positif), and the second uses when stator flux greater than flux reference (error value is negatif). The membership function's input and output use triangular mode membership function , can be viewed in Figure 3.7 below :

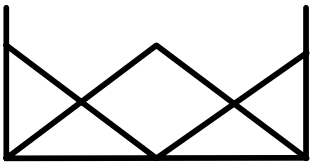

Figure 3.7 Membership function torque error

The values of A, B and C membership function torque error have various values depend on motor characteristic [8], and the values of A, B and C membership function stator flux position are 0, 0.517 and 1.047, base on stator flux position in a sector voltage vector [8].

The membership function stator flux position and duty ratio use as same as membership function torque error, only different in A, B and C values as is shown in figure 3.7

The values of A, B and C membership function *duty ratio* are adalah 0.55, 0.775 and 1, these values are acquired from simulation proses

Application fuzzy rules is used to decrease ripple torque. The *duty ratio* proportional to torque error and stator flux position each its vector along torque deviation level proportional to angle between stator flux and voltage, which is supplied to motor, so that the d*uty ratio* also is influenced by stator flux in each sector. The application of two set the fuzzy set cause when the stator flux greater than stator flux reference , A voltage vector it leads stator flux vector in the two sector will be given by inverter then cause high difference torque level if is compared vector voltage it leads stator flux vector in a sector, when the stator flux less than reference value.

Table 3.3 Fuzzy Rule *duty ratio* Controller[8]

Kesalahan Flux			Kesalahan Torsi		
			Small	Medium	Large
Negatif	Posisi Fluks	Small	Small	Small	Medium
		Medium	Small	Medium	Large
		Large	Small	Medium	Large
Positif	Posisi Fluks	Small	Small	Medium	Large
		Medium	Small	Medium	Large
		Large	Medium	Large	Large

3.6 Block Diagram

The block diagram DTC using can be viewed in Figure 3.10

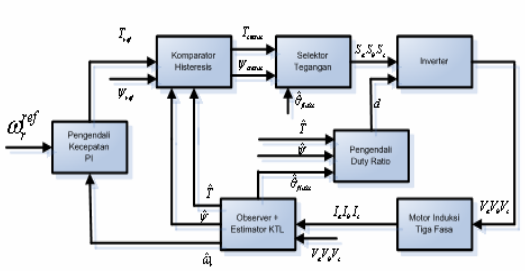

Figur 3.10 The DTC Syistem using *duty ratio*

The *duty ratio* controller acquires input from flux estimate and torque estimate, flux reference, torque and value of flux position estimate. The torque error and value of flux position error in a flux sector as input fuzzy logic controller The duty ratio is produced by proses fuzzification , infference and defuzzification process. .Nevertheless the *duty ratio* value which will be used depend on stator flux error. The *Duty ratio* will modulated triangular signal, then acquire a fixed width pulse .

4. SIMULATION

The results of the three phase induction motor control design using DTC and *duty ratio* is acquired from simulation method and SIMULINK MATLAB program with the various loads and speed. The research's first goal in this paper makes experiment DTC and *duty ratio* using three phase induction with various power, 1,10 and 50 hp is how influence of moment of inertia versus motor dynamic speed.

The sampling time is 10^{-4}seconds, and the modulation frequency in the *duty ratio* is 10^3 hertz.

Speed and Load Simulation

In this simulation the speed is given 100 radian/second at t = 0, then at t=10 second, it is risen till 140 radian/second, and reach nominal motor speed . At time t=0 second is given a balance load it match the motor charcteristic , and at t=14 second, the load is risen till the balance maximum motor torque.

4.1Simulation using Motor Power 1 HP

Table 4.1 The motor parameter 1, 10 and 50 hp is used in simulation program: [3][11][12]

Parameter	value		
Power hp	1	10	50
Num.o.poles Np	2	2	2
Stator Res Rs/Ω	2.76	0.6	0.087
Rotor Res Rs/Ω	2.9	0.4	0.228
Stator Indc.Ls/H	0.2349	0.123	0.0355
Rotor Indc. Lr/H	0.2349	0.127	0.0355
Magn Indc Lm/H	0.2279	0.12	0.0347
M.o.InertiaJ(kgm2	0.0436	0.05	1.6225
D.CoefD(N.msec)	0.0005	0.005	0.1

From this simulation is shown rotor speed ω_r, elektromagnetic torque T_e, single phase stator current i_a and *duty ratio* value. The torque hyteresis constant is 0.08, and flux hysteresis constant is 0.0173, The *observer* constants are acquired from experiment : K = 1.105 ; Kp = 8 ; Ki = 300, the speed control constant, it is used : Kp = 0.5 Ki = 1.2 and maximum torque = 7 Newton .meter.

4.1.1 Speed and Load's Motor

A. Motor Speed with Load variation

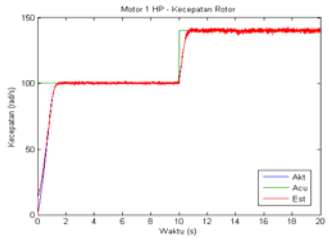

Figure 4.1 motor speed 1 hp with load variation

B. Electromagnetic Torque

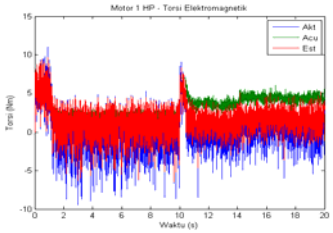

Figure 4.2 Electromagnetic Torque 1 hp with load variation

C. Single Phase Current

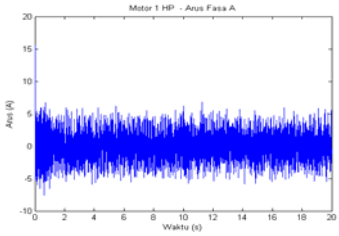

Figure 4.3 Phase A motor current 1 hp with load variation

D. *Duty Ratio*

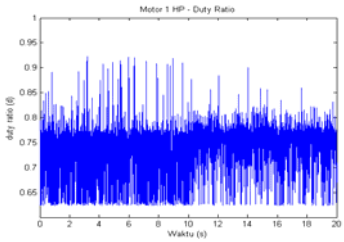

Figure 4.4 duty ratio 1 hp with load variation

4.2 Simulation using Motor Power 10 hp

Besides motor parameters, some constant must be initialized is observer constant gain K = 1.01, speed Kp = 0.8 and Ki = 60. The controller constant speed Kp = 0.1 dan Ki = 0.42. The hysteresis torque 0.1284 and flux 0.0173.

4.2.1 Speed and Load's Motor

A. Motor Speed with Load variation

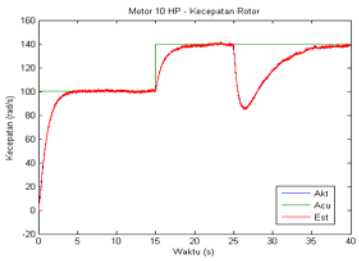

Figure 4.5 motor speed 10 hp with load variation

B. Electromagnetic Torque

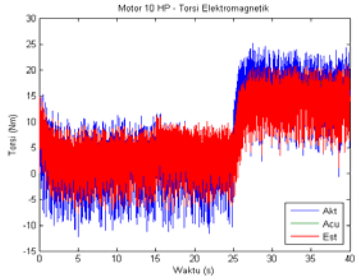

Figure 4.6 Electromagnetic Torque 10 hp with load variation

C. Single Phase Current

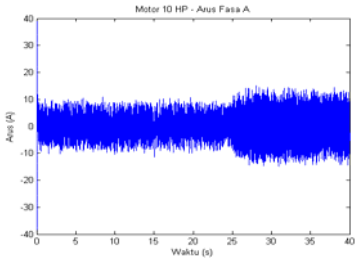

Figure 4.7 Phase A motor current 10 hp with load variation

D. *Duty Ratio*

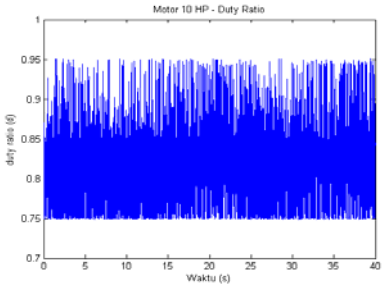

Figure 4.8 duty ratio motor 10 hp with load variation

4.3 Simulation using Motor Power 50 hp

:

The initialization constants are observer, gain K 1.3, *speed* Kp = 0.15 and Ki = 5.0, the controller. speed Kp = 50 and Ki = 50, the hysteresis torque 10 and flux 0.0173. For motor power 50 hp, the fuzzy logic's parameters input torque is 10 and 40 Newtonmeter, and flux position is 0 and 1.047, and output parameter is 0.7 and 1.

4.3.1 Speed and Load's Motor

A. Motor Speed with Load variation

.

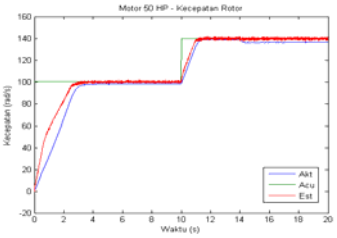

Figure 4.9 motor speed 50 hp with load variation

B. Electromagnetic Torque

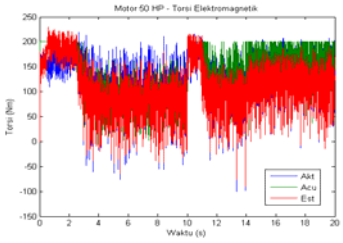

Figure 4.10 Electromagnetic motor Torque 50 hp with load variation

C. Single Phase Current

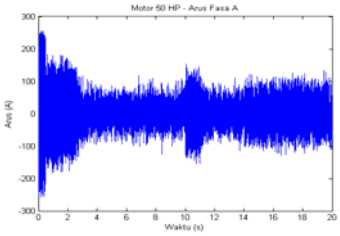

Figure 4.11 Phase A motor current 10 hp with load variation

D. *Duty Ratio*

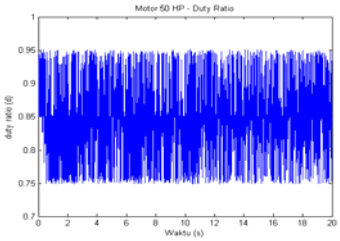

Figure 4.12 duty ratio motor 50 hp with load variation

4.4 Comparison Motor speed 1, 10 and 50 hp.

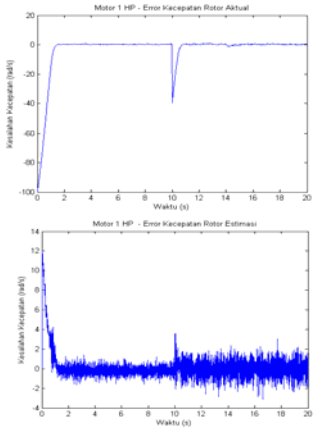

Figure 4.13 The rate actual speed error and estimate speed error motor 1 hp with load variation

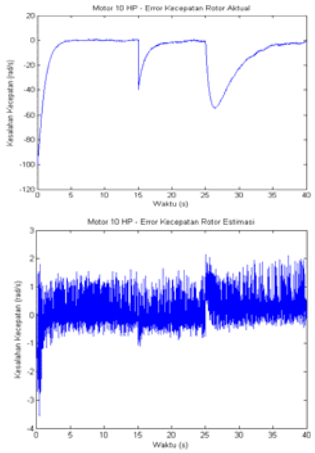

Figure 4.13 The rate actual speed error and estimate speed error motor 10 hp with load variation

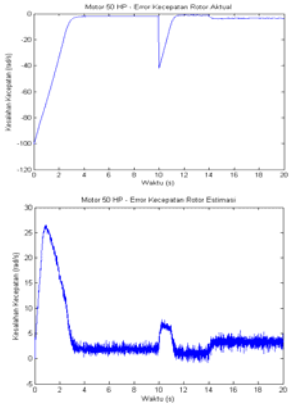

Figure 4.14 The rate actual speed error and estimate speed error motor 50 hp with load variation

Tabel 4.2 Motor speed for power 1, 10 and 50 hp (radian/second)

Power hp	speed err. rad/sec	No Load	Variable Load
1	Actual	0.38	0.317
	Estimate	0.54	0.56
10	Actual	0.93	1.01
	Estimate	0.35	0.33
50	Actual	0.65	2.52
	Estimate	1.22	2.3

The result of the rate actual speed and estimate speed error motor 1, 10 and 50 hp, show the actual motor speed 1 hp is the best, this matter depend on the observer design, it is very important to estimate torque, flux, flux position and motor speed.

4.5 Simulation using variation of Inertia Moment

Table 4.3 Variation of inertia moment induction motor with power 1, 10 and 50 HP

Power hp	1	10	50
time sec.	Moment of Inertia motor Kg.m2		
20	0.005	0.005	0.05
25	0.01	0.01	0.5
30	0.2	1	2.5
35	1	2	5
40	0.0436	0.05	1.622

Table 4.3 describes the variation of inertia moment induction motor with power 1, 10 and 50 hp, which is risen each 5 second begin 20th until 40th second .

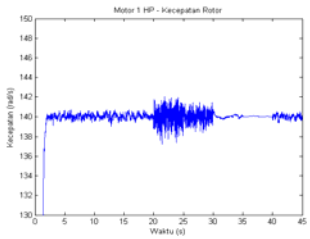

Figure 4.16 motor speed 1 hp with moment inersia variation

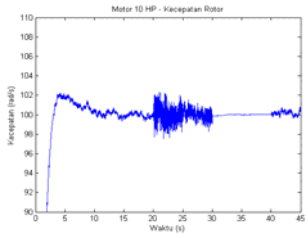

Figure 4.17 motor speed 10 hp with moment inersia variation

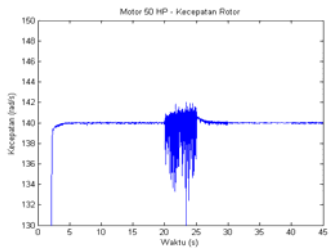

Figure 4.18 motor speed 50 hp with moment inersia variation

5 CONCLUSION

1. The motor with high inertia moment, has rotation more stable if be compared the motor, which has bila dibandingkan dengan motor dengan nilai momen inersia kecil.
2. DTC method using *duty ratio* control can decrease torque *ripple*
3. The *rate actual speed error* motor 1 HP with load variation is 0.317 rad/sec and *estimate speed error* 0.56 rad/sec, for motor 10 HP is 1.01 rad/sec and 0.33 rad/sec. , and for motor 50 HP is 2.52 radian/second and 2.30 radian/second.

REFERENCES

[1] I. Takahashi, T. Noguchi, "A new quick response and high efficiency control strategy of an induction motor", IEEE Trans. Ind. Appl. 1A-22 (October) (1986) pp. 820- 827

[2] M. Depenbrock, "Direct self- control (DSC) of inverterfed induction machine", IEEE Trans. Power Electron. 3 (October (4)) (1988) pp. 420- 429

[3] T. Brahmananda Reddy, J. Amarnath and D. Subba Rayudu1, Direct Torque Control of Induction Motor Based on Hybrid PWM Method for Reduced Ripple: A Sliding Mode Control Approach, ACSE Journal, Volume (6), Issue (4), Dec., 2006

[4] N. R. N. Idris and A. H. M. Yatim, "Reduced torque ripple and constant torque switching frequency strategy for Direct

Torque Control of induction machine," in *Proc. 15th IEEE-APEC*, New Orleans, LA, 2000, pp. 154–161

[5] R.Toufouti S.Meziane ,H. Benalla, Direct Torque Control for Induction Motor Using Fuzzy Logic, ACSE Journal, Volume (6), Issue (4), Dec., 2006

[6] Sanda Victorinne PAȚURCĂ, Aurelian SARCA, Mircea COVRIG, " A Simple Method of Torque Ripple Reduction for Direct Torque Control of PWM Inverter Fed Induction Motor Drives", Annals of the University of Craiova, Electrical Engineering series, No. 30, 2006

[8] Peter Vas, *Sensorless Vector and Direct Torque Control*, Oxford University Press, New York, 2003.

[11] H.F. Abdul Wahab and H. Sanusi, "Simulink Model of Direct Torque

Control of Induction Machine", American Journal of Applied Sciences 5 (8): 1083-1090, 2008

[12] O. Barambones, A.J. Garrido and F.J. Maseda, A Sensorless Robust Vector Control of Induction Motor Drives, Dpto. Ingenier´ıa de Sistemas y Autom´atica E.U.I.T.I Bilbao. Universidad del Pa´ıs Vasco.

ISSN 114-1284

Web Extraction Techniques Advancement: Towards Mashup for Indonesian Electronic Journal Citation Index

Riri Fitri Sari

Department of Electrical Engineering, Faculty of Engineering
University of Indonesia, Kampus Baru UI Depok 16424
Tel : (021) 7270078. Fax : (021) 7270077
E-mail : riri@ui.ac.id

ABSTRACT

This paper reviews the web extraction techniques for Web 2.0 to create a Mashup system to provide information on Indonesia academic citation index. Some web searching and crawling mechanism based search engine optimization system has created an environment for the democratization of information.

Presently the awareness for completeness of data in individual level, publications and to promote and guard the academic publication results have been enforced in order to encourage more publication and citations towards a paper/journal.

This paper describes the user requirement and application design, for the application of Mashup of Citation index for Indonesian Electronic Journal papers. We reviews the existance of personal blog of lecturers, digital online index, wrapper and tools for web extraction and digitalization of libraries in Indonesia. The intented system is expected to provide an award for research paper authors by providing the number of citation to his/her publication.

Keywords
Mashup, Web Extraction, Citation index.

1. INTRODUCTION

Information integration has been flourished during the last five years with the existence of Web 2.0 technologies. Some tools such as wrappers to collect online information on a timely manner have been available on the Internet.

In this work some infrastructure based on Extraction, Transformation and Loading (ETL) have been considered in designing a system to create the Index Citation Mashup. The system has been designed in the form of UML *(Unified Modelling Language)* diagrams, and the making of the prototype using robomaker REST based on OpenKapow. Subsequently the system should be implemented using PHP dan MySQL and web services based on XML standard for the Indonesian e-journal Mashup.

2. WEB EXTRACTION TECHNIQUES

Information technology infrastructure and the facilities development provided use with search engine and indexingsystem. The search engine is designed to make it easy for Internet user to get information from the world wide web. The system is based on the framework that information and knowledge are valuable things that should be used and shared by everyone.

2.1 Web Technologies

The new media has been widely developed with the development of Web 2.0. In order to become a new information society, our society has to change its characteristic and habit from a downloading society to become an uploading society, which provide and share information [2].

The authority to provide information has been moved from publishers, sites, or a knowledge based institution to a common citizen journalism and web based self publishing blog in the Internet. Knowledgeable person will be referred by the Internet users, therefore academician are required to provide complete and up to date information with a good analysis. Internet users will have the capacity to judge information. All information should be digested, analyzed, and evaluated from different perspective. Therefore it could lead to an improvement of human being's quality of life.

Academicians are in the forefront of the knowledge. Critical analysis and evaluation are the main requirement in academic world. A solid work will be based on deep literature review. A citation means an acknowledgement and a milestone in the research result towards a good and innovative research product.

ISSN 114-1284

Presently, there are some citation index tools currently available in the Internet which could provide the track record for academic authors [1, 3, 4, 5,9, 10, 11]. Google scholar [3] and citeseer are some of the indexing system in the form of softcopy which mostly are in English and acknowledge as an international standard of research result. Meanwhile some highly regarded journals is supported by professional organization, in addition to some journals owned by universities, faculties or study program.

International professional organization for researcher in the field of information and communication such as Institute of Electronics and Electrical Engineers (IEEE) and Association of Computing Machinery (ACM) is the highest authority and the most prestigious publication with the advancement of technology which could direct the future development of knowledge in the world. The publication can be searched from search engine, which usually needs a password and paid access to the journal or proceedings publication.

Meanwhile, in Indonesia some researchers and academician need to get the most current information of the citation to their publication. For example for the research publication which has been produced, how many researchers or academic article have referred to that research result. When an article is cited by other people or has been acknowledge as a contribution for the science, the author will be proud with his achievement.

Some places in the Internet has been prepared freely to show the full information such as in encyclopedia which can be updated by every one (note that the IP address of the machine which initiate the changing and adding information will be noted by the system, and when the update has been done). Wikipedia has been the place for the compilation of information which will be very useful, although the correctness of the information has been determined, due to the bias of information and the perspective of the writers. An academic article usually has a neutral characteristic, which is different from free information sources such as from Wikipedia.
The literature searching in the Internet should be carefully conducted to ensure that good quality of references can be gained. Open access journal in the Internet has been provided in the Internet, and many cyber library services have been provided by many universities to support academic communities to gain the most current resources in conducting research.

Web 2.0 technology is very usefull and cheap which can be deployed for the current non Web 2.0 product and services. The Web 2.0 environment enable user contribution to the system.

Search Engine Optimisation (SEO) can be performed better with the web 2.0 delivery mechanism such as Blogs and RSS which significantly can improve the search engine exposure thorugh a distributed mechanism. Wikis for example enable user to build documentation and knowledge based system, with a small investiment.

In Indonesian, a tradition of preservation of Information have come to a long history. The Indonesia National Archive Office kept the national archieval from hundreds of year back. For example many documents can be found from the time where the Malay language was first use in Voolkstraad (Representative Assemby). A Minangkabau Representative named Yahya datuk Kayo, was the first Indonesian member of Voolkstraad (51 members) who deliver his speech in Malay language in 1932.

Documentation and archieve have come to the time when digitalization and the electronic indexing system can help in making the search quicker.

Based on the literature study of the web extraction techniques which is related to the Mashup and its tools such such as Open Kapow, in this work we have created the fundament for a system to implement the system for the electronic journal citation indexing system [6].

Some problems such as the currently available existing standard of pdf files have been faced, which make it difficult to extract information and to evaluate the reference available in the background.

Our studies shows that using the currently available Wrapper such as Open Kapow is not straight forward considering that the reliability of the data extraction is very much dependent on the library at the server of Open Kapow.

2.2 Web Extraction Techniques

Web extraction is a method for mining core information from distributed documents in the Internet. This techniques can help to connect documents with high accuracy. This techniques can help to create a system which can provide credits for the academic paper authors in finding papers written by previous author [16, 17, 18, 19, 21, 22, 23, 24].

OpenKapow and Iopus are some tools which have been explored in this research [15, 16]. Some system such as Robomaker which took data in RSS, atom feeds, REST web extraction and web clip have been analyzed to implement the system. This system will be applied using Open Kapow services. This paper will present the design process of the creation of the Indonesian Electronic Journal Mashup System.

3. LITERATURE REVIEW

3.1. Mashup

Mashup is a hybrid web application which embed data and functionalities from more than one resources. The terminology of digital Mashup can be in the form of digital media file which consists of text, image, audio, video, animation recombined, or modify the result of digital work to create the derivative work. For music, mashup can consist of old songs which consist of other songs. Video Mashup is defined as a video which can be edited from different sources and will look like a complete video [7].

An example of mashup is a cartographic use of data from google maps to add location information to the real estate information, by adding new and different services from the currently available one.

Mashup content can be gained from a third party through public interface or API *(Web Services).* In addition to some method to get content from mashup, web feeds (RSS or Atom) and *screen scraping* can also be used. The term *screen scrapping, web extraction, web harvesting* will be described in more detail later on. Many people experiment using Amazon, eBay, Flickr, Google, Microsoft, Yahoo, or YouTube API, towards mashup editor.
A typical mashup web architecture consist of three part, i.e.:

1. Content Provider: data can be made using different API and web protocol such as RSS, REST, and web service.
2. Mashup sites: web application provides new services using some available data sources.
3. Web browser client: user interface from Mashup. Web content application can divided by web browsers using user language in web client side, for example JavaScript.

Tabel 1 describes the differences between a typical portal and mashup which describe the differences between portal and mashup.

Table 1: Comparison of Portal and Mashup

No	Features	Portal	Mashup
1	Classification	Older technology, using clearly defined approach for web server extension.	Web 2.0 techniques
2	Philosophy/ Approach	Aggregation approach by dividing web server into phases: markup generation and aggregation from markup fragment	Using APIs of available content sites for aggregation and reuse the content.
3.	Content dependent	Oriented towards markup fragment presentation aggregate (HTML, WML, VoiceXML)	Content aggregation can happen and content presentation orientation.
4	Location dependent	Traditional	On server and
5	Style Aggregation	Salad bar style (without overlap)	Melting point style (arbitrary structure)
6	Event Model	Read event model and update	CRUD operation based on REST
7	Relevant Standard	Portlet behaviour based on JSR. 168, 286, WSRP standards	Interchange data PeruXML with semantic REST. RSS and Atom are commonly used. Specific standard will be defined.

3.2. Workflow

Workflow is the description of the operation process which can be described as work result of the staff and machines in an organization, both in simple and complex form [8].

Workflow is a model to represent real time work to be evaluated, for example to describe recurrent operation. Workflow is an activity format which has been made possible by systematic organization of resources, which can be defined by flow of information.

3.3. Citation Index

Citation index is an index from citation on publication which enables user to define which document appears after other ones, from counting the citation of older documents [6].

Currently there are at least five publications of academic citation index available to be subscribed by libraries worldwide:

1. ISI (now part of Thomson Scientific).
   ISI citation index can be found in CD and web site format. The web version is called 'web of science' which is part of WoK data base.
2. Elsevier published Scopus, which is provided online with the same combination of searching subject by browsing citation and literature studies in natural and social sciences.
3. Citeseer system provided citation and other academic literature, particularly in computer and informatics.
4. RePec provided index in economics and other disciplines.
5. Google Scholars (GS) is a free of charge citation index which indexed new articles found in Google search. Currently Google scholar has enough features so that commercial products mention previously may no longer needed [10, 11].

ISSN 114-1284

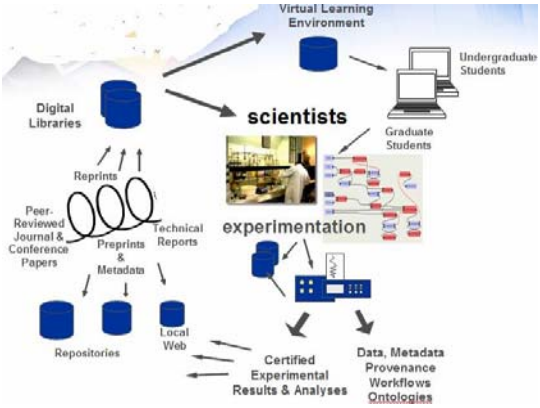

Figure 1: Social Process of Science [27]

Figure 1 shows the social and natural sciences processes, started from research experiment leading to search result repository. The result is published in peer reviewed journals and digital library to create a virtual learning environment.
Citation analysis (Scientometric) is normally conducted for the purpose of information retrieval, and many are used for bibliometrics and other studies for research evaluation [1, 2, 3, 13, 15]. Citation data is the basic information for journal impact factor.

3.4. Mashup Technilogy for Web Extraction

Web extraction is also called web harvesting, web farming, web mining, web scraping [1], dan screen scraping [2]. Extraction is a kind of information search to extract structured information, which is information defined in semantic approach, by context and particular categories of machine readable documents.

The aim of conducting web extraction is to collect information by integrated and automatic manner from heterogeneous resources [4]. The working method of web extraction is similar to the search engine process. Search engine provides information about pages and key words used by user.

The search engine phases conducting searching as follows:
1. *Scan* the web page to search for information.
2. Mark that information.
3. Copy that information.
4. Open other program such as spreadsheet or word processor and paste the copy result.

The limitation in using the search engine is recurrent daily changes of the web pages. To overcome this limitation, web extraction techniques have been created aiming to automate the process of read, copy and paste the information from websites

The web extraction is commonly used for particular information, as defined by web2DB for the following information [5]:
1. Create the contact list and market data.
2. Extract product catalogue.
3. Extract Real Estate information.
4. Automate the searching of advertisement list.
5. Clipping the latest news articles.
6. Automating auction.
7. Extracting betting sites.
8. Server migration.
9. Legal Notices
10. Military purposes

The following is the common extraction technique:
1. Extract information from defined document in a particular manner, such as HTML files, images, email messages, etc. First, the general structure of the document must be evaluated, images, and email messages. This is conducted by learning the general structure of the document, and mapped it with the data model or similar document. The alternative method is by adding more features to the search engine.
2. Conducting analysis to the document structure in relation with other documents. This is due to the fact that many related information can be found in the reference section of a publication.
3. Another alternative is by using recorded data by web server regarding the interaction of the user with a particular document or web page. From this data we can identified interaction pattern between the user and the web page. More over, the interaction pattern in a site can be customized dynamiccaly from the information shown, the depth of the site structure and the resources' format.

Data web extraction is an extraction process of structured data in a web site. The process consist of the following steps:
a. Find the HTML file from a site.
b. Extract relevant part of the data.
c. Process the data.

Most web extraction software is quick and easy to use. Some steps to crawl the designated site, extract structured and integrated data in the web data extraction. Some tools to extract web data have some features such as high speed, multi-thread and high accuracy. Due to the fact that many websites have been arranged with an HTML templates and database in the back, extraction tools must be able to find the information of the template and create an identical copy from the database.

Extracted data from a web site can provide the base for the information acquisition which shows the entity of the document or a web page. Data extraction created the platform for the document retrieval. Other web data extraction tools provided some equipment to generate some automatic

extraction procedure for the pages with repeating elements. Transformation mechanism chosen for this is called *Extensible Stylesheet Language Transformation* (XLST).

Web Content Extractor is an easy to use data extraction software for *web scraping*, *web harvesting*, and data extraction from the Internet. The most frequent changes in HTML design is the change of position of items in the web. The link is conducted by reinserting the page. Web data changes the way information extraction is conducted for business purposes. The combination of conditional statements, general statement, domain specific knowledge, web data extraction tools will eventually lead to intelligent way to find required information. It uses a general statement and contains mapping table to solve the differences between web resources [4].

3.5. Citation Extraction Techniques

Our aim is to create a design to create an application for web extraction in a form of a Mashup to count and update information of how many times citations have been made to a paper.
The following is the steps taken to count the citation to a journal paper [13, 14, 15].

1. Develop a *data-frame library* which consist of the previous information needed for data extraction. Therefore, *data-frame library* consist of historical detail of required information. For example by finding out all electronic journal sites in Indonesia and put the address to the web extraction tools such Open Kapow, Iopus, Lixto atau Marmite.
2. Creating a GUI (*Graphical User Interface*) to enable system users to gather all online paper required. Subsequently an *application-dependent forms*, and algorithm must be created to make sure that data has been gathered automatically from time to time.
3. Producing each component of application ontology (for example object and the connection between rules and bounds, extraction pattern, context, and keyword) by analyzing the page example of a journal and information list.
4. Providing a calculation of the citation number to a journal to evaluate the *ontology-generation system*.

Finding the journal citation is conducted by searching other papers which refers to that particular journal.

Challenges in web site scrapping are how to use the data. Data taken from web data extraction does not follow binary data and complex data format. To solve these problems, web site must provide access to the content through the API and web services.
Other challenge in finding references in Indonesian electronic journal is the fact that some systems prevent the extraction process. Screen/web scraping or web extraction are some method to solve the problem to find the web data by analyzing the structure of the data and wrapping the information.

Web extraction techniques are required to know the layout of the information both in metadata and it the document itself. Layout differences will create the problem to the accuracy of the extraction process. Therefore a model for the pattern should be created so that update and adoption of document manual template can help the process [16, 17, 18, 19, 21, 22].

There are some web extraction technologies to the open source tools. Some free software are available for this such as Yahoo pipes (pipes.yahoo.com), Microsoft popfly, Open Kapow (local computer application), Lixto (Austria), and Iopus [23, 24]. These tools are wrappers with web programming algorithm. The dycotomy of metasearch and google search (search all, including extracting the pdf) is the common problem. We need to also assess when a document received a Digital Object Indentifier (DOI) and where it was published [12].

4. REQUIREMENT AND ENVIRONMENTAL SETTING FOR INDONESIAN E-JOURNAL

The designated system is a web based system to automate the information search on citation of online journals belong to Indonesian universities. From the search result we can gather data and information citation indexing from many areas of knowledge to a database to store information.

Information can be processed so that the identification of the document relationship can be identified. The indexing result can be accessed by authors, researchers, and general public through the Internet. Automation can be done by system through auto update to ensure that the citation information is actual.

The intended system will be a web based system, and from the user side it will be similar to general search engine in which users can provide input in search query in search field provided. After the user executed the command to conduct search, system will search the data base of the processed information, which consist of the number of citation to that paper, the title, and author. The system is designed to provide links which is related to the document title which relate to the user query to be used for the future research.

Automatic web extraction will result ini a mashup. This mashup will integrate and provide relationship information and links between papers found. Figure 2, 3, and 4 depicted some diagrams which show the use case diagram, sequence diagram, and class diagram, of the intended system.

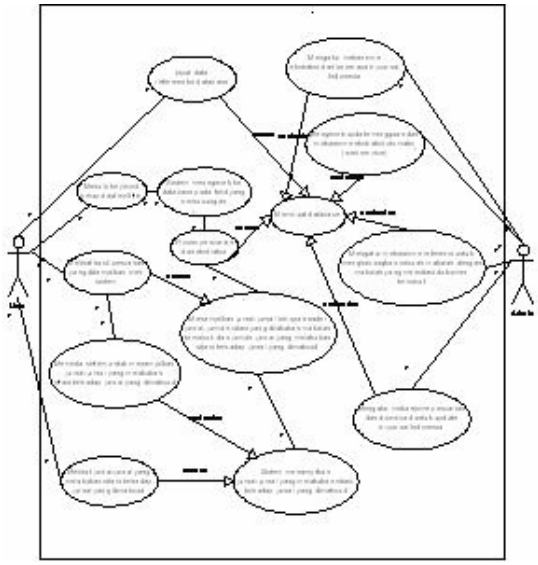

Figure 2: Use Case Diagram

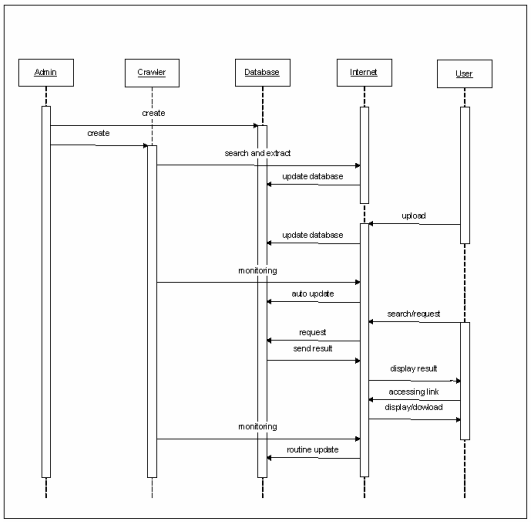

Figure 3: Sequence Diagram

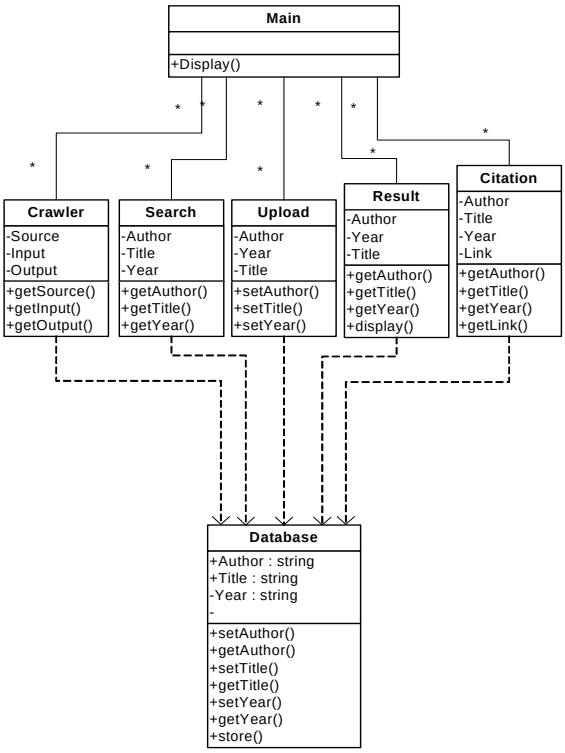

Figure 4: Class Diagram

5. INDONESIAN E-JOURNAL

From the web search of the Indonesian e-journal we have identified that some journals provided full text in the form of pdf file, some only provide abstracts. The following are the journals from Indonesian Universities portal, i.e. Universitas Airlangga (7 Journal), Universitas Negeri Malang (38), Universitas Udayana (31), Universitas Palangkaraya (1), Universitas Kristen Petra Surabaya (14), Universitas Paramadina (1), Universitas Indonesia (1), Universitas Gadjah Mada (5), Intitute Pertanian Bogor (10), Universitas Gunadarma (11).

7. CONCLUSION

Web extraction is a data mining method to retrieved information from distributed documents in the Internet. Using web extraction, user will be able to get the relationship between documents in an accurate manner. Some web extraction techniques will help to create a system to credit authors of research publications. This papers has shown the preliminary approach to design a Mashup for Indonesian electronic journal citation system. The future work will involved the implementation of the web based system using web 2.0 technology and the latest development in web integration methodology.

ACKNOWLEDGMENT

This research is funded by Hibah Kompetensi of the Directorate General of Higher Education, Ministry of National Education of Republic of Indonesia 2008-2009. Thanks to Burhan, Alfa, Bayu, Ruki, and other HCI class 2008 members for their contribution.

REFERENCES

[1] Bollen, J., Van de Sompel, H., Smith, J. and Luce, R, Toward alternative metrics of journal impact: A comparison of download and citation data Information Processing and Management, 41(6): 1419-1440, 2005.

[2] Thomas Friedmand, The world is flat, Gramedia, 2006.

[3] Google scholar, http://scholar.google.com, last last accessed 28 June 2009.

[4] Information Systems institute, ISI, http://www. isinet.com, lat accessed 28 May 2009.

[5] Thomson ISI Website, The impact factor, http://thomsonscientific.com/knowtrend/essay/journalcitationreports/impactfactor/), last accesed 22 March 2008.

[6] Citation index, http://en.wikipedia.org/wiki/ Citation_index, Wikipedia, last accessed March 27, 2008.

[7] Mashup (web application hybrid), http://en.wikipedia.org/wiki/Mashup_(web_application_hybrid), Wikipedia, last accessed August 10, 2008.

[8] Workflow, http://en.wikipedia.org/wiki/Workflow) Wikipedia, last accessed August 10, 2008.

[9] Publish or Perish–Free Citation Software, http://chinmi.wordpress.com/2007/11/23/publish-or-perish-free-citation-software/), last accessed July 10, 2008.

[10] Smith, A. G. Google Scholar as a cybermetric tool, Victoria University of Wellington, New Zealand.

[11] Sadeh, T., Ex Libris. (2006). Google Scholar Versus Metasearch Systems, http://library.cern.ch/HEPLW?12/papers/1/, last accessed March 12, 2006, from

[12] Paskinn, N. (1997). Digital Object Identifier (DOI) System, Tertius Ltd., Oxford, United Kingdom.

[13] Kennan, M. A, Academic authors, scholary publishing and open access in Australia, Learned Publishing, Vol. 20, No. 2, pp 138-146, April 2007.

[14] Meho, L. I., Yang, K. (August 2006). Multi-faceted Approach to Citation-based Quality Assessment for Knowledge Management. http://www.ifla.org/IV/ifla72/index.htm., last accessed July 27, 2006,

[15] Marry Anne Kennan, Scholarly Publishing and Open Access: Searching for understanding of an emerging IS Phenomenon, Proceedings of 15 European Conference on Information System, University of St. Gallen, Switzerland, 7-9 June 2007.

[15] imacros. http://wiki.imacros.net/Data_Extraction. last accessed 10 October 2008.

[16] *Web Data Extraction-The Whats and Whys!* http://www.tethyssolutions.com/web-data-extraction-article.htm, last accessed 10 October 2008

[17] May, Wolfgang; Lausen, Georg. *Information Extraction from The Web*. Institut fur Informatik, Albert-Ludwigs-Universitat, Germany, 2000.

[18] *Web2DB Web Data Extraction Top 10 Uses*. http://www.knowlesys.com/ articles/web-data-extraction/top_10_uses.htm, last accessed 10 October 2008.

[19] Berkowitz, Eric G. and Elkhadiri, Mohamed Reda. *Creation of a Style Independent Intelligent Autonomous Citation Indexer to Support Academic Research*. Departement of Computer Science, Roosevelt University, Schaumburg, IL, 2004.

[20] S´aenz-P´erez, Fernando. *Bib Manager and Word Citer: Bibliography Management and Citation Extraction*. Facultad de Informatica, Universidad Complutense de Madrid, Spain, 2007.

[21] Bollacker, Kurt D.; Lawrence, Steve; Giles, C Lee. *CiteSeer: An Autonomous Web Agent for Automatic Retrieval and Identification of Interesting Publications*, University of Texas, Austin, TX, NEC Research Institute, Princetone, NJ, UMIACS, University of Maryland College Park, MD, 1998.

[22] AnHai Doan, et.al. *User-Centric Research Challenges in Community Information Management Systems.* University of Wisconsin-Madison, Yahoo! Research, 2007.

[23] Mundluru, Dheerendranath. *Automatically Constructing Wrappers for Effective and Efficient Web Information Extraction*. A Dissertation Presented to the Graduate Faculty of the University of Louisiana at Lafayette, 2008.

[24] Zhou, Yuanqiu. *Data-Extraction Ontology Generation by Example*. A Thesis Proposal Presented to the Department of Computer Science Brigham Young University, 2002

[25] *The Scopus Citation Tracker : a powerful way to explore citation information*. http://info. scopus.com/etc/citationtracker/, last accessed 13 October 2008.

[26] *Scopus in detail: How does it work?*. http://info.scopus.com/etc/citationtracker/, last accessed 13 October 2008.

[27] De Roure, E-Science, E-Science and Grid Computing Conference, Bangalore, India, December 2007.

Approaching Distributed Mobile Robot Network in Dynamic Environment by Using Artificial Potential Field Method for Optimized Configuration Solution

R. Mardian[1], W. Jatmiko[1], J. Takahashi[2], K. Sekiyama[2], T. Fukuda[2]

[1] *Faculty of Computer Science*
University of Indonesia, Depok, Indonesia
email: rima56@ui.ac.id

[2] *Departement of Micro-Nano Systems Engineering*
Nagoya University, Chikusa-ku, Japan

ABSTRACT

This paper presents the development of relatively new trend in communication technology addressing mobile ad-hoc network. To deploy the network with highly-mobile characteristic we are going to use distributed robots as media to carry information. The self-deployment algorithm is being constructed to support robots behavior in group. The adaptive method to deliver information within the network is being examined, that mobile robot network tends to suffer the rapid changes in configuration due to the movement of the robots.
The research has been conducted in several phase of implementation. In previous time, the algorithm for configuration process has been established, called self-deployment algorithm with connection priority criteria. In present time, we are going to observe a new way to optimize the algorithm in terms of the success rate of network deployment in minimum number of robots are used. Here we propose the use of artificial potential field method that once is developed to guide autonomous mobile robot in navigation planning.

Keywords
Distributed robot, mobile robot network, artificial potential field

1. INTRODUCTION

Mobile Robot Network (MRN) is relatively new trend in the communication technology development today. This application uses multiple robots as media to carry information throughout the network link which also enables the network with mobility characteristic. By implementing ad-hoc wireless technology and the form of Peer-to-peer communication, robots are capable to communicate each other in order to form network topology [1].
The present research will focus on the design of method to deploy Mobile Robot Network configuration in the given environment. The algorithm used in this research is based on self-deployment with connection priority criteria which supports decentralized and collective behavior among robots in group.
Communication between robots happens in two ways. The first is based on TCP connection as stable communication which is used for error-free data transfer and the second is based on UDP connection as unstable communication which is used to exchange location-information exchange between devices. Robots then need to establish stable connection in order to distribute information through network link [2].
The environment as robot working area is dynamic in which obstacle factors exist that obstruct robot movement. The definition of permitted and prohibited area are being made by using road-map input for each robot in order to model the simulation into the environment as close as the real world. Moreover, the solution for network configuration to be found is expected to be the most optimum solution from the given environment and obstacle definition. This to encounter the limitation often found in real life that the unlimited resource to build Mobile Robot Network is definitely not affordable, or even if we could, it will cost a lot of effort and expense.
The optimum solution of network configuration problem in this research is basically the trajectory with most minimum cost that connecting all given locations. Another requirement is that this trajectory may not violate the obstacles or prohibited area as stated in the road-map definition. For this purpose, we will then use the Artificial Potential Field method to find several possible trajectories. Robot is then to form the formation that follows the derived solution.
For routing problem in this research, we will use Ad-Hoc on Demand Vector Distance method to solve the requirement. This method is sufficient for mobile type ad-hoc network that it supports the capability for quick updating routing table that changes very often. The result that found from simulation activity is then to be evaluated from the sense of the algorithm's capability to find solution from minimum cost and resource in the given environment.

2. MOTIVATION

Artificial Potential Field (APF) is mostly used in several application that related to robot's navigation and motion plan [3][4][5]. The concept of this method is to build trajectory by generating potential-field map from the interaction of robots with its surrounding. Later, this map can be used to guide the movement of the robot. In other cases, this method is also applied for obstacle avoidance activity [6].

In this paper we will then utilize the APF method to find the propitious trajectories from the points that are going to be connected through the MRN communication link. This will provide the possible routes from each point to another within the given environment. By choosing the shortest path among all feasible trajectories, we can then determine the most optimum path to connect the intended points.

3. IMPLEMENTATION FRAMEWORK

Here will be explained how we are going to deliver the MRN application by using Self-deployment algorithm and Artificial Potential Field (APF) method to optimize network link deployment under the limited number of resources.

a. The Self Deployment Algorithm

In order to deploy MRN application, multiple number of mobile robots need algorithm that provide collective behavior to work in group. The self-deployment algorithm will then be capable to handle the decentralized activity of robots in delivering communication network. As this network link subjects to high mobility characteristic due to the movement of the robots, the self-algorithm needs to be adaptive with the changes.

Research in multiple robots' work in group is actually not a new problem to be examined. In several studies, the decentralized algorithm has successfully been implemented to solve hard problem in real life with the utilization collective robots behavior [7][8]. In this phase of research, we will then adapt the usage of self-deployment algorithm with connection priority criteria as this algorithm has successfully solved the cooperative object tracking with sensor network application [1]. This topic is quite similar with the problem we face in this research [2].

The self-algorithm with connection priority criteria treats all objects within the working environment with different priority that reflects the significance of the object for itself. From this priority, robot can decide what to do in the next step of its movement. Robot will then finish its work after all priorities have been fulfilled or whenever the main objective has been reached. To simplify the problem, figure 1 and 2 below will explain how this algorithm works to connect two points in the working environment.

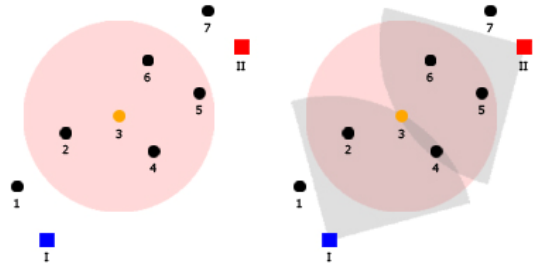

Figure 1 - Robot groups all other objects to determine the priority

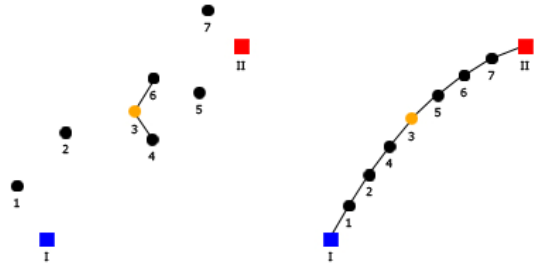

Figure 2 - Robot moves based on the priority

Figure 1 above shows that robot firstly group all other objects in the working environment to determine the priority of each to it. Since the capability of robot to recognize objects in its surrounding is limited, robot will just group objects within its sensing area. This is represented by red circle in left side of figure 1.

As there are two points to be connected through the communication link, robot will create two different groups; the first is the group that will help it connects the 1st target, and the second is the group that help it connects the 2nd target. This is represented in right side of figure 1.

The next activity to be done is deciding the value of priority for each object. This is determined by using distance heuristic that the closest object will be given highest priority. Robot will then approach the object with highest priority from each group, starting from the highest in the first group and then next to the highest in the second group. If there is no object that is grouped within the first or the second group, the priority will be the first or the second target points themselves.

In addition to this, robot also needs to maintain the connection after it is connected to its priority. This will help application to deploy the communication link between the target points whenever all robots have already reached their own movement priority. It is as shown in the right side of figure 2.

The self-deployment algorithm with connection priority criteria has successfully solved the MRN deployment. However, under certain conditions, this algorithm does not ensure the solution to exist; or if there is any solution exists, it is not guaranteed optimum. In other hand, the existence of any obstacle within the working environment will also obstruct this method to find the expected solution. That is why we will try to utilize APF method in order to solve this problem.

b. Artificial Potential Field

It is mentioned that Artificial Potential Field (APF) method has enormously used in term of robot navigation and motion planning. By building the potential-field map of the working environment, robot can then determine the best trajectory to be followed in order to reach the goal of its movement.
As the positions get closer to the goal, they will be given the lower potential value. However, when the positions get closer to the unreachable places or obstacles, they will be represented with the higher potential value. Then, the best trajectory to reach the goal position will be a trajectory that connects the current position of robot with the goal position that in the same time also contains the lowest potential value. It works since the low potential value in field will attract the robot, while the high potential value in field will distract the robot. Figure 3 and Figure 4 below will show the potential field map in case of one obstacle exist between robot and goal position [9].

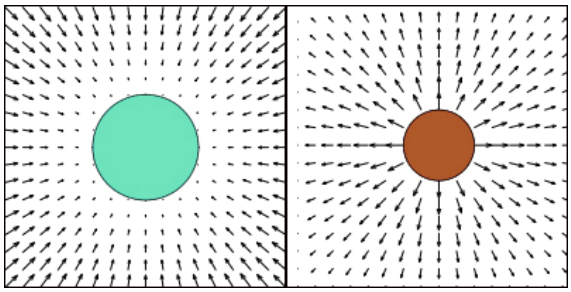

Figure 3 - Attraction from goal position (left) and distraction from obstacle (right)

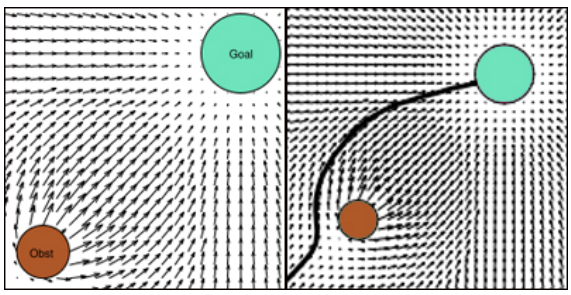

Figure 4 - Attraction and distraction from potential-field value will create directions as trajectories to guide robot's movement

From figure 3 we can see that since robot tends to follow the low potential value, it will create attraction force towards the goal position. It is represented in left side of figure 3 by the arrow that comes into the goal. In the contrary, the distraction force will be created avoiding the obstacles or unreachable position as shown in the right side of figure 3. It is represented by the arrow that comes out of the obstacle. By taking resultant from this both forces as the vector of robot's movement, we will get best trajectory to be followed by robot. It is shown as in figure 4 above.

c. Virtual Force Method

Even APF is expected to be able to find the shortest trajectory for the optimum solution; it still requires information about environment condition in order to generate potential field map. However, in this research we assume that robots do not work within a fixed environment. Therefore, robot first needs to explore its working area in order to get the representation of its circumstances. As the obstacles exist and can obstruct the movement of robots, we will use Virtual Force (VF) method to deal with the problem. This method is actually intended for obstacle avoidance. However, in this research we will exploit the usefulness of this method together with the technique to build the potential-field map in the same time. Figure 5 below is the graphical representation of how Virtual Force works [10].

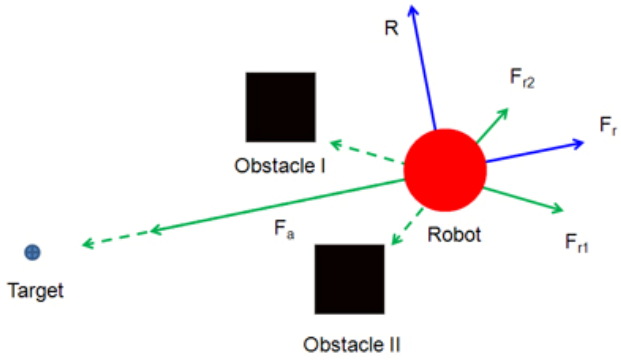

Figure 5 – Virtual force method to avoid obstacle within working environment

From the figure 5 above, robot decides that *R* will be the direction of its movement for the next step. By doing this, robot will be able to avoid obstacle and in the same time to build potential-field map to determine the attraction-distraction force from target and obstacles.

4. FUTURE WORK

This research is actually is still in the progress of development. Through this paper we propose new methods to upgrade the performance of old used method and uplifts the limitation of the research. Recently, the deployment of MRN application still faced the problem regarding to a few number of robot. Here we propose the method to increase the likelihood of finding solution by generating shortest path to be followed to configure the network topology. Therefore, MRN deployment can accommodate solution if the number of available mobile robots is limited.

For the future work, we still need to evaluate the performance of the self-deployment algorithm combined with the utilization of the APF method. In order to do that, we need to develop the simulation and implement the algorithm. Later, we can decide the goodness of this algorithm under several different parameter of experiment. This is expected to bring benefit for the research progression and later we can move on to MRN deployment for multi-points communication link.

5. CONCLUSION

The deployment of MRN application is being investigated through this paper. The research itself has been conducted in several phase of implementation. In previous time, the algorithm for configuration process has been established, called self-deployment algorithm with connection priority criteria. In present time, we are going to observe a new way to optimize the algorithm in terms of the success rate of network deployment in minimum number of robots are used. Here we propose the use of artificial potential field method that once is developed to guide autonomous mobile robot in navigation planning. The proposed method is expected to bring optimum solution.

6. REFERENCES

[1] Takahashi, Junji, Kosuke Sekiyama, Toshio Fukuda. Unknown. *Cooperative Object Tracking with Mobile Robotic Sensor Network*. Nagoya University.

[2] Mardian, Rizki. 2008. *The Handling of Self-configured Multihop Communication by Using Distributed Autonomous Robot*. University of Indonesia.

[3] Qixin, Cao, Leng Chuntao, Huang Yanwen. Unknown. *Evolutional Artificial Potential Field Algorithm Based On the Anisotropy of Omnidirectional Mobile Robot*. Shanghai Jiaotong University.

[4] Vadakkepat, Prahlad, Tong Heng Lee, Liu Xin. 2001. *Application of Evolutionary Artificial Potential Field in Robot Soccer System*. National University of Singapore.

[5] Koren, J. Borenstein. 1991. *Potential Field Methods and Their Inherent Limitations for Mobile Robot Navigation*. University of Michigan.

[6] Sarkar, Saurabh, Scott Reynolds, Ernest Hall. 2007. Virtual Force Field Based Obstacle Avoidance and Agent Based Intelligent Mobile Robot. University of Cincinnati.

[7] Jatmiko, Wisnu et al, 2009. *Evolutionary Computation Approach for Odor Source Localization Problem: Practical Review*, IEEE Transaction on Evolutionary Computation.

[8] Jatmiko, Wisnu et al, 2009. *Niche Robot Based on PSO with Flow of Wind for Multiple Odor Source Localization Problems in Dynamic Environments*, IEEE Transaction on Robotic

[9] Goodrich, Michael. Unknown. *Potential Field Tutorial*.

[10] Takahashi, Junji, Kosuke Sekiyama, Toshio Fukuda. 2007. *Self-deployment Algorithm Based on Connection Priority Criteria with Obstacle Avoidance*. Nagoya University.

ISSN 114-1284

Comparation Measurement Result of IMU and GPS Carried in Vehicle for INS Algorithm

Romi Wiryadinata[a], Th. Sri Widodo[b], Wahyu Widada[c], Sunarno[d]

[a] *Student of Electrical Engineering Dept.*
Gadjah Mada University, Jogjakarta
Email: romi_wiryadinata@yahoo.com

[b] *Electrical Engineering Dept.*
Gadjah Mada University, Jogjakarta
Email: thomas@mti.ugm.ac.id

[c] *Guidance and Control Div.*
National Institute of Aeronautics and Space, Bogor
Email: w_widada@yahoo.com

[d] *Physic Engineering Dept.*
Gadjah Mada University, Jogjakarta
Email: efs_sunarno@yahoo.com

ABSTRACT

GPS precision is excellent in long distance measurement, while it is poor in short distance measurement. IMU (Inertial Measurement Unit) has a different properties, it is excellent in short distance measurement, while it is poor in long distance measurement. Hence, the advantages of both sensors are being integrated by INS (Inertial Navigation System) algorithm using high speed microprocessor. Before being tested in a rocket flying, IMU v2.1 is tested in vehicle. IMU v1.2 has been integrated and a laboratory and field testing with vehicle. The result of this prototype for a while has shown that HPF could result in output stabilization to 0 g (gravity) or in 2.5 volt. Small value of capacitor in second version give fast response to steady position and the characteristics of sensor and signal condition are acknowledged. From this research are identified the amount of noise in zero g state with value ranging from 5 to 12 bit.

Keywords: *Accelerometer, Rate-Gyroscope, 6DOF IMU, INS Algorithm*

1. INTRODUCTION

Natural navigation has exists since thousands years ago in the life of animal or human. Bird, bee, fish and almost all kind of animal use their animal instinct for navigation to recognize their feeding ground and where their live and human who has the intelligence use sun and stars as natural navigation to know their direction and position. [7].

The aim of this research is to determine the level of accuracy between data from the GPS (Global Positioning System) and data from a prototype of IMU (Inertial Measurement Unit) which will be developed as a device for the INS (Inertial Navigation System) algorithm.

INS algorithm that will be developed use for rocket navigation. Later the testing phase in the rocket system, the algorithm testing is done first on the vehicle. Then testing is done using a vehicle with assumption that vehicles move on the surface of the earth that has matrix transformation in the coordinate of body or object reference , which then will be converted into account the reference system to change altitude or coordinate of earth reference .

Previous researches have been done by several people with the object and too many different of research focus. Walchko in 2002 write a paper, which title low cost inertial navigation: learning to integrate noise and find your way, the research has the accuracy of the GPS errors that can be used to reach 10-15 meters per second or equal to 95% in the second [4].

Real-time navigation, guidance, and control of a UAV (Uninhibited Aerial Vehicle) using low-cost sensor which write by Kim et.al on 2006 implemented INS/GPS for GNC (Guidance, Navigation and Control) system on UAV [3].

Design and error analysis of accelerometer-based inertial navigation system, Tan and Park (2002) design INS to computer linear and angular motions of rigid body uses only accelerometer on this paper [2].

Kumar 2004 write that Integration of INS and GPS using Kalman filter with a research focus on creating a INS simulator, where the output GPS processed on FPGA (Field Programmable Gate array) and integration IMU and GPS output processed on DSP (Digital Signal Processing) [10].

Simulation launch vehicle rocket AtlasIIAS also use the INS and the integration of GPS, such as in the paper written by Istanbulluoglu in 2002 [5].

Schumacher (2006) write about the Integration of a GPS aided Strap down INS for land Vehicle, The estimation accuracy and error state of INS be formed and analyzed by EKF (Extended Kalman Filter) [1].

Hjortsmarker (2005) write the experimental system for validating GPS/INS algorithm Integration, which aims to calibrate INS and GPS using the jet coaster so easily be described into three-dimensional space [6].

From some of the above research, this research attempts to analyze and compare the results of INS algorithm experiments testing to use the real-time rocket and a few test vehicles over the (pedestrian), the bicycle, and on the motorcycle with smallest estimation error. Long-term goal of this research is to give a large contribution to missile or guidance rocket at National Institute of Aeronautics and space (LAPAN).

2. INS ALGORITHM

INS or have also a call with INU (Inertial Navigation Unit) consists of several important components in the navigation, which are as Altimeter sensor altitude, GPS navigation as a reference, and IMU (Inertial Measurement Unit) which consists of a sensor and rate-gyroscope and accelerometer sensors added with one component that is most important algorithms Inertial Navigation System (INS), which function as our algorithm to combine the two navigation systems so that the speed and accuracy of the data navigation system can be more accurate. Two navigation systems are the combined GPS and IMU are both similar but not identical in terms sampling data. GPS is a tool for the navigation system based on satellite, while the IMU is not based on satellite but using the body frame and the navigation frame (earth). Altimeter on this research is not used with assume that using sensors accelerometer and three axis rate-gyroscope altitude will obtain from two sensors [8].

(Equation 1) is velocity equation to convert a velocity from body angle (p, q, r - deg / sec) to earth coordinate (– deg), where *c* is *cos* and *s* for *sin*.

$$\begin{bmatrix} \dot{\phi} \\ \dot{\theta} \\ \dot{\psi} \end{bmatrix} = \begin{pmatrix} 1 & s\varphi\ tan\theta & c\varphi\ tan \\ 0 & c\varphi & -s\varphi \\ 0 & s\varphi\ sec\theta & c\varphi\ sec \end{pmatrix} \quad (1)$$

By integration of the above equations we can derive the Euler angles using initial conditions of a known attitude at a given time. But, for pitch angles around ±90°, the error becomes unbounded as tan tends to infinity. Quaternion algebra (equations 2-7) comes to the rescue here. We use four parameters, called the Euler parameters, which are related to the Euler angles as follows [10].

$$\dot{e}_0 = -\frac{1}{2}(e_1 p + e_2 q \quad (2)$$

$$\dot{e}_1 = \frac{1}{2}(e_0 p + e_2 r \quad (3)$$

$$\dot{e}_2 = \frac{1}{2}(e_0 q + e_3 p \quad (4)$$

$$\dot{e}_3 = \frac{1}{2}(e_0 r + e_1 q \quad (5)$$

with the parameters satisfying the following equation at all points of time.

$$e_0^2 + e_1^2 + e_2^2 + e \quad (6)$$

The above equations can be used to generate the time history of the four parameters e_0, e_1, e_2, and e_3. The initial values of the Euler angles are given which are used to calculate the initial values of the four parameters using the following equations.

$$\bar{e} = \begin{bmatrix} c\frac{\varphi}{2}c\frac{\theta}{2}c\frac{\phi}{2} - s\frac{\varphi}{2} \\ s\frac{\varphi}{2}c\frac{\theta}{2}c\frac{\phi}{2} - c\frac{\varphi}{2} \\ c\frac{\varphi}{2}s\frac{\theta}{2}c\frac{\phi}{2} - s\frac{\varphi}{2} \\ c\frac{\varphi}{2}c\frac{\theta}{2}s\frac{\phi}{2} - s\frac{\varphi}{2} \end{bmatrix} \quad (7)$$

Once we have calculated the time history of the four parameters, we can calculate the Euler angles using the following (equations 8-10).

$$\theta = sin^{-1}[-2(e_1 e_3 - \quad (8)$$

$$\varphi = cos^{-1}\left[\frac{e_0^2 - e_1^2 - e_2^2 + e_3^2}{\sqrt{1-4(e_1 e_2 - e_0 e_3)^2}}\right] sign[2(e_1 e_2 - \quad (9)$$

$$\psi = cos^{-1}\left[\frac{e_0^2 + e_1^2 - e_2^2 - e_3^2}{\sqrt{1-4(e_1 e_2 - e_0 e_3)^2}}\right] sign[2(e_1 e_2 - \quad (10)$$

The accelerations (*ax*, *ay* and *az*) of the aircraft along the three body axes, as read by the accelerometers, are given by the (equations 11-14). *U*, *V*, *W* and *p*, *q*, *r* are all available as states. If the acceleration dues to gravity (*g*) model which supplied as a function of location around the earth, then $\dot{U}, \dot{V}$ can be calculated.

$$\dot{U} = a_x + V_r - w_q + \quad (11)$$

$$\dot{V} = a_y - U_r + w_p - g\ cos \quad (12)$$

$$\dot{W} = a_z + U_q - V_p - g\ cos \quad (13)$$

The actual angular rates given by (equation 16), where and is given by (equation 14 and 15).

$$\Omega = \begin{bmatrix} \Omega \\ \_ \end{bmatrix} \quad (14)$$

$$\omega^{i} = \begin{bmatrix} \mu \\ \_ \end{bmatrix} \quad (15)$$

$$\begin{bmatrix} p \\ q \\ r \end{bmatrix} = \begin{bmatrix} p \\ q \\ r \end{bmatrix}_{m} - DCM[i \quad (16)$$

DCM is the direction cosine matrix (transformation matrix), to converting from the local earth or navigation frame to the body frame, given by (equation 17), where *c* is *cos* and *s* for *sin*.

$$DCM = \begin{bmatrix} c\theta c\psi & c\theta s\psi \\ s\theta s\varphi c\psi - c\varphi s\psi & s\varphi s\theta s\psi + c\varphi c\psi \\ s\theta c\varphi c\psi + s\varphi s\psi & c\varphi s\theta s\psi - c\varphi s\theta \end{bmatrix} \quad (17)$$

$$\begin{bmatrix} \dot{X} \\ \dot{Y} \\ \dot{Z} \end{bmatrix} = \begin{bmatrix} V_N \\ V_E \\ V_D \end{bmatrix} - DCM \quad (18)$$

Let and *H* denote the latitude, longitude and height of the aircraft at any instant, then rate of change of latitude is given by (equation 19-21).

(19)

$$\mu = \quad (20)$$

$$\dot{H} \quad (21)$$

3. DESIGN OF SYSTEM

From previous section above diagram block can be described as found in the research (figure 1) following.

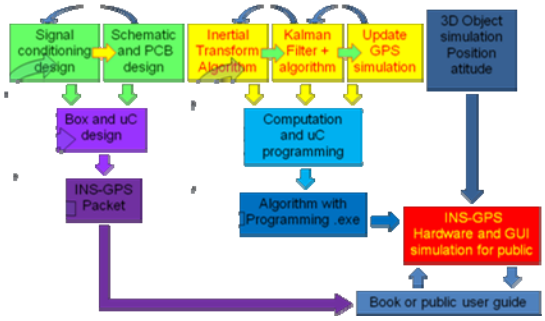

Figure 1: Research plan

This paper is a small part of the research and the beginning of the new algorithm to test the vehicle before entering the next stage in the test with roller coaster, aeromodeling, aircraft, and is implemented directly with the guided rocket at LAPAN. On this research, as there is on (Figure 1) is divided into several stages, including the hardware design, software design in the form of algorithms, box design, simulation software and user guide for public.

In the design of hardware system, IMU v2.1 is designed to experiment with the slow speed for pedestrian, bicycle, motorcycle or car. Previous version of the hardware has been tested and has been published [9].

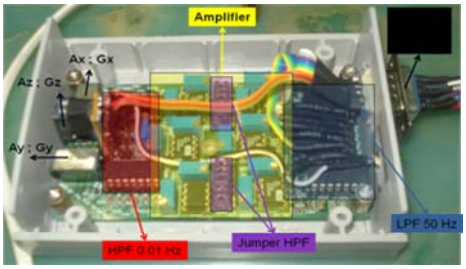

Figure 2: IMU v2.1 and signal processing board

For the data, the microprocessor is used to separate the IMU system because it is still in the experimental stage and should be used to replace the processor. Type of microprocessor used is ATMega8 and ATMega32, depending on the needs and the length of the algorithm is tested.

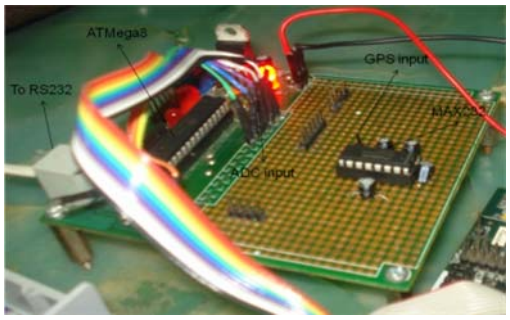

Figure 3: Microprocessor and Max232

Signal conditioning (figure 2) comprises two filters, LPF (Low-Pass Filter) and HPF (High-Pass Filter), which each has custom-made to the needs of the experiment on slow speed. While the amplifier used to increase the output of the sensor. Following (Figure 4) is a schematic of a series of HPF.

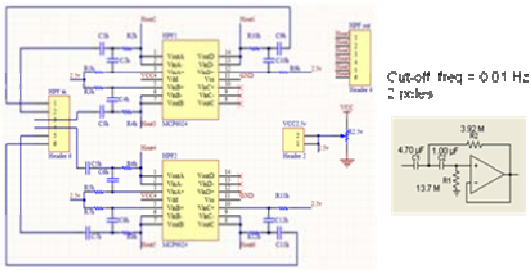

Figure 4: HPF schematic

HPF function to reinstate the position to state the value of 0 g in the system hardware is positioned on the 2.5 volt and also serves to identify the type of changes that occur on the sensors, motion sensors based on whether the real or move because there is a adjust in the position sensor on the body frame coordinate. While the LPF as a function of the output filter sensor. Output from the sensor is not pure value of the sensor but there is noise, bias, and drift of the sensor involved and strengthened, and also to the output system.

Noise, bias, and drift will be removed by digital filter with the following increase and provide initial value and some of the parameters in the algorithm so that navigation is no longer calculated the effects of the hardware system. Following (figure 5) is a schematic of a series of LPF.

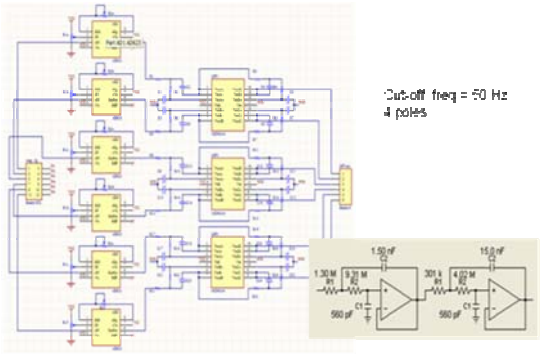

Figure 5: LPF schematic

4. RESULT AND DISCUSS

Research was conducted at guidance and control laboratory. The position of the data as indicated in (figure 6). The data begins when the GPS lock already, start from point 1 to point 2 and then back to point 1

Figure 6: Location collect data

The file saved with different name, this is meant to not only the data stored in each trial but the two data. Only changes the position change. Following (figure 7) is a 6DOF IMU and GPS v2.1 that have been equipped with the INS algorithm for the transformation matrix from body frame to inertial frame or navigation frame.

(a)

(b)

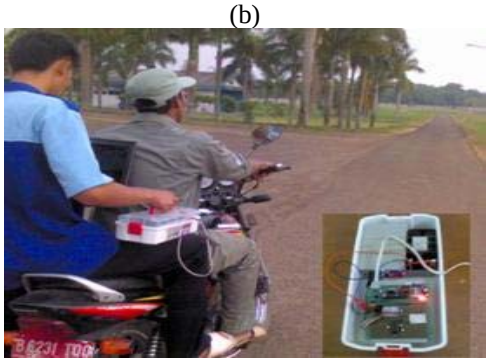

(c)

Figure 7: Testing 6DOF IMU+GPS with pedestrian (a), bicycle (b) and motorcycle (c)

In steady state conditions 6DOF IMU output range is between the following:

ax = 509 to 521 = 12 bit
ay = 511 to 516 = 5 bit
az = 759 to 769 = 10 bit
p = 508 to 515 = 7 bit
q = 484 to 531 = 47 bit
r = 508 to 517 = 9 bit

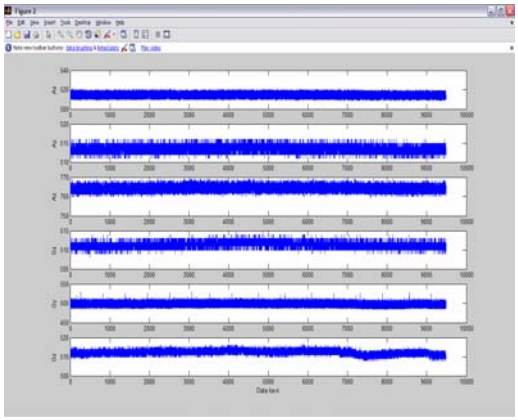

Figure 8: Output 6DOF IMU silence state condition

The value of voltage reference is set on the first, so that the reference voltage and balanced and are between 0 g (see section 3 paragraph 5). 6DOF IMU output value can be seen in (figure 8). Data from the noise, the noise and the big changes of each individual sensor will affect the size of the gain of the amplifier in the signal conditioning.

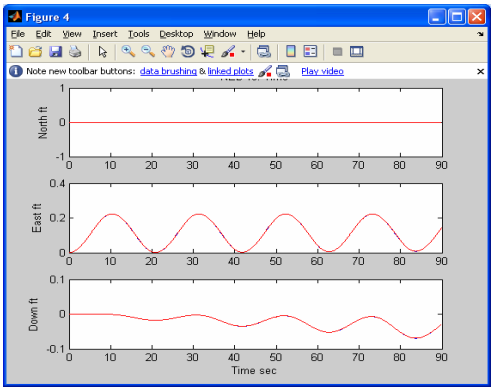

Figure 9: North East and Down Position

The collect data at the time of the vehicle generally will be shifting for initialization, because of the sensor effects. Data for test results by pedestrian, by bicycle and by the motorcycle, do not shown because it can still need to be developed with Kalman filtering. Analysis of data testing will result in the first study on the LAPAN progress report. Here is a picture of output of IMU is converted in the form of position. (North, East, and Down) (Figure 9) and (X, Y and Z) (Figure 10).

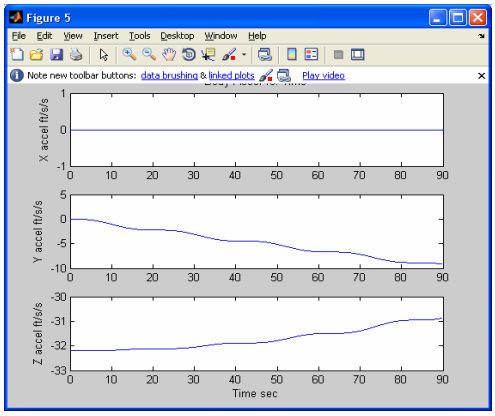

Figure 10: X, Y, and Z position

5. CONCLUSION

IMU v2.1 has been successfully developed and has been tested at low speed with three ways the data is different, with pedestrian, bicycle, and motorcycle. From the results of the experiment may be the characteristics of each and can be the difference in the gain amplifier for each series how the data. Strengthening pedestrian for more gain compared with the bike and compared with the motorcycle. Conclusions from this knowledge need to be research by changing the parameters of gain that have been done on this research and with the effect of noise, drift, and bias of sensor. Small value of capacitor in second version give fast response to steady position and the characteristics of sensor and signal condition are acknowledged. From this research are identified the amount of noise in zero g state with value ranging from 5 to 12 bit. Changes in output at the time the data was due to the effects of drift and bias on the noise.

REFERENCES

[1] A. Schumacher, *Integration of GPS Aided Strapdown Inertial Navigation System for Land Vehicle*, Master Thesis, Royal Institute of Technology, 2006, Sweden. www.ee.kth.se/php/modules/publications/.../XR-EE-SB_2006_006.pdf

[2] C. W. Tan and S. Park, *Design and Error Analysis of Accelerometer-Based Inertial Navigation System*, Research Reports, University of California, 2002, USA. http://repositories.cdlib.org/its/path/reports/UCB-ITS-PRR-2002-21

[3] J. H. Kim, S. Wishart, and S. Sukkarieh, *Real-Time Navigation, Guidance, and Control of UAV using Low-cost Sensors*, The Australian National University, 2006, Australia. www.engnet.anu.edu.au/DEpeople/Jonghyuk.../FSR03-NavGuidCtrl-Kim.pdf

[4] K. J. Walchko, *Low Cost Inertial Navigation: Learning to Integrate Noise and Find your Way*, Master Thesis, University of Florida, 2002, USA. www.mil.ufl.edu/publications/thes_diss/Kevin_Walchko_thesis.pdf

[5] M. Istanbulluoglu, *Performance Tradeoff Study of A GPS-Aided INS for A Rocket Trajectory*, Master Thesis, Air Force Institute of Ohio, 2002, USA. www.stormingmedia.us/12/1293/A129324.pdf

[6] N. Hjortsmarker, *Experimental System for Validating GPS/INS Integration Algorithms*, Master Thesis, Lulea University of Technology, 2005, Sweden. http://epubl.ltu.se/1402-1617/2005/307/index-en.html

[7] R. Wiryadinata and W. Widada, *Development of Inertial Navigation System for Guided Rocket Flight Test*, SIPTEKGAN XI, 2007, Jakarta, Indonesia.

[8] R. Wiryadinata and W. Widada, *Simulasi Penggabungan Data pada Algoritma INS untuk Uji Peluncuran Roket Kendali*, SITIA, 2008, Surabaya, Indonesia.

[9] R. Wiryadinata and W. Widada, *Prototype of A Low-Cost Inertial Measurement Unit for Guided Rocket Flight Test*, SEMNAS UTY 4, 2008, Jogjakarta, Indonesia.

[10] V. Kumar N., *Integration of Inertial Navigation System and Global Positioning System Using Kalman Filtering*, Master Thesis, Indian Institute of Technology, 2004, India. www.casde.iitb.ac.in/Publications/pdfdoc-2004/vikas-ddp.pdf

Analysis of Thermal Characteristics of PVC Cable Rating Voltage of 300/500 Volt under Overload Operation

Rudy Setiabudy[1], Budi Sudiarto[2], Chairul Hudaya[3], Arifianto[4]

[1,2,3,4]*Electric Power and Energy Studies*
Department of Electrical Engineering Faculty of Engineering
University of Indonesia, Depok 16424
http://www.ee.ui.ac.id/epes
E-mail : rudy@ee.ui.ac.id or c.hudaya@nuklir.info

ABSTRACT

Insulation issue is one of the most important things in electrical system distribution. Polyethelene Vynil Chloride (PVC) insulations are widely used as cable insulator in electrical installation because of its good characteristic especially for low voltage application. PVC is light and has high resistance which is suitable for insulator. However, PVC has limited working temperature. The working temperature of PVC is 70°C, its mean that if PVC cable is worked at high temperature (higher than 70°C) the PVC insulator will damage and furthermore it can melt.

We observe the degradation of PVC cable when it operates at high temperature and when the PVC cable starts to melt. We also investigate on what condition this melting may cause a fire. For that purpose, we conducted experiment by applying current to PVC cable 2 x 1.5 mm² using high injection current test. While applying current to the PVC cable, we monitor and record temperature rise on PVC cable every step of current level (every 5 ampere) and then examined the degradation and physical change that is happened to insulator material (PVC) and core.

The results show that the higher current flow is given, the faster cable insulation damage. Conditions in which the cable starts to melt down vary for each cable. For a straight cable, insulation start melt down at 56 A. For a curved cable, insulation start melt down at 54 A.

Keywords : *Insulator, thermal characteristic, PVC Cable, overload operation, maximum temperature.*

1. INTRODUCTION

Insulation issue is one of the most important things in electrical system distribution as its electical and mechanical functions. If the electrical functions break, the electricity supply would stop. Thus, it's necessary to use insulators that are qualified and reliable in an electric power systems to reduce the losses due to disfuction of insulator.

Polymer insulator has the characteristics which are suitable for the demand and fulfill the standard requirements. Besides, it is also having good mechanical and electrical properties,- like lightness, the low of dielectric loss, the low of dissipation factor and the high of resistivity volume. The other advatages of this kind of insulator are easy to be produced and quite cheap if compared with other kind of insulators.

However, the polymer insulators have also the limitations. One of them is its heat resistivity causing the insulator easy to melt down if it's operated on high temperature. At certain condition, the insulator applied in the cables will melt down and finally it will be burned. If arround the cable exists the burnable materials, it will initiate fire. This study investigates the assessment for PVC insulator above its current carrying capacity (CCC) to recognize the insulator degradation.

2. THEORETICAL OVERVIEW

If the temperature rise, the polymer insulator properties may change. This is because the temperature change causes molecular movement inside the insulator material. As the result, structural properties may be altered. If the oxygens and water exist, it will react each other and result in depolymerization, oxydation, and hydrolisys. These will of course change its mechanical, electrical and chemical properties. In this section, we investigate the thermal conductivity, thermal capaicty, heat rate, and expansion coefficient caused by the molecular movements due to increased glass transition temperature (T_g) which consists of melting point temperature (T_m), softing point, and thermal resistivity. Thermal resistivity of polymer material can be seen in Table 1 :

Table 1. Thermal resistivity of Polymers

Polymers	Thermal Resistivity (°C)
Polietilen(low specific mass)	80-100
Polietilen(medium specific mass)	105-120
Polystiren	65-75
Polyvinil chloride	65-75
Resin fenol	150
Resin melamin	160
Resin Urea	90
Polyetilen(high specific mass)	120
Polypropilen	120
Polycarbonate	120
Polyamid	80
Polysulfon	100

2.1 The effect of Curved angle and radius

Figure 1 shows the effect of curved radius R_o against conductor's maximum temperature. The conductor we used in this study was 1 mm in diameter. We got that the critical current (I_{cr}) we applied for straight conductors was 69 A. When the conductor was given 50 A, and curved angle α = 90° at curved Radius R_o = 2 mm, the maximum temperature (T_{max}) will be higher than that of straight conductor. As the curved radius R_o rises, the maximum temperature T_{max} will decrease. The T_{max} with curved angle 90o can be stated as equation below :

$$T_{\max,90}(^{o}C) = -20.56 \ln Ro + 283 \quad (1)$$

The equation (1) can be drawn as a graph below :

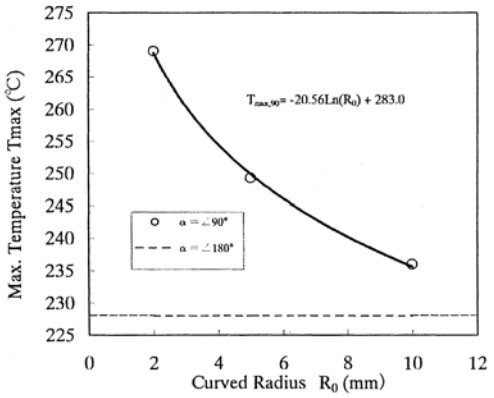

Figure 1. The Effect of R_o against T_{max}

Figure 2 shows the effect of curved angle against maximum temperature of conductor. As the curved angle rises, the maximum temperature decreases.

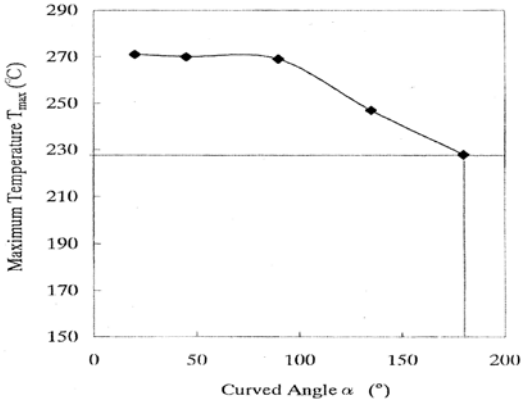

Figure 2. The Effect of α against T_{max}

3. METHODOLOGY

3.1 Measurement Equipments

The measurement equipments of this study consist of :

1) High Current Injector Test Set
2) Voltage AC 220 V
3) Ampere meter
4) Thermocouple
5) Stopwatch
6) Connector cable with capacity of 500 A

3.2 Measurement Circuit

In the experiment, we measured 3 kind of cables; straight cable, curved cable, and non-standard cable. The experiment was carried out by flowing current above its current carrying capacity (CCC). The temperature changes are measured by thermocouple. Figure 3 shows the measurement circuit for increased temperature.

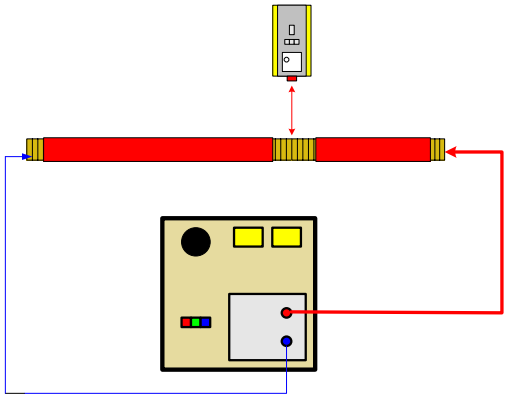

Figure 3. Measurement Circuit for Increased Temperature

4. RESULT AND ANALYSIS

Figure 4 shows the measurement for the straight cable including the temperature at surface insulator, core insulator, and core of conductor. Meanwhile, Figure 5 shows for the curved cable. Figure 6 shows the comparison of straight and curved cable current vs. temperature. We found that the curved cable will start to be smoked when it's given 46 A with the temperature of 156 °C and melt down at 54 A with the temperature of 295 °C. Meanwhile, the straight cable will be smoked at 48 A and melt down at 56 A. Table 2 shows the details of measurement.

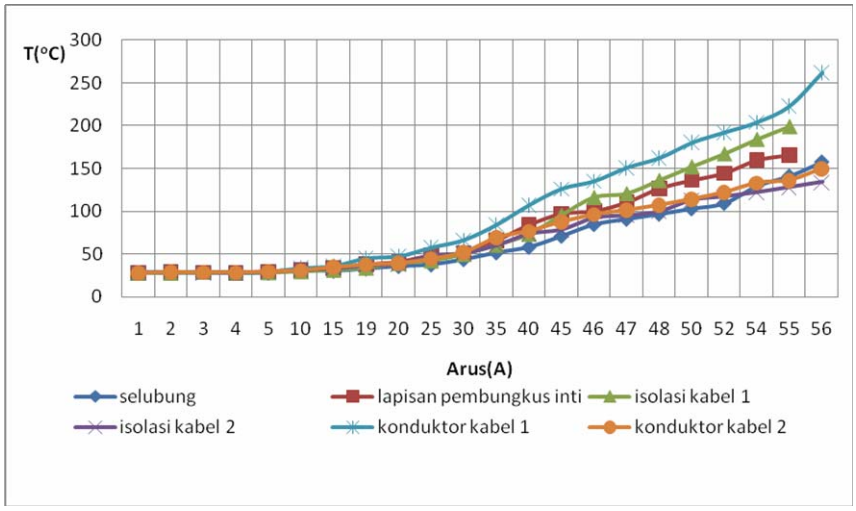

Figure 4. Current vs Temperature on the Straight Cable

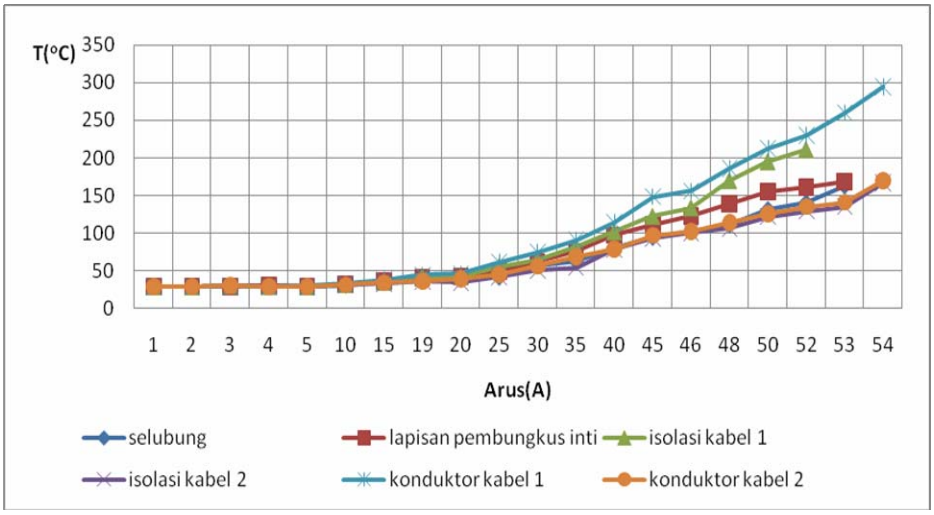

Figure 5. Current vs Temperature on the Curved Cable

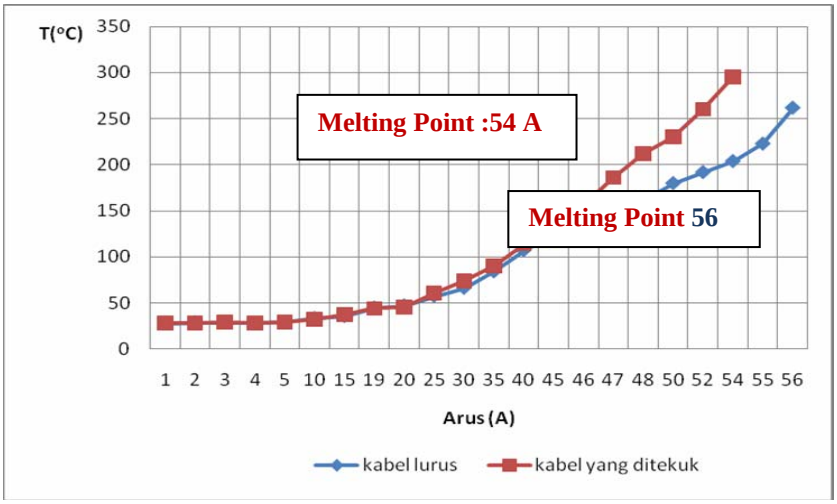

Figure 6. Comparison of Straight and Curved Cable Current vs. Temperature

Table 2. Comparison of Straight and Curved Cable

Current (A)	Tcr Straight Cable (^oC)	Cable Condition	Tcr Curved Cable (^oC)	Cable Condition
46	135	-	156	√
48	162	√	186	√
50	180	√	212	√
52	192	√	230	√
54	204	√	295	×

√ = Smoked × = Melting

According to the measurement, it can be seen that at the same current, the curved cable has higher maximum temperature than straight cable. The temperature distributions on the curved cable are not same. The temperatures are recorded high at the curved section.

5. CONCLUSION

The thermal characteristics of NYM 1.5 mm^2 cable has been investigated. The results show that the higher current flow is given, the faster cable insulation damage. Conditions in which the cable starts to melt down vary for each cable. For a straight cable, insulation start melt down at 56 A. For a curved cable, insulation start melt down at 54 A.

REFERENCES

[1]. Farizandi, Dananto,"*Analisis Karakteristik Penghantar Kabel Fleksibel Dengan Penghantar Kabel Inti Tunggal NYM 2,5 mm2 Dan 4mm2*" Bachelor Thesis, Department of Electrical Engineering, Depok, July 2004.

[2]. Yafang Liu, Kazunari Morita, Toru Iwao, Masao Endo, and Tsuginori Inaba, *"The Temperature Characteristics and Current Conducting Ability of Horizontally Curved Conductors"*, IEEE transaction on power delivery, Vol. 17, No 4,October 2002.

[3]. Yafang Liu, Masao Endo, Tsuginori Inaba, *"The distributions of temperature an magnetic force on a curved conductor,"* IEEE Power Eng. Rev., Vol. 19, pp. 51 52, July 1999.

[4]. Bayliss, Colin, *"Transmission and Distribution Electrical Engineering"*, Oxford, Butherworth-Heinemann, 1996.

[5]. Thue,Williamm, "*Electrical Power cable Engineering*", Marcel Dekkerb Inc, New York, 1999.

[6]. PLN, "*Kabel berisolasi Berselubung PVC tegangan pengenal 300/500V"*, Published in 1992 .

[7]. SVP Indutries, PVC and Fire, <www.svpindustries.com/docs/pvc-and-fire.pdf>

ISSN 114-1284

An Internet Telemetry Design For a medium – scale Manufacturing Company

Sardjono Trihatmo, I Made Astawa, Fachri Reynaldy, Irwan R. Husdi

Center of Communication and Information Technology BPPT
BPPT 2nd Building, 21st Floor, Jl. MH. Thamrin 8, Jakarta 10340
Phone: (021) 316-9815/-9816 Fax: (021) 3169811
E-mail: trihatmo@cbn.net.id

ABSTRACT

This paper introduces a low cost internet telemetry system for controlling and monitoring machines overseas. The system is developed to accommodate the needs of medium scale manufacturing companies so that the design must consider both technical and economical aspect. Unlike the common telemetry systems that implement a client - server communication model, this system uses a client – server – client model. This telemetry communication model is appropriate for controlling and monitoring many slaves that are located in different countries and it can be implemented using a low cost internet service such as a web hosting. Applying this system means creating a value added product and decreasing significantly the cost of after sales services.

Keywords

Internet Telemetry, Control, Manufacturing, SME, web-hosting

1. INTRODUCTION

Manufacturing is a type of industry that is capable to export products. That means a contribution to increase the foreign exchange for Indonesia. One of medium scale manufacturing companies develops machines for food and pharmaceutical processing. After being successful in the domestic market, those machines are exported to several countries such as ASEAN, Middle East and recently Turkey [1.]

Once a machine operates in a foreign country, the company needs to maintain an after sales service. The frequently task is to customize the parameters of the machine according to the demand of customers. Additionally, there is also a requirement that the parameters such as motor speed, gas pressure and chamber temperature need to be monitored all the time to prevent the failure of a product output. Then the company has to send the technicians overseas. According to the company record, there were 10 (ten) after sale services in 3 (three) months in the year 2008. Unfortunately it means a high cost for the company, especially if some machines from the different locations in overseas need to be customized in the same time. Another problem occurs when they apply for an entry permit. It may take several days until weeks to get it. This could affect the credibility of the company because clients need to be treated on time. Most of clients do not know even do not want to know about the permit processing for Indonesian.

A solution for the problem above is to develop a system that is able to monitor the machine parameters remotely. This system is usually called telemetry. A telemetry system is effective and beneficial since it enables 24/7 monitoring, the trend of the parameters of the machine can be online analyzed so that an anticipation against the failure can be taken immediately. For a specific case, a remote parameter setting can be done. However, to do this, a precaution must be taken, especially if the remote process could be danger for human being and environments.

Indonesia has already a national standard in telemetry. It can be seen for example in [4.] The standard is an adoption of the IEC. However, the application of this standard may focus on power distribution line. A publication of this topic can be seen in [5.]. The use of internet for telemetry in power distribution line was introduced in the work of Eichelburg [3.]. He proposed GPRS to connect outlying distribution station with the availability up to 99%. In the commercial area, a remote monitoring has been practiced for a vending machine [2.]. A device is embedded in the vending machine. The device sends machine's condition to a server that belongs to the vendor over GPRS. The owner of the vending machine now connects to the server via internet to check the condition of the vending machine. That inspired us to develop an internet telemetry system

The use of a telemetry system will benefit the company very much. It avoids sending technicians abroad which means reducing the operational cost significantly. In addition, the after sales service can be done on time. However, a cost reduction through the implementation of the telemetry system should not significantly increase the price of the machine and the cost for operating the telemetry system. Otherwise, the

ISSN 114-1284

system would be unused. According to that, the design of a telemetry system must consider both technical and economical aspect.

2. METHODOLOGY

The challenge in the development of this telemetry system is the necessity to consider both technical and economical aspect at the same time. From the economical aspect, it requires the acceptable ratio between the prices of the machine with telemetry system with that of the machine without it. From the technical aspect, the master controller and the controlled slave machine are separated in a very long distance and are not located in the same country. Furthermore number of exported machines may increase.

For the reason above, it is almost impossible to establish a private communication infrastructure. The possible connections are the public phone line and internet. However the use of a direct phone line is not economical solution because the connection is an international connection. So, the internet would be the possible connection.

.There is different kind of internet services. Two of them are the virtual private network (VPN) and web hosting. Technically, the VPN is the most appropriate service for this telemetry system. It offers direct connection to the machine and the machine can be treated as a slave. However, the VPN is still not economical. The price increases with the increasing of the number of connections. For the connection overseas, some internet service provider charge more.

The low cost solution is the use of web hosting as the service. The company needs only to purchase a space and database at ISP's server. The size of it depends on the number of controlled machines. We must assume that the customer overseas has already a local area network so that the machine can be connected to the internet without an extra expense. Web hosting is used for instance in mail server such as yahoo™. Two parties that want to communicate each other must put and take the message in the web server. Since the machine can not be approached directly as a slave/server, then we have to modify the communication model as the client – server – client as can be seen in the following figure.

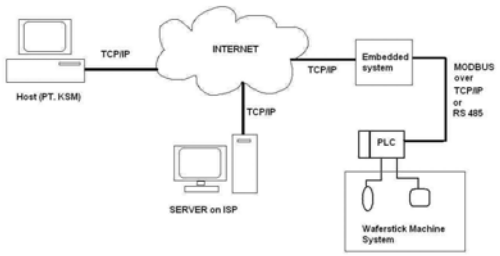

Figure 1: Internet Telemetry Design

Both controllers (in Indonesia) and the machine (overseas) act as a client. In the monitoring process, the machine (as slave client) puts the data into the web server and the controller/observer (as the master client) takes those data and display it. In the setting process the controller/observer puts the data into web server and the machine takes the value and set the parameter according to data. Both clients (controller and machines) initiate the connection. It has an advantage comparing to the client – server model. The local area network where the machine is located does not need to reconfigure the firewall setting because the initiation does not come from outside the network but from the machine itself inside the network.

To implement the client – server – client model through a web hosting service, an interface between the machine and the web server must be developed. The interface can be a single personal computer, an industrial single board computer or even an embedded system. But more important is the development of a program that seeks the address of the web server automatically.

2.1 Sections and Subsections

3. EXPERIMENTS

We limited the experiment so that there is no operating machine because there was no machine available at the moment. Instead of it, we used only a PLC that controls the machine locally. It is justified because the value of the speed of the machine is determined by the PLC.

In the experiments, a system according to the Figure 1 is implemented. All operating systems including the web hosting is a free open source such as Ubuntu©. At the master client a personal computer/notebook with a common specification is used. The function is to display the monitored machine's parameters.

The web server belongs to an internet service provider. Although there are many international ISPs that offer web service cheaply, however an ISP in Indonesia is preferred. When there is a problem with the server/connection, then it is

more convenient and also inexpensive to contact the ISP in Indonesia. The web hosting provides a customized database system. A relational database is programmed using Mysql. An example of the database is shown in the table below:

Table 1:Information about the machine

Field	Type	Null	Key	Default
IDMesin	varchar(12)	NO	PRI	Null
Location	varchar(50)	NO		Null
Other info				

Table 2: Machine's parameters

Field	Type	Null	Key	Default
IDMesin	varchar(12)	NO	FK	Null
DateRead	Date/Time	NO		Null
DateRecv	Date/Time	NO		Null
RpmAdonan1	int			
RpmAdonan2	int			
Other params				
….				
TimeStamp	Date/Time UTC			
Counter	int			

The primary key is the ID machine. There are 23 parameters to be controlled, such as the speed of motors, pressure and temperature. This set of parameters will be sent together. A counter differentiates a set of message and another. Time stamp can be defined by users to determine how often the machine will update its parameter.

At the slave client, an embedded system connects the machine to the internet. In the practice, the machine is controlled locally with a programmable logic controller (PLC). In the experiment a PLC M340 from Schneider Electric is used. The embedded system talks to the machine via PLC using a Modbus protocol. At the early stages of experiments a personal computer substituted the embedded system.

The scheme of the implementation program can be seen in the following figure:

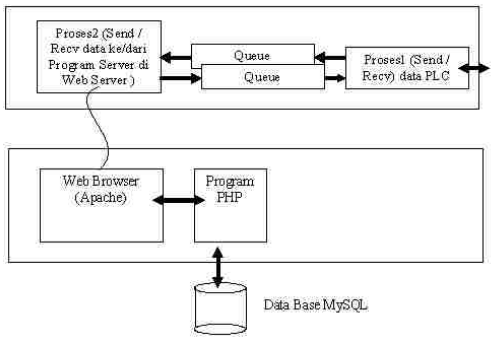

Figure 2: Program scheme

The first block is the program that is developed in the embedded system. There are two sections in the program. The first section communicates with the PLC and the second one connects to the web server. The web browser itself connects data base using PHP.

In the experiment, we developed a simple program that the output of PLC increased its value every 2 minutes and after a defined threshold it reset the value and began to count again. The outputs simulate the speed of motors. Time stamp of telemetry system was set to 1 minute. Then the telemetry system began to monitor and occasionally a parameter change was conducted

4. RESULT AND DISCUSSION

To access the web server, we connect directly to the ISP's web address. In the real application it is strong recommended that the company purchase a domain name so that the access to the web server independent on the change of IP server of the ISP. The picture below shows the connection to the web server that was done by the master client. Values in the left column indicate the value of the output of PLC. For example the speed of 1st motor for *adonan* is 5 rpm at 12:39 pm. The values at the right are the last setting.

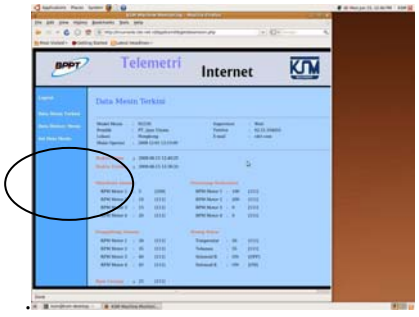

Figure 3: Monitored data at master client (bottom picture was zoomed).at 12:39 pm

To approve the consistency between a monitored value and the real value inside PLC, then we displayed the parameter of PLC using a Unity© vendor specific software.

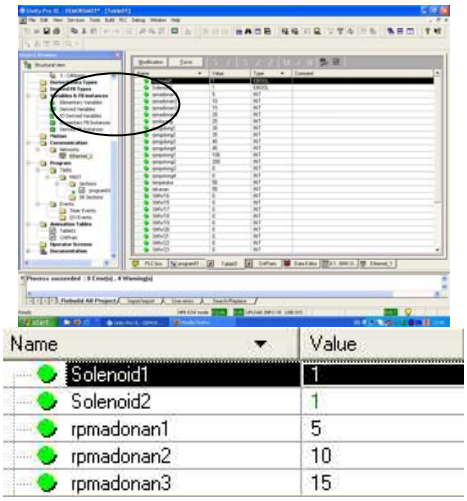

Figure 4 real values inside PLC at 12:39 pm

As can be shown in the picture above, all the real and monitored values are the same. Then in next 2 minutes (12:41 pm) the PLC increased the values as is shown below:

Figure 5: real values inside PLC at 12:41 pm

The speed of motor of *adonan* became 7 rpm. In the master client through web server, all monitored values changed.

Figure 6: Monitored data at master client .at 12:39 pm

Setting process was conducted by the master to specific motors, for instance the speed of 4 motors for cutting (Indonesian: *pemotong*). For setting up parameter, the value must be placed first in the memory address before being transferred to the output. This is important because in the practice, the machine is not in view. There is a risk that the setting may cause an unexpected activity. To minimize the problem, the value must be change gradually and placed in another address other than of output. After the PLC sends back the value to the server, then a real setting can be applied.

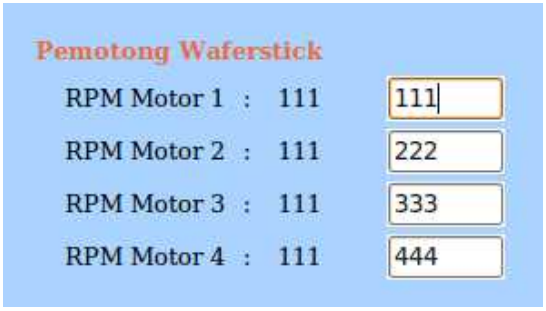

Figure 7: Parameter setting at the master client

As can be seen in the picture using Unity software, the set values were placed in a memory address in the PLC (%MW24 -27).

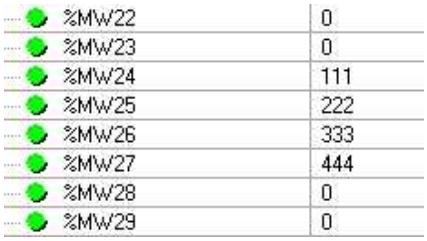

Figure 8: the real value inside PLC

Finally, the process inside the embedded system is documented and for the analysis can be accessed, as shown in the picture below:

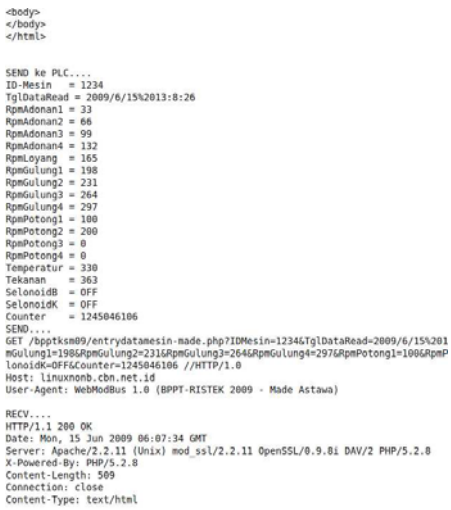

Figure 9 The process inside the embedded system

5. CONCLUTION

Web hosting, as an internet service, can be adapted to implement a low cost telemetry system. With the system, one can monitor and control every where as long as there is an internet connection. A new approach of communication model is a client – server - client model. According to the result of the experiments, the system works properly.

This application has advantages. Firstly, it reduced significantly the cost of after sales services. Secondly, the company has a competitive value added product. Finally all machines can be 24/7monitore so that an early anticipation can be made against the failure. It increases the level of client's satisfaction.

Even though there are some issues that still need to be considered and to be worked out. They are the security and reliability measurement of data. It needs some intensive work in the next step of the research.

REFERENCES

[1.] N.N, www.ksm-machinery.com
[2.] N.N,www.comtechm2m.com/m2m-telemetry-solutions/vending-telemetry-soltion.htm
[3.] Eichelburg, "Using GPRS to connect outlying distribution substation, 18th International Conference on Electricity Distribution, Turin,6 – 9 June 2005
[4.] N.N,"Telemetry Equipments and Systems"(in Indonesian), Document SNI 04-7021.1.1-2004 National Standardization Agency, Vol 1, 2004
[5.] Solida, Asa'ad, " Operating SCADA in he Electricity State Agency" (in Indonesian), National SCADA Workshop, Jakarta 2004

ISSN 114-1284

The Development of an ADS-B Signal Receiver for Civil Aviation in Indonesia

Sardjono Trihatmo, Irwan R. Husdi, Achmad Witjaksono

Centre of Information and Communication Technology BPPT
BPPT 2nd Building 21st Floor, Jl. MH. Thamrin 8, 10340 Jakarta
Phone: (021) 316-9815/-9816, Fax: (021) 316-9811
trihatmo@cbn.net.id

ABSTRACT

This paper introduces a self developed prototype of ADSB receiver. According to International Civil Aviation Organization (ICAO), ADSB technology is considered to substitute radar systems. The purpose of the development of this ADSB receiver is to assess the new technology and to endorse domestic industries. The work includes building the down converter, signal conditioning and message decoding. Since there is a large amount of messages, this paper it does not describe message decoding. At the end it can be concluded that it is highly possible for domestic industries to develop such an ADSB receiver.

Keywords:

Surveillance, broadcast, radar, extended squitter.

1. INTRODUCTION

Radar systems will be substituted by an Automatic Dependent Surveillance Broadcast (ADS-B) system. In contrast to radar system where an aircraft will be scanned and identified by radar, in this new system, an aircraft sends signals (ADSB signal) to the ATC tower actively. It has an advantage that below a certain flight level the aircraft still sends information while radar can not detect it because radar has a fix angle position. In addition, the aircrafts are able to communicate to each other. Furthermore, the operational cost of ADSB is much lower than that of a radar system.

South East Asia nations and Australia are committed to implement the ADSB system. Indonesia needs to adopt this new aviation system. Otherwise the air space over Indonesia is going to be controlled by another country that has implemented the ADSB system. Additionally, Indonesian aircraft may have low priority of service when entering the ADSSB ready country.

Indonesia has relative bigger airspace than all South East Asia nations. To cover the airspace, Indonesia needs to provide a large number of ADSB systems. In a report [1.] of ICAO meeting, 30 ADSB stations will be installed in 2010. Thus it is a potential market for ADSB system providers. All providers are from foreign countries. A problem may occur if their systems are not interoperable. This could happen, since each provider has their own protocol communication in the end system. Additionally, it is important to endorse domestic industry to have knowledge about this new technology so that they are capable develop such system and to maintain the system operation.

Considering the problem above, it is important to assess this new technology, before its implementation. Beginning with study of aviation standard documents, working papers of ICAO workshop we develop such system as a test bed.

ADSB system may include three sub-systems. Those are transmitter-receiver, data link, and network sub system. Since the scope of works is so wide the first approach is focused on an ADSB receiver as the front end system

2. THEORY AND SPECIFICATION

ADSB message [2.] is encoded in 112 bits with the format that is shown in the table below.

Table 1: ADSB Message Format.

Downlink Format (bits)	Target Address (bits)	Message (bits)	Parity Check (bits)
8	**24**	**56**	**24**

First five bits in the downlink format field indicate either the data is an ADSB message or another one. The ADSB message is encoded in “10001” and “10010” or equal to 17 and 18 decimal respectively. A 24 target address is an address that is assigned by the aviation authority as can be seen in the ICAO document [4.] Next field consist the information of the flight. Since there is only 56 bits for message encoding, the complete information must be divided into groups and then transmitted separately. There are 32 groups of message including position, velocity and aircraft status. The determination of 32 groups is accommodated in first five bit of 56 bits message field. The last field contains 24 bits for error detection. It is done by using CRC. The polynomial for the divisor can be found in [3.].

The format of transmitted ADSB data stream according to RTCA document is shown in the picture below. It consists of 4(four) pulses as the preamble and 112 pulses as data. All pulses have duration of 0.5 us with the tolerance at 0.05 us. The second, third and forth preamble pulses are spaced 1.0, 3.5 and 4.5 us respectively from the first preamble pulse. The data block begins 8 second after the beginning of the first preamble's pulse. Like the preamble, the length of a pulse is 0.5 $\pm$ 0.05 us. The data is encoded as using pulse position modulation (PPM) that is often called Manchester encoding. A pulse is transmitted in the first or second half interval of one microsecond tome interval. A time interval consists of a pulse in the first half assigns a “ONE” while in the second half a” ZERO”.

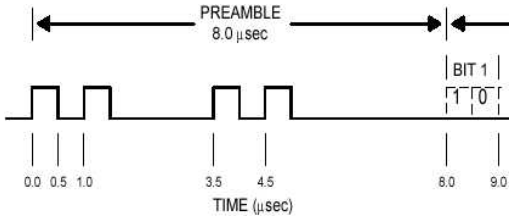

Figure 1: The format of ADSB pulse stream. The preamble.

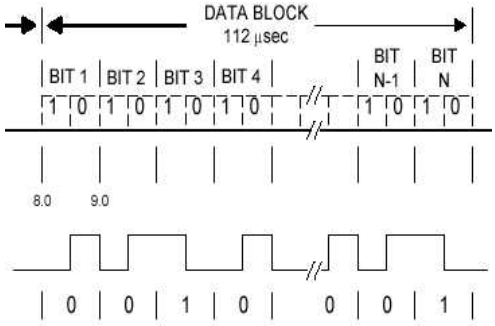

Figure 2: The format of ADSB pulse stream. The data block. PPM encoding.

This data stream is modulated with the frequency at 1090 MHz. A transponder at the aircraft will broadcast the so called the extended squitter.

There are some criteria for the squitter. The important one is the spectrum as can be seen in the Figure 3.

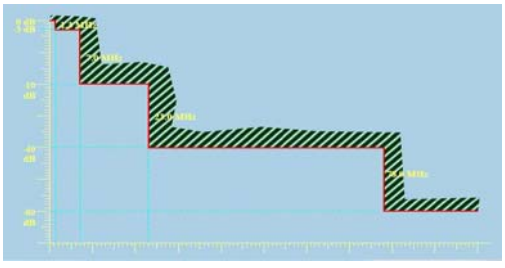

Figure 3: The spectrum of ADSB squitter.

3. DESIGN AND IMPLEMENTATION

To extract and decode the data, a design of the receiver is developed as can be seen in the picture below:

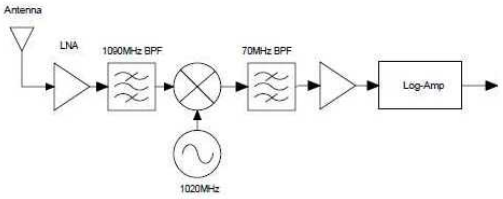

Figure 4: The bock diagram of the receiver (analog section).

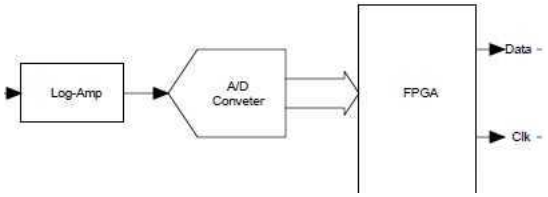

Figure 5: The bock diagram of the receiver (digital section).

The block diagram can be divided into two sections, namely the analog and digital section. The analog section contains a down converter that demodulates the signal. The digital section processes the incoming analog signal so that the ADSB message is validated.

After passing trough a low noise amplifier the 1090 MHz signal will be converted down to an intermediate one. According to the typical spectrum (Figure 3) the signal is demodulated using 1020 MHz signal produced from an oscillator. It represents a bandpass filter with 70 MHz bandwidth inside that is the data signal. The data signal that is still the analog signal is amplified.

Then digital processing begins. The process includes bit confidence determination, preamble detection, retrigerring and ADSB data recognition. First of all, the signal is sampled at 10 MHz. Since a period is one microsecond, then there will be ten sampled value in a period and consequently five sampled value of a pulse. This sample rate is beneficial to determine the bit confidence of PPM code. An alien signal could be superposed to the squitter. It may makes two pulses each in the first and second half interval. In the PPM code that is forbidden. We set so that a valid pulse position (high bit confidence) contains at least 4(four) consecutive sampled values in a half period within a threshold. The threshold is $\pm$ 3 db from the peak. It is under assumption that the interference signal has a short duration of peak time. This has advantage comparing using only peak detection

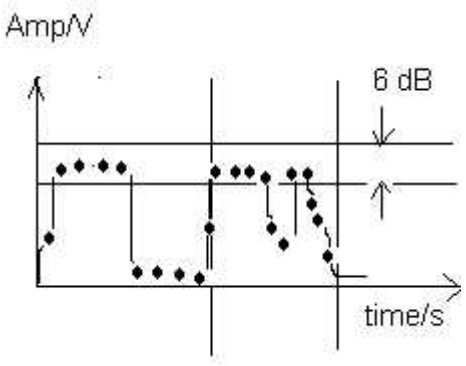

Figure 6: Bit confidence

We can see in the figure that in the first interval the code is clearly ONE. In the second interval, there are two pulses in a period. Using only peak detection, the bit confidence is low so that the data is not valid. However using 10 sample/us, the bit confidence is high. The code is assign as ONE.

Then begin the process to detect the preamble. The process need to recognize the relative transmit time between 4 pulses as it is stated in Figure 2. The pulses must be high confidence. In addition, at least two pulses have a leading edge. It is defined that two consecutive sampled value must be at least 4.8 dB difference for 10 MHz sampling.

It must be reminded that the message from a transponder is a broadcast. It is possible during current preamble recognition, a new but stronger preamble than previous one is detected. Then the new coming preamble must be processed an. If it is valid then the previous message will be discharged. This is a retriggering process that is shown in the Figure 7

Figure 7: The retrigerring

The new coming preamble pulses must be above the threshold area. That is at least 3 dB from the currently being processed preamble pulse. When it is valid then a new threshold must be defined.

The last process is to determine whether the message is the ADSB message or not. According to the previous section, the ADSB message is determined by first five bits of the data. The decimal form of it is 17 or 18. Rather then translating to decimal, it is more efficient if we only inspect the pulses. The binary form of this number has only two bits that its value is ONE. It is the forth and the fifth for 18 and 17 respectively.

After the PPM encoded ADSB message is valid, then the data is converted to a binary stream. The output data is sent in an SPI like protocol. While in the SPI the length of the data usually 16 bits long, in this receiver the data is 112 bit long.

4. RESULT AND DISCUSSION

The result of the ADSB receiver system can be seen in the Figure 8. In the experiment, the data signal was transmitted by an ADSB transponder and the output signal of the ADSB receiver was measured using an oscilloscope of 200MHz bandwidth and with sampling rate 2Gsa/second.

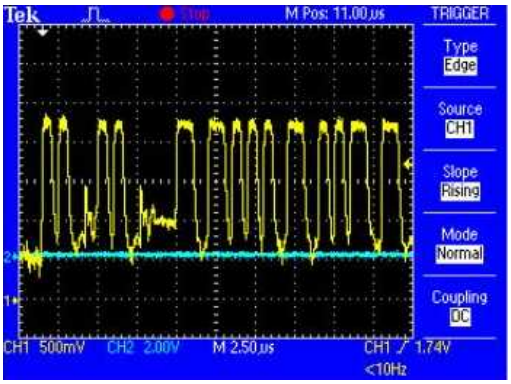

Figure 8: The measured ADSB pulse stream at the receiver.

As the theory said, the demodulated signal contained a preamble that consists of 4 pulses and followed by data. We can see from the oscilloscope display that the difference between second and forth preamble pulse is one division. Since one division is 2.50 microsecond, then the time distance between them is 2.50 microsecond. It is exactly correct according to the standard that is shown in the figure above. It was also said that the data come 8 microseconds after transmitting first preamble pulse. However, the data are encoded in PPM format that has been describe above. It means, the first pulse of data could be 8 or 8.5 microseconds of the first transmitted preamble pulse, depending on the decoded datum is “ONE” or “ZERO” respectively. The picture below is the expanded version of the figure above where the time scale is one microsecond per division. The first pulse of data came 3.50 microseconds after forth preamble pulse that means 8 microseconds from the first transmitted pulse. It indicates us that first datum is a ONE, because the pulse is in the first half interval of one microsecond time period.

ISSN 114-1284

Figure 9: The ADSB first five data in PPM format.

Since the first datum is a ONE, then next four data pulses need to be analyzed, to detect whether the squitter is an ADSB message. The rising edge of the next pulse is about 1.50 microseconds. It indicates us that the pulse is in the second interval of next time period. Thus the second datum is "ZERO". So are the third. The forth pulse may longer than other pulses. Since the maximum accepted length of a pulse is 0.50 + 0.05 microseconds, then it indicates us that the fifth pulse is in the first half interval of a time period what means a "ONE". It concludes that first five bits of data is a consecutive 10001 or in decimal form is 17 (seventeen). According to the standard in figure above, the message is exactly the ADSB message with downlink format 17 (DF 17).

The analysis of the analog signal is proven using the digital signal processing inside the FPGA[5.]. The picture below shows the output of the processing block inside FPGA.

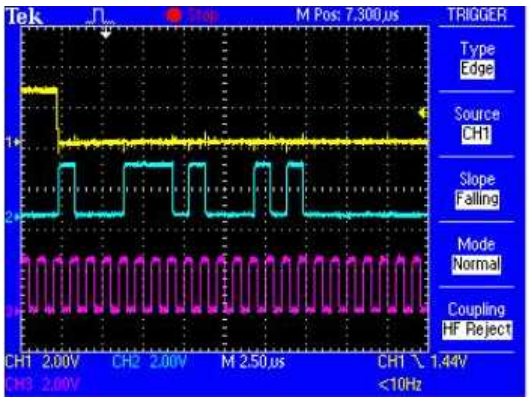

Figure 10: The decoded ADSB data.

There are three output channels. First is a strobe. Second is binary data where high amplitude is ONE and low is ZERO. Last one is the clock with the pulse length of 0.50 microseconds in one microsecond period. After a falling edge of a strobe signal, the data is valid and it is indicated with a rising edge of a pulse. Then in the picture, we can see that the first datum is valid 0.50 microseconds after falling edge of the strobe signal. The first datum is a ONE. The second, third and the forth datum is ZERO and the fifth is already ONE. Thus the code is 10001 what means the DF 17. It concludes that the result from analysis and measurement conform each other.

5. CONCLUTION

The idea of conducting this device engineering is to assess a new technology in civil aviation and to introduce this technology to the domestic electronic industry. Begin from studying the civil aviation standard documents and conducting the experiment, it can be concluded that it is highly possible to develop commercial ADSB receivers in a mass product in Indonesia.

Since the process is a real time and very high speed, then it is highly recommended to use FPGAs as the tools since those are is price competitive in compare with very high digital signal processor.

Finally, the system is still a basic design yet. There are some improvements that must be done, especially in the determination of the bit confidence. A fast but reliable process need to be developed.

ACKNOWLEDMENT

In this occasion, the authors want to thanks PT. compact Microwave Indonesia (CMI) for the collaboration in the development of this receiver, especially for the development industrial standard hardware and packaging.

REFERENCES

[1.] N.N, “Report of the Fourth Meeting of the South East Asia Sub-Regional ADS-B Implementation Working Group (SEA ADS-B WG/4)”, Melbourne, Australia, 9-10 February 2009.
[2.] N.N, “Minimum Operational Performance Standards for 1090 MHz Extended Squitter Automatic Dependent Surveillance – Broadcast (ADS-B) and Traffic Information Services – Broadcast (TIS-B)”, RTCA DO-260A,Vol 1, USA, 2003
[3.] N.N, “Minimum Operational Performance Standards For Air Traffic Control Radar Beacon System/Mode Select (ATCRBS/MODE S) Airborne Equipment”, RTCA DO-181C, USA, June 2001
[4.] N.N, ”Aeronautical Telelecommunication”, ICAO Annex 10 Vol. 4, 3rd Ed, July, 2002.
[5.] Pedroni, ”Circuit Design with VHDL”, MIT Press Cambridge, Massachusetts London, England, 2004

VoDSL Feasibility Analysis and Targeted Applications (Case Study: Bogor and West Jakarta, PT. Telkom, Indonesia)

Sirat, D.*, Prasetio, J.E.*, and Asvial, M*

- *Electrical Engineering Department, Faculty of Engineering, Universitas Indonesia*

Kampus Ui Depok, 16424
Telp: 021-7270078, Fax: 021-7270077
E-mail: sirat@ee.ui.ac.id, and asvial@ee.ui.ac.id

ABSTRACT

VoDSL is a fixed line technology that enables true convergence between multi broadband services and multi voice services into the same pair cable. Actually now, POTS revenue is significantly decreasing in Indonesia, so that the network and feasibility analysis is needed to examine implementation of VoDSL technology especially in PT. Telkom's network. In this paper, the demand projection is developed and analyzed for VoDSL implementation over existing Telkom customers using three models, they are pessimistic, moderate and optimistic. The investment cost, feasibility and payback period during 2008-2013 is analyzed and seek which models suitable for existing infrastructure and demands. The results show that using pessimistic model, VoDSL worth implement as its IRR 6% higher than assumed discount rate and has 80% of CAPEX efficiency that compared to copper investment. From the analysis, VoDSL is supported by existing ATM and IP Network and take in to account for PT. Telkom benefit with seamless migration to broadband services. To guarantee IP quality network implementation, a new strategy with placing voice gateways on intersect locations is needed. VoDSL for both ATM and IP backbone area is feasible that it has positive NPV and IRR above discount rate and payback period from 1 to 2 years.

Keywords

VoDSL, Voice over DSL, G.SHDSL, Voice over ATM, Voice over IP

1. INTRODUCTION

Facing the facts that voice revenue over wireline is decreasing[1]. There are three reasons that PT Telkom should implement VoDSL as a new service with low cost technology. [2] [3]. It could efficiently optimize the copper wired network and generate new services. Some problems in the existing condition of telecommunciation infrastructure and services in Indoensia, they are: First one, there are millions of people in the waiting list asking for cable services, but only thousands of available copper network and the remaining cables are reserved for broadband services such as : IPTV, VoD and high speed internet. VoDSL efficiently could use few cables to answer many demands in telecommunication servcies. Second one, the phone lines requires new copper lines to connect to customers. For every single SOHO or corporate customers and even residentials there are more than one pair of copper supplying phones, faxes, dial-up servers, credit card applications and so on. VoDSL only employs one pair of cable to support all this services up to 16 lines with the same quality as POTS (without compression). And third one, the existing leased lines cannot provide voice services in the same copper wired. VoDSL enables it and can be used to solve te above problems [2]-[5].

In this paper demand projection for VoDSL implementation over existing Telkom customers using three models, they are pessimis, moderat and optimis is developed. In addition, this research is also to build business assessment on VoDSL over existing copper wired network. The investment cost, feasibility and payback period during 2008 – 2013 is calculated and seek which models should be suited to existing infrastructure and demands. Some implementation scenarios consist of topologies of existing and new services that could be served by VoDSL are also to be described and analyzed.

2. VODSL TECHNOLOGY AND NETWORK PLANNING

As shown in Figure 1, VoDSL topology is the same as DSL topology with some added devices, such as IAD (at customer premise) and Voice Gateway (operator site).

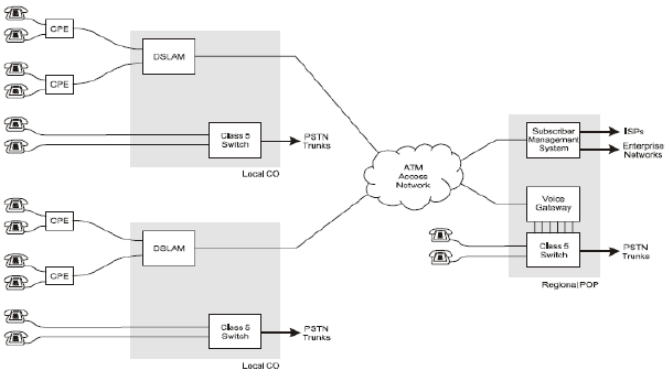

Figure 1. Centralized VoDSL over ATM

Voice Gateway could be located centralized or distributed. Centralized means that only single Voice Gateway serves to all DSLAMs, gives operator low investment and operation cost but QoS guarantee must be well calculated and prepared for end to end network. Distributed means Voice Gateway per DSLAM while Semi Distributed means Voice Gateway for few DSLAMs.

The transport technologies include ATM and IP and use the standardization for voice codecs G.711 or G.726. POTS is to be used in 64kbps and can be compressed to 32kbps. For IP backbone, distributed topology is needed to ensure QoS issues over IP network.

Based on ITU presentation [3], based on derivation from simple IPO (Input Process Output), the network planning model is proposed as shown in Figure 2.

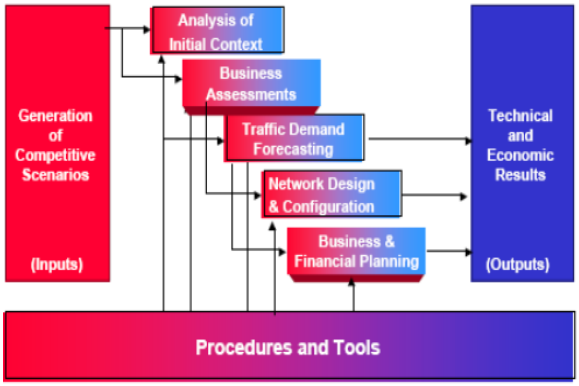

Figure 2. Network Planning Model

1. INPUT
   a) *Generation of Competitive Scenarios* consists of scenarios based on various technology standards.
2. PROCESS
   a) *Analysis of Initial Context*, the basic analysis of scenarios is analyzed using simple tools. In this paper we analyze existing infrastructure and its support for VoDSL.
   b) *Business Assessment*, is used to evaluate the business opportunity on each scenarios.
   c) *Traffic Demand Forecasting*, demand projection and network capacity issues regarding each scenarios.
   d) *Network Design & Configuration*, network reengineering and topology review as required by scenarios.
   e) *Business and Financial Planning*, includes investment and operation cost and feasibility analysis
3. OUTPUT
   a) Economic and Technology Result

This model will be used to analyze VoDSL implementation in Jabodetabek area.

3. Network Architecture

Network utilization in cable networks reach 70% with penetration only 11% of total population JABODETABEK (Jakarta Bogor Depok Tangerang Bekasi) [4]-[5]. Cable network with "ready to broadband" status range between 127 K and 304K for each DATEL (Daerah Telekomunikasi). Total number of DATEL is 8 that serve in JABODETABEK area. The condition of existing condition and the ready to broadband condition is shown in Figure 3.

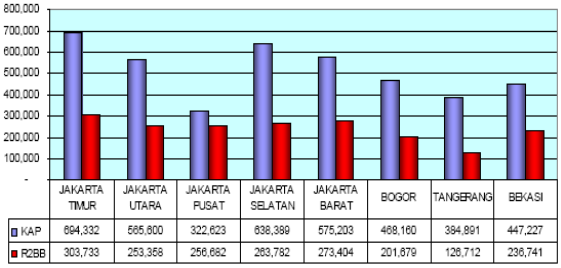

Figure 3. R2BB (Ready to Broadband) vs Existing

There area various access technology employed by Telkom such as : POTS, ADSL, G.SHDSL and backbone technology such as: NG-SDH backbone, SDH backbone, Metro Ethernet backbone and IP Transport. POTS provides the basic telephony services such as phone, fax, dial up access for remote application or credit card payments, and PBX. ADSL supply high downstream bandwidth to customers and one analog phone while G.SHDSL meets corporate customer demand for symmetric bandwidth. VPN or Internet access without any phone services could be delivered over the same copper pair. The demand from POTS waiting list, ADSL office segmen, and G.SHDSL customers are derived in this paper.

4. Demand Projection

The demand projection is built in three models, they are: pesimis, moderat and optimis and consist of POTS, ADSL and G.SHDSL demand combinations.

POTS Waiting list condition is shown in Figure 4. We will calculate status of UN, SI, RE, UO as demands. The UN (Unavailable) means that the network capacity is full; SI means that is is impossible regarding primer cable; RE means that it registered for new cable; UO means that is Unfeasible. POTS growth reach CAGR 10,65% as reported by government in [6]. We will use this as growth condition for POTS projection.

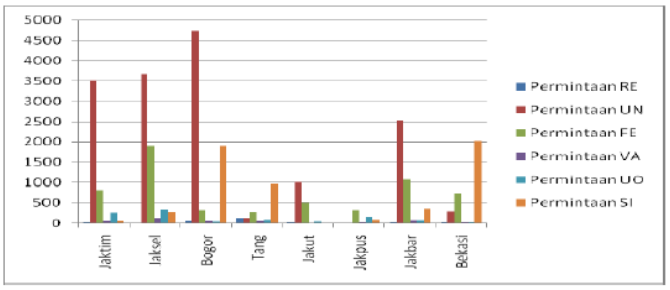

Figure 4. POTS Waiting List

ADSL Network – ADSL services have three base customers, they are residential, office and warnet (internet café). The office customers is focused in the research because they need more than one phone lines for faxes, PBX, and dial-up transaction applications. The office customers are ranging from 2% - 10% of all ADSL customers. From the same source as POTS, 24% of CAGR is used for ADSL.

G.SHDSL network – G.SHDSL customers have more than a pair cable because no phone services could delivered over basic G.SHDSL. G.SHDSL customers pay the higher bill than ADSL office customers for they have symmetric private access in their offices conectivities. G.SHDSL has the same growth as ADSL.

From the data some variables are assumed in the models, they are:

Pesimis – Focusing VoDSL implementation on POTS demand. 10% of growth is sued for POTS, 2% for ADSL and G.SHDSL customers.

Moderat – Focusing on average between POTS and corporate customers. 17% and 5% of growth are used for ADSL and G.SHDS, respectively.

Optimis – Focusing on the higher of POTS and Corporate Customers demand. 24%, and 10% of growth are used for ADSL and all G.SHDSL, respectively. The demand projection is show in Table 1.

Table 1. Demand Projection

		DATA DEMAND			VODSL (a (UN+SI)+2%b+c), yoy = 10%					
	Area	(a) WL POTS	(b) Speedy	(c) G.SHDSL	2008	2009	2010	2011	2012	2013
PESIMIS	Jaktim	3.568	77.257	121	5.234	5.758	6.333	6.967	7.663	8.430
	Jaksel	3.937	85.977	39	5.696	6.265	6.892	7.581	8.339	9.173
	Bogor	6.634	35.840	32	7.383	8.121	8.933	9.827	10.809	11.890
	Tang	1.096	37.857	24	1.877	2.065	2.271	2.498	2.748	3.023
	Jakut	1.030	70.075	20	2.452	2.697	2.966	3.263	3.589	3.948
	Jakpus	100	30.934	116	835	918	1.010	1.111	1.222	1.344
	Jakbar	2.898	72.910	107	4.463	4.910	5.400	5.941	6.535	7.188
	Bekasi	2.309	31.132	10	2.942	3.236	3.559	3.915	4.307	4.738
		21.572	441.982	469	30.881	33.969	37.366	41.102	45.212	49.734

		DATA DEMAND			VODSL (a(UN+UO+SI)+5%b+c), yoy = 10%					
	Area	(a) WL POTS	(b) Speedy	(c) G.SHDSL	2008	2009	2010	2011	2012	2013
MODERAT	Jaktim	3.820	77.257	121	7.804	9.131	10.683	12.499	14.624	17.110
	Jaksel	4.269	85.977	39	8.607	10.070	11.782	13.785	16.128	18.870
	Bogor	6.687	35.840	32	8.511	9.958	11.651	13.631	15.949	18.660
	Tang	1.193	37.857	24	3.110	3.639	4.257	4.981	5.828	6.818
	Jakut	1.072	70.075	20	4.596	5.377	6.291	7.361	8.612	10.076
	Jakpus	258	30.934	116	1.921	2.247	2.629	3.076	3.599	4.211
	Jakbar	2.974	72.910	107	6.727	7.870	9.208	10.773	12.605	14.748
	Bekasi	2.337	31.132	10	3.904	4.567	5.344	6.252	7.315	8.558
		22.610	441.982	469	45.178	52.858	61.844	72.358	84.659	99.051

		DATA DEMAND			VODSL (a(RE+UN+UO+SI)+2%b+c), yoy = 10%					
	Area	(a) WL POTS	(b) Speedy	(c) G.SHDSL	2008	2009	2010	2011	2012	2013
OPTIMIS	Jaktim	3.832	77.257	121	11.679	14.482	17.957	22.267	27.611	34.238
	Jaksel	4.279	85.977	39	12.916	16.015	19.859	24.625	30.535	37.864
	Bogor	6.738	35.840	32	10.354	12.839	15.920	19.741	24.479	30.354
	Tang	1.301	37.857	24	5.111	6.337	7.858	9.744	12.083	14.983
	Jakut	1.085	70.075	20	8.113	10.060	12.474	15.467	19.180	23.783
	Jakpus	261	30.934	116	3.470	4.303	5.336	6.617	8.205	10.174
	Jakbar	2.998	72.910	107	10.396	12.163	14.231	16.650	19.481	22.793
	Bekasi	2.354	31.132	10	5.477	6.792	8.422	10.443	12.949	16.057
		22.848	441.982	469	67.515	82.991	102.058	125.555	154.523	190.245

The service areas as Telephony based customers (Phone majority), Internet based customers (warnet majority) and Corporate based customers (Office building majority) are classified in the analysis. The samples from phone and corporate based is used and from the data, **BOGOR** area is for the most phone customers and **JAKBAR** area is for the most office buildings.

5. Results and Analysis

For calculations, we have to use assumed service rate because VoDSL hasn't delivered elsewhere in Indonesia. Tariff that is used in this analysis is assumed as follow :

- IAD installation : IDR 200K
- Added Voice lines : 0
- Abonemen VoDSL : 80% POTS or IDR 24K
- ARPU per line : IDR 60K
- VoDSLto VoDSL Call Unlimited

We use two scenarios, they are VoDSL over ATM as scenario-1 and VoDSL over IP as scenario-2. Location for both scenario is explained as follows:

Scenario-1 – VoDSL over ATM, Centralized
GW BOGOR : GATOT SUBROTO
GW JAKBAR : SLIPI
Customer ask for 1 phone lines
Scenario-2a – VoDSL over IP, Distributed
GW BOGOR : 10 Locations
GW JAKBAR : 8 Locations
Scenario-2b – VoDSL over IP, Semi Distributed
GW BOGOR : 3 Locations
GW JAKBAR : 2 Locations
Customer ask for 3 phone lines

Revenue Projection

From these assumption we could calculated revenue projection different services as shown in Figure 5 and Figure . We choose as case area is Bogor and Jakarta Barat.

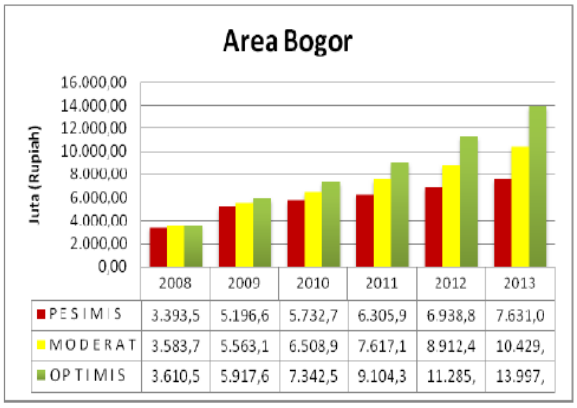

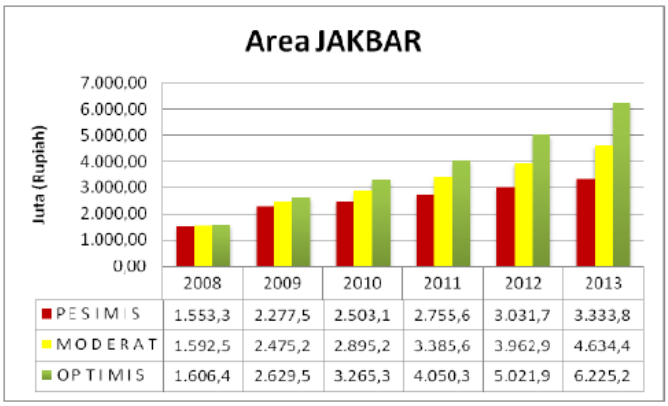

Figure 5. Revenue Projection VoATM

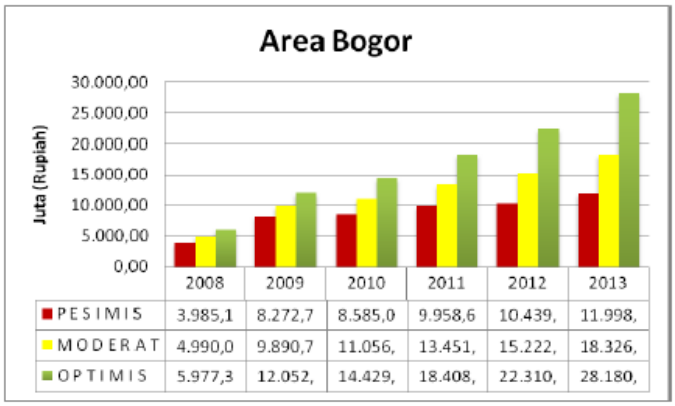

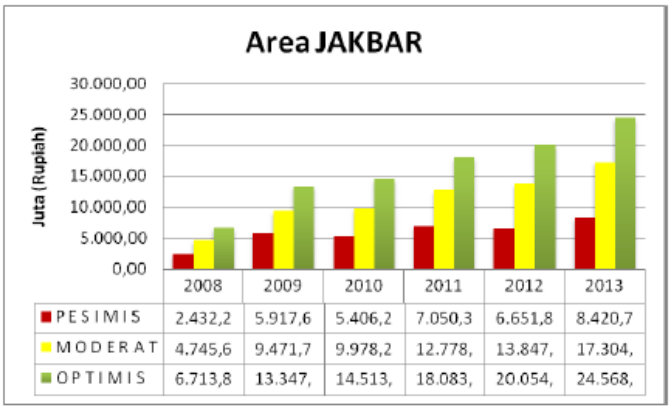

Figure 7. Revenue Projection VOIP

Analysis of Initial Context

For each scenarios, Telkom has all basic network required for copper infrastructure, ATM and IP. Bandwidth available in existing network suits demand calculations with some relocation needed in ATM networks between DSLAM-rich but low demand area and DSLAM-poor but high demand such as : JAKBAR and BOGOR area respectively. The result shot that no investment needed in primer copper, ATM switches and routers.

Table 2. Analysis of Initial Context

Materi	ATM backbone	IP backbone
Konteks Dasar	- ATM-DSLAM mendukung protokol AAL2, AAL5 dan IP - ATM Switch mendukung multi pvc - Dukungan line VoDSL : VoATM codec G.726 : 38.750	IP-DSLAM mendukung protokol AAL2, AAL5 dan IP - Dukungan line VoDSL : VoIP codec G.711 ~ 70.000 ssl
Desain/ Konfigurasi Jaringan	Centralized	Distributed
Demand vs Bandwidth (Bogor + Jakbar) kompresi G.726 (32Kbps)	**1 line telepon/ demand** VoDSL Jakbar *over capacity* : permintaan 8.789 sst dukungan bandwidth 31.000 ssl voDSL- Bogor kapasitas kurang : permintaan 19.753 sst dukungan bandwidth 7.750 ssl	**3 line telepon/ demand G.SHDSL, 2 line telepon/ demand ADSL, 1 line telepon pelanggan baru.** Jakbar : permintaan 35.910 sst Dukungan bandwidth 66.664 ssl Bogor : permintaan 41.811 sst dukungan bandwidth 49.998 ssl

Investment Calculation

Investment cost consist of some parameters as shown in detail price in table 3)

- Voice Gateway (G.711, G.726, VoATM, VoIP)
- Jumper cable

- Optical Patchcord
- IAD
- DSLAM relocation cost

Table 3. Investment Cost

				kurs : 9300	
	Satuan	Vol	Harga	$	Rp
Voice Gateway Cisco MGX8880-CHCL (Chassis and Cooling)	Unit	1	23.465	23.465	
AXSM-32-T1E1-E (32 E1)	Modul	1	30.875	30.875	
AXSM-8-155-E- (8 OC3)	Modul	1	21.613	21.613	
IAD	Unit	6.634	170	1.127.780	
Jumper	Roll	5	900.000		4.500.000
Sarpen Instalasi	Paket	1	2.000.000		2.000.000
Jasa penarikan E1/patchcord	STO	28	500.000		14.000.000
				Total Dollar	1.203.733
				Konversi Rupiah	11.194.712.250
				Total Rupiah	20.500.000
				Jumlah Total	11.215.212.250
				PPn	1.121.521.225
				Total Investasi	Rp12.336.733.475

Copper investment per user reach US$1000. Compare to this VoDSL investment, 80% saving of CAPEX can be achieved and more than copper with lower copper's capacity utilization. One pair cable could serve up to 16 lines (uncompressed). Investment chart year of year is describe in Figure 8.

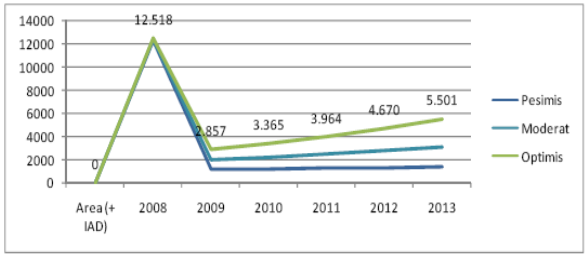

Figure 8. Investment Chart

Operation Calculation

Operation is calculated nd the results is shown in Table 5. Compare to existing condition, OPEX by VoDSL saves 23% from 30% to 7% OPEX.

Table 5. Opex Structure

BIAYA OPERASIONAL	Dalam juta rupiah	0 2008	1 2009	2 2010	3 2011	4 2012	5 2013
BIAYA OPERASI HARIAN							
Marketing		47,51	72,75	80,26	88,28	97,14	106,83
General & administration		23,75	36,38	40,13	44,14	48,57	53,42
O & M		47,51	72,75	80,26	88,28	97,14	106,83
Personnel		23,75	36,38	40,13	44,14	48,57	53,42
Others							
Sub-Total 1		142,53	218,26	240,77	264,85	291,43	320,50
PENGELUARAN LAIN							
cost of Backbone							
RMJ		23,75	36,38	40,13	44,14	48,57	53,42
Building		23,75	36,38	40,13	44,14	48,57	53,42
Power Plant		47,51	72,75	80,26	88,28	97,14	106,83
Sub-Total 2		95,02	145,51	160,52	176,57	194,29	213,67
Total BIAYA OPERASI HARIAN		237,55	363,77	401,29	441,42	485,72	534,17
DEPRECIATION							
TOTAL BIAYA OPERASI		237,55	363,77	401,29	441,42	485,72	534,17

Feasibility Calculations and Analysis

We use NPV, IRR and Payback Period to measure feasibility. NPV includes investment cost, operational expenditures, maintenance cost and revenue projection. NPV is calculated as follows:

$$NPV = \frac{\text{Kas Bersih } 1}{(1+r)^1} + \frac{\text{Kas Bersih } 2}{1+r)^2} + \cdots + \frac{\text{Kas Bersih N}}{(1+r)^n} \quad \ldots\ldots\ldots\ldots\ldots\ldots \quad (4.1)$$

Dimana : r = discount rate, dalam satuan '%'

N = umur investasi, dalam satuan 'tahun'

Payback Period is calculated to get how the project could reach break even for investment.

For IRR, we use discount rate 20%, and calculation result is shown in table 6-8.

Table 6. VoDSL over ATM

		NPV	IRR	Payback Period
Pesimis	Bogor	18.139.521.420	22,30%	1 Tahun 9 Bulan 8 Hari
	Jakbar	7.988.462.408	19,22%	1 Tahun 9 Bulan 12 Hari
Moderat	Bogor	21.364.415.383	17,93%	1 Tahun 9 Bulan 22 Hari
	Jakbar	9.498.931.989	14,86%	1 Tahun 9 Bulan 26 Hari
Optimis	Bogor	24.981.187.464	11,56%	1 Tahun 10 Bulan 8 Hari
	Jakbar	11.110.718.142	8,98%	1 Tahun 10 Bulan 11 Hari

Table 7. VoDSL over IP, Distributed

		NPV	IRR	Payback Period
Pesimis	Bogor	27.050.247.130	12,20%	1 Tahun 9 Bulan 21 Hari
	Jakbar	18.158.318.068	10,10%	1 Tahun 9 Bulan 20 Hari
Moderat	Bogor	36.167.577.392	12,06%	1 Tahun 9 Bulan 29 Hari
	Jakbar	33.829.291.434	17,81%	1 Tahun 9 Bulan 18 Hari
Optimis	Bogor	48.982.180.917	-13,38%	1 Tahun 11 Bulan 10 Hari
	Jakbar	74.246.194.785	1,76%	1 Tahun 10 Bulan 13 Hari

Table 8. VoDSL over IP, Semi Distributed

		NPV	IRR	Payback Period
Pesimis	Bogor	27.050.247.130	27,05%	1 Tahun 8 Bulan 29 Hari
	Jakbar	18.158.318.068	20,28%	1 Tahun 9 Bulan 5 Hari
Moderat	Bogor	36.167.577.392	12,06%	1 Tahun 9 Bulan 29 Hari
	Jakbar	33.829.291.434	20,76%	1 Tahun 9 Bulan 14 Hari
Optimis	Bogor	48.982.180.917	-13,38%	1 Tahun 11 Bulan 10 Hari
	Jakbar	74.246.194.785	2,89%	1 Tahun 10 Bulan 12 Hari

From table 6, Scenario-1 is feasible for BOGOR and JAKBAR with notes, some DSLAM on JAKBAR relocated to BOGOR because phone demand for BOGOR is higher than JAKBAR. While no VoDSL over IP Distributed models is above discount rates on table 7 and therefore scenario-2a not feasible.

We couldn't calculated centralized topology on VoDSL over IP because of QoS issue. Figure 9 and Figure 10 shows the VoDSL for Bogor area and Jakarta Barat area. We could see in Figure 8, why we have to use 10 voice gateways in BOGOR.

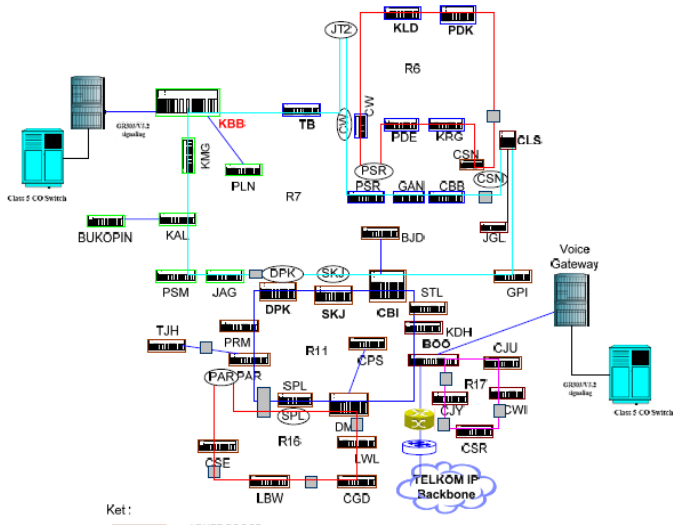

Figure 9. VoDSL BOGOR

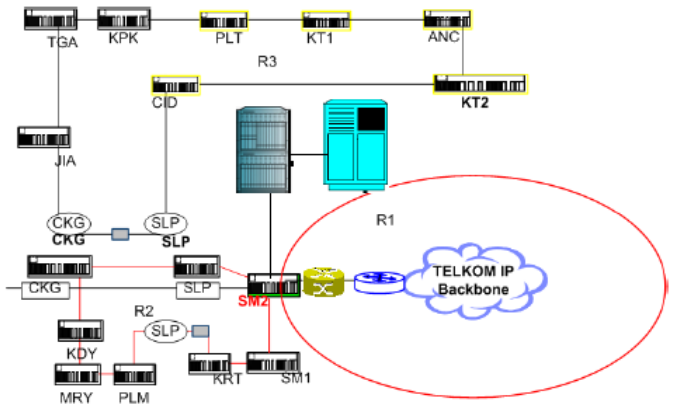

Figure 10. VoDSL JAKBAR

To overcome the problem, we could use semi distributed by "centralized traffic" from buildings across BOGOR and JAKBAR, related to scenario-2b. For example, Buildings across JAKBAR are centralized in SM2 and Slipi area and prposed as redundancy. These two location also intersect locations. That is a location which is part of more than one area. So traffic from other locations within the area directed to these locations. If we applied the same reason to BOGOR, we would have 3 Gateways for BOGOR, the are Cibinong, Depok and Bogor and 2 Gateways for JAKBAR, they are Slipi and Semanggi.
For pesimis model, VoDSL implementation in Bogor and Jakbar over IP is feasible.

Targeted Applications

Residential Connection

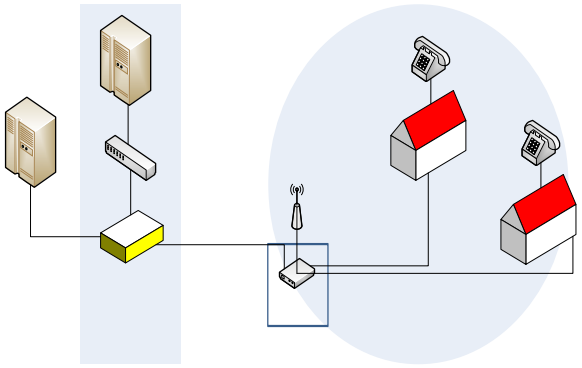

Figure 11. Residensial connection

This architecture as shown in Figure 11 is used to save copper and prepare for broadband connection for customers. IAD is installed in Cable House (no in customer's house) and supply phone lines to several houses. One port of data is connected to

WIFI access Points as a value added for VoDSL. Phone based customers would be educated to use broadband through this connection.

Corporate PBX

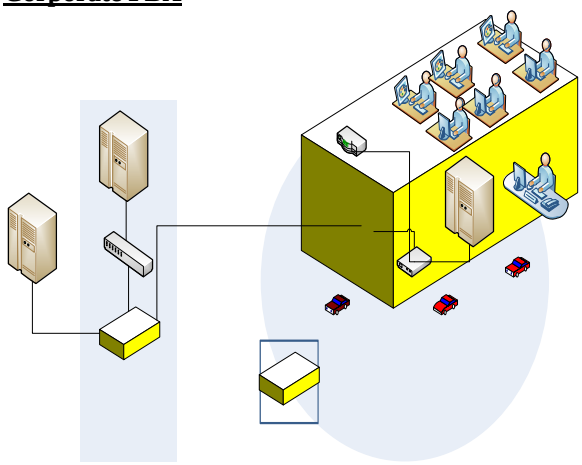

Figure 12. Corporate PBX

This architecture in Figure 12 is used to integrated coppers to a corporate customers. IAD is installed in building and supply phone lines to the company. One port of data is connected to router. By this topology only single copper cable is supplied to building with reduced service rate. Customers will be pleased.

SOHO

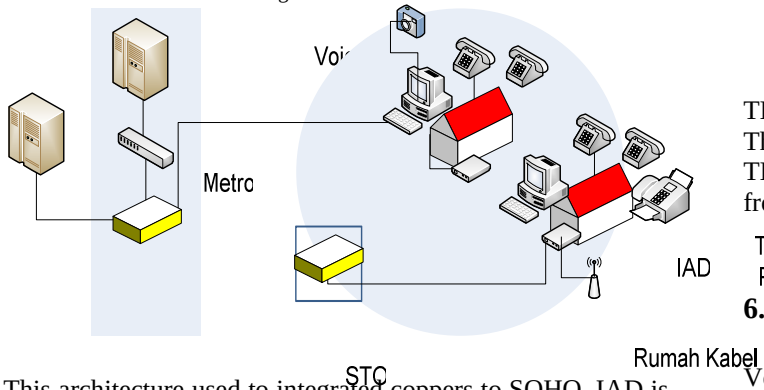

Figure 12. SOHO

This architecture used to integrated coppers to SOHO. IAD is installed in customer premises and supply phone lines to the them. One port of data is connected to access point for internet access. SOHO usually used phone lines for credit card transaction, several bank need several copper lines. By this topology only single copper cable is needed plus lower rate.

WARTEL SPEEDY

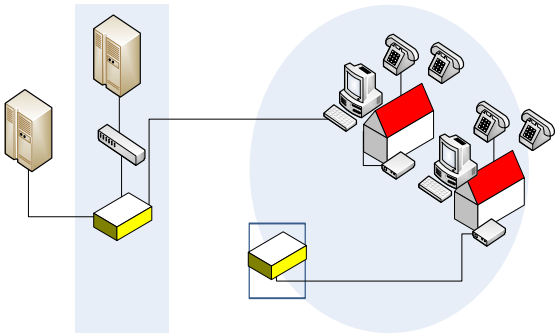

Figure 13. WARTEL SPEEDY

This architecture as shown in Figure 13 is used to integrated coppers to WARTEL and add one internet connection as value added service. By this topology WARTEL partner could reduced opex and monthly cost and even change profit proportion between them and TELKOM.

TELUM

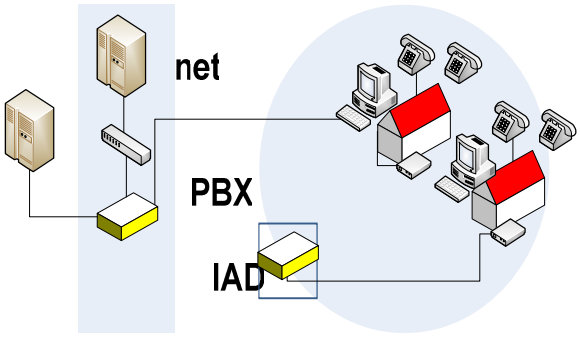

Figure 14. TELUM

TELUM means TELEPON UMUM or Public Telephone. This architecture is used to save coppers supplied to TELUM. TELUM rate could be reduced, and would increase revenue from TELUM. The architecture for this is shown in Figure 14.

6. CONCLUSIONs

VoDSL is supported by existing ATM and IP network own by PT Telkom. POTS waiting list could be served by VoDSL with CAPEX efficiency 80% and payback period of 1 year. This would benefit Telkom with seamless migration to broadband services because IAD has installed in customer premises. VoDSL enables G.SHDSL provides phone-based services; this would efficiently saves copper lines and increase revenues over existing corporate customers. To guarantee IP quality network, implementation strategy is

needed such as placing voice gateways on intersect locations. VoDSL for both ATM and IP backbone area feasible with recommendation, it has positive NPV and IRR above discount rate and payback period from 1 to 2 years.

REFERENCES

[1] "_____", "Revenue Budget & Target", Unit Performansi Divre II PT Telkom, Maret, 2008
[2] "Taylor, Martin", Mastering Voice Over DSL", 1999
[3] "_____",Network Planning, ITU / BDT-COE workshop
[4] "_____", Laporan Tahunan PT Telkom 2007
[5] "_____",indonesia, id.wikipedia.org
[6] Siregar, D, Indonesian Telecommunication Industry, MASTEL, 2008

Proceeding of the 11th International Conference on QiR (Quality in Research)
Faculty of Engineering, University of Indonesia, Depok, Indonesia, 3-6 August 2009
ISSN 114-1284

VIDEO STREAMING CONTENT DEVELOPMENT OVER A PICONET NETWORK BASED ON JAVA API JSR-82

Sri Wahjuni[1], Muhammad Hasannudin Yusa'[2]

Computer Science Department
Faculty of Mathematics and Natural Science, Bogor Agricultural University
Tel/Fax : (0251) 8625584
my_juni04@ipb.ac.id
Computer Science Department
Faculty of Mathematics and Natural Science, Bogor Agricultural University
Tel/Fax : (0251) 8625584
emhayusa@gmail.com

ABSTRACT

Nowdays, a handphone becomes a multipurpose equipment. User can use it to communicate, to capture image or event, as well as to transfer data to another device. Its bluetooth availability increases the inter-device wireless connection usability.

This research design and implement a client-server streaming content constructor over a piconet network in a point-to-point connection using a handphone as client. As an alternative way in recording and delivering data in video format, which is bandwidth consumptive, this paper proposed the recording and sending data in image and video format. The JAVA API JSR-82-based connection is choosen because of its portability. Experiments were done to analyze the camera and voice recording, as well as sending data from client handphone to computer server.

Experiments on camera recording indicated that JPEG encoding of 160x120 pixel resolution produces the highest data transfering speed. The result of voice recording experiment showed commit time to reputed as the best result of audio recording is 5 second. The sending data from client to server experiment showed that delay of sending voice data is bigger than that of image data for similar time. The limitation on processor speed and memory size of the mobile phone influence the delay result while sending image and voice at the same time.

Keywords: *bluetooth, distance learning, piconet, point-to-point, JSR-82*

1. INTRODUCTION

The *handphone* technology increases fastly on the realibility, capability and fetures to satisfy the user [1]. Recently, *handphone* is equipped by additional features such as camera, bluetooth, etc. to meet the user needs. User use h*andphone* not only for voice communication purpose, but for voice recording, photo capture, video player and other purposes. Now, *handphone* becomes a multipurpose equipment. On the other side, long-distance learning also implemented widely. Learning activity does not limited in physical classroom anymore. Using the streaming technology, physical classroom can be replaced by a virtual classroom. A virtual classroom environment aims at simulating a real classroom for remote participants [2]. Then they don't have to meet physically in a classroom. The streaming can be broadcasted through a LAN/PAN/Internet network.

Bluetooth is a flexible and capable technology for providing short-range radio communications between devices in an ad-hoc manner using the 2.4GHz band [3]. Although the bluetooth technology has been established for a long time, there are less applications developed based on it. The common applications are apllications to connect the handphone to the headset or computer [4]. At advanced the audio streaming over bluetooth has been implemented over ACL Links [3] as well as the video streaming [5].

The last two research implemented the bluetooth technology on the computer-based. However implementation of bluetooth-based network on limited device is more complicated. This research proposed an alternative way in feeding the real time video server streaming, by recording the event in image and voice format instead of in video format. Recently, the camera availability together along the bluetooth technology bundled in a handphone provide a challange to use them as streaming content development tools for any purpose, such as long distance learning system as in this research.

In this paper we show how to design and implement streaming content constructor module as part of web-based long-distance learning system. The module consist of two submodules, the client-side (handphone) module and the server-side (computer) module. In supporting that modul development we analyze the file size and the delay information produced by the data recording-and-transfering. This analyzis are needed to choose the right image encoding as well as the voice recording commit time to apply in this application development.

The rest of this paper is organized as follows. Section 2 provides some backgrounds of bluetooth technology. Section 3 presents the design and implementation of streaming content constructor module over a piconet network using JAVA API JSR-82 in a point-to-point connection. Section 4 presents the result of our experiments. Finally Section 5 concludes this paper.

2. BLUETOOTH TECHNOLOGY

2.1 Bluetooth Connection Type

The basic bluetooth network is a piconet, whic is a dynamic ad hoc network. A device calling another to join the piconet is a master and the calee is a slave. The connection can be established through one of three : point-to-point, point-to-multipoint, and scatternet.

Point-to-point connection is established while one *master* and one *slave* perform a communication. When the slave connect to the master are more than one, the connection becomes a po*int-to-multipoint* connection. A device in a piconet can communicate to another device in another piconet to build a scatternet. These type of connections are showed in Fig.1 and Fig. 2 [6].

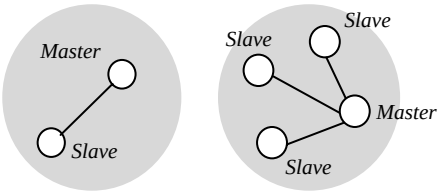

Figure 1: Piconet (a) point-to-point and (b) point-to-multipoint.

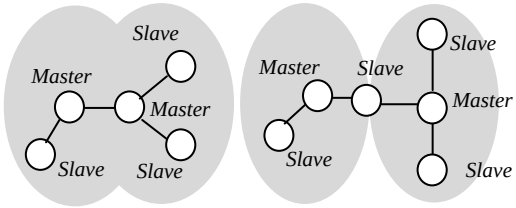

Figure 2: Piconet scatternet.

2.2 Handphone-Computer Bluetooth Connection on JAVA

There are two techniques to build a bluetooth connection between computer and handphone, they are [7] :

a COM-Port-based technique

This technique uses virtual COM-Port as a communication media as shows in Fig. 3

b JSR-82-based technique

The two techniques are similar. The only difference is the API JSR-82 implementation needs additional component that is separated from bluetooth software and operating system. The JSR-82-based architecture is showed in Fig. 4

The mechanism of *Java API JSR-82* implementation includes (Ericsson 2004) : bluetooth stack initialization, in-the-range service and device searching, waiting of connection initialization, connection opening/closing, and running Input/Output operation.

Bluetooth connection created by Java API JSR-82 implement Serial Port Profile (RFCOMM), L2CAP, and OBEX protocols. The JAVA API JSR-82 connection based on Generic Connection Framework (GCF). Fig. 5 shows the state diagram of bluetooth communication mechanism on JSR-82 [8].

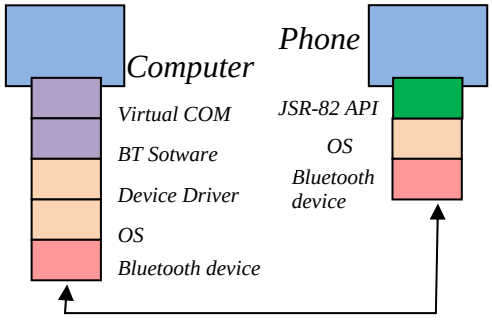

Figure 3: COM-Port-based technique.

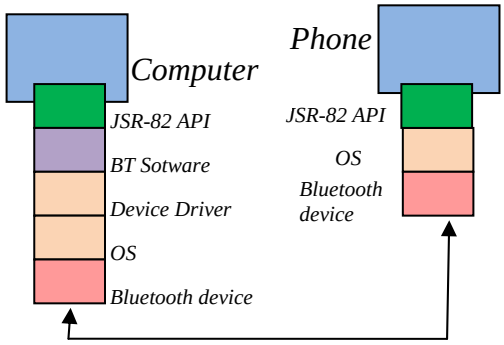

Figure 4: JSR-82-based technique.

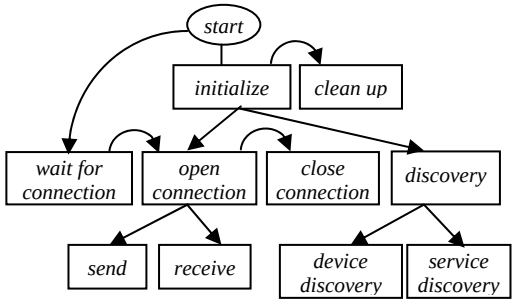

Figure 5: State diagram of Java API Bluetooth (JSR-82) –based connection.

2.3 Mobile Media API (JSR-135)

Mobile Media API (MMAPI) JSR-135 is an optional API packet that application developer has to deploy to access multimedia capability of a JAVA-support handphone. *MMAPI* based on *Java Media Framework* concept in *Java 2 Standar Edition (J2SE)*, built specially for handphone with limited audio/video, processing power, and memory. The *MMAPI* architecture is showed in Fig. 6 [9].

2.4 Video Frame Rate

Video uses frame concept to display a number image per second [10]. The more frames will produce better object movement. For web based application the minimum frame rate is 12 frame per second.

3. DESIG AND IMPLEMENTATION

3.1. Design and Implementation of Streaming Content Constructor Module

There are two submodules in the streaming content constructor module, client-side (handphone) submodule and server-side submodule (computer). The client-side submodule captures image sequence, via handphone's camera, and also records the voice, via handphone's microphone, as specify by user. By the time, this submodule sends the data to the server-side submodule periodically over bluetooth connection.

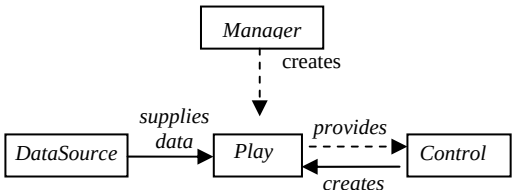

Figure 6: Mobile Media API architecture.

As soon as the data are received by the server, the server-side submodule processes the data to produce a video file and transfering the file to the streaming server.

Based on some literature studies the bluetooth connection is implemented on the JSR-82-based for portability reason.

3.1.1 Design and Implementation of Client-side submodule

Unless configure some connection parameters before sending the data, user open the connection directly using the default configuration. Once the opening connection is established the client will search an available bluetooth service (provide by server).

After the successful opening connection, the client-side submodule will activate a connection handler to control the data sending specified. The available data to send is image, voice, or both of them. Under the control of connection handler client sends the data specified to the server periodically. The process flow is showed on Fig. 7

This submodule is implemented using Java programming language supported by JSR-82 optional package and JSR-135 MMAPI. As pictured in Fig. 8 there are nine section in this submodule, they are :

a Controller, to configure the connection, camera used, and type of data to be transferred,
b Image Capturer, to capture the image and forward it to the image-sender section,
c Bluetooth module, the interface to perform a bluetooth connection,
d Sound Recorder, to capture voice from microphone and forward it to the voice-sender section,
e Device detection, to search in-range another bluetooth device,
f Service detection, to detect a bluetooth service,
g Image-sender, to forward image captured to the server,
h Connection Handler, interfacing communication between bluetooth module and image/voice-sender
i Voice-sender, to forward voice recorded to the server.

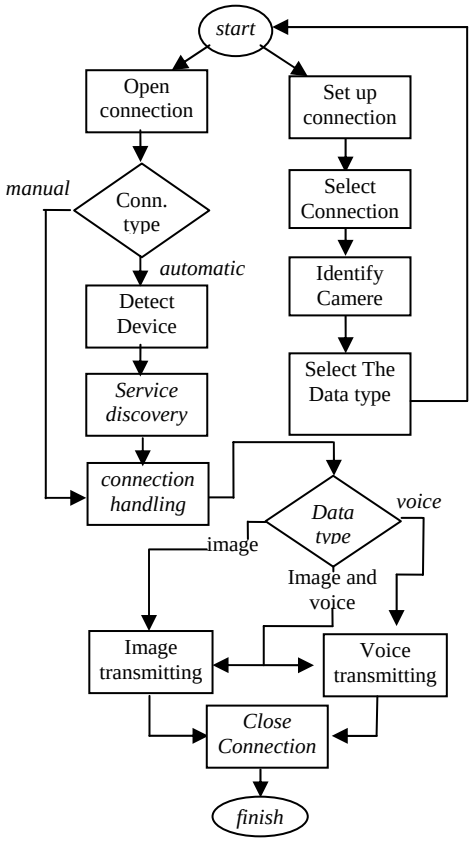

Figure 7: Workflow of client-side submodule.

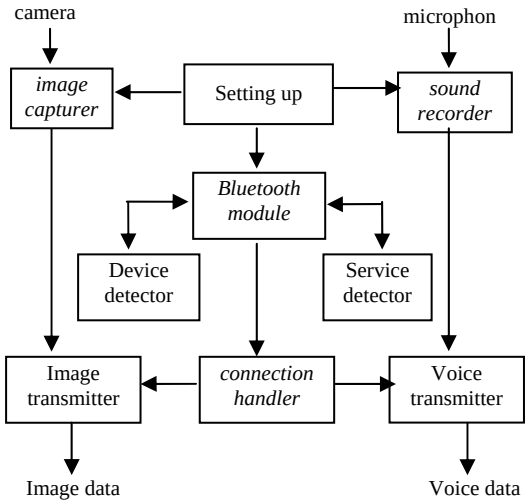

Figure 8: Implementation modules of client-side submodule.

3.1.2 Design and Implementation of *Server-side submodule*

User has to configure teh server before data receiving process, unless he/she activates the server using default

configuration. The server activation is suited to the accepted data type image data, voice data, or both of them. Once the activation is successful, the server-side submodule perform a listening process to capture the connection request from a client. When the connection is established, the server activate a connection handler to save the received data temporarely in the temporary folder.

A special thread is generated to collect the image and voice and merge them altogether into a new file periodically. The next step is transcode the merged file into mp4 format and hintrack it. The last step is move/copy the streaming content file to the root of movie folder of the Darwin streaming server to stream to over the network/internet. Fig. 9 pictures the flowchart of the serve-side (computer) submodule.

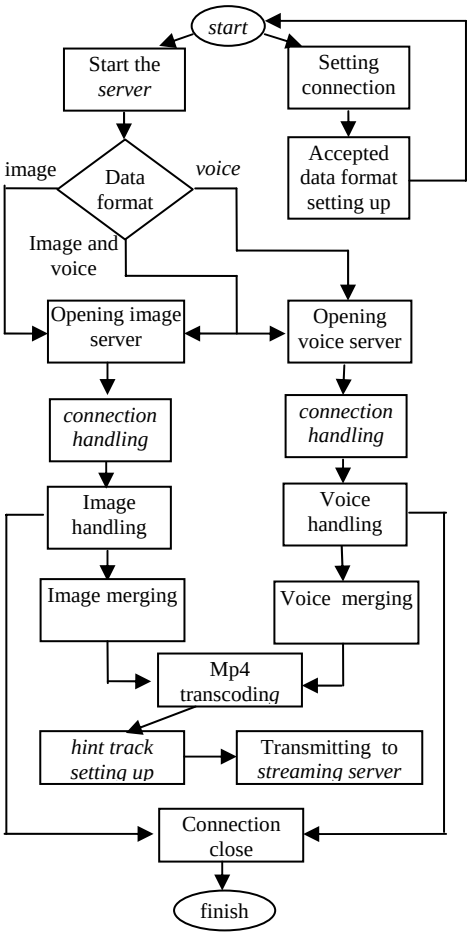

Figure 9: Workflow of server-side submodule.

Server-side submodule implemented using Java programming language supporting by bluecove-2.0.2 library, tritonus share-0.3.6.jar, ,java-getopt-1.0.13.jar, and *Java Media Framework 2.1.1e*. There are seven section in this submodule as pictured in Fig. 10:

a Controller, to configure the accepted data type,
b Connection Handler, to activate the server and to interface to the image/voive receiver,
c Image receiver, to receive image sending by the client,
d Voice receiver, to receive voice sending by the client,
e Display, to display the received image/voice on monitor,
f Video Processing, to process the received file to become a straming content file,
g Streaming content file-sender, to send the streaming content file to the root of movie folder of the Darwin Streaming Server.

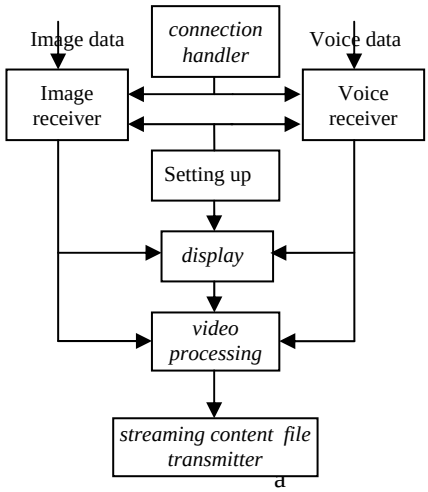

Figure 10: Implementation modules of server-side submodule.

4. PERFORMANCE EVALUATION

The first two experiments are performed to get the best image format and commit time to use in the following tranfering data performance experiments.

4.1 Image Capturing Evaluation

From the various image-encoding capturing in one minute, the result shows that the highest maximum frame number provides by JPEG and BMP encoding. While the best dimension to produce the maximum frame is 160 x 120 pixels as pictured in Fig. 11. Another parameter to analyze is the file size produced by each image encoding for each dimension. Fig. 12 shows that the JPEG encoding has the smallest size for various dimension, while in the contrary for the BMP encoding.

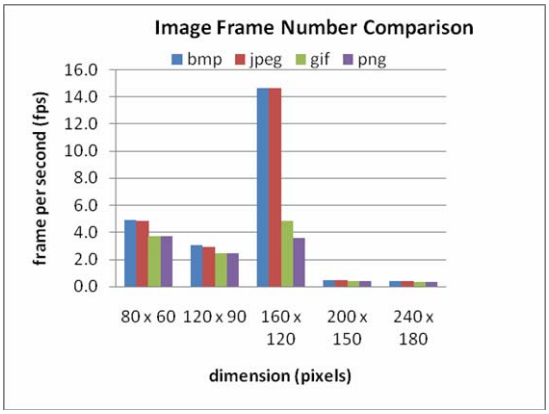

Figure 11: Image frame number for various encoding and dimension.

.As video streaming is a delay-sensitive application, the file to stream should be in minimum size with maximum frame number. The image encoding that meets this requirement is JPEG encoding in 160 x 120 pixels imension.

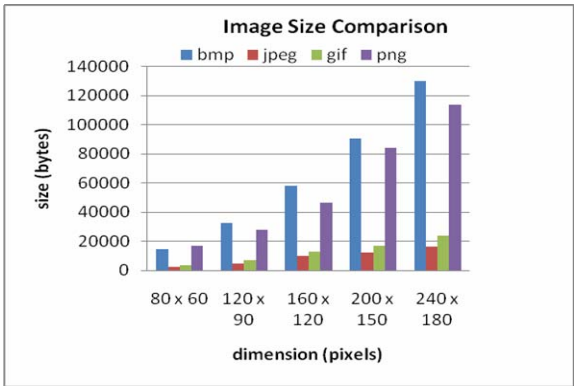

Figure 12: Image file size for various encoding and dimension

4.2 Voice Recording Evaluation

Fig. 13 presents the file size of voice recorded for various commit time, whic is showing the linear relation between them. Other parameters measured in this experiment are recorded file duration and the number of file produced in one minute.

The maximum duration of recorded file provided by voice recording with commit time 5 second as presented in Fig. 14. On the other hand, the number of file produced is less for the longer commit time as presented in Fig. 15.

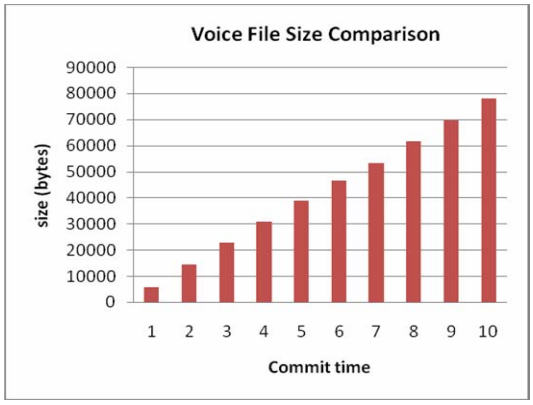

Figure 13: Audio file size for various commit time.

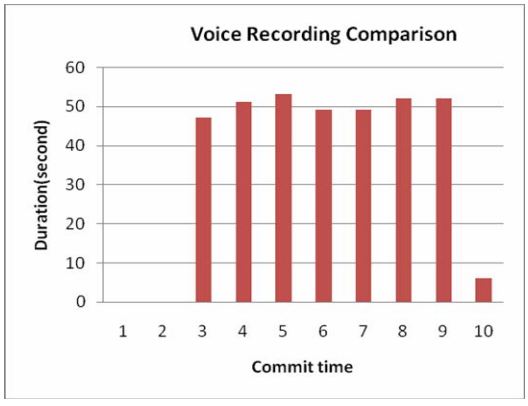

Figure 14: Duration of one minute voice recording for various commit time.

From these experiments the commit time choosen for data transfering is 5 second. This commit time produces the fine combination of duration and number of file.

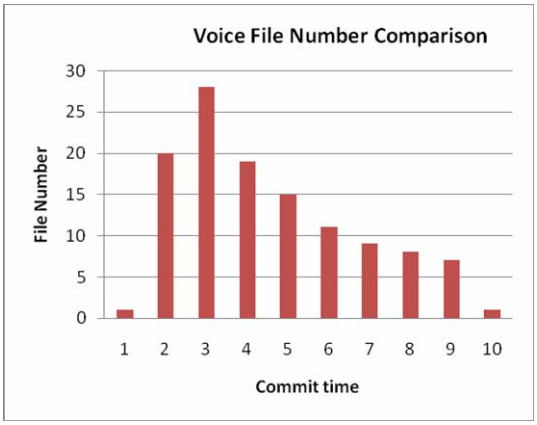

Figure 15: Number of file produced of one minute voice recording.

4.3 Image Transfering Evaluation

The image transfering delays for one minute image recording are 1390-1440 milisecond as pictured in Fig. 16. The delay variation is caused by the various number and size of image file for each capturing.

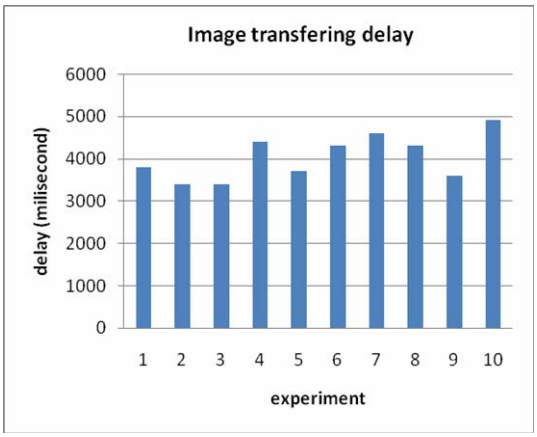

Figure 16: Image data transfering delay

4.4 Voice Transfering Evaluation

Fig. 17 presents the experiment results of one minute voice recording. The transfering delays are 1950-2150 milisecond. In comparing to image transfering delay, the voice transfering delay is higher, because the voice file size is bigger than that of image file. And the voice processing time is longer than that of image.

4.5 Image-Voice Transfering Evaluation

In this experiment, the voice and image transfering is carried out simultanously in one minute period. The transfering delays produced by the both of data are almost the same as pictured in Fig 18. The values are 3000-5000 milisecond, much higher than transfering delay produced

by separated transfering data. This situation is caused by the limited resources of the device.

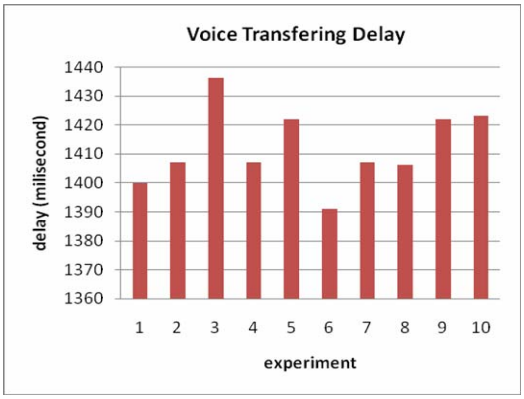

Figure 17: Voice data transfering delay

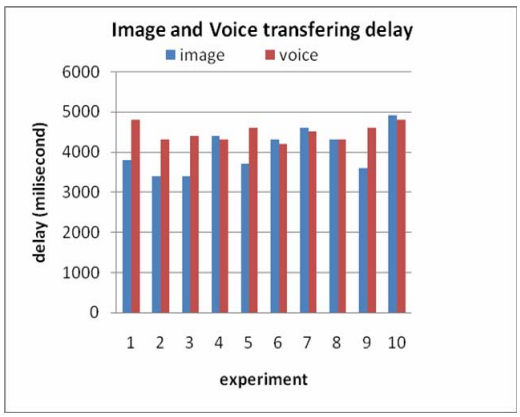

Figure 18: Image-voice transfering delay.

5. CONCLUSION

The handphone equipped with camera and bluetooth connection provides a challenge to build a streaming content for any necessity, such as web-based long-distance learning.

For limited device and connection, the streaming content file can be build from image and voice recorded separately, not as a video file. The image format best suited is JPEG encoding format because of its maksimum number of frame in minimum file size. For this encoding, the recomended dimension is 160 x 120 pixels. While the best commit time for voice recording is 5 second.

Our short-term future involves using point-to-multipoint connection in capturing the image to get the better view of a recorded object.

6. REFERENCES

[1] Djan I and Ruvendi R. 2006. Prediksi Perpindahan Penggunaan Merek *Handphone* di Kalangan Mahasiswa Studi Kasus pada Mahasiswa STIE Binaniaga [jurnal]. Jurnal Ilmiah Binaniaga Vol.02 No.1.

[2] Deshpande S.G, and Hwang J. 2001. A Real-Time Interactive Virtual Classroom Multimedia Distance Learning System. IEEE Transactions on Multimedia, Vol. 3, No. 4

[3] Bilan A.P.P.S. 2003. Streaming Audio Over Bluetooth ACL Links. Proceedings of the International Conference on Information Technology: Computers and Communications (ITCC.03)

[4] Sairam K.V.S.S.S, Gunasekaran N., Reddy S.R.. 2002. Bluetooth in Wireless Communication. IEEE Communications Magazine

[5] Jung S., Chang A., Gerla M. 2006. Video Streaming over Overlaid Bluetooth Piconets (OBP). *WiNTECH'06*. Los Angeles, September 2006.

[6] Nokia. 2003. *Games over Bluetooth: Recommendations to Game Developers*.

[7] Nokia. 2006. *PC Connectivity over Bluetooth in JavaTM Applications.* http://kebo.vlsm.org [24 Juli 2008]

[8] Ericsson. 2004. *Developing Applications with the Java APIs for Bluetooth™ (JSR-82)*.

[9] Goyal V. 2006. *Pro Java ME MMAPI: Mobile Media API for Java Micro Edition*. New York: Appress.

[10] Lee J. 2005. *Scalable Continous Media Streaming System*. Chichester: John Wiley & Sons.

Selecting a Cyclic Redundancy Check (CRC) Generator Polynomial for CEH (CRC Extension Header)

Supriyanto[a], Abidah M. Taib[b], Rahmat Budiarto[c]

[a,c]*School of Computer Sciences*
Universiti Sains Malaysia, Penang Malaysia 11800
[a]*Email: supriyanto@nav6.org*
[c]*Email: rahmat@cs.usm.my*

[b]*Department of Computer Science*
Universiti Teknologi Mara (UiTM) Perlis Malaysia
Email: abidah@perlis.uitm.edu.my

ABSTRACT

Computation and regeneration of CRC code in each router may cause slower IPv6 packet transmission. Utilizing advantages of IPv6 features namely IPv6 extension header and fiber optic medium, we proposed CRC extension header (CEH) to do error control in Network layer rather than in Data Link layer. The purpose is to reduce error checking process in IPv6 packet transmission over high speed networks. The CEH will utilize CRC-32 to do error detection. This paper investigates which CRC-32 generator polynomial would be suitable for CEH. To find out the answer we developed a simulation program in Java that generates IPv6 packet and CRC-32 code. The simulation produced CRC processing time both at the sender and receiver. The result showed that CRC-32 generator polynomial proposed by Castagnoli is the fastest generator polynomial to generate CRC code. We then conclude that Castagnoli generator (CRC-32C) is the best generator to apply in CEH on IPv6 transmission over high speed networks.

Keywords

CRC-32, error, generator polynomial, transmission

1. INTRODUCTION

Internet has been connecting million people in the world. They use Internet not only to communicate each other but also military, business and administration purposes. Sending information from one side to another via Internet is fast and easy but may get some changes on the data due to weakness of the medium or noise affecting the channel. To ensure the data is accurate and free from error, designers have already equipped the protocol stacks such as TCP/IP with error control mechanism.

Error control in TCP/IP is divided into two types: error control in upper layer and lower layer. Upper layer is Transport layer that employ TCP or UDP checksum for segment data. While lower layer is Data Link layer that handle transmission error. This paper focuses on lower layer error control that ensures link by link data transfer of adjacent node is free from error. Transmission errors which change one or more bit of data may be caused by medium used in data transmission. Following the OSI reference model, data from Network layer will be added with header and trailer at the Data Link layer. Trailer is actually frame check sequence (FCS) that contains cyclic redundancy check (CRC) 32 bits to do error checking for the whole fields of link layer frame.

The traditional protocol stacks such as TCP/IP does error checking process by calculating and regenerating the CRC code in each intermediate node. It has to calculate CRC-32 of each IPv6 packet in incoming port of router and regenerate CRC-32 code before forwarding to the next hop. In response to increasing network speed and advance of fiber optic technology, the error checking mechanism in each router eventually become a bottleneck [1]. This study addresses improving IPv6 packet processing by eliminating CRC computation in each router. We proposed a new IPv6 extension header called CRC Extension Header (CEH) to do error checking in Network layer. The CEH uses the same CRC-32 algorithm which is table lookup algorithm. Format of CEH can be seen in figure 1 [2] below.

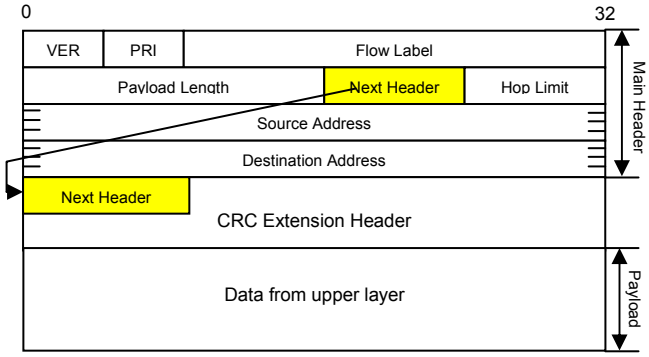

Figure 1 IPv6 packet with CEH

To generate CRC-32 code, it needs certain generator polynomial g(x). There are many generator polynomial have been proposing by researchers. This paper intends selecting the best generator polynomial to be used in CEH. The rest of this paper is structured as follows. Section 2 describes the work by explaining overview of CRC operation. Section 3 discuses the candidates of generator polynomial that will be used in CEH. In Section 4, method of the selection is presented followed with result and discussion in section 5. The end of this paper is conclusion.

2. OVERVIEW OF CYCLIC REDUNDANCY CHECK

Cyclic redundancy check (CRC) is a code that used to detect errors that occur during transmission or storage of digital data information. Error detection is conducted by adding a code on the data transmitted and check the code at the receiver. There are various lengths of CRC codes such as 16 bits (CRC-16) [3] and 32 bits (CRC-32) [4]. This paper focuses on CRC-32 to be used in CEH to detect transmission error in Network layer. This section gives overview of CRC algorithm.

There are many algorithms utilized to generate CRC-32 code. This section introduces the simplest algorithm in order to understand the concept easily. Furthermore, it discusses the fastest algorithm which is table lookup algorithm that widely used today. The simplest way to know CRC code generation is algebraic approach as discussed in [5] and more explanation in [6]. We present a short overview of the algorithm.

In the algebraic approach, an information or message is interpreted as coefficient of polynomial called data word d(x). The data word is divided by pre determined CRC generator polynomial g(x) using equation 1 giving a code word c(x).

$$c(x) = q(x).g(x) + r(x) \quad (1)$$

The operation called modulo two division, meaning that all of the term on equation 1 is base two. q(x) is quotient of the division and r(x) is remainder of the division. CRC operation concerns on the remainder rather than quotient q(x). The remainder also could be obtained using equation 2, which m is the number of bits of the generator polynomial g(x) used or the highest degree of its polynomial. Data word d(x) is appended by 0s and represents with multiplication x^m.

$$r(x) = d(x).x^m \bmod g(x) \quad (2)$$

This operation to obtain r(x) is performed at the transmitter side. Code word c(x) which is d(x) + r(x) is transmitted along the network to reach a destination. Let say the receiver gets a code word c'(x) from the sender. Receiver conducts similar operation using the same generator.

$$c'(x) = c(x) + e(x) \quad (3)$$

There are two ways to justify whether there is an error in the code word received. Firstly, divide c'(x) using the same generator, if c'(x) is divisible by g(x) meaning there is no error or the error is undetected. Secondly, extract r(x) from the code word. Do operation of equation 2 using the same g(x) to get a new CRC code (remainder) r'(x) and then compare the r'(x) obtained with original r(x) extracted from the code word. If the two remainder is the same, there is no transmission error otherwise there is an error in the packet received.

Modulo 2 division generally could be performed by a sequence of shifts register. The division process makes addition and subtraction equal to bitwise XOR. Bitwise XORs are performed for all data including 0s appending till finish and obtain the remainder. The process is equal to shift bit by bit data to register from left most bits. In the hardware implementation uses LFSR (linier feedback shift register) of length m.

The process of bit by bit register needs more time and make it inefficient. To address the problem, engineers implement CRC operation in software using table lookup algorithm. The algorithm processes byte by byte instead of bit. The algorithm proposed by Sarwate [7]. *Firstly*, the CRC value is set to an initial value. Then data word is inputted to data stream byte by byte. *Secondly*, every byte of input stream is performed an XOR operation with the least significant byte of initial value. The result is used as index to access a 256 entry table. *Thirdly*, the value from the table is XORed with the rest of initial value by shifted byte by byte to the right. The result is CRC value to the next iteration.

In term of Ethernet, data word is the whole frame except frame check sequence field (FCS). As shown in figure 2, a standard Ethernet frame consist of destination and source Ethernet address, Ethernet type, data from upper layer and FCS.

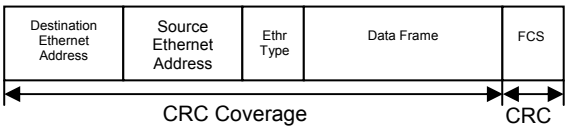

Figure 2 Standard Ethernet frame format

CRC coverage area in figure 2 is data word and FCS is remainder of modulo two division in equation 1. Hence, the whole frame is code word that actually transmitted into the networks.

3. IMPLEMENTATION CRC-32 FOR CEH

Implementation of CRC-32 in CEH uses the same algorithm with the existing CRC in Data Link layer which is table lookup algorithm. The differences of the

new mechanism are coverage area and field of the CRC-32. As mentioned previously, the CRC-32 is used as IPv6 extension header thus it placed between IPv6 main header and upper layer data *(see figure 1)*. The coverage area of CEH is the whole IPv6 packet excluding hop limit and CEH itself as shown in figure 3. From the figure, the size of CEH coverage area consist of 40 bytes IPv6 header minus 2 bytes hop limit field and upper layer data with maximum value 65,535 bytes. However the implementation is adapted with the maximum transmission unit (MTU) of the widely used Data Link layer technology which is Ethernet. Hence, the maximum MTU is 1500 bytes.

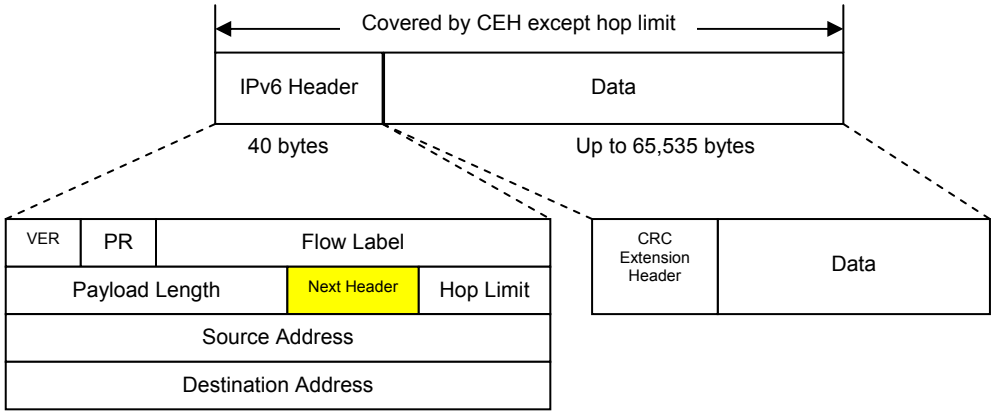

Figure 3 CEH coverage areas for error detection

Using equation 2, the coverage area is divided by g(x) to obtain r(x). r(x) is remainder of the division and represents of CRC code. Then, it is placed in the extension header field as shown in figure 4. Accordingly, pass the IPv6 packet to Data Link layer as usual to transmit through Physical layer without generate link layer trailer.

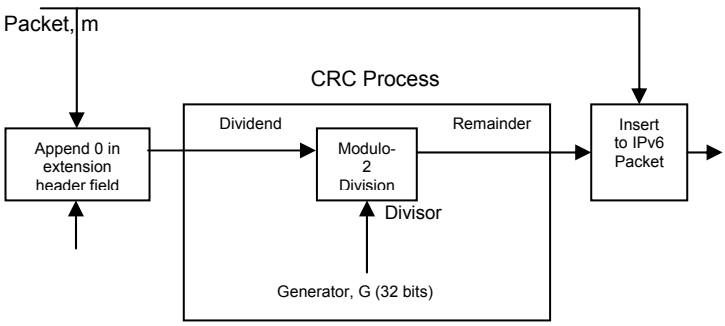

Figure 4 Generation of CEH in transmitter

At the receiver, Data Link layer captures the transmitted packet and pass the packet into Network layer directly. The layer does not compute CRC code any more. In the Network layer of the final destination, the packet will be processed as figure 5. It extracts CEH field from IPv6 packet. The other parts of the packet are divided by a generator to get a new CRC code. The new CRC code is compared with the original CRC inside CEH. If the result is similar, meaning no error. Thus, forward the packet to Transport layer, otherwise reject the packet.

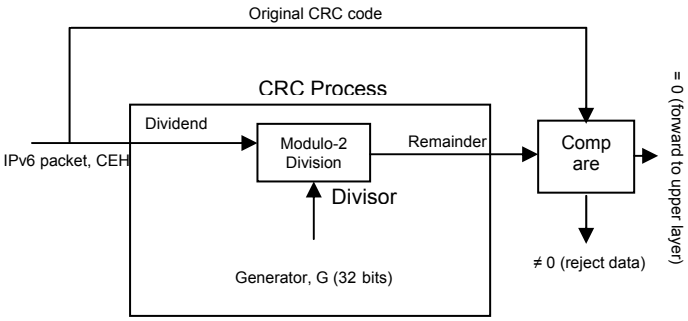

Figure 5 CEH processing in receiver

4. CANDIDATES OF GENERATOR POLYNOMIAL FOR CEH

Generator polynomial is the most important part of CRC code generation. It influences to the result of error detection. Hence selection of the best generator polynomial is also very important. This section discuses three candidates of generator polynomial that will be used in CEH they are standardized generator in IEEE 802.3 (CRC-32E), generator suggested by Guy Castagnoli (CRC-32C) and generator introduced by Philip Koopman (CRC-32K).

4.1 Generator used in Ethernet (CRC-32E)

This generator is widely used in data communication and data storage today. It was standardized by project IEEE 802.3 [8]. It is a polynomial with highest degree 32 and shown as

$$g(x) = x^{32}+x^{26}+x^{23}+x^{22}+x^{16}+x^{12}+x^{11}+x^{10}+x^{8}+x^{7}+ x^{5}+x^{4}+x^{2}+x+1 \quad (4)$$

This polynomial can be formed as binary number as 10000010011000001000111010110111. The left most 1 is coefficient of x^{32} and following bits correspond to coefficient of the polynomial. The number of bits in a generator polynomial is equal to m + 1. The generator can be represented as 32 bit hexadecimal number 0x04C11DB7. However, some CRC implementations use its reverse as 0xEDB88320.

Based on [9], this generator satisfies for 4096≤codeword≤12144 bits. The interval is equal to the size of Ethernet frame (512 – 1518 bytes). For this implementation, it has Hamming distance, HD = 4 meaning the generator are able to detect all 3 bits error and lower.

4.2 Generator Proposed by Castagnoli (CRC-32C)

The name Castagnoli refers to the author of [10]. Castagnoli, Braurer and Herrmann evolved technique of constructing dual code polynomial belong to Fujiwara. They built special purpose hardware to find out new generator to improve performance of IEEE 802.3. Several factorization classes of generator polynomial of size 24 and 32 were evaluated. The evaluation yielded four optimum classes of 32 bits polynomials. *First*, CRC-32/8 code whose factors into $(x + 1)^2$ and three distinct irreducible polynomials of degree 10. The generator equivalent to codes of data length 1023 bits with HD = 8. *Second*, CRC-32/6 is the code of CRC-32 whose factors into $(x + 1)^2$ and two distinct primitive polynomial of degree 15. This generator similar with CRC-32 code for data length 32767 bits and HD = 6. *Third*, generator CRC-32/5 whose consists of one polynomial of degree 32. It gives HD = 5 to 65535 bits data. And the last is generator CRC-32/4. It was resulted from 47000 such codes that factors into (x + 1) times a primitive polynomial of degree 31. This generator keeps HD = 4 but it covers at data words sizes in excess 64 Kb. This generator is represented as

$$g(x) = x^{32}+x^{28}+x^{27}+x^{26}+x^{25}+x^{23}+x^{22}+x^{20}+x^{19}+x^{18}+ x^{14}+x^{13}+x^{11}+x^{10}+x^{9}+x^{8}+x^{6}+1 \quad (5)$$

In the hexadecimal form is 0x1EDC6F41 or 0x82F63B78 in its reverse. RFC 3385 [11] proved this generator to be used in iSCSI (Internet Protocol Small Computer System Interface). Thus we choose the code as a candidate to be used in CEH.

4.3 Generator Proposed by Koopman (CRC-32K)

Koopman did experiment to search a generator polynomial that covers larger data length [4]. He criticized the widely used generator polynomial that is IEEE 802.3. The standard only achieved Hamming Distance (HD) 4 for maximum packet length 12144 bits (Ethernet MTU). Whereas, theoretically it possible to detect HD = 6. The author searched a new generator polynomial that could to be used on HD = 6 for larger data length.

The evaluation was done for several generators including IEEE 802.3 and Castagnoli. The conclusion of the study is a 32 bits generator polynomial whose factors $(x+1)(x^3+x^2+1)(x^{28}+x^{22}+x^{20}+x^{19}+x^{16}+x^{14}+x^{12}+x^9+x^8+x^6+1)$. It constructs a full 32 bits generator represents as

$$g(x) = x^{32}+x^{30}+x^{29}+x^{28}+x^{26}+x^{20}+x^{19}+x^{17}+x^{16}+x^{15}+ x^{11}+x^{10}+x^{7}+x^{6}+x^{4}+x^{2}+x+1 \quad (6)$$

In binary form is 0x741B8CD7 or 0xEB31D82E of its reverse. The authors claimed the generator achieves HD = 6 for 16360 bits data length and HD = 4 to 114663 bits data length.

5. METHOD OF SELECTING GENERATOR POLYNOMIAL

We use two parameters to select the generator suitable for CEH based on previous work and our experiment. The two parameters are error detection capability and processing time to generate CEH in IPv6 packet transmission. The first parameter is analyzed by reviewing previous work on it and the latter analyzed by experiment. We configure small network to do the test bed in order to obtain particular data regarding processing time and delay transmission. The network is shown in figure 6.

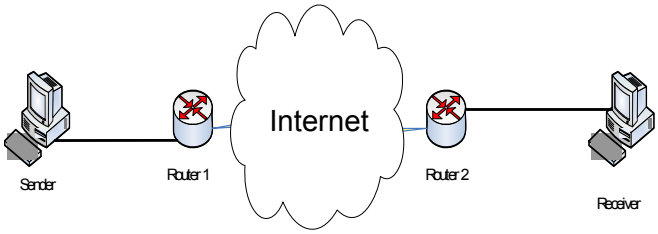

Figure 6 Topology of CRC Generator Polynomial Selection

We develop a program in Java that generates IPv6 packets with CRC extension header. The CRC code is generated from coverage area in figure 3. It is placed between IPv6 main header and TCP header and payload. The complete IPv6 packets are sent through the network. As common extension header, the CEH will not be processed in each router instead of in destination node indicated by destination address field. Another program is run in receiver side to compute the CRC code following figure 5.

6. RESULT AND DISCUSSION

In this section, we present result of our study on data length scope of the three candidates. Capability of generator polynomial to detect transmission error can be measured by its probability of undetected error [9], [10], [12]. This is summarized in table 1.

Based on table 1, HD = 4 and 6 whose available on the three candidates states obviously. This refers to the existing widely generator polynomial which is Ethernet. It uses HD = 4 with minimum data length 4096 (512 bytes) and maximum 12144 (1518 bytes). The data length interval is used in standard IEEE 802.3 for all type of Ethernet. For CEH implementation, we chose to use HD = 4. It means all burst error with 3 bits and below is able to be detected by the generator polynomial.

Table 1 Summary of Data Length

Generator	Factor	HD	Data length (bit)
CRC-32E	32	3	$2^{32} - 1$
		4	**4096 – 12144**
		5	512 – 2048
		6	204 – 300
CRC-32C	1,31	3	-
		4	**5276 – ($2^{31} - 1$)**
		5	-
		6	210 – 5275
CRC-32K	1,3,28	3	-
		4	**16361 – 114663**
		5	-
		6	153 – 16360

Consider to RFC 2460 [12], the minimum MTU in IPv6 transmission over Ethernet is 1280 bytes or 10240 bits. This minimum length is able to be covered by CRC-32E and CRC-32C and it is not covered by CRC-32K. The maximum length of IPv6 MTU over Ethernet is 1518 bytes or 12144 bits. This value is also covered by CRC-32E and CRC-32C. However, for the CRC-32E this value is its maximum. Hence, it is difficult to use for the future because of increasing Ethernet MTU such as jumbo frame implementation. CRC-32C is suitable for larger MTU in the future.

Our experiment used topology in figure 6 to note processing time of each generator polynomial. Processing time of the first packet is different from the following packet. In case of the first packet, it runs full algorithm to generate a table 156-entry. Thus, time processing for the first packet is the biggest one. While other following packets consume fewer time to generate the CRC code. This is because it utilizes the preceding table lookup generated by the first packet.

We sent various sizes of IPv6 packet from sender to receiver: 64, 128, 25, 512, 1024, 1280 and 1492 bytes. The data documented are processing time in sender, receiver and total processing time. Processing time is the time required to generate CRC 32 code and insert it in IPv6 packet as extension header. With an assumption time of IPv6 packet generation is constant value, the processing times represent time to generate CRC code. The result is shown in figure 7, 8 and 9 respectively.

Figure 7 shows graph processing time (ms) vs packet size (bytes) at the sender side. The processing time increases with increasing packet size. This is inline with nature of CRC code that is linier code. Three generator polynomials show tight competition. All of packet size demonstrates small differences. However, the average processing time of CRC-32C is the lowest value that is 0.900 ms compare to CRC-32K 0.918 ms and CRC-32E 0.912 ms.

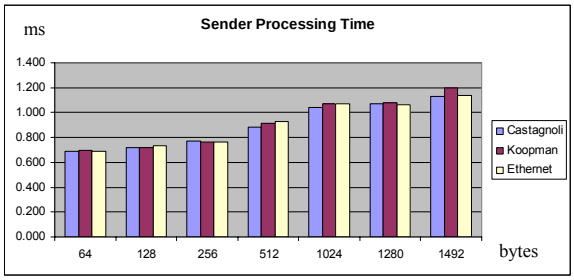

Figure 7 Sender Processing Time

Figure 8 shows processing time (ms) vs packet size (bytes) at the receiver side. The graph also demonstrates similar inclination with sender side. The processing time for the first IPv6 packet in receiver side increases with packet size increasing. However, receiver processing time is smaller than sender side. This is because in the receiver, there is no IPv6 packet generation.

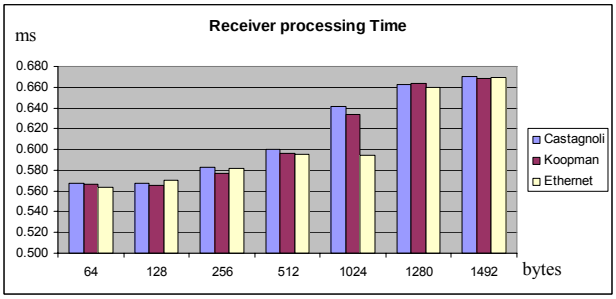

Figure 8 Processing Time in Receiver Side

The smallest average receiver processing time is belonging to CRC-32E that is 0.605 ms and 0.613 ms for CRC-32C and CRC-32K is 0.610 ms.
Total processing time of CRC code generation is shown in figure 9. Similar to previous processing time, the figure also illustrates that the three candidates are homogeny. It means the three generator polynomials are applicable in CEH from processing time point of view. Hence, capability of error detection that is analyzed in early of this section is a good way to determine which polynomial suitable for CEH.

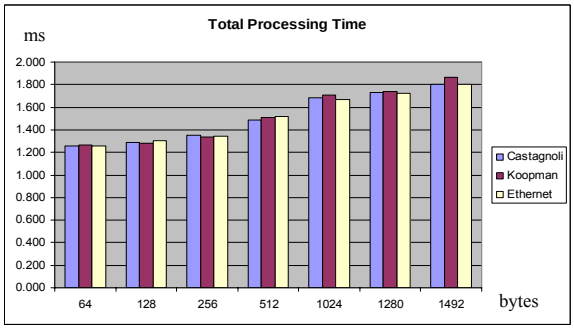

Figure 9 Total Processing Time

As stated earlier, the processing time is based on the first packet. The other following packet need smaller time processing to generate CRC code. This is because there is a CRC code stored on table from the first packet. Figure 10 demonstrates processing time for common Internet packet size that is 1518 bytes. The graph shows time processing for the following packet in exponentially decrease. The three generators shows their trend line enumerated below

$$\text{CRC-32C} = 0.7601x^{-0.9562}$$
$$\text{CRC-32K} = 0.7626x^{-0.9422}$$
$$\text{CRC-32E} = 0.7612x^{-0.9554}$$

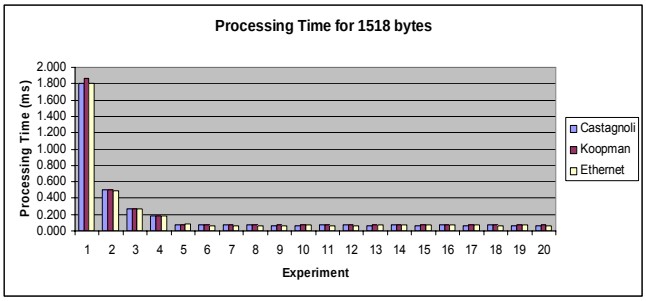

Figure 10 Time Processing for 1518 bytes packet size

The three exponential trend lines demonstrate that CRC-32C has smallest coefficient and power. This means the CRC generator polynomial has the best trend line. The processing time decreases toward smallest value.

7. CONCLUSION

We proposed CRC Extension Header (CEH) as a new mechanism to reduce duplicate error detection in intermediate node. CEH is applied to perform error control in the Network layer. With Network layer error control, we can eliminate error control in each intermediate node which possible to reduce the transmission time. CEH generation needs a generator polynomial. This paper described CEH and how selection of most suitable CRC-32 code generator polynomial for CEH was done. Among the generator used in existing Ethernet (CRC-32E) and two other generator suggested by Castagnoli (CRC-32C) and Koopman (CRC-32K), CRC-32C showed the best result. Its data length range covers larger data and at the same time the minimum data length also smaller than minimum MTU of IPv6 packet. The trend line of CRC-32C has smallest coefficient. We then conclude that CRC-32C suggested by Castagnoli is the most suitable generator polynomial for CRC extension header. Our future works will be implementing the CEH and analyzing its efficiency in handling the error detection in the high speed network.

REFERENCES

[1] F. Braun and M. Waldvogel, *Fast Incremental CRC Updates for IP over ATM Networks*, High IEEE Workshop on Performance Switching and Routing, 2001, pp. 48 – 52.

[2] Supriyanto, Raja Kumar Murugesan, Rahmat Budiarto, Sureswaran Ramadass, *Handling Transmission Error for IPv6 Packets over High Speed Networks*, Proceedings of the 4th International Conference on Distributed Framework for Multimedia Applications (DFMA 2008), Penang, 21-22 Oct., 2008, pp. 159-163.

[3] Castagnoli, G, Ganz, J. & Graber, P. *Optimum cycle redundancy-check codes with 16-bit redundancy*. IEEE Transactions on Communications, Vol. 38**,** 1990, pp. 111-114.

[4] Koopman, P. *32-bit cyclic redundancy codes for Internet applications*. Proceeding of International Conference on Dependable Systems and Networks, 2002.

[5] Martin Stigge, Henryk Plötz, Wolf Müller, Jens-Peter Redlich, *Reversing CRC Theory and Practice.* HU Berlin Public Report, 2006.

[6] Ross N. Williams. *A Painless Guide to CRC Error Detection Algorithms*. ftp://ftp.rocksoft.com/papers/crc_v3.txt, 1996.

[7] Sarwate, D. V. *Computation of Cyclic Redundancy Checks via Table Look-up*. *Commun. ACM,* Vol. 31**,** 1988. pp. 1008-1013.

[8] ANSI/IEEE Standard for Local Area Networks, *Carrier Sense Multiple Access with Collision Detection (CSMA/CD) Access Method and Physical Layer Specifications.* 1984.

[9] Fujiwara, T., Kasami, T. & Lin, S. *Error detecting capabilities of the shortened Hamming codes adopted for error detection in IEEE Standard 802.3*., IEEE Transactions on Communications, Vol. 37**,** 1989. pp. 986-989.

[10] Castagnoli, G., S. Brauer, and M. Herrmann, *Optimization of cyclic redundancy-check codes with 24 and 32 parity bits.* Communications, IEEE Transactions on, 1993. **41**(6): p. 883-892.

[11] Shienwald, D. at. al. *Internet Protocol Small Computer System Interface (iSCSI) Cyclic Redundancy Checks (CRC/Checksum Considerations.* RFC 3385. The Internet Society.

[12] Deering, S. and R. Hinden (December 1998). *Internet Protocol Version 6 (IPv6) Specification.* RFC 2460. The Internet Society

Power Quality of Low Voltage Consumer Loads

Surya Hardi, I. Daut, M.Irwanto, Risnidar Chan, Indra N, Muzamir Isa

Power Electronic and Machine Design Cluster Research
School of Electrical System Engineering, Universiti Malaysia Perlis (UniMAP),
Jl. Pangkalan Asam, Kangar, Perlis
e-mail: surya@unimap.edu.my

ABSTRACT

Power quality is an issue that is becoming increasingly important to electricity consumers at all level of usage. These result from with increasing use of electronic equipment in several sectors for the reason to improve energy efficiency. Almost all power quality issues are closely related with power electronic. Equipment using power electronics in low voltage environments for examples are television, microwave ovens, personal computers, printer, lighting, heating ventilation air conditioners, etc..Using with high efficiency fluorescent lighting with electronic ballast, adjustable speed drive for air conditioning and single phase switch mode power supplies for computers. These equipments are characterized as harmonic sources and also highly susceptible to voltage sag. Harmonics and voltage sags are most frequent among various types of power quality disturbance faced by many consumers. Sources of power quality problems, such as harmonics caused by electronic equipments are characterized as non linear load, whereas voltage sags generally as result from faults (short circuit) in transmission or distribution line. Voltage sags normally do not cause equipment damage, but can easily disrupt the operation sensitive load. Effect produced by voltage sags are variable in generally depending on the magnitude and duration of the sags and type of equipment. A Shaffner "Profline2100" has used for measuring harmonics source and load sensitivity test to voltage sags.

Keywords

Power quality, Harmonics, Voltage Sags, Low voltage consumer loads.

1. INTRODUCTION

With the increasing use of electronic equipment in office buildings and household, power quality issues in low-voltage distribution systems have received much attention from utilities, building owners, tenants and manufacturers. The problems in power quality appeared for the first time in the beginning of the 1980s with the introduction of non linear loads like computers, power electronics, internet, etc [1]-[2]. The power quality problems is defined as any power problem manifested in voltage, current, or frequency deviations that result in failure or disoperation of customer equipment [2].

Many electronics equipment systems are susceptible to disturbances come from the input power supplied to them. Some of the common power disturbances are voltage sags caused by fault in power system, transient over voltage created by the switching of the utility's capacitor banks, voltage waveform distortion generated by the injection of harmonic currents from nonlinear loads is propagate to all distribution circuits [2]-[3].

The harmonic currents interact with the power system impedance creates harmonic voltage distortion on the system. The voltage distortion will continue to increase in the electrical environment as more electronic loads are connected to the power system. For examples the equipment which dominant harmonic sources in commercial building are computers, etc [2]-[5], fluorescent lamps and adjustable-speed drives (ASDs) for heat ventilation AC (HVAC) system and control motor, associated with the diode bridge rectifier circuit having a constant high fundamental power factor [2]-[3]-[4]-[6].

Almost all power quality issues are closely related with power electronic. Equipment presents different levels of sensitive to power quality issues, depending on type of both the equipment and the disturbance. Several surveys have been carried out to determine the relationship between perturbations and damage. The results are not always comparable due to discrepancies in the definition of perturbation characteristics [2].

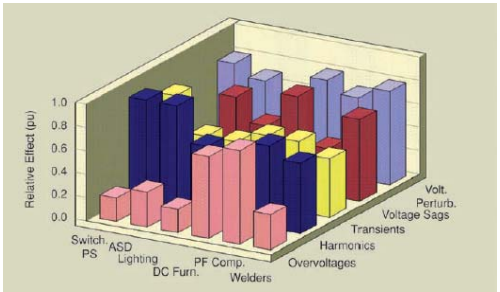

Figure 1(a). PQ issues caused by electronic equipment

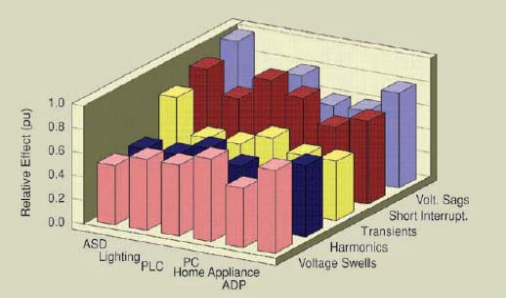

Figure 1(b) Effect of PQ issues on electronic equipment.

The relationship between a typical equipment sensitive and disturbance is shown in Figure 1(a). Furthermore, the effect on power quality of electric power systems due to presence of power electronic equipment, depends on the type of power electronic used. Figure 1(b) shows typical effects of the most common electronic equipment application. From the both of figure, ASDs are extremely sensitive to power quality problems and it's also creates power quality problem.

2. SOURCES OF POWER QUALITY PROBLEMS

2.1. Electronic Power Supplies

Electronic power supplies single phase electronic power supplies are becoming a dominant load in commercial buildings. Personal computers, printers, copiers, and most other single-phase electronic equipment now almost universally employ switch-mode power supplies. The key advantages are the light weight, compact size, and efficient operation. All contain power supplies with similar characteristics [1]-[2]. The personal computer is identified as the most prominent source of harmonics distortion [5,6]. PCs cause power related problems due to the electronic switch mode power supply. They are typical single phase and require low voltage power supply. Almost all electronic power supplies contain a diode bridge rectifier, which supplies d.c power to large d.c filter capacitors. The rectified filter d.c potential is then electronically regulated by a switch mode dc/dc converter before it is passed to micro electronic circuitry.

The percentage of load that contains electronic power supplies is increasing at a dramatic space, with the increased utilization of personal computers in every commercial sector. Commercial loads are characterized by a large number of small harmonic-producing loads.

There are two common types of single-phase power supplies. Older technologies use ac-side voltage control methods, such as transformers, to reduce voltages to the level required for the dc bus. The inductance of the transformer provides a beneficial side effect by smoothing the input current waveform, reducing harmonic content. Newer-technology switch-mode power supplies use dc-to-dc conversion techniques to achieve a smooth dc output with small, light weight components. The input diode bridge is directly connected to the ac line, eliminating the transformer. This results in a coarsely regulated dc voltage on the capacitor. This direct current is then converted back to alternating current at a very high frequency by the switcher and subsequently rectified again.

Figure 2 shows the current and voltage waveforms for a personal computer from laboratory measurement result. It can be shown that the current is pulsed around the peak of the voltage. Odd harmonics have percentage harmonic distortions are much larger than even harmonics. Odd harmonics created are significant until nineteenth harmonics and become small gradually. From harmonic spectrum result obtained the value of total harmonic distortion (THD) of current is 189.4 percent and crest factor (CF) is 5.9. It shows that the computers are a significant as source of harmonics and also generate high crest factor.

2.2. Fluorescent Lighting

The typically accounts for 40 to 60 percent of a commercial building load and it's supplied through low voltage. According to the 1995 Commercial Buildings Energy Consumption study conducted by the U.S. Energy Information Administration, fluorescent lighting was used on 77 percent of commercial floor spaces, while only 14 percent of the spaces used incandescent lighting [3]. Fluorescent lights are a popular choice for energy savings.

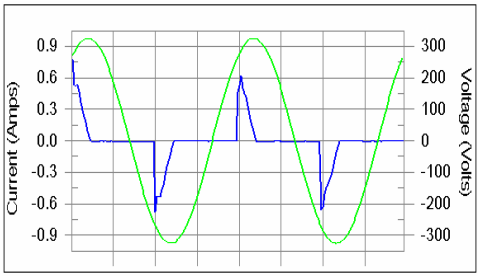

Figure 2(a). Current, voltage waveforms for personal computer.

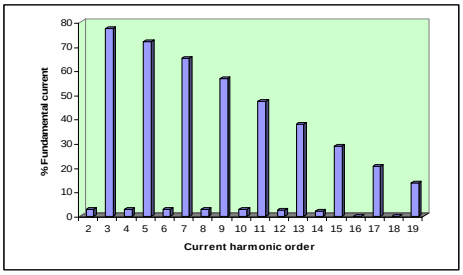

Figure 2(b). Harmonics spectrum for personal computer

Fluorescent lights are discharge lamps which require a ballast to provide a high initial voltage to initiate the discharge for the electric current to flow between two electrodes in the

fluorescent tube. Once the discharge is established, the voltage decreases as the arc current increases. It is essentially a short circuit between the two electrodes, and the ballast has to quickly reduce the current to a level to maintain the specified lumen output. Thus, ballast is also a current-limiting device in lighting applications.

There are two types of ballasts i.e. magnetic and electronic and it does can be supplied at either: 120 volt, 220 volt or 240 volt. Standard magnetic ballast is simply made up of an iron-core transformer with a capacitor encased in an insulating material. Single magnetic ballast can drive one or two fluorescent lamps, and it operates at the line fundamental frequency, i.e., 50 or 60 Hz. The iron-core magnetic ballast contributes additional heat losses, which makes it inefficient compared to electronic ballast.

The lamp voltage and current are at the same frequency of the input ac source, as shown in Figure 3(a). Conventional magnetic ballasts are rapidly being replaced by electronic ballast [3]. Electronic ballast employs a switch-mode–type power supply to convert the incoming fundamental frequency voltage to a much higher frequency voltage typically in the range of 25 to 40 kHz, as shown Figure 3(b). This high frequency has two advantages. First, a small inductor is sufficient to limit the arc current. Second, the high frequency eliminates or greatly reduces the 100 or 120-Hz flicker associated with iron-core magnetic ballast.

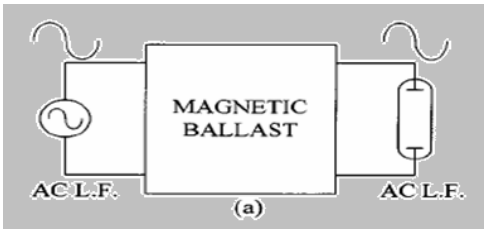

Fig. 3(a). Low-frequency (L.F.) magnetic ballast

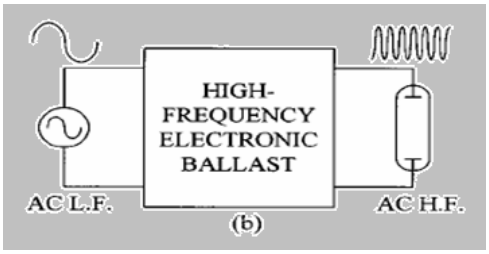

Fig.3(b) High-frequency (H.F.) electronic ballast.

Standard magnetic ballasts are usually rather light source of additional harmonics themselves, because the main harmonic comes from the behavior of the arc [2]. Figures 4 and 5 show a measured fluorescent lamp with magnetic ballast and electronic ballast, respectively. They draw non-sinusoidal current in power system.

The fluorescent lamp with magnetic ballast, the current THD is 17.85 percent and crest factor is 1.6. As a comparison, electronic ballast has current THD of 209 percent and crest factor is 4.3. The both of the lamps generate odd harmonic currents only. Because the fluorescent lamps are significant source of harmonic in commercial buildings, they are usually distributed among the phases in a nearly balanced manner.

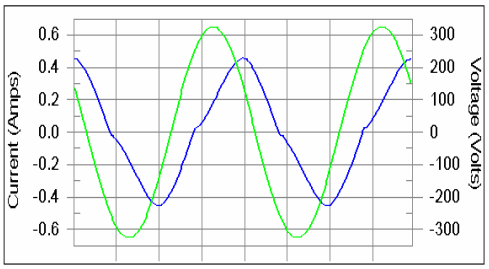

Figure 4(a). The current and voltage waveforms for fluorescent with magnetic ballast

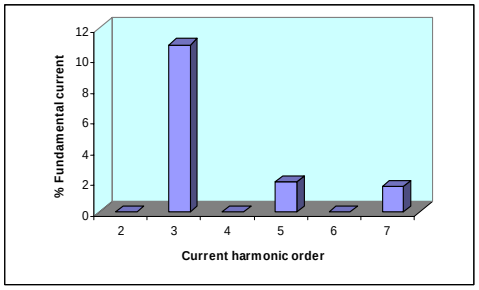

Figure 4(b). Harmonic spectrum for fluorescent with magnetic ballast

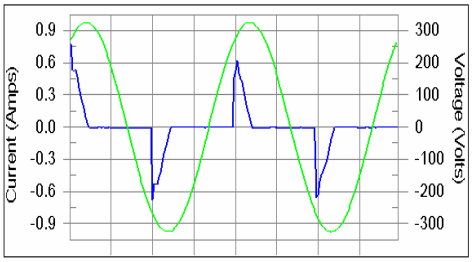

Figure 5(a). The current and voltage waveforms for fluorescent with electronic ballast

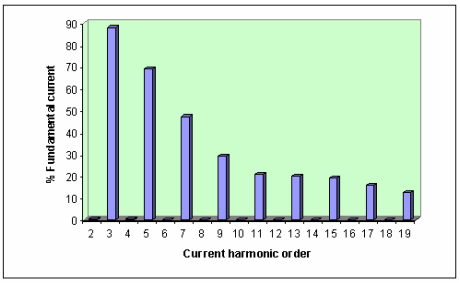

Figure 5(b). Harmonic spectrum for fluorescent with electronic ballast

2.3. Adjustable speed drive (ASD) for HVAC applications

Common applications of adjustable-speed drives in commercial loads can be found in elevator to control motors and in pumps and fans in HVAC systems. An ASD consists of an electronic power converter that converts ac voltage and frequency into variable voltage and frequency. The variable voltage and frequency allows the ASD to control motor speed to match the application requirement such as slowing a pump or fan. Figure 5 illustrates the current waveform and harmonic spectrum for a typical adjustable-speed-drive (ASD) input current [3]. The ASD gives high crest factor too and the current THD of 41.1 percent.

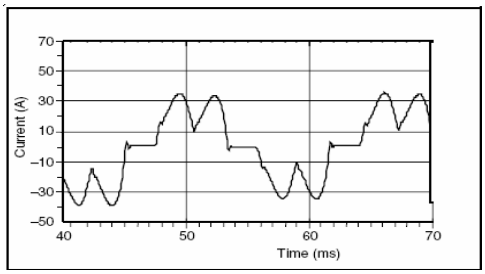

Figure 5(a). Current for an ASD input current

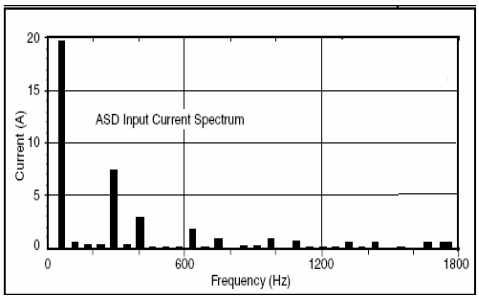

Figure 5(b). Harmonic spectrum for an ASD input

2.4. Voltage sags

Voltage sags are usually associated with system faults but can also be caused by energizing of heavy loads or starting of large motors. The faults on transmission/distribution system can affect even more customers. The customers hundreds of miles from the fault location can still experience voltage sag such as Figure 6, resulting in equipment miss-operation even shutdown [5]. During voltage sag, the voltage is below normal for some period of time that reduces the power and energy delivered to load by the system. The energy lost during a voltage sag event is a function of voltage and the time duration of the sag event.

Voltage sags and momentary interruptions are two of the common power quality concerns for utility customers with sensitive electronic equipment. In power system, disturbances for example voltage sags and service interruptions inevitably occur on some occasions.

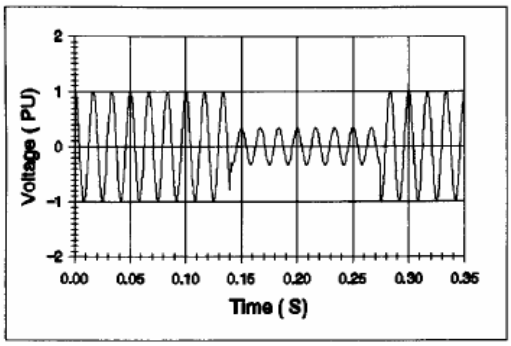

Figure 6. Voltage sag waveform caused by remote fault condition

Customers usually can tolerate complete outages or blackouts since faults in the power system are inevitable. However customers are intolerant if their equipment frequently malfunctions due to voltage sags and momentary interruption in power system. Faults resulting in voltage sags and interruptions can occur within the building installation or on utility system. The voltage sag usually lasts until the fault is cleared by a protective device. This device can be fuse, circuit breaker, re-closer. Table 1 shows types of the protection system used for low voltage system [4].

Table 1. Types of the protection system

Protection Scheme	Sag duration
Fuse	5 to 10 ms
Breaker	80 to 150 ms
Auto re-closing	300 to 700 ms
Back up protection	300 ms to some seconds

3. EFFECT OF POWER QUALITY PROBLEMS

3.1. Effect of Harmonic distortion

The harmonic currents to flow from the harmonic producing load to the power system. The impedance of the power system is normally the lowest impedance seen by the harmonic currents. The harmonic currents interact with the impedances to give rise to harmonic voltage distortion. IEEE Standard 519 [7] provides guidelines for acceptable levels of voltage distortion on the utility system. Evaluations of harmonic distortion are usually performed at a point between the customer and the utility system where another customer can be served. This point is known as the point of common coupling (PCC). The recommended limit the harmonic voltage distortion level for system below 69 kV should be less than 5 percent. If it exceeds the recommended standard limit can influenced on equipment.

The presence additional losses significantly cause increased heating on transformers and motors [3]-[8]. Hysteresis and eddy current losses in the core increase as higher frequency harmonic voltage are impressed on the windings. Hysteresis increase with frequency and eddy current losses increase as the square of the frequency. The current harmonic increases produce additional I^2R losses in the windings. This additional I^2R loss also happened on cables and neutral wires to operate at excessive temperature level. The effective resistance of the cable increase with frequency because of the phenomenon known a skin effect. These increased heating effects can shorten equipment operating life.

The other equipment can be affected by harmonics distortion such as circuit breakers to fail prematurely or malfunction [4]. Capacitor can experience overload and subsequent failure because of absorbe harmonic current. Harmonic currents and highly crest factor influence the operation of protective device [5]-[8]. Fuse and thermal overload relays are prone to nuisance operation when subjected to non linier currents. The relays can operate faster or slower than the expected times for operation at the fundamental frequency alone. Reading error in kWH meters. Computers may exhibit data errors or loss of data and electronic process control may operate out of sequence [4].

The large third harmonic currents in the neutral conductor of rising bus-bar may lead to vibration of joints and cable terminations. If the neutral fails on rising bus-bar system serving single phase loads, over voltage can occur on each single phase board is connected across two phases. Hence, failure of equipment will occur that most common problem is burnt out switch mode power supplies [5].

3.2. Effect of Voltage Sag

Voltage sags normally do not cause equipment damage, but can easily disrupt the operation of sensitive electronic equipment. The voltage sag can be characterized by their magnitude and their duration. The equipment sensitive is determined by the both of values. The sensitivity of the equipment to voltage sags can be expressed by the tolerance curve. Two popular equipment tolerances curve namely the information technology industry council (ITIC) curve and the SEMI F47 curve. Based on reference [9] states more than 62% of disturbance recorded were voltage sags with duration of less than 0.5 s (30 cycles). The effects produced by these disturbances on the equipment are variable depending on equipment types.

3.2.1. Effect on computers.

Voltage sag is normally not a significant problem to single computers unless they are used as servers. In such cases it is relatively easy to protect them, for minor cost by using backup power supply. The problem is not very significant to ordinary single PCs since the lost work not often exceeds 1-2 hours work and often there is a back up or automatic restore of the file. However, there are some PC based offices where disruption will costly greatly. Financial trading and telecommunication offices are typical examples [9]. Two different computers are test to study the effect of voltage sag with specifications of them are shown in Table 4.

Table 4 Specification of the tested computer

	Computer 1	Computer 2
CPU	Intel Pentium III	Intel Pentium IV
RAM	64 MB	512 MB
Hard disk	40 GB	80 GB
Monitor	Dell	Dell
Operating system	Windows 98	Windows 2003

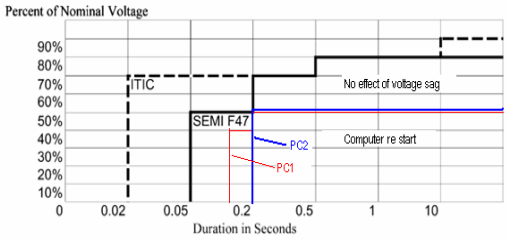

Figure 7. Sensitivity curves for computer

From the Figure 7 for sag of depth 90% to 55%, there are no effects on the both of computers observed during period. However, for sag of depth 50% with duration of 0.2s or more, the both of computers showing restart. For sag of 40%, duration of 0.1s the both of PCs have different sensitive. The 1st computer restarts, while the 2nd computer still in normal operation. Computer 1 shutdown for sag of depth 30% or less, duration 0.1s or more, whereas computer 2 shutdown for sag of 20% or less. It means computer 1 is slightly more sensitive than computer 2. And also can be seen in Figure 7, sensitivity curve for the both of computer is much lower than standard ITIC and SEMI F47 curves. The part above of computer curve denotes that computers do not re start caused by voltage sag.

3.2.2. Effect on Lightings loads

Voltage sags may cause lamps to extinguish. Light bulbs will just twinkle; that will likely not be considered to be serious effect. All lamps, except incandescent lamps, require high voltage across the electrodes during starting. This voltage is essential to initiate the arc. The lamp starting voltage is affected to a large extend by the ambient temperature and humidity levels as well as the supply voltage [9]. Experiments were done two of the most common categories of lightning loads: Fluorescent lamps and Mercury vapor lamp. The specifications of the lamps tested such as in Table 5.

Table 5 Specification of the tested lamp

	Lamp 1	Lamp 2
Type	FCL with magnetic ballast	Mercury vapor lamp
	240 VAC/18 Watt/ 0.37A/PF=0.32	240 VAC/250Watt/ 2.10A/ PF=0.52

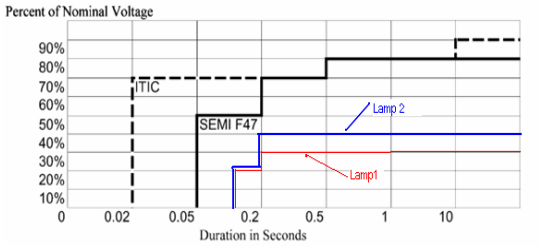

Figure 8 Sensitivity curve for lamps

The Figure 8 shows impact voltage sag on the lamps. Sensitivity of the lamps has response not similar. For examples, for sags of depth until 40% do not cause lamp 1 switch off; whereas lamp 2 when subjected for sag of depth 60 and duration of 10s above will switch off. Its light becomes weaker during the sag period. Sag duration does not affect fluorescent lamp's lightness. The lighting weakness caused by sag depth.

In Figure 8, curves of the fluorescent lamp (lamp 1) and mercury vapor lamp (lamp 2) are much lower than the standard ITIC curve and SEMI F47 curve. Above the line curve, the lamps do not switch off. There may be visible effects like flickering. However, below the line curve the lamps switch off. From this figure also can be shown that the lamp 1 switch off for sags of 30%, duration of 0.2s above. The lamp 2 switches off for sags of 40% and duration of 0.2s above. It's mean that lamp 2 more sensitive than lamp 1.

7. CONCLUSION

Personal computers, adjustable speed drives can be found in elevator to control motors and in pumps and fans in heat ventilations (HV) AC systems, fluorescent lamp with electronic ballast are significant a source harmonics. They inject non sinusoidal current propagate to all circuit of power systems. Interaction of the current with impedance cause harmonic voltage distortion. It can cause detrimental some of equipment in power system and also in consumer.

The computers show almost same affect on the occurrence of voltage sags. The both of computers restart for sag of depth 50% below and duration 0.2 seconds or more. The computers even can shutdown for lower voltage sag.

In the case of lightings show difference behavior on the occurrence of voltage sags. Mercury vapor lamp (lamp 2) more sensitive than fluorescent lamp (lamp 1). They will switch off for voltage sag of 40% and voltage sag 30%, respectively and duration 0.2 seconds or more.

ACKNOWLEDGMENT

The authors would like to acknowledge the help of University Malaysia Perlis (UniMAP) for financial support under research grant (FRGS 9003-00147).

REFERENCES

[1] Kao Chen, "The impact of energy efficiency equipment," IEEE industry application. Conference, 2000.
[2] Marcos, M.M and J.c. Gomez.,"Electric power quality the strong connection with power electronics". IEEE power energy September/October 2003.
[3] R.C. Dugan, Mark F.McGranaghan, Surya Santoso and H. Wayne Beaty.,"Electrical Power Systems Quality", Mc Graw Hill, Second Edition, 2002.
[4] K.S. Philip, Lim P.E., Thomas E., Wyatt, P.E., and Clarence W.Wooddell," Power quality consideration for installing sensitive electronics equipment- A utility's perspective. IEEE 1997.
[5] Eugene Conroy.,"Power monitoring and harmonic problems in the modern building". Power Engineering Journal, April 2001.
[6] McGranachan, M.F, David .Mueller and Mark J.Samotyj.,"Voltage sag in industrial systems. IEEE Trans. On Industry Application, vol.29. no.2, March/April 1998.
[7] IEEE Std. 1159-1995,."Recommended practice for monitoring electric power quality.
[8] C. Sankaran.,"Power quality." CRC Press, 2002.
[9] George G. Karady, Saurabh Saksena, Baozhuang Shi and Nilanjan Senroy."Effect of voltage sags in industrial distribution system". Final report of Power systems engineering research center. October 2005.

ISSN 114-1284

Cognitive Radio as a Regulator of Radios Spectrum

Suzanne A Wazzan

Faculty of Arts and Management Sciences
Um-AlQura University
00966504521678
00966555521074
Email: suwazzi@hotmail.com

ABSTRACT

Nowadays, it is difficult to access radio spectrum because of complicated radio regulation. Large parts of our radio spectrum are sent to licensed radio services. As a matter of fact, a free access to open spectrum, is generally not permitted. However, only some small fractions of the radio spectrum are openly available. These are the unlicensed frequency bands, which build a tiny fraction of the entire radio spectrum, where overlay sharing is commonly used. Spectrum access remains to be a restricting obstacle that may even slow down the development of new radio services that can substantially improve our health, safety, work environment, education of people, and quality of leisure time. This study aims at solving the problem of the difficulty of accessing radio spectrum suffeciently by using the new communication paradigm; cognitive radios. The definition of cognitive radios, system requirements, system architecture and system functions will be discussed.

Cognitive Radios are capable of sensing their spectral environment and locating free spectrum resources. Radios perform local spectrum sensing but Primary User detection and channel allocation is performed in a coordinated manner. This collaborative effort increases the system's ability in identifying and avoiding Primary Users. A group of Cognitive Radios forms a Secondary User Group to coordinate their communication. Each member of this group senses the Spectrum Pool, which is divided into sub-channels. A pair of Secondary Users picks a set of sub-channels spread over multiple Primary User frequency bands to form a Secondary User Link. Sub-channels are picked based on estimated channel gain of a sub-channel and the user's requirements. For group management a number of underlay control channels exists. A Universal Control Channel is used by all groups for coordination and separate Group Control Channels are used by members of a group to exchange sensing information and establish Secondary User Links.

The commercial success of wireless applications in the unlicensed bands indicate that it may be helpful to change our established radio regulatory regime, towards an open spectrum access. We may just want to let radio systems coordinate their usage of radio spectrum themselves, without involving regulation. Cognitive radios overcome this problem as they autonomously manage the usage of spectrum.

In this paper the cognitive radio system which is used to regulate unoccupied frequency bands for the creation of virtual unlicensed spectrum is presented.

Keywords
Cognitive radios, radio spectrum, radio regulation, communication paradigm, wireless communication.

ISSN 114-1284

1. INTRODUCTION

This paper presents a Cognitive Radio approach for usage of Virtual Unlicensed Spectrum (CORVUS), a vision of a Cognitive Radio (CR) based approach that invests allowed spectrum to create "virtual unlicensed bands" i.e. bands that are shared with the primary (often licensed) users on a non-interfering basis. Dynamic spectrum management techniques are used to adapt to immediate local spectrum availability. The system requirements for this approach will be presented, as well as the general architecture and basic physical and link layer functions of CORVUS. This system has been designed by a group of scientists from Berkeley Wireless Research Center, University of California at Berkeley, USA and Telecommunication networks Group, Technical University of Berlin, Germany.

It is commonly believed that there is a crisis of spectrum availability at frequencies that can be economically used for wireless communications, which indicates that a new approach to spectrum licensing is needed. What is clearly needed is an approach, which provides the incentives and efficiency of unlicensed usage to other spectral bands, while accommodating the present users who have higher priority or legacy rights (**primary users**) and enabling future systems a more flexible spectrum access.

An approach, which can meet these goals, is to develop a radio that is able to reliably sense the spectral environment over a wide bandwidth, detect the presence/absence of legacy users and use the spectrum only if communication does not interfere with any primary user. These radios are lower priority **secondary users,** which exploit cognitive radio (CR) techniques, to ensure non-interfering co-existence with the primary users**.** The sensing function is one of the most important attributes of cognitive radios - as it ensures non-interference to licensed users - and should involve more sophisticated techniques than simple determination of power in a frequency band. A CR must sense across the multiple signal dimensions of time, frequency and physical space, of a wireless channel and user networks**. B**est CR operation will allow sensing of the environment and transmission optimized across all of these dimensions and thus allows a truly revolutionary increase in the capacity of spectra to support new wireless applications.

2. COGNITIVE RADIOS

2.1. The Definition of Cognitive Radios

Cognitive radio is a paradigm for wireless communication in which either a network or a wireless connection changes its transmission or reception restrictions to communicate efficiently avoiding interference with licensed or unlicensed users. This alteration of restrictions is based on the active monitoring of several factors in the external and internal radio environment, such as radio frequency spectrum, user behaviour and network state.

2.2. History

The idea of cognitive radio was first presented officially in an article by Joseph Mitola III and Gerald Q. Maguire, Jr in 1999. It was a novel approach in wireless communications that Mitola later described as:

The point in which wireless personal digital assistants (PDAs) and the related networks are sufficiently computationally intelligent about radio resources and related computer-to-computer communications to detect user communications needs as a function of use context, and to provide radio resources and wireless services most appropriate to those needs.

It was thought of as an ideal goal towards which a software-defined radio platform should evolve: a fully reconfigurable wireless black-box that automatically changes its communication variables in response to network and user demands.

Regulatory bodies in various countries (including the Federal Communications Commission in the United States, and Occam in the United Kingdom) found that most of the radio frequency spectrum was inefficiently utilized.[3] For example, cellular network bands are overloaded in most parts of the world, but amateur radio and paging frequencies are not. Independent studies performed in some countries confirmed that observation,[4][5] and concluded that spectrum utilization depends strongly on time and place. Moreover, fixed spectrum allocation prevents rarely used frequencies (those assigned to specific services) from being used by unlicensed users, even when their transmissions would not interfere at all with the assigned service. This was the reason for allowing unlicensed users to utilize licensed bands whenever it would not cause any interference (by avoiding them whenever legitimate user presence is sensed). This paradigm for wireless communication is known as cognitive radio.

3. SYSTEM REQUIREMENTS

The basic premises of the CORVUS system are as follows:

1) Abundance of spectra, which is available and used for spectrum sharing by Secondary Users (SU).

2) SUs use cognitive radio techniques to avoid interfering with Primary Users (PU) when they are present.

We define a PU as an entity that has a high priority in a given frequency band (e.g. cell phone provider, TV station, emergency services, etc). PUs are not cognitive radio aware, i.e. there are no means to exchange information between primary and secondary users provided by a primary system. Specifically, PUs do not provide special signaling in order to access their frequency band. We assume all SUs having cognitive radio capability, i.e. the system only consists of Primary Users and Cognitive Radio capable SUs. Cognitive unaware Secondary Users are treated as noise by this system. In this heterogeneous network, it is assumed that a PU can tolerate interference for no more than at time units. Note that this interference time is dependent on the primary system and may be different for different PUs. After this interference time all SUs have to clear the frequencies belonging to the frequency band of the respective PU. Also, even if a SU is currently using parts of a primary user frequency band, the PU of that band may start the transmission at any time. In case the PU is using a carrier sense access scheme, an SU operating in that band thus has to operate below the carrier sense sensitivity of the PU.

From the above, it is clear that a fundamental requirement for the Secondary User is to continually monitor the presence of Primary Users (or at least every Δt_x). In order to reliably detect primary users, SUs use information based on the Primary User Footprint, which is assumed to be available to the SU System. The primary user footprint includes - but is not limited to - the information from FCC's spectrum inventory table [1]. Additional information could be maximum interference time Δt_x, and local characteristics of PUs such as minimum communication times or time of use.

4. System Architecture

In our system model, SUs form Secondary User Groups (SU Groups) to coordinate their communication. Members of a SU Group use a common control channel for signaling and might communicate with each other in a distributed ad-hoc mode or through a centralized access point. In either mode we assume only a unicast communication, either between a pair of SUs or between a SU and the access point. Direct point-to-point communication between Secondary Users from different SU Group's or broadcast is not supported.
The traffic pattern for the SUs will be initially assumed to have the following characteristics:

1. Centralized, infrastructure based where there has to be a base station or access point providing connection to a backbone connection, as typically found in Internet access networks.
2. Ad hoc networking covers all kinds of ad-hoc traffic that does not assume any infrastructure. Main purpose is to communicate with each other and exchange information within a SU Group.

To support this traffic CORVUS operates over a Spectrum Pool, which could cover from tens of MHz to several GHz creating a "virtual unlicensed band". It is not necessarily a contiguous frequency range and Spectrum Pools of different SU Groups may overlap which implies that SU Groups will compete for the available resources. Each Spectrum Pool will be further divided into N Sub-Channels, which will be the basic resolution used for sensing and transmission.

Figure 2 shows the principle idea of a Spectrum Pooling system in CORVUS. Primary Users own different parts of the spectrum but may not be active at a particular time. The shaded frequency bands indicate that the PU is currently using its spectrum and consequently this frequency band cannot be used by any SU. The figure also shows three different active Secondary User communications. For each communication a pair of SUs picked a pattern of sub-channels to form a Secondary User Link (SU Link). The number of sub-channels in a SU link may vary depending on the quality of the sub-channels, the bandwidth of a single sub-channel and QoS requirement for that connection.

Sub-channels selected to create a SU Link should be scattered over multiple PU frequency. This principle has a double significance. On one hand it limits the interference impact of a SU on a re-appearance of a PU, while on the other hand if a PU appears during the lifetime of a SU Link it would impact very few (preferable one) of the Sub-Channels used by the SU Link. The communication peers using that link would have to immediately clear the affected sub-channel and find a new free sub-channel. In order to maintain QoS, SUs should always have a redundant number of sub-channels for their SU Link.

Within CORVUS, SUs use dedicated logical channels for the exchange of control and sensing information. We envision two different kinds of logical control channels, a Universal Control Channel and Group Control Channels. The Universal Control Channel is globally unique and has to be known to every SU operating in the relevant frequency bands, since access to that channel is pre-requisite for initiating communications. The main purpose of the Universal Control Channel is to announce existing groups and to give the relevant transmission parameters to enable newly arriving users to join a group. Additionally SUs, which want to create a new group can request the local primary user footprints on that channel. Although globally unique the communication range should be locally limited as SU Groups are limited to a local area. In addition to the Universal Control Channel each group has one logical Group Control Channel for the exchange of group control and sensing information.

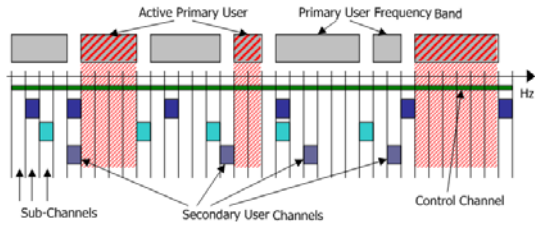

Figure 2. Spectrum pooling idea

Control channels will carry a limited load of low-bit rate signaling which could be located in:

a) dedicated spectrum for this purpose
b) an unlicensed band such as the ISM/UNII bands
c) unlicensed UWB (Ultra Wide Band)

We believe the UWB option is especially attractive if we are considering use of the 3-

10GH band. UWB control channels would be unlicensed but with low impact on other types of communication and with the possibility to operate independently using different spreading codes. There are severe limitations on the power of UWB emissions limiting its range, but the control channel requires very low data rates, so spreading gain will increase the range to be adequate for most applications (more than 10,000 times lower datarate than the commercial UWB systems being envisaged in this band). Note that the Universal Control Channel and the Group Control Channels are logical concepts, which might even be mapped to a single physical channels.

5. SYSTEM FUNCTIONS

Our system design only covers the ISO/OSI layers one (physical layer) and two (link layer). Higher layers will implement standard protocols not specific to cognitive radios and thus are not relevant to our discussion. Figure 3 shows the main building blocks for the deployment of a Cognitive Radio system. We identify six systems functions and two control channels that will implement the core functionality.

5.1. Physical Layer Functions

5.1.1. Spectrum Sensing:

The main function of the physical layer is to sense the spectrum over all available degrees of freedom (time, frequency and space) in order to identify sub-channels currently available for transmission. From this information, SU Links can be formed from a composition of multiple sub-channels. This will require the ability to process a wide bandwidth of spectrum and then perform a wideband spectral, spatial and temporal analysis. Sub-Channels currently used for transmission by SUs have to be surveyed at regular intervals – at least every Δt_x – to detect Primary Users activity on those Sub-Channels ("reclaiming the usage of their Sub-Channels") and if there is activity then those Sub-Channels must be given up.

It will be necessary for the SUs to exchange and merge their local sensing information in order to optimally detect presence of PUs and avoid the hidden terminal problem. This cooperation between SUs within a communicating group will be important to realize adequate accuracy of interference activity. Spectrum sensing is best addressed as a cross-layer design problem since sensitivity can be improved by enhancing radio RF front-end sensitivity, exploiting digital signal processing gain for specific primary user signal, and network cooperation where users share their spectrum sensing measurements.

5.1.2. Channel Estimation:

In order to set up the link, channel sounding is used to estimate the quality of sub-channels between SUs that want to communicate. The transmission parameters (transmit power, bit rate, coding, etc.) are determined based on the channel sounding results. After the setup, the physical layer continuously estimates the quality of sub-channels analyzing the data packets received during ongoing communication.

5.1.3. Data Transmission:

CR's optimally uses the available spectrum as determined by the spectrum sensing and channel estimation functions. Therefore it should have the ability to operate at variable symbol rates, modulation formats (e.g. low to high order QAM), different channel coding schemes, power levels and be able to use multiple antennas for interference nulling, capacity increase (MIMO) or range extension (beam forming). One possible strategy would be based on an OFDM-like modulation across the entire bandwidth in order to most easily resolve the frequency dimension with subsequent spatial and temporal processing.

5.2. Link Layer Functions

5.2.1. Group Management:

We assume that any secondary station will belong to a SU Group. A newly arriving user can either join one of the existing

groups or create a new one through the Universal Control Channel.

5.2.2. Link Management:

covers the setup of a link in order to enable the communication between two SUs and afterwards the maintenance of this SU Link for the duration of the communication. The link layer will initially choose a set of Sub-Channels in order to create a complete SU link subject to the considerations described previously.

5.2.3. Medium Access Control (MAC):

As long as it can be assured that all Sub-Channels are used exclusively, i.e. all Sub-Channels used by one SU Link cannot be used by any other SU Link this problem comes down to a simple token-passing algorithm ensuring that only one of the two communication peers is using the link. However, when considering a multi-group, multi-user system, which may not be centrally organized, making the assumption of exclusively used Sub-Channels is not realistic. So the MAC has to provide means to concurrently access a SU Link by SUs or even to manage the concurrent access of individual Sub-Channels by different connections of different SUs.

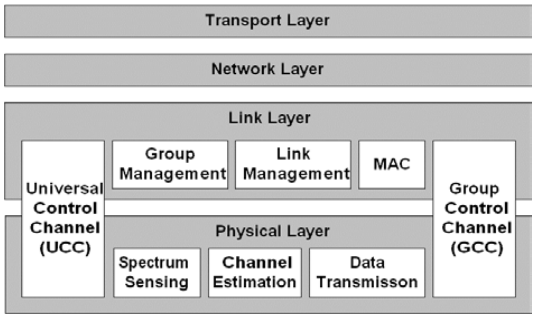

Figure 3. General ISO/OSI Stack for a Cognitive Radi

6. CONCLUSION

In this paper the CORVUS system concepts to harness unoccupied frequency bands for the creation of virtual unlicensed spectrum is presented. The motivation for this approach comes from the enormous success of unlicensed bands and the realization that the present strategy of allocation has resulted in much under-utilized spectra.
Cognitive Radios are capable of sensing their spectral environment and locating free spectrum resources. In CORVUS, these radios perform local spectrum sensing but Primary User detection and channel allocation is performed in a coordinated manner. This collaborative (either centralized or distributed) effort greatly increases the system's ability in identifying and avoiding Primary Users.

In the CORVUS architecture, a group of Cognitive Radios forms a Secondary User Group to coordinate their communication. Each member of this group senses the Spectrum Pool, which is divided into sub-channels. A pair of Secondary Users picks a set of sub-channels spread over multiple Primary User frequency bands to form a Secondary User Link. Sub-channels are picked based on estimated channel gain of a sub-channel and the user's QoS requirements. Furthermore, chosen sub-channels are scattered over the frequency bands of multiple Primary Users to reduce disruption when a Primary User reappears. For group management a number of underlay control channels exists. A Universal Control Channel is used by all groups for coordination and separate Group Control Channels are used by members of a group to exchange sensing information and establish Secondary User Links.

7. REFERENCES:

[1] Ada S. Y. Poon, Robert W. Brodersen and David N. C. Tse. "Degrees of Freedom in Spatial Channels: A Signal Space Approach." submitted to IEEE Trans. on Information Theory, August 2004.
[2] B. A. Fette, Ed., *Cognitive Radio Technology*, Elsevier, 2006.
[3] C. Ting, S. S. Wildman, and J. M. Bauer, "Government Policy and the Comparative Merits of Alternative Governance Regimes for Wireless Services," *Proc. IEEE DySPAN '05*, Baltimore, MD, Nov. 8–11, 2005, pp. 401–19.

[4] C. Jackson, "Dynamic Sharing of Radio Spectrum: A Brief History," *Proc. IEEE DySPAN '05*, Baltimore, MD, Nov. 8–11, 2005, pp. 445–66.
[5] "Cognitive radio." *Wikipedia, The Free Encyclopedia*. 27 Jul 2009, 00:50 UTC. 27 Jul 2009 <http://en.wikipedia.org/w/index.php?title=Cognitive_radio&oldid=304386373>.
[6] DoD 5200.28-STD Trusted Computer System Evaluation Criteria, May 1985; http://csrc.nist.gov/publications/history/dod85.pdf
[7] D.Cabric, S. M. Mishra, R.B. Brodersen, "Implementation Issues in Spectrum Sensing for Cognitive Radios", 38th Annual Asilomar Conference on Signals,Systems and Computers, November 2004.
[8] Fatih Capar, Ihan Martoyo, Timo Weiss, and Friedrich Jondral. Comparison of bandwidth utilization for controlled and uncontrolled channel assignment in a spectrum pooling system." pages 1069–1073, Birmingham (AL), 2002.
[9] IEEE 1900 Std. Committee,IEEE SCC41 home page: http://www.scc41.org
[10] IEEE, "Standard Definitions and Concepts for Spectrum Management and Advanced Radio Technologies," P1900.1 draft std., v. 0.31, June 2007.
[1] S. Haykin, "Cognitive radio: brain-empowered wireless communications Adaptive Syst. Lab", McMaster Univ., Hamilton, Ont., Canada, Feb 2005 Volume: 23 , Issue: 2.
[11] IEEE 1900 Std. Committee,IEEE SCC41 home page: http://www.scc41.org
[7] IEEE, "Standard Definitions and Concepts for Spectrum Management and Advanced Radio Technologies," P1900.1 draft std., v. 0.31, June 2007.
[12] J. Mitola III. "Cognitive radio for flexible mobile multimedia communications. In Sixth International Workshop on Mobile Multimedia Communications", (MoMuC' 99), San Diego, CA, 1999.
[13] J. Mitola III and G. Q. Maguire Jr., "Cognitive Radio: Making Software Radios More Personal," *IEEE Pers.Commun.*, vol. 6, no. 4, Aug. 1999, pp. 13–18.
[14] J. Mitola III. "Cognitive Radio An Integrated Agent Architecture for Software Defined Radio." PhD thesis, KTH Royal Institute of Technology, Stockholm, Sweden, 2000.
[15] M. M. Buddhikot *et al.*, "DIMSUMNet: New Directions in Wireless Networking Using Coordinated Dynamic Spectrum Access," *Proc. IEEE WoWMoM '05*, Taormina -Giardini Naxos, Italy, June 13–16, 2005.
[16] M. Vilimpoc and M. McHenry, 2006, Dupont Circle Spectrum Utilization During Peak Hours; http://www.newamerica. net/files / archive /Doc_File_183_1.pdf
IEEE Communications Magazine, 42:S8–S14, March 2004.
[17] P. Pawelczak, G. J. Janssen, and R. V. Prasad, "Performance measures of Dynamic Spectrum Access Networks," *Proc. IEEE GLOBECOM '06* San Francisco, CA, Nov. 27–Dec. 1, 2006; http://dutetvg.et.tudelft.nl/~przemyslawp/files/prfrmnc.pdf
[18] Timo Weiss and Friedrich Jondral. Spectrum pooling: An innovative strategy for the enhancement of spectrum efficiency.

Palapa Ring Project: Optical Power Budget Supporting Radio over Fiber Technology

Ucuk Darusalam, Purnomo Sidi Priambodo
Dept. of Physics Engineering, University of Nasional, Jakarta 12520
Opto-EAL, Dept. of Electrical Engineering, University of Indonesia, Depok 16424
E-mail: ucuk27@yahoo.com

ABSTRACT

On this paper being analyzed the optical link of Palapa Ring Project in the Region 10 that clustering in the arroud Maluku islands. From the numerical simulation by employing single channel with capacity of rate transmission is 10 Gbps, the maximum of span fiber length is 6 Km while to reach 679 Km away between those cities need 64 EDFA's. By this scheme, regarding combination to Radio over Fiber to reach the rural area so minimum 1 EDFA is also required.

Keywords: *Palapa Ring Project, Radio over Fiber, optical power budget, EDFA*

1. INTRODUCTION

The needs of optical link network that could linking-up the whole region of Indonesia is very essential in order to develop integrity and nationalism. Those whole regions are spread between 5 main islands and 17.000 islands. By looking closer, the many type of social conditions among them not all of them having access to global internet up to date information. The open or free access to information or internet only exist in the main regency such capital of province or center of industry area. This condition influences the economic growth of each region relatively has a great distinction. As an example west region relatively has highest growth that east region. Also the education factor has been influenced by this factor. Internet, communication, and information access is become the fundamental needs to develop the capacity of those region in order to enhance their capability in education and economic.

Palapa Ring Project is the main solution to provide its problem. This project is optical network between 440 Residents (Kabupaten) that launched by Information and Communication Department of Republic Indonesia, also supported by some of telecommunication operator in Indonesia [1]. The launching of this project has begun in 2009 and realizing in the east region first that targeted finish in 2011. The existing of optical network only exist in the west region that connected to Singapore and Hongkong access. This would be integrated with the entire developed network of Palapa Ring. The region of optical link is divided into 11 regions that consist of:

1. Region 1 = West Sumatra
2. Region 2 = Riau, Jambi
3. Region 3 = South Sumatra
4. Region 4 = West Borneo
5. Region 5 = East & South Borneo
6. Region 6 = North Sulawesi
7. Region 7 = South Sulawesi
8. Region 8 = West Papua
9. Region 10 = Bali & Mataram
10. Region 9 = Maluku
11. Region 11 = Java

Those regions would be integrated with optical link via optical communication link. This communication has to consider with the network topology in order to enhance the reliability and access performance. Optical transmission planning is the key to make up those planning. This planning include some optical components (active/passive; laser transmitter, optic receiver, optical amplifier, optical fiber, connector, MUX/De-MUX). Also the heart of optical transmission planning is considering with bandwidth of transmission and parameters that determining the performances and reliability of this network. The main parameter of optical transmission planning are BER (bit error rate) and time of (jitter/wander).

The mature development of communication sytem has reached the broadband scheme. This scheme could be combined in optical fiber communication system called Radio over Fiber [2]. The demand for broadband access has grown steadily as users experience the convenience of high-speed response combined with always-on connectivity. A broadband wireless access network (BWAN) is a cost-effective alternative to providing users with such broadband services since it requires less infrastructure compared to wire-line access networks such as xDSL and cable modem networks [3]. Thus, these days the so-called wireless last miles has attracted much attention. However, it has been concerned mainly with densely populated urban areas. Recent survey shows that although penetration of personal computers in rural areas is significant in some countries most of the users still use low-speed dial-up modem for the Internet access [2] [3]. Since in such case broadband services based on wire-line networks are prohibitively expensive, wireless access network might be the best solution. On the other hand, a radio over fiber (ROF) based wireless access network has been proposed as a promising alternative to BWANs due to its cost-effective network architecture [4]. Hence this scheme could reach the entire region of 440 residents not only restricted to main resident but also could reach the

whole regencies. This hybrid scheme could overcome the geographic condition that has already become main problem to broadcast and open access of communication and information.

On this paper being analyzed the optical power budget that could provide information about the needs and requirement of optic components to build those optical links. Also this analyzes is regarding the possibility to merit with the broadband wireless access network (BWAN).

2. METHOD OF EXPERIMENT

The numerical simulation is taking into account by below diagram:

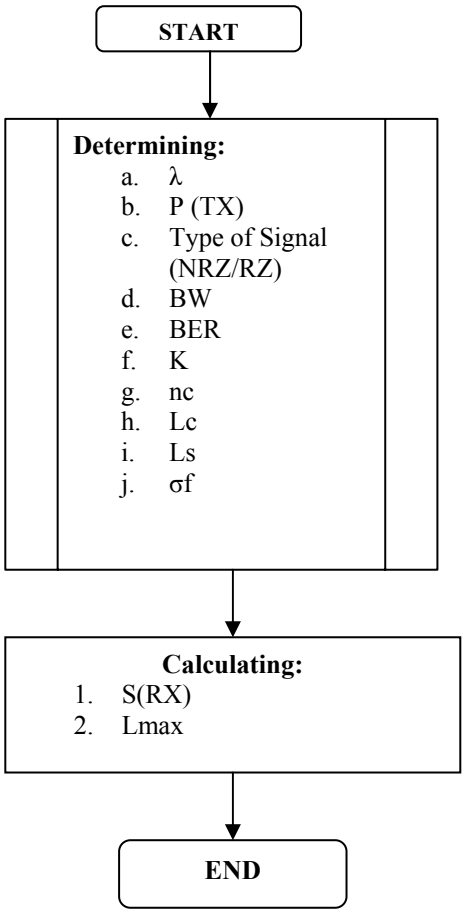

Figure 2.1 Diagram of numerical simulation to find S(RX), L

a. λ the wavelength is chosen at 1300 nm and 1550nm (S and C band)
b. P (TX) is the power of semiconductor laser sources as transmitter in dBm
c. Type of Signal (NRZ/RZ) is the type of digital signal that modulated into laser sources
d. BW is bandwidth of information being broadcasted into network
e. BER is bit error rate
f. K is Excess Noise Factor
g. M is margin of optical link
h. nc is number of connection
i. Lc is loss of connection
j. Ls is loss of splice
k. σf is fiber dispersion factor

The numerical simulation is finding the values of **S(RX)**; sensitivity of photodetector in dBm, **Lmax**; the span of fiber length.

3. RESULT & DISCUSSION

The model of optical link for repeatered submarine fiber optic in the Region 10 (Maluku) as backbone is outlined as figure 3.1.

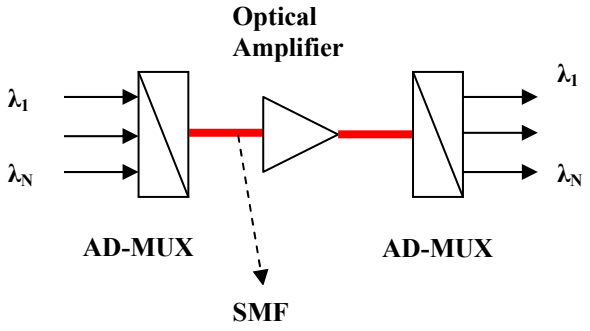

Figure 3.1 The model of Passive Optical Network as backbone.

Figure 3.2 Map of Region 10.

Table 3.1 Span maximum of fiber length for all channel.

λ (Channel)	BW (Gbps)	Lmax (Km)
1	1	6
2	2	6
3	3	6
4	4	6
5	5	6
6	6	6
7	7	6
8	8	6
9	9	6
10	10	6
11	20	6

The calculation as shown as Table 3.1 assumed that channel input to the Add MUX is 10 channels that consist of single wavelength and based on standard ITU - T G.984 Series dan IEEE 802.3ah. Regarding those results if the implementation took place to connecting Kendari City and Ambon City where the total length of span fiber needed is 679 Km then it must use an optical amplifier. The choice of an optical amplifier is EDFA Erbium Doped Fiber Amplifier [5].

Based on numerical simulation of EDFA on the scheme of two level system where the pumping wavelength is 980nm and Pumping power is 20 mWatt, could acquired Gain Spectrum of C-Band wavelength as function of EDFA Length [6]. The maximum Gain is resulted from 1530 nm and 12 m of EDFA length. The minimum case is acquired at the 1560 nm near L-Band for all length (8 m, 9 m, 10 m, 11 m and 12 m).

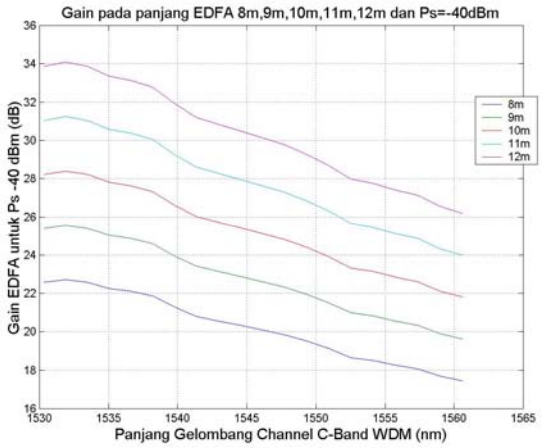

Figure 3.3 Gain profile of EDFA on -40dBm of input signal as function of wavelength (5 channel of C-Band) and length of EDFA.

By assuming the length of EDFA is 8 m based on gain profile of C-Band as shown in figure 3.3, the signal input is -40 dBm and considering the absorption loss is 0.16 dB/Km. Hence the number of EDFA required is 64 one and the power output after traveling 679 Km is -40 dBm. In order to combine those results with Radio over Fiber to reach the rural areas hence minimum 1 EDFA is required to feed the antenna remote unit as outlined in figure 3.4. Each remote unit antenna will share 1 Gbps of via BWAN to user.

The bandwidth that has been planned on Region 10 is 80 Gbps and using 10 channel wavelengths hence each channel wavelength will carry 1 Gbps of rate transmission. If the channel is using C-Band the problem that may arise is fluctuation of gain for every channel. It will arise because each channel has a specific gain for every signal input. The solution to anticipate this problem is using gain flattening method using Bragg Grating Filter. Since the bandwidth doesn't degrade with this method.

The splitting channel then performed in order to feed to antenna remote unit. Each remote unit will receive 1 Gbps data that would already share to user. This technique will overcome the variety of topography in rural area. Hence the high speed connection could be established.

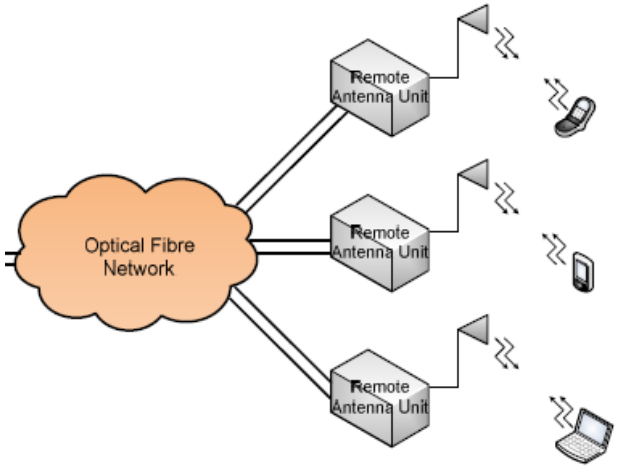

Figure 3.4 Scheme of Radio over Fiber to reach the rural areas [7].

4. CONCLUSION

From the simulation if each single wavelength channel is contained 10 Gbps the maximum span fiber length is 6 Km while to reach 679 kilometer away between Kendari and Ambon Cities within Region 10, so each 10.5 Km need an EDFA.

REFERENCE

[1] www.depkominfo.go.id
[2] H. Bong Kim, Adam Wolisz, A Radio over Fiber based Wireless Access Network Architecture for Rural Areas, Proc. of 14th Mobile & Wireless Communication Summit, Dresden Germany, 2005.
[3] W. Webb, Broadband Fixed Wireless Access as a Key Component of the Future Integrated Communications Environment, IEEE Commun. Mag., pp. 115-121, Sep. 2001.
[4] Implementation frameworks for integrated wireless-optical access networks Deliverable 4, Eurescom, P816-PF, Feb. 2000.
[5] G.P., Agrawal, Fiber Optic Communication Systems, J & W Sons, New York, 1992.
[6] Becker, P. C., N. A. Olsson, J. R. Simpson., Erbium-Doped Fiber Amplifiers: Fundamentals and Technology, Academic Press, 1997, USA.
[7] Francisca Martínez, et al., Transmission of IEEE802.16d WiMAX signals over radio-over-fibre IMDD links, IEEE.

A Comparison between Exponential Filter and FIR Filter On Accelerometer Data Acquisition

Wahyudi [1]), Adhi Susanto [2]), Sasongko Pramono H [2]), Wahyu Widada [3])

[1]*Electrical Engineering, Faculty of Engineering Diponegoro University*
Jln. Prof. Soedarto, SH Tembalang Semarang
Email : wahyuditinom@yahoo.com (the fellow in UGM)
[2]*Electrical Engineering, Faculty of Engineering Gadjah Mada University*
Jln. Grafika no. 2 Yogyakarta
[3]*National Institute of Aeronautics and Space*
Jln. Raya Lapan, Rumpin, Bogor
Email : w_widada@yahoo.com

ABSTRACT

The accelerometer is an acceleration sensor that signal output in voltage/g, where g is the earth gravity. The acceleration is the rate of change of the velocity of an object and the velocity is the rate of change of the position of the same object. The position is the integration of velocity and the velocity is the integration of acceleration. If the data of the acceleration of an object is known, the data of the position can be obtained by applied a double integration. The output of accelerometer has noise and to remove this noise is not enough only use the analog filter but also the digital filter. This paper presents the comparison of two methods of digital filter, they are an exponential filter and a Finite Impulse Response (FIR) filter. The exponential filter is a recursive solution to the process filtering problem, but the FIR is a moving average or nonrecursive filter. A good filtering algorithm can remove the noise from signal, then give the valid information and minimum of error. The estimating of position using the exponential filter is similar to using the FIR filter. The results show that the error average on three axis of position estimation using the FIR filter is 3.0136% and the error average of position estimation using the exponential filter is 3.0087%.

Keywords: *exponential filter, FIR filter, accelerometer, double integration, and position.*

I. INTRODUCTION

An IMU (Inertial Measurement Unit) is the main component of inertial guidance systems used in aircraft, spacecraft, and watercraft, including guided missiles. An IMU works by sensing motion , including the rate and direction of that motion, using a combination of accelerometers and gyroscopes. The data collected from these sensors allows a computer to track a craft's position, using a method known as dead reckoning. An IMU works by detecting the current rate of acceleration, as well as changes in rotational attributes, including pitch, roll, and yaw. This data is then fed into a computer or a microcontroller, which calculates the current speed and position, given a known initial speed and position.[8] On this paper, we done the aquisition of position data from accelerometer on three axis using microcontroller. The goal of this paper is applying the second order of the exponential filter and FIR filter on position estimation use the accelerometer sensor (MMA7260Q) base on microcontroller ATmega 8535. MMA7260Q has three internal accelerometer are placed in a similar orthogonal pattern, measuring position in reference to an arbitrarily chosen coordinate system.

II. THE BASIC OF THEORY

The basic FIR (Finite Impulse Response) filter is characterized by the following two equation, i.e., the FIR difference equation and the transfer function of the filter as below.[1]

$$y(n) = \sum_{k=0}^{N-1} h(k)x(n-k) \qquad (1)$$

$$H(z) = \sum_{k=0}^{N-1} h(k)z^{-k}$$

Where h(k), k=0,1,…,N-1, are the impulse response coefficients of the filter, H(z) is the transfer function of the filter and N is the filter length, that is the number of filter coefficients. It is a time domain equation and describes the FIR filter in its non recursive form: the current output sample, y(n), is a function only of the past and present value of the input, x(n). The exponential filter is a simple IIR (Infinite Impulse Response) filter. Realizable IIR digital filter are characterized by the following recursive equation.

$$y(n) = \sum_{k=0}^{N} a_k x(n-k) - \sum_{k=0}^{M} b_k y(n-k) \qquad (2)$$

Where h(k) is the impulse response of the filter which is theoretically infinite in duration, a_k and b_k are the coefficients of the filter, and x(n) and y(n) are the input and output to the filter. The transfer function of the IIR filter is given as below.

$$H(z) = \frac{\sum_{k=0}^{N} a_k z^{-k}}{1 + \sum_{k=0}^{M} b_k z^{-k}}$$

An important part of the IIR filter design process is to find suitable value for the coefficient a_k and b_k such that some aspect of the filter characteristic, such as the frequency response. Exponential Filter is a simple recursive filter. The first order of exponential filter is shown as below.[2]

$$y(t) = (1-a).y(t-1) + a.x(t) \quad (3)$$

Where $x_{(n)}$ and $y_{(n)}$ are input and output of filter, the value of coefficient α is between 0 to 1. The value of coefficient α can be calculated as below.

$$\alpha = \frac{1}{(1 + 2\pi.\frac{f_c}{f_s})} \quad (4)$$

Where f_c is the cutoff frequency and f_s is the sampling frequency. The second orde of exponential filter is shown as below.

$$y(t)^{[2]} = (1-a).y(t-1)^{[2]} + a.y(t) \quad (5)$$

The features of MMA7260Q are low cost, low current consumption, integral signal conditioning with low pass filter, high sensitivity temperature, selectable sensitivity (1.5g/2g/4g/6g), and low voltage operation. Output of accelerometer is voltage/g that show the acceleration of an object. The functional block diagram is shown in Figure 1[6].

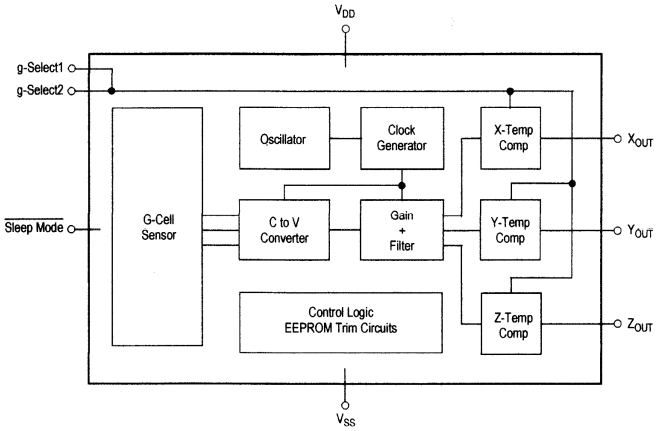

Figure 1 Functional block of MMA7260Q.

The acceleration is the rate of change of the velocity of an object. At the same time, the velocity is the rate of change of the position of that same object. In other words, the velocity is the derivative of the position and the acceleration is the derivative of the velocity, thus:

$$\vec{a} = \frac{d\vec{v}}{dt} \text{ and } \vec{v} = \frac{d\vec{s}}{dt} \text{ or } \vec{a} = \frac{d(d\vec{s})}{dt^2} \quad (6)$$

The integration is the opposite of the derivative. If the acceleration of an object is known, we can obtain the position data if a double integration is applied (assuming initial conditions are zero).

$$\vec{s} = \int \vec{v}dt \text{ and } \vec{v} = \int \vec{a}dt \text{ or } \vec{s} = \int (\int \vec{a}dt)dt \quad (7)$$

One way to understand this formula is to define the integral as the area below the curve, where the integration is the sum of very small areas whose width is almost zero. In other words, the sum of the integration represents the magnitude of a physical variable. The sampling of accelerometer sensor is shown in Figure 2[4].

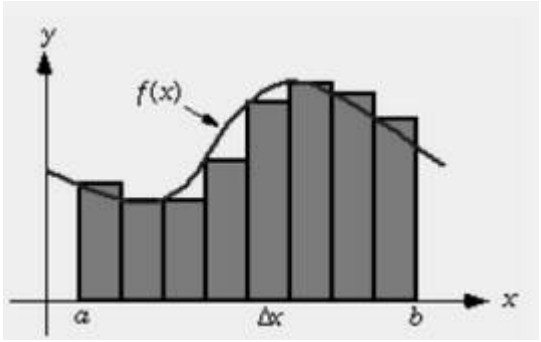

Figure 2. Sampling of gyroscope signal

$$\int_a^b f(x)dx = \lim_{n\to\infty} \sum_{i=1}^{n} f(x_i)\Delta x \quad (8)$$

where $\Delta x = \frac{b-a}{n}$

With the previous concept about "areas below the curve" a deduction can be made: Sampling a signal gets us instant values of its magnitude, so small areas can be created between two samples. In order to create a coherent value, sampling time must always be the same. Sampling time represents the base of this area while the sampled value represents its height. In order to eliminate multiplications with fractions (microseconds or milliseconds) involving floating points in the calculation we assume the time is a unit. Now we know each sample represents an area whose base width is equal to 1. The next deduction could then be that the value of the integral is reduced to be the sum of samples. This assumption is correct if the sampling time tends to be zero. To get the position data, we use the second order of integration trapezoidal method (Runge-Kutta Method) as below.[3]

$$x_k = x_{k-1} + \frac{h}{2}[f(x_k, t_k) + f(x_{k-1}, t_{k-1})] \quad \text{.....(9)}$$

III. DESIGN OF SYSTEM

The microcontroller uses three pin of port A, A.4 A.2 A0, for three inputs from output of accelerometer. Pin A.4, A.2, and A.0 are used as x axis, y axis, and z axis. Output voltage of accelerometer is represented the acceleration and converted to digital data by internal ADC on microcontroller. The accelerometer data is transmitted from microcontroller to personal computer via the serial port RS232. Block diagram of system is shown in Figure 3.

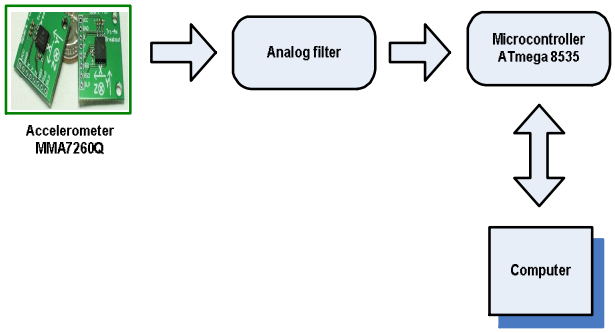

Figure 3 Block diagram of system.

The sub-routine code to get gyroscope data can be exited from CodeWizardAVR as below

```
#define ADC_VREF_TYPE 0x60
// ADC interrupt service routine
interrupt [ADC_INT] void adc_isr(void)
{
unsigned char adc_data;
//Read the 8 most significant bits
//of the AD conversion result
adc_data=ADCH;
//Place your code here
}
Void main(void)
{
// ADC initialization
// ADC Clock frequency: 62,500 kHz
// ADC Voltage Reference: AVCC pin
// ADC High Speed Mode: Off
// ADC Auto Trigger Source: None
// Only the 8 most significant bits of
// the AD conversion result are used

ADMUX=ADC_VREF_TYPE;
ADCSRA=0x86;
SFIOR&=0xEF;
}
```

The design process of FIR filter is to find suitable value for the impulse response coefficients of the filter ,h(k), using the Mathlab FDA Tools. This design use the cut off frequency and sampling frequency of the filter. The cut off frequency of filter is 350 Hz and the sampling frequency is 11 KHz. Block parameter of digital FIR filter design is shown in Figure 4.

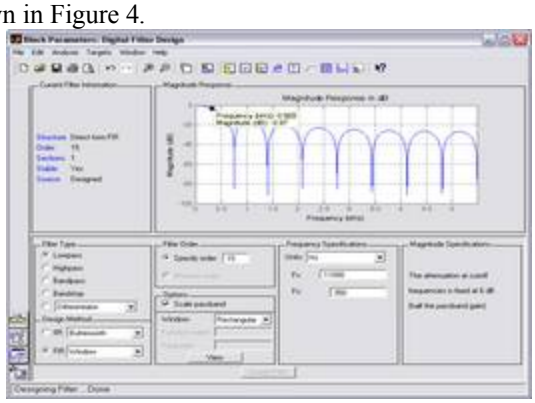

Figure 4 The block parameter of digital FIR filter design.

The impulse response coefficients that obtained from FDA tools is realized for x axis on microcontroller as below.

```
// program FIR x axis
unsigned char FIR_x (unsigned char input)
{
static float
z0x,z1x,z2x,z3x,z4x,z5x,z6x,z7x,z8x,z9x,z10x,z11x,z12x,z
13x,z14x,z15x;
        float output_x,rx,ox,hx;
        z15x=z14x;
        z14x=z13x;
        z13x=z12x;
        z12x=z11x;
        z11x=z10x;
        z10x=z9x;
        z9x=z8x;
        z8x=z7x;
        z7x=z6x;
        z6x=z5x;
        z5x=z4x;
        z4x=z3x;
        z3x=z2x;
        z2x=z1x;
        z1x=z0x;
        z0x=input;
        output_x=(0.0470*z0x+0.0533*z1x+0.05829*z2x
+0.06262*z3x+0.06621*z4x+0.06898*z5x+0.07087*z6x+0
.07182*z7x+0.07182*z8x+0.07087*z9x+0.06898*z10x+0.0
6621*z11x+0.06262*z12x+0.05829*z13x+0.0533*z14x+0.
0470*z15x);
        hx=floor (output_x);
        rx=output_x-hx;
        if (rx<0.5)
        {
        ox=floor (output_x);
        }
        if (rx>=0.5)
        {
```

```
        ox=ceil (output_x);
        }
        return ox;
}
```

The design process of exponential filter is to find parameter (α). A filter parameter (α) can be obtain using equation 4. The exponential filter is used on the cutoff frequency 350 Hz and the sampling frequency 11000 Hz.

$$\alpha = \frac{1}{1 + 2.\pi.350/11000} = 0.83$$

This is a program listing of an exponential filter on microcontroller.

```
float filter_x (char in) //function of exponential filter
{
float ym1,ym2,A1,A2;
static float y1,y2,y12,y22,out1,out2;
A2=0.83;//value of parameter filter
A1=1-A2;
//single exponential filter
y1=A1*in;
y2=A2*out1;
ym1=y1+y2;
out1=ym1;
//double exponential filter
y12=A1*ym1;
y22=A2*out2;
ym2=y12+y22;
out2=ym2;
return ym2;
}
```

IV. EXPERIMENT AND ANALYSIS

The experiment data of position restimation is obtained by using exponential filter and FIR filter. We compare this result on error of estimate position at three axis. Table 1 and Table 2 are the experiment data of x axis using FIR filter and exponential filter.

Table 1. The experiment data of x axis using FIR filter.

No	Estimate distance (cm)	True distance (cm)	Error (cm)	Error (%)
1.	16.664	15	1.664	11.0933
2.	30.732	30	0.732	2.44
3.	44.425	45	0.575	1.2778
4.	60.651	60	0.651	1.085
5.	78.579	75	3.579	4.772
Average				4.1336

Table 2. The experiment data of x axis using exponential filter.

No	Estimate distance (cm)	True distance (cm)	Error (cm)	Error (%)
1.	15.207	15	0.207	1.38
2.	30.483	30	0.483	1.61
3.	46.86	45	1.86	4.1333
4.	60.539	60	0.539	0.8983
5.	73.407	75	1.593	2.124
Average				2.0291

Teble 1 and Table 2 show that the average of error using FIR filter more large than using the exponential filter. The average of error using FIR filter and exponential filter are 4.1336 and 2.0291. Table 3 and Table 4 are the experiment data of y axis using FIR filter and the exponential filter.

Table 3. The experiment data of y axis using FIR filter.

No	Estimate distance (cm)	True distance (cm)	Error (cm)	Error (%)
1.	14.924	15	0.076	0.5067
2.	31.298	30	1.298	4.3267
3.	44.141	45	0.859	1.9089
4.	62.13	60	2.13	3.55
5.	74.107	75	0.893	1.1907
Average				2.2966

Table 4. The experiment data of y axis using exponential filter.

No	Estimate distance (cm)	True distance (cm)	Error (cm)	Error (%)
1.	14.62	15	0.38	2.5333
2.	30.085	30	0.085	0.2833
3.	43.948	45	1.052	2.3378
4.	61.979	60	1.979	3.2983
5.	73.896	75	1.104	1.472
Average				1.9849

Table 3 show that the average of the estimate distance error is 2.2966%. The average error on y axis using exponential filter that shown in Table 4 is 1.9849%. Table 5 and Table 6 are the experiment data of z axis using FIR filter and the exponential filter.

Table 5. The experiment data of z axis using FIR filter.

No	Estimate distance (cm)	True distance (cm)	Error (cm)	Error (%)
1.	15.344	15	0.344	2.2933
2.	20.062	20	0.062	0.31
3.	26.768	25	1.768	7.072
4.	29.172	30	0.828	2.76
5.	39.753	40	0.247	0.6175
Average				2.6106

Table 6. The experiment data of z axis using exponential filter.

No	Estimate distance (cm)	True distance (cm)	Error (cm)	Error (%)
1.	15.92	15	0.92	6.1333
2.	20.094	20	0.094	0.47
3.	22.531	25	2.469	9.876
4.	29.357	30	0.643	2.1433
5.	37.425	40	2.575	6.4375
Average				5.0120

From Table 5 and Table 6, we know that average of the error of estimate distance using FIR filter smaller than using exponential filter. The average error on z axis using FIR filter that shown in Table 5 is 2.1606 and the average error on z axis using exponential filter that shown in Table 6 is 5.0120.

V. CONCLUSION

Design of digital filter in three axis of accelerometer system has been develop to build IMU system. The design process of FIR filter is to find suitable value for the impulse response coefficients of the filter using the Mathlab FDA Tools. The filter characteristic to design FIR filter are the cut off frequency of filter and the sampling frequency. The design process of exponential filter is to find parameter (α).The exponential filter is used on the cutoff frequency 350 Hz and the sampling frequency 11000 Hz. The estimating of position using the exponential filter is similar to using the FIR filter. The results show that the error average on three axis of position estimation using the FIR filter is 3.0136% and the error average of position estimation using the exponential filter is 3.0087% .

REFERENCES

[1] Emmanuel, *Digital Signal Processing Apractical Approach*, Addison-Wesly, 1993

[2] Laviola, J.J., *Double Exponential Smoothing : An Anternative to Kalman Filter-Based Predictive Tracking*, The Eurographics Association, 2003.

[3] Padiyar, K.R., *Power System Dynamics Stability and Control*, John Wiley & Sons, Singapura.

[4] Seifert, K. dan Camacho, O., *Implementing Positioning Algorithms Using Accelerometers*, Freescale Semiconductor, 2007.

[5] ----------, *ATmega 8535 Data Sheet*, http://www. atmel.com, Maret 2004.

[6] ----------, *MMA7260Q Data Sheet*, http://www. freescale.com, April 2008.

[7] ----------, *Solutions Based in Accelerometers*, http://www.freescale.com, Maret 2009.

[8] ----------, http://www.en.wikipedia.org/wiki, Inertial _Measurement_Unit, Januari 2009.

[9] ----------, *Exponential Filter*, http://www. statistics.com, Juli 2008.

PREELIMINARY DESIGN OF FINGER MODEL OF GLUCOSE PERMITTIVIY FOR NON-INVASIVE BLOOD GLUCOSE SENSOR

Yohanes[1], Lukman[2], Djoko Hartanto[3]
EE Departement. Faculty of Engineering. University of Indonesia – Depok, Indonesia
yohanes.calvinus@rocketmail.com, transistor_bipolar@yahoo.com, Djoko@ee.ui.ac.id

Abstract - All parts of our body protected by skin tissues. There are many way to measure glucose rate in a blood for non invasive on this skinned tissue, but one of a part becomes focus which is on fingertip part. A part of fingertip has skin tissue that modestly and comprise of 3 layers which are epidermis, dermis, and subcuttant. This each tissue has a function and existence in the body. Needs to knows to sense glucose rate in blood just looks for part on this tissue that one has vein tissue which is on dermis's layer. On this skinned tissue needs to be analogized into an electronic circuit so is gotten an electronic properties point which is applicable to make a blood glucose sensor. The research done for modeling of tissue electronic circuit to get an electronic properties point (permittivity). The result of electronic properties of skin tissue that will be measured is equivalent by assesses permitivity which is a part of a capacitance point. Using RC circuit will get a permitivity value to figure out an analysis of glucose. Outgrow of permitivity value of glucose that increases in a blood figure out how increase blood glucose rate step-up in a body. To know blood glucose rate that equals to assess permitivity of detectable glucose on fingertip, a RC model that simulate into a graph that figured by matlab programs. Expected by this model can add a scientific contribution for measuring instrument more blood glucose sensor accurately.

Key words: Blood glucose, monitoring tool, non-invasive blood glucose sensor, skinned tissue, modeling of permitivity blood glucose, Matlab Graph

I. INTRODUCTION

As many scientist to research in blood glucose monitoring, there is just for commercial used and not so opened for research in public. So in this research for beginning of all the project were try to describe any blood glucose model at finger skin. Finger skin was choose because it were usuall part wich blood taken for blood glucose invasive methode to measure. There is seen for literatur that describe any analysis of biomedical within electronical engineering that first is blood glucose properties were dielectric equivalent [13]. The second is blood glucose were in β dispersion of dielectric that mean of blood glucose permittivity at of permittivity value [4]. The thirdth is blood glucose were a molecular pyhsically that bond of carbon material ($C_6H_{12}O_6$) [5].

Based on three of literatur to describe what properties of glucose within biomedical and electronic engineering, glucose were described as a capacitive component that equal to permittivity value. If we discuss about dielectric and capacitive there is some of frequency dependent to measure blood glucose. And its permittivity that made of material were diferrences each other. So in this research were make 2 models that can be analysis any changed of glucose effect within dermis or blood parts. Its a simple to analysis if we had a lot of any properties that glucose were been effected it. From any literatur that giving any data of some properties that we need as epidermis, dermis, and blood were giving as seen at Table 1. The data at Table 1 is a constant. In this research we assume that epidermis were human skin dry because part of physically is dead tissue. Assume Dermis were human skin wet that parts of pyhsically is life tissue or life cell that with water concentrated.

Table 1. Data of skin & blood properties [4]

Layers of Skin	(Tipe Data 1)	(Tipe Data 2)	
Epidermis (Human skin Dry)			80
Dermis (Human skin Wet)			30
Blood			20

In dielectric dispersion, there is a point there will be important point that is a relaxation point. The dielectrics will become relaxation when it range between 0-10GHz and will become resonances when it range more than 10GHz. It graph on Graph 1. Resonances in dielectric

means the phase between imaginary part (conductivity) and real part (permittivity) is same or we can assume for 0 and ∞ .

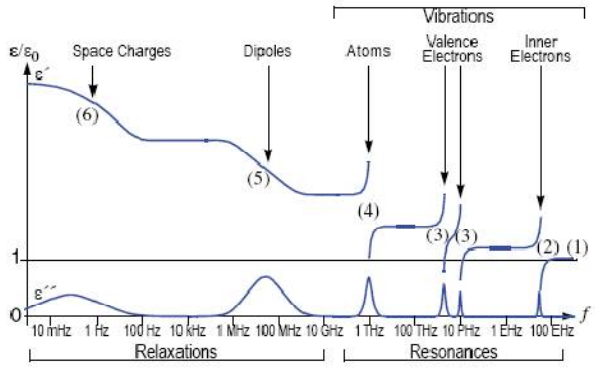

Graph 1. Relaxation & Resonance [22]

II. BODY EQUIVALENT MODEL

Let's we discuss about a common model for macroscopic of body that means our part of body. The circuit model equivalent is RC model circuit with series between every part of our body. It's were drawn on Graph 2. For every cell that our body have, the circuit equivalent is RC model but it more complex than macro's model. For every microscopic model that we must categorize it between intracellular cell or extracellular cell. So model equivalent for extracellular cell is resistance that resist a current that will get into intracellular cell. Capacitance is a model equivalent for intracellular cell that were had a value properties of materials that will permit any of energy to stored. All macroscopic and microscopic model were drawn on Graph 2.

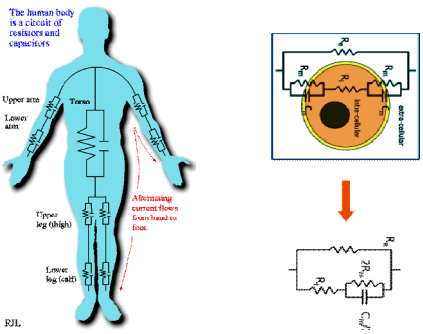

Graph 2. Circuit Model of Macroscopic [23] and Microscopic [4] Equivalent

Many research that do for measure blood glucose at any parts of human body. Harman-Boehm were take their research on ear skin. The model were present at Graph 3. The model were using maxwell-wagner model for two layers. [11]

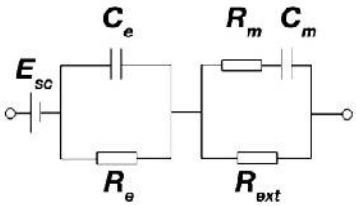

Graph 3. Harman – Boehm Model [11]

III. GLUCOSE AT FINGER SKIN MODEL

Based on Graph 2, we try to make 2 models of finger skin at fingertip. First concept of model were made for describe of glucose change at dermis of skin that had a lot of a tiny blood vessel at dermis of skin. Second concept of model were made for describe of glucose change at blood parts that were the third layer of skin. Both of model were drawn at Graph 4.

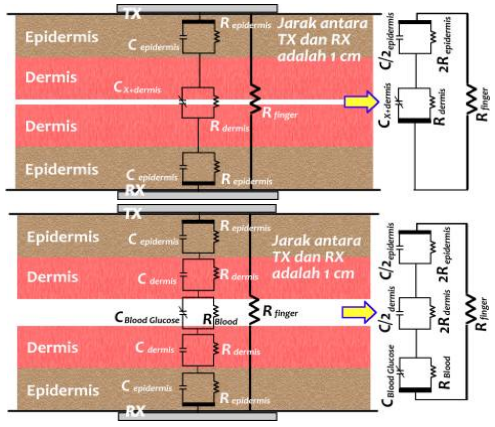

Graph 4. (a). Model 1 (b). Model 2

Simulate both models properties of permittivity with Matlab programming. We can get some of properties like a range frequency of change and relaxation point or resonance point. There is based on maxwell-wagner model to analize both of models and Logarithmic Statisctic that we have a result for permittivity of each which drawn into Graph 5.

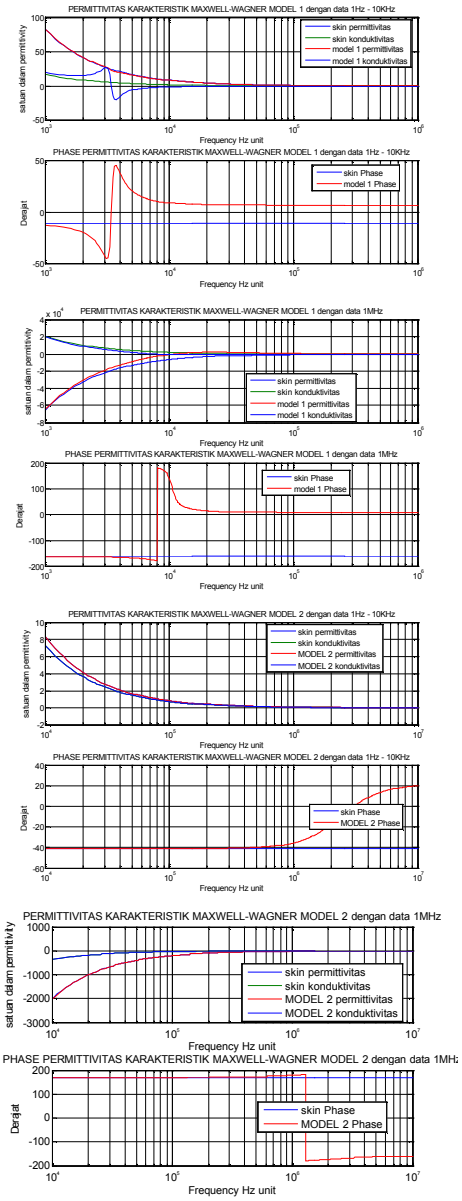

Graph 5. Result of Simulation with Matlab.

IV. CONCLUSION

Based on both of model equivalent, model 1 similar with Harman-Boehm Model that used for ear skin. At model 1 with 1 MHz, it were dispersion relaxation point at 22 KHz frequency. The effect of glucose were relaxation of permittivity at 25 and 0,75 at model 1. The permittivity point of relaxation were describe for a point of glucose value change towards to skin.

REFERENCES

1. *Glucowatch HS Report Outline.* American Diabetes Association.
2. Zuomin Zhao. 2002. *Pulsed Photoacoustic Techniques and Glucose Determination in Human Blood and Tisssue.* Oulu University
3. John D.Enderle. 2006 . *BIOINSTRUMENTATION.* Morgan & Claypool Publisher.
4. Sverre Grimnes. 2008. *Bioimpedance & Bioelectric Basics.* Elsevier Ltd.
5. Faisal Azad. 2008 . *Glukosa dan Metabolisme Energi*. Polton Sport Science & Performance lab.
6. Annex A. 2001. *an overview Bioimpedance Monitoring for Physicians.*
7. Soegianto. 2007. Prinsip Pengukuran Glukosa Darah secara Non-Invasif. *Unpublished.*
8. Caduff, A., Hirt, E., Feldman, Y., Ali, Z., Heinemann, L. 2003. *First human experiments with a novel non-invasive, non-optical continuous glucose monitoring system*, Biosensor and Bioelectronics.
9. Soegianto. 2007. *Biosensor Journal. Unpublished.*
10. Soegianto. 2007. *Simulink Analysis of Blood Glucose Regulation as The Basic Concept of Non-Invasive Blood Glucose Sensor Design.* Quality in Research. University Indonesia.
11. Harman-Boehm. March 2009. *Non-Invasive Glucose Monitoring : a Novel Approach.* Diabetes Technology Society.
12. Saraju P. Mohanty, *Biosensors: A Survey Report,* (November 24, 2001)
13. R. Pethig, 1987. *Dielectric Properties of Body Tissues*. Clinical Physics and Physiological Measurements.
14. Natan van Riel. 2004. *Minimal models for glucose and insulin kinetics: a Matlab implementation,* Eindhoven University of Technology.
15. Francis X.Hart, 2006. *Electric Properties of Tissues*, Wiley Encylopedia of biomedical Engineering. John Wiley & Son, Inc
16. Sverre Grimnes. 2002. *Interface Phenomena and Dielectric Properties of Biological Tissue*, University of Oslo.
17. M. Akimoto. 2006. *Development of the Pulsed Direct Current Iontophoresis and Its Clinical Application*. Progress In Electromagnetics Research Symposium 2006, Cambridge, USA

18. Steven.T. Karris. 2007. *Signals and Systems with MATLAB and Simulink. 3rd edition*. Orchard Publications.
19. Eric. C. Green. 2005. *Design of Microwave Sensor for Non-Invasive Determination of Blood Glucose Concentration.* Baylor University.
20. Kan Ichi Kamiyoshi, Tadao Fujimura, Tsutomu Yamakami. 1967. *Some Characteristic of the Maxwell Wagner Type Dielectric Dispersion.* The Research Institute for Scientific Measurements.
21. Technology Assessment Conference Statement. 1994. *Bioelectrical Impedance Analysis in Body Composition Measurement*. National Institutes of Health.
22. Ken Kundert. *Modeling Dielectric Absorbtion in Capacitor*.
23. RJL system. (2008, Agustus). http://www.rjlsystems.com/

Novel Design Wideband Switched Beam Antenna Array using Modified 3 dB Hybrid Coupler

Yuli Kurnia Ningsih [1,2], E.T. Rahardjo [1], M. Asvial [1]

[1] *Antenna propagation and Microwave Research Group (AMRG)*
Department of Electrical Engineering, University of Indonesia
New Campus UI, Depok , West Java, 16424, Indonesia
yuli_kn@yahoo.com , eko@ee.ui.ac.id

[2] *Department Of Electrical Engineering, Trisakti University*
Kyai Tapa , Grogol , West Jakarta, Indonesia
yuli_kn@yahoo.com

ABSTRACT

The switched beam antenna is one type of the antennas, which consists of the microstrip antenna array and the switch beam network. This feature can help users pointing directly to target or signals direction. In this research, novel design of wideband switched beam microstrip antenna array using a modified 3 dB hybrid coupler in the single layer substrate has been proposed. The results have been achieving a good performance. The return loss is achieved below -25 dB at 9.4 GHz. A wideband characteristic can achieve up to 1 GHz at the center frequency (9.4 GHz)

Keywords
3 dB Hybrid Coupler, switched beam linear array microstrip antenna, wideband

1. INTRODUCTION

Nowadays the need of a broadband channel becomes the most important things in providing wireless infrastructure. Several services in set of devices becomes a absolutely needed for supporting the mobility of wireless telecommication services. The antenna is one of device of wireless system with the fuction is receive and transmit the electromagnetic wave.

Switched beam antenna or so called fixed beam antenna is one kind of the smart antenna which needed more than one beam to select the course of the strongest signal among the exsisting several radiation pattern. With that mentioned ability, the antenna is capable to radiated his energy to appropiate user course. So it is hoped to reduce the interference problem that caused by multipath fading effect.

Switched beam antenna has the ability to reduce of radiation pattern swith the desired target. For that reason, many author has been research the switched beam antenna array because this kind of antenna has the ability of reducing existing interference beside it improved the capacity.

For achieving the switched beam antenna, the simple form to achieve two beams that can be switched according with port that exitate is the integration between array antenna with the hybrid coupler. Array antenna arranged two elements.

Antenna element has an important role in forming and acquiring radiation desires. One type of an antenna element that can be used is by using microstrip antenna.

Antenna microstrip which is arranged in linear array becomes one of the right choice because microstrip antenna has high performances beside easy to combine with active MMIC (Miniatured Microwave Integrated Circuit). So it can be integrated with control system and signal processing.

A linear array antenna consists of identic elements located finite distance apart along a straight line. The total field from the array described by the equation above is made up of an element pattern $f(\theta,\phi)(e^{-jk_o r/4\pi r})$ and the array factor (AF). This is know as pattern multiplication.

Hybrid coupler does make an important role in the design of microwave circuits and their applications are various. It, however, has narrow band characteristic and requires a large circuit area. Now, wideband circuits are in demand.

In order to reduce the size, many authors have suggested several solutions [1] – [3]. Samsinejad et al [1] was resulting in reducing dimension by substitution two pieces of stub which put on an oblique position, an inductor and capacitors. Using this method reduced the size into 27%, however the bandwidth is narrow and by the structure becomes complicated. To achieve a wide band coupler, Chun et al [2] used a cascaded branch line coupler with mixed distributed and lumped distributed elements and Cho at al [3] used N section tandem connected structure. By such methods are resulted a wide bandwidth as wide as 56% and 42% respectively. In fact, it would be desirable to develop an alternative hybrid that can achieve a better tradeoff between bandwidth, size and power handling.

2. NOVEL DESIGN WIDEBAND 3 DB MICROSTRIP HYBRID COUPLER USING CURVE LINE AT THE SERIES ARM

Normally, hybrid coupler consist of a main line which is coupled to a secondary line by two quarter wave length long section spaced one quarter wavelength apart, thus creating a square approximately one wavelength in circumference[4]. The coupling factor is determined by the ratio of the impedance of the shunt and series arms according to Figure 1.

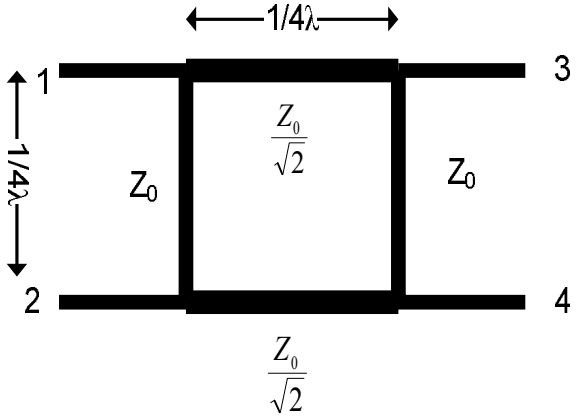

Figure 1: The normal structure 3 dB hybrid coupler

When signal is introduced at a port 1 the signal at the two output arm (port 3,4) are equal in amplitude but have a 90 degree phase difference between each other. Ideally, no signal should appear at the fourth port. The same thing happens of course if a signal enters one of the others port. For 3 dB coupling, the characteristic impedances of the shunt arm is $Z_{sh} = Z_o$ and the series arm is $Z_{se} = Z_0/\sqrt{2}\ \Omega$ respectively for optimum performance of the coupler. The characteristic impedance of input and output port Zo is normaly equal to 50 Ω for microstrip line.

One method to obtain a wideband characteristic was use a thick substrate [5]. Working at high frequency requires proper selection of the substrate. For the new design of hybrid coupler, a substrate with thickness 1.57 mm and dielectric constant (ε_r) 2.2 was selected. This substrate can be categorized as a thick substrate with low permittivity. With increasing in the thickness of the substrate will give higher radiation losses but otherwise it would acquire a wideband characteristic

A novel design of wideband 3 dB microstrip hybrid coupler was proposed which use a substrate with thickness 1.57 mm and dielectric constant (ε_r) 2.2 [6]. The desirable 3dB hybrid coupler should have a good performance such as return loss and isolation loss, wideband characteristic, and a small size on a single layer circuit.

Figure 1 shows the structure of the proposed novel design 90° hybrid coupler with curve line at the series arm.

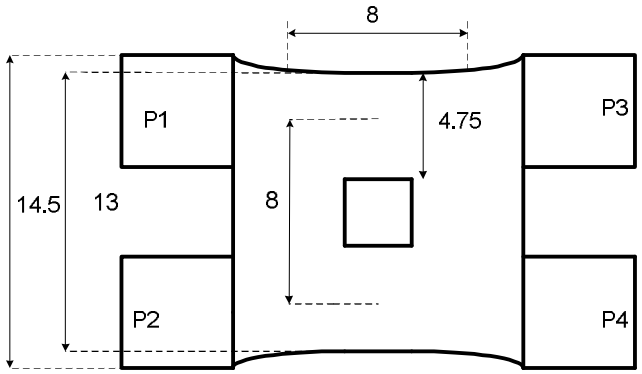

Figure 2 : A New Design 3 dB Hybrid Coupler With Curve Line For f_r = 9 Ghz

A novel design wideband 3 dB hybrid coupler using curve line at the series arm has been simulated. The result takes all the coupling allowing high performance. At 9 GHz, the simulation result shows -3 dB coupling ± 0.3 dB with phase error 3°, return loss below -22.56 dB and isolation below -25.11 dB

3. DESIGN OF SINGLE ELEMENT PATCH ANTENNA

In designing antenna, the first is to decide the working frequency, a bandwidth impedance and the design gain. Further, to select a substrate specification which will used. In designing high frequency antenna which is using microstrip, the kind of selected substrate must according with the requirement [7] those are :

$$f[\text{GHz}]\ h\ [\text{mm}] > 2.14\ \sqrt{\varepsilon_r} \qquad (1)$$

That has been done because the beginning of radiating at high frequency, the course of radiation at the antenna is curved and causing loss. To protecting radiation condition so the selected must conform with (1).
The purpose of the design is the feed line want to located at the same level as the antenna on the single layer, the substrate of antenna used substrate with thickness 1.57 mm and dielectric constant 2.2 .

After gaining the substrate specification, further designing the patch of antenna microstrip. The antenna which is designed here will work at 9.4 GHz .

The design of antenna patch begins with calculate the dimension of the microstrip patch. The designed antenna patch is rectangular shaped. After the calculation, iteration and analysis based on moment method , the effective dimension of patch antenna is resulted, where the length (L) is 10 mm and the width (W) is 12.8 mm as depicted in Figure 3.

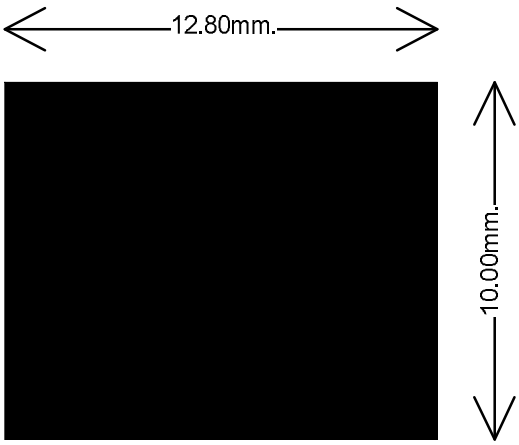

Figure 3: Design of Microstrip Patch Antenna

Resulting from simulation of single element is presented at Figure 4 to Figure 6. It is shown the simulation result at 9.4 GHz.

The return loss for single element achieve below -32.25 dB, The bandwidth achieve 800 MHz from 9.0 GHz to 9.8 GHz. That's mean a good performance for single element can be achieved.

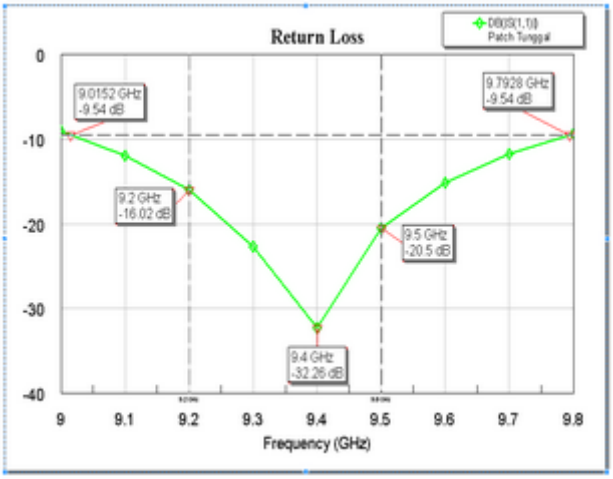

Figure 4 : Return loss for Single Element

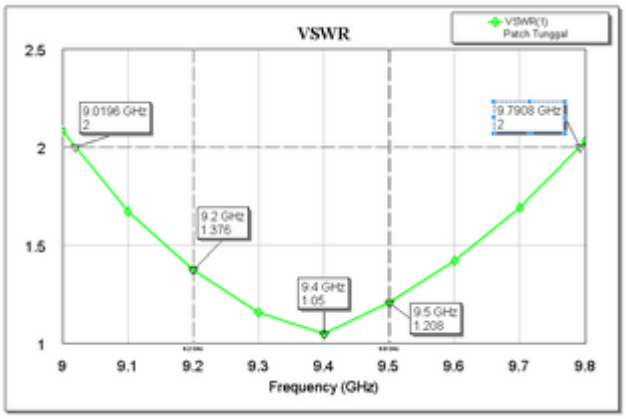

Figure 5: VSWR for Single Element

Figure 6 shown the radiation pattern from the single element. That's not yet produce the required radiation pattern for the swithed beam.

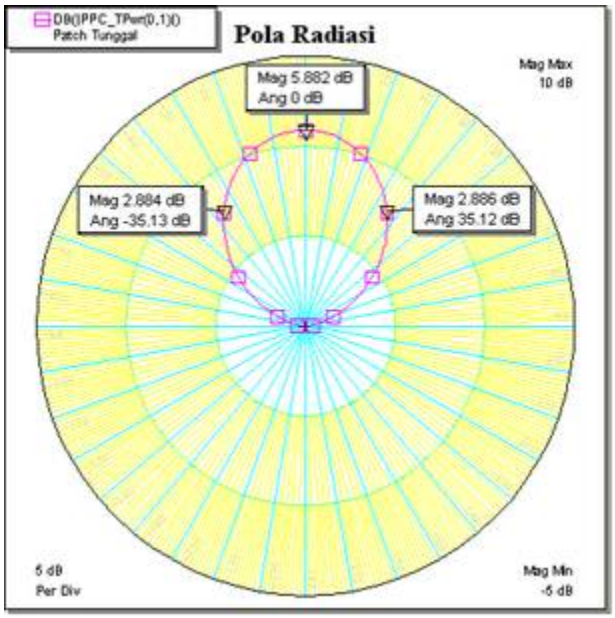

Figure 6: Radiation Pattern for Single Element

4. DESIGNING OF THE SWITCHED BEAM ARRAY ANTENNA

The result of the simulation of single element in question provide a reference to patch that will be integrated with hybrid coupler, that's mean it achieve a microstrip switched beam antenna.

For achieving the switched beam antenna, the simple form to achieve two beams that can be switched according with port that exitate is the integration between array antenna with the hybrid coupler. Array antenna arranged two elements.

Figure 7 shown the design of switched beam antenna array with two radiation patterns that can be changed to diffrent beam. Amount of beam according the amount of port. The distance between the element is ½ λ. This distance is the efficient enough for the effective dimension and it is not make overlapping the other patch element .

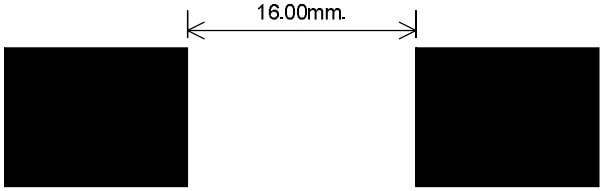

Figure 7: Distance of array antenna 2 elements for f = 9.4 GHz

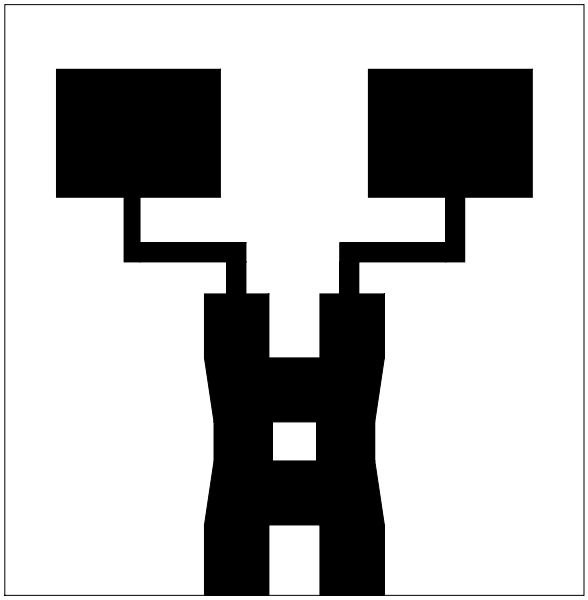

Figure 8: Design of array antenna 2 elements with a hybrid coupler for f = 9.4 GHz

5. RESULT AND ANALYSIS

In this section, simulation results for a novel wideband switched beam antenna array using modified 3 dB Hybrid Coupler are presented. Simulation tools have been used to calculate return loss, VSWR, and radiation pattern, based on the Method of Moments. Simulation results as depicted in Figure 8 are presented in Figure 9 to Figure 11. The ground plane dimension is 45 mm x 46 mm.

5.1. Return Loss

Corresponding to previous port assigning, S_{11}, S_{22}, are the return loss factors. The coupler is designed to keep return loss factor at acceptable level. For the structure forms of a new design are symmetrical so the value of the four ports should be equal. The return loss factor vs frequency is depicted in Figure 9. The reflection coefficient is achieved below -25.29 dB at 9.4 GHz.

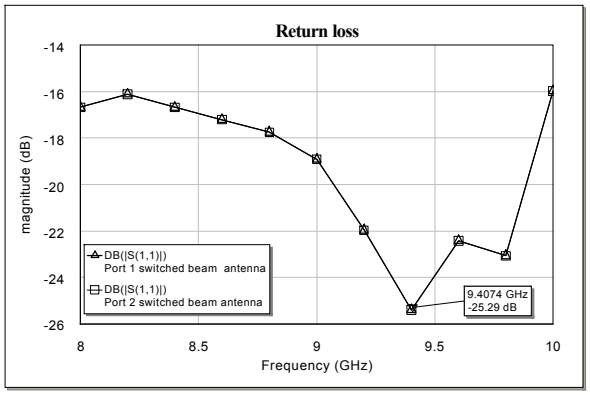

Figure 9: Distance of array antenna 2 elements for f = 9.4 GHz

5.2. Wideband the Switched Beam Array Antenna

Design of the integration between array antenna with a new design of hybrid coupler achieve a wideband characteristic up to 1 GHz, which around 10.6 % the center frequency (9.4 GHz) as shown in Figure 10.

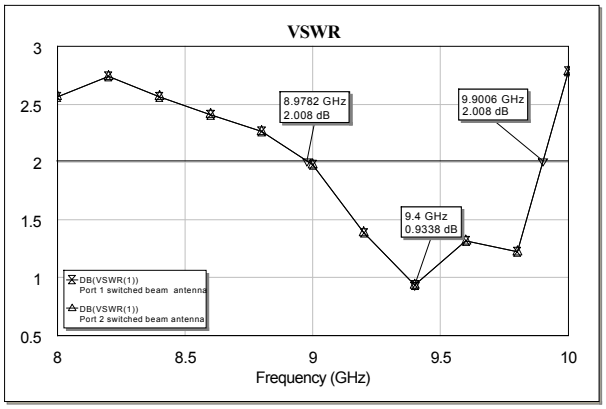

Figure 10: with a hybrid coupler for f = 9.4 GHz

5.3. Switched Beam Antenna Array with Two Radiation Patterns

Figure 11 illustrates the radiation pattern of the switched beam antenna array respectively. From the radiation pattern, it is shown that the angles of the two beams associated with the 2 inputs are -13.5° and 14°.That's mean two beams can be switched according with port that exitate.

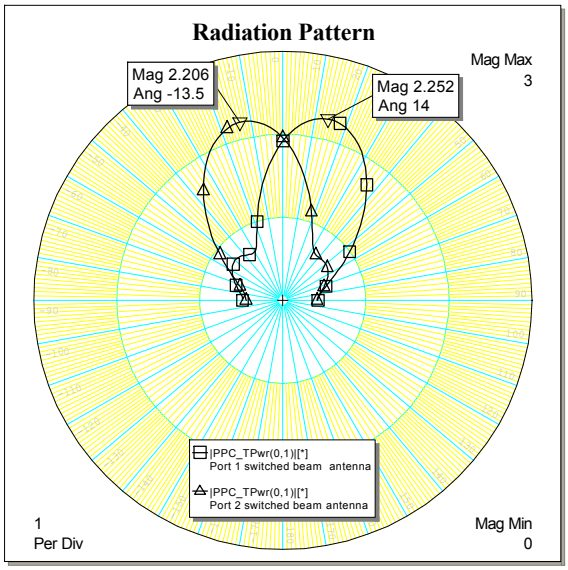

Figure 11: Radiation Pattern of switched beam array antenna for f = 9.4 GHz

6. CONCLUSION

A novel design wideband switched beam antenna array using modified 3 dB hybrid coupler has been studied and simulated. The result takes all the parameters allowing high performance. At 9.4 GHz, the simulation result shows return loss below -25 dB. By printed on the same layer, the integration between array antennas with a new design of hybrid coupler with a curve line at the series, can achieved the excellent bandwidth, up to 10 % centered at 9.4 GHz on a single layer circuit.

REFERENCES

[1] Samsinejad S., M. Soleimani,and N. Komjani,"Novel enhanched and miniaturized 90° coupler for 3G EH mixer", Progress In Electromagnetics Research Letters, Vol. 3, pp 43-50,2008

[2] Chun,Y.H.,J.S.Hong,"Compact wideband branch line hybrid",IEEE Transaction on Microwave Theory and Techniques, Vol 54, No. 2 , pp704-709,2006

[3] Cho, Jeong Hoon, Hee Yong Hwang and Sang Won Yun,"A design of wideband 3 dB coupler with N section microstrip tandem structure",IEEE Microwave and Wireless Components Letters, Vol. 15, No.2, 2005

[4] Collin,R.E,Foundation for Microwave Engineering, 2-nd Edition,Mc Graw Hill International Edition,pp 432-434,1992

[5] Hirasawa ,Kazuhiro; Misao Haneishi, "Analysis,Design and Measurement of Small and Low-Profile Antenna, Artech House,Norwood,1992,pp. 126-135

[6] Y.K. Ningsih, E.T. Rahardjo, "Novel Design Wideband 3 dB Microstrip Hybrid Coupler Using Curve Line at the Series Arm", Proceeding of the International Conference on Electromagnetic Near Field Characterization and Imaging, Taipe, 2009

[7] WR Li, CY Chu,et al," Switched Beam Antenna Based on Modified Butler Matrix with low Side Lobe Level", Electronics Letters 4th, Vol. 40 No. 5 , March 2004

ISSN 114-1284

Performance Comparison of Drop Tail and RED Queueing in AODV ++ for Mobile Ad Hoc Networks

Zulhelman[a], Benny Nixon[b], Riri Fitri Sari[c]

[a, b]*Department of Electric Engineering*
Polytechnic State of Jakarta, Depok 16425
Tel : (021) 7863531 ext 222. Fax : (021) 7863531
E-mail : zuhelman@yahoo.co.id, b3nix@yahoo.co.id

[c]*Department of Electrical Engineering*
University of Indonesia, Depok 16424
E-mail : riri@eng.ui.ac.id

ABSTRACT

Mobile Ad hoc Network (MANET), can be implemented in area that have no telecommunication infrastructure due to its limitation. With MANET, the need for communication in that area can be serviced. For communicating with internet, the MANET must be connected with the nearest telecommunication infrastructure via Gateway. For implementing this, a routing protocol a such as AODV++ has been introduced. This protocol is modification of AODV that was originally designed for only routing packets within the MANET and not between a MANET and a wired network. For measuring performance we use three performance metric packet delivery ratio, end to end delay, and overhead.

In this work, we evaluated the performance comparison between two queuing mechanism that can implemented on a MANET, i.e. Drop Tail and RED. Performance, our hypothesis is that RED perform is better than Drop Tail. To prove this, a scenario has composed as follow; 20 mobile nodes, two gateways, two routers and two hosts. The topology is a rectangular area with 1300 m length and 800 m width. A rectangular area was chosen in order to force the use of longer routes between nodes, compared to a square area with the same node density. The two gateways were placed on each side of the area; their x- and y-coordinates in meters are (200,500) and (1100, 500). All simulations were run for 1000 seconds of simulation time. Since we were interested in studying the behavior of the network in steady state, the first 100 seconds of the simulation were ignored. Ten of the 20 mobile nodes are constant bit rate (CBR) traffic sources sending data packets with a size of 512 bytes, to one of the two hosts, chosen randomly. The sources are distributed randomly within the MANET. The transmission range of the mobile nodes is 250 meters. For overcoming congestion RED Drop Tail queuing algorithm has been used.

Our Simulation result shows that, with adding more mobile nodes, congestion will increased the congestion, and than in comparing both of the queuing mechanism on a MANET, the RED mechanism shows is a better performance than Drop Tail. The AODV ++ evaluation proves that RED is better in management buffer mechanism.

Keyword:
Performance, Comparison, Internet, MANET, AODV++, RED, Drop Tail.

1. INTRODUCTION

A mobile ad hoc network (MANET) can be formed without the need for any established infrastructure or centralized administration. It normally consists of mobile nodes, equipped with a wireless interfaced, that communicate with each other. Due to the fact that kinds of networks are very spontaneous and self-organizing, they are expected to be very useful. It is also highly likely that a user of the network will need to connect to the Internet. There are several routing protocols for MANETs, such as Ad hoc On-Demand Distance Vector (AODV), Dynamic Source Routing (DSR), Optimized Link State Routing Protocol (OLSR) and Topology Dissemination Based on Reverse-Path Forwarding (TBRPF). These protocols were designed for communication within an autonomous MANET, so a routing protocol needs to be modified in order to achieve routing between a mobile device in a MANET and a host device in a wired network (e.g. the Internet). The AODV routing protocol is one of the most developed and implemented routing protocols investigated by the IETF MANET working group. In this work AODV has been modified to achieve routing of packets towards a wired network, which is referred to as AODV+ [1].

ISSN 114-1284

2. AD HOC ON-DEMAND DISTANCE VECTOR (AODV)

Ad hoc On-Demand Distance Vector (AODV) is a reactive MANET routing protocol [1], where the reactive property implies that a mobile node requests a route only when it needs one. Consequently, the node maintains a routing table containing route entries only to destinations it is currently communicating with. Each route entry contains a number of fields such as Destination IP Address, Next Hop (a neighbor node chosen to forward packets to the destination), Hop Count (the number of hops needed to reach the destination) and Lifetime (the expiration or deletion time of the route). AODV guarantees loop-free routes by using sequence numbers that indicate how fresh a route is.

There are two buffer management mechanisms in AODV such as RED (Random Early Detection) and Drop Tail. Floyd and Jacobson introduce RED, a technique implemented at gateways to achieve improved congestion avoidance. The primary goal of RED is to detect and avoid incipient congestion. Essentially, RED monitors and controls the average queue size in order to detect incipient congestion. This reduces the average delay across the gateway. Floyd and Jacobson's algorithm aims to eliminate global synchronization and avoid bias against bursty traffic. TCP senders respond to dropped packets by reducing their window. When the gateway's queue is full, all packets are dropped, and all senders reduce their windows at the same time. This global synchronization results in a loss of throughput and decreased network utilization. Additionally, RED attempts to avoid the bias against bursty traffic inherent to Drop Tail gateways. With Drop Tail gateways, connections with more bursty traffic are more likely to have dropped packets even if they have the same average traffic.
The RED algorithm accomplishes these goals by randomly marking packets such that packets from a particular source are marked with a probability proportional to that connection's share of the bandwidth through the gateway. The algorithm sets up a minimum and maximum threshold for the average queue length (AQL). When the AQL is less than the minimum threshold all packets are forwarded. If the AQL is between the minimum and maximum thresholds, packets are marked with a probability proportional to the AQL. Thus, more packets are marked when the average queue length is longer. For AQLs greater than the maximum threshold, all packets are marked. Marking a packet alerts the sender of congestion and should result in some reduction from the sender. Packets may be marked either by setting a bit in the header or simply dropping the packet.

The former approach requires the recipient to recognize the "congestion" bit and relay this knowledge to the sender. The latter method implicitly alerts TCP of congestion since TCP responds to dropped packets by reducing the window. The goal is for RED gateways to mark packets in fairly even intervals instead of all at once like Drop Tail gateways. This technique avoids biases and global synchronization.

2.1. Operation of RED

RED monitors the average queue size, and checks whether it lies between some threshold minimum and maximum. If it does, then an arriving packet is dropped or marked with probability, p, where p is a function of the average queue size. Several researchers have studied early Random Drop gateways as a method for providing congestion avoidance at the gateway. In the implementation of Early Random Drop gateways in, if the queue length exceeds a certain *drop level*, then the gateway drops each packet arriving at the gateway with a fixed *drop probability*. The drop level and the drop probability should be adjusted dynamically, depending on network traffic.

2.2. The RED algorithm

The algorithm for RED gateways can be explained that the RED gateway calculates the average queue size, using a low-pass filter with an exponential weighted moving average. The average queue size is compared to two thresholds, a *minimum* threshold and a *maximum* threshold. When the average queue size is less than the minimum threshold, no packets are marked. When the average queue size is greater than the maximum threshold, every arriving packet is marked. If marked packets are in fact dropped, or if all source nodes are cooperative, this ensures that the average queue size does not significantly exceed the maximum threshold. The general RED gateway algorithm is as follow [2]:

for each packet arrival calculate the average queue size avg

if min_{th} < = avg < max_{th}__
    calculate probability p, with probability
    p : mark the arriving packet
else if max_{th}_<=_avg
    mark the arriving packet

2.3. Drop Tail

In this gateway mechanism, each congestion period introduces global synchronization in the network. When the queue overflows, packets are often dropped from several connections, and these connections decrease their windows at the same time. This results in a loss of throughput at the gateway [7].

3. SIMULATION RESULTS

For simulating the network, in this work we use ns-2 simulator. This simulator covers a large number of applications of protocol, network types, and network element and traffic models. NS-2 simulator is based on two languages: an object oriented simulator, written in C++ and OTcl (an object oriented extension of Tcl), with one to one correspondence between them. The compiled C++ hierarchy allows us to achieve efficiency in the simulation and faster execution times. This in particular is useful for the detailed definition and operation of protocols and allows one to reduce packet and event processing time.

TCL (Tool Command Language) is used for millions of people in the world. It is a language with a very simple syntaxes and it allows a very easy integration wit other languages. The characteristics of this language are enabling fast development, provide a graphical interface, compatible to many platforms, flexible for integration, easy to use and free [3].

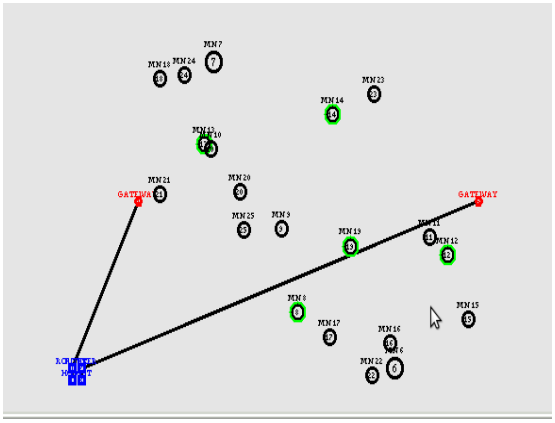

Figure 1 : Scenario of the AODV++ Simulation on Network Animator (NAM)

In analyzing the result we used the fallowing formula that implemented in AWK, this formula are as follow :

1. PDF (Packet Delivery Fraction)
   PDF = (Receive/Send) * 100 %
2. NRL (Normalize Routing Load)
   NRL = Routing Packet/Receive packet.
3. End to end delay

The result of AWK used for analyzing, these result is composed in table 1 and table 2. Table 1 is result of RED queuing mechanism, beside it, table 2 is result from Drop Tail queuing mechanism. Subsequently, using Xgraph these results are displayed. with using Xgraph on NS. The following subsections explain the results.

3.1. Packet Delivery Fraction (PDF)

Table 1 and Table 2 show that PDF values always 100 %, this means that all packets can be delivered to destination. Both Table 1 and Table 2 also show that RED and Drop Tail mechanisms do not influence PDF values. This is confirmed with Casey experiment [5]. Base on these tables using Xgraph tools, we produced Figure 2 which shows that in all time intervals will produce fix PDF. This condition occurred on both of queue mechanism, RED or Drop Tail. This condition occurred because in scenario congestion does not occur, so that all of packets sent, are delivered to MN destination.

The result of this scenario confirmed with the previous hypothesis, because in scenario congestion does not occur because this traffic is lower than the capacity of the network.

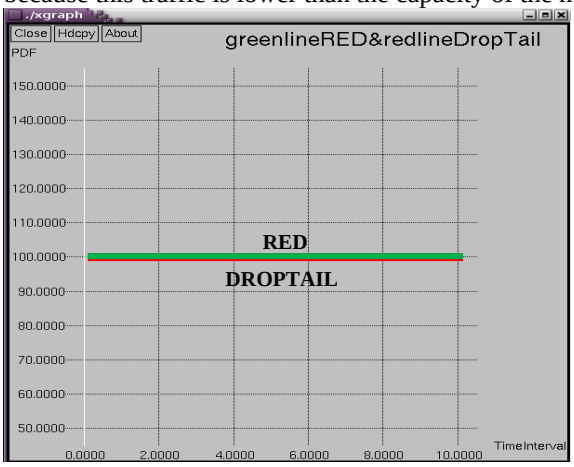

Figure 2: PDF graph for Drop Tail and RED queuing Mechanism.

3.2 Normalized Routing Load (NRL)

The NRL values from simulation result are shown in Figure 3. This graph is made base on both table 1 and table 2. In this graph, green line indicates NRL for RED mechanism, and red line indicate NRL Drop Tail mechanism.

Table 1: The result of simulation with RED Mechanism

Time Interval Traffic (S)	METRIC		
	PDF	NRL	e2n
0.01	100	0.03	265,37
0.1	100	0.03	265,37
0.2	100	0.62	387.58
0.3	100	0.93	383.81
0.4	100	1.21	539.13
0.5	100	1.54	514.13
0.6	100	1.87	489.13
0.7	100	2.13	648.77
0.8	100	2.42	648.77
0.9	100	2.73	648.77
1	100	3.01	648.77
1.1	100	3.01	648.77
2	100	6.03	648.77
4	100	12.06	648.77
6	100	18.05	648.77
8	100	24	648.77
10	100	29.98	648.77

Table 2: The result of simulation with DROPTAIL Mechanism

Time Interval Traffic (S)	METRIC		
	PDF	NRL	e2n
0.01	100	0.03	265,37
0.1	100	0.03	265,37
0.2	100	0.62	387.58
0.3	100	0.62	387.58
0.4	100	0.62	387.58
0.5	100	1.54	514.13
0.6	100	1.87	489.13
0.7	100	2.13	648.77
0.8	100	2.13	648.77
0.9	100	2.73	648.77
1	100	2.73	648.77
1.1	100	3.34	648.77
2	100	3.34	648.77
4	100	12.06	648.77
6	100	12.06	648.77
8	100	24	648.77
10	100	24	648.77

The graph indicates that RED mechanism have NRL is higher then DROPTAIL mechanism. Graph for RED mechanism is indicated with Green line have more overhead then DROPTAIL (red Line). And also is indicated that this trend will increase if rate sending of packet go down (time interval for sending packet go down). Especially for DROPTAIL mechanism, at point time interval 8 s and more, NRL trend to fix.

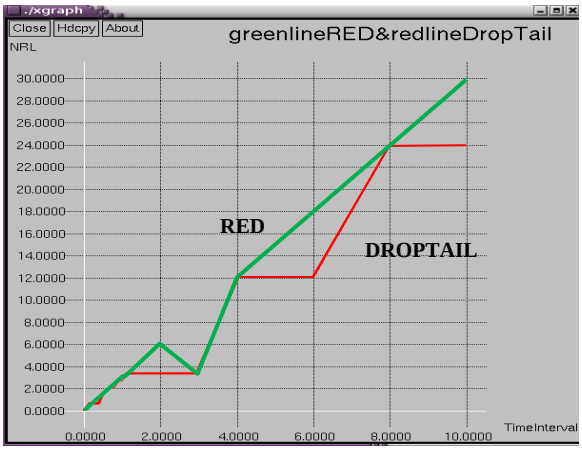

Figure 3: NRL with Time Interval Function

3.3. End-to-end delay

As well as PDF and NRL, End to End Delay for RED and DROPTAIL have different value on time interval low, but if time interval is increased, both queuing mechanism have same value. This is showed in Figure 4. These result can be explained that on Time interval 0.6 s, end to end delay have fix value because on this condition end to end has achieve maximal value. If delay more increase then packet will be discarded (drop).

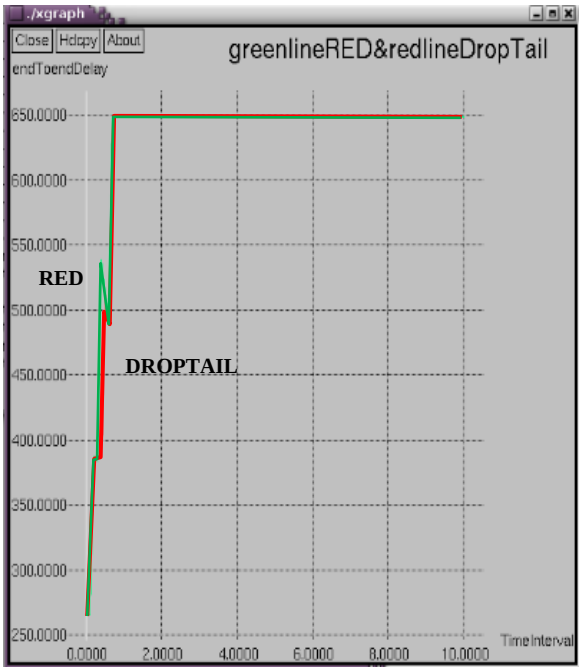

Figure 4: End to end Delay with Time interval Function

4. CONCLUSION

In terms of Normalized Routing Load, in lower time interval data rate, RED mechanism is superior than Droptail, because sending more packet will increase the packet received. On medium time interval data rate, Drop Tail mechanism is superior than RED mechanism, because there are less overhead in Drop Tail mechanism. In the occasion where time interval data rate decreased, both RED and DROPTAIL mechanisms have the different NRL trend, RED mechanisms tends to increase, while DropTail mechanism tend to have a fix NRL.

For Packet Delivery Fraction (PDF), both queue mechanism, RED and Drop Tail have 100% PDF, which indicate that all of packets have been sent, and arrived at destination. This fact indicates that both queuing mechanism do not influence PDF, because in these scenario congestion did not occur.

For end to end delay, in low time interval low, RED's delay is higher than Droptail. In higher time interval both RED and Drop Tail, resulted in similar end to end delay.

REFERENCES

[1] Ali Hamidian, Ulf Körner and Anders Nilsson, Performance of Internet Access Solutions in Mobile Ad Hoc Networks, Department of Communication Systems Lund University, Sweden.

[2] Sally Floyd and Van Jacobson, Random Early Detection Gateways for Congestion Avoidance, Lawrence Berkeley Laboratory University of California,1993.

[3] Aitan Alman, Tania Jaminez, NS Simulator for Beginer, December 2004.

[4] C. Perkins, E. M. Belding-Royer and S. Das. *"Ad hoc On-Demand Distance Vector (AODV) Routing"*. Experimental RFC 3561, 2003.

[5] D. B. Johnson, D. A. Maltz, Y. Hu and J. G. Jetcheva. "*The Dynamic Source Routing Protocol for Mobile Ad Hoc Networks (DSR)"*. Internet experimental RFC 4728, February 2007.

[6] Kenan Casey, and Philip Sitton, "*RED vs. Drop Tail. Buffer Management*", Project of Auburn University,. 2006.

[7] Hashem, E., "Analysis of random drop for gateway congestion control", *Report LCS TR-465*, Laboratory for Computer Science, MIT, Cambridge, MA, 1989, p.103.

Special Issues on Green Infrastructure
for Sustainable Development

Symposium B

PT. NUSANTARA DAYA TEKNOLOGI atau NUSANTARA TECHNOLOGIES didirikan di Jakarta oleh orang-orang yang berkomitmen untuk memajukan pendidikan dan ketrampilan khususnya kejuruan dan kampus-kampus ataupun tempat-tempat pelatihan.

Kami mendedikasikan diri dalam menyediakan jasa layanan dan peralatan praktek. Sebagai perusahaan yang relatif baru, kami memiliki fokus pada bidang pendidikan dan pelatihan:

- Biologi, Kimia dan Farmasi, Fisika,
- Kesehatan dan Kedokteran,
- Industri dan Pabrikasi,
- Komputerisasi.

Kami merupakan pemegang lisensi langsung dari beberapa produsen alat-alat peraga pendidikan dan
ketrampilan dari seluruh dunia, seperti:

- Altay Scientific
- Elettronica Veneta dari Italia
- Cusson Technology dari Inggris
- 3B Scientific dari Jerman.

Visi dan Misi

VISI dari perusahaan kami adalah menjadi partner yang terdepan dan terpercaya dalam memajukan pendidikan dan pelatihan anak bangsa.

MISI kami untuk mencapai VISI tersebut adalah:

- Kami senantiasa mengikuti dan berusaha untuk selalu mengaplikasikan teknologi terkini
- Menjadikan klien sebagai mitra bisnis dan selalu mengedepankan layanan terbaik
- Kami senantiasa memberikan edukasi kepada masyarakat dalam bidang yang sarat dengan Teknologi untuk kepentingan bersama dalam tahun-tahun mendatang



Proceeding of the 11th International Conference on QiR (Quality in Research)
Faculty of Engineering, University of Indonesia, Depok, Indonesia, 3-6 August 2009
ISSN 114-1284

Development of Railway Track Degradation Model for Maintenance Optimization on HSR

Abdur Rohim Boy Berawi[1], Raimundo Delgado[2], Rui Calçada[2], Cecilia Vale

[1]*Transportation System, Massachusetts Institute of Technology (MIT) - Portugal Program, University of Porto, Portugal, E-mail: boy_berawi@yahoo.com*

[2]*Department of Civil Engineering, Faculty of Engineering, University of Porto, Portugal*

ABSTRACT

The implementation of High Speed Railway (HSR) networks involves a large amount of financial support imposing, at the conception and design stage, a complete and rigorous estimation of the total costs involved in the lifecycle of the system. Using appropriated tools for HSR lifecycle costs (LCC) estimation, it is possible to minimize the final cost and, at the same time, to identify the most important aspects, and parameters, that influence the cost evaluation. Research is required not only on LCC modelling but also particularly on the estimation of major degradation factors and on the assessment of its impact on maintenance needs. This paper, which based on the on going doctoral research, will address these objectives by developing improved performance indicators as well as creating a system dynamic for cost effective maintenance strategies.

Keywords:
Track Degradation Model, Dynamic Analysis, Transition zones, train-track interaction, maintenance optimization

1. INTRODUCTION

In recent years, the study on the track degradation in the area of railway has attracted a great deal of attention. The intensive research activity has been carried out by many organizations with aims to secure a high level safety and reliability of the infrastructure system. New technologies and stringent safety standards thus constantly being introduced for several reasons, not only to prevent the assets from failure/damage but also to diminish the risk of loss of human life. Further to that, the other reason is to minimize the main source of problems associated to the performances degradation in terms of ride quality, comfort and etc.

Since failure on the high speed railway system can cause a significant economic losses, many railway infrastructure managers (IMs) thus spent a substantial proportion on the maintenance budget with 60 percent of the total being for track and structure maintenance [1]. Therefore, to have an optimization on track laying and track maintenance is a significant challenge for rail players around the world. The reduction on the maintenance cost would impact to the overall life cycle cost expenditure that can remain rail transport more competitive with respect to road and air transport.

One of the best way to pertain this substance would be by understanding the degradation process of the railway track. Recognizing any changes on the track condition over time and consequences maintenance actions on the track performance enable us to predict residual life time of the asset. The accurate life cycles including any maintenance activities that need to be carried out throughout useful life thus can be drawn and by doing so, the railway company could reduce the operation and maintenance expenditures in the systematic way without endangering the traffic safety.

For this reason, this research aims to develop an approach to predict track degradation in the area of railway infrastructure. The predicted model will be based on the investigation of the dynamic response generated by interaction of vehicle track coupled system and its contribution to the rate of track degradation. Since the major irregularities of the railway track has been revealed in the transition zone, therefore, the adjacent between track embankment and bridges, that represents the stiffness variability, will be served as the places of investigation. Variables that influence the rate of degradation such as traffic characteristics, track parameters and track quality will be analyzed, leading to the development of correlation between the effective parameters and the track degradation. These constructed correlations will define the most influence parameters in the global deterioration model. Furthermore the efforts also will try to identify the threshold value in the general deterioration model that should be kept the performance indicator (vibration, train acceleration etc.) in the range of safety standards, reliability and passenger comforts. This reminder of performance indicator together with predicted degradation model and any other aspect relating to the maintenance activities will be analyzed in order to develop system dynamic for cost effective maintenance.

2. TRACK DEGRADATION CONCEPT

There are many factors that are interconnected and interfaced which may influence track degradation rates. For instance, the interaction between track and train generates the effect of dynamic forces which produce the vibration at many points along the track. As the track growing older, factors such as weather, track condition and component decay rate interact with these forces lead to the track deterioration. Several parameters therefore have been identified as the main contributors on this rate of track degradation. These parameters can be categorized in three areas which are track condition quality (TQI's), traffic and maintenance [2]. Track Quality indices is defined as quantities value that describe the relative condition of the track surface geometries [3]. Sadeghi & Akbari [4] distinguished Track Quality indices to be two dependent variables; Track Geometry Index (TGI) and Track Structure Index (TSI). The TGI indicates only the geometry parameters of the track, such as profile, twist, gauge and alignment that have a direct influence on track riding comfort. This TGI is resulted from the statistical analysis of track geometry data recorded by track inspection cars. The other one, TSI expresses the structural condition of the track, which include the condition of rail, fastening system, sub-grade, and drainage systems. This index refers directly to the actual condition of the track and indicates the track's potential for degradation.

Ferreira and Murray [5] split traffic related deterioration factors into three groups; dynamic effects, speeds and loads. The dynamic effects vary with the type of traffic on the track. Accelerations, retardations, lateral forces in curves, vibrations, and the condition of the rolling stock are examples of factors that affect the track bed. The dynamic forces contribute to the deterioration process as the speed increase while the rates of degradation decrease at low speed. When the train passing along the track, loads give rise to rail wear and fatigue, wheel wear, and increase the strain in rails and sleepers. As a consequence, cracks in the rail appear, the railhead is worn out, sleepers crack, rail fastenings loosen, ballast is redistributed leading to reductions in travel comfort, reduced speeds, increased energy and fuel consumption, higher risks for derailment and delays, and increased needs for maintenance.

The last parameter, maintenance action which involved tamping, grinding, ballast cleaning, lubrication etc, are influencing the quality condition of the track. For instance when the tamping action is performed, the ballast under the ties is re-compacted to provide the proper load bearing. The ties thus distributes the weight of the rail and rolling stock, and keep the track properly aligned, that in turn impede the acceleration of rail degradation rate. As well as tamping, preventive grinding also leads to a significant increase in the service life of rails, slow down the growth of rail corrugation and decrease the traffic noise [6].

3. TRACK SETTLEMENT

Trains, subject to the track structure, are repeated its' loading and unloading as they pass [7]. When the track is in loading cycle, especially to high frequency load variations, the ballast and the layers below can undergo a non elastic displacement. When unloading take a place, the initial geometry does not return exactly and leave a small residual displacement. After several cycles, different parts of the track will accumulate these small settlement lead to a modification of the geometry of the track.

There are two major phases occurs in track settlement. First, its occurred directly after a major maintenance action of the ballast. In this phase, the settlement is relatively fast until the ballast is well compacted and density of the ballast particles is increased. The second phase, the settlement is slower and increases regularly with the number of cycles. In this phase, the settlement mainly governed by several mechanism of ballast and sub-grade behavior for instance continued volume reduction due to the particle rearrangement, sub-ballast or sub-grade penetration into ballast voids, and volume reduction caused by particle breakdown and abrasive wear [8].

The study of track degradation process due to the dynamic load resulted in different track degradation models. Some reviews of them include the modeling of train track interaction are given in Lundqvist and Dahlberg [9], Ishida et al. [10], Iwnicki et al. [11]. However only few papers in this respect modeling the track settlement in transition zone, the places where the stiffness changes are revealed. Therefore, it is important to have a further insights on the mechanism of track deterioration and predict track settlement particularly in the adjacent between two different zones in order to optimize the maintenance decision that respected to the structural safety, track safety and passenger comfort. Beside of this, the improvement of computer capacity and use of numerical methods have made it possible to make more detailed models of train track structure and more reliable prediction on the track settlement.

Thus, there are three main aspects that have been considered important as this research objectives, namely:

A. Identifying the key influencing parameters that may have a great impact on the railway track degradation model.
B. Developing the track degradation model due to the dynamic load in the transition zone
C. Optimizing the way of maintenance strategies (in economical and /or technical way) by developing the system dynamic for cost effective maintenance that leading on the reduction of Life Cycle Cost (LCC).

4. METHODOLOGY

A combination between statistical and engineering approach are adapted for this research equipped by comprehensive track field data with measurement made on the track Porto-Lisboa railway line during the last nine years. The engineering approach consists of establishing the mechanical properties of the entire element that make up the track and the railroads vehicles. By doing so, the appropriate methods of modeling and numerical analysis can be developed to determine the dynamic load that the vehicle will impose on the track as function of train characteristic and track profile. Further to that, the predicted track settlement in the transition zones caused by this load also can be determined. The advantage of this approach is that it gains a deeper insight to understand the interaction between vehicle and track and identify the role of each track and train parameter to the rate of track degradation. The statistical approach involves the analysis of many observations of actual track performance and the corresponding causal parameter. This analysis is used to calibrate the adopted methodologies in engineering analysis by comparing analytical solution with the results presented in the case study. Finally the creation of system dynamic for cost effective maintenance strategies will be carried out in order to find a balance between the maintenance cost (inspection, tamping, grinding activities) on one hand and the consequential cost of failed operation on the other.
With the result of the predicted track degradation model, a general degradation curve will be formed that can be used to optimize the maintenance decisions.

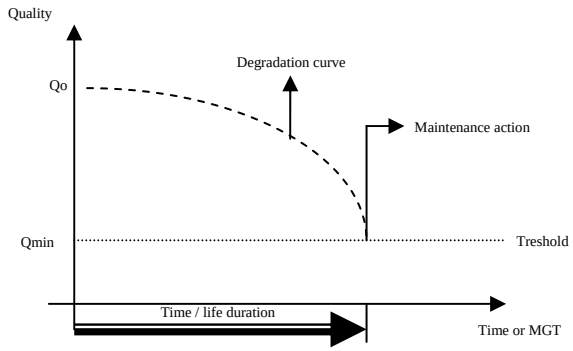

Fig. 1 : Diagram showing general degradation curve

The railway track has initial value or track settlement Qo. During the train operation it degrades/settles because the cumulative of the track loads. If the minimum quality (Qmin) or an intervention level is almost reached, maintenance action (tamping) are carried out.

5. DISCUSSION

In order to quantify the track condition in numerical value, the terms of Track Quality Indices (TQI) is used [12]. This index is defined as a function of one or more of the main geometry parameters such as profile, alignment, gauge, and cant that is obtained from automated geometry vehicles. Profile and alignment are delineated with the track geometry of each rail projected onto the longitudinal vertical and horizontal plane respectively. Gauge is defined as a range between two rails measured at 16 mm below the top surface of the railhead. Cant is used as indicator deviation between the top surfaces of two rail at a given location [13].

By assessing the track condition using TQI formula applied in various countries, the results of trend degradation model on the particular segments of North Line of Portuguese Railways are shown in the following figures. As it can be seen, the trend of degradation is varied between different models. Based on the Five Parameter defectiveness (W5) graphic, the tendency of degradation is quite different with figures presented in J track quality indices (J-coefficient) and Track Geometry Indices (TGI). However, the trend of degradation illustrated in both J-coeff. and TGI even are not totally same but expressed the similar characteristic. This differentiation has been caused due to each of the model employs different weighted values for its particular geometry variables. The other reason is the difference of mid chord measurement that has been conducted by various railway companies to measure the deflection of geometry parameter, for instance the mid chord measurement that has been used by Indian Railway company (TGI) is different with others.

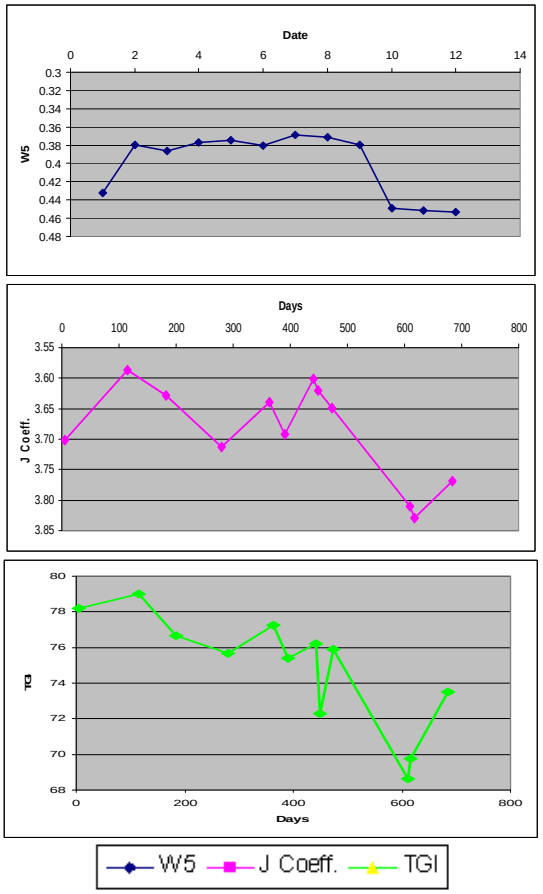

Thus, there are some research priorities that have been revealed concerning this track degradation model:

1. The best track quality indices that represented the true condition of railway track.
2. Mechanism of transmitting these track geometry indices to a value that could assess degradation in terms of track settlement.
3. The level of importance of each particular effective parameters contributing to degradation rates.
4. The minimum quality (threshold value) that should be kept the railway track in the range of safety standards, reliability and passenger comforts, and
5. A mechanism to develop a predicted degradation model and methodology for using it in order to optimizing the maintenance decision.

6. CONCLUSION

This research aims to develop new lifecycle costing models and infrastructure and risk management programs to effectively derive design and maintenance strategies for high-speed rail infrastructures and operations. Some of the future agendas would be developing a Maintenance Management System adapted to HSR and integrating the necessary information from track state, from behaviour models for the life cycle, and from the organization as an active part of the process and assessing the impact on LCC of different design and maintenance strategies for high-speed and very high-speed lines in different operational scenarios.

ACKNOWLEDGMENT

The authors gratefully acknowledge the support given to this project by the " FCT- Fundação para a Ciência e a Tecnologia.

REFERENCES

[1] Nigel Ogilvie, 1999. An A-Z of Reducing Track Maintenance Costs. International Railway Journal.
[2] Iran Ministry of Roads and Transportation (IMRT), 2005. Railway track superstructure general technical specification Standard no. 301. Iran: IMRT Ministry Publication Service, 9-12.
[3] El Sibaie, M and Zhang, Y.J., 2004, Objective Track Quality Indices. 83 TRB Annual Meeting, Washingon DC.
[4] Sadeghi, J. & Akbari, B., (2008)" Development of an improved track geometry indices, Transportation Transaction, Journal of American Society of Civil Engineers (ASCE), Special Edition on Railway, Accepted , in press.
[5] Ferreira, Luis and Murray, Martin H., 1997. Modelling rail track deterioration and maintenance: current practices and future needs**.** Transport Reviews, 17(3). 207 -221.
[6] Van den Bosch, R:A., 2002. Rail Grinding strategies on Netherland Railways, Rail Engineering International, Number 1, pp 8-9.
[7] Lyngby, N., Hokstad, P., and Vatn, J.,2008. RAMS Management of Railway Track. In Misra, K.B. (ed.): Handbook of Performability Engineering. Springer Verlag, ISBN 9781848001305, pp. 1123-1145.
[8] Andrade A.R., 2008. Renewal decision from a Life Cycle Cost (LCC) perspective in Railway Infrastructure : An integrative approach using separate LCC models for rail and ballast components. MSc. Thesis, Civil Engineering Department, Instituto Superiore Tecnico, Portugal
[9] Lundqvist, A. and Dahlberg, T., 2003. Dynamic Train/track interaction including model for track settlement evolvement. Proceedings 18th IAVSD Symposium at Atsugi, Japan, August 24-29, 2003. Vehicle System Dynamics, Vol. 41(Supplement) 2004, 667-676.
[10] Ishida, M., Namura, A and Suzuki, T., 2003. Prediction model of track settlement based on dynamic simulation, Proc. International symposium on speed up and service technology for railway and maglev systems, Tokyo Japan.
[11] Iwnicki S, Grassie S, Kik W., 2000. Track settlement prediction using computer simulation, Vehicle System Dynamics, vol 33, p37-46, Swets & Zeitlinger, Netherlands
[12] Fazio, A.E. and J.L. Corbin, 1986. Track Quality Index for High Speed Track. Journal of Transportation Engineering, Vol 112. No.**I** (American Society of Civil Engineers), pp 46-61.
[13] Sadeghi, J., Fathali, M., and Boloukin, N., 2009. Development of a new track geometry assessment technique incorporating rail cant factor. Proceedings of the institution of Mechanical Engineers, Part F: Journal of Rail and Rapid transit, Vol 223, No. 3, pp 255-263.

ISSN 114-1284

Sustainable Housing Practices in Malaysian Housing Development: Towards Establishing Sustainability Index

Abu Hassan Abu Bakar,PhD[1], **Khor Soo Cheen[2] and Rahmawaty[3]**

School of Housing, Building and Planning
Universiti Sains Malaysia
[1]abhassan@usm.my, [2]s_cheenk@hotmail.com, [3]wawa_archies@yahoo.com

ABSTRACT

This paper presents a study on various sustainable rating systems on sustainable housing that had been developed by various countries around the world. The objective of this study is to develop a framework for a rating system for housing development for Malaysia by taking into account the local requirement. There are numerous sustainable rating systems on building and group of buildings being developed in the built environment around the world. Rating tools like CASBEE, LEED, BREEAM, GB Tool, Green Star to name a few, have great influence over the development of other rating tools over the world. Malaysia too has recently launched a rating system for buildings called Green Building Index (GBI). However, Malaysia is yet to introduce a rating system for measuring the sustainable practices in housing development. Hence, this paper reviews some key available tools that related to the rating of housing developments for the purpose of developing one for Malaysia. Some important factors used for developing a tool for measuring sustainability practices should include sustainability criteria that are related to environment, society, economics, site/land use, communication, transportation and many more. An index for measuring sustainability in housing development will be developed to suit the local context. The formulated index will take into consideration the parameters in sustainable housing developed by various systems around the world. The index that called A Comprehensive Assessment System for Sustainable Housing will be available for further testing.

Keywords: *Sustainable Housing Development, Urban Development, Building (Housing), Sustainability Index, Malaysia.*

1.0 Introduction

Nowadays, sustainable development is a common goal of many worldwide urban (re)development policies (Shutkin, 2000; Berke, 2002; Chan and Lee, 2006). The development of housing sector also include in the policies of urban development. There are many housing schemes have been developed in Malaysia since housing is prerequisite for human habitat settlements. Housing is also a major concern for all people in every corner of the world. In the present context, housing is developing in line with the goals of Habitat Agenda as well as the principles of Agenda 21 which is a blueprint for sustainable development in the 21st Century adopted by 179 nations including Malaysia in Rio de Janeiro in June 1992. (Tosics, 2004) stated that housing is one of the most important public policies affecting urban development and, as such, it has significant potential to contribute to sustainability. Various aspects of housing construction, design, use and demolition can have significant impacts on the environment (Huby, 1998)

According to Islam (1996), the well accepted definition of sustainability was defined by the World Commission on Environment and Development. It is conceived as development "which meets the need of the present without compromising the ability of future generations to meet their needs" (WCED; 1987). This concept must recognize as a safe, secure and universally designed (A Sustainable Housing Forum Report, 2003).

Sustainable development is essential for human settlement development and gives full consideration to the needs of achieving economic growth, social development and environment protection. It is increasingly linked with the concept of quality of life, well being and livability (Moore and Scoott, 2005). It also a dynamic process in which communities participate and accommodate the needs of current and future generations in ways that reproduce and balance local social, economic, and ecological systems and link local action to global concern (Berke and Conroy, 2000). Being sustainable is as much about efficient profit-oriented practice and value for money as it is about helping the environment (BRE Report, 2002)

Sustainable development is unattainable without sustainable building and housing. Chougill (1994) stated that the sustainable housing may be understood in terms of ecological sustainability, economic sustainability, technological sustainability, cultural sustainability and social sustainability. According to Edwards and Turrent (2000) housing is sustainable if everyone has the opportunity of access to a home that is decent; if it promotes social cohesion, well-being and self-dependence.

The aim of this research is to develop a guideline for assessing the residential development in respect to sustainable housing concept for improving the level of sustainable practices in housing development. The formula of sustainability index in housing development will be developed based from the critical factors to the success of

ISSN 114-1284

a sustainable building / housing and the rating system that apply in Japan, United Stated, United Kingdom and else available in others country.

Sustainable housing development should measure the area development within sustainability criteria namely as environmental, society, economics, site/ land uses and facilities of communication and transportation and include the assessment of building forms particularly for housing performance. Therefore, it is possible using two tools separately, independent of the two tools but in simultaneous assessments of the project with the same purpose. For example in Asia, Japan had designed standards and guidelines for sustainable building and urbanization sustainability; it is called as Comprehensive Assessment System for Building Environmental Efficiency (CASBEE for an Urban Area+ Building). These system tools refer to CASBEE for Urban Development and CASBEE for building scale. In the United Stated, a rating system called LEED (Leadership in Energy and Environmental Design) for Neighborhood Development Rating System has been developed. This system is used to evaluate the urban development for sustainability with integrated LEED for building scale assessment system for sustainable building.

1.1 Statement of Problem:

The issues of sustainable housing are still new and still unfamiliar to the public in Malaysia. According to Mohd Jasan (2004) the houses being built in the past decade was not meeting the essential criteria of sustainability and the problem detailed out as follow:

a) The building design do not takes into account of energy efficiency and building green with affordable housing. As building green housing will require specialize design of the building such as materials used either in construction work progress or for building installation purpose, structure of the building and the calculation of energy use of the building. To build the green houses, we need to employ building related professionals with 'extensive residential construction experience, drafting experience, building science backgrounds, indoor air quality investigation training, mechanical ventilation training and much more' (Kibert C., 2005). The problem is we are lack of the green house expertise builders or consultancies in Malaysia.
b) The sustainability of housing development will give greater emphasis on environmental, economic and social issues. The building itself will incur variety of environmental problems such as greenhouse gas emission. The implication of construction activities do cause environmental pollution, mainly because of 'the materials used, nature of design, methods of construction, locations and layout, physical structure and the use to which buildings are put', Ramachandran (1990).
c) The awareness of our public on the important of sustainable housing concept is obscurity. This may result in the difficulty to achieve the objectives of the projects if without the public participation and cooperative in the whole process as they are the end users of the products.
d) The objective of sustainable housing is to make the projects more valuable. With reducing the criteria of building usage such as energy consumption, water and materials used, life cycle cost plus decreasing in the accidents occurrence on sites will improve the quality of life, productivity and user accessibility.
e) The countries of North America, Europe and developed country in Asia do practice the sustainable building with establishment of sustainable rating systems for evaluating each phase of building work of the project. Malaysia does implement the tasks of Agenda 21 as an effort with respond to the sustainable development; however, Malaysia is yet to practice the sustainable building construction, particularly for *residential building*. Recently a green rating tool called the Green Building Index (GBI) of residential was developed, however is yet to be launched.
f) Furthermore, the development of housing sector or housing schemes development, do cover groups of buildings. Not only the building itself but also the whole housing scheme will affect the environmental performance. CASBEE for Urban Development has formulated a tool for this purposed. However, Malaysia is yet to introduce the tool for rating the practice of the sustainable housing development in both urban and suburban.

1.2 Objectives:

The objectives of this paper are as follows:

1. To develop a framework for a comprehensive assessment system for sustainable housing.
2. To identify factors affecting sustainability performance in Housing Development.
3. To formulate a Comprehensive Assessment System for Sustainable Housing (CASSH) for Malaysia.

2.0 The Existing Sustainability Assessment Systems around the World.

Recently, Malaysia has published its own first edition (version 1.0) of Green Building Index (GBI) Assessment Criteria for Non-Residential which measures new building construction since April 2009. The outline for key components of the Green Building Index (GBI) for Residential purpose is yet to be published. The intention of the GBI for Residential is to assess the building and its external area. This system is similar to that of the BREEAM for EcoHomes in the U.K., the LEED for Homes in the U.S., and the CASBEE for Home (detached houses) in Japan, Green Star for Multi-Unit Residential in

Australia and Green Mark for Residential Building in Singapore

This research is conducted with the objectives to establish a sustainability index for rating the housing development in Malaysia. A model for rating the housing development in Malaysia will be established. It will cover a wider scope covering a group of buildings which is similar to that of the assessment of urban development that in practiced in other countries such as Japan (CASBEE for Urban Development) and the U.S. (LEED for Neighbourhood Rating System).

2.1 The currently available building assessment tools around the world

There are several systems for evaluating environmental performance of buildings being developed and established currently. The growth and the use of buildings' environmental performance assessment methods has given great contributions to the building sustainability practices in various stages of building performance. The assessment tools that had been developed worldwide built upon the different evaluation criteria that were based on conditions to suit the countries' own characteristics. The objectives of the tools are to measure the practice of the sustainable building towards realization of sustainable development worldwide. Followings are some of the key assessment systems for buildings developed by various countries around the world such as shown in table 2.0.

Table 2.0: The building assessment tools from various worlds

NO:	Tool name	Country	Year
1	BREEAM	UK	1990
2	GB Tool	International	1998
3	LEED	US	1998
4	CASBEE	Japan	2004
5	HQE	France	1996
6	VERDE	Spain	n/a
7	Green Star	Australia	n/a
8	Green Mark	Singapore	2005
9	Green Building Index	Malaysia	2009
10	BEPAC	Canada	1993
11	Green Globes	US	2004
12	GEM	UK	2003
13	Go Green	Canada	2004
14	HQAL	Japan	2001
15	NABERS	Australia	n/a
16	HK-BEAM	Hong Kong	1996
17	EEWH	Taiwan	1999
18	Green Star SA	South Africa	2008
19	LEED-India	India	2008
20	Green Star NZ	New Zealand	2007
21	FGBC	Florida, US	2002
22	NAHB	US	2005
23	DDC	US	1999
24	Austin Green Building Program	US	1992
25	Colorado Built Green Housing	US	1995
26	EarthCraft House	US	1999
27	Built Green Alberta	US	2001
28	Green Communities	US	2005
29	Minnesota GreenStar	US	2007
30	AccuRATE	Australia	2007
31	ARE Scorecard	Australia	2003
32	BASIX	Australia	2004
33	EnviroDevelopment	Australia	2006
34	Docklands ESD Guide	Australia	2005
35	First Rate	Australia	2008
36	SDS	Australia	1999
37	PassivHaus	Germany	1991
38	The Code for Sustainable Homes	UK	2006
39	BEAT	Denmark	2001
40	EcoCalculator	Canada	2007
41	BEES	US	2007
42	Living Building Challege	US	2007
43	LiderA	Portugal	2005
44	LEED-Brazil	Brazil	2008
45	GOBAS	China	2008
46	DGNB	Germany	2008
47	TeriGriha	India	2008
48	Protocollo Itaca	Italy	2004
49	Leed Mexico	Mexico,US	n/a
50	AQUA	Brazil	n/a

Table 2.1 shows the Primary issues of concern identified in each building assessment tool for various countries around the world. Some key issues were identified as among the most popularly used by these assessment tools are site, indoor environment, energy, material resources and water. Below are summaries of some of the systems that being implemented in various countries.

ISSN 114-1284

1) The BREEAM Method
The BREEAM method is an environmental assessment method developed by the BRE Ltd (Building Research Establishment Limited), in England. It evaluates the environmental performance of buildings in both the design phase as well as the existing buildings in the UK. It is separated according to the building type to BREEAM for offices, Ecohomes, BREEAM retail, industrial BREEAM, BREEAM schools and health buildings. Credits are awarded to each issue according to their performance and are then added together to produce a single overall score. The building is rated on a scale of pass, good, very good or excellent. The method is not available to the public and it involves the participation of the company and the licensed assessors.

2) The GBTool Method
The GBTool is a software system for assessing the environmental and sustainability performance of buildings. It is an implementation of the green building challenge (GBC) assessment method that has been under development since 1996 by a group of more than a dozen teams. The GBC process was launched by Natural Resources Canada, but responsibility was handed over to the International Initiative for a Sustainable Built Environment (IISBE) in 2002.

The method comprises two parts, Module A which includes benchmarks and weights, Module B which results to the sustainability performance of the building. The assessment can be carried out at various phases of the life cycle of a project. The system carries a wide range of issues related to sustainable design. Four phases are included in the tool: pre-design, design, construction and operations. A scale ranging from -1 to +5 is used to express the evaluation in any case. The scale is interpreted as 1 negative performance, 0 minimum acceptable performance (usually but not always defined by regulation), three good practice and five best practice.

3) The LEED Method
The LEED system, developed by the US Green Building Council, is a national standard for developing sustainable buildings. LEED applies to new commercial construction and major renovation projects (LEED-NC), existing buildings operations (LEED-EB), commercial interiors projects (LEED-CI), core and shell projects (LEED-CS), homes (LEED-H) and neighbourhood development (LEED-ND). A number of parameters are evaluated and result to a score, which gives a certification of certified, silver, gold and platinum construction.
The LEED method involves several parties along the process of the evaluation and certification. The verification process consists of four phases, namely inspection, performance testing, rating and certification. In all the phases, the participating of the provider is mandatory.

4) The CASBEE Method
CASBEE is a Japanese environmental labeling method for buildings, based on assessment of their environmental performance. CASBEE is developed based on three major concepts. Firstly, it is designed for the assessment of buildings which corresponds to their lifecycle. Secondly, it is based on a concept that early distinguishes environmental load (L) and quality of building performance (Q) as the major assessment targets. Thirdly, it introduces a new indicator, namely BEE (building environmental efficiency) based on the concept of eco-efficiency. BEE is defined as Q/L to indicate the overall result of environmental assessment of buildings.
CASBEE can be applied to both private and public buildings, which are broadly divided into residential and non-residential and further into building types. The tool comprises of a set of four basic assessment tools, namely CASBEE for pre-design (CASBEE-PD), CASBEE for new construction (2004) (CASBEE-NC), CASBEE for existing buildings (CASBEE-EB) and CASBEE for renovation (CASBEE-RN), which correspond to the individual stages of the building's lifecycle. The tool has introduced a labeling classification of five areas, where class C is regarded as poor in terms of sustainability, class B + , class B - , class A, are regarded as average and class S as excellent.

5) The HQE® method
The HQE® (High Quality Environment) project methodology was developed in France and presents a mostly open character. It integrates a great number of parameters, requires a mode of management of the operations inspired by the international standard ISO 14001, and consists of a project methodology instead of a simple ex-post certification like the majority of the other existing methods. Launched in 1996, the HQE® programme enables developers and project owners to adopt construction options appropriate to sustainable development at all stages of a building's life cycle (manufacture, construction, use, maintenance, conversion and end of life). The HQE Association defined 14 targets specifying the particular environmental requirements that a building, whether new or rehabilitated, must satisfy. The method is applicable in all phases of design. The Environmental management system (EMS) is needed to implement the HQE® method. In fact, most of the builders in France refer to a general declaration without an operative EMS. Few of them are developing a specific approach based on an environmental policy, objectives and targets, requirements and evaluation.

6) Green Building Index
Green Building Index (GBI) is developed by Pertubuhan Akitek Malaysia (PAM) and the Association of Consulting Engineers Malaysia (ACEM). It is a profession driven initiative to lead the property industry towards becoming more environment-friendly. The rating system gives opportunity for developers and building owners to design and construct green, buildings that can provide energy and water savings, a healthier indoor environment, better

connectivity to public transport and the adoption of recycling and greenery for their projects. Buildings are awarded GBI Malaysia Platinum, Gold, Silver or Certified ratings depending on the scores achieved.

Table 2.1 Primary issues of concern identified in each building assessment tool

Assessment Tools	1	2	3	4	5	6	7	8	9	10	11	12	13	14	15
BREEAM	x		x	x	x	X	x								
GBTool	x	X	x	x	x			x	x				x		x
LEED	x	X	x	x	x									X	
CASBEE	x	X	x	x	x					x		x			
HQE	x	X	x	x	x		x			x	x		x		
GBI	x	X	x	x	x	X	x				x				

(Sources: *An International Journal of Management of Environmental Quality: with title 'Present and Future of Building Performance Assessment Tool)*

Notes: 1.Site, 2. Indoor Environment, 3. Energy 4. Material Resources, 5. Water, 6. Transport, 7. Health 8. Social, 9. Economy 10. Comfort 11. Management, 12. Services, 13. Long term performance, 14. Design aesthetics, 15. Functionality.

2.2 The available assessment tools for sustainable urban/ neighborhood development

Several environmental assessment tools for evaluating environmental performance on development of the designated areas are being developed and established currently. The main purpose of establishing these assessment tools is to improve the environmental performance in developed area. It measures the environmental design in multi-angles that are possibly contributed by a group of buildings. Nevertheless, the sustainable urban assessment tool includes the measurement in term of economic and social sustainability level in the development of designated area (housing sector). These assessment tools are built upon different evaluation criteria which based on the countries' conditions to suit the local contents. Followings are some of the key assessment systems developed by various countries around the world such as shown in table 2.2:

Table 2.2: Assessment Tools for Sustainable Urban/ Neighborhood Development in Various Countries

No.	System Name	Country	Year
1	CASBEE for Urban Development	Japan	2007
2	LEED for neighborhood Development	US	2008
3	RHSI (Rural Housing Sustainability Index)	Ireland	2004
4	FGBC-Green Development	Florida, US	2009
5	DDC-Sustainable Urban Site Design	New York, US	2008
6	ACI - Adriatic Common Indicators	Greece, Italy, Slovenia, Other	2004
7	ACTEUR - Analyse Concerté des Transformations et des Equilibres URbains	France	2004
8	Baden-Württemberg-Indicators in the framework of the Local Agenda 21	Germany	2004
9	Catania - State of the Environment Report	Italy	2004
10	Cercle Indicateurs (CI)	Swiss	2004
11	CEROI - Cities Environmental Reporting on the Internet Indicator Database	Czech Republic, Finland, Others	2004
12	Cities21® Assessing Mutual Progress Toward Sustainable Development	Czech Republic, Finland, Latvia, Poland, Others14	2004
13	Core Indicator System of the cities Basel and Zürich	Basle, Zurich	2004
14	Czech Republic - Environmental indicator	Czech Republic	2004
15	Czech Republic - Transport Yearbook 2002	Czech Republic	2004
16	Denmark National Strategy for Sustainable Development	Denmark	2004
17	Nature Balance	The Netherlands	2004
18	EcoBUDGET	Germany, Greece, Italy, Sweden, United Kingdom	2004
19	Ecosistema Urbano	Italy	2004
20	EEA - Core set of environmental indicators	Europe	2004
21	EEA - Environmental Indicators	Europe	2004
22	The Integrated Regional Framework for the North East	North East	2004
23	Environment Explorer Amsterdam	The Netherlands	2004
24	Trends and Indicators for Monitoring the EU Thematic Strategy on Sustainable (TISSUE)	Finland, the Netherlands, UK, France, Italy, Switzerland, Czech Republic	2004
25	SUDEN (Sustainable Urban Development European Network)	France, Italy, Denmark, Romania, Belgium, Poland	2004
26	Indicators for Sustainable Development in Scotland	Scotland	2004
27	Indicators For The Sustainable Development In The Mediterranean Region – ISD	Mediterranean area	2004
28	Quality of Life indicators	United Kingdom	2004

1) CASBEE for Urban Development

Initially, CASBEE is a Japanese environmental labeling method for evaluating and rating the environmental performance of individual buildings. In year 2007, CASBEE has developed another tool which called CASBEE for Urban Development where the assessment tool covers groups of buildings (urban scale) in a designated area. When a project is planned and implemented that comprises multiple buildings and other elements on a single, large-scale site under a unified design concept, assessment can go beyond the environmental design of each building. It also covers identification of new or expanded environmental measures, and their effects, that are made possible by the building group, and thereby contribute to the comprehensive improvement of environmental performance in urban renewal.

Urban Scale

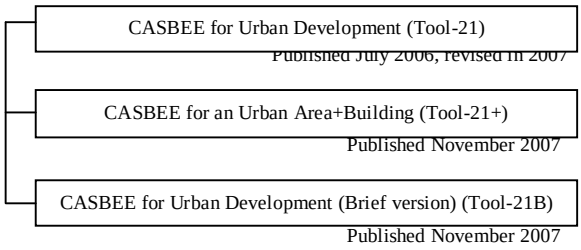

Figure 2.0 The CASBEE expanded tools for specific purposes

(Sources: CASBEE for Urban Development, Technical Manual 2007 Edition)

According to CASBEE for Urban Development, the center of the assessment designation is not the building but the space that surrounds the group of buildings. A hypothetical boundary is set around the area development project to be evaluated. The assessment then addresses both the environmental quality within the boundary and environmental load beyond the boundary. The assessment of buildings themselves is covered by CASBEE (building scale) and is not covered by CASBEE for Urban Development. The figure 2.1 below shows the basic concept of the hypothetical boundary.

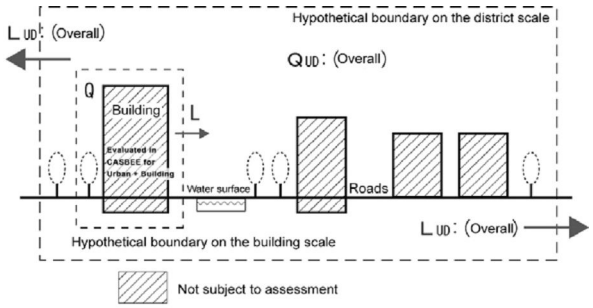

Figure 2.1 Concept of Assessment subjects for CASBEE for Urban Development.

(Sources: CASBEE for Urban Development, Technical Manual 2007 Edition).

Under the CASBEE methodology, which evaluates both environmental quality (Q) within the hypothetical boundary and the environmental load (L) acting outside the boundary, the site boundary is the same as the hypothetical boundary on the building scale. That leads to the approach that "space inside the site" is the environment as a private property under the control of the building owner, designer and the other parties involved in the building, while "space outside the site" is a public property (the public environment), which the building owner cannot control but should consider.

In the same way as the CASBEE (building scale), both Q (environmental quality) and L (outdoor environmental load) are evaluated and scored separately. Q_{UD} (environmental quality in urban development and L_{UD} (outdoor environmental loads in urban development) each comprises three main categories. Table 2.3 below shows the composition of assessment items for both Q (environmental quality) and L (outdoor environmental load).

Table 2.3 Composition of assessment items

Assessment field	Medium-level	Minor category
$Q_{UD}1$ Natural environment (microclimates and ecosystems)	5	17
$Q_{UD}2$ Service functions for the designated area	6	11
$Q_{UD}3$ Contribution to the local community (history, culture, scenery and revitalization)	4	6
$LR_{UD}1$ Environmental impact on microclimates, facade and landscape	6	16
$LR_{UD}2$ Social infrastructure	6	14
$LR_{UD}3$ Management of the local environment	4	13

(Sources: CASBEE for Urban Development, Technical Manual 2007 Edition)

The major categories from $Q_{UD}1$ to $LR_{UD}3$ each comprise 4-6 medium-level categories, and each medium-level category is further divided into minor categories. Each minor category is scored on five levels, according predetermined criteria, and weighting coefficients are applied between assessment fields to calculate the results The tools has introduced a labeling classification of five areas, where class C is regarded as poor in terms of sustainability, class B-, class B+, class A are regarded as Average and class S as excellent.

Table 2.4 The correspondence between ranks based on BEE values and assessments.

Ranks	Assessment	BEE value, etc.	Expressions
S	Excellent	BEE=3.0 or more, Q=50 or more	★★★★★
A	Very Good	BEE=1.5~3.0	★★★★
B+	Good	BEE=1.0~1.5	★★★
B-	Fairly Poor	BEE=0.5~1.0	★★
C	Poor	BEE=less than 0.5	★

(Sources: CASBEE for Urban Development, Technical Manual 2007 Edition)

The assessment procedures are using both of the system tools; there are CASBEE for Urban Development and CASBEE (building scale) to evaluate the target project. While evaluating the building scale with multiple designated buildings, recording the assessment results (point scores) for each building under "Assessment of

ISSN 114-1284

multi-use buildings" using CASBEE for New Construction, then take a weighted average according to the ratio of their floor areas.

2) LEED for Neighbourhood Development

LEED for Neighborhood Development (LEED-ND) is a rating system that integrates the principles of smart growth, new urbanism, and green building into the first national standard for neighborhood design. LEED-ND recognizes development projects that successfully protect and enhance the overall health, natural environment, and quality of life of our communities. Points are available within the LEED for Neighborhood Development rating system for including LEED Certified buildings and for integrating green building practices within the buildings on the project site. These credits relate to energy efficiency, reduced water use, building reuse, recycled materials, and heat island reduction.

According to LEED for Neighborhood Development is a rating system that integrates the principles of smart growth, new urbanism, and green building into the first national standard for neighborhood design. It is being developed by USGBC in partnership with the Congress for the New Urbanism (CNU) and the Natural Resources Defense Council (NRDC).

The rating system encourages smart growth and new urbanizes best practices, promoting the location and design of neighborhoods that reduce vehicle travel that provides work places and public services which are accessible in a walking distance. It promotes more efficient energy and reduced the use of water which is important in urban areas where infrastructure is often overloaded.

Credits are given in the LEED for Neighborhood Development rating system and labeled the LEED Certified buildings for integrating green building practices within the buildings on the project site. These credits relate to energy efficiency, reduced water use, building reuse, recycled materials, and heat island reduction."

Table 2.5 Composition of assessment items

Assessment Field	Prerequisite Assessment	Measurement Criteria Credit (Medium-level)
Smart Location & Linkage (SLL)	6	9
Neighborhood Pattern & Design (NPD)	3	15
Green Infrastructure & Building (GIB)	3	16
Innovation & Design Process (IDP)	NIL	3

(Source: LEED for Neighborhood Development Rating System)

Table 2.5 shows the LEED-ND that comprises four major categories of the assessment field. Each of the main categories has medium level assessment criteria, which the composition distinguished into prerequisite measurement and normal credit measurement in respectively. For the medium–level of prerequisite assessment of each classification comprises a minimum of three to six categories. Then the normal credit measurement can be comprised as maximum as 16 categories.

3) Ireland- A rural housing sustainability index (RHSI)

The rural housing sustainability index is developed by the Minister of the Environment, Heritage and Local Government of Ireland. While the objective of the rural housing sustainability index is to ensure that better-quality and more sustainable housing is constructed in rural areas, while also minimizing the effect of such housing on the rural environment. The index uses 70 criteria or indicators categorized into site, design, construction and social indicators. A score is allocated for each indicator with higher scores allocated for more sustainable actions or options. Threshold scores are set for each category from which the sustainability of the proposed development is determined. This allows planners to more accurately assess the impact of rural development as well as increasing the sustainability of the housing stock. The concept of a trade-off, by allowing more sustainable and sensitive housing in areas where normal housing is inappropriate, is explored.

A detailed list of potential indicators was drawn up from the existing literature and subsequently categorized under four broad groupings, there are: site or environmental indicators, design indicators, building or construction indicators, and finally, social indicators. Thus, as a result the sustainability index is established by comprise 70 indicators of the total of four broad groupings. The criteria used in the selection of sustainability indicators including: policy relevance, simplicity, validity, affordable data, reality, adequate scope and openness. Indicators selected for inclusion in the index had to be policy relevant and satisfy as many of the remaining criteria as possible. The composition of four categorizes of assessment criteria was shown as table 2.6 below:

Table 2.6: Composition of assessment criteria

Assessment Indicator	The quantity of assessment criteria in per categorize
Site (environment)	39
Design	35
Building (construction)	21
Social	13

(Source: A rural housing sustainability index)

4) FGBC-Green Development

The synopsis of the FGBC with stand for Florida Green Building Coalition organization had briefly depicted at the section 2.1 for building assessment tools which currently available around the world. The many resources had offered by the FGBC for green building standards of the certification programs and five in total. Except the developed programs for building's certification, FGBC do develop the assessment program for green development in the designated area, and the certification program is called Green Development Designation Standard Reference Guide.

ISSN 114-1284

The purpose of Green Development Reference Guide is to serve two purposes: to provide information on green development practices and to provide details on how to earn points for complying with the Florida Green Development Designation Standard. The standard requires substantial environmental stewardship beyond typical practice, yet it allows for developers to choose how to meet the standard from a variety of methods. There are enough items to choose from that every developer, through planning and dedication to green development should be able to comply with the standard. This level of planning can only be done through knowledge of the site as well as applying best management practices regarding wildlife preservation, stormwater, transportation, landscaping, and utilities.

The standard was developed by the Florida Green Development Working Committee of the Florida Green Building Coalition, Inc. The committee had active participation from one or more architects, builders, consultants, developers, ecologists, educators, energy raters, government agencies, landscape architects, planners, Realtors, researchers, and water-management district personnel. A number of parameters are evaluated and result to a score, then give the certification based on the score level achieved over a minimum threshold points. It gives the certification of Bronze, Silver, Gold, and Platinum.

The FGBC Green Development Designation Standard of Reference Guidelines does comprise six categories of the main assessment elements. Each of the categories does have the sub-assessment criteria for evaluation. The composition of assessment items are shown in table 2.7:

Table 2.7: Composition of the green development guideline

Category	Assessment criteria	Quantity of sub-assessment items
1	Protect Ecosystems and Conserve Natural Resources	14
2	Circulation	10
3	Green Utility Practices	7
4	Amenities	8
5	Covenants and Deed Restrictions	3
6	Provide Educational Information to Help Achieve and Promote Green Living Practice	10

(Source: FGBC for Green Development)

5) DDC-Sustainable Urban Site Design

The synopsis of the DDC background with stand for Department of Design and Construction had briefly depicted at the section 2.1 for building assessment tools which currently available around the world. As leaders in design and construction, it is DDC responsibility to provide New Yorkers with buildings and services that are socially responsible, progressively designed and environmentally sound. The DDC had published the reference guidelines for building practices and also sustainable urban site design with a purpose of guiding the consultants to successfully navigate the City's design and construction requirements; detail important sustainable strategies; showcase of Design and Construction Excellence policies; and review valued information essential to the design of public facilities.

The Sustainable Urban Site Design Manual offers an introduction to more environmentally, economically, and socially responsible urban site design practices for New York City capital projects. It is conceived as a resource handbook, featuring chapters that marry the unique site conditions encountered on many City projects with appropriate sustainable site design strategies. The contents are addressed to the whole rainbow of NYC DDC project participants, from City administrators to architects and their consultants, to construction managers, contractors, and facility personnel.

The DDC Sustainable Urban Site Design Manual of Reference Guidelines does comprise five categories of the main guidelines in difference aspects. The composition of reference manual is shown in table 2.8:

Table 2.8: Composition of DDC Sustainable Urban Site Design

DDC Sustainable Urban Site Design Manual
1. Sustainable Sites for DDC
2. Maximize Vegetation
3. Minimize Site Disturbance
4. Water Management on Urban Sites
5. Materials in Site & Landscape Design

(Source: The DDC Sustainable Urban Site Design Manual of Reference Guidelines)

6) SURPAM-HK

The SURPAM from Hong Kong is an assessment model developed by Lee and Chan (2007) which is called Sustainable Urban Renewal Project Assessment Model (SURPAM). This assessment model is attempts to generate the most sustainable urban renewal design for an area undergoing urban renewal. The objectives of the model comprised of three aspects namely economic sustainability, environmental sustainability and social sustainability. The design criteria level consists of 17 criteria which are the most important urban design considerations highlighted in previous studies (Chan and Lee, 2007a; Chan and Lee, 2007b; Chan and Lee, 2008). The assessment tool is composed of 34 indicators for 17 design criteria and the composition of the assessment criteria are shown in table 2.9 below:

Table 2.9: Composition of assessment criteria

Assessment element of SURPAM	The quantity of assessment criteria per element
Environment Sustainability	6
Social Sustainability	6
Economic Sustainability	5

(Source: Journal of Facilities "A sustainability evaluation of government-led urban renewal project")

Table 2.10 shows the Primary issues of concern identified in each building assessment tool for sustainable urban development for some countries around the world. Some key issues were indentifies as among the most popularly use by these assessment tools are site, indoor environment, energy, material resources, water, transport, health, social and services.

Table 2.10 Primary issues of concern identified in each assessment tool for sustainable urban area

Assessment Tools	1	2	3	4	5	6	7	8	9	10	11	12	13	14	15
CASBEE	x		x	x	x	x	x	x		x	x	x	x	x	x
LEED	x		x	x	x	x	x	x	x		x	x	x	x	x
RHSI	X	x	x	x	x	x		x	x			x			
FSBC	X	x	x	x	x	x	x	x			x	x	x		x
DCC	X		x	x	x	x	x	x	x		x	x	x	x	x
SURPAM	X	x	x	x	x	x	x	x	x			x			x

Notes: 1.Site, 2. Indoor Environment, 3. Energy 4. Material Resources, 5. Water, 6. Transport, 7. Health 8. Social, 9. Economy 10. Comfort 11. Management, 12. Services, 13. Long term performance, 14. Design aesthetics, 15. Functionality.

3.0 Establishing of the assessing model

The assessment model for housing sustainability index will be addressed as a Comprehensive Assessment System for Sustainable Housing (CASSH). It is made of a hierarchy of three major levels, that is, the outcome, design measurement indicators, and sustainability criteria level. The schematic diagram is as shown below in the theoretical framework in Figure 3.0. The goal level describes the ultimate achievement of the model. It attempts to generate the most sustainable housing development for an area either undergoing new development or renovation. The assessment model is try to evaluate an area of development as a whole, plus evaluates the environmental performance of individual buildings within the designated area as well. The framework requires the assessment method that integrates the neighborhood of building group constructed in the designated area and also consider the assessment of the interior environment performance of the building (housing) itself. The overall format for assessment result is as defined by CASBEE as "Urban Area + Buildings" for the developed area.

The sustainability criteria comprised multiple variables to be evaluated as leverage for achieving housing sustainability in the develop area. They can be categorized in six categories namely; Environment, Society, Economics, Building Forms (Housing), Site/ Land uses, and Communication & Transportation. The design indicators consist of 30 measurement criteria which are important in urban design development or neighborhood development plus building performance considerations highlighted in many other assessment systems. Through the literature review, a total of 131 short listed considerations can be incorporated in the model of assessment after verification through a pilot test for reliability and validity, to suit the local context.

3.1 Toward Establishing a Rating System for Housing Development in Malaysia

Indices are widely used in performance evaluation and have proven useful in locating weaknesses in overall design and system (Bell and Morse, 1999). The index is generally a number that is derived from the collection of a broad range of individually generated values or indicators that are used to characterize or evaluate specific aspects of the system (Gray and Carton-Kenny, 2004).

Rating system (1)

In the building scope Gray and Carton-Kenney (2004) has studied the sustainability index for rural housing. The objective of the study is to ensure a better quality and more sustainable housing is constructed in the rural areas. The sustainability index comprises 70 indicators categorized into site, design, construction and social. The criteria used in the selection of sustainability indicators including: policy relevance, simplicity, validity, affordable data, reality, adequate scope and openness (Gray and Carton-Kenney, 2004).

For example:

$$RHSI = \sum_{i=1}^{n} qi\ wi$$

Where RHSI is the Rural Housing Sustainability Index
n is the number of indicators,
qi is the score of the ith indicators
wi is the weighting attributed to the ith parameter

Rating system (2)

The CASBEE of Urban Development, both Q_{UD} (environmental quality in urban development) and L_{UD} (outdoor environmental loads in urban development) are evaluated and scored separately.

All the categories are also compounded using the formula below to generate BEE_{UD}, and indicator for Building Environmental Efficiency in Urban Development.

Building Environment Efficiency in Urban Development (BEE_{UD})

$$BEE_{UD} = \frac{Q_{UD}}{L_{UD}} = \frac{25 \times (SQ_{UD}-1)}{25 \times (5-SLR_{UD})}$$

Where Q_{UD} is Environmental quality in urban development
L_{UD} is Environmental load in urban development

First the numerator Q_{UD} is defined as $Q=25(SQ_{UD}1)$ to convert the SQ_{UD} scores (1~5 points) for the environmental quality in urban development into the Q_{UD} scale of 0~100. Then the denominator L_{UD} is defined as $L=25(5-LR_{UD})$ to convert the SLR_{UD} scores (1~5 points) for load reduction into the L_{UD} scale of 0~100

Rating system (3)

Lee and Chan (2007) have illustrated the assessment mechanism of the model of the Sustainable Urban Renewal

ISSN 114-1284

Project Assessment Model (SURPAM) on the basis of Hong Kong context to evaluate the sustainability level of individual urban renewal project by assessing the design quality of the projects. The formula for SURPAM as shown below:

$$P_k = jW_j \times S_{kj};$$

where P*k* is the overall score of an urban renewal project *k*,
W*j* is the final weight of criterion *j* in third level,
S*kj* is the score of project *k* on criterion *j*, and *j* is the 17 design criteria.

Proposed an Assessment Model for CASSH

The sustainability level of housing development is represented by the overall score of using formula of CASSH (Comprehensive Assessment System of Sustainable Housing) model. The calculation method is similar to that of the CASBEE for Urban Development and SURPAM of Hong Kong measurement. The calculation of the formula is proposed by multiplying the score indicating the performance of the designated area of each sustainability criterion indicator with the defined weighting of each of the same indicator as well. The weighting coefficients between the assessment criteria will determined by conducting a questionnaire survey to ask the experts who involved in the related fields. It is then use the Analytic Hierarchy Process (AHP) to defining the weighting in numeric which is being done by CASBEE.

The overall score of the sustainable development area is calculated using the formula as shown below:

$$CASSH = \sum SCn \times Wn$$

Where CASSH is Comprehensive Assessment System of Sustainable Housing
n is the numeric indicator for each of the sustainability criteria parameter
SCn is the score of the Sustainability Criteria of each of the n indicator
Wn is the weighting attribute to the n indicator to each Sustainability Criteria

The calculation of final score of CASSH on particular project is as listed below:

$$CASSH = \sum EnxW_{En} + ScxW_{Sc} + EcxW_{Ec} + BxW_B + SxW_S + CTxW_{CT}$$

Where En is represent Environmental criteria
Sc is represent Society criteria
Ec is represent Economics criteria
B is represent Building Forms criteria
S is represent Site/ Land uses criteria
CT is represent Communication & Transportation criteria

In order to calculate the overall score, it is necessary to define the value of the component of each indicator. However, the scores of each criterion will not identify firmly because it vary with performance of the designated area development.

ISSN 114-1284

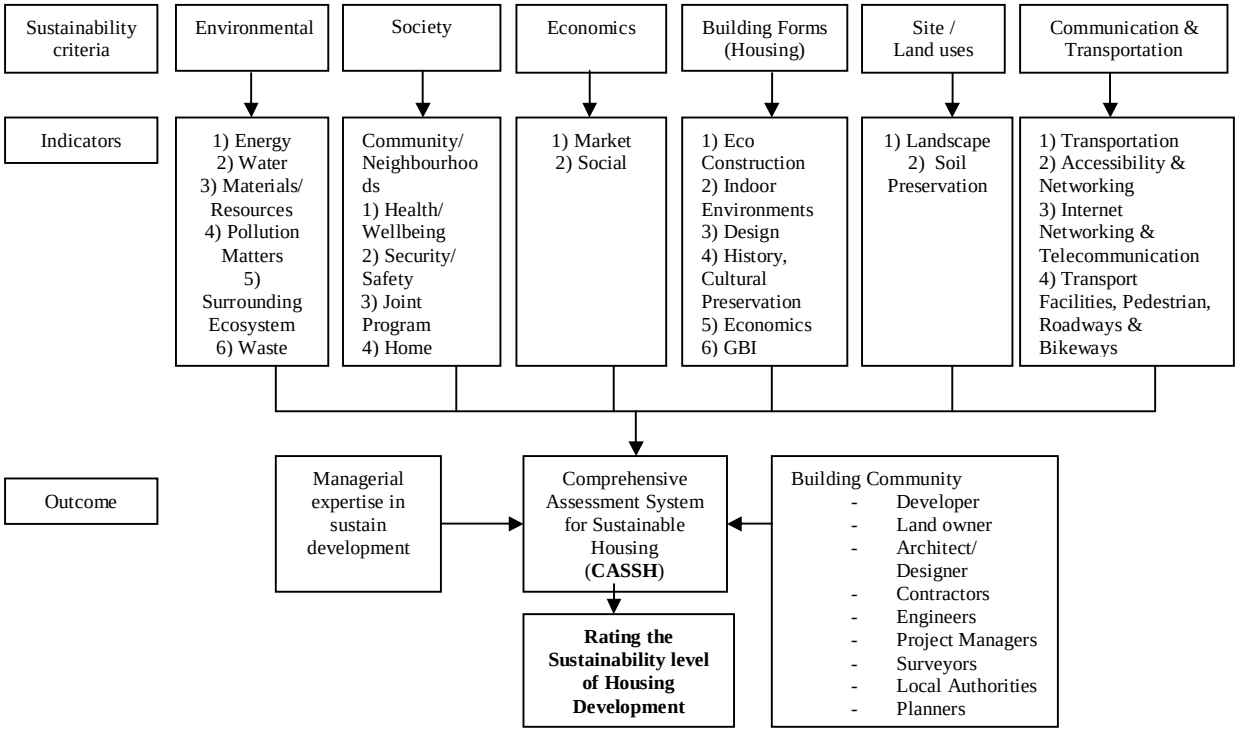

Figure 3.0 Conceptual Frameworks for Comprehensive Assessment System for Sustainable Housing (CASSH)

4.0 Conclusion

Basically, the assessment systems for sustainability from various countries are used to evaluate the building performance. Majority of countries, especially those developed countries, do have their own established building assessment system. For example BREEAM in UK do evaluate buildings by its' type, the BREEAM had formed up the multiple tools for different buildings' design such as, Ecohomes, Healthcare, Industrial, Multi-residential, Prisons, Office, Retail and Education Buildings. However, it is also important to evaluate environmental performance for a group of buildings. This mean evaluation include the surrounding of the designated area, as the assessment activity in Urban Area or in other words, the assessment on the buildings' neighborhood. The common district on buildings within a district can raise environmental quality and performance throughout the area. Thus, the establishment of Comprehensive Assessment System for Sustainable Housing (CASSH) to assess in a wider scope of housing sector development, "encompassing measures deliver through urban renewal and district-wide effort covering multiple buildings", as stated in CASBEE for Urban Development.

The analysis of the existing assessment tools and design methodologies has shown that there is emphasis on environmental issues. However, in the holistic approach, all of the tools will have to consider every aspect of the sustainability parameters and that will result in a more pragmatic effort in preservation of the environment. However, the implementation of the evaluation system will become more complicated and sophisticated.

The assessment tools are intended to be used as guidelines during the design process and as a more general sustainability assessment rather than a more specific architectural evaluation tool. The evaluation of housing sector development not only evaluate the surrounding of building being developed but also should include the assessment of building performance, since the buildings performance also will have significant impact on our environmental. Therefore, the establishment of CASSH, the housing sustainability index, is an assessment tool to evaluate the designated area (exterior spaces on the district scale (roads, plazas and other public spaces, and exterior spaces within building sites) identified by CASBEE Urban Development) and the buildings themselves within the hypothetical boundary of the defined area.

By improving the level of sustainability practices in housing development, this will require to shape up a guideline for rating the residential development in respect to housing sector by using the measurement of housing sustainability index. The formula of sustainability index in housing development will be produced based on adapting the critical factors to the successful practice system tools developed in Japan, United State and United Kingdom. These indicators for sustainability parameters should be recommended to be incorporated in the policy on sustainable built environment and should take into account criteria that compatible to local context.

Lastly, to achieve the sustainability development, it is significant for the development to consider many indicators which includes the following three cores: the Environmental, Social and Economic efficiency.

Reference

[1]. A sustainable Housing Forum Report (2003), *Building Sustainability: How to Plan and Construct New Housing for the 21fst Century*, October 2003.

[2]. Bell, S. and Morse, S., (1999). *Sustainability indicators*, Earthscan Publications Ltd, London.

[3]. Berke, Philip R. and Conroy, Maria Manta, (2000). Are We Planning for Sustainable Development, *Journal of the American Planning Association*, Winter, Vol. 66, No.1, pp.21-33.

[4]. BRE Report (2002). *Reputation, Risk & Reward- The business case for More Sustainable Construction*, Building Research Establishment Ltd (BRE).

[5]. Building grading systems: a review of the state-of-the-art, Publication by Architectural Science Review on 01-MAR-08, retrieves on June 2009, available at: http://goliath.ecnext.com/coms2/gi_0199-7677768/Building-grading-systems-a-review.html

[6]. Bunz, K.R., Henze, P.E and Tiller, D.K.(2006). Survey of Sustaianable Building Design Practices in North America, Europe, and Asia.

[7]. CASBEE (Comprehensive Assessment System for Building Environmental Efficiency) for *Urban Area+Building (2007)*, JSBC (Japan Sustainable Building Consortium), Institute for Building Environment and Energy Conservation (IBEC), Tokyo, retrieved on 3 March 2009, available at: http://www.ibec.or.jp/CASBEE/english/download/CASBEE_UD%2Be_2007manual.pdf

[8]. CASBEE (Comprehensive Assessment System for Building Environmental Efficiency) for *Urban Development (2007)*, JSBC (Japan Sustainable Building Consortium), Institute for Building Environment and Energy Conservation (IBEC), Tokyo, retrieved on 19 December 2008, available at:http://www.ibec.or.jp/CASBEE/english/download/CASBEE_UDe_2007manual.pdf

[9]. CASBEE (Comprehensive Assessment System for Building Environmental Efficiency) for CASBEE *for Building (Detached House) (2007)*, JSBC (Japan Sustainable Building Consortium), Institute for Building Environment and Energy Conservation (IBEC), Tokyo, retrieved on 3 March 2009, available at: http://www.ibec.or.jp/CASBEE/english/download/CASBEE-H(DH)e_2007manual.pdf

[10]. Chan, E.H.W. and Lee, G.K.L. (2008), "A sustainability evaluation of government-led urban renewal projects", Journal of Facilities, Emerald Group Publishing Limited, Vol. 26 No. 13/14, pp. 526-541, retrieved on 23 February 2009, available at: http://www.emeraldinsight.com/Insight/viewPDF.jsp?contentType=Article&Filename=html/Output/Published/EmeraldFullTextArticle/Pdf/0690261304.pdf

[11]. Choguill, C.L. (1994). Sustainable Housing Programme in a World of Adjustment, *Habitat International*, Vol. 18, No. 2, pp 1-11.

[12]. DDC Method, prepared for NYC Department of Design & Construction Office of Sustainable Design by Gruzen Samton Architects LLP with Mathews Nielsen Landscape Architects P, published on June 2008, retrieved on June 2009, available at: http://www.nyc.gov/html/ddc/html/pubs/publications.shtml

[13]. Edwards, B. and Turrent, D. (2000). *Sustainable Housing: Principles and Practice*, E&FN Spon, London.

[14]. FGBC, Green Development Design Standard Version 6 Reference Guide, published on January 2009, retrieved on June 2009, available at: http://www.floridagreenbuilding.org/db/?q=node/5363

[15]. Gray, N.F and Carton-Kenney, M.,(2004). A rural housing sustainability index: background to development, *Municipal Engineering* 157 issue ME.

[16]. Green Building Index, Malaysia system developed by Pertubuhan Akitek Malaysia (PAM) and the Association of Consulting Engineers Malaysia (ACEM). retrieved on 6 May 2009, available arhttp://www.greenbuildingindex.org/

[17]. Huby, M.,(1998). *Social policy and the environment*, Bukingham:Open University Press.

[18]. Islam, N. (1996). Sustainability Issues In Urban Housing in A Low Income Country: Bangladesh, *Habitat International*, Elsevier, Vol. 20, No. 3, pp. 377-388.

[19]. Johari Tun Openg Datuk Amar Abang, State Housing Minister, *RM100mil to construct cheap homes in Sarawak*, Star Paper resources retrieved on 20 May 2009 by http://thestar.com.my/news/story.asp?file=/2009/5/20/nation/3940267&sec=nation

[20]. John Carmody, *Sustainable building rating Systems, Standards and Performance*, Center for sustainable building research of University of Minnesota, published on November 27, 2008, retrieved on June 2009, available at: www.csh.re.kr/sem_board/download.asp?id=J&num=1911,

[21]. LEED (n.d.), Leadership in Energy and Environmental Design for Neighborhood Development Rating System, US Green Building Council, retrieved on 15May 2009, available at: http://www.usgbc.org/ShowFile.aspx?DocumentID=5275

[22]. Mohd Jasan, Yg. Bhg. Dato' Lokman Hakim, Secretary General, Ministry of Housing and Local Government Malaysia, given Forum Speech Title "*GLOBAL AND LOCAL – THE MALAYSIAN RESPONSE TO THE URBAN CHALLENGE*" on 6 July 2004. Retrieve from http://aplikasi.kpkt.gov.my/ucapan.nsf/6c7fcfbe486f405c48256e5a000bd038/38c378de81600ede48256fdc002b27c0?OpenDocumenton 16 September 2008.

[23]. NAHB Model Green Home Building Guidelines, National Association of Home Builders, published on 2006, retrieved on June 2009, available at: http://www.nahbgreen.org/Guidelines/nahbguidelines.aspx

[24]. Parkin, S., F. Sommer and S. Uren (2003). Sustainable development: Understanding the concept and practical challenge, In *Proceedings of the Institution of Civil Engineers, Engineering Sustainability*, 156(ES1), 19-26.

[25]. Philip Kotler, Hermawan Kartajaya, Hooi Den Huan and Sandra Liu, *Rethinking Marketing : Sustainable Marketing Enterprise in Asia*, Prentice Hall: Pearson Education Asia Pte Ltd, 2003.

[26]. Rating Tools Rundown Version 4 updated on November 2007, Center for design, retrieved on May 2009, available at http://cfd.rmit.edu.au/content/download/533/.../Rating Tools Roadmap v2.0.pdf

[27]. Ronald Prinn, study co-author of MIT team, Global warming could be twice as bad as forecast, Star Paper resources retrieved on 20 May 2009 by http://thestar.com.my/news/story.asp?file=/2009/5/20/worldupdates/2009-05-20T021551Z_01_NOOTR_RTRMDNC_0_-397395-1&sec=Worldupdates

[28]. TISSUE browser, System of the current level, Specific Targeted Research for Programme: Integrating and Strengthening the European Research Area, retrieved on June 2009, available at: http://ce.vtt.fi/tissuebrowser_public/index.jsp

[29]. Tonn, Bruce E,(2007). Futures sustainability, *Futures*, Vol.39, pp. 1097-1116.

[30]. Tosics, I.,(2004). European urban development: Sustainability and the role of housing, *Journal of Housing and the Built Environment*, Vol.19, pp.67-90.

[31]. Tom Bigg (Editor), *Survival for A Small Planet*: The sustainable Development Agenda, Earthscan publishes in association with WWF-UK and the International Institute for Environment and Development, 2004.

[32]. Winston, N. (2007). From boom to bust? An assessment of the impact of sustainable development policies on housing in Republic of Ireland, *Local Environment*, Vol.12, No.1, pp.57

ISSN 114-1284

The Trigger of Contractor Associates Involvement in Construction Bidding Process

Ayomi Dita Rarasati[1], Adi Irfan Zidni[2]

[1]*Civil Engineering Department, Faculty of Engineering*
University of Indonesia, Depok 16424
Tel : 62 21 7270029 ext 135. Fax : 62 21 7270028
E-mail : ayomi@eng.ui.ac.id

[2]*Civil Engineering Department, Faculty of Engineering*
University of Indonesia, Depok 16424
Tel : 62 815 48026733
E-mail : airfanzidni@gmail.com

ABSTRACT

In construction project, bidding process is important because it represents early starting construction project. All government bidding projects is executed based on Presidential Decree Number 80/2003 and Region Government Law. In Brebes region, there is incident that bidding process is influenced by Contractor Associates involvement. Contractor Associates links the entire member to get opportunity in following tender with limited emulation.

The aim of this paper is to describe the trigger of Contractor Associates involvement in infrastructure construction bidding process in Brebes Region.

This is a case study research that gather respondent in form of survey and interview with related parties. Data is analyzed with descriptive statistical analysis by using frequency distribution method. The validity and reliability are analyzed with Corrected Total Item Correlation Test and Kruskal Wallis Test.

The results indicate that Contractor Associates involve in bidding process because there are certain work packages requested by government employee, the quality of work is low in terms of low competitiveness in price, the probability to sell the projects is high as a result of few resources, companies have low education background expertise and low skill resources, and the company financial ability is unsteady during tender.

Keywords

Bidding process, contractor associates, involvement

1. INTRODUCTION

Construction projects in both the provincial and district or city, consists of private and government projects. Private sector projects can be conducted through auction or direct appointment and the work is financed with private funds. Meanwhile, the government project, the financing comes from the APBN or APBD, where the responsibility may be attempted carefully and must follow the outlined, because the transparency factors in its implementation is highlighted.

Auction services for government construction projects is technically set in the decree the Presidential Decree No. 80/2003, which refers to the Law No 18/1999 and Law No 5 / 1999, so that it is expected to encourage the creation of a healthy competition, the use of products in the country, reduce the costs, and expanding business opportunities [1].

However, apart from imperfect legislation, and in fact there is behavior controversy contrary to the principles of healthy business competition. Implementation of Presidential Decree No. 80/2003 and Law No. 5/1999 is not realized, this is because there are many cases that occur related to the suspected violations in business competition [2]. Based on the reports, about 60% of reported cases are cases of conspiracy auction construction services suspected. Practices cartel or conspiracy auction often coloring activities auction services in the construction of a number of government institutions [1]. The same phenomenon also occurs in Local Government Brebes Kabupaten (Pemkab Brebes), the violation suspection in the procurement of health equipment Brebes District hospitals in the year 2006. In addition, there is also involvement suspected of individual House of Representatives District Regional Brebes (Brebes DPRD) in the direct appointment of the project [2].

Association of Construction Services is a role in encouraging the creation of business services and construction of health professionalism. Therefore, the association as a delivery vessel communication, coordination, and consultation between public service providers with the construction of construction, are required to improve the capability and professionalism of its members. This is to prevent the occurrence of competition that is unhealthy, because it can often make all parties and rarely cause problems in its implementation, and low quality construction of the resulting [3]. Thus, the associations are expected to play an active role in distributing the aspirations of members to organize and develop the work climate better, which allows the

participation of members in national development [4]. With the opening of the community in the role of business development services result in the construction many associations appear in the construction services sector, which one of them is the Association of Construction Services with the authority to implement the main providers of construction companies. However, often in practice in the field, the authority made it back to the emergence of behavior as opposed to the Law No. 18/1999, which is the difficulty in obtaining a certificate of business and individuals for the construction services business, and many other issues related to business competition in the field of construction services [5].

Association of Construction Services in the Brebes District has an important role, because of suspected involvement in the auction service on the construction of Public Works Brebes District. The indication is the emergence of symptoms similar the cases of prominent auction line-up in the last few years. The involvement of the association is conditioning auctioned, which is coordinating the auction members in construction services. This problem comes from the existence of the association itself, of companies engaged in the construction services sector. This is certainly not going to happen, when service providers compete for construction professionals in an effort to get a project.

In addition, the association is also expected to not get stuck in routines certification members, as a result of many other functions and tasks that have not been optimally implemented. As one of the authorized organization of the setting, guidance, supervision, business development and construction services, the Association of Construction Services in Brebes District not optimal in the running of its duties and functions. In addition, many cases of business competition are not healthy in the construction services sector continues to appear, which usually appear in the form of a conspiracy auction. This can be seen from the establishment that has not been a healthy business competition in the auction service construction, in which associations bridge the interests of its members to create a pseudo-competition condition. Devices such as contract documents and packages prepared in auction are being conditioned with the purpose of the project.

This condition is set in an effort to get the project desired by the members. Due to the involvement of the Association of Construction Services is significant, it should be special attention for the auction as the committee representing the owners to implement the project activities of the goods or services the construction, so it can be expected construction service providers get the best work to given implementation.

2. LITERATURE REVIEW

In project construction, the auction is one important part of a series of project activities. This is because of the success of the auction is the beginning of the start of the implementation of the project construction work. In addition, the auction is also the stage for a very important provider of construction services, as living dead: the company's success depends not in the auction [6]. Given the resources involved and the risk faced, in an effort to obtain the services of construction is expected to carry out work which needs to be done given the tight selection. Auction services are a set of construction activities to provide goods or services in a way to create a healthy competition among providers of goods or services that are equivalent and are eligible, based on the method and procedure which has been set and followed by the parties related to the rule, so that selected service provider is the best construction [7].

Therefore, in this case it is said that the main purpose of the auction is to provide a balanced opportunity for all bidder, resulting in the most affordable price with maximum results. Although generally acknowledged, that cheap is not the sole measure to determine the victory in the auction. However, the mechanism through auction bidding, avoided wherever possible the opportunity to make a conspiracy between competitors or the bidder and the auction committee. Based on Presidential Decree 80/2003, that in every activity of the goods or construction services are required to apply the principles below are efficient, effective, open and competitive, transparent, fair or not discriminatory, and accountable [1].

The selection procedure of service construction process is a series of activities that begins with identifying the needs of service of construction by the owner to prepare and package up to the auction contract for the implementation of physical projects. This process includes research and evaluation work that often reach the internal organization and financial service providers from the construction. This needs to be done, because it will affect the success of the project and the quality of the project [1].

The prequalification process designed correctly should meet things like this. First, ensure that the construction of service is quite competent, responsible, experienced, and have sufficient resources to complete the project. Second, service providers are able to eliminate the construction that has limited resources, over-commitment, and companies that are less or not very experienced, so that reduces the administrative burden and to prevent the owner of difficulty determining the winner. The third is to maximize competition among providers of construction objectives [8].

In the process of decision making on the stage prequalification, project owners must do the steps as follows. First, determine the criteria to be used in the assessment of the participants, of course it depends on the needs of the project. Second, find the data provider of construction services that will be evaluated. This can be done with the construction of service request to submit the data or the way the service providers for the construction or to answer questions that have been prepared. If necessary the data provider of construction services that are less, then be found from other sources. Third, evaluate the data from data-service providers in the construction. Fourth, make the assessment of the data providers with the construction criteria that are used,

already sufficient for decision making. Fifth, if it turns out from these assessments still require additional data, then the next step is the search for additional data, so it is sufficient for decision making. Sixth, decision-making at this stage is a critical step, because the errors in the decision will bring a big impact with the implementation of the project. So in the stages of decision-making, should the data required must be sufficient available [9].

Based on Presidential Decree No. 80/2003, the assessment criteria for construction services performed by the auction committee includes three aspects, namely administrative, technical, and price [1]. System assessments of evaluation service providers should consider the construction of minimum standards for each category, where bid or proposal to auction the documents submitted will be disqualified if it does not meet the standards set. In general, the sale or importation document should include information related to categories such as, the following of the technical approach, management ability, financial capability, personnel qualifications, experience of, the performance of the past, the method of execution, and price information project [10].

Racketeering conspiracy in the auction or services defined as the construction of the cooperative agreement between bidders, which should compete with the goal of winning particular auction participants. This agreement may be made by one or more of the auction participants that are not agree to submit bids, or by auction that a participant with a lower price and then make a bid with a price above the bid price of the company as the winner. The agreement of this kind against the auction process is fair, because the public auction procedure is designed to create equity and to ensure a result with cheap price and most efficient. Therefore, the line-up in the bidding auction is considered inhibit the creation of a healthy competition among the bidder [11].

3. RESEARCH METHODOLOGY

The chosen method of research is survey method with the quantitative approach. The research is based on a theory of reference or some of the literature relevant to the research problems. The category variables are consisting of three criteria as follows, administrative, technical and financial. Meanwhile, to check the validity of research variables, validation is done by specialist construction services by the competent services in the areas of construction and set of research variables used.

Research data collected using the questionnaire as research instrument. The questionnaire was designed in the form of a Likert Scale with the choice of alternative answers to choose one of them as the most appropriate answers. Collecting research data carried out by distributing questionnaire and direct interviews with the respondents.

Methods used to analyze the research data are consists of several methods such as the following statistics. First, test the reliability and validity of the method corrected Item Total Correlation. Second, comparative analysis with the Kruskal Wallis Test methods. Third, the analysis of descriptive statistics with frequency distribution method based on the value of the mode.

After analyzing the research data, then the next stage is to validate the research results to the specialist construction services by the competent services in the areas of construction to ensure that research results are relevant to the facts that occurred in the field.

4. RESULTS

Test results show the validity and reliability Cronbach's Alpha value of 0.479 that is greater than the value for r table df = 23, namely 0.265 and tested questionnaire are proved reliable enough with the reliability level of 47.9%.

Based on the survey that was done, the answers obtained from respondents who agree on the causes of the involvement of association services in the process of implementing the construction auction services in the construction of Public Works Brebes District. The causes are as described in Table 1.

Table 1: Factors in Contractor Associates Involvement Trigger.

Administration Criteria
Requests that a specific work package carried out individual government officials, the complexity of the procedures of certification bodies construction services business, the inconsistency level of competence and ability of business services with the construction certificate, the complexity of the procedures of certification experts and skilled labor, the inconsistency level of competence and ability of experts and skilled workers with a construction certificate services, the complexity of licensing procedures in the field of construction services.
Technical Criteria
Few projects in a year, strict competition because the number of partner services construction, low quality of work due to the price quote that is not competitive, low level of understanding of the scope of partnership work being offered, the size of the project likely to be sold due to limited resources, limited supplies and equipment owned partner, low education level of experts and skilled workers of the partner, low level of attention to the importance of partnership in the K3 system construction project.
Financial Criteria
Low level of ability to make partner in the price quote, the condition of instability in the financial partner auction service construction.

While in the Item Total Correlation Corrected, apparently there are some variables that have a value of r is smaller than the value of r is thus the table, so that to increases the

reliability level up to 85.1% only six grains research variables used, namely the existence of a specific work package request made individual government officials, the complexity of the procedures of certification bodies construction services business, due to low quality of work that is not price competitive bidding, the project likely to be sold due to limited resources, low education level of experts and skilled workers of the partner, and the condition of instability in the financial partner the auction service construction.

Results based on comparative analysis of the membership association, found only one variable that has significant differences, namely the variable complexity of the procedures of certification bodies construction services business with a value Asymp.Sig = 0.046. Then, comparative analysis based on employee status, was found two variables that have significant differences, the variables of a particular work request package made with the individual government officials with a Asymp.Sig value = 0.001 and the variable quality of the work due to the low price bid is not competitive with the value Asymp. sig = 0.022.

5. DISCUSSION

Various phases of research and research data analysis process that includes the validity and reliability testing, comparative analysis, and descriptive statistical analysis, obtained some of findings which is the cause of the involvement of the Association of Construction Services in the process of construction on the auction service Department of Public Works Brebes District is the request packet work that is done a certain individual government officials, the complexity of the procedures of certification bodies construction services business, due to low quality of work that is not price competitive bidding, the project likely to be sold due to limited resources, low education level of experts and skilled workers of the partner, and the instability partner in the financial condition of the auction service construction.

It could not be denied that the auction service in the construction of very large possibility of the occurrence of conspiracy. This often cannot be avoided but cannot be sustained. Conspiracy arising in auction service since construction should be completed early in satisfactory for all parties. If neglected, it will be a bad habit that is considered can decrease the performance of the construction as a whole, in this case will cause a restriction for the construction services business in general.

The request packet of a certain job done individual government officials variable. With demand packages that work done by individual government officials resulted in at least the number of jobs offered. It is not because of the number of projects with a number of service providers that have constructed, the services of the Association of Construction discuss to establish a forum of construction services, called 'faction'. This is done with the intent and purpose to make the way to the fair distribution of projects for each member based on the number of associations that are owned or the nature and type of projects offered. This variable has differences based on respondents' perception of the status of employees, this can only happen due to the directorship of respondents would better understand the problems that occurred in the scope of business in a system of government.

The complexity of the procedures of certification bodies construction services business variable. As is known, that the National Certificate Business Services Construction (SBUJK) is one of the main requirements that must be owned provider of construction services for the construction of the auction services. However, this is often a problem for service providers to get a certificate in construction, both business entities and individuals, so that service providers make the construction activities to do business. In line with the understanding, the variable is also strengthened by previous research on the authority of the Association of Construction Services to develop, in this case carry the certification agency business services construction is still a difficulty for the construction of service [12]. This variable has differences based on respondents' perceptions of the membership association, it is possible for each association has a certification procedure and a different standard.

The low quality of work due to the price quote that is not competitive variable. Based on the experience available, from some of the auction that was conducted with the competitive bidding (free fight), it is possible that the quality of work produced is not good, the price bid submitted by the participants are often very low. So that the Association of Construction Services as the vessel's construction company service providers need to find a way to create a business climate conducive deems. Conditions had a positive impact on the quality of work produced, as with the settings such that the price bid submitted by the participants tends to be higher near plafond budget. On the other hand, it is preferred to prevent entry of the potential and limits competition in general. This is contrary to Law No. 5/1999 Article 22 of the auction process or activity to the goods or services with a competitive price quote and open competition as the broadest. This variable has differences based on respondents' perception of the status of employees, this can only happen due to the directorship of respondents would better understand the business impact and risk of the company owned.

The variable size of the project likely to be sold due to limited resources variable. Not a bit of service construction company that is not competent in conducting business, this can be seen from the many providers of construction only as a role player or a broker in the construction auction services. This means that, easily sell them to buy the work of the project is established, while there is no competence to perform the job. Typically, they lend only other company to partner with a certain amount of compensation in accordance with the agreement. For that is the Association of Construction Services to do a role in the interest of the members and the creation of a conducive business climate. This is starting back with the settings included in Law No. 18/1999 Article 8 of

the business requirements, expertise, skills and business entities and individuals in the field of construction services.

The low level of education experts and skilled workers of the partner variable. Most of the education level of experts and skilled workers of the agency business services construction is very low and does not support the competence in the field of construction services. As is known, that the certificate and Expertise Skills Certificate (SKA-SKT) is one of the main requirements that must be owned provider of construction services for the construction of the auction services. Therefore, the Association of Construction Services to perform the obligation of the workforce that belongs to members. This is certainly in line with what is mandated in Law No. 18/1999 which requires the creation of business professionalism in the field of construction services. This setting is found in Article 9 of the terms of employment, both experts and skilled labor for the construction of business services.

The instability condition of financial partners in the construction auction services variable. Because of the low level of competence construction service providers, especially those related to the ability of financial companies, the goal is to be formed the Association of Construction Services to provide counseling, guidance, help and protect and defend the interests of members. In this case, the association helps members to the financial difficulties of conducting business, so that the expected welfare of the members still guaranteed.

Validation results of research carried out by request and approval of some of the specialist construction services, to ensure that research results are relevant to the facts that occurred in the field. Based on the experts, the demand variables specific work package that the government made an official person can only occur due to weak supervision system and law enforcement officers by the authorities. This problem is actually usual and old case. Almost most of the work required and making fitful construction service providers. System of cooperation in the negative among individual government officials, in this case the many parties concerned to show the impact each other, so that the work request is associated with efforts to defend the budget.

The complexity of the procedures of certification bodies construction services business as a specialist, does not actually relatively complex, even too simple, so it is said less comprehensive. It should forward the process of certification with the facts capability construction service providers in the management of construction, such as production management or field that is expected measurable indication of the capacity in the construction of the project construction.

However, one expert argued that the procedure would still be a certification difficulties experienced construction service providers, because of the complexity of the complex bureaucracy. The fact the process of certification to the private parties in this case the association, does not guarantee the improvement of competence and professionalism of the spirit.

6. CONCLUSION

After several phases of research, such as collect data, process data, interpret data, analyze data, and validate the results of research, the conclusions obtained are as follows: The factors which is the cause of the involvement of the Association of Construction Services in the process of construction on the auction service Brebes District are certain work packages requested by government employee, the quality of work is low in terms of low competitiveness in price, the probability to sell the projects is high as a result of few resources, companies have low education background expertise and low skill resources, and the company financial ability is unsteady during tender.

REFERENCES

[1] Wahyudin, et al., “Petunjuk Pelaksanaan Pengadaan Jasa Konstruksi Oleh Instansi Pemerintah”, Jakarta: BP Cipta Jaya, 2004, pp. 4 – 5.
[2] Komisi Pengawas Persaingan Usaha, “Pembacaan putusan terhadap dugaan pelanggaran UU No 5/1999 yang berkaitan dengan pengadaan alat kesehatan RSUD Brebes tahun anggaran 2006”, Artikel Putusan Perkara KPPU, 2008, Accessed on 1 July 2008 from http://www.kppu.go.id/search/artikel.html.
[3] Kirmanto, Djoko, “Asosiasi Berperan Mendorong Persaingan Sehat Dalam Pengadaan Jasa Konstruksi”, Jurnal Pusat Komunikasi Publik, 2006, Accesed on 20 February 2008 from http://www.pu.go.id/search/jurnal.html.
[4] Ministry of Public Work, “Pembinaan Jasa Konstruksi Berdasarkan Undang-Undang Jasa Konstruksi”, Pembinaan Konstruksi dan Investasi, 2005, Accessed on 20 February 2008 from http://www.kimpraswil.go.id/search/artikel.html.
[5] Witular, Erna, “Perkembangan Usaha Jasa Konstruksi”, Jurnal Jasa Konstruksi, 2001, Accessed on 20 February 2008 from http://www.pu.go.id/search/artikel.html.
[6] Wulfram, I. Ervianto, “Teori Aplikasi Manajemen Proyek Konstruksi”, Yogyakarta: Andi Offset, 2004.
[7] Soeharto, Iman, “Manajemen Proyek Dari Konseptual Sampai Operasional”, Jakarta: Erlangga, 1995.
[8] Bubshait, A. A., & K., Al-Gobali, “Contractor Prequalification in Saudi Arabia, Journal of Construction Engineering and Management, vol.2, 1996.
[9] Jefrey, S. Russell, Skibnieski, M. J, “Decision Criteria in Contractor Prequalification”, Journal of Construction Engineering and Management, vol. 2, 1988.
[10] Gransberg, D. D., “Evaluating Best Value Contract Proposals. AACE International Transactions, vol. 4, 1997.
[11] Tri, Anggraini A. M., “Penegakan Hukum dan Sanksi Dalam Persekongkolan Penawaran Tender”, Artikel Hukum Perdata atau Bisnis, 2007, Accessed on 1 July 2008 from http://www.legalitas.org/search/artikel/2729.
[12] Krisanto, Adi Yakup, “Pelaksanaan Keppres No 80/2003 Tentang Pedoman Pelaksanaan Pengadaan Barang atau Jasa Pemerintah dan Indikasi Persekongkolan Tender di Kota Salatiga”, Jurnal Studi Pembangunan Interdisiplin, vol. XVIII, 2006.

ISSN 114-1284

Application of Green Infrastructure's Approach: an Assessment for Conservation in Peri Urban Area

Cynthia E.V Wuisang, ST.,M.Urb.Hab.Mgt[1]

[1]*Faculty of Engineering*
Sam Ratulangi University, Manado 95114
North Sulawesi, Indonesia
Tel : (0431827578). Fax : (0431) 827578
E-mail : cynthiawuisang@gmail.com

ABSTRACT

Green infrastructure discussed in this paper relates to the connective matrices of green paces found in and around urban and urban-fringe landscapes. The prepositions of this research are fragmented in urbanized landscape area is critical to ecological condition and urban sustainability, green infrastructure hubs and corridors are hostile to a majority of the inhabitants, and natural conditions in urban and peri urban areas are important to be linked.
This paper rapidly assessed and analyzed the schematic views of green infrastructure elements and distribution in peri urban area using a quantitative descriptive as a methodological research. Research conducted in Manado City, North Sulawesi Province and selected peri urban area as a case study. This paper examined a number of diverse research areas that have attributed value to the ideas underpinning green infrastructure planning. A review also is made for assessing the concept of green infrastructure for conservation purpose. Finally, this paper concluded with further development of green infrastructure planning. Through this, I have developed an evidence base and a set of criteria to provide planning solutions for conservation using green infrastructure approach application.

Keywords
Green infrastructure, assessment, adaptive planning, peri urban

1. INTRODUCTION

The rise in green infrastructure research has coincided with a reassessment of what landscapes should be in terms of form and function. Green infrastructure as a term relates to the connective matrices of green spaces that can be found in and around urban and urban-fringe landscapes. They provide a number of complimentary benefits for ecological, economic and social spheres and have been increasingly viewed as concept that both planners and practitioners can draw on.. Policy and planning integration, landscape multi-functionality and organizational cooperation are all ideas that underpin the growth of green infrastructure, but are also important developments in planning policy as a whole. What needs to be solved now is how green infrastructure as a concept and as landscape management process can be implemented in planning practice.

1.1 Green Infrastructure and Conservation

Green Infrastructure is a system, which strategically planned and managed as network of wilderness, parks, greenways, conservation easements, and working lands with conservation value that supports native species, maintains natural ecological processes, sustains air and water resources, and contributes to the health and quality of life for communities and people [Mark *et al* 2008].

The Green Infrastructure network encompasses a wide range of landscape elements, including natural areas - such as wetlands, woodlands, waterways, and wildlife habitat; public and private conservation lands - such as nature preserves, wildlife corridors, greenways, and parks; and public and private working lands of conservation value - such as forests, farms, and ranches. It also incorporates outdoor recreation and trail networks [

Infrastructure is defined as - "the substructure or underlying foundation, especially the basic installations and facilities on which the continuance and growth of a community or state depends" [Webster's New World Dictionary]. Infrastructure is definitely about building roads, electric power lines and water systems as well as social infrastructure such as schools, hospitals and libraries. However, the concept of Green Infrastructure covering elevates air, land, and water to an equal footing with built infrastructure and transforms open space [Bryant 2002].

Green infrastructure is a consideration to ecosystem benefits, storm water management, drinking water protection, ground water recharge, support working-land, increase property values and enhance quality of life. The term green infrastructure have its ability to invoke images of planned networks of green spaces that benefit wildlife and people, link urban settings to rural ones.

2. METODOLOGY

2.1 General Description of Study Area

Research was conducted in Manado City. The city is situated in the Northern part of Sulawesi Island, Indonesia (as shown in figure 1)

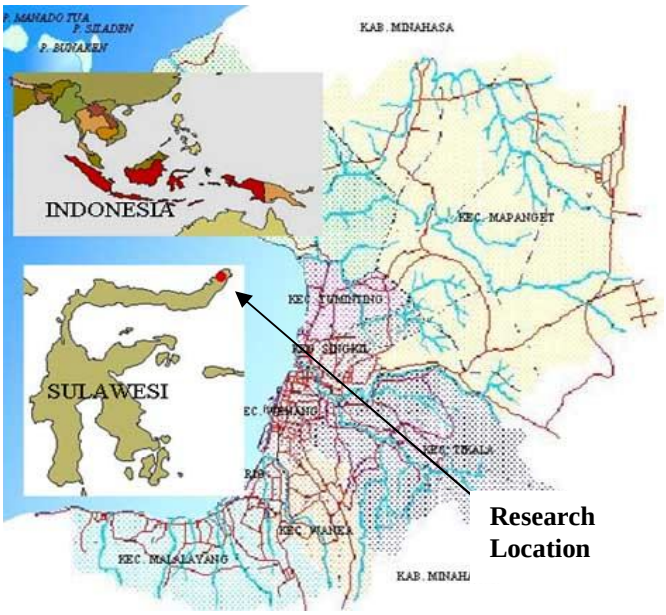

Figure 1. Research location (source: Manado in Figure 2008)

Manado is a capital city of North Sulawesi Province, encompassing 157.126 square kilometres, with the population of 410.033 people reside in 9 districts and 87 sub districts (Manado in Figure 2008). Manado is well known with the spectacular Bunaken Marine National Park, the hospitality of its gentle and friendly people, and diversity in harmony. The city is described as the biggest urban area in the north of east Indonesia region. Hills and plains that meet the coast at Manado Bay frame the plains along western boundary and define the environment of the city. Specifically, Manado has its open water territories that include administratively several small islands i.e, Bunaken Island, Siladen Island and Manado Tua Island. It is a rapidly developing city experiencing urban development in North Sulawesi since 1995. Intense population growth has resulted in extensive and rapid land use changes and the replacement of lands and open spaces with residential, commercial, industrial and infrastructure development.

2.2 Study Site Selection

This study selected peri urban green infrastructure (GI) systems. The GI systems include a range of different GI types including roadsides, pathways, riparian, ponds and patches of green spaces based upon the characteristics of the systems, types and sizes in which they were located. The research began with conducting an evaluation of the existing green infrastructure conditions and sought to provide planning and management frameworks for future consideration. To initiate the research process, secondary data was obtained include air photos and some report data relevant to the study area. The location and extent of all green spaces and GI were the verified in the field.

2.3 Green Infrastructure Survey

This research was conducted by visiting study site over March to May 2009 to observe the patches or hubs and greenway corridors and to assess the biological conditions. To quantify the land use, aerial photography data was applied using ArcView 3.2 software.

3. RESEARCH ANALYSIS

3.1 Rapid Green Infrastructure Assessment

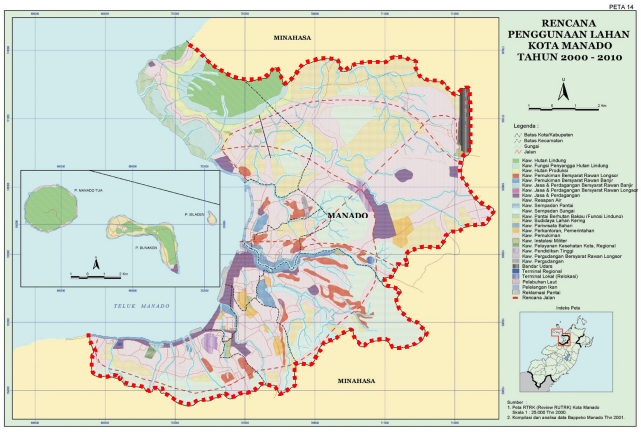

Figure 2. Land Use Planning of Manado City 2000-2010

The purpose of the land use assessment was the identification and mapping of existing green infrastructure in peri urban of Manado City. Land use data were used as the basis for assessment. Map of Manado at scale 1:25.000 and GIS analysis data was used to assess existing GI. This information provided an overview of existing land uses and vegetation within the urban boundary. Existing land use and land cover were categorized using a classification system developed by the National Land Division of Indonesia. Land use and land cover were identified based on what could be "seen" by the satellite. Figure 3 indicates the existing land cover and land use in Minahasa Regency include Manado City and surrounding region. Majority of land are conversed into plantation fields across urban, peri urban and boundary areas.

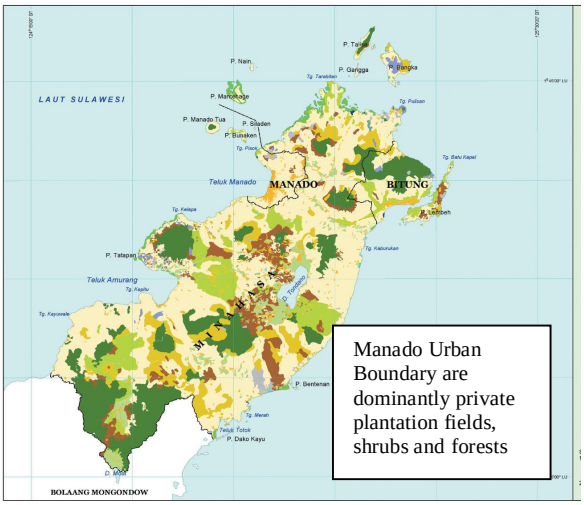

Figure 3. Map of Existing Land Use in Minahasa Regency

3.2 Evaluation of Green infrastructure Systems

A green infrastructure system is best viewed as network or web of open spaces and pathways that provide many benefits and the opportunity for people and animals to travel through the urban environment. Although most greenway corridors are at least partially conserved, the transportation aspects of the suburban greenway and agricultural matrices and hubs fall short of providing a complete or continuous system (as shown in figure 4 below). Many hectares within potential greenway corridors have already been developed for commercial and residential uses. Building blocks or components make up a green infrastructure system. These include greenways, the links in the system, as well as parks, preserves and cultural/ historic sites, which can serve as system hubs, as shown in table 1.

Figure 4. Infrastructure and housing development in Manado

Type of Green Infrastructure	Functions
Landscape Linkages	Linear protected areas that provide sufficient area of space for native plants and animals to flourish while serving as corridors connecting ecosystems and landscapes.
Conservation corridors	Less extensive linear protected areas, serve as biological connecting corridors and also provide outdoor, resource-based recreational opportunities.
Greenbelts	Protected natural lands or working landscape surrounding cities that preserve agricultural productivity as well as to balance and direct urban and suburban growth.
Recreational corridors	Linear open spaces to intense recreational use for residents and visitors.
Scenic corridors	A linear protected corridors and lands for scenic quality and other aesthetic considerations.
Utilitarian corridors	Linear features, such as powerline and pipeline rights-of-way and canals that help connect recreational, cultural or natural system features.
Trails	Designated trails provide access to and appreciation of the values of natural areas, green spaces and historic sites.
Hubs and sites (Reserves, regional parks and preserves, and ecological sites)	The system serves different purposes i.e conserving biological diversity and natural resources, protect important historical and cultural sites and provide some nature-based recreation opportunities, provide ecological benefits, and conserve important or unique natural or geologic features.
Cultural/Historical/ Recreational Sites	Community parks or cultural/historical sites provide recreational opportunities, help protect and interpret cultural heritage and can often serve as a system origin or destination
Urban area	Serve as human hubs for GI systems

The habitat conditions in the green infrastructure system have been assessed in terms of biodiversity conservation purposes without disregard the social and cultural aspects. Based upon indicators of habitat size, vegetation cover, structural diversity and vegetation composition (Jansen and Healey 2003; Parkes *et al* 2003), the actual condition of peri urban area visually assessed and score qualitatively as very small, small, medium and large. Forest patches and riparian corridor are likely to be useful for increasing ecological connectivity and creating green infrastructure network. In the study area, a scale of 0 to 4 was applied for sub-indicator using applicable method of scoring and weighting, as shown in table 2. The result shows significant and potential green infrastructure to be developed and connected between hubs and corridors in peri urban area and create urban greenbelt. Although the majority of land had been conversed into residential, plantation field, there are still opportunities for urban biodiversity conservation.

Table 2. Method of Scoring used to evaluate the green patch condition in study area

Category	Indicator	Sub-Indicator	Score	Method
Patchs/hubs Condition	Patche / hubs Size	Relative patch size	0 - 4	0=non; 1=very small; 2=small; 3=medium; 4=large
	Vegetation Cover	Canopy cover	0 - 4	0=absent; 1=1-20%; 2=21-40%; 3=41-60; 4≥61% cover
		Middlestorey	0 - 4	0=absent; 1=1-20%; 2=21-40%; 3=41-60; 4≥61% cover
		Understorey	0 - 4	0=absent; 1=1-20%; 2=21-40%; 3=41-60; 4≥61% cover
		Ground Cover	0 - 4	0=absent; 1=1-20%; 2=21-40%; 3=41-60; 4≥61% cover
	Structural Diversity	Number of Layers	0 - 4	0=No layers; 1=1 layer; 2=2 layers; 3=3 layers; 4=groundcover, understorey, middlestorey and canopy layers present
		Leaf Litter	0 - 4	0=none; 1=1-29%; 2= 30-50%; 3= 52-65%; 4= >66% groundcover
		Logs and Rocks	0 - 4	0=none; 1= small quantities; 2= abundant but some removed; 3= abundant relatively average intake, 4= abundant relatively large intake
	Composition	Natives in Canopy	0 - 4	0=absent; 1=1-20%; 2=21-40%; 3=41-60; 4≥61%
		Natives in middle storey	0 – 4	0=absent; 1=1-20%; 2=21-40%; 3=41-60; 4≥61%
		Natives in under storey	0 - 4	0=absent; 1=1-20%; 2=21-40%; 3=41-60; 4≥61%
		Natives in Ground Cover	0 - 4	0=absent; 1=1-20%; 2=21-40%; 3=41-60; 4≥61%

Riparian corridors, as part of green space system are primary component in building green infrastructure system. The pattern of Manado City's major streams are eight catchments and riparian systems, which are relevant for developing green infrastructure zones. The open spaces along these streams and their tributaries create opportunities for linking the city's open spaces systems.

Figure 5. Riverine system in Manado City. Tondano river as main stream and small creeks are flow through the urban area and the rivers are include in the Tondano Regional Catchment Development (PWS Tondano).

4. RESULTS

Green infrastructure in the study area was categorized into three classes based upon overall patch conditions evaluation. Class A with high diversity of vegetation and layers are likely to attract wildlife, i.e. birds and small mammals, while class B have moderate and Class C have poor in vegetation-layer density. However, potential patch for conservation purpose can be established by re-vegetation and being connected to a green networks.

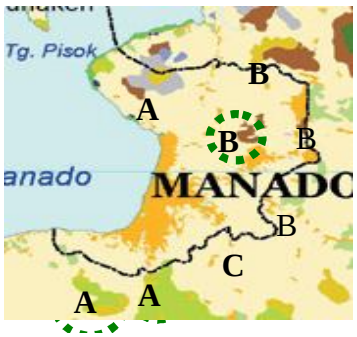

Figure 6. Identification of Potential GI systems

Figure 7. Greenbelt desired

Potential hubs and green corridor in peri urban Manado are described in table 3.

Table 3.Hubs identification and Classification

Patch and potential GI	Classification
Gunung Tumpa Protected Area	A
Pineleng Hills	A
Outer Ring Road Corridor	C
Plantation Fields	C
Swamp and Ponds	B
Shrubs forest	A
Riparian Greenways	A

Limited research time constrained this inquiry and the rigor of the fieldwork, and continuing research on biological condition as well as animal presence and occupant in urban area, particularly pattern and distribution of native species is recommended.

A green infrastructure with ecosystem network can be understood as a set of ecosystem patches, which functionally are connected by flow of organism and interactions within the landscape matrix. Structural components in the matrix include roads, fields and edges. In connection with biodiversity conservation, the ecosystem network is a multi concept include greenways (Ahern 2002), conservation networks (Grove 2003), and ecological networks (Grimm *et al* 2000). Scientists have identified some general design guidelines which can increase biological values of green networks and help minimize the potential negative impacts. Nearly all scientists agree that functional corridors and connectivity and the goal of any green infrastructure planning must be explicitly stated and analyzed (Noss and Coorperrider 1994 in Groves 2003).

5. CONCLUSION AND DISCUSSION

5.1 Planning Strategy

Traditionally, green infrastructures are planned for public utilities, roads, pipes and grey infrastructure, the green space located in leftover or unbuildable land and green space planning limited to development site i.e. lots, internal trails and pocket parks. However, better planning strategies can be developed, by first conduct inventory and assess natural and historic features and functions, secondly, develop a protection and management strategy, third, plan green spaces, such as parks, trails and habitat connections before locating built elements and lastly, connect hubs and green patches across regions and across ownerships. Green infrastructure planning as well as grey infrastructure ideally is plan simultaneously and given equal priority in the planning process. It is also planned as complementary systems and equally considered in the funding process.

A framework of Green infrastructure as a tool for informing decision-making is needed. A set of basic stage is designed as follows:

- Inventory of natural and historic resources
- Identify opportunity and constraints
- Determine risks to identify resources
- Integrate findings and goals into local and regional comprehensive plan
- Amend local ordinances to reflect identified goals

5.2 DISCUSSION

Significant biodiversity conservation is concerned distributed throughout the city, and is particularly concentrated along the outer margin of the city. Urban areas, particularly river ways and mouth adjacent near shore zones are integral to the conservation of urban biodiversity. It is needed to re-thinking and addresses the methods for constructing the conservation blueprint, the distribution of biodiversity features relative to urban areas, and highlight current work of the local government in Manado and nationally Indonesia to address urban threats to biodiversity conservation and knowing that greenways provide a chain of different habitats permeating the urban environment. We suggest that planners can have a positive impact on urban biodiversity by slowing the pace of redevelopment and by not hurrying to tidy up and redevelop brownfield sites, converse land and clear the spaces contain green elements.

5.2.1 Green Infrastructure and Conservation Challenges

Nowadays the accelerated consumption or conversion of open lands in relation with land conservation in Indonesia has been in challenge. The conversion of natural areas and working lands has resulted in increased habitat fragmentation, loss of biodiversity and wildlife populations, disruption of natural landscape processes, impairment of carbon storage and the degradation of air and water resources [Davies et al 2004]. It has also had numerous social consequences including the loss of vital services provided by natural systems, increased public and private costs of providing services to dispersed development, a decreased sense of community and the loss of the connection people feel with nature and with each other [Laurian 2008].

To address these concerns, governments across Indonesia, have developed regulatory approaches to resource conservation, species protection, facilities sitting, air and water quality and land management [www.kehati.or.id]. Local jurisdictions have implemented comprehensive plans; however, many of the communities have not approved the invested heavily in roads, sewers and other public works or "gray infrastructure". Increasingly, communities are investing in parks, open space, farmland and forest protection and in other elements of green space.

Although current approaches can count many accomplishments toward protecting natural systems and processes, improving environmental quality and delivering transportation and other community services, important objectives still go unmet. This patchwork of well-intentioned plans and regulatory approaches by themselves are not sufficient to arrest the decline of species, natural resources and systems or dispel the feeling that we are still losing our quality of life and important measures of the "good life." However, haphazard development as well as haphazard conservation - conservation activities that are reactive, site-specific, narrowly focused or not well integrated with other efforts should be addressed. It is a need of smart growth to strategically direct and influence the patterns of land development and "smart conservation" to direct our nation's

conservation practices [Mark et al 2008]. Green Infrastructure - strategically planned and locally managed networks of protected green space with multiple purposes - is of critical importance to ensuring clean air, abundant clean water, and healthy landscapes for all people today and for future generations. Green Infrastructure provides a solution that ensures environmental protection and a higher quality of life for communities as well as regulatory predictability for landowners and investors.

ACKNOWLEDGMENT

I wish to thank Centre of Minahasa Regency for GIS data and Map Base. I also give thank to Prof. Dr. Sangkertadi, DEA for assistance and suggestion in this research project.

REFERENCES

[1] Ahern, L., Lowe, K., Moorrees, A., Park, G., and Price, R., (in prep.), *Biodiversity Action Plan for the Goldfields Bioregion, Victoria: strategic overview*, Department of Natural Resources and Environment, Melbourne, 2002.

[2] Benedict A. Mark, Mc. Mahon and T. Edward, Green Infrastructure: Smart Conservation for the 21st Century, *Sprawl Watch Clearinghouse Monograph Series*, 2008, viewed 7th April 2009.

[3] Bryant, M.M. "Urban landscape conservation and the role of ecological greenway at local and metropolitan scales", *Landscape and Urban Planning.*,vol 6, pp. 23-44, 2002.

[4] Davies, K. F., Gascon, C. and Margules, C. R, "Habitat fragmentation: consequences, management, and future research priorities", in: *Conservation biology: research priorities for the next decade* (eds M. E. Soule and G. H. Orians), Society of Conservation Biology, Island Press, Washington DC, 2004.

[5] Grimm, B. N, Grove, M.J, Picket, T.A.S and Redman L.C., "Integrated approaches to long- term studies of urban ecological systems", *Bioscience*, 2000, Vol.**50**, No.7.

[6] Groves, C.R 2003, d*rafting a conservation blue print, A practitioner's guide to planning for biodiversity*, Island Press, Washington DC.

[7] Hellmund, P.C and Smith, D S, Greenway ecology and the integrity of landscapes: an illustrated primer, in *Designing Greenways: Sustainable Landscapes for Nature and People*, ch.2, Island Press, Washington DC, pp.42-69, 2006

[8] Heritage Conservancy Organization, *"growing with Green Infrastructure"*, viewed 25 June 2009. http://www.heritageconservancy.org/projects/p-greenway.php.

[9] Hough. M, *City and Natural Process*, NJ: Routedge, 1995, Pp.169.

[10] Kehati-The Indonesian Biodiversity Foundation, http://www.kehati.or.id, view 25 June 2009.

[11] Laurian, L, "Designing Greenways: Sustainable Landscapes for Nature and People" (Book review), *The American Planning Association*, 2008, Vol. 74.1, Pp. 145(1).

[12] Noss, R.F., "Wildlife Corridors", In: D.S. Smith and P.C. Hellmund (Editors), *Ecology of Greenways*. University of Minnesota Press, Minneapolis, MN, 1993, Pp. 43-68.

[13] Parkes, D., Newell, G., Cheal, D., Assessing the quality of native vegetation: the 'habitat hectares' approach, in *Ecological Management Restoration*, 2003, Vol.**4**, S29–S37.

[14] Wuisang, C.E.V, "A Study of Greenways: Issues, Roles and Management Implications for Wildlife in Suburban Adelaide, (master thesis), Bar Smith Library, The University of Adelaide. October 2008.

ISSN 114-1284

Preloading Effects on Shear Strength of Soft Soils Under Consolidated Drained Test

Damrizal Damoerin[1], Wiwik Rahayu[2] and Mira Nurmayani[3]

[1]*Faculty of Engineering*
University of Indonesia, Depok 16424
Tel. : (021) 7270029, Fax : (021) 7270028
E-mail : damrizal@eng.ui.ac.id

[2,3]*Faculty of Engineering*
University of Indonesia, Depok 16424
Tel. : (021) 7270029, Fax : (021) 7270028
E-mail : wrahayu@eng.ui.ac.id

ABSTRACT

Preloading is a method of soil improvement by applying temporary loads on soil layer in the field to increase the shear strength and decrease the settlement at post-construction stage. Laboratory tests was conducted by using triaxial apparatus to simulate the real condition in the field. The soil samples were saturated in the triaxial test until the coefficient B is above 0.97. At the first step of the consolidation stage in the triaxial test, loading is given for 24 hours in amount of 1,5 Pc' and then the cell pressure is released to site pressure condition for another 24 hours, which Pc' value was obtained from consolidation test. And at the second step, loading is given in amount of 2 Pc' for 24 hours and then the cell pressure is released to site pressure condition. Shearing the samples in drained test is carried out slowly under condition of no excess pore pressure until achieving maximum stress and then the test is conducted to strain of 18 %.The test results indicated that the soils parameters under consolidated drained test with preloading are higher than the unconsolidated undrained test and gives a increase the shear strength to support permanent load.

Keywords: *preloading, soft soil, shear strength, consolidated drained, pore pressure, strain*

1. INTRODUCTION

The safety of buildings construction located on soft soil should be ensured against failure and tolerable settlement. One of the applied method in the field is preloading. This method is to increase the shear strength capacity and decrease the settlement during post construction phase by applying load on soil layer.

To simulate the real condition in the field, laboratory study of preloading effect on shear strength in drained condition was conducted on Bekasi soft soils by using triaxial apparatus.

Chin et al. [7] giving detailed information concerning design and construction control of embankment over soft cohesive soils by using preloading or surcharging in the field accompanied with installation of vertical drains to increase the consolidation time. While Damoerin et al. [9] have studied the effect of preloading to shear strength on soft soils with limited consolidation time during 4 hours under consolidated undrained triaxial test. Bouferra et al. [4] have studied on sand under undrained cyclic loading and give information that a large preloading induces a reduction of the resistance of sands to liquefaction.

Consolidated drained triaxial test with preloading on soft soils was conducted to simulate the real condition in the field accompanied with installation of vertical drains to increase the consolidation time. The test results indicated that the soils parameters under consolidated drained test with preloading are higher than the unconsolidated undrained test and gives an increasing shear strength parameters.

2. TEST PROCEDURE

Test on soil samples consist of physical and engineering properties. The engineering properties test consist of consolidation and consolidated drained triaxial test. Pc' value was

obtained from consolidation test and parameter of shear strength was obtained from drained triaxial test.
The soil samples were saturated in the triaxial test until the coefficient B is above 0.97. At the first step of the consolidation stage in the triaxial test, loading is given for 24 hours in amount of 1,5 Pc' and then the cell pressure is released to site pressure condition for another 24 hours. And at the second step, loading is given in amount of 2 Pc' for 24 hours and then the cell pressure is released to site pressure condition. Shearing the samples in drained test is carried out slowly under condition of no excess pore pressure until achieving maximum stress and then the test is conducted to strain of 18 %.

3. TEST RESULTS AND ANALYSIS

3.1 Physical Properties

The physical properties test results are shown in Table 1.

Table 1: Physical properties of Bekasi soft soils.

No.	Physical parameters	value
1	Natural water content	64 %
2	Spesific Gravity	2.639
3	Unit Weight (gr/cm^3)	1.6-1.7
4	Atterberg Limits - Liquid Limit, LL (%) - Plastic Limit, PL (%) - Plasticity Index , PI (%)	 84.137 41.14 40.11
5	Sieve Analysis - Sand (%) - Silt (%) - Clay (%)	 10 71.69 18.31

3.2. Engineering Properties

Generally, the engineering properties are necessary for design of foundation, earth structures and slope.

3.2.1 Consolidation Test

Based on the results of consolidation test, it can be found that the maximum vertical burden pressure has sustained on the sample in the past and it is known as the *preconsolidation pressure* (Pc'). The value of Pc' and overconsolidation ratio (OCR) value which are 137 kPa and 13.564 respectively. The value of Pc' can be used at preloading are 1.5 Pc' and 2.0 Pc' for consolidated drained triaxial test.

3.2.2 Consolidated Drained Triaxial Test

Shearing the samples in drained test is carried out slowly under condition of no excess pore pressure with speed of 0.004 %/minute until achieving maximum deviator stress and then the test is conducted to strain of 18 %. In this test, the effective stress can't be influenced by excess pore water pressure.
Based on the curve about the relation between deviator stress and strain as shown in Figure 1, it can be observed that deviator stress will decrease to strain of 18 % after reaching maximum deviator stress value. The samples reach the maximum deviator stress on strain of < 4 % and it indicates that the soil in over consolidation condition, more stiffer and compact The maximum deviator stress and strain can be seen at Table 2.

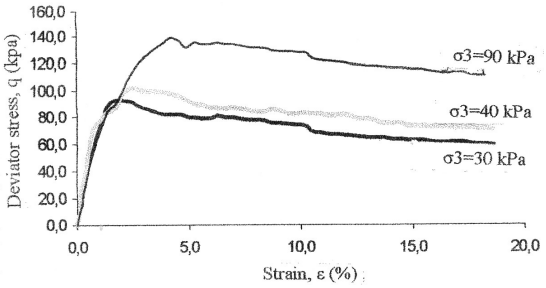

Figure 1: Relation between deviator stress, q and strain, ε.

Table 2: Maximum deviator stress and strain value

σ'$_3$ (kPa)	qmax. (kPa)	ε (%)
30	93,4056	1,76
40	102,4848	2,46
90	139,0411	4,22

3.2.3. Critical State Path

Based on the critical state path method with effective stress of $p' = [1/3(\sigma'_1 + 2\sigma'_3)] = [1/3(\sigma_1 + 2\sigma_3)]$ and deviator stress of $q = (\sigma_1 - \sigma_3)$, illustrated the relationship between deviator and effective stress as shown in Figure 2.

M parameter dan q_o value can be found in Figure 2 and λ_{NCL}, N, λ_{CSL}, Γ parameter can obtained on the curve about the relation between specific volume (v) and ln (effective stress, p') in Figure 3 and 4.

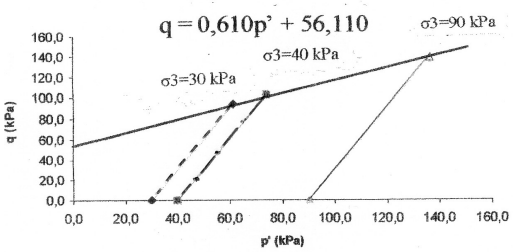

Figure 2: The stress path in q : p' for a drained test on over consolidated sample with a preloading

3.2.4 M Parameter & qo value and C' & Ǿ Parameter

Based on the curve figuring the relation between deviator, q and effective stress, p' as shown in Figure 2, M parameter and q_o value can be obtained. And M parameter can be determined as gradient between q and p' value at failure condition. q_o value is an intersection between gradient line and original point. It indicates that soil in over consolidation condition and have been received the preloading in the past.
M parameter dan q_o value can be used to obtain shear strength parameter of C' and Ǿ by using equation of (1) and (2) as follows:

$$\phi' = \sin^{-1}\left(\frac{3xM}{6+M}\right) \quad \text{..... (1)}$$

$$c' = \left(\frac{3-\sin\phi'}{6-\sin\phi'}\right)q_o \quad \text{..... (2)}$$

Based on the formula 1 and 2 [5], the value C' and Ǿ are given in Table 3.

Table 3: M parameter & q_o value

Parameter	Value
M	0,610
q_o (kPa)	56,110
ϕ' (o)	16,072
c' (kPa)	26,695

3.2.5 Parameter of λ_{NCL}, N, λ_{CSL}, & Γ

These parameter are found from: (i). Graph equations of specific volume (v = 1 + e) versus ln (effective stress, p') on Figure 3 and 4; (ii). Normal Consolidation Line (NCL) with equation of $v = N - \lambda \ln p'$ and (iii). Critical State Line (CSL) with equation of $v = \Gamma - \lambda \ln p'$. By using p = 1 kPa, the value of N , λ *and* Γ can be obtained as shown in Table 4. Normal Consolidation Line (NCL) located on the left of Critical State Line (CSL).
It can be seen from Table 4 that this parameter value by preloading of 2 cycles are smaller than by preloading of 1 cycle. This indicates that volume of soil will be decreasing under preloading.

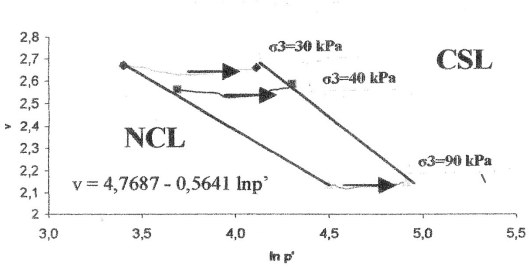

Figure 3: Relation between specific volume, v and ln (effective stress,p') by preloading of 1 cycle (2 Pc').

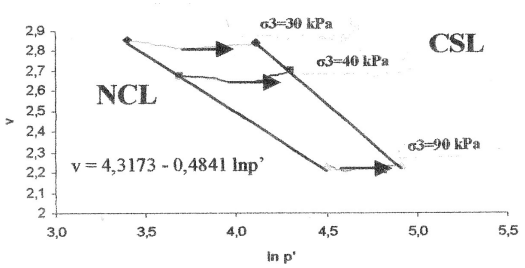

Figure 4: Relation between specific volume, v and ln (effective stress,p') by preloading of 2 cycles (1.5 Pc' and 2 Pc')

Table 4: Parameter of λ_{NCL}, N, λ_{CSL}, & Γ and c' dan ϕ' parameter

Preloading	λ_{NCL}	N	λ_{CSL}	Γ
1.5 Pc and 2 Pc	0.484	4.317	0.633	5.264
2 Pc	0.564	4.768	0.739	5.879

4. Parameter of shear strength under preloading and without preloading.

The particles of soil sample are smaller and more compact than the initial condition. Parameter of shear strength on soil samples under preloading are greater than without preloading as presented in Table 5 as follows:

Table 5: Shear strength parameter

Test type	c′ (kPa)	ϕ′ (o)
UU -Saturation* (without preloading)	17.47	4.28
CU- Saturation **) 4hours preloading (1.5 Pc & 2 Pc)	20.06	12.22
CD - 24hours preloading (1.5 Pc & 2 Pc)	26.695	16.072

(Inti, 2003) *)
(Damoerin et al., 2009) **)

4. CONCLUSION

Influence of preloading with 24 hours consolidation time on shear strength under consolidated drained triaxial test, yielding conclusion as follows:

- Effect of preloading at 1 cycle and 2 cycle on shear strength parameter (C' & Ǿ) is relatively small.
- The increasing of Ǿ value is quite significant and C' value is significant compare to the unconsolidated undrained test.
- M parameter is obtained also quite significant ranging from 0.075 to 0.610.
- qo parameter is obtained quite significant ranging from 17.426 to 56.11.
- Preloading effect on soil samples under consolidated drained test indicated that there is an improvement shear strength parameter value.

ACKNOWLEDGMENT

The authors would like to express the gratitute to the Civil Engineering Departement, Faculty of Engineering – University of Indonesia for the financial support for this study.

REFERENCES

[1] Atkinson, J.H., and Bransby, P.L. (1982), *The Mechanics of Soils*, McGraw Hill Book Company (U.K.) Ltd.

[2] Bowless, J.E. (1979), *Physical and Geotechnical Properties of Soils*, McGraw-Hill, Inc., USA.

[3] Bishop, A.W. and Henkel, D. J. (1982), *The Measurement of Soil Properties in The Triaxial Test*, Edward Arnold Ltd., London.

[4] Bouferra, R., Benseddiq, N. And Shahrour, I. (2007)."Saturation and Preloading Effects on the Cyclic Behavior of Sand". *International Journal of Geomechanics*, ASCE, Vol. 7 No.5, pp. 396 – 401.

[5] Bardet, J. P. (1997), *Experimental Soil Mechanics*, Prentice Hall, Upper Saddle River, New Jersey, 1997.

[6] Craig, R.F. (1987), *Mekanika Tanah (1989).* Terjemahan Budi Susilo Soepandji dari *Soil Mechanics, Fourth Edition* (1987), Erlangga, Jakarta.

[7] Chin, T.Y. and Sew, G.S. (2000), "Design and Construction Control of Embankment Over Soft Cohesive Soils", *SOGISC-Seminar on Ground Improvement-Soft Clay*.

[8] Das, B. M. (1985), *Mekanika Tanah (Prinsip-Prinsip Rekayasa Geoteknik - Jilid I, 1994).* Terjemahan Noor Endah dan Indrasurya B. Mochtar dari *Principles of Geotechnical Engineering* (1985), Erlangga, Jakarta.

[9] Damoerin, D., Prakoso, W. A. dan Ghifari, D. (2009), *Pengaruh Prapembebanan Terhadap Kekuatan Geser Tanah Berdasarkan Uji Triaxial Terkonsolidasi Terbatas Takterdrainasi*, Prosiding Konferensi Nasional Teknik Sipil 3, Universitas Pelita Harapan, Tangerang.

[10] Head, K.H. (1982), *Manual of Soil Laboratory Testing Volume 3*, Pentech Press, Plymouth, London.

[11] Holtz, R.D. and Kovacs. W.D. (1981), *An Introduction to Geotechnical Engineering*, Prentice – Hall Inc., Englewood Cliffs, N.J.

[12] Jurusan Sipil FTUI (2004), *Laporan Akhir Project Grant*, Depok.

[13] Laboratorium Mekanika Tanah FTUI (2001), *Laporan Akhir Penyelidikan Tanah Proyek Bangunan Gedung Sekolah Pondok Pesantren An-Nur Pondok Ungu - Bekasi*, Depok.

[14] Muning, R.R., 2003, Pengaruh Preloading Terhadap Kekuatan Geser dan Indeks Kompresi Pada Tanah Lempung Lunak, Skripsi FTUI, Depok.

Qualitative Study of Conducting Urban Infrastructure after Flood: Case Study of Flood Disaster in Five Regions of Jakarta

Djoko M. Hartono[1] , Evi Novita [1], Irma Gusniani S[1], Imelda Ika Dian Oriza[2]

[1]*Environmental Engineering Study Program, Civil Engineering Department*
Faculty of Engineering, University of Indonesia, Depok 16424
Phone: (021) 7270029. Fax: (021) 7270028
E-mail: djokomh@eng.ui.ac.id, evi_nz@yahoo.com, irma@eng.ui.ac.id

[2]*Faculty of Psychology*
University of Indonesia, Depok 16424
Phone: (021) 7270038
Email: orixza@yahoo.com; oriza@centrin.net.id

ABSTRACT

Jakarta lies in low-lying deltas served by Ciliwung River and many other small rivers. Jakarta also represents over populated area thus open and green areas more and more decreased. Since infiltration capacities of land in Jakarta, decreased, surface runoff has become bigger. As a result, Jakarta often faces flood disaster stricken. Flood disaster affects in human life and properties that includes urban infrastructures. The objectives of this study is to identify and develop a model or mitigation strategy to provide mitigation on urban infrastructures such as water and drinking water supply and also sanitation facilities after floods and to enhance the ability of the community to cope with the flood disaster. Primary data supported with questioner and secondary data obtained by studying the literature. The results of this study show that the height of water flood average a meter and the highest was 4 meter. The flood areas have drained within 5 days. However, the degree of damage on buildings and property is relatively minor during flood. The victims averagely have been living in their house more than 25 years and had experienced hit by floods at least two times. Thus, community learnt from their experience to overcome and prepare themselves in facing next flood in order to reduce the damage, suffering, and losses.

Key word

Floods, water supply, drinking water, sanitation, cope with flooding.

*) This research is Funded by Competitive Based Institution Program (Program Hibah Institusi), University of Indonesia and Directorate General of Higher Education, Department of National Education, 2008.

I. INTRODUCTION

Indonesia generaly has high rainfall, lies in seismic zone and surrounding with many active volcanous. Therefore, Indonesia has more risks to face disasters anytime. That chareacteristic is sensitive for flooded, drought, fire, tsunami and other disasters. The experiences that happen continually and similarly can be reduced the effect as well as the risk.

Jakarta as a capital city of Indonesia with huge population has variety of city infrastructures and facilities such as housing, social facilities, electricity, health services and education as well as transportation. Jakarta lies in low-lying land and as a part of Ciliwung river basin. Therefore, Jakarta will receive water that overflows from surrounding hills or mountain thus discharge into Java Sea. Based on this condition, Jakarta has more risk to face flood disaster and has proved over the last 10 years. Meteorologists forecast five yearly floods at 2002 would repeat at 2007, 2012 and so on. However, the floods occurred at 2008 faster than forecasting before. The forecasting indicates that floods' duration will be more often in the future.

2. OBJECTIVES

The objectives of this study is to identify and develop a model or mitigation strategy to provide mitigation on urban infrastructures such as water and drinking water supply and also sanitation facilities after floods and to enhance the ability of the community to cope with the flood disaster.

The target would be achieved by this study is to encourage the community to compose a guideline in order facing flood disasters.

3. THE STUDY LOCATION

There were five regions of Jakarta would be identified thoroughly by this study, namely West Jakarta, South Jakarta, Center of Jakarta, East Jakarta and North Jakarta. The five region of Jakarta can be seen on Figure 1.

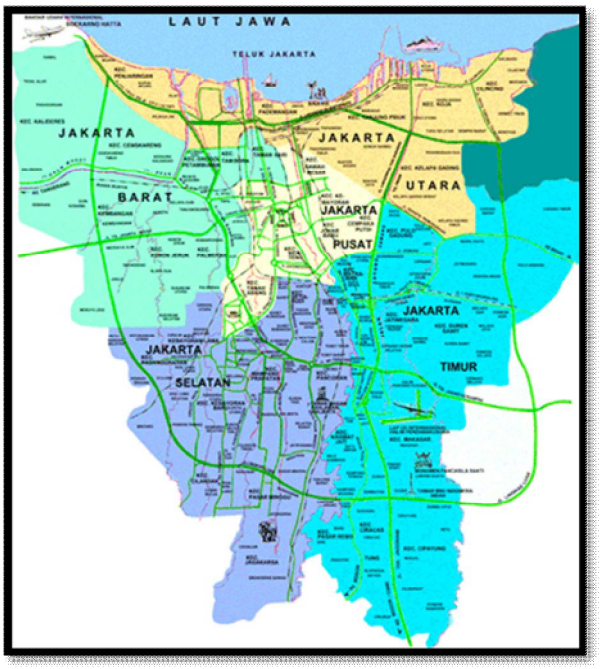

Figure 1. Map of Jakarta [2]

4. LITERATURE STUDY

There are 13 river flow in Jakarta. Ciliwung River is the longest river with length 117 km and divided into five regions [2]. The quality of upstream has shown better than downstream and particularly region that flows through Jakarta is the worse. The water quality of other rivers nor differ from Ciliwung River.
Jakarta Environmental Institution Agency (Badan Lingkungan Hidup Daerah/BLHD) represents a local government to monitor water quality from surface water, such as river and lakes, and groundwater. The quality of river shows as Pollution Index (PI). Based on BLHD monitoring data [1] , the entire region at Ciliwung River indicated moderate to heavy pollution. Not far, 50% of monitored well found contaminated with E. coli.

Clean water supplied by Water Treatment Plant which operated by Local Government Company (PAM JAYA). Therefore, only 60.21% of community served by this company [2]. Meanwhile, 38% community utilizes groundwater as water resource.

Coping mechanism or process is the ability of people to control any inconvenience, danger or emergency condition [5]. This mechanism divided into three strategis namely appraisal focussed strategy, problem focused strategy and emotional focused coping. People can choose one or combining of those strategies which best for themselves. In facing the crisis, people comes through grieving process that divided into five phases as mention on Figure 2 below [5]. People do not have to follow the entire phases but it depends on their endurance.

Figure 2. Phase in Crisis

5. METHODOLOGY

This study use ex-post facto approach and causal comparative method to observe several variables. The purposive sampling method appointed as sampling method in this study. Number of sample calculated by Newbold equation [4] as follow:

$$n = \left[\frac{z_{\alpha/2}\sigma}{B} \right]^2 \qquad (1)$$

Based on that equation, minimum number of sample is 267 whereas in this study, number of sample taken about 500 which divided into 100 samples at each region.

Primary data supported with questioner and field observation. The survey conducted during rainy season on September to November 2008. Meanwhile, secondary data obtained by studying relevance literature.

5. RESULT AND DISCUSSION

5.1. Condition before Floods

There were eleven areas at Jakarta that critical on floods disaster based on aerial view Citra Landsat. Critical area in West Jakarta is Cengkareng, Grogol, Petamburan, and Kalideres. Critical area in South Jakarta is Kebayoran Baru, Mampang Prapatan, and Pasarminggu. Critical area in East of Jakarta is Cipayung, Ciracas, Kramatjati, and Makasar. Critical area in Centre of Jakarta is Tanah Abang, Bendungan Hilir, Karet Tengsin, Kampung Bali, Kebon Melati, Blora and Kebon Kacang.

Observation on respondent in South of Jakarta show that the community in flooded area averagely has been living for 25 years. However, several respondents have been living almost 60 year. Based on that condition, they already had an experience facing floods.

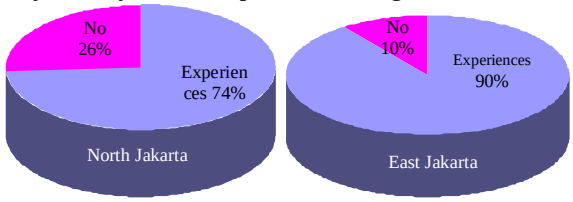

Figure 3. Percentage of respondent who have flood experienced at North and East Region of Jakarta

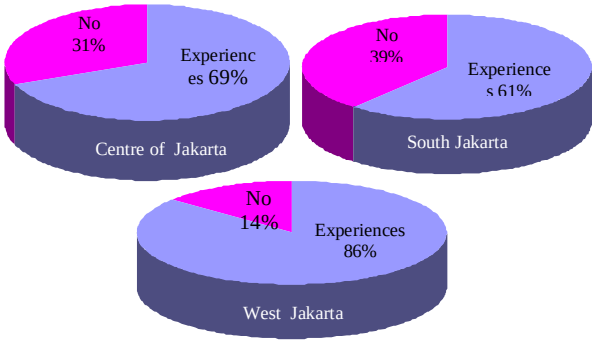

Figure 4. Percentage of respondent who have flood experienced at Centre, South and West Region of Jakarta

Figure 3 and 4 show the percentage of respondents who have flood experienced from East Region of Jakarta higher than other region. Whereas, respondent from South Jakarta is at the least experienced compare with other regions.

Number of people live in a house is about 4 to 5 person in South of Jakarta. Almost every house in the entire regions consists of more than four persons in the house. Table 1 shows length of stay and number of people live in a house among 500 respondent.

People have known how to prepare their house to face floods. Their use some strategies in order to reduce damage, suffering, and losses during floods. One of their strategies is upgrading the house become two levels (storey). Therefore, they can evacuate themselves and rescues their valuable goods to the second floor.

Tabel 1: Length of stay and number of people in a house

Region	Length of stay > 25 years	Number of family > 4 people
West of Jakarta	100	100
South of Jakarta	50	100
Center of Jakarta	50	100
East of Jakarta	100	100
North of Jakarta	100	100

Table 2 below shows the height and wide of respondent house. The entire respondent in Centre and East of Jakarta owning a house with height more than three meters. That height is suitable to anticipate floods which water level could reach more than three meters. However, water level of floods tends to increase that the last occurrence reached up to four meters. In a state of floods, the more of family member will make evacuation process easier and faster. Unfortunately, several respondents have limited space so it is not enough or too crowded for big family.

Table 2: Height and wide of responden house

Region	Height of the house > 3m	Area of house > 40m^2
West of Jakarta	24	50
South of Jakarta	48	100
Center of Jakarta	100	100
East of Jakarta	100	100
North of Jakarta	48	100

Almost the entire respondents already have supplied with water from PAM JAYA. They aware and consider about important of health. Besides, their knowledge about quality and benefit of clean and drinking water is good enough to maintain healthy life. However, in contrary, sanitation facilities such as toilet and septic tank paid less attention to respondent. Most

respondents utilize sharing toilet as well as communal toilet for daily activities. This condition shows on Table 3.

Table 3: The coverage of water supply and sanitation facilities before floods

Region	Water Supplied from PAM JAYA	Sanitation Facilities
West of Jakarta	94	32
South of Jakarta	70	14
Center of Jakarta	93	18
East of Jakarta	74	23
North of Jakarta	94	27

Respondent, which do not get water supplied by PAM JAYA, will try to find another source such as groundwater or buying to other seller.

5.2. Condition during Floods

Beside food and cloth, water supply and sanitation become a big problem during floods. Electricity always shuts down for safety reason. Therefore, people that use electricity equipment such as water pump cannot access clean water from their house or their neighborhoods.

Government and several non-government organizations (NGO) try to help with distributing mineral water to evacuation centre. However, they could reach not the entire flooded area due the difficulties of transportation. Some area is under water so it is not possible to go through that area. Table 4 shows precentage of community that received water supply and sanitation aids.

Table 4: The coverage of water supply and sanitation facilities during floods

Region	Water Supply Facilities	Sanitation Facilities
West of Jakarta	89	75
South of Jakarta	17	14
Center of Jakarta	80	18
East of Jakarta	47	61
North of Jakarta	69	81

There are several water resources that utilize by respondent during floods such as water piping from PAM JAYA, groundwater, package water, and buying to water hawker. They utilize one resource or combining resources to fulfill their needs. The variety of water resources that utilized by respondent can be seen at Figure 5 and 6 below.

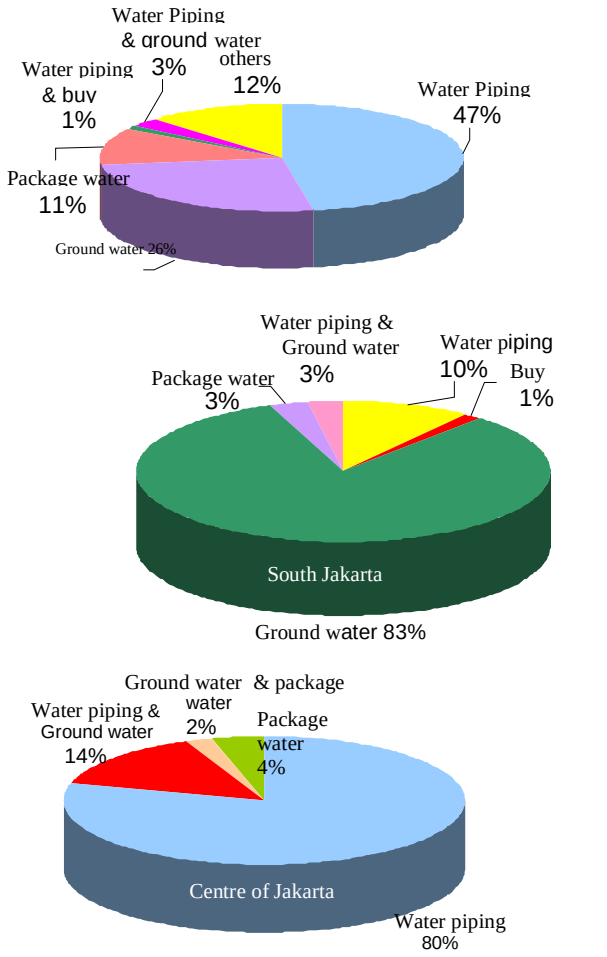

Figure 5. The variety of water resources that utilized by respondent at East, South and Centre of Jakarta

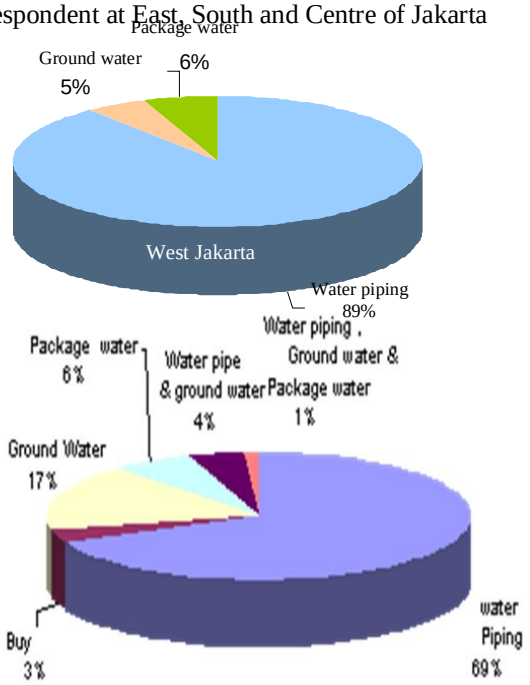

Figure 6. The variety of water resources that utilized by respondent at west and north of Jakarta

Table 4 also indicates the coverage of water supply decreased during floods compare with normal condition before floods. On the other hand, coverage of sanitations facilities increase during floods. This matter caused by government and NGOs aids that provide mobile sanitation equipment. In addition, people, who do not hit by floods, lent their facilities to flood refugee. Consequently, the coverage of sanitation facilities increased.

Flood disaster resulted damage, suffering, and losses to victims. They have to move a while as long as their house is under water. They become a refugee and live in a tent, school, or other public facilities that do not hit by flood until indefinites time. They can go to work or other place because of limited transportation and dried areas during floods. There is no electricity and no income for non-formal worker or non-employee. Consequently, they become dependent on aids.

The condition that mention before gave a sadness to floods victims. Figure 7 depicted what respondents felt during floods. Dominantly, victims become more fatefully in facing floods disasters. Nevertheless, there are several victims felt angry and sad.

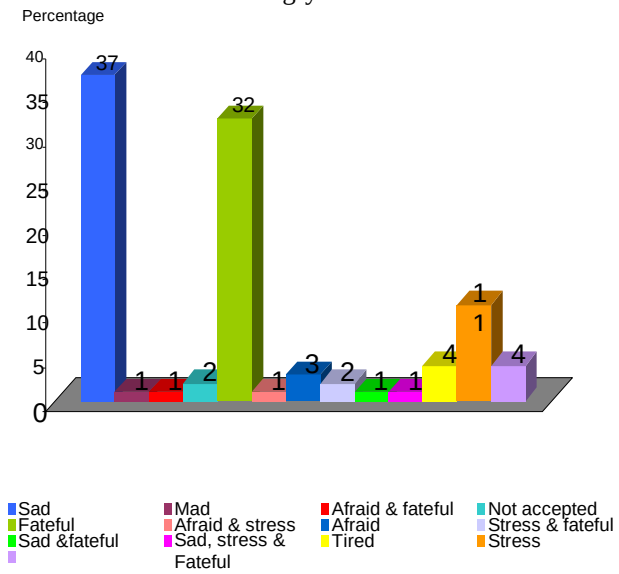

Figure 7. Respondent Feeling Facing Flood Disaster

In order to move back to normal life, the flood victims should get through the entire problem with coping mechanism. Besides, the entire aids from government, NGOs, and other communities will help the victims to cope their sadness, angry, and fateful feeling. With helping, they can overcome their sorrow faster.

CONCLUSION

The community who lived more than 25 years in floods area has experienced to face flood disaster. The government, comunity as well as other parties can not ignore flood risk sincef floods take lives and damage property. They developed strategy to reduce damage, suffering, and losses. One of their strategies is upgrading their height of house. People need water and sanitation facilitates during floods. Government, NGOs, and other community can help victims with providing and distributing water and sanitation facilities. Clean water usually served by PAM JAYA as long as in the state of flood.

Although in Jakarta at there are 12 ponds to catch flood water, however almost all reduced their volume because of sedimentation process and need more rehabilitation and maintaining. However flood control and rehabilitation are very expensive, the local government of DKI Jakarta will continue to finish channel surounding Jakarta, known as East Flooded Channel (Banjir Kanal Timur).

Victims felt angry and sad during floods. Therefore, fateful is dominant feeling for victims. They have to get through the entire problem caused by flood with coping mechanism.

Centre Government as well as local government, community should work together to make a good plan to overcome flooded hazard. Flooding affect people and their property and caused health problem, both physical and emotional, damage building and content of building and landscaping.

REFERENCES

[1] BLHD Jakarta, " Implementation of Pollution Prevention and Destruction of Ciliwung Riverbanks Activities at 2005" (Pelaksanaan Kegiatan Pengendalian Pencemaran dan Kerusakan Daerah Aliran Sungai Ciliwung Tahun 2005)," unpublished.

[2] BR PAM Jaya, "10 Years Cooperation Between Government and Private Sector in Drinking Water at Jakarta 1998-2008" (10 Tahun Kerjasama Pemerintah-Swasta Air Minum di DKI Jakarta 1998-2008), Badan Regulator PAM Jaya Publishing, pp 126, 2008.

[3] Jakarta Public Works Agency, "Concept of Technical Formulation on Environmental Engineering Construction Qualification" (Konsep Rumusan Teknik Kualifikasi Bangunan Teknik Lingkungan), Activities Information Book, pp. 3, 2008

[4] Newbold P; Carlson W.L;, Thorne B.M, Statistic for Bussiness and Economics, Prentice Hall, 2003

[5] W. Loyd, "Coping Mechanism," http//www.wikipedia.com, November 2, 2008.

Proceeding of the 11th International Conference on QiR (Quality in Research)
Faculty of Engineering, University of Indonesia, Depok, Indonesia, 3-6 August 2009
ISSN 114-1284

Situ Gintung Dam Controversy, Rebuilt or Removed?

Dwita Sutjiningsih Kertadikara Marsudiantoro[1], Herr Soeryantono Sahid[2], Toha Saleh[3], Dwinanti Rika Marthanty[4]

Department of Civil Engineering, Faculty of Engineering
Universitas Indonesia, Depok 16424
Tel.: (021) 7270029; Fax.: (021) 7270028
*E-mail:[1]*dwita@eng.ui.ac.id*;[2]*soeryant@eng.ui.ac.id*; [3]*toha.saleh@ui.edu *;[4]*marthanty@yahoo.com

ABSTRACT

On the dawn of March 27, 2009 all of a sudden Situ Gintung Dam in South Tangerang, Banten, Indonesia was being headline on the media allover the world. A 10-meter high earthen dam breached with almost 100-dead toll brings us to a controversy, whether it will be rebuilt or removed. As compare to the situation in the US where around 60 small dams were scheduled for removal in 2008 alone, mostly due to no-longer-served its intended purpose and/or in order to restore its ecological integrity by restoring the free movement of fish and other aquatic organisms. This paper discusses thoroughly the complexity of issues to be considered and the decision-making process to be taken for both possibilities.

Keywords
Situ Gintung Dam controversy; rebuilt or removed; considerations.

1. BACKGROUND INFORMATION

The exact figure of dams allover the world is uncertain, NRC estimated around 2.5 million dams in 1990. According to the latest update by the USACE National Inventory of Dams (NID, 2009), there are 82,642 dams in the US, and approximately one third of these dams pose a "high" or "significant" hazard to life and property if failure occurs. Over one third of these dams are already fifty years old, and in another ten years, more than 60% of these dams will have reached the half-century mark. The deterioration of aging dams creates a financial burden for dam authorities and safety hazards to those living downstream. According to the National Performance of Dams Program at Stanford University, 1,595 significant hazard dams are within one mile of a downstream city.

In the world's record of disasters due to human technical failures, the 1975 collapse of China's Banqiao reservoir dam in Henan province ranked first, which was in a matter of days, 26 dams collapsed one after another, which resulted in massive flooding in nine counties and one town. The total number of deaths recorded was around 240,000. Note that in China there are 85,160 reservoirs, which a total of 3,486 dams collapsed from 1954 to 2005.

As indicated by International River Network, the cause of failure of various types of dams (earthfill, rockfill, gravity, multi-arch, buttress, arch, tailings dam) were either due to overtopping (35%), piping (38%), structural failure or geological/foundation weaknesses (21%), and others 6%. Referring ICOLD (International Committee on Large Dams) Bulletin 109, the statistics of dam failures worldwide (excl. China & USSR) were dominated by overtopping during operation of fill dams, which were less than 30m high.

After the event on the dawn of March 27, 2009, the aging Situ Gintung Dam in South Tangerang, Banten, Indonesia contributed to the statistics of devastating dam failures with almost 100-dead toll, hundreds of victims and missing people. On March 31, 2009, the Directorate General of Water Resources, Ministry of Public Work, has come up with a recommendation to build new check-dam more upstream in order to preserve reservoir function.

According to World Commission on Dams, the consensus among river ecologists is that dams are the single greatest cause of the decline of river ecosystems, since by design dams alter the natural flow regime. Dams also require ongoing maintenance, and can have significant economic impacts on dam authorities, the surrounding community and society in general.

Therefore, despite the long history and importance of dams, there is a growing awareness to remove them. Decommissioning or removal of dams has primarily taken place in the US and Europe, and the trend is likely to go worldwide. Dam “decommissioning” means the deactivation of a dam project’s principle functions and may include: dismantling power generating equipment, permanently opening dam gates, partial breaching of earthen structures, or complete and permanent removal.

The American Rivers organization has documented approximately 750 dam decommissioning since 1912, with the pace picking up to between 20 and 50 each year for the last 10 years. Currently in the United States, more dams are being removed than built. In the year 2008 alone, there were 64 dams removed or scheduled to be removed.

The situation in the US Dam Removal Cited reasons for removal (American Rivers et al., 1999):

- Environmental — 43%
- Safety — 30%
- Economics — 18%
- Failure — 6%
- Unauthorized structure — 4%
- Recreation — 2%

Influencing public opinion can be a lengthy and difficult process, since many groups are involved in dam removal decisions. Scientific information about the benefits and drawbacks of dam removal should be used as the basis of decision making. Dam removal is becoming a new socio-politic-scientific endeavor.

Several tools exist to assist communities and decision makers in evaluating the option of removing a dam. This paper discussing two decision-making guides for dam retain or removal; and exploring the possibility to employ the guidelines for Situ Gintung case.

2. THE DECISION-MAKING MODELS FOR DAM RETAIN OR REMOVAL

Influencing public opinion can be a lengthy and difficult process. Many groups are involved in dam removal decisions; local residents, citizens groups, local government, state government agencies, federal government agencies, businesses and environmental groups. Opponents to dam removal raise concerns such as the effect on property values, recreation, and town identity, while proponents of dam removal raise concerns such as public safety, the cost of maintaining an aging dam, and water quality problems created by dams.

Based on previous work by Stephanie Lindloff, River Alliance of Wisconsin, ten common concerns about dam repair and removal are the following: (1) "If the dam is removed, the river will turn into a mere trickle or even dry up"; (2) "We'll have more flooding problems"; (3) "All that will be left are stinking mud flats"; (4) "If the dam is removed, who will own the 'new' land?"; (5) "If the dam is removed, wildlife habitat will be lost and wildlife will suffer"; (6) "Will property values be affected?"; (7) "Who will pay for the dam's repair or removal?"; (8) "The dam has historical value"; (9) "Dam removal will introduce exotic and/or disease species"; (10) "I've heard you can get sick because of dam repair or removal".

There are several tools exist to assist communities and decision makers in evaluating the option of removing a dam. The following are two tools from two reliable sources, which already approved to be powerful, namely:

- "Exploring Dam Removal: A Decision-Making Guide". A joint project report written by American Rivers and Trout Unlimited for dam removal and river restoration work in 2002.
- "Dam Repair or Removal: A Decision-Making Guide". Document prepared based on a project funded by the Wisconsin Department of Natural Resources and in part by University of Wisconsin-Madison Institute for Environmental Studies.

2.1. Exploring Dam Removal: A Decision-Making Guide Developed by American Rivers and Trout Unlimited (AR & TU)

In exploring whether a dam should be removed or retained, the considerations are structured as follow:

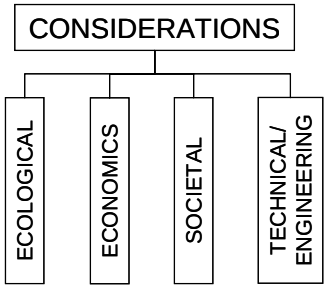

Figure 1: Consideration Structure of AR & TU Decision-Making Guide

Considerations that should be addressed and the bottom line of each issue are summarized in the following table:

Table 1: Considerations, Issues and Bottom Line of AR & TU Decision-Making Guide

	Issues	Bottom Line
ECOLOGICAL CONSIDERATIONS	A. Upstream Flow and Habitat	Will the restored river and riparian habitat upstream outweigh the loss of impounded habitat?
	B. Downstream Flow and Habitat	Is dam removal necessary to restore natural flows to the river? Do the benefits of restored flows outweigh the impacts on species that prefer unnatural flows?
	C. Fish and Wildlife	Is the net impact of dam removal on fish and wildlife populations positive or negative?
	D. Passage and Movement of Fish and Other Species	Will dam removal improve safe passage of migrating fish and movement of resident fish and wildlife? Is dam removal necessary to accomplish this? Can dam removal be done without enabling the spread of undesirable species?
	E. Sediment Movement	What is the current net impact of the accumulated sediment on the impoundment and downstream habitats? How will sediments released during dam removal

	Issues	Bottom Line
		impact the riparian and riverine habitats in the short and long term?
	F. Water Quality	Will dam removal have a net benefit on water quality, taking into account both short-term and long-term impacts and benefits?
	G. Riparian Areas	Will there be a net gain in the amount and quality of riparian habitat as a result of dam removal?
	H. Wetland Areas	How will the wetlands gained by dam removal compare in amount, type, and habitat value to the wetlands lost by dam removal?
	I. Location of the Dam within the Watershed	Will dam removal significantly enhance the river's ecological values, given the location of the dam relative to other dams in the watershed?
ECONOMIC CONSIDERATIONS	A. Dam Owner's Costs and Benefits	Are the long-term costs of operating and maintaining the dam less or more than the costs of removing the dam? Do any benefits of the dam need to be replaced, and if so, by whom?
	B. Societal Costs and Benefits	Are others in the community responsible for any additional costs and benefits of maintaining or removing the dam?
	C. Recreational Costs and Benefits	Will dam removal positively or negatively influence community revenues from recreation?
	D. Environmental Costs and Benefits	Do the net environmental costs (or benefits) of keeping the dam outweigh the net environmental costs (or benefits) of removing the dam?
	E. Property Values	Will dam removal positively or negatively affect property values adjacent to the stream? Will these effects, if any, be short or long term?
	F. Distribution of Costs and Benefits	Who benefits the most from retaining/removing the dam? Who bears the costs for retaining/removing the dam?
	G. Availability of Funding for Dam Repair or Removal	What funds are available to pay for dam maintenance/repair or removal?
SOCIETAL CONSIDERA	A. Community Understanding of the Dam, the River, and Dam Removal	Do the decision-makers and other concerned parties have sufficient information to make an informed decision about dam removal or dam retention?

	Issues	Bottom Line
	B. Service(s) Provided by the Dam	Does the dam provide any services? Are these services as valuable as the services provided by a free-flowing river? If yes, can these services be provided through alternative means?
	C. Who Benefits From and Who Bears the Costs of the Dam	Who benefits from and who bears the costs of the dam? Who will benefit from and who will bear the cost of a restored river?
	D. Community Sentiments Toward the Dam and the River	How do community members feel about the dam? About the river? About dam removal?
	E. Historical Role of the Dam	Does the dam have true historical value, and are there ways to commemorate the historical value without keeping the dam?
TECHNICAL/ENGINEERING CONSIDERATIONS	A. Feasibility of Repairing and Maintaining the Dam	
	A1. Safety Repairs or Upgrades	If the dam is unsafe, will dam removal cost less than repairs and ongoing maintenance? Are repairs to the dam prohibitively expensive?
	A2. Repairs or Upgrades to Continue Efficiently Providing the Dam's Intended Uses	If expensive upgrades are needed to maintain the dam's services, is it more cost effective to remove the dam and find alternatives to replace those services?
	A3. Mitigation of the Dam's Environmental Impacts	If environmental mitigation measures are needed, is it more cost effective to keep the dam and mitigate for its environmental impacts or remove the dam?
	B. Feasibility and Design of Dam Removal	
	B1. Obtaining Dam Removal Permits	Will permitting requirements affect the design, cost or feasibility of the removal? Are there permitting requirements for dam repair, reconstruction, or related to any of the services provided by the dam that will affect the feasibility or cost of keeping the dam?
	B2. Protecting Against Environmental Impacts	What steps must be taken to eliminate or minimize the environmental impacts of the dam removal?
	B3. Managing Sediment	Is there a feasible method of managing the sediment behind the dam?
	B4. Removing Structures	What is the most cost effective and environmentally sound dam removal method?

	Issues	Bottom Line
	B5. Protecting Infrastructure	Are there structures that will have to be stabilized, retrofitted, or relocated if the dam is removed?
	B6. Restoring the Channel	Does the new river channel need to be actively designed or can the river naturally find its own channel?
	B7. Restoring Recovered Land	Will the recovered land need to be actively re-vegetated?

To see the complete checklist questions and toolboxes, one should consult "Exploring Dam Removal: A Decision-Making Guide" in <http://www.americanrivers.org/>.

2.2. Dam Repair or Removal: A Decision-Making Guide Developed by Wisconsin Department of Natural Resources (WDNR) and University of Wisconsin-Madison (UWM)

The document "Dam Repair or Removal: A Decision-Making Guide" is a main reference for The Water Resources Management workshop (WRM) 2000, which is a regular part of the curriculum of the Water Resources Management graduate program at the University of Wisconsin-Madison. The workshop is conducted based on five modules in the document, and involves an interdisciplinary team of faculty and graduate students in the analysis of a contemporary water resources problem.

Considerations of dam retain or removal is structured as follow:

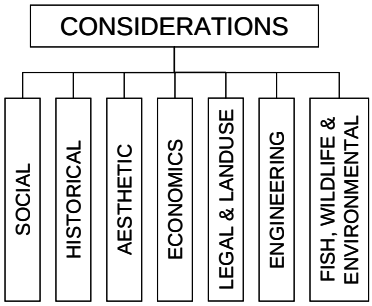

Figure 2: Considerations Structure of WDNR & UWM Decision-Making Guide

The outline of considerations, issues and checklist questions of WDNR & UWM Decision-Making Guide is summarized in the following table:

Table 2: Considerations, Issues and Checklist Questions WDNR & UWM Decision-Making Guide

	Issues	Checklist Questions
SOCIAL	• Community attitudes • Process of decision-making	• What is the social value of the dam and the impoundment? • What are community attitudes toward the dam? • What type of decision-making process will be used for deciding whether to remove or repair the dam?
HISTORICAL	• Historical facts • Historic preservation options	• What is the history of the dam? • Are historical community events hosted at the site? • Is the dam's historical value primarily through association with an adjoining building or structure (for example, a millhouse) versus the impoundment?
AESTHETICS	• Aesthetic concerns • Possible changes in the scenery • Options for enhancing visual appeal	• What are the community's primary aesthetic concerns? • How will the environment of the area change with our decision to repair or remove the dam? • What opportunities exist for enhancing the look of our community as a result of our decision to repair or remove the dam?
ECONOMICS	• Costs Construction costs Safety and liability cost Operation and maintenance costs • Property values Benefits Recreational benefits Environmental benefits • Funding	• What is the cost of repairing or rebuilding the dam? • What is the cost of removing the dam? • If sediment is an issue, what is the cost of addressing the sediment that has accumulated behind the dam? What if the sediments are contaminated? What is the cost of properly disposing the sediment? • Are property values expected to increase or decrease in the surrounding area if the dam and pond are around for another several decades or if the dam is removed? • What funding sources are available to cover construction costs and costs of operation and maintenance with repair or removal?

	Issues	Checklist Questions
LEGAL & LAND USE	• Historical overview of legal regulation on dams • Legal definitions • Repair/removal issues • Role of the Regulatory Commission • Land ownership identification: Dams and flooded lands	• What are the important regulatory considerations? • Who owns the dam? • What are the important land use considerations if the dam is repaired or removed? • What happens to the land submerged by the impoundment if the dam is removed? Who will own the land?
ENGINEERING	• Dam safety and hazard classification • Flood studies • Structure assessment and analysis • Emergency Action Plan • Sediment management	• What is a dam safety inspection? How often does the dam owner need to perform it? • What is the size, type, age and safety condition of the dam? • What is the hazard ranking of the dam (that is, how much potential damage could be caused if the dam were to fail)? • Does the dam provide flood protection? Does the dam meet necessary flood standards? What is the flood passage capacity of the dam? • Would the dam survive maximum headwater conditions (impoundment filled to the top)? Is it possible to see sliding, overturning or foundation failure (such as cracks, holes, crumbled sections, and so forth)?
FISH, WILDLIFE & ENVIRONMENTAL	• Fish/wildlife communities • Effects on fish and other aquatic wildlife habitat • Effect on wetlands • Species of concern • Watershed, water quality, and groundwater	• What is the quality of habitat in the impoundment? Upstream? Downstream? • What is the amount and type of lake or pond habitat that would be lost through dam removal (for example, how many acres of warm-water fishery? How many acres of waterfowl habitat)? • What are the amount and type of reconnected river habitat that would be gained through dam removal? • How would dam removal/repair affect wetlands? • Are the species affected by dam related activities species of concern? Are there endangered species present?

To see the complete checklist questions and toolboxes, one should consult Water Resources Management Practicum 2000: "Dam Repair or Removal: A Decision-Making Guide", in <http://www.ies.wisc.edu/research/wrm00/>.

2.3. Decision-Making Process

A well designed decision-making process can address safety, economic, and environmental concerns and also satisfy the desire of community members and other stakeholders to participate actively in shaping the future of the dam and related natural resources in their community.

The experiences of numerous Wisconsin, USA, communities that have faced the decision-making whether to remove or retain suggest that designing and adhering to a well considered collaborative decision-making process can significantly reduce the conflicts.

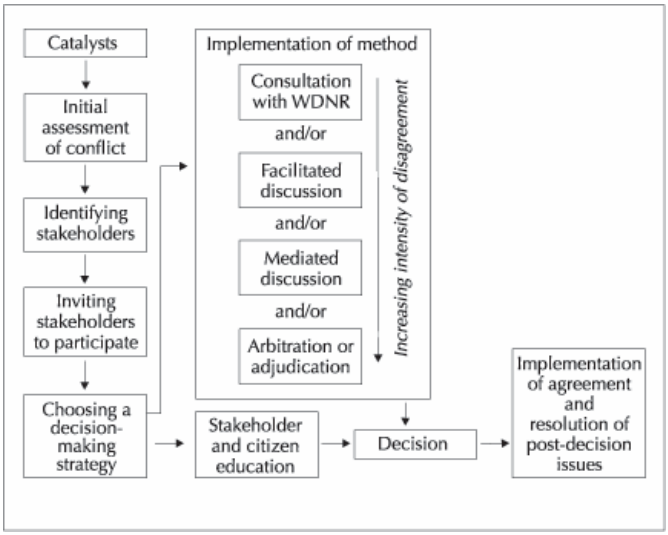

Figure 3: Principal components involved in designing and implementing an appropriate decision-making process.

3. THE SITU GINTUNG CASE

3.1. Situ Gintung Disaster Feature

Situ Gintung Dam was built during the Dutch occupancy in the year 1932-1934. The condition before the dam break was already degraded. The originally 31 Ha reservoir with 10m depth, currently (before its burst) only around 21 Ha left with the depth ranging from 3 to 4 meter.

Located in the vicinity of Jakarta, the storage capacity of the Situ Gintung reservoir diminished gradually within 76 years, mainly due to the pressure of urbanization.

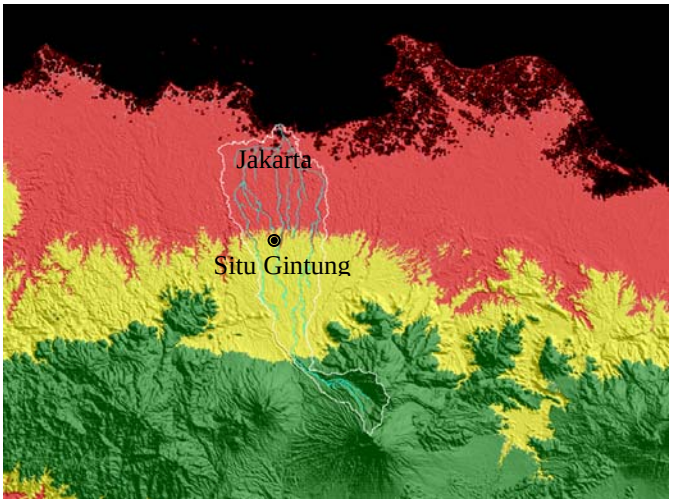

Source: The BPPT, 2009
Figure 4: Location of Situ Gintung Dam.

Based on 1:25,000 Earth Imagery Map, the 2008 land use distribution of the catchment area of Situ Gintung reservoir is dominated by housing (39.70%) and farmland (22.80%). The total catchment area is just around 112.50 Ha.

Source: The BPPT, 2009.
Figure 5: Catchment Area of Situ Gintung Resevoir.

The BPPT (The Agency for the Assessment and Application Technology) has conducted analysis concerning the trigger of Situ Gintung dam failure. Most likely the reason of dam burst was manifold, but the weakest point of the dam was its aging spillway structure. Piping through the spillway crack, and high intensity rainfall brought the dam to collapse.

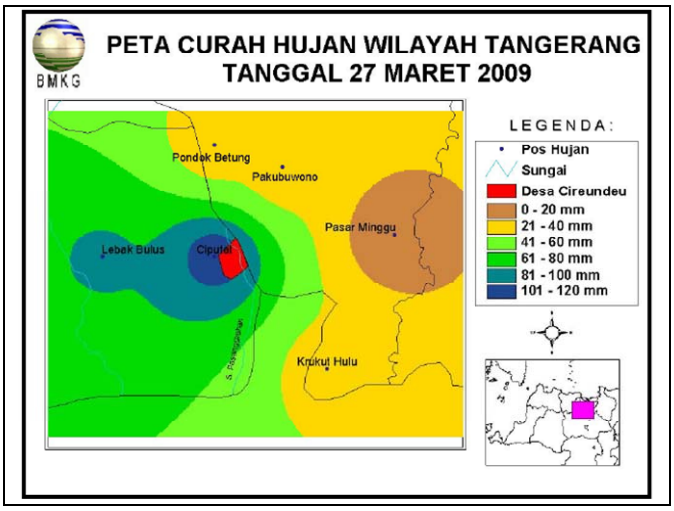

Source: The BMKG, 2009.
Figure 6: Rainfall Distribution on March 27, 2009.

According to the BMKG (Meteorology, Climatology and Geophysics Agency), the total area-rainfall on the preceding day was 113.20 mm.

Although the Situ Gintung dam failure was not the one and only catastrophic event due to human technical failures, the number of dead-toll, hundreds of victims and missing

people was indeed very massive in comparison to i.e. the collapse of Teton Dam in Idaho, USA, where a 90m high dam burst with 'only' 11 dead-toll.

Source: KOMPAS/WISNU WIDIANTORO, 2009
Figure 7: Situ Gintung, Situation Aftermath, March 27, 2009.

The dense housing complexes which occupied floodplains immediately downstream of the dam actually should have never been allowed to be there. People who have chosen to build houses and decided to live there should have known about the regulation and also the most important, about the potential hazard.

The scale of devastating hazard area covered around 11 Ha with 1km in length and 40-150m in width. Within minutes 316 permanent and semi-permanent houses were torn down and billion of rupiahs losses were obvious.

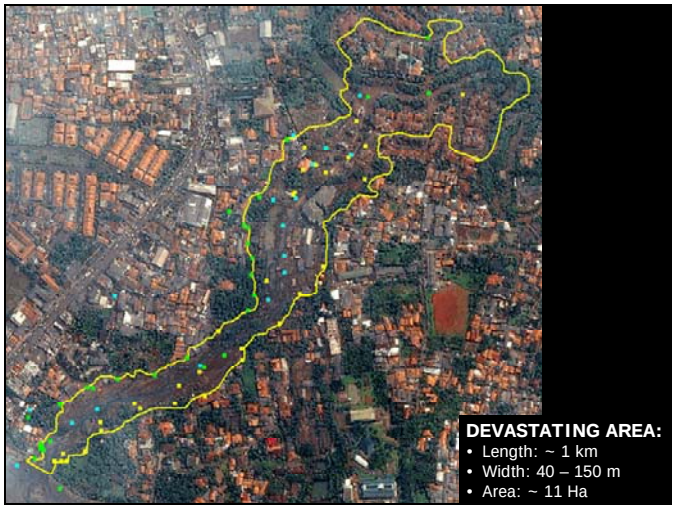

Source: The BPPT, 2009
Figure 8: Devastating Area Downstream of Situ Gintung Dam

3.2. Proposal of Post-Disaster Management

Technical Properties of Situ Gintung Dam/Reservoir can be summarized as follow:

- Dam: ca. 200m-length and ca. 7m-height.
- Appurtenances: one 5mx1.5m spillway and two intakes
- Function: originally for irrigation, then converted into conservation facility utilized for recreation and fisheries.
- Downstream channel: ca. 2m-width channel, tributary of Pasanggrahan river, floodplains occupied by dense housing complexes.

The Directorate General of Water Resource (DGWR), Ministry of Public Works has come up with three options of long-term post-disaster management as summarized on the following table:

Table 3: Proposal of Long-Term Post-Disaster Management

First-Option	Second-Option	Third-Option
Reconstruction alternatives/scenarios: a. Dam location alternatives: rebuild at the same spot (alternative 1); relocate more upstream (alternative 2). b. Select the best fit dam-type. c. Reorganize land usage upstream and downstream area of the dam, in line with the existing regulation; and consider the risk factors of dam safety. d. Enhance the post-construction management approach (dam/reservoir authority, operation and maintenance of dam and reservoir)	Dam decommissioning through: reorganization of previous reservoir area usage and also the downstream part of the dam; river revival; usage of previous reservoir area as public and/or recreational facilities; and cultivation of greenbelt area as aquatic buffer.	Combination of First- & Second-Option by constructing new lower check-dam and its appurtenances more upstream (alternative 2) in order to preserve reservoir function in the form of river-channel (hence smaller) storage. The reservoir serves as conservation facility, which should followed by: reorganizing the land usage upstream and downstream area of the dam, in line with the existing regulation; and consider the risk factors of dam safety. enhancing the post-construction management approach (authority, operation and maintenance of dam and reservoir) utilizing the

First-Option	Second-Option	Third-Option
		previous reservoir area as public and/or recreational facilities; and cultivating greenbelt area as aquatic buffer.

Source: The DGWR, Ministry of Public Work, 2009.

Table 4: Dam Location Alternatives

	Alternative 1	Alternative 2
Dam height	15m	5m
Dam lenght	270m	170m
Inundation area	214,000m^2	161,500m^2
Storage	3,210,000m^3	807,500m^3
Spillway	5x1.5m	5x1m

Source: The DGWR, Ministry of Public Work, 2009.

The dam location alternatives are presented on the following figure.

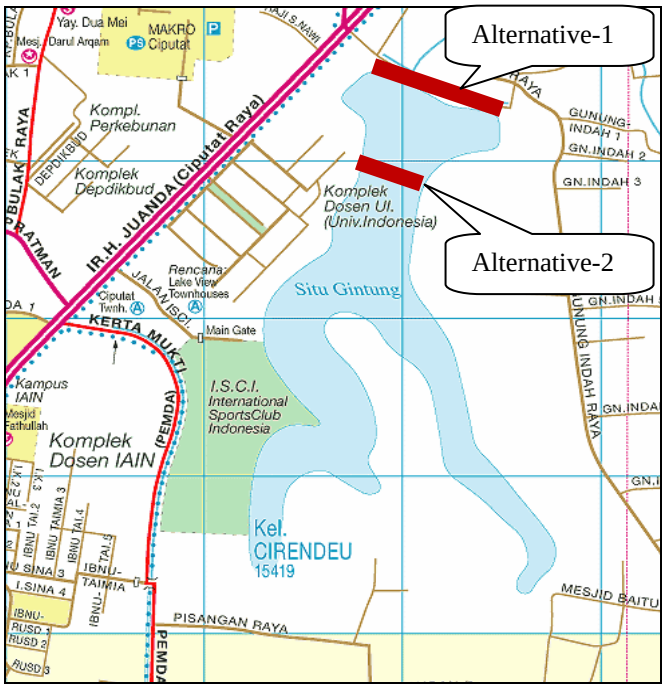

Source: The DGWR, Ministry of Public Work, 2009.
Figure 9: Dam Location Alternatives.

Just within four days after the disaster, on March 31, 2009, to be precise, the DGWR has decided the Third-Option as the most viable one.

4. DISCUSSION

To bear in mind the "Four Spheres" Prism of Sustainability (O'Connor, 2006), there were perfect match to both decision-making guides discussed earlier.

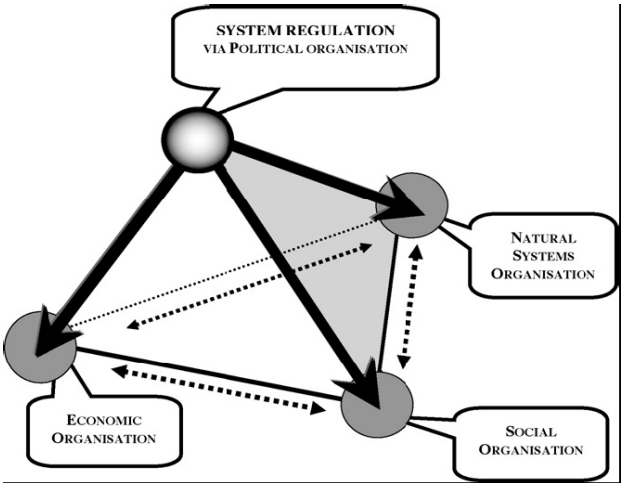

Source: Michelle Graymore, et.al., 2008.
Figure 9: "Four Spheres" Prism of Sustainability.

The "Four Spheres" Prism of Sustainability can accommodate the complexity of interaction and intertwining nature among the issues. I.e. without doing thorough design procedures is impossible to do the estimation of construction costs, safety and other liability risks, as well as operation and maintenance costs; and without conducting surveillances to stakeholders, is impossible to estimate the benefit of recreation, aesthetic, and ecological, as well as property value. Therefore, the economic consideration is a result of manifold preceding thorough assessment of various considerations.

Further discussion is needed as consequence of choosing the third option of DGWR proposal, among others:

Reorganizing the land usage upstream and downstream area of the dam:

- Do the decision-makers and other concerned parties have sufficient information to make decision?
- What is the land-use classification of the land downstream of the dam? What is the level of development at and below the dam site?
- If the properties will be required to carry flood insurance, are property values expected to increase or decrease in the surrounding area? In the flood zone?
- Are property values expected to increase or decrease with the change from lake to river aesthetics?
- How do community members feel about the dam? What is the current level of support for keeping the dam? Do any local/regional/national officials or anybody else support dam retention? How powerful are they?
- Does the dam have true historical value?

Considering the risk factors of dam safety:

- What is the hazard ranking of the dam? Does the National Dam Safety Program Act affect the dam?
- What will be the impacts of dam failure? What are the costs of dam failure flood insurance? For other liability insurance policies?
- How many properties must carry flood insurance because they are in the flood zone if the dam were to fail? Are there buildings below the dam that cannot be occupied because of the dam break analysis?
- What insurance costs will be avoided in relation to the decision? How many homes, buildings, and other properties will be removed from the catastrophic flood zone and no longer be required to carry flood insurance?
- Is there any Emergency Action Plan (EAP) applies? How does it work?
- Does the dam provide flood protection? Does the dam meet necessary flood standards? What is the flood passage capacity of the dam? Would the dam survive maximum headwater conditions?
- Have floodplain studies been administered previously?
- Would there be a need for design or construction of new appurtenances?
- How will the sediment built up behind the dam be handled? How much sediment would potentially be released downstream? How would it impact the stream?

Enhancing the post-construction management approach (authority, operation and maintenance of dam and reservoir):

- What will periodic inspections of the dam cost to prevent future problems?
- Will the dam have appurtenances that require someone to operate them? How much will dam appurtenances operation cost?
- How often will dredging the reservoir need to be done? How much will it cost?
- Will sediment controls need to be maintained? What does the sediment controls maintenance cost?
- Does the reservoir require vegetation control? What does the vegetation control cost?
- If part of the former reservoir is converted into a park or other natural area, how much would be the maintenance cost?

Utilizing the previous reservoir area as public and/or recreational facilities and cultivating greenbelt area as aquatic buffer:

- What type, location, and extent of existing wetlands created by the dam will be lost? What type, location, and extent of lands could be gained? How will the land gained be managed?
- How many people enjoy the activities on the reservoir? On the river? How much do the people value each activity on the reservoir? On the river?
- Do any businesses rely directly or indirectly on recreation at the reservoir? At the river? What is the economic value of the recreational business at the reservoir? At the river?
- What is the economic value of recreating at a new park or natural area?
- Are recreation businesses currently dependent on the reservoir flexible enough to focus on river recreation?
- What are the recreational opportunities associated with the decision? Are new businesses catering to river recreation likely to be established?
- What impact will the decision have on the watershed? Will surface water quality improve/worsen? Does the dam and impoundment affect groundwater levels in the area?
- Will the recovered land need to be actively re-vegetated?

5. CONCLUDING REMARKS

Making a final decision, whether Situ Gintung Dam/Reservoir should be rebuilt or removed, is not a simple task. There are considerable issues need to be taken into considerations. The “Four Spheres” Prism of Sustainability can accommodate the nature of interrelations and intertwining among the issues.

Once all of the data/information is gathered, many factors should be examined thoroughly and comprehensively, in order to understand the influences on the decision, including:

- The societal, economics and ecological circumstances surrounding the case;
- The complexity of the issues;
- The legal and political context in which a decision must be made;
- The amount of controversy surrounding the decision;
- The impetus for considering all possible alternatives;
- The number, identities, and strength of various stakeholders.
- Etc. etc.

ACKNOWLEDGMENT

In preparing this paper, we gratefully acknowledge the assistance from our students Andi, Evi, Yanur and Zainal.

Special thank goes to American Rivers and Trout Unlimited, as well as to Wisconsin Department of Natural Resources and University of Wisconsin-Madison with their generosity in encouraging people to make use their joint project reports.

REFERENCES

[1] Austin, Elizabeth (Lead Author); Robert Sanford (Topic Editor). 2009. "Environmental and social implications of dam removal." In: Encyclopedia of Earth. Eds. Cutler J. Cleveland (Washington,D.C.: Environmental Information Coalition, National Council for Science and the Environment). [Published

in the Encyclopedia of Earth June 23, 2009; Retrieved June 28, 2009].

[2] The River Revival Project of International Rivers Network, 2001. “Reviving The World’s Rivers: The Global View of Dam Removal”.

[3] American Rivers and International Rivers Network. May 2004. “Beyond Dams: Options & Alternatives”.

[4] American Rivers and Trout Unlimited. August 2002. “Exploring Dam Removal: A Decision-Making Guide”.

[5] Kathleen.D.White. “Overview of Current Dam Decommissioning Activities”. Dam Decommissioning Workshop: Options, Opportunities and Challenges. Northwestern Michigan College – Great Lakes Campus, Hagerty Center, Traverse City, Michigan, April 24-25, 2006.

[6] Wisconsin Department of Natural Resources and University of Wisconsin-Madison, 2000. “Dam Repair or Removal: A Decision-Making Guide”. Water Resources Management Practicum (2000).

[7] DGWR, Ministry of Public Works. “Kejadian Bencana Situ Gintung dan Upaya Penanganannya”. Cirendeu, 31 Maret 2009.

[8] Sutopo Purwo Nugroho, 2009. ”Kajian Penyebab Jebolnya Tanggul Situ Gintung dan Antisipasinya”. Tim Mitigasi Bencana BPPT, Pusat Teknologi Pengelolaan Lahan, Wilayah dan Mitigasi Bencana BPPT.

[9] Michelle Graymore, Anne Wallis & Anneke Richards. “Environmental Sustainability: The key to sustainability assessment in South West Victoria, Australia”.School of Life and Environmental Sciences, Faculty of Science and Technology, Deakin University, Warrnambool, Australia. EASY ECO Vienna Conference, 11-14 March 2008.

IMPACT of SALTY WATER to the STRENGTH of BOTH MORTAR and CONCRETE

Eva Azhra Latifa

Jurusan Teknik Sipil
Politeknik Negeri Jakarta Depok - 16425
Telp 021 7863532. Fax 021 7863532
E mail evaall@yahoo.com

ABSTRACT

NaCl as the most active element of seawater which is cause chemical react with Portland cement can decelerate the setting time and reducing strength both of concrete and mortar,. The salty water research using NaCl 2,5% to 7%, influences the compressive and flexural strength of mortar. Mortars composition are 1:4 and 1:5 Portland cement : fine aggregate. Test based on flowtable value 110%. The salty water using NaCl 3,5 % to 7 % is used to mix concrete with w/c ratio 0.5 to observe its compressive and indirect tensile strength. Both of them observed in28 and 56 days

- *The strength of nature mortar's 1:5 is lower than 1:4*
- *Compressive and flexure with 2,5% to 3,5% NaCl increase, but decreases inline with adding NaCl. Increases till 28 days old, but decreases at 56 days.*
- *Slump value and wet density of concrete increase with 3,5% NaCl* but *decreases inline with adding NaCl*
- *Initial setting time of concrete increases with adding 3,5 % and 7 % but the 5% NaCl takes longer than the concrete without NaCl.*
- *Compressive and indirect tensile strength of salty concrete increase with 3,5% NaCl but decreases inline by adding NaCl percentages.*

Keywords: *Mortar, concrete, NaCL, compressive strength, flexural strength, indirect tensile strength.*

1. INTRODUCTION

Houses-building project for the 30 million lower and middle class inhabitants, which consists of 5,9 million head of family approximately 800,000 to 1,000,000 houses.

In accordance to the house-building project, it is not impossible that the contaminated-by-sea water that will be used in the paired-wall and mortar making process may reduce both of the strength and durability of the building which later may caused a violation of minimum building safety terms.

Literature Review

The salt crystal will react with Portland cement until weathering not so long. The same case with ceramic or cement brick because consist of same raw materials, like Al_2O_3, SiO_2 and Fe_2O_3.

NaCl is the easy soluble salt, so the Na^+ and Cl^- ion stay in solution permanently. When the solution evaporated, it can get natrium chlorida (NaCl) crystal.

The following formula says what happen until neutralization or salty react.

$NaCl\ (aq) + H2O\ (l) \longrightarrow HCl\ (aq) +$
(Garam) (Air) (Asam kuat) $NaOH\ (aq)$
Basa lemah)

Water forming: $H^+\ (aq) + OH^-\ (aq) \longrightarrow H2O\ (l)$

Salt forming: $Na^+\ (aq) + Cl^-\ (aq) \longrightarrow NaCl\ (aq)$

The salt behavior is electrolyte, did not change lacmus paper color, and disengage metal and acid leftover ion. The salt reaction happen when acid + alkali = salt + water. Alkali behavior is produce OH^- ion, bitter, and smoothly, electrolyte, corrosive, and reacts with indicator and change it color.

Beside chemical reaction, salt crystallization in void of both mortar and concrete can shattered because of crystallization pressure. Hence salt crystallization occur in water evaporated, salt attack occur in both mortar and concrete on water's surface. Salt turn up with capillary act, so salty attack occurs in permeable of both mortar and concrete. That is although explain the early strength high, but decreases after 28 days.

Methodology

The research method is doing some experiment about material testing base on SNI and ASTM standards to know physical and mechanical behavior both mortar and concrete in laboratories.

Material using for mix both of mortar and concrete involve fine and coarse aggregate with 40mm diameter, Portland Cement, and water polluted NaCl, from 2,5% to 7% with details as follows :

1. For mortar 2,5%; 3,5%; 5%; and 7%
2. For concrete 3,5%; 5%; and 7%

3. TABLES AND FIGURES

Summary data from mortar and concrete testing performance in table and diagram as follows:

Table 1. Summary of mortar testing with and without NaCl

AGE, days	MOR WITHOUT COMPRESSIVE STRENGTH, N/mm²		T A R NaCl FLEXURE STRENGTH, N/mm²		MORTAR WITH NaCl														
					COMPRESSIVE STRENGTH, N/mm²								FLEXURE STRENGTH, N/mm²						
					1:4				1:5				1:4				1:5		
	1:4	1:5	1:4	1:5	2,5%	3,5%	5%	7%	2,5%	3,5%	5%	7%	2,5%	3,5%	5%	7%	2,5%	3,5%	5%
7	159	155	106	86	180	178	173	171	149	129	127	119	100	84	76	64	81	75	71
28	235	186	115	100	226	222	218	214	205	202	182	170	60						
56	252	205	147	110	259	255	246	244	245	220	211	201	124	115	101	80	114	104	81
													73						
													133	125	116	90	125	123	94
													86						

Table 2. Summary of physical behaviour of concrete testing with and without NaCl

Testing	Concrete without NaCl	Concrete with NaCl		
		3,5%	5%	7%
Slump	56 mm	106 mm	89 mm	62 mm
Wet density	21.86 N/mm²	22.75 N/mm²	22.37 N/mm²	19.98 N/mm²
Initial setting time	120 menit	190 menit	175 menit	140 menit

Table 3. Summary of compressive strength of concrete with and without NaCl

	COMPRESSIVE STRENGTH (N/mm²)			
Age, days	Without NaCl	3,5%	5%	7%
7	22.05	20.35	18.40	18.15
28	33.83	32.20	31.79	31.16
56	34.07	33.68	33.08	32,62

Table 4. Summary of indirect tensile strength of concrete with and without NaCl

	INDIRECT TENSILE STRENGTH (N/mm²)			
Age, days	Without NaCl	3,5%	5%	7%
28	2.55	2.48	1.98	1.61
56	3.16	2.83	2.77	2.01

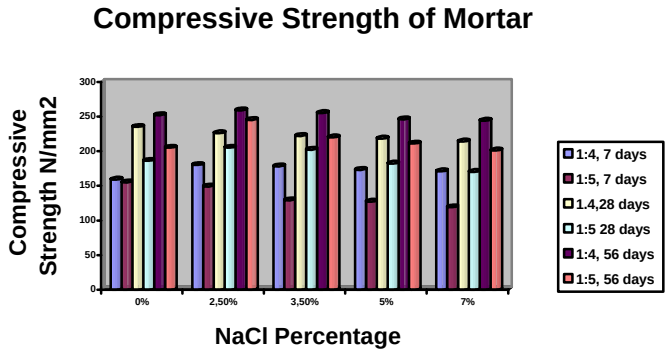

Figure 1. Summary of compressive strength of mortar with and without NaCl

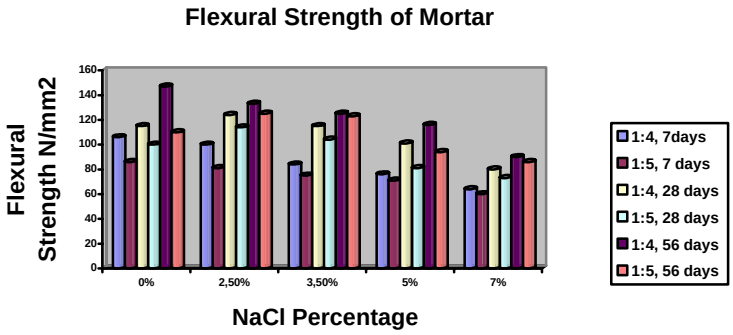

Figure 2. Summary of flexural strength of mortar with and without NaCl

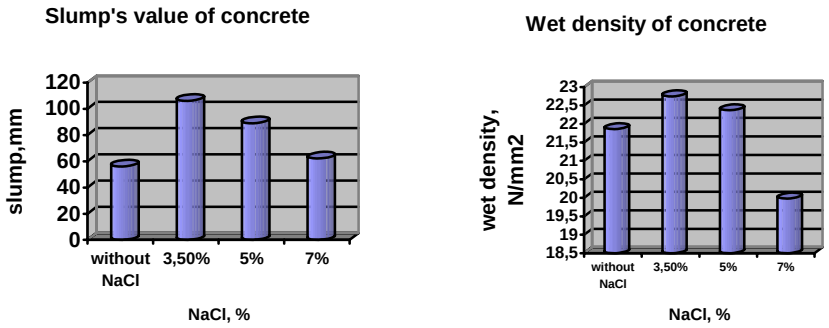

Figure 3. Summary of physical value of concrete with and without NaCl

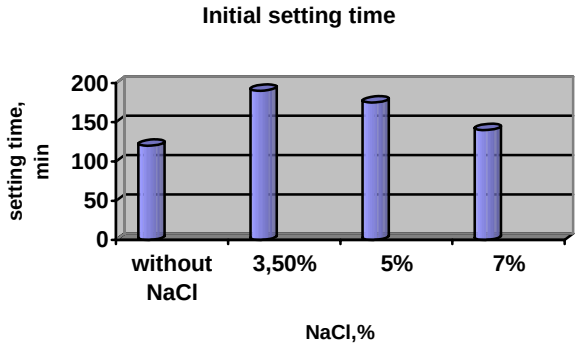

Figure 4. Summary of compressive strength of concrete with and without NaCl

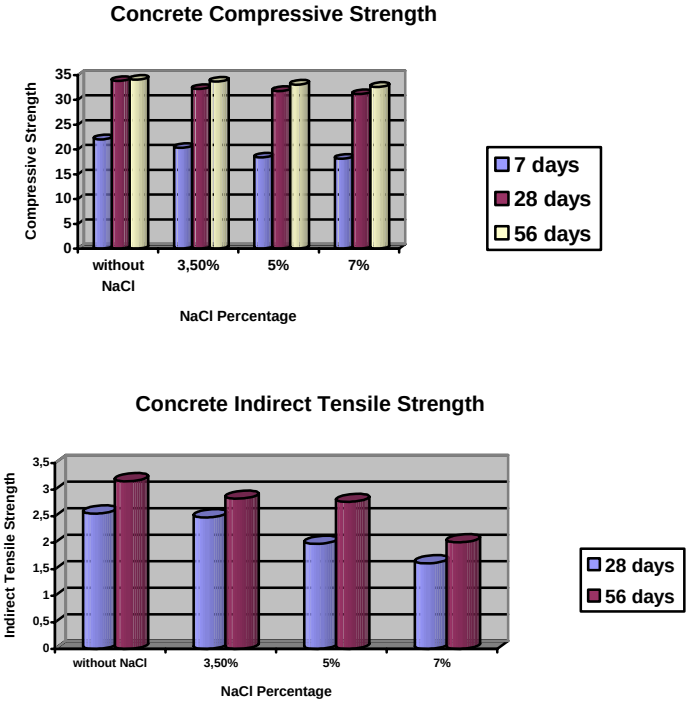

Figure 5. Summary of indirect tensile strength of concrete with and without NaCl

4. DISCUSSION

Workability is an important aspect in mortar. The determination is set by using aggregate with environment condition-suited water level, so the based-on mortar workability strength level determination is subject to ASTM standard. The stirred with contained NaCl water-concrete and mortar, as the matter of fact, have stronger power at the early time, and decrease, although not significant after that, compared to the stirred without NaCl mortars and concrete.

5. CONCLUSION

The conclusions are:

- ❖ Compressive and flexure nature mortar's strength decreases inline with adding fine aggregate. However the strength of 1:5 is lower than 1:4
- ❖ Compressive and flexure salty mortar with 2,5% to 3,5% NaCl increase, but decreases inline with adding NaCl percentages, and increases until 28 and 56 days old.
- ❖ Slump value of concrete increase with 3,5% NaCl but decreases inline with adding NaCl percentages
- ❖ Wet density of concrete increase with 3,5% NaCl but decreases inline with adding NaCl percentages
- ❖ Initial setting time of concrete increases with adding 3,5 %, and 7 % compared to 5% NaCl percentages, but the 5% NaCl takes longer than the concrete without NaCl.
- ❖ Compressive and indirect tensile strength of salty concrete decreases inline by adding NaCl percentages.
- ❖ Ultimately, salty water influences the strength decrease of both concrete and mortar.

ACKNOWLEDGMENT

Thanks to attention and helping from begin of the research until finished this paper to Handoko, Arnida, Waarid Mulyono, Syifa Mulyono, and Mutia Mulyono

REFERENCES

[1] Azizah, Utiya. 2004. Larutan Asam dan Basa. Diambil dari : http://www.google.com [20 Jun 2008].
[2] Davis, HE, Troxell GE, Hauck, GEW, 1982, ***The Testing of Engineering Materials***, Mc Graw Hill New York.
[3] en.wikipedia.org/wiki/***Mortar*** (diakses 13 April 2008)
[4] Latifa, Eva A, 2003, ***Teknologi Bahan II***, Politeknik Negeri Jakarta, Depok
[5] Mulyono, Eva AL , 2002. ***Memaksimalkan Pemakaian Kapur dalam Teknologi Adukan Sebagai Upaya Menghemat Semen***, J: Politeknologi Vol.1 No.3. Jakarta : Politeknik Negeri Jakarta.
[6] Mulyono, Eva AL , 2004 ***Upaya Meningkatkan Sifat Mudah Dikerjakan (Workability) Adukan***

Semen-Pasir Dengan Penambahan FlyAsh, J: Politeknologi Vol.3 No.2. Jakarta : Politeknik Negeri Jakarta.

[7] Neville AM, 1989. ***Properties of Concrete, Third Edition***. English Language Book Society/Longman, London.

[8] SK SNI 03 – 2834 – 2000. ***Tata Cara Rencana Pembuatan Campuran Beton Normal.***

[9] Shetty, MS.2002. ***Concrete Technology Teory and Practice***, S Chand & Company Ltd, NewDelhi.

[10]Skripsi Universitas Kristen Petra. Ion Chlorida. 2002. Diambil dari : http://www.google.com [20 Jun 2008].

[11]Sudjono AS. 2005. Prediksi Waktu Layan Bangunan Beton Terhadap Kerusakan Akibat Korosi Baja Tulangan. Diambil dari: http://www.google.com [20 Jun 2008].

[12]SNI 15-7064-2004. 2004. Semen Portland Komposit. Diambil dari: http://www.google.com [28 Mar 2008

ISSN 114-1284

Review on Public Health Consequences of Indoor Air Pollution to Jakarta Population after Flood

Gabriel Andari Kristanto

Faculty of Engineering
University of Indonesia, Depok 16424
Tel : (021) 7270011 ext 51. Fax : (021) 7270077
Email: gakristanto@gmail.com

ABSTRACT

Poor air quality in indoor environments has been recognized as an important factor that can lead humans to be exposed to different types of pollutants. During the last decade, Jakarta experiences high rainfall intensity causing severe and regular flooding in significant portion of the city due to limited open space and poor drainage. Flood damage varies throughout the city, with some areas flooded to the rooflines while the others might have been spared. Previous studies found that different types of pollutants have been identified in indoor environment such as VOCs, NOx, CO, and bioaerosol pollutants like fungi and bacteria. These fungi and bacteria are not only contaminated indoor environment but also emitted toxin and allergens that can give impact to human health. The objective of this study is to review public health consequences of indoor air pollution to Jakarta population after flood.

Keywords:

indoor air pollution, health, flood, Jakarta

1. INTRODUCTION

Poor air quality in indoor environments has been recognized as an important factor that can lead humans to be exposed to different types of pollutants. There are three factors associated with indoor air quality. Firstly, many studies on human activity pattern showed that people spend more time indoors than outdoors hence there is higher possibility that they expose more to indoor pollutants. A second factor is the negative impact of indoor air quality on human health. The third factor is higher pollutant concentration in indoor rather than outdoor environments. Due to economic development in the last several decades Jakarta faces serious environmental issues like shortage of clean water during dry season, regular flood during rainy season and increased concentrations of air pollutant. With population of more than 8 million and total area of 662 sq km, the city is well known with high population density and urban planning mismanagement. Located in tropical country, Jakarta experiences high rainfall intensity causing severe and regular flooding in significant portion of the city due to limited open space and poor drainage. Almost 40% (265 km2) Jakarta's areas are under sea level and only 17% of those total are has polder system to flood. Flood damage varies throughout the city, with some areas flooded to the rooflines while the others might have been spared.

There are many studies on Jakarta's flood and most of them focused on the condition during the disaster such as the quality of flood water, community coping mechanism, providing clean water and sanitation facilities, etc. On the other hand none of the previous studies mentioned indoor air pollution concern during cleanup and rehabilitation.

Many studies found that different types of pollutants have been identified in indoor environment such as VOCs, NOx, CO, and bioaerosol pollutants like *Penicillium sp* and *Aspergillus*. These fungi and bacteria are not only contaminated indoor environment but also emitted toxin and allergens that can give impact to human health.

The objective of this study is to review public health consequences of indoor air pollution to Jakarta population after flood. Literature reviews and secondary data have been extensively used to identify many factors that contribute to different kinds of diseases that emerge due to Jakarta's flood, choice of housing material, and weather condition. Comparisons among Jakarta conditions with other similar cities around the world were also conducted.

2. INDOOR AIR POLLUTION DUE TO FLOOD

Flooding in Jakarta was not only struck poor but also rich area. During rainy season, regularly the black, smelling water altogether with a lot of garbage poured onto many parts of the city. One of important impact of flood is the length and height of standing water. In 2008 Hartono and Novita investigated that the length of standing water due to Jakarta's flood is varied

ISSN 114-1284

among different areas. From table 1 it is showed that the longest is 30 days and the shortest is 5 days.

Tabel 1. Height and Length of Jakarta's Flood

	West Jakarta	South Jakarta	Central Jakarta	East Jakarta
Length of standing water (days)	8 - 30	6 - 30	5 – 14	14 - 60
Height of standing water (meter)	0.5 - 2	0.5 - 4	0.5 - 2	4 - 10

Source: Hartono and Novita, 2008

It is known that standing water remaining from the flood can be a breeding ground for microorganism. Fungal colonies may develop to visible state in as little as one week. Many fungi occupy surfaces in direct contact with water. These complex communities of fungi, bacteria, protozoa, and algae embedded in mucopolysaccharide matrix called *biofilms* [1] Even after the water recede, bacteria, virus, fungi, mold, and many other contaminants pose a risk to the vulnerable people like the elderly, children, and anyone with chronic disease. Previous investigatiom on flooding in the greater New Orleans found that visible mold growth was significantly associated with flood height 3 ft (0.9 m)[8]. Furthermore study by Solomon *et al.* (2006) estimated 24-hr mold concentrations ranged from 21,000 to 102,000 spores/m3 in outdoor air and from 11,000 to 645,000 spores/m3 in indoor air. They mentioned that the mean outdoor spore concentration in flooded areas was roughly double the concentration in non-flooded areas (66,167 vs. 33,179 spores/m3; $p < 0.05$) with the highest concentrations were inside homes. It was also found that high concentration of indoor fungi and bacteria in flood damaged building contributed to poor indoor air quality more than 3 months after the structures have been reclaimed from flood damaged [3].

Mold and mildew are common terminology used for fungal indoor air pollutant. The predominant fungi indoors were *cladosporium*, *aspergillus* and *penicilium* species although *stachybotrys* was also detected in some studies [9,10]. Previous study found that *Trichoderma* grows optimally in environment with water activity while *Penicillium* sp grows in wide range water activity [2].

Study on Jakarta flood water quality by Oguma (2009) also found viruses and bacteria. These viruses and bacteria are listed in the following table:

Table 2. Viruses and bacteria found in Jakarta's flood water

Viruses	Bacteria
Adenovirus	*Escherichia coli*
Enterovirus	Total coliforms (TC)
Hepatitis A virus	
Norovirus G1	
Norovirus G2	

Source: Oguma, 2009

Those virus listed in Table 2 can cause diarrhea in human and although the bacteria are non pathogenic, but indicate high possibility of fecal contamination.

Furthermore concern of health consequences is not only caused of flood water but also sediment quality. Unfortunately no specific report or scientific studies on Jakarta's flood sediment. However other similar study had been conducted at New Orleans's area after Katrina and Rita[6]. It is found that these sediments came from multiple sources and contain of physical organic, inorganic chemicals, and microbial contamination.

3. FACTORS CONTRIBUTING TO MICROBIAL GROWTH

Different factors contribute to the growth of microbes in indoor environment. Among others are humidity, temperatures, types of building materials, and the availability of carbon as food source. Moisture is probably the most important factor supporting overall indoor fungal growth. With temperature range from 24-30^{o}C during Jakarta's rainy season and humidity can reach more than 100%, fungi can growth very rapidly. In addition most of Jakarta's houses build from bricks and woods that are porous hence reducing moisture can be a big challenge. The distribution of moisture in the material, the type of fungi present, and the material on which the fungi are growing will impact the appearance of surface fungal growth. It has been mentioned that rapid growth of mesophilic or zerotolerant fungi may occur even in the dust when water activity became very high, leading to moldy odors and to drastic changes in the dust populations [1].

4. HEALTH CONSEQUENCES

Different kind of infectious diseases commonly emerge during and after the flood such as dysenteries, asthma, skin rash, etc. Many of these diseases usually traced to the decrease of sanitation condition and lack of clean water. There is lack of studies on fungi or bacteria exposures following flood-damaged housing in Jakarta. Even Crisis Center at Indonesian Health Department only generalized disease such as skin rash and asthma without identifying the source of the diseases.

On the other hand, concerns have been expressed about the potential human health impacts that might have resulted not only from exposure to the growth of fungi and bacteria, but also to the flood sediment during cleanup and rehabilitation of flooded areas. The primary routes of fungal exposures in indoor environment are most likely dermal and inhalation. It was found that exposure to fungal contamination can lead to several infectious and noninfectious health effects impacting the respiratory system, skin, and eyes [4]. Significant exposures probably occur when fungal spores, fungal mycelia, and contaminated growth substrate are aerosolized, especially as a result of handling of moldy material [9]. Furthermore latter

finding mentioned that the allergens of fungi are probably digestive enzymes that are released as the spore germinates [1]. In addition, recent findings also mentioned MVOC (Microbial Volatile Organic Compounds) as chemicals that present in the indoor environment as the result of the metabolic actions of bacteria and fungi. Although they were produced in low concentrations and exposure to MVOCs has not been conclusively linked to health effects but it was suggested that the potential of these chemicals to act ac broad indicators of the ecological state of a building may be realized.

Although adverse health effects of fungal exposure usually categorized as infections, allergic or hypersensitivity reactions, or toxic-irritant reactions but carcinogenicity, induction of tremors, or damage to the immune system or major organs were also reported as the most encountered mycotoxin effects [9]. High respiratory morbidity and allergic complaints had been also reported in occupants mold building structures [2]. Some of hypersensitivity diseases caused by fungi include hayfever and asthma, allergic fungal sinusitis, and hypersensitifity pneumonitis.

5. PREVENTION STRATEGIES

In the aftermath of floods, it is recommended that community and public health department work together to reduce risks of indoor air pollution. Preventing fungi to growth after the flood should be chose as the first option and this can be achieved by removing flood water, controlling humidity, and preventing condensation. Using oxidation agents (such as bleaching) will not only reduce the probability of fungal and bacteria amplification, but also kill them. Note that concentrations of fungal or bacteria aerosols increase during removal activities hence respiratory protection is strongly advised during removal.

Developing cleanup procedures to minimize dust generated from the sediment during rehabilitation of flooded area hence exposure to contaminants such as heavy metals can be reduced.

The development of a public health surveillance strategy among persons repopulating areas after extensive flooding is recommended to assess potential health effects and the effectiveness of prevention efforts.

6. CONCLUSSIONS

Jakarta's populations have been exposed to different kind of diseases due to the regular flooding. Standing water remaining from the flood, flood damaged building materials; flood sediment can be a breeding ground for microorganism such as fungi and bacteria.

Limited study of indoor air pollution and lack of knowledge among Jakarta populations, health workers and government officials on high possibilities of the growth of fungi and bacteria and quality of the sediment in flooded house causes Jakarta populations continually expose to indoor air pollutants even long after the flood receded. It is recommended that many prevention strategies should be conducted to minimize the risks associated with flood.

REFERENCES

[1] Burge, H.A. (2001). *Indoor Air Quality Handbook.* McGraw Hill: USA
[2] Fabian *et al*.(2005). Ambient Bioaerosol Indices for Air Quality Assessments of Flood Reclamation. *Aerosol Science*, 36, 763-783.
[3] Hartono,D.M., and Novita, E. (2008). Qualitative Study of Infrastructure Disaster Mitigation: Case Study of Jakarta Flooding. Civil engineering Department, University of Indonesia
[4] Metts, TA. (2008). Addressing environmental health Implications of mold exposure after major flooding. AAOHN, 56(3), 116-120.
[5] Oguma, K. (2009). Waterborne health risks due to rapid urbanization in Asia
[6] Plumlee *et al*. (2009). Characterization of flood of sediment Katrina and Rita and potential implication for uman health and the environment. *Science and The Storm: USGS Response to Hurricanes*. Downloads from http://www.epa.gov/katrina/testresults/sediments/ summary.html on 12 June 2009
[7] Rao.(2001). *Indoor Air Quality Handbook.* McGraw Hill: USA
[8] Riggs *et al.* (2008). Resident cleanup activities, characteristics of flood-damaged homes and airborne microbial concentrations in New Orleans, Louisiana, October 2005. *Environ. Res*. 106(3):401-409.
[9] Solomon *et. al*. (2006). Airborne mold and endotoxin concentrations in New Orleans, Louisiana, after flooding, October through November 2005. *Environ Health Perspect*. 114(9):1381-6.
[10] Spenger, Samet, and McCarthy. (2001). *Indoor Air Quality Handbook.* McGraw Hill: USA

Evaluation of Pedestrian Characteristics for Different Type of Facilities and its Uses; Case study in the area of Jakarta Indonesia

Heddy R. Agah[1]

[1]*Civil Engineering Department Faculty of Engineering*
University of Indonesia, Depok 16424
Tel: (62-21) 7270029. Fax: (62 21) 7270028
e-mail : agah@eng.ui.ac.id.

ABSTRACT

Pedestrian is vulnerable against traffic accident, due to its speed, maneuver ability to avoid collision and less coverable, which encountered of problems require various forms of guidance, safe separated facilities, and convenience to walk. Pedestrian facilities aimed at segregation, integration and separation, its services and function need primary input comprises of walking speed, density and the area used by individual or platoon, and volume. All of those characteristics are influence by habit, climate and body measure and gender issues. Typical facilities for pedestrian are footpath, crossing, pedestrian bridge, and pedestrian mall. This paper discusses research results related with characteristics of pedestrian in different situations, and facilities in relatively similar area conditions. Some selected areas in the Jakarta Province – Indonesia was observed.

The study is focused on characteristic of pedestrian comprises of speed, flow and density. Observation is done in foot path along the main road and junction in the area of Sarinah - Central Jakarta. It is found that speed range between 47,5 to 71 meter per second, space occupied was relatively bigger than as mention in other references, and density was found 198 people per square meter. Further analysis is on the relationship between parameters, considering gender and age. Density is measured by person per area since pedestrian moving more flexible instead of following straight path lane. The relationship between parameters is similar with the flow phenomena of vehicles flow. Further research is tried to define better characteristic relationship between parameter along a segment of foot path, since in the first stage of research relationship of each two parameter was assumed as linear. It is found that the behavior of pedestrian characteristics is varying among them shelves as well as over time and space, which leads to develop a model suitable to the real condition. Previous model was made under the assumption continuous condition of flow and its facilities regarded the same in terms of time and space. Relationship between parameter is found not always occurred in one same regime, but depend on flow condition. Multi regime model could be more suitable to explain free flow and congested flow condition. With the increase of flow, different type of regime will occurred characterized by discontinuity of curve in one or more points. That means relationship was represented by more than one equation. This observation is undertaken in a special foot path located at University of Indonesia campus.

On the safety aspect, research is undertaken to analyzed interaction between vehicle and pedestrian crossers. The result leads to indentify decision process to across the road safely with a certain time gap of vehicle traffic. It is found 3.75 second as critical gap, neglected the proportion of pedestrian population. Significant variable influencing to decide crossing road are age, physical condition, freedom of maneuver, walking speed and gap situations. If join distribution is ignored, 61%- 73% prefer to across in safe condition identify with age, number of person and walking speed. Considering join distribution, 68%-78% across the road above 3.75 second gap.

Keywords:
pedestrian, characteristics, facilities, multi regime, crossings

1. INTRODUCTION

Pedestrian oriented in urban planning should be used in the planning process to implement environmentally friendly urban space. Physically pedestrian is vulnerable against traffic accident, due to its speed, maneuver ability to avoid collision and less coverable, which encountered of problems require various

forms of guidance, safe separated facilities, and convenience to walk. To provide safety and comfort, pedestrian facilities aimed at segregation, integration and separation. Its services and function need primary input comprises of walking speed, density and the area used by individual or platoon, and flow of pedestrian or flow rate (volume).

Pedestrian's basic characteristic is assumed similar with vehicle traffic flow. It means that when pedestrian travel in linear path and faster speed that is indication of efficient flow, while in congested flow condition provides some disutility to pedestrian [1]. That assumption is reflected the pedestrian real condition but it is not an accurate since pedestrian exhibit complex movement pattern. Pedestrian do not follow a fix lane compare to vehicle movement and tend to have free choice along the route on utility, swerving if encountered any obstructions and previous experience or out of habit. Compare to vehicle movement, pedestrian flows tend to move in a significant degree of randomness. Even flow in pedestrian design analysis makes use of term commonly used in traffic engineering, density or number of pedestrian per unit area is more complicated to be visualized. Flow of pedestrian (u) is estimated from the speed and space occupied (average space per person), relationship between speed and density [2] [3] [4] is linear.

In the basic planning process prediction of spatial movement are often inadequate and to some extent insufficient. This situation is because most of the traffic modeling focused on the vehicles traffic component as transport system and people movement has been to a certain extent dependent of motorized vehicles. To provide pedestrian facilities need knowledge and tools to understand the characteristic of pedestrian by measuring flows, analyzing patterns and identifying function of the movement. Accurate estimation on the impact of plan and pedestrian behavior is required [5].

Sidewalk design [6] provides standard for facility design based of pedestrian level of service (PLOS), in which primary measure of effectiveness is pedestrian space occupancy (density) and flow rates (speed). It indicates free flow movement from the highest to the lowest level of service, while PLOS is noted as "A" indicates the highest level or free flow movement in the other extreme level of "F" means a standstill condition.

Level of service for walkways for pedestrian has been studied by some researchers particularly in the situation ignoring bi-directional flows such as works by Fruin (1987), HCM, (2000), Tanaboriboon and Guyano (1989) in Bangkok, Gerilla GP, Hokao, K, Takayama Y (1955). Most of the results show some similarity between parameter if converted to level of service concepts.

This paper describes characteristics of pedestrian and type of facilities to serve pedestrian movement based on a series of observations in some streets and area in Jakarta - Indonesia. Basic characteristics such as flow, density and space, selection of type of facilities is discussed and identifies the relationship between parameters to estimate average speed and space occupied, and selection type of facilities.

2. METHOD OF SURVEY

Two different places with different type of pedestrian footpath are chosen in the Sarinah area of Central Jakarta and special footpath located at the campus compound the University of Indonesia – Depok. Pedestrian footpath in University Campus is built in the area relatively free from vehicle interferences, with bi-directional flows. Discussion on this topic is divided into two different locations with different condition. In total there are 13 streets in Central Jakarta and one location at Campus of University of Indonesia in Depok.

Criteria to choose observed location are: (i) number of pedestrian; (ii) physical characteristic of facility, separation with vehicle flow; (iii) accommodate peak and off peak flow. Video camera, stop-watch is used to record pedestrian movement, surface pavement is marked, dotted marking horizontally every 70 cm and 500cm longitudinal along the footpath. The length of observed lane is 15.00meter, and period of observation between 09.00 to 10.00 am and 13.00 to 14.00 am.

3. CHARACTERISTIC OF PEDESTRIAN

Observation is undertaken in some pedestrian footpath along some streets. Two different places with different type of pedestrian footpath are chosen, such as road sidewalk in located in some street in the Central City of Jakarta and footpath located at the campus the University of Indonesia – Depok.

3.1 Single Regime

The result of observation at side walk at some stretch of streets in Jakarta [7] (is shown in

Table 1. Parameter is classified by gender, the result shows that average speed for male is higher than female, 51 meter/minute and 50 meter/minute for male and female respectively. However, if we combine both male and female in one group of sample the average speed is higher than speed classified by gender (57 meter/minute). The speed in Jakarta relatively lower compare to the number from some research results observed in Europe [1] (79 meter/minute), United States [2] (81 meter/minute), and in Singapore [8] (76 meter/minutes), which is similar with jaywalking person speed.

Table 1. Parameter of Pedestrian on road sidewalk.

Parameter	Male	Female	Combine
Average speed m/minute	51	50	57
Highest speed m/minute	77	64	77
Lowest speed m/minute	48	41	41
Sample Person	38	25	63

The equation to model pedestrian characteristic assumed that relationship between parameter is linear and apply to all condition which range from free flow to congested flow condition. This phenomenon is called as single regime.

The relationship between pedestrian parameter based on data collected is mathematically written in **Table 2**. Equation is established based on the free flow speed from combination of male and female. Symbol uses for the equation is speed (u), density (k) and flow (u). Since pedestrian movement is not fixed in one lane, it needs to define one additional parameter which is space in unit area per person symbolized as (M).

Table 2. Relationship between parameters

Relationships	Equations
v = f (u)	$v = 4.83(57\text{-}u)\text{-}0.085(57\text{-}u)^2$
v = f (k)	$v = 57k - 11.8k^2$
v = f (M)	$v = 1/(M)^2\ (57M - 11.8)$
u = f (k)	$u = 57 - 11.8k$
u = f (M)	$u = 57 - 11.8/(M)$

The result from observation along the footpath at University campus is shown in **Table 3. Table 3** describe the equation representing relationships between two parameters develop with different model, such as Greenshields, Underwood, and Greenberg. One model is develop to represent the most suit and appropriate with local condition, which represented by row number (4) in **Table 3.**

Table 3. Relationship between parameter for single regime

Speed - Density	Flow – Speed	Flow – Density
Greenshields		
$u = 79.84 - 21.41*k$	$q = 3.729*u - 0.0467u^2$	$q = 79.84*k - 21.41*k^2$
Underwood		
$u = 80.964*e^{(-0.326k)}$	$q = 3.067*u* \ln(80.964/u)$	$q = 80.964*k*e^{(0.326K)}$
Greenberg		
$u = 60.514 - 9.716*\ln(k)$	$q = 507 * u*e^{*(U/9.716)}$	$q = 60.514*9.716*k* \ln(k)$
Alternative Model		
$u = 1/(0.0121 + (0.005*k)$	$q = \{(1/0.005)\text{-}2.42*u\}$	$q=k/\{0.0121+(0.005*k)\}$

Table 4 shows value of pedestrian parameter, compare to result shown in **Table 3** the number are relatively lower. This difference may cause by different characteristic of pedestrian and different environment condition.

Table 4 Parameter of Pedestrian on foot path.

Parameter	Model			
	(1)	(2)	(3)	(4)
Density - congested (ped/m2)	3.73	26.93	506.88 *	16.528
Optimum speed (M/mnt)	39.93	29.79	9.72*	0.005*
Optimum density (ped/m2)	1.86*	3.07	186.42	200*
Maximum flow (ped/m/mnt)	74	91	1812*	200*

Note: (1)Greenshields; (2) Underwood; (3) Greenberg (4) alternative model.

3.2 Multi Regime

Linearization of relationship between parameter is not always occurring for all conditions or variations of flow. To characterize variation of flow in particular when flow becomes higher and almost reach optimum density, it is found the line curve should draw with discontinuity at one particular point reflecting different condition. It means that to represent all variations of flow, equations need to accommodate point of discontinuity. It needs to develop more than one equation for each pair of parameter relationship. The problem is how to determine point of deflect and number of fractions which represented by different equations with different model. This condition is called as multi regime approach.

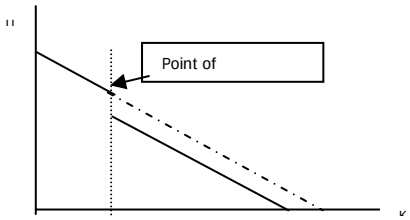

Figure 1 Curve discontinuity

To observe the possibility that condition, one segment of foot-path in Campus of University of Indonesia with bi-directional flow is chosen. **Table 4** shows the value of free flow speed calculated by different analytical model, range between 79.84 to 82,64 meter/minute. This number is relatively similar with speed of pedestrian walking in the city center by means of side road footpath. (9).

Table 4 Free flow speed for model evaluated

Model Analysis	Free flow speed (Meter/menit)	R^2
Greenshields	79.84	0.80
Underwood	80.96	0.812
Greenberg	∞	0.749
Proposed model	82.64	0.811

Multi regime approach is expected to develop relationship between two parameters which closer to the real condition in the field. The key component (parameter K) to develop curve is rely on point of discontinuity. For this particular case based on data collected and trend of curve, it is found that the discontinuity at the value of K equal to 70..

Table 5 Relationship between parameter for model evaluated

Speed - Density	**Flow – Speed**	**Flow – Density**
***Greenberg*- Greenshields; K ≤ 0.70**		
u = 79.72 – 21.37*k	q = 3.73*u – 0.047*u^2	q = 79.72*k – 21.37*k^2
Greenberg – Greenberg; K > 0.70		
u = 58.53 – 25.41*lnk	q = 9.97*u*$e^{(-U/25.41)}$	q = (58.53*k– 25.41*k*lnk)
***Eddi* – Underwood K ≤ 0.70**		
u= 79.84*$e^{(-0.29K)}$	q = 3.45*u*ln(79.84/u)	q = 79.84*k*$e^{(-0.29K)}$
Eddie - Greenberg >0.70		
u = 58.53 – 25.41*lnk	q = 9.97*u*$e^{(-U/25.41)}$	q = (58.53*k– 25.41*k*lnk)
***Proposed* - UI K ≤ 0.70**		
u = 1/(0.0.125+(0.04 *k))	q = 1/(0.04) - 3.125*u	q = k/(0.0125 + 0.004*k)
Proposed Model - Greenberg >0.70		
u = 58.53 – 25.41*lnk	q = 9.97*u*$e^{(-U/25.41)}$	q = (58.53*K– 25.41*k*lnk)

Relationship occur is develop with two models, it verify by level of statistical significant. The set of equation with is shown in **Table 5**, for speed-density, flow-speed and flow-density. **Table 6 is** describes statistical test result from the developed equation as shown in Table 5. From the combination significance level are relatively low, with the two are the highest.

Table 6 Statistical test value of models

Model Analysis	Value		
	R^2	F test	t-test
Greenberg	0.525 0.682	73.62 88.43	66.08 51.45
Eddie	0.545 0.682	301.83 88.43	69.37 51.45
Proposed Model	0.561 0.682	63.68 88.43	74.22 51.45

4. PEDESTRIAN FACILITIES

4.1 Safety Approaches

Pedestrian face high risk when across network segments cause by interaction between vehicles flows and pedestrian flows. **[10]** Accident analysis and modeling is needed to develop in order to characterize the effect for pedestrian crossing road. Attempt to develop the model is not intensively investigate since pedestrian behavior is strongly related to complex human factors. On the other aspect, pedestrians risk exposure is significant when moving across network segment. Difficulties to cross the street reflect aspect of accessibility which is also equal to other transportation mode. [11] It is need to estimate probability for overall approach to model characteristics pedestrian decision to across or to wait until condition allows to safely crossing. Probability to cross is influenced by vehicles flows, gap acceptance between vehicles movement and number of pedestrians which means that pedestrian has a critical gap to cross the street. Dept of Transport UK (**Note TA/10/80**) formulates the possible conflict use the relationship between **V** (flow of vehicles, vehicle per hour) and P (number of pedestrian, person per hour), multiplying **P** with $\mathbf{V^2}$.

Table 8. Type of pedestrian crossing PV^2

Parameter PV^2	**P**	**V**	**Type of Facility**
$>10^8$	80 – 1100	200 - 800	Zebra
$>2 \times 10^8$	80 – 1100	400 -	Divided zebra
$>10^8$	80 – 1100	Over 800	Pelican
$>10^8$	Over 1100	Over 300	Pelican
$>2 \times 10^8$	80 – 1100	Over 760	Divided pelican
$>2 \times 10^8$	Over 1100	400	Divided pelican

Source: Department of Transport, UK – TA/10/80

This value indicates the rate of conflict between vehicles and pedestrian crossers, and use as a mean to select a safe pedestrian crossing type. (**Table 8**).

4.2 Pedestrian Crossing

Facility Type Crossing behavior is determined by the gap acceptance theory which means that pedestrian has a critical gap to safely cross the street. Model based on pedestrian level of conflict however still limited to local behavior. Implementation of approaches and model PV^2 in some observed street in Jakarta proven that range of PV^2 value is higher than value given by DoT. UK. Data for observed street is shown in **Table 9**.

Table 9 P and V values at observation sites

Street name	P	V	PV^2
Senopati	121	1717	3.60E+08
Panglima Polim	197	2832	1.6E+09
Cokroaminoto	248	3195	2.5E+09
Kebon Sirih	352	3671	4.7E+09
Dr. Sutomo	291	4903	7.0E+09
Dr. Sahardjo	366	5061	9.4E+09
Menteng Raya	368	6788	1.7E+10
Rasuna Said	1047	8639	7.8E+10
Gajah Mada	1435	5097	3.7E+10
Hayam Wuruk	1280	5037	3.2E+10
Kramat Raya	250	10918	3.0E+10
Tomang Raya	569	6384	2.3E+10
Pramuka	397	7267	2.1E+10

For the same type of facility, pedestrian and vehicles flows on observed street are higher compare for to value stated by DoT UK. Parameter of PV2 is significantly differ and hence resulting a different type of facilities for safe crossing. High volume of traffic with low speed vehicles allow pedestrian to cross the street resulted in relatively safe.

Table 10 Proposed Type of Pedestrian Facility

PV^2	P	V	Type of Facility
$>5x10^9$	100 - 1250	2000 – 5000	Zebra
$>10^{10}$	100 - 1250	3500 – 7000	Zebra with traffic light
$>5x10^9$	100 – 1250	>5000	Traffic light or bridge
$>5x10^9$	>1250	>2000	Traffic light or bridge
$>10^{10}$	100 - 1250	>7000	Bridge
$>10^{10}$	>1250	>3500	Bridge

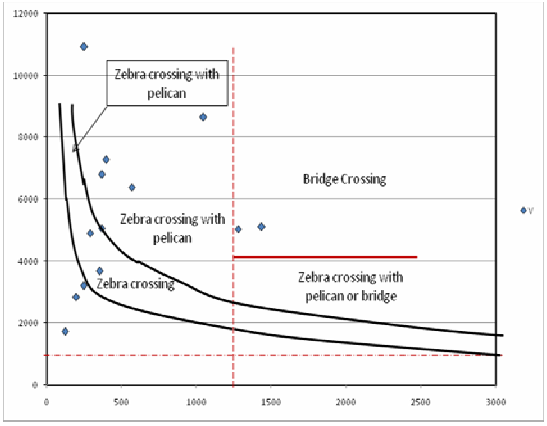

Figure 2 Selection of Pedestrian Facilities based on PV^2 value.

The result of observation and type of pedestrian crossing facility for Jakarta is shown in **Table 10**. [4] [7]

Decision to Cross There are two major factors influencing decision for pedestrian to cross the street: (i) internal factor: age, gender, platoon dimension, physical and mental condition, and freedom to maneuver; (ii) external factors: traffic flow. To characterized decision process, logit model is applied with individual behavior to choose one of best alternatives from at least three possible choices, such as: (i) not to cross; (ii) to cross at critical gap; and (iii) safe crossing. Model develop to accommodate is equitation with utility function: $u = a_0 + a_i x_i + a_n x_n$; ; where n= attribute index, a_0= constanta for utility function; and a_n = utility coefficient function.

From the total sample of 924 people, three utility functions for each possibility is developed and written as follow: (11) (**Sutanto, Agah, Andi, 1999**)

$u_i = -0.324 + 0.263x_i + 0.314x_2 + 0.264x_3 + 0.885x_4 + 0.249x_5 + 0.499x_6 + 0.198x_7$

$u_2 = -0.368 + 0.253x_i + 0.824x_2 + 0.226x_3 + 0.426x_4 + 0.513x_6 + 1.062x_7 + 0.252x_8$

$u_3 = -0.376 + 0.801x_i + 2.941x_2 + 0.292x_3 + 1.628x_4 + 0.559x_5 + 1.760x_5 + 0.533x_7$

The eight variables are: (1)age; (2)speed; (3)gender; (4)freedom to maneuver; (5)gap; (6) delay of pedestrian; (7)platoon; (8)vehicle gaps for safe crossing.

Results shows that about 55.85% pedestrian decide to cross in a critical condition, which means that flow of vehicles, are high and gap is critical. Avoidance of pedestrian for their safety is considered less, since there are some 72,99% of pedestrian crossing the road. The

number of percentage is almost three times comparing to the possibility to cross be a safe condition that is 25,19%.

5. CONCLUSIONS

To provide safe and comfort pedestrian facilities, basic characteristic of pedestrian is important input which influence by behavior of person, environmental conditions and traffic flow. On gender basis is found difference between male and female, in which speed of female is relatively lower compare to male. Relationship between parameter is relatively similar with vehicle flows, however since pedestrian does not follow in fix lane determination of flow must consider space per pedestrian. The relationship of two analytical parameters is found not always linear and can be represented by one model. Combination of two or more model is found to be realistic to represent better condition of pedestrian flow.

Safety factor for pedestrian in observed area (Jakarta) is found not treated as mayor parameter to cross the street. However, compare to the standard develop by DoT, -UK, the facility need to be provided is more moderate. This may cause by high volume with low speed providing small space for pedestrian to cross. Need enforcement both for pedestrian and driver to follow the rule in order to increase road safety.

REFERENCES

[1] Iderlina Mateo-Babiano, Hitoshi Ieda, (2005), Theoretical Discourse on Sustainable Space Design: Towards Creating and Sustaining Effective Sidewalks, Transport Research and Infrastructure Planning Laboratory, Civil Engngr Dept, Univ of Tokyo, *Business Strategy and the Environment Bus Strat* Env.

[2] Fruin (1971), Pedestrian Planning and design, *Metropolitan Association of Urban Designer and Environmental Planners Inc*., New York.

[3] Agah, HR., (1993), Identification of Characteristics and Behavior of Pedestrian at Jakarta, *Proceeding of REAA*, Kuala Lumpur, Malaysia.

[4] Agah, HR, Endang Widjajanti (1990), Identifikasi Kebutuhan Fasilitas Penyeberangan Pejalan Kaki, Proc *Konferensi Regional Teknik Jakan ke-4*. 1990

[5] Kay Kitazawa; Michal Batty, (2004), Pedestrian Behavior Modeling: An Approach to Retail Movement using a Genetic Algorithm, *Center for Advanced Spatial Analysis*, University College London, DDSS 2004

[6] TRB, (2000), *Highway Capacity Manual*, National Research Council, Washington DC.

[7] Agah HR., Endang Widjajanti (1987), Efficiency Pemanfaatan Fasilitas Prasarana Pejalan Kaki Daerah Urban, *Konferensi Tahunan Teknik Jalan ke-3, Himpunan Pengembangan Jalan Indonesia*, Puslitbang Jalan Dep.PU., Bandung.

[8] Tanaboriboon, Y, Hwa. SS., Choor CH.(1986) Pedestrian Characteristics study in Singapore, Journal of Transportation Engineering, ASCE

[9] Agah, HR, Nasir Jalili (2008), Karakteristik Arus Pejalan Kaki berdasarkan Model Mikroskopik, *Simposium XI, Forum Studi Transportasi Perguruan Tinggi*, Universitas Diponegoro, Semarang.

[10] George Yannis, John Golias, Eleonora Papadimitrious, Modeling Crossing Behavior and Accident Risk of Pedestrians, *J of Transportation Engineering, ASCE*, November 2007.

[11] Duncan C., Hakattak A., Hughes R. (2002), Effectiveness of Pedestrian safety treatment for hit-along-roadway crashes, *Proc. TRB 81st Annual Meeting*, Transportation Research Board, Washington DC

[12] Department of Transport, (1980), Design Consideration for Pelican and Zebra Crossing, *Departmental Advice Note No. TA/10/80*, Roads and Local Transport Directorate, UK.

[13] Sutanto Suhodho, Agah, HR., Andi Rahmah (1999), Pengembangan Model Perilaku Pengambilan Keputusan Menyemberang Jalan bagi Pejalan Kaki, *Simposium Forum Studi Transportasi Perguruan Tinggi*, Graha 10 Nopember –ITS, Desember 1999, Surabaya.

ISSN 114-1284

Identification of Deteroriation of Special Lane Flexible Pavement under Repetitive Loading

Heddy R. Agah[1], Sigit P Hadiwardoyo[2]

[1]*Department of Civil Enggr. Faculty of Engineering*
University of Indonesia, Depok 16424
Tel: (62-21) 7270029. Fax: (62 21) 7270028
E-mail: agah@eng.ui.ac.id
[2]*Department of Civil Enggr Faculty of Engineering*
University of Indonesia, Depok 16424
Tel: (62-21) 7270029. Fax: (62 21) 7270028
E-mail: sigit@eng.ui.ac.id

ABSTRACT

Effective and efficient maintenance program and rehabilitation would affect the life cycle and level of service highway pavement. Strategic steps for

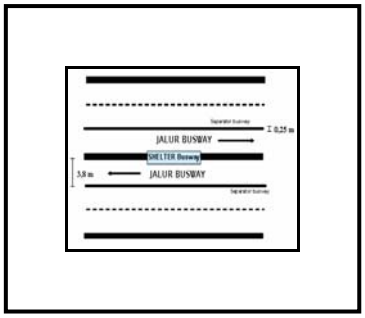

maintenance program understanding and knowledge of the type and severity level of pavement damage is important to be taken into account. This paper discusses deteriorations of the pavement occurred along the corridor of special bus lane as called "busway – lane". This stretch of corridor is experiencing a high frequency of repetitive wheel loads and moving on the relatively same paths. Combination of high frequency, loading characteristic and same wheel paths has resulted in severe distress along the corridor and greater potential acceleration of pavement deterioration on corridor due to buses use. Bus lane use the existing flexible pavement lane, one inner lane occupied from the total of three fast lanes. After open to traffic damage gradually appeared in the pavement surface particularly at the bus stop and wheel path. Total weight of bus including about 80 passengers on board is approximately 15.000 kg. The object of research is Busway lane on corridor Blok M – Stasiun Kota in Jakarta – Indonesia. Total corridor length observed is 12.90 km and 3.80 meter width with total of 20 bus shelters and distance between shelters is 650 meter. There are 91 buses operated in total with the gap of 1.2 to 3.0 minutes during working hours from 05.00 to 22.00.

In order to indentify the type, quantity, and quality of pavement damage, survey is conducted by visual observation. Observation is conducted every 30.00 meters to maximum 150.00 meters length, digital camera used to take picture, map sheet and survey form use to record the surface pavement condition, and straight ruler to measure dimension (length or area) of distress as well as the depth of rut. The recorded data and information would be use as a mean to predict the type of distress, furthermore to find possible solution for the problems encountered refer to measured cracks and other mode of surface pavement damages or distresses. Air and surface pavement temperatures are also measured to analyze the impact and contribution of temperature. Result of visual observation combined with the characteristic of layers beneath pavement surface is analyzed and investigated to estimate contribution of sub-base and base which are mostly granular base materials. From the observed results it is found that the most frequent distress was potholes (33,33%), rutting 19,87% and other types range between 15%-4%. The results show typical damage characteristic, both of single type or combination of several types of distresses while the severity ranged from low to high. However, minimum influence of temperature is found.

Keywords
pavement maintenance, visual observation, distresses, special bus lane.

1. INTRODUCTION

One of the strategic components in pavement management is an ability to estimate and to predict pavement performance distresses and potential failure due to loading and environmental aspects such as temperature and water. This needs objective system and ranking performance criteria to provide comprehensive information to cover type pavement distresses and specific indicative failure condition in particular for the road network system. Pavement condition prediction[1] [2] done through investigation in the field with either using destructive or non destructive testing method. Non-destructive method is relatively faster to undertake and provide initial pavement condition prediction.

This method uses visual observation directly in the field visually by the team of at least three persons and in combination with desk evaluation to interpret any indication and performances from picture taken at the site, or measures pavement surface deflection with one selected equipment types such as Benkelman Beam or Dynaflect, measures skid resistance and surface pavement roughness using roughness meter. [3] [4] [5] Knowledge of the various types and its frequency are important, since it can help in identifying the cause of distresses and also as a means to select most probable repair. It is important to identify the design method and provide pavement management system to find a most effective strategy for maintenance and rehabilitation. [6]

Level of distress is classified with major type such as cracking, patching and potholes, surface deformation, surface defect and other defects [7] [8]. However with a systematic maintenance supported by a consistent, uniform basis data and information collected from the road network of all distresses found in the field will help longer live and more convenient pavement for the rider. Distress is one of the important consideration and primary parameter in pavement design. In particular if mechanistic-empirical method is applied, each failure criterion should be developed separately to overcome or to find proper solution of each specific distress. Typical distress could occur in one specific road condition which experiencing by load with unique types and characteristics. Premature failure will occur due to overloaded vehicles traffic or very high repetition of load (axle load) passing same path or the road pavement surface represented by rutting along wheel path.

As found in some references and previous research [8] [9] [10] typical pattern of deterioration in asphalt pavement is rutting, which develop in relatively rapidly during the first opening to traffic flow and later after reaching a certain period of time or number of vehicles repetition level of deterioration is slower. Other type of distress such as fatigue or cracks normally does not occur in the early stage of services, until sometime after carrying a high number of vehicle wheel repetitions. However, it will develop in relatively rapidly when pavement is weakens. In Indonesia with relatively constant high temperature which creates higher surface temperature compare to air temperature, bleeding will occur if asphalt content is too high, or crack will developed cause by consistency of asphalt.

This paper discusses deteriorations of the pavement occurred along the corridor of special bus lane as called “bus way – lane” located in Jakarta - Indonesia. This stretch of corridor was experiencing a high frequency of repetitive wheel loads and moving on the relatively same paths

2. METHOD OF OBSERVATION

2.1 Distress Survey

Observation is undertaken in combination of direct observation in the site and photograph at selected point coincide with the entire defect found from visual observation. All parts of pavement surface along the corridor are observed and the result is drawing in the map identifying the type, area and distance from a coordinate system. To have a representative distress type and close to real condition [7] [8]**,** team of observer must at least comprises of three persons, observation must have mapping format and distress symbols.

Each segment of observation must not exceed 150 meter, however it is suggested to measure every 30 meter segment of road. The result of this must cover type, number of each distress types and level of severity also the exact location. All of the findings are written in a survey format and drawn in distress map. FHWA method of visual observation to identify type of distress is used as survey format in this research. The result is grouped by the type of distresses to produce a map showing type and frequency as well as location. [4] [9] Referring to the manual from FHWA, deterioration is grouped into 4 (four) of specific groups plus one distress which has different characteristics and geometric as defined

in the first four group. Group classification is: cracking, patching and potholes, surface deformation and surface defects, and to simplify so that easier to note in the field observation code number of distress type is normally used rather than write full name of distress type. (**Table 1**). Severity or level of deterioration is broken down into three levels such as low (L), medium (M) and H (high), e.i: **1-L**, means fatigue cracking (**1**) with low severity (**L**).

Table 1. List of group classification and type of distresses

Code	Group classification	Type of Distress
1	Cracking	Fatigue Cracking
2		Block Cracking
3		Edge Cracking
4a		Longitudinal Cracking (Wheel-paths)
4b		Longitudinal Cracking (Non-Wheel-paths)
5		Reflection Cracking at Joints
6		Transverse Cracking
7	Patching and Potholes	Patch / Patch Deterioration
8		Potholes
9	Surface Deformation	Rutting
10		Shoving
11	Surface Defects	Bleeding
12		Polished Aggregate
13		Raveling
14	Miscellaneous Distresses	Lane To Shoulder Drop-off
15		Water Bleeding and Pumping

2.2 Site Characteristics

Lane Function and the User Since the year of 2003 a new system of public transport has been introduced and offered to the traveler in Jakarta called "Bus Way", which means passenger bus rapid transit, a bus system ride on a special lane of road network system. Bus way in term of infrastructure is designed as a special lane taking one inner lane from the three or more of the existing road lanes and separated by concrete divider to avoid friction and conflict with other traffic vehicles. With this kind of lane, operating speed could be maintained in a constant rate. The first corridor is along the route of Blok M in South Jakarta stretches to Kota located at the business center at North Jakarta with the total length of 12,90 kilometer facilitated with 20 shelters, average lane width is 3.80 meters, and distance between shelters is 650 meters (**Figure 1**). Some widening of road is constructed due to the limit of existing width varies between 0.60 meters to 1.00 meters. The existing pavement is flexible pavement and has been overlaid by hot-mix asphalt concrete several times since the first time of construction to have minimum of 3.80 meter width. However due to the difficulties to find the real condition of existing pavement layer and its overlay surface to maintain good road, detail of layer thickness is not possible to draw in detail. (**Figure 2**)

Bus is operated daily with operating hours started at 05.00 until 22.00, headway time during peak hours is between 1.20 to 3.00 minutes. Maximum gross vehicle weight of bus is 15.000 kilograms and resulted from combination of it is owned weight of 9.340 kilograms and total passenger weight of 4.860 kilograms. Maximum carrying capacity of bus of 85 passengers comprises of 35 sittings and 50 standees with the average body weight of 60 kilograms and approximately another 800 kilogram of goods. Number of buses operating in the observed corridor is shown in **Table 2.**

Table 2. Bus operations for Blok M – Kota corridor

Descriptions	Total number
Number of bus in operations	2.137
Average number buses/day	69
Production/kilometer	464.838
Average kilometer production/day	14.995
Number of Empty kilometer	89.175
Average Km Empty / Hari	2.894
number of kilometer travelled	554.553
average kilometer travelled/day	17.889
Number of trips	17.878
Average trips/days	577
Average trips/bus/day	8,4
Passenger capacity	3.039.325
Number of passenger	1.915.221
Average passenger/day	61.781
Average passenger/Bus/day	896
Passenger/km travelled	3,5
Distance (km)	12,9
Trips (km)	26
Travel time (minute)	45

Source:Badan Layanan Umum Transjakarta, 2008 [11]

2.3 Field observation

Since the early period of opening and bus operation, this special lane experiencing pavement deterioration which may be caused by higher number of traffics from the bus operation compared to the other existing conventional lane in the same flow direction. This situation leads to finding the most possible cause of the distress which in turn will be used as tool to select a proper method to prevent pavement damages. Field observation collects detailed information of each part of the pavement damage and measures it

by the length or area of particular distress type. Type and symbol refer to the FHWA method is used as reference.

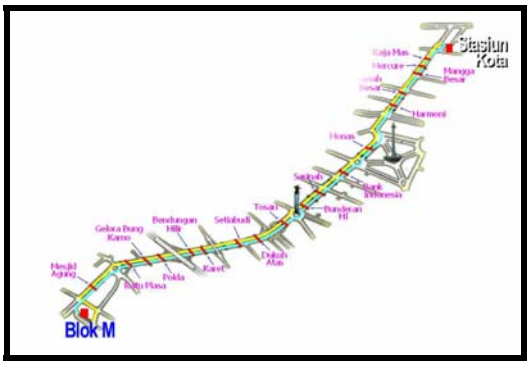

Figure 1 *Map of bus-way lane and shelters on corridor Blok M- Stasiun Kota – Jakarta*

Both air temperature and pavement surface temperature are measure at each part of visual observed segment. However, the measurement is not taken in the same period of time since it follows the measurement of distress. Special observation is done for distress type of rutting. The depth of rut is measured using ruler and taken at every 30 meter, both on the left and right side of bus wheels. From the observation data are collected geometrically, type and location of each distress includes width of bus lane, the width of developed rutting, as well as air and surface temperature. Number of bus traffic flow was taken from the bus authority. Equipment and tool used are: digital camera, thermometer to measure surface pavement temperature, ruler, marking tools and form of data sheet. Distress map sheet is referred to FHWA format and 30 meter segment of observation is applied. From the total of 12.90 km. 2.79 km. was selected as research subject location at corridor I busway (Blok M – Kota).

3. ANALYSIS

3.1 Findings

From the entire stretch of road of 93 sections (30 meters per section) all types of distresses include number of each type is shown in **Table 3**. The number is cumulative of total sections ignoring severity level of deterioration; it is meant that there are 72 locations with fatigue cracking for all type of severity in this classification.

Of the total 15 types of distress observed, the five major types are ranked as the most frequent and detail is shown in **Table 4**. The table also shows two important indicators which are (i) average of each type, and (ii) severity level divided into three levels. Average is calculated from all numbers of type found during observation and depend on the characteristics of each type are measured by area (meter square) or by length (meter length). In the last three columns, level of severity is shown in three different levels (**H=high; M=medium; L=low**), each number in column (in %) is average and calculated from the total length observed road.

Performance of each type is shown in **Figure 2**

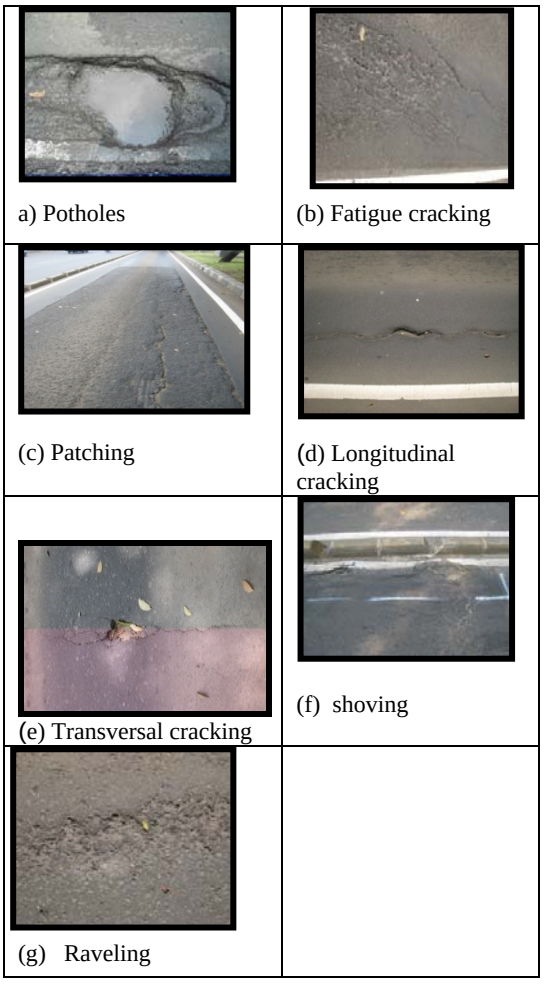

Figure 2. Some types of distresses with high severity level found at sites
Courtesy of: Pietoyo Larastomo (2007) [12]

Table 3 Number of each type of distresses

Code	Classification	Type of Distress	Number	Percent
1	Cracking	Fatigue Cracking	72	16,07
2		Block Cracking	2	0,45
3		Edge Cracking	1	0,22
4a		Longitudinal Cracking (Wheel paths)	38	8,48
4b		Longitudinal Cracking (Non-Wheel paths)	6	1,34
5		Reflection Cracking at Joints	0	0,00
6		Transverse Cracking	23	5,13
7	Patching and Potholes	Patch / Patch Deterioration	65	14,51
8		Potholes	156	34,82
9	Surface Deformation	Rutting	75	16,74
10		Shoving	8	1,79
11	Surface Defects	Bleeding	0	0,00
12		Polished Aggregate	0	0,00
13		Raveling	2	0,45
14	Miscellaneous Distresses	Lane To Shoulder Drop-off	0	0,00
15		Water Bleeding and Pumping	0	0,00

Table 4. Level of severity (%) and average area of the highest distresses observed

Code	Type of Distress	Classification	No	%age	Average Length* Area*	H	M	L
						(%)		
8	Potholes	Patching and Potholes	156	34,82	0.642 m2	42	33	25
9	Rutting	Surface Deformation	75	16,74				
1	Fatigue Cracking	Cracking	72	16,07	1.712 m2	33	39	28
7	Patch / Patch Deterioration	Patching and Potholes	65	14,51	6,25 m2	37	38	25
4a	Longitudinal Cracking (Wheel paths)	Cracking	38	8,48	2,26 m	68	28	3
6	Transverse Cracking	Cracking	23	5,13	1.10 m	17	44	39
	Shoving		10	2.14	1.87 m2			

Table 5. The right and left rut depth of vehicle wheel along the lane.

Path –mm	Right path			Left path		
	Frequency	%	cumulative	Frequency	%	cumulative
1.00	2	2.2	2.2			
2.00	1	1.1	3.2	3	3.2	3.2
3.00	2	1.1	5.4	2	2.2	5.4
4.00	5	5.4	10.8	4	4.3	9.7
5.00	11	11.8	22.6	5	5.4	15.1
6.00	8	8.6	31.2	12	12.9	28.0
7.00	18	19.4	50.5	8	8.6	36.6
8.00	14	15.1	65.6	22	23.7	60.2
9.00	13	14.0	79.6	11	11.8	72.0
10.00	11	11.8	91.4	16	17.2	89.2
11.00	3	3.2	94.6	5	5.4	94.6
12.00	4	4.3	98.9	4	4.3	98.9
15.00	-	-	-	1	1.1	100
16.00	1	1.1	100			
Total	93	100		85	100	

The most frequent and dominant distress along the observed bus-way route is potholes with 33.33%, rutting for about 29.87%, failure cracking of 15.38%, patching of 13,89%, longitudinal cracking of 4,91%. However, bleeding is not found during observation period noted that surface temperature measured is below 53^0C. Surface pavement temperature is between $29,1^0$C – $51,4^0$C. Wide range of measured temperature is influence by the timing of measurement since it is following the visual observation time, some are taken in the morning and the rest are in the mid day. Frequency distribution of surface and air temperature is shown in **Figure 3**.

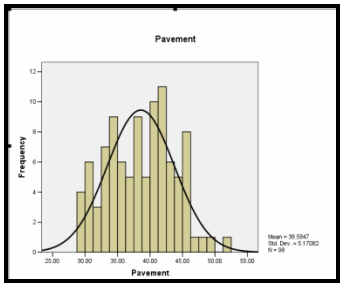

3 (a)

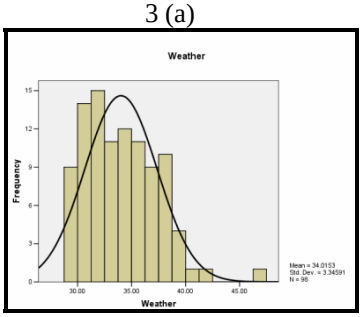

3.(b)

Figure 3 Distribution of measured (a) pavement temperature and (b) air temperature temperature

3.2 Types and Level of Distresses

Rutting This type of distress is a dominant distress found along the observed road after potholes. Rutting is surface depression in the wheel path it will be seen as evident after rain when it is filled by water. This problem normally occurred when pavement in subjected to load from vehicles wheels either overload or riding on the same track, it will create more serious effect when combination of heavy load and riding in relatively the same wheel track. This case is very similar with the lane servicing bus-way system causing phenomena like channeling effect. Detail performance of rutting along the wheel path is shown in **Table 5.** The depth of rut is significant in number ranging between 11.0 mm to maximum 20.0 mm and its frequency which ranges from 11 to 22 from the total number of rut observed. This shows that the effect of traffic is considerable giving strong influence to this type of pavement and vehicle movement characteristics. The depth of rut is approximately 40% -50% of the initial pavement thickness which indicates pavement have been heavily damage.

Further evaluation based on collected data shows there are 375 point or locations of defect, of which some 366 point (97,6% of total defect) are located at wheel path, compare to 9 points defects outside of wheel path. This has proven that load repetitions applied on the same path will influence significant effect to the pavement performance.

Combination of Distresses Failure of pavement does not always show one type, but in many cases, as it is found in this research combination of two or more types failures frequently occurred. In one segment per 30 meter length of observation there also occur in combination of more than one type of distress. As shown in **Figure 4** the most frequent distress is combinations of two types per 30 meter segment, and the highest combination per 30 meter is 19 types. The average combination per 30 meter is found as 4 combination of distresses type, those numbers indicate that distresses always occurred of more than one type and this likely occurs when the maintenance program is delayed. There is time lag between the indication and early stage of distress development and repair action must be done.

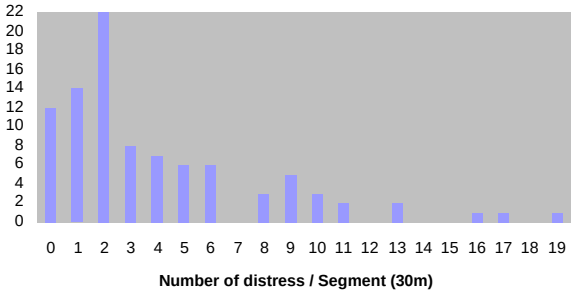

Figure 4 Frequency distribution of distress along the corridor (*horizontal axis representing length of corridor per 30 meter, and vertical shows frequency of distresses*)

Temperature and Distress Hot-mix asphalt concrete is susceptible to temperature which

influence by characteristic of asphalt as binding agent. Temperature affects the resilient modulus of asphalt layers and elastic and viscoelastic properties of hotmix asphalt concrete.

One of the indications of distress caused by high surface temperature is bleeding, however in this research as seen in **Table 6** this type is no found.

Table 6 Correlation between distress classification and temperatures

Location (shelter)	Distress classification		Temperature	
	Type(s)	Number	Pavement	Air
Sawah Besar – Harmoni	Potholes; fatigue cracking patching longitudinal cracking	10	33	33.76
Glodok – Olimo	Potholes, fatigue cracking, longitudinal cracking	9	33	31
Sarinah – Bank Indonesia	Potholes, patching	2	41.8	36.03
Mangga Besar – Sawah Besar	Potholes, fatigue cracking, longitudinal cracking, patching	4	37.6	32.6
Bank Indonesia – Sarinah	Potholes, patching	4	42.4	37

Bus Shelter and Distress Results from field observation shows that distress appear in the area and its surrounding area of shelter are significantly differ from others found along segment. Stop and go bus operation results friction and highly concentrated shear stress in pavement surface. Typically shoving, ruts, raveling and potholes are found, in which shoving are the dominant distress type. (**Figure 5**)

Figure 5 Typical failures in the area of bus shelter

4. CONCLUSIONS

1. Distress type dominating the bus way corridor are potholes (33,33%), rutting (19,87%), fatigue cracking (15,38%), patching (13,89%), transverse cracking (41,9%).
2. Distresses in the area of bus shelter is unique caused by combination of repeated loading and stop and go bus operation causing heavily damage pavement, combination between rutting, shoving and potholes. Higher strength of pavement need to overcome the problem and better drainage to avoid surface filled with still water.
3. Temperature does not contribute to the common problem of higher temperature such as bleeding which may be caused by proper asphalt content in design of asphalt concrete mix.
4. High frequency of load repetition and combined with moving in the same path creates combination of distress in the same segment, with the average of four types of distresses in the same location. Potholes is found as a dominant type of distress is indicates excess of surface water and impact of wheel load.
5. Surface deformation in the form of rutting along the corridor is the effect of wheel load impact, this is caused by less strength of layer both surface and layer beneath.
6. The total of all distresses along the observed corridor as much as 375 point of failures shows that special attention need to taken

into account in term of pavement strength, refer to the number of failure 366 out of 375 occur along the wheel path.

7. Combination of more than two types of distress caused by late action to overcome the problem which lead to foster the deterioration rate and potential to a worst pavement condition

References

[1] Croney, D.,(1977), *The Design and Performance of Road Pavements*, H.M.Stationery Office, London.,

[2] Croner, David; Croney Paul (1991), *The Design and Performance of Road Pavements*, McGraw-Hill Book Europe.

[3] Agah HR (1984), Engineering Performance of Highway Pavement, Master Thesis, *Asian Institute of Technology*, Bangkok

[4]] Sayer, Michael W, (1990), Profile of Roughness, *Measurement of Pavement Surface Condition*, *Transportation Research Record*, no 1260.

[5] Ralph, Haas, (2001), Reinventing The (Pavement Management) Wheel, *proc of the Fifth International Conference on Managing Pavements*, Seattle, Washington, USA.

[6] Goulias, Dimitrias G; Castelo, Humberto; Hudson, W Ronald, (1990), Pavement Distress Surveys in the Strategic Highway Research Program's Long Term Pavement Performance Study, *Measurement of Pavement Surface Conition, Transportation Reserch Board*, no 1260.

[7] Geoplan Consultant Inc, British Columbia MOT, (2002), *Pavement Surface Condition Rating Manual*, Victoria BC

[8] John S Miller, Wiliam Y Belinger (2003), *Distress Identification Manual for The Long Term Pavement Performance Program*. Publication no FHWA RD 03-031, Department of Transport United States Department of Transport, FHWA. June 2003.

[9] Shahin, M.Y. (1994), *Pavement Management for Airports, Roads, and Parking Lots*, Chapman & Hall, New York.

[10] Huang, Yang H. (2004), *Pavement Analysis and Design*, Pearson Prentice Hall, USA

[11] Pietoyo Larastomo, (2007), Identifikasi Kerusakan Perkerasan Busway (Studi Kasus: Koridor I, Blok M-Kota), Tugas Akhir, *Fakultas Teknik Universitas Indonesia* (unpublished).

[12] Badan Layanan Umum Transjakarta, (2008), *Laporan Realisasi Pelaksanaan Operasi Transjakarta Busway*, Februari 2008

ISSN 114-1284

Integration Of Value Engineering And Risk Management to Improving the Efficiency and Efectiveness of Construction Industry in Indonesia

Herawati Zetha R.[1], Yusuf Latief[2], M.A. Berawi[3]

[1]*Faculty of Engineering*
University of Indonesia, Depok 16424
Tel : (021) 7270011 ext 51. Fax : (021) 7270077
E-mail : zetha_r@indo.net.id

[2]*Faculty of Engineering*
University of Indonesia, Depok 16424
Tel : (021) 7270011 ext 51. Fax : (021) 7270077
E-mail : latief73@eng.ui.ac.id

[3]*Faculty of Engineering*
University of Indonesia, Depok 16424
Tel : (021) 7270011 ext 51. Fax : (021) 7270077
E-mail : ale.berawi@gmail.com

ABSTRACK

In general, Indonesian construction industry is still struggling with inefficiency and ineffectiveness which is caused by delayed sechedule and cost overrun. There is a need to improvement the performance of Indonesian construction industry by integrated value engineering and risk management to succeed in the delivery their desired outcomes by maximize value and minimize uncertainty. Value engineering and risk management can assist in creating a culture which enhances project performance by reducing risks. Value Engineering provides an effective process to maximize value in line with the owners and end users requirements; meanwhile risk management provides a process for managing risk. Both processes should be integrated on every significant design, development and construction project. Focusing on the integration of value engineering and risk management applica-tion on the other countries, this paper intends to give clear direction of the subject to be studied, by discussing the scope and approach of both value and risk management. The paper has a conclusion that there is the potential for construction industry in Indonesia to improve the effectiveness and efficiency by implementation the integration of value engineering and risk management. The result of this research is intended to contributing to national construction industry.

1. INTRODUCTION

Construction sector in Indonesia has grown since the beginning 1970's and held an important role in national development. This sector has significantly contributed to other social and economy sector growth. BPS Data 2006 showed that market share on national construction sector has grown to 8,6 % of GDP or equivalent to Rp. 52,3 Trillion in second quarter of 2006 [1]. The importance of this sector is obviously supported a conducive business environment and developed capability.

In general, Indonesian construction industry is still struggling with inefficiency and ineffectiveness during the implementation process of its constructions. Many waste in form of activities which utilizes resources cannot produce expected value, whereas construction project performance should be assessed on how those project management system could contribute added value to the related parties either cost side or time. Abduh (2007) argued that the waste of construction industry in Indonesia has reached 57% whereas the activity which gives additional value is only 10% [2]. This issue is obviously shown inefficiency and ineffectiveness. Alwi et al. (2002) identified the problem of inefficiency and ineffectiveness of Indonesia's construction industry and summed up that the main cause factor is delayed sechedule and impacted to the cost overrun [3]. This condition surely needs contractor's ability to be able to increase effectivity and efectiveness within the management of its construction's project [4],[5]. Contractor shall seek a method, concept, and program to manage project in order to be able reach his goal on vitable period, cost and quality [6].

There are 2 substantial conditions for the success of a project, first; contractor's capability to require expected value by project owner with initial agreed cost of the contract and, second; the effort of minimizing the impact of unavoidable risk and possible project loss [7]. First condition can be fulfilled by *value engineering (VE)* which provides effective ways to maximization value in certain project according to owner expectation. Whereas the second condition is overcome by implementing risk

management contributed to effective process in order to control the risk of a project. Value engineering and risk management within construction industry has been widely applied and accepted as the best tool for effectively management project [8]. The combination of value engineering and risk management within integration process is an excellent strategy which is able to maximize the project value and reduce uncertainty the agreed cost frame. This paper reports a investigated the arguments and the potential for their integration to promote effective and efficient construction industry in Indonesia.

2. METHODOLOGY

A study literature was undertaken to investigate current thinking on the applications of VE and RM in the construction industry in other countries as two discrete disciplines, and to establish the extent to which the literature address for the potential for their integration. This paper explores the procedures and process of VE and RM that has done by others researchers.

3. VALUE ENGINEERING IN CONSTRUCTION INDUSTRY

There is no single definition of VE or VM or of the other terms such as Value Analysis. The pioneer Miles (1961) defined VE as " an organized creative approach which has for its purpose the efficient identification of unnecessary cost" [9]. A definition which encapsulates the principles of VE is as value at systematic, multidisciplinary effort directed towards analyzing the functions of projects for the purpose of achieving the best value at the lowest overall life cycle cost [10]. The same definition was develop by Robinson & John (1997) that VE is a systemic process uses analytical, creative and evaluation techniques on a multi-disciplined basis to achieve the desired functions in a design or process while maximizing value and maintaining or improving required function.

The concept of function is based on the principle that the value of an object is determined by what use is fulfilled and is not related to its cost. VE use to eliminate unnecessary life-cycle costs without sacrificing safety, quality, environmental compliances or other functional requirements and it will increases innovation opportunities, improves cost effectiveness, enhances performance and fosters partnering among the owner, engineering and builder [12].

As a systematic process, VE focused on identifiable steps collectivity known as Job Plan Procedure, which was firstly founded by Miles in 1961 using 40 hour workshop. Developed from Mile's original Job Plan, 6 steps are included from information gathering and criteria setting to decision-making-related to selected options. In current practice, Hannan (1994) developed into three distinct stages of Pre-Study, Main Study (Workshop) and Post-Study activities, all focused on structured problem identification and problem solving [13]. The Society of American Value Engineers or SAVE International published its own job plan in 1997 while Male et al (1998) have their own as well. The different of job plan phases and procedures are as shown in Table 1.

VE is a multi-disciplinary approach based on an interaction of different disciplines providing a collective analysis of all aspects of a project and the cost implications of ideas so as to achieve the best value. Generally VE is applied when there is a well defined scheme in order to optimize costs and benefits. Palmer (1992) support that the earlier in the design process VE studies are carried out, the greater the potential for cost reduction and the lower the extra design cost of implementing proposals, as the majority of cost is committed during the early design stages [17].

Table 1.Job Plan Procedure [8],[15],[16]

LaMiles (1961)	Hannan (1994)	SAVE International (1997)	Male et al (1998)
Orientation Information	Pre Study Phase	Pre-study Phase	Pre-Study Phase
Speculation Analysis	Main Study Phase	Value Study Phase	Information Phase Creativity Phase Evaluation Phase Development Phase
Summary Conclusion	Post-Study Phase	Post-Study Phase	Consensus Phase

Since its introduction into the construction industry, VE has faced resistance. The same problem is happened in Indonesian construction industry. Green (1999) have founded many argue that the confused and inconsistent use the terminology and the lack of a standard definition are barriers to its widespread use [18]. VE is also associated with many misconceptions, such as VE for cost reduction exercise, somehow the aim of VE study is to lower cost whilst retaining or enhancing quality and performance requirements.

We frequently apply value management much earlier in the project lifecycle, in order to embark on the optimal project to provide an exceptionally powerful way of exploring client's needs in depth, addressing inconsistencies and expressing these in a language that all parties, whether technically informed or new to the construction industry [19]. This results in the following benefits:

1. It defines what the owners and end users mean by value and provides the basis for making decisions, throughout the project, on the basis of value. It provides a means for optimizing the balance between differing stakeholders' needs.
2. It establishes the value profile as the basis for clear briefs which reflect the client's priorities and expectations, expressed in a language that all can understand. This improves communications between all stakeholders so that each can understand and respect other's constraints and requirements.
3. It ensures that the project is the most cost-effective way of delivering the business benefits and provides a basis for retaining the business case. It addresses both the monetary and non-monetary benefits.
4. It supports good design through improved communications, mutual learning and enhanced team working, leading to better technical solutions with enhanced performance and quality where it matters. The methods encourage challenging the status quo and developing innovative design solutions.
5. It provides a way of measuring value, taking into account non-monetary benefits, and demonstrating that value for money has been achieved.

Nowadays value engineering is a contraption to render a better utilization of the financial sources, project timing and eventually the betterment of the project value. Value Engineering can be utilized as an appropriate strategy to enhance project implementation and to access the supreme purposes of the project.

4. RISK MANAGEMENT IN CONSTRUCTION INDUSTRY

Risk Management is defined as "the systematic process of identifying, analyzing and responding to project risk, including maximizing the probability and consequences of positive events and minimizing the probability and consequences of negative events to the project objectives" , and also as "an uncertain event or set of circumstances that, should it occur, will have an effect on the achievement on the project's objectives" [20],[21]. The concept of risk management is started with gambling, which is a game of chance, and makes profits based on prediction [19]. Champan & Ward (2002) implies that a source of risk is any factor that can affect project performance, and risk arises when this effect uncertain and significant in its impact on project performance [22]. Risk exists as a consequence of uncertainty while risk management describes the deliberate management of uncertainty or its effects [23],[24].

The aims and objectives of Risk management is to ensure that risks are identified at project inception, their potential impacts allowed for and where possible the risks or their impacts minimized and to improve project performance via systematic identification, appraisal and management of project related risk [22],[24],[25]. In the other word, the aim of risk management is not to eliminate risk but to control it. Successful risk management reduces the uncertainty in achieving a successful outcome to acceptable and manageable levels [19]. Risk Management ensures that risks are identified, reviewed and mitigated accordingly and key stakeholders are made aware of the risks prior to any decision making.

As a systematic process, there are many models used to manage the risks. The standard model is divided into 4 parts namely risk identification, risk analysis, risk response and risk monitoring and review. Meanwhile Baker et al (1999) developed that the methodology encompasses 5 staged: identification, analysis, evaluation, response and monitoring.

Source of risk central to construction industry activities can be grouped under the heading of physical and environmental, design, logistic, cost, legislation and constructability. Also the multiplicity of parties with different roles and aims, the project complexity and the fragmentation of the construction industry are further sources of risk. Project risks are considered to be dynamic and therefore risk assessment should be a continuous process spanning all phases [26].

A formal risk management process delivers the following benefits for the project team [19]:

1. It enables management to embark on innovative, high reward projects in the knowledge that they can control the risks.
2. It requires that the management infrastructure is in place to deliver successful outcomes. This includes setting clear, realistic and achievable project objectives from the outset.
3. It established the risk profile of the project, enabling the appropriate allocation of risk, so that the party best placed to manage it has the responsibility for doing so. Risk allocation is a key component of contract documentation.
4. It allows the team to manage risk effectively, concentrate resources on the things that really matter, resulting in risk reduction as the project proceeds. It also enables them to capitalize on opportunities revealed through use of the process.

On construction industry, risk can have a positive impact upon project performance. Although the current literature has the tendency to present risk as a negative element, but it can be argued that the main benefit of risk management is to help project managers ensure that project objectives are not

affected by adverse effects [7],[15]. Risk management is not a means of removing all the risks, but facilitates explicit decision making which will mitigate the effects of certain risks. This other benefits include: enabling decisions to be more systematic and objective, allowing comparison of the robustness of projects in relation to specific uncertainties, comparing the relative importance of each risk, providing an improved understanding of the project, promoting feedback and information transfer, and heightening awareness of the range of possible outcomes [28].

5. THE POTENTIAL OF INTEGRATED VALUE ENGINEERING AND RISK MANAGEMENT

The idea of integrating Value Management and Risk has started more than ten years ago as many professionals realized that it is impossible to separate between value and risk. Dell'Isola (1997) cited that the opportunity of integrating value management (VM) in conjunction with the formal risk assessment and analysis started in 1993 when a city port authority required a value engineering (VE) effort that would be augmented with an application of a risk assessment [29].

The main idea for integrating VM and RM is to optimize value on a project, minimize the time taken act and to produce results with optimum performance and quality. VE is about articulating what represents value in terms of projects benefits while risk management is about identifying causes of uncertainty and what can go wrong. Thus to optimize value, that is essential that the construction industry actively manage both value and risk. It is necessary to take risks to maximize value. Both activities complement each other to maximize the chances of project success, which is VE can reduce risk and risk Management provides opportunities to increase value.

Value engineering and risk management are two well-established disciplines recognized as a part of best practice [15]. The links between them are strong. Risk is managed it is possible to achieve a cost saving and an enhancement in value, while value is considered there may be risks associated with each phases. Norton & McElligott (1995) suggest that risk management may be enhanced by VE, using the VE team to either audit or produce a project's risk management plan [10]. In a combined approach there is potential to benefit from the assembled multidisciplinary team and also to promote the introduction of risk management into an organization [30]. Since the risk management is mainly perceived as a negative process a combined approach could mean that advantage could be taken of the creative, positive atmosphere of value engineering study to generate ideas to mitigate risks or identify opportunities.

In the construction industry, both VE and RM are well and widely accepted as best practice tools for effective management of projects [31],[25]. Griffin (2006) said that the issue is no longer about whether they should be used but whether the processes should be integrated [32]. The application of VE will help client to identify the best way of meeting business need while RM is used to manage the risks associated with the solution that offers the best whole-life value to the business and should not be seen as barrier to innovation [25].

It is arguable that the integration of RM and VM can be used to reduce the negative impact on projects and to assist value improvement [8]. While this is so, the risk of available alternatives will influence the decision about project objectives and preferred outline designs which strengthen the idea of combining RM and VM [30]. Furthermore, Othman (2004) supported the idea of integration of VM and RM as two complimentary disciplines, saying that best value could not be achieved unless associated risks have been managed. The reasons why there is a need to integrate between VM and RM is as follows [26], [30],[34],[35]:

1. Utilisation of the same resources/multi-disciplinary team hence avoiding duplication of effort.
2. Involvement of stakeholders in the workshops.
3. Good way of introducing VM and RM into an organization.
4. Maintain and improve future appraisals and assessment of projects.
5. Influences the VM proceeds in this case-option appraisal, by allowing the users to consider specific options used in the past similar projects.
6. Makes them aware of their weakness and strengths.
7. Shortening he time taken to develop viable solutions based on the risks facing a project.
8. Identifies specific risk allocation structures in association to contrast strategies.
9. Provides in-depth assessment process.

5.1. Advantages of Integrating Value and Risk

There are four advantages in integrating value and risk management practices [31]:

1. Integration enables value and risk issues to be considered together. From the very beginning of the project a full picture is available to help decision-makers develop an understanding of opportunities and uncertainties.
2. Integration is more efficient, not only from the depth and quality of the discussion process, but

also because fewer workshops and meetings are required.

3. The use of this integrated discourages the use of ambigious and inconsistent language and so promote a common team understanding and coordinated effort to realize the client's objectives. This should reduce the levels of confusion in the industry and make it easier for facilitators and others to work within project team.
4. Any value management, value analysis, value engineering or risk management tool or other relevant business management tool can be incorporated where, and whenever desired.

5.2. How to Integrated Value Engineer-ing and Risk Management; Learn from Other

Workshops are useful way of identifying project risk and therefore it possible to combine risk and value engineering in the some workshop [30]. There are some papers published which strongly suggest integrating the risk management with value engineering. Kirk (1995) introduces the probabilistic estimating concept by combining range estimating and Monte Carlo Simulation instead of traditional Determining estimating [36]. This practice also gives the decision-maker a better confidence when determining the contingency for the project. Mootanah (1998) also made a very intensive study on the interactive strategy for value and risk management framework, and he proposed the possible interface as shown in Figure 1 [37].

In the UK, a general guide in integrating value and risk management is provided by OGC, identified as The Gateway Process. This process helps to reduce overall project risk by examining the project at critical stages in its life cycle to provide assurance that it can progress successfully to the next stage [25]. Kirk (1995) and Thompson (2004) suggested that value and risk management could be integrated in a workshop through the job plan process with risk considerations in each phases as shown in table 2 [35],[36].

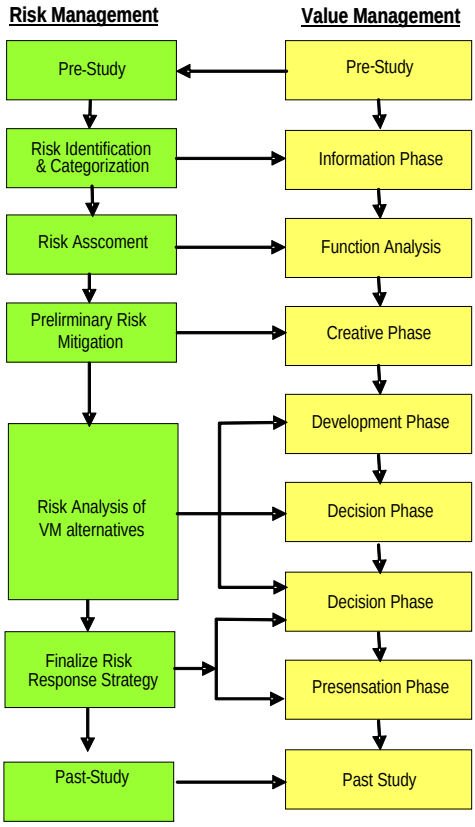

Figure 1 : Possible Interface of Value and Risk Management (Mootanah, etc)

Dallas (2006) developed the milestones for integrated value and risk management and found that to reflect project progress the objective of value and risk studies change as the project moves from stage to stage [19]. The evolution of most Development and Construction Project is, by their nature, an interactive process as shown on Figure 2 [8]

Although there are different approaches towards the use of integrated value and risk management, this literature study found out many similarities on integration (Berawi et al, 2007). The first similarity is about aims and objectives whereby all projects have clear sets of aims and objectives to be achieved after the workshop. Secondly, the workshops were conducted according to the basic principles which consist of techniques like job plan and brainstorming.

Table -2
Risk considerations and activities in Job Plan phases

Job Plan Phase	Risk Considerations	RM Activities
Information Phase	Listing of known risks, issues, problems associated with the project Project may have been initiated as a result of a problem or a risk	Identify risk issues Determine risk impact Perform risk analysis of designer cost estimate
Function Analysis Phase	Some functions may address or be influenced by know risks	Brainstorming Risk mitigation
Creative Phase	Ideas may address how to get around known or possible risks	
Evaluation Phase	Evaluation criteria should include risk items to eliminate ideas which have a very high risk associated with them	Consider risk as a weighted criterion
Development Phase	Risk allowances associated with each proposal at all stages of a project, especially during the construction and operation and maintenance will give a better comparison of proposals during any cost/ benefit analysis using whole life costing Time implications	Conduct RA of VA alternative design
Presentation Phase	The risk that not everyone will sign up to the preferred proposal and how to deal with it	Present RA with suggested mitigations Recommend project cost & contingency
Implementation Phase		Perform second risk analysis of final reconciled proposal

Job plan and brainstorming played vital part in conducting VE studies to generate ideas, evaluate and develop them during the workshops. The third similarity concerns on the risk aspect and risk management workshops.

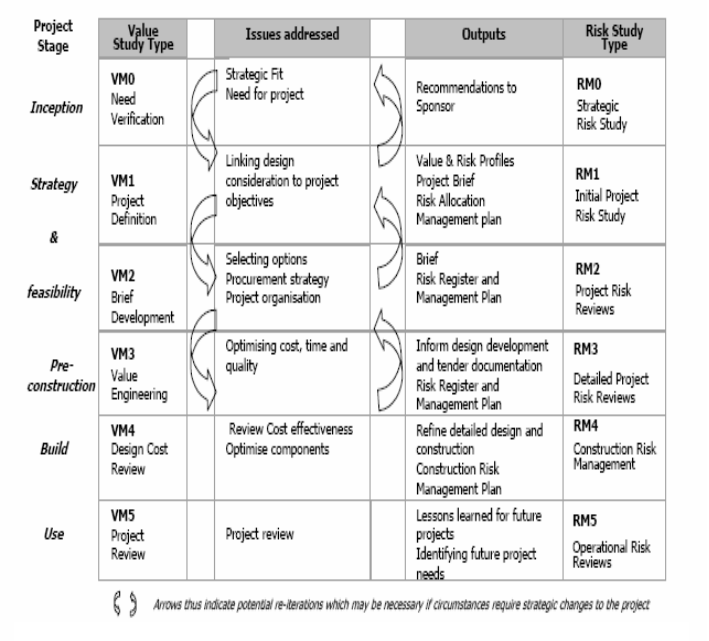

Figure 2. Milestones for Integrated Value and Risk Management Reviews

6. INTEGRATED VALUE AND RISK MANAGEMENT ON INDONESIA CONSTRUCTION INDUSTRY

VE has an important role on industry to continually improve the innovative construction management which is implemented on many construction projects and infrastructure in developed countries such as UK and Iran, especially for the high cost projects (Palmer et al, 1996, Bytheway & Charles, 1971, Berawi & Woodhead,2005). In the Indonesia construction industry, the implementation of value engineering, risk management and also infrastructure projects are still not popular (Marzuki, 2007, Soemardi, 2006). Eventually if we pointed on normative aspect, the implementation of value engineering was defined at Article 23 Law No. 18/1999 about Construction Services which declares that if it is found any inefficiency indication occurred because of unusual construction price, design construction or construction method, therefore it will be recommended to use the value engineering.

This statement is being strengthened by Peraturan Pemerintah RI Nomor 29/2000 which declares that for high risk construction project is shall be conducted a pre-feasibility study, feasibility study, general and technical planning. Meanwhile Peraturan Menteri Pekerjaan Umum no. 45/PRT/M/2007 about the Technical Guidelines of the Government Building Construcion stated that Indonesia's government wish to increase efficiency and effectiveness of construction industries by implemented value engineering. Regarding to Article 2, The technical guidance aims to render a government building accords to its function,

requirement the safety, health, convenience, easily and efficient on resource purpose with effective and efficient.

Based on the fact that the delay and cost overrun happened on many Indonesia's construction industries, this paper is aimed as a preliminary study on how the integration of VE and risk can improve the value and minimize the risk. Therefore, it will improve the eficiency and efectiveness of Indonesia construction industry as it was applied on other countries. Hereafter it will be conducted a sequel study to find how it is implemented on Indonesia construction industry as its condition and the readiness of the construction industries stakeholder.

7. CONCLUSION

This paper concerns on the integrated value and risk management that have been conducted on other countries to be studied and implemented on Indonesia construction industry. As the literature study which has been done, it is concluded that the integration of value engineering and risk management in a project at various countries was applied and widely accepted as a best tool for improvement better effective project management (Weatherhead and Griffin, 2006). Combination of both within one integration process is a good strategy to maximize value of a project meanwhile reducing risk in a cost frame that was already conducted. Thus it can be concluded that the implementation of value and risk management on a construction industry project in Indonesia should be improved the efficiency and effectiveness throughout the value maximization and the risk minimization. The next research will be focused on how to integrate the value and risk management on Indonesia construction industry as its own consideration.

References:

[1] BPS , "Berita Resmi Statistik", No.40/IX/14 Agustus 2006

[2] Abduh M., "*Konstruksi Rampng untuk Mencapai Konstruksi yang Berkelanjutan"*, Proceeding Seminar Nasional Sustainability dalam Bidang Material, Rekayasa dan Konstruksi Beton, KK Rekayasa Struktur FTSL, Desember 2007.

[3] Alwi, S., Hampson, K., Mohamed, S. (2002), *Non Value-Adding Activities : A Comparative Study of Indonesian and Australian Construction Projects*, Proceedings of the 10th annual conference of the IGLC, Gramado, Brazil.

[4] Hendrickson, C.,"*Project Management for Construction"*, 2nd Edition, Prentice Hall, 2000

[5] Oberlender, Garold D,"*Project Management for Engineering and Construction*,, 2nd Edition, McGraw-Hill, 2000

[6] Yohanes L.D. Adianto, Danu Tirta Gunawan, Linna (2007), "Studi Pemahaman dan Penerapan Constructability Kontraktor di Bandung", Jurnal Teknik Sipil Volume 7 No.1 Oktober 2007,page 27-39.

[7] Ray R. Ventakaraman, Jeffery K.Pinto, " Cost and Value Management in Project," John Wiley & Sons, Inc, 2008

[8] Saipol Bari Abd Karim, Mohammed AM Berawi, Imran Ariff Yahya, Hamzah Abdul-Rahman and Othman Mohamed,"The Integration of Value and Risk Management in Infrastructure Projects: Learning From Others", Proceeding Quantity Surveying International Conference, 4-5 September, 2007, Kuala Lumpur

[9] Miles, L.D,"Techniques for Value Analysis and Engineering," Mc Graw-Hill , 1961

[10] Norton, B.R. & McElligott,W.C.,"Value Management in Construction: A Practical Guide", Macmillan London, 1995

[11] Yuh Huei Chang," Implementing The Risk Analysis in Evaluation Phase to Increase the Project Value", SAVE Knowledge Bank, 2006

[12] Davis Langdon LLP, "Getting Value for Money from Construction through Design – How Auditors can Help, National Audit Office (NAO), Commission for Architecture in the Built Environment, OGC, 2004

[13] Hannan, D.,"The value Management Workbook: A Standard Approach for Project Managers", Proceeding of the SAVE Annual Conference, 1994.

[14] Male S, Kelly J & Fernie S. et al,"The Value Management benchmark : A Good Practice Framework for Clients and Practitioners," Thomas Telford Publishing, UK, 1998.

[15] HIlley & Paliokostas, P.P.,"Value Management and Risk Management: An Examination of The Potential For Their Integration and Acceptance as a Combined Management Tool in The UK Construction Industry,"COBRA 2001 Conference Paper.

[16] Sutrisno M.,"An Investigation of Private Sector Participation Project Appraisal in Developing Countries using Elements of Value and Risk Management", PhD Thesis; Manchester Centre for Civil and Construction Engineering, UMIST, 2004.

[17] Palmer, A.,"An Investigative study of Value Engineering in USA and its relationship to UK cost control procedures," PhD Thesis, Loughborough University of Technology, 1992

[18] Green, S.D," Towards an integrated script for Risk and Value Management", Proceeding. CIB W-55 & W-56 Joint Triennial Symposium, Customer Satisfaction: A Focus on Research and Practice in Construction, 1999

[19] Michael F. Dallas,"Maximising Project Value Through Integrated Risk and Value Management", SAVE Knowledge Bank, 2006

[20] Project Management Institute, PMI,"A Guide to the Project Management Body of Knowledge, PMBOK guide, 2nd Ed, Project Management Institute, Inc, 2000

[21] Chapman, C , & Ward, S ,"Transforming Project Risk Management into Project Uncertainty Management", International Journal of Project Management, 21, pg. 97-105, 2003

[22] Chapman, C , & Ward, S,"Project Risk Management: Processes, Techniques and Insight", John Willey & Sons Ltd, 2002.

[23] Association for Project Management (APM),"Project Management Body of Knowldege", 4th Ed, 2000
[24] Ward SC, Klein JH, Avison DE, Powell PL & Keen J,"Flexibility and the Management of Uncertainty: A Risk Management Perspective", The International Journal of Project & Business Risk Management, 1[2], pg. 131-145, 1997.
[25] OGC,"Office of Government Commerce-Achieving Excellence in Construction, Procurement Guide 04: Risk and Value Management, 2003
[26] Smith N.J., Merna T & Jobling P," Managing Risk in Construction Projects", 2nd Ed, Blackwell Science Ltd, 2006
[27] Kim,S. & Bajai, D,"Risk Management in Construction: An Approach for Contractors in South Korea", Cost Engineering VOl,42 No.1, 2000
[28] Edwards,L.,"Practical Risk Management in The Construction Industry", Thomas Telford,London 1995
[29] Dell'Isola, A,"Value Engineering: Practical Applications for Design, Construction, Maintenance & Operations", R.S. Means Company Inc, 1997
[30] Connaughton J.N. & Green, S.D.,"Value Management in Construction: A Client's Guide, CIRIA, London, 1996
[31] Marion Weatherhead et al,"Integrating Value And Risk in Construction", CIRIA C639, London, 2005
[32] Griffin, L,"Taking Project by S.T.O.R.M – A Model for Integrating Value, Opportunity and Risk Management," Value Magazine, Feb 2006, Institute of Value Management, UK.
[33] Othman A.A.E.,"Value and Risk Management for Dynamic Brief Development in Construction", Proceeding of the CII-HK Conference, 2004
[34] Paliokostas,G.P.,"The Integration of Value Management and Risk Management (MSc Dissertation)", Dept. of Civil and Construction Engineering, UMIST, 2000
[35] Thompson, M,"Value Solutions- A Path to Sustain Infrastructure; Incorporating risk into Value Engineering", CSVA Conference, Toronto, 2004
[36] Kirk,D.Q.,"The Integration of Value Management and Risk Management", SAVE Proceeding, 1995
[37] Mootanah, D. P. & Poynter-Brown, R. & Jefferyes, M. "A Strategy for Managing Project Risks in Value Management Studies" *SAVE International Conference Proceedings 1998*, p 266-274.

ISSN 114-1284

A COMPARISON STUDY OF FACADE DESIGNS IN LEO BUILDING AND ZEO BUILDING IN MALAYSIA

Hong, Wan Thing [1], Aminuddin, A.M.R [2], Rao, S.P [3]

Post Graduate Student, Faculty of Built Environment,
University of Malaya, 50603 Kuala Lumpur, Malaysia
Tel: (+6012)3469950. Fax: (+603)79809496
E-mail: ashleyhwt@yahoo.com [a]

Faculty of Built Environment,
University of Malaya, 50603 Kuala Lumpur, Malaysia
Tel: (+603)7967 5398. Fax: (+603)7967 5713
E-mail: asrulmahjuddin@um.edu.my [b]

Faculty of Built Environment,
University of Malaya, 50603 Kuala Lumpur, Malaysia
Tel: (+603)7967 6826. Fax: (+603)7967 5713
E-mail: raosp@um.edu.my [c]

ABSTRACT

Building facades and their design strategies play a significant role in achieving optimal thermal performance. The aim of the design is to provide an adequate quality of thermally and visually comfortable environments to the occupants by utilising minimal energy consumptions. Opaque walls and glazed windows should have should have the ability to attenuate and modulate the solar heat received at their surfaces. They should also allow sufficient day lighting for the building. The usage of glass facade has become a standard design in most office buildings due to its high aesthetics, high visible and modular systems. This paper investigates the facade designs of low energy office buildings in Malaysia. A comparison study on how these passive designs contribute to energy efficiency in the tropical country is conducted in LEO Building and ZEO building in Malaysia. It will also highlight the occupants' perception on the building interior comfort and aesthetic value relative to the surrounding glass facade. This paper is presenting a detailed comparison study of LEO Building and ZEO Building, based on the facade design considerations, performances and environmental comforts. It is expected to give further insight on effective facade design for such low energy office buildings.

Keywords:
Aesthetic value, environmental comfort, energy efficiency, facade design, low energy office.

1.0 INTRODUCTION

Malaysia has consumed approximately 50% of the total energy consumption for air-conditioning in non-residential buildings. The electricity demand in Malaysia is expected to grow 6% to 8% per annum [1]. As a result, the development of energy efficient building is urgently needed! Besides M&E system, responsive building facade is one of the important components to achieve energy efficiency by reducing the need for cooling, lighting and ventilation [5]. Facade design and construction has great potential in controlling its interior environment, through the high levels used of insulation, energy efficient windows and passive solar design techniques. Furthermore, the usage of glass facade has become a standard design for office buildings due to its high visible, high aesthetic and modular system.

The design strategies of Low Energy Office Buildings in Malaysia have integrated high performance building facades which provide high quality and comfortable environment for the occupants. This paper investigates the facade design in Low Energy Office (LEO) Building and Zero Energy Office (ZEO) Building in Malaysia by means of comparative analysis in reducing the energy consumption.

2.0 LOW ENERGY OFFICE (LEO) BUILDING

The Low Energy Office (LEO) Building is the building of Ministry of Energy, Water and Communication (MEWC). It is the first example of a government building in Malaysia which demonstrates the integration of the best energy efficiency measures, and low environmental impact without compromising on user comfort. The ultimate goal of LEO Building is to achieve energy savings of more than 50% compared to conventional office buildings in Malaysia.

This building has become the Winner of 2006 ASEAN Energy Award for the New and Existing Energy Efficient Buildings. The design aspects that brought LEO building to the Award are:

i. Passive building design (building orientation, shape, natural ventilation, etc.),
ii. Active design of M&E systems (air-conditioning and lighting), and
iii. Low Energy office equipments

The main focus of this paper falls on LEO Building's passive building design connecting to its facade significance.

3.0 ZERO ENERGY OFFICE (ZEO) BUILDING

The Zero Energy Office (ZEO) Building is the new headquarter for Malaysia Energy Centre. The building consumes very low amount of energy and it is experimental proven that ZEO is 80% more energy efficient than a typical office building. The building energy consumption will become net zero only when the Building Integrated Photovoltaic (BIPV) is attached.

To achieve this, the integrated whole building design approach and systems are being implemented with the following main strategies:-

i. Passive building design (building orientation, shape, natural ventilation, etc.)
ii. Renewable energy supply system (photovoltaic systems)
iii. Active design of M&E systems (air-conditioning and lighting)
iv. Low energy office equipments

Nevertheless, the main focus of this paper falls on ZEO Building's passive building design with its advance facade design such as thermo wall and double low-e glazing in order to maintain the occupants' comfort.

4.0 THE SOLAR STUDY OF FACADE DESIGN

There are various components of space heat gains from internal and external sources. The external heat gains into the building are mainly from the external sources (solar radiation). The external heat gets in the building through the processes of conduction and convection from the building envelopes i.e. wall and windows. Internal sources such as occupants, electric lights and equipments also provide heat inside the building as they are actively operated [2].

A sun path diagram is a plot of the path of the sun across the sky using the sun's elevation in the sky for one axis and the azimuthal position of the sun for the other axis [3]. Figure 1 shows the sun path in Kuala Lumpur which is beneficial to the facade design to maximize daylight used but decrease solar heating load in a building.

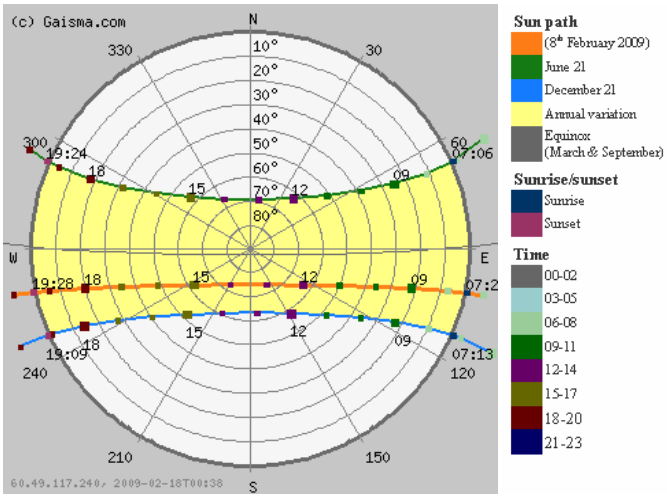

Figure 1: Sun Chart plotted for determining the sun path in Kuala Lumpur for the whole year and also the daily sun path from 7am to 7pm [4].

As solar radiation impinges on the non-shaded window glass, approximately 10% of the radiant heat of clear glass is reflected back outdoors, part of it (5-50%, depending on composition & thickness of glass) is absorbed by the glass and the remainder is transmitted directly indoors [2].

Figure 2 shows the absorption, reflection and transmission of solar radiation in glass.

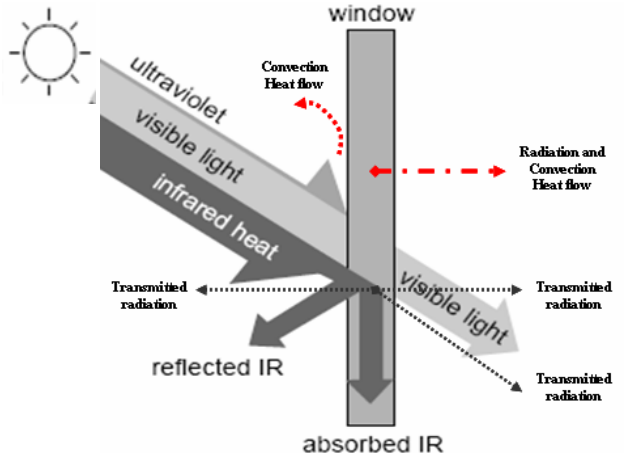

Figure 2: The absorption, reflection and transmission of solar radiation in glass [8].

The Sun provides the daylight in two ways. Part of the sun's energy reaches the earth's surface as direct sunlight. Some of the other part is scattered by the atmosphere and produces the blue sky. This is called as diffused sunlight. The direct sunlight may cause excessive brightness which may contribute to visual discomfort or what we called as glare.

5.0 PASSIVE DESIGN STRATEGIES FOR FACADE

i. A building design should firstly understand how climate response can influence its facade performance. Tropical climate buildings would require a facade that able to keep the building cool however the cold countries would prefer to keep the building warm.
ii. Besides the climate, the site condition and landscape are also important design factors. The facade may be warmed up by the hot air through convection. Green roof, green wall and water features may lower down the surrounding air temperature and provide higher moisture in the air. Trees are also good shading devices to protect glazing from direct sunlight, and lower the indoor air temperature [9].
iii. A building shape, form and orientation may determine the receipt of solar radiation. It was found that a spherical building consumes lesser energy. In Malaysia, east and west facing windows are getting direct absorption of heat into the building. Thus, most building windows are facing north or south.
iv. Office buildings are major glazed facade building. In Malaysia, the work stations shall be located along the building perimeter to encourage the full use of daylight and good views. The secondary function rooms shall be located at the core of the building.
v. Insulated material is essential to act as a barrier from heat transferring in and out from the building. There are few commonly available insulating materials in Malaysia:
    - Aerated Concrete
    - Mineral Wool
    - Low-e double glazing
vi. The recommended maximum window to wall ratios for Malaysian buildings are always high for south & north facades but lower for east & west facade [9].
vii. The shading devices are preventing direct sunlight for good visual and thermal comfort. Punch hole window with light shelves is best in shading direct radiation, and also bounces natural light deeper into building interiors. The adjustable louvers with shading fins are widely used at most of the office building windows [9].
viii. Designing the facade with more openings between two building blocks, big opening at facade, ample size and number of windows and sufficient ventilation louvers may assist in cross-ventilation.
ix. Windows may influence occupant thermal comfort by heat gain or heat loss through the glass, which either raises or lowers the room air temperature, and by radiation exchange between occupant and the glass and other surroundings.
x. The application of glass facade can influence the charm of a building through the exterior outlook, high visible for indoor and outdoor views and good visual comfort

6.0 A COMPARISON CASE STUDY ON FAÇADE DESIGN AND ENERGY PERORMANCE

6.1 Facade passive design strategies

Table 1 compares the passive design features for LEO Building and ZEO Building. It was found that LEO Building is greater in the passive design aspects with its green roof design, internal cooling items and the atrium design for thermal stack effect. All these features are not found in ZEO Building.

However, ZEO Building has a unique design feature which is not found in LEO building i.e. the self-shading facade, which shades against the direct solar radiation into the building.

Figure 3 and figure 4 show both buildings are L-shape on plan with the main facades are facing north and south. Most office areas are designed along the facades to maximise the use of daylight.

Figure 3: The interior space layout of LEO Building shows the office areas are designed along the facades to maximise the use of daylight. It is L-shape on plan with and the main facades are facing north and south.

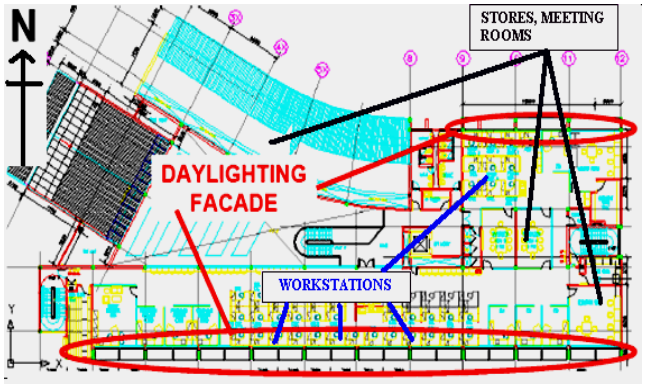

Figure 4: The interior space layout of ZEO building shows the workstations are designed along the facades. The building is also L-shape on plan and the daylighting facades are also facing north and south.

Table 1: The comparison of facade design strategies in LEO Building & ZEO Building.

Design Factors	Ministry of Energy, Water and Communications - LEO	Malaysia Energy Centre - ZEO
Climate Conditions	• Putrajaya: Hot & high humidity • Daily temperature: 27°C - 35°C	• Bangi: Hot & high humidity • Daily temperature: 27°C - 35°C
Site condition	Well planned office complex	Low density area with manufacturing companies & shop lots
Landscape design	Low-rise plants & young trees	Low-rise plants, young trees, negligible water feature
Roof garden	Roof garden exists	No roof garden
Building orientation	Main facades are facing north and south	Main facades are facing north and south
Internal cooling effects	Artificial water wall, interior landscape	Limited low-rise pots plants
Window to wall ratios	Minimum number of windows at east and west facades	Minimum number of windows at east and west facades
Building size	GFA: 38,700m^2 (height: 7-storeys)	GFA: 4,000m^2 (height: 3-storeys)
Building form and shape	• L-shape on plan • Affected by punch hole windows, light shelves & overhangs	• L-shape on plan • Affected by split windows, light shelves & self shading facade
Interior space layout	Perimeter – Workstations Core – secondary function rooms	Perimeter – Workstations Core – secondary function rooms
Natural ventilation	Atrium – thermal stack effect	Atrium – open air concept

6.2 Opaque wall design, material & thermal performances

Table 2 compares the wall energy performances in LEO Building and ZEO Building. The designs of the wall in both of the buildings lead to high reduction in the use of electricity for cooling.

However, .the solar absorption, U-Value, conductivity, internal and external surface temperatures of Thermowall in ZEO building were generally showing more energy efficient results compared to the Aerated Lightweight Concrete Wall in LEO Building.

Table 3 compares the glass energy performances in LEO Building and ZEO Building. The spectrally selective low-e double glazing used in ZEO Building windows is greater compared to the light green tinted tempered glass in LEO building, as its low-e coating is able to reflect majority of the infrared (IR) and ultraviolet (UV) light back to the ambient. The Argon gas layer between the panes decreases the heat transfer activity through conduction and convection.

Table 2: The comparison of thermal performance of wall in LEO Building & ZEO Building.

OPAQUE WALL	MEWC LEO Building 200mm Aerated Lightweight Concrete Wall	PTM ZEO Building 100mm Thermowall
Wall surface area	Large (7-storey high)	Small (3-storey high)
Solar absorption	Low (light brown/ grey & white painted surfaces)	Lower (white and nearly white painted surfaces)
U-Value	0.6 W/m^{2}K	0.56 W/m^{2}K
Conductivity	0.12 W/mK	0.056 W/mK
Internal Surface Temperature	Average: 27.79 °C	Average: 27.02 °C
External Surface Temperature	Average: 34.13 °C	Average: 34.86 °C

Table 3: The comparison of glazing performances in LEO Building & ZEO Building.

BUILDING	MEWC LEO BUILDING	PTM ZEO BUILDING
Type of Glass	12mm Light green tinted tempered glass (Single)	6mm Tempered Coated Low-E Glass + A16 with Argon gas + 4mm Clear Tempered Float Glass
Window to wall ratios	• North & south – High (30-40%) • East – Low (≈ 25%) • West – Lowest (negligible)	• North & south – High (30-40%) • East – Low (≈ 20%) • West – Lowest (negligible)
Window shading systems	• Punch hole windows with light shelves (lower floors) • Exterior louvres (higher floors)	• Split windows with mirror light shelves
Daylight penetration	Punched hole windows and light shelves reflecting some of the light further into the room.	Diffused daylight →mirror light shelves → highly reflected fixed blind (top of split window) → reflective mirror at the ceiling → inside the building for a deeper distance.
Illuminance (Lux)	• Full Daylit area – average 959 lux (without internal shading devices) • Semi Daylit area – average 686 lux (with the aid of artificial lights)	• Full Daylit area 1– average 695 lux (without internal shading devices) • Full Daylit area 2– average 488 lux (with the aid of skylights)
VT (%)	63.1	50.0
SHGC	0.50	0.29
U-Value	5.70 W/m^2/K	1.10 W/m^2/K
Conductivity	0.068 W/mK	0.029 W/mK
Int. surface temperature	Average: 29.7^{o}C	Average: 27.6^{o}C
Ext. surface temperature	Average: 35.8^{o}C	Average: 33.7^{o}C

6.3 Glass facade design, material, lighting effect & thermal performances

The comparison study results on their SHGC, U-Value, conductivity, internal and external surface temperatures also demonstrate greater thermal performance of the spectrally selective low-e double glazing. Besides, the spectrally selective low-e double glazing VT is only 50%. Hence the illuminance readings obtained from ZEO are lower compared to LEO Building, but has achieved the visual comfort for all clerical and office works. However, the illuminance taken for LEO building is higher and not within the visual comfort range for all clerical and office works. Therefore, internal shading devices are always applied in LEO Building.

Figure 5 shows the window shading systems provided in LEO building and ZEO building. The punch hole window with light shelf in LEO Building blocks the direct sunlight and reflects part of the sunlight further into the room. The split window system with mirror light shelf at north and south facades of ZEO Building allow deeper daylight penetration and without glare. The diffused daylight collected at the mirror light shelves will be reflected through the highly reflected fixed blind (top of split window), and blinds reflecting light upwards to the reflective mirror at the ceiling, and subsequently reflects it back into the building for a deeper distance.

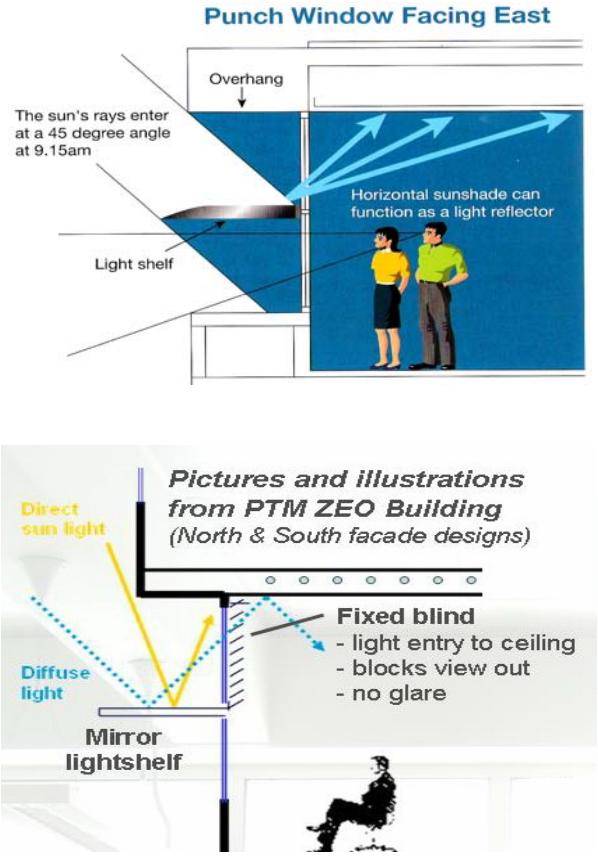

Figure 5: Punch hole windows with light shelf in LEO Building (top) and split window system with mirror light shelf in ZEO Building (bottom).

7.0 COMPARISON SURVEY ON BUILDING INTERIOR COMFORTS & AESTHETIC VALUE

Table 4: The comparison of occupants' viewpoints on the building interior comforts and aesthetic value of the application of glass facade in LEO Building & ZEO Building.

SURVEY QUESTIONS	MEWC LEO BUILDING	PTM ZEO BUILDING
Respondents' sitting position	Majority 49% - east	Majority 60% - south
Importance of glass facade	Majority 76% agree	Majority 80% agree
Reason of glass facade is highly preferred	Maximisation of daylight use - 76% agree	Maximisation of daylight use - 100% agree
Most comfortable factor of sitting nearby the glass facade	Sufficiency of visible daylight - 73% agree	Sufficiency of visible daylight - 100% agree
Improvement of health & productivity	58% agree	52% agree
Lighting condition	▪ 39% preferred combination of both natural daylight & artificial light ▪ 46% are using natural daylight only	• 56% preferred natural daylight only • 64% are using combination of both natural daylight & artificial light
Frequency of internal shading devices are opened	Majority (55%) - seldom	Majority (52%) - always

Daylight quality & visual comfort nearby the glass facade	• 58% – daylight provided is ideal for PC work • 55% – never feel glare from daylight source • 48% – experienced the shadow for all clerical and office works • 39% – experienced insufficient daylight for both paper work and PC work.	• 60% – daylight provided is ideal for PC work • 68% – never feel glare from daylight source • 48% – never experience the shadow for all clerical and office works • 48% – experienced insufficient daylight for paper work
Reason of glass facade is aesthetic	67% – elegant of its transparency & modular system & can observe outdoor view and scenery	68% – elegant of its transparency & modular system
Thermal comfort of sitting nearby glass facade	48% – unbiased (not warm and not cool)	44% – unbiased (not warm and not cool)
Factors affecting thermal comfort	67% – indoor air temperature (air-conditioning temperature)	92% – indoor air temperature (air-conditioning temperature)

Table 4 compares the occupants' perception on the building interior comforts and aesthetic value on the application of glass facade in LEO Building and ZEO Building.

Generally, ZEO Building respondents were more satisfied on the daylight quality in their working place compared to LEO Building respondents, where they preferred to use daylight more than other lighting sources for all clerical and office works. This indicates positive remark for the spectrally selective low-e double glazing, which provides ample daylight without discomfort glares into the building, based on the occupant perceptions.

Most of the LEO Building and ZEO Building respondents did not comment on the thermal condition around the glass facade. However, more respondents from ZEO Building did not feel warm when sitting nearby the glass facade compared to LEO Building respondents.

In addition, more respondents from ZEO Building felt that the indoor air temperature is the main factors that affecting the thermal comfort in their working place. This reveals the spectrally selective low-e double glazing in ZEO Building is better in thermal resistance compared to the light green tinted tempered glass in LEO Building, based on the occupant perceptions.

Most of both buildings' occupant opined that glass facade is aesthetic due to its elegant, high transparency and modular system. However, ZEO Building respondents were slightly more in favour to this factor compared to LEO Building respondents. This reveals the occupants were more satisfied with the building exterior outlook compared to the view from the internal office.

8.0 CONCLUSIONS

Although ZEO Building is more energy efficient on the overall performance compared to LEO Building, however the facade design considerations with natural environment are greater in LEO building. The design features of green roof, internal landscape and the atrium design for thermal stack effect in LEO Building are not found in ZEO building.

Both buildings facade designs have contributed to very little energy consumption by reducing the use of electricity mainly for lighting and cooling. However, the thermowall with rockwool insulation, split window system with spectrally low-e double glazing and mirror light shelves in ZEO building are found to be more advanced compared to the aerated lightweight concrete wall and punch hole window with light shelves in LEO Building.

More respondents in ZEO Building opined that glass facade at their working place is providing high quality daylight, better thermal performance, better thermal comfort and well exterior outlook compared to the respondents in LEO Building.

9.0 ACKNOWLEDGMENT

The authors wish to acknowledge the financial support from the University of Malaya for this research.

10.0 REFERENCES

[1]. Abdul Rahman, Samirah & Zain-Ahmed, Azni (2005), Energy in buildings, Pusat Penerbitan Universiti (UPENA), UiTM

[2]. Ameen, Ahamadul (2006), Refrigeration and Air Conditioning, Prentice Hall of India Private Limited, New Delhi.
[3]. Environmental Health Perspectives, Student Edition, August 2005, http://ehp.niehs.nih.gov/science-ed/2005/sun.pdf, Natural Institute of Environmental Health Sciences, cited 5th October 2008.
[4]. Gaisma, http://www.gaisma.com/en/dir/location/Malaysia/Kualalumpur.html, cited 18th February 2009.
[5]. Kibert, Charles J. (2005), Sustainable Construction: Green Building Design and Delivery, John Wiley & Sons, Inc.
[6]. Kristensen, Poul., Sustainable Buildings for the future – FUTURARC Forum 2008, IEN Consultant Malaysia.
[7]. Ministry of Energy, Water and Communications (2004), Low Energy Office: The Ministry of Energy, Water and Communications Building.
[8]. O'Connor, Jennifer., Lee, Eleanor., Rubinstein, Francis., Selkowitz, Stephen. (2008), Tips for Daylighting with Windows – The Integrated Approach, Ernest Orlando Lawrence Berkeley National Laboratory, California, U.S.
[9]. Tang, C.K., Kristensen, Poul E. & Lojuntin, Steve A. (April 2004), Design Strategies for Energy Efficiency in New Buildings (Non Domestic), The Ministry of Energy, Water and Communications Malaysia & Department of General Public Works Malaysia.

ISSN 114-1284

Barrier-free Infrastructure for Disabled People Sustains Green Infrastructure

Inge Komardjaja, PhD

Research Center for Human Settlements
Department of Public Works
Jl. Panyawungan, Cileunyi Wetan, Kab. Bandung 40393
Tel.: + 62 22 779-8393 Fax : + 62 22 779-8392
E-mail: ikomard@gmail.com

ABSTRACT

Green infrastructure in cities is essential for the citizens to improve their health and to develop social, cultural, and commercial interaction. Disabled people, however, are excluded from these opportunities because of their difficulties in surmounting any physical barriers. By providing barrier-free infrastructure for disabled people, the green infrastructure is sustained, as inhabitants may opt for walking, bicycling, and using public transport, while leaving their own motor vehicles at home. To analyze this topic, the author employs the qualitative method with a heuristic orientation that allows the use of personal experience of being impeded by barriers. Casual talks with few disabled people about their personal experience in dealing with barriers, and a thorough review of relevant texts support the analysis. The result reveals that the realization of barrier-free infrastructure will take time to happen, which is attributable to the constraint of economic struggle for survival. But, barrier-free infrastructure will have a significant effect on the sustainability of green infrastructure. In conclusion, the inclusion and exclusion of disabled people regarding the green infrastructure is a question of how well they are accepted by the general public. The degree of mutual public acceptance of different social groups is a yardstick of social sustainability.

Keywords: *disabled people, ambulant disability, barrier-free infrastructure, green infrastructure, universal design*

1. INTRODUCTION

Public urban green spaces hold a vital role in people's lives. Parks, for example, offer green environments that are open to the public, usually without charge. Parks are places where people come for sport, recreation, and social interaction with all kinds of people. Not only does the green scenery engender people's appreciation of nature, but natural green also improves their health. While green infrastructure is so beneficial for all lives on planet earth, it does not completely serve disabled people who have special needs in regard to their limited mobility. A careful observation about the parks in Bandung, the city where the author lives and works, shows that it is unlikely for disabled people to enjoy the green and fresher air of the parks. The hilly parcel of land, the narrow footpath, the uneven surfaces, the dirty benches, and the step(s), are impediments for disabled people. They can hardly walk or wheel their chair in a park. The physical barriers are not only difficult to surmount for personal independent mobility, but also for the carers.

It has been claimed that parks are the lungs of the city. Certainly, this is undeniable, particularly with the high level of pollution in the air that stems from emissions of carbon dioxide from motor vehicles. This is one of the reasons that in Jakarta once a month, environment authorities enforce a "Motor-vehicle-free Day"[1]. The implementation of such a day is quite effective in keeping the level of pollution down. The benefit for the community is the opportunity to walk, jog, bike, play, and just have fun, without disturbances from motor vehicles that produce much commotion. This all aim at leading a healthier life for the citizens, which ultimately reduce the cost of health problems and slow down the energy consumption. In this lifestyle of health and recreation, disabled people are disregarded. They do not have the physical capability to take part in outdoor pleasure. The core of green infrastructure is to recognize the value of nature for the human environment [1], which disabled people are also entitled to delight in.

1.1 The purpose

Against this background and problem, the purpose of the paper seeks how the barrier-free infrastructure sustains green infrastructure. One approach is the "low impact development", which in this paper is defined as barrier-free infrastructure that does not prompt people to damage and pollute the environment. Instead, the barrier-free infrastructure sustains the green and natural environment by motivating citizens to opt for walking, cycling, and using public transportation, while leaving their motor vehicles at home. This is in line with the program of

[1] Translated from *Hari Bebas Kendaraan Bermotor* (*HBKB*)

HBKB which target is to convert private car owners to using public transportation. To achieve this, the built environment ought to be cleared from unnecessary impediments. If builders create such physical environment, disabled people will have the same opportunity as the non-disabled people to lead a more meaningful and healthier life.

2. METHODOLOGY

Data collection for this paper is carried out by employing four forms: text reading, informal talks, careful observation, and personal experience. These four forms are intertwined and each form should not be analyzed of its own. The text is obtained from books, internet, journals, and an unpublished article. Adding to the text are personal talks with some ambulant disabled people who live in Bandung. The talks were done in the past, but they are still valid to be included in this paper, because problems with physical barriers do not change through the passage of time. Personal opinions of being ambulant disabled and the challenges of confronting physical and attitudinal barriers have enriched the analysis and interpretation of this study. Observations about the built environment encompasses the residences of those disabled people; public buildings (banks, hospitals, religious worship places, universities, government offices); public open spaces (streets, sidewalks, parks); and the public transport (mini vans, tricycled pedicabs, motorcycle cabs). Other observations are about the manner disabled people overcome physical barriers. With their physical limitation, they maneuver their way among the obstacles to reach the place they intend to go. These detailed observations are done, because the author of this paper is physically disabled and thus, might claim to have an intimate knowledge of disability issues. Furthermore, she has been studying these issues for over a decade. Social research that uses personal experience is called heuristic, an orientation of the qualitative inquiry.

3. DEFINING DISABILITY

Indonesia holds the premise that a disability is a physical or/ and mental impairment endured by the individual. The impairment is perceived as a 'personal tragedy' with all the oppressions that follow [3]. In Ototake's words "poor darling," which lead parents to become overprotective towards their disabled children. With this negative outlook, these children might develop the thought that a community needs to feel sorry for them [4]. Focusing on the disabled persons, professionals are obliged to facilitate them, so they are able to function better in society.

The provision of accessible environments is thus essential in the lives of disabled people. To be independently mobile is, in fact, a basic human need. Referring to the design of the built environment and independent mobility, there are four categories of disabled people [5]:

a) mobility-impaired: ambulant and non-ambulant (wheelchair user);
b) sensory: visual and hearing impairment;
c) cognitive: mental illness, and developmental or learning disability;
d) multiple: a combination of any or all of the above.

Ambulant disabled people are those who are able to walk, either with or without crutches, walking sticks, braces, or walking frames. The non-ambulant disabled people are the wheelchair users, who are unable to walk and depend solely on a wheelchair for mobility. While all four categories are in need for special designs to participate fully in society, this paper highlights the people with mobility impairment. This category has often been the target of various technological strategies and adaptations [6] to alleviate the difficulties caused by their limited mobility and to give them equal opportunities in integrating into mainstream society.

3.1 The ordinances

Efforts to improve the quality of life of disabled people have been done in Indonesia. In relation to the built environment, the Department of Public Works", through the Directorate of Building and Environment Planning, Directorate General of Housing, has formulated and published Ordinance Number 30/PRT/M/2006 of the Republic of Indonesia about "Technical Guidelines for Facilities and Accessibilities of Buildings and Environments." For the welfare of disabled people, the Department of Social Affairs, through the Bureau of Law, has made the publication of Ordinance Number 43 Year 1998 of the Republic of Indonesia about "Improving the Social Welfare of Disabled People." The application of the ordinances is far from its accomplishment. Most disabled people do not receive government aid and do not get assistive devices or the necessary medical treatment for their mobility. "There are few legal and social pressures to promote a non-discriminatory stance on disability," according to Byrne [7]. An example of this is the Department of Public Works that publicized Decree Number 469/KPTS/1998 of the Republic of Indonesia about "Technical Requirements of Accessibilities for Public Buildings and Environments" in 1998. Eight years on, the 2006 ordinance was made public. After a lapse of eight years, there are no significant changes of the built environment. Another example is the pilot project of Gambir train station in Jakarta. In 2000, authorities equipped the station with standard facilities for disabled people, such as ramps, talking elevators, a special bell for asking help, train schedules in Braille, lowered phone booths for people in wheelchair, special toilets, and a parking space reserved for disabled people [8]. Now, 2009, these standard facilities do not function at all. Inevitably, there must be stricter enforcement of existing rules to provide barrier-free environments.

3.2 The social challenge

Disabled people in general make little or no progress in their lives. The causes are many; it may be problems of economy, social situation, education and employment opportunities, or/ and the lack of volition of the disabled persons. The last point is central in their lives. Everything they do and everything they think is a product of their volition. If they have no strong desire to make progress, not much can be done, for outsiders are only in the capability to provide facilities and to give them support.

The causal link between the country's economic crisis and the minimal services and facilities for disabled people, means that they have to make the best out of their 'personal tragedy' by themselves and their family. Their dependence on others is obvious. As they do not earn a reliable income, family members are responsible for their livelihood. Furthermore, society at large often perceives disabled people as an embarrassment and there is little empathy to encourage them to develop personally. This kind of judgment and stigma affect the lives of disabled people who are not considered valuable members of the community. They remain housebound, uneducated, and unskilled [7]. As no one assists and guides them, they become passive and may think that their impairment is a personal tragedy or is valued as "poor me" [4]. How can this social challenge be overcome? By removing the mental barriers of the people, that is mostly provoked by "sheer unfamiliarity" [4] with disabled people. This may engender the premise that disabled people are different, helpless, and weird. Educating a society, particularly targeting at children, is important. Disability is simply a physical trait of the person, like wearing glasses, being fat/ thin, short/ tall, dark/ light [4]. Instead of thinking that disabled people are different and weird, society ought to accept them as unique individuals.

4. ENVIRONMENTS THAT "DISABLE" PEOPLE

Mobility and accessibility are two inseparable factors that are of great concern for disabled people. The current physical condition of Bandung is nothing but barriers, not only for disabled people, but for all citizens as well. The difference between the two groups, the disabled and the non-disabled people, is that the latter is often not aware of the barriers as they have no difficulties surmounting them. These barriers and hindrances are physical and human-made, and inhibit the easy passage of people. Real examples encompass the:
- sidewalk: narrow and high sidewalks with loosened tiles; busy thoroughfares that are not equipped with standard sidewalks;
- vehicular road: open holes on vehicular roads due to torrential rains and the passing of heavy trucks;
- public transport: public vans that stop suddenly to wait for passengers;
- environment: the dusty air in dry seasons and the muddy streets during monsoons;
- road users: motor-cyclists who drive at excessive speed;
- negligence: absence of fences or barricades at the edge of descent continuous water flow; haphazard construction.

The above examples are not exhaustive, but they give an idea about the disorders that occur on the streets. This is one of the reasons that many citizens choose to use their own private motor vehicles, cars and motorcycles, for their destinations, which of course will add the level of pollution in the air. People on main streets that lack shady trees will find it uncomfortable to walk. Even for short distances, younger people opt for public transport rather than walking through dust or under the scorching weather. In such environments people with mobility problems are less capable to take part in the hustle and bustle of the city. But, on the other hand, the non-disabled people can still enjoy the city's life despite the tumult and barriers.

4.1 Movement on the streets

Streets in Asian cities are "places where people spend most of their lives" [9], an indication that citizens value more outdoors activities than indoor life. On the streets, people endure difficulties to move in a straight line. Pedestrians face impediments in front and underfoot [10] and they have to stay alert to possible harms caused by the different speed of vehicles that maneuver for space. The slow pace of a tricycled pedicab that uses human energy results in the congestion of other vehicles, while the faster speed of motor vehicles scares off pedestrians. The continuous flow of traffic and the quick timing of the red traffic light engender pedestrians to be careless and violate the rules of crossing the street properly. They cross at any time and from any spot they wish, as waiting for the traffic flow to subside is futile. Pedestrians assume drivers to be responsible for their safety. As vehicles literally cover the road, pedestrians have to thread their way between cars and motorcycles [11].

Sidewalks along main roads and thoroughfares are strategic sites for economic activities of low-income and informal traders who hardly leave space for pedestrians. Added to this are the cars and motorbikes parked along the edge of the vehicular street. At dawn, we can find wet markets that occupy half the width of the vehicular road which may continue until late morning. Only when most of the items are sold out do hawkers and vendors vacate the space, leaving behind a huge mound of litter. Walking down the street is often a sequence of interruptions and encounters that disrupt smooth passage [9].

In a disabled-unfriendly city like Bandung, there is hardly space for the limited mobility of disabled and elderly people. The middle- and higher-income people have their domestic helpers and private chauffeurs to run

errands for them. While some disabled people strive for independent living, they also appreciate helpers who save them from troubles on the streets. On the streets, people with limited mobility have to nerve themselves to walk along the edge of vehicular roads, of getting on and off the public van, of crossing the street, and of walking on uneven sidewalks. These difficulties are not so much caused physical disability, since everyone on the street is likewise struggling for any form of survival.

5. THE LACK OF STATISTICAL INFORMATION

There are no reliable and updated statistics for the number of disabled people in Indonesia. The World Health Organization (WHO) estimates that ten percent of the population is disabled [8]. Without accurate data, this paper has limitations to analyze completely and convincingly regarding the importance of providing accessible urban infrastructure. Nonetheless, the sound logic of the current design requires such infrastructure indeed. Statistics would support the agreement on the necessity of barrier-free infrastructure, if figures on the following aspects were available, that is the number of: ambulant disabled people, those who live in the city, the level of education, the type of employment, those who work in the formal sector, those who use their private motor vehicle or public transport, and those who live with a family. Such elaborated information may not be available for a long time. This pessimistic view derives from the indication that the entity and need of disabled people are not a preference for the government compared with other social groups. Disabled people have to make their own concerted effort to make progressive changes in their lives without the government's support. Disability is indeed not a crucial topic to be included in the government's priority list, compared with the alleviation of the inhabitants' poverty. As Indonesia is still struggling with the country's economic crisis, services and facilities for disabled people are minimal [7]. However, we cannot disregard the fact that disabled people have their share in making up the plurality of a society. To neglect disabled people means to ignore human potentials. We should bear in mind that to become disabled is not a person's choice and individuals may not want to live with a disability.

6. ANALYZING GREEN INFRASTRUCTURE AND UNIVERSAL DESIGN

Indonesia is well-known for its tropical lush green nature which can be sustained, if only people resist the temptation to transform a large part of the natural environment into "a new shape" [5], called the built environment. The green infrastructure has to be planned in advance, before the transformation of land begins. By doing so, land can be designated appropriately for recreation and doing physical exercise, improving the community's health, and energy savings. For the benefit, of people, green infrastructure in cities "forms a tapestry of open space that serves and guides smart growth" [1]. In cities, parks, trails, green ways and other open spaces serve the human need for social contact. As social beings, we reach maturity through harmony and friction with people surrounding us; the quality of our personality will not fully develop in isolation. In Bandung some parks are filled with citizens who do mainly exercise, like walking, while inhaling the fresh morning air. Communication among them is vital for the development of social, commercial, and cultural interaction; personal contact provides the fundamental part of such links [13]. As they regularly meet and communicate, an active community of morning walkers could be formed. If such is the case, the green infrastructure has achieved its purpose. People with disabilities, however, hardly receive the benefits of this infrastructure, because [12]:
- the design of the green infrastructure are full of physical barriers: footpaths with staircases, width of footpaths does not cater for the need of persons on wheelchair and people with walking sticks;
- the public transport is inaccessible for most ambulant disabled people.

These barriers cause many disabled people prefer staying indoors [12]. An effective solution to the problem of excluding disabled people is to implement the universal design which principle does not discriminate against any potential user of the green infrastructure. The former approach, barrier-free environment, aims at easing the difficulties that disabled people face. It is often referred to as "designing for special needs" [13]. Because green infrastructure is used by various groups of inhabitants, the provision of separate routes for disabled people is unnecessary and socially not acceptable. Universal design, on the other hand, does not attempt to make separate provision for these people, but emphasizes that the design of the built environment provides accessibility and usability for all sectors of the society simultaneously [13].

6.1 Universal design

Universal design means designing buildings and exterior spaces that can be used by all people, regardless of their level of ability or disability. The term "universal design" was coined in 1980 by the late Ronald L. Mace, who founded the Center for Universal Design in North Carolina, USA.

Universal design or inclusive design is not a design style, but an orientation to design that is based on the premises that:
- Disability is not a special condition of a few people;
- If the design works well for disabled people, it works better for everyone;
- Usability and aesthetics are mutually compatible.

The ability to move around comfortably, conveniently, and safely, must be the standard of a well-designed

infrastructure. The provision of such infrastructure will generate low impact development. It will be most likely that people prefer walking to driving a car or riding a motorcycle and this purpose reduces environmental damage and air pollution. As the universal design gives value to all individuals, they enjoy the opportunities and amenities with minimum constraints. It is therefore imperative to create infrastructures for all kinds of people and should not just be provided for the sake of the city planning requirement.

7. CONCLUSION

As a member of the United Nations, Indonesia has heeded the mandate of ESCAP (Economic and Social Commission for Asia and the Pacific) to remove physical barriers [5]. As a response, the government has publicized ordinances, has built ramps on campus of the Department of Public Works, and has conducted national conferences. These actions, however, do not lead to the realization of constructing barrier-free infrastructure in public spaces. One of the causes of this failure is attributable to the constraint of economic struggle for survival. All sorts of economic trade occur on public spaces, such as sidewalks and parks, which are tolerated at the expense of more chaotic traffic and increasing jaywalkers. On the streets, ambulant disabled people are ignored and street users are so immersed in their own struggle, that there is hardly room for unselfish concern. Furthermore, the government has to prioritize the improvement of per capita income, education, employment, health, sanitation and clean water, low cost housing, and land acquisition. Its preoccupation with coping and surviving leaves hardly any resource for the development of equity, social justice, basic human needs, environmental awareness, and welfare. It is not surprising that the needs of disabled people are not a priority in the list of survival concerns [11].

When basic human needs are met, and social justice and equity assured, disabled people can demand barrier-free infrastructure. For now, disabled people should make use of human assistance by asking passers-by for help when they are not able to surmount physical barriers.

7.1 A note on green infrastructure

The inclusion and exclusion of disabled people regarding the green infrastructure is a question of how well they are accepted by the general public. Today, the inhabitants of a city are made up of diverse people, who are often very different from each other. With a low degree of mutual acceptance of using public infrastructure may lead to conflict and in the long run will create an unsustainable society. This does not only apply to disabled people, but also other marginalized social groups, such as ethnic minorities. The degree of mutual public acceptance of different social groups is a yardstick of social sustainability [12].

REFERENCES

[1] Wiki, "Green infrastructure," *http://www.greeninfrastructurewiki.com/*, internet opened March 2009.
[2] Metropolitan, "HBKB menjadi ajang sosialisasi," *Kompas*, p. 26, June 26 2009.
[3] L. Crow, "Renewing the social model of disability," The disability archive UK, *http://www.leeds.ac.uk/disabilities-studies/archiveuk/archframe.htm*, 1992, internet opened August 17 2001.
[4] H. Ototake, *No one's perfect*, Tokyo, New York, London: Kodansha International, 2000.
[5] "Promotion of non-handicapping physical environments for disabled persons: guidelines," *UNESCAP*, New York: United Nations, ch. 2, pp. 7-23, 1995.
[6] B. Gleeson, "A place on earth: technology, space, and disability," *The Journal of Urban Technology*, vol. 5, no. 1, pp. 87-109, 1998.
[7] J. Byrne, "Life is challenging for people with disabilities in Indonesia," Inside Indonesia, *http://www.insideindonesia.org/content/view/303/29*, 2002, internet opened May 7 2009.
[8] B. Sirait, "Jakarta's disabled are striving for a better deal," Inside Indonesia, *http://www.insideindonesia.org/content/view/1046/ 47*, 2008, internet opened May 7 2009.
[9] J. D. Harrison & K. J. Parker, "Pavements for pedestrians: Asian city streets for everyone," paper presented in New York Conference "Designing for the 21st century," June 18-21 1998, unpublished.
[10] T. Edensor, "The culture of the Indian street" in N. R. Fyfe (Ed) *Images of the street*, London & New York: Routledge, pp. 205-221, 1999.
[11] I. Komardjaja, "The malfunction of barrier-free spaces in Indonesia," *Disability Studies Quarterly*, vol. 21, no. 4, www.cds.hawaii.edu, 2001.
[12] K. Seeland & S. Nicolè, "Green spaces to meet disabled people's needs: an empirical survey on the Isle of Mainau in Southern Germany," http://www.openspace.eca.uk/conference/proceedings/PDF/Seeland.pdf, internet opened March 29 2009.
[13] J. D. Harrison & K. J. Parker, "The stepless city concept: an urban planning tool for accessible environments," paper presented in the third International Convention on Urban Planning, Housing and Design (ICUPHD) "Cities for the 21st century," Singapore, September 22-24 1997, unpublished.

STUDY OF PARTICIPATIVE CONCEPT WITHIN DESIGN OF GREEN INFRASTRUCTURE* (Integrated Solid Waste, Water Resources, and Urban Transportation Management): Case Study of Sukmajaya District, City of Depok.

[1]Irma Gusniani, [2]Dwita S.M., [3]Sulistyoweni, [4]Tri Tjahyono

[a,c]*Environmental Engineering Study Program, Civil Engineering Department*
Faculty of Engineering, University of Indonesia, Depok 16424
Tel : (021) 7270029 Fax : (021) 7270028
[a]*E-mail irma@eng.ui.ac.id,* [c]*E-mail sulistyoweni1@yahoo.com*

[b,d]*Civil Engineering Study Program, Civil Engineering Department*
Faculty of Engineering, University of Indonesia, Depok 16424
Tel : (021) 7270029 Fax : (021) 7270028
[b]***Email : dwita@eng.ui.ac.id,*** [d]***Email :tjahjono @eng.ui.ac.id***

ABSTRACT

Land use changes reduced the pervious fraction of watershed area. An alternative to solve this problem is introducing concept of Low Impact Development (LID). LID is technology in managing surface runoff starting from its sources (rainfall). This approach is known as off-stream approach. The implementation of LID concept will only be effective if all people who live especially on the upper part of the watershed take part. However, this situation most likely can generate sentiment of unfairness, since the upstream people have to bear the cost of the program, while the beneficiaries are the people who live in the downstream part of the watershed. Implementing new paradigm with 3R principles (reduce, reuse, recycle) will decrease the quantity of solid waste disposed to final disposal site (TPA.) Simultaneously, implementing traffic calming and managing urban transporter is aimed to improve quality of life to resettlement region as urban transport un-regularity. These three activities will ask people to contribute to achieve the program aim to improve the environment in Depok.. A research with respondent survey method is intended to know people participation in these programs. The research result is a recommendation to decision makers in developing implementation policies regarding solid waste management, rainwater management, and also urban transportation management in the City of Depok. In water resource management research, people agree that they are also responsible to contribute to flood disaster mitigation, even though they realize that they gain no direct benefit from such program. In case of solid waste management, the result of a research shows that people are willing to participate within solid waste management with 3R principles. The results of transportation management research show that respondents are agree that "the road hump" as speed limit marker.

Keywords

water resources, solid waste, urban transportation, Low Impact Development, 3R, road hump

**) Funded by Competitive Based Program (Program Hibah Kompetisi B) Directorate General of Higher Education, Department of National Education, 2008*

1. INTRODUCTION

Kecamatan Sukmajaya, in the year 2006 has population density around 6,600 per square kilometer, and it is starting to face environmental problems for example in managing its water resources, solid waste and also urban transportation.

In the year 2006 Department of Civil Engineering FTUI was successful in competing for B-Program grant launched by the Directorate General of Higher Education. The B-Program Competitive Grant (*PHK-B: Program Hibah Kompetisi B*) last from 2007 up to 2009. The program proposed to perform "*green infrastructure by design*" research and community outreach focusing in the field of: integrated solid waste management, water resources management and also urban transportation management. The aim of the program is promoting improvement of Kecamatan Sukmajaya environment with "*green design*" concept.

Parallel with increasing population growth of Sukmajaya, number of solid waste is also increasing, and now become major problem for city of Sukmajaya. For example, solid wastes are in many places such as in a river bank makes the river contaminated. Others are limited of solid waste infrastructure; human resources and budget are making it worse for solid waste management. Lastly, solid waste collecting services has limited coverage, accumulated solid

waste increased and no more land available for final disposal (TPA) are crucial points to develop solid waste management for city of Depok

Implementing new paradigm such as 3R (reduce, reuse, recycle) principles and optimization solid waste treatment in every *kelurahan* with building solid waste plant unit (*Unit Pengolahan Sampah = UPS*), will decrease the quantity of solid waste disposed to TPA and also reduced solid waste infrastructure. Join activities has been made between University of Indonesia (UI) and Division of Clean and Environment, Local Government of Depok to implement program of 3R and empowered people in this program. Program faced difficulties such as people lacked of knowledge how to live healthy and how to activate 3R, and also people refuse local government program to build UPS in several locations.

Land use changes reduced the pervious fraction of watershed area. An alternative to solve this problem is introducing concept of Low Impact Development (LID). LID is technology in managing surface runoff starting from its sources (rainfall). This approach is known as off-stream approach. The implementation of LID concept will only be effective if all people who live especially on the upper part of the watershed take part. However, this situation most likely can generate sentiment of unfairness, since the upstream people have to bear the cost of the program, while the beneficiaries are the people who live in the downstream part of the watershed.

To encourage the upstream people to implement the LID program, a compensation scheme should be developed. The compensation is based on the implemented LID facilities. The implementation scale is grouped into three categories namely: individual (household), communal and region. The compensation rate is based on the budget needed for construction, and operation & maintenance of the facilities for each scale. The form of compensation at individual (household) scale is numerous, namely: design and technical specification for operation & maintenance of facilities, construction material (or in-cash), construction workers (or in-cash), turn-key project, land compensation (in-cash or tax deduction).

Relates to transportation aspect, the unsustainable infrastructure development is reflected in the high level of traffic jam, air pollution, and of road accident. In Indonesia, the condition of urban environment is getting worse because of the public transportation operational pattern.

Two research programs have been conducted:

1. Developing of traffic calming is for making a liveable street and socialization improvement in neighborhoods.
2. Rationalization of public transport to improve urban public transport quality.

Key success of those three programs depends on the level of people participation in running those programs. Therefore a research of people participation in form of people willingness to support those programs should be conducted.

Study on water resources management is aimed: (1) to know the willingness of people to participate in flood disaster mitigation and their responsibility; (2) to know the preference of upstream people relating to the compensation form in order to optimize the result; (3) to decide people, characteristic of compensation preferred by upstream based on its implementation scale.

The water resources management research was conducted in *Kecamatan* Sukmajaya covering *Kelurahan* Sukmajaya, Abadijaya, and Mekarjaya. Target respondents were community member as benefeceries.

The aims of study of integrated domestic waste management are (1) to know people willingness to participate in domestic waste management with 3R concept; (2) to be familiar with participation form of people within domestic waste management with 3R concept.

The study of integrated domestic waste management is implemented at in *Kecamatan* Sukmajaya covering *Kelurahan* Kalibaru, Abadijaya and Mekarjaya. Target respondents were community member as benefeceries

The research result is a recommendation to decision makers in developing implementation policies regarding rainwater management, solid waste management, and also urban transportation management in the City of Depok.

2. METHODS

2.1 Integrated Domestic Waste Management Based On 3R Principle.

Respondent's questioners for domestic waste management survey are arranged in orderly fashion from recommendation of integrated domestic waste management model. The questioners are divide into 3 parts consist of (1) questions which intend to see community participation level in domestic waste management; (2) questions which intend to see form of community participation in domestic waste management; (3) questions which intend to see community recompense for services of domestic waste management. All questions cover:

- Willingness to separate domestic waste which materials can be recycled.
- Willingness to accomplish organic domestic waste treatment turn into compost.
- Form of community contribution on domestic waste management implementation with 3R basis.
- Form of domestic waste management organization with 3R basis.
- Willingness to separate domestic waste and sell it to collector
- Willingness to pay domestic waste management retribution.

The result were analyzed with descriptive approach with discussing quantitative and qualitative data to figure out research synthesis

2.2 Water Resources Management

Respondent survey method was conducted using a set of questionnaire as instrument. The control variables employed were economics and education. The inquiry covering:

- *Willingness to participate in flood disaster mitigation*

- *Willingness to implement LID concept based on land and financial availability*
- *Acceptance to implement LID concept in relation to the responsibility in flood mitigation and its benefits resulted from LID implementation*
- *Preference form of compensation for implementing LID concept*
- *Respondent identities in relation to their motivation to implement LID concept at individual (household), communal, and region scales.*

Individual respondents were categorized based on their land ownership. 100 of respondents were divided into 3 categories:

- *Category I is respondents with land ownership < 90 m2.*
- *Category II is respondents with land ownership > 90 m2 up to < 150 m2.*
- *Category III is respondents with land ownership > 90 m2.*

The survey result was processed using Frequency Distribution and Cross Tabulation methods. Frequency Distribution was aimed to figure out the number of responses for each question, and Cross Tabulation was aimed to know interrelation among responses. The analysis and synthesis of research result were conducted using descriptive approach based on quantitative and qualitative data.

2.3 Urban Transportation Management

Transportation strategies require changes in public attitudes and behavior. The more a particular scheme is supported by the groups affected, the more likely will the implementation of the scheme be successful. There is also of strong evidence that local support will also possible to provide additional tangible and intangible benefits e.g. additional financial support in particular for maintaining the scheme and improving quality of the neighborhood and therefore will increase housing values and quality of life. For these reasons a series of meeting were carried out to the resident in *Kecamatan* Sukmajaya.

3. RESULT AND DISCUSSION

3.1. Integrated Domestic Waste Management Based On 3R Principle

Division of Clean and Environment, Local Government of Depok has their strategies with new paradigm year 2008 recently. Their strategies consist of:

1. Implementing new paradigm with 3R principles (reduce, reuse, and recycle) and people empowerment in this program
2. Performing most favorable of domestic waste at TPA at each sub-district with construct domestic waste treatment unit (UPS)
3. Executing to lessen domestic waste at TPA with undertakes domestic waste management at first in UPS will be built.
4. Improving people empowerment to undertake domestic compost
5. Preparing and implementing Local Government Decree regarding clean management in accordance to Decree No. 18 Year 2008 on Domestic Waste Management.

Division of Clean and Environment is facing problems where people have no ability to understand clean life style and implementation of 3R. Limited of infrastructure, human resources and financing are other problems faced by government and these situation must have more pay attention. Other, people refuse government program to build UPS. All repudiate can cause building UPS are behind schedule, therefore target of building UPS can not be accomplished

The survey results were analyzed covers:

a. People participation level within domestic waste management.

- People willingness to accomplish domestic waste separation develops into several parts that can be recycled.
- People willingness to treat organic domestic waste to develop into compost

b. Form of people participation within domestic waste management

- Contribution Form can be achieved within domestic waste management implementation based on 3R principles.
- People keen to split domestic waste and sell it to collector.

c. Willingness to pay in Domestic Waste Management

- Organization for Domestic waste manager based on 3R principles
- Willingness to pay domestic waste retribution

a. People participation level within domestic waste management

- *Willingness to separate domestic waste turn into small parts and it can be recycled.*

The survey result shows that people willingness to participate within domestic waste separation consist of 42% respondent throw domestic waste including several parts can be recycled, and other, 57% respondent has already separated material can be recycled which this material can be sold (14%), reuse almost 7% and give material to people who needed (36%). Basically, 91% respondents have knowledge that domestic waste must be separated before they pitch it, but only 24% respondents carry out material separation for recycle purpose. Based on question of respondent willingness to participate in integrated domestic waste management with 3R basis, almost 85% respondent willing and able to participate in this program, only 9% respondents said no to participate and 6% respondent no answers.

Other question such as how people willing to separate material turn into recycle process, number of respondent answer this question was 71% said yes, and the rest said no. The result of survey showed that people can be empowered in domestic waste management with 3R principles. Recently, people had already split domestic waste to become organic and an-organic domestic waste, even though they don't really understand the purpose of domestic waste separation. For that reason, government officer have

to clarify and disseminate domestic waste management with 3R principles means and also to introduce the economic value of domestic waste has been separated.

- *Willingness to treat organic domestic waste turn into compost*

In this moment, some people had already treated their own domestic waste to develop into compost. Conducting organic domestic waste to become compost is only 11% respondent performed it, converted into livestock food is 3% respondent give this answer, and filing it is almost 86% respondents answered this question. In addition, number of respondents which is agree to treat their domestic waste turn into compost in their house is 59% respondents, and respondent who is disagreed is only 2%.

Based on the study area, most people deny making compost because of they have not land. The other reason is that they have little information and knowledge to make compost right, no odor, benefit for them and compost has big value.

b. People Participation Form Within Domestic Waste Management

- *People Participation Form*

People have a choice to contribute during domestic waste management program with 3R basis such as make a payment (31%), clean up domestic waste in their environment (29%), carry their own domestic waste to generation point (15%), or split their own domestic waste into 2 parts i.e. organic material and an-organic material (13%), and split organic material which is a form of their contribution (9%). In brief, pay and clean domestic waste in their environment is the greater choices among them. For that reason, it should be figure out another their contribution form to carry on domestic waste management program, and people obtain to recognize it.

- *Willingness to split domestic waste and sell it to collector*

Respondent response to question of what should they do after splitting their domestic waste, the answer are they will give the product after splitting to collector (39%), sell it to scavenger-collector (28%), sell it to collector (28%) and no answer (2%).. From respondents who is agree to sell recycled material to collector and get money, 39% respondents are in agreement that the money should be save in RT/RW for gathering needs, the other said that the money should be a payment for domestic waste manager. From the result of survey shows that people concur to that recycled material is sold it to scavenger or collector and the money is utilized to pay domestic waste management services and/or for gathering needs.

c. Willingness to Pay for Domestic Waste Management

- *Form of organization for domestic waste management with 3R basis.*

Respondents propose domestic waste management organization in RT/RW region are a new form of free organization (85%), other disagree (14%) and no answer (1%). Therefore, a proposed form of organization is to have board of RT/RW or board of Head of Sub-district to become a member of that organization (32%), voluntary (23%), and *Pemuda Karang Taruna* as a member of organization board (13%).

The result of survey showed that people agreed that domestic waste management organization in their neighborhood should be formed and work independently with head of *RT/RW* or *kelurahan* as prime mover and also a member o organization board

- *Willingness to pay for domestic waste management retribution.*

People generally recognize that to manage domestic waste needs money, which is showed from answer of respondents (91%), other they are not familiar with (3%) and no answer (6%). People who pay for their retribution, almost 87% respondents disburse routinely for domestic waste management services, and the rest are not. The number of 50% respondents pay the bill of domestic waste management services less than Rp. 10.000,- and 24% respondents pay approximately Rp. 10.000,- up to Rp. 20.000,-.

For people who do not disburse for domestic waste management services, they do not get a billing payment or notice to pay (35%), other respondents (24%) felt unsatisfied with its services, and 12% respondents have no money to pay, and also about 12% respondents had different reasons.

People really understand and realize that domestic waste management needs money that means they will get a good services and the consequences they have to pay. The bill for domestic waste management services is varied depend on type of services, for that reason this payment should be made standard. This means people willing to pay based on its services they get and the management of domestic waste can work their jobs with sufficient budget available. Furthermore, the local government officers have assignment to socialize a number of payments for domestic waste management services per month to their people.

3.2 Water Resources Management

The analysis and synthesis of survey result covers:

a. Community responsibility concerning flood disaster mitigation

b. Community willingness to participate individually

- *Willingness to participate in form of devoted land and financial contribution*
- *Individual preference of compensation form*

c. Community willingness to participate communally

- *Willingness to participate in form of financial contribution*
- *Communal preference of compensation form*

a. **Community Responsibility Concerning Flood Disaster Mitigation**

87% of respondents are aware that flood disaster mitigation is everybody responsibility. They are also aware that not only the downstream people are responsible for the flooding in the downstream area. The upstream people committed to contribute to conservation effort through their contribution in form of land and financial commitment, although they realized that direct benefit will go to the downstream people.

The form of preferred compensation for their active participation in flood mitigation were: 67% of respondents wanted a reward system such as improvement of public services, 16% wanted tax deduction, and 14% wanted increasing their land valuation.
For respondents who do not want to participate in the program, an intensive socialization program should be conducted in order to develop their awareness, that the flood disaster mitigation needs a holistic approach, which needs participation (also) from upstream people, who occupy the recharge area.

b. **Community Willingness to Participate Individually**

• *Willingness to participate in form of devoted land and financial contribution*

The willingness to participate in form of devoted land depends on the availability of excess on their land parcels. That is why the category III respondents (76%) are dominantly ready to devote their land for implementing LID program. In general more than 50% of all categories respondents are committed to participate. They are aware that they should not convert the whole parcel area into impervious cover, since rainwater can only infiltrate into the ground through pervious area. In most cases the reason for objection is unavailability of excess land (89.7%), and the rest criticize, that individual initiatives will not be effective.
The willingness to participate in form of financial contribution depends on their income per month. It is understandable that only 29% of category I respondents willing to participate, since 67.6% of them have income less than Rp. 4,000,000.-. Even the category III respondents only 55% are ready to contribute. The objection mostly due to no extra budget (63%); it should be bear by the government (35%); extra money will be used for other purposes (20%).

• *Individual preference of compensation form*

Preference of respondents is dominated by turn-key-project, since most of them are government officials or private employees, who do not have enough time to supervise the construction.

People Participation	Category I	Category II	Category III
Land and Financial	• Const. Material • Design & Technical Specification • Const. Workers • Turn Key Project	• Turn Key Project	• Design & Technical Specification • Const. Material • Const. Workers • Turn Key Project
Land	• Turn Key Project	• Turn Key Project	• Design & Technical Specification • Const. Material • Const. Workers • Turn Key Project
Financial	• Turn Key Project	• Turn Key Project	• Design & Technical Specification • Const. Material • Const. Workers • Turn Key Project

c**. Community willingness to Participate Communally**

• *Willingness to participate in form of financial contribution*

Willingness to participate communally in form of financial contribution for construction conservation facilities is high. Only 3% are refusing to participate. This high level of participatory is a good starting point to emerge a social capital or strength social bounding in the community system. In fact, it means those community has capability to support development and improvement of social capital.
Collective financial contribution is preferred, since this is more affordable.

• *Communal preference of compensation form*

The form of preferred compensation is reward system. It means, government should improve their services capacity and pay more attention to the community needs.

3. 3 Urban Transportation Management

Speed is a significant factor in accidents. A safer speed for built up areas is not more than 20 km/h and no aggressive acceleration or stop and go movements occurs by the traffic. The quality of life can be affected by growing volumes of traffic and traffic traveling at inappropriate speeds. One way to solve the problem is by introduce traffic calming. Various instruments for traffic calming and the most important are road humps for reducing travel speed of vehicles.
A series of meeting were carried out to the resident in *Kecamatan* Sukmajaya. Basically support depends on their personal conditions. For example, residents in the more affluent area are prefer totally ban of through traffic or “rat run” and not interest whatever of traffic calming benefits. They do not bother the fact that street network in Depok is limited. On the other hand people living in less affluent area are enthusiastic with the concept of traffic calming.
Issues of who are the publics are important understood. Basically there are three groups can be represented (IHT, 1997):
1. Those who are users of transport services and networks, by any mode of transport ;
2. Those who are affected by the scheme in the area concerned; and
3. Those who provide transport infrastructure or operate the transport services.

In the case the second sub group is the target of public involving because traffic calming is more area concerned rather than transport services users. Consultation leaflets and questionnaires were carried out by the team and the results are follows:
1. Residents in the concerned areas agreed that the existing road humps are not properly design. Instead of to protect the neighborhood, the actual conditions, the road becomes dangerous to the traffic in particular to motorcycles and deteriorates the road structure because the road humps are blocking the drainage channels.
2. Residents also agreed that motorcycle riders are the most concern of why residents installed road humps. Because there no local government guidelines and involvement, the road humps are not properly designed.

3. Residents are hoping that local government will adopts UI's design and through the regulation becomes the formal guidelines for installing road humps as a part of traffic calming programs
4. As a result, traffic calming program must be formally binding as a local act (*Peraturan Daerah*) and the guidelines must be adopted as a part of the regulation.

4. CONCLUSION

4.1 Integrated Domestic Waste Management Based On 3R Principle

(1) People recognize that domestic waste that parts can be recycled should be separated before going to final generation point. People also willing to participate implementing 3R principle at sources point when integrated domestic waste management based on 3R put into practice. To enforce people understanding on 3R principle and its advantage, hence government should do an elucidation on integrated domestic waste management based on 3R and also introducing economic value comes from domestic waste separation. From socialization program of 3R principle and other programs that implemented by government of Depok city therefore those programs will support reducing domestic waste in final generation point and promote to do domestic waste preparation at treatment plant unit (UPS).
(2) Recently, several people in community had already recycled organic domestic waste turn into compost. On the other hand, many people do not agree making compost at their place, because there is not land available and also they do not know the advantages and economic value of compost. For that reason, government should made identification which region is appropriate to produce compost and provide more information on using compost for their interests. In addition, there is no possibility to make compost at domestic waste sources, then build UPS will be imposed at that region.
(3) Community is agreed that they have to form a self standing unit of domestic waste management organization and the member and board come from RT/RW organization.
(4) People recognized that they have to pay domestic waste collecting services. The billing payment for its service is varied depends on type of services. Therefore, it should be made a standard of billing payment equal to its service, and the management of domestic waste work properly because the finance is always available. To enforce community willing to pay domestic waste services, government should decide the number of payment correctly.

4.2. Water Resources Management

(1) People realize that flood disaster mitigation is responsibility of all stakeholders. This can be seen when upstream people build conservation facilities as part of flood disaster mitigation in down-stream region.
(2) Community willingness to participate individually is shown in form of devoted land and financial contribution. Based on land ownership category (category I < 90 m2; category II > 90 up to < 150 ; and category III > 150 m2) it can be concluded that: In general more than 50% of all categories respondents are committed to participate. They are aware that they should not convert the whole parcel area into impervious cover. In most cases the reason for objection is unavailability of excess land (89.7%). Only 29% of category I respondents willing to participate, since 67.6% of them have income less than Rp. 4,000,000.-.
(3) Preference of respondents is dominated by turn-key-project.
(4) Willingness to participate communally in form of financial contribution for construction conservation facilities is higher than individual participation. Only 3% are refusing to participate. This high level participatory is a good starting point to emerge a social capital or strength social bounding in the community system. Collective financial contribution is preferred, since this is more affordable.
(5) Communal preference of compensation form is reward system.

4.3 Urban Transportation Management

(1) Residents in the concerned areas agreed that the existing road humps are not properly design and that motorcycle riders are the most concern of why residents installed road humps. The road humps are not built properly designed, since there is no local government guidelines and involvement
(2) Traffic calming program must be formally binding as a local act (*Peraturan Daerah*) and the guidelines must be adopted as a part of the regulation.

REFERENCES

[1] Pasanen, E, and Salmivaara, H., "Driving speeds and pedestrian safety in the City of Helsinki". Traffic Engineering & Control, 34, 308-310, 1993.
[2] Institution of Highway and Transportation (IHT), "Road in Urban Environment"1997
[3] Dimitriou, Harry T., *Transport Planning for Third World Cities*. Routledge. London, 1990.
[4] Ogden, K. W., Bennet D. W. *Traffic Engineering Practice (third edition)*. Departement Civil Engineering Monash University. Australia, 1984
[5] Bappenas,'"Kajian Kebijakan Penanggulangan Banjir di Indonesia" Final Report. 2003.
[6] Tchobanoglous, "Integrated Solid Waste Management", 1998.
[7] Forbes Mc Dougall, "Integrated Solid Waste Management : a life cycle Inventory", 1998.

ISSN 114-1284

The Model of Toll Road Length to Population in East Asia

Ir. Lukas B. Sihombing, MT[1)]
Prof. Dr. Ir. Budi S. Soepandji [2)]
Dr. Ir. Ismeth S. Abidin [2)]
Dr. Ir. Yusuf Latief, MT [2)]

[1]*Faculty of Engineering*
University of Indonesia, Depok 16424
Tel : (021) 7270011 ext 51. Fax : (021) 7270077
E-mail : lukas_sihombing@yahoo.com

[b]*Faculty of Engineering*
University of Indonesia, Depok 16424
Tel : (021) 7270011 ext 51. Fax : (021) 7270077

ABSTRACT

The length of toll road in China so fantastic, there are currently 53,600 km of toll road traversing the country – the second longest in the world behind the United States, which has 89,000 km. And China plans to have 85,000 km of toll road by 2020.
Meanwhile, in East Asia including Indonesia, Malaysia, Philippines, and Thailand, in 2006 there were respectively 608 km, 2,332 km, 181 km, and 176 km.
In this paper wants to see the relationship of length of toll road to population as independent variable and foreign direct investment (FDI), Toll road investment, land area, gross domestic product (GDP) as dependent variable.
The method of this study use econometric analysis on pooled data.
The result of this study will see how China and Malaysia maintain their toll road investment to sustain their GDP, and how the length of toll road growth in Indonesia, Philippines, and Thailand lower than China or Malaysia.

Keywords
Example:
toll road, econometric analysis, pooled data.

1. INTRODUCTION

Analysis at this paper will use panel data or pooled data as estimation method to compare the relationship of inter-residue and to identify and measure effects that are simply not detectable in pure cross-section or pure time-series data [1]. The case of this paper is toll road infrastructure as an equation of residue structure. Basically, this estimation is General Least Square (GLS) as an equation of system. Pooled data or panel data analysis at this paper considered to be equation system with certain residual covariant matrix structure.

1.1. Population and Sample

Population in this research is: firstly, equation model of toll road length ratio as population of country and toll road length. Second, FDI ratio as toll road investment and land area. Third, GDP in a country. And sample of countries are China, Indonesia, Malaysia, Filipina, and Thailand. Totally sample are 50,starts the year 1996 until 2006.

1.2. Sources of Data

The countries that applied in this research are China, Indonesia, Malaysia, Filipina, and Thailand for toll road length, population, Foreign Direct Investment (FDI), toll road investment, and GDP, start began 1996 until 2006.
Data collected by using pooled data, where time-series and cross-section data was merged so that number of observations to become number of years is multiplied with number of states. Data type applied is secondary data where: a) length of toll road in China (CCB International , China Toll Road, China and Hong Kong Equity Research, and Chinadaily [3], Indonesia [4], Malaysia [5], Philippines [6], [7], [8], Thailand [9]; b) Population [10], [11], [12], and [13]; (c) FDI [14]; d) Toll Road Investment [15]; e) Land Area [16]; f) GDP [17]. Data can be seen on Table 1.

1.3. Econometric Model

1.3.1. General Structure Model

Model Structure in general is given as follows:
$lnrtoll_{it} = \alpha_1 + \beta_{i1} lnrfdi_{it} + \beta_{i2} lngdp_{it} + \varepsilon_{it}$

where:
$lnrtoll_t$ *:* ratio between turnpike lengths with population
$lnrfdi_t$ *:* ratio between multiplications between FDI (million dollars) with invesment of turnpike (million dollars) divided soil; land;ground wide (square km)
$lngdp_t$*:* GDP (million dollar)
α_1 = intercept, β_1 *until* β_k = slope, ε_{it} = stochastic disturbance term and i = number of individuals. Pays attention to that α and β varies for all individual. This model indicates that parameter α and β varies. Successively in part of this will be studied:
1). Model Structure I (called as also common model / common) what indicates that all effect from variable in each same individual (uniform) so that we are not akam sees effect from individual, hence model becomes:
$lnrtoll_{it} = \alpha_1 + \beta_1 lnrfdi_{it} + \beta_2 lngdp_t + \varepsilon_{it}$
2) Model Structure III / V that is economical indicates that effect from variable in each individual differs in. Model structure who applied is for following:
$lnrtoll_{it} = \alpha_1 + \beta_{i1} lnrfdi_{it} + \beta_{i2} lngdp_t + \varepsilon_{it}$
Pays attention to that α and β varies for all individual.
Where structure Model III applies solution is using heterokedastic condition without existence of correlation between units (GLS) while Structure Model V applies solution is using heterokedastic condition with existence of correlation between units (SUR).
3). Model Structure IV where effect from every unique variable is specified according to assumption of its(the economics. If we assume that effect from same lnrfdi to all states while effect from lngdp differs in to all states.

Workmanship procedure at Eviews applies pooled data:

2. ESTIMATION WITH STRUCTURE COVARIAN

2.1. Structure Common (Model I)

To finalize econometric model like this there are some methods as according to assumption condition of this V structure that is condition A) homokedastic, B) heterokedastic structure, C) autocorrelation structure, D) structural existence of correlation between error term. This condition will be explained one by one at part following.

2.1.1.Homocedastic Structure

Solution of this model can apply GLS or OLS. Estimation with OLS has been studied at Estimation random coefficient. Estimates for this Model structure can be done either at object pool or object system.

Way of pooled data called as procedure at pool data where:

- Dependent of Variable : lnrtoll?
- Sample : 1996 2006
- Common Coefficient : lnrfdi? lngdp? Shows coefficient? same for every individual
- Specific Coefficient :
- Intercept : common, shows intercept ? 1 differs in every individual.
- Weighting: No Weights shows applied [by] method OLS with assumption Homokedastik.

2.1.2. *Object System* (OLS)

Specification of at object system is written:

LNRTOLL_CH = C(1) + C(2)*LNRFDI_CH + C(3)*LNGDP_CH

LNRTOLL_IND = C(1) + C(2)*LNRFDI_IND + C(3)*LNGDP_IND

LNRTOLL_MSIA = C(1) + C(2)*LNRFDI_MSIA + C(3)*LNGDP_MSIA

LNRTOLL_PH = C(1) + C(2)*LNRFDI_PH + C(3)*LNGDP_PH

LNRTOLL_TH = C(1) + C(2)*LNRFDI_TH + C(3)*LNGDP_TH

- Estimation methods : ordinary Least Square
- Iteration Control : Iterate Coefficient to convergence
- Sample : 1996 2006

2.1.3. Heterokedastic Structure and There Is No Cross Sectional Correlation

For solving of GLS/WLS, eviews memeberikan facility with weighting: bawah weights with iterate to

convergence, where ? 21 anticipated by doing iteration so that is gotten value ? which most efficient.

2.1.3.1. *Object Pool* (GLS/WLS : *Cross Sectional Weight*)

Estimator WLS/GLS with procedure pool applies Weighting : cross sectional weight shows applied [by] method GLS with assumption Heterokedastik.
If it is applied White Heteroskedasticity-Consistent Standard Errors & Covariance, happened at errors standard.
Result Of Estimation:
Estimator WLS/GLS and iterate to convergence gives result of estimation as follows:
Measurement of errors standard based on e'e/(nT). We will differentiate result of this with result of regression with other method hereunder.

2.1.3.2. *Object System* (GLS/WLS)

For estimator GLS/WLS, procedure at object system done as:

- **Estimation methods** : *Weighted Least Square*
- **Iteration Control**: *Iterate Coefficient to convergence*

For estimator GLS/WLS with iteration, procedure at object system done as:

- **Estimation methods** : *Weighted Least Square*
- **Iteration Control**: *Simultaneous Updating*

Both giving the same estimation with above pool object. Difference happened at Standard Error.

2.1.4. Heterokedastic Structure and There Are Cross Sectional Correlation (SUR)

Much the same to with heterokedastic model which has been studied, main difference with model before all is that there is correlation at errors between equations . Means diagonal OFF filled by bilinear covariant is not null.

Solution of estimation can apply good of feasible generalized least square (FGLS) and also maximum likelihood estimator (MLE)
Eviews provides this structure choice Pooled Estimator with procedure SUR, while at System Estimation with procedure estimation methods SUR.
Other solution by using FGLS is obtained by doing estimation beforehand at ? 2i, where Maximum likelihood estimator is generalized least square. Estimation with method FGLS, eviews applies procedure SUR and estimation with method maximum likelihood estimator (MLE), eviws applies procedure SUR with iteration. Procedure workmanship at Eviews can apply two procedures that is pooled data or apply system equation.
2.1.4.1. Object Pool (SUR /FGLS) dan MLE
Estimator SUR with procedure pool applies weighting : SUR shows method GLS with assumption Heterokedastik with existence of correlation between units.
Way of pooled data conceived of procedure at pool data where:

- Dependent Variable *: lnrtoll?*
- Sample : *1996 2006*
- Common Coefficient : *lnrfdi? lngdp? Menunjukkan coefficient β* sama untuk setiap individu
- Cross Section Specific Coefficient :
- Intercept : *common*, menunjukkan intercept α1 berbeda untuk setiap individu.
- Weighting : *SUR*
- Iteration Control:

Estimator SUR with iteration (MLE) with procedure pool applies Weighting: SUR and Iterate Coefficient to convergence.

- Dependent Variable : *lnrtoll?*
- Sample : *1996 2006*
- Common Coefficient : *lnrfdi? lngdp? Menunjukkan coefficient β* sama untuk setiap individu
- Cross Section Specific Coefficient :
- Intercept : *common*, menunjukkan intercept α1 berbeda untuk setiap individu.
- Weighting : *SUR*
- Iteration Control: *Iterate to convergence*

Result Of Estimation without White Heteroskedasticity-Consisntent Standard Errors & Convergence as follows:

Measurement of errors standard based on e'e/(nT). We will differentiate result of this with result of regression with other method hereunder.
2.1.4.2. Object System (SUR(FGLS) dan MLE)
For estimator FGLS (SUR), procedure at object system done as:

- Estimation methods : *SUR*
- Iteration Control : *Iteration Coefficient to convergence*

Persamaan:
LNRTOLL_CH = C(1) + C(2)*LNRFDI_CH + C(3)*LNGDP_CH

LNRTOLL_IND = C(1) + C(2)*LNRFDI_IND + C(3)*LNGDP_IND
LNRTOLL_MSIA = C(1) + C(2)*LNRFDI_MSIA + C(3)*LNGDP_MSIA

LNRTOLL_PH = C(1) + C(2)*LNRFDI_PH + C(3)*LNGDP_PH

LNRTOLL_TH = C(1) + C(2)*LNRFDI_TH + C(3)*LNGDP_TH
Result Of Estimation:
For estimator MLE, procedure at object system done as:

- Estimation methods : *SUR*
- Iteration Control : *Simultaneous Updating*

2.1. Random Structure (Model III/V)

As explained to be above, Structure III/V that is economical indicates that effect from variable in each individual differs in. Model structure who applied is as follows:

$lnrtoll_{it} = \alpha_1 + \beta_{i1}\, lnrfdi_{it} + \beta_{i2}\, lngdp_{it} + \varepsilon_{it}$
Pays attention to that ? and ? varies for all individual. Estimates for this Struktur Model can be done at object pool and object system. In procedure at object pool is:
Way of pooled data conceived of procedure at pool data where:

- Dependent Variable : *lnrtoll?*
- Sample : *1996 2006*
- Common Coefficient :
- Cross Section Specific Coefficient : *lnrfdi? lngdp? Menunjukkan coefficient β* sama untuk setiap individu
- Intercept : *Fixed*, menunjukkan intercept α1 berbeda untuk setiap individu.
- Weighting : *(choose)*
  - No Weighting if using method GLS with homokedastic assumption.
  - Bawah weight if using method GLS (heterokedastic without existence of correlation between units). In classification of model as Model III
  - SUR if using method GLS (heterokedastic with existence of correlation between units). In classification of Model as Model V.
- Iteration Control: (select;chooses)
  - Without iteration control if using not to apply method MLE
  - Iterate Coefficient to convergence if using not to apply method MLE

Way of system conceived of procedure System where specification at object system is written:
LNRTOLL_CH = C(11) + C(12)*LNRFDI_CH + C(13)*LNGDP_CH

LNRTOLL_IND = C(21) + C(22)*LNRFDI_IND + C(23)*LNGDP_IND

LNRTOLL_MSIA = C(31) + C(32)*LNRFDI_MSIA + C(33)*LNGDP_MSIA

LNRTOLL_PH = C(41) + C(42)*LNRFDI_PH + C(43)*LNGDP_PH

LNRTOLL_TH = C(51) + C(52)*LNRFDI_TH + C(53)*LNGDP_TH

- Estimation methods: (select;chooses)
  - OLS juka menggunkan method OLS with homokedastic assumption
  - WLS bawah weights if using method GLS (heterokedastic without existence of correlation between units). In classification of model as Model III
  - SUR if using method GLS (heterokedastic with existence of correlation between units). In classification of model as Model V
- Iteration Control : (select;chooses)
  - Iterate Coefficient to convergence: if using not to apply method MLE
  - Simulation Updating: if using applies method MLE

2.1.2.1. Estimation MLE

Here made as Model V, where it is assumed that economic model has relationship (correlation) residue between banks (individual), so that at procedure pool we apply way following:

- Specific Coefficient: lnrfdi? lngdp? Shows coefficient ? differs in every individual

- Intercept: Fixed, shows intercept ? 1 differs in every individual

- Weighting :
  - SUR if using method GLS (heterokedastic with existence of correlation between units)
- **Iteration Control:**
  - Simultaneous Updating if using applies method MLE

Result Of Estimation is as follows:
While at procedure system we apply procedure:

- Estimation methods:
  - SUR if using method GLS (heterokedastic with correlation between units)

- Iteration Control:
  - Simultaneous Updating: If using applies method MLE

Result Of Estimation is as follows:

2.1.5. Random Structure (Model IV)

2.1.5.1. Estimation SUR/FGLS

At Model Structure IV-A, we assume that effect from lnrfdi differs in to turnpike length ratio while effect from same lngdp to turnpike length ratio.

Model is assumed [by] there is relationship (correlation) between individuals (SUR). Model structure who applied is as follows:

$$lnrtoll_{it} = \alpha_1 + \beta_1 lnrfdi_{it} + \beta_{i2} lngdp_{it} + \varepsilon_{it}$$

Note: ? permanent 1 for all individual and ? 3 varies for semuaindividu. Estimated for this Model structure can only be done at object system.

Way of system conceived of procedure System where at object system is written:

LNRTOLL_CH = C(11) + C(12)*LNRFDI_CH + C(13)*LNGDP_CH

LNRTOLL_IND = C(21) + C(22)*LNRFDI_IND + C(13)*LNGDP_IND

LNRTOLL_MSIA = C(31) + C(32)*LNRFDI_MSIA + C(13)*LNGDP_MSIA

LNRTOLL_PH = C(41) + C(42)*LNRFDI_PH + C(13)*LNGDP_PH

LNRTOLL_TH = C(51) + C(52)*LNRFDI_TH + C(13)*LNGDP_TH

Note: Pays attention to that permanent lngdp parameter for all individual

- **Estimation methods:**
  - SUR if using metodeGLS (heterokedastic with existence of correlation between units) In classification of model as Model V
- **Iteration Cotrol:**
  - Iterate Coefficient to convergence: if using not to apply method MLE

Test Statistic	Value	df	Probability
Chi-square	41536.70	4	0.0000

Null Hypothesis Summary:

Normalized Restriction (= 0)	Value	Std. Err.
C(13) - C(53)	-5.530420	0.216005
C(23) - C(53)	-8.901487	0.253040
C(33) - C(53)	-7.039943	0.302901
C(43) - C(53)	-8.235944	0.214723

Restrictions are linear in coefficients.

Result of Estimation is as follows:

3. Determination of Model

3.1. Choosing A Model IV-A and V

In determining model who is better is done [by] examination with testing in the large Wald at equation of system (system equation) Formulation of hypothesizing is as follows:

$H_0 : \beta_{2CH} = \beta_{2IND} = \ldots = \beta_{2TH}$: is model IV-a with MLE
H_1 : not H_0 : is model V with MLE
Note: we can only differentiate to model with the same bilinear covariant structure. Here we take example that there are correlation of residue between individuals (

SUR) with estimator MLE. By paying attention to above hypothesizing formula, model restriksi is model IV-A and model restriksi do not be model V.

Way of system conceived of procedure System where specification at object system is written:

LNRTOLL_CH = C(11) + C(12)*LNRFDI_CH + C(13)*LNGDP_CH

LNRTOLL_IND = C(21) + C(22)*LNRFDI_IND + C(23)*LNGDP_IND

LNRTOLL_MSIA = C(31) + C(32)*LNRFDI_MSIA + C(33)*LNGDP_MSIA

LNRTOLL_PH = C(41) + C(42)*LNRFDI_PH + C(43)*LNGDP_PH

LNRTOLL_TH = C(51) + C(52)*LNRFDI_TH + C(53)*LNGDP_TH

Initial step, we are estimation beforehand model structure which more unrestriksi (Model V), then we are restriksi at test wald:

C(13)=C(23)=C(33)=C(43)=C(53)
Got result:

Wald Test:
System: SYST_MDL3_SUR1

Showing above examination is rejection H_0 : $\beta_{2CH} = \beta_{2IND} = \ldots = \beta_{2TH}$: that is model IV-A dg MLE. So model who is better is model where effect GDP is not uniform to lnrtoll from every state (individual).

3.1.2. **Choosing A Model II and V**

At this examination , we test better which model to explain variable dependen that is model by assuming existence of idividu V (individual effect α differs in and variable effect β is same) with model without existence of individual effect (individual effect ? differs in and variable effect ? differs in), Model V. Examination here is done with testing in the large Wald at equation of system (system equation).

Hypothesizing formula is as follows:

$H_0 : \beta_{1CH} = \beta_{1IND} = \ldots = \beta_{1TH}$

$\beta_{2CH} = \beta_{2IND} = \ldots = \beta_{2TH}$
: that is model IV-A dg MLE

H1 : non H0 : that is model V with MLE

Wald Test:
System: SYST_MDL3_SUR1

Test Statistic	Value	df	Probability
Chi-square	633074.8	8	0.0000

Null Hypothesis Summary:

Normalized Restriction (= 0)	Value	Std. Err.
C(12) - C(52)	-0.406834	0.013409
C(22) - C(52)	-0.084310	0.025852
C(32) - C(52)	-0.201638	0.066396
C(42) - C(52)	-0.128286	0.022314
C(13) - C(53)	-5.530420	0.216005
C(23) - C(53)	-8.901487	0.253040
C(33) - C(53)	-7.039943	0.302901
C(43) - C(53)	-8.235944	0.214723

Restrictions are linear in coefficients.

Note: we can only differentiate to model with the same bilinear covariant structure. Here we take example that there are correlation of residue between individuals (SUR) with estimator MLE. By paying attention to above hypothesizing formula, model restriksi is model II and model restriksi do not be model V.

Way of system conceived of procedure System where specification at object system is written:

LNRTOLL_CH = C(11) + C(12)*LNRFDI_CH + C(13)*LNGDP_CH

LNRTOLL_IND = C(21) + C(22)*LNRFDI_IND + C(23)*LNGDP_IND

LNRTOLL_MSIA = C(31) + C(32)*LNRFDI_MSIA + C(33)*LNGDP_MSIA

LNRTOLL_PH = C(41) + C(42)*LNRFDI_PH + C(43)*LNGDP_PH

LNRTOLL_TH = C(51) + C(52)*LNRFDI_TH + C(53)*LNGDP_TH

Initial step, we are estimation beforehand model structure which more unrestriksi (Model V) then we are restriksi at test wald:

c(12)=c(22)=c(32)=c(42)=c(52),
c(13)=c(23)=c(33)=c(43)=c(53)
Got result:

Showing above examination is rejection H_0 : $\beta_{1CH} = \beta_{1IND} = \ldots = \beta_{1TH}$: that is model II dg MLE. So model who is better is model where effect of all variables is not uniform to lnrtoll from every state (individual).

3.1.3. **Choosing A Model II and I**

Kitapun can do examination of model between common, that is model where effect from all same variables to dependent variable of all individuals and there is no fixed effect (Model I) with model existence of individual effect (Model II). Examination here is done with testing in the large Wald at equation of system (system equation). Hypothesizing formula is as follows:

H_0 : $\alpha_{CH} = \alpha_{IND} = \ldots = \alpha_{TH,}$: yaitu model I (common) dengan GLS
H1 : $\alpha_{CH} \neq \alpha_{IND} \neq \ldots \neq \alpha_{TH,}$: yaitu model II (fixed efect) dengan GLS
Note: we can only differentiate to model with the same bilinear covariant structure. Here we take example that there are correlation of residue between individuals (SUR) without estimator MLE. By paying attention to above hypothesizing formula, model restriksi is model I and model restriksi do not be Model II. In examination of this Wald, usage of procedure pool cannot be done. For the purpose is applied procedure system.

Initial step, we are estimation beforehand model structure which more unrestriksi (Model II).

Specification of model is:

LNRTOLL_CH = C(11) + C(2)*LNRFDI_CH + C(3)*LNGDP_CH

LNRTOLL_IND = C(21) + C(2)*LNRFDI_IND + C(3)*LNGDP_IND

LNRTOLL_MSIA = C(31) + C(2)*LNRFDI_MSIA + C(3)*LNGDP_MSIA

LNRTOLL_PH = C(41) + C(2)*LNRFDI_PH + C(3)*LNGDP_PH

LNRTOLL_TH = C(51) + C(2)*LNRFDI_TH + C(3)*LNGDP_TH

And the graph of that model can be seen on Figure 1.

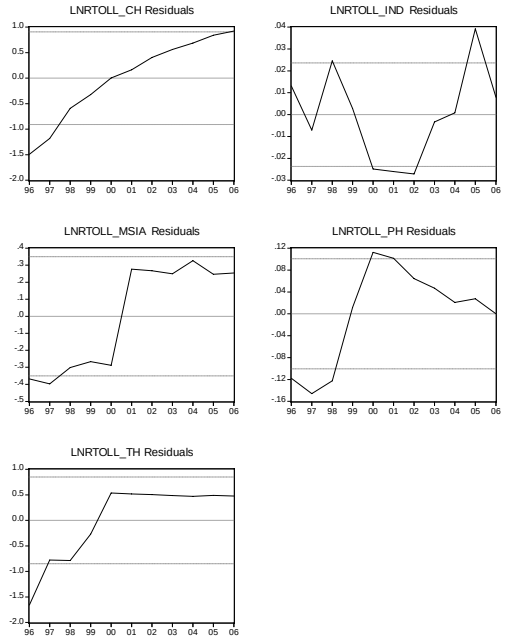

Figure 1. Model II and V

Test Wald as follows:
C(11)=C(21)=C(31)=C(41)=C(51)

Showing above examination is rejection H_0 : $\alpha_{CH} = \alpha_{IND} = \ldots = \alpha_{TH}$: that is model I (common). So model who is better is model where effect of all variables is not uniform to lnrtoll from every state (individual).

4. CONCLUSION

Model who is better is Model V with MLE
Specification Of Model:

LNRTOLL_CH = C(11) + C(12)*LNRFDI_CH + C(13)*LNGDP_CH
LNRTOLL_IND = C(21) + C(22)*LNRFDI_IND + C(23)*LNGDP_IND
LNRTOLL_MSIA = C(31) + C(32)*LNRFDI_MSIA + C(33)*LNGDP_MSIA
LNRTOLL_PH = C(41) + C(42)*LNRFDI_PH + C(43)*LNGDP_PH
LNRTOLL_TH = C(51) + C(52)*LNRFDI_TH + C(53)*LNGDP_TH

And the graph of that model can be seen on Figure 2.

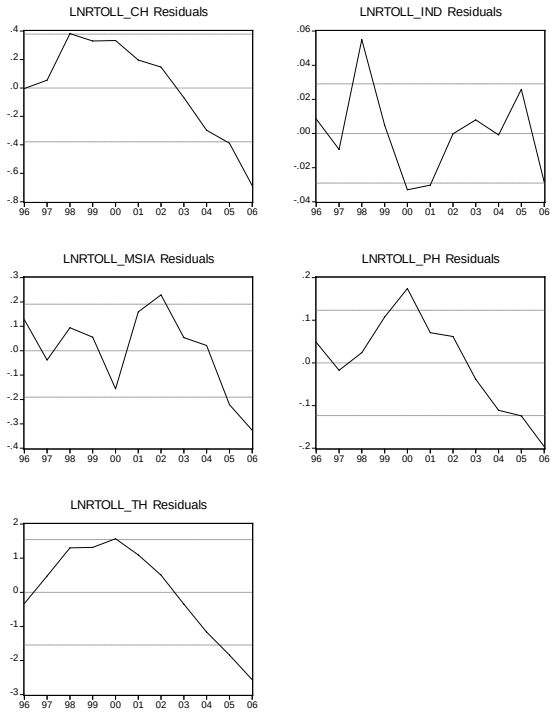

Figure 2. Model V with MLE

REFERENCES

[1] Baltagi, Badi. H., "Econometric Analysis of Panel Data," John Wiley & Sons, Ltd., 2005, pp. 11-104
[2] The World Bank, (1999)., "Asian Toll Road Development Program," Japan, pp. I-2
[3] http://www.chinadaily.com.cn/bizchina/2008-01/07/content_6374334.htm, accessed on June 6, 2008.
[4] www.bpjt.net, accessed on October 2007.
[5] http://www.llmnet.gov.my/serverpages/highway/highway_info.aspx, accessed on June 12, 2008.
[6] http://www.mntc.com/, accessed on June 12, 2008
[7] http://65.163.15.183/index.asp, accessed on June 12, 2008
[8]http://www.ap-infra.org/cgi-local/inter/section_top.pl?fnm=phil-e.htm&s1no=6&s2no=2, accessed on June 12, 2008.
[9] Statistical Year Book Thailand 2004
[10] http://pwt.econ.upenn.edu/php_site/pwt62/pwt62_form.php, accessed on June 12, 2008, for year 1996-2004.
[11] http://data.un.org/Data.aspx?d=CDB&f=srID%3a29070, accessed on June 12, 2008, for year 2005.
[12] *Economic and Social Survey of Asia and the Pacific* 2008: Sustaining Growth and Sharing Prosperity for year 2006.
[13] https://www.cia.gov/library/publications/the-worldfactbook/geos/tt.html for year 2008, accessed on June 12, 2008, for year 2008.
[14] (http://data.un.org/Data.aspx?d=CDB&f=srID%3a29070), accessed on June 12, 2008.
[15] http://ppi.worldbank.org/explore/ppi_exploreCountry.aspx?countryId=67, accessed on June 12, 2008.
[16] https://www.cia.gov/library/publications/the-worldfactbook/geos/tt.html, accessed on June 12, 2008.
[17] http://data.un.org/Data.aspx?d=CDB&f=srID%3a29923, accessed on June 12, 2008.

Table 1. Variables Time Series

YEAR	TOLL_CH	TOLL_IND	TOLL_MSIA	TOLL_PH	TOLL_TH	POP_CH	POP_IND	POP_MSIA	POP_PH	POP_TH
1996	3422	532.65	913.5	130	18.7	1218.257	209.2728	20.04456	73.38606	59.6083
1997	4771	532.65	913.5	130	45.8	1230.299	212.9757	20.47609	75.01299	60.3112
1998	8733	544	1017	136.477	45.8	1241.891	216.6676	20.91198	76.57618	61.0029
1999	11605	551.25	1084.7	159.275	77.8	1252.766	220.3427	21.35446	78.13392	61.6835
2000	16314	551.25	1092.6	181.435	175.9	1262.474	224.1384	21.79329	79.73982	62.352
2001	19437	560.32	1942.1	181.435	175.9	1271.085	227.7414	22.22904	81.36975	63.0069
2002	25130	560.32	1992.1	181.435	175.9	1279.161	231.3261	22.66237	82.99509	63.6453
2003	29745	590.62	2002.1	181.435	175.9	1286.975	234.8935	23.09294	84.61997	64.2653
2004	34288	608.12	2227.7	181.435	175.9	1294.846	237.8366	23.52542	86.15125	64.8242
2005	41005	608.12	2252.7	181.435	175.9	1312.979	226.063	25.653	84.566	63.003
2006	45339	608.12	2331.7	181.435	175.9	1320.864	228.864	26.114	86.264	63.444

YEAR	INVTOLL_CH	INVTOLL_IND	INVTOLL_MSIA	INVTOLL_PH	INVTOLL_TH	FDI_CH	FDI_IND	FDI_MSIA	FDI_PH	FDI_TH
1996	6266.26	867.93	3848.26	467.93	556.76	40180	6194	5078.41	1517.00	2335.88
1997	7917.73	867.93	4893.69	739.27	556.76	44237	4677	5136.51	1222.00	3894.74
1998	8809.93	867.93	5177.33	739.27	562.66	43751	-241	2163.40	2287.00	7314.76
1999	9181.55	1607.77	5327.77	784.11	576.66	38753	-1866	3895.26	1247.00	6102.68
2000	10013.96	1607.77	5940.08	786.98	576.66	38399	-4550	3787.63	2240.00	3365.99
2001	10301.21	1607.77	6267.80	1309.52	676.16	44241	-2977	553.95	195.00	5067.17
2002	11243.61	1607.77	6267.80	1326.77	676.16	49308	145	3203.42	1542.00	3341.61
2003	12602.48	1607.77	7020.01	1394.03	686.00	47077	-597	2473.16	491.00	5232.27
2004	13010.40	1610.65	7183.87	1394.03	782.00	54937	1896	4624.21	688.00	5860.26
2005	16357.11	1610.65	7465.11	1394.03	782.00	79127	5260	3966.01	1854.00	8964.27
2006	20045.53	3335.72	7719.52	1509.00	782.00	78095	20752	6063.55	2345.00	10749.90

YEAR	GDP_IND	GDP_MSIA	GDP_PH	GDP_TH	LAND_CH	LAND_IND	LAND_MSIA	LAND_PH	LAND_TH
1996	584678.2	161068.499	250208.4	377427	9326410	1826440	328550	298170	511770
1997	622382.5	175750.558	267578.7	378469	9326410	1826440	328550	298170	511770
1998	546691.2	164625.306	268991.3	342455	9326410	1826440	328550	298170	511770
1999	558978.2	177254.108	282146	362855	9326410	1826440	328550	298170	511770
2000	599264.4	197162.996	305503.3	388376	9326410	1826440	328550	298170	511770
2001	636060	202554.764	318355.1	406351	9326410	1826440	328550	298170	511770
2002	676311.1	214647.899	338339.3	435449	9326410	1826440	328550	298170	511770
2003	723064.1	231469.265	362244.3	476035	9326410	1826440	328550	298170	511770
2004	779368.2	254726.086	394738.6	519202	9326410	1826440	328550	298170	511770
2005	848504.7	275946.322	426869	558858	9326410	1826440	328550	298170	511770
2006	921241	300816.123	462960.4	603937	9326410	1826440	328550	298170	511770

ISSN 114-1284

Transport Planning Around Conservation Forest Area at Supiori as a New Expanding Regency of Biak Island

R. Didin Kusdian

Civil Engineering Departement
Faculty of Engineering
University of Sangga Buana YPKP
E-mail: kusdian@yahoo.com

ABSTRACT

Supiori was appearing as new regency on west side of Biak Island in Papua Province, Eastern of Indonesia. As a new autonomic administrative area Supiori Regency has some vision, mission, objectives, and goals, to improve the community live in all sectors by development programs. This is a unique point to be discussed, because before legitimated as one autonomic regency separated from Biak Numfor regency, the area of Supiori is dominated by conservation forest area. The first activity to reach this regency vision is arrange the area land use planning which still keep the boundary of conservation forest area. So this is interesting problem to arrange the development planning to increase the quality of community live in all sectors and at the same time the green area which covered by the law as the conservation forest must be kept at it boundary lines. After area land use planning arranged and reviewed, the second step must be arranged as a derivation of it, is transportation system planning. In the fact Supiori regency has only limited transportation infrastructure, with low quantity of dimension and low quality of structure. This study will explore the quantitative and qualitative aspects of transport planning analysis of Supiori regency in Biak Island. Data collecting is done in January, 2009 including land use planning review, traffic and existing transport infrastructure investigation, and social economics data. The data is got from the site as primary data and also from local government office in the form of statistical printed data and also maps as secondary data. For quantitative analysis of planning this study use the most known model of Four Step Transport Planning Model, especially the three steps including Trip Generation, Trip Distribution and Modal Split. The models were derived in form of mathematical model which can be processed in numerical data and output with use computer. Trip generation was estimated from population and number of household data, and trip distribution calibrated with use primary traffic data which transform to be prior origin-destination matrix and distance matrix which transform to be cost matrix with negative exponential function, processed with gravity model and multi regression calibration to determine cost function parameter. The result using the model is quantity estimating of person and freight movement demand in Supiori Regency area in the form of future origin destination matrix which describes the movement from zone to zone inside this regency. From estimating results the transport planning and future program policy in transportation for this regency was stated. The resume of this are: port infrastructure, road and bridges and terminals planning for connecting each districts and separated little islands. All of these infrastructures prepared and controlled to be kept out of forest conservation area.

Keywords: *conservation forest boundary, new regency development, person and movement estimation model, transport planning, future policy program*

1. INTRODUCTION

The development planning of Supiori Regency transportation network is derived from land use planning and policy, which arranged with basic principle of development as follows:

- **Hierarchies**
  Transportation network is develop with consider the hierarchies of a nodes as acitivity centers which is already stated in land use planning. This can be told that transportation network must be planned in order to make work or estabish the nodes hierarchies stated in land use planning.
  In this case system base of analisys must be held as the principle of qualitative and quantitative analysis process. Systemic relationship must be viewed both between transportation network and land use, also between nodes inside transportation network it self.

ISSN 114-1284

- **Geography**

  The geographical basic principle mean that transportation network system development determination factor of shape, configuration, quantity and quality of network systems to be develope. Several aspects of these principles are: morphology, hydrology, natural disaster, and conservation forest.

- **Economy**

  The economy basic principle issues a declaration that transportation system arrangement for one region must consider the economic system behaviour of it. This economic system behaviour will be key factor of the role and function of transportation network inside region system that being developed.

  For the region with progressive economic system the role and function of transportation network is to supply the demand of peoples and freights movements derived from progressive economic activity, this agree with the philosopy as well known as " ships follow the trade". But for developing region the role and function of taransportation network accidentally is to generate the economy progress of the region. And for most new regency region, this role of transportation network is, of course, more appropriate, especially according with the acceleration of East Indonesia development.

  But in this case the carefully attention must be held in the transportation planning, because of many regions are play the role as the conservation area, and have the important tropical forest as the part of pneumonia of the earth. This role is very important for the sustainability of it region development and for whole people in the world whose live now even next generation that will be born. [1]

- **To Support The Region Development**

  The basic principle of region development issue the declaration that the arrangement of transportation network must take attention and support to the development of the region according with the concept and development planning of region space and it land use. With refer to Regency's RTRW (Indonesian: Recana Tata Ruang Wilayah, that mean is Regional Land Use Planning), the transportation network development will more clear, optimal and harmonic with the direction of future it regency land use and activity. The purpose of transportation network development planning is not allowed to make opposite with space and land use planning, and also it regency's economic characteristic. It must be in one must be consider geographical capacity limit. Geographical capacity limit act the role as

  coordinating view, legality, and also integrated with future ecological sustainability thinking. [2][3][4][5]

2. TRANSPORTATION SYSTEM PLANNING OF SUPIORI REGENCY

According to bacis principles above, the first and important step of transportation planning for Supiori Regency is to identify and state center points of regional planning. The analysis done for determine hierarchy pattern of activity system of those center points and derive it to identify support patern in the shape of transportation system configuration. In determination of activity centers, the main reference is strartegic policy of local government which is already state and legalited.

Due to basic thinking above, there is conclusion as follows:

1. Because of Supiori Regency's administrative area boundary is new transport boundary system which just begin to growth, the estimation of transport demand used the method of scenario.
2. The calculation of travel pattern base on origin-destination zone (according activity center as a center point of zone) inside the region.
3. Transport demand estimation calculated with use four step method. [6]
4. The meanning of transport demand estimation, in this case, is included the direction of above scenarios.

With refer to The RTRW of Supiori Regency that has established in It local government policy, the activity center point which in modelling act as the center point of zone an in model calculation mean as nodes, identify according to following Criterias :

A. Hierarchy of cities system which satated in RTRW
B. Transportation system policy stated in RTRW
C. Distribution of center of district
D. Distribution of recidence centers at recidenced islands outside main island of Supiori (Biak).
E. Already act as existing transportation nodes.

The result of analysis is as shown in Table 1. And the transport system component established in each nodes is identified as shown in Table 2.
Map of Supiori Regency is shown in figure 1.

Table 1
Transportation Nodes In Supiori Regency

Number	Nodes					
		A	B	C	D	E
1	Sorendiweri	O	O	O		O
2	Korido	O	O	O		O
3	Sabar Meokre	O	O	O		O
4	Yenggarbun		O			O
5	Sowek	O	O	O		
6	Rani				O	
7	Aruri				O	
8	Mapia				O	
9	Befondi	O		O	O	

Table 2
Transportation Fasility Components At Each Nodes

Number	Nodes	Surface Transportation Supporting Fasility	Crossing Over Transportation Supporting Fasility
1	Sorendiweri	Regency Terminal	Pier
2	Korido	District Terminal	Pier
3	Sabar Meokre	District Terminal	Pier
4	Yenggarbun	-	Pier
5	Sowek	District Terminal	Pier
6	Rani	-	Pier
7	Aruri	-	Pier
8	Mapia	-	Pier
9	Befondi	-	Pier

Source : Communication Office of Supiori Regency

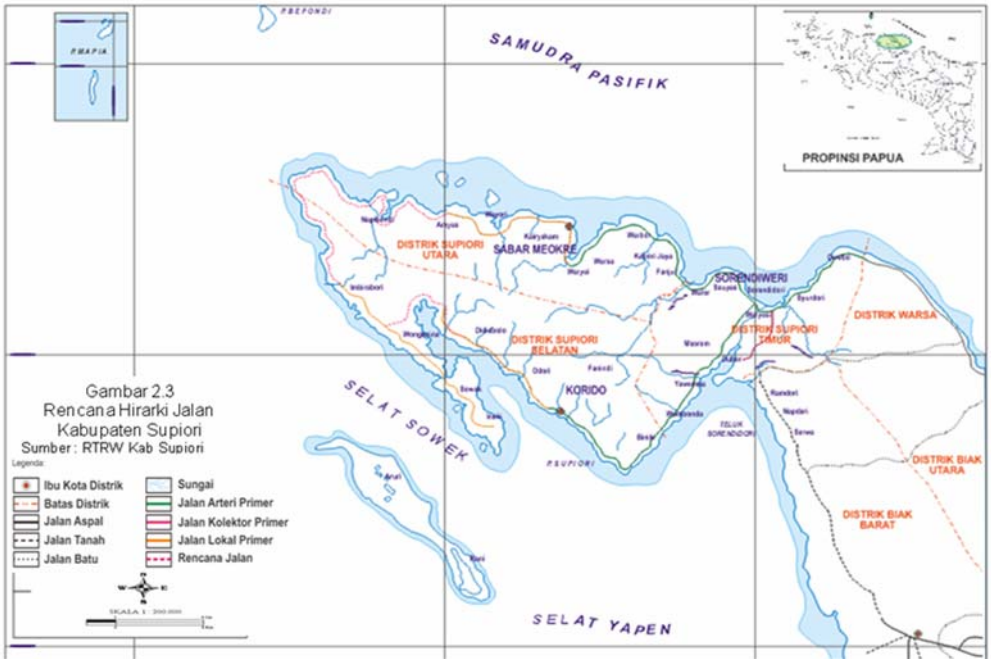

Figure 1 Map of Supiori Regency

2.1 Estimated Person Transport Demand of Supiori Regency

Calculation and analysis result from secondary data, which use atraction and production index, is derived numerical estimation of production and atraction of transport demand as described in Table 3. Accelerated with the recent policy that establised Supiori as a new regency, the amount of population increased and growth fast enought, as shown in Table 4. Population growth than adopted as the growth factor for production and atraction of person transport movement, this can be draw the estimating amount of transport demand in next the year of 2014, and 2024, as shown in Table 5 and Table 6, respectively.

This simple estimation give the description that transportation demand in Supiori Regency will be continuous increase in next 20 years until the year of 2024.

Table 3 Production and Attraction of People Movement in Supiori Regency 2009

Center of activity	District	Population	Family (Home)	Village	Index of Product	Index of Attraction	Production (People/day)	Attraction (People/day)
INTERNAL								
Sorendiweri	Supriori Timur	3918	845	10	0.17	0.52	654	440
Korido	Supriori Selatan	2589	533	7	0.17	0.21	432	551
Yenggarbun	Supriori Utara	1020	296	5	0.37	0.52	378	531
Sabarmiokre	Supriori Barat	1874	357	7	0.17	0.52	313	186
Sowek	Kep Aruri	4912	1046	9	0.17	0.52	820	545
Befondi	Kep Aruri						164	178
Mapia	Kep Aruri						163	155
Rani	Kep Aruri						159	189
Aruri	Kep Aruri						145	158
EXTERNAL:						TOTAL	3227	2932
Biak Numfor							557	581

Source:Analysis result

Table 4 Population Growth of Supiori Regency

Year	Population	Growth	i	i per year
2005	12201			
2006	12410	0.01713	1.71 %	
2007	14313	0.173101	17.31 %	8.66 %

Source : Center of Statistic Berau (Indonesia: Biro Pusat Statistik, BPS)

Table 5 Estimated Person Transport Demand of Supiori Regency In The Year of 2014

Activity Center	District	Production (person/day)	Attraction (person/day)
INTERNAL			
Sorendiweri	Supriori Timur	990	666
Korido	Supriori Selatan	654	654
Yenggarbun	Supriori Utara	573	804
Sabarmiokre	Supriori Barat	474	282
Sowek	Kep Aruri	1242	825
Befondi	Kep Aruri	248	270
Mapia	Kep Aruri	247	235
Rani	Kep Aruri	241	286
Aruri	Kep Aruri	220	239
EXTERNAL			
Biak		810	880

Source:Analysis result

Table 6 Estimated Person Transport Demand of Supiori Regency In The Year of 2024

Activity Center	District	Production (person/day)	Attraction (person/day)
INTERNAL			
Sorendiweri	Supriori Timur	2272	1529
Korido	Supriori Selatan	1502	1502
Yenggarbun	Supriori Utara	1314	1846
Sabarmiokre	Supriori Barat	1087	646
Sowek	Kep Aruri	2849	1893
Befondi	Kep Aruri	570	619
Mapia	Kep Aruri	567	539
Rani	Kep Aruri	553	657
Aruri	Kep Aruri	504	549
EXTERNAL			
Biak		1858	2019

Source:Analysis result

2.2 Estimated Freight Transport of Supiori Regency

In this case the estimation of freight movement inside and outside of Supiori Regency is base on daily basic freight demand of population. The standar for this have issued by Ministry of Communication of Republic of Indonesia, as describe in Table 7. From Table 7 can be determine basic consumption demand of population for each district. Freight transport demand estimation calculating result in the form of freight production-atraction for future until the year of 2014, 2019, and 2024, is shown in Table 8, Table 9, Table 10, respectively. Also in these table stated the demand of freight vehicles in according with 12 ton capacity of trucks. The growth of freight transport demand in future will attend to the demand of higher capacity of trucks.

Table 7 Standard of Consumption per capita per year

No	**commodity**	**Consumption/person/year (kg)**
1	Beras	145,47
2	Gula	14,04
3	Garam	7,88
4	Tepung	7,39

Source: Ministry of Communication Republic of Indonesia

Table 8

Freight Production-Attraction until the Year of 2014

Production Growth Coefficient = 1.03
Dependency Decreasing Coefficient = 0.9

Activity Center	District	Production (Ton/year)	Attraction (Ton/year)	Truck 12 ton cap.	
				Production	Attraction
INTERNAL					
Sorendiweri	Supriori Timur	1665.01	933.57	140	78
Korido	Supriori Selatan	1810.52	616.90	152	51
Yenggarbun	Supriori Utara	768.11	243.04	65	20
Sabarmiokre	Supriori Barat	1316.64	446.53	111	37
Sowek	Kep Aruri	395.58	1170.42	34	98
Befondi	Kep Aruri	79.12	382.59	8	32
Mapia	Kep Aruri	78.67	333.16	8	28
Rani	Kep Aruri	76.74	406.23	7	34
Aruri	Kep Aruri	69.98	339.60	7	28
EXTERNAL	Total	6260	4872	531	406
Biak		2923	3756	244	314

Source:Analysis result

Table 9

Freight Production-Attraction until the Year of 2019

Production Growth Coefficient = 1.03
Dependency Decreasing Coefficient = 0.9

Activity Center	District	Production (Ton/year)	Attraction (Ton/year)	Truck 12 ton cap.	
				Production	Attraction
INTERNAL					
Sorendiweri	Supriori Timur	2597.79	2545.47	217	212
Korido	Supriori Selatan	2824.81	934.47	236	78
Yenggarbun	Supriori Utara	1198.43	368.16	101	31
Sabarmiokre	Supriori Barat	2054.24	676.40	172	56
Sowek	Kep Aruri	617.20	1772.92	52	148
Befondi	Kep Aruri	123.44	579.54	11	48
Mapia	Kep Aruri	122.74	504.66	11	42
Rani	Kep Aruri	119.73	615.35	11	51
Aruri	Kep Aruri	109.19	514.42	10	43
EXTERNAL	Total	9768	8511	823	709
Biak		3405	2930	284	245

Source:Analysis result

Table 10
Freight Production-Attraction until the Year of 2024

Production Growth Coefficient = 1.03
Dependency Decreasing Coefficient = 0.8

Activity Center	District	Production (Ton/year)	Attraction (Ton/year)	Truck 12 ton cap.	
				Production	Attraction
INTERNAL					
Sorendiweri	Supriori Timur	4053.12	9253.97	339	771
Korido	Supriori Selatan	4407.33	1132.41	368	94
Yenggarbun	Supriori Utara	1869.81	446.14	157	37
Sabarmiokre	Supriori Barat	3205.07	819.67	268	68
Sowek	Kep Aruri	962.96	2148.46	81	179
Befondi	Kep Aruri	192.59	702.30	17	59
Mapia	Kep Aruri	191.51	611.55	17	51
Rani	Kep Aruri	186.81	745.70	17	62
Aruri	Kep Aruri	170.36	623.39	15	52
EXTERNAL	Total	15240	16484	1270	1374
Biak		5769	4572	481	382

Source:Analysis result

2.3 Transportation Development Program of Supiori Regency

The development program stated for Supiori Regency in order to anticipate it transport demand above is included surface transport and water (sea) transport. For surface transport the main program is develope the new road on west area of Biak Island, in order to make out island link road.
Freight transport growth in another side need to be anticipate, if the estimating amount of freight calculated above is happend in future, of course the exsisting bridges that recent planted in Supiori Regency all must be replaced by steel or concrete bridges, which will stronger enought to use by heavy trucks.
Another program besides surface transport development is port development at Marsram Village, East Supiori Distric. For Air transport the important program is take place in surface transport that is the demand in improving the road to be use from all districts inside Supiori Regency to be arrived in Biak Airport in time, according with flying schedule.
The piers or traditional little port need to be developed at each separated island (Mapia, Aruri, Rani, Befondi, and Sowek) in order to establish an easy communication with main land of Supiori Regency area, or the western side of Biak Island.

3. DISCUSSION

The important think to discuss in this paper is according to the special characteristic of Supiori Regency in case of that this regency is growth from conservation forest. Until the research of this topic held in the field, there is still the strictly rule that must be keep, about the boundary line of conservation forest in Supiori Regency. The discussion is have done too with RTRW planner team, and the commitment is make the development planning of this regency with still keep the boundary of conservation forest. So the future development area of regency capital city of Soriwendari is made in the shape of long line to southest direction, out side and following the shape of conservation forest boundary land.

Some key developments in reaching target audiences are now pinpointed because of their potential importance for the field and for transportation. Then a diverse set of threads, “catalyzing a future,” are identified which show promise for energizing the field of road ecology, as well as noticeably improving both surface transportation and nature on the land around us [7]. The quality targets are the starting point when the desirable long-term state of the existing road network is formulated for important natural and cultural heritage assets [8]. The relation between new road development even can be integrated with more details conservation program [9] [10]. New road projects are not only aimed at alleviating congestion created by the growing population pressures, but are concurrently viewed in relation to the natural landscape. As future roadway alignments are considered, planners and designers are using the environmental landscape as a tool to design sustainable roadway projects in an effort to preserve a healthy interconnected landscape for future generations. [11]

4. CONCLUSSIONS

There are 3 conclusion come from this study, as follows:

1) Transport demand of Supiori Regency is still low.
2) The development of transportation network in Supiori Regency, Biak Island is necessary to anticipate the population and economic growth till meet the optimum equilibrium between population-economic activity-ecology.
3) Out line island ring road development at western of Biak Island, still need to make the back up transportation facilities beside water (sea) transportation that can be used 24 hours per days along the year, and not depend on the seasons. Is this case boat transportation not always available if the sea wave is too high.
4) New link road that across in direction of south-north in the middle of Supiori Regency is not allowable, because this can be destroy the conservation forest. Also in the same time, as have studied from topography data, it is not technically feasible too.

REFERENCES

[1]. Soemarwoto, Otto, 1997, *Ekologi, Lingkungan Hidup, Dan Pembangunan*, Penerbit Djambatan.
[2]. Jayadinata, Johara T., 1992, *Tata Guna Tanah Dalam Perencanaan Pedesaan Perkotaan dan Wilayah*, Penerbit ITB Bandung.
[3]. Vasconcellos, Eduardo, 2001, *Urban Transport, Environment, and Equity*, Earth Scan, London and Sterling VA.
[4]. Winarso, Haryo; Pradono; Zulkaidi, Denny; Miharja, Miming, 2002, *Pemikiran dan Praktek Perencanaan Dalam Era Transformasi di Indonesia*, Departemen Teknik Planologi Institut Teknologi Bandung, Yayasan Sugianto Soegijoko.
[5]. Nurzaman, Siti Sutriah, 2002, *Perencanaan wilayah di Indonesia pada masa sekitar krisis*, Penerbit ITB, Bandung.
[6]. Tamin, O.Z.(2008), *Perencanaan, Pemodelan, & Rekayasa Transportasi,Teori, Contoh Soal, dan Aplikasi*, Penerbit ITB, Bandung.
[7]. Forman, Richard T. T., 2003,"Road Ecology: A Look Behind The Book and The Field", *Proceedings of International Conference of Ecology and Transportation (ICOET)*, Lake Pacid- New York
[8]. Nilsson, Lars, 2003, "Targets and Measures For Consideration of Natural And Cultural Heritage Assets In The Transport System", *Proceedings of International Conference of Ecology and Transportation (ICOET)*, Lake Pacid- New York
[9]. DiGregoria, John, 2005, "Integration Transportation Conservation with Regional Conservation Planning", *Proceedings of International Conference of Ecology and Transportation (ICOET)*, San Diego
[10]. Austin, John M.; Viani, Kevin; Hammond, Forrest; Slesar, Chris, 2005, "A GIS Based of Potentially Significant Wildlife Habitats Associated With Roads in Vermont", *Proceedings of International Conference of Ecology and Transportation (ICOET)*, San Diego
[11]. Burn, Joseph, 2007, "Application of Ecological Assessments to Regional and Statewide Transportation Planning", *Proceedings of International Conference of Ecology and Transportation (ICOET)*, Little Rock-Arkansas

.

PERCEPTION OF URBAN COMMUNITY CONCERNING THE EXISTENCE AND PERFORMANCE OF PUBLIC OPENSPACES

Reny Syafriny[1] ,Cynthia Wuisang[2], Sangkertadi[3]

[1,2]Laboratory of Housing & Human Settlement,
Faculty of Engineering, Sam Ratulangi University
Manado – 95115 , Indonesia
Tel : (0431) 852959 Fax : (0431) 854511
Email : renysy@yahoo.com , cynthiawuisang@gmail.com

[3]Laboratory of Science & Technology,
Faculty of Engineering, Sam Ratulangi University
Manado – 95 115, Indonesia
Tel : (0431) 852959 Fax : (0431) 854511
Email : t_sangkertadi@yahoo.com

ABSTRACT

Urbanization process, especially population growth and construction development do not proportionally balance with public space provision for accomodate the community activities. This situation will subsequently lead to unsatisfactory condition of urban society. The objectives of this research are to describe various perception of people about the existence of public space available in town and to observe their behavioral pattern in using public area, which is later on able to contribute basic concept for developping the appropriate urban space design and management system. Three samples of public open spaces taken for the study are in Manado, Indonesia. This study focusses firstly on, how the existence of public space can function with the demand and expectation of people in town ; Secondly is, how far, the urban space design available has been able to accommodate all the public expectations. Method used in this research are interview, questionnaire, and behavioral mapping. The research findings, in general, show that there are negatives perceptions and complain concerning the design of public space and amenities. Meanwhile behavioral mapping conclude that some activities are taken in wrong places and some elements of public open spaces are properly unused and inattentive while some other are over capacity.

***Key words** : public openspace, urban space design, human perception, spatial behavior.*

1. INTRODUCTION

Urban regeneration and construction development tend to sacrify urban land areas which are formerly reserved for public facility including urban public openspace. Meanwhile public openspaces play important role for urban life, because it has social and psychological values to support daily activities for inhabitant.

Provision and management of public openspace recently do not reach the main problems yet, especially to give properly response against actual needs of the people who live in urban area.

Carr, 1992, finds that planning and designing public openspace must convey 3 values, those are :
1). Responsive , means it should respond the basic needs of users ; comfort, relaxation, engagement active/passive, and discovery.
2). Democratic , means freely accessible for all the people
3). Meaningful, means having strong relationship between users and its millieu .

Carr also define that good design of public openspace is when there is harmony between physical environment and social dimension, which can stimulate users activities, comfort, and encourage social relation among users.

Rishbeth, 2001, observed and remarked that certain etnisgroups living in the urban area, prefer to make their own public space in the neighbourhood openspace. It conclude that the existence of public openspace in the urban area raised on different perception of the respective users .

Some groups assume that the existence of public open space give positive contributions for their daily living, on the other hand, it often brings anxious, fears and other negative impact. Unpleasant things might happened in it. Furthermore, the relationship between users activities and setting system of an openspace will build specific behavior which are definitely different from one place to another.

2. OBJECTIVES

In general, this research try to expand theory and models of urban design setting in term of urban development and

management based on perceptions and behavior study of urban society as users. Whereas specifically the objectives of the research focused on two issues.
First issue is, to gather some information about human perception concerning openspace available in town and secondly is to develop behavior mapping method by doing Post Occupancy Evaluation (POE) on public openspace in Manado.

Furthermore, the research findings will be useful to develop theory and models of urban development and planning which may contribute to urban development evaluation and policy for Manado and other medium size cities.

Within the most of discussions about architecture, environment and behavior studies, terms of behavior setting was defined in 2 categories, that is system of setting and system of activity. Both are strongly related to compose behavior setting. (Haryadi and Setiawan, 1995). System of setting , also called system of place and space, represents a series of physical elements linked eachother and formed certain relation and can be functioned for certain activities. Meanwhile system of activity figure out a series of human behavior deliberately performed by people individually or in groups.

3. METODOLOGY

Methods used in this reseach are physical observation on the spot by recording the whole elements exist into worksheets, distribution the questionnaires, and interview some visitors. The application of behavioral mapping used place-centered mapping method. Physical observation method try to figure out performance of a place which will define the environmental quality of public space. Meanwhile questionnaires dan interviews with the visitors try to explore public opinion about the existence of the place.
Bevahior mapping is relatively new in urban planning and design approach. Yet, it still limited on several models explored by reseachers, and place-centered mapping is one of favourable model to figure on human behavior using its millieu.

3.1. Reseach Location

Research conducted in Manado, the capital city of North Sulawesi. It is a medium size city with population about 450 inhabitants. Manado is located in the coastal area, at the edge of Manado bay. For the last 10 years, construction development grew rapidly and changes happens in parts of the city.

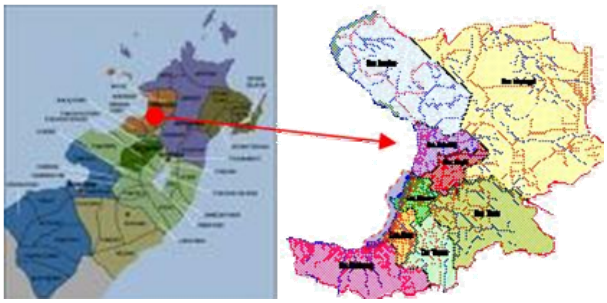

Figure 1 : Map of North Sulawesi & Manado City

3.2. Questionnaires

Substances of the questionnaires classified by :

- Participants personal background
- Various kind of activities and its frequency
- Impression and response about the situation.
- Public opinion concerning the performance.

Questionnaires were distributed proportionally depend on the capacity of 3 different object in Manado. Execution considered the intensity of people who participate and benefit the objects. Number of respondent was assumed 20% capacity of the millieu, so that composition of respondents are different in each objects. Operation took place on office hours and holiday.

3.3 Behavior Mapping

Behavior mapping is built based on the result of observation human activities, during a certain period which produce spatial activities pattern, restricted by some elements in the object.
This study proposed place-centered method from behavior mapping, for exploring which elements in the setting are dominantly give influence and support main activities.
Four steps of mappings are :

1. Prepare a worksheet as basic map by recording all physical elements presumed to stimulate some action in the setting.
2. Making a list of actions and decide the symbols for each activities .
3. In a certain time period, register the whole activities occurs using symbols on the worsheet prepared.
4. Transform whole information in the informative map.

4. FINDINGS AND DISCUSSION

4.1. Description of Research Objects

Research conducted at 3 main objects of public openspace in Manado, the capital city of North Sulawesi. There are Taman Kesatuan Bangsa (TKB), Sparta Tikala, and Bahu Mall. Those 3 public openspaces are the favourite place that people prefer to visit during their free time, mostly on the weekend.

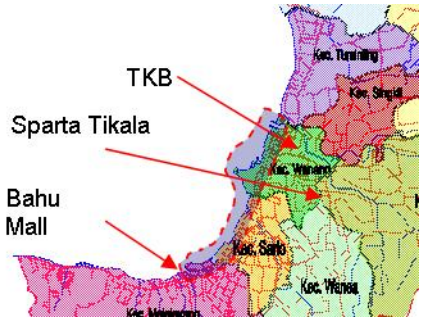

Figure 2 : Locations of Research Objects

a. Taman Kesatuan Bangsa (TKB)

TKB is an old square plaza on the Central Bisiness District area in Manado. Surrounded by commercial building, this square has historical background and become an important place because it has been designed since early period of urban growth. It has been renoved from times to times according to urban redevelopment process.

On the peak hours, this square is intensively occupied. Most of the visitors use the square as a pedestrian way to move from one side to another. Some others used as a resting area. There are some coffee shops on the site available for spending breaktimes. For the last few years , local authority has built an open theatre in the square for making this square more attractive. On the evening hours, the place become so quiet because all the stores adjecent were closed, and no activities around.

Extension of central commercial modern towards the seaside area had slowly removed economic activities and reduced density of this area.

Figure 3 : TKB and it's surroundings

b. Lapangan Spata Tikala

Sparta Tikala is a formal openspace, a small park with grass and trees, created in front of local government official buildings. It has jogging track and benches insides. There are different elements and functions on the site. People use the park for playing or doing some exercises, rendez-vous, ceremony, or other social affairs. Sometimes they use for exhibition and promotion affairs.

During the day, this place is relatively quiet. On the north and south sides, outside the park, there are pedestrian ways with benches and big trees that formed comfortable space for shading.

Although the park has lower density of usage, the existence of place give particular impression for the citizens.

Figure 4 : Lapangan Sparta Tikala

c.Bahu Mall Seaside Area

Another kind of openspace in the city is coastal zones that exist along 20 kms of Manado coastal lines. One of the most successful design for public openspace is Bahu Mall recreation center. People of Manado enjoy much having meal in many circumstances, particularly during recreation time. This social phenomenon lead the authority provides many cafetaria in the recreation center like Bahu Mall seaside area.

Conception of the reclamation area in coastal zones is multifunction area consist of recreation, commercial and sporting facilities. Morning hours, people do some exercises regularly, and during the day, commercial and cafetaria predominant the whole area. In the afternoon, teenagers occupied some interesting spot area just to chat or relaxation. They enjoy the beatiful scenery of the sun goes down to the earth, and it is the best moment in this .

On Sunday morning or holidays, the place is more crowded because some people from the region come to visit the area.

Figure 5 : Bahu Mall seaside area

Table 1
Existing Condition at 3 objects

Situation	TKB (1)	TIKALA (2)	BAHU MAL (3)
Spatial Shapes	Square 74 x 33 m	Trapesium 105 x 93 m	Square 62 x187m
Access	2 entrance gates on east and west sides	Main entrance at the east and west sides.	Main entraces from south dan east sides
Border lines	Fences and trotoir arround and shopping arena in north and westsides	Streets arround with high traffic density	Coastal line in northwest , street and parking area and commercial buildings surrounding.
Dimension of space	2442 m2	9765 m2	11594 m2
Materials used	beton floor with decorative garden	Grass court in the middle, surrounding by pedestrian /beton and decorative garden	Asphalt and ground covered
Height	30 cm from street level	10 - 20 cm from street level	100 - 120 cm from sea level

4. 2 Spatial Behavior of Urban Community

Behavior setting as design approach simply define as interaction between human action and its millieu or surrounding matters. Thus, behavior setting consists a group of people doing some actions or activities, taking place in a particular spaces, spending duration and in the restricted conditions .
Behavior mapping in public openspace could be applied by observing every movement produced periodically and drawing it into a sketch of maps.
The research observed 3 different locations in Manado and conducted at 3 different occasions; early in morning hours (06.00 – 10.00) , at noon (12.00-14.00) , and in the afternoon (16.00-18.00) Those were conducted on working days and holidays.

Table 2
Examples of Behaviour Mapping Process at Taman Kesatuan Bangsa (TKB)

System of Activity	Location : TKB Time :	Behavior Mapping
1.Standing in group and talking		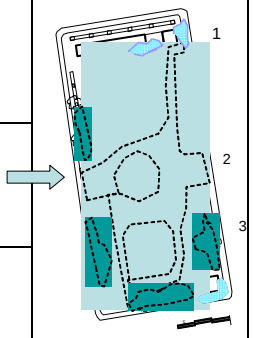
2. Walking/ Passing Through		
3. Sitting, talking, eating	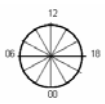	

The result indicates that people used public openspace only for passive activities, and follows setting available. Eventually some elements are ignored and unused like some benches at Tikala, and open theatre at TKB.

Figure 6 : community behavior in openspace of Manado

Urban Community in Manado generally use the openspace available for leisure or doing some exercises in the morning. For particular groups, especially teenagers, the needs of public space is important for social activities or special ocassion like playing and friendship gathering. For new couple, the existence of public openspace is necessary for doing some sport or playing with children and other family.

Obviously, the importance of openspace is to refresh urban air quality, however it has to be taking into account its social aspect for accomodate the needs of expression and education for urban community.

Constructions of behavior mapping on 3 locations as case studies, there are some different pattern in using the place.

Tabel 3
Users activities in Public Openspace

DIFFERENT AGE GROUPS	Spatial Function		
	TKB	SPARTA TIKALA	BAHU MAL
Teenagers (15 – 21)	Walking/ Passing through Sitting/eating	Sitting , talking Excescise/ sport	Walking Sitting. talking Sport /games
Adult (21 – 45)	Walking/Passing through Sitting/take rest Standing/Talking	Sitting, talking Sport activity	Walking Sport Sitting/talking
Elders (>45)	Sitting	Sitting	Sitting Walking

4.3 Openspace Performance

Space performance in architecture, either indoor or outdoor, determined by seveval things. In case of outdoors, it could be designed by provision supporting elements likes trees, sculpture, pond, or benches. All these elements should be well interpreted by individual senses. Exploration about human perception against space performance examines how far the combination elements enable to stimulate the positive feelings of human being.

Community perception about existence of pulic openspace in Manado generate some understanding about the needs and types of openspace suitable for their habitual life. 180 participants have been involved with the interviews and questionnaires. They were grouped on 3 catagories :
teenagers (15 – 19 years old) – 63 participants
adult (20 – 45 years old) – 101 participants
and elders (> 45 years old) - 16 participants
Percerption of openspace is represented by components : Personal interest, spatial impression and importance of spatial equipments.

Table 4 shows that some element of openspace have been perceived differently by each groups.

Table 4
Users Perceptions of 3 locations based on different age groups

Perception Variable	Components	% of each groups		
		(15-19)	(20-45)	(> 45)
Personal Interest	Atmosphere	49	22	44
	Accessibility	21	29	44
	Supporting Facility	27	29	13
Spatial Impression	Temperature	38	43	31
	Cleanliness	33	39	63
	Safety	13	10	0
Importance of equipments	Lights	10	14	13
	Benches	24	12	0
	Public telephone	25	29	13
	Waste disposal	43	27	38
	Shelter	29	42	19

Personal Interest

First group is interested in atmosphere of the object. They think nuance is important things in the object (49 %), and so the third group. They marked that ambience can influence the attractiveness of a place. It shows that teenagers and elders need more atmosphere in the openspace to support their activities outdoors. Furthermore, teenagers need more dynamics, colorful and pleasant space, while the elders prefer peaceful and comfortable place. Second group (20 – 45 years old), in fact, do not even care about the atmosphere as long as they could easily do their activities like sports and playing.
Table 4 also shows that only third groups pay more attention about accesibility (44%). It it obvious that elders have handycap in mobility compared to others.

All respondents perceived that supporting facility of public openspace has no relationship with attractiveness of a public openspace. Therefore, supporting facilities are not the reason why they visit a public openspace.

In such a case, human interest, especially teenagers group against space performance is when the openspace offers ambience which can support their outdoor activity. Whereas the elders prefer openspace completed with atmosphere and good accesibility.

Spatial Impression

. Most of the respondent felt inconvenient being in the objects because it is hot and dirty. Although there are some trees for shading, they do not fucnctioned well to reduce temperature. Local authority has provided some waste disposal box in each corner, but trash and wastepapers are scattered around.

63% of the elders complain that objects are very unclean. It indicates that elders is more concern about cleanliness compare to other groups. In the future, local government should pay more attention concerning shading and cleanliness of parks and squares in town.

4.3.3 Urban Amenities & Equipments

Benches, Shelters, garbage trays, telephone box, light fixtures are some equipment needed for outdoor activities. Their existences will support various activities outdoors .
Most of the teenagers and the elders proposed improvement of waste disposal system of public openspace. While the young couples concern about shading and shelter. (42%)

5. CONCLUSION AND RECOMMENDATION

Spatial behavior of urban community in Manado depends on system of setting available. Limitation of its usage caused by its design of elements. Lacks of shading area caused people could not enjoy the scenery of sunset. Limitation of number and various activities are caused by spatial condition which could not represent the real need of users. Some activities are taken in wrong places like playing on the parking area. Some elements of public open spaces are properly unused and inattentive while some other are over capacity, like pedestrian and paving for doing exercises.

In case of 3 objects observed, spatial design and supporting facilities could influence human behavior in two ways, it means , if design product could be perceived well, there will be positive behavior of users. On the contrary, if it was perceived negatively, there will be negative reaction of users. Spatial quality of public openspace depends on elements offered in respective area. In such cases, 3 object observed have many aspects ignored that generate negative impression from users. Negative impression concerning architectural design is, complain about microclimate and maintainance/ cleanliness.

Application of behavior mapping combined with interview about spatial impression supposed to be representation of real needs of existences of public space in Manado. It should be concidered by designers and policy makers to make a decision for urban change.

Behavior mapping method has been used for building design evaluation, and it is important to expand the application for outdoor facilities, especially for public facilities. Public space design should consider interaction between users and its millieu, so that it will help to stimulate positive behavior of the users.

REFERENCES

[1] Haryadi dan Setiawan, *"Arsitektur Lingkungan dan Perilaku : Teori, Metodologi dan Aplikasi"*, 1995, Proyek Peningkatan Pusat Studi Lingkungan Hidup, Dirjen Dikti Depdikbud.

[2] Poluan S J, Syafriny R, , *"Kualitas Ruang Terbuka di Manado, Studi Kasus di Beberapa Kompleks Kampus dan Sekolah Menengah Umum"*, 1999, Laporan Penelitian DIK – Lembaga Penelitian Unsrat, Manado.

[3] Rahmi, Wibisono H. Bambang and Setiawan B.*"Rukun and Gotong Royong: Managing Public Places in an Indonesian Kampung"*. Public Places in Asia Pacific Cities : Current Issues and Strategies. *The Geo-Journal Library*. Dordrecht/Boston/London: Kluwer Academic Publisher. 2001. Volume 60

[4] Rappoport, A, "*Human Aspects of Urban Form*", Pergamon Press, 1977.Oxford.

[5] Setiawan, *"Pengembangan Pertanian Perkotaan untuk Meningkatkan Produktivitas Lingkungan Perkotaan perkotaan dan Menuju Kota yang Berkelanjutan"*, Jurnal Manusia dan Lingkungan, 2000, PSLH,UGM Vol VII no.2..

[6] Setiawan, B. (A), *"Integrating Environmental Goals into Urban Redevelopment Schemes: Lessons from the Code River, Yogyakarta"* . Jurnal Water Science & Tecnology. IWA Publishing and the Authors, 2002, Vol 45 No 11 pp 71-76.

[7] Sommer, R, dan Sommer, B., *"Behavioral Mapping: A Practical Guide to Behavioural Research"*, Oxford University Press. 1980 New York.

[8] Syafriny R, Sangkertadi, , *"Kajian Kenyamanan Termal Pada Pengguna Pedestrian di Ruang Publik Pusat Kota Manado"*, 1998 [unpublished] Laporan Penelitian DIK – Lembaga Penelitian Unsrat

[9] Syafriny R, Sangkertadi, *"Pengaruh Naungan Pada Pedestrian Terhadap Kenyamanan Termis Pejalan kaki di Pusat Kota Manado*". Journal of Research & Development Lembaga Penelitian Unsrat, 1999, Manado,

ISSN 114-1284

FAILURE ANALYSIS OF NYLON MESH AS BEAM CONFINEMENT BASED ON FRACTURE MECHANICS APPROACH

Rr. M.I. Retno Susilorini[1]

[1]*Department of Civil Engineering*
Faculty of Engineering
Soegijapranata Catholic University
Tel : (024)844155 hunting Fax : (024)8445265
E-mail : retno_susilorini@yahoo.com; susilorini@unika.ac.id

ABSTRACT

Nylon mesh has been proven to give higher ductility for beam compared to unconfined one. This research takes a fracture based approach as failure analysis because fracture mechanics has become a solution to prohibit a catastrophic failure of structure. This research refers to previous experiment data. The data is analyzed further in this paper by analytical method. The experiment method was run by third point flexural test of specimens. The specimens consisted of four concrete beams with dimension of 15x20x600 mm, two beams were confined with nylon mesh and two other beams were unconfined. The concrete beams were designed with compressive strength f'_c about 30 MPa. The analytical method calculates longitudinal and transversal strain and also determines a fracture parameter, it is stable crack length. The research meets conclusions that: (a) transversal strain of confined beams is higher compared to unconfined ones; (b) the deformation of nylon mesh is going to achieve stable crack until it is failure; (c) failure analysis shows that those values of transversal strain of specimens (0.12-0.13) mentioned in Table 1 are laid on stage of transition; and (d) the previous model fit to the experiment results, that the stable crack length achieved for specimens is about 36-40 mm.

Keywords
Failure, nylon, confinement, beam, fracture

1. INTRODUCTION

The confinement takes an important role in improving beam's ductility. Nylon mesh has been proven to give higher ductility for beam compared to unconfined one. Previous research reported by ([1],[2]) noticed that nylon has great value of tension strength and elongation. Nylon also has unique characteristic of 'yield point elongation' which provides optimal stable crack length when it is embedded in cementitious matrix.

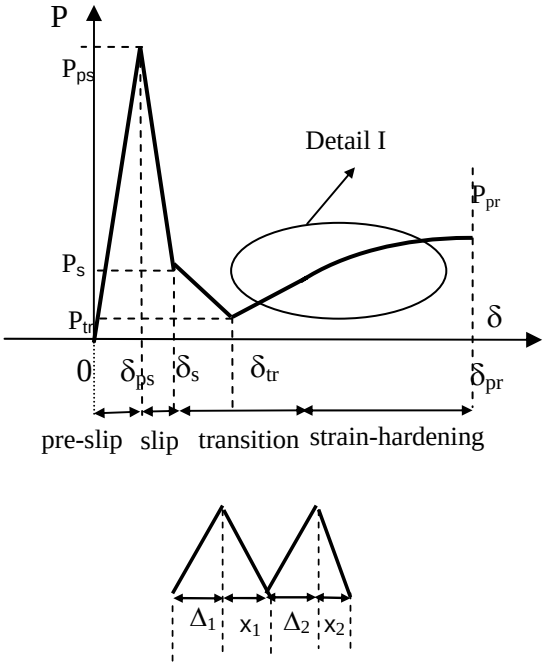

Detail I

Figure 1 : Relation of load-displacement of fractured pullout
([1],[2])

Recall [1],[2]. The model of fractured pullout ([1],[2]) is formulated by equation (1) and result a P-δ (load-displacement) curve (Figure 1). The curve consists of 4 (three) stages: (a) Stage of pre-

ISSN 114-1284

slip, (2) Stage of slip, (3) Stage of transition, and (4) Stage of strain-hardening.

$$P_n = \left(r_{\Delta I}\frac{a_1}{a_2}E_{ps}A\right)+\left(r_{\Delta II}\frac{a_1}{a_2}E_sA\right)+\left(r_{\Delta III}\frac{a_1}{a_2}E_{tr}A\right)+\left(r_{\Delta III}\frac{a_1}{a_2}E_{pr}A\right) \quad (1)$$

Where:

P_n = load (N)
A = fiber section area (mm^2)
E_{pr} = modulus of elasticity at stage of strain-hardening (MPa)
E_{ps} = modulus of elasticity at stage of pre-slip (MPa)
E_s = modulus of elasticity at stage of slip (MPa)
E_{tr} = modulus of elasticity at stage of transition (MPa)
a_1 = total displacement of a stage (mm)
a_2 = initial length of specimen or fiber that is specific for every stage (mm)
$r_{\Delta I}$ = ratio of total free-end fiber displacement of free-end at stage of pre-slip
$r_{\Delta II}$ = ratio of total free-end fiber displacement of free-end at stage of slip
$r_{\Delta III}$ = ratio of total free-end fiber displacement of free-end at stage of strain-hardening

The fracture phenomenon happened during pullout process can be explained as follow ([1],[2]). During the stage of pre-slip, the fiber is fully embedded in cementitious matrix, thus the fracture process phenomenon has not already happened yet. After critical matrix stress $\overline{\sigma}_m$ exceeded, a crack is created and the stage of slip and unstable fracture process begin. The normal fracture generated instantaneously and then followed by lateral fracture after the separation of specimen. Hence, the unstable fracture process change into stable fracture process when the stable crack length reached at the end of slip stage or transition stage. The stable fracture process will initiate the stage of strain-hardening with 'jagged' phenomenon. During the stage of strain-hardening, the increase of strain ε will increase the stress σ along the fiber until the fiber gets broken.

The theoretical modeling of fractured pull-out is covering all the phenomenon exists during the experimental test. The phenomenon is captured as fracture phenomenon, hence, the unstable crack will always exist ([1],[2]). This unstable crack will change to be stable crack only if the crack arrester is emerged.

Stable crack length of fractured pullout ([1],[2]) defined as follow.

$$l_2 = \frac{0.5c}{\overline{\varepsilon}} \quad (2)$$

Where:

l_2 = stable crack length (mm)
c = crack width (mm)
$\overline{\varepsilon}$ = critical fiber strain

Transversal strain can be expressed by

$$\varepsilon_{tr} = \frac{(h+\delta)-h}{h} \quad (3)$$

Where:

ε_{tr} = transversal strain
h = height of beam (mm)
δ = deflection of beam (mm)

Longitudinal strain can be expressed by

$$\varepsilon_l = -\kappa\delta \quad (4)$$

Where:

ε_l = longitudinal strain
κ = curvature of beam (mm^{-1})
δ = deflection of beam (mm)

While the curvature of ductility [4] is expressed by equation (5) as follow.

$$\kappa = \frac{1}{\rho} = \frac{M}{EI} \quad (5)$$

Where:

κ = curvature of beam (mm^{-1})
ρ = the radius of curvature at a specific point on elastic curve (mm)
M = internal moment (Nmm)
E = material's modulus of elasticity (MPa)
I = beam's moment of inertia computed about the neutral axis (mm^4)

The mechanism of confining effect [7] can be explained as follow. Transversal reinforcement is lightly stressed at lower compressive stress, hence, the concrete is not influenced by the

reinforcement. When ultimate stress is almost reached, the transversal strain of concrete is rapidly increasing, that is caused by crack propagation. Therefore, concrete will expand and compress the transversal reinforcement. If compressive area is confined by closed transversal reinforcement such as hoops, ties, or spiral reinforcement, then the ductility of beam will be increased very fast. Later, the beam performance is more ductile in ultimate stage.

Several previous researches noticed about the importance of confinement for raising higher performance of beam with various media such as meshes, sheets, jackets, etc, but no research try to use nylon mesh to confine the beams but This research referred to previous experiment data ([3]-[6]). The data is analyzed further in this paper by analytical method. The previous research shows good performance of confined beams with nylon mesh This research referred to previous experiment data ([3]-[6]). The data is analyzed further in this paper by analytical method. Hence, it is interesting to investigate further the failure of nylon mesh as beam confinement by fracture mechanics approach.

The fracture mechanics approach has been implemented in many concrete structure failure analyses ([8]-[22]). According to [21], the problem of strain-softening and strain-hardening is engaged to crack distribution. This crack distribution takes a role as a trigger of structure failure because of the improvement of localized crack to be fracture. The suppression of concrete fracture can be implemented by increasing the toughness and tension ductility [22].

The fracture mechanics analysis is also applied to pull-out problem that is closely tight to bond mechanism and interface characteristic of fiber-cementitious matrix. [23] explains that interface bond becomes a significant factor in improving the performance of fiber cementitious composites. Hence, the behaviour of bond between fiber and cementitious matrix can be characterized by pull-out test. The result of pull-out test is giving descriptions of whole composites, selecting the main ingredient of composites, and predicting the structure failure of composites [24].

This research takes a fracture based approach as failure analysis of unconfined and confined beams of previous research ([3]-[6]). It is necessary to conduct fractured based failure analysis because fracture mechanics has become a solution to prohibit a catastrophic failure of structure. By using fracture mechanics, the design is going to achieve more safety margin for structure and higher economic value as well as structural benefit.

2. METHODS

This research refers to previous experiment data ([3]-[6]). The data is analyzed further in this paper by analytical method. The experiment method of previous research ([3]-[6]) was run by third point flexural test of specimens. The specimens consisted of four concrete beams with dimension of 15x20x600 mm, two beams were confined with nylon mesh and two other beams were unconfined ([3]-[6]). The concrete beams were designed with compressive strength f'_c about 30 MPa. The analytical method calculates longitudinal and transversal strain and also determines a fracture parameter, it is stable crack length.

Nylon mesh dimension ([3]-[6]) described by Figure 2. The confined specimen is described by Figure 3 ([3]-[6]), while the setting of third point flexural test is described by Figure 4 ([6]).

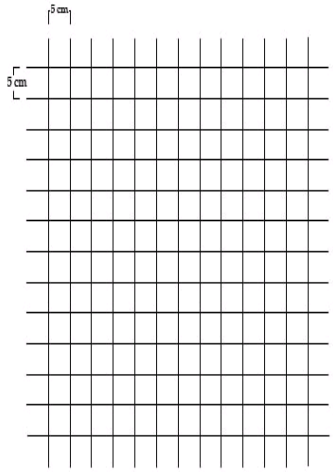

Figure 2 : Dimension of nylon mesh ([3]-[6])

Figure 3 : Specimen with nylon mesh confinement
([3]-[6])

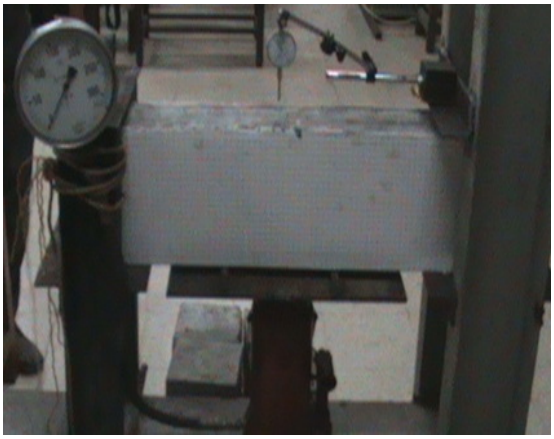

Figure 4 : Third point flexural test setting
([3]-[6])

3. RESULTS AND DISCUSSION

Previous research ([3]-[6]) show (Figure 5) that the ultimate load of confined beams increase about 30-40% (1489,6 N, 1421 N) compared to the unconfined ones while its displacement also increase about 40-70% (24 mm, 26,7 mm). It is proved that the increase of displacement emphasizes that the ductility of beams also increases at ultimate load until beams collapse.

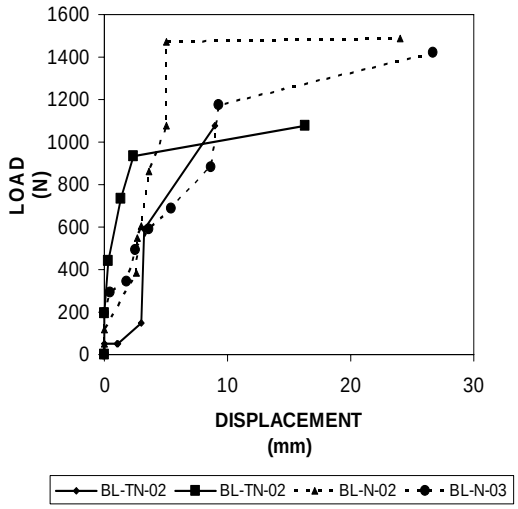

Figure 5 : Load-Displacement Relationship during the Loading History
([3]-[6])

The strain of confined and unconfined beams is shown by Table 1. Table 1 shows that transversal strain of confined beams is higher compared to unconfined ones. Transversal strain for unconfined beams (BL-TN-02 and 03) is about 0.04-0.08, while for confined beams (BL-N-02 and 03) is about 0.12-0.13. Longitudinal strain unconfined beams is about 0.00000042-0.00000077, while for confined beams is about 0.0000015-0.0000016.

Table 1 : Strain of confined and unconfined beams

SPECIMEN CODE	LONGITUDINAL STRAIN	TRANSVERSAL STRAIN
BL-TN-02	-0,0000004275	0,045
BL-TN-03	-0,0000007743	0,0815
BL-N-02	-0,0000015744	0,12
BL-N-03	-0,0000016714	0,1335

Table 2 : Stable crack length of confined beams

SPECIMEN CODE	STABLE CRACK LENGTH (mm)
BL-N-02	41,67
BL-N-03	37,45

According to ([1],[2]), the nylon itself has maximum strain of about 1.1. Stable crack length of confined beams based on Equation 2 is about 37-41 mm and described more clearly in Table 2.

Previous model of ([1],[2]) that is fractured pullout with full embedded nylon fiber l_f = 100 mm (that means it the specimen has 50 mm each part) conveys strain of 0.04966-0.342 for its stage of transition. Hence, failure analysis shows that those values of transversal strain of specimens (0.12-0.13) mentioned in Table 1 are laid on stage of transition. It could be said that whenever transversal strain achieved, stable crack length occured. Stable crack length of previous model is 36.44 mm while the confined beams are about 37-41 mm. Hence, the previous model fit to the experiment results, that the stable crack length achieved is about 36-40 mm.

4. CONCLUSIONS

The research meets conclusions that:

a) transversal strain of confined beams is higher compared to unconfined ones;
b) the deformation of nylon mesh is going to achieve stable crack until it is failure;
c) failure analysis shows that those values of transversal strain of specimens (0.12-0.13) mentioned in Table 1 are laid on stage of transition;
d) the previous model fit to the experiment results, that the stable crack length achieved for specimens is about 36-40 mm.

REFERENCES

[1] Susilorini, Retno, M.I., *Model Masalah Cabut-Serat Nylon 600 Tertanam dalam Matriks Sementitis yang Mengalami Fraktur*, Dissertation, Unika Parahyangan, Bandung, 2007.

[2] Susilorini, Retno, Rr. M.I., *Pemodelan Cabut-Serat Berbasis Fraktur*, Unika Soegijapranata Press, 2009.

[3] Susilorini, Retno, Rr. M.I., Setyanegara, E., dan Adhitya S, S., "The Advantage of Nylon Mesh for Beam Confinement - Smart material for beam repair", Proceeding of First International Conference on Rehabilitation and Maintenance in Civil Engineering (ICRMCE), Solo, 21-22 March, Universitas Sebelas Maret, pp. 208-212, 2009.

[4] Susilorini, Retno, M.I. Rr.,. "'Green' Technology to Enhance the Ductility of Concrete Beam - The Advantage of Nylon Mesh Confinement", Proceeding of Second Annual International Conference Green Technology and Engineering, 15-17 April, Universitas Malahayati, Lampung, pp. 96-9, 2009.

[5] Susilorini, Retno, M.I. Rr., 'A Miracle' of nylon Mesh Confinement, Penerbit Unika Soegijapranata, Semarang, 2009.

[6] Setyanegara, E. dan Adhitya S, S. *Kinerja Kuat Lentur pada Balok Beton* dengan Pengekangan Jaring-Jaring Nylon, Tugas Akhir, Program Studi Teknik Sipil, Unika Soegijapranata, Semarang, 2008..

[7] Park, R., and Paulay, T., *Reinforced Concrete Structure*, John Wiley & Sons Inc., New York, 1975.

[8] Susilorini, Retno, Rr. M.I., "Fractured Based Approach for Structural Element Design – Safe Building, Safe City", Proceeding Third International Conference on Economic and Urban Management "City Marketing, Heritage, and Identity", PMLP Unika Soegijapranata, Semarang, pp. 451-465, 2007.

[9] Susilorini, Retno, Rr. M.I., "Integral-J Kritis untuk Model Elemen Hingga pada Cabut Serat Fraktur Nylon 600", Tiga Roda Forum "Perkembangan Terkini Teknologi dan Rekayasa Konstruksi Beton di Indonesia", 12 Desember, Hotel Bumi Karsa - Bidakara, Jakarta, pp. 1-14, 2007.

[10] Susilorini, Retno, Rr. M.I., "Analisa Kegagalan Struktur Berbasis Fraktur untuk Penyelamatan Bumi dan Pembangunan Berkelanjutan", Makalah, Seminar "Save The Forest, Save The Earth, 5 February, Fakultas Teknik, Unika Soegijapranata, Semarang, pp. 1-11, 2008.

[11] Susilorini, Retno, Rr. M.I., "The Role of Shear-Friction on Pull-Out Fractured Based Modeling of Nylon 600 with Clumped Fiber End", Seminar Nasional Teknik Sipil IV, 13 Februari, Program Pascasarjana – Jurusan Teknik Sipil, Surabaya, pp. B91-B101.

[12] Susilorini, Retno, Rr. M.I., "Fracture to Failure, a Fracture Mechanics Approach for Bridge Failure Analysis", Proceeding of International Seminar "The Technology of Long Span Bridge to Strengthen the Unity of Nation", 8-9 July, pp. M.20.1-20.6, 2008.

[13] Susilorini, Retno, Rr. M.I., "A Fractured Based Pull-Out Model of Short Nylon 600 Embedded in Cementitious Matrix", *Jurnal Ilmiah Semesta Teknika* (Terakreditasi), Universitas Muhammadiyah Yogyakarta, Vol. 11, No. 1, May, 2008.

[14] Susilorini, Retno, Rr. M.I., "Stable Crack Length on Pull-Out Problem – Significant Factor of Pull-Out Modeling for Concrete Pavement Structure's Element", Proceeding of International Symposium XI FSTPT, 29-30 October, Universitas Diponegoro, pp. 1-9, 2008.

[15] Susilorini, Retno, M.I. Rr, "Striving For 'Green Concrete' with Nylon 600 Fiber - A Review of Pull-Out Model with Nylon 600", Proceeding of Second Annual International Conference Green Technology and Engineering, 15-17 April, Universitas Malahayati, Lampung, pp. 52-56, 2009.

[16] Susilorini, Retno, M.I. Rr, "Model Cabut-Serat Nylon 600 Tertanam dalam Matriks Sementitis Berbasis Fraktur", *Jurnal Dinamika Teknik Sipil* (Terakreditasi), published on Vol. 9 No. 1, July Jurusan Teknik Sipil, Universitas Muhammadyah Surakarta, 2009.

[17] Li, V.C., Chan, Y.W., Wu, H.C., "Interface Strengthening Mechanism in Polymeric Fiber Reinforced Cementitious Composites", Proceedings of International Symposium on Brittle Matrix Composites, (eds. Brandt, A.M, Li, V.C., Marshall, L.H), IKE and Woodhead Publ, Warsaw ,pp. 7-16, 1994.

[18] Clements, M., "Synthetic as Concrete Reinforcement", Concrete Magazine, United Kingdom, September, pp. 37-38, 2002.

[19] Martinez-Barrera, G., "Concrete Reinforce with Irradiated Nylon Fibers", *Journal of Material Research*, Vol.21, No. 2, February, pp. 484-491, 2006.

[20] Nadai, A., *Theory of Flow and Fracture of Solid*s, Volume I, McGraw-Hill Company. Inc, New York, USA, 1950.

[21] Bazant, ZP., "Fracture Mechanics of Concrete: Concepts, Models, and Determination of Material Properties – State of the Art Report", Proceedings, First International Conference on Facture Mechanics Concrete Structure (Framcos 1), (Ed. Bazant, ZP), Colorado, USA, pp. 6-140, 1992.

[22] Li, V.C., and Wang, S., "Suppression of Fracture Failure of Structures by Composite Design based on Fracture Mechanics", corresponding paper in Compendium of Papers CD ROM, Paper 5543, 2005.

[23] Kawamura, M., Igarashi, S.I., "Fluorescence Microscopic Study of Fracture Process of the Interfacial Zone Between a Steel Fiber and Cementitious Matrix Under Pullout Loading", *ACI SP-156* on Interface Fracture and Bond, (eds. Buyukozturk, O., Wecharatana, M.), pp. 173-190, 1995.

[24] Sun, W., Lin, F., "Computer Modelling and FEA Simulation for Composite Single Fiber Pullout", *Journal of Thermoplastic Composite Materials*, Vol. 14, No. 4, pp. 327-343, 2001.

ISSN 114-1284

FRACTURE BASED APPROACH FOR FAILURE ANALYSIS OF NYLON 600 FIBER

Rr. M.I. Retno Susilorini[1]

[1]*Department of Civil Engineering*
Faculty of Engineering
Soegijapranata Catholic University
Tel : (024)844155 hunting Fax : (024)8445265
E-mail : retno_susilorini@yahoo.com; susilorini@unika.ac.id

ABSTRACT

The research purposes to implement fracture based approach in failure analysis of nylon 600 fiber and also partly embedded nylon 600 fiber in cementitious matrix. The methods are experiment and analytical by modeling. The experiment activities consist of tension test of nylon 600 fiber and pullout test of partly embedded nylon 600 fiber in cementitious matrix with length 150 mm and 180 mm. The research meets conclusions: (1) Whenever fracture takes place, it is always an unstable crack; (2) Stable cracks are established by the presence of crack arrester; (3) After the establishment of stable cracks, increasing strain beyond strain ε_1 will not increase stress σ_1, hence do not induce additional fracture; (4) Increasing of strain ε after the establishment of stable cracks in point g will increase stress, the second slip will not take place; (5) Broken nylon fibers have a longer embedded length because of the possibility of crack arrester presence is bigger than the shorter ones; and (6) Since the middle right side of matrix is at the intersection point with fiber acts as crack arrester in the beginning of pull-out process, then the load-displacement (P-δ) and stress-strain (σ–ε) curves of pull-out test will be the same as the load-displacement (P-δ) and stress-strain (σ–ε) curves of fiber tension test.

Keywords
Fracture, failure, nylon 600, pullout

1. INTRODUCTION

Nylon 600 fiber has great value of tension strength, elongation, tension strength, and also elastic modulus ([1], [2], [11]). The embedded nylon 600 fiber provides optimal stable crack length, and improves strain-hardening property ([1]-[11]). Because of its advantages, nylon 600 is believed to be applied into cementitious matrix to achieve best performace of cementitious matrix or concrete.

A popular approach to fracture problems is fracture mechanics. Fracture mechanics is very important in case of fiber cementitious composites. The improvement of fiber cementitious composites such as FRC, HPRFCC, and ECC seldom implements the fiber application such as nylon, which is categorized as synthetic fiber. It should be noted that fiber takes an important role in determining whole fiber-reinforced cementitious composite (FRC) performance. Previous researches have proved a better performance of ECC using various synthetic fiber surfaces [12], high performance as alike steel performance [13], and even higher compressive stress for irradiated nylon fiber by gamma [14]. The nylon fiber has a special characteristic of multiple constrictions at stretching condition [15] called 'yield point elongation' that has magnitude of 200%-300% of initial fiber length.

According to Bazant [16], the failure of concrete structures should consider the strain-softening related to distributed cracking, localized crack that grows to larger fracture prior to failure, and also bridging stresses at the fracture front. Therefore, the suppression of fracture of concrete can be implemented by improving higher toughness and higher tensile ductility [17]. Hence, the application of nylon 600 fiber into cementitious matrix is proper effort to achieve ductility performance.

It is important to recognize the properties of interfaces between fiber and cementitious matrices by a pull-out test and then takes failure analysis by fracture based approach. The research purposes to implement fracture based approach in

ISSN 114-1284

failure analysis of nylon 600 fiber and also partly embedded nylon 600 fiber in cementitious matrix.

2. METHODS

This research conducts experiment and analytical methods. The experiment activities consist of tension test of nylon 600 fiber and also pull-out test of partly embedded nylon 600 fiber in cementitious matrix. The analytical method conveys pull-out modeling.

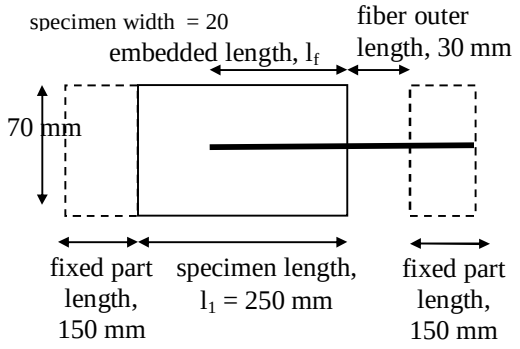

Figure 1: Dimension of specimen

The dimension of specimens is shown by Figure 1 while the setting of pullout test by Figure 3. The pull-out test is provided by computerized Universal Testing Machine "Hung Ta". The nylon 600 fiber is made in Indonesia with 1.1. mm in diameter and embedded length 150 mm and 180 mm for partly fiber embedded specimens. Mix design for cementitious matrix is cement : sand : water ratio of 1:1:0.6. Analytical method applied by modeling and formulation of theoretical model ([1], [2], [11]). The analytical models are built based on experiment result.

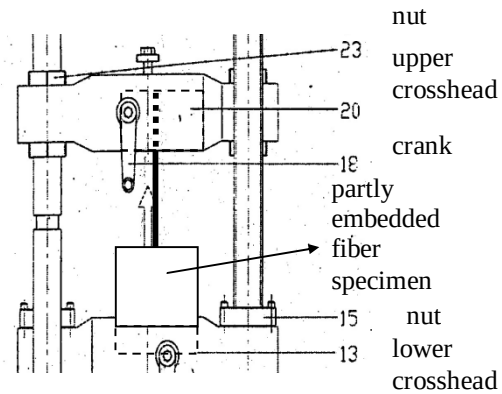

Figure 2 : Setting for pullout test

3. RESULTS AND DISCUSSION

3.1. Results

The results show that nylon 600 fiber has average maximum tension stress of 1471.21 MPa. Figure 3 shows relation of stress-strain of nylon 600 tension test with average maximum strain of 0.89, average maximum elongation of 84.11%, and average maximum tension load of 1398.13 N. A unique property of nylon fiber is shown by 'jagged' phenomenon on stress-strain ($\sigma-\varepsilon$) curves as also shown by Figure 3. This phenomenon is caused by the yield point elongation and the viscosity of nylon itself.

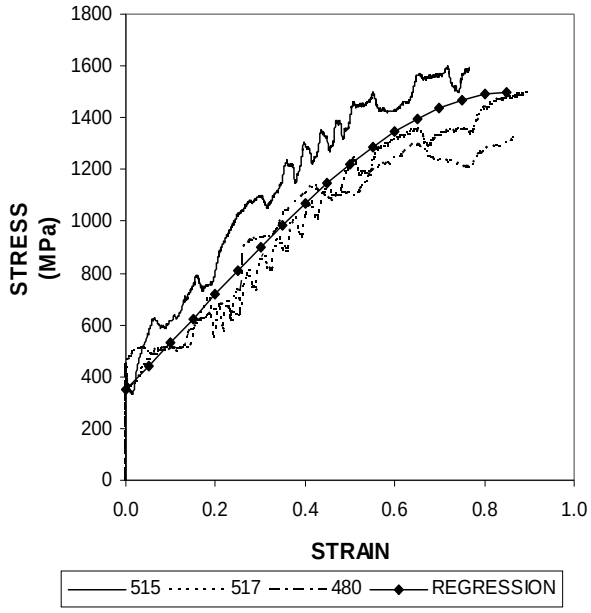

Figure 3 : Relation of stress-strain of nylon 600 tension test

The results of pullout test are shown below. Firstly, the experiment results show that the pullout test represent fracture phenomenon in some stages during pull-out process. Figure 4 describes the stages: (a) Pre-slip stage, (b) Slip stage, and (c) Strain-hardening stage. The pre-slip loads are about 400-430 N and pre-slip displacements are no more than 0.1 mm. The slip loads are in the same range of pre-slip loads with displacements of 3-4 mm. The strain-hardening loads are observed as 1300-1500 N and its displacement about 150-190 mm.

ISSN 114-1284

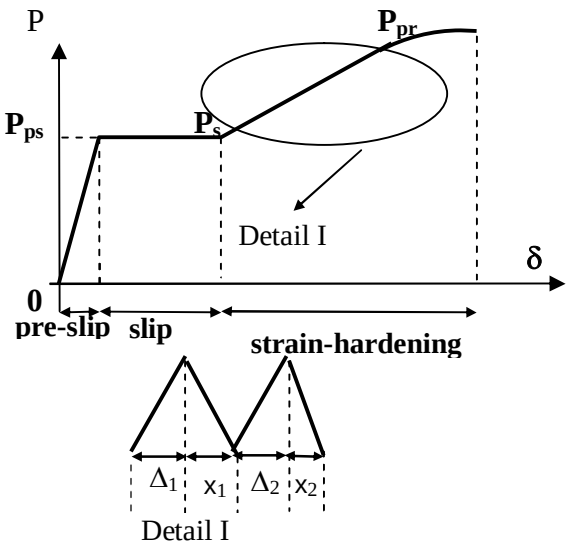

Figure 4 : The stages during pullout process

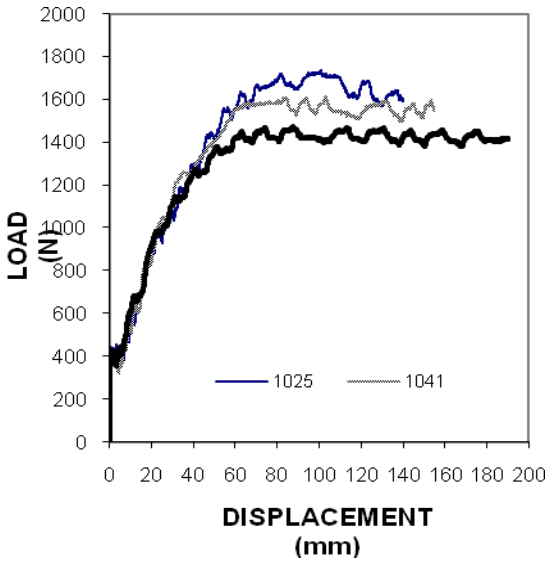

Figure 5 : Relation of load-displacement of specimen with embedded length (l_f) of 150 mm and 180 mm

Figure 5 describes relation of load-displacement of specimen with embedded length (l_f) of 150 mm and 180 mm. Specimen 1025 and 1041 have embedded length l_f = 150 mm while specimen 2438 has l_f = 180 mm. Specimen with l_f = 180 mm has bigger displacement (190.2 mm) than l_f = 150 mm (140.08 and 154.76 mm). On the contrary, specimen with l_f = 180 mm has lower ultimit load (1400 N) than l_f = 150 mm (1500-1600 N).

Relation of stress-strain of specimen with embedded length (l_f) of 150 mm and 180 mm is described by Figure 6. Specimen with l_f = 180 mm has bigger strain (2.8) compared to l_f = 150 mm (2.06 and 2.28). On the contrary, specimen with l_f = 180 mm has lower ultimit stress (1500 N) than l_f = 150 mm (1600-1800 N).

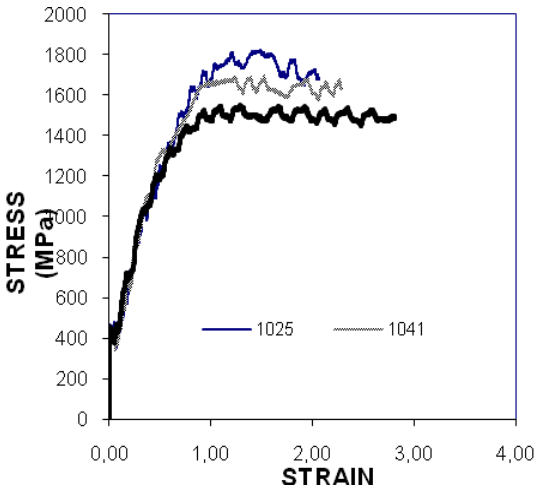

Figure 6 : Relation of stress-strain of specimen with embedded length (l_f) of 150 mm and 180 mm

The results were analyzed to become basis of pullout modeling. Several aspects have been considered in the modeling: (1) Fracture capacity of embedded fiber is a function of Poisson's ratio of fiber, (2) Some stages exist during the pull-out and fracture pull-out process, (4) A 'jagged' phenomenon exists on strain-hardening part of load-displacement (P-δ) and stress-strain (σ–ε) curves of pull-out, and (4) Unstable and stable

ISSN 114-1284

fracture process phenomenon exist during the pull-out process.

Pullout modeling conceives a formulation of load which is a function of displacement that is expressed by Equation 1.

$$P_n = \left(r_{\Delta I}\frac{a_1}{a_2}E_{ps}A\right) + \left(r_{\Delta II}\frac{a_1}{a_2}E_sA\right) + \left(r_{\Delta III}\frac{a_1}{a_2}E_{pr}A\right) \quad (1)$$

Where:

P_n = load (N)
A = fiber section area (mm^2)
E_{pr} = modulus of elasticity at stage of strain-hardening (MPa)
E_{ps} = modulus of elasticity at stage of pre-slip (MPa)
E_s = modulus of elasticity at stage of slip (MPa)
a_1 = total displacement of a stage (mm)
a_2 = initial length of specimen or fiber that is specific for every stage (mm)
$r_{\Delta I}$ = ratio of total free-end fiber displacement of free-end at stage of pre-slip
$r_{\Delta II}$ = ratio of total free-end fiber displacement of free-end at stage of slip
$r_{\Delta III}$ = ratio of total free-end fiber displacement of free-end at stage of strain-hardening

The range value of E_s, E_{ps}, dan E_{pr} for pull-out model is described by Table 1.

Tabel 1 : Range value of E_s, E_{ps}, and E_{pr}

	STAGE OF PRE-SELIP	STAGE OF SLIP		STAGE OF STRAIN-HARDENING
		INITIAL SLIP	POST SLIP	
l_f (mm)	E_{ps} (x 10^3 MPa)	E_s (x 10^3 MPa)	E_s (MPa)	$E_{pr} = E_n$ (MPa)
150	500 - 650	3000 - 4000	500 -1500	400 - 2500
180	500 - 650	4000 - 5000	500 -1500	400 - 2500

Pullout modeling also conveys a formulation for stable crack length as expressed by Equation 2.

$$l_2 = \frac{\bar{\delta} - \bar{\varepsilon} l_0}{\bar{\varepsilon}} \quad (2)$$

Where:

l_2 = stable crack length (mm)
l_0 = initial outer fiber length (mm)
$\bar{\delta}$ = fiber displacement at time of stable fracture achieved (mm)
$\bar{\varepsilon}$ = critical fiber strain

Stable crack length for each embedded length can be calculated based on experiment results as explained by Table 2.

Tabel 2 : Stable Crack Length of Specimens

l_f (mm)	l_2 (mm)
150	37,7375
180	37,7375

The pullout model then built based on experiment results and described by Figure 7-10 as follow.

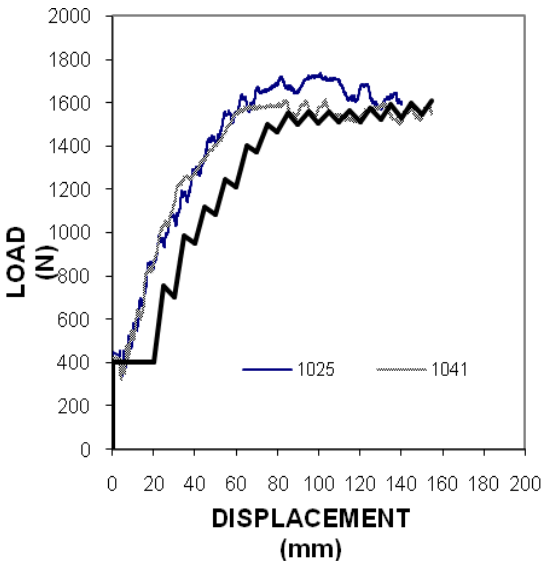

Figure 6 : Relation of load-displacement of experiment results and model with embedded length l_f = 150 mm

ISSN 114-1284

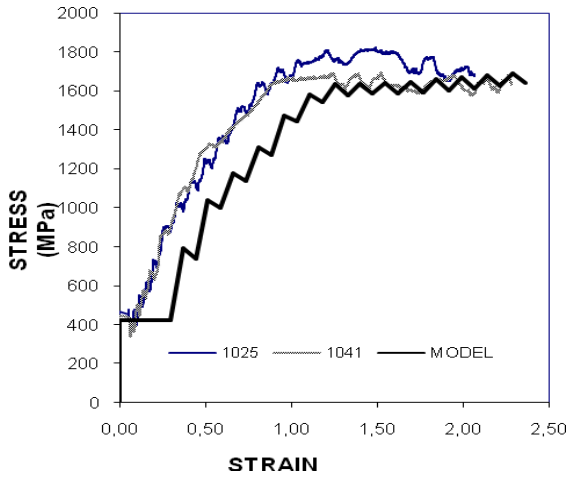

Figure 7 : Relation of stress-strain of experiment results and model with embedded length l_f = 150 mm

Figure 6 and 7 show that the model fit to the experiment results. For relation of load-displacement of experiment results and model with embedded length l_f = 150 mm (Figure 6), the model achieves stage of with load of about 400 N and stage of strain hardening with load of about 1500 N. Figure 7 shows that for stress-strain relation the model achieved stress at stage of slip with load about 400 MPa and stage of strain-hardening with load about 1600 MPa.

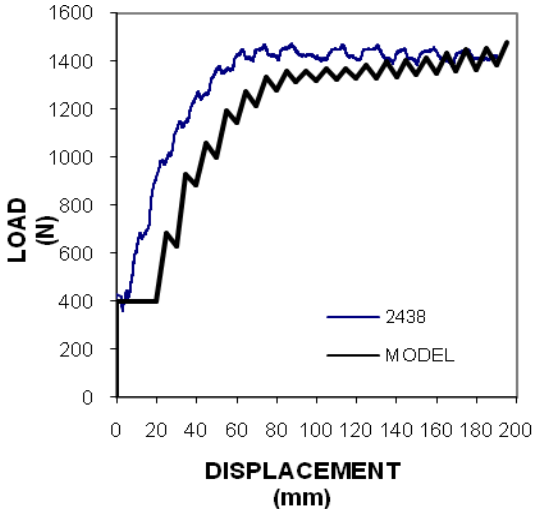

Figure 8 : Relation of load-displacement of experiment results and model with embedded length l_f = 180 mm

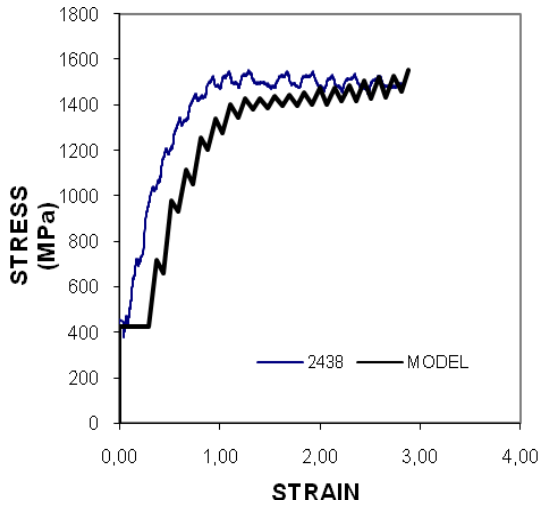

Figure 9 : Relation of stress-strain of experiment results and model with embedded length l_f = 180 mm

Figure 8 and 9 also describe that the model fit to experiment results. Figure 8 shows that the model also achieve stage of slip with load of about 400 N and stage of strain-hardening with load of about 1350 N. It is lower than the loads achieved by the specimens with embedded length of l_f = 150 mm.

The same phenomenon happened for stress-strain relation of Figure 9. The model achieve stage of slip with load of about 400 MPa and stage of strain-hardening with load of about 1400 MPa. It is lower than the loads achieved by the specimens with embedded length of l_f = 150 mm.

3.2. Discussion

Whenever fracture takes place, it is always an unstable crack. Unstable crack will change into stable crack with certain condition. Stable crack length will be occured when the crack arrester presents. It means, the phenomenon of unstable fracture that happened at the stage of pre-slip will change into stable fracture at the stage of slip.

It is interesting that the load and stress of embeded length l_f = 180 mm are lower compared to l_f = 150 mm. However, the displacement for embeded length l_f = 180 mm is bigger compared to l_f = 150 mm. It can be explained as follow. The long embedded length (150 mm and 180 mm)

produces broken fiber when specimen gets failure. It should be noted that long embedded length of specimen is related to the possibility of crack arrester presence. Because of that bigger possibility makes the strain-hardening part in load-displacement curve is longer for long embedded fiber length. The stable crack length will be achieved in stable fracture.

For both embedded length l_f = 150 mm and l_f = 180 mm, the stable crack length are the same, l_2 = 37,7375 mm (Table 2). It can be seen (Figure 7-10) that they achieve same critical load and stress at the stage of slip that the stable fracture occured. Hence, the modeling represents the fracture phenomenon in appropriate way.

4. CONCLUSIONS

The research meets conclusions:

a) Whenever fracture takes place, it is always an unstable crack;
b) Stable cracks are established by the presence of crack arrester;
c) After the establishment of stable cracks, increasing strain beyond strain ε_1 will not increase stress σ_1 (the slip stage exists), hence do not induce additional fracture;
d) Increasing of strain ε after the establishment of stable cracks in point g will increase stress σ (the strain-hardening stage exist), the second slip will not take place;
e) Broken nylon fibers have a longer embedded length because of the possibility of crack arrester presence is bigger than the shorter ones;
f) Since the middle right side of matrix is at the intersection point with fiber acts as crack arrester in the beginning of pull-out process, then the load-displacement (P-δ) and stress-strain (σ–ε) curves of pull-out test will be the same as the load-displacement (P-δ) and stress-strain (σ–ε) curves of fiber tension test

ACKNOWLEDGMENT

The author gratefully acknowledges UBCHEA (United Board of Higher Christian Education) for supporting research grant (2005-2007); and to Prof. Ir. Moh. Sahari Besari, MSc., PhD as Promotor; and also to Prof. Bambang Suryoatmono, PhD. as Co-Promotor; for their great contributions of ideas, discussions, and intensive assistance to the dissertation.
.

REFERENCES

[1] Susilorini, Retno, M.I., *Model Masalah Cabut-Serat Nylon 600 Tertanam dalam Matriks Sementitis yang Mengalami Fraktur*, Dissertation, Unika Parahyangan, Bandung, 2007.

[2] Susilorini, Retno, Rr. M.I., *Pemodelan Cabut-Serat Berbasis Fraktur*, Unika Soegijapranata Press, 2009.

[3] Susilorini, Retno, Rr. M.I., "Fractured Based Approach for Structural Element Design – Safe Building, Safe City", Proceeding Third International Conference on Economic and Urban Management "City Marketing, Heritage, and Identity", PMLP Unika Soegijapranata, Semarang, pp. 451-465, 2007.

[4] Susilorini, Retno, Rr. M.I., "Integral-J Kritis untuk Model Elemen Hingga pada Cabut Serat Fraktur Nylon 600", Tiga Roda Forum "Perkembangan Terkini Teknologi dan Rekayasa Konstruksi Beton di Indonesia", 12 Desember, Hotel Bumi Karsa - Bidakara, Jakarta, pp. 1-14, 2007.

[5] Susilorini, Retno, Rr. M.I., "Analisa Kegagalan Struktur Berbasis Fraktur untuk Penyelamatan Bumi dan Pembangunan Berkelanjutan", Makalah, Seminar "Save The Forest, Save The Earth, 5 February, Fakultas Teknik, Unika Soegijapranata, Semarang, pp. 1-11, 2008.

[6] Susilorini, Retno, Rr. M.I., "The Role of Shear-Friction on Pull-Out Fractured Based Modeling of Nylon 600 with Clumped Fiber End", Seminar Nasional Teknik Sipil IV, 13 Februari, Program Pascasarjana – Jurusan Teknik Sipil, Surabaya, pp. B91-B101.

[7] Susilorini, Retno, Rr. M.I., "Fracture to Failure, a Fracture Mechanics Approach for Bridge Failure Analysis", Proceeding of International Seminar "The Technology of Long Span Bridge to Strengthen the Unity of Nation", 8-9 July, pp. M.20.1-20.6, 2008.

[8] Susilorini, Retno, Rr. M.I., "A Fractured Based Pull-Out Model of Short Nylon 600 Embedded in Cementitious Matrix", *Jurnal Ilmiah Semesta Teknika* (Terakreditasi), Universitas Muhammadiyah Yogyakarta, Vol. 11, No. 1, May, 2008.

[9] Susilorini, Retno, Rr. M.I., "Stable Crack Length on Pull-Out Problem – Significant Factor of Pull-Out Modeling for Concrete Pavement Structure's Element", Proceeding of International Symposium

XI FSTPT, 29-30 October, Universitas Diponegoro, pp. 1-9, 2008.

[10] Susilorini, Retno, M.I. Rr, "Striving For 'Green Concrete' with Nylon 600 Fiber - A Review of Pull-Out Model with Nylon 600", Proceeding of Second Annual International Conference Green Technology and Engineering, 15-17 April, Universitas Malahayati, Lampung, pp. 52-56, 2009.

[11] Susilorini, Retno, M.I. Rr, "Model Cabut-Serat Nylon 600 Tertanam dalam Matriks Sementitis Berbasis Fraktur", *Jurnal Dinamika Teknik Sipil* (Terakreditasi), published on Vol. 9 No. 1, July Jurusan Teknik Sipil, Universitas Muhammadyah Surakarta, 2009.

[12] Li, V.C., Chan, Y.W., Wu, H.C., "Interface Strengthening Mechanism in Polymeric Fiber Reinforced Cementitious Composites", Proceedings of International Symposium on Brittle Matrix Composites, (eds. Brandt, A.M, Li, V.C., Marshall, L.H), IKE and Woodhead Publ, Warsaw ,pp. 7-16, 1994.

[13] Clements, M., "Synthetic as Concrete Reinforcement", Concrete Magazine, United Kingdom, September, pp. 37-38, 2002.

[14] Martinez-Barrera, G., "Concrete Reinforce with Irradiated Nylon Fibers", *Journal of Material Research*, Vol.21, No. 2, February, pp. 484-491, 2006.

[15] Nadai, A., *Theory of Flow and Fracture of Solid*s, Volume I, McGraw-Hill Company. Inc, New York, USA, 1950.

[16] Bazant, ZP., "Fracture Mechanics of Concrete: Concepts, Models, and Determination of Material Properties – State of the Art Report", Proceedings, First International Conference on Facture Mechanics Concrete Structure (Framcos 1), (Ed. Bazant, ZP), Colorado, USA, pp. 6-140, 1992.

[17] Li, V.C., and Wang, S., "Suppression of Fracture Failure of Structures by Composite Design based on Fracture Mechanics", corresponding paper in Compendium of Papers CD ROM, Paper 5543, 2005.

ISSN 114-1284

Thermal Impact of Pedestrian Environment Materials to Dynamic Discomfort in Tropical Humid Environment

Sangkertadi [1], Reny Syafriny [2], Cinthya Wuisang [2]

[1] *Laboratory of Building Science & Technology, Department of Architecture, Faculty of Engineering, Sam Ratulangi University, Manado, Indonesia*
Tel 0431 852959
t_sangkertadi@yahoo.com

[2] *Program Study Urban & Regional Planning, Department of Architecture, Faculty of Engineering, Sam Ratulangi University, Manado, Indonesia*
renysy@yahoo.com
cynthiawuisang@gmail.com

ABSTRACT

This paper contains the intention of thermal discomfort of pedestrian area in tropical humid environment, especially for the people in walking activity. This study applied field measurements, questionnaires and calculations. Day time thermal measurements of outdoor spaces and pedestrian ways were realized. At the same time we distributed questionnaire on thermal feeling to the people who walked on pedestrian way. Thermal measurement includes air temperature, radiant temperature, wind and humidity. Scale of thermal feeling refer to the AHSRAE definition. We had 24 subjects who filled the questionnaire on comfort feeling. They walked on pedestrian way for 5 minutes or of about 300 m long distance. Three types of pedestrian way were examined. Type-1 is pedestrian well protected under trees canopy, type-2 is pedestrian partially protected by trees canopy, and type-3 is pedestrian totally exposed to solar radiation. The study was done at noon under clear sky, when temperature is assumed to be maximum in a day. The results, in general show that there is different up to 3 scales between thermal comfort under trees and without trees shading. Beside, the dynamic discomfort was found for the people in walking activity.

Keywords
Outdoor comfort, Tropical humid, Open-space

1. INTRODUCTION

Architect or urban designer's major task is to create the best possible outdoor environment to the people's activities. Soft and hard materials implemented for outdoor spaces, play important role determining convective and radiant temperature of its environment. Outdoor thermal comfort is therefore depends on utilization of landscape material. A good thermal performance that gives comfortable microclimate of urban space will be one of primary point of interest for the visitors or even for the migrants to do their outdoor activities: parking, relaxing, walking, retailing, etc. The landscape materials such as grass, trees, asphalts, concrete-block,. etc, which are implemented at and surround of pedestrian ways, may influence the microclimate and thermal comfort at urban space. In hot and humid areas, a state of discomfort is often caused by ambient atmosphere which are too hot and very humid, with a higher solar radiation. Under these conditions, sweat rate and skin evaporation are considered to be primary factors for feelings of thermal comfort. Such active control is not possible exteriorly, but some degree of control is needed for human comfort. Wind, solar radiation and precipitation are factors to be considered. Since the solar radiation can be controlled using vegetation or man-made shelter constructions, wind velocities play an important role to increase comfort feelings by evaporative cooling.

Each site has its own microclimate, determined by its local surrounding, by the weather, and by the character of urban area. Many of scientific studies have shown that the city is warmer than the surrounding countryside. This effect is known as the urban heat island. Urban activity without good control may cause of increasing of air temperature insides city and its hinterland. Vast enhanced hard material covering the ground and utilizes metal for roofing that has reflectance towards sun radiation push acceleration the happening of urban heat island. In urban areas, natural vegetation is often removed and replaced by non-evaporating, non-transpiring impervious surfaces. Under such alteration, the partitioning of incoming solar radiation into fluxes of sensible and latent heat is skewed in favor of increased sensible heat flux as evapotranspirative surfaces are reduced.

Open space or exterior facilities are an essential element of urban design, and they are not just part of a beautification program. Rather, they are a comfort system as well as a support element for retailing, pedestrian ways and others vitalities of urban spaces. Soft and hard materials covering park space, roofing and wall, play important role determining convective and radiant temperature of its environment. Outdoor thermal comfort is therefore also depends on utilization of surface material.

It is always of interested to study the exterior thermal performance of the cities in tropical humid countries. Many of developing countries are located in the tropical zones. The global era in 21st centuries and the warning of climate

ISSN 114-1284

changes may influence the direction of agglomeration strategy of the cities. Development policy to make grow up the cities is therefore oriented to the friendly environment principles. Nowadays green technology or friendly environment is common strategy to develop many sectors. By the 21st century 70-80 per cent of the world's population will live in cities and towns, demanding higher standards of comfort, goods and wealth. At present, the only means mankind knows of meeting these demands is by increasing output and pillaging the earth's resources. Although both the tools and technologies exist to build new cities with minimum impact on the environment, not many examples exist [1]

In hot and humid areas, a state of discomfort is often caused by ambient atmosphere which are too hot and very humid, with a higher solar radiation. Under these conditions, sweat rate and skin evaporation are considered to be primary factors for feelings of thermal comfort. Such active control is not possible exteriorly, but some degree of control is needed for human comfort. Wind, solar radiation and precipitation are factors to be considered. Since the solar radiation can be controlled using vegetation or man-made shelter constructions, wind velocities play an important role to increase comfort feelings by evaporative cooling.

From the view point of coordinated city and energy planning efforts, it must be considered that the potential for natural thermal conditioning of spaces in buildings is not only a function of building technology, but also of the city's volumetric pattern, including non-built elements such as trees and grass. From the view point of urban climatology and energy efficient building, trees have multiple effects on potential utilization of conservation and passive design strategies, that can be summed up as follows:

- Reduction of the urban heat island effect, as consequence of lower heat flows absorbed and released by concrete-block, paving-stone, wall and roofs due to the shading provided by tree crowns and the reduction of the air temperature due to evapotranspiration.
- Reduction of cooling loads caused by reduced incident radiation on glazed surfaces, reduction of sol-air temperature on roofs and walls shaded by trees and lower ambient temperature as previously described.

This paper contains the intention of thermal performance of outdoor environment in the center town of Manado city, Indonesia, located in humid tropical climate zone. Manado is the capital of North Sulawesi Province in Indonesia, and actually is being prepared to be an important international city supported by its favorable geographical position and its industry and tourism attractions. Manado is one of some Indonesia's cities which will face a remarkable urbanization in 21st centuries.

The objective of the study is to know outdoor thermal impact of materials and vegetation covering pedestrian area in the tropical environment

2. BRIEF THEORY AND REFERENCES

In agreement with ASHRAE (American Society of Heating, Referigerating and Air Conditioning Engineers) thermal comfort for a person is here defined as "*that condition of mind which expresses satisfaction with the thermal environment*". Thermal neutrality for a person is defined as the condition in which the subject would prefer neither warmer nor cooler surroundings. The reason for creating thermal comfort is first and foremost to satisfy man's desire to feel thermally comfortable, in line with his desire for comfort in other directions. Man's intellectual, manual and perceptual performance is in general highest when he is in thermal comfort. The most important variables which influence the condition of thermal comfort are: activity level (heat production in the body), thermal resistance of the clothing (clo-value), air temperature, mean radiant temperature, relative air velocity and water vapor pressure in ambient air.

The discomfort associated with exposure to warm and humid environments is attributed to the conscious awareness of perspiration and an elevated body temperature. The secretion of sweat onto the skin surface permits the dissipation of metabolic heat from the body by evaporation when the loss of heat by radiation and convection is insufficient to maintain thermal balance. In warm conditions in the resting, individual and with increased metabolic levels associated with work and exercise; it was recognize that unpleasantness and thermal discomfort are associated with sweating, rather than skin or body temperature.

The DISC scale that represent a correlation introducing sweat rate and percentage of skin wetness is more adapted to be used for prediction of thermal feeling in hot and humid environment [3],[5]

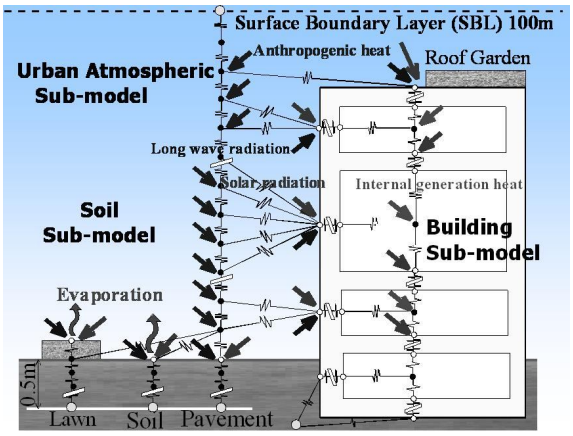

Figure.1. Analogical thermal modeling of city environment [2].

ISSN 114-1284

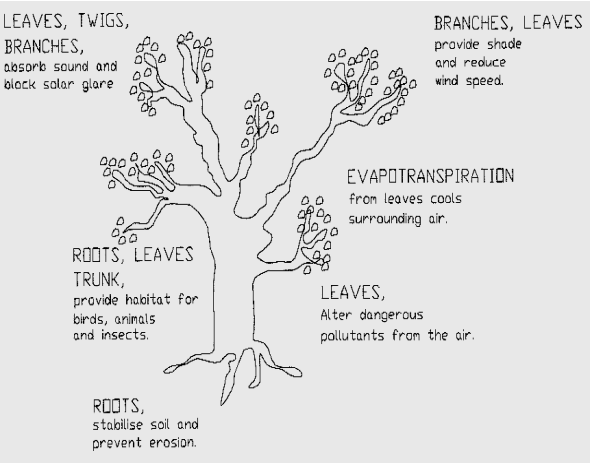

Figure.2. Role of trees component in reducing thermal effect and save living environment [4]

The environmental parameters affecting thermal comfort conditions outdoors, even-though similar to indoors, are encountered within a much wider range and are more variable. Therefore due to this complexity, in terms of variability, temporal and spatial, as well as the great range of activities people are engaged in, there have been very few attempts to understand comfort conditions outside
Trees are recommended as considerable shade component, because its organic material is both non-reflection and non-transmission to heat penetration. A very large area of non-shading open space using hard covering may cause increasing of urban heat island effect. Since the city is too hot, it is therefore needed more of energy to make cool-down the environment. There is a close relation between design strategy of open space and impact of energy demand of city. Covering ground with grass vegetation may give a reduction of one scale of thermal comfort at noon [6]

Table.2. Thermal feeling definition of DISC and ASHRAE scales

PMV	DISC	Definition
-3		Cold
-2		Cool
-1		Slightly Cool
0	0	Neutral
+1	1	Slightly Uncomfortable
+2	2	Uncomfortable
+3	3	Very Uncomfortable
+4	4	Untolerable

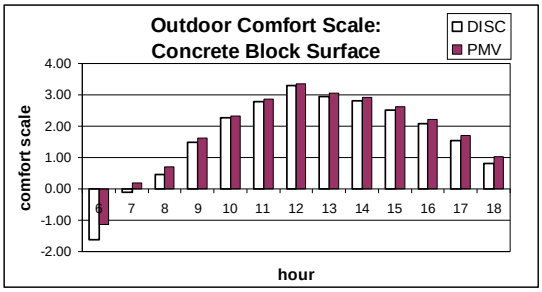

Figure.3. Calculation of comfort scale of open-space environment using Concrete-block for surface [6]

The measurements realized by Jörg Spangenberg [7] in Brazil, indicated that a public park with good vegetation has a cooling effect with around 2°C lower than its surroundings. The surface temperature measurements also showed that natural surfaces are considerably cooler than commonly used construction materials such as concrete and asphalt. The results from the simulations presented in the study clearly show that vegetation in the form of trees has a great potential of improving the microclimate and mitigate heat stress in a hot humid climate. The leaf area index (LAI) and leaf area density (LAD) of the canopy proved to be important metrics, which have a significant influence on the microclimate. The denser the tree canopy (higher LAI and LAD), the lower the air and surface temperatures and the better the thermal comfort for hot-humid climate. In general, trees provide, under their canopies (locally restricted), significant improvements on thermal comfort principally during midday and in the early afternoon as they provide overhead shading by attenuating the solar radiation. The crucial benefit of shade, resulting in considerably lower mean radiant temperatures, has more influence on the thermal comfort.

3. METHODS

This research focuses the relations between urban design variables and thermal comfort. The research objects are the empirical and rational predictive models of outdoor thermal comfort for walking activity. The urban environment of Manado city, Indonesia was chosen as locations of the study. Three areas of open space located in the centre of the city were taken place as sample geographic. This study applied field measurements, questionnaires and simple calculations. Day time thermal measurements of outdoor spaces and pedestrian ways were realized. The field research consists of 3 different pedestrian way variables and 24 applied questionnaires. Three types of pedestrian way were examined. Type-1 is pedestrian well protected under trees canopy, type-2 is pedestrian partially (± 50%) protected by trees canopy, and type-3 is pedestrian totally exposed to solar radiation. All of the pedestrian way ground surface is covered by paving concrete. This field study was done at noon under clear sky, when temperature is assumed to be maximum in a day. Calculation of thermal comfort applying DISC was also realized applying parameters obtained by field measurement. A form (questionnaire) was designed to record human thermal impact on a comfort scale along with other information of interest such as location; date; time; age; sex; height, weight and dressing of subject; and climatic measurements: wind, air temperature, mean radiant temperature and air humidity. Subjects (pedestrians) were asked their state of thermal comfort each 1 minute for along of 5 minutes in walking activity (1.8 met). They started answer the question after about 2 minutes walked on a shadowed open-space. Each respondent need 7 minutes in this field experiment. They clothed of tropical style dress.

The frequency distribution of experienced thermal stress on a comfort scale is shown in Table.2

Table.2. Distribution of the respondents

	Pedestrian Type-1	Pedestrian Type-2	Pedestrian Type-3
Men	3	4	5
Women	5	4	3
Total	8	8	8

Climatic measurement equipments were used are : infrared thermometer, thermo-hygrometer, and anemometer.

A proposed regression model called dynamic discomfort scale (DISC $_{dyn}$) was developed by exploration of the results from questionnaires, time-exposure, climatic measurements and combined with DISC formulation. The term of dynamic is to be correlated to the function of time along activity, or:

$$DISC_{dyn} = f\{DISC, t\} \; ; \; t \text{ in minute}$$

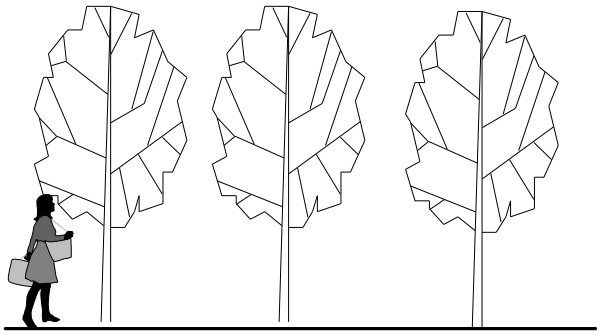

Pedestrian way type-1

Pedestrian way type-2

Pedestrian way type-3

Figure.4. Types of pedestrian examined

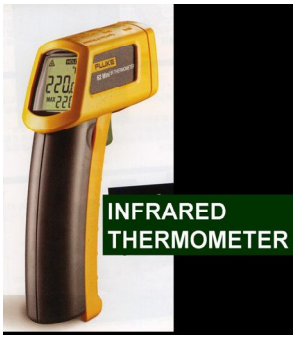

Thermohygrometer

Anemometer

Figure.5. Equipments for climatic measurement

4. RESULTS AND DISCUSSION

Thermal feel responds recorded from questionnaires indicate influence of time-exposure of the body to the climatic environment, especially for the case of sun exposed pedestrian. With the same climatic condition, after 5 minutes exposed to the sun in walking activity, human feel very uncomfortable. It was also noted that there is a linear increasing respond of thermal feeling from first minute to the fifth (from comfortable scale to very uncomfortable). For the case where pedestrian way is not totally exposed to the sun (about 50% protected from the sun), it was found that there is a small change of the respond from first minute to the fifth. Table 3 to 5 show the result from measurement and questionnaires for all types of pedestrian way. Respondents filled the questionnaire of thermal comfort in terms of syntax: *slightly cool, comfort, slightly uncomfortable, uncomfortable, very uncomfortable, or feel head pain (untolerable).*

ISSN 114-1284

Table 3. Results of pedestrian way type-1

Resp. No	Time (min)	Ta (^{0}C)	Trm (^{0}C)	v (m/s)	RH (%)	Vote of Resp value	Vote of Resp def.
1	1	32	32	0.2	71.3	0.0	comfort
	2	31.2	31.2	0.2	70.5	0.0	comfort
	3	31.2	31.2	0.1	70	0.0	comfort
	4	31.1	31.1	0.2	72.6	0.0	comfort
	5	31.1	31.1	0.1	72.6	0.0	comfort
2	1	32	32	0.2	71.3	0.0	comfort
	2	31.2	31.2	0.2	70.5	0.0	comfort
	3	31.2	31.2	0.1	70	0.0	comfort
	4	31.1	31.1	0.2	72.6	0.0	comfort
	5	31.1	31.1	0.1	72.6	1.0	slightly uncomfortable
3	1	31.5	31.5	0.3	72.4	0.0	comfort
	2	31.4	31.4	0.2	72.1	0.0	comfort
	3	31.7	31.7	0.3	72.6	0.0	comfort
	4	31.7	31.7	0.2	72.4	0.0	comfort
	5	31.9	31.9	0.5	73.2	0.0	comfort
4	1	32.1	32.1	0.4	72.7	0.0	comfort
	2	31.7	31.7	0.4	72.5	0.0	comfort
	3	31.6	31.6	0.3	72.8	0.0	comfort
	4	31.5	31.5	0.3	72.1	0.0	comfort
	5	31.5	31.5	0.3	72.5	0.0	comfort
5	1	32.1	32.1	0.4	71.5	0.0	comfort
	2	32.1	32.1	0.5	71.6	0.0	comfort
	3	31.7	31.7	0.3	72.6	0.0	comfort
	4	31.6	31.6	0.2	71.9	1.0	slightly uncomfortable
	5	31.6	31.6	0.2	72.1	1.0	slightly uncomfortable
6	1	31.6	31.6	0.3	71.5	0.0	comfort
	2	31.3	31.3	0.5	71.3	0.0	comfort
	3	31.3	31.3	0.6	71.3	0.0	comfort
	4	31.6	31.6	0.5	71.6	0.0	comfort
	5	31.9	31.9	0.6	71.7	0.0	comfort
7	1	32.1	32.1	0.4	72.1	0.0	comfort
	2	32.4	32.4	0.7	72.4	0.0	comfort
	3	32.3	32.3	0.6	72.1	0.0	comfort
	4	32.1	32.1	0.6	72.7	0.0	comfort
	5	31.7	31.7	0.2	72.5	1.0	comfort
8	1	31.9	31.9	0.6	72.4	0.0	comfort
	2	31.9	31.9	0.8	72.4	0.0	comfort
	3	32.2	32.2	0.3	72.8	0.0	comfort
	4	32.2	32.2	0.6	72.9	0.0	comfort
	5	32.3	32.3	0.4	73.3	0.0	comfort

Table 4. Results of pedestrian way type-2

Resp. No	Time (min)	Ta (^{0}C)	Trm (^{0}C)	v (m/s)	RH (%)	Vote of Resp value	Vote of Resp def.
1	1	32.4	39.7	0.4	71.5	0.0	comfort
	2	32.5	40.4	0.6	70.5	0.0	comfort
	3	32.2	41.8	0.3	70.1	1.0	slightly uncomfort
	4	32.5	42.0	0.3	72.6	1.0	slightly uncomfort
	5	32.5	41.8	0.3	73.4	2.0	uncomfort
2	1	32.1	40.1	0.3	71.3	0.0	comfort
	2	32.1	41.5	0.2	70.5	0.0	comfort
	3	31.2	41.1	0.2	70.1	1.0	slightly uncomfort
	4	31.1	40.6	0.2	72.6	1.0	slightly uncomfort
	5	31.1	40.4	0.4	73.4	1.0	slightly uncomfort
3	1	32.3	41.2	0.3	71.1	0.0	comfort
	2	32.3	41.6	0.4	70.5	0.0	comfort
	3	32.3	40.7	0.5	71.2	0.0	comfort
	4	32.1	40.2	0.5	70.2	1.0	slightly uncomfort
	5	31.9	41.9	0.6	70.5	1.0	slightly uncomfort
4	1	32.2	41.5	0.4	72.4	0.0	comfort
	2	32.2	41.1	0.2	72.5	0.0	comfort
	3	32.4	42.1	0.3	72.1	0.0	comfort
	4	32.3	40.3	0.3	72.1	1.0	slightly uncomfort
	5	32.1	41.1	0.3	72.5	1.0	slightly uncomfort
5	1	32.6	41.0	0.5	66.2	0.0	comfort
	2	32.1	39.7	0.6	68.3	0.0	comfort
	3	32.5	41.3	0.3	68.1	1.0	slightly uncomfort
	4	32.5	41.7	0.2	67.5	1.0	slightly uncomfort
	5	32.5	40.4	0.2	67.5	1.0	slightly uncomfort
6	1	32.7	41.4	1.1	69.8	0.0	comfort
	2	32.6	40.5	1.2	70.8	0.0	comfort
	3	32.6	40.0	0.6	70.4	1.0	slightly uncomfort
	4	32.6	39.8	0.5	71.6	1.0	slightly uncomfort
	5	32.6	40.8	0.1	71.7	1.0	slightly uncomfort
7	1	32.7	42.3	0.8	72.1	0.0	comfort
	2	32.7	43.2	0.7	72.3	0.0	comfort
	3	32.8	41.9	0.6	72.1	0.0	comfort
	4	32.7	42.7	0.6	72.4	1.0	slightly uncomfort
	5	33.1	42.7	0.2	71.9	2.0	uncomfort
8	1	32.8	41.8	0.6	72.4	0.0	comfort
	2	32.8	41.4	0.8	72.4	0.0	comfort
	3	32.2	41.2	0.6	72.8	0.0	comfort
	4	32.6	40.4	0.4	72.9	1.0	slightly uncomfort
	5	32.6	40.8	0.4	73.1	1.0	slightly uncomfort

For the case of pedestrian way type-1 (Table 3) that was fully protected to direct solar radiation, most of people feel enough comfortable after 5 minutes in walking activity. There were only 4 responds (10%) that fill slightly uncomfortable after 5 minutes walking. This is may be caused by effect of low wind velocity that influence feel of comfort or decrease comfort level by evaporative process. In that case the wind velocity was of 0.1 to 0.2 m/s with air temperature of 31 to 32^{0}C.

For the case of pedestrian way type-2 (Table 4) it were found significant different values compared to the case of type-1. Situation slightly uncomfortable and uncomfortable were found several times after 4 to 5 minutes of walking activity. This is certainly impact of radiant temperature from direct solar gain on the pedestrian area. People feel uncomfortable when radiant and air temperatures are relatively high with low air velocity.

People feel more uncomfortable and very uncomfortable when they walk on the pedestrian way that is totally exposed

to direct sun shine. Even they may feel intolerable condition and feel of pain head due of solar radiation penetration after 5 minutes of walking (Table 5)

Table 5. Results of pedestrian way type-3

Resp. No	Time (min)	Ta (^{0}C)	Trm (^{0}C)	v (m/s)	RH (%)	Vote of Resp value	Vote of Resp def.
1	1	33.4	55.8	0.3	66.9	0.0	comfort
	2	33.3	57.2	0.3	66.6	2.0	uncomfort
	3	33.5	60.6	0.3	67.7	2.0	
	4	33.8	60.8	0.3	66.6	3.0	very uncomfort
	5	33.5	60.4	0.2	66.4	4.0	untolerable
2	1	33.2	56.9	0.3	69.6	0.0	comfort
	2	33.3	60.1	0.4	69.5	2.0	uncomfort
	3	32.3	60.2	0.4	68.4	2.0	
	4	32.3	59.2	0.2	68.5	2.0	
	5	32.3	58.7	0.2	66.5	4.0	untolerable
3	1	33.1	59.2	0.3	71.1	0.0	comfort
	2	33.6	60.1	0.4	70.5	2.0	uncomfort
	3	34.3	58.2	0.4	68.5	2.0	
	4	34.7	57.2	0.2	67.1	2.0	
	5	34.5	61.1	0.2	66.4	4.0	untolerable
4	1	33.7	60.1	0.4	62.8	0.0	comfort
	2	35.2	59.2	0.5	59.7	1.0	slightly uncomfort
	3	34.6	61.2	0.4	63.4	2.0	very uncomfort
	4	32.5	57.2	0.5	69.1	2.0	
	5	33.7	59.2	0.4	67.2	4.0	untolerable
5	1	33.6	58.5	0.4	66.2	1.0	slightly uncomfort
	2	32.8	56.2	0.4	68.3	1.0	
	3	32.9	59.2	0.4	68.1	2.0	uncomfort
	4	33.7	60.1	0.3	67.5	2.0	
	5	33.8	57.3	0.4	67.5	3.0	very uncomfort
6	1	32.5	59.3	0.4	69.8	0.0	comfort
	2	32.7	57.3	0.4	70.8	1.0	slightly uncomfort
	3	32.9	56.2	0.4	70.4	2.0	uncomfort
	4	32.5	55.9	0.4	71.6	2.0	
	5	33.1	58.1	0.4	67.6	3.0	very uncomfort
7	1	33.4	61.3	0.3	66.6	1.0	slightly uncomfort
	2	33.7	63.2	0.4	67.2	3.0	very uncomfort
	3	33.4	60.2	0.4	66.9	3.0	
	4	33.2	62.2	0.6	68.8	4.0	untolerable
	5	35.5	61.7	0.4	67.9	4.0	
8	1	33.5	60.1	1	66.5	1.0	slightly uncomfort
	2	33.8	59.3	0.2	67.7	2.0	uncomfort
	3	32.2	59.4	0.4	69.9	2.0	
	4	32.6	57.1	0.4	68.1	3.0	very uncomfort
	5	33.7	58.1	0.5	69.8	3.0	

From the results of questionnaires and climatic measurements, we developed three regression correlations of dynamic discomfort scale ($DISC_{dyn}$) using statistic method. The equations are as follow:

For pedestrian totally exposed to the sun:

$DISC_{dyn} = ABS\ [DISC - 6.45 + 0.0402\ t + 6.541\ log\ (t) - 2.5096\ (log(t))^2\ ]$

For pedestrian partially ($\pm$ 50%) exposed to the sun:

$DISC_{dyn} = ABS\ [DISC - 4.42 - 0.0525\ t + 0.8193\ log\ (t) + 1.8047\ (log(t))^2\ ]$

For pedestrian totally protected from the sun:

$DISC_{dyn} = ABS\ [DISC - 3.75 - 0.0372\ t - 0.3109\ log\ (t) + 2.0962\ (log(t))^2\ ]$

Where :

$DISC$ = $3.9338\ Sw + 0.0158\ Ds - 0.3348$ [5]

t = time of exposure to outdoor environment (minute), $t > 0$

Sw = Percentage of skin wettedness

Ds = Sweat rate (g/h)

Note: equations to calculate Sw and Ds may be obtained from some references related to physiological comfort.

Figure.6 is a x-y graphic that shows a comparison of thermal feel scale obtained by equation of $DISC_{dyn}$ and thermal feel from questionnaires for the case of pedestrian way type-3 (totally exposed to sun shine).

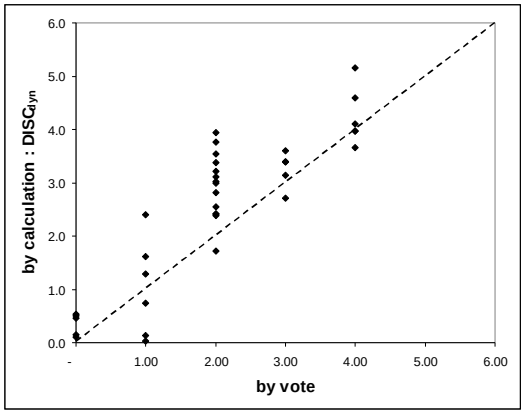

Figure.6. Comparison of Comfort feeling by DISCdyn and from questionnaires

Figures 7,8, and 9 show three types of non-linear line of dynamic discomfort ($DISC_{dyn}$) as the function of time exposure for subject adult (ADU = $\pm$ 1.6 m^2) wearing tropical cloth (0.6 clo), in walking activity (1.8 met), wind 0.4 m/s, and RH=70%.

Looking at the figure 8, we get a state of very uncomfortable (scale=3) after 4 minutes walking at noon for the case of pedestrian totally exposed to direct solar gain. While for the case of pedestrian under trees protection, we may get situation slightly uncomfortable after 5 minutes walking (Figure 7).

Using these graphics we may decide where we must implant the trees and to know the distance each others. If a state of uncomfortable (scale=2) is assumed as the limited value of comfort, then we can decide to implant vegetations or trees after 2 minutes walking, or of about each 100 meters maximum (man speed walking is about 3 km/h). If a state of slightly uncomfortable (scale=2) is to be assumed as the

ISSN 114-1284

limited situation of minimum comfort, then we get a distance of about 50 to 75 meters between trees.

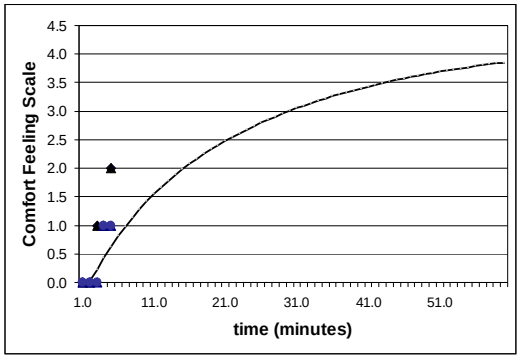

Figure 7. Application of $DISC_{dyn}$ in humid and tropical environment on pedestrian way type-1.

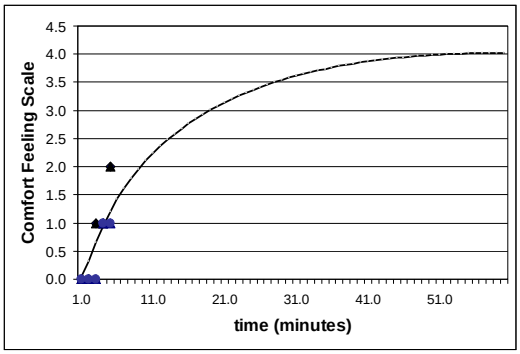

Figure 8. Application of $DISC_{dyn}$ in humid and tropical environment on pedestrian way type-2.

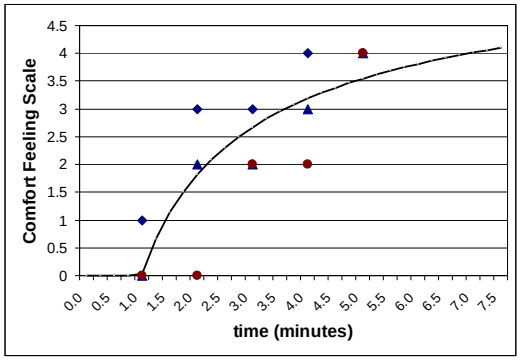

Figure 9. Application of $DISC_{dyn}$ in humid and tropical environment on pedestrian way type-3. Comparison with values from questionnaires (scatter points)

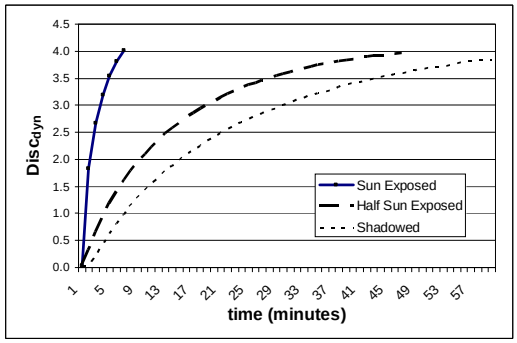

Figure.10. Comparison of increasing line of discomfort for 3 types of pedestrian environment.

5. BRIEF CONCLUSION

This study explores situation of outdoor discomfort that is dynamically changed as function of time in minutes. We may know the respond feel of the body that is exposed to certain climatic environment along certain times. Pedestrian materials such as trees, vegetations and paving concrete may influence significantly the situation of discomfort. We may stated that the positive impact of trees is more significant to increase thermal comfort feel, comparing to the influence of materials of pedestrian way. Influence of radiant temperature is enough strong to make the body feel uncomfortable.

Other results of this study are three non-linear regression equations of the dynamic discomfort scale ($DISC_{dyn}$) for the people in walking activity, representing the three types of pedestrian way which were examined. We may use the equation to decide the position of trees for pedestrian ways.

Finally we may make statement that this study give a valuable contribution for the research on outdoor thermal comfort especially to make green the pedestrian way in the tropics and humid cities.

REFERENCES

[1] Guy Battle, Chris McCarthy, "Tropical Sustainability", in *Architectural Review*, Vol. 196, September 1994.

[2] Aya Hagishima, Jun Tanimoto, Tadahisa Katayama, "An Intrigued Analysis to Quantify the Causes for Urban Heat Island", Kyushu University, 2009

[3] Berglund L.G, Cunningham D J, "Parameters of Human Discomfort in Warm Environment", in *ASHRAE Transaction*, vol 92 part 2B, 1986

[4] Naeem Irfan, Adnan Zahoor, Nadeemullah Khan, "Minimising The Urban Heat Island Effect Through Lanscaping", in *NED Journal of Architecture and Planning*, Vol One, November, 2001.

[5] Sangkertadi, *"Contribution a l'etude du comportement thermoaeraulique des batiments en climat tropical humide. Prise en compte de la ventilation naturelle dans l'evaluation du confort"*. These Doctorat, INSA de Lyon, 1994.

[6] Sangkertadi, "Thermal Effect of Materials for Ground Covering and Roofing in Tropical City Environment", paper accepted for the *Second Annual International Conference on*

Green Technology and Engineering 2009, Bandar Lampung, 15-17 April 2009

[7] Jörg Spangenberg, Paula Shinzato, Erik Johansson and Denise Duarte, "Simulation of The Influence of Vegetation on Microclimate and Thermal Comfort in The City of Sao Paulo" in Rev. SBAU, *Piracicaba, Vol.3, no.2, june. 2008.*

Evaluation Model Development on Jakarta Transportation System by Dynamic System Simulation

Siti Nur Fadlillah[1], Nunung Nurhasanah[2], Bahtiar Abbas Saleh[3], Bambang Sugiharto[4]

[1,2,3,4] *Industrial Engineering Department, Science and Technology Faculty*
Jl. K.H. Syahdan No. 9, Kemanggisan, Jakarta
E-mail : nofadila@yahoo.com; nunung@binus.edu; bahtiars@binus.edu; b_sugiharto@yahoo.com

ABSTRACT

Jakarta has experienced every complex problems related to its transportation system. Problems of transportation in Jakarta Metropolitan is felt more days are are more problems. Now, problem related to existing public vehicles in Jakarta is bad public transportation system management, especially the balance of total public transportation fleet with total passengers. This research is to rationalize amount of public transportation in certain routes in Jakarta, so ideal ratio can be gotten between fleets and passengers. Data processing is carried out by using AHP method to choose research location and determine priorities of project as research object. System Modeling of Problems is carried out by using dynamic Program, in this matter, by using Powersim Software. Based on result of model developed, total public transportation rationally in Tanjung Priok – Cilincing (M-14) Route is 30 vehicles. Those amounts will give high load factor value if they are integrated with innovation as public transportation scheduling system, so they can increase drivers' income as amount of Rp. 940.650,-, and can decrease traffic jam.

Keywords
public transportation, route, priority, system, dynamic simulation

1. INTRODUCTION

1.1 Background

Transportation problems in Jakarta Metropolitan City have been felt that more days are more problems. Any efforts are tried by DKI Government, but those are not carried out comprehensively, so the result cannot give real effect. The grow of total vehicles in DKI Jakarta for last 10 years is 6% per year and millions of vehicles from outside of Jakarta come into Jakarta and cause traffic jam in many roads in Jakarta. Repair of public transportation system constitutes main solution which should be immediately carried out by Local Government of DKI. Safe, comfortable and proper and timely public transportation constitutes target that should be implemented.

1.2 Research Purpose

This research purpose is to rationalize amount of public transportation vehicles in every public transportation route in Jakarta, so ideal ratio can be gotten between fleets and passengers

2. DISCUSSION

2.1 Research Methodology

Approach in these activities is system approach. This approach is chosen because model of policy in determining balance between amount of mode and passengers is influenced by many interrelated elements between one and another and dynamics in nature.

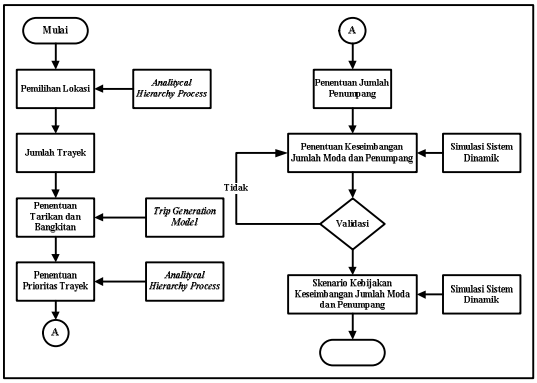

Picture 1. Mind frame flow diagram

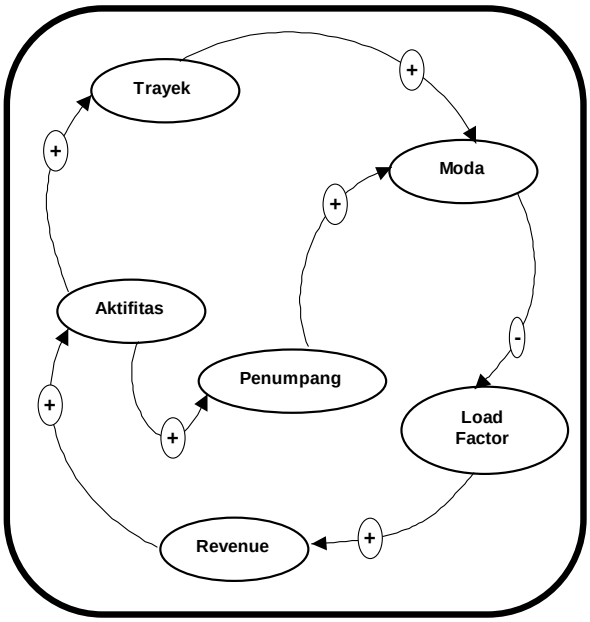

Picture 2 : Causal Loop Diagram model mental

2.2 Research Result

Discussion in this research will be carried out in phases, firstly by determining research location by choosing alternatives of research location, namely Central Jakarta, West Jakarta, East Jakarta, North Jakarta, and South Jakarta. Then after location is chosen, project priorities should be determined as object in this transportation research. Then, calculation of passengers and total fleet determining model are carried out to determine balance between total mode or fleet needed with total passengers. Then, scenario of policy is made to determine balance between total mode and total passengers.

2.3 Determine Research Location

Determine research location is carried out by using AHP Method. Hierarchy Structure of Problems in this selection can be seen in Picture 3.

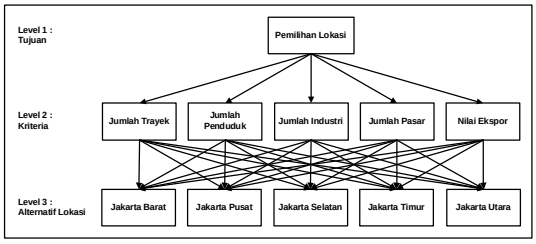

Picture 3. Hierarchy Structure research location determination

Selection process is carried out by holding discussion with experts; consist of academicians, namely, Mr. Ir. Edi Santoso Msc, Lecturer of Industrial Engineering, University of Bina Nusantara, and also constitutes researcher from BPPT. The second and third experts are practitioners, namely, staff from Jakarta Transportation Agency and Planning Bureau, Transportation Department.

Result from software expert choice is that load criteria of total route is 0,398, load criteria of total population is 0,245; load criteria of total industries is 0,156; load criteria of total market is 0,136, and load criteria of total export is 0,064. Based on load values, the highest load criterion is for total route. So in order to choose location as research object based on location with the highest total route is North Jakarta with total route is 37 routes.

2.4 Determine total passenger on 5 routes in North Jakarta

From 37 routes in North Jakarta, 5 routes are chosen as the highest amount of passengers by considering that the highest amount of passengers indicate route with the more need of public transportation amount. Based on selection result, 5 routes with highest amount of total passengers are Tanjung Priok – Blok M, Tanjung Priok – Embrio, Tanjung Priok – Kota, Tanjung Priok – Cililitan, Tanjung Priok – Cilincing.

Determine total passengers in these routes are carried out by making Origin Destination (O-D) Matrix, to find how many the highest amount of total passengers is determined. Reference to total passengers, research priority is Tanjung Priok – Blok M.

Tabel 1: Amount of passengers from origin to destination 5 selection trajec

Origin	Destination						Oi
	Tj. Priok	Blok M	Embrio	Kota	Cililitan	Cilincing	
Tj. Priok	-	1.376	1.112	1.088	992	952	**5.520**
Blok M	1.186	-	217	2.030	1.987	270	**5.690**
Embrio	1.150	220	-	276	150	234	**2.030**
Kota	1.123	2.023	245	-	1.089	350	**4.830**
Cililitan	1.023	1.856	174	1.134	-	347	**4.534**
Cilincing	983	254	270	332	365	-	**2.204**
Dj	**5.465**	**5.729**	**2.018**	**4.860**	**4.583**	**2.153**	-

2.5 Determine Route Priority in North Jakarta

From 5 routes chosen, there are other route priorities that should be chosen as research objects because of time limitation in research. Selection process is carried out by using AHP method. Hierarchy structure of problems in route alternative chosen can be seen in Picture 4.

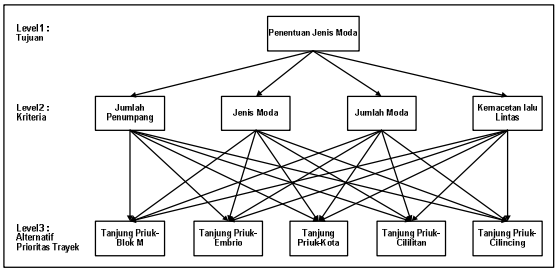

Picture 4. Hierarchy structure of moda selection

Criteria in choosing this route are type of mode, total mode, total passengers and traffic jam. As a result of software, load criteria of mode type is 0,338; load criteria of total mode is 0,220; load criteria of total passengers is 0,083; load criteria of traffic jam is 0,359.
Based on those load values, the highest criterion is traffic jam. So in order to choose route as research object based on route, the highest potential traffic jam is route of Tanjung Priok – Cilincing, passed by *Mikrolet M-14*.
From O-D Matrix, it can be known that Dj value is 2,153 passengers and total Oi is 2.204 passengers. So total passengers in route Tanjung Priok – Cilincing will be an input in the model for the further step; namely, to choose between both values as the highest value, and total passengers in this route is 2.204 passengers per day.

2.6 Determine Balance Model of Total Mode and Passengers

In order to determine balance of total mode and passengers, modeling and simulation is carried out by using dynamic system simulation.

2.7 Balance Model Simulation on Total Mode and Passengers by Using Dynamic System Simulation

Simulation made in route transportation model of mode M14 is to generate 3 big systems, namely income for vehicles' owners, income for drivers, and income for drivers based on ratio.

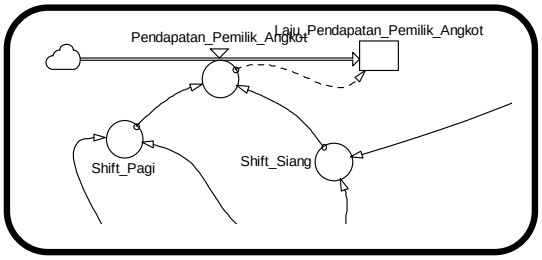

Picture 6 : Drivers' income system

System in Picture 6 is formed based on drivers' income for morning and noon shift. An assumption used in system served in Picture 7 is for vehicles' owners who as mode fleet M14, not vehicles' owners individually.

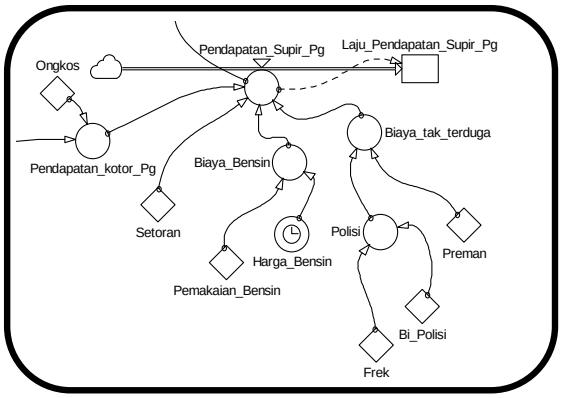

Picture 7. for vehicles' owners income system

Drivers' income is net income of drivers after being deducted with other expenses. Discussion and analysis carried out then is for morning income of drivers, and this condition is also valid for noon income of drivers, but dynamic system simulation model used in both existing conditions are morning and noon shift. Assumed that on morning and noon shift, total drivers drive mode M14 is one person. Net income is gotten by deducting net income with combination of variable and deposit constant, gasoline expense and undetermined expense. Other expenses in this system are deposit, gasoline expense and undetermined expense. Total deposit constant constitutes obligatory deposit data given by public transportation vehicle to the owners, namely Rp 100.000,- Gasoline is gotten from variable of gasoline price and constant of total gasoline consumption. Constant average of gasoline consumption based on interview result with public vehicles' driver is 19,2 liters for each shift.
Gasoline price is become variable because as it is known, gasoline price is not stable and always experience fluctuation, so gasoline variable uses step function, namely on 31st period, there is addition for 500. Variable of gasoline expenses is gotten by multiplying constant of gasoline consumption with variable of gasoline price. Based on simulation, expenses paid by public vehicle's driver starting from 31st period will decrease Rp 500,-
Undetermined expense comes from police variable (pay police because of traffic trespassing carried out) and constant of street kids. In one day, any drivers get traffic ticket in route M14

from police because of any reasons. The most reason is waiting passengers or stop more than 5 minutes not in the usual place. In addition, passengers motor and go down not in the usual place in the location of Cilincing Street and Yos Sudarso Street.

Total traffic ticket averagely is Rp 15.000,- based on interview with several public vehicles' drivers. While frequency is determined in constant informed is that one week or 5 monitoring days, there is possibility to get traffic ticket 3 times, so its value is 0,6.

The final variable is morning gross income. This income constitutes combination between constant of expenses with variable of total morning passengers. Constant of expenses is gotten based on average expenses paid by passengers, namely Rp 2.500,-. Variable of total morning passengers is described in model served in Picture 8.

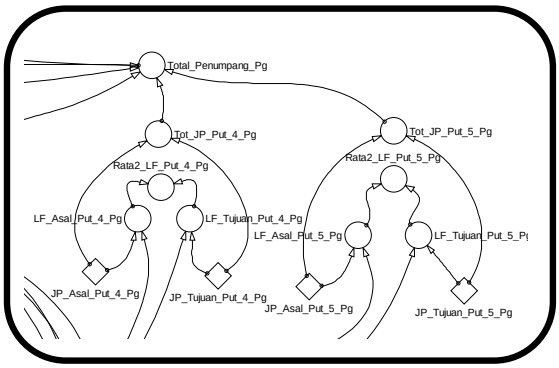

Picture 8. Variable of total morning passengers

Variable of total morning passengers means total passengers who motor M14 in the morning shift, namely from 5 o'clock in the morning up to 12 o'clock at noon. It means that there are 5 times passengers' rotations by using this mode from Tanjung Priok Terminal to Cilincing Terminal.

The abovementioned model only represents 4th and 5th morning shifts. The following explanation will only describe total passengers in morning shift for the 4th rotation. Total passengers in 4th rotation are gotten by adding constant of total passengers from origin and destination. Total passengers from origin and destination are determined as constant in this model. Because passengers motor are assumed in the fixed amount.

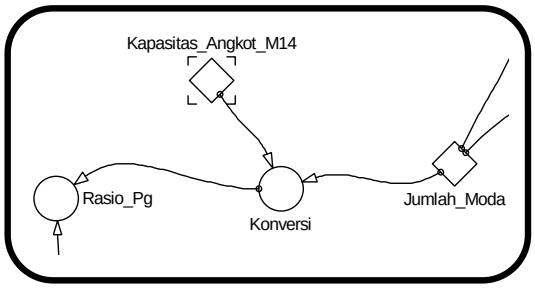

Picture 9. Load Factor model determination

Determining risk is carried out separately for morning and noon shifts. The following ratio constitutes load factor happen in the morning shift. This statement is same with served in Picture 10

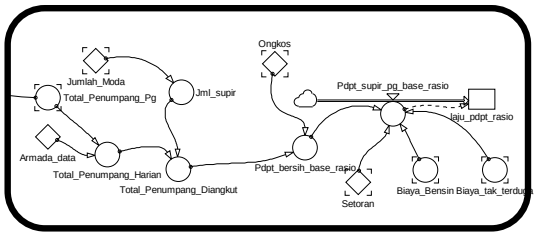

Picture 10. Total passengers and mode comparison

The abovementioned model constitutes determination of total drivers' income influenced by ratio; in this matter is load factor. If it is influenced by ratio, so variable, of course, should be known, is total drivers. Because there are many fleet together with total vehicles' drivers. So variable of total drivers is added by entering constant of total mode.

2.8 Analysis of Simulation Result

Based on simulation result between total mode, ratio and drivers' income described in Table 2, it is known that more available mode is lower load factor ratio, as a result of more drivers' income, and otherwise.

Tabel 2: Simulation Result

Total Mode	Load Factor Ratio	Net driver's income (Rp.)
79	0,114	90.400
50	0,180	273.100
30	0,300	604.900
12	0,750	1.849.150

Based on modeling result to determine balance between total mode and total passengers by using dynamic system simulation, it is known that total mode optimally is 30 modes, and ratio between total passengers and transportation capacity is 0,3000 and driver's income per day is Rp

604.900,- Based on simulation result, condition of transportation amount right now is 79 vehicles, and they are not realistic compared with those amounts, because load factor ratio will be low, and as a consequence, driver's income will also low.

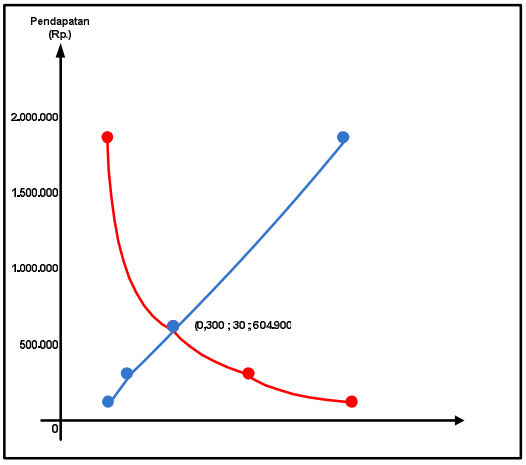

Picture 5.17. Total mode and driver's income relation

2.9 Scenario of Balance Policy between Total Mode with Passengers

Balance scenario between mode and total passengers is to develop scheduling for mode in route M14. Mode scheduling meant here is to schedule arriving and leaving of mode from one stasion to other stopping place.

Trip carried out by Mode M14 is basically without scheduling. There are 79 vehicles operated to bring passengers from the morning up to noon. Every vehicle does not have exact stopping place. Vehicle will be stopped where passengers want to stop. Based on monitoring result along route of Tanjung Priok – Cilincing, it is known that there are 18 roads passed by this mode. It is also known that every time vehicle stops need averagely one minute or 60 seconds. And length of trip from one stopping place to other stopping place is at least 1,6 minutes or 96 seconds. So average time needed from on stopping place to another stopping place is 2,6 minutes or 156 seconds. If mode M14 leaves in the morning at 5.00 o'clock from Tanjung Priok Terminal, so this mode will arrive in Cilincing at 5.23 o'clock.

Basically, scheduling may not be carried out by operating 79 vehicles all at once. If so, of course, traffic jam cannot be avoided, and load factor is very small, as proven in the previous model.

2.10 Mode Scheduling Policy without Adding Stopping Place

This policy will be carried out in the scenario of total mode of 79, 30 and 20. This scenario will not be carried out by adding stopping places. First scenario will be valid for total mode of 79 with traffic jam condition. So length of time needed to pass with this traffic jam is 300 seconds. Stopping time does not change, namely 60 seconds, but length of running mode is 240 seconds, because there are several traffic jam points. Picture below serves SFD in accordance with actual condition.

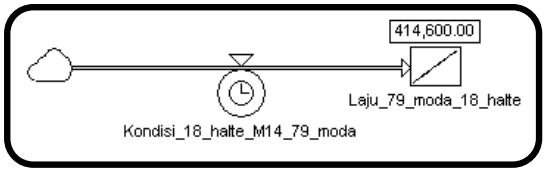

Picture 11. System 79 Mode with 18 Halte

From abovementioned simulation, it is known that it is impossible to schedule 79 modes in one day, because time needed for 79 modes operated are around 116 hours after 5 o'clock.

Therefore, there is mode accumulation along Tanjung Priok – Cilincing route. And there is unfair competition among public vehicles' drivers. Based on simulation result, if fleet operated is 79 vehicles, to driver' s income is very low, that is Rp 90.400,- It is if driver drives in the morning shift. Actually, there are 4 up to 5 drivers drive fleet.

Second scenario will be valid for total modes as amount of 79 vehicles if there is no traffic jam. It means that trip period should be passed from one stopping place to another stopping place is 156 seconds. Third scenario is to operate 30 vehicles in 18 stopping places, and conditions are traffic jams. There are 30 vehicles chosen because they are fitted with harmony between load factor and best driver's income.

From simulation result, it is known that the 30th vehicle actually finishes its trip 43,67 hours. The following will be carried forth scenario if there is no traffic jam, assumed that length of time needed to pass from one stopping place to another is 156 seconds. The fifth and sixth scenarios are to operate 20 modes in 18 stopping places in traffic jam and non traffic jam conditions. If traffic jam happens, so the following is its simulation result. From those conditions, it is known that the 20th mode will arrive in Cilincing around 29,08 hours from the first mode leaving time at 5 o'clock in the morning. The 6th scenario is if for 20 modes in fluently traffic, and there are 18 stopping places. From those condition that the 20th mode will

arrive in Cilincing around 15,12 hours from the first mode leaving time at 5 o'clock in the morning. It is meant that the 20th mode can finish its trip at 22.12 o'clock.

Tabel 3: Scenario recapitulation

Scenario	Moda (unit)	Head Way (second)	Time Cycle last (hour)	Condition
I	79	300	115,00	Macet
II		156	59,89	Tidak Macet
III	30	300	43,67	Macet
IV		156	22,71	Tidak Macet
V	20	300	29,08	Macet
VI		156	15,12	Tidak Macet

2.11 Mode Scheduling Scenario By Adding Stopping Places

The second big scenario constitutes scenario to implement stopping place development as amount of 10 places along M14 mode route from Tanjung Priok – Cilincing. Total modes simulated are 70, 30 and 20. Conditions are if there is traffic jam and there is no traffic jam.

If the second scenario is chosen, so of course, there is consequence should be gotten by government, there are 10 stopping places should be developed as public service facilities. In this matter, stopping places are not to arrange M14 mode scheduling, in order that drivers do not stop to motor and go down passengers, as well as to decrease traffic jam along those routes.

The first scenario carried out for M14 mode is 79 vehicles, and operated based on schedule by using 10 stopping places, as well as assumed that several traffic jams happen along those routes. So length of time to pass those routes from one to another stopping place is 300 seconds.

From simulation, it is known that first mode leaves Tanjung Priok is at 5 o'clock, and arrives in Cilincing at 5.45 o'clock. So length of time to pass from Tanjung Priok to Cilincing is 45 minutes. The last mode is the 79th arrive in Cilincing on 62,5 hours.

The second scenario is carried out for M14 mode of 79 vehicles, and operated based on schedule by using 10 stopping places, as well as assumed that there is no traffic jam along routes. So trip time needed from one to another stopping place is 156 seconds.

From simulation, it is known that first mode will leave Tanjung Priok at 5 o'clock, and arrive in Cilincing at 5.23 o'clock, so average trip time passed from Tanjung Priok to Cilincing is 23 minutes. Last time the 79th mode arrive in Cilincing is at the 32,5 hours.

Third scenario is carried out for M14 mode is 30 vehicles, and operated based on schedule by using 10 stopping places, as well as assumed there are several traffic jam along routes. So trip time needed from one to another stopping place is 300 seconds.

From simulation, it is known that first mode leaves Tanjung Priok at 5 o'clock, and arrives in Cilincing at 5.23 o'clock, so average trip time passed from Tanjung Priok to Cilincing is 23 minutes. Last time the 30th mode arrives in Cilincing is at the 23,67 hours.

The forth scenario is carried out for M14 mode is 30 vehicles, and operated based on schedule by using 10 stopping places, as well as assumed there is no traffic jam along routes. So trip time needed from one to another stopping place is 156 seconds.

From simulation, it is known that first mode leaves Tanjung Priok at 5 o'clock, and arrives in Cilincing at 5.23 o'clock, so average trip time passed from Tanjung Priok to Cilincing is 23 minutes. Last time the 30th mode arrives in Cilincing is at the 12,31 hours.

The fifth scenario is carried out for M14 mode is 20 vehicles, and operated based on schedule by using 10 stopping places, as well as assumed there are several traffic jams along routes. So trip time needed from one to another stopping place is 300 seconds.

From simulation, it is known that first mode leaves Tanjung Priok at 5 o'clock, and arrives in Cilincing at 5.23 o'clock, so average trip time passed from Tanjung Priok to Cilincing is 23 minutes. Last time the 30th mode arrives in Cilincing is at the 15,75 hours.

The sixth scenario is carried out for M14 mode is 20 vehicles, and operated based on schedule by using 10 stopping places, as well as assumed there is no traffic jam along routes. So trip time needed from one to another stopping place is 156 seconds.

From simulation, it is known that first mode leaves Tanjung Priok at 5 o'clock, and arrives in Cilincing at 5.23 o'clock, so average trip time passed from Tanjung Priok to Cilincing is 23 minutes. Last time the 30th mode arrives in Cilincing is at the 8,19 hours.

From abovementioned sixth scenario of simulation result, the following Table 4 will provide its recapitulation.

Table 4:. Sixth scenario recapitulation

Scenario	Moda (unit)	Head Way (second)	Time Cycle Last Moda (hour)	Condition
I	79	300	62,50	Macet
II		156	32,50	Tidak Macet
III	30	300	23,67	Macet
IV		156	12,31	Tidak Macet
V	20	300	15,75	Macet
VI		156	8,19	Tidak Macet

Based on calculation result of harmony for amount of mode, ratio and total driver's income, so best ratio or load factor is 0,30. This value is become indicator to develop scenario in line with two abovementioned big scenarios. Simulation result to operate M14 route is 30 modes provided in the following table.

Table 5: 30 Moda schedulling with halte adddition

Cyclus	Starting Time	Finishing Time	Cycle Time (Hour)
I	05.00	06.18	1,30
II	06.18	07.36	
III	07.36	08.54	
IV	08.54	09.12	
V	09.12	10.30	
VI	10.30	11.48	
VII	11.48	13.06	

By applying scenario to operate 30 modes and additional stopping places, so there is one rotation in the morning shift, and driver can carry out 7 rotations, while of there is no schedule, driver only can carry out 5 rotations. So it will influence driver's income significantly. The following is the comparison.

Table 5: Comparison driver's income with policy

Policy	Moda	Rasio (Load Factor)	Number of Cyclus in 1 Shift	Drivers' Revenue (Rp./day)
Without adding shelter	30	0,300	5	604.900
With adding shelter	30	0,421	7	940.650

From abovementioned table, it is known that additional stopping places for 30 vehicles will generate ratio lower than additional stopping places for additional stopping places, namely 0,421. Refer to this policy, driver's income increase from Rp 604.000,- to become Rp 940.650,- because rotation will increase also, namely from 5 rotations to become 7 rotations. The following SFD simulation result indicates the increase in driver's income.

3. CONCLUSION AND SUGGESTIONS

3.1 Conclusion

1. Based on developed model result, total public transportation vehicles for Tanjung Priok – Cilincing (M-14) rationally are 30 vehicles. Those amounts will give the highest load factor if they are integrated with innovation as public transportation scheduling system, so they can increase driver's income and will decrease traffic jams.
2. Based on policy and scenario made, suggested policy is to schedule 30 vehicles by adding 10 stopping places. Additional stopping places will increase government's fund as amount of Rp 100.000.000,- and they will increase driver's income become Rp 940.650,-

3.2 Suggestions

In view of conditions, there are 79 M-14 vehicles with average trip feasibility are for 60 vehicles. System evaluation of licenses for M-14 routes may be carried out.

REFERENCES

[1]. Aminullah, E. 2004. Berpikir Sistemik : Untuk Pembuatan Kebijakan Publik, Bisnis dan Ekonomi. PPM, Jakarta.
[2]. BPS. 2007. Jakarta Barat dalam Angka. BPS. Jakarta.
[3]. BPS. 2007. Jakarta Pusat dalam Angka. BPS. Jakarta.
[4]. BPS. 2007. Jakarta Selatan dalam Angka. BPS. Jakarta.
[5]. BPS. 2007. Jakarta Timur dalam Angka. BPS. Jakarta.
[6]. BPS. 2007. Jakarta Utara dalam Angka. BPS. Jakarta.
[7]. Chung, W.C. 1999. *A System Dynamic Simulation Model in The System Support Organization of A Speedy Printing Company* (ABC/CND/Powersim Project). Thesis. *Systems Management College of Notre Dame*. (on-line) dalam http://.www.rondo.com/capstone/Paper/
[8]. Eriyatno, 2003. Ilmu Sistem: Meningkatkan Mutu dan Efektifitas Manajemen. Bogor: IPB Press.
[9]. Mainheim, 2000. *Fundamental and Transportation Analysis*, McGraw Hill, New York.
[10]. Marimin. 2004. Teknik dan Aplikasi Pengambilan Keputusan Kriteria Majemuk. Gramedia Widiasarana Indonesia, Jakarta.
[11]. Muhammadi, E. Aminullah, dan B. Soesilo. 2001. Analisis Sistem Dinamis : Lingkungan Hidup, Sosial, Ekonomi, Manajemen. UMJ Press, Jakarta.
[12]. Nurhasanah, Nunung, dan Siti Nur Fadlilah. 2008. Pemodelan trategi Pemasaran Produk Barang Jadi tekstil berdasarkan Pendekatan Simulasi Sistem Dinamik pada Industri kecil Menengah di Kota Bogor. Proceeding Seminar Nasional INSAHP5. ISBN:978-979-97571-4-2. p:B12-1.
[13]. Radzicki, M.J. 1994. Powersim, *The Complete Software Toll For Dynamic Simulation*. User's Guide and Reference. Modell Data AS, Norway.
[14]. Saaty, T.L. 1993. Pengambilan Keputusan Bagi Para Pemimpin. Terjemahan. Pustaka Binaman Pressindo, Jakarta.
[15]. Sterman, J.D. 2000. *Business Dynamics : Systems Thinking and Modeling for A Complex World*. McGraw Hill, USA.

ISSN 114-1284

CONCEPT STUDY OF SOLID WASTE MANAGEMENT (PILOT PLANT IN NEIGHBORHOOD (RW) 04, MEKARJAYA SUB-DISTRICT, SUKMAJAYA DISTRICT, CITY OF DEPOK)

Soelistyoweni Widanarko[1], Evy Novita[2]

Environmental Engineering Study Program, Department of Civil Engineering
Faculty of Engineering, University of Indonesia
Phone: (021) 787 5031
Email [1]sulistyoweni1@yahoo.com, [2]evi_nz@yahoo.com

ABSTRACT

The City of Depok produces solid waste up to 3,000-3,400 m^3/day. The amount of solid waste transportable to landfill is only 1,200m^3/day, approximately 35% of total amount produced. Solid waste is transported to Cipayung Landfill, an area of 11.1 hectares, which is predicted to be packed by 2010. The objective of this research is to implement the 3Rs (Reuse, Reduce & Recycle) concept in providing inputs and feedback for the Government City of Depok in order to minimize the amount of solid waste and prolonging landfill operational period. There are 3 activities in this research which are observing a location already implementing 3Rs concept, outlining an integrated solid waste management (ISWM-3Rs) concept model and developing solid waste pilot plant. The ISWM-3Rs concept model can be successfully implemented through community socialization activities, with the assist during the implementation process. The ISWM-3Rs concept model is proven to reduce amount of solid waste transported to landfill. This program will generate revenue to the RW (Rukun Warga). ISWM-3Rs Cadres and agents play an important role to successfully the ISWM-3Rs concept.

Keywords

Solid waste, ISWM-3Rs, pilot plant, Neighborhood Organization (RW)

1. INTRODUCTION

The City of Depok is located in West Java with an area of 200,9km^2 and population reaching 1,503 million people [1]. The city is constantly growing and producing solid waste up to 3,000-3,400m^3/day [1]. However, the amount of solid waste transportable to landfill is only 1,200m^3/day, approximately 35% of total amount produced. The source of solid waste originates from residential (62%), traditional market (21%) and others (17%). Solid waste transported to Cipayung Landfill, the 11.1 hectares final disposal area, predicted to be packed by 2010 [1].

Waste management is managed by the Office of Cleanliness and Landscaping (OCL) City of Depok. OCL has a strategy which used in solid waste management as follow: a) implementing a new 3Rs (reduce, reuse and recycle) concept basis paradigm with the community's involvement; b) optimizing the waste treatment in every sub-district through developing Waste Treatment Unit (WTU); c) reducing the amount of solid waste sent to landfill (TPA) through proper treatment at WTU; d) increasing the community's involvement in producing compost at their home site; and e) composing and implementing Local Government Decree (Perda) on cleanliness management and in line with Law no. 18 (2008) on Solid Waste Management [1].

OCL has built 5 WTU's in 2007 and at this moment is still operational. In 2008, an additional 18 WTU's were built where 5 have been operational. By 2011, OCL is planning to have added an additional 40 WTU's thus totalling 60 WTU's in Depok. Each WTU has a capacity of 30 m^3/day except the one located at landfill (90 m^3/day) [1].

The obstacle faced by OCL , amongst, are the low level of community's awareness on clean and healthy living and the implementation of 3Rs [1]. The limitation of infrastructure, human resources and funding is also part of the obstacles that needs to be addressed, along with the community's refusal of having WTU built in their neighbourhood. An example of community refusal is seen at Taman Cipayung Residence and Bukit Rivaria Residence. These refusal cause a delay in delivering WTU and thus not able to meet the target set in the early stages.

The obstacle in solid waste management faced by the Government of Depok addreses the needs to develop a waste management model that reflects the community's involvement. The model that will be developed is aimed to reduce the amount of solid waste directly from its main source, which is residential. This, in turn, will also reduce the amount of waste send to the landfill.

ISSN 114-1284

2. OBJECTIVES

The objective of this research is to implement the 3Rs (*Reuse, Reduce* & *Recycle*) concept in providing inputs and feedback for the Government City of Depok in order to develop an Integrated Solid Waste Management System (ISWM-3Rs). These inputs and feedback could minimize the amount of solid waste send to landfill, thus prolonging its operational period.

3. METHODOLOGY

There are 3 activities in conducting this research: 1) Observation at location which already implementing 3Rs concept for its solid waste management; 2) outlining an integrated solid waste management concept model with 3Rs basis; and 3) developing solid waste pilot plant with 3Rs basis.

3.1. Observation

Observation conducted as input and comparator in developing integrated solid waste management base on 3Rs (ISWM-3Rs) at pilot plant. Observation will be conducted at location which are already implementing 3Rs concept in their solid waste management. The object of this observation, amongst, is socialization process which have been conducted, implementing 3Rs concept process, solid waste separation, supplying the facilities, composting and recycle process, organization, funding aspect and obstacles.

Observation in the field conducted at house as source of solid waste and the activity of composting and separating took place. Hereinafter, result of observation noted and became materials to analyze the outlining ISWM-3Rs concept model and it's implementing process.

3.2. Outlining an Integrated Solid Waste Management Concept Model with 3Rs Basis

The concept model is developed based on the community's needs and requirement, which is then utilized to facilitate during try-out phase.

3.3. Developing Solid Waste Pilot Plant with 3Rs Basis

The practice of ISWM-3Rs does not conduct in wide area but only in one RW. RW 04, which resides at Mekarjaya Sub-district, was chosen as pilot plant location base on their good response during socialization process.

The ISWM-3Rs model that will be conducted should be appropriate with the local community requirement. The selection of model will be discussed with the entire community member, thus, the chosen model is a collective decision within the community.

The practice of ISWM-3Rs model includes the following three activity phase which are preparation phase, implementing phase and improvement phase as shown in Table 1.

Table 1: Phase of ISWM-3Rs practice

PREPARATION	IMPLEMENTATION	IMPROVEMENT
Exploring potential location and solid waste composition	Model building	Monitoring
Program briefing and explanation	Discussing	Evaluating
Survey of community needs	Organization building	
Planning to fulfill community needs	Implementing	
	Management	

4. RESULTS AND DISCUSSIONS

4.1. Observation Results

Observation was conducted at the Griya Pancoran Mas Residence within Rangkapan Jaya Sub-District, Pancoran Mas District. This residence is located in one RW that consists of 7 RT's, comprise of 360 middle-income housing units and is seen in Figure 1 below.

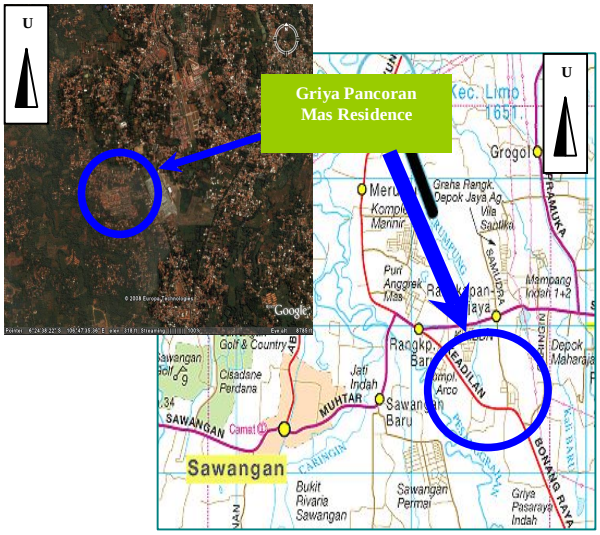

Figure 1: Observation location at Griya Pancoran Mas Residence, Rangkapan Jaya Sub-district [2, 3]

Waste management at Griya Pancoran Mas Residence was first socialized in October 2007 through participating in various residence activities such as neighborhood meetings. Work Groups (WG) and Environmental Cadres (EC) were formalized, where WG would be the person in charge, proctor and enforcement whenever EC face challenges. EC were chosen based on their ability and willingness to implement ISWM-3Rs. EC is responsible for briefing, monitoring, coordinating with housing units within their supervising area, managing recycled materials such as selling these materials to recycle agent and sales bookkeeping.

The ISWM-3Rs model was implemented starting in May 2008. Each RT had 4 EC, totalling 28 for the entire residence area. Each EC recieves Rp 30.000/day from OCL for the first 3 months. This funding is provided since it is an OCL work program, and in addition, OCL also provides bins for individual composter for seperating inorganic waste, drill to create bio-pore and poster and banner for campaigning.

Observation was conducted on each EC and houses as the main subject of waste management, where the observation is required to see how EC performs their duties with consistency. The observation items for EC include whatever actions taken when dealing with recycled material, ability to motivate the housing unit within their supervising area in order to seperate waste and composting, along with level of consistency shown in implementing the model in their own home. The observation in each housing include level of awareness and consistency in dealing with waste seperation, making compost, usage of recycled material, and their views toward WG and EC.

The observation period lasted for approximately 2 months, and the ISWM-3Rs model implemented at Griya Pancoran Mas is as follow:

a. Each house conducted waste separation for organic and inorganic waste
b. Organic waste consist of three types, which are yard waste, unprocessed food waste and processed food waste
c. Yard waste is converted to compost by forming a rounded wire mesh and the waste is inserted into the rounded area
d. Unprocessed food waste is converted to compost via takakura method
e. Processed food waste is converted to compost via bio-pore
f. Inorganic waste recyclable is collected in the bins provided, collected every 7-10 days by EC, sold to recycle agent and bookkeeped the amount sold
g. Waste that cannot be converted to compost or as recycled material will be collected by waste collector and taken to temporary station

Figure 2: Solid waste separation, bio-pore and composting with Takakura method in Griya Pancoran Mas Residence

In the early stages of implementation, it is observed that the EC are still active in controlling and briefing the houses under their supervision. But later in the program, inconsistancy begins to grow. Some EC in RT 05 and 07 shows sign of boredome and demotivated, EC in RT 04 shows inconsistency in compost processing especially shredding the waste. But on the other hand, EC in RT 02 and 03 still shows consistency in motivating their resident as well as within their homes for waste separating and composting.

Based on house observation, it is seen that waste seperating went well with the exception some houses were inconsistent in performing this act. Composting via takakura method also went well at the early implementation stage, but reaching the end of observation period it is seen that the community's motivation started to wear out especially during the shredding process. The common reasoning being the fact that this process is time consuming, where the bulk of their time is allocated towards their family or full-time job. In addition, some resident complain that the takakura method is difficult to perform. The roles and responsibility of WG and EC were shown positive, with the exception that some thought WG didn't provide sufficient support to implement ISWM-3Rs.

There were several difficulties that the resident felt in implementing this system, which are:

a. Shredding takes too much time, thus demotivating resident to perform this task
b. Minimum knowledge on composting via takakura method resulting compost produced being too wet, too dry or containing maggot, thus causing lack of interest from resident
c. Composting via bio-pore attracts mouse and rodent, thus causing lack of interest from resident
d. Duration between recyled material collection is too long, thus creating a sense that the resident's house is filled with garbage

These feedbacks from Griya Pancoran Mas residence will be utilized in the model development at pilot plant.

4.2. An Integrated Solid Waste Management Concept Model with 3Rs Basis Results

The 3Rs concept has very important role in an integrated solid waste management system. One of its benefits is to reduce solid waste volume that enters into landfill, thus prolonging the landfill operational period. The 3Rs concept related with solid waste management hierarchy resides on top of hierarchy. This concept can be developed based on solid waste type to separate, garbage bin type and location, and composting methods used. The ISWM-3Rs concept could be seen in Figure 3 below.

Solid waste separation was conducted to dissociate waste deemed for reused, recycled or composted based on its originate being organic or inorganic waste. Inorganic waste will be further separated into paper, plastic, glass, textile and metal.

Solid waste that has been separated will not be mixed when transferred to temporary station (TPS). Bins and transportation system are needed to dissociate the waste types. The bins could be individually or communally provided.

Figure 3: Integrated solid waste management concept model

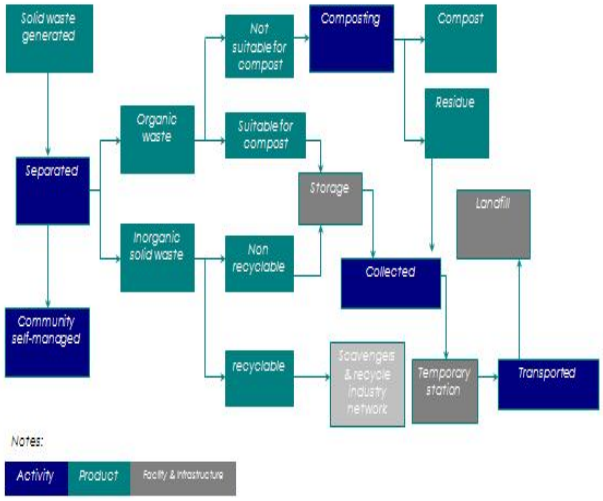

with 3Rs basis in general

The bins to be utilized must be strong enough, waterproof, inexpensive, easily made or obtained, and easily emptied. The suitable materials that could be used include plastic, fiberglass, metal, wood, cane or bamboo. Indonesian National Standard (SNI) No.19-2454-2002 could be followed for waste bin material and size. The amount of bins utilize is exactly the same amount of waste separated. The waste bins are placed in front of each residence or house and accessible to waste collector and owner. The alternatives of waste bins location can be seen at Figure 4.

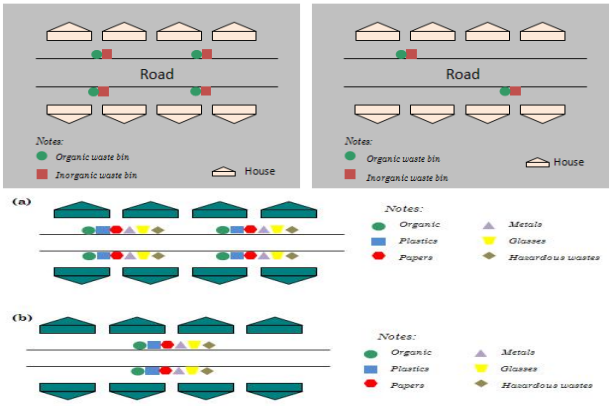

Figure 4: Alternatives of waste bins location at residence area

Transportation type and period that will be performed refers to ISWM-3Rs model. Waste transportation will be divided into two transportation types, each for organic and inorganic waste. Organic waste will be carried away to temporary station daily or every two days. Should organic waste will composted communally, it should be carried away daily. But the other hand, the waste doesn't have to be carried away daily if individually composted since it is not economical.

Organic waste will be composted and becomes fertilizer. There are several methods in composting depending if individual or communal. Takakura method is performed for individual composting, whereas open windrow method is performed for communal composting. Bio-pore, both individually and communally, could be useful to make compost for yard waste.

According to the explanation above, therefore a models has

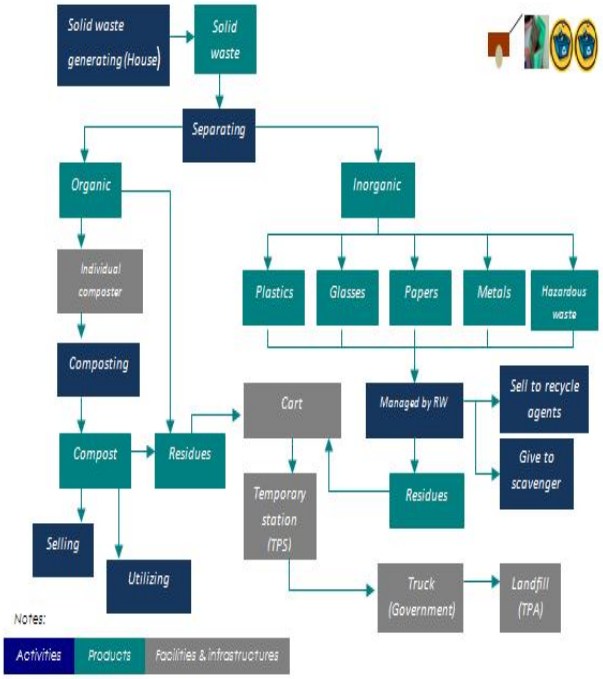

been developed as shown at Figure 5 below.

Figure 5: The ISWM-3R model of integrated solid waste management that implemented at RW 04 Mekarjaya Sub-District

The ISWM-3Rs model has been developed base on:

a. Composting methods: individually or communally
b. Type of waste separated which consist of two waste types (organic and inorganic waste) or six waste types (organic, plastic, paper, glass, metal, and hazardous waste)
c. Management of inorganic recycled materials conducted by waste owners or local organization (RW/PKK)

4.3. Solid Waste Management Pilot Plant Results

The Pilot Plant was conducted at RW 04 in Mekarjaya Sub-District, started with initial phase of socializing the model. Socialization were done during several meetings with local

organization (RW/RW Siaga/Ketua RT/PKK), where in the meetings formal organization was formed and in line with the already local RW/RW Siaga/Ketua RT/PKK organization. In addition, Environmental Cadres were appointed to assist the community during ISWM-3Rs practice.

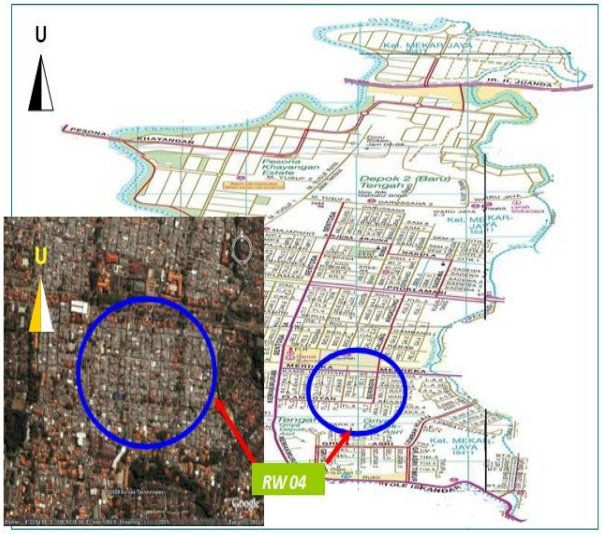

Figure 8: Pilot plant location at RW 04 Mekarjaya Sub-District [3, 4]

The materials needed to implement this model consist of plastic bag utilized as temporary storage of inorganic recycled material and plastic bin utilized as individual composter. This initial try out will be conducted only on 75 houses, with the hope that other residents will be inspired to emulate this program and provide their own materials.

The ISWM-3Rs model chosen for RW 04 is using model 4 with some minor alterations to accomodate the community's current condition. Model 4 is based on seperating the waste into 2 categories, which are organic and inorganic waste. Organic waste deemed for composting is immediately fed into the composter and utilized in the try-out, whereas the ones undeemed are trashed and taken to temporary station at Merdeka Road.

Figure 9: The practice of ISWM-3Rs at RW 04 Mekarjaya Sub-District

Inorganic waste is delivered by its owner weekly to RW office, and then sold off to recycle agent. The alteration performed on model 4 accomodates recycled material managed by RW and PKK organization and not by owner/source of waste.

5. CONCLUSIONS

The ISWM-3Rs concept model is applied successfully through socialization and supervision during implementation process at all time and consistently. Socialization activities were performed during community's monthly meeting, thus eliminating the need for additional meetings. Socialization was necessitated to conduct in order to enhance and shift the community's paradigm on solid waste so they can better understand waste treatment and management correctly. The other successful key of socialization is community's awareness towards the importance of solid waste management.

At the starting period of ISWM-3Rs practice, local organization which includes RW, PKK and EC should be formed. This organization and EC will implement the model and maintain ISWM-3Rs consistenly and sustainably.

The implementation of ISWM-3Rs is able to reduce the amount of waste tranported to temporary station and landfill while simultaneously converting organic waste into compost as value added material and also recycling inorganic waste.

Other succesful ISWM-3Rs factor includes the presence of recycle agents to support the inorganic recycled material chain, connecting the owner/source to recycle factory. Collaborating with these agents is an additional source of income for RW/PKK organization.

REFERENCES

[1] Herwandi, W. "Solid waste management at City of Depok" (Pengelolaan Sampah Di Kota Depok), unpublished.
[2] Google Earth, "Aerial View of Rangkapan Jaya Sub-District", http://www.googleearth.com, October 2, 2008.
[3] G.H. Holtorf, "Jakarta. Jabodetabek. Street Atlas and Index. Version2.0, 2005/2006 edition," Macromedia, 2005.
[4] Google Earth, "Aerial View of Mekarjaya Sub-District", http://www.googleearth.com, October 2, 2008.

ISSN 114-1284

HEURISTIC SOLUTION OF MINIMUM CONCAVE-COST MULTICOMMODITY FLOW PROBLEM

Prof. Dr. Ir. Sutanto Soehodho, MEng. [1] , Ir. Nahry, M.T. [2]

[1] *Professor in Transportation*
Dept of Civil Engineering,
Faculty of Engineering,University of Indonesia
Kampus UI Depok 16424. Ph: 021-7270029
Email : ssoehodho@yahoo.com

[2] *Doctoral Candidate*
Dept of Civil Engineering,
Faculty of Engineering,University of Indonesia
Kampus UI Depok 16424. Ph: 021-7270029
Email : nahry@eng.ui.ac.id

ABSTRACT

This study is concerned with the solution approach of Minimum Concave cost Multicommodity Flow (MCMF) problem. The proposed MCMF makes use of transportation and production cost as well as revenue as its component and it takes form of multisource multidestination system. Concave cost function of our model is associated with transportation and production cost. The objective function of the model is minimization of negative profit.

The particular issue considered in our MCMF model is the use of network representation (NR) in order to solve the model. All the components of the model are represented in link cost functions of links of NR and Flow Requirement of nodes of it. This paper will be focused on the heuristic solution of the problem.

Due to the complexity of the model, the solution approach takes form of bi-level model. The objective of first level is to cluster NR into some sub networks in order to modify multisource network problem into some single source network problem. The objective of second level is to solve the NR, but at this level the NR is already clustered into some sub networks that takes form of single source.

Keywords

Minimum Concave-cost Multicommodity Flow problem, multi sources, network representation.

1. INTRODUCTION

The problem of Minimum Concave-cost Multicommodity Flow (MCMF) arises in many application areas. One of them is its application in the optimization of freight distribution system. Its task is how to assign some amount of products to particular plant to satisfy demand at some points in order to minimize cost of the system.

Concave-cost function arises usually due to the encountered economies of scale in considering some components of cost, such as transportation and production cost. In practice, the unit cost of transporting (or producing) freight usually decreases as the amount of freight increases. Hence, in economies of scale, the marginal cost of transporting (or producing) products is presumed as a decreasing function over the usual operating range. Consequently, in actual operations the transportation (or production) cost can usually be formulated as a concave cost function.

A key mathematical difficulty in analyzing the minimum concave cost network problem is the optimal flow x^* may be a relative minimum and not a global minimum. That is, x^* may minimize the objective function over the intersection of the feasible region and a neighborhood of x^*, but may not minimize the objective function over the entire feasible region.

The MCMF problem proposed in this work is characterized by particular issue regarding the approach used in model solution. We are employing Network Representation (NR) in order to solve the problem. Our NR is originally formed by associated physical network which represents production and demand points, as well as intermediate points (e.g. warehouses). Links between those points denote transportation facilities between those points, such as roads, waterways, railways and airways. Furthermore, we add dummy links and nodes to such physical network, if it is needed, to represent all of the cost components of the model. By using this NR, we solve the problem of MCMF of such NR through the algorithm that is developed in this work.

Due to the complexity of the problem of minimization of concave cost function, especially due to the multisource network and multicommodity problem, we try to approach our MCMF solution by bi-level model. Bi-level model stratify MCMF problem into 2 (two) levels. The objective of first level is to cluster NR into some sub networks in order to modify (original) multisource network problem into some single source networks. The objective of the second level is to solve the original MCMF problem,

but at this level the NR is already clustered into some sub networks. Each of sub network takes form of single source multidestination network.

The organization of the paper is as follows. Section 2 provides an overview of current literature on MCMF problem; section 3 presents our model and discusses its formulation; section 4 proposes algorithm to solve our model, and finally section 5 summarizes the research undertaken and propose some recommendation.

2. LITERATURE REVIEW

Traditionally, minimum concave cost network flow problems have usually been solved in the following 3 ways [7]:

1. By solving a series of Linear Programming approximations to the original problem
2. By local search methods designed to send an extreme flow by searching among candidate solutions
3. By metaheuristic methods, such as Tabu Search, Genetic Algorithm, Simulated Anealling.

Zangwill [8] argue that although concave functions can be minimized by an exhaustive search of all the extreme points of the convex feasible region, such an approach is impractical for all but the simplest of problems. He proposes some theorems which explicitly characterize the extreme points for certain single commodity networks. Algorithms are developed to determine the solution for networks with single source multiple destination networks and single destination multiple source.

Gallo [3] proposes that there is a one-to-one correspondence between the set of extreme flows and Destination Spanning Tree, where the root is source node , each terminal node is a destination, and the remaining destinations (if any) appear as intermediate nodes. Solving the problem of minimum concave cost network flow is based on an implicit enumeration of the elements of Destination Spanning Tree, using a Branch and Bound method. He employs uncapacitated and single source multidestination network.

Guisewite and Pardalos [4] discuss a wide range of results for minimum concave-cost network flow problem, including related applications , complexity issues, and solution techniques. They show that that problem is NP-hard for cases with cost functions other than fixed charge. Algorithms for the general problem are exact or approximate. Exact techniques are efficient only for specific subclasses of problems, and are usually based on branch-and-bound or dynamic programming techniques. Approximation algorithms are based on local search or solving a related linear or convex problem.

Larsson, Migdalas and Rönnqvist [5] propose a heuristic solution technique for the capacitated concave minimum cost network flow problem based on a Lagrangean dualization of the problem. The Lagrangean dual is solved by a subgradient search procedure.

Yan and Luo [7] employ the techniques of simulated annealing and threshold accepting to develop several heuristic that would efficiently solve the concave cost transportation network problems, which take form of . single stage and capacitated network.

Fontess and Gon□alves [2] address the single source uncapacitated minimum concave cost network flow problem. They present a hybrid approach combining a genetic algorithm with a local search.

Yan, Juang, Chen and Lai [7] propose utilization of Genetic Algorithm to develop a global search algorithm for solving concave cost transshipment problems. Efficient encoding, initial population generation, as well as cross over and mutation strategies have been developed to deal with characteristic of the model as single commodity and multisource multidestination problem.

3. MODEL FORMULATION

Our MCMF problem employs transportation cost, production cost as well as "negative revenue" as its cost components. The formulation is set up as cost minimization problem with quantity of products distributed on each link of NR as decision variable. As the transportation and production cost are designed as concave cost function, hence our proposed model follows the nature of MCMF problem. MCMF is aimed to minimize cost in order to deliver some amounts of products from origin to destination, whereas it is limited by some constraints in capacity. The formula of our MCMF problem is as follows :

$$\min Z(x_{ijm}) = \sum_{i \in I} \sum_{j \in J} \sum_{m \in M} \varphi_{ijm}(x_{ijm}) \qquad (1)$$

subject to :

$$\sum_i x_{ilm} - \sum_j x_{ljm} = q_{lm} \quad \forall\, l \in N,\ \forall\, m \in M \qquad (2)$$

$$x_{ijm} \geq 0 \quad \forall (i,j) \in A,\ \forall\, m \in M \qquad (3)$$

where :

x_{ijm} : is aggregate flow on link $i - j$ of product - m

$\varphi_{ijm}(.)\ \forall i \in I, j \in J, \forall m \in M$: is link cost function of link $i - j$ of product-m

q_i : is flow requirement of node-i

N : is set of nodes of network representation

A : is set of links of network reprsentation

M : is set of products

Equation 1 shows the objective function of minimizing total cost of all links on the network which associated to all types of products. The optimization is limited by Flow Requirement on each node, that is total inflow minus total outflow of the node (equation 2). Finally, non negative flow is guaranteed in this optimization.

ISSN 114-1284

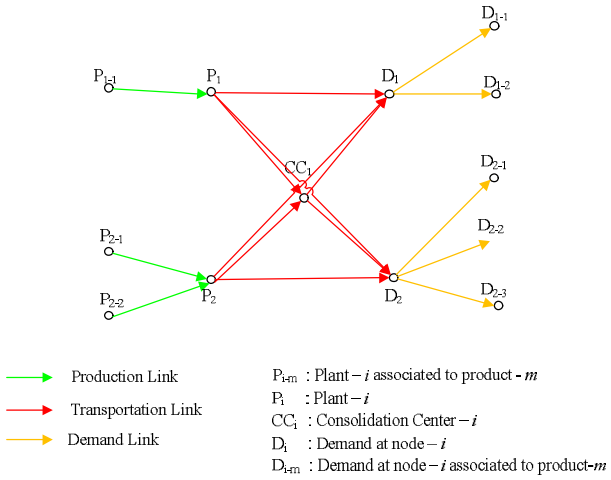

Figure 1. Example of Network Representation

NR associated to our proposed model is denoted in figure 1. Our NR consists of 3 types of links, those are production links which represent production cost, transportation links which represent transportation cost and demand links which represent revenue. Each of production links is associated to production cost of certain type of product, while each of demand links is associated to revenue obtained from selling certain type of product on that node. Both production and demand links are product-exclusive. Furthermore, transportation link is assigned to deal with all types of products aggregately since it is assumed that unit cost to transport any type of products in certain transportation link is similar.

Solving MCMF problem of such NR is similar to solving minimization model of equation 1. All of the constraints of equation 2 are satisfied by the Flow Requirements determined to all of nodes of NR.

4. HEURISTIC SOLUTION OF MCMF PROBLEM

Due to the complexity of solution of MCMF problem, particularly caused by multisource as well as multicommodity problem of the model, we approach the solution by bi-level model. Figure 2 shows the step-wise of our bi-level model.

At the first level, we focus on clustering the destination nodes, based on the associated production point which is the best-suited to be assigned to. At this level, we consider our model as a linear model. It implies that the cost to transport (or produce, or sell) one unit of product from one point to another point is constant, not depend on the quantity of product it deals with. Such unit cost is defined through the associated link cost function, that is by corresponding one unit of flow to its associated cost function.

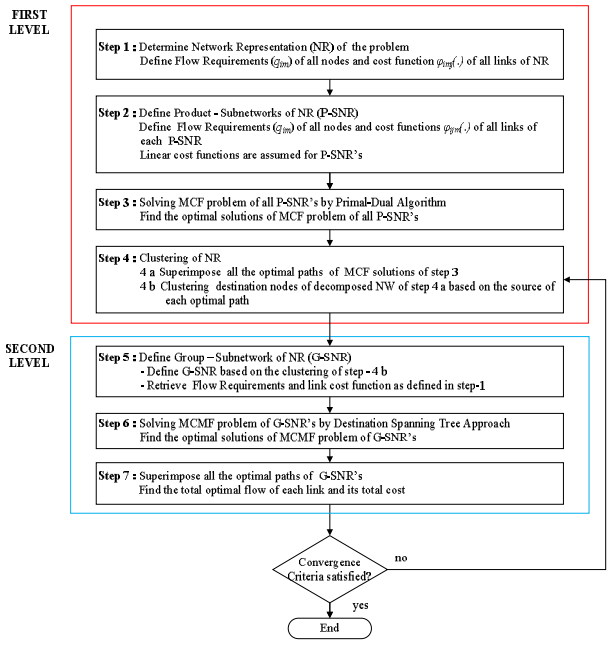

Figure 2. Step-wise of Bi-Level Model

At this level, NR is decomposed into M – Product Sub Network Representation (P-SNR) , where M is the number of types of products. Each of P-SNR represents all the possible links and nodes to be assigned to serve distribution of certain product from origin to destination. P-SNR of product-*x* (for example) consists only of links and nodes of NR in which product *x* can pass through them.

Figure 3a shows the example of one NR that consists of 2 production points (P_1 and P_2) , 7 demand points (D_1~D_7) and it deals with 2 types of products (product 1 and 2). P_1 produces both types of product, whereas P_2 only produces product 1. P-SNR's of such NR are shown in figure 3b and 3c. Figure 3b denotes P-SNR of product 1 and figure 3c denotes that of product 2. Due to product-exclusivity of production links (or demand links) , it is shown that in P-SNR 1 there are no link $P_{2-2} – P_2$ and D_1-D_{1-2} as well as other links associated to product 2. Whereas, there are no link $P_{1-1} – P_1$, $D_1 – D_{1-1}$ and other links associated to product 1 in P-SNR 2.

Due to the linear assumption, the first level concerns to Minimum Cost Flow (MCF) problem. MCF problem of P-SNR's are solved by Primal-dual algorithm. The algoritmic strategy of the Primal-dual is at every iteration it solves a shortest path problem and then solves a maximum flow problem that sends flow along all shortest path [1]. The Primal-dual also maintains a pseudoflow that satisfies the reduced cost optimality conditions and gradually converts it into a flow by augmenting flows along shortest path.

Furthermore, at the end of first level, MCF solutions of all P-SNR's are superimposed to find total optimal flow of first level. The superimposing is allowed to find total flow due to 2 (two) reasons :

1. Unit cost of transportation link of any type of products in certain transportation link is similar.

2. Eventhough the unit cost of production and demand link of all product may not be similar, there exists independency between production link (or demand link) of certain product and the others (due to product-exclusivity of production or demand links) .

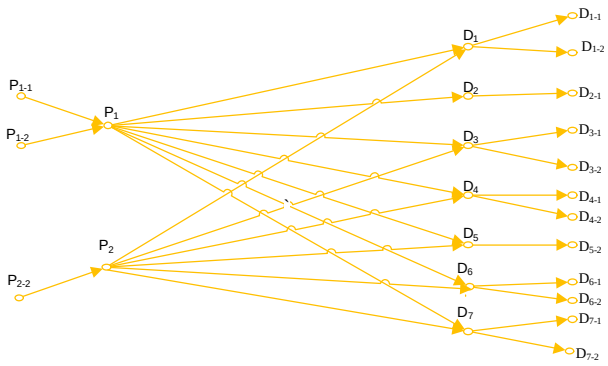

Figure 3a. An example of Network Representation (NR)

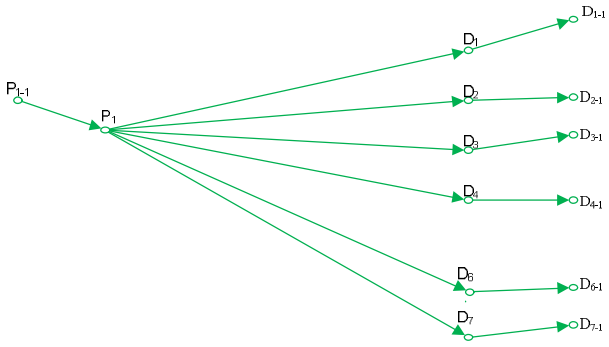

Figure 3b. Product-Subnetwork Representation (P-SNR) of product 1

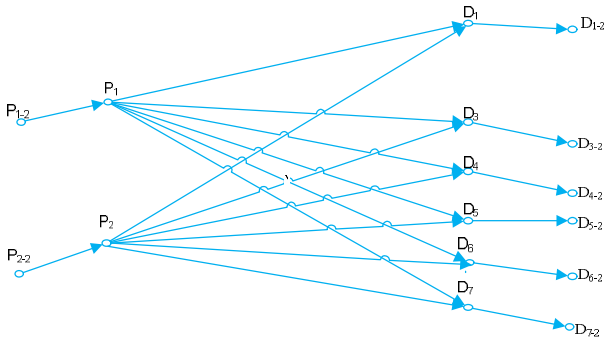

Figure 3c. Product-Subnetwork Representation (P-SNR) of product 2

Notes :

Possible links of Network Representation (NR)

Possible links to be assigned product 1

Possible links to be assigned product 2

Link between P_{i-m}- P_i : Production Link

Link between P_i – D_i : Transportation Link

Link between D_i – D_{i-m} : Demand Link

P_{i-m} : Plant – *i* associated to product - *m*

P_i : Plant – *i*

D_i : Demand at node – *i*

D_{i-m} : Demand at node – *i* associated to product-*m*

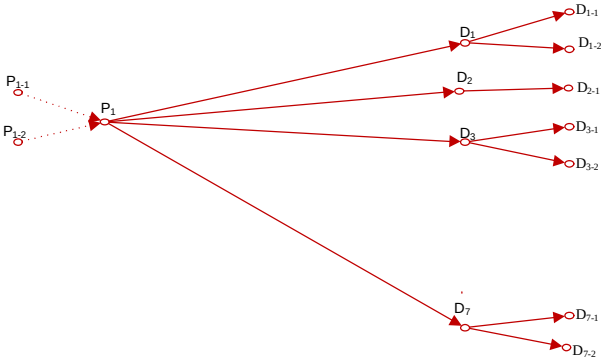

Figure 4a. Group-Subnetwork Representation (G-SNR)-1

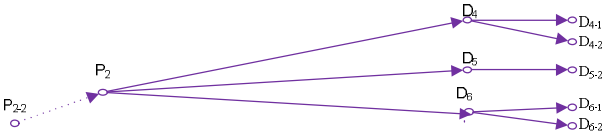

Figure 4b. Group-Subnetwork Representation (G-SNR)-2

Notes :

Possible links of G-SNR 1 (supplied by plant 1)

Possible links of G-SNR 2 (supplied by plant 2)

Production cost-assigned dummy links of P_1

Production cost-assigned dummy link of P

Link between P_i – D_i : Transportation Link

Link between D_i – D_{i-m} : Demand Link

P_{i-m} : Plant – *i* associated to product - *m*

P_i : Plant – *i*

D_i : Demand at node – *i*

D_{i-m} : Demand at node – *i* associated to product-*m*

Justified by the optimal solutions of first level, we proceed to cluster the destination nodes into S - Group Sub Network Representation (G-SNR), where S is the number of source nodes. Figure 4a and 4b show one possible clustering of NR discussed in figure 3a. Figure 4a represents G-SNR 1 which consists of links that are originated in node P_1, whereas figure 4b shows that of node P_2. Production links of G-SNR are not employed directly in the structure of G-SNR, hence each of G-SNR's forms single source multidestination system, where node P_i is designed as a source. Production links just functioned at the algorithm to assign production cost of certain product that consumed at node D_{i-m} and supplied by associated production point.

At second level, all or some of link cost functions are taken into account as concave functions.. Hence, the second level is dealing with Single Source Multidestination MCMF problem. The problem of each G-SNR is solved by heuristic algorithm related to Destination Spanning Tree solutions [3].

The following description will explain the step-wise more clearly.

Step 1 is aimed to define the NR of MCMF problem. NR is composed of links and nodes which represent all of the cost components of the mathematical model. In step 1, all link cost functions are defined, as well as flow requirements of all nodes. Special assignment is carried out to the production and demand links. To each of production links (and demand links), we assign cost function associated to certain product. Whereas, each of transportation links is assigned to cover all types of product, hence its link cost function is defined in aggregate form, no matter the type of product transported.

In association to the production link cost function assignment described above, flow requirement of production point (P_{i-m}) is numbered as production capacity of node-*i* on product-*m* , where *m* is the-*m* of associated production link. The similar treatment is carried out to the demand point (D_{i-m}), where the flow requirement of demand point denotes the quantity of product consumed at node-*i* on product-*m* and *m* is the-*m* of associated demand link. Flow requirement of intermediate nodes should be assigned as zero, since the inflow and outflow at such nodes are always designed in balance.

Step 2 is aimed to define Product – Subnetwork (P-SNR), included Flow Requirement of all nodes as well as link cost function of all links. P-SNR is originally formed by NR. Each of P-SNR is associated to certain type of product. P-SNR of certain product is distinguished to the other P-SNR only in the amount of Flow Requirement of both production point and demand point. When we assign flow requirement of production points of P-SNR of product-*x* (for example), we just number the flow requirement of production points that related to production links which are associated to product-*x*.

The similar assignment is carried out to Flow Requirement of Demand Points. When we assign Flow Requirement of demand points of P-SNR of product-*x*, we just number the Flow Requirement of demand points that related to demand links which are associated to product-*x*.

Flow Requirement of the remaining nodes of Production Points and Demand Points are set as zero. This zero value is due to no product is considered in P-SNR of *x* except product-*x* itself.

At step 3, we solve Minimum Cost Flow problem of each P-SNR of step 2 by Primal-dual Algorithm. In general, Prima-dual algorithm employs shortest path and maximum flow algorithm to optimize the assignment of distribution in order to minimize total cost.

Having the optimal paths of all P-SNR's, at step 4 we superimpose optimal paths of all P-SNR's and find total optimal flow of NR in the first level. From such path pattern of total optimal flow of NR, we heuristically cluster the destination nodes into some groups, depend on the number of origin nodes of NR. Therefore, clustering makes NR grouped into *S* Group – Sub Network (G-SNR), where *S* is the number of origin nodes. Accordingly, each G-SNR takes form of single source multidestination network.

Using G-SNR's of step 4, we proceed to second level to solve MCMF problem of G-SNR's. At step 5, Flow Requirements and Link Cost Functions of G-SNR are defined by retrieving all information of step 1. Thus, link cost function of G-SNR takes form of concave function.

At step 6, we solve the MCMF problem of each G-SNR by Destination Spanning Tree algorithm. DST algorithm developed by Gallo [3] is employed at this step.

Step 7 is aimed to superimpose all the optimal paths of G-SNR's and find the associated optimal flows of NR.

Due to the heuristic approach of clustering destination nodes (step 4), in which it may produce more than one possible set of clustering, step 7 could be continued by rearrangement the clustering of step 4 and carry out step 5 to step 7 in similar ways to the first iteration. The process will be ended when the convergence criteria is satisfied.

5. CONCLUSION

Due to the complexity of problem of Minimum Concave-cost Multicommodity Flow, particularly of multisource network, this research work proposes one heuristic solution which takes form of bi-level model. The principle of that approach is the assumption of linear cost function of first level and concave cost one of second level. Those are assumed in order to change the problem of multi source into single source one. It is realized that the proposed step-wise is merely an attempt to come close to the global optimum solution. This research work is essentially intended to make contribution to research field of freight distribution. Further works may be carried out in order to make comparation between some approaches that have been developed by previous researchers with this work.

6. REFERENCES

[1] Ahuja, R.K., Magnanti, T.L. and Orlin, J.B., *Network Flows*. Prentice Hall , New Jersey, 1993

[2] Fontes, D.B.M.M. and Gonzalves, J.F. " Heuristic solutions for general concave minimum cost network flow problem", *Networks 2007-DOI 10.1002/net,*, www. interscience. wiley.com., 2007.

[3] Gallo, G., Sandi, C. and Sodini, C. , " An algorithm for the min concave cost flow problem" , *European Journal of Operational Research 4*, 248-255,1980.

[4] Guisewite, G.M. and Pardalos, P.M., "Minimum concave-cost networl flow problems : applications, complexity , and algorithms", *Annals of Operations Research*, 25, 75-100, 1990.

[5] Larsson,T., Migdalas, A. and Ronnqvist, M., "A Lagrangian heuristic for the capacitated concave minimum cost network flow problem", *European Journal of Operational Research 78*, 116-129, 1994.

[6] Yan, S., Juang, D.S., Chen, C.R. and Lai, W.S., " Global and local search algorithms for concave cost transshipment problems", *Journal of Global Optimization 33*, 123-156, 2005.

[7] Yan, S. and Luo, S.C., "Theory and methodology. Probabilistic local search algorithms for concave cost transportation network problems", *European Journal of Operational Research 117*, 511-521, 1999.

[8] Zangwill, W.I., "Minimum concave cost flows in certain networks", *Management Science* , Vol.14, No.7, 1968

ISSN 114-1284

Preliminary Study on the Potential of Developing High Speed Train in Jawa Island

Suyono Dikun[1] and Jack Suprapto[2]

[1]*Associate Professor, Department of Civil Engineering*
University of Indonesia, Depok 16424
Tel : (021) 7270029. Fax : (021) 7270028
E-mail :sdikun@eng.ui.ac.id

[2]*Doctorate Student*
University of Indonesia, Depok 16424
Tel : (021) 3453946, Fax : (021) 3813972
E-mail : jack_suprapto@yahoo.com

ABSTRACT

In its long-term effort to revitalize Indonesia railway, government is also looking at the possibility to develop a high speed passenger railway transport system in Jawa. The Jawa High Speed Train (JHST) will form an important element of multimodal transport system in the region and in the same time is expected to reduce over-congestion and over-saturation of Jawa's road network in many years to come. But Indonesia has no experience on high speed train and its implementation will have to be based on studies and experiences of many different aspects and perspectives in other countries. While high speed train technology is now available in Japan and some European countries and can be imported and borrowed, the socio-economic and political conditions of contemporary Indonesia are somewhat distinct and deserve investigation.

This paper reports the literature reviews of studies and practical experiences about high speed rail transport that had been done elsewhere in the world and that had been widely published in the international journals. The paper will also identify the various factors that can lead to the successful implementation of the system as well as its shortcomings, once it is decided the system will be built in Indonesia. Special focus is given to Jawa island, where economic and population consideration matters and political support could be influential in building up policy consensus and determination in national scale. The paper also takes a look at the possibility of financing scheme to search for the best option available. Public-private partnership and its corresponding project financing would be examined accordingly. Early findings of the study will serve as basic and background information to the policy makers in transport sector and will serve as both basic academic and practical guidance for the future rail-based transport development in Indonesia.

Keywords

High-speed train, Jawa's rail, public-private partnership, project financing

1. INTRODUCTION

1.1. The People Movement

There are at least two academic rationales for implementing a high speed train in Jawa island. First, is the steady increase of population and its consequences for high demand of traveling in the island. Second, is the heavy reliance of Jawa's economic mobility on road system which had been oversaturated, overcongested, and consistently deteriorated. A long-term perspective of Jawa's economy reveals the unchallenged trend of the dominance of the region in the national economy. This strongly indicates that economic mobility in Jawa will still be growing steadily in the future. The road system in Jawa, however, cannot be continuously burdened as the major transport mode to carry the additional future passenger urban and inter-urban traveling, without reasonable modal shares from other modes, especially railway. With 151 million people in 2025, passenger trips in Jawa would be growing tremendously high and it is believed that only the combination of road, rail, air, and coastal sea transport as an integrated system would be able to ease the burden of intra- and inter island people traveling.

Indonesia is now embarking on the railway revitalization programs to put the rail transport in the economic perspectives and to make rail as the backbone of national transport, especially for national distribution and logistic system. It is perceived that the high speed rail system would significantly contribute to more efficient passenger movements in Jawa and would be instrumental to the

revitalization efforts in the longer term, and in the same time also the economic efficiency of the country. A high speed rail transport in Jawa would also be a significant step toward a multimodal transport system, which is now lacking from national transport configuration.

1.2. Population Growth

One of many outstanding political economic issue of contemporary Indonesia is its population growth and dispersion. Indonesia population grew by 1.36 percent between 2000-2005, leading to total number of population of 220 million in 2005. Although growth rate is projected to decline to an average of 1.25 percent between 2005-2015 and 1.05 percent between 2015-2025, total population will still reach more than 234 million in 2010, 248 million in 2015, 261.5 million in 2020, and 273.6 million in 2025 [1]. Figure 1 shows the population imbalance in which Jawa island with only 7 percent of Indonesia total land area will be inhabited by 151.5 million people in 2025. In contrast, Papua with 17 percent of land area and with all the relatively unexploited wealth and treasures of its land, sea, and forest will only be inhabited by 3.7 million people, 20 years from now.

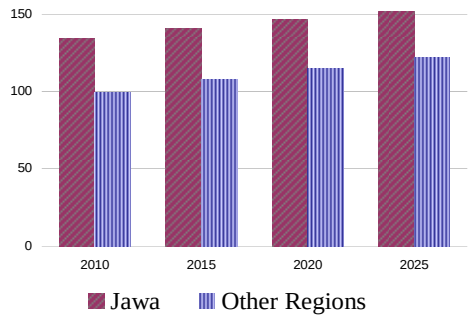

Figure 1 : Projection of Jawa Population
Source : Bappenas, BPS, UNFPA, 2005

Another demographic issue in Indonesia is the massive urbanization that has long been occurring in a rather alarming rate, as shown in Figure 2. In Jawa, around 82 percent of its population on the average is projected to live in urban areas by 2025, increase significantly from 57 percent in 2000. Bali is the second largest region in term of urbanization rate with 79.6 percent followed by Kalimantan 59.8 percent, Sumatera with 57.3 percent, and Sulawesi by 46.2 percent [2]. Figures 1 and 2 clearly show a very-skewed population distribution between regions that has been occurring for so many years in the past and that is still persistently prevailing until 2025, and probably longer. Population growth, *per se*, is probably not really the main issue here as well as its distribution over regions could be made more evenly and regional economy is growing well to absorb

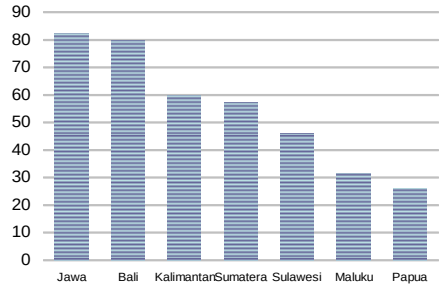

Figure 2 : Projection of 2025 Urbanization Rate
Source : Bappenas, BPS, UNFPA, 2005

increasing labor forces from every region in the country. But in Indonesia dispersed population and more even economic development have never been the case. Since Jawa's population is growing rapidly and its corresponding people mobility is also increasing significantly, it is imperative for Jawa to have a modern rail-based transport system that is capable to carry millions of person-trips in a much faster mode and more efficient manner.

As the sustainable carrying capacity of Jawa has declined steadily, it is not an exaggeration to put Jawa as the main focus of national efforts to ease the burden of population pressures and its following social, economic, and mobility problems. But population policy measures cannot be effectively implemented without other policy measures, including the transportation measures, a rather total solution for long suffering of Jawa's over-crowdedness, over-saturated, and transport inefficiencies . Table 1 shows the population figures of the provinces in Jawa for 2005 and 2025 and its corresponding percentages of urban population in provincial levels. Table 1 clearly shows the increasing numbers of provincial population in Jawa and its corresponding urbanization rates. West Jawa is the province that will be experiencing the highest population rise and 81.4 percent of the population will inhabit urban areas in 2025.

With only 7 percent of total national land area, Jawa island will be the home for more than 151 million people in 2025. But this most populous island in the country has been for many years contributing almost 60 percent to the national economy and will most likely stay that way for the unforeseeable future. The combination of demographic and economic advancement has placed Jawa as the central of national economic development. As such, the regional transport system must also be put in the economic perspective and cannot be singled out from economic policy stream. Overall, urbanization rate in Jawa will go well over 80 percent and will put about 120 million people in its urban areas.

Table 1: Jawa Population Configuration

	2005	2025
Banten	9,309.0 (60.2%)	15,343.5 (81.5%)
DKI Jakarta	8,699.6 (100.0%)	9,259.9 (100.0%)
West Jawa	39,066.7 (58.8%)	52,740.8 (81.4%)
DI Yogyakarta	3,280.2 (64.3%)	3,776.5 (82.8%)
Central Jawa	31,887.2 (48.6%)	33,152.8 (73.8%)
East Jawa	35,550.4 (48.9%)	37,194.5 (73.7%)
Total	127,793.1 (63.5%)	151,468.0 (82.2%)

Source : BPS, Bappenas, UNFPA, 2005
Population in million people, numbers in parentheses are % of urban population.

1.3. Regional Economic Disparity

Regional economic disparity in Indonesia is a latent phenomenon, as latent as the population imbalance. Although regions have their own regional budgets assembled from regional taxes and central government grants, nevertheless, sector budgets were so predominantly larger that regions had frequently been depending upon to build large scale projects in the regions. As a result, gaps between regional and sector and gaps among regions rapidly escalated and the lack of sector-regional linkages had somehow contributed to the regional economic disparity. For many years, sector priorities and their budget allocation tend to focus on more developed regions where economic benefits are more obvious while less developed and remote regions tend to be left behind. This explains why the regional economic disparity in Indonesia is so persistent and its record can be traced back to 1980 and 1990 decades to look at the share of each region in national economy.

This phenomenal fact about economic gap can be seen from Figure 3 which shows extremely skewed share of regional GDP between Western and Eastern Indonesia and between Jawa and off-Jawa in the period of 1975-2006. Assembled from regional economic data collected by Bappenas in the pre-decentralization years and the latest data from BPS, the figures clearly depict the facts that imbalance was so persistent that for many decades Western Indonesia- Jawa, Sumatera, and Bali- had been contributing around 80 percent to national GDP, and Eastern Indonesia, the rest of the archipelago which in fact are very rich in natural, marine, and mineral resources, contribute only about 20 percent [3].

Out of 80 percent of western Indonesia contribution to the national GDP, 58 percent on the average was created from Jawa economy alone. According to BPS report on September 2007, the 2006 GDP at current market price was Rp.3,338 trillion, out of which Jawa economy contributed Rp.1,855 trillion, Sumatera shared Rp.697.9 trillion, and Bali shared Rp.37.4 trillion [4]. Jawa with almost 60 percent share to the economy was becoming increasingly dominant as the origin of export, while the role of Sumatera was decreasing, and the role of other regions were relatively the same. More than that, these figures also confirm the fact that economic disparity will presumably prevail far beyond 2006 as there was no major policy effort whatsoever has ever been done recently to address the issue.

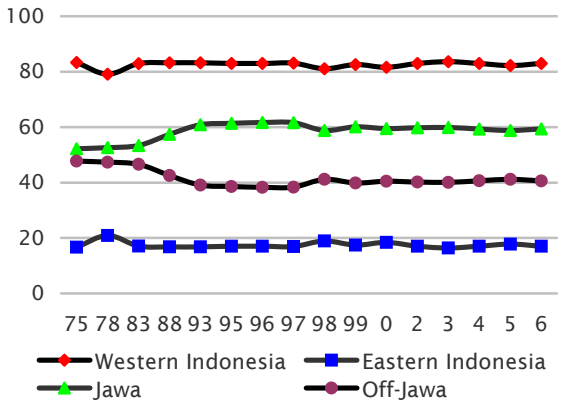

Figure 3 : Regional Distribution of GRDP (%) average of 1975-2006
Source :: Bappenas, 1980-1990 & BPS 2007

1.4. Lack of Transport Intermodalism

Export, investment, and consumption by both public sector for capital goods and by public at large for consumables will continue to drive the economic growth of the country. For the past several years following the crisis, growth had been primarily driven by consumption and not by investment. These economic activities had been served reasonably well by transport system when economy grew by an average of 7 percent during two decades before the 1997 crisis. In this sense, the role of transportation is absolutely important in supporting the social and economic development of the country. But following the crisis, transport infrastructure was deteriorated rapidly to the extent that transport has failed to support the efficient mobility of the nation.

Economic movement in Indonesia, especially in Jawa has long been heavily dependent on road system. Although railway transport had been operating in Jawa since the colonial time, its role in transporting people had been consistently declining from time to time due primarily to rapid development of road networks and the declining rail networks. The national modal share for both passenger and freight transports can be seen from Figures 4 and 5. In 2005, total passenger trips reached 2.38 billion people and total cargo 2.76 million tons. But shares of rail transport in national mobility constitute only 7.32 percent for passenger movement and a negligible 0.67 percent for freight. Figures 4 and 5 also reveal the dominance of road transport in Indonesia with 84.13 and 91.25 percent

respectively for passenger and freight [5]. This modal share situation does not
seem to change much in 2009 due mainly to the lack of major infrastructure investment and no enhancement in public sector spending in the railway sector.

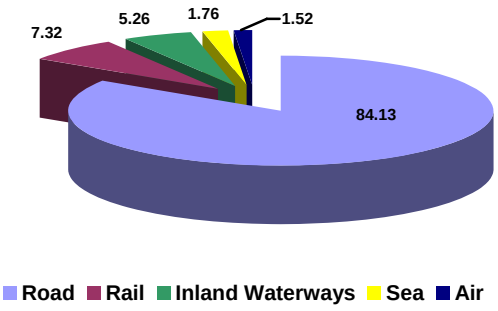

Figure 4: National Modal Share of People Movement (%, 2005)
Source : Dept. of Transport, 2005

For the past fifteen years, railway sector in Indonesia had been governed by Law Number 13/1992 which authorized public monopoly and extremely sector oriented. Public sector is the owner, the provider, the financier, and the operator of the national railway system and services. Monopoly by the state and its delegation to the state-owned enterprise (SOE) had been the core of all the railway business and services, whose financing had long been relying on the state budget. Government regulations and other operating regulations had not given enough rooms for private partnership, and if any, only in a small scale business. Despite of its comparative advantages of being energy efficient, congestion free, and mass transport, railway sector in the past had been under tight regulation, socially oriented, and had never been put in the center of economic activities

The fact that the majority of economic mobility in Jawa is carried out by road reveals the policy shortcomings where transport intermodalism has never existed and transport development has long been focussed on road. Unfortunately, this road-heavy policy had been there for a long time and Indonesia had come to the situation where road network has been under heavy burdens and other modes such as rail and coastal shipping had been kept insignificant.

2. LITERATURE REVIEW

2.1. Early Research

The very first emerging idea of high speed train can probably be traced back to 1904 when Robert Goddard, who was a college freshman at the time, wrote a paper proposing a form of frictionless travel by raising train cars off the rails by using electromagnetic repulsion roadbeds [6]. In the early 1920s, a German scientist named Hermann Kemper pioneered a work in attractive-mode magnetic levitation levitating (Maglev) trains. Kemper continued to research and pursue his concept through the 1930s and 1940s and established the basic design for practical Maglev in a 1953 paper [7]. Since then, research on high speed train continued to be developed and the system started to be implemented. At the beginning of 2008, there were about 10,000 kilometers of new high speed lines in operation around the world and, in total more than 20,000 kilometers of the worldwide rail network was devoted to high speed services [8].

Early study on high speed rail in Jawa was started in 1996 when HSR-200 Management with Halcrow Fox undertook a study of Jawa's rail and its possibility to build a 200 to 300 km/h speed train to shorten a travel time of Jakarta-Surabaya to around 3 to 4 hours. For speed and procurement reasons the

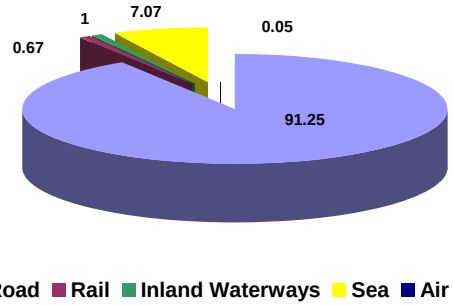

Figure 5: National Modal Share of Freight Movement (%, 2005)
Source : Dept of Transport, 2005

study indicated the need for a standard gauge and will therefore be entirely new track and require total separation from all cross traffic. The north corridor length, the size of the population served, and the continuing economic growth of the region all indicate that at some time in the future, the high sped train with 300 km/h speed will become both economically and financially viable in Jawa [9].

At about the same time, a feasibility study on High Speed Train on Java North Line was also conducted by SYSTRA-SOFRETU-SOFRERAIL (SSS Study) in March 1996. The study investigated three scenarios for the corridor: (1) S-160M, a system with 160 km/h commercial speed for both passengers and cargo on the existing 1,067 mm narrow gauge track; (2) S-200M with a 200 km/h commercial speed on a standard gauge of 1,435 mm track for both passengers and cargo; and (3) S-300P a passenger only train with a commercial speed of 300 km/h, possibly up to 360 km/h, on a standard gauge track.

Table 1 shows the configuration of the scenarios.

Table 1 : The Scenarios' Configuration

Scenarios	Track length (km)	Travel time (hours)	Projected traffic in 2022 (mill. pax)	Estimated Costs (1996 mill. US$)
S-160M	722	5.4	14.6	1,800
S-200M	687	4.0	17.8	8,900
S-300P	687	2.5	21.5	10,600
Option at 360 km/h	687	2.2	26.0	10,600

Source : The SSS Study, 1996

shortened to only about 2.2 to 5.5 hours only, compared, for example, by using the Argo Bromo express line with 9 hour travel time. Each of the scenarios had its own advantages and disadvantages, viewed from different aspects: generated traffic, total costs, sociology, environment, and strategic perspectives. The government at that time selected the S-300P alternative although still expressing the desire to improve the existing narrow gauge network. Using a multi-criteria analysis, the study recommended the S-300P as the ultimate system for future Jawa rail transport system. With 300 km/h train speed, the service will be very competitive compared to airplanes. In France, Japan, and Spain, the 300 km/h speed has demonstrated to be technically, commercially, and financially successful based on the latest and proven technology. In staging, the existing system must be enhanced by some elements of S-160M for improving the quality of current passengers and cargo regional rail transport. The study had also indicated the need for building the 683 km line between Jakarta-Surabaya with a commercial speed up to 360 km/h using a standard gauge [10].

A more recent study on JHST was done by a consortium of Japanese consultant firms (JJJA Study) in 2008 which coined the system as "Argo Cahaya", a system with 300 km/h commercial speed on 1,435 mm standard gauge with the estimated total costs of more than 2 trillion Japanese Yen [11]. The technical specification is displayed in Table 2 below. The study has also identified four scenarios of financing schemes of using public-private partnership and the study went further by setting the technical modern project financing techniques.

It appears that railway in the world has gained new momentum. In Spain, the first HSR was inaugurated in April 1992 on the Madrid-Seville route with great success. In the paper published in 2007 on the network economies, Coto, Inglada, and Rey [12] concluded that high speed rail implies a significant reduction of generalized cost in the rail mode. This reduction produces two clearly differentiated effects, known as induction and substitution, which correspond to those trips which would not have been made if this new service did not exist and those which would have been made in another mode of transport. Further, they concluded that the introduction of high speed rail produces a dramatic change in demand patterns for different modes of transport. Modal split will change dramatically in the affected corridor as the generalized cost of the railway is lower than the generalized cost of air transport. Table 3 shows this modal split changes. The HSR market share is correlated with rail commercial speed. In those lines where the average speed of rail is around 200 km the market share of the HSR is higher than 80 percent.

With the three scenarios, Jakarta-Surabaya could be

In the US, a high speed train has been envisioned to be constructed in the 168 km Richmond-South Hampton Corridor, Virginia. The HSR is determined to operate in 2025 with maximum allowed speed between 130 and 180 km/h speed [13]. But RSH Corridor was only the beginning; it was a small stretch in the massive development plan of US HST determined in 2008 and 2009. The nationwide HST network would include the Northeast Corridor, California Corridor, Empire (NY) Corridor, Pacific Northwest Corridor, South Central Corridor, Chicago Hub Network, Florida Corridor, Keystone (PA) Corridor, Northern New England Corridor, Southeast Corridor, and Gulf Coast Corridor. With the allocated federal funding of around US$ 9.5 billion in 2008 and 2009 and future additional funding anticipated due to national importance placed by Obama Administration, HST development was really on the national agenda of the US [14].

Table 2 : Technical Specification of JHST

Train length	8 cars @ 25 meters = 200 meters
Body width	3,380 mm
Maximum speed	300 km/h
Total weight	About 400 tons at 100% passenger volume
Maximum axle loads	< 14 tons at 100% passenger volumes
Capacity	Executives : 50 seats, economy class 580 seats, total 630 seats
Gauge	Standard 1,435 mm
Power	AC 25 kV, 50 Hz
Control system	Digital ATC with onboard braking patterns

Source : The JJJA Study, 2008

Morocco is moving forward with plans to expand its rail network by building a high-speed rail service linking Tangier to Casablanca. A new TGV line will cut travel times between the two cities from more than five hours to a bit more than two hours. Some 8 million passengers per year are expected to use the new train by 2016. These agreements relate to the

design, construction, commissioning, use of rolling stock, the commercial services to be offered by the high-speed rail link, and the maintenance of a 200 km stretch of track allowing a running speed of 320 km/hour [15].

Table 3 : Travel Time and Market Share of HSR in Europe

	Length (km)	Travel time (h)	Speed (km/h)	Market Share (%)	
				Rail	Air
Madrid-Barcelona	630	2.75	229	50	50
Madrid-Seville	471	2.42	195	83	17
Paris-Amsterdam	450	4.00	113	45	55
Paris-Brussels	310	1.42	219	95	5
Paris-London	444	2.25	197	81	19
Paris-Lyon	430	2.00	215	90	10
Rome-Bologna	358	2.50	143	75	25
Rome-Milan	560	4.50	125	35	65
Stockholm-Gotteborg	455	3.00	152	62	38
Tokyo-Osaka	515	2.42	213	85	15

Source : Milan, Inglada, Rey, 2007

In China, it is determined that the Beijing-Shanghai high-speed railway will be put into operation in 2010. The new rail line will allow passenger trains to run at the speed of 350 km/h, meaning the whole trip will take only five hours, or nine hours less than that at current speed. The 1,464 km Beijing-Shanghai main railway line is one of the most important in China, connecting two of the country's most prominent economic areas and forming the busiest railway route. The new line, upon its completion in five years, will have a one-way line capacity to 80 million passengers and more than 100 million tons of cargo annually.

With an investment of US$ 31.6 billions, the railway was the most expensive construction project in one lump sum China had started since 1949. About 50 percent of the investment came from the state-owned Beijing-Shanghai High-Speed Railway Co. Ltd. The remainder would be raised through share offerings, bank loans and foreign investment. Indigenous and foreign strategic investors would have a chance to invest in the railway as the government intended to diversify the investors. [16].

The study on the economic impacts of high speed rail investment was done by Gines de Rus [17] who studied the costs and benefits of a new high speed line. Rus found out that while the engineering aspect of high speed train is complicated, its economic analysis is very simple. The lack of private sector participation, however, increases the risk of losing the net benefits in the best alternative use of public money. Rus pointed out that the construction of a new line of HSR of a length within the range of 400-600 km has a significant impact on air transport.

High speed rail track is a civil engineering infrastructure. As such the construction of such system will have to undergo strength of material and other structural analyses on the strength, durability, and safety of the system. Studies on these matters have also been conducted elsewhere. The main challenges for civil engineers are to select the corridor, develop an economical drawing for it, construct it and finally do the inspection and maintenance works of it. Engineers have to study the design and operational requirement of high-speed track, effect of high speed on track and vehicle, and salient features of high-speed track. Mechanical and electrical engineers will also to get involve in the construction of a HST project. The new corridor will usually be of double electrified lines for high-speed passenger traffic. The signaling system shall have cab signaling with automatic train control, solid state interlocking device, centralized traffic control, and non insulated track circuits. The telecommunication shall be with latest technology consisting of fibre optic system, train radio control and tele-printer and facsimile arrangement. For electrification, the power supply system will have auto transformer system of 2x25 kV with OHE system of maximum span of 60 m and current carrying capacity of 920 Amperes [18], [19].

2.2. High Speed Train in Operation

2.2.1. Japanese System

The early high speed train line operating in Japan was the Tokaido-Shinkansen line which started operation in 1964 and since then has expanded considerably. Its success also prompted the development of high speed trains in the west. But the Japanese public demanded an even faster form of high speed rail travel. The Shinkansen used a conventional train design, with motors and other equipment mounted on the rolling stock, electric power gathered from overhead wires, and wheels running on rails.

It was impossible to increase the speeds much more. Some of the limitations included: greater size and weight of on board equipment, difficulty in collecting electric power, and reduced adhesion between wheels and rails at higher speeds that may cause wheel slipping. There had to be some new sort of technology that could create faster trains that were

just as safe as or even safer than the trains running on the Shinkansen lines [20].

The former Japanese National Railways (JNR) began conducting Maglev research and development in 1970. The Miyazaki Test Track was built in southern Japan and test runs were being conducted on the tracks. In 1979, the prototype ML-500 test train reached an unmanned speed of 517 km/hour on the 7 km track, which proved that Maglev had a great potential for reaching higher speeds than any other train built before that. At this stage of development, the government started funding the project. The MLU001 was the first Maglev developed with government financial aid. Other models were built and continued to be tested and experimented on the Miyazaki test track. But there was a problem with the track. It was too short and only had a single guide way with no tunnels and no gradients. The experimental data gathered on the Miyazaki test track would be too limited to verify trains commercial potential and use [21].

Maglev stands for Magnetically Levitated and could be regarded as the latest technology of high speed train. Maglev trains will not have to touch the tracks in order to move, i.e. they will travel frictionless. That creates the potential for speeds faster than all the conventional rail travel used today. Maglev vehicles are designed for operating speeds up to 500 km/hour, a tremendous speed advantage over conventional rail travel. Since Maglev trains do not actually touch the rails when they travel, there is no mechanical contact and wear, so that Maglev guide-ways could last up to 50 years or more with very little maintenance at all. Maglev vehicles will have longer lifetimes than conventional rail travel for this reason. They will also have longer lifetimes than automobiles, trucks, and airplanes.

After the JNR was split and privatized in 1987, the Tokaido Shinkansen experienced an increase in passengers which led to more calls to build a commercial Maglev line as soon as possible. As a result, the Yamanashi Test Line was constructed in Tamanashi Prefecture, approximately 100 km west of Tokyo. The Yamanashi test line was 18.4 km long and supported a wide range of tests to determine the commercial feasibility of the Maglev train. The track was made up 16 km of tunnels and an open section that was 1.5 km long in the middle of the track. A substation for power conversion and other facilities were located in the 1.5 km stretch of open section. Part of the line was double tracked to simulate trains going in opposite directions at super high speeds.

Trial runs began on the Yamanashi Test line in April 1997. The cars were not levitated but instead were driven at low speeds on rubber tires. Once tests confirmed that there were no defects in the vehicles or the guideway itself, levitation runs began at the end of May 1997. The speeds were increased incrementally to monitor car movement and verify braking performance. On December 12 1997, a new world record of 531 km/hour was set for manned train travel. A maximum speed of 550 km/h was set for unmanned travel 12 days later [22].

2.2.2. The TGV System

From the first service with fare-paying passengers in September 1981, the French train *à grande vitesse* (TGV) has set the pace in European high-speed (initially above 200 km/h) rail operations. The *lignes à grande vitesse* (LGV) network remains perceived as environmentally sound compared to short and medium-haul air travel or mass use of private cars. Not only has the TGV developed with successive fleet orders, the dedicated high-speed network on which they are primarily designed to run, the LGV, continue to expand within France and across borders. By mid-2008, the French government had made a new commitment to high-speed rail that, if carried through, will see the format break out from the main Paris-centered radial routes, well on the way to being a true national network. The TGV/LGV system evolved from several projects aimed at cutting rail travel times, with hover and magnetic levitation systems and gas turbine propulsion being discarded along the way.

With reduced point-to-point travel times and attractive pricing policies, domestic air traffic has fallen or air routes have ceased completely. Unlike the Japanese Shinkansen counterpart that largely evolved due to the limitations of narrow gauge lines and thus became an entirely separate network, LGV were created and developed within the context of the wider SNCF operation. To prolong the life of track formations, strict 17-ton axle weight limits are imposed where TGVs run. While many communities lobbied to be included in the LGV network, mindful of the noise and visual intrusion of high-speed rail operations, SNCF adopted a range of measures aimed at reducing noise disturbance in adjoining new lines. The majority of TGV operate at a maximum service speed of 300 km/h to 320 km/h

2.2.3. The Korea High Speed Train

Korea's first high-speed line, the 300 km/h KTX trains, based on the French TGV, complete the Seoul-Busan journey in 2 hours 40 minutes compared to 4 hours 10 minutes by conventional train. In 2008, a further 120 km is completed (total 412 km), to further reduce travel time The project was developed over 12 years with total cost of $ 15.3 billion. There are 46 trains, 12 made in France by Alstom, and the rest in Korea by Rotem. They are

388 meter long with 18 coaches, 935 passenger seats, and weigh 771 tons. Korea's first high-speed railway will open April 1st. French TGV trains reaching 300 km/h will cover the 409 km between Seoul and Pusan in just 2 hours 40 minutes, against 4 hours 10 minutes with current trains and track. When the second phase, Taegu - Pusan, is complete in 2008, trip time will be 2.17 hours. Fares set by the construction and transportation ministry have been set at 124-148 % of the existing high-speed train service, and 63-72 % of airline tickets. Korea will start running domestically designed and built 300 km/h trains, known as G7, in 2007

2.2.4. The Taiwan High Speed Train

The first four cars of the 700T Shinkansen trains destined for Taiwan have been unveiled. They will be formed as 12-car sets and have a maximum operating speed of 300 km/h. Services on the Taiwan High Speed Line are scheduled to start in 2005. East Japan Railway will build two prototype bullet trains capable of a top speed of 400 km/h and test them from 2005 to 2008 in northeastern Japan. It aims to launch the trains by 2013 and run them at a maximum speed of 360 km/h, which could be the fastest in the world for commercial trains [23]

3. JAWA RAIL TRANSPORT

The Indonesia Railway

In spite of massive studies that had been undertaken in the past and the issuance of formal planning documents such as mid-term development planning, transport blue-prints, the National Transport System (Sistranas), and their corresponding legal and regulation frameworks, rail transport in Indonesia has been stagnant for decades. Public monopoly, dualism in government agencies between Department of Transport and State Ministry of State Owned Enterprises (SOE), and heavy reliance on state funding had made the SOE, PT KAI behaved like public organization and had been in a difficult position to run the rail business in an efficient and effective fashion.

The transport system in Jawa, however, has been far from sufficient to transport future passenger trips in the region, especially when population has reached more than 150 million in 2025. Jawa rail system, therefore, must be modernize and revitalized as to be able to gain much more share in passenger transport which is currently very small in the national level. Table 4 shows the existing rail network in Indonesia in which 1,610 km out of 6,797 km (23.7 percent) is not in operation. Indonesia had been experiencing the decline of its railway network and services for long. The rail network had decline from 6,797 km in 1939 to 6,096 km in 1955 and only 4,675 km in 2006. The decline was due to the closing of some railroad links resulted from less demand or infrastructure damages. Number of stations and shelter also declined from the 1.516 units in 1939 to only 571 units in 2001. The number of locomotives was also sharply declining from 1.314 units in 1939 to 530 units in 2000.

It is legitimate to assume that public monopoly of Indonesia railway has to be regarded as to come to an end due to declining services, safety, and maintenance budget where government is no longer able to provide sufficient public service obligation (PSO) and infrastructure maintenance. Therefore railway reforms must be undertaken to establish a new railway industry and services which is modern, safe, professional, effective, efficient, and reliable. The path to railway reforms has been opened by the issuance of the new Railway Law (Number 23/2007) which dismantles the public monopoly of railway provision in Indonesia and opens the door for railway provision by private sectors and local governments [24]. This new law marks the beginning of new era in Indonesia railway where private investors are now allowed to invest in railway infrastructure, industry, and services without the obligation to cooperate with the SOE. Railway industry and services are considered vital to the economy. Under the forthcoming new law, railway sector will be freed from natural monopoly and will embark on a more liberalized market structure.

With 3,327 km network in service, Jawa rail is the biggest rail transport in the country for passenger trips. Table 5 demonstrates the number of 2005 passenger volumes for six major corridors in Jawa. Therefore, market restructuring and unbundling for Indonesia railway are urgently necessary to revitalize the sector which is now declining over time. Opportunity will soon be widely opened to invest in different market segment of rail industry, including an extensive system of high-speed passenger and freight rails in Jawa and other big islands. Preparation works to the railway revitalization programs has been undertaken by the Technical Team of the railway revitalization coordination team and has been outlined in its interim report [25]. In the report, revitalization programs will include revitalization of the railway sector, its institutions, corporate restructuring, and human resources development of railway sector.

The main objectives of the railway revitalization program are twofold. First is to increase the railway shares in the national passenger and freight movements. Second is to make railway as the backbone for the national transport, logistic, and distribution systems. As such, railway will closely interact with the economy. Government is now

working on the national railway revitalization programs but many things on what direction and how much government will take on the reform programs are remained to be seen in the near future.

Table 4 : Indonesia Rail Network, 2006

The current rail network in Jawa, Sumatera, and Madura 6,797 km	In operation 4,675 km;	Sumatera 1,348 km	Main Line 1,329 km	North Sumatera 516 km
			Secondary Line 19 km	West Sumatera 169 km South Sumatera 663 km
		Jawa 3,327 km	Main Line 2,966 km	West Jawa 1,125 km
			Secondary Line 361 km	Central Jawa 1,130 km East Jawa 1,072 km
	Non operation 2,122 km;	Sumatera 512 km; Jawa and Madura 1,610 km	North Sumatera 428 km	West Jawa 410 km
			West Sumatera 80 km	Central Jawa 585 km
			South Sumatera 4 km	East Jawa & Madura 615 km

Source : DG Railway, September 2006

Table 5 : Passenger Volumes in Jawa (millions)

Jakarta – Bandung	37,750,470
Jakarta – Surabaya	3,693,895
Jakarta – Cirebon	3,252,824
Jakarta – Semarang	2,295,466
Semarang – Surabaya	839,138
Bandung - Yogyakarta	507,109
Total	48,338,902

Source : National O-D Survey, R&D DOT, 2006

4. PRELIMINARY FINDINGS

4.1. The Benefits of High Speed Train

High Speed Train (HST) is a new technology that allows the train moving at a very high speed between 300 to 350 kilometers per hour. In Japan as well as in European countries, HST had been implemented as a transport mode with the objective to change the modal split of passenger transport with the aim to reduce travel time, congestion, traffic accidents, and environmental damage. But besides of modal choice changes, a HST would have other economic and environmental benefits. The ultimate implementation of high speed train in Jawa would reduce air and highway congestion, air pollution, and inefficient energy use, the transport parameters that have becoming worse over time. Although the investment would be tremendously high in the beginning, long-term economic benefits to the society would outweigh the costs.

4.2. Jawa HST Early Findings

Table 7 lists a summary of the characteristics of JHST that can be concluded so far from the previous studies. A further study needs to be undertaken to refine these characteristics and to investigate the real economic and technical feasibility of such a system. The proposed JHST Line passing through Jakarta – Cirebon – Semarang – Surabaya, for example, will serve for the predicted demand of about 20 million passengers per year in 2023.

5. MANAGEMENT AND FINANCING SCHEMES

Investing in JHST system is on the frontline of government effort to revitalize the Indonesia railway. The ultimate objective is to change the modal split in passenger transport from road to rail with the aim of reducing congestion, accidents, and environmental externalities. But the system requires high quality infrastructure, meaning that new dedicated track has to be built at a cost substantially higher than the conventional rail line. Consequently, a very large infrastructure project such as the JHST cannot be solely financed by the government. It is envisaged that some sort of public-private partnership (PPP) must be employed with a non- or partial recourse modern project financing as the means to fund the project.

It is difficult at this time to formulate the management organization and project financing arrangement for the JHST project. Although it is clear that a careful PPP scheme must be established from the beginning. But for the interest of an academic satisfaction, this study proposes project management and its corresponding financing schemes as shown in Figure 6 as a preliminary arrangement. Figure 6 llustrates a typical PPP project structure involving many parties united in a vertical chain from suppliers, contractors, advisors, to insurers through many contractual agreements. This structure can be adopted with some modifications along the line to the JHST project. To develop an IPP, a developer or the special purpose vehicle (SPV) of the JHST project typically needed to sign four primary contracts: (1) a construction or equipment contract usually on a fixed-price, turnkey basis with an experienced contractor; (2) a long-term operation & maintenance contract; (3) a long-term power

purchase agreement with a creditworthy public utility; and (4) a long-term contract for track and stations management and supervision. Project financing of JHST project can be constructed from both debt and equity financings.

Table 7 : Summary of JHST Characteristics

Maximum Speed	300 km/h
Reduce travel time	JHST with cruise speed up to 300 km per hour would be able to traverse Jakarta-Surabaya (684 km) within just 2 hour and 45 minutes, comparable favorably with air transport and the current conventional train. Access time to Jakarta and Surabaya airports are getting longer from time to time due to heavily congested roads. JHST offers the advantage of railways by getting rid of access time to the airports, waiting times in the airports for check-in, boarding, baggage claim, etc., thereby reducing the total time for point to point traveling.
Low energy consumption	JHST would be powered by electricity supply and no fossil-based energy would be consumed. As such, the system would be very energy efficient and environmentally friendly. The system does not burn oil but instead uses electricity, which can be produced from coal, nuclear, hydro, wind, or solar power plants.
Axle loads	< 14 tons
Gauge width	1435 mm standard gauge and UIC 60 rail
Alignment & Tracks	New double track, built as far as possible within the railway right of way with. Sleepers are made from concrete twin block.
Signaling System	The latest technology, computer based, radio links, and satellite system, engineered to the highest international high speed standards. The entire system will be controlled from a single control center.
Overhead Power	Electric power transmitted from the grid to the trains via an overhead line system. The 25 kV AC modern system to be installed and should be capable of 300 km/h train operation.
Rolling Stocks	Initial train fleet of 25 sets, each set consists of 8-12 cars with power car at one end and a driving trailer car at the other. Made from lightweight construction using monocoque design in which the entire vehicle body is a structural element. Axle load should not exceed 17 tons.. The power car will be energized from the overhead catenary system at 25 kV.
Estimated Costs	In the range of US$ 10-20 billion

6. THE NEED FOR FURTHER STUDY

In Indonesia, the idea of building a high speed train seems to be far away from realization. But the completion of 5.4 km Suramadu bridge between Jawa and Madura Islands might prove it otherwise. The country is also considering to link up Jawa and Sumatera islands by building a more than 30 km long span bridge that utilizes a rail passage. Imagine a high grade economic linkage between Madura, Jawa, and Sumatera with high speed traveling for both people and cargo. So, high speed railways are probably on the horizon already.

Technology for high speed rail had been well developed in France, Japan, and Germany. The common characteristics can now be concluded that a high speed rail with more than 300 km/h speed would need a very special purpose infrastructure and rolling stock combined with specific operating conditions. In dense populated areas such as urban and suburban, it is necessary to install 2 metre-high fencing to provide a secure environment for high-speed lines and to minimize the risks of collision with people, animals and road vehicles; at grade road crossings are not allowed so that the lines must be built on a separate grade.

Despite of the construction costs, it is preferable to build double tracks workable in both directions, allowing trains to operate at full speed, irrespective of the direction, on either track. Each high-speed train should have an axle load not exceeding 17 tons, with a power car at each end of the rake of articulated trailers. The driver receives the speed limit indications on his cab-signal display. These are fed in as coded frequencies or digital messages carried in the current flowing in the rail strings. The driver's role is not limited to watching automatic controls operate; human beings remain “in the driving seat” and are therefore still able to react, if the situation suddenly deteriorates. On the other hand, driving aids make the driver's task easier and the continuous speed control system trips emergency braking if the train's speed becomes incompatible with safety. It takes three kilometer stopping distance to stop a high sped train running at full speed. Accordingly, when it must be slowed, decrementing speed limit indications are transmitted to the driver in the form of a restrictive sequence.

After the railway renaissance in Japan and European countries, many other countries including China and America have revived their railways by building a Maglev high speed rail system. They have proven to

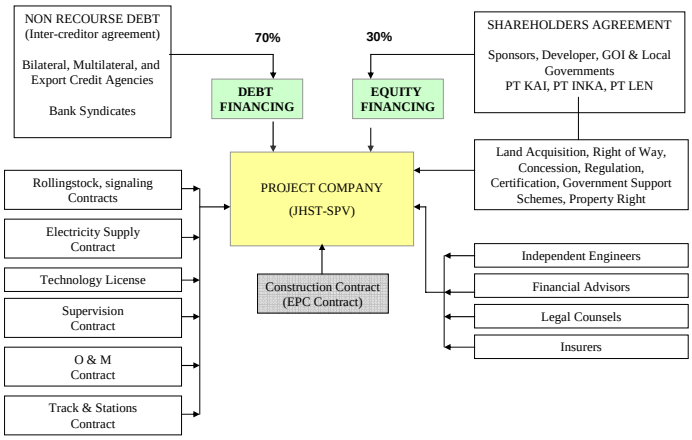

Figure 6: Typical Proposed JHST Project Financing

be faster than traditional railway systems that use metal wheels and rails and are slowed by friction. The low maintenance of the Maglev is an advantage that should not be taken lightly. When you don't have to deal with the wear and tear of contact friction you gain greater longevity of the vehicle. Energy saved by not using motors running on fossil fuels allows more energy efficiency and environmental friendliness. Maglev will have a positive impact on sustainability. Using superconducting magnets instead of fossil fuels, it will not emit greenhouse gases into the atmosphere. Energy created by magnetic fields can be easily replenished. The track of a Maglev train is small compared to those of a conventional train and are elevated above the ground so the track itself will not have a large effect on the topography of a region. Since a Maglev train levitates above the track, it will experience no mechanical wear and thus will require very little maintenance. Overall, the sustainability of Maglev is very positive. Although the relative costs of constructing Maglev trains are still expensive, there are many other positive factors that overshadow this..

Indonesia, however, is still in the beginning. Research and studies need to be undertaken to investigate further what would be the best option for high speed rail in terms of technology, environment, investment, and financing. This paper only provides a slight insight and creates more awareness to the transport planners in this country of the necessity of more efficient, reliable, and modern way of traveling. Such research is collaborative in nature involving many disciplines and requires government support in both political and funding matters.

REFERENCES

[1] Indonesia Population Projection. Badan Pusat Statistik, Bappenas, and UNFPA.. Jakarta, July 2005.
[2] Ibid.
[3] Regions in Numbers. Bappenas, 1980-1990 & BPS 2007
[4] Badan Pusat Statistik. Gross Regional Domestic Product of Provinces in Indonesia by Industrial Origin 2002-2006, September 2007.
[5] The Blue Print of Indonesia Railway. Directorate General of Railways, Dept. of Transport, 2005.
[6] Thai Luu, T. and D. Nguyen. Maglev : The Train of the Future. University of Pittsburgh Annual Conference, April 2005. thl11@pitt.edu and ddn4@pitt.edu
[7] Elhorst, J.P. and J. Oosterhaven. Integral Cost Benefit Analysis of Maglev Projects Under Market Imperfections, The University of Groningen. Journal of Transport and Land Use, Summer 2008, pp. 65-87. Available also in http://www.jtlu.org.
[8] Campos, J. de Rus, G. and I. Barron. Some Stylized Facts About High Speed Rail. A Review of HSR Experiences Around the World. Proceedings of the 11th. World Conference on Transport Research, Berkeley, 2006.
[9] North Java High Speed Rail. Technical Annex. HSR Two Hundred management Ltd. and Halcrow Fox. February 1996.
[10] Master Plan and Feasibility Study for High Speed Train on Jawa North Line. SYSTRA-SOFRETU-SOFRERAIL and DDA Consultants. March 1996.
[11] Study on Java High Speed Railway Construction Project. JTC Co., JARTS, JEC Co., and ALMEC Co. November 2008.
[12] Milan, Pablo-Coto , Inglada, V., and B. Rey. Effects of Network Economies in High Speed Rail : The Spanish Case. Publishe on line on August 9, 2007, Springer-Verlag, 2007.
[13] Richmond to South Hampton Roads High-Speed Rail Feasibility Study. Virginia Department of Rail and Public Transportation and Parsons Transportation Group, April 2002.
[14] Florida High Speed Rail Authority Update. Orange County Board of County Commissioners, April 2009.
[15] Hassan Benmehdi for Magharebia in Casablanca.http://www.railway-technology.com /projects/beijing/.
[16] http://www.china.org.cn/english/travel/164388.htm. Xinhua News Agency April 3, 2006.
[17] Gines de Rus. The Economic Effects of High Speed Rail Investment. Discussion Paper No. 2008-16 prepared for the Round Table on Airline Competition, Systems of Airports, and Intermodal Connections. OECD and International Transport Forum Joint Research, October 2008.
[18] Ei-Sibaie M. Jamieson D. , Tyreil, D and J.C. Dorsey. Engineering Study in Support of the Development of High Speed Track Geometry Specifications.Federal Railroad Administration, Washington, DC 20590.
[19] Coenraad Esveld. The Development of High Speed Track Design. Delft University of Technology, 1993
[20] Sawada, Kazuo, "Magnetic Levitation (Maglev) Technologies 1. Supderconducting Maglev Developed by RTRI and JR Central", Japan Railway & Transport Review, No. 25, 58-61.

ISSN 114-1284

[21] He, J. L., Coffey, H. T., Rote, D.M. Analysis of the Combined Maglev Levitation, Propulsion, and Guidance System. IEEE Transactions on Magnetics, Vol 31, No. 2, March 1995, pp 981-987.
[22] Ibid.
[23] http://en.wikipedia.org/wiki/Taiwan_High_SpeedRail.
[24] Undang-undang Nomor 23 Tahun 2007 Tentang Perkeretaapian. Jakarta, 2007.
[25] Revitalisasi Perkeretaapian Nasional. Laporan Interim, TRKA, Maret 2009.

ISSN 114-1284

Toward the Establishment of Jabodetabek Rail-Based Urban Public Transport System

Suyono Dikun[1], Tommy Ilyas[2] , and Ghoefron Koerniawan[3]

[1]*Associate Professor. Department of Civil Engineering University of Indonesia. Depok 16424*
Tel : (021) 7270029. Fax : (021) 7270028
E-mail :sdikun@@eng.ui.ac.id

[2]*Professor. Department of Civil Engineering. University of Indonesia. Depok 16424*
Tel : (021) 7270029. Fax : (021) 727002
E-mail : t_ilyas@rad.net.id

[3]*Doctorate Student. Department of Civil Engineering. University of Indonesia. Depok 16424*
Tel : (021) 3506204 Fax : (021) 3506204
E-mail : ghoefron.k@gmail.com

Abstract

By the year 2025 Jakarta population will reach 9.26 million people, while the day population is believed to be much more than that due to commuting people to and from its supporting cities of Bodetabek. By now the total population of Jabodetabek is believed to be more than 20 million. This situation is of course getting worse when road infrastructures and other means of public transport cannot keep up with the increasing population and its travel demand.

The provision of safe. convenient and reliable rail-based public transportation services is a must to solve the problem of urban transportation in the Jabodetabek region and to help increase its economic sustainability. As the share of urban railway services in the Jabodetabek transportation system is only of a small portion. it is rather imperative for the region to have an efficient rail-based urban public transport system. Currently, rail transport contributes only around 7 percent of national people mobility. Government is now revitalizing the railway sector following the issuance of Law Number 23/2007 in which public monopoly is abolished and market for rail industry and services is open for competition.

Government through the Railway Revitalization Team is now working on enhancing Jabodetabek rail system and services as a means to increase the share of rail transport on the national public transport and hence on the regional economy of Jabodetabek. The study will function as a background study on the implementation of enhanced Jabodetabek Rail-Based public transport system.

This paper presents various factors that can lead to the improvement of economic and people movements in the Jabodetabek area by means of rail-based public transport. The factors include the level of service of the Jabodetabek Rail, the access to the system, the improvement in infrastructure and rolling-stock performances, and the quality and capability levels of management and human resources needed to operate such a system. The performance indicators of such system to better serve the demand would be the quality of people movement using the rail system (comfort, access, affordability, safety, security) and the efficiency of the people movement (access time, travel time, egress time, and speed). The study will preliminarily look at the possible modal shift that could happen as a result of the system. The paper will also take a look at the possibility of private participation and financing scheme to search for the best option available.

Keywords : *Jabodetabek. railway revitalization. urban mobility. public-private partnership. project financing*

1. INTRODUCTION

1.1. The Complexity

Jakarta expanded from 180 square kilometers in 1960 to a fully urbanized metropolis in the 1970s. At about the same period of time, Jakarta and its neighbor cities-Bogor, Depok, Tangerang, and Bekasi-(Bodetabek) agglomerated into one greater Jakarta area called Jabodetabek (Figure 1). Since then. Jabodetabek becomes the largest urban agglomeration in Indonesia. But the expansion of the city and the acceleration of the development of its physical economic and business facilities have not been accompanied by the enhancement of transport infrastructure and services that can serve the city's mobility accordingly. The result is that the urban

transport problems in the greater urban region have been accumulated and becoming more complex from time to time. The traffic congestion is so massive that the region is now under constant threat of total urban gridlock.

Traffic congestion problem is so severe that it will need a dynamic, significant, brave, fast, and smart solution. Ordinary and conventional approach simply is not going to work. The solution must be dynamic to keep up with the uncontrollable growth of population and its increasing vehicle ownership and utilization. It must be significant and brave because the unstoppable growth of population and vehicle ownership is highly influenced by the socio-economic activities of the city which are believed to occupy a significant amount of national productivity. The solution must also be fast because the cities are getting worse from time to time or threatened to head for a total gridlock. Brave and smart solution will be absolutely necessary due to the political complexity of the problems. And one critical solution to the problems would be to establish an integrated rail-based public transportation in the greater area as the backbone to accommodate millions of person trips generated every day in the region.

Figure 1 . Jabodetabek Greater Area

1.2. The Study Area

Table 1 shows that with only 6.580 square kilometers of land area. the population of the agglomeration increased dramatically from 8.34 million people in 1971 to 24.93 million in 2007. The land area of original Jakarta is 656 square kilometers and was inhabited by about 9.0 million people in 2007. The Bodetabek area which is 5.925 square kilometers in size is the house for 15.877 million people. During the working days. Jakarta population is believed to be much more to reach 10 to 12 million people due to commuting people to and from its supporting cities of Bodetabek.

Table 1 : Jabodetabek Propulation Growth

Regions	Area (sq.km)	Population in 1971	Population in 2007
DKI Jakarta	655.7	4.579	9.057
Bogor & Depok	3.380.7	1.863	6.529
Tangerang	1.259.8	1.067	5.076
Bekasi	1.284.2	831	4.268
Jabodetabek	6580.4	8.340	24.930

Source : BPS-2008

Figure 2 depicts the population density of the agglomerated region. The figure shows that with only 656 square km land area. DKI Jakarta has the size of population density of 13.500 people per square kilometer. made it the densest region in Indonesia. The Jakarta city center was the most populated region with the density of 18.618 persons per square kilometer.

As in many other big cities in Indonesia, urbanization is still consistently progressing in the Jabodetabek region. Urban population increased by 1.27 times during the period 1990-2000 from 13.1 millions to 23.0 million people. Urban area expanded by 1.41 times during the same period from 1,660 square kilometer to 2,339.4 square kilometer. The share of urban areas within the region increased from 25 percent to 35 percent in the 1990s. Projections made by BPS, Bappenas,,and UNFPA [1] show an alarming number; that more than 80 percent of Jawa population will reside in urban areas in 2025. This means more than 120 million people in Jawa will be urban inhabitants sixteen years from now.

There are several factors leading to the condition. First, is the marginalization of rural economy where agriculture, the biggest sector absorbing workforce so far, has consistently declined, forcing farmers and peasants to sell their agricultural land and gradually turning them into landless sporadic workers. When they have spent up their money for consumption purposes and finally found that rural economy can no longer provide opportunity for them to survive, they invade urban areas as the last resort to earn money with whatever means they have. Second, the urban-centered economic development in the last several decades had widened the urban-rural gap in such a way that urban areas had generated big employment opportunity for rural people to work. And third, despite excellent development planning this country has had in the past, massive economic and political centralization and the lack of workable regional economy strategy and implementation to strengthen regional economy had left rural development in the sideline.

There are a lot of consequences of the massive urbanization on the economic carrying capacity of the city and the quality, capacity, and efficiency of urban transport. The transport system simply cannot keep up

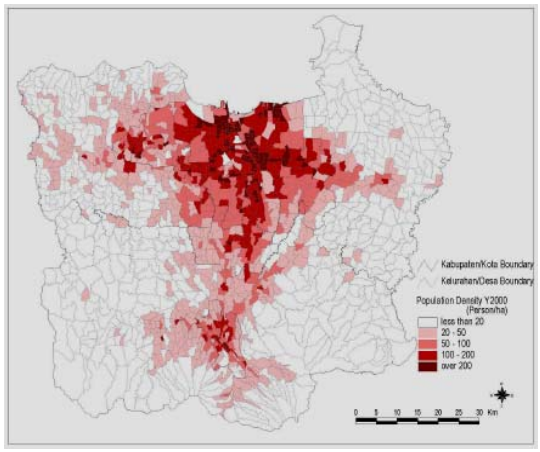

Figure 2 : Population Density

Source : SITRAMP Study 2004

with the increasing demand and keeps deteriorating over time and in some extent becomes a contributing factor to the process of urban decay. These phenomena have been taking place in Jabodetabek greater area where the quality of life of its population had been gradually declining.

1.3. The Traffic Problems

Massive traffic congestion has been taking place day by day in Jakarta's road network for so many years without any significant mitigation measures at sight. The city administration has always blaming the unbalanced growth between road network (only a negligible 0.01 percent per year) and traffic (9 percent per year) as the major cause of congestion. But the imbalance is only one factor of the many contributing factors to the creation of the massive congestion. Another factor is the uncontrollable growth of motorized vehicles. Figure 3 reveals the fact that only in 5 year period between 2002 to 2007. the number of registered vehicles has risen from 4.1 million to 5.8 million. out of which 3.58 millions were the motorcycles. So far city government. including Bodetabek regions do not have any measures to mitigate the increasing number of motorized vehicle on the road, including any traffic demand management strategy to curb the use of vehicular traffic during the working days.

In 2002. there were 7.3 million commuting trips that required public transport services. The numbers is estimated to grow to 9.9 million trips by 2010 and 13 million trips in 2020. Jakarta intra urban trips constitute the largest portion of the total daily trips and the rest are external commuting trips generated from the Bodetabek areas. As many as 3.6 million person trips will commute to inner Jakarta city in 2020. Based on the traffic and road network data, the city government has forecast the total gridlock will happen in 2014 when the number of four-wheeled motorized vehicles (about 3.3 millions) fills the road space totally, if no major actions is undertaken to mitigate the use of private cars [2].

With only 7.650 km road length or 6.3 percent of total land area, Jakarta generated about 17.1 million person trips per day in 2008 and the trips were served by 5.6 million private cars, including motorcycles, and by only 86.435 public transport vehicles, buses in all sizes, paratransit, and rail. The private cars which constitute 98.5 percent of total vehicles in Jakarta carry 44 percent of the total person trips, while public transport with only 1.5 percent fleet carries 56 percent of total person trips. Only about 3 percent of the trips were served by Jabotabek rail. Because there is no policy to curb the rapid growing of car ownership and usage, more than 1.100 new vehicles was added to the city street every single day in Jakarta

Many studies on Jakarta urban transport had been undertaken and recommendation on policy measures and transport infrastructure development had also been made to the government but implementation had so far been so poor. Decisions that had been made, however, rarely followed the policy recommendation of the studies, indicating the missing links between conceptual framework and political decision making process. The uncontrollable traffic growth in Jakarta and the resulted massive traffic congestion can be seen as policy shortcomings that have been around for so many years without any major correction measures on place. The failures of good policy combined with the imbalances between supply and demand of transport facilities had made the traffic situation in Jabodetabek area gets worse from time to time.

Another important policy development in the Jabodetabek traffic problems is the transport demand management (TDM). The complexities of urban transport problems in the area have been contributed also from the inconsistencies of land use implementation. The interaction between transport facility and land use that can result in an efficient

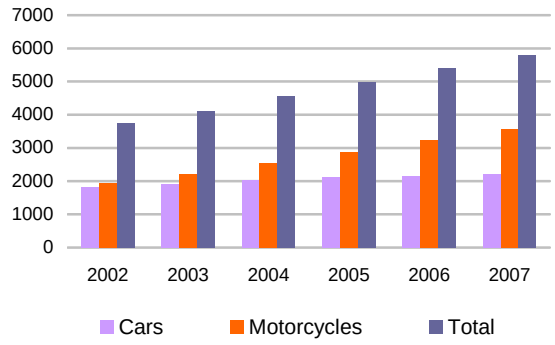

Figure 3 : Number of Registered Vehicles in Jakarta
(1.000) Source : Jakarta City Report, 2008

urban structure and movements simply does not exist. Integration of transport modes and between transport and land use had also been very poor as an integrated institution is also lacking from the policy making process.

1.4. The Economic Lost

Economic lost resulting from heavy congestion is clearly a primary concern of all parties, government. road users, and industry. But everybody seems to get stuck in the middle of congestion and does not seem to understand what to do. SITRAMP study [3] in 2004 had estimated the annual congestion costs which is also the economic lost to amount to Rp. 3.000 billion for vehicle operating costs and Rp. 2.500 billion for the value of travel time. The study further projected that should there be no improvement undertaken in the period up to the year 2020, accumulated economic lost would amount to Rp. 65.000 billion, which consists of Rp. 28.100 billion for additional vehicle operating costs and Rp. 36.900 for longer travel times at the present value discounted by 12 percent. This estimated economic lost, even limited merely to vehicle operating cost and travel time, would be more than the development cost proposed in the master plan.

In accordance with the anticipated growth in population and vehicle ownership in the next 20 years, total number of trips is expected to grow even more rapidly. The total number of trips made in Jabodetabek in 2020 will increase at about 37 percent compared to 2002. A total person trip per day was 36.7 million in 2002. The number will rise to 45.2 million in 2010 and 50.4 million in 2020. Person trips generated from Bodetabek areas constitute a slightly more than a half of the total trips; the other half will be generated from the city of Jakarta, including from and to the central business districts at the central city.

At present, the modal share of public transport in total passenger trips is about 60 percent (excluding non-motorized transport). If no action is taken. modal share of public transport, especially the share of the bus, will fall to less than half of the total motorized share because of the low level of service. and the modal share of the private car, which is more convenient in mobility, will rapidly increase.

2. THE EXISTING JABODETABEK RAIL

2.1. Poor Services

Jabodetabek Rail is currently running an urban commuter system of about 160 km operating length, connecting major cities in Jabodetabek, Bogor in the south, Bekasi in the east, Tangerang in the west, and Serpong in the southeast. Figure 4 shows the existing rail network. Seven lines are in operation, including the new revived line to Tanjung Priok. This system currently carries about 400.000 passengers per day or about 0.2 percent of the total passenger travel demand. The quality of the urban railway, however, is poor with low level of service in almost every aspect such as low train and line capacity, low frequency, delayed schedules, damaged and uncomfortable train cars, poor station facilities, and insufficient station plazas and access roads. Buses, on the other hand, play a dominant role in the region's public transportation; however, the quality and level of bus service at present is also poor in many aspects such as unscheduled departure, unexpected stoppage of operation, long waiting time, sense of insecurity on board by passengers, and dirty condition inside the buses. These urban public transport problems in Jabodetabek can be attributed to lack of effective public transport planning, insufficient maintenance funding, lack of good public policy, and insufficient monitoring on operation.

Jabodetabek Rail, however, has been experiencing some structured problems in train operation. The major problems include shortage of line capacity, poor safety, shortage of electrical spare parts, and signaling problems. Due to the shortage in line capacity. overcrowded passenger on the trains had been a chronic phenomenon. The current level crossing equipment for safety was installed by Japan in 1980's and has been maintained rather improperly. However. collision accident with electric car occurs frequently due to deterioration caused by long year use and damages. Meanwhile, because of the frequent and unexpected strong lightning, signaling system in Jabodetabek has many faults and it may cause train accident.

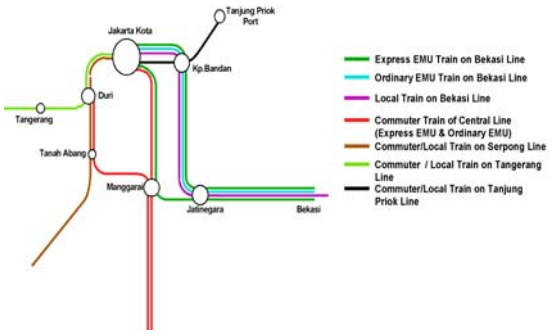

Figure 4 : The Existing Jabodetabek Rail Network
Source : Daop Jabotabek PT KAI

The electrification of the Serpong and Tangerang Lines had been completed in 1995 and 1998 respectively with financed by France Loan. There are four DC traction power substations on each line with 3.000 KW capacities respectively. Meanwhile. electrification of adjacent line as Western Line had been operated since 1986 financed by Japanese Loan.

The different DC outgoing voltage between France and Japan substation systems were confirmed by investigation team on 1997. which is measured of 1.720 V DC nominal on France area and 1.650 V DC nominal on Japan area.

This performance indicates that the existing rail facility have much room to be improved to maximize its potential. In addition to the existing rail network. an independent mass transit system has been planned to operate at around 2015. This new rail system is expected to provide quality rail transportation services for the next generations leading to enhancement of business and commercial activities in the capital region.

2.2. Shortage of Capacity

Table 2 depicts the passenger volumes of Jabodetabek Railway from 2001 to 2007. The volumes declined from 121.5 millions in 2001 to 100.5 in 2004 and picked up a little bit to 108.1 million in 2007. This passenger volumes in Jabodetabek rail constitute about 70 percent of total national rail passenger volumes and had been creating shortage of capacity for the system. Jabodetabek rail is always in short supply against increased demand due to the shortage of rolling stock and poor management. The shortage of capacity in 2002 is shown in Table 3. The table clearly shows that load factors during morning peak hours amounted from 207 percent in the Serpong Line to 340 percent in Bogor Central Line. Bogor-Central Line has the highest passenger volumes.

Table 2 : Jabodetabek Passenger Volumes 2001-2007

Year	Economy Class	Air Conditioned	Total
2001	115.610.243	5.860.925	121.471.168
2002	111.482.152	5.935.313	117.417.465
2003	95.386.433	6.654.454	102.040.887
2004	91.565.130	9.018.413	100.583.543
2005	92.367.502	8.601.896	100.969.398
2006	94.780.400	9.644.320	104.424.720
2007	104.915.164	13.180.533	118.095.697

Source : DG Railway, 2008

2.3. Saturated Stations

Gambir station was so crowded with long distance train passengers and commuter that PT KAI has been forced to cancel using this station for all ordinary commuter trains. In double-double tracking project. Manggarai Station is planned to be the only terminal for long and middle distance trains. The routes of these trains will be arranged and simplified without conflict with the commuter trains. There are extremely shortages of the access roads to the station, which is because of no station plaza on Jabotabek railway station. PT.KA (Persero) have managed valuable and enormous land in Jabotabek area, but these lands have not been used sufficiently, especially as station square can count a little.

2.4. Freight Transport

The freight train in the Jabotabek area is operated on Western line, Eastern line, Tanjungpriok line, and Bekasi line. The coal train is operated on Serpong line, Western line, Eastern line, and Bekasi line. The container train is operated on Tanjungpriok line, Eastern line, and Bekasi line. The share of railway freight transportation, however, is small and diminishing. Jabodetabek rail is probably focusing on passengers while freight transport will be the domain of separate freight rail operator.

2.5. Mixed Land Use

Historically the railway in Jabotabek was developed for cargo transportation connecting Jakarta Kota and Tanjung Priok with the other regions, and also for middle and long distance trains connecting Jakarta to the other regions. In other words, until recently, the railway network had not been developed for passenger travel within urban areas. Currently land use surrounding the railway stations is not appropriate for a railway transport system. In order to attract rail passengers, highly dense urban facilities should ideally be located within walking distance from the stations. However at present there are few high-rise office buildings and commercial facilities. At present. the land near the stations is usually occupied by low-class housing in urban areas. Consequently sufficient passenger demand for the railway cannot be expected from the existing urban land use.

2.6. Lack of Integration between Modes of Transport

Integration between railway and other modes of transport can be made at an interchange transport node. Furthermore integration between railway and road transport is provided by access roads to railway stations. However, these transport facilities for integration between rail and road have not been well developed and integration does not really exist. It is unfortunate that for many years the arrogance and ignorance of both rail operator and city government had kept Jabodetabek rail and busway, for example, separated to each other and passengers have been unable to reap he benefit of inter modal transport. Efforts have been done to integrate these two modes of passenger transport in Jabodetabek but strong leadership seems lacking.

Table 3 : Commuter Transport (Morning Peak 2 Hours). 2002

Line	Number of train	Headway (minutes)	Train Capacity	Passenger Volume	Load Factor
Bogor -Central Line	18	6.7	15.224	51.744	340 %
Bekasi Line	13	9.2	8.448	22.240	263 %
Serpong Line	7	17.1	6.800	14.089	207 %
Tangerang Line	2	60	800	2.275	284 %

Source : DG Railway. 2004

2.7. Lack of Access Roads to Railway Station

Except for big stations such as Gambir and Kota, smaller railway stations at Jabodetabek are suffering from poor access roads. Station squares have not been well developed even though lands for station squares are available at many stations. The available squares in fact have been occupied by vendors and activities not related with railway traveling. The width of access road to Serpong Station is very narrow. Passengers have to walk on the railway along access road from level crossing without walking on access road.

2.8. Safety and Security

In general, the railway transport is the safest mode of transport compared with other modes. But Jabodetabek rail transport is probably the exception. The reasons are obvious; shortage of technical staff, the deferred maintenance of facilities and rolling stock, and poor attitudes of passengers. It is extremely dangerous for a train beyond capacity to operate with no door or opened door. A lot of passengers are still riding the train on top of the railcars. Between 2000-2002, railway accidents record shows 12 accidents and 43 collisions with cars or public transport vehicles occurred.

3. LITERATURE REVIEW

3.1. Past Studies

Many studies on urban transportation in Jakarta and other cities in Indonesia had been undertaken in the past. Reports of the studies had been widely published. All of those studies in general come to the conclusions that cites' transport condition will be greatly improved if the city governments build a mass rapid transit as a backbone of urban transport system. Since cities population grew very rapidly. there is no more land available for road network expansion and if there is any, land acquisition is usually very expensive and socially and politically sensitive. Transportation demand management, therefore, is critically needed. Unfortunately, none of those recommendations has never been implemented seriously by the city administrations.

The lack of integration of modes is partly attributable to the lack of access roads to railway stations and subsequently lack of feeder bus services. At present many access roads to the stations in Jabodetabek are either in a poor condition or simply do not exist. Part of the station space is also frequently occupied for non-rail business purposes.

Cities are now trapped in the middle of heavy congestion as a result of wrong consistent policies and do not really know what to do or being ignorance of the policy recommendations. On the contrary, no full-scale study has so far ever been conducted on the railway transport, especially study on the enhancement of Jabodetabek rail. This paper will not describe the past studies in detail. And instead will focus on the findings and recommendation of SITRAMP Study on the integrated transport master plan for Jabodetabek, finalized in 2004 by JICA and Bappenas [3].

3.2. The Spatial Planning

The future Jabodetabek transport system, including its rail-based transport system must be based on the consolidated spatial plan dedicated for the Jabodetabek region and its upstream areas, the Bopunjur (Bogor-Puncak-Cianjur). The Jabodetabek Bopunjur spatial plan has been prepared by the Department of Public Works and has been approved as the Presidential Regulation. The plan, shown in Figure 5, shall be the principal guidelines for the region's spatial development including transportation system development. The plan maintains the common regional planning issues to provide a guiding principles of population dispersion in the Bodetabek area, to restrict development in southern water catchment areas, and to promote linear

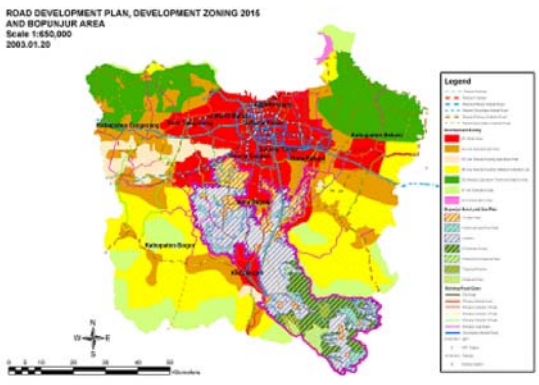

Figure 5 : Jabodetabek Bopunjur Spatial Planning
Source : SITRAMP Study. 2004

development along the East-West axis (Bekasi-Tangerang).

Figure 6 shows major destinations of home-to-work trips in year 2002. The largest attraction center is located in the central area of DKI Jakarta. and its sphere of influence reaches the neighboring cities of Bodetabek. To achieve sustainable urban growth in Bodetabek area, the Master Plan proposes that urban center development should be encouraged to realize balanced residence-employment suburban development. This should be supported by a strict urban development control of the designated land use plan and development zoning. Following this guideline, planning issues in transportation sector should be identified and an efficient trunk transportation system must also be established.

3.3. Transit Based Development

Figure 7 shows the trunk transport network proposed by the study on the ground of rail-based scenario. The scenario was prepared to emphasize the mass transit oriented system because the heavy burden by vehicle traffic is expected in the center of Jakarta due to difficulty in road capacity expansion by road construction including the high mobility highway network and ordinary arterial roads. The scenario

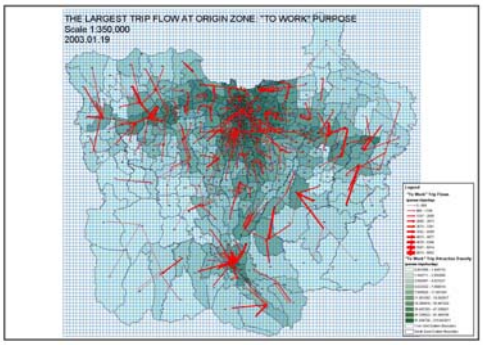

Figure 6 : Major destinations of Home-to-

was constructed based on the development of: (1) Double Double Tracking of the Western Line between Karet and Manggarai; (2) Double Tracking of Tangerang Line between Tangerang and Duri and extension to the Soekarno-Hatta Airport; (3) Construction of New West-East Mass Transit Line between Duri and Cikarang; (4) Double Tracking of Serpong Line between Serpong and Tanah Abang; (5) Jakarta MRT between Kota; Fatamawati/Lebak Bulus; and (6) New Mass Transit Line between Ciledug and Blok M.

3.4. Policy Recommendation

The development of a full-scale Jabodetabek Railway must be supported by the implementation of some policy measures, especially with respect to the management and operational aspects. Among policy measures recommended by SITRAMP was the enhancement of maintenance system for electric traincars, improvement of the quality of management of railway operation, and railway financial reform. Government was also urged to establish multimodal transport system with the provision of extensive public transportation network and with rail as the primary mode. To improve the attractiveness of railway business, it is necessary to serve high intensity land development in the surrounding area of railway stations.

3.5. Transport Demand Management

The Jabodetabek megalopolitan area has no well-structured transport demand management strategies so far. This is understandable, however, due to the lack of an integrated transport planning and integrated transport authority in the area. A small scale traffic improvement programs such as optimization of traffic signal controls, intersection improvement programs, and law enforcement for traffic violation by paratransit (ojek. angkot. and micro buses) had never been undertaken consistently. Travel demand management strategy such as the 3-in-1 scheme seems generally effective in reducing the number of vehicles entering the restricted zone; but the scheme has become ineffective due to the facts that congestion moved to the alternative streets and car users picked a person on the street to fulfill 3- passenger requirement. The current 3-in-1 scheme can actually be transformed to a road pricing scheme with an aim to generating part of funds to develop transportation infrastructures and to improve public transport services. But the strategy has never been implemented so far.

3.6. Integrated Transport Authority

An integrated public transportation in Jabodetabek area would need an integrated transport authority to take care the coordination in planning process and development fund raising between respective government agencies and foreign lending organizations. Indonesia transport sector is now

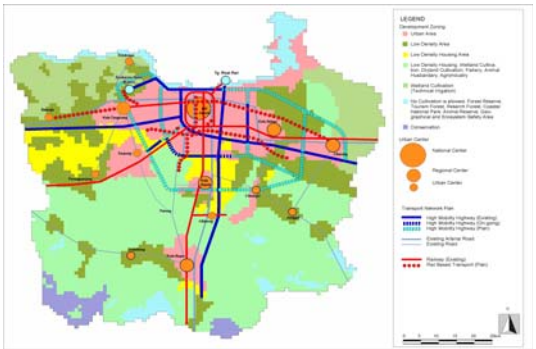

Figure 7 : Rail-Based Jabodetabek master Plan
Source : SITRAMP 2004

lacking of effective coordination in planning between different transportation sub-sectors and between the central and local governments. Furthermore, there is almost no coordination in planning between transportation sector and other development sectors such as housing development and railway system development. These facts suggest it is very necessary to institute an organization with a strong power for authorization of region-wide plans that covers multiple local governments, equipped by solid planning and supported by sufficient technical staff and funds.

4. THE NEW JABODETABEK RAIL

4.1. The Background

As many as 120 million people will reside in urban areas in 2025 in Jawa. It is imperative therefore for government to prepare rail-based urban public transportation which is efficient, reliable, and able to fulfill the demand in a more convenience manner. The development of a full-scale Jabodetabek rail-based transport system is therefore imperative for the agglomeration. The 24.9 million people in 2007 and probably 30 million in the years ahead would not be served adequately by the existing road-base public transport. A full-scale rail transport will not only ease the massive congestion of road traffic and is therefore critical for sustaining the economic mobility of the region, but will also mark the most critical step of the national railway revitalization efforts.

4.2. The Railway Master Plan

Government is now preparing a national level railway master plan projected until 2025 [4]. In the master plan, it was projected that rail passenger trips in Jawa would increase from the current 6 percent of national passenger volumes to 8.49 percent in 2010 and 12.0 percent in 2025. In the national level it was projected that rail passengers would constitute 15 to 17 percent of national passenger volumes. The projected number of rail passengers in 2025 is shown in Table 4. In Jawa Bali alone, there would be almost 245 million passenger volumes by rail, consisting of intra- and inter provincial, including urban rail passengers. Jabodetabek rail is presumably the biggest part of the total national rail passenger. To serve the nationwide projected demand, it was projected that 6.800 km tracks must be available for service, meaning that as long as 3.473 km new track must be built until 2025 in Jawa. This must also be accompanied by 669 locomotives and 6.690 train sets to serve the 2025 demand.

Table 4 : Projection of National Rail Passenger Volumes by Regions (2025)

Regions	2006	2010	2015	2020	2025
Jawa Bali	127.519.723	155.158.347	184.299.294	214.417.082	244.673.991
Sumatera	2.566.924	4.366.143	6.401.799	8.653.562	11.103.851
Kalimantan	-	-	479.468	781.226	1.120.520
Sulawesi	-	-	2.483.369	3.902.371	5.406.375

Source : Draft II. National Railway Master Plan. DG Railway. April 2009

For urban rail, the master plan has laid out a long-term development plan for Jabodetabek Rail until 2025. With 5.790 square kilometer land area, Jabodetabek rail would need around 900 km double track to serve passenger demand in 2025. With the assumption of 18 hours daily operation, 15 minute headway, four major routes, and average speed of 30 km per hour, it was estimated that Jabodetabek would need 128 trains, with flexible number of railcars, to utilize the tracks optimally.

4.3. The On-Going Rail Projects

The works of Jabodetabek rail network enhancement programs have actually been progressing. Figure 8 schematically illustrates this work of network enhancement. Table 5 lists rail projects that have been constructed or on-going. In addition to the list and as a part of the long-term development programs outlined in the Railway Master Plan, the following rail projects can be considered as strategic actions to achieve the objectives.

4.3.1. Track Elevation of Eastern Line

The Eastern line is now passing through the highly populated urban districts of Jakarta with at grade intersections with the crossing roads. This has a severe adverse effect on train operation in terms of safety and punctuality and at the same time causing traffic congestion around the level crossing by obstruction of traffic flow and poor safety. The road congestion will furthermore increase, which leads to compelling the train to reduce speed near the level crossing. The elevation of the line will include 5.4 km track between Pasar Senen and Kampung Bandan, a rehabilitation of Kota Station, and an extension of 2 km elevated railway between Jakarta station and new station at Kali Besar Barat.

4.3.2. Double Tracking and Electrification of Serpong Line

Upgrading of 23.4 km railway line between Tanah Abang-Serpong into a double track electri-fied line has partially been done. With this improvement the Serpong line will be able to transport more passengers as a commuter railway.

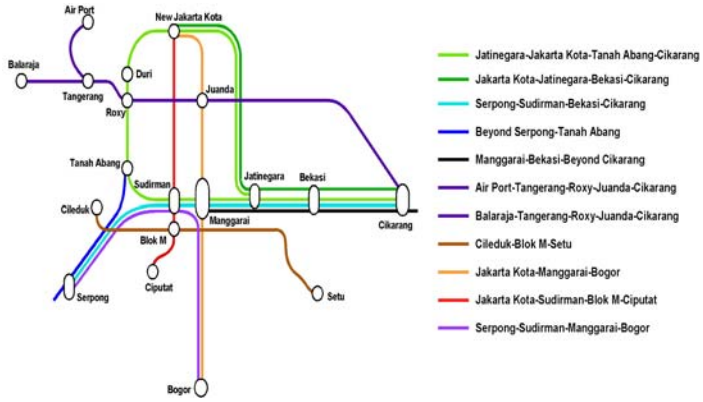

Figure 8 : The Railway Network Enhancement Program
Source: SITRAMP Study 2004

4.3.3. Double Tracking and Electrification of Tangerang Line

Track improvement and the electrification of Tangerang Line's single track were completed in 1999. Since land and other facilities are already available for the double tracking and electrification. the work can be started immediately. There is a plan to extend the Tangerang Line to Soekarno Hatta international airport to provide direct rail access from central Jakarta to the airport.

4.3.4. Tanjung Priok-Citayam-Parung Panjang New Railway Line

This line is planned to transport cargo by connecting Tanjung Priok, Cakung (Bekasi Line), Nambo (Cibinong Cement), Citayam (Bogor Line), and Parung Panjang Merak Line) . The section between Citayam and Nambo has been completed with a single non-electrified track. The rehabilitation and improvement of the line will revive freight rail movement that has been decreasing in recent years.

4.3.5. Grade Separation at Manggarai Central Station

Regional long distance train operation at Gambir and Jakarta Kota stations will be terminated in order to use the semi-loop line as an urban railway. The middle and long distance trains will stop at the Manggarai station and urban rail services will be provided in a semi-loop operation. To provide frequent urban rail service on the semi-loop line, it is necessary to separate the semi-loop line from the middle and long distance line, as well as the central line, by grade separation at the Manggarai station. This project is to be included in the double-double tracking project of the Bekasi line. With that, Manggarai station is prepared for bigger and better station and is projected to play a larger role as central station in the city.

4.4. The New Rail Network

It is necessary to improve the overall performance of services in which the existing network should be expanded to accommodate greater passenger carrying capacity, to increase frequency, and accordingly to increase fleet size by adding more railcars. Figure 8 depicts one alternative of the basic networking concept for future Jabodetabek rail services. In addition to or in replacement of the existing services. several new lines and services were added to the existing network. The coverage of the new network was much larger and included the linkages of major points previously not connected. Among the important lines include the airport link which connects the airport with Cikarang, Ciputat, to Jakarta Kota Line via Sudirman, and a looping line of Jatinegara to Cikarang via Kota. Tanah Abang and Sudirman.

The basic networking concepts applied to new rail system which possibly be developed by other private operators should cover existing and emerging urban centers and should work as part of the distribution system of the existing main commuter system. Its inter-modality, however, must be carefully taken into consideration. More than that quality of the new system should meet the passenger demand of urban middle- and high-income class people in future.

With the new lines and services added to the future rail network, passenger carrying capacity will be increased incrementally in accordance with increases of the demand. To accommodate prospective demand of middle and upper high income people, the express commuter trains will be introduced and will be equipped with air conditioning system; hence, the service is provided with a higher fare than that of the normal rail services in anticipation of higher willingness and affordability to pay of the users. The demand for this type of service seems to be very high at present and it is a promising business opportunity to improve commuter train services when private operators come to the market. It is imperative, however, that the new services will provide convenience of transfer between the north-south operation and east-west operation, minimizing the headways, and maximizing passenger carrying capacity. Attention should also be given to the airport rail access and maintain inter-modality with other rail other systems such as MRT.

The new Jabodetabek will provide extensive services for east-west corridor with three new lines. The first line starts from Cikarang through Bekasi and reaches Serpong. This line has intra-modal transfer points at

Manggarai and Sudirman stations with the MRT north-south line and the Bogor-Central line. The second east-west line also starts from Cikarang. passing the northern area of Kota Bekasi then reaches Balaraja in the west. This line connects new development area in Southern Bekasi and the airport. and will promote the development of Western Tangerang Area. There are several intra-modal points at Juanda and near Harmoni with south-north lines. Bogor-Central Line and MRT. And the third East-West Line starts from Bekasi through the southern area of Cikampek Arterial Road, Blok M, Ciledug and reaches Tangerang. This line has an important role to reduce the congestion of the Cikampek road network and the road between Blok M and Ciledug.

Table 5 : Jabodetabek Rail Enhancement Projects

Projects	Project Cost (US$ million)
Depok Electric Railcar Depot	102.7
Parungpanjang-Citayam New Railway Line	121.6
Tanah Abang-Serpong Double Tracking	83.1
Construction of 50 Electric Railcar Trainset	245.0
Grade Separation at Manggarai	58.38
Railway Electrification of Jawa Main Line	678.0
Engineering Design of Jakarta MRT	30.0
Double Double Tracking Manggarai-Bekasi Line	645.0
Total costs	1,963.78

Other important features of the new Jabodetabek rail network will be the new Jakarta Kota Station that will be constructed on the Loop Line and the first line of Jakarta Mass Rapid Transit (MRT) line. At this new station passengers can transfer to the Loop Line and MRT. It is possible to shorten headway of Central Line to 3 minutes. This line's train operation is undisturbed by the Western Line train operation by grade separation at the Manggarai Station. The MRT is provided along the major arterial roads in the central part of DKI Jakarta, namely, Sudirman-Thamrin corridor, connecting Blok M and Kota. This line has multiple transfer points with other rail systems.

4.5. The Spin-off

The current Jabotabek rail is operating as a regional division of PT KAI, the incumbent operator. In July 2008, the Jabotabek rail was spin-off and transformed into PT KAI Commuter Jabodetabek (PT KCJ) and will be gradually transformed into a separate entity with the main purpose to make rail as the backbone of public transport in Jabodetabek area. The current Jabotabek rail transport carries about 400.000 passengers per day or 70 percent of total rail passengers but constitutes only 4 percent of Jabodetabek total public transport demand. In its railway master plan. it is projected that up to 900 km new tracks will be developed until 2025. adding around 720 km to the existing tracks. This projection would probably fit within the network expansion projected by the SITRAMP Study described above. The expansion of the rail network will be accompanied by 128 unit trains. It is also projected that the full-scale Jabodetabek operation in 2025 will require around 1.4 million Kwh electricity power per day, a demand that could be fulfilled by the future power supply when 20.000 MW new generations have been completely entered the power grid at that time.

4.6. Investment and Financing

Unlike other infrastructure projects such as power generation, toll roads, and telecommunication, rail projects are usually not so attractive for private investors to invest. At least for the first ten years of railway revitalization programs, government investment and public expenditures would be very critical for building the basic infrastructure, providing support, and bearing the risks of investment.

5. CONCLUSION

Jabodetabek greater region is envisioned to have a consolidated rail-based transport system as the backbone for more than 30 million people and probably more than 50 million daily person trips in 2025. As long as 900 km rail network would be developed until 2025 along with its corresponding trains and railcars, energy needs, and management. In terms of organization, steps have been taken to go to that direction by spinning-off the current Jabotabek rail into the a new separate entity, the PT KAI Commuter Jabodetabek. This new urban rail operator is expected to be the embryo for a full-scale modern rail urban operator in the near future.

According to the railway law, new railway infrastructure and services could be provided by local governments and private investors. Enhanced by the decentralization policy, local and city governments are responsible for the provision of its own transport service, including for rail service. The crucial issue is how to ensure that the strategies and policies stipulated based on these individual spatial plans are mutually consistent and well coordinated at the region and city level. It is probably still the responsibility of central government. i.e. Department of Transportation. to integrate the national and regional rail infrastructure and services and to provide technical and management guidance to local governments. It is also necessary for central government to reconcile the disputes that could arise because of the differences in the infrastructure planning at the local level.

ISSN 114-1284

With regard to the institutional aspect of transportation management in the Jabodetabek region, it is urgently needed to clearly define the rationale of the establishment and conceptual structure of a transportation authority to deal with an integrated transportation master plan and management. This could be achieved by either strengthening the existing institution, establishing new metropolitan transportation authority, and by forming a metropolitan transport planning commission. Coverage of such an institution could also be enhanced to include the integration of transportation system and land use, in particular land use and urban development control.

Financial constraint is considered as the major obstacle for rail infrastructure development in the Jabodetabek region. For the next ten years. government would need to invest rather heavily in the railway revitalization program since rail market is probably not sweet enough for private investors to enter. After the extended basic infrastructure accompanied with adequate and conducive regulations have been in place. the market would probably be mature to invite large-scale private investment.

REFERENCES

[1] BPS. Bappenas. and UNFPA. Indonesia Population Projection 2000-2025. July 2005.
[2] Kebijakan Integrasi Angkutan Antar Moda di Jakarta. Makalah disampaikan oleh Asisten Pembangunan Sekda Provinsi DKI Jakarta pada rapat koordinasi PT KAI dan Pemda DKI Jakarta tentang pengembangan Kereta Api Jabodetabek. Jakarta. 16 Juli 2008.
[3] The Study on Integrated Transportation Master Plan for Jabodetabek (SITRAMP Phase II). JICA and Bappenas. Technical Report. March 2004.
[4] Rencana Induk Perkeretaapian Nasional. Draft 1. Direktorat Jenderal Perkeretaapian Departemen Perhubungan. April 2009.

ISSN 114-1284

Building a Knowledge Sharing Culture for Successful Lessons Learned in Construction

Yudi Arminto [1], Mohammed Ali Berawi [2], Yusuf Latief [3]

[1] *Civil Department, Faculty of Engineering*
University of Indonesia, Depok 16424
Tel : (021) 7270011 ext 51. Fax : (021) 7270077
E-mail : yudiarm@yahoo.com

[2] *Civil Department, Faculty of Engineering*
University of Indonesia, Depok 16424
Tel : (021) 7270011 ext 51. Fax : (021) 7270077
E-mail : ale.berawi@gmail.com

[3] *Civil Department, Faculty of Engineering*
University of Indonesia, Depok 16424
Tel : (021) 7270011 ext 51. Fax : (021) 7270077
E-mail : latief73@eng.ui.ac.id

ABSTRACT

The construction industry appears to adopt innovative concepts and protocols from other industries such as lean production, supply chain management, total quality management and value management in targeting improved efficiencies. But the 'culture of manufacturing' is seen to be largely derived from the respective organization culture, whereas 'the culture of construction' is reflected in each 'project culture'. This may be one of the reasons why concepts and protocols from 'manufacturing' cannot be directly transplanted in construction. While some of them may be adapted for one project, the same 'adjusted formats' cannot be used in other projects. This requires separate, if not unique, adjustments of various/ different ideas to suit project specific requirements.

This paper discusses some theoretical issues concerning an ongoing research project which aim to build a knowledge sharing culture that supports successful lessons learned within construction organization in Indonesia. The theories on project learning and the concept of organizational culture are presented and discussed. Furthermore the paper demonstrates links between a culture that influences of project behavior and the perception of team members and how this tie can be used to foster the development of construction process and lessons learned.

Keywords
Organization Culture, Process, Lessons Learned,Contractor

1. INTRODUCTION

Managing knowledge effectively is critical to the survival and advance of a company especially in project-based industries such as construction (Kamara, Anumba, and Carillo, 2002). Effective knowledge management can reduce project time and cost, improve quality and provide a major source of competitive advantage for the construction organizations (Shelbourn, Bouchlaghem, Anumba, Carrillo, Khalfan, and Glass, 2006; Kivrak, Arslan, Dikmen, and Birgonul, 2008). Stoddart (2001) argues that knowledge sharing can only work if the culture of the organization promotes it. Studies by De Long and Liam (2000), shows that culture influence knowledge sharing by as much as 80%.

The construction industry is being viewed as one with poor quality emphasis compared to other sectors like the manufacturing and service sectors (Kubal, 1994; Kanji and Wong, 1998; Wong and Fung, 1999). It not only the final product that is subject to criticisms but the processes, the peoples, the materials etc are under tremendous pressure for better quality in construction. One of the common reasons for the failure of TQM is the cultural position of the company. If the TQM effort is inconsistent with the organizational culture, the effort will be undermined (Dean and Evans,1994 in Adebanjo and Kehoe, 1998). However, addressing culture change has not been easy since most people are unclear about exactly what this means and how it should be approached (Smith, Tranfield, Foster, and Whittle, 1993). Williams et al. (1993) in Adebanjo and Kehoe

(1999) addressed that, despite the growing awareness of cultural issues, comparatively little attention has been paid to the practical, day-to-day processes involved in creating, managing and changing organisational culture. A cultural and behavioral shift in the mind-set of all participants in the construction process especially top or senior management is necessary if the construction industry is to improve its performance (Kanji and Wong, 1998; Love and Heng, 2000; Haupt and Whiteman, 2004).To bring about this change the organization must identify the elements that contribute to the development of knowledge sharing in construction organization.

An Ernst and Young study identified culture as the biggest impediment to knowledge transfer, citing the inability to change people's behaviors as the biggest hindrance to managing knowledge (Watson, 1998). In another study of 453 firms, over half indicated that organizational culture was a major barrier to success in their knowledge management initiatives (Ruggles, 1998). Studies on the role of culture in knowledge management have focused on such issues as the effect of organizational culture on knowledge sharing behaviors (DeLong & Fahey, 2000; Jarvenpaa & Staples, 2001). Similarly, Gold, Malhotra, & Segars (2001) found While studies have shown that culture influences knowledge management and, in particular, knowledge sharing, there is little research on the broader aspects of the nature and means through which organizational culture influences the overall approach taken to knowledge management in a firm.

The construction industry presents particular challenges for the design of lessons-learned systems, as it encompasses multiple contexts - those of business, technology, process and the separation of the design and construction stages, to name a few - and multiple stakeholders with often competing interests. Its processes are idiosyncratic (i.e. different parties improvise different solutions to unique challenges) and contextual (i.e. different types of projects pose different kinds of challenges).

The paper aim to build a conceptual knowledge sharing culture that supports successful lessons learned within construction organization in Indonesia.

2. CULTURE OBSTACLES TO SUCCESSFUL KNOWLEDGE SHARING

Since culture has the potential to impact on business activities of companies, knowledge management practices can also be affected by cultural. Davenport and Prusak (1998), knowledge management is the process of creating value from an organization's intangible assets. Culture are important issues for every organization in every industry. There are many different definitions of culture. The definitions differ greatly according to the research fields. Barthorpe *et al*. (2000) presented an overview of the literature published on the subject of culture and defined it simply as ''what we are and what we do as a society''. A research carried out by Abeysekera (2002) showed that culture in the construction industry is considered to be about the "characteristics of the industry, approaches to construction, competence of craftsmen and people who work in the industry, and the goals, values and strategies of the organizations they work in". Holden (2002) defined culture as varieties of common knowledge. He suggested that cross-cultural management can be viewed as a form of knowledge management, and culture as an organizational knowledge resource which can be managed.

The notion of knowledge sharing has attracted much attention in the knowledge management literature. Themes, such as attitudes to knowledge sharing, actual knowledge sharing behavior, media and means for knowledge sharing, barriers to knowledge sharing have been among the topics discussed both in the published literature and at academic and practitioner-oriented conferences. On the other hand, there have been several studies that showed an impact on knowledge management practices (Voel and Han 2005; Ford and Chan, 2003). Finestone and Snyman (2005) found that cultural diversity in companies result in barriers in knowledge sharing. Similarly, Sackmann and Friesl (2007) assessed the cultural influences on knowledge sharing behavior in project teams. They determined that different cultural backgrounds of team members due to different ethnicities, gender, national culture or functions create a context of cultural complexity, which might affect knowledge sharing in a negative way. Thiessen *et al.* (2007) found that cultural differences increase the difficulties of transferring explicit knowledge whereas the increase is smaller for those associated with the tacit knowledge transfer.

Ma, Qi, and Wang (2008) also examined the impact of some key contextual factors that affect

knowledge sharing within project teams in the Chinese construction sector. They found that trust is positively related to knowledge sharing. In their study, Dhanaraj, Lyles, Steensam, and Tihany (2004) also found that tie strength, trust and shared values are important in tacit knowledge transfer in international joint-ventures. Some other studies also showed that knowledge sharing, communication, and learning in organizations are strongly influenced by cultural values of individual employees (Hutchings and Michailova, 2004; Ardichvili, Maurer, Li, Wentling, and Stuedemann, 2006).

King (2008) focused on the various levels of culture in terms of how they can affect knowledge management practices and outcomes. He developed a conceptual framework that can be used by a firm to address culture-knowledge management relationship issues. Ang and Massingham (2007) examined the affect of national culture on knowledge management for multinational companies and proposed a framework for standardization and adaptation of knowledge management processes based on differences in national culture. They found that the level and nature of impact will vary by knowledge management's processes or sub-processes. Pauleen *et al*. (2007) developed a model to explain the influence of national culture on organizational knowledge management processes. Their model proposes that national culture affects organizational knowledge management processes both directly and indirectly.

Marshall, Prusak, & Shpilberg (1996) indicate that it is not easy to encourage voluntary sharing of knowledge by employees, particularly in financial trading firms where competition is fierce. Davenport and Pursak (1997); Kluge, Stein and Licht (2001); Kankanhalli, Tan and Wei (2002); Keong and Al-Hawamdeh (2002), all refer to the 'knowledge is power syndrome'. If the view of employees is that knowledge is power this will make sharing of knowledge 'an unnatural act in most organizations', and if knowledge is seen as a valuable resource then any situation that may allow knowledge to become public could be seen as threatening (Keong and Al-Hawamdeh 2002). Kluge, Stein and Licht (2001) refer to the 'not invented here' syndrome which they explain as 'the tendency to neglect, ignore or, worse still, disparage knowledge that is not created within your own department' and say the situation can arise through a mistrust of external knowledge. Keong and Al-Hawamdeh (2002) also make reference to the 'not invented here' attitude saying that this attitude can have a detrimental impact when striving to promote knowledge sharing.

Concern about job security is another aspect of sharing that brings a strong resistance to sharing of knowledge (Darling 1997). Darling continues, 'A knowledge culture devotes itself to increasing and sharing knowledge and involves every person in those vital tasks' Resistance to knowledge sharing is evident in comment referred to by Darling, 'this stuff about knowledge sharing is nothing more than me dumping what I know in a pool so I will become dispensable' It may be that if their employment is threatened people will not be inclined to share their knowledge and may even leave the organization taking with them the very knowledge that could have given value to it. The ageing population of many industrial countries is a further aspect of knowledge sharing that needs to be addressed and is raised by Keong and Al-Hawamdeh (2002). So often the knowledge accumulated over many working years is not captured so that the considerable pool of knowledge and experience possessed by such employees is lost to the younger generation. They also indicate the detrimental effect on the organization of the loss of knowledge when resignations, and promotions occur. However, for those who are made redundant there is perhaps a more difficult situation to deal with—they frequently feelings of resentment and asking them to share their knowledge before leaving is likely to be a difficult task.

Resistance or lack of interest in sharing knowledge deprives others of the opportunity to gain knowledge and can in fact rebound on those who are not very willing to share. Many organizations have intranets to enable employees to share, exchange, and access knowledge, but if a non-sharing culture exists there will be little benefit for the organization or its employees. It is possible that employees may not find the intranets user friendly, therefore, there is likely to be resistance to sharing knowledge through that system, or for some it may simply be too much of a hassle to try to find what is being sought (Mitchell 2003). Where resistance to sharing knowledge attitudes exist, organizations need to consider undertaking an approach to implementing behavioral patterns amongst staff that are conducive to knowledge sharing. Regular meetings for the purpose of discussing work-related experiences provide an avenue for sharing knowledge that generates a collaborative environment and one through which everyone benefits.

3. PREVIOUS STUDIES

Previous studies and experiences in the construction industry showed that cultural have an impact on knowledge sharing, either negative or positive of construction enterprises working. However, exactly how culture affects management is still a difficult question to answer (Shore and Cross 2005).

Countries		*Previous literature*
Malaysia	:	Lisa Low Seow Wei and Abdul Hakim Mohammed (2004);
United Kingdom	:	Liz Blankson-Hemans (2006); School of NKM, Trieste (2008); Serkan Kivrak, Andrew Ross, Gokhan Arslan, (2009); Mark Marlin, PMP PM WORLD today – featured Paper (2008)
USA	:	David Gurteen (1999)
Lisboa, Portugal	:	Francisco Loforte Ribeiro (2008)

Table 1: Summary of previous studies on knowledge sharing culture, project learning, and lessons learned

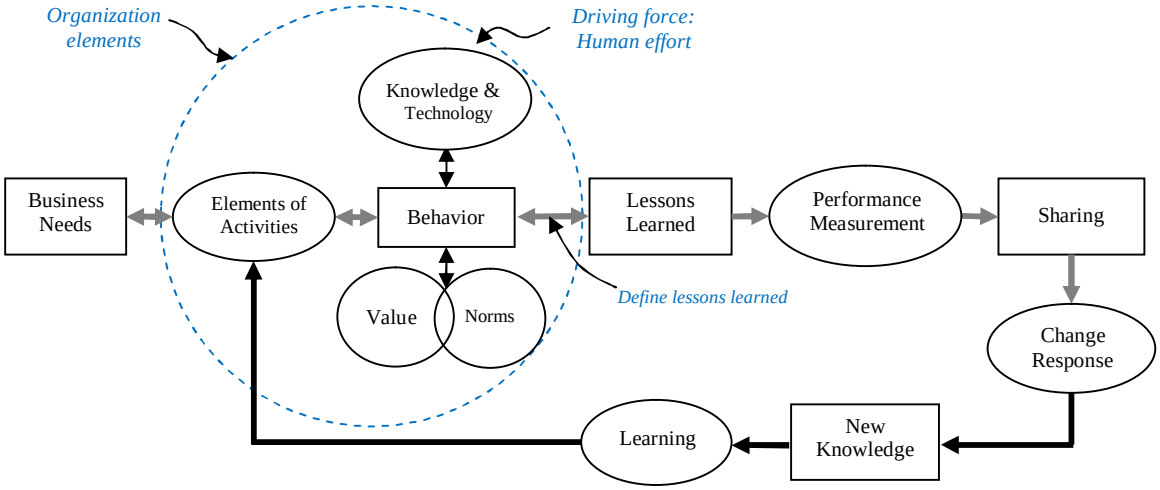

Figure 1 : An Overview of Organization Elements Driven Successful lessons

4. UNDERSTANDING THE KEY DRIVERS FOR SUCCESSFUL LESSONS LEARNED

By understanding how culture influences knowledge sharing in their organizations, can be illustrated specific actions for adapting the organization's culture to support the behaviors needed as overview figure 1:

4.1 Business Needs

Define the activities of business: Coming up with new ideas; Improving implementation and processes. Identify the business needs e.g. reduce project time and cost, improve quality. Finding the gap between the status quo and these activities; Tie the needs to strategic objectives.

Determine what the organization wants to be able to do. e.g. improve efficiency, provide a better quality service. Identify who could provide the requirement; consider potential options for meeting the need.

4.2 Elements of Activities

Element of activities or practices are the formal or informal routines used in the organization to accomplish work. Practices include project implementation processes, key activities, team meetings, time sheets, career paths, compensation plans, etc. Each practice – formal or informal – has specific roles and rules (often unspoken) guiding how they are carried out (Trice and J.M. Beyer, Cliffs, 1993). Work processes: include encourage people to work together more effectively, to collaborate and to share - ultimately to make organizational knowledge

more productive (David Gurteen, 1999). But we need to remember a few things.

4.3 Knowledge and Technology

The ultimate goal of knowledge management is the sharing of knowledge (Tserng and Lin, 2005). The majority of the managers also highlighted the importance of knowledge sharing and pointed out the direct relationship between knowledge sharing and culture. Previous studies and experiences in the construction industry showed that cultural differences have an impact on daily businesses, either negative or positive, of construction enterprises working nationally or internationally. However, exactly how culture affects management is still a difficult question to answer (Shore and Cross 2005).

Gurteen(1999) state that Knowledge Management is fundamentally about people – not technology. But absolutely no way that you can share knowledge effectively within an organization without using technology. The role of IT in a KM system is as a facilitator as previous attempts to capture personal experiences proved unsuccessful (Carrillo *et al.* 2004). There is a need to incorporate technologies that augment existing work practices, with the development of an IT strategy being important in improving its effectiveness (Egbu and Botterill 2002). *"IT systems don't manage knowledge; they manage data and information (Prusak, 2006)."*

The Knowledge content generation tools include various authoring tools (Bergeron, 2003) – word processing editors, multimedia editors, graphics programs, image and sound editors, video editing systems, as the focus is put on time-saving and efforts-saving technologies facilitating the process of creation of relevant high-quality content. Another technology allowing the generation of knowledge from data is knowledge discovery, defined in (O'Leary, 1998) as "nontrivial extraction of implicit, previously unknown, and potentially useful information from data."
Knowledge discovery is a method that includes different tools and approaches to analyze both text and numeric data. As an example of a class of technologies for knowledge discovery could be mentioned data mining tools or the process of extracting meaningful relationships from usually very large quantities of seemingly unrelated data. Specialized data mining tools allow managers to perform competitive analysis, market segmentation, trend analysis, sensitivity analysis, and predictions based on information in the corporate database (Bergeron, 2003).

4.4 Elements of Organization Culture

Schein (1985) defines organizational culture as a set of implicit assumptions held by members of a group that determines how the group behaves and responds to its environment.
These tacit values and beliefs determine the more observable organizational norms and practices that consist of rules, expectations, rituals and routines, stories and myths, symbols, power structures, organizational structures, and control systems (Bloor & Dawson, 1994; Johnson, 1992). In turn, these norms and practices drive subsequent behaviors by providing the social context through which people communicate and act (DeLong & Fahey, 2000). Putting this into the context of knowledge management, organizational culture determines the social context (consisting of norms and practices) that determines "who is expected to control what knowledge, as well as who must share it, and who can hoard it" (Delong & Fahey, 2000). Figure 1 illustrates this conceptual linkage between culture and knowledge management behavior.

Culture exists at different levels of the organization. Values are deeply embedded, tacit assumptions that are difficult to talk about and even more difficult to change. Norms and practices, on the other hand, are more directly observable and easier for employees to identify. Thus, norms and practices around knowledge use are more amenable to change. In fact, practices are the most visible symbol of culture, and they provide the most direct levers for changing behaviors needed to support knowledge management objectives. Changing behaviors around knowledge use is the most direct way to alter organizational norms, which will reinforce the necessary behaviors over time.

Values

Values indicate what an organization's members believe is worth doing or having. They indicate preferences for specific outcomes or behaviors, or what the organization aspires to achieve. It is important to differentiate espoused values, which are talked about but that don't influence behavior, from values that truly motivate behavior in a firm (Trice and J.M. Beyer, Cliffs, 1993). Schein (1992) state that value can be understood as the stated and unstated preferences and principles shared by members of an organization. Examples include loyalty, customer satisfaction, innovation,

diversity, and teamwork. Schein's rationale can be summarized thus: once the (a) espoused values become (b) employees' shared values and beliefs, they can turn into (c) expected behaviors and attitudes. After they do so, those behaviors and attitudes develop into (d) shared assumptions or basic underlying assumptions. Around the entire process there are artifacts, which are helpful illustrations of values. Values are beliefs on how people should behave with regard to such matters as care and consideration for colleagues, customer service, the achievement of high performance and quality, and innovation (Handy, 1993). Green. S (2005) state that there are three attributes to a core competence: it adds value to customers, it is not easily imitated and it opens up new possibilities in the future (Youker, 2006).

Newcombe (1997) defined a project's culture as: 'the shared values, beliefs and assumptions of the stakeholders involved in a project'. Its positive consequences include: enhanced project effectiveness; reduced parochialism and rivalry; and ability to reconcile conflicting project strategies. Its negative consequences include difficulty to introduce change and innovation.

Norms

Norms are the shared beliefs about how people in the organization should behave, or what they should do to accomplish their work. Norms represent the *expected* patterns of behavior. For example, they describe how employees *actually* create, share, and use knowledge in their work (Trice and J.M. Beyer, Cliffs, 1993). Norms are unwritten but accepted rules which tell people in organizations how they are expected to behave. They may be concerned with such things as how managers deal with their staff (management style), how people work together, how hard people should work or the extent to which relationships should be formal or informal (Handy, 1993).
A norm is a behavior (way of doing things, custom) that the group practices on an ongoing basis. A norm serves as a "ground rule" for the group's behavior. Through a process of consciously creating norms for the group, positive norms can be selected (Rochelle Kopp, 2005; http://www.japanlink.com/en/business/pdf/hybrid.pdf).

The following are some general examples of the types of topics that can be addressed when creating norms for a hybrid culture. However, the specific issues that should be addressed for a given team will depend on its situation and challenges.

- What language should be used when?
- How should documents and correspondence be handled?
- How should information be reported? To whom? How often? In what format (oral, written, meeting?)
- What should be the frequency and type of regularly scheduled meetings?
- How to ensure that meetings and conversations are readily understandable for non-native speakers of English?
- How to ensure that all participants contribute equally to the discussion, and that the discussion is not dominated by individuals who are more vocal or fluent in English
- What degree of *nemawashi* (consensus-building pre-meetings) should be conducted prior to meetings? Will decision-making be done by consensus, majority rule, or determination of the senior individual present?

What then does it mean to create a Knowledge Sharing Culture?" Well it's about making knowledge sharing the norm. To create a knowledge sharing culture you need to encourage people to work together more effectively, to collaborate and to share - ultimately to make organizational knowledge more productive David Gurteen (1999). But we need to remember a few things:

- We are talking about sharing knowledge and information – not just information.
- The purpose of knowledge sharing is to help an organization as a whole to meet its business objectives. We are not doing it for its own sake.
- Learning to make knowledge productive is as important if not more important than sharing knowledge. Michael Schrage in a recent interview said that he thinks, "knowledge management is a bullshit issue" as "most people in most organizations do not have the ability to act on the knowledge they possess".

Changing a culture is tough. Not only does it mean change – which has always been tough – it means seeing the world in a different way. It means revealing our hidden paradigms like the tacit acceptance that "knowledge is power".

4.5 Lessons Learned

The aim of lessons learned is to convey knowledge gained through experience, in some specific field of action, as means to enhance future performance. Few studies provide a definition of the lessons they present or explore the concept of lessons learned. The *PMBOK® Guide* defines Lessons Learned as "The learning gained from performing the project. Lessons Learned may be identified at any point." Learning can come from successes where we did something creative or imaginative and we would like to see it repeated on future projects and learning can come from our failures where something failed to meet our expectations and we would like to improve and not make the same mistake again. It would be nice to say most of the learning comes from our successes, but the reality is that most of the learning comes from our failures. Cowles (2004) state that a lessons learned is knowledge or understanding gained by experience contain negative experience and positive experience. A lesson must be significant, valid, applicable, and could describe a problem or issue that the organization will investigate. "*A lesson learned is knowledge or understanding gained by experience. The experience may be positive, as in a successful test or mission, or negative, as in a mishap or failure…A lesson must be significant in that it has a real or assumed impact on operations; valid in that is factually and technically correct; and applicable in that it identifies a specific design, process, or decision that reduces or eliminates the potential for failures and mishaps, or reinforces a positive result* (Secchi, 1999 in Weber 2001)*.*"

Lessons learned is forms of knowledge artifacts. *A knowledge artifact is a defined piece of recorded knowledge that exists in a format that can be retrieved to be used by others. A process drawn on a napkin at lunch can become a knowledge artifact if it can be recorded for someone else to use. Typically artifacts are something more tangible – i.e. a document, a picture or graphic, a video, an audio, a project plan, a presentation, a template … to name several (Seiner, Robert S., 2001).* What one user may consider a valuable lesson learned another may consider inconsequential or non-relevant information. It is critical to establish a common understanding as to what type of information (i.e., knowledge artifact) is a candidate for sharing using this system.
"The lack of leadership involvement in and commitment to the learning process is the most critical barrier." (Dressler, 2007) An effective Lessons Learned process means having a disciplined procedure that people are held accountable to follow. It means encouraging openness about making mistakes or errors in judgment. It often means cultural or organizational change, which does not come easy in most organizations. It means leading by example. If management is unwilling to learn from their mistakes, it is unlikely that the rest of the organization will be willing to admit to mistakes. In fact, management must reward people for being open and admitting to making mistakes, bad decisions, judgment errors, etc. This, of course, flies in the face of many corporate cultures.

Lessons Learned captured on a project seldom benefit that project. They benefit future projects. Often, a project manager sees capturing Lessons Learned as simply another chore that provides his or her project with little value, especially if the Lessons Learned procedure is complex, takes a fair amount of resources and time to implement, and management has not provided adequate resources to perform the work. The solution here is to have a simple procedure, ensure projects have the resources and time to implement the procedure, and hold project managers accountable for following the procedure. The "lack of value to my project" problem can be alleviated by proving to people the value of Lessons Learned to the organization and by ensuring that projects in the planning stages incorporate Lessons Learned from prior projects.

4.6 Performance Measurement

In an attempt to address successful lessons learned, characteristics of emerging performance indicators have been proposed by different researchers (Kaplan and Norton, 1992; Lynch and Cross, 1995; Neely, 1999; Love and Holt, 2000; Neely and Adams, 2001). It is of agreement that the formation of indicators should start with analysis of both the organizational complexity and the operating environment characteristics. Common issues that are used to describe these include:

- The changing nature of work;
- Increasing global competition;
- Specific improvement initiatives;
- National and international quality awards;
- Changing organizational roles;
- Changing external demands; and
- The power of IT.

Further, the indicators should have the following essential characteristics:

- Measures should be able to identify causes of problems;
- Measures should be able to address all possible performance drivers (in broad, complex and dynamic nature of the construction industry business environment);
- Measures should be able to identify potential opportunities for improvement; and

Information they provide should arrive in time to take actions. Characteristics of emerging performance measurement systems.

4.7 Sharing

One approach to defining knowledge-sharing success focuses on the degree to which the knowledge is re-created in the recipient. Consistent with the innovation literature but on more micro basis, knowledge can be seen as knowledge packages embedded in different structural elements of an organization, such as in the people and their skills, the technical tools, and the routines and systems used by the organization, as well as in the networks formed between and among these elements (Argote & Ingram, 2000; Leonard-Barton, 1992). Successful knowledge sharing results in firms mastering and getting into practice product designs, manufacturing processes, and organizational designs that are new to them (Nelson, 1993).

The concept of knowledge management has narrowed the definition of knowledge sharing as being essentially a process of capturing a person and organization's expertise wherever it resides and distribute it to wherever it can help produce the biggest returns for the individual and organization (Krogh, 2000). According to Wang (1999), knowledge sharing is the conversion between tacit knowledge to explicit knowledge and vice versa while the knowledge 'oscillates' from individuals to the organizations and back. When, employees shared tacit and explicit knowledge through their daily interaction and activities, the original knowledge spread out.

4.8 Change Response

After the knowledge has been acquired or "sourced," it normally cannot be used in its raw form and must be transformed in order to become a valuable knowledge asset and to facilitate its further application and re-use (Liebowitz, 1999). Knowledge can be transformed in many ways, specifically to conform to the format of the target repository. Traditionally, knowledge has been collected, compiled, verified, validated, and organized by an "end user", who embeds it into intermediate products, new customer products, or educational programs.

4.9 New Knowledge

New knowledge is a result of sharing and change response among project employees and stakeholders

4.10 Learning

America's Construction Industry Institute conducted a large-scale investigation of lessons learned processes, carried out by its Modeling Lessons Learned Research Team (Fisher,, Deshpande and Livingston, 1998). Out of the 2400 organizations surveyed, they found strong evidence that most organizations were using insufficient dissemination processes. Such lessons learned system has grown through popular concepts such as the "learning organization" (Senge, 1990), through developments in knowledge management (Davenport and Prusak, 1998), and through technological advancements that hold the promise of wider, more efficient distribution of lessons within an organization. Lessons learned systems supported by knowledge management and organizational learning approaches can be used to develop validated experiential lessons (Fong & Yip, 2006)

Knowledge Sharing is not about giving people something, or getting something from them. That is only valid for information sharing and occurs when people are genuinely interested in helping one another develop new capacities for action; it is about creating learning processes (Peter Senge, 1990). Knowledge sharing is seen as occurring through a dynamic learning process where organizations continually interact with customers and suppliers to innovate or creatively imitate. Lessons learned can be shared amongst parties that have a vested interest in ensuring that positive experiences are repeated and while avoiding the recurrence of negative experiences (Kim & Nelson, 2000).

Furthermore, to create a true learning culture, learning must not be for the sake of the individual alone, but for the team and the wider organization, as Fifth Discipline Field Book points out: *Learning in organizations means the continuous testing of experience, and the transformation of that experience into knowledge*

– accessible to the whole organisation, *and relevant to its core purpose*
Creating a climate in which staff naturally share their learning is a significant part of building a learning culture.

5. DISCUSSION

After identifying the factors expected to influence knowledge-sharing culture, we then proceed to detail the key people management practices that, according to theory and research, should be most effective in fostering knowledge sharing in construction organizations to gain successful lessons learned.

The conceptual frameworks knowledge sharing culture for successful lessons learned, namely:

1. Cultures which driven knowledge sharing behavior are:
   - Norms produce behavior which strongly influence works climate, management style and how people work together.
   - Core values are the basic beliefs about what is good or best for organization, and about what management thinks is important, what should or should not happen.
   - Practices are the formal or informal routines used in the organization to accomplish work.
2. Knowledge sharing base on behavior will create a good or best lessons learned.
3. Effectiveness lessons learned must be measured to make matching with business objective
4. Sharing lessons learned knowledge include of mistake and successful to all project employees
5. There are response of audience to increase performance through improvement value, norms and practices. Ultimately to create a new knowledge
6. Transfer knowledge and skill individually to organization will change element of activities
7. All of organization elements driving force by human effort

A cultural and behavioral shift in the mind-set of all participants in the construction process especially top or senior management is necessary if the construction industry is to improve its performance

6. CONCLUSION

This paper firstly deals with the conceptual framework of knowledge sharing culture for successful lessons learned and its critical success factors. It also examines the preferred practices of knowledge sharing as illustrated in the Figure 1. At the end, the factors that promote the development of knowledge sharing culture will be identified, which can be followed by element of organization culture to change their employees behavior driven successful lessons learned within the organization.

ACKNOWLEDGMENT

Many thanks go to Mr. Mohammed Ali Berawi, PhD my supervisor who giving supported to accomplish this paper and beloved my family who motivated me.

REFERENCES

1. Adebanjo, D., and Kehoe D.,(1998), An evaluation of quality culture problems in UK companies, *International Journal of Quality Science*, vol. 3, no. 3, pp. 275-286.
2. Adebanjo, D., and Kehoe D.,(1999), An investigation of quality culture development in UK industry, *International Journal of Quality and Reliability Management*, vol. 19, no. 7, pp. 633-649
3. Ang, Z., and Massingham, P. (2007). ‘‘National culture and the standardization versus adaptation of knowledge management’’. *Journal of Knowledge Management*, Vol. 11, No. 2, pp 5-21.
4. Ardichvili, A., Maurer, M., Li, W., Wentling, T., and Stuedemann, R. (2006). ‘‘Cultural influences on knowledge sharing through online communities of practice’’. *Journal of Knowledge Management*, Vol. 10, No. 1, pp 94-107.
5. Baltahazard, P. A., & Cooke, R. A. (2003). *Organizational culture and knowledge management success: Assessing the behavior-performance continuum* (Working Paper). Arizona State University West.
6. Barrie, D.; Paulson, B. (1992) *Professional Construction Management*, New York: McGraw-Hill.
7. Darling, MS 1997, ‘Knowledge Cultures’, *Executive Excellence*, February, pp. 10-11.
8. Davenport, T. & Prusak, L. (1998). *Working knowledge: How organizations manage what they know.* Harvard Business School, Boston
9. Davenport, TH, Prusak, L & Wilson, HJ (2003), *What’s the Big Idea?* Harvard Business School Press, Boston, Massachusetts.

10. DeLong, D. W., & Fahey, L. (2000). Diagnosing cultural barriers to knowledge management. *Academy of Management Executive*, *14*(4), 113-127.
11. Dhanaraj, C., Lyles, M.A., Steensam, H.K., and L. Tihany. (2004). ''Managing tacit and explicit knowledge transfer in IJVs: the role of relational embeddedness and the impact on performance''. *Journal of International Business Studies*, Vol. 35, pp 428-442.
12. Finestone, N., and Snyman, R. (2005). ''Corporate South Africa: making multicultural knowledge sharing work''. *Journal of Knowledge Management*, Vol. 9, No. 3, pp 128-41.
13. Fisher, D., Deshpande, S. and Livingston, J. (1998). *Modeling the lessons learned process* (Research Report 123-11). Albuquerque, NM: The University of New Mexico, Department of Civil Engineering.
14. Ford, D.P., and Chan, Y.E. (2003). ''Knowledge sharing in a multi-cultural setting: a case study''. *Knowledge Management Research in Practice*, Vol. 1, No. 1, pp 11-27.
15. Gold, A. H., Malhotra, A., & Segars, A. H. (2001). Knowledge management: An organizational capabilities perspective. *Journal of Management Information Systems*, *18*(1), 185-214.
16. Haupt, T. C., and Whiteman, D. E., (2004), Inhibiting factors of implementing total quality management on construction sites, *The TQM Magazine*, vol. 16, No. 3, pp. 166-173.
17. Hofstede, G. (1991), "Cultures and Organizations: Software of the Mind, Intercultural Cooperation and its Importance for Survival," New York, NY: McGraw-Hill.
18. Hofstede, G. (2005) *Cultures and Organizations: Software of the Mind*, (2nd Ed.), New York: McGraw-Hill.
19. Hutchings, K., and Michailova, S. (2004). ''Facilitating knowledge sharing in Russian and Chinese subsidiaries: the role of personal networks and group membership''. *Journal of Knowledge Management*, Vol. 8, No. 2, pp 84-94.
20. Jarvenpaa, S. L., & Staples, S. D. (2001). Exploring perceptions of organizational ownership of information and expertise. *Journal of Management Information Systems*, *18*(1), 151-183.
21. Jarvenpaa, S. L., & Staples, S. D. (2001). Exploring perceptions of organizational ownership of information and expertise. *Journal of Management Information Systems*, *18*(1), 151-183.
22. Kamara, J.M., Anumba, C.J., and Carillo, P.M. (2002). ''A Clever approach to selecting a knowledge management strategy''. *International Journal of Project Management*, Vol. 20, pp 205-211.
23. Kanji, G. & Wong, A., (1998), Business Excellence model for supply chain management, *Total Quality Management*, vol. 10, no.8, pp. 1147-1168.
24. Kankanhalli, A, Tan, BCY, Wei, K 2002, 'Managing Knowledge Workers: A Technological Perspective', *Journal of Information and Knowledge Management*, March, vol. 1, no. 1, pp. 18-25.
25. Kaplan R. S., and Norton D. P. (1992). The Balanced Scorecard – Measures That Drive Performance, Harvard Business Review, **70**, pp.71-79.
26. Keong, LC & Al-Hawamdeh, S 2002, 'Factors Impacting Knowledge Sharing', *Journal of Information and Knowledge Management*, vol. 1, no. 1, pp. 49-56.
27. King, W.R. (2008). ''Questioning the conventional wisdom: culture-knowledge management relationships''. *Journal of Knowledge Management*, Vol. 12, No. 3, pp 35-47.
28. Kivrak, S., Arslan, G., Dikmen, I., and Birgonul, M.T. (2008). ''Capturing knowledge in construction projects: knowledge platform for contractors''. *ASCE Journal of Management in Engineering*, Vol. 24, No. 2, pp 87-95.
29. Kivrak, S., Ross, A., Arslan, G., (2009). Impacts of Cultural Differences on Knowledge Management Practices in Construction.
30. Kluge, J, Stein, W & Licht, T 2001, *Knowledge Unplugged: The McKinsey & Company global survey on knowledge management*, Palgrave, Basinstoke, UK.
31. Krogh, V. G., Kazuo Ichijo and Ikujiro Nonaka (2000). *Enabling Knowledge Creation: How to Unlock the Mystery of Tacit Knowledge and Release the Power of Innovation*. New York: Oxford University Press. P. 25 & 29.
32. Kubal, M (1994), *Engineered quality in construction : partnering and TQM*, McGraw-Hill, New York.
33. Leidner, Alavi, Kayworth (2006). *The Role of Culture in Knowledge Management: A Case Study of Two Global Firms*
34. Love P.E.D. and Holt G.D. (2000) Construction business performance measurement: the SPM alternative. Business Process Management Journal, **6** (5), pp. 408-416.
35. Love, P.E.D. and Heng, L. (2000), Total quality management and the learning organization: a dialogue for change in construction, *Construction Management and Economics*, Vol. 18 No. 3, pp. 321-31.
36. Lynch R.L. and Cross K.F., 1995). Measure Up! How to Measure corporate Performance. 2nd Edition. Blackwell Publishers: Oxford.
37. Ma, Z., Qi, L., and Wang, K. (2008). ''Knowledge sharing in Chinese construction project teams and itsaffecting factors - an empirical study''. *Chinese Management Studies*, Vol. 2, No. 2, pp 97-108.
38. Marshall, C, Prusak, L & Shpilberg, D 1996, 'Financial Risk and the Need for Superior Knowledge Management', *California Review*, Spring, vol. 8, no. 3, pp. 77-101.
39. Neely A. (1999). The performance Measurement Revolution: Why now and What next?

International Journal of Operations and Production management, **19:2**, 205-228.

40. Neely A. and Adams C. (2001). Perspectives on Performance: The Performance Prism. Handbook of Performance Measurement (ed Bourne, M). Gee Publishing, London.
41. Patrick S.W. Fong & Jimmy C.H. Yip (2006), An Investigative Study of the Application of Lessons Learned Systems in Construction Projects
42. Pauleen, D.J., Wu, L.L., Dexter, S. (2007). ''Exploring the relationship between national and organizational culture, and knowledge management'', In Pauleen, D.J. (ed.), *Cross-Cultural Perspectives on Knowledge Management*, Libraries Unlimited, Westport, USA, pp 3-19.
43. Peter Anthony, Managing Culture, Open University Press, 1994. p29.
44. R. Weber, D. W. Aha and I. Becerra-Fernandez (2001) Intelligent lessons learned systems. Expert Systems with Applications Volume 20, Issue 1, January 2001, Pages 17-34
45. Riley, M., Clare-Brown, D. (2001) Comparison of Cultures in Construction and Manufacturing Industries. *ASCE Journal of Management in Engineering*, July 2001, 149- 158.
46. Rowlinson, S.M. & Walker, A. (1995) *The Construction Industry in Hong Kong* (Hong Kong, Longman).
47. Ruggles, R. (1998). The state of the notion: Knowledge management in practice. *California Management Review 40*(3), 80-89.
48. Ruggles, R. (1998). The state of the notion: Knowledge management in practice. *California Management Review 40*(3), 80-89.
49. Sackmann, S.A., and Friesl, M. (2007). ''Exploring cultural impacts on knowledge sharing behavior in project teams – results from a simulation study''. *Journal of Knowledge Management*, Vol. 11, No. 6, pp 142-156.
50. Schein, E. H. (1992). *Organizational culture and leadership*. (2nd ed.). San Francisco, CA: Jossey-Bass management series. Jossey-Bass social and behavioral science series.
51. Schultzel, H.J. & Unruh, V.P. (1996) *Successfiil Partnering—Fundamentals for Project Owners and Contractors* (New York, John Wiley and Sons).
52. Secchi, P. (Ed.) (1999). Proceedings of Alerts and Lessons Learned: An Effective way to prevent failures and problems (Technical Report WPP-167). Noordwijk, The Netherlands: ESTEC
53. Seiner, Robert S. (2001), Meta Data as a Knowledge Management Enabler. The Data Administration Newsletter (TDAN.com)
54. Senge, P. (1990). *The fifth discipline: The art and practice of the learning organization*. New York: Doubleday Currency.
55. Shelbourn, M.A., Bouchlaghem, D.M., Anumba, C.J., Carrillo, P.M., Khalfan, M.M.K., and Glass, J. (2006). ''Managing knowledge in the context of sustainable construction''. *Journal of Information Technology in Construction*, Vol. 11, pp 57-71.
56. Smith, S., Tranfield, D., Foster, M. and Whittle, S. (1993), Strategy for managing the TQ agenda, *International Journal of Operations and Production Management*, Vol. 14 No. 1, pp. 75-88.
57. Sommerville, J. (1994) Multivariate barriers to total quality management within the construction industry, *Total Quality Management*, vol.5, no.5, pp. 289-298.
58. Stoddart, L. (2001). Managing Intranets to Encourage Knowledge Sharing: Opportunities and Constraints. *Online Information Review*. 25(1): 19-28.
59. Thiessen, M.S.W., Hendriks, P.H.J., and Essers, C. (2007). ''Research and development knowledge transfer across national cultures'', In Pauleen, D.J. (ed.), *Cross-Cultural Perspectives on Knowledge Management*, Libraries Unlimited, Westport, USA, pp 219-243.
60. Trice and Beyer, 1993, provided material for defining "subcultures;" also see "Three Cultures of Management: The Key to Organizational Learning" by E.H. Schein, *Sloan Management Review*, (Fall 1996):9-20, for an excellent discussion of the role of subcultures as a barrier to improving organizational effectiveness.
61. Tserng, H.P., and Lin, Y.C. (2005). ''A knowledge management portal system for construction projects using knowledge map''. *Knowledge Management in the Construction Industry: A Socio-Technical Perspective*, pp 299-322, Idea Group Publishing, Hershey, Pa
62. Voel, S.C., and Han, C. (2005). ''Managing knowledge sharing in China: the case of Siemens ShareNet''. *Journal of Knowledge Management*, Vol. 9, No. 3, pp 51-63.
63. Wang F. H. (1999). *Knowledge Management*. China: Economy Shan Xi Publisher. P.218-222.
64. Watson, S. (1998). Getting to "aha!" companies use intranets to turn information and experience into knowledge — And gain a competitive edge. *Computer World, 32*(4), 1.
65. Wong, A. & Fung, P., (1999) Total quality management in the construction industry in Hong Kong: a supply chain management perspective, *Total Quality Management*, vol. 10, no .2, pp. 199-208.
66. Youker. R (2006), Project Management as a Core Competency (PM World Today – Second Edition – December 2008)
67. Kamara, J.M., Anumba, C.J., and Carillo, P.M. (2002). ''A CLEVER approach to selecting a knowledge management strategy''. *International Journal of Project Management*, Vol. 20, pp 205-211.
68. Newcombe, R. (1997) Procurement paths: a cultural/political perspective. In Davidson, C.H. and Meguid, T.A.A. (eds), *Procurement: A Key to Innovation*, I. F. Research Corporation, Montreal, pp. 523–34.

COPYRIGHT

All papers submitted must be original, unpublished work not under consideration for publication elsewhere. Authors are responsible to obtain all necessary permission for the reproduction of tables, figures and images and must be appropriately acknowledged. The paper is not defamatory; and the paper does not infringe any other rights of any third party.

The authors agree that the Technical Committee's decision on whether to publish the paper in the Conference's proceedings shall be final. The authors should not treat any communication from the Technical Committee members who reviewed their work as an undertaking to publish the paper.

Prior to final acceptance of the paper, authors are required to confirm in writing that they hold all necessary copyright for their paper and to assign this copyright to the Conference Organizer.

Symposium on Tropical Eco-Urbanism

Symposium C

QiR

PT. PURI FADJAR MANDIRI

Konsultan Teknik dan Bisnis

PURI

Teknik Sipil

Penyelidikan Tanah

Analisa Dampak Lingkungan

Geodesi/GPS-Topografi

dan Hidrografi

Study Finansial & Ekonomi

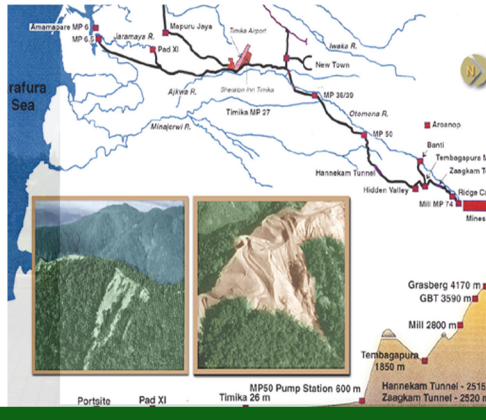

Gedung Puri
Jl. Warung Jati Barat No. 75A Jakarta 12740, Indonesia
Tel. : 62(0)21 – 7974766 (Hunting) Fax. : 62(0)21 – 7974765
email : purimail@rad.net.id

Proceeding of the 11th International Conference on QiR (Quality in Research)
Faculty of Engineering, University of Indonesia, Depok, Indonesia, 3-6 August 2009
ISSN 114-1284

The Images of Jakarta: View from *Kampungs*

Antony Sihombing

Department of Architecture, Faculty of Engineering,
University of Indonesia 16424
Tel (021) 7863512, Fax (021) 7863514
E-mail; a.sihombing@eng.ui.ac.id

ABSTRACT

Jakarta is a complex city, a city of conflicts and a city of differences: the traditional and modern, the informal and formal, the unplanned and planned, the rich and poor, and the sacred and the worldly, often standing side by side. It presents as a complex of kampungs and, at the same time, a kota. This paper responds to the question: Why do people want to continue living in kampungs despite the tensions and conflicts they experience, seemingly caused by excessive and ever-encroaching development of kota? The question will be addressed through exploring the lived experiences of people in kampungs. This paper discusses Jakarta, view of both kampung and kota, from the perspective of kampungs. Images that Jakarta inhabitants have of their own kampungs, which reported not only the views of the residents and the informal sector workers, but also the views of the NGOs who work in the kampungs of Jakarta.

Key words: kota, kampung, and images of Jakarta.

1. INTRODUCTION

An article in *Kompas* on 19 February 2000 titled '*Kampung Kagak Kampungan'* (*kampung* is not *kampungan*) reminded us of the meaning of *kampung* by distinguishing it from *kampungan*. A *kampung* is simply a traditional, spontaneous and diverse settlement in an urban area. *Kampungan* has two meanings: primitive, and bad mannered. This article was a critique of the Government of the Province of *DKI* (Special Region of Capital City) Jakarta, which tends to view *kampungs* only as ugly, poor and informal settlements; they are seen as weakening the attractiveness of Jakarta, just as they are also interrupting the urban development of Jakarta towards a modern metropolitan city.

Jakarta is indeed, at one level, a *kampung* and at the same time a *kota*. It is a complex city or city of contrasts: the traditional and the modern, the rich and the poor, the sacred and the worldly, often standing side by side in a bustling metropolis. Jakarta is a big city and, as well, a big *kampung* [1]. Leaf makes this point:

> …Jakarta is also *perkampungan yang besar*, the big village, and [this is] a reference to both its physical forms as a multitude of small *kampung* settlements or villages grown together as well as its social role as a receptor of immigrants from throughout the country.

2. KOTA

2.1. A Bulldozer

The image of the bulldozer is not unfamiliar to *kampung*[1] residents, particularly those who have faced the threat of having their *kampungs* demolished. They view the government and developers as a bulldozer or destructive machine, which has flattered their houses in the *kampungs*. It is an image of power on one side and of powerlessness on the other. The image of the inability of *kampungs* to fight against the bulldozer is the image of their weakness against *kota*. Rosello tells a similar story of the *bidonvilles* (in France, which are similar to *kampungs* in Jakarta), when residents cannot stay to defend themselves from the power of 'bulldozers'[2]. He stressed that:

> There was nothing more important than the complete erasure of *bidonvilles*. This included making them less visible, hiding them behind

1 K*ampung* is an unstructured, unorganized and informal settlement in relation to the broader socio-economic system. It can also be realized as a settlement in an urban area without infrastructure, planning or urban economic networking. Poverty and poor of quality of life are the features of *kampungs*.

ISSN 114-1284

> smokescreens of words and physical barriers: fences and walls were built, bulldozers piled up earth to create artificial hills [high-rise buildings or new developments in Jakarta] that compounded the inhabitants' serious drainage problems but successfully hid unsightly *bidonvilles* from richer neighbourhoods (p. 249).

From the perspective of *kampung* residents, *kota* is a bulldozer that has excessive power over *kampungs*. According to Urban Poor Consortium (UPC) the government has removed 200,000 families from river banks because of their alleged contribution to flooding in Jakarta.

2.2. Expensive and Restricted Space, but Place for Working

Large numbers of people from *desas*[2] or other cities have moved to Jakarta to improve their income and seek a better future. To reduce their costs (of both transport and housing) and also minimize the time to get to their office places, they live in *kampungs* close to the city or even in the city centre. In this sense, Han argued that *kampung* is 'a settlement "in" or "around" a city where…urban characteristic is noticeable, and high density [and] low servicing account for some general environmental and housing problems'[3].

The informal sector in *kota* must pay an 'informal daily tax', which is collected by *premans*.[3] If they do not pay this 'tax' to the *premans*, they will not be safe working in the area, or may even lose their jobs. The *premans* are employed by a mafia or godfather[4] who illegally controls particular areas in *kota*.

Kota is high-cost space and every square metre is costly, so people from middle to low income groups cannot afford to live there. *Kota* is also seen as modern (high-tech, sophisticated, and the centre of information), and is the locus of the new culture of modernity. *Kampung* inhabitants cannot gain access to these matters, which are alien to them. People struggle for work and for the right to live.

Another sign of the exclusiveness of *kota* is when government includes in the master plan the idea of privatization of large areas, roads and recreation places. Fenced, gated settlements and a divided city are exclusive space and place, and express another characteristic of *kota*. Toll-road developments in Jakarta become exclusive, while the government is reluctant to revitalize the public transport system and its facilities, which are needed for most Jakartans. *Kampungs*, the informal and poor settlements, feel that *kota* is restricted space and place. From the perspective of *kampungs*, *kota* is also impermeable or exclusive for them.

The trend to separate *kota* from *kampungs* is another form of exclusiveness. These separations can occur through demolishing *kampungs* and relocating the inhabitants to the outskirts of the city, or putting them into low cost flats. However, most *kampung* residents choose to live 'on earth' or 'on land' because earth or land is the symbol of power, prosperity, and harmony. And they sense that flats are enclosed (walled and rigid) settlements. Thus both of these separations—out of the city or into the flats—are problematical.

In line with the view of *kota* as a place for working, *kampung* inhabitants, particularly those working in the informal sector, feel that *kota* is a restricted zone for them. The government has issued many *Perdas* (urban regulations) to restrict the operation of the informal sector such as those on *becaks* and *PKL* (*pedagang kaki lima*) or pedestrian vendors mentioned earlier.

Jakarta as a restricted city, for example for *becak* and *PKL*, is in some sense a contradiction of the people's freedom to come, move, or live in Jakarta from different *desas* or cities, at various socio-economic levels, and from various socio-cultural backgrounds. Every year after *Idul Fitrie*[5] Jakarta gets an additional population (1–2%) of people coming to work in the informal sector. In anticipation of this migration, *Pemprov DKI* Jakarta established a new *Perda* to sort out people migrating to Jakarta. Thus, besides a restricted space being established for the

---

2 *Desa* is a traditional settlement in the rural area.

3 *Preman* comes from the phrase 'free man'. The word '*preman*' is a term used in Medan (North Sumatera) to indicate the local mafia.

4 Prof Sahetapy, a member of parliament, suggests (*Kompas*, 13 March 2003) that there are 'untouchable godfathers' found in this country, particularly in Jakarta, who control the city, and the police are unable to arrest them.

5 *Idul Fitrie* is Islamic Great Celebration

ISSN 114-1284

informal sector, the *Perda* also designates Jakarta as a 'forbidden city' for people from other Indonesian *desas* and cities, through checking the identity cards of migrants during this season (after *Idul Fitrie*) in train stations and bus terminals.

As a result of centralization of socio-economic activities in *kota*, the opportunity to find jobs is greater in *kota* than in *kampung*s themselves. *Kota* is a place where elites run their businesses, generating a lot of jobs in both the formal and the informal sectors. Many *kota* employees, particularly the young and single, who work in formal jobs (secretaries, middle management, junior professionals, etc) choose to live in the *kampungs* behind *kota*. Some of them are from *kampungs* who have succeeded in moving up the socio-economic ladder.

However, many *kampung* inhabitants are from uneducated and unskilled backgrounds, so they find it difficult to get formal jobs in *kota*. The informal sector enables them to solve this problem, because they do not need a large amount of capital and training to do these jobs. They can work in the informal sector to serve *kota* activity as supporting staff, drivers, servants, pedestrian vendors, etc. (Figure 1). For example, Wati from *kampung* Anyer (Central Jakarta) protested against the Jakarta government, because in her view: 'government has never understood the people, we would not stay on illegal land (close to or along the railway) if we had the money to buy houses in permitted settlements'.

Ordinary people want to live in the city centre close to their work place, but the government has removed many of them to the outskirts of the city, for example to *Perumnas* (National Housing Agency) estates or peripheral settlements. However, as a result of poor planning of these new settlements in the outer city they have difficulty in getting to work in *kota*. Because of inadequate public transport they need more time to get to their work in the morning and to get home in the evening. Johan Silas (*Kompas*, 22 Juni 1996) criticized the inefficiency of Jakarta. He argued that people need two hours to get to work places (offices) in *kota* and another two hours to get home. They have to get up early in the dark (at about four or five a.m.) to catch public transport and arrive at work on time, and they arrive home in the dark.

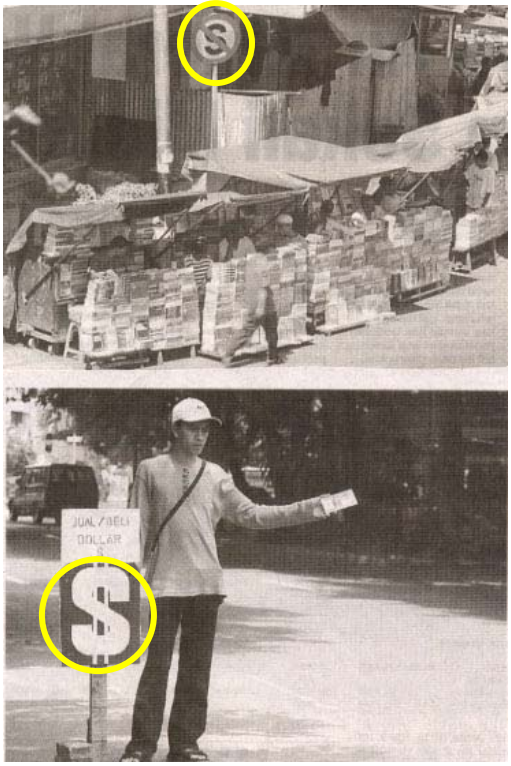

Figure 1: Activities of the informal sector in Jakarta

Note: The on-street informal sector: selling books on a pedestrian area with 's' traffic sign, which means 'no standing' (top); and selling dollars with another 's', which means please stop to buy dollars (bottom)

Source: Photographs by author

2.3. Center of Power and Basis of Conflicts

Non Government Organizations (NGOs) suspect that the implementation of *RTRW* in city developments does not take the side of the public. Elites can design the results of public opinion surveys according to their own wishes, just as if that opinion had come from Jakarta's citizens, the majority of whom live in *kampungs*. NGOs view *kota* as the centre of power to control the whole city through city planning and design. This view was also stressed by Michel Foucault when he described architecture (including planning and design) as an intermediary of 'the relationship of power and space' and 'as a political "technology" for working out the concerns of government through the spatial "canalization" of everyday life' [4]. So planning and design are tools of government or elites to maintain power over *kampungs*, as Low and Lawrence–Zuniga quote from Rabinow (1982) and Foucault (1975) [5]:

ISSN 114-1284

> …architecture and planning function as spatial tactics contributing to the maintenance of power of one group over another at a level that includes the control of the movement and surveillance of the body in space as well as the transformation of spatial ideologies. They do not focus, however, on individuals' everyday resistance to spatial forms of social control.

When the elites use excessive power over the city, particularly over *kampungs*, by manipulating city planning and design, *kota* becomes a basis of conflicts between the formal and the informal sector or *kota* and *kampungs*, consistent with the suspicions of the 36 NGOs.

The central and provincial governments, supported by the private sector, practise such social, economic and political power on the people of Jakarta. Socio-economically, elites manage most of the markets and the formal economy of the city, control most strategic spaces in the city, and also try to persuade government to change public space to private. And hence they also effectively manage the constraints within which the informal economy also must function.

Socio-politically, elites use their power by exploiting Jakarta's citizens for their personal interests, or for the interests of their group or party. As Ward [6] argues, 'the crime is political or economic gain from the exploitation of the ignorance or hardship of others'. It is now widely believed that many social conflicts that have occurred in Jakarta have been provoked by the elites. For example, in the Manggarai elites (developers) established their power in the business area. Moreover, Ward stressed that 'the criminal is usually the promoter or developer' [7]. As well, in Kebon Kosong, members of the Kemayoran delegation and the NGO activists alleged to me that elites paid *premans* to intimidate and build fear among people to cause them to accept relocation from this *kampung* more easily. Building the *Masjid* Akbar in Kebon Kosong is also a kind of 'soft' persuasion from developers, by using their power (money and intelligence) to persuade inhabitants to accept the plan. Furthermore, religion is an easy tool with which to persuade people. Elites often use this to create horizontal social conflicts between different groups. Social harmony between religions had been building in Indonesia for a long time, but is now deteriorating. Destroying churches, banning Christian services in communities, and banning the building of new Christian churches are examples of the abuse of power by elites over citizens to promote their own (invariably economic) ends.

Social conflicts have occurred often between one *kampung* and another and between *kampungs* and *kota*. According to Low and Lawrence–Zuniga [8], such 'contested spaces' are generated by political struggles, conflicts of characteristics between elites and residents, and bringing together race, poverty, and place in urban communities. Low and Lawrence–Zuniga [9] quote Kuper's experience of Swazi sites:

> … some sites have more power and significance than others; "these qualities need have no fixed relationship to a physical, empirical dimension," although "political influence may manifest itself in bestowing these qualities through the manipulating of forms"… sites are social spaces that function in politicized dramas as a condensed symbol operating within complex social and ideational structures (p. 19).

Kota seems more powerful than *kampungs*, even though there are more residents in *kampungs* than in *kota*. Socio-culturally, *kampungs* are more powerful than *kota*, but politically and economically, *kota* is more powerful than *kampungs*. Thus, *kampungs* and *kota* not only influence each other, but also come into conflict based on their power.

3. KAMPUNG

3.1. Tiny and Unfenced Space but Public and Recognizable

For *kampung* residents their homes, even though small, have the real value of settling or dwelling beyond their walls. Nugroho [10][6] argued that for *kampung* residents the psychological value of living or settling in *kampungs* is greater than for people living in *kota*:

> …something beyond the walls of a house in *kampungs*, which cannot be seen by the eye, has a psychological value contributing to the real value of the house or settlement. The value of the house or settlement for the people in a *kampung* might be higher than for the people from middle-to-up classes in the *kota* (p. 43)

6 This is translated from a paper by R. P. Nugroho (1997), Sebuah Rumahkah Rumah Kumuh? Suatu Study Tentang Arti Sebuah Rumah, *Kilas*, Jurnal Arsitektur FTUI, Jakarta, Indonesia

ISSN 114-1284

Reflecting the middle to low income status of residents, *kampungs* are low-rise settlements with an effective and tight use of space. These characteristics, along with the kinship tradition in *kampungs*, encourage openness and friendly relationships among inhabitants. As a consequence of limited space in *kampung*s, all spaces outside houses such as lanes, streets, *warungs*[7], *masjid* (mosque), and tiny open spaces between the houses become public spaces. Hilda Kuper in Low and Lawrence-Zuniga [11] notes that these kinds of spaces can be accepted as 'social spaces'. Even though the public and organic spaces in *kampungs* are tiny and poor, they are social spaces because, according to Kuper, social spaces are experiential, 'whereby individuals attach values to space through social and personal experiences, and culturally as a conceptual model'.

In *kampungs*, the public and social spaces on lanes or streets are produced by the connection between socio-cultural activities and relationships, and the built environment itself. This is somewhat similar to social spaces in *desa*, which are naturally established by kinship (socio-cultural relationship) and also the built environment, but which are of lower density and larger in area than in *kampungs*. This in part happens because most *kampung* residents originally practised a traditional way of life, often from the *desa*s of rural areas (many of which have in fact been transformed into urban areas, e.g. in old Jakarta, and in my present *kampung* in Pondok Labu). Additionally, as a result of the tiny space in their houses and also the tropical climate, the residents often socialize and even work outside their houses (Figure 2).

Kampungs are unplanned and 'no barrier' settlements. They originally did not consider boundaries and fences. As a consequence of the fluidity of the functioning of space, *kampungs* have no fixed land-use, so it is difficult to identify particular functions, sizes and forms. Even though *kampungs* are not on the formal (city) map and have no planned land-use, nevertheless we have seen in the cognitive maps of residents that they do identify their land, area, or even the territory of their community or neighbourhood. From my experiences and the surveys in *kampungs*, the residents recognize each other well in a community. They do know who their neighbours are, and even their names, the number of family members, and their jobs.

Figure 2: Public space on the lane: walking trader with children

Source: Photograph by author

The houses are divided only by a wall between one and another, and their doorways open straight on to the lanes (Figure 3).

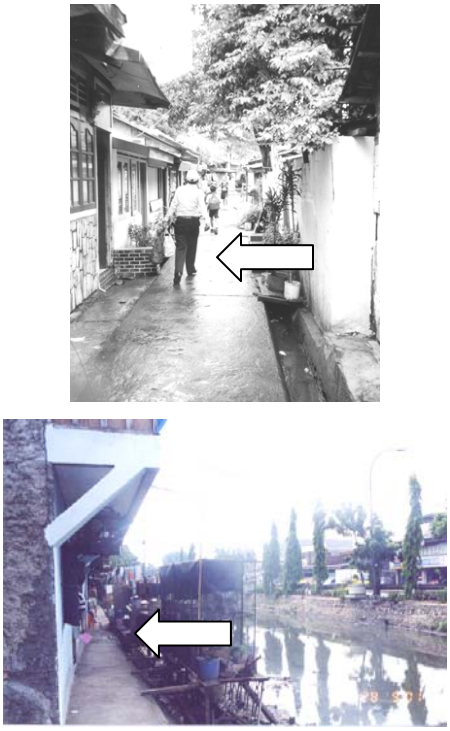

Figure 3: Unfenced kampong in kampung Manggarai (top) and kampung Pejagalan (bottom)

Source: Photographs by author

7 *Warung* is a traditional local shop/kiosk in a *kampung*, which usually provides the daily needs of people in the *kampung*.

3.2. Unprotected but Secure

Legally, *kampungs* have no protection. The system of land rights in Indonesia is based on the Basic Agrarian Law (BAL) of 1960 [12]. According to MacAndrews, the two types of land system in Indonesia are informal registration of *hukum adat* (traditional law) and written land titles and land registrations. The first originated from traditional law and the second, which was created by the colonial government, has remained mainly in urban areas up to the present. Thus the written land rights system is dominant in urban areas. The implementation of this system does not cover the *kampung* areas of Jakarta, however, but focuses much more on *kota*.

Because ownership certificates give evidence of their rights, land owners, developers, or users have security to develop and commercialize their areas. All activities and buildings in *kota* are developed and built on legal land with land certificates and building certificates. These certificates also give an assurance of protection of urban regulation and future city planning, including essential city services of infrastructure and public facilities.

From my investigations in *kampungs*, most of the people in *kampungs* own their own houses. However, the majority of them have no right-of-ownership (*hak milik*) certification (Figure 4). This indicates that most people in *kampungs* live on illegal land. This uncertainty of right to the land creates land conflicts in *kampungs*, between people and people, people and the formal private sector, and people and government. In these conflicts, ordinary people always lose either by force or by law in court [13].

Most buildings in *kampungs* are also built without building certificates, because a building certificate cannot be applied for by people while they have no ownership certificate for their land. Thus, legally, people are insecure; and their buildings or even whole *kampungs* can be demolished easily by *kota* development. Conversely, however, the government allows *kampungs* as part of city administration by establishing *RT*s and *RW*s in *kampungs*. In view of this form of municipal administration, residents in areas with this status feel that they have some legal security in their *kampungs*.

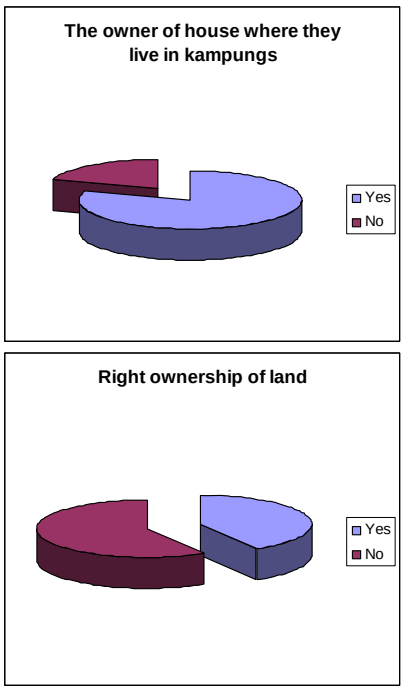

Figure 4: Ownership of houses (top left); of land rights (top right) in *kampungs*

Source: Survey by author

In reality, *kampungs* are unprotected by law and government. Fires, floods, social conflicts, and demolition of *kampungs* occur because of poor protection by government. The government is reluctant to construct better infrastructure and facilities in *kampungs* which are going to be demolished. As a result of poor public facilities and lack of infrastructure, *kampungs* are not only insecure; they are also uncomfortable.

However, in another important sense, *kampungs* are secure for the residents, because socially they are recognized by and are friendly with each other. They manage their own local or community security system, *hansip* (*pertahanan sipil* or civil defence) and *ronda kampung* (*kampung* guarding), supported by security posts and *RW* posts. This system is based on the mutual self-help tradition among communities or neighbourhoods, *gotong royong*[8] and *rukun*[9], in which people are not paid for any tasks in

8 Gotong royong is the custom of cooperation, mutual self-help, the sharing of burdens, or solidarity in *kampung* communities

9 *Rukun* is understood as 'good' and 'peace' in connection with relationships. It also means 'one mind' or 'one interest', or unanimous.

ISSN 114-1284

guarding their community. From my own lived experience in *kampungs* and from my survey, I found another reason why the community residents feel secure living in *kampungs*: they are close to their relatives or friends; thus, socio-economically, they can survive living in the city.

3.3. Self-Sufficient

A community is a place and space where a group of people live together, consequent on two needs: interests and territories. *Kampung* as community of interest practises *gotong royong*, *rukun*, democracy, and friendship among inhabitants, establishing adaptability among residents. *Kampung* as community of territory covers informal, unregulated, and uncontrolled space, and place is flexible. The remarkable system of social relationships in *kampung*s, built on the concepts of *gotong royong*, *rukun*, *arisan*, and *koperasi*[10], is also the basis of self-sufficiency in *kampungs.*

Kampung residents do not find it too difficult to change their jobs because they do not need special skills for the jobs that they seek, whether those are in the *kampung* or even in the formal sector represented by *kota*. Thus in a crisis they are likely to be able change their jobs more easily than the residents of *kota*, to adapt to a new situation. For example: Wati was a nurse in a hospital, but now she works together with her husband in *warung makanan* (meals) (Figure 5, no 1); Iyah was a garment labourer, but now she works as a car-park attendant; etc. (Figure 5, no.2).

Through this characteristic of adaptability to different situations, it seems that *kampungs* are able to manage their problems or crises better than *kota*.

As a result of irregular and unpredictable earnings, many people in *kampungs* have multiple jobs, because they need extra revenue from the second job. A teacher can run a *warung* in his house; a labourer working in a market in the morning can be a *satpam* (security) in *kota* in the evening; an office boy in *kota* in the day time can be a *bakso* vendor in the evening, etc. Another example is the 'three in one job': one person can work in three different places and at three different times in the day (morning, afternoon and evening) in one particular job: formal and informal, such as *satpam*, teacher, car-park attendant, etc.

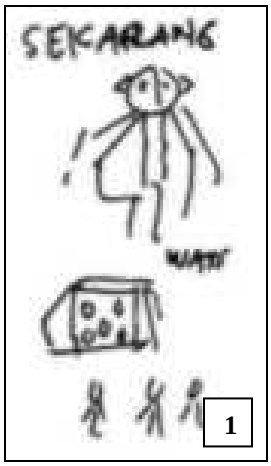

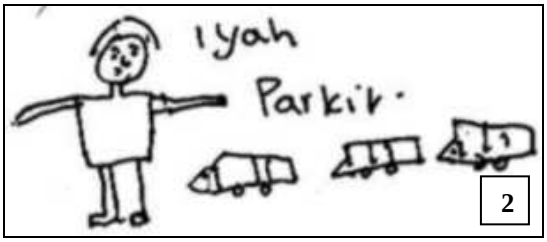

Figure 5: Adaptability of *kampung* residents

Source: UPC, 2000
Note: (1) From nursing to *warung*, (2) From garment worker to car park attendant.

3.4. Behind Kota

Socio-economically, *kampungs* are settlements for middle to low socio-economic classes. The main reason why most ordinary people choose to live in *kampungs* close to *kota* is because they want to be close to their workplaces. As argued in previous discussion, in the everyday life of Jakarta, *kampung*s support *kota* lives 'from behind'. For instance, behind *Jalan* Thamrin, Sudirman and other grand avenues can be found *kampungs* that contain many *warungs* and much low-cost rental housing to support *kota* lives Another form of dependency of *kota* on *kampung*s is from *kampung* residents with portable shops who walk to *kota* to sell various kinds of fresh food (Figure 6). The dependency

2

10 *Koperasi* is Indonesian traditional banking; and *arisan* is the local and traditional banking system in a community.

of *kota* on the *kampungs* has increased since the Indonesian economic crisis. The ability of people (including formal workers in *kota*) to afford to buy things through the formal sector is decreasing, while their daily needs remain the same.

Figure 6: The informal sector supports *kota* life: portable shops in Menteng (bottom) move from *kampung* Manggarai (top)

Source: Photographs by author

4. CONCLUSIONS: JAKARTA AS A KOTA KAMPUNG

This was demonstrated that from the perspective of *kampung* there were different and often conflicting images between *kampung* and *kota*: private and public, formal and informal, restricted and open space, or the power of elites and mutual self-help.

The image of Jakarta from the *kampung* perspective is also one of contrast, as it was from the perspective of *kota*. It seems like white and black or good and bad. Nevertheless, it is clear that *kota* provides job opportunities for many *kampung* residents, in both the formal and the informal sector, while the *kampungs* provide cheap and accessible labour. Thus in reality the relationship between *kampung* and *kota* is to a large extent symbiotic—it is arguable that neither could exist without the other (though the *kampungs* might indeed survive, albeit transformed). Therefore, people want to continue living in *kampungs* despite the tensions and conflicts they experience, seemingly caused by excessive and ever-encroaching development of kota.

5. REFERENCES

[1] Leaf, M. L., *Land Regulation and Housing Development in Jakarta, Indonesia: From the 'Big Village' to the 'Modern City'*, Doctoral Dissertation, University of California at Berkeley, USA, 1991, p. 1.

[2] Rosello, M., 'French bidonvilles around 1960s Paris: Urbanism and individual initiatives', in N. Leach (ed.), *The Hieroglyphics of Space*, Rouledge, London and New York. 2002.

[3] Han, V, *Housing and Development: an evaluation of concepts and ideas with case studies focusing on housing policies and spontaneous settlement in third world cities*, unpublished PhD dissertation, The University of Washington, 1979, p.2.

[4] Foucault, M., *Discipline and Punish: The Birth of the Prison*, Vintage, New York, 1975

[5] Low, S M and Lawrence-Zuniga, D, 'Locating Culture', in Low and Lawrence-Zuniga (ed.), *The anthropology of space and place*, Blackwell Publishing, Berlin, 2003, p.30.

[6] Ward, C, 'Planners as vandals', *Ekistics*, vol. 39, no. 231, 1975, p. 81.

[7] Ward, C, 'Planners as vandals', *Ekistics*, vol. 39, no. 231, 1975, p. 81.

[8] Low, S M and Lawrence-Zuniga, D, 'Locating Culture', in Low and Lawrence-Zuniga (ed.), *The anthropology of space and place*, Blackwell Publishing, Berlin, 2003, p. 19.

[9] Low, S M and Lawrence-Zuniga, D, 'Locating Culture', in Low and Lawrence-Zuniga (ed.), *The anthropology of space and place*, Blackwell Publishing, Berlin, 2003, p.19.

[10] Nugroho R. P., 1997, Sebuah Rumahkah Rumah Kumuh?: Suatu Study Tentang Arti Sebuah Rumah, *Kilas*, Jurnal Arsitektur FTUI, Jakarta, Indonesia

[11] Low, S M and Lawrence-Zuniga, D, 'Locating Culture', in Low and Lawrence-Zuniga (ed.), *The anthropology of space and place*, Blackwell Publishing, Berlin, 2003, p.19.

[12] MacAndrews, C, 'Central Government and Local Development in Indonesia: An Overview', in MacAndrews (ed.), *Central government and Local Development in Indonesia*, Oxford University, Singapore–Oxford–New York, 1986, p. 13

[13] Suyanto, B, 'Pembangunan *Kota* Sengketa Tanah: Kasus *Kotamadya* Surabaya', *Prisma*, vol. XXV, no. 9, pp. 37-39, 1996.

ISSN 114-1284

Considerable Study: Application of Leadership in Energy and Environmental Design for Existing Building 2.0 version (LEED-EB 2.0) USGBC In Indonesia Case Study: Faculty of Computer Science Buildings (CSB), University of Indonesia

Dyah Nurwidyaningrum
Sri Kurniasih
Azwan Aziz

Master Student
Building TechnologyProgram
Departement of Architecture
Faculty of Engineering
University of Indonesia, Depok 16424
Tel : (021) 7270011 ext 51. Fax : (021) 7270077
E-mail : Nurwidyaningrum@yahoo.com

ABSTRACT

In order to save the earth from global warming, USGBC (United State Green Building Council) uses LEED (Leadership in Energy and Environmental Design) as a green building standard rating system for sustainable design. LEED for Existing Building maximizes operational efficiency while minimizing environmental impacts. To achieve LEED certification, buildings must meet all Perquisites in the Rating System and a minimum of 32 points. In this research, we study how a Computer Science Building (CSB) operation relates to LEED USGBC Values. How far implementation of green building standard. This study concentrates on perquisites for existing building criteria version 2.0. CSB is one of the best buildings in technology facilities for the University of Indonesia. It has a chance to have a good rating score. The data collection method includes surveying, interviewing, and obtaining literature related to LEED. Standards Research methods include a qualitative description for CSB and quantitative measurement.

Keywords

LEED, USGBC, Green Building

1. INTRODUCTION

In green building design, LEED USGBC become one of standard to evaluate the quality of building using energy efficient performances and controlling environmental impacts. LEED for Existing Buildings (LEED EB) maximizes operational efficiency while minimizing environmental impacts. As a leading-edge, consensus-based system for certifying green building performance, operation, and maintenance. LEED for Existing Buildings addresses exterior building site maintenance programs, efficient/optimized use of water and energy, purchasing of environmentally preferred products, waste stream management and ongoing indoor environmental quality (IEQ). In addition, LEED for Existing Buildings provides sustainable guidelines for whole-building cleaning/maintenance, recycling programs and systems upgrades to improve building energy, water, IEQ and materials use.

This study focuses on 6 (six) LEED USGBC values related to CSB building operations. The six values are Sustainable Site, Water Efficiency, Energy & Atmosphere, Material Resources, Indoor Environmental Quality and Innovation in Upgrades, Operation & Maintenance. The results of the study can be used as a parameter to improve building interior and exterior quality for peoples and environment.

2. LEED REQUIREMENT

In favor of the sustainable site aspect, there are 14 possible points for green building sub criteria. The subcriterias are Erosion and Sedimentation Control, Age of Building, Plan for Green Site and Building Exterior Management, High

ISSN 114-1284

Development Density Building and Area, Alternative Transportation: Public Transportation Access, Bicycle Storage & Changing Rooms, Alternative Fuel Vehicles and Car Pooling & Telecommuting, Reduced Site Disturbance: Protect or restore Open Space, Storm water Management: Rate and Quantity Reduction, Heat Island Reduction, Light Pollution Reduction. Each sub criteria has LEED-EB standard point. The two earlier sub criteria have to be required to evaluate other sub criteria.

Water Efficiency aspect have 5 possible points standard. Sub criteria in water efficiency aspect are Minimum Water Efficiency, Discharge Water Compliance, and Water Efficient Landscaping: Reduce Water Use, Innovative Wastewater Technologies, and Water Use Reduction. The first and second sub criteria have to be required before evaluate others.

For Energy & Atmosphere aspect, green building has to get minimum 23 possible points. It has 12 sub criteria, they are Existing building Commissioning, Minimum energy performance, Ozone Protection, Optimize energy performance, On-site and off-site renewable energy, Building Operation and Maintenance: Staff education, Building System Maintenance & Monitor, Performance Measurement: Enhanced Metering & Emission Reduction Reporting, Documenting Sustainable Building Cost Impacts. The first three sub criteria have to be required.

In Material Resources aspect, building have to get minimum possible 16 points in Source Reduction and Waste Management: Waste Management Policy and Waste Stream Audit, Storage & Collection of Recyclables, Toxic Material Source Reduction: Reduced Mercury in Light Bulbs, Construction, Demolition and Renovation Waste Management, Optimize Use of Alternative Materials, Optimize Use of IAQ Compliant Products, Sustainable Cleaning Products and Materials, Occupant Recycling, Additional Toxic Material Source Reduction: Reduced Mercury in Light Bulbs. The first three sub criteria have to be required to continue other sub criteria evaluation.

Indoor Environmental Quality aspect have 22 possible points. It consists of Outside Air Introduction and Exhaust System, Environmental Tobacco Smoke (ETS) Control, Asbestos Removal or Encapsulation, Polychlorinated Biphenyl (PCB) Removal, Outside Air Delivery Monitoring, Increased Ventilation, Construction IAQ Management Plan, Documenting Productivity Impacts : Absenteeism and Healthcare Cost Impacts & other impacts, Indoor Chemical and Pollutant Source Control : Non-Cleaning-Reduce Particulates in Air Distribution & Non-Cleaning-High Volume Copying/Print Room/Fax Stations, Controllability of System : Lighting & Temperature & Ventilation, Thermal Comfort : Compliance & Permanent Monitoring System, Day lighting and Views : Day lighting & Views, Contemporary IAQ Practice, Green Cleaning : Entryway System, Isolation of Janitorial Closets, Low Environmental Impact Cleaning Policy, Low Environmental Impact Pest Management Policy & Low Environmental Impact Cleaning Equipment Policy. The first four sub criteria have to be required.

Innovation in Upgrades, Operations and Maintenance aspect has minimum 4 possible points and 1 point for LEED Accredited Professional.

3. IMPLEMENTATION RESULT

The result study shows that CSB has lower score than LEED certified point. In design, CSB has good quality planning even though some materials has lower quality than other Campus buildings. CSB has been already designed with energy efficiency building standard in Indonesia. LEED has higher and more detail standard than building regulation in Indonesia.

For sustainable aspect, CSB has meet almost all points required, except one on Alternative Transportation: Car Pooling & Telecommuting. For the other sub criteria, CSB still doesn't get full point so for this aspect; CSB gets 9 points than 14 standard points or 64% value.

Table 1. CSB Points Result for Sustainable Sites

CRITERIA	STANDARD POINTS	RESULT
Erosion and Sedimentation Control	Required	√
Age of Building	Required	√
Plan for Green Site and Building Exterior Management	2	1
High Development Density Building and Area	1	1
Alternative Transportation: Public Transportation Access	1	1
Alternative Transportation: Bicycle Storage & Changing Rooms	1	1
Alternative Transportation: Alternative Fuel Vehicles	1	1
Alternative Transportation: Car Pooling & Telecommuting	1	-
Reduced Site Disturbance: Protect or Restore Open Space	2	1*
Storm water Management: Rate and Quantity Reduction	2	1*
Heat Island Reduction: Non-Roof	1	1
Heat Island Reduction: Roof	1	1
Light Pollution Reduction	1	1
Total Point	**14 points**	**9 points**

Notation * shows that data is not complete

For water efficiency aspect, CSB get only one points of 5 standard points or 20%. In CSB operation, it has used water equipment as Indonesian National Standard (SNI) but not propose for water efficiency yet.

Table 2. CSB Points Result for Water Efficiency

CRITERIA	STANDARD POINTS	RESULT
Minimum Water Efficiency	Required	√
Discharge Water Compliance	Required	√
Water Efficient Landscaping: Reduce Water Use	2	1*
Innovative Wastewater Technologies	1	-
Water Use Reduction	2	-
Total Point	**5 points**	**1 points**

Notation * shows that data is not complete

Energy & Atmosphere aspect is the most important aspect for green building standard. CSB acquires only 4 points of 23 standard points (16,7%). It hapens cause in Energy & Atmosphere aspect requires measurement control in building operation. CSB doesnot has this requirement.

Table 3. CSB Points Result for Energy & Atmosphere

CRITERIA	STANDARD POINTS	RESULT
Existing building Commissioning	Required	√
Minimum energy performance	Required	√*
Ozone Protection	Required	-
Optimize energy performance	1-10	-
On-site and off-site renewable energy	1-4	-
Building Operation and Maintenance: Staf education	1	-
Building Operation and Maintenance: Building System Maintenance	1	1
Building Operation and Maintenance: Building System Monitor	1	1*
Additional Ozone Protection	1	-
Performance Measurement: Enhanced Metering	3	1*
Performance Measurement: Emission Reduction Reporting	1	-
Documenting Sustainable Building Cost Impacts	1	1*
Total Point	**23 points**	**4 points**

Notation * shows that data is not complete

In Material Resources, CSB acquires only 2 points of 16 standard points (12,5%). This aspect requires some criteria that concerns to safety and nontoxic materials for peoples. This requirement is not be required yet by CSB operation.

Table 4.CSB Points Result for Materials &Resources

CRITERIA	STANDARD POINTS	RESULT
Source Reduction and Waste Management: Waste Management Policy and Waste Stream Audit Required	Required	√
Source Reduction and Waste Management: Storage & Collection of Recyclables	Required	√
Toxic Material Source Reduction: Reduced Mercury in Light Bulbs	Required	-
Construction, Demolition and Renovation Waste Management	2	1
Optimize Use of Alternative Materials	5	1
Optimize Use of IAQ Compliant Products	2	-
Sustainable Cleaning Products and Materials	3	-
Occupant Recycling	3	-
Additional Toxic Material Source Reduction: Reduced Mercury in Light Bulbs	1	-
Total Point	**16 points**	**2 points**

For Indoor Environmental Quality aspect, GSB gets 12,5 points of 22 standard points (57%). This aspect requires controlling documentation for evaluating building indoor quality. In design, CSB has already required but it has not do documentation evaluating for improve indoor quality.

Table 5.CSB Points Result for Indoor Environmental Quality

CRITERIA	STANDARD POINTS	RESULT
Outside Air Introduction and Exhaust System	Required	√
Environmental Tobacco Smoke (ETS) Control	Required	√
Asbestos Removal or Encapsulation	Required	-
Polychlorinated Biphenyl (PCB) Removal	Required	-
Outside Air Delivery Monitoring	1	-
Increased Ventilation	1	1
Construction IAQ Management Plan	1	1
Documenting Productivity	1	-

Impacts : Absenteeism and Healthcare Cost Impacts		
Documenting Productivity Impacts : Other Impacts	1	1
Indoor Chemical and Pollutant Source Control : Non-Cleaning-Reduce Particulates in Air Distribution	1	1
Indoor Chemical and Pollutant Source Control : Non-Cleaning-High Volume Copying/Print Room/Fax Stations	1	0,5 *
Controllability of System : Lighting	1	1
Controllability of System : Temperature & Ventilation	1	1
Thermal Comfort : Compliance	1	1
Thermal Comfort : Permanent Monitoring System	1	-
Day lighting and Views : Day lighting	2	2
Daylighting and Views : Views	2	1
Contemporary IAQ Practice	1	-
Green Cleaning : Entryway System	1	1
Green Cleaning : Isolation of Janitorial Closets	1	1
Green Cleaning : Low Environmental Impact Cleaning Policy	1	-
Green Cleaning : Low Environmental Impact Pest Management Policy	2	-
Green Cleaning : Low Environmental Impact Cleaning Equipment Policy	1	-
Total Point	**22 points**	**12,5 points**

Notation * shows that data is not complete

For the last aspect, Innovation in Upgrades, Operations and Maintanance, CSB has not done improvement yet and It has not submitted for LEED sertificatification yet. So for this aspect CSB doesnot get point.

Table 6.CSB Points Result for Innovation in Upgrades, Operation And Maintenance

CRITERIA	STANDARD POINTS	RESULT
Innovation in Upgrades, Operations and Maintenance	4	-
LEED Accredited Professional	1	-
Total Points	**5 points**	**0 point**

Finally, In favor of all criteria, the summary is represented in table below. CSB gets better point for aspects: sustainable sites and Indoor Environmental Quality. CSB meet very lower value for the other aspects. This result indicates that CSB has been good in physical design but has to improve energy efficiency planning.

Tabel 7.CSB Complete Points Result

CRITERIA	STANDARD POINTS	RESULT	Persen t points
Sustainable Sites	14	9	64 %
Water Efficiency	5	1	20 %
Energy & Atmosphere	23	4	16,7 %
Materials & Resources	16	2	12,5 5
Indoor Environmental Quality	22	12,5	57 %
Innovation In Upgrades, Operations & Maintenances	5	0	0
Total Point	**85 points**	**28,5 points**	**100 %**

4. CONCLUSION

Based on the analysis, there are some conclusions of LEED EB implementation on CSB:

1. Design based on building regulation and SNI is not meet LEED standard points yet.
2. Limitation of CSB Documentation causes the research cannot measure others important data that possibly effecting the total point.
3. This LEED certified points can improve Indonesian building quality in energy efficiency, but It needs government support to implement green bulding that can save environment.
4. There are some contraimplementation between design and operation in CSB, so they cannot get along. Building operation have to be improved to get first aim design bulding so energy efficiency can be reached.
5. LEED EB 2.0 version doesnot intent yet to firesafety as energy efficiency in green building concept. We think that firesafety is very important aspect in building design completeness.

ACKNOWLEDGMENT

We say thank to CSB management faculty that has given completely documentation and lecturers who has supported for this study.

REFERENCES

[1] Green Building Rating System for Existing Building Upgrade, Operation and Maintenance Version 2 (LEED-EB), Updated July 2005, USA.

[2] Holcim Award for Sustainable Construction: *Holcim Award Competition* 2007-2008.

[3] Lechner, Norbert, *Heating, Cooling and Lighting Design Methods for Architecture,* 2001.

[4] *Egan, David M., Concepts in Thermal Comfort,* New Jersey, 1975.

[5] Watson, Donald. 1993. The Energy Design Handbook. AIA Press

[6] http://uk.geocities.com/standarisasi/sni-033.html

ISSN 114-1284

Energy-Efficient Window Concept For Classroom in Warm Tropical Area

Floriberta Binarti[1]

[1]*School of Architecture*
Engineering Faculty, Univ. of Atma Jaya Yogyakarta, Yogyakarta 55281
Tel : (0274) 487711 ext 1261. Fax : (0274) 487748
E-mail : floriberta_binarti@yahoo.com

ABSTRACT

Shading device, window to wall ratio, window height, and glazing are important factors in determining building energy consumption in the tropics. This study employed the four factors in designing energy-efficient window for classroom to reduce the energy consumption for supplemented lighting and mechanical ventilation. The main parameter is classroom's cooling load or heat transfer through the building skins (< 10 watt/m^2) incorporated with secondary parameters, i.e. indoor illuminance level (200-400 lux) or daylight factor (2-3%), and horizontal illuminance distribution. Relationship among window to wall ratio, window to floor ratio, height of clerestory, clerestory to wall height ratio, and classroom's orientation, width and length are examined using Ecotect simulation program to establish a concept for energy-efficient classroom's window. Window with projected clerestory is the most energy efficient. It transfers minimum solar radiation and creates the most even horizontal illuminance distribution with sufficient level. Small difference in energy performance but lower cost can be achieved by window with glass-block clerestory or with lightshelf. Three kinds of clerestory should be applied on classroom with considering the window to wall ratio (20%), the clerestory head height to room height ratio (11%), the head height clerestory to room width ratio (around 5%).

Keywords: *clerestory, cooling load, daylight factor, illuminance distribution, window.*

1. INTRODUCTION

Three main issues in window design for warm tropical area are uneven horizontal illuminance distribution, glare and high solar heat gain. Window design is one of the factors, which affects the building energy consumption for lamps and air conditioning [1]. An energy-efficient window, then, should be able to distribute horizontal illuminance more evenly, avoid glare and reduce solar heat gain.

A determinant factor of window design in the transmission of solar radiation into indoor space is window to wall ratio (WWR). Proper shading devices and/or replacing the window glazing property with the lower solar admittance can modify WWR in order to achieve low thermal transmission and sufficient indoor illuminance. Shading devices function as effective shields for solar radiation, but in some cases they cannot create even horizontal illumination distribution and even block occupant's view to outside.

To maintain the view through the window, while at the same time let daylight penetrate into the deepest side of the room, side window is divided into two parts. The lower window functions as view window with shading device surrounding the window to shade the indoor space from direct sunlight, rainfall, and glare. The upper window which called as clerestory allows daylight to penetrate into the deepest side of the room.

Lightshelf introduces internal shelf upper the view window to bounce daylight more deeply by reflecting the light up to the ceiling and to avoid direct glare to occupants. Many studies proved the advantages of lightshelf in creating even daylight distribution and reduce penetration of solar heat gain [10][8][3].

Special glass for the clerestory can replace the internal shelf to avoid glare and creates uniform indoor illuminance [9]. The glass should have low thermal transmission, but high or medium visible transmittance.

Projected clerestory is another idea to allow daylight coming into the deeper side of the room and functions as solar shading for the lower window.

In this study the three possibilities would be examined by using Ecotect simulations to find optimum model/form, dimension, and position with suitable glazing properties. The aim is to generate a concept of energy-efficient window, that can be applied on classrooms with varied dimension in Yogyakarta.

This paper reports results of two experiments. The first experiment examined 48 models of classroom with 3 variations in window design. These models have similar (not the same) window to wall ratio (WWR) and window to floor ratio (WFR). Fifty six models with the same WWR and WFR were constructed in the second experiment to improve the first experiment results. As the results of models with projected clerestory in the second experiment seem

unreasonable, disscussion will combine results of the two experiments.

2. METHOD

Energy-efficient window will be designed on classroom models with variation in capacity. It was assumed that classrooms rely on mechanical ventilation to achieve the indoor thermal comfort. Models are located in Yogyakarta, which is renowned as a student city with many educational buildings. Located on 8^0 south latitude and 110^0 east longitude, the city belongs to a tropical region with very bright sky and abundant solar radiation.

Ecotect simulation program were used to examine their thermal and visual performances. Comprehensive facilities provided by Ecotect offer possibility to analyze the solar, thermal and daylight aspects in relative short time without reconstruction of the model. The same procedure was applied in the first and the second experiments.

2.1 Define Classrooms with Variation in Capacity

Classroom models with three variations in capacity were designed by following principles of classroom design requirements. Calculation of the classroom area was based on National Standard of classroom area, i.e. 2 m^2/person [7]. Classroom length must be no more than six times of screen height to maintain its visual comfort for learning. The width should be more than the screen width. The screen sill height is between 1.22-1.83 m'. The minimum ceiling height is 3.05 m' [4].

Table 1: Area of classroom models

CAPACITY (p)	MIN. CLASSROOM AREA (m^2)	CLASSROOM AREA (m' x m')
The first experiment		
25	50	6.1 x 8.4
50	100	8.5 x 12
75	150	9.5 x 16.5
The second experiment		
25	60.2	7.0 x 8.6
40	82.0	9.3 x 9.0
60	123.0	11.7 x 10.5
75	154.0	11.0 x 14.0

2.2 Define Classrooms and the Height of Clerestory

The classroom height was determined by the minimum standard of air flow rate for classroom and the minimum height of clerestory. A classroom should have 4-12 times of Air Change per Hour and provide 15 cfm per person of air-flow rate [2]. In order to illuminate the deepest side of the classroom, clerestory head height must have 1.5 times in height of the classroom width for window without internal shelf and 2.5 times for window with internal shelf [12]. Considering net (occupancy) area of classroom, in the the second experiment clerestory head height became 1/3 times of the classroom width.

Table 2: Height of classroom models

CAPACITY (p)	CLASSROOM AREA (m' x m')	CLASSROOM HEIGHT (m')	CLERESTORY HEAD HEIGHT (m')
The first experiment			
25	6.1 x 8.4	3.2	6.1/2.5 ≤ 3.1
50	8.5 x 12	3.5	8.5/2.5 ≤ 3.4
75	9.5 x 16.5	4	9.5/2.5 ≤ 3.9
The second experiment			
25	7.0 x 8.6	3.0	8.6/3 ≤ 2.9
40	9.3 x 9.0	3.2	9.0/3 ≤ 3.0
60	11.7 x 10.5	3.6	10.5/3 ≤ 3.5
75	11.0 x 14.0	3.8	14.0/3 ≤ 3.7

2.3 Designing Energy-efficient Windows

Window affects the building energy consumption in two ways.

First, it can transfer heat energy into the building. Energy flows through window in a building by three physical effects, i.e. (1) conductive and convective heat transfer between the outer window surface and the adjacent air due to temperature difference, (2) net long-wave radiative heat exchange between outer window surface and the sky, ground, or adjacent objects; and (3) short-wave radiative heat exchange incident on the window [1]. Window to wall ratio (WWR) can determine the rate of conductive, convective and radiative heat transfer through the window and the wall. Design of the shading device (width, form, and thermal properties) can reduce radiative heat transfer rate. Whilst, glazing properties affect conductive and radiative heat transfer rate through the window.

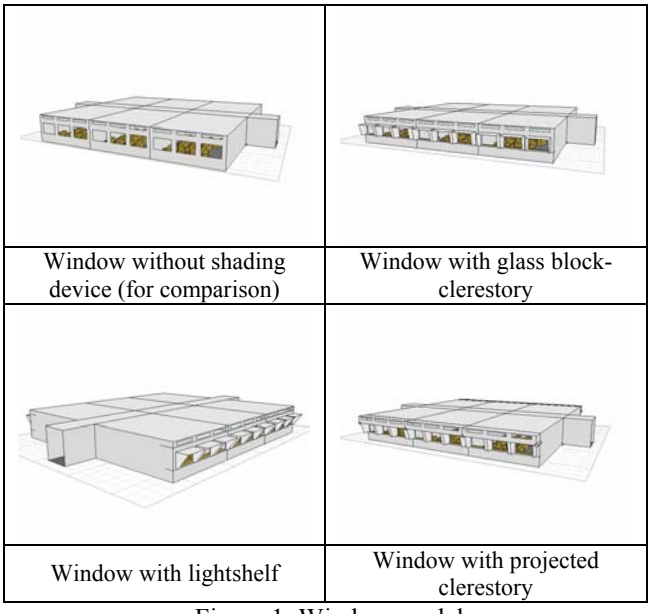

Figure 1: Window models

The second, daylight incoming through the window can reduce electrical energy demand for artificial lighting during sunshine. Window area, form (including shading device), position, and the optical properties of window materials (visible transmittance) are important factors in creating proper illuminance level and even horizontal distribution.

This study proposed three window models. First model is window with 1 m'-lightshelf. Second model is view window with clerestory made of glass block. This kind of glass is considered as affordable material with low thermal transmitance (U_v = 2.9 W/m^2.K) and medium visible transmitance (0.55). The third is view window with projected clerestory. Shading devices on view windows were designed by "shading design wizard" tool in Ecotect. The calculation was based on the sun path diagram. Material properties of each model remain constant except glass-block clerestory.

2.4 Heat flows through the building fabrics

Ecotect's "Thermal Analysis" provides "Losses and Gains" as a facility to simulate relative contribution of different heat flow paths. Actual hourly fabric gains distribution can show the amount of heat flows through the external surface of each zone. The calculation is based on Admittance method. This method is based on the concept of cyclic variation. It is not as physically accurate as the response factor or finite difference methods. However, it can be very helpful in desicion making of building design process in conditions where the temperature swing and energy inputs are changing steadily. This method is suitable to the models condition, where mechanical cooling is applied to achieve indoor thermal comfort. Simulation of fabric gains can describe relative accurate results, because the simulation calculates incident solar radiation passing through an aperture as part of space load and fabric load based on internal admittance values.

2.5 Illuminance Level and Daylight Factor

Ecotect analyzes illuminance level and daylight factor based on Building Research Establishment (BRE) Split-Flux method. Standard overcast sky illuminance distribution is used to calculate the illuminance level and daylight factor in order to represent a worst-case scenario to be designed for. Therefore, values will not change with different dates or times and not be affected by changing model orientation. Ecotect also provides link to Radiance for physically accurate and comprehensive lighting analysis.

3. RESULTS AND DISCUSSIONS

3.1 Projected Clerestory for Low Heat Transfer

At the first time total glass area had 34-39% of the exposed wall area and height of clerestories are between 25% and 34% of the classroom height. Only window with projected clerestory can reach the standard of thermal transfer. Windows with lightshelf transfer solar radiation relative low, but still above 45 W/m^2.

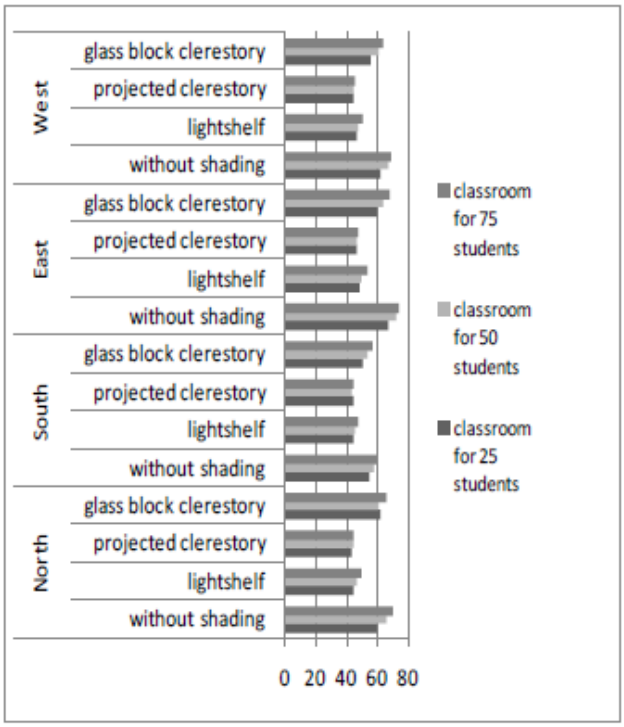

Figure 2: Hourly thermal transfer value (W/m^2) of window with 34-39% WWR (the first experiment)

Results of daylight factor simulations show very high value. Windows with projected clerestory create daylight factor above 5%. Windows with lightshelf have higher value (more than 6.5%). These results are too high for classroom which the standard of DF is 2-3.5% [5]. Low daylight factor is considered as more comfortable, because the calculation of daylight factor is under the worst-case (overcast sky condition).

Table 3: Dimension of Windows

CLASSROOM CAPACITY (persons)	VIEW WINDOW (m' x m')	CLERESTORY HEIGHT (m')
The first experiment		
25	3 @ 1.3x1.0	0.35
50	3 @ 2.0x1.0	0.40
75	3 @ 3.0x1.0	0.45
The second experiment		
25	3 @ 1.75 x1.10	0.250
40	4 @ 1.75 x1.10	0.305
60	5 @ 1.75 x1.10	0.410
75	6 @ 1.75 x1.10	0.465

In order to reduce thermal transfer value and daylight factor, window areas are decreased into 20% of exposed wall areas. This value was also applied in the the second experiment. All models in the the second experiment have 20% WWR and 20% WFR. The height of view window remain constant in 1.10 m' with 1'm sill height.

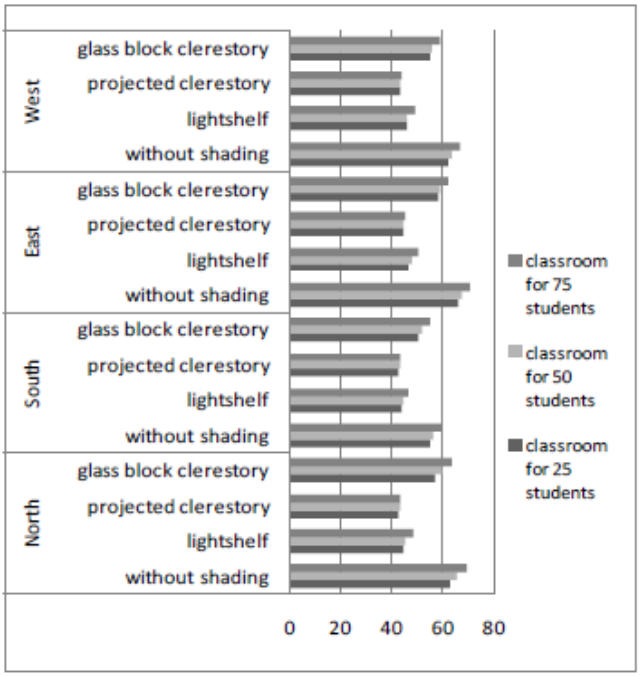

Figure 3: Hourly thermal transfer value (W/m^2) of window with 20% WWR (the first experiment)

New dimensions reduce the rate of heat transfer insignificantly (< 10%), but can create acceptable daylight factors. Only windows with projected clerestory transfer solar heat below the standard. Some windows with lightshelf facing to North or South can raise the standard of thermal transfer value. Others are still above 45 W/m^2.

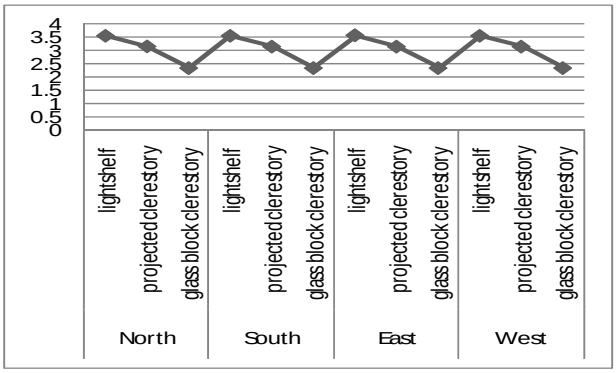

Figure 4: Average daylight factor (%) of windows for 25-students classroom (the first experiment)

Uneven daylight distribution potentially creates glare in area with high level illuminance or needs more electrical lighting to supplement daylighting in area with low illuminance level. Daylight distribution can be considered as uniform if the distribution value is not less than 80% [11]. Some windows with projected clerestory facing to north and south have more uniform daylight distribution (76%). Daylight factor distributions of windows facing to west and east are still difficult to handle.

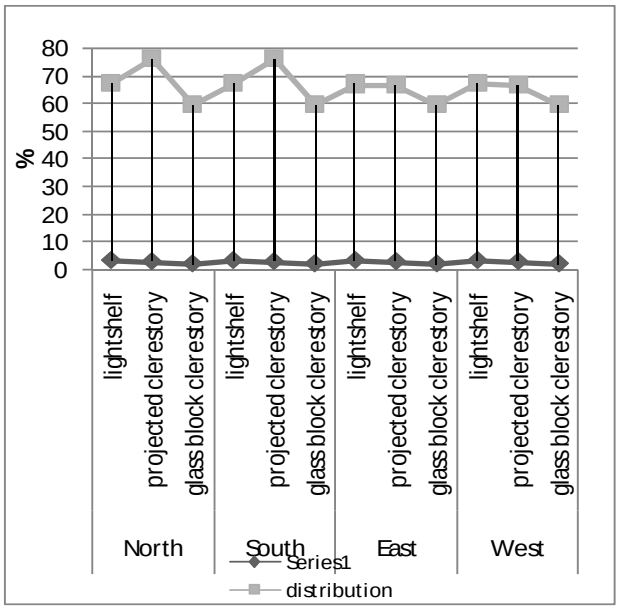

Figure 5: Distribution of daylight factor of window for 25-students classroom (the first experiment)

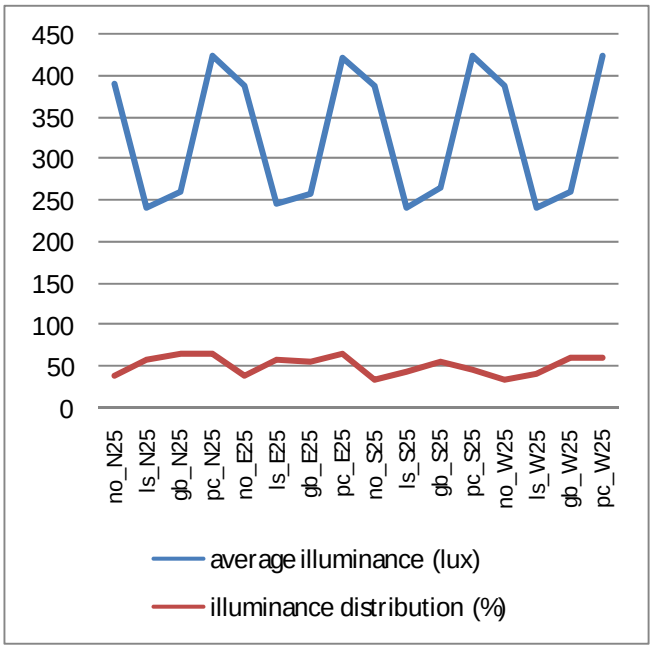

Figure 6: Average illuminance and illuminance distribution of windows for 25-students classroom (the second experiment)

Daylight performances of windows simulated in the second experiment show regular patterns. Windows with lightshelf create the most comfortable illuminance level. The average illuminance levels of windows with glass-block clerestory are still acceptable/comfortable. Similar patterns in illuminance distribution indicate there is insignificant improvement in classrooms with shading device. The best improvement occurs in small-capacity classrooms. Results of window with projected clerestory, however, seem unreasonable. Window with any shading device should have lower average illuminance level than window without shading device. There may be an error in the model construction.

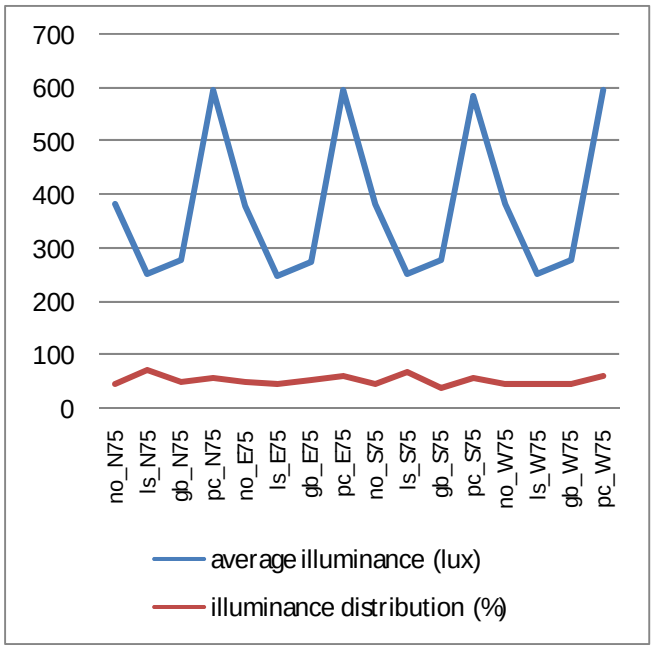

Figure 7: Average illuminance and illuminance distribution of windows for 75 students classroom (the second experiment).

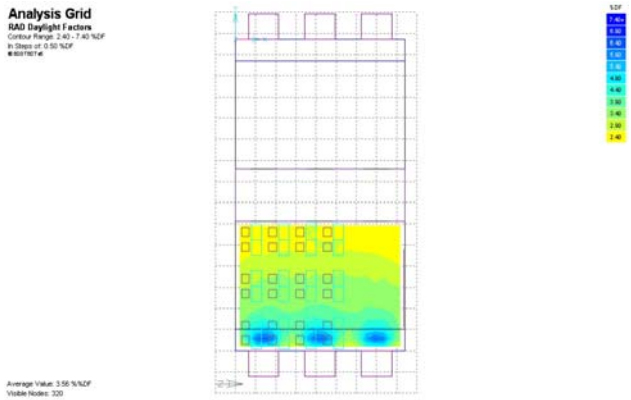

Figure 8: Daylight Factor in a classroom for 25 students with lightshelf facing to East (the first experiment)

Figure 8 and figure 9 show that high daylight factors (> 7%) or illuminance level (> 600 lux) are located on the area near the windows, because large amount sunlight passed through view windows directly. Two alternatives to improve daylight distribution without reducing window area in order to maintain comfortable view angles:

- Enlarge the shading device. This alternative seems to be unrealistic, as the recent shading devices are large enough.
- Change glass of view window with low visible transmittance glass, such as: tinted glass.

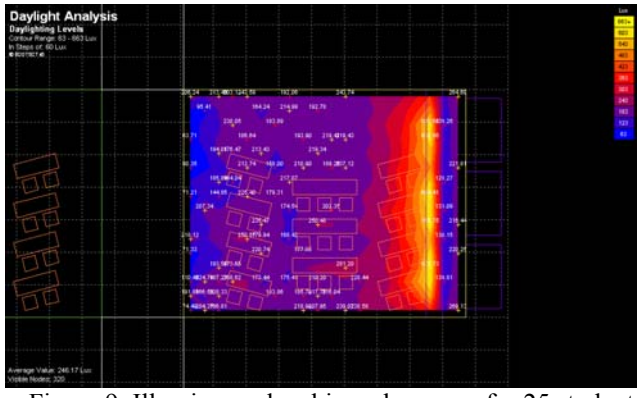

Figure 9: Illuminance level in a classroom for 25 students with lightshelf facing to East (the second experiment)

3.2 Heat gains through the building fabrics

Simulation results of hourly heat flowing through the building fabrics (figure 10) show similar conclusion. Window with projected clerestory is the most energy-efficient. Windows with glass block-clerestory perform better in heat gains comparing to windows with lightshelf. This is opposite to results produced by simulations of thermal transfer value through exposed wall surfaces.

Interesting results were shown by comparing results of classroom for 50 students to those of classroom for 25 students. Three window models have the same pattern. Heat energy flowing through classroom models for 25 students has higher rate than those for 50 students if window models applied are glass block clerestory, lightshelf and without shading. These make sense, because classrooms for 25 students have bigger WWR, window to floor area ratio, window to wall height ratio, clerestory height to room width ratio, and smaller room width to window height ratio.

Classrooms with projected clerestory show opposite results. Higher value of classroom for 50 students than its classroom for 25 students may be related to the ratio of the room width to the room length. The ratio of classroom for 25 students is 0.73 (0.02 higher than the ratio of classroom for 50 students). Relative narrow space allows higher penetration of solar radiation. Ratio of room width to room height seems to work in a room with projected clerestory.

A classroom having 10 W/m^2 heat loads through the building fabrics with adequate daylight level can be considered as energy-efficient if it is compared with 15 W/m^2 for energy standard of lighting for classroom [5].

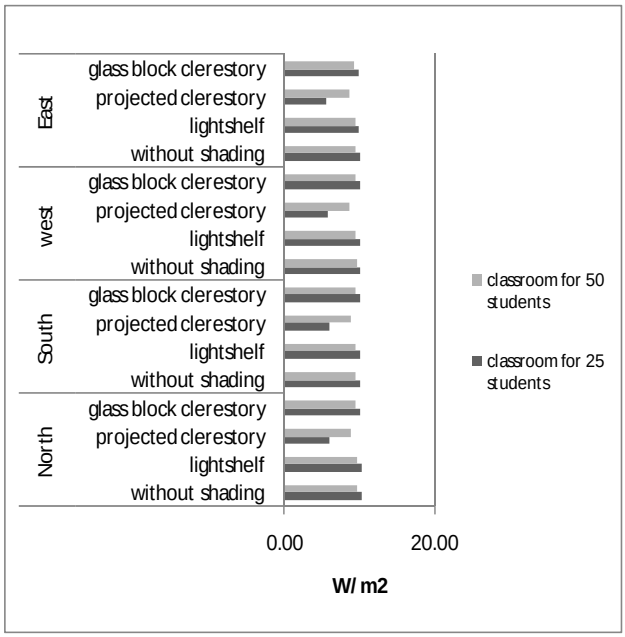

Figure 10: Hourly heat flows through the building fabrics (the first experiment)

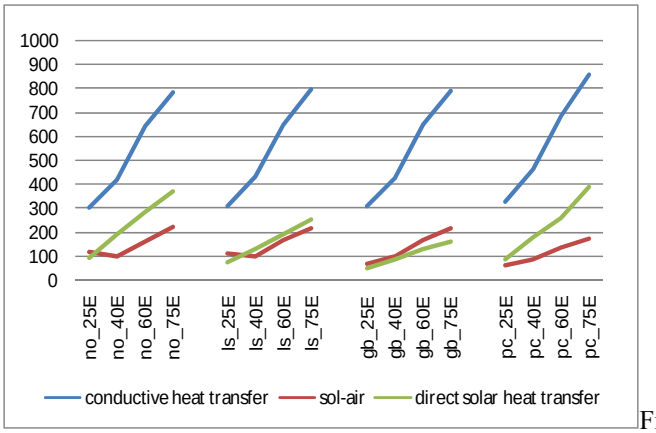

Figure 11: Heat Transfer Through The Building Skins of Classrooms Facing to East (in Watt)

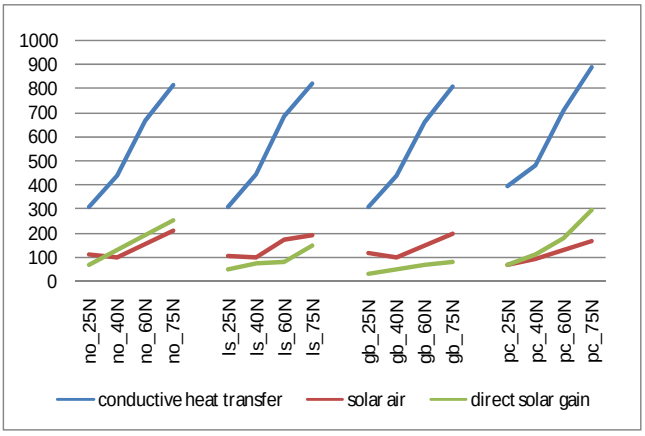

Figure 12: Heat Transfer Through The Building Skins of Classrooms Facing to North (in Watt)

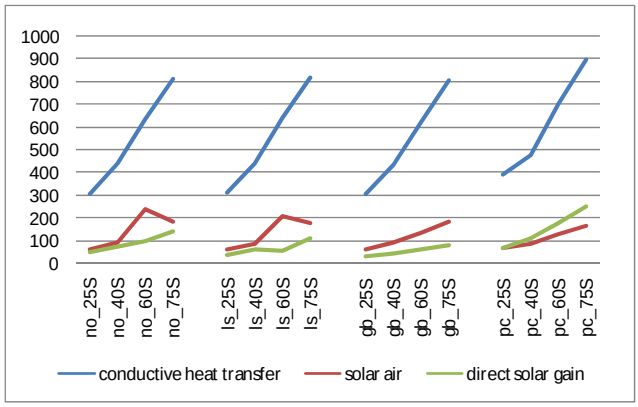

Figure 13: Heat Transfer Through The Building Skins of Classrooms Facing to South (in Watt)

Results of the second experiment show the effect of shading device on the heat transfer. The present of shading device reduces direct solar gain of the classrooms. Window with glass-block clerestory reduces the greatest direct solar gain. Lightshelf can decrease the direct solar gain. Window facing to south admits the lowest direct solar gain, but the greatest effect occurs on windows facing to east. Projected clerestory gives unreasonable results again. Its energy performance is worse than without shading device.

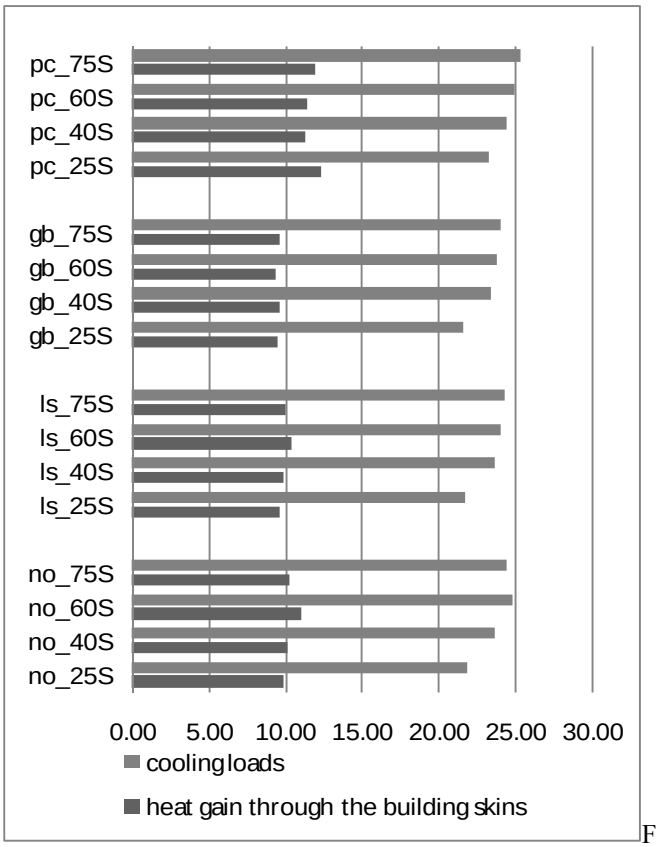

Figure 14: Energy profile of classrooms facing to South (W/m2)

Calculations of classrooms cooling load in the the second experiment show similar pattern. Window with glass-block clerestory or lightshelf has the best energy performance.

Glass-block clerestory can reduce solar heat gain until below 10 W/m^2 for the window facing to south. Relative high energy performance of classroom can be reached by applying lightshelf on its windows. Lightshelf can reduce cooling load a little bit lower than glass-block clerestory. However, it can distribute daylight more evenly, especially in classrooms with big capacity. Application of glass block on clerestory has an advantage in construction cost. Lightshelf and more even projected clerestory are still much more expensive. However, the internal shading device which presents on lightshelf and projected clerestory can prevent annoying glare that may appear on its clerestory.

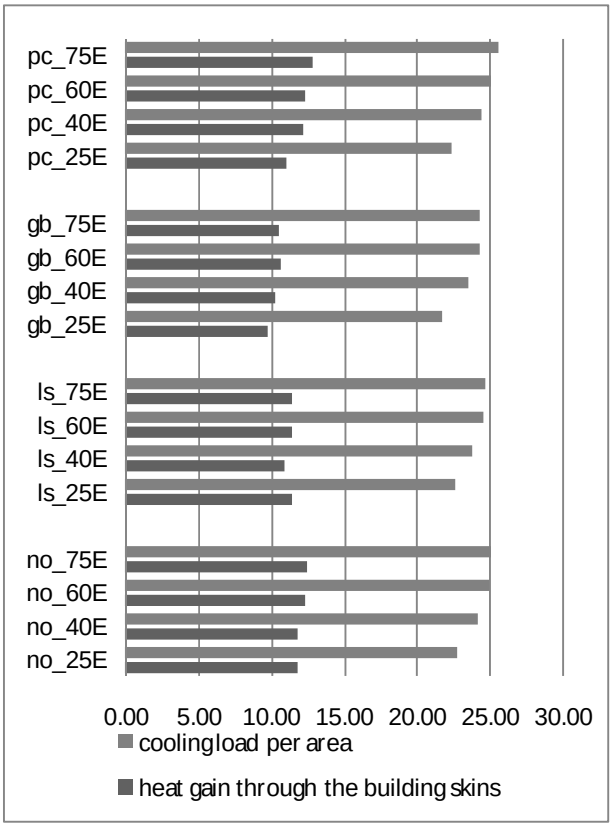

Figure 15: Energy profile of classrooms facing to East (W/m2)

3.3 Window glazing

Low-e double glass replaced clear glass on view windows in order to achieve the most energy efficient window. However, low-e double glass on view windows cannot improve their thermal performances. The amount of solar radiation transmitted through building envelope remains the same as those of view windows with clear glass. Low emittance glass cannot work effectively if there is only small temperature difference between the indoor and the outdoor (naturally ventilated room), but it work effectively in mechanically ventilated room.

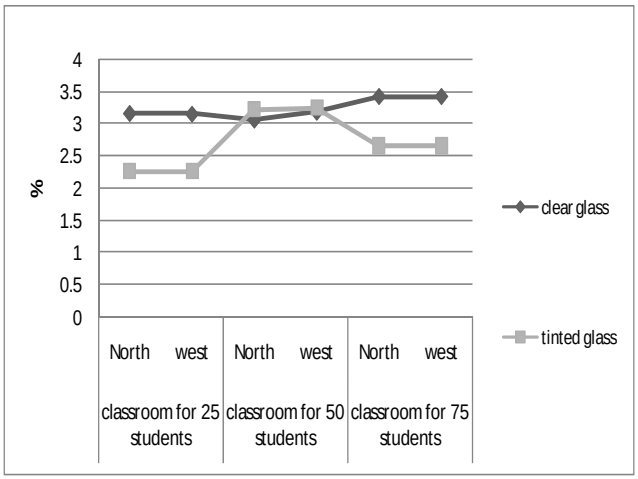

Figure 16: Comparison of average daylight factor between projected clerestory window with clear glass and with tinted glass (the first experiment)

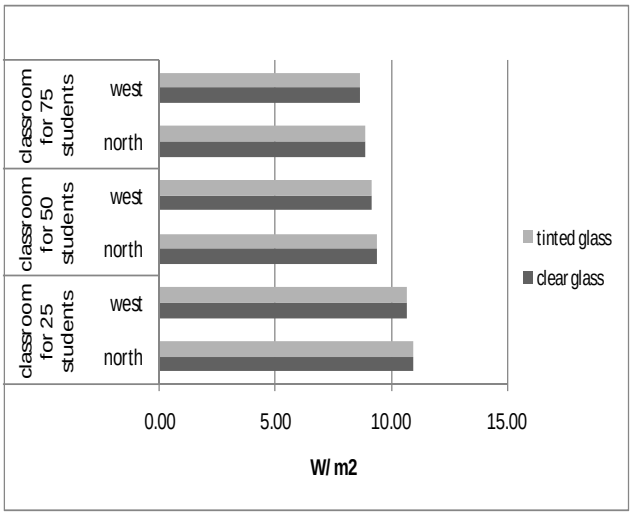

Figure 17: Comparison of hourly heat gains through the building fabrics between projected clerestory window with clear glass and with tinted glass (the first experiment)

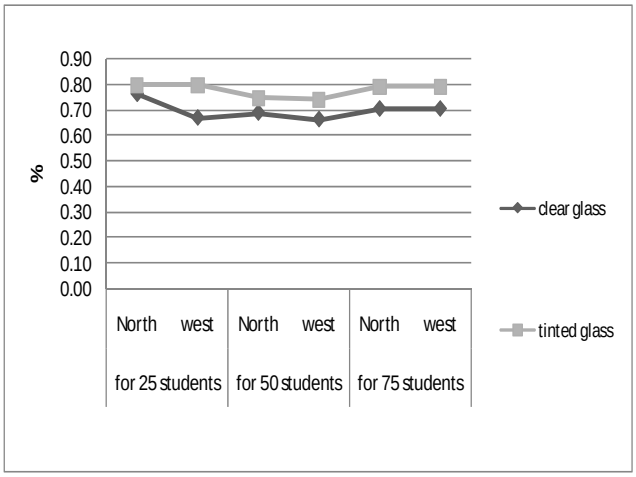

Figure 18: Comparison of daylight distribution between projected clerestory window with clear glass and with tinted glass (the first experiment).

Figure 19: Three dimensional picture of a classroom for 25 students with projected clerestory is resulted by Radiance (link to Ecotect) simulation.

Replacing clear glass with tinted glass on view window can improve the average and the distribution of daylight factor. All windows with projected clerestory and tinted glass on their view windows produce uniform daylight distribution (> 75%) and suitable daylight factors for learning activity (reading and writing). However, different interior illumination levels created by placing clear and tinted glass on the same wall plane cause a feeling of gloom.

4. CONCLUSION

Projected clerestory can protect the indoor area from direct solar radiation. Horizontal surface of the projected clerestory also functions as horizontal shading for view window below the clerestory. Its horizontal surface reflects sunlight into the deep side of the room depending on the ratio of clerestory height to room width. Less expensive alternatives are lightshelf and glass-block clerestory.

A window with 20% WWR can be considered as an optimal window area for classroom with reflectances 0.95 for the ceiling, 0.85 for the internal wall, 0.7 for the floor, 0.85 for the desks and 1.0 for the shading device; both for energy-efficiency and to maintain proper view to outside. Lower average classroom reflectance needs higher WWR, clerestory height, and window to floor area.

Comparing the results of the first and the second experiment, for classroom's window without obstruction from adjacent wall or building, the clerestory head height should be around 0.4 of the room width to achieve low energy classroom. One meter height view window with around 11% of clerestory head height to room height and 5% of clerestory head height to room width can distribute daylight evenly. Higher view window creates hotspot on area near the window. View window glazing with low visible tranmittance can improve the horizontal illuminance distribution.

ACKNOWLEDGMENT

The author wishes to thank Univ. of Atma Jaya Yogyakarta for financial support to conduct this research.

REFERENCES

[1] ASHRAE, *ASHRAE Fundamentals*, 2003, pp. 27.1-27.2.
[2] ASHRAE, *ASHRAE Ventilation Standard for Schools*, 2001.
[3] F. Binarti, "Lightshelf for improving indoor horizontal illuminance distribution", *Jurnal Teknik Universitas Brawijaya*, XII (1),1-7, 2005.
[4] H. Burnett, J. Wagner, G. Gyorkos, B. Horn, *Classroom Guidelines for the Design and Construction of Classrooms at the University of California, Santa Cruz*, UCSC Media Service, California, 2003, pp. 7-13, 27.
[5] Dept. PU, *Tata Cara Perancangan Pencahayaan Alami pada Bangunan Gedung*, SNI 03-2396-2001, 2001.
[6] E. Ghisi, and J. A. Tinker, "An ideal window area concept for energy efficient integration of daylight and artificial light in buildings", *Journal of Building and Environment*, 40 (1),51-61, 2005.
[7] Keputusan Menteri PU no. 441/kpts/1998.
[8] M. Laar, "Lightshelf and fins – carrying on where the tropical modernism left off", *Proceedings of Seventh International IBPSA Conference*, Rio de Janeiro, Brazil, August 13-15, 2001.
[9] M. Laar, "Daylighting systems for the tropics the example of laser cut panels (Australia) and plexiglas daylight (Germany)", *Proceedings of Seventh International IBPSA Conference*, Rio de Janeiro, Brazil, August 13-15, 2001.
[10] P. A. Muniz, *The Geometry of External Shading Devices as Related to Natural Ventilation, Daylighting and Thermal Comfort, with Particular*, Dissertation for degree of Doctor of Philosophy in Virginia Polytechnic Institute and State University, UMI Dissertation Information Service, Michigan, 1985.
[11] D. C. Pritchard (ed), *Interior Lighting Design*, 6th ed., The Lighting Industry Federation Ltd. And The Electricity Council, London.
[12] B. Stein, J. S. Reynolds, W. T. Grondzik, A. G. Kwok, *Mechanical and Electrical Equipment for Buildings*, John Wiley & Sons, New York, 1986, pp. 938-950.

Quality of Life Status in Multi-storey Low Income Housing

Moediartianto [1)], Ita Sulistyawati[2)], Inneke Hantoro[2)]

[1] *Department of Architecture, UNIKA Soegijapranata Semarang*
[2] *Department of Food Technology, UNIKA Soegijapranata Semarang*
E-mail: aant@unika.ac.id, aant_id@yahoo.com

ABSTRACT

For most people live in small walk-up flat units in Indonesia, aspect of thermal comfort and food safety is not considered as a quality of life element. Nonetheless, satisfaction with their thermal environment and food safety has a place to influence the expectation about what their "dream" house is. The quality-of-life issues discussed in this paper were limited to thermal comfort and food safety and conducted in two multi-storey public housings in Semarang. This study assesses the inhabitant perception to their thermal environment, level of food safety knowledge including how appropriates the food hygienic practices applied in their daily life and propose some recommendations to improve it to advance their quality of life. Houses of each typical flat unit (27 m², 36 m², 54 m²) will be assessed through observation and interview using questionnaire. Thermal comfort was measured using method of Field Studies of Thermal Comfort (FSTC). The level of food safety knowledge was measured based on USDA/Partnership for Food Safety Education. The findings of study indicate lower satisfaction of thermal comfort and lower level of food safety knowledge among occupants who live in smaller flat units, while was lower.

Keywords*: thermal comfort, food safety, satisfaction, quality of life, public housing*

1. INTRODUCTION

According to the Indonesia Central Statistic Bureau [1] 45.6% of total 206 million populations in Indonesia are living in urban area. Almost 70% of those urban populations are the middle low and low income groups [2]. With the urban population growth rate 4.2% per annum during 1990-2000; urban development in Indonesia is characterized by rapid land-use changes in its urban center as well as by the conversion of prime agricultural lands to residential areas and other urban land use to the peripheries [3]. It follows that the need of new houses in urban area is raised about 800.000 units per year, not included the backlog of house units from the years before. Simultaneously, the increase of urban population growth in Indonesia have created seriously implications on the need of land for living space and shelters as the result of market forces because lands especially those in inner-city areas became scarce and more expansive.

Since the development of housings in urban area in line with population growth is not fit with the provided lands, the vertical-housing development has been promoted by Indonesian government as one of appropriate alternatives. For middle-low income groups, *Rumah Susun (Rusun)* has been built-up intensively in some major cities in Indonesia such as Semarang.

Unfortunately, Indonesia has not come close yet to solve neither its quantitative nor qualitative housing problems after three decades of development. Those quantitative problems may actually be influenced by the qualitative problems since the most Indonesians have miss-perception with respect to live in public residential buildings like *Rusun*. For many people, built-up for low income community means sometimes low cost construction (unsecured), low environmental quality (unhealthy) and low design quality (uncomfortable) [4].

1.1 QOL indicators

With respect to healthy city concept, housing conditions are part of the most general quality of life (QOL) indicators [5]. Nonetheless, in Asian developing countries such as Indonesia, studies on QOL especially in housings have been scarce and infrequent. Seik [6] mentioned that research efforts in this field are mainly focused on urban QOL originated from scholars in Western world who were from various disciplines such as sociology and psychology.

Eight essential indicators of housing quality components is identified by Lawrence [5] i.e. (1) site characteristics, (2) residential buildings as a shelter, (3) safe supply of water, sewage and solid waste disposal, (4) neighborhood ambient atmospheric conditions and indoor air quality, (5) household occupancy conditions which avoid transmission of infections and the occurrences of injuries (6) access to community facilities and services, (7) food safety and (8) control of vectors of disease that can propagate in the building structure.

To measure those indicators, researchers usually conduct the form of either objective or subjective measurements. The first is employed to assess the level of various basic needs of life as Maslow stated such as food and shelter. These needs are common human needs to all cultures, which indicated by objective conditions and settings (such as physical, social, and economics settings). On the contrary, Morris & Coombes argue subjective indicators are more at individual´s level of satisfaction indicated by psychological state [6]. Although both types of measurement assess QOL differently, they are interrelated. With regard to Maslow and Lawrence [6, 5] theory mentioned above, this research assesses thermal comfort

using subjective measurement while for level of food safety knowledge using objective measurement.

1.1.1 Thermal Comfort

ASHRAE Standard 55-2004 describes thermal comfort as "that condition of mind which expresses satisfaction with thermal environment" [7]. This standard aims to identify the combinations of indoor space environment (temperature, thermal radiation, humidity and air speed) and personal factors (activity and clothing) that will produce thermal environmental conditions acceptable to 80% or more of the occupants within a space [8]. In like manner, Fountain *et al* [9] suggest an alternative theory of thermal perception i.e. the adaptive model. It states that the match between one's expectations about indoor climate in a particular context and what actually exist will convince thermal sensation, satisfaction and acceptability. In terms of QOL, Malkina-Pykh and Pykh [10] mentioned that subjective satisfaction is usually described in strongly relation to one's expectations of it. One's satisfaction level of thermal environment explains one's expectation of a better condition than he/se feels at the moment.

A method so called Field Studies of Thermal Comfort (FSTC) is expounded by Nicol and Roaf [7] as an appropriate approach to evaluate thermal comfort environment in building. The focus of this method is more concerned with the responses to a building of its occupants. In the FSTC, the occupant is asked to express his/her own feeling at the time such as "how do you feel about temperature now?"

1.1.2 Food Safety

Obtaining safe food is everyone's right. Winarno [11] emphasized that food safety is the ultimate, first and most important prerequisite aspect must be fulfilled before other requirements of food. It means if food is no longer safe to be consumed so its nutritional content, deliciousness, appearance and quality have no meaning anymore, in fact that kind of food have to be destroyed. In addition to that, Act of The Republic Indonesia Number 7 of 1996 on Food [12] stated that food safety is included as one of QOL's elements. It stated that sufficient availability of safe, nutritious and quality food is a main pre-requisite, which must be met in the effort to arrange a system, which provides protection for the purpose of health, and to play a larger role in increasing the prosperity and welfare of the people. Food safety itself is defined as food safety is the condition and efforts required to prevent food from possible biological, chemical-contamination and contamination by other objects which may disturb, harm, and endanger the human health.

Human population consists of different age, living experience, healthiness, cultural knowledge, sex, political view, nutritional need, family states, type of work, and educational background. This condition will result in different perception on food safety [13]. Bappenas [14] reported that the first cause of food poisoning insidents in Indonesia during 2004-2005 comes from household food (food processed at household scale), see Table 1. One of the reasons of this occurrence is because of insufficient food safety knowledge of the food preparer in the household, as one of stakeholder in the food supply chain.

Table 1. Causes of Food Poisoning in Indonesia in 2004-2005

Cause	Number (%)	
	2004	2005
Household food	53,7	42,4
Processed food	15,2	15,2
Catered food	15,2	21,2
Snack food	12,2	17,9
Not reported	3,7	-
Miscellaneous	-	3,3

Source: Bappenas (2007)

This study assesses the inhabitant perception to their thermal environment, level of food safety knowledge including how appropriates the food hygienic practices applied in their daily life and propose some recommendations to improve it to advance their quality of life.

2. METHODOLOGY

The study described was conducted in two multi-storey public housings in Semarang. The buildings were built under different initiative programs and concepts since the problem of housing for low and middle income groups in Semarang was issued to be solved.

1. The first was *Rusun* Pekunden was built in 1996 using "top down" design approach in which the population has no experience on participatory decision-making to plan their environment. Situated on a central district of city, it comprises 92 flat units disposed in five blocks which have 4-storey height.
2. The second was *Rusun* Bandarharjo, which is located in an urban fringe of Semarang nearby the national harbor Tanjungmas, about 2 kilometers to the north from city centre, and orientated at 22 degrees to the true north. Around the housing some villages called kampongs are exist which has high density of land occupancy. It comprises 210 flat units disposed in three blocks, which has 4-storey heights.

Figure 1 : Building facades of *Rusun* Pekunden & Bandarharjo

This study is conducted in "different period", which is during April – May 2006 for thermal comfort measurement and during May – July 2009 for the level food safety knowledge measurement. The second part of this study is an extension of the first, since QOL assessment need to be measured in more aspects to attain more complete QOL status. This research was done in

three steps, which are observation, development of questionnaire and interview of respondents using the questionnaire.

Climatic condition

Questionnaire surveys on thermal comfort were conducted in a season characterized by hot and humid days and nights. The daily average temperature recorded during that "period" fell within 25.6-29.1°C and the maximum RH was higher than 60%, occasionally reaching 90%. As recorded by Semarang climatology station, hot winds blow from Southeast direction to Northwest direction during that "period". The monthly wind magnitude is only up to 3.6 m/s with the average value 2.3 m/s at the height of 10.0 m above ground level

Sampling

To asses thermal comfort aspects, a total of 165 respondents from two multi storey low income housings were asked to participate in a questionnaire survey. More than 50% of them involve in all observation seasons. The objective is to investigate the degree of thermal comfort based on the occupant's perception.

Table 2. Demographic data of respondents for thermal comfort

.

Housing	Flat Unit	Gender	Age groups					Sub total	Total
			<20	21-30	31-40	41-50	>50		
Pekunden	27	M	3	17	7	7	9	43	
		F	9	15	13	6	6	49	
	54	M	5	0	1	3	4	13	
		F	1	0	3	2	1	7	112
Bandarharjo	27	M	1	5	5	4	1	16	
		F	4	5	5	0	1	15	
	36	M	0	1	2	1	3	7	
		F	1	9	1	2	2	15	53

Table 3: Sampling distribution

	Hot season
Number of subjects	165
House type (number of subjects)	27(31) 36(22) 54(33)
Date of survey	1 April 2006 – 22 May 2006
Time of survey (number of subjects)*	M(105) A(87) E(94)

**) M = morning (07.00 -11.00 am), A = afternoon (13.00 -16.00), E = evening (18.00 -22.00)*

Simultaneously, questionnaires about the level of food safety knowledge were also conducted to housewives as respondent samples. The housewives were chosen since they have important role in food supply for their family. The number of respondents used from *Rusun* Bandarharjo are 49 respondents (type 27) and 16 respondents (type 36); whereas from *Rusun* Pekunden are 68 (type 27) and 9 (type 54.)

The key questions in food safety knowledge questionnaire are divided into three parts, which are background; basic information related to food safety; food safety knowledge and food handling practices. This knowledge questions was developed based on the 4 elements (separate, cook, chill, and clean) of food safety identified in the USDA/Partnership for Food Safety Education, Fight Bac!® program [15]. The response for basic food safety knowledge and food handling practices questions was agree, disagree or don't know. Knowledge based questions were graded as right or wrong. For purposes of statistical assessment, "don't know" was considered as an incorrect answer. Whereas for food handling practices 1 – point is given for the proper handling practice (right answer) and 0 – point is given for improper practice (wrong and don't know answer.)

In addition to that, there was a close observation conducted during data collection using questionnaires, which acquire information about typical flat unit plan. This information is needed to find out the use of existing rooms related to food hygiene practices.

3. RESULTS AND DISCUSSION

3.1 Thermal Comfort Aspect

3.1.1 Comparison between seasons

Fig. 2 shows that for all seasons, the thermal acceptability is below to 80%. Surprisingly, it is not like what expected, with mean thermal sensation (ASHRAE/Tsv) vote of 0.434, the evening session can satisfy only 44% of people.

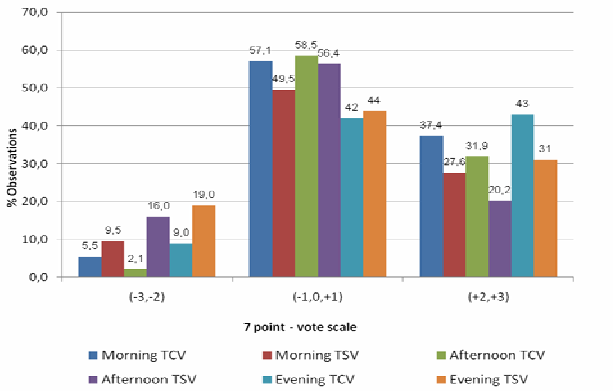

Figure 2 : Thermal comfort acceptability for different sessions indentified on ASHRAE scale and Bedford scale [N (M) = 105, (A) = 87, (E)= 94)]

Distribution of those thermal sensation votes is seen have a correlation with wind sensation scale as shown in Fig. 3. It describes a high 29.8% of occupants have a feeling that the air movement for evening season was in motionless condition.

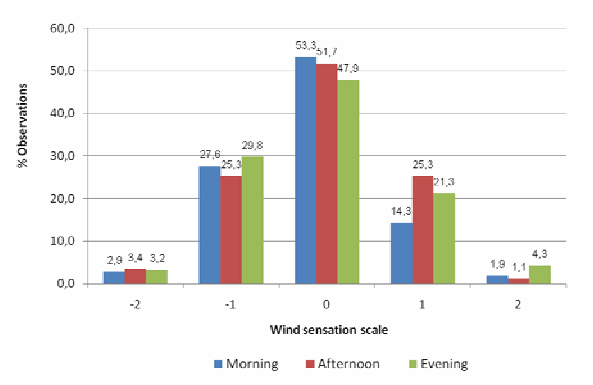

Figure 3 : Wind sensations for different sessions
[N (M) = 105, (A) = 87, (E)= 94)]

3.1.2 Comparison between flat types

Based on the ASHRAE scale, none of occupants in all flat types is able to achieve an acceptable thermal condition with 80%, whereas with Bedford scale, only they who live in flat type 54 (83.3%) expressed satisfaction with their indoor thermal environment. It confirms that a comfortable condition of a house is usually described in relation to type, size and location.

Inspection to a correlation between thermal sensations with wind sensation, occupants living in flat type 27 units seem to experience an extreme condition. A high percentage of respondents (76.7%) in left categories (-2,-1) feel the low wind speed in their indoor environment.

During the visit of the field survey, evidence was found dealing with the unused bedroom in the bedtime. By a deeply interview**,** the occupants mentioned that this bedroom occupied by 5 people was uncomfortable for sleeping due to the high temperature and lack of fresh air inside. It follows that they prefer to sleep in living room at the floor.

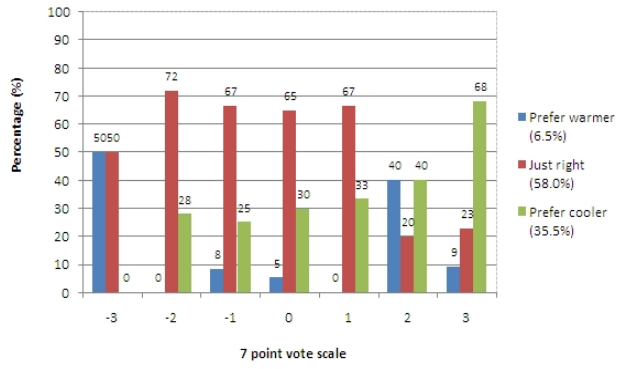

Figure 4: Thermal comfort preference (N=165)

From Fig. 4 we can see that there is a tendency for occupants to perceive coolness or cold sensation as comfortable condition. It is reflected that occupants wanted to be cooler is relatively higher compared to the percentage of occupants wanted to be warmer by 35.5%. Hence, occupants who voted cool (-2), slightly cool (-1) and neutral (0) said that those conditions are just right for their bodies. It might indicate that people living under tropical hot humid region wish a cooler environment since they have expectation about the better condition in cool level.

Evaluating human response to their real environment in building, some complex factors of human being such as culture, gender, economic status, preference and expectation may be not included in human heat balance method [8]. Accordingly, currently approaches are more suggested to view human as active subjects who can modify their environment and behavior for attaining a state of comfort.

Fig. 5 illustrates various adaptive actions which are commonly employed by the occupants when they feel uncomfortable inside. Going out from indoor rooms to outdoor space is highly preferred by occupants with the percentage of 39%. Other favored action in this case is the usage of fan with the percentage of 33%.

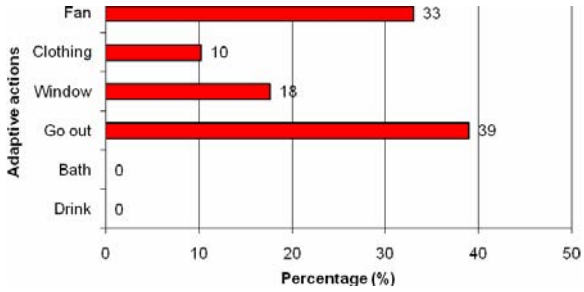

Figure 5: Adaptive behavior (N=138)

Interestingly, the environmental control by opening window is less favorable for occupants with the percentage of only 18%. Compared to finding results from previous natural ventilation studies conducted in tropical hot humid region such as Wong & Huang [16]; Feriadi [17] & Wong [18], this different phenomenon can be explained with these following arguments. Firstly, the low percentage of window indicates a real problem that the current available window is insufficient for improving the uncomfortable condition inside as mentioned in earlier discussion. Secondly, the unique characteristic of observed buildings should be considered where the sheltered skywalks can facilitate not only social engagement for low-middle income groups but also provide open and airy feeling.

On the other hand, relatively higher preference for the use of fan can signify that in facts occupants also want to experience comfort sensation due to wind or air movement inside their flat units. Also, this result shows a good agreement with the common phenomenon in Indonesia where the most homes has at least one fan unit to control their environmental thermal comfort.

A significant correlation between the favorable action and the most comfortable space is found where occupants prefer to go to terrace for obtaining more comfortable condition at outdoor space compared to indoor environment such as at living room or bedroom by

percentage of 51%. This condition may be due to the following reasons. Firstly, natural ventilation cannot work well within small flat units due to inappropriate design in which the cross ventilation pattern was changed to be single-sided ventilation pattern. In other
word, there is insufficient air contact due to inappropriate room organization. Secondly, dense occupant with high activity in afternoon, for instance, creates heat accumulation that cannot be transferred well to outside due to the lack of air movement. Thirdly, terraced corridor provides airy spaces for various forms of activities.

3.2 Food Safety Aspect

3.2.1 Floorplan observation

From the conducted observation on typical flat unit plan, it is revealed that all three types of flat unit have kitchen that is relatively near the toilet and not good enough air circulation within (see Fig. 6) One of the consequences of having limited area of living is higher risk of cross contamination of microorganism among the existing rooms. In the case of toilet, there is high possibility to leave unoccupied toilet open, which will lead to microbial spreading inside the flat. Activities in the kitchen influent the introduction or removal of air, such as cooking drives off oxygen, while stirring, mixing, and beating foods introduce oxygen. Some bacteria grow rapidly only in the presence of free oxygen; others require the absence of oxygen; some grow in both atmospheres and even others may have special atmospheric requirements [19]. Nonetheless, the occurrence of cross contamination via hands was already prevented through washing-before produce-food behavior practiced by more than 75% inhabitants.

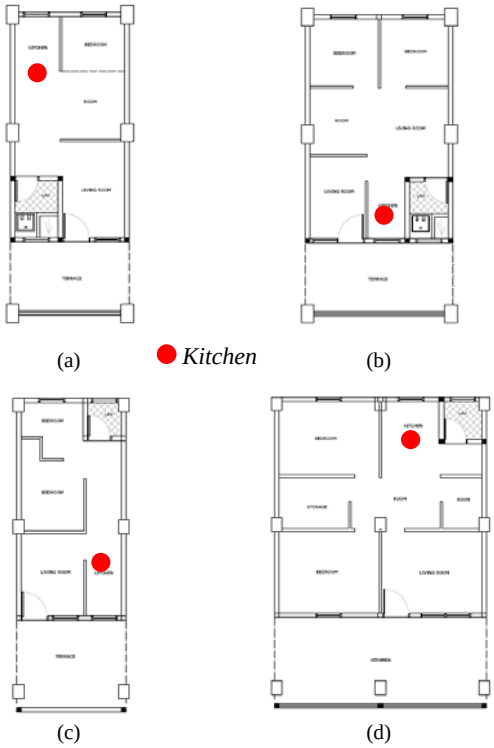

Figure 6: Typical Floorplan of four existing flat unit in *Rusun* Bandarharjo (a) type 27 (b) type 36 and Pekunden (c) type 27, (d) type 54.

3.2.2 Food Safety Knowledge

Housewives represent a family member which is mainly involved in preparing and providing meal in their family. Thus, level of food safety knowledge of housewives is crucial. Housewives assumed as home food preparer is a critical link in the food production to consumption to prevent food-borne illness [20].

Studies have estimated that between 50% and 87% of reported food borne disease outbreaks have been associated with the home. Identified common mistakes identified include serving contaminated raw food, cooking/heating food inadequately, having infected persons handle implicated food and practice poor hygiene. However it is known that a part of food borne illnesses in the home result from eating raw foods of animal origin or engaging in unsafe food preparation practices in the home [21]. Therefore, home food preparer need to know how to minimize the presence of pathogens or other risky contaminants in food.

Table 4 . Distribution of the right answers given by respondents from different multi storey housings to questions related with general food safety knowledge

Questions	The percentage of true answers (%)			
	B-27	**B-36**	**P-27**	**P-54**
• All harmful bacteria are destroyed by thorough and complete cooking	**93.9**	**81.3**	**83.8**	**100**
• Moldy food is safe to eat if you scratch the mold off the surface of the food	**93.9**	68.8	**94.1**	**88.9**
• It can take only a small number of harmful bacteria to make the person sick	**81.6**	**75.0**	60.3	44.4
• Unsafe foods can be identified by the way they look and smell	*4.1*	*0.00*	*4.4*	*0.00*
• In the kitchen, food can be contaminated with harmful bacteria during handling and storage	*69.4*	*68.8*	*69.1*	*66.7*
• Bacteria can grow and survive in refrigerated food	**77.6**	56.3	52.9	44.4
• It is safe to eat raw cookie dough or cake batter that contains raw eggs	*44.9*	*25.0*	*45.6*	*66.7*
• Meat that has been handled and/or prepared properly can be kept in the freezer for 6 months and still be safe to eat	**87.8**	0.00	61.8	**88.9**
• It is safe to place cooked meat on the same unwashed plate you used for the uncooked food	**95.9**	**75.0**	**97.1**	**100**
• It is safe to thaw meat in the room temperature	*28.6*	*25.0*	*19.1*	*44.4*
• The color changes of meat indicate meat quality deterioration	**98.0**	**87.5**	**88.2**	**77.8**
• It is safe to consume half-cooked meat	**83.7**	**87.5**	**86.8**	66.7
• It does not necessary to wash vegetable or fruit before we consume it	**95.9**	**87.5**	**98.5**	**88.9**

Note: B = Bandarharjo (B-27: type 27; B-36: type 36)
P = Pekunden (P-27: type 27; P-54: type 54)

Table 4 presents the right answers given by respondents to the questions about general food safety knowledge of housewives from *Rusun* Bandarharjo and *Rusun* Pekunden. The result shows that most of respondents have no sufficient basic knowledge on food safety. Only respondents from B-27 showed adequacy in food safety. It is indicated with the percentage of correct answers that reached 75% of 9 out of 13 given questions. While, other respondents from B-36, P-27, and P-54 only can answer 5 - 6 out of 13 questions with 75% correct answers (the limit of subject proficiency.) The result implies that people with low income, which is associated with *rusun* inhabitants, not always has lack of food safety knowledge.

Almost all of respondents agreed that harmful bacteria could be eliminated by thorough complete cooking (81.3-100%.) However, many of them stated that it is safe to consume raw food that contains raw eggs. Microbial hazards include food poisoning bacteria such as *Salmonella*, *E.coli*, *B. cereus*, *S. aureus* and many others can spread from raw foods such as meat, poultry and unwashed vegetables either directly or via food preparers, work surfaces and equipment [22]. Eggs can carry harmful bacteria inside and on their shells. Salmonella is often found as a threatening contaminant in eggs. Salmonella – positive eggs present another risk of which many food preparers are unaware – cross contamination. Cracking, separating, or beating an egg can spread Salmonella over a wide area in the kitchen, contaminating work surfaces, utensils, mixing bowls, and hands. Moreover, the numbers of live Salmonella in a contaminated egg can become dangerously elevated if the egg has been mishandled – high enough that traditional cooking methods may not kill all of the Salmonella organisms [23]. Therefore, egg or food contained with egg should not be consumed raw. These raw foods can be made safe by cooking which kill bacteria [20].

Most of respondents also believed that it is not safe to place cooked food on the same unwashed plate, which has been used for the uncooked food (75 – 100%.) However, the respondents seem do not have good understanding on cross contamination. Most of them do not aware that harmful bacteria contamination can occur during food handling and storage in the kitchen. The presence of pathogens in raw meat, poultry and eggs places the burden of ensuring food safety on the shoulders of food preparers. Insufficient and improper storage conditions can cause the growth of microbial contamination. Clearly the home kitchen can be a dangerous place. Cross contamination of the pathogen microorganisms from storage places to production area can occur if food preparers pay less attention on hygiene practices. Poor attention to hand washing, inadequate cleaning of utensils and work surfaces, and use of contaminates sponges can contribute to cross contamination [24, 23].

Moreover, most of them do not know that thawing meat in room temperature can cause bacterial the growth of microbial contaminant. Food poisoning bacteria can grow in food that is not defrosted properly. Food can be thawed at room temperature, but it should be done quickly as harmful bacteria could grow if the food gets too warm while thawing. Ideally thawing or defrosting is done in the fridge. Putting food in the fridge will keep food at a safe temperature while it is defrosting. Microwave or putting the food in a container with a lid and then place it under cold running water also can be alternatives [22].

Most respondents also stated the changes of food color denote the degradation of food quality (77.8 – 97.9%.) However, it seems that respondents only rely on the visual observation to detect the degradation of food. As a matter of fact, microbial contamination on food cannot be examined only by the way the food look and smell. The presence of pathogenic bacteria or toxin in food has to be found out through laboratory testing.

Table 5. Distribution of the right answers given by respondents from different multi storey housings to questions related with food handling practices

Questions	The percentage of true answers (%)			
	B-27	B-36	P-27	P-54
• When grocery shopping, you always choose good quality of food	**98.0**	**100**	**97.1**	**100**
• You always wash fruit or vegetable before further processing	**100**	**100**	**97.1**	**100**
• You always wash fruit and vegetable by soaking it in water	53.1	18.8	44.9	33.3
• You always wash raw meat and fish before further processing	**98.0**	**93.8**	**97.1**	**100**
• After cutting raw food, you wash the cutting board and knife first before cutting cooked food	**95.9**	**93.8**	**84.1**	**88.9**
• You separate raw meat and fish from ready-to-eat food	**93.9**	**93.8**	**97.1**	**100**
• It is important to wash your hand after cracking an egg	**85.7**	**81.3**	**88.4**	**100**
• You or your family consumes raw egg	46.9	12.5	28.9	33.3
• You cook egg and make sure that the egg yolk is well cooked	**93.9**	**87.5**	71.0	**88.9**
• You wash your hand with soap before processing foodstuff	**81.6**	**75.0**	**76.8**	**77.8**
• It is safe to eat snack while you preparing food	57.1	43.8	47.8	55.6
• It is safe to use the same spoon to taste then stir the food without washing it	**83.7**	**81.3**	7.3	11.1
• After handling raw meat, fish, and/or poultry, wiping hands on a paper towel is sufficient to clean hands	**93.9**	**81.3**	17.4	11.1
• It is safe to clean your hand using the same towel to clean kitchen utensils	**93.9**	**87.5**	17.4	11.
• You often wash towel that you use for hand cleaning	59.2	**75.0**	69.6	55.6
• It is safe to keep cooked rice in room temperature more than four hours	**77.6**	62.5	50.7	11.1
• It is safe for person who suffer from typhus, diarrhea, cough, influenza and dysentery to produce food	51.0	37.5	33.3	11.1
• It is important to have short and clean hand nails while produce food	**87.8**	**75.0**	**84.1**	**100**
• It is safe to consume food that is already keep for more than six hours in room temperature and reheating it	28.6	31.3	46.4	44.4

Note: B = Bandarharjo, P = Pekunden

In general, respondents only apply appropriate food handling practices for eight out of nineteen questions with

minimum 75% of true answers. The result reveals that respondents from smaller flat unit tend to aplly more food handling practices than the bigger one (See Table 5.)

We also can see from Table 5 that the respondents answer five out of nineteen questions with less than 75% correct answer. Most of them do not understand that cleaning fruits and vegetables by soaking will cross contaminate microorganism among the washed food and also the soaking water. Interestingly, more than 97% of the respondents surely choose good quality food and they also wash fruit and vegetable before they consume or process it. Meanwhile, eating raw eggs become the habit of less then half of the inhabitants (12.5 - 47%); this condition is risky to cause bacterial infection as it is explained earlier. Consuming snack during food production will increase risk of microbial contamination, since the preparer's hand sometimes touch his lips and may cross contaminate the food produce. Many bacteria and viruses found in the mouth can cause disease, especially if an employee is ill. For instance, the preparer who suffers from typhus, diarrhea, cough, influenza and dysentery produce food, the pathogenic microbes can be transported from the person to food via hand or air. During a sneeze, some bacteria from the mouth are released into the air. The microorganisms may infect other people or may land on food while it is being handled [26]. Citing Buckland and Tyrell (1964) in Lelieveld *et al.* [27], they reported that sneezing and blowing the nose were more than 1000 times more efficient than coughing in producing infectious aerosols from nasal secretions.

Some housewives assume that consuming food that is already keep for more than six hours in room temperature and reheating it is still safe (28.6 – 46.4%.) As a matter a fact, the number of microorganism within the food will increase exponentially during room temperature storage. Even after reheating the food, it should not be consumed since the food is already decayed. They do not understand that most foods spoil easily because they have the nutrients that microbes need to grow. One way to inhibit counts of microbes is by cold storage, which only allows facultative microorganisms and psychrotrophs to survive [26].

Although it is important for people to distinguish safe food and to develop food safety knowledge, behaviors, and practices; there are only a few studies conducted on food safety knowledge and perceptions of consumers in Indonesia. Hence, it is required to carry out further research on food safety literacy, especially focusing on people who act as food preparer. Later on, it is required to develop food safety education program for every element involved in food supply chain, including home food preparers.

4. CONCLUSIONS AND RECOMMENDATIONS

- Since the shortage of land inline with the growth of cities in developing countries like Indonesia will dictate the development of buildings vertically, it is worthy to enhance the design quality of multi-storey public housings with respect to local climate characteristics and room layout.
- From the subjective measurement results, it can be concluded that people who live in tropical hot humid regions have expectation to reach a better thermal condition in cooler environment. Nevertheless, they can accept slightly warmer condition by carrying out some adaptive behaviors. In terms of Quality-of-Life, this subjective satisfaction can enlighten one's expectation of a better condition. If building occupants are given opportunity to modify their environment, they will make themselves comfortable.
- Dealing with building design of multi storey public housings in Indonesia, it is important to be mentioned that providing flat units with small area i.e. type smaller than 27 m^2 is no longer suggested. In fact, it is a difficult task to create a comfortable environment in a small unit by utilizing natural ventilation optimally. It retains a retrograde image of uncomfortable building for living.
- Most of respondents have no sufficient basic knowledge on food safety, except for B-27 respondents. It implies that people with low income, which is associated with *rusun* inhabitants, not always has lack of food safety knowledge. Moreover, respondents from smaller flat unit tend to apply better food handling practices than the bigger one.
- It is suggested to conduct further research on microbial air quality and microbial density on food and kitchen utensils. The result will give more complete picture on food safety status as one of QoL indicators.
- It is required to carry out further research on food safety literacy, especially focusing on people who act as food preparer.

ACKNOWLEDGMENT

The authors would like to thank Sherly Ardiany Subarjo and Nancy Yustina for their valuable contribution in conducting the survey and data input of the level of food safety knowledge.

REFERENCES

[1] Anonim, "Percentage of Population by Area, Province and District 2000" , Indonesia Central Statistic Bureau, Retrieved from http://www.datastatistikindonesia.com/component/option,com_tabel/kat,1/idtabel,118/Itemid,165/

[2] H.Winarso, "Inner City Redevelopment Strategy: The Role of Agents in the Development Process, Learning from Two Cases in Indonesia", 1999, Retrieved 12 September 2006 from http://www.wmin.ac.uk/builtenv/maxlock/Core_Areas/Studies/Band Sam.pdf

[3] T. Firman, Major Issues in Indonesia´s Urban Land Development, *Land Use Policy 21*, pp. 347-355. 2004

[4] Moediartianto, "Natural ventilation performance of multi-storey low income housings in a hot humid climate: Assessment of thermal comfort and indoor air quality", 2006, unpublished

[5] D.C.C.K. Kowaltowski, V.G. da Silva, S.A.M.G. Pina, L.C. Labaki, R.C. Ruschel, and D.C. Moreira, "Quality of life and sustainability issues as seen by the population of low-income housing in the region of Campinas, Brazil", *Habitat International 30*, pp. 1100–1114, 2006

[6] F.T. Seik, "Subjective assessment of urban quality of life in Singapore (1997-1998)", *Habitat International 24*, pp. 31-49, 2000.

[7] F. Nicol, and S. Roaf, "Post-occupancy evaluation and field studies of thermal comfort", *Building Research & Information 33(4)*, pp. 338–346, 2005

[8] R.J. de Dear, and G.S. Brager, "Thermal Comfort in Naturally Ventilated Buildings, Revisions to ASHRAE Standard 55", *Energy and Buildings* 34, pp. 549-561. 2002

[9] M. Fountain, G. Brager, and R. de Dear, "Expectations of indoor climate control", *Energy and Buildings Volume 24, Issue 3*, pp. 179-182, 1996

[10] I.G. Malkina-Pykh, and Y.A Pykh, "Quality-of-life indicators at different scales: Theoretical background", *Ecological Indicators 8*, pp. 854 – 862, 2008

[11] F.G. Winarno, *Naskah Akademis Keamanan Pangan*, Bogor, 1997

[12] Anonim. "Act of The Republic Indonesia Number 7 of 1996". Jakarta, 1996

[13] R. A. Seward, "Definition of Food Safety", John Wiley and Sons, Inc. USA, 2003

[14] Bappenas. "Rancangan Aksi Nasional Pangan dan Gizi 2006-2010", 2007. Retrieved from http://www.bappenas.go.id/node/62/88/rencana-aksi-naional-pangan-dan-gizi-2006-2010-/

[15] L.F. Pivarnik, M.S. Patnoad, N.L. Richard, R.K. Gable, D.W. Hirsch, J. Madaus, S. Scarpati, and E. Carbone, "Assessment of Food Safety Knowledge of High School and Transition Teachers of Special Needs Students", *Journal of Food Science Education 8*, pp. 13-19, 2009

[16] N.H. Wong, and B. Huang, "Thermal Comfort Evaluation of Naturally Ventilated Public Housing in Singapore", *Building and Environment 37*, pp. 1267 – 1277, 2002

[17] H. Feriadi, (), *Thermal Comfort for Naturally Ventilated Houses in Indonesia*, Proceeding of International Symposium Building Research and the Sustainability of the Built Environment in the Tropic, Tarumanegara University, Jakarta, pp. 215 – 227, 2002

[18] N.H. Wong, "Comparative Study of the Indoor Air Quality of Naturally Ventilated and Air-Conditioned Bedrooms of Residential Buildings in Singapore", *Building and Environment 39*, Elsevier, pp. 1115-1123, 2004.

[19] Idaho Department of Health and Welfare, " Food Safety and Sanitation Manual". Idaho. 2005

[20] L. Mederios, V. Hillers, P.. Kendall and A. Mason, "Evaluation of Food Safety Education for Consumers", *Journal of Nutrition Education and Behaviour, 33 (S1)*, pp. 27-34, 2001

[21] N. Unusan, "Consumer Food Safety Knowledge and Practices in The Home in Turkey", *Food Control 18*, pp. 45–51, 2007

[22] Food Standards Agency Scotland, " Cook Safe Food Safety Assurance System". Scotland. 2005

[23] P. Entis, "Food Safety Old Habits, New Perspectives", ASM Press. Washington DC. 2007

[24] B., Ergönül & G. Pelin, "Application of HACCP system in catering sector in Turkey" *Internet Journal of Food Safety 3*: pp. 20-24, ____

[25] Food Standards Agency Northern Ireland, "Safe Catering – Your Guide to Making Food Safely". Ireland. 2007

[26] N. G. Marriot, "Essentials of Food Sanitation" Chapman and Hall. New York, 1997

[27] H. L. M. Lelieveld, M. A. Mostert, J. Holah and B. White (Eds.), "Hygiene in Food Processing" CRC Press. Cambridge, 2003

Identification of Environmental Factors Influencing the Quality of Housing Environment

Ninin Gusdini, Laila Febrina

Environmental Engeneering
Sahid Jakarta University,
Jl. Prof.Dr.Soepomo no. 84.Tebet.Jakarta Selatan 12870
Telp.(021) 8312813-15 Fax. (021) 835476
Email : adhe_tl@yahoo.com, laila_febrina@yahoo.com

ABSTRACT

The uncontrolled growth of population has influenced some pressure to space and environment. As an effect, we must making serious efforts of the housing demand and its facilities. Meanwhile, good quality of the healthy housing is everyone's need. The land limitedness sometimes brings some quite bad impacts to the quality of the environment itself and eventually will cause the decrease of the quality of environmental housing and people's living quality.

This research is aimed to analyze some factors which influence the quality of housing environment. This research is implemented in a local/self-supporting and formal housing in district of North and South Cikarang.We obtain data from the survey result and questionnaires addressed to some samples of people around the location. We use descriptive and discriminated analysis to find out the significant factors of the housing quality and get discriminated equation to estimate the quality of the housing environment. The result of the research states that the quality of air/noise, reforestation/greening, road width, transportation and numbers of places worship are the main factors which determine the quality of the healthy housing whether it is good or not. Also we get the discriminated equation as follow:
Y = 0,601X1 + 0,165X2 + 0,1615X3 + 0,590X4 + 0,471X5 – 0,662X6 – 4,835

Cutoff point of group of housing environment health is -0.6. This means that the environment can be included in good health of environment if Y> 0.6. Classification accuracy is 67.8%.

Keywords
Housing, health of environment, diskriminan,cutoff point

1.INTRODUCTION

Housing area have been increasing about 50% during ten years ago, and most of them as formal housing at urban area. An Uncontrolled of housing growth cause the decreasing of environmental quality of residential

The growth of residential are not followed the development of infrastructure which to serve the residential for basic needs such as water, to maintain environmental sustainability and support the flow of goods and people between internal and external regions in the city can cause of degradation for quality environment of residential.

This research carried out at Cikarang District of North and South. The reason for choosing the location is as these districts are located in Bekasi Regency, which borders directly with Jakarta, so Bekasi obtain additional population of DKI Jakrta

The research focused on studying the factors influencing the quality of housing environment. The objectives of the research were: (1) to evaluated the residential quality based on standard guidelines by Department of Health (2) to identify the factor assosieted to quality of housing environment, (3) to make the descriminan formulation of housing environmental quality

1.1.Housing and Residential

Housing according to Decree of The Minister for Public Health of RI Number 829/MENKES/SK/VII/1999 is functioning house group as residence environment or dwelling provided with environmental facilities and basic facilities.

Residential according to Minister for Public Health of RI number 288/MENKES/SK/III/2003 is housing, hostel, dormitories, kondomonium / apartment, mansions and of a kind him.

According to SNI concerning Procedures Planning of residential defined that housing environment is a group of houses with environmental facility. Environmental facilities are road/street, drinking water channel, drainage,

solid waste disposal, electrics network. And the infrastucture at residential consists of educational facilities, healthy facilities, commercial, governance,public service, recreation, and culture.

1.2.Environmental Quality of Housing

Environmental Quality of Housing consists of physical and non physical component (social of economics). Direktorat Cipta Karya(1979) specified level of quality of housing environment use parameter such as . (1)furnerability of location against natural disasters; (2)quality of fresh water resource; (3)quality of air and noise pollution; (4)greening/penghijauan; and (6)facilities and infrastructure consisting of sanitation, waste management, drainage/sewerage system, condition of roads, transportation, education and worshipping facilities.

Identification of Housing Environmental Health Quality level of each type of residential areas was evaluted based on basic standard of Minister of Health Republic of Indonesia no:829/Menkes/VII/1999 regarding criteria of Housing Environmental Health Quality covering six aspects: critical areas, quality of air and noise pollution, reforestation/greening, disease vectors, and environmental facilities, and infrastructure such as transportation facility, school, worship facilities and vector of disease

2.METHODOLOGY

2.1.Stage sampling

Type of the research used is analytic descriptive research. Amount of Sample is taken pursuant to formula of Slovin, 1994 as follows:

$$n = \frac{N}{(1 + N e^2)}$$

in this case:
n = amount of sample every types housing
N= amount of populations every housing type in one segment
e = diffuseness of carelessness because of mistake of intake of sample which can be tolerated. To the amount of populations 500-2500, assess e gyrate 2 - 10%.

2.2 Phase of Identification and Classification of Health of Environment Housing

Factor Physical and non physical at indicator mount the quality of health of housing environment is given by score 1 to 5 at propagated questionnaire to resident in region of North and South Cikarang.

Classification analysis result of calculation of health of housing environment is based on the amount of variable scores health of housing environment and factor of scale is later; then calculated by highest and the lowest score. According To Direktorat Cipta Karya(1979), classes amount made by classification 4 class health of environment that is:
class 1 : very good,
class 2 : good,
class 3 : rather good,
class 4 : unfavorable.

Formula used in class interval is:
class interval =

$$\frac{\text{The highest score – The lowest score}}{\text{The amount of class}}$$

Class 1 : very good	(75 – 60)
Class 2 : good	(59 – 44)
Class 3 : rather good	(43 – 28)
Class 4 : unfavorable.	(27 – 15)

Hereinafter to discriminan, analysis to know variable having an effect on (variable of predictor) at forming of health of environment housing of dab obtained also equation of model of its discriminan.

Through analytical method will be identified and tested by variable data in each housing environment:

1. Variable which is enough significant statistically as predictor variable (with f value < 0.05) so automatically process of analysis will be discontinued
2. Model of Discriminan used is
   $Y= C + B_1X_1 + B_2X_2 + B_3X_3 + B_nX_n$

Where:

- Y is the level of quality of health of housing environment at selected housing
- C is number of Constanta of equation of discriminan
- B1, B2, B3 and of Bn is the level of function value from each predictor variable X1, X2, X3, and Xn 3. Critical point is boundary value determining what is type health of housing environment including very good classification, good, rather good, unfavorable, according to Santosa and Tjiptono (2004), and and determined based on the calculation formula:

$$Z_{cu} = (Nb.Za + Na.Zb)/ (Na + Nb)$$

3.DATA ANALISYS

The health of environment housing data obtained from propagated questionnaire to 182 houses in district of North and south Cikarang.

3.1.Health of Environment Housing

Measurement of health of housing environment is meant to know how condition of quality of environment which is in

district of North and South Cikarang. Measurement of health of housing environment is based on some physical variables and non-physical. Pursuant to field survey obtained data that without differentiating self-supporting housing and foral housing explained that counted 22 boxes of sample which in district of North South Cikarang and enter in criterion health of good housing environment (Class of II) and 2 boxes of sample enter in criterion health of rather good housing environment (class of III).

Meanwhile for the district of North Cikarang that counted 20 boxes of sample, existing enters in criterion health of good environment (class 2) and 5 boxes of sample enter in criterion health of rather good housing environment (class 3).

3.2.Analysis of Discriminan

Analysis of discriminan is aimed to know some phenomenon that is how relation of level the quality of health of housing environment with characteristic variable at housing area. What kind of variable of having an effect on or becoming variable of predictor at level of quality of health of housing environment.

Analysis Discriminan of Health of Environment Housing
Health of housing environment in North and South Cikarang reside in two conditions that is health of good housing environment (class 2) with score value range between 46 - 59 and health of rather good environment (class 3) with value 30 - 45.

Pursuant to analysis of discriminan for the health of housing environment, obtained data that from 13 variable found on health of housing environment, there are 6 most differentiating variables to class health of good housing environment (class 2) with class health of rather good housing (class 3). This matter can be seen at table 1.

Variable with value of significant F 0.05 meaning there is difference between environmental class 2 with environmental class 3. Variable differentiating is the quality of air / noise, tree protector of road, green space, wide environmental road, transportation medium and Places worship. Meanwhile variable which cannot differentiate between rather good and good environmental quality is location, quality of ground water, sanitary, solid waste disposal, drainage, condition of environmental road, amount of school and vector diseases

Table 1. Significancy Score
Health Of Environment Housing

Tests of equality of group means

	Wilks' Lambda	F	df 1	df 2	Sig.
Quality air, noise	,846	10,358	1	57	,002
Tree protector of road	,911	5,591	1	57	,021
Green Space	,865	8,898	1	57	,004
Wide of road	,901	6,294	1	57	,015
Transportation facility	,922	4,830	1	57	,032
Places worship	,900	6,351	1	57	,015

Process hereinafter is to look for equation of discriminan. It is approach model of calculation of class type of health of housing environment
table 2. Tables of discriminan function of health of housing environment.

Table 2. Canonical Discriminant Function Coefficients

	Function
	1
Air quality	
Noise, Vibration	,601
Tree protector of road	,165
Green Space	,615
Wide of road	,590
Transportasi	,471
Places worship	-,662
(Constant)	-4,835

Unstandardized coefficients

Pursuant to table 2 obtained by equation of discriminan for the health of housing environment shall be as follows:

$Y = 0{,}601\ X_1 + 0.165\ X_2 + 0{,}615\ X_3 + 0{,}590\ X_4 + 0{,}471\ X_5 - 0.662\ X_6 - 4{,}835$ (equation 1)

Where:
Y = Class of health of environment that is class 2 (good) or class 3 (rather good)
X1 = Quality of air, noise
X2 = Tree Protector road
X3 = Green Space
X4 = Wide of environmental road
X5 = Medium Transportation
X6 = Places worship

Explanation of distinguishing variable between qualities of health rather good and good environmental shall be as follows:

Noise at housing with good environmental quality relative peaceful with gyration < 50 dB, and air quality tends to cleaner of cause far from motor vehicle pollution and noise. Meanwhile the noise quality at housing with rather good quality is ranging from 51-60 dB. Analogical from fisrt equation obtained positive sign (+) at X1, this matter mean that good progressively air quality of housing hence will have good progressively also the quality of health of housing environment.

Protector tree road for good category have amount of above 50% from existing housing area, meanwhile for rather good category have 25-50% protector tree at housing area. Based on first equation obtained positive sign (+) at X2, matter this means more and more protector trees road of housing environment will compare diametrical with environmental quality of housing.

Green Space meant to improve the environmental quality, comfort, freshness and avoid environmental degradation for sustainable development. Green spaces at housing are with category health of good environment between 25 - 50% from housing area. Meanwhile Green spaces at housing with rather good environment class gyrate less than 25% from housing area. Based on first equation is obtained positive sign (+) for the X3, matter this means more and more green space at one particular housing environment hence will good progressively also the quality of health of housing environment.

Transportation medium at housing with quality health of good environment, more complete, generally they use ojek (rent motorcycle), private vehicle or made available by city transport residing in at elbow main road. Meanwhile at environmental quality of rather good housing is generally only one just city transport type to especial road/downtown. Equation 1 is obtained by positive sign (+) at X4, of matter this means complete progressively transportation medium which there is at one particular housing environment, hence will be good progressively also the quality of housing environment.

Wide for environmental road at housing with good quality tend to more wide and can passed by vehicle of wheel four and road of its environment has been concreted. Wide meanwhile environmental road at housing with environmental quality rather good 2- 4 meters and cannot passed by vehicle of wheel four. Based on first equation obtained positive sign (+) at X5, matter this means wide progressively environmental road of housing environment hence will good progressively also the quality of health of housing environment.

Places worship at housing with health of good environment has amount less than two places worship. Meanwhile the amount of places worship at housing with health of rather good environment generally has more than two places worship, Based on first equation where obtained negative sign (-)at X6 (amount of places of worship) which means the more places worship at one housing environment hence environmental quality of the housing is not yet good of course. Process hereinafter is to look for critical point (cut off Point) as constrain to determine a housing type come into environmental class 2 (good environmental class) or 3 (rather good). To calculate to search score boundary value or critical point follows formula of Santosa and of Ciptono, (2004), as follows:

$$Z\,cu = (Nb.\ Za + Na.Zb) \ / \ (Na + Nb)$$

Coefficient value center group (Z) obtained from value of centroid pursuant to calculation of SPSS. Assess Centroid for the health of housing environment can be seen at table 3.

Tabel 3. Cenntroid Score of Health Environment

Functions at Group Centroids

Class of Environment	Functions
	1
2,00	,408
3,00	-1,008

Unstandardized canonical discriminant functions evaluated at group means

As for detailed calculation to look for score boundary value or critical point shall be as follows:

$$Z\,cu = (Nb.\ Za + Na.Zb) \ / \ (Na + Nb)$$

Where:

Zcu= Critical point of level health of housing environment.
Na = Amount of sample which enter environmental class category 2 (good) = 42
Nb = Amount of sample which enter environmental categories 3 (rather good) = 17
Za= Function of Centroid environmental class 2= 0,408
Zb= Function of Centroid environmental class 3=-1,008.

$$Z\,cu = (Nb.\ Za + Na.Zb) \ / \ (Na + Nb)$$
$$= (17 . 0{,}408) + (42 . -1{,}0081) \ / \ (17 + 42)$$
$$= - 0{,}6$$

Tabel 4. Critical Value Boundary (Cuttoff Point) health of housing environment

health of housing environment	Number of group member	Core Coefisien of Group (Z)	Critical value boundary (Z_{cu})
Class 2 (good)	42	0,408	- 0,6
Class 3 (rather good)	17	-1,008	

Pursuant to table 4, hence critical value boundary (cutoff point) of group of health of housing environment is - 0.6,. Matter this means an environmental type of housing tends to come into class category 2 (good) if value of Y is - 0.6. Meanwhile an environmental type of housing tends to come into class category 3 (rather good) if value of Y is - 0.6.

After conducted cross validated like at table 5, hence accuracy of estimation equation of discriminan of class 2 (good) and class 3 (rather good) shows number 67.8%. This matter means that function of discriminan can classify 67.8% from existing variables.

Table 5. Result of Classification Health of Environment Housing

Classification Results[b,c]

		Environment Class	Predicted Group Membership		Total
			2.00	3.00	
Original	Count	2,00	28	14	42
		3,00	0	17	17
	%	2,00	66,7	33,3	100.0
		3,00	0	100,0	100.0
Cross-validated[a]	Count	2,00	28	14	42
		3,00	54	12	17
	%	2,00	66,7	33,3	100.0
		3,00	29,4,0	70,6	100.0

a.Cross validation is done only for those cases in the analysis. In cross validation, each case is classified by the function derived from all cases other than that case.
b.76,3 % of original grouped cases correctly classified.
c.67,8 % of cross-validated grouped cases correctly classified

CONCLUSION

Based on the research result in District of North and South Cikarang can be concluded that variable health of housing environment is divided into two classes, those are health of good environment (class 2) and health of rather good environment (class 3). Variable differentiating between class health of environment 2 and class 3 is the quality of air/noise, reforestation/greening,, green area, wide environmental road, transportation facility and amount of Places worships. Equation of discriminan obtained is:

$$Y = 0.601\ X_1 + 0{,}165\ X_2 + 0.615\ X_3 + 0.590\ X_4 + 0.471\ X_5 - 0662\ X_6 - 4.835$$

Meanwhile boundary assess score (cutoff point) for the health of housing environment is - 0.6. This matter means that an environmental type of housing comes into environmental class 2 (good) if value of Y is the same or bigger than - 0.6. Meanwhile an environmental type of housing tends to come into class 3 (rather good) if value of Y is less than 0.6. Accuracy of classification for the health of housing environment is 67.8% where analysis of its discriminan can classify existing variable counted 67.8%.

REFERENCES

(1) Anderson, E.R, *Multivariate Data Analysis.Fourth Edition*,Ed Englewood, NJ: Prentice-Hall, 1995.
(2) Badan Perencanaan Pembangunan Daerah dan Badan Pusat Statistik,*Kabupaten Bekasi Dalam Angka.Kabupaten Bekasi, 2005*
(3) Departemen Pekerjaan Umum, *Persyaratan Kesehatan Perumahan*, Cetakan ke II, Direktorat Jenderal P2M & PL.Jakarta.
(4) Direktorat Jenderal Cipta Karya, *Pedoman Perencanaan Lingkungan Permukiman*, 1979.
(5) Menteri Perumahan dan Prasarana Wilayah, *Pedoman Teknis Pembangunan Rumah Sederhana Sehat (Rs SEHAT)*,Jakarta,2002.
(6) Sutanto, Penginderaan Jauh dan Sistem Informasi Geografis: *Perkembangan Mutakhir dan Terapannya.Seminar Nasional Penginderaan Jauh Untuk Kesehatan Pemantauan dan Pengendalian Terkait Kesehatan Lingkungan*, Yogyakarta hlm16-29, 1997
(7) Santosa, *Kajian Kualitas Lingkungan Perumahan dan Perubahan Penggunaan Lahan Pertanian Kota Yogyakarta dengan Bantuan Foto Udara*,Desertasi,Pascasarjana,Institut Pertanian Bogor, 1993.
(8) Supranto,J, *Analisis Multivariat*, PT. Rinaka Cipta,Jakarta, 2004

ISSN 114-1284

Landscape Analysis to the Informal Settlement on the Code Riverfront in Yogyakarta – Indonesia

Suparwoko

Department of Architecture, Faculty of Civil Engineering and Planning
Islamic University of Indonesia, Yogyakarta – parwoko@ftsp.uii.ac.id
Tlp. 0274-881621 dan Mobile. 0813.9226.0855

ABSTRACT

On the rapid process of urbanization in developing countries it is not surprising that many spots in urban areas could be found informal settlements particularly squatters on riverbank in most Indonesian cities, such as Jakarta, Surabaya, Palembang, Semarang, Yogyakarta, etc. The informal settlement is any residential activities in any areas that are conducted without formality aspect relating to the government, such as tax, regulation, location permit, license, etc. This paper will analyze the landscape of the informal settlement on the Code Riverbank in Yogyakarta to respond the urban heat island issue. Landscape is characterized by a broad area of common unique visual character based on physically landform, vegetation, waterfront, and land use pattern. Urban landscapes with a high content of vegetation elements in particular, have thus potentials to perform a variety of social functions and as such to establish or regain a role of healthy, desirable and restorative urban landscapes. However, on the Code Riverbank in the city of Yogyakarta, there are many informal settlements that dominate the land use pattern of the urban riverfront. The physical component of the high density of the informal housing represents a variety of social functions of urban land uses. The high density of the informal settlement on the Code riverfront has avoided the ecological function of the Code watershed. The high density of the informal housing is able to influence the urban temperature in Yogyakarta that support the issue of urban heat island issue as a part of global warming phenomena. "Urban Heat Island" (UHI) refers to the tendency for a city to remain hotter than its surroundings. The casual factors of the UHI are mainly building density, more paving, and less vegetation. The research suggests that the informal housing density in urban riverfront has visually represented a low content of natural landscape, particularly landform, vegetation and water and this visual has reduced the uniqueness of the natural potential of the Code Riverfront. This phenomenon has a contribution to the higher level of urban temperature as an aspect of the UHI effect. Another finding is that the proposed balance landscape development between natural and man-made construction on the river watershed of the Code Riverfront will support the cooler urban landscape.

Key Words: *Urban informal settlement, Code Riverfront*

1. INTRODUCTION

Landscape study has been practiced in the earliest time, when human pointed out where is the best location for agricultural field, trading center, or even residential uses. Historically, it was found that urban settlements or other development centers located close water resources, such as lakes, beaches or rivers. Ecologically, the river should be treated as a main water resource and played as a natural drainage system on continuous water cycle. Due to the population growth, urbanization, and technology inventions in many sectors including constructions, urban population need more housing, paved streets, and other built area. This growth has reduced vegetation and increased building density in urban areas. One of the basic urbanization problems in developing countries is illegal settlement. A slum is a house especially built on public or private land illegally. Due to the economic and social conditions, taking down of these slums owned by low income persons is very difficult. [1] In Indonesia, this phenomenon has been the way how people try to occupy more land that people can found in urban areas, including riverbanks that referred to be watershed and not permitted for construction.

The development created by current urbanism in Indonesian cities caused serious changes to the quality of the riverfront landscape. River Code, one of three main rivers in the city of Yogyakarta has been degraded with loosing its function as a water resource and watershed. This river has many houses occupy land on the riverbank and most buildings are informal settlements. Therefore, the quality of the Code riverfront landscape has formed a slum area that has more illegal housing constructions and not much vegetation. Any urban areas with many building construction and with little vegetation will be hotter compared with its surrounding areas.

2. ISSUE AND OBJECTIVE

The current development on the Code riverside in the city of Yogyakarta does not concern with ecological development. The Ecological development is respecting to the value of river as natural drainage system and as protected area on riverside. Intensive development on the riverside has created very high density of people and building houses, mostly informal settlements. This development pattern has reduced green areas of vegetation increased pavement along the Code riverfront in the city of Yogyakarta. This development phenomenon will support the issue of Urban Heat Island where the city of Yogyakarta is hotter compare with surrounding areas, particularly rural areas. Therefore, Yogyakarta needs some alternative of development model constructing any human settlements along the river, particularly on the Code River in Yogyakarta.

The objective of this paper is to (1) analysis the current development along the Code riverside by using a river as natural drainage system, (2) analysis the current development of informal settlements (on the Code riverfront in the Yogyakarta municipalities) relating to the casual factors of the urban heat island issue, (3) suggests a development model of informal settlements on the Code riverside that is likely able to reduce the problems of Urban Heat Island in urban areas. The method of analysis is using the qualitative approach. The analysis model consists of three concurrent flows of activities including data reduction, data display and conclusion drawing or verification. [2]

3. RIVERFRONT LANDSCAPE

Natural conditions of river landscape providing a proper drainage system and well-continuous water cycle. When rainfall occurs, the water is absorbed by vegetation that covering the soil surface (for itself and groundwater) and the others gently returned to surface water such as river or lake. By the river stream, the water journey continued to the sea, which a great evaporation take place, form a clouds, and thus become a rainfall again.

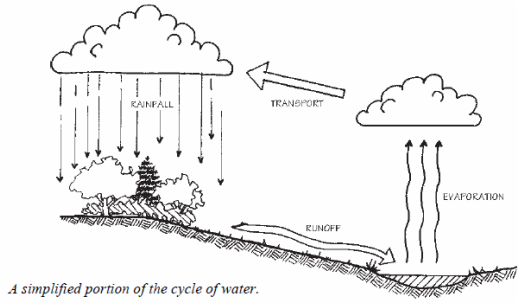

Figure 1. Natural Water Cycle

By the change of human development, the contours are smoothed and the landscape is comprised of hardened surfaces (rooftops, paved streets, etc.). These changes resulting in higher run off velocity that increased erosive potential. Hence, at a high concentration of rainfall, it can be resulting as floods or landslide [3]

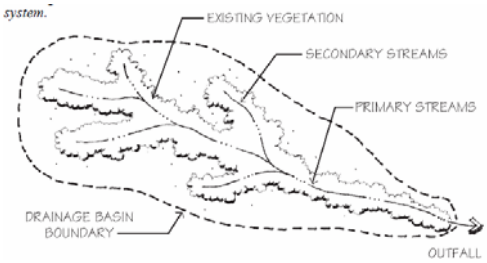

Figure 2. River as natural drainage system

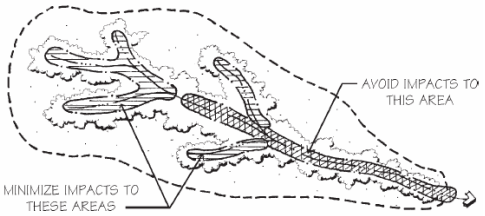

Figure 3. Areas must be protected along the riverside

The riverfront natural landscape gives the basic concept for analyzing the current Code riverside development, particularly the existence of informal settlements, based on the value of river as water cycle as natural drainage system, and to protected river watershed.

4. URBAN HEAT ISLANDS EFFECT

Urban Heat Island (UHI) effects are created when natural vegetation is replaced by heat-absorbing surfaces such as building roofs and walls, parking lots, and streets. Through the implementation of measures designed to mitigate the UHI, urban people can decrease their demand for energy and effectively "cooler" the urban landscape. [4] [5] The analysis of the UHI issues will focus on the natural aspect of environment particularly vegetation, that is crucial component of the cooler urban landscape and it is able to reduce the demand of cooling energy when it is placed on the proper area in the urban landscape. Urbanization that followed by rapid development that make less vegetation in order to be replaced by concrete materials was determined as significant factors that causing urban heat island.

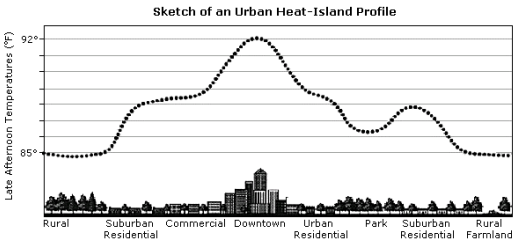

Figure 4. Urban Heat Island Profile

Heat islands develop when a large fraction of the natural land cover in an area is replaced by built surfaces (building and paving) that trap incoming
solar radiation during the day and then re-radiate it at night [6] [7]. This means that building and paving on urban areas replace land vegetated land cover will increase heat on the area.

The mitigation measures to reduce the heat island effect provide a link to local as well as global issues. The economic cost of implementation strategies is not only by the cooling energy savings, but also by the reduction in greenhouse gas emissions, esthetic value of urban forestry, and the increased quality of human health [8]. Therefore, the UHI issue recommends that urban areas are (1) to decrease building density and provide more open space for public, (2) to decrease paved land surface, and (3) to increase vegetation. This suggestion is relevant to the case study of the Code riverside that has been a very dens residential building with little vegetation.

5. INFORMAL SETTLEMENTS and URBANIZATION

The main reason of the urbanization movement, where rural people move to urban areas, is the insured job, high salary, and the other facilities such as education, health, culture etc. Primary objectives of the rural people migrating to urban areas is having a guaranteed and permanent job and then having a shelter. Nevertheless, if the financial inefficiencies of the local authorities, the level and quality of the services have been low, especially the lack of convenient residential areas has led to construction of informal settlements [1].

Informal settlements are usually a phenomenon which mostly occurs in developing and newly industrializing countries [9]. The UN [10] defines **informal settlements** as:
„*Areas where groups of housing units have been constructed on land that the occupants have no legal claim to, or occupy illegally; 2. unplanned settlements and areas where housing is not in compliance with current planning and building regulations (unauthorized housing).*“

Based on its conceptual categorization, informal settlements were classified into three types, (1) Unauthorized land development or informal subdivision, (2) squatter settlements, and (3) informal rental housing [11]. Those concept reflected most of informal settlements concept that marked it as visual pollution and social economic problem. The other concepts of informal settlements rely on the paradigms that informal settlements is a kind of solution for poor and marginal urban people to live in urban areas.

Table 1. Population Density and Flat Housing Need [12]

Population Density and Flat Housing Need			
Low	Medium	High	Very High
<150 jiwa/ha	150 - 200 jiwa/ha	200 - 400 jiwa/ha	>400 jiwa/ha
As ALTERNATIVE for special area	As RECOMMENDATION for urban central activities and special are	As REQUIREMENT for urban revitalization	As REQUIREMENT for urban revitalization

Source: Badan Stadarisasi Nasional, 2004

Informal settlements could be viewed as great intelligence in the use of resources, in shifting single use to mixed use, from low density to high density, and from absence of infrastructure to full infrastructure [13]. Therefore, the informal settlement on the Code riverfront is crucial to be analyzed by measuring the landscape based on the main causal factors of the UHI issue which are (1) building density, (2) vegetation, and (3) paving.

Table 1 will be used to analyzing the population density on the Code Informal Settlement and the need for flat housing development.

6. INFORMAL SETTLEMENT ON THE CODE RIVERFRONT AS A CASE STUDY AREA

Based upon regional administration, Code river is located in three local administrations which are the Sleman Districts, the Bantul District, and the Yogyakarta Municipality. The upper stream is drawn from north side of the mount Merapi until its lower downstream in the south that relate to a cross section with Opak River in the Bantul Ditrict. The middle downstreen of the Code River is situated in the Yogyakarta district where the riverside of Code is fully occupied by informal settlements [14]. Based on the Yogyakarta Statistic Office in 2005, from 151,420 households living in Yogyakarta Municipality, 2.14% of them lived next to riverside including in Code riverside called Code community. Code community consisted of 71% native people and 29% migrants. Most of them (53%) have been living there for more than 25 years. [15].

The expansion of Code riverside by squatters was determined by two reasons. The first one was the independent status of land, encouraging people to squatter. While the second reason for Code riverside expansion was represented cultural, economic, and social demands [16]. Based on the survey, it was found that the reason in choosing Code riverbanks as their settlements were compiled and classified into three main reasons, as an economic motivation (33%), for comfort living (40%), and as a forced movement option because they didn't have any alternative place for living (27%).

With high density and high population indeed, waste become an ecological problem. Littering it away to the river was an easy and cheap way for Code community. By recent years, it became a more serious problem causing degradation of river quality and higher risk of flood. From the other Code's study, it was founded that an area with high density would also raise the risk for groundwater pollution [17]. It was reported by Harian Jogja, 26 December 2007 that Code is the most polluted river among three main rivers in the Yogyakarta Province.

The two previous paragraphs proofs:
(1) The Code riverside is not treated a natural drainage as suggested by the North Carolina Department of Environment and Natural Resources Division of Water Quality
(2) The Code riverside is not protected to avoid any intensive development and make the Code River as the most polluted river in Yogyakarta.

According to government riverside policy that laid down by Indonesian Ministry of Civil Works in 1993, minimum space required between a river and built up area is 15 meters. However, by considering that the existing development growth on the Code watershed has been a high density informal settlement, the official government of the Yogyakarta Municipality has determined 3 meters space between river and built area on the Code riverside. This government policy does not concern with the value that rivers to be protected as a natural drainage system as suggested by the North Carolina Department of Environment and Natural Resources Division of Water Quality. This also suggests that the Yogyakarta municipality is not aware with the long term issue if the river conservation.

The term of informal could be determined as anything conducted without formality or ceremony [18]. Using this as analogy, informal settlements then referred as settlements without any supported formality aspects relating to the government. Informal settlement were often remarked with its illegal status of land ownership. Reported on this definition, most of dwellings settled on Code riverbanks were marked as an illegal or informal settlements. From data survey collected by the direct observation, it was founded that less than 50% of settlements have legal documents. Only 38% of settlements in Code riverbank already have the SHM (Certificate of Land Ownership) and 9% only have HGB (Right to Use the Property). Most of them (40%) have to pay for living in those areas by renting lands or rooms. The remaining precentage of Code community (11%) still lived in "Magersari"[1] landstatus. In term of rights for build property, 61% of them don't have IMB (Rights to Construct Building) that means, 61% of building settlements on Code riverbanks are illegal. Hence, the survey reported that 47% of people lived in Code riverbanks get their land as an inheritance land.

RT 69/RW 19 Dusun Karang Anyar Kelurahan Bronto Kusuman was recorded density value for 481 people/hectares, made it classified as very high density area. Within this area, more than 60% of settlements were too small to be noted as dwellings. Most houses on the Code riverbank have a mixed-use, commonly for economic and residential functions. Visually, the main characteristics of informal settlements in Code riverside were high density, small size houses, lack of ventilation, and narrow streets [19]. In the recent observation on April 2009, the population density in the kampung Jogoyudan was 480 persons/hectare. The research found that:
(1) Based on the Indonesian Standard of Urban Settlement (SNI 03-1733-2004) the population density in the Kampung Jogokaryan can be categorized as very high density and this will be required for revitalizing the Code settlement to flat housing.
(2) With the high density of population, the Code riverside also has a high density of building houses mostly one story building. This construction building density is contributing to the urban heat island. This fact also suggest that lowering building density and increasing more space for public activities more vegetation could reduce urban heat island problem in Yogyakarta city.
(3) The Code informal settlement is very high density of people and building creates the area lack of vegetation. This fact also supports to increase the urban heat of Yogyakarta (See Figure 5).

A crucial concept to transform horizontal housing to be vertical one can be adopted from [1] (See Figure 6). The concept suggests that the government should develop a new law put into practice to formalize illegal or informal settlements.

[1] Yogyakarta Province has a special policy referred to its special status that acknowledge Sultan's land for people to live in. People that lived in Sultan's Land called "magersari". They don't have any payment for live or settled on the Sultan land, form as Sultan's pity for his people in the previous time. The status of "magersari" is still debated by local government and national government.

Figure 5. Code River in Yogyakarta

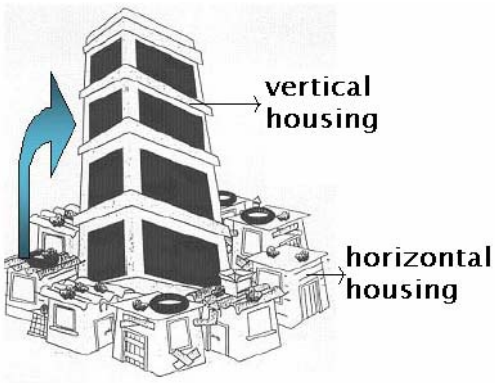

Figure 6. Transforming Horizontal to Vertical Housing

The urgent recommendations are as follows:

a. Slums or informal settlements are constructed in a low-qualified manner , not meet with river conservation, and support urban heat island effect. Therefore, the transformation of the informal settlement to horizontal building should be provided to support river conservation and reduce the UHI problems.
b. Instead of leaving settlement right to slum owner completely, this right should be shared with public authorities. In other words, slum or informal settlement owners should not be given all development right on building plot; instead, they should only be given a single flat.
c. Building contractors, called as land developer, which works according to the general rule of 'giving flats to land owners for their landownership', the remaining flat dwelling can be rented of sale with a long scheme of payments to other migrants who have no land or building certificate on the Code riverside area.

The scheme of transforming horizontal to vertical housing is appropriate with the government policy plan of "**one million towers**" for revitalizing urban slums and fulfilling the current and future urban housing need, especially for urban community with the low income segment.

7. CONCLUSIONS

Urbanization in Yogyakarta creates informal settlements on the riverside. The growth of informal settlement in Yogyakarta is due to lack of balance development between urban and rural improvement.

The informal settlements on the riverside perform a high density of population and buildings, and reduce open space with rich of vegetation in Yogyakarta urban riverfront, such as the Code river. The Code River with informal settlement proofs that imbalance landscape (between natural and man made construction) has occurred in Yogyakarta. This phenomenon has supported the problem of urban heat island in Yogyakarta urban area. The government policy on the Code riverside so far does not improve significantly the ecological landscape quality.

To mitigate the Urban Heat Island Effect in Yogyakarta, the local community, investor, and the government are to work together in transforming horizontal to vertical housing construction from now end then. This transformation suggests: (1) The Code riverside is to be protected from the intensive development, (2) vertical housing on the Code Riverside will give more open space and more vegetation to be planted., (3) paving can be used if necessary and porous paving is better construction.
By increasing the transformation of horizontal informal settlement to formal vertical housing, open space, public, and vegetation in urban areas will increase in urban areas, including the landscape on the riverside. This action will make the urban environment cooler and be able to mitigate the UHI problem.

REFERENCES:

[1] Bayram UZUN and Mehmet CETE, *A Model for Solving Informal Settlement Issues in Developing Countries*, FIG Working Week 2004, Athens, Greece, May 22-27, 2004
[2] MB. Miles & AM. Huberman, *Qualitative Data Analysis* (2nd edition), Thousand Oaks, CA: Sage Publications, 1994.
[3] North Carolina Department of Environment and Natural Resources Division of Water Quality, 1998, *Storm Water Management: Site Planning, North Carolina Stormwater Site Planning Guidance Manual,* State of North Carolina: North Carolina Department of Environment and Natural Resources Division, 1998
[4] V. Gorsevski,, H. Taha, , D. Quattrochi, and J. Luvall, *Air Pollution Prevention Through Urban Heat Island Mitigation*: *An Update on the Urban Heat Island Pilot Project*, 1998 accessed

on February 8, 2009 at http://wwwghcc.msfc.nasa.gov/uhipp/epa_doc.pdf

[5] Y. Yamamoto, *Measures to Mitigate Urban Heat Islands in Japan*, article on Global Change and Sustainable Development, Vol. 1, No. 2, July 2007

[6] D. Quattrochi, J. Luvall, D. Rickman, M. Estes, C. Laymon, and B.Howell, *A decision support information system for urban landscape management using thermal infrared data. Photogrammetric Engineering and Remote Sensing*. 66 (10), p.1195-1207. 2000

[7] T.R.Oke, *The energetic basis of urban heat island. Journal of the Royal Meteorological Society*. 108 (455), 1-24, 1982

[8] WD. Solecki, C. Rosenzweig, G. Pope, M. Chopping, R. Goldberg, and A. Polissar A, *Urban Heat Island and Climate Change: An Assessment of Interacting and Possible Adaptations in the Camden, New Jersey Region*, Research project summary on Environmental Assessment and Risk Analysis Element STATE OF NEW JERSEY*:* Division of Science, Research & Technology, 2004

[9]. Hofmann, J. Strobl, T. Blaschke, and H. Kux, *DETECTING INFORMAL SETTLEMENTS FROM QUICKBIRD DATA IN RIO DE JANEIRO USING AN OBJECT BASED APPROACH*, 2006 accessed on June 15, 2009 from http://www.commission4.isprs.org/obia06/Papers/05_Automated%20classification%20Urban/OBIA2006_Hofmann_et_al.pdf

[10] United Nation Statistics Division, *Environment Glossary, Informal Settlements*, Copyright © United Nations, 2006 accessed on June 20, 2009 http://unstats.un.org/unsd/environmentgl/gesform.asp?getitem=665

[11] Alain Durand-Lasserve, *MARKET-DRIVEN EVICTION PROCESSES IN DEVELOPING COUNTRY CITIES: THE CASES OF KIGALI IN RWANDA AND PHNOM PENH IN CAMBODIA*, Global Urban Development Magazine, Volume 3, Issue 1, November 2007

[12] Badan Standarisasi Nasional, *Tata cara perencanaan lingkungan perumahan di perkotaan*; SNI 03-1733-2004, Jakarta: Badan Standarisasi Nasiona,

[13] 2004 Srilestari Niniek Rosalia, *Squatter Settlement? Vernacular Or Spontaneous Architecture? Case Study: Squatter Settlement In Malang And In Sumenep, East Java*, published on Dimensi Teknik Arsitektur Vol. 33, No. 1, Desember 2005: 125 – 130

[14] Suparwoko, 2009, Revitalisasi Kawasan Sungai Code Yogyakarta: Konservasi Alam dan Pengembangan Pariwisata, paper delivered on the Workshop on REVITALISASI KAWASAN SUNGAI CODE" June 1, 2009 Islamic University of Indonesia, Jl. Cik Di Tiri 1 Yogyakarta

[15] Peduli Sampah, *Pengelolaan sampah di daerah bantaran sungai Kali Code* Minggu, 03-Juni-2007, accessed on May 19, 2009 from http://www.pedulisampah.org/mod.php?mod=publisher&op=viewarticle&artid=19

[16] Arif Budi Solihah, *'Typology and Morphology Study of Waterfront Housing Characters; Code River Housing Case Study, Research Report* High Education General Directorate, National Education Department, Unpublished, No. 199/P4T/DPPM/DM.SKW/SOSAg/III/2004,

[17] F. Yorhanita, (2001). *Zonasi Potensi Pencemaran Air Tanah Pada Teras Sungai Code Yogyakarta*, article on Manusia dan Lingkungan Journal 2001, Vol. VIII

[18] M. Webster, *Merriam Webster Dictionary & Thesaurus*, Bulington: Franklin Electronic Publisher, Inc., 1999

[19] A. Chrysantina, H. Kusnanto, A. Fuad, *Analisis Spasial dan Temporal Kasus Tuberkulosis di Kota Yogya, Juli - Desember 2004, accessed on March 23, 2009, from* http://anis.fuad.googlepages.com/analisisspasialTBkotayogya.pdf.

ISSN 114-1284

Rebalancing Our Perspectives in Looking at and Interpreting Urban Spatiality through Thirdspace

Yulia Nurliani Lukito

Department of Architecture Faculty of Engineering
University of Indonesia, Depok 16424
Tel : (021) 7863512. Fax : (021) 7863514
E-mail : yulianurliani@yahoo.com

ABSTRACT

This paper aims to investigate the idea of cityspace through third space, or as fully lived space, as an alternative in understanding a city. My argument is modernist visions of a city like Howard;s Garden City, Frank Lloyd Wright's Broadacre City, and Le Corbusier's Contemporary City have same fundamental principles such as segregation of use, dominance of private over public space, and focus on auto. The next generation learns that these utopias not only had sterile and suburban character but also disintegrated the street as the community's habitable common ground. According to Edward Soja, there is an alternative approach to a city that use the production of cityspace in its combined expression as contextualizing form and process By understanding a city as both form and process, or as third space, hopefully I can open up new understanding of a city by rebalancing our perspective in understanding complexity of our social, historical, and spatial dimensions of a city.

Keywords
modernist city, urban spatiality , thirdspace

1. INTRODUCTION

Our cities and its communities are at a critical point in terms of they will grow and deal with increasingly urgent environmental and social concerns. Ever since the modern time, new theories of cities emerged and stressed on the importance of technology and industry in our living space. They all have the same basic principles of segregation of use, focus on auto, and dominance of private over public space. Since then, our cities continue growing auto-dependent city, sprawls, and facilitating the loss of natural landscapes.

At the beginning, what modernist planners and architects proposed for our cities seems to be environmentally friendly. Ebenezer Howard defined a vision of small towns surrounded by a greenbelt. Le Corbusier developed urban and suburban areas for living and leisure all in blocks and surrounded by green areas. Frank Lloyd Wright proposed decentralization combining urban and suburban areas in green environment.

There are some critiques addressed to the ideas of modern cities proposed by architects and planners above. Even though all planners proposed the same idea about the importance of green areas in the city, all of the cities above has awareness that automobile will be the center for our lives. The cities have sterile character, disintegration between street as the community's habitable common ground, and lack of real living experience considerations. As a result, there is lack of fundamental qualities of real cities such as defined public space, pedestrian scale, and integrated diversity of use and population (Caltharpe, 1993). Sprawls and suburbs are also two problems that modern cities have to deal with.

Still there is a hope that our cities will be compact and green and become places that provide good social, cultural and recreational activities, and a feeling of community. The last idea of cities concerns ecological sustainability connects human settlement patterns to ecological conditions. Moreover, a new perspective in understanding our cities also should combines expression as contextualizing form and process.

In relation to rebalancing our perspectives in understanding cities, I want to further discuss some classic theories of city, including how they become the basic of modern cities and comparison between these theories. I then want to discuss how the next generation thinks these

utopias disintegrate the street as the community's habitable common ground. There should be an alternative vision of place and community that not only emphasizes physical form of a city but also unifies concerns about the environment and the quality of life. Here I want to investigate an alternative idea of understanding a city through the ecology of place, and also understanding a city through thirdspace or as fully lived space (Soja, 2000)[1]. Hopefully, there is an alternative concept of sustainable places that suggest a better model for planning our cities in the future that unites both social and environmental goals..

2. MODERNIST IDEAS OF A CITY

Ebenezer Howard envisaged his Garden City as a tightly organized urban center for 30,000 inhabitants, surrounded by a perpetual "green belt" of farms and parks[2]. In the city there would be both quiet residential neighborhoods and facilities for a full range of commercial, industrial and cultural activities. Howard thought the great cities of his time decreasing to insignificance as their people desert them for a new way of life in a decentralized society. The urban population would be distributed among hundreds of Garden Cities whose small scale and diversity of functions represent a world in which the little man has finally won out. No longer would a single metropolis control a whole region. The agricultural belt prevents the town from sprawling out into the countryside and make sure that the citizens enjoy both a compact urban center and ample open countryside.

There is a Central Park located at the center of the town, which gives recreation grounds within very easy access of all the people. This park is surrounded by a glassed-in arcade where manufactured goods are exposed for sale. Since Howard wanted to balance individualism and central organization, he rejected the idea of cooperative department stores. He proposed many small shops that offer only one for each category of goods.

There are two kinds of centers in the Garden City namely the neighborhood centers and the civic center. The neighborhood centers are slices in circular pie with the most substantial homes would be arranged in crescents bordering Grand Avenue. In the middle of Grand Avenue is the most important neighborhood institutions. Howard put the factories at the periphery of the city, adjacent to the circular railroad that surrounds the town and connects it to the main line. The factories would be close to the homes.

Howard's emphasis on the importance of a permanent girdle of open and agricultural land around the town soon became part of British planning doctrine that eventually developed almost into dogma. Its most impressive application was the plan for Greater London in 1944 and--following passage of the New Towns Act of 1946--the creation of a ring of new towns beyond the London Greenbelt. On practical grounds at least as strong a case could be made for an urban configuration based on wedges of open space thrusting inward and confining development to the intervening corridors.

Howard's verbal pictures and accompanying diagrams show his own beliefs about how a model garden city should be laid out. The ring and radial pattern of his imaginary Garden City was a plan that many other writers of the time also favored, because of its perceived superiority from both engineering and architectural viewpoints.

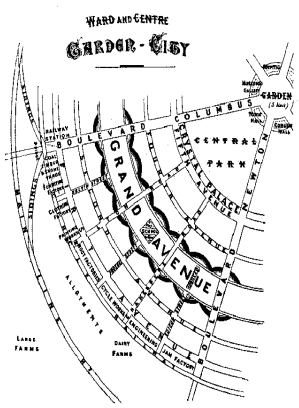

Figure 1: Howard's Garden City, Sources www.library.cornell.eduReps/DOC/Howard.html

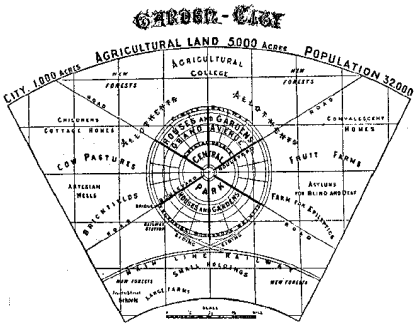

Figure 2: Howard's Garden City, Sources www.library.cornell.edu/Reps/DOC/Howard.html

There are six excellent boulevards, each 120 feet wide. The boulevards cross over the city from centre to circumference and divide the city into six equal parts or wards. In the centre is a circular space containing about five and a half acres, laid out as a beautiful and well- watered garden. Surrounding this garden, each standing in its own ample grounds, are the larger public buildings--town hall, principal concert and lecture hall, theatre, library, museum, picture-gallery, and hospital.

In *the City of Tomorrow and Its Planning* Le Corbusier stated that a city should consist of skyscrapers for commercial use surrounded by parks. In the center there would be a train station, the "hub" of the city, and three-story buildings with "luxury shops, restaurants and cafés." Surrounding the center there would be a belt of residential buildings, with small communities offering domestic services. Le Corbusier use zoning to accommodate "the exodus of city dwellers" from the centers of great cities, and the "replacement by business." His vision of a modern city is the idea that the center should be for business and some public services surrounded by two belts of residential areas – one with "blocks of dwellings on the 'cellular' system", and one outer garden city.

In the Contemporary City all dwellings are mass-produced, but they are not all alike. Every building's location depends upon one's position in the hierarchy of production and administration. The elite houses were in the center while the workers houses were at the periphery. Le Corbusier wanted to create a comprehensive environment in which man, nature, and the machine would be reunited. For Le Corbusier, order is expressed by pure forms, which is expressed in a perfectly symmetrical grid of streets. He designed an richly coordinated system of transportation; highways, even bicycle paths and pedestrian walks. The center of the city is a multilevel interchange for the whole system that serves people in motion. Surrounding the central terminal are twenty-four glass-and-steel skyscraper, each sixty stories high. The skyscraper allowed Le Corbusier to unite the apparent opposites of urban design: density and open space. The skyscrapers free the ground for greenery; they also are a fitting symbol for the grandeur of the functions they house.

The Contemporary City is a city of administration. The great towers would be the headquarters of the intellect as well as industry. To provide an appropriate setting for the public gatherings of the elite, Le Corbusier made the administrative center also the cultural and entertainment center. The proletarians in their satellite cities have none of the special privileges of the elite.

The Contemporary City grew out of this new conception of capitalist authority and a pseudo-appreciation for workers' individual freedoms. The plan shows clearance of the historic cityscape and rebuilding utilizing modern methods of production. The apartment was pre-fabricated with *les unites*, were available for everyone at the center of "urban" life based upon the needs of each particular family. The business center was located to the north of *les unites* and consisted of glass & steel skyscrapers every 400 meters. The skyscrapers were to provide office space for 3,200 workers per building. Sunlight and circulating air were also part of the design. The building would be placed upon pilotis, five meters off the ground, so that more land could be given over to nature. Setback from other unites would be achieved by *les redents*, patterns that Corbusier created to lessen the effect of uniformity.

Figure 3: Le Corbusier's Contemporary City, source http://tesugen.com/archives/04/06/corbus-city-of-tomorrow

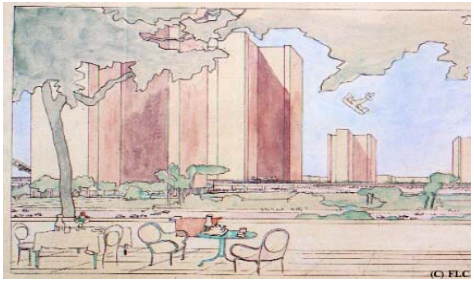

Figure 4: Le Corbusier's Contemporary City, source http://tesugen.com/archives/04/06/corbus-city-of-tomorrow

Inside *les unites* were the vertical streets, i.e. the elevators, and the pedestrian interior streets that connected one building to another. Corridor streets were destroyed. Automobile traffic was also to circulate on pilotis supported roadways

five meters above the earth. The entire ground was given to pedestrians, with pathways running in orthogonal and diagonal projections. Other transportation modes, like subways and trucks, had their own roadways separate from automobiles.

Each apartment block was equipped with supporting section in the basement, like catering and laundry. This would enable the individual to think, or utilize the play and sports grounds which covered much of the city's land. Children were to be dropped off at *les unites'* day care center. Transportation systems were also made to save the individual time

Many scholars thought Le Corbusier's vision of modern city was a compact and high-tech city. However, they have failed to consider individual freedoms. Certainly, Corbusier provided leisure activities that he enjoyed. There can be no extravagance or chaotic excess. Individuals were not allowed to have a voice in the governance of their lives; they are able to behave, but not to act. Additionally, there is no room in the Le Corbusier's City for individuals to act non-rationally, while in reality, it is improbable that humanity will ever behave in so-called rational ways. Thus, Corbusier's vision suffers from an naive conception of human nature.

Le Corbusier's idea of authority is both patriarchal and bureaucratic, what Richard Sennett refers to as the authority of false love and the authority of no love (Sennett 1980). Corbusier argued, following Plato, that universal truth, beauty, and goodness could be ascertained by those who had divorced themselves from matter (human bodies). *Les grand inities* could then prescribe a plan grounded in objective calculations and scientific facts. There could be no debate, i.e. no politics regarding the precepts of the plan. Humanity was to accept this discipline as a necessary, objective ordering of reality by a doting, paternalistic authority. Corbusier put it like this, "Authority must step in, patriarchal authority, the authority of a father concerned for his children," (Le Corbusier 1967: 152).

Le Corbusier saw himself as the one could step outside of history and uncover the good society through the glory of rationalism and established orthogonal order. This is the essence of utopian thought, the reliance on scientific fact and removal of memory. Any other thing is disorder and must be brought into line. Le Corbusier's designs for the city are grounded in the desire to escape the earth. The vertical street, the skyscraper, the death of the street, the destruction of the sensuality of city life are all proof positive that he was terrified of the earth and others. In the Contemporary City, Corbusier describes the view from the skyscraper as not of this earth; it is placid, serene, and harmonious.

Broadacre City was an urban or suburban development concept proposed by Frank Lloyd Wright late in his life. He presented the idea in his article *The Disappearing City* in 1932. A few years later he unveiled a very detailed model representing an hypothetical 10 km² community. The model was made by the student interns who worked for him at Taliesin.

Broadacre City was the antithesis of a city and the apotheosis of the newly born suburbia, shaped through Wright's particular vision. It was both a planning statement and a socio-political scheme by which each U.S. family would be given a one acre (4,000 m²) plot of land from the federal lands reserves, and a Wright-conceived community would be built anew from this. There is a train station, few office and apartment buildings in Broadacre City, but the apartment dwellers are expected to be a small minority. All important transport is done by automobile and the pedestrian can exist safely only within the confines of the one acre plots where most of the population dwells. Wright's emphasis on the completely detached house standing on its owner's ground derived from his belief in a society where the individual would enjoy the independence that comes from self-sufficiency.

Wright intended Broadacre City to be the place where this contradiction would be overcome. He wanted a city without spiritual or material walls, which would nonetheless be a secure community. In his ideal city, Wright made the family the central institution of his new society with the family as the key to the stability of the whole community. Broadacre City is thus as much a prevention of as it is a solution to its central problem: how can freedom and democracy be preserved in an industrial society?

Wright assumed that modern man had a car. If properly planned, cities could spread over the countryside and still not lose their cohesion or efficiency. The diffusion of population would generate conditions for the universal ownership of land. The world of concentrated wealth and power would be replaced by one in which the means of production would be widely held. The open plan of Broadacre City was a authentic departure from the neat concentric circles of the Garden City. Wright's idea is there must no longer be a physical separation between urban and rural areas.

All buildings are in the midst of farmland and forest with transportation system unites the citizens with many points of community exchange that provide the urban experience.

The merging of town and country, physical and mental labor, work and leisure – these were all part of Wright's effort to reduce the fragmentation of modern life from Broadacre City. Factories and other economic institutions were thus spread explicitly as “support units” for the family. Wright had hoped that decentralization would preserve the social value he prized most highly – individuality. The houses he designed ranged in size from “one-car houses” to “five-car houses.”

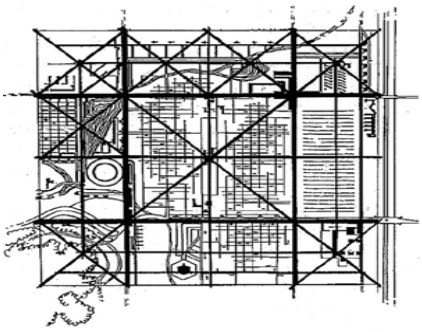

Figure 5: Wright’s Broadacre City, source: www.fba.fh-darmstadt.de

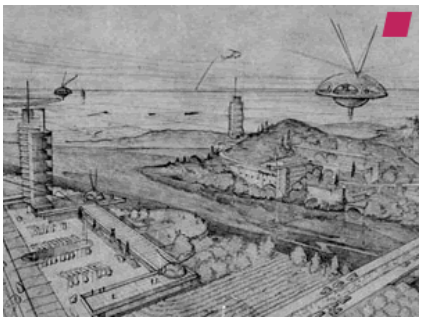

Figure 6: Wright’s Broadacre City, source: www.fba.fh-darmstadt.de

3. DISCUSSIONS: CRITIQUES OF MODERN CITIES

Howard, Wright and Le Corbusier based their ideas on the technological innovations that inspired their age, the express train, the automobile, the telephone and radio, and the skyscraper [3]. Howard realized that the railroad system that had contributed to the growth of the great cities could serve the planned decentralization of society equally well. Wright understood that the personal automobile and an elaborate network of rads could create the conditions for an even more radical decentralization. Le Corbusier looked to technology to promote an opposite trend. He made use of the skyscraper as a kind of vertical street which would permit intensive urban densities while eliminating the “soulless streets” of the old city.

Wright's and Le Corbusier's ideal cities confront each other. Both believe in industrialization had produced the conditions for a new era . This era would commence with the replacement of existing cities by new forms of community suited to the new age. Wright wanted to decentralize society, replacing existing cities with a continuous union of town and country where the individual and his family could flourish. Both recognized the city as the natural home of centralized power. Le Corbusier placed a corresponding faith in organization, and predicted a very different fate form modern society. For him industrialization meant great cities where large bureaucracies could coordinate production. Le Corbusier had the elite live in luxurious high-rise apartments close to the center while their subordinates were relegated to satellite cities at the outskirts. For Le Corbusier, the future would be a Radiant City of glass and steel skyscrapers set in parks. Both Radiant City and Broadacre city are an attempt to revitalize work and reconcile man with nature. Howard's deepest value was cooperation and Wright's indiviudalism, Le Corbusier's aim was a society in which both cooperation and individualism could find simultaneous expression.

In *The Death and Life of Great American Cities* (1961), Jacobs rejects Le Corbusier's concept of urban surgery, for it means imposing his one plan over everyone else's [4]. She argues that Le Corbusier’s neatly arranged skyscrapers in the park are a terrible oversimplification of urban order. Their rigid division of functions makes a true diversity impossible, their inhuman scale and vast empty spaces destroy the close-knit vitality of an attractive city. Above all, Jacobs believes that the planner must no longer try, as Howard, Wright, and Le Corbusier once tried, to define the central goals of his society and offer a unified plan for reaching them. The common good is served through maximizing the individual's opportunity to pursue his own ends. For Jacobs, the cities are already built. They can be renovated but never transformed.

Lewis Mumford;s phrase “Yesterday's City of Tomorrow” for all three ideal cities means the very concept of the ideal city appears to belong to the past [5]. The plans of Howard, Wright, and Le Corbusier suppose that conflict will eventually be overcome in a harmonious industrial society; that human understanding can resolve the problems of society. Sennett thinks the planners' search for harmony is not only bad urban policy but even worse psychology [6]. Sennett doubts that municipal authorities in a dense, uncontrollable human settlement might nevertheless try to force their own version of order. He wants to promote direct social life that people would be required to deal with people different from themselves and to experience in their own lives the movement from conflict to agreement.

A sustainable city is a city designed with consideration of environmental impact, inhabited by people dedicated to minimisation of required inputs of energy, water and food, and waste output of pollution. A sustainable city can feed itself with minimal reliance on the surrounding countryside, and power itself with renewable sources of energy. The sustainable city is specifically non-utopian. The authority of this city is one of quintessence in a place and space. Knowledge does not exist outside time and space. It is an authority of political education, where the knower and the known become one. Diversity is respected, and nature is not an object of gratification. Howard, Wright, and Le Corbusier see nature as fulfilling unlimited human needs and wants. Nature becomes "other" in their plans. A sustainable city would take the notion of inter-connectedness between men and nature: the deep ties that weave our lives together with the natural world. Nature is respected for its balance seeking process and its limits.

The idea of the city in the future is about nurturing sustainable cities, and sustainable places. Sustainable places seek more broadly to minimize the extent of their ecological footprint. The application of sustainability concepts to the field of urban planning is a relatively recent phenomenon. There are several dimensions in community planning stated by Beatley and Manning namely scale, sectoral and venues or spheres [7]. In the first dimension, there should be a multiscale approach such as vertical sustainability (the sustainability of a particular development project) and horizontal sustainability (the location of people and activities over space). In sectoral dimension, in order to create sustainable places we need concerted effort in policy arenas, including transportation,economic development and housing. In the last dimension sustainable places will require actions and in a number of different places in the community.

There are consequences associated with current growth patterns and approaches to city. The low-density, sprawling development patterns are very expensive in terms of the costs of public infrastructure, and dealing with environmental and social problems. This sprawling patterns of growth threaten our environmental resources. Sprawl breeds social isolation and undermines a sense of community and respect and appreciation for “otherness.” Langdon (1994) mentions about disconnection challenge the social ties that give individuals pleasure and invigorate community life. Living in gated communities reflects a lack of concern for the future of our society at large. The privatization of many functions of traditional government such as private security guards suggests a serious reduction of our social contracts. The greater our separation from the public the easier it is to believe that we Have few ethical obligations to others.

In *Thirdspace,* Edward Soja defines his concept of “Thirdspace,” a notion of space that combines spatiality with sociality and historicality [8]. Thirdspace is an interdisciplinary idea of space, history, and society that treats the micro-geographies of the everyday with as much seriousness as it treats the macro-geographies of larger historical trends. Both of these geographies are crucial for a nuanced interpretation of the site under investigation. For Soja, Thirdspace is “an-Other” space, a sprawling, radical zone created and populated by the marginalized. Thirdspace can be used as a radical, libratory concept of space, including our cities.

At the heart of critical spatiality is the recognition that, like history and society, space is not encountered as a transparent or objective “reality,” but is constructed in social practice and must therefore be theorized. Firstspace shows the concrete materiality of spatial forms or things that can be empirically mapped. Secondspace is ideas about space or thoughtful re-presentations of human spatiality in mental or cognitive forms. Thirdspace might be partially encapsulated in the notion of lived realities as practiced. Lefebvre in *the Production of Space* names these categories perceived space (or spatial practice), conceived space (or representations of space), and lived space (or spaces of representation) [9].

4. CONCLUSION

To conclude, Howard's, Le Corbusier's, or Wright's urban thought has had a direct effect on city planners. Some of their notions have made their way into urban renewal logic: clearance, the destruction of memory, the plan as scientific fact, sub-standard housing, etc. Certainly, their aseptic view of the city has destroyed the street theater that Jane Jacobs so lovingly describes. The landscapes of Howard, Wright, and Corbusier, regardless of its evocation of nature, are unsensual, ahistorical. None of them engage Thirdspace or lived space that embodies the real and imagined life world of experiences, emotions, events, and choices. Sustainable cities offer a better worldview, one that connects humans, nature, history, and place with a viable vision for the future. In this alternative or Third perspective, the spatial specificity of urbanism is investigated as fully lived space, a simultaneously locus of structured individual and collective experience and agency. Not like materialist approach, here city space is physically and empirically perceived as form and process, as measurable configurations and practices of urban life.

REFERENCES

[1] E. Soja, *Thirdspace: Journeys to Los Angeles and Other Real and Imagined Spaces*, Cambridge, MA:: Blackwell, 1966
[2] Fishman, *Urban Utopias in the Twentieth Century*, Cambridge, Mass: The MIT Press, 1977
[3] Fishman, *Urban Utopias in the Twentieth Century*, Cambridge, Mass: The MIT Press, 1977
[4] J. Jacobs, *The Death and Life of Great American Cities*, New York: Random House, 1961
[5] R. Sennet, *The Uses of Disorder: Personal Identity & City Life*, New York, 1970
[6] R. Sennett, *Authority*,. New York: W.W. Norton and Company, 1980
[7] T. Beatley, K Manning, *The Ecology of Place*, Washington DC: Island Press, 1997
[8] E. Soja, *Thirdspace: Journeys to Los Angeles and Other Real and Imagined Spaces*, Cambridge, MA: Blackwell, 1996
[9] H. Lefebvre, *Production of Space*, translated by Donald Nicholso-Smith, Willey-Blackwelll Publication, 1992
[10] L. Mumford, "Yesterday's City of Tomorrow," *Architectural Record* 132, no. 5 (Nov. 1962)
[11] W. Curtis, *Le Corbusier: Ideas and Forms*, New York: Rizzoli International Publications, 1986.
[12] R. Fishman, *Urban Utopias in the Twentieth Century*, Cambridge, Mass: The MIT Press, 1977
[13] Le Corbusier, *The City of Tomorow And Its Planning*, Trans. by Frederick Etchells. Cambridge Mass: The MIT Press, 1971.
[14] Le Corbusier, *The Radiant City*, Trans. by Pamela Knight, Eleanor Levieux, and Derek Coltman. New York: The Orion Press, 1967
[15] R. Sennett, *Authority*,. New York: W.W. Norton and Company, 1980
[16] P. Serenyi, ed., *Le Corbusier in Perspective*, Englewood Cliffs, NJ: Prentice Hall Publishers, 1975
Wikipedia
http://www.gunnzone.org/Space/BenSira_Space.htm
http://www.terrain.org/articles/13/strategy.htm
http://amst.umd.edu/About%20Us/Research/cultland/annotations/Soja.html

Symposium in Energy Conservation Through Efficiency in Design and Manufacturing

Symposium D

Center for Materials Processing & Failure Analysis

Dept. of Metallurgy & Material
Faculty of Engineering – University of Indonesia

CMPFA
Center for Material Processing and Failure Analysis

Center for Materials Processing & Failure Analysis (CMPFA), established in 2001, is a business unit of Dept. of Metallurgy & Material, Faculty of Engineering, University of Indonesia that provides services to oil and gas industries, chemical industries, power generating plants, steel fabricators and automotive industries. We are supported by high qualified staff (4 professors, 10 doctors & 13 masters) who have years of experience in dealing with clients' demand.

CMPFA is equipped with facilities of laboratories including chemistry lab, mechanical testing lab, metallography & heat treatment lab, metal forming lab, foundry lab, corrosion lab, non-destructive test lab, scanning electron microscope (SEM) & X-Ray Diffraction (XRD).

Since the beginning of 2008, CMPFA has been trying to implement Laboratory Management System (ISO 17025) to fulfill the customer need of accredited laboratory under the name of LABORATORIUM UJI MATERIAL.

CMPFA is divided into several divisions:

1. Material Testing Division

This division handles the clients' request for various material testing, material characterization and metallurgical analysis.
Some of the tests are but not limited to:

- Chemical Analysis
- Mechanical Testing
- Heat Treatment & Metallography
- Corrosion Test & Environment Simulation
- Non Destructive Testing

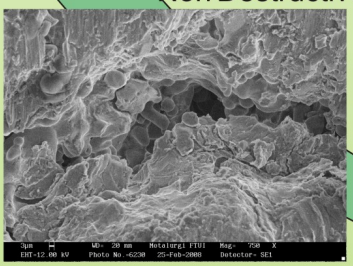

2. Training Division

The center also offers various in-house training or short course with the following subject areas:

- Basic metallurgy for non metallurgist
- Materials selection for design construction
- Metal heat treatment
- Mechanical testing for material
- Corrosion testing and prevention
- Metallography technique
- Foundry technology and mold design
- Welding metallurgy
- NDT radiation and non-radiation technique
- Polymer materials & technologies
- Costumized syllabus & curricullum depend on costumer request

3. Consultation & Analysis Division

The consultation & analysis group specializes in root-cause analysis, problem solving & product development. Our special expertise is in quantifying all aspects of failure analysis, forensic analysis, product comparison, performing in-depth investigations using material engineering analysis, metallurgy and materials testing.

This division offers several services:

- Failure analysis
- Insitu metallography
- Insitu NDT
- Casting assessment & reject reduction
- Welding procedure standard
- R & D support analysis

4. Approved Training Body (ATB) for welding certification

ATB is a special division for welding training that has been certified by Indonesian Welding Society (IWS) as Authorized Nation Body (ANB) - International Institute of Welding (IIW).

Conduct welding trainig activity including theoretical lectures and practical welding training for the following categories:

- International Welding Engineer (IWE)
- International Welding Technologist (IWT)

Contact:
Center for Materials Processing and Failure Analysis
Departemen Metalurgi dan Material
Fakultas Teknik Universitas Indonesia
Kampus Baru UI Depok 16424
Phone: (021) 78849045
Fax: (021) 78888111
email: cmpfa@metal.ui.ac.id
web: http://www.metal.ui.ac.id
CP: - Deni Ferdian
- A. Ivan Karayan

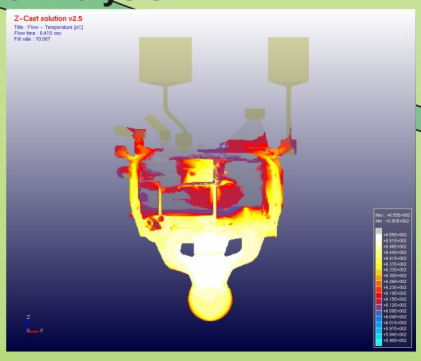

Proceeding of the 11th International Conference on QiR (Quality in Research)
Faculty of Engineering, University of Indonesia, Depok, Indonesia, 3-6 August 2009
ISSN 114-1284

Study of Characteristic Experimental Combustion of Coconut Shell in a Fluidized Bed Incinerator UI

Adi Surjosatyo

Mechanical Engineering Dept.
Faculty of Engineering
University of Indonesia, Depok 16424
Tel : (021) 7270032. Fax : (021) 7270033
E-mail : adi.surjosatyo@ui.edu

ABSTRACT

Fluidized bed insineration of biomass, such as coconut shell and branch trees or waste wood, has been conducted in University of Indonesia town jungle. This technology converts biomass to a useful and a cleaner energy, such as, heat for drying purpose. Observation finding the characterization of fluidization bed combustion is through primary air blower variation and coconut waste feeding variation. Results show that fluid bed combustion system worked properlu as expexted. Bed temperature during combustion test reached 800^{o}C to 850^{o}C.

Keywords
Fluid bed combustor, fluidization, self- sustaining combustion, good mixing

1. INTRODUCTION

Fluidized bed incineration systems can burn any kind of waste and have been proved to be highly efficient and environment friendly than other incineration systems. Fluidized bed reactors operate at relatively lower temperatures than other types. Complete combustion of the gases is ensured in the integrated combustion chamber with sufficient excess oxygen. The chamber is sized to ensure at least 2 second flue gas residence time at 850 ^{o}C or the temperature required by local legislation.

Fluidized bed incinerators are primarily used for liquids, sludges and shredded solid wastes. Fluidized bed incinerator consists of a vertical steel cylinder, usually refractory lined, with a sand bed on a supporting grid plate and air injection nozzles. *FB incineration of hospital waste*

2. RESEARCH METHODOLOGY

Conducting this research there are some important steps such as follows:

2.1. Preparation
- 2.1.1. Problem identification
- 2.1.2. Literature survey
- 2.1.3. Define the solid fuel waste type and size

2.2. Set Up Preparation
- 2.2.1. Laboratorium Set up
- 2.2.2.Defining solid fuel dimension & screening
- 2.2.3. Instrumentation Calibration

2.3. Testing and Data Collection
- 2.3.1. Measuring speed variation on screw feeding
- 2.3.2. Measuring mass-flowrate of solid fuel in screw-feeder.
- 2.3.3. Measuring air blower speed.
- 2.3.4. Measuring temperature at freeboard area with variation of solid fuel and air blower.

2.4. Data Interpretation and Plotting Graphs
- 2.4.1. Variation of feeding waste
- 2.4.2. Variation of Primary Air Blower
- 2.4.3. Analyzing of Ploting Graphs

2.5. Experimental Set-up

For this purpose a method has been done as follows. A fluidized bed combustion system has built & tested properly for this project. Figure 1 shows the complete installation of this system as follows:

Figure 1. Installation Fluidized Bed Combustion system.

3. RESULTS AND DISCUSSION

3.1. Characteristic of Feeder System

There are variation of feeding speed that depends on fuel solid size as shown on Figure 1. For fuel small size on average length (l) = 5-10 mm, width (w) = 5-10 mm and thickness (t)= 4-5 mm, the feeder will work on motor speed of 17 rpm or about 0.235 kg/s. For bigger size with average length (l) = 20-25mm, width (w) = 20-25 mm and thickness (t) = 4-5 mm, and the feeder will work on motor speed of = 21 rpm or about 0.527 kg/s.

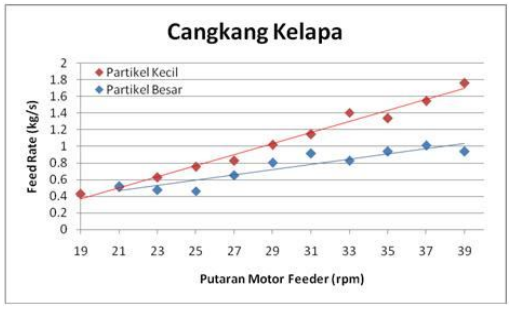

Figure 1. Feedrate of coconut shell against motor speed (upper graphs for small size & lower graph for big size)

Figure 2. Coconut shell as waste fuel (left: big size; right: small size)

For smaller size, increasing of feed rate is lower than bigger size, but at the same feeding-speed the feed rate of smaller size is higher than bigger size. This is due to density of smaller size is higher density than bigger size. Minimum feed rate of smaller size is 0.4 kg/s of 19 rpm and bigger particle is 0.5 kg/s at 21 rpm.

3.2. Characteristics of Blower

Figure 3 shows the minimum fluidization reachs 2.6 m^3/min at blower speed 2700 rpm. In this study working area where fluidization occurred, air blower supplies flowrate of 4.9 to 5.3 m^3/min.

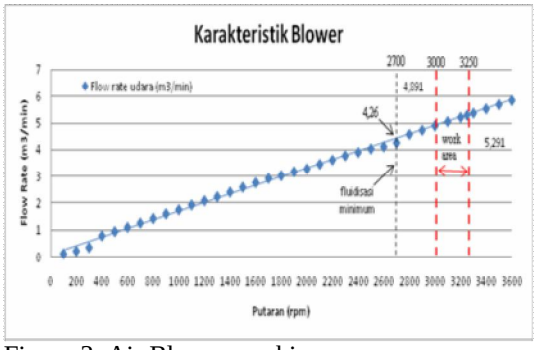

Figure 3. Air Blower working area.

3.3. Temperature Distribution inside the Furnace

There are five (5) Thermocouples corresponding to the height of furnace. Temperature are collected from thermocouples are average value after fuel burned. Fuel flowrate and air blower are varied so that temperature distribution along the height can be evaluated. Figure 4 is ploting, the commencing the combustion was used LPG gas burner for around 30 minutes, while this gas burner works in 20 minutes, coconut shell as support fuel was injecting in to the hot bed. After 10 minutes bed temperature T1 increases to around of 800°C, then LPG burner switch off immediately. From this point a *self-sustainable combustion* has started.

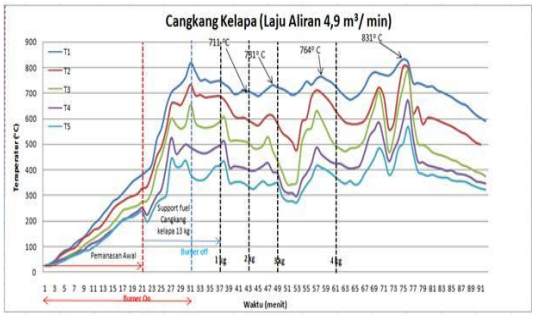

Figure 4. Temperature distribution from start-up to finish the operation combustion process.

Then bed temperature slightly decreases until reaching a steady state condition. On this condition starts feeding 1 kg/min of solid waste, and bed temperature T1 decreases around of 80°C or T1 is 700°C. But in the short time temperature increases again to 720°C. This transient

temperature indicates a burning process from a'cold' solid fuel, or heat from bed environment was needed to burn the solid fuel. Feeding process gradually rises to 4 kg/min, this followed by increasing the bed and freeboard temperature as shown in Figure 4 as well.

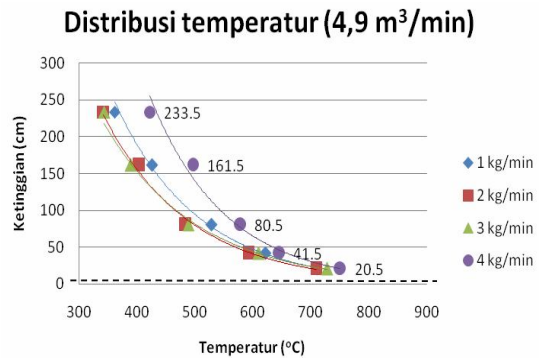

Figure 5. Temperature distribution inside the furnace at air flowrate 4.9 m^3/min corresponding to thermocouple height

Variation of furnace temperature at different fuel feeding speed and primary air blower (4.9m^3/min) is shown in Figure 5. The highest temperature reaches at bed temperature of 760^{o}C and the lowest is around of 233.5^{o}C. Also increasing of waste fuel feeding leads a higher temperature at thermocouple near the furnace outlet.

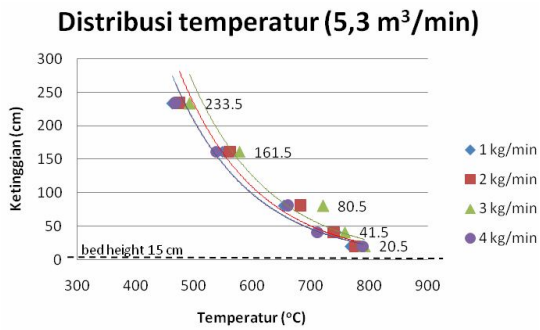

Figure 6. Temperature distribution inside the furnace at air flowrate 5.3 m^3/min corresponding to thermocouple height

Further rising of air supply to 5.3 m^3/min, increases average bed and freboard temperature. This indicates that increasing of air supply gives better combustion process. It is possible a secondary air could be needed to achieve a higher and cleaner combustion.

4. CONCLUSION

A fluidized bed combustion system has successfully constructed and tested for burning coconut shell as solid waste in Faculty Engineering University of Indonesia. General conclusion can be deducted as follows:

4.1. Increasing of feeding speed motor rises directly the feed rate of solid waste as well.

4.2. Rising the air supply influences the increasing of bed and freeboard temperature

4.3. A self sustainable combustion is achieved at temperature around 715 to 750^{o}C.

ACKNOWLEDGMENT

The authors are grateful to final year Mecahnical Engineering student 2009, namely, Arsya, Darma and Davin who have worked very hard and for their support during carry out the research work.

REFERENCES

1. Bruce R. Munson, Donald F. Young, *Mekanika Fluida*, terj. Harinaldi, Budiarso (Jakarta: Erlangga, 2003).
2. Christian, Hans. "Modifikasi Sistem Burner dan Pengujian Aliran Dingin *Fluidized Bed Incinerator* UI." Skripsi, Program Sarjana Fakultas Teknik UI, Depok, 2008.
3. "Experimental Operating & Maintenance Manual – Fluidisation and Fluid Bed Heat Transfer Unit H692," P. A. Hilton Ltd.
4. Geldart, D., *Gas Fluidization Technology*, (New York: John Wiley & Sons, 1986).
5. Howard, J. R., *Fluidized Beds – Combustion and Applications*, (London: Applied Science Publishers, 1983).
6. Kunii, Daizo & Octave Levenspiel, Fluidization Engineering, (New York: Butterworth-Heinnemann, 1991).
7. Robert H. Perry, Don W. Green, Perry's Chemicsl Engineers' Handbook 7th Ed., (Singapore: McGraw-Hill Int., 1997.
8. Surjosatyo, Adi. "Fluidized Bed Incineration of Palm Shell & Oil Sludge Waste." Tesis, Program Magister Engineering Universiti Teknologi Malaysia, 1998.
9. Warren L. McCabe, Julian C. Smith, Peter Harriott, Unit Operasi Teknik Kimia, terj. E. Jasjfi (Jakarta: Erlangga, 1987).

ISSN 114-1284

The Calculation of Water Filtration System with Capacity 10 liter/minute for Flood Water Filter Application

Anggito P. Tetuko[1], Deni S. Khaerudini[1], Muljadi1, and P. Sebayang[1]

[1]*Research Centre for Physics, Indonesian Institute of Sciences*
Kawasan PUSPIPTEK Serpong Tangerang 15314
Email: angg005@lipi.go.id

ABSTRACT

The analytical calculations of fluid mechanic in water filtration system have been done. This water filtration system consists of cyclone pre filter and several filters using media, such as: silica sand, manganese greensand, granulated activated carbon (GAC), sediment filter, porous ceramic, and post carbon. This system also completed with reverse osmosis (RO) system and two pumps (submerge and RO high pressure pump). The calculations were done using Darcy laws for porous medium; Stoke laws for particulate medium, and Reynold formulae to calculate the Reynold number and fluid flow type in the water filtration system. From the result it can be concluded that the flow rate and Reynold number inside cyclone pre filter, and filter using media: silica sand, manganese greensand, granulated activated carbon, sediment filter, porous ceramic, post carbon, and also reverse osmosis systems are the following, for flow rate capacity: 200.0, 160.7, 42.1, 32.9, 6.1, 3.1, 11.8, and 12.3 liter/minute. The Reynold number: 69359.4; 19478.1; 5101.4; 9674.3; 1123.7; 561.8; 3482.3; and 2247.4. From the calculations also, it can be concluded that the filtration system can reach for minimum 10 liter/minute capacity.

Keywords

Flood water, filtration, Darcy law, Stoke Law, Reynold number

1. INTRODUCTION

Flood is one of the disasters that have a lot of effect in human life, especially can cause illness and disease, because the rareness of drinking water. After a flood, water can be contaminated and can not be use by human, unless it proven safe. To solve this problem, the technology such as water filtration is needed. Water filtration is the process of removing undesirable chemical and biological contaminants from raw water. Filtration also remove solid particle from a fluid by passing the fluid through a filtering medium or septum, on which the solids are deposited **[1]**. The solid particle may be coarse, fine or aggregate, such as: silica sand, manganese greensand, granulated activated carbon and post carbon (figure 1) **[2]**.

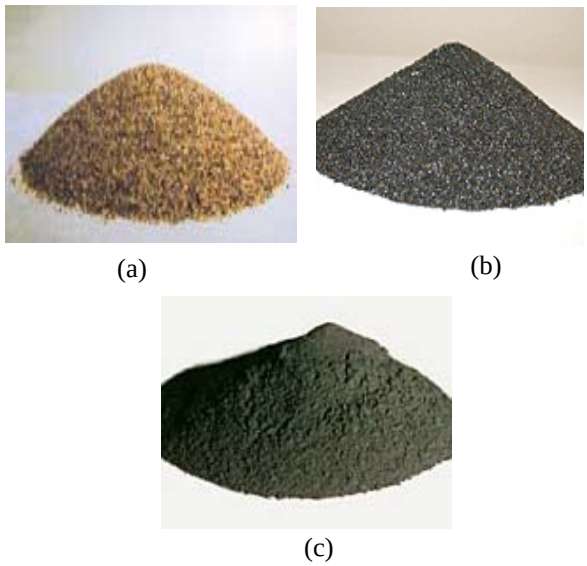

(a) (b)

(c)

Figure 1. (a). Silica sand, (b). Manganase greensand and (c). Post carbon

In water filtration system, sand is an extremely effective filter media because its ability to hold back coagulum or precipitates containing impurities. Filter sand size, angularity and hardness are the important filter sand characteristics to ensure proper filtering **[3]**. Manganese greensand is a purple – black filter medium that is used for the removal of soluble iron, manganese and hydrogen sulfide from well water supplies. It also has the capacity to remove radium and arsenic. There are several sizes of carbon media that is used for filter media, granulated or fine. The use of carbon in water filtration is to remove chlorine and organic contaminants from tap water, also for color and taste removal in water **[4]**. Beside coarse, fine or aggregate media in filtration system, there is also other media to make sure the water filtered completely and to remove the suspend in water that not well for human body. The media are: sediment, porous ceramic and reverse osmosis (figure 2).

(a) (b)

Figure 2. (a). Sediment and (b). porous ceramic as filter media **[5],[6]**

Filters can be divided into two types: pressure and gravity. Pressure filters consist of closed vessels containing beds of sand or other granular material through which water is forced under pressure. These filters are frequently used in certain industrial situations, and a number have been installed for public water supplies. Gravity filters consist of an open-topped box (usually made of concrete) drained at the bottom, and partly filled with a filtering medium (normally clean sand). Raw water is admitted to the space above the sand, and flows downward under the action of gravity **[7]**.

The goal of water filtration is to produce water fit for a specific purpose. Most water is filtered for human consumption (drinking water) but water filtration may also be designed for a variety of other purposes, including to meet the requirements of medical, pharmacology, chemical and industrial applications. In general the methods used include physical process such as filtration and sedimentation, biological processes such as slow sand filters or activated sludge, chemical process such as flocculation and chlorination and the use of electromagnetic radiation such as ultraviolet light. The filtration process of water may reduce the concentration of particulate matter including suspended particles, parasites, bacteria, algae, viruses, fungi; and a range of dissolved and particulate material derived from the minerals that water may have made contacted after falling as rain **[8]**. Water filtration also relatively inexpensive and improves the overall taste of tap water as well as the smell, and appearance. Many filtrations will also remove some harmful chemicals found in drinking water.

2. DESIGN

This filtration system consists of cyclone pre filter, ceramic filter, reverse osmosis and several filters with media: sand, manganese greensand, granulated activated carbon, sediment, and post carbon. This filtration system also companied by submerge pump and reverse osmosis pump with capacity 200 and 50 liter/minute to make sure the target of 10 liter capacity can be revealed. The water filtration system was shown in figure 3.

The calculation of the system was used formulae from Darcy's law to calculate the flow in porous medium, Stokes's law to calculate the flow in particle medium, continuity law and Reynold number to calculate the velocity and flow rate in the system

In cyclone pre filter, the flow rate in pre cyclone filter was designed suitable with submerge pump (200 liter/minute) and the velocity can be calculated using formulae 1 **[10]**.

$$Q = A \times v \tag{1}$$

$$\mathrm{Re} = \frac{\rho \times v \times d}{\mu} \tag{2}$$

In formulae 2 **[10]**, water physical properties, such as density (ρ), dynamic viscosity (μ) and velocity must be substituted to calculate Reynold number (Re).

In sand filter media, manganese greensand, granulated activated carbon and post carbon, the velocity must be calculated first using Stoke law, formulae 3 **[3]** with media and water physical properties (density and dynamic viscosity). Then the flow rate and Reynold number in sand, manganese green sand, granulated activated carbon and post carbon media can be calculated using formulae 1 and 2 **[10]**.

The calculation of flow rate in sediment, ceramic and reverse osmosis can be calculated using formulae 4 **[11], [12**] by substituting permeability, pressure, area, density, gravity and length. Then Reynold number and flow rate in those media can be calculated using formulae 1 and 2

$$v_s = \frac{g \times (\rho_s - \rho) \times d_p^{\,2}}{18 \times \mu} \tag{3}$$

$$Q = \frac{K \times P \times A}{\rho \times g \times L} \tag{4}$$

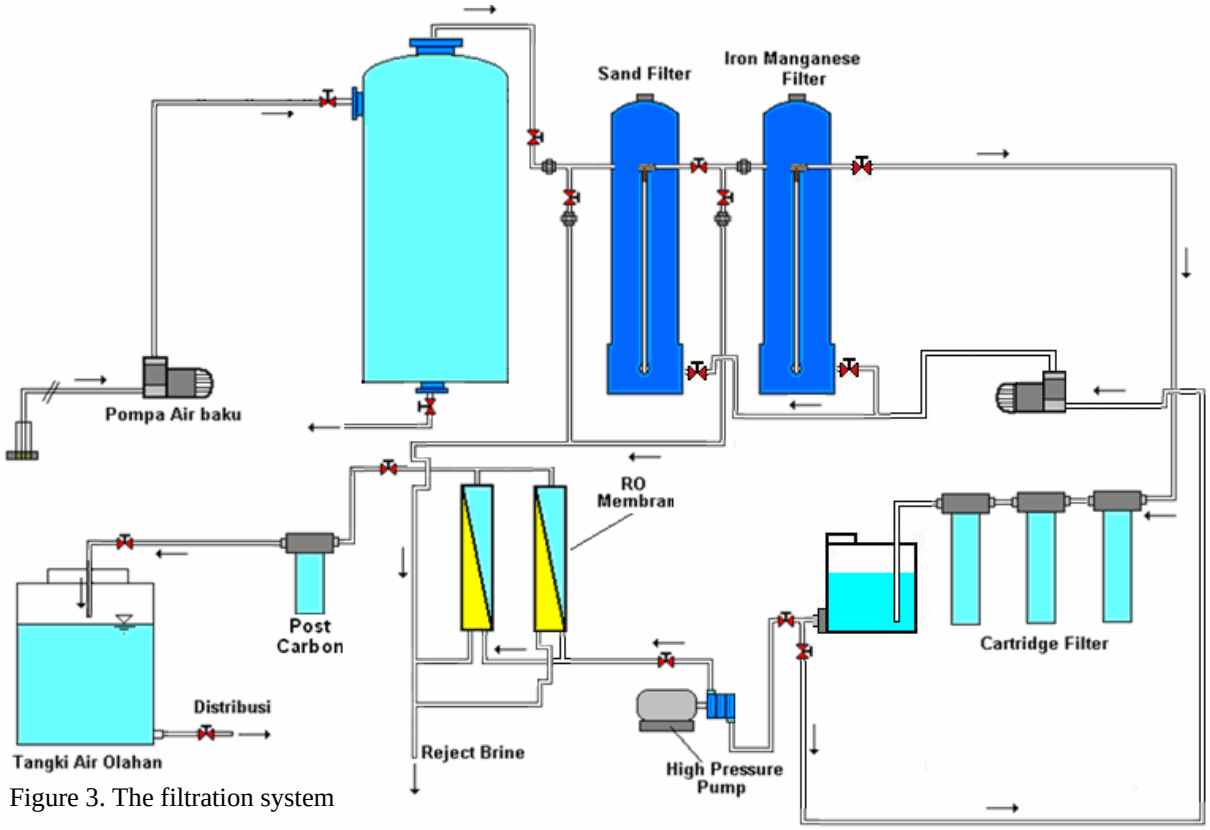

Figure 3. The filtration system

3. RESULT AND DISCUSSION

Cyclone separators are designed to remove suspended solids from liquids. The separating efficiency depends on the flow velocity and the density of the particle. Liquid enters the upper chamber and separated because of the density difference between water that has less density with sludge that has bigger density. The separating efficiency varies from 22 -70 μm and depends on the density of the solids, higher density leads to finer separation. Separated solid are removed with an automatic purge system or with manual purge valves. The separating efficiency in cyclone filter was shown in figure 4

In Darcy law for calculating fluid in porous media, permeability is very affected the flow in the system. Permeability depends on the combination of the fluid and porosity in porous media. Permeability describes how easily a fluid is able to move through the porous material.

In Stoke law for calculating fluid in particle medium, the density of media and particle diameter is very affected the overall flow rate and velocity in the system.

Beside that the velocity in the system is affected by surface area and design of the media itself. Velocity also affected by fluid physical properties, such as density and viscosity, the increase in velocity can make higher pressure drop in the system. In filter system, the velocity is maintained not too fast to ensure the media can filter the media well. Based on the calculation, it can be concluded that the flow type in cyclone pre filter, sand, manganese greensand, granulated activated carbon and post carbon are turbulence. And the flows in sediment, ceramic and reverse osmosis are laminar. This flow type different is cause by the permeability of the material and velocity, because higher permeability and velocity can result to higher Reynold number, resulting the flow type into turbulence.

The calculation result of velocity, and Reynold number in the filtration system was shown in table1. Based on the flow rate calculation, it can be concluded that the flow rate is decreasing from 200 liter/minute in cyclone pre filter to 3.07 liter/minute in ceramic filter, after flowed in several media: sand, manganese greensand, granulated activated carbon, sediment, and ceramic. The flow was increased again after pumped by reverse osmosis pump with flow rate 50 liter/minutes. Finally the flow rate was decreased until 11.83 liter/minute after passed in reverse osmosis and post carbon. This flow rate reduction can be cause by the fluid friction and pressure drop across the media to filter the water inside the water filtration system. The flow rate in the system after passed to several media was shown in figure 5.

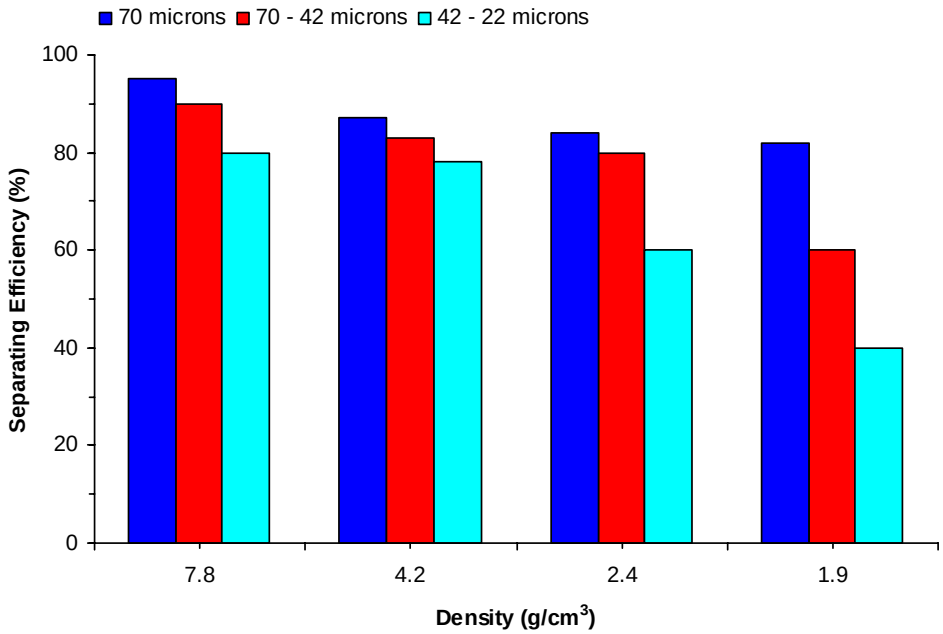

Figure 4. Separating efficiency in cyclone pre filter

Table 1. The calculation result of fluid mechanic in filtration system

Filter	v (m/s)	Re
Cyclone	0.73	69359.4
Sand	7.14×10^{-2}	19478.14
Manganese greensand	186.97×10^{-4}	5101.42
Granulated activated carbon	8.61×10^{-2}	9674.83
Sediment	1×10^{-2}	1123.67
Ceramic	5×10^{-3}	561.84
Reverse osmosis	2×10^{-2}	2247.35
Post carbon	3.1×10^{-2}	3482.27

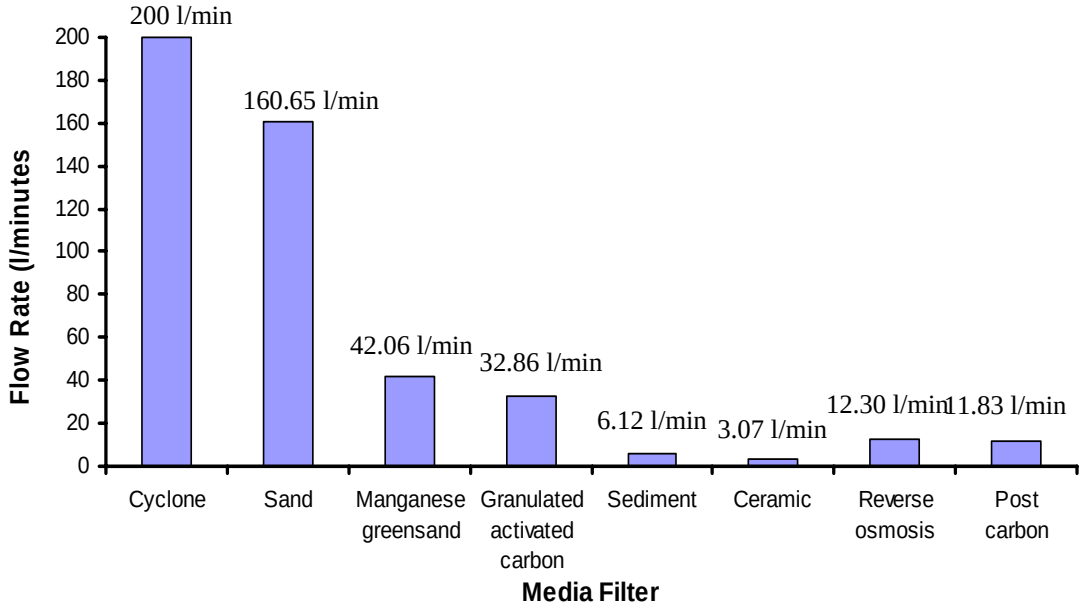

Figure 5. Flow Rate in several filter media

4. CONCLUSION

From the water filtration fluid mechanic calculations, it can be concluded that the filtration system can reach minimum 10 liter/minute capacity after flew in cyclone pre filter and several media, such as: silica sand, manganese greensand, granulated activated carbon, sediment, ceramic, reverse osmosis and post carbon.

5. REFERENCES

[1] W.L. Mc Cabe, "Unit Operations of Chemical Engineering Third Edition", Mc Graw Hill, 1996.
[2] http://www.northernfiltermedia.com
[3] K.J.Ives, "Filtration of Clay suspensions Through Sand", Clay Minerals (1987) 22, 49-61
[4] http://www.allwaterfiltrationsystems.com/
[5] http://sentryfilter.com/sediment
[6] A.P. Tetuko, D.S. Khaerudini and P. Sebayang, "Pembuatan dan Karakterisasi Keramik Berpori dari Tanah Liat dan Limbah Lumpur Padat (Sludge) sebagai Filter Air", Prosiding Seminar Nasional Metalurgi dan Material, Agustus, 2007.
[7] http://en.wikipedia.org/wiki/Water_purification
[8] I. Huisman, "Slow Sand Filtration", World Health Organization, 1998
[9] http://www.bernoulli.se
[10] B.R. Munson, "Fluid Mechanic, Fourth Edition", John Wiley and Sons Inc, 2002
[11] J.G.I. Hellstrom, T.S.Lundstrom, "Flow through Porous Media at Moderate Reynolds Number, International Scientific Colloquium, Modelling for Material Processing, Riga, June 8 -9, 2006.
[12] L. Pal, M. K. Joyce and P.D. Fleming "A Simple Method for Calculation of the permeability Coefficient of Porous Media", TAPPI Journal, September 2006.

Proceeding of the 11th International Conference on QiR (Quality in Research)
Faculty of Engineering, University of Indonesia, Depok, Indonesia, 3-6 August 2009
ISSN 114-1284

Calculating Thermodynamic properties of Dioxin Formation by Gaussian '98

Annisa Bhikuning[1]

[1] *Faculty of Industrial Technology*
Mechanical Engineering Department
Trisakti University, Jakarta 11440
Tel : (021) 5663232 ext 434. Fax : (021) 5605841
E-mail : annisabhi@gmail.com

ABSTRACT

Dioxin is the most toxic chemical known in our environment. This group of compounds comprises 75 Polychlorinated dibenzo-p-dioxins (PCDDs) and 125 Polychlorinated dibenzofurans (PCDFs). Many of them are toxic substances, particularly from combustion of waste materials in incinerators and process high stability under various conditions. Many researchers calculated thermodynamic properties of dioxin with used different kind of methods. And each method has it own limitations. In this research, thermodynamic properties such as enthalpy, entropy and Gibbs free energies of PCDD/Fs were calculated using Gaussian '98 based on ab initio quantum chemistry B3LYP/6-311+G(2d,p)//B3LYP/6-31G(d) as a basis set. In the comparison with other methods show that this research has corrected value for thermodynamic of PCDD/Fs. The small errors appeared because of the differences model chemistry and methods. To make more accuracy of this thermodynamic calculation, it recommends to use higher level of theory using B3LYP/6-311+G(3df,2df,2p)//B3LYP/6-31g(d).

Keywords: *Thermodynamic properties, combustion, dioxins, enthalpy, Gibbs free energy*

1. INTRODUCTION

Dioxin is the most toxic chemicals known in our environment and the name it's given to a group of molecules made up of two chlorinated benzene rings connected by one or two atoms of oxygen. This group of compounds comprises 75 Polychlorodibenzo-*p*-dioxins (PCDDs) and 125 related compounds called Polychlorodibenzo furans (PCDFs). Characteristic of all the compounds is a high melting point, a low vapour pressure, a low water solubility and a reasonable solubility in and affinity for apolar media.

Chemical Structure of a few the most toxic dioxins: PCDD and PCDF

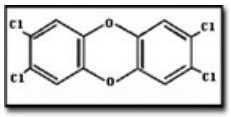

2,3,7,8-Tetrachlorodibenzo-p-dioxin

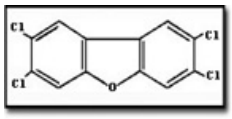

2,3,7,8-Tetrachlorodibenzofuran

Dioxins occur in the environment in complex mixtures of the 226 congeners. Most of the 226 dioxin congeners are thought to pose no risk to human health, and only 17 congeners with chlorine are reported to have potential health effects. An International system has been developed which assigns toxicities to each congener relative to the most toxic form (2,3,7,8 TeCDD).

Dioxins are not manufactured as commercial products or ingredients. They occur in combustion process and certain chemical processes. It is now believed that dioxins and furans are formed in the low-temperature combustion region of incinerators through heterogeneous catalytic reactions occurring in the fly-ash environment. However, the detailed chemical reactions are not understood.

Study for dioxins formation in incinerator process would be very significant in determining the formation mechanism of polychlorinated dioxins (PCDDs) and furans (PCDFs), and would assist in design of strategies to effectively control or eliminate emissions of these compounds.

Unfortunately, the thermodynamic data from other researchers and experimental information on their thermodynamic properties is difficult to obtain.

In this research, all the thermodynamics of polychlorinated dibenzo-*p*-dioxins and dibenzofurans (PCDD/Fs) were calculated by *Gaussian '98*. Study for dioxin formation is very important to understand the formation mechanism of PCDD/Fs in thermal processes and It

would assist in the effective control or elimination of the PCDD/Fs emissions during the thermal combustion and reduction processes.

2. LITERATURE REVIEW

There are several investigations in calculating thermodynamic data in combustion process.

Shaub [6] calculated heats of formation at 298 K for 75 PCDD isometric species through the 'group additivity method' which Benson (1976) contrived, and estimated the values of standard entropy and heat capacity at constant pressure for Dibenzo-p-dioxin (C12H8O2), 1-Chlorodibenzo-p-dioxins (C12H7O2Cl), 2-Chlorodibenzo-p-dioxin (C12H8O2Cl)1, 2,3,7,8-Tetrachlorodibenzo-p-dioxin (C12O2Cl4), Octachlorodibenzo-p-dioxin (C12O2Cl8). However, the evaluation of thermodynamic functions through Benson's group additivity method is unreliable for the dibenzo species. This entropy values appear to contain considerable errors since they were derived from rough estimates of their molecular structures and vibration frequencies. As an example, Shaub estimate value of heats formation at 298 K of 2,3,7,8 TCDD is -345.14 kJ/mol, which is quite different from Domalski and Hearing (1993) estimated value of -168.2 kJ/mol. However, Domalski estimates for these thermodynamic parameters of heats of formation, entropy and heat capacity at constant pressure are limited only to those at 298 K, which prevent their use in the thermodynamic calculations at higher temperatures used in incineration and pyrometallurgical process. Thus, the earlier thermodynamic calculation using Shaub's estimates appears to be unreliable.

Huang [9] predicted the enthalpies and Gibbs free energies of formation of PCDDs by several methods. These included three semi-empirical methods (MNDO, AM1 and PM3); three different implementations of Benson's group additivity method were also evaluated. Huang reported that the CHETAH program is the best for evaluating gaseous enthalpies of formation of PCDDs.

Saito and Fuwa [8] calculated the thermodynamic parameters of heats of formation at 298 K using the semi-empirical molecular orbital method with the PM3 Hamiltonian. Their study aimed to determine thermodynamic data bases for these substances within a scientific error range.

Andrew McLennan [5] calculated the thermodynamic data using Gaussian '94 and used the MNDO semi-empirical and DFT/ab initio method in his calculations. The semi-empirical methods computed the heats of formation of PCDDs in their solid states.

Pengfu Tan [10] predicted of the toxic PCDD/Fs isomer distribution using the three different databases were compared with measured values from the industrial incinerator, wood combustion system, electric arc furnace, and iron ore sinter plant. The comparison showed that the MNDO method predicts more reliable isomer distribution than PM3 method and the Group additivity method.

2.1 An overview Of Computational Chemistry

There are two broad areas within computational chemistry devoted to the structure of molecules and their reactivity: *molecular mechanics and electronic structure theory*. They both perform the same basic types of calculation:

a. Computing the energy of particular molecular structure (spatial arrangement of atoms or nuclei and electrons).
b. Performing geometry optimizations, which locate the lowest energy molecular structure in close proximity to the specified starting structure. Geometry optimizations depend primarily on the gradient of the energy-the first derivative of the energy with respect to atomic positions.
c. Computing the vibrational frequencies of molecules resulting from interatomic motion within the molecule. Frequencies depend on the second derivative of the energy with respect to atomic structure, and frequency calculations may also predict other properties which depend on second derivatives. Frequency calculations are not possible or practical for all computational chemistry methods.

2.1.1 Molecular Mechanics

Molecular mechanics simulations use the laws of classical physics to predict the structures and properties of molecules. Molecular mechanics methods are available in many computer programs, including MM3, HyperChem, Quanta, Sybyl and Alchemy. There are many different molecular mechanics methods. Each one is characterized by its particular *force field*.

Molecular mechanics calculations don't explicitly treat the electrons in a molecular system. Instead, they perform computations based upon the interactions among the nuclei. Electronic effects are implicitly included in force fields through parametrization.

This approximation makes molecular mechanics computations quite inexpensive computationally, and allows them to be used for very large systems containing many thousands of atoms. However, it is also carries several limitations as well. Among the most important are these:

a. Each force achieves good results only or a limited class of molecules, related to those for which it was parametrized.
b. Neglect of electrons means that molecular mechanics methods can not treat problems where electronic effects predominate.

2.1.2 Electronic Structure Methods

Electronic structure methods use the laws of quantum mechanics rather than classical physics as the basis for their computations. Quantum mechanics states that the energy and other related properties of a molecule may be obtained by solving the Schrödinger equation:

$$H\Psi = E\Psi \qquad (1)$$

For any but the smallest systems, however, exact solutions to the Schrödinger equation are not computationally practical. Electronic structure methods are characterized by their various mathematical approximations to its solution. There are two major classes of electronic structure methods:

a. *Semi-empirical methods*, such as AM1, MINDO/3 and PM3, implemented in programs like MOPAC, AMPAC, HyperChem and Gaussian, use parameter derived from experimental data to simplify the computation. They solve an approximate form of the Schrödinger equation that depends on having appropriate parameters available for the type of chemical system under investigation. Different semi-empirical methods are largely characterized by their differing parameters sets.
b. *Ab initio methods,* unlike either molecular mechanics or semi-empirical methods, use no experimental parameters in their computations. Instead, their computations are based solely on the laws of quantum mechanics- the first principles referred to in the name ab initio –and on the values of a small number of physical constants:
    - The speed of light
    - The masses and charges of electrons and nuclei
    - Planck's constant

Gaussian offers the entire range of electronic structure methods. This work provides guidance and examples in using all of the most important of them. *Ab initio* methods compute solutions to the Schrödinger equation using a series of rigorous mathematical approximations.

Semi-empirical and *ab initio* methods differ in the trade-off made between computational cost and accuracy of results. Semi-empirical calculations are relatively inexpensive and provide reasonable qualitative descriptions of molecular system and fairly accurate quantitative predictions of energies and structures for systems where good parameter sets exist.

In contrast, ab initio computations provide high quality quantitative predictions for a broad range of systems. They are no imitated to any specific system. Early ab initio programs were quite limited in the size of system they could handle. However, this is not true for modern ab initio programs. On a typical workstation, Gaussian '98 can compute the energies and related properties for systems containing a dozen heavy atoms.

2.2 Methods

The Gaussian program contains a hierarchy of procedures corresponding to different approximation methods (commonly referred to as different levels of theory).

Table 1. Approximation Method of Gaussian Program

Keyword	Method	Availability
HF	Hartree-Fock Self-Consistent Field	Through 2nd derivatives
B3LYP	Becke-style 3-Parameter Density Functional Theory (Using the Lee-Yang-Parr correlation functional)	Through 2nd derivatives
MP2	2nd Order Moller-Plesset Perturbation Theory	Through 2nd derivatives
MP4	4th Order Moller-Plesset Perturbation Theory (including Singles, Doubles, Triples and Quadruples by default)	Energies only
QCISD(T)	Quadratic CI (Single, Double and Triples)	Energies only

2.3 Isodesmic Reaction

In this research ΔHf°of PCDD/Fs are calculated by using isodesmic reaction. An isodesmic reaction is one in which the total number of each type of bond is identical the reactants and products. Here is a simple example

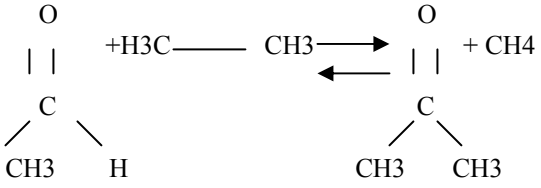

In this reaction, there are twelve single bonds and one (C-O) double bond in both the reactants and products. Because of this conservation of the total number and types of bonds, very good results can be obtained relatively inexpensively for isodesmic reactions due to the cancellation of errors on the two sides of reactions.

In addition, isodesmic reactions may be used to predict the heats of formation for compounds of interest by predicting □H for the reaction and then computing the desired heat of formation by removing the known heats of formation for the other compounds from this quantity.

From the previous studies there are no paper reported the thermodynamic properties from all 226

ISSN 114-1284

congeners of PCDD/Fs. The thermodynamic properties of PCDFs are not easy to find. Therefore, in this paper the PCDFs data were compared with experimental data from incinerator.

The thermodynamic properties are calculated by using Gaussian '98. Thermodynamic properties such as enthalpy, entropy and Gibbs free energies of PCDD/Fs were calculated based on ab initio quantum chemistry using the B3LYP/6-311+g (2d,p)//B3LYPD/6-31 g(d) basis set.

3. CALCULATION PROCEDURE

3.1 Calculation Enthalpy From Gaussian'98

From out put of Gaussian '98 we can get E (Sum of electric and thermal energies). The calculations of enthalpies of PCDD/Fs are isodesmic reactions, the reactions we can see above:

Reactant (A) + n*HCl = Product (B) + n*H2

For example:

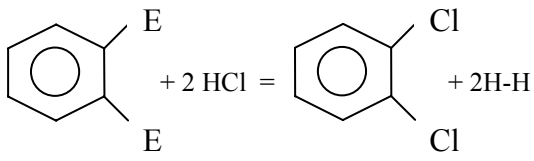

ΔHf°(Dichlorobenzene) ={E (Dichlorobenzene)+ E(H2) - E(Benzene) - E(HCl)} + ΔHf°(Benzene)

Where:

ΔHf° = standard enthalphy
E = Sum of electronic and thermal energies from output file of gaussian'98

The condition of isodesmic reaction is the number of atoms and bonds of reactants are the same as one of products respectively.

The standard formation enthalpy of the objective is calculated as following:

ΔHf°(Dichlorobenzene) ={E (Dichlorobenzene)+ E(H2) - E(Benzene) - E(HCl)} + ΔHf°(Benzene)

3.2 Calculation of Thermodynamics PCCD/Fs

From the output file of Gaussian, enthalpies are calculated and NASA Polynomial table are made after. In NASA polynomial table the thermodynamic values are calculated based on JANAF table.

Molar specific heat capacity C_{pj}^0, molar enthalpy H^0,molar entropy S^0, and Gibbs free energy G^0 at given temperature under the standard pressure can be calculated by using a NASA polynomial based on JANAF table.

Molar specific heat capacity C_{pj}^0 for species j at standard pressure (1 atm) is defined as a function of temperature T as follows

$$\frac{C_{pj}^0}{R} = a1 + a2T + a3T^2 + a4T^3 + a5T^4 \qquad (T \geq 1000K) \quad (2)$$

$$\frac{C_{pj}^0}{R} = a8 + a9T + a10T^2 + a11T^3 + a12T^4 \qquad (298K(Tb) \leq T < 1000 \quad (3)$$

As molar enthalpy,

$$H_j^0 = \int_{Tb}^{T} C_{pj}\,dt + H_j^0(Tb) \quad (4)$$

As for molar entropy,

$$S_j^0 = \int_{Tb}^{T} C_{pj}^0\,d\ln T + S_j^0(Tb) \quad (5)$$

And The Gibbs free energy:

$$G_j^0 = H_j^0 - TS_j^0 \quad (6)$$

4. RESULT

4.1 Data of PCDDs and PCDFs

First of all we compared ΔHf° datas of the PCDDs with another methods.

Table 2. Calculated Ideal Gas Enthalpy of Formation for PCDD Compared to another methods

ΔHf° (kJ/mol)						
	This research (Gaussian '98)	MNDO Andrew's (Gaussian '94)	Shaub 1982	PM3 (Huang et al) 1996	Chetah (Huang et al) 1996	Fuwa Saito
1CDD	-89.594	-115.64	-94..9	-82.76	-91.63	-61
2 CDD	-97.043	-123.91	-137.6	-86.17	-91.63	-67.1
1,3DCDD	-124.045	-142.24	-161	-86.17	-112.13	-87
2,3DCDD	-121.945	-141.95	-165.6	-88.29	-121.34	-89.1
1,2,3 TrCDD	-136.245	-148.71	-223.1	-104.49	-132.6	-105
1,2,4 TrCDD	-139.758	-150.14	-187.47	-102.41	-141.8	-103,3
1,2,3,6 TeCDD	-154.51	-168.15	-255.27	-124.7	-162.34	-125.7
1,2,3,4 TeCDD	-143.83	-169.83	-278.68	-114.63	-162.34	-115.5
2,3,7,8 TeCDD	-181.673	-186.38	-344.9	-136.3	-162.34	-137.2
1,2,3,4,6 PeCDD	-175.124	-171.62	-273	-140.56	-182.8	-141.5
1,2,4,6,7 PeCDD	-189.9	-184.65	-287.7	-144.58	-192.05	-145.6
1,2,4,8,9 PeCDD	-189.7	-184.5	-250.2	-144.57	-192.05	-145.5
1,2,3,4,6,7 HxCDD	-198.19	-187.17	-339.1	-162.5	-203,.4	-163.5
1,2,4,6,8,9 HxCDD	-211.83	-198.4	-312.25	-163.66	-221.8	-164.7
1,2,3,4,6,7,8 HeCDD	-217.81	-199.91	-401.15	-183.74	-223.84	-184.8
1,2,3,4,6,7,9 HeCDD	-219.83	-200.6	-365.54	-181.54	-233.05	-182.6
OCDD	-227.77	-202.41	-418.8	-199.36	-244.35	-200.5

From PCDDs data showed that this work accurate enough with MNDO semi-empirical method by Andrew's [6]. For the comparison between shaub's have very big differences. The numbers of studies have been reported that shaub's data is inaccurate and unsatisfactory. Because the enthalpy formations have very big differences compared to others studies.

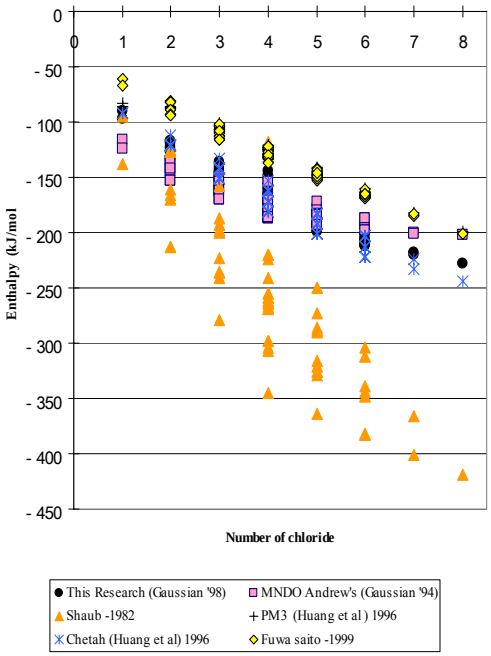

Figure 1. The Enthalpy Comparison of PCDDs at 298.15 K

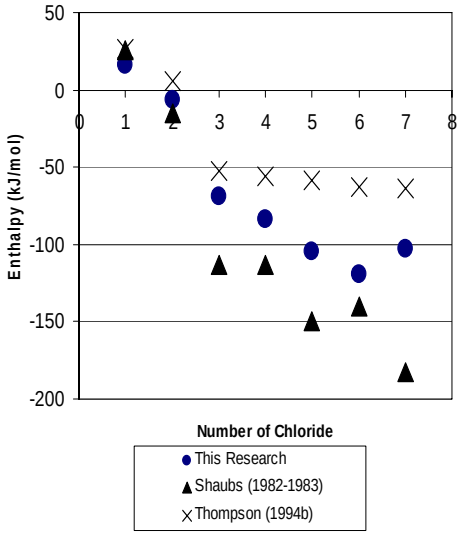

Figure 2. The Enthalpy Comparison of PCDFs at 298.15 K

In comparing between this research and shaub's, its correlation is shown very big and inaccurate. The discrepancy between shaub's value and this research become larger as the number of Chloride in horizontal axis. It is clear that the shaub's method overestimates. The change in heats of formation caused by chlorine allocation change estimated in shaub's study is unrealistically large compared with this research. For example, Shaub's heats of formation difference between 2,3,7,8-TeCDD. In this research -181.673 kJ/mol and shaubs is -344.85 kJ/mol, which is obviously unrealistic for the difference caused of chlorine atom allocation.

4.2 Comparison with Experimental Value

The experimental values of the enthalpies of PCDD/Fs are limited. Therefore, in this research the comparison of PCDD/Fs are compared with the available datas.

Table 3. Comparison with Experimental Value

Products	Enthalpy (kJ/mol)				
	MNDO (1998) Andrew	This Research	Exp Value Pedley (1994)	Exp-Andrew (%)	Exp-This Research (%)
Methane	-50.08	-89.9	-	-	-
Benzene	88.75	71.108	82.6	6.93	16.16
Chlorobenzene	55.92	-	52	7.01	-
1 CDD	-115.64	-89.594	-85.7	25.89	4.35
2 CDD	-123.91	-97.04	-74.1	40.20	23.64
2,3 DCDD	-141.95	-121.94	-111.9	21.17	8.23

From table 3 shows that this research has a good agreement in comparing with experimental value. The errors values are small than using MNDO method.

5. DISCUSSION

The differences results of enthalpy PCDD/Fs from other research because each researcher used their own method. And for discussion in this research, the results of enthalpy are influenced by B3LYP/6-311+G(2d,p)//B3LYP/6-31G(d) as a basis set

5.1 Discussion of Differences Basis sets

A basis set is the mathematical description of the orbitals within a system used to perform the theoretical calculation. Larger basis sets more accurate approximate the orbital by imposing fewer restrictions on the locations of the electrons in space.

Standard basis sets for the electronic structure calculations use linear combinations of Gaussian functions to form the orbitals. Basis sets assign a group of basis functions to each atom within a molecule to approximate its orbitals.

In Andrew's calculation using a semi-empirical method (MNDO), the basis set did not need to be specified since a basis set is inherent in the method.

In this research using the ab initio method, the basis set was B3LYP/6-311+G(2d,p). It means puts 2d functions and 1 function on heavy atoms (plus diffuse functions), and 1p function on hydrogen. Basis sets with diffuse functions are important for systems where electrons are relatively far from the nucleus: molecules with lone pairs, anions and other systems with significant negative charge, systems in their excited states, systems with low ionization potentials, descriptions of absolute acidities, and so on.

In this research was using the B3LYP/6-311+G(2d,p)//B3LYP/6-31G(d) for basis set because it has high level theory than others but to calculate the data it took more than 8 hours to finish.

5.2 Discussion of B3LYPD/6-311+G(2d,p)//B3LYPD/6-31G(d)

The calculated data in this research were accurate enough because of these reasons:

a. B3LYPD/6-311+G(2d,p)//B3LYP/6-31G(d)is also include as high level single point energy calculation. The most highest is B3LYP/6-311+G(3d,2df,2p)//B3LYP/6-31G(d) and the second is B3LYP/6-311+G(2d,p)//B3LYP/6-311+G(2d,p). The basis set is very important to have accuracy data. The more high level of theory will get more accuracy of the results.
b. The Mean Absolute Deviation from Experiment (MAD): The average differences between the computed and experimental values have very small errors.

6. CONCLUSION

1. Calculating Thermodynamic with gaussian'98 by using B3LYP/6-311+G (2d, p)//B3LYP/6-31G (d) as a basis set is accurate enough.
2. The small errors appeared because of the differences model chemistry and methods.
3. This method has a good agreement in comparing with experimental value because the small error values appeared.
4. To make more accuracy of this thermodynamic calculation, it recommends to use higher level of theory using B3LYP/6-311+G(3df,2df,2p)//B3LYP/6-31g(d).

ACKNOWLEDGMENT

I wish to express sincere appreciation and gratitude to Professor Yoshihara Yoshinobu for his support, advices and encouragement help me in this research. The last, I would like to say deepest sincere to my husband and my son and also my father and my mother whose support me and giving me advice for many things in my life.

REFERENCES

[1] P.W.Atkins. *Physical Chemistry*; fourth edition, Oxford University Press, 1996.
[2] James B.Foresman and Eleen Frisch, *Exploring Chemistry With Electronic Structure Methods*, Second Edition, Gaussian Inc, Pittsburgh, PA, 1996.
[3] Y. Yoshinobu, *Chemical Equilibrium and Thermo-chemical Data*, lectures, 2002.
[4] J.Ishizu, *Investigation of Dioxin Formation in Municipal Solid Waste Inceration Based On Chemical Equilibrium*, Eco-Technology, Research Center, Ritsumeikan University, 1-1-1 Nojihigashi, Kusatsu, Shiga 525-8577, Japan
[5] A. Mc Lennan, *Thermodynamic of Dioxin Formation*, Thesis and Seminars, Department of Chemical Engineering, University of Queensland, 1998.
[6] W.M.Shaub, Thermochemica acta, Vol.58, 11-44 (1982)
[7] O.V.Dorofeera, *Thermodynamic Properties of Dibenzo-p-dioxin, Dibenzofurans,and Their Polychlorinated Derivatives in The Gaseous and Condensed Phases.Thermodynamic Poperties of Gaseus Compound*s, Journal of Chemical and Engineering Data, Vol 44, No.3, 1999.
[8] N.Saito and A. Fuwa, *Prediction for Thermodynamic Function of Dioxins for Gas Phase Using Semi-Empirical Molecular Orbital Method With PM3 Hamiltonian*, Chemosphere 40 (2000) 131-145,1999.
[9] Huang et al, *Gibbs Free Energies of Formation of PCDDs: Evaluation of Estimation Methods and Application For Predicting Dehalogenation Pathways,* Environmental Toxicology and Chemistry, Vol.15,No.6,pp.824-836,1996.
[10] Peng Fu Tan et al, *Thermodynamic Modeling of PCDD/Fs Formation in Thermal Processes*, Environmental Science Technology, 2001,35 1876-1874.

INFLUENCE OF ANHYDROUS ETHANOL ADDITION ON THE PHSYCOCHEMICAL PROPERTIES OF INDONESIAN REGULER UNLEADED GASOLINE

Atok Setiyawan[1], Bambang Sugiarto[2] & Yulianto S. Nugroho[3]

[1]*Faculty of Engineering*
University of Indonesia, Depok 16424
Tel: (021) 7270011 ext 51. Fax: (021) 7270077
E-mail : atok_s@me.its.ac.id

[2]*Faculty of Engineering*
University of Indonesia, Depok 16424
Tel: (021) 7270011 ext 51. Fax : (021) 7270077
E-mail : bangsugi@eng.ui.ac.id

[3]*Faculty of Engineering*
University of Indonesia, Depok 16424
Tel: (021) 7270011 ext 51. Fax : (021) 7270077
E-mail : yulianto.nugroho@ui.edu

ABSTRACT

Ethanol is one of the most populer and attractive fuel alternative for Spark Ignition Engine (SIE). The addition of ethanol to gasoline will change most of the physicochemical properties of gasoline-ethanol blends. The properties change of gasoline-ethanol blends lead to alter engine performances, and emissions. The tested fuel of gasoline-ethanol blends compose the Indonesian regular unleaded gasoline and anhydrous ethanol in diferent compositions. The gasoline was blended with ethanol to get 10 test blends ranging from 0% to 40% by volume of ethanol with an increament of 5%. The blends were tested based on the ASTM standards. The results are the addition of ethanol to gasoline lead to increase in the RVP up to a maximum of 71.3 kPa – increased by 11.3% compared with the gasoline - with 5% of ethanol added and tends to decrease with percentage over 10%. The RON of gasoline-ethanol blends increased proportionally with the addition of ethanol. In average the addition of 5% volume of ethanol increased 1.95 point of RON.

***Key words**: gasoline-ethanol blends, properties, vapor pressure, and RON*

1. INTRODUCTION

Gasoline as a fuel of Spark Ignition Engine (SIE) is a complex mixtures composed hundreds volaitile and flammable hydrocarbons ranging from 4 to 12 carbon atoms per molecule. Gasoline can be classified as parafanic, naphtanic and aromatic had a boiling point between 30°C and 220°C. The properties of gasoline are influenced by the origin of crude oil (API and chemical composition), refinement process (distilation, alkylation, hydrocracking, and catalitic cracking process), specification and properties that fit to a climate, requirement and specification of automotive manufacturer (based on applied technology of engine), and emission standards. Recently most gasoline the contain octane booster compound to improve anti knock properties, such as: MTBE, ETBE, TAME, ethanol (oxygenate octane booster), toulene, xylene or iso-octane and other additives.

Ethanol is one of the compounds that improve octane booster for gasoline and one of the most populer alternative and renewable fuel for a Spark Ignition Engine (SIE). As an alternative fuel, ethanol can be used as a dedicated or blending fuel. As an octane booster, ethanol is the most effective to increase octane number of gasoline compared to other compounds such as: ETBE, MTBE, iso-octane and toluene[1] as seen in Fig. 1. The advantages of ethanol addition into gasoline are not only increase the octane number effectively but also improve a combustion process due to containing oxygen molecules.

The effects of addition of ethanol into gasoline has been reported by many researchers,

in which it reduces emission pollutans: CO (in the range of 5-90%) and HC (in the range of 7-85%)[1,2,3,4,5] depend upon the engine technologies applied and proportion of ethanol in the gasoline-ethanol blends. On the other hand, the impact of the addition ethanol into gasoline toward engine performance are increase a torque/power and fuel consumption by 3-9% and 3-21% respectively compared to the reference fuel[3,4,5,6].

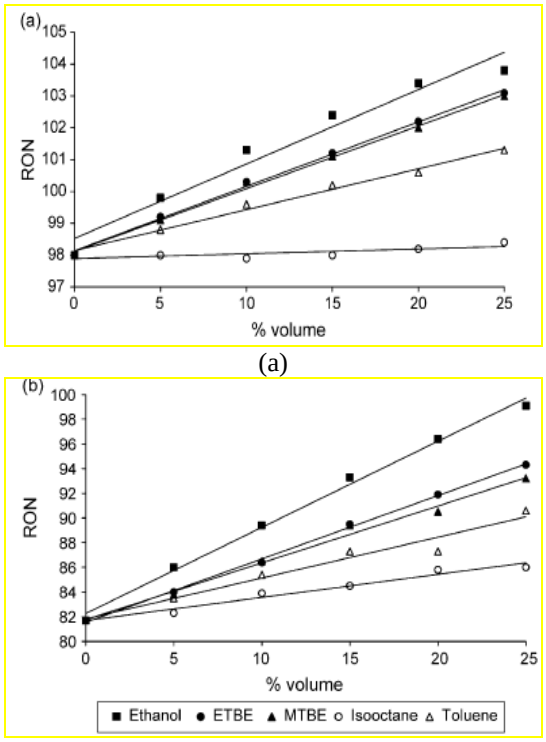

Figure 1. Motor Octane Number graphics for (a) Gasoline A dan (b) Gasoline B containing octane booster coumponds– specification of Gasoline A dan B are available on Table 2[6]

The addition of ethanol to gasoline will change phsycochemical properties significantly, mainly: volatility, density, viscosity, heat of combustion and octane number. The significancy of the properties change depend on the percentage presents influence of anhydrous ethanol addition (up to 40% v/v) on the physcochemical properties of Indonesia reguler unleaded gasoline (premium). and purity of ethanol as well as the chemical composistion of gasoline[7,8,9,10,11]. This paper presents influence of anhydrous ethanol addition (up to 40% v/v) on the physcochemical properties of Indonesia reguler unleaded gasoline (premium).

2. MATERIALS AND METHODS

2.1 Materials

An anhydrous ethanol is obtained directly from one of the Indonesian ethanol manufaturers located in Malang and did not experience the denaturation process. The denaturation process is the addition of a small quantity (less than 5%) of hydrocarbon fuel into ethanol. The denaturated anhydrous ethanol ussually call as ”fuel grade ethanol”[12]. The specification of anhydrous ethanol used for a research can be seen in the Table 1.

Table 1. Specification of anhydrous ethanol

Parameter	Specification	Test Method
Appearance	clear colorless liquid free of suspended matter	Visual
Strength at 15°C	Min 99.7 % v/v	Alcoholmeter
Total Acid as Acetic Acid	Max 30 ppm	Test by Titrimetry
Moisture Content	Max. 0.30 % w/w	Karl Fischer titration
Density at 20°C (at point of production)	Max. 0.792	Hydrometer
Material non volatile at 105°C (at point of production)	Max. 30 ppm	Gravimetry

The gasoline used for a research is the Indonesian reguler unleaded gasoline (premium) with specification as stated in the Table 2 and obtained from the Pertamina Gas station labeled ”Pasti Pas” in order to attain an accurate and good quality of product. The Table 2 also gives specification of other gasoline used for some researchers.

Table 2: Specifications and properties of gasoline

No.	Properties	Unit	Method	Spec. of Indonesian Reguler Unleaded Gasoline (Premium)[13]	Spec. of Brazilian Gasoline Type A (Non Commercial) Takeshita[11]	Spec. of Brazilian Gasoline (Commercial)[11]	Properties of Gasoline A da Slva[6]	Properties of Gasoline B da Slva[6]	Properties of Gasoline Heish[14]
1	Molecular weight								
2	Lead	gr/l	ASTM D3237-97	0.013	0.005-Max	0.005-Max	111	98	< 0.0025
3	Sulphur	%(w/w)	ASTM D2622-98	0.05	0.12	0.1			0.0061
4	Density (15/15°C)	kg/m^3	ASTM D3237-97	715 -780	-	-	734	706	757.5
5	Vapour pressure	kPa at 38°C	ASTM D5191	62-Max	45 - 62	69-Max			53.7
6	Distilation		ASTM D86-99a						
	10% Evaporated (v/v)	°C		74-Max	65-Max	65-Max	56	81	54.5
	50% Evaporated (v/v)	°C		125-Max	120-Max	120-Max	105	98	
	90% Evaporated (v/v)	°C		180-Max	155-190	155-191	152	109	167.3
	Final Boiling Point (FPB)	°C		215-Max	220-Max	220-Max	168	126	
	Residu	%vol.		2	2	2			1.7
7	Oxygen content	%(w/w)	ASTM D4815-94a	2.72 Max					
8	Ethanol content	%(v/v)	NBR13992						
9	Octane Number								
	RON		ASTM D2699-86	88-Min			90	79	94.5
	MON		ASTM D2700-86	-	82-Min	82-Min	98	82	
10	Gum	(mg/100 ml)	ASTM D381	5	5-Max	5-Max			0.2
11	Hydrocarbon		ASTM D1319						
	Aromatic	%(v/v)			57-Max	45-Max	33	9	
	Olefins				38-Max	30-Max			
	n-Paraffin						12	14	
	i-paraffin						48	57	
	Naphtene						4	17	

2.2 Methods

To verify the volatility (Reid Vapor Pressure - RVP), distillation curve, octane rating, density and kinematic viscosity of premium-ethanol blends, equipment approved by the American Society for Testing Materials – ASTM was used. The RVP tests were performed using a Grabner Instruments Minivap VPS device, following the ASTM D 5191 standard. The RON tests were carried out with a CFR engine according to the ASTM D-2699-96. The density tests were conducted following the ASTM3237-97 procedures as well as the kinematic viscosity tests were based on the ASTM D-445. Heat of combustion tetst were carried out with a Parr bomb calorimeter.

3. RESULTS AND DISCUSSIONS

All of the tests were carried out using the ASTM procedures and standards as tabulated in Table 3.

Table 3: Properties of premium, ethanol and premium-ethanol blends.

No.	Properties	Unit	Method	E-0 (Premium)	E-5	E-10	E-15	E-20	E-25	E-30	E-35	E-40	E-100 (Ethanol)
1	Density (15/15 C)*)	gr/cm^3	ASTM D 323	0.7204	0.7224	0.7249	0.7288	0.7327	0.7361	0.7383	0.7446	0.7475	0.793
2	Vapour Pressure*)	kPa at 38 C	ASTM D 5191/D	63.9856	71.363	68.881	67.34	66.882	66.468	66.399	65.0199	52.126	15.5827
3	Heat of combustion**)	MJ/l		29.07	28.666	28.264	27.863	27.461	27.06	26.658	26.2565	24.249	21.04
4	Viscosity*)	cSt at 40°C	ASTM D 445	0.48	0.49	0.5	0.52	0.55	0.57	0.6	0.63	0.72	1.11
5	Distillation*)		ASTM D 86-99a										
	Initial Boiling Point (IBP)	C		38	38	39	41	39.5	40.5	44	40.5	43	77.25
	10% Evaporated (v/v)	C		49	48	48	49	49	49.5	51	50	52.5	77.25
	50% Evaporated (v/v)	C		73	74	63	63.5	65	66.5	68.5	70.25	71.5	77.25
	90% Evaporated (v/v)	C		148	159	154	147	144.5	138	143	140.5	78.5	77.5
	Final Boiling Poin (FBP)	C		183	183	185	182	183.5	182.5	182	180.5	173.3	78
6	RON***)		ASTM D 2699-86	88.62	90.61	91.89	94.70	97.06	98.35	99.50	102.28	104.21	127.43

Note: *) tested at Unit Produksi Pelumas Surabaya Laboratory (UUPS), PT Pertamina

**) tested at ITS Chemical Engineering Laboratory

***) tested at Unit Produksi Pelumas jakarta Laboratory (UPPJ), PT Pertamina

3.1. Research Octane Number (RON)

The quality of gasoline is constantly based on its octane number, which indicates its antiknocking strength. Research Octane Number (RON) is one of the extremely important property of SIE fuel concerning antiknocking during combustion occurs in the cylinder combustion chamber. The combustion of gasoline in the SIE occurs initiation by sparking from spark plug and flame propaggate to burn mixture of gasoline and air while combustion mixture by compression/ autoignition is prohibited. Gasoline having a high octane number produces more effective combustion in Spark Ignition Engine. The efficiency of a gasoline fueled engine is highly influenced by the fuel's antiknock characteristics. The RON of anhydrous ethanol is much higher - i.e. around 127 - compared to the premium as shown in the Table 3.

The addition of ethanol into gasoline caused a linear increase in the RON as shown in Fig. 1. The increase of the RON of gasoline-ethanol blends are influenced by some factors such as, RON of the based gasoline, chemical composition of gasoline and the proportion of ethanol in the blend. The increase of RON improves combustion procces lead to efficiency of engine rise.

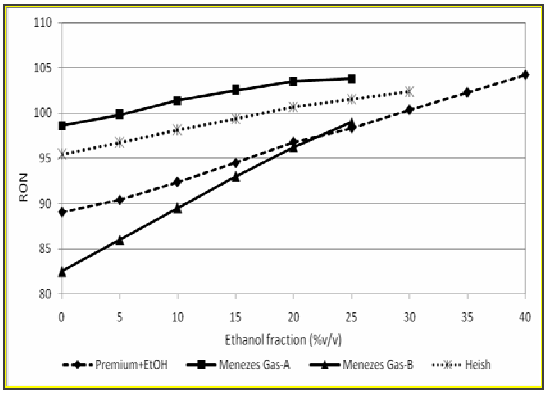

Figure 1: Octane Number for several gasolines

Every 5% v/v addition of ethanol into premium increased around 1.9 point of the RON and at the 40% of ethanol in the blend, the RON reached 104 point. The Fig. 1 shows that a higher RON of the base gasoline tends to decrease the effectiveness of ethanol addition for increasing RON of the premium-ethanol blends and vice versa. The addition of 5% volume of ethanol into the Menezes type A gasoline that has RON of 82.5 increased around 3.3 point of the RON. On the other hand for the Menezes type B gasoline that has RON of 95.4 only increased around 1.7 point of RON for every 5% volume of the ethanol addition.

3.2. Volatility and Reid Vapor Pressure (RVP)

Volatility can be undestood as the ease with wich fuel evaporates. The volatilty expressed as vapor pressure is the most important of property of fuel for SIE due to the combustion process take place in a gaseous environment. In inside of combustion chamber of SIE, where the gasoline must first vaporized and mixed with air so that combustion can occur. The vapor pressure can be determined by a variety of methods, most of them are based on the properties of Reid Vapor Pressure (RVP) and distillation curve.

Gasoline contains hundreds volatile and flammable liquid hydrocarbon compounds from light fractions (C_4) to medium fractions (C_{12}) each having a boiling point that interfres with the others when mixed.The RVP is an indicator of the volatility of the lightes fraction of the gasoline (i.e. of the most volatile compounds) meanwhile the distilation curve gives an idea of the volatility of the gasoline throughout the range of distillation.

Figure 2 describes an evolution of vapor pressure in kPa measured at 37°C (RVP) of the addition of ethanol into gasolines. In general, the addition of ethanol into premium lead to a significant increase with the first 5% of ethanol volume added. Cotinuoesly increasing the percentage of ethanol in the blends more than 5% by volume into gasoline tends to decrease vapor pressure steadily – the same result obtained by API[15]. Some researchers found that the highest increase of vapor pr**e**ssur occur between 5% and 10% the addition of ethanol[6,10,11]. The vapor pressure of blending premium and ethanol which is higher than each of vapor pressure of compossed fuels called as azeotrope effect. The hydrocarbon structure of gasoline-ethanol which cause azeotrope is not yet known. However, the vapor pressure, being an indicator of fuel volatility, is closely related to the molecular interaction of the mixture components[16]. Some researchers consider that the polar molecular structure of ethanol is responsible for increasing vapor pressure of gasoline-ethanol blend due to molecular interaction between ethanol and gasoline (non-polar structure) becomes weak[2,11].

The addition of 5% anhydrous ethanol into premium increased Reid Vapor Pressure by 11.5% from 64 kPa (pure premium) to 71.3 kPa. Azeotrope effect of gasoline-ethanol blends are influenced by chemical compistions of gasoline. Gasoline has a high concentration of paraffin and naphtene provide a higher azetrope effect, the RVP increade by 30% with the addition of ethanol. Meanwhile gasoline contains a rich of aromatic lead to a 15% increase in the mixture's RVP[6]. In term of the spesification of a base gasoline (Table 2) used by the author and Takeshita are similar to the commercial Brazilian gasoline, the azeotrope effects of them are also similar as showed in Fig. 2.

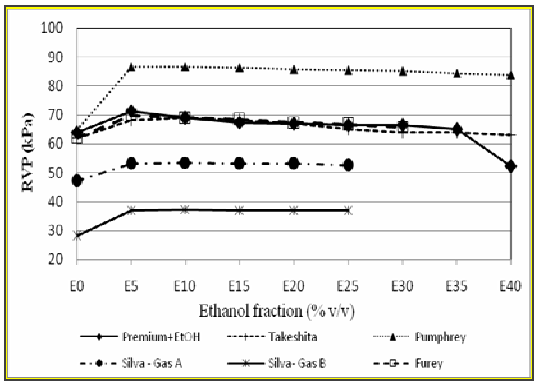

Figure 2: Reid Vapor Pressure for several gasolines

The vapor pressure is related to evaporative emissions occur by a wide variety of mechanisms, including fuel spillage and vapor displacement during refuelling, venting of fuel tank vapor as ambient temperature change, fuel evaporation from engine compartment of parked vehicles due to residual engine heat, liquid leaks in vehicles fuel systems, and so on[2]. However, the presence of ethanol into gasoline mixture increase the mixture's vaporization enthalpy, rendering vaporization difficult and reducing the temperature in the intake haeder, thus allowing a greater mass of fuel to enter the cylinder. In addition, the ethanol consist of oxygenate compounds show a lower combustion enthalpy which, in some cases, compensate for the increase in density of the mixture in intake header lead to maintaining the engine's power. The vapor pressure property is related to safety, transport, and storage of fuel.

The vapor pressure of pure premium and premium-ethanol blends is higher than vapor pressure specified in the Decree of Directorate Generale of Energy and Natural Resources. Based on the specification, the maximum vapor pressure either for pure gasoline (premium) or oxygenate gasoline is 62 kPa, as stated in (Table 2). It is recommended that the specification for oxygenate gasoline (bio-premium contains 3-5% v/v of ethanol) should be revised in order to fit the tested RVP as well as apllied in the Brazilian oxygenate gasoline.

3.3. Volatility and Distilation Curve

Volatility can also be determined by using distillation curve according to the ASTM D-86 standard and procedure. The distillation curve gives an idea of the volatility of gasoline throughout the range of distillation (light up to heavy fraction of hydrocarbon), since the RVP vapor pressure is just a good indicator of the volatility of light fraction of the gasoline. The distillation curve can, in simple terms, be represanted by three points: T10, T50 and T90 which represent the temperatures at which 10, 50 and 90% vaporization of the gasoline's initial occurs. These temperatures characterize the volatility of the fuel's light, medium and heavy fraction. These fractions, in turn, affect the engine's different operating regimes.

Figure 3, shows the distillation curve for the anhydrous ethanol and gasoline used by author and Takeshita. Temperature of vaporization of the both ethanol is similar at around 78°C for a whole volume of vaporization. Ethanol, being a pure compound, has a single distillation point, unlike the other compounds which are mixtures of hydrocarbon.

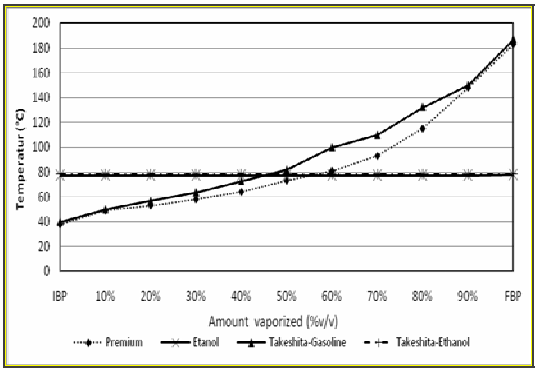

Figure 3: Distillation curves anhydrous ethanol and gasoline

Based on the specification of gasoline (Table 2), premium and gasoline used by Takeshita for the research is similar as well as the distillation curve for the both gasoline. The

slight different occurs in the middle of the curve in which the vaporization temperature of medium fraction is slightly higher compared to premium. It indicates that a higher concentration of medium fractions for the Takashita's gasoline than the premium.

Figure 4 shows the distillation curve for the premium, anhydrous ethanol and premium-ethanol blends, these curves as reference in the analysis of the effect of the addition of ethanol to premium. The distillation of premium shows continuous and smooth increase in temperature as the distillation process progresses (Fig. 3). In general, except for the addition of 5% v/v of ethanol, the increase of addition of ethanol to premium tends to increase the Initial Boiling Point (IBP). The addition of ethanol did not change the Final Boiling Point (FBP).

The addition of 5% v/v of ethanol to premium a sudden change in temperature can be observed, which occurred after 40% distillation of the initial volume. With the addition of 10% v/v of ethanol to premium the same sudden change occurred, however, after a distillation of 50% of the initial volume. With the consecutive increase in the proportion of ethanol in the blends, the location of this sudden increase in temperature tends to occur closer and closer to the final percentage of distillation.

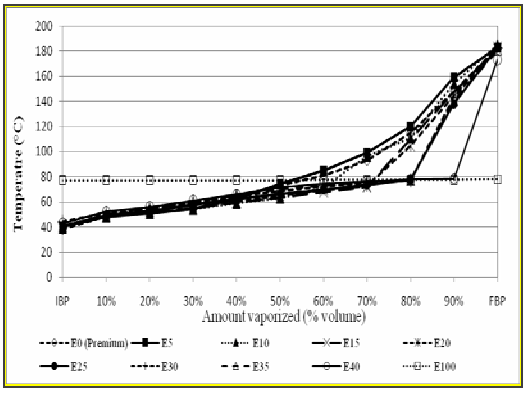

Figure 4: Distillation curves for anhydrous ethanol-premium blends (E0-E40 and E100)

The distillation point that corresponds to 10% of the evaporated volume is related to the engine ignition, mainly for the cold start. The addition of ethanol into gasoline that increases the volatility of the gasoline-ethanol blends can cause the formation of vapor bubbles in the fuel, interrupting the flow and resulting in the engine stalling. In addition, the 50% distilled limit is monitored by its relation with the heating and accelerating of the engine and with the fuel economy. The maximum limits established for the temperature of a 90% evaporated volume and of the FBP aim to control the quantity of high boiling point compounds and to avoid the formation of carbon deposits inside the engine[17].

3.4 Viscosity

Viscosity is defined as the easy with which is fuel can flow. Kinematic viscosity test was carried out correponding to the ASTM D-445 at 40°C. The kinematic vicosity of ethanol is much higher as much as two fold than compared to the premium. The addition of ethanol to premium caused the vicosity of mixture increase is not proportionally with the percentage of ethanol in the mixture. More ethanol in the mixture much more increase in the kinematic viscosity as shown in Fig. 5.

Viscosity is related to droplet formation and development when fuel is injected into manifold or combustion chamber. In general, the higher viscosity of fuel tends to make a bigger dropplet size and spray properties change. Although the gasoline-ethanol blends has higher viscocity than pure gasoline, based on the Gao's research there was no significant change in the spray developing pattern for different blends of gasoline-ethanol (25%, 50%, 75% and 100% ethanol) compared to gasoline[18].

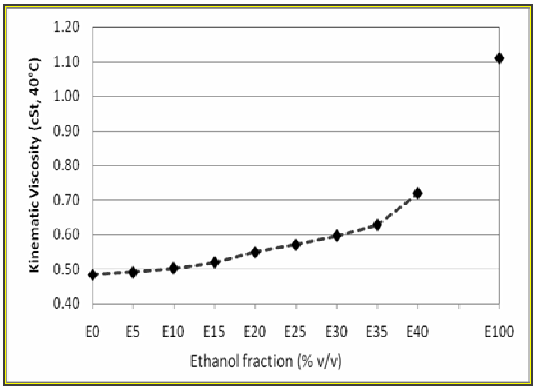

Figure 5: Kinematic viscosity curve for anhydrous ethanol-premium blends (E0-E40 and E100)

3.5. Density

Figure 6, gives density among gasoline-ethanol blends at 15°C used by some researchers. As can be seen in the Figure 6, the increase in the addition of ethanol in the gasoline increase the density of the mixtures,

which may attributed to the higher density of the ethanol. The increase of mixtures is propositional to the amount of ethanol addition. Changes in the density affect the quantity of fuel that is injected into the combustion chamber during each cycle, lead to altering the ideal-fuel burning ratio. In general the mixture that has a higher density, the burning will be incomplete, resulting in the emission pollutants increase also. In the case of ethanol in which a density compound is higher than the premium, due to ethanol contains oxygen so it will improve the combustion efficiency. In other words, without any reduction air combustion, it makes the ratio of fuel-air of gasoline-ethanol mixture becomes lean.

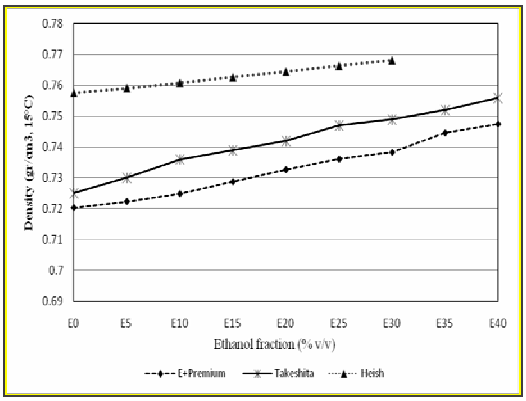

Figure 6: Density of gasoline-anhydrous ethanol blends

3.6. Heat of Combustion

Heat combustion is the amount of heat releases per unit mass or unit volume of a substance when the substance is completely burned. Heat combustion of the anhydrous ethanol is 21.04 MJ/liter - only around 72% of the heat combustion of premium (Table 2). The heat combustion of the tested premium tends to low compare the other gasoline used by other researchers in which the heat of combustion of gasoline in the range of 31-33 MJ/liter[1,3,4,57].

Heat of combustion is important properties of fuel for the Spark Ignition Engine (SIE), in which most of the SIE are used for automotive. One of the most important prerequisite of fuel for the automotive engine is having a high energy density. If there is no change in the gasoline engines modifications when using ethanol fuel, the engines consume 30% more than gasoline. However, some researchers have been succeeded to reduce fuel consumption for the SIE using ethanol by engine modifications and setting engine operational parameters[3], even fuel consumption of gasoline-ethanol blends for the SIE is lower than pure gasoline[1].

4. CONCLUSION

The main results of experiment are the addition of ethanol to gasoline lead to increase in the RVP up to a maximum of 71.3 kPa – increased by 11.3% compared with the gasoline - with 5% of ethanol added and tends to decrease with percentage over 10%. The RON of gasoline-ethanol blends increased proportionally with the addition of ethanol. In average the addition of 5% volume of ethanol increased 1.95 point of RON.

ACKNOWLEDGMENT

The authors would like to thank to Heads and staffs of the Laboratory of Surabaya Lubrication Production Unit (UPPS) and Jakarta Lubrication Production Unit (UPPJ) PT. Pertamina (Persero) which allowed us to conduct test of fuel properties according to the ASTM standard and procedures.

REFERENCES

1. Al-Hasan M,"Effect of ethanol-unleaded gasoline blends on engine performance and exhaust emissions" Journal of Energy Conversion and Management (44) 1547-61, 2003, Pergamon.
2. Balabin R.M, R.Z. Syunyaev and A.A. Karpov,"Molar enthalpy of vaporization of ethanol-gasoline mixture and their colloid state", Fuel Vol. 86, pp: 323-7, 2007, Elsevier.
3. Bang-Quan He, and Jian-Xiin Wang," A study on emission characteristics of an EFI engine with ethanol blended gasoline fuels", Atmospheric Environmet Vol. 37, pp. 949-957, 2003, Elsevier.
4. Jia, Li-Wei, and Mei-Qing Shen," Influence of ethanol–gasoline blended fuel on emission characteristics from a four stroke motorcycle engine", J of Hazordous Materials Vol,123, pp. 29-35, 2005, Elsevier.
5. Wei-Dong Hiesh, Rong-Hong Chen," Engine performance and pollutant emission of an SI engine using ethanol-gasoline blended fuels", Atmospheric Environment Vol.36, pp. 403-410, 2002, Elsevier.

6. Da Silva R., Renanto Cataluna, Eliana W.eber de Menezes, Dimitrios Samios, and Claisse M. Sartori Piatnicki,"Effect additives on the antiknock properties and Reid vapor pressure of gasoline", Fuel Vol. 84., pp. 951-9, 2005, Elsevier.
7. Chan-Wei Wu, Rong-Horg Chen," The influence of air-fuel ratio on engine performance and pollutant emission of an SI engine using ethanol-gasoline-blended fuels", tmospherin Environmet Vol.38, pp. 7093-1700, 2004, Elsevier.
8. Kar Kenneth, T. Last, C. Haywood and R. Raine,"Measurement of vapor Pressure and Enthalpies of vaporization of gasoline and ethanol blends and their effects on mixture preparation in an SI Engine", SAE 2008-01-0317, 2008.
9. Lanzer T., O.F. von Meien, C.I. and Yamamoto,"A predictive thermodynamic model for the Brazilian gasoline", Fuel Vol. 84, pp. 1099-104, 2005.
10. Pumphrey J.A., J.I. Brand and W.A. Scheller, "Vapour pressure measurement and predictions for alcohol-gasoline blends", Fuel Vol. 79, pp. 1405-11, 2000, Elsevier.
11. Takeshita, E.V., R.V.P. Rezende, and S.M.A Guelli U. De Souza,"Influence of solvent addition on the physicochemical properties of Barzilian gasoline", Fuel Vol. 87, pp. 2168-77, 2008, Elsevier.
12. Prihandana Rama, Kartika Noerwijari, P.G. Adinurani, D. Setyaningsih, S. Setyadi, and R. Hendroko, "Bioetanol Ubi Kayu – Bahan Bakar Masa Depan", AgroMedia Pustaka, 2007, Jakarta.
13. Pertamina,"Bahan Bakar Minyak Untuk Kendaraan Bermotor, Rumah tangga, Industri dan marine", PT Pertamina (Persero), 2008, Jakarta, Indonesia.
14. Hiesh Wei-Dong, and Rong-Hong Chen,"Engine performance and pollutant emission of an SI engine using ethanol-gasoline blended fuels", Atmospheric Environment (36), pp. 403,10, 2002, Pergamon.
15. American Petroleum Institute (API), "Alcohol and Ethers: A Tecnical assessment of their application as fuel and fuel components. API Publication 4261. 2001, Third edition.
16. Menezes EWD, Rosangela da Silva RC, and Ortega RJC, "Effects of ethers and ether/alcohol additives on the psychochemical properties of diesel fuel and on engine tests,", Fuel, Vol.85, pp. 505-9, 2006..
17. Delgado RCOB, Araujo AS, and Fernandes Jr. VJ, "Properties of Brazilian gasoline mixed with hydrated ethanol for flex-fuel technology", Fuel Process Technology, 2006, doi:10.1016/ i.fuproc.2006.10.010.
18. Gao Jian, Deming Jian, and Z. Huang,"Spray properties of alternative fuels: A comparative analysis of ethanol-gasoline blends and gasoline, Fuel, Vol. 86, Issue 10-11, July-August, pp 1645-50, 2007.
19. Ranajit, Sahu,"Technical paper on the introduction of the greater than E-10 gasoline blends"- internet access on July 2007.

ISSN 114-1284

Performance of an Air Conditioning as Hybrid Refrigeration Machine Uses Hydrocarbons Refrigerant (HCR22) As Substitutes For Halogenated Refrigerant (R22)

Azridjal Aziz

Department of Mechanical Engineering, Faculty of Engineering
University of Riau, Pekanbaru 28293
Tel: (0761) 566786. Fax : (0761) 66595
E-mail : azridjal@yahoo.com, azridjal@unri.ac.id

ABSTRACT

Hybrid refrigeration machine is the machine with refrigeration principle and heat pump in one machine, so-called the hybrid refrigeration vapor compression. Air-conditioning and refrigerating industries weathered the phase out of chlorofluorocarbons (CHCs) and hydro chlorofluorocarbons (HCFCs), which caused from the ozone layer depletion, by developments of hydro fluorocarbons (HFCs) as alternative refrigerants. However, the HFCs will also phase out because they are greenhouse gases as a cause of global warming. Therefore, natural substances, such as ammonia, hydrocarbons, carbon dioxide, are getting great interest. The research result is indicated that the use of mass HCR22 (hydrocarbon refrigerant of substitution R22) at hybrid refrigeration machine more economical 57.78% compared to R22 (halocarbon refrigerant), because HCR22 has the higher level of latent heat compared to R22. Cooling rate and heating rate by HCR22 compared to R22, is more efficient too. The Power consumption of compressor use of HCR22 is more economical 25.12% compared to hybrid refrigeration machine that use R22. In conclusion using of hydrocarbon refrigerant can economize of electrical energy consumption and environmental friendly.

Keywords

refrigeration, refrigerant, hybrid, hydrocarbon, halocarbon

1. INTRODUCTION

Refrigeration machine generally is used for conditioning room as cooling effect from evaporator that give comfortable and chilly sense for human in working room or office building, houses, apartment, industry, office, hospital, etc. Refrigeration machine is one of energy conversion machine type, where a number energy is needed to result refrigeration effect [1]. On the other side, heat losses waste by system goes to environment as requirement thermodynamics principle that machine can be function. Heat from the condenser escaped to environment usually castaway off hand without exploited. And so do at heat pump machine, a number of energy required to give the warming effect by absorbing heat from environment. Absorbing heat from the environment can be exploited to make cool something, but usually tend to let castaway [2].

Starting from case of refrigeration machine and heat pump machine above, hence various effort have been done to develop a system using principle of refrigeration and heat pump in one machine. At this machine, cooling effect and heating effect can be yielded and exploited simultaneously, so that useful power of machine becomes higher. Inwrought machine with the this double function is recognized as hybrid refrigeration machine, because refrigeration machine generally operating with the vapor compression cycle, hence this machine is referred as refrigeration machine vapor compression cycle [3].

To operate the refrigeration machine with hybrid vapor compression cycle is required the refrigerant as working fluid. The refrigerant usually used is the halogenated refrigerant; one of them is type HCFC-22 /Hydro chlorofluorocarbon or R-22. But from the result of research, halocarbon refrigerant show the nature of which can destroy the ozone layer and have big potency to make-up of global warms effect, so that the use refrigerant will be discontinued inclusive of also making and its usage [4].

One of alternative refrigerant for substitution of halocarbon refrigerant is hydrocarbon refrigerant. Some excess owned by the hydrocarbon refrigerant, that is serve the purpose of direct substitution (drop in substitute) without component replacement, environmental friendly (do not damaged the ozone layer), a little usage refrigerant, economize the energy, and fulfill the international standard [5].

This research aim to know the parameter influencing performance of air conditioning, what modification have become the hybrid refrigeration machine, among other things is cooling capacities, warming capacities, energy for compressor, coefficient of performance (COP) and performance factor (PF). This Research is done because exploiting of evaporator and condenser simultaneously of course will be give the trouble or change to influence the machine performance. At this research is used hydrocarbon refrigerant as replacement of halocarbon refrigerant (R-22). With hydrocarbon refrigerant, the air conditioning apparatus

remain to admit of used without component replacement and expected do not go down the system performance.

2. RESEARCH METHOD

The refrigeration machine used in this research, is modification from air conditioning machine become the hybrid refrigeration machine. This apparatus, evaporator and condenser use water as cooling and heating load.

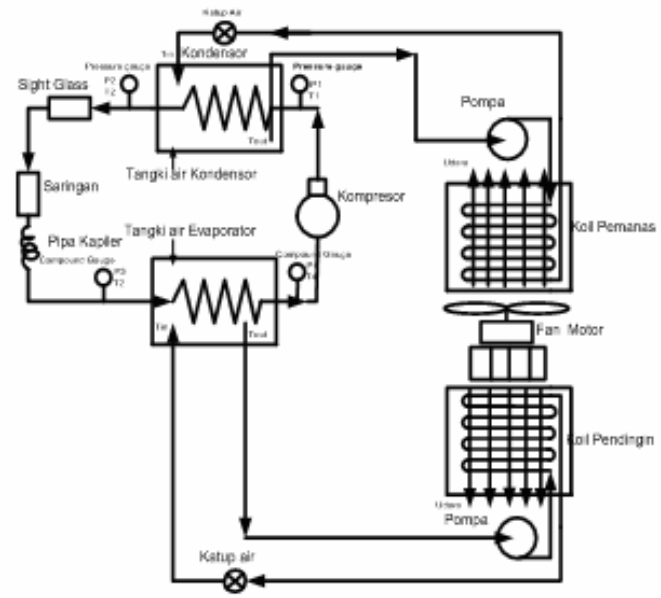

Figure 1: Simple scheme of hybrid refrigeration machine of vapor compression cyle.

Research method done through few step in the following is:

1. Phase of Research Preparation.

This step is done by literature study and understanding to concept of refrigeration machine of vapor compression cycles that using hydrocarbon as refrigerant, by learning book and relevant recent of research journal.

2. Phase of Design and Apparatus Making Test.

At this step is done design of test apparatus base on literature study or recent research journal publication. Furthermore, result of design is realized by doing equipment making test that is a refrigeration machine of vapor compression

3. Phase of Test Data Result

At this step is done data record that needed by using some kinds of measuring instrument for example: pressure gauge, thermometer, millimeter, stopwatch, etc. Data taken cover the power of compressor, temperature input and output from the evaporator, temperature input and output from the condenser, flow rate of water in to cooling and heating water tank, pressure input and output from the compressor, pressure of condenser and pressure of evaporator

4. Phase of Data Analysis

Data obtained will be tabulation and done calculation according to principles of thermodynamics, the data will be plotted in graphics which can give the information about influence of temperature input and output from evaporator, influence of temperature input and output from condenser, water flow rate from heating and cooling water tank, pressure input and output from compressor, pressure from condenser and evaporator, that compared to system performance.

5. Phase of expression about conclusion

At this step the entire result obtained from step 1 to step 4 previously concluded to become the final conclusion obtained from this research, and suggestion for the perfection of next research.

3. RESULT AND DISCUSSION

3.1 Result of Design the Hybrid Refrigeration Machine

The result of design the hybrid refrigeration machine is:

1. Compressor, in this machine used hermetic compressor, with rotary type, the power of compressor is 1 HP.
2. Evaporator, in evaporator used copper pipe 3/8 “, that have one pass with 31 cm long. The entire evaporator have 66 pass with 11 level. Each level have 6 pass. The design data from evaporator :
   a. Temperature of outer pipe surface, *Ts* is 9.17 ^oC
   b. Total surface area of pipe, *Ao* adalah 0.6175 m^2
   c. Lenght of pipe, *L* adalah 20.69 *m*
   d. Coefficient of mean heat transfer, h_0 = 219.018 $W/m^2.^0C$
   e. Overall heat transfer coefficient, U_0 = 172.7496 $W/m^2.^0C$
3. Condenser, in condenser used copper pipe 3/8”, that have one pass with 33 cm long. The entire evaporator have 66 pass with 11 level. Each level have 6 pass. The design data from evaporator :
   a. Temperature of outer pipe surface, *Ts* is 40.93 ^oC
   b. Total surface area of pipe, *Ao* adalah 0.6489 m^2
   c. Total Lenght of pipe, *L* adalah 21,74 *m*
   d. Coefficient of mean heat transfer, h_0 = 315.738 $W/m^2.^0C$
   e. Overall heat transfer coefficient, U_0 = 236.649 $W/m^2.^0C$
4. Capillary pipe, the diameter of capillary pipe is 1.7 mm, that working at condensation temperature 45 ^oC and evaporation pressure 5 ^oC, the lenght of capillary pipe is 1.65 m.

3.2 Data Processing of Test Result

Data obtained from testing through measurement is in the form of nature of from refrigerant, water, and electrics data. Nature of the among other things is temperature, pressure, mass, time, speed and also voltage and electrics current.

Calculation Sample:

Power of compressor:

$$W_k = \eta_m \times \sqrt{3} \times V \times I \times Cos\phi = 0.82kW$$

Where: η_m = 0.8, $\cos\phi$ = 0.83, V = 223 volt,
I = 3.2 A

Cooling capacity in the evaporator box:

$$Q_e = \dot{m}_{ae} \times C_{P,ae} \times \Delta T_{ae} = 2.17kW$$

Where: $\dot{m}_{ae}$ = 0.1234 kg/s,

C_{Pae} = 4.183 kJ/ (kgK),

ΔT_{ae} = 4.2 ^{o}C

Heating capacity in condenser:

$$Q_k = \dot{m}_{ak} \times C_{P,ak} \times \Delta T_{ak} = 2.91kW$$

Where: $\dot{m}_{ak}$ = 0.0883 kg/s,

C_{Pak} = 4.178 J/ (kgK),

ΔT_{ak} = 7.9 ^{o}C

Coefficient of performance:

$$COP = \frac{\dot{Q}_e}{\dot{W}_k} = 2.64 \quad , \; PF = \frac{Q_k}{W_k} = 3.55$$

$$TP = \frac{(q_k + q_e)}{w_k} = 6.19$$

3.2 Discussion

At this research will be analyzed influence of water mass flow rate in evaporator water tank to performance of hybrid refrigeration machine (COP, PF and TP). Analyze also will learn about the water mass flow rate in evaporator to cooling effect, heating effect, and the power of compressor. Furthermore watch closely about change of water mass flow rate in evaporator/condenser to water temperature input and output, temperature and pressure in refrigeration machine

3.2.1 Mass of Refrigerant R22 and HCR22

Comparison of between amount of R22 refrigerant mass to HCR22 refrigerant (figure 2), the optimum mass of R22 is 900 gram at COP 2.42, while the optimum mass of HCR22 is 380 gram at COP 2.55. So the uses of HCR22 refrigerant, the refrigerant mass more efficient 57 percent to the mass of refrigerant R22.

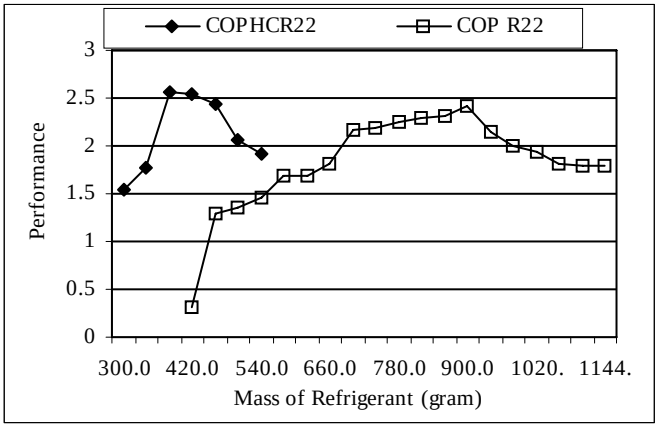

Figure 2: Optimum mass and optimum COP of refrigerant HCR22 and R22

3.2.2 Cooling Rate and Heating Rate

At transient condition that is condition of moment of hybrid refrigeration machine at first start run until steady condition, figure 3 shows that cooling rate of HCR 22 compared to faster than cooling rate of R22.

The cooling time until steady condition for HCR22 around 40 minutes at temperature 7.1 ^{o}C, whereas R22 need time around 60 minutes at temperature 8.3 ^{o}C. Heating rate until steady condition for HCR22 around 40 minutes at temperature 44.8 ^{o}C whereas R22 need time around 60 minutes at temperature 44.4 ^{o}C. Appear that cooling rate and heating rate for HCR22 faster than R22 with cooling time and heating time almost at the same period.

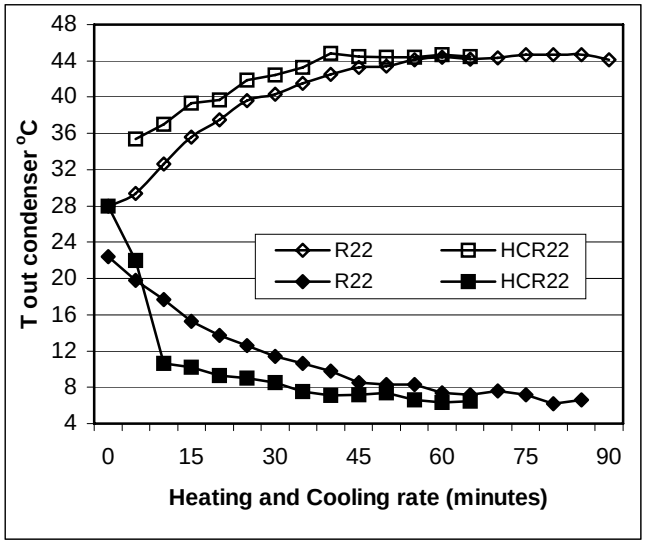

Figure 3: Cooling rate and heating rate of refrigerant HCR22 and R22

Performance of hybrid refrigeration machine : COP, PF and TP at water speed rate in evaporator and condenser at 0.067 kg/s and 0.088 kg/s, with R22 refrigerant and HCR22 refrigerant.

3.2.3 Performance of Hybrid refrigeration machine (COP, PF, TP)

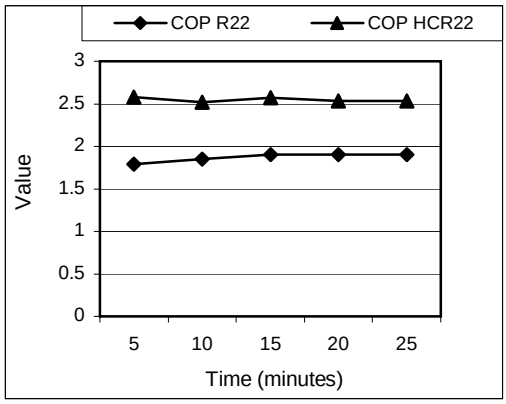

Figure 4: COP hybrid refrigeration machine with HCR22 and R22 refrigerant

The performance of hybrid refrigeration machine is COP, PF and TP at water speed rate in evaporator and condenser at 0.067 kg/s and 0.088 kg/s, with R22 refrigerant and HCR22 refrigerant (figure 4).

From the figures, we knows that COP, PF, ITP with HCR22 at hybrid refrigeration machine higher than R22. COP, PF and TP is 2.548, 3.203 and 5.751 for HCR22. COP, PF and TP is 1.834, 2.62 and 4.454 for R22. HCR22 can absorb energy bigger than R22 at the same pipe volume refrigerant.

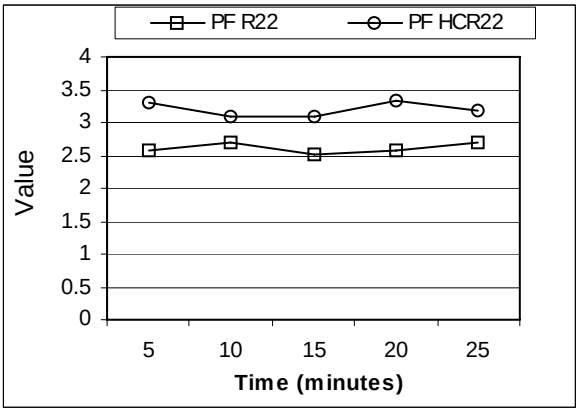

Figure 5: PF hybrid refrigeration machine with HCR22 And R22 refrigerant

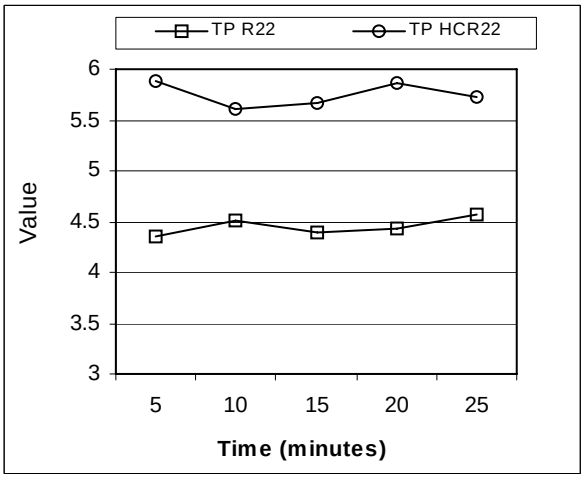

Figure 6: TP hybrid refrigeration machine with HCR22 and R22 refrigerant

3.2.4 Cooling Capacity, Heating Capacity and Power of Compressor

Cooling capacity with HCR 22 higher than cooling capacity with R22, because HCR22 can absorb heat higher than R22, HCR22 have latent heat higher than R22. For the same cooling capacity HCR22 need refrigerant mass lower than R22 (about 50% mass for HCR22 compared to R22). Figure 7 shows cooling capacity between HCR22 and R22 is 1.943 kW and 1 834 kW.

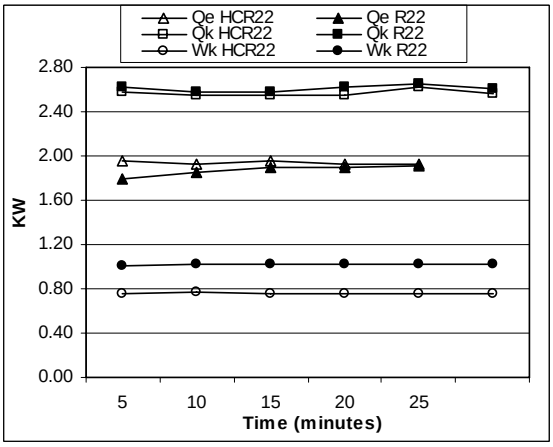

Figure 7: Cooling capacity, heating capacity and power of compressor with HCR22 and R22

Table 1 shows the experimental data form this research, this table summary data from the research.

Table 1: Experimental data research with HCR22 and R22

Description	Refrigerant	Value	Unit	Result	Efficiency%
Refrigerant Mass	HCR22	380	gram		57.78
	R22	900			
Cooling Rate	HCR22	40	minutes	faster	33.33
	R22	60			
Heating Rate	HCR22	40	minutes	faster	33.33
	R22	60			
COP	HCR22	2.548	unit	Increase	38.93
	R22	1.834			
PF	HCR22	3.203	unit	Increase	22.25
	R22	2.62			
TP	HCR22	5.751	unit	Increase	29.12
	R22	4.454			
Cooling Capacity	HCR22	1.943	kWatt	Increase	5.94
	R22	1.834			
Heating Capacity	HCR22	2.567	kWatt	decrease	-1.69
	R22	2.611			
Condenser Pressure	HCR22	260	Psig	decrease	-18.60
	R22	319.4			
Compressor Power	HCR22	0.763	kWatt	decrease	-25.12
	R22	1.019			

Heating capacity with HCR22 is lower than heating capacity R22. Because pressure at condenser with R22 higher than HCR22 (figure 8). At higher pressure condenser, the temperature higher too, so heating energy for water at condenser bigger at higher temperature. Figure 7 shows that heating capacity that comparison HCR22 and R22 with heating effect between HCR22 and R22 whereas heating capacity for HSR22 and R22 is 2.567 kW compared to 2.611 kW.

The mean pressure of compressor with HCR22 refrigerant is 260 Psig and the mean pressure of compressor with R22 is 319.4 Psig. Figure 7 shows that the comparison between power of compressor with HCR22 (0.763 kW) to R22 (1.019 kW). The power of compressor with HCR22 more efficient compared to R22 about 25%.

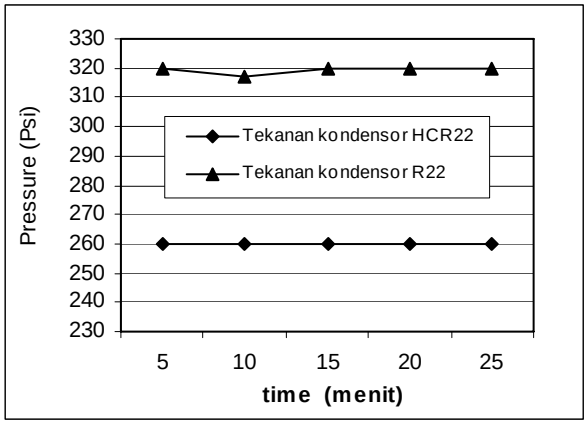

Figure 8: Pressure at condenser with HCR22 refrigerant and R22 refrigerant

4. CONCLUSION

At this research, from result of design and discussion done to experimental data, can conclude that:

1. Design output from the experimental apparatus is : the length of evaporator pipe is 20.69 *m* with surface area 0.6175 m^2 and heat transfer coefficient 172.7469 $W/(m^2.^0C)$. The length of condenser pipe is 21.74 *m* with surface area 0.6489 m^2 and heat transfer coefficient 236.469 $W/(m^2.^0C)$. The length of capillary pipe is 1.65 m with 1,7 mm diameter.
2. The use mass of hydrocarbon refrigerant HCR22 more efficient 57.78 % compared to R22 refrigerant, because latent heat of HCR22 higher than R22.
3. Cooling rate and heating rate with HCR22 faster than 33.33 % compared to R22. Performance of HCR22, the COP increase 38.93%, PF increase 22.25% and TP increase 29.12% compared to R22.
4. At the use of hydrocarbon refrigerant HCR22, cooling rate increase 5.94%, while heating rate decrease 1.69% because the pressure of condenser decrease 18.6%. The power of compressor with hydrocarbon refrigerant HCR22 more efficient 25.12 % compared to R22.

ACKNOWLEDGMENT

Authors gratefully acknowledge financial support for the reported work under the HEDS JICA grant scheme.

REFERENCES

[1] W. F. Stoecker and J.W. Jones, “Refrigeration and Air Conditioning”, Erlangga, 1994.
[2] C. P. Arora, ‘Refrigeration and Air Conditioning”, Mc Graw-Hill International Edition, 2001.
[3] Amrul, “Experimental Study of Characteristic of Hybrid Refrigeration Machine Vapor Compression Formation Paralel and Seri using Hydrocarbon Refrigerant HCR12”, Thesys, Mechanical Engineering Department ITB, Bandung, 2001.
[4] A.D. Pasek, N.P. Tandian, and W. Adriansyah, ‘Training of Trainers Refrigerastion Servicing Sector”, LPPM-ITB, 2004.
[5] Suamir, I Nyoman, “Design and Making Performance of Test Apparatus Hydrocarbon Refrigerant R-12 Substituted”, Thesis, Mechanical Engineering Department ITB, Bandung, 1999.

Proceeding of the 11th International Conference on QiR (Quality in Research)
Faculty of Engineering, University of Indonesia, Depok, Indonesia, 3-6 August 2009
ISSN 114-1284

Dimensionless Investigation of Air Mixed and Displacement Ventilation Systems Based on Computational Fluid Dynamics for Indoor Air Quality Improvement in Office Room

Bambang Iskandriawan

Faculty of Civil Engineering and Planning
Institut Teknologi Sepuluh Nopember, Kampus ITS Keputih Sukolilo Surabaya 60111, Indonesia
Tel. +62-31-5931316 Fax. +62-31-5931147
iskandriawan10@yahoo.co.id

ABSTRACT

Air ventilation system is needed in the purpose of maintaining clean and fresh air. It will improve the comfort, wealthy and productivity of occupant. This research investigates the influence of fresh air diffuser position to the indoor air quality (IAQ) where it focuses on CO_2 gas contaminant concentration. The aim of this investigation is to explore the establishment of the flow pattern uniqueness depend of the diffuser position which is discussed in convection heat transfer and fluid dynamics fields.

Using Fluent 6.2 as computational fluid dynamics, several variables will be exploited. The specify boundary types room model is established in GAMBIT software generating such a specific office room. The full scale experiment is accomplished to obtain the research validation. The dimensionless analysis derived from the ratio between the distance of diffuser to the wall and the length of the ventilated room. The CO_2 gas contaminant in the exhaust diffuser are always higher in the displacement ventilation, therefore they are lower inside the room with the displacement ventilation system. The displacement ventilation is more effective in the treatment of indoor contamination.

Keywords:

Dimensionless, contaminant, mixed, displacement, diffuser

1. INTRODUCTION

Air ventilation system is activated to take outside contaminant immediately from the room. The achievement of ventilation design needs the system which is not suffering overload with adequate capacity.

What kinds of performance characteristics are required in analyze of air displacement ventilation system should be paid close attention from the preceding research. The researches focus to the displacement ventilation system was done by some researchers (Figure 1).

King and Clements [6] concluded that the accurate application of stratification air conditioning system for the building where the indoor air quality increases could offer some benefit. In case study, 1.138.195 kilowatt per annum electrical power operation could be saved, 50.55% of the operation cost prediction with the conventional system.

Stratification air temperature and ventilation effectiveness are some significant characteristics of displacement ventilation in accordance with Hu and Glicksman [8]. Nielsen [9] accomplished an experiment with air terminal device which is mounted next to the lower wall.

The purpose of Xu, Yamanaka and Kotani [13] is investigating the influence of heat loss through the wall to temperature gradient and contaminant concentration inside the room with the displacement ventilation.

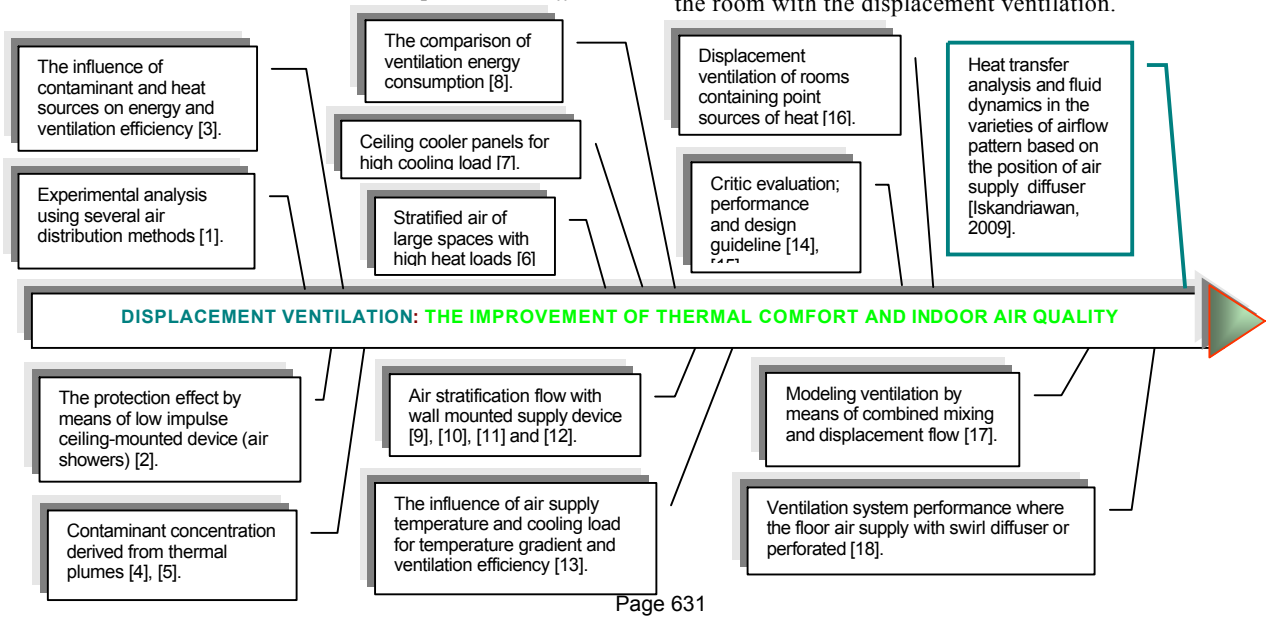

Figure 1. The fish bone diagram of displacement ventilation system research

Lau and Chen [18] examine the performance of displacement ventilation where the air is supplied at floor area with swirl diffuser is compared to perforated diffuser in the high cooling load (about 90 W/m^2). Experiment method as the validation is applied used for comparison. Some considerations are implemented such as air change hour, the diffuser number and location also occupant, furniture, partition and the exhaust location.

The aim of this research is to explore the establishment of unique airflow depend of the position of air supply diffuser (locally behavior) is linked to the convective heat transfer knowledge based on computational fluid dynamics method. The result of this investigation is expected could contribute the long journey to obtain the substantial enhancement to improve the thermal comfort and indoor air quality (IAQ).

2. METHOD

This research based on the simulation of CFD (Fluent 6.2) with makes use of the location of fresh air diffuser parameter. The CFD simulation is set up with the design of ventilation system and the interior of office room derived from the existing principle. The office room model is generated in GAMBIT (Geometry and Mesh Building Intelligent Toolkit) software subsequently meshing process is completed. In the Fluent 6.2 is clarified boundary condition system. There are four types of viscous flow: laminar flow also k-epsilon standard, RNG and realized. In this case k-epsilon standard is selected by reason of the most similarity toward the air ventilation experimentation.

Based on the air ventilation experiment room (Figure 2), the model of office room with the air ventilation system is created as we can see at Figure 3. The dimension of the room is x_L=4.315m × z_W=3.81m × y_H=3m.

Figure 2. Experiment room of the air ventilation system

There are a number of heat sources in the room: occupants, lamp and computer. The air duct installation possibly it is used the same as the air mixed or displacement ventilation system. The CO_2 contaminant gas is sprayed from the mouth of occupants to spread inside the room.

Table 1 shows us the validation of CFD simulation by means of the measurement of air temperature in air ventilation experiment. The measurement is conducted for the extreme position of supply air diffuser: mixed centre (mc), mixed side (ms), displacement centre (dc) and displacement side (ds).

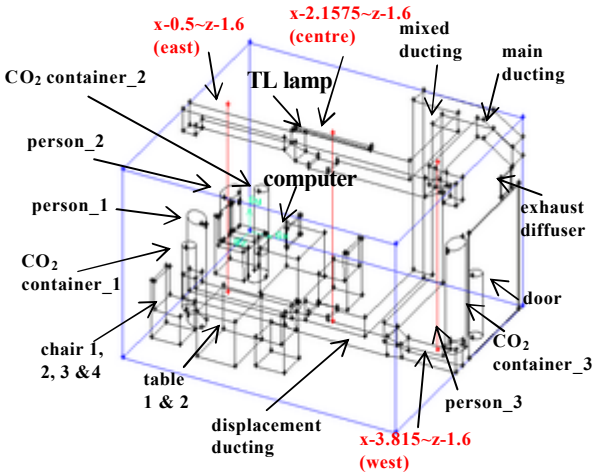

Figure 3. Established office room model in GAMBIT software which is exported to Fluent 6.2 CFD

Table 1 The difference of air temperature between experiment and CFD simulation for air mixed centre (mc), mixed side (ms), displacement centre (dc) and displacement side (ds) ventilation system as the validation

Method	No.	Height room (m)	Air temperature (°C)			
			mc	ms	dc	ds
Experiment	1	2.5	24.85	26.25	25.61	24.69
	2	2.0	23.73	25.78	24.48	24.47
	3	1.5	24.30	25.50	24.63	23.89
	4	1.0	23.52	23.24	22.65	23.36
	5	0.5	22.46	23.41	21.65	22.32
Simulation	1	2.5	20.72	23.15	21.35	24.55
	2	2.0	20.73	23.16	21.34	24.55
	3	1.5	20.76	23.16	21.32	24.54
	4	1.0	20.77	23.17	21.30	24.53
	5	0.5	20.78	23.18	21.27	24.52
Δ (%)			14.57	7.22	11.66	3.23
$\Delta_{average}$ (%)			7.34			

Dimensionless study

There are five variables of a/A: ≈0, 1/5, 1/4, 1/3 and 1/2. The extreme positions are where the location of supply air diffuser at side (a/A≈0) and at centre (a/A=1/2). Where *a* = the distance of supply air diffuser to the side wall and *A* = the room length (see Figure 4). We need to recognize the performance of air ventilation where the positions of air supply diffuser are not simply at the side or at the centre of the room, that's why the dimensionless analysis of air ventilation is required to examine.

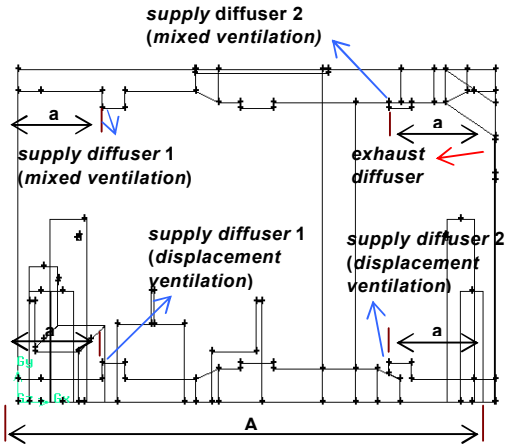

Figure 4. Dimensionless analysis of air ventilation system with a/A variables

In addition it is accomplished some assessment of thermal comfort and indoor air quality aspects that are velocity, heat energy at the exhaust and the intensity of CO_2 contaminant gas inside the room. The investigation is accomplished for two systems of air ventilation: mixed and displacement system.

3. RESULT AND DISCUSSION

The airflow pattern is identifiable for each condition of the supply air diffuser position derived from the value of ratio a/A (Figure 5). They have a tendency to change from badly behaved toward fine arrangement while the dimensionless ratio increase moreover in mixed or displacement ventilation. There is a low behavior of airflow pattern due to wall effect where the air supplies diffuser too adjacent to the side wall. Air supply near the wall boundary layer tends to generate separation zone henceforth it leads to death air area inside the room.

Supply air distribution flow is improved whereas the supply diffuser moves to the centre.

A number of air conditioning designers still decide to place the air supply diffuser close to the wall perhaps the reason of the aesthetic parameter merely.

Air velocity

At the centre of room, the higher the value of ratio a/A the velocity tends to increase (see Figure 6) since the location which is measured is more close to the air supply source. The contradictory situation is happen at the east and west location where the greater the value of ratio a/A, the velocity will decrease (see Figure 7 and 8) for the reason that the air supply diffuser more far away.

There is a broken velocity at the centre of room where the velocity is decline that is at the room height about 0.5m (lower zone) in displacement centre and about 2.5m (upper zone) in mixed centre ventilation.

At the room east side, the air velocity in ratio a/A =1/3 is lower than that of ratio a/A=1/2 (mixed centre) in the area less than the height about 1.5m. This phenomenon will influence the quality of ventilation such as room air temperature and exhaust heat energy.

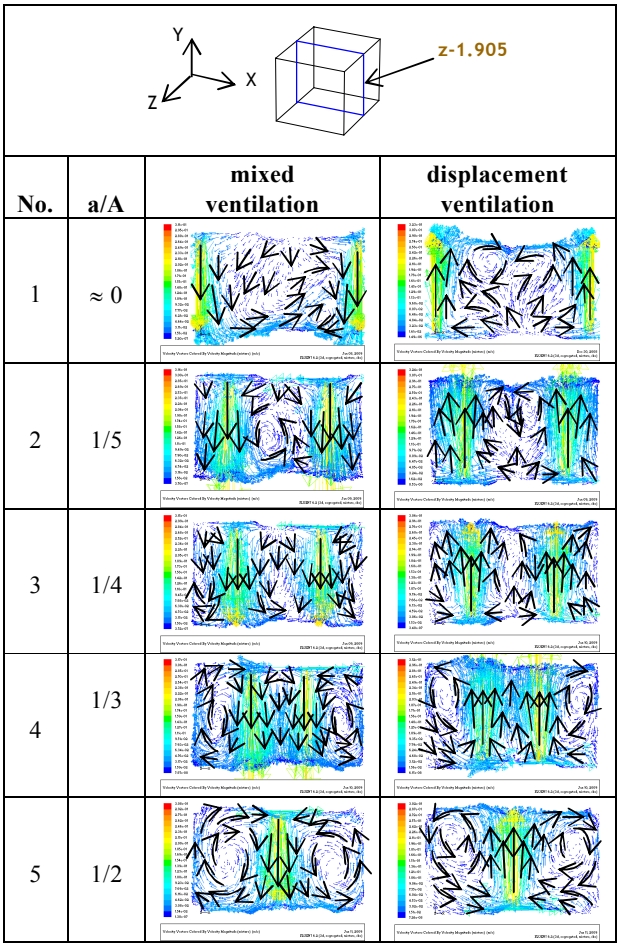

Figure 5. Room air velocity vector at z-1.905 vertical plane (centre of width) through some a/A variables

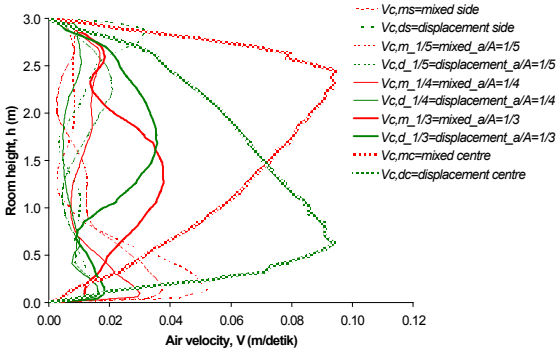

Figure 6. Air velocity at the centre of room with some a/A variables

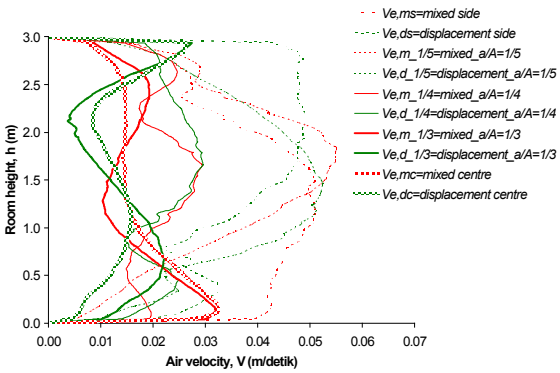

Figure 7. Air velocity at the east side of room with some a/A variables

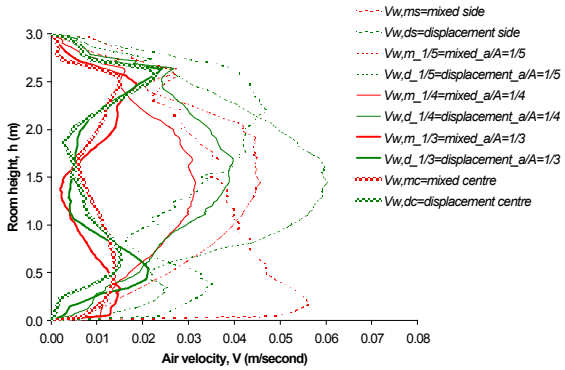

Figure 8. Air velocity at the west side of room with some a/A variables

Exhaust heat energy

It can be seen from Figure 9 that the higher the ratio a/A (supply air diffuser moves to the centre of room), the room air temperature is go down moreover in mixed or displacement ventilation. The circumstances in a/A ≈ 0 where the supply air diffuser close to the side wall are not so do well. As a result of death air area which is created by the wall boundary layer tends to develop separation zone therefore the room air temperature is high.

The greater the value of ratio a/A, the exhaust heat energy, Q_e tends to improve likewise in mixed or displacement ventilation. The higher the value of Q_e, the room air temperature tends to decrease. The exception is come about in a/A =1/3 mixed ventilation, the Q_e is larger than that in a/A =1/2(mixed centre), that means there is an optimum value of supply diffuser movement which is related to the exhaust heat energy. Moreover, it is better than displacement ventilation of a/A =1/4.

As well there is no significant escalating of exhaust heat energy, Q_e within a/A =1/3 compare to a/A = a/A in displacement ventilation.

There is no effect of heat energy generated by means of person_2 in displacement centre ventilation (a/A =1/2) even in ratio a/A =1/3 displacement ventilation in the height of occupation zone (around 1.5m). Only person_1 and person_3 have an effect on the raising of room air temperature. It means that they more effective compare to the others which is linked to the task of air ventilation to reduce the room air temperature.

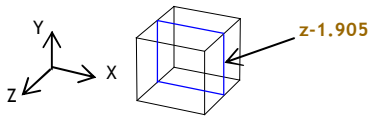

No.	a/A	mixed ventilation	displacement ventilation
1	≈ 0	Q_e=110.72 Watt	Q_e=118.46 Watt
2	1/5	Q_e=118. 08 Watt	Q_e=123.95 Watt
3	1/4	Q_e=120.59 Watt	Q_e=125.73 W
4	1/3	Q_e=126.65 Watt	Q_e=131.13 Watt
5	1/2	Q_e=122.91 Watt	Q_e=131.25 Watt

Figure 9. Room air temperature contour at z-1.905 vertical plane (centre of width), T= (18-22)^{o}C and exhaust absorbed heat, Q_e (Watt) among some a/A variables

Displacement centre constructs the lowest room air temperature at the centre of room (Figure 10). It creates a stratification temperature even though it is not excessively significant. The hot zone in the upper region and the cold zone in the lower region are generated by means of the accurate displacement ventilation system.

Unfortunately, the room temperature rise at the height below about 0.5m for displacement centre. It is suspected that the airflow is not passing through the area since the displacement supply air diffuser too high. It is can be reduced with the using of floor air supply diffuser.

At the east side of room, the displacement ventilation with a/A =1/2 and a/A =1/2 are the best particularly in the area only higher than more or less 1m. This is happening because several obstacles such as table, chair and person_2 block the fresh air supply at the east side. At the height area lower than 1m, the outstanding ventilation are the mixed ventilation of a/A =1/2, a/A =1/3 and a/A =1/5.

At the west area, the existing of person_3 damage the action of displacement ventilation especially for a/A =1/2 and a/A =1/3. Possibly the most excellent operation are mixed ventilation for a/A =1/4 and a/A =1.5 in the west area of room.

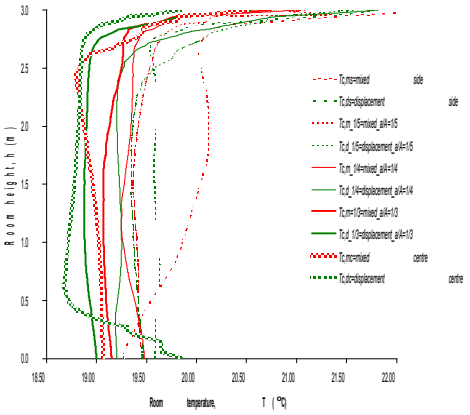

Figure 10. Air temperature at the centre of room with some a/A variables

CO_2 contaminant gas

The amount of contaminant gas in this case CO_2 inside the room influences the indoor air quality as well as the comfort for occupant. Too many CO_2 gas will give the terrible effect to the work attitude of the occupant. The problem is how the ventilation system could optimum to reduce the gas concentration. In this paper, the sources of CO_2 gas are the mouth entrance of person_1, person_2 and person_3.

As we can see at Figures 11, 12 and 13, the displacement ventilation for a/A=1/2 and a/A=1/3 are the most excellent compare to the others. Moreover they are able to bring the largest CO_2 gas which is shown in the exhaust diffuser area. Especially in the displacement ventilation, the upper the value of a/A, the higher CO_2 gas concentration in the exhaust diffuser. Again the position of supply diffuser close to the wall should be prevented because it creates unsuccessfulness in the task to reduce the contaminant gas. Figure 14 present us, at the centre of room the displacement ventilation system with a/A =1/3 is the most doing well to cut down CO_2 gas concentration.

At z-0.43 vertical plane the displacement ventilation for a/A=1/3 compete together with that for a/A=1/2 create the low CO_2 gas concentration in the room. Some of them display us the concentration of CO_2 gas are thick at the area close to the exhaust diffuser.

At a/A≈0 and a/A=1/5 the quality of indoor air are the worst in support of mixed ventilation as well as displacement ventilation. That's mean the location of supply diffuser close to the wall are not respectable in case of air ventilation mission to transport the gas contaminant leave out from the room point of view.

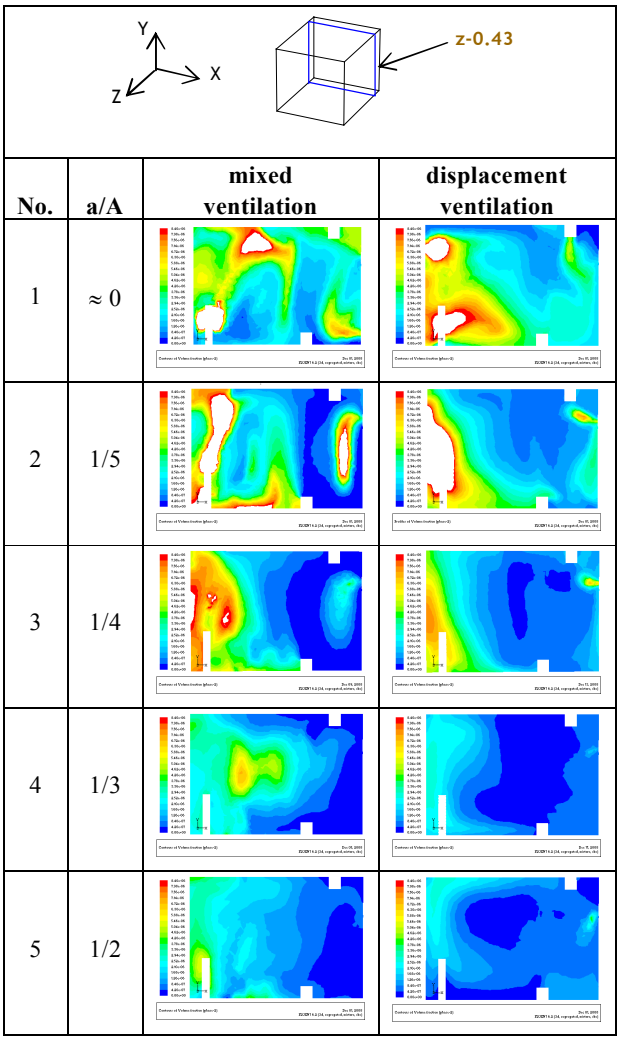

Figure 11. CO_2 gas contaminant contour at z-0.43 vertical plane (exhaust diffuser area), C=(0-8.4)ppm with some a/A variables

At x-4.3 vertical plane displacement ventilation, the maximum CO_2 gas concentration is existent in the area close to the exhaust diffuser. The higher the ratio a/A, the CO_2 gas concentration will increase in the exhaust diffuser. Particularly in the displacement ventilation for a/A≈ 0, the direction of air supply velocity is not effective to drive the contaminant as a result the CO_2 gas is still in the lower zone. On the other hand, it is complicated to draw closing

stages in the mixed ventilation because the maximum CO_2 gas concentration is not occurring in some of the exhaust diffuser.

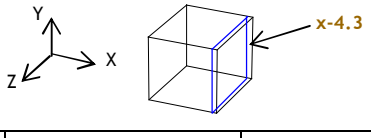

No.	a/A	mixed ventilation	displacement ventilation
1	≈ 0	C=(0~32.9)*ppm*	C=(0~2.6)*ppm*
2	1/5	C=(0~5.3)*ppm*	C=(0~5.2)*ppm*
3	1/4	C=(0~23)*ppm*	C=(0~8.6)*ppm*
4	1/3	C=(0~0.91)*ppm*	C=(0~10.6)*ppm*
5	1/2	C=(0~0.9)*ppm*	C=(0~11.3)*ppm*

Figure 12. CO_2 gas contaminant contour at x-4.3 vertical plane (exhaust diffuser area) with some assessment of contaminant, C and a/A variables

At y-2.2 horizontal plane, the displacement ventilation system always achieve succeeds to move CO_2 gas contaminant close to the exhaust diffuser. The area size of CO_2 gas concentration increase whiles the ratio a/A enlarges. Faithfully, the accurate implementation of displacement ventilation will create the clean zone in the lower region and the polluted zone in the upper region.

Based on the result of CO_2 gas contaminant at the room centre, it is better to comprehensive correlated for all time the relation between CO_2 gas concentration with the air velocity vector at the certain location. Of course we need moreover to confirm them in the others area of room before we determine the best location of air supply diffuser.

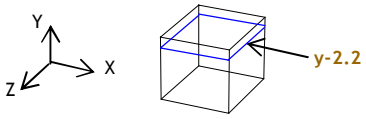

No.	a/A	mixed ventilation	displacement ventilation
1	≈ 0		
2	1/5		
3	1/4		
4	1/3		
5	1/2		

Figure 13. CO_2 gas contaminant contour at y-2.2 horizontal plane (exhaust diffuser area), C= (0~14)ppm with some a/A variables

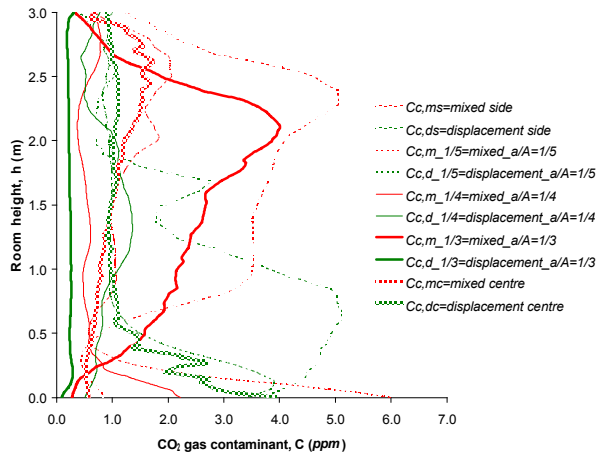

Figure 14. CO_2 gas contaminant at the centre of room through some a/A variables

4. CONCLUSION

The position of air supply diffuser will determine the performance of ventilation. The air flow patterns of ten air ventilation systems are contradictory considerably.

At the position where fresh air supply diffuser is present, the air velocity decrease with the room height increase for displacement ventilation system. The opposite condition in the mixed ventilation, the velocity decrease when the position decreases. Rely on the dimensionless ratio the air velocity are change. They increase or decrease is depending on the position toward the supply air diffuser.

The room air temperature is lower in the value of dimensionless ratio where the supply air diffuser around the centre moreover in the mixed or displacement ventilation. However high quality distribution is essential that's why the mixed centre is quiet better compare to the mixed and displacement side. There is an optimum value of dimensionless ratio where the fresh air could absorb heat energy in the exhaust diffuser.

In line to the result of room air temperature, the displacement ventilation systems within highest dimensionless ratio are the supreme to transport CO_2 contaminant gas out the room through exhaust diffuser.

In displacement centre, the height of ducting need to be considered because of the supply air couldn't get through to the hot air commencing the heat source especially in the lower zone.

The wall boundary layer could generate separation zone which is easily construct the death air area. The supply air diffuser is placed nearby to the side wall perhaps only aesthetic parameter purpose.

The arrangement of furniture and the other equipment in the room interior is crucial with displacement ventilation. The existence of them can block the fresh airflow to transfer heat to the exhaust diffuser.

The thermal comfort and indoor air quality are compared for mixed and displacement ventilation system with several value of the dimensionless ratio. The exploration can be continued to obtain the better variable for the best ventilation system such as the position of exhaust diffuser, ventilation capacity and the room form.

ACKNOWLEDGMENT

This work has been supported in part by The Research and Technology Official Ministry (*KNRT*) of The Republic of Indonesia, Practical Research Incentive Program in 2007 and 2008.

REFERENCES

[1] Holmberg, R.B., K. Folkesson, L.G. Stenberg and G. Jansson. 1987, *"Experimental Analysis of Office Climate Using Various Air Distribution Methods"*. Proceedings of ROOMVENT 1987.

[2] Kristensson, J.A. and Lindqvist, O.A. 1993, "*Displacement Ventilation Systems in Industrial Buildings*", [Conference Paper] ASHRAE Transactions. Publ by ASHRAE, Atlanta, GA, USA. V 99 pt 1 p 992-1008.

[3] Chen, Q. 1988, *"Indoor Airflow, Air Quality and Energy Consumption of Buildings"*. Ph.D. Thesis, Delft University of Technology, The Netherlands.

[4] Stymne, H., Sandberg, M. and Mattsson, M. 1991, "*Dispersion Pattern of Contaminants in a Displacement Ventilated Room"*, Proocedings of the 12th AIVC Conference.

[5] Mundt, E. 1996, "*The Performance of Displacement Ventilation Systems "*, Ph.D. Thesis, Royal Institute of technology, Sweden.

[6] King, A.R., Kronfalt, M. & Clements, R.F. 1993, "Stratified Air Conditioning of Large Spaces with High Heat Loads", *Australian Refrigeration, Air conditioning & Heating* 47 n 2, 24-29.

[7] Skistad, H. 1994, "*Displacement Ventilation"*, Research Studies Press Ltd. England.

[8] Hu, S., Chen, Q. & Glicksman, L.R. 1999, "Comparison of energy consumption between displacement ventilation systems for different U.S. buildings and climates*"*, *ASHRAE Transactions* 105 (PART 2), 453-464.

[9] Nielsen, P.V. 1994, "Stratified Flow in a Room with Displacement Ventilation and Wall-Mounted Air Terminal Devices", *ASHRAE Transactions*, ASHRAE, Atlanta, GA, USA, 1163-1169.

[10] Nielsen, P.V. 1996, "*Temperature Distribution in a Displacement Ventilation Room"*, Proceedings of ROOMVENT 1996 (3); 323-330.

[11] Mattsson, Magnus. 1999, "On The Efficiency of Displacement Ventilation with Particular Reference to The Influence of Human Physical Activity", Doctoral Thesis, Centre for Built Environment Royal Institute of Technology Gavle, Sweden.

[12] Yuan, X., Chen, Q. and Glicksman, L.R. 1999a, "Models for Prediction of Temperature Differences and Ventilation Effectiveness with Displacement Ventilation", ASHRAE Transactions 105 (PART 1), 353-367.

[13] Xu, M., Yamanaka, T. & Kotani, H. 1999, "Vertical Temperature gradient and Ventilation Efficiency in Rooms with Displacement Ventilation – Influence of Supply Air Temperature and Heat Load", *Technology Reports of Osaka University* 49 n 2348, 179-188.

[14] A Yuan, X., Chen, Q. and Glicksman, L.R. 1998, "*Critical Review of Displacement Ventilation"*, ASHRAE Transactions, ASHRAE, Atlanta, GA, USA, 78-89 4101.

[15] Yuan, X., Chen, Q. and Glicksman, L.R. 1999b, "*Performance Evaluation and Design Guidelines for Displacement ventilation"*, ASHRAE Transactions 105 (PART 1), 340-352.

[16] Iskandriawan, Bambang. 2001, *"Displacement Ventilation of Rooms Containing Point Sources of Heat"*, Master Dissertation, University of Wollongong, Australia.

[17] Waters, JR and Simons, MW. 2002, *"Modelling Ventilation by means of Combined Mixing and Displacement Flow"*. Building Serv. Eng. Res. Techol. 23,1, pp, 19-29.

[18] Lau, J. And Chen, Q. (2007), "Floor Supply Displacement Ventilation for Workshops" *Building and Environment*, 42 (4), 1718-1730.

[19] Awbi, H.B. (1995), "Ventilation of Buildings" *E & FN SPON an Imprint of Chapman & Hall.*

Proceeding of the 11th International Conference on QiR (Quality in Research)
Faculty of Engineering, University of Indonesia, Depok, Indonesia, 3-6 August 2009
ISSN 114-1284

Optimization of Heating Characteristic and Energy Consumption at Bearing Heater U Model 220 Volt using Induction Electromagnetic Principle based on Taguchi Method

Candra Bachtiyar, Golfrid Gultom, Manan Ginting

Mechanical Industry Technology Department
Pendidikan Teknologi Kimia Industri, Medan 20228
Tel : (061)7867810. Fax : (061) 7862439
E-mail : candra-b@depperin.go.id

Mechanical Industry Technology Department
Pendidikan Teknologi Kimia Industri, Medan 20228
Tel : (061)7867810. Fax : (061) 7862439
E-mail : golfridg@yahoo.com

Mechanical Industry Technology Department
Pendidikan Teknologi Kimia Industri, Medan 20228
Tel : (061)7867810. Fax : (061) 7862439
E-mail : mananginting@yahoo.com

ABSTRACT

In this study, The Taguchi method is used to find the optimal heating characteristic and energy consumption of bearing heater U model that it make in Electronic Laboratory of PTKI Medan. An orthogonal array, the signal to noise (S/N) ratio, and the analysis of variance (ANOVA) are employed to investigate the heating characteristic and energy consumption of bearing heater U model 220 volt using bearing type 6308. Through this study, not only can the optimal the heating characteristic and energy consumption be obtained, but also the main parameter that effect the heating time and energy consumption can be found. As shown in this study, the Taguchi method provides a systematic and efficient methodology for design optimization of heating characteristic and energy consumption. It has been shown that heating characteristic and energy consumption can be improved significantly. The confirmation experiments were conducted to verify the optimal heating time and energy consumption. The improvement of the optimal heating time and energy consumption from initial parameter to the optimal parameter is about 794 %.

Keywords : *Taguchi method, Optimization, Bearing Failure, Induction Electromagnetic*

1. INTRODUCTION

The reliability of machine is of paramount importance in industry. Bearing play an important role in the reliability and performance of machine. Due to the closed relationship between machine development and bearing assembly performance, it's difficult to imagine the progress of modern rotating machinery without consideration of wide application of bearings. In additional faults a rising in machinery are often linked to bearing faults. The result of various studies show that bearing problems accounts for over 40 % of all machine failures [1]

The main factor of bearing faults is dust and corrosion. Dirt and other foreign matter that is commonly present often contaminate the bearing lubrication. Bearing corrosion is produced by presence of water, acids, deteriorated lubrication and even perspiration from careless handling during installation. Bearing problems are also caused by improperly forcing the bearing onto the shaft. This produces physical damage in the form of brinelling or false brinelling of the race way, which lead to premature failure [2]

In practically, the way to maintenance and the best process during installation of bearing are tools to avoid the failure this component. Study of bearing show premature failure at bearing cause of the way during installation bearing use a simple method (improperly forcing the bearing) contribute 25 % until 30 % from total failure at bearing [3]. Failure this part will disturb working efficiency of machine and this condition create new problem at industry. To reduce and solve this problem, studying bearing and method of installation become important. A recent method during installation of bearing had been developed by induction electromagnetic principles. Methods use bearing heater which is heating by winding of wire through current

electricity. These methods will generated energy then use induction process to transfer of heat and change the dimension of bearing. Research had been done by Candra Bachtiyar and Golfrid Gultom (2008) at Electronic Laboratory – Pendidikan Teknologi Kimia Industri (PTKI - Medan) success made bearing heater Umodel at laboratory scale and observed this equipment [4,5,6]. Recent bearing research shown prevent failure focused on condition based on monitoring. Advantages this monotoring is prevent catastropic breakdown and eficiency during production. Application this method on motor using vibration monitoring, current analysis, and thermal analysis [7,8,9,10]. On other side, mounting bearing to shaft to reduce failure focus on chossing type of bearing, tolerance and prevent missaligment. In 2009, this equipment increased a number of winding that can connect to 220 volt [11]. Study installation of capasitor at electric equipment could improve power factor [12]. Through this study, implementation of capasitor and Taguchi method at this equipment will adopt to improve power factor and get optimum design parameter.

Basically, the Taguchi method is a powerful tool for the design of high quality systems. It provides a simple, efficient and systematic approach to optimize designs for performance, quality, and cost. The methodology is valuable when the design parameters are qualitative and discrete. Taguchi parameter design can optimize the performance characteristics through the settings of design parameters and reduce the sensitivity of the system performance to sources of variation. In recent years, the rapid growth of interest in the Taguchi method has led to numerous applications of the method in a world-wide range of industries and nations [13]. In the following, the Taguchi method is introduced first. The experimental details of using the Taguchi method to determine and analyze the optimal parameters are described next. The optimal heating characteristic and energy consumption parameters with regard to performance indexes such as heating time and energy consumption are considered. Finally, the paper concludes with a summary of this study.

2. DESCRIPTION OF THE TAGUCHI METHOD

Taguchi is the developer of the Taguchi method. He proposed that engineering optimization of a process or product should be carried out in a three-step approach, i.e. system design, parameter design, and tolerance design. In system design, the engineer applies scientific and engineering knowledge to produce a basic functional prototype design, this design including the product design stage and the process design stage. In the product design stage, the selection of materials, components, tentative product parameter values, etc., are involved. As to the process design stage, the analysis of processing sequences, the selections of production equipment, tentative process parameter values, etc., are involved. Since system design is an initial functional design, it may be far from optimum in terms of quality and cost. Following on from system design is parameter design. The objective of parameter design is to optimize the settings of the process parameter values for improving quality characteristics and to identify the product parameter values under the optimal process parameter values. In addition, it is expected that the optimal process parameter values obtained from parameter design are insensitive to variation in the environmental conditions and other noise factors. Finally, tolerance design is used to determine and analyze tolerances around the optimal settings recommend by the parameter design. Tolerance design is required if the reduced variation obtained by the parameter design does not meet the required performance, and involves tightening tolerances on the product parameters or process parameters for which variations result in a large negative influence on the required product performance. Typically, tightening tolerances means purchasing better- grade materials, components, or machinery, which increases cost. However based on the above discussion, parameter design is the key step in the Taguchi method to achieving high quality without increasing cost. To obtain high cutting performance in turning, the parameter design proposed by the Taguchi method is adopted in this paper. Basically, experimental design methods were developed originally by Fisher [13,14]. However, classical experimental design methods are too complex and not easy to use. Furthermore, a large number of experiments have to be carried out when the number of the process parameters increases. To solve this problem, the Taguchi method uses a special design of orthogonal arrays to study the entire parameter space with a small number of experiments only. The experimental results are then transformed into a signal-to-noise (S/N) ratio. Taguchi recommends the use of the S/N ratio to measure the quality characteristics deviating from the desired values. Usually, there are three categories of quality characteristic in the analysis of the S/N ratio, i.e. the-lower-the-better, the-higher-the-better, and the nominal- the-better. The S/N ratio for each level of process parameters is computed based on the S/N analysis. Regardless of the category of the quality characteristic, a greater S/N ratio corresponds to better quality characteristics. Therefore, the optimal level of the process parameters is the level with the greatest S/N ratio. Furthermore, a statistical analysis of variance (ANOVA) is performed to see which process parameters are statistically significant. With the S/N and ANOVA analyses, the optimal combination of the process parameters can be predicted. Finally, a confirmation experiment is conducted to verify the optimal process parameters obtained from the parameter design.

To summarize, the parameter design of the Taguchi method includes the following steps: (1) identification of the quality characteristics and selection of design parameters to be evaluated; (2) determination of the number of levels for the design parameters and possible interactions between the design parameters; (3) selection of the appropriate

orthogonal array and assignment of design parameters to the orthogonal array; (4) conducting of the experiments based on the arrangement of the orthogonal array; (5) analysis of the experimental results using the S/N and ANOVA analyses; (6) selection of the optimal levels of design parameters; and (7) verification of the optimal design parameters through the confirmation experiment. Therefore, three objectives can be achieved through the parameter design of the Taguchi method, examples: (1) determination of the optimal design parameters for a process or a product; (2) estimation of each design parameter to the contribution of the quality characteristics; and (3) prediction of the quality characteristics based on the optimal design parameters [13,14].

3. PROCESS EXPERIMENT

Researchers decide to divide activity become 4 steps during experiment to find contribution parameter that chosen during heating time and energy consumption at bearing heater U model :

1. Literature study. Consist of collecting books, especially related with bearing, failure at bearing, induction electromagnetic process topic, and Taguchi method
2. Journal. Collect journal also activity to support literature study which is information from journal will use to support final report in this paper.
3. Collect data of experiment. Activity collect data of experiment based on lay out experiment to find heating time and energy consumption
4. Conclusion of Experiment. After study data of experiment, the next step is concluding of experiment based on orthogonal array, signal-to-noise (S/N) ratio and analysis of variance (ANOVA).

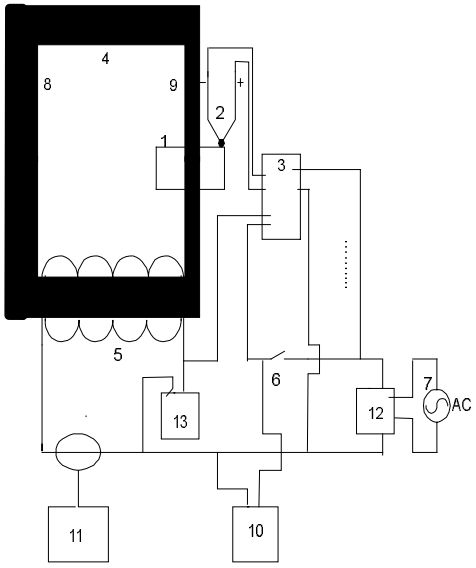

Note :

1. Bearing
2. Thermocouple
3. Temperatur controller
4. Core
5. Winding
6. Push bottom
7. Power Supply
8. Heating area 1
9. Heating area 2
10. Cos Phi
11. Clamp on meter
12. Vari Ac
13. Capasitor

Figure. 1 Design experiment

3.1 Selection of parameter and their level

The experiments were carried out on bearing heater U model 220 volt and bearing type 6308. The initial parameters were as follows: capasitor, sensor location and ratio heating area and inner diameter bearing 6308. The feasible space for parameters was defined by varying the capasitor in the range 0-64 μF , sensor location rate in the range inner side of bearing, middle and outer side, and ratio in the range 0.016-0.033. In the parameter design, three levels of the parameters were selected, shown in Table 1.

Table 1: Parameter and their level

Symbol	Parameter	Unit	Level 1	Level 2	Level 3
A	Capasitor	μF	0	48 [a]	64
B	Ratio heating area and diameter bearing	-	0.016	0.025 [a]	0.033
C	Sensor Location	mm	Inner	Mid [a]	out

a initial parameter , mid = middle and out = outer

3.2 Performance measurement

Heating characteristic of bearing heater consist of three parameter, heating time and energy consumption. Heating time measured from heating bearing until reach set point temperature. Energy consumption measured from variable of voltage, current, cos phi and time to reach set point of this equipment during heating bearing.

4. DESIGN AND ANALYSIS OF PARAMETER

In this section, the use of an orthogonal array to reduce the number of the experiments for design optimization of the heating characteristic and energy consumption parameters is reported. Results of the experiments are studied using the S/N and ANOVA analyses. Based on the results of the S/N and ANOVA analyses, optimal settings of the parameters for heating time and energy consumption are obtained and verified [13].

4.1 Orthogonal Array Experiment

To select an appropriate orthogonal array for the experiments, the total degrees of freedom need to be computed. The degrees of freedom are defined as the number of comparisons between design parameters that need to be made to determine which level is better and specifically how much better it is. For example, a three-level design parameter counts for two degrees of freedom. The degrees of freedom associated with the interaction between two design parameters are given by the product of the degrees of freedom for the two design parameters [13,14]. In the present study, the interaction between the heating characteristic and energy consumption parameters is neglected. Therefore, there are eight degrees of freedom owing to there being three parameters. Once the required degrees of freedom are known, the next step is to select an appropriate orthogonal array to fit the specific task. Basically, the degrees of freedom for the orthogonal array should be greater than or at least equal to those for the design parameters. In this study, an L_9 orthogonal array with four columns and nine rows was used. This array has eight degrees of freedom and it can handle there -level design parameters. Each parameter is assigned to a column, nine parameter combinations being available. Therefore, only nine experiments are required to study the entire parameter space using the L_9 orthogonal array. The experimental layout for the three heating characteristic and energy consumption parameters using the L_9 orthogonal array is shown in Table 2. Since the L_9 orthogonal array has four columns, one column of the array is left empty for the error of experiments: orthogonality is not lost by letting one column of the array remain empty.

Table 2 : Experiment Layout using L 9 an orthogonal array

Experiment No.	Heating Characteristic Parameter Level			
	A	B	C	D
	Capasitor	Ratio	Sensor Location	Error
1	1	1	1	
2	1	2	2	
3	1	3	3	
4	2	1	3	
5	2	2	1	
6	2	3	2	
7	3	1	2	
8	3	2	3	
9	3	3	1	

4.2 Analysis of S/N Ratio

In the Taguchi method, the term 'signal' represents the desirable value (mean) for the output characteristic and the term 'noise' represents the undesirable value (S.D.) for the output characteristic. Therefore, the S/N ratio is the ratio of the mean to the S.D. Taguchi uses the S/N ratio to measure the quality characteristic deviating from the desired value. The S/N ratio η is defined as

$$\eta = -10 \log (\text{M.S.D.}) \qquad (1)$$

where M.S.D. is the mean-square deviation for the output characteristic. As mentioned earlier, there are three categories of quality characteristics, the-lower-the-better, the higher- the-better, and the-nominal-the-better. To obtain optimal heating characteristic and energy consumption, the-lower-the-better quality characteristic. The mean-square deviation (M.S.D.) for the-lower-the-better quality characteristic can be expressed as:

$$\text{M.S.D.} = \left[\frac{1}{n} \sum_{i=n}^{n} Y_i^n \right] \qquad (2)$$

where n is the number of tests and Y_i is the value of heating time and the i the test [13]. Table 3 shows the experimental results for heating time and the corresponding S/N ratio using equation (Eqs. (1) and (2)). Since the experimental design is orthogonal, it is then possible to separate out the effect of each parameter at different levels. For example, the mean S/N ratio for the capasitor at levels 1 and 2 can be calculated by averaging the S/N ratios for the experiments 1–3, and 4–6, respectively.

Table 3 : Experiment result for heating time and S/N ratio

Experiment No.	Capasitor	Ratio	SensLoct	Heat. time (s)	S/N ratio (dB)
1	0	0.016	In	1614	-64.15
2	0	0.025	Mid	5040	-74.04
3	0	0.033	out	918	-59.25
4	48	0.016	Out	8190	-78.26
5	48	0.025	In	3240	-70.21
6	48	0.033	Mid	1420	-63.04
7	64	0.016	Mid	5670	-75.07
8	64	0.025	Out	3331	-70.45
9	64	0.033	In	1051	-60.43

Ratio = ratio heating area and diameter of bearing
Sens Loct = Sensor location
Heat time = Heating time

The mean S/N ratio for each level of the other parameters can be computed in the similar manner. The mean S/N ratio for each level of the parameters is summarized and called the S/N response table for heating time (Table 4). In addition, the total mean S/N ratio for the four experiments is also calculated and listed in Table 4. Fig. 2 shows the S/N response graph for heating time.

Table 4 :S/N response for heating time

Symbol	Parameter	Mean / SN Ratio (dB)			
		Level 1	Level 2	level 3	Max -Min
A	Capasitor	-65.82	-70.50	-68.65	4.68
B	Ratio	-72.49	-71.57	-60.91	11.5
C	Sensor Location	-64.93	-70.72	-69.32	5.78

The total mean S/N ratio = - 68.32 dB.

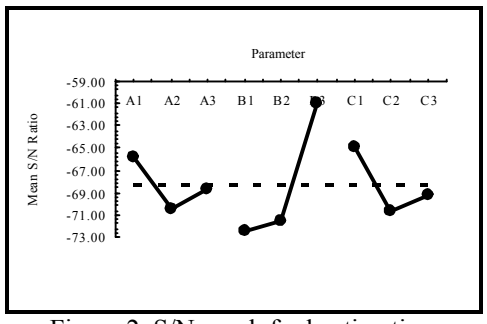

Figure 2 :S/N graph for heating time

On the other hand, the-lower-the-better quality characteristics for energy consumption should be taken for obtaining optimal energy consumption during heating period. The M.S.D. for the the-lower-the-better quality characteristic.

Table 5: Experiment result for energy consumption and S/N Ratio

Experiment No	Capasitor	Ratio	Sens Loct	Energy Cons	S/N ratio (dB)
1	0	0.016	In	69.04	-36.78
2	0	0.025	Mid	176.4	-44.93
3	0	0.033	out	39.27	-59.25
4	48	0.016	Out	268.63	-48.58
5	48	0.025	In	106.27	-40.52
6	48	0.033	Mid	46.576	-33.36
7	64	0.016	Mid	339.06	-50.60
8	64	0.025	Out	199.19	-45.98
9	64	0.033	In	62.84	-35.96

Ratio = ratio heating area and diameter of bearing
Sens Loct = Sensor location
Energy Cons = Energy consumption

Table 5 shows the experimental results for energy consumption and the corresponding S/N ratio using Eqs. (1) and (2). The S/N response table and S/N response graph for energy consumption are shown in Table 6 and Fig. 3. Regardless of the-lower-the-better of the the higher-the-better quality characteristic, the greater S/N ratio corresponds to the smaller variance of the output characteristic around the desired value (Eqs. (1)–(2)).

Table 6 : S/N response for energy consumption

Symbol	Parameter	Mean / SN Ratio (dB)			
		Level 1	level 2	level 3	Max-Min
A	Capasitor	-46.98	-40.82	-44.18	6.16
B	Ratio	-45.32	-43.81	-42.86	2.46
C	Sensor Location	-37.75	-42.96	-51.27	13.51

The total mean S/N ratio = - 44.00 dB.

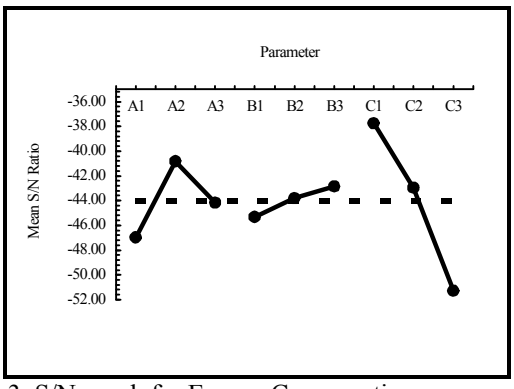

Figure 3 :S/N graph for Energy Consumption

4.3 Analysis of Variance

The purpose of the analysis of variance (ANOVA) is to investigate which design parameters significantly affect the quality characteristic. This is to accomplished by separating the total variability of the S/N ratios, which is measured by the sum of the squared deviations from the total mean S/N ratio, into contributions by each of the design parameters and the error. First, the total sum of squared deviations SS_T from the total mean S/N ratio η_m can be calculated as:

$$SS_T = \sum_{i=1}^{n} (\eta_i - \eta_m)^2 \qquad (3)$$

where n is the number of experiments in the orthogonal array and η_i is the mean S/N ratio for the i the experiment.

The total sum of spared deviations SS_T is decomposed into two sources: the sum of squared deviations SS_d due to each design parameter and the sum of squared error SS_e. The percentage contribution r by each of the design parameters in the total sum of squared deviations SS_T is a ratio of the sum of squared deviations SS_d due to each design parameter to the total sum of squared deviations SS_T. Statistically, there is a tool called an F test named after Fisher to see which design parameters have a significant effect on the quality characteristic. In performing the F test, the mean of squared deviations SS_m due to each design parameter needs to be calculated. The mean of squared deviations SS_m is equal to the sum of squared deviations SS_d divided by the number of degrees of freedom associated with the design parameter. Then, the F value for each design parameter is simply the ratio of the mean of squared deviations SS_m to the mean of

squared error. Usually, when F >4, it means that the change of the design parameter has a significant effect on the quality characteristic [13,14,15,16]. Table 7 shows the results of ANOVA for heating time. It can be found that capasitor and location of sensor are the un significant parameters for affecting heating time. The change of ratio heating area and diameter of bearing in the range given in Table 1 has an significant effect on heating time. Therefore, based on the S/N and ANOVA analyses, the optimal parameters for heating time are the capasitor at level 1,ratio heating area and diameter of bearing at level 3, and the location of sensor at level 1.

Table 7 : Analysis of Variance (ANOVA) for heating time

Smb	Parameter	*DOF*	*Sum of Square*	*Mean Square*	F	Contr
A	Capasitor	2	33.41	16.70	0.87	8.91
B	Ratio	2	248.72	124.36	6.53	66.33
C	Sens Loct	2	54.73	27.36	1.43	14.59
Error		2	38.05	19.02		10.14
Total		8	374.93			100

Smb = Symbol, DOF = degree of freedom,
Contr = Contribution, Sens. Loct = Sensor location
Ratio = ratio heating area and diameter of bearing

Table 8 shows the results of ANOVA for energy consumption. capasitor, ratio heating area and diameter of bearing, and location of sensor are the un significant energy consumption parameters for affecting energy consumption. However, the contribution order of the parameters for energy consumption is location of sensor, then capasitor, and then ratio heating area and diameter of bearing. The optimal parameters for energy consumption are the capasitor at level 1, ratio heating area and bearing diameter at level 3, and the location of sensor at level 1.

Table 8 : Analysis of Variance (ANOVA) for energy consumption

Smb	Parameter	*DOF*	*Sum of Square*	*Mean Square*	F	Contr
A	Capasitor	2	57.16	28.58	0.28	10.50
B	Ratio	2	9.24	4.62	0.04	1.69
C	Sens Loct	2	278.84	139.42	1.40	51.25
Error		2		198.79	99.3	
Total		8	544.04			100

Smb = Symbol, DOF = degree of freedom,
Contr = Contribution, Sens. Loct = Sensor location
Ratio = ratio heating area and diameter of bearing

4.4 Confirmation Test

Once the optimal level of the design parameters has been selected, the final step is to predict and verify the improvement of the quality characteristic using the optimal level of the design parameters. The estimated S/N ratio using the optimal parameters for heating time can then be obtained and the corresponding energy consumption can also be calculated by using Eqs. (1) and (2).

Table 9 shows the comparison of the predicted heating time with the actual heating time using the optimal parameters, good agreement between the predicted and actual heating time being observed. The increase of the S/N ratio from the initial heating time parameters to the optimal heating time parameters is 18 dB, which means also that the heating time more fast about 7,94 times.

Table 9 : Results of the confirmation experiment for heating time

	Initial Parameter	Optimal Parameter	
		Prediction	Experiment
Level	A2B2C2	A1B3C1	A1B3C1
Heating time (s)	3600	182.78	453
S/N Ratio (dB)	-71.12	45.23	-53.12

Improvement of S/N ratio = 18 dB

Table 10 shows the comparison of the predicted energy consumption with the actual energy consumption using the optimal parameters. The increase of the S/N ratio from the initial energy consumption parameters to the optimal energy consumption parameters is 15.98 dB and therefore the energy consumption value is improved by 6.09 times. In other words, the experiment results confirm the prior design and analysis for optimizing the heating time and energy consumption parameters.

Table 10 : Results of the confirmation experiment for energy consumption

	Initial Parameter	Optimal Parameter	
		Prediction	Experiment
Level	A2B2C2	A1B3C1	A1B3C1
Energy consumption	118.08	19.37	19.37
S/N Ratio (dB)	-41.44	-25.7463	-25.7463

Improvement of S/N ratio = 15.98 dB

5. CONCLUSION

This paper has discussed an application of the Taguchi method for optimizing the heating characteristic and energy consumption at bearing heater U model 220 Volt. It has been shown that heating time and energy consumption can be improved significantly. The confirmation experiments were conducted to verify the optimal parameters. The improvement of heating characteristic and energy consumption from the initial parameters to the optimal parameters is about 794 %.

6. ACKNOWLEDGMENT

This research is supported by Pendidikan Teknologi Kimia Industri Medan – Ministry of Industry, Republic of Indonesia under research grant 2009

7. REFERENCES

[1] Schoen. R. R, Habetler. T. G, Kamran F, Bartheld. R. G, "Motor Bearing Damage Detection using Stator Current Monitoring," *IEEE Trans. Ind. Appl, Vol. 31,* pp. 1274-1279, 1995.

[2] Sciferl, R.F & Melfi, M.J., "Bearing Current Remediation Option," *IEEE Industry application Magazine,* Vol 10, no 4 , pp 40-50, July-August, 2004.

[3] www.machinerylubrication.com/ *article_detail.asp?articleid=1863*

[4] Bachtiyar. Candra, Gultom. Golfrid, "Perancangan Alat pemanas Bearing Model U dengan Prinsip Induksi Elektromagnetik," *Seminar Nasional Perkembangan Riset di Bidang Industri XIV*, 17 Juni 2008, PSIT FT UGM, Jogjakarta, PPM-4, Hal : 40-46, 2008.

[5] Bachtiyar. Candra, Gultom. Golfrid, "Effect Extended Heating Area on Heating Characteristic of Bearing at U Model Bearing Heater Using Electromagnetic Induction Principle," *Soehadi Reksoewardojo 2008*, 3-4 November 2008, Chemistry Departement, ITB, Bandung, Teknologi Produk Bersih Hal : 1-6, 2008.

[6] Bachtiyar. Candra, Gultom. Golfrid, "Desain Optimasi Alat Pemanas Bearing Model U Menggunakan Prinsip Dasar Induksi Elektromagnetik dengan Metode Taguchi," *SMART 2008*, 27 Agustus 2008, Laboratorium Sistem Produksi, Jurusan Teknik Mesin dan Industri, UGM, Jogjakarta, Produk Design, Hal : 27-34, 2008.

[7] Onel,.I.Y & Benbouzid, M.E.H., "Induction Motor Bearing Failure Detection and Diagnosis : Park and Concordian Transform Approches Comparative Study", *Electric Machines & Drives Conference, IEMDC '07, IEEE International*, 3-5 May 2007, Vol 2, 1073-1078 , 2007.

[8] Onel, I.Y., Dalci, K.B., Senol, I., "Detection of bearing defects in three-phase induction motors using Park's transform and radial basis function neural networks", *Sadhana,* Vol. 31, Part 3,. 235–244, 2006.

[9] Arkan, M., Calis, H., Taglug, M.E., "Bearing and misalignment fault detection in induction motors by using the space vector angular fluctuation signal", *Electrical Engineering (Archiv fur Elektrotechnik),* Vol 87 , no 4, 197-206, 2004

[10] Yang, D. M., Stonach, A. F., MacConnell, P., "The Application of Advanced Signal Processing Techniques to Induction Motor Bearing Condition Diagnosis"**,** *Meccanica*, Vol 38**,** 297–308, 2003.

[11] Bachtiyar. Candra, Gultom. Golfrid, "Alat Pemanas Bearing Model U menggunakan Prinsip Induksi Elektromagnetik," *Lomba Rancang Bangun Teknologi 2008*, 21 Agustus 2008, BPPT, Jakarta, 2008.

[12] www.te.ugm.ac.id/~bsutopo/pari3.pdf

[13] Ross. Philip J, *Taguchi Techniques for Quality Engineering*, Second Edition. New York , Mc Graw Hill, 1996.

[14] Yang. W.H, Tarng. Y.S, "Design optimization of cutting parameters for turning operations based on the Taguchi method," *Journal of Materials Processing Technology* , Vol. 84, pp. 122-129, 1998.

[15] Phadke. M.S, *Quality Engineering Using Robust Design*, New York. Prentice Hall International, 1989.

[16] Montgomery. D.C, *Introduction to Statistic Quality Control*, 2nd ed., New York, Jhon Willey and Sons, 1999.

Dynamic Analysis Experimental Investigation of Vibration Characteristic Generated by Looseness of Bearing the Internal Combustion Engine

Fransiskus Louhenapessy [1], Achmat Zubaydi [2], Suharjono [3], I. Made Ariana [4], A.A. Masroeri [5]

1. Student Doctor Program, b. Promoter, c. Co Promoter, d. Co Promoter
2. e. Lecturer in Doctor Program in Marine Technology

Graduate Program in Marine Technology
Ocean Engineering Faculty
Sepuluh Nopember Institute of Technology
Surabaya 2009
E-mail : frans@na.its.ac.id

Faculty of Engineering
University of Indonesia, Depok 16424
Tel : (021) 7270011 ext 51. Fax : (021) 7270077
E-mail : authora@@ui.edu

ABSTRACT

This research was conducted with the purpose to analyze according to the dynamic and experiment investigates of vibration characteristics in the bearing clearance result on internal combustion engine. Inertia force mass due motion to engine components that work on the bearing as a component of rotation, translation and swung. Experimental results showed the condition of engine static amplitude biggest impact in the vertical direction at a frequency of 200 Hz and amplitude 1.14 m/sec2/N horizontal direction while the 0.03 m/sec2/N, obtained stiffness and attenuation vertical direction k_{eqv} = 11150 N/m and c_{eqv} = 1750 Nm / s, horizontal direction k_{eqh} = 374 390 N/m and c_{eqh} = 20525 Nm/s. Results of measurement clearance 0:33 mm in the cylinder, 0.26 mm in the small gudgeon pin, 0.65 mm in biggest the gudgeon pin and 0:20 to 0:40 µm to the main bearing. Dynamic experimental results are obtained after reconstruction signal characteristic vibration due to imbalance of force amplitude signal 0:05 m/sec2 horizontal direction and vertical direction 0:11 m/sec2 engine on circle 15 Hz or 900 rpm, on the condition does not use compression. This research is useful as an initial study, the application of technology for predictive maintenance in the main engine ships based monitoring vibration signals according to periodically.

Key word : *Main engine, Amplitude, Force, Compression, Reconstruction Signal*

1. INTRODUCTION

As a means product of power the engine component composed of a static like engine body and dynamic like components s piston, connecting rod, crank shaft and bearing. Use of bearing on the dynamic component is to connect the components one with another and provide flexibility for them to trick movement. Bearing on the gudgeon-pin connecting rod to receive the of the piston load is the load due to combustion and other load such as inertia force, gravity force of the engine components motion. Forces are forwarded to the crankshaft through the connecting rod and main bearing, the forces in to provide bearing house (engine body), like in [1].

Impulsive load due to compression and combustion of the causing presence contact load that will occur when the engine operates. This mentioned resulting in over heating and clearance on the bearing ball. Lubrication condition that does not perfect and presence pattern of movement that can also cause clearance on the main bearing ball and the bearing on the gudgeon-pin connecting rod. Clearance on all of the bearing exceeds the maximum value that can be received, then specific actions should be taken, or damage from the engine shattered likely occurs. Therefore, the need to developing techniques to detect damage diagnosis damage on all the conditions bearing on the engine before damaged.

This research is useful as a basic to develop maintenance technology on base monitoring the vibration signals periodically, as an effort to replace conventional maintenance in the field of marine power in Indonesia. Conventional maintenance is not accurate because the repair was based on visual, hearing and schedules operational main engines.

Maintenance main engine like this is very harmful the owner because to predictive as faulty which the engine is still in the normal at repair, the components are still good in the change. With maintenance technology based measurement of the vibration signal main engine breakdown time can be predicted.

2. METHOLOGY DYNAMIC ANALYSIS EXPERIMENTAL INVESTIGATION of VIBRATION CHARACTERISTIC

Main problem is how to do in order to obtain experimental vibration response signals in the form of time-domain and frequency influence inertia force. Measurement results analyzed to obtain the vibration characteristics at a frequency that is lower than 0 to 100 Hz. The characteristics vibration problem is depending on the engine that is n = 900 rpm, which is obtained from this revolution of frequency n/60 = 15 Hz. These frequency as a basis 1xrpm then harmonic next 2xrpm of up to 6xrpm.

The vibration is in the form of a waveform that is focused on the relationship between the acceleration as a function of time, which is the acceleration magnitude can be scale in the simulation curve as Figure 13, Figure 14 waveform in the FFT to frequency spectrum to be make in MATLAB and can be read in curve as Figure 15, Figure 16. The characteristics vibration comes from the physical nature of the dynamics of engine components and the nature of the physical components bearing.

Experimental frequency characteristics of vibration is coming from the physical nature of the engine components to provide force imbalance and roller main bearing, such as ball pass frequency outer (BPFO), inner ball pass frequency (BPFI), ball spin frequency (BSF), fundamental train frequency (FTF) and waviness. As a result of the many signals that the record was held by the accelerometer vibration response analysis of the experimental gradually, as in [2].

2.1 Dynamic Modeling

Determining the vibration response in the house pad holder is determined based on the style of the work on the main bearing. Based on the actual condition of the vibration response can be determined by using dynamic modeling, as shown in Figure 1 and Figure 2.

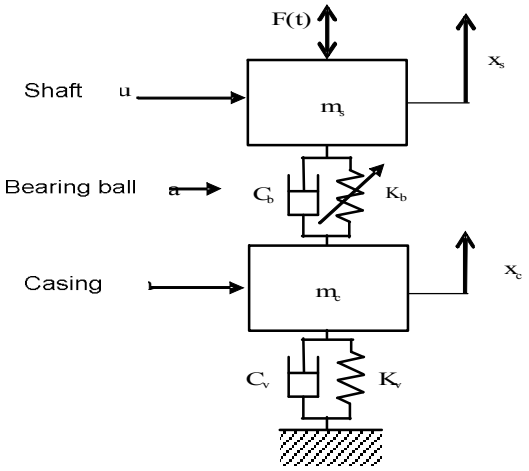

Figure 1 : Dynamic model main bearing

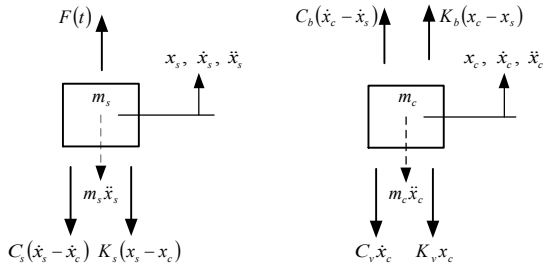

Figure 2 : Free body diagram ball bearing

Force F(t) that work on the model of the ½-axis is the force that works on the main bearing. This occurs because the axis on the vertical cylinder model is supported by 2 ball roller fruit. Dynamic modeling is done on the system axis applies to a main bearing modeling is also valid for the main bearing to two.

Modeling system is used with two degrees freedom (two-degree-of-freedom system). View from the physical nature of the system the rigidity crankshaft bearing ball can be assumed that with the settlement of non-linear system. Force is excogitation force $F(t)$, the force that inertia $m_s\ddot{x}_s$ meets the legal Newton to two, due to attenuation $c_s(\dot{x}_s - \dot{x}_c)$ and force due to stiffness $k_s(x_s - x_c)$. Diagram of free mass with 2 classified in the two-degree-of-freedom system can appear as movement equation 2 below.

$$m_s\ddot{x}_s + C_b(\dot{x}_s - \dot{x}_c) + K_b(x_s - x_c) = F(t) \qquad (1.a)$$

$$m_c\ddot{x}_c - C_b(\dot{x}_c - \dot{x}_s) + C_c\dot{x}_c - K_b(x_c - x_s) + K_c x_c = 0 \qquad (1.b)$$

2.2 Modeling Load on Ball Bearing

Depending on the size of the load zone on the following scale (1) the value force of work, (2) geometry bearing and (3) the value of diametrical clearance (Cd). By using the method of contact Hertzian and know geometry, the cushion stiffness can be determined. Cushion stiffness on the condition of dry contacts can be developed based on the relationship Hooke, so that relationships can be expressed in the equation (2).

$$K_{br} = \frac{\partial F_r}{\partial \delta_r} \qquad (2)$$

As a preliminary approach, the condition of dry contacts can be used so that the Hertzian contact model can be applied by the elastic force is assumed only dependent on the deflection. Relationship can be expressed in equation 3, as in [3].

$$Q = K_n.\delta^n \qquad (3)$$

Value of *n*, on the condition of the contact line (roller bearing) is 1:11 and a condition for the contact point (ball bearing) is 1.5. Depending on the value of KN geometry cushion material and the wheel can be determined using equation (4).

$$K_n = \frac{4}{3\pi\left(h_1 + h_2\right)}\sqrt{\bar{R}} \qquad (4)$$

Where :

$$\bar{R} = \frac{R_1 R_2}{R_1 + R_2}; \qquad h_i = \frac{1-\upsilon_i^2}{\pi E_i}, \qquad \text{i = 1, 2}$$

Harris, simplify the equation (3) into equation (4), as in [3].

$$K_n = \left[\frac{1}{(1/K_{pi})^{1/n} + (1/K_{po})^{1/n}}\right]^n \qquad (5)$$

K_{po} and K_{PI} values elements of the ball to contact with the steel roller line as the equation (5) can be determined using equation (6).

$$K_{pi/o} = 2{,}15\ x\ 10^5\ \Sigma\rho^{-1/2}\left(\delta^*\right)^{-3/2} \qquad (6)$$

Where is the curvature summing $\left(\Sigma\rho\right)$, it can be determined using the equation 7.a, equation 7.b as below.

$$\Sigma\rho_i = \frac{1}{D}\left(4 - \frac{1}{f_i} + \frac{2\gamma}{1-\gamma}\right) \qquad (7.a)$$

$$\Sigma\rho_o = \frac{1}{D}\left(4 - \frac{1}{f_o} - \frac{2\gamma}{1+\gamma}\right) \qquad (7.b)$$

$$\gamma = \frac{D\cos\alpha}{d_m} \qquad (7.c)$$

Dimensionless contact deformation (δ), determined by using a table that had been developed by Harris based on the curvature difference. Curvature difference is determined by using equation 7.a, equation 7.e.

$$F(\rho)_i = \frac{\frac{1}{f_i} + \frac{2\gamma}{1-\gamma}}{4 - \frac{1}{f_i} + \frac{2\gamma}{1-\gamma}} \qquad (7.d)$$

$$F(\rho)_i = \frac{\frac{1}{f_i} + \frac{2\gamma}{1-\gamma}}{4 - \frac{1}{f_i} + \frac{2\gamma}{1-\gamma}} \qquad (7.e)$$

When the radial direction of the working force of co-linear with the position of roller elements bearing, the deflection at the point roller contact elements can be determined using equation 8, as in [3].

$$F_r = ZK_n\left(\delta_r - \tfrac{1}{2}C_d\right)^{1,5} Jr\left(\varepsilon\right) \qquad (7.f)$$

$$\left(\delta_r - \tfrac{1}{2}C_d\right)^{1,5} = \frac{F_r}{ZK_n\, Jr\left(\varepsilon\right)} \qquad (7.g)$$

$$\left(\delta_r - \tfrac{1}{2}C_d\right) = \sqrt[1,5]{\frac{F_r}{ZK_n\, Jr\left(\varepsilon\right)}}\ ; \ \left(\delta_r - \tfrac{1}{2}C_d\right) \text{ is } \delta_{\max} \qquad (7.h)$$

$$\delta_{\max} = \sqrt[1,5]{\frac{F_r}{ZK_n\, Jr\left(\varepsilon\right)}} \qquad (8)$$

$$\delta_r = \sqrt[1,5]{\frac{F_r}{ZK_n\, Jr\left(\varepsilon\right)}} + \frac{1}{2}C_d \qquad (9)$$

Deflection on the ball bearing by the because of the total radial force, Fr, can be defined as a deflection from resultant two elements bearing ball. Deflection of each element is calculated based on the force of co-linear elements that work on the bearing by using the equation 10, as in [3].

$$\delta = \left(\frac{Q}{K_n}\right)^{1/n} \qquad (10)$$

Deflection of the roller ball is determined as resultant deflection of each element by using the equation. (9).

$$\delta_\phi = \sqrt{\delta_A^2 + \delta_B^2 - 2\delta_A\,\delta_B\cos(180 - \theta)} \qquad (11)$$

Thus the force of the work on radial roller ball can be determined using equation 12.

$$F_r = \frac{1-E_\phi}{1+E_\phi} Z\,K_n\,\delta_{\max}^n\, Jr(\varepsilon) \qquad (12)$$

Where $E\Phi$ is the error factor due to the position of the element ball of force radial direction of the work. Value Φ can be determined using equation 13.

$$\phi = (\omega_i - \omega_c).\Delta t \qquad (13)$$

In the experimental knowledge, accelerometer placed on the bearing house with the horizontal direction x, and vertical y. Modeling force of the work on the bearing shown in Figure 7. Observed radial force and analysis in vertical or horizontal direction and the load that zone. Refer to the model the system stiffness in the system x and y can be written on equation 12.

2.3 The Process of Loading the Ball Bearing

Study experimental conducted to measure the vibration response in the vertical direction (y), and the horizontal direction (x). By the influence of the load of the dynamic force imbalance, then the total angle style radial oscillation can. This is shown in Figure 3 where the angular position of the angle of load zone will be changed according to the total

force radial direction. Thus, the stiffness bearing a global system of coordinates (x, y) will be affected. Stiffness value in such conditions can be determined using equation 17.

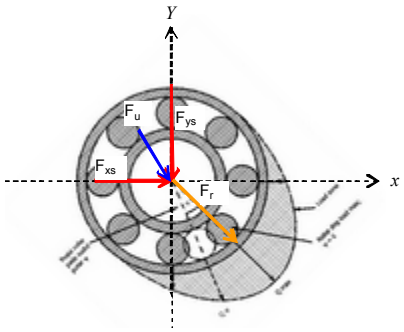

Figure 3 : Curve load zone of bearing

$$k_{bij} = \frac{\partial F_i}{\partial \delta_j}, \text{ i, j = x, y} \qquad (14)$$

Where :

$$\begin{Bmatrix} F_x \\ F_y \end{Bmatrix} = F_r \begin{Bmatrix} \cos\alpha_o \cos\psi \\ \cos\alpha_o \sin\psi \end{Bmatrix} \qquad (15)$$

$$\begin{Bmatrix} F_x \\ F_y \end{Bmatrix} = \frac{1-E_\phi}{1+E_\phi} Z\, Jr(\varepsilon) K_n \delta_{\max}^n \begin{Bmatrix} \cos\alpha_o \cos\psi \\ \cos\alpha_o \sin\psi \end{Bmatrix} \qquad (16)$$

Hence,

$$K_b = \begin{bmatrix} K_{bxx} & K_{bxy} \\ K_{byx} & K_{byy} \end{bmatrix} = \frac{1-E_\phi}{1+E_\phi} n Z\, Jr(\varepsilon) K_n \delta_{\max}^{n-1} \begin{bmatrix} \cos^2\psi & \cos\psi\sin\psi \\ \cos\psi\sin\psi & \sin^2\psi \end{bmatrix} \qquad (17)$$

2.4 Stiffness and Attenuation Bearing House

Attenuation and stiffness bearing is determined through the identification process. In regard to study experimental frequency response function of the system test bearing ball and the home supporters made. Curve function frequency response function of the system of multi-degree freedom "MDOF" can be obtained with assumption as a combination of several systems "SDOF". Thus the system of reacceptance "MDOF" can be expressed in equation 18, as in [4].

$$\alpha_{jk}(\omega) = \sum_{s=1}^{N} (SDOF)_s = \sum_{s=1}^{N} \frac{{}_sA_{jk}}{\omega_s^2 - \omega^2 + i\eta_s \omega_s^2} \qquad (18)$$

2.5 The Dynamic Model

Studies theoretic developed can be directed to build a dynamic system modeling slider crank. The truth model is the dynamic response, vibration fitness model with the measurement of vibration response. Based on the dynamic model as shown in Figure 1, the movement equation can be written as the system in equation 19.

$$m_s \ddot{x}_s + C_v (\dot{x}_s - \dot{x}_c) + K_v (x_s - x_c) = 0 \qquad (19.a)$$

$$m_c \ddot{x}_c + C_b (\dot{x}_c - \dot{x}_s) + K_b (x_c - x_s) = F_s \qquad (19.b)$$

Equation 19.a, equation 19.b, can be expressed in matrix form as written in equation 20 below.

$$\begin{bmatrix} m_s & 0 \\ 0 & m_c \end{bmatrix} \begin{Bmatrix} \ddot{x}_s \\ \ddot{x}_c \end{Bmatrix} + \begin{bmatrix} C_v + C_b & -C_b \\ -C_b & C_b \end{bmatrix} \begin{Bmatrix} \dot{x}_s \\ \dot{x}_c \end{Bmatrix} + \begin{bmatrix} K_v + K_b & -K_b \\ -K_b & K_b \end{bmatrix} \begin{Bmatrix} x_s \\ x_c \end{Bmatrix} = \begin{Bmatrix} 0 \\ F_s \end{Bmatrix} \qquad (20)$$

By using the equation 20, the reacceptance system dynamic model can be expressed as in equation 21, as in [4].

$$\alpha_{jk}(\omega) = \sum_{r=1}^{N} \frac{(\psi_{jr})(\psi_{kr})}{(K_r - \omega^2 M_r) + i(\omega C_r)} \qquad (21)$$

Where,

$$\{\psi\}^T [m] \{\psi\} = [M_r];$$

$$\{\psi\}^T [c] \{\psi\} = [C_r];$$

$$\{\psi\}^T [k] \{\psi\} = [K_r]$$

Thus, the vibration response of the system can be expressed in equation 22.

$$\begin{Bmatrix} x_s(t) \\ y_s(t) \\ x_c(t) \\ y_c(t) \end{Bmatrix} = \begin{bmatrix} \alpha_{11} & \alpha_{12} & \alpha_{13} & \alpha_{14} \\ \alpha_{21} & \alpha_{22} & \alpha_{23} & \alpha_{24} \\ \alpha_{31} & \alpha_{32} & \alpha_{33} & \alpha_{34} \\ \alpha_{41} & \alpha_{42} & \alpha_{43} & \alpha_{44} \end{bmatrix} \begin{Bmatrix} f_{xs} \\ f_{ys} \\ f_{xc} \\ f_{yc} \end{Bmatrix} \qquad (22)$$

2.6 Bearing Vibration Response

From equation 19.a and 19.b, can be simplified and written in the form of the following;

$$\begin{bmatrix} m_s & 0 \\ 0 & m_c \end{bmatrix} \begin{Bmatrix} \ddot{x}_s \\ \ddot{x}_c \end{Bmatrix} + \begin{bmatrix} c_b & -c_b \\ -c_b & c_b + c_v \end{bmatrix} \begin{Bmatrix} \dot{x}_s \\ \dot{x}_c \end{Bmatrix} + \begin{bmatrix} k_b & -k_b \\ -k_b & k_b + k_v \end{bmatrix} \begin{Bmatrix} x_s \\ x_c \end{Bmatrix} = \begin{bmatrix} F(t) \\ 0 \end{bmatrix} \qquad (23)$$

With assume that,

$$x = Xe^{i\omega t}; \dot{x} = i\omega Xe^{i\omega t}; \ddot{x} = -\omega^2 Xe^{i\omega t}$$
$$F(t) = F_o e^{i\omega t} \quad (24)$$

Equality applied to 23 of 24 that can be re-written as:

$$-\omega^2\begin{bmatrix} m_s & 0 \\ 0 & m_c \end{bmatrix}\begin{Bmatrix} \ddot{x}_s \\ \ddot{x}_c \end{Bmatrix}e^{i\omega t} + i\omega\begin{bmatrix} c_b & -c_b \\ -c_b & c_b + c_v \end{bmatrix}\begin{Bmatrix} \dot{x}_s \\ \dot{x}_c \end{Bmatrix}e^{i\omega t} + \begin{bmatrix} k_b & -k_b \\ -k_b & k_b + k_v \end{bmatrix}\begin{Bmatrix} x_s \\ x_c \end{Bmatrix}e^{i\omega t} = \begin{Bmatrix} F(t) \\ 0 \end{Bmatrix}e^{i\omega t} \quad (25)$$

$$-\omega^2\begin{bmatrix} m_s & 0 \\ 0 & m_c \end{bmatrix}\begin{Bmatrix} \ddot{x}_s \\ \ddot{x}_c \end{Bmatrix} + i\omega\begin{bmatrix} c_b & -c_b \\ -c_b & c_b + c_v \end{bmatrix}\begin{Bmatrix} \dot{x}_s \\ \dot{x}_c \end{Bmatrix} + \begin{bmatrix} k_b & -k_b \\ -k_b & k_b + k_v \end{bmatrix}\begin{Bmatrix} x_s \\ x_c \end{Bmatrix} = \begin{Bmatrix} F(t) \\ 0 \end{Bmatrix} \quad (25.a)$$

$$\begin{bmatrix} k_b + i\omega c - \omega^2 m_s & -(i\omega c_b + k_b) \\ i\omega c_b + k & (k_b + k_v) + i\omega(c_b + c_v) - \omega^2 m_c \end{bmatrix}\begin{Bmatrix} X_s \\ X_c \end{Bmatrix} = \begin{Bmatrix} F_o \\ 0 \end{Bmatrix} \quad (26)$$

By using the Kramer theorem, then the equation 26 can be completed and obtained as follows:

$$\Delta = \left(k_b + i\omega c - \omega^2 m_s\right)\left\langle (k_b + k_v) + i\omega(c_b + c_v) - \omega^2 m_c \right\rangle - \left\langle (i\omega c_b + k)(i\omega c_b + k_b) \right\rangle \quad (27)$$

$$X_s = \frac{F_o\left\langle (k_b + k_v) + i\omega(c_b + c_v) - \omega^2 m_c \right\rangle}{\Delta} \quad (28)$$

$$X_c = \frac{F_o(i\omega c_b + k_b)}{\Delta} \quad (29)$$

Thus, the response ancillary casing (bearing house) can be written in the following equation.

$$X_c(t) = \frac{F_o(i\omega c_b + k_b)}{\Delta}e^{i\omega t} \quad (30)$$

And,

$$X_c(t) = \frac{(i\omega c_b + k_b)}{\Delta}F_o(t) \quad (31)$$

Structure has a close cushion that can be assumed as attenuation hysteretic, by 'Lim'

2.7 Reconstruction Vibration Response

Reconstruction in the frequency response is selected is 15, 30, 45, 60, 75 and 90 Hz above equation can be done with the synthesis, such as below and the results shown in the picture below. Equation 32, equation 33 below apply to the test with the condition of spark plugs for condition of horizontal and vertical angle and phase, as in [2].

$$R_x = m_{gh}\cos(\omega t) + \phi_h \quad (32)$$

$$R_y = m_{gv}\cos(\omega t) + \phi_v \quad (33)$$

Figure 16, Figure 17, the waveform is measured on the accelerometer due to the multi-complex derived from the multi-component engine. Waveform reconstruct this signal is derived from the pure components of the engine measured on the vertical and horizontal direction, the condition of spark plugs is closed or open and use. Waveform is what is used as a signal reverence for validation. The picture above can be used as engine vibration and the response is validated with the standard response to vibration theoretic technology for use in predictive maintenance.

3. EXPERIMENTAL

Internal Combustion Engine

Main component is a piston engine composer, the piston, , connecting rod, Crank shaft , cylinder block and engine block as Figure 4, piston has a translation movement, Crank shaft rotation and movement to connecting rod the movement has a swing that is more complex, as in [1], [7] . On this research, the process does not involve data compression and force from the combustion engine because it played by AC motor, so that the work is inertia force.

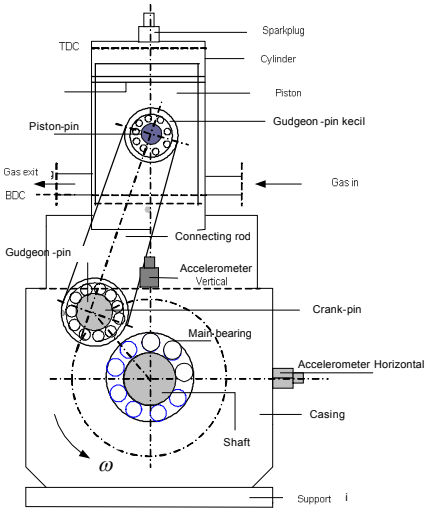

Figure 4 : Construction Engine

Bearing Data

Study computing conducted in this research refers to the test device is used. Test the device using the bearing ball that has the following specifications: Trademarks: Koyo 6205, type: Ball bearing, in Diameter (in): 25 "mm", Diameter outside

(do): 50 "mm", Diameter pitch (dm :) "mm", Diameter ball (D): 7.6 "mm", roll number of elements: 9, Corner contact (α): 0, Basic load rating: Dynamic (C): "N", Static (Co) : "N". Radial load of work on the bearing ball is determined through study kinematical. Movement by the slider crank happen because of the electric motor on 900 rpm.

Measuring Clearance

The problems that clearance is very dominant, so the diameter measurement was held at the cylinder, piston, bearing piston and piston-pin, is to analyze the loose (clearance) the cylinder and bearing piston. Results obtained for loose cylinder is 0:33 mm, and to bearing is 0:19 mm. Earned a respite on the price obtained at the reference (dedy Satria 1995). Looseness between the road and bearing pen crank pen is 0.65 mm while the main bearing is 20 μm.

Dynamic Characteristics Measurements

Research conducted on the engine on the dynamic characteristics of measurement methods excitation cushion shock (shock excitation). With the method, excitation force form impulse force given to the measured object, so hopefully the system will vibrate at a frequency of free personality. Set up a test frequency response function shown in Figure 5 is as follows: 1.Computer system, 2. Hammer exits (impact hammer), and 3. Amplifier conditioning, 4. Accelerometer, 5. Power amplifier, 6. IO port, 7. Multi channel spectrum analyzer.

Impulse force given to the engine body is done by using the impact hammer with a strike near the accelerometer on the vertical and horizontal directions so that the response vibration measured by accelerometer. Giving force impulse engine on the body caused by the region at the assumed close to the ball. Results and measurement data processed by signal analyzer multi "MSA" and the result displayed on the computer system.

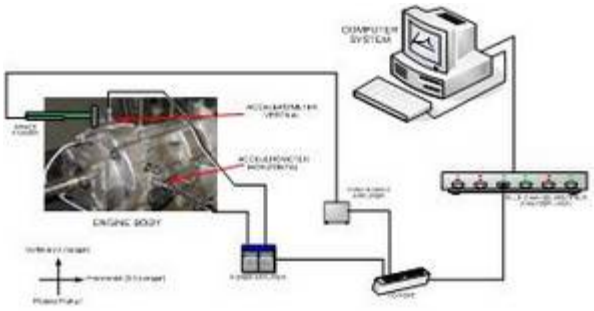

Figure 5 : *Set up* experimental for investigate frequency respons function

Vibration Response Measurement

Set up a vibration measurement instrumentation used in this research as shown in Figure 6 below. Body around the engine crankshaft is assumed as the ball home in the area because there is a bearing ball (ball bearing) as the main bearing support crankshaft. Measurements conducted on the bearing house at the crank at 0 degrees on the piston reaches tdc direction by 90 degrees vertical and horizontal direction at the position began to exhaust of the doors open.

Accelerometer placement on the position so that the signal caused record response vibration direction is vertical and horizontal. Control engine settings can be done with the change of motor cycles (ac motor) use a converter, also inserted key phase as optical pulse generator for measurement of vibration. Charge amplifier is used to signal control vibration measurement by accelerometer, which is very dominant "Multi Signal Analyzer" is a working process for the measurement signal to obtain the frequency spectrum and waveform. Then the computer system by a signal formed by MSA is shown in the image signal of the vibration response.

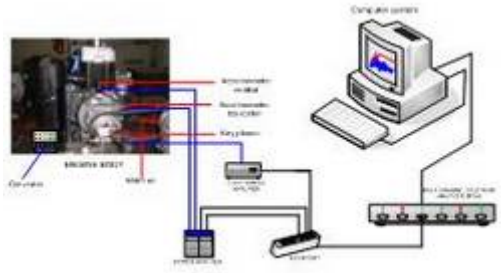

Figure 6 : Set up Experimental dynamic vibration

4. RESULTS AND DISCUSSION

4.1 Force on Main Bearing

Correction of determining the vibration response using the modal synthesis with the force that comes from the main bearing as shown on curve below. Observed in Figure 7, Figure 8 is that the force of the maximum occurs at the vertical direction of the work on the main bearing to the slider crank case under study, 90 N, the force is at least 15 N. Thus, by using test cases obtained curve stiffness, as shown in Figure 9, as in [6]. The size of the force shown in this curve stiffness is 100 N and the maximum amount of the maximum value of stiffness is 10e +6, curve is a form of non-linier.

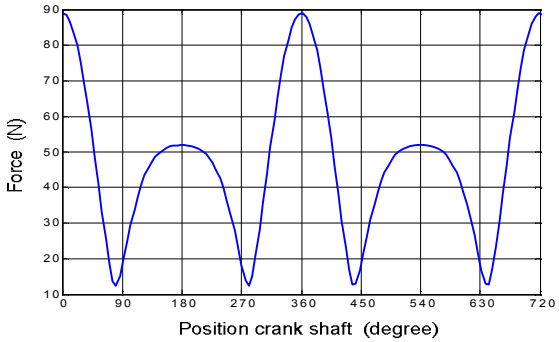

Figure 7 : Curve force vertical direction computation simulation result

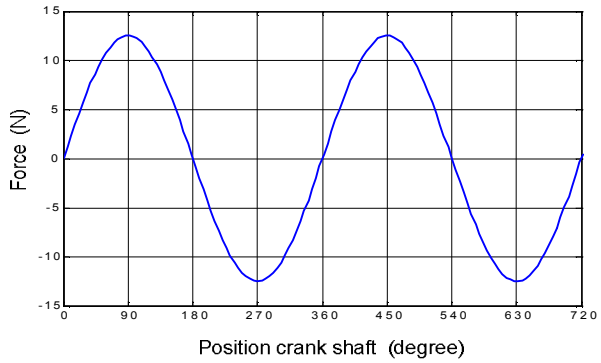

Figure 8 : Curve force horizontal direction computation simulation result

4.2 Stiffness Bearing Ball

Computing studies the determination of stiffness bearing test is done by using mathematical modeling. Condition that represents the diametrical clearance bearing and tears on the ball used computational knowledge that is 20 µm. Knowledge computational results are shown in Figure 9. Curve stiffness as a function of radial force ball bearing on the shows that are on the stiffness values from 0 to 9.6e +6 N/m with a range of force values from 0 to 100 N as Figure 7, Figure 8.

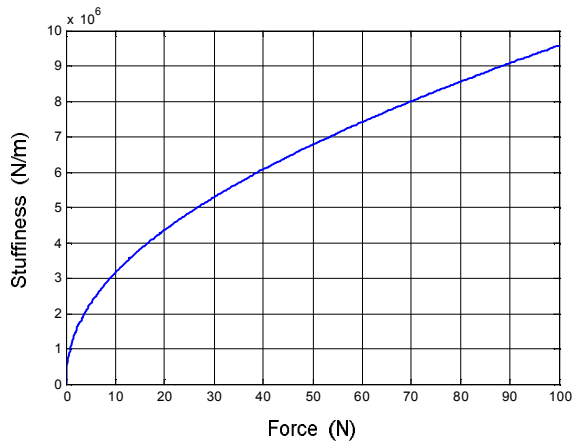

Figure 9 : Stiffness Curve versus radial force

4.3 Results Static Test

Length Crank shaft one-cylinder engine test object between the two is quite short, as observed in Figure 4. Because of the short axis, then stiffness be high so that it can be observed as a rigid axis (rigid shaft). Thus the dynamic stiffness model of the system can be dimodelkan two-degree freedom system as shown in Figure 1, Figure 2. Model underpinning the value of stiffness can be determined with knowledge computational using Hertzian contact rule, home cushion while stiffness is determined through the identification process. Study conducted with the knowledge FRF analysis results in a frequency of 100 Hz (about 6 x frequency circle) using circle-fit method. Knowledge results in the frequency response function horizontal and vertical direction can be observed in Figure 10, Figure 11.

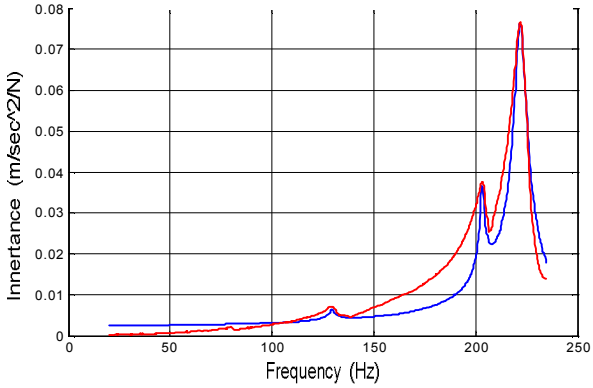

Figure 10 : Circle fit result on vertical direction

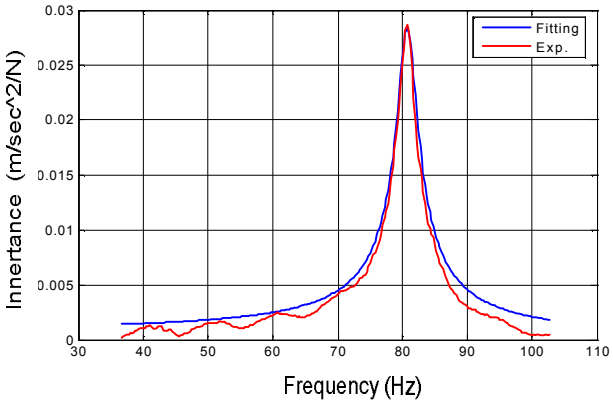

Figure 11 : Circle fit result horizontal direction

Characteristic of bearing house in the research is determined through process identification. Circle-fit method used to obtain stiffness values and attenuation system based on the home support in the data frequency response function. Plot data penguin frequency response function and the circle-fit in Figure 10, Figure 11 shows 2 curve each with a circle-fit and curve point frequency response function experimental results for vertical and horizontal direction. Value of dynamic parameters of the circle-fit will be used in modeling the response to the vibration direction is vertical k_{eqv} = 11150 "N/m" and c_{eqv} = 1750 "Nm/s" and the horizontal direction k_{eqh} = 374 390 "N / m" and c_{eqh} = 20525 "Nm/s".

4.4 Results of Dynamic Experiment

Engine driving by motor cycles with 900 rpm in the condition of spark plugs open so that it does not happen all the compression in the cylinder. Figure 12, Figure 13, the signal is measured on the accelerometer due to the multi-complex derived from the multi-component engine. Signal with the color blue is the signal transient measured in horizontal and vertical direction, with the condition of spark

plugs do not use open burning, Signal red with a key derived from the phase of the time to reach the 1 cycle of crankshaft .. Waveform of record this signal is coming from the engine components and parts dynamic main bearing. Super position of this signal with the signal clear in the frequency domain like in Figure 14, Figure 15 indicates the signal in the frequency domain measured on the accelerometer due to the multi-complex derived from the multi-component engine that is the result of the function of the Fourier transport waveform is created in the program Mat lab. This describes the frequency domain nature of the physical components of the engine vibrates, the condition of spark , open or does not use combustion, which is measured on the vertical and horizontal direction.

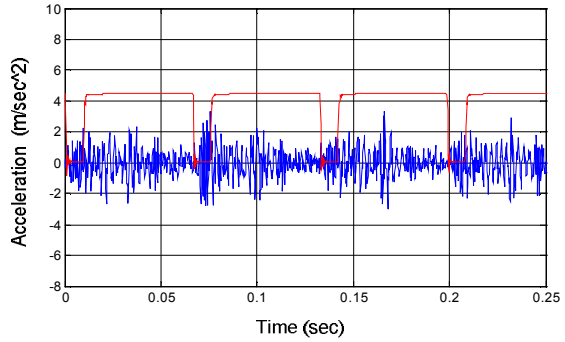

Figure 12 : Result Experimental curve on horizontal direction

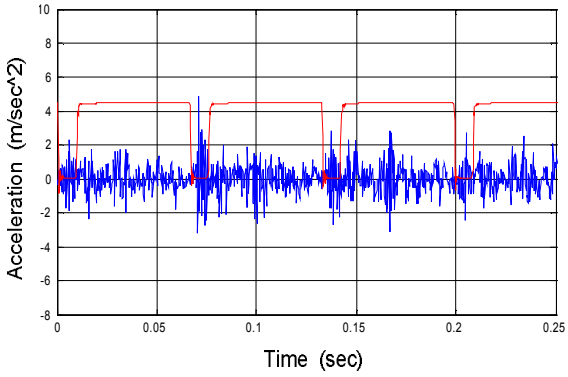

Figure 13 : Result Experimental curve on vertical direction

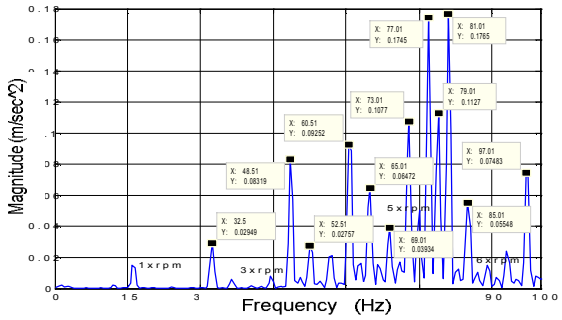

Figure 14 : Result experimental curve in horizontal direction on frequency domain before reconstruction

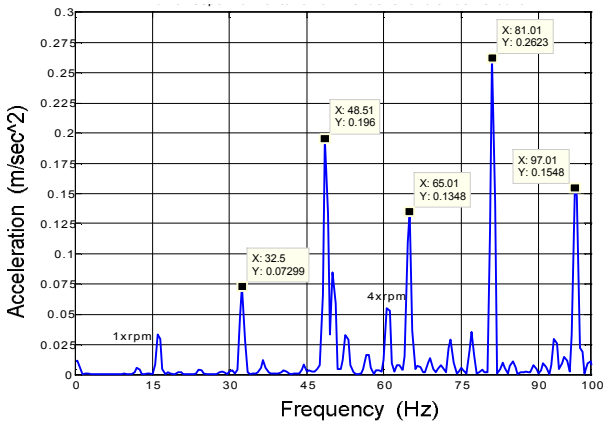

Figure 15 : Result experimental curve in vertical direction frequency domain before reconstruction

5. RECONSTRUCTION RESULTS DISCUSSION SIGNAL VIBRATION

Signals obtained from the results of reconstruction of the movement of engine horizontal direction, due to the force of the imbalance that occurred at the time of engine operation. In Figure 16, observed that the signal is not purely sinusoidal, but no signal going to the super position amplitude that varies from 0 to 0.0175 m/sec2 is the acceleration in the horizontal direction. Movement direction of the horizontal acceleration with the engine this is the case for a round of crankshaft within 0:05 seconds.

Can be observed in Figure 17, that the size of the style of the work on the crankshaft in a different round of dimension. Position on the Super curve signal that describes the position on a particular style of fluctuations occurs in the crankshaft. Force engine of the shake (shaking) the direction to the left or to the right with amplitude and acceleration as shown in the curve, the conditions on the open plug (not compression). Movement of the engine in the horizontal direction in which work force shake (shaking) is smaller/less than the vertical direction, as in [8], [9].

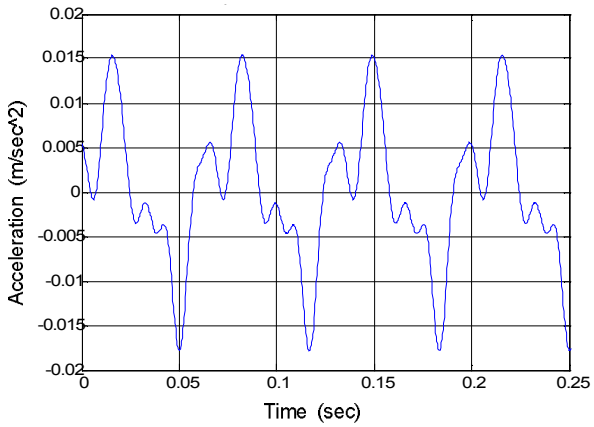

Figure 16 : Result experimental curve in horizontal direction on frequency domain after reconstruction

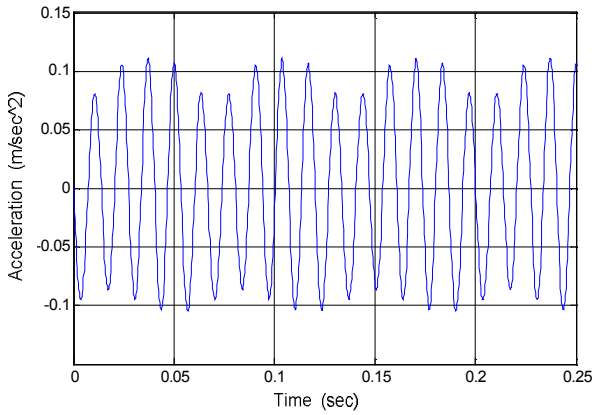

Figure 17 : Result Experimental curve in vertical direction time domain after reconstruction

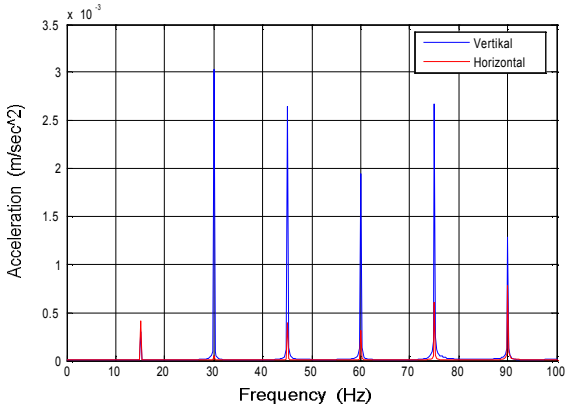

Figure 18 : Result Experimental curve in horizontal and Vertical direction on frequency domain after Reconstruction

Figure 17, the signal is curve vibration caused by shake-force vertical direction (towards the top and down direction), with a pure sinusoidal shape. 1 cycle on the crank with 0:05 seconds of time going three sinusoidal waves, amplitude achieve 0:13 m/detik2, on the condition of all spark plugs (do not use compression pressure). Movements of the engine in the vertical direction in which work style shake (shaking) more than the horizontal direction.

Figure 18, is curve frequency domain response of the reconstruction plug open vertical and horizontal. At the direction of vertical acceleration of 0:31 m/sec^2 at a frequency of 30 "Hz", in the horizontal direction is smaller than the vertical direction of 0:01 m/sec^2 on the same frequency. The frequency of the waveform and the other can be seen in this curve.

6. CONCLUSION

Results of dynamic analysis and experimental knowledge characteristic vibration due to looseness in the bearing internal combustion engine such as the above can be conclusion that signals obtained from the experimental multi-effects, namely the physical nature of the main bearing and imbalance of the piston crank system, this can be seen curve in the waveform and frequency domain. This research is useful as an initial study, the application of technology for predictive maintenance in the main engine ships in based monitoring vibration signals.

REFERENCE

[1] Wiranto Arismunandar, *Penggerak Mula Motor Bakar Torak*, Penerbit ITB Bandung, 1988.

[2] Carolus Bintoro, MT., *Analisis Teoritik Dan Kaji Eksperimental Ciri Getaran Mekanik Akibat Keausan Pada Bantalan Rol Silindrik,* Disertasi Doktor, Program Studi Teknik Mesin, Institut

[3] Harris A.T., *Rolling Bearing Analysis*, John Willey & Son Inc. 1991.

[4] Ewins D.J., *Modal Testing*, Theory and Practice, John Wiley & Sons Inc, 1981.

[5] Biezeno C. B. And Grammel R., *Engineering Dynamics, T*he book was first published in German in one volume entiled, Technische Dynamic, 1939. Teknologi Bandung, 2006.

[6] Holowenko A. R., *Dynamics of Machinery*, Associate Professor of Mechanical Engineering Purdue University, Wiley Trans-Edition. 1980.

[7] Hamilton H. Mabie, Fred W. Ocvirk, *Mechanism and Dynamics Machinery,* Third Edition, Wiley International Edition. 1975.

[8] Maleev V.L., M.E., DR, A.M., Ir. Bambang Priambodo, *Operasi Dan Pemeliharaan Mesin Diesel*, Penerbit Erlangga, 1986.

[9] Arend Schwab L., 2002: Dynamic of Flexible Multibody Systems, Small Vibration Superimposed on a General Rigid Body Motion, Ph.D thesis, Delft University The Netherlands, April 2002.

Proceeding of the 11th International Conference on QiR (Quality in Research)
Faculty of Engineering, University of Indonesia, Depok, Indonesia, 3-6 August 2009
ISSN 114-1284

Multi-axis Milling Optimization through Implementation of Proper Operation Strategies in Machining Processes

Gandjar Kiswanto, Zulhendri, Benito H, Priadhana E

Department of Mechanical Engineering – University of Indonesia
Kampus Baru – UI Depok, 16424
gandjar_kiswanto@eng.ui.ac.id

ABSTRACT

Multi-axis (5-axis) milling is used in the machining of complex shaped surfaces in a wide range of industries such as aerospace, automotive and ship building. Commercial CAM systems have however limited functionality. These limited functions restrict users to obtain high quality product in a efficient manner. Most of provided milling strategies still need user interactions and decisions which are often very troublesome. This paper describes the research conducted to enhance the CAM-system functionality and eventually optimize multi-axis milling processes. Three machining operation strategies are investigated and the results are implemented in the CAM-system based on faceted models developed by Laboratory of Manufacturing Technology and Automation, Department of Mechanical Engineering – University of Indonesia. These strategies are : 1) proper combination of tool type and cutting feed direction for 3-axis roughing and 5-axis finishing, 2) curvature based milling (feed direction) direction and segmentation, and 3) inclination angle control.

Keywords: *Multi-axis Milling, Milling Optimization, CAM-system*

INTRODUCTION

Current existing CAM-systems are still lack of functionalities that needs to optimize milling operation in order to enhance quality and minimizing machining time. The optimization means obtaining higher efficiency in machining processes and better surface quality. This research was investigating three strategies that can greatly improve machining operation functionalities. First, when 5-axis machining needs to be used following the common 3-axis roughing. In this case, the appropriate combination of tool-type and feed direction during 3-axis roughing and 5-axis finishing play important role. Furthermore, strategy when machining sculptured/contoured surfaces on which surface features (e.g. concave, convex, saddle and flat) are exist. In this kind of surfaces, each surface feature has its optimal tool type and feed direction. The last strategy is possibilities and condition to use multi-axis milling with dynamic inclination angle. The investigation of the above strategies is explained as the following.

FIRST MILLING STRATEGY for OPTIMISATION

The first strategy is to implement optimal combination of cutting directions and tool types during 3-axis roughing and 5-axis finishing process, since most of roughing and finishing processes are conducted using 3-axis and 5-axis machining, respectively.

In most practical cases, when the 5-axis machining is needed after the 3-axis roughing, the operator would simply assign the feed direction without considering the appropriate direction and tool type which result best machined quality. In order to know the influence of using different feed direction and cutting tool type, in this research, three type of cutting tools (Flat-end, Ball-nose, and Thoroidal cutter) are combined with two feed directions for 3-axis roughing and 5-axis finishing.

Experimental Setup

Cutting Tools
Material : solid carbide cutter, diameter : 10 mm. Total flute : 4. Type : 1. *Flat-end :* 2. Thoroid with 1,0 mm corner radius and 3. 5 mm Ball nose radius, as seen at following figure.

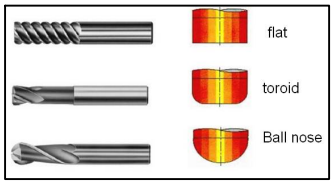

Figure 1. Cutter type, flat end, toroid dan ball-nose

Cutting Condition :
- Cutting velocity (V_c) = 150 meter per minute, for mild steel material
- Cutting speed per tooth (f_z) = 0,04 - 0,1 mm/flut, for 10 mm diameter
- spindel speed (n) is n = 4500 rpm
- the feed rate (Vf) is 700 mm/min
- *roughing process,* depth of cut : 0.5, *scallop* 0.3 mm
- *finishing process,* no additional cutting, *scallop* 0.2 mm
- cutter *Overhang* 35 mm

Factor and Test Level
Factor and test level can be seen in table 1:

Tabel 1. Factors and Test Level

FACTOR / LEVEL	Tool Type roughing	Tool Type finishing	Feed Direction
Level 1	Flat	Thoroid	*across*
Level 2	Thoroid	Ball Nose	*parallel*

Because of there were 3 factors; and 2 levels, so that the amount of test based on full factorial is 2^3 = 8. In roughing process, the test was done in 2 ways, across and parallel. The finishing proses was done by machining across to roughing direction. The optimal combination is the one that produce higher quality of the machined surfaces. The following table shows the results of the combination.

Table 2. Machine surface quality produced by several combination of tool-type and machining direction during 3-axis roughing and 5-axis finishing

No	Tool type Roughing	Tool type Finishing	3-axis vs 5-axis Direction	Ra (μm)	Wt (μm)
1	Flat	Ball nose	Across	0.419	1.839
2	Flat	Ball nose	Parallel	0.279	1.486
3	Flat	Toroidal	Across	0.697	2.205
4	Flat	Toroidal	Parallel	0.332	1.060
5	Toroidal	Ball nose	Across	0.709	2.628
6	Toroidal	Ball nose	Parallel	0.439	1.442
7	Toroidal	Toroidal	Across	0.797	2.546
8	Toroidal	Toroidal	Parallel	0.475	1.419

The results are as the following :
1. For *finishing*, ball-nose cutter produces lower Ra than toroidal type
2. For cutting direction, parallel direction produces lower Ra than across direction.

For *roughing* and *finishing interaction* :
1. *Roughing* with *flat*-end tool and *finishing* with ball-nose produces lower Ra than *roughing* with *flat-end* and *finishing* with *toroidal*.
2. *Roughing* with *toroidal* and *finishing* with ball-nose cutter produce lower Ra than *roughing toroidal* and *finishing toroidal types*.
3. The combination that produces lowest Ra is between *roughing* with *flat* and *finishing* with ball-nose cutter

For interaction of *finishing* and direction :
1. *finishing* ball-nose cutter type and parallel direction produce smoother Ra than *finishing* ball-nose cutter type and across direction
2. *finishing toroidal* cutter type and parallel direction produce smoother Ra than *finishing toroidal* type and across direction
3. The lowest Ra is produced by combining *finishing* ball-nose cutter type with parallel direction, but the difference is very small to *finishing toroidal* type with parallel direction.

The effect to The Machined Surface Waviness (Wt)
For cutting direction, parallel direction produces smaller Wt than across direction. In more detail :
for interaction of *finishing* and direction :
a. *finishing* ball-nose type and parallel direction produce smaller Wt than *finishing* ball-nose type and across direction
b. *finishing toroidal type* and parallel direction produce smoother Wt than *finishing toroidal* type with across direction.
c. The smoothest will be produced by combining *finishing* toroidal type with parallel direction

SECOND MILLING STRATEGY for OPTIMISATION

The next strategy is conducting the optimal 5-axis finishing direction on each surface contour classified by convex, concave and saddle region identified in the workpiece that would produce higher quality machined surface with lower machining time. The identification is done by curvature evaluation of the model. Once the surface feature (contour) is identified, an appropriate milling direction can be applied.

In this research, the curvature estimation methods, modified *Spherical Image* and Gauss-Bonnet Scheme, are combined and implemented to determine the shape of the model as the characteristic of curvature and then segment it based on the shape of surface model, where an area would be put in the same segment if it has the same curvature characteristics and adjacent location.

Developed Methods

Approximations to the surface normal and Gaussian curvature of a smooth surface are often required when the surface is defined by a set of discrete points rather by a formula (Meek et al., 2000). In this study, the used objects are 3D faceted models where they are composed by discrete points forming mesh of triangles. This approximation is only valid for smooth surface; a surface that is continue, is not coarse, and does not make angle in any area (Figure 2).

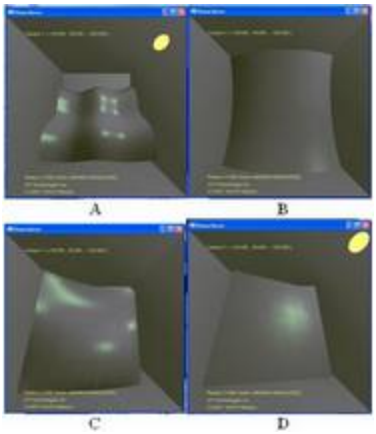

Figure 2: 3D faceted models that were used for curvature estimation tests

Surfa ce Curvature

Curvature is a deviation of an object or of space from a flat form and therefore from the rules of geometry codified by *Euclid*. At any point on the surface, one may consider surface curves passing through that point; locally such a curve lies in some plane intersecting the surface at that point (Kresk P et al., 2001).

Theorem 1. Meusnier's theorem :

$$k_C = k_n \cos\Theta \qquad (1)$$

where :

k_c = curve curvature; curvature of the curve
k_n = normal curvature; the curvature of any curve lying in an intersection plane which contains the surface normal direction at the given point
θ = the angle between the intersection plane and the surface normal.

Principal curvatures are primary and secondary directions and magnitudes of curvature. A given direction in the tangent plane is chosen and θ is defined as the angle between this preferred direction and the intersection plane. For θ (0, π) the function $kn = f(\theta)$ has two extrema. These extrema are called the principal curvatures (Kresk P, et al).

Theorem 2. Euler's theorem :

$$k_n = k_1 \cos^2\alpha + k_2 \sin^2\alpha \qquad (2)$$

where :

k_1 & k_2 = principal curvatures
k_n = normal curvature
α = the angle between the direction of k_1 and desired direction

Gaussian curvature (global curvature) is the product of principal curvatures k1 and k2 as follows:

$$K = k_1 \bullet k_2 \qquad (3)$$

And mean curvature is the average of principal curvatures:

$$H = \frac{(k_1 + k_2)}{2} \qquad (4)$$

Modified Gauss-Bonnet Scheme

Gauss-Bonnet Scheme is usually called Angle Deficit Method, because this method uses the total

of angle which is surrounding a vertex in an area, compared to the full circumference angle 360°. If an area, or a curvature calculation zone, is convex or concave, then the surrounding angle is less then 360°. Furthermore, if the area is flat, then the angle is +/- 360°. On the other hand, if the area is rather wavy or saddle, or formed a hyperbolic shape, then the angle is more than 360°.

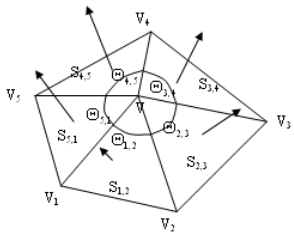

Figure 3: Surface of angle deficit method

Area of every triangle (which is represented by symbol $S_{x,y}$ in Figure 3) can be partitioned into three equal parts, one corresponding to each of of its vertices, so that the total area of a path on the surface around V on the polyhedron is

$$total\ area = \frac{1}{3}\sum S_{i,i+1} \qquad (5)$$

where $S_{i,i+1}$ is the area of triangles, formed by vertices V, V_i, dan V_{i+1} (Meek, et al., 2000).

The total angle of the triangles on the vertex V (in figure 3) is angle deficit of the polyhedron which are formed from the related triangles,

$$angle\ deficit = 2\pi - \sum \Theta_{i,i+1} \qquad (6)$$

Then total is the angle deficit in equation (6), compared with the area related to the vertex V in equation (5),

$$K = \frac{2\pi - \sum \Theta_{i,i+1}}{\frac{1}{3}\sum S_{i,i+1}} \qquad (7)$$

Modified Spherical Image

The estimation of the curvature value using Spherical Image method is conducted by creating a closed curve on the surface, surrounding a vertex which is being a chosen point to determine the value of the curvature. On the path that has been created, some points should be put (Figure 3), whereas the surreounding points are adjacent with the center point.

Vertices which compose the path and the center vertex will form a polyhedron that consists of triangles of the faceted model, just like the triangles that are used in Gauss-Bonnet Scheme (Figure 4).

After the vertices for curvature estimation have been acquired, then the next step is creating normal vectors on the surface for every vertex, and that is center vertex, as well as the surrounding vertices. If the tails of the unit normals to the surface along the path are placed at the origin, then the heads of those unit normals are the vertices located on the top of the normals. If the vertices on the top are connected, then a path called *spherical image* of the vertices located on the surface is formed.

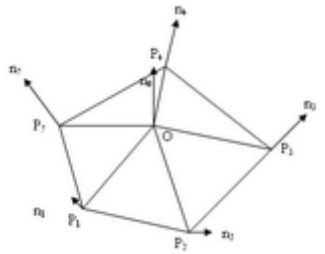

Figure 1: Surface of spherical image method

The theorem states that the curvature at the given point on a surface (in figure 4, the vertex is characterized with 'O') is the limit of the area of the spherical image of the path divided by the area of the path as the path shrinks around the point (Meek, et al). In Figure 4 above, a path that forms spherical image is a closed curve which surrounds a non-planar polygon $P_1P_2...PnP_1$. And then spherical image of this path is a polygon $n_1n_2..n_nn_1$, where n_i is unit normal of P_i. The ratio of the area of all triangles $n_in_0n_{i+1}$ over the area of all the triangles is an approximation to the total curvature at point O.

$$K = \frac{\sum L_{n_i n_o n_{i+1}}}{\sum L_{P_i P_o P_{i+1}}} \qquad (8)$$

The experiment is conducted to the several faceted models. Every model represents the shape which has been divided, concave, convex, saddle and flat. The experiment models can be seen in figure 2.

The value of curvature estimation method is determined in every point of calculation. The value of curvature shows the shape of surface on the specific location.

Using the Spherical Image method, the value of +/- 1 shows that the shape of the surface is flat or saddle, while the value which is less than 1 means that the surface is concave. If the value from the calculation is more than 1, then the surface which is located at that point is convex. The example of the result using the spherical image method for the model that has been shown in Figure 1(A) can be seen in Table 1. Every cell represents the location of every point of calculation of the model. The visualization by using some colors in every point of the model which represents the result of the calculation can be seen in Figure 5.

In Figure 5, the result of the points which show value less than 1 means the shape is concave, are colored by blue, whereas the result which value is more than 1 (convex) is colored by red. If the value is +/- 1 (the shape is flat or saddle) then the color would be white. The presentation by using colors are meant to make easier to understand what the value is trying to tell, since visual approach is often clearer than the series of numbers for a human.

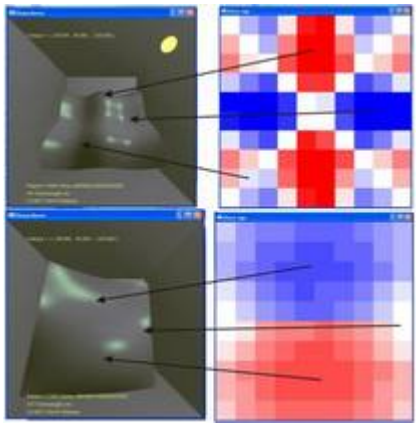

Figure 5: Segmentation of models using Spherical Image

For Gauss-Bonnet Method, the value of +/- 0 indicates that the shape of the surface is flat, and the negative value indicates that the shape is saddle. If the value is positive, then it means that the shape is convex or concave. Same as above, every cell represents the location of every point of calculation of the model. The visualization of the result by using colors can be seen in Figure 6.

Table 3 . The example result of spherical image method for the faceted model in Figure 2(A)

Row/ Col	1	2	3	4	5	6	7	8	9	10
1	1.001	0.980	0.973	1.009	1.047	1.051	1.007	0.972	0.984	1.000
2	1.016	1.001	0.984	1.026	1.070	1.077	1.027	0.986	0.995	1.015
3	1.027	1.008	0.998	1.039	1.091	1.088	1.039	0.998	1.010	1.027
4	0.989	0.972	0.960	0.998	1.042	1.041	0.998	0.960	0.974	0.991
5	0.946	0.926	0.911	0.959	0.997	0.993	0.956	0.920	0.929	0.948
6	0.951	0.929	0.916	0.959	1.003	0.999	0.962	0.914	0.926	0.949
7	0.991	0.972	0.963	1.001	1.046	1.035	0.999	0.962	0.971	0.991
8	1.025	1.010	0.999	1.039	1.092	1.084	1.037	0.998	1.011	1.028
9	1.017	0.993	0.986	1.030	1.074	1.069	1.023	0.988	1.003	1.015
10	0.998	0.9809	0.9721	1.0098	1.048	1.053	1.0086	0.974	0.9819	0.999

In Figure 6, the red color represent that the result of the curvature calculation is positive, which means the shape of the surface is concave or convex. On the other hand, if the color is blue, then then the value of the curvature is negative and the shape is saddle. The shape of flat will be indicated by white color and the value is +/- 1.

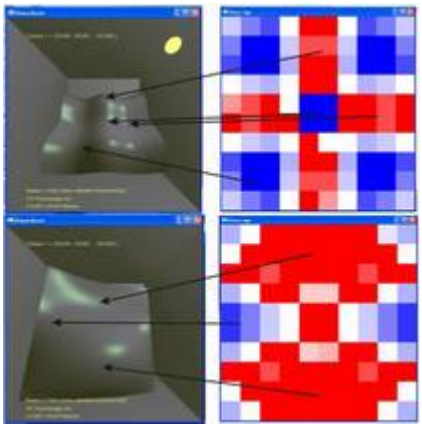

Figure 6: Segmentation of models using Gauss-Bonnet

Segmentation will be done based on the result of the curvature estimation. For each point which has the same / similar curvature value and is adjacent to each other will be included in the same segment. An example is shown in the visualization of the result in Figure 5 and 6. In the figure, some points in an area which has the same color can be included in a segment. On the other hand, the neighboring area which is covered by the same color, but different color with its neighbor will be included in the other segment. From this result, there will be one or more segment(s) in a model which will become a hint to make a tool path and determine each segment's the best milling direction based on its curvature characteristic which has been known. The result of the surface-shape (contour) identification is shown below.

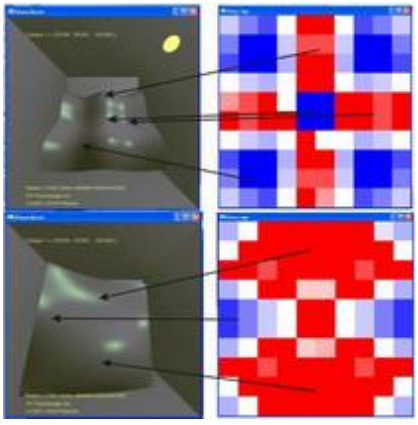

Figure 7. Surface feature (contour) identification by curvature analysis

Once the surface feature (curvature value) can be identified, the appropriate feed direction must be known for each surface feature.

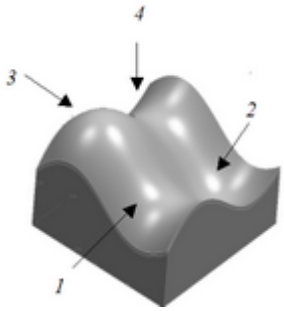

Figure 8. Sculptured surface with concave-convex combination

The milling operation is conducted into the surface model (Figure 8) in order to know the relation between the curvature and appropriate milling direction. The result is shown in Figure 9.

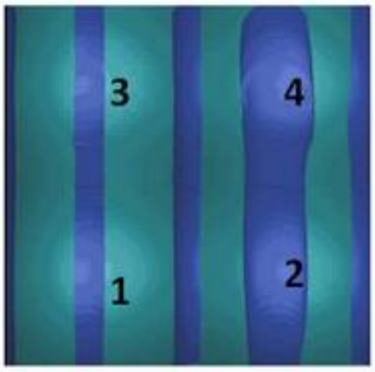

Figure 9. Cut width area w.r.t milling direction

As shown in Figure 9, milling direction (4-to-2) would result larger cut width area compared to the one using milling direction (3-to-1). The larger the cut width area the larger the material removed. Since, point 4 and 1 resemble the same curvature (and applied with different milling direction), therefore, it is clear that milling direction along minimum curvature direction is more preferred.

THIRD MILLING STRATEGY for OPTIMIZATION

The third or last strategy is to apply optimal tool orientation (inclination angle) during the 5-axis finishing with respect to the surface contour. In this part, the relationship or influence of changing inclination angles to the machined surface roughness is investigated.

ISSN 114-1284

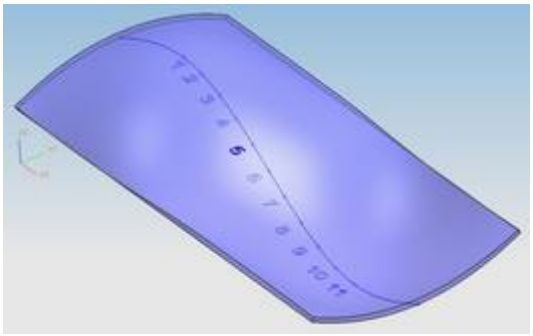

Figure 10. A surface model having covex/concave region

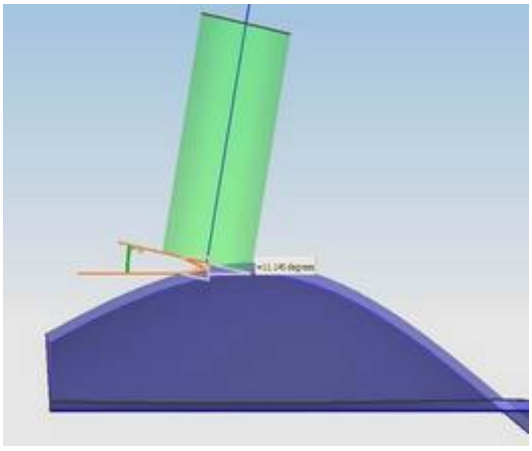

Figure 11 . Inclination angle influencing the cut-area

A contoured surface/model as shown in the Figure 10 is used on which the tool paths are generated along the surface with various inclination angles which are 10, 15, 20, 25, and 30. Each tool inclination angle is used along the tool path, and the cut-area (Figure 12) at several positions on the surface which having different curvatures are measured. The result shows in Figure 13.

It can be seen that, the lower the inclination angle the higher the cut area is produced. Furthermore, with the same inclination angle, the cutting tools cut more material at the concave region compared to the convex one. In other words, the highest cut-areas are on the concave region of the surface model.

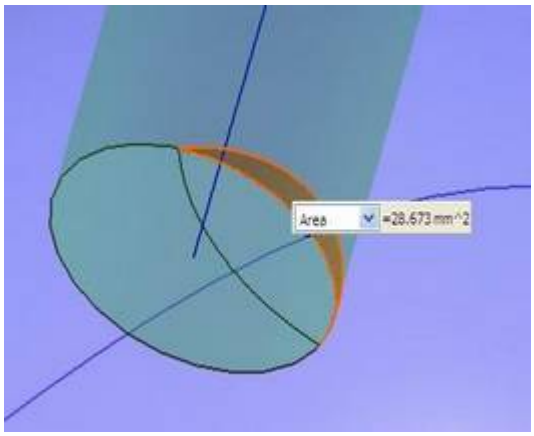

Figure 12. Cut area at the tool end

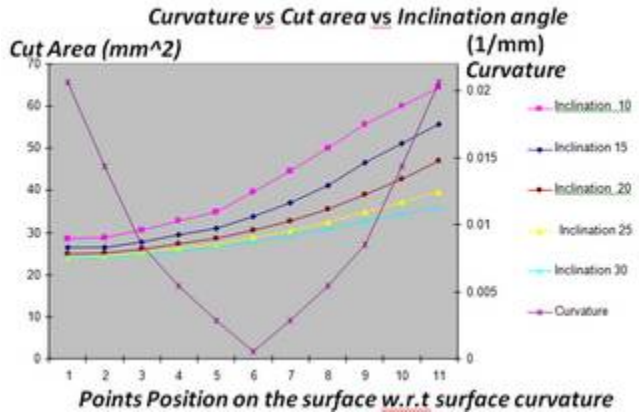

Figure 13. Inclination angle vs Curvature vs Cut-area

CONCLUSION AND FURTHER RESEARCH

The research investigates three milling optimization strategies:

a. Proper combination of tool-type and cutting direction during 3-axis roughing and 5-axis finishing
b. Feature (curvature) based optimal milling direction
c. Optimal inclination angle

The above three strategies can be implemented to improve the CAM-system functionalities.

Further research is needed to intelligently analyze the surface and provides suggestion for the optimal machining strategies.

REFERENCES

Back Day Kyun, et.al (2006) *Chips volume prediction using a numerical control verification model*, International Journal of Machine Tools & Manufacture, Vol. 46 Elsevier.

Choi, B., Jerard, R.B. (1998). Sculptured Surface Machining. *Dordrecht : Kluwer Academic Publishers*.

Gatzke, T., Grimm, C. (2003). Tech Report WUCSE-2004-9 : Improved Curvature Estimation on Triangular Meshes. *Eurographics Symposium on Geometry Processing*.

Kilgard, M. (1996). The OpenGL Utility Toolkit (GLUT) Progarmming Interface. *Silicon Graphics*.

Kiswanto, G. (2005). Pengembangan dan Pembuatan Sistem CAM (Computer Aided Manufacturing) yang Handal Berbasis Model Faset 3D untuk Pemesinan Multi-axis dengan Optimasi Orientasi Pahat dan Segmentasi Area dan Arah Pemesinan. *Laporan Kemajuan RUT XII Tahap II*.

Kresk, P., Lukacs, G., & Martin, R.R. (2001). Algorithm for Computing Curvatures from Range Data. *Technical Report – Prague Computer and Automation Research Institute, Budapest Cardiff University*.

Meek, D., & Walton, D. (2000). On Surface Normal and Gaussian Curvature Approximations Given Data Sampled from A Smooth Surface. *Computer Aided Geometric Design*, (17), 521-543.

Surazhky, T., Magid, E., Soldea, E., Elber, G., & Rivlin, E. (2003). Comparison of Gaussian and Mean Curvatures Estimation Methods on Triangular Meshes. *IEEE Transaction on Robotics and Automation*, (1), 1021-1026.

Yang, John L & Chen, Yoseph C (2001), *A Systematic Approach for Identifying Optimum Surface Roughness Performance in End-Milling Operations*, Journal of Industrial Technology, Taiwan.

Wallner, Johanes & Glaeser, Georg & Pottman, Helmut, *Geometric Contributions to 3–Axis Milling of Sculptured Surface*, Jurnal of Technology, Institut fur Geometric, Technische Universitat Wien, Austria, 2000.

Proceeding of the 11th International Conference on QiR (Quality in Research)
Faculty of Engineering, University of Indonesia, Depok, Indonesia, 3-6 August 2009
ISSN 114-1284

Prediction on High Strain Rate Properties for Nylon and GFRP Composite Materials

Gatot Prayogo[1], Danardono A.S[1]

[1]*Mechanical Engineering Department,*
University of Indonesia, Depok 16424, Indonesia
Tel. 021-7270032 (ext. 246), Fax. 0217270033,
E-mail: gatot@eng.ui.ac.id

ABSTRACT

High strain rate properties measurement of polymer materials has been limited due to difficulties in the measuring equipment, although high strain rate properties data is very essential as constitutive material for impact simulation. This work is aimed to get suitable visco-elastic data at desired high strain rate for impact simulation using Finite Element Analysis (FEA). Dynamic Mechanical Properties Testing in tensile oscillation at frequency of 10 Hz and 100 Hz was performed for Nylon and GFRP materials. Experimental data from that testing shown as tensile storage and loss moduli was converted to shear storage and loss moduli based on principle corresponding between Young's modulus, shear modulus and Poison's ratio. High strain rate properties data for both materials at desired frequency, about 2500 Hz, indicated as Short time shear modulus (G_0), Long time shear modulus (G_∞) was obtained by extrapolation technique on experimental result performed at low to moderate strain rate material properties. The extrapolation is based on a linear relationship between several mechanical properties (visco-elastic data) and logarithm of its strain rate. The result showed that high strain rate properties data for nylon and GFRP composite material, at desired frequency are suitable enough for impact simulation.

Key words
Visco-elastic data, high strain rate, impact simulation, finite element analysis.

1. INTRODUCTION

Since the 1960s, composite materials have been a major factor in weight reduction of structural components in the aerospace and automotive industries. Fiber-reinforced composites (FRC) are still regarded as relatively new materials within the mechanical engineering field and often lack the detailed material property data associated with metals. In particular, the use of composites in safety critical applications, such as an aircraft structure, leads to uneasiness since the mechanical response in crash applications is not well understood.

Composite materials have high specific strength, stiffness and excellent resistance against fatigue. Unfortunately, the materials are very sensitive to impact damage due to impingement of raindrops, hailstones, debris, and tools dropped by maintenance personnel. These impacts can generate significant damage inside composite materials called Barely Visible Impact Damage (BVID). When the long term usage of structures fabricated by composite materials is considered, an impact of single raindrop at velocity of 200 m/sec may produce no damage but repetition of the raindrop impact will bring about erosion on the materials [1)].

An experimental research of repeated raindrop impacts using nylon beads as impactor and GFRP as target materials has been conducted [2)]. Damage generated from that experiment is ring crack at front surface of specimen, star crack at back surface of specimen, and internal damage showing as debonding, matrix cracking, and delamination.

In order to analyze above impact damage, a series of attempts should be conducted. One of those attempts is to do impact simulation to get internal and surface transient stresses , contact duration, etc., using FEM. Since, Nylon and GFRP materials behave as visco-elastic materials at high strain rate deformation, therefore it is necessary to obtain visco-elastic data as a constitutive materials during simulation.

High strain rate testing has been used widely in the test of FRC material properties, However, at high crosshead rates, up to and above 2 m/s, inertial disturbances become inherent and cause inaccuracies in the analysis [3)]. These disturbances are due to the phenomenon of mechanical resonance and control problems that the test equipment acquires at high speeds. Therefore, the objective of this research work is to estimate high strain rate properties data at desired frequency, which is about 2500 Hz.

2. EXPERIMENT AND METHOD

2.1 Experiment

Dynamic mechanical properties testing was carried out based on ASTM Standard D 4065-1 using Visco-elastometer [4]. Due to limitation of experimental apparatus, selected frequency for this testing were 10 Hz and 100 Hz, and the range of testing temperature was between 15°C to 150°C. A typical data of tensile storage mudulus and tensile loss modulus for nylon and GFRP materials can be seen in Fig.1 and Fig.2, respectively, as shown below. Element of viscoelastic data for Nylon and GFRP composite materials can be shown in Table 1 and Table 2, below.

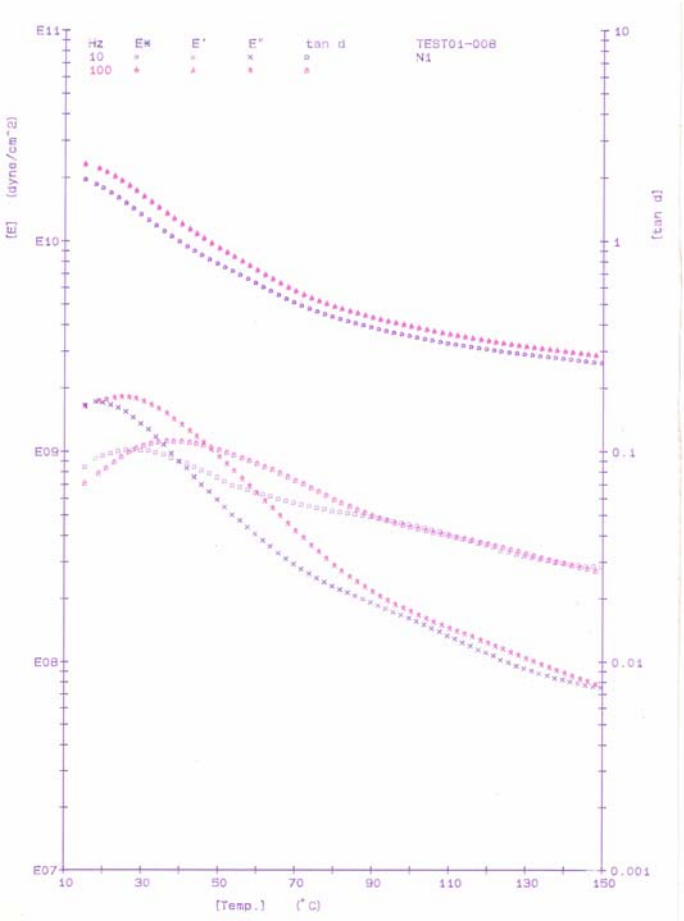

Fig. 1, Storage and loss tensile moduli of nylon materials

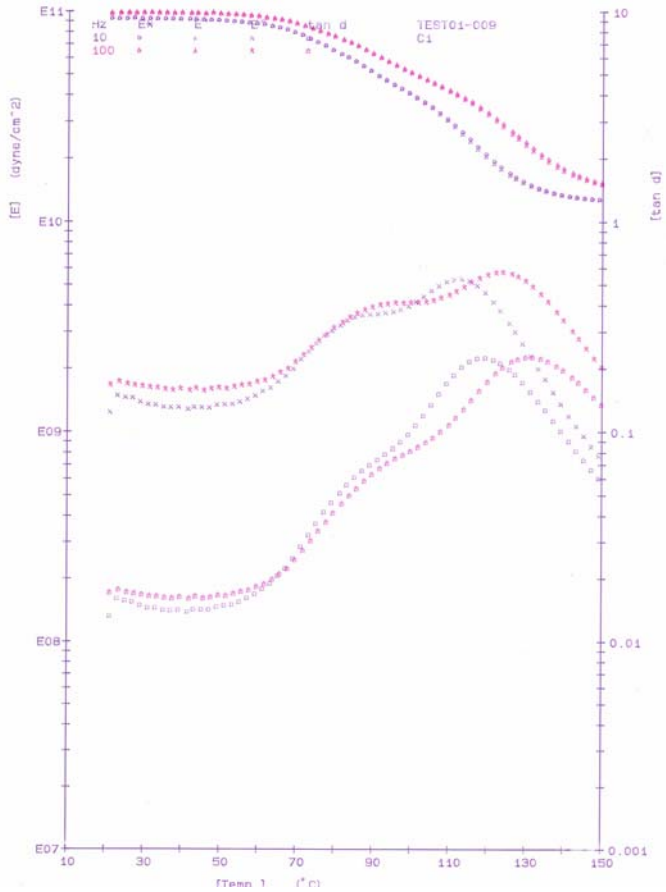

Fig. 2, Storage and loss tensile moduli of GFRP materials

ISSN 114-1284

Table 1, Element of viscoelastic data for Nylon.

No.	温 度 °C	周波数 Hz	E* dyne/cm^2	E' dyne/cm^2	E" dyne/cm^2	tan d	ΔF gf	Ld cm
9	23.9	10	1.61E+10	1.61E+10	1.61E+09	0.1005	1.01E+03	0.014
10	24.7	100	1.93E+10	1.92E+10	1.81E+09	0.0942	1.08E+03	0.015
11	25.9	10	1.52E+10	1.51E+10	1.54E+09	0.1020	9.62E+02	0.016
12	26.7	100	1.83E+10	1.82E+10	1.80E+09	0.0991	1.04E+03	0.016
13	27.8	10	1.43E+10	1.43E+10	1.45E+09	0.1017	9.07E+02	0.018
14	28.5	100	1.73E+10	1.72E+10	1.78E+09	0.1034	1.00E+03	0.018

Table 2, Element of viscoelastic data for GFRP composite materials.

No.	温 度 °C	周波数 Hz	E* dyne/cm^2	E' dyne/cm^2	E" dyne/cm^2	tan d	ΔF gf	Ld cm
1	21.2	10	9.32E+10	9.32E+10	1.24E+09	0.0133	1.52E+03	0.001
2	21.3	100	9.77E+10	9.77E+10	1.66E+09	0.0170	1.53E+03	0.008
3	23.2	10	9.28E+10	9.28E+10	1.49E+09	0.0160	1.48E+03	0.009
4	23.6	100	9.81E+10	9.81E+10	1.73E+09	0.0176	1.54E+03	0.008
5	25.2	10	9.28E+10	9.28E+10	1.46E+09	0.0157	1.48E+03	0.009
6	25.8	100	9.82E+10	9.82E+10	1.68E+09	0.0171	1.54E+03	0.009

2.2 Method

In order to predict high strain rate properties of Nylon and GFRP composite materials, experimental data from Dynamic Mechanical Properties testing above shown as tensile storage (E') modulus and loss modulus(E") was converted to shear storage modulus and shear loss modulus based on principle corresponding between Young's modulus, shear modulus and Poison's ratio [5].

Furthermore, high strain rate dynamic mechanical properties shown as shear storage modulus (G_0) and shear loss modulus (G_∞), etc., for Nylon and GFRP composite materials is predicted based on linear extrapolation of logarithm of the rate of strain on the material properties to provide the data at high strain rates as discussed by Okoli et.al. [6,7]. For the data acquired from dynamic mechanical properties testing as shown in Table 1 and Table 2 of Nylon and GFRP Composite Materials. Selected testing temperature was very similar to the temperature during impact testing, around 25º C, its frequency were 10Hz and 100 Hz, due to limitation of experimental apparatus. In this case, required frequency used for determining the value of high strain rate properties is about 2500 Hz, which is related to contact duration between impactor and target material, about 40 micro-second for impact velocity of 200 m/s. As instance, the result of extrapolation can be shown in Fig. 1, Fig. 2 and Fig. 3, for Nylon material. The same technique of extrapolation were also performed for viscoelastic data of GFRP composite materials. Complete result of extrapolation can be seen in Table 3 below.

ISSN 114-1284

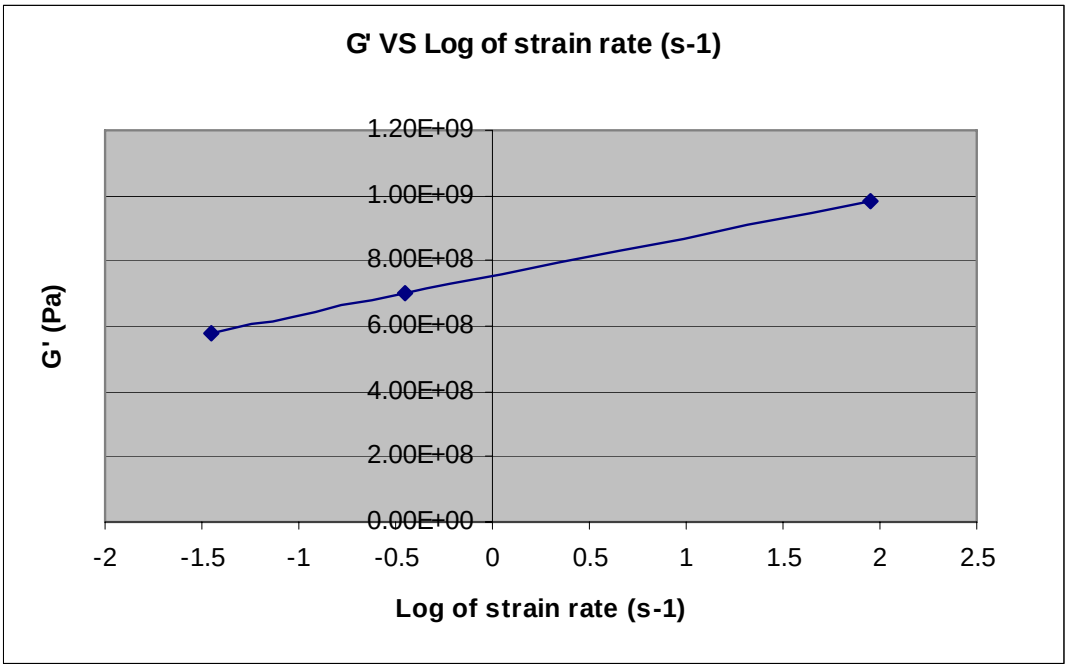

Figure 3, Shear storage modulus G' VS Log of strain rate (s^{-1}) untuk Nylon.

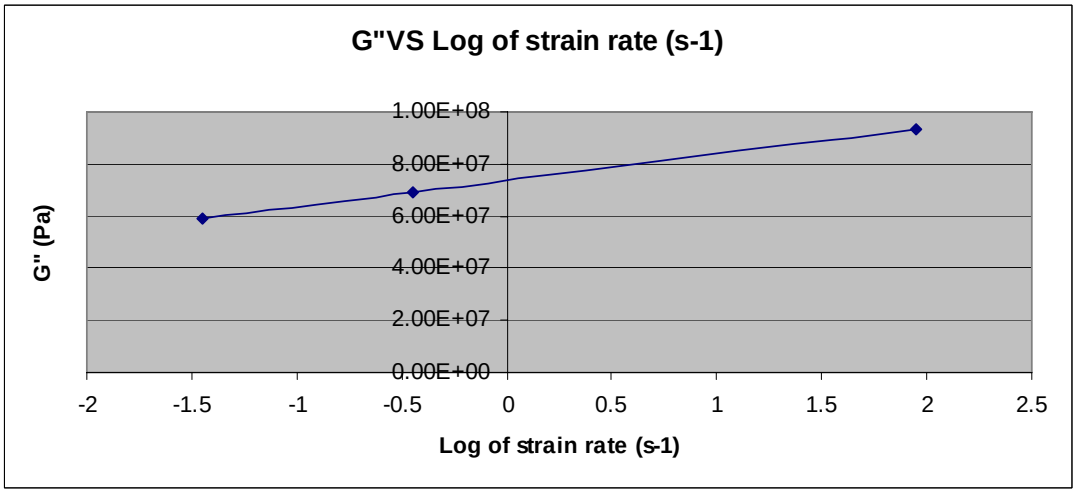

Figure 4, Shear loss modulus G" VS Log of strain rate (s^{-1}) untuk Nylon

ISSN 114-1284

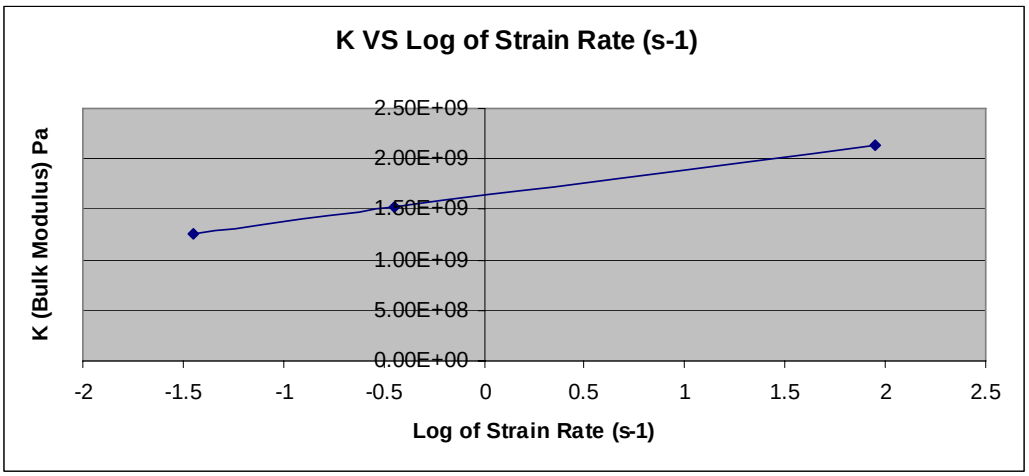

Figure 5, Bulk modulus (K) VS Log strain rate (s^{-1}) untuk Nylon

3. RESULT AND DISCUSSION

From the experimental result, as shown inTable 3 below that dynamic mechanical properties for Nylon and GFRP composite material increase from that at low strain rate (10 Hz) to moderate strain rate (100 Hz). For certain polymer materials, dynamic mechanical properties increase with increasing testing frequency due to occurrence of strain hardening [3)]. Dynamic mechanical properties at high strain rate (25000 Hz) is obtained from extrapolation technique. This technique of extrapolation is valid enough since it is very difficult to measure this properties at high strain rate experimentally due to limitation of experimental measurement. The inertia force problem during experiment of dynamic mechanical properties at high strain rate become main reason.

The data resulted from this extrapolation technique will be used for impact simulation using FEM. Contact duration resulted from impact simulation will be compared and discussed to that from impact testing. Impact simulation work is still underway right now.

Table 3, complete result of extrapolation for Nylon and GFRP composite materials

Mech. Properties	Nylon Material			GFRP Composite Materials		
	10 Hz	100 Hz	25000 Hz	10 Hz	100 Hz	25000 Hz
Go (Pa)	5.81E+08	7.00E+08	9.85E+09	3.57E+09	3.78E+09	4.28E+09
G∞ (Pa)	5.92E+07	6.92E+07	9.32E+07	5.62E+07	6.46E+07	8.47E+07
K (Pa)	1.26E+09	1.52E+09	2.14E+09	7.73E+09	8.18E+09	9.26E+09
β			1.06E+01			5.05E+01

Where *Go* is short time shear modulus in Pa, *G*∞ is long time shear modulus in Pa, K is bulk modulus in Pa and β is decay constant which is equal to *Go*/*G*∞.

4. CONCLUSION

From this research work, it can be concluded that extrapolation technique based on a linear relationship between several mechanical properties (visco-elastic data) and logarithm of its strain rate is valid enough. The value of dynamic mechanical properties at high strain rate i.e. at 25000 Hz, will be used in impact simulation.

ACKNOWLEDGMENT

I would like to thank to Industrial Research Institute of Aichi Prefecture Government, Nishishinwari, Hitotsugi-cho, Kariya City 448, Aichi Prefecture, Japan, for conducting Dynamic mechanical properties testing.

5. REFERENCES

[1] Zukas J.A., Limitations of Elementary Wave Theory, in ed. Zukas J.A., et.al, Impact Dynamics, John Wiley & Sons, 1982, USA.

[2] Gatot Prayogo, Hiroomi Homma, Yasuhiro Kanto, Repeated Rain-drop Impact Damage in Glass-Fibre Reinforced Plastics, 2nd ISIE (International Symposium on Impact Engineering), Beijing, China, 1996

[3]. Walley S.M, Field J.E., Pope P.H.,Safford N.A., A Study of the Rapid Deformation Behaviour of a Range of Polymers, Philosophical Transactions of the Royal Society of London. Series A, Mathematical and Physical Sciences, Vol. 328, No. 1597 (Apr. 5, 1989), pp. 1-33.

[4]. Standard Practice for Plastics : Dynamic Mechanical Properties: Determination and Report of Procedures, ASTM D 4065.

[5] Gatot Prayogo, Danardono A.S., On The Estimation of Visco-elastic Properties for Nylon and GFRP Materials, Proc. of The 10th International Conference on Quality in Research (QIR), Faculty of Engineering, University of Indonesia, Jakarta, Indonesia, 2007.

[6]. Okoli O.I, and Smith G. F., "High Strain Rate Characterization of a Glass/Epoxy Composite," Journal of Composites Technology & Research, JCTRER, Vol. 22, No. 1, January 2000, pp. 3–11.

[7]. Okoli O.I, Abdul latif Ainullotfy, Failure in Composite Materials : overview in attempt of prediction, Composite Part A: applied science and manufacturing, 33 (2002) 315 – 321.

ISSN 114-1284

Aggregate Planning of Airbrake at the Machining Department, PT "X" – Bandung

Gatot Yudoko[1], Iqsan Diaz[2]

[1]*School of Business and Management*
Bandung Institute of Technology, Bandung 40132
Tel : (022) 2531923 ext 219. Fax : (022) 2504249
E-mail : gatot@sbm.itb.ac.id

[2]*School of Business and Management*
Bandung Institute of Technology, Bandung 40132
Tel : (022) 2531923 ext 219. Fax : (022) 2504249

ABSTRACT

PT "X" – Bandung is a state-owned companies and one of its products is vehicle. One of the important subassemblies of the vehicle is the airbrake. This paper is aimed at formulating an aggregate plan for the Machining Department for the production of airbrake for the upcoming scheduled three consecutive periods, namely period 1 (12 days), period 2 (12 days), and period 3 (27 days). The formulation of the aggregate plan began with rough-cut capacity planning to see whether the available resources would be able to meet the demand. It turned out that the available resources was unable to meet the demand. Therefore, we developed four alternatives. The first alternative was trying to meet the demand using the available resources by accepting the lateness in which penalty costs would have to be calculated based on the contract agreement. The second alternative was adding capacity through overtime and in this regard the overtime costs would be calculated. The third alternative was adding capacity by purchasing new machines in which the capital required would be calculated. And the last alternative was a mix of overtime and the addition of new machines and the related costs would be calculated as well. The alternative with the least cost would be selected. Based on our analysis, we conclude that the last alternative is the best aggregate production plan for the company in meeting the demand of airbrake for the upcoming three periods.

Keywords: *aggregate planning, rough cut capacity planning, airbrake*

1. INTRODUCTION

One of various products produced by a state-owned manufacturing company in Bandung was vehicle. One of important subassemblies for making vehicle is airbrake. The Machining Department had order of airbrake for three consecutive periods, namely period 1 consisting of 12 days, period 2 with 12 days, and period 3 with days. Each working day had eight hours. To make these orders, the department could use 18 machines as shown in Table 1. The objective of this paper is to propose an aggregate plan for the three periods.

Table 1. Type and number of machine

Machine	Number (units)
Regular lathe	9
Special lathe	6
Regular drill	3
Special drill	1
Regular mill	1
Special mill	1

2. METHODOLOGY

We adopt rough-cut capacity planning [1] to see whether the existing machines would be able to meet the orders or not. If the existing capacity could meet the demand, then we could show the calculation. If not, we would explore alternatives [2] in order to meet those orders. Based on our observation and discussion with the Machining Department in 2008 we finally came up with four alternatives: (1) fulfilling the orders using the existing capacity, but with lateness, (2) using possible overtime, (3) adding the existing capacity by purchasing new machines, and (4) a mix of overtime and adding new machines.

All required data were collected in the Machining Department in 2008. Data gathered include parts for making airbrake, routing data, overtime capacity, overtime wage, machine price. Recognizing the confidentiality of parts, we were allowed to use only part initials, instead of their full names.

It was stated in the contract that the buyer would terminate its orders if the company failed to deliver the orders at the maximum allowable lateness amounting to 5% of the contract value.

ISSN 114-1284

3. RESULTS

Rough cut capacity plan for nine regular lathes for the three periods are shown in Tables 1, 2, and 3. The required hours for period 1, 2, and 3 were 1,531.2; 2,692.2; and 3,692.8 hours respectively. The capacity of regular working hours for period 1 and 2 was 864 hours each and for period 3 was 1,944 hours. For the three periods, the total capacity available was 3,672 hours. Therefore, the existing capacity of regular lathes was less than the required one.

Table 1. RCCP for regular lathe for period 1

Component	Units required	Hours required
B1	135	72.0
B2	135	43.2
B3	135	58.0
B4	135	72.0
B5	135	72.0
CDV	135	90
COO	135	108.0
PT	105	56.0
DB	270	144.0
BH	65	270.0
TC	190	190
RP	105	56.0
CI	270	180.0
P	105	120.0
Total		1,531.2

The existing capacity of special lathe for periods 1, and 2 was 576 hours each, and 1,296 hours for period 3. The required hours for the same periods are shown in Table 4, 5, and 6. The capacity of periods 1 and was less than the required one, while the capacity for period 3 was more than the required one. For the overall three periods, the total existing capacity (2,448 hours) was less than the required capacity (2,949.2 hours).

Table 2. RCCP for regular lathe for period 2

Component	Units required	Hours required
B1	169	90.1
B2	169	54.1
B3	515	206.0
B4	169	90.1
B5	169	90.1
CDV	169	112.7
COO	169	135.2
PT	279	148.8
DB	338	180.2
BH	230	460.0
TC	432	432.0
RP	279	148.8
CI	338	225.3
P	279	318.9
Total		2,692.3

Table 3. RCCP for regular lathe for period 3

Component	Units required	Hours required
B1	216	115.2
B2	216	69.1
B3	216	115.2
B4	216	115.2
CDV	216	144.0
COO	216	172.8
PT	50	26.7
LNFN	1,500	2,333.4
DB	432	230.4
RP	50	26.7
CI	432	288.0
P	50	57.1
Total		3,693.8

Table 4. RCCP for special lathe for period 1

Component	Units required	Hours required
LH1	145	46.4
LH2	145	23.2
LH3	145	89.2
LH4	145	46.4
CDV	135	90.0
DCP	65	17.3
VB	145	46.4
FL	145	46.4
COO	135	72.0
Total		477.4

For three regular drills, the existing capacity for periods 1 and 2 was 288 hours, and for period 3 was 648 hours. The required hours for periods 1, 2, and 3 are shown in Tables 7, 8, and 9 and these exceed the existing capacity.

Table 5. RCCP for special lathe for period 2

Component	Units required	Hours required
RH1	515	164.8
LH1	515	164.8
RH2	515	82.4
LH2	515	82.4
RH3	515	316.9
LH3	515	316.9
CDV	169	112.7
DCP	450	120.0
VB	515	164.8
FL	515	164.8
TH	140	44.8
RH4	515	164.8
LH4	515	164.8
COO	169	90.1
Total		2,155.0

Table 6. RCCP for special lathe for period 3

Component	Units required	Hours required
CDV	216	144.0
DCP	216	57.6
COO	216	115.2
Total		316.8

Table 7. RCCP for regular drill for period 1

Component	Units required	Hours required
CDV	135	108.0
CI	135	108.0
DB	135	72.0
B1	135	72.0
Total		360.0

Table 8. RCCP for regular drill for period 2

Component	Units required	Hours required
CDV	169	135.2
CI	169	135.2
DB	169	90.1
B1	169	90.1
Total		450.6

Table 9. RCCP for regular drill for period 3

Component	Units required	Hours required
CDV	216	172.8
CI	216	172.8
DB	216	115.2
B1	216	115.2
LNFN	500	200.0
Total		776.0

The existing capacity for special drill, special mill, and special mill was the same because each had one machine. The existing capacity for periods 1 and 2 was 96 hours each, and 216 hours for period 3. The required hours for special drill, regular mill, and special mill are shown in Table 10, 11, and 12 respectively. The required hours for special drill were higher that the existing capacity for all three periods. The required hours for regular mill were less than the existing capacity for all three periods. The required hours for special mill were higher than the existing capacity in period 3.

Table 10. RCCP for special drill

Component	Units required	Hours required
COO	Period I: 135	216.0
	Period II: 169	270.4
	Period III: 216	345.6

Table 11. RCCP for regular mill

Component	Units required	Hours required
COO	Period I: 135	54.0
	Period II: 169	67.6
	Period III: 216	86.4

Table 12. RCCP for special mill

Component	Units required	Hours required
LNFN	Period III: 500	1,333.3

Because the existing capacity was unable to meet the order, we then explore and analyze possible consequences for each alternative. In this sense, we simply analyze the total capacity and required hours for the three periods. A summary of alternative 1, fulfilling the orders using the existing capacity, is shown in Table 13. As we can see, the total shortage of regular lathe was 4,245 hours. Using nine machines and eight hours per day, this shortage equals 59 working days late. For special lathe, the shortage was 501.2 hours or 11 days late. By the same calculations, the lateness for regular drill, special drill, and special mill were 16, 52, and 116 days respectively.
Alternative 2 sought to meet the orders using overtime. Each working day allowed four overtime hours. Therefore, using nine regular lathes, the shortage of 4,245 hours equals 118 days. With daily overtime wage of 60,000 rupiahs, the total overtime cost would be 63.72 million rupiahs. The similar calculations for the other machines are summarized in Table 14.

Table 13 . Consequences of alternative 1

Regular lathe	
Total hours required	7,917.3
Total hours available	3,672.0
Total shortage	4,245.3
Lateness (days)	59
Special lathe	
Total hours required	2,949.2
Total hours available	2,448.0
Total shortage	501.2
Lateness (days)	11
Regular drill	
Total hours required	1,586.7
Total hours available	1,224.0
Total shortage	362.7
Lateness (days)	16
Special drill	
Total hours required	832.0
Total hours available	408.0
Total shortage	424.0
Lateness (days)	53
Regular mill	
Total hours required	208.0
Total hours available	408.0
Total shortage	0
Special mill	
Total hours required	1,333.3
Total hours available	408.0
Total shortage	925.3
Lateness (days)	116

Table 14. Consequences of alternative 2

Regular lathe	
Total hours required	7,917.3
Total hours available	3,672.0
Total shortage (hours)	4,245.3
Overtime/day (hours)	36
Overtime required (day)	118
Overtime cost/day (rupiah)	60,000
Total overtime cost (rupiah)	63,720,000
Special lathe	
Total hours required	2,949.2
Total hours available	2,040
Total shortage	909.2
Overtime required	24
Overtime per day	38
Overtime cost/day	60,000
Total overtime cost	13,680,000

Table 14. continued.

Regular drill	
Total hours required	1,586.7
Total hours available	1,224.0
Total shortage	362.7
Overtime required	12
Overtime per day	31
Overtime cost/day	60,000
Total overtime cost	5,580,000
Special drill	
Total hours required	832.0
Total hours available	408.0
Total shortage	424,0
Overtime required	4
Overtime per day	106
Overtime cost/day	60,000
Total overtime cost	6,360,000
Special mill	
Total hours required	1,333.3
Total hours available	408.0
Total shortage	925.3
Overtime required	4
Overtime per day	232
Overtime cost/day	60,000
Total overtime cost	13,920,000

Alternative 3 is adding the existing capacity by purchasing new machines. For nine regular lathes with a total of 51 regular working days and hours per day, the shortage of 4,245.3 hours as shown in Table 15, equals 11 machines. The price of each machine was 100 million rupiahs. The new machines would require 11 new operators. There was not any problem with additional space required for the new machines. The remaining calculation for the other machines can be seen in Tables 15, 16, 17, 18, and 19.

Table 15. Consequences of alternative 3 for regular lathe

Total hours required	7,917.3
Total hours available	3,672.0
Total shortage	4,245.3
Number of machine required	11
Number of operator required	11
Machine price (rupiahs)	100,000,000
Salary/day (rupiahs)	60,000
Total machine cost (rupiahs)	1,100,000,000
Total operator cost (rupiahs)	33,660,000
Total additional cost (rupiahs)	1,133,660,000

Table 16. Consequences of alternative 3 for special lathe

Total hours required	2,949.2
Total hours available	2,040.0
Total shortage	909.2
Number of machine required	3
Number of operator required	3
Machine price	100,000,000
Salary/day	60,000
Total machine cost	300,000,000
Total operator cost	9,180,000
Total additional cost	309,180,000

Table 17. Consequences of alternative 3 for regular drill

Total hours required	1,586.7
Total hours available	1,224.0
Total shortage	362.7
Number of machine required	1
Number of operator required	1
Machine price	35,000,000
Salary/day	60,000
Total machine cost	35,000,000
Total operator cost	3,060,000
Total additional cost	38,060,000

Table 18. Consequences of alternative 3 for special drill

Total hours required	832.0
Total hours available	408.0
Total shortage	424.0
Number of machine required	2
Number of operator required	2
Machine price	35,000,000
Salary/day	60,000
Total machine cost	70,000,000
Total operator cost	6,120,000
Total additional cost	76,120,000

Table 19. Consequences of alternative 3 for special mill

Total hours required	1,333.3
Total hours available	408.0
Total shortage	925.3
Number of machine required	3
Number of operator required	3

Machine price	25,000,000
Salary/day	60,000
Total machine cost	75,000,000
Total operator cost	9,180,000
Total additional cost	84,180,000

Alternative 4 is a mix of overtime and adding new machines. We recognize that there many combinations of this mix and we did not enumerate them one by one. Instead, we firstly use the overtime during the 51 days and then the remaining shortage would be met by adding or purchasing new machines. For nine regular lathes as shown in Table 20, the overtime capacity for 51 days with 4 hours each day was 1,836 hours and thus the shortage after using the overtime would be 2,409.3 hours. This shortage could be fulfilled by adding four new machines and their overtime for 49 days. Adding three machines would result in overtime days more than 51 days, and adding five machines would be more expensive. The calculations for the other machines are summarized in Table 21 for regular drills, and Table 22 for special mill.

Table 20. Consequences of alternative 4 for regular lathe

Total hours required	7,917.3
Total hours available	3,672.0
Total shortage	4,245.3
Overtime	1,836
Shortage after overtime	2,409.3
Additional 4 machines	1,632
Shortage after adding new machine	777.3
Overtime with new machines (days)	49
Machine cost (4 units)	400,000,000
Operator cost (4 workers)	12,240,000
Overtime cost (9 workers)	36,720,000
Overtime cost 4 workers in 49 days	15,680,000
Total additional cost	464,640,000

Table 21. Consequences of alternative 4 for regular drill

Total hours required	832.0
Total hours available	408.0
Total shortage	424.0
Additional 1 machine	408
Shortage after adding 1 machine	16
Overtime with new machine (days)	2
Machine cost	35,000,000
Operator cost (1 worker)	3,060,000
Overtime cost for 2 workers for 2 days	320,000
Total additional cost	38,380,000

Table 22. Consequences of alternative 4 for special mill

Total hours required	1,333.3
Total hours available	408.0
Total shortage	925.3
Additional 2 machines	816.0
Shortage after adding new machines	109.0
Overtime with new machines (days)	14
Machine cost (2 units)	75,000,000
Operator cost (2 workers)	6,120,000
Overtime cost for 3 workers for 14 days	3,360,000
Total additional cost	84,480,000

4. DISCUSSION

Based on the analysis, we can see that alternative 1, operating with the existing capacity, would be unacceptable because the lateness exceeds the maximum allowable limits and this would result in termination of the contract which is unwanted by the company. The similar situation would occur with alternative 2, adding capacity using overtime in which shortages in regular lathe, special drill, and special mill would also cause lateness which would result in contract termination. Therefore, this alternative was unwanted as well by the company. Alternative 3, adding capacity by purchasing new machines can meet the required hours and therefore fulfill the order as scheduled. The total cost for this alternative was 1.641 billion rupiahs. The last alternative, adding capacity by using overtime and purchasing new machines could fulfill the order and the schedule. The total additional costs of this alternative would be 606.76 million rupiahs. Therefore, among the four alternatives, alternative 4 would be the best one. The summary of the four alternatives are shown in Table 23.

5. CONCLUSIONS

The orders for the three periods would be unable to meet either using the available capacity or using overtime. These orders could be fulfilled as scheduled through purchasing six new machines or a mix of overtime and purchasing four new machines. The best alternative would be the mix of overtime and purchasing four new machines. We acknowledge that this alternative might not be the optimal one. In addition, our analysis did not include holding costs since because of our inability to get the necessary data.

Table 23. Summary of all alternatives

Alternative	Cost (rupiahs)	Consequences
1. Operating with the existing capacity		
Regular lathe	0	Contract terminated due to lateness
Special lathe	0	Contract terminated due to lateness
Regular drill	0	Contract terminated due to lateness
Special drill	0	Contract terminated due to lateness
Regular mill	0	Contract terminated due to lateness
Total	0	Contract terminated due to lateness
2. Adding capacity using overtime		
Regular lathe	63,720,000	Contract terminated due to lateness
Special lathe	13,680,000	Can fulfill the order
Regular drill	5,580,000	Can fulfill the order
Special drill	6,360,000	Contract terminated due to lateness
Special mill	13,920,000	Contract terminated due to lateness
Total	103,260,000	Contract terminated due to lateness
3. Adding capacity by adding new machines		
Regular lathe	1,133,660,000	Can fulfill the order
Special lathe	309,180,000	Can fulfill the order
Regular drill	38,060,000	Can fulfill the order
Special drill	76,120,000	Can fulfill the order
Special mill	84,180,000	Can fulfill the order
Total	1,641,200,000	Can fulfill the order
4. Adding capacity through a mix of overtime and adding new machines		
Regular lathe	464,640,000	Can fulfill the order
Special lathe	13,680,000	Can fulfill the order using overtime
Regular drill	5,580,000	Can fulfill the order using overtime
Special drill	38,380,000	Can fulfill the order
Special mill	84,480,000	Can fulfill the order
Total	606,760,000	Can fulfill the order

Table 23. continued.

REFERENCES

[1] B. J. Finch, *Operations Now: Supply Chain Profitability and Performance*, Third Edition, International Edition. Singapore: McGraw-Hill, 2008.

[2] R. B. Chase, F. R. Jacobs, and N. J. Aquilano, *Operations Management for Competitive Advantage with Global Cases*. Eleventh Edition, International Edition. Singapore: McGraw-Hill, 2007.

ISSN 114-1284

HYDROGEN ABSORPTION PROPERTIES OF THE Mg-Ti ALLOY PREPARED BY MECHANICAL ALLOYING

Hadi Suwarno

Center for Technology of Nuclear Fuel– BATAN
Building 20, Puspiptek Area, Setu, Tangerang Selatan 15314, Banten, Indonesia

ABSTRACT

Metal hydrides are applied for reversible solid-state hydrogen storage at low pressures with high volumetric capacity, i.e. it should contain several kg of the metal hydride powder. Magnesium based has been researched for years due to the high hydrogen capacity. Although magnesium can absorb hydrogen up to 7.6 wt%, high operating temperatures and slow kinetics prevent them from practical application. Therefore, alloyed with other metals are being considered.

The synthesis and characterizations of Mg–Ti alloys prepared by mechanical alloying technique in toluene solution and the hydrogen absorption properties of the synthetic yielded have been performed. The Mg and Ti powders are milled with the variation of milling time 10, 20, and 30 h, in a Spex 8000 high energy ball mill. The milled specimens are analyzed with an X-ray diffractometer, Philip, type PW 1710, using Cu as the anode tube and = 1.5406 Å. Qualitative and quantitative analysis are calculated using Rietveld method developed by Fuji Izumi. The microstructure of the specimens after milling and hydriding are identified with a scanning electron microscope, Philip type 550.

The refinement analysis of the x-ray diffractions results show that the mechanical alloying of the Mg–Ti alloy under toluene solution result in the formation of four phases, namely Mg, Ti, TiH_2 and Mg_2Ti. Quantitative analysis show that the mass fractions of TiH_2 and Mg_2Ti phases are 62.90 wt% and 30.60 wt%, while the rests are Mg (2.6 wt%) and Ti (1.25 wt%). On hydriding at 300 ^oC, the milled powders are transformed into Mg_2TiH_4, TiH_2 and -MgH_2 phases with the mass fraction of 25.48 wt%, 64.0 wt%, and 10.52 wt%, respectively. Measured hydrogen capacity of the specimens is about 6.7 wt%.

INTRODUCTION

Magnesium is a promising material as hydrogen storage media because it can store 7.6 mass% of hydrogen. Various Mg-based alloys and compounds have been studied to improve its hydriding temperature and rate of hydrogenation. Among those materials, Mg_2Ni intermetallic compound is well known to form Mg_2NiH_4 hydride with high reaction rate, which has hydrogen storage capacity of 3.6 mass% [1-4]. Unfortunately the hydriding-dehydriding rate of the alloy is relatively at high temperature and therefore alloying of magnesium with other metal is considered.

Working with magnesium needs a special attention since it is difficult to cast at accurate desirable composition, especially by conventional melt-cast methods. The low melting point, the high vapor pressure, and the activity against oxygen are the most reason for magnesium when alloyed with other metals by melting methods. To solve the above problems, synthetic alloying with high energy ball milling has been introduced by many researchers. During mechanical alloying of two elemental powders, a binary mixture will be formed depends on the energy formation. An amorphous alloy powder will be formed if the heat of mixing in the liquid state has large negative heat and a crystalline powder will be formed if the heat of mixing is positive. The advantages of mechanical alloying in the synthesis of these powders can be defined as follows: (a) can be used to alloy elements having vastly different melting temperature, which cannot be easily done by conventional techniques such as arc melting, (b) is mature powder synthesis technique, and the method can be easily scaled from laboratory to industry.

In this paper magnesium alloyed with titanium with the atomic ratio of Mg:Ti = 2:1 prepared in a high energy ball milling in order to study the interaction of the alloy formed with hydrogen is discussed.

EXPERIMENTAL

The starting material consisted of elemental crystalline powders of titanium at purity of 99.5% and particle size of -100 mesh purchased from Aldrich and magnesium at purity of 99.7% and particle size of -325 mesh purchased from Merck. About 15 grams of Mg and Ti elements with the atomic ratio of Mg:Ti = 2:1 are mixed together with balls and then poured into a vial together with the toluene. The ball-to-specimen ratio is 8, and the milling is performed every 10, 20, and 30 h at room temperature in the toluene solution. The vial is made of stainless steel with a diameter of 5.1 cm and is 7.6 cm in length. The balls are also made of stainless steel with a diameter of 12 mm. The vial is then put into a high energy milling (HEM) Spex type 8000. One cycle of milling of the Spex type 8000 consists of normal blending speed of 4500 rpm, run time 90 minutes, and off time 30 minutes. This means that 10 h of milling needs 5 cycles of milling operation.

The hydriding experiment is conducted in a Sievert system that can be operated under high vacuum condition with a maximum operating pressure of 1000 mbar. The procedure of the experiment has been published

elsewhere[5]. About 3 gram of specimen obtained after milling is put into the hydriding system and then heated for 1 h at temperature of 430 oC for removing the toluene from the powder and recrystallization. After cooling down to room temperature the weight of Mg-Ti powder is measured. To avoid direct contact the powder with air during removing the powder from the system fro weighing purposes, hydrogen is admitted to the system. Hydrogen absorbed by the specimen can be calculated from the pressure changes during measurements.

The quality and quantity of the phases formed are analyzed using an x-ray diffractometer (XRD), Philip, type PW 1710, with Cu as the anode tube and □ = 1.5406 Å. Continuous scanning is conducted at 0.02° step size and 0.5 second/step. The scanning results are analyzed using *Rietveld method* developed by Fuji Izumi[6].

RESULT AND DISCUSSION

Figure 1 shows the XRD refinement result of the Mg-Ti alloy with the atomic ratio of Mg:Ti = 2:1 before milling, where only Mg and Ti peaks are identified. Quantitative analyses of the XRD refinement result yields a mass fraction of Mg and Ti are 62.76% and 37.24%. This result equals to the previous composition of the Mg and Ti metal powders.

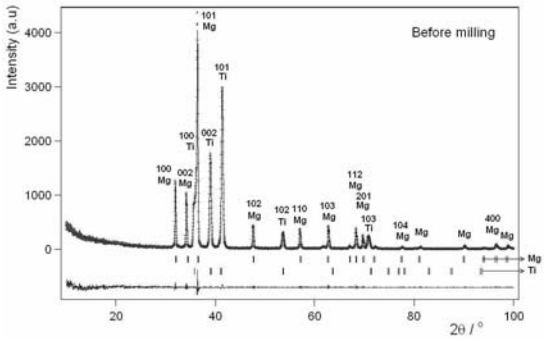

Figure 1. The XRD refinement result of the Mg and Ti before milling.

Figure 2 shows the XRD refinement result of (a) Mg-Ti alloy after 10, 20 and 30 h of milling and (b) after hydriding at temperature of 300 ^{o}C. Compared to the XRD of Mg-Ti before milling, it shows that the sharp peaks from Mg and Ti disappear and the new peaks formed. The low intensities of the new peaks formed are caused by a crystal structure changes of the specimens into amorphous state and a new phase formation. The refinement result of these new peaks appear at 2 . close to 19^{o}, 35^{o}, 40^{o}, 45^{o}, 59^{o}, and 70^{o} can be identified as Mg, Ti, TiH_2 and Mg_2Ti phases. Quantitative analyses on the XRD refinement result points out that the mass fraction of the Mg, Ti, TiH_2 and Mg_2Ti are 5.26 wt%, 1.25 wt%, 62.90 wt% and 30.60 wt%, respectively. The formation of TiH_2 in the specimen is suggested from the specimen preparation i.e. during removing the specimen from the hydriding system for weighing purposes, where hydrogen is used to avoid direct contact the specimen with oxygen. The grain sizes of individual crystallite calculated using Scherrer formula obtained that the Mg_2Ti, TiH_2, and Mg are 5.7 nm, 5.4 nm and 3.5 nm, respectively. The formation of binary Mg_2Ti informs us that mechanical alloying can be used to alloy elements having vastly different melting temperature, which cannot be easily done by conventional techniques such as arc melting. After hydriding, the elemental components of Mg_2Ti, Mg, Ti and TiH_2 are converted into new hydrided ones, i.e. MgH_2, Mg_2TiH_4 and TiH_2. Beside the peaks of TiH_2 incline, new peaks at 2θ = 31^{o} and 39^{o} can be identified as new phases from □-MgH_2 and Mg_2TiH_4 and the mass fraction of TiH_2, Mg_2TiH_4 and MgH_2 in the specimen equal to 64.0 wt%, 25.48 wt%, and 10.52 wt%, respectively.

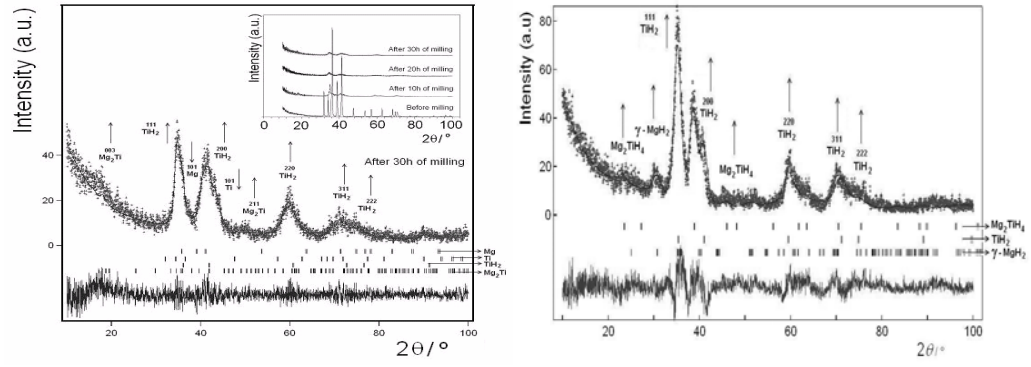

(a) (b)

Figure 2. The XRD refinement results of (a) Mg and Ti after 30 h of milling and (b) after hydriding at 300 ^{o}C.

Figure 3 shows the *P-W-T* (pressure, weight gained, temperature) diagram represents the hydrogen sorption properties of the Mg-Ti alloy. From the figure in can be seen that only one plateau pressure is obtained, an indication that absorption on hydrogen into this alloy is very fast. Microstructure of the specimen also plays an important role in the performance of the material, where the fine microstructure increases the surface contact of the powder with hydrogen. The pressure versus wt% of

hydrogen in Fig 3 depicts that the hydrogen capacity is high, about 6,7 wt%. Compared to that of the Mg_2Ni[7,8], which absorbed hydrogen up to 3.6 wt% and Mg-Al, which absorbed hydrogen up to 3.2 wt% for □-phase and 4.9wt% for □-phase alloys [9,10], the Mg-Ti alloys looks more promising to be used as hydrogen storage material. For all Mg-based materials it is observed that mechanical alloying accelerates the hydrogenation kinetics of the magnesium based materials at low temperature, but a high temperature must be provided to release the absorbed hydrogen from the hydrided magnesium based materials. It is believed that the dehydriding temperature is largely controlled by the thermodynamic configuration of magnesium hydride. In addition, the rate of dehydriding is also depends on the milling time, where the longer milling time gives faster kinetics of dehydriding[12].

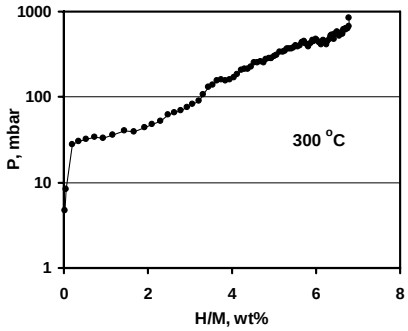

Figure 3. The *P-W-T* diagram of the Mg-Ti alloy at 300 °C.

Figure 4 shows the hydriding rate of the Mg_2Ti alloy measured at temperature of 300 °C. It is showed that maximum hydrogen content of about 6.7 wt% after 1270 seconds. Although the time needed to absorb hydrogen relatively long (21.16 min), the high capacity of hydrogen should be considered. Lomness et al. reported that in their experiment on Mg-Ni-Ti alloy they obtained the hydrogen capacity was about 11 wt% [13], almost twice as much as the present experiment. The high hydrogen capacity is closed connection to the nanosize particle used. Compared to other Mg-other metals alloy (Mg-Al, Mg-Ni, and Mg-Fe) the present result shows higher hydrogen capacity. Therefore, Mg-Ti can be considered in the future development of Mg-based material.

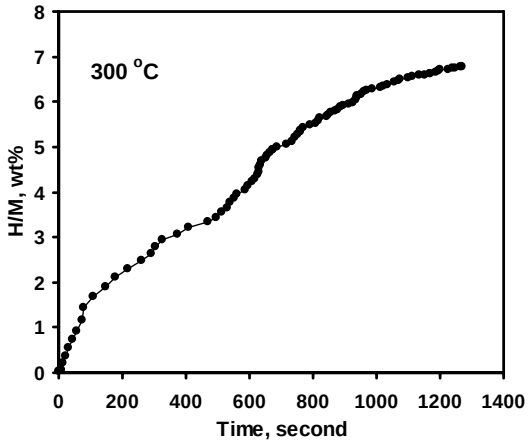

Figure 3. The hydriding rate of the Mg-Ti alloy at 300 °C.

CONCLUSION

Investigation on the hydrogen absorption properties of Mg-Ti alloy prepared by mechanical milling has been carried out. After 30 h of milling the elemental Mg and Ti powders can be synthesized into Mg_2Ti. The formation of TiH_2 is suggested from the use of hydrogen as media during alloy preparation. After hydriding, the specimens consist of TiH_2, Mg_2TiH_4 and MgH_2 phases with the mass fraction equal to 64.0 wt%, 25.48 wt%, and 10.52 wt%, respectively. Hydrogen capacity of the Mg-Ti alloy about 6.7 wt% is a good prospect for further investigation in developing Mg-based for hydrogen storage materials.

ACKNOWLEDGMENT

The Author would like to express his gratitude to the State Minister of Research and Technology for provisioning financial support through the Incentive Program, KNRT, fiscal years 2007-2009; PT. BATAN Teknologi for providing facilities and supports for this research program; the Director of the Center for Nuclear Fuel Technology, BATAN and the Director of the Center for Nuclear Industry Material Technology, BATAN.

REFERENCES

1. T.T. Ueda, M. Tsukahara, Y. Kamiyaa, S. Kikuchi, ., *J. Alloys Comp* 386 (2005) 253–257.
2. H. Suwarno, "Preparation and characterization of Mg_2NiH_4 for Hydrogen Storage", *Indonesian Journal of Material Science*, Dec. 2008, Special Edition, pp. 153-157.
3. J. Bystrzcki, T. Czujko, R.A. Varin, D. Oleszak, T. Durejko, W. Darlewski, Z. Bojar and W. Przetaiewicz, *Rev. Adv. Mater. Sci*., 5 (2003) 450-454.
4. Z. Dehouche, R. Djaozandry, J. Goyette, T.K. Bose, *J. Alloys Comp.*, 288(1999)312-318.
5. H. Suwarno, A.A. Wisnu, I. Andon, *Int'l Conf Solid State Ionic*, Proc, PTBIN, Serpong, Indonesia, 2007.
6. F. Izumi, Rietan Manual, 1994 (private communication).
7. Ming Au, Savannah River Technology Center Aiken, SC 29803, "Hydrogen Storage Properties of Magnesium Base

Nanostructured Composite Materials", WSRC-TR-2003-00239.
8. H. Suwarno, "Preparation and Characterization of Mg2NiH4 for Hydrogen Storage", *Indonesian Journal of Material Science*, Special Edition, Dec. 2008, pp. 153-157.
9. S. Bouaricha et al., *J. Alloys Comps.*, 297 (2000) 282.
10. J.C. Crivello, T. Nobuki, S. Kato, M. Abe, T. Kuji, *J. Advanced Science*, 19 (2007) 3.
11. H. Suwarno, "A Study on Preparation and Hydriding of □-Mg_2Al_3 and □-$Mg_{17}Al_{12}$", *Indonesian Journal of Nuclear Fuel*, to be published in July 2009.
12. G. Barkhordarian, T. Klassen, R. Bormann, *J. Alloys Comps.*, 407 (2006) 249.
13. J.K. Lomness, H.D. Hampton, L.A. Giannuzzi, *Int J Hydrogen Energy,* 27 (2002) 915.

Proceeding of the 11th International Conference on QiR (Quality in Research)
Faculty of Engineering, University of Indonesia, Depok, Indonesia, 3-6 August 2009
ISSN 114-1284

Determination of Residence Time in the Flow Exchange Between Recirculation Zone Behind A Sudden Expansion and Outer Region Using High-Speed Visualization Method

Harinaldi [1] and Y. Sakai [2]

(1) Departement of Mechanical Engineering
Faculty of Engineering University of Indonesia
Kampus Baru-UI, Depok, Jawa Barat, 16424
E-mail: harinald@eng.ui.ac.id

(2) Graduate School of Science and Technology, Keio University
3-14-1 Hiyoshi Kohoku-ku, Yokohama-shi,
Kanagawa-ken 223-8522, Japan

ABSTRACT

The present paper is devoted to an investigation of the problems of mass exchange behind the flame holder by utilizing a novel high-speed visualization technique based on laser sheet imaging. The experimental work was done in a flame holder model having a sudden expansion configuration in the form of a backstep. The model was placed in a horizontal small-scale wind tunnel and since the main objective is to determine the residence time, the experiment was done under isothermal (non reactive) flow. The visualization of the flow field was done with a laser-sheet based technique, where a planar image of the flow field, which was illuminated by a thin laser, was captured by a video camera. The visualization set-up consisted of a 4 W Argon-ion laser beam with a wavelength output of 514.5 nm (Coherent Innova 70-4) and a high-speed video camera (Motion scope HR series, Red Lake Imaging) which could be set to capture video images of 1000 frame/s. The continuous motion of the gas in the flow field could be visualized with sufficient temporal and spatial resolutions. Self-developed image processing software was used to conduct direct luminance intensity measurement on recorded image. The assessment of the residence time was done by analyzing the time history of the luminosity of recirculation zone on frame by frame basis.

Keywords: *Time residence, recirculation zone, high-speed visualization*

1. INTRODUCTION

Flame holding mechanism in a high speed air flow deals with maintaining the flame in the flow field at the condition that the flame which is formed is in the same degree as if it is in a low speed flow field. In order to hold a flame in a high speed and usually highly turbulent flow, one must either uses a small hot pilot flame or relies on recirculation holding. Of the standard flame holding techniques employed in subsonic combustion chambers, most involve the formation of recirculation zones in the flow field which assist in stabilizing flame structures. Strehlow [1] mentioned that these recirculation regions can be produced in a number of ways. These recirculation regions, which are typically formed behind bluff body (rod or sphere), V-gutter flame holders, by introducing a region of backflow using an opposed flow, or behind a sudden expansion of the duct area by introducing a step, are usually very low speed regions and provide conditions for a continuous source of ignition through the entrainment of hot combustion products. The diffusion flame then formed is mainly controlled by the mixing process of the utilized fuel and oxidizer (mostly air), as the time constant for mixing τ_{mix} is 5-6 orders of magnitude higher than the time constant for the chemical reaction τ_{cheml}. This means that mixing is the leading control parameter for the flame stabilization as well as for the efficiency of technical combustion process.

Furthermore, the stability of the process of combustion behind the flame holder greatly depends on the amount of heat received by the fresh mixture from recirculation zone. It is therefore advisable to investigate the flame holder operation with a study on the flow exchange between the zone and the outer flow. Proceeding from the peculiarities of the stream behind a sudden expansion, the exchange between the zone and flow has been usually assumed to take place mainly as a result of turbulent diffusion. However, there is no such effective way of directly determining the turbulent exchange coefficient for the recirculation zone. One of the possible methods is to determine it indirectly from the mean time of the presence of gas in the zone behind flame-holder. The residence time is then defined as mean time of exchange which describing the ratio of volume of the zone to that of the gas flowing through this zone per unit of time. Knowing the residence time and the dimension of the zone, it is possible to compute the mean coefficient of turbulent diffusion.

Bovina [2] mentioned that the connection between the zone diffusion coefficient D_z, the upstream flow diffusion coefficient D_f, flow velocity V_f and the size of the flame-holder d_{fh} is expressed by the following simple relationship

$$\frac{D_z}{V_z} = K_1 \frac{D_f}{V_f} + K_2 d_{fh} \quad (1)$$

In this case K_1 and K_2 are coefficients of proportionality. However, he did not succeed in finding away of directly determining the turbulent exchange coefficient for the recirculation zone and eventually proposed an indirect method based on the mean time of the presence of gas in the zone behind the flame holder (residence time, τ_{res}). Then in diffusion exchange

$$\tau_{res} = \frac{V_z r_m}{S D_z} \quad (2)$$

Where V_z , S and r_m are the volume, the surface and the mean radius of the zone respectively. The residence time and the dimension of the zone being known, it is possible to compute the mean coefficient of diffusion.

While there are abundant works devoted to determine the size of recirculation zone [3-6], to obtain the residence time was of considerable interest by itself. The dependence of its magnitude on various factors, such as the velocity and turbulence of the upstream flow, the dimension of the flame-holder and the composition of the mixture, have not as yet been comprehensively elucidated. The general physical consideration in determining the time residence is as follow. Some foreign admixture easily carried away by the turbulent displacement of the medium, whose presence can be fixed in some way is introduced into the zone behind the flame holder. After a stationary process between inflow and the discharge of the admixture has been established, its feeding is abruptly stopped and the change is recorded in its concentration in time from the equilibrium C_o to practically nil. The change in concentration occurs in accordance with the following equation:

$$C = C_0 e^{-\frac{t}{\tau_{res}}} \quad (3)$$

In the physical sense and numerically this value is equal to the mean time of the presence of gas during the stationary process (residence time). From Equation 3 we can obtain the magnitude of the residence time.

The present paper is devoted to an investigation of the problems of mass exchange behind the flame holder by utilizing a novel high-speed visualization technique based on laser sheet imaging. The continuous motion of the gas in the flow field could be visualized with sufficient temporal and spatial resolutions. Self-developed image processing software was used to conduct direct luminance intensity measurement on recorded image. The assessment of the residence time was done by analyzing the time history of the luminosity of recirculation zone on frame by frame basis.

2. EXPERIMENTAL METHOD

2.1 Apparatus and Test Condition

The present work was conducted in an experimental set-up as described in Fig. 1. The air was driven by a vortex blower into a horizontal small-scale wind tunnel and then flowed into a test section. The cross section of the test section upstream of the step was 50 x 80 mm2. The step height, H was 20 mm and the length of the test section was 300 mm. In the base wall, a gas injection port with 1 mm-slot exit spanned across the test section was installed at a distance lf from the step. Through the slot injection port, nitrogen gas from a high-pressure gas tank was injected upward into the test section after passing through a capillary manometer system for flow rate adjustment. The injected gas flow line was firstly passed through a particle seeding system, so that the injected nitrogen gas seeded with scattering particles entered the recirculation flow field in the test section. After a stationary process between inflow and the discharge of the seeded nitrogen has been established, the feeding is abruptly stopped and the change of luminosity of images is recorded.

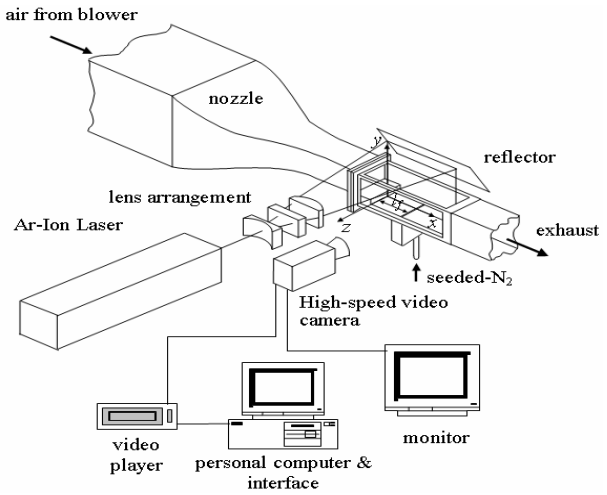

Figure 1. Sketch of Experimental Set-up

The test section was fixed to a transverse arrangement that allowed three-dimensional movement. Throughout the entire experiments of the present study, the upstream main airflow velocity was maintained constant at U_o = 10 m/s. In the experiments, the principal parameters were the ratio of specific momentum between the injected nitrogen and the main airflow ($I = \rho_{N2} V_{N2}^2 / \rho_o U_o^2$) and the stream wise

distance from the step to the injection slot (l_f). The specific momentum ratio of injection (I) was varied from 0.04 to 0.5 by altering the seeded-nitrogen injection velocity. Two locations of gas injection were selected within the recirculation zone, where the flow structure was different. In case (a), the nitrogen was injected at near step position ($l_f/H = 2$) where the recirculating flow was predominant. While in case (b) it was at near reattachment position ($l_f/H = 4$), where the shear turbulence was predominant.

The visualization of the flow field was done with a laser-sheet based technique, where a planar image of the flow field, which was illuminated by a thin laser, was captured by a video camera. The visualization set-up consisted of a 4 W Argon-ion laser beam with a wavelength output of 514.5 nm (Coherent Innova 70-4) and a high-speed video camera (Motion scope HR series, Red Lake Imaging) which could be set to capture video images of 1000 frame/s. The continuous motion of the gas in the flow field could be visualized with sufficient temporal and spatial resolutions, though images at the flow region with especially high local velocity would locally blur.

2.2 Assessment Method

Self-developed image processing software was used to conduct luminosity measurement on recorded image at a certain local point within the recirculation zone. Figure 2 represents an example of a captured image. To determine the residence time, the luminosity history at several points were tracked starting from the initial frame when the seeding is still introduced until several instants after the seeding is completely stop. In this method, images from about 2000 frames for each parameter condition were examined. The historical data of luminosity were then plotted into graphs to determine the magnitude of residence time.

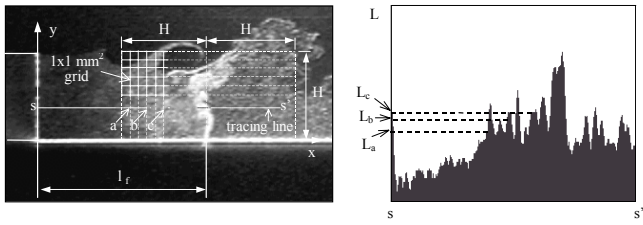

Figure 2. Assessment Method of Image luminosity

3. RESULTS AND DISCUSSION

Examples of luminosity signal history taken from image analysis are shown in Fig. 3 for the case of $l_f/H = 2$ and I = 0.04. From the figure it can be seen that the signal of luminosity indicates expected time history pattern for a recirculation region behind the step. The origins of the graphs show the cut-off point of the seeding process after a constant seeding. Afterwards, the graphs follow an exponential decrease until the intensity of luminance in the

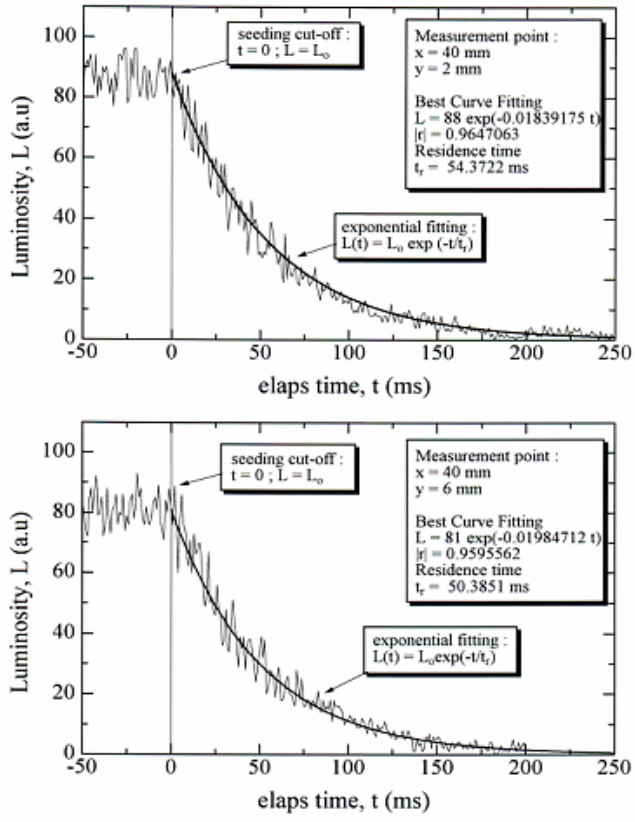

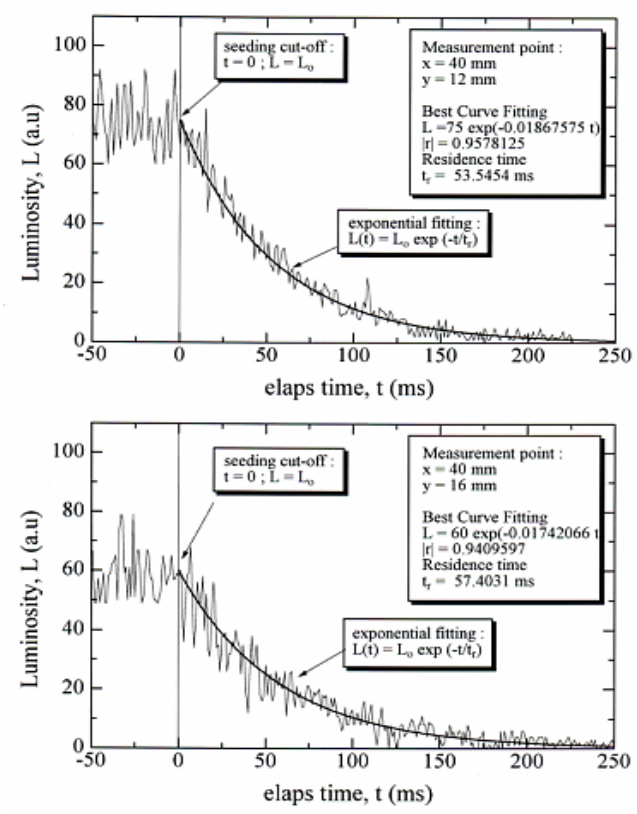

Figure 3. Example of luminosity signal history (U_o=10 m/s; l_f/H = 2; I = 0.04)

image vanishes. From the exponential fitting, the residence times are then determined.

Figure 4 summarize the residence times measured for all the case of specific momentum ratio of injection in the present study I = 0.04 – 0.5 when the nitrogen gas injection is at l_f/H = 2. For each case of specific momentum ratio, the measurements of luminosity is taken at several vertical position (y/H = 0.1 – 0.8) at horizontal position above the injection point (x/H = 2). The average magnitudes of residence times are also given. From the figure it can be seen that for the lowest momentum of injection (I = 0.04), local time residences are significantly scattered with standard deviation about 3 ms. However, for higher specific momentum of injection, the data show more constant value of residence time magnitude. Furthermore, the figure also indicates an obvious effect of the specific momentum injection to the shorten of residence time as the average magnitude drops about 27 % from 54 ms to 41 ms when the specific momentum is increased from 0.04 to 0.5. As implied by Equation (2), this result suggests that a higher specific momentum injection supports a faster flow exchange between the recirculation zone and the outer region.

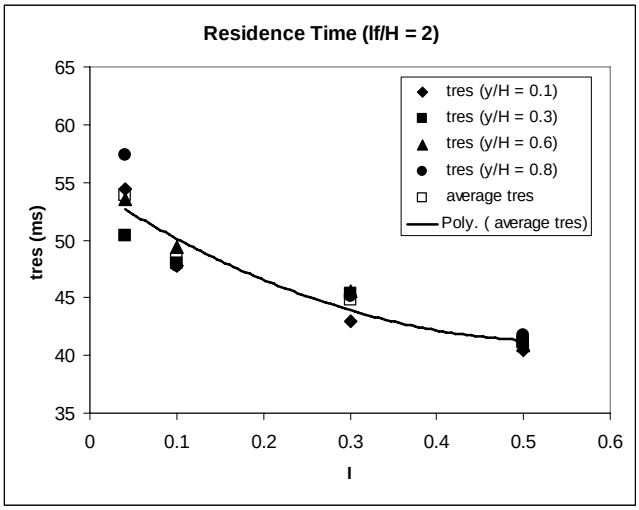

Figure 4. Effect of Injection Momentum to the Residence Time magnitue (U_o=10 m/s; l_f/H = 2; x/h = 2; I = 0.04-0.5)

Meanwhile, Fig. 4 summarize the residence times measured for all the case of specific momentum ratio of injection in the present study I = 0.04 – 0.5 when the nitrogen gas injection is at l_f/H = 4. Again, for each case of specific momentum ratio, the measurements of luminosity is taken at several vertical position (y/H = 0.1 – 0.6) at horizontal position above the injection point (x/H = 4). The average magnitudes of residence times are also given. From the figure it can be seen that shifting the injection position of the gas toward downstream direction and approaching reattachment point will shorten the residence time for the whole range of specific momentum of injection. When we compare the average magnitudes of residence times for the corresponding specific momentum injection in the previous case (l_f/H = 2), the decrease are ranging from 26 % for I = 0.04 to 11 % for I = 0.5. Moreover, it is apparent from the figure that injection near the reattachment point will make the influence of varying the specific momentum ratio becomes less significant. This result suggests a dominant effect of the shear turbulence with high intensity to the flow exchange between the recirculation zone and the outer region.

Furthermore, in a flame holding application those two trends could be the main aspect to be considered in maintaining the flame stability within the recirculation region.

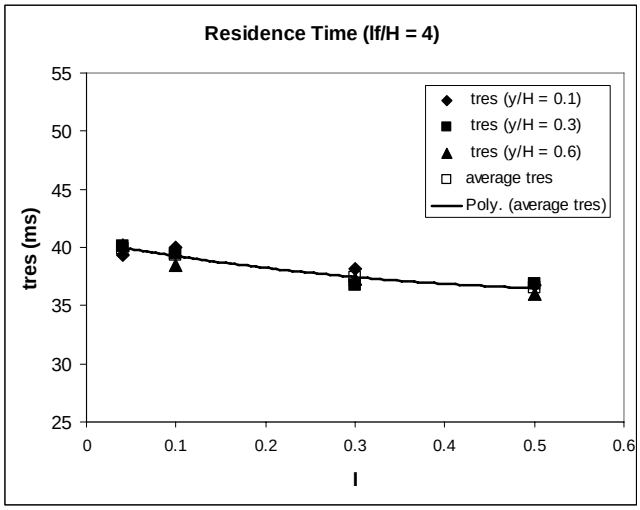

Figure 5. Effect of Injection Momentum to the Residence Time magnitue (U_o=10 m/s; l_f/H = 4; x/H = 4; I = 0.04-0.5)

4. CONCLUSION

In the present work, an investigation of the problems of mass exchange behind the flame holder has proposed a novel high-speed visualization technique based on laser sheet imaging to determine the residence time inside a recirculation flow region. The experimental work was done in a flame holder model having a sudden expansion configuration in the form of a backstep in which a seeded nitrogen gas is injected to simulate a fuel injection to a combustion chamber. The conclusions are as follows:

(1) The proposed method has been effectively used to measure the residence time which can be further analyzed to determine the turbulent exchange coefficient
(2) When the specific momentum ratio of the injection is increased, the time residence decreases which suggest a faster flow exchange between the recirculation zone and the outer region.
(3) Shifting the injection to approach the reattachment point will make the influence of varying the specific momentum ratio becomes less significant to the magnitude of time residence. This suggests a dominant effect of the shear turbulence with high intensity to the flow exchange between the recirculation zone and the outer region.

REFERENCES

1. Strehlow, R.A., **Combustion Fundamental**, McGraw-Hill,Inc., pp.360-361, 1985
2. Bovina, T.A , "Studies of Exchange Between Re-Circulation Zone Behind The Flame-Holder and Outer Flow", The 12th International Symposium on Combustion, The Combustion Institute, pp.692-696, 1970.
3. Chiang, T.P. and Sheu, T.W.H., "A numerical revisit of backward-facing step flow problem," Physics of Fluids, 11, , pp. 862-874, 1999
4. Yang, J.T., Tsai, B.B and Tsai, G.L., "Separated-reattaching flow over a backstep with uniform normal mass bleed," Trans. ASME, J. Fluid Engineering, 116, , pp. 29-35, 1994
5. Coats, C.M, Richardson, A.P. and Wang, S., "Nonpremixed combustion in turbulent mixing layers part 2: recirculation, mixing and flame stabilization," Combustion and Flame, 122, pp. 271-290, 2000)
6. Asanuma, T., Handbook of Flow Visualization, New ed. (in Japanese: Nagare no Kasika Handobuku), Asakura Shoten, Tokyo, , pp. 78-79 and pp.158-164. 1986

ISSN 114-1284

Burner Tip Temperature on Flame Lift-up Phenomenon

I Made Kartika Dhiputra[1], Cokorda Prapti Mahandari[2]

[1,2,]*Flame and Combustion Research Group Thermodynamic Laboratory,*
Mechanical Engineering Department Faculty of Engineering
University of Indonesia, Depok 16424
Tel : (021) 7270032. Fax : (021) 7270033
E-mail : [a]dhiputra_made@yahoo.com
: [b]pmahandari@yahoo.com

ABSTRACT

Flame lift-up phenomenon was proposed to overcome the overheating problem on burner tip. This phenomenon was initiated on the premix combustion using Bunsen burner built-in a ring above the tube burner. This work would be focused on measuring tip burner temperature. Temperature measurement was done utilizing two different method; platinum rhodium thermocouple and infra red thermograph. The infra red thermograph camera was connected to a computer to analysis the image using image processing software. It has been found that burner tip temperature of Bunsen flame was greatly influenced by the AFR or equivalent ratio. The highest burner tip temperature was nearly on AFR stoichiometric or equivalent ratio of 1. Burner tip temperature after flame lift-up indeed was lower than burner tip on Bunsen flame without lift-up. The proposition to apply this phenomenon seems appropriate to diminish the tip burner problem. However ring temperature look have yield on burner tip temperature due to the radiation heat loss. Simulation of heat loss from Bunsen flame based on flame temperature had been studied. This finding needs to be implemented on revealing the heat loss from flame lift-up phenomenon to clarifying burner tip temperature variation.

Keywords
Premixed combustion, flame lift-up, tip burner, temperature

1. INTRODUCTION

Damaged on burner tip due to high temperature stimulate the application of flame lift-up phenomenon on burner design. Flame lift-up phenomenon initially found on premix combustion using Bunsen burner slotted in a ring above the tube burner. This phenomenon was similar to lifted flame on diffusion flame. It retained the lifted flame using ring. The occasion when the flame jump to the ring was called lift-up phenomenon. So far a preliminary research on flame lift-up phenomenon had been done to investigate Air Fuel Ratio (AFR) for flame lift-up and the effect of ring position on AFR. Flame lift-up would appear on AFR above AFR blow-off without ring. It means that flame lift-up is on a lean combustion process. Position of ring or distance of ring from the exit tube burner was also play a part on determining AFR for lift-up. Closer ring position would provide greater AFR for lift-up [1].

In order to implement this phenomenon on design of burner, flame height had also been investigated. Research on flame height of flame lift-up has been done on the basis of AFR, position of ring, inside diameter of ring and material of ring [2,3,4]. Flame height was directly affected by AFR in reverse. This finding match up the Rokke correlation for premix flame that express flame height is proportional to mass fuel fraction and Froude Number [5].

Position of ring from the exit tube burner has also altered the flame height. It seems that flame height of flame lift-up was equivalent to position of ring. Research on flame height has also been done in term of inside diameter of ring employing 3 different inside diameter. It demonstrated that on low flow rate of fuel, inside diameter of ring nearly proportional to flame height. Nonetheless there was an optimum inside diameter that resulted in maximum flame height.

Further experimental study on material of ring particularly temperature of ring had also been carried out. Currently the impact of material ring has been investigated. Two different materials on the same dimension of ring have been applied [4,6,7]. For ring made of ceramic, AFR for lift-up was much lower contrast to ring made of stainless steel. Flame height would also vary. It has been found that flame height on ring made of ceramic was higher compare to flame height on ring made of stainless steel. Temperature of ring made of ceramic is lower than temperature of ring made of stainless steel when lift-up appeared. From AFR for lift-up, it seems that the raising of AFR is proportional to the raising of ring temperature. This result is match with the previous study, that lower AFR means lower flame temperature, and so was the ring temperature [7].

But, in the same burning load, it did not show the same thing. In the previous study it was found that AFR was defined by ring position on same burning load. Closer ring position means higher AFR. In term of the fuel flow rate, higher fuel flow rate did not affect the ring temperature when lift-up happened. On lower ring position, ceramic or stainless steel, show constant ring temperature. For stainless steel ring, on high position and high fuel flow, ring temperature is slightly raise, and this is in contrast with ceramic ring.

Correlation between ring temperature and flame length still cannot be defined since there is a jumping data for

those two materials. But for correlation between flame length and AFR for lift-up is match, for ceramic and stainless steel ring.

Measurements of burner tip temperature have never been reported to consider the phenomenon to be practically implemented. Therefore in this work burner tip temperature with and without flame lift-up phenomenon was measured using two different methods. The result can be used to estimate weather this phenomenon could be considered as the improvement on burner design. The experimental result was also evaluated based on simulation.

2. EXPERIMENTAL

This research was carried out using propane as a fuel. A Bunsen Burner Flame Propagation and Stability Unit which consist of air flow meter and gas flow meter, fan and AC motor were used to create flame and control the propane and air flow rate. The tube of Bunsen burner is 14 mm diameter and 38 cm height. A ring made of stainless steel AISI 304 with outside diameter of 30 mm and thickness of 5 mm was placed above the burner tube concentrically using a ring adjuster.

Thermocouple and infra red thermograph were used to measure the tip burner temperature. Infrared thermograph was directly connected to a computer so that the image can be analyzed using an image processing software as it is shown on Figure 1.

Flow rate of propane and flow rate of air were measured using rotameter and recorded whenever lift-up happened. The rotameter had been calibrated using a wet gas meter. Experimental was started without ring. Gas valve was open and it was kept on a fix value

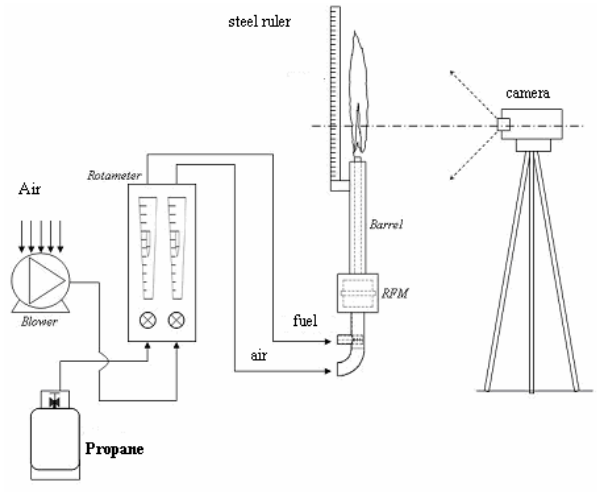

Figure 1. Experimental set-up

that can be seen from the rotameter. Ignition can be done and air valve was open slowly. Tip burner temperature and air flow rate was recorded. Air valve was further increased slowly until a fix value then tip burner and air flow rate was recorded. Experiment was done until flame was blow off.

Experimental expand with ring that put above the exit tube burner concentrically using ring adjuster. Gas valve was open and it was kept on a fix value that can be seen from the rotameter. Ignition can be done and air valve was open slowly until lift-off. Then within a few second flames will jump from the exit tube burner to the ring and 'sit on the ring'.

AFR was calculated based on regular propane flow rate. Air flow rate was regulated until the flame lift-up phenomenon came out. Air flow rate, tip burner temperature were recorded simultaneously.

Experiment was done on four positions of ring from the burner tube that is 10 mm, 20 mm, 30 mm and 40 mm respectively. For each position of ring, six variation of propane flow rate was carried out. The heat release of the flames studied ranges between 1.5 KW and 2.5 kW.

3. RESULT AND DISCUSSION

Image from the measurement of tip burner temperature without ring that had been done using infra red thermograph was presented on Figure 2. It shows that emissivity of the burner tip can be set on 0.44. The value for tip burner temperature was taken on the center of tip burner surface since this location is perpendicular to the infra red camera. AFR of each data was calculated and presented on Table 1.

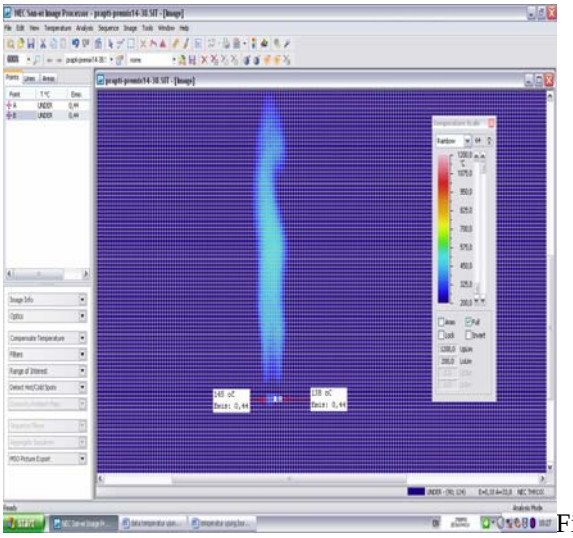

Figure 2: Image of the measurement of tip burner temperature without ring

Table 1: Tip burner temperature on AFR variation

AFR	Temperature (^{o}C)
17.3	101
19.2	137
21.2	144
23.2	148
25.4	147
27.6	146
29.9	144
32.2	138
34.6	137

Image from the measurement of tip burner temperature after lift-up or with ring was presented on Figure 3. and all the data were showed on Table 1

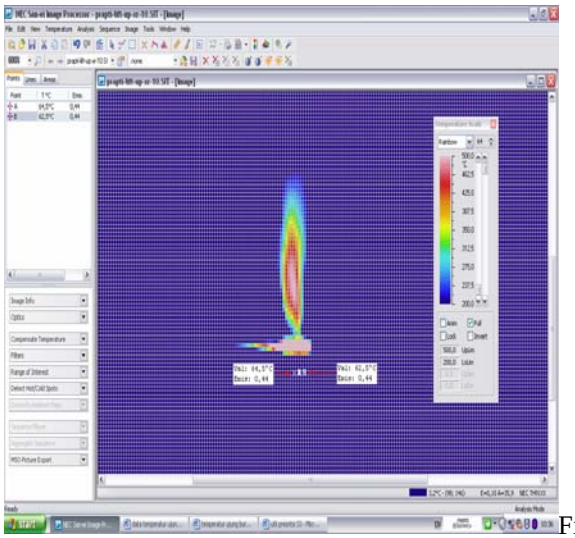

Figure 3: Image of the measurement of tip burner temperature after lift-up

Table 2: Tip burner temperature on after lift-up

x_r= 10 mm		x_r= 20 mm		x_r= 30 mm		x_r= 40 mm	
AFR	T(C)	AFR	T(C)	AFR	T(C)	AFR	T(C)
32	96	33	97	32	74	32	71
34	88	35	88	33	51	33	70
37	71	36	74	35	54	34	62
39	67	38	71	37	61	36	60
41	63	40	65	38	57	37	56
43	62	42	50	40	50	39	50

Burner tip temperature on Bunsen flame without flame lift-up would be compare to burner tip temperature after lift-up. It is showed on the same chart as on Figure 4.

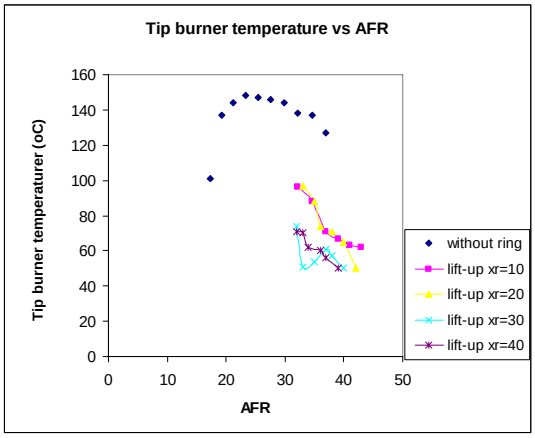

Figure 4. Tip burner temperature with and without ring or after lift-up

Tip burner temperature without ring followed flame temperature distribution that nearly maximum on AFR stoichiometric. In this experiment as propane was used as a fuel then the AFR stoichiometric was about 24.

However distribution of tip burner temperature after lift-up was hardly difficult to figure out. Definitely tip burner temperature after lift-up were lower compare to tip burner temperature without lift-up. Not only because the higher AFR that decrease the temperature, but also heat radiation to material of ring that absorb a certain thermal energy of combustion. This result was corresponded to previous experimental result on flame length of flame lift-up using two different material of ring [4].

Position of ring from the tip burner is also affected the tip burner temperature. The closer position of ring higher tip burner temperature will be. This result is consistent with the simulation result on tip burner temperature without ring that considers the standoff distance of the flame as it is shown on Figure 5 [10].

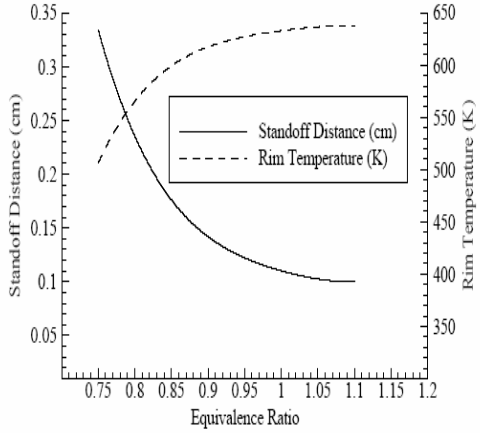

Figure 5: Rim temperature on equivalence ratio variation

4. CONCLUSION

Distribution of tip burner temperature on Bunsen flame was similar to the distribution of flame temperature. It depends on the AFR of equivalence ratio and it is the highest on its stoichiometric mixture.

Flame lift-up phenomenon was decrease the tip burner temperature. The longer distances of ring from the tip burner also decrease the tip burner. Therefore application of this phenomenon on burner design could be possible to overcome the overheating problem on premix burner.

REFERENCES

[1] Cokorda P.M., I Made Kartika Dhiputra, Flame Lift-up on A Bunsen Burner; A Preliminary Study" *Proceedings of the 10th International Conference on Quality in Research (QIR)* Engineering Center University of Indonesia, December 2007, pp EPE-13

[2] I Made Kartika Dhiputra et all "Flame Height of Propane the Propane Flame lift-up", *Proceeding of the 1st International*

Meeting on Advanced in Thermo-Fluid, UTM Johor, Malaysia 26 August 2008

[3] I Made Kartika Dhiputra, Hamdan Hartono A, Cokorda Prapti Mahandari, 2008, "Perubahan Panjang Nyala Api pada Fenomena "Flame Lift-up" Akibat Letak Ketinggian Posisi Ring 'Flame-Hold', *Proceeding Seminar Nasional Teknik Mesin 3*,UK Petra , Surabaya, Indonesia, pp101-104

[4] I Made Kartika Dhiputra, Bambang Sugiarto, Amri Parlindungan Sitinjak, Cokorda Prapti Mahandari, 'Pengaruh Material Ring Pada Fenomena Nyala Api Lift-up', *Proceeding Seminar Nasional Teknik Mesin* ITENAS Bandung, 28 Oktober, 2008

[5] Nils A Rokke, 'A Study of Partially Premixed Unconfined Propane Flames, *Combustion and Flame* 97:88-106

[6] I Made Kartika Dhiputra, Bambang Sugiarto, Cokorda Prapti Mahandari, 'The Influence of Ring on AFR and Flame Height of Flame Lift-up Phenomenon; an Experimental Study", will be published on this Proceeding

[7] I Made Kartika Dhiputra, et al, "Temperature Rong pada Fenomena Flame lift-up", *Proceeding Seminar Nasional Teknik Mesin* ITENAS Bandung, 28 Oktober, 2008

[8] I Made Kartika Dhiputra, Cokorda Prapti Mahandari, 'Karlovitz Number for Predicting A flame lift-up on Propane Combustion", *Proceeding The 1st International Meeting on Advances in Thermo-Fluid* 26th August 2008, Universiti Teknologi Malaysia, Johor, Malaysia

[9] I Made Kartika Dhiputra, Eko Warsito, Cokorda Prapti Mahandari, 'Karakteristik Temperatur Maksimum Nyala api Pembakaran Non Difusi Gas Propana dengan Teknik Pencitraan Nyala (Infra Red Thermography)', *Proceeding Seminar Nasional Teknik Mesin 3*,UK Petra Surabaya, Indonesia hal. 89-92

[10] Ludwig Christian Haber, An investigation into the origin, measurement and application of chemiluminescent light emissions from premixed flames, Master's Thesis, Virginia Polytechnic Institute and State University, 2000

Proceeding of the 11th International Conference on QiR (Quality in Research)
Faculty of Engineering, University of Indonesia, Depok, Indonesia, 3-6 August 2009
ISSN 114-1284

Influence of Air-Injection to the Alteration of Lifted-Distance Of A Propane Diffusion Flame

I Made K Dhiputra[1)], Harinaldi [2)], NK.Caturwati[3)]

"Flame and Combustion Research Group", Thermodynamics Laboratories
Mechanical Engineering Department University of Indonesia, Depok-Jakarta
Phone number : (021) 7270032 & 7864089 - Fax. (021) 7270033
E-mail : dhiputra_made@yahoo.com, harinald@eng.ui.ac.id, n4wati@yahoo.co.id

[1),2)] Mechanical Engineering Department, University of Indonesia.
[3)] Mechanical Engineering Department, Sultan Ageng Tirtayasa University,
Ph.D Cand. of Mechanical Engineering Department, University of Indonesia

ABSTRACT

Combustion of gas with diffusion system is generally used in industrial furnaces. Base flame of a diffusion flame usually departs from the burner tip. Such condition is called lifted-flames. The distance between base-flame to burner tip is called as lifted-distance. Lifted distance of diffusion flames generally increase linearly as the velocity of fuel gas injection from burner tip is increased. This is called as lift-off condition. The paper discuses the alteration of lifted-distance due to an air-injection around the jet flow of propane. Propane flowed through a 1.8 mm burner diameter with ejected combustor type and cone nozzle type at burner tip. The propane was burned in quiescence air until lift-off condition was reached. Furthermore air was injected around the jet of propane. The injection angles were 15^0, 30^0, 45^0, 60^0 and 75^0 from propane flow direction.
Lifted distance of a diffusion flames has strong correlation with characteristic of air diffusivity to the fuel. A shorter lifted-distance means greater air diffusivity to fuel gas. Injection of air around fuel flow at low flow rate produces flame with lower lifted distance than flames in quiescent air. Air injection with 45^0 direction gives the lowest lifted distance of diffusion flame.

Keywords: *diffusion combustion, base-flames, lifted-flames, lifted-distances*

1. INTRODUCTION

Combustion is process to convert chemical energy to thermal energy. There are two kind of combustion process: namely premixed combustion where fuel and oxidizer are mixed completely before their entering to combustion chamber and non-premixed or diffusion combustion where fuel and oxidizer flow into the combustion chamber separately.

Generally, the non-premixed combustion is preferred to be applied in industries for safety and reliability reasons, because in a diffusion flame, lifted phenomena often takes place early. With the base at a distance from burner tip, the flame gives an advantage to avoid thermal contact between the flame and the nozzle which would lead to erosion of the burner material. The disadvantage of this flame stabilization technique is that lifted flame blow off more easily than attached flame and therefore must continuously be controlled [1].

Liftoff distance defined as the distance between burner tip and base of flame will increase with additional velocity until the flame blows out [2]. The criteria for establishing the liftoff height are different for each theory and can be given as follows:

1. The local flow velocity at the position where the laminar flame speed is a maximum and matches the turbulent burning velocity of a premixed flame.
2. The local strain rates in the fluid exceed the extinction strain rate for laminar diffusion flame let.
3. The time available for back mixing by large scale flow structures of hot products with fresh mixture is less than a critical chemical time required for ignition.

Liftoff heights for free and confined jets at propane diffusion combustion have investigated by Cha M.S and Chung S.H. [3] and they found that the ratio of the liftoff height at blowout to the nozzle diameter maintains a near-constant value of 50 for free and confined jets. Result of observation indicates that liftoff heights x_f for free jets are proportional to the nozzle exit mean velocity u_i and are independent of the nozzle diameter and the data can be fit to equation (1):

$$\bar{x}_f = 0{,}002245u_i - 0{,}01663 \qquad (1)$$

While liftoff height for confined jets the data can be fit to equation (2).

$$\frac{\bar{x}_f}{d_i} = u_i\left(1{,}02 + \frac{0{,}0976}{d_d - 0{,}35}\right) \qquad (2)$$

Where d_i = nozzle diameter, d_d = shroud diameter.

L.K. Su et al. [4] investigated lifted jet diffusion flame by planar laser-induced fluorescence and particle image velocimetry. They delineate that there is high temperature region at the base of lifted flame.

Watson et al [5] performed simultaneous CH and OH PLIF measurements at the flame base. The CH radical is short-lived and is thought to mark the instantaneous reaction zone, while OH is removed by slower three-body reactions and marks regions containing hot combustion products. Maurey et al.[6] also observed high-temperature region outside and upstream of the reaction zones.

Some of research result suggested that at base flame has high temperature beside brightness; hence determination of base flame from flame photograph is determined as the position with highest brightness level.

2. EXPERIMENT

This research investigated the effect of air injection to alteration of lifted distance on a propane diffusion flame. Initially, propane was supplied to the quiescent air and a chemical reaction occurred. Flow rate of propane was increased gradually until liftoff condition reached. With propane flow rate at 69 ml/s, lifted distance reached 130 mm. Furthermore, air was injected around of propane flow through guide ring having various angles. Figure 1 shows the scheme of propane and air flow at the tip burner before entering the combustion chamber.

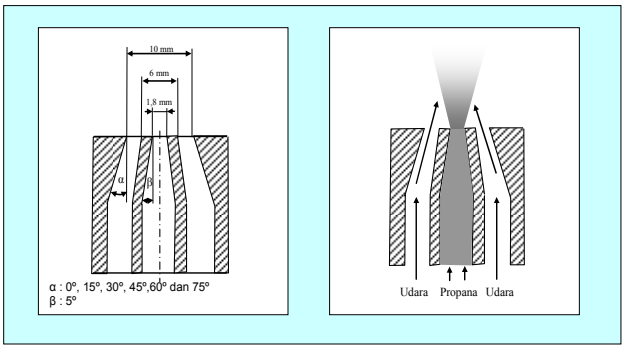

Figure 1: Scheme of propane and air flow at burner tip before entering the combustion chamber.

Propane flowed through cone nozzle type with exit diameter 1.8 mm and angle of cone nozzle 5^0. Air was injected around of propane through a gap between outer cone nozzles with outer diameter 6 mm and guide ring with inner diameter 10 mm. Guide ring has various angles of 0^0, 15^0, 30^0, 45^0, 60^0 and 70^0. Co-flow of air injected to propane occurred in case of the angles of guide ring was 0^0.

For each angles of guide ring, air injected was increased gradually and the alteration lifted distance was perceived. The sketch of experimental equipment is presented at Fig.2.

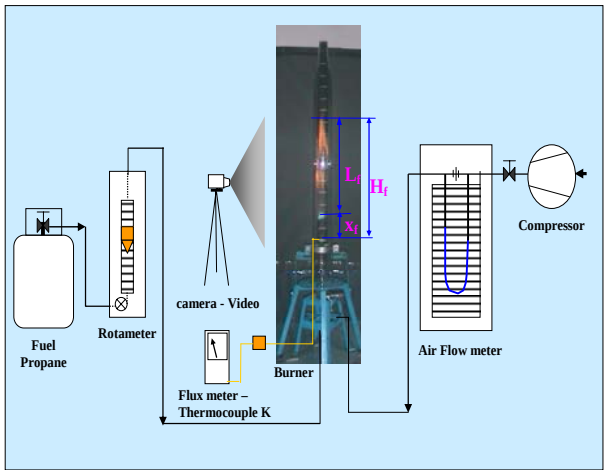

Figure 2. Schematic of experiment appliances

Propane flowed through a flow meter which has been calibrated by Wet Gas meter prior to the experiment. Flow of propane is controlled by a flow meter. Then, propane flowed into the nozzle burner for ejection into the combustion chamber. Air from compressor reservoir was delivered through orifice flow meter which have calibrated previously by Wet Gas meter before injected to the burner which passes through gap between guide ring and cone nozzles of burner tip.

Glass shroud with 82 mm of diameter and 1 m of length was installed to serve as the wall of combustion chamber for combustion with air injection. The image of flame was captured by camera, and then from the photograph some measurements of flame dimension were conducted including flame height, H_f , flame length, L_f, and Lifted distance, X_f.

3. RESULTS AND DISCUSSION

When Propane ejected to quiescence air and combusted at certain flow rate of propane, camera records the flame shape. From the captured images, the dimension of flame is determined. Figure 3 show lifted distance for propane's flame in quiescence air for some value of propane flow rate. Lifted distance is proportional to flow rate of propane. Lifted distance X_f (mm) is linearly dependent with flow rate of propane Q_f(l/s) as show as equation (3)

$$X_f = 2719.8Q_f - 59.698 \quad (3)$$

Meanwhile, Equation (5) present lifted distance X_f in meters and mean exit velocity of propane u_i in m/s when ejected from nozzle burner.

$$u_i = \frac{4.Q_f}{\pi.d_i^{\,2}} \quad (4)$$

$$X_f = 0.00691\,.u_i - 0.0597 \quad (5)$$

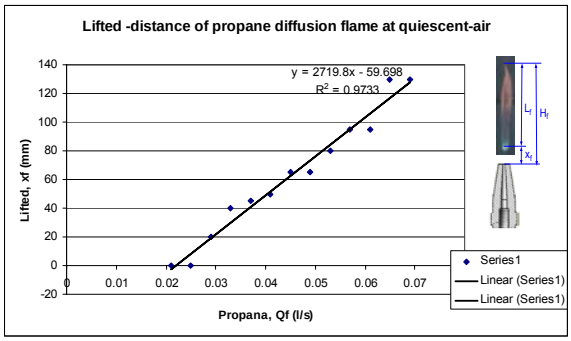

Figure 3. Lifted distance for Propane flame in quiescence air.

Equation (5) has similarity with observation result by Cha M.S and Chung S.H for free jet flames [3]. Hereinafter at propane flow rate is 69 ml/s air injected around propane stream, the alteration of lifted distance by air injection is presented in Figs. 4-9. It have the same tendency with the case of shortest lifted distance at low air injection flow rate and increases again when increased air injection. By gentle air injection, mixing between fuel and air is faster. Diffusion time become shorter than jet propane at quiescence air.

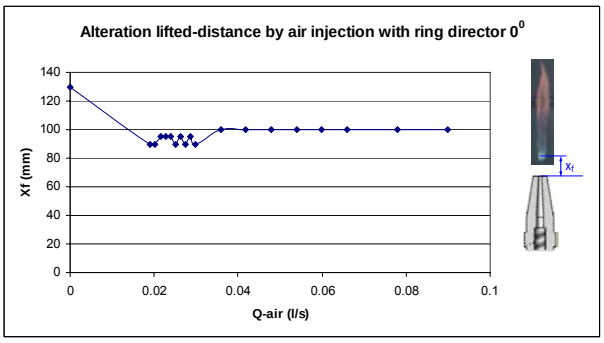

Figure 4. Alteration lifted distance by air injection through Ring director with angle 0^0.

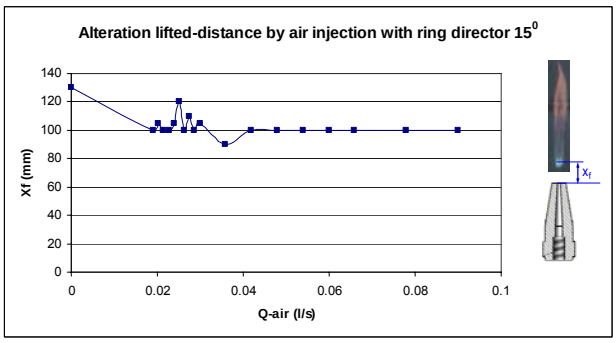

Figure 5.Alteration lifted distance by air injection through guide ring with angle 15^0.

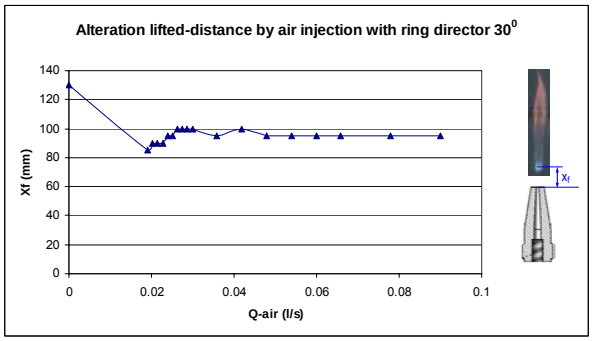

Figure 6. Alteration lifted distance by air injection through guide ring with angle 30^0.

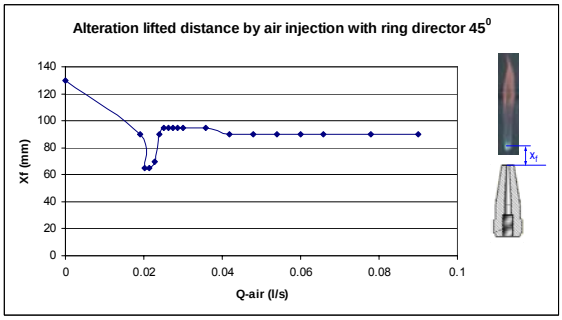

Figure 7.Alteration lifted distance by air injection through Ring director with angle 45^0.

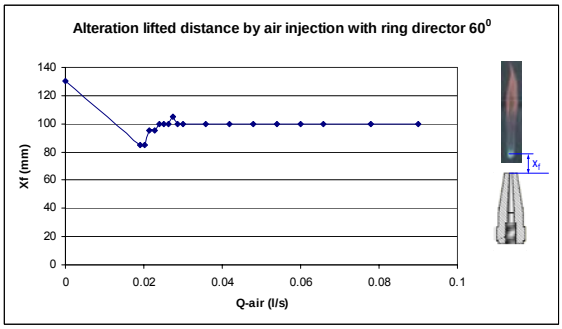

Figure 8. Alteration lifted distance by air injection through guide ring with angle 60^0.

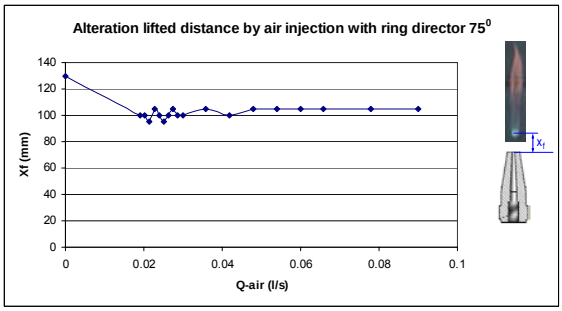

Figure 9. Alteration lifted distance by air injection through guide ring with angle 75^0.

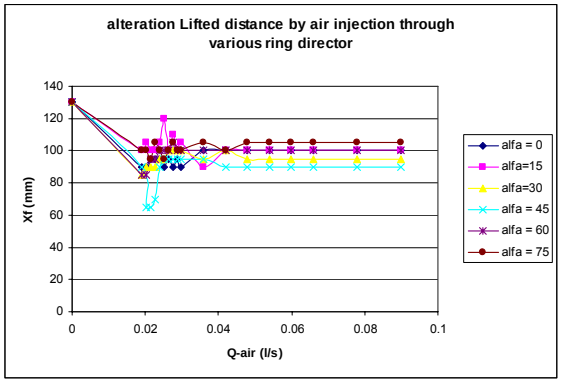

Figure 10. Alteration lifted distance by air injection through various guide rings.

The tendency of lifted distance decrease along with the increase of air injection reaches the maximum value for air flow rate 19.1 – 20.3 ml/s or air to fuel ratio is equal to 0.28 – 0.29. The decrease of maximum lifted distance decreases by air injection for various guide rings is presented at Fig. 11. Ring directors have 45^0 angles to propane stream give maximum value for alterations of lifted distance.

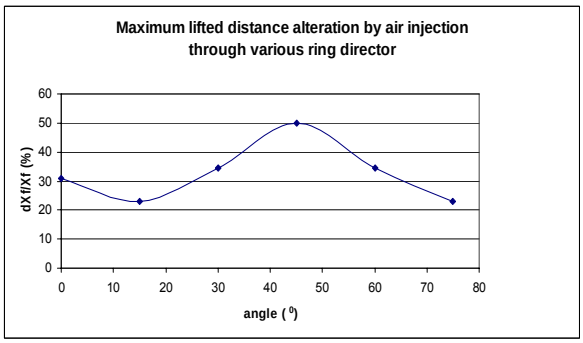

Figure 11.Maximum lifted distance alteration by air injection through various ring directors

Moreover, some numerical simulations were also conducted for propane jet injected into a combustion chamber with air injection through guide ring having various angles of 0^0, 30^0, 45^0 and 60^0. Figure 12, 13 and 14 show some results from the simulation in case of propane flow rate at 69 ml/s, and air injected flow rate at 20 ml/s. The numerical model solver is steady-state, axisymmetrical, viscous model is k-epsilon and species transport model inlet diffusion.

Figure 12 shows that mass-fraction of propane for guide ring with 45^0 angles decreases faster than the other ring. This proves that guide ring with 45^0 angles improves diffusion process of air into propane. Beside that Fig.13 shows that guide rings with angles 45^o produces highest turbulence kinetic energy compared to other angle.

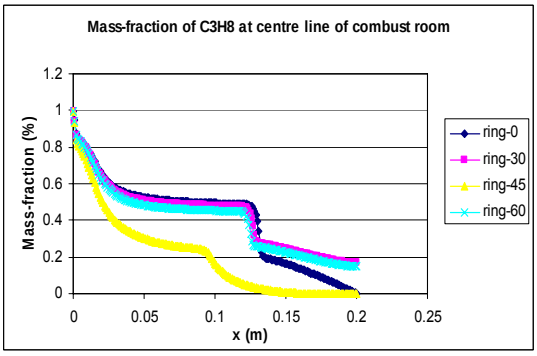

Figure 12.Mass Fraction of C_3H_8 at centre line of combust-room

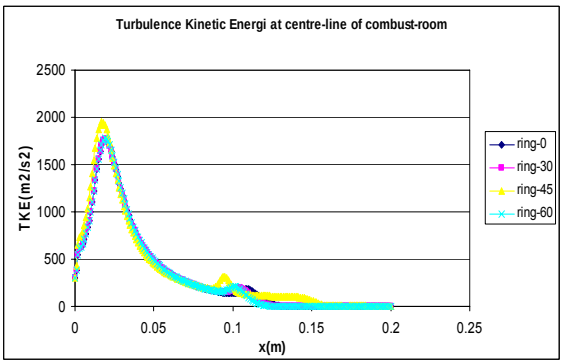

Figure 13.Turbulence Kinetic Energy at centre-line combust-room.

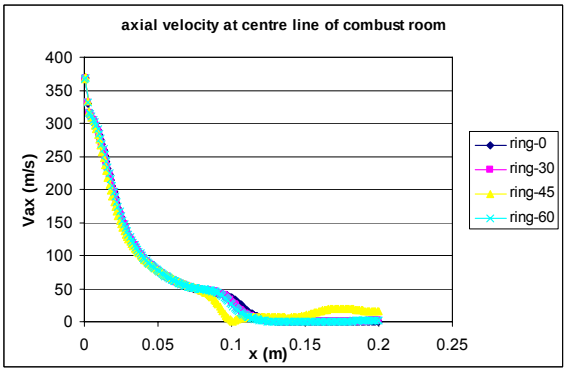

Figure 14.Axial velocity at centre-line combust-room.

Figure 14 shows axial velocity along the axis symmetry. In case of guide ring with 45^0 angles, the velocity initially reaches the minimum values which indicates that propane have radial flow, this support mixing between propane and air.

4. CONCLUSION

Air guide ring directors with angles of 45^0 to propane stream increases the diffusion process of air to propane. Numerical simulation proved that mass fraction of propane for 45^0 angles decreases faster than the other angle and the flow field has maximum turbulence kinetic energy distribution and reach minimum axial velocity earlier.

REFERENCES

1. Peter, N., Turbulent Combustion, Cambridge University Press, Cambridge, 2000, p. 238.
2. Stephen R.Turns, "An Introduction to Combustion", McGraw-Hill, Inc.(1996).
3. Cha M.S. and Chung S.H.,The Combustion Institute, 121-128 (1996)
4. L.K.Su,O.S.Sun, M.G.Mungal, Combustion and Flame 144(2006)494-512.
5. K.A.Watson, K.M.Lyons, J.M.Donbar, C.D.Carter, Combustion and Flame 119(1999)199-202.
6. C.Maurey, A. Cessou, B.Lecordier, D.Stepowski, Proc.Combust.Inst. 28 (2000) 545-551
7. Made K Dhiputra, Harinaldi, NK.Caturwati, "Characteristics of lifted flame at diffusion combustion of Propane with various dimensions of nozzles burner" Proceedings of The 1st International Meeting on Advances in Thermo-Fluids, Universiti Teknologi Malaysia, 2008.

ISSN 114-1284

Application of CFD software to analysis of air velocity and temperature distribution in hospital operating theater

Ispa Firmazona[1], Nasruddin[2], Budihardjo[2]

[1]*Faculty of Engineering*
Refrigeration and Air Conditioning Laboratory Mechanical Engineering Department
University of Indonesia, Depok 16424
Tel : (021) 7270011 ext 51. Fax : (021) 7270077
E-mail : kai_zona@yahoo.com

[2]*Faculty of Engineering*
Refrigeration and Air Conditioning Laboratory Mechanical Engineering Department
University of Indonesia, Depok 16424
Tel : (021) 7270011 ext 51. Fax : (021) 7270077
E-mail : nasruddin@eng.ui.ac.id, budihardjo@eng.ui.ac.id

ABSTRACT

Air flow distribution and temperature in the hospital operating theater play a very important role in maintaining staff and patient comfort. Air temperature and velocity inside the older operating theater hospital are not matching with given standards. These limitations are due to the site constraint and also financial aspect.

The FLOVENT is one of the Computational Fluid Dynamics (CFD) software which has proven its validity in simulating airflow distribution in operating theaters. The engineering judgment has to be carefully selected to a successful CFD modeling job and must be taken to include all the relevant physics in the model.

Model visualization and simulation result shows that many factor has to be taken into account before using the software. The appropriate selection of the design parameters such as temperature, velocity and volumetric flow of fresh air have to be clearly defined to ensure accurate results.

A CFD model of airflow distribution is developed and its validation with the existing operating theater is already conducted. Furthermore, this model can be used as a reference in the earlier design of air flow modeling in operating theater.

Model analysis and thermal behavior in one of hospital operating theater in Indonesia will be explained specifically in this paper.

Keywords: *Flovent, Ventilation, Operating Theater, Visualization Model, Laminar Flow, Clean Room.*

1. INTRODUCTION

One of the basic differences between the air conditiong systems for health care facilities including the operation room and that for other building types is the high risks of bacterial and viral infections into the rooms. Design and construction of the operation room have been regulated with some institutions in order to increase the hospital health management systems. Some technical specifications including other general requirements such as air conditioning system, ventilation and indoor air quality (IAQ) have been regulated with thoses institutions, but actually in some cases it is necessary to provide a specific design criteria for clean room or operating room.

The air conditioning system for clean room is designed for : maintaining the conditioned room temperature, relative humidity and filtering air to reduce the airborne particle contamination flowing into the room. The type of those airborne contaminants in the health care air conditioning system such as viable particle, which causes some infections and allergy for human. The examples of viable particle which are transported by air such as bacteria, fungi, spore and pollen. The airborne sources from outside air which could flow into the conditioned room are from air conditioning system, infiltration through window/door, piping system and hood. The viable particle could be controlled by air filtering system, positive pressure and isolation from all of infiltration sources. Meanwhile the particle sources from conditioned room/clean room itself are from human skin, breathing process, hair and cosmetic materials. The contaminated dust, particles control and air flow system are the main subjects to maintain the clean room conditions. The clean room performance conditions highly depend on quality and distribution of particle concentration, temperature, relative humidity, flow pattern and system construction.

The air conditiong and ventilation system for cleanroom which comply the medical and technical requirements is one the main aspects to improve public health services.

2. OPERATING THEATER

Operating room and operating theater are the special room which faciltitaed with some medical equipments to do some operations for the patient. Operating room is catagorized as cleanroom based on the guidelines and standards such as from US Federal Standard 209E (cancelled on November 29, 2001), BS 5295 and ISO 14644 Part 1 which can be defined as enclosed room where the airborne particle concentrations are controlled for a specific limit.

3. VENTILATION

The 100% fresh air system ventilation is normally required for health care facilities especially for cleanroom or operating theater. Air conditiong system could contribute to spread micro organisms. Normally in the healthcare air conditioning systems especially in cleanroom is equipped with some air filter with efficiency from 30%, 90% and 99.7% (HEPA). Air flow pattern inside the opearting room should flow from laminar flow canopy downward to operating table and then flows into return air grille and door. It is necessary to protect air change inside operating room with other rooms around the building. The air change factor is important for controlling temperature, relative humidity, to exhaust the anestetic gases dilluted in air, to reduce and remove bacterial contamination and also to control air movement in the mini zone, micro environment and sterilized zone.

ASHRAE has generally recommended for air ventilation in the cleanroom as follow : air change per hour between 20-30 times, air circulation inside the room is 80% of intake air volume, using filter with 90% and 99.7% efficiency which can filter particle with size 0.5 micron, positive air pressure inside the room 12.5 Pa (5 cm H_2O), relative humidity 40%-60% and inside room temperature around 20 $^oC \div 24\ ^oC$.

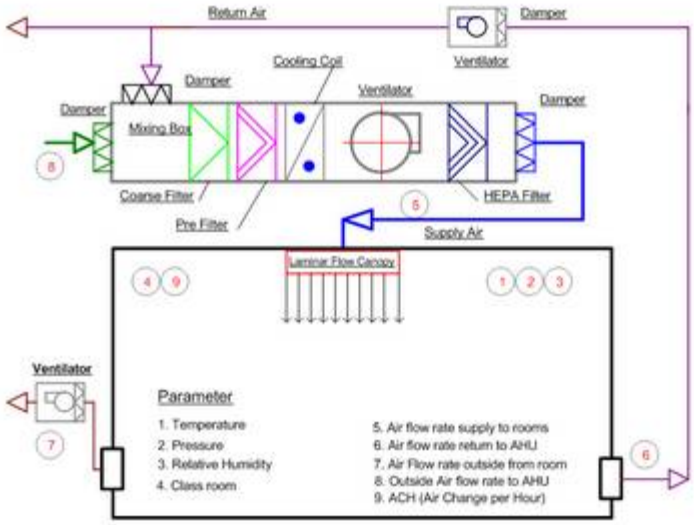

Figure 1. Typical Air Distribution system for Operating Theater

4. AIRFLOW MODELING

Flovent is 3D software using finite element method for *Computational Fluid Dynamics* (*CFD*) applications, developed by *The Mechanical Analysis Division of Mentor Graphics Corporation* from *United Kingdom* (former *Flomerics*).

This software usually uses as a simulation tool in the engineering design processes including heat transfer and fluid flow.

In air conditioning and ventilation system, Flovent could be used for temperature distribution optimization and contaminant control inside and outside the building. Air flow modelling could help the designer of air conditioning system for performance prediction of the air flow pattern in the clean room before the construction, the effect of room change architectural design and sufficient air change inside the room.

5. CASE STUDY

The temperature dan velocity distribution inside the operating room in one of the hospital in Jakarta is simulated by Flovent V7 with the following data :

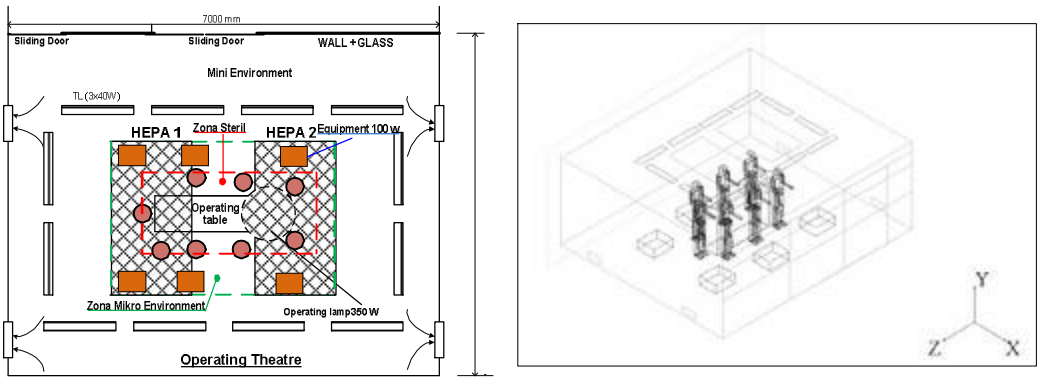

Figure 2. Operating Theater sketch and Model Visualisation

a) Room Dimension and Material
Operating room is located in the ground floor with volume 7 m x 6 m x 2.8 m.

Table 1. Dimension and item Operating Theater

Item	unit	Dimension
operating table	1	1900 mm x 500 mm x 1200 mm
operating lamp	1	300 mm x 300 mm x 100 mm
Doctor, nurse and patient	8	170 mm (5 ft 7 in) weight 77 kg (170 lb)
Overhead Lights	12	1000 mm x 200 mm
HEPA	2	2100 mm x 1200 mm
Exhaust	4	600 mm x 200 mm
others equipment	6	500 mm x 500 mm x 500 mm

b) Supply Air
Using 2 HEPA filters with the following specifications 1500 m^3/h with 25 ACH at temperature 20 °C

c) Exhaust
Four Exhaust with capacity 588 m^3/h.

d) Person
Three medical doctors, one anasthesist, one instrumention person, two nurses assistent (instrument), and one patient. Every person has average heat source 170 W

e) Lamp
Operating lamp 350 W and TL lamp 3 x 40W

f) Other electronic equipments
6 unit with 100 W/equipment

g) Operation table
Material alumunium

h) Cooling load estimation
Cooling load calculation is important to predict and estimate the heat generation inside the room and to select refrigeration equipments.

Table 2. Estimated of Cooling Load

item	unit	source (watt)	total source (watt)
Operating lamp	1	350	350
Overhead Lights	12	120	1440
People	8	170	1360
Others equipment	6	100	600
Total Cooling Load			3750

6. SIMULATION ANALYSIS

The initial data are collected from the operating room actual condition with assumption that outlet air distribution laminar flow canopy with unidirectional air flow and air temperature is same in all part of the room. Supply air intake flows into laminar flow canopy is designed for 3000 m^3/h at constant temperature 20°C.

From the above data, the simulated air flow velocity and air temperature are shown in the Figure 3 and Table 3.

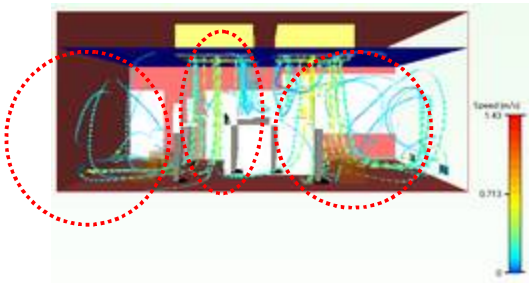

Figure 3. Flow distribution at first trial

Table 3. Mean temperature, pressure and velocity at the first trial

sumbu x	2,8	3	3,2	3,3	3,5	3,6	3,8	4	4,2	4,3	rata-rata
temperatur awal	20,5	20,9	21,4	22	23	23,3	23,2	22,6	21,8	21,6	22,03
pressure awal	39	39	38,9	38,9	38,9	38,9	38,9	39	39,1	39,1	38,97
velocity awal	0,275	0,175	0,107	0,0918	0,318	0,355	0,397	0,412	0,325	0,282	0,27

For the first simualation, the data are based on the actual conditions in the sample hospital with supply fresh air at 20^{o}C and debit 3000 m^{3}/h, with power for lighting 120 W.

The simulation result of air flow outside the laminar flow canopy (LFC) is shown that there are 3 parts of the flows : *non uni directional air flow* and even tends to form a *mixed flow* near the wall. It is because of the change of air flow after disturbance with some obstacles such as person, medical equipments, operation table, which cause turbulence around the wall. This phenomenon is possibly caused by the long distance between the two LFC and also mixed air flow. The outlet air velocity from LFC is around 0.30 ÷ 0.35 m/s and near the operating table around 0.27 m/s. Outlet average air temperature from LFC 20^{o}C and near the table is 22^{o}C. It is also shown that the pressure is 38.97 Pa inside the room but it does not comply with ASHRAE Standard which is 12.5 Pa at positive pressure.

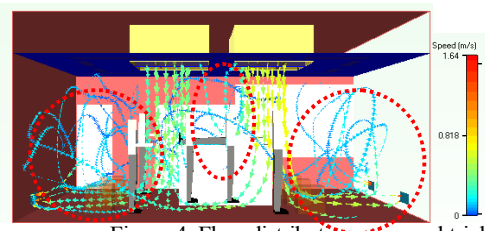

Figure 4. Flow distribution at second trial

Table 4. Mean temperature, pressure and velocity at the second trial

sumbu x	2,8	3	3,2	3,3	3,5	3,6	3,8	4	4,2	4,3	rata-rata
temperatur 1	20,5	20,9	21,6	22,3	22,9	23,1	23	22,9	22	21,9	22,11
pressure 1	28,9	28,9	28,9	28,9	28,9	28,9	28,9	28,9	29	29	28,92
velocity 1	0,29	0,185	0,11	0,091	0,215	0,216	0,297	0,329	0,33	0,37	0,24

In the second simulation we increased the outlet flow from exhaust and only 10% of return air. The result shows that air temperature and velocity tend to same as the first simulation but the pressure becomes 28.9 Pa. It is because the opening exhaust incraeses but not yet complied the ASHRAE Standard.

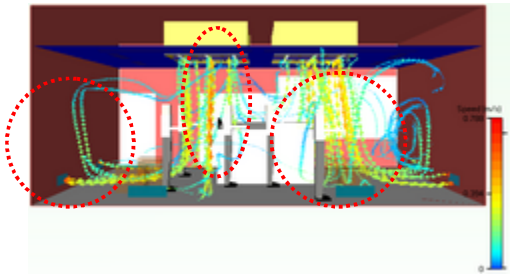
Figure 5. Flow distribution at third trial

sumbu x	2,8	3	3,2	3,3	3,5	3,6	3,8	4	4,2	4,3	rata-rata
temperatur 2	21	21,2	21,4	21,7	21,9	22	22,5	22,8	24,3	24,1	22,29
pressure 2	4,02	4,02	3.99	3.99	3.98	3,97	3,97	3,97	3,97	3,97	3,98
velocity 2	0,38	0,2081	0.18	0,172	0,19	0,215	0,32	0,153	0,104	0,09	0,20

Table 5. Mean temperature, pressure and velocity at the third trial

In the third simulation with increasing exhaust air flow and only 10% of return air and add the number of exhaust into 8 unit. It is shown that the flow is much better than before but the flow pattern is still *"non uni directional air flow"*, and average pressure inside the room decreases of 3.98 Pa.

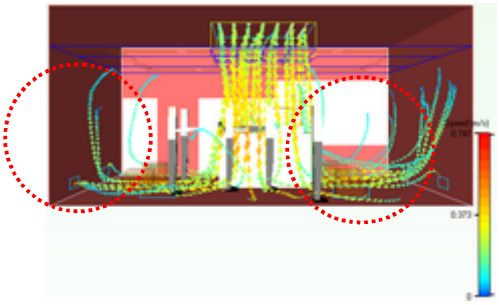
Figure 6. Flow distribution at fourth trial

Table 6. Mean temperature, pressure and velocity at the fourth trial

sumbu x	2,8	3	3,2	3,3	3,5	3,6	3,8	4	4,2	4,3	rata-rata
temperatur 3	20	20,1	20,8	20,5	21	21,1	22,1	22,3	25	24,4	21,73
pressure 3	72,7	72,7	72,6	72,6	72,6	72,6	72,6	72,6	72,6	72,6	72,62
velocity 3	0,29	0,247	0,19	0,192	0,2	0,218	0.31	0,208	0.189	0,106	0,21

In the fourth simulation with 1 HEPA, exhaust air flow with 20% return air and increasing exhaust into 8 unit. It shows that the flow pattern is *"uni directional air flow"* on the table surface where as the sterilzed place but still forms *"non uni directional air flow"* and average pressure 72.62 Pa.

Figure 7. Flow distribution at fifth trial

Table 7. Mean temperature, pressure and velocity at the fifth trial

sumbu x	2,8	3	3,2	3,3	3,5	3,6	3,8	4	4,2	4,3	rata-rata
temperatur 4	20	20,1	21	20,9	21,1	21,4	22,2	22,4	24,8	23,4	21,73
pressure 4	17,6	17,7	17,7	17,7	17,7	17,6	17,6	17,6	17,7	17,6	17,65
velocity 4	0,32	0,303	0,19	0,195	0,17	0,186	0,21	0,178	0,2	0,12	0,21

The fifth simualtion with 1 HEPA and exhaust air flow increasing, 10% return air and number of exhaust 4 unit. It is shown that flow pattern is "*uni directional air flow"* at the surface of the operation table and in the right hand side of the figure, but in the left "*non uni directional air flow"* and average pressure inside the room of 17.65 Pa where the ASHRAE Standard is 12.5 Pa.

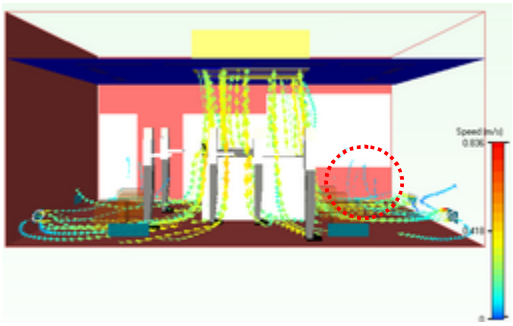

Figure 8. Flow distribution at sixth trial

Table 8. Mean temperature, pressure and velocity at the sixth trial

sumbu x	2,8	3	3,2	3,3	3,5	3,6	3,8	4	4,2	4,3	rata-rata
temperatur 5	20	20,1	20,3	20,4	20,9	21	22	22,3	24,2	24	21,52
pressure 5	11,7	11,8	11,8	11,8	11,8	11,8	11.8	11,7	11,7	11,7	11,76
velocity 5	0,302	0,245	0,2	0,196	0,301	0,219	0,301	0,205	0,57	0,134	0,27

In the sixth simulation with 1 HEPA and exhaust air flow, 10% return air and exhaust 4 unit. It shows that the flow pattern is "*uni directional air flow"* at all part of the room and average pressure 11.76 Pa as follows the ASHRAE Standard.

7. CONCLUSION

Model visualization and simulation using Flovent V7 as a CFD Model shows that pressure and temperature distribution in the operating room are not well confirmed with the requirements of any standard. The appropriate selection of the design parameters such as temperature, velocity and volumetric flow of fresh air have to be clearly defined to ensure accurate results.

The influence of difference design parameters on volumetric flow of supply air, layout of HEPA filter and position and number of return air grille can have a major impact on the air flow distribution pattern. It has been shown from the last trial that the flow has a type of unidirectional air flow.

REFERENCES

[1] Departemen Kesehatan RI: Keputusan Menteri Kesehatan RI No:1204/Menkes/SK/X/2004 Tanggal : 19 Oktober 2004 :PERSYARATAN KESEHATAN LINGKUNGAN RUMAH SAKIT

[2] Federal Standard 209 E, 1992 : Federal Standard Airborne Particulate Cleanliness in Clean Rooms and Clean Zones.

[3] ISO 14644-1, 1999: Cleanrooms and associated controlled environments--Part 1: Classification of air cleanliness.

[4] British Standard 5295,1989: Environmental cleanliness in enclosed spaces. General introduction, terms and definitions for clean rooms and clean air devices.

[5] DIN 1946-2, 1994-01 : Ventilation and air conditioning; technical health requirements (VDI ventilation rules).

[6] DIN 1946-4, 1999-03 : Ventilation and air conditioning - Part 4: Ventilation in hospitals (VDI Ventilation rules).

[7] ASHRAE HANDBOOK, 2007 : HVAC Applications

[8] FloVent V7, 2007 :The Mechanical Analysis Division of Mentor Graphics Corporation, United Kingdom.

[9] ASHRAE. 2003. HVAC Design Manual for Hospitals and Clinics. Atlanta : ASHRAE special project 91.

[10] Budihardjo. 2009. Aplikasi "FLOVENT V7" Sebagai Model Pola Distribusi Aliran Udara dan Temperatur Pada Perancangan Awal Operating Theater. Depok.: University of Indonesia.

Proceeding of the 11th International Conference on QiR (Quality in Research)
Faculty of Engineering, University of Indonesia, Depok, Indonesia, 3-6 August 2009
ISSN 114-1284

Optimal Tool Orientation for Positional Five-axis Machining of Molding Die Surface

Yeong Han Cho[1], Seong Jin Yang[2], Hyun Wook Cho[3], Sang Hoon Lee[4], Jung Geun Lee[5], Jung Whan Park[6]

School of Mechanical Engineering,
Yeungnam University, Gyeungsan, Korea
+82-53-810-3524
[1]E-mail: tigerjr@ynu.ac.kr
[2]E-mail: theshell@ynu.ac.kr
[3]E-mail: hyun8046@nate.com
[4]E-mail: uandi012@ynu.ac.kr
[5]E-mail: willtechcom@chol.com
[6]E-mail: jwpark@yu.ac.kr

ABSTRACT

The paper presents the study on a CAPP(computer-aided process planning) system that suggests optimal tool orientation with which positional five-axis machining of sculptured surface in a molding die manufacturing. The positional five-axis machining is operated on a five-axis NC machine, with the cutting tool orientation being fixed during the cutting operation. This type of machining operation is effective in machining separated areas (geometric features) on a molding die. The optimal tool orientation for a machining area is obtained through two steps: (1) the local optimal tool orientation on each cutter-contact point is obtained, which is based on the machinability condition, then the angular range of global tool orientation is obtained by the union of the local angles; (2) the tool length map for the indicated global tool orientation range is computed via interference check (collision and stroke-over), and the tool orientation with the minimum tool length is selected as an optimal tool orientation. The research was implemented on the basis of a commercial CAM system(I-Master) in the Windows XP environment, and was tested for positional five-axis machining of molding dies for automotive parts in a local company.

Keywords

Positional 5-axis machining, optimal tool orientation angle, CAPP

1. INTRODUCTION

Five-axis machining of molding dies has more benefits such as fewer set-ups and better machining accuracy resulting from shorter tool length [1,2]. It may be classified into positional five-axis and continuous five-axis depending on cutter orientation change (see Figure 1). The positional five-axis machining is a fixed-axis machining on a five-axis NC machine with the cutter-axis tilted, while the continuous five-axis machining is the conventional simultaneous five-axis machining.

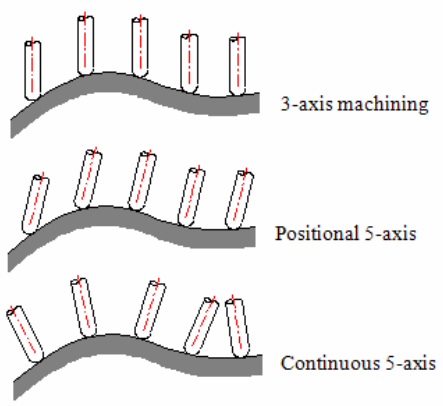

Figure 1: Machining types

Machining process of a molding die consists of several unit machining operations(UMOs), which is a combination of conventional three-axis, positional and continuous five-axis machining operations. An NC programmer determines most suitable machining type to each machining feature area.

Simultaneous five-axis machining can adaptively change cutting speed and tool posture at each CC(cutter contact) point by continuously varying tool-orientation, but it requires somewhat complicated interference avoidance and computing time. It should be noted that the positional five-axis machining is well applied to machining of molding die surface, due to consistent tool posture and simple interference avoidance compared to continuous five-axis machining [3].

According to a commercial CAM software developer [4], distinct machining types on a five-axis machine are: 73% of positional five-axis machining, 22% of multi-face three-axis machining, and 5% of continuous five-axis machining. It can be said that continuous five-axis machining operation using a five-axis machine may well be applied to where fixed-axis

machining is either infeasible or inefficient.

The tool length should be as short as possible without interference (e.g., collision) in order to enhance machining accuracy and surface finish, due to tool deflection and chattering. In positional five-axis machining of a certain surface area, it is imperative to select a tool orientation that minimizes tool length of the applied cutter but also causes no collision. A few existing commercial CAM systems provide such functionality, but requires complicated user interactions or fairly much computing time.

The research developed a system that computes the optimal tool-orientation with minimum tool-length for a ball-end milling case, given a surface area to be machined. Section 2 describes the key procedure, followed by an illustrated case in Section 3.

2. CONVENTIONAL PROCESS

A conventional process to determine the tool orientation and length by which a certain surface area is to be machined is described in figure 2. Tool orientation is usually designated by setting up a local coordinate system in a commercial CAM system. As shown in the figure, the process requires NC programmer's insight and experience, tool-path generation and collision avoidance through interactive as well as iterative operations.

The similar process should be repeated for each feature surface that needs positional five-axis tool-path generation, which is tedious and time consuming job. In addition, it does not always generate optimal tool orientation with minimum tool length, which may result in non-optimal machinability.

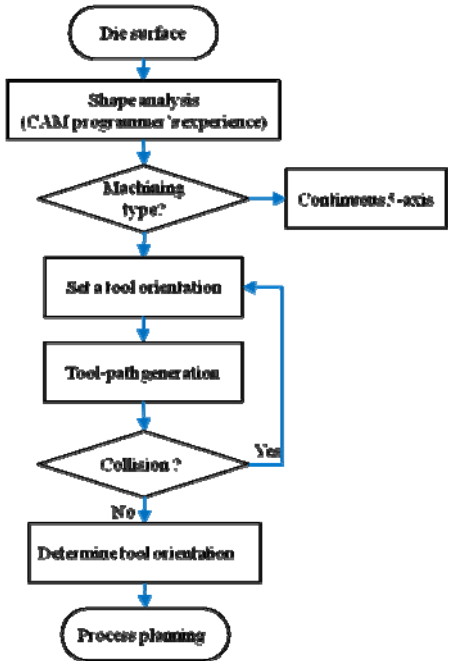

Figure 2 : Conventional process of work coordinate set-up

3. PROPOSED PROCESS

3.1 Overall view

Figure 3 depicts overall procedure of the proposed process, which is summarized as follows:

< Phase 1 >
(1) Sampling CC points on the defined surface area,
(2) For each CC point, determine preferred tool-orientation range,
(3) Obtain overall preferred tool-orientation range for all CC points,
< Phase 2 >
(4) Select feasible tool-orientation range from the preferred tool-orientation range for all CC points by checking stroke-over and collision,
(5) Determine the optimal tool-orientation angle with minimum feasible tool-length.

In the 1st phase, the preferred tool-orientation range for each CC point is determined based on a previous study which considered cutting force and surface finish in a ball-end milling case [5]. In the 2nd phase, the feasible tool-length for a specified tool-orientation is computed via interference check (i.e., stroke-over and collision check), the tool-orientation with minimum feasible tool-length is selected as an optimal tool-orientation. The collision check process considers cutter shank, tool holder, machine spindle, and machine table. Following sections describe more details about the process.

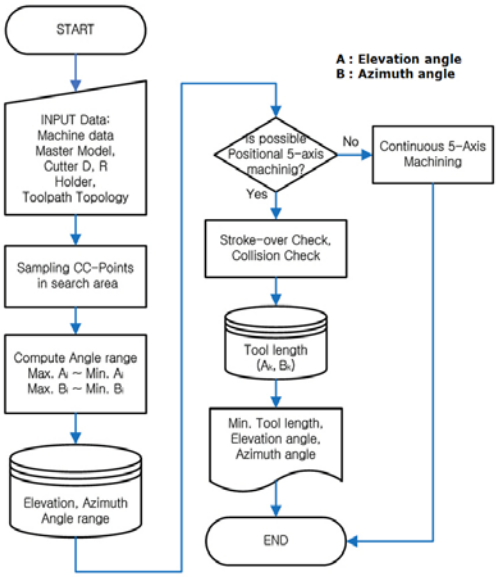

Figure 3 : Overall procedure

3.2 Phase 1: preferred tool-orientation

The 1st phase of the overall process determines preferred range of acceptable tool-orientation by aggregating each preferred tool-orientation at a single CC point. A previous study [5] depicted that the acceptable tool inclination angle (ball-ended milling) at a CC point should be 15˚ to 45˚ measured from the surface normal, which is based on cutting force and surface finish. This concept can be represented by a cone (see figure 4), since the applied cutter is a ball-ended mill. Being measured in the local coordinate system of a CC point, the tool inclination angle is converted to tool-orientation of the global coordinate system, which is represented by elevation and azimuth angles (see figure 5). The elevation and azimuth angles (A,B) corresponding to a tool inclination vector **n'** is represented by equation (1).

$$\text{A (elevation angle)} = a\tan 2(\sqrt{n'^2_x+n'^2_y},\ n'_z) \quad \text{(1a)}$$

$$\text{B (azimuth angle)} = a\tan 2(n'_y,\ n'_x) \quad \text{(1b)}$$

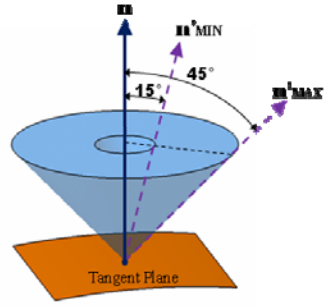

Figure 4 : Local acceptable range of tool-orientation

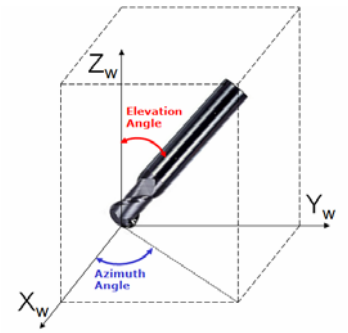

Figure 5 : Elevation and azimuth angles to define tool-orientation

The overall range of acceptable tool-orientation for all CC points is obtained by summing up each tool-orientation range of a single CC point, which is represented by ranges of elevation and azimuth angles such as $(A,B)_{MIN}$~$(A,B)_{MAX}$. Figure 6 depicts a schematic diagram of the phase 1.

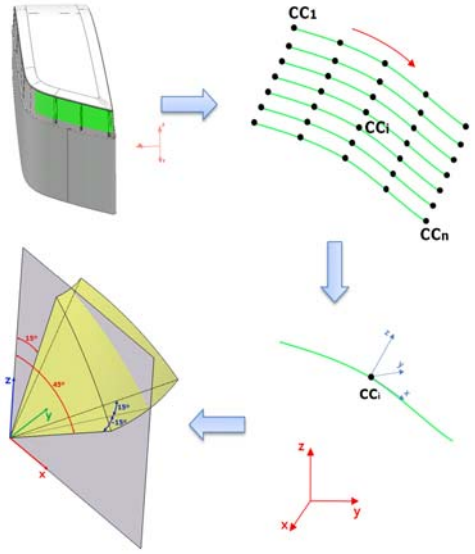

Figure 6 : Overall preferred range of tool-orientation

3.3 Phase 2: optimal tool-orientation

The overall preferred range of tool-orientation $(A,B)_{MIN}$~$(A,B)_{MAX}$ obtained in the 1st phase can be thought of as an initial filtering out process for efficient computation. The 2nd phase determines the optimal tool-orientation by computing minimum feasible tool-length at each tool-orientation among the given preferred range. The procedure is summarized as follows:

(1) For a tool-orientation $(A,B)_k$ among the overall range $(A,B)_{MIN}$~$(A,B)_{MAX}$, compute feasible tool-lengths for all CC points, and find the minimum tool-length L_k,
(2) Find the minimum tool-length L_m at $(A,B)_m$ among L_k, and set the optimal tool-orientation to be $(A,B)_m$.

The feasible tool-length at a tool-orientation $(A,B)_k$ at CC point is obtained via interference check including machine axis stroke-over, machine collision and tool collision. The machine axis stroke-over can be verified by considering inverse kinematics of the target NC machine. The machine and tool collision consider collisions between components such as machine spindle, table, cutter shank, and tool holder. The tool-length computation is based on the previous study [6]. Figure 7 describes overall procedure of phase 2.

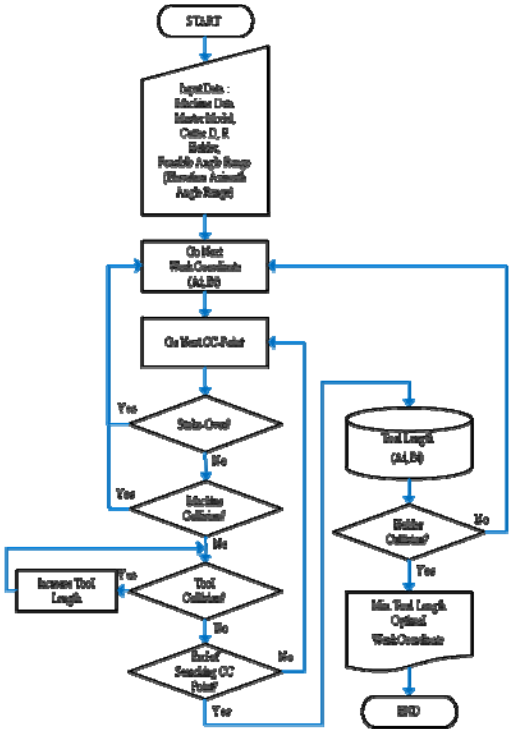

Figure 7 : Search of the optimal tool-orientation

4. ILLUSTRATED EXAMPLE

The proposed system has been implemented by Visual C++ and OpenGL in Windows XP environment. Figure 8 shows an example molding die surface, where the red colored face is the machining area. Figure 9a depicts preferred tool-orientation range (in elevation & azimuth angles), figure 9b illustrates the optimal tool-orientation.

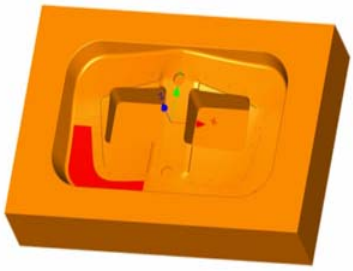

Figure 8 : Molding die surface and machining area

(a)

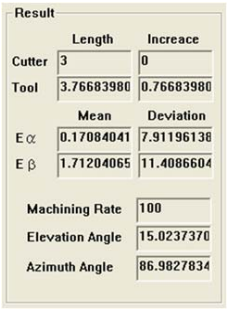

(b)

Figure 9: Preferred range of tool-orientation and search result

5. DISCUSSION

The research has developed a system that determines the optimal tool-orientation for positional five-axis machining of molding die surface. It provides a CAM programmer with an optimal work coordinate system and minimum tool-length information, thereby enabling objective and efficient process planning for five-axis machining tool-path generation.

It should be noted that the tool-length is not the only factor affecting machinability. As a previous study depicts [5], the tool inclination angle itself is an imperative machining condition. Therefore, another criterion including tool-length and tool inclination angle can be considered as an error function at a CC point as follows:

$$\varepsilon_T = \omega_\alpha\left(\frac{\varepsilon_\alpha}{\Delta a}\right) + \omega_L\left(\frac{\varepsilon_L}{\Delta L}\right);$$

where ε_α = angular deviation of inclination angle from given value,
ε_L = tool-length deviation (L_i-L_0, L_0 = minimum tool-length),
ω_α, ω_L = weighting factors,
$\Delta\alpha$, ΔL = scaling factors.

Considering the above combined error function at each CC point should be dealt in the further research.

REFERENCES

[1] Mason, F., "5×5 for High-productivity Airfoil Milling", American Machinist, Nov, pp.37-39, 1991.
[2] Tonshoff, H.K., Hernaadex-Camacho, J., "Die manufacturing by 5-and 3-axis milling", Mechanical Working Technology, Vol.20, pp.105-119, 1989.
[3] Hopkin, B., "Benefits of positional five-axis machining", Moldmacking Technology, May 2005.
[4] Delcam Korea, http:\\www.delcam.co.kr.
[5] Kang, I.S., Kim, S.W., Kim, J.S., Lee, K.Y., "A study on the machining characteristics according to tool position control for

5-axis high speed mold machining", Journal of Korea Society of Machine Tool Engineers, Vol.16, No.5, pp. 63~69, 2007.

[6] Lee, J.G., Yang, S.J., Cho, Y.H., Yoo, S.K., and Park, J.W., "Development of a System to Generate Tool Orientation Information for Positional 5-Axis Machining of Die and Mold", Computer Aided Design and Applications, Vol. 5, pp. 434-441, 2008.

THE EFFECTS OF ETHANOL MIXTURE IN GASOLINE (BIOETHANOL) E-20 TO MOTORCYCLE PERFORMANCE

Lies Aisyah[1], Riesta Anggarani[2], Lutfi Aulia[3]

[1]*KPRT Aplikasi Produk*
PPPTMGB "LEMIGAS", Jakarta 12230
Tel: (021) 7394422 ext. 1645. Fax: (021) 7398278
E-mail: laisyah@lemigas.esdm.go.id

[2]*KPRT Aplikasi Produk*
PPPTMGB "LEMIGAS", Jakarta 12230
Tel: (021) 7394422 ext. 1645. Fax: (021) 7398278
E-mail: riesta@lemigas.esdm.go.id

[3]*KPRT Aplikasi Produk*
PPPTMGB "LEMIGAS", Jakarta 12230
Tel: (021) 7394422 ext. 1639. Fax: (021) 7398278
E-mail: laulia@lemigas.esdm.go.id

ABSTRACT

One of biofuel which is possible to be used as a replacement fuel and as a mixture for gasoline is ethanol, due to its characteristics similarity with gasoline. This research purposed to know the performance of RON 88 gasoline and ethanol fuel mixture (bioethanol) at 20% (E-20) ethanol concentration on 4 stroke engine.

The research started with conducting the physical-chemical characteristic test of RON (Research Octane Number) 88 gasoline and bioethanol E-20. And then, the performance test conducted to those fuel using two motorcycles on 5000 km road test.

There were two cycles of 5000 km road test for each motorcycle, using RON 88 gasoline at the first cycle as reference and using bioethanol E-20 at the second cycle. In the beginning of each cycle, the overhaul and engine spare part replacement for each motorcycle were conducted to optimize the motorcycles engine. In each cycle, at 2500 km cover distances, the performance test to measure acceleration power, fuel consumption, and emission rate were conducted using chassis dynamometer test engine.

The result showed that the use of bioethanol not only affected the physical-chemical characteristic of gasoline but also affected the fuel performance test. The use of bioethanol E-20 had increase the fuel consumption by 27.15%. For the emission test, the use of bioethanol had decrease the CO emission by 35.80%. The CO_2 emission was also decrease by 22.27%. The hydrocarbon (HC) particulate emission was decrease by 18.5%, while the NOx emission was decrease by 53.7%. The bioethanol E-20 performance also showed by the acceleration and power, that in general, the use of bioethanol had decrease these two parameters of the motorcycles tested.

Keywords
Bioethanol, engine, performance, road test, RON 88 gasoline

1. INTRODUCTION

During the past five years, Indonesian oil production has been declining due to the natural decline of oil reservoirs on production wells. On the other hand, the increase of Indonesian population has intensified the need of transportation means and industry activities that implies to the rise of national refined fuel oil (BBM) consumption and demand. In order to meet the fuel demand, the government has to import some fuel. According to the Directorate General of Oil and Gas, the import of petroleum keeps rising significantly from 106.9 million barrels in the year 2002 to 116.2 million barrels in 2003 and 154.4 million barrels in 2004 [1].

By the end of 2007, fuel consumption is estimated to have reached 1.189 million barrels per day and will continue to increase in line with the population growth rate reached 1.6% per year. Currently, the highest fuel consumption in Indonesia is in the transportation sector. Data from the Ministry of Energy and Mineral Resources (DESDM) as in Table 1 shows the consumption of gasoline for transportation in Indonesia

has a tendency to continue to increase in the period 2000 – 2007 [2].

Table 1 : Indonesian fuel consumption in the year 2000-2007

Year	Fuel Consumption (kL)
2000	12.059.026
2001	12.705.861
2002	13.323.304
2003	14.211.145
2004	15.928.928
2005	16.959.594
2006	17.068.237
2007	17.878.569

By means of those conditions, the government has disseminated a plan to reduce the dependence of Indonesia upon refined fuel oil by introducing President's regulation of Number 5, 2006 pertaining to National Energy Policy to develop an alternative energy as a substitution for refined fuel oil. Despite the fact that the policy stresses on the use of gas and coal, this policy also states the use of renewable energy resources such as biofuel as an alternative energy to replace fossil fuels. The Indonesian government has also given a serious concern of biofuel development by issuing President Instruction of No. 1, 2006 on 25 January 2006 about providing and using biofuel as an alternative energy.

In this study, fuel that examined is bioethanol for gasoline substitution. Bioethanol is an alcohol compound, in this case ethanol (C_2H_5OH), which is made from the fermentation agriculture products, so that become the renewable energy. Indonesia is rich with natural resources to produce ethanol, for example, sugar cane, maize, and cassava. We must learn this possibility so that it can produce profit as big as for the welfare of the Indonesian people.

From previous studies that have been done show that the performance of motorcycle using alcohol as fuel is close to the performance of the motorcycle using fuel gasoline [3]. The research purposed to determine the performance (acceleration, power, specific fuel consumption, and exhaust emissions) of gasoline RON 88 mixture with 20% ethanol (bioethanol) E-20 when used on a 4 stroke engine motorcycle.

2. EXPERIMENTAL METHODS

Research begins with the physical-chemical characteristics of RON 88 gasoline, the ethanol FGE with purity 99.5% volume, and gasoline-ethanol mixture in the percentage of 20% ethanol (E-20). Physical-chemical characteristics tested include distillation, water contents, oxygen contents, copper strip corrosion, oxidation stability, Reid vapor pressure, density, and octane number. Testing method used in this research accordance with the specification of gasoline in Indonesia, which is set by the government.

Further test is the 4 stroke engine motorcycle (as seen in Table 2) performance test using a static test bench chassis dynamometer. Prior to the performance test, those motorcycle were over haul and there were replacement of spare part to the new one. The expectation was the engine condition would have optimal performance [4]. After finished all the tests, the road test was been done for each motorcycle as far as 5.000 km.

Table 2 : Technical specification of fuel gasoline vehicles

No.	Description	Motorcycle 1	Motorcycle 2
1.	Engine Type	4 Stroke	4 Stroke
2.	Manufacturing Year	2005	2005
3.	Volume of Cylinder	125	110
4.	Capacity of Lubricant	0.8	0.8

Road test for each motorcycle consists of 2 cycle. First cycle, motorcycle is using RON 88 gasoline as its fuel. Second cycle, motorcycle is using bioethanol (E-20) as its fuel. After the distance cover 2.500 km, there were performance tests for both motorcycles using chassis dynamometer test bench.

Table 3 : Physical-chemical characteristic of RON 88 Gasoline, bioethanol E-20, and pure ethanol.

Fuel Characteristics	Result Analysis			Limit *)		ASTM Methods
	Gasoline	E-100	E-20	Min.	Maks.	
Research Octane Number	88,3	> 118	96,3	88,0	-	D 2699
Oxidation Stability, merit	> 360	> 360	30	480	-	D 525
Oxygen Content, %m/m	-	34,73	7,34	-	2,7	D 4815
Distillation :						D 86
10% vol. evaporation, ^oC	50,0	77,2	49,0	-	74	
50% vol. evaporation, ^oC	80,5	77,3	67,0	88	125	
90% vol. evaporation, ^oC	154,0	77,4	150,5	-	180	
Final Boiling Point, ^oC	186,0	82,2	185,5	-	215	
Residue, % vol.	1,0	1,0	1,0	-	2,0	
Reid Vapor Pressure, kPa	56,5	19,29	64,75	-	62	D 323
Density @ 15^oC, kg/m^3	730,7	793,8	746,3	715	770	D1298/D4052
Water Content, % volume	NIL	NIL	NIL	-		
Copper Strip Corrosion, merit	1a	1a	1a	Class 1		D 130

***)** Indonesian RON 88 Gasoline Spesification [5]

Performance test conducted in the chassis dynamometer that has following technical specifications.

- Brand: Dynojet
- Type: 250i
- Year: 2004

Testing equipment with the above parameters is used to measure speed and acceleration, whereas specific fuel consumption (SFC) and emission levels conducted in the laboratory performance of Applications Product Research Program Group, LEMIGAS. Specific fuel consumption and emissions tests were conducted on the condition of the idle position (neutral gear).

Specific fuel consumption method test is explained as follows. Motorcycle switched on idle position. Measure the fuel that will be tested with a 100 mL cylinder graduate. Use a fuel hose to connect the cylinder graduate with motorcycles carburettor. Note the time that needed to make 100 mL of fuel in the cylinder graduate out. Specific fuel consumption is calculated with the formula:

SFC (L / hr) = 0.1 x 3600/time (seconds) [4]

Emission test conducted in a way to measure the actual CO, CO2, HC, and NOx in the motorcycle exhaust output using *Autocheck* exhaust gas analyzer.

3. RESULTS AND DISCUSSION

3.1 Physical-Chemical Characteristics

In Table 3 it can be seen the physical-chemical characteristics of RON 88 gasoline, bioethanol E-20, and pure ethanol. The distillation parameter of 50% distillate (T50) of E-20 did not meet the specifications set by the government. T50 distillation effect on the motorcycle acceleration. Since the T50 of E-20 was lower than gasoline, it was predicted that in the performance test, motorcycle using bioethanol would have lower acceleration than the one using RON 88 gasoline [6].

Furthermore, oxygen content exceeds the E-20 specification because ethanol is one of the oxygenat which can increase the amount of oxygen in the fuel. The presence of oxygen will affect the formation of deposits in the combustion chamber because the oxidation reaction will occur and resulted oxide in the form of a deposit. The formation of this deposit can only be viewed with the rating engine which is not done in this research.

In addition, oxidation stability is also outside of specifications related to the existence of oxygen in E-20. This states that the bioethanol is easier to oxydize than gasoline. The result is the same as the influence of high oxygen contents, which is the formation of deposits in combustion chamber [6].

On the other hand, the addition of ethanol gives a benefit as seen in the increasing of gasoline octane number. With the addition of 20% ethanol in RON 88 gasoline, research octane number of bioethanol become 96,3 equivalent to RON 95 gasoline. The increase of octane number can occur because ethanol has a higher octane number than RON 88 gasoline, which is > 118.

3.2 Acceleration

3.2.1 Acceleration Rate

Acceleration rate is measured from minimum torque (gear 1) until the motor reach maximum torque (gear 4) at a certain speed. Motor acceleration is measured by using chassis dynamometer test bench. The results showed 4.48% decrease in the acceleration rate. This is shown by Figure 1.

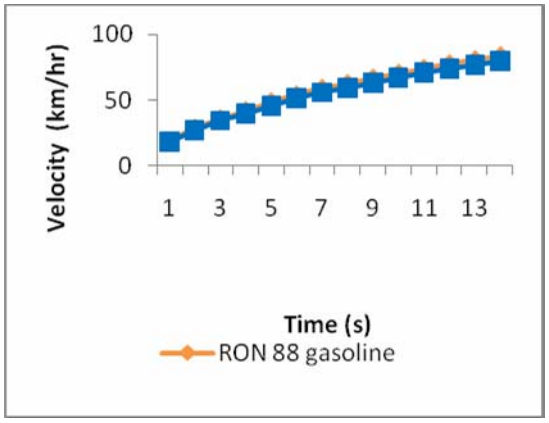

Figure 1 : Effect of bioethanol E-20 to acceleration time

3. 2. 2 Acceleration Power

Results from the chassis dynamometer test also indicate the decreasing of acceleration power in the motorcycle. The effect of bioethanol E-20 mixture in RON 88 gasoline decreased the acceleration power 2.24 % as showed in Figure 2.

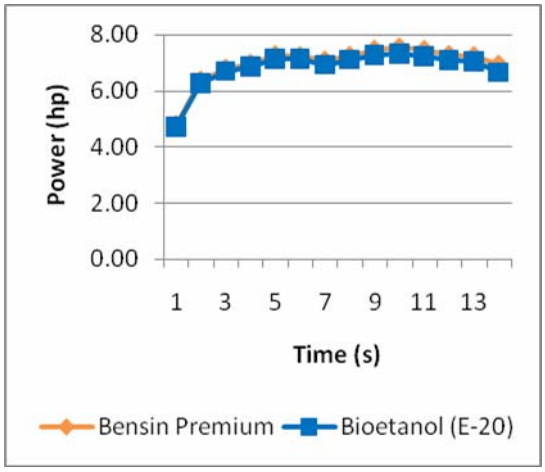

Figure 2 : Effect of bioethanol E-20 to acceleration power

3.3 Fuel Consumption

To see the effect of bioethanol (E-20) as a motorcycle fuel compare to RON 88 gasoline, the fuel consumption measurements carried out on the idle condition. This is to avoid the influence of external factors that can reduce the measurement accuracy. The results showed that the use of bioethanol (E-20) as a motorcycle fuel increase 27.15% consumption when compared to RON 88 gasoline. This is shown by Figure 3.

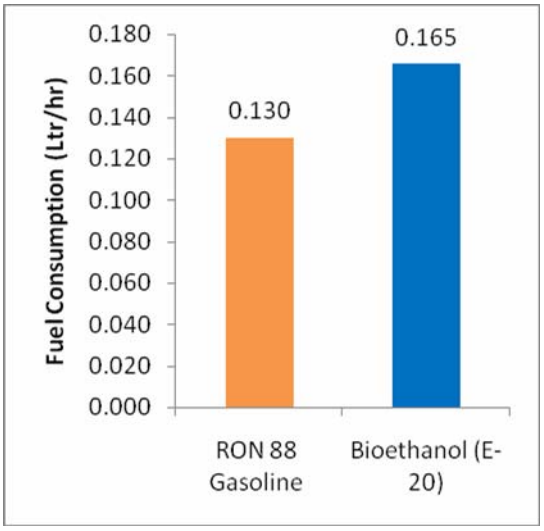

Figure 3 : Effect of bioethanol E-20 to specific fuel consumption

One of the causes of increased fuel consumption when using bioethanol is the calorie of bioethanol is lower then the calorie of gaoline. In addition, there are differences of physical-chemistry characteristics of the fuel such as viscosity and distillation.

3.4 Exhaust Gas Emissions

Exhaust gas emission tests on motorcycle were conducted on the condition of the idle position. Parameter of gas emissions that are measured consist of carbon monoxide (CO),carbon dioxide (CO_2), hydrocarbon (HC), and nitrogen dioxide (NOx). From the results of the test indicates the use of bioetanol gives a positive effect on the environment. There is a decline of bioethanol's exhaust gas emissions compared to RON 88 gasoline. CO emission is lower 35.8%, CO_2 emission is lower 22.26%, HC is lower 18.5%, and NOx is significantly decrease to 53.7%. This is shown in the Figure 4 to Figure 7.

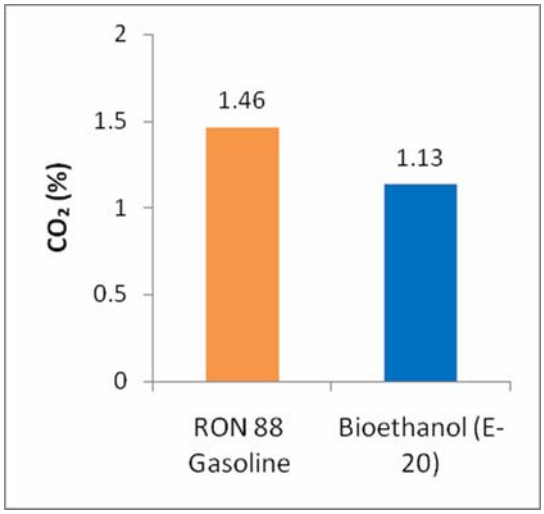

Figure 4 : Effect of bioethanol E-20 to the decline of CO_2

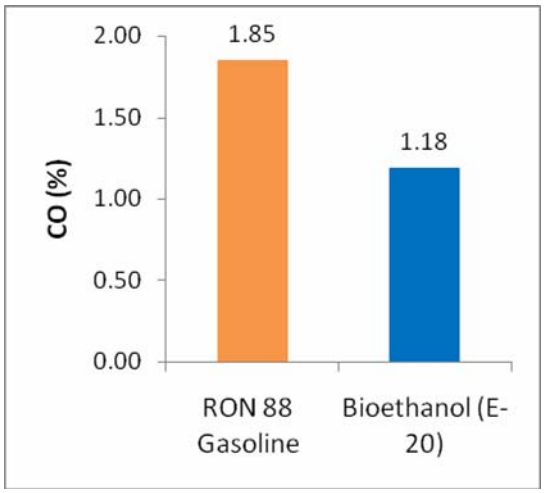

Figure 5 : Effect of bioethanol E-20 to the decline of CO

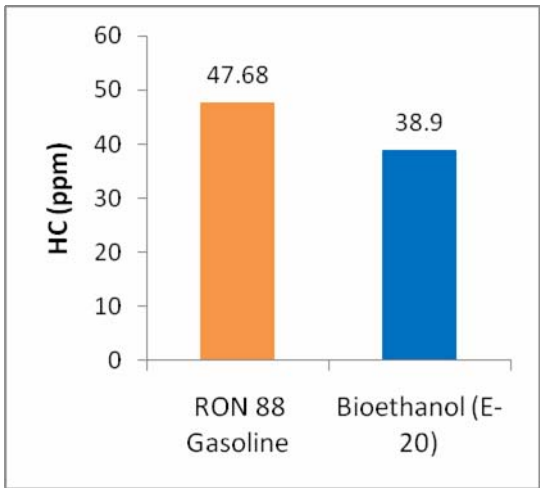

Figure 6 : Effect of bioethanol E-20 to the decline of hydrocarbon

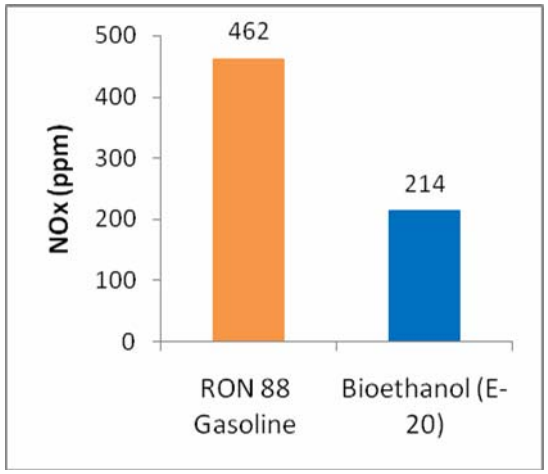

Figure 7 : Effect of bioethanol E-20 to the decline of NOx

4. CONCLUSION

1. Some parameters of phisycal-chemical characteristic of RON 88 gasoline were changed when mixed with ethanol:
   a. Octane number increased
   b. Distillation at T50 decreased
   c. Oxygen content increased and related to the decreasing of oxidation stability

2. Effect of ethanol addition in RON 88 gasoline to motorcycle performance can be defined into three parameters:
   a. Motorcycle acceleration :
      - Acceleration rate decreased to 4.48%
      - Acceleration power decreased to 2.24%
   b. Specific fuel consumption of motorcycle using E-20 is 27.15% higher than RON 88 gasoline.
   c. Exhaust gas emissions of E-20 compare to RON 88 gasoline is lower 35.8% of CO, 22.26% of CO_2, 18,5% of HC, and 53.7% of NOx.

REFERENCES

[1] A. Shintawaty, "The Prospect of Biodiesel and Bioethanol Development as the Alternative Fuel in Indonesia," *Economic Review*, no. 203, March 2006.
[2] Ministry of Energy and Mineral Resources, "Key Indicator of Indonesia Energy and Mineral Resources", Centre for Data and Information on Energy and Mineral Resources, 2007.
[3] Riesta A, et.al, "Study on The Bioethanol Application as Motorcycle Fuel and Its Effect On The Lubrication System" (in Bahasa), LEMIGAS Study Report, Dec 2008.
[4] Pallawagau La Puppung, "Fuel Consumption Analysis of Gasoline Vehicle using Chassis Dynamometer" (in Bahasa), *Lembaran Publikasi LEMIGAS*, vol. 39, no.1, pp. 26-36, 2005.
[5] Indonesian RON 88 Gasoline Spesification based on SK Dirjen Migas No. 3674K/24/DJM/2008 (in Bahasa), 17 March 2006, www.migas.esdm.go.id
[6] E. Jasjfi, "Development of Gasoline Quality Using Oxygenates" (in Bahasa), Material Sheet on The Course of Fuel and Lubricant Effect on The Engine Performance, LEMIGAS, 1991.

ISSN 114-1284

Production Sharing Contract (PSC) Scheme Model For Coalbed Methane (CBM) Development

Mahmud Sudibandriyo, Lestantu Widodo

Department of Chemical Engineering, Faculty of Engineering
University of Indonesia, Depok 16424
Tel : (021) 7863516. Fax : (021) 7863515
E-mail : msudib@che.ui.ac.id

ABSTRACT

Due to declining of oil and gas production and increasing the demand, in 2006, the Government of Indonesia issued Regulation Number 033/2006 to encourage the development of Coalbed methane (CBM) for alternative energy sources. Regarding to this issue, some specific terms and conditions must be applied for the CBM contract, therefore, an economic calculation model is needed to be used as a reference in evaluating or appraising CBM working area blocks in bid. In this study, a suitable model for CBM Production Sharing Contract (PSC) scheme is developed by modifying appropriate terms and conditions in economic model for oil and gas contract. CBM development scenario in South Sumatra is used for an example case with two base scenarios. In this case, total gas production during 23 years of operation is estimated to be 609,000 MMScf, while total expenditures is about US$ 745,130,000. In South Sumatra - Case I, where First Trenched Petroleum (FTP) is set 5% (shareable), Cost Recovery Ceiling (CRC) is 100% for 1-5 years and 90% for 6-end years, Split (after tax) is 55:45, Tax 44%, and Price of Gas is US$ 4.3 /MMBTU, the results show that Internal Rate of Return (IRR), Pay Out Time (POT), Net Present Value (NPV) @ 10% p.a and % profit for contractors are 12.9%, 15.4 years, US$ 44,000,000 and 41.87% respectively; while NPV @ 10% p.a and % profit for Government are US$ 160,000,000 and 58.13% respectively. Furthermore, our sensitivity analysis shows that yearly gas production and gas price are very sensitive economic parameters upon the change of IRR, NPV, and Government take, while Split and CRC are sensitive policy parameter upon the change of IRR and Government take. In order to make IRR close to 20%, the only way is to increase the wellhead price gas to be US$ 7.00/MMBTU. No policy parameters can be used to obtain this value.

Keywords: *Coalbed Mathane (CBM), PSC, economic evaluation, economic parameter, policy*

1. INTRODUCTION

Indonesia possesses in place CBM resources potential to a number of 453 TCF [1,2,3]. Assuming 10% of this value, or as much as 45 TCF, can be produced, Indonesia will not be bothered anymore with the issue of increasing energy demand. Therefore, to boost the development of CBM for alternative energy sources, the Government of Indonesia issued Regulation Number 033/2006.

The regulation for CBM production is similar to the one applied in the production of oil and conventional natural gas, using a production sharing contract (PSC) scheme. The only difference is that in the CBM development, specific characters such as cost and longer time needed for production need to be considered. Therefore, an economic calculation model is needed as tool for the government to evaluate and to estimate the value of the blocks offered. This model can be developed from an economic calculation model usually used for conventional natural gas by modifying the model with specific requirement and characteristics for the CBM production. This model should be able to simulate the best scheme for the CBM production sharing contract that can satisfy both government and investor.

2. METHODS OF STUDY

The scheme of the study can be illustrated in Figure 1, and described as folllows.

a. Collecting data of typical CBM dewatering and gas production, estimated cost parameters which has been evaluated based on a pilot project. These data include the data obtained from the CBM field development in South Sumatra [4,5]. The cost parameters considered in this study include:
   - Number of wells
   - Annual gas production
   - Water gas production

- Production facilities (well facilities, piping network, future plan (compressor, process facilities, etc)
- Project investment cost, including:
  - Well drilling and related facilities
  - Gathering station
  - Low pressure compressor
  - Production tools and gas sales compression system
  - Tangible, intangible, capital and non capital project cost applied to the *PSC* accounting
- Depreciation schedule for tangible and capital cost according to *PSC*
- Operating Cost including:
  - Well maintenance
  - Production cost
  - Processing unit
  - Water treatment and Compression/ gas transportation

b. Reviewing the above data, and selecting appropriate production and development cost parameters
c. Modifying the model from oil and gas economic calculation by using appropriate parameters applied for CBM production
d. Economic evaluation of CBM field development including IRR, POT, and NPV.
e. Perform sensitivity analysis of economic calculation to obtain the most affecting variables upon economic parameters.
f. Making conclusions an recommendations

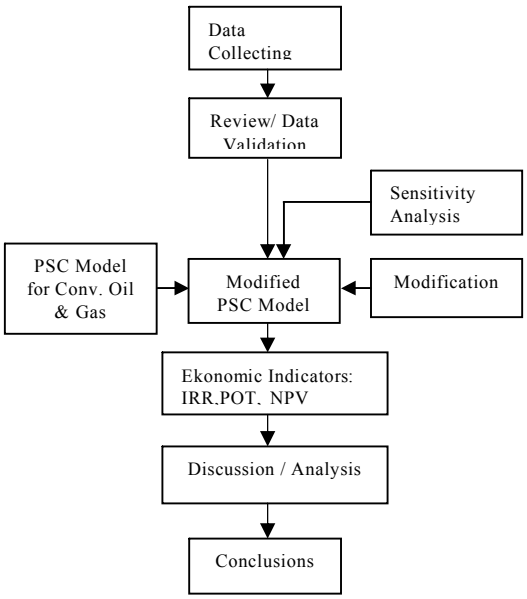

Figure 1. Research methods Scheme

3. RESULTS

Based on the cost components usually encounter in conventional gas development together with the data obtained from the CBM, the CBM field development, its production facilities and input data used in the economic evaluation can be described as follows.

3.1 Field Development

In this study, 367 wells will be drilled in two steps of development. In the first step, about 210 wells will be drilled. Pilot wells will also be used as a part of development system. Horizontal pilot scale wells will also be made in the development step. The main target of this development step is to obtain the optimum production.

In the second step, the number of wells is expanded. The main goal of this step is to maintain production rate during the contract time. The addition wells are around 10 to 24 wells annually. Horizontal drilling and special treatment might be applied to support gas production and sale.

Production Facilities

The CBM production facilities are slightly different from the conventional gas production. These include:

- *Well facilities*
  Well production system consists of *PCP screw* type pump moved by electrical motor set on surface to produce water from tubing and gas from annulus. This pump type is selected because of four reasons: (a) big capacity, (b) intermittent, (c) resist on high gas concentration and coal flakes and (d) cheaper than other types.
- *Piping Network*
  Gas compressor at capacity of 2-3 MMSCFD is needed near the well hole and set at the gathering station. Inlet pressure is 10 to 20 psig and the outlet is 150 psig to gather gas from 10 to 20 wells to the sales point. P*olyethylene* (PE) pipe is used at low pressure section to reduce investment cost.
- *Future Plan*
  Main compressor for gas sales will be set near the field. Several clusters with the capacity of 5 to 10 MMSCFD processing gas will be set up in the project area. Each cluster will serve 20 wells.

Input Data

Input data needed in the model includes investment data, annual gas and water production

, number of wells and number of production facilites needed. Furthermore, two cases are studied based on the specified above data.

***Case* I**

In this case, the following conditions are considered:

a. *FTP* = 5 % (shared for government and contractor)
b. *CRC* = 100 % for year 1 to 5, 90% for year 6 to the end of the contract
c. *Split* = 55 : 45 (after tax)
d. *Tax* = 44 %
e. Gas and water production is shown in Table 1 and Tabel 2.
f. Wellhead gas price is US$ 4.30/MMBTU

***Case* II**

In this case, the following conditions are considered:

a. *FTP* = 10 % (only for government)
b. *CRC*= 90 % for year 1 to the end of contract, or 80% for year 1 to the end of contract
c. *Split* = 55 : 45 and 60 : 40 (after tax)
d. *Tax* = 44 %
e. Gas and water production is shown in Table 1 and Tabel 2.
f. Wellhead gas price is US$ 4.50/MMBTU or US$ 5.00/MMBTU.

3.3.1 Production Rate

Annual gas and water production are estimated based on the reservoir simulation as shown in Table 1 and Table 2 [4,5].

Table 1. Annual Gas Production Estimation (MMSCFY)

Year	Gas Production	Year	Gas Production
2008		2023	32000
2009		2024	32000
2010		2025	32000
2011		2026	32000
2012	1500	2027	32000
2013	1500	2028	32000
2014	1500	2029	32000
2015	3000	2030	32000
2016	3000	2031	32000
2017	15000	2032	32000
2018	15000	2033	32000
2019	25000	2034	30000
2020	25000	2035	26500
2021	25000	2036	26500
2022	32000	2037	26500

3.3.2 Investment Cost and Operating Cost

In general, operating cost of CBM production is higher than a conventional gas production at the early stage. This is because CBM production has longer dewatering stage (5-7 years compared to 1 year in conventional gas). After this stage, the CBM production cost is estimated US $ 0.03/MCF lower than a conventional one. Exploration cost for one well in CBM is estimated about US$ 400.000 [6,7], lower than the one in oil or conventional gas (US$ 1 – 2 million).

Table 2. Annual Water Production Estimation (Thousand of Barrel)

Year	Water Production	Year	Water Production
2008		2023	20000
2009		2024	19000
2010		2025	17000
2011		2026	16000
2012	33000	2027	15500
2013	36500	2028	15000
2014	42000	2029	14500
2015	39500	2030	14000
2016	36000	2031	13500
2017	34000	2032	13000
2018	30000	2033	13000
2019	27500	2034	11000
2020	25000	2035	10700
2021	24000	2036	10600
2022	22000	2037	10500

Meanwhile, compression and power plant cost is about 2-8 % and 5 % of the total production respectively. Therefore, only 87-93 % of the total production can be sold. Transportation and distribution cost should be covered by *end user*.

Project investment starting from year 1 up to year 23 consisting of drilling related facility cost, gathering pipeline, low pressure compressor, production and sales compression system is described in Table 3.

Detail description of the above cost parameters is as follows:

a. Well and facilities
- Core and *coring* analysis is US$ 125.000 per well
- Well and facilities is US$ 425.000 per well consisting the following components:

- Access road, US$ 50.000. *Flow line,* US$ 25.000
- Drilling, completion and cracking, US$ 250.000 per well
- *PCP* pump and installation, US$ 100.000 per well.

b. *Pipelines* and production facilities (including water treatment)
- Low pressure gas gathering and compressor for each station consisting of modulo system @ 5-10 MMSCFD, US$ 1.200.000
- Water-gas separation system for 100 MMSCFD of gas, US$ 15.000.000

Tabel 3. Biaya Investasi dan Operasional Proyek

Year	No of Wells	Descriptions
Pilot Stage		
2008	4	3 core hole & 1 exploration well
2009	1	Facilities for Pilot Project
2010		Dewatering, prod. testing, gas market study, POD
Development Stage		
2011	4	
2012	37	
2013	36	P/L, compressor, separator
2014	36	P/L, gathering plant, compressor, separator
2015	36	P/L, gathering plant, compressor, separator
2016	36	P/L, gathering plant, compressor
2017	24	P/L, gathering plant, compressor
2018	18	Gathering plant
2019	18	Gathering plant
2020	18	Gathering plant
2021	12	
2022	12	
2023	12	
2024	10	
2025	10	
2026	10	
2027	10	
2028	10	
2029	8	
2030	8	
2031- 37		None

c. *Pipelines* and Compressor for gas sales
The following data is used for information only, and not used for calculation, because we use *wellhead price* in this study.
- Compressor with the capacity of 100 MMSCFD, US$ 45 million
- Piping, US$ 12 million, consisting of:
  - 25 km of 24 inch piping to send the gas to PGN & PLN pipe, US$ 9 million.
  - Piping for other market (5-6 location @ 5 MMSCFD), US$ 3 million.

Because CBM gas content high purity of methane (>90%) with N2 and CO2 impurities (without H2S), investment for gas treating facilities is not included [9,10].

Operating cost consists of existing well maintenance, production cost, water treatment cost, and gas compression/transportation. Those cost components are:
- Well maintenance and production cost, US$ 25.000 per well per year.
- Water production and treatment, US$ 0.30 per barrel.

Other cost component is US$ 15.000 for restoration per well per year.

3.4 Economical Calculation of CBM Contract

Economical evaluation of the CBM production is calculated based on the PSC model as shown in Figure 2 [8].

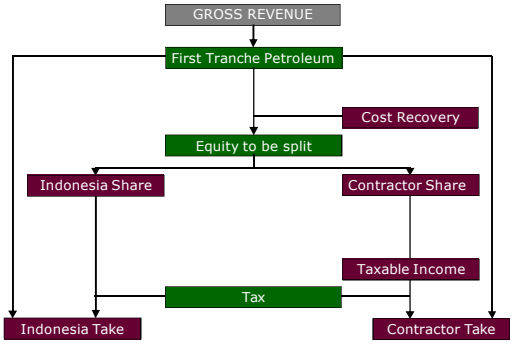

Figure 2. PSC Model for CBM Production

3.4.1. Results for *Case* I

Using conditions described in Case I, the following Tables 4 and 5 shows the economic indicators results.

Table 4. Economic Indicators of CBM Development on Case I

Economic Indicators	Value
Expenditure, MM US$	745.13
NPV @ 10% p.a, MM US$	44.00
% Gross of Revenue	30.00
Internal Rate of Return (% IRR)	12.90
Profit to Investment Ratio (PIR), Fract.	2.82
Pay Out Time (POT) Year	15.40
Contractor Take, % of Profit	41.87
GOI Take, % of Profit	58.13
NPV @ 10% p.a MM US$	160.00
% Gross of Revenue	41.59

Table 5. Revenue Distribution on Case I

Revenue Distribution	Contractor (MM US$)	Government (MM US$)
Gross Revenue	2618.70	
Net Cash Flow	784.48	1089.09
Cost Recovery	632.95	0
Total FTP Share	105.22	25.72

Table I shows that, based on Case I, contractor does not get reasonable IRR, i.e. 12.9%.

3.4.2. Results for *Case* II

Using conditions described in Case II (*CRC* 90%, Split 55:45 and Gas price US$ 4.50/MMBTU), the following Tables 6 and 7 show the economic indicators results.

Table 6. Economic Indicators of CBM Development on Case II

Economic Indicators	Values
Expenditure, MM US$	745.13
NPV @ 10% p.a, MM US$	29.00
% Gross of Revenue	25.9
Internal Rate of Return (% IRR)	12.00
Profit to Investment Ratio (PIR), Fract.	2.54
Pay Out Time (POT) Year	15.00
Contractor Take, % of Profit	35.52
GOI Take, % of Profit	64.48
NPV @ 10% p.a MM US$	194.00
% Gross of Revenue	46.95

Table 7. Revenue Distribution on Case II

Revenue Distribution	Contraktor (MM US$)	Government (MM US$)
Gross Revenue	2740.50	
Net Cash Flow	708.73	1286.64
Cost Recovery	625.38	0
Total FTP Share	0	274.05

As on Case I, the results shown in Table 6 also shows that, based on Case II, contractor does not get reasonable IRR, i.e. 12.0% (lower than Case I). For gas price US$ 5.00/MMBTU, IRR is obtained 13.4%.

3.4.3 Results on Sensitivity Analysis

Effects of economic variables on economic parameters are studied further to observe the sensitivity of each variable, following are the results.

a. Sensitivity Analysis on Case I

Figure 3 shows effect of gas production rate, gas price, Capex, and Opex on IRR. This figure shows that gas production rate and gas price give very sensitive effect on the IRR, while both Capex and Opex do not give significant effect on the IRR. For instance, increasing production rate or gas price by 20 % will increase the IRR from 12.9 to 15.3%.

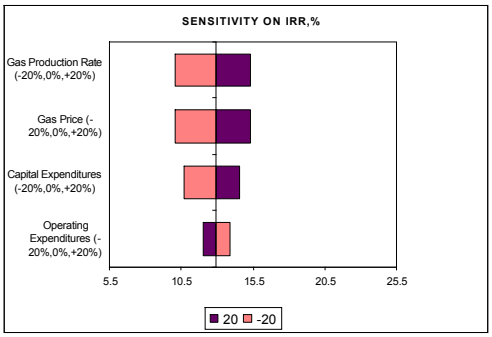

Figure 3. Effect of Gas Production, Gas Price, Capex and Opex on *IRR* in Case I

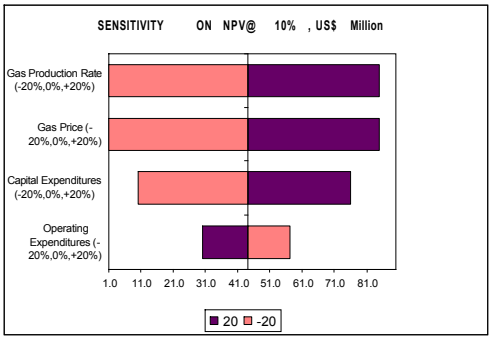

Figure 4. Effect of Gas Production, Gas Price, Capex and Opex on *NPV* in Case I

Figure 4 shows effect of gas production rate, gas price, Capex, and Opex on NPV for contractor. This figure shows that gas production rate and gas price give very sensitive effect on the NPV, while both Capex and Opex do not give significant effect on the NPV. For instance, increasing production rate or gas price by 20 % will increase the NPV from US$ 44 million to US$ 85 million.

Table 8 shows the sensitivity of the policy parameters on IRR. From the investor side of view, Split ratio is a very sensitive parameter on IRR. If the investor wants 19% of IRR, the Split ratio (Government: Contractor) should be 10 : 90, which is practically impossible, or the CRC is increased up to 120%, which is also impossible. Meanwhile FTP is not a significant factor on the change of IRR.

Table 9 shows the sensitivity of the policy parameters on Government Take. Similar to the above results, Split and CRC are important factors affecting the Government Take (in the reverse direction), while FTP is not a significant factor.

Tabel 8. Change of IRR on Policy Parameters In Case I

SPLIT PEMERINTAH : KONTRAKTOR	IRR (%)
0 : 100	19.6
10 : 90	18.7
20 : 80	17.6
30 : 70	16.5
40 : 60	15.2
50 : 50	13.8
55 : 45, BASE CASE	12.9
60 : 40	12
70 : 30	9.9
COST RECOVERY CEILING (%)	
100% (1-5); 90% (6-AKHIR KONTRAK), BASE CASE	12.9
100% (1 - AKHIR KONTRAK)	14
110% (1 - AKHIR KONTRAK)	15.9
120% (1 - AKHIR KONTRAK)	19.3
F T P (%)	
5 (SHAREABLE), BASE CASE	12.9
10 (SHAREABLE)	13
15 (SHAREABLE)	13
20 (SHAREABLE)	13
5 (NON SHAREABLE)	12.2
10 (NON SHAREABLE)	

Tabel 9. Change of Government Take on Policy Parameters In Case I

SPLIT PEMERINTAH : KONTRAKTOR	IRR
0 : 100	18.5
10 : 90	17.6
20 : 80	16.6
30 : 70	15.5
40 : 60	14.2
50 : 50	12.8
55 : 45, BASE CASE	12.0
60 : 40	11.2
70 : 30	9.1
COST RECOVERY CEILING (%)	
100% (1-5); 90% (6-AKHIR KONTRAK), BASE CASE	12.0
100% (1 - AKHIR KONTRAK)	13.2
110% (1 - AKHIR KONTRAK)	15.1
120% (1 - AKHIR KONTRAK)	18.5
F T P (%)	
5 (SHAREABLE), BASE CASE	13.4
10 (SHAREABLE)	13.5
15 (SHAREABLE)	13.5
20 (SHAREABLE)	13.6
5 (NON SHAREABLE)	12.7
10 (NON SHAREABLE)	12.0

b. Sensitivity Analysis on Case II

Figure 5 shows effect of gas production rate, gas price, Capex, and Opex on IRR in Case II. As in Case I, gas production rate and gas price also give very sensitive effect on the IRR, while especially Opex does not give significant effect on the IRR. For instance, increasing production rate or gas price by 20 % will increase the IRR from 12.0 to 14.4%.

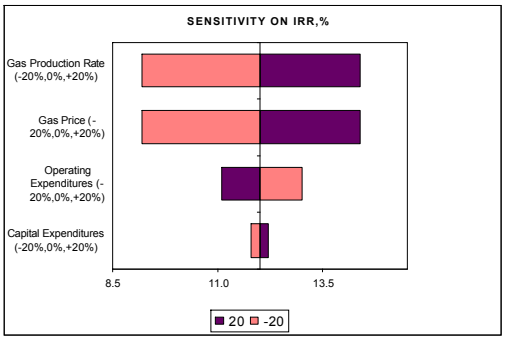

Figure 5. Effect of Gas Production, Gas Price, Capex and Opex on *IRR* in Case II

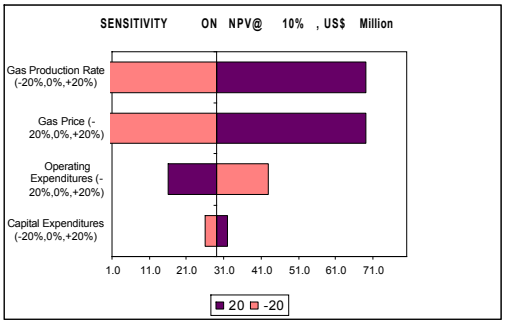

Figure 6. Effect of Gas Production, Gas Price, Capex and Opex on *NPV* in Case II

Figure 6 shows effect of gas production rate, gas price, Capex, and Opex on NPV for contractor. This figure shows that gas production rate and gas price give very sensitive effect on the NPV, while especially Opex does not give significant effect on the NPV. For instance, increasing production rate or gas price by 20 % will increase the NPV of contractor from US$ 29 million to US$ 65 million.

Table 10 shows the sensitivity of the policy parameters on IRR. As in Case I, split ratio is the most sensitive parameter on IRR for Case II. If the investor wants 19% of IRR, the government will gets nothing, or the CRC is increased up to 125%, which is also impossible. Meanwhile FTP is not a significant factor on the change of IRR.

Table 11 shows the sensitivity of the policy parameters on Government Take. Similar to the above results, Split and CRC are important

factors affecting the Government Take (in the reverse direction), while FTP is not a significant factor.

Table 10. Change of IRR on Policy Parameters In Case II

.

4. CONCLUSIONS

1. Base on Case I, IRR for CBM development in South Sumatra is 12.9%, and on Case II, IRR is obtained 13.4% at CRC = 90% and gas price US$ 5.00/MMBTU (the highest reasonable CRC and gas price).
2. Sensitivity analysis shows that Gas production rate and gas price give more significant effect on IRR and NPV, compared to the effect of Capex and Opex. Meanwhile, among the policy parameters, Split and CRC give significant effect on IRR, and FTP shows the least effect, both for Case I and Case II.

Tabel 11. Change of Government Take on Policy Parameters In Case II

SPLIT PEMERINTAH : KONTRAKTOR	GOV. TAKE (%)
0 : 100	13.73
10 : 90	22.96
20 : 80	32.19
30 : 70	41.41
40 : 60	50.64
50 : 50	59.87
55 : 45, BASE CASE	64.48
60 : 40	69.09
70 : 30	78.32
COST RECOVERY CEILING (%)	
100% (1-5); 90% (6-AKHIR KONTRAK), BASE CASE	64.48
100% (1 - AKHIR KONTRAK)	61.18
110% (1 - AKHIR KONTRAK)	54.67
120% (1 - AKHIR KONTRAK)	13.73
F T P (%)	
5 (SHAREABLE), BASE CASE	58.15
10 (SHAREABLE)	57.98
15 (SHAREABLE)	57.87
20 (SHAREABLE)	57.76
5 (NON SHAREABLE)	61.35
10 (NON SHAREABLE)	64.48

3. From the government point of view, Split and CRC give significant effect on Government take, and FTP shows the least effect, both for Case I and Case II.

4. In order to get IRR = 20%, the following schenarios can be used:

Base Case I :

a. Gas price is increased to US$ 7,53/MMBTU, IRR = 20,6%
b. Gas price US$ 6,88/MMBTU, CRC = 100%, IRR = 20,2%

Base Case II :

a. Gas price is increased to US$ 8,10/MMBTU, IRR = 20,2%
b. Gas price US$ 7,65/MMBTU, CRC = 100%, IRR = 20,2%
c. Gas price US$ 6,75, FTP=10% (shared), CRC=100%, IRR = 20,0%

REFERENCES

[1] *Advanced Resources International, Inc., Indonesian Coalbed Methane – Resource Assessment, Unpublished Report, Prepared foe Asian Development Bank, Manila – MIGAS, Jakarta, 2003*
[2] *Ephindo-MedcoEnergi, Presentation of CBM Project, South Sumatra Joint Evaluation, April 2007*
[3] *Hydrocarbon Asia, Indonesia Coalbed Methane : resources and development potential, Report CBM July/August 2006*
[4] *Institut Teknologi Bandung, Joint Evaluation Study on CBM, Overlapping Area of Medco-Ephindo, South Sumatera, May 2007*
[5] *Kurnely, Kun, Budi Tamtomo, Salis Aprilian, A Preliminary Study of Development of Coalbed Methane (CBM) in South Sumatra, SPE 80518, 2005*
[6] *Widodo, Lestantu, Studi Komparatif Berbagai Kontrak Kerjasama Eksplorasi dan Eksploitasi Minyak Bumi di Asia Pasifik, Tugas Akhir S1, Institut Teknologi Bandung, 1996*
[7] *Widodo, Aruman, Peluang CBM Sebagai Energi Alternatif di Masa Depan, Ikatan Sarjana Ekonomi Indonesia, Jakarta, 2007*
[8] *PT. Suhartama Multijaya, Penyusunan Kebijakan Pengembangan Pengusahaan Coalbed Methane (CBM), 2006*
[9] *Sosrowidjojo, Iman B., Coalbed Methane Potential in the South Palembang Basin, Jakarta 2006 International Geosciences Conference and Exhibiton, 2006*
[10] *Lin, Whenseng, Min Gu, Anzhong Gu, Xuesheng Lu, Wensheng Cao, Analysis of Coal Bed Methane Enrichment and Liquefaction Processes in China, Shanghai Jiaotong University, Poster PO-37*

ISSN 114-1284

Development of Thermoelectric Generator Utilization Waste Heat from Combustion Engine

Nandy Putra, RA Koestoer, M Adhitya, R M Agizna, Ricky F Gazali

Heat Transfer Laboratory, Department of Mechanical Engineering
University of Indonesia
Kampus UI Depok, Jakarta
email: nandyputra@eng.ui.ac.id

.

ABSTRACT

The increasing of demand for energy sources and the decreasing of fossil energy sources then needed new alternative energy sources. And from this research, the use of Thermoelectric Generator (TEG) is one solution for this issue. TEG is a module that can convert heat energy into electrical energy by utilizing the velocity difference between each electron of the two types of semiconductor which conduct different potential. This principle is known as Seebeck effect that reversing way of Peltier effect on Thermoelectric Cooling (TEC). And the focus of this research is to know the power generated efficiency of TEG by using exhaust waste gas of motorcycle as a source of heat. In this research, 100 cc 4 strokes motorcycle is applied, the 8 TEG modules were employed for generating electricity and the motorcycle will be simulated run steadily up to speed 20 km/ hour with 3 kinds of variations RPM. This research gives maximum power output 3.15 W at ΔT of 65.56 ^{O}C.

Keywords: *Heat Waste, Thermoelectric Generator, Energy Conservation, Hybrid Car, Differences Temperature.*

1. Introduction

It was realized that the need of energy day after day is increasing proportional to. Since energy sources have limited quantities, many researchers have been developing new method in order to increase the efficiency of energy utilization, especially in the field of transportation. And the Hybrid car was made to fulfill those demands.

A hybrid vehicle is a vehicle that uses an on-board rechargeable energy storage system (RESS) and a fuel based power source for vehicle propulsion. These vehicles use much less fuel than their counterparts and produce less emissions. In general hybrid vehicles recharge their batteries by capturing kinetic energy through regenerative braking. Some hybrids use the combustion engine to generate electricity by spinning a generator to either recharge the battery or directly feed power to an electric motor that drives the vehicle.

The hybrid car that used the electric motor as the support engine, use the electricity from the battery to run. The baterry is recharged when the driver manage the car to be decelerated, such as step off the accelerator lever or push the brake lever. Either the car is stop at the traffic light or traffic jam, it is also recharged. This condition reduces the fuel consumption that supports the combustion engine. For example, while the vehicle stops at the traffic lights, the combustion engine automatically turned off and change to electric engine.

Hybrid engine works with an additional sensor which is programmed to rechange automatically choosing between combustion engine or electrical engine. This is the preeminent engine from other conventional engines which more efficient because less gasoline are needed to reach the same distances.

Nowadays the hybrid car are still depent on the usage of regenerative breaking to produce the electricity, and the heat waste were not utilized. By using Seebeck principle of a thermoelectric generator, the waste heat energy from combustion of a hybrid engine can be converted into electrical energy which can be used for charging the battery. It was found out that the combustion temperature range from 100-250^{o}C, and the ambient temperature reach at 30-35

^{o}C. This condition makes a temperature difference that is required for Seebeck Principle to produce electricity[1].

The aim of this research is to develop a better way of utilizing the waste heat from combustion engine for generating electric power by using thermoelectric module.

2. Thermoelectric Generator (TEG)

Seebeck in 1822 discovered the thermoelectric effect. He observed an electric flow when one junction of two dissimilar metals, joined at two places, was heated while the other junction was kept at a lower temperature [2]. The electrical output produced was initially very small magnitude and there was no significant value in electric power generation. With the development of semiconductors material, it is founded that the output could be magnified significantly and this field began to be developed [3]. Renewable energy, such as solar energy, wind energy or hydropower is preferred, but it has limited use and is dependent on weather and topography. Thermoelectric Generator can convert heat energy to electrical power directly [4]. In additional, thermoelectric power generation has the advantages of being maintenance free, silent in operation and involving no moving or complex parts [5].

The available space to install a thermoelectric generator in an automobile is normally reduced because of the tendency to put more equipment in less space. There are mainly three possible locations for the TEG [6]:

1. Just behind the exhaust manifold
2. Between the manifold and the catalyst converter
3. After the catalyst converter

Figure 1 explained the TEG's structure which consist of type-n and type-p semiconductors. Those semiconductors are flanked between ceramic wafers where the cold and hot side will conduct and release heat. Heat source conducts heat on hot side and even though the cold side releases heat to environment. When temperature differences applied on this module between hot side and cold side, with the Seebeck Principle, it will produce electricity depend on its efficiency, called figure of merit. Iofee [2], who first studied thermoelectric module, found from the thermodynamic analysis that this ratio is function of the parameter called figure of merit (which is a function of only the thermoelectric material) and the temperature differences across the two parts of module. Generally, voltage is produced proportional to temperature gradient.

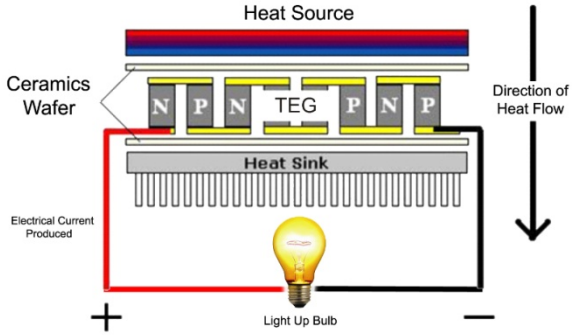

Fig 1. Thermoelectric Structure [6]

The efficiency of power generated by TEG depends on temperature difference. High power generated produced at higher temperature difference. When the temperature difference is getting wider, it effect to power income which is getting higher. So generally, a cooler such as heat sink, water jacket etc, applied together with TEG. Otherwise, increase the temperature of heat source. Thermoelectric generator can be connected each other as serial or parallel similar to a battery module to generate more voltage or current.

Many experiments have developed to explore the utility of thermoelectric power generator more widely. Rida Y. Nuwayhid et.al 2004 [7] developed a thermoelectric power generator using waste heat of a woodstove. Testing was undertaken under a controlled woodstove firing rate and temperatures, and open circuit voltages were monitored over extended periods. The maximum steady state matched load power was 4.2 W using a single module. The use of multiple modules with a single heat sink was found to reduce the total power output relative to single module case as a result of reduced hot to cold surface temperature differences. Because of this condition, higher voltages can be realized at some losses in available electric current, Eakburanawat et.al 2006 [4] developed a thermoelectric power generation to charge a battery with microcontroller based. The proposed system has maximum charging power of 7.99 W. That is better than direct charging by approximately 15%. This thermoelectric generation module is also applicable on notebook. Steven J W [8] presented Derivations and expressions for the optimal internal thermal resistance of a small ΔT thermoelectric generator with steady and time varying external thermal resistance.

Since the exhaust gas combustion as the heat source, it must be concern about the fluctuate amount of heat flux that transferred on hot side. So the temperature difference always changes during combustion. Because of that, the power generated is also become fluctuate as the temperature difference change each seconds. And when the maximum efficiency of TEG is reach at given temperature difference, the power income become a highest result for the TEG to generates power, even the temperature difference increasing. So, it's possible that when temperature difference is high, but the power income is remain low.

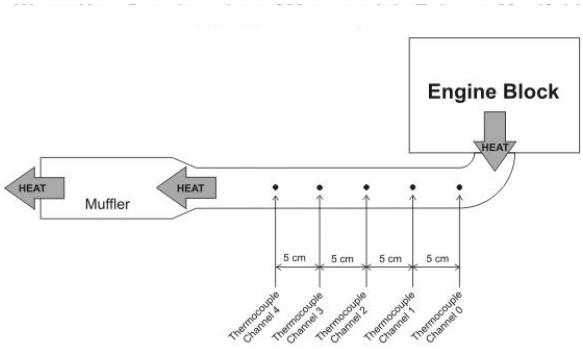

Fig 2. Scheme installation of thermocouple on motorcycle muffler

Figure 2 shows the placement of thermocouples on the muffler of motorcycle. It is done in order to know the temperature distribution of the muffler heated by the exhaust gas.

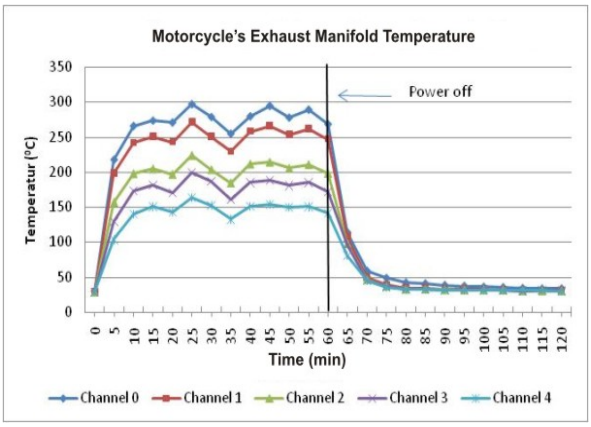

Fig 3. Temperature distribution on exhaust manifold of combustion engine

Figure 3 shows the temperature distribution on exhaust manifold, with the different position one and anothers to know about the temperature changes in any place as the comparison to placed the module for TEG. The experiment conducted on 110 cc motorcyle 4 strokes. Thermocouples are attached at given length on surface of the muffler.

The temperature distribution are range from 150 to 300 ^{o}C. The highest temperature is at the closest length to the exhaust manifold of the engine. And then it decrease until the tip of the muffler. Even when the engine is turned off, the muffler temperature is still higher than the ambient temperature. So, temperature difference still occur and produced electricity until the muffler temperature is similar to ambient temperature. But not as high as at higher temperature difference. This circumstance is another considerable for using TEG on muffler.

3. Design of Experimental Instrument for Thermoelectric Generator

In this research, it is realized that needs a support structure or bracket for TEG to be connected after exhaust manifold and before pipe or muffler. The bracket support structure is designed to be compatible with the exhaust manifold of the motorcycle engine and fit to the conventional muffler. Figure 4 shows construction of the designed bracket support structure where the TEG elements are placed.

The bracket is an aluminum block, which has dimension of 180 x 48 x 48 mm. The block was bored for flowing exhaust gas. The diameter of the hole is 30 mm that similar with diameter of pipe or muffler. In order to assemble easily the bracket into the exhaust manifold and pipe, the flans (5) are positioned on the top and bottom of the bracket.

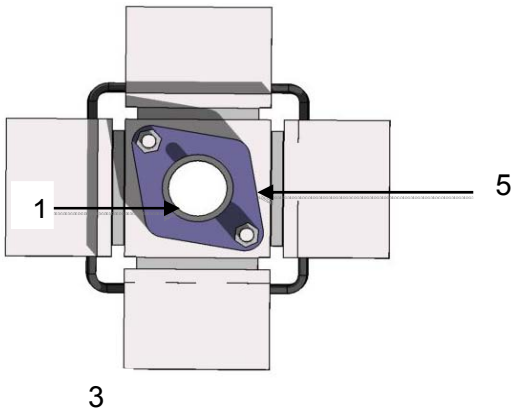

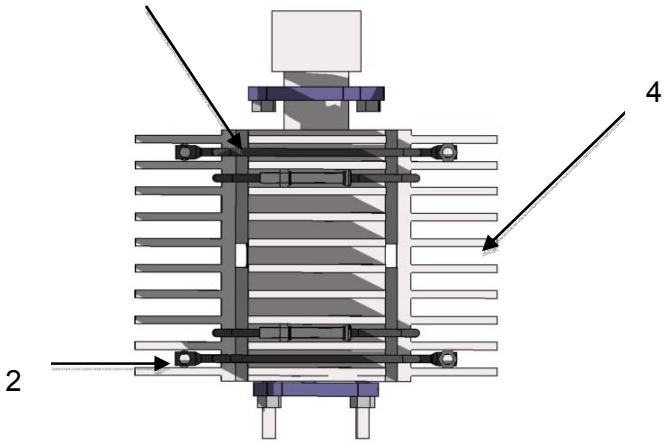

Fig 4. Bracket support structure

Eight TEGs (3) were used in this experiment. Each side of block was designed to hold two TEGs. The exhaust gas will flow through inside the bracket and heat will transfers to TEG. The heat will conduct through this aluminum bracket and reach the hot side of TEG. To have high temperature difference between hot and cold side of TEG, heat sinks (4) must be attached on the cold sides of TEG in order to absorbed heat and accelerated the released of heat to the environment. Fin heat sinks made of aluminum were used in this experiment

In this case, the using of bolts to tight heat sink and the TEG on the block is avoided in order to reduce heat conduction from the block to cold side of the TEG. These bolts will conduct more heat on cold side and affected decreasing of temperature difference between hot side and cold side. Rubber clams (1), clamps (2) are used to tight all TEGs and heat sink on the block.

4. Experimental Setup

The TEG system was tested with some variations such as electrical circuit analysis (serial, parallel, and series-parallel) and also based on the rotation of the engine (idle, middle, and high). This aims to represent the possible conditions of data logged with the conditions that might be faced when the motor run.

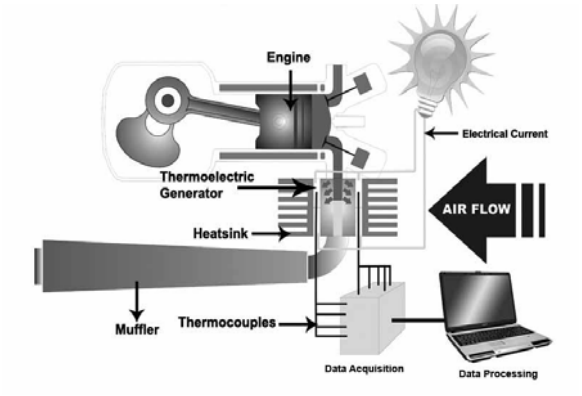

Fig 5. Schematic of experimental setup of TEG on motorcycle

The figure 5 shows the experimental setup of TEG on motorcycle. The bracket is attached after the exhaust manifold, to obtaining higher temperature on hot side.

To acquire temperature data, 11 thermocouples types K are employed, the thermocouples connected into PC based data acqusition system, (National Instrument Data Acquisition DAQ 9172). These thermocouples are placed on hot side and cold side of TEG, ambient temperature, and exhaust manifold.

All TEGs cable are connected with many kind of combination such as serial, parallel, and serial-parallel circuit module. Each experiment will conduct with different mode, in order to know the value of power which is generated by TEG. A multimeter is connected to the module to show voltage and current generated by TEG. In these experimental, 12 volt bulb is used as load.

The experimental is carried out on motorcycle which is simulated run. Therefore, to create this condition this experiment 160 watt, 30 inch fan is applied in order to blow the air similar to the situation when the motorcycle runs at 20 km/h. This air flow is to absorb the heat on heatsinks.

The test consists of a motor cycle with cylinder capacity of 100 CC – 4 strokes. Obtained data from experiment consists of output currents, output voltage, output power, the temperature data the heat and cold, are all comparable with the function of time. The data itself is done until the system is stable.

Beside the circuit combination, the experiment is also run in three kind of engine rotation, that's high RPM ranged from 3000-3500 RPM, middle RPM ranged from 2000-3000 RPM, and idle condition ranged from 1000-2000 RPM.

5. Result and analysis

Figure 6 shows the temperature distribution in each condition of RPM, as can be seen that the high RPM condition provided highest temperature difference. The change of temperature value is linear to the changes of RPM. The biggest temperature difference is 70 ^{o}C. It is clear that with high RPM, flow rate of exhaust gas will flow more gas through the block. Then the block will absorb more heat. As shown in fig 6 temperature difference was influenced by type of RPM. When the RPM was high, bigger temperature will occurred on hot side of TEG.

After several time, the engine was shouted down, then the difference temperature between hot side and cold side for all condition will decrease rapidly.

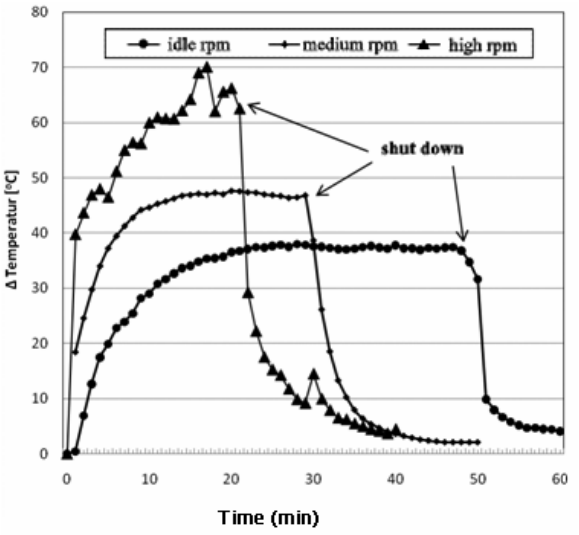

Fig 6. Comparison temperature difference versus time of TEG in each type of RPM

Figure 7 and 8 show the measurement of voltage and electric current as variation of circuits at high rotation of engine respectively. The serial mode electricity circuit gave highest voltage, it reached 7 volt. The parallel mode provided the lowest voltage. Meanwhile as depicted in Fig 8, the highest electric current is provided by parallel mode. In this research 3 Ampere was obtained in parallel mode. From the figure, it can be noted that even the engine has already been shouted down, the potential voltage and current still occurred because there are still temperature different on this system.

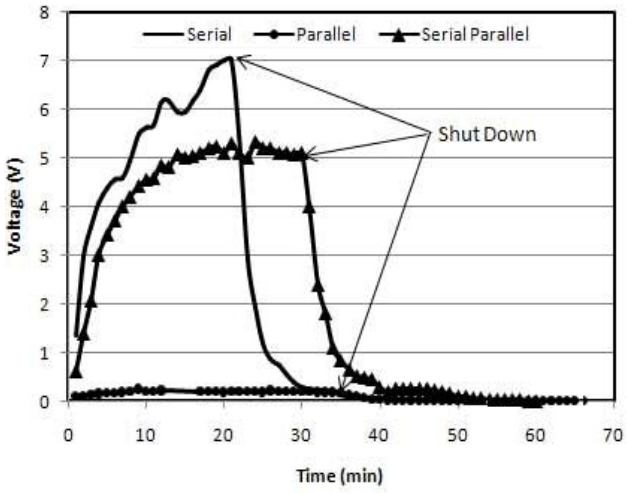

Fig 7. Comparison of voltage versus time in each circuit combination

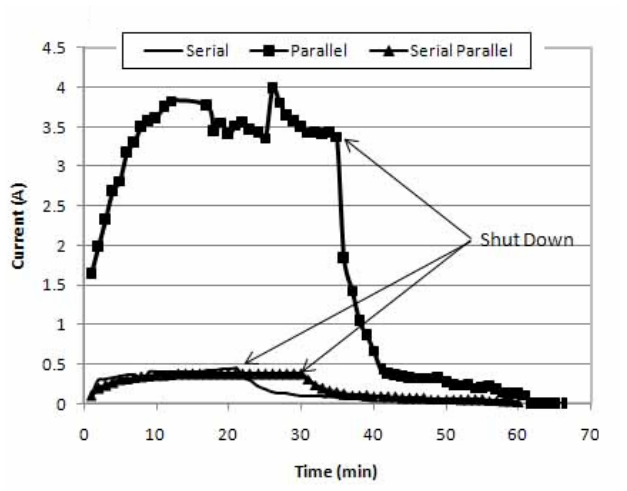

Fig 8. Comparison of current versus time in each circuit combination

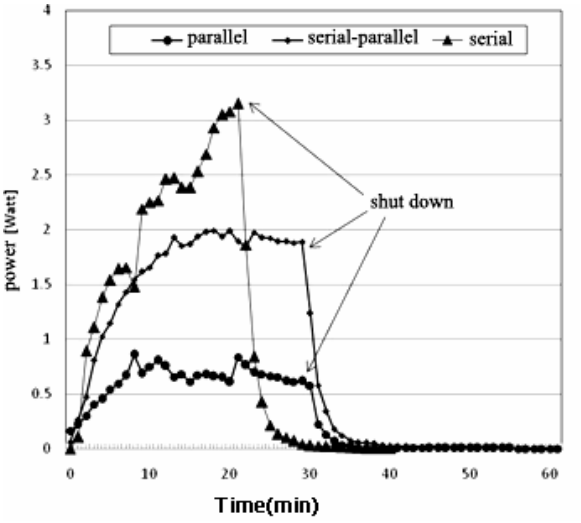

Fig 9. Comparison of power generated in high rpm on each type of module

Fig 9. is the comparison of the power that can be produce by each circuit in high RPM condition. The maximum power generated of this test is 3.2 watt in serial mode circuit and high rpm condition that produce 65^{o}C temperature differences. While at parallel and combination circuit, the power that produced is 0.9Watt and 2Watt, with 38^{o}C and 48^{o}C temperature difference.

Figure 10 displayed the comparison of power generated of TEG in serial module of thermoelectric generator at variation of engine rotation. It shows that the high electrical power will produce at the high rpm. As showed in Fig 6. High rpm acquire high difference temperature.

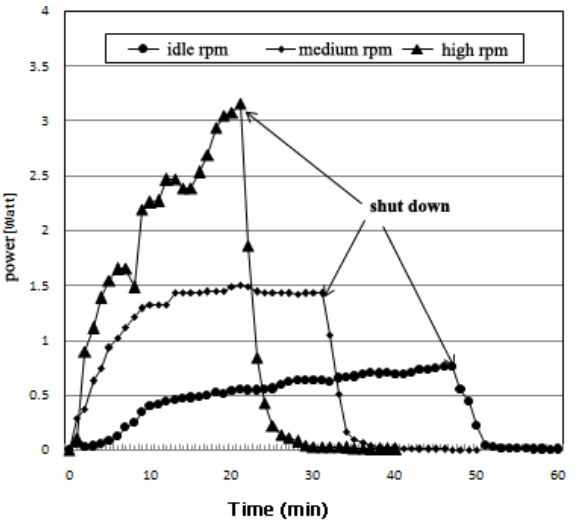

Fig 10. Comparison power generated versus time of TEG in each type of RPM in serial module

Nurwayhid et.al,[7] stated that the increasing of the amount of TEG may not be warranted that the power that can be produced will increase linearly too. On that research, one module produce 4W of electricity while when two modules is used only 3,8W that can be produced. This condition is also might be happen in this research, the increasing of TEG module is not influenced the amount of power that can be produced.

6. Conclusions

From the experimental results, it can be concluded that thermoelectric module is able to generate a number of electrical energy, utilizing the existing temperature difference. By using 8 TEG modules, it can produce power at about 3.2 watt at ΔT 62.5 ^{0}C (in serial circuit). The circuit can be adjusted by purpose, if needed to get a bigger current, parallel module circuit of TEG could be more effective. On the other hands, the serial circuit is used to obtain a bigger voltage. The experiment bought a result of high voltage in serial circuit in the high RPM condition. Meanwhile, high current was obtained in parallel module. The heat sinks on the cold side play an important role to obtain higher temperature difference and to produce higher electricity.

Acknowledgement

The author would like to thank RUUI 2008 for funding this project.

References

[1] S. Chatterjee and K.G.Pandey, Thermoelectric cold-chain chests for storing/transporting vaccines in remote regions, Applied Energy, Volume 76, Issue 4, December 2003, pp. 415-433

[2] Iofee AF. Semiconductor Thermoelements dan Thermoelectric Cooling. In: Phys Semicond. London: Infosearch Ltd; 1957

[3] Rowe DM. Thermoelectric Power Generation-an update. In: Vincenzini P, editor 9th Cimtec-World Forum on New Materials, Symposium VII-Innovative Materials in Advanced energy Technologies, Florence, Italy 1998, p.649-64.

[4] Eakbuarawat J, Boonyaroonate I.Development of a thermoelectric battery-charger with microcontroller-based maximum power point tracking technique, Applied Energy, October 2005.

[5] Vazquez J, Miguel A, Bobi S, Palacios R, Arenas A. State of the art of thermoelectric generators based on heat recovered from the exhaust gases of the automobiles.

[6] Min G Rowe DM, Peltier devices as generator, CRC handbook of thermoelectric, London CRC Press, 1995.

[7] Nurwayhid RY, Shihadeh A, Ghaddar N. Development and testing of a domestic woodstove thermoelectric generator with natural convection cooling. Energy Conversion and Management 46 (2005) page 1631-1643

[8] James W. Stevens Optimal design of small ΔT thermoelectric generation systemsEnergy Conversion and Management, Volume 42, Issue 6, April 2001, Pages 709-720

Proceeding of the 11th International Conference on QiR (Quality in Research)
Faculty of Engineering, University of Indonesia, Depok, Indonesia, 3-6 August 2009
ISSN 114-1284

EFFECTIVENESS OF PLATE HEAT EXCHANGER ON SPLIT AIR CONDITIONING WATER HEATER SYSTEM

Nandy Putra, Luky Christian, Dwi Ananto Pramudyo

Heat Transfer Laboratory
Mechanical Engineering Department, Faculty of Engineering University of Indonesia
Kampus Baru UI Depok
E-mail : ***nandyputra@eng.ui.ac.id***

ABSTRACT

As the government's instruction about energy savings, some efforts need to be done to succeed this program. In household areas, energy savings can be done by so many ways, from turning off unused lamps until utilizing waste heat from air conditioning system to produce hot water which is known as Air Conditioning Water Heater (ACWH). ACWH is a heat recovery system that utilizes waste heat from refrigerant to produce hot water simultaneously through of a heat exchanger which is very suitable to be implemented at residence apartments. The existing ACWH system needs to be developed to reach an optimum result. Some problems of ACWH systems nowadays are low efficiency, insufficient hot water temperature, long period of heating, and increasing of evaporator temperature. The objective of this research is to maximize the performance of ACWH using Plate Heat Exchanger which has highest efficiency among all type of heat exchanger. The water flow rate and cooling load are variables to be tested. The result of ACWH system shows that the system with 2600W of cooling load can produce 50L/hr hot water with 46^{0}C temperature in open loop method.

Keywords *: Energy, Heat Recovery, Efficiency, Plate Heat Exchanger, Water Flowrate, Cooling Load*

1. Introduction

Indonesia has tropical climate which has high ambient temperature and humidity. Almost all houses, residences, and apartments in big cities use Air Conditioner (AC) to produce thermal comfort for human beings. Another demand for residences is water heater unit to produce hot water for many purposes such as bathing, washing, etc. System that is mostly used nowadays is the usage of 2 discreet systems, AC and water heater units, which each of those consume lots of energy.

Another alternative available is using water heater unit that doesn't consume any energy such as Solar Water Heater (SWH) and Air Conditioning Water Heater system (ACWH).

ACWH is not a new system. It has been developed for the last 50 years. ACWH recovers waste heat from air conditioning system to produce hot water. With this system, we can get 2 benefits simultaneously, cooling effect and water heating effect that consumes less power.

In subtropical climate (US), ACWH system are claimed to produce hot water with no additional energy at all [1]. Further studies shows that ACWH system will reach breakeven point with its initial cost in 2-3 years period [2].

Nowadays ACWH system has been developed in many countries, most of them in countries with tropical and subtropical climate. Ji et al [3] developed ACWH system that can produce hot water up to 50^{0}C in China (subtropical climate). In subtropical climate, ACWH system has another additional benefit as room heater. For tropical climate, ACWH system has been tested and developed by Techarungpaisan et al [4], and Putra et al [5, 6, 7]. In tropical countries ACWH is not used as room heater due to the high ambient temperature, so most systems developed in tropical countries only have 2 functions, as air conditioner and as water heater.

ACWH systems have several problems, such as temperature of hot water, long heating time, up to malfunction of cooling effect of the system itself. All of these problems made ACWH systems rarely used during 1980-1990 period.

As the technology developments, ACWH problems can be reduced and eliminated so that ACWH system is commonly used nowadays, especially in Europe [8]. By this research, the researchers want to develop an ACWH system that can be applied at residence apartments so that the energy consumption can be minimized.

2. Objective

The aim of this research is to develop, and optimize Split Air Conditioning Water Heater (S-ACWH) system with plate heat exchanger to produce better performance. S-ACWH performance is measured by 2 main parameters, hot water temperature and COP

3. System Description

Testing apparatus schematic can be seen at figure 1. Residence apartments is simulated as closed cabin with dimension 3 x 1,5 x 1,5 m. Cooling loads in the apartments such as humans, electric appliances, etc are simulated with lamps that can be varied from 0 – 2600 W. With this testing apparatus, we hope the testing condition resembles the real conditions at the apartments where the ACWH system is to be applied.

Main parameters to be measured in this testing are temperature (water and refrigerant) and pressure of the refrigerant.

Thermocouples (type K) are installed at inlet & outlet of working fluids of the Plate Heat Exchanger (PHE), outlet of condenser, inlet & outlet of evaporators. All thermocouples are connected to data acquisition module which connected to the computer. While pressure gauges are installed at inlet & outlet PHE (to measure pressure drop of PHE), compressor suction and evaporator inlet.

Thermocouples and pressure gauges are installed so that the information gained can be used to draw the system at P-h diagram.

4. Results and Analysis

Water flow rate variation has a significant effect to the hot water produced as seen at figure 2. Hot water temperature produced decrease as the water flow rate increase due to lesser contact time between water and PHE as water velocity inside PHE increased.

Another factor is gate valve opening. As water flow rate increase, gate valve is opened lesser. Gate valve can't be fully closed to maintain compressor suction pressure in its optimum range (60-70 psi). If the suction pressure decreases, the system will lose its cooling effect. Partially opened gate valve limits the amount of refrigerant flow to the PHE

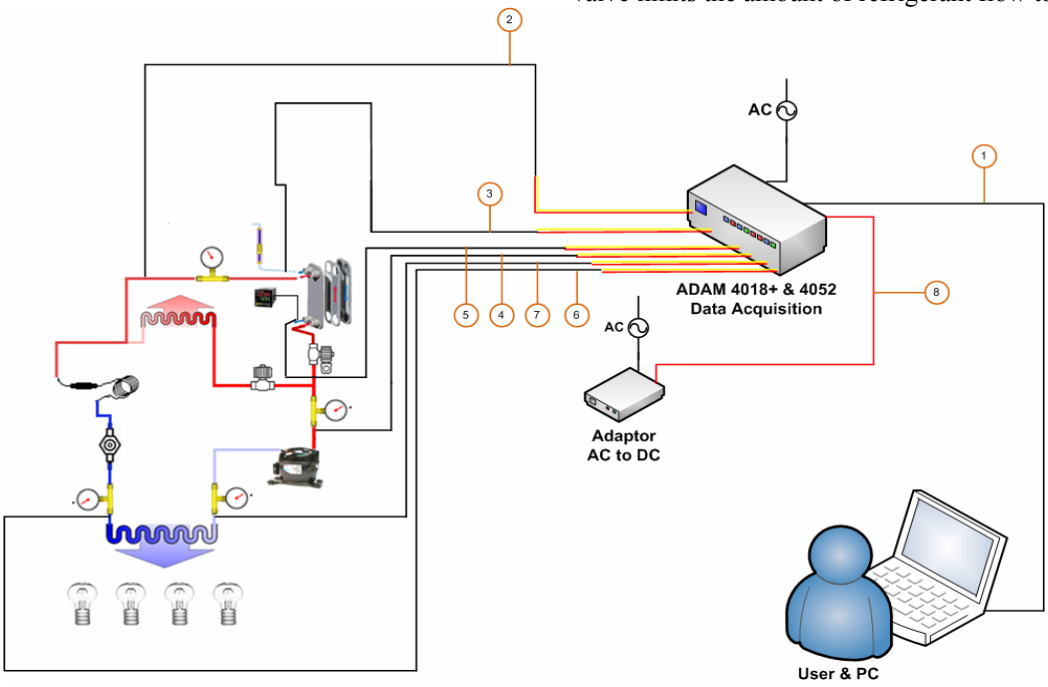

Figure 1. Testing apparatus schematic

ISSN 114-1284

Refrigerant inlet temperature also decreases due to increased heat recovery in the system. Enthalpy is a function of temperature. If the enthalpy of refrigerant decreases due to heat recovery, the temperature will also decrease.

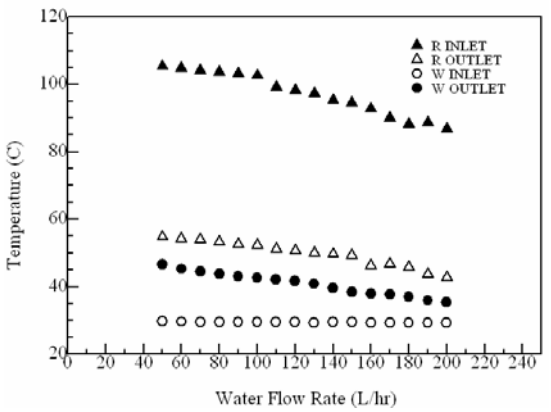

Figure 2. Working fluids temperature at PHE inlet & outlet

Decreasing hot water temperature produced doesn't indicate that the heat absorbed by water also decrease. Decrease of hot water temperature will decrease the temperature difference (ΔT). But the mass flow rate will increase. Mass flow rate increasing rate is bigger than temperature difference decrease rate. The result is an increase in heat absorbed by water.

Increased water flow rate will result in increased Renolds number (Re) of the flow. As the Re increase, the flow will switch from laminar flow into turbulent flow. Turbulence flow will result in higher heat transfer coefficient.

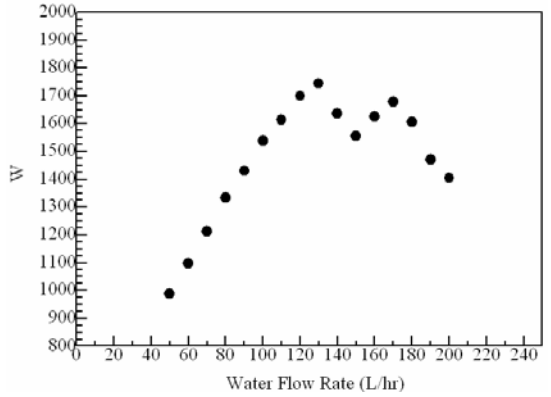

Figure 3. Heat absorbed by water

Heat absorbed by water can be maximized up to condenser capacity. As seen in figure 3, maximum heat absorbed by water is about 1750 W, much lesser than condenser capacity which is 3000W. Several developments will be done in the upcoming research to solve this problem.

In figure 4, we can see that the compressor work tends to decrease as the water flow rate increase. As stated before, heat absorbed by water increase as the water flow rate increase. The more heat absorbed by water, the more enthalpy of the refrigerant dropped. Refrigerant temperature will also decrease

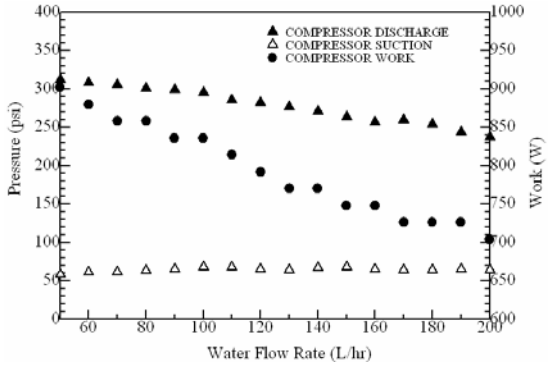

Figure 4. Compressor performance

The temperature of refrigerant at compressor inlet and outlet are decreasing. The decreasing rate of refrigerant temperature at compressor outlet ($\Delta T_{R,o}$) is greater than the decreasing rate of refrigerant temperature at compressor inlet ($\Delta T_{R,i}$) which results in decrease of refrigerant temperature difference ($T_{R,o} - T_{R,i}$). Lesser temperature difference means lesser enthalpy difference (Δh). Compressor work is a multiplication of refrigerant mass flow rate and enthalpy difference between compressor inlet and outlet refrigerant. Lesser Δh will result in lesser compressor work.

Decreasing compressor work is followed by decreasing discharge pressure due to heat recovery. Suction pressure is maintained constant by varying gate valve opening.

Overall system performance (COP_{ch}) increases as the water flow rate increase. COP is a ratio between effects gained compared to works done. In this system, the effects gained are the cooling effect and water heating.

Cooling effect is assumed constant as the cooling load is constant at 2600 W (heat transferred from the cabin is constant). System's cooling performance (COP_c) will increase as the compressor work decrease.

Water heating effect increases as water flow rate increase, which is shown by higher amount of heat absorbed by water. System's heating performance (COP_h) will increase due to higher heating effect gained and decreasing compressor's work.

Overall system performance (COP_{ch}) is addition of cooling performance and heating performance. Increased both performance will result in increase overall system performance. Overall system performance in S-ACWH increases 37,5% - 100% compared to normal AC system.

ISSN 114-1284

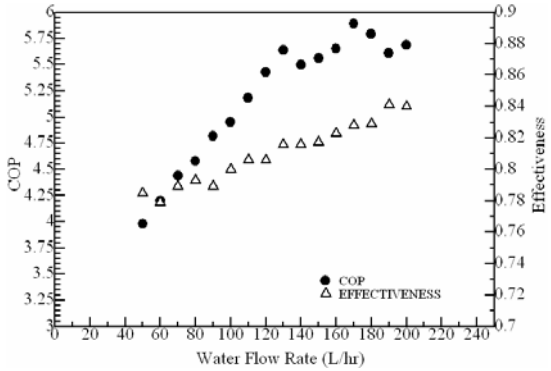

Figure 5. S-ACWH performance for water flow rate variation

PHE effectiveness in this system is not as high as normal PHE effectiveness. In calculation, refrigerant mass amount to the PHE is assumed same with refrigerant mass amount of the system. In fact, some refrigerant will flow to condenser (bypass) because gate valve is opened. This assumption is made due to the limited testing apparatus. In this testing, we were unable to get refrigerant flow meter. If refrigerant flow rate to PHE is decreased to its actual condition, PHE effectiveness will increase to its ideal condition (>0,9). PHE effectiveness increases due to increased heat absorbed by water as water flow rate increase. System's COP and effectiveness for water flow rate variation testing is shown at figure 5.

In figure 6, we can see that cooling load variation does have effect on hot water temperature produced, but the effect is not as significant as water flow rate variation in previous testing. Even there is increase in hot water temperature, the increase is very small, so that it can be considered constant.

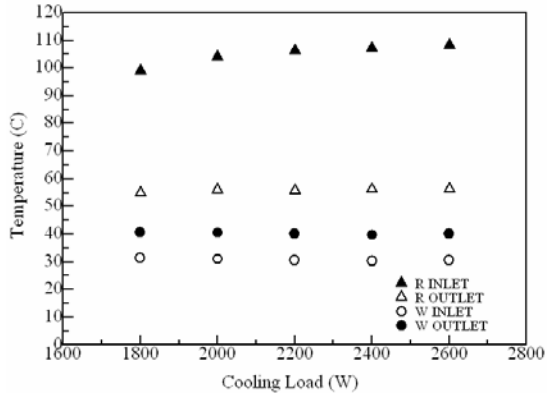

Figure 6. Working fluids temperature at PHE inlet & outlet

Increased cooling load means that more heat need to be transferred from the cabin and more heat to be rejected. More heat to be rejected means more heat available to heat the water.

Refrigerant temperature also increases as the cooling load increase. More cooling load will increase refrigerant enthalpy more, which result in higher refrigerant temperature.

Constant hot water temperature is followed by constant amount of heat absorbed by water. There is an increase, but quite small that in can be considered constant. In this testing, water flow rate is maintained constant at 100L/hr. Same water flow rate means same water flow which result in same Re and overall heat transfer coefficient. In this testing, heat absorbed by water tends to increase as cooling load increase. The amount of heat absorbed by water can be seen at figure 7.

As seen in figure 8, compressor's work tend to increase even the increase is not significant. The higher the cooling load, the enthalpy of refrigerant at compressor's suction will also increase which results in higher compressor's work.

Suction and discharge pressure tends to be constant during testing. There is increase in suction and discharge pressure, but again, not significant.

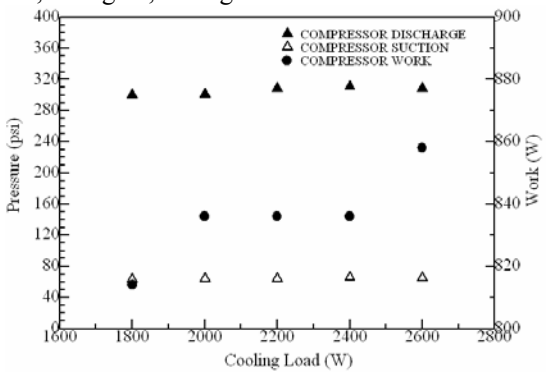

Figure 7. Compressor's performance

Discharge temperature increase as compressor's work increase and suction temperature increase as more enthalpy increase due to higher cooling load must be transferred from the cabin.

Overall ACWH performance (COP_{ch}) tends to increase as cooling load increase, but the increase is not as significant as in water flow rate testing. ACWH's overall performance for this testing can be seen at figure 9.

The cooling effect increase as the cooling load increased. But increased cooling effect is followed by increased compressor's work. This will result in increase in cooling performance (COP_c) but, the increase is not very significant.

The heating effect tends to be constant. The heating performance (COP_h) will decrease due to increase in compressor's work.

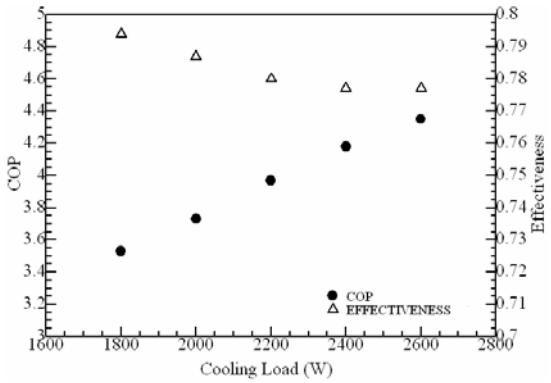

Figure 8. ACWH performance for cooling load variation

Increase in cooling performance and decrease in heating performance result in increase in overall ACWH performance. The increase rate in cooling effect is greater than the decrease rate in heating effect. ACWH performance increases 20 – 49,5 % compared to normal AC.

PHE effectiveness tends to decrease as water flow rate increase. Increase in cooling load is not followed by increase in hot water temperature produced.

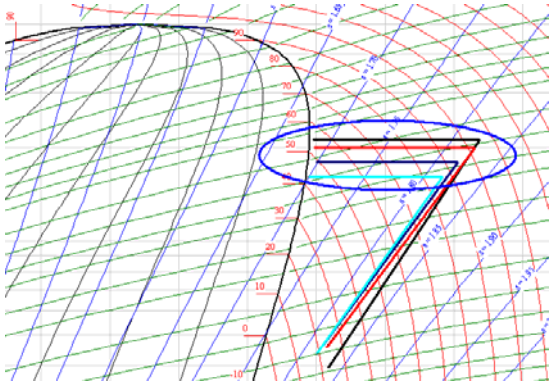

Figure 9. ACWH's Heat Recovery in P-h diagram (50L/hr, 100L/hr, 150L/hr, and 200L/hr)

As seen in figure 10, heat that should be rejected at the condenser is utilized to heat the water. The refrigerant used is the refrigerant which has highest enthalpy, at the compressor outlet. Refrigerant exiting the PHE is still at superheated phase. This refrigerant is mixed together with refrigerant exiting condenser before expanded together.

5. Comparison with existing ACWH systems.

As known, ACWH systems have been developed in the last 50 years. Many investigations have been done to have better ACWH's performance. Compared to previous research, modifications are done by modifying the testing schematic and changing the heat exchanger to gain best performance.

As seen in table 1, the highest heat exchanger effectiveness is gained using plate heat exchanger with this testing configuration. If the main parameter is hot water temperature, we can use helical triple shell pass heat exchanger to minimize the initial cost. Compared to plate heat exchanger, helical heat exchanger is cheaper. But as that heat exchanger's effectiveness is low, it may disturb the ACWH performances; especially it will decrease the cooling effect which results in higher cabin temperature.

Considering system performance and initial cost, the best option is using ACWH with plate heat exchanger. High effectiveness of heat exchanger will prevent malfunction of the system.

Table 1. Comparison of ACWH systems with various heat exchangers and testing schematic

Parameters	PHE	Triple Shell Pass [7]	Double Shell Pass [6]	Single Shell Pass [5]
T water in (^{0}C)	29.64	23	28	27
T water out (^{0}C)	46.59	60	47	47
ε (%)	78.5	59	22	27
COP	3.98	3.78	2.76	N/A

6. Conclusions

Based on data and analysis gained during testing, some conclusions can be concluded as the results of this testing:

- Using 1 PK rated Air Conditioner, water flow rate 50 – 200 L/hr and 2600 W cooling load, ACWH system can produce hot water with 35 – 47 ^{0}C. Higher water flow rate will result in lower hot water temperature
- With 100 L/hr water flow rate and 1800 – 2600 W of cooling load, the system can produce hot water at 39 – 41 ^{0}C temperature. The higher the cooling load, the higher hot water temperature produced.
- S-ACWH system will decrease compressor's work compared to normal AC system due to heat recovery
- S-ACWH system will produce higher performance than normal AC. Performance will increase 20 – 100 % compared to normal AC performance.

Acknowledgment

This research has been funded by Hibah Bersaing DIKTI 2008.

7. References

[1] E.F. Gorzenik. Heat water with your air conditioner. Electrical World 188 (11) (1977), 54-55

[2] O'Neal et al. Energy and economic effects on of residential pump water heater. CONF-790107-2, Oak Ridge National Laboratory, USA, 1997

[3] Jie Ji, Tin-tai Chow, Gang Pei, Jun Dong, Wei He, Domestic air-conditioner and integrated water heater for subtropical climate, Applied Thermal Engineering, Volume 23, Issue 5, April 2003, pp.581-592

[4] P. Techarungpaisan, S. Theerakulpisut, S. Priprem, Modeling of a split type air conditioner with integrated water heater, Energy Conversion and Management, Volume 48, Issue 4,2007, pp.1222-1237

[5] Nandy Putra, Dian Mardiana, Muliyanto, Kinerja Alat Penukar Kalor pada Air Conditoner Water Heater, Prosiding Seminar Nasional Efisiensi dan Konservasi Energi (FISERGI) 2005, 12 Desember 2005, ISSN 1907-0063, Universitas Diponegoro, Semarang, Indonesia.

[6] Nandy Putra, Amry D Hidayat, Nasruddin, Karakteristik Unjuk Kerja Penukar kalor Double Shell pada sistem aur conditioniner Water Heater, Seminar Nasional Perkembangan Riset dan Teknologi di Bidang Industri Universitas Gajah Mada Yogyakarta, 27 Juni 2006. ISBN 979-99266-1-0

[7] Nandy Putra, Nasruddin, Handi, Agus LMS, Sistem Air Conditioner Water Heater dengan Tiga Alat Penukar Kalor Tipe Koil disusun Seri, Seminar Nasional Tahunan Teknik Mesin 6, 2007, Banda Aceh, Universitas Syah Kuala, 20-22 Nopember 2007, ISBN 979 97726-8-0

[8] H.J. Laue, Regional report Europe: ''Heat pumps—status and trends'', International Journal of Refrigeration 25 (2002) 414–420

ISSN 114-1284

Application of Modified Equalizer Signal Processing for Enhancing Incipient Damage Signal from Solid Machine Element

Nirbito W.[1], Sugiarto B.[2], Priadi D.[3]

[1,2]*Dept. of Mechanical Engineering*
Faculty of Engineering
University of Indonesia, Depok 16424
Tel : (021) 7270032. Fax : (021) 7270032
E-mail : wahyu.nirbito@ui.edu; bangsugi@eng.ui.ac.id

[3]*Dept. Of Metallurgy and Material Engineering*
Faculty of Engineering
University of Indonesia, Depok 16424
Tel : (021) 7270011. Fax : (021) 7270077
E-mail : dedi@eng.ui.ac.id

ABSTRACT

Since incipient damage in solid was in the state of microstructure disintegration and did not vibrate the body yet, therefore common practice to detect failures by detecting its vibration could not be applied. So there were 2 major efforts must be done in order to detect such incipient damage. Firstly was the designing and manufacturing of sensor which could sense the stress waves generated due to the microscopic disintegration of the solid material. Secondly was the developing of signal processing techniques which could enhance and show up the signals of the incipient damage, i.e. microscopic damage.
The propagating stress waves as the so called Acoustic Emissions were captured by a specially designed AE sensor. However, the signals were corrupted or buried under the background signals, i.e. noise. Many attempts to clean up such noise have been done in various researches were based on conventional adaptive noise cancelling that applying mathematical methods. The authors of this paper had researched the so-called equalizer which was a technique to reconstruct the convoluted signal into a delayed form of the original signal by implementing iterative process. However, some modification should be made in the routines of the common basic structure in order to suit with the characteristics of the stress wave. The simulation gave satisfactory results, as well as the tests with real data from real time experimental.

Keywords: *signal processing, blind deconvolution, vibration, condition monitoring.*

1. INTRODUCTION

In machines maintenance practice, the ability to detect the occurrence of early damage before a catastrophic failure happen will improve the utilization performance of the machines since its failures can be predicted better and the machines can be utilized most to the real limits.
Microscopic disintegration would be present first in the solid material of a machine element before fractures occurred. As the crystalline molecules started to disintegrate, energy would be released as wave of stresses. This wave would propagate throughout the solid material in a form of longitudinal Raleigh waves. Since the wave was propagating in same form of sound wave, this stress propagation was also called as Acoustic Emission. From vibration point of view, the stress wave had very high frequency but with very low amplitude. Therefore, the wave was not strong enough yet to vibrate the machine element or been detected by common sensors such as accelerometers or velocity transducer. Even though the stress wave was present but it was totally buried under other vibration signal sources as noise. If the presence of the stress wave could be detected, it means that the incipient damage was known since this wave was generated due to the disintegration of the crystalline molecules of the solid material prior the real sensible fracture occurred.
A specially designed sensor had been developed and successfully been used in this research to capture signals of incipient damage from the solid material of a machine element [1]. However, other means were still needed to reveal the real stress wave that originated from the incipient damage out of the noise. Many attempts had been done in various researches but still with unsatisfactory results. The main problem was the ability to differentiate between the real stress wave and the other wave as noise. Most researchers used mathematical methods directly as well as noise cancelling methods in trying to clean the noise from the real signal. Mathematical methods such as Hillbert Transform, Least Mean Square (LMS), Griffith algorithm, Estimation Maximization algorithm as well as the Auto Regressive methods were used as the core of the Adaptive Noise Cancelling technique. Many authors had reported

ISSN 114-1284

such researches for the noise removal process. However, the application of such methods were still not yet ready for real practice since many difficulties and unsatisfactory results were found [2]. Other techniques regarding noise removal or signal cleaning in other fields such as communication, mobile telephones etc. had been explored and studied in this research. In mobile communication there was the so-called equalizer for reconstructing convoluted signals. Basically it was a technique to reconstruct the convoluted signal into a delayed form of the original signal by implementing iterative process. The process involved a parallel Finite Impulse Response Filters, which were iteratively calculated and analyzed. By treating the signal, which captured by the specially developed sensor, as a digitized discrete time series then the original stress wave signal had been successfully revealed [3,4].

2. ANALYTICAL MODEL

In the real practical situation, the observed signal from a measurement was not the original input signal, but was the convolution result of the original input signal $x[n]$ with the impulse response system $h[n]$ plus corrupted by noise $s[n]$. The original input signal was inaccessible and the impulse response system was unknown. The system or the channel was comprised the physical transmission media and channel as well as the transmit and receive filters. In Digital Signal processing, convolution was the computation of the output signal $y[n]$, given knowledge of both the input signal $x[n]$ and the impulse response $h[n]$ of the system. Just the opposite, deconvolution refers to the determination of the impulse response of the system $h[n]$ or the input signal $x[n]$ whereas the output of the system $y[n]$ was typically accessible. With the availability of a reliable model of the system, the unknown input signal could be estimated. Since convolution was commutative, the deconvolution problems were mathematically equivalent and the solution was relatively straight forward [5,6]. In the efforts to enhance incipient damage signal from solid machine element, the original signal of the solid machine element was inaccessible directly, whereas the channel impulse response was unknown. To capture the original signal, this situation raised the need for a deconvolution process without any a priori knowledge of the channel/system or the original input signal. Since this process was performing "blindly", it was called as the blind deconvolution. Figure 1 below showed a basic configuration of a blind deconvolution. In order to reconstruct the original signal, a system that optimally removed the distortion that an unknown channel induced on the transmitted signal was needed .

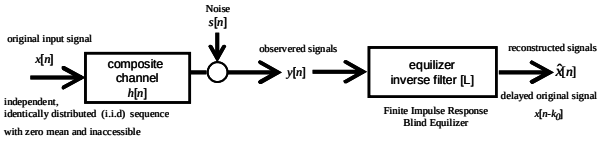

Figure 1 blind deconvolution system model for enhancing incipient damage signals

This system was classically known in mobile communication field as equalizer. Unlike the ordinary equalizer, this blind equalizer performed without access to the original input or any known training sequence, target or desired signal in terms of adaptive filtering. The objective was to deconvolve the receiver input $y[n]$ to retrieve the channel input $x[n]$. The output of the blind equalizer was denoted $\hat{x}[n]$. It could be restated as to find the Finite Impulse Response (FIR) of the inverse filter $e[n]$ that will give $\hat{x}[n]$ was as close as possible to the delayed original signal $x[n-k_0]$ in the Mean Square Error (MSE) sense [2, 3, 4] :

$$\mathrm{MSE}(e,k_0)\underline{\Delta}\sum\{|\hat{x}[n]-x[n-k_0]|\}^2 \Rightarrow \text{minimum} \qquad (1)$$

The process for enhancing the corrupted signals, involved a parallel Finite Impulse Response Filters, which were iteratively calculated and analyzed. Figure 2 below showed the block diagram of blind deconvolution (blind equalizer) iterative system model [7].

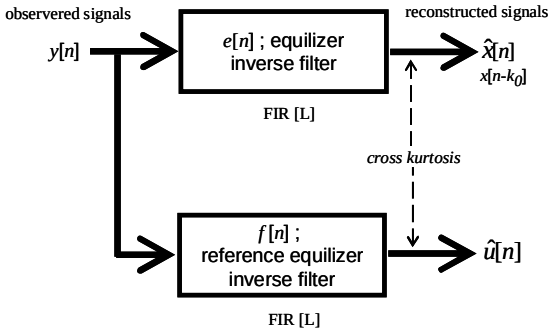

Figure 2 Block Diagram of Blind deconvolution iterative system

Basically by using the analog-digital signal acquisition, the total observed signals were digitized to be time series. Then it was processed as statistical cummulants as Shalvi and Weinstein higher order statistics operation methods. However, the algorithm required pre-knowledge of the excitation signal such as kurtosis and mean value and the convergence was generally slow because their method was based on stochastic gradient algorithm. To overcome those hindrances, beside an equalizer with $e[n]$ was the equalizer impulse response, was introduced to the channel output $y[n]$ to produce an output signal, a second parallel inverse filter with the same order was introduced as a reference system filter. The task of the second filter was to generate an implicit sequence of reference data for the iteration process. The impulse response of second filter was denoted by $f[n]$. The solution to blind deconvolution was based on the maximum "cross kurtosis" quality function [8]. Cross kurtosis between $\hat{x}[n]$ and $u[n]$ could be used as a measure of equalization quality. Using the convolution between the equalizer input and output signals, the cross-cumulant of the observed signal $y[n]$ and the reference signal $u[n]$, could be used to maximize the quality function [8,9]. Numerical techniques that been used to solve the iterative higher order

statistics operation were the Eigen calculation in Eigen Values determination method which was originating from the Blind Deconvolution method. The eigenvector algorithm (EVA) method originally developed by Kammeyer and Jellonek [9,10]. It based on cross kurtosis of two higher order cumulants and maximized the kurtosis criterion. Using this method, the characteristic of the inverse channel could be estimated directly from a number of samples of the observed signal. The iterative procedures consisted of calculating the blind equalizer impulse response and the outputs of the filters. After a certain number of iterations (based on the received data samples), both the reference and the equalizer systems will have a set of coefficients very close to the Minimum Mean Square Error equalizer [10].

Using the convolution between the equalizer input and output signals, the cross-cumulant of the observed signal $y[n]$ and the reference signal $u[n]$, can be used to maximize the quality function [10]. The cross cumulant of the output signal $u[n]$ and observed signal $y[n]$, denoted as C_4^{uy} could be calculated as written below.

$$C_4^{uy} = E\{|u(k)|^2 y_k y_k^*\} - E\{|u[k]|^2\}E[y\{y_k y_k^*\} - ..... \\ .....E\{u[k]y_k\}E\{u[k]^* y_k^*\} - E\{u[k]^* y[k]\}E\{u[k]y_k^*\} \quad (2)$$

" * " denoted the convolution operator.

As a Hermitian cross cumulant matrix, C_4^{uy} could be rewritten as scalar cross-cumulants where the symmetry property $C_4^{uy}(i_1,i_2) = [C_4^{uy}(i_2,i_1)]^*$ was exploited as:

$$C_4^{uy} = \begin{bmatrix} C_4^{uy}(0,0) & [C_4^{uy}(-1,0)]^* & ... & [C_4^{uy}(-l,0)]^* \\ C_4^{uy}(-1,0) & C_4^{uy}(-1,-1) & ... & [C_4^{uy}(-l,-1)]^* \\ ... & ... & ... & ... \\ C_4^{uy}(-l,0) & C_4^{uy}(-l,-1) & ... & C_4^{uy}(-l,-l) \end{bmatrix} \quad (3)$$

If R_{yy} represented the Toeplitz autocorrelation matrix of the observed signal $y[n]$, e was the equalizer impulse response and σ_d^2 denoted variance of the signals, then,

maximized $\left|e^* C_4^{uy} e\right|$ was subjected to $e^* R_{yy} e = \sigma_d^2$ (4)

$$C_4^{uy}{}_e = \lambda\, R_{yy}\, e \quad (5)$$

$$R_{yy}^{-1}\, C_4^{uy}\ e_{EVA} = \lambda\ e_{EVA} \quad (6)$$

Equation (5) and (6) were the Eigen Vector Algorithm EVA equations for determining the coefficient vector $e_{EVA} \underline{\Delta} [e_{EVA}(0),.....,e_{EVA}(l)]^T$. It could be obtained by choosing the eigenvector of $R_{yy}^{-1} C_4^{uy}$ associated with the maximum magnitude Eigen value λ, and was called the EVA-(l) solution to the problem of blind equalization. The e_{EVA} were calculated by choosing the most significant eigenvector of the estimated $R_{yy}^{-1}\, C_4^{uy}$. The calculation process gave the result as the MMSE (minimum mean square error) criterion was met in the iteration. These eEVA results were denoted then as $e_{EVA}^i[n]$ of the blind equalizer. Iteratively, load back the $e_{EVA}^i[n]$ into the reference system as a new estimation of $f[n]$. This iteration process produced the latest $e_{EVA}^i[n]$, until a sufficient equalization result was obtained (controlled by a relative error value set up), or the equalizer coefficient did not change anymore, i.e. the relative error is smaller than the set value [8,9,10]. The calculations routines were prepared and written on the Matlab® platform.

However, some modification should be made in the routines of the equalizer structure in order to suit with the characteristics of the stress wave. Since the method required a Bayesian type of series, a modification to remove the mean value or to shift the time domain signal to zero mean axis had been added prior the numerical processes stated above could begun. Numerical method steps for doing this were called as "remmean" subroutine, which was written in Matlab® as well. The maximum number of iteration was set to 120 times or the MSE value of 0.005 was reached whatever came first. This set up value was a reasonable value based on time, cost, affectivity and efficiency of an iteration operation with an acceptable result. Since the SNR were not known and with a variety due to the nature of the defects, a "moderate" value of 32 was taken for the FIR filter length [11,12]. The signals of the incipient damage could be detected as pulses showed in the time domain signal waves. This signal pulses, were defined as The Crest Factor, i.e. a ratio of the maximum peak of the signal over the RMS value. The Crest Factor could be regarded as a feature in condition monitoring or fault diagnosis.

$$\text{Crest Factor} = \frac{\text{Maximum Peaks}}{\text{RMS}} = \frac{X_{peak}}{\sqrt{\frac{1}{N}\sum_{i=1}^{N} X_i^2}} \quad (7)$$

The Crest Factors were good indicators to assess the property of the output signals. Even though a large amount of data is needed to be captured for accuracy, in the processing only some percentage of the total numbers was needed. This would be a significant saving in time and calculation efforts if the optimum percentage of samples could be determined first. The EVA approach in detecting signals had sensitivity in a range of SNRs in terms of Crest Factor and Energy. The signal energy levels stay relatively constant for SNRs less than 0.5 whereas the crest factors were hovering in a certain range. But at low SNR, interesting results were shown with a low Crest Factor and a high Energy. However, these relationships could not be used straightforward directly for determining the optimum number of samples data based on the high Crest factor since the Energy level could not be directly related to the number of samples [12,13]. The highest crest factor was appeared from processing an optimum percentage of data samples. For best practices, data samples should be captured at least twice the maximum frequency of interest times he capturing time, e.g. 3 revolutions. But it already revealed that by using too many samples data, i.e. more than 50%, the enhancement process would fail to show the original signals up. Therefore, the first step was to find the optimum percentage of the data sample points according to the

ISSN 114-1284

maximum crest factor value was found. Then after the optimum numbers of samples to be processed were determined, the real Blind Deconvolution full process were run to reconstruct or to enhance the original desired signals. So, the usage of all series data of the signal could be avoided to save the iteration time as well as to improve the result. Figure 3 on next page showed the Flow Chart of Digital Signal Processing for enhancing signal from incipient damage of solid machine element [13,14].

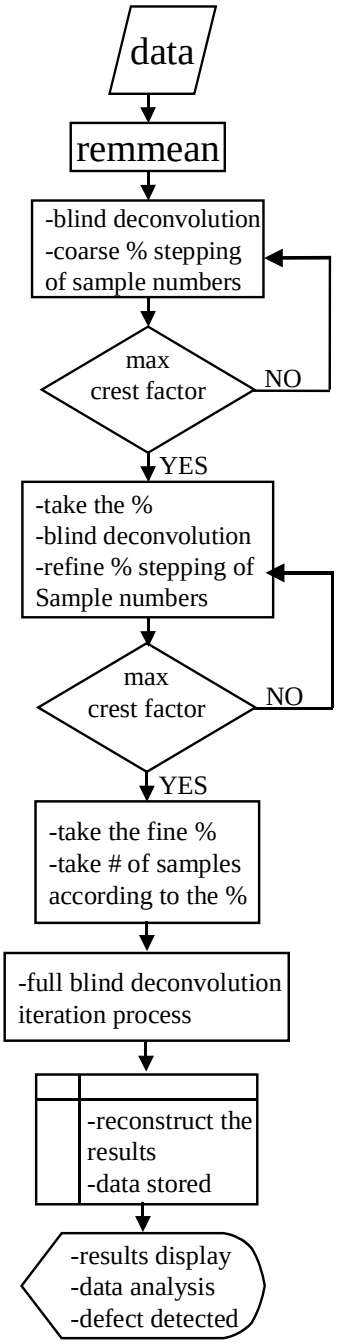

Figure 3 DSP flow chart to enhance signal of incipient damage from solid machine element

3. EXPERIMENTAL

Computer simulation data were firstly used to test the function ability and the reliability of the method. An experimental rig was constructed to test the feasibility of using the EVA blind deconvolution to detect a simulated rolling element bearing failure under controlled conditions. The bearing was set to rotate at a fixed rpm rate that gave its bearing defect frequency.). A schematic of the modeling process was shown in figure 4 below. A constant impulsive response $h[n]$ were provided by the machine element. Simulated noise signal data were generated using the series generator of a DSP software and sinusoidal wave generator via PZT actuator. Number of data points, spacing, values range, mean values and standard deviation were parameters that been set up when generating the simulated noise [12,13].

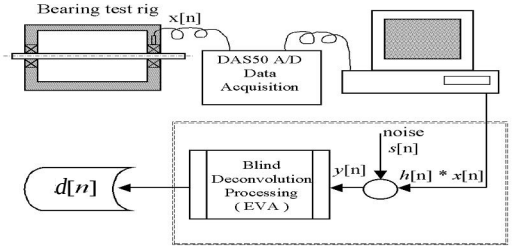

Figure 4 Schematic Diagram of the simulation experimental system set up

After that, real data from real time laboratory experimental tests were used as the experiment stage 2. Figure 5 below showed the real time experimental set up.

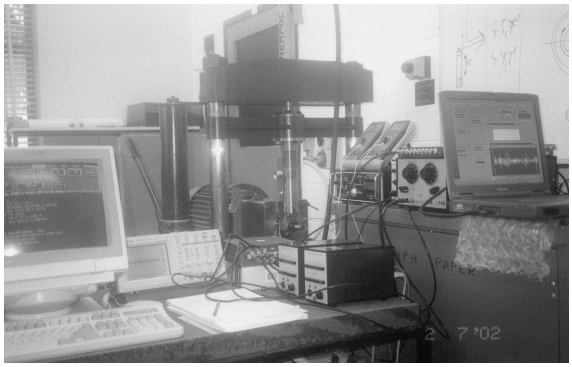

Figure 5 real time experimental and observation test rig

A test rig consisted of a hydraulic press and an electric motor and a set of sensors mounting were built. A new ball bearing, which installed on the output shaft of the electric motor, was loaded radially by the hydraulic jack and simultaneously was rotated at a normal operating speed by the electric motor. It was set up for a simulated extreme real operation condition. By using the bearing life/performance calculation procedures, i.e. from the manufacturer-operating manual, it was predicted that the ball bearing would last for 117 hours in that extreme operation condition. Specially designed AE sensor and common

accelerometer sensor were used to detect the signal and to compare the capability of both sensors in detecting incipient damage. With real time observation and offline signal processing, then the ball bearing condition was monitored and analyzed every hour. Reconstructed signals were extracted from the observed signal after the observed data were processed offline with a computer with the application of the Blind Equalizer Digital Signal Processing method. The method had succeeded to reveal the stress wave from the noise-corrupting signal [11,12,13,14].

4. RESULTS AND DISCUSSION

A numerical iteration procedure was executed with blind deconvolution calculation for refining number of samples in order to find the optimum samples numbers to be used in the Blind Equalization steps. These iterative calculation processes were based on the maximum Crest factor determination with regard to the optimum sample numbers been used. Figure 6 below showed that the optimum percentage of data samples were needed to enhance signal pulses, i.e. Crest Factor, significantly were in the range of 30% to 40%. The optimum percentage of data samples were the one that gave the highest crest factor value. It also showed that the enhancement process would fail to show the

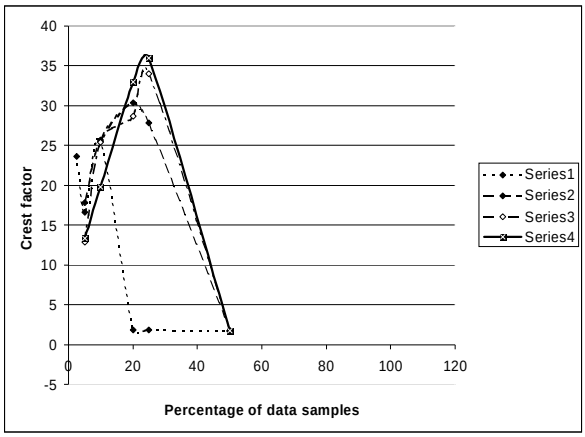

Figure 6 Percentage of data samples been used according to the maximum Crest Factor value

original signals up if using too many samples data [13, 14].

The simulation gave satisfactory results, as the reconstructed signal was so similar to the original simulated signal data. A number of tests were conducted to test the sensitivity of the technique in detecting a minute defect masked by a range of corrupting with varying SNRs. The amplitudes to mask the bearing signal were adjusted to give a range of signal-to noise ratios (SNR). It was evident that the generated noise has masked the bearing signal. However, higher SNR above 0.738 were not used in the test, as the bearing signal became more prominent and was clearly visible. Figure 7 showed the corrupted signal at low-level noise (SNR=0.738) and the reconstructed signal output after blind equalization process. Figure 8 showed the corrupted signal by high level noise (SNR=0.262) and the original signal after blind equalization reconstruction process. Both outputs, from low level noise and high level noise, distinctly showed the defective bearing signal with an impact rate corresponding to an outer-race bearing defect. Figure 9 showed the original signal from a simulated outer race defect bearing. From figure 7 and 8, it could be seen that the Crest Factors and signal energy levels of the reconstructed signals were similar to that of the original bearing as shown in figure 9.

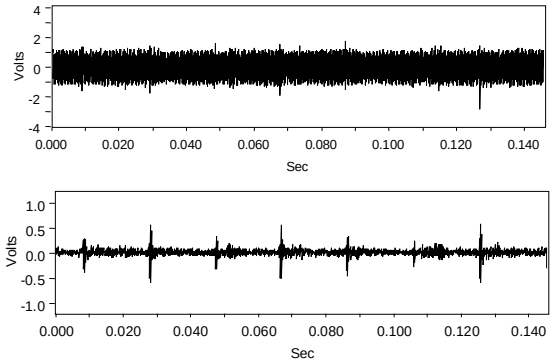

Figure 7 Corrupted signal at low level noise and result from blind equalization reconstruction process

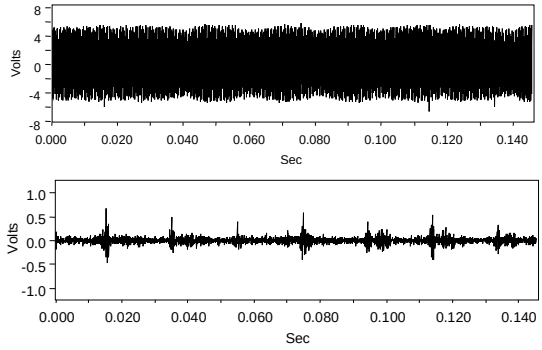

Figure 8 Corrupted signal at high level noise and result from blind equalization reconstruction process

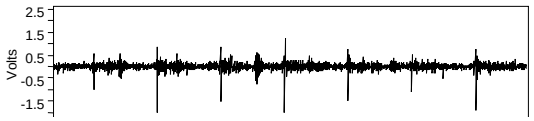

Figure 9 Original signals from simulated defect bearing

For the real practical tests, a new ball bearing which was installed on the output shaft of an electric motor and simultaneously rotated at a normal operating speed, was loaded radially by a hydraulic jack. With real time

ISSN 114-1284

observation and offline signal processing, then the ball bearing condition was monitored and analyzed every hour. Reconstructed signals were extracted from the observed signal after the observed data were processed offline with a computer using the blind equalization technique. Figure 10 on next page showed firstly the observed signal after 115 hours run, captured by the AE sensor, which contained the original signal of the microscopic defects, electric line noise as well as other noise, and secondly the reconstructed signal as a result from the blind equalization process. It was quite clear that all noise, including noise due to the electricity frequency were cleaned up and the little pulses were enhanced and appeared as the microscopic defect signals.

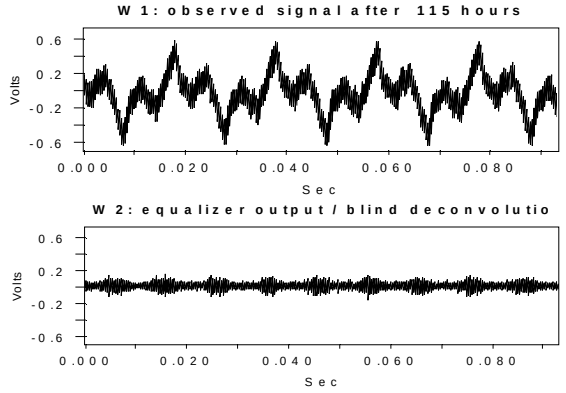

Figure 10 Corrupted signal after 115 hours test run and result from blind equalization reconstruction process

For next test, another new type of bearing was installed on the electric motor shaft and rotated, was extremely loaded to shorten its operating life hours in order to have efficient and effective observation time. 2 types of sensors were installed, i.e. AE sensor and common accelerometer sensor. Accelerometer sensor was used to get a comparison of the signals in order to prove that the signals which captured by the AE sensor were came from incipient damage, since incipient damage signal could not been detected by common accelerometer because the stress waves from such incipient damage were very low in amplitude so therefore had not vibrate the machine element body yet.

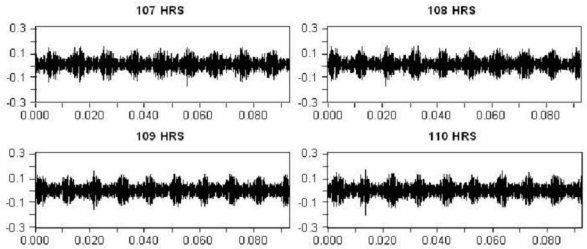

Figure 11 Reconstructed signals as result from blind equalization reconstruction process on observed signals after 107 to 110 hours test run

Figure 11 above showed that the blind equalization method had successfully eliminated the corrupting noise. The shape of the reconstructed time domain signal changed where signs of impacts clearly appeared. These impulsive signals were due to the AE signals from incipient damage in the bearing. These reconstructed bearing signals with pulses suggested that the bearing had a localized incipient defect. Whereas from figure 12, it showed the facts that the reconstructed signals were unchanged from that the observed or measured signals by the common accelerometer for the same bearing. No sign of impacts in the bearing that was detected by common accelerometer. This was due to the reality that the bearing was not vibrating since it had not had physical damage yet.

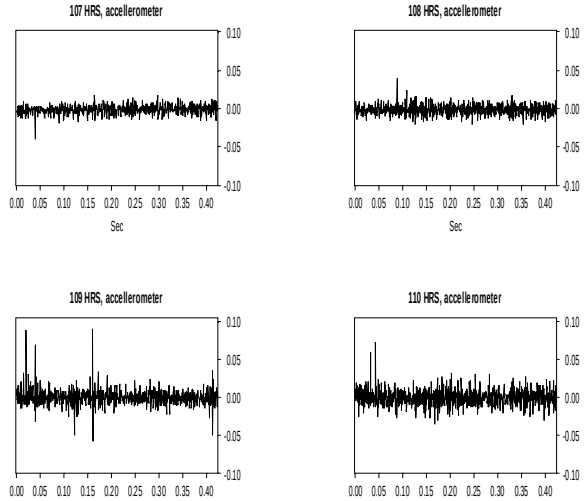

Figure 12 Reconstructed signals as results from blind equalization reconstruction process after 107 to 110 hours test run, from same bearing, detected by common accelerometer

Physical checks on the bearing showed nothing significantly to be the defect. This bearing was relatively still in a good condition, even the pulses in the signals were very clear. The number of pulses, which appeared in a certain time, would show the frequency of the impact/pulses. The vibration frequency told us that the incipient defect was in the outer race but still in a microscopic level since no significant sign of defect on the outer race could be seen visually. This was due to the facts that the frequency of the pulses in the time domain waveform was matched with the frequency of BPFO (Ball Passing Frequency Outer) of the test bearing. The reconstructed bearing signal with pulses suggested that the incipient defect was localized and in microscopic level, i.e. microstructure disintegration, in the solid material of the bearing outer race [13,14,15].

5. CONCLUSION

The advantages of blind equalization as a technique to recover the original signal of a typical faulty solid machine element, i.e. rolling elements bearing, which corrupted by noise and distorted by the transmission path were revealed. This technique that been developed with the numerical iteration method had shown its capability to enhance the

signal of incipient damage in the solid material of a machine element. The Blind deconvolution/equalization had been successfully developed based on Eigen vector approach (EVA) to enhance the incipient damage signals from the observed signals. The results showed the superiority of the technique in extracting the signals from a total observed signal that was corrupted by noise. It was found that there was a good agreement between the graph to determine the optimum percentage of sample numbers and the results of the blind equalization processes. The optimum values from the graph were matched with result from the preprocessing calculation which gave the values in a range of 30%-40% number of optimum samples. It was found that this procedure worked well and the incipient damage signals had been recovered from the observed signal. This technique clearly reproduced the original signal and worked very well with periodic noises, which could be very suitable from rotating machine elements. Since the characteristic frequencies contained very low energy, and usually are overwhelmed by noise and higher levels of macro-structure vibration, than it was difficult to identify them in the frequency spectrum. However, the defect could be detected directly from its time domain waveform, i.e. the equalizer outputs, even at an early stage of failure, still in microscopic level, far before the significant real defects could appear. The research would be developed later on to be a new technique in detecting very early damage, which no technique could do before. The most benefit of this method meanwhile was the contribution in improving the performance and the best practice of the vibration condition monitoring in the predictive or reliability centered maintenance.

6. ACKNOWLEDGMENT

The authors would like to acknowledge and appreciate highly the assistances and supports from Prof. Andy Tan of Mech. Eng. QUT, and the research facility supports from Dynamics and Vibration Laboratory of QUT, Brisbane-Australia, where most of the works regarding this research were done there. The authors would like also to acknowledge and appreciate highly the permission granted, via email, to explore, apply, adjust, enhance and/or improve the EVA technique for the Blind Deconvolution method as well as to use it in the authors' research for academic purposes; from Prof. Kammeyer and all his assistants at the University of Bremen West Germany.

7. REFERENCES

[1] A.C.C. Tan, M. Dunbabin and W. Nirbito. "Piezoceramic Sensors and Actuators for Vibration Detection and Control". in the 2nd ACSIM. 2000, 23-25 August. Nanjing - ROC.

[2] Tan A.C.C., and Mathew J. The Adaptive Noise Cancellation and Blind Deconvolution Techniques for Detection of Rolling Elements Bearing Faults – A Comparison. in the 3rd ACSIM. 2002, 25-27 September. Cairns, QLD - Australia: QUT.

[3] Tan, A.C.C., Nirbito, W., Mathew, J., "Detection of Incipient rolling element bearing failure by blind deconvolution", Keynote paper, Asia-Pacific Vibration Conference, APVC 2001, October 2001

[4] Nirbito W., Tan C. C., Mathew J., "Detection of the Incipient Rolling Elements Bearing Defects, Directly from Time Domain Vibration Signals, by Using a Non- Mechanical Sensor", 7th Quality In Research (QIR) International Conference, FT-UI Depok, 2004

[5] Haykin, S.S., "Blind Deconvolution". Prentice-Hall information and system sciences series. 1994, Englewood Cliffs, N.J: PTR Prentice Hall,. ix, 289.

[6] Oppenheim, A.V., R.W. Schafer, and J.R. Buck, "Discrete-Time Signal Processing". 2nd ed. 1999, Upper Saddler River, N.J.: Prentice Hall,. xxvi, 870.

[7] Nirbito, W., A Strategy of Determination of The Machine Elements' Incipient Defects By Detecting The Acouctic Emissions/ Stress Waves Propagation, 4th Annual National Conference on Mechanical Engineering, Bali, Indonesia November 2005.

[8] Kammeyer, K.-D. and B. Jelonnek. "Eigenvecto Algorithm for Blind Equalization". in IEEE Signal Processing Workshop on Higher-Order Statistics. 1993. Lake Tahoe, California USA: ELSEVIER Signal Processing.

[9] Kammeyer, K.-D., B. Jelonnek, and D. Boss, "Generalized Eigenvector Algorithm for BlindEqualization". ELSEVIER Signal Processing, 1997. 61(No. 3, September): p. 237-264.

[10] Boss, D., B. Jelonnek, and K.-D. Kammeyer, "Eigenvector Algorithm for Blind MA System Identification". ELSEVIER Signal Processing, 1998, April. 66 (No. 1): p. 1-28.

[11] Nirbito, W., A.C.C. Tan, and J. Mathew. "The Enhancement of Bearing Signals Corrupted by Noise Using Blind Deconvolution - A Feasibility Study". in the 2nd ACSIM. 2000, 23-25 August. Nanjing - ROC.

[12] Nirbito, W., Tan, A.C.C., and Mathew, J., "Detecting The Bearing Signals in Noise by The Application of Blind Deconvolution – a Simulation", Asia Pacific Vibration Conference (APVC), Gold Coast, Queensland –Australia, 2000.

[13] Nirbito, W., Tan, A.C.C., and Mathew, J., "Detecting Incipient Defect Of Rolling Elements Bearing By Applying The Blind Deconvolution Method In Numerical Technique". in the 4th International Conference on Numerical Analysis in Engineering, April, Yogyakarta-Indonesia: IC-STAR USU and JICA, 2005.

[14] Nirbito, W., Sumardi T.P., Tan C.C. "Improving the Enhancement of Corrupted Signal in Noise: An Optimation of Blind Deconvolution EVA Method by Reducing Samples Size on Maximum Crest Factor", in the 5th International Conference on Numerical Analysis in Engineering, May, Padang-Indonesia: IC-STAR USU and JICA, 2007.

[15] Nirbito W., Priadi D., Sugiarto B., "The Development of New Technique to Detect Incipient Damage in Machine Component", in the International Conference On Materials and Metallurgical Technology (ICOMMET), June, Surabaya-Indonesia, ITS, 2009

ISSN 114-1284

Fireproofing Required Area at Process Train

Nugrahanto Widagdo

SHE-Q Department
PT Badak NGL, Bontang 75324
Tel : (0548) 552952. Fax : (0548) 552320
E-mail : nugrahantow@badaklng.co.id

ABSTRACT

As one of passive fire protection application in industry, fireproofing practice is quite beneficial to provide a degree of fire resistance for protected structures and equipment during emergency condition. Normally this practice was conducted at the design phase of constructing a new plant. However in an operating plant, fireproofing application shall be inspected regularly by conducting a fireproofing survey. From this survey, further evaluation is required to review the application.

During 2008 Full Risk Insurance Survey in PT Badak NGL, this practice was also highlighted. Since PT Badak NGL as widely recognized company is highly concern on safety for plant operation, therefore efforts to review the application and standardize the area required fireproofing at Process Trains was introduced. By using API 2218 as guidance, evident parameters and methods used to determine fireproofing area is stated. Methods used for determining the area in this paper consist of identifying type of fire that might occur, developing scenarios and analyzing consequences of each impact of scenarios on Process Train areas. Based on the result, a fireproofing required area mapping could be generated.

Keywords:

Passive fire protection, fireproofing, pool fire, consequence analysis, Process Train

1. INTRODUCTION

As like any other industries that deal in flammable liquids and gases, PT Badak NGL also concerns on the hazards of the fluid. These kinds of risk shall be managed to avoid undesired events such as explosions and fires. Therefore a system to protect the plant during emergency must be ready at all times. One of protection system which available in PT Badak NGL is fireproofing that could provide protection on equipment and structures to withstand fire exposure for certain amount of time.

During PT Badak NGL extensive experience, fireproofing practices which has been applied are maintained by conducting inspection, review and assessment. On fireproofing survey at Process Trains conducted internally, it was identified that several locations shall be determined whether those locations shall be fireproofed or not. Based on that purpose and also from external Insurance inspection recommendations in 2008, a review is needed on fireproofing requirements based on risk that exposed to the equipment or structures. The review is referred to API Publication 2218 – Fireproofing Practices in Petroleum and Petrochemical Processing Plants to generate the guidance and fireproofing mapping at Process Trains.

2. REQUIREMENTS

The term of Fire-Proof, as mentioned in the API Publication 2218, does not mean totally safe from the effects of fire. Fireproofing refers to the systematic process (including materials and the application of materials) that provides a degree of fire resistance for protected substrates, therefore it is also categorized as the passive fire protection. On the publication it is stated that to provide protection, the severity and duration of the fire scenarios shall be determined. However PT Badak NGL had determined that the fireproofing materials shall resist from fire for 90 minutes, referred to PT Badak NGL General Specification No. B.2.6 regarding Fireproofing.

This API document specifically addresses property loss protection for pool fires scenarios but not jet fires or vapor cloud explosions. Pool fires mainly selected due to intense and prolonged heat exposure that could cause collapse of unprotected equipment and lead to the spread of burning liquids. However the limit of the structures and equipment to withstand the heat radiation shall be determined.

Further consideration is derived from the publication that the computer modeling equates 300°C (572°F) to an exposure of approximately 12.5 kW/m^2 (4000 $BTU/hr\text{-}ft^2$) for exposure without fireproofing or water spray. This figure is applied for most of equipment, however since the other temperature limitation is higher and will be covered within the calculation, for instance for steel structure that can reach 538°C (1000°F), therefore heat flux of 12.5 kW/m^2 (4000 $BTU/hr\text{-}ft^2$) is selected for computer simulation.

In addition, related concern was also taken to generate mapping through layout of the plant rather than side view since it has already been covered in the standard. From all

above descriptions, it is obvious that this paper will emphasize on area required to be fireproofed rather than selection of fireproofing material.

3. METHODS

Since the fire type, heat flux and several considerations have been determined, the next step is to generate the fire scenarios. By considering pool fire as previously mentioned, the objective is searching the scenarios that provide intense and prolonged heat exposure of burning liquid. Several large lines, pressure vessel and tanks were then identified. Large pipelines were chosen since it could release tremendous amount of liquid hydrocarbon, while pressure vessels and tanks were selected by considering that they could hold level of flammable liquid. Vessels that were identified are shown on below table. Train H, as indicated in the table, was used in the calculation to provide the worst scenario effect since the Train has the biggest capacity among the others.

Table 1. Volume of Vessels Containing Flammable Liquid

Tag No.	Description	Tank Type	Total Volume (m^3)
H2C-1	Drier Separator Decanter	Vertical	26.18
H3C-1	Scrub Column	Vertical	14.80
H3C-2	Scrub Column Condensate Drum	Vertical	18.40
H3C-4	Deethanizer Column	Vertical	19.96
H3C-5	Deethanizer Condensate Drum	Horizontal	6.52
H3C-6	Depropanizer Column	Vertical	12.57
H3C-7	Depropanizer Condensate Drum	Horizontal	18.43
H3C-8	Debutanizer Column	Vertical	7.10
H3C-9	Debutanizer Condensate Drum	Horizontal	17.27
H4C-1	Propane Accumulator	Horizontal	149.08
H4C-2	High Level Propane Flash Drum	Vertical	89.63
H4C-3	Medium Level Propane Flash Drum	Vertical	72.71
H4C-4	Low Level Propane Flash Drum	Vertical	177.92
H4C-12	High Level Propane Knock Out Pot	Vertical	27.37
H4C-7	MCR First Stage Suction Drum	Vertical	42.64
H4C-8	MCR Second Stage Suction Drum	Vertical	71.59
H5C-1	High Pressure MCR Separator	Vertical	62.25
H5C-2	LNG Flash Drum	Vertical	47.08

During identification, vessels and lines on Plant 1 - CO_2 Removal Plant and Plant 2 - Dehydration Plant (except 2C-1 - Drier Separator Decanter) shall be excluded. Plant 1 was left out since the amine solution is not categorized as flammable liquid (as seen on its MSDS). As for Plant 2, there is no significant amount of hydrocarbon liquid observed that could stay for 90 minutes fire.

A release calculation then was performed to measure the size of liquid pools from various sources listed. During calculations, some assumptions were used such as using full bore release area for the leak size and 100% level of the flammable liquid in the vessel. At any instant in time, the rate of liquid spreading can be found by use of a simple hydrodynamic model,

$$\frac{dr}{dt} = \alpha\sqrt{h}$$

$$r = \alpha \int_0^t h^{1/2}\, dt \qquad (1)$$

where: r = pool radius at time t, m
t = time, s
α = constant = $\left[2g\left(\rho_s - \rho_{liq}\right)/\rho_s\right]^{1/2}$
h = pool height, m
g = gravitational acceleration, 9.8m/s^2
ρ_s = density of solid or ground, kg/m^3
ρ_{liq} = density of liquid, kg/m^3

The total volume of liquid released is measured with

$$V_{liq} = \int_0^t \frac{dV_{liq}}{dt}\, dt \qquad (2)$$

where: V_{liq} = volume of liquid in pool at any time t, m^3

Since the liquid pool size has been determined then the surface flux of the pool fire is calculated using the following equation,

$$q_{sf} = \dot{m}.\Delta H_c\left(1 - e^{-bD}\right) \qquad (3)$$

where: q_{sf} = surface flux of fire, kW/m^2
m = mass burning flux, kg/(m^2.s)
ΔH_c = the heat of combustion for the burning liquid, kJ/kg
b = extinction coefficient, dimensionless
D = diameter of the liquid pool, m

The surface of the flame is divided into numerous differential areas. The following equation is then used to calculate the view factor from a differential target, at a specific location outside the flame, to each differential area on the surface of the flame.

$$F_{dA_t - dA_f} = \frac{\cos(\beta_t)\cos(\beta_f)}{\pi r^2}\, dA_f \qquad (4)$$

where: $F_{dA_t - dA_f}$ = view factor from a differential area on the target to a differential area on the surface of the flame, dimensionless

dA_f = differential area on the flame surface, m^2
dA_t = differential area on the target surface, m^2
r = distance between differential areas dA_t and dA_f, m
β_t = angle between normal to dA_t and the line from dA_t to dA_f, degrees
β_f = angle between normal to dA_f and the line from dA_t to dA_f, degrees

The radiant heat flux incident upon the target is computed by multiplying the view factor for each differential area on the flame by the appropriate surface flux, atmospheric transmittance, then summing these values over the surface of the flame

$$q_{ai} = \sum_{A_f} q_{sf} \cdot F_{dA_t - dA_f} \cdot \tau \qquad (5)$$

where: q_{ai} = attenuated radiant heat flux incident upon the target due to radiant heat emitted by the flame, kW/m^2
A_f = area of the surface of the flame
q_{sf} = surface flux of fire, kW/m^2
τ = atmospheric transmittance, dimensionless

Equations (4) and (5) are repeated to achieve 12.5 kW/m^2 on each scenario.

4. DISCUSSION

All calculation was executed using Canary computer simulation as a supporting tool. By utilizing this software time required to calculate all scenarios was reduced significantly. Results of the calculation were sorted by scenarios that provided large impact. Summary of the top list results from the simulation are described in the table below.

Table 2. Major Impact Results of Pool Fire Cases for Heat Flux of 12.5 kW/m² (4000 BTU/hr-ft²)

No.	Source of Fire	Distance (Meters)
1	H4C-2	55.8
2	H4C-1	51.2
3	H5C-2	45.9
4	H4C-4	38.6
5	H4C-3	28.4
6	H5G-1A/B	28.1
7	H3C-1	25

From the table it can be seen that all of the results providing the largest impact were occurred from the vessels leak cases. It can be understood since vessels store large number of liquid that could sustain the heat radiation during 90-minute fire exposure. Therefore by these results, more attention on establishing and maintaining existing protection system on these vessels surroundings should be performed.

The last step was plotting those simulation results into plot plan of Process Trains. Each of the calculation was put together into one plot plan of Process Train and removed the similar overlapped radius of heat fluxes. The result of this plotting is shown below.

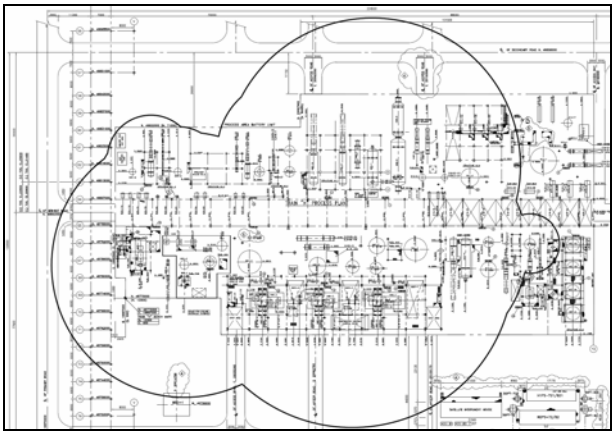

Figure 1. Fireproofing Required Area at Process Train

Hence as we can see, the area covered with radius of collective heat fluxes from all scenarios is the area that could be exposed to fire for at least 90 minutes, therefore fireproofing shall be applied within this area. In general, Plant 1 and Plant 2 (except 2C-1) as mentioned previously is not recommended to be fireproofed, however on the mapping, several areas (right side of the figure) at those plants still require fireproofing because those certain areas could also receive heat flux impacts from previous determined other scenarios.

Furthermore the result can be used as guidance for fireproofing application at other Process Trains. Besides the results, the methods used can be implemented to other areas such as storage tanks, loading docks and knock out drums at Storage & Loading areas.

5. CONCLUSIONS

The API Publication 2218 is a beneficial reference to determine fireproofing required area at the Process Trains, since some requirements have been clearly mentioned such as pool fire cases with heat exposure of approximately 12.5 kW/m^2 (4000 $BTU/hr\text{-}ft^2$). Therefore further sequential steps to identify and calculate the pool fire scenarios have been more structured.

From the calculation result, it can be deduced that the scenarios that provided large impact occurred on the vessels leak cases. Hence besides the fact that those vessels could hold certain amount of liquid which should

be well monitored, assessment on existing protection system at surroundings of the vessels shall be established and maintained.

Although the standard also provides guidance for fireproofing application on dimension of fire scenario envelope, the overall mapping on the plant could not be known directly from it. Through the mapping generated from all identified scenarios calculated in this paper, the required area to be fireproofed which in this case at Process Trains could be justified.

REFERENCES

[1] American Petroleum Institute, *Publication 2218 – Fireproofing Practices in Petroleum and Petrochemical Processing Plants*, 2nd Edition, August 1999.
[2] PT Badak NGL, *General Specification Volume IV B.2.6 Revision 2*, November 2001.
[3] Center for Chemical Process Safety (CCPS) of American Institute of Chemical Engineers (AIChE), *Guidelines for Consequence Analysis of Chemical Releases*, New York, First Edition, 1999.
[4] Quest Consultant Inc., *Canary by Quest User's Manual*, Quest Consultant Inc., Oklahoma, 2004.

ISSN 114-1284

Finite Element Analysis of Heavy Duty Truck Chassis Subjected by Cyclic Loading

Ojo Kurdi[2], Roslan Abdul Rahman[a] and Mohd Nasir Tamin[a]

[a] *Faculty of Mechanical Engineering*
Universiti Teknologi Malaysia
81310 UTM Skudai, Johor Bahru, Malaysia

[b] *Mechanical Engineering Department*
Faculty of Engineering, Diponegoro University
Kampus Baru UNDIP Tembalang
Semarang, Indonesia 50239
Tel: (024) 7460059
E-mail : ojokurdi@yahoo.com

ABSTRACT

The chassis of trucks is the backbone of vehicles and integrates the main truck component systems such as the axles, suspension, power train, cab and trailer. The truck chassis has been loaded by static, dynamic and also cyclic loading. Static loading comes from the weight of cabin, its content and passengers. The movement of truck affects a dynamic loading to the chassis. The vibration of engines and the roughness of road give a cyclic loading. Next, the materials and methods should be explained briefly. The chassis used in the truck have almost the same appearance since models developed 20 or 30 years ago, denoting that they are a result of slow and stable evolution of these frames along the years. The manufacturers of these chassis, in the past, and some still today, solve their structural problems by trial and errors. Conducting experimental test in the early stage of design is time consuming and expensive. In order to reduce the cost, it is important to conduct simulation using numerical methods by software to find the optimum design. Determination of static, dynamic and fatigue characteristic of a truck chassis before manufacturing is important due to the design improvement.. This paper presents the Finite Element Analysis (FEA) of heavy duty truck chassis subjected by cyclic loading using Finite Element (FE) software. The out put of this analysis is useful for failure analysis of chassis and as a preliminary data for fatigue life prediction of chassis. The both analysis are the important steps in design of chassis.

Keywords:
Finite Element Analysis, Truck Chassis, Cyclic Loading, Component Design, Stress Analysis

1. INTRODUCTION

The chassis of trucks is the backbone of vehicles and integrates the main truck component systems such as the axles, suspension, power train, cab and trailer. The truck chassis has been loaded by static, dynamic and also cyclic loading. Static loading comes from the weight of cabin, its content and passengers. The movement of truck affects a dynamic loading to the chassis. The vibration of engines and the roughness of road give a cyclic loading. The existing truck chassis design is normally designed based on static analysis. The emphasis of design is on the strength of structure to support the loading placed upon it. However, the truck chassis has been loaded by complex type of loads, including static, dynamics and fatigue aspects. It is estimated that fatigue is responsible for 85% to 90% of all structural failures [1]. The knowledge of dynamic and fatigue behavior of truck chassis in such environment is thus important so that the mounting point of the components like engine, suspension, transmission and more can be determined and optimized.

Many researchers carried out study on truck chassis. Karaoglu and Kuralay [2] investigated stress analysis of a truck chassis with riveted joints using FEM. Numerical results showed that stresses on the side member can be reduced by increasing the side member thickness locally. If the thickness change is not possible, increasing the connection plate length may be a good alternative. Fermer et al [3] investigated the fatigue life of Volvo S80 Bi-Fuel using MSC/Fatigue. Conle and Chu [4] did research about fatigue analysis and the local stress-strain approach in complex vehicular structures. Structural optimization of automotive components applied to durability problems has been investigated by Ferreira et al [5]. Fermér and Svensson [6] studied on industrial experiences of FE-based fatigue life predictions of welded automotive structures.

ISSN 114-1284

The objective of the work in this paper is mainly to focuses on the application of FEA of cyclic loading on the heavy duty truck chassis. Sub modeling technique has been applied on the critical area in order to find the more reliable, more accurate and faster way of simulation.

2. MODEL OF TRUCK CHASSIS

The model is depicted in Figure 1. The model has length of 12.350 m and width of 2.45 m. The material of chassis is Steel with 552 MPa of yield strength and 620 MPa of tensile strength [7].

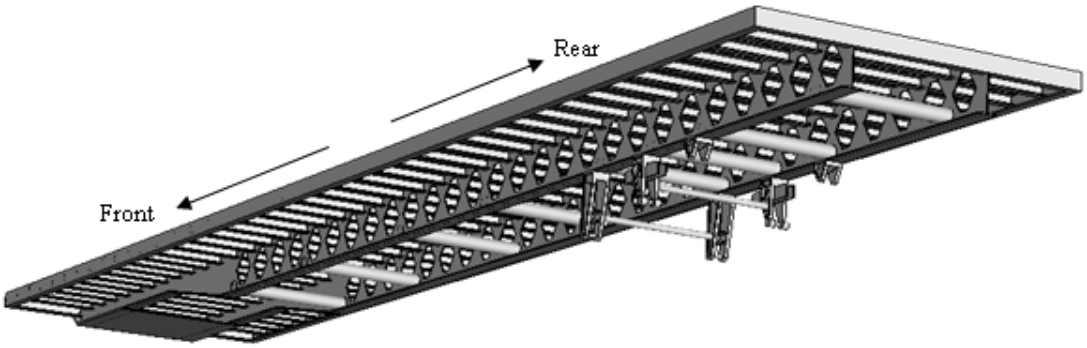

Figure 1. Model of truck chassis

The material properties of chassis are tabulated in Table 1. The truck chassis model is loaded by static forces from the truck body and cargo. For this model, the maximum loaded weight of truck plus cargo is 36,000 kg. The load is assumed as a uniform pressure obtained from the maximum loaded weight divided by the total contact area between cargo and upper surface of chassis. In order to get a better result, locally finer meshing is applied in the region which is suspected to have the highest stress.

Table 1: Properties of truck chassis material [7]

Modulus Elasticity E (Pa)	Density ρ (kg/m3)	Poisson Ratio	Yield Strength (MPa)	Tensile Strength (MPa)
207 x 109	7800	0.3	550	620

2.1 Boundary Condition of the Model

There are 3 boundary conditions (BC) of model; the first BC is applied in front of the chassis, the second and the third BC are applied in rear of chassis, as shown in Figure 2. The type of BC 1 is pinned (the displacement is not allowed in all axes and the rotation is allowed in all axes) that represent the contact condition between chassis and cab of truck. The BC 2 represents the contact between chassis and upper side of spring that transfer loaded weight of cargo and chassis to axle. In the BC3, the displacement and the rotation is zero in all axes on all of bolt's body. This condition is called fixed constrain. The bolt in BC 3 is assumed perfectly rigid. This assumption was realized by choosing a very high modulus Young value of the bolt properties.

2.2 Location of Critical Area

Based on the previous paper, The location of maximum Von Misses stress is at opening of chassis which is contacted with bolt as shown in Figure 3. The stress magnitude of critical point is 386.9 MPa. This critical point is located at element 86104 and node 16045 [8].

2.3 Submodeling Technique Application

Sub modeling technique is used to achieve efficiency in finite element analysis when details are required in sub-regions of a large structure. The sub modeling is also known as the cut boundary displacement method or the specified boundary displacement method.

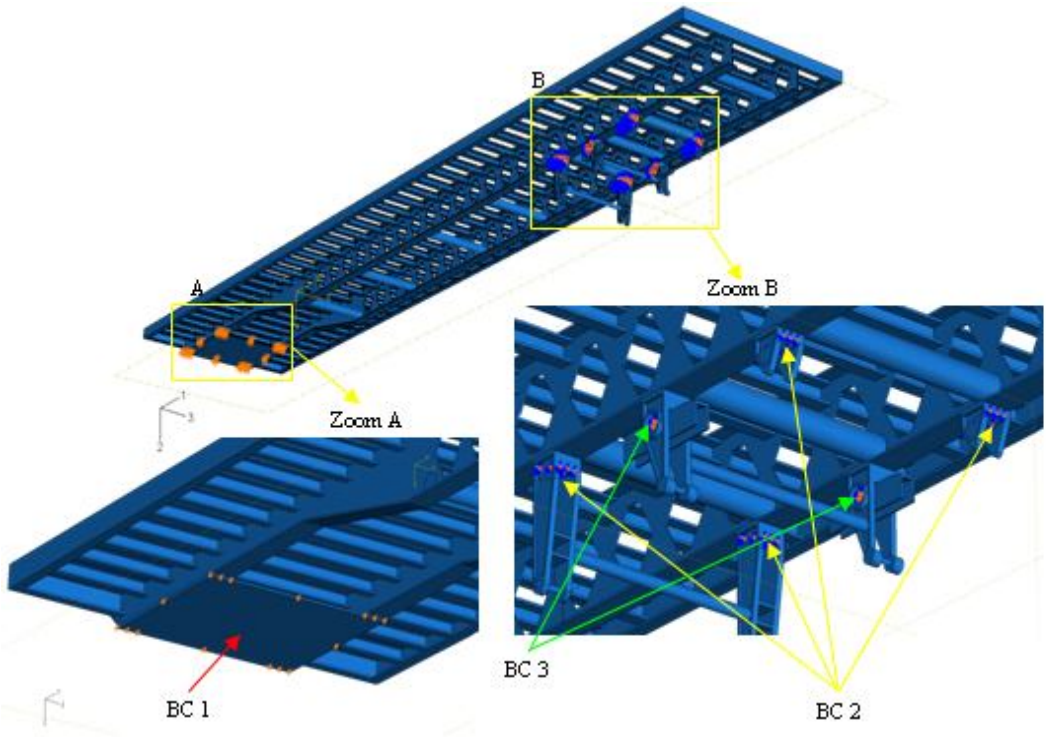

Figure 2. Boundary conditions representation in the model

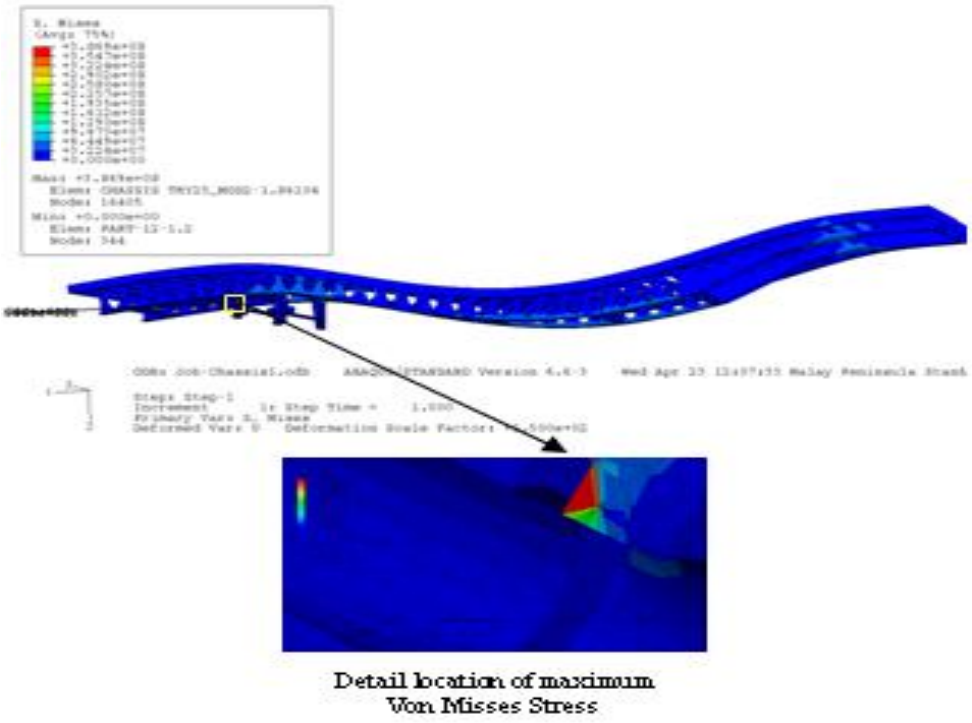

Figure 3. Von Misses stress distribution and critical point location

Based on the Von Misses highest stress area location obtained from previous paper [9], some part of chassis area is taken as a sub structure component where the cyclic loading from the roughness of road will be applied. The sub structure component is shown in Figure 4.

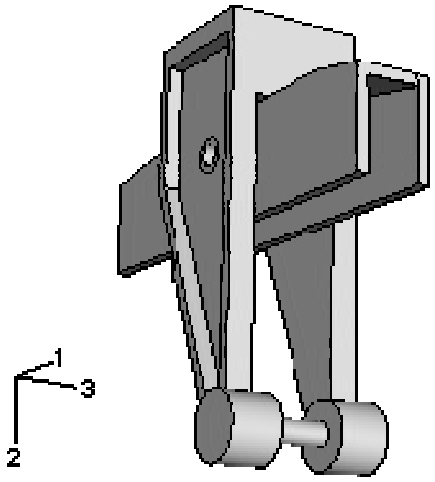

Figure 4. Sub structure Component of Truck Chassis

2.4 Cyclic Loading

Figure 5 – Figure 7 show the response of vehicle suspension due to roughness of road. These data are obtained from direct measurement of some accelerometer placed on the some point on the vehicle. These data converted to the force that will be applied on the sub structure component of truck chassis as cyclic loading .

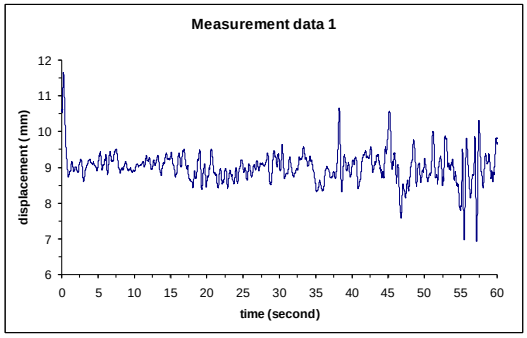

Figure 5. Response of sprung front left suspension of vehicle due to road roughness

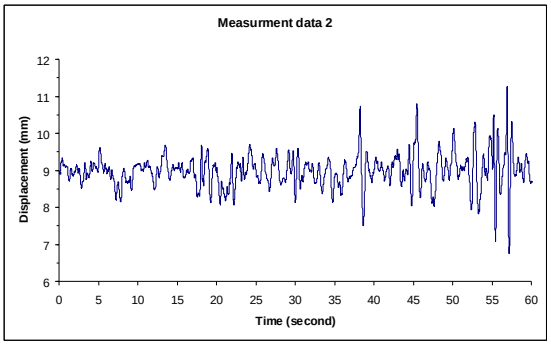

Figure 6. Response of sprung front right suspension of vehicle due to road roughness

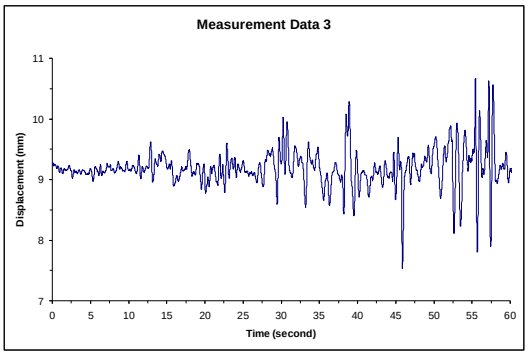

Figure 7. Response of sprung rear left suspension of vehicle due to road roughness

3. RESULT AND DISCUSSION

Figure 8 shows the Von Misses stress distribution of sub structure component subjected by static loading whereas Figure 9 shows the Von Misses stress distribution of the same model subjected by cyclic loading obtained by direct measurement from moving vehicle. The location of highest stress area for both model is same, namely at node 15951 whereas the magnitude of highest stress is little different, the stress of model subjected by cyclic loading is higher than the result of model subjected by static loading. The differences of highest stress magnitude of both model is not significant, just 0.05 %. It shows that the dominant loading on the truck chassis is comes from cargo and its content as static loading; the road roughness does not give significant effect to the stress of component.

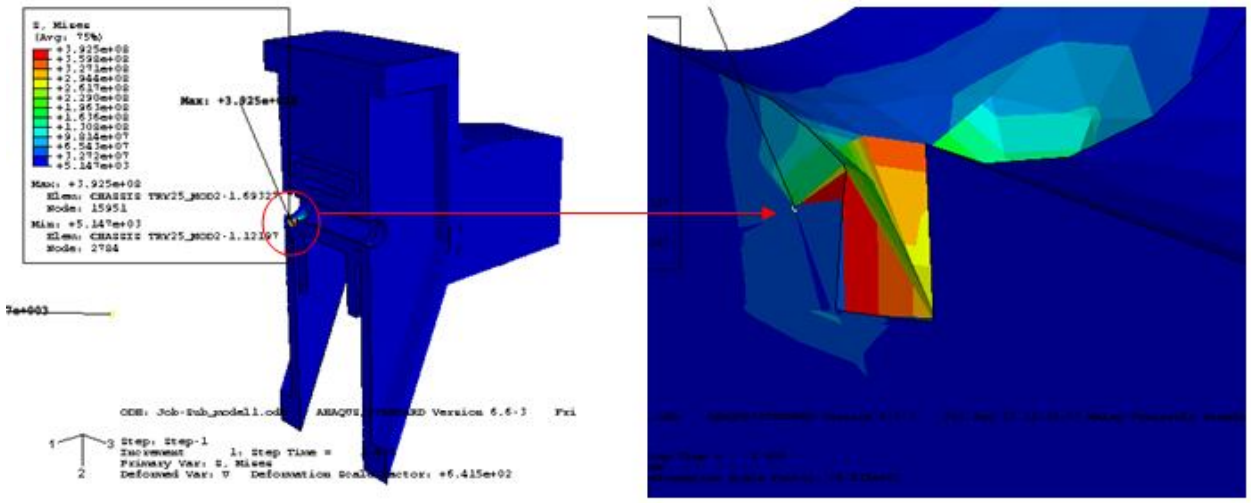

Figure 8. Von Misses result of sub modeling technique without cyclic loading

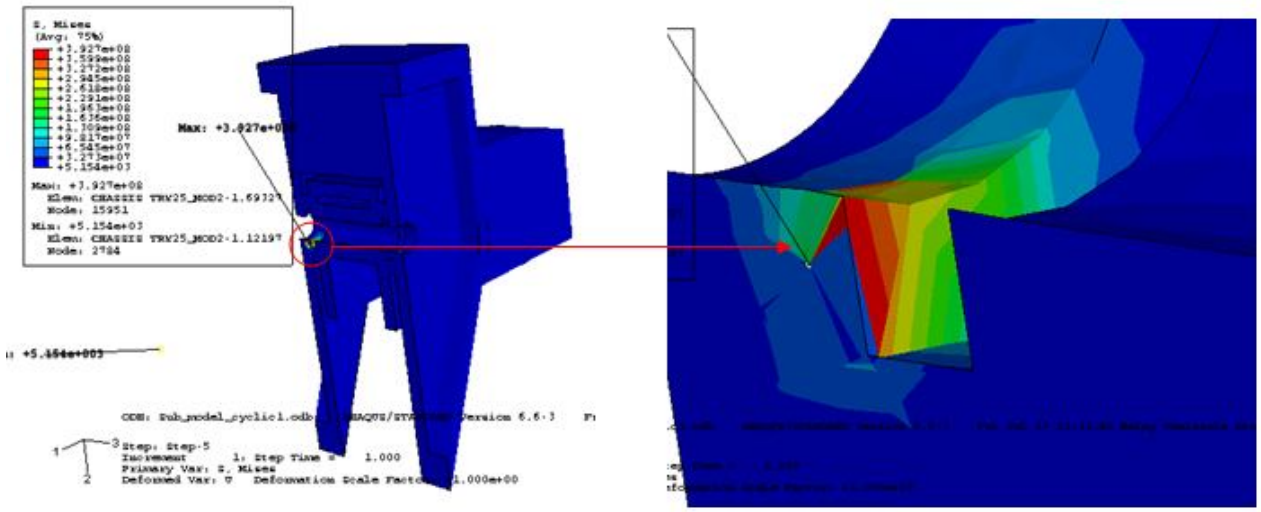

Figure 9. Von Misses result of sub modeling technique with cyclic loading

7. CONCLUSION

The finite element simulation of cyclic loading from the road roughness has been done successfully on the sub structure truck chassis component. The result shows that no significant effect of cyclic loading to the stress of the model, so it can be concluded that the static load is a dominant factor that cause a high stress in the truck chassis. The result need to validate by experiment and it is needed to do further research to look for other effect of cyclic loading to the failure of chassis such as effect of cyclic loading to fatigue life of component. The stress distribution of chassis can be used as preliminary data for fatigue life prediction of truck chassis.

.

ACKNOWLEDGMENT

The authors would like to thank the Ministry of Science, Technology and Innovation (MOSTI) for funding this research via project no. 04-01-06-SF0109. Our gratitude also goes to the members of Sound and Vibration Laboratory and Computational Solid Mechanics Laboratory of Universiti Teknologi Malaysia for their helpful discussions throughout the completion of this work.

REFERENCES

[1] MSC.Fatigue [Encyclopedia]. Los Angeles (CA, USA): MacNeal Schwendler Corporation, 2003.

[2] C. Karaoglu and N. S. Kuralay, "Stress Analysis of a Truck Chassis with Riveted Joints", *Elsevier Science Publishers B. V. Amsterdam, the Netherlands*, 2000, Volume 38, 1115 – 1130.

[3] M. Fermer, G. McInally and G. Sandin, "Fatigue Life Analysis of Volvo S80 Bi-Fuel using MSC/Fatigue", *Worldwide MSC Automotive Conference*, Germany, September, 1999.

[4] F. A. Conle and C.-C. Chu, "Fatigue Analysis and the Local Stress-strain Approach in Complex Vehicular Structures", *International journal of fatigue (Int. j. fatigue)*, 1997.

[5] W. G. Ferreira, F. Martins, S. Kameoka, A. S. Salloum, and J. T. Kaeya, "Structural Optimization of Automotive Components Applied to Durability Problems", *SAE Technical Papers*, 2003.

[6] M. Fermér and H. Svensson, "Industrial Experiences of FE-based Fatigue Life Predictions of Welded Automotive Structures", *Fatigue & Fracture of Engineering Materials and Structures* 24 (7), 2001, 489–500.

[7] R. C. Juvinall and K. M. Marshek, "Fundamental Machine Component Design", *John Willey & Son, Inc*., USA, 2006.

[8] Kurdi, O., Abd-Rahman, R., Tamin, M. N., "Stress Analysis of Heavy Duty Truck Chassis Using Finite Element Method", *2nd Regional Conference on Vehicle Engineering and Technology* 2008 Kuala Lumpur, Malaysia, 15-17 July 2008.

[9] Kurdi, O., Abd-Rahman, R., Tamin, M. N., "Sub Modeling Technique in Stress Analysis of Heavy Duty Truck Chassis", *International Conference on Science & Technology: Applications in Industry & Education (2008)*, Permatang Pauh, Pinang, Malaysia, 12 – 13 December 2008.

ISSN 114-1284

Enrichment Combustion of South Sumatra Non-Carbonized Coal Briquette

Pratiwi, D.K.[1], Nugroho, Y.S.[2], Koestoer, R.A.[3], Soemardi, T.P.[4]

[1]*Post Graduate Student, Mech. Eng. Dept. Engineering Faculty, Indonesia University,*
Lecturer of Engineering Faculty, Sriwijaya University
E-mail : pratiwi.diahkusuma@yahoo.com

[1.2.3] *Lecturer of Post Graduate Program, Mech. Eng. Depart.,*
Engineering Faculty, Indonesia University
E-mail : yulianto@eng.ui.ac.id[2], koestoer@eng.ui.ac.id[3], tresnasoemardi@yahoo.com[3]

ABSTRACT

Indonesian coal is unique among internationally traded coal for its low ash and sulphur contents. However, despite generally favourable quality characteristics, the majority of Indonesian coals have a relatively high moisture content and consequently low calorific value.Indonesia's domestic demand for coal is currently small relative to its production. In 2007, coal production was 213 million tonnes. Of this production, about 47 million tonnes was consumed domestically, mainly for power generation and for cement production. Today, due to extremely high price of oil in international market, it is believed that coal share in domestic electricity generation and cement production will follow an increased trend. Coal is becoming the most important choice among proven energy resources to sustain the required national economic growth in Indonesia. However, the utilization of the low rank coal fraction of Indonesian coal is depend on the ability to provide appropriate technologies for coal up-grading and efficient combustion processes

This paper presents the initial study of enrichment-combustion of non-carbonized briquette. The motivation of this work is that flame temperature of coal briquette by natural drag combustion is low and not enough to be used for heat source in manufactures processes. The flame temperatures could be increased by the increasing of oxygen concentration in the intake air, known as enrichment-combustion. The results are quite promising since coal temperatures above 1350 ℃ can be achieved.

Keywords
enrichment-combustion, flame mean temperature
non-carbonized coal briquette

1. INTRODUCTION

In domestic market, low rank coal which is from Bukit Asam South Sumatra is purchased in form of non-carbonized coal briquette. The proximate analysis of that is shown in Table 1.

Table 1. The proximate analysis data of Non-carbonized coal briquette

No	Parameter	Results
1.	Total Moisture	20.84 %
2.	Proximate Analysis	
	- Inherent Moisture	10.75 %
	- Ash Content	17.34 %
	- Volatile Matter	35.36 %
	- Fixed Carbon	38.55 %
3.	Sulphur	1.87 %
4.	Calorific Value	6214

Data from research before (*Diah .et.al, Sisest, UNSRI 2009*) shown that flame temperature maximum that can be reached by natural drag combustion is 1200 °C, for 2000 g of the briquette, but the increasing of the coal weight is not have significant effect for the char temperature. The temperature tend to constant (see Fig. 2).

This maximum char temperature of non-carbonized coal briquette is not enough as thermal energy resources for manufacturing industries. Because of that, for this application and to increase the char temperature until over 1000 °C, there is need to another technology for combustion processes.

According to According to *Kelly Thambimuthu* flame temperature can be increased over than dapat 1300 °C by oxygen-enrichment in the intake air to combustion chamber, Fig. 2.

ISSN 114-1284

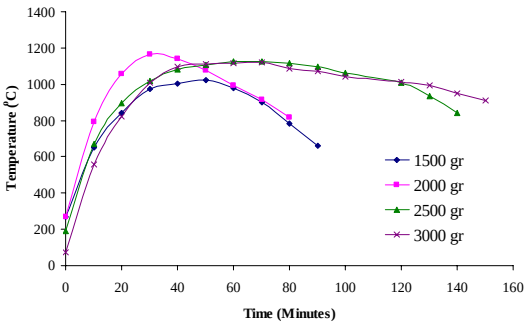

Fig. 1 Time-temperature history of a non-carbonised coal briquette combustion in a natural draft furnace for various coal loadings

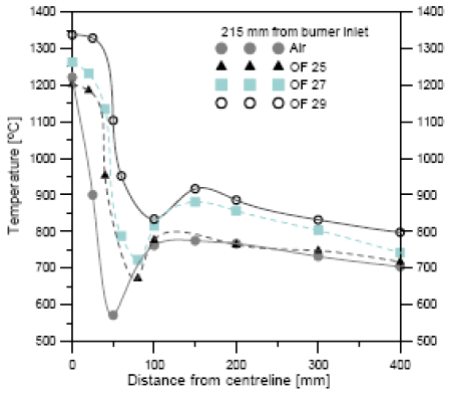

Fig.2. Temperature in combustion chamber

In order to look for the appropriate way to increase the char temperature, so this paper will presented about analytical study of South Sumatra non-carbonized coal briquette combustion by oxygen enrichment.

2. THEORITICAL REVIEW

In this study, intake air to combustion chamber from air tank is compressed air which is control by regulator at 0.5 atm pressure gauge. This is using natural air with 21 % oxygen and 79 % nitrogen and than oxygen composition is increased until 30 %.

For this study, the compressible gas formulas is using as basic equation about the relationship between pressure drop from compressed air in the tank and the air velocity that flow from nozzle to combustion chamber.

$$p_1 - p_2 = 2\rho^2 \frac{v^3 l^2}{\mu g d}$$

Where :
p_1 = air pressure in tank (Pa)
p_2 = air pressure discharge (Pa)
v = air velocity (m/s)
ρ = density (kg/m^3)
l = pipe length (m)
d = pipe diameter (m)
μ = kinematic viscocity

Than, air velocity flow from nozzle to combustion chamber ia :

$$v = \sqrt[3]{\frac{\Delta p.\mu g d}{2\rho^2 l^2}}$$

Than Mach Number is used to compute mass flow rate of oxygen from nozzle

$$\frac{1}{2}\rho v^2 = \frac{1}{2}\rho M^2 a^2$$

Where :
M = Mach Number
$v = Ma$
and

$$a = \sqrt{\frac{\gamma P}{\rho}}$$

Each of chemical composition in briquette will react with oxygen to perform combustion product and releases heat as the result of the combustion reaction process. However, if the process is carried out at a constant pressure or constant volume, it will determined only by the initial and final states of the system.The heat of reaction at standard state is follow :

$$\Delta H_{reac\,tan\,ts} + \Delta H_{r,T_2} = \Delta H_{r,T_1} + \Delta H_{product}$$

$$\Delta H_{reac\,tan\,ts} = \sum_{i=1}^{N} v_i' \int_{T_1}^{T_2} c_{p.M_i} dT$$

c_p *is* a constant average specific heat at constant pressure, M_i is total mass of species i, *v'* is stoichiometric coefficient for species i as a reactant and *v''* as a product.

$$\Delta H_{products} = \sum_{i=1}^{N} v_i'' \int_{T_1}^{T_2} c_{p,M_i} dT$$

Hence, the heat evolve from the combustion process is :

$$\Delta H_{r,T_2} - \Delta H_{r,T_1} = \int_{T_1}^{T_2} \sum_{i=1}^{N} (v_i'' c_{p,i}) dT - \int_{T_1}^{T_2} \sum_{i=1}^{N} (v_i' c_{p,i}) dT$$

By using those formulas, the chemical reaction of combustion will be simulated by using CFD (*Computational Fluid Dynamic).*

3. DISCUSSION

Simulation is conducted for fixed bed condition, where primary stream of air contain 30 % more oxygen composition than natural air with pressure inlet is 0.5 atm. Secondary stream is natural drag air with inlet velocity is 0.005 m/s. The pressure outlet of exhaust gas is 0 atm pressure gauge. Equipment is setting as Fig.3.

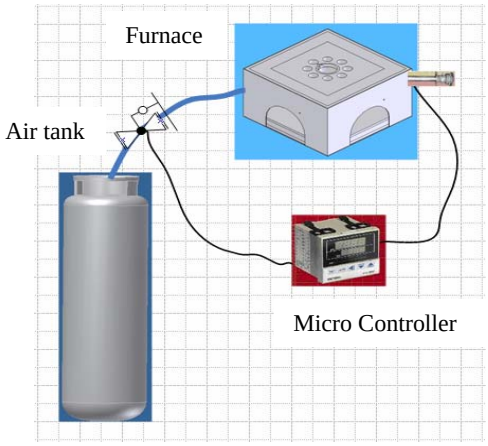

Fig. 3. Equipment set up for experiments

From simulation, the relationship between fuel mixture fraction and mean temperature char is shown on Fig. 4

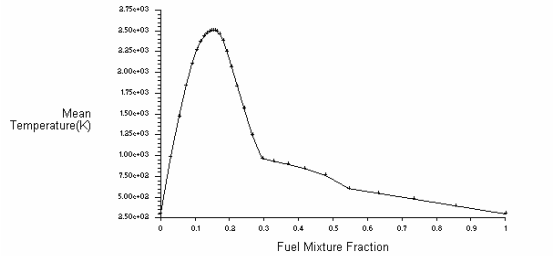

Fig.4.The relationship between *Fuel Mixture Fraction* of Non-Carbonized Coal Briquette with *Mean Temperature (K)*

On the Fig.4, mean temperature char max that could be reached is 2565 K at fuel mixture fraction 0.18. Than, the temperature will be decrease until fuel mixture fraction 0.3 at mean temperature 900 °C, and 1 at 300 K.

The CO_2 contains in exhaust gas will be max at fuel mixture fraction 0.18. This means that the combustion reaction will complete at this value and the composition of CO will be at minimum level., Fig. 5.

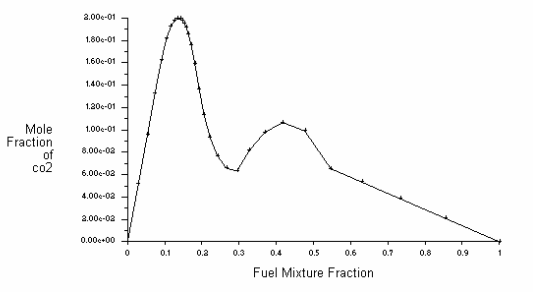

Fig. 5. The correlation of *Fuel Mixture Fraction with Mole Fraction of* CO_2

4. CONCLUSION

Data from analytical study of non-carbonized coal briquette combustion by oxygen enrichment in intake air, known that :

1. Briquette char mean temperature maximum at 2565 K will be reached at 0.18 *Fuel Mixture Fraction*
2. Composition of CO_2 will be at maximum level in the exhaust gas at 0.18 *Fuel Mixture Fraction*
3. The oxygen enrichment combustion technology for non-carbonized coal briquette is appropriate for manufacturing industries application.

REFERENCES

[1]. PT. Tambang Batu Bara Bukit Asam, *"Analisis Batubara non Karbonisasi",* Pelabuhan Tarahan

[2]. Pratiwi DK, Nugroho SN, Koestoer RA, Soemardi TP,*'Experimental Study of Non-Carbonized Coal Briquet Combustion*', Sisest Unsri 2009

[3]. Kelly Thambimuthu ,"*Developments in Oxy-fuel Combustion",* Presentation to 1st ISCDRS, Seoul, January 18, 2005

[4]. Kuo, K Kenneth, *"Principles of Combustion",* John Wiley & Sons,.Inc, Singapore, 1986

Proceeding of the 11th International Conference on QiR (Quality in Research)
Faculty of Engineering, University of Indonesia, Depok, Indonesia, 3-6 August 2009
ISSN 114-1284

Unsteady Load Analysis on a Vertical Axis Ocean Current Turbine

Ridho Hantoro[(1)], I.K.A.P. Utama[(2)], Erwandi[(3)]

[(1)] Departement of Engineering Physics ITS,
presently Ph.D Student at The Faculty of Marine Technology ITS
hantoro@ep.its.ac.id

[(2)] Professor, Departement of Naval Architecture ITS
kutama@na.its.ac.id

[(3)] Senior Research Fellow, Indonesian Hydrodynamics Laboratory, Surabaya
erwandi@gmail.com

ABSTRACT

The current energy demand and its dramatic rate of growth related to the increasing impact of developing countries, clearly indicate the necessity to consider renewable energy as a primary mean to alleviate the needs of a large number of communities around the world. One of those source with potentials opportunity is ocean current. Since unsteady hydrodynamics is the main source that drives the turbine into destructive vibration modes, it could lead to high cycle fatigue structural failures of the turbine after long exposure to unsteady loadings.

The current work presents preliminary analysis of unsteady load on a Vertical Axis Ocean Current Turbine (VAOCT) including changes of forces in its rotation. The work is conducted numerically, where the forces are created in every 5 degrees of turbine rotation at velocity variations of 0.5. The simulation results indicate the force fluctuation in its rotation which can cause unbalanced of turbine. NACA 0018 foil is used as straight rectangular blade model and simulated with nBlade=3 and shaft without pitch control. The comparison values of Cd and Cl of a blade was made, resulting the maximum error of 2.6411% for Cd and 0.7261% for Cl. Two phenomena of periodic dynamics force fluctuation pattern according to the vector resultant formed in a full 360^0 rotation. The result of the recent work will be developed and use as a tool to understand more the phenomena of fluid-structure interaction on VAOCT in order to minimize the effect of vibration according to its reliability.

Keywords: *ocean current, unsteady load, vibration, VAOCT*

1. INTRODUCTION

The motivation for this project arose from an expected vibration source of a small-scale vertical axis wind turbine currently undergoing field-testing. Vertical-axis turbine that is fully submerged and subject to an incoming flow caused by a marine current. Each blade has a straight rectangular, high-span plan form and it is connected to the rotor shaft by two arms. Conversion of streaming water energy into mechanical and electrical energy is based on a simple mechanism.

The hydrodynamic force acted by the incoming flow on the blades generates a torque that force blades, and hence the turbine, to rotate about its shaft. Using an electric generator, mechanical shaft power can be converted into electric power. An important aspect is that a vertical-axis turbine of this type can produce power regardless of the direction of the onset flow and producing force fluctuation subjected to fluid-solid interaction. From the above description it is apparent that production of power from water currents is primarily related to the hydrodynamic forces that are acted on blades.

Nonetheless, the global performance of the turbine results from an interplay of several components. Thus, a successful turbine design can derived only from a multi-disciplinary work, in which turbine hydrodynamics represent the first necessary step. Maximizing the turbine power output can be achieved only if the mechanism of generation of the hydrodynamic force on the blades is clearly identified and tools to design high-performance rotors are developed. In view of the complexity of physical aspects affecting the turbine performance, the most appropriate approach is to combine experimental activity and theoretical studies. This paper carry out a distinct investigation of assessing computational tools to understand more the hydrodynamic forces acting on vertical-axis turbine.

The turbine consists of 1 metre long vertically aligned blades each fixed to the central shaft by two horizontal arms and separated from one another by an angle of θ=120º. The blade profile is a NACA 0018 with a chord length of 0.1 metre fixed at zero angle of attack to the support arms. The turbine optimally operates at a blade-tip speed ratio (the ratio of the blade rotational velocity to the ambient wind velocity) of 2.3. As the blades turn about the central shaft, they encounter

an incident flow that is composed of the ambient flow and the flow due to rotation (Figure 1). This incident wind results in lift and drag forces on the blades resulting in both a thrust force and a radial force on the turbine arms. Note that in this paper, lift is defined as the force perpendicular to Uwind, and drag is defined as the force parallel to Uwind.

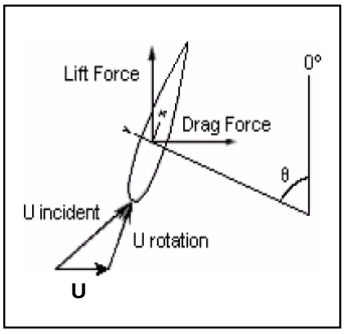

Figure 1: Lift and Drag components on the blade

It is evident that the lift and drag forces on the blade will then vary in time resulting in cyclic loading on the blades. There is also an expected decrease in flow momentum on the downwind side of the turbine as a result of the passing of the upstream blades.

Initial field tests on the turbine show the existence of significant vibration at three times the frequency of rotation, indicating that hydrodynamic loading on the blades may be the cause. In order to better understand the nature of this excitation source, a computational fluid dynamic (CFD) simulation was performed.

2. Fluid-Solid Interaction (FSI)

Structures in a fluid flow will generally induce fluctuating components. These fluctuating or flow-induced oscillations are important aspects of the flow pattern which may in turn excite natural modes of the structure. Such feedback loops in the fluid-structure system are highly nonlinear and under certain conditions may dominate the motion of the fluid-structure system. For each vibrational mode, data usually include the amplitudes of deflection, velocity and acceleration. These responses are linear and translational for bending modes and angular for torsional modes.

When each vibrational mode is independent, the system may be described by studying each mode separately. In general however, systems have two or more degrees-of-freedom and the response can be analyzed only by solving a system of simultaneous differential equations. As strongly emphasized by Naudascher [1] and Sarpkaya [2], the engineer is advised to carry out a detailed preliminary investigation in which all sources providing hydrodynamic loading are identified and their *effect* assessed., several classes of fluctuating hydrodynamic forces.

Naudascher develops a very workable scheme for distinguishing the sources of hydrodynamic loading and we use the terminology and classifications developed by Naudascher. There are four broad categories of fluctuating fluid forces, as shown in Figure 2.

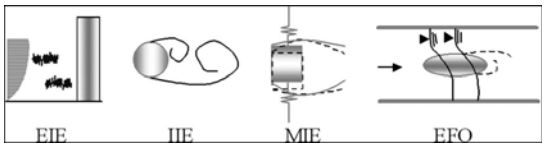

Figure 2. Examples of sources of excitation mechanisms (Naudascher [3])

These categories are fluctuations from:
1) Extraneously Induced Excitations (EIE);
2) Instability Induced Excitations (IIE);
3) Movement Induced Excitations (MIE), and
4) Excitations due to fluid oscillators (EFO)

From structural point of view, there are many research has explored the phenomena of rotating and vibration structure. Khader [4] investigating a simple structural model is adopted to study the stability of a rotating cantilever shaft with uniformly distributed mass, mass moment of inertia and stiffness, and make evaluation of effects of the gyroscopic moment associated with the mass moment of inertia of the rotating shaft-disk system, and of external damping forces and moments, which restrain the translation and tilting of the shaft's cross-section. The research continued by Behzad and Bastami [5] who investigated the effect of shaft rotation on its natural frequency. Apart from gyroscopic effect, the axial force originated from centrifugal force and the Poisson effect results in change of shaft natural Frequency.

Beedor and Qaisia [6] studies the forced vibrations of a flexible rotating blade under the excitation of shaft torsional vibration. A reduced order nonlinear dynamic model is adopted, wherein the torsional vibration degrees of freedom is substituted by a simple harmonic motion with a frequency that is function of the system rotating speed. The resulting system of second-order ordinary differential equation with harmonically varying coefficients is solved using the method of harmonic balance. The solution is useful for defining dangerous operating speed ranges and for quantifying the relationship between shaft torsional and blade bending natural frequencies.
Lau [7] conducted An analysis of a turbine blade fatigue life that includes the physics of fluid–structure interaction on the high cycle fatigue (HCF) life estimate of turbine blades. The rotor wake excitation is modeled by rows of Karman vortices

superimposed on an inviscid uniform flow. The vortex-induced vibration problem is modeled by a linear cascade composed of five turbine blades and the coupled Euler and structural dynamics equations are numerically solved using a timemarching boundary element technique. The analysis can be applied to any blade geometries; it is not limited to the blade geometry considered here.

Geometric analysis and flow characterization are performed together in making an assessment of potentials for flow-structural interaction. Unsteady fluid loads are either motion-independent or motion-induced *as* broken down in Figure 3. Motion-independent loads may be periodic or random, whereas motion-induced loads are primarily periodic. Periodic fluid forces include those resulting from vortex shedding. Random fluid oscillations include turbulence and acoustics.

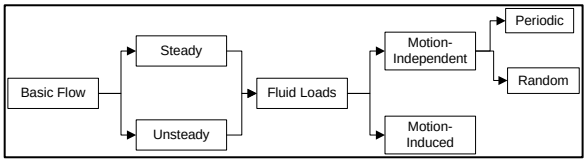

Figure 3. Characteristics of the Flow and its Interaction with Structure [8]

In some cases, the fluid forces are altered by the structural response, and motion-dependent fluid loads must be considered. These are cases of flow/structural interaction. Motion-induced unsteady fluid loads occur in the closed-loop feedback response of an elastic structure. Flow-structural interaction problems occur in specific regimes of reduced velocity. Quick estimates of Strouhal numbers at critical Reynolds numbers are possible to determined reference to basic geometry classifications and to fluid added mass. In many cases it is possible to quickly categorize the actual geometry in some design problem or some problem of high cycle fatigue in an operating system as being close to one of these basic fundamental geometries and thereby obtain the needed estimates.

4. Results

4.1. Numerical Model

The 3D numerical domain was designed to simulate the conditions of the turbine blade flow. A Steady State simulation with rotating wall was performed. Three turbine blade was then located within the domain at a radius of 0.5 metre from the axis of rotation (Figure 4). The inlet flow condition was fixed at U-flow = 0.5 m/s normal to the boundary, with turbulent intensity of 5%.

The outlet of the stationary domain was set at an opening. The upper and lower surfaces of the domain were also set with an opening. The surface of the blade and shaft was modelled as a smooth no-slip surface. The rotational velocity of the rotating wall was set at 2.3 rad/s giving a blade-tip speed ratio (TSR) of

$$TSR = \frac{\omega.r}{U} = \frac{1.15}{0.5} = 2.3$$

The initial conditions for the domain were the same as the inlet conditions.

Turbulence was modelled using the k-ω model near the blade and shaft.

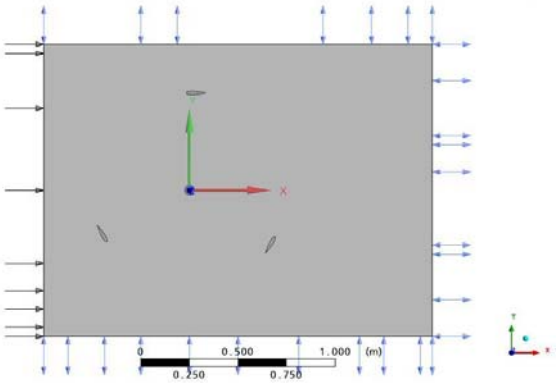

Figure 4. Numerical Domain showing the blade and shaft contained.

4.2. Force Fluctuation

The model was validated for theta of 0^0 to 12^0 and compared with literature results of a NACA 0018 airfoil [9]. As shown in Figure 5, the numerical results appear to match the literature data well.

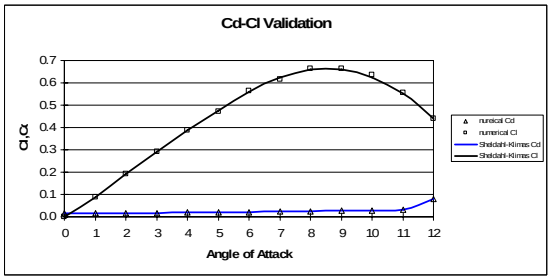

Figure 5. Validation of the model against literature [9]

There are differences dynamics behavior in comparison of force components on a foil in assembly (three turbine and shaft) and stand alone rotation.

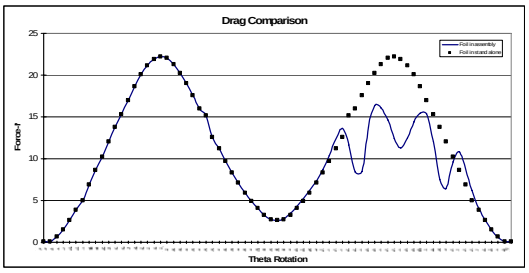

Figure 6. Drag Force Fluctuation on a foil at U:0.5 m/s and 22 rpm

The dynamics of drag and lift force characteristics shown in Figure 6 and Fig 7. There is no force fluctuation for stand alone condition along 180^0 of rotation as the foil to rotate without any disturbance in its upstream.

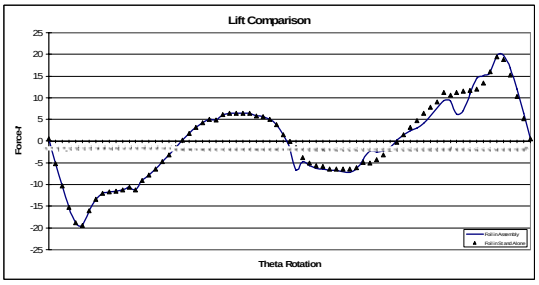

Figure 7. Lift Force Fluctuation on a foil at U:0.5 m/s and 22 rpm

Different behavior force fluctuations occurred for assembly condition at the position of rotation > 180^0. This fluctuation mainly because of the unstable flow pattern received which has been disturbed by others foil and/or shaft in its upstream. In the aspect of fluid force, this is subject to the increase of turbulence intensity by the movement of the body immersed and classified in Movement induced Oscillation [3].

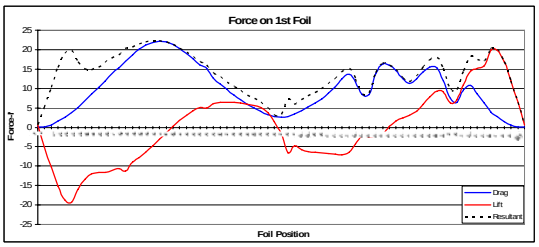

Figure 8. Force Fluctuation on a foil at U:0.5 m/s and 22 rpm

Complete forces fluctuation including its force resultant produce from of a foil and shaft at assembly condition in full 360^0 is shown in Figure 8 and Figure 9.

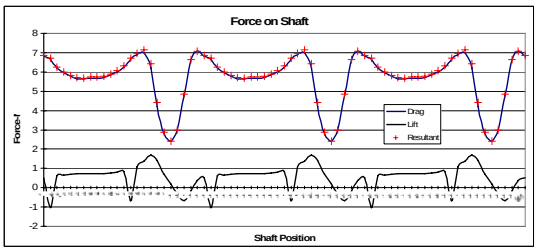

Figure 9. Force Fluctuation on shaft at U:0.5 m/s and 22 rpm

Optimization of total forces and the vector directions was made by estimate the total forced resultant acting on all of turbine components and describe in Figure 10.

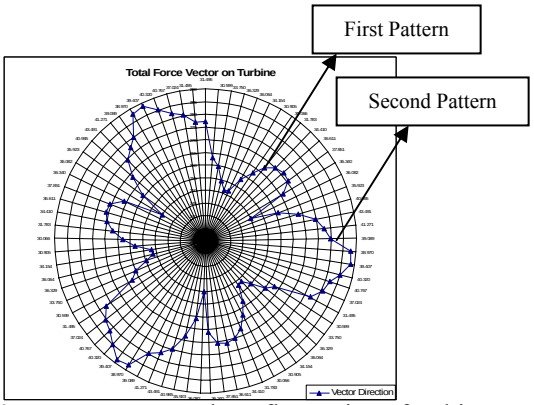

Figure 10. Force vector resultant fluctuation of turbine at U:0.5 m/s and 22 rpm

Two periodic dynamics force fluctuation pattern according to the vector resultant formed in a full 360^0 rotation, the first pattern occurred at Theta rotation of 25^0 - 65^0 , 145^0 - 185^0, and 265^0 - 25^0, while the second pattern occurred at Theta rotation of 65^0 - 145^0 , 185^0 - 265^0, and 305^0 - 25^0.

4.3. Torque Fluctuation

An intrinsic, mechanical phenomenon associated with the operation of ocean current energy conversion systems is given to the time variations
components of a ocean current turbine ideal conditions of a steady called “torque ripple”. Torque ripple is a name in torque which are transmitted through the various drive train ultimately to its load. Torque ripple in a vertical axis ocean current turbine is caused by continuously changing angles of attack between the apparent wind and the turbine blades [10,11]. Other events which contribute to the development of torque ripple include variations in ocean current magnitude and direction, blade dynamics, blade stall and torsional slack in the drive train.

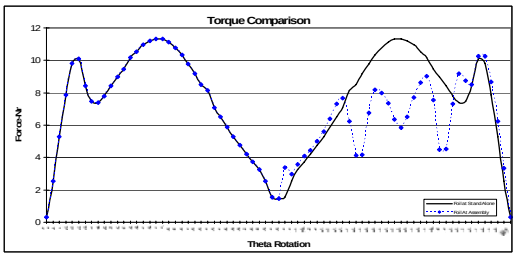

Figure 11. Torque Fluctuation on a foil at U:0.5 m/s and 22 rpm

As a consequence of force fluctuation, the resulted torque also experience the unsteady value and has direct impact to shaft which to be main load support since turbine will rotate 24 hours in ocean environment. The comparison of dynamic behavior of torque on a foil in full 360^0 is showing a similar phenomena with the force fluctuation and shown in Figure 11. Deviation of torque fluctuation between foil in stand alone and assembly condition also occurred at the position of rotation > 180^0.

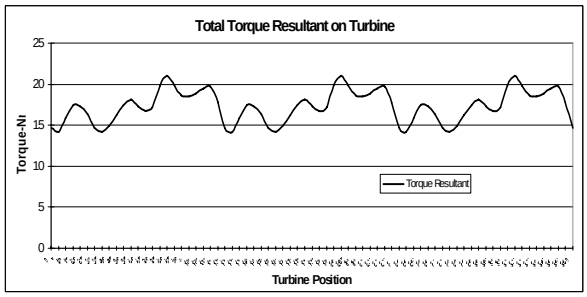

Figure 12. Total torque resultant fluctuation of turbine at U:0.5 m/s and 22 rpm

If sufficiently large, torque ripple may have a detrimental effect on fatigue life of various drive train components (such as shafts, couplings and transmissions) and on output power quality. It may also cause the generator pull-out torque to be exceeded, resulting in a sudden loss of load and possible turbine run-away. Torque ripple is clearly a concern of vertical axis ocean current turbine proponents, and deserves the attention of detailed investigations.

5. Conclusions

A CFD simulation of a vertical axis ocean current turbine blade has been developed and validated using static experimental data. Simulations then confirmed the existence of vibration driving forces generated from hydrodynamic forces. These results indicate that the majority of the force on the blade is in the radial direction. Furthermore, the dominant frequency of this vibration driving force is equal to the frequency of rotation, resulting in a driving force for all three blade and finally to the shaft as main support and mechanic power transmission.

Conversely, only a small portion of the force is actually used to drive the turbine and this is achieved in an unsteady oscillating manner. Future simulations with structural responds will be performed to study the effect of mode shapes generated by unsteady load. These simulations will be validated against experimental data obtained from the turbine prototype. Once validated, the CFD model will be used to predict hydrodynamic and vibration characteristics of future designs.

References

[1] Naudascher, E., "Flow-Induced Streamwise Vibrations of Structures", Journal of Fluids and Structures (1987) 1, 265-298
[2] Sarpkaya, T., "A Critical Review of the Intrinsic Nature of Vortex-Induced Vibrations", Journal of Fluids and Structures 19 (2004) 389–447
[3] Naudascher, E., *AIRH Design Manual: Hydrodynamic forces*. Rotterdam: A.A. Balkema Publishers, 1991.
[4] N. Khader, Stability Of Rotating Shaft Loaded By Follower Axial Force And Torque Load, Journal of Sound and Vibration 1995 182(5), 759-773
[5] M. Behzad, A.R. Bastami, Effect of centrifugal force on natural frequency of lateral vibration of rotating shafts, Journal of Sound and Vibration 274 (2004) 985–995
[6] B.O. Al-Bedoor, A.A. Al-Qaisia, Stability Analysis of Rotating Blade Bending Vibration Due To Torsional Excitation, Journal of Sound and Vibration 282 (2005) 1065–1083
[7] Y.L. Lau, R.C.K. Leung, R.M.C. So, Vortex-induced Vibration Effect On Fatigue Life Estimate of Turbine Blades, Journal of Sound and Vibration 307 (2007) 698–719
[8] B.-L. Liu and J.M. O'Farrell, High Frequency Flow/Structural Interaction in Dense Subsonic Fluids, NASA Contractor Report 4652
[9] Sheldahl, R.E. and Klimas P.C., Aerodynamic Characteristics of Seven Symmetrical Airfoil Sections through 180-Degree Angle of Attack for Use in Aerodynamic Analysis of Vertical Axis Wind Turbines. Sandia National Laboratories Unlimited Release, 1981.
[10] B. F. BlackWell, L. V. Feltz, "Wind Energy - A Revitalized Pursuit," Sandia Laboratories Report No. SAND75-0166, March 1975.
[11] B. F. Black'well,W. N. Sullivan, R. C. Reuter,J. F. Banas,"EngineeringDevelopment Status of the Darrieus Wind Turbine," Journal of Energy, Vol. 1,No. 1, Jan.-Feb. 1977.

ISSN 114-1284

ANALYTICAL STUDY OF SELF-EXCITED VIBRATION ON TWO DEGREE OF FREEDOM VIBRATORY TILLAGE

Soeharsono[a], Radite PA Setiawan[b], I Nengah Suastawa[c]

[a]*Mechanical Engineering Deptartment*
Trisakti University, Jakarta 11440
Graduate Student of Agricultural Machinery Dept IPB
Kampus IPB Darmaga Bogor 16680.
gatotsoeharsono@yahoo.com

[b]*Agricultural Machinery Deptartment*
Bogor Agricultural University
Kampus IPB Darmaga Bogor 16680. iwan_radit@yahoo.com

[c]*Agricultural Machinery Deptartment*
Bogor Agricultural University
Kampus IPB Darmaga Bogor 16680. nsuastawa@yahoo.com

ABSTRACT

Analytical and experimental study on vibratory tillage by adding an external energy to tillage-tool has been widely applied. This method would significantly reduce soils resistance; unfortunately it uses a lot of energy. Self-excited vibration phenomenon on vibratory tillage has also been shown experimentally reduce soils resistance though not as much as the former. However, no analytical study of the latter method in detail can be found. This paper discusses analytical study of self-excited vibration of tillage-tool on vibratory tillage due to natural excitation of varying cutting forces. The Vibration of vibratory tillage was modeled as vibration with two-degree of freedom system, i.e. the motion of tillage-tool and the motion of swinging-mass arm. The tillage-tool is connected to an implement by an elliptic spring while the swinging-mass arm is connected to the tillage-tool by an elastic bar, which has functions as a spring. The natural excitation of varied cutting force was modeled as a periodic function, which can be expressed as a Fourier series. The elasticity of the elastic bar and the mass of swinging arm are optimized further, so that the tillage-tool vibrates violently at its resonant frequency. This condition will decrease both the soils resistance and the draft force needed for loosening soil density due to self-exited vibration during tillage operation.

Keywords: vibratory tillage, self-excited, vibration, soils resistance, Fourier series.

1. INTRODUCTION

Soil compaction reduces rooting, infiltration, water storage, aeration, drainage, and crop growth. To loosen the compact soil however high draft force and energy consumption is needed. It is well-known that tillage-tool vibration will reduces draft force during tillage operation if the maximum velocity of oscillation is higher than the velocity of the implement. Other advantages of this system is reduced clods size and increased number of crack in soil. This condition will facilitate penetration of plant roots, nutrients, water and air circulation in all soil that is necessary to plant growth.

There are two methods to oscillate tillage-tool. The first method is done by adding a mechanical energy while the second method is to take advantage of the elascity of tillage tolls combined with a varied cutting forced so that the tillage-tool will vibrate in accordance with self excited vibration phenomenon. The first method would reduce soils resistance significantly; unfortunately it uses a lot of excessive energy. The increase of energy consumption is caused by the amount of energy that is needed to drive inersia of tillage-tool and its mechanism.

The first method has been studied analytically [1-4] and experimentally [5-8]. Yow J. et.al. [1] investigated a substantial reduction in draught force about 30 % at velocity ratio about 2 and the overall power consumption will then only increase up to 50% above that for a non-oscillating tool. Butson et.al. [5] reported draft ratio about 0.58 at the velocity ratio about 3 but the power ratio increased until 3.2

The second method has been studied experimentally [9-11]. All author reported that this method will reduce the draft force though not as much as the former. Decreasing the draft force is depending only on the elasticity of the spring. Soeharsono *et al*. [12] conducted an analitycal study of self excited vibration on single-degree of freedom system of vibratory tillage. The excitation caused by varied cutting force was model as a periodic function which expands against as a Fourier series. The spring constant was varied and Soeharsono *et al*. [12] reported that the system will resonance at natural

frequency closed to twice the value of the excitation frequency.

This paper discusses analytical study of self excited vibration on a new model of vibratory tillage. The vibration of vibratory tillage was model as a vibration with two degree of freedom system i.e. angular rotation of tillage-tool θ_1 and angular rotation of swinging-mass arm θ_2. Tillage-tool was connected to main frame by a semi elliptic bar which has function as main spring while swinging-mass arm was connected to tillage-tool by elastics bar which had function as swinging spring. The natural excitation of varied cutting force was modeled as a periodic function, which can be expressed as a Fourier series and the graph was based on the quantitative data of unconfined test conducted in soil mechanics laboratory of agricultural machinery department IPB.

Differential equation of vibration shows that mass matrix $\boldsymbol{M}$ and stiffness matrix $\boldsymbol{k}$ will cause the coordinates θ_1 couples to coordinates θ_2. By modal analysis method, the coordinates θ_1 and θ_2 converted to new uncouple coordinates, namely η_1 and η_2. Thus, the solution becomes the solution of two vibration equation with one degree of freedom systems in η_1 and η_2 which transformed again into coordinates θ_1 and θ_2.

Elasticity of the main spring k_1 and inertia of the tillage tolls J_1 were kept constant while elasticity of connecting spring k_2 and mass of swinging mass m_2 were varied. This condition will effect to vibration of tillage-tool θ. This vibration will represent in graph of maximum displacement of the tillage-tool d_3 as function of time t and θ as function of m_2. At a certain condition, the tillage-tool will vibrate violently so the velocity ratio will greater than unity. There for the possibility of decreasing both soil resistance and draft force are visualized.

2. METHODOLOGY

2.1 Governing Differential Equation

The model of vibratory tillage is shown in figure 1. It consist of semi elliptic bar (which has function as main spring), tillage-tool, elastics bars which has function as connecting spring and swinging arm. A mass of m_2 is located on swinging arm. The model was installed on a carriage which has forward speed of V_0. The vibration of tillage-tool was induced by variation of soil resistance. During forward motion of carriage, tillage-tool press the soil and high resistance encounter, the tillage-tool displaces and the energy is store as potential energy in the main spring. When soil break up, soil resistance decreases, the restoring force of the spring return the tillage-tool to the original position and tillage-tool will be oscillated in accordance with self excited vibration phenomenon.

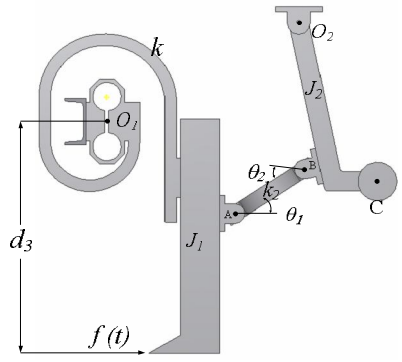

Figure1: Physical model of vibratory tillage

It is clear that the vibration of vibratory tillage could model as self excited vibration with two degree of freedom system as shown in figure 2. Due to soils viscous-elastics behavior, the soil was modeled as viscous damper c_s and soil stiffness k_s. All structure were made from steel therefore the damping coefficient are neglected. If θ_1 and θ_2 are angular displacement of tillage-tool and swinging arm, the differential equation of motion of the system is:

(1)

or

Where:

(2)

$f(t)$: draft force

J_1: mass inertia of tillage-tool and main spring

k_1: angular stiffness of main spring
k_2: linear stiffness on connecting spring
d_1: Distance from center of rotation of tillage-tool O_1 to point A
d_2: Distance from center of rotation swinging arm O_2 to point B
l_2: Distance from center of rotation swinging arm O_2 to point C
d_3: Distance from center of rotation tillage-tool to damping force of soil.

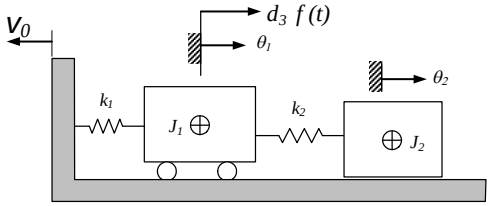

Figure 2: Vibration model of vibratory tillage

Equation 1 shows that coordinate θ_1 is coupled to coordinate θ_2, by modal analysis method, the coordinates θ_1 and θ_2 converted to new uncouple coordinates, namely η_1 and η_2. The natural frequency and eigen-vector of equation 1 are ω_{n1}, ω_{n2}, $\{Q\}_1$ and $\{Q\}_2$. Modal matrix $\boldsymbol{Q}$ defined as:

$$\boldsymbol{Q} = [\{Q\}_1\{Q\}_2] = \begin{bmatrix} Q_{11} & Q_{12} \\ Q_{21} & Q_{22} \end{bmatrix} \quad (3)$$

The orthogonal principle of $\boldsymbol{Q}$ to mass matrix $\boldsymbol{J}$ and stiffness matrix $\boldsymbol{k}$ written as:

$$\boldsymbol{Q^T J Q} = \boldsymbol{M} \text{ and } \boldsymbol{Q^T k Q} = \boldsymbol{\kappa} \quad (4)$$

Where $\boldsymbol{M}$ and $\boldsymbol{\kappa}$ are general mass matrix and general stiffness matrix respectively

$$\boldsymbol{M} = \begin{bmatrix} M_1 & 0 \\ 0 & M_2 \end{bmatrix} \quad \boldsymbol{\kappa} = \begin{bmatrix} \kappa_1 & 0 \\ 0 & \kappa_2 \end{bmatrix} \quad (5)$$

$$\kappa_j / M_{j=}\ \omega_{n,j}^2 \quad j = 1,2$$

Modal analysis method requires transforming the couple coordinate $\boldsymbol{\theta}$ to new uncouple coordinate $\boldsymbol{\eta}$

$$\theta = Q\eta \qquad \eta = \begin{Bmatrix} \eta_1 \\ \eta_2 \end{Bmatrix} \quad (6)$$

Substitute equation (5) and (6) to equation 1 and pre multiply by $\boldsymbol{Q^T}$ obtained two equations of vibration with one single degree of freedom system:

$$M_1\ddot{\eta}_1 + \kappa_1\eta_1 = Q_{11}M(t),$$

and

$$M_2\ddot{\eta}_2 + \kappa_2\eta_2 = Q_{12}M(t) \quad (7)$$

$M(t)$ is a periodic function with period of T and frequency of ω expresses as a Fourier series [13-14]:

$$M(t) = \frac{a_0}{2} + \sum_{n=1}^{\infty} a_n Cos(n\omega t) + b_n Sin(n\omega t) \quad (8)$$

Where:

$$a_0 = \int_0^T M(t)dt, \ ,$$

$$a_n = \frac{2}{T}\int_0^T M(t)Cos(n\,\omega t dt$$

$$b_n = \int_0^T M(t)Sin(n\omega t)dt$$

$$\eta_1 = \frac{a_0}{2\kappa} + \sum_{n=1}^{\infty} \frac{a_n Cos(n\omega t) + b_n Sin(n\omega t)}{\kappa_1(1-(n\omega/\omega_{n1})^2)}$$

$$\eta_2 = \frac{a_0}{2\kappa} + \sum_{n=1}^{\infty} \frac{a_n Cos(n\omega t) + b_n Sin(n\omega t)}{\kappa_2(1-(n\omega/\omega_{n2})^2)}$$

Thus the response of $\boldsymbol{\theta}$ is:

$$\theta_1 = Q_{11}\eta_1 + Q_{21}\eta_2 \quad \text{And} \quad \theta_2 = Q_{21}\eta_1 + Q_{22}\eta_2 \quad (9)$$

Equation 8 and 9 show that the system will vibrate violently if $(n\omega/\omega_{n2})^2$ closed to unity.

2.2 Dynamical Parameter

The dynamic parameters of vibratory tillage in figure 1 are as follow: Angular stiffness of main spring k_1 was 32086 *Nm/rad* and the mass inertia of tillage-tool J_1 was 2.486 *N-m*^{2} inertia mass of swinging arm j_2= *0.404 kg-m*^{2}. Other parameters are d_1 = 0.4 m, $d2$ = 0.38 m, $d3$ = 0.6 m, l_2 = 0.448 m, angle $\theta_1 = 28^0$ and $\theta_2 = 21^0$. Two different connecting springs were used for simulation, i.e. connecting spring with stiffness k_2 = 70312.5 N/m and k_2 = 132629 N/m. swinging mass m_2 was varied and depending on connecting spring used for simulation. Both main spring k_1 and connecting spring k_2 were made from alloy steel which have yield strength about 400 MPa, other material were made from structural steel. Substituted above dynamical parameter to equation 1 will obtain differential equation of vibration as:

$$\begin{bmatrix} 2.486 & 0 \\ 0 & 0.363 + 0.18m_2 \end{bmatrix}\begin{Bmatrix} \ddot{\theta}_1 \\ \ddot{\theta}_2 \end{Bmatrix} + \begin{bmatrix} 32086 + 0.353k_2 & -0.355k_2 \\ -0.355k_2 & 0.337k_2 \end{bmatrix}\begin{Bmatrix} \theta_1 \\ \theta_2 \end{Bmatrix} = \begin{Bmatrix} d_3 f(t) \\ 0 \end{Bmatrix} \quad (10)$$

Draft force $f(t)$ was modelled as a periodics function as shown in figure 3. The draft force is devide into 4 step. The vibration cycle starts point 1 (t= *0)* with the tillage-tool stationary and about to move forward. From point 1 to point 2 the tillage-tool moves forward through tilled soil (loosen soil) and from point 2 to point 3 the tillage-tool move forward cut the untilled soil (dense soil). From point 3 to point 4 and 5 the tillage-tool moves backward through tilled soil. For each step, the model of draft force was based on the qualitative data of unconfined test which had conducted in soil physics laboratory of agricultural machinery department IPB.

- For tilled soil (loosen soil), the draft force is constant and closed to zero.
- For untilled soil (dense soil) the draft force is in the form of three order polynomial of t.

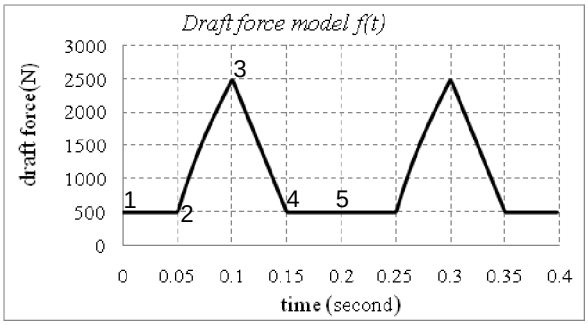

Figure 3: Draft force model for depth tillage of 0.25 m

Maximum draft force (point 3) was calculated with Gill model [15], for tillage depth of 0.3 m, the draft force is about 2500 N. Assumed that the period of draft force is

0.2 second (excitation frequency fe = 5 Hz) so the draft force is modeled as:

$$f(t) = 500\ N \qquad 0<t<0.05$$
$$= 3.2E6\ t^3 - 960000\ t^2 + 128000\ t^2 + 3900\ (N) \qquad 0.05<t<0.1$$
$$= -4000\ t + 6500\ (N) \qquad 0.1<t<0.15$$
$$= 500\ N \qquad 0.15<t<0.2 \qquad (11)$$

2.3 Simulation Procedure

Simulation was based on equation (1) to equation 9 and focused on steady state response of tillage-tool. Detail of simulation is shown in table 1. For spring stiffness k_2= 44762 N/m, swing mass m_2 was varied from 1 kg to 3 kg while for spring stiffness k_2 = 132629 N/m, swing mass m_2 was varied from 2 kg to 4 kg

Fable 1 Dynamics parameter used for simulation

Stiffness k_1 Nm/rad	Inertia J_1 Kg-m^2	Inertia J_2 Kg-m^2	Stiffness k_2 N/m	Swing mass m_2 kg
32086	2.486	0.404	70312.5	0 to 3 kg
32086	2.486	0.404	132629	0 to 4 kg

Displacement of tillage-tool, swing mass and connecting spring is plot as functions of swing mass and plot in time domain. For high displacement, the stress of spring is check again. This is important to avoided excessive strain in the spring and to avoid the spring going to plastic. All graphs are analyzed further to determine the possibilities of draft force reduction during tillage operation.

3. RESULT and DISCUSSION

Frequency was calculated first, for excitation period about 0.2 second, the excitation frequency f_e is 5 Hz. As swinging mass varied, the fundamental frequency is varied too. For k_2 = 70312.5 N/m, the fundamental frequency f_{n1} is varied from 16.42 Hz (m_2=0 kg) to 14.17 Hz (m_2 = 3 kg) while k_2 = 132629 N/m the fundamental frequency f_{n1} is varied from 16.54 Hz (m_2=0 kg) to 14.11 Hz (m_2=4 kg).

For maximum force about 2500 N, Statics deflection of tillage-tool is 29 mm. Contribution of swinging arm and swinging mass m_2 to statics deflection is very small and can be omitted. The graph of maximum deflection of tillage-tool, swinging mass and connecting spring as function of m_2 caused by varied cutting force *f(t)* is shown in figure 4 (for k_2 = 44762 N/m) and in figure 5 (for k_2 = 132629 N/m).

For k_2 = 70312.5 N/m, high displacement of tillage-tool is encounter in range of swinging mass m_2 from 1.5 kg to 2.0 kg or in the range of fundamental frequency f_{n1} from 15.24 Hz to 14.87 Hz while maximum tillage-tool deflection about 75 mm occurred at m_2 about 1.8 kg or at resonance frequency f_r about 15.02 Hz. For m_2 = 1.5 kg the displacement of tillage-tool is 34.4 mm while the displacement of connecting spring is 19.6 mm. At this condition, the equivalent stress in main spring is 180 MPa while the equivalent stress in connecting spring is 400 MPa closed to yield strength of material. For m_2 = 2.0 kg, the displacement of tillage-tool is 35.2 mm while displacement of connecting spring is 22 mm. At this condition, the equivalent stress in main spring is 182 MPa while the equivalents stress in connecting spring is 406 MPa higher than yield strength of material.

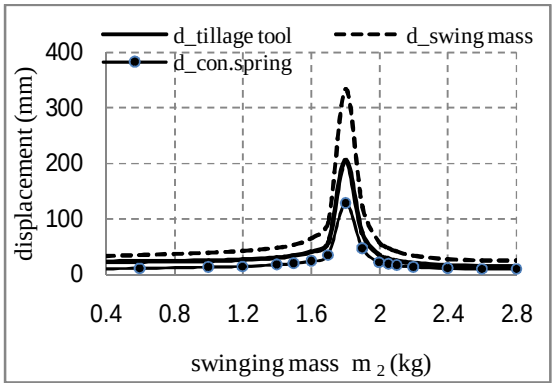

Figure 4: Maximum displacement for k_2 = 70312 N/m

For k_2 = 132629 N/m, high displacement of tillage-tool is encounter in the range of swinging mass m_2 from 2.1 kg to 2.6 kg or in the range of fundamental frequency from 15.15 Hz to 14.88 Hz while maximum tillage-tool deflection about 148 mm occurred at m_2 about 12.4 kg or at resonance frequency about 15.0 Hz. For m_2 = 2.1 kg the displacement of tillage-tool is 42 mm while displacement of connecting spring is 17 mm At this condition, the equivalent stress in main spring is 220 MPa while the equivalent stress in connecting spring is 375 MPa. For m_2=2.6 kg, the displacement of tillage-tool is 40.2 mm while the displacement of connecting spring is 17 mm. At this condition, the equivalent stress in main spring is 218 MPa while the equivalents stress in connecting spring is 375 Mpa. All stress conditions is lower than yield strength of material.

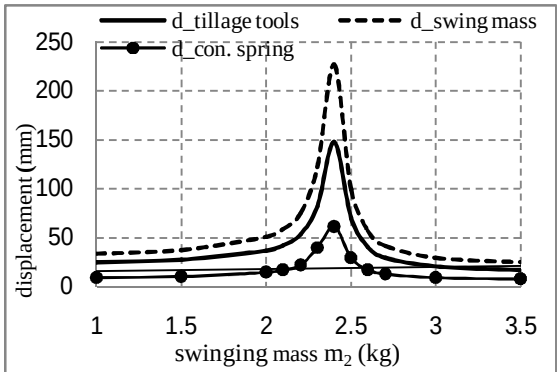

Figure 5: Maximum displacement for k_2 = 132629 N/m

Condition of velocity ratio greater than unity or condition of draft force reduction is correlated to high tillage-tolls deflection, thus simulation is continuing with two conditions (table 2). First is simulation with connecting spring k_2 = 70312 N/m and swing mass m_2 = 1.5 kg and m_2 = 1.5 kg, others is simulation with connecting spring k_2 = 132629 N/m and swing mass m_2 = 2.1 kg and m_2 = 2.6 kg. Possibilities of draft force reduction during tillage operation are investigated by analyzing time response of tillage-tool for both conditions.

Table 2: Condition of simulation

Spring stiffness k_2 (N/m)	Swing mass m_2 (kg)	Condition
70312	1.5	$f_{n1}>f_r$
	2	$f_{n1}<f_r$
132629	2.1	$f_{n1}>f_r$
	2.6	$f_{n1}<f_r$

Time response for *k2* = 70312 N/m is shown in figure 6 while time response for *k2* = 132629 N/m is shown in figure 7. All graph shows that tillage-tool vibrates in excitation frequency and in its fundamental frequencies. Fundamental frequency of graph 1 and graph 3 is higher than its fundamental frequency while fundamental frequency of graph 2 and graph 4 is lower than its resonance frequency.

From t = 0 s to 0.05 s, tillage-tool retract tilled soil, all graph shows that tillage-tool vibrates in half cycle. The importance thing in this step is the tillage-tool cut the clod in a smaller size.

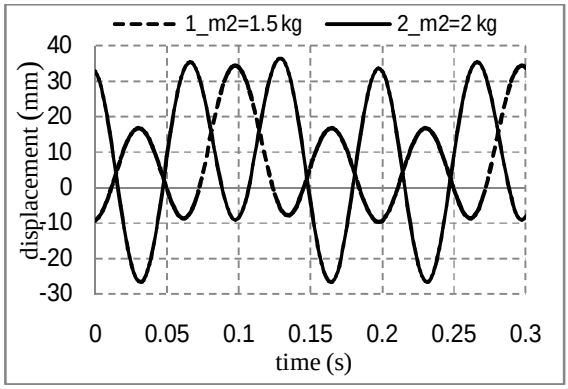

Figure 6: Displacement of tillage-tool for k_2 = 70312 N/m

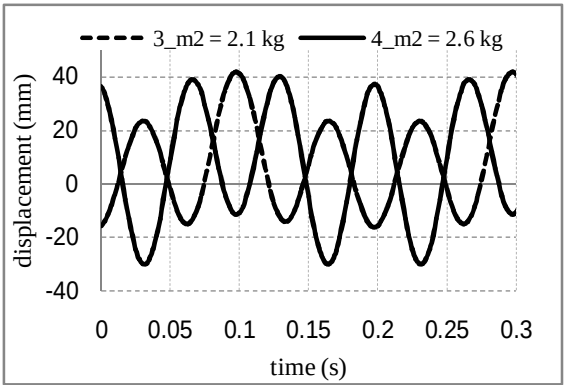

Figure 7: Displacement of tillage-tool for k_2 = 132629 N/m

From t = 0.05 s to 0.1 s tillage-tool cut untilled soil. For vibration with frequency higher than its resonance frequency (graph 1 and graph 3), the tillage-tolls vibrates in low energy level. Compact soil presses the tillage-tool to move backward until the soil break up. This phenomenon is similar to phenomenon on conventional tillage that's why no draft forces reduction in this step. For vibration with frequency lower than its resonance frequency (graph 2 and graph 4), the tillage-tolls vibrates in high energy level in half cycle. First, compact soil presses the tillage-tool to move backward until the soil break up, soil resistance decreases and the restoring force of the spring pushed the tillage-tool to move forward. This phenomenon is similar to vibratory tillage resulting draft force reduction [1]

From t = 0.1 to t = 0.2, all graph shows that the tillage-tool vibrates pass through tilled soil. This is important for tillage-tool to cut the soil clod to smaller size.

4. CONCLUSION

In this work, the simulation of self excited vibration phenomenon on vibratory tillage has successfully been demonstrated. The vibration of vibratory tillage was modeled as vibration with two degree of freedom system

while the excited force was modeled as periodic function. The tillage-tool was vibrated periodically at excitation frequency and at its fundamental frequency. The value of resonance frequency was found three times than that the value of excitation frequency.

The possibilities of high displacement of tillage-tool or the possibility of draft force reduction is happen if the system vibrates around its resonance frequency. In this case, two important conditions were note:

- For vibration with frequency higher than its resonance frequency, there were no draft force reduction were predicted but the quality of soil were increased i.e. the size of soil clod become smaller.
- For vibration with frequency lower than its resonance frequency, both draft force reduction and smaller size of soil clod were predicted

REFERENCE

[1] Yow J., and Smith U.J., 1976, Sinusoidal Vibratory Tillage, Journal of Terramechanies, Vol. 13, No. 4, pp. 211 to 226

[2] Butson. J. M.dan Rackham, H.D., 1981a, Vibratory Soil Cutting II. An Improved Mathematical Model, J. agric. Engng Research, 26, 419-439

[3] Kofoed S. S., 1969, Kinematics and Power Requirement of Oscillating Tillage-tool, J. agric. Eng. Res. 14 (1) 54-73.

[4] Radite P.A.S dan Suastawa I.N., 1998. Analisis gerak dan Karakteristik Penggetar Togel untuk Bajak Singkal., Seminar dan Kongres PERTETA, Yogyakarta

[5] Butson, J. M.dan Rackham, H.D., 1981b, Vibratory Soil Cutting I. Soil Tank Studies of Draught and Power Requirements, *J. agric-. Eng Res.* (1981) 26, 409-418

[6] Bandalan E.P., Salokhe V.M., Gupta C.P., Niyamapa T., 1999, Performance of an oscillating subsoiler in breaking a hardpan. Journal of Terramechanics 36, 117-125

[7] Niyamapa, T., Salokhe, M. V., 2000a, Force and pressure distribution under vibratory tillage-tool, Journal of Terramechanics 37, 139±150.

[8] Niyamapa T. and V.M. Salokhe M. V., 2000b, Soil Disturbance and Force Mechanics of Vibrating Tillage-tool, Journal of Terramechanics 37 151±166

[9] Szabo B., Barnes F., Sture S. and Ko J. H., 1998, *Effectiveness of Vibrating Bulldozer and Plow Blades on Draft Force Reduction*, Transaction of the ASSAE vol.41(2):283-290.

[10] Qiu Lichun and Li Baofa, 2000, Experimental Study on the Self-Excited Vibration Subsoiler for Reducing Draft Force, Transaction of the Chinese Society of Agricultural Engineering 116 960 72-76

[11] Berntsen R., Berre B., Torp T., Aasen H., 2006, Tine force established by a two-level and the draught requirement of rigid and flexible tines. Soil and Tillage Research 90 230-241

[12] Soeharsono, Radite P.A.S., Tineke Mandang, 2008, Self excited vibration phenomenon on vibrating subsoiler coused by natural excitation of varied cutting force, Jurnal TeknikMesin vol 10 No 1 pp 46-51

[13] Kreyszig E., 1988, *Advanced Engineering Mathematics*, John Willey & Son, Singapore

[14] Meirovitch. L., 1986, Element of Vibration Analysis, McGraw-Hill inc, Singapore

[15] Gill W.R. and Vanden Berg. 1968, Soil Dynamics in Tillage and Traction. USDARS Agriculture Handbook No. 316 U.S., Washington D.C 20402: Government Printing Office

,

Proceeding of the 11th International Conference on QiR (Quality in Research)
Faculty of Engineering, University of Indonesia, Depok, Indonesia, 3-6 August 2009
ISSN 114-1284

Modified Particle Swarm Optimization for Multi Odor Localization with Open Dynamics Engine

W. Pambuko, W. Jatmiko

Faculty of Computer Science
University of Indonesia, Depok 16424
Tel : (021) 7270011 ext 51. Fax : (021) 7270077
E-mail : wulung.pambuko@ui.edu

ABSTRACT

The new algorithm based on Modified Particle Swarm Optimization which is robots could change its niche membership is investigated. Then, ODE (Open Dynamics Engine) library is used for physical modeling of the robot like friction, balancing moment and others. This research has a purpose of validation for that MPSO in previous result is applicable in real robot. Simulations prove that newly proposed algorithm can solve diversity lackness problem in multi source problem.

Keywords

Example:
Modified Particle Swarm Optimization (MPSO), Open Dynamics Engine (ODE), Niche Characteristics

1. INTRODUCTION

This research has a purpose to improve MPSO algorithm proposed in the previous research by A. Nugraha [1]. This research also upgraded simulator created which was still in 2D. The 3D simulator developed in this research, its program based on the 2D simulator from the previous research as its result shown in Figure 1. It used ODE library to make the 3D version. This purpose is to reduce gap between software and real hardware. In 2D simulation, robot's movement is drawn by drawing a circle which represents the robot from one coordinate to another. And where there is a collision between 2 robots, these robots do not need to change their direction. Robots are just colliding like if they are balls in pool table.

Algorithm proposed in this research is called Draft Niche-PSO. The word "draft" here is taken from the new behavior of niche that now neutral robots and charged robot could draft from 1 niche to another. For this drafting behavior, there is new robot, main robot which has an attract area. This purpose is to increase the divergence of MPSO algorithm.

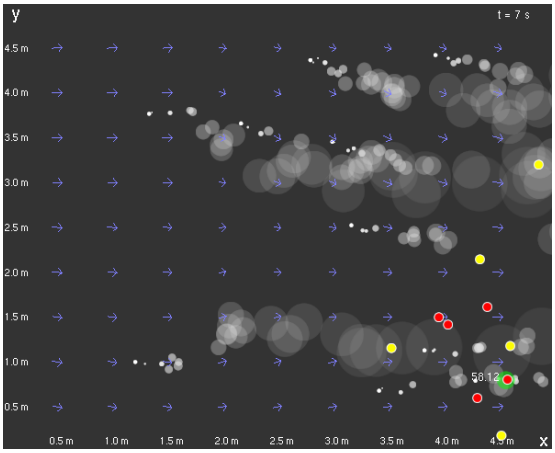

Figure 1: 2D Version Simulator

In Figure 1, neutral robots are the red robots and charged robots are the yellow robots. Main robots did not exist in the previous research.

2. ODE MODELING

Robot(s), field, odor source(s), and plumes are here to be modeled with ODE.

2.1 Robot Modeling

Robot's design is shown in Figure 2 and Figure 3. Robot's principal of changing direction is shown in Figure 4 that robot has to turn each wheel in opposite direction. Robot's changing direction has pivot which is the center of the robot itself. Robots here do not changing their direction while moving forward, they are spinning.

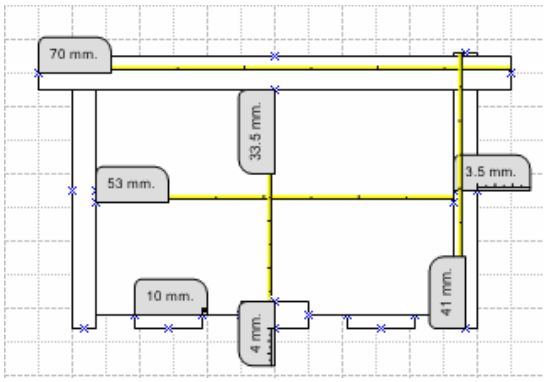

Figure 2: Robot Design (Front)

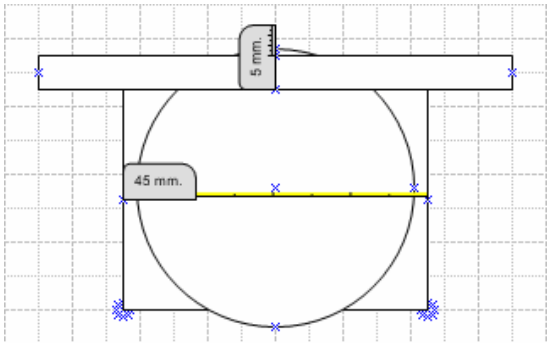

Figure 3: Robot Design (Side)

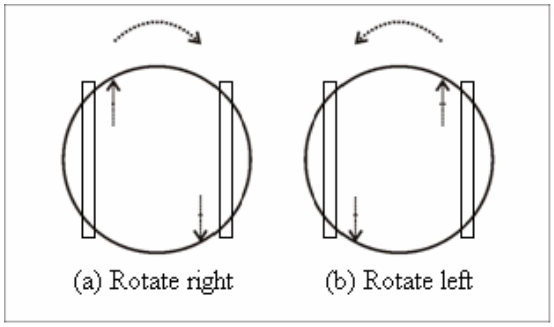

Figure 4: Robot Rotation

The result of robot modeling is shown in Figure 5. Color for each neutral, charged and main robot are shown in Table 1.

Table 1: Robot Color

Robot	Color	RGB
Neutral	Red	(1.0, 0.0, 0.0)
Charged	Yellow	(1.0, 1.0, 0.0)
$CHCl_3$	Purple	(0.8, 0.2, 1.0)

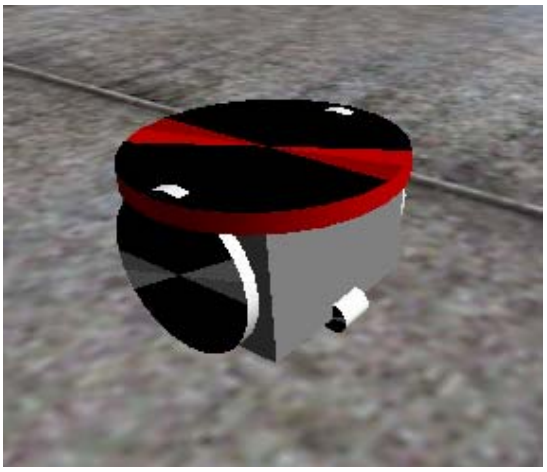

Figure 5: Robot in ODE (Neutral Robot)

2.2 Field Modeling

Field are design as square if viewed from right above. It is build with 4 block with each edge connected as shown in Figure 6. Field has transparency so that robots, odor source(s) and plumes can be seen from side.

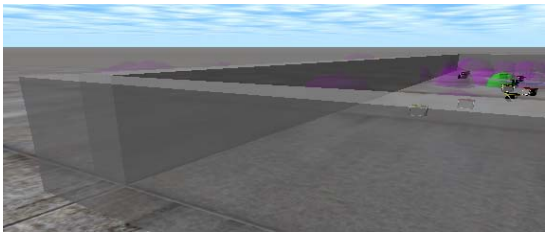

Figure 6: Field in ODE

2.3 Plumes Modeling

Plumes in this research has characteristic as:
[1]. Transparent
[2]. Do not have any collision with any other objects
[3]. Drawn as a sphere
Plumes will become more and more transparent as time running. By the time it has just emitted from its source it transparency is 0, and this transparency will increased until its value is 1 and plumes will become invisible. Plumes are gas material so that it does not have any collision with any other objects. Plumes are drawn as a sphere. Plumes in real life are an enormous number of dust particles for that it is nearly impossible to draw. The size of the sphere will become bigger and bigger as time running. Plumes design result is shown in Figure 7.

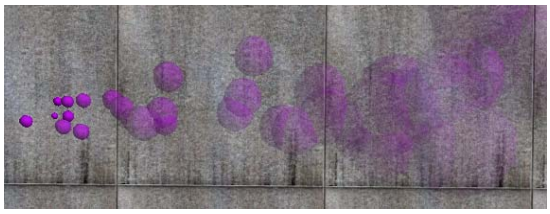

Figure 7: Plumes

2.4 Odor Source Modeling

Odor source in this research simply modeled with half sphere. Actually it is a full sphere, but half below part is under the ground so that it could not be seen. Odor source's color is purple, the same with plumes' color. Odor source model is shown in Figure 8.

Figure 8: Odor Source

Odor source once it had been found by a robot, it will be closed. Odor source closing is illustrated with changing its color into grey as shown in Figure 9.

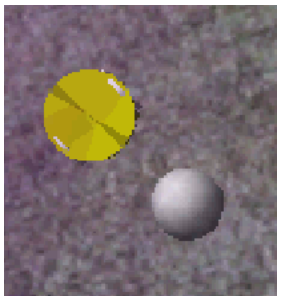

Figure 9: Odor Source Declaration

3. DRAFT NICHE-PSO

Newly proposed algorithm in this research is called Draft Niche-PSO. In Draft Niche-PSO there is possibility for neutral or charged robot to draft to another niche, to change its membership of niche. Robot newly introduced here is main robot which control drafting procedure.

3.1 Main Robot

Main robot has an attract area where other niche's neutral or charged robot whom entered this area will become its niche member. Unlike neutral robots or charged robots, main robots only have local best, and like charged robots, they have charge, too, but only effects with other main robots. Main robot design is shown in Figure 10. The blue circle shows the attract radius. The R Core line in the simulator will not be drawn.

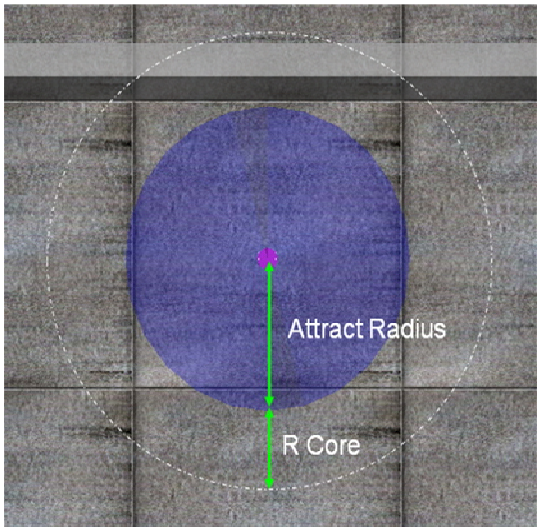

Figure 10: Main Robot

Main robot will reject other main robot if their R Core limit intercepted. The amount of rejection is shown in equation (1).

$$u_{jk}(t) = \begin{cases} \dfrac{Q_j Q_k (x_j(t) - x_k(t))}{(AttractRadius + RCore)^2 \left\| x_j(t) - x_k(t) \right\|} \\ 0 \end{cases} \quad (1)$$

Where μ is the amount of rejection, Q is the amount of charge.

μ will become 0 or main robot do not reject any other main robot if their R Core radius is not intercepted.

4. RESULT

After implementing robot and its environment in 3D simulation including physical model, we utilized MPSO algorithm for searching multiple odor source in dynamic environment. Its results show that MPSO is applicable in real situation.

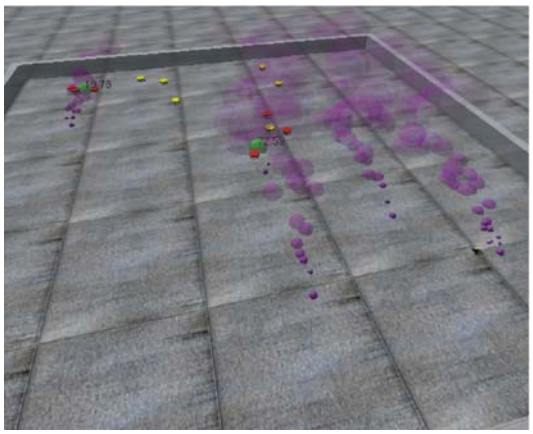

Figure 11: MPSO with ODE

Draft Niche-PSO also shows a good result for increasing the diversity of previous PSO algorithm. Now, we see the comparison of them with initial condition shown in Figure 12 and Figure 13.

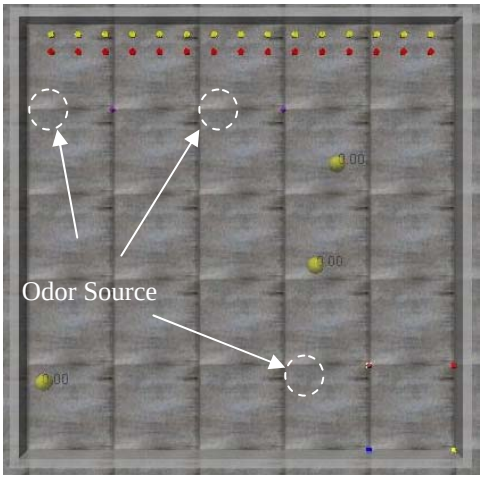

Figure 12: Original MPSO (Initial)

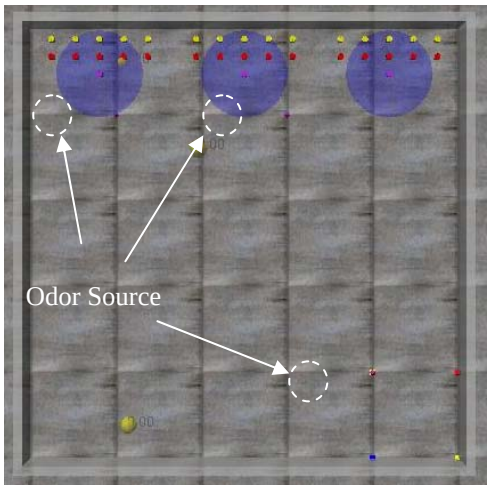

Figure 13: Draft Niche-PSO (Initial)

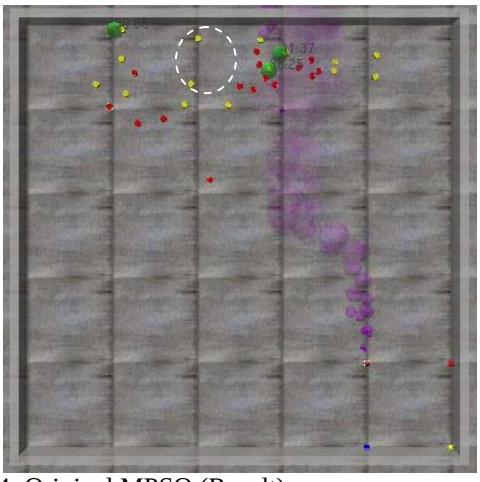

Figure 14: Original MPSO (Result)

Figure 14 shows the result of original MPSO. We can see that 2 niche still toward the same odor source with their global best near each other.

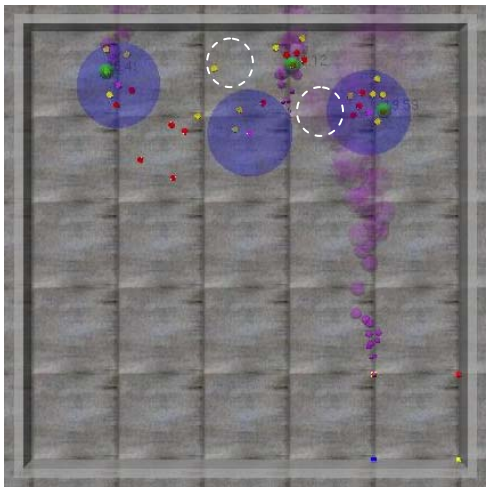

Figure 15: Draft Niche-PSO (Result)

Figure 15 shows the result of Draft Niche-PSO. We can see that middle niche and right niche were moving toward the different odor source.

7. CONCLUSION

We have implemented MPSO algorithm in 3D environment in order to model robot movement and environment in searching multiple odor sources. We have moved one step further to implement MPSO in real robot for searching odor source in real world. The result of this simulation is not analyzed yet. Furthermore, this simulation must be analyzed in order to assess its effectiveness.

ACKNOWLEDGMENT

This work was supported in part by the Science and Technology 2007 by Indonesia Toray Science Foundation and the Incentive Research Program 2008-2009 by the Ministry of Research and Technology Republic of Indonesia.
The authors also are grateful to Prof. J. A. Farrell from the University of California, Riverside, U.S.A., for his support in advanced turbulent-environment source-code.

REFERENCES

[1] A. Nugraha, Modified Particle Swarm Optimization for Multi Odor Localization, Faculty of Computer Science, University of Indonesia, 2008.
[2] Kousei Demura, Easy! Practical! Robot Simulation (Book style). Morikita Publisher, Tokyo, 2008.
[3] W. Jatmiko, A. Nugraha, W. Pambuko, B. Kusumoputro, K. Sekiyama, T. Fukuda, Localizing Multiple Odor Sources in Dynamic Environment using Niche PSO with Flow of Wind Based on Open Dynamics Engine Library, paper presented in The Second International Conference on IT Application and Management, University of Indonesia, 2009.

Proceeding of the 11th International Conference on QiR (Quality in Research)
Faculty of Engineering, University of Indonesia, Depok, Indonesia, 3-6 August 2009
ISSN 114-1284

Optimal Tool Orientation for Positional Five-axis Machining of Molding Die Surface

Yeong Han Cho[1], Seong Jin Yang[2], Hyun Wook Cho[3], Sang Hoon Lee[4], Jung Geun Lee[5], Jung Whan Park[6]

School of Mechanical Engineering,
Yeungnam University, Gyeungsan, Korea
+82-53-810-3524
[1]E-mail: tigerjr@ynu.ac.kr
[2]E-mail: theshell@ynu.ac.kr
[3]E-mail: hyun8046@nate.com
[4]E-mail: uandi012@ynu.ac.kr
[5]E-mail: willtechcom@chol.com
[6]E-mail: jwpark@yu.ac.kr

ABSTRACT

The paper presents the study on a CAPP(computer-aided process planning) system that suggests optimal tool orientation with which positional five-axis machining of sculptured surface in a molding die manufacturing. The positional five-axis machining is operated on a five-axis NC machine, with the cutting tool orientation being fixed during the cutting operation. This type of machining operation is effective in machining separated areas (geometric features) on a molding die. The optimal tool orientation for a machining area is obtained through two steps: (1) the local optimal tool orientation on each cutter-contact point is obtained, which is based on the machinability condition, then the angular range of global tool orientation is obtained by the union of the local angles; (2) the tool length map for the indicated global tool orientation range is computed via interference check (collision and stroke-over), and the tool orientation with the minimum tool length is selected as an optimal tool orientation. The research was implemented on the basis of a commercial CAM system(I-Master) in the Windows XP environment, and was tested for positional five-axis machining of molding dies for automotive parts in a local company.

Keywords

Positional 5-axis machining, optimal tool orientation angle, CAPP

1. INTRODUCTION

Five-axis machining of molding dies has more benefits such as fewer set-ups and better machining accuracy resulting from shorter tool length [1,2]. It may be classified into positional five-axis and continuous five-axis depending on cutter orientation change (see Figure 1). The positional five-axis machining is a fixed-axis machining on a five-axis NC machine with the cutter-axis tilted, while the continuous five-axis machining is the conventional simultaneous five-axis machining.

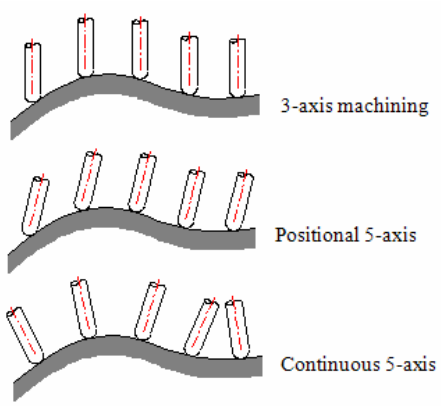

Figure 1: Machining types

Machining process of a molding die consists of several unit machining operations(UMOs), which is a combination of conventional three-axis, positional and continuous five-axis machining operations. An NC programmer determines most suitable machining type to each machining feature area.

Simultaneous five-axis machining can adaptively change cutting speed and tool posture at each CC(cutter contact) point by continuously varying tool-orientation, but it requires somewhat complicated interference avoidance and computing time. It should be noted that the positional five-axis machining is well applied to machining of molding die surface, due to consistent tool posture and simple interference avoidance compared to continuous five-axis machining [3].

According to a commercial CAM software developer [4], distinct machining types on a five-axis machine are: 73% of positional five-axis machining, 22% of multi-face three-axis machining, and 5% of continuous five-axis machining. It can be said that continuous five-axis machining operation using a five-axis machine may well be applied to where fixed-axis

machining is either infeasible or inefficient.

The tool length should be as short as possible without interference (e.g., collision) in order to enhance machining accuracy and surface finish, due to tool deflection and chattering. In positional five-axis machining of a certain surface area, it is imperative to select a tool orientation that minimizes tool length of the applied cutter but also causes no collision. A few existing commercial CAM systems provide such functionality, but requires complicated user interactions or fairly much computing time.

The research developed a system that computes the optimal tool-orientation with minimum tool-length for a ball-end milling case, given a surface area to be machined. Section 2 describes the key procedure, followed by an illustrated case in Section 3.

2. CONVENTIONAL PROCESS

A conventional process to determine the tool orientation and length by which a certain surface area is to be machined is described in figure 2. Tool orientation is usually designated by setting up a local coordinate system in a commercial CAM system. As shown in the figure, the process requires NC programmer's insight and experience, tool-path generation and collision avoidance through interactive as well as iterative operations.

The similar process should be repeated for each feature surface that needs positional five-axis tool-path generation, which is tedious and time consuming job. In addition, it does not always generate optimal tool orientation with minimum tool length, which may result in non-optimal machinability.

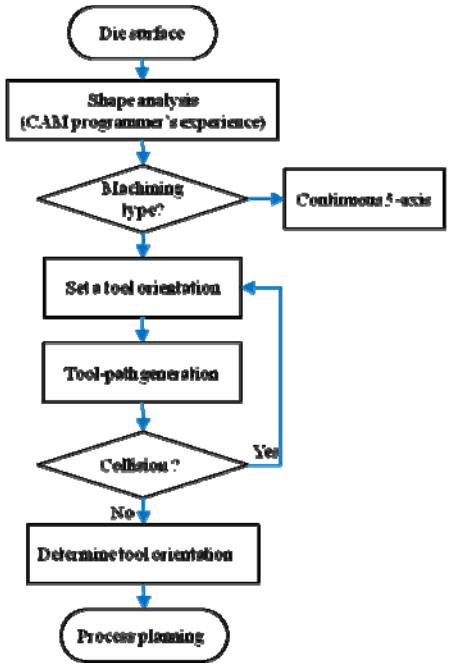

Figure 2 : Conventional process of work coordinate set-up

3. PROPOSED PROCESS

3.1 Overall view

Figure 3 depicts overall procedure of the proposed process, which is summarized as follows:

< Phase 1 >
(1) Sampling CC points on the defined surface area,
(2) For each CC point, determine preferred tool-orientation range,
(3) Obtain overall preferred tool-orientation range for all CC points,
< Phase 2 >
(4) Select feasible tool-orientation range from the preferred tool-orientation range for all CC points by checking stroke-over and collision,
(5) Determine the optimal tool-orientation angle with minimum feasible tool-length.

In the 1st phase, the preferred tool-orientation range for each CC point is determined based on a previous study which considered cutting force and surface finish in a ball-end milling case [5]. In the 2nd phase, the feasible tool-length for a specified tool-orientation is computed via interference check (i.e., stroke-over and collision check), the tool-orientation with minimum feasible tool-length is selected as an optimal tool-orientation. The collision check process considers cutter shank, tool holder, machine spindle, and machine table. Following sections describe more details about the process.

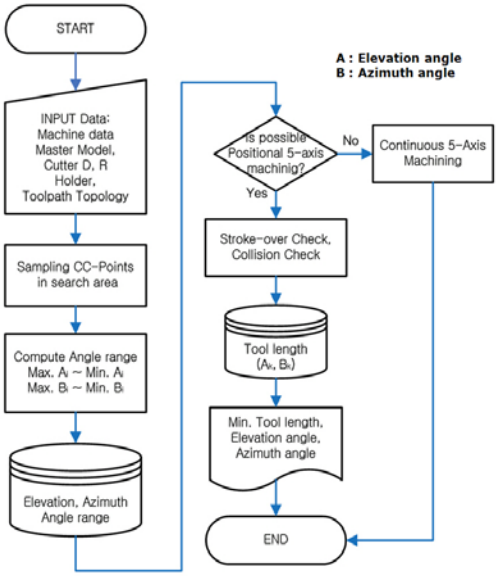

Figure 3 : Overall procedure

3.2 Phase 1: preferred tool-orientation

The 1st phase of the overall process determines preferred range of acceptable tool-orientation by aggregating each preferred tool-orientation at a single CC point. A previous study [5] depicted that the acceptable tool inclination angle (ball-ended milling) at a CC point should be 15˚ to 45˚ measured from the surface normal, which is based on cutting force and surface finish. This concept can be represented by a cone (see figure 4), since the applied cutter is a ball-ended mill. Being measured in the local coordinate system of a CC point, the tool inclination angle is converted to tool-orientation of the global coordinate system, which is represented by elevation and azimuth angles (see figure 5). The elevation and azimuth angles (A,B) corresponding to a tool inclination vector **n'** is represented by equation (1).

$$\text{A (elevation angle)} = a\tan 2(\sqrt{n'^2_x + n'^2_y},\ n'_z) \quad (1a)$$

$$\text{B (azimuth angle)} = a\tan 2(n'_y,\ n'_x) \quad (1b)$$

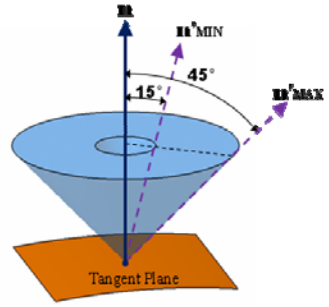

Figure 4 : Local acceptable range of tool-orientation

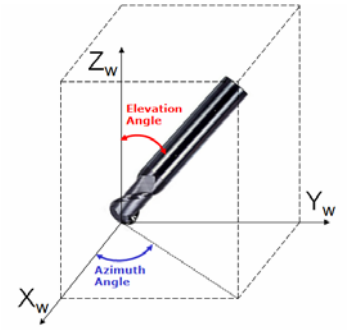

Figure 5 : Elevation and azimuth angles to define tool-orientation

The overall range of acceptable tool-orientation for all CC points is obtained by summing up each tool-orientation range of a single CC point, which is represented by ranges of elevation and azimuth angles such as $(A,B)_{MIN}$~$(A,B)_{MAX}$. Figure 6 depicts a schematic diagram of the phase 1.

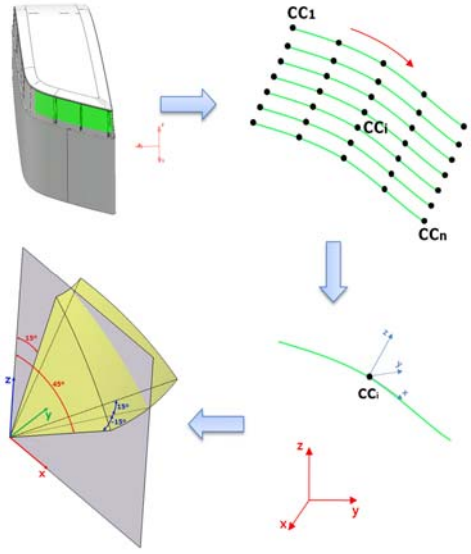

Figure 6 : Overall preferred range of tool-orientation

3.3 Phase 2: optimal tool-orientation

The overall preferred range of tool-orientation $(A,B)_{MIN}$~$(A,B)_{MAX}$ obtained in the 1st phase can be thought of as an initial filtering out process for efficient computation. The 2nd phase determines the optimal tool-orientation by computing minimum feasible tool-length at each tool-orientation among the given preferred range. The procedure is summarized as follows:

(1) For a tool-orientation $(A,B)_k$ among the overall range $(A,B)_{MIN}$~$(A,B)_{MAX}$, compute feasible tool-lengths for all CC points, and find the minimum tool-length L_k,
(2) Find the minimum tool-length L_m at $(A,B)_m$ among L_k, and set the optimal tool-orientation to be $(A,B)_m$.

The feasible tool-length at a tool-orientation $(A,B)_k$ at CC point is obtained via interference check including machine axis stroke-over, machine collision and tool collision. The machine axis stroke-over can be verified by considering inverse kinematics of the target NC machine. The machine and tool collision consider collisions between components such as machine spindle, table, cutter shank, and tool holder. The tool-length computation is based on the previous study [6]. Figure 7 describes overall procedure of phase 2.

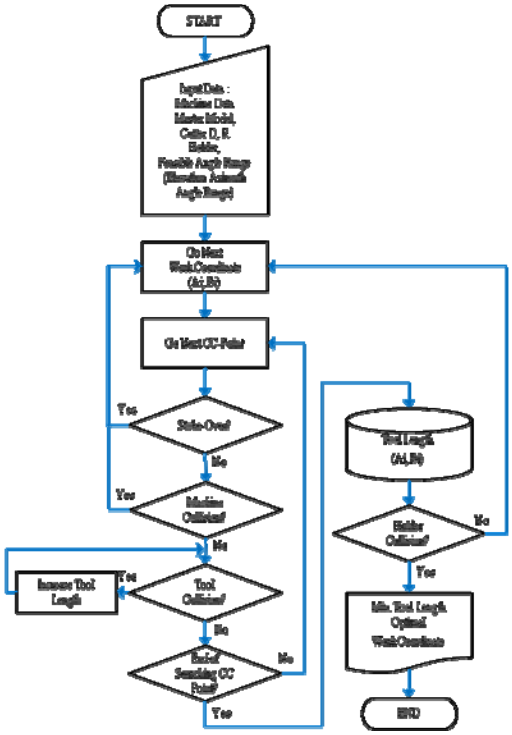

Figure 7 : Search of the optimal tool-orientation

4. ILLUSTRATED EXAMPLE

The proposed system has been implemented by Visual C++ and OpenGL in Windows XP environment. Figure 8 shows an example molding die surface, where the red colored face is the machining area. Figure 9a depicts preferred tool-orientation range (in elevation & azimuth angles), figure 9b illustrates the optimal tool-orientation.

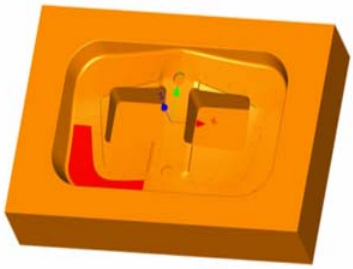

Figure 8 : Molding die surface and machining area

(a)

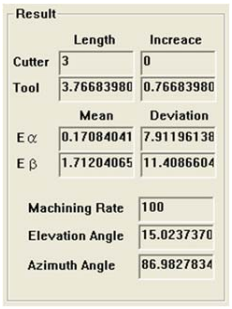

(b)

Figure 9: Preferred range of tool-orientation and search result

5. DISCUSSION

The research has developed a system that determines the optimal tool-orientation for positional five-axis machining of molding die surface. It provides a CAM programmer with an optimal work coordinate system and minimum tool-length information, thereby enabling objective and efficient process planning for five-axis machining tool-path generation.

It should be noted that the tool-length is not the only factor affecting machinability. As a previous study depicts [5], the tool inclination angle itself is an imperative machining condition. Therefore, another criterion including tool-length and tool inclination angle can be considered as an error function at a CC point as follows:

$$\varepsilon_T = \omega_\alpha\left(\frac{\varepsilon_\alpha}{\Delta a}\right) + \omega_L\left(\frac{\varepsilon_L}{\Delta L}\right);$$

where ε_α = angular deviation of inclination angle from given value,
ε_L = tool-length deviation (L_i-L_0, L_0 = minimum tool-length),
ω_α, ω_L = weighting factors,
$\Delta\alpha$, ΔL = scaling factors.

Considering the above combined error function at each CC point should be dealt in the further research.

REFERENCES

[1] Mason, F., "5×5 for High-productivity Airfoil Milling", American Machinist, Nov, pp.37-39, 1991.
[2] Tonshoff, H.K., Hernaadex-Camacho, J., "Die manufacturing by 5-and 3-axis milling", Mechanical Working Technology, Vol.20, pp.105-119, 1989.
[3] Hopkin, B., "Benefits of positional five-axis machining", Moldmacking Technology, May 2005.
[4] Delcam Korea, http:\\www.delcam.co.kr.
[5] Kang, I.S., Kim, S.W., Kim, J.S., Lee, K.Y., "A study on the machining characteristics according to tool position control for 5-axis high speed mold machining", Journal of Korea Society of Machine Tool Engineers, Vol.16, No.5, pp. 63~69, 2007.

[6] Lee, J.G., Yang, S.J., Cho, Y.H., Yoo, S.K., and Park, J.W., "Development of a System to Generate Tool Orientation Information for Positional 5-Axis Machining of Die and Mold", Computer Aided Design and Applications, Vol. 5, pp. 434-441, 2008.

Symposium on Advanced Materials and Processing

Symposium E

CCIT
FAKULTAS TEKNIK
UNIVERSITAS INDONESIA

Kelas Eksekutif (Jum'at-Sabtu)
Program Pendidikan Profesional 2 tahun
bidang Teknologi Informasi

becoming world class IT professional

CCIT-FTUI telah berdiri sejak tahun 2002. Di CCIT-FTUI anda akan dididik menjadi seorang profesional handal di bidang IT (*Information Technology*) berkelas internasional. Kurikulum pendidikan yang dipakai adalah kurikulum terkini yang diberi nama MasterMind Series (MMS). Kurikulum ini memberikan fleksibilitas untuk memilih jalur peminatan ***Software Engineering*** atau ***Network Engineering***, dengan pilihan *platform open source* atau *proprietary*.

Excellent is not destination, but becoming a professional is a must

NIIT
World Leading IT Institute

www.ccit.eng.ui.ac.id

potongan 50% biaya pendaftaran dengan membawa pamplet ini

Master Mind Series (MMS) Curriculum

MASTERMIND SERIES

Software Engineering | **Network Engineering**

Semester 1

- Office Applications
- Programming Fundamentals
- Understanding IT Applications
- Operating Systems Fundamentals
- Networking Fundamentals

Software Engineering	Network Engineering
Introduction to Relational Database Design	Introduction to Relational Database Design
Implementing Database Using SQL Server 2000	Implementing Database Using SQL Server 2000
Introduction to WEB Content Development	Implementing and Administering MS Windows XP Professional
Developing Object based Client Server Applications	Administering MS SQL Server 2000 Databases

(2 Semester)

Semester 3 (Software Engineering)	Semester 3 (Network Engineering)
Fundamentals of Linux	TCP/IP Fundamentals and Concept
Understanding Sofmare Business Processes and Development Life Cycle Development	Managing and Maintaining a MS Windows Server 2003 Environment / **linux 05**
Developing Portable Web Applications Using XML Tchnology	Implementing, Managing and Maintaining an MS Windows Server 2003 Network Infrastructure / Linux System Administration
Object Oriented Analysis and Design Using UML	Planning and maintaining an MS Windows Server 2003 / Linux Networking & Security Admin

Semester 4 (Software Engineering)	Semester 4 (Network Engineering)
Developing Enterprise-Wide Applications part I	Planning, Implementing and Maintaining an MS Windows Server 2003 Active Directory Service
Developing Enterprise-Wide Applications part II	Designing Security for an MS Windows Server 2003 Network
Developing Enterprise-Wide Applications part III	Information Security Essentials
Understanding Application Development Life Cycle and Architecture	Software project Managemant
Understanding Site Design Methodology and Management	

(4 Semester)

FASILITAS

- Ruang belajar yang nyaman (full AC) dengan kapasitas kecil sehingga penyampaian materi pengajaran lebih maksimal.
- Buku-buku / Courseware gratis
- Sertifikasi CCIT-FTUI dan Sertifikasi international dari NIIT
- 1 orang 1 komputer dengan akses internet.
- Perpustakaan mini dengan buku-buku terbaru dan berbagai majalah serta tabloid IT yang up to date.
- Fasilitas Web-based training melalui website http://www.netvarsity.com
- Angsuran pembayaran fix
- Coffe break

e-mail : ccit@eng.ui.ac.id

RINCIAN BIAYA PENDIDIKAN

BULAN	ANG	Rp
Agu 2009	1	4.000.000
Sep 2009	2	2.000.000
Okt 2009	3	2.000.000
Nov 2009	4	2.000.000
Des 2009	5	2.000.000
Jan 2010	6	2.000.000
Feb 2010	7	2.000.000
Mar 2010	8	2.000.000
Apr 2010	9	2.000.000
Mei 2010	10	1.500.000
Juni 2010	11	1.500.000
Juli 2010	12	1.500.000
Agu 2010	13	1.500.000
Sep 2010	14	1.500.000
Okt 2010	15	1.500.000
Nov 2010	16	1.500.000
Des 2010	17	1.500.000
Jan 2011	18	1.500.000
Feb 2011	19	1.500.000
Mar - Juli 2011		FREE

INFORMASI & PENDAFTARAN

Gedung Engineering Center Lt. 1
Fakultas Teknik Universitas Indonesia
Kampus UI Depok 16424, Indonesia
Phone / Fax : 021 - 7884 9047 / 786 3508
021 - 6865 6258 / 985 23311

Hotline **021-686 56258**
021-788 49047

ISSN 114-1284

The Effect of Fatiguing on the Polarization Profiles of Ferroelectric Polymer Films

Albinur Limbong

Faculty of Information Technology
Adventist University of Indonesia, Parongpong-Bandung
Tel.: (022)2700032, Fax. (022): 2700162
Email: alimbong@unai.edu

ABSTRACT

When ferroelectric materials are subjected to repeated reversal of polarization, the magnitude of the reversed polarization is observed to decrease. This phenomenon is referred to as fatigue and is generally ascribed either to space charge effects or to the pinning of domain walls at defects.

In recent times several techniques have been developed which allow the study of polarization profiles in thin, insulating films. In the present work, the polarization profiles in fatigued ferroelectric polymers were measured using the laser intensity modulation method (LIMM).

The polymers studied were polyvinylidene fluoride (PVDF) and its copolymers with trifluoroethylene (TrFE). The polymers were fatigued by reversing the polarization many times using a cyclic field with an amplitude above the coercive field. For some of the polymers, this leads to a decrease in the magnitude of the reversed polarization, while for others, the magnitude remained reasonably constant.

It was found that those polymers which showed most fatigue in their hysteresis loops had a more symmetrical distribution of polarization after fatiguing. The lack of fatigue and asymmetrical polarization profiles seem to be associated with materials which contain the non-polar α crystal form.

Keywords:

Polarization, Fatigue, Ferroelectric, Pyroelectric, LIMM

1. INTRODUCTION

This year marks the fortieth anniversary of the announcement of the piezoelectric properties of the ferroelectric polymer polyvinylidene fluoride [1]. In the period since this announcement, there has been a large amount of research into the ferroelectric nature of PVDF and some of its copolymers. Ferroelectrics find applications in a range of electronic devices, arising from their high dielectric constant, piezoelectric, pyroelectric and switching properties. In the case of switching an important property is fatigue; the reduction of the observed reversed polarization with repeated cycling of the applied electric field. This property is of particular importance in the recent application of ferroelectrics in memory chips [2].

In order to better understand the causes of fatigue, polarization profiles were prepared for ferroelectric polymer films which had been fatigued. The method used was the LIMM technique [3-5]. In this technique light, with periodically varying intensity is directed onto the surface of a sample. The frequency of variation determines the spatial distribution of temperature fluctuation in the sample and hence the magnitude and phase of the pyroelectric current. Deconvolution of the current allows the extraction of the polarization profile in the sample.

2. BACKGROUND THEORY of LIMM

A complete description of the theory underlying LIMM is readily available in the literature [3-8]. For completeness, a brief outline is given here.

The basic arrangement for LIMM is shown in figure 1. It consists of a free standing pyroelectric film, with electrodes on both surfaces. The distance through the sample is denoted x. The back surface (x=d) of the film is thermally isolated, while the front surface (x=0) is illuminated by a modulated laser beam.

ISSN 114-1284

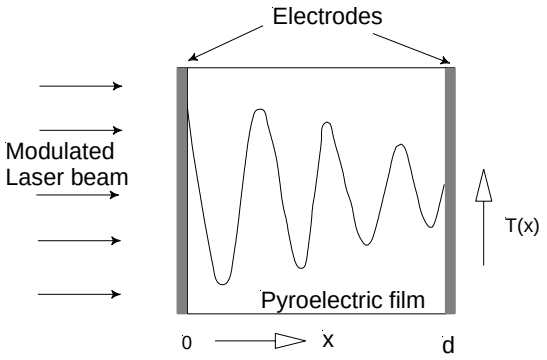

Figure 1: Thermal wave inside a pyroelectric film. Sample is heated from x=0, while the other surface (x=d) is thermally isolated.

The temperature fluctuation $\Delta T_\omega(x,t)$ at the point x, is given by [4]:

$$\Delta T_\omega(x,t) = \frac{\eta W_\omega}{\mu G_t}\frac{\cosh[\mu(d-x)]}{\sinh(\mu d)} e^{j\omega t} \qquad (1)$$

where $\mu = (1+j)\sqrt{\frac{\omega}{2\delta_t}}$, δ_t is the thermal diffusivity, W_ω is the laser beam power, η is the emissivity and G_t is the thermal conductivity and ω is the frequency of the thermal wave.

The thermal waves generated by the optical excitation create a pyroelectric current ($I_p(t)$) between the two electrodes of the sample. There are several mechanisms contributing to the pyroelectric effect [7], such as the temperature dependence of the dipolar polarization (primary pyroelectric effect), thermal expansion of the crystallites (secondary pyroelectric effect), thermal expansion of the amorphous regions, temperature dependence of the crystallinity, and temperature dependence of the space charge distribution. In LIMM measurements, it is not possible to separate the effects of these contributions [4].

If permanent dipoles are compensated by an appropriate charge density, the time dependent pyroelectric current, I(t), is given by [3,8]:

$$I_p(t) = I_{p\omega} e^{j\omega t} = \frac{\alpha_p A}{d}\int_0^d P(x)\frac{\partial \Delta T_\omega(x,t)}{\partial t}dx \qquad (2)$$

where P(x) is the unknown, spatially dependent polarization distribution and $\alpha_p = \frac{1}{P}\frac{dP}{dt}$ is the relative temperature dependence of the polarization. The product of α_p and P(x) is the spatial variation of pyroelectric coefficient (p(x)). Inserting the temperature profile from equation (1) into equation (2) yields the pyroelectric current:

$$I_{p\omega} = \frac{A\alpha_p \eta W_\omega}{\rho c d}\frac{\mu}{\sinh(\mu d)}\int_0^d P(x)\cosh[\mu(d-x)]dx \qquad (3)$$

In a LIMM experiment the pyroelectric current is measured as a function of modulation frequency ω. To obtain the spatial polarization distribution equation (4) has to be deconvoluted. A convolution integral is given by:

$$g(y) = \int f(x) r(y-x) dx \qquad (4)$$

where the function f(x) is convolved with a response function r(x). The convolution theorem states that:

$$G(y)=F(y)R(y) \qquad (5)$$

where F, G and R are the Fourier transforms of the functions in equation (4). The Fourier transforms of g(y) and r(y) can be calculated by dividing G(y) by R(y), and an inverse Fourier transformation is calculated. Mathematically, this calculation is readily done. In practice however, this is an ill-posed problem. Since g(y) always contains some experimental noise, there exists an infinite set of function, f(y), which after convolution with r(y), agree with g(x) within the uncertainty.

Several deconvolution techniques, each with its own advantages and disadvantages, have been developed [4,5]. The first is a Fourier filtering method. By expanding the solution of the heat conduction equation (3) as a Fourier series, the distribution P(x) can be calculated from the measured pyroelectric current [5].

The second method is the regularization method [6]. In this method, in order to get a reasonably smooth polarization profile, it is necessary that the integral over the second derivative should be minimised, i.e.

$$\int_0^d \left|P''(x)\right|^2 dx = \min \qquad (6)$$

A disadvantage of this method is that one has to find the right compromise between suppressing unphysical oscillations and smoothing out the solution too much [7]. In practice, one often encounters a strong polarized layer near the surface, giving rise to a rapidly changing P(x), and a much smoother distribution deep inside the sample.

Both Fourier filtering and regularization methods often produce artefacts and require a large computational effort. Ploss *et al*. [7,8] proposed an approximation technique. Near the surface of the sample, an approximate solution of the heat conduction can be used to obtain an analytical expression for the polarization distribution. Referring to equation (1) the

spatial temperature change at high frequencies ($\omega > 2\delta_t/d^2$) is approximated as [7]

$$T_\omega(x) = \frac{\eta W_\omega}{\mu G_t} e^{-\mu x} \quad (7)$$

From equations (2) and (7) the pyroelectric current at high frequencies can be written as:

$$I_{p\omega} = \frac{\eta \alpha_p A W_\omega}{\rho c d} \int_0^\infty P(x) \mu e^{-\mu x} dx \quad (8)$$

The difference between the real ($I_{p\omega re}$) and imaginary (I_{pim}) components of this current is given by [8]

$$P_a(x_t) = \int_0^\infty P(x) \frac{2}{x_t} \sin(x/x_t) e^{-x/x_t} dx \quad (9)$$

where $P_a(x_t)=I_{p\omega re}-I_{p\omega im}$ and $x_t(=2\delta_t/\omega^{-1/2})$ is the thermal diffusion depth. Ploss *et al*. [7] defined the function $[2\sin(x/x_t)/x_t]e^{-x/xt}$ as a thermal scanning function ($f(x,x_t)$). Based on the analysis of the properties $f(x,x_t)$ they found that the temporal derivation of the temperature amplitude has all the properties of a scanning function for the pyroelectric profile. The function $P_a(x_t)$ which is calculated from the measured pyroelectric current is an approximation of the pyroelectric distribution $P(x_t)$ for small x_t. Therefore, the approximation $P(x_t) \approx P_a(x_t)$ is only valid near the heated surface of the sample. With the approximation method the component of the measured pyroelectric spectrum gives an approximation for the pyroelectric profile without the necessity for a mathematical inversion [8]. This enables LIMM to be used as an on-line procedure, where the pyroelectric coefficient at a given depth on the sample is obtained directly from the current measured at a particular frequency.

The strength of the approximation method is its accuracy in showing the polarization profiles near the heated surface [8].

3. EXPERIMENTAL

The polymers used were PVDF and its copolymers with trifluoroethylene (TrFE). The samples were of two types. The first type consisted of commercial films of 25 μm thickness. 25 μm films of PVDF were obtained from Kureha and Solvay, and 65/35 and 75/25 mol% VDF/TrFE copolymers in 25 μm thickness were obtained from Solvay. The second type of sample were sub-micron films, prepared by spinning a solution of the polymer onto a metallised glass substrate. Such spun-cast samples typically had a thickness of the order of 0.1 μm. It may be possible to produce samples with thickness less than 0.1 m. [9,10].

Hysteresis loops for the films were generated in conventional Sawyer-Tower type circuits. The 25 μm films required maximum voltages around 2 kV in order to generate the loops. For these films, the period of cycling of the field could not be reduced below a few tens of seconds, because of slew rate limitations in the high voltage supply. For the spun-cast films, the required voltages were much lower, and readily supplied by an ordinary signal generator. The period used was normally less than a second. If the period was greater than one second, then the loops tended to balloon in shape - presumably as a result of leakage in the films.

LIMM measurements were made by illuminating the samples either with a modulated IR laser diode or with a chopped laser beam. The pyroelectric current thus generated was measured using a lockin amplifier. The currents were measured over the frequency range from 10 Hz to 10 kHz.

4. RESULTS

The effects of fatigue on the hysteresis loops of the commercial 25 μm films are illustrated in Figures 2 and 3. Figure 2 shows the effect of repeated cycling on the loops of the Kureha 25 μm PVDF films. The period of these loops was 100 s. Neither of the PVDF films (i.e. Kureha and Solvay) showed a significant reduction in reversed polarization with repeated cycling. Both materials produced loops which were reasonably symmetric about the zero polarization axis.

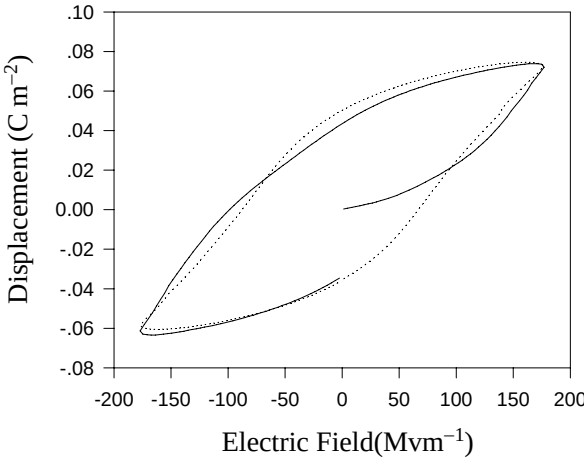

Figure 2: The first (solid) and 100th (dotted) loops for 25 μm Kureha PVDF. The loop period was 100 s.

In contrast, both the 65/35 and 75/25 copolymers displayed fatigue, which was clearly evident even during the first couple of cycles. The copolymers would normally display a large initial loop, lying entirely above the polarization axis, (Figure 3) and subsequent loops would maintain this initial offset.

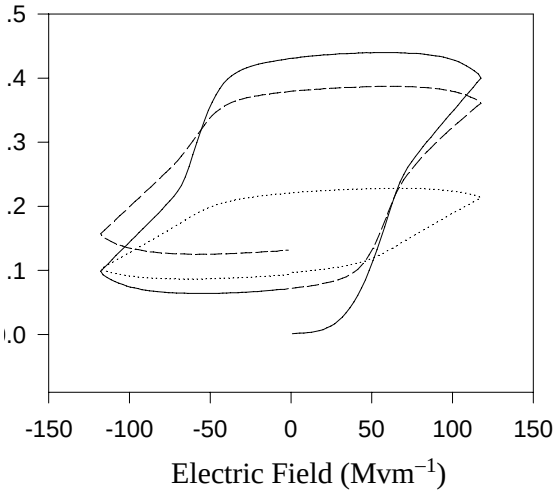

Figure 3: The first (solid), second (dashed) and tenth (dotted) loop for a 25 μm Solvay 65/35 copolymer film. The loop period was 100 s.

Figure 4 shows the loops for a 230 nm spun-cast film of the 65/35 VDF/TrFE copolymer. The sample was initially cycled 9×10^4 times, then left for eight days with short-circuited electrodes, after which another 4×10^4 loops were run. The period of the loops was 0.03 s. Figure 4 shows the shape of the first and the 9×10^4th loop obtained from the initial run on this sample.

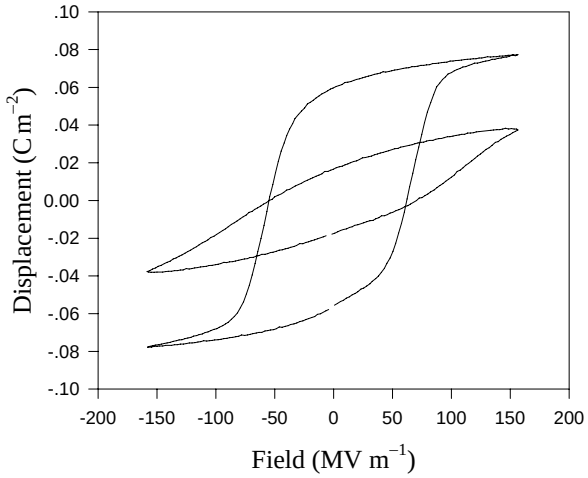

Figure 4: Hysteresis loops for a 230 nm film of 65/35 VDF/TrFE copolymer. The larger loop was the initial loop, the smaller one is the 90,000th loop. The loop period was 0.03 s.

Figure 5 shows the magnitude of the switched polarization obtained in the initial run of 9×10^4 loops and in the subsequent run of 4×10^4 loops run after eight days resting. The spun-cast films displayed a fairly constant polarization for the first thousand or so loops, then a steady decrease in the amount of reversed polarization. If a sample was rested for some time, then re-cycled, the reversed polarization continued at a value close to that of the last cycle in the previous run.

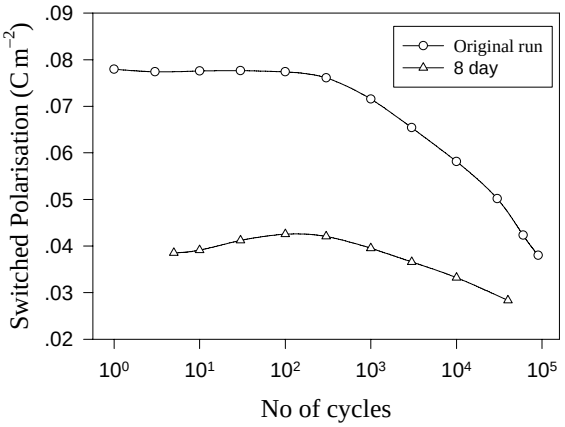

Figure 5: The switched polarization, as measured from the hysteresis loops, for the sample of figure 4. The upper plot shows the polarization observed in the initial 90,000 loops. The lower plot shows the polarization observed after eight days resting.

Because of the limitation in resolution of the LIMM measurement, it was only possible to obtain meaningful polarization profiles in the 25 μm samples. The polarization profiles in the Kureha and Solvay PVDF and both copolymer films, before any poling treatment, is shown in Figure 6.

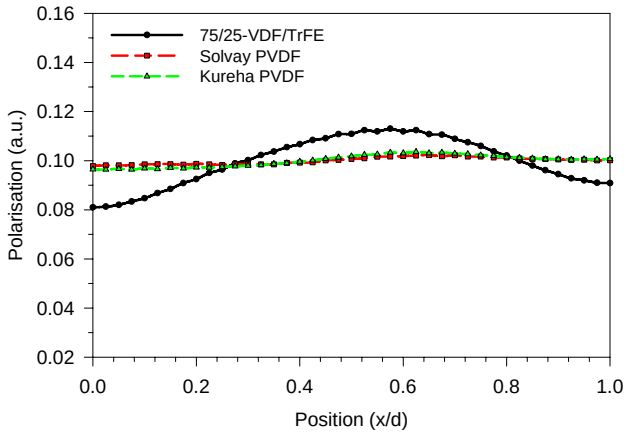

Figure 6: Polarization profiles in unpoled 25 μm films of PVDF and DVF/TrFE copolymers.

The horizontal axis in this plot represents the position through the thickness of the film as a fraction of the total thickness. The Solvay 25 μm PVDF film showed similar behaviour to the Kureha film and is not shown separately.

In the deconvolution process the mean polarization is set to 0.1 and the polarization fitted around this value by a least-squares fitting [3]. Thus the vertical scale in figures 6 and 7 has an unknown offset and only the variation of the polarization through the thickness can be inferred from these plots.

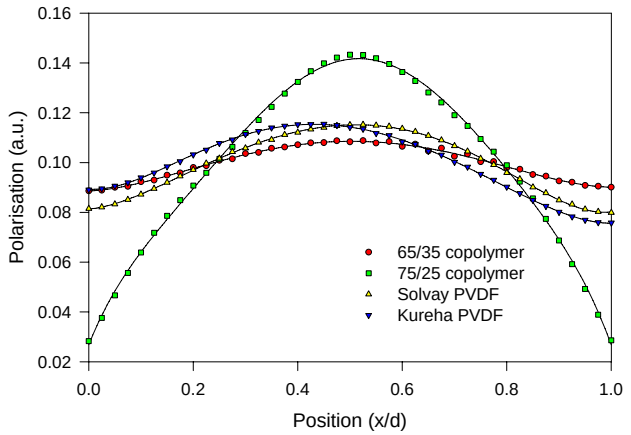

Figure 7: Polarization profiles in PVDF and copolymer films which have been exposed to several cycles of poling.

The polarization profiles obtained for samples of unpoled, half, one, ten and two hundred cycle poled Kureha PVDF films, with thickness of 25 μm, are shown in figure 8. Poled or fatigued samples were subjected to a maximum field 180 MVm^{-1}. While the polarization profiles for unpoled, poled and fatigued 65/35-P(VDF/TrFE) films are shown in figures 9. For the copolymer, the field amplitude was 140 MVm^{-1}.

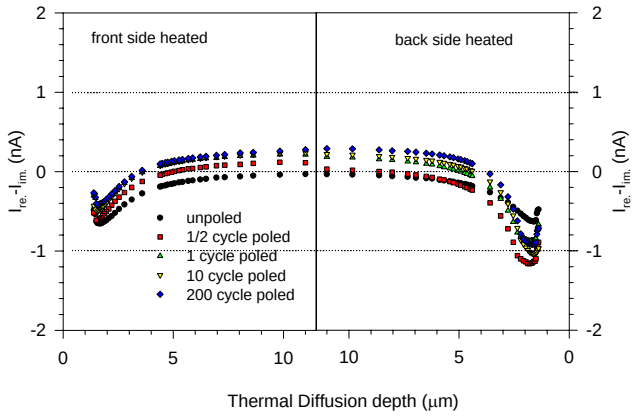

Figure 8: Polarization profiles near the heated surfaces of unpoled, poled and fatigued Kureha PVDF.

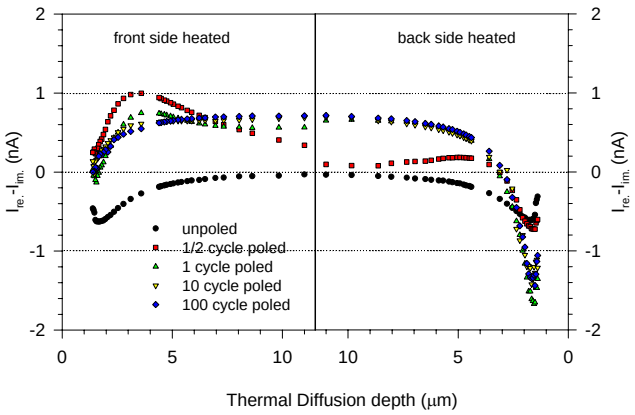

Figure 9: Polarization profiles near the heated electrodes of unpoled, poled and fatigued Solvay 65/35-P(VDF/TrFE) samples.

It is seen from figures 8 and 9 that all of the unpoled polymer films had some initial polarization. The nature of this initial polarization was similar for all films; it was symmetrical and was located near the electroded surfaces. It is assumed that this initial polarization arises from a diffusion of electrons from the metal electrodes into the surface regions of the polymers. This migration would result in regions of space charge accumulation near the electrodes and would be the same for both surfaces of the polymers. As the samples were poled, the effects of these space charge regions remain visible, however they become quite asymmetrical. The space charge region on the left in the figures, becomes much less prominent and, for the copolymer samples, virtually disappears with large numbers of field cycles. This is the surface of the film which becomes positive when the field is first applied. On the right hand side, the space charge layer becomes more prominent and also becomes much narrower, meaning that it is much more localized in the vicinity of the electrode. These effects are much more noticeable in the Solvay PVDF and the copolymers than they are in the Kureha PVDF. It can be recalled that the Kureha PVDF is the film with the highest content of the α crystal form.

The polarization in the bulk of the polymers, before the application of the field, was essentially zero. This is as expected, suggesting that there is random orientation of the dipoles in the bulk of the polymer. As the samples became poled, the net polarization in the bulk increased and was always largest and most uniform after several hundred field cycles. In the early stages of poling there was often some non-uniformity in the profiles, especially in the copolymers. The results for the 65/35 copolymer, shown in figure 9 show this effect very prominently. For most samples there were occasional discontinuities when the two halves of the plots were joined. This is a result of the poorer resolution of the approximation method for positions deep within the films.

ISSN 114-1284

5. DISCUSSION

The thin polymer films exhibit similar fatigue behaviour to that observed in ceramic ferroelectrics [11]. The polarization remains reasonably constant for about one thousand cycles, then drops with repeated cycling. In ceramics the number of cycles before the reduction is usually more than this, and indeed for memory applications efforts are directed towards reducing fatigue. The effects of fatigue appear to be reasonably permanent, in that the switched polarization did not recover after resting the sample for eight days.

In the 25 μm films the situation appears more complex. In the 25 μm PVDF films it appears at first that there is no fatigue. However these films contain significant amounts of the non-polar α crystal form. IR spectroscopy [12] indicates that continued reversal in these films leads to a steady conversion of the α form to the polar β form. It is the β form which is thought to be responsible for the reversible polarization, and an increase in β content would increase the switchable polarization. Thus in the PVDF films it may be that the increased β content masks the effects of fatigue. In copolymer films with VDF content in the range from 70% to 80%, the crystal form is almost entirely β [13]. Thus it appears that the films with significant β content and little, if any, α content are the ones which display fatigue.

The pre-existing polarization in the films, as shown in fig. 5, is similar to that observed by others [14]. In ref. [14] this initial polarization was found to be independent of electrode material and to have a magnitude in the range from 0.01 to 0.02 Cm^{-2}. In previous studies the variation in poled films, even those which have been poled in one direction, then reverse poled, show distinct asymmetries [13,14]. In the case of copolymer films studied here (figure 9), the polarization is quite symmetric after several reversals, while that in the PVDF films is not. After fatigue, we might expect that the polarity of the last half cycle would be evident, but the fatigued copolymer samples all display a final polarization which is quite symmetric.

Since fatigue appears in the first few loops if the loop period is large (figure 3), but does not appear for several hundred loops if the period is small (figures 4 and 5), it would seem that the important factor is the time of exposure to the field, rather than the actual number of reversals. This would tend to indicate a space charge migration as being the underlying cause, rather than domain wall effects. Space charge has been thought to inhibit the switching in PVDF and a model of space charge attachment to the polar crystals has been used to explain this inhibition [14]. If space charge is the cause of the fatigue, then it seems that presence of the α crystal form in a sample may inhibit the motion of space charge, hence prevent it moving to the β crystals.

To date, equipment limitations have prevented running loops of the same period on both thick and thin films, although it is hoped to be able to do this in the near future. It would also be very interesting to be able to look at the polarization profiles in the sub-micron films. Unfortunately at the moment it seems that no techniques are available to probe polarization with the precision required.

6. CONCLUSION

The polarization distributions in ferroelectric polymer films, with 25 μm thickness, have been presented in this chapter. The polarization was generated by applying a cyclic field for up to several hundred cycles. The effects of differing numbers of field cycles have been observed.

The most reliable measurements of the polarization distributions are felt to be those proposed by Ploss *et.al*. [8], obtained by the approximation method. This is in spite of the poor resolution of this method in the central regions of the films.

It is apparent that when electrodes are deposited on unpoled films, some charge diffusion occurs, leading to space charge regions in the vicinity of the electrodes. Cyclic poling of the films leads to the development of significant polarization in the bulk of the films and also has an affect on the space charge regions. While this suggests that space charge is involved in the fatigue process, the mechanism by which it operates is not obvious.

In the present context, the results of this chapter indicate that cyclic poling produce films with a uniform distribution of pyroelectric activity through their thickness, although there are significant surface charge layers at the negative electrode.

ACKNOWLEDMETS

I acknowledge support for this work from the Macquarie University Research and am thankful to Adventist University of Indonesia for the support to join this QIR seminar.

REFERENCES

[1] H. Kawai, “The Piezoelectricity of Polyvinylidene fluoride,” *Jpn. J. Appl. Phys.*, vol. 8, pp. 203-205, 1969.

[2] H. S. Nalwa, *Ferroelectric Polymers: Chemistry, Physics and Applications*, NY: Marcel Dekker, 1999, ch. 6, pp. 435-470.

[3] S. B. Lang and D. K. Das-Gupta, Laser Intensity Modulation Method (LIMM): A Technique for Determination of Spatial Distribution of Polarization and Space Charge in Polymer Electrets,” *J. Appl. Phys*,. vol. 59, pp. 2151-2160, 1986..

[4] S. B. Lang, “Laser Intensity Modulation Method (LIMM): Experimental Techniques, Theory and

Solution of the Integral Equation", *Ferroelectric*, vol. 118, pp. 343-361, 1991.

[5] S. B. Lang, "An Analytical Integral Equation of the Surface Laser Intensity Modulation Method Using the Constrained Regularization Method", *IEEE Trans. Dielec. Elec. Insul.*, vol. 5, pp. 70-76, 1998.

[6] D. K. Das-Gupta and J. S. Hornsby, "A non-destructive Technique for the Determination of Spatial Charge and Polarization Distributions in Insulating Polymers," *J. Phys. D: Appl. Phys.*, vol. 25, 1485-1490, 1992.

[7] B. Ploss, "Pyroelectric and Nonlinear Dielectric Properties of Copolymers of Vinylidene fluoride-Trifluoroethylene," in *Ferroelectric Polymers: Chemistry, Physics and Applications*, H. S. Nalwa, ed. Marcel Dekker, 1999, ch.4 pp. 182-220.

[8] B. Ploss, R. Emmerich, and S. Bauer, "Thermal Wave Probing of Pyroelectric Distributions in the Surface Region of Ferroelectric Materials: A New Method for Analysis," *J. Appl. Phys*., vol. 72, pp. 5363-5370, 1992.

[9] A. Limbong, I. L. Guy, Z. Zheng, Afifuddin, and T. Tansley, "Properties of Thin Ferroelectric Polymer Films," *Ferroelectrics*, vol. 230, pp. 61-66, 1999.

[10] A. Limbong, *An Investigation of the Pyroelectric Properties of Ferroelectric Polymer Films*, PhD Thesis, Macquarie University, Sydney-Australia, 2000, pp. 85-90.

[11] Q. Jiang, W. Cao, L. E. Cross, Electric Fatigue in Lead Zirconate Titanate Ceramics, *J. Am. Cer. Soc.*, vol. 77, pp. 211-215, 1994.

[12] I. L. Guy and J. Unsworth, "Conformational and Crystallographic Changes Occuring in Polyvinylidene Fluoride during the Production of D-E Hysteresis Loops," *J. Appl. Phys.*, vol. 61, pp. 5374-6378, 1987.

[13] K. Tashiro, "Crystal Structure and Phase Transition of PVDF and Related Copolymers", in *Ferroelectric Polymers: Chemistry, Physics and Applications*, H. S. Nalwa, Ed. NY: Marcel Deker, 1993, ch. 3, pp. 63-181.

[14] S. Ikeda, T. Fukada and Y. Wada, "Effect of Space Charge on Polarization Reversal in a Copolymer of Vinylidene Fluoride and Trifluoroethylene", *J. Appl. Phys.*, vol. 64, pp. 2026-2030, 1988.

Effect of Firing on Producing SiC/Al Ceramic Matrix Composite by Directed Melt Oxidation (DIMOX)

A.Zulfia, F. Isabela. G.N. Anastasia

Department of Metallurgy and Materials, Faculty of Engineering
University of Indonesia, Depok 16424
Tel : 021-7863520, Fax : 021-7872350
Email anne@metal.ui.ac.id

ABSTRACT

This research is to study the effect of firing and holding time on characteristic of SiC/Al Ceramic Matrix Composite produced by Directed Metal Oxidation (DIMOX). The firing temperature and holding time used were various from 900°C to 1300°C for 10 and 20 hours respectively. The characteristic of composites were examined such as density, porosity, hardness, and microstructure analysis. The results showed that SiC preform has been infiltrated by Al liquid and occurred optimally at 1100°C for 20 hours. This ceramic composites possess highest density of 3,54 gram/cm^3, while porosity tents to increase with increasing firing temperature. Porosity within the channels is associated primarily with insufficient Al flow to feed the solidification shrinkage. The highest hardness obtained at 1300°C for 10 hours i.e. 1820 VHN. The distribution of SiC particles spread over SiC/Al composites and new phases present containing of spinel ($MgAl_2O_4$), Al_2O_3 and Mg_2Si analyzed by EDS.

Key words *: CMC's, firing temperature, holding time, DIMOX*

1. INTRODUCTION

Ceramic Matrix Composite (CMC's) of SiC/Al is one of the important candidate materials for use in airplanes, automobiles and the first wall of fusion reactors[1]. Directed metal oxidation (DIMOX) is one of the methods to produce CMC's which have high toughness and good thermal shock resistance, as well as high stiffness, good wear resistance and high temperature stability. Further more, the method allows production of near net shape at a low cost. The process has been developed commercially by the Lanxide Corporation[2,3] . The process involves the oxidation of a bulk molten metal by a gas through a directed growth process to produce an interconnected ceramic reaction product that may contain several percent of residual metal. This process mostly used for some space application[4]. Solid-liquid interface energy reduces by holding time for all of ceramic particle-Al alloy system. Some of the surface energy change and occurred faster interface reaction at higher temperature. Decomposition of oxide coat in the solid ceramic phase either physically or chemically has also been considered as one of influencing factor that affect the wetting kinetics[5]. Molten metal start to infiltrate when the solid-liquid interface energy decreasing.

In many cases, the great improvement of wettability can be observed in the 900°C temperature for ceramic/Al-alloy system[6,7]. This behavior has been explained by decomposition of thin coating of Oxide on the ceramic surface[7,8] and also by the change of the Oxide coating on the liquid metal surface. Temperature will affect the viscosity, and the viscosity effect of molten Alloys Al to the infiltration is shown by intrinsic parameter (Φ) that is developed by Martins[9] and expressed as:

$$\Phi = \frac{(\gamma \cos \theta)}{2\mu} \quad \text{.....(1)}$$

For which : γ = Surface energy (mNm^{-1})
θ = Liquid-Solid contact angle
μ = molten viscosity

High intrinsic parameter value is used as the description of infiltration speed improvement for the lower viscosity of molten Alloys Al.

Although the stability of ceramic phase in the Metal-Ceramic system is usually only allowing a few solubility, but the small amounts of solution can reduce solid-liquid interface energy. Adsorption is a surface reaction that is depends on concentrate, temperature and diffusivity. The relationship between the adsorption, temperature, surface energy, and concentrate is expressed by the Gibbs equation:

$$\Gamma = -\frac{1}{RT}\frac{d\gamma}{\ln dX} \quad \text{.....(2)}$$

For which:

Γ = Adsorbs (m/^{o} mol)
R = Gas constant (8.3144 joules /^{o} mol
γ = Surface energy (mNm^{-1})
X = Solute Mole faction .

The greater the adsorption more the solute tends to lower the surface energy. The time dependence of wetting can be explained in terms of reaction kinetic in ceramic-metal system, for a system of high reactivity interfacial reaction proceed quickly after physical contact between liquid and solid phases.

Generally, wetting ability is poor and wetting process is slow for less reactive system, so that needed by the longer time to reach the wetting. Analyzing of the oxide layer on the ceramic phase considered one of the factors affecting the kinetics of wetting[7,8]. The liquid metal starts infiltration if decrease of the solid-liquid interfacial energy.

Almost linear decreasing of wetting angle with time for the SiC/Al system was observed by Halverson et al[10]. Aghajanian in its research prove that detention time influence the kinetics infiltrate, the longer holding time with the same process give the greater kinetics infiltrate[11].

2. Experimental Procedure

Materials used are Al alloy block with composition showed in **Table 2.1**, analyzed by Spectrometer, SiC powder (94,23%) and Mg powder (98,5%). All these materials then were arranged as in **Figure 2.1**. The prepared samples were heated in muffle furnace at temperature of 900, 1100 and 1300^{o}C with ramp temperature of 10^{o}C/minute. This temperature was maintained for 10 and 20 hours then furnace cooled.

Tabel 2.1. Chemical Composition of Al alloy (%wt).

Al	Si	Cu	Mg	Zn	Fe	LOI
86,3	9,91	1,56	0,23	0,405	1,01	-

The characterization of composites produced was examined such as density and porosity (ASTM C 373-88), micro hardness Vickers (ASTM E 384), and microstructural analysis by SEM link to EDS..

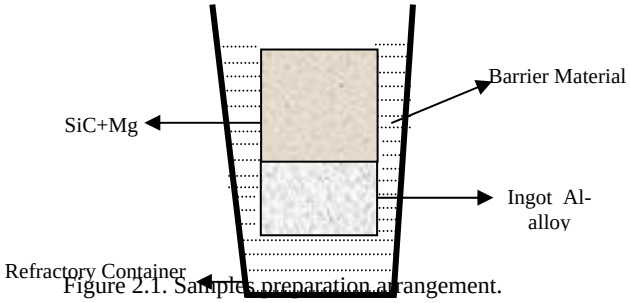

Figure 2.1. Samples preparation arrangement.

3. Result and Discussions

3.1. Effect of Firing Temperature and Holding Time on Density

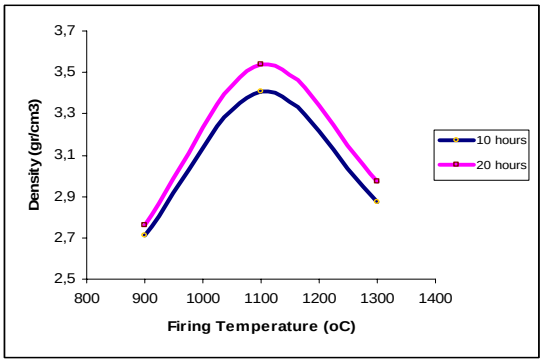

Figure 3.1 Effect firing temperature and holding time to density

The density increase significantly from temperature 900^{o}C to 1100^{o}C with value from 3,2 gr/cm^3 to 3,6 gr/cm^3, while after 1100^{o}C the density decrease for both holding time as shown in **Fig. 3.1**, but the value is still higher than 900^{o}C. This is indicated that Al alloy block mostly has been infiltrated into ceramic powder at higher temperature, as we know that the density of Al was lower than the density of SiC (2.7 kg/m^3 Vs 3.12 kg/m^3 respectively). This higher value than that of the matrix SiC might be caused by Al_2O_3 product created as the effect of Al oxidation.

At higher temperature and longer holding time create molten Al more infiltrate because Mg which is mixed with SiC has oxidized with air to form MgO. Interdiffusion MgO with alumina layer on the surface of Al changed MgO into un protective spinel ($MgAl_2O_4$) so that it can be wetted by molten Al[12-14].

3.2 Effect Firing Temperature and Holding Time on Porosity

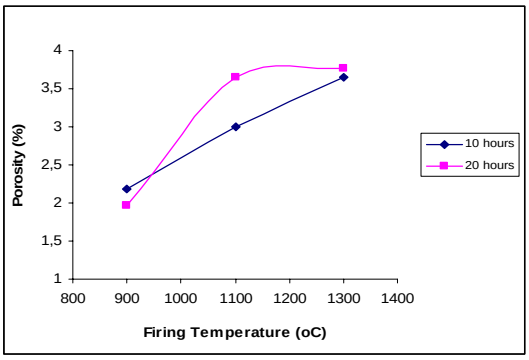

Figure. 3.2 Effect firing temperature and holding time to porosity

At higher firing temperature and longer holding time generated higher porosity, it seems that the value slightly odd. It should be the porosity content tends to decrease with higher temperature. Microstructural observation showed that porosity locate dominantly on the interface of Al block or on the base of CMC's. Area around interface is an area of pre-form which poor contain of oxygen so that according to Manor et al.[15] the growth of matrix initiated by spinel ($MgAl_2O_4$) formation. $MgAl_2O_4$ which does not occur will give the space amongst pre-form particles which then cause such a porosity formation. Three dimension interconnected ceramic structure also can cause the formation of porosity on the product caused by interconnected ceramic structure, so that Al can not fill all remain space on ceramic matrix.

3.3 Effect Firing Temperature and Holding Time on Hardness

The hardness of CMC's is shown in **Fig. 3.3.** The micro hardness of CMC's will decrease with longer holding time. The highest hardness value is obtained at firing temperature of 1300°C and holding time for 10 hours.. Increasing hardness due to less porosity and high density. At 1300°C for 10 hour, the phases present giving increasing hardness due to the formation of $MgAl_2O_4$. The spinel is form on the outer layer of SiC as the product of reaction

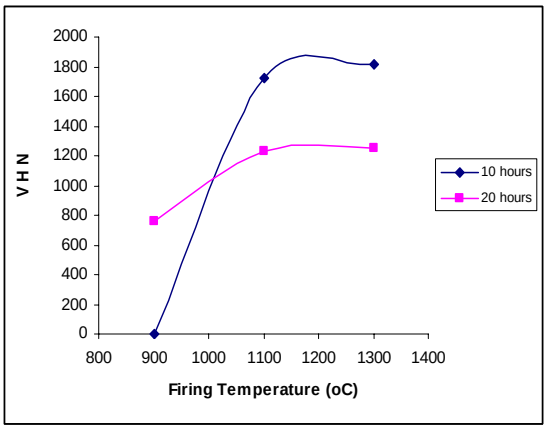

Figure. 3.3. Effect firing temperature and holding time to hardness

At firing temperature of 1100°C and 1300°C for 20 hours, the hardness were decrease due to increasing porosity and more molten Al infiltration to perform.

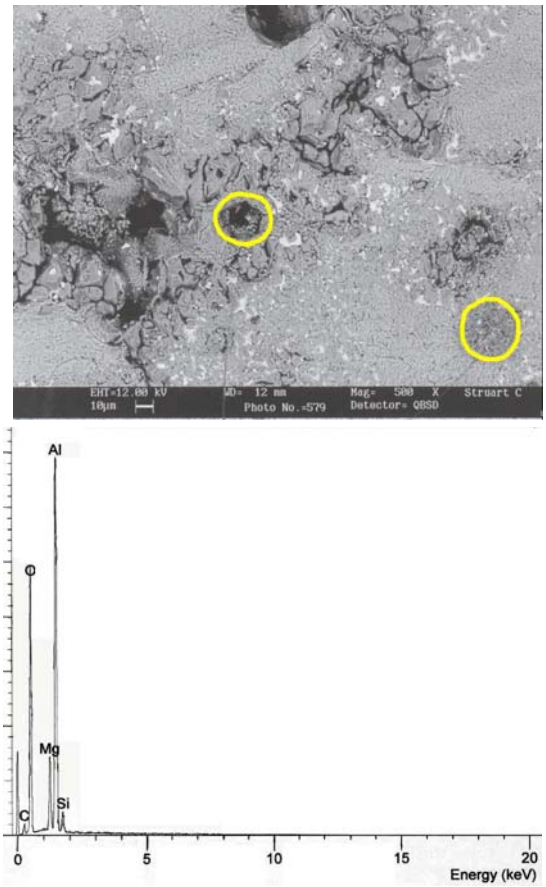

Figure 3.4. SEM link to EDS indicated the phases present on CMC's product during firing at temperature of 1300°C for 10 hours.

CMC's produced in this research has hardness in the range between 1200VHN (1100 °C for 10 hours) and 1800VHN (1300 °C for 10 hours) as

mentioned above that increasing hardness also is affected by a new phase present in CMC's such as Al_2O_3 (possess hardness between 1500 – 1650 VHN).

3.4. Microstructural Analysis

The formation of Al_2O_3 on the SiC surface due to oxidation of SiC at temperature 1100°C react with Al analysed by EDS (**Fig. 3.5**). The particles SiC seem to be uniform distribution on the microstructure (**Fig. 3.6**).

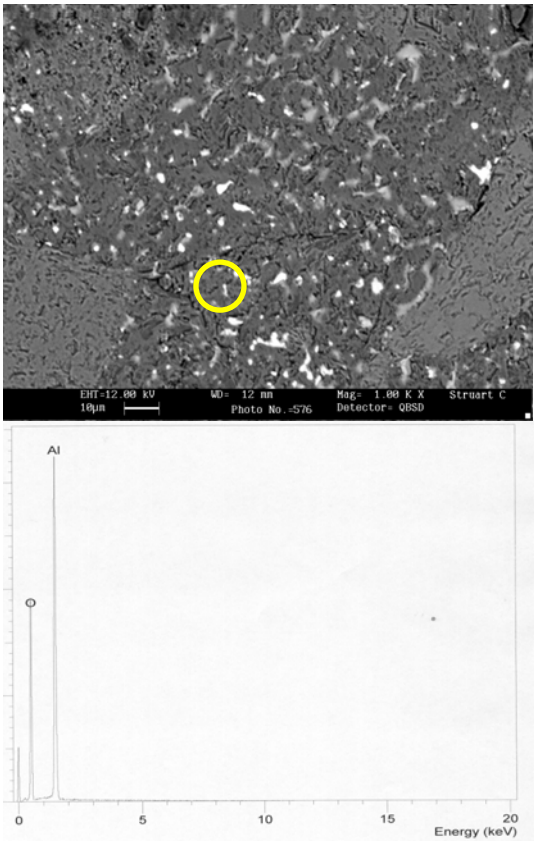

Figure 3.5. Microstructure of CMC's after firing at 1100°C for 20 hours, Al_2O_3 zone is found in the structure analyzed by EDS

The present of Cu might be originated from Al alloy block with light phase can reduce the Mg_2Si solution in SiC/Al system.[16]. Mg content in this CMC promoted the formation of spinel ($MgAl_2O_4$) and also present in the formation of Mg_2Si. These new phases occurred after firing at 1100 °C for 20 hours.

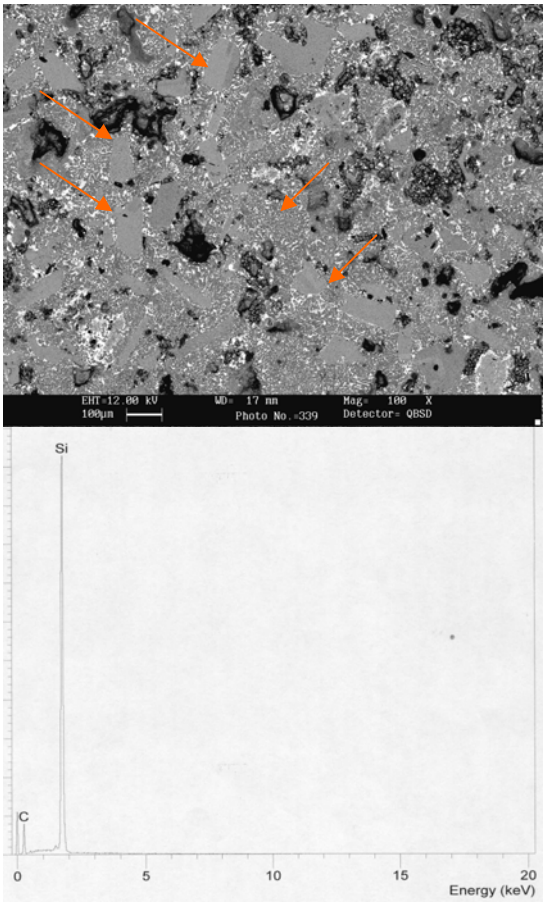

Figure 3.6. SiC distributed uniform and the light phase is channel Al. after firing at 1100°C for 20 hours**.**

4. Conclusions

- The optimum properties of CMC's found at condition of firing temperature at 1300°C for 10 hours..
- The distribution of SiC particles spread over SiC/Al composites, and microstructural analysis found new phases produced during firing containing Al_2O_3, $MgAl_2O_4$ and Mg_2Si analysed by SEM link to EDS.

References

1. T. Iseki, T. Kameda and T. Muruyama, Interfacial Reaction between SiC and Aluminium during Joining, Chapman and Hall, 1984. pp1692-1698.
2. Newkirk, M.S. Urquhart, A.W & Zwicker, H.R, Formation of Lanxide ceramic Composite materials, J. Matter Res. 1 (1986). pp.81-89.
3. Pickart, S. M., The mechanical properties of ceramic composite produced by melt oxidation. Acta. Metall. Mater, 40 (1992) pp.177-184.

4. Composite Materials Handbook Vol. 5, Ceramic Matrix Composite, USA, Department of Defense, June 2002
5. Oh. S.Y. " Wetting of Ceramic Particulates with Liquid Aluminium Alloys : Part II , Study of Wettability ". Metallurgical transaction Vol. 20A. 1989. PP. 533-541.
6. H. John H. Hausner, Influence of oxygen partial pressure on the wetting behavior in the system Al/Al_2O_3, Journal of Material Science Letters, 1986 pp 549-551.
7. B.C. Allen and W.D. Kingery;Trans AIME, 1959, Vol.215, pp 30-36
8. R. Warren and C.H. Anderson, Composites, 1984, pp 101-111
9. G.P. Martins, D.L. Olsen and G.R. Edwards" metallurgical Transactions" volume 19B,1988, P.96.
10. D.C. Halverson, A.J. Pyzik and LA. Aksay. " Ceramic Engineering and Sains Proceeding". American Ceramic Society. July-Augusts , 1985 pp. 736-744
11. Aghajanian M. K. et al., Properties and Microstructures of Lanxide Al_2O_3 – Al Ceramic Composite Material ; Journal of materials Science, USA, (1989) pp.658-670.
12. X.Gu & R.J. hand, " The Production of Reinforced Alumina/Aluminium Bidies by Directed Metal Oxidation, Journal of the European Ceramic society, (1995) pp. 823 – 831.
13. Xio, P. & Derby, P, The formation of Al_2O_3/Al composite by oxidation. Proc. Br. Ceram. Soc,.., 50 (1993) pp. 191-199.
14. Zhang P. et al., Interdifusion in the MgO-Al_2O_3 Spinel with or without some Dopant , Metallurgical & Materials Transactions, Abstracts vol. 27A, 1996.
15. Manor et al., Microstructure Evaluation of SiC/Al_2O_3/Al Alloys Composites Produced by Melt Oxidation, Journal of The American Ceramic Society, Vol. 76, 2001, pp 1777-1787.
16. Murayama, M. dkk., *The Effect of Cu Additions on the Precipitation Kinetics in an Al-Mg-Si Alloy with Excess Si*. Metallurgical and Materials Transactions A Vol. 32A, page 239, February 2001.

Morphological, Thermal, and Viscoelastic Characteristic of Polypropylene-Clay Nanocomposites

Achmad Chafidz[1], Mohammad Al-Haj Ali[1*], Saeed AlZahrani[1], Rabeh Elleithy[2]
1. Chemical Engineering Department – King Saud University – Riyadh – Saudi Arabia
2. SABIC Polymer Research Chair – King Saud University – Riyadh – Saudi Arabia

ABSTRACT

Polypropylene-clay nanocomposites were prepared. A commercial homopolymer polypropylene was melt blended with commercial nano-clay masterbatch at different concentration using Laboratory Mixing Extruder (LME). The influence of three different concentrations of nano-clay on the morpholofy structure, the non-isothermal crystallization, and the viscoelastic properties were investigated. These properties were characterized using Scanning Electron Microscope (SEM), Differential Scanning Calorimetry (DSC), and Dynamic Mechanical Analysis (DMA). The results show that the melting temperature of the PP-clay nanocomposites were not significantly affected by the presence of nano-clay material. However, the dispersion of nano-clay in the PP matrix increases the crystallinity of PP- clay nanocomposites, which reached maximum crystallinity at 5 wt% nano-clay loading. DMA curves show an increase in storage modulus of nanocomposite material, which indicate that the incorporation of nano-clay into PP matrix remarkably enhances its stiffness and thermal stability.

Keywords
Nanocomposites, polypropylene, nano-clay, masterbatch, melt blend

1. INTRODUCTION

Polypropylene (PP) is one of the most widely used polyolefin polymers. It is used in different applications as automotive parts, and cable insulation. The properties of polypropylene are significantly enhanced using different fillers. Although, traditional fillers such as $CaCO_3$ and talc improve PP properties, there are many limitations as poor fillers dispersion. The use of fillers in nano-scale is believed to overcome such limits.

Polymer nanocomposites consist of a polymeric and a reinforcing nanoscale material. Because the nano-materials are so small, limited amounts are sufficient to enhance the polymer properties. Thus, the use of such materials has no effect on polymer density, transparency and processability compared to the traditional composites. This feature counterbalanced the negative effect of high cost of nanofillers [1,2,3].

Recently, commercial nanocomposite masterbatches have been already manufactured. Using commercial masterbatch becomes a promising alternative in the production of polymer-nanocomposites compared with using bulk nano-materials. Besides dust free, masterbatch also has a less healthy and safety risks. Another advantage of masterbatch is the elimination of difficulty in dispersion process and also easy handling because the nano-materials are bounded inside the polymer matrix. Therefore, masterbatch process is considered to be one of the simplest and most economical methods in processing of polymer-nanocomposites. However, literature survey revealed that the investigation reports which studied polypropylene-nanocomposites using masterbatch are limited compared to direct incorporation of nano-material into polyolefin that makes it an attractive area for research [4,5].

Among the entire potential nanomaterials, nano-clay (layered silicate) has attracted great interest among researchers, because clay materials are easily available, environmentally friendly, and their intercalation chemistry has been investigated for a long time. This make nano-clay one of the most widely accepted and effective nano-reinforcements [1,3]. One of the most widely used methods to prepare PNs is melt intercalation method. This method is compatible with current industrial processes as extrusion and injection molding. Besides, it is environmental friendly because no solvent is used [1,6,7].

In the present work, two series of PP-clay nanocomposites were prepared. The aim of this work will be studying the influence of composition (nano-clay content) on the properties of PP-clay nanocomposites. We will investigate the morphology by SEM , the crystallinity with DSC analysis, and viscoelastic behavior in a wide range of temperature using DMA tests.

2. MATERIALS AND METHODS

2.1. Materials

A commercial homopolymer polypropylene (PP) were used as matrix materials for the polyolefins nanocomposites which were investigated in this work. The polypropylene was acquired from the local market (product name : PP70) which has MFI 8 g/10 min. The melt flow index (MFI) was measured at 230 ^oC at a load of 2.16 kg, according to ASTM-D1238. Commercial PP nano-clay masterbatch with 50 wt% concentration of nano-clay (product name : NanoMax, from Nanocor) was used for the preparation of the nanocomposites. The nano-clay is organophillic montmorillonite (MMT)

which has been modified with dimethyl-dihydrogenated tallow ammonium.

2.2. Preparation of polypropylene-organoclay composites

In this work, polypropylene/nano-material composites were prepared by diluting highly concentrated nano-material masterbatch pellets in polypropylene matrix using melt blend technique. Laboratory Mixing Extruder (LME), made by Dynisco, was used at constant chamber temperature of 260 ^{o}C, die temperature of 265 ^{o}C, and rotor speed of 250 rpm. The melt blend process was done in two steps. The first step was the pelletization step where the nano-material masterbatch was blended with polypropylene matrix then pelletized. The next step was to use these pellets to extrude ribbons. These two steps were necessary to avoid the lack of mixing that was observed on the ribbon surface when the masterbatch was used directly to produce ribbons without the pelletization step. Prepared polypropylene nanocompostie materials (both pellets and ribbons) were characterized. The specimen will be called PP70-5 for the sample obtained using PP70 and nano-clay 5 wt%, etc.

For the morphology of the nanocomposties, scanning electron microscopy (SEM) images were obtained using a JEOL JSM-6360A scanning electron microscope operated at an acceleration voltage of 15 kV. Calorimetric measurements were carried out using a differential scanning calorimetry DSC-60 from Shimadzu. The samples used here were the pellet extrudates from LME. They were cut into small pieces and maintained at the weight of about 5-10 mg. All materials were treated in the same way : For 1st heating scan, they were heated with a constant heating rate of 10 ^{o}C/min from ambient temperature up to 200 ^{o}C, to erase their previous history, they were held for 10 min at 200 ^{o}C, subsequently cooled down to 30 ^{o}C with the cooling rate 10 ^{o}C/min. Then for the 2nd heating scan, the samples were heated again at rate of 10 ^{o}C/min up to 350 ^{o}C, and the corresponding thermogram was recorded. The melting temperature, T_m was taken as the maximum in the transition endotherm. The non-isothermal crystallization analyses were carried out from the melt at 150 ^{o}C with a cooling rate of 10 ^{o}C/min down to 50 ^{o}C. The crystallinity of the specimen may be calculated from the experimental heat of fusion ΔH_m and the literature value of 100% crystalline polymer material, ΔH_m^o and for PP, ΔH_m^o is 207 J/g [17]. In order to estimate the percentage of crystallinity (Xc), the following equation was used :

$$X_c = \frac{\Delta H_m}{\Delta H_m^o} . 100\ [\%] \qquad (1)$$

Dynamic Mechanical Analysis (DMA) was performed using AR-G2 instrument made by TA Instruments. The analysis was carried under torsion mode at a controlled angular frequency of 1 rad/s and 1% strain. The samples were heated with intervals of 3 ^{o}C from 30 ^{o}C up to 140 ^{o}C. The specimens used here were the ribbon extrudates from LME machine which has a thickness about 0.3 mm.

3. RESULTS AND DISCUSSIONS

3.1. Dispersion of the organoclay in polypropylene

Figure 1(a),(b) and Figure 2(a),(b) shows the SEM micrographs of PP70-clay nanocomposites respectively with nano-clay content 5% and 15% with different magnification. The study of the SEM images revealed that all the samples showing a good dispersion of both nano-clay loading in polypropylene matrix. It is because the processing conditions like high screw speed rotation which generated high shear forces. Additionally double cycle processing were used at sample preparation which generated more shear forces. As for the extent of intercalation or exfoliation of the nanocomposites still need further investigation.

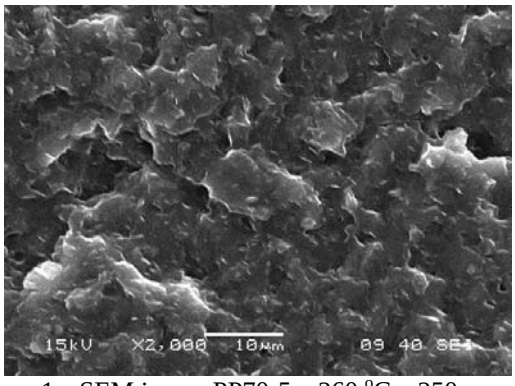

Figure 1a. SEM image PP70-5 – 260 ^{o}C – 250 rpm

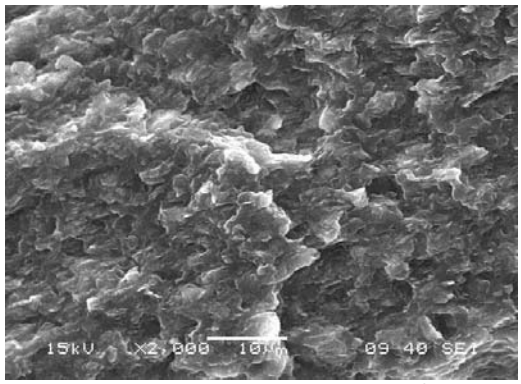

Figure 1b. SEM image PP70-15 – 260 ^{o}C – 250 rpm

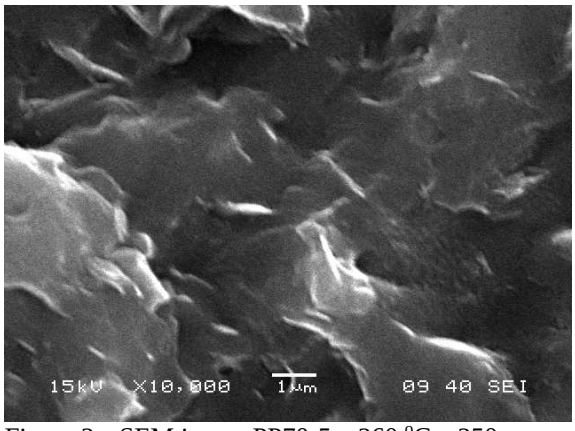

Figure 2a. SEM image PP70-5 – 260 °C – 250 rpm

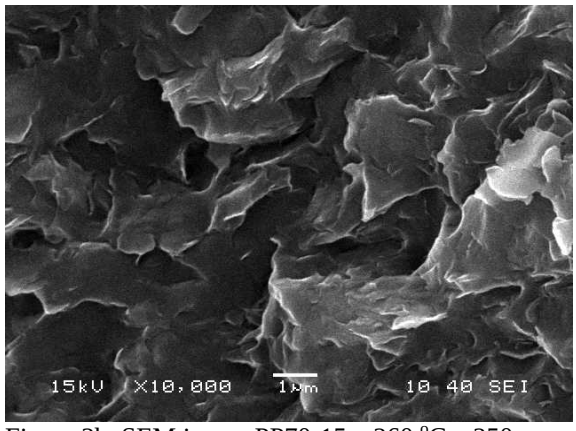

Figure 2b. SEM image PP70-15 – 260 °C – 250 rpm

4.2. Thermal properties

The heating thermograms of the PP-clay nanocomposites are presented in Figure 3. The DSC results in terms of melting temperature (T_m), heat of fusion (ΔH), and the percentage of crystallinity (X_c) are summarized in Table 1. The corresponding cooling thermograms of the non-isothermal crystallization are presented in Figure 4. The DSC measurements show that the melting peak of PP-clay nanocomposites is not significantly affected by the changes in the nano-clay content in PP matrix. While, the heat of fusion (attributed to crystallinity content) of PP70-clay nanocomposites increased up at 5% wt nano-clay loading but then decreased at higher loading (see Figure 3 – see also Table 1), but still most of them higher than the pure PP. There were also the shifting of the crystallization temperature to higher temperatures (from 11 up to 13 °C) of the corresponding exotherm of Figure 4.

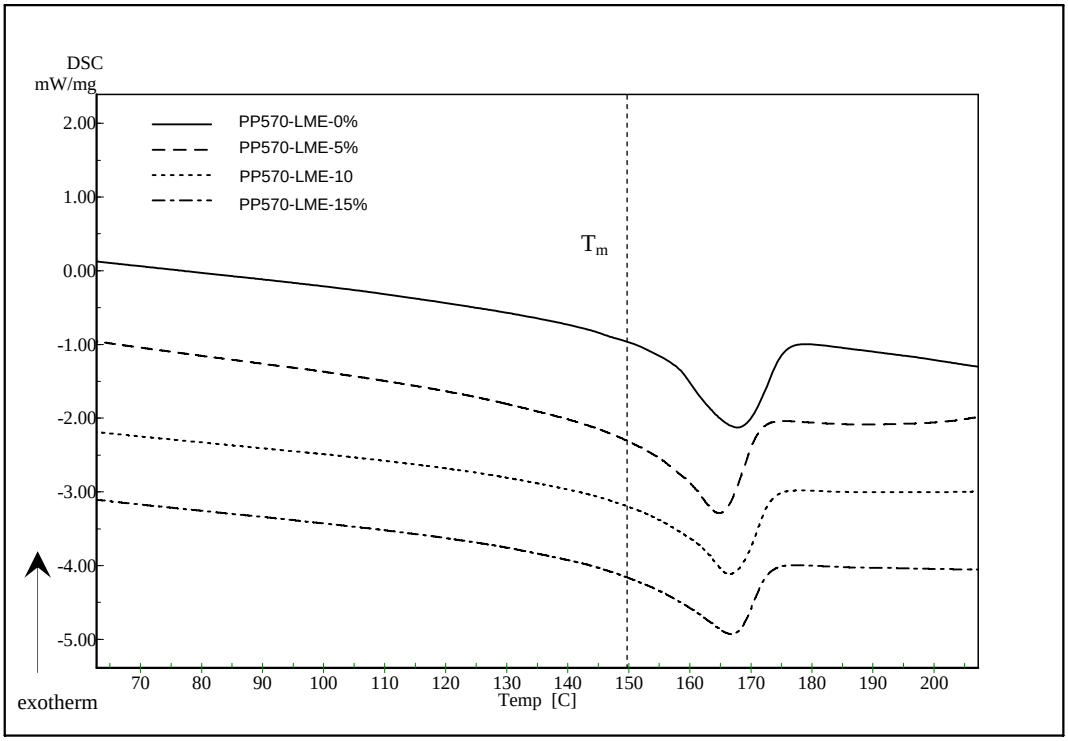

Figure 3. DSC thermograms of PP70-clay nanocomposites at a heating rate of 10 °C/min. The curves have been shifted in the *y*-direction to make them distinguishable

The explanation of this phenomena is that the presence of nano-clay platelets dispersed in the PP matrix significantly reduce the crystallization time of PP. It was proposed that clays enchance the nucleation process of the matrix by acting as heterogenous nuclei during the crsytallization of PP [8]. Thus making the crystallinity to increase and crystallization temperature shifting to higher temperature (see Table 1). But, there is no further increasing of crystallinity in PP-clay nanocomposites at nano-clay loading higher than 5 wt% (it reached maximum of 72.96 %). The decreasing of the crystallinity degree can be explained by the presence of an excessive number of nano-clay platelets which can hinder the motion of the polymer chain segments and thus, retard crystal growth [9].

It was proposed that the explanation above also describe another peak (beside Tc_1) which appear on the crystallization diagram of both PP-clay composite materials (see Figure 4 - Tc_2). If we observe carefully, most of Tc_1 for all the samples (pure and the nanocomposites – both of PP) are almost same (110 – 113 ^oC). But, in nanocomposite samples there is Tc_2 with higher temperature of Tc_1. It is proposed that Tc_2 could be attributed to heterogenous crystallization caused by the presence of nano-clay, while Tc_1 could be attributed to homogeneous crystallization by PP itself. So, in the crystallization diagram of nanocomposite samples we found two populations of crystallites. This postulation needs further investigation.

Table 1. DSC results for PP70-clay nanocomposites

Sample (nano-clay)(wt%)	T_m (°C)	Heat of Fusion (J/g)	X_c (%)	Tc_1 (°C)	Tc_2 (°C)	T onset (°C)
0	167.62	130.33	62.96	111.06	-	115.16
5	164.74	151.03	72.96	113.24	123.14	127.11
10	166.31	138.96	64.23	113.24	124.63	128.31
15	166.67	126.41	61.07	113.24	122.2	126.75

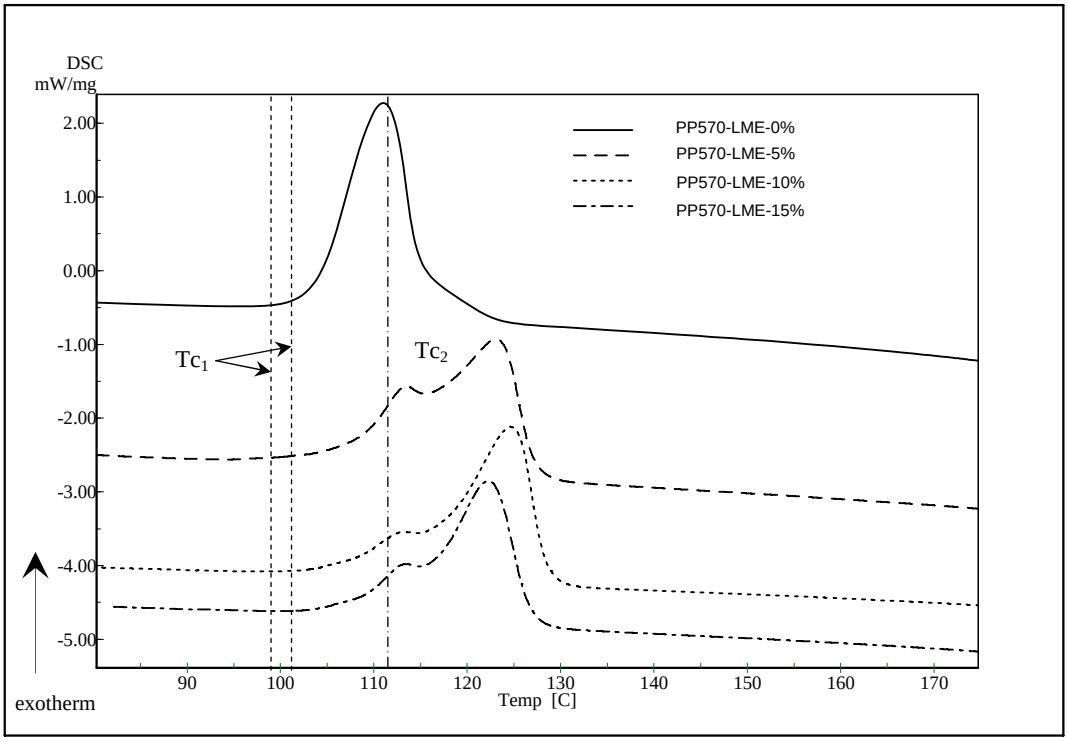

Figure 4. DSC thermograms of non-isothermal crystallization for the PP570-clay nanocomposites at a cooling rate of 10 ^oC/min.

4.3. Viscoelastic properties

To study the reinforcing effect of nano-clay material in a wide temperature range, dynamic mechanical analysis (DMA) of nanocomposites has been carried out at a fixed frequency 1 Hz, 1 % strain in the temperature range 30 – 140 ^oC. The dynamic mechanical results were obtained in terms of storage modulus (G') and plot of storage modulus (G') versus loss modulus (G''). In Figure 5, the temperature dependencies of the dynamic storage modulus G' are shown for the neat PP and PP-clay nanocomposites containing 5%,10% and 15% wt of nano-clay. It can be observed that the storage modulus G' of the nanocomposites were higher that those of the corresponding neat PP. This behavior can be explained as follows :

The matrix of the composites can be assumed that consists of two parts. One of them is the free part, where the state of the macromolecular chains is the same as that in the pure PP matrix. The other is the interphase. The larger the interfacial area and the stronger the interaction between the matrix and the fillers, the greater the volume of the interphase. Because the macromolecular chains of the interphase are restricted to the surface of the fillers, the molecular motion is greatly limited. As a result, the storage modulus of the interphase is higher that of the free part. It was proposed that increasing of nano-clay material enlarges the interfacial area and results in an increasing volume of interphase which improves the storage modulus of the materials [9].

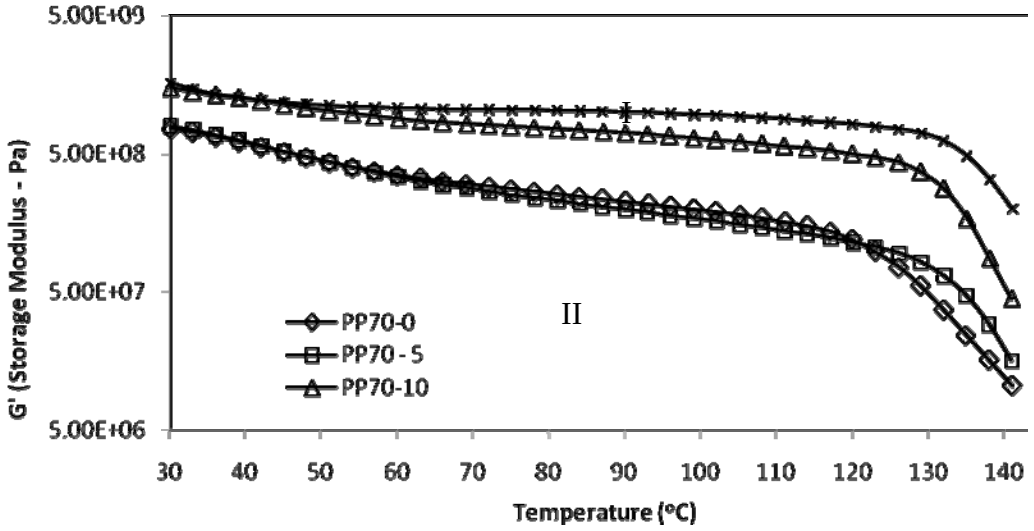

Figure 5. Storage modulus (G') versus temperature of PP70-clay nanocomposites at frequency 1 Hz.

If we observe again in Figure 5, there are two different types of curve, curves I (PP70-10 and PP70-15) and curves II (PP70-0 and PP70-5). In each of the curves we divided into two region, flat region and steep region. From the flat region we calculate the slope of the curves. And in the steep region we calculate the "softening temperature", the temperature where the storage modulus start to fall, by using tangent. If we observe carefully the curve of neat PP falling steeply than the nanocomposites. The curve of nanocomposite materials looks like more flat. It shows us that the presence of nano-clay gives a good thermal stability on the resulting nanocomposite materials. And also the "softening temperature" of the nanocomposites material are higher than the neat PP. It shows us that the addition of nano-clay material made the resulting nanocomposite material has a wider range temperature of usage than neat PP.

From the Figure 6. (G' versus G" curve), it can be observed that there are two different types of curve. The neat PP and PP70-5 curves are similar. However, in the higher loading of nano-clay (PP70-10 and PP70-15) the curves look different and have greater value than before. It shows that the presence of nano-clay material in higher loading made the resulting nanocomposite materials have different molecular structure that the neat PP, as results of interaction between nano-clay and PP matrix [10].

Table 2. DMA results of PP70-clay nanocomposites at different loading of nano-clay

Sample	G' (@51 °C), Pa	G' (@75 °C), Pa	G' (@102 °C), Pa	Slope of the flat region x E-2	Softening Temp, °C
PP70-0	4.31E+08	2.75E+08	1.89E+08	-1.84	123
PP-70-5	4.30E+08	2.52E+08	1.62E+08	-2.06	130
PP-70-10	1.02E+09	7.82E+08	6.30E+08	-1.09	131
PP70-15	1.11E+09	1.04E+09	9.47E+08	-0.513	133

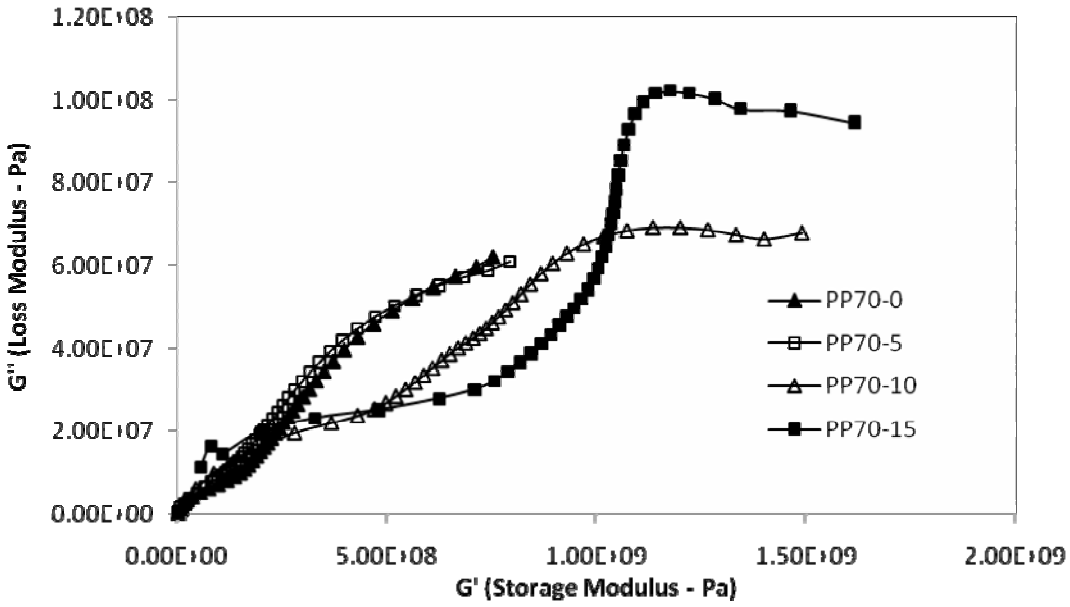

Figure 6. G' (Storage Modulus) vs G" (Loss Modulus) of PP-clay nanocomposites at different nano-clay loading

5. CONCLUSIONS

Melt blended PP-clay nanocomposites were obtained using different compositions, in order to study the effect of nano-clay loading on the thermal behavior, viscoelastic properties and morphology of the nanocomposites prepared. The presence of organo-clay nano-material cause a great enhancement of the crystallinity because the nano-clay act as nucleating agents, thus promoting heterogeneous crystallization. Furthermore, there was also shifting of crystallization temperature to a higher temperatures. While, any significant effect of the clay loading on the dispersion of the clay in the composites properties was not revealed. DMA curves show marked improvement of storage modulus of the nanocomposites; the increase is affected by the presence of nano-clay, especially at higher loading. It is also found that the addition of nano-clay material gives a good thermal stability and wider temperature range of usage on the resulting nanocomposite materials.

6. ACKNOWLEDGEMENT

The authors are grateful to the SABIC Polymer Research Chair, King Saud University for their financial support and laboratory facilities.

REFERENCES

1. ALexandre, M., Dubois, P., Polymer – layered silicate nanocomposites : preparation, properties and uses of a new class of materials, Journal Materials Science & Engineering, 28(2000)1-63
2. Giannelis, EP., Polymer Layered Silicate Nanocomposites, Journal Advance Materials, 1996, 8, No.1
3. Lei, S.G., Hoa, S.V., Ton-That M-T., Effect of clay types on the processing and properties of polypropylene nanocomposites, Journal Composites Science and Technology 66(2006)1274-1279
4. Prasantha, K., et al., Masterbatch-based multi-walled carbon nanotube filled polypropylene nanocomposites : Assessment of rheological and mechanical properties, Journal Composites Science and Technology 2008
5. Lee, S.H., Kim, M.W., Kim, S.H., Youn, J.R., Rheological and electrical properties of polypropylene /MWCNT composites prepared with MWCNT masterbatch chips, European Polymer Journal 44(2008)1620-1630
6. Modesti, M., Lorenzetti, A., Bon, D., Besco, S., Effect of processing conditions on morphology and mechanical properties of compatibilized polypropylene nanocomposites, 46(2005)10237-10245
7. Pavlidou S., Papaspyrides, C.D., A review on polymer – layered silicate nanocomposites, Journal Progress in Polymer Science 33(2008)1119-1198
8. Nwabunma, D., Kyu, T., Polyolefin composites, New Jersey : John Wiley & Sons, Inc, 2008 – 18
9. Kontou, E.,Niaounakis, M. Thermo – mechanical properties of LLDPE/SiO2 nanocomposites, Journal Polymer 47(2006)1267-1280
10. Azizi, H., Ghasemi, I., Karabbi, M., Controlled-peroxide degradation of polypropylene : Rheological properties and prediction of MWD from rheological data, Journal of Polymer Testing 27(2008)548-554.

Continuous Transesterification by Biocatalytic Membrane Microreactor for Synthesis of Methyl Ester

Achmadin Luthfi [1], Siswa Setyahadi [1], Misri Gozan [2], and Mohammad Nasikin [2]

[1] *Center for Bioindustrial Technology, BPP Technology, MH Thamrin 8, Jakarta 10340*
Phone (021) 3169513, Fax (021) 3169510
Email: achmadin.luthfi@ui.ac.id

[2] *Department of Chemical Engineering, Faculty of Engineering, University of Indonesia, Depok 16424*
Phone: (021) 3863516, Fax: (021) 3863515

ABSTRACT

We developed a new concept of biocatalytic microreactor for continuous transesterification by utilizing the pores of membrane as a matrix for enzyme immobilization. Microreactors have become a promising technology in biotechnology and chemical engineering field. The membrane pores as a kind of microreactor was modified by simple adsorption with lipase from **Pseudomonas sp** *which is suitable for a highly efficient biocatalytic transesterification. A lipase solution was allowed to permeate through the Biomax™ membrane with NMWL 300,000 made of polyethersulfone (Millipore). The performances of biocatalytic membrane microreactor (BMM) have been studied in biodiesel synthesis through transesterification of triolein with methanol. Transesterification was carried out by passing solution triolein and methanol through porous of the membrane. The degree of triolein conversion using these microreactors was about 80% with a reaction time 19 minute. The stability of BMM system showed very good results, with no activity decay during 3-days period of continuous operation. This BMM system might be suitable for triglycerides transesterification (commercial production of biodiesel), which produce no waste stream.*

Keywords:
Microreactor, Immobilization, Biodiesel, Biocatalytic, Membrane

1. INTRODUCTION

Development in biocatalyst application (enzymes, whole cells, antigens or antibodies) requires continuous reactor to be used. In such operations immobilization is necessary. Common immobilization techniques include physical adsorption onto a solid support [1], covalent bonding to a solid support [2] and physical entrapment within a polymer matrix support [3]. The synthetic utility of lipases can be greatly improved when lipase are adsorbed onto micropores membrane due to the special characteristics of a membrane which separates the two phases thus avoiding emulsion formation; it also provides a means for immobilizing the lipase thus enhancing enzyme activity, stability and recyclability of lipase [4].

A simple method of immobilizing enzymes onto porous membranes modified using long time adsorption has been suggested. Support for the enzyme is achieved by using a sponge layer and porous asymmetric membrane made of polyethersulphone. Permeation of the substrate solution through the membrane minimizes diffusional mass-transfer resistance of the substrate to the immobilized enzyme, and hence enhances the overall biocatalytic reaction. To our knowledge, biocatalytic membrane reactor for applications in synthesis of methyl ester (biodiesel) has not been reported.

Among various studies on lipase catalyzed for biodiesel production, two main problems have been reported. First, inactivation of the enzyme due to methanol excess during reaction [5] and adsorption of glycerol on the enzyme surface[6]. A second problem is correspond to the reaction time is still unfavourable if compared to the alkali catalyzed homogeneous processes, in order to achieve product yield of ≥ 90% it was necessary to utilize reaction time greater than 40 hours [7]. Therefore several attempts have been made to develop an effective system to commercialize the lipase-catalyst process in biodiesel industrial application.

In this study, a new concept of biocatalytic membrane microreactor is developed for synthesis of methyl ester. By utilizing the pores of membrane as a kind of microreactors was prepared by a simple surface modification. The nanostructure formed by simple adsorption of membrane porous with lipase. When an immobilized enzyme adsorbed on the inner wall of the membrane pores is used for transesterification reaction, the activity of immobilized enzyme is predicted to increase because the pores act as microreactor.

The objective of this study were twofold: (i) to immobilize lipase originating from a *Pseudomonas sp* onto porous membrane using long time adsorption; and (ii) to evaluate of conversion degree of substrate during permeation of triolein solution dissolved in methanol. The membrane pores could function as microreactors and as nanocatalist system to produce a high rate of transesterification reaction.

2. MATERIAL AND METHODS

2.1. Materials

Commercially available disk membranes made of polyethersulphone (PES) with NMWL 300 kDa were used as matrix for enzyme immobilization and then act as a kind of microreactors. The membranes were supplied by Millipore Inc. (USA). Lipase D from *Rhizopus oryzae* was purchased from Valley Research (South Bend, India), Lipase Y from *Candida rugosa* were purchased from Sigma-Aldrich (Japan). Lipase PS and Lipase AK from *Pseudomonas sp* were purchased from Amano Enzyme (Nagoya, Japan). Triolein from Sigma-Aldrich (Belgium) were used as substrate triglyceride. All the chemicals were analytical grade and used without further purification.

2.2. Immobilization

0.5–0.75 g of crude lipase were dissolved in 50 ml of 50mM phosphate buffer (pH 7.0) and the solution was gently stirred using a magnetic stirrer for 2 h. Afterwards the solution was centrifuged at 3000 rpm for 10 min to remove the insoluble substances. Enzyme immobilization onto membranes was carried out following the two main steps: (i) simple adsorption on the support layer and (ii) permeation through the membrane. Firstly, a membrane sample 63.5 mm diameter was fixed in filtration cell (Amicon, model 8200, Fisher Scientific, Loughborough, UK) so that only sponge layer was in contact with the lipase solution while the membrane layer was placed upside down prevented from contact by the enzyme solution.

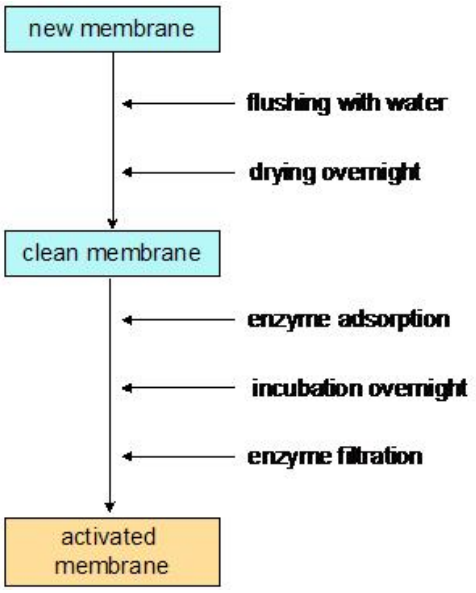

Fig 1. General procedure for the preparation of active membranes with immobilized enzymes

20 ml of lipase solution in phosphate buffer (pH 7.0) was poured in to filtration cell. Membrane samples were incubated with lipase solution for 18 h at 20°C. After incubation overnight the lipase solution was permeated through the sponge layers of the membranes in dead-end filtration cell under a pressure of 2 kPa without stirring. A lipase solution was allowed to permeate through the membrane, and lipase molecule adsorbed on the inner wall of the membrane pores. After immobilization, membranes were rinsed with 50mM phosphate buffer (pH 7). The amount of lipase adsorbed onto the sponge layer and retained in the membrane pores was determined as the amount of protein in solution before and after permeation and in washing using Lowry method. The amount of lipase adsorbed in the membrane was calculated as follows:

$$E = (C_0 - C)v \qquad (1)$$

where C_0 and C are the concentrations of lipase solution before and after filtration (mg/L), respectively. ν is the volume of lipase solution.

2.3. Transesterification reaction

Figure 2 is a diagram of experimental setup, which consisted of a stirred cell, a hot plate magnetic stirrer and peristaltic pump to provide driving force (vacuum) for permeation.

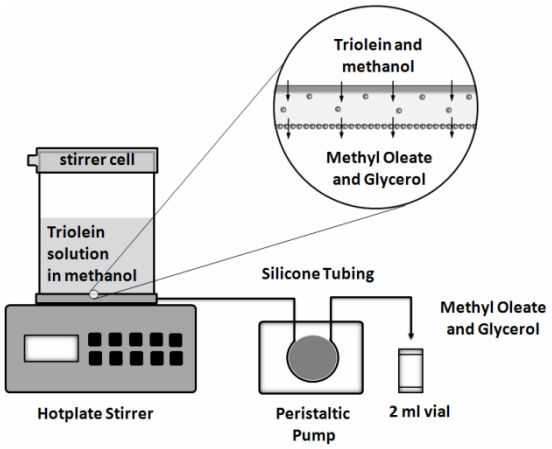

Fig 2. Experimental setup of microreactor for transesterification reactor

Continuous agitation was provided just above the membrane surface by a magnetic spin bar suspended from the cell top and driven by an external magnetic stirrer. The membrane microreactor was designed on a base of utilize a membrane pores as microreactor. The 300 kDa membrane consists of immobilized lipase in the pores (40 nm) with an effective area of 28.7 cm2. The disk membranes were placed in Amicon filtration cell. Enzyme-loaded side of membrane sponge was placed at the bottom side therefore no direct contact with feed solution. The peristaltic pump was used for driving forces (vacuum) of permeate streams at a flow rate of 5 ml/min. Fifty millilitres of solution containing of triolein in methanol used as a feed stream.

The feed and receiving reservoirs were kept at a constant temperature of 35±1 °C.

Transesterification started by forcing the solution phases through the membrane microreactor. Triolein solution in methanol was diffuse through the biocatalytic membrane microreactor then converted to methyl oleate and glycerol. Trans-esterification reactions occurred as a result of catalytic action of immobilized lipase in the membrane pores.

2.4. Analysis

The concentrations of FAMEs in the reaction mixture were determined using HPLC with a UV detector at 205 nm. The analytical HPLC system consisted of two Shimadzu LC-9A pumps and a SPD - 10A variable - wavelength UV detector (Shimadzu, Kyoto). For this analysis, a LiChroCART RP-C18 analytical column of 2504 mm (Merck, Darmstadt, Germany) was employed. The mobile phase consisted of three different components: hexane, isopropanol and methanol. Reservoir A contained methanol and reservoir B contained a mixture of isopropanol and hexane (5:4, v/v). The gradient went from 100% A to 50% A 50% B linearly over 30 min. The flow rate of the mobile phase was 1 ml/min and the sample injection volume was 10. This nonaqueous RP-HPLC method was modified from the method reported by Holcapek et al. [8].

3. RESULTS AND DISCUSSION

3.1. Types of Lipase

Lipases were screened for their ability to transesterification triolein with short-chain alcohols to alkyl esters. The lipase from *Pseudomonas cepacia* (PS) was most efficient for converting triolein to methyl oleate with primary alcohols, whereas the lipase from *Candida rugosa* (AY) was not efficient for transesterification triolein with primary alcohols to give methyl oleate.

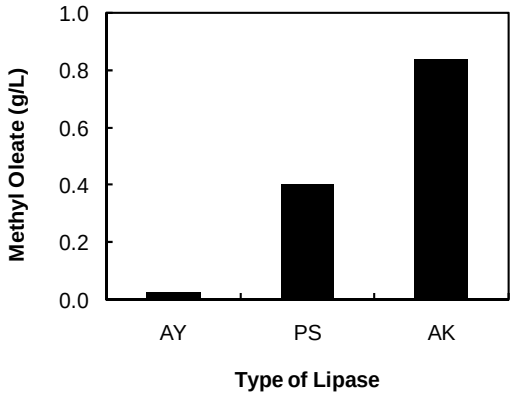

Fig 3. Lipase screening on transesterification

Reactions were carried out in erlenmeyer glass (100 ml) containing mixture of 10 g triolein, 3 x 0.37 g methanol (methanol to oil molar ratio of 3), and 0.25g dried lipase. The reaction mixture was incubated at 40°C, 220rpm, and 24h reaction time in a shaker incubator. The screening results for the tested lipase are presented in Fig. 3. Reaction products are presented as g/L of methyl oleate in the reaction mixture.

3.2. Lipase Immobilization

Physical adsorption of lipase for immobilization is one the most widely used methods [Balcao 1996]. The lipase was immobilized into the sponge layer of PES 300 kDa membrane by long time adsorption and filtration of 50 g/l of lipase in buffer solution (pH 7.00) at room temperature. In this way, lipase becomes adsorbed on the sponge layer and in the membrane pores. Consider a protein (lipase) with diameter d and a pore of diameter d_p. When $d << d_p$ the protein can enter most pores, deposit on the pore walls, and thus increase enzyme loading [9]. Scanning Electron Microscopy (SEM) was used to produces images of cross section of both new membrane and lipase immobilized membrane (Fig 4).

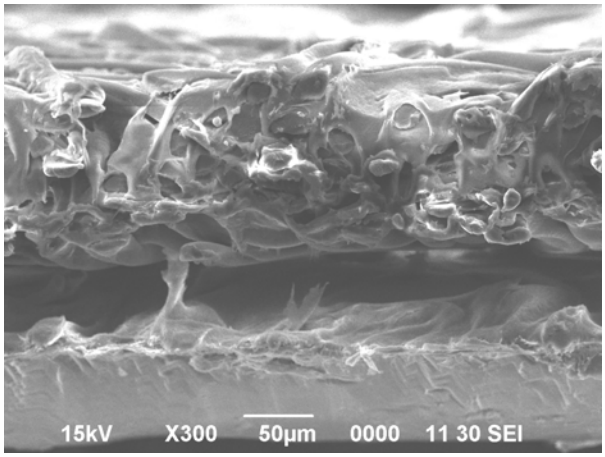

(a)

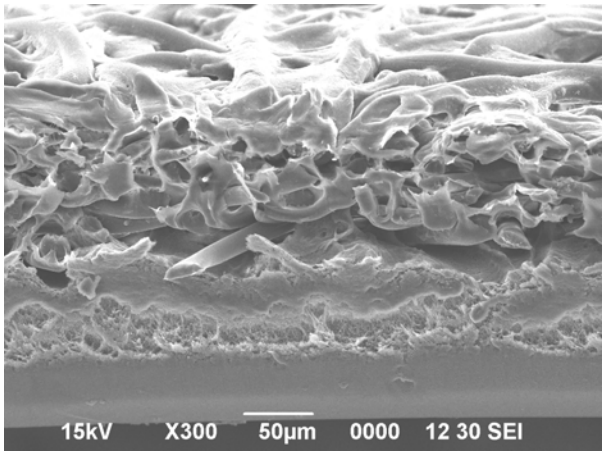

(b)

Fig 4. SEM micrograph of new mwmbrane (a) and lipase immobilized membrane (b)

3.3. Influence of permeate flux

The conversion of triolein to methyl oleate occurs within membrane pores, where act as microreactors, during the

permeation of the substrate solution through the membrane. In this type of operation mode, the permeate flux is an important parameter. In fact, high flux means low residence time of substrate solution within the microreactor. The reaction were carried out using triolein 10 gram in 3 g methanol, the value of vacuum pump scale were between 1-3, corresponding to permeate flux 0.5 to 2.2 litre/m^2.h, respectively. The value of permeate fluxes were then plotted versus conversion as illustrated in Fig 5. The amount of immobilized enzyme is another important parameter to consider. According to Fig 5, the best performance was attained using a concentration of protein within membrane pores of about 3.2 g/m^2.

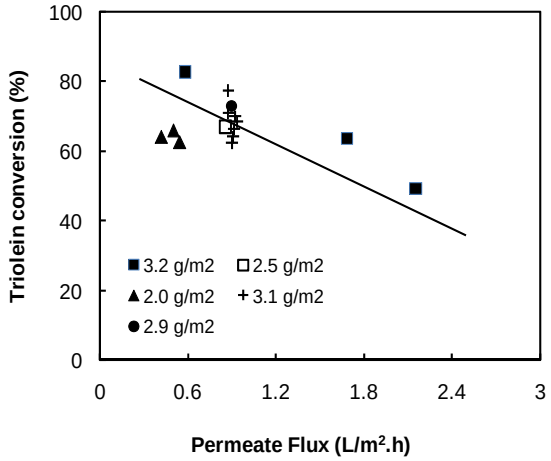

Fig 5. Experimental setup of microreactor for transesterification reactor

Fig 5 also demonstrate that, at the higher flux (lower residence time) conversion decreased, and this effect was particularly significant for 3.2 g/m^2 of immobilized enzyme. From these values the corresponding residence time were calculated and reported that the degree of triolein conversion using these microreactors was about 80% with a reaction time 19 minute. The results clearly show that reaction time of enzymatic transesterification in membrane microreactor system was faster than in conventional system., in order to achieve product yield of $\geq$ 90% it was necessary to utilize reaction time greater than 40 hours [7].

3.4. Stability of biocatalyst membrane microreactor

The stability of enzyme was measured using 2.042 g/m2 and 3.115 g/m2 of immobilized enzyme. Experiments were carried out continuously for 3 days. During the experiments there was no evidence of activity decrease in the microreactor and the conversion was constant at about 65% for 1st stage and 85% for 2nd stage (Fig. 6). In order to calculate the half-life experiments will need to be carried out for a longer time; nevertheless the results show that microreactor maintained good stability for at least 3 days.

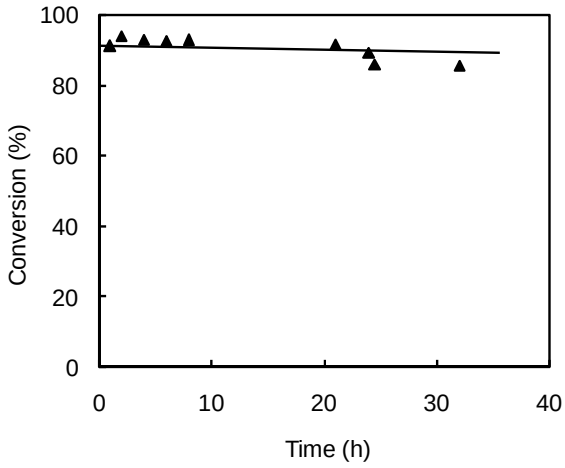

Fig 6. Stability of lipase immbilized membrane during transesterification reaction

4. CONCLUSIONS

In this study, a new concept of membrane microreactor is developed for trans-esterification reaction. The influences of various parameters such as permeate flux, enzyme loading and stability was investigated.

The degree of triolein conversion using these microreactors was about 80% with a reaction time 19 minute. Most significantly, the enzymatic microreactor exhibited far superior activity than the crude enzyme. The stability of enzymatic microreactor system showed very good results, with no activity decay during 3-days period of continuous operation. This system might be suitable for triglycerides transesterification (commercial production of biodiesel), which produce no waste stream.

5. REFERENCES

[1]. A. Bosley, and A. Pielow, “Immobilization of lipases on porous polypropylene: reduction in esterification efficiency at low loading”, Journal of American Oil Chemists Society 74 (1), 107–111 (1997)

[2]. D.R. Walt, and V. Agayn, “The chemistry of enzyme and protein immobilization with glutaraldehyde”, Trends in Analytical Chemistry 13 (10), 425–430 (1994).

[3]. C. Pizarro, M. Fernandez-Torroba, C. Benito and J. Gonzalez-Saiz, “Optimization by experimental design of polyacrylamide gel composition as support for enzyme immobilization by entrapment”, Biotechnology and Bioengineering 53 (2), 497–506 (1997).

[4]. GM. Rios, MP. Belleville, D. Paolucci, J. Sanchezet, “Progress in enzymatic membrane reactors – a review”, Journal of Membrane Science 242, 189–196 (2004)

[5]. S.J. Kim, S.M. Jung, Y.C. Park, and K.M. Park, “Lipase catalyzed transesterification of soybean oil using ethyl acetate, an alternative acyl acceptor”. Biotechnol. Bioproc. Eng. 12: 441-445 (2007).

[6]. V. Dossat, D. Combes, and A. Marty, Continuous enzymatic transesterification of high oleic sunflower oil in a packed bed reactor: influence of the glycerol production. Enzyme Microb. Technol. 25, 194–200 (1999).

[7]. A. Hsu, K.C. Jones, T.A. Foglia, and W.N. Marmer, "Continuous Production of Ethyl Esters of Grease Using an Immobilized Lipase." Journal of the American Oil Chemists Society, 81 (8), 749-752 (2004).
[8]. M. Holcapek, P. Jandera, J. Fisher, and B. Prokes ,"Analytical monitoring of the production of biodiesel by high-performance liquid chromatography with various detection methods". J. Chromatogr. A, 858, 13–31 (1999).
[9]. P. Aimar, M. Meireles, P. Bacchin, and V. Sanches, "Fouling and concentration polarization in ultrafiltration and microfiltration", NATO ASI Ser. E, 272, 27-57 (1994)

Proceeding of the 11th International Conference on QiR (Quality in Research)
Faculty of Engineering, University of Indonesia, Depok, Indonesia, 3-6 August 2009
ISSN 114-1284

Preparation and Characterization Nano Catalyst from Pyrite (FeS_2) for Coal Liquefaction

Agus Wahyudi[1], Sariman[1], Bambang Sunendar[2], Ahmad Nuruddin[2]

[1] *R&D Center for Mineral and Coal (Puslitbang TekMIRA)*
Jl. Jend. Sudirman 623 Bandung, INDONESIA
E-mail: wahyudi@tekmira.esdm.go.id

[2]*Department of Physical Engineering, Institute of Technology Bandung*
Jl. Genesha 10 Bandung, INDONESIA

ABSTRACT

Liquid coal is a future energy which keeps being developed to replace fossil based unrenewable energy source. One of the most important factor to run this process is the role of catalyst. This requirement leads to question how to provide low cost catalyst in abundant.

In this research, pyrite mineral (iron-sulfide) from gold mining waste has been employed. Pyrite which its content has been increased to 92%, was measured its activity by sulfidazing test. The product, active compound pyrhotite ($Fe_{1-x}S$) was characterized by XRD and crystal size was determined by Scherer equation. This pyrite sulfidazing test at coal liquefy's temperature (400 ^0C) resulted pyrhotite crystal with size 33.13 nm.

Next investigation, pyrite mineral activation was conducted at temperature 400, 500 and 600 ^0C to obtain hematitee. This hematitee then was milled by HEM (high energy milling) resulted 50-300 nm in size. After sulfidazing test at temperature 400 ^0C, active compound pyrhotite was acquired with crystal size 24 nm. Crystal size of pyrhotite affects coal liquefy's rate and yield. Smaller the sizes, the better influence to coal liquefy conversion process. Finally, hematitee as a nano catalyst used for coal liquefaction process and reached the conversion up to 91.05%.

Keywords: *nano catalyst, pyrite, sulfidizing test, pyrhotite crystal, coal liquefaction.*

1. INTRODUCTION

As a big country, Indonesia was faced with a big problem in fuels supplies, especially from oil resources where the deposition was predicted only for 30 years later. Coal liquefaction is one of technology wich keep being developed to gain liquid fuel from coal. It is very important to change fossil fuel from petroleum where the deposition is growing decrease.

On coal liquefaction process, catalyst has important roles to increase the yield product and speed up the convertion process. It used for assist hydrogen put into coal or coal-solvent mixtures to increase active hydrogen availability. Hydrogen has function for hydrogenize aromatic compound, promote cracking reaction and stabilize free radicals. Figure 1 gives ilustration for coal hydrogenation mechanism.

Synthetic catalist such as Co-Mo is the most effective catalyst for this pupose since it's reactivity but the price is very expensive. Another source wich has eligible low price and good ability for coal liquefaction is catalyst based on iron (Fe). This catalyst has better activity when transform to pyrhotite coumpound ($Fe_{1-x}S$), which occured when added together with sulfur in liquefies reaction condition.

This research aimed to prepare catalyst in nano scale for coal liquefaction pupose from gold mining waste, pyrite (FeS_2) rich, which has not been used optimaly.

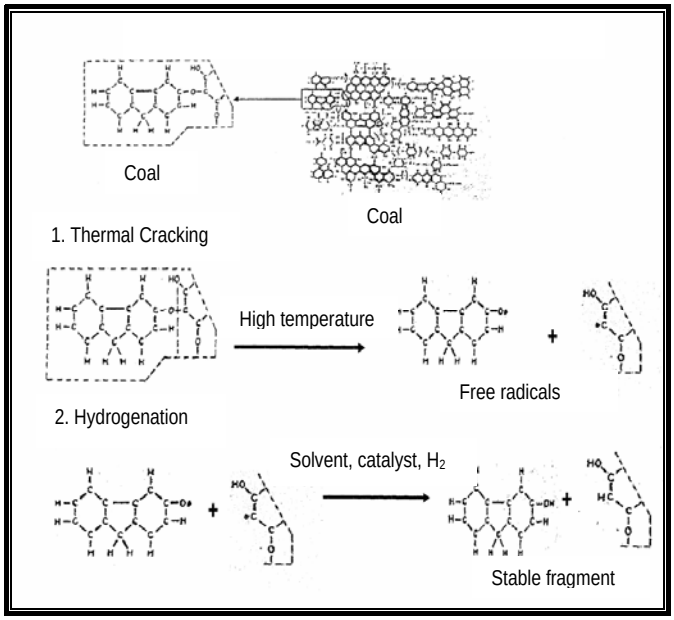

Figure 1. Coal hydrogenation mechanism

2. EXPERIMENTAL

Experimental steps shown in figure 2 below.

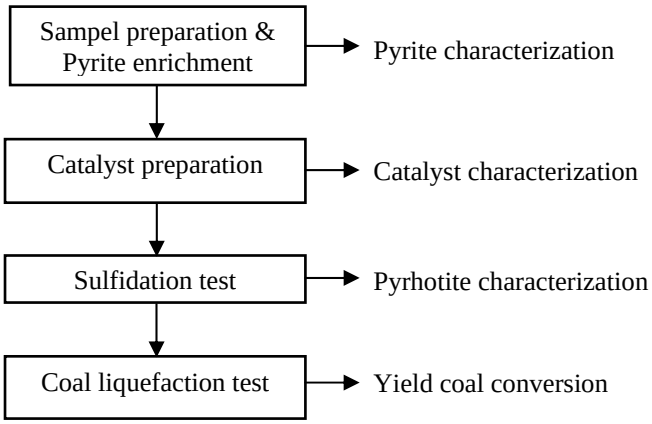

Figure 2. Flow diagram of the research

Preparation of raw materials from bulk size by crushing and milling using jaw crusher and ball mill until -200 mesh in size (76 micron). After that, pyrite enriched by flotation method with two variation, i.e. solid percentage and collector value.

Catalyst synthesized by roasting pyrite at several temperatures: 400, 500 and 600 ^{0}C. The resulted material then milled with high energy milling (HEM) to get higher surface area.

To obtain the catalyst convertion to pyrhotite, processed in sulfidazing test using autoclave unit, mix together catalyst, sulphur, antracen oil, without coal, and injected with hydrogen gas (100 bar), set at 300, 350, and 400 ^{0}C. To measure the size of pyrhotite crystal formed, used XRD and calculated with Scherer equation.

Finally, to confirm the liquefaction conversion conducted by coal liquefaction test using apparatus and the same condition with sulfidation test, using coal from Berau - East Kalimantan.

3. RESULTS AND DISCUSSION

3.1 Sample Preparation and Pyrite Enrichment

Table 1 shows chemical composition of raw materials.

Table 1. Chemical composition of raw material (%wt)

Si	Al	Fe_{Tot}	Ca	Mg	K	Na	S	LOI
10.70	1.24	33.7	0.11	0.028	0.49	0.041	38.0	25.2

From that composition, Fe_{Tot} 33.7%, it is potential used pyrite for coal liquefaction catalyst based on iron (Fe). To enrich the pyrite value, it was done by flotation method with two variations, solid percentage and collector value. Table 2 shows the flotation condition.

Table 2. Flotation condition

Condition	% Solid variation	Collector value variation
Feed size	-200 mesh	-200 mesh
Collector (Xanthat)	200 g/ton	-variation-
Frother	Phini oil	Phini oil
% solid	-variation-	20%

The optimal condition occured at 20% solid and 200 g/ton collector value, gained 91.50% pyrite value with 93.80% recovery.

3.2 Preparation and Characterization Catalyst

Catalyst for coal liquefaction was prepared from pyrite which has already enriched. Activation was done at several temperatures: 400, 500 and 600 ^{0}C as long as 2 hours, regarding TGA/DTA test result (Figure 3).

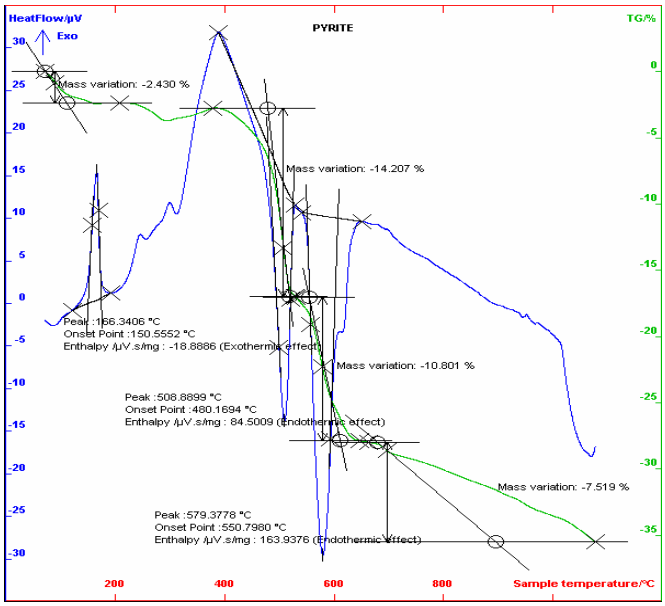

Figure 3. TGA/DTA curve of pyrite

Regarding information from TGA/DTA analyzed at 500 ^{0}C pyrite significantly transform to hematite, shown by the most extreme slope. This phase transformation phenomenon effects in it's physical properties, i.e. surface area and pore size. Table 3 shows the value of spesific surface area and avarage pore size of hematite (pyrite activated) measeured by BET method.

Tabel 3. Spesific surface area and avarage pore size of hematite

	T=400 ^{0}C	T=500 ^{0}C	T=600 ^{0}C
Spesific Surface Area	1,75 m^2/g	4,57 m^2/g	2,51 m^2/g
Avarage Pore Radius	108 nm	133 nm	110 nm

As catalytic puposes, surface area is one of the most important factors which influence the effectivness process. The highest surface area, the highest effectivness of catalyst's role. Therefore, to increase the surface area can be done by size reducing by using high energy milling apparatus (HEM) in several hours. The result can be measured by SEM as shown in figure 4.

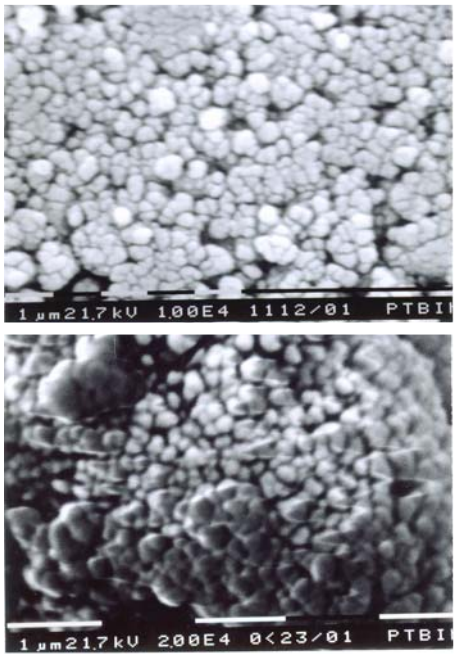

Figure 4. SEM photograph of hematite milled in 18 hours by using HEM

From above picture shows that the smallest particle size about 50 nm and the biggest about 300 nm.

3.3 Sufidazing Test

Sulfidazing test used hematite as catalyst succesfully formed pyrhotite crystal ($Fe_{1-x}S$), shown by pyrhotite peak in XRD difractogram (figure 5). While using pyrite as catalyst, only a few has converted to pyrhotite but the rest still in pyrite (FeS_2) phase (figure 6).

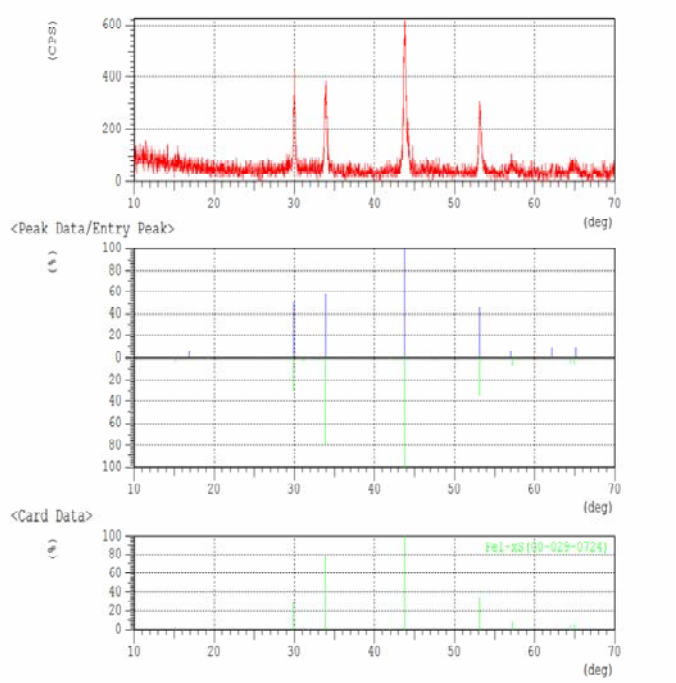

Figure 5. XRD difractogram of sulfidazing test result using hematite as catalyst

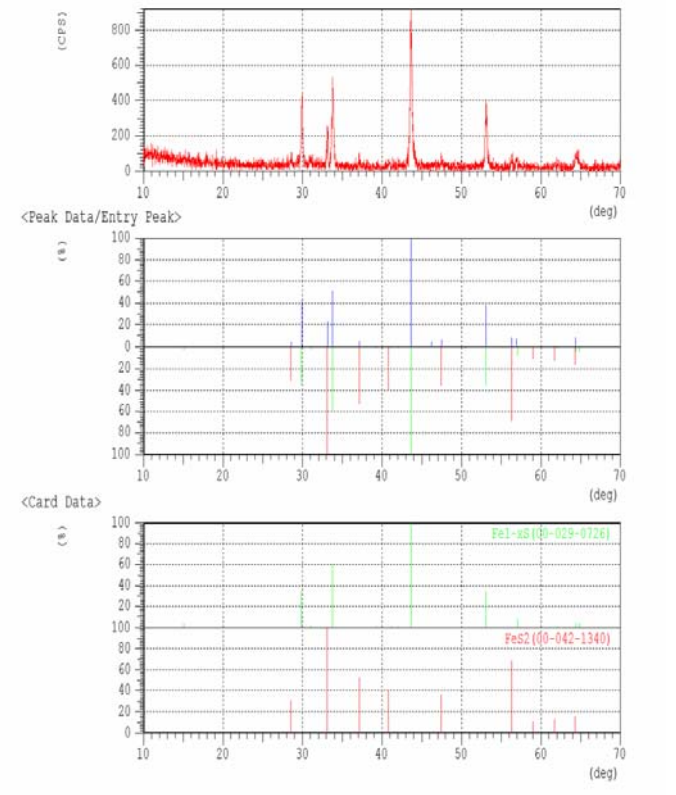

Figure 6. XRD difractogram of sulfidazing test result using pyrite as catalyst

By using Scherer equation, the size of pyrhotite crystal can be obtained as shown in figure 7.

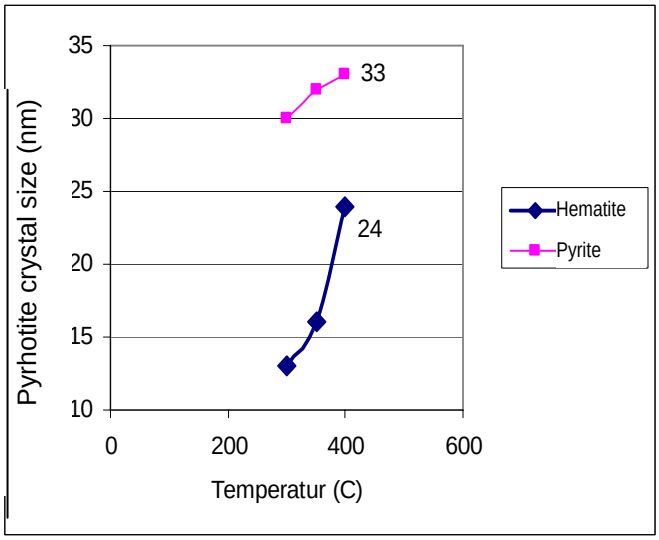

Figure 7. The growth of pyrhotite crystal resulted from sulfidazing test by using hematite and pyrite as catalyst at 300, 350 and 400 ^{0}C

As the result, hematite catalyst able to form pyrhotite crystal with the better size (24 nm) than by using pyrite (33 nm) at 400 ^{0}C. That caused Fe in hematite (Fe_2O_3) has oxidation number +3 so easier formed pyrhotite than Fe in pyrite (FeS_2) which only has oxidation number +2. Beside that, surface area in hematite is higher than pyrite, by milling treatment until sub-cron/nano scale.

3.4 Coal Liquefaction Test

The result of coal liquefaction using hematite catalyst shown in table 5 below.

Table 4. Yield coal conversion to liquid

Product	% Conversion
Liquid coal	91,05
Unreacted coal	8,95

From the data above, liquefaction coal from Berau-East Kalimantan gained total liquid coal 91.05% consist of light oil , water and gas reached up to 45.77%, asphalten 23.03% and preasphalten 22.25%. The rest is unreacted coal 8.95%.

4. CONCLUSSION

Preparation of catalyst hematite was carried out by activing pyrite at 500 ^{0}C and milling using high energy milling (HEM) apparatus resulting hematite with particle size 50-300 nm from 76 micron. By using this catalyst in sulfidazing test formed pyrhotite crystal 24 nm in size, and succesfully convert solid coal into liquid coal reached up to 91.05%.

REFERENCES

1. Ningrum, S.N., dkk. (2005), Program pencairan batubara menambah pasokan BBM di Inodonesia, *Majalah Mineral & Energi*, **3**, 14-17.

2. Anonim, Departemen Energi dan Sumber Daya Mineral. (2005), Batubara cair gantikan minyak bumi, *Majalah Wartabara*, **1**, 10-11.

3. Ningrum, S.N., Tirtosoekotjo, S. (2004), Prospek pencairan batubara peringkat rendah Indonesia dengan teknologi brown coal liquefaction, *Majalah Mineral dan Energi*, **2**, 41-47.

4. Sariman. (2005), *Pemanfaatan Katalis Limonit untuk Proses Pencairan Batubara*, Puslitbang Tekmira, Bandung, 5-20.

5. Kaneko, T., Tazawa K., Okuyama N., Tamura M., Shimasaki K. (2000) Effect of highly dispersed iron catalyst on direct coal liquefaction, *J.Energi and Fuels*, **79**, 263-271.

6. Ngurah, A. (1990), *Percobaan Peningkatan Kadar Pirit Kalimantan Selatan Cara Gravimetris dan Flotasi*, PPTM, Bandung, 1-3.

7. Dutta, J., H. Hofmann. (2003), *Nanomaterials*, E-book, 37-39.

8. Satterfield, C.N. (1991), *Heterogoneus Catalyst in Industrial Practice*, Second Edition, McGraw-Hill Inc., 87-128.

Proceeding of the 11th International Conference on QiR (Quality in Research)
Faculty of Engineering, University of Indonesia, Depok, Indonesia, 3-6 August 2009
ISSN 114-1284

Investigation into the nanostructural evolution of TiO_2–polymethyl methacrylate nanohybrids derived from the sol–gel technique

Akhmad Herman Yuwono [1*], Donantha Dhaneswara [1]
Yu Zhang [2] and John Wang [2]

[1]*Department of Metallurgy and Materials Engineering, Faculty of Engineering*
University of Indonesia, Depok-West Java, Indonesia 16424
Tel : +(62-21) 7863510. Fax : +(62-21) 7872350
E-mail : ahyuwono@@metal.ui.ac.id

[2]*Department of Materials Science and Engineering Faculty of Engineering*
National University of Singapore, Singapore 117574
E-mail : msewangj@nus.edu

ABSTRACT

In this research, the nanostructural evolution of TiO_2 crystallite upon in situ sol−gel process of titania–polymethyl methacrylate (TiO_2–PMMA) nanocomposites was systematically investigated. The main objective is to understand the mechanisms responsible for the amorphous nature of the sol−gel derived TiO_2−polymethyl methacrylate (PMMA) nanohybrids. For this purpose, two sol−gel parameters i.e. the coupling agent concentration, water content or hydrolysis ratio (rw), and pH value of the titania precursor solution were varied. On the basis of XRD analysis, it has been found that the modification of those parameters can enhance the nanocrystallinity of pure TiO_2 phase. However, this could not be applied when the titania precursor was mixed with the PMMA segment. On the basis of XRD and FTIR analyses, it was found that the largely amorphous TiO_2 state is related to the fast development of stiff Ti−OH networks during the hydrolysis and condensation stages in sol−gel process, worsened by the entrapment of the rigid PMMA matrix.

Keywords

Example:
Nanohybrids, TiO_2, PMMA, hydrolysis ratio, pH, nanostructural evolution.

1. INTRODUCTION

Poly(methylmethacrylate) or PMMA is well-known as an excellent optical polymer for use in optical fibers, optical disks and lenses [1]. However, the refractive index (n_o) of PMMA is limited to only 1.49. On the other hand, titanium oxide (TiO_2, titania) has been recognized as an inorganic material having high refractive index, *i.e.* ~2.45 (anatase) and ~2.70 (rutile). Therefore, an incorporation of TiO_2 nanoparticles into PMMA has been considered for preparing high-refractive index polymers. Accordingly, titania-poly(methyl methacrylate) or TiO_2-PMMA nanohybrids have been studied previously by several researchers. Zhang *et al*. [2] synthesized TiO_2-PMMA nanohybrid using chelating ligand as a coupling agent. A further study on preparation and optical properties of PMMA-titania thin films was performed by Chen *et al*., [3,4] who synthesized thin film TiO_2-PMMA nanocomposites by *in situ* sol-gel process of trialkoxysilane-capped PMMA-titania combined with spin coating and multi-step annealing process. The refractive indices of thus prepared films were reported in the range of 1.505-1.867, provided the loading of titanium alkoxide in the precursor solution was up to 90 wt%.

In our previous works, it has been shown that the TiO_2−PMMA nanohybrids derived from *in situ* sol-gel polymerization exhibits a very fast recovery time of ~1.5 picosecond and a large third order nonlinear optical susceptibility, $\chi^{(3)}$, as observed [5,6]. Therefore, the nanocomposites are promising for several potential applications in optoelectronic devices such as nonlinear optical switching devices in photonics and real-time

coherent optical signal processors [7,8]. However, it is realized, that TiO_2−PMMA nanohybrids are limited by the occurrence of amorphous TiO_2 nanoparticles, which cannot be avoided under the conditions tolerable by the polymer matrix upon the low temperature sol−gel process. Therefore, it is thus of our main interest to investigate the factors causing the amorphous nature of TiO_2 phase in PMMA matrix. For this purpose, two synthesis parameters involved in the *in situ* sol−gel polymerization, including the water content or hydrolysis ratio (*rw*), and pH value of the titania precursor solution were systematically investigated.

2. EXPERIMENTAL

In this work, we used an *in-situ* sol-gel polymerization technique, which is basically a thorough mixing process between a pre-hydrolyzed TiO_2 precursor (titanium isopropoxide, Ti-iP) and pre-polymerized PMMA. First, the monomers, methyl methacrylate (MMA, 99%, Acros) and coupling agent 3-(trimethoxysilyl)propyl methacrylate (MSMA, 98%, Acros), and initiator benzoyl peroxide (BPO, 98%, Acros) in solvent tetrahydrofuran (THF, 99%, Acros) were added into a reaction flask and polymerized at 60°C for 1 hour. The molar ratio of MSMA to MMA+ MSMA was controlled at 0.25 and the amount of BPO added to the mixture was fixed at 3.75 mol%. Furthermore, a TiO_2 based sol solution was prepared by mixing titanium isopropoxide (Ti-iP, 98%, Acros) with ethyl alcohol (EtOH, 95%, Merck) in a container and stirred for 30 minutes. A mixture of de-ionized water and hydrochloric acid (HCL, 36%, Ajax) was then added under stirring condition into the transparent solution to promote hydrolysis. The Ti-iP concentration in the solution was controlled at 0.4 M. It should be noted that for investigation purposes, first we varied the coupling agent concentration since this agent governs the interaction between inorganic and organic moieties in nanohybrids. For further investigation, three different sols with different pH value i.e. 3.08, 1.08 to 0.33 were prepared under the same ratio of water to Ti-iP (*rw*) or hydrolysis ratio of 0.82. At the same time, other sols with varying hydrolysis ratio of 0.82, 2.00 and 3.50 under the same pH value of 0.78 were also synthesized. All of these parameters were thoroughly varied while maintaining the stability of sol solutions to be clear and transparent. Finally, this transparent sol solution was carefully added drop by drop over a duration of 30 minutes into the partially polymerized monomers with rigorous stirring to avoid local inhomogenities. The reaction was allowed to proceed at 60°C for another 2 hours. In this study, the weight ratio between the inorganic and organic precursors in the reaction mixture was fixed at 60:40.

The fabrication of thin film was performed by spin coating the hybrid solution onto glass substrates at 3000 rpm for 20 seconds. The coated films were then annealed in two stages of curing temperatures, *i.e.* at 60°C for 30 minutes and 150°C for 3 hours. The nanohybrids characterization was carried out with X-ray diffraction (XRD) measurements on Bruker AXS θ–2θ diffractometer using Cu K-α radiation (1.5406 Å) operated at 40 kV, 40 mA and with a step-size of 0.02° and time/step of 20 seconds. The incidence angle between the beam and film plane was fixed at 1.5°. Further analysis was performed using Fourier Transform Infrared (FTIR) spectroscopy at room temperature in the range of 4000-400 cm^{-1} using Bio-Rad model QS-300 spectrometer, which has a resolution of $\pm$ 8 cm^{-1}.

3. RESULTS AND DISCUSSION

Effect of coupling agent concentration. In the present study, 3-(trimethoxysilyl)propyl methacrylate (MSMA) is introduced as a coupling agent between the inorganic titanium alkoxide precursor and the organic MMA matrix. In our previous work [5,6] a constant MSMA/(MSMA+MMA) molar ratio of 0.25 was used in the nanohybrid preparation. Thermal gravimetric analysis (TGA) and FTIR studies confirmed that the thus derived nanohybrids demonstrated a strong interaction between the inorganic and organic moieties. For optical properties, this can be beneficial since the resulting nanohybrid is transparent in the visible region. On the other hand, however, such a strong bonding may have a reverse effect on the TiO_2 formation, *i.e.,* the strong hindrance experienced by the hydrolyzed titanium alkoxide (Ti−OH networks) in PMMA gave rise to largely amorphous TiO_2 phase. Therefore it is of further interest to investigate whether an incorporation of a lower concentration of coupling agent at the solution preparation stage can provide a higher flexibility for the hydrolyzed titanium alkoxide to undergo densification in the PMMA matrix during the subsequent annealing process. By having so, it is expected that Ti−O−Ti bonds will be able to

develop a long-range order, such that nanocrystalline TiO_2 particles can be formed. The amount of MSMA/(MSMA+MMA) molar ratio was reduced down to 0.05 and the resulted nanohybrid was compared to that derived from 0.25

Figure 1 is the XRD traces for both nanohybrids showing two broadened phase peaks at 2θ angles of 25.35 and 48.12° that can be assigned to (101) and (200) crystal planes of anatase phase. The nanohybrid derived from the coupling agent ratio of 0.05 shows slightly stronger diffraction peaks than those derived from the coupling agent ratio of 0.25.

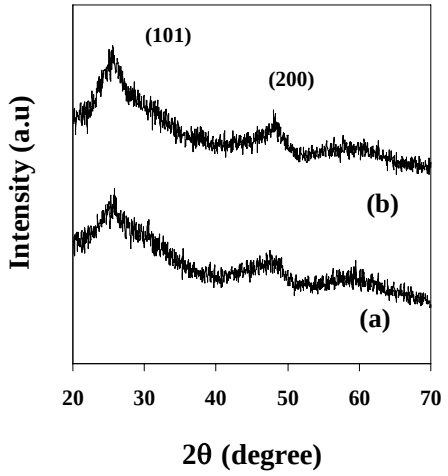

Figure 1. XRD traces of nanohybrid derived from ratio MSMA/(MSMA+MMA) ratio of (a) 0.25 and (b) 0.05.

For further confirmation, FTIR spectroscopy of the two nanohybrids was investigated. The stretching vibrations for both samples are shown in Figures 2 and 3, for both low wavenumber range (1100−400 cm^{-1}) and high wavenumber range (4000−2400 cm^{-1}), respectively. Figure 2 shows the occurrence of absorption bands located at 450 and 650 cm^{-1} which can be assigned to Ti−O and Ti−O−Ti stretching vibrations, respectively as the characteristic of nanocrystalline TiO_2 in short and long range order [9,10]. In addition, there is an additional band at 910 cm^{-1}, corresponding to the stretching vibration of Ti−O−Si bond [11]. Although the two nanohybrids show similar intensities, however a careful comparison reveals that there occurs a considerably higher band intensity in the range of 1000−1200 cm^{-1} in spectrum "(b)", in comparison to spectrum "(a)". This band, with the strongest absorption peak located at ~1080 cm^{-1}, is assigned to the Ti−O−C stretching mode originated from the remaining unhydrolized alkoxy groups [12,13]. Although there is a possibility of overlapping with C−O−C bonds originated from the PMMA matrix in the range of 1039−1192 cm^{-1} [3], however the same amount of MMA monomer was incorporated into both nanohybrids. This was further confirmed by checking the stretching vibration of C−H bond at 2950 cm^{-1} as shown in Figure 3.15. Both spectra "(a)" and "(b)" are very similar in intensity. Therefore it can be concluded that the enhanced intensity at ~1080 cm^{-1} in spectrum "(b)" of Figure 3.14 is related to the higher number of Ti−O−C bonds in the nanohybrid derived from the lower coupling agent ratio.

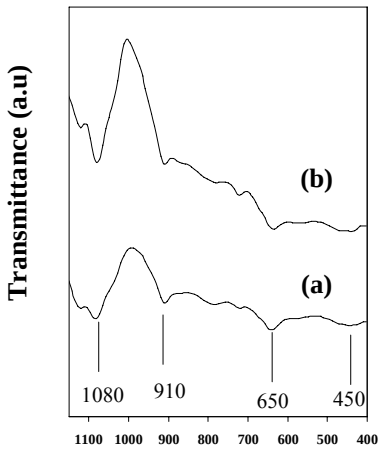

Figure 2. FTIR spectra of the nanohybrid derived from MSMA/ (MSMA+MMA) ratio of (a) 0.25 and (b) 0.05, respectively, in the low wavenumber range of 1100−400 cm^{-1}.

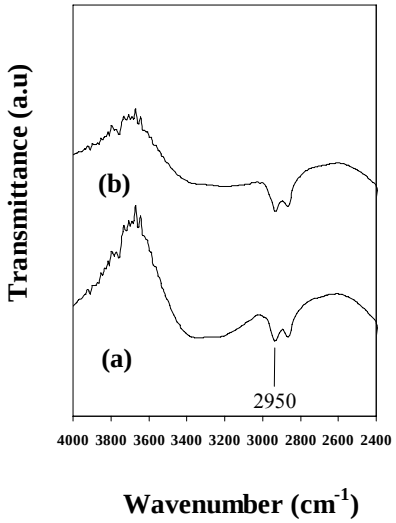

Figure 3. FTIR spectra of the nanohybrid derived from MSMA/(MSMA+MMA) ratio of (a) 0.25 and (b) 0.05, respectively, in the high wavenumber range of 4000−2400 cm^{-1}.

It is of further interest to investigate the reason behind the enhanced nanocrystallinity shown by the nanohybrid derived from the lower coupling agent ratio. One approach is to look at the three absorption bands, *i.e*. Ti−OH at ~3400 cm^{-1}, Ti−O−C at 1080 cm^{-1} and Ti−O−Si at 910 cm^{-1}. As seen in Figure 3, the intensity of Ti-OH band for the nanohybrid derived from the coupling agent ratio of 0.05 is lower than that derived from 0.25, while a higher intensity of Ti−O−C band (Figure 2) is demonstrated by the former. In contrast to these differences, both nanohybrids show more or less the same intensity for Ti−O−Si band. As proposed by Brinker and Hurd [14] and Langlet *et al.* [15], the largely amorphous TiO_2 thin films obtained at low temperatures is due to the formation of stiff Ti−OH networks resulted from the fast condensation of titanium alkoxide precursor, which in turn hinder the densification of crystallite TiO_2 phase. In this connection, therefore, the low intensity of Ti−OH observed for the nanohybrid derived from the lower coupling agent ratio suggests a reduced amount of amorphous phase. On the other hand, the high intensity of Ti−O−C stretching mode from the unhydrolized alkoxy groups in this sample is related to the high number of interfacial sites for TiO_2 nucleation. The interfacial bond is not as stiff as Ti−OH network and is therefore sufficiently flexible to take part in the densification of TiO_2 phase, *i.e*., by the arrangement of Ti−O−Ti bonds in the long-range order and thus an enhancement in TiO_2 nanocrystallinity was resulted, as detected by XRD. Zhang *et al.* [13] has reported that Ti−O−C bond, together with Ti−O and Ti−OH, can lead to connected networks of TiO_2 nanoparticles in titania-poly(phenylenevinylene) or TiO_2−PPV nanocomposites. The interfacial phase plays an important role in providing the necessary dispersion function and thus preventing the agglomeration of TiO_2 nanoparticles in polyvinyl alcohol (PVA) matrix [16].

The effects of different coupling agent concentrations on nanohybrids were further investigated by TGA. Figure 4 shows that both samples have similar response upon heating up to 850 ^oC. It is clearly demonstrated that the nanohybrid derived from the lower coupling agent ratio decomposes at a lower temperature than that derived from the higher coupling agent ratio. This can be accounted for by the high number of interfacial Ti−O−C bonds of unhydrolized alkoxy groups in the former, as has been confirmed by FTIR spectroscopy. On the other hand, the similarity in TGA behavior up to 300 ^oC shown by both samples can be related to the similar intensity of Ti−O−Si band at 910 cm^{-1} shown in Figure 2. With further heating beyond 300 ^oC, however, the difference in mass change becomes more remarkable when both samples underwent the second stage of mass loss. This suggests that once the unhydrolized alkoxy groups had been decomposed, there occurred a higher number of organic segments, dissociated from the inorganic networks in the former. This is further supported by the reduced amount of char yields at 850 ^oC produced by this sample, suggesting a lower number of remaining organic moieties that could be trapped in the inorganic network. Based on this observation, it is confirmed that a lower concentration of coupling agent can lessen the binding strength between the inorganic and organic moieties upon heating, particularly at temperatures beyond the decomposition temperature T_d of PMMA matrix (345 ^oC).

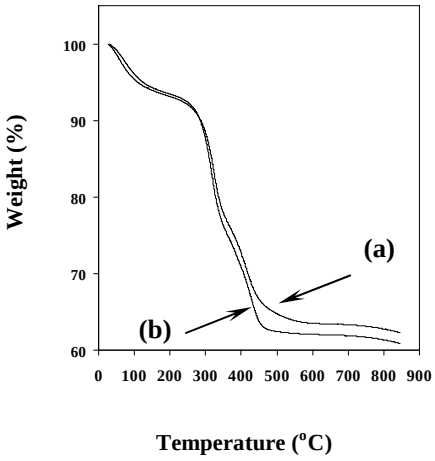

Figure 4. TGA curves of the nanohybrid derived from MSMA/(MSMA+MMA) ratio of (a) 0.25 and (b) 0.05, respectively.

Effect of pH value. Brinker and Hurd [14] and Langlet *et al.* [15] proposed that the amorphous state of TiO_2 was caused by the formation of stiff Ti−OH arising from fast condensation. In line with this understanding, Yoldas [17] also suggested that if the rate of condensation process is faster than hydrolysis, the alkyl groups are incorporated into the structure and sterically hinder the formation of

ordered structure. Therefore, in order to enable the precursor to crystallize into an equilibrium structure, the condensation should proceed slowly after the completion of hydrolysis. Lowering the pH value of the titania solution has been considered effective in enhancing the rate of hydrolysis and to inhibit the condensation [18]. This is made possible since the −OR groups in alkoxide are protonated by H^+ ions, making their charges more positive. Being positively charged, the metal ions repel the −OR groups and prefer to be attached to the −OH groups. Consequently, this promotes the hydrolysis process and at the same time decreases the rate of condensation significantly since the protonated species reduce their interaction by repelling each other. Yoldas [19] and Kallala *et al.* [20] have shown a difference in the inhibition ratios can lead to sols, transparent gels, turbid gels or precipitates. Accordingly, Gopal *et al.* [21] and Watson *et al.* [22] have reported the formation of anatase and rutile TiO_2 synthesized directly from an acid-catalyzed solution at temperatures close to room temperature. For the nanohybrids investigated in this study, however, a question remains as to whether a slow condensation rate of the protonated titanium hydroxide can lead to the densification of TiO_2 during the subsequent annealing process, while at the same time polymerization of the MMA monomers takes place effectively. The latter is responsible for the fast trapping effect causing a largely amorphous TiO_2 phase in the polymer matrix. Therefore, it will be of further interest to investigate the effect of pH value on the nanocrystallinity of TiO_2 phase in nanohybrids. For the investigation, TiO_2−PMMA nanohybrids were derived from TiO_2 sol solutions of pH value varying in the range of 3.08 to 0.33. This was done by adjusting the amount of hydrochloric acid (HCl) added, the function of which is to control the hydrolysis and condensation rates of titanium alkoxide [20,23]. The water to titanium alkoxide ratio (r_w) in each solution was kept at 0.82. Prior to mixing with the organic constituent, the sols were stirred at room temperature for 72 hours, aimed at providing sufficient time for the protonation of titanium alkoxide to take place, in accordance with the amount of hydrochloric acid added into the sol precursors. The XRD traces of the thus derived nanohybrids are given in Figure 5. It is shown that the nanohybrid derived from the inorganic sol solution of pH 3.08 (trace "(a)") is highly amorphous as indicated by the occurrence of two broadened humps in the 2θ ranges of 20−35° and 40−55°. By contrast, diffraction peaks at 2θ of ~25 and 48° corresponding to (101) and (200) crystal planes of anatase titania were observed for the nanohybrids derived from the inorganic sol solution of pH 1.08 and 0.33 (traces "(b)" and "(c)").

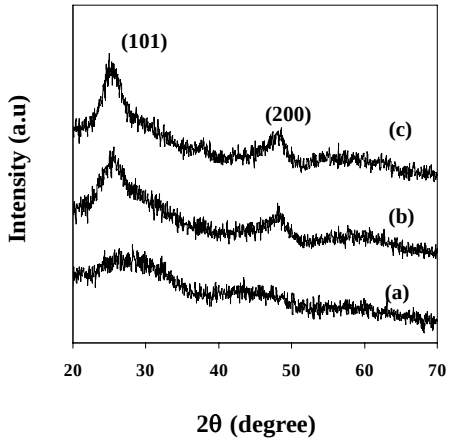

Figure 5. XRD traces of the nanohybrid derived from inorganic sol solution with pH value of (a) 3.08, (b) 1.08, and (c) 0.33, respectively.

The results observed above can be interpreted by considering the role of H^+ ion in providing repulsion forces among the protonated inorganic species. It is known that a highly acidic protonation leads to a stronger repulsion force and thus formation of extended structure from the hydrolyzed alkoxide [24]. By using small-angle X-ray scattering (SAXS), Xiong *et al.* [25,26] investigated the structure of inorganic species in trialkoxysilane-capped acrylic-titania hybrids derived from titania sols under three typical pH values of 4.4, 7.0 and 8.8, representing acid, neutral, and basic conditions, respectively. They observed that under the basic condition the inorganic domains can reach a radius of gyration (R_g) and fractal dimension (D) of 7.3 nm and 1.35. However, under the acid condition, the values were only 2.4 nm and 0.18, respectively. The smaller sizes in the latter were associated with the restriction of inorganic chain-like structure into open regions of the mesh produced by the crosslinked polymers [25,26]. This was more or less similar to the situation of the amorphous nanohybrid derived from titania sol with a pH value of 3.08 investigated in the present work (trace "(a)" in Figure 5). On the other hand, however, the notable diffraction peaks in the XRD traces "(b)" and "(c)" for the nanohybrids derived from titania sols with a much lower pH value

(1.08 and 0.33) suggest a rather different mechanism in comparison to what has been proposed by Xiong *et al.* [25, 26] for acid catalyst condition. In the system investigated in this project, the linear chain-like structures of hydrolyzed inorganic precursors were able to perform further self-densification in the solution stage. It proceeded up to the stage when the nanohybrid sample was annealed, whereby a rigid organic PMMA network was formed. The nanocrystallinity of the sample derived from the sol solution with a much lower pH value, *i.e.*, 0.33 (trace "(c)") is slightly higher than that of 1.08 (trace "(b)"). It suggests that the stronger repulsion force created among the protonated species at lower pH values can induce a better densification for titania phase in the TiO_2−PMMA nanohybrid system.

Effect of water to alkoxide ratio. The water to alkoxide (R_w) or often called as *hydrolysis ratio* determines the potential functionality of inorganic monomers in building the network [27]. In the previous investigation, a R_w of 0.82 was consistently used for the titania sol which is stable and did not turn into a gel, prior to mixing with polymer matrix. However, this ratio is less than the required stoichiometric value, *i.e.*, 4. As a result, the alkoxide precursor experienced an incomplete hydrolysis process. It is therefore of interest to find out whether the amount of water during sol preparation can favor a more completed hydrolysis and thus provide a higher nanocrystallinity for the titania phase in nanohybrid. For investigation, three different sols with R_w of 0.82, 2.00 and 3.50 under the same pH value of 0.78 were prepared. All the titania sol solutions were transparent and stable. An attempt to increase R_w to 4.00 led to the formation of immediate gel which could not be incorporated homogenously into pre-polymerized PMMA. Therefore, the first three compositions were used for further investigation. The XRD traces of the resulting nanohybrids are given in Figure 6. It is shown that when R_w is 0.82, the resulting nanohybrid (trace "(a)") demonstrates two broadened diffraction peaks at 2θ of ~25.35° and 48.12° corresponding to (101) and (200) crystal planes of anatase titania phase. An increase in R_w to 2.00 did not lead to a significant enhancement in nanocrystallinity for the respective nanohybrid (trace "(b)"). However, there was an onset of additional two peaks at 2θ of 38.63° and 55.08° corresponding to (112) and (211) crystal planes. Further increase of R_w to 3.50 gave rise to an un-expected occurrence of amorphous titania phase.

The above observation can be analyzed by considering that an increase in R_w gives rise to a stronger nucleophilic reaction between water and alkoxide species, and thus more −OR groups bonded to metal were substituted by −OH network structure. A larger and more compact structure of inorganic domains, as a result of the formation of a three-dimensional network structure, is therefore expected with the completion of −OH network [25,26].

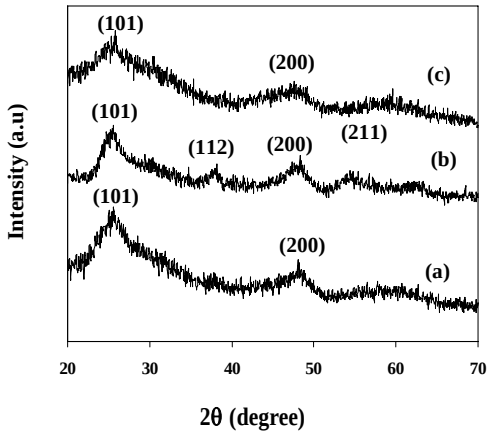

Figure 6. XRD traces of the nanohybrid derived from inorganic sol solution with R_w of (a) 0.82, (b) 2.00, and (c) 3.50, respectively.

Based on the XRD results, however, such increase in the inorganic domain size to form bigger nanocrystallites was not clearly indicated when R_w was increased from 0.82 to 2.00, as shown by diffraction peaks intensity at 2θ of ~25.35° and 48.12°. Yu *et al.* [28] has proposed a transition model of the inorganic domains in TiO_2−SiO_2 nanohybrid whereby chain-like structures transformed into particle-like clusters when R_w was varied from a value below the stoichiometric ratio (<4) to that of above the critical value (>4). The appearance of two additional peaks at 2θ of 38.63° and 55.08° suggested that the high number of −OH groups generated at R_w of 2.00 had provided more TiO_2 nuclei which furthermore grew as nanocrystals of different directions in addition to what has been formed at R_w of 0.82. It is of interest to compare the current result with a previous work performed by Xiong *et al*. [29] who employed SAXS technique to investigate the effect of water content on the structures of thermoplastic acrylic resin−titania hybrids. They

observed that hybrids derived from R_w of 1 and 2 demonstrated shallow linear regions in the Guinier and Porod plots, indicating little phase separation. Besides, the difference in scattering intensity between hybrids derived from R_w of 1 and 2 was small. This is very similar to the nanohybrids with R_w of 0.82 and 2 in the present study, as revealed by XRD results in Figure 6. However, at high R_w, a discrepancy occurs between the current result and what has been observed by Xiong *et al.* [29]. In their case, further increase of R_w up to 4 led to a denser inorganic phase with a larger size. In contrast, the nanohybrid derived from the hydrolysis ratio, R_w of 3.50, is highly amorphous when compared with those of derived from 0.82 and 2.00. Again, this is associated with the trapping of the hydrolyzed alkoxide groups by rigid PMMA network during and after annealing at 150 ^{o}C. It is highly possible that although a great number of –OH groups were generated through the relatively complete hydrolysis, however due to the strong constraint effect by organic polymer matrix, they failed to proceed to the subsequent densification and hence nanocrystalline TiO_2 phase was not achieved. In connection with the discrepancy observed between the two studies, it should be noted that Xiong *et al.* [25,26,29] relied on the SAXS scattering patterns in order to determine the sizes of inorganic phase in the hybrid composition. Indeed, several variations in their synthesis process such as pH value, water content and solvent mixture which led to different levels of hydrolysis and condensation for titania precursor could result in different levels of phase separation and thus scattering patterns accordingly. It was not confirmed whether the inorganic network formed in the hybrids were amorphous Ti−OH, nanocrystalline TiO_2 or a mixture of both. Therefore, the observed scattering pattern can be considered as a response from cumulative quantity of inorganic phases, regardless of their amorphous or crystalline nature. As a result, the SAXS studies of Xiong *et al*. [25,26,29]were not affected by the trapping mechanism of titania phase by the polymer matrix, as encountered in the nanohybrids investigated in the current study.

4. CONCLUSION

In an attempt to understand the mechanism responsible for the largely amorphous nature of the TiO_2 phase in the nanohybrids, several processing parameters involved in sol−gel and *in situ* polymerization were investigated, including coupling agent concentration, pH value and water to alkoxide ratio. Variation of these processing parameters did not effectively lead to a significant enhancement in the nanocrystallinity of TiO_2 phase in the nanohybrids. They were not adequately effective to compete with the formation of stiff Ti−OH structures, which were trapped by the rigid network of polymerized PMMA matrix. This mechanism has resulted in a largely amorphous structure for TiO_2 phase in nanohybrids.

REFERENCES

1. H.A. Hornak, Ed. *Polymers for Lightwave and Integrated Optics*, Marcel Dekker, New York, 1992
2. J. Zhang, S. Luo and L. Gui, *J. Mater. Sci*. **32**, 1469 (1997)
3. W. C. Chen, S. J. Lee, L.H. Lee and J. L. Lin, *J. Mater. Chem*. **9**, 2999, (1999)
4. L. H. Lee and W.C. Chen, *Chem. Mater*. **13**, 1137 (2001)
5. A.H. Yuwono, J.M. Xue, J. Wang, H.I. Elim, W. Ji, Y Li and T.J. White, *J. Mater. Chem.* **13**, 1475 (2003).
6. H.I. Elim, W. Ji, A.H. Yuwono, J.M. Xue, J. Wang, *Appl. Phys. Lett*., **82 (16)**, 2691 (2003).
7. B. Wang, G.L. Wilkes, J.C. Hedrick, S.C. Liptak and J.E. McGrath, *Macromolecules*, **24**, 3449 (1991).
8. G.L. Fischer, R.W. Boyd, R.J. Gehr, S.A. Jenekhe, J.A. Osaheni, J.E. Sipe and L.A. Weller-Brophy, *Phys. Rev. Lett*. **74 (10)**, 1871 (1995).
9. Y. Djaoued, S. Badilescu, P.V. Ashrit, D. Bersani, P.P. Lottici and R. Brüning, *J. of Sol-Gel. Sci. Tech.* **24**, 247 (2002).
10. S.X. Wang, M.T. Wang, Y.Lei and L.D. Zhang, *J. Mater. Sci. Lett*. **18**, 2009 (1999).
11. A. Leaustic, F. Babonneau and J. Livage, *Chem. Mater*. **1**, 240 (1989).
12. W. Que, Y. Zhou, Y.L. Lam, Y.C. Chan, S.D. Cheng, Z. Sun and C.H. Kam, *J. Sol−Gel. Sci. Technol*. **18**, 77 (2000).
13. J. Zhang, X. Ju, B.J. Wang, Q.S. Li, T. Liu and T.D. Hu, *Synth. Met*. **118**, 181 (2001).
14. C.J. Brinker and A.J. Hurd, *J. Phys. III France* **4,** 1231 (1994).
15. M. Langlet, M. Burgos, C. Couthier, C. Jimenez, C. Morant and M. Manso, *J. Sol−Gel. Sci. Technol.* **22**, 139 (2001).
16. X.C. Chen, *J. Mater. Sci. Lett*. **21**, 1637 (2002).
17. B.E. Yoldas, *J.Mater. Sci*. **14**, 1843 (1979).
18. J. Livage, M. Henry and C. Sanchez, *Prog. Solid State Chem*. **18**, 259 (1988).
19. B.E. Yoldas, *J.Mater. Sci*. **21**, 1086 (1986).
20. M. Kallala, C. Sanchez and B. Cabane, *J. Non-Crys. Solids* **147-148**, 189 (1992).

21. M. Gopal, W.J. Moberly Chan and L.C. De Jonghe, *J. Mater. Sci*. **32**, 6001 (1997).
22. S. Watson, D. Beydoun, J. Scott and R. Amal, *J. Nanopart. Res*. **6**, 193 (2004).
23. M. Burgos and M. Langlet, *Thin Solid Films* **349**, 19 (1999).
24. C.L. Chiang, C.C. Ma, D. L. Wu and H.C. Kuan, *J. Polym. Sci. Polym. Chem*. **41**, 905 (2003).
25. M. Xiong, S. Zhou, L. Wu, B. Wang and L. Yang, *Polymer* **45**, 8127 (2004).
26. M. Xiong, S. Zhou, B. You and L. Wu, *Polymer* **43**, 637 (2005).
27. M. Kallala, C. Sanchez and B. Cabane, *Phys. Rev. E* **48**, 3692 (1993).
28. H. F. Yu and S.M. Wang, *J. Non-Cryst. Solids* **261**, 260 (2000).
29. M.N. Xiong, S.X. Zhou, B.You, G.X. Gu, L.M. Wu, *J. Polym. Sci. Polym. Phys*. **42**, 3682 (2004).

Influence of Cr addition on Fe-Al coating obtained by high energy milling

Alfian Noviyanto[1*], Sri Harjanto[2], Agus Sukarto Wismogroho[3], Dedi Priadi[2], Nurul Taufiqu Rochman[1]

[1]*Advanced Material and Nanotechnology Laboratory,*
Research Center for Physics, Indonesia Institute of Sciences
Komp. PUSPIPTEK Serpong 15314
**alfiantep@yahoo.com*

[2]*Department of Metallurgy and Materials Engineering,*
Faculty of Engineering, University of Indonesia
Kampus UI Depok 16424

[3]*Department of Advanced Material and Nanostructure,*
Graduate School of Science and Engineering, Kagoshima University

ABSTRACT

Fe-Al coating on steel has been fabricated by mechanical alloying method using high energy milling HEM-E3D. The resulted will be utilized in carbon steel coating process in order to improve its corrosion resistance and its resistance of both chemically and mechanically degrading environment. The properties of its compound were predicted to be improved by the addition of Cr in Fe-Al coating process. Mixture composition of Fe-40at.%Al and Fe-40at.%Al-3at.%Cr was used as initial coating agent of steel plate. Stainless steel vial of 100 ml was used for milling process under argon condition for 32 h. The grinding media were stainless steel balls of 10 mm and 5 mm in weight composition of 1:5. Milling speed was maintained at 263 rpm. To observe coating evolution, carbon steel substrate were also milled in milling process. The ball to powder ratio was 8:1. The microstructure of milling results was characterized using SEM-EDS, XRD and micro hardness tester. SEM results showed the coating exist after 8 hours of milling time. The thickness of coating is depending on milling time, the coating will become thick as longer milling time.

Keywords: *High Energy Milling, Coating, Fe-Al, Cr addition.*

1. INTRODUCTION

Fe-Al alloys known have a structural superiority in high temperature condition because their resistant to oxidation, sulphidation and corrosion [1-4]. This alloys posses a high strength because a high attractive force between element composer [5]. On the other hand, the mixing of this powders become intermetallic alloys with various combination. Because their superiority, this alloys is hoped to assume substitute the use of stainless steel and Ni base superalloys in several case [6-13]. The lack of this alloys are brittle in room temperature and strength decrease when the temperature above 600^{o}C. Several approaches has been developed to decrease the lack of this alloy, one of the approach is adding element like Cr [14-15]. The other approach is nanostructured material that can be increase the ductility of intermetallic [16].

Coating Fe-Al with nanostructured on steel has been done by Grosdidier *et al*. [16], Ji Gang *et al*. [17] and Guilemany [18]. The temperature is used for thermal spray as high as 2350^{o}C [16]. Intermetallic FeAl was formed on coating and have a nanostructured [16-18]. The recent research showed combination of ball mill and pack cementation was used to coating the steel [19]. Intermetallic Fe_2Al_5 was formed after 15-120 minute at temperature 400-600^{o}C. This result is faster if compare with the conventional pack cementation. Ball mill was used is responsible to form the nanostructure coating.

This research is to investigate the intermetallic Fe-Al coating on structural steel. Beside that, this research was investigated the form of nanostructure powder and coating of Fe-Al powder.

2. EXPERIMENTAL METHOD

Materials used in this research are Al (purity above 90%) and Fe (purity more than 99% with size 10 µm) obtained from Merck Co. Ltd. Cr powder (purity above 99% with size -200 mesh) obtained from Soekawa Chemical. Composition of powder are Fe-40at.%Al and Fe-40at.%Al-3at.%Cr.

Coating conducted by using high energy milling HEM-E3D for 32 hours in inert condition by using argon gas with the speed determined at 263 rpm. Milling use the vial with the volume 100 mL made from stainless steel. Ball mill was used are made from chrome steel with size 10 mm and 2 mm. The comparison between big ball and small ball is 1:5 with the ball to powder ration (BPR) is 8:1. To keep the temperature during milling is lower (25-50^{o}C), every 5 minute HEM-E3D taken a rest for 1 minute. Result of the milling was characterized using SEM Leo 430 and XRD Philips with anode tube CuKa.

3. RESULT AND DISCUSSION

Figure 1 showed the XRD patterns of substrate surface is coated the powder mixture of Fe-40at.%Al in the initial state and after different milling times. From Figure 1, one can perceive coated layer occurring in the powder samples during milling. From Figure 1, it can be seen that at the early stage of MA process (0–8 h), only Fe peaks can observed and no Al peak. After milling for 16 h, Al peaks was observed with small intensity. On further milling, Al peaks was disappear and only small intensity of Al (111) was observed. This indicates that solid solution is formed since Al atoms dissolves into Fe lattice [20].

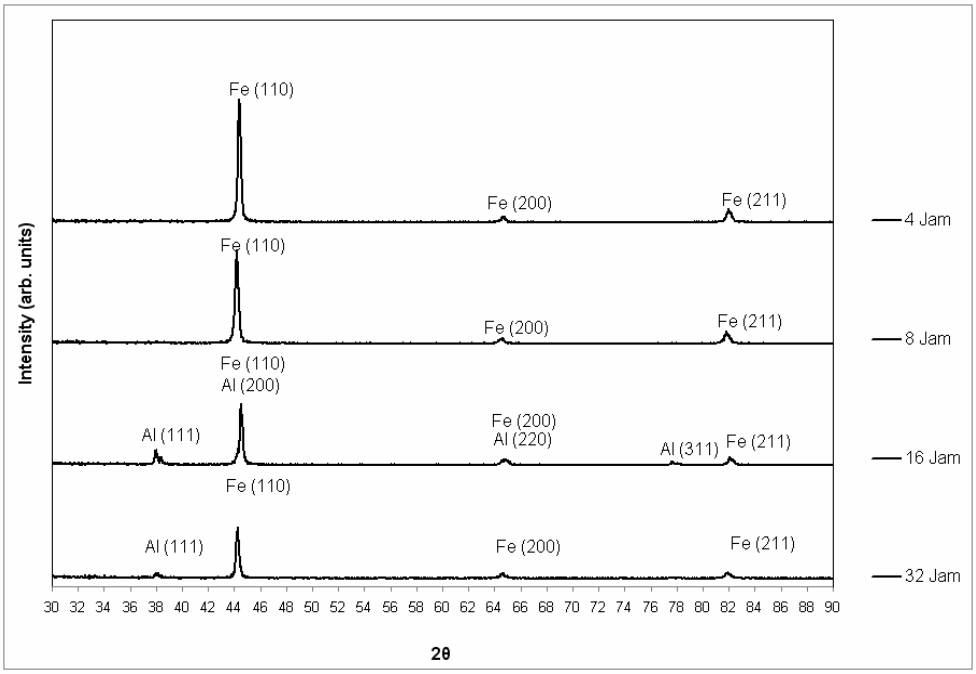

Figure 1. XRD Result of Substrate surface was coated with Fe-40at%Al powder

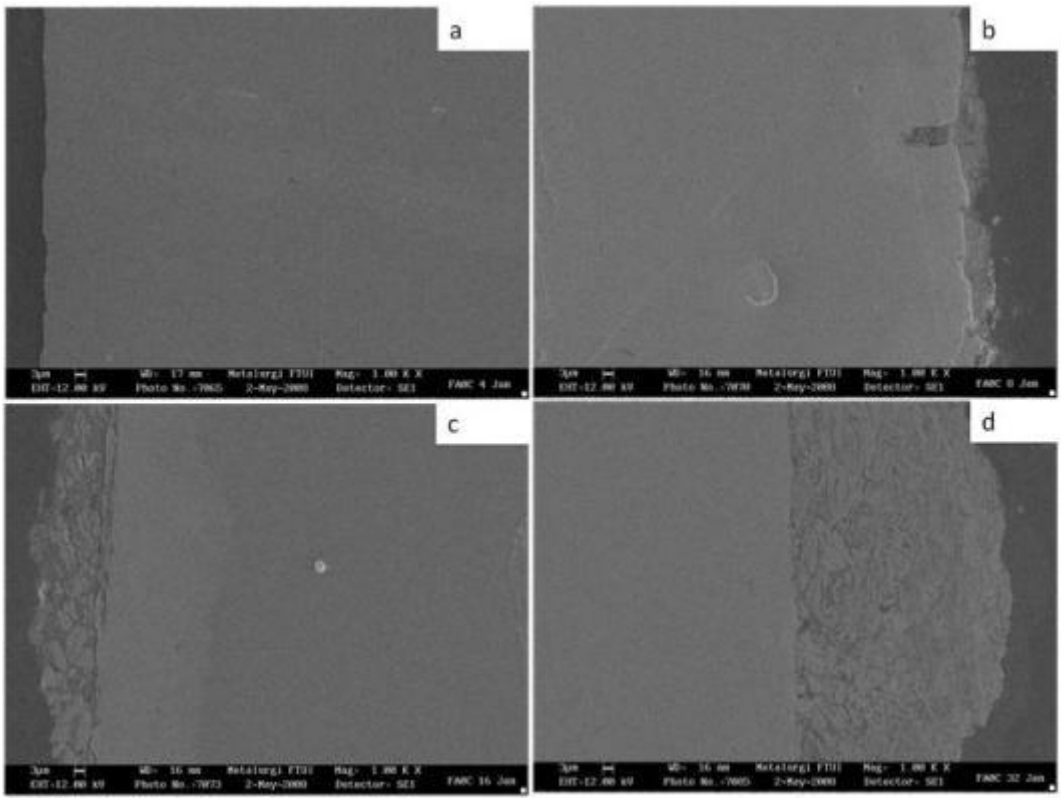

Figure 2. SEM Image of Substrate was coated with Fe-40at.%Al (a) 4 hours, (b) 8 hours, (c) 16 hours and (d) 32 hours

Figure 2 showed the cross section of substrate with Fe-40at.%Al coating. This result was appropriate with XRD result. In the early time of milling (0-8 h), there is no coating layer. Only small of powder stick on substrate found at milling time 8 hours. According to XRD result, this powder is Fe. On further milling (16 h), the coating layer is formed. The powder was coated still rough and have a big size. After milling time 32 h the coating became thick and the structure of coating smooth than before.

Figure 3 showed XRD result of substrate surface was Coated with Fe-40at.% Al-3at.% Cr. On the addition 3at.% Cr, MA process seen more quickly. This indicated with the shift to the left at the peak of the Fe (110) starting from milling time 16 h. This shift of peak indicated phase transformation of Fe-Al to FeAl or Fe_3Al. In addition, the peak Al (311) is not appear on the milling time 16 hours. This is different with Fe-40at.%Cr in which the Al (311) peak still observed in milling time 16 hours.

Cr addition effects have observed on layer thickness as showed in Figure 4. The coating layer became thickness on further milling time. There is different between Cr addition and without Cr addition. Coating layer with Cr addition thicker than without Cr addition.

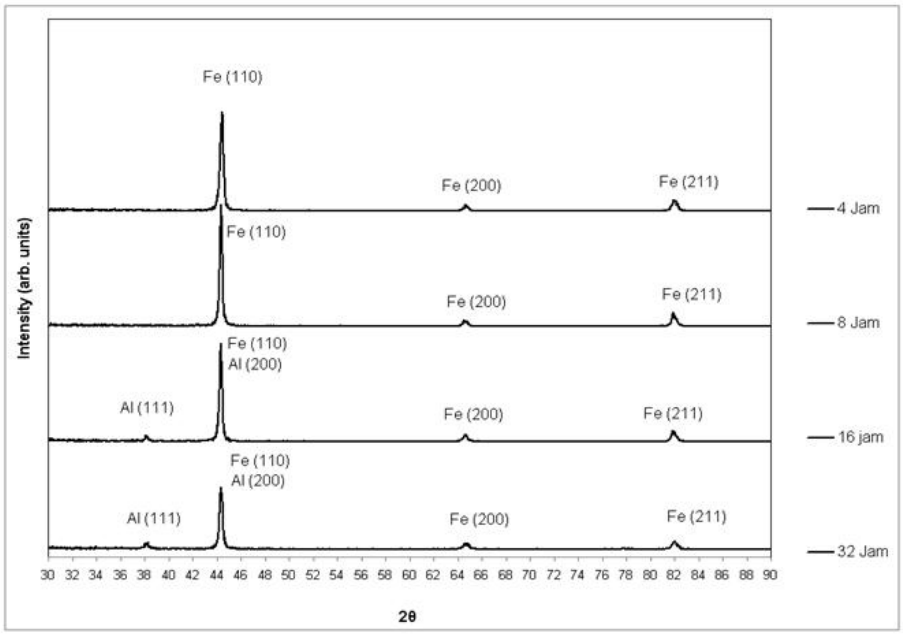

Figure 3. XRD Result of Substrate surface was coated with Fe-40at%Al-3at.%Cr powder

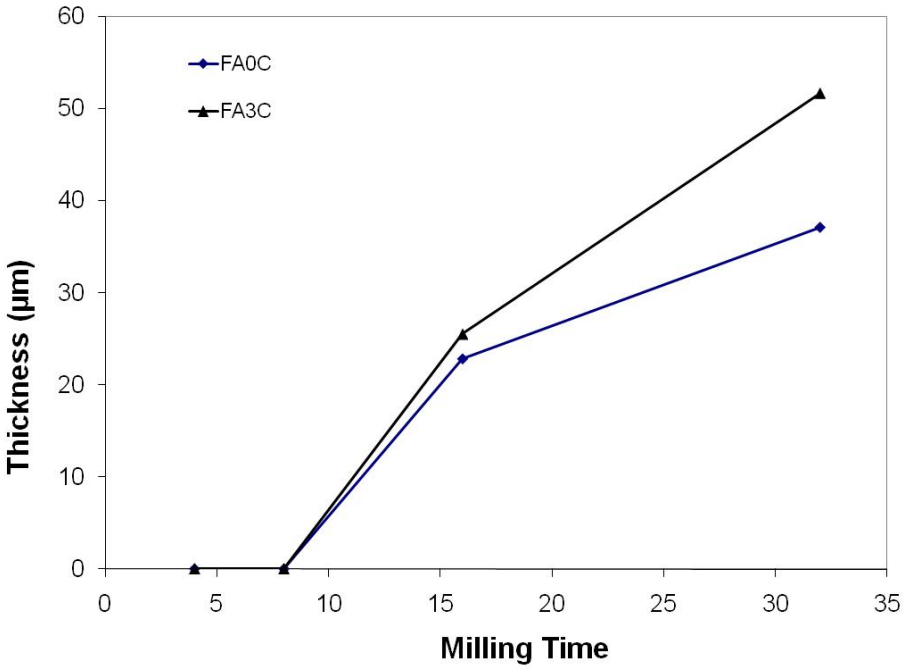

Figure 4. Coating Layer Thickness

4. CONCLUSION

1. The coating layer was formed after milling time 8 hours.
2. Influence of Cr addition was observed on pulverized of Al and thickness of coating layer.

5. REFERENCES

[1] S.C. Deevi, V.K. Sikka, Intermetallics **4** (1996), pp. 357-375.

[2] C.G. McKamey, N.S. Stoloff, V.K. Sikka, "Physical metallurgy and Processing of Intermetallic Compounds, (1996), Chapman and Hall, London, pp.351-391.

[3] S.C. Deevi, V.K. Sikka, P.J. Maziasz, R.W. Cahn, Proceedings of the International Symposium on Nickel and Iron Aluminides: Processing, Properties, and Applications, ASM, Materials Park, OH, (1996), pp. 145-156, 361-375.

[4] M. Hashii, Y. Hosoi, "Characterization of FeAl Intermetallic Compound in the Process of Mechanical Alloying, TMS, (1998), pp. 2425-2430

[5] P.H Shingu, K.N. Ishihara, "Non-Equlibrium materials by Mechanical Alloying", Material Transaction, JIM, Vol. **36**, 2, (1995), pp. 96-101.

[6] N.S. Stoloff. MRS Symp.Proc., MRS, **39** (1985), pp. 3-27.

[7] C.G. McKamey, J.H. De Van, P.F. Tortorelli, and V.K. Sikka, J. Mater.Res, **6** (1991), 1779-1805.

[8] N.S. Stoloff, C.T. Liu, Intermetallics, **2** (1994), 75-87.

[9] C.G. McKamey, P.J. Maziasz, G.M. Goodwin, T. Zacharia, Matls. Sci. and Engin.,**A174** (1994), 59-70.

[10] P.J. Maziasz, G.M. Goodwin, D.J. Alexander, S. Viswanathan, Proceedings of the International Symposium on Nickel and Iron Aluminides: Processing, Properties, and Applications, (1996), 157-176.

[11] R.H Rabin, R.N. Wright, Metall. Trans., **22A**, (1991), 277-286.

[12] J.S. Sheasby, Int. J. Powder Metall. Powder Technol., **15(4)**, (1979), 301-305.

[13] D.J. Lee and R. M. German, Int. j. Powder Metall. Powder Technoll. **12** (1985), pp.9-21.

[14] G. Sharma, R. Kishore, M. Sundararaman, R.V. Ramanujan. Materials Science and Engineering **A419** (2006) 144-147

[15] C.G. McKamey, C.T. Liu, Scripta Metall. Mater. **24** (1990) 2119–2122.

[16] Thierry Grosdidier, Albert Tidu and Han-Lin Liao. Scripta mater. **44** (2001) 387–393

[17] Ji Gang, Jean-Paul Morniroli, Thierry Grosdidier. Scripta Materialia **48** (2003) 1599–1604

[18] J.M. Guilemany, C.R.C. Lima, N. Cinca, J.R. Miguel. Surface & Coatings Technology **201** (2006) 2072–2079

[19] Zhaolin Zhan, Yedong He, Deren Wang, Wei Gao. Intermetallics **14** (2006) 75–81

[20] Hongwei Shi, Debo Guo, Yifang Ouyang. Journal of Alloys and Compound **455** (2008) 207-209.

Material Properties of Novelty Polyurethane Based On Vegetable Oils

Anika Zafiah Mohd Rus

Faculty of Machanical and ManufacturingEngineering
University Tun Hussein Onn,86400, Johor, Malaysia
Tel : (012) 7282205, (006) 07 4537823
E-mail : zafiah@uthm.edu.my, anika63@hotmail.com.my

ABSTRACT

Bio-polymer from vegetable cooking oils was synthesis to substitute petrochemical derivatives polymer in a specific treatment in order to ease the degradation pathways. Treatment with titanium dioxide (TiO_2) was found to affect the physical properties of this solid polymer in a systematic way. As the loadings of TiO_2 were increased (up to 10% of monomer weight), large strain responses were obtained; thus the stress vs. strain curves plotted by the Instron tensile test showed an increase from 5% to 31%. This study also revealed a remarkable characteristic in the pigmented polymer exhibiting soft – but – tough behaviour at high TiO_2 loading. The DMTA test also showed that the properties of the sample loaded with 10 % TiO_2 increased its tan delta peak (damping factor) from 0.43 to 0.7. The tan delta peak showed that the damping properties of the material were improved markedly upon loading with TiO_2. This is useful since noise is radiated by vibration, and the application of damping materials to the vibrating surface converts the energy into heat, which is dissipated within the damping materials rather than being radiated as airborne noise.

Keywords: *Polyurethanes, 4,4'-methylen-bis-(phenylisocyanate), damping, titanium dioxide, rapeseed.*

1. INTRODUCTION

In recent years, the use of polymers made from renewable materials has been developed in diverse areas especially in furniture, mattresses, automotive or building components. Polyurethanes (PU′s) made from renewable materials are one of the most important groups of polymers because of their versatility and they can be manufactured in a wide range of grades, densities and stiffness. In this project, polymers based on renewable materials such as rapeseed (RS) and sunflower oil (SF) were synthesized and cross-linked with methylene di-*p*-phenyl diisocyanate (MDI) to form highly crosslink polymer name as polyurethanes.

Currently, fossil or petroleum-based is used as raw materials needed to make industrial chemicals and nearly all types of plastics. However, nowadays plants could provide a renewable, biodegradable source of high value speciality product such as nylon, glue, paints, cosmetics, lubricants, components of detergents or plastics. These could all be produced from plants rather than fossil or petroleum-based materials. The sustainability of this industrial sector is dependent in the long term on a fundamental shift in the way in which resources are used, from non-renewables to renewables, from high levels of waste to high levels of reuse and recycling, and from products based on lowest first cost to those based on life cycle costs and full cost accounting, especially as applied to waste and emissions from the industrial processes that support construction activity [1].

1.1 Modification of Polymers using fillers

Fillers, either particulate or of fibrous nature, as glass, metal oxides, natural fibres and metals, have been added to thermoplastics and thermosets for decades to form polymer composites. Fillers are used in polymers for a variety of reasons: cost reduction, improved processing, for example in curing with a cross-linking agent such as in sulphur vulcanization, density control, optical effects, thermal conductivity, control of thermal expansion, electrical properties, magnetic

ISSN 114-1284

properties, flame retardancy and improved mechanical properties, such as hardness and tear resistance and many more reasons.

The term 'functional filler' is often used to describe materials that do more than provide cost reduction. Examples of functional fillers include carbon black and precipitated silica reinforcements in tyre treads, the role of stabilisers to reduce in-process degradative effects, and many more miscellaneous additives for polymers such as blowing agents, impact modifiers, lubricants or antimicrobials. Increased polymer consumption over the past twenty years has not only stimulated developments in manufacturing plant, but has also led to a parallel growth in the usage of a large variety of liquid and solid modifiers, including fillers and reinforcements [2]. Fillers may be classified broadly as organic or inorganic substances, and further subdivided according to chemical family.

2. METHODOLOGY

2.1 Preparation of Novelty Hydroxylated Monomer

The development of novel feedstocks for polyurethane monomer derived from renewable materials has become important because the use of polyurethane polymers is increasing at a rate of 1 million tonnes a year [3]. This level is unsustainable in the long term without the development of alternative sources. Oils from vegetable crops can be manipulated chemically to produce a variety of polymeric materials, including polyurethane products.

The reaction of organic isocyanate with compounds containing OH (hydroxyl) groups is capable of wide application in polymer formation [2]. Thus the urethane linkage, –(NHCOO)- can be produced by reacting compounds containing active hydrogen atoms with isocyanate, where polymer formation can take place if the reagents are di- or polyfunctional. The preparation of the hydroxylated monomer was divided into two stages, beginning with the preparation of catalyst (hydrogen peroxide / tungsten powder / phosphoric acid) to generate the epoxides from the unsaturated fatty compounds, while the second stage comprised the acid-catalysed ring-opening of the epoxides to form polyols

2.2 Preparation of Novelty Polyurethanes Polymer

Viscous polyurethanes find application in their liquid state as adhesives or sealants. The polyol monomers can be further polymerised or 'cured' to higher molecular weight solid materials. The curing process involves the addition of a cross-linking agent such as MDI, which allows the polyol group to form a urethane bridge.

The test specimens were prepared according to the standard dumb-bell shape of the tensile test. The dimensions of the samples are as type 1A and 1B (BS EN ISO 527-2:1996). The method is appropriate for use with rigid and semirigid thermosetting moulding and cast materials, including filled and reinforced compounds. The samples for the dumb-bell tensile test were prepared by mixing 15 g (3 g equivalent) of polyol and an appropriate amount of 4,4′-methylene-bis- phenylisocyanate (MDI), different percentages of titanium dioxide (such as 2.5, 5.0, 7.5 and 10.0 % equivalent weight of polyol) and pouring the mixture into the dumb-bell shaped mould.

2.3 Testing of Novelty Polyurethanes Polymer

Polymers can be characterised by a variety of means such as tensile test (disclosing the stress-strain relationships), Dynamic Mechanical Thermal Analysis (DMTA) and many more. The tensile testing of dumb-bell shaped samples was carried out according to ISO 527-2:1996 using an Instron tensile testing machine Model 4303 with installed computer programme. The machine was run at a crosshead speed of 5 mm/min.

A Tritec 200 DMTA (Triton Technology) instrument was employed for dynamic evaluation of the novelty polyurethane. Rectangular test pieces of polyurethane (~15 mm long, 10 mm wide, 2.3 to 2.4 mm thick) were tested in a standard air oven with a single cantilever mode using test frame L and clamp type C at a frequency of 0.5 Hz with a heating rate 5°C/min. In this system, a sinusoidal stress is applied to a vibrator unit using a sinusoidal current. The stress imposed upon the specimen is therefore directly related to the amount of current delivered to the vibrator. All the specimens were studied between 25° C and 150° C.

3. RESULTS AND DISCUSSION

3.1 Effect of addition of TiO_2 on DMTA for Novelty Polyurethanes Polymer

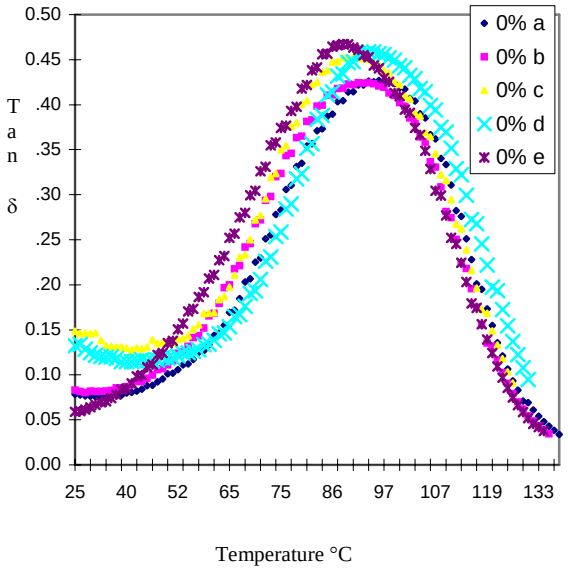

Figure 3.1. Value of tan δ determined by DMTA for 5 samples of neat novelty Polyurethane

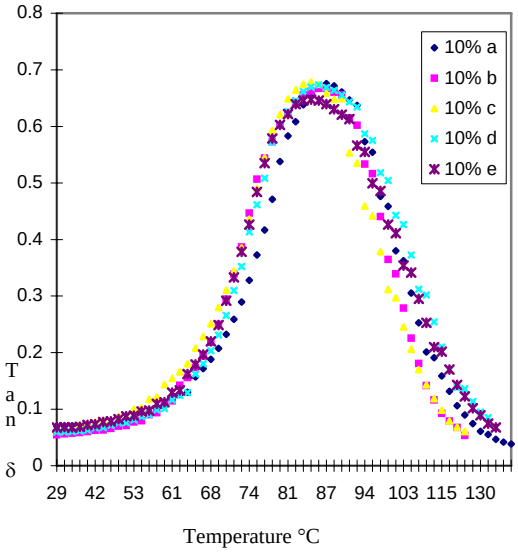

Figure 3.2 Value of tan δ determined by DMTA for 5 samples of novelty Polyurethane loaded with 10% of TiO_2

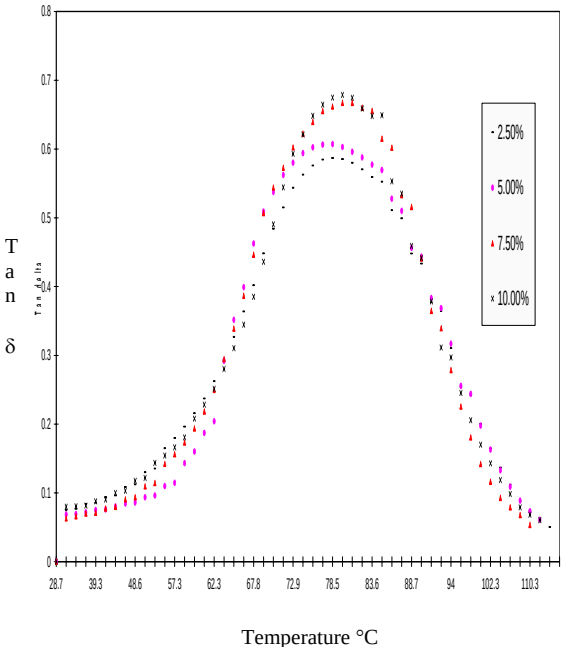

Figure 3.3 Value of tan δ determined by DMTA for novelty Polyurethane loaded with different percentages of TiO_2

The temperature at the maximum value of tan δ corresponds to T_g at which the tan δ value indicates the damping response of the resins. The temperature range for efficient damping (tan δ >0.3) for most of the common homopolymers is around 20 to 30°C [4]. A high tan delta (δ) value is essential for good damping properties. Damping refers to the capacity of a material to dissipate energy during vibration, and is often linked to the mobility of microstructural defects. Polymeric materials with a high damping factor play an important role as insulating or automotive interior components [5]. Commercially, polymers may be applied to the surface of a vibrating substrate to increase damping [6].

The glass transition temperature (T_g) of a composite is important to analyse because the interaction modes between the polymer and the added components can be determined. The glass transition region is the region of maximum damping, at which stage the polymer changes from the glassy to the rubbery state. The broadening of the glass-to-rubber transition is partly due to a broad distribution in the chain length distribution between crosslinks (7-8).

Referring to Figure 3.1 and Figure 3.2 for neat and loaded with TiO_2 (10% of monomer weight) respectively, the results shows the composite of novelty Polyurethane increased its average tan δ peak from 0.45 to 0.7. The sharply increasing the value of tan δ peak showed that the damping properties of the material were improved marked upon progressive loading with TiO_2 but narrowing the glass-to-rubber transition curve. This interesting result may be attributed to both the inherent characteristics of TiO_2 and the development of chemical interactions between the polymer and TiO_2. The T_g value of a polymer is related to the movement of segments of polymer chains in free spaces [9-11].

3.2 Effect of addition of TiO_2 on Tensile Strength for Novelty Polyurethanes Polymer

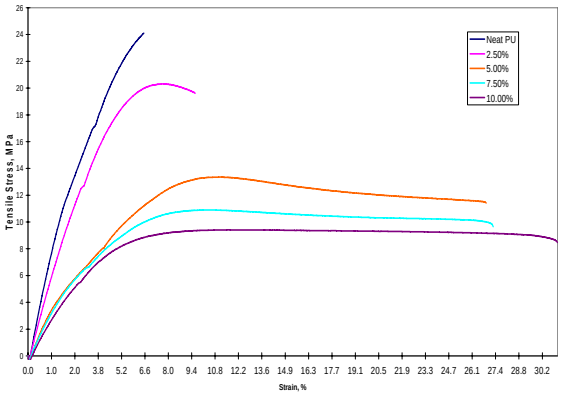

Figure 3.4 Influence of TiO_2 loading for tensile strength of Novelty Polyurethanes samples

Figure 3.4 shows the tensile strength of Novelty Polyurethanes upon loading with TiO_2. The tensile strength decreases, and the elongation to break (%) increases, with increasing levels of TiO_2 composites. Treatment with TiO_2 was found to affect the physical properties of the polyurethane in a systematic way. As the loadings of TiO_2 increased (up to 10% of monomer weight), large strain results were obtained; thus the stress vs. strain curves plotted by the Instron tensile test showed an increase from 5% to 31%. Increase in elongation to break showed a remarkable characteristic exhibiting soft – but – tough behaviour [12], where the toughness of the material is the area under the stress-strain curve.

4. CONCLUSION

Polyurethanes (PUs) have been synthesised successfully from renewable resources namely vegetable oils (rapeseed, sunflower), using MDI as the cross-linking agent. The triglycerides in these vegetable oils provide the alkene functionality as the basis for ultimate conversion to reactive hydroxyl groups. Epoxides can be readily prepared by treatment of the alkenes with a peroxide (for example, hydrogen peroxide, H_2O_2). The ring-opening of the epoxides to yield hydroxylated triglycerides was achieved using hydrochloric acid. The mechanism of urethane formation in the final step is via a nucleophilic attack of the hydroxyl group on the isocyanate groups of MDI.

The tensile test was conducted with different PU samples composites from different batch preparations. As the loading of TiO_2 was increased (up to 10 % of monomer weight), the elongation to break was improved as the TiO_2 loading was increased from 5 % to 31 % (for polyurethanes loaded with 10 % TiO_2). Therefore by increasing the level of TiO_2, one can alter the mechanical properties of the polymer as desired.

A single loss tangent peak was observed in the DMTA test. A high tan delta peak is essential for a good damping material. The loss tan δ peaks for the polymer loaded with 2.5, 5, 7.5, 10 % of TiO_2 were 0.58, 0.6, 0.68, and 0.71 respectively as compared with neat novelty polymer at only 0.43. These data shows that the damping ability is enhanced through the introduction of TiO_2 into the polymer.

ACKNOWLEDGMENT

The author would like to thank Universiti Tun Hussein Onn Malaysia (UTHM), Johor, Malaysia for supporting this research under Short Term Research Grant.

REFERENCES

[1] Kibert C.J., Sendzimir J., *Construction Ecology: Nature as a basis for green buildings,* , J & Guy, London and New York: Spon Press, 2002; pp. 7.
[2] Robert S. M., Chambers D., Balazs B., Cohenour R., Sung W., *Polym. Degrad. Stab.*2003;82: 193-196.
[3] Andrew J. C., *Private Communication (Final Report)*, 2003.
[4] K. Ueberreiter, G. Kanig, *J Chem Phys.* 1950:**18**,399-406.
[5] W. Chang, T. Baranowski, and T. Karalis, *J. Appl. Polym. Sci*. **51**, 1077-1085 (1994)
[6] *J. Mater. Chem*., 2-000: 2666-2672.
[7] Z. Petrovic, M. Ilavsky, K. Dusek, M. Vidakovic, *J. Appl. Polym. Sci*. 1991: **42**, 391-398.

[8] P. Bonardelli, G. Moggi and A. Turturro, *Polym*, 1986:27, 905.
[9] A.R. Shultz and A. L. Young, *Macromolecules*, 1980:13, 663.
[10] R. F. Boyer, *J. Polym. Sci., Part C: Polym. Symp*., 1966:14, 267.
[11] R. W. Warfield and B. Hartmann, *Polym*, 1980: 21, 31.
[12] J.M.G. Cowie, *Polymers: Chemistry & Physics of Modern Materials*, 1991,Chapman & Hall.

Proceeding of the 11th International Conference on QiR (Quality in Research)
Faculty of Engineering, University of Indonesia, Depok, Indonesia, 3-6 August 2009
ISSN 114-1284

Design of Diethyl Carbonate Reactive Distillation Column Process

Anisatur Rokhmah, I-Lung Chien, Renanto Handogo

Chemical Engineering Department
Sepuluh Nopember Institute of Technology, Surabaya 60111
E-mail : a.rokhmah@gmail.com

ABSTRACT

This research introduces a study about reactive distillation column system to produce diethyl carbonate by using ASPEN PLUS ™. Further study about reactive distillation system is required to be developed in order to gain industrial process improvement, especially in diethyl carbonate (DEC) production. Suitable thermodynamic and kinetic model parameters from ASPEN PLUS ™ regressions are used to describe this process. The purpose of method is to obtain the optimum process design and operating condition. The optimum process design and flowsheet is shown by minimal total annual cost (TAC). For a steady state condition, optimal condition is reached by 8:1 feed ratio of EtOH:DMC, 38 total trays of distillation column, feed location of dimethyl carbonate (DMC) at 29th stage and feed location of ethanol (EtOH) at 3th stage. From previous system we create one more system to recycle EtOH in order to complete overall system.

Keywords : *ASPEN PLUS™, diethyl carbonate, dimethyl carbonate, process design, reactive distillation*

1. INTRODUCTION

Reactive distillation (RD) is a combination of separation and reaction in a single vessel. Reactive distillation is important in industries because of its benefits that represent in improvements of process efficiency and economic. Advantages of the using of reactive distillation are : increase process efficiency and reduction of investment and operational costs, chemical equilibirium limitations can be overcome, higher selectivities can be achieved, auxiliary solvents can be avoided, azeotropic or boiling mixtures can be more easily separated. This research focusing on diethyl carbonate (DEC) production. DEC is one of the promising candidates for oxygen-containing fuel additive, which has been reported by many researchers. It has more oxygen content than methyl tert-butyl ether (MTBE) (40.6 versus 18.2) and hence not so much needed to have same effect. Engine texts show that DEC reduces particulate emissions almost 50% when the engine is under load. Without load, particulate emissions are reduced by approximately 30% **.** The gasoline/water distribution coefficient of DEC is more favorable than that of dimethyl carbonate and ethanol. So DEC is readily miscible with fuel and does not phase separate. It is also more readily biodegradable. All the properties make DEC an attractive alternative oxygen-containing fuel additive (Wang et al., 2007).

2. THERMODYNAMIC MODEL

Chemical reactions, phase equilibrium characteristic, and transport phenomenon are required to be concerned to obtain a perfect reactive distillation system design. In order to have best operation condition, that is providing production efficiency and reducing energy cost, it is needed to carefully selecting the thermodynamic models in a reactive distillation column system. In this research, UNIQ–RK model is chosen for the description of the thermodynamics of mixture. Experimental data from literatures are used to enhance the thermodynamic predictability of ASPEN properties by using regression.

This systems includes five components: dimethyl carbonate (DMC), ethanol (EtOH), ethyl methyl carbonate (EMC), methanol (MeOH), dimethyl carbonate (DMC). They does not have miscibility gaps, however three binary azeotropes appear in this system, that are : MeOH-DMC, EtOH-MEC, and EtOH-DMC.

This research provides regression for vapor-liquid equilibrium data by using UNIQ-RK model parameter. The UNIQ-RK model can describe strongly nonideal liquid solutions and liquid-liquid equilibrium. Several literatures have conducted the experimental data for components in this system. Regression is required to have a high accuracy prediction model compared to experimental data.

Experimental data for components is obtained from papers. Methanol-DEC vapor liquid equilibrium experimental data is provided from Rodriquez (Rodriguez et al., 2003); EtOH-DMC and MeOH-DMC vapor liquid equilibrium experimental data are also provided by Rodriguez (Rodriguez et al., 2002) in different paper; EtOH-EMC, EtOH-DEC, and DMC-DEC vapor liquid equilibrium experimental data are obtained from Luo (Luo et al., 2000). The other vapor-equilibrium plots for MeOH-EMC, EMC-DEC, and DMC-EMC that have no experimental data in any literatures are based on UNIFAC model parameter from ASPEN built in system. ASPEN offers many built in model parameters; UNIFAC model parameter that used to predict vapor liquid equilibrium for remained components is one of features that support by ASPEN. Thus, all the vapor equilibrium plots can be accomplished.

Table 1 : Boiling Temperatures of Pure Components

Components	Boiling points (°C)
MeOH	64.7
EtOH	78.4
DMC	90.4
EMC	107.9
DEC	126.5

Table 2 : UNIQ-RK model parameters

i	DMC	MeOH	EtOH	EtOH	EtOH
j	DEC	EtOH	DMC	DEC	EMC
T	K	K	K	K	K
bij	-432.23	-291.81	-53.32	0.311	-53.70
bji	253.10	196.451	-120.39	-164.97	-123.79

i	MeOH	MeOH	EMC	EMC	EMC
j	DEC	DMC	MeOH	DEC	DMC
T	K	K	K	K	K
bij	75.89	-29.27	-288.63	13.195	18.12
bji	-422.75	-245.43	69.21	-22.28	-24.61

Table 3. Azeotropes

	P (KPa)	T(°C)		mole (%)	
		a	b	a	b
MeOH + DMC	25.6	32.16	31.8	82.91	80.82
	38.65	40.89	40	83.98	82
	53.09	48.01	47.8	84.81	83.23
	101.33	63.7	62.7	86.56	86.77
	101.3	63.7	63.43-63.9	86.56	85.03-86.8
	102.52	64	64.1	86.59	85.04
	273.24	91.46	91.4	89.27	88.97

	P (KPa)	T(°C)		mole (%)	
		a	b	a	b
EtOH + DMC	24	41.64	40	61.16	57
	101.33	75.39	74.9-75.31	70.26	66-70.55

	P (KPa)	T(°C)		mole (%)	
		a	c	a	c
EtOH + EMC	101.3	77.9	78.9	90.87	95

a. ASPEN split (UNIQ-RK).
b. Gmehling et al.
c. Luo et al.

3 KINETIC MODEL AND PARAMETERS

Transesterification of dimethyl carbonate (DMC) with ethanol to produce diethyl carbonate (DEC) occurs in this reactive distillation system. This system consists of two consecutive reactions with the intermediate product of ethyl methyl carbonate (EMC). The main product is DEC that known as an important reactant and solvents for many chemical processes. Hu-Ping Luo and Wan-De Xiao in 2001 have determined some expressions to represent the kinetic of this reactions and in the year of 2004, another kinetic parameters of this reactions that has been used by Mueller and Kenig (Mueller and Kenig, 2007). This research uses Richter kinetic parameter (Mueller and Kenig, 2007) in ASPEN simulation.

DMC + EtOH ⇔ EMC + MeOH (a)

EMC + EtOH ⇔ DEC +MeOH (b)

Homogeneous catalyst that applied to reactive distillation system complicates in product purification. Heterogeneous catalyst provides significant conversion, selectivity, and solve purification problems. Potassium carbonate (K_2CO_3) is used in this system as suggested as an appropriate catalyst by Angeletti (Mueller and Kenig, 2007). This reaction is a reversible reaction, the reaction rate type is as follows:

$$r_1 = k_{+1} x_{DMC} - k_{-1} x_{EMC} x_{MeOH} \quad (3.1)$$

$$r_2 = k_{+2} x_{DMC} - k_{-2} x_{EMC} x_{MeOH} \quad (3.2)$$

$$k_{+m} = k_{0,m} \exp\left(\frac{-E_{A,m}}{RT}\right) \quad (\text{for } m = 1, 2) \quad (3.3)$$

$$k_{-m} = \frac{k_{+m}}{K_{reac,m}^{eq}} \quad (\text{for } m = 1, 2) \quad (3.4)$$

Where :

K_{reac}^{eq} = reaction equilibrium constant

K = reaction velocity constant [mol.kgcat^{-1} .s^{-1}]

R = gas constant [J .mol^{-1} .K^{-1}]

T = temperature [K]

r = reaction rate related to catalyst mass [mol .kgcat^{-1} s^{-1}]

x = liquid-phase mole fraction [mol/mol]

Table 4 : *Kinetic parameters*

Reaction	Activation energy E_A (J/mol)	Frequency factor k_0 (mol s^{-1} $kgcat^{-1}$)
a	39971	2.54×10^5
b	37258	2.02×10^4

6. DISCUSSION

Figure 1: Design system of reactive distillation column process

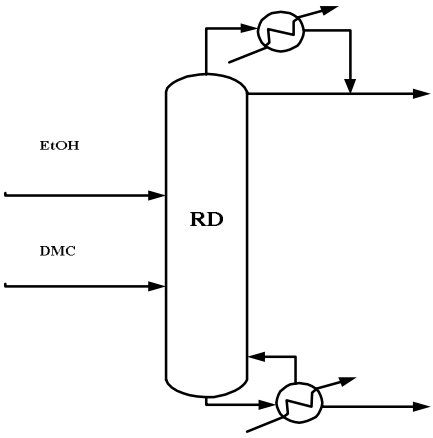

This is system of reactive distillation system to produce DEC. We set design specs and varies for this system by fix mole purity of DEC at bottom is 0.995 and conversion od DMC is 0.995 %. This system is run by using ASPEN PLUS ™ to design proper distillation system and achieve design specs and varies. Optimum design is determined by calculation of TAC. By changing feed ratio of EtOH and DMC, minimum TAC can be reached.

This figure shows total annual cost (TAC) for several feed ratio. From that figure, it is known that total annual cost minimum for this process is obtained in 8:1 feed ratio of EtOH:DMC with reactive section from 3rd tray until 29th tray. From this feed ratio, it observed later to get a specific feed location that provides optimum design of DEC production in reactive distillation column system.

Figure 2: TAC minimum by varying the feed ratio of EtOH/ DMC

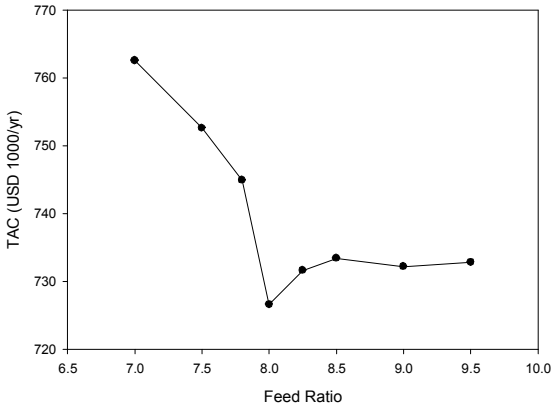

Figure 3: TAC minimum by varying the feed location of EtOH and DMC

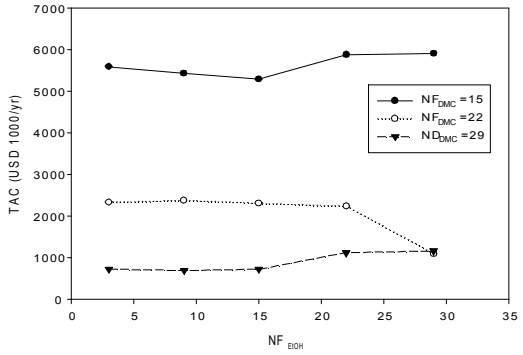

From that figure, total annual cost minimum is obtained by 8:1 ratio of EtOH : DMC and feed location of DMC is at 29th tray and feed location of EtOH 9th tray. Total annual cost minimum is 692.33 (USD 1000/yr).

7. CONCLUSION

Reactive distillation is becoming an important part of industrial improvement. It provides efficiency production and several advantages that develop conventional distillation system. This research is one case of reactive distillation column system in producing diethyl carbonate (DEC) that has been known as important product in industry. By using ASPEN PLUS ™, we design a system to obtain minimum total annual cost. Thermodynamic model and kinetic parameters are chosen accurately to fit the simulation and experimental data. From simulation, total annual cost minimum for optimum design are determined by set feed ratio of EtOH/DMC to 8:1 and feed location of DMC is at 29th t tray and feed location of EtOH 9th tray.

REFERENCES

[1] Rodriguez, J. Canosa, A. Dominguez, J. Tojo., "Fluid Phase Equilibria", vol 201, pp 193-194, 2002.
[2] A. Rodriguez, J. Canosa, A. Dominguez, J. Tojo, Isobaric Phase Equilibiria of Diethyl Carbonate with Five Alcohols at 101.3 kPa", Journal of Chemical and Engineering Data, Vol. 48, No. 1, 2003.
[3] D. Wang, B. Yang, X. Zhai, L. Zhou, "Synresearch of diethyl carbonate by catalytic alcoholysis of urea", Fuel Processing Technology, vol. 88, pp. 807–812, 2007.
[4] H. P. Luo and W. D. Xiao, "A reactive distillation process for a cascade and azeotropic reaction system: Carbonylation of ethanol with dimethyl carbonate", Chemical Engineering Science, vol 56, 2001.
[5] H. P. Luo, W. D. Xiao , and K. H. Zhu, "Isobaric Vapor-Liquid Equilibria of Alkyl Carbonates with Alcohols," Fluid Phase Equilibria., vol 175, 2000.
[6] I. Mueller and E. Kenig, " Reactive Distillation in a Dividing Wall Column : Rate-Based Modeling and Simulation". Ind. End. Chem. Res., vol 46, pp. 3709-3719. 2007.
[7] J. Gmehling, J. Menke, J. Krafczyk, K. Fischer, "Azeotropic Data", Germany :Wiley VCH, 2004.
[8] Okasinski, J. Matthew, and M. F. Doherty, "Design Method for Kinetically Controlled, Staged Reactive Distillation Columns," Ind. Eng. Chem. Res.,vol 37 (7), pp 2821–2834,1998.
[9] Okasinski, J. Matthew, and M. F. Doherty, "Thermodynamic Behavior of Reactive Azeotropes," AIChE. Journal, vol 43 (9), pp. 2227-2238, 1997.

Proceeding of the 11th International Conference on QiR (Quality in Research)
Faculty of Engineering, University of Indonesia, Depok, Indonesia, 3-6 August 2009
ISSN 114-1284

Characterization of Composite Membranes Synthesized by Photo-Grafting Polymerization of Polysaccharide with Methyl Methacrylate

Asep Riswoko

Centre for the Technology of Material, BPPT
Jl. MH Thamrin 8, Jakarta 10340
Tel : (021) 3169887. Fax : (021) 3169873
E-mail : asepriswoko@webmail.bppt.go.id

ABSTRACT

Composite membranes were synthesized by photo-grafting polymerization of polysaccaharide celulosic palmitat with a functional monomer methyl methacrylate (MMA) and a photoinitiator (darocure 1173) using UV irradiation. As result, polysaccharide-polymethylmethacrylate compo-site membranes with several weight ratio composition were obtained. The membranes' surface texture, mechanical performance and capacity to adsorb 2-(4-isobutyl-phenyl)-propionic acid (ibuprofen) from methanol solution was evaluated yielding information regarding the effect of the concentration of functional monomer on the resulting membranes' properties.

The composited membranes showed significantly higher mechanical and sorption capability to ibuprofen than that of uncomposited polysaccharide membrane. With the composite insitu polymerization technology, high mechanical properties of the hydrophilized membrane could successfully be combined with the synthetic polymer, yielding substance-specific polymer composite membranes. By the inexpensive preparation provides a good basis for the development of applications of composite membrane polymers in separation processes such as solid-phase selective permeation.

Keywords

Composite membrane; Photo-initiated graft copolymerization; Solid-phase selective permeation

1. INTRODUCTION

A membrane is a layer of material which serves as a selective barrier between two phases and remains impermeable to specific particles, molecules, or substances when exposed to the action of a driving force. Some components are allowed passage by the membrane into a permeate stream, whereas others are retained by it and accumulate in the retentate stream. In the chiral separation technology, membrane is also attractively developed especially for mass production application due to low consumption of chemical agent, good reliability, and high effectiveness for the separation process [1]. The membrane for the chiral separation process is necessary to have a good chiral recognition, mechanical property and high productivity.

As an approach to obtain a good reliability and mechanical property of chiral membrane, polysaccharide which is known as a high chirality of natural resource polymer attempted to be functionalized with monomer methyl methaacrylate. The reaction of monomer methylmethaacrylate may lead us to obtain polymerization product, as well as poly methyl metha acrylate by using a radical polymerization. However the condition is tend to produce a bulk of homopolymer. In order to develop the physical properties of polysaccharide membrane derived from palmitoyl cellulose, a photo grafting polymerization using UV irradiation will be used as an in situ polymerization method. However, many reaction variables may influence the properties of the polysaccharide-polymethyl-methaacrylate membrane. Here, the effect of weight ratio composition and irradiation time on the producing membrane properties as well as surface texture, mechanical performance and capacity to permeate 2-(4-isobutyl-phenyl)-propionic acid (known as ibuprofen) from methanol solution will be evaluated and discussed.

2. EXPERIMENTAL SECTION

Membrane development has been carried out covering synthesis, mechanical as well as tensile strength and elongation characterization, and permeation performance. The synthesis and permeation experiment processed in BPPT laboratorium, and the mechanical testing was done in BATAN laboratorium.

2.1 Synthesis

Methyl metha acrylate (0,5 g) was poured into palmitoyl cellulose (0,5 gram) solution in dichloromethane (10 ml) in Petridis (diameter 7 cm). After darocure 1173 (0,2 ml) dropped into the mixture, the solvent was evaporated in situ at ambient temperature for 1 hour. The pre-casted membrane

was irradiated under UV lamp (Phillips 20W x 3) for 1, 3 and 5 hours, respectively.

2.2 Mechanical testing

Mechanical testing was carried out following with ASTM-D-1822-L using cutting machine of Dumb Bell Ltd., SAITAMA JAPAN. The cutted samples were then measured by Strograph-R1 (Toyoseiki) to provide the data of tensile strength and elongation ratio.

2.3 Permeation experiment

As feeding sample, 0,1M solution of ibuprofen in methanol (200 ml) was poured into the feeding chamber equipped with the composite membrane at the bottom of the chamber. The concentration of the permeated solution was calculated from obtained specific weight-concentration correlation graph after 1 to 4 hours of permeation.

Table 1. Equipment of chamber for permeation

No.	Equipment's item	Scale
1	Membrane's active area	4,9 mm
2	Diameter	2,5 inch
3	Chamber length	200 mm

3. RESULT AND DISCUSSION

3.1 Synthesis

Synthesized two types of solid flat sheet membranes, those are palmitoyl cellulose and palmitoyl cellulose-g-PMMA membranes were considered to be evaluated to understand the relationship between the membranes's consisted material and their physical properties. Obtained membranes were visually transparent as well as showed in figure 1 below.

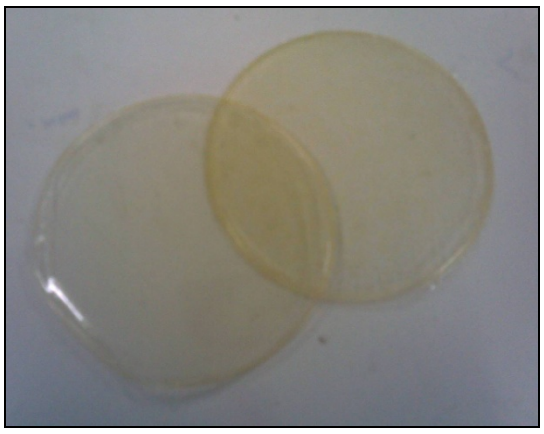

Figure 1. Palmitoyl cellulose base membranes

The preparation of membranes by UV photo grafting might provided a covalently and three-dimensionally cross linked macromolecular substances [2]. By cross linking of methyl methacrylate monomer in bulk within palmitoyl cellulose, it is possible to obtain either compact networks or swellable and/or, respectively, porous, networks with a defined interstitial structure. The effectiveness of this preparation method should be considered with their provided physical properties as well as mechanical strength and elongation ratio.

3.2 Physical properties

3.2.1 Mechanical characterization

Mechanical characterization was carried out to know the strength and the elongation ratio of the prepared membranes. The results of the mechanical test were summarized in graph (Figure 2) below.

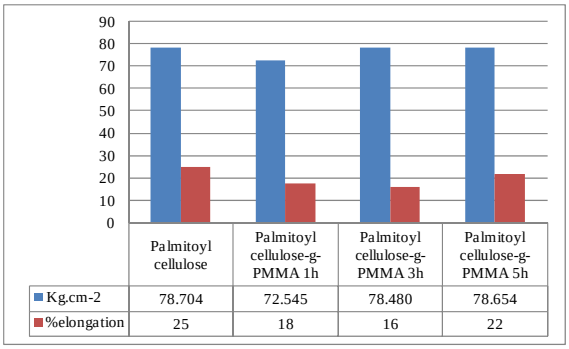

Figure 2. Mechanical properties of membranes

The graph showed a little different value between the mechanical strength of the membrane prepared purely from palmitoyl cellulose and those from grafting with poly methyl methacrylate. However, the grafting process by 1 hour UV irradiation provided the membrane with the lowest strength's value. It indicates that a longer time of irradiation was necessary to complete the polymerization process of MMA monomer. By elongation of the irradiation time for 3 and 5 hours, the mechanical strengths tend to increase up to 8.4%.

As shown in figure 2, the membrane purely prepared from palmitoyl cellulose showed the highest elongation ratio. It indicates that the palmitoyl cellulose membrane has a good plasticity. Due to the polymerization of monomer might occur completely, the closest elongation ratio to that of the palmitoyl cellulose membrane showed by the product of grafting with 5 hour irradiation. It suggests that the bulk polymerization of methyl methacrylate has worked properly in palmitoyl cellulose by enough time of UV irradiation and provided a networked macromolecular substance.

3.2.2 Surface characterization

The membranes synthesized either from palmitoyl cellulose or palmitoyl cellulose-g-PMMA showed a good full-dense membrane as seen in SEM's figure below, with have relatively a lower porosity. From the SEM's characterization, it is known that palmitoyl cellulose and PMMA were miscible each others, and no delaminating effect were observed.

The character is necessary to develop the membranes as permeation medias that distinguish each isomers of ibuprofen which have same structure and size of molecule. By inter-molecular recognition mechanism, those isomers would be separated to passage only one of the isomers.

3.3 Permeation evaluation

As the research purpose that is to develop membranes for separation, permeation of subject has been done using 2-(4-isobutyl-phenyl)-propionic acid (known as ibuprofen) from methanol solution. However, in this paper, only the permeation rate of rasemat (mix of the isomers) would be evaluated without any consideration about the enantiospecific separation.

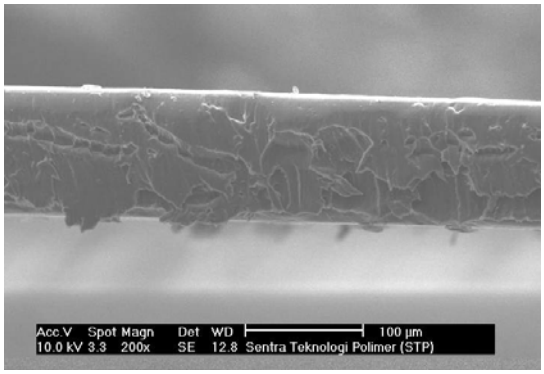

(a). Palmitoyl cellulose

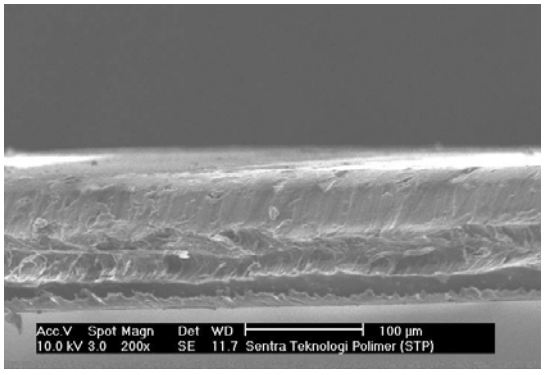

(b). Palmitoyl cellulose-g-PMMA (1 h)

Figure 3. Cross-section of membranes by SEM

With the equipment as described in table 1 and showed in figure 4 below, the permeation process has worked following to the vertical mechanism. By this mechanism, the reverse flow of the passage permeate from receiver solution might be prevented. As the result, the permeation experiment has provided a better yield of the passage permeate than that of the permeation by horizontal mechanism [3].

Figure 4. Permeation chamber

***Table 2**. Permeation result of membranes*

Membrane name	**Palmitoyl cellulose**	**Palmitoyl cellulose-g-PMMA**		
Preparation	**pure**	**1 hour**	**3 hours**	**5 hours**
Average of membrane thickness (mm)	**0.15**			
Object of permeate	**Ibuprofen**			
Solvent	**Methanol**			
Concentration of feeding (M)	**0.1**			
Volume of feeding (mL)	**200**			
Permeation rate (10^{-5} x $g \cdot m \cdot m^{-2} \cdot h^{-1}$)	**9.8**	**28.2**	**7.0**	**15.3**
Yield of passage ibuprofen (%) (first 1 hour permeation)	**1.95**	**7.56**	**0.47**	**2.74**

As shown in table 2, by the membranes which have average thickness around 150 micrometer, ibuprofen as permeate have allowed to passage away to the receiver with different permeation rate. Although, all of the membranes seem to play

as full dense as they were observed by cross-sectional SEM's character, their permeation rates depended on their preparation condition. The membrane consisted with only palmitoyl cellulose showed a moderate level than others. Around 2 % of ibuprofen passages the membrane after 1 hour permeation. By inserting methyl methacrylate and polymerized bulkily within the base material, the obtained composite membrane showed an enhancement of permeation behavior. This might be considered that the phenomenon could occur due to the polymerization process forming of some nodular inside the base material [4].

4. CONCLUSION

A series of composite membranes has been prepared from palmitoyl cellulose and methyl methacrylate by irradiation under UV lamp using conventional photoinisiator. The performances of the composite membranes were evaluated and compared with base membrane prepared purely from palmitoyl cellulose. The composite membranes have good mechanical properties, however respect to their strength and elongation ratio compared with base material, no enhanced properties were observed. On the other hand, the composite membrane showed a better performance on their permeation rate than that of the base membrane. In the future, further development on their composite preparation method is necessary to obtain the composite membrane with a higher strength but remain their good permeation performance.

ACKNOWLEDGMENT

We would like to thanks to Indonesian Ministry of science and technology for funding our research.

REFERENCES

[1] Robert Beyerlein, 2005, available from http://www.atp.nist.gov/focus/membrane.htm.
[2] D. Braun, H. Cherdron, M. Rehahn, H. Ritter, B. V, 2005, "Polymer Synthesis: Theory and Practice Fundamentals, Methods, Experiments" pp. 324, Springer-Verlag Berlin Heidelberg 2005.
[3] Asep Riswoko "Enantiomeric separation of Ibuprofen using polysacharide membranes", Proceeding of ICCS 2007, Mat/22-2, Jogjakarta.
[4] Kailash C. Khulbe, C.Y. Feng, Takeshi Matsuura, 2008, "Synthetic Polymeric Membranes Characterization by Atomic Force Microscopy", pp. 5, Springer-Verlag Berlin Heidelberg 2008.

REDUCTION KINETIC CHARACTERISTIC OF LATERITIC IRON ORE

Basso D. Makahanap[1], A. Manaf[2]

[1]*Faculty of Mathematics and Natural Science*
University of Indonesia,
Kampus UI, Jl. Salemba Raya No 4, Jakarta 10430, Indonesia
Postgraduate Program of Materials Science
e-mail: bassod.makahanap@krakatausteel.com

[2]*Faculty of Mathematics and Natural Science*
University of Indonesia
Kampus UI, Jl. Salemba Raya No 4, Jakarta 10430, Indonesia
Postgraduate Program of Materials Science
e-mail: azwar@ui.edu

Abstract

A laboratory investigation was carried out to study the reduction behavior of the lateritic iron ore with anthracite coal under isothermal condition in the temperature range 800 ^{0}C to 1100 ^{0}C.

The main mineral content of investigated lateritic iron ore was found as the following: Goethite : 62.8%, Hematite : 18.3% and Magnetite (Fe_3O_4) : 6.2% and other oxide minerals like Alumina : 6.6%, Silica : 4.5% , Chromate : 3.3% and others. The ores and anthracite coal as the reducing agent were co-milled to -60 mesh. The milled mixture material was then heated isothermally att temperatures 800, 900, 1000 and 1100^{0}C for reduction time varied from15 to 90 minutes of each reduction temperature It was found that both temperature and reduction time determine the metallization kinetic in which the maximum value were obtained at higher temperatures and a longer reduction time. The kinetics of metallization at an isothermal temperature showed two stages relation with reduction times, two constant rates (K) were derived. This suggests that two different reduction mechanisms occur during the lateritic iron ore reduction.

Keywords: *iron ore; coal; kinetics; metalization; mixed grinding; reduction*

1. Introduction

Laterites are the products of intensive and long lasting tropical rock weathering which is intensified by high rainfall and elevated temperatures. One of the lateritic ore species is lateritic iron ore, which has significant amount in the world. But so far lateritic iron ore contribution on iron and steel industry is very small or even can be neglected, due to its low Fe content (less than normal requirement 60% Fe). Recently, due to shortage of iron ore raw material, the lateritic iron ore is starting to be utilized as raw material for iron and steel making industry by reducing with suitable technology for example rotary kiln.

Indonesia has much enough lateritic iron ore deposits but so far this lateritic iron ore deposits is not utilize yet as main raw material for Indonesian iron and steel industry. In order to utilize the lateritic iron ore, the research in laboratory and pilot plant scale should be started.

The investigated lateritic iron ore consist mainly of Goethite, a hydrated iron oxide FeO(OH), 62.8%.

If the Goethite is heated, the dehydroxilation will be occurs at about 200 – 350^{0}C

$$FeO(OH) = Fe_2O_3 + H_2O \quad (R1)$$

This is a step which naturally occurs in the reduction precess as a result of heating.

The milled mixture material was then heated isothermally at four different temperatures 800, 900, 1000 and 1100^{0}C for reduction time varied from15 to 90 minutes of each reduction temperature. All reduced materials were analyzed quantitatively with X-ray diffractometer (XRD) in

order to analyze the minerals content in order to study their reduction kinetics characteristic.

The reduction parameter used is metallization (M).

Metallization (M) = $(Fe_R/Fe_T) \times 100\%$. (1)

Where Fe_R = reduced or metallic iron in the reduced material sample

Fe_T = total iron in the ore sample

It was found that both temperature and reduction time determine the metallization kinetic in which the maximum value were obtained at higher temperatures and a longer reduction time. The kinetics of metallization at an isothermal temperature showed two stages relation with reduction times, expressed by two kinds of kinetic curve from which two constant rates (K) were derived. This suggests that two different reduction mechanisms or models occur during the lateritic iron ore reduction.

2. Lateritic Iron Ore Reduction And Kinetic Model

Reaction kinetics in iron ore reduction deal with the rate which iron oxides are converted by the removal of oxygen. The reaction mechanism in lateritic iron ore and coal mixtures is very complex with respect to simultaneous reaction steps due to the following reasons:

1. a system of many particles and many phases, i.e. iron, iron oxide, coal, carbon etc;
2. a system of many gases i.e. CO, CO_2, H_2, H_2O, etc;
3. a system of many chemical reactions, i.e
   a. dehydroxylation of Goethite
      $2FeO(OH) = Fe_2O_3 + H_2O$
   b. reduction of hematite to magnetite:
      $3Fe_2O_3 + CO = 2Fe_3O_4 + CO_2$ (R2)
   c. reduction of magnetit to wustite :
      $Fe_3O_4 + CO = 3FeO + CO_2$ (R3)
   d. reduction of wustite to iron :
      $FeO + CO = Fe + CO_2$ (R4)
   e. Carbon gasification, Boudouard reaction :
      $C + CO_2 = 2CO$ (R5)
   f. Coal devolatilization, coal to carbon;
      Coal = C + voaltile matter (R6)

The reduction of hematite to wustite (R2, R3) is condidered as a complex gas-solid reaction influenced by complex structural changes in the intermediate oxides.

2.1 Reduction Mechanism

The reacting mixture under study is a multiple phase heterogenous system. Heterogeneous chemical reactions take place at interface which move spatially and change their character with reaction time. Heat and mass transfer are not only active within each phase, but also between phases.

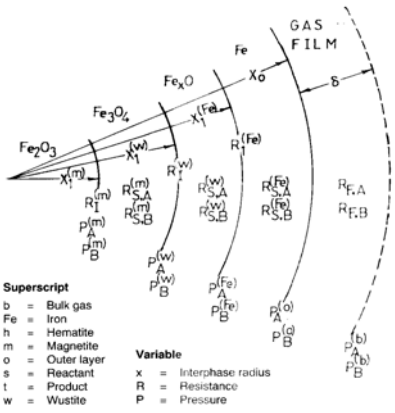

Figure1- Reprsentation of model with three concentric shells [14]

The fundamental steps involved in the reduction of iron oxide are as follows:

1. diffusion of the reducing gas across the boundary layer;
2. intraparticle diffusion of the reducing gas to the reaction interface;
3. phase-boundary reaction, migration of Fe^{++} and electrons to the iron nucleus;
4. intraparticle diffusion of oxidized gas from reaction interface;
5. diffusion of oxidized gas across the boundary layer;

These steps are shown in **Figure 1**.

Dutta et.al [3] shows that reduction of iron ore fines with carbonaceous material consist of two stages reduction as shown in **Figure 2**, the **first** is conversion of hematite to wustite (reaction R2 – R3) and the **second stage** is the reduction of wustite to Fe (reaction R4).

2.2 Iron Ore Kinetic Reduction Model

The complexity of reactions involved in the carbothermic reduction of iron oxide has led to difficulty in the selection of an appropriate reduction model.

There are several methods generally used to describe the kinetics of carbothermic reduction of iron oxide, such as:

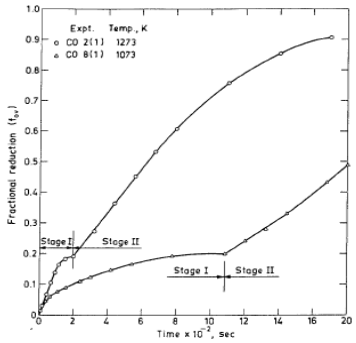

Figure2, Overall fractional reduction vs time [1]

1. Nucleation and growth model. This model consist of several varian models :
   a. The first order reaction,
      $Ln (1-M) = -kt$ (2)
   b. Prout and Tompkin model [Prakash 1996]
      $Ln (M/[1-M]) = kt$ (3)
   c. Avrami-Erofe'ev equation for phase change model
      $[-ln(1-M)]^{1/2} = kt$ (4)

   Where M = metallization
   k = rate constant
   t = reduction time

   The equation (2) – (4) is based on general equation, Avrami equation
   $R = 1 - e^{-Kt\wedge n}$ (5)

   $Ln (1-R) = -Kt^n$ (6)

   Where R = reduced fraction
   K, n = rate constant
   t = reduction time
2. Equation for phase boundary-controlled reaction model
   $1 - (1-M)^{1/3} = kt$ (7)

   Where M = reduced fraction
   k = rate constant
   t = reduction time

Nucleation and growth model typically shows four stages as shown in **Figure 3**:

1. induction period at the beginning of reaction, during which stable nuclei are formed;
2. acceleratory period, which extends up to fractional extents of reaction between 0.1and 0.5, during which some of the nuclei become active and grow;
3. linier period, where the extent of reaction proceed linierly with time;
4. decay period, which appears at high degrees of decomposition.

In order to compare the result of each model and to determine the suit model for the reduction of lateritic iron ore, the root-mean square deviation (RMSD) were applied.

$$RMSD = [(\sum(R_{Fitt} - R_{exp})^2/m]^{1/2} \quad (8)$$

Where
R_{Fitt} = calculation result of reduced fraction
R_{exp} = experimental data of reduced fraction
m = number of experimental data

The model with the lowest RMSD value is the suit model for the lateritic iron ore reduction.

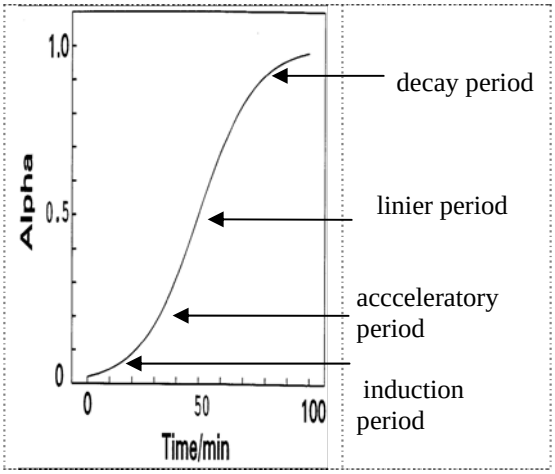

Figure 3, Kinetics steps of nucleation process

3. Experimental Procedure

The experimental procedure is the following:

1. The ore and antrachite coal as reducing agent were milled to -60 mesh by a ball mill. The ore and antrachite coal was mixed with mol ratio between ore and carbon in the antrachite is 1:2, asumption all of the ore is hematite (Fe_2O_3);
2. The milled mixture material was then heated isothermally at four different temperatures 800, 900, 1000 and 1100^0 C for reduction time varied from 15 to 90 minutes of each reduction temperature. The heating curve is shown in **Figure 4**;
3. The ore was heated up to 250^0C for 30 minutes seperately from the milled mixture material in order to analyze the goethite and hematite content changing due to ore heating.

isothermal temperature was increase if the

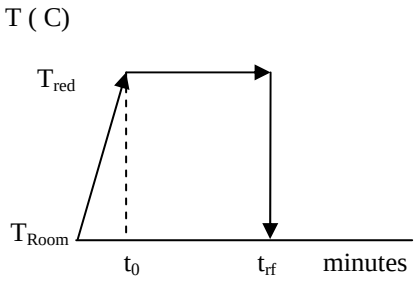

Figure 4, Experimental heating curve. T_{red} = isothermal reduction temperature, T_{room} = room temperature, t_0 = isothermal reduction time start, t_{rf} = isothermal reduction time finish**.**

4. The fresh ore, heated ore and all of the reduced materials were analyzed with XRD and the result was analyzed quantitatively with GSAS (General Structure Analysis Sytem) software.

The antrachite composition is Fixed Carbon : 85.57%; Ash : 10.88%; Lost of ignition (LoI) : 89.12%; Volatile matter : 5.5%; Water content : 1.84%.

4. Result And Discussion

The fresh lateritic ore XRD data was analyzed quantitatively, it was found that the lateritic iron ore consist mainly of Goethite, a hydrated iron oxide FeO(OH), 62.8%. The other iron minerals are Hematit (Fe_2O_3) : 18.3%, Magnetit (Fe_3O_4) : 6.2% and other oxide minerals like Alumina (Al_2O_3) :6.6%, Silika (SiO_2) : 4.5%, Chromite (Cr_2O_3) : 3.3% and others also found in small amount (less than 1%) with Fe total : 54.34%.

If the ore was heated at 250^0C for 30 minutes, the goethite and hematite content would be change, goethite content was reduced very significantly while hematite and Fe content were increased very significantly due to dehydroxylation of goethite (R1), as shown in **Table 1**.

The XRD data of reduced material in this case metallic Fe and total Fe were then coverted into metallization by using **equation (1)**.

During heating from room temperature to the reduction temperature, reduction occurs which was expressed by metallization as shown in **Table 2.**

Figures 5A and **5B** plots the correlation of metallization and time under isothermal condition (800, 900, 1000 and 1100^0C). It was obsereved in these figures that reduction time and temperature determine the metalization, metalization at an reduction temperature and time were increased.

Table 1. The fresh lateritic iron ore and 30 minutes 250^0 C heated ore.

Mineral	Content (%)	
	Fresh ore	Heated ore
Goethite, FeO(OH)	62.8	9.15
Hematite, (Fe_2O_3)	18.3	81.70
Magnetit , (Fe_3O_4)	6.2	9.15
Fe	54.34	69.57

Table 2, Metalization at reduction time = t_0 or M_0.

Temperature (C)	M_0 (%)
800	0.0
900	1.7
1000	12.5
1100	41.2

Metalization at an isothermal temperature showed two stages relation with reduction times, means that the reduction of lateritic iron ore consist of two stages, similar to reduction stage of iron ore fines reduction in **Figure 2**, in this case first stage is conversion of goethite, FeO(OH), to wustite, FeO, and the second stage is conversion of wustite to Fe. This suggest that two different constant rates (K) and two reduction mechanism or models occur during the lateritic iron ore reduction.

From **Figure 5A, 5B** also obtained that the conversion time of goethite, FeO(OH), to wustite, FeO, was shorter if the reduction temperature was increase, the conversion at 1100^0C occurs before the isothermal period was achieved (before t_0). The conversion time is shown in **Table 3.**

Table 3, Convertion time of goethite to wustite

Temperature (C)	Convertion time of goethite to wustite (min)
800	60
900	45
1000	30
1100	Before t_0

It was also observed in **Figure 5A, 5B** that the reduction pattern follow the nucleation and growth pattern shown in **Figure 3**. For the reduction temprature 800^0, 900^0 and 1000^0C induction, acceleratory and linier period, no decay period were observed, means the conversion of goethite , FeO(OH), to wustite or first stage reduction and conversion of wustite, FeO, to Fe occurs in these temperature and reduction time range. The two

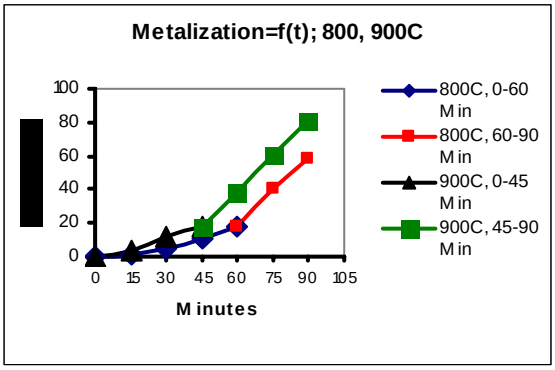

5A

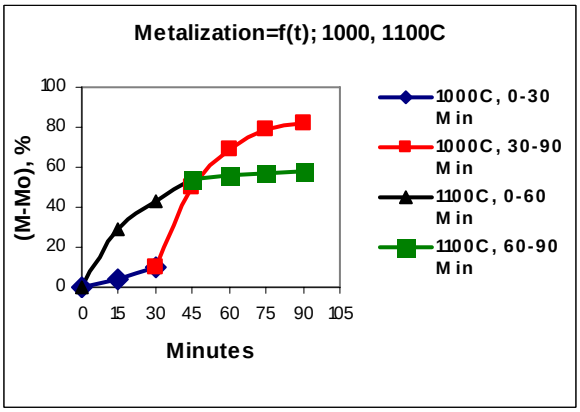

5B

Figure 5A, 5B; Reduction result. M= metalization at reduction time = t minutes, M_0 = metalization at reduction time = t_0. (M-M_0) = metallization at isothermal reduction period.

constant rates (K) were for first stage and second stage reduction.

At the reduction temperature 1100^{0}C no induction and acceleratory period were obsereved, just linier period and decay period were observed means that no conversion of goethite to wustite or first stage reduction was observed, just conversion of wustite to Fe was obsereved in this reduction time range. The two constant rates were for linier and decay periods.

The isothermal reduction metallization (M-M_0) data was correlated with nucleation and growth model, equation (2), (3), (4) and phase boundary-controlled reaction model, equation (7) in order to determine the suit model for lateritic iron ore reduction root mean square deviation (RMSD) parameter (**equation 9**) was applied. The correlation plot of metalization, reduction time and reduction temperature for each model is shown in **Figure 6A – 9B.** Root mean square deviation (RMSD) for each model is shown in and **Table 4** for temperature 800^{0}C, 900^{0}C and

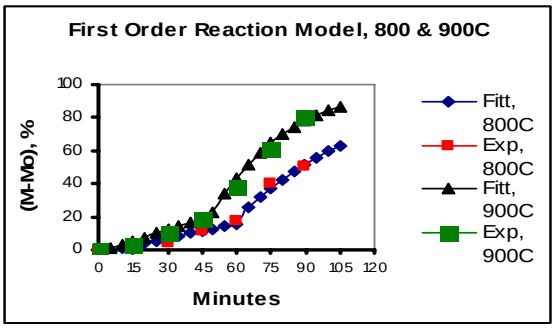

6A

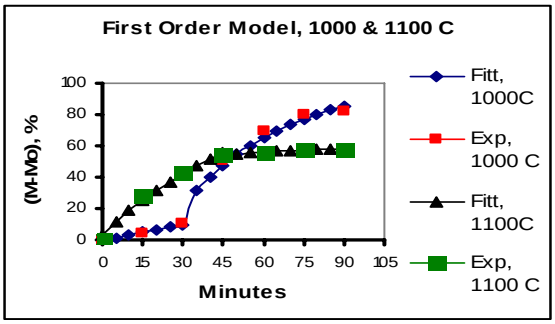

6B

Figure 6A, 6B; First order model. Fitt = calculation result. Exp = experimental result.

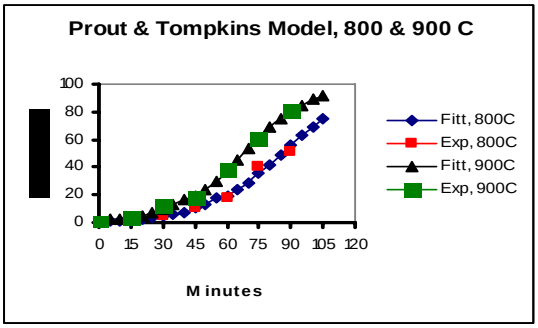

7A

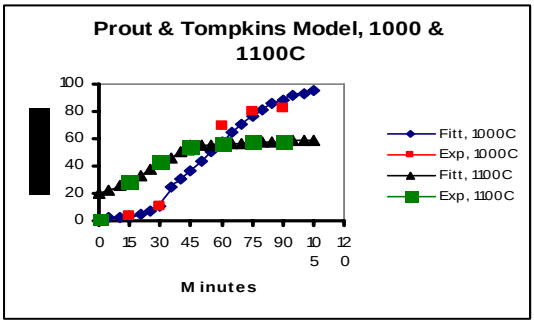

7B

Figure 7A, 7B: Prout & Tompkins model. Fitt = calculation result. Exp = experimental result.

1000^{0}C. Root mean square deviation (RMSD) for each model at temperature 1100^{0}C is ahown in **Table 5.**

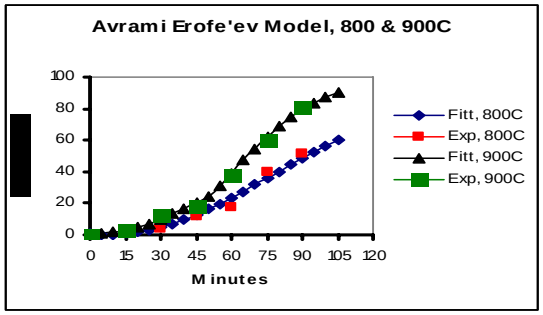

8A

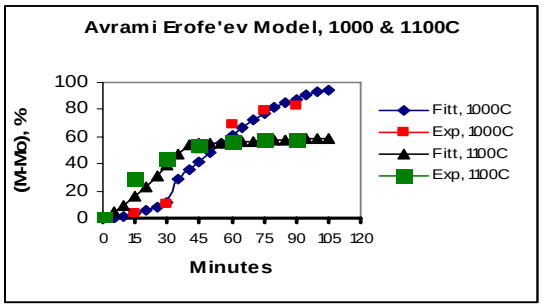

8B

Figure 8A, 8B: Avrami Erofe'ev model. Fitt = calculation result. Exp = experimental result.

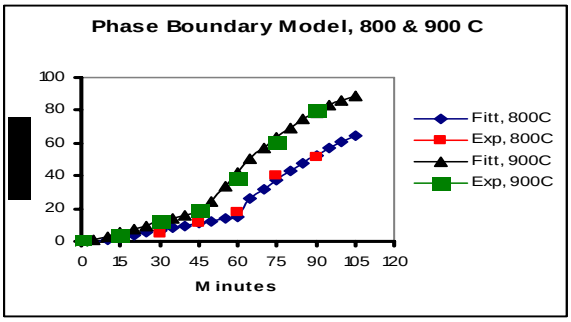

9A

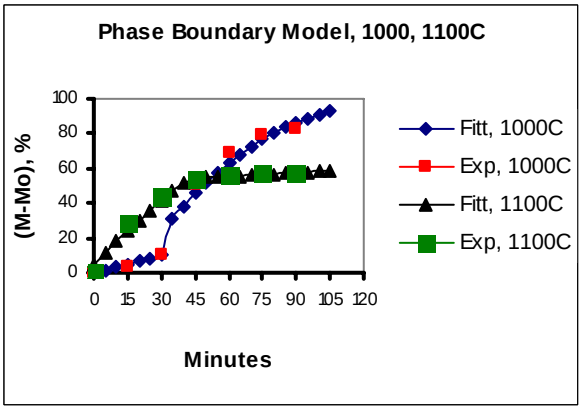

9B

Figure 9A, 9B: Avrami Erofe'ev model. Fitt = calculation result. Exp = experimental result.

Table 4, Root mean square deviation (RMSD) data for reduction temperature 800^0, 900^0 and 1000^{0}C for First Order Reaction Model (FO), Prout & Tompkins model (PT), Avarmi Erofe'ev model (AE) and Phase Boundary model (PB).

T (C)	RMSD			
	FO	PT	AE	PB
First Stage				
800	1.373	4.092	2.912	1.819
900	1.347	2.421	1.644	1.301
1000	0.800	0.718	0.500	0.777
$\sum$ First stage	3.521	7.231	5.052	3.898
Second Stage				
800	1.37	4.092	4.546	2.117
900	5.072	0.592	1.291	3.473
1000	5.383	9.550	7.880	6.889
$\sum$ Second stage	11.829	14.234	13.717	12.479

Table 5, Root mean square deviation (RMSD) data for reduction temperature 1100^{0}C for First Order Reaction Model (FO), Prout & Tompkins model (PT), Avarmi Erofe'ev model (AE) and Phase Boundary model (PB).

T (C)	RMSD			
	FO	PT	AE	PB
1st stage				
1100	2.482	9.800	7.882	3.225
2nd stage				
1100	0.363	0.373	0.408	0.758

Figures 6A – 9B shows that the reduction models mentioned above were fitt to the experimental result, means the lateritic iron reduction fitt to those models.

Table 4 shows that at the temperature range 800^0 – 1000^{0}C among the reduction models mentioned above, for first stage or conversion of goethite to wustite and second stage or conversion of wustite to Fe, First Order Reaction model had a smallest RMSD compare to the others, 3.521for the first stage and 11.829 for the second stage. Means that the suit reduction model for lateritic iron ore reduction model at temperature 800^0 - 1000^0 is Nucleation and Growth - First Order Reaction Model.

Table 5 shows that at the temperature 1100^{0}C among the reduction models mentioned above, for the conversion of wustite to Fe during linier period

and decay period, First Order Reaction model has a smallest RMSD value compare to the others, 2.482 for the linier period and 0.363 for the decay period. Means that the suit reduction model for lateritic iron ore reduction model at temperature 800^0 - 1000^0 is Nucleation and Growth - First Order Reaction Model.

The constant rate (K) acording to First Order Reaction Model is shown in **Table 6** and **Figure 10.**

Figure 10, The constant rate according to First Order Reaction Model, Ln (1-M) = -kt. K_1 = constant rate for conversion of goethite to wustite, K_2 = constant rate for conversion of wustite to Fe.

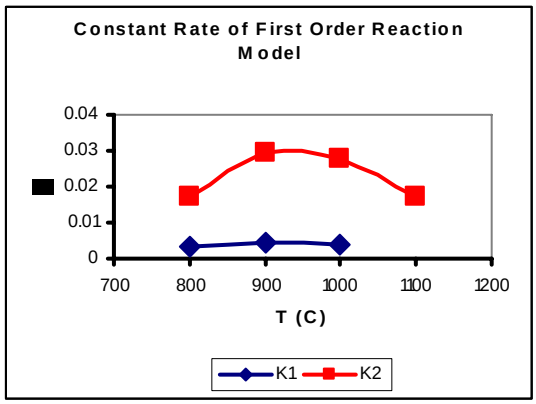

Table 6, The constant rate according to First Order Reaction Model, Ln (1-M) = -kt. K_1 = constant rate for conversion of goethite to wustite, K_2 = constant rate for conversion of wustite to Fe.

T (C)	K_1 (%/min)	K_2 (%/min)
800	0.0032	0.0174
900	0.0047	0.0295
1000	0.0037	0.0276
1100	--	0.0173

Figure 10 and **Table 6** shows that the contant rate conversion of of goethite to wustite was less compare to conversion of wustite to Fe due to less complexity of conversion of wustite to Fe (R4) compare to conversion of goethite to wustite (R1-R3). Constant conversion rate of both conversion goethite to wustite and wustite to Fe, K_1 and K_2 increased if the reduction temperature was increase from 800^0 to 900^0C then decreased from 900^0 to 1100^0C due to decreasing of Fe oxide in the ore.

Conclusion

The reduction kinetics of lateritic iron consist of two conversion stages. Conversion of goethite to wustite and conversion of wustite to Fe, each stage has its own constanta rate (K)

The reduction kinetics of lateritic iron ore fulfill several kinetics model i.e., first order reaction model, Prout & Tompkins model, Avrami-Erofe'ev modeland phase boundary model. By applying the root means square (RMSD) parameter the first order reaction model was determine as the suit model of the reduction kinetics of lateritic iron ore.

Constant conversion rate of wustite to Fe (K_2) was higher compare to constant conversion rate of goethite to wustite (K_1).

Constant conversion rate, (K_1, K_2), was increased if the reduction temperature increased from 800^0 to 900^0 and then decreased if the temperature increasedfrom 900^0 to 1100^0.

Acknowledgement

This reduction research was carried out at chemical laboratory of PT KRAKATAU STEEL, Cilegon and the XRD analysis was carried out at Postgraduate Program of Materials Science laboratory, Jl. Salemba Raya 4, Jakarta.

Thank you to PT KRAKATAU STEEL management where the first author is being employed as Process And Product Research And Development Manager for providing facilities for experimental work. Also thank you to Postgraduate Program of Materials Sciencewhere the first author is being studied for providing facilities for analysis work.

References

[1] Dutta, S.K., Ghosh, A., *"Kinetics of Gaseous Reduction of Iron Ore Fines"* ISIJ International, Vol. 33 (1993), No 11, pp. 1168 – 173.

[2] Brown, M.E., *"The Prout-Tompkins rate equation in solid state kinetics"*, Thermochimica Acta 300 (1997) 93-106.

[3] Brown, M.E., Glass, B.D., *"Pharmacetical application of the Prout-Tompkins rate equation"* Thermochimica Acta 190 (1999) 129-137.

[4] Feinman, J., Mac Rae, D.R., *"Direct Reduced Iron, Technology and Economics of Production and Use"*, The Iron & Steel Society.

[5] Stephenson, R.L., Smailing, R.M., *"Direct Reduced Iron, Technology and Economics of Production and Use"*, Iron & Steel Society of AIME.

[6] Donskoi, E., McElwain, D.L.S., *"Estimation and Modelling of Parameters for Direct Reduction in Iron/Coal Composites: Part I. Physical Parameters"*, Metallurgical And Materials Transaction B, Volume 34B, February 2003, p.93-102.

[7] Piotrokowski, K., et.al., "*Effect of Gas Composition on the Kinetics of Iron Oxide Reduction n a Hydrogen Process"*, International Journal of Hydrogen Energy, vol. 30, Isue 15, December 2005, p.1543-1554.

[8] Donskoi, E., McElwain, D.L.S. and Wibberley, L.J., *"Estimation and Modelling of Parameters for Direct Reduction in Iron/Coal Composites: Part II. Kinetic Parameters"*, Metallurgical And Materials Transaction B, Volume 34B, April 2003, p.255-266.

[9] Lee, J.C., Min, D.J., Kim, S.S., *"Reaction Mechanism on The Smelting of Iron Ore by Solid Carbon"*, Metallurgical and Material Transaciton B, Volume 28B, December 1997, p.1019-1028.

[10] Lu, W.K., Huang, D.F., *"The Evolution of Iron Making Process Based on Coal-Containing Iron Ore Agglomerates*", ISIJ International, Vol. 41 (2001), No 8, pp. 807 – 812.

[11] Moon, J., Sahajwalla, V., "*Kinetic Model for the Uniform Conversion of Self Reducing Iron Oxide and Carbon Briquettes"* . ISIJ International, Vol. 43 (2003), No 8, pp. 1136 – 1142.

[12] Moon, J., Sahajwalla, V., *"Investigation Into The Role of Boudouard Reaction in Self-Reducing Iron Oxide and Carbon Briquettes"*, Metallurgical and Material Transaciton B, Volume 37B, April 2006, p.215-221.

[13] O'Connors, F., Cheung, W.H, Valix, M., *"Reduction Roasting of Limonite Ores: Effect of Dehydroxylation*", International Journal Of Mineral Processing, 80 (2006) p.88 – 99.

[14] Prakash, S., *"Reduction and sintering of fluxed iron ore pellets – a comprehensive review"*, The Journal of The South African Institute of Mining and Metallurgy, January/February 1996.

[15] Ray, H.M., *"Kinetics of Metallurgical Reactions"*, International Science Publisher, New York.

[16] Sun, S., Lu, W.K., "*Mathematical Modelling of Reactions in Ore/Coal Composites*", ISIJ International, Vol. 33 (1993), No10, pp. 1062 – 1069.

[17] Sun, S., Lu, W.K., "*A Theoritical Investigation of Kinetics and Mechanism of Iron Ore Reduction in an Ore/Coal Composites*", ISIJ International, Vol. 39 (1999), No 2, pp. 123 – 129.

[18] Sun, S., Lu, W.K., "*Building of a Mathemathical Model for the Reduction of IronOre Reduction in an Ore/Coal Composites "*, ISIJ International, Vol. 39 (1999), No 2, pp. 130 – 138.

Fading of Al-5Ti-1B Grain Refiner of 0.081 and 0.115 wt. % Ti in AC4B Alloy Produced by Low Pressure Die Casting

Bondan T. Sofyan[1] and Lulus Basuki[1]

[1]*Department of Metallurgy and Materials Engineering*
Faculty of Engineering University of Indonesia,
Kampus UI Depok 16424
Tel : (021) 786 3510. Fax : (021) 787 2350
E-mail : bondan@metal.ui.ac.id,

ABSTRACT

AC4B alloy (Al-8Si-2.4Cu) is one of the most desirable cast aluminium to be processed through low pressure die casting (LPDC). However, there are many problems, particularly shrinkage and porosity, that need to be resolved. One way to solve this problem is by using grain refiner. Another constraint is the duration of one cycle LPDC process of ~ 450 kg capacity may take up 4 hours, that causes fading. This research is aimed to understand the fading mechanism of Al-5Ti-1B grain refiner of 0.081 and 0.115 wt. % Ti during LPDC. Fading was observed through the changes of hardness, tensile strength and microstructure.

The results show that the longer the holding time, the lower hardness and the tensile strength of AC4B alloy. On the other hand, the longer the holding time, the higher the ductility and the secondary dendrite arm spacing (SDAS). This indicates that fading occurred before 1 hour. In addition, microstructure observation by using Scanning Electron Microscopy (SEM) and Energy Dispersive X-Ray Analysis (EDAX) showed the presence of titanium in the alloy which indicates that titanium may act as the nucleant for solidification process.

Keywords
Grain refiner, fading, AC4B, LPDC, Al-5Ti-1B

1. INTRODUCTION

One way to improve the quality of aluminium casting products is by using grain refiner [1-3]. Grain refiner reduces grain size of aluminium casting by resisting the growth of columnar grains and promoting equiaxed grains [4-6]. The grain in aluminium casting can be refined by forming as much dendrites as possible during initial solidification, and maintain that they all grow at the same rate. This only can be achieved if the nucleation starts near to liquidus temperature, or minimum undercooling, by providing particles on which dendrites can readily nucleate and grow [3, 7-8].

There are several types of grain refiner available for aluminium alloys, such as aluminium-titanium, aluminium-titanium-boron master alloys, and titanium or titanium-boron containing salt tablets [7]. The aluminium-titanium and aluminium-titanium-boron master alloys are the most popular to use, such as Al-10Ti, Al-6Ti, Al-3Ti-1B, Al-5Ti-1B, Al-5Ti-0.6B, Al-10B, Al-5B, and Al-3B [9].

The mechanism of grain refinement is related to the nucleant particles which is contained in the grain refiner, i.e. TiB_2 or $TiAl_3$ particles. If titanium is present in the alloy at the levels greater than ~0.15 %, then on cooling, nucleation of $TiAl_3$ occurs before aluminium. Aluminium then nucleates on $TiAl_3$ reducing the undercooling and thus producing a smaller grain size [7,10]. When using aluminium-titanium-boron master alloy as the grain refiner, $TiAl_3$ particles will dissolve and introduce solute titanium in to the melt, while TiB_2 remains as a solid dispersion in the melt [6-7,11]. TiB_2 particles have the order of 0.5 to 5 μm. Although there is still a debate about precise nucleation mechanism, however, for wrought alloys it is generally thought that the mechanism involves nucleation of aluminium on layers of $TiAl_3$ which are formed and stabilised on specific facets of TiB_2 particles [7, 11-12].

The weakness of grain refiner is the fading that occurs within a period of time. Fading may be caused by settling, agglomeration and poisoning of nucleant particles [6-7]. The density of TiB_2 (4.5 g/cm^3) is larger than molten aluminium (2.3 g/cm^3), that makes the particles settle down the furnace [7,13-14]. Presence of borid particles may lead to agglomeration that speeds up the settling

process. During the fast settling the large agglomerate also collides with the smaller one and becomes larger [6-7,13]. Agglomeration also occurs when TiB_2 combines with oxide film and make fast settling [15]. While poisoning of Al-5Ti-1B grain refiner is commonly caused by other elements such as silicon, zirconium, chromium, iron and tantalum [7-8,11-12,16]. When the melt has silicon content exceed 2 %, the coarsening effect will start and extend with the higher silicon content [17-18]. It is also known that addition of AlTiB grain refiner to zirconium containing melt would result quick poisoning. $TiAl_3$ layer can be displaced in the presence of zirconium and tantalum. The poisoning can happen by subtitution of element in $TiAl_3$ layer [7,12]. This research was purposed to study the fading mechanism of Al-5Ti-1B grain refiner in AC4B alloys produced by low pressure die casting (LPDC) process.

2. EXPERIMENTAL METHOD

The melting of AC4B was conducted in reverberatory furnace with the capacity of 500 kg at 810 ± 5 °C. Then aluminium was poured in to the preheated ladle and trapped hydrogen was eliminated by using Gas Bubble Floatation (GBF) for 8 minutes. Rod Al-5Ti-1B grain refiner was added at the begining of the GBF process, with the amount of 0.081 and 0.115 wt. % Ti. Molten metal was then injected through LPDC machine at 700 – 710 ^oC. Fading was observed through the changes of hardness, tensile strength and microstructure for a period of 0 – 2 hour. Samples were taken from thick and thin area of the component to see effect of heat transfer on grain refinement and fading.

3. RESULTS AND DISCUSSION

The microstructure of Al-5Ti-1B grain refiner is presented in Figure 1. The microanalysis of each position is tabulated in Table 1. There are white and grey phases as the matrix. Small white phase is found evenly distributed in the matrix. The white phase has 20.47 wt. % Ti and 53.91 wt. % B. By converting this value to atomic percentage, the white phase can be assume as TiB_2 particle. The similar method was also used to point 2 and 3, point 2 is AlB_2 and point 3 is AlB_2 combined with TiB_2. According to solute paradigm, boride and the other particles can act as nucleating subtrate[19].

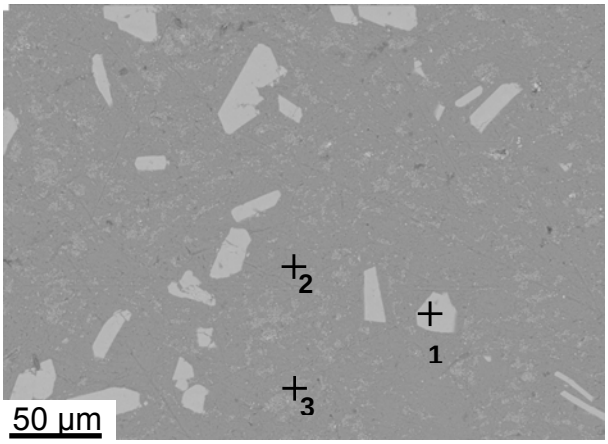

Figure 1. Microstructure of Al-5Ti-1B grain refiner.

Table 1. Microanalysis of Al-5Ti-1B grain refiner at positions shown in Figure 1.

Posi-tion	Content (wt. %)			Color	Phase
	Al	Ti	B		
1	25.62	20.47	53.91	white	TiB_2
2	36.43	0.34	63.23	grey	AlB_2
3	33.24	9.66	57.10	white	$Al\ B_2$ and TiB_2

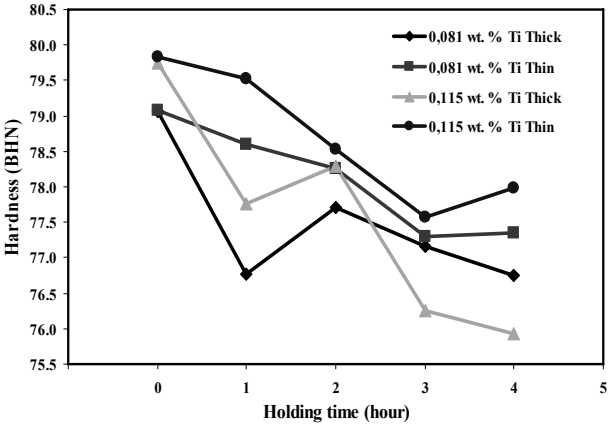

Figure 2. The effect of Ti addition and the sample position on the hardness of AC4B alloys produced by LPDC process for 4-hour period.

The change of hardness with the increase in holding time is provided in Figure 2. The hardness of thin section is generally higher than thick section due to higher solidification rate.

Samples with addition of 0.081 wt. % Ti at thick section shows that the longer the holding time, the lower the hardness of LPDC products. After 4 hours, the hardness dramatically decreased to 78 BHN. Similar trend was found for thin section, as well as for addition of 0.115 wt. % Ti.

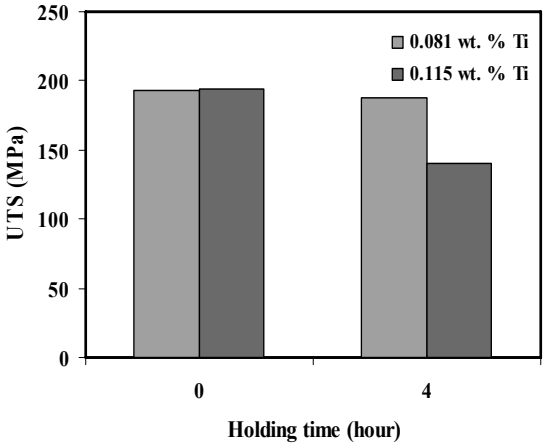

Figure 3. The change of ultimate tensile strength (UTS) of AC4B alloy produced by LPDC after 0 and 4 hours, with addition of 0.081 and 0.115 wt. % Ti.

The change of tensile strength of AC4B alloy produced by LPDC after 0 and 4 hours can be seen in Figure 3. This shows the declining of ultimate tensile strength for both 0.081 and 0.115 wt. % Ti after 4 hours. After 4 hours of LPDC process, the alloy with addition of 0.081 and 0.015 wt. % Ti underwent a decline in tensile strength for 5.6 and 54.1 MPa, respectively. The tendency in tensile strength is similar with that in hardness. Both hardness and tensile strength are parameters of resistance of materials to plastic deformation, so the values are generally proportional [20].

Microstructures of AC4B alloy processed by LPDC with 0.081 and 0.115 wt. % Ti addition are provided in Figures 4 and 5, respectively. It is clear that the dendrites are smaller in the thin section than those in the thick section. Both sections show that the longer the holding time, the larger the dendrites, confirming the results of hardness and tensile tests.

The secondary dendrite arm spacing (SDAS) was quantitatively measured and the results are presented in Figure 6. After 4 hours of LPDC, the size of dendrites in alloy with 0.081 wt. % Ti addition rises by 5.4 μm and 12.7 μm at thick and thin sections, respectively. Alloys with addition of 0.115 wt. % Ti also showed similar results, in which the size of SDAS increases by 14 μm and 7.7 μm at thick and thin sections, respectively.

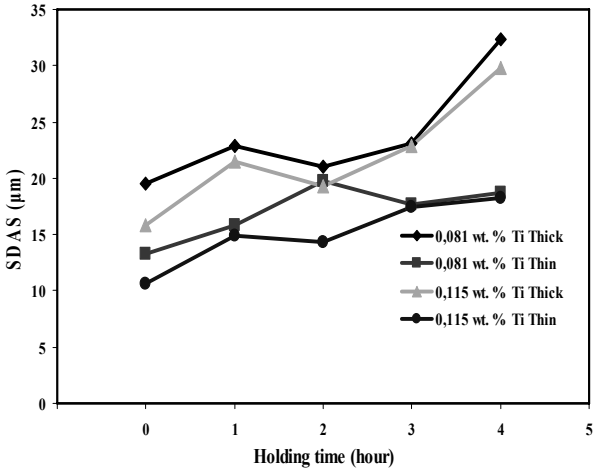

Figure 6. Change in secondary dendrite arm spacing (SDAS) in 4 hours in AC4B alloys added with 0.081 and 0.115 wt. 5 Ti in thick and thin areas.

The change of microstructure of AC4B alloy with addition of 0.081 wt. % using SEM and EDAX for 4 hours period is shown in Figure 7. The results of microanalysis of each point are tabulated in Table 2. The results show that the longer the holding time, the more sparsely distributed the Al_2Cu phase. This tendency is shown both in thick and thin samples. While the Al-Si eutectic phase tends to be coarser by the increase in holding time. The larger size of Al_2Cu, Al-Si eutectic phases and dendrites is correlated with the decrease in hardness and tensile strength of the alloys. Trace of titanium was observed for 0.64 % at point 5 of thick sample of 0 hour (Figure 7 (a)). This may indicate the presence of $TiAl_3$ particle at this point. Therefore, it confirms the mechanism of grain refinement by the presence of nucleant particles in the microstructures that seed the growth of dendrites in the molten metal.

ISSN 114-1284

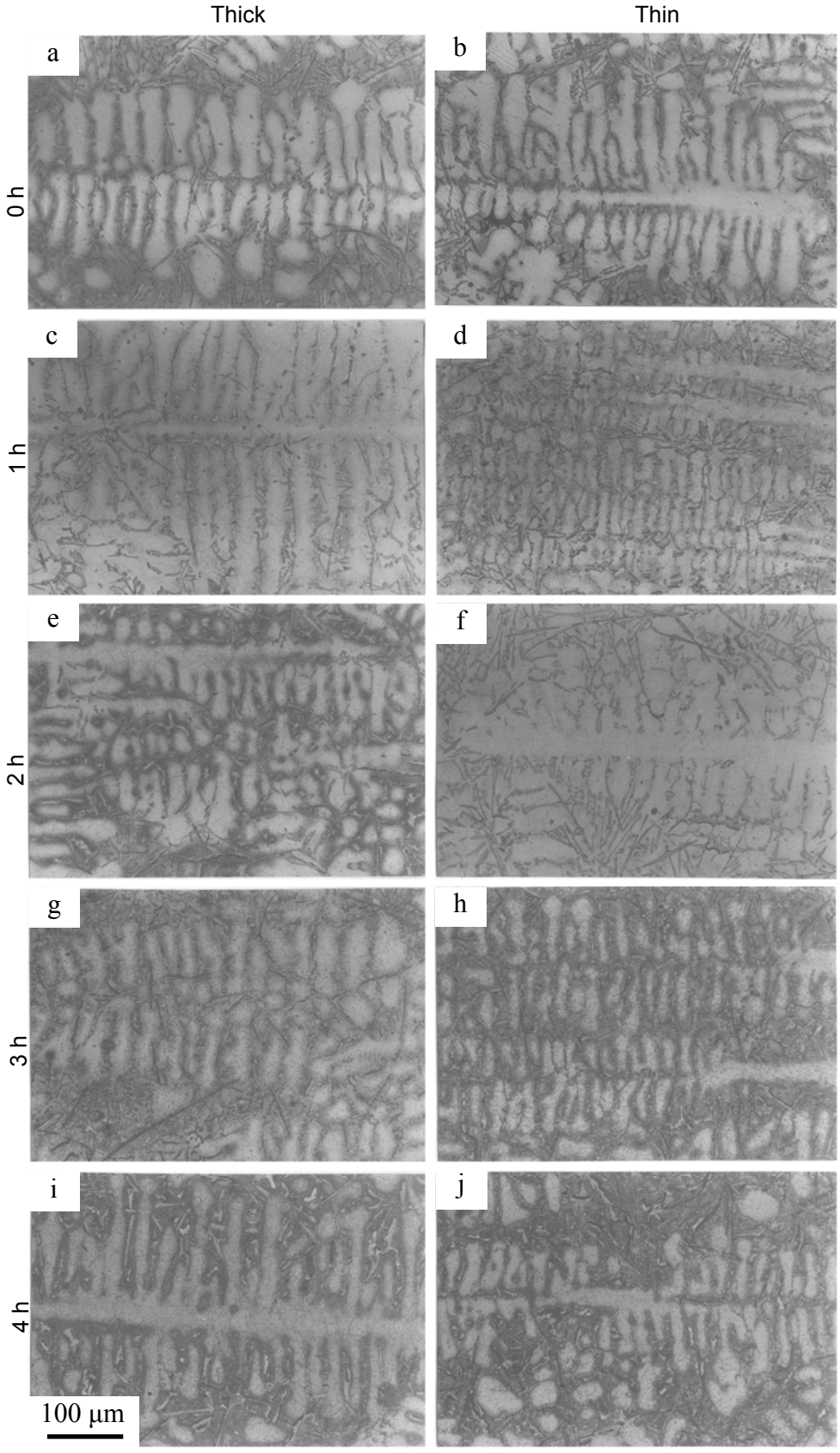

Figure 4. The change of microstructure of AC4B alloy with addition of 0.081 wt. % after (a-b) 0 hour; (c-d) 1 hour; (e-f) 2 hours; (g-h) 3 hours; (i-j) 4 hours, from thick and thin areas.

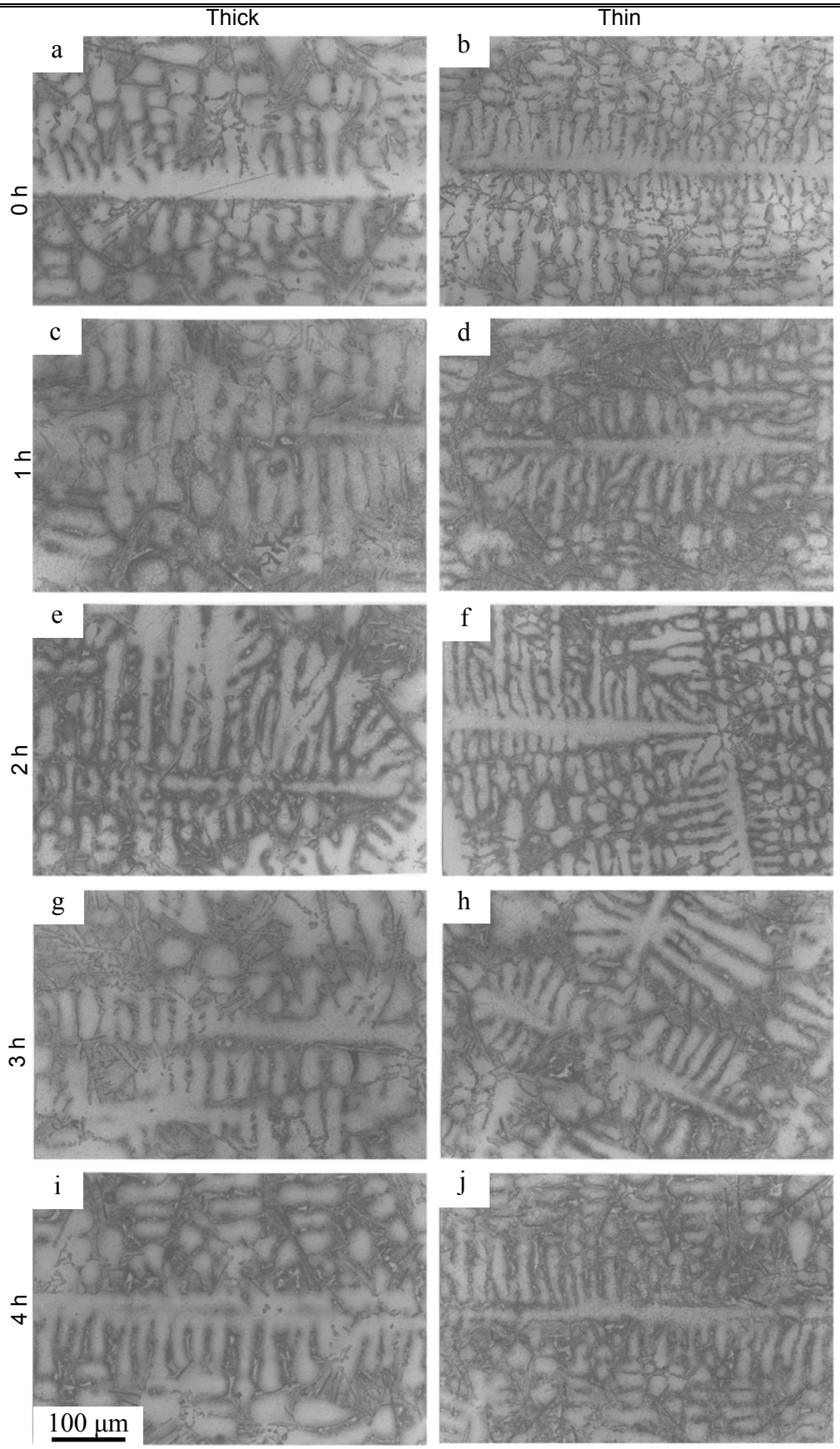

Figure 5. The change of microstructure of AC4B alloy with addition of 0.115 wt. % after (a-b) 0 hour; (c-d) 1 hour; (e-f) 2 hours; (g-h) 3 hours; (i-j) 4 hours, from thick and thin areas.

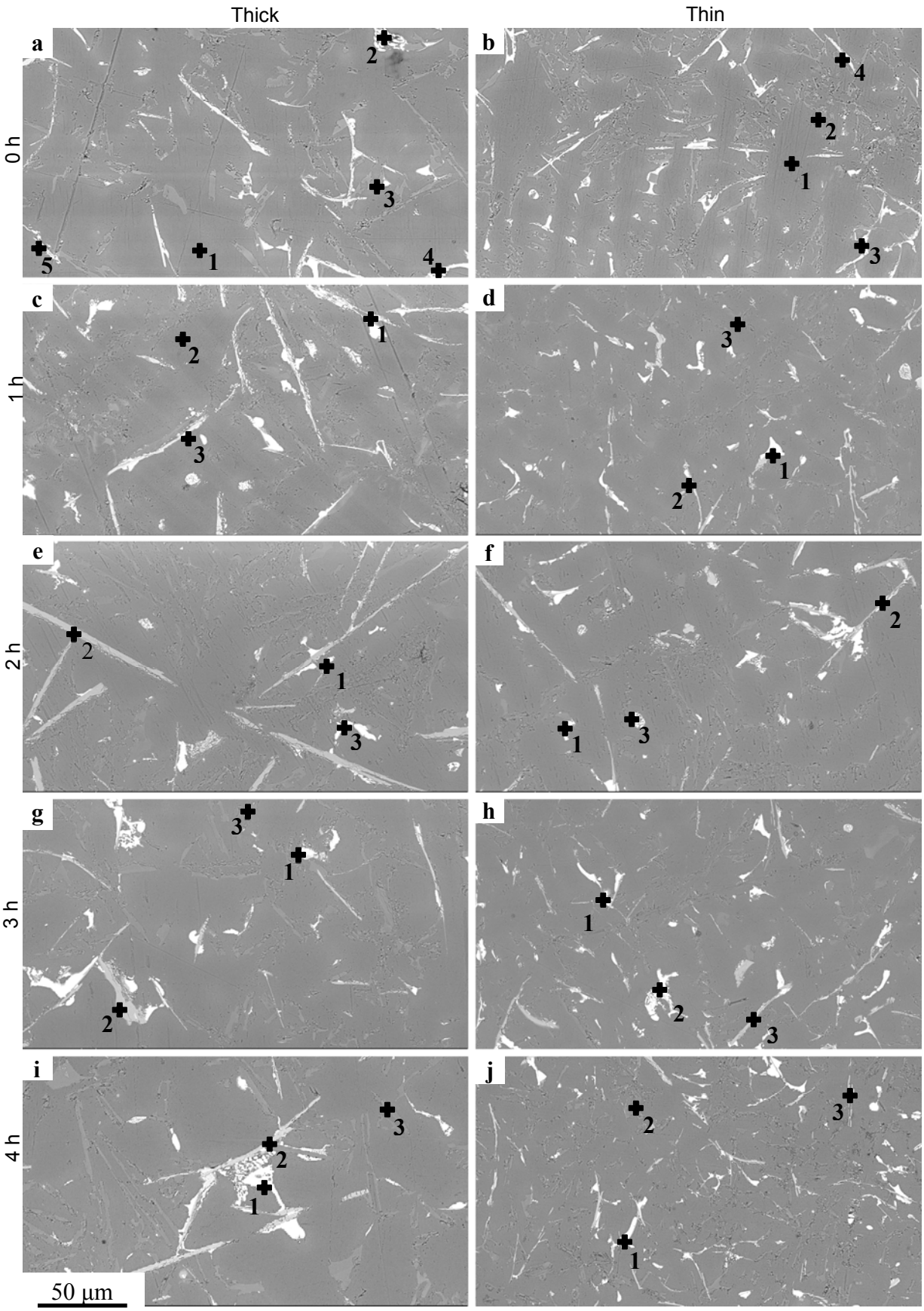

Figure 7. The change of microstructure (SEM) of AC4B alloy with addition of 0.081 wt. % Ti after (a-b) 0 hour; (c-d) 1 hour; (e-f) 2 hours; (g-h) 3 hours; (i-j) 4 hours, in thick and thin samples. The results of microanalysis of each point are tabulated in Table 2.

Table 2. Results of microanalysis of AC4B alloy with addition of 0.081 wt. % Ti at the points shown in Figure 7.

Sample	Point	Element (wt. %)			Color	Phase
		Al	Si	Cu		
0 hour, thick section	1	94.48	1.90	-	grey	Al
	2	64.88	2.74	29.36	white	Al_2Cu
	3	19.49	82.34	-	grey	Al-Si
	4	64.13	5.27	24.05	white	Al_2Cu
	5	57.66	11.65	16.18	white	Al_2Cu
0 hour, thin section	1	94.88	1.88	-	grey	Al
	2	15.24	80.60	-	grey	Al-Si
	3	91.05	0.95	7.27	white	Al_2Cu
	4	32.91	63.03	-	grey	Al-Si
1 hour, thick section	1	89.70	1.48	6.86	white	Al_2Cu
	2	94.80	2.00	-	grey	Al
	3	57.17	11.56	-	grey	Al-Si
1 hour, thin section	1	38.36	5.87	45.20	white	Al_2Cu
	2	59.15	14.91	21.82	white	Al_2Cu
	3	52.37	42.09	-	grey	Al-Si
2 hours, thick section	1	88.11	1.27	8.47	white	Al_2Cu
	2	60.53	11.68	-	grey	Al-Si
	3	42.71	0.51	56.26	white	Al_2Cu
2 hours, thin section	1	88.13	2.34	8.28	white	Al_2Cu
	2	72.20	22.63	-	grey	Al-Si
	3	93.84	1.76	-	grey	Al-Si
3 hours, thick section	1	70.22	11.91	11.48	white	Al_2Cu
	2	57.09	11.19	-	grey	Al-Si
	3	88.60	1.23	8.93	white	Al_2Cu
3 hours, thin section	1	87.10	1.36	7.59	white	Al_2Cu
	2	29.21	0.17	60.83	white	Al_2Cu
	3	93.93	1.59	-	grey	Al-Si
4 hours, thick section	1	30.04	0.19	59.94	white	Al_2Cu
	2	93.06	1.50	-	grey	Al-Si
	3	11.83	83.11	-	grey	Al-Si
4 hours, thin section	1	88.95	1.27	8.13	white	Al_2Cu
	2	88.63	2.34	7.62	grey	Al-Si
	3	87.95	1.16	9.16	white	Al_2Cu

4. CONCLUSIONS

1. The longer the holding time, the lower hardness and the tensile strength of AC4B alloy. On the other hand, the longer the holding time, the higher the secondary dendrite arm spacing (SDAS).
2. The examination using SEM and EDAX shows the presence of titanium that indicates the presence of nucleant particles, particularly $TiAl_3$.
3. The result shows that there is a fading phenomenon in AC4B alloys produced by LPDC process which occurred after 0 hour.

ACKNOWLEDGMENT

The authors would like to thank University of Indonesia for the granting of Riset Unggulan Universitas Indonesia 2008 that funded this research.

REFERENCES

[1] Nafisi, Shahrooz.& Ghomashchi, Reza. "Grain refining of conventional and semi-solid A356 Al–Si alloy" *J. Mat. Processing Tech*. Vol. 174, no. 1, pp. 371 – 383, 2006

[2] Zhang, Z, Bian, X., Wang, Y, and Liu, X "Microstructure and Grain Refining Performance of Melt-Spun Al- 5Ti- 1B Master Alloy" *Mat. Sci. Eng. A,* Vol. 352, no. 1, pp. 8-15, July 2003.

[3] Lee Y.C., Dahle, A.K., StJohn, D.H., Hutt, J.E.C. "The effect of grain refinement and silicon content on grain formation in hypoeutectic Al–Si alloys". Mat. Sci. Eng. A, Vol. 259, no. 1, pp. 43-52, Jan 1999.

[4] Easton, M. and StJohn, D, *Grain Refinement of Aluminium Alloys: Part I. The Nucleant and Solute Paradigms—A Review of the Literature*. Australia. University of Queensland. 1999.

[5] Schneider, W.A., Quested, T.E., Greer, A.L., and Cooper, P.S. *A Comparison of the Family of AlTiB Refiners and their Ability to Achieve a Fully Equiaxed Grain Structure in DC Casting*. (n.d). Metallurg Aluminum. 2003.

[6] Schaffer, P.L. and Dahle, A.K. "*Settling behaviour of different grain refiners in aluminium"*. Mat. Sci. Eng. A, Vol. 413, pp. 373 – 378, Dec 2005.

[7] Metallurg Aluminum. (1998). *Grain Refinement of Al-Si Foundry Alloys*. (n.d). Metallurg Aluminum.

[8] Binney, M.N, StJohn, D.H., Dahle, A.K., Taylor, J.A., Burhop, E.C., and Cooper, P.S. *Grain Refinement of Secondary Aluminum-Casting Alloys*. (n.d). Metallurg Aluminum. 2003.

[9] Ramachandran, T.R., Sharma T.R., and Balasubramanian K. *Grain refinement in light alloy*. India. Nonferrous Materials Technology Development Centre. 2008.

[10] Kashyap, K. T. and T. Chandrashekar. *Effects and Mechanisms of Grain Refinement in Aluminium Alloys*. India. Indian Academy of Sciences. 2001.

[11] Greer A.L. *Grain Refinement of Alloys by Inoculation of Melts*. UK. JSTOR. 2003.

[12] Kearns, M.A., Thistlethwaite, S.R, and Cooper, P.S. *Recent Advances in Understanding The Mechanism of Aluminum Grain Refinement by TiBAl Master Alloys*. USA. Metallurg Aluminum. 1996.

[13] Oishi, K., Sasaki, I. and Otani, J. "Effect of silicon addition on grain refinement of copper alloys"

Materials Letters, Vol. 57, no. 15, pp.2280-2286, Apr 2003.

[14] Naglic ,I. , Smolej, A and Dobersek, M. *Remelting of Aluminum With The Addition of AlTi5B1 and AlTi3C0.15 Grain Refiners*. Slovenia. Metalurgija. 2007.

[15] Thistlethwaite, S.R. and Fisher, P. *Recent Development in Grain Refinement Technology*. Australia. Metallurg Aluminum. 1995.

[16] Asenio-Lozano, J, and Suarez-Pena, B. "Efect of The Addition of Refners and/or Modifers on The Microstructure of Die Cast Al–12Si Alloys". *Scripta Materialia,* Vol. 54, pp. 943 – 947, 2006.

[17] Qiu, D., Taylor, J.A., Zhang, M-X., and Kelly, P.M. "*A Mechanism for The Poisoning Efect of Silicon on The Grain Refinement of Al–Si Alloys"*. Acta Materialia. Vol. 55, no. 4, pp. 1447 – 1456, Feb 2007.

[18] Bermingham, M.J., McDonald, S.D., Dargusch, M.S. and StJohn, D.H. **"**The mechanism of grain refinement of titanium by silicon"**,** *Scripta Materialia*, Vol. 58, No. 12, pp.1050-1053, Jun 2008.

[19] Limmaneevichitr, C. and Eidhed, W., "Fading mechanism of grain refinement of aluminum-silicon alloy with Al-Ti-B grain refiners" *Mat. Sci. Eng. A*, Vol. 349, no. 1, pp.197-206, May 2003

[20] Callister, W.D. (2003). *Material Science and Engineering An Introduction*. Singapura. John Wiley Sons.

Proceeding of the 11th International Conference on QiR (Quality in Research)
Faculty of Engineering, University of Indonesia, Depok, Indonesia, 3-6 August 2009
ISSN 114-1284

Titanium Effect on Aluminum Alloy AA3104 Against the Drawn Wall Ironing During Can Body Making Process

Caing[1*], Bambang Sugiono[1], Dedi Priadi[2]

[1]*Materials Science, Physics Department, Universitas Indonesia*

[2]*Metallurgy and Materials Department, Universitas Indonesia*

Kampus UI Depok 16424

*Caing
Email : caing@unitedcan.com
Phone: 08161101271

Abstract

The purpose of this research is to find a suitable aluminum alloy for two-piece carbonated soft drink can body material in order to reduce the material thickness from 0.280 to 0.270 mm and thus a production cost. Aluminum alloy AA3104 has been used for many years as a carbonated soft drink can material through deep drawing process followed by wall ironing process until a specific desired can height is obtained. Due to inside pressure on the filled can, the can need to have enough strength to prevent deformation, especially on the bottom area of the can (dome). By reducing material thickness, the strength of the can will also reduce dramatically. For this reason, the material needs to be developed to get a suitable strength, while at the same time retains its good formability. In this research, aluminum alloy AA3104 containing 3 variations of titanium composition were prepared, i.e. Ti 0.00%, Ti 0.010% and Ti 0.013%. The analysis including chemical composition, surface roughness, microstructure, and precipitate resulted from the addition of titanium were carried out. Mechanical properties including tensile, LDR, and formability also have been done. Analyses on the final cans including dome reversal pressure, axial load, and can dimension were also included. The can body measuring data to find the average chart, range chart and Cpk index were done by using a commercial software. As a production process simulation, the strength test also has been done after heating the material at 210°C for 10 minutes. Surface roughness analysis shows that the addition of titanium results in better sheet surface of aluminum alloy AA3104. Microstructure analysis shows that the addition of titanium promotes precipitation on aluminum alloy AA3104. XRD analysis shows that the addition of titanium forms Ti_3Al precipitate while the sample containing 0.013% of titanium has better distribution of Ti_3Al precipitate. Mechanical properties test results show that the addition of titanium increases yield strength, tensile strength and elongation of aluminum alloy AA3104. By increasing the yield strength and tensile strength will also increase the strength while increasing of elongation will increase formability of aluminum alloy AA3104. On the deep drawing and wall ironing processes simulation by using aluminum alloy AA3104 containing 0.013% titanium with 0.270 mm thickness, the results show that the tear off rate reduces from 60 ppm to 23 ppm, dome reversal pressure increases 4.3% and axial load increases 6.74%. Heating the material at 210°C for 10 minutes reduces the yield strength, tensile strength, increases the elongation, and reduces the dome reversal pressure and axial load. Stability and capability study case with 0.270 mm thickness indicates that the material confirms customer requirements. It then can be concluded that the aluminum alloy AA3104 containing 0.013% of titanium with the thickness of 0.270 mm can be used in commercial production for two-piece carbonated soft drink cans.

Keywords : *Two-piece can, deep drawing, drawn wall ironing, aluminum alloy AA3104, formability, yield strength, tensile strength, dome reversal pressure, elongation, axial load strength, tear off rate.*

Introduction

Aluminum alloy AA3104 is commonly used for carbonated soft drink can body with drawn wall ironing (DWI) process, this alloy is called $Al_{12}(Fe,Mn)_3Si$. The reason of using aluminum alloy

is because easy to form and non toxic[1]. The weakness of aluminum is low strength, so that will effect to the low strength of the dome of can when the thickness is reduced for production cost saving purpose. In the DWI can industry, 70% of production cost is from aluminum material. In order to reduce the thickness from 0.280 mm to 0.270 mm, small amount of titanium is added to the alloy to catch the can strength within the desired specifcation.

Experimental.

Three types of aluminum alloy AA3104 with variation titanium content are prepared for this research, i.e. Ti 0.00%, Ti 0.010%, Ti 0.013%, and the following composition is measured using Spark OES.

Table 1 Chemical Composition of Sample

Element	Alloy 1	Alloy 2	Alloy 3
	Content (weight %)	Content (weight %)	Content (weight %)
Si	0.130	0.130	0.130
FE	0.420	0.420	0.420
Cu	0.220	0.210	0.210
Mn	1.000	1.000	1.000
Mg	1.120	1.120	1.120
Zn	<0.0001	<0.0001	<0.0001
Ti	**<0.0001**	**0.010**	**0.013**
Cr	0.030	0.031	0.034
Ni	0.016	0.016	0.016
Pb	0.003	0.002	0.003
Sn	0.002	0.001	0.002
V	0.011	0.011	0.012
Cd	0.002	0.001	0.002
Al	97.040	97.050	97.040

Results and Discussion

Figure 1, 2 and 3 showed that the precipitation area of aluminum sheet alloy AA3104 on the top and longitudinal surface increase by adding of titanium up to 0.013%. This precipitation influence of the material strength.

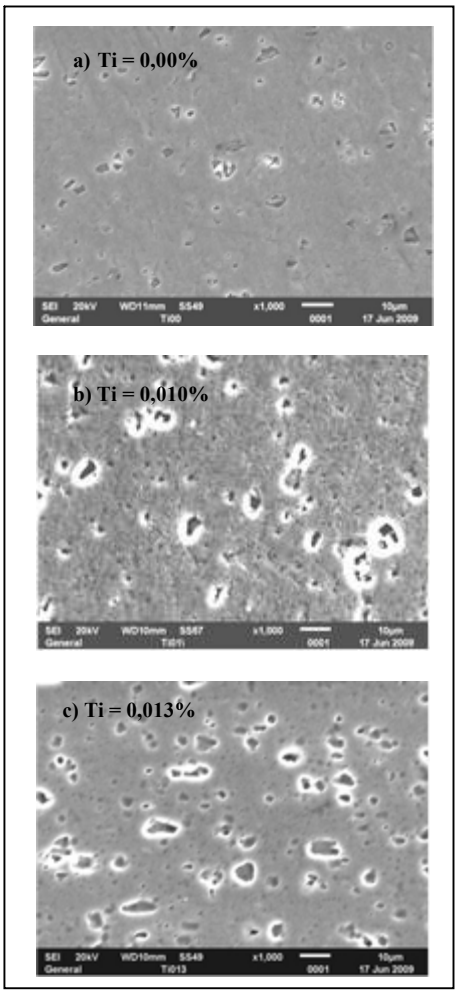

Figure 1. Micro Structure of Top Surface Aluminum Alloy Sheet AA3104 a) Ti = 0,00%, b) Ti = 0,010% and c) Ti = 0,013%

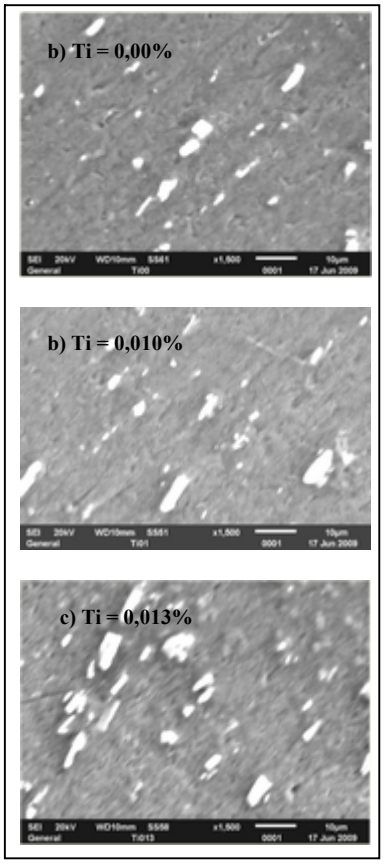

Figure 2. Micro Structure of Longitudinal Surface Aluminum Sheet Alloy AA3104 a) Ti = 0,00%, b) Ti = 0,010% and c) Ti = 0,013%

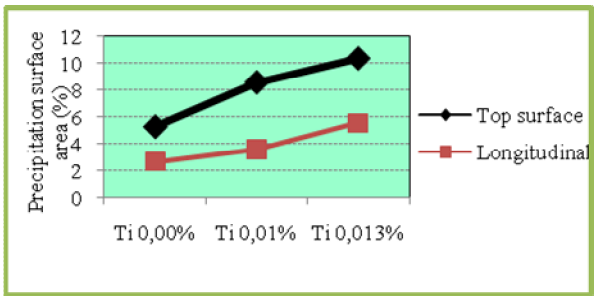

Figure 3. Precipitation Area of Top and Longitudinal Surface Aluminum Sheet Alloy AA3104 with Ti content 0,00%, 0,010% and 0,013%

Figure 4, showed that the sheet surface of Aluminum Alloy AA3104 with Ti content up to 0.013% has uniform particles and less roughness for both Ra and Rz scale, in this case titanium influences the grain size of aluminum alloy or titanium as the grain refiner of aluminum alloy[2]. The fine grain on sheet has an effect to increase of elongation and make a better formability during drawn wall ironing process (DWI).

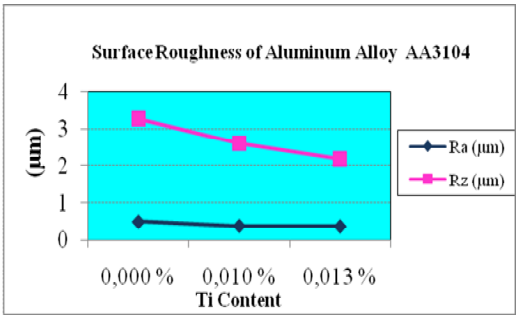

Figure 4 Surface Roughness Aluminum Alloy AA3104 with Ti = 0.00%, Ti = 0.010% and Ti = 0.013%

Figure 5 and 6, showed the tensile and yield strength test result for aluminum alloy AA3104 with the content of Ti = 0.00%, Ti = 0.010% and Ti = 0.013%. For this analysis, the sample was prepared according to the standard JIS 2201 (13B). The sample with titanium content up to 0.013% has tensile strength 3.02% and yield strength 3.52% above the sample without titanium. This is because the titanium formed intermetallic phase $AlTi_3$ and changed the rectangular grain to globular [3]. Tensile and yield sterngth are needed in relation to the can strength, as far as in good formability during DWI process.

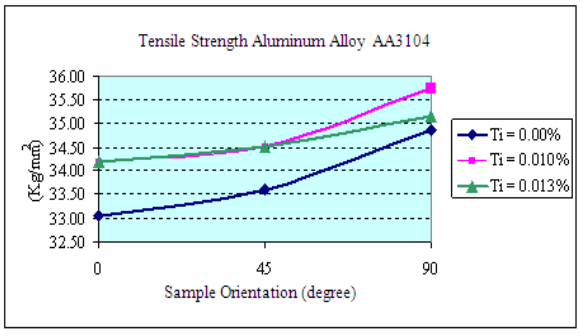

Figure 5 Tensile Strength Aluminum Alloy AA3104 with Ti = 0.00%, Ti = 0.010% and Ti = 0.013%

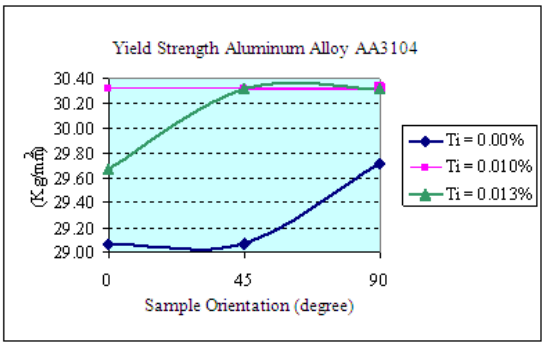

Figure 6 Yield Strength Aluminum AlloyAA3104 with Ti = 0.00%, Ti = 0.010% and Ti = 0.013%

The elongation test result as shown on figure 7 also increase about 46.32% compared to the sample without titanium, this phenomena is related to the finer grain size for sample with titanium content. The material with higher elongation should have better formability for deep drwing process.

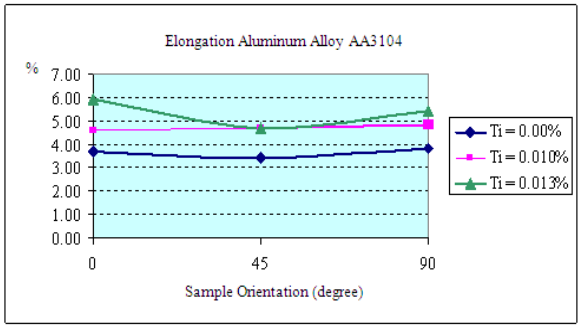

Figure 7 Elongation Aluminum AlloyAA3104 with Ti = 0.00%, Ti = 0.010% and Ti = 0.013%

Figure 8 is the analysis result of Limiting Drawing Ratio for the aluminum alloy AA3104 versus tear off rate during DWI process using Minster Cupper DAC-150-84 and Ragsdale Body maker machine. This analysis is conducted to find out the best LDR ratio in order to have the best tear off rate during DWI process. The best LDR ratio is 1.50.

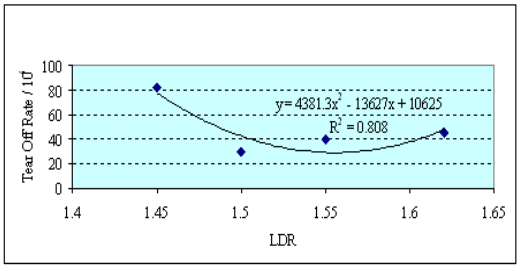

Figure 8 Limiting Drawing Ratio VS Tear Off Rate for DWI Process

Dome reversal pressure (DRP) is the plastic deformation on the dome area after the can is pressured from inside. Since the can will has inside pressure after filling, DRP is the important parameter on carbonated soft drink can. International standard for DRP is minimum 90 PSI.

Figure 9, showed the dome reversal pressure (DRP) for the two-piece aluminum DWI cans are made using aluminum alloy AA3104 with Ti = 0.00%, Ti = 0.010% and Ti = 0.013% before and after baking 210°C for up to 10 minutes. The result shown that the titanium content on the aluminum alloy AA3104 effected to increase the DRP. This is related to the above explanation regarding to the tensile and yield strength.

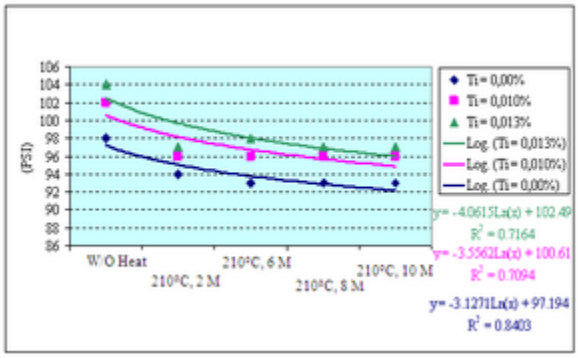

Figure 9 Dome Reversal Pressure (DRP) Without and With Heating Process of Finished Can

Axial load is the can body strength against the verical load. The weak point is in the middle of can body area. This simulation test is related to the closing process with double seaming system. Figure 10 showed that the axial load resistand of can body using aluminum alloy AA3104 with titanium content up to 0.013% have higher axial load resistance compared to the 0.00% titanium content , and reduced after baking for all of them.

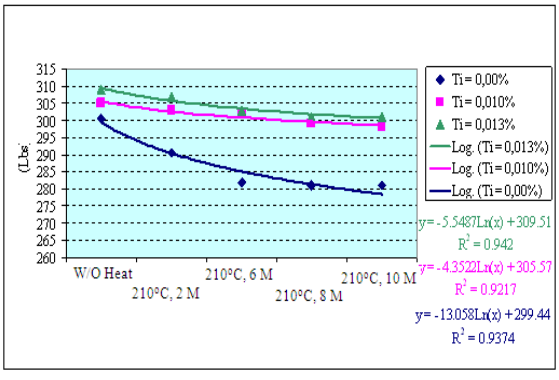

Figure 10 Axial Load Resitance Without and With Heating Process of Finished Can

Tear off rate is the total failure of the cans per million (ppm) during DWI process. Figure 11 showed that the tear off rate for the aluminum alloy AA3104 with titanium content up to 0.013% is better compared to the 0.00% titanium content. This is related to the elongation of material as already explained earlier.

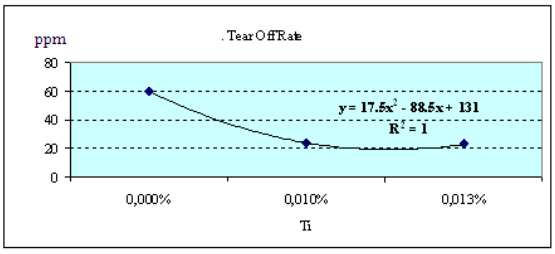

Figure 11 Tear Off Rate of DWI Process Using Aluminum AlloyAA3104 with Ti = 0.00%, Ti = 0.010% and Ti = 0.013%

The stability and capability process also was investigated on this research using SPC software – (NWA Quality Analyst 5.1) for aluminum alloy AA3104 with 0.013% Ti content, 0.270 mm thickness. Using the specific formula, the result was stable and capable, that is mean the material able to use for commercial production [4].

Conclusion

Based on the above investigation, by adding titanium up to 0.013% on the aluminum alloy AA3104 effected to the increasing of precipitation, finer grain size, more uniform particle, formed the intermetallic phase $AlTi_3$ and changed the rectangular grain to globular. These phenomena influence to the mechanical properties of material, i.e. increase tensile strength, yield strength, and elongation.

References

[1] S Smith, W.F. (1979). *Materials and Engineering Instituite*. Columbia: ASM International.
[2] Morris, J. G., Merchant, H. D., Westerman, E. J., Morris, P. L. (1993). *Aluminium Alloys for Packaging*. TMS. Pennsylvania.
[3] Zeren, M., & Karakulak, E. Microstructural Characterisation of Al-Si-xTi Cast Alloys. *Journal of Material Science and Technology*. *Material*. Jakarta.
[4] Gasversz, Vincent. (1998). Statistical Process Control Penerapan Teknik-Teknik Statistikal Dalam Manajemen Bisnis Total. Jakarta: PT. Gramedia Pustaka Utama.

Proceeding of the 11th International Conference on QiR (Quality in Research)
Faculty of Engineering, University of Indonesia, Depok, Indonesia, 3-6 August 2009
ISSN 114-1284

Electrical Characteristics of TiO_2 Added-Fe_2O_3 Ceramics For NTC Thermistor

Dani Gustaman Syarif[1], Dessy Yanti Maesaroh[2], Wiendartun[2]

[1]PTNBR-BATAN, Jl. Tamansari 71, Bandung 40132, INDONESIA.
Telp.:62-22-2503997, Fax.:62-22-2504081, Email:danigusta@yahoo.com
[2] Department of Physics, Indonesia University of Education (UPI), Jl. Setiabudhi 228, Bandung.

ABSTRACT

A study of the effect of TiO_2 addition on electrical characteristics of Fe_2O_3 ceramic for NTC thermistor has been performed. The aim was to know whether or not the TiO_2 addition can be made as a method for controlling electrical characteristics of the Fe_2O_3 ceramic for NTC thermistor. Powder of Fe_2O_3 derived from mineral containing Fe_2O_3 and TiO_2 with concentration of 0, 10 mole % and 20 mole % were mixed homogeneously. The mixed powder was pressed with pressure of 4 ton/cm^2 to form pellets. The green pellets were sintered at 1200^{o}C for 2 hours in air. After sintering, some pellets were analyzed by using an x-ray diffractometer (XRD) and a scanning electron microscope (SEM). Electrical resistivity of the pellets was measured at different temperatures. The XRD data showed that the pellets crystallized in Fe_2O_3 hematite. A second phase of Fe_2TiO_5 was found in the ceramics added with TiO_2. The SEM data showed that the grain size of the ceramics decreased with increasing TiO_2 concentration. It was known from the electrical data that the thermistor constant (B) and room temperature resistivity (ρ_{RT}) of the ceramics increased following the increase of the concentration of TiO_2. The value of (ρ_{RT}) and (B) of the Fe_2O_3 ceramics made in this work fits the market requirement.

Keywords: *Thermistor, NTC, Fe_2O_3, TiO_2, ceramic.*

1. INTRODUCTION

NTC thermistors are widely used for many kinds of instruments due to its special characteristic [1]. An NTC thermistor works based on the fact that the resistance of the thermistor decreases/increases when the surrounding temperature increases/decreases. Generally the NTC thermistors are made of spinel ceramics consist of transition oxide such as MnO, NiO, CuO, ZnO and CoO [2-12]. However, the thermistor can also be made from Fe_2O_3 ceramics due to its semiconductive characteristic[13-15].

In order to get capability in thermistor production and to step up the added value of mineral abundant in Indonesia, some researches have been carried out [13-15]. In our previous works [13], Fe_2O_3-based thermistor ceramics from yarosite mineral (containing Fe_2O_3) had been well produced and characterized. It was found that those Fe_2O_3 ceramics had relatively low resistivity. The resistivity of intrinsic Fe_2O_3 ceramic should be large due to its large band gap. So, the low resistivity may be due to the presence of TiO_2. It was found in our previous study that TiO_2 can lower the resistivity of the Fe_2O_3 ceramics [15].

In order to get Fe_2O_3 based-NTC thermistor having variable resistivity some efforts can be done. One of them is by adding additive. The addition of additive such as TiO_2 can be used as a method for controlling resistivity. Theoretically the capability of TiO_2 in lowering the resistivity will be limited by the solubility of TiO_2 in Fe_2O_3. Therefore the addition of TiO_2 with concentration larger than the solubility may increase the resistivity of the Fe_2O_3 ceramics. In this study the effect of TiO_2 addition with concentration of 10 mole % and 20 mole % on the electrical characteristics of the Fe_2O_3 was studied.

2. METHODOLOGY

Powder of Fe_2O_3 derived from yarosite mineral was mixed with TiO_2 powder with concentration of 0, 10 and 20 mole % TiO_2. The processing method for deriving Fe_2O_3

from mineral can be found elsewhere [13]. The mixture was mixed in an electrical blending machine. The homogeneous mixture was pressed with pressure of 4 ton/cm^2 to form pellets. The green pellets were sintered at 1200^{o}C for 2 hours in air. A structural characterization was done by using x-ray diffraction (XRD). Microstructure of the pellet was examined using a scanning electron microscope (SEM). Electrical characteristics were evaluated by measuring the resistivity of the pellets at various temperature from room temperature to 100^{o}C. Thermistor constant (B) and room temperature resistivity (r_{RT}) were determined from ln Resistivity versus 1/T curve based on equation (1) while sensitivity (a) was calculated using equation (2).

$$\rho = r_o \exp (B/T) \quad \ldots\ldots (1)$$

where, ρ = resistivity (ohm.cm), ρ_o = a constant (ohm.cm), B = Thermistor constant and T = temperature in Kelvin (K).

$$\alpha = B/T^2 \quad \ldots\ldots (2)$$

where, α = sensitivity (%/K), B = Thermistor constant in Kelvin (K) and T = temperature in Kelvin (K).

3. RESULTS AND DISCUSSION

3.1 XRD analyses

Figure 1-3 shows that all ceramics crystalized in Fe_2O_3 hematite (JCPDS 33-0664). The major peaks are from the Fe_2O_3 hematite, however, some additional peaks are clearly seen in Figure 2 and 3. These figures are belong to the samples containing 10 % mole and 20 mole % TiO_2. These additional peaks are from second phase. The second phase may be additive of TiO_2 or a reaction product of TiO_2 and Fe_2O_3. The result of analyses shows that the second phase is Fe_2TiO_5 (JCPDS 41-1432). During sintering a part of Fe_2O_3 reacted with TiO_2 additive following a reaction of equation (3).

$$Fe_2O_3 + TiO_2 \rightarrow Fe_2TiO_5 \quad \ldots\ldots (3)$$

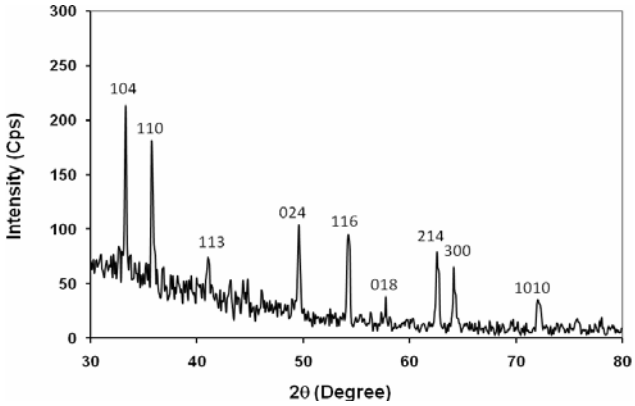

Figure 1: XRD profile of Fe_2O_3 ceramic without TiO_2.

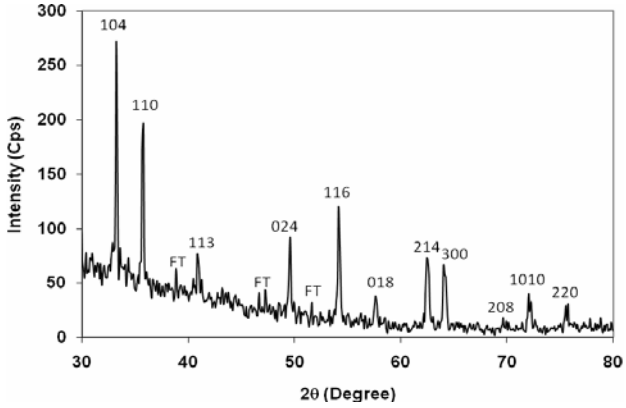

Figure 2: XRD profile of Fe_2O_3 ceramic with 10 mole % TiO_2 addition. FT is peak from the second phase of Fe_2TiO_5.

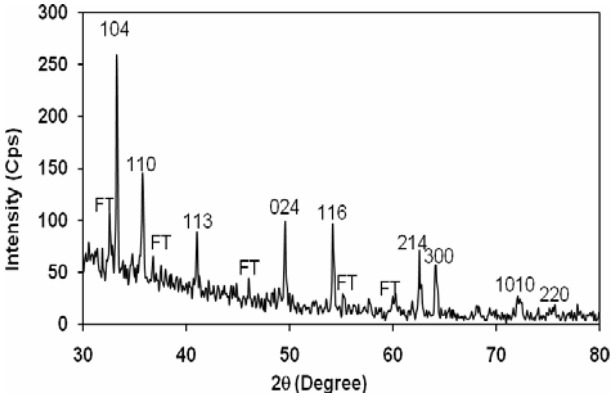

Figure 3: XRD profile of Fe_2O_3 ceramic with 20 mole % TiO_2 addition. FT is peak from the second phase of Fe_2TiO_5.

ISSN 114-1284

a. SEM analyses

It can be seen from Figure 4 that grain of the Fe_2O_3 ceramic containing TiO_2 is smaller than that of the ceramic without TiO_2. The grain becomes smaller following the increase of the concentration of the TiO_2 added. Quantitatively the decrease of grain size of the ceramic as function of the TiO_2 concentration is shown in Table 1. The decrease of the grain size is caused by the presence of the second phase of Fe_2TiO_5 which are segregated at grain boundaries. The second phase inhibited the grain growth during sintering.

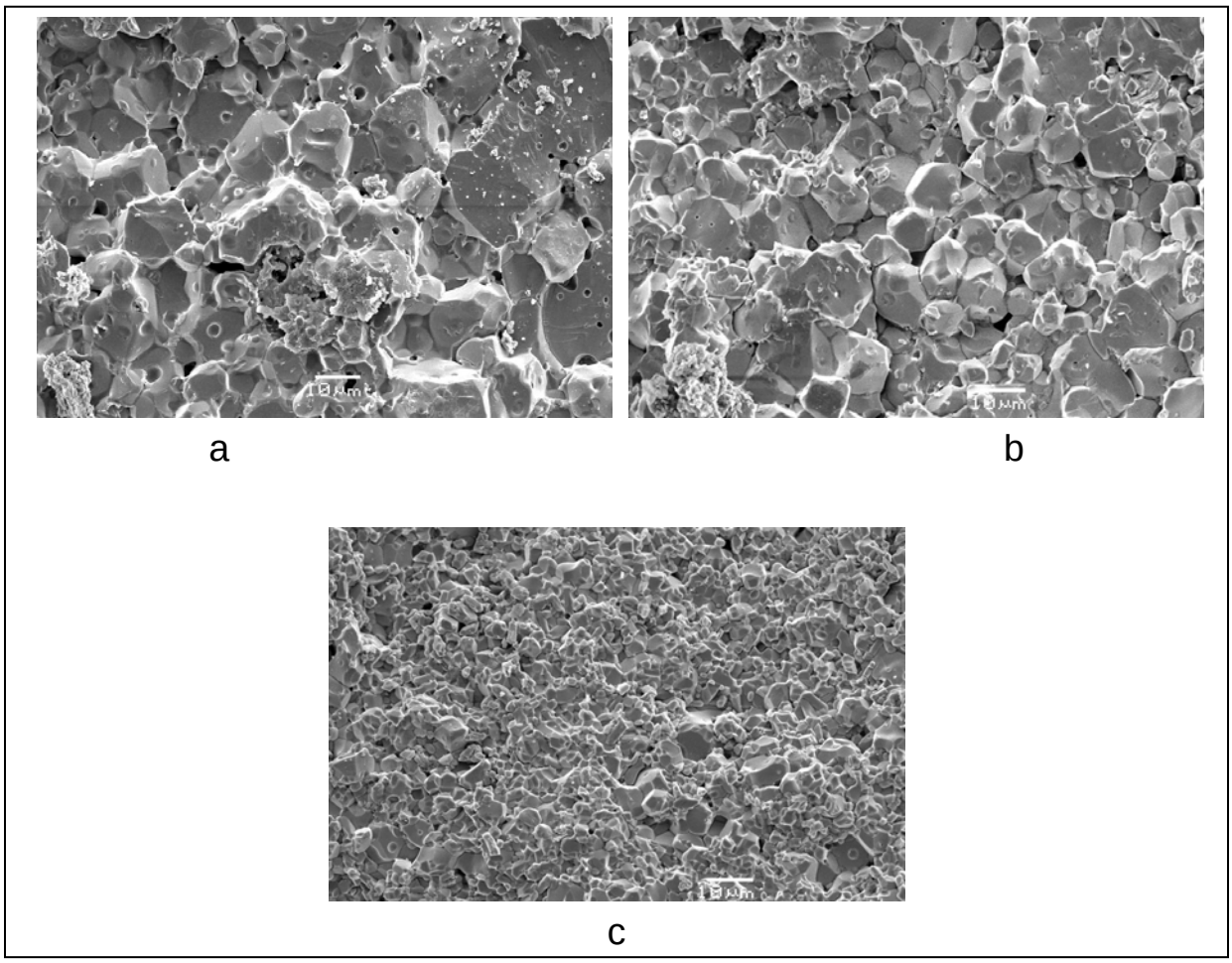

Figure 4: Microstructure of Fe_2O_3 ceramics with and without TiO_2 addition.

a. Without TiO_2, b. With 10 mole % TiO_2 and c. With 20 mole % TiO_2.

Tabel 1. Grain size of Fe_2O_3 ceramics as a function of TiO_2 concentration.

No.	Concentration of TiO_2 (Mole %)	Grain size (μm)
1.	0	19.6
2.	10	14.4
3.	20	9.3

b. Electrical Characteristics

Electrical data of the TiO_2 added-Fe_2O_3 ceramics is shown in Figure 5 and Table 2. The electrical data of Fig. 5 shows that the electrical characteristic of the ceramics follows the NTC tendency expressed by an Arrhenius equation of eq. 1 [2,3,7-15]. As shown in Table 2 and Fig. 5, the room temperature, thermistor constant and sensitivity of the ceramics increases with the increase of TiO_2 concentration. The responsible factor for increasing the resistivity, thermistor constant and sensitivity is the presence of second phases Fe_2TiO_5 which is segregated at grain boundaries. The presence of the second phase resulted in ceramics with small grain. The grain boundaries are scattering center for charge carrier, so the many the grain boundaries are, the large the resistivity is. This situation also causes the thermistor constant and sensitivity become large. Comparing to the value of room temperature resistivity, B and α for the industry (where the room temperature resistivity is not larger than 1 Mohm, B and α are equal or larger than 2000K and 2.2%/K, respectively)[6], the room temperature resistivity, B and α of all ceramics fit the requirement.

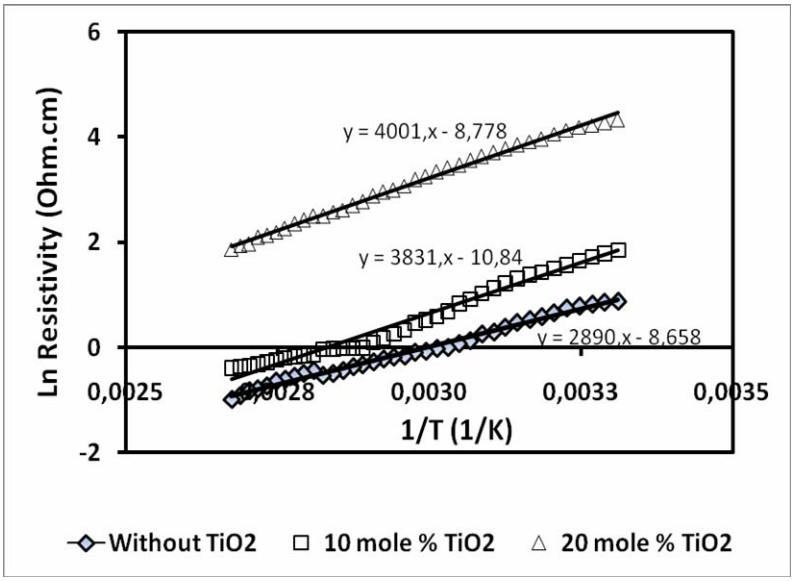

Figure 5: Ln Resistivity vs 1/T for Fe_2O_3 ceramics with and without TiO_2.

Tabel 2. Electrical characteristics of Fe_2O_3 with and without TiO_2 addition.

No.	Composition	B (K)	α (%/K)	ρ_{RT} (Kohm)
1.	Without TiO_2	2890	3,21	0,98
2.	10 mole % TiO_2	3831	4,26	1,93
3.	20 mole % TiO_2	4001	4,45	4,56

4. CONCLUSION

The grain size of the Fe_2O_3 ceramics decreases by addition of TiO_2 because the added TiO_2 reacted with a part of Fe_2O_3 forming Fe_2TiO_5, segregated at grain boundaries and inhibited grain growth during sintering. The addition of TiO_2 increased the room temperature resistivity (ρ_{RT}), the thermistor constant (B) and sensitivity (α) of the Fe_2O_3 ceramics through changing the microstructure. The value of (ρ_{RT}), (B) and (α) of the Fe_2O_3 ceramics made in this work fits the market requirement.

AKCNOWLEDMENT

The authors wish to acknowledge their deep gratitude to Mr. M. Yamin for his help in preparation of Fe_2O_3 from yarosite mineral.

REFERENCES

[1]. BetaTHERM Sensors [on line]. Available: http://www.betatherm.com.

[2]. M. Parlak, T. Hashemi, M.J. Hogan, A.W. Brinkman, "Electron beam evaporation of nickel manganese thin film negative temperature coefficient thermistors", Journal of materials science letters, Vol.17, p.1995, 1998.

[3]. E. S. Na, U. G. Paik, S. C. Choi, "The effect of a sintered microstructure on the electrical properties of a Mn-Co-Ni-O thermistor", Journal of Ceramic Processing Research, Vol.2, No. 1, 2001, p 31-34.

[4]. Y. Matsuo, T. Hata, T. Kuroda, "Oxide thermistor composition", US Patent 4,324,702, April 13, 1982

[5]. H. J. Jung, S. O. Yoon, K. Y. Hong, J. K. Lee, "Metal oxide group thermistor material", US Patent 5,246,628, September 21, 1993.

[6]. K. Hamada, H. Oda, "Thermistor composition", US Patent 6,270,693, August 7, 2001.

[7]. K. Park, "Microstructure and electrical properties of $Ni_{1.0}Mn_{2-x}Zr_xO_4$ ($0 \leq x \leq 1.0$) negative temperature coefficient thermistors", Materials Science and Engineering, B104, 2003, p. 9-14.

[8]. K. Park, D.Y. Bang, "Electrical properties of Ni-Mn-Co-(Fe) oxide thick film NTC thermistors", Journal of Materials Science: Materials in Electronics, Vol.14,2003, p. 81-87.

[9]. S. G. Fritsch, J. Salmi, J. Sarrias, A. Rousset, Shopie Schuurman, Andre Lannoo, "Mechanical properties of nickel manganites-based cermics used as negative temperature coefficient thermistors", Materials Research Bulletin, Vol. 39, 2004, p. 1957-1965.

[10]. R. Schmidt, A. Basu, A.W. Brinkman, "Production of NTCR thermistor devices based on $NiMn_2O_{4+\delta}$", Journal of The European Ceramic Society, Vol. 24, 2004, p. 1233-1236.

[11]. K. Park, I.H. Han, "Effect of Al_2O_3 addition on the microstructure and electrical properties of $(Mn_{0,37}Ni_{0,3}Co_{0,33-x}Al_x)O_4$ ($0 \leq x \leq 0.03$) NTC thermistors", Materials Science and Engineering, B119, 2005, p. 55-60.

[12]. Wiendartun, D. G. Syarif, The Effect of TiO_2 Addition on the Characteristics of $CuFe_2O_4$ Ceramics for NTC Thermistors, Proceeding of the International Conference on Mathematics and Natural Sciences (ICMNS) 2006, ITB, Bandung, 2006.

[13]. D. G. Syarif, A. Ramelan, "Electrical Characteristics of NTC Thermistor Ceramics made of Mechanically Adtivated Fe_2O_3 Powder derived from Yarosite", Proceeding of the 2007 International Conference on Neutron and X-ray Scattering (ICNX 2007), Bandung Institute of Technology, Indonesia, 2007.

[14]. D. G. Syarif, "Fabrication of thick film ceramics for NTC thermistor using Fe_2O_3 derived from mineral", International Conference on Instrumentation, Communication and Information Technology (ICICI 2007) Proc., 271-274, 2007.

[15]. D. G. Syarif, Karakterisasi keramik Fe_2O_3:1mTi hasil sinter dan perlakuan panas, Jurnal Mesin Trisakti (in Bahasa Indonesia), Vol.9, No.1, 2007.

Proceeding of the 11th International Conference on QiR (Quality in Research)
Faculty of Engineering, University of Indonesia, Depok, Indonesia, 3-6 August 2009
ISSN 114-1284

Resin flow on Manufacturing Process of Kenaf/Polyester Composite by Vacuum Assisted Resin Infusion (VARI) Method

A.H. Dawam Abdullah, M. Karina, H. Onggo, A. Syampurwadi

Research Center For Physics,
Indonesian Institute of Science (LIPI), Bandung 40135
Telp : (022) 2503052, Fax : (021) 2503050
E-mail : dawamdullah@yahoo.com

ABSTRACT

This research is aimed to investigate the detail process of Vacuum Assisted Resin Infusion (VARI), which the most important method in composite manufacturing. The Kenaf fiber is used as reinforce, whereas as matrix is used Unsaturated Polyester Resin (UPR). There are two preform used here, they are woven and uni-directional (UD). VARI method is performed to get high quality impregnation composite. Parameter to be identified are the inlet-outlet position and type of preform. Several tests and characterization have done to revealed the properties of composite and its mixture elements. SEM analysis is done to identified the fiber's morphology and degree of impregnation. Viscosity of resin is measured by brokfield test to found out time needed during VARI process. Front flow pattern of resin is observed by camera image incrementally. For woven preform, wetting process done easier than uni-directional (UD). And Diagonal inlet-outlet position let the most efficient of wetting process.

Keywords : *Composite, vacuum, preform, resin flow*

1. INTRODUCTION

The vacuum assisted resin infusion (VARI) offers many advantages over the traditional resin transfer molding such as lower tooling cost and room temperature processing [1]. VARI has chiefly been used to produce large component in short series, such as boats, offshore structures, vehicle body panel, front end for high speed train engines [5]. VARI process simply can be divided into 3 (three) steps: First, pre-molding, fiber preform is put inside the flexible vacuum bag. In this step, inlet and outlet is adjusted to avoid cavity that could make the leakage. Next, vacuum process, by adequate vacuum pressure the resin will pull-in and get into vacuum so the resin will flow and impreg into fiber preform. Finally, at certain time, the curing process will occurred and resin will get solidified. So composite is taken out of the mold. Schematically, steps are described by fig.1 [1].

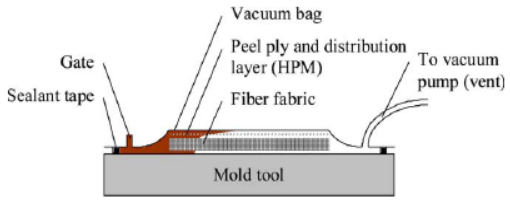

Figure 1 : VARI method

This study focuses on flow pattern of fiber preform and composite properties. Wetting process is the critical point in Vacuum Assisted Resin Infusion (VARI). Incomplete impregnation will lead to defective parts containing dry spots. So processing parameters such as the number and location of inlet and outlet parameter need to be properly set [1]. Preform role as a significant parameter wheather difficult or ease to be flowed by resin. There are two methods in approaching VARI process. They are experimental observation and modeling/simulation. Experimental describe more detail the process and without any simplification at circumstance condition. But, it is very costly due to many experiments that must be done. In other hand, simulation approach give more sophisticated analysis of process. Of course, need to be implemented complex mathematical model, in spite of simplification maybe applied to make it possibly countable.

2. METHOD

Morphological properties of fiber and preform were carried out by using Scanning Electron Microscope - SEM (type JEOL 330). In term of resin curing, the reaction is exotermic. As resin flow, time elapsed before solidification is critical point at pre-cure analysis. Time vs viscosity of resin is plotted by measuring viscosity of the catalized-resin by Brokfield Inst (manufactured Brookfield Engineering Analysis, Inc). In making composite, it was prepared two type of preforms, they are woven and uni-directional (UD) of kenaf fibers. Numbers of fibers stacking here are single layer and 2 (two) plies. During resin flowing, wetting process is recorded incrementally. So by marking the sign, each step/front flow of

resin flowing will be recorded. Degree of impregnation of resin through the fibers is a analyzed by scanning electron microscope. VARI process is powered by vacuum pump with the capacity of vacuum 4 cfm, 5x10-1 Pa.

3. RESULT

3.1. VARI system

VARI system that was designed consist of single vacuum pump, as schematically seen at fig.2. On between port outlet and the pump is placed resin-trap to avoid unintended suck of resin through the pump. On the figure, resin inlet is dummy, whereas the actual experiment will be described later. Vacuum bag with fiber preform inside is placed on the glass table as half molding. As we know another half molding is roled by the vacuum bag.

.

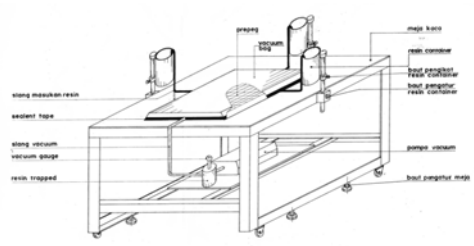

Fig 2 : VARI designed

3.2 Resin curing properties

As mentioned before, to identified the curing properties of resin , we measure the viscosity of resin by Brookfield method. And the result as fig.3 showed that resin curing time is about 15 minutes, which is occurred at 0.1 % hardener. This mean, to process the composite, resin should be completely distributed on whole preform shorter than 15 minutes. Otherwise, the resin will get stuck before complete wet process.

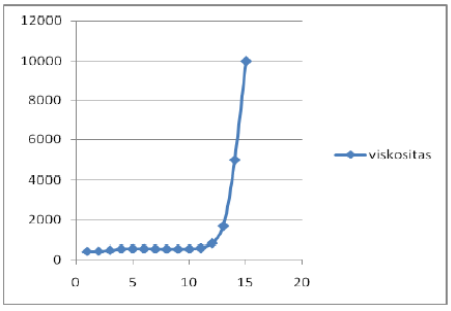

Figure 3: Time vs viscosity of resin

3.3 Fiber - Preform geometry

As received , the fiber is identified regarding the geometry and surface morphology. Figure 4 & 5 describe below more detail. Geometry of preform is given by camera image, whereas surface morphology of fiber is resulted from SEM characterization.

(a) (b)

Fig 4 : camera image of preform : (a) woven ; (b) unidirectional-UD

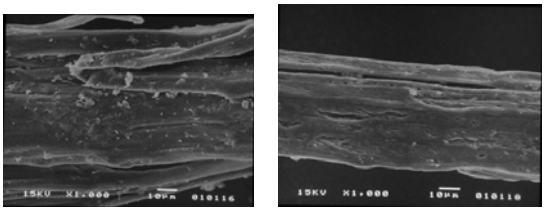

(a) (b)

Fig 5 : SEM image of fiber from prefom : (a). woven ; (b). unidirectional-UD

3.4 Resin front flow patterns

Incrementally observation of resin flow is aimed to understand how does the resin geometrically flowing. This is beneficial to predicting resin wet flow pattern for the specific shape composite.. Here, the result for several type resin front flow profile

3.4.1 Unidirectional (UD) ; I-port vs Y-port ; 1 (one) layer ; time process ± 13 minutes

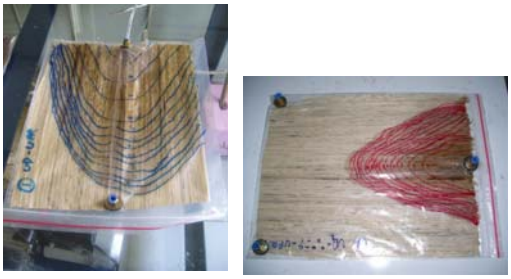

(a) (b)

Fig 6 : Camera image of wetting process : (a) I- port ; (b). Y-port

3.4.2 Woven ; I-port vs Diagonal-por ; 2 (two) layer ; time process 8 minutes

Fig 7 : Camera image of wetting process : (a) I- port ; (b). Diagonal-port

3.4.3 Woven : Diagonal-port vs Y-port, 2 (two) layer, time process > 5 minutes

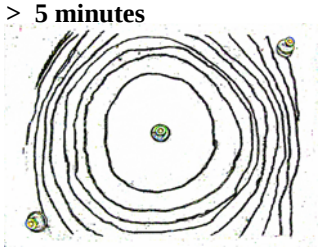

Fig 8 : Image view resin flow of Diagonal port . (the curve line refer to front flow for each minute, dimension 29x34 cm)

by measuring wetting area incrementally we could tabulate the data as given in Table 1 and fig 8.

Table 1 : Resin flow of diagonal port, woven

Time (minute)	Wetting Area (cm2)	Percent area (%)
1	178	27
2	336	51
3	442	68
4	529	81
5	653	100

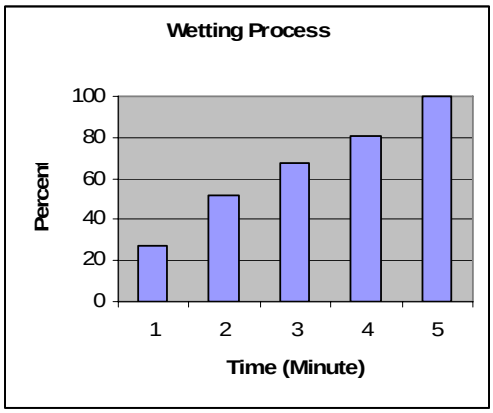

Fig 9 : Chart of resin flow of Diagonal-port, woven .

Whereas, by different condition, for Y-port, image view of resin flow is given by fig 10.

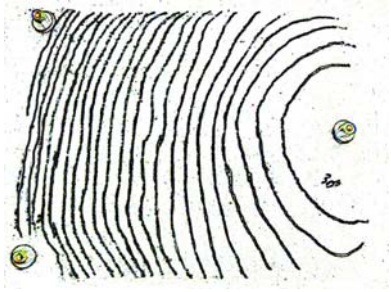

Fig 10 : Image view resin flow of Y-port . (the curve line refer to front flow, where for each line gaps mean 1/2 minutes; dimension 29x34 cm)

So did before, we can measure the area incrementally as given in Table 2 and Fig 11.

Table 2 : Resin flow of Y- port , woven

Time (minute)	Wetting Area (cm2)	Percent Area (%)
1	129	23
2	223	40
3	283	51
4	342	62
5	396	71
6	443	80
7	485	88
8	521	94
9	554	100

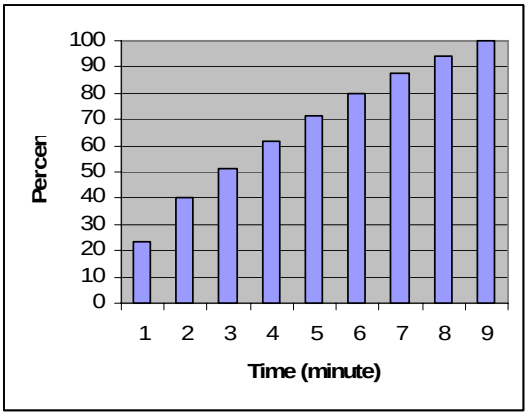

Fig 11 : Chart of resin flow of Y port ,woven

3.5 Resin Impregnation

After resin cured, a better way to identified degree of resin impregnation is observeing cross section of composite. For this purpose, SEM analysis was performed to reveal microstructure of composite as seen the result at fig. 12

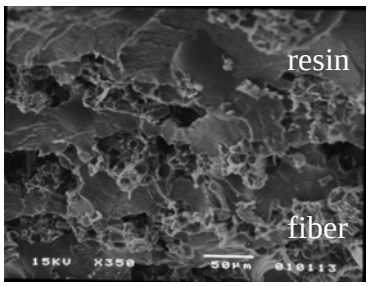

Fig 12 : SEM image of composite's cross section

4. DISCUSSION

As mentioned on previous section, here we can analyze several matter through the research. At first, by fig.3, it is simply said that for hardener content 1%, the resin will solidify by less than 15 minutes. Dramatical rise-up of viscosity after 15 minute (mixing resin + hardener) as evidence for it. Theoritically, short after this glassy state, resin change its phase from liquid into solid. This phenomena occurred due to crosslink mechanism of the resin. [4]

Fig 4 and 5 tell about fiber condition of both preform, they were woven and unidirectional (UD). Although raw material of both preform are the same, kenaf fiber, there were slightly difference between them. As a woven preform, the fiber are perpendicular to each other. Naked eye observation revealed that big portion area of vacancies inside the preform. Those big vacancies role as resin pathway. This is lead to efficient process during resin flow. Resin will flow rapidly even without resin flow media. On the other hand, for UD preform, the fibers lay on paralell manner as it's very dense condition. Through these preform, composite may has a good fiber volume fraction due to rather big portion. But as a drawback, upon manufacturing process, resin will get difficult to wet the preform due to less vacancies. And when observing fiber diameter by SEM, the image exhibit both are have the same diameter $\pm$ 50µm, fit to the previous research about kenaf fiber [3].

Fig 6 describe front flow of resin flow on UD preform. The image explain how the position inlet-outlet lead to different sucking mechanism. With the elapsed time 13 minutes (just before curing), outermost front flow of I- port reach longer distance than Y-port. It mean, I-port give more efficient wetting process than Y-port on uni-directional (UD) preform. Fig 7 show different thing. By these figure, it can be compared wetting process on woven preform according to inlet-outlet position. It was resulted that Diagonal-port has better wetting process than I-port. Where, to accomplishment of total layer, diagonal-port need sorter time than I-port, within $\pm$ 3 minutes.

Fig 8-11 describe wetting mechanism on woven preform. By those, It is clearly explained that for flowing process, resin are linearly flowing. It is proven by chart on fig. 9 and 11 : time vs percent wetting area relation. Mechanically meaning that, gradient of pressure inside the vacuum merely constant during flowing. As we know, source power that make resin to flow into the preform is gradient of pressure from inlet to otlet port due to vacuum pump. Fig 8 and 10 show that on the same preform (woven) resin flow at Diagonal – port resulted in higher efficiency. The time process cut almost 50%, so make it is highly distinct. One reason as hypothesis to explain about that is, condition of pressure gradient Diagonal-port is distributed more homogenously than I-port.

Fig 12 is SEM image of cross section of UD kenaf fiber/ UPR composite. Clean (black) area refer to resin formation after curing. Whereas white rough area represent the fiber inside resin. These observing reveal information that resin successfully impreg to the vacancies between fibers. They role as a binder among fiber. where each bundle fiber enclosed perfectly. Furthermore, at given magnification, no void observed after curing. This is as respectly achievement by VARI, to get high-fiber fraction volume for enlarging the role of fiber on composite [2].

5 . CONCLUSION

Keneaf/UPR composite has successfully manufactured by VARI method. Several parameters were performed and observed. It is reveal some conclusion. First, by comparing woven and uni directional fiber, we got that VARI process for woven preform run easier than unidirectional (UD). Second, Diagonal-port for woven reach more efficient wetting than Y-port. And third, through VARI, resin good impreg onto the fiber as seen by SEM image.

6. ACKNOWLEDGMENT

We appreciate to Research Center for Physics, Indonesian Institute of Science (LIPI) who kindly fund all matter for this research. And special thank to Herlan Abbas, who dedicated support all technical problem we have.

REFERENCES

[1] C.J. Dong, Development of a process model for the vacuum assisted resin transfer molding simulation by the response surface method in Composites, Part A : Applied Science and Manufacturing, Elsevier, 2006, part A 37 :1316-1324

[2] X. Song, Vacuum Assisted Resin Transfer Molding (VARTM) : Model Development and Verification, Dissertation in Virginia Polytechnique Institute and State University, Virginia, 2003,

[3] A. H . Dawam Abdullah, Hermawan J, Holia, Study of Morphology and Mechanical Properties of Kenaf Fiber, Proceeding in Indonesian Polymer Association VII, Jogjakarta, 2007

[4] I.K. Varma and V.B. Gupta, Thermosetting Resin-Properties, Comprehensive Composite Materials, Vol 2, pp : 1-56, Elsevier, 2000

[5] B.T. Astrom, Manufacturing of Polymer Composites, Chapman & Hall, Sweden, pp : 229-231, 1997

Synthesis and Characterization of Macro Pores Ceramics Based on Zeolite and Rice Husk Ash

Deni S. Khaerudini[1], Anggito P. Tetuko[1], and P. Sebayang[1]

[1]*Research Centre for Physics, Indonesian Institute of Sciences*
Kawasan PUSPIPTEK Serpong Tangerang 15314
Email: deni008@lipi.go.id

ABSTRACT

The characterization of ceramic pore membrane prepared by dry casting was investigated. The ceramics were made with zeolite and rice husk ash at various compositions: 100:0, 90:10, 80:20, and 70:30 %wt. The average particle size of raw material is about 70 µm. The porous ceramics were produced in several stages: zeolite and rice husk ash powder are mixed using ball mill for 0.5 h; then porous compact are formed by packing suspensions into "green" compact with a certain shape at 20 MPa using hydraulic press, and the green compact is consolidated by sintering at 900°C and 1000°C for 1 h. The porous ceramics were characterized using various parameters, such as: firing shrinkage, porosity, density, compressive strength, bending strength, Vickers hardness, as well as XRD and SEM for microscopic analysis. Experimental results indicate that the method and compositions have strong effects on the crystallinity type, physical, and mechanical properties of the synthesis products. Firing shrinkage and density test result are tend to decrease with increasing of RHA content addition and sintering temperature, but for the others test result such as porosity, compressive strength, bending strength, and hardness Vickers are linear with increasing of RHA content addition and sintering temperature.

Keywords

Porous ceramics, zeolite, rice husk ash, porosity, density

1. INTRODUCTION

Zeolites are hydrated crystalline aluminosilicates with open three-dimensional framework structures, made up of SiO_4 and AlO_4 tetrahedral linked by sharing their oxygen atom to form regular intracrystalline cavities and channels of atomic dimensions. The framework structure encloses cavities occupied by large ions and water molecules, both of which have considerable freedom of movement, permitting ion exchange and reversible dehydration. Zeolit can be represented by the formula $M_{2/n}.O.Al_2O_3.a.SiO_2.b.H_2O$ or $M_{c/n}.\{(AlO_2)_c(SiO_2)_d\}.b.H_2O$ where M is the compensating cations with valence n, a and b is silicate dan water molecule, c and d is the amount of tetrahedra of alumina and silica. Rasio d/c or SiO_2/Al_2O vary from 1 to 5.

Natural zeolites have been widely used because of their unique physical-chemical characteristics such as ion-exchange property and selectivity in sorption [4, 5]. Zeolites are the aluminosilicate minerals that have a porous structure. Zeolite pores consists of 8, 10, 12 and 14 membered of oxygen ring systems to form tube-like structure and pores that interconnected to each other. Tube-like structure can exists as one, two or three direction with different sizes. Zeolites can be classified based on their pore size; small pore within 5Å; medium pore, within 4.5 Å to 6.4 Å; and large pore within 6.5 Å - 7 Å [1] Zeolites are widely used as ion-exchange beds in domestic and commercial water purification, softening, and other applications. In chemistry, zeolites are used to separate molecules (only molecules of certain sizes and shapes can pass through), as traps for molecules so they can be analyzed. Nowadays, zeolites are also employed as alternative heterogeneous catalysts to substitute homogenous catalysts in many organic processes such as in Friedel-Crafts reaction because of its more efficient and environmentally-friendly which can eventually reduce plant corrosion and eliminate environmental problems.

It is well known that many plants have an ability to accumulate silicon compounds. One example is rice (Oryza sativa), one of the major cultivated plants in the world including in Indonesia. It is a fibrous material containing cellulose as the major constituent, lignin, and ash [2]. As the main component in the rice husk ash is the silica, it can be used as a source or added component in preparing advanced materials like SiC, Si_3N_4, elemental Si and Mg_2Si. During production of rice, huge amounts of rice husk are left as waste product. Husk is usually disposed of by combustion, thus giving rice husk ash (RHA). This by-product is produced in many places world-wide and constitutes an environmental problem due to air and water pollution. On the other side, chemical analysis shows that a white variety of RHA can contain up to 90–99% silica. It is, therefore, not unusual that this cheap source of silica may be of interest for numerous industrial uses, including the large-scale

synthesis of porous ceramics. Previously, the content of rice husk ash at different combustion temperatures has been studied. The white ash that was obtained from combustion is generally 10 -15 % of the total dry weight of rice husk. The abundant rice husk ash in Indonesia is giving alternative economical sources for synthesizing zeolite pore ceramics.

Porous ceramic have potential for applications as critical components in many industries because of their inert, strong, reusable, and temperature resistant capabilities. These properties may open various field for applications, such as in thermal insulation purposes, building materials, gas separation, water treatment, and etc. A great deal of research work has been devoted to porous ceramics in the past few decades, including various fabrication techniques with different starting materials [3]. At present, porous ceramic membranes used as separation media are usually made from high purity powders such as Al_2O_3, ZrO_2, SiC, and mullite. However, high cost resulted from the expensive starting materials and high sintering temperature, which limit their applications, especially in water treatment application. Therefore, searching for cheaper starting materials with lower sintering temperature is meaningful. Porous ceramics are produced within a wide range of porosities and pore sizes depending on the application intended. The manufacture of porous ceramic is concerned with macro pores (above 0.1 μm in diameter) for microfiltration, micro pores (ranging from 0.1 μm to 2-3 nm) for ultrafiltration, and nano pores (less than 3 nm) for nanofiltration [4]. Porous ceramic are especially suitable for processes with high temperatures and harsh chemical environments or for processes were sterilizability of the membrane is important [5, 6].

In this paper, our objective was focused on preparation of the wide-pore zeolite, a potentially interesting aluminosilicate for many catalytic applications. The objective of this paper is to explore the synthesis of zeolite using white rice husk ash as the silica source. In this study the synthesis of zeolite pore ceramics using amorphous rice husk ash which was obtained by controlled burning of rice husk, as silica sources. The brief discussion on manufacture and modification of porous ceramic with special attention to zeolite and rice husk ash are presented. The effect of each composition on performance of the ceramics not only in porosity but also in others properties, such as: firing shrinkage, density, compressive strength, bending strength, Vickers hardness, XRD, and SEM are discussed.

2. METHOD

Natural zeolite powder was obtained from Pahae, Simangumban, North Sumatera, Indonesia (figure 1.a). The main chemical compositions of the natural zeolite pahae was 60.18% SiO_2, 14.25% Al_2O_3, 11.61% CaO, 3.96% MgO, 4.41% Fe_2O_3, 3.47% K_2O, 1.64% Na_2O, 0.48% TiO_2 by weight. Meanwhile, the rice husk (figure 1.b) was obtained from Gunung Sindur, Bogor, West Java, Indonesia. Rice husk was cleaned with water and boiled with 1 N HCl for 3 h to remove impurities. Then it was burned at 900 ^oC for 2 h under oxygen atmosphere. The obtained ash was found to be an amorphous phase having the following chemical compositions: 94.18% SiO_2, 0.20% Al_2O_3; 1.50% CaO, 1.58% K_2O, and 2.54% Fe_2O_3 by weight. The average particle size of the zeolite and rice husk ash is about 70 μm (as shown in figure 1.a and 1.b). The synthesis of zeolite ceramic pore membrane was prepared by dry casting method. The mixture of zeolite and rice husk ash at various compositions: 100:0, 90:10, 80:20, and 70:30 in %wt ratio with sodium silicate (Na_2SiO_3 5 %wt) as binder agent was ball milled for 0.5 hour. After mixing process, zeolite and rice husk ash powder was then placed in cylindrical steel to obtained porous compact (green body) with a certain shape at 20 MPa using hydraulic press. Final process of synthesis, the green compact was consolidated by sintering in electrical furnace at 900 ^oC and 1000 ^oC for 1 h. After soaking the samples were furnace cooled and the specimens are ready for tested.

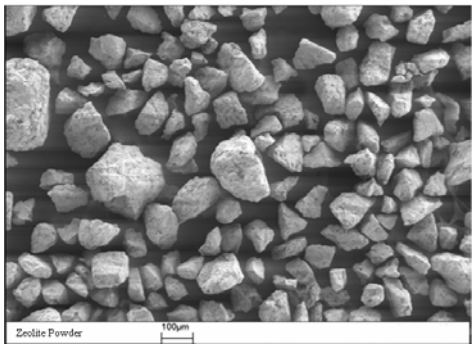

(a)

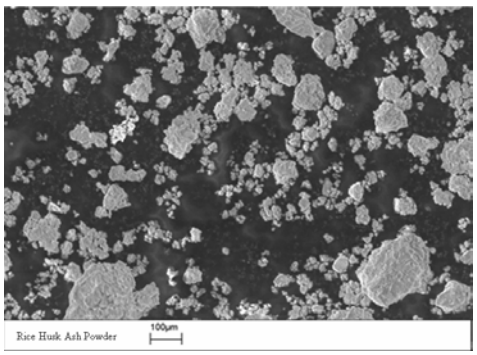

(b)

Figure 1. Photomicrograph of (a) natural zeolite and (b) rice husk ash as raw material

In the casting (shaping) process of ceramics, it usually used the additive (binder agent) to simplify casting process and also to control the microstructure of the material that will be produced. The main function of binder is to increase the strength before heat treatment process applied as green body. Sintering is densification process of particle in high temperature below the melting point, to increase the density and strength of material. In drying process, microstructure changes occur. The green

body obtained from dry casting process is sintered to decrease water content and eliminate the binder which is still remaining in specimen.

The density and porosity of the sintered specimens was determined by Archimedes' method. Analysis of the crystalline phases present in the sintered specimens was based on their X-ray diffraction (XRD) patterns with CuK radiation. Types of zeolite were identified by comparing the peak positions (2 and their intensities from the obtained XRD-pattern with that of pure phase). The microstructure photographs were observed on Scanning Electron Microscopy (SEM). The measurement of compressive, bending strength, hardness, and firing shrinkage were performed to confirm the mechanical properties of specimens.

3. DISCUSSION

The density and porosity of the sintered specimens were measured using Archimedes water displacement method at room temperature. The porosity and density as a function of RHA content at different sintering temperature is shown in figure 2.

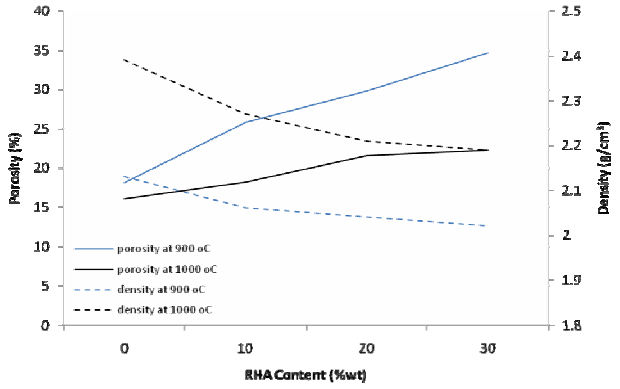

Figure 2. Effect of RHA content to the density and porosity behavior at sintering temperature 900 °C and 1000 °C

The RHA concentration addition strongly affected the porosity and density. This indicates that the porosity and density result can be widely controlled by the RHA concentration addition to the specimen. On the other hand, the density and porosity of the sample is determined almost entirely by the intrinsic Si addition of RHA itself. Porosity test results of specimen for sintering 900 °C were 18.08, 25.78, 29.69, and 34.59 %; and for sintering 1000 °C were 16.07, 18.19, 21.51, and 22.22 % measured by Archimedes method, for RHA content 0, 10, 20, and 30 wt% respectively. Density test results of "green" compact specimen were 1.45, 1.42, 1.35, and 1.34 g/cm^3 measured by Archimedes method, for RHA content 0, 10, 20, and 30 wt% respectively. After sintering process, density test results of specimen for sintering 900 °C were 2.13, 2.06, 2.04, and 2.02 g/cm^3; and for sintering 1000 °C were 2.39, 2.27, 2.21, and 2.19 g/cm^3, for RHA content 0, 10, 20, and 30 wt% respectively.

This observation is based on considering not only the porosities and pore sizes but also other mechanical properties testing. The mechanical properties of porous ceramics are shown in figure 3, 4, and 5 in sequence. The compressive and bending strength as a function of RHA addition at different sintering temperature is shown in figure 3. The influence of RHA addition and especially sintering temperature changed the distribution of compressive and bending strength significantly. The higher sintering temperature, the higher compressive and bending strength is at the same given weight fraction of the RHA increase. Compressive strength test results of specimen for sintering 900 °C were 8.48, 15.82, 17.50, and 27.59 MPa; and for sintering 1000 °C were 35.25, 49.34, 70.87, and 74.08 MPa, for RHA content 0, 10, 20, and 30 wt% respectively. Bending strength test results of specimen for sintering 900 °C were 4.03, 5.77, 6.38, and 7.25 MPa; and for sintering 1000 °C were 17.87, 18.09, 18.58, and 20.46 MPa, for RHA content 0, 10, 20, and 30 wt% respectively.

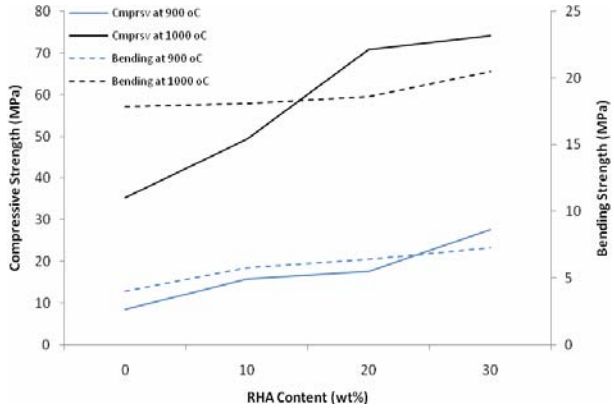

Figure 3. Effect of RHA content to the compressive and bending strength behavior at sintering temperature 900 °C and 1000 °C

The hardness Vickers and firing shrinkage as a function of RHA addition at different sintering temperature is shown in figure 4. Hardness is an indicator of a materials resistance to permanent deformation. Hardness is increase with increasing of RHA content and sintering temperature. For specimen at sintering temperature 900 °C, the influence of RHA addition and especially sintering temperature changed the distribution of hardness Vickers slightly (liable flat). However, at temperature 900 °C, the hardness Vickers was increased slightly. This may be due to the pore structure of the specimens (as evidenced in SEM photomicrograph at figure 7) that have good distribution of porosity. This investigation also indicated that substantial improvements were apparent in sintering temperature process. Meanwhile, the shrinkage is an unwanted phenomenon, because it causes deformation of material. Hence, ceramics pore should be design in a way that doesn't allow the local shrinkage or deformation when it applied in industry. The participation hard phase Si from RHA to hardness and

shrinkage phenomenon has a significant influence. The higher is percentage participation of RHA the lower shrinkage percent of specimen. Firing shrinkage test results of specimen for sintering 900 ^oC were 27.22, 18.01, 11.84, and 9.65 %; and for sintering 1000 ^oC were 40.64, 31.09, 27.89, and 11.95 %, for RHA content 0, 10, 20, and 30 wt% respectively. Meanwhile, hardness test results of specimens for sintering 900 ^oC were 339.14, 340.48, 344.08, and 346.22 HVN; and for sintering 1000 ^oC were 354.34, 355.62, 375.18, and 452.32 HVN measured by micro hardness tester with pyramidal diamond 1 kgf load, for RHA content 0, 10, 20, and 30 wt% respectively.

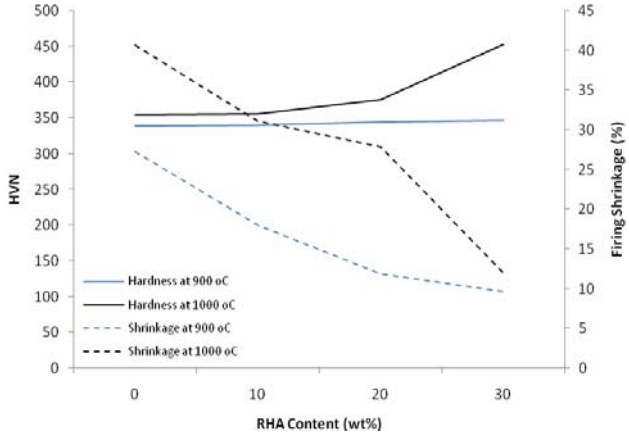

Figure 4. Effect of RHA content to the hardness vickers and firing shrinkage behaviour at sintering temperature 900 ^oC and 1000 ^oC

The last step of researches for produced material was microstructure evaluation. This was carried out in scanning electron microscope (SEM) and X-ray diffraction (XRD). The X - ray diffraction (XRD) pattern analysis of the specimen at 30 %wt RHA addition and sintering temperature 900 ^oC investigated in this work is shown in figure 5. The specimen which has showed maximum porosity was chosen for X-ray analysis as well.

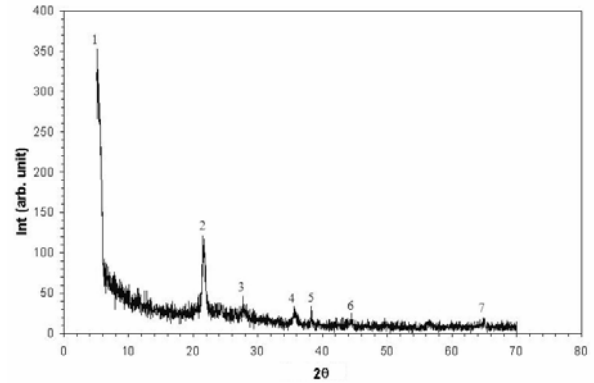

Figure 5. X-ray diffraction of 30 %wt RHA specimen fired at sintering temperature 900^oC

As seen, the phases in the diffractograms presenting mainly on the presence, in sequence: Sodium Silicate ($NaSi_7O_{13}$), Aluminium Silicate ($Si_{7276}Al_{2772}O_2$), Silimanit (Al_2SiO_5), Andalusit ($Al_2(SiO_4)O$), Zeolite ($Si_{11,96}Al_{0,04}O_{24}$), Silikon Dioksida ($SiO_2$), and Mulite ($Al_2(Al_{2,5}Si_{1,5})O_{9,75}$) peaks. The main characteristic signals of specimen are at 5.7588^o, 21.598^o, 27.9006^o, 35.6551^o, 38.3257^o, 44.3925^o, and 64.6558^o, respectively. The possible phases were also searched and confirmed by x-ray diffractogram database (JCPDS).

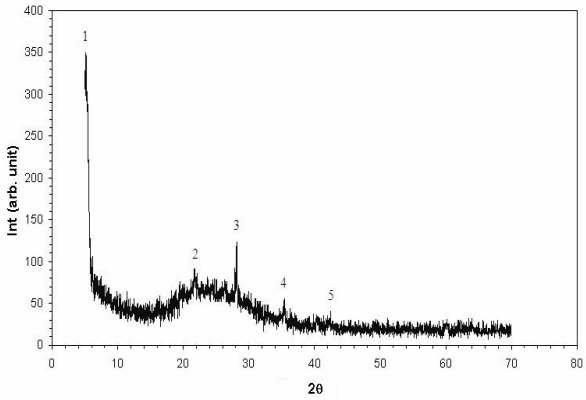

Figure 6. X-ray diffraction of 0 %wt RHA specimen fired at sintering temperature 1000^oC

Meanwhile, the X - ray diffraction (XRD) pattern analysis of the specimen at 0 %wt RHA addition (100 %wt natural zeolite) at sintering temperature 1000 ^oC investigated in this work is shown in figure 6. The specimen, which has showed minimum porosity as the extreme comparison, was chosen for X-ray analysis as well. The phases in the diffractograms presenting mainly on the presence, in sequence: Aluminium silicate ($Al_2Si_{24}O_{51}$), Zeolite ($Si_{11,96}Al_{0,04}O_{24}$), Zeolite ($Si_{11,96}Al_{0,04}O_{24}$), Zeolite ($Si_{11,96}Al_{0,04}O_{24}$), and Zeolite ($Si_{11,96}Al_{0,04}O_{24}$) peaks. The main characteristic signals of specimen are at 5.4161^o, 21.6651^o, 28.0789^o, 35.7085^o, and 38.2659^o, respectively. The possible phases were also searched and confirmed by x-ray diffractogram database (JCPDS). These are typical of the main phases found in the natural zeolite and confirmed further in experiments now.

In order to examine the morphology of obtained specimen in XRD patterns were viewed under scanning electron microscope. Figure 7 shows the scanning electron microscope (SEM) images of the specimen with 30 %wt RHA which is fired at sintering temperature 900 ^oC. It shows the best distribution of porosities and pore size of the specimens. The sintering temperature and RHA addition changed the distribution of porosities and the pore size significantly (as also shown in figure 1); the higher RHA addition (30 %wt) and sintering temperature at 900 ^oC increased the porosities from 18.08 percent to 34.59 percent but it decreased the diameter pore size of about below 1 □m. In one of their earlier studies [6], the author observed the influence of sintering temperature on porosity and pore size with particle shaped by uniaxial pressing; at temperature of about 960 ^oC was found good enough for filter fabrication. In the present study, all fabricated materials (sintered at 900 and 1000 ^oC) are found useful for

filtration applications which have the pore size above 0.1 μm in diameter, its mean the classification of porous ceramics is concerned with macro pores which is suitable for microfiltration application. Sintering also is a crucial parameter for successful fabrication. It needs reliable characterization technique to provide information on the formation of porosity at the sintering temperature applied.

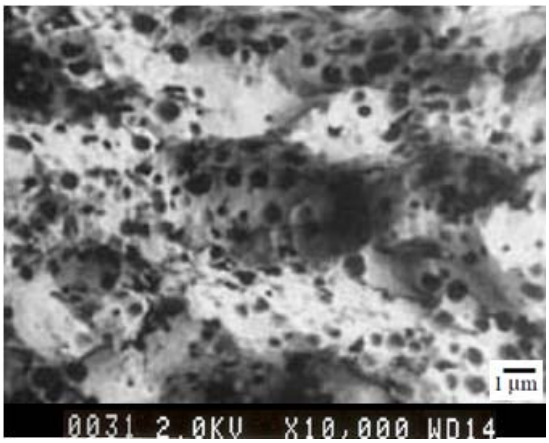

Figure 7. SEM photographs of 30 %wt RHA specimen fired at sintering temperature 900 ^{o}C

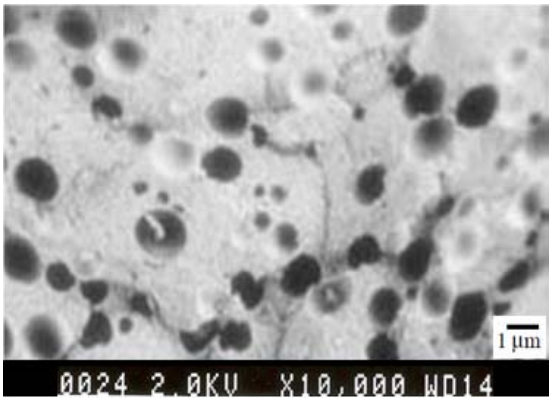

Figure 8. SEM photographs of 0 %wt RHA specimen fired at sintering temperature 1000 ^{o}C

Meanwhile, for the specimen with 0 %wt RHA (100 %wt natural zeolite) at sintering temperature 1000 ^{o}C, as shown in figure 8, it shows less distribution of porosities. The sintering temperature and specimen compositions changed the porosities only slightly, but it has significant increasing the median pore size of about above 1 □m. The explanation was supported by the ratio of Si/Al in natural zeolite in which has the influences to the new seed porosity

4. CONCLUSIONS

In this study, macroporous zeolite materials were successfully prepared from natural zeoilte and rice husk ash. Rice husk ash is a cheaper and environmental friendly alternative silica source in mass production of versatile macroporous materials. Thus, further studies on the synthesis of other types of porous microporous materials from RHA and their application will be investigated.

5. REFERENCES

[1] X. Zhang, G. Meng, and X. Liu, "Preparation and Characterization of Tubular Porous Ceramics from Natural Zeolite," *Journal of Porous Matter*, vol. 15, pp. 101-106, 2008.

.[2] D. Prasetyoko, Z. Ramli, S. Endud, H. Hamdan, and B. Sulikowski, "Conversion of Rice Husk Ash to Zeolite Beta," *Elsevier-Waste Management,* vol. 26, pp. 1173-1179, 2005.

.[3] J. Caro, M. Noak, and P. Kolsch, "Zeolite Membranes: From the Laboratory Scale to Technical Application," *Springer Science*, vol. 11, pp. 215-227, 2005.

[4] T. Fukasawa, Z.Y. Deng, M. Ando, T. Ohji, and Y. Goto, "Pore Structure of Porous Ceramics Synthesized from Water-based Slurry by Freeze-Dry Process," *Journal of Material Science*, vol. 36, pp. 2523-2527, 2001.

[5] O. San, C. Ozgur, and C. Karguzel, "Preparation and Characterization of a Highly Hydrophilic Glassy Pore Wall Membrane Filter," *Journal of Ceramics Processing Research,* vol. 9, no. 3, pp. 296-301, 2008.

[6] X. Yao, S. Tan, and D. Jiang, "Fabrication of Hydroxyapatite Ceramics with Controlled Pore Characteristics by Slip Casting," *Journal of Material Science: Material in Medicine*, vol. 16, pp. 161-165, 2005.

Synthesis of Iron Oxide Nanoparticle with Polymer Stabilizer

Dewi Sondari, Ahmad Randy, Agus Haryono

Polymer Chemistry Group, Research Center for Chemistry
Indonesian Institute of Sciences
Kawasan Puspiptek Serpong, Tangerang 15314 - INDONESIA
Phone : +62-21-7560929, Fax:+62-21-7560549
e-mail: sondaridewi@yahoo.com

ABSTRACT

Magnetic nanoparticles have been of great interest because of their extensive applications. For many of their applications, the synthesis of controlled sized particles is of key importance. This work prepares magnetite particles through relatively simple method of coprecipitation. To control particle size in coprecipitation method, this work tried to use polymer stabilizer to obtain more uniform magnetite particle size. Polymer used in this study was poly(ethylene glycol methacrylate-*co*-methacrylic acid) (poly(EGMA-*co*-MAA). The methacrylic acid unit in the polymer was expected to interact with the surfaces of the iron oxide particles. The ratio of iron salt:polymer was varied between 1:0.85, 1:0.7, and 1:0.42. The smallest average particle size is 182.3 ± 72.3 nm (Fe:poly = 1:0.85) and the largest average particle size is 907.8 ± 222.1 nm. Since the polymer synthesized was insoluble in water, it is less effective in controlling magnetite particle size prepared by coprecipitation method.

Keywords
Magnetite, coprecipitation method, polymer,

1. INTRODUCTION

Magnetite is common ferrite that has a cubic inverse spinal structure with the formula of Fe_3O_4. The compound exhibited unique electric and magnetic properties based on the transfer of electrons between Fe^{2+} and Fe^{3+} in the octahedral sites [1]. Magnetic nanoparticles have been of great interest because of their extensive applications in high density data storage, biochemistry, hyperthermia, in vivo drug delivery and MR contrast reagent [2-7]. For many of these applications, the synthesis of controlled sized particles is of key importance, because the electrical, optical, and magnetism properties of these particles depend strongly on their dimensions. The magnetic structure of the surface layer usually is greatly different from that in the body of nanoparticle, and the magnetic interactions in the surface layer could have a notable effect on the magnetic properties of nanoparticles.

Various synthetic procedures have been used to synthesize magnetic nanoparticles. Magnetite (Fe_3O_4) nanoparticles dispersed in solvents are frequently used as ferrofluids [8]. Magnetic nanoparticles have often been synthesized by the coprecipitation of ferrous (Fe^{2+}) and ferric (Fe^{3+}) ions under basic conditions [9]. This coprecipitation method could also be done with ultrasonic irradiation [10]. Other synthetic methods include the thermal decomposition of an alkaline solution of an Fe^{3+} chelate in the presence of hydrazine, and the sonochemical decomposition of an Fe^{2+} salt followed by thermal treatment [11]. Recently, the synthesis of monodisperse and sized-controlled magnetic ferrite nanoparticles has been reported by several groups. Hyeon and co-workers reported the synthesis of monodisperse and highly crystalline γ-Fe_2O_3 and cobalt ferrite nanoparticles without the need for a size selection process [12]. Alivisatos and co-workers synthesized γ-Fe_2O_3 nanoparticles from direct decomposition of $FeCup_3$ [13]. Uniformly sized magnetic nanoparticles were synthesized by the high temperature reaction of iron (III) acetylacetonate [14].

This work prepares magnetite particles through coprecipitation method. It is extensively used method for preparing magnetite. To control particle size with coprecipitation method, this work tried to use polymer stabilizer to obtain more uniform magnetite particle size.

2. MATERIAL AND METHOD

2.1 Material

tert-Butyl methacrylate (Aldrich, 98%), ethylene glycol methyl ether methacrylate (EGMA)

ISSN 114-1284

(Aldrich, 99%), methyl 2-bromopropionate (MBP) (Aldrich, 98%), 2,2'-bypyridyl (Bipy) (Aldrich, 99%), iron(III) chloride hexahydrate ($FeCl_3.6H_2O$, Aldrich), iron(II) chloride tetrahydrate ($FeCl_2.4H_2O$, Aldrich), ammonium hydroxide solution (25%, Fluka), copper(I) chloride (Merck), and fuming hydrochloric acid (Merck).

2.2 Synthesis of poly(EGMA-*co*-*t*BMA)

Copper chloride (70 mg) and 2,2'bipyridyl (218 mg) were added in three-necked flask. The flask was purged with nitrogen gas for a few minutes. Then a mixture of *tert*-butyl methacrylate (3.96 g), ethylene glycol methyl ether methacrylate (20 g), and 2.4 mL of ethanol were added to the flask. Last, methyl 20bromopropionate (117.5 mg) was added. The mixture was heated at 60°C in an oil bath for 3 h. The experiment was stopped by opening the flask and exposing the catalyst to air. The final mixture was diluted in ethanol and passed through a silica column (70-230 mesh) to remove copper catalyst. The filtered solution was dried in low-pressure oven. The polymer obtained appeared as a yellowish rubbery material.

2.3 Hydrolysis of poly(EGMA-*co*-*t*BMA)

Twenty grams of poly(EGMA-*co*-*t*BMA) and 180 mL of 1,4-dioxane were added in a round bottom flask. The mixture was stirred to dissolve the polymer. Then 10 mL of concentrated HCl (37%) was added and the flask was capped with a condenser. The mixture was refluxed for 6 h and subsequently cooled to room temperature. Then the filtered solution was diluted with water. Water was removed by rotary evaporation. The polymer obtained appeared as a brownish rubbery material.

2.4 Preparation of Fe_3O_4 particles

The magnetic nanoparticles were tried to synthesized via conventional precipitation methode in the presence of the copolymer poly(EGMA-*co*-MAA), used as a particle stabilizer. Iron(II) chloride and iron(III) chloride ($[Fe^{3+}]/[Fe^{2+}] = 2$) were added in a round bottom flask under nitrogen atmosphere and were subsequently diluted in water (overall iron concentration in water approximately 6 g/L). The polymer was added in the reaction mixture under nitrogen atmosphere. The ammonium hydroxide solution was slowly added under strong stirring conditions, resulting in the formation of a dark precipitate. This mixture was purified by dialysis in water.

2.5 Particle characterization

Prepared particles were dried in a vacuum oven for Fourier transform infrared spectroscopy (FT-IR) analysis. The present of Fe_3O_4 were analysed with x-ray diffraction (XRD). Particles morphology was characterized with scanning electron microscopy (SEM). Particles sizes were analyzed with particle size analyzer (PSA).

3. RESULT AND DISCUSSION

In this work, magnetite particles were prepared by coprecipitation method. Mixed solution of Fe^{3+} and Fe^{2+} were reacted with ammonium hydroxide solution to form Fe_3O_4, as swhon in eq. 1.

$$2FeCl_3 + FeCl_2 + 8NH_3 + 4H_2O \rightarrow Fe_3O_4 + 8NH_4Cl \quad (1)$$

Coprecipitation method is a common method of producing magnetite particles, because its relatively simple procedure. However, with this method, a suitable particle surface treatment is needed to form stable magnetite particles. To obtain controlled particle size, this work attempted to use polymer stabilizer. The polymer studied was random copolymer of poly(ethylene glycol methacrylate-*co*-methacrylic acid) (poly(EGMA-*co*-MAA). The methacrylic acid unit in the polymer was expected to interact with the surfaces of the iron oxide particles [15]. The ratio between polymer particles and total iron concentration (Fe:polymer) was varied by 1:0.85, 1:0.7, and 1:0.42.

The infrared spectra showed at Fig. 1. The three FT-IR spectra showed key absorption of Fe_3O_4 particles at around 500-575 cm^{-1} [16]. Specific band at 590 cm^{-1} assigned to Fe-O vibration was also noticed [17]. The XRD pattern of magnetite particles obtained is shown in Fig. 2.

From the SEM images of obtained magnetite particles (Fig. 3), it was difficult to determine the single particle size. The SEM images showed what might be the occurrence of magnetite particle agglomeration.

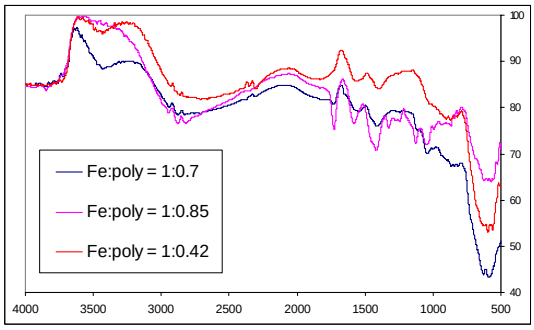

Figure 1. FT-IR spectra of prepared magnetite particles.

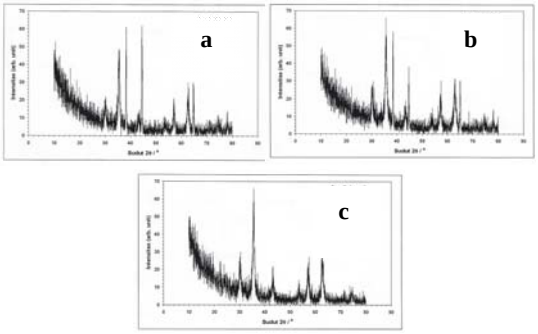

Figure 2. XRD pattern of prepared magnetite with Fe:poly ratio of: a) 1:0.85, b) 1:0.7, and c) 1:0.42

Table 1 shows PSA measurement of three batches of magnetite particles prepared in this work. Obtained particle sizes are relatively large and did not belong to the scale of nanoparticles. The smallest average particle size is 182.3 ± 72.3 nm (Fe:poly = 1:0.85) and the largest average particle size is 907.8 ± 222.1 nm.

The polymer we tried to use was random copolymer of poly(EGMA-*co*-MAA). It appears that this copolymer is not soluble in water. Water solubility of the polymer stabilizer is important in order to polymer to be dispersed among magnetite particles and to make sure that the methacrylic acid unit interacts with the surface of iron oxide particles. This work use ethylene glycol methacrylate as one of monomer in the random copolymer. Reference [18] shows that in the case of poly(EGMA-*co*-MAA), the copolymer is not soluble in water since the single ethyleneglycol unit is insufficient to solubilize the hydrophobic polymer backbone. Thus, poly(oligo(ethylene glycol) methacrylate-*co*-methacrylic acid) (poly(OEGMA-*co*-MAA) is more soluble in water than poly(EGMA-*co*-MAA). The large particle size measured from PSA and SEM suggest that the copolymer used in this work can not act as a particle stabilizer because of its insolubility in water. It was shown by the tendency of prepared magnetite particles from coprecipitation method to precipitate when kept at shorter time. Thus, nanoscaled magnetite particles did not occur. Correlation between obtained magnetite particle size and Fe:polymer ratio can not be taken as the polymer rarely involve in stabilizing the magnetite particles.

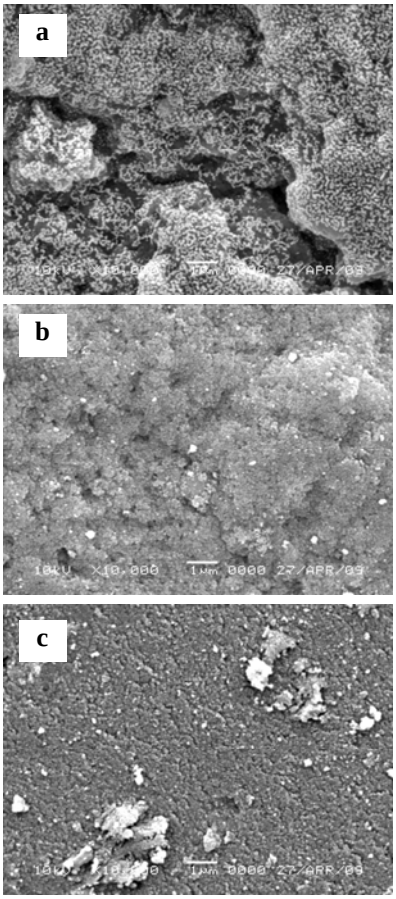

Figure 3. SEM image of magnetite with Fe:poly ratio of: a) 1:0.85, b) 1:0.7, and c) 1:0.42

Table 1. Particle size of the magnetite particles prepared in the present of polymer stabilizer

	Iron salts/polymer Fe:poly (w/w)	Mean diameter (nm)
1	1:0.85	182.3 ± 72.3
2	1:0.7	907.8 ± 222.1
3	1:0.42	797.3 ± 196.2

4. CONCLUSION

The random copolymer used in this study of preparing magnetite particle is insoluble in water. This happen because the single ethyleneglycol unit is insufficient to solubilize the hydrophobic polymer backbone. Thus, this random copolymer is less effective in stabilizing magnetite particles and can not be used to control magnetite particle size.

REFERENCES

[1] S. Si, C. Li, X. Wang, D. Yu, Q. Peng, Y. Li., "Magnetic monodisperse Fe_3O_4 nanoparticles," *Crystal Growth & Design,* vol. 5, no.2, pp. 391-393, (2005).

[2] A.K. Gupta, A.S.G. Curtis, "Surface modified superparamagnetic nanoparticles for drug delivery: Interaction studies with human fibroblasts in culture," *J. Mater. Sci. Mater. Med*, vol. 15 pp. 493-496, 2004.

[3] R. Hergt, R. Hiergeist, I. Hilger, W.A. Kaiser, Y. Lapatnikov, S. Margel, U. Richter, "Maghemite nanoparticles with very high AC-losses for application in RF-magnetic hyperthermia," *J. Magn. Magn. Mater.*, vol. 270, pp. 345-357, 2004.

[4] R.H. Kodama, "Magnetic nanoparticles," *J. Magn. Magn. Mater.*, vol. 200, pp. 359-372, 1999.

[5] M. Johannsen, A. Jordan, R. Scholz, M. Koch, M. Lein, S. Deger, J. Roigas, K. Jung, S. Loening, "Evaluation of magnetic fluid hyperthermia in a standard rat model of prostate cancer," *J. Endourol.*, vol. 18, pp. 495-500, 2004.

[6] G.X. Li, V. Joshi, R.L. White, S.X. Wang, J.T. Kemp, C. Webb, R.W. Davis, S.H. Sun, "Detection of single micron-sized magnetic bead and magnetic nanoparticles using spin valve sensors for biological applications," *J. Appl. Phys.*, vol. 93 no. 10, pp. 7557-7559, 2003.

[7] H. Zeng, J. Li, Z.L. Wang, J.P. Liu, S.H. Sun, "Bimagnetic core/shell $FePt/Fe_3O_4$ nanoparticles *Nano Lett.*, vol. 4, pp. 187-190, 2004.

[8] A.B. Nicholas, B.J. Katie, C.J. Dean, E.B. Arthur, "Preparation and properties of an aqueous ferrofluid," *JchemEd*., vol. 76 no. 7, pp. 943-948, 1999.

[9] T. Fried, G. Shemer, G. Markovich, "Ordered two-dimensional arrays of ferrite nanoparticles," *Adv. Mater.*, vol. 13, pp. 1158-1161, 2001.

[10] E.H. Kim, H.S.Lee, B.K.Kwak, B.K.Kim, "Synthesis of ferrofluid with magnetic nanoparticles by sonochemical method for MRI contrast agent," *J. Magn. Mag*. *Mater*., vol. 289, pp. 328-330, 2005.

[11] T. Hyeon, S.S. Lee, J. Park, Y. Chung, Y.-W. Kim, B.H. Park, "Synthesis of highly crystalline and monodisperse cobalt ferrite nanocrystals," *J. Phys. Chem.*, vol. 106, pp. 6831-6833, 2002.

[12] J. Rockenberger, E.J. Scher, A.P. Alivisatos, "A new nonhydrolytic single-precursor approach to surfactant-capped nanocrystals of transition metal oxides," *J. Am. Chem. Soc.*, vol. 121, pp. 11595-11596, 1999.

[13] S. Sun, H. Zeng, "Size-controlled synthesis of magnetite nanoparticles," *J. Am. Chem. Soc.*, vol. 124, pp. 8204-8205, 2002.

[14] S.H. Gee, Y.K. Hong, D.W. Erickson, M.H. Park, "Synthesis and aging effect of spherical magnetite (Fe_3O_4) nanoparticles for biosensor applications," *J. Appl. Phys.*, vol. 93, no. 10, pp. 7560-7562, 2003.

[15] J.F. Lutz, S. Stiller, A. Hoth, L. Kaufner, U. Pison, R. Cartier, "One-pot synthesis of PEGylated ultrasmall iron-oxide nanoparticles and their in vivo evaluation as magnetic resonance imaging contrast agents," *Biomacromolecules*, vol. 7, pp. 3132-3138, 2006.

[16] R. Balasubramaniam, A.V. Ramesh Kumar, P. Dillmann, "Characterization of rust in ancient Indian iron," *Current Science*, vol. 85, no. 11, pp. 1546-1555, 2003.

[17] M. Raileanu, M. Crisan, C. Petrache, D. Crisan, M. Zaharescu, "Fe_2O_3-SiO_2 nanocomposites obtained by different sol-gel routes," *J*. Optoelectron. Adv. *Mater*., vol. 5 no. 3, pp. 693-698, 2003.

[18] C.R. Becer, S. Hahn, M.W.M. Fijten, H.M.L. Thijs, R. Hoogenboom, U.S.Schubert, "Libraries of methacrylic acid and oligo(ethylene glycol) methacrylate copolymers with LCST behaviour," *J. Polym. Sci. Part A: Polym. Chem*., vol. 46, pp. 7138-7147, 2008.

Efficacy of Chitosan-based Antimicrobial (AM) Packaging

Endang Warsiki[1] and Titi C. Sunarti[1]

[1]*Faculty Agriculture Technology*
Bogor Agriculture University, Bogor 16002
Tel : (0251) 8621974,. Fax : (0251) 8621974
E-mail : warsiki@yahoo.com.au
titibogor@yahoo.com

ABSTRACT

Chitosan is a chitin derivate matter that called multifunction groups because it has three groups, i.e. amine-acid, primary hydroxyl, and secondary hydroxyl groups. Chitosan has ability to kill bacteria. Its polycation is able to restrain the growth of molds and bacteria. On the other hand, the using of chitosan as material for biodegradable packaging film has already proven and even already been applied commercially for food. The two functions of the material as packaging and as antimicrobial agent can be called antimicrobial packaging. However, so far, the scientific research of the efficacy of chitosan base film as antimicrobial packaging is very rare. In this research, a film was developed from chitosan and tested to its efficacy of selected microorganism.

The purposes of this research was to investigate the efficacy of chitosan-based antimicrobial film against Staphylococcus aureus (S. aureus)s, Escherichia coli(E. coli) and Salmonella typhimurium (S. typhimurium). The methodology used in this research were (i) producing antimicrobial film and (ii) antimicrobial assay of the film for selected microorganism.

The efficacy of chitosan antimicrobial film for E. coli and S. thyphimurium were greater than S. aureus. Efficacy of antimicrobial film was also influenced by storage temperature. Results from efficacy test conducted for those selected microorganism was storage at 5°C had greatest effect whereas storage at 37°C had the smallest effect.

Keywords
Chitosan, antimicrobial film, Staphylococcus aureus, Escherichia coli, Salmonella typhimurium,

1. INTRODUCTION

As a result of consumer demand on packaging, it has encouraged the creation of innovative packaging to maximize benefits and minimize the negative impact of packaging. The function of packaging to protect food products to be the main guarantee for consumers. Antimicrobial (AM) packaging is a concept that combines innovative materials and packaging materials in an anti-microbe system. In principle, the AM agent can be added to any polymer material. The AM agent will released slowly from the packaging to product to prevent the damage of food packaged causing by microbe growth such as fungi, bacteria and others. Antimicrobial packaging materials are increasing of interest as a potential technique for safely preserving food products. On the other hand, AM packaging is also a simplify of the producing packaging by manufacturing packaging materials and AM agent in one stage.

AM packaging has been developed trough research in the last few years. However the implementation of packaging in commercial scale is very rare. Hence, more research should be done to trigger to speed up its application. The present work will concentrate on fabrication of the AM film-chitosan base. The film then it assayed under different temperature of storage against , *E. col,i S. typhimurium* and *S. aureus.*

2. MATERIAL AND METHODS

2.1. Material and Apparatus

The material used in the research were chitosan, acetate acid, glycerol and aquadest. Other chemicals was ethanol. The apparatus needed for analysis were test plate, test tube, drops pipette, mixer, spatula, magnifying glass, glass beaker, erlenmeyer and incubator.

2.2. Methods

The chitosan AM film was produced by the modification of Vodjani and Torres method [1]. Chitosan of 3 g was diluted on 1% (v/v) of acetic acid and heated on the temperature of 50^{o}C for 60 min. When the solution was homogen, immediately 0.5% (v/v) of glycerol was added. After the solution has been prepared, the solution is poured to the top of the film frame. The sheet of chitosan AM film and then is dried in the oven of 40°C for 24 h. The flow process of producing AM film is shown in Figure 1.

The films were tested for their inhibition against the selected microorganisms: *E. Coli*, *S. Typhimurium* and *S. aureus* by using an agar disc diffusion method [2]. Each film sample was cut into a circle of 5 mm in diameter and sterilized with UV light for 2 min prior to being placed on an agar plate surface seeded with 1 mL of test culture. The plates were incubated for 7 days at the temperature of 5, 15, 27 and 30^{o}C. The clear zone formed around the film disc in the media was recorded as an indication (Figure 2) and inhibition index was calculated by the equation (1) [3].

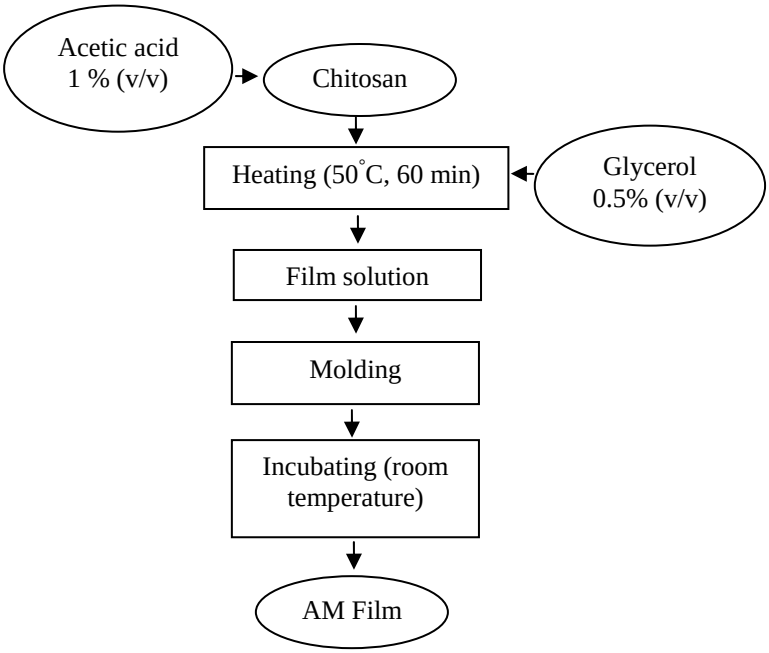

Figure 1. Flow process for chitosan AM fim producing

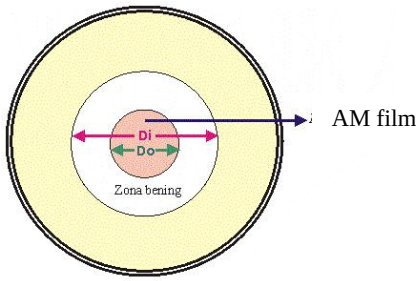

Figure 2. Clear zone

$$\text{Inhibition index (\%)} = \frac{(Di - Do)}{Do} \times 100\ \% \text{.....(1)}$$

Where :
Di = internal diameter
Do = ekstenal diameter

3. RESULT AND DISCUSSION

AM against bacteria is shown by perform the clear zone on the agar plate. Clear zone is a zone where bacteria can not grow and proliferate as a result of active material in the film, while the zone indicated microbe growing was shown by colours colony. Figure 3 presents the graph index of inhibition of the AM film against E. coli. It is shown that a decreasing in the index of retardation during the storage for all temperature of 5, 15, 27 and 37°C tested in this study. It means that the longer storage of the film, the active substance from chitosan used to prevent the *E. coli* bacteria is also reducing. The higher temperature of storage the film, the lower the effect of retardation obtained, indicated by the low index retardation. A similar results was also obtained in literature [4].

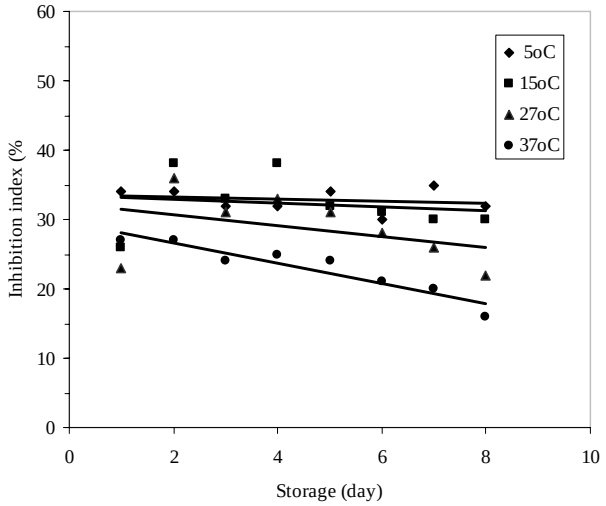

Figure 3. Inhibition index of AM film against *E. coli*

In the graphs presented in Figure 4, it appears that the film activity against *S. typhimurium* also decreased during storage, however, at low temperatures, namely 5 and 15°C, the decreasing in the index is not too significant. The declining might occurred more rapidly in line with the increasing temperature of storage. It means that the ability of chitosan AM film to kill banteria is low in high temperature.

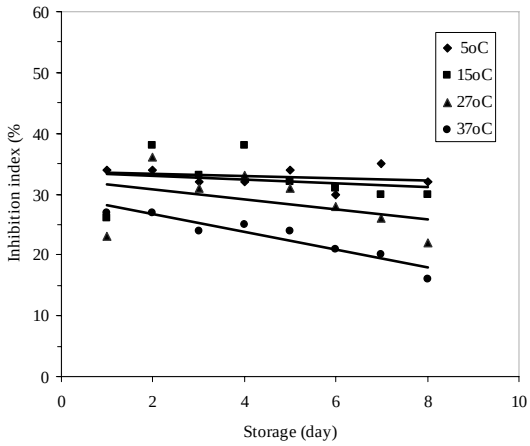

Figure 4. Inhibition index of AM film against *S.. typhimurium a*

Figure 5 shows that the longer the film storage, the lower activity of the AM film against *S. Aureus*. The higher temperature storage of AM film is also resulted on the lower the effect of retardation obtained as indicated by the low index of inhibition.

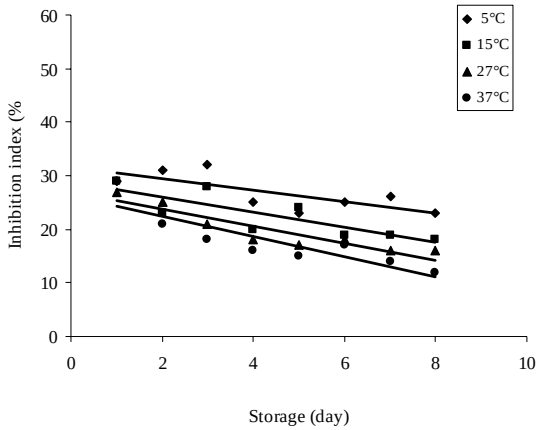

Figure 4. Inhibition index of AM film against *S. aureus*

However, from the Figure 3, 4 and 5 above shows that the retardation film of the *E. coli* and *S. typhimurium* was greater compare to *S. aureus*. According to literature [5], the gram-negative bacteria (*E. coli* and *S. typhimurium*), has more negative ion in its cell and thinner peptidoglican thus it makes more sensitive to chitosan.

As it is shown that the reducing of inhibition index are linear along the storation. Hence, it can calculate the slopes as indicates a decreasing rate of active substances containing in AM film material and estimate the shelf life of the AM agent in days as displayed in Table 1.

Tabel 1. Shelf life of chitosan AM film

Temterature of storage (^{0}C)	Shelf life (days)		
	E. coli	*S. typhimurium*	*S. aureus*
5	24,10	90,72	29,77
1	19,66	78,29	20,50
25	18,99	38,73	17,18
37	16,92	20,13	13,86

4. CONCLUSION

The results of the present study highlighted the promising potential and feasibility of chitosan base films for use as AM packaging materials. Chitosan film is evidently able to prevent microorganisms. The level of inhibition index of the bacteria growth are depending on the temperature and the period of storage. The AM film could inhibit *E. coli* and *S. typhimurium* greater than *S. aureus*.

5. REFERENCES

[1] Vojdani, F. and Torres, J. A. 1990. "Potassium sorbate permeability of methylcellulose and hydroxypropyl methylcellulose coatings: effect of fatty acids', *Journal of Food Science, 55:* p. 841-846.
[2] Appendini, P. dan J. H. Hotchkiss. 2002. Review of Antimicrobial Food Packaging. *Innovative Food Sci & Emerg Technol*. 3: 113-126.
[3] Sanla-Ead, N., A. Jangchud, V. Chonhenchob dan P. Suppakul. 2006. Antimicrobial Activity of Cinnamon, Clove and Galangal Essential Oils and their Principal Constituents, and Possible Application in Active Packaging. *The Proceedings of 15th IAPRI World Conference on Packaging (WorldPak2006)*: 216.
[4] Chung, Y., Y. Su, C. Chen, G. Jia, H. Wang, J. C. Gaston dan J. Lin. 2004. Relationship between Antibacterial Activity of Chitosan and Surface Characteristics of Cell Wall. *Acta Pharmacol Sin.* 25(7):932-936.
[5] Tsai, G. J. dan W. H. Su. 1999. Antibacterial activity of shrimp chitosan against Escherichia coli. *J. Food Prot*. 62:239–24

Proceeding of the 11th International Conference on QiR (Quality in Research)
Faculty of Engineering, University of Indonesia, Depok, Indonesia, 3-6 August 2009
ISSN 114-1284

Preliminary simulation of temperature evolution in comminution processes in ball mills

F. Nurdiana[1], Muhandis[2], A. S. Wismogroho[3], N.T. Rochman[3], L.T. Handoko[1,2]

[1]*Group for Nuclear and Particle Physics, Department of Physics, University of Indonesia, Kampus Depok, Depok 16424, Indonesia*

[2]*Group for Theoretical and Computational Physics, Research Center for Physics, Indonesian Institute of Sciences, Kompleks Puspiptek Serpong, Tangerang 15314, Indonesia*
E-mail : laksana.tri.handoko@lipi.go.id

[3]*Group for Nanomaterial, Research Center for Physics, Indonesian Institute of Sciences, Kompleks Puspiptek Serpong, Tangerang 15314, Indonesia*

ABSTRACT

A model for comminution processes in ball mills is presented. The model provides an empirical approach using the physically realistic modelization of the ball mill system, but also deployes the statistical method to extract relevant thermodynamics observables. Those physical observables are investigated by treating the whole system as a statistical macroscopic ensemble.

Keywords
nano process, ball-mill, canonical ensemble, modelling

1. INTRODUCTION

The comminution processes in recent years attract the attention among scientists and engineers due to the increasing demand of ultrafine powders for nanotechnology applications in many areas. The demand then requires the improvement of comminution equipments like ball mills, roller mills and so on. Unfortunately, the development of such comminution equipments always contains a lot of uncertainties due to a wide range of unknown parameters. These, in fact, lead to significant statistical errors. In order to overcome such problems, several models have been developed to quantitatively describe comminution process in various types of mills [1,2,3,4,5].

On the other hand, mathematical modeling and simulation may provide prior information and constraint to the unknown parameter ranges which should be useful to develop more optimized experimental strategy in comminution processes. However, in most cases of mathematical models, the physical observables like grain-size etc are extracted from a set of equation of motions (EOM). Such EOM's are considered to govern as complete as possible the dynamics of the system, from the mechanical motions to the evolution of grain-size distribution. This approach is obviously suffered from the nonlinearities of the equations under consideration, and then the requirement of high computational power to solve them numerically. This fact often discourages a quantitative and deterministic approach for the simulation of such system. These nonlinear effects like chaotic behavior of the sphere motions within the mill encourages some works modeling the system using semi-empirical approaches [6]. However most of semi-empirical models require a large number of experimental data based on prior observations [7], or measured variables obtained from simulation results by other authors [8,9].

In this paper we deploy a novel model and approach developed recently which is combining the deterministic approach for milling bodies motion, and the statistical approach to relate them with considerable macroscopic physical observables [10].

2. THE UNDERLYING MODEL

The whole system is modeled empirically using hamiltonian method. It is represented by a total hamiltonian describing all aspects of dynamics in the ball mills. It is further used to calculate the partition function and extracting the relevant thermodynamics observables.

The dynamics of each 'matter' in the system, i.e. balls and powders inside the vial, is described by a hamiltonian $H_m(r,t)$. The index m denotes the powder (p) or ball (b) and $r = (x,y,z)$. The hamiltonian contains some terms representing all

relevant interactions working on the matters inside the system [10],

$H = H_0 + V_{int} + V_{ext}$ (1)

with v denotes the vial, while H_0 is the free matter hamiltonian and V's are the internal and external potentials.

The internal potential contains all considerable interactions among matters, i.e. among powder-powderm, powder-ball, ball-ball, powder-vial and ball-vial. The details of all potentials can be found in [10].

Using statistical mechanis, the hamiltonian is related to the partition function,

$Z \propto \exp [- \beta H]$, (2)

with $\beta = 1/k_B T$ for temperature T independent H. Further, the partition function is used to extract some statistical observables, for instance Helmholz free energy,

$F_H = -1/\beta \ln Z$, (3)

and pressure,

$P = -F_H/V$. (4)

Please note that the above equations hold for classical and general system. For a canonical system like our case, it is represented in a continue form in term of space displacement x and momentum p respectively [10].

Considering the normalized partition function, finally we found the pressure to be,

$P = 1 - F \beta \ln^{-1} (2m\pi\beta)$, (5)

where the auxiliary function F represents all geometrical contribution of vial and its motions.

3. RESULT AND DISCUSSION

Making use of Eq. (5) we can draw general behavior of pressure in term of system temperature. Note that this result is independent from the geometrical form and motions of vial. The behavios is depicted in Fig. 1 as a function of system temperature T.

From the figure, it is clear that the pressure depends highly on the system temperture. Its rough behavior is same for any ball mills, but the shapes are determined completely by the function F characterizing the geometrical structures and motions in the inertial system. Therefore Eq. (5) provides a general behavior for temperature-dependent pressure in the model, while the geometrical structure and motion of vial is absorbed in the function F. Its physically meaningfull region is depicted in Fig. 1 for any temperature along the horizontal axis.

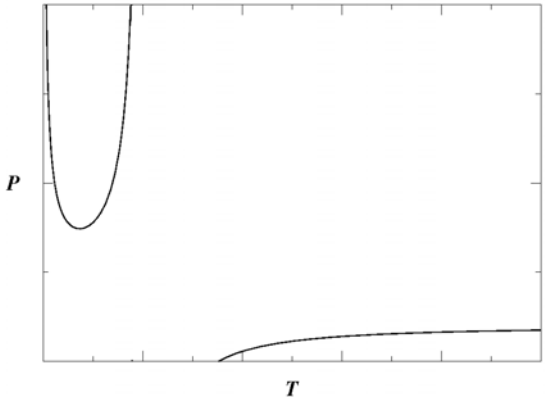

Fig. 1 The normalized temperature-dependent pressure in the system of any ball mills.

From the figure, the physically meaningful region is between $0 < T < 1/(2m\pi k_B)$, and $T > T_{th}$ where the threshold temperature is always greater than $1/(2m\pi k_B)$ respectively.

7. CONCLUSION

We have considered a model for communution processes in ball mills using hamiltonian approach. This approach has a great advantage on extracting the physical observables directly from the hamiltonian without a need to solve a set of equation of motions of the whole system which always leads to unsolvable non-linear problems.

More complete numerical calculation is required to take into account the contribution of geometrical shapes and motions of vial represented by the function F.

ACKNOWLEDGMENT

The work is supported by the Riset Kompetitif LIPI in fiscal year 2009. Muhandis thanks the Group for Theoretical and Computational Physics LIPI for warm hospitality during the work.

REFERENCES

[1] B. K. Mishra, R. K. Rajamani, "The discrete element method for the simulation of ball mills", *Applied Mathematical Modeling* 16 (1992) 598-604.
[2] B. K. Mishra, R. K. Rajamani, "Simulation of charge motion in ball mills", *International Journal of Mineral Processing* 40 (1994) 171-186.
[3] B. K. Mishra, "Charge dynamics in planetary mill", *Kona Powder Particle* 13 (1995) 151-158.
[4] B. K. Mishra, C. V. R. Murty, "On the determination of contact parameters for the

realistic {DEM} simulations of ball mills", *Powder Technology* 115 (2001) 290--297.

[5] T. Poschel, C. Saluena, "Scaling properties of granular materials", *Physical Review* E64 (2001) 011308.

[6] G.Manai, F.Delogu, M.Rustici, "Onset of chaotic dynamics in a ball mill : atractor merging and crisis induced intermittency", *Chaos* 12 (2002) 601-609.

[7] R.M. Davis, B.McDermott, C.C. Koch, "Mechanical alloying of brittle materials", *Metallurgical Transactions* A19 (1988) 2867.

[8] D.Maurice, T.H. Courtney, "The physics of mechanical alloying : a first report", *Metallurgical Transactions* A21 (1990) 289-302.

[9] D.Maurice, T.H. Courtney, "Milling dynamics, Part II : dynamic of a spex mill in a one dimensional mill", *Metallurgical Transactions* A27 (1996) 1981.

[10] Muhandis, F. Nurdiana, A. S. Wismogroho, N. T. Rochman, L. T. Handoko, "Extracting physical observables using macroscopic ensemble in the spex-mixer/mill simulation ", *American Institute of Physics Proceeding* (2009) in press.

The Effect of Tensile Loading on Time-Dependent Strain Development in Low Alloyed TRIP Steel

Fatayalkadri Citrawati[1,2], Lie Zhao[2,3] and Jilt Sietsma[2]

[1]*Research Centre for Metallurgy*
Indonesian Institute of Sciences, Kawasan PUSPIPTEK, Tangerang 15314
Phone : (021) 7563205 ext 201 Fax : (021) 7560553
email : fatayalkadri.citrawati@lipi.go.id

[2]*Departement of Materials Science and Engineering*
Delft University of Technology
Mekelweg 2, 2628 CD Delft, The Netherlands

[3]*Materials Innovations Institute M2i*
Mekelweg 2, 2628 CD Delft, The Netherlands

ABSTRACT

It is found that under mechanical loading, Transformation Induced Plasticity (TRIP) steel shows a time-dependent strain under a constant applied stress, the strain keeps increasing during the holding process. This phenomenon was previously assumed due to temperature decrease during the holding process, thus the temperature decrease should take place at the same time scale as the strain variation. However, no experimental evidence confirming this relation was observed. To investigate this, a thermocouple was attached to the tensile specimens and recorded the temperature variation while the specimen was being tensiled with different loading schedule at the fixed stress rate, 5 MPa/s. The loading modes used for the tests were stepwise loading, loading-unloading and loading-holding for 72 hours. The retained austenite volume fraction of each specimen after tensile tests was measured using Vibrating Sample Magnetometer (VSM). From the present study, the temperature effect on strain development during the holding process only plays a role in the beginning of the holding process and it will end when the temperature reaches room temperature, afterwards isothermal martensitic transformation (IMT) mechanism is observed to take place.

Keywords
Tensile loading, martensitic transformation, TRIP steels, plastic deformation, time-dependent effect.

1. INTRODUCTION

TRIP Steel is well-known for its properties combination between strength and ductility, it becomes a favorite material for automotive application due to its ability to absorb energy during crashing and the low cost. The existence of TRIP effect in the material is due to the transformation of retained austenite phase to martensite when a certain amount of external stress is applied to the material. The easiness of retained austenite phase to transform to martensite becomes an important factor to produce TRIP effect in a material and it will depend on the retained-austenite stability. It will be affected by its chemical composition, size and orientation [1, 2]. A certain amount of heat will be generated in the material, when it is tensiled to a certain stress level. It can be determined by assuming that all the energy absorbed during straining was converted to heat [3]. It was assumed previously [4], in a stepwise tensile test during the holding process, that the subsequent decrease in the temperature delivers the driving force of austenite transformation. The adiabatic heat evolved was calculated and the temperature decrease during holding process was simulated to have similar time constants to the strain increase. The present work is to observe the factors influencing the strain development during the holding process when a certain amount of external stress applied to the material in a stepwise tensile loading.

2. EXPERIMENTAL

2.1 Experimental Material

The material used in this work was galvanized TRIP steel with chemical composition shown in Table 1. The yield stress, ultimate tensile stress and uniform elongation of the material are 468 MPa, 738 MPa and 22% respectively.

Table 1: Chemical composition of TRIP Steel

Elements	C	Mn	Si	Al	P	Fe
%wt	0.185	1.610	0.352	1.100	0.089	Bal.

The M_s temperature of the material was calculated and the result is 439 K. The material was machined to get tensile test specimens as stated in ASTM E8 standard.

2.2 Tensile Loading and Temperature Measurement

Three different tensile loading were carried out, stepwise loading, loading-unloading and loading-holding for 72 hours. The schematic illustration of stepwise and loading-unloading test can be seen in Figure 1. It was performed in a Zwick Z100 100 kN at the same stress rate, 5 MPa/s. It was chosen due to its load cell capability considering the strength of the TRIP steel. The specimen was gripped using a serrated-wedge grip with screw-like fastener. It was chosen considering the smoothness of the specimen surface. This kind of grip can tightly hold the specimen and eliminate slip during the test.

For the stepwise loading test (Fig. 1(a)), the specimens were tensiled starting from 100 MPa until 700 MPa, held for 20 minutes for every 100 MPa higher. During this holding process the temperature and strain variation were observed.

In the loading-unloading test (Fig. 1(b)), the specimens were tensiled until the tensile load reached 400 MPa, 500 MPa, 600 MPa or 700 MPa. After the specimen reached the target stress level, it was held for 10 minutes, and then unloaded to 0.6 MPa (10 N). After the specimen reached this stress level it was loaded again to the previous target level and held for another 10 minutes. The temperature and strain variation during holding were also observed. This loading-holding-unloading cycle was carried out three times for each specimen at each target stress level.

The third tensile test was loading to 700 MPa and held for 72 hours.

In order to observe the temperature variation during tensile loading, a type-K thermocouple was attached to the tensile specimens and the temperature variation was recorded using Yokogawa DL750 ScopeCorder. The Cu-wire was spot-welded only in the middle of the specimens since other locations show the same behaviour of temperature evolution during the tensile test. The wire was attached between the extensometer needles, the thinnest part of the specimen when it was loaded. The ScopeCorder was set to record temperature in the range of 273 K to 373 K, the frequency chosen was 10 Hz and the duration was varied between 15 min/div and 30 min/div.

2.3 Magnetic Test

The retained austenite volume fraction of each specimen after tensile tests was measured using Lake Shore 7307 Vibrating Sample Magnetometer (VSM). The 2 x 2 x 1.25 mm^3 sample weight was measured and afterwards it was put in the sample holder. During the measurement, the specimen inside the holder vibrated vertically, with an amplitude 0.7 mm and frequency 82 Hz, due to a sinusoidal signal from the transducer. This signal made the specimen to undergo a sinusoidal motion. The pick-up coils on both sides of the sample holder recorded the signal from the sample motion. Method used for data acquisition was point by point, with a maximum field of 2 T. The average time per point was 10 seconds and the number point was 41. From this measurement, the relation between field and magnetic moment per mass was obtained. The values of saturation magnetization (M_{sat}) can be used as indication of retained austenite phase fraction in the specimen by using equation [5]:

$$f_\gamma = 1 - \beta \frac{M_{sat}(c)}{M_{sat}(f)} \quad (1)$$

where f_γ is the volume fraction of retained austenite, β is a constant equal to 0.989 [5] to consider the contribution of cementite on magnetization at room temperature, $M_{sat}(f)$ is the saturation magnetization of austenite-free sample and $M_{sat}(c)$ is the saturation magnetization of austenite-containing sample.

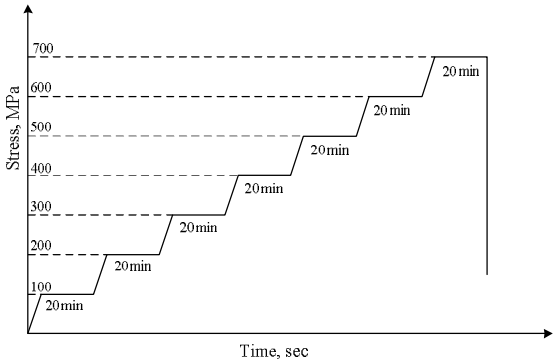

(a)

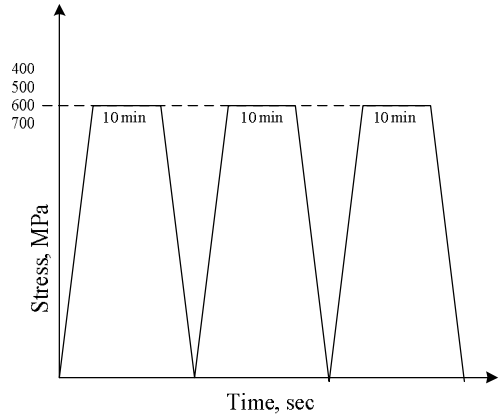

(b)

Figure 1: Schematic illustration of (a) stepwise tensile test (b) loading – unloading tensile test.

3. RESULTS

The plot of stress vs. time, strain vs. time and temperature vs. time can be seen in Figure 2.

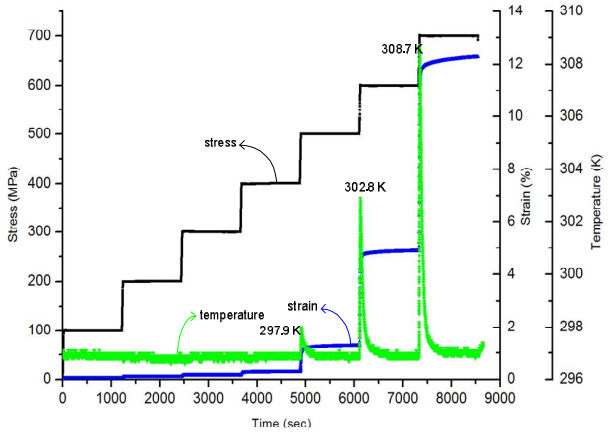

Figure 2: Plot of stress-time, strain-time and temperature-time of stepwise tensile tests.

The plots between strain – time and temperature – time for each stress level, 400, 500, 600 and 700 MPa, can be seen in Figure 3. The $\Delta\varepsilon$ in the figure represent the strain increase during holding process, it was calculated by subtracting the end strain (ε_{end}), where the holding process finished, with the initial strain ($\varepsilon_{initial}$), where the holding process started. Similarly ΔT represent the temperature difference between room temperature when the experiment were carried out and the highest temperature reached when the specimen was tensiled.

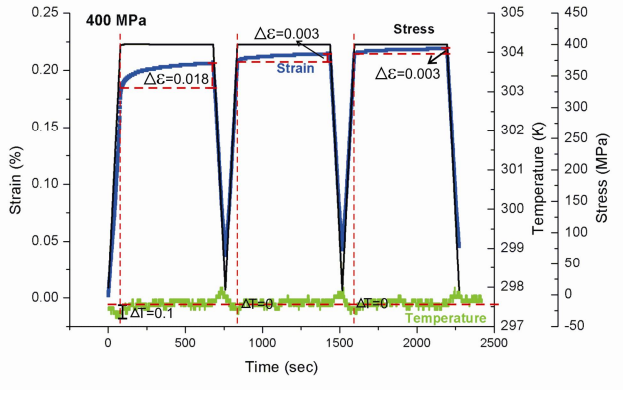

(a)

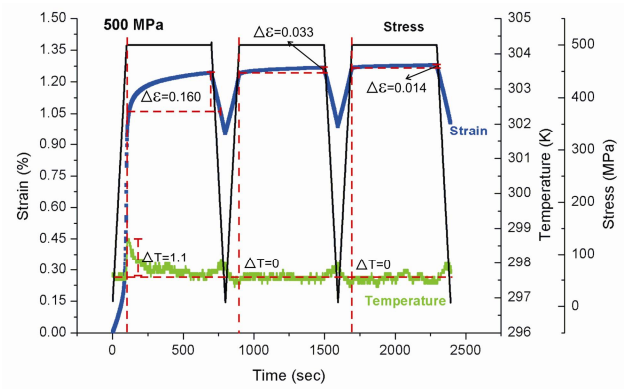

(b)

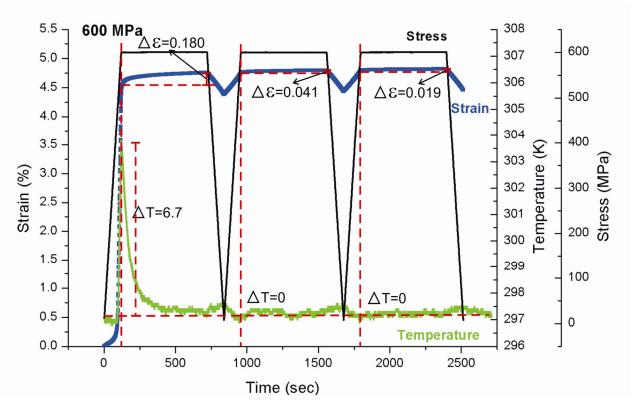

(c)

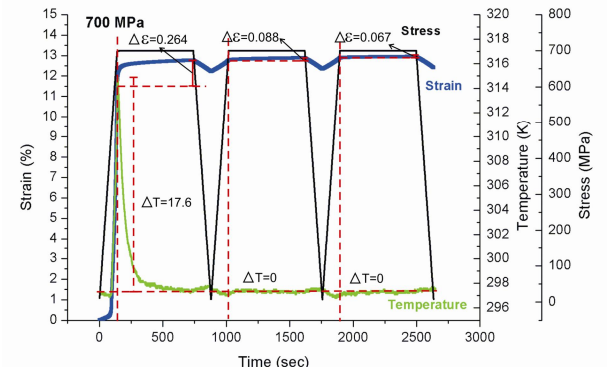

(d)

Figure 3: Plots of strain – time and temperature – time in loading – unloading tensile test for (a) 400 MPa (b) 500 MPa (c) 600 MPa (d) 700 MPa.

The plot of strain vs. time during the third tensile test is depicted in Figure 4. The strain increase during the 72 hours holding process is summarized in table 2 for the first 30 minutes of holding and the rest of the holding process. The data for the first 30 minutes of the holding process are divided into three parts, the first consecutive 10 minutes.

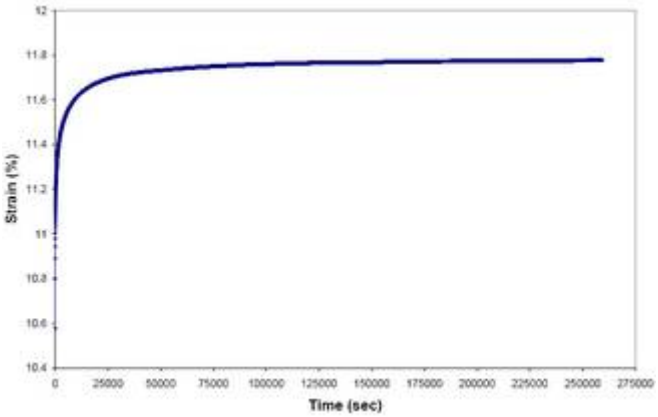

Figure 4: Plot of strain – time in loading – holding tensile test. The material was hold for 25900 sec (72 hours)

Table 2: Delta strain and average strain rate values during 72 hours holding in loading-holding tensile test.

Test duration (sec)	$\Delta\varepsilon$ (%)	Average strain rate (s^{-1})
0 – 600 sec (first 10 minutes)	0.712	1.2×10^{-5}
601 – 1200 sec (second 10 minutes)	0.077	1.3×10^{-6}
1201 – 1800 sec (third 10 minutes)	0.047	7.8×10^{-7}
1801 – 259.200 (71 hours and 30 minutes)	0.363	1.4×10^{-8}

The retained austenite calculation results from magnetic test can be seen in Figure 5.

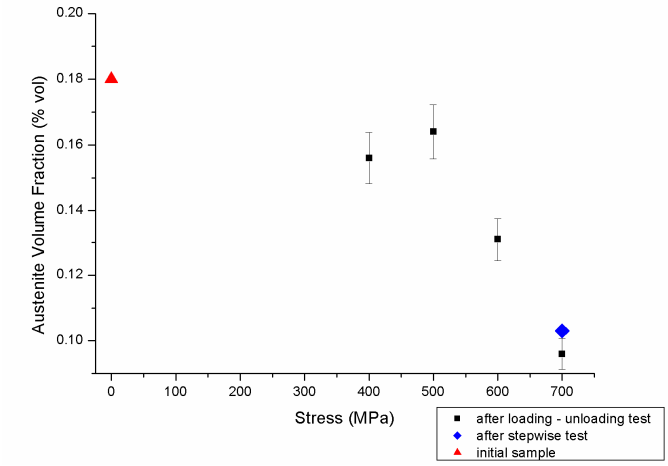

Figure 5: Plots between austenite volume fractions remained in the specimen after loading – unloading and stepwise tests vs. stress level used during the tensile test. The austenite volume fraction in the initial specimen was also measured and plotted in the graph.

4. DISCUSSION

4.1 Temperature Effect on Strain Development during Holding Process

The evolution of temperature during tensile will decrease as the holding process started. The plots between strain – time and temperature – time during the holding process can be seen in Figure 6. For the loading – unloading test, the heat only evolved during the tensile process before the first holding process but not before the second and third holding processes. From Figure 6, the relation between strain increase and temperature decrease is not linier, as one can see in Figure 7. The strain value used in this graph is normalized to the initial strain. It shows that the time scale for both processes is not the same, and that the strain continues to increase when the temperature has become equal to room temperature.

The increase in strain can be correlated to martensite formation. Martensite grains will form a larger volume compared to austenite, thus, martensite formation will have a contribution to the change of the specimen dimension by increasing the strain. The austenite transformed can be correlated to the austenite volume fraction reduction from its initial amount in the initial specimen. It can be seen from the magnetic test result (Figure 5), the loading-unloading specimens and stepwise specimens show smaller amounts of retained austenite than the initial one, thus, there was an austenite transformation in the specimen during the test.

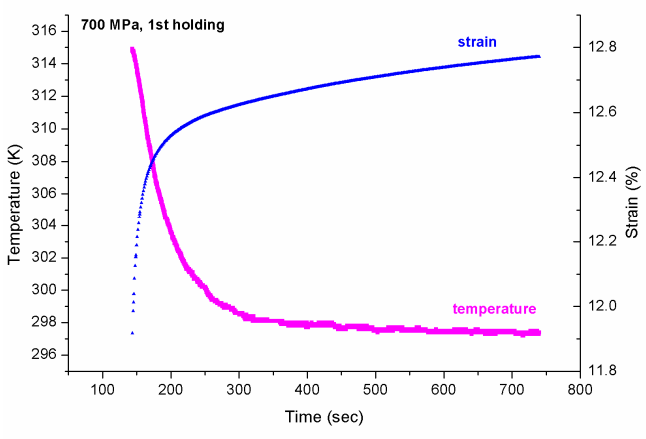

Figure 6: Plots between temperature – time and strain – time during the first holding process in loading – unloading tensile test, tensiled to 700 MPa.

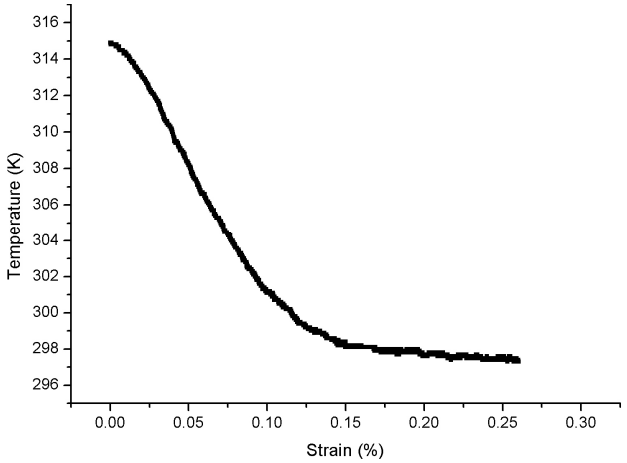

Figure 7: Plots of temperature vs. strain in loading – unloading tensile test, tensiled to 700 MPa, at the first holding process.

The decrease in temperature will increase the chemical driving force for martensite formation and increase the formation of shear bands [6]. The decrease in temperature can affect both the ΔG^{ch}, the free-energy difference providing the chemical driving force, and the rate of shear band formation both will increase. The increase in shear band formation will lead to an increased number of shear band intersections which become the nucleation site of martensite. Thus, it will tend to promote the martensite formation during the temperature decrease.

After approximately 100 seconds of holding, the rate of increasing strain becomes lower as well as the rate of temperature decrease. It is observed [7] from micrographs of TRIP steel deformed in tension to a strain of 0.02, partially transformed grains can easily be found which is evidence that autocatalytic effect is very weak or absent in TRIP Steel. In the absence of autocatalytic effect during the martensite formation, the transformation rate to achieve full martensite formation over austenite grains in the material becomes lower.

A prior tensile loading applied to the material is likely to have an effect on the strain development and heat evolvement in the material during tensile process. For a specimen tensiled to 700 MPa, the stepwise test shows ΔT-value as much as 11.8 K, whereas in the loading – unloading test the value of ΔT is 17.6 K. The difference in the highest temperature reached at the moment in which the holding process started has correlation with its initial strain. The stepwise has lower initial strain value than the loading – unloading test, which is 10.9% for stepwise and 11.3% for loading-unloading test (Figure 8). If the condition was assumed to be adiabatic, the area formed under stress – strain line in the stress – strain plot show all amount of energy absorbed during straining which was converted to heat.

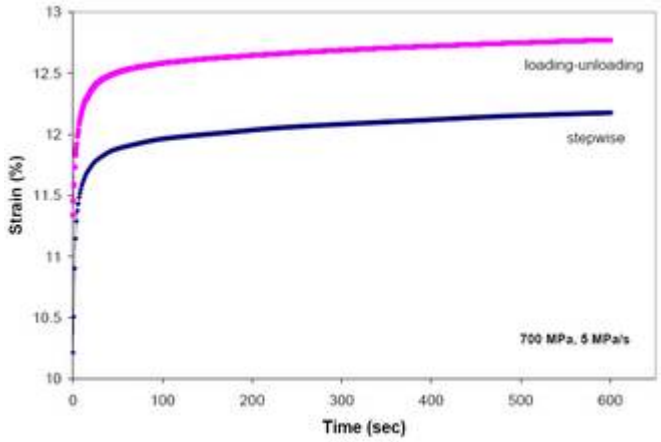

Figure 8: A strain – time plot of a stepwise tensile test when it reaches 700 MPa and loading-unloading tensile test to 700 MPa.

In the stepwise test, the previous deformation will have a work-hardening contribution to the austenite which will possibly make it less stable, and hence lower the initial strain value when the holding process starts. The rate of transformation in stepwise test tends to lower as the stress value increases (Figure 9). It might be due the least stabile fraction of austenite already being transformed at a lower stress level, the austenite becomes more stable and less amount of austenite can be transformed under certain level of deformation.

4.2 Isothermal Effect on Strain Development during Holding Process

In loading-unloading tensile test, at the second and the third loading process, the temperature increase due to tensile process in average was close to zero. It was only observed in the first 50 seconds of the holding process, the increase of temperature is approximately 0.3 K and afterwards the temperature value remains constant. This condition is observed for both second and third holding process. The time – strain and time – temperature plots for the second and the third loading process can be seen in Figure 10 and Figure 11. During this holding process, the relation between strain and time is logarithmic rather than linear, especially in the first several seconds of the holding process. The transformation process is faster in the beginning of holding than in the end of it. The strain still continued to increase whereas the temperature stays at constant value. This process can also be identified as isothermal martensitic transformation (IMT). The IMT process has its own critical temperature, denoted as M_{si}. Below this temperature the IMT process can proceed at a constant temperature

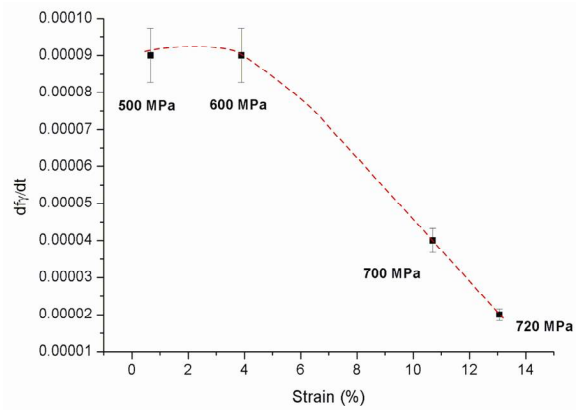

Figure 9: A plot between austenite transformation rate during holding at 500, 600, 700 and 720 MPa with strain, which corresponds to the holding stress level.

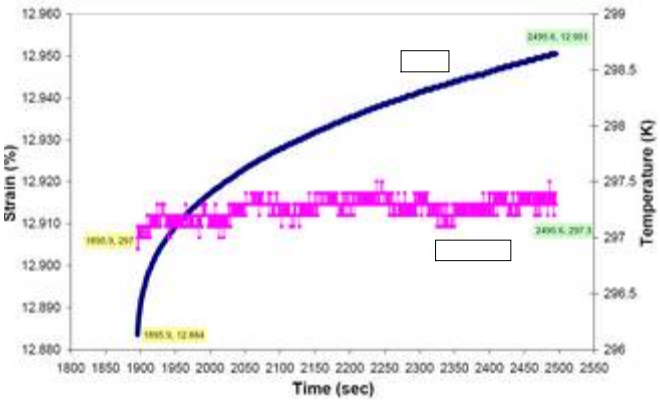

Figure 11: Strain development in the third loading process, holding for 10 minutes. The temperature value stays constant during the holding. The data was obtained from tensile test to 700 MPa.

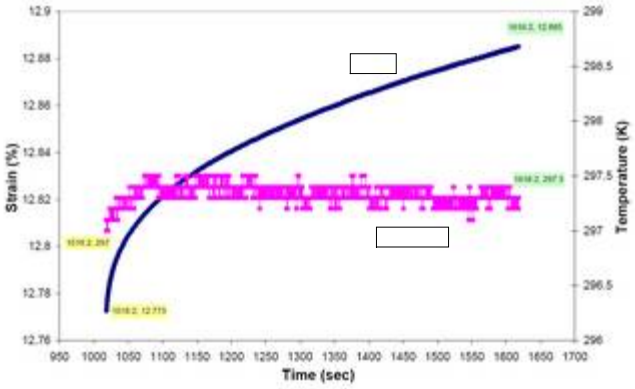

Figure 10: Strain development in the second loading process, holding for 10 minutes. The temperature value stays constant during the holding. The data was obtained from tensile test to 700 MPa.

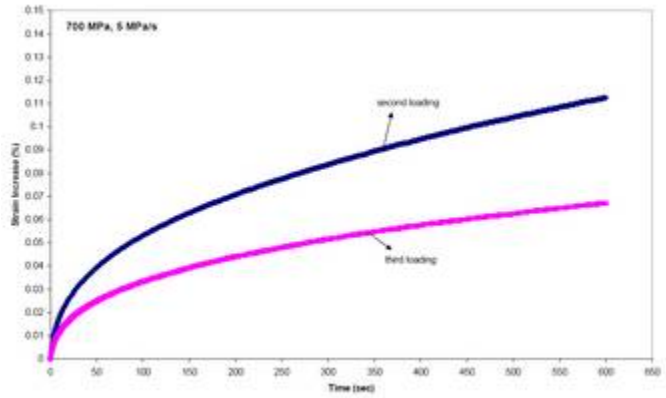

Figure 12: Strain development in the second and third loading process for tensile test to 700 MPa. The third loading process shows a slower development rate than the second one.

Even though the shape of the time-strain plot looks the same, the rate of strain development between the second holding and the third one is different. From Figure 12, it is seen that the third one has lower rate than the second one. This plot is obtained by normalizing the time to zero and normalizing the strain to the strain value at the beginning of the holding process (initial strain). The transformation rate can be very low but also very fast, depending on the M_s temperature of the material and the difference between M_s temperature and the temperature at which the IMT process is carried out [7].

In the third, when the material was held for 72 hours, the strain kept increasing even though at very low rate (Table 2). It shows that holding the material under mechanical loading at room temperature for TRIP Steel counted as a low rate IMT process. The rate can be altered due to some external factors, one of it is pre-strain. The more pre-deformation applied to the material, the lower the IMT rate will be [7]. This effect is already seen in Figure 12. The third loading has lower development rate than the second loading since the material has already suffered more deformation than the second one. Compared to the M_s temperature of this material, room temperature where the tensile test was carried out has a difference of 142 K and the test can be counted as low temperature situation, where the IMT process is likely to occurred.

The effect of prior deformation on the transformation can also be seen from stepwise and loading-unloading test results. For instance at 700 MPa, even though the initial strain value is higher in the first holding process of loading – unloading test than in stepwise test, when the IMT starts, the rate to form martensite becomes higher in the stepwise than in one step

tensile test (Figure 13). This behavior can be explained using martensite nucleation rate equation proposed by Raghavan-Entwisle-Pati-Cohen [8,9] and IMT activation energy equation [7] :

$$\dot{N} = \left\{ n_i + f\left(p - \frac{1}{\bar{V}} \right) \right\} \upsilon \exp\left(-\frac{\Delta W_a}{RT} \right) \quad (2)$$

$$\Delta W_a = W_0 - k\Delta G \quad (3)$$

where $\dot{N}$ is martensite nucleation rate, n_i is the initial density of nucleation sites, f is martensite volume fraction, p is the parameter of autocatalytic effect, $\bar{V}$ is the mean volume of the martensite plates after the test, υ is lattice vibration frequency, ΔW_a is activation energy for nucleation, R is gas constant and T is test temperature. a and k are constants, W_0 is extrapolated value for ΔG to zero at linear relation of ΔG vs. ΔW_a .

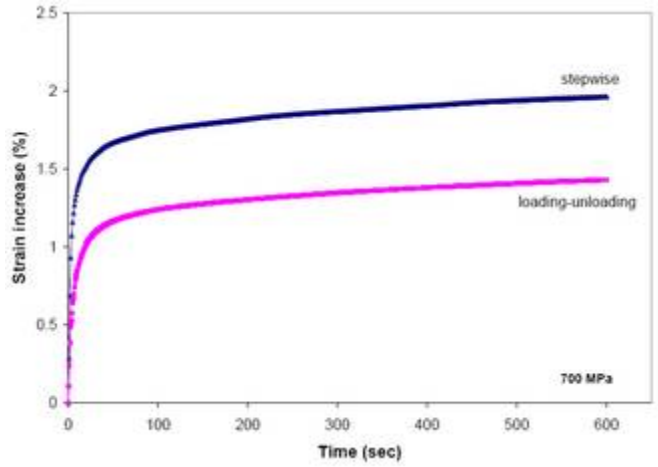

Figure 13: The strain development rate in stepwise and loading-unloading tensile test, loading to 700 MPa.

By assuming that k , a and T_a have the same value in both conditions, lower temperature will result in higher temperature difference with the M_s temperature, thus the thermodynamic driving force becomes higher and according to equation (3), the activation energy will be lower. From equation (2), since the value of testing temperature is the same at both situations, the exponential factor in the equation will be lower when the activation energy is higher. It is assumed that both conditions will have the same density of initial nucleation sites, lattice vibration frequency and autocatalytic parameter. It is being calculated previously [10] that this parameter will have the same value if the testing temperature and the stress level used are the same. The contribution of volume fraction of martensite and martensite plate mean volume will increase the nucleation rate as its values are increasing. In stepwise test, these two parameters are lower than in loading-unloading tensile test, however it is observed in Figure 13 that the strain rate development is higher than the loading-unloading tensile test. Hence, the activation energy has higher effect in the nucleation rate of martensite. IMT process under mechanical loading at room temperature, besides being affected by the test temperature, will also be affected by the heat generation and the consequent temperature increase during the loading process.

At lower stress level, 400 MPa, in stepwise test and loading – unloading test, the activation energy for IMT process is the same, since there is no heat generation in the material. According to equation (2), the nucleation rate will be only affected by martensite volume fraction and martensite plate mean volume, while the rest of the parameters are assumed to be the same in both conditions. Since the stepwise test possessed higher initial strain value than the loading-unloading tensile test, thus the strain development rate of stepwise test will also be higher than the loading-unloading tensile test, as shown in Figure 14. In the stepwise test, loading and afterwards holding at 100, 200 and 300 MPa is assumed to have a contribution to the formation of martensite in the material before the loading reaches 400 MPa. Some austenite might be work-hardened but more austenite is transformed to martensite. The fraction of martensite becomes higher than the loading-unloading tensile test to 400 MPa

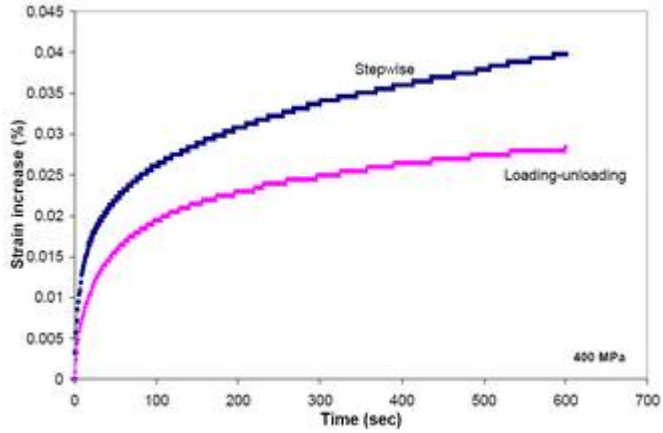

Figure 14: The strain development rate in stepwise and one step tensile test, loading to 400 MPa at 5 MPa/s

5. CONCLUSIONS

The conclusions that can be drawn from the present work are:

- The temperature effect on strain development during the holding process only plays a role in the beginning of the holding process.
- Driving force of martensite formation and rate of shear band formation, are temperature-dependent parameters, they will increase as the temperature decreases. Their contribution during the holding process is to promote the martensite formation.
- The IMT mechanism takes place after the temperature reaches constant value at room temperature.

- Martensite formed from the previous mechanism will have an effect on the IMT activation energy. At the same temperature, the martensite nucleation rate under IMT mechanism will tend to increase when the prior-martensite in the material is higher.
- The activation energy of IMT has a strong relation with thermodynamic driving force of martensite formation.
- The effect of stress rate on the strain will differ depending on the amount of heat generated in the material.
- The effect of previous deformation in the material, e.g. the effect of lower loading step to the higher loading step strain value in stepwise test, tends to lower the strain value and heat generation in the material.

REFERENCES

[1] E. Jimenez Melero, N.H. van Dijk, L. Zhao, J. Sietsma, S.E. Offerman, J.P. Wright and S. van der Zwaag, "Characterization of individual retained austenite grains and their stability in low alloyed TRIP steel," *Acta Materialia*, no. 55, pp. 6713-23, 2007.

[2] S. van der Zwaag, L. Zhao, S. O. Kruijver and J. Sietsma, "Thermal and mechanical stability of retained austenite in aluminium-containing multiphase TRIP steels," *ISIJ International*, vol. 42, no. 12, pp. 1565-70, 2002.

[3] A.K. Sachdev and J.E Hunter Jr., "Thermal effects during uniaxial straining of steels," *Metallurgical Transaction A*, vol. 13A, pp. 1063-7, 1982.

[4] L. Zhao, B. Mainfroy, M. Janssen, A. Bakker and J.Sietsma, "Time-dependent strain development under constant stress in TRIP steels," *Scripta Materialia*, no. 55, pp. 287-290, May 2006.

[5] L. Zhao, N.H. van Dijk, E. Bruck, J. Sietsma and S. van der Zwaag, "Magnetic and x-ray diffraction measurements for the determination of retained austenite in TRIP steels," *Materials Science and Engineering A*, vol. 313, pp. 145-152, 2001.

[6] J. Talonen,"Effect of strain-induced α'-martensite transformation on mechanical properties of metastable austenitic stainless steel," Doctoral Dissertation, Laboratory of Engineering Material, Department of Mechanical Engineering, Helsinki University of Technology, 2007.

[7] V.A. Lobodyuk and E.I. Estrin,"Isothermal martensite transformation," *Physics-Uspekhi*, vol. 48, no. 7, pp. 713-732, 2005.

[8] S.R. Pati and M. Cohen,"Kinetics of isothermal martensitic transformations in an iron-nickel-manganese alloy," *Acta Metallurgica*, vol. 19, pp. 1327-1332, 1971.

[9] V. Raghavan and A.R. Entwistle,"Physical properties of martensite and bainite," *Iron and Steel Institute Spec*, rep. 93, pp. 30, 1965.

[10] G. Ghosh and V. Raghavan,"The kinetics of isothermal martensitic transformation in an Fe-23.2wt. %Ni-2.8 wt.% Mn alloy," *Materials Science and Engineering*, vol. 80, pp. 66-74,1986.

[11] T.Y. Hsu (Xu Zuyao),"Martensitic transformation under stress," *Materials Science and Engineering A*, vol. 438, pp. 64-68, 2006

[12] W. F. Hosford and Robert M. Caddell,"Metal forming : Mechanics and Metallurgy," Second Edition, Engelwoods Cliffs: Prentice-Hall, 1993.

[13] A. K. Sachdev and J. E. Hunter, Jr, "Thermal Effects during Uniaxial Straining of Steels," *Metallurgical Transaction A*, vol. 13A, pp. 1063-1067, 1982

ISSN 114-1284

Ionic Species Study of $PM_{2.5}$ and PM_{10} under Stagnant Atmospheric Conditions in the GIST Area, Gwangju, South Korea

Gatot Suhariyono

Aerosol Laboratory, Center for Technology of Radiation Safety and Metrology (PTKMR),
National Nuclear Energy Agency (BATAN), Jl. Lebak Bulus Raya, Pasar Jum'at, Jakarta Selatan 12440, Indonesia,
Tel: 62-21-7513906, Fax: 62-21-7657950
Email: g_suhariyono@batan.go.id

ABSTRACT

In GIST (Gwangju Institute of Science and Technology) area, data on particulate matter concentrations ($PM_{2.5}$ and PM_{10}), and chemical compositions concentrations are important and useful to know air quality, particularly for urban areas, Gwangju city, South Korea, under stagnant atmospheric conditions, especially on the daytime and on the nighttime. The objective of this study was to investigate the chemical composition concentration of the air ion species (Na^+, NH_4^+, K^+, Mg^{2+}, Ca^{2+}, Cl^-, NO_3^-, and SO_4^{2-}) in fine particles ($PM_{2.5}$) and to study concentrations of PM_{10} in the GIST area on September 24 to October 7, 2007. Measurement of $PM_{2.5}$ concentration was carried out by using an Medium Volume $PM_{2.5}$ Particulate was collected with a $PM_{2.5}$ cyclone inlet in twice every day during 12-hour, every 9.00 am and 9.00 pm. Concentrations measurement of PM_{10} were obtained real time by using the Beta Gauge monitor. The Teflon filters from the $PM_{2.5}$ cyclone sampler were used for the analysis of ionic species (anion (Cl^-, NO_3^-, and SO_4^{2-}) and cation (Na^+, NH_4^+, K^+, Mg^{2+}, Ca^{2+})) by ion chromatography. The average concentrations of $PM_{2.5}$ and PM_{10} were on the night (from 9.00 pm to 9.00 am) higher than the concentrations on the day (from 9.00 am to 9.00 pm). The highest concentration of $PM_{2.5}$ and PM_{10} were on the nighttime of October 4, 2007, and the contents were SO_4^{2-}, Ca^{2+}, NH_4^+, Cl^-, and K^+. While the contents of $PM_{2.5}$ and PM_{10} on the daytime of October 4, 2007 were Na^+, Ca^{2+}, K^+, NH_4^+, and SO_4^{2-}. The average concentrations of NO_3^-, Cl^-, K^+, Mg^{2+} on the nighttime were higher than the ones of NO_3^-, Cl^-, K^+, Mg^{2+} on the daytime. The average concentrations of NH_4^+, SO_4^{2-}, and Ca^{2+} on the daytime were almost closed to the concentrations on the nighttime.

Keywords: *$PM_{2.5}$, PM_{10}, ion species, Gwangju, South Korea*

1. INTRODUCTION

Particulate matter, also known as particle pollution or PM, is a complex mixture of extremely small particles and liquid droplets found in the air. Some particles, such as dust, dirt, soot, or smoke, are large or dark enough to be seen with the naked eye. Particles can only be detected using an electron microscope. Particle pollution is made up of a number of components, including acids (such as nitrates and sulfates), organic chemicals, metals, and soil or dust particles [1].

The size of particles is directly linked to their potential for causing health problems. Environmental Protection Agency **(**EPA) is concerned about particles that are 10 μm in diameter or smaller, because those are the particles that generally pass through the throat and nose, and enter to the lungs [1]. Once inhaled, these particles can affect the heart and lungs, and cause serious health effects. EPA groups particle pollution into two categories:

1. Inhalable coarse particles, such as those found near roadways and dusty industries, are larger than 2.5 μm and smaller than 10 μm in diameter.
2. Fine particles, such as those found in smoke and haze, are 2.5 μm in diameter and smaller. These particles can be directly emitted from a source, such as forest fires, or the particles can form, when gases emitted from power plants, industries and automobiles react in the air.

The average diameter of single human hair is about 70 μm, around 30 times larger than the largest fine particle (2.5 μm). These particles come in many sizes and shapes, and can be made up of hundreds of different chemicals. Some particles, known as primary particles are emitted directly from a source, such as construction sites, unpaved roads, fields, smokestacks or fires. Others form in complicated reactions in the atmosphere of chemicals such as sulfur oxides (SOx) and nitrogen oxides (NOx) that are emitted from power plants, industries and automobiles. These particles, known as secondary particles, make up most of the fine particle pollution in the country.

Small particles less than 2.5 μm in diameter pose the greatest problems, because they can get deep into lungs, and some may even get into bloodstream and cause serious health problems (Fig. 1). Fine particles ($PM_{2.5}$) also are the major cause of reduced visibility (haze). Numerous scientific studies have linked particle pollution exposure to a variety of problems, including increased respiratory symptoms, such as irritation of the airways, coughing, or difficulty breathing, for example; decreased lung function; aggravated asthma; development of chronic bronchitis; irregular heartbeat; nonfatal heart attacks; and premature death in people with heart or lung disease. People with heart or lung diseases, children and older adults are the most likely to be affected by particle pollution exposure.

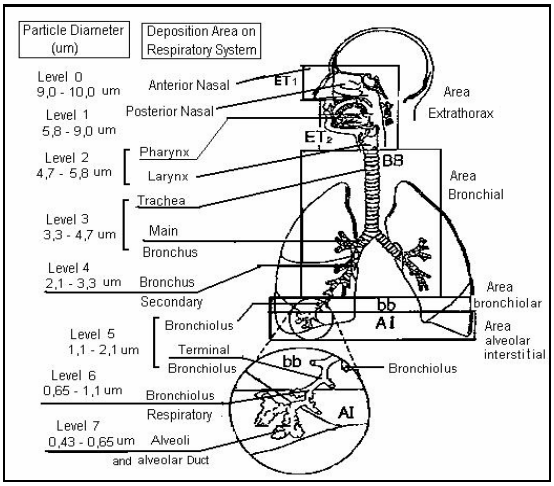

Figure 1. Deposition of the aerosol particles in respiratory system.

The Clean Air Act, which was last amended in 1990, requires EPA to set National Ambient Air Quality Standards (NAAQS) for widespread pollutants from numerous and diverse sources considered harmful to public health and the environment. The Clean Air Act established two types of national air quality standards. Primary standards set limits to protect public health, including the health of "sensitive" populations such as asthmatics, children, and the elderly. Secondary standards set limits to protect public welfare, including protection against visibility impairment, damage to animals, crops, vegetation, and buildings. EPA revised the air quality standards for particle pollution in 2006. The NAAQS standards in 2006 tighten the 24-hour fine particle ($PM_{2.5}$) standard from the current level of 65 $\mu g/m^3$ to 35 $\mu g/m^3$, and retain the current annual fine particle standard at 15 $\mu g/m^3$. The Agency decided to retain the existing 24-hour PM_{10} standard of 150 $\mu g/m^3$ and the Agency revoked the annual PM_{10} standard, because available evidence does not suggest a link between long-term exposure to PM_{10} and health problems [1].

Airborne particulate matter is one of the important markers of air quality and is of important health concern in urban areas, especially with respect to a number of chronic respiratory diseases. There is an abundance of epidemiological evidences associating increased air particulate pollution with the incidence of adverse human health effects [2, 3]. Fine particles ($PM_{2.5}$) as well as particle components such as sulfate ion (SO_4^{2-}) and strong acidity (H^+) also are strongly associated with increased mortality and other adverse health effects [4]. Ion-ion sulfate (SO_4^-), nitrate (NO_3) and ammonium (NH_4^-) are the most common component of secondary particles in the atmosphere. These particles are formed in the atmosphere from direct emissions of sulfur dioxides (SO_2), nitrogen oxide (NO_x) and ammonia (NH_3) gases. Ion-ion SO_4^{2-}, NO_3^- , and NH_4^+, dominate the identifiable components within the fine fraction ($PM_{2.5}$) [5]. In large urban areas, nearly half of NO_x emissions are caused by automobile exhaust. HCl is mainly produced by coal combustion and refuse incineration, and industrial waste incinerations primary pollutant, and by the reaction of HNO_3 with NaCl in sea-salt particles as a secondary pollutant [6].

In GIST (Gwangju Institute of Science and Technology) area, data on particulate matter concentrations ($PM_{2.5}$ and PM_{10}), chemical compositions and gaseous concentrations are important and useful to know air quality, particularly for urban areas as Gwangju city under stagnant atmospheric conditions, especially on the daytime and on the nighttime. The objective of this study was to investigate the chemical composition concentration of the air ion species (Na^+, NH_4^+, K^+, Mg^{2+}, Ca^{2+}, Cl^-, NO_3^-, and SO_4^{2-}) in fine particles ($PM_{2.5}$) and to study concentrations of PM_{10} in the GIST area, Gwangju, South Korea.

2. METHODS

Aerosol sampling was collected on September 24 to October 7, 2007 in Samsung Building, the GIST area, Gwangju, South Korea (35.10 N, 126.53 E). As shown in Fig. 2, the sampling site is located in the city of Gwangju, which is the fifth largest city in Republic of Korea and located 330 km south of Seoul. Its population of approximately 1.4 million people occupies an area of 501.4 km^2 in which there are 0.3 million motor vehicles [7]. Aerosol sampling was conducted in a mobile laboratory trailer at the Gwangju Institute of Science and Technology (GIST), which is located in a northern suburb of Gwangju and surrounded by rural areas from north to east of the sampling site. The Hanam industrial complex is located several kilometers southwest from the sampling site.

Measurement of $PM_{2.5}$ concentration was carried out by using an Medium Volume $PM_{2.5}$ Particulate was collected with a $PM_{2.5}$ cyclone inlet in twice every day during 12-hour, every 9.00 am and 9.00 pm. Cyclones system are airborne system of diameter size selective inlets that create a circular air motion. This circular motion separates fine and coarse particles. Cyclones are Teflon coated to minimize the loss of reactive gases (e.g. HNO_3, NH_3) to the internal surfaces of the cyclone [8]. A $PM_{2.5}$ cyclone inlet is integrated with gooseneck adapter, coupler, and 47 mm Teflon filter pack with quick release at outlet. The Teflon filter with 47 mm diameter and 2.0 µm pore size was placed in filter pack. Aerosol samplers were operated with flow rate 16.7 lpm. The flow rate was calibrated with dry test gas meter, and to know aerosol volume. The filter was put in Petridis, then wrapped with Teflon tape and aluminum foil, and stored in a refrigerator after sampling.

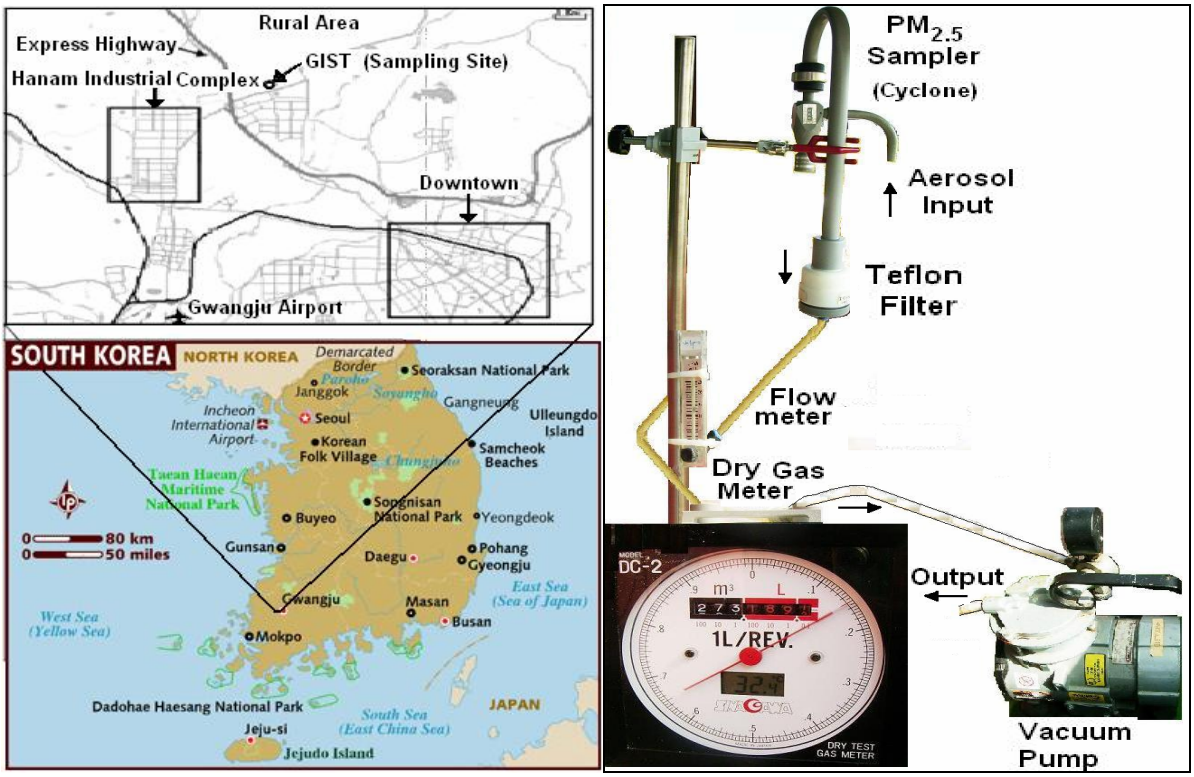

Figure 2. Location of the sampling site and the sampling instruments of $PM_{2.5}$.

All samples were refrigerated between collection and analysis after sampling to minimize losses due to volatilization and evaporation during transportation. Aerosol mass of fine particle fraction were measured by the gravimetric method using an electronic microbalance with a sensitivity of one µg. $PM_{2.5}$ concentration (C) was calculated with divide between difference of particle mass after and before sampling with sampling volume. m_t is filter mass after sampling (µg), m_0 is filter mass before sampling (µg), t is sampling time (minute), and F is the flow rate of sampling (m^3/minute).

$$C = \frac{m_t - m_0}{t \cdot F} \quad \mu g/m^3 \qquad (1)$$

The teflon filters from the $PM_{2.5}$ cyclone sampler were used for the analysis of ionic species by ion chromatography (IC), made in Dionex, DX-120 type (Figure 6). Each sampled filter that collected in Petridis was put into a 20 ml vial, wetted with 15 ml distilled deionizer water (DDW) and shaken with shaker machine during 1 hour with speed 200 rpm. Then each solution of sample was taken 4 ml for anion (Cl^-, NO_3^-, and SO_4^{2-}) analysis and 4 ml for cation (Na^+, NH_4^+, K^+, Mg^{2+}, Ca^{2+}) analysis. All solution was entered into special vial for the analysis of IC. At the same time standard eluent solution, 4 ml was made also to calibrate anion and cation with the concentration of 1, 5, 10 and 20 ppm respectively. The eluent solution for anion measurement is sodium carbonate (Na_2CO_3) 600 mM (15.90 g / 250 ml) and sodium bicarbonate ($NaHCO_3$) 680 mM (14.28 g / 250 ml) with flow rate 1.2 ml/min. The eluent solution for cation measurement is Methane Sulfonic Acid (CH_3SO_2OH) 1 M (96.10 g/l) with flow rate 1 ml/min. Total conductivity for anion is between 16 and 20 µS (µSiemens) and for cation 3 µS. Blank solution of distilled deionizer water is made also as control solution. All solution was analyzed by IC average 20 minutes for ionic concentration.

Concentrations measurement of PM_{10} were obtained real time by using the Beta Gauge monitor at the distance of about one kilometer from the $PM_{2.5}$ sampling site in the GIST eastside. Some meteorological data in the Gwangju area, such as temperature, pressure, wind speed, wind direction, and relative humidity, were obtained from website (www.kma.go.kr) of the Korean Meteorological Administration (KMA) [9].

3. DISCUSSION

The measurement results of $PM_{2.5}$ and PM_{10} concentration in the GIST area were shown in Figure 3. The average concentration and its standard deviation of $PM_{2.5}$ were 39.838 ± 17.265 µg/m^3 on the night (from 9.00 pm to 9.00 am) higher than 35.557 ± 8.920 µg/m^3 on the day (from 9.00 am to 9.00 pm). The maximum and minimum concentrations of $PM_{2.5}$ were 85.173 and 18.796 µg/m^3 on the night respectively, and on the day 47.747 and 21.002 µg/m^3 respectively. This case is similar with the study of Haobo Wang and David Shooter, which found that nighttime of particle matter concentrations were higher than their daytime
concentrations in Christchurch, New Zealand [10]. The highest concentration of $PM_{2.5}$ was 85.173 µg/m^3 on the night (Oct. 4, 21.00 to Oct. 5, 9.00 am (Night 11)). This was possibly, because underway building making at southeast

side of the sampling site and the wasteland at east side of the sampling site releases fine particles, so that the fine particles of dust can be collected by the filter. The occurrence of these fine particles was proved by the low visibility on October 5, at 3.00 am to 7.00 am which is only 2.5 to 4 km. In Korea, it is commonly defined that the haze occurs, if the visibility range is less than about 5 km by the eye [9]. The increase of fine particles ($PM_{2.5}$) and acidic gas pollutants were associated with the rate of incidence of adverse human health effects as well as visibility impairment. The average weather condition on October 4, 21.00 to October 5, 9.00 am (Night 11) is brune (haze), temperature (18.18 ^oC), relative humidity (90.75 %), wind speed (0.9 m/s = 3.24 km/h), wind direction (45^o / North-East). In addition, the mean $PM_{2.5}$ concentrations of the haze episodes was lower than those of other cities such as Athens, Greece (80.7 μg/m^3 (1990)), Mexico city, Mexico (94.4 μg/m^3 (1992)), Beijing, China (127 μg/m^3 (2001)), Seoul, South Korea (131 μg/m^3 (2001), 50.3 μg/m^3 (1996), 75 μg/m^3 (spring), 95 μg/m^3 (summer), 90 μg/m^3 (fall), 85 μg/m^3 (winter, 2003-2004) [9, 11].

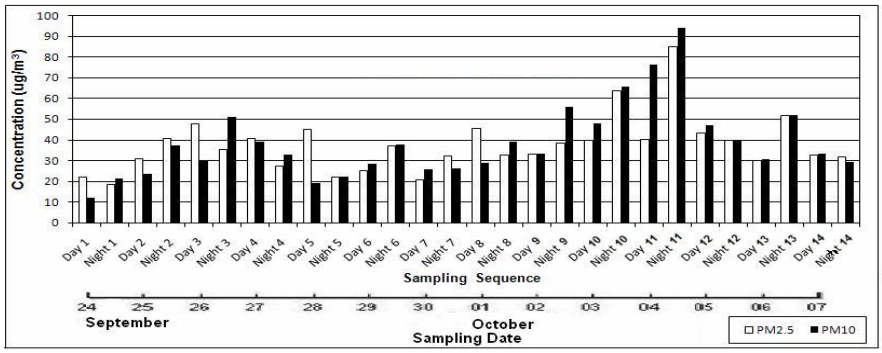

Figure 3. The measurement results of $PM_{2.5}$ and PM_{10} concentration.

The highest concentration of $PM_{2.5}$ on October 4, 21.00 to October 5, 9.00 am (Night 11) can be caused by Asian Dust. According to KMA, Korea, the Asian dust measurement results of PM_{10} concentration on Night 11 were also in fact the highest, even the concentration were high on the daytime and the nighttime. The air mass trajectory on September 24 to 30, 2007 was originated from the desert areas of Mongolia and China (northen) passed through the northeastern part of China, where highly polluted areas and agricultural areas are located. Agricultural burning occurs especially at these areas during the fall season [9]. The air mass trajectory on September 24 to 30, 2007 also was originated from southern China, which includes the major industrial areas [11]. The air mass trajectory on October 1 to 7, 2007 was originated from the China (northeastern) where highly polluted areas and agricultural areas are located. Therefore PM_{10} concentrations on Night 11 were reality the highest, because the air mass concentration from China was the highest on that time. The measurement results of PM_{10} concentration by Beta Gauge monitor in the GIST eastside was similar with the Asian dust measurement results of PM_{10} concentration by KMA. The average PM_{10} concentrations and its standard deviation on the day and the night were 34.018 ± 15.676 μg/m^3 and 43.274 ± 19.581 μg/m^3 respectively.

The highest contributors to the $PM_{2.5}$ mass are major ionic species such as NO_3^-, SO_4^{2-}, and NH_4^+ [9]. The measurement results of nitrate (NO_3^-) anion concentration can be shown Figure 4. The average NO_3^- concentration on the daytime was lower than the one on the nighttime. The average NO_3^- concentrations and its standard deviation on the daytime and the nighttime were 0.636 ± 0.327 μg/m^3 and 1.144 ± 0.791 μg/m^3 respectively. The highest concentration of NO_3^- was 2.825 μg/m^3 on nighttime of Oct. 3, 2007 and 1.136 μg/m^3 on daytime of Sept. 27, 2007. The NO_3^- ions are related with visibility impairment [9]. If the NO_3^- concentration is increase, so the visibility is decrease. This case was proven the low visibility on October 3, 2007 the nighttime until 3 km and the daytime until 11 km. Nitrates are used by plants as nutrients, exploited in agriculture as a fertilizer and chemical manufacturing. Based on the wind direction (average South-West and on Sept. 27, and Oct. 3, 2007), that cases were probably caused by the existance of NO_3^- from chemical process of Hanam Industrial.

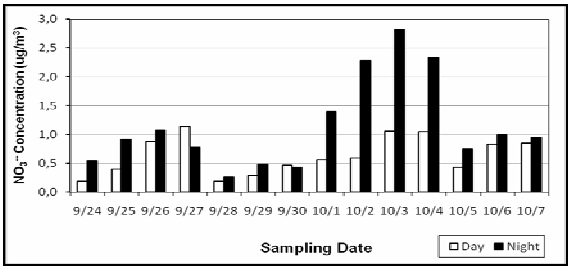

Figure 4. The measurement results of NO_3^- anion concentration.

The measurement results of anion concentration and calibrate of sulfate (SO_4^{2-}) can be shown Figure 5. The average SO_4^{2-} concentration on the daytime was almost closed to the one on the nighttime. The average SO_4^{2-} concentrations and its standard deviation on the daytime and the nighttime were 2.605 ± 2.377 μg/m^3 and 2.734 ± 2.671 μg/m^3 respectively. The highest concentration of SO_4^{2-} was 11.151 μg/m^3 on the night and 9.561 μg/m^3 on the day of Oct. 4, 2007. The SO_4^{2-} ions are related with visibility impairment also [9]. If the SO_4^{2-} concentration is increase, so the visibility is decrease. This case was proven the low visibility on October 4, 2007 the nighttime until 2.5 km and the daytime until 7 km.

Sulfates are important in both the chemical industry and biological systems. Based on the wind direction (South-West on the daytime and North-East on the nighttime of Oct. 4, 2007), that cases were probably caused by the existance of chemical process in Hanam Industrial on the daytime and of biological systems (a agricultural area) on the nighttime.

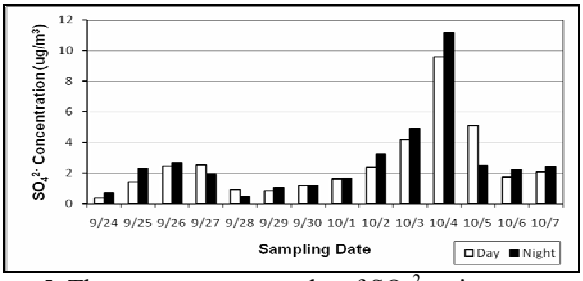

Figure 5. The measurement results of SO_4^{2-} anion concentration.

The concentration measurement results and calibrated of ammonium cation (NH_4^+) can be seen Figure 6. The average NH_4^+ concentration on the daytime was almost closed to that on the nighttime. The average NH_4^+ concentrations and its standard deviation on the daytime and the nighttime were 1.105 ± 1.027 μg/m^3 and 1.362 ± 1.359 μg/m^3 respectively. The highest concentration of NH_4^+ was 5.292 μg/m^3 on the night and 4.038 μg/m^3 on the day of Oct. 4, 2007. The distribution of ammonium ion is from a localized source into the soil. Based on the wind direction (South-West on the daytime and North-East on the nighttime of Oct. 4, 2007), the highest NH_4^+ concentration was probably originated from in the automobile exhaust of Highway and from in the combustion processes of Hanam industrial on daytime and from agricultural biomass burning of a rural area on nighttime.

The average Na^+ concentration on the daytime was higher than that on the nighttime (Fig. 7). The average Na^+ concentrations and its standard deviation on the daytime and the nighttime were 0.660 ± 0.316 μg/m^3 and 0.535 ± 0.213 μg/m^3 respectively. The highest concentration of Na^+ was 0.836 μg/m^3 on the night of Oct. 7, 2007 and 1.064 μg/m^3 on the day of Oct. 1, 2007. Sodium ions are the principal cation in sea salt vapor and chemical process. Based on the wind direction (North on the daytime of Oct. 1, and on the nighttime of Oct. 7, 2007), the highest Na^+ concentration was probably originated from the Japan Sea.

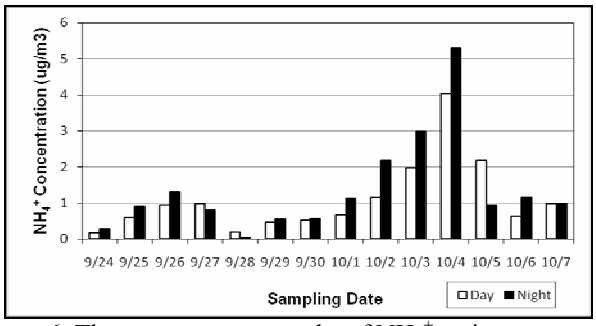

Figure 6. The measurement results of NH_4^+ cation concentration.

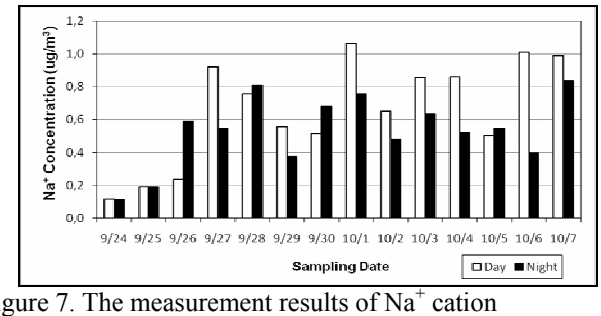

Figure 7. The measurement results of Na^+ cation concentration.

The average Cl^- concentration on the nighttime was higher than that on the daytime (Fig. 8). The average Cl^- concentrations and its standard deviation on the daytime and the nighttime were 0.306 ± 0.067 μg/m^3 and 0.389 ± 0.099 μg/m^3 respectively. The highest concentration of Cl^- was 0.591 μg/m^3 on the night of Oct. 4, 2007 and 0.507 μg/m^3 on the day of Sept. 27, 2007. Cl^- (chloride) ions are the principal anion in sea salt vapor and chemical process. Based on the wind direction (South-West on the daytime of Sept. 27, and North-East on the nighttime of Oct. 4, 2007), the highest Cl^- concentration was probably originated from chemical process in Hanam Industrial on the daytime and from the Japan Sea on the nighttime.

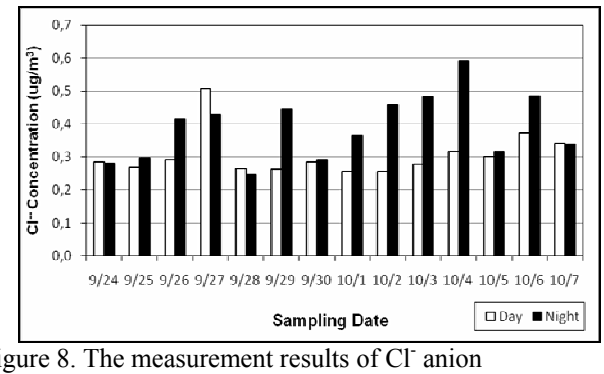

Figure 8. The measurement results of Cl^- anion concentration.

The average K^+ concentration on the nighttime was higher than that on the daytime (Fig. 9). The average K^+ concentrations and its standard deviation on the daytime and the nighttime were 0.365 ± 0.074 μg/m^3 and 0.416 ± 0.082 μg/m^3 respectively. The highest concentration of K^+ was 0.629 μg/m^3 on the night and 0.564 μg/m^3 on the day of Oct. 4, 2007. Potassium ion is primarily used in fertilizers and the chemical industries. Based on the wind direction on Oct. 4, 2007, the highest K^+ concentration was probably originated from chemical processes of Hanam industrial on daytime and from agricultural biomass burning of rural area on nighttime.

The average Mg^{2+} concentration on the nighttime was higher than that on the daytime (Fig. 10). The average Mg^{2+} concentrations and its standard deviation on the daytime and the nighttime were 0.484 ± 0.030 μg/m^3 and 0.522 ± 0.151 μg/m^3 respectively. The highest concentration of Mg^{2+} was 1.041 μg/m^3 on the night of Sept. 29, 2007 and 0.560 μg/m^3 on the day of Sept. 27, 2007. Based on the wind direction

(North-East on Sept. 29, and South-West on Sept. 27, 2007), that cases were probably caused by the existence of Mg^{2+} ion from Hanam industries on Sept. 27, 2007 and the dust existence of agricultural biomass burning on Sept. 29, 2007.

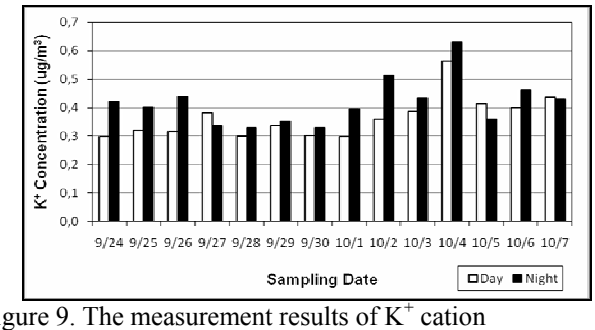

Figure 9. The measurement results of K^+ cation concentration.

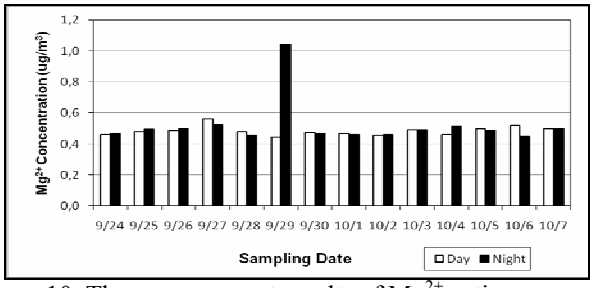

Figure 10. The measurement results of Mg^{2+} cation concentration.

The average Ca^{2+} concentration on the nighttime was closed to that on the daytime (Fig. 11). The average Ca^{2+} concentrations and its standard deviation on the daytime and the nighttime were 0.548 ± 0.073 μg/m^3 and 0.550 ± 0.080 μg/m^3 respectively. The highest concentration of Ca^{2+} was 0.711 μg/m^3 on the night and 0.675 μg/m^3 on the day of Oct. 6, 2007. Calcium ion is as an alloying agent used in the metal production, and cement factory. Based on the wind direction (North-East on the daytime, and South-East on the nighttime of Oct. 6, 2007, that cases were probably caused by the existence of Mg^{2+} ion from building materials on the nighttime and the dust existence of agricultural biomass burning on the daytime.

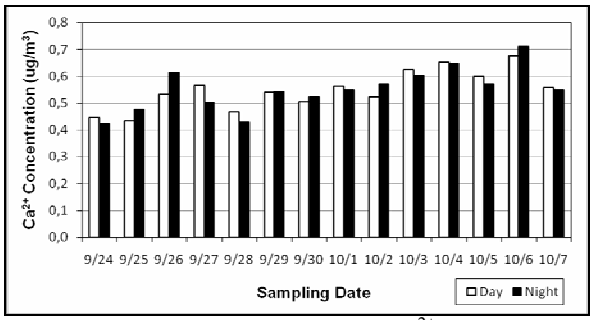

Figure 11. The measurement results of Ca^{2+} cation concentration.

4. CONCLUSION

The average concentrations of $PM_{2.5}$ and PM_{10} were on the night (from 9.00 pm to 9.00 am) higher than those on the day (from 9.00 am to 9.00 pm). The highest concentration of $PM_{2.5}$ and PM_{10} were on the nighttime of October 4, 2007, and the contents were SO_4^{2-}, NO_3^-, Ca^{2+}, NH_4^+, Cl^-, and K^+. While the contents of $PM_{2.5}$ and PM_{10} on the daytime of October 4, 2007 were Na^+, Ca^{2+}, K^+, NH_4^+, and SO_4^{2-}. The average concentrations Na^+ on the daytime were higher than those on the nighttime. The average concentrations of NO_3^-, Cl^-, K^+, and Mg^{2+} on the nighttime were higher than the ones on the daytime. The average concentrations of NH_4^+, SO_4^{2-}, and Ca^{2+} on the daytime were almost closed to those on the nighttime. The average concentrations of PM_{10}, were lower and the average $PM_{2.5}$ concentrations were a little higher than the ones of the US NAAQS standard respectively.

ACKNOWLEDGMENT

Many thanks to Prof. Young Joon Kim, Dr. Suil Kang, Dr. Suthipong Sthiannopkao, all administrative staffs of IERC (International Environmental Research Center) and GIST, and all members of Air Quality Monitoring Laboratory, GIST as well as all of internship students for their kindly help and support.

REFERENCES

[1] Environmental Protection Agency (EPA), "Particulate Matter, " http://www. epa.gov/air/particles/, 2007.

[2] D.W. Dockery, and C.A. Pope, "Acute Respiratory Effects of Particulate Air Pollution," *Annu. Rev. Public Health*, 15, pp. 107-132, 1994.

[3] D.W. Dockerey, C.A. Pope III, X. Xu, J.D. Spengler, J.H. Ware, M.E. Fay, B.G. Ferris, and F.E. Speizer, "An Association between Air Pollution and Mortality in six U.S. cities," *New Engl. J. Med*., 329, pp. 1753 – 1759, 1993.

[4] L.M. Neas, D.W. Dockery, P. Koutrakis, D.J. Tollerund, , and F.E. Speizer, "The Association of Ambient Air Pollution with Twice Daily Peak Expiratory Flow Rate Measurement in children," *American Journal Epidemiology* 141, pp. 111-122, 1995.

[5] J. J. Lin, Characterization of water-soluble ion species in urban ambient particles, *Environment International 28*, pp. 55-61, 2002.

[6] A. Bari, V. Ferraro, L. R. Wilson, D. Luttinger, L. Husain, "Measurement of gaseous HONO, HNO_3, SO_2, HCl, NH_3, particulate sulfate and $PM_{2.5}$ in New York", NY, *Atmospheric Environment 37*, pp. 2825-2835, 2003.

[7] S.Y. Ryu, B.G. Kwon, Y.J. Kim, H.H. Kim, K.J. Chun, "Characteristics of Biomass Burning Aerosol and its impact on regional air quality in the summer of 2003 at Gwangju, Korea", *Atmosphere Research 84*, pp. 362 – 373, 2007.

[8] University Research Glassware, "URG Parts Catalog", http://www.urgcorp.com/cyclones/ how.html, USA, 2006.

[9] C.M. Kang, H.S. Lee, B.W. Kang, S.K. Lee, Y. Sunwoo, "Chemical Characteristics of acidic gas pollutants and $PM_{2.5}$ species during hazy episodes in Seoul, South Korea, " *Atmosphere Environment 38*, pp. 4749 – 4760, 2004.

[10] H. Wang, and D. Shooter, "Coarse-fine and day-night differences of water-soluble ions in atmospheric aerosols

collected in Christchurch and Auckland, New Zealand," *Atmosphere Environment 36*, pp. 3519 – 3529, 2002.

[11] H.S. Kim, Jong-Bae Huh, P. K. Hopke, T.M. Holsen, S.M. Yi, "Characteristics of the major chemical constituents of PM2.5 and smog events in Seoul, Korea in 2003 and 2004," *Atmosphere Environment 41*, pp. 6762 – 6770, 2007.

Temperature and pH effect in Carbon Steel Corrosion Rate using Hydrogen Sulfide gas environment

Haipan Salam[1], Agus Solehudin[2]

[1,2] *Mechanical Engineering Education Department,*
Indonesia University of Education, Bandung 40154, Indonesia
Telp. (022) 2020162 / Fax. (022) 2020162
[1]*E-mail: Haipansalam@gmail.com*
[2]*E-mail: asolehudin@upi.edu*

ABSTRACT

Geothermal energy is an alternative energy to replace oil and gas energy. In its development, geothermal fluid contains compounds that corrosive to carbon steel pipe. This corrosive compounds are carbon dioxide (CO_2), chloride compounds, and hydrogen sulfide as the most corrodent. API 5LX65 carbon steel was used as a test specimen. This specimen was put in 3.5 %b/v NaCl with H_2S gas to get corrosion process. The pH value was varied by addition of acetic acid. Corrosion rate was calculated based on weight loss. Result of corrosion rate calculation at pH 3.2 demonstrated an increasing of corrosion rate with an increasing temperature at 25°C – 75°C and decreasing at 97°C. This decreasing in corrosion rate may be attributed to the fact that sulfide iron film was composed as corrosion product. Meanwhile, at 75°C with variation of pH value, the calculation result demonstrated that corrosion rate was decrease with an increasing of pH value from 3.2 to 6.1, and then increase at pH 6.6. The increasing of H_2S gas concentration causes the increasing of corrosion rate. Corrosion layer as corrosion product was known from SEM and EDS. Results of SEM and EDS showed that the surface morphology demonstrate a pitting corrosion.

Keywords: *Corrosion rate, Carbon steel, Temperature, pH, Hydrogen Sulfide.*

1. INTRODUCTION

Geothermal energy is an alternative energy to replace oil and gas energy. In its development, geothermal fluid contains compounds that corrosive to carbon steel pipe. This corrosive compounds are carbon dioxide (CO_2), chloride compounds, and hydrogen sulfide as the most corrode [1]. Existence of H_2S in aqueous can cause corrosion at carbon steel pipe and yield solid sediment in the form of sulfide iron or dissolve ion and cause thinning corrosion or pitting corrosion.

Internal corrosion of oil-producing equipment by carbon dioxide has been thoroughly investigated by many workers [2-3]. Materials selection for installations handling well fluids with CO_2 and H_2S is often dictated by the H_2S concentration alone, according to accepted standards. For short-life wells, this may lead to over-specification and unnecessarily high construction costs. Normal carbon steel could be a candidate for pipelines carrying an H_2S containing water phase. Lyle and Schutt explain corrosion at carbon steel that effect of dissolve H_2S gas is localize corrosion and at the surface of carbon steel formed sulfide iron coated. The character of iron sulfide coat is porous so that can be corroded [2]. Sridhar, N., et all, supporting that sulfide iron represent less sulfide corrosion product that can improve corrosion rate. Result of research above can be concluding that H_2S gas can cause corrode at surface of material [3].
Some experiment study has been conducted and publication in many literature such as Ikeda al et., 1984, Videm. Et al, 1994, Valdes, Et al, 1998 is limited to attempt of laboratory experiment from size to condition of experiment which adapted by the condition in field. The addition a few of H_2S gas at CO2 environment can cause local corrosion and thinning corrosion improvement radically [4]. Russell D.Kane, explain that stress corrosion cracking is happened in API 5CTN-80 steel at geothermal environment because of hydrogen embrittlement. These hydrogen atoms produce by sulfidation process at metal surface [5]. Basuki, E.A. dan Martojo,W., tells that the tendency of gas and oil produce which progressively mount requiring carbon steel pipe with high strength to detain oil fluid pressure. Carbon steel with higher C content will improve strength of steel, but it can cause degradation of toughness fracture. So it can be decrease of sulfide stress cracking [1].

The aim of this research was to study the variation of temperature and pH in carbon steel corrosion rate at hydrogen sulfide environment. The corrosion rate was calculated using weight loss method.

2. EXPERIMENTAL

API 5LX56 Carbon steel were use as spesiment. The dimenstion of speciment is 29.48 mm x 11.29 mm x 2.94 mm. The test solution was distilled water with 3.5% NaC1 saturated with H_2S gas mixture. The corrosion processes were done for 24 h. Acetic acid use to arranged pH value and temperature process between 25-100°C. The corrosion rate was calculated using weight loss of specimen. After exposure, the steel specimen was removed from the test section, dried and stored in a desiccators. The corroded steel surfaces were examined by scanning electron microscopy (SEM), and energy

dispersive spectroscopy (EDS) was used to determine the composition of the corrosion film.

3. RESULT

Figure 1 shows the temperature dependence of steady-state corrosion rates on carbon steel at pH 3.5. The corrosion rate increase with increasing of temperature from 25°C to 75°C and at higher temperature the corrosion rate value decreased. This is because of sulfide iron coated in the surface of the specimen. At figure 1 also shows the higher corrosion rate is 0.694 mpy at 75°C.

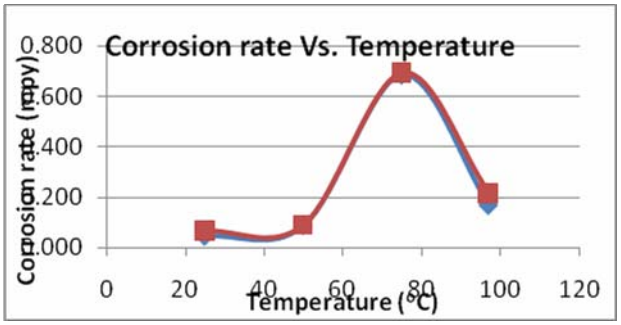

Figure 1. Corrosion rate vs. temperature, at pH 3.5 and 24h.

The temperature at highest corrosion rate from figure 1 was used to fine correlation of corrosion rate at various pH. Figure 2 shows the pH dependence of steady-state corrosion rates on carbon steel at 75°C. However, only the highest value is cited in figure 2. Corrosion rates in H_2S environments were significant decrease from pH 3.2 to 6.1 and increase at pH 6.6. The corrosion rate was increase because effect of amount H_2S in environments.

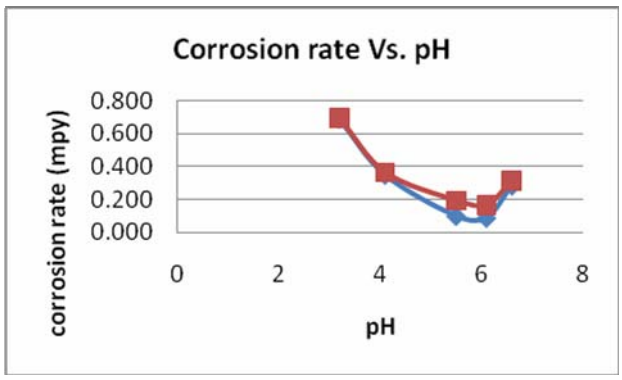

Figure 2. Corrosion rate vs. pH, at temperature 75°C and 24 h.

This result is strengthened with surface morphology result from SEM analysis (Figure 3). Figure 3.a shows surface morphology of carbon steel before corrosion test. The dark black from that figure is morphology of carbon steel from the specimen. On the other hand, Figure 3.b and 3.c reveal the morphology of the layer formed on carbon steel after corrosion test for pH 6.1 and pH 3.2 at temperature 75°C during 24 h. it can be noticed that the layer in not uniform. SEM observations at high resolution have revealed numerous cracks and porosities as shown in Fig. 3.c. These indicate that thinning and localize pitting corrosion product. The chemical composition of specimen determined by SEM/EDS is given in Table 1. The chemical composition of the matrix and the nodular graphite was determined in carbon steel, as shown in Fig. 3.a. regarding the matrix, iron, manganese, nickel, vanadium, chrome and titanium were detected whereas the nodular graphite contains carbon (4.88 at.%). The surface layer formed after corrosion test (Figure 3.b and 3.c) includes mainly iron, sulphur and oxygen.

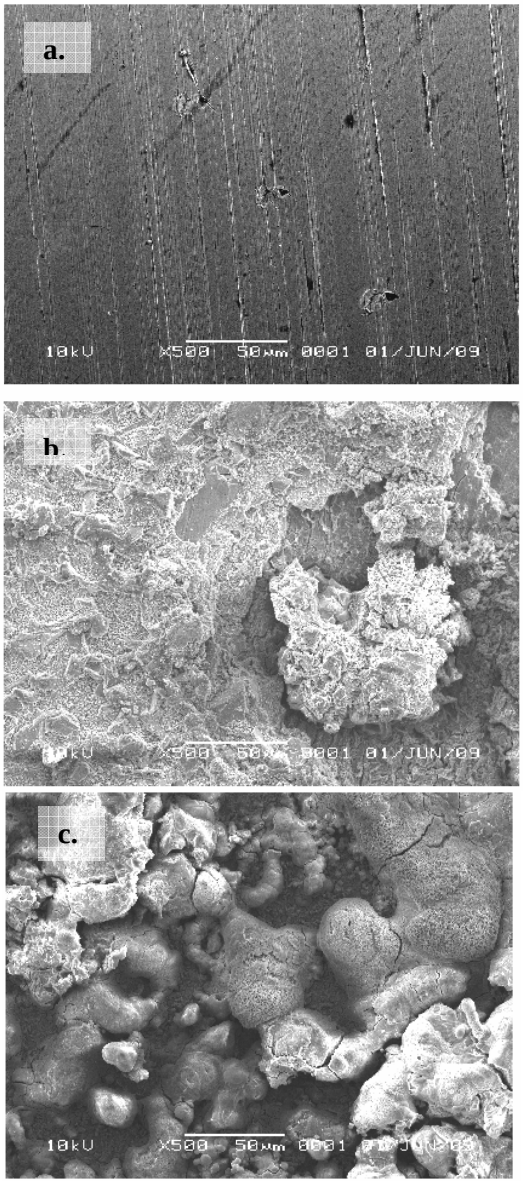

Figure 3. Surface morphology of Carbon Steel API 5LX65: (a) Before corrosion test (b) After corrosion test at temperature 75°C, and pH 6.1, 24 h, (c) After corrosion test at temperature 75°C, and pH 3.2, 24 h,

Table 1. Chemical composition of the sites reported in Fig. 3 obtained from SEM/EDS examinations (in at.%)

Speciment	Fe	C	Ti	V	Cr	Mn	Ni	O	S
Carbon steel	91.98	4.88	0.10	0.40	0.28	1.04	1.32	-	-
After corrosion test, at pH 6., 75°C, 24 h	42.27	-	-	-	-	-	-	28.09	29.64
After corrosion test, at pH 6., 75°C, 24 h	40.63	-	-	-	-	-	-	58.95	0.42

Compared to the content of elements in the layer formed on carbon steel after corrosion test at pH 6.1 and pH 3.2 is characterized by significant enrichment in sulfur (between 29.64 and 0.42 at.%) and oxygen (between 28.09 and 58.95 at.%), as determined on Fig. 3.b and 3.c and reported in Table 1. This result can be notice that corrosion test with pH 6.1 formed sulfide and oxide compound which seen from SEM/EDS analysis (Table 1). Meanwhile, SEM/EDS for specimen after corrosion test with pH 3.2 notice that iron oxide was formed in the surface of specimen.

4. DISCUSSION

4.1. Corrosion mechanism effect of H_2S

The H_2S-promoted increase in corrosion rate is almost one order of magnitude. Similar results have been reported by others. Reaction that happened in system when there are H_2S in system shall be as follows:

$$H_2S_{(g)} = H_2S_{(l)} \quad (1)$$

The dissociation reaction in H_2S aqueous shall be as follows:

$$H_2S_{(aq)} + 4e^- \rightarrow H_2S^-_{(aq)} \quad (2)$$

$$H_2S^-_{(aq)} + H^+_{(aq)} \rightarrow H_2S...H_{(aq)} \quad (3)$$

$$H_2S...H_{(aq)} \rightarrow H_2S_{(aq)} + H_{(aq)} \quad (4)$$

Molecules of H_2S adsorb on the metal surface and react with free electrons from the metal (eqn.2). These intermediates act as bridge-forming ligands with adsorbed protons (eqn. 3). Finally, hydrogen is liberated on disintegration of the complexes (eqn. 4) [6-8]

Consequently, H_2S can increase the hydrogen evolution rate without taking part in the net reaction. Since corrosion behavior deteriorated after H_2S addition on carbon steel, it appears to be unaffected by the presence of nonferrous compounds in the corrosion products. Thus, the catalytic mechanism given by eqns (1-4) seems to be a more probable cause of the increased corrosion rates.

4.2. pH Effect

At low pH value (< 2.0), dissolved iron and iron sulfide do not precipitated at metal surface. These should be dissolved and precipitated at high solubility of iron sulfide phase at lower pH than 2.0. In this case, H_2S play a role as accelerator at solubility of iron. At pH value 3.0 to 5.0, H_2S can inhibit iron to $FeSH^+$ as mackinawite.

At pH value 3.0 to 5.0, H_2S is become $FeSH^+$ as mackinawite that can be as an inhibition effects of corrosion. This metastable mackinawite could change into another sulfide compound which more protective such as troilite. Protectiveness or inhibition effect of H_2S depends on stability and protectiveness of formed sulfide [7]. H_2S concentration has a great effect to the protectiveness of sulfide layer. The higher concentration of H_2S, the more the amount of mackinawite in the layer [8]. This formation of mackinawite cause defect structure that cannot prevent iron corrosion effectively. At high concentration of H_2S, there will be more mackinawite precipitated on metal surface.

According to mechanism of corrosion in CO_2/H_2S environment, corrosion can be anticipated with some environmental factor such as chemical solution, rate of flow, temperature, pressure, H_2S concentration and any other factor that influence metal corrosion rate. The formation of corrosion product layer depends on environment condition as diffusion barrier for corrosive specimen which has significant effect to metal corrosion rate.

Commonly, structure and composition of FeS protective layer depend on concentration of H_2S in environment system. $FeSH^+$ at electrode surface can be directly mixed into mackinawite layer [8], or hydrolyzed to become Fe^{2+} that depends on solution pH value [7, 9]. At a range pH value 3.0 to 5.0 with low concentration of H_2S, FeS protective layer inhibit corrosion rate at metal sample [7]. Mackinawite formed through solid phase reaction at pH value 7.0 to 7.4 and room temperature. But, at pH value 5.5 – 7.0 precipitation of FeS was produced imperfectly [10](Harmandas dan Koutsoukos, 1996).

4.3. Temperature Effect

Temperature increases the rate of almost all chemical reactions. Figure 1 illustrates common observations on the effect of temperature on the corrosion rates of carbon steel metals. That is, an almost negligible temperature effect is followed by a very rapid rise in corrosion rate at higher temperatures [11].

Perhaps the most important single factor in corrosion is the effect of temperature. Accordingly, if is very important that the temperature of the surface of the specimen (which is the corroding temperature) be identified and known. Figure 1, shows corrosion increases from low rate to several mils per years as a result of increasing the temperature.

5. CONLUSION

Corrosion measurements of carbon steel and pure iron in the presence of H_2S were performed in a flow loop. Result of corrosion rate calculation at pH 3.2 demonstrated an increasing of corrosion rate with an increasing temperature at 25°C – 75°C and decreasing at 97°C. This decreasing in corrosion rate may be attributed to the fact that sulfide iron film was composed as corrosion product. Meanwhile, at 75°C with variation of pH value, the calculation result demonstrated that corrosion rate was decrease with an increasing of pH value from 3.2 to 6.1, and then increase at pH 6.6. The increasing of H_2S gas concentration causes the increasing of corrosion rate. Corrosion layer as corrosion product was known from SEM and EDS. Results of SEM and EDS showed that the surface morphology demonstrate a pitting corrosion.

6. ACKNOWLEDGEMENT

The financial support of the DP2M DIKTI and Corrosion Laboratory Mechanical Engineering Education Department, Indonesia University of Education are appreciated.

7. REFERENCES

[1] Basuki, E.A., and Martojo, W. *Ketahanan pipeline terhadap sulfide hydrogen (H_2S)*, *Proceeding of Indonesian Pipeline Technology*, ITB, 2004.

[2] Gerus, B.R.D., *Detection and Mitigation of weight loss corrosion in Sour gas gathering system*, Shell Canada Ltd., 1974.

[3] Sridhar, N., Dunn, D.S., Anderko, A.M., Lenca, M.M., and Schutt, H.U., *Effect of water and gas compositions on the internal corrosion of gas pipelines modeling and experiment studies*, *Corrosion Journal*, 2001, Vol. 57, No 3.

[4] Videm K., Kvarekval J., *Corrosion of Carbon Steel in CO_2 Saturated Aqueous Solution Containing Small Amount of H_2S*, Corrosion, 1994, papper no. 12.

[5] Russel D. Kane, Evaluation of geothermal production for sulfide stress cracking and stress corrosion cracking", CLI International, Inc. Texas, USA, 2001.

[6] J. KVAeEKVAL, *The Influence of Small Amounts of H_2S o n CO_2 Corrosion of Iron and Carbon Steel*, Advance in Corrosion Control and Materials in Oil and Gas Production, European Federation of Corrosion Publications, SPIRES Design Partnership, 1999, No 26, part 2, Ch. 10.

[7] Ma *et al*., *The Influence of H_2S on Corrosion of Iron under Different Condition*, Corrosion Science, 2000, 42, p 1009.

[8] D. W. Shoesmith, P. Taylor, M. G. Bailey, & D. G. Owen, *The formation of ferrous monosulfide polymorphs during the corrosion of iron by aqueous hydrogen sulfide at 21 °C,* J. Electrochem. Soc., 1980, 125, p. 1007-1015.

[9] Shilpha R. Parakala, *EIS investigation of carbon dioxide and hydrogen sulfide corrosion under film forming conditions*, Thesis, Ohio University, 2005.

[10] Harmandas dan Koutsoukos, *The Formation of Iron(II) Sulfide in Aqueous Solution*, Journal of Crystal Growth, 1996, 167, p. 719.

[11] Fontana, M.G. Corrosion Engineering, Third edition, McGraw-Hill, New York, USA. 1987, p 26, 167-179.

Finite element micro mechanical modeling of the plasticity of dual phase steel

Haryanti Samekto[1], Caroline Tan Yifung[2]

[1,2] Faculty of Mechanical and Manufacturing Engineering,
Universiti Tun Hussein Onn Malaysia (UTHM), Batu Pahat 86400, Malaysia
Phone: +60 7 4537717. Fax: +60 7 4536080
E-mail: haryanti@uthm.edu.my

ABSTRACT

The application of dual phase steel is growing due to the increasing demand of light weight structure. Dual phase steel has an excellent property combination of high strength, ductility and formability which is favourable for metal forming processes. As dual phase steel consists of ferrite matrix and martensite islands as strengthening particles, it is important to understand the interaction between the two phases with very dissimilar mechanical properties. This paper reported the results from finite element simulation and experimental studies which were carried out to investigate the behaviour of dual phase steel under plastic deformation. Metallographic and SEM observation were done for specimens under 10% to30 % engineering strain. After measuring the ferrite grain size and the martensite particle size, finite element method was applied to represent the microstructure into two dimensional micro mechanical model. Experimental study confirmed that the grain of ferrite underwent elongation meanwhile the distance amongst martensite particles became shorter. Micro voids then occurred in the area of martensite concentration. Finite element analysis results demonstrated that ferrite phase experienced higher strain than martensite particles and stress concentration took place in the boundary interface between phases.

Keywords
Dual phase, finite element, micromechanical.

1. INTRODUCTION

In the last decade the application of the sheet forming technology in industries has changed rapidly due to the increasing demand of geometrical complexity and high performance of the metal parts required by design. To fulfill these needs, the advanced high strength steel - dual phase steel - has been developed. The excellent features of this material are its high tensile strength and its good formability. Therefore, the use of dual phase (DP) steel is increasing, especially in automotive industry [1, 2, 3].

Dual phase (DP) steels consist of a ferritic matrix containing a hard martensitic second phase in the form of islands or particles obtained by heat treatment processes. The volume fraction of hard second phases determines its strength and the soft ferrite phase gives this steel excellent ductility. In some instances, hot-rolled DP steels can have a microstructure also containing significant quantities of bainite which is required to enhance its stretching capability.

Although many studies [4, 5, 6, 7] has been carried out to investigate the metallurgical aspects and to optimise the mechanical properties and formability of dual phase steel, unfortunately the material behavior under plastic deformation have not been studied sufficiently. This paper will discuss the interaction of ferritic matrix and martensite particles subjected to uniaxial stress. To understand the interaction, experimental studies as well as simulation using finite element method (FEM) were carried out which was focused on elastic plastic behaviors of the two phases in micro scale. The results from micro mechanical modeling could be then used to optimize the grain size, particle distribution and to predict failure.

2. TENSILE TEST AND MICROSTRUCTURE OBSERVATION

2.1 Material

DP steel used for this study was from commercial brand Docol 800DP supplied by Swedish Steel Manufacturer SSAB. Docol 800DP is classed into advanced high strength steel since its ultimate strength is about 800 MPa. The material was delivered in from of cold rolled sheet with nominal thickness 0.75mm. Table 1 shows its chemical composition.

Table 1: Chemical composition of Docol 800DP.

Chemical Components	composition in w%
Carbon, C	0.12
Silicon, Si	0.20
Manganese, Mn	1.50
Phosphorus, P	0.015
Sulfur, S	0.002
Niobium, Nb	0.015
Aluminium, Al	0.04

2.2 Uniaxial tensile testing

Uniaxial tensile tests were carried out following the ASTM E8 standard. Tensile specimens of dog bone shape

were cut from the sheet and oriented 0^o, 45^o and 90^o of the rolling directions in order to assess the anisotropy factor.

Figure 1 shows the true stress-strain curve obtained from tensile test with strain rate 0.05 s^{-1}. From the graph, the material could be assumed isotropy as the true stress strain curves from rolling directions 0^o, 45^o and 90^o demonstrated no significant variation. The ultimate engineering strength was slightly below 700 MPa and total elongation was about 30%. The engineering stress-strain was converted into true stress-strain and the ultimate true stress was 870 MPa and total elongation was 27%.

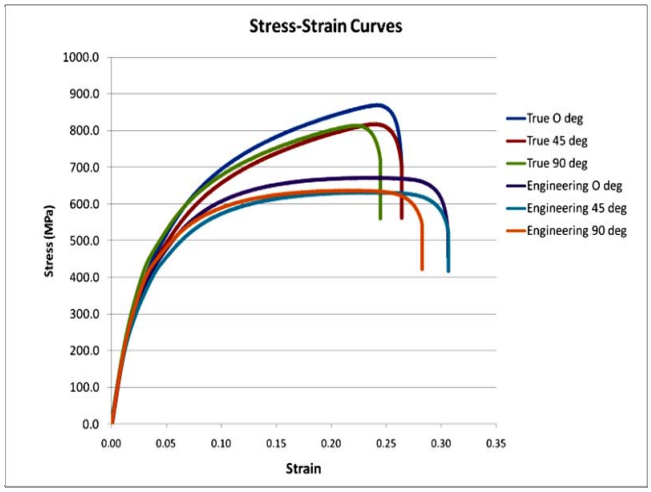

Figure 1: Stress strain curve of DP steel

2.3 Microstructure observation

Optical metallographic as well as scanning electron microscope (SEM) examinations were carried out whereby the microstructure was to reveal. Figure 2(a) shows the as-delivered microstructure in which the martensite particles were not so well distributed. However, the mechanical properties were satisfactory according to tensile test results.

Figure 2(b), 2(c) and 2(d) show microstructures after specimens were 9.5%, 18% and 26% plastically deformed (equivalent to 10%, 20% and 30% engineering strain). From micrographs, it can be seen that ferrite grains elongated meanwhile martensite particles shifted only. The higher the deformation the more martensite particles assembled in certain areas. Micrograph from the area near the failure zone in Figure 2(e) shows that voids grew in the interface between ferrite and martensite.

Grain and particle size measurement were conducted according to ASTM standard E 112. The mean size of ferrite grain was 9 μm and the mean size of martensite particle was 2 μm.

3. FEM MICRO MECHANICAL MODELING

Dual phase steel can be categorized as multiphase steel for it has two separate phases. For multiphase material, it is important to understanding the local mechanics and mechanisms governing the elastic–plastic deformation as heterogeneous solids. By using micro-modeling approach, phase combinations of different size, morphology, phase distribution and volume fraction can be analyzed by only having the properties of each existing phase.

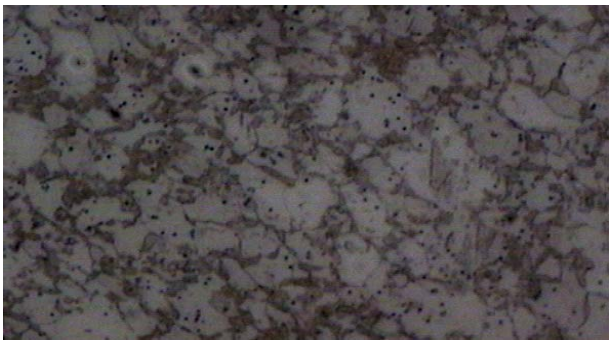

(a) As delievered. 1000X

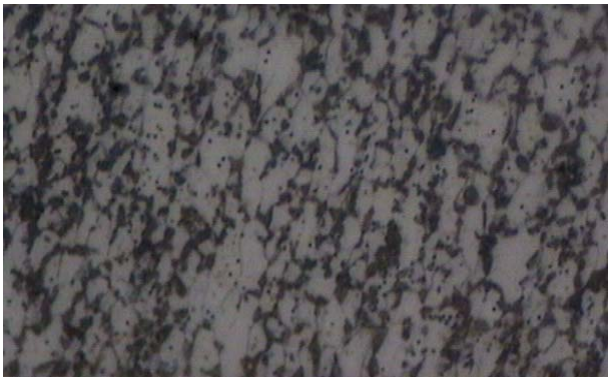

(b) After 18% deformation. 1000X

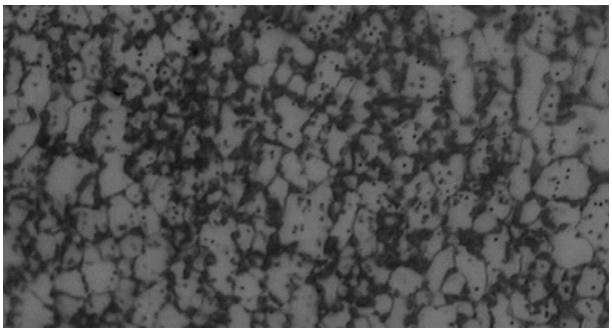

(d) After 26% deformation. 1000X

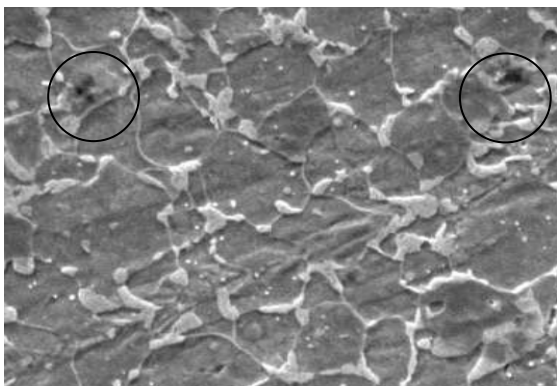

(e) Voids at failure area. SEM 2000X.

Figure 2: Microstructures of DP steel. Nital.

3.1 Wilson-Theta method for time integration

In this study, material was subjected to tensile stress. Because the force in the uniaxial tensile testing was gradually increased, tensile testing could be considered as dynamic problem, or time function problem. The general representation of dynamic problems in FEM is as follow:

$$F = [K]\,u + [C]\,\dot{u} + [M]\,\ddot{u} \tag{1}$$

Where F is the external force, K is the stiffness matrix, C is the damping matrix, M is the mass matrix, u, $\dot{u}$ and $\ddot{u}$ are the displacement, velocity and acceleration respectively.

FE implicit time integration using Wilson-Theta method was applied in this study. Wilson's method is a linear acceleration method in which the acceleration is assumed to vary linearly within each time interval from t to $t + \Theta\Delta t$, where $\Theta \geq 1.0$. If $\Theta = 1.0$, the linear acceleration will be reduced. In practice, $\Theta = 1.4$ is often selected [8]. Displacement, velocity and acceleration at the time $t + \Theta\Delta t$ are then written as follow:

$$\dot{u}_{i+1} = \dot{u}_i + \frac{\Theta\Delta t}{2}(\ddot{u}_{i+1} + \ddot{u}_i) \tag{2}$$

$$u_{i+1} = u_i + \Theta\Delta t\,\dot{u}_i + \frac{\Theta^2(\Delta t)^2}{6}(\ddot{u}_{i+1} + 2\ddot{u}_i) \tag{3}$$

FE method seeks u_{i+1} to solve the equilibrium equation (1) which becomes:

$$F_{i+1} = Ku_{i+1} + M\ddot{u}_{i+1} \tag{4}$$

Substituting acceleration $\ddot{u}_{i+1}$ from (2) and (3) gives:

$$F'_{i+1} = F_{i+1} + \frac{M}{(\Theta\Delta t)^2}\left(6u_i + \Theta\Delta t\,\dot{u}_{i+1} + 2(\Theta\Delta t)^2\ddot{u}_i\right) \tag{5}$$

By combining the similar terms and rewriting (5) into load vector expression, the general equation becomes:

$$F_{i+1} = F_i + \Theta(F_{i+1} - F_i) \tag{6}$$

3.2 Geometrical representation and discretization

Determination of geometrical representation is a decisive step in micro-mechanical modeling to guarantee an effective transition from a solid with a repetitive microstructure to an equivalent homogeneous continuum which represents the two phase microstructure. A representative volume element; could be a cylinder, a sphere etc, is assumed to compose the solid in a repetitive way and each small volume matches its neighboring cells in all aspects. This is indeed a simplifying assumption, but has proved to be satisfactory and is widely accepted.

Modeling the microstructure as a plane element or axisymmetric cell reduced the complexity of 3D modeling and minimizes the computational cost. Representative elements in form of a cylinder for the matrix and sphere for the particle have been reported very effective to model DP steel with variation in phase composition [9, 10]. A single cell was decomposed from a homogenous stacked hexagonal array which represented grain structure. Figure 3 shows the simplified geometrical representation.

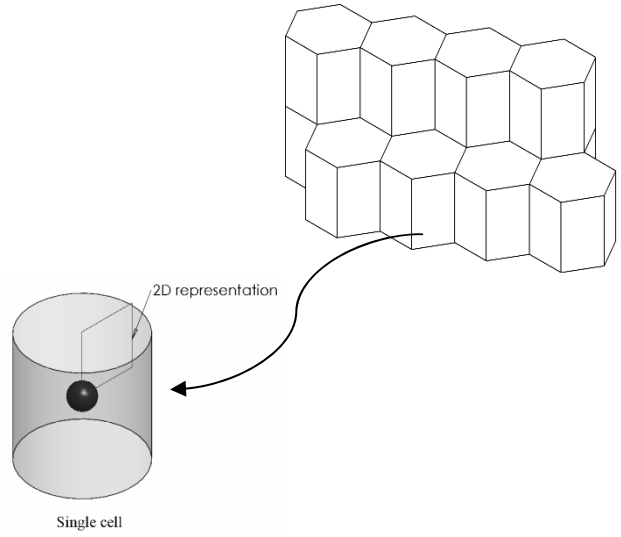

Figure 3: Stacked hexagonal array and a single cell of representative volume element

In this study, multi cell model was introduced instead of single cell although the stacked hexagonal array approach was still used. The configuration of the representative elements in multi cell as well as FE discretisation can be seen in *Figure 5* and Figure *6*. The multi cell model was thought to be capable to model not only the grain elongation but also the movement of the islands and the occurrence of voids. Multi cell mechanical model managed to effectively simulate fracture in multiphase steel, as reported in [11].

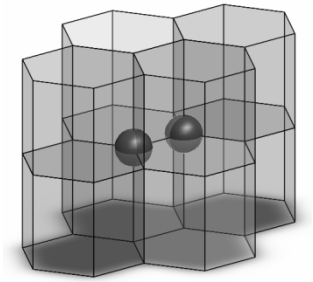

Figure 4: Configuration of multi cell volume representation

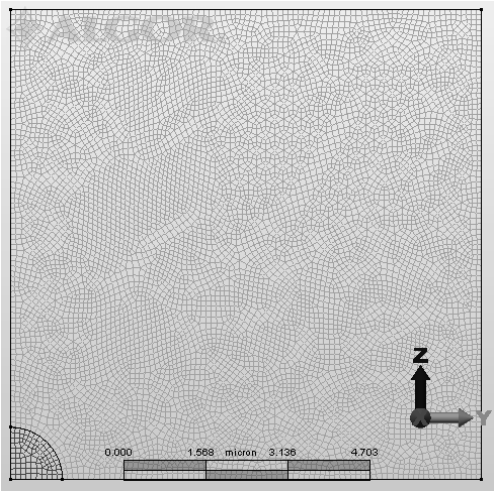

(a) 2D discretization single cell

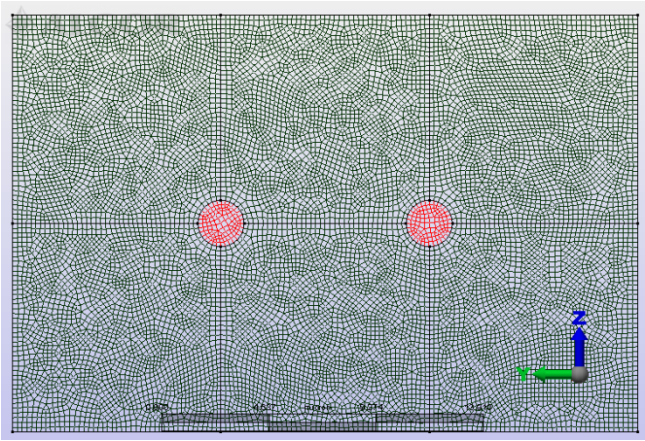

(b) 2D discretization of multi cell

Figure 5: Single and Multi cell configuration and its 2D representation.

3.3 Elastic plastic hardening model

Stress-strain curve from tensile testing (Figure 1) indicates that dual phase steel deformed not only elastic-plastically but also hardened isotropically. Therefore the constitutive model for isotropic elastic plastic hardening can be used to represent the material behavior.

In the elastic plastic approach, total strain 'rate' tensor is decomposed into elastic and plastic components:

$$\dot{\varepsilon}_{ij} = \dot{\varepsilon}_{ij}{}^{e} + \dot{\varepsilon}_{ij}{}^{p} \tag{7}$$

The elastic strain $\dot{\varepsilon}_{ij}{}^{e}$ is described by Hooke's law. On the other hand the plastic strain $\dot{\varepsilon}_{ij}{}^{p}$ may occur only if the flow criterion below is fulfilled.

$$\text{If} \begin{cases} f < 0, & \dot{\varepsilon}_{ij}{}^{p} = 0 \\ f = 0, & \dot{\varepsilon}_{ij}{}^{p} = \dfrac{3}{2}\dfrac{\dot{\varepsilon}^{p}}{\sigma}\sigma'_{ij} \end{cases} \tag{8}$$

The Von Misses yield function f can be written as:

$$f = \sigma - \bar{\sigma} \tag{9}$$

where $\bar{\sigma}$ is the flow stress and the equivalent stress σ is defined by Von Misses is as follow:

$$\sigma = \sqrt{\frac{3}{2}\sigma'_{ij}\,\sigma'_{ij}} \tag{10}$$

Where σ'_{ij} is the deviatoric stress. The equivalent plastic strain $\dot{\varepsilon}^{p}$ can be found from expression:

$$\dot{\varepsilon}^{p} = \sqrt{\frac{2}{3}\varepsilon_{ij}{}^{p}\,\varepsilon_{ij}{}^{p}} \tag{11}$$

The hardening factor is described by the increase of flow stress $\bar{\sigma}$ as function of plastic strain according to the material model:

$$\bar{\sigma} = K\left(\varepsilon_0 + \dot{\varepsilon}^{p}\right)^{n} \tag{12}$$

The values of material parameters for ferrite matrix and martensite particle used for FE model are presented in Table 2.

Table 2: Material parameters for ferrite and martensite [12]

Parameters	Ferrite	Martensite
Stress constant K	597 MPa	2409 MPa
Elastic limit ε_0	0.002	0.002
Strain hardening coefficient n	0.07	0.31
Poisson's ratio r	0.28	0.28

True stress-strain curves for ferrite and martensite were created by using material model equation (10) and parameters in Table 2. The comparison of the stress-strain curves of the two phases can be seen in *Figure 6*. From the curves, the mechanical properties dissimilarities can be clearly depicted.

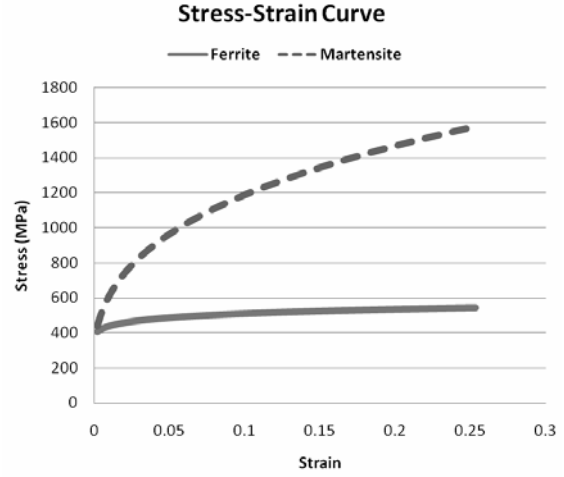

Figure 6: Stress strain curves of ferrite and martensite plottet from material model in equation (10)

3.5 Simulation results

Contour plots of the equivalent stress and strain for both single cell and multi cell models can be seen in *Figure 7* and *Figure 8*. The red areas correspond to the highest stress or strain and blue areas correspond to the lowest.

In the single cell model as well as in the multi cell model, martensite phase had higher stress than ferrite, but lower strain. When an external force was applied into the ferrite-martensite structure, the stress conveyed from ferrite matrix to martensite second phase. Because the ferrite had higher formability than the martensite, ferrite matrix had higher strain or deformation. However due to the higher strength, the martensite bore stress more.

Grain boundary or transition area was the area with the highest strain concentration or the most critical zone. In this model, the surface contact between martensite and ferrite was defined as bounded interface. In this contact definition, the nodes in the interface were matched. If stress was conveyed from ferrite to martensite and cause deformation or strain, strain was accumulated in the transition areas and could initiate failure. Table 3 presented the values of the stress and strain at different areas.

Table 3: Stress and strain values at 26 % deformation

Area	Stress	Strain
Ferrite	0.130 N/μ^2	0.51
Martensite	0.205 N/μ	0.48
Grain boundary	0.135 N/μ^2	0.69

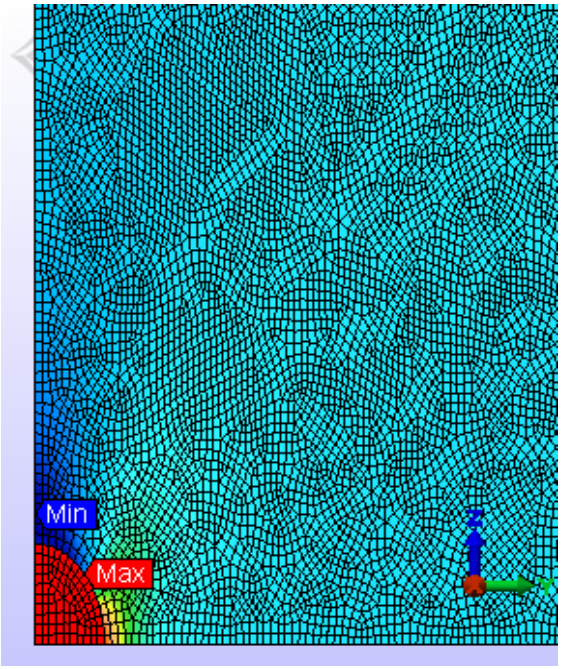

(a) Stress distribution from single cell model

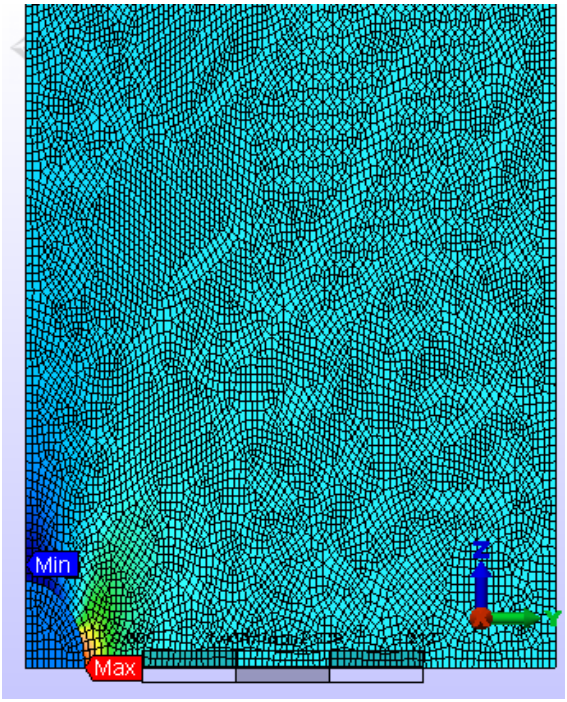

(b) Strain distribution from single cell model

Figure 7: FE simulation results from single cell

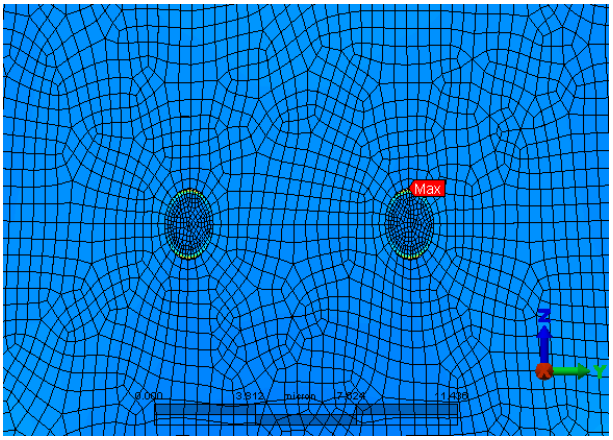

(a) Stress distribution from multi cell model

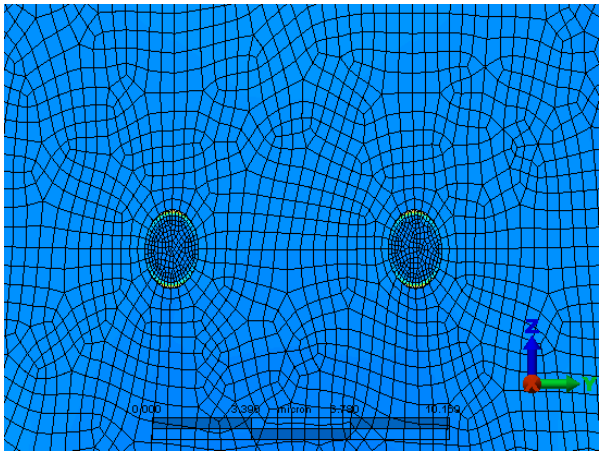

(b) Strain distribution from multi cell model

Figure 8: FE simulation results for multi cell

The FE results from multi cell model in *Figure 8* show that the large elongation of the ferrite caused the martensite particles moved closer. The same phenomena could also be clearly observed in the photographs of microstructures in *Figure 2*. If the martensite particles concentrated in a certain area, the strengthening function of the particles in the steel declined. Multi cell model came out with different area of stress and strain concentration although still on the grain boundary.

Figure 9 show the stress and strain profile graph of the two phases and a node in the boundary. The graph depicted that the differences of stress and strain grew with the increase of deformation

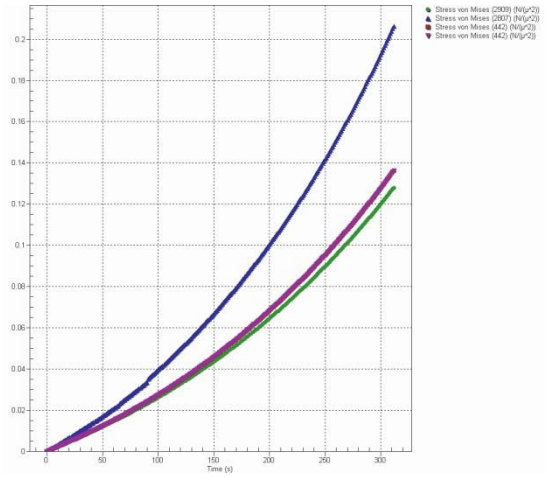

(a) Stress profile

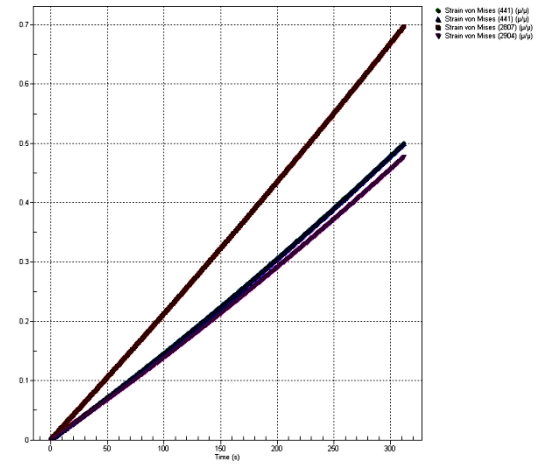

(b) Strain profile

Figure 9: Stress and strain profile at ferrite and martensite

7. CONCLUSION

Experimental observation as well as FE simulation of micro mechanical model were conducted to study the behavior of the dual phase steel under deformation. Conclusions drawn from the study are:

1. Boundary interface between ferrite matrix and martensite second phase was the most critical area due to the strain accumulation. This was recognized in the FE simulation and supported by SEM micrograph.
2. The multi cell micromechanical model was considered better regarding the representation of the behaviour of the dual phase steel under plastic deformation.
3. The difference of stress and strain in the martensite, ferrite and phase interface grew with the increase of deformation.

ACKNOWLEDGMENT

The authors thank to the financial support provided by Malaysian Ministry on Higher Education (MOHE) under Fundamental Research Grant Scheme (FRGS) Project No. 0369.

REFERENCES

[1] AISI/DOETechnology Roadmap Program. *Characterization of Formability of New Generation High Strength Steels for Automotive Applications.* Final Report, Southfield: American Steel and Iron Institute (AISI), 2003, 1-12.

[2] AISI. *UltraLight Steel Auto Body-Advanced Vehicle Concepts (ULSAB–AVC).* Engineering Report, Southfield: American Iron and Steel Institute (AISI), 2002, 1-149.

[3] WorldAutoSteel - World Steel Association. "AHSS Application Guidelines." *www.worldautosteel.org.* Edited by S. Keeler. http://www.worldautosteel.org/Projects/AHSS-Guidelines.aspx (accessed June 22, 2009).

[4] Liedl, U, S Traint, and E. A. Werner. "An unexpected feature of the stress–strain diagram of dual-phase steel." *Computational Materials Science* 25, no. 1-2 (2002): 122-128.

[5] Soto, R, W Saikaly, X Bano, C Issartel, G Rigaut, and A Charai. "Statistical and theoretical analysis of precipitates in dual-phase steels microalloyed with titanium and their effect on mechanical properties." *Acta Materialia* 47, no. 12 (1999): 3475-3481.

[6] Tavares, S. S. M., P. D. Pedroza, J. R. Teodosio, and T Gurova. "Mechanical properties of a quenched and tempered dual phase steel ." *Scripta Materialia* 40, no. 8 (1999): 887-892.

[7] Szewcyk, A. E., and J. Gurland. "A Study of the Deformation and Fracture of a Dual-Phase Steel." *Metallurgical Transaction A* 13A (1982): 1821-1826.

[8] Logan, D. L. *First course in the finite element method , 3 rd Edition.* Pacific Groove: Brookscole, 2003.

[9]Al-Abbasi, F. M., and J. A. Nemes. "Characterizing DP-steels using micromechanical modeling of cells." *Computational Materials Science* , no. 39 (2007): 402-415.

[10] Al-Abbasi, F. M., and J. A. Nemes. "Micromechanical modeling of dual phase steels." *International Journal of Mechanical Sciences*, no. 45 (2003): 1449–1465.

[11] Uthaisangsuk, V, U. Prahl, and W. Bleck. "Micromechanical modelling of damage behaviourof multiphase steels." *Computational Materials Science*, no. 43 (2008): 27-35.

[12] Davies, R. G. "The mechanical properties of zero carbon ferrite plus martensite structures." *Metallurgical and Materials Transactions A* 9, no. 3 (1978): 451-455.

Proceeding of the 11th International Conference on QiR (Quality in Research)
Faculty of Engineering, University of Indonesia, Depok, Indonesia, 3-6 August 2009
ISSN 114-1284

Study of Aggregation and Orientation of Photo-Responsive Molecule of Disperse Red 19 Film Deposited On Silane Substrate Surface

Heindrich Taunaumang [1], Donny Royke Wenas [1]

[1]*Physics Department, Mathematics and Sciences Faculty, Manado State University*,

ABSTRACT

Study of aggregation and orientation of photo-responsive molecules such as Disperse Orange 44, Disperse Red 1 have been carried out for optimizing optical properties for application photonics devices such as optical switching and optical data storage. Usually the photo-responsive molecules are available in form of powder, however, for photonics devices application this material must be prepared in form of film with good quality i.e., smooth surfaces, homogenous thickness, good optical stability, transparency and good optical properties. In this research the photo-responsive material of Disperse Red 19 film was deposited on silane substrate surface by using physical vapor deposition (PVD). The relationship between the property and structure of the Disperse Red 19 film is mainly focused of this study. The result of vacuum deposited Disperse Red 19 film shows a smooth surface with homogeneous thickness. Furthermore, the results of FTIR and UV-VIS measurements and also XRD measurement are performed. These results indicated that the Disperse Red 19 film show a specific aggregation and orientation which is promising for developing photonics devices application.

Keywords *: Disperse Red 19, vacuum deposition , silane, aggregation, orientation*.

1. INTRODUCTION

Photo-responsive molecule with its structure consists of donor, acceptor and azobenzene bridging groups have been subjected to the optical material research for optimizing optical properties in order to be suited for photonics technology application. When this molecule is exposed to light (photon), this molecule undergoes trans-cis isomerization phenomenon that caused a changing in index refraction. This phenomenon is utilized as a basis of photonics devices such as optical switching, optical data storage [1,2].

The photo-responsive materials such as Disperse Orange 44, Disperse red 1 and Disperse Red 19 have been known as a nonlinear optical chromophore in the developing of nonlinear optical and photorefractive polymer [3,4,5], because of its high nonlinear optical properties (hyperpolarizability) due to -electron clouds delocalization.

For photonics devices application, the photo-responsive molecule should be performed in film with good quality that possesses smooth surfaces, homogenous thickness, and good optical stability.

This research is to study the relationship between the molecular structure and the

property of Disperse Red 19 photo-responsive film. This film was deposited on silane substrate surface produced by using Physical Vapor Deposition (PVD) method.

The film was characterized by means of UV-VIS , FTIR and XRD measurements.

2. EXPERIMENT

a. Sample preparation

Photo-responsive material used in this research is Disperse Red 19 (DR19). This material purchased from Aldrich supplier in form of powder. This molecules has molecular weight of 330,35 and melting point of about 300^{o}C [6]. The structure of this molecule is shown in figure 1.

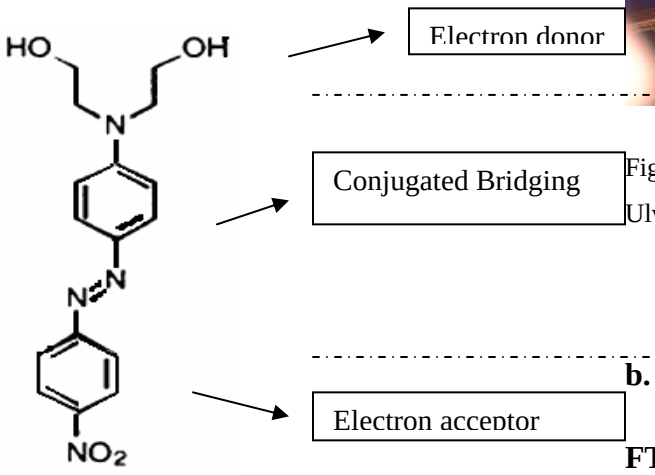

Figure 1. The molecular structure of Disperse Red 19

This molecules is available in form of powder and then prepared in form of solution and film. The solution of DR19 sample was prepared by dissolving DR19 powder into N-methyl pyrollidinone (NMP) solvent. The homogeneous solution of DR19 was obtained by stiring the solution for about one hour by using a magnetic stirer. The film sample was prepared by using the Physical Vapor Deposition (PVD) method. The crucible temperature was used 173^{o}C. The DR19 film was deposited on silene substrate surface. The substrate surface temperature was chosen to be 26^{o}C. The evaporator equipment used in this experiment was VPC-type from Ulvac Sinku Kiko as shown in figure 2.

Figure 2. Evaporater of VPC-410 type from Ulvac Sinku Kiko.

b. Sample Characterization

FTIR measurement

In this research the FTIR spectra was obtained by using FT-IR 801 Single Beam Spectrophotometer. The FTIR characterization was measured in range of 4600-400 cm^{-1}. For this measurement, the sample preparation of

ISSN 114-1284

DR19 powder was prepared in KBR matrix and for sample of film was deposited on silicon wafer. Before the measurement was carried out, the background of the sample was first measured, in order to avoid any moda which appear from the KBr matrix or substrate. The experimental results are shown in Figure 3 and 4.

UV-VIS measurement

The optical characteristics of DR19 molecules in form of solution and film were obtained from UV-VIS spectra. This measurement was carried out using an instrument of Beckmen DU-7000 Single Beam Spectrophotometer. This measurement obtained UV-VIS spectra in range of 250-800 nm. The background of the sample was first measured. The solvent used for DR19 solution sample was N-methyl pirrolidinone (NMP). For the DR19 film sample was deposited on silicon substrate. The experimental results are shown in Fifure 5 and 6.

XRD measuremet

The X-Ray Diffraction (XRD) measurement is intended to investigate the physical structure i.e., crystal structure and crystallinity of DR19 film. The XRD measurement was carried out by using instrument of Philips Diffractometer in the range of measurement : 2 (3.5-75^o). The XRD spectra was recorded by scan 2 at 30 kV, 30 mA with the radiation source CuK (= 1,5406 Angstrom). The sample of DR19 film on silane substrate was prepared for this measurement. The experimental results is shown in Figure 7.

3. RESULTS AND DISCUSSION

The experimental results of FTIR measurement of DR19 powder and DR19 film are shown in Figure 3 and 4. The identification of the FTIR absorption peak are shown in Table 1 and 2.

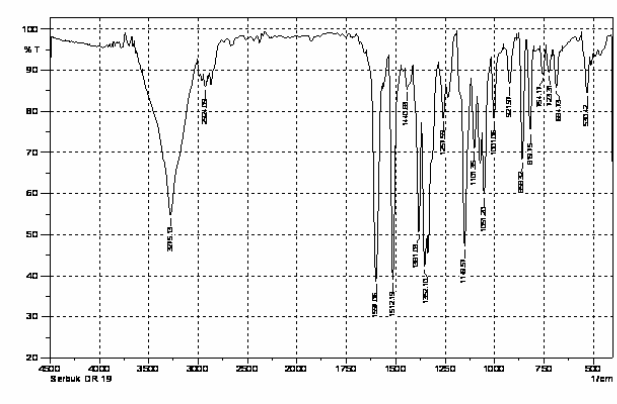

Figure 3 . Spectra of FTIR measurement of Disperse Red 19 powder

ISSN 114-1284

Table (1). Identification of FTIR absorption peak for Disperse Red 19 pristine powder in KBR matrix

Position (cm^{-1})	Transmission Intensity	Identification [7,8]
3481	S, wide	O-H stretching of bounded intermolecular
2924	Vw	C-H asymmetric stretching of CH_2
2854	Vw	C-H symmetric stretching of CH_2
2962	Vw	C-H asymmetric stretcting of CH_3
2873	Vw	C-H symmetric stretching of CH_3
1589	Vs	C=C stretching of phenyl ring
1512	Vs	NO_2 asymmetric stretching
1440	Vw	C-H stretching of CH_3
1381	S	N=N stretching
1340	Vs	NO_2 symmetric stretching
1185	Vw	C-N stretching of phenyl
1142	S	Phenyl-N stretching of aliphatic amine
1107	W	C-N stretching of aliphatic amine
1101	S	C-N (str.) in aliphatic amine
1051	W	C-O stretching of C-OH group
858	S	C-H out-of-plane bending of NO_2
824	S	C-H out-of-plane bending
754	W	CH_2-N stretching
723	W	CH_2 rocking vibration
681	W	C-C Ring out of plane bending
617	W	OH wagging

Note : Vs: very strong, S: strong, W: weak, Vw: weak.

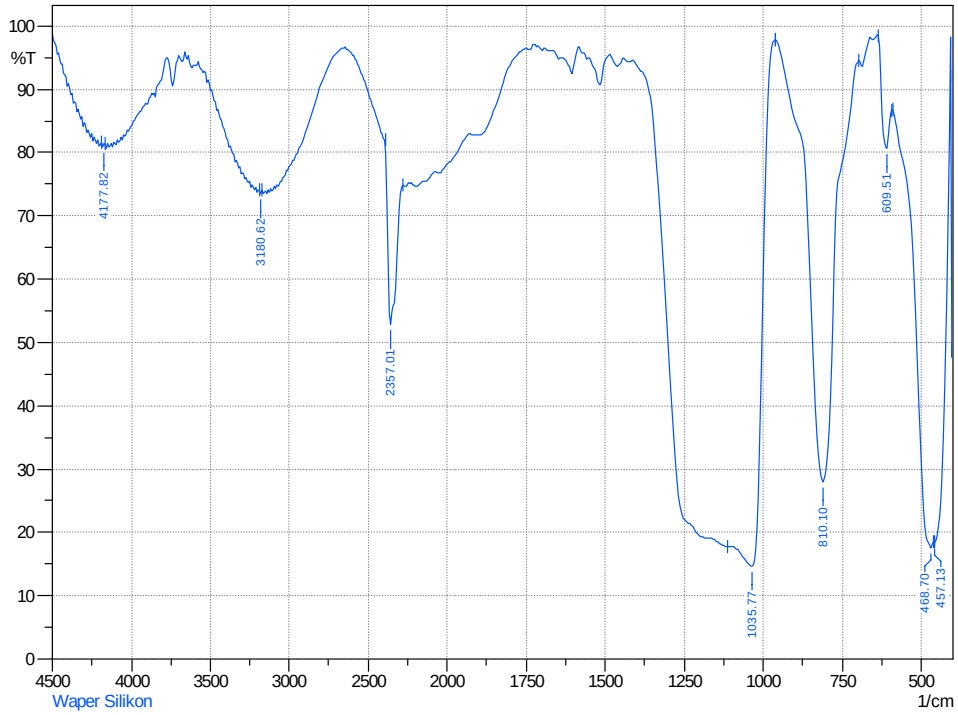

Figure 4. Spectra of FTIR measurement of Dispersed Red 19 Film

Table (2). Identifiation of FTIR absorption peak for Disperse Red 19 film

Frequency (cm^{-1})	Transmission Intensity	Identification [7,8]
4177	S, wide	O-H stretching intermolecular bounded
3180	W	O-H stretching intermolecular bounded
2357	S	N-C-O stretching
1600	Vw	C=C stretching of phenyl ring
1519	Vw	NO_2 stretching asymmetric
1512	Vw	C=C stretching of phenyl ring
1400	Vw	N=N stretching
1181	Vs	Phenyl-N stretching
1153	Vs	Phenyl-N stretching
1142	Vs	Phenyl-N stretching
1107	Vs	Phenyl-N stretching

ISSN 114-1284

1051	W	C-O stretching of C-OH group
810	S	C-H out-of-plane bending of phenyl
609	Vw	OH wagging
457	Vw	C-C Ring out-of-plane bending

Note : Vs: very strong , S: strong , W: weak, Vw: very weak.

The FTIR spectra for DR19 film exhibit very weak absorption band of NO_2 stretching (1512 cm^{-1}) and C=C of phenyl ring (1589 cm^{-1}) due to orientation of this group perpendicular to the substrate surface. The very weak of this NO_2 stretching is probably restricted by hydrogen bonding as indicated by a board absorption band in range of 1250-1000 cm^{-1}.

Figure 5 shows UV-VIS spectra for sample of DR19 solution (NMP solvent). This figure shows a maximum absorption (λ_{max}) at 506 nm. The maximum absorption at 506 nm corresponding to electronic energy transition of 2.5 eV. This spectra exhibits a broad absorption band with high intensity which indicates of strong oscillator of DR19 molecule. This absorption band corresponding to π-π* electronic transition from the donor group to the acceptor group in DR19 monomer.

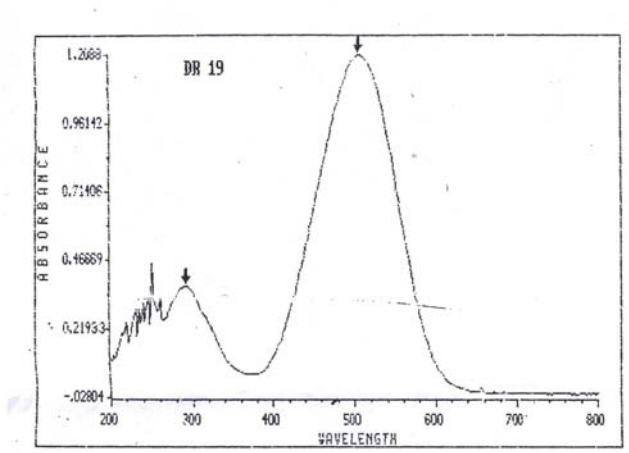

Figure 5. Spectra of UV-VIS measurement of solution of Disperse Red 19 Powder

Figure 6 shows UV-VIS spectra for the 19 film deposited on silane substrate surface. This spectra shows a broad absorption band in the visible region with high intensity which is significantly different compared to absorption band of DR19 solution (Figure 5). This differences due to in DR19 film the inter-molecules distance is more closer then in solution (isolated molecules) its mean that the inter-molecules interaction in the film is more stronger as well.

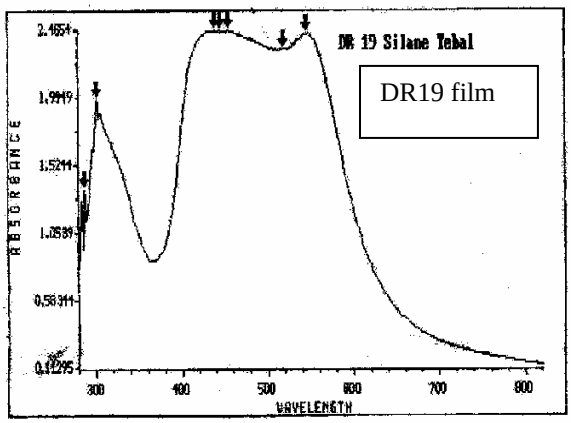

Figure 6. Spectra of UV-VIS measurement of vacuum deposited film of Disperse Red 19 on silane substrate

The UV-VIS spectra shows two absorption peaks in visible region i.e., at λ_1 = 444 nm and λ_2 = 544 nm which corresponding to electronic energy transition of E_1 = 2.8 eV and E_2 = 2.3 eV respectively. Figure 6 also clearly shows a shifting in absorption peak to the longer wavelength (red-shift) of about 38 nm and shifting to the shorter wavelength (blue-shift) of about 62 nm compared to the absorption peak in solution (506 nm). This is as indication of molecules aggregation in the DR19 film. As reported that the blue shift and a red shift in absorption peak are correlated to dipolar aggregation H-type and J-type respectively [9]. According to the point-dipole model that the shifting of absorption peak strongly depends on a magnitude of angle between dipole moment transition and aggregate stacking direction. If the angle between moment dipole transition and stacking direction equal or smaller then 54^o, so the maximum absorbance aggregates is called red-shift (J-aggregation). And if the angle between dipole moment transition and aggregates stacking direction is bigger then 54^o so this maximum absorbance aggregates is called blue-shift (H-aggregation). Based on this results indicate that some of molecules in the film are oriented in parallel and others oriented in perpendicular to the substrate surface.

Figure 7 shows XRD spectra of the DR19 film on silane substrate. This spectra indicates that the physical structure of the DR19 film is amorphous. This is as indication of the order of molecular orientation on the substrate surface which are randomly. This result is supported by the UV-VIS measurement.

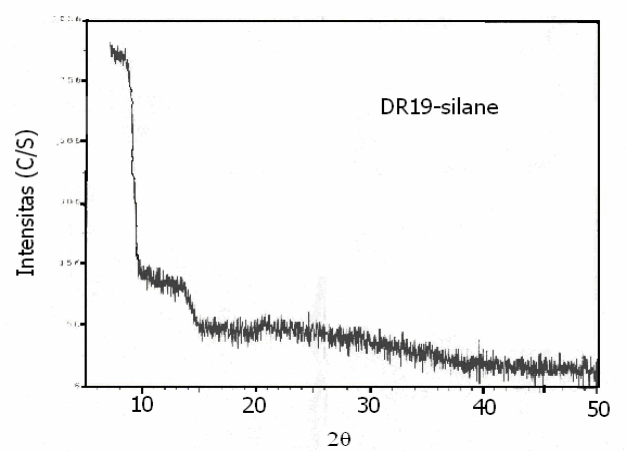

Figure 7. The XRD spectra of DR19 on silane substrate.

4. CONCLUSION

The DR19 film on silane substrate surface was obtained by physical vapor deposition method possesses a smooth surface and homogeneous thicknesses. A broad absorption of the FTIR spectra of the DR19 film in range of 1250-1000 cm^{-1} as indication of strong intermolecular interaction due to hydrogen bonding.

This UV-VIS measurement indicates that the DR19 film consist of combination of H-type and J-type molecular aggregation. This phenomenon is supported by the XRD measurement results for DR19 film on silane substrate which are amorphous.

ACKNOWLEDGMENTS

We thank Dr. Herman and Prof. Tjia May on for helpful discussion. Thank for Directorate High Education of Indonesia (Dikti) for funding this research with contract number No: 032/SP2H/PP/DP2M/III/2008.

REFERENCES

[1]. Natanshon, A., P. Rochon, M-S.Ho, and C. Barret. 1995, *Azopolymer for reversible Optical Storage. 6. Poly[4[2-(methacryloyloxy)ethyl]azobenzene]*. Macromolecules. 28, 4179-4183.

[2]. Meng, X., A. Natanshon, C. Barret, and P. Rochon. 1996, *Azopolymer for Reversible Optical Storage.10. Cooperative Motion of Polar Side Groups in Amorphous Polymers*, Macromolecules.29, 946-952..

[3]. Chen, J.P., F.L. Lebarthet, A. Natanshon, and P. rochon.1999, *Highly Stable Optically Induced Birefringence and holographic Surface Grating on a New Azocarbazole Based Polyimide*, Macromolecules, 32, 8572-8579.

[4]. Choi, D.H., KJ.Chao, YK.Cha, and J.J. Oh.2000, *Optically Induced Anisotropy in Photoresponsive Sol-Gel Matrix Bearing a Silyleted Disperse Red 1*, Bull. Korean Chem.Soc. 21, 1222-1226.

[5]. Delaire, A.J., K. Nakatani.2000, *Linear and Nonlinear Optical Properties of Photochromic Molecules and materials*, Chem. Rev. 100, 1817-1845.

[6]. Sigma. 1993.

[7]. Buffeteau, T., A. Natanshon, P. Rochon, M. Pezolet. 1996, *Study of Cooperative Side Group Motions in Amorphous Polymers by Time Dependent Infrared Spectroscopy*, Macromolecules, 29, 8783-8790.

[8]. Ho, M-S., A. Natanshon, and P. Rochon.1996, *Azo Polymers for Reversible Optical Storage.9, Copolymers Containing Two Types of Azobenzene Side Groups*, Macromolecules.29, 44-49.

[9]. Kim, B.J., S.Y. Park, and D.H. Choi. 2001, *Effect of Molecular Aggregation on the Photo-Induced Anisotropy in Amorphous Polymethacrylate Bearing an Aminonitrobenzene Moeity*, Bull. Korean Chem. Soc. 22, 271-275.

Proceeding of the 11th International Conference on QiR (Quality in Research)
Faculty of Engineering, University of Indonesia, Depok, Indonesia, 3-6 August 2009
ISSN 114-1284

The Thermodynamic Analysis of Direct Synthesis of Dimethyl Ether by Using Chemcad 5.2

Heri Hermansyah, Slamet, Darmaji Setiawan, Oktovan Andriyanda

Chemical Engineering Department, Faculty of Engineering
University of Indonesia, Depok 16424
Tel. 021-7863156
Email : heri@chemeng.ui.ac.id

Abstract

Dimethyl Ether as an alternative energy which is synthesized from syngas has been improved in some countries. The need of energy fulfillment becomes the significant attention considering the fact that energy supply in form of fuel has become less and less in quantity so that the technology innovation is required to solve this problem. To help better understanding on thermodynamic characteristic of direct synthesis reaction of Dimethyl Ether, we have to analyze the thermodynamic effect on operation variable namely temperature, pressure, and equation of state H2/CO toward the reaction activity, such as conversion, selectivity and yield. The thermodynamic analysis can be accomplished by using simulator that use Gibbs Reactor module on Chemcad Software. On Gibbs module, we find that the possible reactions do not have to be specified. However, we are justified to classify the components which are possible getting involved in the reaction activity. The products of potential reactions, then, are based on the altering of the minimum Gibbs free energy from those reactions. Therefore, Gibbs module is more effective and appropriate to be applied on the simulation of balanced chemical equation.

Key word:
Dimethyl Ether Synthesis, Thermodynamics analysis, Gibbs reactor

1. Background of the study

The energy crisis has become an interesting topic to debate since the past century over many countries around the world. The requirement of energy completion for the sake of human life could absolutely not be granted only by available natural resources. This problem has won the awareness of so many researchers to create and seek for substitution energy. Many inventions on technological aspects have been formed to help solving this problem. The newest energy substitution of the natural energy is not only expected to discharge the human needs effectively but also have to be more efficient in cost. One of the energy substitutions is Dimethyl Ether which is made of the synthesis process of syngas (synthetic gas).
Dimethyl Ether (DME) is considered as the twenty-first century energy, which can be applied on diesel truck, generator, and is also tempted to substitute LPG (liquefied Petroleum Gas) or gas for cooking [1]. It can also be used to operate diesel machine because it has simple molecular formula so it is not less productive to form emission of such components on burning process. The components are exactly named NO_x, CO, and SO_x. They are produced in the lowest level so it supports the realization of the environmental standard in some countries including Europe (EURO5), U.S. (U.S. 2010) and Japan (2009 Japan), and is also supposed to be applied because it has higher cetane number than that of oil for burning process. It numbered about 55-60 higher than oil which has only 40-50 [2]. By using this kind of alternative energy, we expect to have cleaner environment due to the less-contaminated of pollutant it produced which is also smaller that that of oil [3]. In addition, the DME can be applied to substitute LPG. It is becoming the most important alternative energy in develop countries especially China, India, and Brazil because they require portable fuel (tank packed fuel). They need it to supply for the suburban society which is living in distant from city and facilities. Another important thing is that DME which is regarded as environmentally-friendly fuel contains no toxin and burn without producing particulate emission.
DME can be synthesized from natural gas, coal, and also natural residue (biomass). There are two kinds of synthesis process that has so far been performed to produce DME. The first is called traditional process that is done through the synthesis process of methanol and continued by dehydration system [4]. The second method is by using catalyst which can produce methanol and ether from synthetic gas in the same reactor [5]. To get the optimum condition of operation we have to observe the thermodynamic of DME synthesis reaction first.

2. Basic of the Theory

Dimethyl Ether, or is best known as methoximethane, oxybismethane, methyl ether, wood ether, and DME, is colorless and odor of smell. Dimethyl Ether can also be soluble with water [6]. Its formula is patterned below CH3OCH3. The empirical formula of DME is patterned below C2H6O (the same with that of ethanol). Dimethyl Ether is also used as aerosol fuel and consumed together with propane to give thermal expansion within low temperature of -60ºC. This character is useful for cryogenic freeze. It is a valuable alternative energy for perfect burning process of petrol liquefaction, natural gas

liquefaction, diesel and gasoline. Again, Dimethyl Ether can be made of natural gas, coal and biomass.

Conventional DME is produced by using methanol dehydration method. Nowadays, many researchers are still busy seeking and developing new method in order to be able to produce DME in immense scale. However, they put their main concern on making DME by synthesizing hydrogen and CO which are commonly called by syngas. It is produced from methanol by combining two molecules of methane to create two new molecules, DME and water. This reaction is identified as reversible reaction (see equation of the 4th reaction).

DME can be used as fuel to diesel machine, petrol (30 % DME and 70 % LPG) and turbine. DME works better on diesel machine because it has high cetane number, which is higher than that of oil for diesel which has only 38-53. However to make a diesel machine which needs DME as its fuel, we have to change and modify some part of it. And as a synthetic fuel, the result of burning activity produced by DME is relatively cleaner than that of oil (without black carbon) which can also replace conventional diesel, LPG or is able to be changed into hydrogen for fuel cell. Beside that, DME can be decomposed for some hours at troposphere and surprisingly has no cause of greenhouse effect and the eroding of ozone stratum. Moreover, it is not characterized as corrosive at some metals. Consequently, DME is considered as an environmentally-friendly fuel and is promisingly safety for our surroundings.

The Reaction of DME Synthesis

DME product which is common to use involves the methanol dehydration reaction (see equation 4 below), however recently in five years the researchers have established the technology of direct synthesis of DME from syngas (hydrogen and monoxide carbon) with the aim of producing DME in huge scale with little money in order to use it as fuel.

Direct synthesis of DME needs temperature of 210-290ºC and pressure about 3-10MPa; intervention catalyst is also used to get synthesis and dehydration of methanol. The chemical reactions and heat reaction for synthesis of DME are listed below:

$$3CO + 3H_2 \Leftrightarrow CH_3OCH_3 + CO_2 + 246.0 \ kJ/DME \quad \cdots (1)$$

$$2CO + 4H_2 \Leftrightarrow CH_3OCH_3 + H_2O + 205.0 \ kJ/DME \quad \cdots (2)$$

$$2CO + 4H_2 \Leftrightarrow 2CH_3OH + 182.6 \ kJ/DME \quad \cdots (3)$$

$$2CH_3OH \Leftrightarrow CH_3OCH_3 + H_2O + 23.4 \ kJ/DME \quad \cdots (4)$$

$$CO + H_2O \Leftrightarrow CO_2 + H_2 + 41.0 \ kJ/DME \quad \cdots (5)$$

The synthesis of DME from syngas at equation (1) has three main steps: reaction of methanol synthesis at equation (3), dehydration reaction at equation (4) and changing reaction at equation (5). If the rate of changing reaction is slow, combination of reaction (3) and (4) produce the reaction of (2). Entirely, the reaction is exothermic reaction, and to the core, the increasing of temperature reaction is caused by the formation process of methanol. Due to the characteristics of exothermic reaction, the problem of minimizing heat that are created from synthesis of DME is becoming a major problem to be seek for the best technology as a solution to overcome with. The JFE Corporation (Japan) has improved the synthesis of DME by using Slurry Reactor since 1989. Slurry consists of inert solvent and catalyst particle. Reactant gas formed bubbles and is diffused to solvent liquid. In here, the chemical reaction happens in catalyst. The heat of the reaction will quickly be absorbed by solvent liquid which has high capacity and conductivity of heat, consequently the distribution of temperature in reactor become homogeny. Another technology which has advanced using DME as its alternative fuel, is Haldor Topsoe [7] (U.S.) by applying fixed bed reactor.

3. Methodology

Thermodynamic analysis of Dimethyl Ether reaction directly from syngas is focused on using the Chemcad software Batch Version 5.2 (Chemstation Inc. 2901 Wildress Drive, Suite 305 Houston, Texas 77042 U.S.A.). The analysis is aimed to determine the condition of optimum operation that will be applied to fixed bed reactor. From all of the available reactor module on Chemcad module, Gibbs module reactor is chosen based on fully consideration of effectivity from Gibbs reactor module in thermodynamics analysis by reducing the Gibbs free energy in each possible reaction [8].

In the Gibbs reactor the number of product that are produced, the composition and condition of heat reaction are calculated based on free Gibbs energy minimally, appropriate with all complementary mass. All of the components which are used on the flow sheet must be written on the component list which subsequently is required to count the minimum free Gibbs energy, except which are specifically not joined along with (identify as inert).

The flow diagram of thermodynamic analysis is shown in figure 1. On that diagram, firstly we have to do the step of making model (flow diagram) then accomplish the input data standard component database, pressure, and temperature of feed input. Whereas, the minimum information which is needed by Gibbs reactor is bait input and rate input. If we want such a different state with the feed input, we can arrange the temperature and pressure. The reactor can also be utilized to liquid fuse or vapor or the mixture of both things. This reactor can also be used for isothermal state at particular temperature or is adjusted with feed temperature. For adiabatic reactor, the amount of stagnant heat can be attached or even eliminated, so that the temperature border can be set. The analysis of thermodynamics which has been done in this article is by arranging isothermal reactor mode.

The simulation is done to know exactly the influence of variable operation state, such as temperature, pressure, and feed ratio (H_2/CO). The result of simulation which vary from data of composition product, yield and conversion, are analyzed to get the data of optimum operation state for Dimethyl Ether synthesis.

ISSN 114-1284

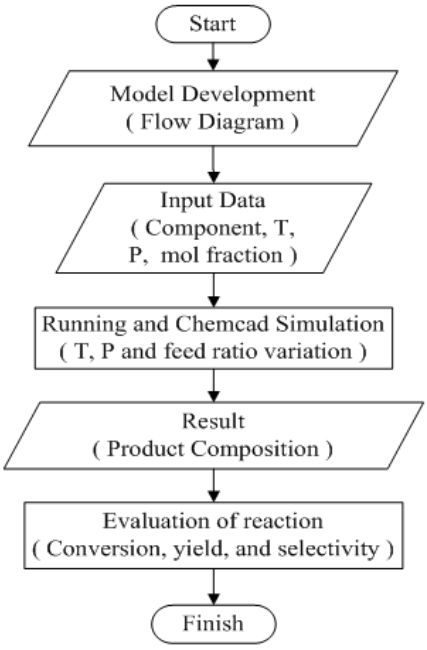

Figure 1. *Flow diagram of thermodynamic simulation*

4. Result and Discussion

4.1 The Influence of Pressure

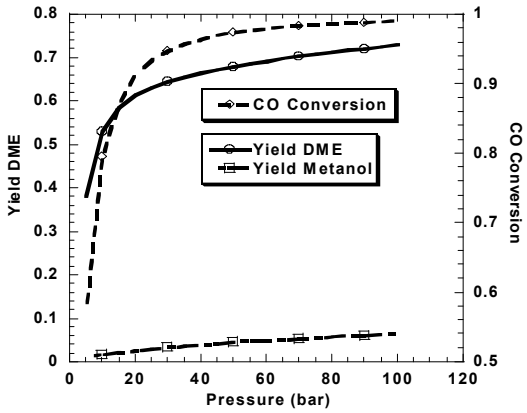

Figure 2. *Effect of pressure to performance of reaction at temperature 250℃ and feed ratio (H_2/CO) 2:1*

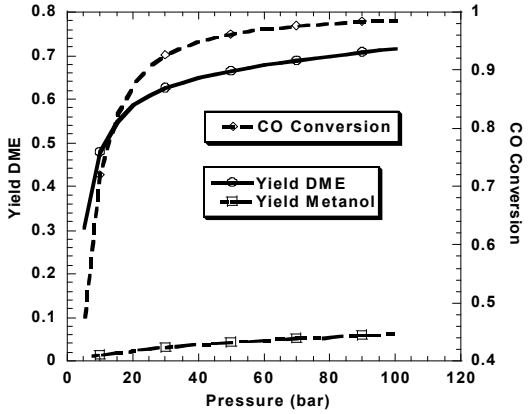

Figure 3. *Effect of pressure to performance of reaction at temperature 260℃ and feed ratio (H_2/CO) 2:1*

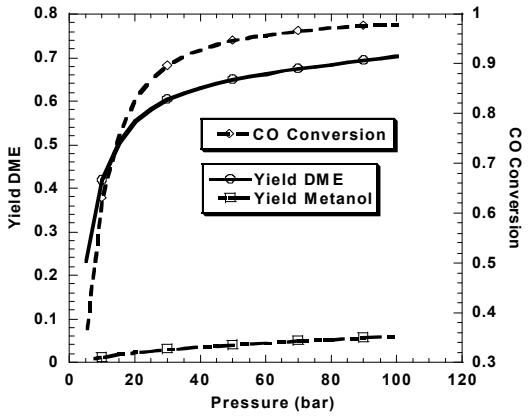

Figure 4. *Effect of pressure to performance of reaction at temperature 270℃ and feed ratio (H_2/CO) 2:1*

The simulation is executed in any stable temperature that is because it is really shown reaction activity influenced only by parameter of pressure from simulation result (picture 2-4) we can see that until the pressure of 60 bar CO conversion, DME yield occur an acutely raise, after 60 bar pressure, the rising will still be happened but in relatively lower number rather that that of the previous pressure. From the simulation result, we can also see that in whatever pressure exert, the prominent produced is DME in which the yield is higher that methanol.

Appropriately with the balance reaction principal, that pressure is set to be higher as a result the balance reaction incline to move to the part which has smaller molecule. On the direct synthesis of DME (Equation on reaction 1 and 2), the reactant component has greater number of molecule than that on product molecule. So it can be proved that DME position in the product can easily increase when the pressure is up.

The result of the simulation above, can also illustrate that the conversion is moving up significantly at the interval of pressure 60 bar, this case happens because the synthesis reaction of methanol become the border of all the reactions. This also indicates that the reaction of DME formation can also be done at the same pressure interval in the synthesis reaction of methanol.

ISSN 114-1284

On simulation graphic above, we can also find that the DME is also constructed as the first product adjacent to methanol [9]. This is for the reason that in the direct synthesis reaction of DME, methanol will conversed straightforwardly to DME and water. Thermodynamically, the degree of which a chemical reaction can be estimated from Gibbs energy cost in each reaction. According to journal literature, the data Gibbs energy for reactions which in involved to the DME formation is listed below:

$$CO + 2H_2 \Leftrightarrow CH_3OH, \Delta G_{600\,K} = 45.4\,{}^{kJ}/_{mol} \quad \cdots(6)$$

$$2CH_3OH \Leftrightarrow CH_3OCH_3 + H_2O, \Delta G_{600\,K} = -10.7\,{}^{kJ}/_{mol} \quad \cdots(7)$$

From Gibbs energy data above, we can see that Gibbs energy for synthesis reaction of methanol. So, thermodynamically the DME compound will be easier to be formed (liked) than methanol compound.
From this simulation, we can conclude that operation of DME synthesis is on 30-70 pressure.

4.2 The Influence of Temperature

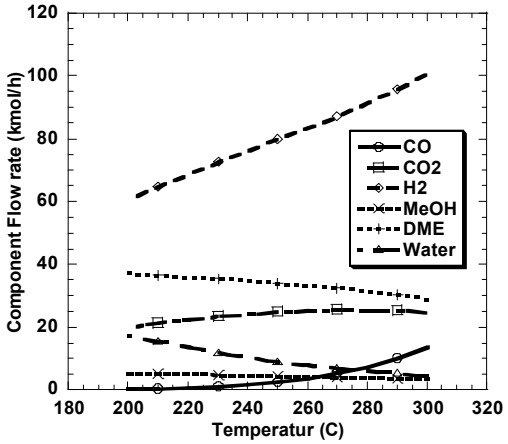

Figure 5. *Product composition as a temperatur function (at pressure 50 bar and feed ratio 2:1)*

The result of simulation above is accomplished with variation of temperature between 200 to 300 ºC with pressure of 50 bar and of bait ratio of H_2/CO in proportion to 2:1. From that result, we can see also that the product of DME occurs in a descending within the increasing of reaction of temperature. This case can be explained by looking up the synthesis reaction of DME as exothermic reaction (see equation of reaction 1 and 2) by which the increasing of temperature will effect on the balance reaction which tempted to move to the reaction which characterized as endothermic, to which the reaction will shift to the reactant. The water gas shifts reaction 9WSGR) [10] in which CO is the real product that experience enlarger amount as the increasing of the temperature reaction or we can say as endothermic (see equation of reaction 5). This simulation is done by pressure state of 50 bar, by which the election of pressure as optimum condition of synthesis reaction of DME is principally based on the reaction activity when CO conversion experience significant increase until 50 bar. And for the next, it will still increase but not as much as before. The pressure effect has undeviating proportion to product DME so in whatever amount of pressure that are produced by DME, the yield is still higher rather than other product such as methanol, CO2, and water. According to simulation result of the temperature influence to the product composition, we determine the optimum temperature in 270ºC, output composition of CO2 become greater than water. It is clear that this case is not necessitated since the character of CO is as pollutant on air.

4.3 The Influence of Feed Ratio H_2/CO

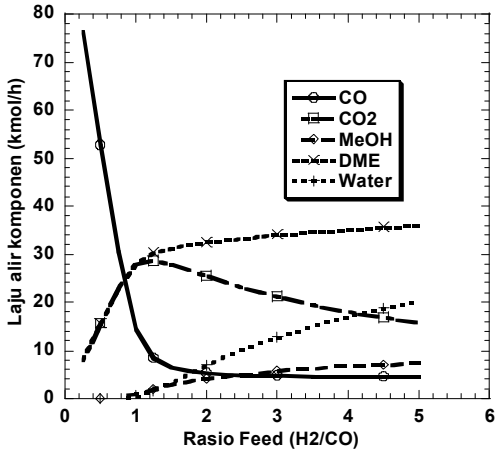

Figure 6. *Product composition as a feed ratio function (at temperatur 250℃ and pressure 50 bar)*

Simulation of feed ratio H_2/CO influence is performed by marking from 0,5 to 5 to see how it effects on the reactor and the product composition. According to simulation, we can see that DME will be increased along with the ratio mark which is increasing too. Whereas, CO conversion is significantly enhancing until reaching 2:1 feed ratio, then conversion experience relatively at constant cost. CO_2 occurs in maximum condition when feed ratio in the reactor is as big as 1:1 proportion. This case can be explained by giving attention on equation of the first reaction that is written before and that of direct synthesis reaction of DME with 1:1 proportion. H_2/CO produces DME and CO_2 as the main product. While for the equation of the second reaction with 2:1 feed ratio will result on DME and water has higher yield than water. From the simulation result we can conclude that the optimum feed ratio state for synthesis reaction of DME is about 2:1. It is regarding to the proportion when feed ratio reach 2:1 or we called it as CO conversion which is determined as nearly constant and that of the last product of DME which will be closely to constant distance.

5. Conclusion

Thermodynamically, direct synthesis reaction is more dominant than synthesis reaction of methanol that

participates along with it. It is proved with the data of Gibbs which is obtained from the literary journal restating that number of Gibbs energy on synthesis of DME reaction is about -10,7 Kj/mol (see equation of reaction 7) much smaller than Gibbs energy from synthesis reaction of methanol which has only 45.4 Kj/mol (see equation of reaction 6). The pressure of operation opted about 50 bar, which is because of security reason and simulation of reaction activity can be concluded that CO conversion is experiencing the significant raising until 50 bar. The temperature of operation is chosen for 270ºC regarding to the catalyst stability that has limitation of operation temperature distance, besides it is also because this temperature produce higher CO rather than water that indicate unwanted pollutant produced in higher number. Bait Ratio (H2/CO) that is chosen for research condition in proportion of 2:1 due to he sthyochiometric condition for direct synthesis reaction of DME has to be fulfilled that effect on distance formation of DME becoming relatively constant if the bait ratio become mere numerous.

REFERENCES

[1]. Qingjie, G. Xiaohoang Li, *Direct Synthesis of LPG from Synthesis Gas over Pd-Zn-Cr/Pd-β hybrid catalysts,* Elsevier (2007)
[2]. Ogawa, T., Norio Inoue, Tutomo Sikada, Yotaro Ohno, *Direct Dimethyl Ether Synthesis – Journal of Natural Gas Chemistry* (2003)
[3]. Fleisch T. SAE 950 061, (1995)
[4]. G. Qi, X. Zheng, J. Fei. Hou, *A Novel Catalyst for DME Synthesis from CO hydrogenation,* J. Mol. Catal. 176 (2001)
[5]. Air Products and Chemicals. DOE/PC/90018-T7, (1993)
[6]. *DuPont Talks About its DME Propellant,* Aerosol Age (1982)
[7]. Dybkjar, I. and Hansen, J.B., Large Scale Production of Alternative Synthetic Fuels from Natural Gas, *Natural Gas Conversion IV: Studies in Surface Science and Catalysis,* Amsterdam: Elsevier (1997)
[8]. Sunarya, S., *Studi Termodinamika Reaksi Hidrogenasi CO_2 dan CO menjadi Metanol dengan Chemcad*, (1998)
[9]. Fujimoto, K., Kenji Asami, Tsutomu Shikada, and Hiro-o Tominaga, *Selective Synthesis of Dimethyl Ether from Synthesis Gas*, (1984)
[10]. W. Ligang, F. Deren, H. Xingyun, *Influence of Reaction Conditions on Methanol Synthesis and WGS Reaction in the Syngas to DME Process,* Journal of Natural Gas Chemistry (2006)

ISSN 114-1284

Preparation and characterization of Chitosan/Montmorillonite (MMT) nanocomposite systems

Hery Haerudin[1], Andika W. Pramono[2], Dona Sulistia Kusuma[1], Aisyiyah Jenie[1], Nicolas H. Voelcker[3], Christopher Gibson[3]

[1]*Research Center for Chemistry, Indonesian Institute of Sciences,*
Kawasan PUSPIPTEK, Serpong, Tangerang 15314, Indonesia
Tel: (021)7560929. Fax: (021)7560549
E-mail: d_sulistia@yahoo.com

[2]*Research Center for Metallurgy, Indonesian Institute of Sciences,*
Kawasan PUSPIPTEK, Serpong, Tangerang 15314, Indonesia
Tel: (021)7560562 ext 3268. Fax: (021)7563205
E-mail: andika_pram@yahoo.com

[3]*School of Chemistry, Physics and Earth Sciences, Flinders University of South Australia*
GPO Box 2100, Bedford Park, South Australia, 5042, Australia
Tel: +61 (08) 8201 5338. Fax: +61 (08) 8201 2905
E-mail: nico.voelcker@flinders.edu.au

ABSTRACT

A natural based nanocomposite film consisting of chitosan, montmorillonite (MMT) and cashew nut shell liquid (CNSL) was synthesized. The nanocomposite was prepared by mixing suspension of clay particles (filler, MMT) with a solution containing chitosan as macroscopic polymer matrix. In this study, it was proposed that non-ionic long chain-alkyl molecules with possible interactions with the amine group of chitosan could be used as plasticizer. As natural source for these compounds, an extract of CNSL was used. A series of chitosan/MMT composite samples containing two different clay contents and sample with an additional CNSL are prepared. FTIR spectroscopy of the nanocomposite films indicated that by addition of CNSL amide groups of the chitosan are probably less attached and have more space for vibration. CNSL seems to provide intermolecular spaces between the chitosan molecules. AFM analysis showed that the composite has particle size of 100 nm and less, which confirmed that nanocomposite has been successfully produced by this method. Addition of CNSL as plasticizer improved the tensile strength by 10% and the elastic modulus by almost 18%. Cell growth was observed on all the nanocomposite samples studied here.

Keywords
montmorillonite (MMT), chitosan, CNSL, nanocomposite

1. INTRODUCTION

The use of biopolymer as component of composite for packaging materials is very much studied recently. Studies regarding to the improvement of composite properties such as brittleness, low heat distortion temperature; gas permeability, etc. for a wide range application are very much interested. Additionally, the development of biobased nanocomposites are carried out with intention to provide physical protection for food, improving food integrity as well as protection from microbes and fungi [1].The use of biobased nanocomposites for packaging material has been reviewed [2,3].

Chitosan as biopolymer is also very much studied for development of new composite material with montmorillonite (MMT) clay. Various experiments including the modification of MMT properties by converting the MMT into organo-montmorillonite (OMMT) prior to the nanocomposite preparation [4], as well as the variation of MMT concentration [5] and different dimension were studied [6] to enhance the properties of chitosan/MMT composite. Studies on interaction of small molecules such as glycerol as plasticizer with chitosan in chitosan film was also thoroughly studied [7,8]. Regarding to the limited water resistant and mechanical properties of original biopolymer, studies on the improvement of those properties by including hydrophobic material into the biopolymer composite [9,10] or by addition of other small molecules to enhance hydrophobicity [11,12,13] or plasticity [14,15] were carried out. Since application of the chitosan composite as packaging material for food is strongly considered, especially regarding to the its antimicrobial activity, most studies of chitosan/clay nanocomposite have also included antimicrobial activity test.

It is known that the properties polymer/clay composite are strongly afftected by addition of surfactant into the composite. On those system, the typical molecules are

long-chain alkyl quaternary ammonium chlorides [16,17,18], which is easily incorporated into the clay structure. Large molecule additions, except the use of long-chain alkyl quartenary amines or pollyglycol [19,20], in order to manipulate the composite properties are seldom studied. In the present study, it was proposed that non-ionic long chain-alkyl molecules with possible interactions with the amine group of chitosan could be used as plasticizer. As natural source for these compounds, an extract of cashew nut shell (cashew nut shell liquid-CNSL) was used. A series of chitosan/MMT composite samples containing two different clay contents and sample with an additional CNSL are prepared. CNSL is known as a source for cardol, cardanol and anacardic acid, phenolic compound with a long-chain alkyl group. A typical solvent-extracted CNSL contains anacardic acid (60-65%), cardol (15-20%), cardanol (10%) and traces of methylcardol [21]. Addition of CNSL as a source of relatively big molecules into the composite was intended also to improve the hydrophobicity as well as the mechanical properties of resulted composites.

2. EXPERIMENTAL

2.1 Materials

Montmorillonite (MMT) employed in this study was K10 montmorillonite from Sigma-Aldrich. This montmorillonite is well known as having a CEC of 70-100 meq/100 g. Chitosan purchased from Sigma-Aldrich (Cat Nr. C3646) had a degree of deacetylation of 85% minimum. Commercial cetyltrimethyl ammonium bromide (CTAB) from E-Merck (Cat. No. 1.02342) was employed for this study. Cashew Nut Shell Liquid (CNSL) was extracted from cashew nut shell originated from Sumba Island, Indonesia. Prior to the use for composite preparation, chitosan was pretreated in basic solution of 10% NaOH. The extraction procedure for CNSL was as follows: Adequate of fresh redistilled n-hexane was added to the cashew nut shell in a round glass flask. Extraction was carried out by refluxing 100 g cashew nut shell in 250 ml of n-hexane for 2 hours and followed by filtration and evaporation of n-hexane.

2.2 Preparation of Na-Montmorillonite and organo-montmorillonite (OMMT)

The OMMT was prepared by cation exchange between Na-MMT galleries and CTAB in an aqueous solution. MMT (2 g) was dispersed using a stirrer in distilled water to obtain clay suspension, and allowed to stand for 24 h after vigorous stirring for 30 min. CTAB (2 g) was dissolved in distilled water, and then dropped slowly into the MMT suspension at 85°C under stirring. After stirring for 4 h, the product was washed several times with distilled water and filtered to ensure the complete removal of bromide ions, which were detected with $AgNO_3$ until no AgBr precipitate was found. The product was dried at 85°C to yield OMMT.

2.3 Preparation of Chitosan/Montmorillonite Composite

The chitosan solution was prepared using a 1% acetic acid solution. 4 g chitosan was dissolved in 100 ml acetic acid solution (1%) and stirred for 4 hours to obtain a homogeneous mixture. A 2% clay suspension in acetic acid solution (1%) was also prepared. The suspension was added into the resulted gel such that a 1% and 3% MMT content in the mixture was obtained. The mixture was stirred at 50°C for 2 days to obtain a homogeneous chitosan/MMT suspension. This procedure was carried out using K10 montmorillonite (Sigma-Aldrich), Na-exchanged K10 and CTAB exchanged K10. For samples containing CNSL, a solution of 25 mg CNSL in 100 ml ethanol was prepared separately. The CNSL solution was added accordingly into the chitosan/MMT mixture after a rigorous 2 days mixing, that a final 1% CNSL content was obtained.

2.4 Characterization

2.4.1 Infrared (IR) Spectroscopy

All IR spectra were obtained using a Nicolet Avatar 370MCT (Thermo Electron Corporation, USA) equipped with a standard transmission accessory. Spectra of the composite films were recorded and analysed using OMNIC version 7.0 software, in the range of 650–4000 cm^{-1} at a resolution of 1 cm^{-1}, the background was taken using an original chitosan powder. IR of the composite film was performed in transmission mode with crushed powders in KBr discs in the range of 650–4000 cm^{-1} at a resolution of 1 cm^{-1}.

2.4.2 Atomic Force Microscopy (AFM)

Tapping mode AFM was performed on a Multimode Nanoscope IV microscope (Veeco Corporation, USA). Commercial Si cantilevers (FESP, Veeco Corporation, USA) were used for all experiments. The images were processed and analysed using the Nanoscope 5.31r1 software (Veeco Corporation, USA).

2.4.3 Differential Scanning Calorimetry (DSC)

In the present work, DSC 2920 (TA Instruments) was used for the measurement. The instrumental cell constant and temperature calibration were performed using indium. Chitosan/MMT samples were analysed under continuous heating conditions (10°C min^{-1}) between room temperature and 200 °C. 8-10 ± 0.1 mg of sample was weighed into a standard aluminium pan and placed onto the DSC cell platform.

2.4.4 Mechanical Properties

The mechanical properties of chitosan/ MMT nanocomposites were tested using an Universal Testing Machine, Orientec Co. Ltd., Model UCT, 5-T. The specimens were prepared according to ISO 527-2. All specimens were tested using a crosshead speed of 1 mm/min.

2.4.5 Cell Growth-Test

1 cm^2 membranes were transferred to wells of a 12 well Iwaki tissue culture plate (cat# 3815-012). Membranes were seeded with HEK 293 cells at density 10^5 cells/cm^2 (3.85 x 10^5 cells per well in a 2 mL volume) in DMEM (Invitrogen) +10% FCS (JRH) + 2 mM L-glutamine + 100 U/ mL penicillin 100ug/mL streptomycin (Invitrogen). HEK 293 cells were grown in the presence of the membranes for 20 hours at 37C 5% CO_2. At 20 hours media was removed and replaced with 2 ng/mL Hoescht 33342 (Sigma) stain in complete media and incubated at 37°C 5% CO_2 for 0.5 hours. Staining was visualized under appropriate fluorescent excitation/emission conditions for Hoescht stain. The photographs were taken with a 20 X objective on a Leica laborluxD fluorescent scope.

3. RESULTS AND DISCUSSION

Table 1 as shown below gives the list of sample used for the studies. . Each sample contains 3% of clay or its modified one. CNSL was added as a solution in ethanol, 1% w/w of the chitosan used for film preparation.

Table 1. List of samples tested for the studies. Each sample contains 3% of clay or its modified one. CNSL was added as a solution in ethanol, 1% w/w of the chitosan used for film preparation.

Clay type		CNSL Addition
K10	Untreated	No
K10-CTAB	Organic clay	No
K10-CN	Untreated	Yes
K10-CTAB-CN	Organic clay	Yes

3.1 Infrared spectroscopy

FTIR analysis of the composite films were performed to study the structural changes causes by modification of clay component prior to the preparation of composite. The IR spectra were taken by transmission as well as DRIFT method. The spectrum of chitosan is characterized by broad and intense band at 3450-3200 cm^{-1} (hydrogen bonded OH stretching overlapped with N-H stretching bands); C-H stretching band at 2783 cm^{-1}, The N-H deformation band of chitosan was found at 1559 cm^{-1} .The strong bands at 1656 cm^{-1} and 1599 cm $^{-1}$ are ascribed to the amide I (C=O stretching) and amide II (N-H bending modes) of the chitosan.

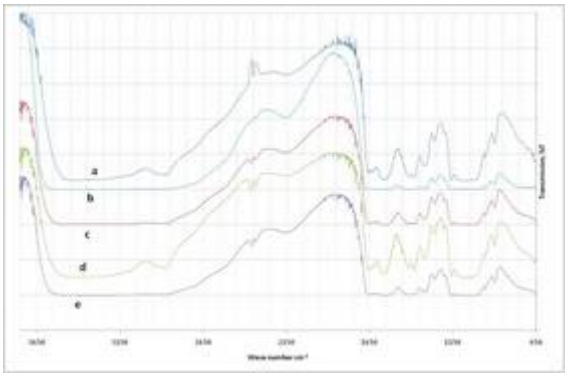

Figure 1. Transmission FTIR spectra of (a) pure chitosan (CS) film; (b) CS/3% K10; (c) CS/3% K10-CN; (d) CS/3% K10-CTAB; and (e) CS/3% K10-CTAB-CN composites

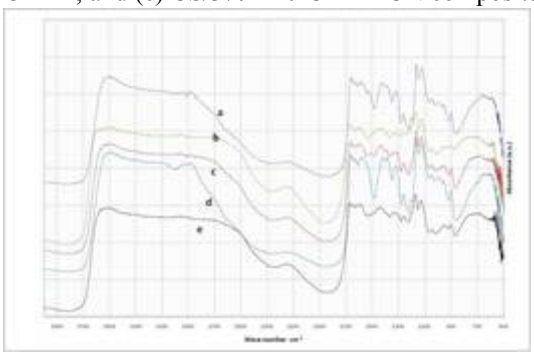

Figure 2. DRIFT spectra of (a) pure chitosan (CS) film; (b) CS/3% K10; (c) CS/3% K10-CN; (d) CS/3% K10-CTAB; and (e) CS/3% K10-CTAB-CN composites

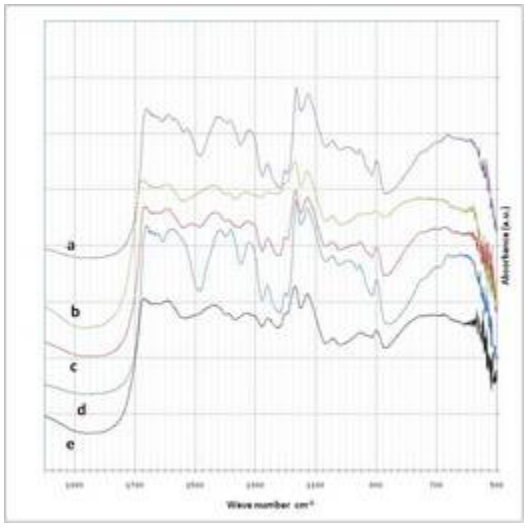

Figure 3. DRIFT spectra of (a) pure chitosan (CS) film; (b) CS/3% K10; (c) CS/3% K10-CN; (d) CS/3% K10-CTAB; and (e) CS/3% K10-CTAB-CN composites.

Generally, the amide bands are shifted to the higher wave number by addition of the CNSL. By addition of CNSL amide groups of the chitosan are probably less attached and have more space for vibration. CNSL seems provide intermolecular spaces between the chitosan molecules. This should be result in a higher plasticity of the resulting material. The C-O stretching band around 1160 cm^{-1} remained undisturbed by the addition of CNSL.

3.2 Atomic Force Microscopy (AFM)

AFM analysis was conducted to determine the nanoscale structure of the composite synthesized.

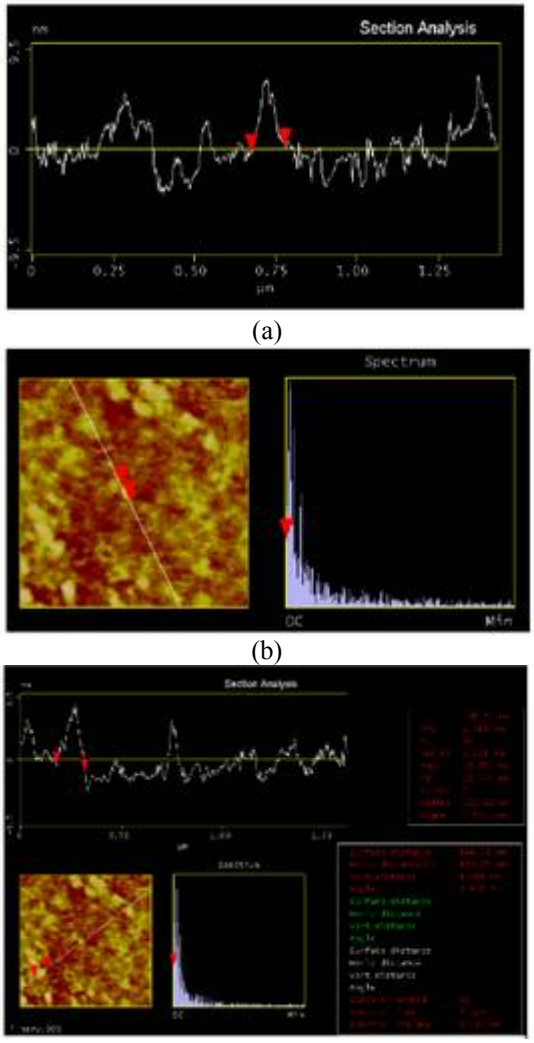

Figure. 4 Morphology analysis of longitudinal section of CS/K10-CTAB using AFM (a) Particle horizontal size of 103 nm (b) Area of analysis (c) Particle horizontal size of 139 nm

As shown in Fig. 4, the MMT particle forming the composite has the length of 103 nm (Fig. 4a) and 139 (Fig. 4c). However, the surface height is less than 9,5 nm. This can be explained as follows. The MMT particles forming the composite only consist of a few layers, resulting the MMT particles thickness of less than 10 nm. Although the length of the particle is more than 100 nm, the formation of particles of less than 10 nm indicates the presence of exfoliation from the MMT particles. Since the MMT are used as fillers, then most likely the composite synthesized was in the form of *ordered intercalated nanocomposite.*

3.3 Differential Scanning Calorimetry

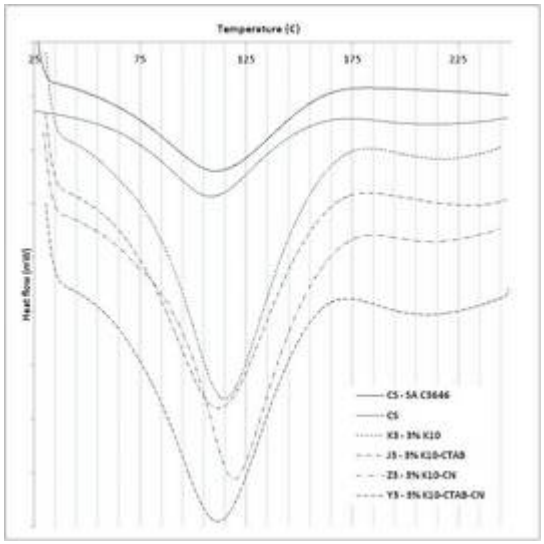

Figure 4. DSC thermogram of samples. From above downwards: (a) chitosan (CS) powder (C3636, Sigma-Aldrich), (b) CS film, (c) CS/3%-K10, (d) CS/3% K10-CTAB, (e) CS/K10-CN and (f) CS/K10-CTAB-CN.

As shown by the thermogram, glass transition in DSC was not observed. That indicates that amorphous structure does not exist. No thermoset cure temperature was observed from 25°C to 250°C. Most probably no crosslinking, formation of new bonds occured in the material at that temperature range. DSC thermograms show only that water released from the film at similar temperature range as on the original chitosan when the formula of composite film was containing CTAB. It could be explained, that the preparation of organo-montmorillonite (OMMT) has removed most of the trapped water molecules from the MMT, such that less water existed in the MMT as well as in the resulting composite film. It was expected that the hydrophobicity would be increased by the addition of CNSL, which means, it was also expected that water molecules would be released at much lower temperature from the film containing CNSL in the formulation. The thermograms shows that there was no effect for OMMT, but on composite containing plain unmodified MMT (c and e) water molecules were released at higher temperature, CNSL addition into the formula seems result in

stronger water retention in the film. The CNSL component molecules has retained the trapped water molecules on montmorillonite.

3.4 Mechanical Properties

Table 2. Tension test result of nanocomposite samples

Sample code		Yield strength [Mpa]	Tensile strength [Mpa]	Rupture [Mpa]	Elastic Modulus [Mpa]
CS/K10-CTAB	avg	59.4	76.9	75.9	2470
	std. dev.	1.5	8.4	9	220
CS/K10-CTAB-CN	avg	66.8	84.6	84.5	2910
	std. dev.	3.9	10.6	10.7	250

From the measurements shown in Table 2, it is shown that the addition of CNSL increases the modulus elasticity, yield strength, tensile strength as well as the rupture of the composite. The tensile strength is improved by 10% and the elastic modulus by almost 18%.

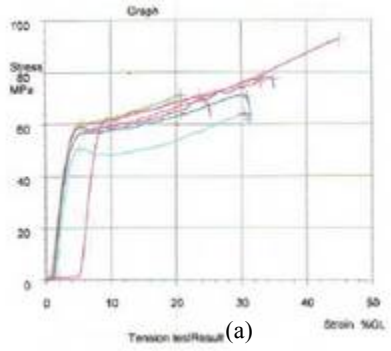

(a)

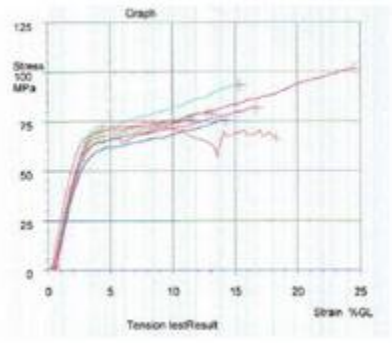

(b)

Figure 5. Tension test graphic result (a) CS/K10-CTAB (b) CS/K10-CTAB-CN

3.5 Cell Growth-Test

It was difficult to differentiate the living cell from the film, since the chitosan film gives a strong background fluorescence using this particular method. Despite of this problem, it could be conclude that cell growth were observed on all the samples studied here.

ISSN 114-1284

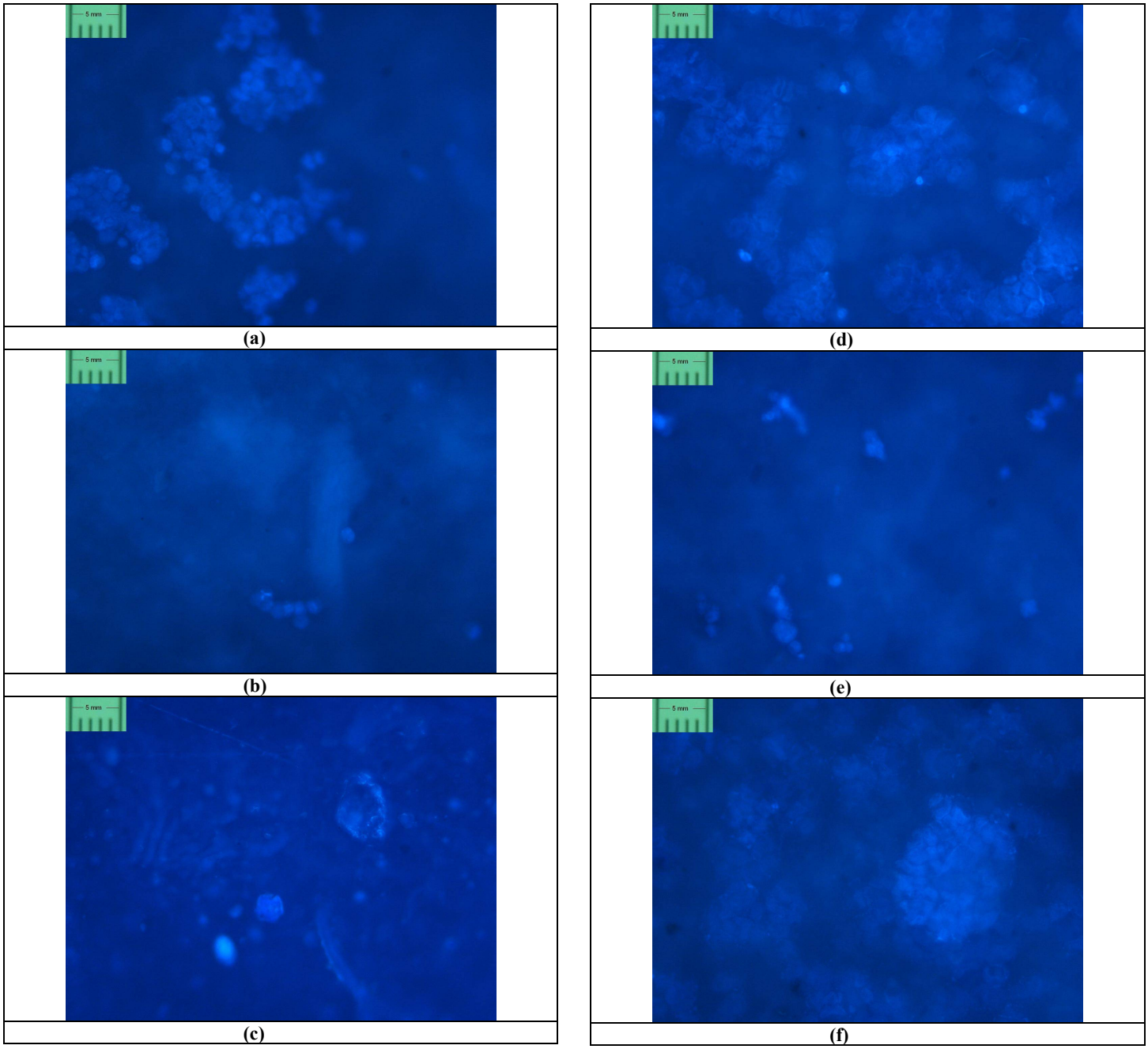

Figure 6. Cell growth test on chitosan film (a) CS (Chitosan film): ++ (b) Z3 (3% K10-CN): + (c) J3 (3% K10-CTAB): No cells (d) K3 (3% K10): + (e) Y3 (3% K10-CTAB-CN): + (f) J3 (3% K10-CTAB): ++

4. CONCLUSION

A natural based nanocomposite film consisting of montmorillonite, chitosan and cashew nut shell liquid (CNSL) has been successfully synthesized. It has been proven that CNSL seems to provide intermolecular spaces between the chitosan molecules. AFM analysis showed that the composite has particle size of 100 nm and less, which confirmed that nanocomposite has been successfully produced by this method. The preparation of organo-montmorillonite has removed most of the trapped water molecules from the montmorillonite, such that less water existed in the montmorillonite as well as in the resulting composite film, as shown by the DSC analysis. However, the addition of CNSL component molecules has retained the trapped water molecules on montmorillonite. Addition of CNSL as plasticizer improved the tensile strength by 10% and the elastic modulus by almost 18%. Cell growth was observed on all the nanocomposite samples studied here.

ACKNOWLEDGMENT

The present work was co-sponsored by the Endeavour Program of the Australian Government.

REFERENCES

[1] J. W. Rhim, S. I. Hong, H. M. Park, and P. K. W. Ng, "Preparation and Characterization of Chitosan-Based Nanocomposite Films with Antimicrobial Activity", *J. Agric. Food Chem*., vol. 54, no. 16, pp. 5814-5822, 2006.

[2] Z. Akbari, T. Ghomashchi, and S. Moghadam, "Improvement in Food Packaging Industry with Biobased Nanocomposites", *International Journal of Food Engineering,* vol. 3 : Iss. 4, Article 3., DOI: 10.2202/1556-3758.1120, 2007.

[3] P.K. Dutta, S. Tripathi, G.K. Mehrotra, J. Dutta, "Perspectives for chitosan based antimicrobial films in food applications", *Food Chemistry,* 114, pp.1173–1182, 2009

[4] X. Wang, Y. Du, J. Yang, Y. Tang, J. Luo, "Preparation, characterization, and antimicrobial activity of quaternized chitosan/organic montmorillonite nanocomposites", *J. Biomed. Mater. Res. A*, vol. 84, no. 2, pp.384-390, Feb. 2008.

[5] X. Y. Wang, Y. M. Du, J. H. Yang, X. H. Wang, X. W. Shi, and Y. Hu, "Preparation, characterization and antimicrobial activity of chitosan/layered silicate nanocomposites", *Polymer*, vol. 47, pp. 6738–6744, 2006.

[6] C. Tang, N. Chen, Q. Zhang, K. Wang, Q. Fu, and X. Zhang, "Preparation and properties of chitosan nanocomposites with nanofillers of different dimensions", *Polym. Degrad. Stab.,* vol. 94, no. 1, pp. 124-131, Jan. 2009.

[7] I. Quijada-Garrido, V. Iglesias-González, J.M. Mazón-Arechederra, J.M. Barrales-Rienda, "The role played by the interactions of small molecules with chitosan and their transition temperatures. Glass-forming liquids: 1,2,3-Propantriol (glycerol)", *Carbohydrate Polymers*, vol. 68, pp. 173–186, 2007

[8] E. Ruiz-Hitzky, M. Darder, and P. Aranda, "Functional biopolymer nanocomposites based on layered solids", *J. Mater. Chem.*, vol. 15, pp. 3650–3662, 2005.

[9] Y. L. Liu, C. H. Yua, K. R. Leea, and J. Y. Lai, "Chitosan/poly-(tetrafluoroethylene) composite membranes using in pervaporation dehydration processes", *J. Membrane Sci.*, vol. 287, no. 2, pp. 230-236, Jan. 2007.

[10] K. Gabrovskaa, A. Georgievaa, T. Godjevargovaa, O. Stoilovab, and N. Manolova, "Poly(acrylonitrile)chitosan composite membranes for urease immobilization", *J. Biotech.,* vol. 129, no. 4, pp. 674-680, May 2007.

[11] C. Caner, P. J. Vergano, and J. L. Wiles, "Chitosan Film Mechanical and Permeation Properties as Affected by Acid, Plasticizer, and Storage", *J. Food Sci.*, vol. 63, no. 6, pp. 1049-1053, 1998.

[12] G. E. Luckachan and C.K.S. Pillai, "Chitosan/oligo L-lactide graft copolymers: Effect of hydrophobic side chains on the physico-chemical properties and biodegradability", *Carbohydrate Polymers,* vol. 64, no. 2, pp. 254-266, May 2006.

[13] S. Rivero, M.A. García, and A. Pinotti, "Composite and bi-layer films based on gelatin and chitosan", *J. Food Eng.,* vol. 90, no. 4, pp. 531-539, Feb. 2009.

[14] H.K. No, S.P.Meyers, W. Prinyawiwatakul, and Z. Xu, "Applications of Chitosan for Improvement of Quality and Shelf Life of Foods: A Review", *J. Food Sci.*, vol. 72, no. 5, pp. 87-100, 2007.

[15] N. E. Suyatma, L. Tighzert, A. Copinet, and V. Coma, "Effects of Hydrophilic Plasticizers on Mechanical, Thermal, and Surface Properties of Chitosan Films", *J. Agric. Food Chem.*, vol. 53, pp. 3950-3957, 2005

[16] W. Xie, J. Y. H. M. Hwu, G. J. Jiang, T. M. Buthelezi, and W. P. Pan, "A Study of the Effect of Surfactants on the Properties of Polystyrene-Montmorillonite Nanocomposites", *Polym. Eng. Sci.*, vol. 43, no. 1, pp. 214-222, Jan. 2003.

[17] M. C. Costache, M. J. Heidecker, E. Manias, and C. A. Wilkie, "Preparation and characterization of poly(ethylene terephthalate)/clay nanocomposites by melt blending using thermally stable surfactants", *Polym. Adv. Technol.*, vol. 17, pp. 764–771, 2006.

[18] S. B. Bae, C. K. Kim, K. Kim, and I. J. Chung, "The effect of organic modifiers with different chain lengths on the dispersion of clay layers in HTPB (hydroxyl terminated polybutadiene)", *European Polymer Journal*, vol. 44, pp. 3385–3392, 2008

[19] J. Bajdik, M. Marciello, C. Caramellab, A. Domjánc, K. Süveghd, T. Mareke, and K. Pintye-Hódi, "Evaluation of surface and microstructure of differently plasticized chitosan films", *J. Pharm. Biomed. Analysis*, vol. 49, pp. 655–659, 2009.

[20] C. L. Silva, J. C. Pereira, A. Ramalho, A. A. C. C. Pais, and J. J. S. Sousa, "Films based on chitosan polyelectrolyte complexes for skin drug delivery: Development and characterization", *J. Membrane Sci.,* vol. 320, pp. 268–279, 2008

[21] P. P. Kumar, R. Paramashivappa, P. J. Vithayathil, P. V. Subba Rao, and A. S. Rao, "Process for Isolation of Cardanol from Technical Cashew (Anacardium occidentale L.) Nut Shell Liquid", *J. Agric. Food Chem.*, vol. 50, pp. 4705-4708, 2002.

ISSN 114-1284

The Stabilization of Soft Clay and Coconut Fiber Increases the Bearing Capacity of Highway Subgrade

Indra Nurtjahjaningtyas[1]

[1]*Faculty of Engineering*
University of Jember
Faculty of Engineering University of Jember
Tel : (0331) 484977 ext 112; (0331) 410241 Fax : (0331) 410240
E-mail : indranurtj.tekniksipilunej@gmail.com

ABSTRACT

In the development of highway, the most important thing is subgrade, because the subgrade is the most important factor to determine the density needed for flexible pavement. If the subgrade is soft clay that has low and sensitive bearing capacity toward the change of water concentration, it will cause the instability of the highway. Therefore, chemical stabilization is needed to improve the subgrade. This research concerns with the chemical stabilization of soft clay and coconut fiber. The result shows that the addition of coconut fiber can increase 3.19% CBR (California Bearing Ratio) of the soft clay. The 10% and 20% addition of coconut fiber can increase 220% bearing capacity of the subgrade. The test result indicates that the highest density of subgrade takes place in the 20% addition of coconut fiber with 1.21 gr/cm^3 MDD (Maximum Dry Density) but the real soil increases 20% bearing capacity. Then, the smallest value of Swelling Potential takes place in the 20% addition of coconut fiber with 11.11% regression compared to the real soil.

Keywords

chemical stabilization, bearing capacity, soft clay, coconut fiber

1. INTRODUCTION

Soil is a material consisting of aggregate (grain) solid minerals that are not tied to each other chemicals and organic material from the mold was. Soil as a useful building material in a variety of civil engineering works in addition to the Soil also serves as a foundation of the building. (Braja M. Das, Noor Endah, Indrasurya B. Mochtar, 1988). Soil is the part that is not separated from human life, most human activity associated with the Soil. For example, among other farming activities on the plant and the structure of road.

At the first break even until now in remote areas have been using coconut fiber which is the rest of the coconut harvest crops up to the road that damaged when exposed to rain as they often passed by and the road is not paved. But after a while the road is dry and the coconut fiber to filled earlier integrates with the Soil and the Soil on the road crust, and logged more time on the ground does not damage before to filled with coconut fiber, then Soil on the road to be stable. Soil treatment is to give thought to examine how far coconut fiber can increase the bearing capacity soil stabilization method with the chemical.

A very important factor in determining the thick pavement needed on the road asphalt (flexible pavement) is a subgrade. When Subgrade is a clay soil which has bearing capacityed the low and very sensitive to changes in water level, will cause instability road. Therefore, the required improvements to the Soil. improvements to the soil carried out among the chemical stabilization. Stabilization is a process to improve the nature of Soil in a way to add something on the soil in order to increase resources to bearing capacity. Stabilization method that is widely used mechanical stabilization and chemical stabilization. Stabilization is to add mechanical strength and resources to bearing capacity improvements to the way Soil and improvements to the nature of the structure-mechanical nature of the Soil, while the chemical stabilization is to add strength and strong bearing capacity to the Soil to reduce or eliminate the way the nature of the technical nature of soil-less mix in a way beneficial to the soil material chemicals such as cement, lime or pozzolan. Subgrade layer is 50 cm - 100 cm thicks which is the bottom of surface construction pavement a road or runway aircraft. Subgrade must have the high bearing capacity and able to maintain the volume changes during the service even though there are differences in environmental conditions. Subgrade can be a base soil can compacted native Soil if the original well, the Soil that brought from other places and then or soil material with stabilization.

ISSN 114-1284

Primary function is to receive Soil pressure due to the traffic load on the surface so that the Soil should have the high bearing capacity an optimal fashion so that a result is able to receive the traffic load without changes and damage that means. Bearing capacity of Subgrade can be estimated with the practice or the classification results of the CBR test, plate loading test, and so on (Sukirman, 1995).

In this research tried to make improvements to the Soil with chemical stabilization using coconut fiber. As with the coconut fiber is a waste (waste product) that is very rarely used, easily obtained than the amount of coconut fiber and relatively much cheaper price compared with lime, cement and sand. It tried to take advantage of this coconut fiber as a soil stabilization material. And is expected to use the coconut fiber, the ground water level can be reduced so that it can be used as subbase and subgrade materials. From the background above can be formulated as a problem, Whether stabilization of soft clay with coconut fiber can increase the bearing capacity of Soil? And How many percent of the addition of coconut fiber on the soft clay soil that produces the highest bearing capacity

2. REFERENCES

2.1 Soil

Soil is a material consisting of aggregate (grain) solid minerals that are not tied to each other chemicals and organic material from the mold was. Soil as a useful building material in a variety of civil engineering works in addition to the Soil also serves as a foundation of the building. (Braja M. Das, Noor endah, Mochtar B. Indrasurya).

2.2 Soil Stabilization

Soil stabilization is to make efforts to meet the Soil requirements and the needs of a particular technique. If the Soil has been stable, the Soil will have the strength, kemampumampatan (compressibility), created for ease of building on it (Dr. Ir. Hapsoro Tri Suryo Utomo). Stabilization is a process to improve the nature of Soil in a way to add something on the Soil with the goal to get the changes the physical nature of Soil to the better, for example:
a. Stabilization in the soil volume (volume stability)
b. Increase resources to bearing capacity Soil (strength or bearing capacity
Stabilization method that is widely used:

1) Mechanical stabilization (mechanical stabilization of soil) Stabilization method is used on Soil that has great run-down flower. Stabilization of soil mechanics can be done in a way:
a) basic soil mix with good soil. This can be done with a mix of native soil akan distabilisasi with sand with a certain amount so that the run-down nature of the flower's native Soil to be reduced.
b) the use of opium Subgrade (soil compaction) Use of opium is a process in which material dipadatkan Soil, so that the volume of empty space (void) of Soil in the first place will be off the air so heavy volume of soil will be increased.

2) stabilization Chemicals (chemical stabilization of soil) Chemical soil stabilization in soil stabilization is a way to add or blend with the native Soil of other chemicals. Of chemical soil stabilization include:

a) soil stabilization with lime (lime stabilization)
b) soil stabilization with cement (cement stabilization)
c) soil stabilization with asphalt (bituminous stabilization)
d) and stabilization with other materials such as fly ash.

2.3 Mineral Particles Of Clay

Soil is a clay sized less than 0.002 mm. Particles is the main source of cohesion in a cohesive soil (Bowles, 1991). Loam soil is the Soil that is up to the microscopic size of the sub microscopic corrosion that comes from the chemical elements of rock composer, is very hard clay soil in the dry and the water level in the plastis are. At the higher water content clay is sticky (cohesive) and very soft (Das, 1994)
Nature of the clay soil was as follows (Hardiyatmo, 1999):

a. Fine grain size, less than 0.002 mm,
b. Low permeability,
c. The increase in capillary high water,
d. Are very cohesive,
e. Rate decrease of flowers,
f. Slow process of consolidation.

Fine grain soil, especially clay soil akan much influenced by the water. The nature of the soil clay will compacted greater on the clay in the dry compacted than the optimum compacted the optimum wet. In compacted the clay that is relatively dry optimum water shortages because of the clay has a greater tendency to sink in the water as a result is easy to use nature (Hardiyatmo, 1999).

The influence of water content is very big on the strength of clay soil. The addition of water will cause the distance between long distant grain tensile strength so that the interesting inter-grain will be reduced. Conversely, if the water content in soil is reduced to (dry), then the water will form a thin layer of water (water film) around the cavity between the grain and cause a high voltage capillary. Capillary voltage was formed by the surface tension of water will increase the strength of clay soil slide.

2.4 Coconut fiber

Coconut fiber, coconut skin and consists of fibers embedded in the skin in between the hard (coconut shell), in which approximately - approximately 35% of the total weight of mature coconut, coconut for a different variety of Percentage above will be different too. (Budi Lestariyo).

Composed of coconut fiber on mineral and organic elements, namely; hemisellulose and pectin (which is a component dissolved in water), lignin and sellulose (components that are not soluble in water), potassium, calcium, magnesium, nitrogen and protein. Comparison of the components depending on the age of fiber kelapanya. Lignin in coconut fiber fiber ranged from 40 to 50%.

Fibers are relatively short-fiber, fiber cells throughout approximately - approximately 1mm diameter with 15 micron fiber a strand and consists of 30 to 300 cells or more, viewed from the cross cut. Fiber length of fibers ranging 15 to 35 cm diameter with 0.1 to 1.5 mm. Fiber fiber has a high floating power, resistant to bacteria, salt water and cheap, are the weakness is, can not pelleted with both the fiber and are rigid. (Budi Lestariyo).

2.5 Pavement Road

Pavement road is layers of material are placed on the Subgrade to receive the traffic load so that the burden of these (plus pavementnya own weight) can stand up by Subgrade. The goal of creating a structure pavement way to get a flat surface so that the vehicle can be through in all weather conditions. There are two types of pavement way, namely:

a. Pavement rigid (rigid pavement), in which the concrete material in general, have the strength to withstand the voltage enough so it would keep the traffic load.
b. Pavement flexible (flexible pavement), where only material mainly spread the traffic load to the bottom of the field with a wider base so that the Soil does not receive the load exceeds the bearing capacity..

To see pavement flexible arrangement can be seen in the image on 1 as follows:

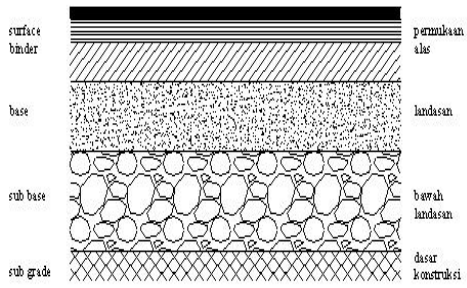

Figure 1. Structure pavement flexible

Flexible Pavement layer stack consists of:

1) surface course
Surface layer is created with the purpose of security and comfort of road users. Surface layer should be resistant to damage due to load and non load (Wear and tear). Asphalt is the material most appropriate for the additional surface layer pavement pelekat is flexible because the aggregate material and water-resistant.

2) base course
This section is located under the surface layer, working to prevent voltage collapse due to the high concentration of wheel load. Besides, the base layer provides for the surface layer.

Given the need to directly receive the wheel of a high voltage, then the quality of the material foundation layer must be high also. CBR is the minimum value of 80%. To get a high CBR value required gradation well.

For the foundation layer of aggregate is used preferably from the broken stone (stone crused). Aggregate of this kind have a high corner of the slide from the rounded aggregate (rounded) because the interlocking between the grains become more powerful.

3) subbase course
Layer beneath the foundation is part pavement that lies between the Soil basis (subgrade) and Lapis foundation (base course). Main function of this layer is part of the structure to spread the burden pavement wheels. Layer beneath the foundation to use this material, which is relatively cheap, so save the cost of construction.

Materials used in the foundation layer is a material non plastis, form there, silt or sand clayey. Layer below the foundation should have a CBR value of 25 when compacted with the water content field. However, if the material is good not much found, then the 10 cm top foundation layer can be replaced with lower-quality materials have provided CBR> 8 on the bad condition.

Layer beneath the foundation is not required if the Soil CBR basically more than 25. When CBR is <25, the necessary foundation layers down to the minimum thickness 10 cm.

4) Subgrade
Subgrade in the pavement is the original Soil surface has been improved with the use of opium or quality with stabilization chemicals. Strength and duration pavement road structure is highly dependent of the nature and resources to bearing capacity the Subgrade. According to requirements, minimum subgrade CBR road is 5%, while for the airport between 6% and 10%.

Improve the quality of the Subgrade (subgrade) will pavement structure provides a more economical. This included use of opium, but not often need to be a chemical stabilization.

2.6 Indek Propertis Soil

Testing Index Propertis Soil consists of testing the water content, weight and content and specific gravity which aims to see the physical attributes of Soil.

2.7 Atterberg Limit

Very important kind of grain on the ground is fine plastisitasnya. This is because the clay minerals in the soil. Plastisitas Soil is the ability to adjust to the changes in the form of a constant volume without fracture or fracture-crash. Depending on the degree of water, Soil can be liquid, plastis, semi-solid, or solid. Physical position on the smooth hard-ground water level is a certain consistency. (Qunik Wiqoyah, 2006).
Atterberg, 1911 (in Hardiyatmo, 1999), providing a way to describe the boundaries of the Soil of consistency with the hard-smooth considering the actual water content. Boundary is the limit of the liquid (liquid limit), limit plastis (plastic limit), and limit decrease (shrinkage limit). index elasticity (plasticity index) (PI) is the difference between liquid limit (LL) and the limit plastis Soil (PL)

2.8 Optimum Density

Aracteristics of soil can be assessed from the standard laboratory test called the Proctor test. This soil density test to determine the relationship between water content and density of Soil so that it can be a maximum density and optimum water content. Density is highly dependent on soil water content, the smaller the water content of the soil will be the greater, as well as reverse it. Its calculation using the equation 2.7 and 2.8 below:

a. content of heavy wet soil;

$$\gamma = \frac{B2 - B1}{V} \quad \text{.....(2.7)}$$

$B1$ = berat mold

$B2$ = berat tanah + mold

V = volume mold

b. content of soil dry weight

$$\gamma d = \frac{\gamma x 100}{(100 + w)} \quad \text{.....(2.8)}$$

w = water content after the use of opium

2.9 CBR (California Bearing Ratio)

CBR is a comparison between the burden of a material against the penetration of the standard depth of penetration and speed of the same. CBR is an empirical way to determine the strength of the Soil, other than the CBR is also useful to have boosted the value of Soil resources in densely maximum. CBR value is the price of the basic quality of the soil compared with the standard form of broken stones that have CBR value of 100% in the shoulder the burden of traffic. CBR can be divided in accordance with an example how to get the Soil that is the field CBR (CBR field inplace or CBR), CBR field rendaman (undisturbed soaked CBR) and CBR laboratory (laboratory CBR). CBR laboratory can be divided into two kinds, namely laboratory rendaman CBR (soaked laboratory CBR) and CBR laboratory without rendaman (unsoaked laboratory CBR) (Soedarmo and Purnomo (1997), Determining the value of CBR soil samples carried out against the use of opium is compacted with the standard. If the CBR value is determined with the soaking rendaman held for 4 days (96 hours). CBR rendaman test method is to asumtion the rain or when bad condition in the field that will provide the influence of the addition of water on the ground water has been reduced, so that it will lead to the development of a (swelling) and a decrease in strong bearing capacity of Soil.

Test results can be obtained by measuring the size of the load on a certain penetration. The amount of penetration as the basis for determining CBR penetration is 0.1 "and 0.2", is calculated with the equation 2.9 and 2:10 the following:

Penetrasi 0,1" (0,254 cm)

$$\text{CBR (\%)} = \frac{P1}{3x\,1000} x\,100 \ \% \text{.....(2.9)}$$

b. Penetration 0,2" (0,508 cm)

$$\text{CBR (\%)} = \frac{P2}{3x\,1500} x\,100 \ \% \text{.....(2.10)}$$

with:
P1: pressure test on the penetration of 0.1 "(g/cm3)
P2: pressure test on the penetration of 0.2 "(g/cm3)
From the second value is used in calculating the value of the largest

2.10 Swelling Potential

Clay minerals, grain size of soil, water content and index plastisitas highly influential on the swelling potential of clay

No	Test Type	Test No			Average
		1	2	3	
1	Water content	53.404	52.741	53.179	53.108
2	Unit Weight	1.623	1.408	1.495	1.509
3	Specific Gravity	2.631	2.525	2.463	2.5398

soil. Increasing the percentage of grain size based on the faction clay (0.002 mm) and index plastisitas on various clay minerals will increase the percentage of swelling potential (Chen, 1975). The addition of water in the ground kind of grain or fine clay will soil volume changes (swelling). Relationship between the swelling of the index plastisitas can be seen in Table1

Table 1 Relationships between the swelling potential of the index plastisitas

Swelling Potential	Indeks plastisitas
Low	0 - 15
Medium	10 - 35
High	20 - 55
Very high	>35

The addition of water in the ground kind of grain or fine clay akan soil volume changes (swelling). More details, the situation can be seen in Figure 2

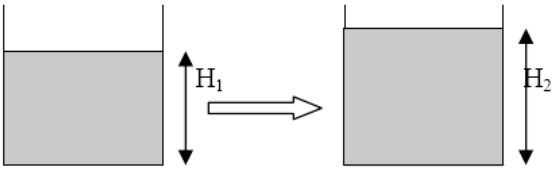

Figure 2. The influence of addition of ground water in hard-smooth

Swelling value can be calculated that occurred with 2:11 of the following:

$$\text{Swelling} = \frac{\Delta H}{H1} x100\ \% \text{.....(= 2.11)}$$

With:
ΔH=H2-H1
ΔH:he swelling due to increased water (cm), H1:high test substances before the addition of water (cm), H2:higher test object after the addition of water (cm).

4. RESULTS AND DISCUSSION

4.1 Data Material Testing Results

Test material consists of Index Propertis (water content, unit weight, specific gravity), soil particle gradation, and atterberg limit. This test aims to see the technical nature of the Soil that will be used in research. The test results index propertis and atterberg limit can be seen in Tabel 2 to 3 as follows:

Table 2 Analysis of Index Propertis Soil

No	Test Type	Test No			Average
		1	2	3	
1	Water content	53.404	52.741	53.179	53.108
2	Unit Weight	1.623	1.408	1.495	1.509
3	Specific Gravity	2.631	2.525	2.463	2.5398

Table 3 Analysis of Atterberg Limit

No	Test Type	Test result		
		LL	PL	PI
1	Atterberg Limit	52,33	44,94	7,39

Results of testing (Table 2) obtained water content from an average of three sample is 53.108% and the Unit Weight of soil on average is 1.509 gr / cm ³ and the average weight of soil types from three sample is 2.5398. With the value of 53.108% water content the soil including soil with high water content. In general, GS loam soil ranged from 2.5 to 2.9, the soil including clay.

Index Plastisitas very influential on the development potential of Soil that is the higher the index plastisitas akan large development potential.

Results of testing (Table 3) LL values obtained 52.33%, 44.94% PL. Based on the equality of 2.4 obtained Plastisitas Index (PI) 7.39%, according to the Atterberg, 1911, (Table 3) including the clay soil silty with plastisitas are.

3.2 Soil Testing

Testing consists of the Soil use of opium (Modified Proctor), and swelling potential CBR (California Bearing Ratio). The test aims to test the making of objects. test results opium den, swelling potential, and the CBR can be seen in sub-section 3.2.1 to 3.2.3 as follows:

3.2.1 Test for use of Modified Proctor

Soil use of opium is very dependent on the value of the volume of dry weight, the greater the value of the volume of dry Soil will be more compact. In data processing for Soil use of opium, to look for relationships between the degree of water (Water Content) and the volume of dry weight (Dry Density). This is useful to know the value of MDD (Maximum Dry Density) and OMC (Optimum moisture Content).
The value of MDD (Maximum Dry Density) and OMC (Optimum moisture Content) for each soil mix - coconut fiber can be seen in table 4 following:

Table 4 Results of each comparison test optimu mix

No	Comparison of Mixed	MDD (gr/cm³)	OMC (%)
1	100 % : 0 % (soil: coconut fiber)	1.11	34
2	90 % : 10 % (soil: coconut fiber)	1.20	30
3	80 % : 20 % (soil: coconut fiber)	1.21	29
4	70 % : 30 % (soil: coconut fiber)	1.19	31
5	60 % : 40 % (soil: coconut fiber)	1.03	44
6	50 % : 50 % (soil: coconut fiber)	1.09	39
7	40 % : 60 % (soil: coconut fiber)	1.08	35

MDD value is used to find the weight of the mixture for CBR (California Bearing Ratio) value by multiplying the volume of the MDD. While the value of OMC, is the number of degree of water required to obtain maximum density. So, when CBR test, the water depends on the value of OMC. To see the value of MDD (Maximum Dry Density) and OMC (Optimum moisture Content) on the comparison of each soil mixture - coconut fiber are presented in picture 4.2 and 4.3 below:

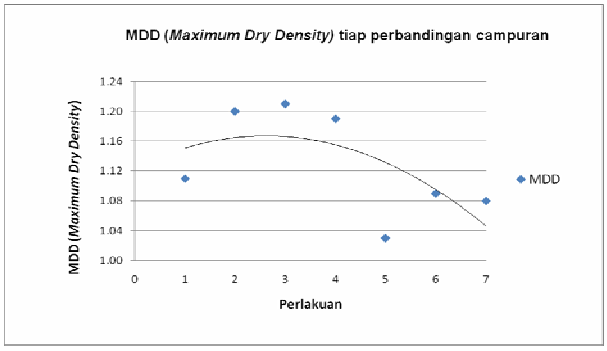

Figure 3. Graph MDD (Maximum Dry Density) for each comparison of a mixture

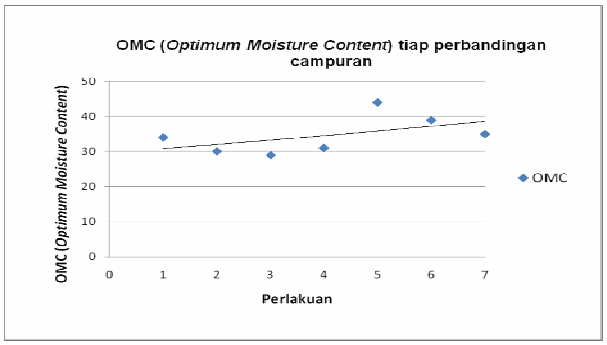

Figure 4. Graph OMC (Optimum moisture Content) for each comparison of a mixture

Graph of MDD (Maximum Dry Density) for each comparison mixture (picture 3) obtained a value MDD (Maximum Dry Density) occurred in a mixture of the highest 80%: 20% (soil: coconut fiber) with a value of MDD 1.21 gr / cm ³. MDD (Maximum Dry Density) compared to the native Soil, Soil with MDD mixture of coconut fiber to increase 10%. However, the addition of coconut fiber greater than 30% does not increase the effective density of Soil, can be seen from the picture MDD to decrease the value of 4.2 after mixing exceeds 30%.

Graph of OMC (Optimum moisture Content) of the comparison showed that the value of a mixture of OMC (Optimum moisture Content) occurred at the highest mix of 60%: 40% (soil: coconut fiber), as shown in Figure 4.

3.2.2 Test swelling Potential

Potential development of Soil resources to the very influential bearing capacity. If the potential to decrease the development of Soil resources to bearing capacity improved Soil. Swelling potential testing, soil testing after the use of opium in the Modified Proctor soaked Soil for 4 days. Then the swelling potential value can be searched with the equation 2.9. The swelling potential value for each comparison of soil mix - coconut fiber can be seen in table 5 below:

Table 5 Results of each comparison swelling potential mix

No	Comparison of Mixed	Swelling Potential (%)
1	100 % : 0 % (soil: coconut fiber)	66.67
2	90 % : 10 % ((soil: coconut fiber)	61.54
3	80 % : 20 % ((soil: coconut fiber)	55.56
4	70 % : 30 % ((soil: coconut fiber)	74.29
5	60 % : 40 % ((soil: coconut fiber)	71.43
6	50 % : 50 % ((soil: coconut fiber)	70
7	40 % : 60 % ((soil: coconut fiber)	75.67

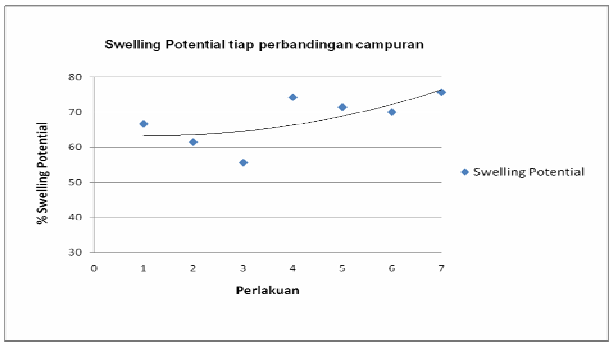

Figure 5. Graph swelling potential for comparison of each mixture

Figure 5 shows the relationship between the size of the development and comparison of Soil in the mixture after rendam for 4 days. Figure also shows that the lowest potential value of swelling occurred in a mixture of 80%: 20% (soil: coconut fiber) with swelling potential value of 55.56%. Large decrease compared to the native Soil that is 11.11%.

3.2.3 Tests for CBR (California Bearing Ratio)

Resources to bearing capacity the Subgrade can be estimated, among others, the practice of CBR checks. CBR value is one of the parameters used to identify resources to bearing capacity Soil planning in the basic layer pavement. When the Subgrade has a high CBR value, will reduce the practical thickness pavement which is located on the Subgrade (subgrade).

The value of CBR (California Bearing Ratio) for each comparison of soil mix - coconut fiber can be seen in table 6 below:

Table 6 Results of each comparison CBR test mixture

No	Comparison Value Mixed	CBR
1	100 % : 0 % (soil: coconut fiber)	0.99
2	90 % : 10 % (soil: coconut fiber)	3.19
3	80 % : 20 % (soil: coconut fiber)	3.19
4	70 % : 30 % (soil: coconut fiber)	2.98
5	60 % : 40 % (soil: coconut fiber)	1.29
6	50 % : 50 % (soil: coconut fiber)	1.10
7	40 % : 60 % (soil: coconut fiber)	2.10

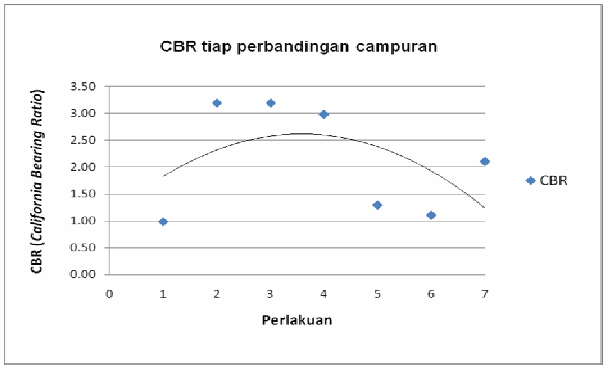

Figure 6. Graph CBR value for each comparison of a mixture

Mixing soil material with coconut fiber stabilizer which can increase the stability of the Soil value of CBR. Figure 6 shows the relationship between the size of the CBR value and the comparison mix. Figure also shows that the addition of coconut fiber is very good to increase the bearing capacity loam soil.

Figure 6 also shows that the highest values occur in the CBR mixture 90%: 10% and 80%: 20% (soil: coconut fiber) with a CBR value of 3.19%. Large increase compared to the native Soil that is 220%.

4. CONCLUSION

From the results of the research and analysis that was done then the conclusion can be drawn as follows:

1. The addition of coconut fiber in the clay soil can increase the bearing capacity of Soil, that is can be seen from the CBR test results obtained at the highest CBR value of the addition of 10% and 20% coconut fiber with the CBR value 3.19%, with large increase of 220%. 10% and 20% coconut fiber is the addition on the ground, because the composition of soil and coconut fiber is balanced.

2. Test results from use of opium obtained the highest density of Soil on the addition of 20% coconut fiber with a value of MDD (Maximum Dry Density) 1.21 gr / cm ^{3}, compared with the original Soil was increasing by 10%. Swelling of the test results obtained Potential Potential smallest value of swelling occurred on the addition of 20% coconut fiber, with a large decrease in 11.11% if compared with the native soil.

REFERENCES

[1] Bobby H. Ir. 1982, *Teori- penyelesaian mekanika tanah,* Terjemahan lengkap dari buku solution of problem in soil mechanics b h c sutton Surabaya, Yustadi ofset.

[2] Bowles. J.E., 1984, *Sifat-sifat Fisis dan Geoteknis Tanah (Mekanika Tanah)* edisi kedua, Jakarta, Erlangga

[3] Das, B.M., Endah N., Mochtar., I.B., 1988, *Mekanika Tanah (Prinsip-prinsip Rekayasa Geoteknis)* Jilid 1, Surabaya

[4] Hardiyatmo H.C , 2002, *Teknik Pondasi 1* , edisi kedua,Yogyakarta, Beta offset

[5] Lestariyo., B, '*Sabut Kelapa Sebagai Bahan Baku Interior Tekstil*', www.ikaittsttt.org

[6] N. Indra, Ambarwati Dwi., 1992, " *Studi Kemungkinan Abu Ampas Tebu Sebagai Bahan Stabilisasi Tanah,*" Tugas Akhir, Program Studi Diploma III Perhubungan Jurusan Teknik Sipil, Fakultas Teknik Sipil dan Perencanaan , Institut Teknologi Sepuluh November, Surabaya.

[7] Shirley LH, Ir. 1994, *Penuntun Praktis Geoteknik dan Mekanika Tanah (penyelidikan lapangan dan laboratorium)* ,Bandung, NOVA.

[8] Smith. M. J , 1992, Seri Pedoman Godwin, *Mekanika Tanah,* edisi keempat, Jakarta, Erlangga

[9] Wiqoyah, Q., 2006, dinamika TEKNIK SIPIL, Volume 6, Nomor 1,
Januari 2006 : 16-24 *Pengaruh Kadar Kapur, Waktu Perawatan dan Perendaman Terhadap Kuat Dukung Tanah Lempung,* Surakarta., eprints.ums.ac.id.

ISSN 114-1284

Predicting Crack Initiation Location on Adhesive Joint due to Multi-axial Loading

Irfan Hilmy

Mechanical Engineering Dept.
National Institute of Technology, Bandung 40124
Tel : (022) 7272215 ext 139. Fax : (022) 7202892
E-mail : irfan@itenas.ac.id

ABSTRACT

The behavior of damage parameters in adhesive bonding has been investigated in order to predict the location of the initial crack in the adhesive region. The research was started by investigating the interaction between the adhesive and its substrate in different types of joint configuration. The first natural choice was the simplest adhesive joint configuration known as Single Lap Joint (SLJ). It was found that although simple in loading condition which was tensile loading, stress state that occurred in the adhesive region was relatively complex. From analysis of the adhesive region it was found that damage initiated at a location where the von-Mises stress and Triaxiality have a maximum value. Although SLJ only expanded on axial load, the stress state that occurred can be categorized as multi-axial as indicated by the variation of the Triaxiality value. From this finding, it can be stated that for multi-axial stress states, Triaxiality is an important factors for crack initiation. Several adhesive joint configurations were considered, starting with the Butt-joints (BJ), the Cleavage Joints (CJ) and finally the Scarf Joints (SJ). The SJ was chosen since a simple relationship existed between triaxiality and adhesive bondline angle. Triaxiality can be determined numerically using finite element analysis and experiments. Finally, the damage parameters were constructed as a function of von Mises stress and triaxiality.

Keywords
Triaxiality, Damage Evolution, Finite Element, Experimental

1. INTRODUCTION

The definition of adhesive bonding is a process of joining two parts/structures using a non-metallic material (adhesive). The number of applications for adhesives in bonding structural components is rising rapidly. Interest is high in aerospace, infrastructure, automotive, marine, and biomedical communities.

The advantages of adhesive bonding are: a) microstructure unaffected, b) load distributed uniformly at right angles to loading direction, c) different materials and very thin parts can be joined, d) high strength in combination with riveting, e) metals with different electrochemical properties can be joined (insulating effect of adhesive), f) distortion-free joining and g) weight saving and light constructions.

The disadvantages are: a) limited form stability, process parameters must be held within very narrow range, b) change of properties of joint with time (ageing of adhesive layer etc.), c) complicated strength calculation, repair possibilities limited, d) low peeling strength, e) creep sensitive, f) complicated control of process, g) low adhesive layer strength must be compensated by large joining area, h) influence of time on process properties and i) low tolerance pre-treatment of joining parts surfaces.

1.1 Triaxiality of Adhesive Joints

Structural engineer in general considers that a uniaxial tensile test is suitable to describe the behaviour in structures. But, in a multi-axial loading state, this understanding needs to be updated. Scaffer et al. [1] stated that the void nucleation, void growth, and void coalescence models depend on the triaxiality. If the triaxiality value rised, tendency to failure increased. He also stated that a proper calculation of the triaxiality needs 3D non-linear analysis.

A unique behaviour of triaxiality is that it can be controlled by adjusting the geometry or loading mode. Barsoum [2] had performed research where triaxiality was controlled and was kept constant during the test by maintained the ratio between tension and torsion fixed. Decreasing the torsion will also decrease the triaxiality and vice versa. Seppala et al. [3] explained that void growth occurs because system tries to relax from an applied tension load in order to minimize the elastic energy. Material around the void will deform plastically to accommodate the void growth. Naturally, a plastic deformation emerges because of local shear stress that might occur from an applied load or from a stress field around the void, even if it is a hydrostatic stress.

Dutta and Kushwaha [4] found that a stress state is an important factor in a crack initiation and the strain failure. The stress state generally can be presented by the stress triaxiality, which has a very important role in ductile failure. Higher triaxiality value show how dominate a hydrostatic stress in stress field. On the contrary, a stress deviatoric component has important role compared to the hydrostatic stress at low triaxiality values. Void growth rate related directly to the stress triaxiality value and plastic strain accumulation. Scahfer et al [1] has performed a non-linear finite element analysis of a round bar with a notch, which was subjected to a small-scale tension load. They analysed

the stress levels at failure and found that the failure locations are consistent with the locations where the stress triaxiality are higher in all cases considered.

1.2 Investigation of SJ

Among many types of different adhesive joint configuration, a scarf joint has been investigated extensively and became a theoretical and experimental subject. This is due to a good mechanical property of this joint, regardless the type of loading applied. In fact, because of a substrate bevel shape, the loading due to bending moment caused by bad alignment can be reduced. Objois et al. [5] has researched the behavior of the SJ. The research is based on an analytical theory developed by Wasiama [6]. The theoretical equation is based on the following assumptions: (1) adhesive layer was far enough from ends of specimen where the load was applied so Saint-Venant assumption was still valid, (2) on the cross section of substrate, the normal stress distribution was homogeneus, (3) because thickness was small enough compare to other two dimensions, a plane strain assumption can be applied, (4) material of adhesive and substrate were assumed homogenous and isotropic whilst mechanical behavior was linear elastic and (5) on adhesive-substrate interface, where strain field was continuous, adhesion was assumed perfect.

2. TRIAXIALITY CHARACTERISTIC

Lemaitre proposed that in the field of damage mechanics, the stress triaxiality, not the von Mises equivalent stress, governs the damage process [7]. This is to say, to analyze a mechanical response of a construction with high constraint, such as the solder joints in electronic packaging where a thin ductile layer of solder alloy constrained by the surrounding rigid elastic substrates, the concept of stress triaxiality should be introduced [8,9].

A study about triaxiality is based on the fact that this variable has a very important role to determine a generalized damage solution. Because of its part in the damage evolution formula as one of the independent variable, theoretically, triaxiality can be controlled. In an experimental level, this means that the experiment should be designed and developed to such extent where triaxiality also can be controlled. To choose which adhesive joint is suitable for this purpose, an analysis whether theoretically or numerically should be carried.

Practical choice is of course a Finite Element (FE) analysis. Since calculation of triaxiality need a von-Mises equivalent stress and a hydrostatic stress at any point in adhesive layer, those values can be extracted directly. With the finite element analysis, no matter how complex the structure is, the triaxiality value can be obtained. It is contrary to an analytical solution where only limited solutions available for simple structures.

In the formula to calculate triaxiality, there is a variable T_x, which contains a von-Mises equivalent stress and a hydrostatic stress. The hydrostatic stress is a stress that can make an element shrink or grow without change in shape. Hydrostatic stress itself can be extracted from the principal stresses. Since the principle stresses are three stresses in three-dimensional direction, it raises question whether to use three-dimensional or two-dimensional analysis to extract stresses. Is it enough to model a joint as a two-dimensional element without sacrifying its accuracy? If triaxiality calculation can be performed in two dimensions, for example by using a plane-stress or a plane-strain assumption, the complexity and the computing time can be reduced.

The triaxiality is like a map of stress state of a structure in this case is an adhesive joint. The triaxiality is predicted unique belong to a particular type of the adhesive joint. The main issue presented in this chapter is the selection process of joint that has a good and simple relation between changing the load or geometry correlated with the triaxiality value. The triaxiality from several types of adhesive joints in three-dimensional model is evaluated and compared. Continue with a comparison between the three-dimensional and two-dimensional model.

3. TRIAXIALITY OF SLJ

SLJ geometry is shown in Figure 1. In this model, the adherends were made from 2014-T6 Aluminium with Young Modulus, E = 70000 N/mm, Poisson's Ratio, v = 0.33. The adhesive was made from FM-73™ film-form from Cytec. The material properties of FM-73 are as follow: Young Modulus (E) = 1211.25 N/mm^2, Poisson's Ratio, v = 0.38. The model uses a multilinear kinematic hardening material.

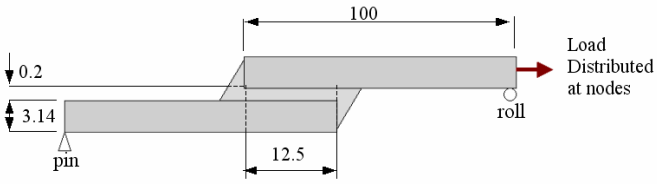

Figure 1: Geometry of single lap joints with boundary conditions

Several assumptions of FE modeling of a SLJ have been made. The SLJ has been modeled using a 2D plain strain element (Plane82 from ANSYS element library). This is a 2D higher order element. With the presence of nodes in the middle of element, this element has advantages: a) more accurate results for mixed (quadrilateral-triangular) automatic meshes and b) irregular shapes can be tolerated without much loss of accuracy [10]. Final meshing is shown in Figure 2.

In ANSYS, a hydrostatic stress is defined as NLHPRE. The following values are calculated from the two stresses results presented above.

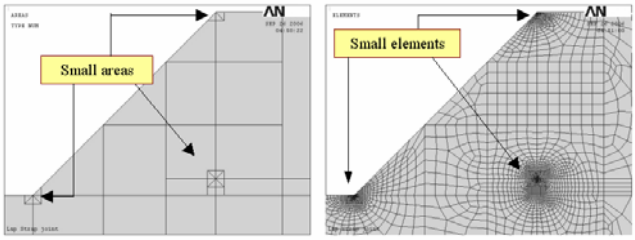

Figure 2: (a). Areas where the finest meshing sizes are located (b). Final Meshing

A triaxiality ratio is defined as:

$$T_x = \frac{\sigma_H}{\sigma_{Eq}} \quad (1)$$

The triaxiality function is defined as follow:

$$R_v = \frac{2}{3}(1+\nu) + 3(1-2\nu)T_x^2 \quad (2)$$

Where ν is *Poisson's Ratio* and T_x is *Triaxiality Ratio*. If the hydrostatic stress and the equivalent stress values are already available, a triaxiality contour of *Tx* (triaxiality ratio) and R_v (triaxiality function) can be calculated. Both stress results should be saved in a table so called the Element Table (ETAB), a facility available in ANSYS. With the Element Table, several mathematical manipulations of the stored data can be performed with its functions. For this purpose, the following functions are used: *Exponentiation*, *Multiply* and *Add* items. Triaxiality function is shown in Figure 3.

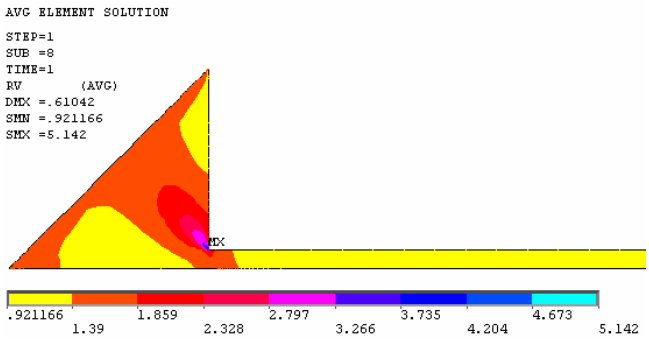

Figure 3: Contour of Triaxiality function (Rv) at load level 60%

4. TRIAXIALITY OF BJ

4.1 BJ under Tension loading

The first natural choice to analyze was a BJ under tension load. The BJ is modeled based on ASTM STP standard adapted from Prakash [11]. Based on the standard geometry, a three-dimensional model was developed as shown in Figure 4 by using Solidedge™. Model consists of four solid geometries. First two solid geometries represent substrate (upper and lower) and two other represent adhesive layer.

There are two reasons behind this modeling technique: (1) Firstly, an adhesive was modeled using two solids geometries because a finer meshing in the adhesive region was required. Since in ANSYS Workbench the stresses values in three layers of adhesive are needed. First and third layer are layers represent contact interface between the adhesive and the substrate (upper and lower). The second layer represents the adhesive layer in the middle of adhesive. (2) Secondly, it is easier to extract those stresses after the geometry model was imported to the finite element application; in this case is ANSYS Workbench.

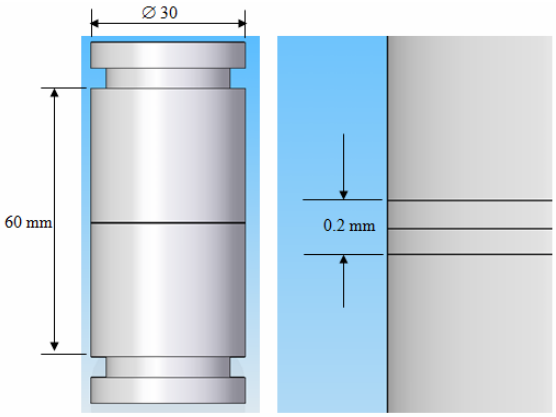

(a) (b)

Figure 4: CAD model of BJ (a) Overall model and (b) Zoom at Adhesive region

Next, the CAD model was saved in an IGES format because the ANSYS recognized this model as a solid model. To check that the contact between solids is attached properly, a continuity analysis is done by giving the same material property to all solid model, in this case is mild steel. If the contact regions were properly attached each other, no discontinuity in stress or displacement occurred. Figure 5 shows a comparison between a stress contour (a) before and (b) after real adhesive property (FM 73) was applied to the joint. From those analyses results, we can quite confident that the model is reasonable and the contact between solid models is perfectly match each other.

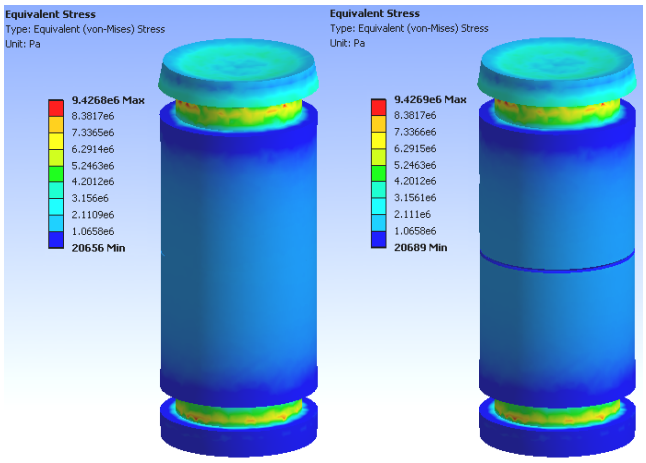

(a) (b)

Figure 5: Equivalent stress (a) before and (b) after including adhesive layer

After a contact model has been validated, next step was to extract stresses needed for calculating the triaxiality: a von-Mises equivalent and the three principal stresses since hydrostatic stress can be calculated by averaging all of the principal stresses. Using the function *Meshgrid*, a triaxiality result then is plotted as surface function and shown in Figure 6.

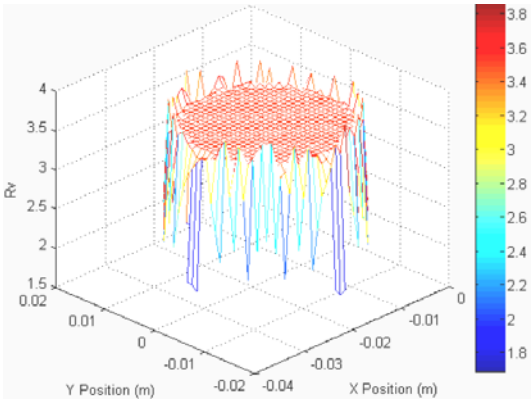

Figure 6: Triaxiality values of mid-layer adhesive BJ under tension load after refinement, F = 1000N

From Figure 6, it is shown how an edge effect contributes to the curve shape. At the edge, singularity problem exists and raised von-Mises equivalent stresses. As a consequence, the triaxiality values drop at the edges. If a finer meshing applied, the amount of dropped triaxility values will decrease. Now, consider values in the middle, the triaxiality values are nearly constant at 3.5. From the result, conclusion can be made that when an adhesive is subjected to a pure tension, the triaxiality will be 3.5. To check whether the triaxiality change when the tension load was changed, another analysis was performed with tension load was raised to 2000 N. No changes in triaxiality were found.

4.2 BJ under Torsion Loading

The analysis continued with a BJ with a torsion loading. The torsion is a common load for a circular shape beam like the shaft. The BJ will suffer a pure shear so it was predicted that a different triaxiality value with the one from tension load would exist. The result of triaxiality after mesh refinement is shown in Figure 7. A peak arise at the center of BJ where there is no torsion in that point. But the triaxiality value at peak is not much different and still at value 0.92. From this analysis, a conclusion has been made that for the case of pure shear, the triaxiality value was fixed at 0.92. From both tension and torsion analysis, general conclusion can be made that the triaxiality values for both cases lies in extreme values. A prediction has been made that the values of triaxiality always lie in between extreme values, 0.92 and 3.5.

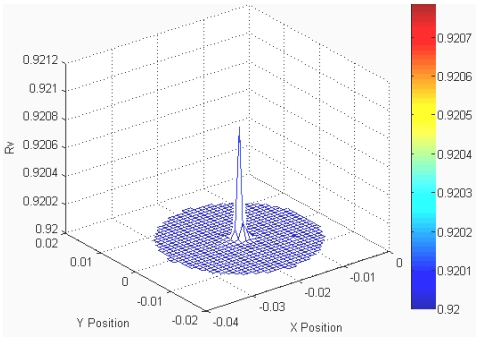

Figure 7: Triaxiality values contour of BJ under torsion T = 150 N.m after refinement

4.3 BJ under Mixed Loading

From the previous analysis, a prediction has been made that in order to control the triaxiality values in a BJ, a mixed loading between tension and torsion should be applied. To prove the prediction, two analyses will be compared. First load combination was torsion 150 N.m and tension 1000 N. The triaxiality result is shown in Figure 8. The result was nearly similar with the one in Figure 7 except the two observations: Firstly, the spike is not as sharp as the previous one which means more points have affected its values; Secondly, the peak had higher value, which is near 1.2. An interesting fact is majority of triaxiality still at value 0.92. It means that triaxiality for this case is still dominated by the torsion load.

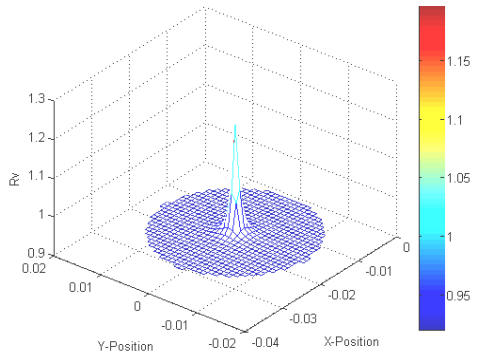

Figure 8: Triaxiality values contour of mid-layer adhesive BJ under mixed load torsion T = 150 Nm and tension L = 1000 N

A second load combination is considered with lowering the torsion became 15 N.m and held the tension at the same value 1000 N. The triaxiality result is shown in Figure 9. It is shown that the peak arises to maximum value nearly 3.5, which is a value at pure tension condition. More points also increase its value around the center and follow the parabolic shape. From this plot we can say that for this case the torsion is less dominant than the first case.

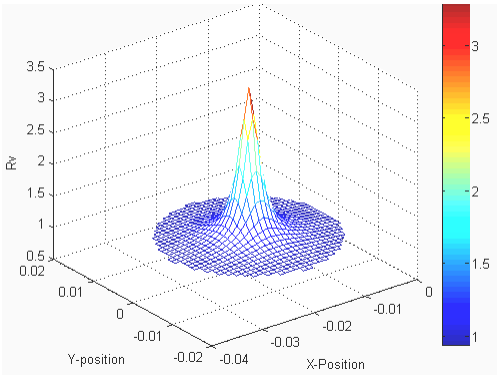

Figure 9: Triaxiality values contour of BJ under mixed load, torsion = 15 Nm and tension = 1000 N

From the two analyses, the effect of mixed loading can be seen and can be controlled by adjusting the combination values of both tension and torsion load. From all of the figures considered, the transition of triaxiality from different loading can be seen and understood.

5. TRIAXIALITY OF CJ

A CJ is a joint that can receive a mixed loading even tough it is only subjected to a tension load. The geometry of joint as shown in Figure 10 that makes one line of the tension load can be transferred into the tension and the bending. From its geometry profile, it is easily to predict that half layer of an adhesive bondline will suffer compression whilst the other half will suffer tension.

Analysis is performed to the CJ model, which is referring to the standard CJ adapted from ASTM D 1062 [12]. A modification has been made by change the thickness to 5 mm. The purpose of this changing is to lower the tension load needed to make this joint fail. Meshing is shown in Figure 10 (a). Boundary conditions were given with a tension load 1000 N distributed at the upper area of the hole in the upper substrate and fixed support at the lower area of the hole in the lower substrate as shown in Figure 10 (b).

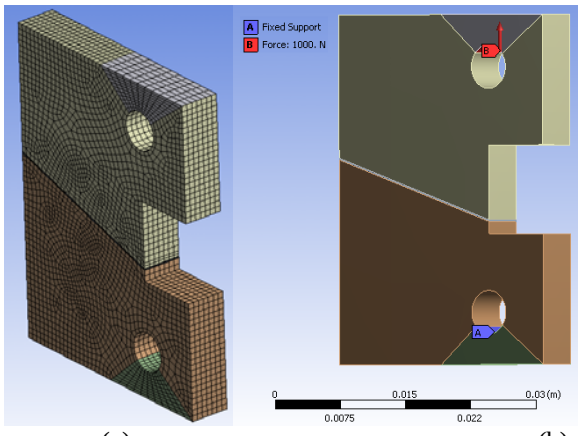

(a) (b)

Figure 10: Model of 3D CJ after modification: (a) Meshing, (b) Boundary conditions

As usual, to verify that the geometries have perfectly match at contact region, an analysis with material mild steel for all solid models, including the adhesive region, has been performed. The result is quite satisfying where no discontinuity values of the von-Mises contour stress across the adhesive region can be observed. The result then is compared with the one after the adhesive material insertion, FM 73. Now the adhesive layer can be seen from the von-Mises contour stress as shwon in Figure 11. Two observations can be noted as follow: (1) the stress concentration occurs near the hole was not affecting the adhesive region and (2) half of the adhesive layer suffer compression (left region of bondline) and half other suffer tension (right region of bondline). Like any structure, which was subjected to bending moment, there was a point along bondline somewhere near the middle that carries no moment.

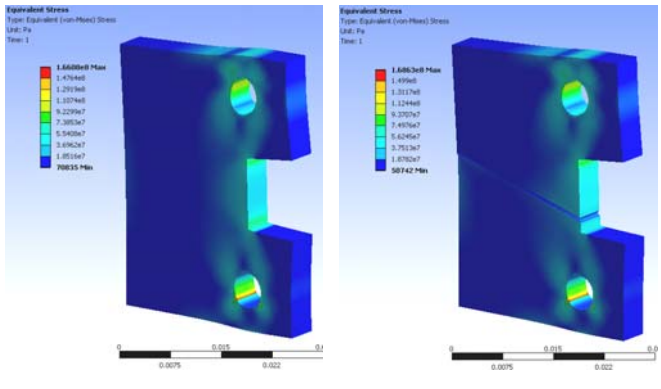

(a) (b)

Figure 11: Equivalent stress Contour and total deformation: (a) Continuous mild steel and (b) after adhesive material replacement

The result from a finer model is shown in Figure 12. As predicted before, there is a line across the thickness that has zero moment, which now is clear that this related to minimum triaxiality value, which is 0.92. From the legend, it can be seen that the range of triaxiality values is between 0.92 and 3.6, which is still consistent with the result from BJ.

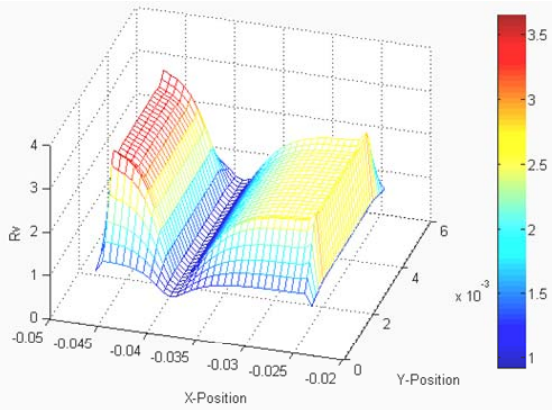

Figure 12: Triaxiality values of CJ in middle layer after refinement, bondline angle 18.5^{O}

A comparison will be made with a two-dimensional model using the plane-strain element. The purpose of this

comparison was to check whether its two-dimensional model can be used instead of the three-dimensional analysis. In region where singularity has no effect, it is likely that the two-dimensional model will be fit with the three-dimensional model. To compare both models, firstly, triaxiality values extracted from line in the middle by averaging triaxiality along two lines L1 and L2 as shown in Figure 13. The three points indicated reference points.

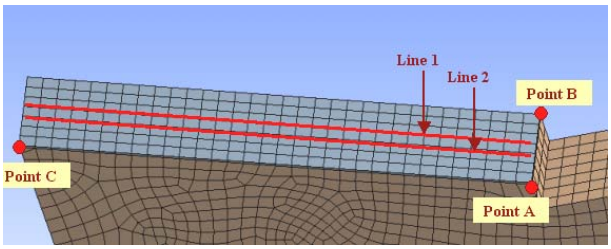

Figure 13: Notations in mid-layer of CJ model.

The result of average triaxiality value compared to the one from plane-strain analysis is shown in Figure 14. It is shown that the triaxiality profile along bondline from both results show good agreement. Discrepancy arises at edge because of the differences in meshing size. Small shifting of low region also occurs because the loading condition does not exactly have the same distribution. A load condition in three-dimensional model was applied on a surface while the load in two-dimensional model was applied at nodes.

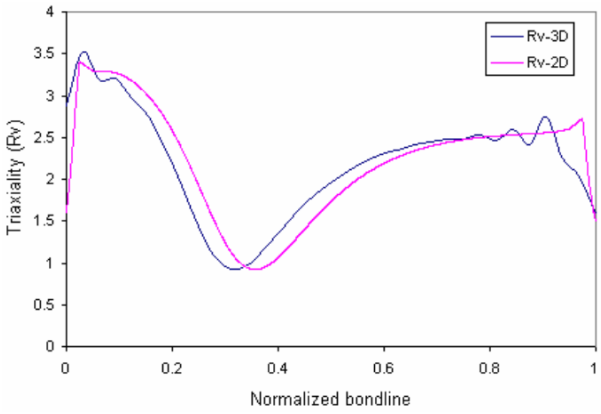

Figure 14: Comparison of triaxiality values of CJ between 3D and plane strain model, bondline angle 18.5^{O}

After a good agreement has been made between the three-dimensional and the two-dimensional analysis, for the next analysis, two-dimensional model will be used. Finally, it is important to check the effect of a changing orientation angle between the bondline and the horizontal line. The triaxiality of four different bondline orientation angles has been computed and displayed in Figure 15.

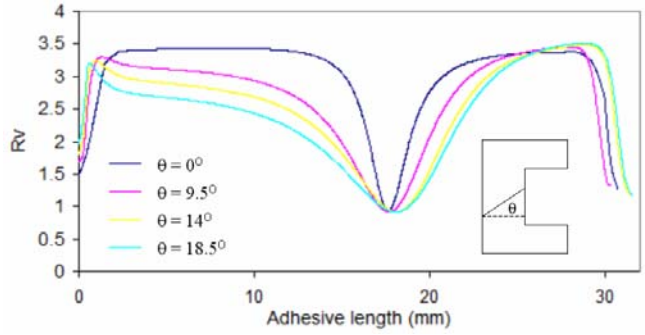

Figure 15: Effect of orientation to triaxiality value along bondline.

Figure 15 shows four triaxiality profiles along the bondline. Note that different end points existed because the bondline line is not the same and is not normalized. It was shown that at the elevation zero hence bondline is along horizontal line, majority of values were at maximum (like pure tension in BJ's case) except the narrow low peak at neutral line where the bending moment is zero. The change of the triaxiality profile can be seen here as the elevation rises.

6. TRIAXIALITY OF SJ

Another type of an adhesive joint, which has a simpler profile compared to the CJ, is the SJ. The load applied to the SJ is tension and co-linear hence no bending moment occurs. But, since the construction similar to the CJ where the orientation angle exists, the load applied transferred into tension and shear stress. The use of the SJ is quite common because larger contact area makes the joint stronger and can split the loading as described before. SJ model has been developed using the same technique as the CJ modeling and has shown in Figure 16.

After meshing is done, boundary conditions are applied in the green region with a fixed support at upper hole surface of upper substrate and force a 1000 N distributed at lower hole surface of lower substrate

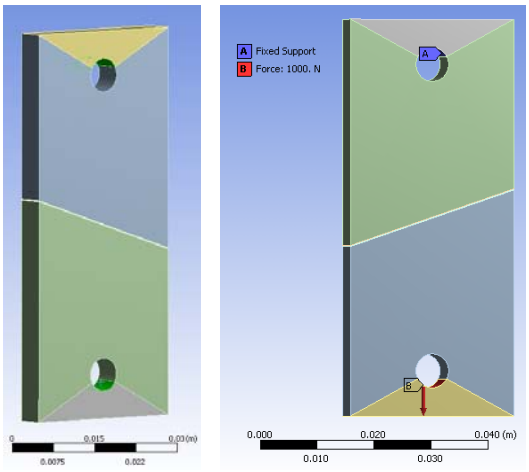

Figure 16: SJ model (a) Loading contact, (b) boundary conditions: Fixed support and distributed load

A static analysis of SJ with a mild steel properties applied to all solid models has been performed and are shown in Figure 17 (a). The contour of von-Mises equivalent stress is continues across adhesive geometry, which shows that a solid region adjacent to each other are in contact properly. Second analysis with real adhesive property, FM 73, is then performed and is shown in Figure 17 (b). Now the adhesive region can be seen. From this analysis, also it can be seen that the stress concentration near the hole does not affect adhesive region.

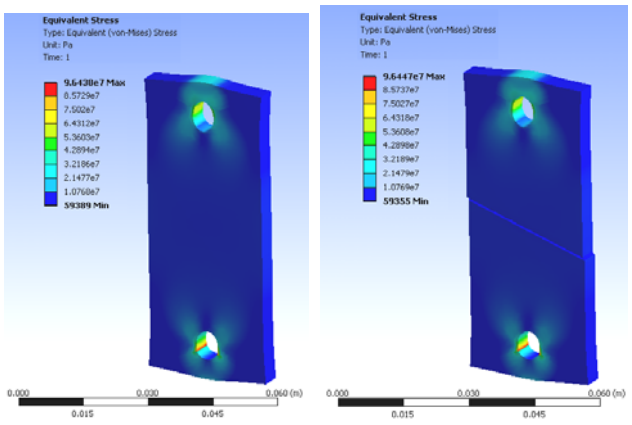

(a) (b)

Figure 17: Von-Mises equivalent stress contour of SJ (a) full mild steel, (b) after FM 73 inserted

The finer mesh have been made and analyzed with the triaxiality result is shown in Figure 18. Now, the triaxiality shape changes with the middle region far from the edge have nearly constant value of 1.67. Near the edge, the triaxiality values drop and a ripple effect also occurs. This ripple effect will be seen clearly in two-dimensional analysis comparison. The legend shows that range of triaxiality lies between 1 to nearly 1.8.

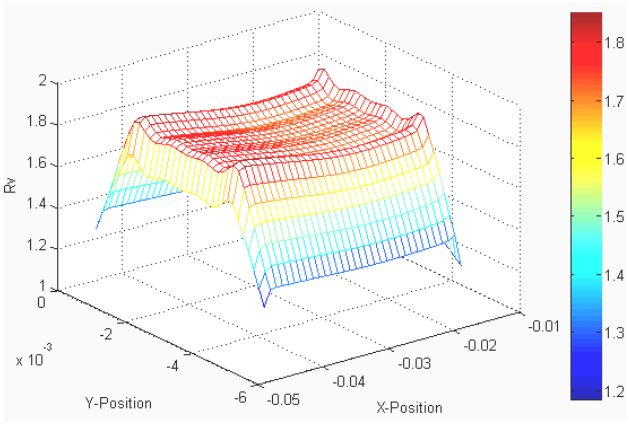

Figure 18: Triaxiality values of SJ in adhesive layer after refinement, bondline angle =18.5^{O}

With the same method as in a CJ, in order to compare a three-dimensional analysis with a two-dimensional analysis, the triaxiality value along the mid line needs to be extracted. Two-dimensional analysis has been performed using a plane-strain element. The comparison is shown in Figure 19. A slightly different result also occurs just like the one from the CJ result. The reasons of the difference are the fact that the boundary conditions are not exactly the same, which is the same reason behind the difference in CJ. From here, it is quite confident to state that the two-dimensional analysis can be used to represent the SJ model.

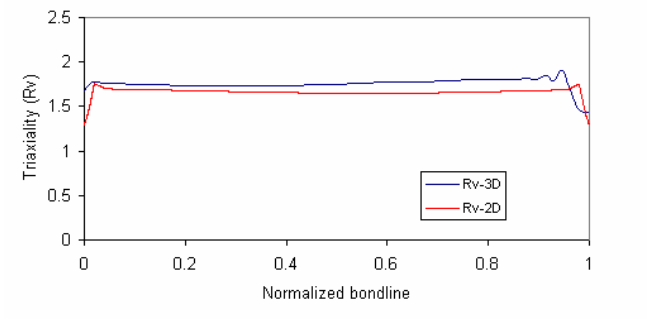

Figure 19: Comparison of triaxiality values of the SJ between 3D and plane strain model

Analysis continued for other orientation of bondline. Five different elevations /orientation angles are considered and the triaxiality results are shown in Figure 20.

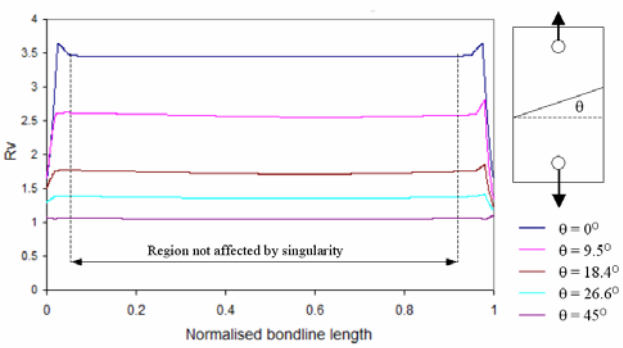

Figure 20: Triaxiality of the SJ as a function of orientation angle

It is clear now how a triaxiality profile change from no elevation specimen, where a maximum the triaxiality value exists, to the highest elevation, where the triaxiality value has minimum value. It is also shown that for every orientation, the triaxiality has constant value along its bondline region where the singularity has no effect.

7. CONCLUSION

After analyzing the three cases of loading in a three differents joint which are BJ, CJ and the SJ, conclusion can be made as follow:

1. The triaxiality (Rv) is not constant along bondline for two cases of joint: BJ and CJ

2. In a practical or a laboratory scale, adjusting and maintaining torsion-tension load combination at fixed value for BJ is a bit hard to implement.
3. Characterize of the triaxiality is influenced by the loading state and not just the geometry.
4. For a laboratory scale, a BJ and CJ are not easily implemented but from the finite element analysis, several important aspects related to the triaxiality behavior are covered and understand.
5. The triaxiality values along its bondline are constant for all orientation considered except a small region at ends, the triaxiality drops as the effect of singularity.
6. The constant value of triaxiality along its bondline is a good feature of this joint. Based on results in Figure 20, the triaxiality value versus angle can be fitted using least square method so the other triaxiality value for particular angle can be extracted.

REFERENCES

[1] BW Schafer and MS Zarghamee, *Triaxiality and Fracture of Steel Moment Connections*, Journal of Structural Engineering, October 2000
[2] I Barsoum, *Ductile Failure And Rupture Mechanisms in Combined Tension and Shear*, Licentiate Thesis No. 96, TRITA, HFL – 0407, KTH Solid Mechanics, Stockholm, Sweden, 2006
[3] ET Seppala, J Belak, RE Rudd, *Effect of Stress-Triaxiality on Void Growth In Dynamic Fracture of Metals: a Molecular Dynamics Study*, October 13, 2003
[4] BK Dutta and HS Kushwaha, *A Modified Damage Potential to Predict Crack Initiation: Theory and Experimental Verification*, Engineering Fracture Mechanics 71:263–275, 2004
[5] A Objois, J Assih, JP Troalen, *Theoretical Method to Predict the First Microcracks in a Scarf Joint*, The Journal of Adhesion, 81:893–909, 2005
[6] A Wasiama, *Analyse Theorique et Experimentale des Contraintes dans uns Assemblage colle a simple recouvrement du type sifflet, sollicite en traction simple en et fatigue*, PhD Dissertation, 1991
[7] J Lemaitre, *A Course on Damage Mechanics*, New York: Springer-Verlag, 1996.
[8] AG Varias, Z Guo, CF Shih, *Ductile Failure Of A Constrained Metal Foil*, Journal of Mechanics and Physics of Solids, vol. 39, pp. 963-986, 1991
[9] Y Huang, KX Hu, CP Yeh, NY Li, KC Hwang, *A Model Study of Thermal Stress-Induced Voiding in Electronic Packaging*, ASME Journal of Electronic Packaging, vol. 118, pp. 229-234, 1996
[10] Material Reference, ANSYS ver. 9.0
[11] V Prakash, CM Chen, A Engelhard, G Powell, *Torsional Fatigue Test for Adhesive Bonded Butt Joints*, Journal of Testing and Evaluation, Volume 23, Issue 3, May 1995
[12] ASTM D 1062-02, *Test Method for Cleavage Strength of Metal-to-Metal Adhesive Bonds*, Vol. 15.06, 2003

ISSN 114-1284

Crystallinity of Hydroxyapatite Made of Eggshell's Calcium and Diammonium Hydrophosphate

Kiagus Dahlan, Rahmi Solihat, Akhiruddin Maddu, Yessie Widya Sari

Department of Physics, Bogor Agricultural University, Kampus IPB Darmaga, Bogor, Indonesia
E-mail: kdahlan@ipb.ac.id

ABSTRACT

Most of eggshell nutrients contain $CaCO_3$ and, therefore, this calcium rich material could be used as bone implant starting material. The obtained calcium can be reacted with phosphate compound to produce hydroxyapatite (HA), a biomaterial whose composition and structure are almost similar to those of bone minerals. This research reported that hydroxyapatite (HA) derived from eggshell using hydrothermal method had been synthesized. Hydrothermal synthesis was held in a closed autoclave under controlled temperature and pressure. The starting material was chicken eggshell heated at 1000°C for 5 hours to remove their organic components and decompose the calcium carbonate into calcium oxide (CaO). CaO solution resulted from 5 hours calcination was then dropped by $(NH_4)_2HPO_4$ solution of several concentrations which were 0.06 M, 0.3 M and 0.6 M. This mixture remained for 8 hours inside the hydrothermal autoclave under two different pressures, 2 atm and 5 atm. Sample was then sedimentized through an aging process of 12 hours. Characterization using X-ray diffraction showed that the most crystalline HA in this experiment was resulted from 1 M calcined eggshell solution added with 0,6 M diammonium hydrophosphate solution at hydrothermal pressure of 5 atm. XRD analysis also showed that the HA volume fraction of this sample was very high. The same trend was also shown by FTIR spectra. SEM image presented that the particles were homogeneous and non-agglomerated.

Keywords
Eggshell, hydroxyapatite, hydrothermal, calcination, crystallinity

1. INTRODUCTION

About 95% eggshell nutrients contain $CaCO_3$. Therefore, this calcium rich material could be used as bone implant starting material to produce hydroxyapatite (HA), bone substituted biomaterial.

There are several methods for synthesizing HA. Some of them are wet method, dry method, hydrothermal method, and flux method. Hydrothermal method was chosen in this study in order to get well crystallized and non-agglomerated HA with homogeneous in size and shape. This method also has advantages like rapid heating, fast reaction and high yield [1-4].

HA is chemically similar to the mineral component of bones and hard tissues in mammals; its chemical formula is $Ca_{10}(PO_4)_6(OH)_2$. Several methods of characterization, which are X-Ray Diffraction (XRD), Fourier Transform-Infra Red (FT-IR), Scanning Electron Microscopy (SEM) and Energy Dispersive X-Ray Analysis (EDXA, may be employed to confirm the formation and characterize the material.

HA is a bioactive material. It has the ability to integrate in bone structures and support bone ingrowths without breaking down or dissolving. Therefore, it could be used as bone fillers in the forms of powders, porous blocks or beads to fill bone defects or voids [5-8].

This research was conducted to synthesize HA from chicken eggshells. Bio-based HA crystal is a potential biomaterial to serve as a biocompatible bone implant. Moreover, this implant might have its economical value as it uses chicken eggshells waste as the starting materials.

2. MATERIALS AND METHODS

The materials used in this research were chicken eggshells, diammonium hydrophosphate, $(NH_4)_2HPO_4$, and aquabides.
This research consisted of three experimental steps, which were eggshell calcination, hydrothermal synthesis and HA characterization.

2.1 Eggshell Calcination

Eggshells, firstly, were cleaned and heated at 1000°C to remove their organic components and decompose the calcium carbonate into calcium oxide. The sample color became white after heating. To find out the optimum duration of heating indicated by the largest amount of calcium oxide obtained, the heating was performed during 5, 10 and 15 hours. The optimum time was then chosen for further experiments.

2.2 Hydrothermal Synthesis

The calcined eggshells consisting the largest content of CaO was diluted by aquabides in three different molarities, which were 0.1 M, 0.5 M and 1 M. The CaO solutions were then dropped by $(NH_4)_2HPO_4$ solutions stoichiometrily keeping the ratio of Ca/P being 1.67. The concentrations of $(NH_4)_2HPO_4$ solutions, therefore, were 0.06 M, 0.3 M and 0.6 M. Each of these 3 solutions containing CaO and $(NH_4)_2HPO_4$ remained at pressure of 2 atm (120°C) and 5 atm (150°C) for 8 hours, respectively, in a hydrothermal autoclave.

After heating, sample was sedimentized through an aging process for 12 hours. Then, the sediment was gained by a process of filtering before heating at 110°C for 3 hours to remove water from sample. Finally, HA was obtained as white dried powder.

2.3 Characterization

XRD characterization used PHILIPS model APD 3520 diffractometer. FTIR characterization used BRUKER model TENSOR 37 FTIR Spectroscopy. SEM-EDXA characterization used JEOL JCM-35C scanning electron microscope. The sample was coated by gold-palladium (80% of Au and 20% of Pd) beforehand. Coating processes used an Ion Sputter JFC-1100 machine.

3. RESULTS AND DISCUSSIONS

3.1 Characteristics of Calcined Precursor

FTIR characterization resulted that there were some carbonate contents in all samples indicated by the presence of IR carbonate's group bands around wave number 1450 cm^{-1} and 875 cm^{-1}. Table 1 shows the percentage of transmission of carbonate groups. Samples heated for 5 hours had the least content of carbonate groups indicated by high transmission percentage which were 52% transmission at 875 cm^{-1} and 38% transmission at 1450 cm^{-1}.

Table 1: Percentage of transmission of carbonate groups

Heating time (hrs)	Percent transmission (%)	
	1450 cm^{-1}	875 cm^{-1}
5	38	52
10	38	47
15	23	33

This finding was emphasized by XRD results. Figure 1 shows the XRD patterns of eggshells heated at 1000°C for 5 hours. It was also found from volume fraction calculation that 68.27 % of the samples heated for 5 hours were calcium oxides.

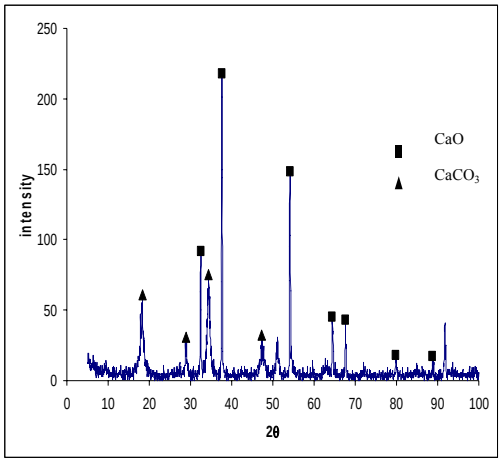

Figure 1: XRD patterns of eggshell heated at 1000 °C for 5 hours

Calcination processes of eggshells, that liberate CO_2 and leave CaO molecules, are reversible. Once the calcium oxide product has cooled, it immediately begins to absorb CO_2 from air. After a certain time, it is reconverted into $CaCO_3$ since Gibbs free energy decreases. Experimentally, therefore, cooling process has to be conducted rapidly.

3.2 Characteristics of HA

3.2.1 X-Ray Diffraction (XRD)

XRD characterization presented that all samples had similar peaks corresponding to hydroxyapatite (JCPDS 9-432), type A-carbonated apatite (JCPDS 35-180), type B-carbonated apatite (JCPDS 19-0272), and octa calcium phosphate (JCPDS 44-778). There were also two low intensity peaks indicating calcium oxides at 2θ > 50 degrees.

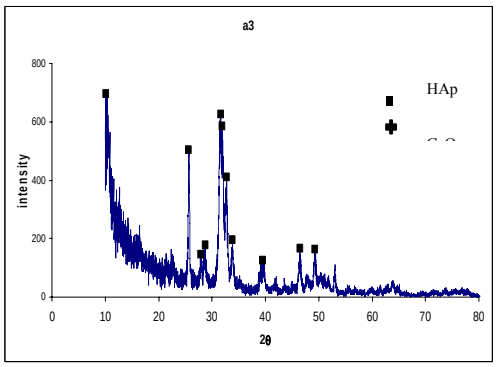

Figure 2: XRD patterns of highest precursor concentration samples pressurized at 2 atm.

Figure 2 shows the XRD patterns of 1 M CaO added with 0.6 M $(NH_4)_2HPO_4$ solutions pressurized at 2 atm.

Lattice parameters for hexagonal structure of HA were determined by using Cohen's method. Table 2 shows lattice parameters of the samples which are very close to reference. This high accuracy lattice parameters supported the conclusion that the samples were composed of HA.

Table 2: Lattice parameters of samples (reference: a =9.418 Å, c = 6.884 Å)

Pressure (atm)	Molarities (M)		Parameters (Å)	
	CaO	$(NH_4)_2HPO_4$	a	c
2	0.1	0.06	9.54	6.94
2	0.5	0.3	9.74	7.13
2	1	0.6	9.23	6.74
5	0.1	0.06	9.42	6.86
5	0.5	0.3	9.49	6.92
5	1	0.6	9.37	6.82

Volume fraction calculation revealed that samples with higher molarity precursor yielded higher mass product. Samples containing 1 M CaO and 0.6 M $(NH_4)_2HPO_4$ solutions pressurized at 2 atm resulted 8.6169 g mass product, while samples containing the same concentrations but pressurized at 5 atm resulted 8.436 g mass product.

Table 3: Mass product and volume fraction of all samples.

Pressure (atm)	Molarities (M)		Mass product (g)	Volume fraction (%)
	CaO	$(NH_4)_2HPO_4$		
2	0.1	0.06	0.6672	93.75
2	0.5	0.3	4.6104	96.13
2	1	0.6	8.6169	94.02
5	0.1	0.06	0.5811	92.05
5	0.5	0.3	5.023	89.00
5	1	0.6	8.436	95.61

Table 3 shows the mass product and the volume fraction. All samples showed volume fraction of more than 92%. Table 4 shows crystal size and crystallinity of all samples. Crystal size was varied and ranged from 28.37 nm to 106.37 nm. High crystallinity was presented by all samples with the degree of crystallinity more than 95%.

Table 4: Crystal size and crystallinity of all samples

Pressure (atm)	Molarities (M)		Crystal size (nm)	Crystallinity (%)
	CaO	$(NH_4)_2HPO_4$		
2	0.1	0.06	85.16	96.99
2	0.5	0.3	32.74	96.95
2	1	0.6	106.37	96.20
5	0.1	0.06	28.37	96.56
5	0.5	0.3	32.75	95.53
5	1	0.6	30.40	96.59

3.2.2 Fourier Transform-Infra Red (FT-IR)

All IR spectra showed the stretching and vibrational modes of OH^- groups at 3570 cm^{-1} and 635 cm^{-1}, whereas the bands derived from 635 cm^{-1} indicated groups of HA [9]. Considering sharp band at 635 cm^{-1}, 2-atm pressurized samples had less HA than 5 atm-pressurized samples. Another parameters corresponding to HA were the presence of PO_4^{3-} groups at 1090 cm^{-1}, 1034 cm^{-1}, 962 cm^{-1}, 603 cm^{-1}, 565 cm^{-1} and 472 cm^{-1}. Vibrational modes at 1090 cm^{-1} and 1034 cm^{-1} were categorized as asymmetry vibrational band indicating crystalline phase calcium phosphate compound. These two bands also explain that all samples performed crystalline phase. Figure 3 shows the FTIR spectra of all samples. The appearance of crack structure of phosphate absorption band at 565 cm^{-1} and 603 cm^{-1} also demonstrated the crystalline phase of the samples. Figure 3 shows that all samples had their cracks.

However, FTIR spectra also shows that there are some impurities, such as CH_3^+, OH^- stretch in H_2O and CO_3^{2-}. All samples indicated the existence of OH stretch, as a broad band at 3400 cm^{-1} and as a split band at 3570 cm^{-1}. The presence of carbonate also indication of type A- and type B-carbonated apatite. As the transmission is high, the presence of type A- or type B-carbonated apatite is minor.

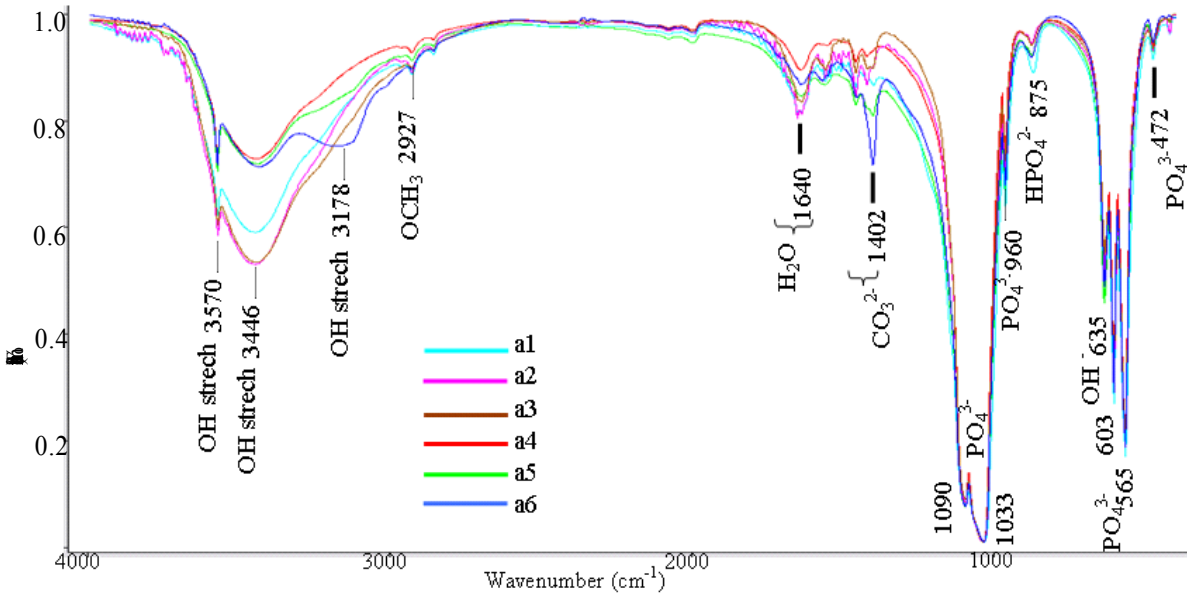

Figure 3: FTIR spectra of all samples (a1, a2, a3 containing low, high, higher precursor concentration, respectively, pressurized at 2 atm; a4, a5, a6 containing low, high, higher precursor concentration, respectively, pressurized at 5 atm).

3.2.3 EDXA and SEM

The results of EDXA are shown at Table 5, all samples had Ca/P value in the range of 1.3 – 1.7. Furthermore, EDXA emphasized XRD result in which samples are dominated by HA. EDXA also showed the compound exist in sample, which are CaO and P_2O_5 indicating precursor materials. Figure 4 shows SEM image with 20000-times magnification. It shows the homogeneous and densely arranged microcrystalline particles.

Table 5: Ca/P ratio of all samples

Pressure (atm)	Molarities (M)		Ca/P
	CaO	$(NH_4)_2HPO_4$	
2	0.1	0.06	1.675
2	0.5	0.3	1.726
2	1	0.6	1.420
5	0.1	0.06	1.354
5	0.5	0.3	1.644
5	1	0.6	1.531

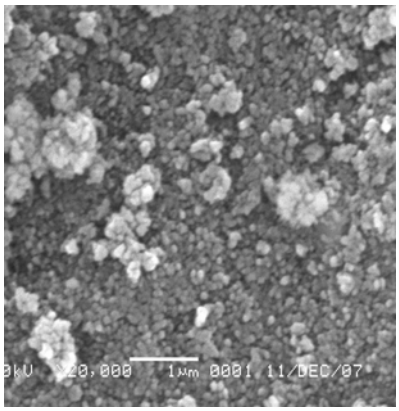

Figure 4: SEM picture of samples pressurized at 5 atm.

4. CONCLUSION

Hydrothermal method pressurized at 2 atm and 5 atm seemed to result highly crystalline HA indicated by XRD peaks and supported by lattice parameters very close to pure HA. However, some calcium oxide as starting materials still existed on samples. FTIR spectra also showed the presence of type A and type B carbonated apatite.

High precursor concentration and hydrothermal pressure resulted high volume fraction and mass product of HA. High crystallinity and small crystal size of HA were also obtained in the experiments. SEM image of this sample showed homogeneous and non-agglomerated particles.

5. REFERENCES

[1] K. Ioku, S. Murakami, T. Atsumi, Jeyadevan, and E. H. Ishida," Porous composite with tunnel like interconnecting pores of hydroxyapatite with magnetite particles," *J. Eng. Mater*, vol. 309, pp. 1039-1041, 2000.

[2] K. de Groot, "Bioceramics consisting of calcium phosphate salts," *Biomater*., vol. 1, pp. 47-50, 1980.

[3] M. Ashok, S. N. Kalkura, N. M. Sundaram, and D. Arivuoli, "Growth and characterization of hydroxyapatite crystals by hydrothermal method," *J. Mater. Sci.*, vol. 18, pp. 895-898, 2007.

[4] J. K. Han, H. Y. Song, F. Saito, and B. T. Lee, "Synthesis of high purity nano-sized hydroxyapatite powder by microwave-hydrothermal method," *Mater. Chem. Phys*., vol. 99, pp. 235-239, 2006.

[5] T. V. Thamaraiselvi, K. Prabakaran and S. Rajeswari, "Synthesis of hydroxyapatite that mimic bone minerology," *Trends Biomater. Artif. Organs*, vol. 19, pp. 81-83, 2006.

[6] Y. Z. Wan, Y. Huang, C. D. Yuan, S. Raman, Y. Zhu, H. J. Jiang, F. He, and C. Gao, "Biomimetic synthesis of hydroxyapatite/bacterial cellulose nanocomposites for biomedical applications," *Mater. Sci. Eng.*, vol. 27, pp. 855-864, 2007.

[7] M. Sivakumar, T. S. S. Kumart, K. L. Shantha, and K. P. Rao, "Development of hydroxyapatite derived from Indian coral," *Biomater*., vol. 17, pp. 1709-1714, 1996.

[8] M. Wang, "Bioactive materials and processing," in *Biomaterials and Tissue Engineering*, D. Shi, Ed. Springer, Berlin, 2004, ch. 1, pp.1-26.

[9] A. Siddharthan, S. K. Seshadri, and K. T. Sampath, "Rapid Synthesis of Calcium Deficient Hydroxyapatite Nanoparticles by Microwave Irradiation," *J. Trends. Biomater. Artif. Organs*, vol. 18, pp. 2-6, 2005.

ISSN 114-1284

Characterization of Aluminum Metal Matrix Nanocomposites Produced by Powder Metallurgy Process

Koswara[1], B. Soegijono[1] , Dedi Priadi[2].

[1]*Materials Science Graduate Programs, Faculty of Math and Sciences, University of Indonesia, Depok 16424*
[2]*Department of Metallurgy and Materials Engineering, Faculty of Engineering, University of Indonesia. Depok 16424*

E-mail : koswara@ymail.com, fadhil_net@yahoo.com

ABSTRACT

Aluminum metal matrix nanocomposites has been produced by powder metallurgy process. The aluminum powder and 10%, 20% and 30% weight of the SiC nanoparticles mixed in a mixing unit. The green body billet was obtained after the mixed particles pressed in a 10 mm diameter cylinder with a unidirectional 1 ton/cm^2 compacting force. The billets were sintered in an innert atmosphere at 620^{0}C that was known as solid state sintering and at 720^{0}C that was known as liquid phase sintering. The sintering was done in 2 hours time. The microstructures of nanocomposites when was sintered in 620^{0}C exhibit alpha grain of pure aluminum surrounded with nanocomposites. The nanocomposites that were obtained after sintering process in 720^{0}C exhibit homogeneous nanocomposites microstructures.

Keywords
Alumunum metal matrix nanocomposite, Powder metallurgy process

INTRODUCTION

Aluminum metal matrix nanocomposite is metal matrix composite that use nanoparticle to act as strengthening element. There are two type of manufacturing metal matrix nanocomposite. Powder process method and liquid process method. The powder process method have several type, such as mechanical alloying or mechanical attrition method, vapor deposition method and mixing method.
Generally, powder processes of metal matrix nanocomposites produced by mechanical attrition. This processes introduced the nanoparticulates into the metal powder by the use of planetary ball mill. The ball to powder weight ratio is at about 40 to 1. After the powder compacted and sintered, the particulates act as strengthening component in the metal matrices and increase the mechanical properties of the composite.
Differs from general powder metallurgy processes, this research use mixing process of SiC nanoparticles and aluminum particles in a mixing unit. Mixing process was done in 2 hours. The mixed powder then pressed in a cylinder and sintered in 620^{0}C and in 720^{0}C at 2 hours time in vacuum condition.
Because of the easy of manufacturing process, the mixing process can be done in larger quantity and can be applied to manufacture several industrial product.

EXPERIMENTAL

Samples consisting of 10 grams of aluminum powder each mixed with different content (10%, 20% and 30%) of nanoparticles SiC in a mixing unit. Mixing processes were done in 2 hours time. The mixer rotate at 3 rpm. The aluminum powder was obtained from Merck and the SiC nanoparticles was obtained from NaBond Technologies, Co, Limited, China. The samples then pressed in a cylinder to obtain 10 mm diameter to 30 mm length green body billet. Pressing force was carried out at unidirectional compacting force of 1 tons/cm^2. Before the mixed powders were poured to the cylinder, the cylinder wall was lubricated with zinc stearate.
The 10 mm diameter green body billets were inserted into a pyrex tube to undergo sinter process. The process was carried out in a vacuum condition. The tube was heated in a muffle furnace. Sinter processes at 620^{0}C and 720^{0}C were done 2 hours time. After sinter process, the billets were cut for metallographic investigation. Also, samples were taken from sintering process have undergone

microhardness testing. The tests were carried out in Vickers methods using 25 grams weight.

RESULTS AND DISCUSSIONS

Metallographic examinations in samples that were taken after sintering process indicated that some porosity occurs. Metallographic examinations used optical method. Figure 1 show that the porosity occurs in all areas of the samples.

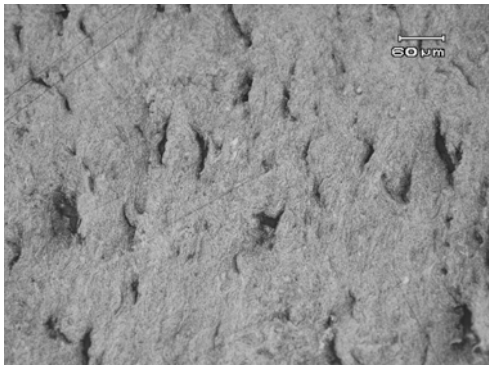

Optic, unetch, 200x

Figure 1. Porosity of the sample contain of aluminum and 10% SiC after sintering at 720^0C

Figure 2 shows metallograpic result of sample that was taken after sintering process at 620^0C. There are two types of microstructures, alpha grain of pure aluminum and composite microstructures surrounding alpha grains. The composite microstructures consist of SiC nanoparticles and aluminum matrix. The appearance of composite microstructures means that the outer areas of the aluminum particles liquefy and intrude the SiC nanoparticles and surrounded it with aluminum at the time of sintering process.

The hardness of the composite microstructures is similar between the samples at 100 to 120 Vickers Hardness Number. The hardness of the aluminum grain is at about 33 VHN

Figure 3 shows metallograpic result of sample that was taken after sintering process at 720^0C. Composite microstructures found over all of the sample area. It is indicating that the aluminum liquefy at the sintering time and intrude to all of SiC nanoparticles cluster and surround it with aluminum. Optical method in metallographic examination to the samples sintered in 720^0C can not differentiate the microstructures of different SiC content. It is because of lower magnification ability of the optic microscope.

The porosity which was still found in the samples sintered at 720^0C as can be seen in figure 1 indicated that the melting of the aluminum particles occurs at limited area. It is caused by the present of nanoparticles which thickens the aluminum liquid when aluminum liquid mixed with nanoparticles at liquid phase sintering time.

The porosity formerly comes after compaction process. The high ratio between length to diameter of billet at 3:1 causes this porosity. The application of zinc stearate can not resolve the problem if the ratio is too high. The porosity distributed evenly in all of the area of the billet. It indicate that compression force is not sufficient at all of the billet body and as the result of higher ratio of length to diameter. To eliminate the porosity, the ratio between length to diameter of billet must be maximum 1:1.

Also, the porosity was caused by the lack of sintering time. Although the sintering temperature at 720^0C or beyond the liquidus temperature and applied at 2 hours sintering time, it is apparently clear that the full density result is far from being reached. Finally, the porosity is still found after hot rolling process.

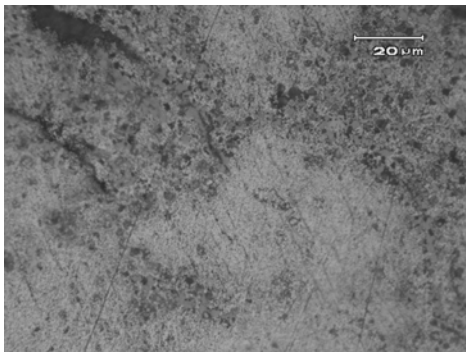

Optic, unetch, 1000x

Figure 2. Microstructure of sample contain with aluminum and 10% SiC after sintering at 620^0C. White area indicate alpha grain of pure aluminum surrounded with grey area of composite structure

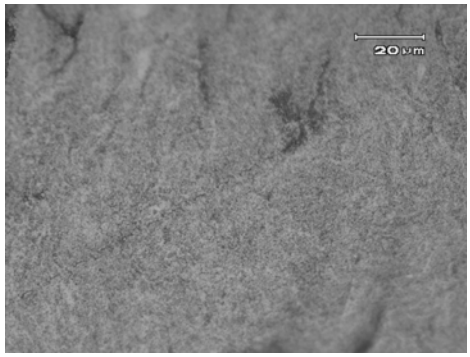

Optic, unetch, 1000x

Figure 3. Microstructure of sample contain with aluminum and 10% SiC after sintering at 720^0C sintering. Sample indicate homogenous grey area of composite structure

CONCLUSSION

Aluminum metal matrix nanocomposite can be manufactured by powder metallurgy process using mixing method. Sintering at solid state phase produce two types of microstructures, alpha grains of pure aluminum and composite microstructures surrounding the alpha grains. Sintering at liquid phase produces homogeneous nanocomposite microstructures.
Porosity is still found although sintering is done at liquid phase and after hot rolling process. The porosity can be eliminated if the ratio between length and diameter of billet maximum 1:1.

REFERENCES

1. Dr Josep Costa, J Fort, P Roura, G Viera, E Bertran, Ludo Froyen, *Microstructural Study of Mechanical Alloyed Aluminum with Nanometer Size Silicon Carbide Powder*, 1998 PM World Congress Metal Matrix Composites, Granada, Spain, 1998
2. Sie Chin Tjong, *Novel Nanoparticle-Reinforced Metal Matrix Composites with Enhanced Mechanical Properties*, Advanced Engineering Materials **2007**, *9*, No. 8
3. Claudio L. De Castro, Brian S. Mitchell, *Nanoparticles from Mechanical Attrition*, in *Synthesis, Functionalization and Surface Treatment of Nanoparticles*, Edited by M.-I. Baraton, American Scientific Publishers, 2002
4. Suk-Joong L.Kang, *Sintering, Densification,Grain Growth, And Microstructure*, Elsevier Butterworth-Heinemann, Oxford, Great Britain, 2005

Proceeding of the 11th International Conference on QiR (Quality in Research)
Faculty of Engineering, University of Indonesia, Depok, Indonesia, 3-6 August 2009
ISSN 114-1284

ANALYSIS OF MICROSTRUCTURE FORMATION IN AISI 304/316L DISSIMILAR STAINLESS STEEL WELDS

M. Anis* and B. Munir

Department of Metallurgy & Materials Engineering University Indonesia
Kampus UI Depok 16424 Indonesia
** Correspoding Author; email: anis@metal.ui.ac.id*

Abstract

*A welding of austenitic stainless steels of different types, AISI 304 and AISI 316 L was carried out using GTAW (Gas Tungsten Arc Welding) method with a straight polarity. A single-*V *groove was chosen and filler metals of E308 and E316 were used with argon shield. Weld metal's microstructure was evaluated using an optical microscope. The Cr_{eq}/Ni_{eq} ratio of the weld metal was found to be about 1.67 with ferrite number (FN) about 10. The microstructure was identified to have a ferritic-austenitic (FA) solidification mode termed type B. The morphology of delta ferrite formed was vermicular (skeletal) type. This type of microstructure has a typically good resistance to hot cracking and corrosion.*

Keywords: stainless steel, welding, microstructure

INTRODUCTION

Welding of austenitic stainless steels or commonly grouped as 300-series, contains 15-32% chromium and 8-37% nickel is one of the most practically carried out in industry. More than 90% of stainless steel welding involves the 300-series, mostly due to the good weldability of austenitic stainless steels. They are readily weldable with common arc processes such as; gas tungsten arc welding (GTAW), shielded metal arc welding (SMAW), gas metal arc welding (GMAW) processes and other techniques. Other important factors are the good corrosion resistance and mechanical properties both at low and high temperature. Weldments of 300-series stainless steels possess high toughness, even at the as-welded condition. Welding of dissimilar metals is usually applied for transitional joints in many equipment and constructions for economic reasons [1].

However, problems may arise in dissimilar metals welding such as improper choice of electrodes and welding parameters will result in welding defects. This work reports the microstructure formation in the weldment of dissimilar stainless steel 300-series using different electrodes/filler metals [2].

EXPERIMENTAL DETAILS

Plates of stainless steels AISI 304 and 316L 6mm in thickness were welded by Gas Tungsten Arc Welding (GTAW) Esab-Aristotig200 Sweden using E308 and E316L filler metals. A single V-type groove was applied in each specimen. The electrode is EWTh-2 2,4mm diameter using straight polarity. Argon was used as the shielding gas at 15 ft3/hour flow rate. The heat input for welding was controlled by varying the electric current and welding speed.

Microstructure characterization of the resulting specimens was carried out by optical microscope. All of the experiment and characterization was done at The Department of Metallurgy and Materials Engineering University of Indonesia - Depok.

RESULTS AND DISCUSSION

The area for microstructure evaluation in this report includes weld deposit and heat affected zone (HAZ) of both E304 and E316L.

As seen in figure 1 (a) and (b), it was found that the structure of weld deposit is dominated by austenite phase (bright area) with few delta ferrite (darker area). For the HAZ area, the structure is also dominated by austenite phase, as seen in figure 2 (HAZ of AISI 304) and figure 3 (HAZ of AISI 316L). The grain size of the HAZ is typically bigger than that of the base metals. This is mainly due to heating process during welding.

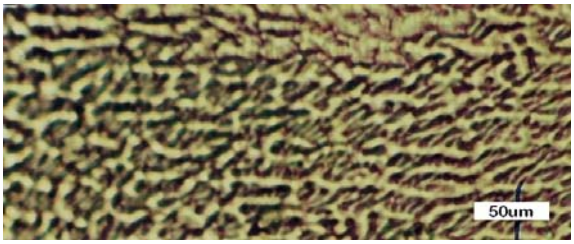

(a)

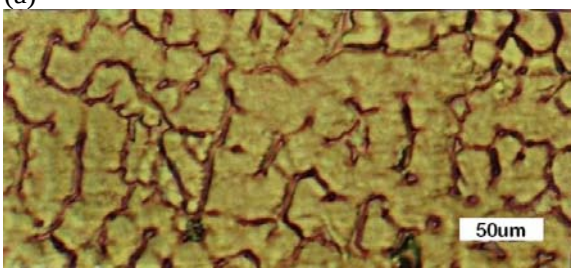

(b)

Figure 1. Microstructure of weld deposits, the dominant vermicular (a) and lathy (b) structure.

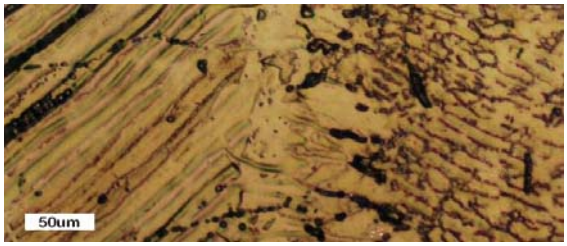

Figure 2. HAZ microstructure of AISI 304

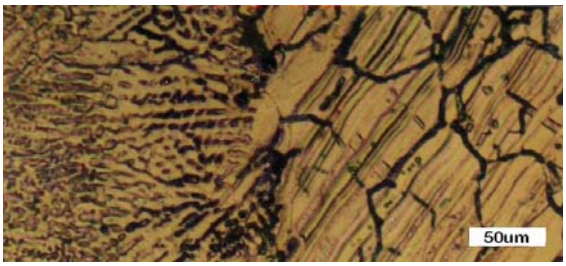

Figure 3. HAZ microstructure of AISI 316L

The weld deposit of AISI 300 steels can be classified into 3 types A, B, C based on their microstructure and the morphology of delta ferrite structure [3]. Nickel equivalence (Ni_{eq}) is the term used for the cumulative effects of austenite stabilizing elements as a weighted summation of their respective concentration levels while chromium equivalence (Cr_{eq}) is similarly the term used for the ferrite stabilizers [4]. The ratio of the two terms, i.e., equivalency ratio, is usually taken as Cr_{eq}/Ni_{eq}, based on the actual chemical composition of the steels involved, and can be used as a quantitative indicator for predicting the primary mode of solidification for arc (fusion) welded 300 series stainless steel. Since a small but finite amount of ferrite in the finished weldment is desired, weld pool solidification as primary ferrite is preferred to prevent the likelihood of encountering hot cracking during welding.

The use of applicable formula to calculate Cr_{eq} and Ni_{eq} is critical to predict the resulting microstructure [5]. A low Cr_{eq} / Ni_{eq} ratio produces austenitic solidification mode with type-A microstructure, while a high Cr_{eq} / Ni_{eq} ratio can produce a primary ferrite solidification mode with type-C microstructure. However, due to limited specimen availability in this research, only one method was applied for analysis of the microstructure.

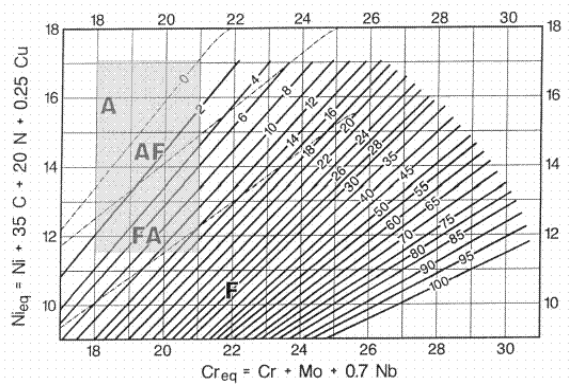

Figure 4. the WRC-1992 diagram for Cr_{eq} / Ni_{eq} of AISI 300 stainless steels

According to the specimen chemical composition and welding parameters, calculated heat input at 0.3 – 0.8 kJ/mm, the Cr_{eq} / Ni_{eq} ratio can be estimated at ~1.67 using Schaeffler formula. Hence, the microstructure can be classified as type B using the criteria proposed by Suutala [3], with ferrite content up to 10% dominated by vermicular morphology [6]. Moreover, using the WRC-1992 diagram [7-8] shown in figure 4, the weld deposit is predicted to have FN (ferrite number) ~10.

Referring to the Fe-Cr-Ni constitution diagram and putting the Cr_{eq} / Ni_{eq} ratio value to the diagram at the figure 4, the solidification mode of weld deposit is predicted to be Ferritic-Austenitic (FA). The FA solidification starts with delta-ferrite formation situated at the dendrites' axis and prefers to have vermicular or lathy structure depended on the value of Cr_{eq} / Ni_{eq} ratio.

The type B solidification starts with primary delta-ferrite solidification followed by

ternary phase reaction between liquid metal, delta-ferrite and austenite. Austenite formed between the ferrite dendrites through peritectic or eutectic reaction and then grew towards liquid metal and ferrite. The growth of austenite towards liquid metal promotes segregation of microstructure, while the growth towards ferrite through equiaxial or acicular mechanism caused drastic drop of ferrite volume fraction.

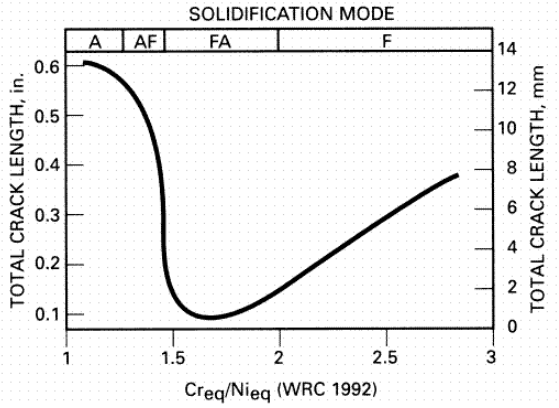

Figure 5. Cracking susceptibility based on WRC-1992 and Cr_{eq}/Ni_{eq} ratio [8]

Refer to the diagram shown in figure 5, the type-B solidification weld deposits produced in this research can be predicted to have good cracking resistance. The welding handbook describes the possibility for encountering weld solidification cracking increases dramatically at Cr_{eq}/Ni_{eq} ratios slightly less than 1.5 as the total crack length increases [9].

CONCLUSION

1. Welding of dissimilar stainless steels AISI 304\E308/316L and AISI 304\E316L/316L was carried out successfully.
2. Microstructure of the welds consists of ferrite at 10 vol-% in the austenite matrix.
3. The weld deposit has a Cr_{eq}/Ni_{eq} ratio ~1.67, which gives a type-B solidification. The ferrite number (FN) value was 10 and the morphology shows a *vermicular* structure.

ACKNOWLEDGEMENT

Special thanks to Mr. Z. Ismail and RH. Prabowo for specimen preparations.

REFERENCE

[1] Mersereau, C., Welding Journal, 77 (11), November 1998.
[2] Omar, A.A., Welding Journal, 77 (2), February 1998.
[3] Suutala, N., Takalo, T., and Moisio, T., Met.Trans.A, vol.10A, 1979.
[4] Suutala, N., Met.Trans.A, vol.14A, 1983.
[5] Suutala, N., Met.Trans., vol.13A, 1982
[6] Suutala, N., Takalo T, and Moisio T., Met,Trans.A, vol.11A, 1980.
[7] _____, American Society for Metals, Metals Handbook, 9th, vol.6, Metals Park, Ohio, 1983.
[8] Korinko, P and Malene, S , U.S. Department of Energy Reports WSRC-MS-2001-00544, 2001
[9] Anon, Welding Handbook, 8th Ed, Vol. 4., Materials and Applications Part 2., AWS, Miami, FL. 1998

Proceeding of the 11th International Conference on QiR (Quality in Research)
Faculty of Engineering, University of Indonesia, Depok, Indonesia, 3-6 August 2009
ISSN 114-1284

Failure Analysis of Automotive Lateral Control

M. Anis, Deni Ferdian, Winarto

Dept. Metallurgy and Material, Faculty of Engineering
University of Indonesia,
Kampus Baru UI Depok 16424
Tel : (021) 7863510. Fax : (021) 7872350
E-mail : deni@metal.ui.ac.id

ABSTRACT

Lateral control rod, which is a part of automotive differential system were failed during services. The lateral control rod system consists of a single rod with mass dumper welded and two joint at each side attached to the wheel system. Experiment procedure begins with examination by visual method followed by chemical composition of base metal. In addition, cross section of failed part was prepared for metallographic evaluation with hardness profile measurement accomplished by micro Vickers method. SEM equipped with EDS analysis was used for fractography and microanalysis examination. Observation of the fracture surface showed brittle fracture mode with beach mark propagation and chevron mark along the rod circumference. The lateral control rods at one point have a direct surface contact to the mass dumper which later on becomes a stress concentration. Lateral rod failure was initiated from the bottom area between the rod and the mass damper. The repeated load receive creating a radial or beach mark pattern and followed by chevron mark as the final fracture.

Keyword :
Lateral control, welding, stress concentration, brittle fracture

1. INTRODUCTION

Lateral control rod, which is a part of automotive differential system were failed during services. The unit was failed after three months in services. No information regarding the serviceability of the part or operational condition. The rod was made from carbon steel complied with JIS G 3445 - STKM 11A [1]. The lateral control rod system consists of a single rod with mass dumper and two joint at each side attached to the wheel system, as seen in Figure 1. The failed section of the rod was located at the area adjacent to mass dumper, as seen in Figure 2. The lateral rod part system was joined by welding method.

Figure 1. Lateral control rod (pointed) position in rear wheel system

Figure 2. As receive condition of failed lateral control rod

2. EXPERIMENT

Experiment procedure begins with examination by visual method and macro photograph on the failed part. Chemical composition of base metal was analyzed by optical emission spectrometer. In addition, cross section of failed part was prepared for metallographic evaluation with Nital 2% used as etching agent. Mechanical properties were conducted by performing tensile testing and hardness testing which accomplished by micro hardness Vickers method. SEM equipped with EDS analysis was used for fractography and microanalysis examination of the failed surface section.

3. RESULT AND DISCUSSION

3.1 Visual Examination

Visual observation of the failed part showed that the main fracture took place at the rod, above the mass dumper plate, as seen in Figure 3. Fracture area occurs at 1/3 of the total length of the rod, adjacent to the mass damper.
Observation of the fracture surface showed brittle fracture mode with beach mark propagation and chevron mark along the rod circumference. The fracture started from the bottom area of the rod, which can be noticed from the dark color of the fracture surface (mark by a circle), as seen in Figure 3. The dark color at fracture area indicated that corrosion already occurred.

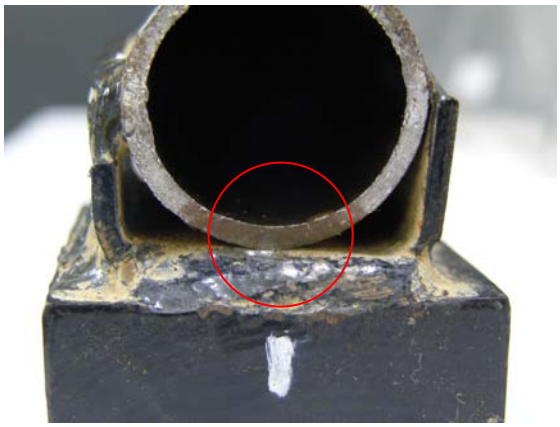

Figure 3. The main fracture showed at the bottom area of the rod. Dark color (corrosion product) covered the area of crack origin

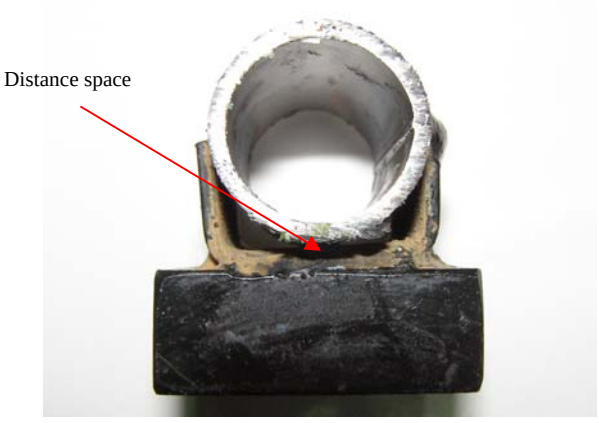

Figure 4. The gap between rod and mass damper

Visual observations also revealed there was a distance space approximately 2 mm between the rod and mass dumper, as seen in Figure 4. However, at the failed location those spaces were not existed. Observation at fracture origin showed an area indicated as point contact between the rod and mass dumper, as seen in Figure 5.

Figure 5. Point contact between the rod and mass damper, notice the bright appearance and slightly deformed

3.2 Chemical Analysis/Identification and Mechanical Properties

Some portions of the lateral control rod were subjected to the chemical analysis using optical emission spectrometer (OES). Chemical composition was complied with the specification JIS G 3445-STKM 11A.

Table 1. Chemical composition result of the failed sample in comparison to the standard JIS G 3445 - STKM 11A

	% C	% Si	% Mn	% P	% S
JIS G 3445-STKM 11A	0.12 max	0.35 max	0.6 max	0.04 max	0.04 max
Failed sample	0.042	0.011	0.192	0.013	0.007

The tensile testing was conducted at the base material of failure rod using a Shimadzu Universal Testing Machine. The average result of the tensile testing is 372 MPa for ultimate tensile strength (UTS) and 274 MPa for yield strength with the elongation of 38%. The ultimate tensile strength and the elongation conform to the specification of JIS G 3445 which minimum tensile strength required is 290 MPa and minimum elongation is 35%.
The hardness test was carried out on the cross section of lateral rod. This test was carried out in accordance with Vickers hardness testing method. The result, showed a value of 126 HV in average.

3.3 Metallography Examination

The microstructures of lateral rod were taken at the base metal, under a magnification of 100x and 500x, respectively. Based on the results, it can be seen that the microstructure of low-alloy carbon steel is dominated by ferrite and small amount of pearlite, as seen in Figure 6 and 7. No indication of abnormal non-metallic inclusion was found.

Figure 6. Microstructure in base metal of rod, mag 100X, 2% Nital etched, consist of ferrite and small amount pearlite

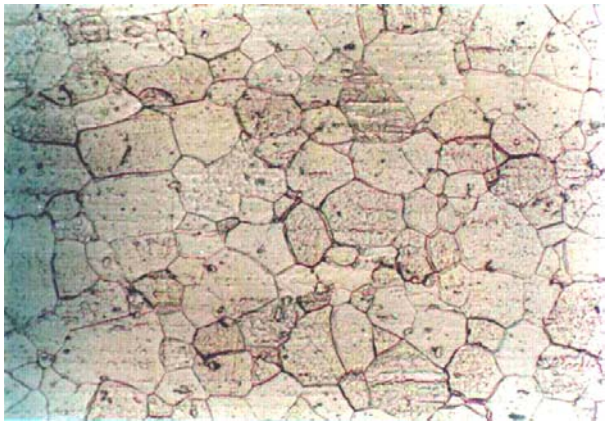

Figure 7. Microstructure of rod with higher magnification (500x) showed ferrite phase matrix.

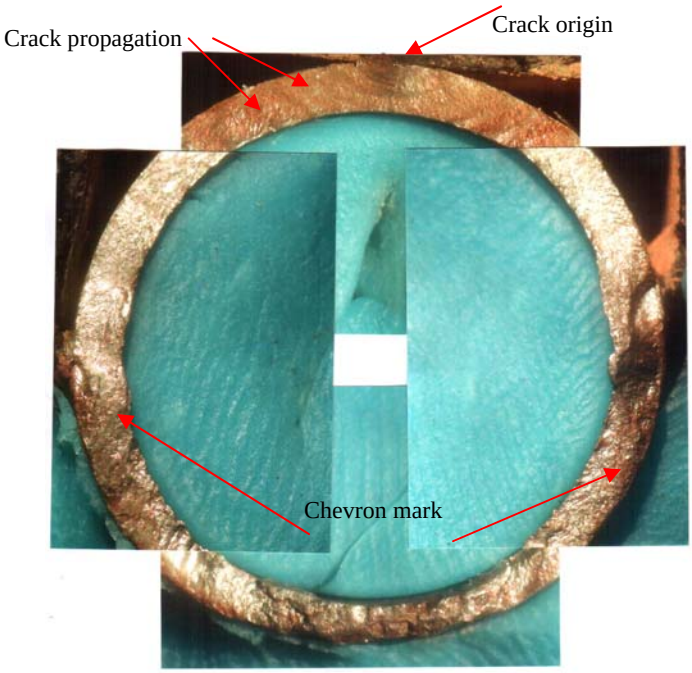

Figure 8. Surface fractography of failed rod, notice arrest line at crack origin and followed by chevron mark, mag 7x.

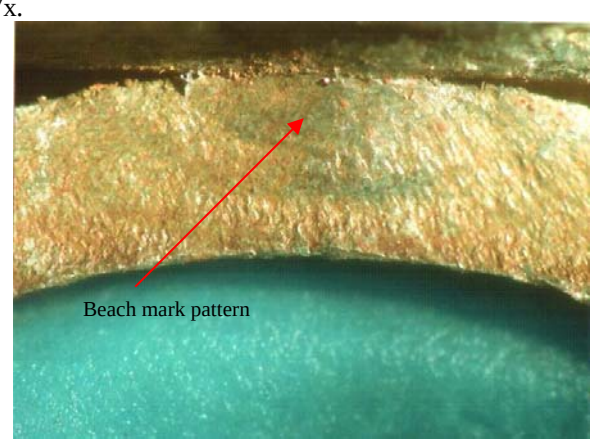

Figure 9. Closer examination at the crack origin showed a beachmark pattern, mag 20x

3.4 Fractography Examination

Fractography examination revealed that the facture occurred in two different modes, the fracture was initially a brittle mode, which can be recognized from the fracture mark creating a repeated line or beachmark as seen in Figure 8 and 9, and this was subsequently followed by chevron mark pattern. However, the SEM macrofractography result indicated that the surface of failed part was already covered with the corrosion product which makes it difficult to determine and examined the fracture origin, as seen in Figure 10 and 11.

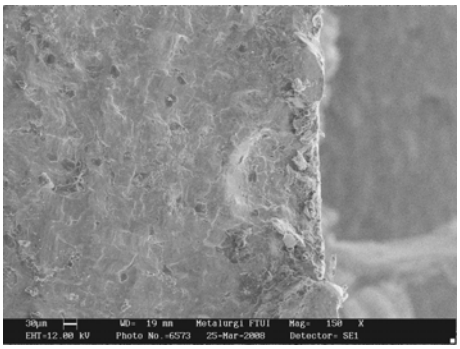

Figure 10. SEM fractography of the failed surface, taken at the chevron mark region, mag 150x.

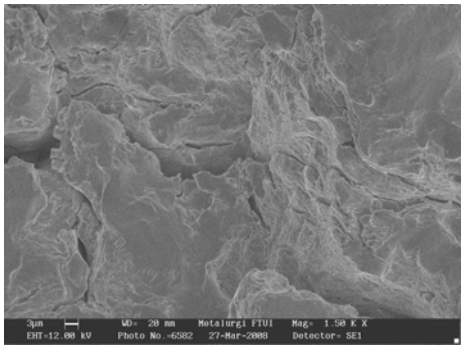

Figure 11. Closer examination revealed micro crack at the failed surface, mag 1500x.

A lateral control rod is a unit attached to the axle (differential) house and car body (chassis). It functions as a wheel stabilizer and therefore it has a vertical load modeling to balance the movement of the back wheels. Ideally, load or stress in the lateral control rod will be distributed uniformly along the lateral rod. The mass damper as a vibration reducer will help stabilizing the movement to prevent the damage caused by vibration. Mechanical testing and metallographic examination of the rod found conformity to the material standard.
Based on visual examination, the crack initiated from the bottom of rod adjacent to the mass damper then propagates upward until final failure occurred. Visual examination showed indication of fatigue failure. Fatigue damage result in progressive localized permanent structural change and usually occurs in materials subjected to fluctuating stress and strain [2]. Fatigue failures are caused by the simultaneous action of cyclic stress, tensile stress, and plastic strain. If any of one of theses three is not present, fatigue crack will not initiate and propagate [3-4].

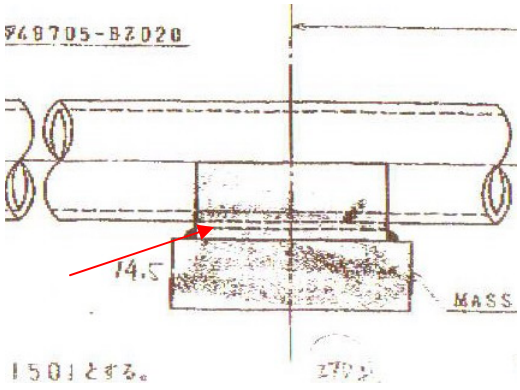

Figure 12. Clearance indication in the mechanical drawing of the lateral rod (mark by dash line).

Referring to the technical drawing of the lateral control as seen in Figure 12, it has been found that there is a differentiation between schematic and actual condition. The observation from the failed part showed that there is no clearance in one side of the mass damper as in the schematic. In other words, the mass damper is in outright position. This condition indicated that improper manufacturing process has already occurred. The lateral control rod which directly connects to the mass damper in one point contact will give a number of forces to the rod and mass damper themselves and therefore it become a stress concentration initiator.
When the car wheel moves, the cyclic (up and down) stress or load is received by the lateral control rod and is distributed evenly across the rod. However, in this failure case, the stress is disturbed and can not be distributed properly to the whole rod. One point contact becomes the point which receives the highest stress. As the wheels move, the cyclic stress or load will be frequently transmitted until the crack initiated. Load received at the lateral rod can be seen in Figure 13.
Crack initiation occurred in the body that has lower strength than other parts in the system. In this case, the mass damper has a better strength than the lateral control rod.

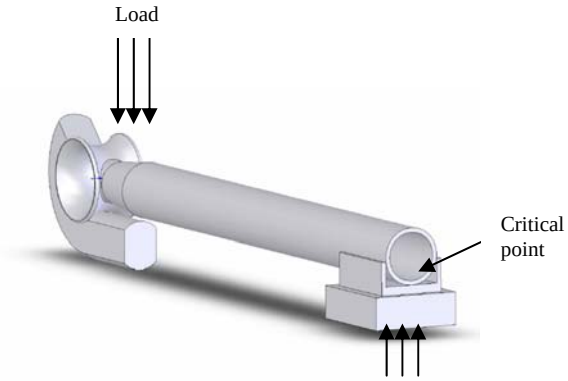

Figure 13. Schematic of load system received at the lateral rod.

The repeated load receive creating a radial or beach mark pattern and then they propagated slowly upward until the rod cannot accommodate the stress and failed in brittle manner indicated by chevron mark at the final fracture.

4. CONCLUSIONS

Based on the results of investigation, it was found that the lateral rod failure due to fatigue mechanism. The crack was initiated from the bottom area between the rod and the mass damper. This condition was occured due to the lack of clearance between them which created a high stress point at the rod. The stress received from the normal service condition was concentrated at that point, instead of being distributed along the rod. The repeated load receive creating a radial or beach mark pattern and followed by chevron mark as the final fracture. Improper and lack awareness in manufacturing during the welding process of lateral rod joint lead to this failure.

REFERENCES

[1]. JIS Handbook, *G 3445: Carbon steel tube for machine structure purposes*, Ferrous Material and Metallurgy II, Japan Standard Association, 2005, pp 1565-1575.

[2]. ASM Handbook, *Fatigue failure*, In : ASM Handbook Vol 11, Failure Analysis and Prevention, ASM Ohio, 2002, pp 700 – 727

[3]. E. B. Howard, *Atlas of fatigue curves*. In: American Society for Metals, 2nd ed. (Ed. E.B. Howard), John Wiley and Sons, New York, 1986. pp 1-15.

[4]. W.D. Callister Jr, *Crack initiation and propagation*. In: Materials Science and Engineering: an Introduction, 4th edition. (Ed., W. D. Callister, Jr.), John Wiley & Sons, Inc., New York, USA, 1997, pp 208-227.

An X-ray diffraction study of the effects of sintering on bovine hydroxyapatite

Muhammad Sontang*[a], Eny Kusrini[b], M.I.N. Isa[a]

[a] Department of Physical Sciences, Faculty of Science and Technology

Universiti Malaysia Terengganu, 21030 Kuala Terengganu, Terengganu, Malaysia

[b] Department of Chemical Sciences, Faculty of Science and Technology

Universiti Malaysia Terengganu, 21030 Kuala Terengganu, Terengganu, Malaysia

*Corresponding authors: Tel : 60-9-6683332; Fax : 60-9-6683326; E-mail: msontang@umt.edu.my.

ABSTRACT

A bovine bone has been sintered at temperatures up to 1100°C and the mineral content examined in detail by powder X-ray diffraction (XRD), energy dispersive X-ray spectroscopy (EDX) and scanning electron mcroscopy (SEM). XRD profile analysis data has been determined to characterize the microstructural features of the bovine bone at varying temperatures from 500 to 1100°C. The best XRD profile of bovine hydroxyapatite (HA) was obtained upon sintering treatment in vacuum at 1000°C for 3h. The crystal structure of HA from powder bovine bone is refined on powder XRD using the Rietveld analysis with molecular formula of $[Ca_{10}(PO_4)_6(OH)_2]$. The unit cell of HA is hexagonal with space group $P6_3/m$, a = b = 9.435 Å and c = 6.895 Å, v = 531.60 $Å^3$ and Dx =3.13 g cm^{-3}. The powder pure bovine bone had the interconnecting pore network in the surface structure. The findings are discussed in the context of potential bone substitute as well.

Keywords: Bovine Bone; Hydroxyapatite; Rietveld analysis; Sintering; XRD

ISSN 114-1284

1. Introduction

Bone is a complex, composite material with a mineral matrix commonly thought of as carbonated calcium hydroxyapatite (CHA) [1]. Because of the role of calcium phosphate in many biological processes they have been extensively investigated. This mineral has microstructural characteristics such as crystallite size, strain and stochiometry that are critical to bone physiology and function [2]. Operative treatment to replace bone that is lost due to accident or bone defects resulting inflammantion has remained a challenge for orthopedic surgeons. Due to the limited supply of natural bone for grafting, the need for bone substitutes which has the similar physicochemical and biological properties as a nature bone is ever increasing [3]. For example, the alternative treatment for bone defects is the use of xenogenous bone which is morphologically and structurally similar to human bone. Xenogeneous bone is usually from bovine bone and it is low cost.

The bovine bone is easy to obtain as a bio-waste, and available in unlimited supply. The organic part of bovine bone contains collagen and proteins while the inorganic part is mainly hydroxyapatite (HA) [4]. HA was derived from powder processing route has a great potential for bone substitute owing to its excellent biocompatible and high osteoconductive and osteoinductive non-toxicity, non-inflammatory behavior and non-immunogenicity properties [5,6].

Two factors important that can be affect the HA properties, i.e. (i) the temperature, and (ii) duration of heat treatment [7]. Therefore, the influence of heat treatment on bovine bone at low and high temperatures is of great important, thus it is not disrupt the HA phase stability.

In the paper we report the effect of sintering on bovine bone and phase purity of the HA by powder X-ray diffraction studies. The HA directly was prepared from bovine bone through sintering treatment. This study also attempted to investigate the physicochemical properties of the resulting HA when sintered in vacuum at different temperatures. The resulting HA is expected for use as a potential bone substitute.

2. Experimental

2.1. Sample preparation

A femur of an adult bovine (2 years 9 months old) was procured from Darma Jaya (Jakarta, Indonesia). The bone samples were cleaned to remove visible tissues and substances on the bone

surface. The clean bovine bone samples were defatted using a boiling followed with sun drying to remove the organic substances. This was done to avoid soot formation in the material during the heating treatment. The dried bovine bone samples were cut into rectangular prism shape of approximate size 10 mm x 10 mm x 10 mm. The bovine bone samples were sintered in vacuum by an electric Bohler furnace an automatic digital and rotary vacuum pump with pressure of 10^{-3} torr at different temperatures between 500°C and 1100°C using heating rate of 5°C/min for 2, 3 and 4 hours. The bovine bone pieces were cooled to room temperature by a slow furnace cooling followed by crashed using a mortar pestle and that sieved to obtain bovine HA powder (60 mesh).

2.2. Characterization

A powder specimen was spread on a non-reflective quartz specimen holder with a well depth of 0.2 ram. X-ray diffraction (XRD) intensity patterns for Rietveld refinement were obtained from an automated X-ray diffractometer. Phase analysis of bovine HA samples by XRD Shimadzu ZD 610 was carried out at room temperature using Cu Kα as the radiation source at a scan speed of 7°/min and a step scan of 0.05°. The crystalline phase compositions were identified with reference to standard JCPDS data available in the system software [8]. Crystallographic parameters of HA were determined based on the refinement of these XRD data by the Rietveld analysis and a computer program developed by Izumi [9] and Rigaku Limited Company. The unit cell parameters were refined together with several non-structural parameters; a zero correction of the 2θ experimental scale, the U, V, W and m profile function parameters defining the FWHM (full width at half maximum). The values of the refined non-structural parameters and the unit cell parameters are listed in Table 1. The refined fractional atomic coordinates and the occupation for the resulting HA when sintered at 1000°C for 3h are summarized in Table 2.

The microstructure of the sintered bovine bone was performed using a scanning electron microscopy (SEM Philips XL 30 series). Chemical analysis was also carried out using an energy dispersive X-ray spectroscopy (EDX) at 20 kV.

Table 1 Summary of crystallographic data for HA

Recording conditions	
Radiation	Cu Kα
Divergence aperture (°)	1
Receiving aperture (°)	0.2
Beam width (mm)	10
Angular range (°, 2 θ)	20-60
Step width (°, 2θ)	0.02
Count time (s per step)	30
Temperature	Room
Crystal data	
Molecular formula	$Ca_{10}(PO_4)_6(OH)_2$
System	Hexagonal
Space group	$P6_3/m$
$a = b$ (Å)	9.43505
c (Å)	6.89557
$\alpha = \beta$ (°)	90°
γ (°)	120
Z	1
Rwp and Rp	6.53 and 5.06

Table 2 Refined structural parameters and generalized coordinates of HA when sintered at 1000℃ for 3h

ISSN 114-1284

Atom	m	*x*	*y*	*z*	B (Å^2)
O(1)	6	0.33	0.47(7)	0.25	2.02
O(2)	6	0.59(9)	0.45(7)	0.25	1.84
O(3)	12	0.33(5)	0.25(5)	0.25	0.0
OH	2	0.00	0.00	0.00	1.0
P	6	0.40(4)	0.36(7)	0.06(5)	0.2
Ca(1)	4	0.3(3)	0.66(7)	0.25	0.6
Ca(2)	6	0.24(1)	0.00(5)	0.66(7)	1.2

Note:

m = number of atom

x,y,z = structure parameters

B = magnetic induction

3. Results and Discussion

3.1. Characteristic and general observation

The properties of HA produced by sintering in vacuum was evaluated over temperatures range from 500 to 1100^{o}C. A direct observation that was made upon sintering treatment at different temperatures was the color change of the bovine bone powder. The color of bovine bone at room temperature is light yellow. Upon sintering treatment at temperatures of 500, 600 and 700°C the color of bone samples changed to black and grey. After sinter treatment in the ranges 800-1100°C, the color of bone samples is white, indicating that complete removal of organic matrix (e.g. collagen and proteins).

3.2. XRD studies

The XRD profiles of HA between 900°C and 1100°C were similar and showed a substantial increase in peak height and a decrease in peak width. There is a marked decrease in peak widths between 500°C and 600°C and then a steady decrease to 800°C. Apparent at the higher

temperatures, the peak widths is sharper than at the lower temperatures. This indicates an increase in crystallinity and crystallizes size [3]. All the XRD data of the bone samples were in good agreement with the earlier report of the XRD structure of HA characteristic pattern (XRD JCPDS file No. 9-432) [8]. Comparison XRD profiles of synthetic HA and the resulting HA when sintered at 1000°C for 2, 3 and 4h are shown in Figure 1.

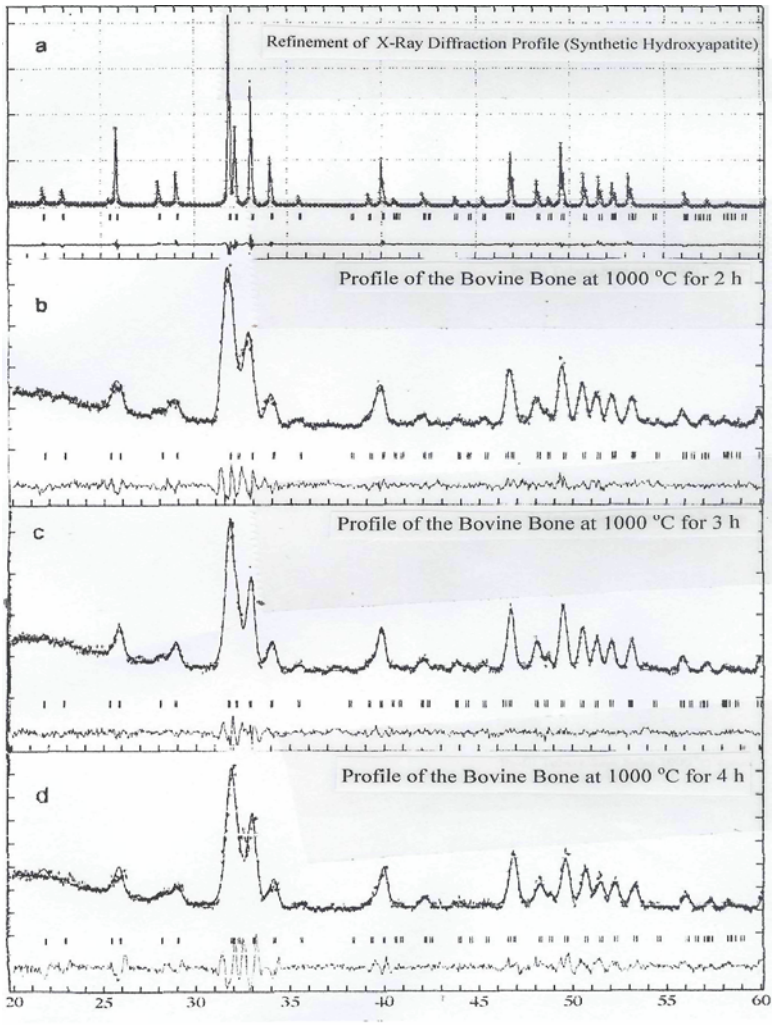

Figure 1 Comparison X-ray diffraction profiles of synthetic HA (a) and HA at 1000°C for 2h (b), HA at 1000°C for 3h (c) and HA at 1000°C for 4h (d)

ISSN 114-1284

Although decomposition of HA phases was not observed in bovine bone powder sintered up to 1100°C, dehydoxylation of HA has taken place. This can be observed by simply comparing the XRD peaks position of the sintered HA with the standard JCPDS data for stiochiometric HA [10]. The position of three diffraction peaks which corresponds to the (211), (300) and (202) reflection of sintered HA are very similar in position at temperatures between 900°C and 1100°C. These results indicate that dehydroxylation of the HA phase in bovine bone has occurred during sintering. The sintered bovine bone is hydroxyl carbonate apatite, which is benecial for biomedical purposes due to its similarity with the bone apatite. The position XRD peak of bovine bone exhibited 2θ angles of 31.65, 32.50 and 34.55° with the (211), (300) and (202) reflection, respectively. Upon sintering treatment at 1000°C for 3h, the position of XRD peaks of HA showed peak shifting due to dehydroxilation with 2θ angles of 31.85, 32.90 and 34.00° with the (211), (300) and (202) reflections, respectively (Figure 2). The best XRD profile of HA was obtained when sintered in vacuum at 1000°C for 3h.

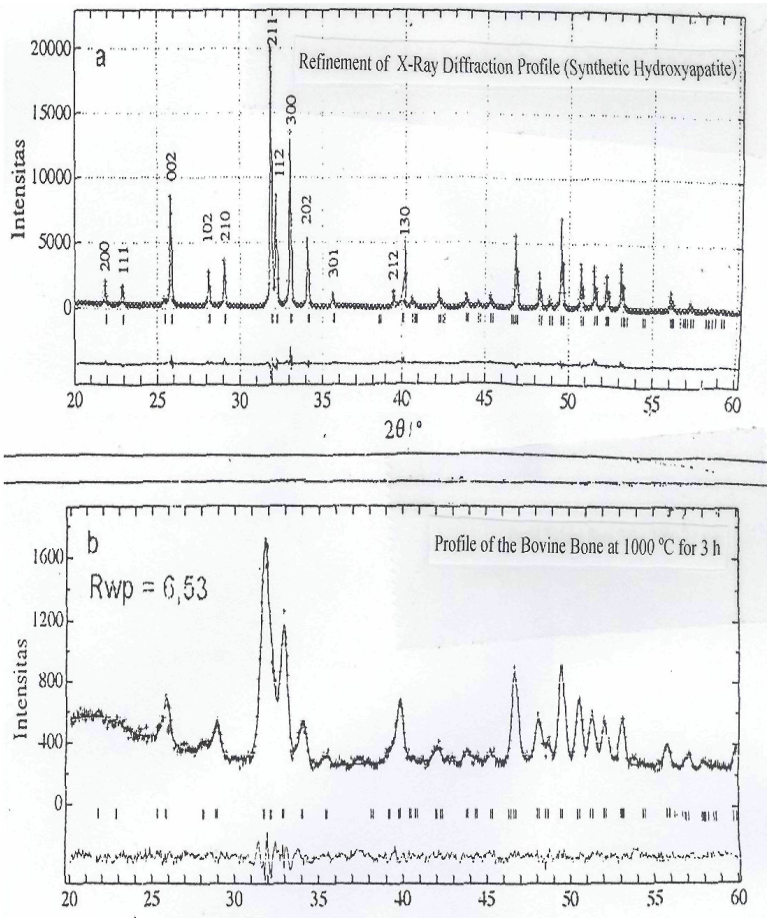

Figure 2 Comparison XRD patterns between the synthetic HA (a) and the resulting HA when sintered at 1000°C for 3h.

As the sintering temperature increased to 1100°C, the intensity of the characteristic peaks for β-tricalcium phosphate (β-TCP), which are located at 2θ angles of 27.75°, 31.65°, 45.55° and 48.0°, were observed to gradually increase. There is no evidence of β-TCP at lower temperatures. The present powder XRD data results suggest that the resulting HA stability in the bone matrix was not disrupted when sintered in vacuum up to 1000°C. XRD analysis also indicated the absences of secondary phases, such as calcium oxide (CaO). Thus, it suggested that bovine HA powder results in high crystallinity and single phase HA and is also believed to be pure natural HA as indicated by the peak of the diffraction patterns (XRD JCPDS file No. 9-432) [8].

All of the carbonated calcium hydroxyapatite (CHA) peaks (002) are clearly broader than those of the IRF (instrument resolution function). Line profile XRD analysis produced quantitative estimates of crystallite size at each temperature. The CHA peak is described in Figure 2 for the (002) diffraction peak.

In the present study, the crystal structure of natural HA is only observed upon sintering treatment at 1000°C for 3h. It is therefore interesting to compare the present results with previously refined cell parameters from HA. The refined values of a and c are in agreement with the earlier reported in the structural analysis of HA [11]. The crystal structure of HA has been reported by Aoki [11]. The bovine HA is crystallized in hexagonal with, $a = b = 9.43505$ Å and $c = 6.89557$ Å, $\alpha = \beta = 90°$ and $\gamma = 120°$, space group $P6_3/m$ and $Z = 1$ (Table 1). Molecular formula of HA from bovine bone has been characterized by powder XRD using the Rietveld analysis that is $[Ca_{10}(PO_4)_6(OH)_2]$ with number of calcium (Ca) = 10, phosphor (P) = 6, oxygen (O) = 24 and hydroxyl ion (OH^-) = 2 (see Table 2). The Rietveld analysis is particularly useful for obtaining accurate estimates of the unit cell parameters since they result from an overall optimization process involving strongly correlated effects such as the zero correction. The crystalline phase composition of sintered bovine bone is

similar with the natural bone mineral which is composed by [$Ca_{10}(PO_4)_6(OH)_2$], [hydroxyapatite, HA] of about 93% and $Ca_3(PO_4)_2$, [β-tricalcium phosphate, β-TCP] of 7% has been also reported by Martin [12].

The Ca(1) atom is lying on the threefold axis and coordinated to six oxygen atoms, which forms a twisted triangular prism. The Ca(2) atoms are situated around the hexagonal screw axis and are in an irregular sevenfold coordination with six phosphate oxygen atoms and the hydroxyl ion. The position of hydroxyl oxygen is shifted above or below the centre of the Ca(2) triangles. Only the one molecule HA in unit cell dimension was observed.

3.3. EDX analysis

A typical EDX spectrum shows the various elements that are present in the powder bovine bone matrix. The analysis indicated that the inorganic phases of pure powder bovine bone composed mainly of Ca and P as major constituents with some minor components comprising that are Na, Mg and O. The chemical compositions of pure bovine bone and human bone were similar. Thus, the resulting HA from pure bovine bone can be used for medical application as a potential bone substitutes. According the molecular formula of the standard HA, the Ca/Pa molar ratio is approximately 1.67 [3]. The Ca/P ratio of natural HA from bovine bone is approximately 1.65. This value lies within the acceptable for the HA.

3.4. Microstructure analysis

The microstructure of the pure powder bovine bone appears to be dense due to the presence of organic substances in the bone matrix. The morphology of pure bovine bone showed a porous network. From the surface morphology, the porous structure appears to be interconnected.

4. Conclusion

The natural hydroxyapatite (HA) has been obtained from the bovine bone bio-waste. The crystal structure of resulting HA is hexagonal with space group $P6_3/m$. The powder XRD data of HA shows that the intensity of major three peaks of HA which corresponds to the (211), (300) and (202) reflection are very similar in position at temperatures between 900°C and 1100°C which may be indicative of the dehydoxylation of HA during

sintering. The resulting HA can be used for medical application as a potential bone substitutes.

Acknowledgements

The author wishes to thank University of Indonesia for the facilities. Special thanks are devoted to Dr. Ellyza Herda and Dra. Nazly Hilmy, PhD, APU from Department of Material Sciences University of Indonesia and The National Atomic Energy Agency (Badan Tenaga Atom Nasional or BATAN), for their assistance in preparing this research.

References

[1] A. Bigi, G. Cojazzi, S. Panzavolta, A. Ripamonti, N. Roveri, M. Romanello, K. Suarez, L. Moro, J. Inorg. Biochem. 68 (1997) 45.

[2] K.D. Rogers, P. Daniels, Biomater. 23 (2007) 2577.

[3] C.Y. Ooi, M. Hamdi, S. Ramesh, Ceramics Int. 33 (2007) 1171.

[4] S.R. Krishna, C.K. Chaitanya, S.K. Seshadri, T.S.S. Kumar, Trends Biomater. Artif. Organs 12 (2002) 15.

[5] W. Suchanek, M. Yoshimura, J. Mater. Res. 13 (1998) 94.

[6] L.M. Rodríguez, M. Vallet, J.M.F. Ferreira, M.P. Ginebra, C. Aparicio, J. Planell, J. Biomed. Mater. Res. 60 (2002) 159.

[7] S. Joschek, B. Nies, R. Krotz, A. Gofpferich, Biomater. 21 (2000) 1645.

[8] JCPDS Card File No. 9-432 (Hydroxyapatite), Joint Committee on Powder Diffraction Standards, Swathmore, PA, 1996.

[9] F. Izumi, Rietveld Analysis System, Japan, 1989.

[10] P.E. Wang, T.K. Chaki, J. Mater. Sci.: Mater. Med. 4 (1993) 150.

[11] H. Aoki, Science and Medical Applications of Hydroxyapatite, Takayama Press System Centre Co, Inc., Tokyo, 1991.

[12] R.B. Martin, Biomaterials, in: R.C. Dorf (Ed.), The Engineering Handbook, CRC Press, Boca Raton, 2000.

ISSN 114-1284

Production Sharing Contract (PSC) Scheme Model For Coalbed Methane (CBM) Development

Mahmud Sudibandriyo, Lestantu Widodo

Department of Chemical Engineering, Faculty of Engineering
University of Indonesia, Depok 16424
Tel : (021) 7863516. Fax : (021) 7863515
E-mail : msudib@che.ui.ac.id

ABSTRACT

Due to declining of oil and gas production and increasing the demand, in 2006, the Government of Indonesia issued Regulation Number 033/2006 to encourage the development of Coalbed methane (CBM) for alternative energy sources. Regarding to this issue, some specific terms and conditions must be applied for the CBM contract, therefore, an economic calculation model is needed to be used as a reference in evaluating or appraising CBM working area blocks in bid. In this study, a suitable model for CBM Production Sharing Contract (PSC) scheme is developed by modifying appropriate terms and conditions in economic model for oil and gas contract. CBM development scenario in South Sumatra is used for an example case with two base scenarios. In this case, total gas production during 23 years of operation is estimated to be 609,000 MMScf, while total expenditures is about US$ 745,130,000. In South Sumatra - Case I, where First Trenched Petroleum (FTP) is set 5% (shareable), Cost Recovery Ceiling (CRC) is 100% for 1-5 years and 90% for 6-end years, Split (after tax) is 55:45, Tax 44%, and Price of Gas is US$ 4.3 /MMBTU, the results show that Internal Rate of Return (IRR), Pay Out Time (POT), Net Present Value (NPV) @ 10% p.a and % profit for contractors are 12.9%, 15.4 years, US$ 44,000,000 and 41.87% respectively; while NPV @ 10% p.a and % profit for Government are US$ 160,000,000 and 58.13% respectively. Furthermore, our sensitivity analysis shows that yearly gas production and gas price are very sensitive economic parameters upon the change of IRR, NPV, and Government take, while Split and CRC are sensitive policy parameter upon the change of IRR and Government take. In order to make IRR close to 20%, the only way is to increase the wellhead price gas to be US$ 7.00/MMBTU. No policy parameters can be used to obtain this value.

Keywords: *Coalbed Mathane (CBM), PSC, economic evaluation, economic parameter, policy*

1. INTRODUCTION

Indonesia possesses in place CBM resources potential to a number of 453 TCF [1,2,3]. Assuming 10% of this value, or as much as 45 TCF, can be produced, Indonesia will not be bothered anymore with the issue of increasing energy demand. Therefore, to boost the development of CBM for alternative energy sources, the Government of Indonesia issued Regulation Number 033/2006.

The regulation for CBM production is similar to the one applied in the production of oil and conventional natural gas, using a production sharing contract (PSC) scheme. The only difference is that in the CBM development, specific characters such as cost and longer time needed for production need to be considered. Therefore, an economic calculation model is needed as tool for the government to evaluate and to estimate the value of the blocks offered. This model can be developed from an economic calculation model usually used for conventional natural gas by modifying the model with specific requirement and characteristics for the CBM production. This model should be able to simulate the best scheme for the CBM production sharing contract that can satisfy both government and investor.

2. METHODS OF STUDY

The scheme of the study can be illustrated in Figure 1, and described as folllows.

a. Collecting data of typical CBM dewatering and gas production, estimated cost parameters which has been evaluated based on a pilot project. These data include the data obtained from the CBM field development in South Sumatra [4,5]. The cost parameters considered in this study include:

- Number of wells
- Annual gas production
- Water gas production
- Production facilities (well facilities, piping network, future plan (compressor, process facilities, etc)
- Project investment cost, including:
  - Well drilling and related facilities
  - Gathering station
  - Low pressure compressor
  - Production tools and gas sales compression system
  - Tangible, intangible, capital and non capital project cost applied to the *PSC* accounting

- Depreciation schedule for tangible and capital cost according to *PSC*
- Operating Cost including:
  - Well maintenance
  - Production cost
  - Processing unit
  - Water treatment and Compression/ gas transportation

b. Reviewing the above data, and selecting appropriate production and development cost parameters.
c. Modifying the model from oil and gas economic calculation by using appropriate parameters applied for CBM production
d. Economic evaluation of CBM field development including IRR, POT, and NPV.
e. Perform sensitivity analysis of economic calculation to obtain the most affecting variables upon economic parameters.
f. Making conclusions an recommendations

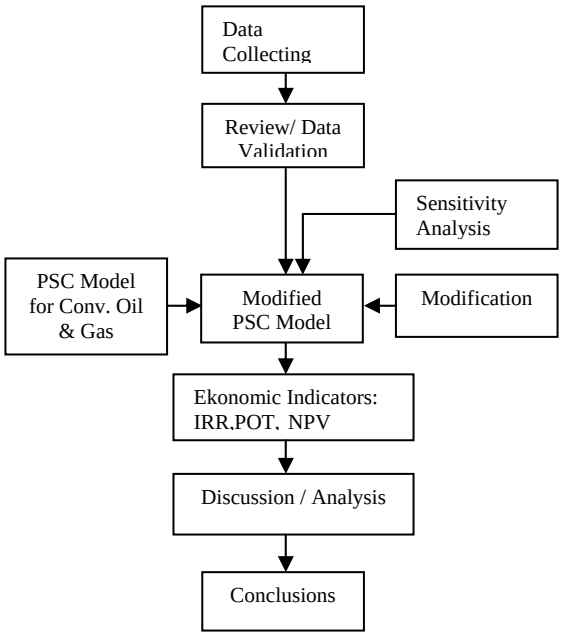

Figure 1. Research methods Scheme

3. RESULTS

Based on the cost components usually encounter in conventional gas development together with the data obtained from the CBM, the CBM field development, its production facilities and input data used in the economic evaluation can be described as follows.

3. 1 Field Development

In this study, 367 wells will be drilled in two steps of development. In the first step, about 210 wells will be drilled. Pilot wells will also be used as a part of development system. Horizontal pilot scale wells will also be made in the development step. The main target of this development step is to obtain the optimum production.

In the second step, the number of wells is expanded. The main goal of this step is to maintain production rate during the contract time. The addition wells are around 10 to 24 wells annually. Horizontal drilling and special treatment might be applied to support gas production and sale.

Production Facilities

The CBM production facilities are slightly different from the conventional gas production. These include:

- *Well facilities*
  Well production system consists of *PCP screw* type pump moved by electrical motor set on surface to produce water from tubing and gas from annulus. This pump type is selected because of four reasons: (a) big capacity, (b) intermittent, (c) resist on high gas concentration and coal flakes and (d) cheaper than other types.
- *Piping Network*
  Gas compressor at capacity of 2-3 MMSCFD is needed near the well hole and set at the gathering station. Inlet pressure is 10 to 20 psig and the outlet is 150 psig to gather gas from 10 to 20 wells to the sales point. P*olyethylene* (PE) pipe is used at low pressure section to reduce investment cost.
- *Future Plan*
  Main compressor for gas sales will be set near the field. Several clusters with the capacity of 5 to 10 MMSCFD processing gas will be set up in the project area. Each cluster will serve 20 wells.

Input Data

Input data needed in the model includes investment data, annual gas and water production , number of wells and number of production facilites needed. Furthermore, two cases are studied based on the specified above data.

***Case* I**

In this case, the following conditions are considered:

a. *FTP* = 5 % (shared for government and contractor)
b. *CRC* = 100 % for year 1 to 5,
   90% for year 6 to the end of the contract
c. *Split* = 55 : 45 (after tax)
d. *Tax* = 44 %
e. Gas and water production is shown in Table 1 and Tabel 2.

f. Wellhead gas price is US$ 4.30/MMBTU

***Case* II**

In this case, the following conditions are considered:

a. *FTP* = 10 % (only for government)
b. *CRC*= 90 % for year 1 to the end of contract, or 80% for year 1 to the end of contract
c. *Split* = 55 : 45 and 60 : 40 (after tax)
d. *Tax* = 44 %
e. Gas and water production is shown in Table 1 and Tabel 2.
f. Wellhead gas price is US$ 4.50/MMBTU or US$ 5.00/MMBTU.

3.3.1 Production Rate

Annual gas and water production are estimated based on the reservoir simulation as shown in Table 1 and Table 2 [4,5].

Table 1. Annual Gas Production Estimation (MMSCFY)

Year	Gas Production	Year	Gas Production
2008		2023	32000
2009		2024	32000
2010		2025	32000
2011		2026	32000
2012	1500	2027	32000
2013	1500	2028	32000
2014	1500	2029	32000
2015	3000	2030	32000
2016	3000	2031	32000
2017	15000	2032	32000
2018	15000	2033	32000
2019	25000	2034	30000
2020	25000	2035	26500
2021	25000	2036	26500
2022	32000	2037	26500

3.3.2 Investment Cost and Operating Cost

In general, operating cost of CBM production is higher than a conventional gas production at the early stage. This is because CBM production has longer dewatering stage (5-7 years compared to 1 year in conventional gas). After this stage, the CBM production cost is estimated US $ 0.03/MCF lower than a conventional one. Exploration cost for one well in CBM is estimated about US$ 400.000 [6,7], lower than the one in oil or conventional gas (US$ 1 – 2 million).

Table 2. Annual Water Production Estimation (Thousand of Barrel)

Year	Water Production	Year	Water Production
2008		2023	20000
2009		2024	19000
2010		2025	17000
2011		2026	16000
2012	33000	2027	15500
2013	36500	2028	15000
2014	42000	2029	14500
2015	39500	2030	14000
2016	36000	2031	13500
2017	34000	2032	13000
2018	30000	2033	13000
2019	27500	2034	11000
2020	25000	2035	10700
2021	24000	2036	10600
2022	22000	2037	10500

Meanwhile, compression and power plant cost is about 2-8 % and 5 % of the total production respectively. Therefore, only 87-93 % of the total production can be sold. Transportation and distribution cost should be covered by *end user*.

Project investment starting from year 1 up to year 23 consisting of drilling related facility cost, gathering pipeline, low pressure compressor, production and sales compression system is described in Table 3.

Detail description of the above cost parameters is as follows:

a. Well and facilities
- Core and *coring* analysis is US$ 125.000 per well
- Well and facilities is US$ 425.000 per well consisting the following components:
  - Access road, US$ 50.000. *Flow line*, US$ 25.000
  - Drilling, completion and cracking, US$ 250.000 per well
  - *PCP* pump and installation, US$ 100.000 per well.

b. Pipelines and production facilities (including water treatment)
- Low pressure gas gathering and compressor for each station consisting of modulo system @ 5-10 MMSCFD, US$ 1.200.000
- Water-gas separation system for 100 MMSCFD of gas, US$ 15.000.000

Year	No of Wells	Descriptions
Pilot Stage		
2008	4	3 core hole & 1 exploration well
2009	1	Facilities for Pilot Project
2010		Dewatering, prod. testing, gas market study, POD
Development Stage		
2011	4	
2012	37	
2013	36	P/L, compressor, separator
2014	36	P/L, gathering plant, compressor, separator
2015	36	P/L, gathering plant, compressor, separator
2016	36	P/L, gathering plant, compressor
2017	24	P/L, gathering plant, compressor
2018	18	Gathering plant
2019	18	Gathering plant
2020	18	Gathering plant
2021	12	
2022	12	
2023	12	
2024	10	
2025	10	
2026	10	
2027	10	
2028	10	
2029	8	
2030	8	
2031- 37		None

Tabel 3. Biaya Investasi dan Operasional Proyek

c. *Pipelines* and Compressor for gas sales
The following data is used for information only, and not used for calculation, because we use *wellhead price* in this study.
   - Compressor with the capacity of 100 MMSCFD, US$ 45 million
   - Piping, US$ 12 million, consisting of:
     - 25 km of 24 inch piping to send the gas to PGN & PLN pipe, US$ 9 million.
     - Piping for other market (5-6 location @ 5 MMSCFD), US$ 3 million.

Because CBM gas content high purity of methane (>90%) with N2 and CO2 impurities (without H2S), investment for gas treating facilities is not included [9,10].

Operating cost consists of existing well maintenance, production cost, water treatment cost, and gas compression/transportation. Those cost components are:
- Well maintenance and production cost, US$ 25.000 per well per year.
- Water production and treatment, US$ 0.30 per barrel.

Other cost component is US$ 15.000 for restoration per well per year.

3.4 Economical Calculation of CBM Contract

Economical evaluation of the CBM production is calculated based on the PSC model as shown in Figure 2 [8].

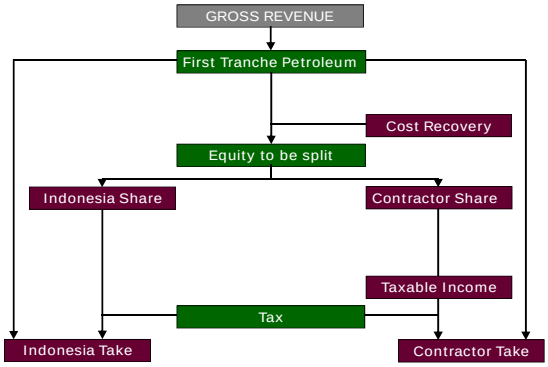

Figure 2. PSC Model for CBM Production

3.4.1. Results for *Case* I

Using conditions described in Case I, the following Tables 4 and 5 show the economic indicators results.

Table 4. Economic Indicators of CBM Development on Case I

Economic Indicators	Value
Expenditure, MM US$	745.13
NPV @ 10% p.a, MM US$	44.00
% Gross of Revenue	30.00
Internal Rate of Return (% IRR)	12.90
Profit to Investment Ratio (PIR), Fract.	2.82
Pay Out Time (POT) Year	15.40
Contractor Take, % of Profit	41.87
GOI Take, % of Profit	58.13
NPV @ 10% p.a MM US$	160.00
% Gross of Revenue	41.59

Table 5. Revenue Distribution on Case I

Revenue Distribution	Contractor (MM US$)	Government (MM US$)
Gross Revenue	2618.70	
Net Cash Flow	784.48	1089.09
Cost Recovery	632.95	0
Total FTP Share	105.22	25.72

Table I shows that, based on Case I, contractor does not get reasonable IRR, i.e. 12.9%.

3.4.2. Results for *Case* II

Using conditions described in Case II (*CRC* 90%, Split 55:45 and Gas price US$ 4.50/MMBTU), the following Tables 6 and 7 show the economic indicators results.

Table 6. Economic Indicators of CBM Development on Case II

Economic Indicators	Values
Expenditure, MM US$	745.13
NPV @ 10% p.a, MM US$	29.00
% Gross of Revenue	25.9
Internal Rate of Return (% IRR)	12.00
Profit to Investment Ratio (PIR), Fract.	2.54
Pay Out Time (POT) Year	15.00
Contractor Take, % of Profit	35.52
GOI Take, % of Profit	64.48
NPV @ 10% p.a MM US$	194.00
% Gross of Revenue	46.95

Table 7. Revenue Distribution on Case II

Revenue Distribution	Contraktor (MM US$)	Government (MM US$)
Gross Revenue	2740.50	
Net Cash Flow	708.73	1286.64
Cost Recovery	625.38	0
Total FTP Share	0	274.05

As on Case I, the results shown in Table 6 also shows that, based on Case II, contractor does not get reasonable IRR, i.e. 12.0% (lower than Case I). For gas price US$ 5.00/MMBTU, IRR is obtained 13.4%.

3.4.3 Results on Sensitivity Analysis

Effects of economic variables on economic parameters are studied further to observe the sensitivity of each variable, following are the results.

a. Sensitivity Analysis on Case I

Figure 3 shows effect of gas production rate, gas price, Capex, and Opex on IRR. This figure shows that gas production rate and gas price give very sensitive effect on the IRR, while both Capex and Opex do not give significant effect on the IRR. For instance, increasing production rate or gas price by 20 % will increase the IRR from 12.9 to 15.3%.

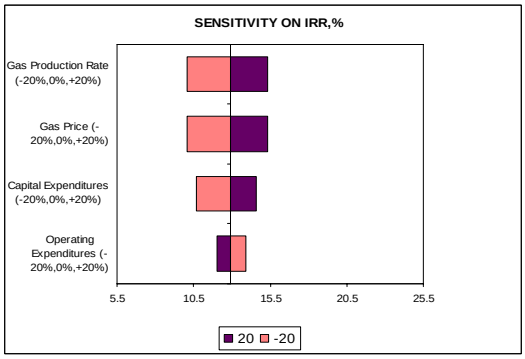

Figure 3. Effect of Gas Production, Gas Price, Capex and Opex on *IRR* in Case I

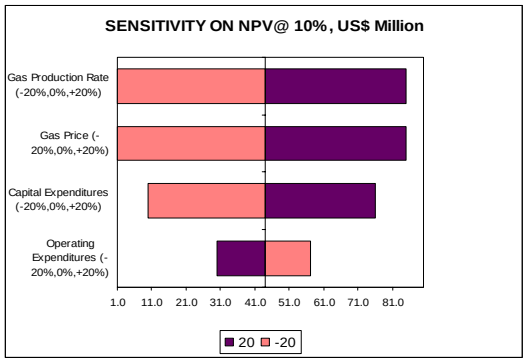

Figure 4. Effect of Gas Production, Gas Price, Capex and Opex on *NPV* in Case I

Figure 4 shows effect of gas production rate, gas price, Capex, and Opex on NPV for contractor. This figure shows that gas production rate and gas price give very sensitive effect on the NPV, while both Capex and Opex do not give significant effect on the NPV. For instance, increasing production rate or gas price by 20 % will increase the NPV from US$ 44 million to US$ 85 million.

Table 8 shows the sensitivity of the policy parameters on IRR. From the investor side of view, Split ratio is a very sensitive parameter on IRR. If the investor wants 19% of IRR, the Split ratio (Government: Contractor) should be 10 : 90, which is practically impossible, or the CRC is increased up to 120%, which is also impossible. Meanwhile FTP is not a significant factor on the change of IRR.

Table 9 shows the sensitivity of the policy parameters on Government Take. Similar to the above results, Split and CRC are important factors affecting the Government Take (in the reverse direction), while FTP is not a significant factor.

Tabel 8. Change of IRR on Policy Parameters In Case I

SPLIT PEMERINTAH : KONTRAKTOR	IRR (%)
0 : 100	19.6
10 : 90	18.7
20 : 80	17.6
30 : 70	16.5
40 : 60	15.2
50 : 50	13.8
55 : 45, BASE CASE	12.9
60 : 40	12
70 : 30	9.9
COST RECOVERY CEILING (%)	
100% (1-5); 90% (6-AKHIR KONTRAK), BASE CASE	12.9
100% (1 - AKHIR KONTRAK)	14
110% (1 - AKHIR KONTRAK)	15.9
120% (1 - AKHIR KONTRAK)	19.3
F T P (%)	
5 (SHAREABLE), BASE CASE	12.9
10 (SHAREABLE)	13
15 (SHAREABLE)	13
20 (SHAREABLE)	13
5 (NON SHAREABLE)	12.2
10 (NON SHAREABLE)	

Tabel 9. Change of Government Take on Policy Parameters In Case I

SPLIT PEMERINTAH : KONTRAKTOR	GOV. TAKE (%)
0 : 100	0
10 : 90	10.27
20 : 80	20.91
30 : 70	31.54
40 : 60	42.18
50 : 50	52.81
55 : 45, BASE CASE	58.13
60 : 40	63.45
70 : 30	74.08
COST RECOVERY CEILING (%)	
100% (1-5); 90% (6-AKHIR KONTRAK), BASE CASE	58.13
100% (1 - AKHIR KONTRAK)	54.73
110% (1 - AKHIR KONTRAK)	47.64
120% (1 - AKHIR KONTRAK)	1.3
F T P (%)	
5 (SHAREABLE), BASE CASE	58.13
10 (SHAREABLE)	58.02
15 (SHAREABLE)	57.90
20 (SHAREABLE)	57.79
5 (NON SHAREABLE)	61.44
10 (NON SHAREABLE)	

b. Sensitivity Analysis on Case II

Figure 5 shows effect of gas production rate, gas price, Capex, and Opex on IRR in Case II. As in Case I, gas production rate and gas price also give very sensitive effect on the IRR, while especially Opex does not give significant effect on the IRR. For instance, increasing production rate or gas price by 20 % will increase the IRR from 12.0 to 14.4%.

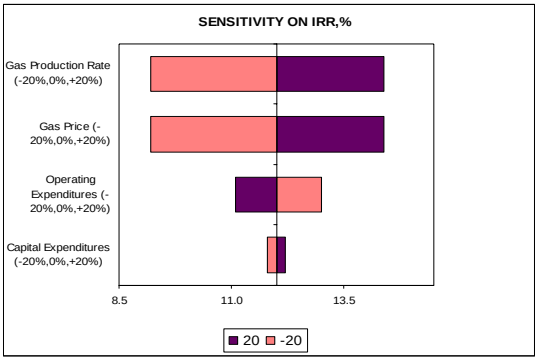

Figure 5. Effect of Gas Production, Gas Price, Capex and Opex on *IRR* in Case II

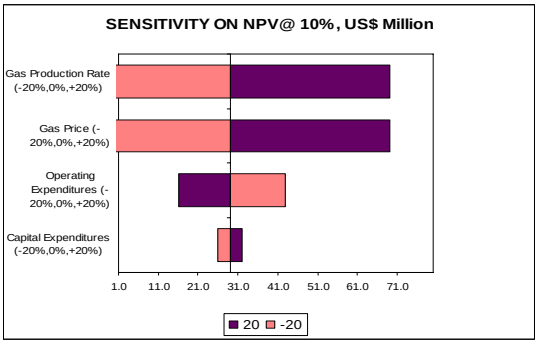

Figure 6. Effect of Gas Production, Gas Price, Capex and Opex on *NPV* in Case II

Figure 6 shows effect of gas production rate, gas price, Capex, and Opex on NPV for contractor. This figure shows that gas production rate and gas price give very sensitive effect on the NPV, while especially Opex does not give significant effect on the NPV. For instance, increasing production rate or gas price by 20 % will increase the NPV of contractor from US$ 29 million to US$ 65 million.

Table 10 shows the sensitivity of the policy parameters on IRR. As in Case I, split ratio is the most sensitive parameter on IRR for Case II. If the investor wants 19% of IRR, the government will gets nothing, or the CRC is increased up to 125%, which is also impossible. Meanwhile FTP is not a significant factor on the change of IRR.

Table 11 shows the sensitivity of the policy parameters on Government Take. Similar to the

above results, Split and CRC are important factors affecting the Government Take (in the reverse direction), while FTP is not a significant factor.

Table 10. Change of IRR on Policy Parameters In Case II

SPLIT PEMERINTAH : KONTRAKTOR	IRR
0 : 100	18.5
10 : 90	17.6
20 : 80	16.6
30 : 70	15.5
40 : 60	14.2
50 : 50	12.8
55 : 45, BASE CASE	12.0
60 : 40	11.2
70 : 30	9.1
COST RECOVERY CEILING (%)	
100% (1-5); 90% (6-AKHIR KONTRAK), BASE CASE	12.0
100% (1 - AKHIR KONTRAK)	13.2
110% (1 - AKHIR KONTRAK)	15.1
120% (1 - AKHIR KONTRAK)	18.5
F T P (%)	
5 (SHAREABLE), BASE CASE	13.4
10 (SHAREABLE)	13.5
15 (SHAREABLE)	13.5
20 (SHAREABLE)	13.6
5 (NON SHAREABLE)	12.7
10 (NON SHAREABLE)	12.0

.

4. CONCLUSIONS

1. Base on Case I, IRR for CBM development in South Sumatra is 12.9%, and on Case II, IRR is obtained 13.4% at CRC = 90% and gas price US$ 5.00/MMBTU (the highest reasonable CRC and gas price).
2. Sensitivity analysis shows that Gas production rate and gas price give more significant effect on IRR and NPV, compared to the effect of Capex and Opex. Meanwhile, among the policy parameters, Split and CRC give significant effect on IRR, and FTP shows the least effect, both for Case I and Case II.

Tabel 11. Change of Government Take on Policy Parameters In Case II

SPLIT PEMERINTAH : KONTRAKTOR	GOV. TAKE (%)
0 : 100	13.73
10 : 90	22.96
20 : 80	32.19
30 : 70	41.41
40 : 60	50.64
50 : 50	59.87
55 : 45, BASE CASE	64.48
60 : 40	69.09
70 : 30	78.32
COST RECOVERY CEILING (%)	
100% (1-5); 90% (6-AKHIR KONTRAK), BASE CASE	64.48
100% (1 - AKHIR KONTRAK)	61.18
110% (1 - AKHIR KONTRAK)	54.67
120% (1 - AKHIR KONTRAK)	13.73
F T P (%)	
5 (SHAREABLE), BASE CASE	58.15
10 (SHAREABLE)	57.98
15 (SHAREABLE)	57.87
20 (SHAREABLE)	57.76
5 (NON SHAREABLE)	61.35
10 (NON SHAREABLE)	64.48

3. From the government point of view, Split and CRC give significant effect on Government take, and FTP shows the least effect, both for Case I and Case II.

4. In order to get IRR = 20%, the following schenarios can be used:

Base Case I :

a. Gas price is increased to US$ 7,53/MMBTU, IRR = 20,6%
b. Gas price US$ 6,88/MMBTU, CRC = 100%, IRR = 20,2%

Base Case II :

a. Gas price is increased to US$ 8,10/MMBTU, IRR = 20,2%
b. Gas price US$ 7,65/MMBTU, CRC = 100%, IRR = 20,2%
c. Gas price US$ 6,75, FTP=10% (shared), CRC=100%, IRR = 20,0%

REFERENCES

[1] Advanced Resources International, Inc., Indonesian Coalbed Methane – Resource Assessment, Unpublished Report, Prepared foe Asian Development Bank, Manila – MIGAS, Jakarta, 2003

[2] Ephindo-MedcoEnergi, Presentation of CBM Project, South Sumatra Joint Evaluation, April 2007

[3] Hydrocarbon Asia, Indonesia Coalbed Methane : resources and development potential, Report CBM July/August 2006

[4] Institut Teknologi Bandung, Joint Evaluation Study on CBM, *Overlapping Area of Medco-Ephindo*, South Sumatera, May 2007

[5] Kurnely, Kun, Budi Tamtomo, Salis Aprilian, *A Preliminary Study of Development of Coalbed Methane (CBM) in South Sumatra*, SPE 80518, 2005

[6] Widodo, Lestantu, *Studi Komparatif Berbagai Kontrak Kerjasama Eksplorasi dan Eksploitasi Minyak Bumi di Asia Pasifik*, Tugas Akhir S1, Institut Teknologi Bandung, 1996

[7] Widodo, Aruman, Peluang CBM Sebagai Energi Alternatif di Masa Depan, Ikatan Sarjana Ekonomi Indonesia, Jakarta, 2007

[8] PT. Suhartama Multijaya, Penyusunan Kebijakan Pengembangan Pengusahaan Coalbed Methane (CBM), 2006

[9] Sosrowidjojo, Iman B., *Coalbed Methane Potential in the South Palembang Basin*, Jakarta 2006 International Geosciences Conference and Exhibiton, 2006

[10] Lin, Whenseng, Min Gu, Anzhong Gu, Xuesheng Lu, Wensheng Cao, *Analysis of Coal Bed Methane Enrichment and Liquefaction Processes in China*, Shanghai Jiaotong University, Poster PO-37

ISSN 114-1284

Design & Economic Analysis of Small LNG Plant From Coalbed Methane

Mahmud Sudibandriyo, Hans Wijaya
Department of Chemical Engineering, Faculty of Engineering
University of Indonesia, Depok 16424
Tel : (021) 7863516. Fax : (021) 7863515
E-mail : msudib@che.ui.ac.id

ABSTRACT

Coalbed Methane (CBM) is a new methane resources abundanty available in Indonesia. In this study, we evaluate the possibility of developing a small LNG plant from CBM at Rambutan Field through purification process and liquefaction. Due to low impurities and low pressure characteristic of CBM, we selected to use Pressure Swing Adsorption (PSA) method with eight columns in rows for purification process. Meanwhile, we used a Single MRC (Single Mixed Refrigerant Cycle) of Black and Veatch PRICO for liquefaction processes which are more suitable for a small scale LNG plant. Our economic analysis shows that the small LNG plant needs an investment as much as US$ 438.031.452,06. At the price of coalbed methane raw material US$3/MMBTU, the price for LNG product should be sold at US$8/MMBTU in order to get Internal Rate of Return (IRR) value 24.34 %, and payback period of 5.49 years from starting the construction or 3.49 years after operation of the plant

Keywords: *Coalbed Methane, PSA, LNG Process, Natural Gas Purification, Economic Evaluation*

1. INTRODUCTION

Coalbed Methane (CBM) is a new methane resources abundanty available in Indonesia. Only at one location (Rambutan Field), in South Sumatra, 0.8 TCF of methane reserve from CBM has been indicated with the purity of more than 90 % of methane [1]. This methane reserve might be potentially produced as energy resources for transportation need in Palembang which is 165 km away from the CBM resources. Considering the distance from the consumer and the rate of production which is estimated to be 50.9 MMcfd, this methane resources might be utilized through a small LNG (Liquified Natural Gas) plant and transported using LNG trucking [2].

In this study, economic feasibility of developing a small LNG plant from CBM source at Rambutan Field involving purification and liquifaction units is analyzed. This is a unique case, considering its specific CBM gas contents and conditions.

2. METHODS OF STUDY

This study is initiated by collecting the characteristics of the gas produced by CBM, including its condition and composition. The requirement of the LNG, which will be produced, should also be specified. Then, types of suitable unit processes are selected according to the above conditions and specifications.

Once the process is selected, the simulation is performed manually and by using Hysis software in order to obtain the specific size of each unit process and its energy consumption. This information will be used to calculate the CAPEX (Capital Expenditure) and OPEX (Operation Expenditure). All the prices are extrapolated for year 2015 as a reference year when the plant is expected to be built.

Profit is obtained by subtracting revenue from LNG sales and the OPEX, depreciation, and tax. Therefore, cash flow of the company can be determined and analyzed its economical feasibility. In this case, IRR, NPV and Payback Period, are calculated using suitable formula [3] and evaluated. Sensitivity analysis is performed using spider chart and tornado chart method [4].

3. RESULTS

The plant is designed for the average capacity of 50,9 MMcfd, which is enough for transportation energy need in Palembang and vacinity. Considering the methane reserve available at Rambutan field, which is 0.8 TCF, and 50% recovery, this plant is expected to operate up to 21 years. The life time of this LNG plant also agrees with the normal life time of typical LNG plant in the world [5]. The *small scale* LNG *Plant* at Rambutan Field is assumed to be constructed in 2015 and start producing LNG in the beginning of 2017.

The average temperature and pressure of CBM source at Rambutan Field are 43 ^{o}C and 7.83 atm, and its composition is shown in Table 1 [6,7]. Meanwhile, the specification of the LNG produced should meet the requirement shown in Tabel 2 [8].

Table 1. Gas Content and Composition of CBM Well Head

Components		Mol Percent			
		Seam 2	Seam 3	Seam 5	Average
Carbon Dioxide	CO_2	0.19	0.2	4.25	1.55
Nitrogen	N_2	2.25	2.37	0.15	1.59
Methane	CH_4	96.16	96.55	93.8	95.50
Ethane	C_2H_6	1.04	0.72	1.26	1.01
Propane	C_3H_8	0.28	0.21	0.33	0.27
Iso-Butane	i-C_4H_{10}	0.02	0.07	0.1	0.06
n-Butane	n-C_4H_{10}	0.01	0.01	0.01	0.01
Iso-Pentane	i-C_5H_{12}	0.01	0.01	0.01	0.01
n-Pentane	n-C_5H_{12}	0.01	0.01	0.01	0.01
Hexanes	C_6H_{14}	0.01	0.01	0.02	0.01
Heptanes plus	C_{7+}	0.02	0.02	0.06	0.03
Ave. Gas Content (m3/t)		1.61	3.6	2.92	2.71
Coal Thickness (m)		10	10	11	10.33

Table 2. Specification of LNG

Physical Properties	
Properties	**Value**
Phase	Liquid (at T= -159 ^oC, P = 0,07 kg/cm^{2}g)
Appearance	colorless
Smell	LNG like
Density	Average 453 kg/m^3
Heating Value (HHV)	1105 - 1165 BTU/SCF
Composition	
Component	**Composition**
C_1 (Methane)	min 95 %
C_2 +	max 4,8 %
N_2	max 1 %
CO_2	< 100 ppmv
H_2S	<4 ppmv
H_2O	<1 ppmv
Hg	max 0,01 μgr/Nm3

3.1 Selected Proses

Figure 1 shows Block Flow Diagram of the LNG plant selected based on the condition and composition of the CBM available. Due to its low pressure and low nitrogen and carbondioxide contents, the CBM gas is purified using Pressure Swing Adsorption (PSA) process in molecular sieves 5 A at pressure 300 psia and temperature of 25 ^oC. Eight adsorption columns are used for the adsorption process and the other eight columns are used for regeneration. The capacity of adsorption is calculated based on the adsorption isotherm obtained by Wakasugi [9].

Total gas of 940,63 ton/day or 48,46 MMCFD will be produced from the PSA unit. As much as 12 % of total gas (112,87 ton/day) is used for fuel consumption in the gas turbine to generate electricity and 6,16 ton/day is used for regeration purpose in the PSA unit. Therefore, only 821,6 ton/day will be processed further in the liquifaction unit.

Liquifaction process uses a *single mixed refrigerant* method patented by Black and Veatch PRICO [10]. Table 3 shows the composition of mixed refrigerant used.

Tabel 3. Mixed Refrigerant Composition

MR Component	% Mole
N2	10
C1	24
C2	28
C3	16
i-C4	5
i-C5	17

3.2 Economic Analysis and Sensitivity

The CAPEX needed [11] for building a small scale LNG plant is listed in Table 4. Total CAPEX is $ 157.152.784,50 for total LNG production of 821,6 ton/day or 0,299 MTA (Thousand of Ton Annual). Ratio of CAPEX to the LNG production is $ 524,03 MM/MTA, which is higher than normal ratio for building a *base load* LNG *plant* ($ 300 MM/MTA) [5]. This result is not unexpected, considering that unit cost for bigger scale plant always less than the smaller scale.

Tabel 4. CAPEX Esitmation

UNIT	Investment (US$)	%
PSA Purification	4,323,551,57	2.69
Liquefaction Process	4,220,691,35	2.69
Power Plant	75,246,062,76	47.88
Piping, Instrumentation & Control	3,333,011,37	2.12
Land	15,000,000,00	9.54
Service Facilities	14,505,386,17	9.23
Site Development	2,901,077,23	1.85
Contractors	14,505,386,17	9.23
Engineering, Supervision, Start Up	8,703,231,70	5.54
Others	14,505,386,17	9.23
TOTAL CAPEX	157,152,784,50	100.00

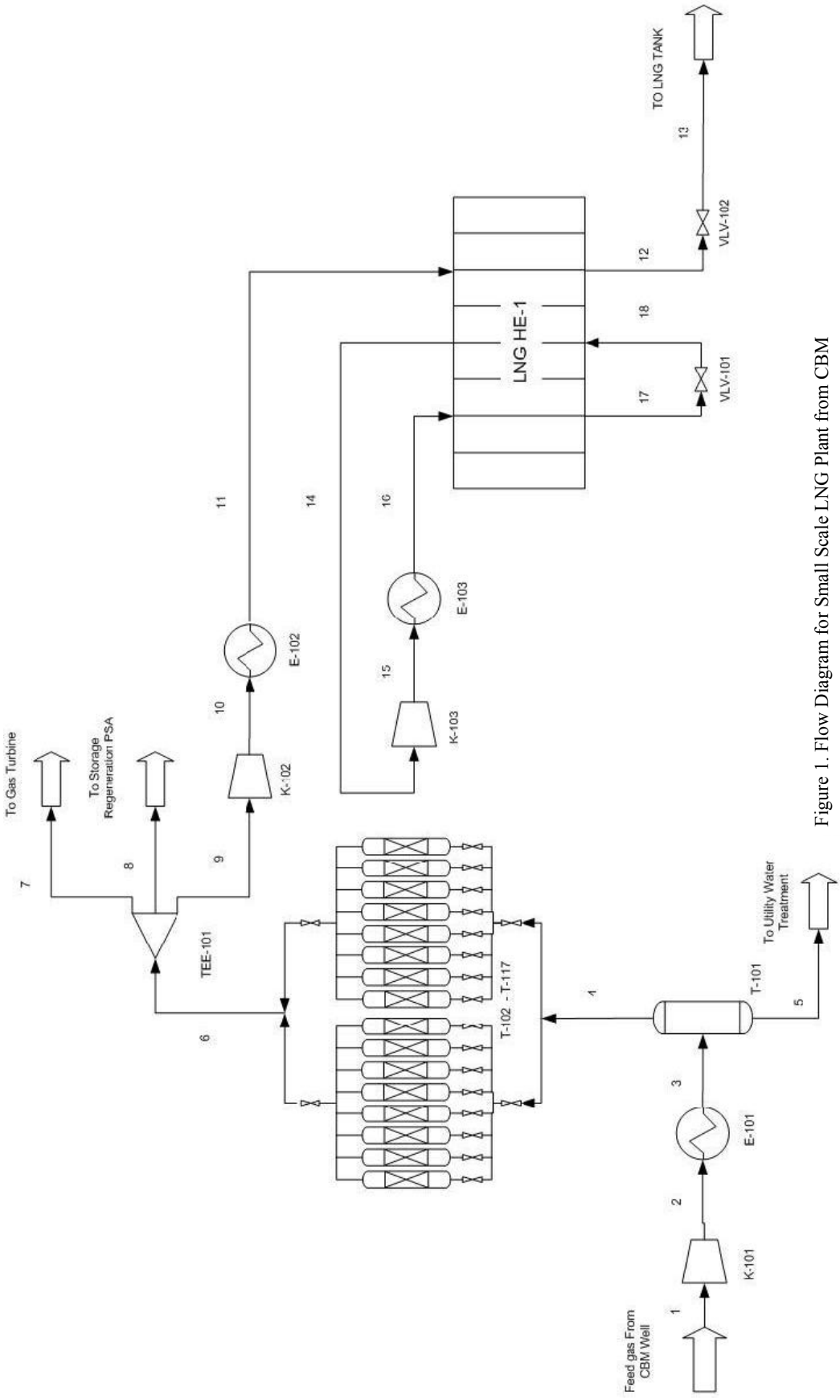

Figure 1. Flow Diagram for Small Scale LNG Plant from CBM

Estimation of OPEX and its components can be seen in Table 5. This estimate is calculate based on literature [11] and recent market situation.

Tabel 5. OPEX Estimates

Component	Cost (US$)
Direct Cost & Utilities	5,563,014,59
Insurance	1,813,173,27
Marketing & Administration	3,000,00
Labors & Office	553,200,00
TOTAL OPEX	7,932,387,86

OPEX per MMBTU production can be calculated as $ 0,54 / MMBTU. According to literature [5], OPEX per MMBTU for base load LNG plant is about $ 0.2 / MMBTU (excluding purification process). Comparing the two values, and considering the difference in scale and cost in purification process, the OPEX estimates in our small LNG plant is quite reasonable.

Assuming the price for raw natural gas is $ 3/MMBTU and the selling price is $ 8/MMBTU based on Free On Board (FOB), profit can be calculated by substructing revenue with the operating cost and depreciation. The profit is obtained as much as $ 4 / MMBTU.

Based on the calculated CAPEX, OPEX and depreciation, the cashflow can be made, assuming that equity of this plant comes from 100 % self funding, the inflation rate is 2,8% and government tax (PPH No 22) is 30%. The IRR for the above standard price is obtained to be 24,34%. The NPV at 2015 is obtained as much as $ 438.031.452,06. *Payback period* is 5,49 years since the construction begin, or 3,49 years after LNG production. Therefore, this small LNG plant is feasible to be developed.

Changing -20% to 20% upon selling price of LNG, CBM price, CAPEX and OPEX gives the following effects on IRR:

IRR increase up to 35.5% by changing 20% of LNG price and decrease to 12.5% by changing
-20% of LNG price.
IRR increase up to 29% by changing -20% of CBM price and decrease to 19% by changing 20% of CBM price.
IRR increase up to 31% by changing -20% of CAPEX and decrease to 20% by changing 20% of CAPEX.
IRR increase up to 25% by changing -20% of OPEX and decrease to 23% by changing 20% of OPEX.
The above results show that the LNG price is the most sensitive parameter in the economic feasibility of the plant studied, and the OPEX is the least sensitive one. Similar results are also obtained for the effect of NPV on the change of -20% to 20% upon selling price of LNG, CBM price, CAPEX and OPEX.

Simulation on the cash flow based on the fixed OPEX and CAPEX and varying GMB and LNG prices gives the following equations (in US$) for different IRR:

For IRR = 20%
Selling LNG price = CBM price + 4,13

For IRR = 15 %
Selling LNG price = 1.03 CBM price + 3,85

For IRR = 10 %
Selling LNG price = 1.02 CBM price + 3,60

The above equations can be used to estimate the price of LNG for a specific price of CBM price and at the rate of return required.

4. CONCLUSIONS

1. Based on the CBM price of US$ 3 and the selling price of LNG at US$ 8, the IRR for the above standard price is obtained to be 24,34%. The NPV at 2015 is obtained as much as $ 438.031.452,06. *Payback period* is 5,49 years since the construction begin, or 3,49 years after LNG production. Therefore, this small LNG plant is feasible to be developed.
2. Sensitivity analysis shows that the LNG price is the most sensitive parameter in the economic feasibility of the plant studied, and the OPEX is the least sensitive one.

3. Feasible price for the LNG produced can be estimated according to the price of the CBM at a certain IRR required, as follows:

   For IRR = 20%
   Selling LNG price = CBM price + 4,13

   For IRR = 15 %
   Selling LNG price = 1.03 CBM price + 3,85

   For IRR = 10 %
   Selling LNG price = 1.02 CBM price + 3,60

REFERENCES

[1] Coal Report Indonesia 2000 American Embassy Jakarta Indonesia, October 2000.

[2] Hetland Jens, NATO Science Series "*Economical limitation of natural gas transportation* Hetland" . Accessed on December 1, 2008 from http://books.google.co.id/books?id=CAjgMBrZ0ZsC&pg=PA330&lpg=PA330&dq=Economic+limitation+of+natural+gas+transportation+Hetland&source=bl&ots=y4L3B4bNxd&sig=6lO0QCNT-ZIi3iCKfK6FkmlFG-I&hl=id&sa=X&oi=book_result&resnum=1&ct=result#PPR14,M1

[3] P. E. Degarmo, W.G. Sullivan., J.A. Bontadelli, E.M. Wicks, "Engineering Economy", 11Ed, PT. Prenhallindo Jakarta Indonesia, 1997.

[4] L. Widodo, "Keekonomian Pengusahaan Gas Metana-B Di Wilayah Sumatera Selatan Dan Kalimantan Timur" Thesis, Program Pasca Sarjana Fakultas Teknik UI, Jakarta, Indonesia, 2008.

[5] V. Chandra, "Fundamental of Natural Gas: An International Perspective", Penn Well Corporation Oklahoma USA, 2006.

[6] E.H. Legowo, I.B. Sosrowidjojo and E. Syahrial," *Current Status of Coalbed Methane (CBM) Development in Indonesia*," Research and Development Centre for Oil and Gas Technology, LEMIGAS, Jakarta, Indonesia, April 18, 2006.

[7] I.B. Sosrowidjojo, "On Going Coalbed Methane (Cbm) Development In South Sumatra Basin," *Lemigas Scientific Contribution*, Vol. 29. No.3, pp 15-24. Dec. 2006

[8] A. Anisa "Laporan Kerja Praktek PT. Badak Natural Gas Liquefaction , Co." Laporan Kerja Praktek, Program Sarjana Fakultas Teknik UI, Depok 2008.

[9] Y. Wakasugi, S. Ozawa, and Y. Ogino, "Physical Adsorption of Gases at High Pressure V". An Extension of Generalized Adsorption Equation to Systems with Polar adsorbents, *Journal of Colloid and Surface Science*, 79(2), 1981.

[10] A.J., Mathias, et.al. "*Process For Cooling A Product In A Heat Exchanger Employing Microchanels For The Flow Of Refrigerant And Product*" US PATENT No. 6,622,519 B1, Velocys, Inc, USA Sep.23,2003.

[11] M.S. Peters & K.D. Timmerhause, "Plant Design And Economics For Chemical Engineering", 4TH Edition, McGraw-Hill, Inc Colorado USA, 1991.

QUANTUM STATES AT JUERGEN MODEL FOR NUCLEAR REACTOR CONTROL ROD BLADE BASED ON Th_x DUO_2 NANO-MATERIAL

Moh. Hardiyanto
Large Hadron Collider (LHC) Laboratory – Muon Hadron Division
Betha Group Section CANDU – CERN Nanomaterial Experiments
CERN – Lyon, France
E-mail : mohamadhardiyanto@ yahoo.com

ABSTRACT

The functional of a multi purpose research nuclear reactor control rod blade nuclear reactor is stabilized and controlling devices for nuclear chain reactions, the existing of Cerenkov's radiation impact and thermal neutron flux in reactor chamber. This research was conducted in Large Hadron Collider (LHC) – Muon Hadron Division at CERN, Lyon – France under International Research between Canadian Deuterium Uranium (CANDU) – Nuclear Reactor and Betha Group Section for sub-particles for nanomaterial. Using Juergen Model with quantum states approaching and testing by Muon-Hadron Stirrer equipment had determined the Th_xDUO_2 derivatives materials. This material shown the strength of thermal neutron flux absorbed about 2.1 x 10^5 – 1.8 x 10^6 Ci/mm, the value of Electrical Conductivity is 26.62 – 29.98 in 800º - 890º C temperature, however at 2.1 x 10^5 Ci/mm thermal neutron flux condition is 29.44 – 37.88 in IAEA standard. At 450 tesla magnetic field and 2.1 x 10^5 Ci/mm thermal neutron absorber, the crystalline structure reduction is 6.88% until 10.95% for 25 years period in 45.7 megawatts with UO_2 more enrichment and Pu_2O also Th_2O_y nuclear fuel element matrix.
Keywords : Cerenkov's Effect, Quantum states, Fast neutron floating, Juergen Model, Muon-Hadron Stirrer

1. INTRODUCTION

This research involves a multi purpose research nuclear reactor with increasing of its adjusted power from 30 megawatts (MW) to 50 MW. This process has changed the nuclear fuel element matrix from UO_2 to be UO_2 more enrichment with Pu_2O and Th_2 O_y buffer element. This matter could be increasing of thermal neutron flux up to 2.1 x 10^5 currie/mm in normal condition, much more Cerenkov's radiation figure out and several quantum states in reactor chamber (Stuart, Thomas P., 2001).

The shape and dimensions of control rod blade include 5 meters length, 0.80 meters diameter and thickness fit on 0.10 meters. Moving on normally with 76 mm/second speed and reached above on reactor yield is 1.6 meters for normal condition. These values have fixed on International Atomic Energy Agency (IAEA) regulation (CANDU, 2001).
At present time, the control rod blade material is Zircalloy-4, and according of IAEA recommendation, this material have to change with best substance fitted on 50 MW adjusted power. The eliminary investigations show that material has found from Sr_2 Al_xO_y types (Moh Hardiyanto, 2001) consists are three types including Th_x DUO_2 , Th_{x-1} DUO_2 and Th_{x-2} DUO_2 materials. From basic testing with Super Muon-Magnetic equipment in few conditions ; normal, sub critical, critical phase 1 and phase 2 have eliminary result such as the highest thermal neutron flux absorber value could reached by Th_x DUO_2 with much more stability in graduation points. Another thing, when the Cerenkov's radiation shown up, this material expression the more ordered electron clouds track, then could be count to facing neutrino, μ, and anti-neutrino particles bombarding around the reactor chamber.

2. LITERATURE AND FORMULATION

2.1 Juergen Model

The IAEA standard for software and programming to multi purpose nuclear research reactor was written in Modula's language consists are 4 main programmes including numerical processing, begin to simulation, advanced simulation and establishing calculations also display. Additional for this software, Ising Model has 38,700 sub-programmes consists are 8,700 formulations and calculations especially in physics, chemistry and other nuclear reactions. Thereby, include 10,000 sub-programmes for various databases. More completed with 15,000 sub-programmes for making simulations. After that working, this software was completed with 5,000 sub-programmes to display with interactive processing, specific in nuclear chain reactions at reactor chamber with all devices (Durant, W.C., 2001).

2.2. Super Muon-Magnetic

The equipment has developed especially for multi purpose nuclear reactor. Advanced devices will be connected and integrated with reactor chamber and shielding of its reactor and generates with 150 kilowatts power non-stop electrical force, commonly by 2.1 grams Thorium-331, one isotope species from Trans-Uranium series (Waghmare, Y.R., 2001). Various parts will be connected with this equipment test including premier properties such as:

- Thermal neutron flux luminosity between 1.9 x 10^4 currie/mm to 2.1 x 10^6 currie/mm with Na_2SO_3 liquid moderator.
- Magnetic field between 400 tesla up 610 tesla of thermal neutron flux existence in reactor chamber when adjusted power increasing around 50 MW.

- The magnetic frequency around 410 MHz until 550 MHz for each chain reaction based on UO_2 more enrichment nuclear fuel.
- Existing of v and v$^-$ particles and more muon-hadron particles when Cerenkov's radiation coming up in reactor chamber.
- The value of temperature around 800° - 890° C, when adjusted power increase to 50 MW.

This part was connected with special device, *catch-nuc power*; the equipment will be generated electrical power amount 70 kilowatts per hour.

Through by Super Muon-Magnetic and Juergen Model will be determined the derivation of Th_x DUO_2 covering are Th_x $DUO_{1.7,}$ Th_x $DUO_{1.8}$ and Th_x $DUO_{1.9}$ types with involving the quantum states.

2.3. Quantum States Approaching

Most formulations will be used in this research based on relativistic quantum mechanics, Einstein's condition, and a few interstellar quantum statistics until the derivation from BCS theory in super-conductivity state (Gomiez, J.A., 2001).

Begin from standard formulation for relativistic wave length, forward to spectrum of nuclear analysis up to super-conductivity state with Fermi, Fermi-Hall condition (Beiser, Arthur, 1998). The first of Compton's wave length in Einstein-Dirac state expressed by:

$$\frac{\{hf_0 - hf + m\}^2}{c^2} - m_0^2 c^2 = \left\{\frac{h}{\lambda_0}\right\}^2 + \left\{\frac{h}{\lambda}\right\}^2 - \frac{2h^2}{\lambda_0 \lambda}\cos\theta \qquad (1)$$

Considering the total energy in relativistic states is:

$$E^2 = p^2 c^2 - m_0^2\ c^4 \qquad (2)$$

Meanwhile the formulation of Einstein-Dirac could be written in muon-hadron particle with:

$$E_\varphi = \frac{e^4 \sin\phi}{4\pi\varepsilon_0 c^2 r} \qquad (3)$$

In this case, considering that the speed of the electron is small in comparison it the speed of neutron particle, the electric field of Electrical Conductivity (EC) flowing at Einstein-Sommerfeld field in an point H_{11} with polar coordinates

$$\left(\frac{E_\varphi}{E}\right)^2 = \frac{e^4 \sin^2\phi}{(4\pi\varepsilon_0)^2 m_n^2 c^4 r^2} \qquad (4)$$

As the intensity is directly proportional to the square of the electric field. The total amount of energy scattered per unit volume of the scattered per second is given by

$$U_s = \int_0^\pi I_s (2\pi r^2 \sin\theta) d\theta \qquad (5)$$

$$U_s = \left(\frac{1}{2}\right)\left[\frac{2\pi n e^4 r^2}{(4\pi\varepsilon_0)^2 m^2 c^4 r^2}\right] \int_0^\pi (1+\cos^2)\sin\theta\, d\theta \qquad (6)$$

The first formulation investigated by Arthuro J. Gomiez (Gomiez, J. Arthur, 2001) shown that the crystalline structure will be derived from BCS theory such as

$$H_1 = \sum_i J\left\lfloor C_{ki\uparrow}^F C_{ki\downarrow}^F \right\rfloor \qquad (7)$$

The early equation was given by Abrikosov, Balseiro and Russel in matched on superconductivity crystalline structure (Kempster, M.H.A., 1999) using Fermi's state non reactive electron cloud and Fermi-Hall reactive electron cloud. The completed equation was given by

$$H_{II} = \sum_i J\left\lfloor C_{ki\uparrow}^F C_{ki\downarrow}^F \right\rfloor + k\sum_i \sum_j \left\lfloor C_{kij\uparrow}^F C_{kij\downarrow}^F \right\rfloor \qquad (8)$$

Consider of quantum relativistic field and existence of Gell-Mann's specification particles (Valli, G., 2000) and based on Bose-Einstein state. Begin from electron potential energy up to Rydberg's constant, derived such as:

$$K = \frac{1}{8}\frac{me^4}{\varepsilon_0^2 h^2 n^2} \qquad (9)$$

$$V_{(r)} = \frac{-1}{4}\frac{me^4}{\varepsilon_0^2 n^2 h^2} \qquad (10)$$

From both Equations (9) and (10) will be found total energy on the *n*-th shell in crystalline structure displacement (Chattopadhyay, C., 1998) at semi-relativistic quantum condition, is:

$$\frac{1}{\lambda_c} = \frac{1}{8}\frac{m_e e^4}{\varepsilon_0^2 h^3 c}\left\{\frac{1}{n_2^2} - \frac{1}{n_1^2}\right\} \qquad (11)$$

Reviewing from a few formulations, it is clear that by measuring σ the value of *n*-th can be determined

$$n = \left(\frac{3}{8\pi}\right)\left[\frac{(4\pi\varepsilon_0)^2 m_n^2 c^4}{e^4}\right]\sigma \qquad (12)$$

At 2.1 x 10^4 currie/mm thermal neutron flux absorption for minimal condition in reactor chamber, the value of *n*-th stage begin from 1 up 2 according the Fermi's interference condition, expressed :

$$E_{n1} - E_{n2} = \frac{1}{8}\frac{m_n e^4}{\varepsilon_0^2 h^2}\left\{\frac{1}{n_2^2} - \frac{1}{n_1^2}\right\} \qquad (13)$$

In this Equation found the value of Rydberg's constant for thermal neutron flux at reactor chamber, the amount is 1.097373 x 10^7 m^{-1}. Based on the Rydberg's constant and wearing the Compton's nuclear wave length for thermal neutron flux scattering in crystalline structure, Pfund at Princeton University (Vasudeva, D.N., 1999) found the new

series near in "Doublet-Natrium" red-infra closest with derivation of Dirac's Mirror equation such as:

$$E(eV) = -\frac{1}{e_c}\frac{m_e e^4 z^2}{8\varepsilon_0^2 h^2}\frac{1}{n^2} \qquad (14)$$

When "z" is value for moment-magnetic spin of angular electron in solid state.

According these equations and seem to reactor chamber flow from nuclear fuel reaction until shown up the Trans-Uranium series with DUO_2 fuel element, then a few device of Super Muon-Magnetic will be recorded a lot of data with many serial repeated reaction. For precisely calculations, many equations will be transferred in group-theory, one of modern mathematical tools in quantum-relativistic phenomena.

In this part will be described the changing of the semi-relativistic formulation to quantum's group-theory, develop by Dirac, Gell-Mann, and other famous physicians (Beiser, Arthur, 1998). Start by the steady force law in relativistic magnetic field up to the connection of phonon-electron cloud in solid state structure. Describing such as:

$$H_{II} = \sum \varepsilon_k C_{kt}^F - \hbar\Delta\sum\left\{C_{k\uparrow}^F\, C_{k\downarrow}^F x\hbar c\right\} \quad (15)$$

Derivation of BCS's theory break by Abrikosov-Balseiro-Russel formulation energy potential expressed as:

$$\Delta = g_{BCS}\sum_k \left\langle C_{k\downarrow} \bullet C_{k\uparrow}\right\rangle \qquad (16)$$

Analysis by Vitalli Ginsburg (Harold, Thomas S., 2001) using with Superconducting Quantum Interference Device (SquID) shown that Fermi's interference displacement caused by UO_2 nuclear fuel in 400 tesla magnetic field reactor chamber.

3. RESULT AND DISCUSSIONS

Ultimate testing for the three types materials including are $Th_x\ DUO_{1.7}$, $Th_x\ DUO_{1.8}$ and $Th_x\ DUO_{1.9}$ covering the Cerenkov's radiation impact existence at reactor chamber. This moment was happened at moderator pool, so to be reactive with Na_2SO_3 liquid. The element of nuclear fuel matrix was using UO_2 with Pu_2O and Th_2O_y buffer element could be increasing for thermal neutron flux until 4.7 x 10^9 currie/mm. In this picture on below, has shown the Cerenkov's radiation was happened at reactor chamber, when the nuclear fuel element covered UO_2 more enrichment.

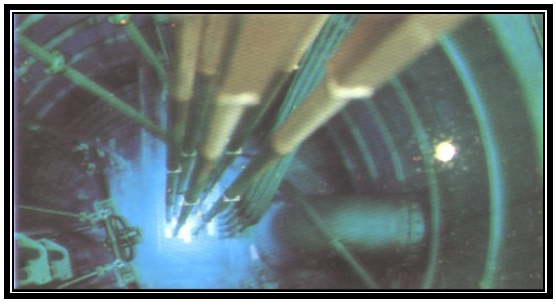

Figure 1-Cerenkov's radiation moment at 45.7 MW with DUO_2 more enrichment

(Courtesy and special permission of CERN, Lyon)

From the picture above, it has shown the blue color deep at reactor chamber, if look from reactor's yield bottom. It has biggest thermal neutron flux until 5.3 x 10^{10} currie/mm and coming up of v,v^- particles in amount is 2.6 x 10^4 mol per 1 activation reaction. This particles has known as Dirac's particle couldn't shield or barrier with Pu or Th up to 10^{10} light-years thickness.

After through the ultimate test by Cerenkov's radiation, the material of $Th_x\ DUO_{2-x}$ derivatives has tested in quantum magnetic-spin and magnetic-resonance at 450 tesla magnetic field on 45.7 MW and detecting by *Electron Spectroscopy for Chemical Analysis to Neutron* (ESCA-N). The picture from its tested has figured out below.

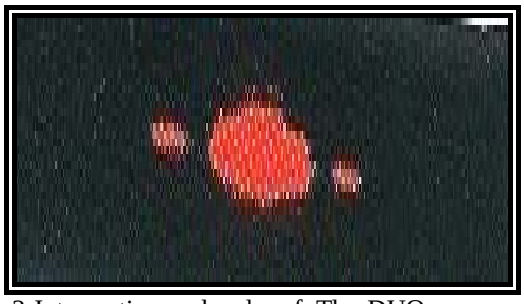

Figure 2-Intersection molecular of $Th_x\ DUO_{2-x}$ in 450 tesla magnetic field
(*Courtesy of CERN, Lyon*)

Looking forward the picture, find out the nucleus of greatest mass from $Th_x\ DUO_{2-x}$ assemble to making a center of gravity's mass surrounding by two interstellar mass. Hosted by Dirac, these interstellar are phonon-electron's active cloud and always pairing together. It will be explained how the quantum magnetic-spin keep on steady state for long period as long as there isn't loosing mass, however a much little bit value. The value is 2.426 x 10^{-12} m and to converted to relativistic-mass unit by Bose-Einstein multiplier.

Based on a few Equations shown that the post result by Super Muon-Magnetic experimental with magnetic-spin frequency at 550 MHz and rolling shield of 450 tesla magnetic field, the quantum density from inactive Fermi-Hall's paired cloud has connected with plane wave is homogenous state. Figure out by Bohr-Sommerfeld's formulation has calculated wrote by

$$\mu_{BS} = \frac{e\hbar}{2m_e}$$

$$= \frac{1.6021892x10^{-19}\,x\,6.626176x10^{-34}}{4\pi\left(9.109534x10^{-31}\right)}$$

$$= 9.274078\ \ x10^{-24}\ JT \qquad (17)$$

Comparison by the value of Magneton-Bohr's formulation

$$\mu_B = eh/2m_e$$

= magneton Bohr
= 9.273 x 10^{-24} J/T (18)

there is very tight difference, but a much little value has enough to making Fermi's effect on intersectionthe value of

nucleus magneton, μ_N, has described by Equation (15) but in group-theory of quantum relativistic, for seem not to be complicated, take a look for semi-relativistic formulation, using :

$$|\mu_N| = |g_N| \frac{e}{2m_p} \sqrt{I(I+1)\hbar} \qquad (19)$$

When $\sqrt{I(I+1)\hbar}$ is quantum moment magnetic-nucleus as describing by Einstein and Sommerfeld (Weigner, Karl P., 2002)0 took place of the v particle, and making a good simplify calculation for nucleus magneton such as

$$\mu_N = \frac{e\hbar}{2m_p}$$

$$= \frac{1.6021892\,x10^{-19}\,x\,6.626176\,x10^{-34}}{4\pi\,1.6726485\,x10^{-27}}$$

$$= 5.50824 \text{ x}10^{-27} \text{ JT}^{-1} \qquad (20)$$

Therefore nucleus magneton $\approx \frac{1}{1836}$

From Bohr's magneton, it can be divided of interstellar ensemble for a few micro-substances. These was explained how the thermal neutron for 450 tesla magnetic field could reach the quantum boundary layer and affected the Fermi's effect increasing so depth in the crystalline structure.

The phenomena about this matter could see for picture below making by *Kaon* detector, which is integrated by Gell-Mann spectroscopy and connected to Magnetic Stirrer for reactor chamber, was adjusting its power.

The picture has shown one magneton nucleus and five interstellar consists are thousands phonon-electron's paired making a barrier for thermal neutron luminosity and its bombarding, was given such as

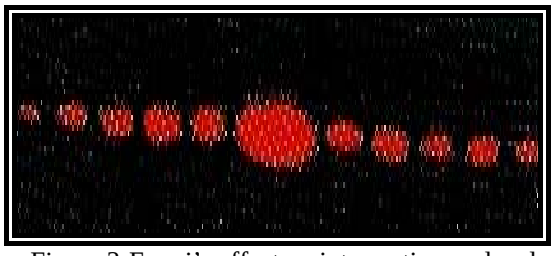

Figure 3-Fermi's effect on intersection molecular of Th_x DUO_{2-x} in 450 tesla
(*Courtesy of CERN, Lyon*)

Remaining of Anderson's tunnel fields has found the fluxoid and based on Equations (19) and (20) for deflection requirement crystalline structure, having found the value for distance between one interstellar to other side as written by

$$R_e = \sqrt{\frac{I}{\mu}} = \sqrt{\frac{2.643x10^{-47}}{1.62668x10^{-27}}} = 1.275x10^{-10}{}_m \quad (21)$$

In quantum magnetic-spin for relativistic field, the reliability of crystalline structure depends on Bohr-Sommerfeld formulation, Fermi-Dirac's state, and Bose-Einstein statistic condition, and reference to Equations (15) and (21), will have investigated each interstellar by :

$$N_i = g_i e^{-\varepsilon_{1/kT}} / \sum_i g_i e^{-\varepsilon_{1/kT}} \qquad (22)$$

Remaining those impact and based on the study about reliability of crystalline structure of substitution material, Th_x $DUO_{1.8}$, then this substrate made to a pellet and to be testing in Super Muon-Magnetic tray connected to reactor chamber. According to Equations (10) until (18) above, there is must be existing of quantum magnetic-rotate also magnetic-spin simultaneously from crystalline structure caused by EC effect at the 10^3 nm area depth. Using with ESCA-N, involves bombarding the surface with high-energy of thermal neutron in 45.7 MW adjusting power to emit phonon-electrons cloud pairing together, then making of Fermi-Dirac's state in outer-boundary layer, so it could be analyzed for information on the elemental of the depth surface.

The picture below could be shown how the enough strongest of Th_x $DUO_{1.8}$ material facing the impact of the EC's value at semi-relativistic quantum magnetic-spin and magnetic-rotate for reliability of its crystalline structure, and also facing to thermal neutron flux bombarding at 2.1 x 10^5 currie/mm amount. For better viewing, take a look about its graph comparison between present material, Zircalloy-4, and the substances at thermal neutron bombarding for IAEA standard around is 1.9 x 10^5 currie/mm and just only 400 tesla quantum magnetic-rotate and magnetic-spin frequencies, when moderator liquid has still same condition, Na_2SO_3 and the state of muon-hadron particles there weren't detected by *Kaon* and Gell-Mann detectors, and the picture on below

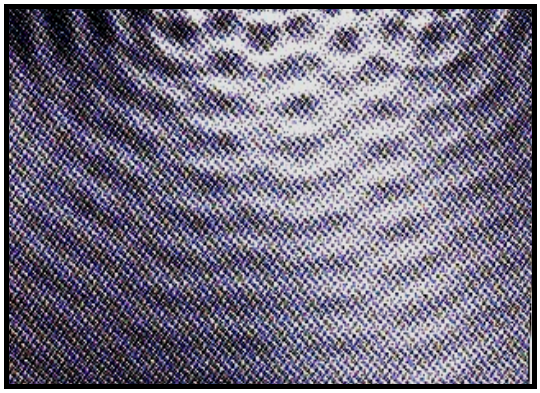

Figure 4-Cross-section effect of EC on sub critical phase based on Th_x $DUO_{1.8}$
(*Courtesy of CERN, Lyon*)

Observing that picture, and concerning of crystalline structure for Th_x $DUO_{1.8}$ material for it's crystalline structure reliable value, there is a few points for analyzing that phenomena such as:

a. The Compton's displacement wave length has very smooth waving on top side, it means for 0.811752 / 10^{-3} amu magneton's nucleus, the phonon-electron cloud together with Fermi-Dirac state and neither of one pieces of thermal neutron could be breaking the barrier on 10^3 nm depth area.

b. At adjusted power 45.7 MW and 2.1 x 10^5 currie/mm luminosity of thermal neutron, the interstellar of this material able to conduct of quantum semi-relativistic electrical charge, the amount is 7.8114/eV. It can be calculated by Equations (2.45) and (2.47) in group-theory, but with quantum coupling rotation for magnetic-rotate has shown by

$$P^2 = J(J+1)\hbar^2;$$

requirement : **J** = 0,1,2,… (23)

$$P_Z^2 = M^2\hbar^2 \quad ; \text{requirement:}$$

M = 0, ±1, ±2, …**J** (24)

$$P_k^2 = K^2\hbar^2 \quad \textbf{;} \text{ requirement:}$$

K = 0, ±1, ±2, …**J** (25)

$$E_{FD} = J(J+1)\frac{\hbar^2}{8\pi^2 I_{FD}} + K^2\left(\frac{1}{I_F} - \frac{1}{I_D}\right)\frac{\hbar^2}{8\pi^2} \quad (26)$$

c. At bottom side it looks that the electron-neutron cloud in active reaction, then the electrical charge line could be an ensemble together with notation C ; which one of parity coefficient is up arrow, there is possibility to grew up much more interstellar neighboring as far as 0.001127 x 10^{-10} meter, and fixed on Einstein-Sommerfeld predictable.

d. For magnetic field has reached 450 tesla, the value for quantum magnetic-spin of Th_x $DUO_{1.8}$ is 7.8114/eV thereby the resonance of spin-rotate has matched with formulation and more completed in quantum states. Additional result, after testing Th_x DUO_{2-x} derivative, there is tabulation to indicate that the Th_x $DUO_{1.8}$ has bigger value than another derivative themselves.

Table 1 : The properties of quantum magnetic field states

Materials	Quantum magnetic-spin value	Quantum states
Th_x $DUO_{1.7}$	7.1006/eV	$C^F_{kij\uparrow}; E_{(FD,J)}$
Th_x $DUO_{1.8}$	7.8114/eV	$C^F_{kij\uparrow}; E_{(FD,P,J)}$
Th_x $DUO_{1.9}$	7.7221/eV	$C^F_{kij\uparrow}; E_{(FD,J)}$

Source: Experimental test at 1.0 μ m Fermi-Dirac area (*Courtesy of Betha Group LHC, CERN, Lyon*)

According of quantum magnetic-spin and magnetic-resonance which are expressed by Equations (11) until (22) that was describing about how strongest impact from thermal neutron bombarding to Fermi-Dirac interstellar area wide. However, the wide is 0.001127 x 10^{-10} meters having magnetic field deflection on resonance of spin-rotate around 6772.55 cm per each Fermi's cloud active reaction. This matter in 500 MHz up to 550 MHz magnetic-spin frequency with Na_2SO_3 liquid moderator's water cooling at reactor chamber. For show up the impact and existing of Fermi-Dirac's surface effect caused by Anderson's tunnel for floating of thermal neutron electrical charge in quantum magnetic-spin also resonance, it has figure out from Gell-Mann spectroscopy and ESCA-N devices below

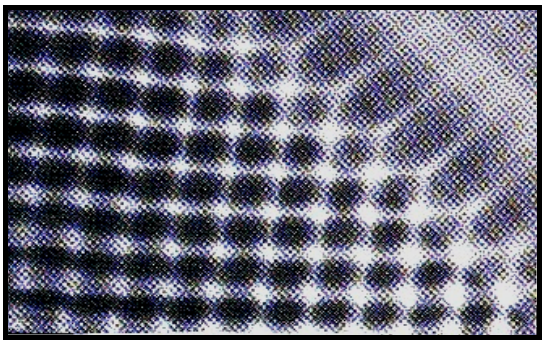

Figure 5 – Flux of thermal neutron effect cross-section caused by Fermi-Hall state at 2.1 x 10^5 currie/mm on 450 tesla in critical phase based on Th_x $DUO_{1.8}$ in 45.7 MW (*Courtesy of CERN, Lyon*)

Based on the resonance of magnetic-spin and is rotate. Then using a few formulation will be found the joining between Coulomb nuclear force with Bohr's centripetal force in relativistic quantum area, which is 2.1 x 10^4 currie/mm thermal neutron flux absorption for minimal condition in reactor chamber, the value of *n*-th stage begin from 1 up 2 according the Fermi's interference condition. Based on the formulation for Fermi-Dirac's active cloud in coherent Compton's wave length, will be adjoined of critical modulation phonon's vibration and Cooper's pair cloud, there was written by $\varpi = \exp(-i\vec{p} \bullet \left[\vec{r}\, x\, \hbar\right])$ (27)

If using the Einstein-Sommerfeld deflection requirement for the thermal neutron flux from Compton's nuclear wave length after first chain ordered reaction, could be wrote by

$$\oiiint_J \vec{p}\, x\hbar\, x\left[-\vec{i}\, x\left\{\vec{j}\, x\hbar\right\} dr\, dl\, dS\right] \bullet \oiiint_p \Phi < \xi_F > \quad (28)$$

Through by Anderson's tunnel field could be found of fluxoid value with Einstein-Sommerfeld deflection effect of mesonic in positive charge and lambda point in magnetic field, bring the Equations (18) until (27) in simple value, written by

$$\Phi = \frac{2\pi\ \hbar\ c\ S_{II}}{q^{\pm}_{\uparrow}} \quad (29)$$

$$\Phi^{\pm}_{\uparrow\downarrow} = \vec{\Phi}_0 \bullet S_{II} \quad (30)$$

When the value is 2.0678 x 10^{-7} gauss cm^2 and was called the earlier fluxoid reaction in quantum magnetic-spin and magnetic-rotate just like the Figure 5 especially in bottom plane.

In a few Equations (27) until (30) have shown Ae^{ik_0x} represents the wave traveling along the *x*-axis with amplitude A and Be^{-ik_0x} represents the reflected Compton's wave along negative *x*-axis with amplitude B for quantum resonance state.

4. CONCLUSIONS

Investigations and research using by Juergen Model programming also Super Muon-Magnetic equipment based on Th_x $DUO_{1.8}$ material for control rod blade nuclear reactor 45.7 megawatts have a few result, expressed:

a. The strength of thermal neutron flux absorbed is 2.1 x 10^5 – 1.9 x 10^6 currie/mm.
b. The values of Electrical Conductivity (EC) about 26.62 – 29.98 in 800º - 890º C temperature for IAEA standard. At thermal neutron flux amount 2.1 x 10^5 currie/mm then the value of EC is 29.44 – 37.98 in IAEA standard. For magnetic field has reached 450 tesla, the value for quantum magnetic-spin is 7.8114/eV and Anderson's tunnel between interstellar area around 0.001127 x 10^{-10} meters, then the thermal neutron electrical charge could be flowing smoothly.
c. For magnetic field is 450 tesla and thermal neutron absorption exactly 2.1 x 10^5 currie/mm, the crystallization structure reduction is 6.88% - 10.95% for 25 years period in 45.7 megawatts.

REFERENCES

1. Betingthon, Dominique F., (2001) Making of Control Rod Blade in Magnetic Stirrer, CANDU Reactor of Canada Atomic Journal, 18, pp. 111-125.
2. Chalotra, G.P., (1999). Electrical Engineering Materials, Khana Publishers, New Delhi.
3. Chattopadhyay, C., and Rakshit P.C., (1998). Quantum Machanics and Solid State Physics, Mc-Graw Hill Book Co., New York.
4. Durant, W.C.,(2000). Manufacturing of Control Rod Blade by Simulation, Journal of PWR and BWR Reactor, 15, pp. 156-164.
5. Gomiez, Arthuro J., (2001). Idle Time and Power in Sr_2O_3 . H_2O for High Energy, British Atomic Energy Journal, 44, pp.110-123.
6. Harold, Thomas S., (2001). Unsteady Condition for Sr in Multi Purpose Reactor, British Atomic Energy Journal, 44, pp. 137-151.
7. Kempster, M.H.A., (1999). Materials for Engineers, Mc-Graw Hill Book Co., New York.
8. Moh. Hardiyanto, (2001). Eliminary Study for Control Rod Blade Nuclear Reactor Based on Sr + Al Alloy, CERN Proceeding, ISBN 979-8554-51-8.
9. Stuart, Thomas P., (2001). Muon Particle to be Absorbed by Sr_2Cr_3O in PWR, IAEA Journal, 34, pp. 85-99.
10. Thorton, Ian, (2001). Preorientation Sr_2O_2 Compound in Control Rod Blade",CANDU Reactor of Canada Atomic Journal, 18, pp. 77-89.
11. Valli, G., (2000). The Experimental Programme for the Development of The Multi Purpose Reactor, IAEA Journal, 21, pp. 141-145.
12. Vasudeva, D.N., (1999). Fundament als of Magnetism and Electricity, S. Chand and Company Ltd., New Delhi.
13. Vialli, T., (2000). Ising Model for Control Rod Blade Moderator, IAEA Journal, 27, pp. 187-199.
14. Waghmare, Y.R., (2001). Strontium Elements in Multi Purpose Reactor at 25 MW, CANDU Reactor of Canada Atomic Journal, 17, pp. 56-69.
15. Weigner, Karl P., (2002). Buffer Element of Thermal Neutron Flux in CANDU, CANDU Reactor of Canada Atomic Journal, 2, pp. 44-57.

About Author:

Researcher at Betha Group for Muon-Hadron LHC, CERN, Lyon, France.

Etchant Selection for the High Metallographic Quality of HSLA-0,037%Nb Prior-Austenite Grain Boundaries

Myrna Ariati, W Narottama Putra, Sutopo and D Febriani

Dept. Metallurgy and Material, Faculty of Engineering
University of Indonesia,
Kampus Baru UI Depok 16424
Tel : (021) 7863510. Fax : (021) 7872350
E-mail : myrna@metal.ui.ac.id

ABSTRACT

Prior Austenite is an important phase in high strength low alloy (HSLA) steel , before it being transformed by cooling to room temperature from austenite temperature of reheating process. in Thermo Mechanical Control Process.(TMCP) . However, the observation of prior austenites is limited due to the difficulty to find an appropriate etchant solution. The present study is aimed at overcoming this problem therefore the behavior of the austenite grain during hot working, can be monitored.
In this experiment, a single composition of HSLA-0.037Nb with 0.048%C, was heated to various austenization temperatures of 1000, 1100, 1200 and 1300°C, fast cooling by water quenching. .Metallography. examination were performed using five different composition of picric acid , aquadest or Alcohol, $CuCl_2$, HCl and wetting agents .
Visual observation shows that the higher the reheating temperature, prior austenite grain boundaries can be observed more clearly as can be observed in samples reheated to 1300°C for all etchant solution composition and techniques .
The most optimum etchant solution for revealing prior austenite grain boundary for this type of steel is supersaturated picric acid solution in alcohol, with small amount of HCl and modified with additional of small amount of Dodecylbenzenesulfonat (DBS) as the wetting agent . More over, additional of Dodecylbenzenesulfonat (DBS) makes picric acid solution works better significantly.

Keyword: *Etchant Composition , Prior Austenite, Grain boundaries, HSLA-Nb,., Thermo Mechanical Control Process (TMCP)*

1. INTRODUCTION

High Strength Low Alloy Steel (HSLA) or Microalloy Steel with small amount of Nb,V or Ti has high structural Strength, with minimum tensile strength of 350 MPa[1,2]. The strength of this kind of steel can be improved by various mechanism such as solid solution strengthening,grain refining, precipitate strengthening and work hardening (dislocation hardening) [2].. The Strength of HSLA steel is affected by the final microstructure and final grain size. For this purpose, Thermo Mechanical Control Process (TMCP) has been applied to control the microstructure and mechanical properties of HSLA Steel

The Interest in controlling the thermomechanical process on the materials mainly has the following reason [3,4];

a. To have the higher quality of product by a precise control process.
b. To reduce the cost production,especially in the development of new production techniques or improvement of existing techniques.

These reason become more important since with increasing demand of metallic products, and energy crisis is increasing worldwide , saving energy during hot forming has attracted to do.
For this purpose, the quantitative metallographic method can be used to calculate the austenite grain size . However, the observation is limited with the difficulty to find an appropriate etchant solution. The present study is aimed at overcoming this problem so that the behavior of the austenite grain during hot working, can be monitored.
Metallography techniques to reveal the prior austenite grain boundaries is unique since the observed austenite structures actually had been transformed to ferrite or martensite. Various prior austenite etching techniques had been applied by some researchers , but those techniques applied to HSLA with higher Carbon content and only at a certain reheating temperature[5,6] . The present study focuses on the effect of reheating temperature of steel and composition of etchant solution to the metallographic quality of prior austenite of HSLA-Nb.

2. EXPERIMENT

In this experiment, a single composition of HSLA-0.037Nb with 0.048%C, was heated to various austenization temperatures of 1000, 1100, 1200 and 1300°C, holding for 30 minutes in the Muffle Furnace with heating capability up to1600°C,follows with fast cooling using cold water quenching .Metallography examination wew performed using five different composition of picric acid , aquadest or Alcohol, $CuCl_2$, HCl and wetting agents .

The composition of HSLA Steel is as follows;

Table 1. HSLA Steel observed in research (wt%)

Ti	C	Si	Mn	P	S	Al
0,002	0,048	0,266	0,706	0,01	0,007	0,037
Cu	*Nb*	**V**	**Ni**	**Cr**	**N**	**Cu+Cr+Ni**
0,052	0,037	0,003	0,022	0,018	0,004	0,092

The material is HSLA steel slab**,** with dimension of working samples are cubes with axes of 1 cm as follows;

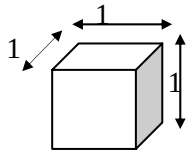

Figure 1. Working samples dimension

After heating and quenching process with cold water (0^oC), metallographic sample preparation starts with grinding,polishing and etching. Fast cooling from austenization temperature is to have martensite microstructure which according to some literatures , will makes easier to reveal the prior austenites grain boundaries. Etching solution and techniques applied in this research are as follows;

Tabel 2. Etchant techniques and solution composition,

Etching Solution	***EtchingTemp. (^oC)***	***Etching time Sample 1 (1000^oC)***	***Etching time Sample 2 (1100^oC)***	***Eching time Sample 3 (1200^oC)***	***Etching time Sample 4 (1300^oC)***
Saturated Picric acid 30%[7] *30 gr asam* picric + *100 ml alkohol + 1 drop of HCl+ DBS(modified)*	*Temp ruang 25 –27*	*5 mnt*	*5 mnt*	*3 mnt*	*2.5 mnt*
Etsa Jepang:[8] *2 gr asam* picric + *0,5 gr* $CuCl_2$ *+ 2 ml* teepol + *100 ml aquades + 1 drop of HCl*	*Temp ruang 25 –27*	*4 mnt*	*4 mnt*	*6 mnt*	*5 mnt*
Etsa Super Picral:[9] *2 gr asam* picric + *100 ml aquades + 3 ml* teepol	*70 – 80*	*4 mnt*	*3.5 mnt*	*3 mnt*	*2.5 mnt*
Super Picral (modifikasi): *2 gr asam* picric + *100 ml aquades + 3 ml* teepol + *3 drops of HCl*	*70 – 80*	*3.5 mnt*	*3 mnt*	*2.5 mnt*	*2 mnt*
Etsa Saturated Picric Acid:[10] *10 gr asam* picric + *100 ml aquades + 3 ml* teepol	*70 – 80*	*4 mnt*	*4.5 mnt*	*3.5 mnt*	*3 mnt*

•

Etching Solution composition has adopted from previous researchers which had applied to different composition steels [7,8,9,10], while etching time and temperatures applied with trial and error in this observation. One of these techniques also modified with additional of wetting agents like dodecylbenzenesulfonat (DBS)

After etching process, metallographic examination under optical microcope with some magnification has done, and austenite grain boundaries appearance were observed and compared each other.

3. RESULT AND DISCUSSION

Metallography examination with five different etching solution and techniques shows prior austenite appearance as photomicrographs as follows;

3.1 Prior Austenite with various etching techniques of samples with heating temperature of 1000^oC

3.1.1 Saturated Picric Acid 30%

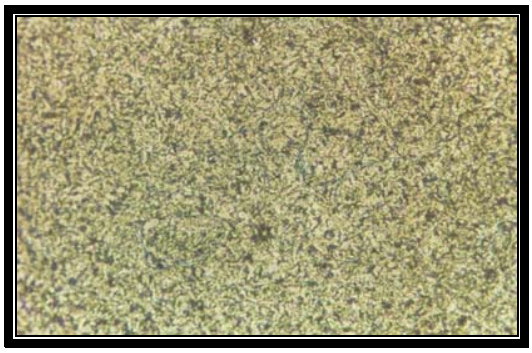

Figure 2. Prior Austenite Grain Boundaries saturated Picric Acid 30%, sample no 1,200x Magnification

3.1.2 Japanese etching Solution

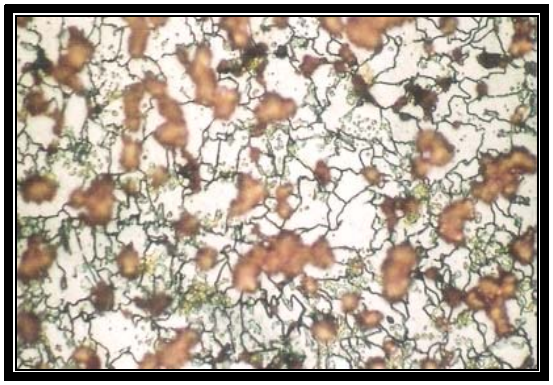

Figure 3. Prior Austenite Grain Boundaries ,Japanese etching, sample no 1,500x Magnification

3.1.3 Super Picral Solution

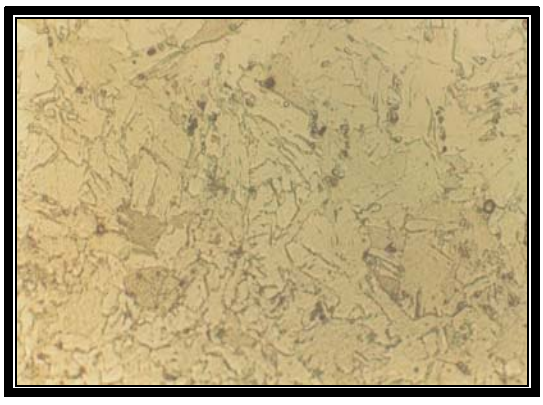

Figure 4. Prior Austenite Grain Boundaries ,super picral etching ,sample no 1,500x Magnification

3.1.4. Modified Super Picral Solution

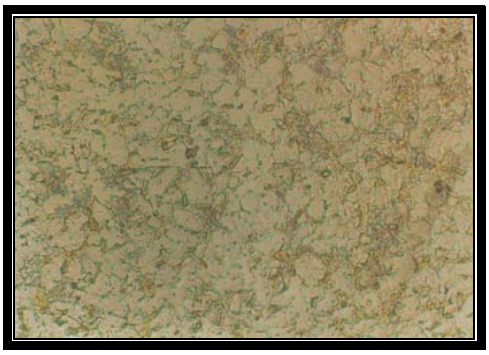

Figure 5. . Prior Austenite Grain Boundaries, Modified super picral etching ,sample no 1,500x Magnification

3.1.5 Saturated Picric acid 10% Etchant solution

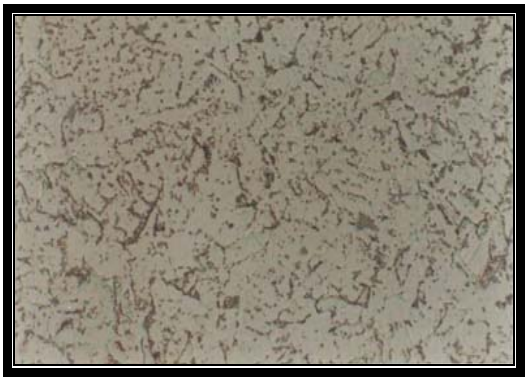

Figure 5. . Prior Austenite Grain Boundaries saturated ,picric 10% acid etching,,sample no 1,500x Magnification

3.2.Prior Austenite with various etching techniques of samples with heating temperature of 1100^{o}C

3.2.1 Saturated Picric Acid 30%

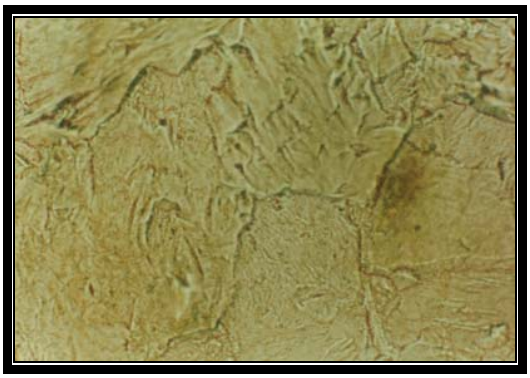

Figure 6. Prior Austenite Grain Boundaries saturated Picric Acid 30%, sample no 2,500x Magnification

3.2.2 Japanese etching Solution

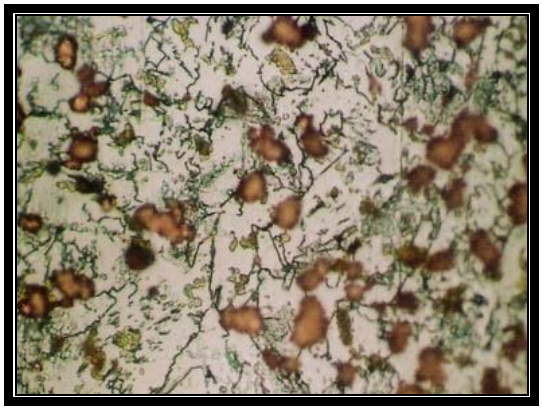

Figure 7.Prior Austenite Grain Boundaries ,Japanese etching, sample no 2,500x Magnification

3.2.3 Super Picral Solution

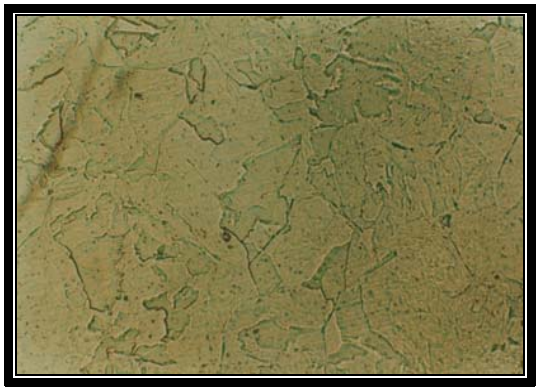

Figure 8. Prior Austenite Grain Boundaries ,super picral etching ,sample no 2,500x Magnification

3.2.4. Modified Super Picral Solution

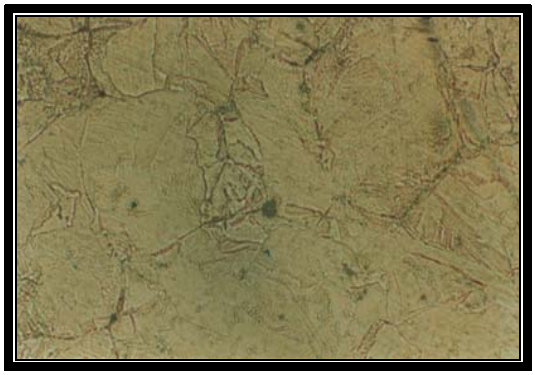

Figure 9 Prior Austenite Grain Boundaries, Modified super picral etching ,sample no 2,500x Magnification

3.2.5. .Saturated Picric acid 10% Etchant solution

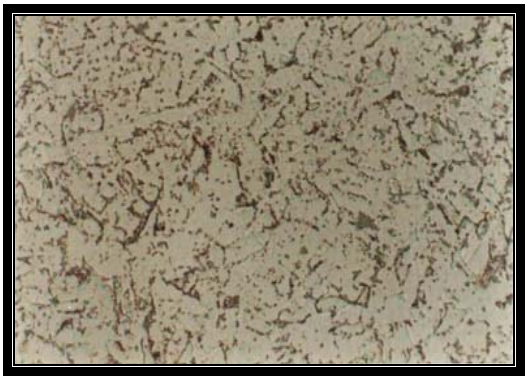

Figure 10. Prior Austenite Grain Boundaries saturated ,picric acid 10% etching,,sample no 2,500x Magnification

3.3.Prior Austenite with various etching techniques of samples with heating temperature of 1200^{o}C

3.3.1 Saturated Picric Acid 30%

Figure 11. Prior Austenite Grain Boundaries saturated Picric Acid 30%, sample no 3,100x Magnification

3.3.2 Japanese etching Solution

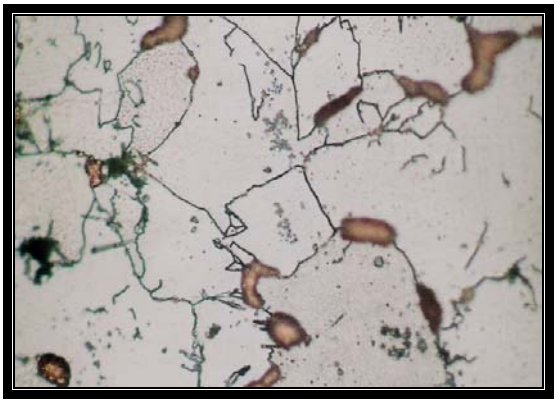

Figure 12.Prior Austenite Grain Boundaries ,Japanese etching, sample no 3,500x Magnification

3.3.3 Super Picral Solution

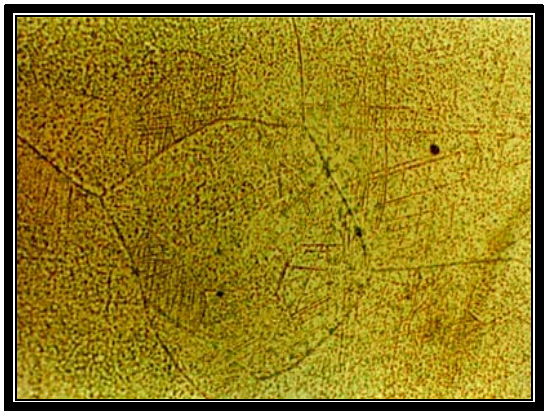

Figure 13.Prior Austenite Grain Boundaries ,super picral etching ,sample no 3,500x Magnification

3.3.4. Modified Super Picral Solution

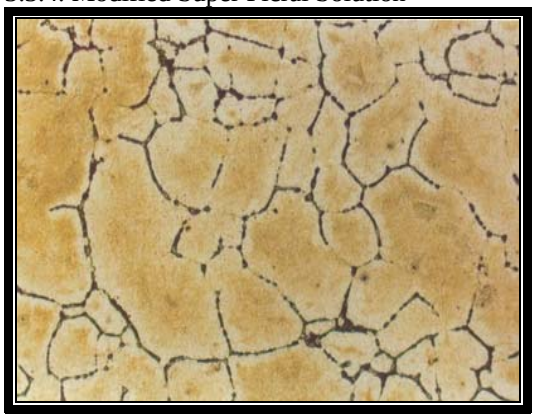

Figure 14. Prior Austenite Grain Boundaries, Modified super picral etching ,sample no3,100x Magnification

3.3.5. .Saturated Picric acid 10% Etchant solution

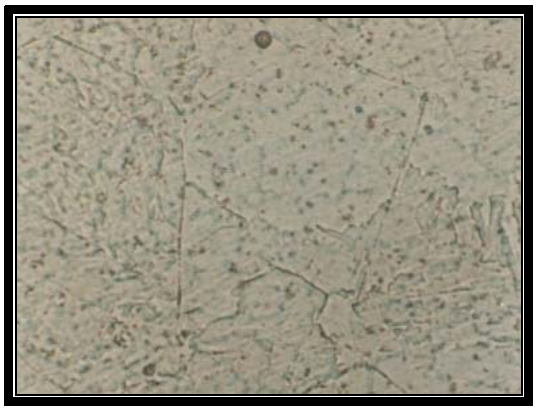

Figure 15. Prior Austenite Grain Boundaries saturated ,picric acid 10%etching,,sample no 3,500x Magnification

3.4.Prior Austenite with various etching techniques of samples with heating temperature of 1300°C

3.4.1 Saturated Picric Acid 30%

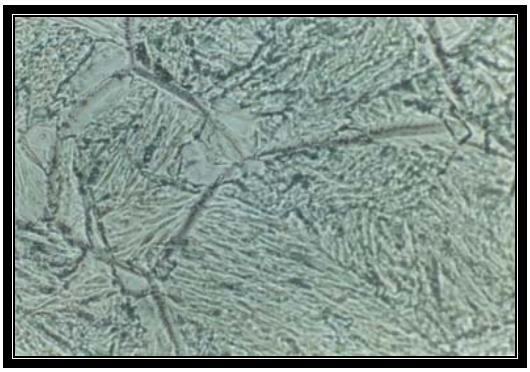

Figure 16. Prior Austenite Grain Boundaries saturated Picric Acid 30%, sample no 4,500x Magnification

3.4.2 Japanese etching Solution

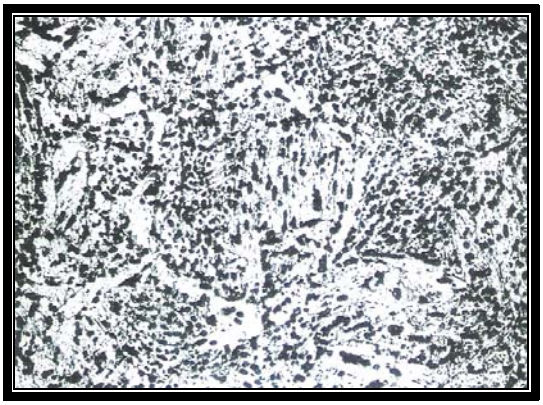

Figure 17. Prior Austenite Grain Boundaries ,Japanese etching, sample no 4,100x Magnification

3.4.3 Super Picral Solution

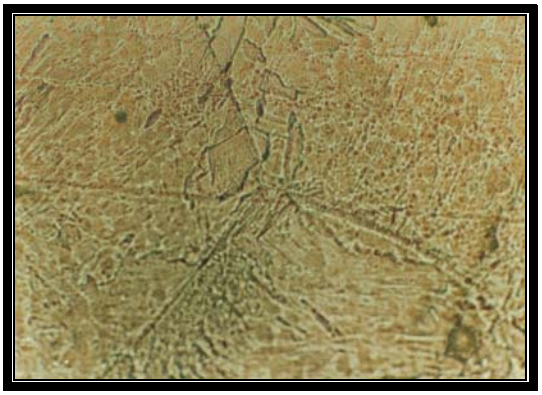

Figure 18.Prior Austenite Grain Boundaries ,super picral etching ,sample no 4,500x Magnification

3.4.4. Modified Super Picral Solution

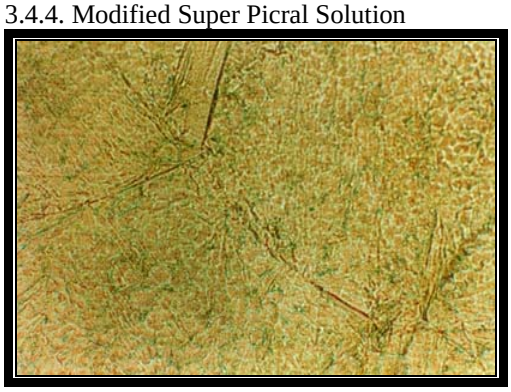

Figure 19. Prior Austenite Grain Boundaries, Modified super picral etching ,sample no4,500x Magnification

3.3.5. .Saturated Picric acid 10% Etchant solution

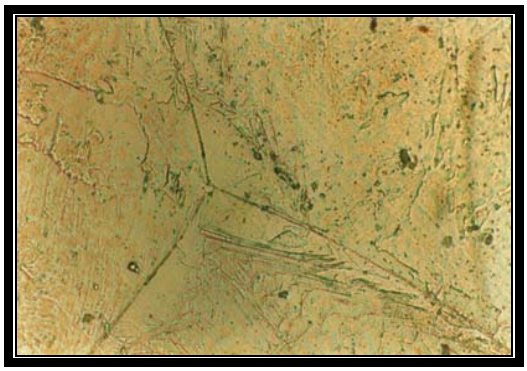

Figure 20. Prior Austenite Grain Boundaries saturated ,picric acid 10%etching, sample no 4,500x Magnification

Photomicrographs aboves, shows that the prior austenite grain boundaries can be revealed by all the etching solutions and techniques observed, but in different qualities.

A very good prior austenite grain boundaries appearance can be obtained by saturated picric acid 30% modified by additional of wetting agent Dodecylbenzenesulfonat(DBS). This etching solution not only reveal the prior austenite grain boundaries , but also the grain structures.Besides this kind of etching, Japanese etching solution also reveal austenite grain boundaries, however It also reveal some phases with brown colours at the grain boundaries of austenites. Super picral solution and its modification can reveal the austenite grain boundaries, although it looks like should be at the longer etching time, as it looks as only thin grain boundary appearance. Saturated picric acid 10% etching solution also reveal thin grain boundaries appearance, as it is difficult to reveal in photomicrograph with low magnification.

These visual observations shows that prior austenite grain boundaries are very sensitive to the etchant solution composition, methods and in the same time also affected by austenization temperature of steel. .

For HSLA-0.037Nb which was previously austenized at 1000 °C, the prior-austenite grain boundaries almost can not be clearly revealed by any etchant solution composition and methods.(figure 2 to figure 5). Almost the same appearance can be observed for samples with

austenizing temperature of 1100°C, which prior austenite revealed with low quality appearance (figure 6-figure 10) With higher austenization temperature, as samples with austenization at 1200°C and in the first place at 1300 °C , austenite grain boundaries become easier to reveal and can be observed clearly (Figure 11-figure 18). This observation also shows that an etching solution consisting of saturated picric acid 30% in alcohol with an additional of small amount of HCl is the most effective etchant solution to reveal the prior austenite grain boundaries in comparison to other combination of etchant solution , at almost all austenizing temperature except at 1000°C. It was also found that a modification on that etching solution with small amount of dodecylbenzenesulfonat (DBS) as the wetting agents , is significantly more effective in revealing the prior-austenite grain boundaries of high metallographic quality

4.CONCLUSIONS

Based on analysis to these photomicrographs aboves, it was found that reheating temperature in Thermo Mechanical Control Process (TMCP) influences the ability of etchant solution in revealing prior austenite grain boundaries. The higher the reheating temperature, prior austenite grain boundaries can be observed more clearly as can be observed in samples reheated to 1300°C.

The most optimum etchant solution for revealing prior austenite grain boundary for this type of steel is supersaturated picric acid 30% solution in alcohol, with small amount of HCl and modified with additional of small amount of Dodecylbenzenesulfonat (DBS) as the wetting agent . Additional of Dodecylbenzenesulfonat (DBS) makes picric acid solution works better significantly.

REFERENCES

[1]. Yang H. Bae, et al., "Effects of Austenite Conditioning on Austenite/Ferrite Phase Transformation of HSLA Steel," *Jurnal Teknologi*, 45(1) 2004: hal. 137-142

[2]. B.K Panigrahi, "Processing of low carbon steel plate and hot strip-an overview," *Jurnal Teknologi*, 24(4) 2001: hal. 361-371

[3] C.M Sellars "Static Recrystallization and Precipitation During Hot Rolling of Microalloyed Steels" *Mat Science Seminar* 23-24 Oct, 1982,pp 1-18

[4]I.V Samarasekera and EB Hawbolt," Overview of Modelling The Microstructureal state of Steel Strip during Hot Rolling,", *The Journal of The South African Institute of Mining and Metallurgy*, August, 1995, pp 157-165

[5]G.F Vander Voort, *Metallography-Principles and Practice* (USA: McGraw-Hill, 1984), hal. 166-170;219-223

[6] Chris North, "Etching to reveal grain boundaries," *Experts Metallography Forum*, 11 Februari 2007

[7] Eddy S.Siradj, "*Strain induced precipitation kinetics of Nb(CN) in Nb-HSLA Steel as a function of thermomechanical history,*" Ph.D Thesis, The Department of Engineering Materials University of Sheffield, 1997, pp 9

[8] Myrna Ariati, E.S.Siradj, *"Evaluasi Proses Etsa untuk Menampakkan Batas Butir Austenit Prior pada Baja HSLA,"* Jurnal, Fakultas Teknik UI Jurusan Metalurgi, Depok, 2000.

[9]Chris North, *"Etching to reveal grain boundaries,"* Experts Metallography Forum, 11 Februari 2007

[10] Bruce L. Bramfitt, Arlan O. Benscoler, *Metallographer's Guide, Practices and Procedures for Iron and Steels* (ASM International, 2002), pp 7-8;33;70-73;219-221;229-230

Proceeding of the 11th International Conference on QiR (Quality in Research)
Faculty of Engineering, University of Indonesia, Depok, Indonesia, 3-6 August 2009
ISSN 114-1284

Carbon Analysis produced by High Rise Combustion of Palm Fibre

Nanik Indayaningsih[1, 2], Anne Zulfia[1], Dedi Priadi[1], Sunit Hendrana[2]

[1] *Department of Metallurgy and Material – Faculty of Engineering, University of Indonesia*
Depok 16424; Phone: 021 7863510; Fax: 021 7872350
indaya@plasa.com; anne@metal.ui.ac.id; dedi@metal.ui.ac.id

[1,2] *Research Center For Physics, Indonesian Institute of Sciences*
Kawasan Puspiptek Serpong 15314; Phone: 021 7560570; Fax: 021 7560554
nani005@lipi.go.id; suni002@lipi.go.id

ABSTRACT

Carbon can be used in many applications for example: as electrode of energy device, conductive material, reinforced plastics, as well as structural composites. Natural carbon can be in the form of the diamond, graphite, or coal with possessed the different carbon rate. The aim of this research is to analyze and produce carbon by High Rise Combustion of Palm Fibre. This carbon will be used for electrode of energy device. Carbon has been processed by using high rise warm-up technique. The carbon produced then analysis using EDS and SEM techniques to observe the element content and morphology of carbon as well as the diameter. Results showed that after obstetrical warm-up of carbon element gyrate contain of 32% - 57%. While in the form of good hollow tube before and after warm-up, the diameter of carbon was approximately 2μm - 8μm, and there were a hole at the tube wall with the size of 1μm - 2μm. Based on the specification of the carbon analysis currently was probably matched as a carbon to be used for an electrode materials conducting gas.

Key words: *carbon, pyrolysis, palm fibre, fixed carbon*

1. INTRODUCTION

Carbon is an element that resides in several polymorphic forms, thus, it can be in an amorphous form [1]. Carbon is not always in one certain group, it can be in a metal, ceramic, polymer. Several types of carbon: charcoal, active carbon, graphite and diamond. A carbon element can be found anywhere, in solid matter (human being, animals, plants), liquid (alcohol), gas (methane) and its existence is in a connection, forming a compound, such as hydrocarbon. Carbon can occur from a result of a decomposition process. The public better knows it as charcoal. Charcoal or active charcoal usually occurs as it is deliberately made, whereas coal and diamond is naturally formed in the nature. A natural fiber consists of several compounds, including cellulose, lignin and hemicelluloses. These compounds contain an element of carbon that can be decomposition by a certain process of heating, thus it can produce charcoal of approximately 35% with a porosity of 70%, whose carbon content is approximately 80 to 90% [2].

Technological development enables carbon to be applied for various types of needs, among others, hydrogen storage, biomedical, medical treatment for broken bones [3], super-capacitor, textile industries [4], conductive or reinforced plastics [5], energy storage, conductive adhesives and connectors, molecular electronics, thermal materials, structural composites (aircraft, spacecraft, and suspension bridges), catalyst supports, air, water and gas filtration, reinforced tennis rackets, baseball bats, field emission, field-effect transistors, fibers and fabrics [6], batteries and fuel cell.

Carbon, when it is used a fuel cell PEM electrode component, resembles a "frame", forming porous or hollow sheets or plates or composite sheets/plates that are arranged from a line of carbon in a solid cylinder or tube. Pores are needed in fuel cell electrodes to conduct and distribute gas fuel in all electrolyte surfaces, Figure 1 [7]. Various forms of carbon as “frames” of this PEMFC electrode can be made using a chemical vapor deposition (CVD) method [8, 9, 10], laser ablation, arch method, ball milling, plasma-enhanced chemical vapor deposition [11], usually from powder of pure carbon materials.

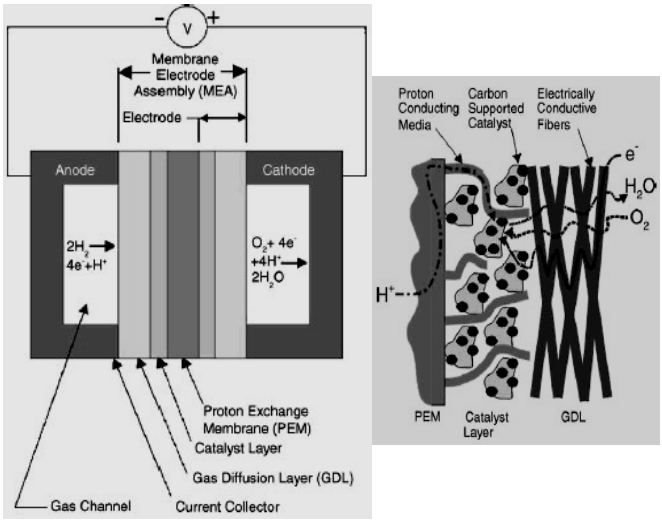

Figure 1: Electrode frame that has a function to conduct and distribute gas

In this research carbon is made from palm fibers through a process of carbonization or pyrolysis. As natural fibers contain several compound (including lignin, cellulose and hemicelluloses) whose existence may form a line along its stem, the leveled heating it is estimated or expected to be in a

form of "carbon wire" or "carbon tube." The use of carbon in this form in the creation of electrode sheets is estimated to form a frame or texture that has large porosity and is evenly distributed, of which it is a requirement as a PEMFC electrode.

2. EXPERIMENT

The basic material for the carbon making is palm fibers. Before being processed, palm fibers as natural materials, an thermal analysis is carried out in a room with a temperature of up to 900^0 using DTA-TG to find out at what temperature and what reaction that occurs, and to find out the percentage of weight loss due to the heating.

Carbon is made of palm fibers using a heating method in limited air (pyrolysis) in the temperature of 275^0 for 2 hours. The carbon content of the charcoal that occurs is analyzed using a fixed carbon method (ASTM D 1762-64) and EDX, and a microstructure is observed using SEM and XRD. Heating is continued in the temperature of 500^0 for 1 hour, and the same analysis is carried out.

3. RESULT AND DISCUSSION

A DTA TG analysis result on palm fibers with a temperature of up to 900^0C can be seen in Figure 2, showing there are 2 large peaks of an exothermic reaction in the temperature of between 272^0C - 324^0C and between 399^0C - 530^0C with a weight loss of 45% and it drops to 75%. According to Euro Sjostrom [12] in a range of the first peak of hemicelluloses and cellulose, this is degraded in the range of the second peak of degraded lignin. Heating of between these temperatures, natural materials are disentangled gradually, producing a large number of distillates, especially acid acetate and methanol, and then a number of tar and gas products.

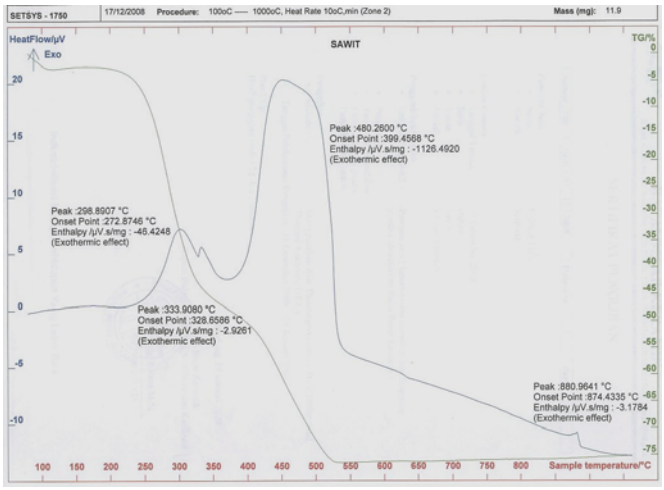

Figure 2: A curve of palm fiber DTA-TG analysis is carried out on a room temperature of 900^0C.

A result of a microstructure analysis suing XRD is shown in Figure 3, showing that charcoal, which is made, has an amorphous structure, and sharp peaks can be seen and they are most likely minerals or compounds that are contained in the palm fibers. The compounds are natural compounds in natural materials, thus it is difficult to be removed although they are heated up to 900^0C. The diffraction curve, which forms a hill or hillock, shows that the structure of the materials is amorphous. The 2θ position of the peak of the hill or hillock (amorphous structure) is nearly the same with the 2θ position of the graphite crystal structure in accordance with the XRD analysis of the graphite materials (Figure 4). This indicates that charcoal that is made dominantly contains an element of C and has an amorphous carbon structure.

Figure 3: Photos of the palm fiber basic material (left), after being carbonized (right).

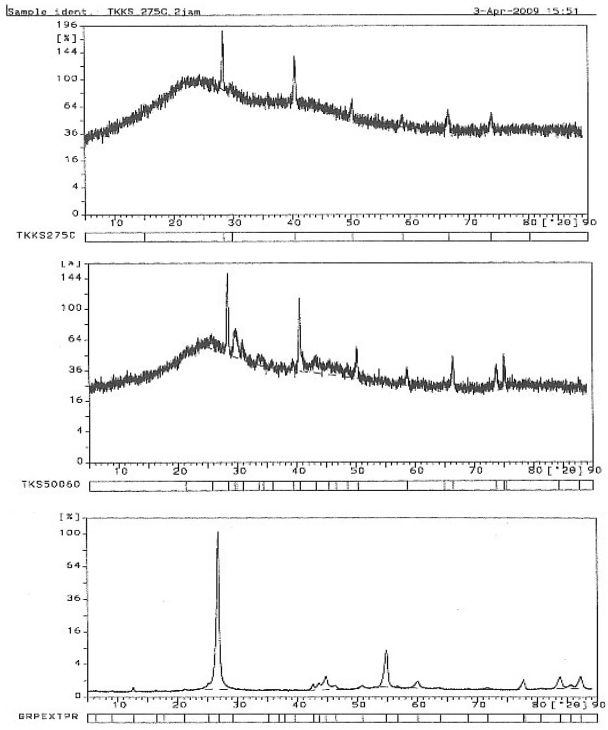

Figure 4: Diffraction curve and data on a palm fiber sample that has been heated (in limited air) at the temperature of 275^0 for 2 hours (above) 500^0 for 1 hour (middle), and pure graphite materials (below).

Tabel 1: EDX analysis Data on palm fibers that have been heated with a temperature of 275^0 for 2 hours

Angle [°2θ]	d-value α1 [Å]	d-value α2 [Å]	Peak width [°2θ]	Peak int [counts]	Back. int [counts]	Rel. int [%]	Signif.
15.080	5.8702	5.8848	0.480	32	600	6.0	0.97
28.375	3.1428	3.1506	0.120	543	480	100.0	2.94
29.765	2.9991	3.0065	0.320	40	433	7.3	1.34
40.525	2.2242	2.2297	0.240	266	272	48.9	4.85
50.210	1.8155	1.8200	0.200	59	166	10.9	1.38
58.670	1.5723	1.5762	0.400	22	119	4.1	1.68
66.440	1.4060	1.4095	0.280	46	98	8.5	2.12
73.685	1.2846	1.2878	0.320	31	90	5.8	1.32
80.270	1.1950	1.1980	0.280	5	85	0.9	0.94

Table 2: EDX analysis data on palm fibers that have been heated with a temperature of 500^0 for 1 hour

Angle [°2θ]	d-value α1 [Å]	d-value α2 [Å]	Peak width [°2θ]	Peak int [counts]	Back. int [counts]	Rel. int [%]	Signif.
21.210	4.1855	4.1959	0.960	26	515	3.4	1.25
25.690	3.4648	3.4734	0.480	79	484	10.2	1.58
28.430	3.1368	3.1446	0.180	773	392	100.0	10.03
29.490	3.0264	3.0340	0.120	185	365	23.9	0.83
29.840	2.9917	2.9992	0.240	199	357	25.7	1.92
30.855	2.8956	2.9028	0.160	117	328	15.1	0.79
33.520	2.6712	2.6779	0.480	41	272	5.3	1.07
34.265	2.6148	2.6213	0.480	42	262	5.5	0.92
35.955	2.4957	2.5019	0.320	23	237	3.0	0.84
39.455	2.2820	2.2877	0.320	32	207	4.2	0.88
40.585	2.2210	2.2265	0.200	445	199	57.6	10.78
43.170	2.0938	2.0990	0.560	59	180	7.7	2.44
45.440	1.9944	1.9993	0.640	42	164	5.5	1.05
46.630	1.9462	1.9510	0.140	35	159	4.5	0.93
48.545	1.8738	1.8785	0.400	30	146	3.9	1.07
50.265	1.8137	1.8182	0.060	110	139	14.3	0.83
58.705	1.5714	1.5753	0.320	37	100	4.8	1.69
64.885	1.4359	1.4394	0.480	11	86	1.4	0.83
66.410	1.4066	1.4101	0.100	83	85	10.7	1.14
73.730	1.2839	1.2871	0.160	49	77	6.3	1.05
75.020	1.2650	1.2682	0.100	76	79	9.8	2.46
75.275	1.2614	1.2645	0.080	40	79	5.1	2.18
84.270	1.1482	1.1510	0.960	5	69	0.7	1.07
87.645	1.1124	1.1152	0.320	12	64	1.6	0.87

Table 3. EDX analysis data on graphite

Angle [°2θ]	d-value α1 [Å]	d-value α2 [Å]	Peak width [°2θ]	Peak int [counts]	Back. int [counts]	Rel. int [%]	Signif.
6.380	13.8422	13.8766	0.720	117	620	0.1	3.01
9.080	9.7313	9.7555	0.560	110	392	0.1	2.57
12.590	7.0251	7.0425	0.080	610	289	0.5	1.25
16.445	5.3859	5.3993	0.480	64	240	0.1	1.74
17.750	4.9928	5.0052	0.480	26	234	0.0	1.01
21.080	4.2110	4.2214	0.240	74	262	0.1	1.97
25.075	3.5484	3.5572	0.280	562	303	0.5	3.67
26.835	3.3195	3.3278	0.260	113232	279	100.0	281.99
29.145	3.0615	3.0691	0.400	106	246	0.1	0.97
35.175	2.5492	2.5556	0.640	22	166	0.0	0.95
36.910	2.4333	2.4393	0.480	24	156	0.0	1.30
37.850	2.3750	2.3809	0.320	18	151	0.0	1.10
39.500	2.2795	2.2852	0.400	13	146	0.0	0.77
42.645	2.1184	2.1236	0.060	310	144	0.3	0.75
43.560	2.0760	2.0811	0.280	376	146	0.3	4.46
44.690	2.0261	2.0311	0.100	967	146	0.9	0.83
46.425	1.9543	1.9592	0.440	185	151	0.2	6.86
50.895	1.7927	1.7971	0.120	142	182	0.1	1.09
54.850	1.6724	1.6765	0.280	4789	225	4.2	54.59
56.690	1.6224	1.6264	0.240	76	190	0.1	1.30
60.080	1.5387	1.5425	0.280	353	169	0.3	5.56
63.795	1.4578	1.4614	0.640	35	132	0.0	3.01
68.530	1.3681	1.3715	0.400	14	106	0.0	1.25
71.705	1.3151	1.3184	0.480	50	104	0.0	2.72
77.685	1.2282	1.2312	0.100	369	94	0.3	1.54
77.910	1.2252	1.2282	0.100	174	94	0.2	1.05
80.530	1.1918	1.1947	0.320	24	102	0.0	0.95
83.765	1.1538	1.1567	0.140	529	117	0.5	2.47
85.580	1.1339	1.1367	0.480	110	112	0.1	3.79
87.210	1.1169	1.1196	0.140	520	108	0.5	2.90

Palm fibers and charcoal of a leveled heating result with limited air are shown in the Figure 5. This charcoal of the heating result is observed using SEM and it shows that diameters of the palm fiber charcoal vary between 100μm and1000μm. A morphology from the palm fiber charcoal shows that there are hollows in the form of alleys or tubes, which are parallel with the fibers with various diameters of hollows or tubes, between 2μm - 8μm, and at alley wall there are hole with the diameter about 1μm - 2μm. Morphology and a lot of pores in this charcoal/carbon are very attractive, it can be likely applied for a basic material of electrode in PEMFC.

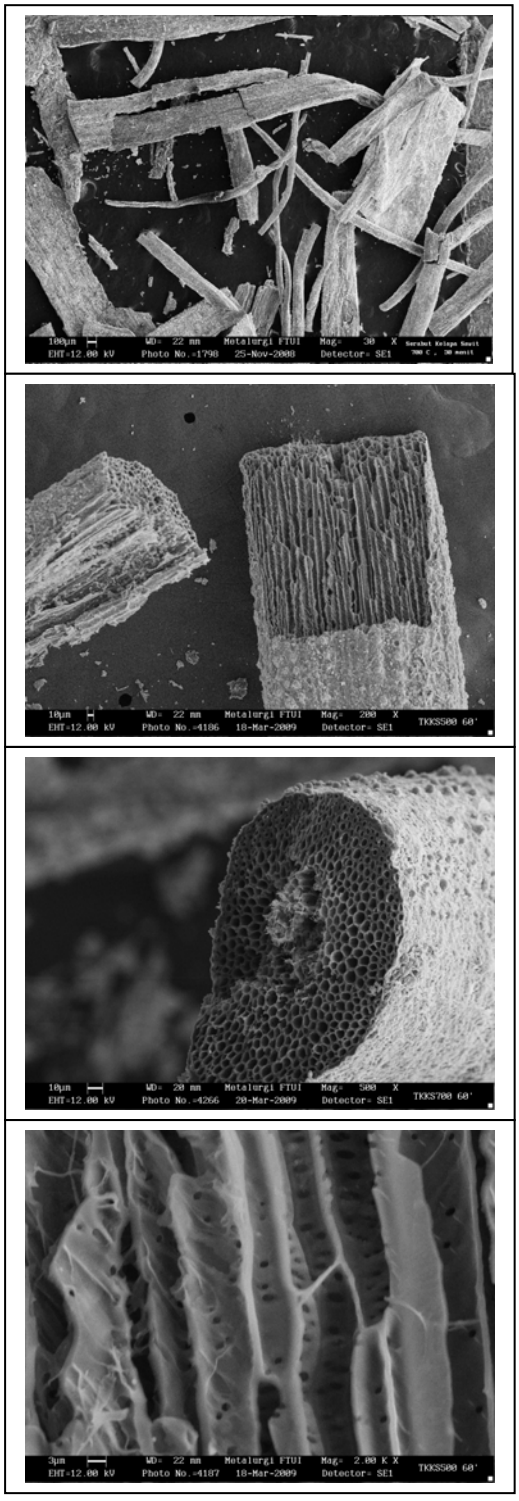

Figure 5: SEM observation result on palm fibers that have been heated , Enlargement of 30X, 200X, 500X, 2000X (from top to downwards)

An ash analysis result of palm fiber charcoal, which has been heated with a temperature of 500^0 for 1 hour, shows that its carbon content is between 56.4% - 58.6%, the average is 57%. The rest is in accordance with a qualitative and quantitative analysis result using EDX, showing there are several compounds that are contained in the palm fiber

charcoal such as K_2O, CaO, SiO_2, MgO, ZnO and other. Table 1 shows a comparison of the total weight percentage (Wt%), which is detected for carbon from materials that are heated with a temperature of 275^0C, having an average C content of 47%, and Table 2 for carbon from materials that are heated at the temperature of 500^0, having an average C content of 32%. As a comparison, pure graphite is analyzed using the same equipments EDX, and data of the analysis result in the Table 3 shows that graphite has an average C content of 91%.

Tabel 1. EDX analysis Data on palm fibers that have been heated with a temperature of 275^0 for 2 hours

Element	Spect. type	Element (%)	Atomic (%)
Observation in position 1			
C K	ED	55.66	78.57
Mg K	ED	3.12	2.18
Si K	ED	7.97	4.01
Zn K	ED	33.25	14.44
Total		100	100
Observation in position 2			
C K	ED	46.55	73.47
Si K	ED	3.43	2.31
K K	ED	49.98	24.21
Total		100	100
Observation in position 3			
C K	ED	38.01	66.40
Si K	ED	0.62	0.62
Cl K	ED	23.51	13.63
K K	ED	36.02	19.35
Total		100	100

Table 2: EDX analysis data on palm fibers that have been heated with a temperature of 500^0 for 1 hour

Element	Spect. type	Element (%)	Atomic (%)
Observation in position 1			
C K	ED	47.03	73.23
Mg K	ED	1.20	0.92
Si K	ED	1.50	1.00
Cl K	ED	36.32	8.51
K K	ED	33.95	16.24
Total		100	100
Observation in position 2			
C K	ED	24.49	49.97
Mg K	ED	2.49	2.50
Si K	ED	2.69	2.35
P K	ED	4.56	3.85
Cl K	ED	8.65	8.12
K K	ED	39.59	24.79
Ca K	ED	17.05	10.45
Total		100	100
Observation in position 3			
C K	ED	25.22	50.51
Mg K	ED	1.98	1.97
Si K	ED	2.24	1.93
P K	ED	3.03	2.37
S K	ED	1.44	1.09
Cl K	ED	17.39	11.57
K K	ED	36.20	22.46
Ca K	ED	12.43	7.51
Total		100	100

Table 3. EDX analysis data on graphite

Element	Spect. type	Element (%)	Atomic (%)
Observation in position 1			
C K	ED	75.62	92.83
Si K	ED	9.85	4.93
Zn L	ED	10.53	2.26
Total		100	100
Observation in position 2			
C K	ED	97.31	98.93
Si K	ED	2.69	1.17
Total		100	100
Observation in position 3			
C K	ED	96.75	98.59
Si K	ED	3.25	1.41
Total		100	100

IV. CONCLUSION

Charcoal that is made from palm fibers forms an amorphous carbonic structure, and the diameters of the palm fiber charcoal vary between 100µm - 1000µm. The morphology of the carbon/charcoal from palm fibers is in a form of alleys, which are parallel with the stem of the palm fibers, with diameters of between 2µm - 8µm, and the wall of the alleys has holes of between 1µm - 2µm in diameter. The carbon content in the charcoal, which is made from palm fiber is 32% - 57%.

ACKNOWLEDGMENT

The authors would like to express their gratitude for the financial support by Insentive Program of RISTEK.

REFERENCES

[1] William D.Callister , “Materials Science and Engineering”, 3 edition, John Willey & Son, 1993.
[2] D Fengel and G Wegner, “Wood: Chemistry, Ultrastructure, Reactions“, University of Munich, Institute for Wood Research, Divisionof Wood Chemistry and Ultrastructure Research, Walter de Gruyter & Co, 1989.
[3] http://www.physorg.com/news5239.html, July 2008.
[4] Nature, 423, 703, 2003.
[5] http://www.nanovip.com/node/2077, December 2008
[6] R.H. Baughman, Science 290, 1310 (2000) in http://www.cheaptubesinc.com/cnt101.htm
[7] S. Litster1, G. McLean, “PEM fuel cell electrodes”, Review, Journal of Power Sources 130, p.61-76, Elsevier, 2004.
[8] http:www.forest.umaine.edu/image/PDF%20file/CNT%Poster.pdf
[9] Junbing Yang, Di-Jia Liu and David J. Gosztola, “Functionalized Aligned Carbon Nanotubes as a Novel Catalytic Electrode for PEM Fuel Cells”, Chemical Engineering Division and 2Chemistry Division, Argonne National Lab., 9700 S, Cass Ave, Argonne, IL 60439, USA.
[10] M. Wilson *et al*, “*Nanotechnology: Basic Science and Emerging Technologies*”, Chapman and Hall, ISBN 1-58488-339-1, 2002.
[11] http://www.ornl.gov/info/ornlreview/v34_2_01/carbon.htm, July 2008.
[12] Euro Sjostrom, “Wood Chemistry, Fundamentals and Applications”, Lab. Of wood Chemistry, Porest Product Dep., Helsinki Univ.of Tech., Espoo, Finland, Academic Press, 1993.

ISSN 114-1284

DEVELOPMENT AND CHARACTERIZATION OF MAGNETIC MATERIAL BARIUM HEXAFERRITE FOR MICROWAVE ABSORPTION

Priyono and Azwar Manaf
Material Science Study Program PPS - FMIPA University of Indonesia
Kampus UI, Jl. Salemba Raya No. 4, Jakarta, Indonesia

Abstract

Ferrite is widely known as a material which is used as hard magnet and soft magnetic materials and for various applications such for magnetic data storage, computer, radio wave tools, television and microwave. In addition, ferrite is also used as electromagnetic impedance (EMI) particularly for the ultra high frequency. This research develops Type-M hexaferrite as an absorbing material through nanostructure engineering by the method of mechanical milling route. The formation of phase $BaFe_{12-2x}(MnTi)_xO_{19}$ (x varies from 0.0 to 2.5) is through a two-stage mechanism which starts with the formation of $(Fe,Mn,Ti)_2O_3$. The synthetic result is tested by X-ray Diffraction and TEM to determine its structure and formation phase. Meanwhile, the magnetic characteristic is tested by permeagraph in saturating field of up to 2.15 Tesla. Network Analyzer (1 GHz to 6 GHz) is used to compute the reflection and transmission coefficients as well as reflection loss in that range of frequency. Formation through a two-stage mechanism occurs perfectly at the temperature of 1200 C. The Synthetic result shows that the partial substitution of Fe^{+3} ions with Mn^{+2} ions and Ti^{+4} influences the change

in the lattice parameter from c = 23.2093 nm to c =22.8146 nm, meanwhile the value of a tends to be constant. The research result shows that there is a change in magnetic properties particularly coercivity which significantly decreases as the number of Mn^{+2} and Ti^{+4} ions increase. Besides, there is a shift in resonance microwave absorption in the frequency range 1 GHz to ~ 4Ghz and it is characterized as multiband.

Keywords*: M-Type Barium Hexaferrite, Substitution, Microwave Absorption*

1. Introduction

The development of high frequency microwaves experiences an expository growth particularly the one which applies wireless technology. The development of electronics and electronic devices with high frequency application should always be accompanied with technology of electromagnetic absorption. To remove the bias field which normally occurs in various electronic tools, in a relatively low frequency it can be done by placing a ferromagnetic metal which can reduce the low frequency electromagnetic interference (EMI); however, it cannot be used for very high frequency such as application microwave and ferrite material becomes one alternative to reduce it. Although various ferrite materials are known as permanent magnet, ferrite is also used as a soft magnet such as in high frequency transformers, circulators, isolators, tunable filters and phase shifters, antenna and radar absorbing material (RAM) and stealth material, [1][2]

Spinnel Mn-Zn ferrite magnet is frequently used for application in microwave with lower frequency and Garnet is used for applications with higher frequency [3], meanwhile Hexagonal magnet class is mostly promoted for even higher frequency. Hexaferrite structure has six classes

which are distinguished on the basis of their chemical composition and structure. Type Y and Type Z are often utilized for applications with high frequency, yet only few research has used Type M because Type M has a higher crystal anisotropy which is more suitable for permanent magnet. Research on single crystal by Karim et all [4] shows that the resonance frequency of $BaFe_{12}O_{19}$ takes places in the frequency range of ~ 42 GHz. Thus, substitution of Fe^{+3} ion with various transitional metals can reduce the magnetocrystaline anisotropy[5][6].

Addition of a small number of additive ions from other transitional metals can significantly change magnetic properties such permeability, magnetic saturation, remanence, magnetic cooercivity, as well as the Curie temperature.

2. EXPERIMENTAL PROCEDURE

Barium ferrite which is substituted by Mn^{+2} ions and Ti^{+4} ions is synthesized through two mechanisms. The first mechanism begins with the formation of $(Fe,Mn,Ti)_2O_3$ by using the components forming $MnCO_3$ and TiO_2 as well as Fe_2O_3 in the heat of 1300 C and the next stage is the formation of $BaFe_{12-2x}Mn_xTi_xO_{19}$. The two stages are conducted by using mechanical alloying method.

The study on the formation of $BaFe_{12-2x}Mn_xTi_xO_{19}$ is conducted by heating it in various temperatures from 850 C to 1200 C at the pressure of 1 atm. The phase formation result is analyzed using XRD C_0 K_α (PW-1830 Philips Netherlands) at the angle of $2\Theta = 20^0$ to 80^0 with the step width of 0.02^0. Magnetic properties are analyzed using Permeagraph in the external field up to 2.15 Tesla. Nanostructure material is conducted by using Transmission Electron Microscope (TEM) which is equipped with electron diffraction tool, whereas the transmission and reflection of electromagnet waves is examined by using Network Analyzer (HP8735ES) at the frequency range of 1 GHz to 6 GHz.

3. RESULTS AND DISCUSSIONS

The substitution using Mn^{+2} ions and Ti^{+4} ions in Fe_2O_3 uses the oxide components of Fe_2O_3, TiO_2 and $MnCO_3$ in various temperatures have been conducted and analyzed deeply and the result shows that the optimum temperature in which the substitution takes place is at 1300 C[7].

3.1 Structural Analysis

Ionic substitution process may occur when the balance of ions can be achieved. Ion balancing process is achieved when the number of Fe^{+3} ions are substituted by the same number of ions and those ions are from Mn^{+2} and T^{+4}. As a result, the substation process is likely to occur to 2 Fe^{+3} ions which are substituted by one Mn^{+2} ion and one Ti^{+4} ion. It has been proved previously that if the number of fractions of Mn^{+2} ions exceeds the number of fractions of Ti^{+4} ion atoms there will be formed two $(Fe,Mn,Ti)_2O_3$ and $MnFe_2O_4$ and if the number of fractions of Mn^{+2} atoms is fewer than the fraction of Ti^{+4} atom ions, $(Fe,Mn,Ti)_2O_3$ and Fe_2TiO_5 are formed. This condition may be maintained until the number of Fe^{+3} ions which are substituted reach 21.8% of the atoms [8].

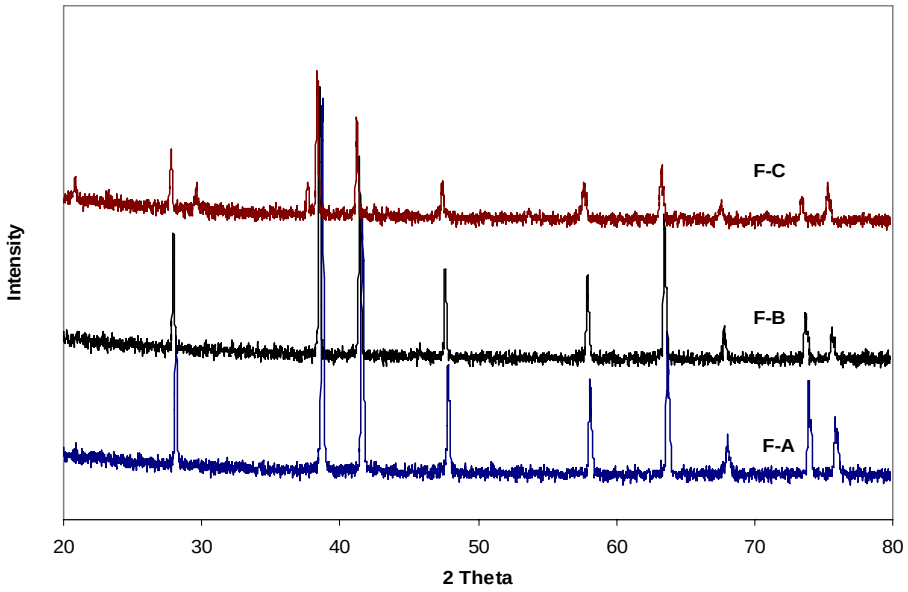

Figure 1 Diffraction pattern of substitution of Mn ions and Ti ions in phase Fe_2O_3. F-A represents Fe_2O_3, F-B represents $Fe_{1.5}Mn_{0.25}Ti_{0.25}O_3$ and F-C represents $Fe_{1.10}Mn_{0.45}Ti_{0.45}O_3$ with the heating of 1300 C for 4 hours.

Figure 1 shows the result of partial substitution of Mn ions and Ti ions for the formation of $Fe_{1.5}Mn_{0.25}Ti_{0.25}O_3$ and $Fe_{1.25}Mn_{0.325}Ti_{0.325}O_3$ and Fe_2O_3. Fe^{+3} ions which are partially substituted by Mn^{+2} ions and Ti^{+4} ions, Mn^{+2} ions on the subskin of $3d^5$ more prefers to substitute in the spin down position of Fe^{+3} ion in the subskin of 3d0, meanwhile Ti^{+4} ion in the subskin of $3d^0$ will substitute the position of Fe^{+3} in its spin up position. The difference of position of ions partially substituting Fe ions will have an impact on the lattice parameter in the previous condition[9].

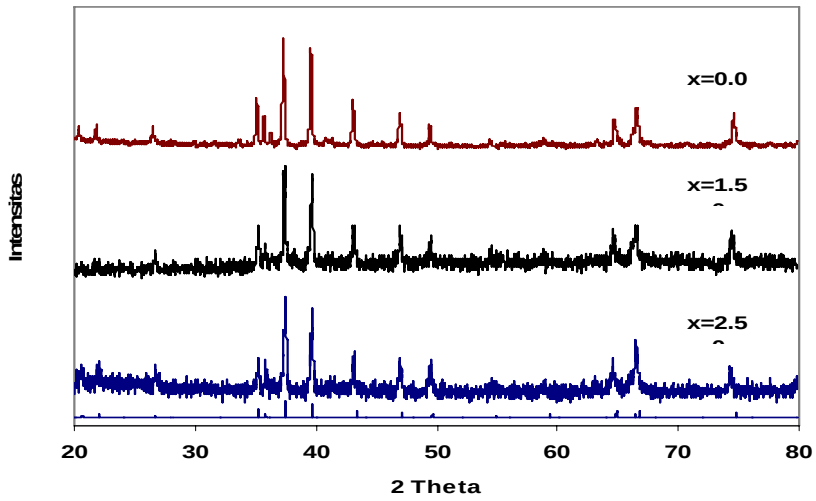

Figure 2 and X-Ray powder difraction patterns of $BaFe_{12-2x}Mn_xTi_xO_{19}$ (x=0.0 and 1.5 as well as 2.5) in 1200 C

ISSN 114-1284

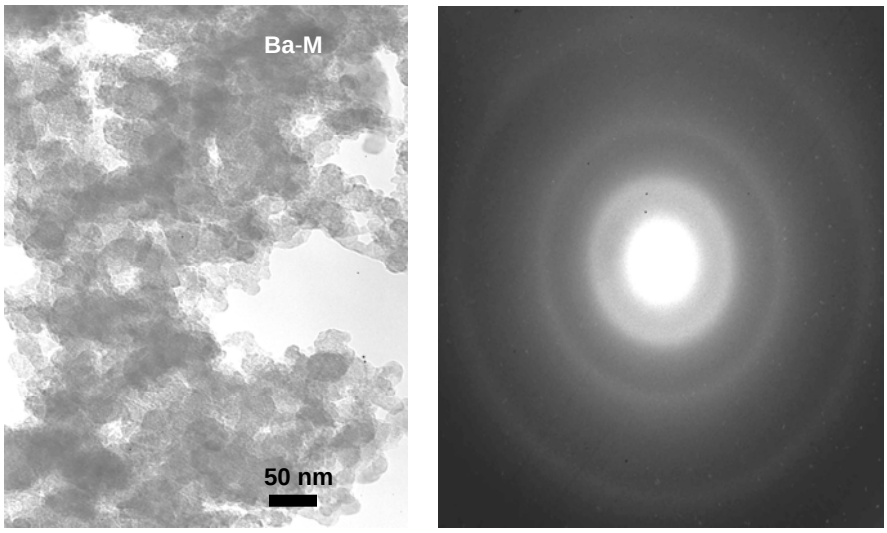

Figure 3. Braigh fild image and Selected Area Electron Difraction (SAED) of TEM $BaFe_{12-2x}Mn_xTi_xO_{19}$ (x = 1.5) in 1200 C

Figure 2 shows the diffraction pattern of compound $BaFe_{12-2x}Mn_xTi_xO_{19}$ for various composition of x =0.0 and 1.5 as well as 2.5. Generally, the three substitute compounds have the same diffraction pattern as the diffraction pattern of compound BaO.6 (Fe_2O_3), which is a single phase with magnetoplumbit structure. The presence of the substitute ion only results in a change in the intensity pattern. This result indicates that the formation of temperature of barium ferrite formation can be done in the temperature of 1200 C. Whereas according to Ghasemi[10] formation through composing compounds directly can only take place if the temperature is above 1250 C. The difference in the formation temperature is likely to be caused by the difference in the methodology used. In the first method, the substitution is conducted first while in the second method the substitution is conducted simultaneously. Using the first method, the growth of the size of crystal particle can be slowed down to the size of nanocrystal. The photo result of TEM shows that using the first method, the size of crystal particle is smaller than 50 nm.

Based on the result of calculation on the change in lattice parameter it is found that the presence of Mn^{+2} ions and Ti^{+4} ions do not significantly change in lattice parameter a = 5.8487 nm, yet the same thing does not happen to value of lattice parameter c = 675,8681 (for x = 0 the result is 5,8862 nm and c = 696,4060 nm[7]. Consequently, the change in the lattice parameter has an impact on the constant value of crystal anisotropy so that the magnetic properties of a material such as coersivity and magnetic saturation will change.

3.2 Magnetic Properties

Hysteresis loop of the magnet sample $BaFe_{12-2x}Mn_xTi_xO_{19}$ in which x = 0, 1.5, and 2.5 is shown in Figure 5. It is obvious that as the number of Mn^{+2} and Ti^{+4} atom fractions increase, the remanence and the saturation magnetization linearly decreases, unlike the decrease in the coercivity value.

ISSN 114-1284

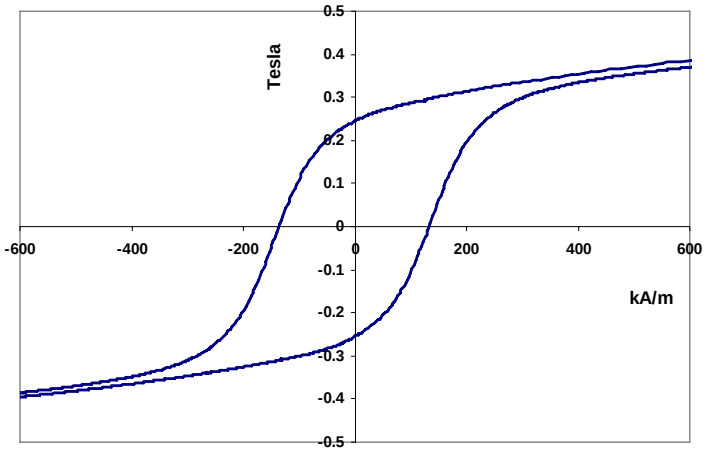

Figure 4. Hysteresis $BaFe_{12-2x}Mn_xTi_xO_{19}$ (x=0.0) with the growth temperature of 1200 C.

Systemically decrease in magnetic properties in the structure of $BaFe_{12-2x}Mn_xTi_xO_{19,}$ which is shown in Figure 5 results from the substitution of Fe^{+3} ions with Mn^{+2} ions and Ti^{+4} ions. Mn^{+2} ions occupy the spin down position of Fe^{+3} ions ($3d^0$) in tetrahedral (4fl), while Ti^{+4} ions position themselves in the position of Fe^{+3} in its octahedral lattice. Since Mn^{+2} is paramagnetic in nature, it is suspected that it may cause the decrease in total magnetic moment which has an impact on the decrease in magnetic properties particularly in its coercivity and magnetic saturation. It also applies on the substitution by Ti^{+4} ions in the oxtahedral position of F_e^{+3} ions. The substitution of Fe ions with Ti and Mn ions which has caused the decrease in the volume of cell units, by referring to the research result by Mones, it can be concluded that the pace of the decrease in the total magnetic moment of the main phase because of substitution of Ti ions is bigger than the pace of the decrease in the volume of cell units so that the total magnetization of the main phase becomes lower.

3. 3 Losses Study in Microwave frequency

Figure 6 shows that reflection coefficient (S_{11}) and transmission coefficient (S_{21}) for x = 1.5 and 2.5 at the frequency range of 1 GHz and 6 GHz. Both values indicate a difference in resonance. Both of the samples are multyband because they have a number of resonance peaks. At the frequency range of 1 GHz and 2 GHz, both samples have relatively similar resonance frequency, meanwhile for x=2.5 there is a shift in frequency, exceeding 4 GHz. The transmission coefficient which is relatively high compared to the transmission coefficient is more likely to be caused by the size of the sample which is quite thick (~12 mm) so that more radiation is absorbed.

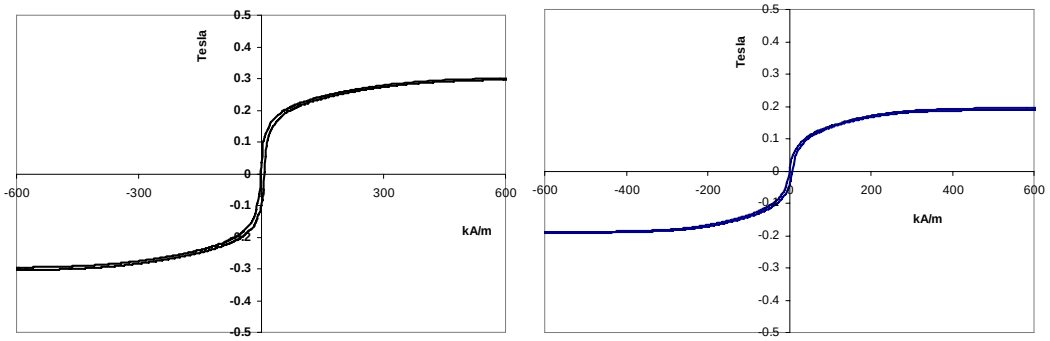

Figure 5 Hysterisis $BaFe_{12-2x}Mn_xTi_xO_{19}$ (x = 1.5 and 2.5) with the growth temperature of 1200 C

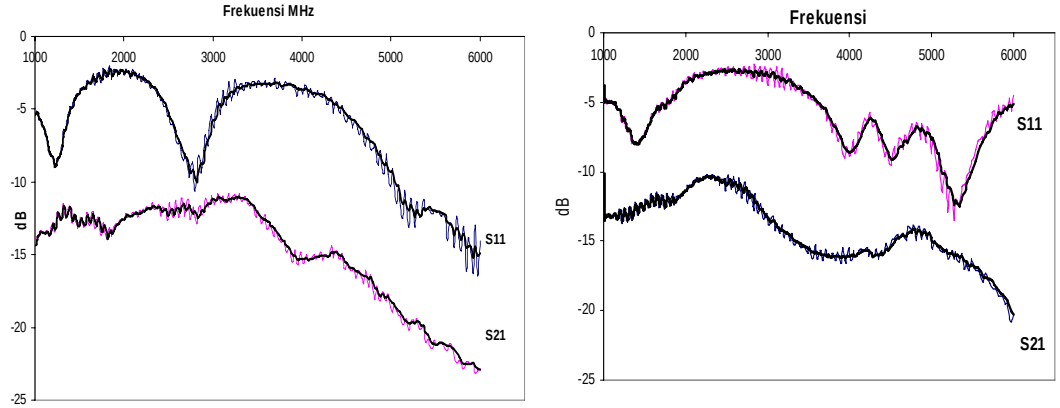

Figure 6 The graph of reflection coefficient (S11) and transmission coefficient (S21). The electromagnetic wave of $BaFe_{12-2x}Mn_xTi_xO_{19}$ ((a) x = 1.5 and (b) x = 2.5)) is measured by Network Analyzer using Coaxial wave guide

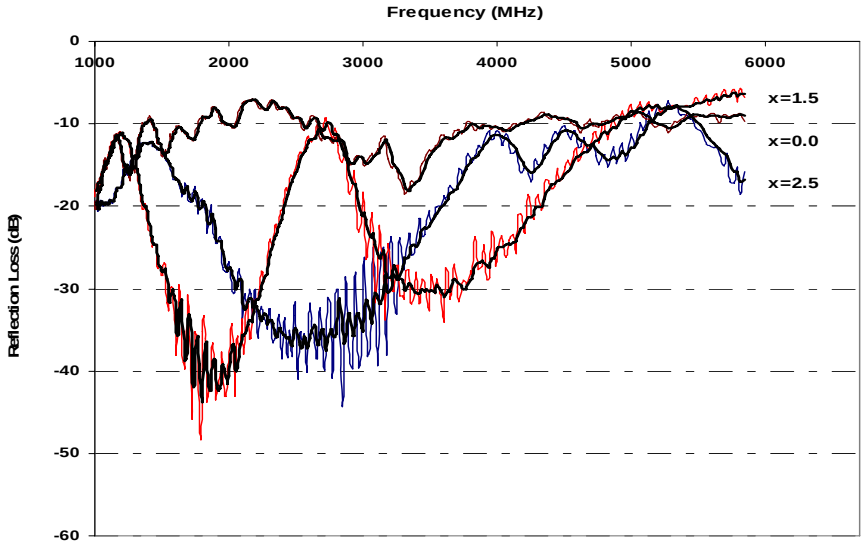

Figure 7 Reflection loss in material $BaFe_{12-2x}Mn_xTi_xO_{19}$ (x=y= 0.5; 1.0 and 1.5) in the thickness of ~ 12 mm

The calculation of reflection loss in total is shown in figure 7. Material which is not substituted has the lowest reflection of the other materials which have been substituted.

Conclusions

Formation of $BaFe_{12-2x}Mn_xTi_xO_{19}$ can be achieved by mechanical integration from the composing components Fe_2O_3, $MnCO_3$ and TiO_2 and $BaCO_3$ which is conducted through two stages of treatment can be perfect in the heating of 1200 ^{0}C. The synthetic result which is preceded with the formation of $(Fe,Mn,Ti)_2O_3$ has a lower temperature formation of $BaFe_{12-2x}Mn_xTi_xO_{19}$ than the temperature in one-stage treatment.

$BaFe_{12-2x}Mn_xTi_xO_{19}$ has a lower volume of unit cells as the number of Mn^{+2} ions and Ti^{+2} ions compared to materials which are not substituted. The decrease in the value of the lattice parameter from c = 23.2093 nm to c = 22.8146 nm with the value of a which is relatively the same can have an impact on a number of properties particularly on the magnetic properties and electromagnetic wave absorption particularly in the microwave frequency.

A change in the lattice parameter is accompanied with the decrease in coercivity and the total magnetization value as well as the shift in the microwave absorption frequency. Microwave absorption in the magnetic material barium ferrite which is substituted by Mn ions and Ti ions in the range of 1 GHz and 6 GHz is multiband and occurs in the range of 1 GHz to 4 GHz.

REFERENCES

[1].Li,W. and Linfeng Chen, C.K. Ong, 2002, Studies of Static and High Frequency magnetic Properties for M-Type Ferrite Ba(Co Zr)$_x$ $Fe_{12-2x}O_{19}$, Journal of applied Physics Vol 92, 3902-3907

[2] Dubrunfaut, D, S. Zouhdi, A. F. Fourier Lamer, E. brando and H. Vincent, 1999, Study of Microwave absorptions in M-Hexaferrite for anti-radar Application, Eur Phys. J. 8. 159-162

[3] Doo Whan Kang, Hak Gue Yeo, 2005, Preparation and Properties of Polyorganosiloxane rubber Nanocomposite containing Ultra fine manganese Zinc Ferrite Powder, J. Ind. Eng. Chem. Vol. 11 No. 4, 567-572

[4] Karim, R., S.D. Bell, J.R. Truedson, and C.E. Patton (1993). Frequency dependence of The ferromagnetic resonance line width and effective line width in manganese substituted single crystal barium, J. Appl. Phys.73(9), pp 4512-4515,

[5] Bai, Y., Jing Zhou, Zhilun Gui, Zhenxing Y., Long Tu li, 2003, Complex Y-Type hexagonal ferrites: an ideal material for high frequency chip magnetic Components, J. of Magn. Magn Material 264 pp. 44-49

[6] Ravinder, D., P. salami, P. Mahesh B.S. Boyanov,2004, High temperature Thermoelectric power studies of Cobalt and titanium Substituted Barium Hexagonal Ferrite, journal of Magn. Magn. Materials,268, 154-158

[7] Piyono, A. Manaf, 2007, Substitusi Mn dan Ti Pada Struktur Fasa Fe_2O_3 Melalui Teknik *Mechanical Alloying", Proc. Kentingan physiscs forum 4th,pp 25-30*

[8] Priyono dan Azwar Manaf ,2007, Substitusi Mn dan Ti pada Struktur Fasa Magnetik Barium Hexaferrite Melalui Teknik Pemaduan Mekanik (Mechanical Alloying). J. Jusami,

[9 Toyoda, T., K.Kitagawa, K. Yamawaki, T. Hanashima, S. Sasaki, P.D. Siddons, Site preference Study of Ti-Mn and Ti-Co for Fe^{+3} in Ba Hexagonal Ferrites by Means of X-Ray Diffraction and Absortion Measurement, J. of The Ceramics Society of japan Supplement 112-1, pp 1455-1458, 2004

[10]Ghasemi A., A. Saatchi, M. Saleh, A. Hossienpour, A. Morisako and X. Lia, 2006, Influence of matching thickness on The absorption properties of doped barium ferrite at microwave frequencies, Phys. Stat. Sol.(a) 203,No.2, pp. 358-365

ISSN 114-1284

Development of Pt-Ni/C Alloy Nanocatalysts For The Proton Exchange Membrane Fuel Cell

Rusnaeni N.[1], Hendrajaya L.[2], Purwanto W.W.[3] and Nasikin M.[3]
[1] Indonesia Institute of Sciences
[2] Institute of Technology Bandung
[3] University of Indonesia

ABSTRACT

Pt-Ni/C alloy nanocatalysts synthesized by polyol method with atomic ratio, are investigated to find the origin of the enhanced activity of the oxygen reduction reaction (ORR) for fuel cell applications. Prepared catalysts are characterized by various techniques, such as X-ray diffraction (XRD), Scanning Electron Microscopy (SEM-EDX), and cyclic voltammetry (CV). XRD analysis shows that all prepared catalysts with different atomic ratio exhibit face centered cubic and have smaller lattice parameters than pure Pt catalyst. The mean particle size of the catalysts are between 4.3 to 6.3 nm. Electrochemical experiments using CV, are conducted to test the ORR activity of the Pt-Ni/C catalysts. Cyclic voltammograms (5 mV s^{-1}) at 25°C obtain the electrochemical active area and activity of electrocatalysts Pt-Ni/C in the potential range 900 mV versus RHE.

Keywords : *alloy catalyst; oxygen reduction reaction (ORR); fuel cell*

1. INTRODUCTION

Fuel cells are becoming a subject of intense applied research for portable, stationary and electric vehicle applications due to their high conversion efficiencies, high power density and low pollution. Among the various types of fuel cell, the proton exchange membrane fuel cells (PEMFC) are attractive power sources and the most suitable candidates for electric vehicles and residential applications as they can be operated at a low temperature of <100°C. Platinum supported on a carbon is widely used as the electrocatalyst in PEMFC. However, platinum is expensive and the world's supply of Pt is limited and to promote alternatives for reducing the use of Pt.

Therefore, how to improve the electrocatalytic activity is a very important issue [1,2,3]. The search for oxygen reduction reaction (ORR) catalysts that are more active, less expensive and with greater stability than Pt has resulted in the development of Pt based transition metal alloys [4, 5]. Some platinum-based binary alloys have the best prospect for use as a cathode catalyst such as PtCr, PtZr, PtTi exhibit a higher catalytic activity for ORR in pure acid electrolytes than pure platinum [3]. Although for improved performance from the Pt-based metal alloys, it is necessary to taylor the electrocatalyst layer to achieve the optimum Membrane Electrode Assembly water balance under the selected PEMFC operating conditions. Such alloy catalysts could improve the activity toward oxygen

ISSN 114-1284

reduction by a direct four-electrons reaction without involving the intermediate hydrogen peroxide step. The mechanisms for the enhanced activity of platinum alloy catalysts toward oxygen reduction have been studied extensively in recent years [4]. Mukerjee S. have explained the improvement in the PtCo catalytic activity based on an increase in the d-orbital vacancy promoting a stronger metal-oxygen interaction, particle size, and the inhibition of formation of Pt-OH at potentials above 800 mV vs RHE [5]. The stronger Pt-O_2 bond can cause a weakening and lengthening of the O-O bond and an easier scission of the O-O bond resulting in an increase in the reaction rate. But the other side, an increase the d-band vacancy in Pt makes it difficult to loose an electron for oxygen reduction. The enhanced electrocatalytic activity of the PtCr, PtCo, PtCu and PtNi can be explained by an electronic factor, i.e. the change of the d-band vacancy in Pt upon alloying and/or by geometric effects (Pt coordination number and based on the decrease in the Pt-Pt distance) [6].

In the present research, we use transition metal nickel, which has received little attention, to synthesize the Pt alloying catalyst because nickel has similar atomic radius to Co, Fe or Cu. Ni had been studied for oxygen cathode in anode PEMFC but the critical issues of improving the ORR activity was not analyzed completely. Therefore, we prepare Pt-Ni/XC-72R and characterize by various techniques. X-ray diffraction (XRD) characterization is carried out to determine the mean crystalline size and the lattice parameter of these Pt-Ni/C catalysts. Energy Dispersive X-ray spectroscopy (EDX) is used to investigated the bulk composition. Electrochemical experiments including cyclicvoltammetry (CV), are also conducted to characterize these Pt-Ni/C catalysts, to determine the electrochemical area of the catalysts, and to test the ORR activity of the catalysts.

2. EXPERIMENT

2.1. Preparation of the electrocatalysts

The carbon supported Pt-Ni catalysts are prepared by the Ethylene Glycol Method. H_2PtCl_6 and transition metal precursor solution is mixed well and added to carbon ethylene glycol solution alloy metal loading : 30 wt%, Pt:Ni = 1:1; 3:1; 4:1 in atomic ratio) under mecanically stirred conditions. 2.5M NaOH is added to adjust the pH of the solution to about 10. The temperatur is then increased to 190^{o}C for 2 hour.

2.2. Characterization

All catalysts are characterized by recording their powder XRD pattern on an X-ray diffractometer using CuKα radiation with a Ni filter and step scanning. The tube current is 30 mA and tube voltage is 40 kV. Using XRD we can do qualitative analysis. The Pt diffraction peaks are used to calculate the mean size of the Pt particles according to Scherrer's formula.

$$D = 0.9\lambda_{K\alpha 1} / B_{2\theta} \cos\theta$$

D is mean size of Pt particles, λ is the X-ray wavelengh, B is the half-peak width for the peak in radians, θ is the maximum angle of the peak. The metal composition of these PtNi/C catalysts determined by EDX. Electrochemical characterization is performed on a Instruments , in which reference working and counter electrodes are separated, is used for CV measurements. An Ag/AgCl electrode is used for the reference electrode and a platinum wire is used for the counter electrode. The catalysts layer of the working electrode is prepared as follows : a mixture containing PtNi/C catalysts, ethanol and 5 wt% Nafion are ultrasonically blended in a glass vessel for half an hour to obtain a homogeneous ink. The ink is spread on the surface of Carbon electrode and dried in an oven at 80°C for 10 min to obtain a thin active catalytic layer. The electrolyte is 1 M $HClO_4$ solution. CV is obtained after using high purity nitrogen to clean the electrolyte solution for 20 min. The scan rate is 50 mV/s and scan range is from -0.2 to 1.2V (Ag/AgCl). ORR tests are obtained after oxygen bubbling for 20 min. The scan range is from 1.2V to -0.2V (Ag/AgCl)

3. RESULT AND DISCUSSION

The metal bulk composition of these PtNi/C catalysts determined by EDX are shown in Table 1. From this table, the sample 13 can be found to have higher Pt loading than sample 2 and 12. The Pt loading of all samples are lower than the setting value. Figure 1 compare the X-ray diffraction patterns of the Pt/C and PtNi/C catalysts. The diffraction peaks of the PtNi/C alloy catalysts shift to higher angles as compared to that of Pt/C, indicating a lattice contraction arising from the substitution of the smaller Ni atoms for the larger Pt atoms. All the XRD peaks can be indexed as face centered cubic (FCC) structure [7, 8]. The lattice parameters and the mean PtNi/C particle sizes were calculated from Scherrer's formula based on Pt(111) peak and listed in Table 1.

Table 1. Metal composition of Pt-Ni/C

Sample Number	Pt:Ni atomic ratio	Lattice parameters (°A)	Particle size (nm)
Sample 2 Pt : Ni = 1 : 1	23 : 77	3.64	5.7
Sample 13 Pt : Ni = 3 : 1	37 : 63	3.66	6.3
Sample 12 Pt : Ni = 4 : 1	29 : 71	3.81	4.3
Pt/C Commercial	-	3.93	5.9

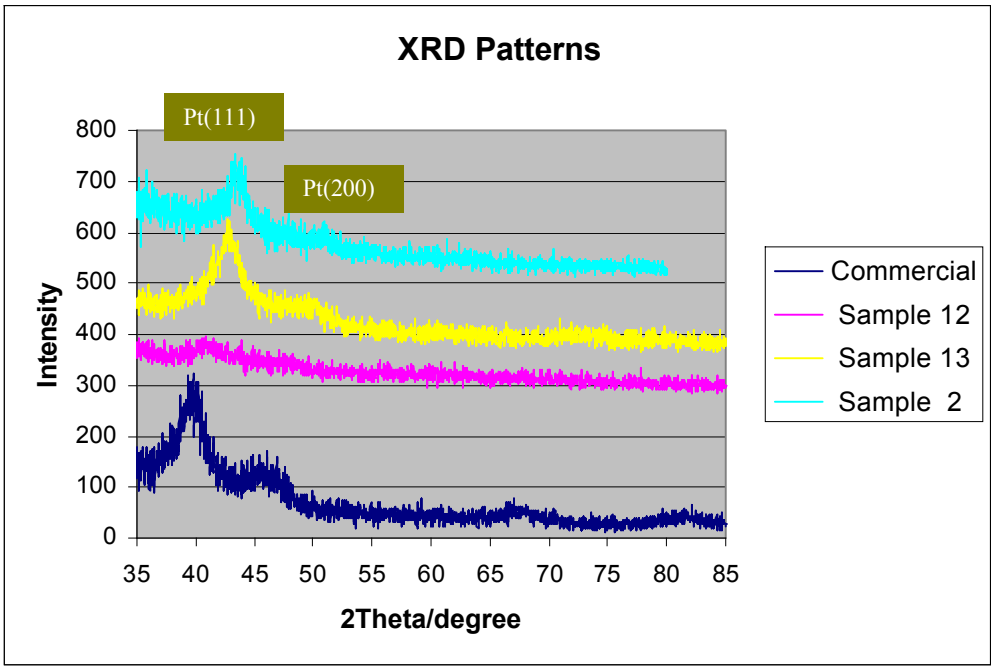

Figure 1 : XRD patterns of Pt/C and Pt-Ni/C prepared by EG method

With the data given in Table 1, the lattice parameter and hence the average Pt-Pt distance is decrease as the ratio atomic Pt is increased. The PtNi system under this composition is known to exhibit a $PtNi_3$ type structures for sample 13 as evident from the phase diagram, an for sample 2 and 12 exhibit a PtNi type structure. The $PtNi_3$ and the PtNi have a cubic structure in which the Pt atoms occupy all corner positions and the Ni atoms occupy all the face centered positions [9, 10, 11]. Because the shoulder around $2\Theta = 71^{o}$ do not appear in the XRD results, we speculate that the Pt-Ni has a disordered phase of face centered cubic structure in which the Pt and Ni atoms are randomly distributed at the corner and face centered positions.

ISSN 114-1284

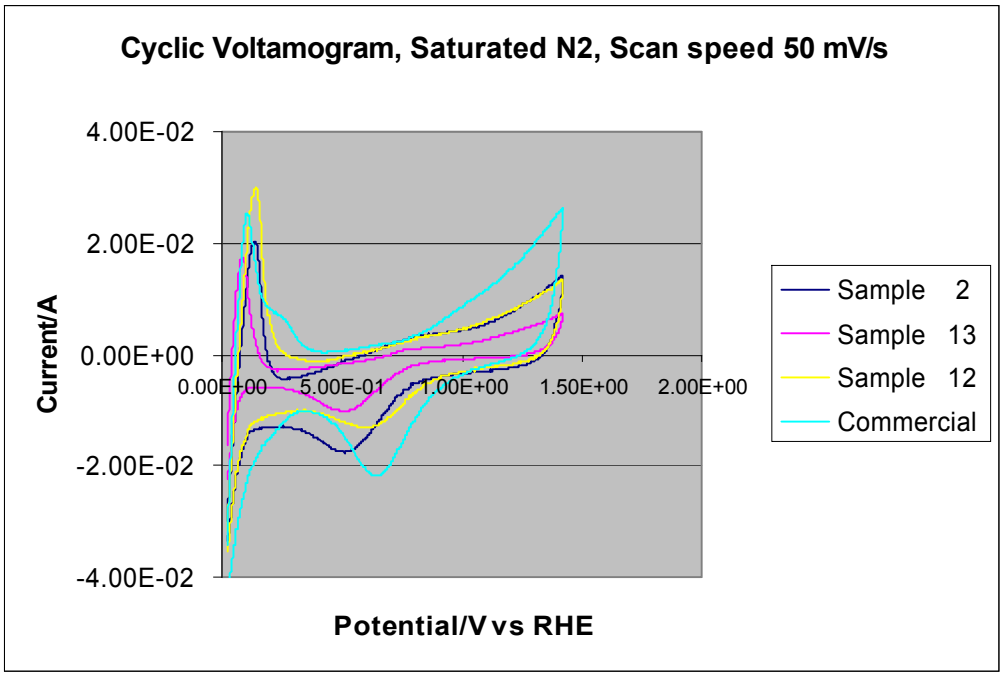

Figure 2 : Cyclic voltammograms for Pt/C commercial and Pt-Ni in 1M $HClO_4$, saturated N_2, The potential scan is 50 mV/s

Figure 2 compare the voltammetric behavior of the sample 2, 13, 12, and commercial. The cyclic voltammetry (CV) tests are performed in 1.0M $HClO_4$. From hydrogen desorption peak areas in yhe CV curve and the Pt single crystalline activity surface area transition constant Q_m = 0.21 mC/cm2Pt, the electrochemical surface area for these catalysts can be calculated. The results are shown in Table 2. Pt/C commercial has the largest surface area. But when the transition metal is added, the surface area becomes smaller. ORR tests are conducted in 1.0M $HClO_4$, which is a weak anion adsorption acid and can be used to evaluate the catalytic activity [12]. There are generally two ways to express the catalytic activity : One is mass activity (MA), which is the current per unit amount of catalyst and MA has practical implications in fuel cells because the cost of the electrode is largely dependent on the amount of platinum used.

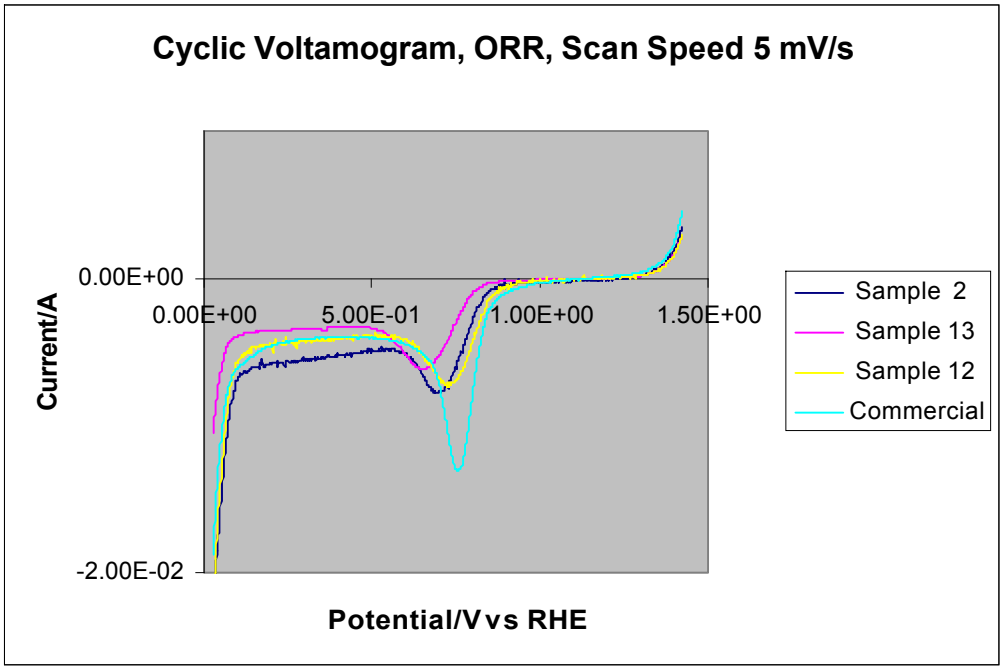

Figure 3 : The polarization curves for ORR on Pt/C commercial and Pt-Ni in 1M $HClO_4$, The potential scan is 5 mV/s

Table 2. Electrochemical characterization for Pt/C and PtNi catalysts, scan speed 5 mV/s

Catalysts	H_2 desorption (Q_H) mC	Ic pd 0,9V mA	Electrochemical Surface area (EAS)(cm^2/mg)	At 900 mV vs RHE)	
				Mass Activity (MA) (mA/mg Pt)	Specific Activity (SA) (mA/cm^2)
Sample 2	2.38	1.01	40.66	3.61	0.09
Sample 13	1.78	0.47	123.38	6.71	0.55
Sample 12	4.1	1.01	164.16	8.42	0.05
Pt/C Commercial	7.4	1.05	160.54	4.77	0.03

The other is specific activity (SA), which is the current per unit surface area of catalyst and the specific activity provides a measure of the electrocatalytic activity of platinum atoms in the particle surface. The MA and SA can be obtained through equation below :

MA (mA/mg) = $i_{0.9V}$ / W, W is the mass of Pt calculated

SA (mA/cm^2) = $i_{0.9V}$ /S, S is the electrochemical surface area

The ORR current is negative, the absolute values of ORR for these catalysts are used. The activity results are shown in Table 2. The ORR test results of the catalysts are shown in Figure 3. Since we are concerned with the electrichemical kinetic effects, the attention will be focused on

the region where the potential exceeds 0.9 V vs RHE. From Figure 3 and Table 2, it is found that Sample 12 has the highest MA of 8.42 mA/mg and the highest EAS of 164.16 cm^2/mg, but Sample 13 has the highest SA of 0.55 mA/cm^2. Moreover PtNi/C show a higher ORR activity than that of Pt/C. This may be attributed to the adition of Ni to Pt/C catalyst. The more electropositive transition metal Ni,

to which the oxygen species is attached, provides an electrochemical force that favor the four electron oxygen reduction electrochemical pathway, and consequently improves the ORR activity of the catalyst. This phenomenon results from the adsorption property of oxygen on Pt surface by dual site mode. Therefore the Pt-Pt nearest-neighbor distance plays an important role in determining the adsorption behavior. The addition of Ni to Pt/C catalyst not only reduces the Pt lattice parameter, but also enhances the catalytic activity. Therefore the alloying effect is an important factor affecting the catalitic activity toward ORR.

4. CONCLUSIONS

In this study, we use transition metal nickel to synthesize Pt alloying catalyst. X-ray diffraction (XRD) characterization is carried out to determine the mean crystalline size, these Pt-Ni/C catalysts. Electron Dispersive X-ray Spectroscopy is used to determine the bulk composition of catalyst. Electrochemical experiments including cyclic voltammetry (CV) are also conducted to characterize these PtNi/C catalysts, to determine the electrochemical area of the catalysts and to test the ORR activity of the catalysts. Samples 2, 13, and 12 produces by the lattice parameter, and the PtNi alloy effect of using EG method, has a competitively mean size particle, EAS, MA and SA value than that of Pt/C commercial.

REFERENCES

[1] Tsou Y.M., T. Zawodzinski, S. Mukerjee, M. Roelofs, M. Litt, N. Kalkhoran, O. Polevaya, Progress Report FY Departement of Energy, Hydrogen Programme , USA (2006).

[2] Huerta-Gonzales R.G., Carvayar-Chavez J.A., Feria-Solorza O., Electrocatalysis of Oxygen Reduction on Carbon Supported Ru-Based Catalysts in Polymer Electrolyte Fuel Cell, J. Power Source 153, 11-17 (2006)

[3] Ralph T.R., M.P. Hogarth, Platinum Met. Rev. 46 (3), (2002) 117 – 135

[4] Tada T., The Current State of the Development of Electrocatalysts for Use in Fuel Cell, 1st International Fuel Cell Expo (2005).

[5] Mukerjee S., Reducing Overpotensial Losses for Oxygen Reduction Reaction with Pt Based Alloys : a RRDE and in situ synchrotron XAS Investigation, Unpublish.

[6] Ross P.N.,Progress Report FY 2006 Departement of Energy,Hydrogen Program USA

[7] Patel K., S. Kapoor, D. P. Dave, T. Mukherjee, Synthesis of Pt, Pd, Pt/Ag, Pd/Ag Nanoparticles By Microwave Polyol Method, J. Chem.Sci., 117, 4, 311-316 (2006)

[8] Oh H.S., J.G. Oh, Y.G. Hong, N. Kim, Investigation Of Carbon-Supported Pt Nanocatalyst Preparation By The Polyol Process For Fuel Cell Application, Electrochemica Acta, 52, Issue 25, (2007) 7278-7285

[9] Radillo-Diaz A., Coronado Y., Perez L.A., Garzon I.L., Structural and electronic properties of PtPd and PtNi nanoalloys, Eur. Phys. J. D 52, 127-130 (2009)

[10] Schmid M., Stadler H., Varga P., Direct Observation of Surface Chemical Order by Scanning Tunneling Microscopy, Phys. Rev. Lett., vol. 70, No. 10. (1993).

[11] Gauthier Y, Dolle P, Baudoing-Savois R., Hebenstreit W., Platzgummer E., Schmid M., Varga P., Chemical Ordering and Reconstruction of $Pt_{25}Co_{75}$(100): an LEED/STM Study, Surface Science 396, 137-155 (1998).

[12] A. Pazio, M. De Francesco, A. Cemmi, F. Cardellini, L. Giorgi, Comparison of High Surface Pt/C Catalysts by Cyclic Voltametry, J. of Power Source 105, 13-19 (2002)

Proceeding of the 11th International Conference on QiR (Quality in Research)
Faculty of Engineering, University of Indonesia, Depok, Indonesia, 3-6 August 2009
ISSN 114-1284

AFM Lithography: A Simple Method for Fabrication of Silicon Nanowire Transistor

Kam C. Lew, Sabar D. Hutagalung[1]

School of Materials and Mineral Resources Engineering, Engineering Campus,
Universiti Sains Malaysia, 14300 Nibong Tebal, Penang, Malaysia
Tel : (604) 5996171. Fax : (604) 5941011
[1]E-mail: mrsabar@eng.usm.my

ABSTRACT

Atomic force microscopy (AFM) was used as a lithography technique to create nanoscale oxide patterns for nanoelectronic device fabrication. The AFM lithography has been performed using a conductive AFM tip to produce the silicon oxide nanopatterns on silicon on insulator (SOI) wafer. The parameters such as tip-sample voltage, writing speed and oxidation time were well controlled to form silicon nanowire transistor patterns. The tetra methyl ammonium hydroxide (TMAH) was used as the etching reagent for silicon machining, whereas, hydrofluoric acid (HF) for oxide removal. A silicon nanowire transistor with structures of a nanowire channel, a source (S) and a drain (D) pads, and a lateral gate (G) has been successfully fabricated via AFM lithography followed by chemical etching processes.

Keywords

AFM lithography, chemical etching, silicon nanowire, transistor

1. INTRODUCTION

Nanotechnologies had become one of the promising research areas by which might bring a significant progress into material and device development. To get specific nanoobjects and their properties, particular techniques should be selected. For the surface microscopy, scanning probe microscopes (SPM) has been using in fabrication of nanostructures and nanodevices as well. The microscope worked in standard SPM modes as in the STM mode, contact, non-contact and tapping AFM mode, magnetic mode (MFM) and lateral force mode (LFM) [1]. Atomic force microscope (AFM) had become useful tools not only for observing surface morphology and nanostructure topography but also for fabrication of various nanostructures. There were several methods for nanopatterning such as dip-pen nanolithography (DPN), chemo mechanical surface patterning and local anodic oxidation (LAO) patterning.

For local anodic oxidation (LAO) patterning method, the oxide will grow on a chemically reactive substrate by the application of a voltage between a conductive AFM tip and a substrate surface which acted as an anode. There was a threshold voltage at which the anodic oxidation started. The water molecules adsorbed on a substrate dissociates due to high electric field ($E > 10^7$ V/m) into fragments (e.g. H^+, OH^- and O^{2-}) and acted as an electrolyte [1]. The reaction of the LAO patterning was happened as shown by Equation 1:

$$Si + 2OH^- + 4H^+ \rightarrow SiO_2 + 2H^+ \quad (1)$$

LAO method was influenced by some parameter such as tip radius, air humidity, tip sample voltage, tip writing speed and oxidation time [2-7].

2. EXPERIMENTAL

Silicon oxide (SiO_x) pattern was formed on silicon-on-insulator (SOI) wafer by means of AFM nanolithography, which is, localized anodization induced by a conductive AFM tip followed by etching processes. These anodic SiO_x patterns could serve as masks for the chemical etching of Si in alkaline solution. The commercially available SOI wafer (Soitec) has the top Si layer of 100 nm in thickness, buried oxide (SiO_2) layer of 200 nm, and bottom Si substrate of 6.25μm. The SOI wafer was cut to smaller size of 1 cm x 1 cm followed by cleaning process from any contaminant and native oxide that could influence the performance of the device fabrication. Briefly, the RCA cleaning procedure was used to clean the SOI wafer and then followed by the surface passivation with 2% HF for 1 min. The objectives of this treatment are to remove the native oxide naturally existing on the wafer surface and passivating the silicon layer by metastable hydrogen terminated surface. During this step the Si–O bonds are replaced by low energy Si–H bonds.

After wafer cleaning and passivation process, the nanoeletronic devices were designed on SOI surface by AFM lithography via local anodic oxidation patterning. Experimental work was carried out using an environmentally controlled scanning probe microscope (SPM) machine (SII SPI3800N). This SPM is equipped with CAFM mode with a nanotechnology software package to control the tip-sample voltage and tip movement according to pre-designed patterns. The anodic oxidation process was performed in the chamber with relative humidity in the range of 40-50% at room temperature. A conductive AFM with a gold-coated conductive tip (diameter ~ 20 nm) was operated at -7 to 9V bias relative to the sample at writing speed of 6 to 9 μm/s.

Wet chemical etching process was performed to the patterned sample to obtain silicon nanowire transistor devices. Tetra methyl ammonium hydroxide (TMAH, $(CH_3)_4NOH$)) containing no alkaline metal was used as the etching reagent for Si machining, whereas, hydrofluoric acid (HF) for oxide removal. In the first etching stage, patterned sample was etched in an aqueous solution of 25 wt% TMAH at 60°C for 10s to remove Si layer that not cover by oxide patterns. In this process, TMAH reagent is choosing due to its etching behavior that very high selectivity ratio between Si/SiO_2 (etching rate ~ 2000:1). After TMAH etching, the patterns were characterized by AFM and FESEM. The second etching stage is removing the oxide mask layer by HF etching process. Sample was immersed in 2% HF solution for 20s to produce a SiNW transistor device.

The size, topography and microstructure of device were characterized by AFM and FESEM analysis. Figure 1 shows a schematic diagram of the fabrication of SiNW transistor device.

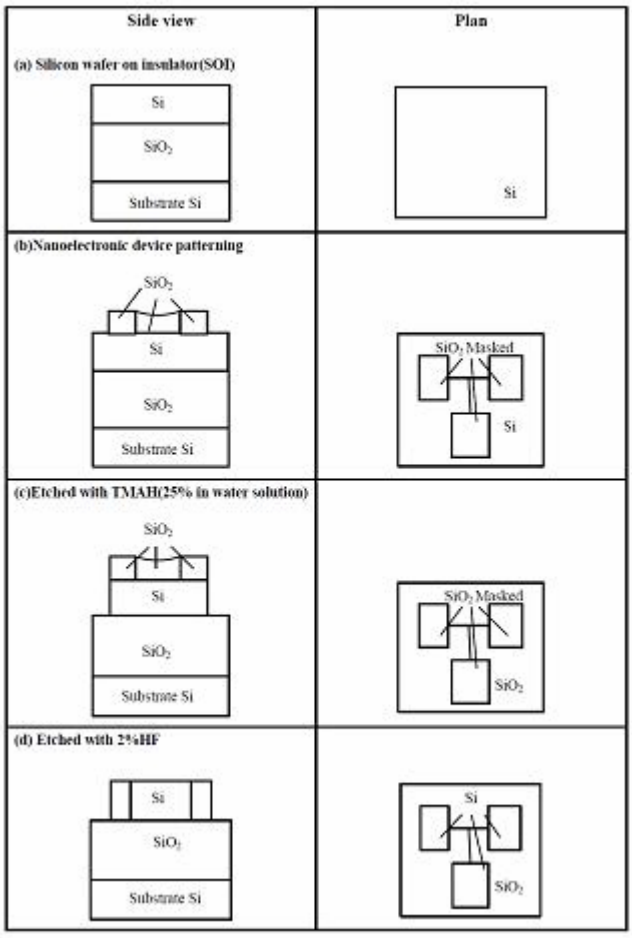

Figure 1: Schematic procedure of silicon nanowire (SiNW) transistor fabrication.

3. RESULTS AND DISCUSSION

The applied tip-sample voltage is one of the important parameter that will influence the local anodic oxidation (LAO) patterning result [1-7]. It was found that the tip-sample voltage will affected the size (width and height) of the patterned nanoscale oxide where the width and height of the pattern are increases with the tip-sample voltage [1].

Figure 2 shows the effects of applied tip-sample voltage and tip writing speed to the size of the patterned oxide nanowires. In this case, the nanowire patterns were drawn by applied tip sample voltage from 7 to 9 V at two different tip writing speed, 6um/s and 9um/s. The measurement results indicate that the width of the oxide nanowires is increasing linearly with increment of the tip sample voltage. For tip writing speed of 9 um/s, the width of the oxide wires is increase from 86.91 nm at tip sample voltage 7 V to 175.17nm and 290.81 nm for tip sample voltage 8 V and 9 V.

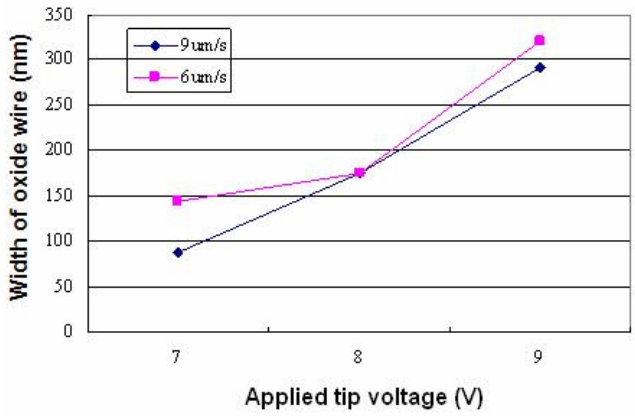

Figure 2: Graph of the width of the oxide nanowires at different applied tip sample voltage for two different tip writing speed, 9 um/s and 6 um/s.

Figure 3 shows the graph of the height of the oxide nanowires that drawn by tip sample voltage from 7 to 9 V at two different tip writing speed, 9 um/s and 6 um/s. From the measurement, the height of the oxide wires also increase linearly due to the increasing of the tip sample voltage. For tip writing speed of 9 um/s, the height of the oxide nanowires increase from 1.25 nm to 2.35 nm for tip sample voltage 7 V and 8 V. The height of the oxide wires further increase to 4.50 nm for tip sample voltage 9 V.

Tip writing speed also influenced the result of the local anodic oxidation patterning. Cervenka *et al.* [1] has found that beside the tip sample voltage, tip writing speed also affected the width and height of the oxide nanowires. It was found that the tip writing speed and applied tip sample voltage have to be well controlled in order to produce good result of oxide nanowires via local anodic oxidation patterning. Therefore, the suitable tip writing speed and applied tip sample voltage with other parameters should be found during the patterning process.

As shown in Figure 2 the lower tip writing speed of 6um/s produced bigger of the oxide nanowires if compared to the higher tip writing speed of 9 um/s at the same applied

tip sample voltage. For tip writing speed 6 um/s, the width of the oxide wires increase from 144.89 nm at tip sample voltage 7 V to 174.49 nm and 321.40 nm for tip sample voltage 8 V and 9 V. The result shows that the 6 um/s tip writing speed was produced more highly in the width of the oxide wires compare to the tip writing speed 9 um/s. But, the more lower the tip writing speed, the more of the time had been taken for patterning.

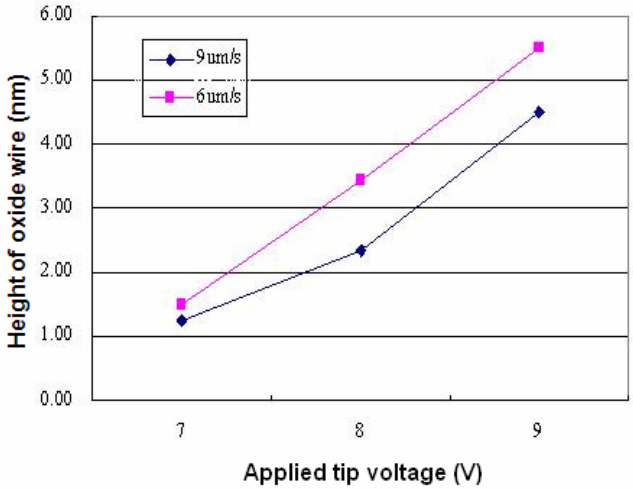

Figure 3: Graph of height of the oxide nanowires at different applied tip sample voltage for two different tip writing speed, 9 um/s and 6 um/s.

Figure 3 shows the graph of height of the oxide wires which had been drawn by tip writing speed, 6um/s and 9um/s with tip sample voltage from 7 to 9 V. From the graph in the Figure 3, the height of the oxide wires will increase due to lower down the tip writing speed which applied to the same tip sample voltage. The graph also shows that the height of the oxide wires will increase due to the increase of the tip sample voltage for the two different tip writing speed. So, the more lowly the tip writing speed, the more highly the height of the oxide wires

Figure 4 shows that the two dimensional (2D) and three dimensional (3D) images of the simple nanoelectronic structure drawn by AFM lithography patterning via local anodic oxidation (LAO) method. The designed of the nanoelectronic (Silicon nanowire transistor) was patterned at tip sample voltage of 7V with tip writing speed of 6um/s. The device has the source (S), drain (D) and lateral gate (G) with a silicon nanowire as a channel. The size of patterned oxide wire are 3 nm in thickness, 160 nm width and 1.744 µm in length which determined in situ by AFM topographic analysis. Meanwhile, the square pad size is about 5µm x 5µm. These oxide patterns will be used as mask system to protect Si layer underneath during the chemical etching process by using TMAH.

The TMAH etched of unmasked Si layer produced the oxide covered device structure as shown in Figure 5. Lastly, a completed SiNW transistor device was formed by removing the oxide layer via HF etching process. Figures 6 and 7 show the AFM and FESEM images of completed formation of silicon nanowire transistor after final stage of etching process by HF.

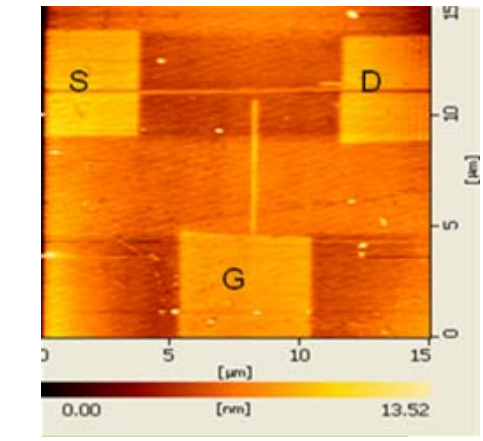

(a)

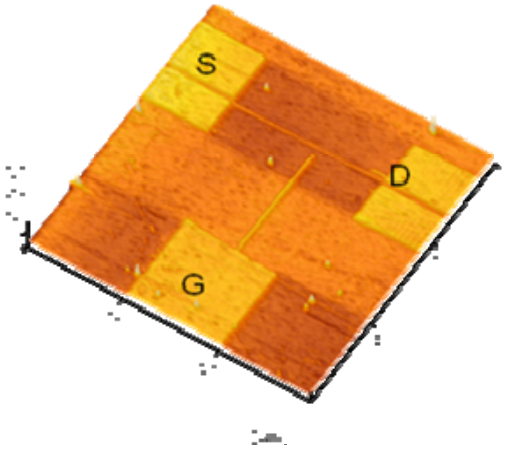

(b)

Figure 4: (a) 2D and (b) 3D AFM images of SiNW transistor patterned by AFM lithography.

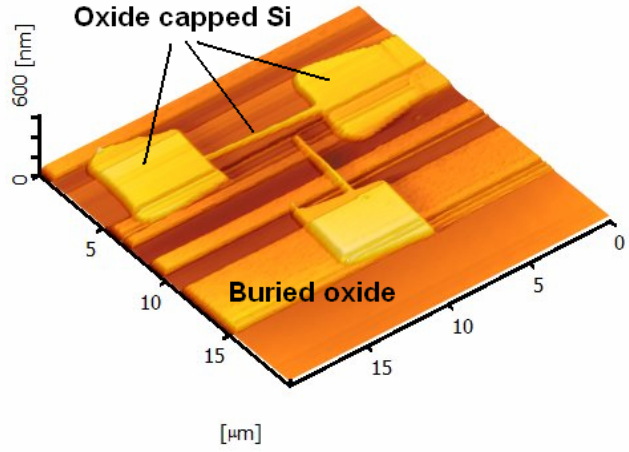

Figure 5: AFM image of device structure taken after etched with TMAH for 10 s

From the AFM topographic analysis obtained the diameter of nanowire is 45.80 nm with 6810.16 nm lengths. The surface of the fabricated device is very smooth observed from the AFM analysis (Figure 6).

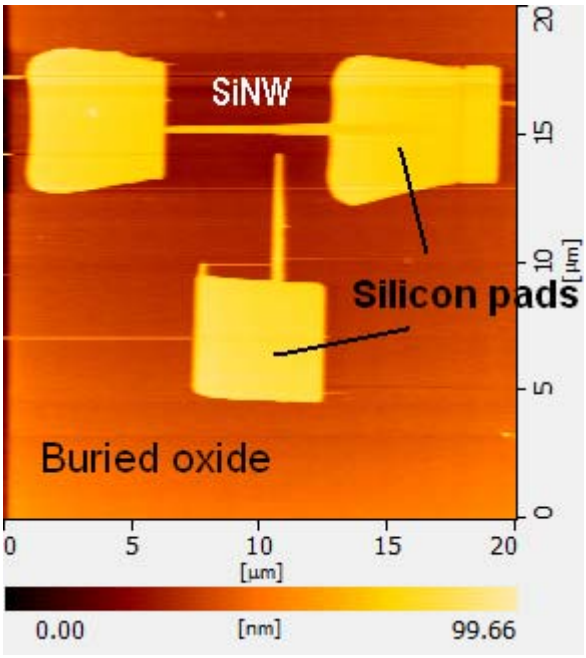

(a)

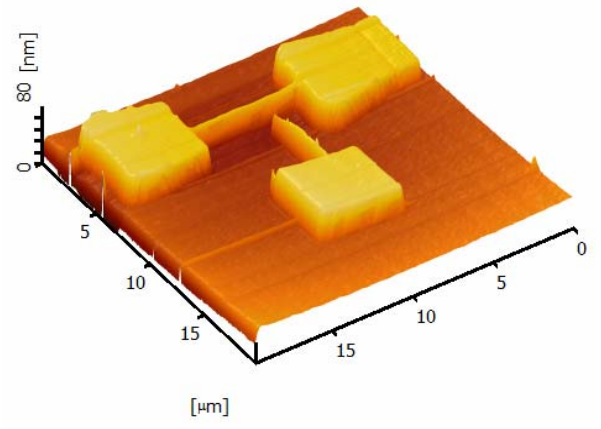

(b)

Figure 6: (a) 2D and (b) 3D AFM images of completed formation of silicon nanowire transistor after final stage of etching process by HF.

4. CONCLUSION

As a conclusion, a simple nanoelectronic device (silicon nanowire transistor) using a silicon nanowire as a channel with source (S), drain (D) and lateral gate (G) pads has been successfully fabricated by AFM nanolithography process. The lithography process via LAO using conductive AFM is influenced by certain parameters such as applied tip sample voltage, tip writing speed, and environment humidity. In this work, the lithography patterning of simple nanoelectronic device had been drawn at 7 V tip sample voltage and 6 um/s tip writing speed. These parameters have been chosen based on the optimum condition from experimental results of the height and width of the oxide nanowires at different applied tip sample voltage and tip writing speed.

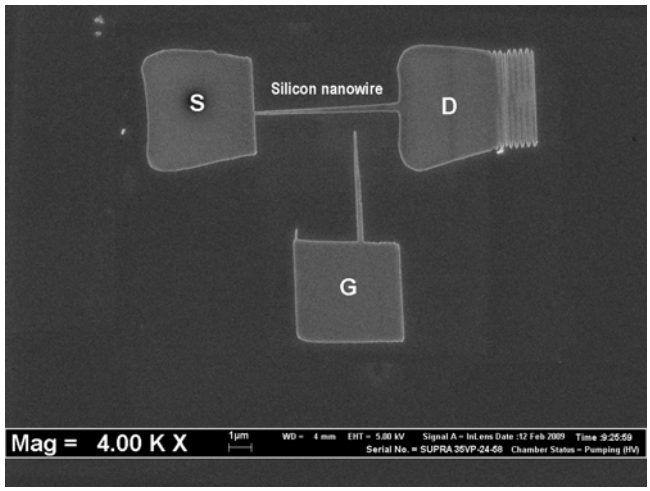

Figure 7: FESEM image of fabricated silicon nanowire transistor.

ACKNOWLEDGMENT

This work was supported by the Science Fund Research Grant, Ministry of Science, Technology and Innovation (MOSTI), Malaysia under project number 03-01-05-SF0384 and USM-RU-PGRS Grant. K.C. Lew wishes to thank Universiti Sains Malaysia for the fellowship schemes.

REFERENCES

[1] J. Cervenka, R. Kalousek, M. Bartosik, D. Skoda, O. Tomanec and T. Sikola, "Fabrication of nanostructures on Si(100) and GaAs(100) by local anodic oxidation", *Appl. Surf. Sci.*, vol. 253, pp. 2373-2378, 2006.

[2] T. H. Fang, "Mechanisms of nanooxidation of Si (100) from atomic force microscopy", *J. Microelectronics*, vol. 35, pp. 701-707, 2004.

[3] R. Held, T. Heinzel, P. Studerus, K. Ensslin, "Nanolithography by local anodic oxidation of metal films using an atomic force microscope", *Physica E*, vol. 2, pp. 748-752, 1998.

[4] S. D. Hutagalung, T. Darsono, K. A. Yaacob, Z. A. Ahmad, Zainal, "Effects of tip voltage and writing speed on the formation of silicon oxide nanodots patterned by scanning probe lithography", *J. Scann. Probe Microsc.*, vol. 2, pp. 28-31, 2007.

[5] S. Lee, J. Kim, W. S. Shin, H. J. Lee, S. Khoo, H. Lee, "Fabrication of nanostructures using scanning probe microscope lithography", *Mater. Sci. Eng. C*, vol. 24, pp. 3-9, 2004.

[6] X. N. Xie, H. J. Chung, C. H. Sow, A. T. S. Wee, "Nanoscale materials patterning and engineering by atomic force microscopy nanolithography", *Mater. Sci. Eng. R*, vol. 54, pp. 1-48, 2006.

[7] F. S. S. Chien, W. F. Hsieh, S. Gwo, A. E. Vladar, J. A. Dagata, "Silicone nanostructures fabricated by scanning probe oxidation and tetra-methyl ammonium hydroxide etching", *J. Appl. Phys.*, vol. 91, pp. 12-16, 2002.

Proceeding of the 11th International Conference on QiR (Quality in Research)
Faculty of Engineering, University of Indonesia, Depok, Indonesia, 3-6 August 2009
ISSN 114-1284

Aluminium foam fabrication by means of powder metallurgy and dissolution process

Sri Harjanto[1], Ahmad Effendi

[1]*Departement of Metallurgy and Materials Engineering, Faculty of Engineering*
University of Indonesia, Depok 16424
[*]*E-mail : harjanto@metal.ui.ac.id*

ABSTRACT

Metal foams or also known as cellular materials are widely used in many applications due to their attractive properties, especially in excellence good damping capacity, high impact energy absorption and very high specific stiffness. In this paper, aluminium metal foam was manufactured by powder metallurgy process route and dissolution in water. NaCl particles were added up to 90%wt and employed as cell structure former. The aim of the study is to produce and to characterize the properties the aluminium foam. The results show that aluminium foam was successfully fabricated by this method. In general, the density and porosity increase with the higher addition of NaCl to the mixture. Addition of 50wt% of NaCl to the mixture gives the density of 0.81 g/cm^3 compared to 2.25 g/cm^3,i.e. the density of the sintered product without NaCl addition. The porosity shape is almost similar with that of NaCl particles. It can be distinguished from the porosity due to imperfection during compaction by its shape.

Keywords

Cellular materials, Al, metal foam, metallic powder, lower density, porosity

1. INTRODUCTION

Metallic foam materials or also known as cellular metallic materials are categorized as new materials since a few decades with unique properties combination [1]. There are many applications of metallic foam in a great diversity industrial field, such as in automotive, energy, chemical, aerospace industries and so on [1-3]. The manufacturing process of this material is available practically in several routes for many kinds of metallic materials, for instance aluminium, copper, iron, titanium and others [2,3].

In case of aluminium foam, it can be manufactured, for instance by gas injection, foaming agent addition, powdered metal [1-4]. Zao and Sun (2001) have developed a powder metallurgy and dissolution process, which is also known as sintering and dissolution process (SDP) [5]. This process consists of three steps. Firstly, the mixture of Al, NaCl and additives is compacted to form a green compaction at a certain pressure. Secondly, the green is sintered at above or below the melting temperature of Al to form well-bonded structure. Finally, the NaCl particle is removed from sintered by leaching in hot water, leaving a foam structure of Al. Further study of SDP process optimization has been also conducted [6, 7]. Zao et al. (2004) showed that the optimum range of compaction pressure is 200 – 250 MPa and sintering temperature at 670 – 680^{o}C [6].

Based on the previous works of Zao et al. [5], the present study aims to produce aluminium foam by using powder metallurgy and dissolution process. The raw materials morphology used in this study is flake aluminium powder and acicular NaCl. It is different from Zao *et al.*'s works, which utilized atomized aluminium particles and round NaCl [6]. Physical and mechanical characterizations of aluminium foam are undertaken to the products after finishing the process.

2. EXPERIMENTAL METHOD

2.1 Materials

Aluminium powder (purity > 90%) and NaCl (technical grade) were used as main raw materials in this study. Al_2O_3 particles was also added to

the mixture in a certain amount as matrix strengthener. Zinc stearate was added in the mixture as a lubricating agent.

Fig. 1 shows the morphology of aluminium (flaky) and NaCl powders (acicular). The mean size of aluminium particle was 65.9 μm, whereas the size range of NaCl was 67 -667 μm.

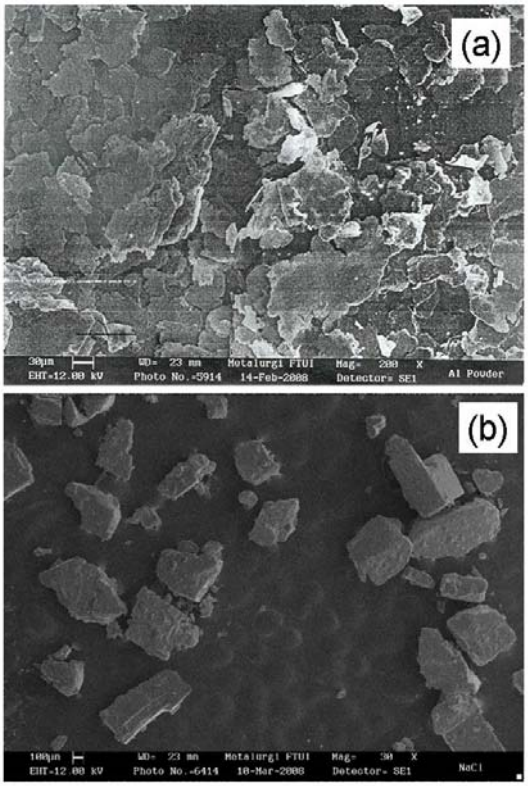

Figure 1: Raw materials utilized in this study. (a) aluminium and (b) NaCl powders.

2.2 Procedures

The aluminium powder was mixed with NaCl in the proportion of 0, 30, 50, 70 and 90 mass%. The additives were also admixed to the mixture by using rotary mixer for about 5 minutes. The homogenous powder mixture was then compacted at 200 Bar at room temperature. The sintering process of green compacted powder was conducted at 650^{o}C for 2 hours. After cooled down in room temperature, the sintered product was dissolved in warm water to remove NaCl from the products.

The metallic foam products were characterized their density and porosity. Scanning electron microscope (SEM; Leo, Oxford Instruments) was utilized to observe the structure of metal foam.

3. RESULTS AND DISCUSSION

Fig. 2 shows the sintered product (a) and leached product (b) of aluminium foam. It was also observed in some of the sintered product that a little portion of Al melts out on the surface of the sintered product in the form of globule. It is because actual sinter temperature in the furnace is still higher than aluminium melting point, even the heating element was set at 650^{o}C. Some part of the sample product was degraded during water dissolution. To avoid these conditions, attention should be paid during the process to obtain optimum condition.

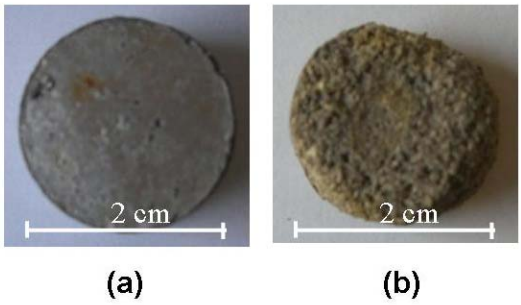

Figure 2: The sintered product (a) and the leached product (b) of aluminium foam.

Fig. 3 illustrates the structure of the foam after water dissolution process for 50% NaCl addition. It is observed that foam or cell structure was produced by using this process. The cell shape is relatively similar with the shape of NaCl, i.e. acicular form. The cell size, in case of 50% NaCl addition, is in the range of 350-687 μm, which is still in the range of NaCl size. Qualitatively, the amount of cell structure increases with increasing in addition of NaCl in the mixture. Some interconnection cell in the structure is also observed. It means that open cell structure was partly produced in this study.

Fig. 4 shows the effect of NaCl addition to the metal foam density. Actually, without NaCl addition, the density of sintered aluminium powder (2.25 g/cm^3) was still lower than that of aluminium bulk density (2.70 g/cm^3). It indicates that the porosity was formed as a defect of powder metallurgy process. Gradually, the density of aluminium foam is decreased with increasing in NaCl addition. Addition 30-90% NaCl into

aluminium powders mixture decreases the density of aluminium foam to the range of 1.58 – 0.22 g/cm^3.

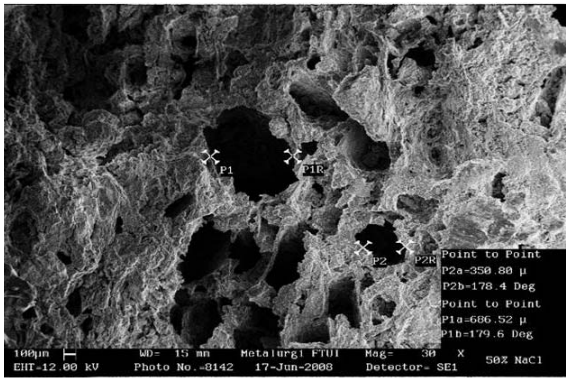

Figure 3: Microstructure of aluminium foam with 50% addition of NaCl.

On the contrary, the population of cell structure, in term of porosity percentage, is increased with increasing in NaCl portion in the mixture, as shown in Fig. 5. About 17% of porosity was formed as the defect of powder metallurgy process. Addition of 30 – 90% NaCl increases the porosity in the form of cell structure to the range 41.37-91.7%. The percentage of the measured porosity is still higher than NaCl addition in each condition. It indicates that the porosity in aluminium foam consists of defect porosity of powder metallurgy process and porosity which is formed during dissolution process. It also means that most of NaCl was removed during dissolution process.

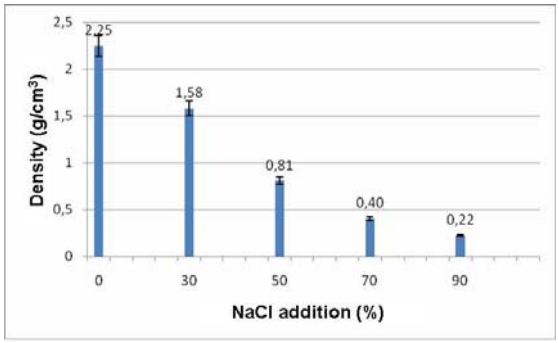

Figure 4: Effect of NaCl addition to the aluminium foam density.

4. CONCLUSION

The results of the present study show the reproducibility of the powder metallurgy and dissolution process to produce aluminium foam. More than 41% of density reduction compared with aluminium bulk density can be produced in the form of aluminium foam. The morphology and size of NaCl, as perform cell structure, should be considered to obtain a certain form of cell structure.

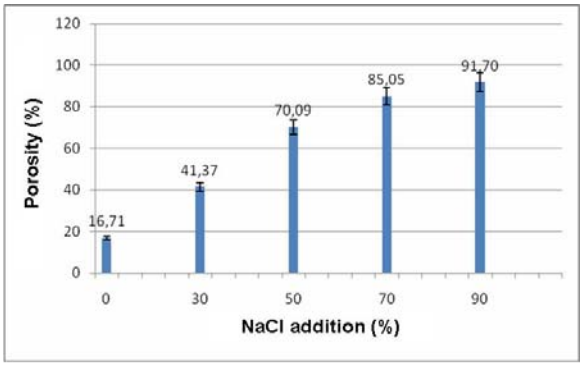

Figure 5: Effect of NaCl addition to the porosity in the aluminium foam.

REFERENCES

[1] J. Banhart, "Manufacture, characterisation and application of cellular metals and metal foams". *Progress in Materials Science*,46, pp. 559–632, 2001.

[2] J. Banhart, " Foam Metal: The Recipe", *Europhysics News*, Jan/Feb, pp. 17-20, 1999.

[3] H. N. G. Wadley, " Cellular Metals Manufacturing", *Advanced Engineering Materials*, vol. 4, no. 10, pp. 725-733, 2002.

[4] V.C. Srivastava, K.L. Sahoo ,"Processing, stabilization and applications of metallic foams. Art of science." *Materials Science*-Poland Vol. 25, 3, pp. 734-751, 2007.

[5] Y.Y. Zhao dan D.X Sun, "A Novel Sintering-Dissolution Process for Manufacturing Al Foams", *Scripta Materialia*, 44, 105-110, 2000.

[6] Y.Y. Zhao, F. Han, and T. Fung, "Optimization of compaction and liquid state sintering in sintering and dissolution process for manufacturing Al foams", *Material Science Engineering*, A364, pp. 117-125, 2003.

[7] D.X. Sun dan Y.Y. Zhao, "Phase Changes in Sintering of Al/Mg/NaCl Compacts for Manufacturing Al Foams by Sintering and Dissolution Process", *Material Letters*, 29, pp. 6-10, 2004.

Proceeding of the 11th International Conference on QiR (Quality in Research)
Faculty of Engineering, University of Indonesia, Depok, Indonesia, 3-6 August 2009
ISSN 114-1284

AFM and Ellipsometry Study of Thin Film Monolayer Organic using Langmuir-Blodgett Methode for Nano Technology

Sri Vidawati[a], Ulrich Rothe[b], Bambang Soegijono[a], and M. Hikam[a]

[a]*Department of Physics, Faculty of Mathematics and Natural Science, University of Indonesia, Depok 16424 Indonesia E-mail* : sri.vidawati@ui.edu

Physiological Chemistry, University of Matin Luther, Hollystraße 1, 06097 Halle , Germany

ABSTRACT

We report on the deposition by Langmuir-Blodgett process of thin film monolayer organic Tetraether lipids were transferred onto Silicon wafer substrates. Langmuir experiments were performed with the Langmuir trough from a commercial film balance (Riegler & Kirstein GmbH, Mainz, Germany) . The surface pressure was measured with a filter paper Wilhelmy balance. The experiments were performed at a temperature of 19˚C ± 1˚C. The subphase was pure water. The Tetraetherlipid were dissolved in chloroform in concentration 1 mMol for the film balance experiments. Thin film monolayer organic were made onto substrate Silicon wafer which Hydrophobic, Hydrophilic and Aminosilanisated properties. Ellipsometry Measurements show that the thickness and optical properties of monolayer films, The surface morphology with Atomic Force Microscoy (AFM) as results showed that in all films domains are present and that the thickness of the observed domains films varies between 2 nm and 5 nm. From all films the hydrophobically transferred showed the most homogeneous organization on the substrates. After transfer on hydrophilic and aminosilanisated surfaces the lipids are arranged in small islands on the substrates.

Keywords :

Thin Film Monolayer Organic, Tetraethelipid, Langmuir-Blodgett, AFM, Ellipsometry, Hydrophobic, Aminosilanisated, Hydrophilic

1. INTRODUCTION

Organized molecular films at the air-water interface as well as on solid substrates of great importance to a number of nanotechnology , nanoelectronic, biosensor, material science, biomimetic chemistry, biomedical and drug-delivery applications.

The application of nanotechnology principles and methodology is providing an exciting will generate a revolution of novel applications in several arenas. Applications of nanotechnology range from novel nanosensors, to novel methods for sorting and delivering bioactive molecules, to novel drug-delivery systems. Supported membrane systems are key features of emerging nanotechnologies.

Self-assembled phospholipid membranes play an important role in biological processes. Mimicking these natural thin films lipid-coated surfaces are of great importance to a number of biomedical applications, including intravenous drug delivery, biomaterials, and biosensors. Surface-supported lipid layers are also interesting as model surfaces in studies of protein adsorption or biophysical membrane studies.

Regarding the behavior at the air-water interface, monofunctional amphiphilic molecules are the most commonly used model compounds which have been extensively studied. In a monolayer of amphiphiles, the hydrophilic headgroups are immersed in the water and the hydrophobic tails jut out into the air. Supported membrane systems are key features of emerging nanotechnologies, because these tetraether lipids self-assemble into ordered structures with extraordinarily stability against chemical and microbial degradation.

Our work has several flavors, indicated in the title. The first how large area the homogeneous of monolayer film organic onto Silicon wafer substrate with some kind properties of substrate (Hydrophobic, and Aminosilanisated) which using Langmuir-Blodgett technique and also characterization using Atomic Force Microscopy and Ellypsometric equipment the reason of the present investigation was to find out while bolaamphiphiles tetraether lipids may also great potential in applied science especially in the field of nanotechnology a detailed physicochemical characterisation of tetraether lipid films at the air-water interface or after deposition onto solid supports (Silicon wafer subtrate).

2. MATERIALS AND METHODS

2.1 THE LIPIDS AND OTHER MATERIAL

The archaea were grown in semicontinuous fermentor (Biostat 50D, Braun, Melsungen, Germany) cultivation according to Freisleben et al. (1994) at temperatures between 39°C and 59°C in sulfuric acid medium at pH 2. The main tetraether glycolipid (MGL) was extracted and purified from H.-J. Freisleben and E. Antonopoulos as described by Blöcher et al. (1984) modified by a two-step chromatography with DEAE-cellulose and silica columns eluted with chloroform/methanol. Analyses of the lipid composition was carried out by a high performence liquid chromatography (HPLC). The purity of the MGL fraction was 99%. The Langmuir film balance experiments were accomplished with MGL-extracts from cultures grown at 39°C (MGL39) and 59°C (MGL59). The lipid was lyophilized at 10^{-2} torr overnight and stored at room temperature over phosphopentoxide in an exsiccator. All chemicals were obtained from Merck (Damstadt) or Sigma (Deisenhofen) at the highest purity available.

2. 2 LANGMUIR-BLODGETT (LB)

The monolayer investigations were carried out with a commercial film balance (Riegler & Kirstein GmbH, Mainz, Germany) with a rectangular thermostatted Teflon trough. The surface pressure was measured with a filter paper Wilhelmy balance. The lipids were dissolved in chloroform in a concentration 1 mMol for the film balance experiments. The subphase was pure water of Milli Q quality (18.2 MΩ, pH 5.6). The experiments were performed at a temperature of 20°C. After spreading, the lipid films were equilibrated for different times at zero surface pressure before starting the measurements. All films were compressed with a constant speed of 0, 1 mm/s.

2.3 WAFER MODIFICATION AND PURICATION

The Hydrophobic substrates were prepared using SiO_2 wafer which were cleaned with Piranha Method. For activation of the wafer surface a Hydrophobisation Method was used. Put into Dimethyl C_{18} – Chlorsilan. The hydrophobicity of the substrates thus prepared were reasonably good with the layer should be 1,5 nm and a contact angle 90˚ resulted.

The aminosilanisated substrates were prepared using SiO_2 wafer which were cleaned with Piranha Methode. For activation the wafers were cleaned using UV-lamp (Xeradex, Lampenwerk

Wipperfürth, Germany) for 5 minutes and than put into aminopropyldimethylethoxysilane. An aminosilanisation ot the substrate a layer of 1 nm and a contact angle 70˚ resulted.

2. 4 ELLIPSOMETRY MEASUREMENTS

Ellipsometry Measurements were accomplished with a mapping single wavelength ellipsometer SE–400 (Sentec Instrument, Germany, Berlin). As light source a He/Ne laser with a wavelength $\lambda = 632,8$ nm was used. The angle of incidence was 60˚. A substrate refractive index of 3,874 used for Silicon. The upper layer refractive index were determined by 1,46. The bolaamphiphiles (Archaebacterial tetraetherlipid) were transferred onto Silicon wafers (1cm x 1cm). The surface was scanned in a single line direction from the pure silicon oxide layer into the lipid layer. The distance between the measurement points is 200µm, the are of one spot is 250 μm^2.

2. 5 ATOMIC FORCE MEASUREMENTS

The morphology of the transferred film were investigated in the contact mode using an AFM image were obtained on NanoWizard (JPK Instruments, Berlin, Germany) under atmospheric conditions. The samples were examined within one our after preparation.

3. RESULT

3. 1. FILM BALANCE

We have transferred the bolaamphiphiles from air/water films on silicon substrates by Langmuir Blodgett technique at the highest surface pressure. Caldarchaeol in concentration 50µl 1 mMol at temperature 20°C had surface pressure about 20 mN/m.

We have transferred the monolayer Bolaamphiphiles on silicon substrates by Langmuir Blodgett technique at various type of transfer (Y-type for Aminosilanisated substrates and X-type for Hydrophobic substrates).

We have attempted to transfer the monolayer films onto hydrophobic (X-Type) and aminosilanisated substrates (Y-type transfer). The monolayer of these bolaamphiphiles are transferred at the surface pressures given in Figure 1

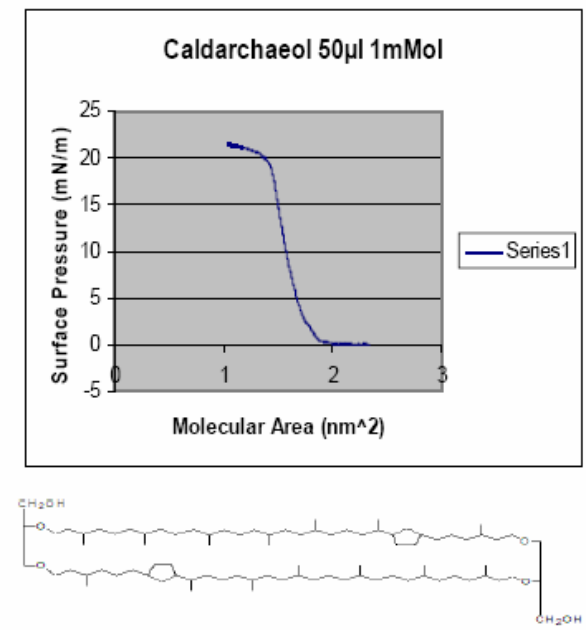

Figure 1 Representative Surface Pressure/ Area isotherms at 19°C,for Caldarchaeol 50µm 1mMol

3.2. ELLIPSOMETRY

he ellipsometry gives a mean film thickness over a large spot area of 250 μm^2 and therefore can not discriminate between different morphological substructures. Therefore, only 75% of the total surface areas of the substrates were covered by the lipid layer. The surface was scanned in a single line direction from the pure silicon oxide layer into the lipid layer.

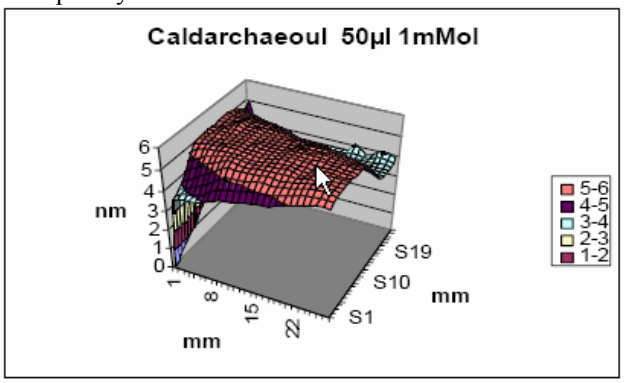

Figure 2. Ellipsometry for Caldarchaeol 50µm 1Mol YType transfer onto Amino-silanisated wafer

3. 3. ATOMIC FORCE MICROSCOPY (AFM)

The surface morphology of monolayer films were studied by means of AFM. The AFM images for the Langmuir-Blodgett monolayer films of bola amphiphiles on hydrophobic substrates and aminosilanisation substrates with the respective height profiles along a chosen line are shown in Fig 3.

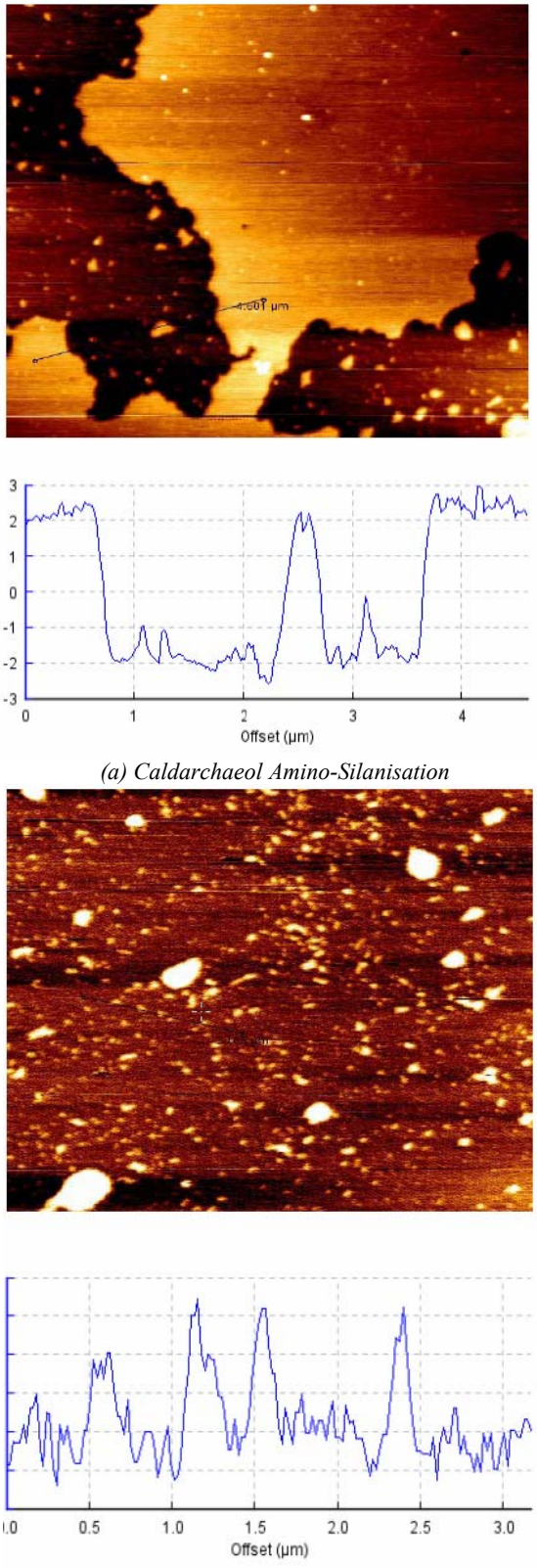

(a) Caldarchaeol Amino-Silanisation

Figure 3 (a) Caldarchaeol Amino-Silanisation (Y-Type Transfer) and (b) Caldarchaeol Hydrophobic (X-Type Transfer)

4. DISCUSSION AND CONCLUSION

The phase behavior and the molecular organization of natural and synthetic archaeal tetraether lipids has been investigated for more than 20 years . At present the phase behaviour and the molecular organization of the tetraetherlipids from thermoacidophilic archaea become of special importance, because these lipids can be form very stable monomolecular model membrane systems . To establish a organization-model for natural tetraether lipids in dependence on the living conditions of the archaea we investigated monomolecular films of these lipids on the air-water interface by using a combination of Langmuir-Blodgett film balance, ellipsometric and AFM experiments.

The Surface pressure vs Area per molecular isotherms (Fig.1) for caldarchaeol in our experiments, bolaamphiphiles form metastable liquid-expanded monolayers where one molecule occupied an area of nearly 1, 4 nm² forms a stable liquid-expanded monomolecular film. Compression of the monolayer leads to a homogeneous condensed phase and then to a collapsed state.

For the symmetric bolaamphiphile Caldarchaeol the film collapsed at a pressure near 20 mN/m and a molecular area of about 1,4 nm². Caldarchaeol gives the most instable lipid films therefore we could not plot a compression-decompression curve. Nevertheless a transfer has been tried. The ellipsometric data showed a thickness of the film after hydrophobic (X-Type) transfer of about 2,8 nm, whereas the film-thickness after transfer onto amino-silanisated (Y-Type) wafer the thicknes reached only 1,5 nm. This points for all films to a horseshoe-conformation.

Ellipsometry even in the mapping technique is unable to resolve single higher standing domains, because the smallest spot cover an area of 250 μm^2 and therefore the data only represent a combined mean value of horseshoe and upright standing domains.

According to the ellipsometric data our AFM results showed that for Hydrophobic substrates had in all films domains are present and that the thickness of the observed domains films (almost 100% was covered lipids) varies between 2 nm and 5 nm. This is consistent with the assumption of coexisting upright standing and horse-shoe like conformations. But for Aminosilanisated substrates had only 40% was covered lipid. From films the hydrophobically transferred showed the most homogeneous organization on the substrates than transfer on amino-silanisated surfaces the lipids are arranged in small islands on the substrates. The large area was covered films onto Slicon Wafer Substrates which importants for applications.

ACKNOWLEDGEMENTS

This study was supported by the DAAD. The authors would like to thank the group of Dr. Ulrich Rothe (Institute of physiological chemistry University Halle) for the technical support.

REFERENCES

[1]. U. Bakowsky, U. Rothe, E. Antonopoulos, T.Martini, Lutz Henkel, H.J. Freisleben, *Monomolecular organization of the main tetraether lipid from Thermoplasma acidophilum at the water-air interface, Chem.* Phys. Lipids 105 (2000), 31-42

[2]. Marc Ernst, H.J. Freisleben, Emmanouil Antonopoulos, Lutz Henkel, Walter Mlekusch, Gilbert Reibnegger, *Calorimetry of archaeal tetraether lipidindication of a novel metasable thermotropic phase in the main phospholipid from Thermoplasma acidophilum cultured at 59°C*, Chem. Phys. Lipids 94 (1998) 1-12

[3]. M. Frant, P. Stenstad, H. Johnsen, K. Dölling, U. Rothe, R. Schmid, K. Liefeith, *Anti-infective surfaces based on tetraether lipids for peritoneal dialysis catheter systems*, Mat-wiss. u. Werkstofftech (2006) 37, no. 6

[4]. A. Papra, F. Penacorada, J. Reiche, S. Katholy, L. Brehmer, H. G. Hicke, *Structure and stability of Langmuir monolayers and Langmuir-Blodgett films of bisaroyl azide bolaamphiphiles, Supramolecular* Science 4 (1997) 423-426

[5]. R. Rolandi, H. Schindler, M. De Rosa, Gambacorta, *Monolayers of ether lipids from archaebacteria*, Eur Biophys J (1986) 14:19-27

[6]. Peter Böhme, Hans-Georg Hicke, Christoph Boettcher, Jürgen-Hinrich Fuhrhop, *Reactive and rigid monolayers of bisaroyl azide diamide bolaamphiphiles on polyacrylonitrile surfaces*, J. Am. Chem. Soc. (1995), 117: 5824-5828

[7]. H. Franz, S. Dante, Th. Wappmannsberger, W.Petry, M. de Rosa, F. Rustichelli, *An X-ray reflectivity study of monolayers and bilayers of archae lipids on a solid substrate,* Thin Solid Film 327-329 (1998), 52-55

[8]. Mario De Rosa, Archaeal lipids*: structural features and supramolecular organization*, Thin Solid Films 284- 285 (1996) 13-17

[9]. Raj Kumar Gupta, K.A. Suresh, *AFM studies on Langmuir-Blodgett film of cholesterol*, Eur. Phys. J. 14 (2004): 35-42

[10]. Jürgen-Hinrich Fuhrhop, Hans-Hermann David, Joachim Mathieu, Ulrich Liman, Hans-Jorg Winter, Egbert Boekema, *Bolaamphiphiles and monolayer lipid membranes made from 1, 6, 19, 24-Tetraoxa-3, 21cyclohexatriacontadience-2,5,20,23-tetrone*, J. Am. Chem. Soc.(1986) 108:1785-1791

[11]. Karen Köhler, Annete Meister, Bodo Dobner, Simon Drescher, Friederike Ziethe, Alfred Blume, *Temperature-dependent aggregation behaviour of symmetric long-chain bolaamphiphiles at the air-water interface*, Langmuir 22 (2006), 2668-2675

[12]. L. Fittabile, M. Robello, A. Relini, M. De Rosa, A. Gliozzi, *Organization of monolayer-formed membranes made from archaeal ether lipids,* Thin Solid Film 284-285 (1996): 735-738

[13]. Jerome L. Gabriel, Parkson Lee Gau Chong, *Molecular modeling of archaebacterial bipolar tetraether lipid membrans*, Chem. Phys. Lipids 105 (2000) 193-200

[14]. Moira L. Bode, Subash R. Buddoo, Sanet H. Minnaar, Chris A. Du Plessis, *Extraction, isolation and NMR data of the tetraether lipid calditoglycerocaldarchaeol (GDNT) from Sulfolobus metallicus harvested from a bioleaching reactor*, Chem. Phys. Lipids 154 (2008), 94-108

[15]. J.L. Dote, W.R. Barger, F. Behroozi, E. L. Chang, S.-L. Lo, C. E. Montague, M. Nagumo*, Monomolecular film behaviour of tetraether lipids from a thermoacidophilic archaebacterium at the air/water interface, Langmuir* (1990), 6:1017-1023

[16]. Yi Y. Zuo, Eleonora Keating, Lin Zhao, Seyed M. Tadayyon, Ruud A. W. Veldhuizen, Nils O. Petersen, and Fred Possmayer, *Atomic Force Microscopy studies of functional and dysfunctional pulmonary surfactant films.I. micro- and nanostructures of functional pulmonary surfactant films and the effect of SP-A*, Biophys. J.(2008) 94:3549-3564

ISSN 114-1284

The Effect of Ultrasonic Wave on Reduction of particle size Process of Silica

Suryadi[1], Wahyu B.W. [1], Agus Sukarto[2], Nurul T.R. [1]

[1]*Research Center for Physics, PUSPIPTEK Serpong*
[2] *Graduate School of Engineering, Kagoshima University, Japan*
suryadi_sun@yahoo.com

Abstract

Has been done research of the effect of ultrasonic wave (sonication) on reduction of particle size of domestic silica of kalimantan (SDK) to produce silica nanoparticles. In this research, sonication was done at frequency 20 kHz with dissociation energy intensity (power) ± 60 watts. In order to observe the effect of sonication, the samples were sonicated using time variable of 0 minute, 180 minutes and 300 minutes which were then named as SDK0, SDK180 and SDK300 sample, respectively. The obtained samples were then characterized using X-Ray Diffractometer (XRD), Scanning Electron Microscope (SEM) and Particle Size Analyzer (PSA). The comparison of XRD analysis of the samples shows no significant crystal structure change on each sample. SEM analysis of SDK0 sample shows microstructure in the form of relatively big agglomerate. Whereas, the microstructure of SDK180 and SDK300 sample show the scale tendency of smaller agglomerate. In addition, PSA analysis shows quantitatively the occurred reduction of particle size process. PSA analysis shows the reduction of average particle size of SDK0, SDK180, and SDK300 samples, where the longer sonication time the smaller particle size is. Besides, the sonication was observed can conduct reduction of particle size without making any crystal structure damage of the samples.

Keywords : ultrasonic wave, reduction of particle size, silica, sonication

INTRODUCTION

Silica is the oxide form of silicon which usually found in nature in the form of quartz and opal [1]. Silica (SiO2) was known to have abrasion resistance, electrical insulation and high thermal stability properties which has been applied widely in industry. This mineral has great abundance in Indonesia, however still not utilized maximally. Silica nanoparticle posses superior novel properties which cannot be achieved in bulk particle size. Besides, silica nanoparticle is a real expensive material ($10000/ton) [2] and cannot be produced in Indonesia. Therefore, the research to yield silica nanoparticle absolutely have a real strategic and high economic value.

One of common way utilized to yield nanoparticle is mechanical milling method. This method can yield nanoparticle by giving mechanical force in the form of collision, shear, and strain. However, though this method is applicable to yield nanostructured material, the utilization of this method often less effectively in yielding nanoparticle which primarily caused by agglomeration phenomenon causing particle size exactly bigger and bigger. Therefore, another method is required to yield nanoparticle more effectively which one of them is sonication method using ultrasonic wave.

The main advantage of sonication method is its ability in breaking the agglomeration. In solution, ultrasonic wave generate cavitation phenomenon. Cavitation is the event of formation, growth and implosive breakage of bubble in fluid. According to Suslick (1998), the event of bubble collapse produce an intense local heating (~ 5000 K), high pressure (~ 1000 atm), high heating and cooling rate (> 109 K/s), and fast liquid flow (~ 400 km/jam) [3]. This process sequence finally will break particle and also agglomerate in the sample.

EXPERIMENTAL SETUP

The samples used for this experiment were obtained from local silica rocks. The silica rocks were crushed manually to yield smaller size of about 1 cm. The crushed silica rocks were the milled using disk mill for 20 minutes. The yielded powder was then dissolved in techinal ethanol solution. The solution was then sonicated with energy intensity of 60 W for 0, 180, and 300 minutes. The obtained samples were then characterized using XRD, SEM, and PSA.

RESULTS AND DISCUSSION

XRD pattern comparison SDK0, SDK180, and SDK300 samples is shown in Figure 1. From Figure 1, it can be seen that sonication process gives no significant on XRD pattern of the three samples. Neither the appearance of new peak nor disapperance of initial peak was observed from those three XRD pattern. This condition imply that there is no mechanical reaction like usually it is in common mechanical milling process. Moreover, there is no significant intensity decrement which shows no deformation on the crystal structure of the processed samples. There is also no peak shifting which shows no significant lattice strain.

ISSN 114-1284

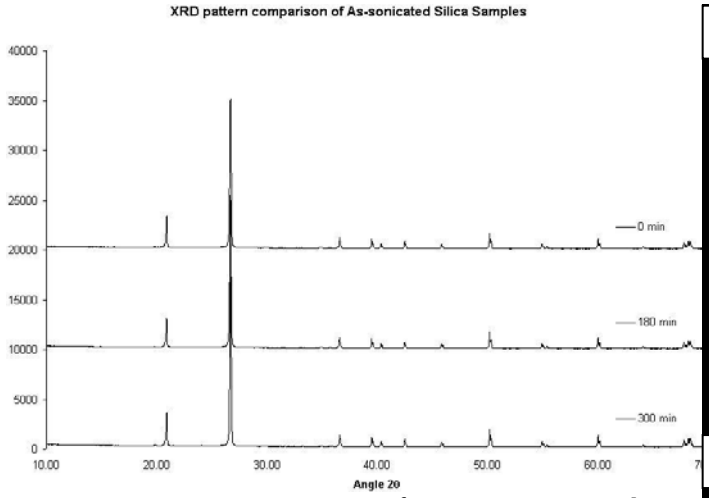

Figure 1. XRD pattern comparison of SDK0, SDK180, and SDK300 samples

Microstructure of the three samples is compared using SEM photograph as shown in Figure 2. From the comparison of the three SEM photograph, it can be seen clearly that separation process and breakage of particle were happened. It also can be seen from Figure 2(a) that unsonicated sample seems to form particle groups with morphology showing that there are still weak bondings between particles. After 180 minutes sonication, those particle groups seem to break and change into particle clusters with various size, from 19µm to some hundred nanometers. This breakage process was continued for 300 minutes sonication time, yielding smaller size particle clusters. In general, it can be seen that the breakage process of weak bondings and reduction of particle size was happened simultaneously for 300 minutes sonication time. The yielded particle size is relatively more homogeneous compared to 180 minutes-sonicated sample. However, reduction process of particle size was still incomplete so that there are still relatively big particle clusters remaining compared to average particle size.

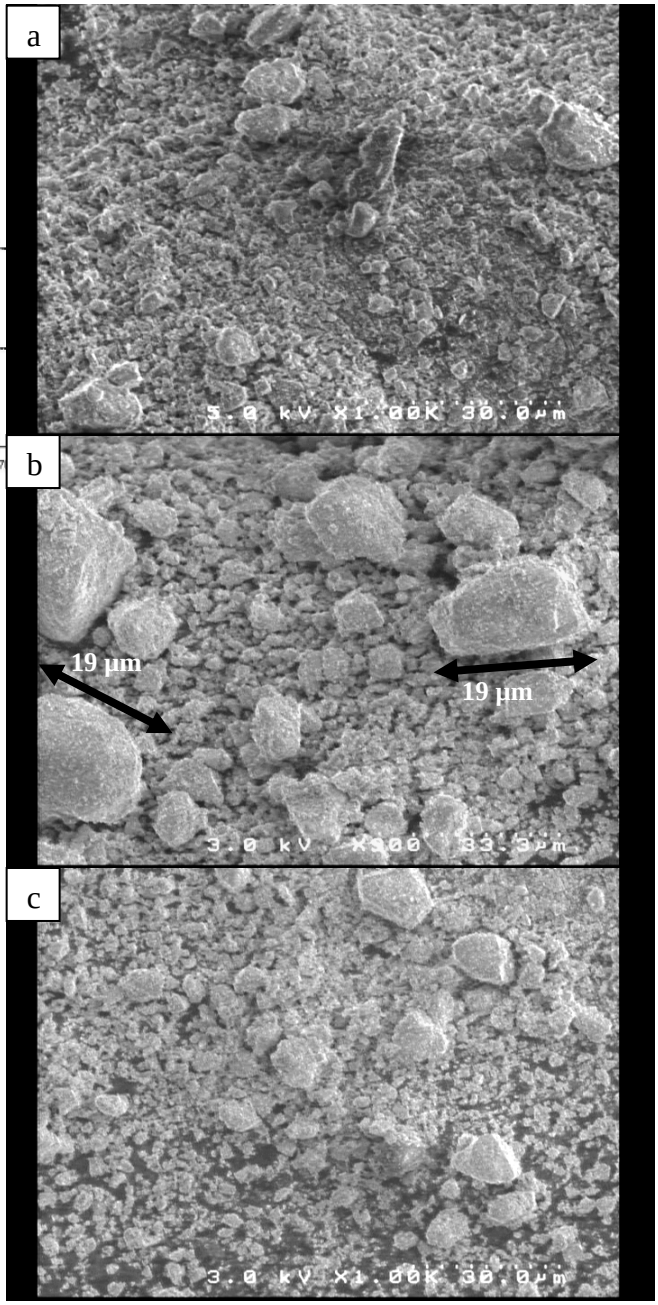

Figure 2. SEM photograph of sonicated samples for: a. 0 minute b. 180 minutes c. 300 minutes

SEM photograph of the sonicated sample with magnification of 25000X is shown in Figure 3. From Figure 3, it can be seen that unsonicated sample has particle clusters which are tied by weak bondings among particles as also shown in Figure 2. After 180 minutes sonication, those weak bondings are broken, caused the disconnection of particle clusters from the bonding. However, reduction process of particle size was still not happened effectively because the dissociation energy of sonication process is applied firstly to break the bonding among the clusters. The circle parts of Figure 3(b) indicate that there are some particle which still in process of disconnection of weak bonding among particles. The disconnection process of weak bonding among particles was continued with the next step e.g. reduction process of

ISSN 114-1284

particle size after 300 minutes sonication time as shown in Figure 3(c). It can be seen clearly in Figure 3(c) that there are particle size distributions, showing clearly the occurrence of reduction process of particle size. However, as can be seen from Figure 2(c), the reduction process of particle size was still incompleted so that some relatively large particles are still remaining.

The results of particles size measurements using PSA are shown in Figure 4 and Figure 5. From those measurements, the initial sample has particle size of about 2.25 µm. After 180 minutes sonication the average size was reduced to 478.7 nm. Whereas, 300 minutes-sonicated sample has average particle size of about 207.7 nm. It is then clear reduction of particle size has already happened. However, though reduction of particle size has already happened, the XRD shows no crystal structure transformation on the samples. This can be happened because reduction process of particle size during sonication doesn't include plastic deformation process which usually can be observed on conventional mechanical milling process [4-9]. Thereby, reduction process of particle size prepared by sonication method has an advantage over conventional mechanical milling process in avoiding the crystal structure of the sample from destruction.

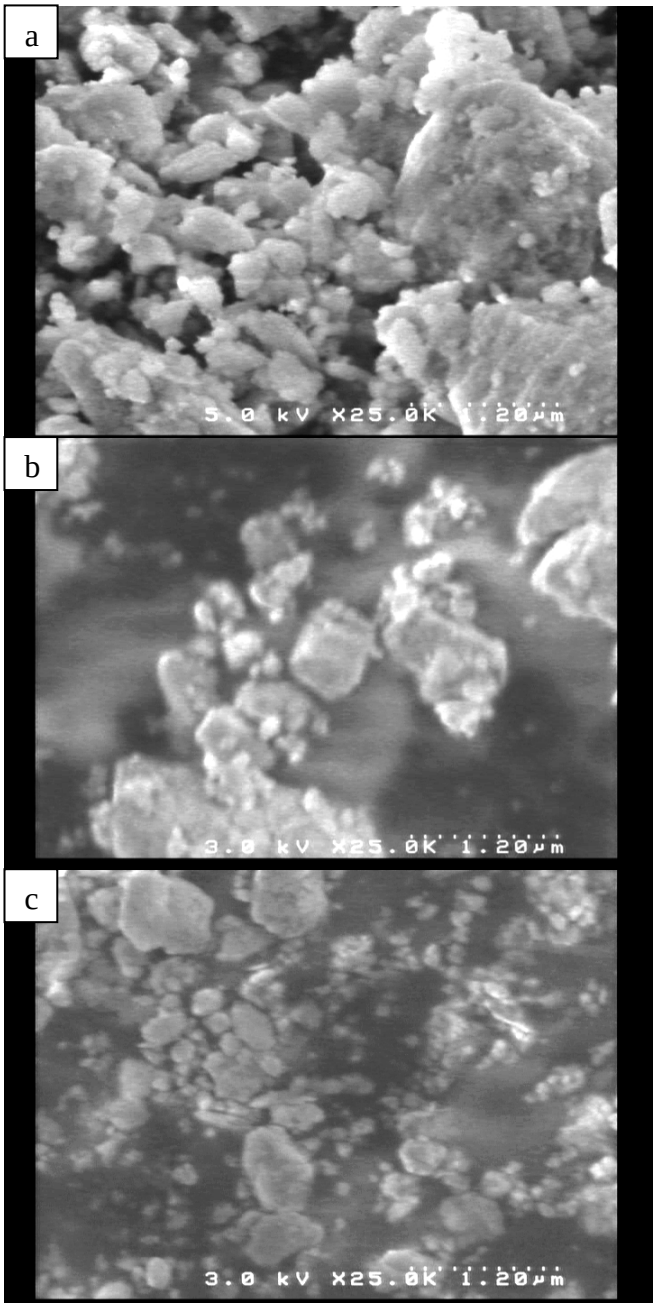

Figure 3. SEM photograph of sonicated sample with magnification 25000X: a. 0 minute b. 180 minutes c. 300 minutes

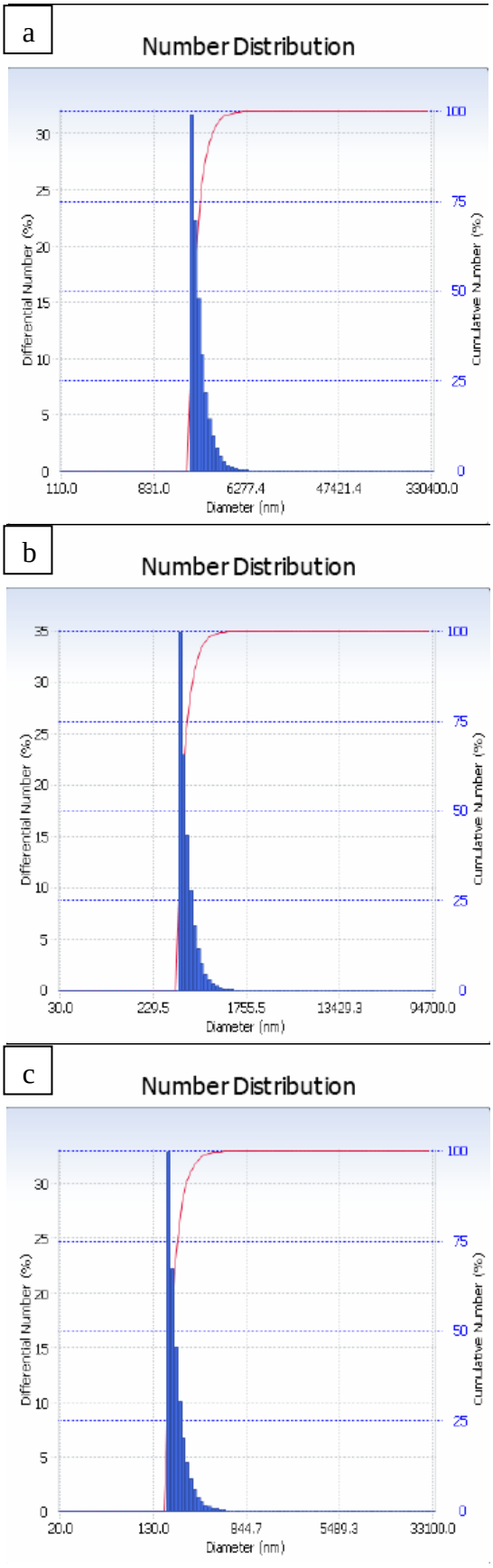

Figure 4. Result of particle size measurements: (a) 0 minute (b) 180 minutes (c) 300 minutes

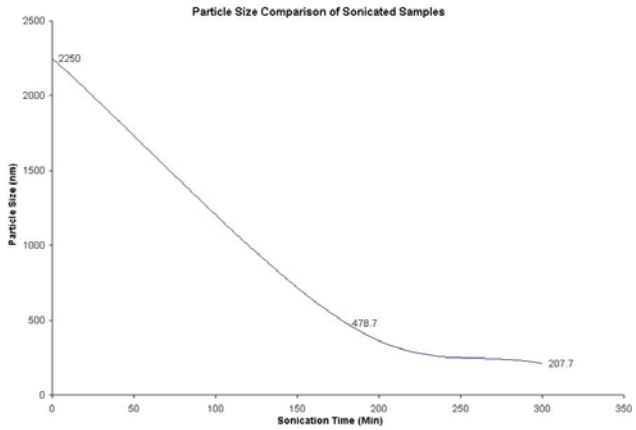

Figure 5. Comparison of sample particle size which has been sonication during 0, 180, and 300 minutes.

CONCLUSION

1. The ultrasonic wave gives micro scale effect on sonication process in term of reduction of particle size which correlates linearly with sonication time.
2. The conducted sonication process was able to do reduction of particle size without changing crystal structures of the processed sample.

REFERENCES

[1] Vlack, L.H.V., Ilmu dan Teknologi Bahan, 5th ed., Jakarta, p. 136-151, 231-236, 317-322, 1994.
[2] Jang, D.H. et.al, Colloids and Surfaces A: Physicochem. Eng. Aspects 313-314, p.121-125. 2008.
[3] Suslick, S.B. et.al, Nature 353 (1991) 414. Taken from Gedanken, 2004.
[4] N. T. Rochman, K. Kawamoto, H. Sueyoshi, Y. Nakamura and T. Nishida: J. Japan Soc. Heat Treatment, 39, p. 312 (1999).
[5] N. T. Rochman, K. Kawamoto, H. Sueyoshi, Y. Nakamura and T. Nishida: J. Mat. Proc. Tech., 89-90, p. 367 (1999).
[6] Y. Kimura and S. Takaki: "Proc. 1998 Powder Metallurgy World Congress & Exhibition", Granada, Spain, 1 (1998), p. 573.
[7] D.Maurice and T.H.Courtney: Metallurgical and Materials Trans. A, 25A, p. 147 (1994).
[8] E.J.Fasiska and H. Wagenblast: Trans. Metallurgical Society of AIME, 239 p.1818 (1967).
[9] Suryanarayana, C. Mechanical Alloying and Milling. Marcel Dekker. 2004.

ISSN 114-1284

Performance of Portland-Blended Cement as future's *'Green Cement'*

V.Indrawati and A.Manaf

Postgraduate Program of Materials Science, University of Indonesia
e-mail: vera.indrawati@ui.ac.id

ABSTRACT

Supplementary cementing material (SCMs) of local resources was used for partial replacement of the Portland clinker in attempt to reduce CO_2 emission in the cement production. Replacement of Portland clinker up to 20 wt.% with SCMs in the normal cement has reduced CO_2 emission by 0.18 Ton CO_2/Ton cement. However, when compared with that of normal cement, the property is still comparable in which almost 80% of the mechanical strength of the normal cement was achieved (32 MPa vs 40 MPa). In this paper, performance of portland blended cement was evaluated through mechanical strength, phase identification and microstructure.
Key words: portland cement; SCMs; CO_2 emission; portland-blended cement; mechanical strength

INTRODUCTION

Since 19th centuries, Portland cement has been commonly used in the construction. Its performance in term of mechanical strength and durability are assumed as the best. Unfortunately, its sintering process has negative effects to the environment because of CO_2 emission. Research on cementing materials which refers to Roman cement has given a new direction to new type of cement which is called blended cement. This kind of cement is not only related to the environment aspects but durability of concrete structures is also included[1]. Blended cement is produced by mixing Portland clinkers with other Supplementary Cementing Materials (SCMs). These SCMs could be natural or artificial such as slag, flyash, silica fume, metakaolin[1][2]. Trass is natural SCM which its deposit abundantly in the country. In this paper, we report results of replacement of up to 40 % trass to portland cement

EXPERIMENT

Trass from two different sources were characterized by XRF and XRD to identify the chemical and mineral compositions. Trass materials were ground together with portland clinker and gypsum to produce blended cement. Replacement of 20, 30 and 40% of portland clinker were prepared. Compressive strength of its cement mortar were measured and microstructures of cement pastes were investigated by SEM. Water to cement ratio(W/C) used is 0.485

RESULT AND DISCUSSION

Figure 1 showed the compressive strength of blank portland cements compared with that of blended cements of 20, 30 and 40% trass. Refer to 40 Mpa as mechanical strength of normal cement, replacement up to 20 % trass has values of 32 and 40 Mpa strength at 28 and 56 days curing. By calculation, CO2 reduction of 20, 30 and 40% clinker replacement are 0.18, 0.27 and 0.36 T/Tcement respectively. Microstructures by SEM of cement pastes at 56 days age also showed insignificant difference between portland and blended cement. Figures 2 to 5 showed microstructures of calcium silicate hydrate (CSH) originated from hydration of calcium silicate (C3S) from portland clinker which responsible for mechanical strength of cement. In portland blended cement deduction of C3S portion is replaced by CSH formed from reaction of silica in SCMs with Ca(OH)2 as site product of C3S hydration.

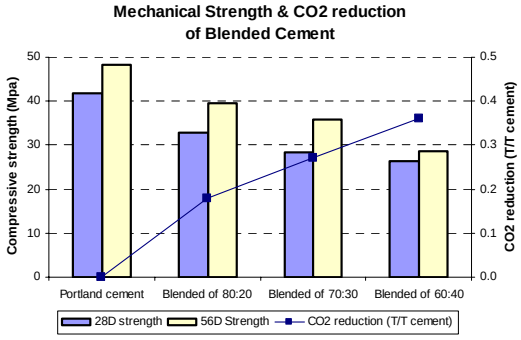

Figure 1. The compressive strength of cements

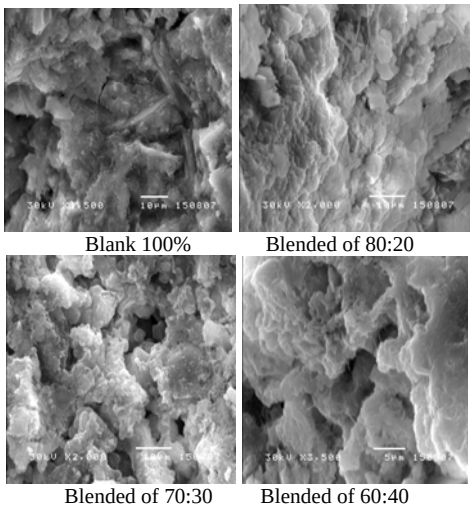

Blank 100% Blended of 80:20

Blended of 70:30 Blended of 60:40

Figure 2-5 Micrograph of cement pastes at 56 days

ISSN 114-1284

CONCLUSION

Replacement of up to 30 % trass to portland cement still gives good mechanical strength makes portland blended cement is promising for future's cement as well as contribute in reducing CO_2 emission.

REFERENCES

1. L.Turanli et.al, Effect of material characteristic on the properties of blended cement containing high volumes of natural pozzolans, Cement and Concrete Research 34 (2004) 2277-2282

2. Luca Bertolini et.al, Corrosion of Steel in Concrete, Part I. Properties of Cementitious Materials, Wiley-VCH GmBH & Co (2004)

ISSN 114-1284

Effect of Boron Addition on the As-cast Structure and Mechanical Properties of 6.5% V-5 % W High Speed Steel

Vita Astini, Yus Prasetyo[1], and E.R. Baek*
***erbaek@ynu.ac.kr**

School of Materials Science and Engineering
Yeungnam University, 214-1, Dae-dong, Gyeongsan-si, 712-749, Korea
Tel : +82 53 8102539
Email : vitaastini@ynu.ac.kr

[1]KT Roll Reasearch Engineer, #436-18, Changgok-Ri, Paltan-Myeon,
Hwasung City, Kyungki-Do, Korea
Tel: +82 31 354-8400
Email : yus_prasetyo@ktroll.co.kr

ABSTRACT

High speed steel (HSS), widely used for tools, because of excellent hardness, wear resistance, and high temperature properties. HSS rolls consist of martensitic matrix, hard carbide such as MC, M_2C, M_7C_3, and M_6C and secondary carbides the matrix. The most decisive microstructure in HSS fracture toughness is intercellular carbide and their distribution together with matrix characteristics. Direct micro fracture observations show that micro cracks initiate at hard carbides formed along in cell boundaries, and that fracture proceeds along these carbides [1]. Connected carbide can easily propagate the microcrack on the cell boundary. In order to develop HSS fracture toughness without decrease the wear resistance, boron is used for alloying element. We investigate the boron effect on the HSS properties using HSS alloy with ± 0.04 wt% boron. Boron can segregate in austenite cell boundaries and occupy vacancy sites induced by deformation so as to prevent the formation and propagation of microcracks at boundaries [2]. Bending test was performed to study the effect of boron on HSS strength. Microstructure characterization; phase identification, carbide identification, boron segregation and fractography of the materials was performed using SEM/EDS, XRD. The cell size and carbide volume fraction is examined using image analysis software. Boron addition increase around 10% bending strength of the material. Matrix hardness and overall hardness also increased. There are no differences of carbide morphology with addition of boron.

Keywords
Boron addition, high speed steel, segregation, bending test, cell refining

1. INTRODUCTION

High speed steel has excellent hardness, wear resistance, and also high-temperature properties. These properties make HSS become suitable material for roll material. Roll material must have excellent wear resistance because of the application of this material. These HSS rolls have different microstructure and characteristic from high speed tool steels. When manufacturing tool steels, the structure is destroyed in the subsequent deformation such as forging, and the final microstructure after heat treatment consists of tempered martensite containing fine and well distributed carbide [1]. The cast structure of HSS contains of coarse carbide, and the matrix will transform to temper martensite after heat treatment.

Carbides on HSS material contribute to the hardness of HSS. If volume fraction of carbide increases, the hardness of the HSS also increases. Coarse carbides are generally segregated along cell boundaries, therefore, overall roll hardness increases, but fracture toughness tends to deteriorate [1]. Consequently, the microstructural factors such as size, volume fraction, distribution of coarse carbides, and the characteristics of the martensitic matrix play important roles in enhancing the roll properties.

Boron has a strong tendency to segregate to the grain boundaries but not to cavity (free) surfaces, and enhance grain boundary cohesion [3], segregation of boron can be found as a component of Fe2B [4]. Segregation of boron and enhancing of the grain boundary cohesion causes cell refinement and winding of grain boundaries. Boron is enhancing of the grain boundary cohesion that obstructs grain growing at annealing course [5]. K.N.Kim [5] investigated that with the increase of boron addition the RT bend strengths also increase. S.H Song [6] investigated effect boron on the C-Mn steels and austenitic stainless steels. It has been shown that boron can segregate to

Table 1
Chemical composition of HSS investigated (wt %)

Tbale

Sample	Chemical Composition (%wt)								
	C	Si	Cr	Ni	Mo	Mn	W	V	B
Target	1.918	0.835	6.076	0.488	3.034	0.444	5.026	6.527	0.04
Alloy 1									
With boron	1.98	1.02	5.94	0.58	4.09	0.53	5.21	6.9	0.04
Without boron	2.20	0.72	6.68	0.58	4.27	0.59	5.34	7.35	-
Alloy 2									
With boron	1.85	0.96	6.1	0.474	3.79	0.57	4.58	6.24	0.056
Without boron	1.84	0.96	5.74	0.482	3.42	0.55	4.35	6.37	0.004

austenite grain boundaries and occupy vacancy sites induced by deformation so as to prevent the formation and propagation of micro cracks at boundaries and in turn improve the steel hot ductility.

The complexes diffuse from the matrix to the boundary causes the boundary segregation since the boundary is a sink for vacancies. Therefore, when a specimen is cooled to a lower temperature from a higher temperature, solute atoms will segregate to austenite grain boundaries. Since the diffusion rate of B-vacancy complexes is far faster than that of P-vacancy complexes [8], B vacancy complexes arrive at the grain boundary more quickly than P-vacancy complexes do in the process of continuous cooling, which suppresses the segregation of phosphorus. As shown in [8], the binding energy of boron with the grain boundary is approximately twice of that of phosphorus.

In order to develop HSS fracture toughness without decrease the wear resistance, boron is used for alloying element. The purpose of this study is to investigate the effect of boron on the casting HSS alloy sample properties. The addition of boron is 0.04 wt %.

2. EXPERIMENTAL PROCEDURE

Materials used in this study were four HSS manufactured by casting method, whose chemical composition listed in table 1. The basic composition of the HSS is 1.9C-6.5V-6Cr-0.8Si-0.4Mn-3-Mo-5W (wt. %) and this alloy design to be able to investigate the effect of boron addition by addition 0.04 wt % boron in some alloy. The HSS alloys were manufactured by a laboratory scale induction furnace casting apparatus with the capacity 2.5 kg. The melt was charged into the mold and then equilibrium solidified.

The samples were polished and etched in vilella and marble's [10] (10 g CuSO, 450 mL HCl, 50 mL water) and were observed by an optical microscope and scanning electron microscope (SEM). Compositions of carbides and the matrix were quantitatively analyzed by energy dispersive spectroscopy (EDS). Carbides were examined using Murakami etchant [10] (10 g K3Fe (CN), 10g NaOH, 100 ml water), in which M2C (black), M7C3 (light pink), and M6C (pink) carbides are selectively etched but not the matrix and MC carbides. The cell size and the volume fraction of respective carbides were quantitatively analyzed using an image analyzer.

An X-ray diffractometer was used to confirm the kind of carbides and to measure the amount of retained austenite (γ). Microhardness of the matrix was measured by a vickers hardness tester under 25 g loads.

Sample with dimension 3x3x30 mm were used for room temperature bend testing using three point bending method.

3. RESULT AND DISCUSSION

Fig. 1(a) through (d) are optical micrographs of the four as-cast HSS. It is known that boron generally has major effect on cell size. Figs. 1 show the effect of boron on the cell size for the foundry samples. In alloy 1, sample with boron (Fig.1 (a)) produce smaller cell size than sample without boron (Fig.1 (b)). This phenomenon also happened in alloy 2, sample with boron (Fig.1 (c)) produce smaller cell size than sample without boron (Fig.1 (d)). Boron has a strong tendency to segregate to the grain boundaries but not to cavity (free) surfaces, and enhances grain boundary cohesion [5]; segregation of boron can be found as a component of Fe_2B [4]. So the segregation of boron and enhancing of the grain boundary cohesion causes cell refinement. Increasing of boron content can reduce the solubility of carbon on γ phase (reduce the γ loop) [16]. Boron also can make C replacement on γ phase and also cementite. Another mechanism of cell refining is because of boron act like C, together with C and high contain of V, W it will promote MC carbide formation on the liquid in high temperature. The formation of MC carbide became nucleating agent for solidification process. So additional of boron will increase the MC carbide content on the liquid, it means that increasing nucleating agent on the liquid. From what has been mentioned above, it will refine the cell size gives cell size refining effect. The calculation of cell size shows in table 2. In alloy 1, the addition of boron reduces the cell size 46 %. In alloy 2 the addition of boron reduces the cell size 17 %.

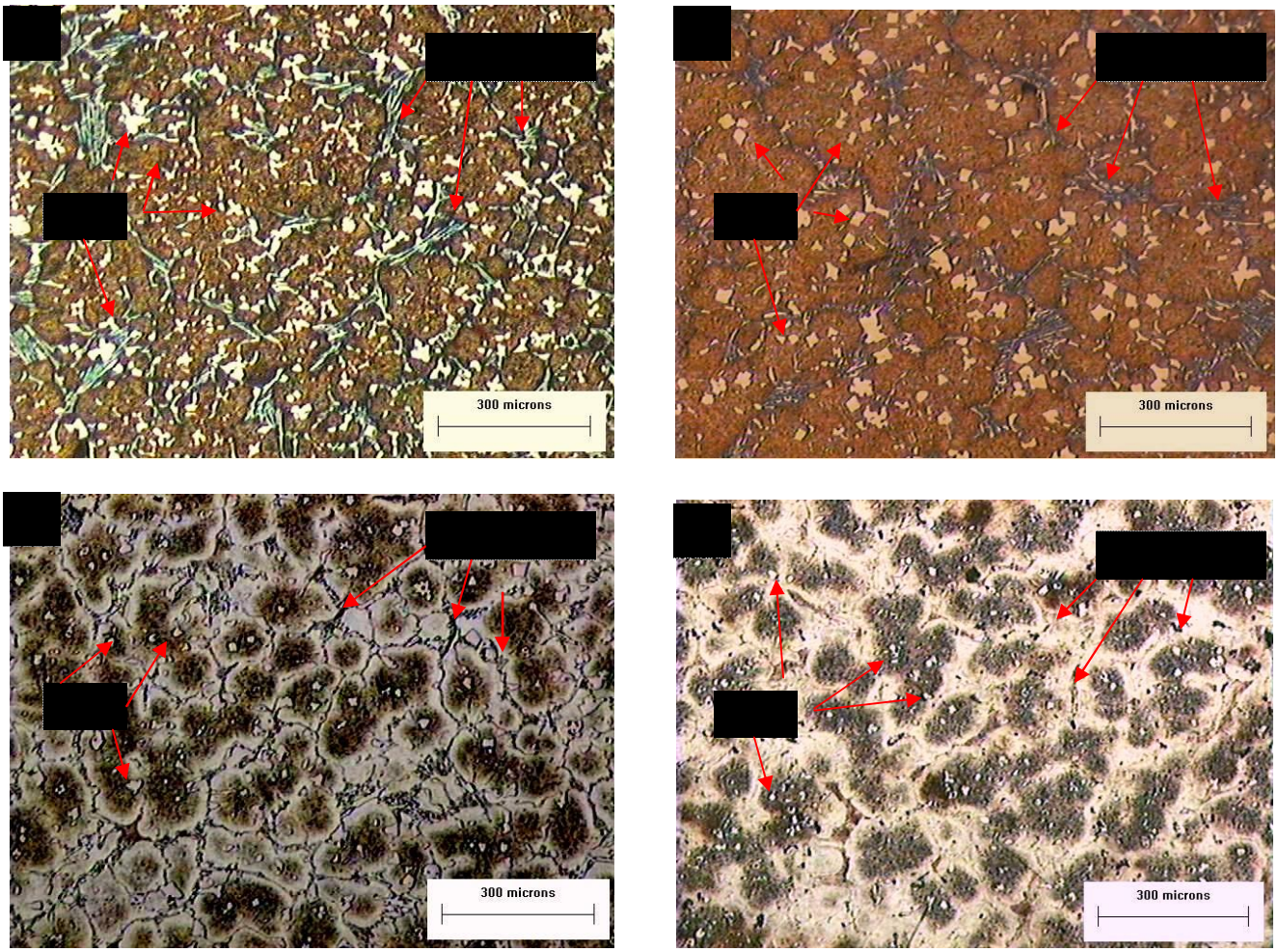

Figure 1: (a) through (d), Optical micrographs of four as-cast HSS, Vilella etched.
(a) alloy 1 with boron (b) alloy 1 without boron (c) alloy 2 with boron (d) alloy 2 without boron

Table 2
Cell Size Calculation

Sample	Cell Size (μm)	
	alloy 1	alloy 2
With boron	34.52	39.64
Without boron	63.52	47.58

Table 3
Microhardness Calculation

Sample	Microhardness (HV)	
	alloy 1	alloy 2
With boron	480	535
Without boron	400	493

Table 4
Carbide Volume Fraction Calculation

Sample	Carbide Volume Fraction All (%)		Carbide Volume Fraction MC (%)		Carbide Volume Fraction (M2C+M7C3) (%)	
	Alloy 1	Alloy 2	Alloy 1	Alloy 2	Alloy 1	Alloy 2
With boron	17.44	18.57	7.2	8.91	10.24	9.66
Without boron	15.98	17.36	6.64	8.54	9.34	8.82

ISSN 114-1284

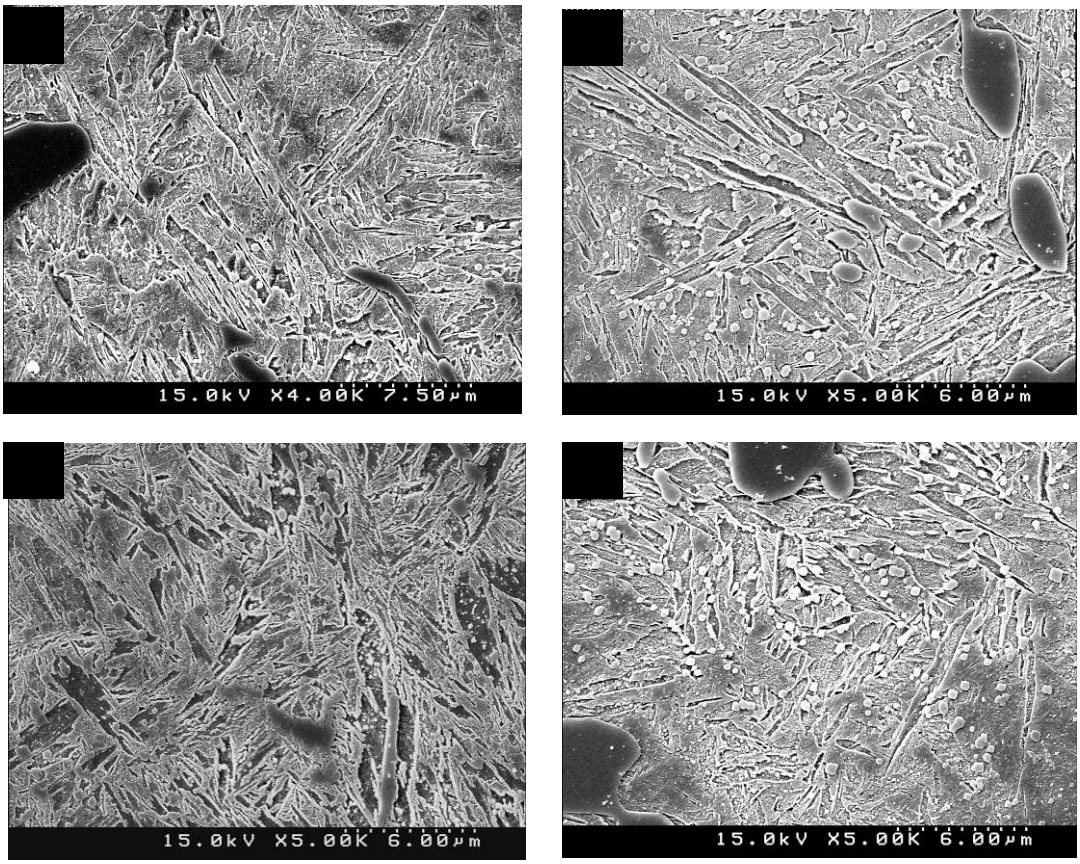

Figure 2: (a) through (d), SEM micrographs Analysis of four as-cast HSS, Marble's etched.
(a) alloy 1 with boron (b) alloy 1 without boron (c) alloy 2 with boron (d) alloy 2 without boron.

Boron has lower solubility on the Fe matrix for ± 10 ppm on 900°C, confirm by T.B.Cameron [4]. T.B Cameron found that the solubility of boron in the austenite is higher than in the ferrite at the invariant temperature. Therefore it will produce eutectoid reaction. During cooling, eutectoid reaction will happen because of the difference of boron solubility on austenite and ferrite (Fig.3). The reaction is:

$$\gamma \rightarrow Fe_2B + \alpha$$

In alloy 1 and alloy 2 with boron sample we found formation of Fe_2B that confirm from the XRD data (Fig 7 (a) and (b) with low peak intensities.

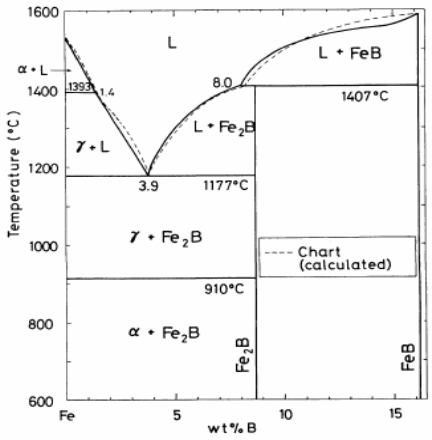

Figure 3: Calculated equilibria in Fe-FeB phase diagram [16]

In Table 3, the average hardness values of the four HSS samples are provided in HV units (Hardness Vickers). The hardness values of without boron samples are observed to be lower than those of with boron samples. This is because samples that contain boron have smaller cell size compare with without boron sample. And also in boron sample there are $M_{23}(C,B)_6$. From the XRD results (Fig.7), we found the formation of $M_{23}(C,B)_6$. It has been reported [11] that only soluble B can segregate and then later precipitate as $M_{23}(B,C)_6$ at grain boundaries. These particles act like other interstitial alloying elements which are able to fill the unfavorable gaps on grain boundary and stabilize the grain boundary surfaces [11]. Likewise, it has been shown that boron atoms tend to migrate to austenite grain boundaries (segregation), a fact that can be associated to B-vacancies interactions [8,11]. Boron can also act as interstitial atom in Fe site that can also increase the hardness of the material.

MC carbides are V-rich carbides (V_4C_3 in chemical stoichiometry) containing mostly V with small amounts of W, Mo, Cr, and Fe. M_2C and M_6C carbides are carbides containing Mo and W, and M_7C_3 carbides are Cr-containing ones. Because of high content of Cr, W and Mo, M_7C_3 type or M_2C type carbides are located along solidification cell boundaries (Fig.1). Most of MC type carbides are formed inside cells (Fig.1). This is happened for entire samples. HSS with boron samples contain higher % carbide volume fraction than HSS without boron samples (Table 4).

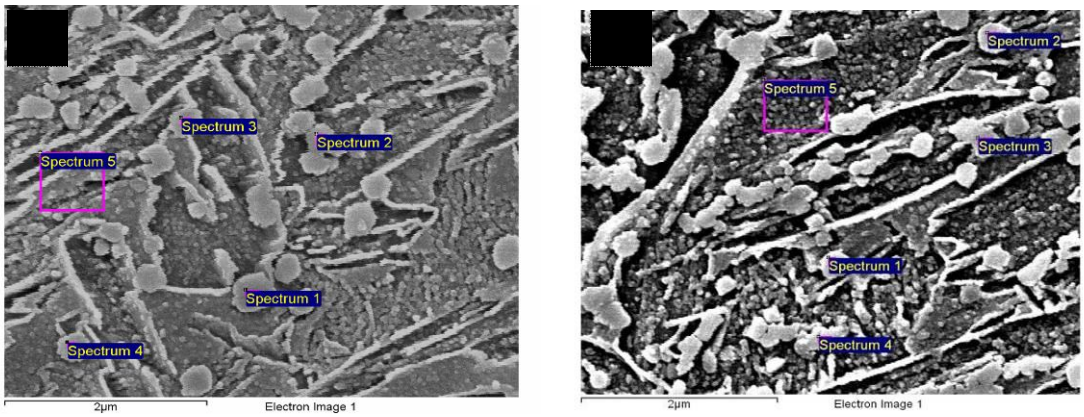

Figure 4: EDS composition Analysis of Alloy 2 HSS (A) With boron (B) Without boron , Marble's etched.

Table 5
EDS Composition Analysis

Spectrum A	Element V	Cr	Fe	Mo	W		Spectrum B	Element V	Cr	Fe	Mo	W	
1	16.5	6.59	57.2	4.75	14.96	carbide	1	14.07	6.08	60.3	4.04	15.52	carbide
2	9.07	5.09	69.7	3.21	12.92	carbide	2	9.9	5.1	66.11	3.22	15.68	carbide
3	8.31	5.64	71.7	2.85	11.51	carbide	3	8.35	6.35	67.72	3.71	13.87	carbide
4	2.22	6.69	81.66	2.22	7.21	carbide	4	9.68	5.04	66.49	4.1	14.69	carbide
5	4.84	5.86	78.36	2.21	8.74	matrix	5	3.13	6.66	81.08	0	9.13	matrix

Table 6
Effect Boron on Bending Strength

Sample		Size of the samples (±0.005)(mm)	Most load (average) (kgf)	Bending Strength (Mpa)
Alloy 1	With boron	3 x 3 x 30	243.45	270.50
	Without boron	3 x 3 x 30	219.44	243.82
Alloy 2	With boron	3 x 3 x 30	130.43	146.64
	Without boron	3 x 3 x 30	118.00	128.61

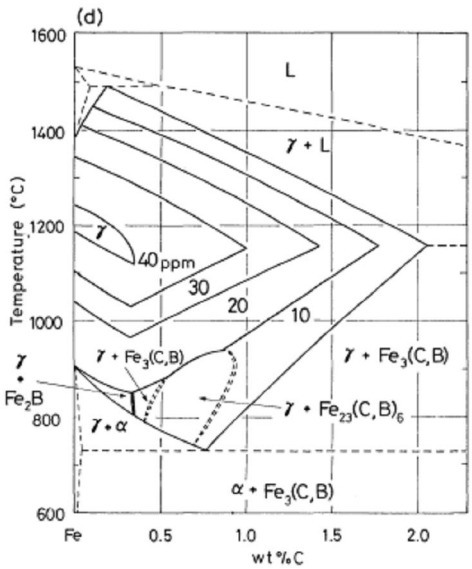

Figure 5: C-B system and carbon limitation for pure austenite [16]

In alloy 1, with boron sample produce 1.13 % higher carbide volume fraction than without boron sample. In alloy 2, with boron sample produce 1.38 % higher carbide volume fraction than without boron sample. This is because boron decreases the solubility of the carbon on austenite phase (Fig.5) [16]. Rejected carbon will tend to form carbide. So additional of boron will increase the carbide content. It was confirm from the XRD data (Fig.7) that with boron samples have higher peak intensity of carbide than without boron sample. For entire samples, from the calculation, the quantity of M_7C_3 type or M_2C carbides is higher than MC carbide. This is because of high containing of Cr, W and Mo, so M_7C_3 type or M_2C carbide is easier to form.

Fig.2 (a) and (b) are SEM micrographs of matrices of Alloy 1 with boron (a) and without boron (b). It can be confirmed that the as-cast matrix is lath martensite in both alloy. The carbon content in the HSS rolls is generally 1.5–2.0%, most of which is combined with such strong

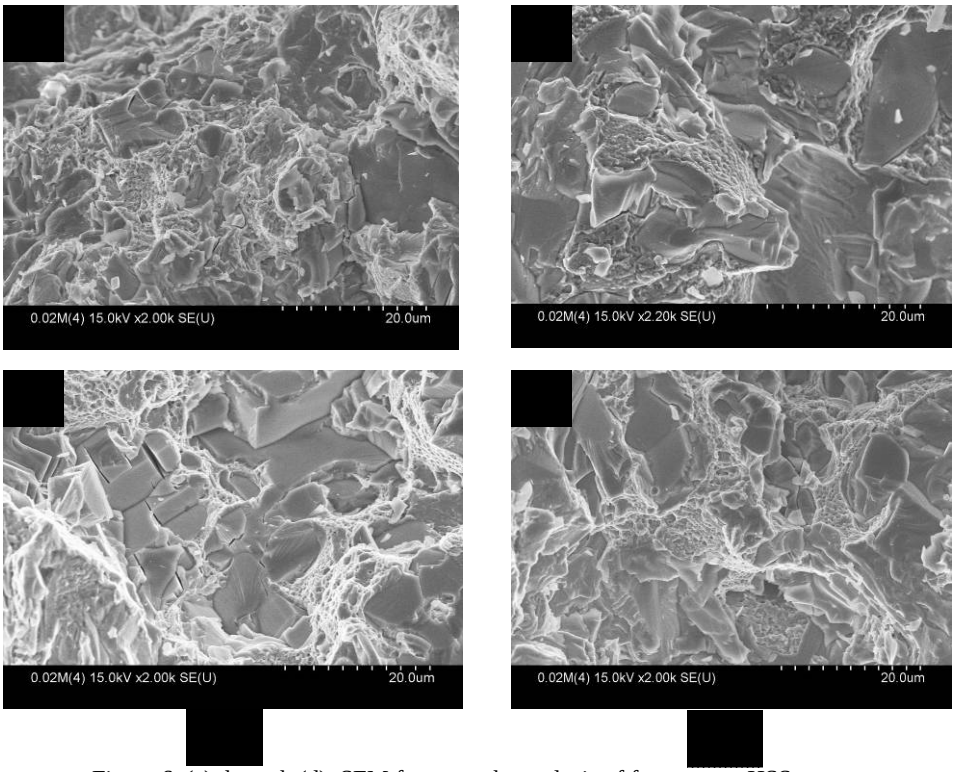

Figure 6: (a) through (d); SEM fractographs analysis of four as-cast HSS.
(a) alloy 1 with boron (b) alloy 1 without boron (c) alloy 2 with boron (d) alloy 2 without boron.

carbide formers as V, W, and Mo [1]. The rest of carbon,0.3–0.6%, is contained inside the matrix, and forms lath-type martensite when the carbon content is below 0.4%, while plate-type martensite when it is above 0.4% [1]. Fig.2(c) and (d) are SEM micrographs of matrices of alloy 2 with boron (c) and without boron (d). It can be confirmed that the as-cast matrix is lath martensite in both alloys. Evenly distributed inside the matrix are quite fine spherical carbides (Fig. 4). This fine carbide analyzed using EDS. The result of qualitative and quantitative EDS analysis shown in Table 5. This fine carbide contains higher vanadium, tungsten, and molybdenum than the matrix. The fine carbide formed during slow cooling on solidification process. This fine carbide distributed on the matrix.

The result of room temperature bend test of sample made form casting are shown in table 6. From the table shows that sample contain of boron tend to have higher bending strength than without boron sample. The RT bend strength of with boron alloy is higher than without boron alloy by about 10 % in alloy 1 and alloy 2. It shows that additional of boron improves the ductility of the alloy; the mechanisms of boron ductilizing effect may include: (1) boron enhances grain boundary cohesion [3]; (2) boron modifies grain boundary structure that allows slip accommodation and transmission across the boundaries at lower levels of stress accumulation [5].

We analyze the fractographs of bending sample. For entire sample bending-tested at room temperature. As we know, HSS contain high carbide volume fraction. Fracture easily happen on the eutectic carbide that segregated on the grain boundary. In alloy 1 with boron (Fig.6 (a)), when the specimen is fractured there appears to be ductile fracture with small and large dimples and with small apparent grain boundary facets. In alloy 1 without boron (Fig.6 (b)), the material exhibit intergranular failure on the carbide site and also there are small dimple. Fracture most happened on carbide. In alloy 2 with boron (Fig.6 (c)), when the specimen is fractured there appears to be mix between ductile fracture with small and large dimples and also we can find intergranular fracture in some part. In alloy 2 without boron (Fig.6 (d)), the material exhibit mix between intergranular failure and also ductile fracture, but with boron sample has more dimple than this sample. From the fracture surface appearance shows that for material with boron tend to has fracture on the matrix (ductile fracture) with small and large dimples, but for the material without boron fractures tend to happen on the carbide site (intergranular). It shows that boron tend to increase the ductility because of boron enhances grain boundary cohesion.

Fig. 7(a) through (b) are X-ray diffraction results of alloy 1 and 2 after casting. At the as-cast state, peaks of martensite, MC, M_2C, and M_7C_3 are dominant, together with a small amount of austenite for entire samples. We found the peak of $M_{23}(C,B)_6$ and Fe_2B in with boron sample(Fig.7(a) and (b)). In this alloy, the peak intensity of retained austenite is very small, shows the small contain of retained austenite in the samples.

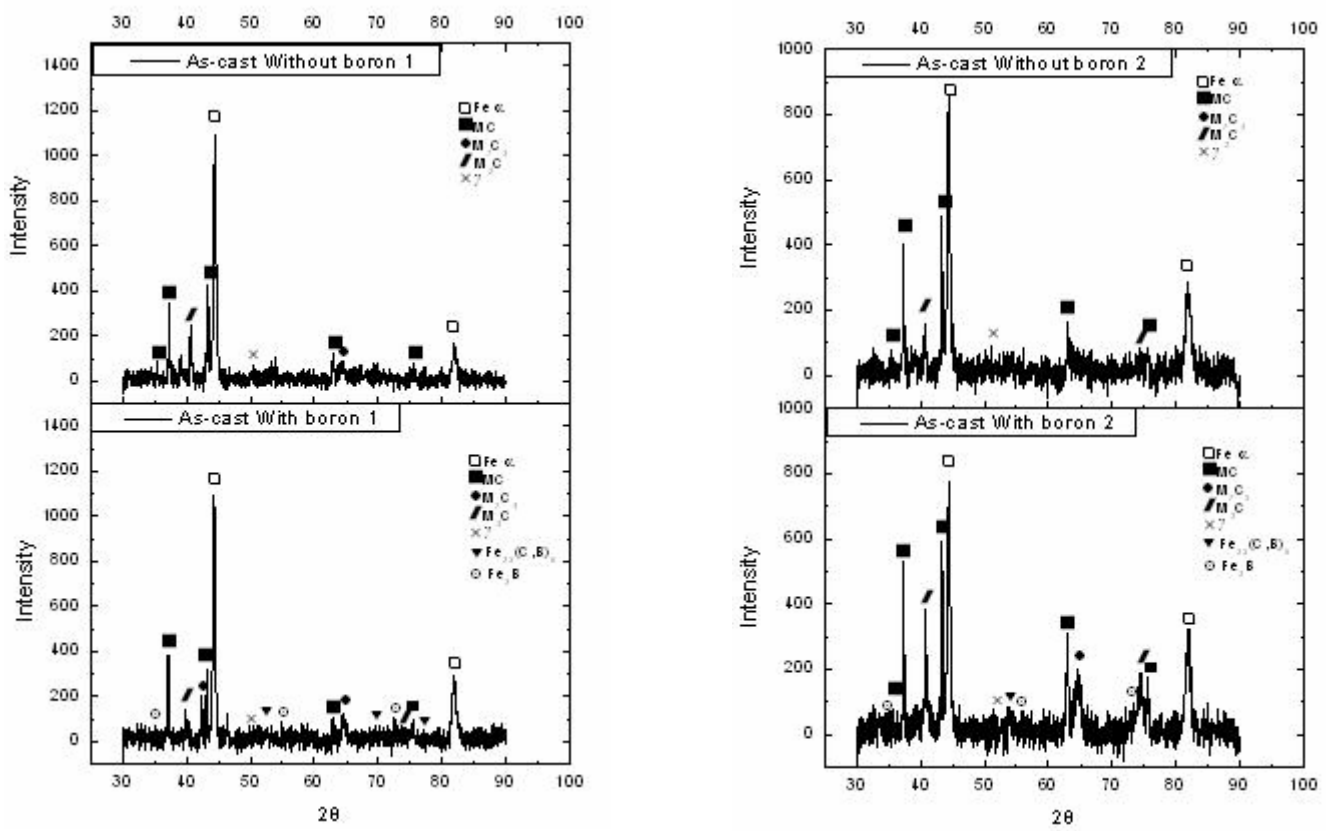

Figure 7: XRD Result (a) Alloy 1 (b) Alloy 2

4. CONCLUSION

In this study, the effect of Boron on properties of HSS alloy was investigated.

1. Additional boron 0.04 % on the HSS alloy shows cell refining effect on the sample. With boron sample produce cell size ± 30 % smaller than without boron sample. This is because boron increase nucleating agent by increasing formation of MC carbide. It is also increase the % carbide volume fraction for with boron sample.
2. Additional boron 0.04 % on the HSS alloys increases the bending strength ± 10 %. The improved ductility for the studied alloy is because of the enhanced grain boundary cohesion by boron.
3. Additional of boron tend to increase the hardness of the material. This is because boron gives cell refining effect and also boron can act as interstitial atom on Fe site.

5. REFERENCE

1. K.C.Hwang, Lee Sunghak, H.C.Lee, *J. Mater.Science* , **A245**, 296-304 (1998).
2. S.Suzuki, M.Tanino, Y.Waseda, ISIJ International, Vol.42 (2002).
3. C. L. White, R. A. Padgett, C. T. Liu, *Scripta Metallurgica*, Vol. 18 (1984) 1417-1420.
4. T. B. Cameron , J. E. Morral, Metall.Trans. A 17 (1986) 1481.
5. K.N.Kim, et al., *J. Magnetism and Magnetic Mterials*, 227 (2004) 331-336
6. S.-H.Song, et al., *J.Mater.Science*,A360(2003)96-100.
7. T. Mega, J. Shimomura, E. Yasuhara, Mater. Trans. JIM, 36 (1995) 1206.
8. K.C.Hwang, Lee Sunghak, H.C.Lee, *J. Mater.Science* , **A245**, 282-295 (1998).
9. W.Garlipp, M.Cilense, S.I.Novan, *J.Mater.Proces. Tech.*,144(2001)71-74
10. ASTM E 407-07 "Standard Practice for Microetching Metals and Alloys
11. E.Lopes C.et al.. *J.Mater.Science*, A480(2007) 49-55.
12. E.Wachowicz, A.Kiejna, *J.Computational Material Science*, 432008)736-743.
13. Tasgih Yahya et al., *J. Material and Design*, (2009).
14. J.Hardell et al.,*Wear*, 264 (2008) 788-799.
15. J.E.Morral, W.F.Jadeska, *J. Metal and Matallurgical Transaction A*, 11 A (1980) 1682.
16. Ontani, Hiroshi, et al. Calculation of Fe-C-B Ternary Phase Diagram (ISIJ),(1998).

17. Nack J.,Kim, *J.Mater.Science*,A 449-451(2007)51-56.
18. J.Laigo, et al., *J.Materials Characterization*, 59 (2008)1580-1586.
19. Wang, Mingjia, *J.Mater.Science and Engineering*,A 438-440 (2006)1139-1142.
20. Kim, Ji Hui, *J.Mater.Science and Engineering*, A 477 (2008)204-207.

Comparison of Porosity Defects on Duralumin Produced with Permanent Mold at Conditioned Atmosphere and Vacuum Castings

Wahyono Suprapto[1], Bambang Suharno[2], Johny Wahyuadi Sudarsono[2] , Dedi Priadi[2]

[1]*Doctor Candidate, Faculty of Engineering, University of Indonesia*
Faculty of Engineering, Brawijaya University, Malang 65145
Telp: (0341) 569103, Fax : (0341) 553286
E-mail : wahyos_metftub@yahoo.com

[2]*Faculty of Engineering*
University of Indonesia, Depok 16424
Tel : (021) 7270011 ext 51. Fax : (021) 7270077
E-mail : @ui.edu

ABSTRACT

Mostly, duralumin is used extensively as a material in aerospace, automotive, and other industry, i.e. petroleum to cryogenic materials. Porosity defect until now consists in metals casting especially in duralumin that would reduce its mechanical properties. The Researchers and Foundry mans reports about porosity had conclude that it is affecting solution hydrogen in casting. Several processes; fluxing, vacuum following induced argon gas, high isostatic pressure, and high pressure die casting have been tried to eliminate the hydrogen solution in duralumin casting. This article will explain the method to reduce hydrogen solution by vacuum system in casting process to eliminate hydrogen absorption in metal melt and trapped in solidification, respectively. The objective of this experiment research is to compare porosity defect included porosities density and morphology on duralumin casting process by melting, followed by solidification in atmosphere and vacuum conditions. Pure aluminum ingot (99.5%Al) and pure copper scrap (98.5%) as raw materials are melted on stainless-steel crucible and pouring at 700 ^{o}C for cooling in isothermal process. Specimen casting made by permanent mold to near net shape is aimed to lessen removed materials and reduced its thermal effect. The porosity was studied with Picnometry method, and then would be confirmed with optic method and scanning electron microscopy. Present work is focusing on qualitative and quantitative analysis (QQA) of casting product specimens. The experimental result also gives explanation of birthed casting defect especially in duralumin casting.

Keywords
Porosity, vacuum, solidified, isothermal, picnometry, QQA

1. Introduction

Metal casting is one method of manufacturing process, and this method history has begun since 4000 BC, but aluminum casting was not founded until 1825 and its major usage was to produce kitchen tools. Research and products development of aluminum casting continuously running to explore aluminum alloys, so in 1901-1906 Dr. Alfred Wilm succeed to find Al-Cu with spectacular characterization and it is named Duralumin [1]. Because, it is Duralumin is significant properties for strength to weight ratio (σ_t: 190 MPa for O, and σ_t: 470 MPa for T4), good quality in corrosion resistance and thermal conductivity, and *fracture toughness* and *fatigue* is excellent. In 1973 – 1999 periods, several experiments have been tried vacuum casting method to improve the quality of aluminum alloys casting products [2]. And now, casting of aluminum alloys especially duralumin is commonly used in automotive and aerospace industries, and in petroleum industry for cryogenic pipe. However, Designer and Foundry-man have constrains with porosity defects that is difficult to eliminate.

The matter of porosity formation must be detected and avoided in melting and solidifying processes, in order to produce high quality of Duralumin casting. When aluminum alloy casting is done in atmospheric condition, oxygen, nitrogen, hydrogen gases always follows it. The atmospheric humidity and the mixture of additions, such as constitute element ingots to increase its gasses contents in casting process. And then hydrogen is the only gas dissolved to a significant extent in the melt that would affect fatally on Duralumin casting. In the literatures, porosity forms when there is a gas entrapment, solidification shrinkage due to failure of inerdendritic feeding, and/or precipitation of dissolved gas from the molten metal. Most research jobs have been done until now to decrease of porosity with several methods, i.e. fluxing, continued vacuuming, only

to melting process, and can would to optimal produce. This article is an innovative process that hopefully would be an improvement of Duralumin casting of melted and solidified is done by simultaneously.

Porosity is casting defect especially in duralumin, it includes morphology and density and would effected on mechanical properties. Generally, porosity in metals would be reduced in mechanical properties is where some incident because it's unknowable. It's is always consist of every aluminum alloy casting and nothing null but only decreased or elimination. Now, urgently some question about of porosity is first questions, limits of porosity casting is allowable in duralumin. The second question is the length of term effect Duralumin porosity in atmospheric and vacuum casting conditions. For, the answered of important two questions is needed statistic knowledge to explained porosity phenomenon. So then descriptive in qualitative and quantitative test, and statically interpretation until inferential is crucial to explored thus comparison.

2. Materials and Experimental Setup

2.1. Material Processing

Initially, the research design is to compare between duralumin porosity at atmospheric condition and vacuum condition to determine quality and quantity of porosity in metallograpy, i.e., using microstructures, so information from its porosity can be correlated with mechanical properties. However, the actual research until now just for duralumin casting from aluminum ingot and copper pipe as the raw materials in reveberatory furnace, and this is done as the pre research on dissertation. This involves; a). Measurement of element content substance will be done with spark spectrometry, b). Casting of raw materials to made duralumin, c). Measurement of duralumin casting mass will be done with digital electric balance, and d). Porosity characterization is done with picnometry and optic microscopy. Each of the above experiments for duralumin casting while three replications to data precision, and made data accuracy would be uncertainty test is to compared of research instruments with it's in metal laboratory at University of Indonesia. Result of uncertainty test is multiplying factors would used in research data.

2.2. Casting Procedure

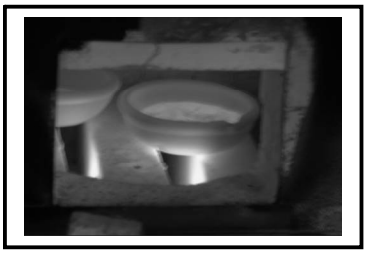

Figure 1: Duralumin melt in crucible.

There are preparations to make duralumin casting products in this research which are mass analysis, melting process, pouring, and solidification, and testing of the specimens. The calculation and weight balance of one kg aluminum ingot which contains 995 grams of pure aluminum to produce Al-Cu with composition of 2.5, 3.0, 3.5, 4.0, 4.5 % Cu need addition of 25.90, 31.24, 36.64, 42.09, 47.60 grams of copper scrap in a series. To simplify the analysis, other elements will be ignored since the composition is less than 0.5% in the raw materials i.e.; Mg, Fe, Si, Zn etc. Raw materials which have been measured with the same proportion will be put in a ceramics crucible for melting process in reveberatory furnace. The first period raw materials will be melted in seventy five until eighty five minutes and the next periods of raw materials will be melted in twenty minutes. Then, melted duralumin in crucible will be poured and solidified by gravity and atmosphere condition in permanent mold. As presented on the figure 1 is duralumin melt in crucible on casting process.

2.3. Porosity Test

Qualitative and quantitative of porosity defect of duralumin casting are respectively measured by microscope optic and Picnometry apparatus (mass balance). Microscope optic by 50 magnitude is used to get image, and Picnometry to determine the percentage of porosity defects. The experimental are the Picnometry apparatus for density test of duralumin cast can be expressed as; $\gamma_C = \frac{Wa}{Wa - Ww} x\gamma_W$ (1)

where Wa and Ww is specimen weight on air and specimen weight in water, γ_c dan γ_w is casting density and water density. And experiment porosity test of duralumin cast can be expressed as;

$$P = \frac{\gamma_{IC} - \gamma_C}{\gamma_{IC}} x100\% \qquad (2)$$

where γ_{IC} is ideal casting density is find analytical from chemical content of specimen from spark spectrometry. As presented on the figure 2 the Picnometry apparatus as measured weight balance on experiment. The measured weight of specimen is dipped in water media

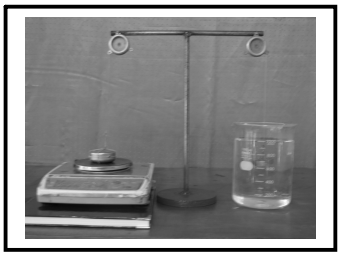

Figure 2: Picnometry apparatus

3. Data and Discussion

A. Chemical Content

The material balance data of this experiment are appearance on the chemical composition of raw material and duralumin shown in Table 1.

Table 1. Mass balance of materials

Elements	Weight [%]						
	Raw Materials		Al-Cu alloy with % Cu				
	Al ingot	Cu scrap	2.5	3.0	3.5	4.0	4.5
Al	99.5	<0.002	96.20	95.9	95.4	95.4	95.1
Cu	0.006	98.5	2.25	2.74	3.00	3.31	3.71
Mn	0.108	0.003	0.088	0.084	0.098	0.089	0.087
Si	0.28	0.245	0.324	0.368	0.290	0.365	0.290
Mg	0.008	0.001	0.157	0.166	0.179	0.163	0.156
Zn	<0.005	0.280	0.048	0.043	0.073	0.046	0.049
Fe	<0.001	0.358	0.661	0.483	0.758	0.500	0.424
Ti	0.001	-	0.012	0.014	0.010	0.010	0.015
Cr	0.029	0.002	0.007	0.007	0.012	0.009	0.004
Ni	0.023	0.100	<0.005	<0.005	<0.005	<0.005	<0.005
Pb	<0.002	<0.005	0.014	0.010	0.008	0.008	0.006
Sn	<0.01	<0.005	0.112	0.112	0.105	0.069	0.109
P	-	0.011	-	-	-	-	-
Co	-	0.042	-	-	-	-	-
Bi	-	0.363	-	-	-	-	-

Shown Table 1 is proportion goal of alloyed Al-Cu not yet success because copper and aluminum are decrease, and increasing of ferrous. Effect of alloy elements and density measure density by Picnometry is shown of Figure 4a. Highest heating temperature and long period duralumin melt are caused reducing aluminum element. The ideal produce of casting is importance to added primary substance (Al and Cu) because in metal casting it's will be change to slag and gas specially materials with low melt point. Generally, aluminum alloy casting is added 10 to 15% primary material and 5 to 7.5% material alloy from mass balance account by stociometry [3].

Fluid flow in interdentritic capillary depend of primary dendritic arm spacing (PDAS) and secondary dendritic arm spacing (SDAS), it's crucial as variable in solidification mechanism to predict of formed microposity. The other factor is added alloy composition, content gas of air, casting dimension, thermal conductivity of mold is depended solidification process. In experiment of duralumin casting, added substance in raw material have high melting point like it ferrous and silicon is increased. It's will be made new compound (fe intermetalic) in aluminum alloy is harmed by complex marphology, i.e.; $Al_{15}(Fe,Mg)_3Si_2$ phase [4]. Certainty, $Al_{15}(Fe,Mg)_3Si_2$ and other phases on duralumin will be detected by scanning electron microscopy [5].

B. Microstructure and Porosity

Duralumin microstructure or porosity of the optic microscopy is shown in Figure 3. They generally consist of structural grains and porosities is differential in fraction volume, which exhibits relatively smaller contrast compared to casting area. By figure 3, increased trend of porosities on each added copper ratio in duralumin is cleared.

Figure 3 and 4b showing optic microscope of duralumin micro porosity and porosity of duralumin. Aluminum alloy, bronze, eutectic Al-Si alloy have short-freezing-range to make excellent surface of casting. To make the channel open wider we have to make first solidification and continuing to fill in the liquid. In the end of the internal pressure become lowest cause by the minimize fill in inside the pore of liquid nucleation.

Solidification and nucleation continuously to driving force on the growth of inside the pore beside the casting surface. The casting area porosity generally consists of the smallest and contrast round grains. In the lowest temperature (on solidification) porosity as the sign of solubility(hydrogen).According to (6), porosity inside the casting solidification cause to liquidation or the capable porosity inside the casting solidification cause to liquidation or the capable to fill in interdendritic out-let finally became shrinkage.

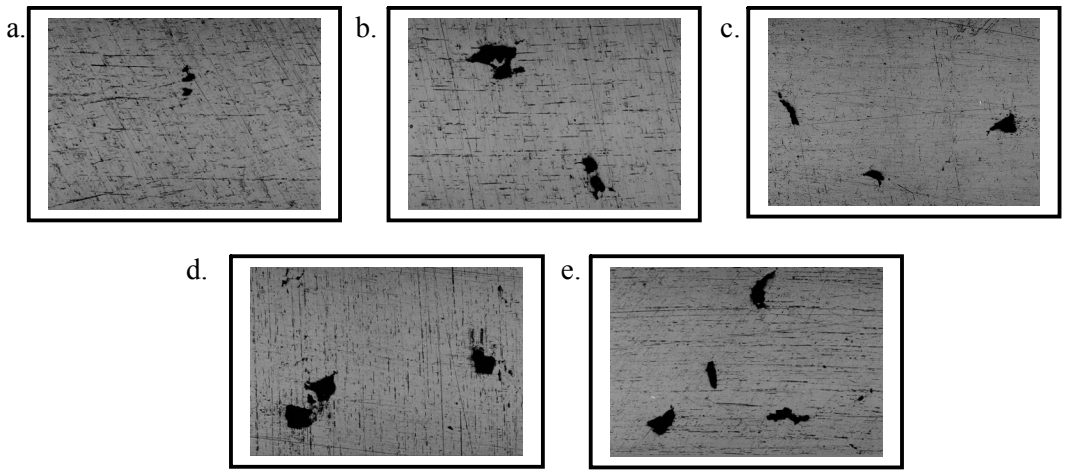

Figure 3: Porosity in duralumin casting, a. alloyed 2.5% Cu, b. alloyed 3.0% Cu, c. alloyed 3.5% Cu, d. alloyed 4.0% Cu, e. alloyed 4.5% Cu

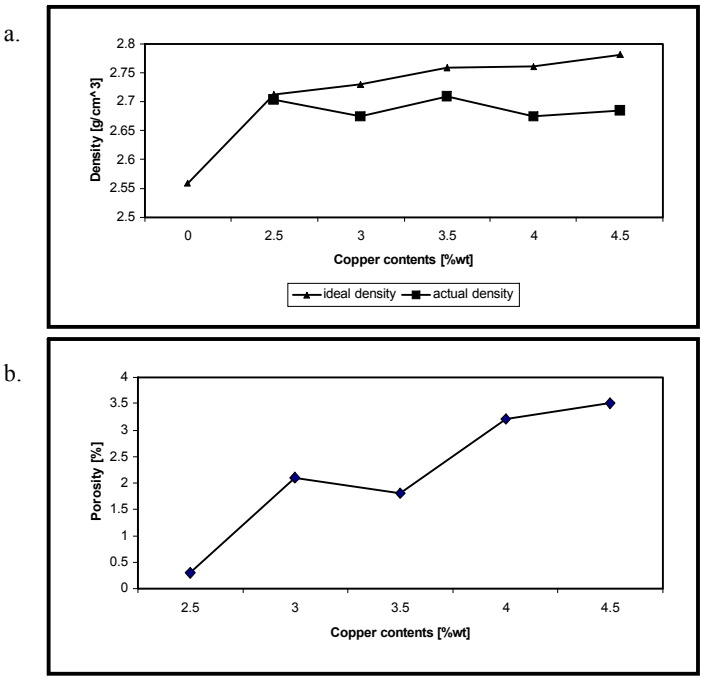

Figure 4: Physic performance of duralumin casting diagram, a. density comparison, b. porosity vs copper on duralumin

4. Conclusion

The melt recycling of Aluminum ingot the variations of added copper scrap in reveberatory furnace with respect to density and porosity was done. The contents of aluminum and copper in duralumin decreased and ferrous increased from casting designs. But it's copper continuously to trend be promote of higher copper ratio each alloying. The trend of porosity will be increase of high than low copper ratios, and aluminum has trend inversed.

References

1. TU-Wien, "Development of Al-Si-Mg Alloys for Semi-Solid Processing and Silicon Spheroidization Treatment (SST) for Al-Si Cast Alloys", A dissertation submitted for the degree of Doctor of Technical Sciences, SWISS FEDERAL INSTITUTE OF TECHNOLOGY ZURICH, 2002.

2. Serope Kalpakjian, Steven Schmid, ”Manufacturing Engineering and Technology”, Fifth Edition in SI Unit, Published by Prentice Hall, Pearson Education South Asia Pte Ltd, Singapore, 2006.

3. Z. LI, A. M. SAMUEL, F. H. SAMUEL, C. RAVINDRAN, and S. VALTIERRA, “Effect of alloying elements on the segregation and dissolution of CuAl2 phase in Al-Si-Cu 319 alloys”, JOURNAL OF MATERIALS SCIENCE 38 : 1203 – 1218, 2003.

4. G. Garcia-Garsia, J. Espinoza-Cuadra, H. Mancha-Molinar, “Copper Content and Cooling Rate Effects Over Second Phase Particles Behavior in Industrial Aluminum-Silicon Alloy 319”, Materials and Design 28 (2007) 428-433, Elsivier, 2007.

5. V. Raghavan, “Phase Diagram Evaluations: Section II : Al-Cu-Zn (Aluminum-Copper-Zinc)”, JPEDAV 28:183–188, DOI: 10.1007/s11669-007-9025-x 1547-7037 © ASM International, 2007.

6. M. L. N. M. MELO, E. M. S. RIZZO, R. G. SANTOS,”Predicting dendrite arm spacing and their effect on microporosity formation in directionally solidified Al-Cu allo”, JOURNAL OF MATERIALS SCIENCE 40, 1599 – 1609, 2005.

Formation Mechanism of Nano Sized Geometry on Mechanical Alloying of Bi-Mn System

Wahyu B. W.[1], Agus S.W.[2], Nurul T.R.[1]

[1]*Pusat Penelitian Fisika LIPI, Kawasan PUSPIPTEK Serpong, 15314*

[2]*Graduate School of Engineering, Kagoshima University, Japan*

wahyubw@gmail.com

Formation mechanism of nanosized geometry in Mechanical Alloying process is very interesting field of study which hasn't revealed and studied intensively. Compared to the micro-structured bulk material, nano-structured material has large surface energy which gives significant influences to the thermal stability. Many previous researches have reported the increases of strength and hardness of nano-crystalline materials which have been consolidated into bulk material, compared to the conventional large-grain size bulk material. In order to study the formation mechanism of nanosized geometry, we proceed Mechanical alloying experiment of stoichiometric composition of Bi-50%atMn from pure Bi and Mn powder using High Energy Milling (HEM) for different specified time. The processed powders were then characterized using X-Ray Diffraction (XRD), Scanning Electron Microscopy (SEM) and Energy Dispersive Spectroscopy (EDS). The X-ray diffraction pattern shows structural change and formation of new phase which then became rapidly since 32 h. The comparison of SEM images gives better visualization which can be concluded for overall process as process evolution from the existence of mechanical bonding into chemical bonding.

Keywords: *Nanosized geometry, Mechanical Alloying, Bi-Mn system.*

Introduction

Bi-Mn has been known as a metallic alloy with suitable characteristics to be applied as permanent magnet. This alloy is affected easily by external magnetic field because of its high magnetic anisotropy energy [1]. The phenomena of highly negative Kerr Polar rotation (-1.2˚) in the range of UV spectrum and high perpendicular magnetic anisotropy of MnBi, the stable phase of Bi-Mn system up to 550˚C, is the characteristics that makes MnBi good candidate for magneto-optic data recording [2-3]. $BiMnO_3$ and $BiMn_2O_5$ as possible phase of Bi-Mn or Bi-Mn-O system are known to have rare multiferroic phenomenon that has novel functional potential for micro/nano devices[2]. On the other hand, Mechanical Alloying is one method of material synthesis which is very interesting to explore for some phenomena such as particle refinement, amorphous formation, and solid solution [5]. However, there are still limited studies which discover the formation mechanism of nanosized geometry, conducted by mechanical alloying process. For those purpose, this paper describes the formation mechanism of nanosized geometry in correlation of mechanical alloying process. This study is aimed to study the microstructural evolution of Bi-Mn system alloy during mechanical alloying process.

Experimental Procedure

The material used for this experiment is 99.5% purity needle-shaped Bi flakes which were firstly powdered using Siebtechnik blast mill (disk mill) to reach micron-size powder. The powdered Bi then mixed with 99.5% purity manganese in initial composition of Bi-50%atMn and were MA-ed using High Energy Milling E3D (HEM E3D). The process was carried in argon condition with BPR (Ball to Powder Ratio) of 10:1 at normal speed of 300 rpm. The mixed powders were sampled for MA time of 1, 4, 8, 16, 32, and 64 jam which then characterized using Digital Rigaku Geigerflex XRD, ESEM tipe XL30CP- Philips, and HR-SEM (JEOL JSM-6510LA). The overall step of the experimental is shown in Figure 1.

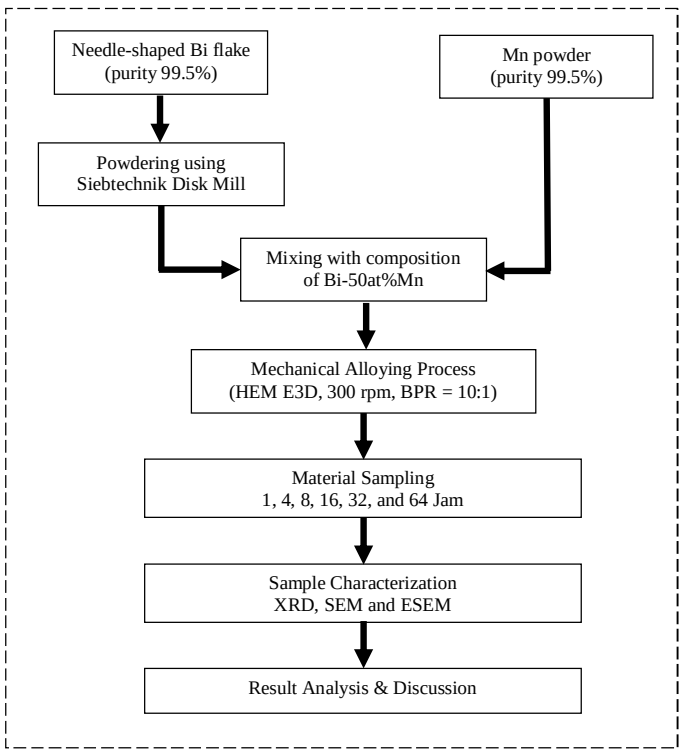

Figure 1 Experimental Flowchart

Results and Discussion

X-Ray Diffraction pattern of MA-ed Bi50at%Mn is shown in Figure 1. Before MA process, the pattern is dominated by Bi peaks and there's only one strongest Mn peak detected, relative to overall peak intensities. After 1 hour MA, there can be seen the occurrence of new phases which identified as $Bi_{24}Mn_2O_{40}$ (222) and Bi_2Mn (002). This shows the mixing and initial reaction between Bi and Mn particles has occurred since 1 h MA time. The processes were accompanied by the inclusion of oxygen particles through the process, resulted the formation of new phase.

There is no drastic change on the XRD pattern alter 4 h milling, yet some peaks intensity started to decrease. Meanwhile, new phase peak which occurred firstly afear 1 h milling experienced no significant change after 4 h milling. The similar result was also happened after 8 h milling time, yet the intensity decrement of Bi main peaks continued to occur. After 16 h milling, $Bi_{24}Mn_2O_{40}$ (310) which close to Bi (012) peak and Bi_3Mn_2 (002) started to occur, whereas $Bi_{24}Mn_2O_{40}$ (222) and Bi_2Mn (002) peaks were getting higher. As new phases occurred, almost all Bi and Mn peaks decreased accompanied by peak broadening. This could happen because of advanced reaction among powder particles, including oxygen particles.

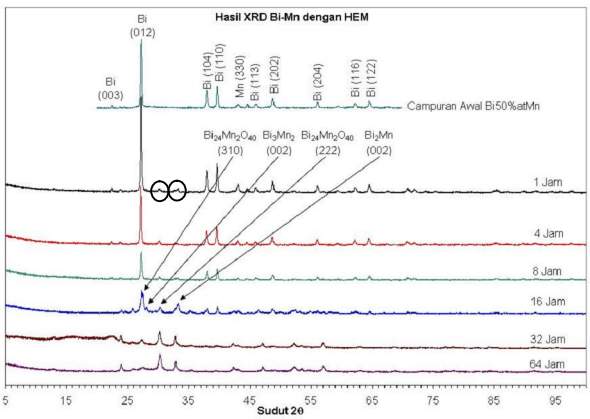

Figure 2. XRD pattern of Bi50at%Mn prepared by HEM

After 32 h milling time, $Bi_{24}Mn_2O_{40}$ (310) and Bi_3Mn_2 (002) phases were vanished which followed by significant intensity decrement and peak broadening of Bi (012), whereas $Bi_{24}Mn_2O_{40}$ (222) and Bi_2Mn (002) peaks were getting stronger. The

occurrence of $Bi_{24}Mn_2O_{40}$ (310) and Bi_3Mn_2 (002) phases were then triggered the decrement of Bi (012) intensity and not the advanced reaction for phase formation. On the other hand, Bi (104) and Bi (110) peaks were also vanished without pre-formation of new phase. In advance, there is no significant XRD pattern difference between 64 h simple and 32 sample, except for the broadening of Bi (012) peak. In addition, there is little increment of $Bi_{24}Mn_2O_{40}$ (222) peak. By analyzing these result, it can be concluded that the formation reaction of $Bi_{24}Mn_2O_{40}$ (222) started to stop. The process was then stepped to the next process i.e. grain refinement process.

Figure 3 shows the microstructure evolution of as-milled Bi-50%atMn. After 1 h milling the powder grains began to mix heterogeneously, yet the individual particles still dominated the microstructure. However, after 4 h milling there are many kind of morphologies which dominated by flaky shape with maximal length of around 28 µm and only small amount of particles which still in their original shape. This could happen because of the plastic deformation from the collision of milling balls which is the initial stage of milling process. By comparing the difference of morphology size between 1 h and 4 h, it can be proved that almost all parts of particles grain have made clusters instead of exist individually. Therefore, the process after 4 h milling is plastic deformation which conducted by balls collision.

After 8 milling microstructure photograph shows many lumps which form big cluster. There are no flaky shapes as we can seen for 4 h milling remaining and replaced by big cluster which came from the joining of those flaky shapes. This joining was not followed by chemical reaction yet only included the process of morphology and particle structure deformation. This can be confirmed by comparing XRD pattern of 4 h and 8 h, where there is no significant difference between those two patterns. The intensity decrement of Bi (012) peak was caused by mechanical deformation on some structure of Bi (012) particles.

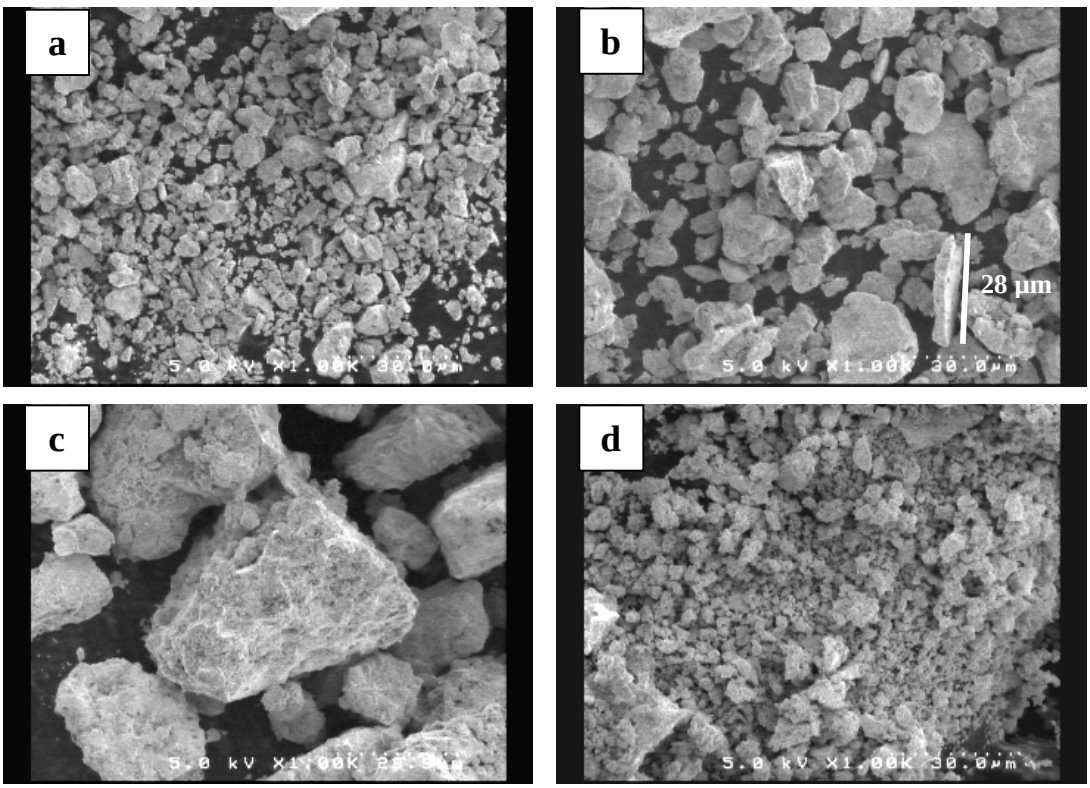

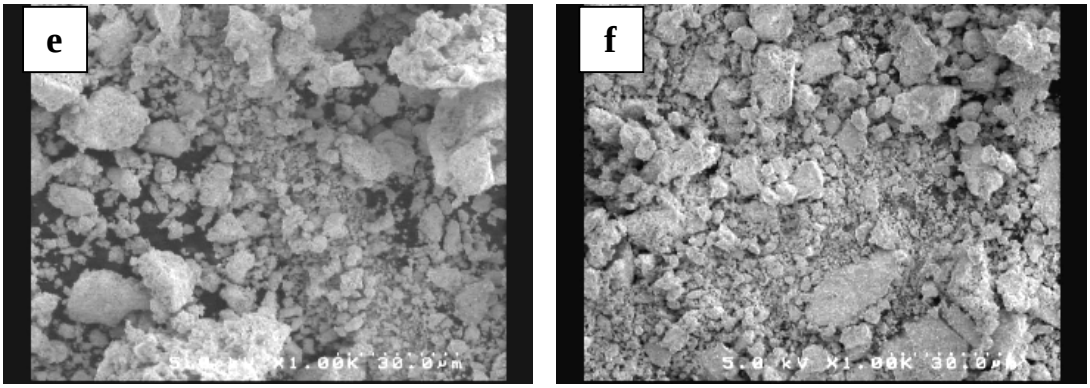

Figure 3. Microstructure evolution of as-milled Bi-50%atMn prepared by HEM E3D (1000X magnification) a. 1 h b. 4 h c. 8 h d. 16 h e. 32 h f. 64 h

After 16 h milling, the particles were broken into smaller cluster which inferred intensive particle refinement and the beginning of new phase formation if we compare with XRD pattern. This could be happen because the lump formation after 8H milling is the saturation point that makes further joining could not happen. Therefore, the actual process after particle agglomeration is particle fracturing which is the preliminary stage before reaction for new phase formation. This could be happen because the smaller particle size will increase surface to volume ratio which ismore unstable in thermodynamics point of view and makes chemical reaction easier to happen [6]. After 32 h milling, some of grains were going to re-agglomerate with brighter color compared to smaller grains and different morphology appearance compared to grains cluster in 8 h milling time. Compared to XRD pattern of 32 h milling, those grains cluster were predicted as new phase of $Bi_{24}Mn_2O_{40}$ (222) and Bi_2Mn (002). The description agree with sample's diffraction pattern where after 32 h milling, the main Bi peak of (002) decrease significantly meanwhile $Bi_{24}Mn_2O_{40}$ (222) and Bi_2Mn (002) phase peaks is getting higher. In conclusion, after 32 milling time most of Bi (012) particles and all of Bi (202) particles experienced particle refinement that make them able to react and change into $Bi_{24}Mn_2O_{40}$ (222) and/or Bi_2Mn (002) phases. After 64 h, bright phases seem increase in number with more homogeneous size, whereas darker particles seem not too dominant. XRD pattern of 64 h sample shows the disappearance of all of Bi and Mn peaks whereas new phase peaks show no significant intensity change. From the result, and by comparing XRD pattern of 64 h sample, it can be concluded that phase transformation was no longer happened and turned into particle size homogenization. The illustration of the process for each milling time is described globally in Figure 4.

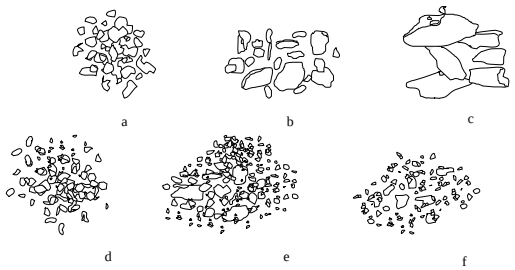

Figure 4. The illustration of the process for each milling time a. 1 h b. 4 h c. 8 h d. 16 h e. 32 h f. 64 h

The as-milled Bi-50%atMn micrograph with 50000X magnification is shown in Figure 5. After 4 h milling, the surface microstructure is dominated by fiber geometry that seems to attach because of collision force from milling balls that conduct morphology deformation. At that time, mixing and particle size refinement have not happened yet that can be concluded by looking the various morphology and wide distribution of particle size. Mixing and particle size refinement process which is accompanied by the formation of new phases was happened after 16 h milling, showed by the appearance of various morphologies such as fibers, flakes, rods, and spheres.

ISSN 114-1284

The particle size refinement and formation of new phase process was still continued after 32 h milling, showed by the appearance of two main morphologies i.e. spheres and fibers which is smaller than fiber geometry in 4 h milling. After 64 h milling, the geometry patterns appear more homogeneous and show no different morphology and no significant particle size. Size and particles morphology homogenization process can be seen more clearly as can be seen in microstructure photograph with 1000 X magnification.

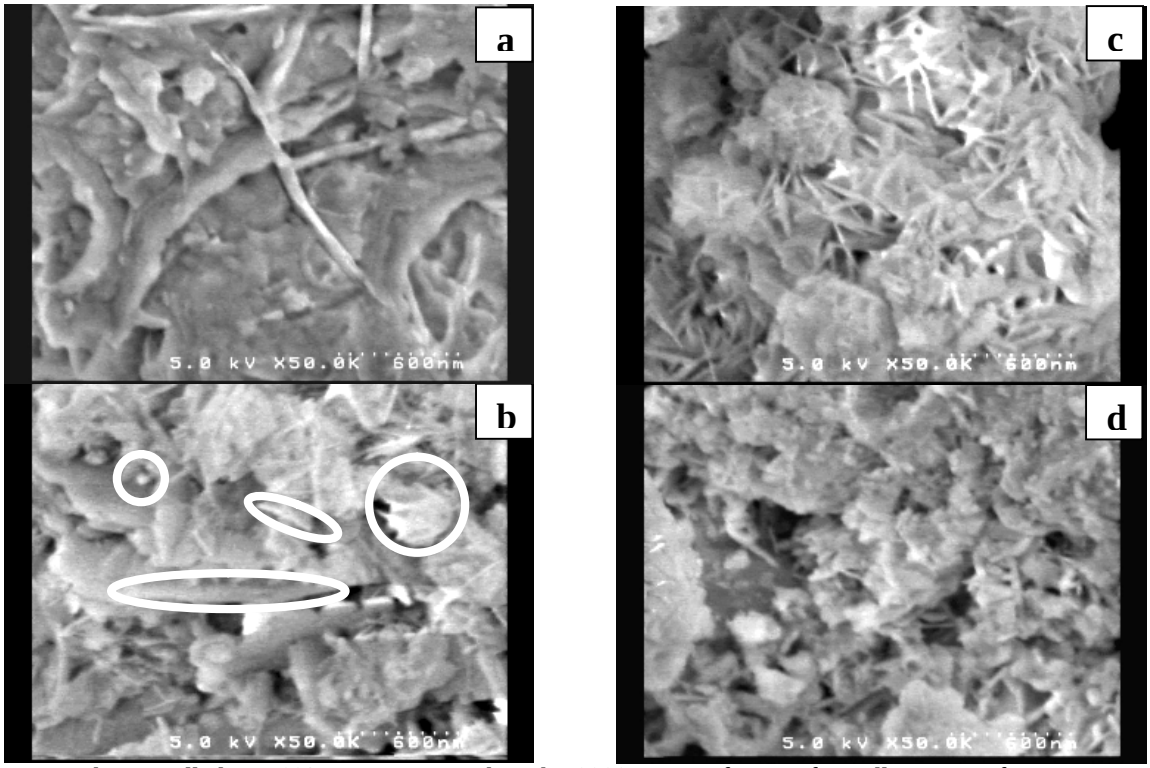

Figure 5 The as-milled Bi-50%atMn micrograph with 50000X magnification for milling time of a. 4 h b. 16 h c. 32 h d. 64 h

Conclusion

From the discussion of the obtained results, it can be concluded that the stages and processes by which the Bi-50%atMn samples experienced different microstructure change are:

1. Heterogeneous mixing process
2. Plastic deformation process
3. Agglomeration process
4. Particle size refinement process
5. The reaction process for phase transformation
6. Homogenization process of particle size distribution

Acknowledgment

Authors would like to thank to Dr. Azwar Manaf for the guides and warm discussion.

References

[1] B.W. Roberts, Phys. Rev. 104(1956) 607-616.

[2] D. Chen, J.F. Ready, E.. Bernal, J. Appl. Phys. 39 (1968) 3916.

[3] P.M. Oppeneer, V.N. Antonov, T. Kraft, H. Eschrig, A.N. Yaresko, A.Y. Perlov, J. Appl. Phys, 80(1996) 1099.

[4] R.J. Jia, J.T. Han, X.J. Wu, C.L. Wu, Y.H. Huang, W. Huang, Mat.Res. Bulletin 43 (2008) 1702-1708.

[5] C. C. Koch, Mat. Transactions, JIM, 36 (1995) 2, 85-95.

[6] G. Cao, Nanostructures & Nanomaterials: Synthesis, Properties, & Applications, Imperial

DEVELOPMENT OF DIRECT REDUCTION PROCESS OF IRON SAND INTO PIG IRON

Wahyu Firmansyah[1,2], Alfian N[2], Agus S.W[2], dan Nurul T.R[2].
[1]*Departemen Fisika, Program Material Sains Universitas Indonesia*
[2]*Lab Material Lanjut dan Nanoteknologi*
Pusat Penelitian Fisika- LIPI
Kawasan PUSPIPTEK Serpong Tangerang 15314
Telp. (021)68483137 Fax (021)70933137
Email : wahyufirmansyahdinasty@yahoo.com

ABSTRACT

In this experiment has been done processing of iron sand to be iron igot by direct reduction using electric arc furnace at 1700°C. The pellet was constituted by iron sand, graphite, limestone, and bentonite with composition of 74:20:5:1 wt % respectively. NaF was also added to composite pellet funcitioned as sludge catcher and aggregation agent. From the experiments, iron ingot in the form of pig iron with iron content of 96,58 % and carbon content of 3,40 % has been yielded. The metallization process yielded 61,47 %. In the sludge, there are still remain iron in the form of Fe_2TiO_4 and FeO compounds, which has proved that reduction process was still not conducted perfectly.

Keyword *: Iron sand, Iron ingot, Electric arc furnace, Sludge.*

INTRODUCTION

Steel or iron is a vital raw materials in industry, almost 95% of metal-made product is dominated by steel which is used in every dailly life activity, such as electrical power plant, building structure, bridge structure, car body etc. In correlation with the demand of steel as a raw material in every field, the lack of iron ores deposit was the most problem to solve in steel industry. Indonesia has an abundance iron ores resource, but existing technology can not be applied to process it. Indonesia's iron ores has no significant Fe content, or it is categorized as low grade iron ores.

Iron sand is availabled in Indonesia abundantly, but it is only used to produce low economic value purposes. Whereas is very potential to process to be special purposes, for example coloration [1], toner [2], magnetic recording [3]-[5], magnet ferit [6] and iron steel [7]. The goal of this experiment is to study possibility of direct reduction process of iron sand pellets into ingot iron and used graphite as reductant.

EXPERIMENT

Graphite powder and iron sand (after being purified by magnetic separator) were inserted with milestone and bentonite with composition of 74:20:5:1 wt % respectively. The mix component and then were refined by disc mill for 10 minutes. Whereas during being refined by disc mill 5 wt % (7.34 g) Sodium Flouride was added to the mix component. To make a composite pellet compact was used sugar cane extract which is dissolved in water with composition 1:1. Cylinderical composite pellet was shape used PVC pipe with about 3 cm diameter and 6 cm height. Pellet was burnt use electric arc furnace with 50 volt and 125 Ampere

for 20 minutes, and temperature during burning process was 1700-1800^{o}C measured by optical pyrometer. The ingot iron and sludge yielded from metalization were analyzed by XRF, XRD, SEM and EDS.

DISCUSSION

1. Preparation and Analysis of Raw Material.

Iron sand was separated based on magnetic properties by magnetic separator. Separation used magnetic separator is better than conventional process used sieve mesh. Elemental analysis of iron sand is shown by Table.1

Based on literature [8][9] iron oxide contented on iron sand after separation were magnetite (Fe_3O_4) and ilmenite ($FeTiO_3$). By varying magnetic field which was used, magnetite (Fe_3O_4) and ilmenite ($FeTiO_3$) could be separated. Compound analysis using XRD shown that magnetite is a major component and ilmenite as a minor component. By comparing with database ICDD every peaks shown can be define, and the comparing result is shown by Table. 2. From ICDD database Fe_3O_4 has cubic of crystal system and Fd3m of *space group* with lattice parameter a = 8,41 Å, in correlation with PDF no. 02-1035. Meanwhile $FeTiO_3$ Rhombohedral of crystal system and R3c of *space group* with lattice parameter a = 5,123 Å and c = 13,760 Å in correlation with PDF no 83-0192.

Table.1. XRF analysis of Iron sand before and after separation

No. Atom	Name of Atom	Iron sand before magnetic separation (wt %)	Iron sand after magnetic separation (wt %)
12	Mg	1.6856	1.6319
13	Al	1.4674	1.8889
14	Si	3.2633	1.3394
20	Ca	0.5941	0.1110
22	Ti	14.1864	9.8348
23	V	0.4766	0.5337
24	Cr	0.0493	0.0683
25	Mn	0.6780	0.8253
26	Fe	77.5112	83.3887
52	Te	0.0880	-

Tabel. 2. Diffraction Peaks Identification Of Magnetic Component of Iron Sand

No of Peaks	d_{hkl}		hkl	Compounds	ICDD
	ICDD	Experiment Data			Reff. No
1	4,8479	4,9421	111	Fe_3O_4	021035
2	2,9800	3,0121	220	Fe_3O_4	021035
3	2,7186	2,7562	104	$FeTiO_3$	830192
4	2,5400	2,5527	311	Fe_3O_4	021035
5	2,4300	2,4460	222	Fe_3O_4	021035
6	2.0900	2,1181	400	Fe_3O_4	021035
7	1,7100	1,7204	422	Fe_3O_4	021035
8	1,6037	1,6265	018	$FeTiO_3$	830192
9	1,4800	1,4896	440	Fe_3O_4	021035
10	1,2808	1,2829	220	$FeTiO_3$	830192
11	1,2600	1,2680	622	Fe_3O_4	021035

By using GSAS, the composition of $FeTiO_3$ and Fe_3O_4 can be known. Iron sand after separating by magnetic separator content of 8.96 wt % $FeTiO_3$ and 91.04 wt % Fe_3O_4. Result of GSAS Analysis is shown by Picture. 1. The picture shows that peaks result from GSAS analysis was correctly fit with the peaks result from XRD instrument.

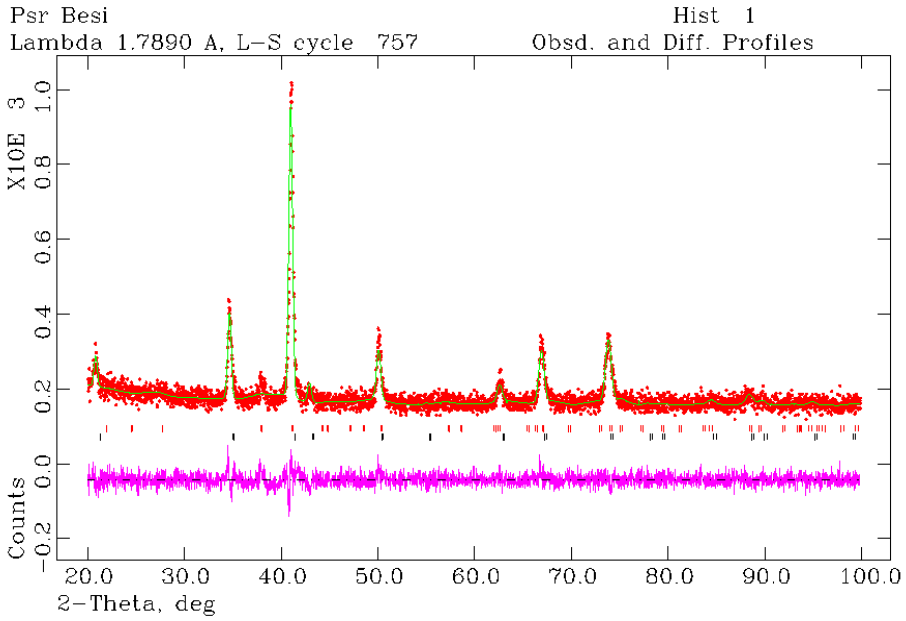

Picture 1. GSAS plot analysis of XRD patern of iron sand after magnetic separation.

ISSN 114-1284

2. Production and Burning of Pellets.

Pellets composition which was made to produce hot-metal/pig iron with 1 kg capacity is shown by Table 3. NaF was added as aggregation agent to facilitate sludge separation from molten iron and increase hot metal viscosity. Nurul (2004) [10] reported that by adding aggregation agents and sludge catcher impurities can be separated from hot metal effectively.

On burning process of pellets, amount of pellets which is entered on furnace is shown by table 4.

Tabel 3. Composition of Pellets was Made.

	Iron sand (g)	Graphite (g)	Bentonite (g)	Limestone (g)	NaF (g)
Sampele of pellet	108.04	29.2	1.46	7.3	7.34

Picture. 2. Pellet with diameter of 3cm, and high of 6cm.

Table 4. Variation of Burning process of Pellets.

No	Pellet	Iron	Time	Current	Voltage	Temp
1	400 gr	103 gr	20 mnt	125 A	50 V	1700 ^{o}C
2	400 gr	95 gr	23 mnt	125 A	50 V	1700 ^{o}C
3	400 gr	98 gr	25 mnt	125 A	50 V	1700 ^{o}C
Average	400 gr	99 gr	23 mnt	125 A	50 V	1700 ^{o}C

Based on table 4, for every 400 gr pellets which was burnt, it would be yielded 100 gr metal iron. The Product of burning of iron sand pellets is shown by Picture 3.

ISSN 114-1284

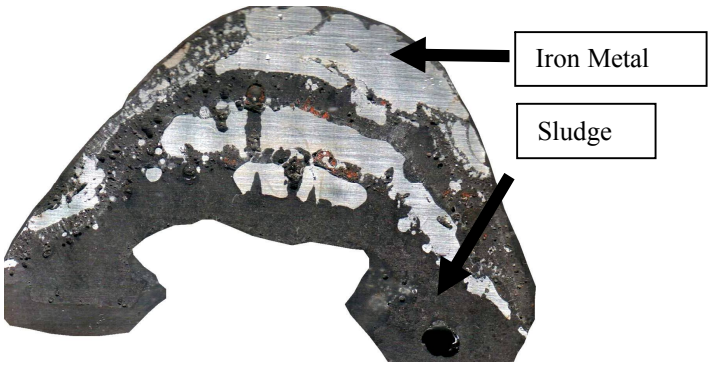

Picture. 3. The Product of Burning of Iron Sand Pellets.

3. The Calculation of Metallization.

To calculate percent of metallization from process of pellets burning, consider two chemical reaction that represent two reaction of iron formation. Calculation by using stoichiometry on chemical reaction (1.1) dan (1.2)

Total of Pellets weight = 400 gr

Total of iron sand weight on pellets = 70,46% x 400 gr = 281,84 gr

Total of iron weight on iron sand (based on XRF data) = 83,38 % x 281,84 gr = 235,00 gr.

Weight fraction of Fe_3O_4 (Based on GSAS Resulted) = 91,04 %

Weight of Fe_3O_4 on iron sand = 91,04 % x 235,00 gr = 213,94 gr

Weight fraction of $FeTiO_3$ (Based on GSAS Resulted) = 08,96 %

Weight of $FeTiO_3$ on iron sand = 21,06

$$Fe_3O_4 + 4C \rightarrow 3Fe + 4CO_{(g)} \quad (1.1)$$

Weight of iron which is yielded from reduction reaction magnetite (Fe_3O_4) by graphite based on chemical reaction (1.1) is :

3 x mol Fe_3O_4 = mol Fe

$$3 \times \frac{wFe3O4}{Mr.\mathrm{Fe3O4}} = \frac{wFe}{Ar.\mathrm{Fe}}$$

$$\text{w Fe} = 3x\frac{wFe3O4}{Mr.\mathrm{Fe3O4}} \text{ x Ar. Fe}$$

$$\text{w Fe} = 3x\frac{213{,}94}{232} \text{ x } 56$$

w Fe = 154,92 gr

weight of iron resulted is 154,92 gram

$$FeTiO_3 + C \rightarrow Fe + CO_{(g)} + TiO_2 \quad (1.2)$$

Weight of iron which is yielded from reduction reaction ilmenite ($FeTiO_3$) by graphite based on chemical reaction (1.2) is :

mol $FeTiO_3$ = mol Fe

$$\frac{wFeTiO3}{Mr.\mathrm{FeTiO3}} = \frac{wFe}{Ar.\mathrm{Fe}}$$

$$\text{w Fe} = \frac{wFeTiO3}{Mr.\mathrm{FeTiO3}} \text{ x Ar. Fe}$$

$$\text{w Fe} = \frac{21{,}06}{152} \text{ x } 56$$

w Fe = 7,76 gr

weight of iron resulted is 7,76 gram

So that total of iron resulted from iron sand pellets which containt Fe_3O_4 and $FeTiO_3$ is 162,68 gram.

Total of metallization percent is:

ISSN 114-1284

$$\frac{wFeExperiment}{w.Fe.Calculation} \text{ x } 100\ \%$$

$$\frac{100}{154{,}92 + 7{,}76} \text{ x } 100\% = \frac{100}{162{,}68} \text{ x } 100\%$$

So that percentage of metallization process of burning of iron sand pellets is 61,47 %

4. Analysis of Pig Iron and sludge Resulted.

a. Analysis of Pig Iron

Pig iron which was resulted of iron sand burning at 1700°C in electric arc furnace is shown by Picture 4. Elements analysis of pig iron is shown by Table 5, and give information that pig iron contains 96,05 wt % of Fe, and contains Si as a major impurity. Another impurities was also existed but could be neglacted. Compounds analysis by XRD showed that pig iron which was resulted is closed to iron synthesis which is listed in ICDD database with PDF no. 01-1267. The correlation between pig iron resulted from experiment and iron synthesis from ICDD database is shown by Table 6.

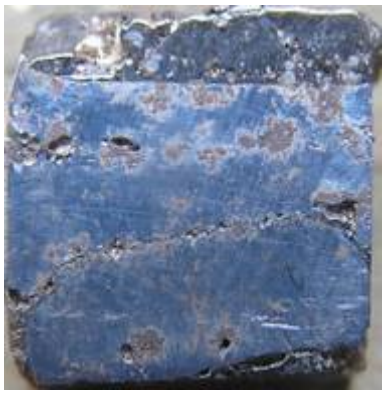

Picture 4. Pig iron resulted

Table. 5. Pig iron element analysis by XRF

No. Atom	Nama Atom	(wt %)
13	Al	0.5469
14	Si	1.7592
16	S	0.5106
19	K	0.1546
20	Ca	0.5381
22	Ti	0.4384
26	Fe	96.0523

Tabel 6. Correlation experiment resulted and ICDD Database for Iron.

No. Peak	d_{hkl}		hkl	Compound	ICDD
	ICDD	Experiment			Reff. No
1	2,0100	2,0345	110	Fe	011267
2	1,4300	1,4366	200	Fe	011267
3	1,1700	1,1721	211	Fe	011267

ISSN 114-1284

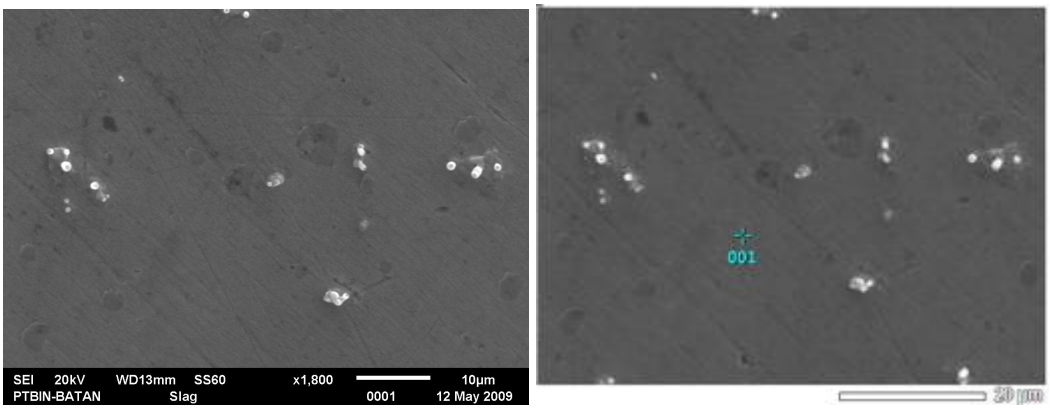

(a) (b)

Picture 5. Microstucture of Pig Iron.

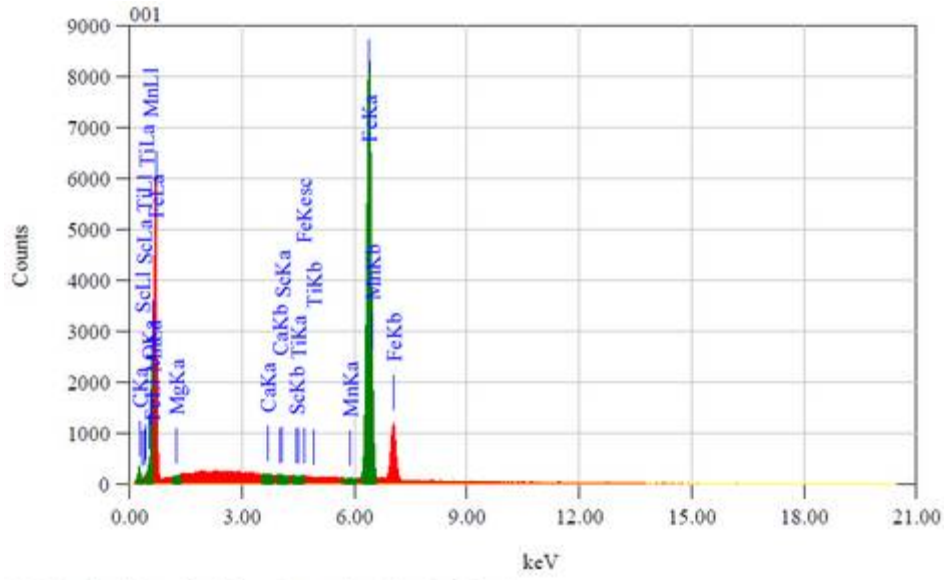

ZAF Method Standardless Quantitative Analysis
Fitting Coefficient : 0.1571

Element	(keV)	Mass%	Error%	Atom%	Compound	Mass%	Cation	K
C K	0.277	3.40	0.10	14.07				0.7793
O K								
Mg K								
Ca K	3.690	0.02	0.12	0.02				0.0217
Sc K								
Ti K	4.508	0.00	0.13	0.00				0.0025
Mn K								
Fe K	6.398	96.58	0.25	85.90				99.1964
Total		100.00		100.00				

Picture 6. EDS analysis of Pig Iron.

Microstructure analysis of pig iron was shown by Picture 5, and give information that one phase was resulted in a product. That can be concluded iron was formed and separated effectively from sludges. Elements analysis by EDS ensure that pig iron was really formed with 3.40 wt % is contained.

ISSN 114-1284

b. Analysis of sludges

Surface of sludge resulted is shown by Picture 7. Based on XRF analysis known that sludge still contains iron with high concentration, it is almost 59 wt % and also contains 17 wt % Ti follow by 6.45 wt % Na and 6.02 wt % Ca. Analysis of compound for sludge by XRD show that Fe, Ti and Ca were formed as Fe_2TiO_4, $CaTiO_3$, FeO and TiO with composition of 35.08, 46.40, 18.51, and < 0.01 wt % respectively. Correlation Table is shown by Table 8.

Picture 7. Sludge resulted

Tabel 8. Correlation experiment resulted and ICDD Database for sludge.

No. Peak	Titik d_{hkl}		Hkl	Senyawa	ICDD
	ICDD	Data Penelitian			Reff. No
1	4,9275	5,0231	111	Fe_2TiO_4	751380
2	3,0175	3,0309	220	Fe_2TiO_4	751380
3	2,6834	2,7312	110	$CaTiO_3$	752100
4	2,5733	2,5767	311	Fe_2TiO_4	751380
5	2,4878	2,5117	111	FeO	772355
6	2,1910	2,2240	111	$CaTiO_3$	752100
7	2,1545	2,1692	200	FeO	772355
8	2,1337	2,1313	400	Fe_2TiO_4	751380
9	2,0390	2,0383	101	TiO	820803
10	1,8975	1,9254	200	$CaTiO_3$	752100
11	1,7421	1,7381	422	Fe_2TiO_4	751380
12	1,6425	1,6380	511	Fe_2TiO_4	751380
13	1,5493	1,5598	211	$CaTiO_3$	752100
14	1,5234	1,5291	220	FeO	772355
15	1,5087	1,5023	400	Fe_2TiO_4	751380
16	1,2992	1,2944	311	FeO	772355
17	1,2163	1,2122	201	TiO	820803

CONCLUSION

Pig iron was resulted from iron sand pellets by burning at 1700°C in electric arc furnace, and percentage of metallization process is 61.47 %. In the sludge, there are still remain iron in the form of Fe_2TiO_4 and FeO compounds, which has proved that reduction process was still not conducted perfectly.

ACKNOWLEDGEMENT

Dr. Azwar Manaf, M.Met as tutor

Research Centre for Physics as a place for an experiment.

REFERENCES

[1] Ozel, E., Unluturk, G., dan Turan, S., (2006). Production of brown pigments for porcelain insulator applications, journal of the European ceramic society, 26, 735-740.

[2] Brezoi, D.V., dan Ion, R.M., (2005). Phase evolution induced by polypyrrole in iron oxide-polypyrrole nanocomposite, Sensors and Actuators B: Chemical, 109 (1), 171-175.

[3] Peng, Y., Park, C., dan Laughlin, D.E., (2003). Fe_3O_4 thin film sputter deposited from iron oxide targets, Journal of Applied Physic, 93 (10), 7957-7959.

[4] Aso, K., Sato, T., dan Ishibashi, M., (1999). Magnetitc Force microscopic study of magnetic tapes recorded at MHz frequencies, Journal of Magnetism and Magnetic Materials, 193, 430-433.

[5] Yamamoto, S., Hirata, K., Kurisu, H., Matsuura, M., Doi, T., dan Tamari, K., (2001). High coercivity ferrite thin-film tape media for perpendicular recording, Journal of Magnetism and Magnetic Materials, 235, 342-346.

[6] Parkin, I.P., Elwin. G., Kuznetsop, M.V., Pankhurst, Q.A., Bui, Q.T., Foster, G.D., Barquin, L.F., Komarov, A.V., dan Morozov, Y.G., (2001). Self-propagating high temperature synthesis of $MFe_{12}O_{19}$ (M=Sr,Ba) from the reaction of metal superoxides and iron metal, Journal of Materials Processing Technology, 110 (2), 239-243.

[7] Muta'alim, Tahlili, L., Purwanto, H., dan Subiantoro, (1995). Pembuatan Prereduced Pellet Pasir Besi, Laporan Penelitian (in house research), PPTM, Bandung.

[8] Yulianto, A., Bijaksana, S., Loeksmanto, W., dan Kurnia, D. (2003). "Extraction and purification of magnetit (Fe_3O_4) from iron sand", Proceeding of the Annual Physics Seminar, ISBN: 979-98010-0-1, 102.

[9] Manaf, A. (2005). "Kegiatan Litbang Pasir Besi (Iron Sand) di Universitas Indonesia", Seminar Lokakarya Pemanfaatan Bahan Baku Lokal untuk Industri baja Nasional, PT Krakatau Steel, Cilegon.

[10] Nurul, T. R., Suehiro, S., Higashiiriki, K., Nakano, A., Yamada, K., Hamaishi, K., Nakamura, S., Sechi, Y., Matsuda, T., dan Sueyoshi, H., (2004). "Pb-Free Brass from Scrap by Compound-Separation Methode", Transactions of the Materials Research Society of Japan, Vol. 29, No. 5.

Proceeding of the 11th International Conference on QiR (Quality in Research)
Faculty of Engineering, University of Indonesia, Depok, Indonesia, 3-6 August 2009
ISSN 114-1284

Electrical Characteristics $CuFe_2O_4$ Ceramics With and Without Al_2O_3 for Negative Thermal Coefficient (NTC) Thermistor

Wiendartun[1)], Dani Gustaman Syarif[2)], Arief Permadi[1)]

[1)] *Physics Department, UPI, Jl.Dr Setiabudhi 229 Bandung, email: wien@upi.edu*
[2)] *PTNBR BATAN, Jl.Tamansari 71 Bandung,, email: danigusta@yahoo.com*

ABSTRACT

In order to get capability in thermistor production in Indonesia, a study on electrical characterization of $CuFe_2O_4$ base-ceramics with Al_2O_3 addition has been performed.. The Al_2O_3 addition was done with various concentrations namely 0, 1 dan 5 mole %. Powder of CuO, Fe_2O_3 and Al_2O_3 was mixed and ground. The mixture was pressed with pressure of 3,9 ton/cm^2 to form pellets. The pellets was then sintered at 1100^{0}C for 2 jam in air. After sintering, two sides of some sintered pellets were coated with silver paste and fired at 600^{o}C for 10 minutes. Some of coated samples were heat treated at 500^{o}C for 5 minutes in N_2 gas. These pellets were analyzed using x-ray diffraction (XRD). R-T and ageing characteristics were evaluated. From the XRD data, it was known that the $CuFe_2O_4$ ceramics produced crystallized in tetragonal spinel. According to the electrical data, the thermistor constant (B) and sensitivity (a) increases due to the addition of Al_2O_3. It was known from the ageing test that only the ceramics with 0 and 1 mole % Al_2O_3 fit the electrical stability condition.

Keywords *: Ceramic, $CuFe_2O_4$, Al_2O_3, thermistor, NTC, ageing.*

1. INTRODUCTION

NTC thermistor are widely used due to its capability to be applied in many applications such as temperature sensor, electric current limiter, flowrate meter and pressure sensor[1]. It is known that generaly the NTC thermistor is made of ceramic having structure of spinel of AB_2O_4 where A is the ion occupies tetrahedarl position and B is the ion occupies octrahedral position[2-10]. Many works have been performed in order to improve the characteristic of the NTC thermistor having spinel structure [6,7,11]. Theoritically, the addition of additive such as Al_2O_3 may change the electrical characteristics of $CuFe_2O_4$ ceramic.

When the additive of Al_2O_3 is added to the $CuFe_2O_4$ ceramic, the characteristics of the $CuFe_2O_4$ ceramic may cange because two conditions may accur namely, the first, Al_2O_3 dissolves in the $CuFe_2O_4$ through substituting Cu ions or Fe ions, the second, Al_2O_3 does not dissolve and segregate at grain boundaries. When the substitution of Fe or Cu ions results in an increase of electron in the conduction band, the electrical resistivity of the $CuFe_2O_4$ will decrease. On the contrary, when the second condition occurs, the electrical resistivity may increase due to a change in microstructure. In this work, the effect of the Al_2O_3 addition on the electrical characteristics, especially the electrical stability, of the $CuFe_2O_4$ ceramic was studied.

2 . METHODOLOGY

Powder of CuO, Fe_2O_3 and aditive of Al_2O_3 (0, 1 and 5 mole %) were mixed and ground. The composition is shown at Table 1. After calcination at 800^{o}C for 2 hours, the mixture was ground. The ground powder was pressed with pressure of 3,9 ton/cm^2 to form pellets. The green pellets were sintered at 1100^{0}C for 2 hours in furnace air. Two sides of some sintered pellets were coated with silver paste. Some silver coated samples were heat treated at 500^{o}C for 5 minutes in N_2 gas. Structure of the sintered pellet was analyzed using x-ray diffraction (XRD). For electrical characterization, the electrical resistance of the pellets was measured at various temperatures. The measurement was done before and after ageing test. The ageing test was conducted by measuring the resistance of the pellet at room

temperature after heating at 150°C in every several hours. Thermistor constant (B) is the gradient of the ln Resistivity vs 1/T curve which is constructed based on equation (1) [2-11] expressing NTC characteristic. Sensitivity (α) was calculated using equation (2)[6].

$$R = R_0 . Eksp.(\frac{B}{T}) ……..(1)$$

where R = thermistor resistance (Ohm), R_0 = a constant (Ohm), B = Thermistor constant (K) and T = Temperature (K).

$$\alpha = \frac{-B}{T^2} ……(2)$$

where α = Sensitifitas termistor,

B = Koefisien termistor dalam °K

T = suhu dalam °K

Activation energy can be calculated using equation (3)[6],

$$B = \frac{\Delta E}{k} ……..(2)$$

Dengan B = Konstanta termistor (°K)

ΔE = Energi aktivasi (eV),

k = Konstanta Boltzmann $(\frac{eV}{°K})$

Table 1. Sample composition in mole %.

No.	CuO	Fe_2O_3	Al_2O_3
1.	40	60	0
2.	40	59	1
3.	40	55	5

4. RESULTS AND DISCUSSION

4.1 XRD Analyses

XRD profiles of $CuFe_2O_4$ base-ceramics added with Al_2O_3 are shown at Fig. 1 and Fig.2 as the representative. All the $CuFe_2O_4$ base-ceramics crystallized in tetragonal structure (JCPDS No.34-0425). In all XRD profiles peak of Fe_2O_3 was observed indicating that a part of the Fe_2O_3 could not form $CuFe_2O_4$ solid solution. Peak from Al_2O_3 was not observed in all XRD profiles. This fact gives a possibility that the Al_2O_3 was dissolved.

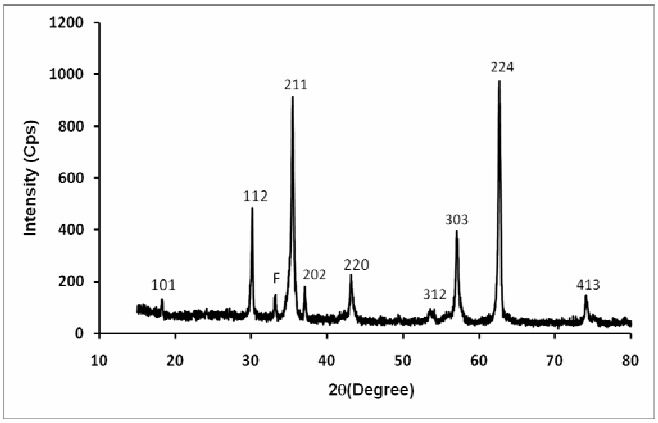

Fig.1. XRD profile of $CuFe_2O_4$ base-ceramic ($40CuO-60Fe_2O_3$) without Al_2O_3 addition. F is peak from Fe_2O_3.

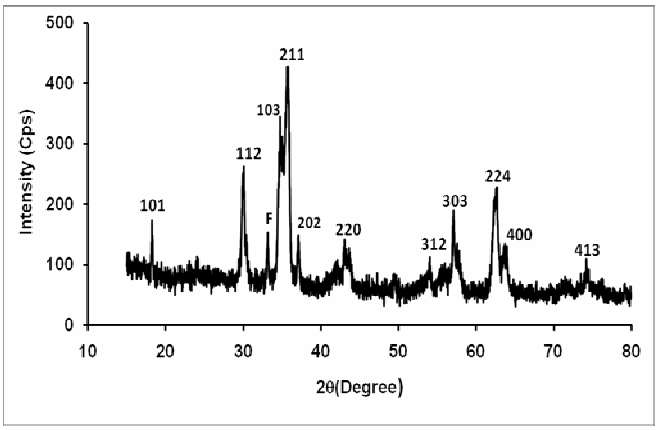

Fig.2. XRD profile of $CuFe_2O_4$ base-ceramic ($40CuO-60Fe_2O_3$) with 1 mole % Al_2O_3. F is peak from Fe_2O_3.

4.2 Electrical Characteristics

Curves of ln Resistivity vs 1/T in Fig. 3 are linear indicating that the $CuFe_2O_4$ base-ceramics obey the NTC characteristic of the thermistor. As shown in Table 1, thermistor constant (B) and sensitivity (alpha) of the ceramics added with Al_2O_3 are larger than those of the ceramics without Al_2O_3. This means that the addition of Al_2O_3 icreased the thermistor constant and sensitivity of the ceramics. Large B and α is good for the NTC thermistor. The value of B and α of the ceramics fit the market requirement

(larger than or equal 2000K(B) and 2.2%/K(α,alpha)). The mechanism of the increasing the thermistor constant and sensitivity is as follow. The Al_2O_3 segregates at grain boundaries and impeded grain growth during sintering. The ceramics then contains small grains or many grain boundaries. Because the grain boundaries are scattering center for electron, the electrical resistivity and thermistor constant of the ceramics increase.

The ageing test result is shown in Fig. 4. As can be seen, for sample without Al_2O_3, from 0 to 100 hours ageing test, the resistivity change rapidly following the aging time. From 100 hours to 1000 hours, the resistance tends to stable. Below 100 hours, the ions in the ceramics tend to rearrange during heating at 150°C[12]. Here, some Fe^{2+} oxidizes to Fe^{3+}. So, the resistance has not been stable. In the range 100-1000hours, the resistance tends to stable though slightly fluctuates. The time to reach a stability condition is different depending on the concentration of Al_2O_3. For sample added with Al_2O_3 the time to reach the stable condition is about 200 hours. It is clear that the addition Al_2O_3 worsen the stability. The fluctuation of the resistance becomes larger as the concentration of Al_2O_3 increases. The value of 200 hours can be taken as a time for preparing a stable $CuFe_2O_4$ base-ceramics for NTC thermistor.

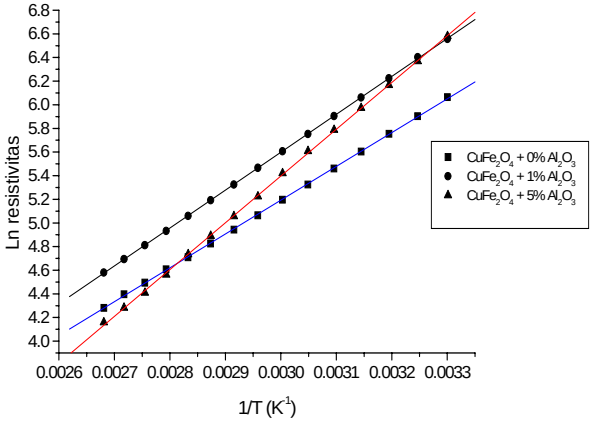

Fig.3. The relation between ln Electrical Resistivity and 1/T.

Table 1. Electrical characteristics of the ceramics.

No.	Penambahan Al_2O_3 (mole %)	B (^{0}K)	α (%/ ^{0}K)
1.	0	2862	3,22
2.	1	3208	3,61
3.	5	3958	4,46

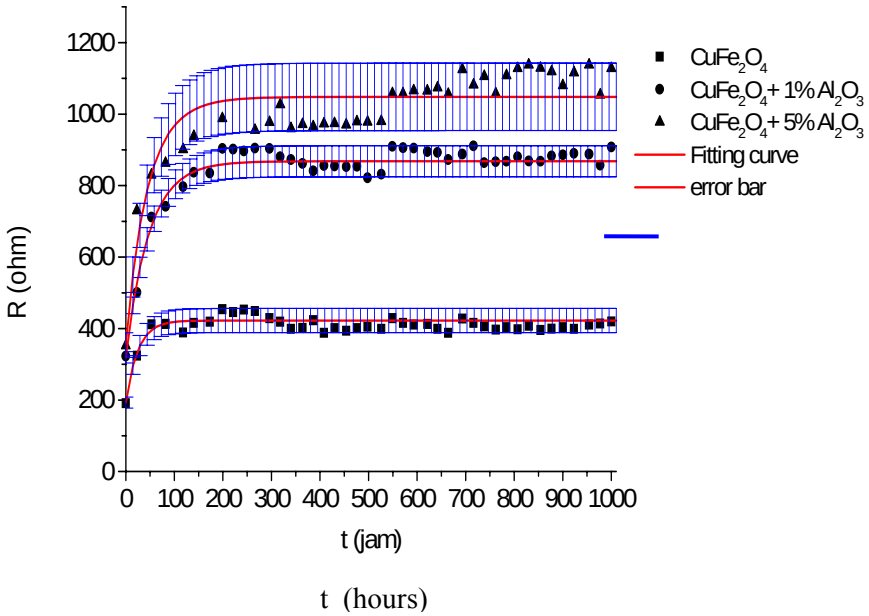

t (hours)

Fig. 4. Electrical resistance as function of time as the result of ageing test.

5. CONCLUSION

All $CuFe_2O_4$ base-ceramic crystallized in tetragonal structure. Thermistor constant (B) and sensitivity (a) of the $CuFe_2O_4$ base-ceramics increase with the increase of Al_2O_3 concentration. This means that the additionof Al_2O_3 can be used as a controlling parameter. However, the addition of Al_2O_3 decreases the electrical stability of the $CuFe_2O_4$ base-ceramics. Only sample without Al_2O_3 and that added with 1 mole % Al_2O_3 fit the electrical stability condition. Heating at 150^oC for 200 hours can be used to make $CuFe_2O_4$ base-ceramic stable electrically.

AKNOWLDGMENT

The authors wish to acknowledge their deep gratitude to DIKTI, Department of National Education of Indonesian Government for financial support under hibah PEKERTI program with contract No. 014/SPP/PP/DP2M/II/2006 April 24, 2006.

REFERENCES

[1]. BetaTHERM Sensors [on line]. Available: http://www.betatherm.com.

[2]. E.S. Na, U.G. Paik, S.C.Choi, "The effect of a sintered microstructure on the electrical properties of a Mn-Co-Ni-O thermistor", Journal of Ceramic Processing Research, Vol.2, No. 1, pp 31-34, 2001.

[3]. Y. Matsuo, T. Hata, T. Kuroda, " Oxide thermistor composition, US Patent 4,324,702, April 13, 1982

[4]. J. H. Jung, O. S. Yoon, Y. K. Hong, J. K. Lee, "Metal oxide group thermistor material", US Patent 5,246,628, September 21, 1993.

[5]. K. Hamada, H. Oda, "Thermistor composition", US Patent 6,270,693, August 7, 2001.

[6]. K. Park, "Microstructure and electrical properties of $Ni_{1.0Mn2-x}Zr_xO_4$ ($0 \le x \le 1.0$) negative temperature coefficient thermistors", Materials Science and Engineering, B104, pp. 9-14, 2003.

[7]. K. Park, D.Y. Bang, "Electrical properties of Ni-Mn-C0-(Fe) oxide thick film NTC thermistors", Journal of Materials Science: Materials in Electronics, Vol.14, pp. 81-87, 2003.

[8]. S.G. Fritsch, J. Salmi, J. Sarrias, A. Rousset, S. Schuurman, Andre Lannoo, "Mechanical properties of nickel manganites-based cermics used as negative temperature coefficient thermistors", Materials Research Bulletin, Vol. 39, pp. 1957-1965, 2004.

[9]. R. Schmidt, A. Basu, A.W. Brinkman, Production of NTCR thermistor devices based on $NiMn_2O_{4+\delta}$", Journal of The European Ceramic Society, Vol. 24, pp. 1233-1236, 2004.

[10]. K. PARK, I.H. HAN, "Effect of Al_2O_3 addition on the microstructure and electrical properties of $(Mn_{0,37}Ni_{0,3}Co_{0,33-x}Al_x)O_4$ ($0 \le x \le 0.03$) NTC thermistors", Materials Science and Engineering, B119, pp. 55-60, 2005.

[11]. Wiendartun, D. G. Syarif, The Effect of TiO_2 Addition on the Characteristics of $CuFe_2O_4$ Ceramics for NTC Thermistors, International Conference on Mathematics and Natural Sciences (ICMNS) 2006, ITB, Bandung, October 2006.

[12].M. M. Vakiv, Aging Behaviour of Electrical Resistance in Manganite NTC ceramics, Jurnal of the European Ceramics Society, 2004.

ISSN 114-1284

Modification of Microstructure of AC4B Aluminium Cast Alloys by Addition of 0.004 wt. % Sr

Willy Handoko[1] and Bondan T. Sofyan[1]

[1]*Department of Metallurgy and Materials Engineering, Faculty of Engineering*
University of Indonesia, Depok 16424, Indonesia
Tel : (021) 786 3510, Fax : (021) 787 2350
E-mail : bondan@eng.ui.ac.id

ABSTRACT

Cylinder heads of motorcycles are produced by low pressure die casting (LPDC) process using AC4B aluminium cast alloy. Rejects that are often found in this component are misrun due to the inadequate fluidity of molten metal to fill up cavity of LPDC die. Fluidity of molten metal may be enhanced through modification of microstructure by adding Sr. This research studied the effects of Sr addition of 0.004 wt. % on the as-cast properties of AC4B alloys.

Addition of Sr was conducted by adding rod Al-10 Sr master alloy in the holding furnace. Injection temperatures of LPDC process were varied 680, 700 and 720 ^{o}C. Fluidity of molten metal was measured by spiral method, and porosity was observed through vacuum porosity tests. Tensile and hardness tests were conducted as well as observation on the microstructure of the materials in as-cast condition by using light microscopy and SEM (scanning electron microscope) equipped with EDS (energy dispersive spectroscopy).

Fluidity of AC4B aluminium alloys increases by addition of 0.004 wt. % Sr. The higher the injection temperature, the higher the fluidity of the molten metal. Addition of Sr seems to increase the porosity level, which then decreases the hardness of the alloy. However, the distribution of porosity is random, and no particular mode is able to detect. The presence of Sr modify the accicular Si eutectic into fine fibrous. Injection temperature seems to have little effects on the modification of mircostructure by addition of Sr.

Keywords
AC4B, Sr, low pressure die casting, fluidity, modification

1. INTRODUCTION

One foundry alloy that is popular for use in automotive application is AC4B aluminium alloy, due to its excellent castability and mechanical properties. Its excellent corrosion resistance and low cost of recycling are also important considerations from an environmental point of view. Aluminium alloy AC4B is essentially a hypoeutectic Al-Si alloy with two main solidification stages, formation of aluminium rich dendrites followed by development of silicon phase. Two major disadvantages of these alloys. The first is the sharp edges of the coarse acicular silicon phase that occurs in the microstructure, promoting crack initiation and propagation which leads to poor mechanical properties. Another disadvantage is their long freezing range, which leads to feeding difficulties in the interdendritic region, resulting in increased porosity [1].

Strontium is added to hypoeutectic aluminium-silicon alloys in order to transform the morphology of the silicon phase from acicular flakes to a fibrous rodlike form, thereby improving mechanical properties, especially fracture toughness and elongation [2]. At a given cooling rate, Sr decreases nucleation and growth temperatures of the (Al)-Si eutectic and this effect is higher the higher the cooling rate [3]. Addition of Sr does not affect primary deposition of (Al) but apparently modifies reactions occurring after

the (Al)-Si precipitation. DTA work by Martinez *et al.* [3] confirmed that Sr addition has a direct influence only on the growth mechanism of the (Al)-Si eutectic. Small changes in overall eutectic kinetics due to Sr modification also results in subtle modification during final stages of solidification as well as in the precipitation of iron and manganese rich phases.

However, Sr addition is also associated with porosity formation. In this connection, Dahle *et al*. [4] suggested the change in the mode of eutectic nucleation – from that occurring near the a-Al dendrites in the Sr-free alloy, to that taking place within the eutectic liquid itself in the Sr-containing alloy. The mode in operation controls the distribution of the remaining liquid in the last stages of solidification when feeding becomes extremely difficult. This distribution, in turn, will define the connectivity of the feeding channels, and thus determine the resultant porosity profile in the solidified casting.

The aim of the present study is to understand the changes in the microstructure due to 0.004 wt. Sr addition to AC4B alloy produced by LPDC process. Fluidity of the molten metal and the resulting porosity was observed. Effect of injection temperature was also studied.

II. EXPERIMENTAL METHOD

An Sr-containing alloy was cast by using commercial AC4B as the base alloy and the resulting nominal composition is presented in Table 1. The charge materials consist of 70 % of ingot and 30 % of return scrap. These alloys were melted in an industrial furnace and gas bubble floatation process by using argon was performed for 8 minutes to remove trapped air from the molten metal. Master alloy Al-10Sr was added into the molten metal just before injection with the amount of 0.004 wt. % Sr. Injection temperatures were varied 680, 700 and 720 ^{o}C, and molten metal was injected into metal mould with resin-coated sand cores possessing the shape of cylinder head, therefore, it is expected that heat transfer in different position within the mould will be different. Hardness of the LPDC products was measured by using Rockwell B method with 1/16 inch diameter of indenter at 150 kg of load. Measurement was conducted around the studbolt region with 7 identation.

Fluidity test was conducted by using spiral mould with gravity method, in which molten metal was poured into the spiral mould, and the length of spiral was measured by using measuring tape. Microstructures at the tip of the spiral were observed to compare them with the LPDC structures.

Table 1. Nominal composition (wt. %) of alloys in this study

Alloy	Si	Cu	Mg	Fe	Mn	Sr	Al
Base	8.2	2.3	0.11	0.78	0.12	-	rem
Modified	8.9	2.6	0.13	0.88	0.13	0.004	rem

Tensile specimens were made by pouring molten metal into dog-bone-shaped metal mould in accordance with JIS Z2201, test piece no. 4. Hardness measurements were performed by Brinnel method at clamp area of the tensile specimens, by using steel ball indenter of 1/16 inch diameter. Seven indentations were taken for each hardness measurement.

Samples of each alloy were taken at three different positions of the cylinder head, representing area with high, medium dan low solidification rate, designated as area 1, 2, and 3, respectively. Samples were cut into 10 x 10 mm blocks for microstructural and microanalysis. Modification of microstructure was observed by means of a light microscope and LEO 420 SEM. Samples for microstructural analysis were prepared by etching with 0.5 % hydrogen fluoride.

III. RESULTS AND DISCUSSION

A. Effects of Sr on Fluidity and Porosity

Fluidity is an important factor in casting processes to reduce misrun. Results in Figure 1 show that at all injection temperatures, addition of 0.004 wt. % Sr increased fluidity of molten AC4B alloys. This is in correlation with previous studies that the role of Sr in solidification process is to decrease the eutectic temperature so that shorten the solidification range and resulting in higher fluidity [5]. Strontium is also known to reduce interfacial energy of molten aluminium that allows better fluidity [6]. As has been widely known, the higher the pouring temperature, the higher the fluidity of the molten metal. Another observation is that AC4B alloys containing Sr showed brighter silvery colour.

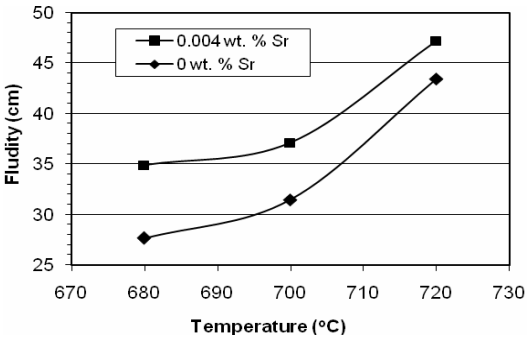

Figure 1. Effect of Sr addition and injection temperature on fluidity of AC4B alloys.

Figure 2 shows the intersection of vacuum porosity sample of the Sr-free and Sr-containing alloys. The presence of Sr seems to increase the amount of porosity. This has been shown by Amberg et al. [7] that modifier increase dissolution of hydrogen in molten metal, and decrease eutectic temperature that leads to longer period of solidification. The addition of 0.004 wt. % Sr increases porosity level from #5 to #7 in ASM standard. Figure 3 further confirms that the porosity increases in size and distribution by addition of Sr. This figure also shows that the porosity changes to transgranular and more rounded in the Sr-containing alloy.

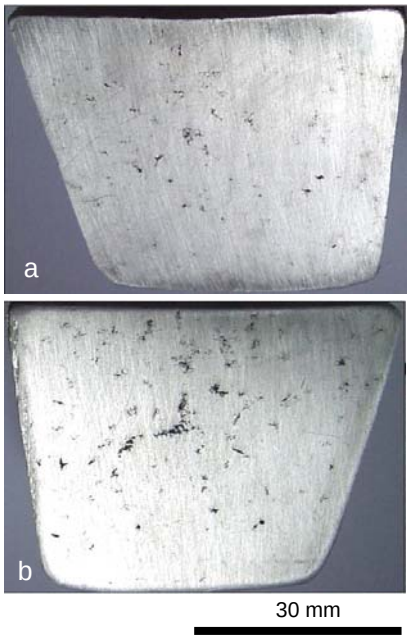

Figure 2. Porosity content in AC4B alloys with (a) 0 wt. %, and (b) 0.004 wt. % Sr.

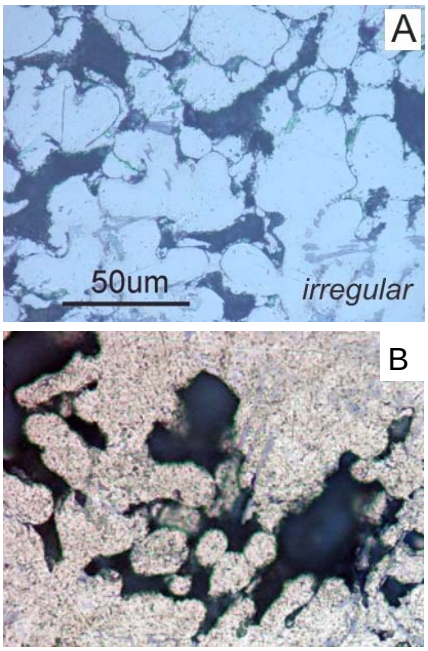

Figure 3. Morphology of porosity in (a) Sr-free, and (b) 0.004 wt. % Sr-containing AC4B alloys. Microstructures were taken from fluidity samples.

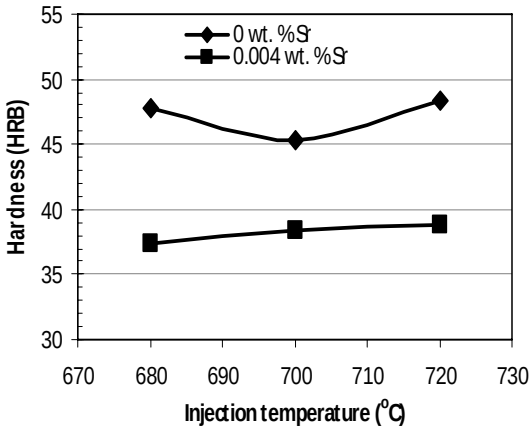

Figure 4. Effect of Sr content and injection temperature on the hardness of AC4B cylinder head.

B. Effects of Sr on Mechanical Properties and Microstructures

Figure 4 show the effect of 0.004 wt. % Sr addition on the hardness of AC4B alloys as LPDC products at different injection temperatures. It is clear that addition of Sr decreases the hardness for ~ 20 %, and there was no significant effect of injection temperature. This is in contrast with the

tensile strength which shows slight increase for 0.8 % from 196.1 MPa to 197.8 MPa (Figure 5). This peculiarity was further observed by measuring the hardness at the clamp area of the tensile samples. The result is provided in Figure 6. The hardness shows an increase by addition of 0.004 wt. % Sr, in line with the tendency in tensile strength. Observation on microscopy on the LPDC products and the tensile samples showed that LPDC products possess more porosities than the tensile samples. Different mould materials may be the reason for the difference.

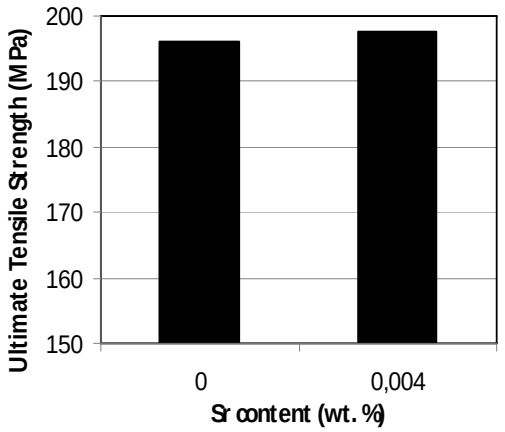

Figure 5. Effect of addition of 0.004 wt. % Sr on strength of AC4B alloy.

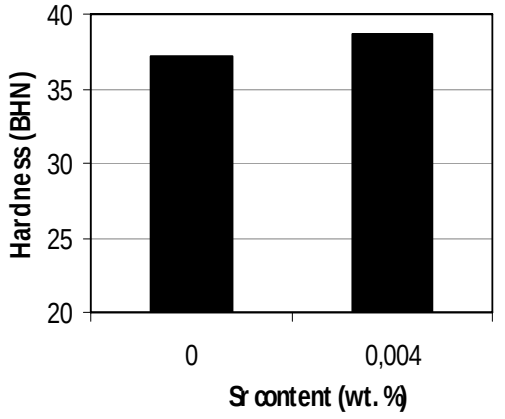

Figure 6. Hardness measured on tensile strength samples with different Sr content.

A series of microstructural analysis on the effect of Sr addition and injection temperatures is presented in Figure 7. These micrographs were taken from samples cast at 680 ^{o}C. In general, microstructure of AC4B alloys in as-cast condition consists of α-aluminium dendrites with interdendritic second phases. This is in correlation with the fact that solidification of hypoeutectic Al-Si starts with formation of α-aluminium dendrites, followed by eutectic reaction and formation of second phase particles, such as Mg_2Si and Al_2Cu. Aside from that, second phase particles containing Mn and Fe also form, such as Al_5FeSi (during slow solidification) and $Al_{15}(Mn,Fe)_3Si_2$ (during rapid solidification) [9]. As has been widely known, rate of solidification determines dendrite arm spacing (DAS), the higher the rate, the smaller the spacing, and this is confirmed in Figure 7.

Modification of microstructure by Sr can be clearly seen at position 3, which has the lowest solidification rate. Eutectic silicon structure was modified from coarse acicular into fine fibrous, similar to class C (modified) in accordance to ASM standard. At position 1, the microstructure is readily modified during high rate of solidification. Therefore, degree of further modification by Sr addition is not as apparent as that at positions 2 and 3. Quantitative measurement shows that modification also resulted in the decrease in DAS, which in turn increase the strength and hardness of the alloys. Observation revealed that varying injection temperature for 680, 700 and 720 ^{o}C did not affect the microstructure and level of modification of the alloys.

Detailed micrographs of AC4B alloys at position 1, which has the highest solidification rate, are presented in Figure 8. Identity of each phase was confirmed by EDXS analysis, tabulated in Table 2. Change of interdendritic structure due to modification is clearly revealed, in which the morphology of Al-Si eutectic transforms from acicular into fine fibrous structure. No alteration of morphology was detected in α-Al(Fe,Mn)Si phase (position 3 and 4). The small amount of Sr may be the reason for this. The pocket Al_2Cu structure was modified into massive blocks (position 1 and 2). This phase was initially well dispersed within the matrix, but upon addition of 0.004 wt. %, it tends to segregate at particular locations. This segregation may be caused by the lowering of eutectic temperature for $\pm$ 10 ^{o}C by addition of Sr, so that shorten remaining solidification time for Al_2Cu formation.

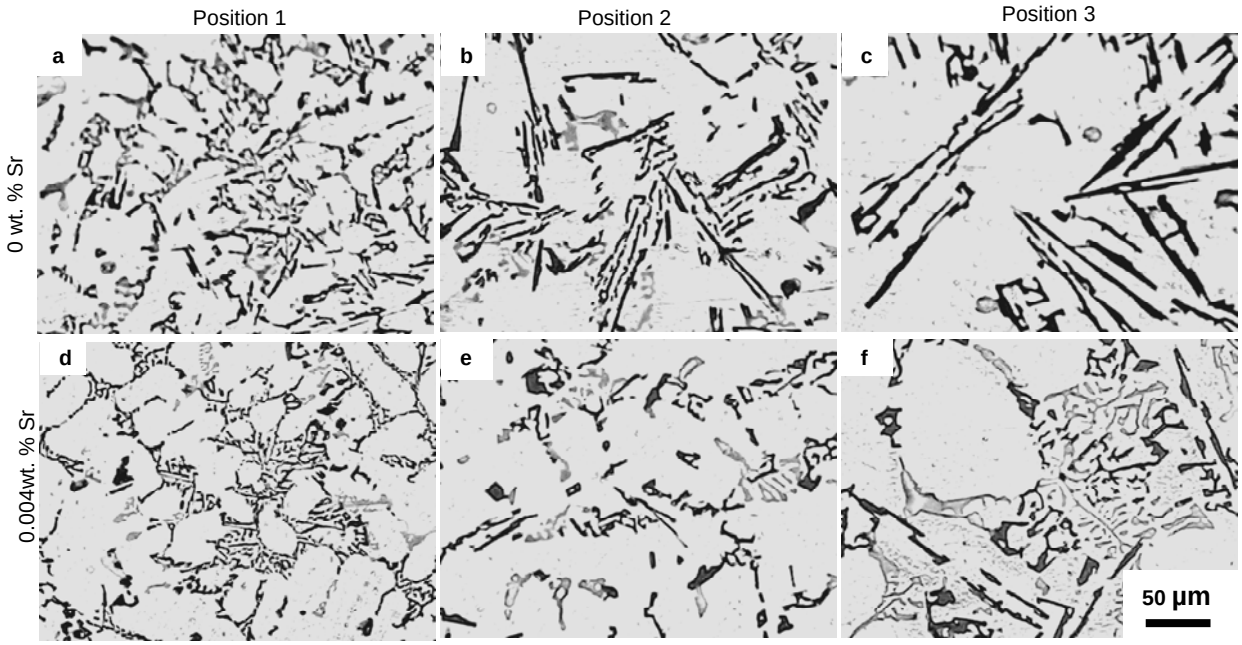

Figure 7. Effects of addition of (a-c) 0 wt. %, and (d-f) 0.004 wt. %, Sr on modification of AC4B alloys produced by LPDC process at 680 ^{o}C at different positions. Position 1, representing high solidification rate; position 2, representing medium solidification rate; and position 3, representing low solidification rate.

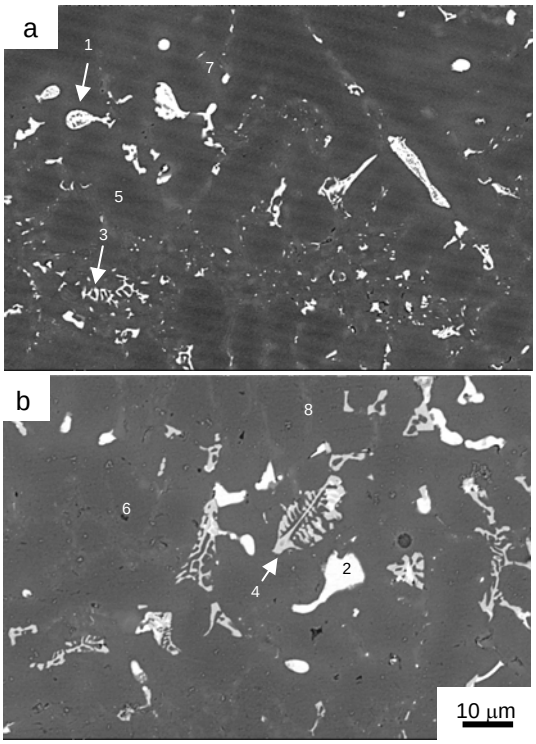

Figure 8. SEM micrographs of AC4B alloys added with (a) 0 wt. % Sr, and (b) 0.004 wt. % Sr, taken from position 1, which has the highest solidification rate.

Table 2. Microanalysis result on positions shown in Figure 8.

No	Element (wt. %)					Phase
	Al	Si	Cu	Fe	Mn	
1	81.60	5.73	12.67	-	-	Al_2Cu
2	84.55	2.41	13.04	-	-	Al_2Cu
3	57.00	6.50	0.62	32.40	3.48	Al(Fe,Mn)Si
4	61.00	6.29	0.57	30.19	1.94	Al(Fe,Mn)Si
5	7.91	92.09	-	-	-	Al-Si eutectic
6	29.97	70.03	-	-	-	Al-Si eutectic
7	98.32	1.68	-	-	-	Al matrix
8	98.59	1.41	-	-	-	Al matrix

CONCLUSIONS

1. Addition of 0.004 wt. % Sr to AC4B alloys processed by LPDC increases the porosity level from 5 to 7 (ASM scale), and reduces the hardness of LPDC products at all injection temperatures.
2. Addition of 0.004 wt. % Sr to AC4B alloys processed by gravity casting as tensile samples, increases tensile strength and hardness. Porosity in tensile samples was found less than in LPDC products.
3. Addition of 0.004 wt. % Sr increases fluidity of AC4B alloy. Increase in injection

temperatures also increases fluidity of the alloys.

4. Addition of 0.004 wt. % Sr modifies the silicon eutectic from acicular to finer fibrous in class C (modified).
5. Injection temperatures do not have significant impact to the microstructure and mechanical properties of the alloy.

ACKNOWLEDGMENTS

This research was partly funded by Ministry of National Education, the Republic of Indonesia through Hibah Bersaing XIII scheme.

REFERENCES

[1] W. LaOrchan, J.E. Gruzleski, "Grain Refinement, Modification and Melt Hydrogen – Their Effects on Microporosity, Shrinkage and Impact Properties in A356 Alloy", *AFS Transaction*, Vol. 39, pp. 415-424, 1992.

[2] C.M. Dinnis, M.O.Otte, A.K.Dahle and J.A.Taylor, "The Influence of Strontium on Porosity Formation in Al-Si Alloys", *Met. Mat. Trans. A*, Vol. 35A, pp. 3531-3541, November 2004.

[3] E.J.Martinez D., M.A. Cisneros G., S. Valtierra, and J. Lacaze, "Effect of strontium and cooling rate upon eutectic temperature of A319 alloy", *Scripta Mat*., Vol. 52, pp. 439 – 443, 2005.

[4] A .K. Dahle, J. Hjelen and L. Arnberg, *Proc. 4th. Decennal Int. Conf. on Solidification Processing 1997*, University of Sheffield, UK, 1997, p. 527.

[5] P.R. Beeley, *Foundry Technology*, London, Butterworth, 1972.

[6] J.E. Gruzleski and B.M. Closset, *The Treatment of Liquid Aluminium-Silicon Alloys*, Illinois, AFS, 1999.

[7] L. Arnberg, L. Backerud, and G. Chai, *Solidification Characteristics of Aluminium Alloys: Vol. 3, Dendrite Coherency*, Sweden, AFS, 1990.

[8] J. Lozano, P. Asensio, and S. Beatriz, Effects of addition of refiners and/or modifiers on the microstructure of die cast Al-12Si alloys, *Scripta Mat*., Vol. 54, pp. 943-947, 2006.

[9] L. Bakerud, G. Chai, J. Tamminen, *Solidification Characteristics of Aluminium Alloys: Vol. 2, Foundry Alloys*, Stockholm, Skan Aluminium, 1990.

Proceeding of the 11th International Conference on QiR (Quality in Research)
Faculty of Engineering, University of Indonesia, Depok, Indonesia, 3-6 August 2009
ISSN 114-1284

Effect of Cooling Rate on Microstructure & Hardness in the Solution Annealing of Duplex Stainless Steel Welds

Winarto [1] and Muhammad Anis [2]

[1, 2]*Metallurgy & Materials Engineering Department – University of Indonesia*
Kampus Baru – UI, Depok – 16424
Tel : (021) 7863510. Fax : (021) 7872350
E-mail : [1] winarto@metal.ui.ac.id; [2] anis@metal.ui.ac.id

ABSTRACT

Duplex stainless steels have a mixed microstructure consisting of ferrite (bcc) and austenite (fcc) phases. When duplex stainless steels have the optimum phase balance, which is usually approximately equal proportions of ferrite and austenite phases, they exhibit higher resistance to stress corrosion cracking and higher strength than austenitic stainless steels. However, the melting and solidification associated with fusion welding processes destroy the favorable duplex microstructure of these stainless steels, which causes the loss of low-temperature notch toughness and corrosion resistance in the weld. This situation suggests that the favorable duplex microstructure of the duplex stainless steel should be maintained, but there have been few papers dealing with the effect of cooling rate of solution annealing of duplex stainless steel. In this study, the microstructure and hardness properties of fusion welded duplex stainless steel were examined. High-quality welds were successfully produced in the duplex stainless steel by Gas Tungsten Arc Welding (GTAW) process. The base material had a microstructure consisting of the ferrite matrix with austenite islands, but weld annealed duplex stainless steel with water quench have a dominantly coarse grains of ferrite phases in the HAZ and weld metal zone in comparing with air cooling. The smaller grain sizes of the ferrite phases caused increases hardness within the HAZ and weld metal zone.

Keywords:
Duplex Stainless Steel, Annealing, Cooling Rate, Microstructure and Hardness

1. INTRODUCTION

Duplex Stainless Steels composed of ferrite and austenite in similar amount. They have good corrosion properties, high yield strength and good toughness in the temperature range -50 to 250°C. Above 400°C several structures changes occurs in duplex stainless steel during isothermal and anisothermal heat treatments.

Welding process usually change the phase composition balance between austenite and ferrite phase. The weldment phase balance highly influenced by the chemical composition and cooling rate at the weldment. At the HAZ region usually a coarse microstructure was formed with high fraction of ferrite phase. Numerous works already presented regarding the cooling rate and carbide phase formation. Work by Ogawa and Koseki [(1)] showed that equilibrium composition between ferrite and austenite are continually changing according to austenite and ferrite solvus line. Tavares *et.al* [(2)] studied the cooling rate effect morphology, toughness and microstructure of duplex stainless steel UNS S 31803. Solution treatment and furnace cooling remove the carbide from grain boundary and promote increase toughness. Work by Badji *et.al*[(3)] studied faster cooling rates affect the microstructure at fusion line even with same heat input.

Several papers regarding the duplex stainless steel failure attribute to welding process already well documented. Work by Battacharya and Sigh [(4)] studied the susceptibility Duplex Stainless Steel grade to Stress Corrosion Cracking can be attributed to heating process during manufacturing especially welding.

This paper focused on studied the effect of cooling rate on microstructure and hardness properties in the solution annealing of welded duplex stainless steel UNS S 31803 (SAF 2205) pipes, welded by manually TIG Welding process.

2. EXPERIMENTAL METHOD

The research was carried out using duplex stainless steel UNS S 31803 (SAF 2205) pipes, 10 inch diameter with 12.7 mm thickness. The sample then welded by GTAW method with welding parameter which refers to ASME sec IX as follow:

Method : GTAW (Gas Tungsten Arc Welding) manual type
Joint Design : Butt joint with 60 ° V- groove.
Filler type : ER 2209
Filler size : Diameter 2.0/2.4 mm
Interpass temp : 150°C max
Gas : Argon 99.995 %
Current : 80 – 130 Ampere (Root Pass) & 90 – 250 A (Filler Cap)
Voltage range : 8 – 15 Volts
Travel speed : 70 – 190 mm/min
Heat Input : 0.5 – 1.5 kJ/

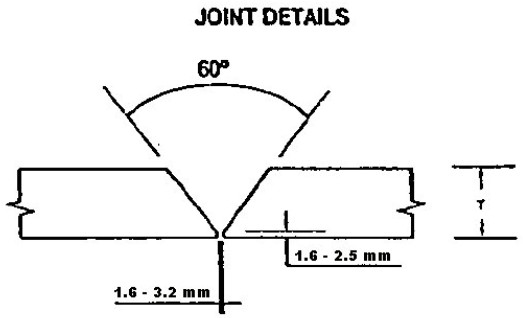

Fig 1. Schematic of weld joint design

The welded sample then cut into into three different heat treatment processes which are as-welded, water quench-annealed and air cooling annealed. The annealing process of welded samples was carried out at temperature of 1100°C and held for 90 minutes. After that those were quenched by water and air. Metallurgical characterization performed by micro vickers hardness test under 300 gr load for 15 second. Microstructure examination performed using light optical microscope. Ferrite content was measured by Scion™ image analysing sofware at 500x magnification on sample etched with electrolytic 50 mol KOH etching.

Table 1. Typical chemical compostion for S 31803 (SAF 2205) and Filler wire ER 2209

Material	C	Mn	Si	Cr	Ni	Mo	N
UNS S 31803	0.022	1.65	0.51	22.02	5.23	3.25	0.183
Filler ER-2209	0.014	1.63	0.53	22.55	8.94	3.11	0.13

3. RESULT AND DISCUSSION

3.1. Metallographic Examination

All the samples revealed the typical austenite-ferrite duplex structure, as can be seen in Fig. 2.

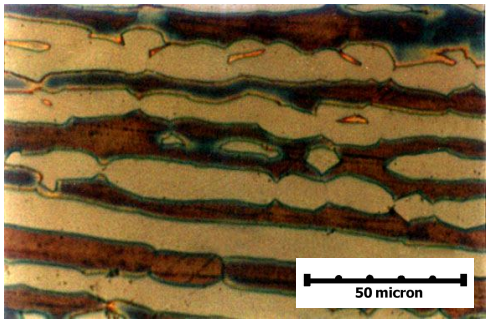

Fig 2. Microstructure of the base metal duplex stainless steel of UNS S 31803 (SAF 2205).

During solidification, basically duplex stainless steel solidified as ferrite, the transformation of austenite phase start below the ferrite solvus line along the ferrite grain boundaries [5]. Normally, welded areas have a high cooling rate which suppresses the austenite formation. However, multi pass welding process created a reheating condition and promotes secondary austenite formation.

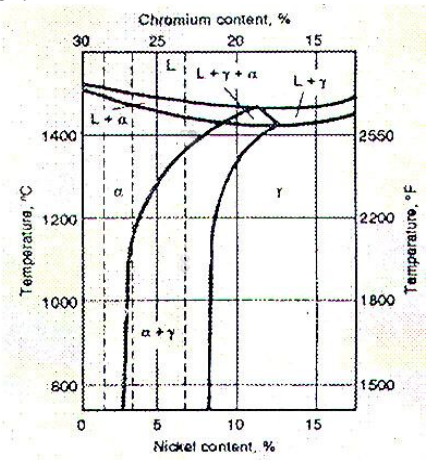

Fig 3. Diagram Pseudo-binary of Duplex SS (68% Fe)

ISSN 114-1284

In water quenched samples (fast cooling) new grain of austenite start growing at the α/α grain boundaries. Due to rapid cooling austenite can not develop fully.

The performance of DSS can be highly influenced by welding process. Several parameter used during the process could alter and change the microstructure morphology of the duplex stainless steel joint. The proper welding method, filler metal and inter-pass temperature are needed to ensure proper phase balance and avoid the formation of precipitate or inter-metallic phase. Shielding gas also could play and important factor for obtaining optimal phase balance between austenite and ferrite [6-7]. Phase balance at the weld is required to avoid, excessively high ferrite content could cause brittleness, whereas a lack of ferrite could cause a loss of resistance to stress corrosion cracking [5].

Metallographic examination by light optical microscope was taken at weld and HAZ. Microstructure of the weld showed a different phase and balance between ferrite and austenite. The entire sample also showed secondary austenite at their joint area. Cooling rates have a significant impact to the welded microstructure morphology such as austenite – ferrite phase balance or precipitate and carbide formation, as seen in Fig 4 and Fig 5.

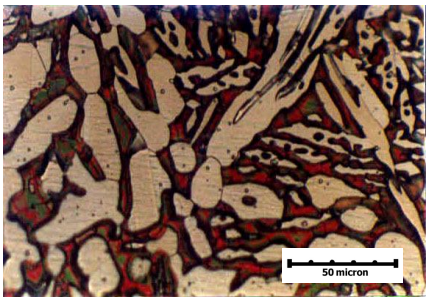

(a)

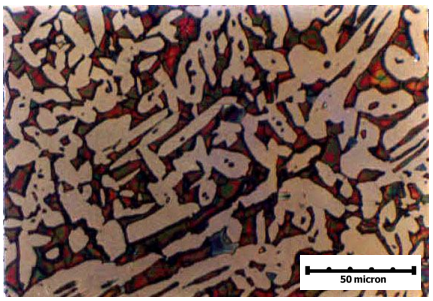

(b)

Fig 4. Microstructure of Weld Metal on UNS S 31803 welds with (a) water cooling and (b) air cooling

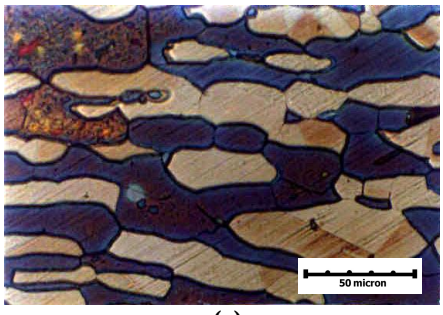

(a)

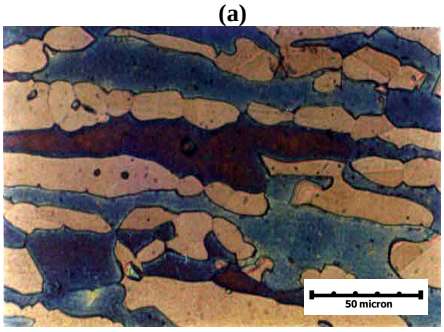

(b)

Fig 5. Microstructure of HAZ on UNS S 31803 welds with (a) water cooling and (b) air cooling

Microstructures at weld metal taken from air cooling sample have a vermicular appearance (Fig. 4) and finer dendrite of secondary austenite. Ferrite content analysis is 43.4 % which is lower compared to the water cooling sample (53.8 %). The cooling rates of water quenched samples are highly influenced by the capability of quench medium to drive out the heat of the sample. Normally, water quench have a higher cooling rate compared to air (atmosphere). The microstructures of HAZ taken from water cooling sample have a round and coarser appearance of secondary austenite (Fig. 5) and the ferrite content is 56 % which is higher than air cooling samples.

Table 2. Ferrite Content Calculation for S 31803 Welds

Weld Area	Water Quench		Air Cooling	
	% α	% γ	% α	% γ
HAZ	56.0	44.0	53.8	46.2
Weld Metal	52.3	47.7	43.4	56.6

3.2. Hardness Testing

The quench medium creating different cooling rate and lead to changes in different hardness value. In general assumption, the cooling rate from water medium is higher compared to air atmosphere.

The ferrite contents increase with increasing the cooling rate, hence the hardness increased with increasing cooling rate, as seen in Fig. 6.

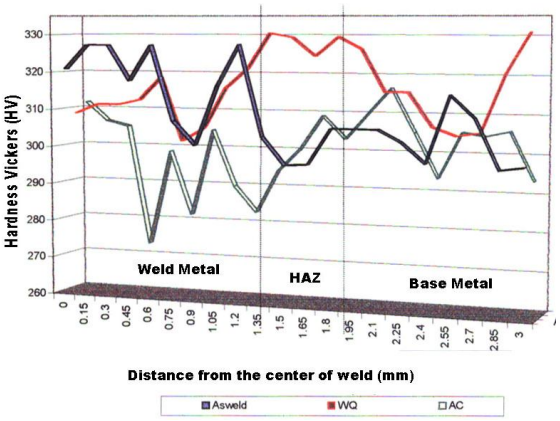

Fig 6. The effect of cooling rate to the hardness distribution of weldments UNS S 31803.

4. CONCLUSION

The cooling rate of solution annealing for welded duplex stainless steel of UNS S 31803 have a significant impact to microstruture morphology. This occured due to different cooling rate from each quenching medium. The changes can be seen for the microstructure shape and ferrite content. Higher cooling rate yields a secondary austenite growth, but the increasing the ferrite content. The hardness increased with increasing cooling rate.

REFERENCES

[1] Ogawa, T., Koseki, T., Effect of composition profile on metallurgy and corrosion behavior of duplex stainless steel weld metals, *Welding Journal*, Vol. 68 No. 5, (1989) pp.181-191.

[2] Tavares, S.S.M., Terra, V. F., Pardal, J.M, Cindra Fonseca, M.P, Influence of the microstructure on the toughness of a duplex stainless steel UNS S31803, *Journal of Materials Science*, Vol 40. No. 1, (2005), pp 145 – 154

[3] Badij R., Belkessa B., Maza H., Bouabdallah M, Bacroix B,. Kahloun C., *Mater Sci Forum* 217(2004) pp.467

[4] Bhattacharya. A., Singh., P.M., Stress Corrosion Cracking of Welded 2205 Duplex Stainless Steel in Sulfide-containing Caustic Solution, *Journal of Failure Analysis and Prevention*, Vol 7 No.5 (2007), pp 371-377.

[5] Lippold J.C and Kotecki D.J, *Welding Metallurgy and Weldability of Stainless Steel*, (2005) pp. 231 John Wiley and Sons Inc.

[6] Wiktorowicz R., and Crouch J., Shielding gas developments for TIG welding of duplex and super duplex stainless steels, *Welding and Metal Fabrication*, vol. 62, No. 9, (1994), pp. 379-382.

[7] Sathiya, P., Aravindan, S., Soundararajan, R,. and Noorul Haq, A., Effect of shielding gases on mechanical and metallurgical properties of duplex stainless-steel welds, *Journal of Material Science*, Vol.44 n.1 (2009).pp 114-121.

Symposium on Industrial Engineering Approach for Productivity

Symposium F

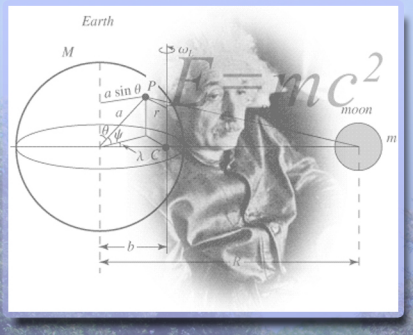

QiR

Quality in Research

THE 12th INTERNATIONAL CONFERENCE ON QiR (QUALITY IN RESEARCH)

4 – 7 July 2011
UNIVERSITY OF INDONESIA, DEPOK, INDONESIA

SPECIAL ISSUES ON:
- Advanced Materials Processing and Technology
- Industrial Engineering Approach for Productivity Improvement

SYMPOSIUM IN:
- Energy Conservation through Efficiency in Design and Manufacturing
- Information and Communication Technology
- Green Infrastructure for Sustainable Development

IMPORTANT DATES

· Extended Abstract	: 15 February 2011
· Notification of Abstract Acceptance	: 1 March 2011
· Submission of Camera-Ready Paper	: 1 April 2011
· Early Bird Registration	: 1 May 2011
· Conference Date	: 4-7 July 2011

Supported by:
Materials Research Society – Indonesia (MRS-Indonesia)
Masyarakat Nanomaterial Indonesia (MNI)
Badan Kerja Sama Perguruan Tinggi Teknik Industri Indonesia (BKSTI)

Organized by:
Faculty of Engineering, University of Indonesia
Gedung Dekanat Lt. 3
Kampus UI, Depok 16424, Indonesia
Phone : +62 – 21 - 786 3503 / 9114 5988
Fax : +62 - 21 – 7270050
Email : qir@eng.ui,ac.id, qir.ftui@gmail.com
Website : http://qir.eng.ui..ac.id
Chair Person : Dr. Bondan T. Sofyan,
bondan@eng.ui.ac.id

QiR

http://qir.eng.ui.ac.id

ISSN 114-1284

Hybrid Heuristic For Minimization of Cell Load Variation Within Group Technology

Agus Ristono

Industrial Engineering Department, Faculty of Industrial Technology
University of Veteran National Development, Yogyakarta 55281
Tel : (0274) 485363. Fax : (0274)486256
E-mail : agus_ristono@yahoo.com

ABSTRACT

Group technology (GT) has been proposed to increase productivity in manufacturing. The basic idea of GT is to exploit the similarity between parts and manufacturing processes. Parts similar in design and manufacture are grouped into part families. Machines are organized into machine cells to process part families. The problem of forming part families and machine cells is referred to as the GT. In this paper, we develop a new optimization algorithm that combines the simulated annealing and tabu search called the hybrid heuristic. The resulting hybrid algorithm retains the global perspective of the simulated annealing and the local search capabilities of the tabu search. We also present a detailed application of the proposed algorithm to solving cell load problem in GT and it is found empirically to outperform a pure simulated annealing algorithm implementation, particularly for large problems. The computational experience is also reported.

Keywords

Group technology, family, machine cell, cell load, hybrid heuristic, tabu search, simulated annealing

1. INTRODUCTION

Machine layout in a tradisional production system is mainly process (function) oriented where machines performing similar processes are grouped together. Parts requiring more than one process travel from one section of a production system to another until their operation requirements are completed. Long and uncertain throughput times are usually the major problems in such a system. Other problems include an increase in inventory holding cost, untimely product delivery and loss of sales [20]. Manufacturing firms have to look for better layout approaches to increase productivity.

Group Technology (GT) can be defined as a concept for increasing production efficiency by grouping various parts and products with the same or similar characteristics [12]. The set of similar parts can be called a part family. The application of GT results in the mass production effect to multi products and small-lot-sized production. The important areas of GT applications are classification and coding, process planning, part family and machine cell design, GT layout, group scheduling, and cell loading. For successful implementation of GT may involve the use of classification and coding which describes the basic characteristics of a given part with respect to its manufacturing process [11].

There are two type of machine layout in GT, namely, logical and physical machine layout [4]. In a logical machine layout, machines are dedicated to part families but their positions in a factory are not altered. In a physical machine layout, dedicated machine cells containing different machines are grouped together to exploit flow shop efficiency in processing part families. Although clustering concepts for physical layout are discussed in this paper, many of these concepts can be easily applied to a logical layout.

Ideally, all operations of parts in a part family should be completed within a machine cell. However, such ideal physical machine layouts are rare in practice. In most actual layouts, there are usually exceptional parts and exceptional machines. An exceptional part requires processing on machines belonging to more than one machine cell. An exceptional machine processes parts from more than one part family. To effectively implement GT, a good clustering algorithm is needed such that the number of exceptional parts and exceptional machines are minimized and improved measure for minimization of cell load variation within GT.

Many GT applications involve combinatorial optimization, that is, obtaining the optimal solution among a finite set of alternatives. Such optimization problems are notoriously difficult to solve. One of the primary reasons is that in most applications the number of alternatives is extremely large and only a fraction of them can be considered within a reasonable amount of time. As a result, heuristic algorithms are often applied in combinatorial optimization. Among the most successful such heuristics are evolutionary algorithms, genetic algorithms, tabu search, and neural networks. All of these algorithms are sequential in the sense that they move iteratively between single solutions or sets of solutions.

However, in some GT applications it may be desirable to maintain a more global perspective, that is, to consider the

entire solution space in each iteration. In this paper we propose a new optimization algorithm to address this difficult class of problems. The new method converges to a global optimum of combinatorial optimization problems in finite time and is very robust. We also present a detailed application of the method to a product design problem. Numerical results demonstrate the effectiveness of our proposed method.

In this paper, we use meta-heuristic such as simulated annealing and tabu search to evaluate several cases for the GT using minimization of cell load variation and Grouping efficiency as performance measurement. Minimization of cell load variation was proposed by Venugopal and Narendran [21], while Grouping efficiency proposed by Chandrasekharan and Rajagopalan [15].

2. PROBLEM FORMULATION

GT is an assignment-type problem and can be summarized as follows: given n items and m resources, the problem is to determine an assignment of the items to the resources optimizing an objective function and satisfying a stated set of additional side constraints. An objective function provides the basis for evaluating the machine groupings arrived at by a searching method. In the present work, one problem formulation (objective function) model was implemented. The model is based on the minimization of cell load variation.

2.1. Minimization of cell load variation model

This model is based on the model proposed by Venugopal and Narendran [21]. In this model we define m as the number of machines, k as the number of cell, and n as the number of parts. W = [w_{ij}] is an m*n machine component incidence matrix where w_{ij} is the workload on machine *i* induced by part *j*. X = [x_{ij}] is an (m*k) called as cell membership matrix, where

$$x_{ij} = \begin{cases} 1 & \text{if machine is in cell } i \\ 0 & \text{otherwise} \end{cases}$$

M = [m_{ij}] is an (k*n) matrix of average cell load, where

$$m_{jl} = \frac{\sum_{i=1}^{m} x_{il} w_{lj}}{\sum_{i=1}^{m} x_{il}}$$

The total load of cell i induced by part j is given as:

$$\sum_{i=1}^{m} x_{il} w_{lj}$$

The number of machines in cell i is given as:

The mathematical programming formulation of the grouping problem is as follows:

$$\text{Minimize } z_1 = \sum_{i=1}^{m}\sum_{i=1}^{k}\sum_{i=1}^{n}(w_{ij} - m_{ij})^2 \qquad (1)$$

Subject to:

$$\sum_{l=1}^{k} x_{il} = 1 \quad \forall i \qquad (2)$$

$$\sum_{i=1}^{m} x_{il} \geq 1 \quad \forall l \qquad (3)$$

The expression $\sum_{i=1}^{m}\sum_{i=1}^{k}\sum_{i=1}^{n}(w_{ij} - m_{ij})^2$ is the objective function. Equation (1) gives the extent of variation of the load on machine i in cell l (induced by all parts) from the mean load of cell i. The objective function z1 adds this quantity for all the machines and cells. Hence this formulation requires a solution for which the total cell load is minimized such that every machine belongs to exactly one cell and no cell is empty. Equation (2) ensures that for particular i, machine i is assigned to one cell only. Equation (3) ensures that no cell is empty.

2.2. Model Illustration

As an illustration, consider a 3x3 problem whose workload incidence matrix is given as:

$$w_{ij} = \begin{pmatrix} 0{,}3 & 0 & 0{,}2 \\ 0 & 0{,}9 & 0 \\ 0{,}5 & 0 & 0{,}5 \end{pmatrix}$$

where rows represent machines and columns represent parts. Suppose the machine grouping arrived at by the searching algorithm is:

Machine	1	2	3
Cell	1	2	1

This means that machines 1 and 3, respectively are in cell 1, while machine 2 is in cell 2. This implies:

$$x_{il} = \begin{pmatrix} 1 & 0 \\ 0 & 1 \\ 1 & 0 \end{pmatrix}$$

Since

$$Z= x_{11}(w_{1j} - m_{1j}) + x_{12}(w_{1j} - m_{1j}) + x_{21}(w_{2j} - m_{2j}) + x_{31}(w_{3j} - m_{3}) + x_{32}(w_{3j} - m_{3j})$$

and

$$m_{lj} = \frac{\sum_{i=1}^{m} x_{il} w_{lj}}{\sum_{i=1}^{m} x_{il}}$$

then:

$$m_{11} = \frac{x_{11}w_{11} + x_{31}w_{31}}{x_{11} + x_{31}} = \frac{0,3 + 0,5}{2} = 0,4$$

$$m_{12} = \frac{x_{11}w_{12} + x_{31}w_{23}}{x_{11} + x_{31}} = \frac{0 + 0}{3} = 0$$

$$m_{13} = \frac{x_{11}w_{13} + x_{31}w_{33}}{x_{11} + x_{31}} = \frac{0,2 + 0,5}{2} = 0,35$$

$$m_{21} = \frac{x_{22}w_{21}}{1} = 0$$

$$m_{22} = \frac{x_{22}w_{22}}{1} = 0,9$$

$$m_{23} = \frac{x_{22}w_{23}}{1} = 0$$

$$m_{lj} = \begin{bmatrix} 0,4 & 0 & 0,35 \\ 0 & 0,9 & 0 \end{bmatrix}$$

The matrix m_{lj} is then used to evaluate the objective function value.

3. HYBRID HEURISTIC

3.1. Motivation for the hybrid heuristic

Tabu search (TS) was introduced by Glover [8] as a technique to overcome local optimality. The strategic principles underlying TS have been more broadly formulated and extended which leads to the modern form of TS. Since then, TS has gained attention due to its potential for solving combinatorial problems including scheduling [6], transportation [3], layout [13] and telecommunications [14], etc. TS is a potential approach for solving the cell design problem.

Tabu search has its antecedents in methods designed to cross boundaries of feasibility or local optimality, which are normally viewed as barriers towards global optimality for existing optimal solution approaches. It systematically imposes and releases constraints to permit exploration of otherwise forbidden regions, thus, the search is able to move in and out of various intermediate local optima and explore good solutions closer to the global optimum.

A move in TS refers to a search action that perturbs the current solution to another solution. TS methods operate under the assumption that a neighbor-hood can be constructed to identify `adjacent solutions' that can be reached from any current solution through a move. Frequently, pair-wise exchanges (moves) are used to construct neighbor-hoods in permutation problems. To prevent the search from repeating exchange combinations tried in the recent past, potentially reversing the effects of previous moves by exchanges (moves) that might return to previous positions, the moves are classified tabu for a particular number of iterations called the tabu tenure. A tabu list is maintained to keep record of the attributes that are classified as forbidden (tabu). The size of the tabu list is equal to the tabu tenure and is simply referred to as tabu size. The attributes reside in the tabu list for a specified number of iterations and then are removed, freeing them from their tabu status. Several aspiration criteria may be used to override tabu status.

The tabu list is usually a circular list in which elements are added in sequence in positions 1 through tabu tenure and then started over at position 1. Empirical results have indicated that a robust range of values for tabu size exist for which such a simple tabu list performs very effectively for driving the search beyond local optima and obtaining progressively improved solutions [8]. The best value of tabu size seems to be an increasing function of the size of a problem. If it is too small, cycling will occur and if it is too big, it will constrain the search enough to skip the `deeper valleys' (i.e. better local minima) of the objective function value space [13].

Simulated annealing (SA) is a randomized version of local search that was first proposed by Kirkpatrick et al. [19]. It is based on certain analogies that exist between problems of combinatorial difficulty and large systems with many degrees of freedom, such as those normally encountered in statistical mechanics. Readers are referred to Kirkpatrick et al. [19], Van Laarhoven et al [16] and Jajodia et al [18] for the details of SA and its potential applications in solving optimization problems.

Traditionally, a sequential search method for finding an optimum begins with an initial solution and sequentially moves to a better solution in the neighbourhood until no improvements can be made. The search is frequently terminated at a local, not global, optimum. Simulated annealing (SA) is an algorithmic approach attempting to avoid the search being trapped at a local minimum by occasionally allowing unimproved moves. The generic SA procedure is outlined below.

Step 1. Define an initial solution *S*.

Step 2. Set an initial high temperature $T > 0$, cooling ratio $0 < r < 1$, and the number of times L.
Step 3. Do steps 4 and 5 until T approaches 0.
Step 4. Do L times for the following:
Step 4.1. Pick a random neighbouring solution S 0 of S.
Step 4.2. Compute Δ = cost (S') - cost (S)
Step 4.3. If $\Delta < 0$ then set $S = S$'.
Step 4.4. If $\Delta \geq 0$ then set $S = S$' with probability $\exp(-\Delta/T)$.
Step 5. Set $T = rT$ and go to step 4.
Step 6. Return solution S.
Note that the above generic SA algorithm returns only the last (best) solution obtained. In order to increase the probability of obtaining a global optimum, Rich and Knight [5] modified the generic SA to allow several good solutions to be kept in addition to the last. All these good solutions are candidates for future perturbations. The proposed algorithm utilizes a similar idea to increase the search space.

3.2. Proposed Procedure

As discussed in Section 3.1, tabu search has shown a lot of promise in the past in solving combinatorial optimization problems such as sequencing and facility layout. However, the direct application of TS to solve the GT problem requires a high degree of computational effort. In conventional TS all the pair-wise exchanges are evaluated and the exchange (move) that provides the best solution (lowest objective value) is chosen as the candidate move to perturb the present solution. For the GT problem, the neighbourhood is defined as the $\binom{n}{2}$ adjacent solutions that can be obtained by pair-wise exchanges (swaps).

Such a procedure is time consuming when applied to the integrated shortcut design problem, since ($\binom{n}{2}$-tabu size) separate optimization (GT design) problems need to be solved to identify the best move in each iteration (without considering the aspiration criterion). Moreover, some exchanges may result in infeasible sequences as discussed in Section 3. In addition, TS starts with an initial solution and improves it. Though it is a highly constrained neighbour-hood search method that overcomes the limitations of simple descent methods, some bias may exist due to the choice of the initial solution. Simulated annealing on the other hand has proven to be capable of overcoming the bias caused by different initial solution [17]. SA also requires less computation effort per iteration than TS.

The suitability of TS to solve the GT problem together with SA's computational efficiency and robustness to initial sequence motivated the development of a hybrid procedure that unites the features of these two search procedures. The hybrid procedure is likely to provide good solutions to the GT design problem in a timely fashion due to the highly constrained search process employed by the procedure together with the randomization aspects used to search the solution space. A detailed description of this combined TS and SA procedure is presented in Figure 1.

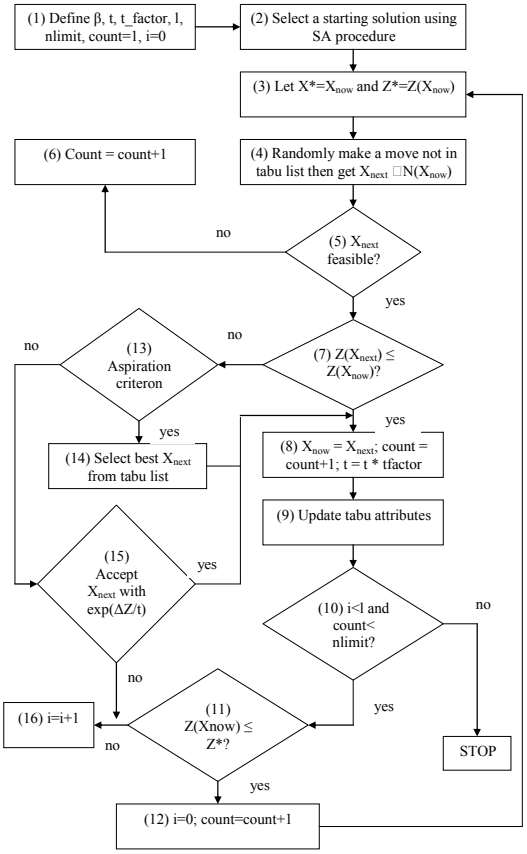

Figure 1: Flow-chart of the proposed procedure

4. COMPUTATION ANALYSIS

The proposed algorithm written in Pascal 7.0 and runs on PC with a Pentium 133 MHz. The proposed algorithm execution illustration is first given, then several set of problem types which were used are presented to compare the results with other algorithms.

		Parts														
		1	2	3	4	5	6	7	8	9	10	11	12	13	14	15
Machines	1	0	1	0	0	0	0	0	0	0	1	1	1	0	0	0
	2	0	0	1	0	1	0	0	1	0	0	0	0	1	0	1
	3	1	0	0	0	0	1	0	0	1	0	0	0	0	1	0
	4	1	0	0	1	0	0	0	0	1	0	0	0	0	1	0
	5	0	0	1	0	1	0	0	1	0	0	0	0	1	0	1
	6	1	0	0	1	0	1	0	0	1	0	0	0	0	1	0
	7	0	1	0	0	0	0	1	0	0	1	1	1	0	0	0
	8	0	0	1	0	1	0	0	1	0	0	0	0	1	0	1
	9	0	0	0	1	0	1	0	0	1	0	0	0	0	1	0
	10	0	1	0	0	0	0	1	0	0	1	1	1	0	0	0

Figure 2. Incidence matrix [11]

4.1. Algorithm execution illustration

This section provides an illustration of all internediate solutions arrived at in the solving of a machine grouping problem using the proposed algorithm. The set of input data used in this illustration is from Chan and Milner [11]. The input incidence matrix is shown in Figure 2. Number of machines is 10, number of parts is 15, minimum number of machines in a cell is 2, maximum number of machines in a cell is 6. The option for minimization of cell load variation is considered (objective function model). The results are plotted in Figure 3.

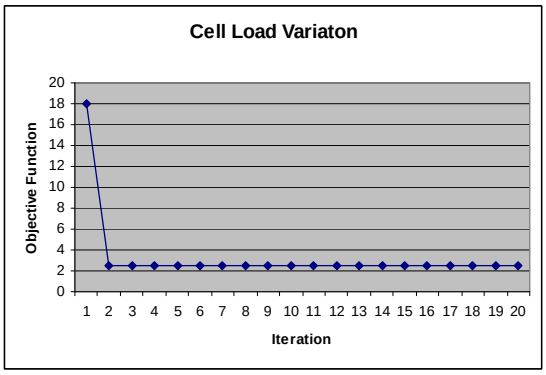

Figure 3. The proposed algorithm's objective function plots using Chan and Milner [11] data

The cell load variation drops from a value of 18 at the initial solution-state to 2.5 at the second solution state and settles at that value. This means that in the actual sense, the optimum solution was found at the fifteenth solution state even though the user indicated that the SA algorithm search through 20 solution states. The machine part grouping for the solution corresponding to the global is given in matrix form in Figure 4. The clustering efficiency is 92%.

	1	4	6	9	14	3	5	8	13	15	2	7	10	12
3	1		1	1	1									
4	1	1		1	1									
6	1	1	1	1	1									
9		1	1	1	1									
2						1	1	1	1	1				
5						1	1	1	1	1				
8						1	1	1	1	1				
1										1		1	1	1
7										1	1	1	1	1
10										1	1	1	1	1

Figure 4. Final solution

4.2. Extention computational results

We further tested the results of our algorithm with those of the TSP-based heuristic [4] and GA [9] for 5 data sets from literature. The detailed results of the further experiments are presented in Table 1. The measures frequently used in the literature are used in the present comparative study. One is grouping efficiency [15], which is defined as follows:

$$\eta = w\,\eta_1 + (1-w)\,\eta_2 \qquad (4)$$

where :
η = grouping efficiency (GE)
η_1= (o-e)/(o-e+v)
η_2= (M*P-o-v)/(M*P-o-v+e)
M= sum of machines
P = sum of parts
o= sum of 1's elements in solution matrix $\{a_{pm}\}$
e= sum of exceptional's elements in solution matrix
v= sum of *void* in solution matrix
w= weight (we use 0.5)

Table 1. Performance of the algorithm compared to TSP and GA

Number	Source	Size	Grouping efficiency (%)		
			TSP Cheng et al [4]	GA Onwubolu and Mutingi [9]	Proposed Algorithm
1	Seifoddini and Wolfe [10]	5 x 18	86.76	86.76	86.76
2	Kusiak and Chow [2]	5 x 7	87.5	87.5	87.5
3	Kusiak and Chow [3]	7 x 11	73.7	74.24	74.24
4	Boctor [7]	7 x 11	88.06	88.06	88.06
5	Carrie and Kusiak and Rajagopalan [15]	8 x 20	71.66	84.6	71.66

Table 1 shows that the proposed algorithm favorably competes with that of Onwubolu and Mutingi [9] and that both algorithms produce better solutions than Cheng et al [4], espcecially on third case [2], which is the commonly used reliable algorithm in comparative studies. In some cases our algorithm produces the same results as Onwubolu and Mutingi [9] for example solution in problems 1, 2, 3 and 4. The solutions from our algorithm in Table 1 are based on automatically generated cell size and there is the possibility that we can obtain better solutions by specifying different cell sizes and cell size capacities. Another point that needs to be addressed is that the authors of the TSP-based algorithm under the section of comparative study say:"it is not appropriate to use our objective function to evaluate the other solutions". This means that their objective function is solely dependent on the distance measures that belong to the family of Minkowski metric. In practice, a manufacturing systems engineer may want to consider only total cell load variation as objective function, or only intercellular moves as objective function, or a combination of both. This is what we have built into our algorithm: flexibility for the manufacturing systems designer.

5. CONCLUSION

This paper presents a hybrid tabu search and simulated annealing procedure for solving the GT design problem for fabrication facilities designed. A hybrid approach was developed to unite the best features of both TS and SA. This approach efficiently yields good solutions and tends to be insensitive to starting solutions. The proposed hybrid procedure can also solve many other cellular system design problems, since the cell formation, on which it is based, are commonly seen in practice. Therefore, the proposed design procedure promises to be a valuable approach for solving system design integration problems not only in GT but also in more general cellular manufacturing systems.

REFERENCES

[1] A. Gunasekaran, S.K. Goyal, I. Virtanen and P. Yli-olli, "An investigation into the application of group technology in advanced manufacturing systems," *International Journal of CIM*, Vol.7, no. 4, pp.215-228, 1994.

[2] A. Kusiak and M. Cho, "Similarity coefficient algorithm for solving the group technology problem," *International Journal of Production Research*, Vol. 30, pp.2633-2646, 1992.

[3] A. Kusiak and W.S. Chow, "Efficient solving of the group technology problem," *Journal of Manufacturing Systems*, Vol. 6, pp.117-124, 1987.

[3] B. Cao and G. Uebe, "Solving transportation problems with nonlinear side constraints with tabu search," *Computers and Operations Research*, Vol. 22, no. 6, 593-603, 1995.

[4] C.H. Cheng, C.H. Goh and A. Lee, "Designing group technology manufacturing systems using heuristics branching rules," *Computers and Industrial Engineering*, Vol. 40, pp.117-131, 2001.

[5] E. Rich and K. Knight, *Artificial Intelligence*, Second Edition, McGraw-Hill, ch. 3, pp. 71-72, 1991.

[6] E.H.L. Aarts, J.K. Lenstra. and N.L.J. Ulder, "A computational study of local search algorithms for job shop scheduling," *ORSA Journal on Computing*, Vol. 6, no. 2, pp. 118-25, 1994.

[7] F.F. Boctor, "A linear formulation of the machine part cell formation problem," *International Journal of Production Research*, Vol. 28, pp.185-196, 1991.

[8] F. Glover, "Future paths for integer programming and links to artificial intelligence," *Computers and Operations Research*, Vol. 5, pp.533-49, 1986.

[9] G.C. Onwubolu and M. Mutingi, "A genetic algorithm approach to cellular manufacturing systems," *Computers and Industrial Engineering*, Vol. 39, pp.125-144, 2001.

[10] H. Seifoddini and P.M. Wolfe, "Application of the similarity coefficient method in group technology," *IIE Transactions*, Vol. 18, pp.271-277, 1986.

[11] H.M. Chan and D.A. Milner, "Direct clustering algorithm for group formation in cellular manufacture," *Journal of Manufacturing Systems*, Vol. 1, no. 1, 64-76, 1982.

[12] I. Ham, K. Hitomi and T. Yoshida, *Group technology*. Boston: Kluwer-Nijhoff, USA, 1985.

[13] J. Skorin-Kapov, "Extensions of a tabu search adaptation to the quadratic assignment problem," *Computers and Operations Research*, Vol. 21, no. 8, pp.855-65, 1994.

[14] M. Laguna and F. Glover, "Bandwidth packing: a tabu search approach," *Management Sciences*, Vol. 39, no. 4, pp.492-500, 1993.

[15] M.P. Chandrasekaran and R. Rajagopalan, "An ideal seed non-hierarchical clustering algorithm for cellular manufacturing," *International Journal of Production Research*, Vol. 24, pp.451-464, 1986.

[16] P.J.M. Van Laarhoven, E.H.L. Aarts and J.K. Lenstra, "Job shop scheduling by simulated annealing," *Operations Research*, Vol. 40, no. 1, pp.113-125, 1992.

[17] R.D. Meller and Y.A. Bozer, "A new simulated annealing algorithm for the facility layout problem," *International Journal of Production Research*, Vol. 34, no. 6, pp.1675-1692, 1996.

[18] S. Jajodia, I. Minis, G. Harhalakis and J.M. Proth, "CLASS: computerized layout solutions using simulated annealing," *International Journal of Production Research*, Vol. 30, no. 1, pp.95-108, 1992.

[19] S. Kirkpatrick, Jr.C.D. Gflat and M.P. Vecchi, "Optimization by simulated annealing," *Science*, Vol. 220, pp.671-680, 1983.

[20] T.J. Greene and R.P. Sadowski, "A review of cellular manufacturing assumptions, advantages and design techniques," *Journal of Operations Management*, Vol. 4, pp.85-97, 1984.

[21] V. Venugopal and T.T. Narendran, "A genetic algorithm approach to the machining grouping problem with multiple objectives," *Computers and Industrial Engineering*, Vol. 22 no. 4, pp.469-480, 1992.

ISSN 114-1284

The Influence of Collaboration to the Supply Chain Performance (A Survey on Modern Retails at DKI Jakarta and Bandung City)

Agus Purnomo
Industrial Engineering Department
Engineering Faculty – Pasundan University Bandung 40153
e-mail : nrpsga@yahoo.com ; aguspurnomo@unpas.ac.id

ABSTRACT

The competition paradigm in modern retail has recently been changed, from the former, intercorporate competition into inter supply chain network. The improvement of Retail Supply Chain Performance seem to be the main demand to win high competition. Some questions of the study include : first, how does The Collaboration happen ? Second, how does The Supply Chain Performance happen ? And third, how far is the influence of Information Collaboration, Decision Synchronization Collaboration, Incentive Alignment Collaboration, and Organization Collaboration to The Modern Retailer Supply Chain Performance either partial or simultaneous. The study was conducted as descriptive and verification method in which the causality was used as a type of investigation. This study was under taken in Hypermarket, Supermarket, and Minimarket. Number of sample are 207, while the empirical way of testing to examine hypotheses, the author used Structural Equation Modeling (SEM) processed by Lisrel 8.30 software for windows NT. Research findings indicate that; (1) There are some positive and significant influence between Information Collaboration to The Modern Retailer Supply Chain Performance; (2) There are some positive and significant influence between Decision Synchronization Collaboration to The Modern Retailer Supply Chain Performance; (3) There are some positive and significant influence between Incentive Alignment Collaboration to The Modern Retailer Supply Chain Performance; (4) There are some positive and significant influence between Organization Collaboration n to The Modern Retailer Supply Chain Performance; (5) There are some simultaneously positive and significant influence between Information Collaboration, Decision Synchronization Collaboration, Incentive Alignment Collaboration, and Organization Collaboration to The Modern Retailer Supply Chain Performance. Based on the findings above the author concludes that Collaboration in Supply Chain between Modern Retailers and Key Suppliers are significantly able to enhance The Modern Retailer Supply Chain Performance.

Keywords : *Information Collaboration, Decision Synchronization Collaboration, Incentive Alignment Collaboration, Organization Collaboration, Supply Chain Performance.*

1. INTRODUCTION

Supply chain collaboration has become a new imperative strategy for companies to create competitive advantage [12]; [25]. A closer relationship enables the participating companies to achieve cost reductions and revenue enhancements as well as flexibility in dealing with supply and demand uncertainties [5]; [18]. Hewlett-Packard (HP), for instance, initiated collaboration with one of its major resellers [7]. These collaborative efforts, which focused on co-managed inventory by considering different levels of demand uncertainty, enabled both parties to improve fill rate, increase inventory turnover, and enhance sales. Similarly, Wal-Mart collaborated in demand planning and replenishment with its major suppliers to increase inventory turns, reduce inventory costs, reduce storage and handling costs, and improve retail sales [21]. Supply chain collaboration requires a reasonable amount of effort from all participating members to ensure the attainment of potential benefits [3]; [9]. The chain members also search for better practices and ideas through benchmarking their current collaborative practices to other collaborative supply chains. To achieve higher supply chain efficiencies, the various members of the supply chain are presumed to share information and trust one another. According to Supply Chain Management (SCM) theory, the level of collaboration depends on the nature of relationships (e.g., the frequency of the contact, the level of trust, etc.) and the application of advanced information technologies such as collaborative forecasting [11]; [19]. Improving relationships among the members of the supply chain in turn leads to cost reductions and higher levels of customer service [26].

The growth of modern retail in DKI Jakarta and Bandung is higher than the other cities in Indonesia. This certainly will cause the level of competition inter modern retailer become more and more tight. Thus the retail supply chain performance seems to be the most important demand to win the strict competition. The increase of retail supply chain performance would expectedly reached through collaboration with suppliers in form of information Collaboration, Decision Synchronization Collaboration, Incentive Alignment Collaboration, and Organization Collaboration. Some questions of the study include : first, how does The Collaboration happen ? Second, how does The Supply Chain Performance happen ? And third, how far is the influence of Information Collaboration, Decision Synchronization Collaboration, Incentive Alignment Collaboration, and Organization Collaboration to The Modern Retailer Supply Chain Performance either partial or simultaneous.

2. LITERATURE REVIEW

Collaboration between supply chain partners has been covered extensively in the strategic management literature [6]; [16]. Other researchers have examined the

theoretical implications of supply chain collaboration through unilateral supply policies [14]; [27]. Other researchers have employed theoretical models to examine bilateral information exchange rather than unilateral policy incentives [10]; [20]. The practitioner-oriented research into supply chain collaboration tends to focus on the emerging concept of Collaborative Planning, Forecasting and Replenishment (CPFR) and Vendor Managed Inventory (VMI) [1]. Though rigorously reported empirical data are rare, [15] presents results for 31 grocery retail chains that adopted Campbell's continuous replenishment process and showed a significant improvement in inventory turns and a simultaneous reduction in stock-outs. Sharing of physical assets as suggested by our concept of structural supply chain collaboration has been examined in pieces but not holistically. For example, [8] examine the benefit of coordinated shipments to improve truck utilization.

The definitions of collaboration made by researchers as well as column writers in business magazines are not incongruous, nor are they ever the same; it seems extremely difficult to develop a general one-sentence definition of collaboration [4]. Collaboration can (similar to [19]) understanding of the SCM term), be considered to contain two different things. First, collaboration can be characterized as a certain type of relationship between independent companies or functions in a company where trust, win-win thinking, commitment and openness are important ingredients [20]; [21]; [22]. Second, collaboration also consists of activities that are performed by the participating actors within the collaboration [19]. Collaboration within the logistics area, which is the focus in this dissertation, typically means sharing information and jointly negotiating and deciding upon logistics activities in the supply chain such as transportation and inventory. This means a two-way communication with jointly, voluntary agreed goals [23]. Since collaboration should contribute to improvements in the supply chain, the possibility for the involved parties to influence the collaboration is important; otherwise there is a risk that major opportunities for improvements can be lost as well as the win-win situation [13]; [24]

Collaboration variable in the research is grouped as follow :

1) *Information Collaboration*
   Cooperation amongst collecting and disseminating relevant and functual information using all resources to make decision, planning, and supply chain operation. The collaboration indicators include : Demand Forecasting, Sales Administration, Inventory level, Promotion Plan, Delivery Schedule, Information Technology [23].
2) *Decision Synchronization Collaboration*
   Cooperation of decision making is based on adjustment of planning and supply chain operation standard. Collaboration indicators include : Purchasing, Target Market, Price Policy, Service Level [22]; [2].
3) *Incentive Alignment Collaboration*
   Cooperation of risk equivalent regulation and benefit which is caused by planning and supply chain operation. Administrative fee and utilizing technology are normally handed together amongst members of supply chain to keep commitment. Collaboration indicator include: Discount Program, Research & Development, Inventory Management, Product Warranty [22]; [2]
4) *Organization Collaboration*
   Collaboration organization and making use of cross firm function focusing on planning and supply chain operation. The collaboration indicators are : Information Technology Implementation, Supply Chain Design, Customer Satisfaction Measurement [2].

Based on the problem faced by modern retailers and relevant literature study. The research paradigm shows as follow :

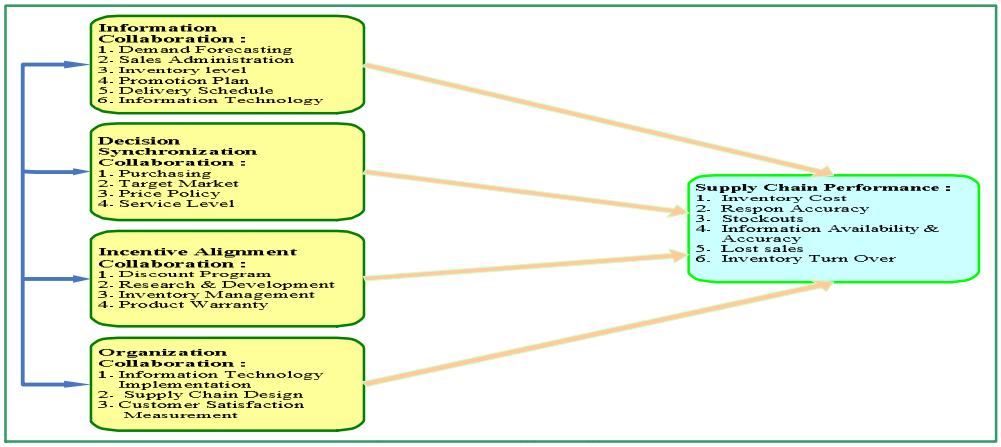

Figure 1. Research Paradigm

State of the art for this research presented in table 1 below:

Table 1. Research State of The Art

No	Authors	Year	Research Title	Type of Collaboration				Analysis Technique
				Infor-mation	Decision Synchronization	Incentive Alignment	Organi-zation	
1	Patnayakuni and Patnayakuni	2002	Towards a Theoritical Framework of Digital Supply Chain Integration	✓				Linier Regres-sion
2	Dooley and King	2004	Efficient Consumer Response and the Importance of Collaboration for Supermarkets	✓				Linier Regres-sion
3	Simatupang and Ramaswami Sridharan	2005	The collaboration index: a measure for Supply Chain collaboration	✓	✓	✓		Index
4	Prabir K. Bagchi and Tage Skjoett-Larsen	2005	Supply Chain Integration: a European Survey		✓	✓	✓	Path Analysis
5	J. Taco Van der Vaart and Dirk Pieter Van Donk	2007	Supply Chain Integration and Performance : The Impact of Business Conditions.	✓				Correla-tion
6	Agus Purnomo	2008	The Influence of Collaboration to The Supply Chain Performance (A Survey on Modern Retails at DKI Jakarta and Bandung City)	✓	✓	✓	✓	SEM

3. RESEARCH METHOD

Research methods used in this study are descriptive and explanatory survey. In descriptive survey, the researcher wants to have a description about level of collaboration which aims to headwaters (key distributor). It has been conducted by retailers from DKI Jakarta and Bandung. Explanatory survey is captured out in to 250 head gerai hypermarket, supermarket, and mini market in DKI Jakarta and Bandung as sample. The purpose of the survey is to know how is the correlation inter variable amongst information collaboration, Decision Synchronization Collaboration, Incentive Alignment Collaboration, and Organization Collaboration to The Modern Retailer Supply Chain Performance, through hypothesis test. Investigation type used in the research is causality, a kind of research type stating the existence of causal correlation of research variable between independent variable and dependent variable. Data analysis has been completed by using quantitative method. It is statistically tested the hypothesis used Structural Equation Modeling (SEM) processed by software Lisrel 8.30 for Window NT.

Stuctural Equation Model shows the correlation between endogenous latent variable and exogenous latent variable as following formula:

$$Y = \gamma_{Y1}X_1 + \gamma_{Y2}X_2 + \gamma_{Y3}X_3 + \gamma_{Y4}X_4 + \zeta_y$$
……..……(1)

Where : Y=Supply Chain Performance; X_1= Information Collaboration; X_2= Decision Synchronitiozan Collaboration; X_3= Incentive Alignment Collaboration; X_4= Organization Collaboration; $\gamma_{1y}\, s.d\, \gamma_{4y}$ = influence value exogenous latent variable to endogenous latent variable.

Figure 2 below describes a research model for all variables in SEM diagram form.

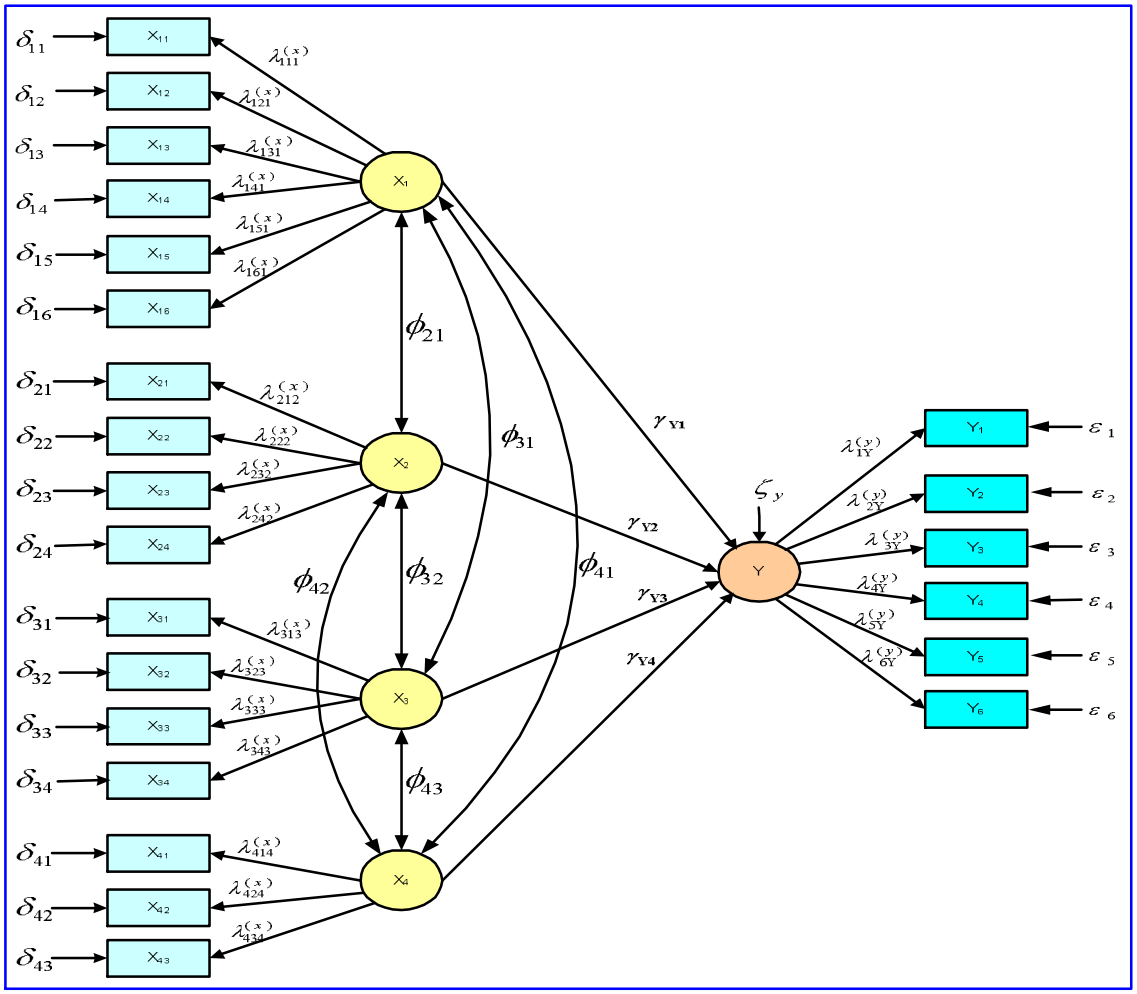

Figure 2. Research Model in the Form of SEM Diagram for All Variables

4. FINDINGS

Based on 207 respondent, the retailer characteristic description based on communication and information technology which is used in collaboration with key suppliers (figure 3) shows that 100% of minimarkets used telephone/facsimile to have communication and information exchange when they collaborate with their key suppliers. While 85,33% supermarket used telephone/facsimile in the same time with 14,67% electronic data interchange (EDI) to exchange information and communication when collaborating with key suppliers, 41,54% hypermarkets used telephone/facsimile, Electronic Data Interchange/EDI (41,54%) and 16,92% esupply Chain Management / eSCM to have communication and information exchange when collaborating with key suppliers.

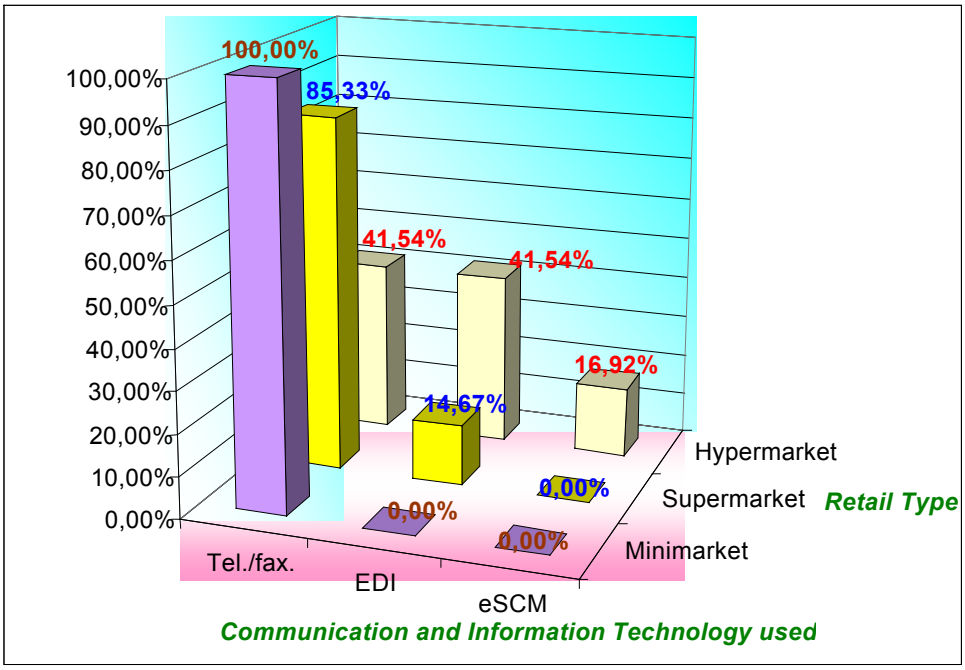

Source : questioner (n=207), 2009

Figure 3. Characteristics of Retailers according to Communication and Information Technology used in Collaboration with Key Suppliers

The description of retailers characteristic according to arrangement collaboration constraint with key suppliers (figure 4) are: first, insufficiency of information and technology equipment (25,12%), second, unsynchronized in decision making (23,19%), third, unequivalency of giving risk and benefit (19,81%), fourth, interfims unreliability and fifth, less of logistic competency (14,01%). According to the description above, we find that the insufficient of information technology equipment has placed the first constraint in collaboration with suppliers. It is relevant to communication and information technology which is used by retailers collaborating with key suppliers mostly used telephone/facsimile.

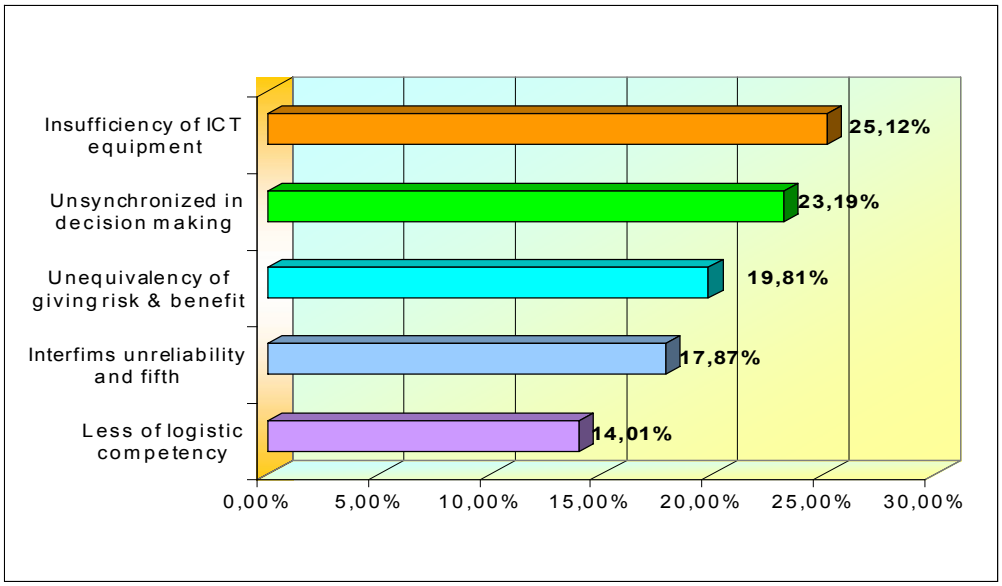

Source : resulted from questioner (n=207), 2009

Figure 4. Retailer characteristic according to the arrangement of collaboration constraints with key suppliers

The result of validity test in correlation with product moment and reliability test using Alpha Cronbach Test, show that each value is significant, the data is valid to be processed with Structural Equation Modeling (SEM) using software Lisrel 8.30.

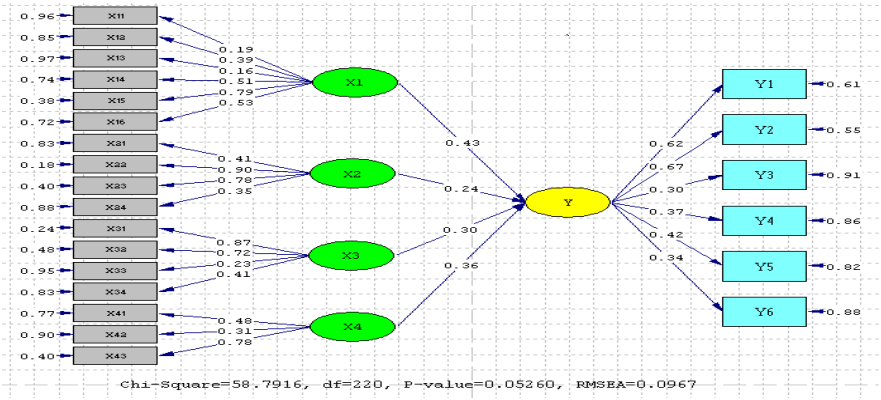

Source : Processed from questioner (n=207) with *software* Lisrel 8.30, 2009

Figure 5. Complete Stripe Diagram Standardized Solution
The Effect of Collaboration to Supply Chain Performance

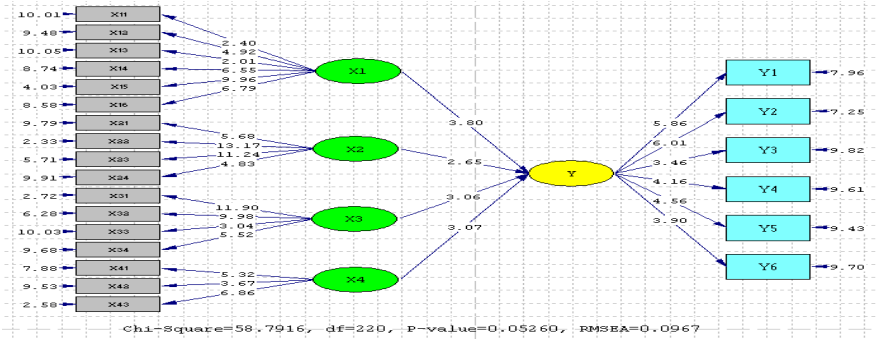

Source : Processed from questioner (n=207) with *software* Lisrel 8.30, 2009

Figure 6. T – Value Complete Stripe Diagram
The Effect of Collaboration to Supply Chain Performance

Structural model test is done according to Figure 6 the result shows the existence of positive and significant correlation Exogenous Latent Variable (Information Collaboration / X_1, Decision Synchronization Collaboration / X_2, Incentive Alignment Collaboration / X_3 and Organization Collaboration X_4 with Endogenous Latent Variable (supply chain performance / Y). The model compatibility test used Goodness – of – Fit – Test (GOF) presented in table 2.

Table 2. Goodness-of-Fit-test Summary

GOF Value	Estimation	Critical value	Test Result
Nilai *P*	0.0526	*P* > 0,05 : model *fit*	Model fit to data
RMSEA	0.0967	RMSEA < 0,8 : model *fit*	
GFI	0.9710	GFI > 0,9 : model *fit*	
AGFI	0.9876	AGFI > 0,9 : model *fit*	
NFI	0.9763	NFI > 0,9 : model *fit*	
NNFI	0.9725	NNFI > 0,9 : model *fit*	

Source : Processed from questioner (n=207) with *software* Lisrel 8.30, 2009

The result of computation influence decomposition between exogenous latent variable and endogenous latent variable supply chain performance (Y), can be concluded that exogenous latent variable (information collaboration (X_1) showed the bigger total causal effect (TCE) compared to endogenous latent variable supply chain performance (Y), namely 0,4269. Meanwhile, exogenous latent variable of decision synchronization collaboration (X_2) showed the smallest TCE compared to endogenous latent variable supply chain performance (Y), it is 0,2390. While exogenous latent variable organization collaboration (X_4) and incentive

alignment collaboration (X_3) showed the averaged TCE compared to endogenous latent variable supply chain performance (Y) one after the other, 0,3644 and 0,3010.

The explanation of hypothesis test found that information collaboration, decision synchronization collaboration positively and significantly influenced to the modern retailer supply chain performance, meaning that descriptively collaboration, decision synchronization collaboration, incentive alignment collaboration and organization collaboration have been applied and appropriately used by the modern retailer and key supplier in DKI Jakarta and Bandung. The successful of implementing collaboration, decision synchronization collaboration, incentive alignment collaboration and organization collaboration will hopefully increased the modern retailer supply chain performance inform of : lower inventory cost, accuracy respond, lower stock outs, information availability and accuracy, lower lost sales and higher inventory turn over.

5. Conclusion

The research has completely considered the collaboration aspect related to supply chain performance between the modern retailers and key suppliers namely about information collaboration, decision synchronization collaboration, incentive alignment collaboration and organization. The result of the study shows that there are some partial and simultaneously positive and significant influence between Information Collaboration, Decision Synchronization Collaboration, Incentive Alignment Collaboration, and Organization Collaboration to The Modern Retailer Supply Chain Performance. Based on the findings above the author concludes that Collaboration in Supply Chain between Modern Retailers and Key Suppliers are significantly able to enhance The Modern Retailer Supply Chain Performance.

Information Collaboration resulted the biggest TCE compared to supply chain performance, it means that employing the appropriate information and communication technology would become the main determination to improve the modern retailer chain performance.

REFERENCES

[1]. Aviv, Y. : Gaining benefits from joint forecasting and replenishment processes: the case of auto-correlated demand. *Manufacturing & Service Operations Management,* 4(1), 2002, pp. 56-74.

[2]. Bagchi, P. K. and Skjoett-Larsen,T. : Supply Chain Integration: a European Survey. *International Journal of Logistics Management*, 16(2), 2005, pp. 275-294.

[22]. Skjoett-Larsen, T., C. Thernoe and C. Andresen : *Supply chain collaboration Theoretical perspectives and empirical evidence.* International Journal of Physical Distribution and Logistics Management, 33 (6), 2003.

[23]. Simatupang, T. M. and R. Sridharan : *The collaborative supply chain.* International Journal of Logistics Management, 13 (1), 2002.

[3]. Barratt, M. and Oliveira, A. : "Exploring the experiences of collaborative planning initiatives", International Journal of Physical Distribution & Logistics Management, Vol. 31 No. 4, 2001, pp. 266-89.

[4]. Barratt, M. : *Understanding the meaning of collaboration in the supply chain.* Supply Chain Management: An international journal, 9 (1), 2004, pp. 30-42.

[5]. Bowersox, D.J. : "The strategic benefits of logistics alliances", *Harvard Business Review*, Vol. 68 No. 4, 1990, pp. 36-43.

[6]. Bradenburger, A. and B.J. Nalebuff : Co-opetition: A revolutionary mindset that redefines competition and cooperation in the marketplace. New York. Doubleday, 1996.

[7]. Callioni, G. and Billington, C. : "Effective collaboration: Hewlett-Packard takes supply chain management to another level", OR/MS Today, Vol. 28 No. 5, 2001, pp. 34-9.

[8]. Cheung, K.L. and H.L. Lee. : The inventory benefit of shipment coordination and stock rebalancing in a supply chain. *Management Science,* 48(2), 2002, pp. 300-306.

[9]. Corbett, C.J., Blackburn, J.D. and van Wassenhove, L.N. : "Partnerships to improve supply chains", Sloan Management Review, Vol. 40 No. 4, 1999, pp. 71-82.

[10]. Governing, S. : Information flows in capacitated supply chains in fixed ordering costs. *Management Science*, 48(5), 2002, pp. 644-651.

[11]. Handfield, Robert B. and Ernest L. Nichols. *Introduction to Supply Chain Management.* Upper Saddle River, NJ*:* Prentice Hall, 1998.

[12]. Horvath, L. : "Collaboration: key to value creation in supply chain management", Supply Chain Management: An International Journal, Vol. 6 No. 5, 2001, pp. 205-7.

[13]. Ireland, R. and R. Bruce : *CPFR Only the beginning of collaboration*. Supply Chain Management Review, Sept/Oct, 2000.

[14]. Klastorin, T.D., K. Moinzadeh, et al. : Coordinating orders in supply chains through price discounts. *IIE TransactionsI,* 34(8), 2002, pp. 679-689.

[15]. Lee et al. : "The bullwhip effect in supply chains", Sloan Management Review, Vol. 38 No. 3, 1997, pp. 93-102.

[16]. Laseter, T.M. : *Balanced sourcing: cooperation and competition in supplier relationships.* San Francisco. Jossey-Bass Publishers, 1998.

[17]. Lee, H.G., T. Clark, et al. : Research report. Can EDI benefit adopters? *Information Systems Research*, 10(2), 1999, pp.186-195.

[18]. Lee, H. L. and S. Whang : *Information sharing in a supply chain.* International journal of Technology Management, 20 (3/4), 2000, pp. 373-87.

[19]. Mentzer, et al. : "Defining Supply Chain Management." *Journal of Business Logistics,* 22(2), 2001, pp. 1-25,

[20]. Moinzadeh, K. :. A multi-echelon inventory system with information exchange. *Management Science,* 48(3), 2002, pp. 415-426.

[21]. Parks, L. : "CRP investment pays off in many ways", Drug Store News, Vol. 21 No. 2, 1999, pp. 26.

[24]. _____. : Benchmarking supply chain collaboration. *Benchmarking: An International Journal*, Vol. 11 No. 5, 2004, pp. 484-503.

[25]. Spekman et al. : "An empirical investigation into supply chain management", International Journal of Physical Distribution & Logistics Management, Vol. 28 No. 8, 1998, pp. 630-50.

[26]. Svensson, Goran. "A Firm's Driving Force to Implement and Incorporate a Business Philosophy into its Current

Business Activities: the Case of ECR." *European Business Review,* 14(1), 2002, pp. 20-29,

[27]. Taylor, A.T. : Supply chain coordination under channel rebates with sales effort effects. *Management Science*, 48(8), 2002, pp. 992-1007.

ISSN 114-1284

Integration of ISO/ IEC 17799:2005 and ISO/ IEC 2700:2005 in the Information Technology Department of a Bank's Balanced Scorecard to become 4th Generation Balanced Scorecard

Akhmad Hidayatno[1], Distya Tarworo Endri[2]

[1]*Industrial Engineering Department, Faculty of Engineering*
University of Indonesia, Depok 16424
Tel : Tel : (021) 78888805 Fax (021) 78885656
E-mail : akhmad.hidayatno@ui.edu

[2]*Industrial Engineering Department, Faculty of Engineering*
University of Indonesia, Depok 16424
Tel : (021) (021) 78888805 Fax (021) 78885656
E-mail : distya_ti@yahoo.com

ABSTRACT

In accordance with advancement of technology, so does incremental business interconnectivity of Bank D through Information Technology . This will bring along a larger amount and variation of threats and vulnerabilities towards IT security. Therefore, support system and IT resources enhancement becomes critical. With this concern, the requirements of ISO/ IEC 17799:2005 and ISO/ IEC 27001:2005 on Information Security should be integrated to Information Technology Department of Bank D Balanced Scorecard. This is known to be 4th generation of Balanced Scorecard. This research is dedicated to find methods of putting 4th generation of Balanced Scorecard into practice at Bank D.
The methods that we have developed is based on Analytical Hierarchy Process, which complementing the risk management process that is the heart of ISO requirements.

Keywords

4G Balanced Scorecard, Information Security, Risk Management, Analytical Hierarchy Process, ISO 27001:2005

1. INTRODUCTION

In order to attain the vision and mission while completing major duties of Bank D, information technology support is required. Therefore, vision and mission at Information Technology Department was established. The vision and mission make use of 3rd generation of Balanced Scorecard as management and measurement system of information technology. Balanced Scorecard helps organization to define key success, determine relationship between the key success, and develop the measurement that is appropriate to evaluate information technology performance.[1]

On the other hand, Bank D strives to increase information security performance by implementing Information Security Management System (ISMS) of ISO/ IEC 27001:2005 certification. The certification is able to control information technology based on practice guidance in ISO/IEC 17799:2005. [2]

If we could combine both requirements, the organization could benefits from more effective and efficient performance measurement which is related to risk management. The 4th generation of Balanced Scorecard which balance the profit earning strategy and the internal control strategy based on Sarbanes-Oxley do this. [3]

Fourth generation of Balanced Scorecard brings benefits to improve internal control, further understanding to entity of process, detect risk in internal process earlier, as tool of making effective internal audit program, increase transparency and accountability, show the gap between target and real condition of internal process, increase organization's value, and assure internal process control that is easy to be traced and improved in the next periods or is called Kaizen.

This research aims to obtain integration methodology of ISO/ IEC 17799: 2005 and ISO/ IEC 27001:2005 into Information Technology Department's Balanced Scorecard to become 4thBalanced Scorecard.

2. METHODS

Risk is the condition where there is a gap between result and expected outcome.[4] Risk of information technology based on Internasional Standard Organization is potential condition that threat will cause vulnerability to an asset or more so that the asset lost or broken.[5] Asset in information system is something that is attempted to be protected [6].

Operational risk is the lost risk of insufficient or failure of internal process, people, and system, or external events [7]. Components of operational failures are operational failure risk in running business and operational strategy risk from external factor [8]. Operational risk could be classified by people, relationship, process and technology, physical, and other external risks[9].

Threat is potential of vulnerability from threat source. Threat source is any condition or event that potentially causes lost in information technology. Vulnerability is the lack of security system in procedure, design, implementation, or internal control that can make security policy disruption. Likelihood is the probability where there is any potential vulnerability that can happen because of threat in an environment. Impact is the result of vulnerability that can be described as one or combination of integrity, availability, and confidentiality.

Steps of Information Security Management System (ISMS) implementation [5] are planning ISMS, implementing and conduction ISMS, monitoring and evaluating ISMS, and maintaining and improving ISMS.

Balanced Scorecard is a method to translate mission and strategy of company to a comprehensive measurement and give framework of strategic management and measurement. Four perspectives of Balanced Scorecard are financial, customer, internalbusiness process, and learning and growth.

The Balanced Scorecard for Sarbannes Oxley Act (4th generation of Balanced Scorecard) as the improvement of 3rd generation of Balanced Scorecard that has been applied by many companies. [3] The previous generations is as follows [10]:

a) 1st generation "Multimodal Assessment Tool" the additional nonfinancial perspectives to measure performance–learning and growth, internal business, process, and customers – to represent major stakeholders in business [11]
b) 2nd generation "Top Down Management Tool" that is the beginning of strategic goal concept where there is additional essential of organization strategy to each perspective of 1st generation of Balanced Scorecard [12]
c) 3rd generation "Knowledge-creating and Strategic Communication Tool" (based on strategy map) where there is strategy map that can give illustration of critical aim of organization and relationship between Key Performance Indicator from each perspective

Since risk that is related to daily operation changes everyday, company has to communicate important information and monitor every risk sign to prevent failure of external audit. Balanced Scorecard for SOX canhelp company, top management, director, and stakeholder. It makes use of 3rd generation of Balanced Scorecard as the basis. Profit earning strategy is still reflected but then added by internal control. Based on risk control matrix, key risk indicator (KRI) of each risk has a role as lagged indicator and key control indicator (KVI) of each control has a role as leading indicator.

The selection of indicators is important. Some consideration of indicator selection are metric that is suitable to risk, represent stakeholders, has support from senior management, understand risk indicator versus performance indicator, simple and understandable, consistent framework, quantifiable, invest in technology, use escalation criteria, and indicator as work in progress [13]. Other considerations include characteristics and effective key risk indicators are based methodology and consistent standard; related to risk factor: source, likelihood, impact, and correlation; quantifiable; could be traced by time; support goal, risk owner, and risk standard category; balance between leading and lagging indicators; useful to the decision and management action; could be compared internally and externally; time and cost efficient; and risk could be simplified without losing its real meaning [14].

Recommended steps to make indicator are identify indicators in organization, gap assessment, indicator improvement, validation and target level determination, dashboard design, make a control plan and escalation criteria [15].

In order to simplify the fulfillment of multiple criteria, we will use the priority matrix [16]

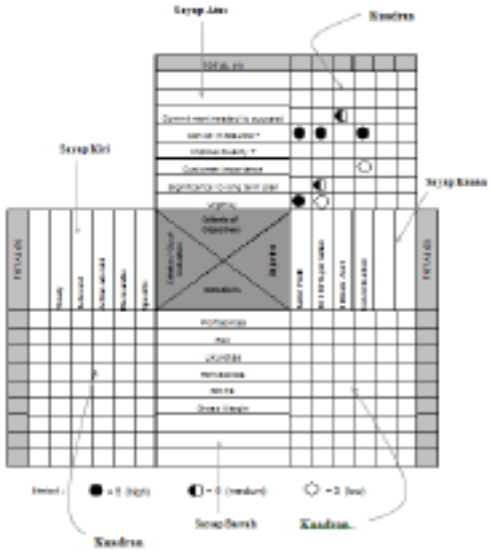

Figure 1: Example of Priority Matrix [14]

We can identify all potential indicators to measure each perspective.. Priority matrix was designed so that company just need 1 simple matrix to select the alternatives with

ISSN 114-1284

scoring: 9 for strong relationship, 6 for medium relationship, 3 for weak relationship, and 0 for no relationship.

Since Bank D is the 1st bank in Indonesia that has applied 3rd generation of Balanced Scorecard and ISO/ IEC 17799:2005 and ISO/IEC 27001:2005, research uses expertise judgment in those two fields. Experts criteria are very important in AHP. [17]

The respondents of research are:

a) Information Technology Department of Bank D that has been and had been KPI manager of Information Technology of Bank D and security officer ISO/ IEC 17799:2005 and ISO/ IEC 27001:2005
b) Project leader of ISO/ 27001:2005 certification project.

Based on the educational background, four respondents have information technology, Telecommunication and Balanced Scorecard background. They also have been employees there for 11 – 14 years with experience as KPI manager of Information Technology of Bank D for ±3 years. Beside that, the experience of ISO/IEC 17799:2005 and ISO/ 27001:2005 is ranging between 1 until 3 years.

Based on Saaty, (personal communication, October 12, 2003) if there is no expert in a subject of research, a lot amount of respondents won't be enough. If there is just 1 expert who knows everything, it is sufficient to make a good scaling.

3. DISCUSSION

Figure 2 show the complete methodology by combining all the elements necessary from all perspectives. Each process and aspect of ISO/ IEC 17799:2005 and ISO/ IEC 27001:2005 that is integrated into Balanced Scorecard to become 4th generation Balanced Scorecard used experts that make use of both qualitative – problem definition – and quantitative aspects – judgment and importance level.

Risk selection criteria determination was based on input from 1st step of ISMS implementation which is ISMS planning and 3rd step deliverable which is risk profile. On the other hand, indicator selection criteria alternatives are from Budgeting Planning and Performance Management of Bank D with flexibility of additional criterion.

Indicator selection criteria weighting was conducted by pair wise comparison from Analytical Hierarchy Process (AHP) method. From this weighting result, we could recognize the importance level of each criterion to be consideration of Information Technology Department to make decision of selecting implemented KRI and KCI.

After selecting risk, KRI and KCI determination made use of priority matrix. Input of KRI and KCI were from 4 steps of ISO/ IEC 17799:2005 and ISO/ IEC 27001:2005. Selected KRI and KCI would be the input for risk control matrix creation.

Risk control matrix is a requirement that is needed for developing Balanced Scorecard. It was from Risk Assessment of Policy Division, Operational Division, and Administration Division of Information Technology Department selected KRI and KCI.

Relationship determination between KRI, KCI, and KPI of Information Technology Department of Bank D is the basis for identifying and assessing ISMS implementation support to KPI from internal business perspective. It is also the development of 3rd generation of Balanced Scorecard to become 4th generation of Balanced Scorecard at Information Technology Department of Bank D.

Then criteria of risk and indicator were selected. Criteria for risk are risk happens to critical assets and it has to controlled risk. Criteria for indicator are align to strategic target of department and can be controlled, quantifiable, capable of illustrating previous performance and current performance, specific and explicit, data could be quantified periodically, realistic, time bound, and understandable.

Data processing for weighting indicator selection criteria was conducted by averaging all respondents' score by geometric average [18]. Then, by using Expert Choice Software, weight for each criterion and inconsistency ratio was assessed based on distributive mode.

Using priority matrix, all risks of Policy Division, Operational Division, and Administration Division of Information Technology Department 26 risks are selected based on criteria.

In indicator selection several steps were conducted:

a) Make total of 1st quadrant – respondents' assessment of selected risk and KRI- and 2nd quadrant – respondents' assessment and KCI. After that, sorting KRI and KCI which has highest and 2nd highest total with minimum score of 24.
b) Make total of 3rd quadrant – KRI and indicator selection criteria – and 4th quadrant – KPI and indicator selection criteria. Both quadrant are for assessing the ability of

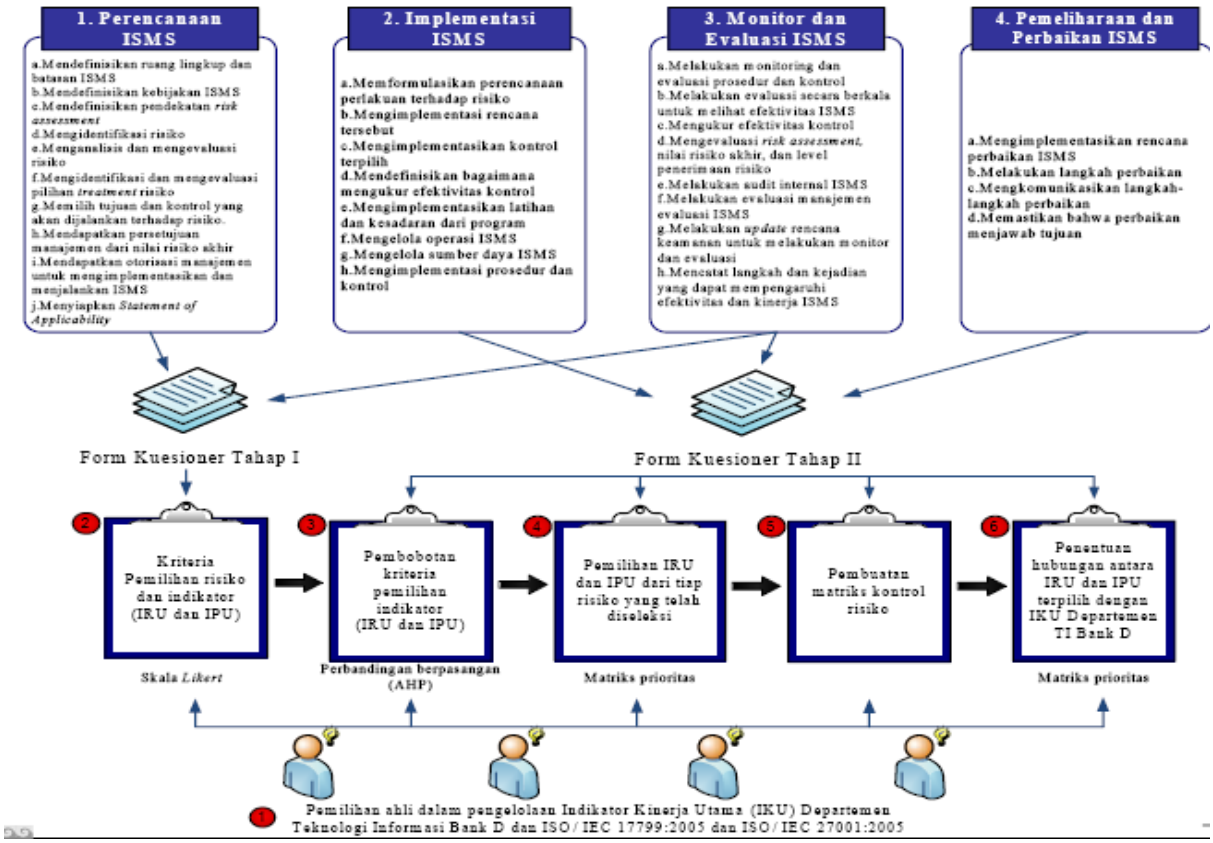

Figure 2 Methodology for the integration of Risk Management from ISO/IEC 27001:2005 into the Balanced Scorecard

c) KRI and KCI to fulfill indicator selection criteria. After that, the total was multiplied by weight of each criterion
d) Confirm those selected KRI and KCI to the respondents

Table 1 Example of Selected KRI and KCI

No	Risk	Key Risk Indicator (KRI)	Key Control Indicator (KCI)
1	The lack of physical security of Director's and Vice Director's Room causes unexpected access that affects authorization process	Measurement of Losing and Damaged Asset in Director's and Vice Director's Room	Measurement of Access Control Compliance
2	Unappropriate asset maintenance causes thermal control can not be used because of damaged components	Measurement of thermal Control Availability	Measurement of Asset Maintenance Level
			Measurement of Incident Corrective effectiveness

After KRI and KCI of each risk had been selected, risk control matrix of Information was constructed. The example of risk control matrix can be seen in table 2. The aim for creating risk control matrix is to identify KRI, KCI, and whole plan of risk mitigation.

Data processing to determine the relationship between KRI and KCI and KPI of Information Technology Department of Bank D was conducted by making total of 3rd quadrant that contains assessment of relationship between KRI and KPI and 4th quadrant that contains assessment of KCI and KPI.

The example of this relationship is the relationship between KRI "performance level of mainframe" and KCI "maintenance level of asset" with KPI "downtime percentage of critical applications and email".

No	Asset	Risk Classification	Description	Likelihood	Impact	KRI	Control Activities	KCI
9	Director and Vice Director's Room	Operational Risk	Lack of control in access control could potentially cause unexpected access to Director and Vice Director's room so that results in authorization process of Informatio Technology Department (e.g. missing information)	Level 7	Level 7	Measurement of Losing and Damaged Asset in Director's and Vice Director's Room	- Bank D Regulation about Registration and Nonactivation of Access Rights of User - Access Rights Evaluation Regulation - Physical Access Control	Measurement of Access Control Compliance

Table 2 Example of Risk Control Matrix

4. CONCLUSION

ISO/ IEC 27001:2005 into Information Technology Department Balanced Scorecard to become 4th generation of Balanced Scorecard could be applied by these steps:

a) Selection of Expert Respondents
b) Determine risk selection criteria (Likert scale)
c) Weighting of indicator (KRI and KCI) selection criteria based on pairwise comparison of Analytical Hierarchy Process (AHP) method.
d) Key Risk Indicator and Key Control Indicator setting that use priority matrix
e) Risk control matrix making
f) Determination of relationship between KRI and KCI with KPI of Information Technology Department of Bank D

REFERENCES

[1] Epstein, Marc J. & Rejc, Adriana. How to measure and improve the value of IT. Strategic Finance. 2005
[2] Brenner, Joel. ISO 27001: Risk Management and Compliance. Risk Management ABI/INFORM Global, 2007, 54, page 24.
[3] Tomura, Tomonori. Beyond Sarbanes-Oxley: Improving Corporate Value with a 4th generation Balanced Scorecard Approach. www.bptrends.com. 2006.
[4] Vaughan, Emmet J. Risk Management. John Wiley & Sons. Canada. 1997.
[5] ISO/IEC/TMB SAG-Security Secretariat.ISO/IEC 27001:2005, Information technology – Security techniques --Information security management systems– Requirements. Geneva: ISO/IEC/TMB SAG-Security Members. 2005.
[6] Dube, D.P. Information System Audit and Assurance, New Delhi: Tata McGraw-Hill Publishing Company Ltd. 2005.
[7] Basel Committee on Banking Supervision. The internal rating – based approach (supporting document to the new basel capital accord), Consultative Document. 2001
[8] Crouhy, Michel, Galai, And, & Mark, Robert. (2001). Risk Management. McGraw-Hill.
[9] Hoffman, D. Managing Operational Risk. Canada: John Wiley and Sons, Inc. 2002.
[10] Simon, Steven John.Balanced Scorecard: A Tool to Improve IS Department Planning and Evaluation. Journal of Information Technology Case and Application Research. 2005.
[11] Kaplan, Robert S., & Norton, David P. Balanced Scorecard: Translating Strategy Into action. Boston, Massachusetts: Harvard Business School Press. 1996
[12] Kaplan, Robert S., & Norton, David P. Strategy Maps: Converting Intangible Assets Into Tangible Outcomes. Boston, Massachusetts: Harvard Business School Press. 2004.
[13] Davies, Jonathan, and Haubenstock, Michael. Building effective indicators to monitor operational risk. The RMA Journal. 2002.
[14] Lam, James et al. Developing key risk indicators and ERM reporting. USA Emerging best practices. Inc. Cognos. 005. 2006.
[15] Immaneni, Aravind, Mastro, Chris, & Haubenstock, Michael. A structured building key risk. Operational Risk: Special Edition of The RMA Journal. 2004.
[16] Hidayatno, Akhmad and Christine Chandra. Using Hoshin Kanri to Select and Prioritizes PERTAMINA's Evaluation of its Strategic Business Units (SBU), Journal of Technology, Faculty of Engineering University of Indonesia, July 2001.
[17] Saaty, Thomas L. Decision making for Leaders - the Analytic Hierarchy Process for Decisions in a Complex World. Pittsburgh: RWS Publications. 1999.
[18] Saaty, Thomas L. The Seven Pillars of the Analytic Hierarchy Process. Kobe: Proceedings of the Fourth International Symposium on the Analytic Hierarchy Process. 1999.

Product Miniature Quality Design with Multi Responses Taguchi Method

Ali Parkhan[1], Ceria Mustika[2], I. D. Widodo[3]

[1,2,3]*Industrial Engineering Study Program,*
Islamic University of Indonesia

ABSTRACT

One of the important factors that influence the firm sustainability is product quality. The quality of temple miniature product can be measured using the product shrinkage and strength. Factors that influence the temple miniature are resin composition (A), cobalt composition (B), catalyst composition (C), talk composition (D), and mixing duration (E). Besides, there is an uncontrollable factor namely room temperature. Initial parameter setting is the factor level combination of $A_1B_1C_1D_1E_1$ (combination of 55% resin, 0.4 % cobalt composition, 0.6 % catalyst composition, 44% talk composition and 5 minutes mixing duration). For this combination, its shrinkage is 2.625 % and the strength average is 120.437 kg/cm^2. Taguchi method is applied to improve product performance. Based on Taguchi method, the optimal factor level combination is $A_1B_2C_2D_1E_2$ (55% resin composition, 0.3 % cobalt composition, 0.4 % catalyst composition, 44% talk composition and 10 minutes mixing duration). It can successfully improve quality and reduce cost. The shrinkage can be reduced to 1.875 % and strength average can be improved to 136.875 kg/cm^2. This combination also reduces cost to Rp. 30.5/ product.

Keywords: *quality, Taguchi, level factor combination, cost*

1. INTRODUCTION

In globalization era, product and process efficiency and quality have become main consideration for industry that aware of competition. Nowadays, many products have used fiber glasses, including temple/statue miniature. Temple miniature quality is determined by strength of getting impact and shrinkage.

By considering this phenomenon, temple miniature industry should be able to produce product that has maximum strength and minimum shrinkage with minimum cost/price. Therefore, industry must improve its product quality by maintaining its pricing. Taguchi method is applied to minimize experiment cost and time applied. Multi responses Taguchi method is used because there are 2 variables being involved, strength and % shrinkage.

2. LITERATURE REVIEW

2.1 Quality definition

Conventional definition of quality usually reflects some direct characteristics of product, such as, performance, reliability, easy to use and aesthetic. Whereas, strategic definition of quality is anything that can satisfy customer need [1].

2.2 Quality control

Quality control is defined as measurement process done in period of product and process design. Quality control involves every phase of product research and development, production process design and customer satisfaction. Quality control is divided into:

a. Off line Quality Control

Off line quality control consists of [2, 3, 4] three steps, as follow:

Step 1: Concept Design

In this step, product design and development idea from customer, are generated. Model and method applied in this step are Quality Function Deployment, Dynamic Signal-to-Noise Optimization, Theory of Inventive Problem - Design of Experiments, Competitive Technology Assessment -, Pugh Concept Selection.

Step 2: Parameter Design

This step is to optimize level of control factor to some effect appeared by other factors so that product will be robust from noises. Therefore, this step is also called by robust design. Model and method applied in this step are Engineering Analysis, The System P Diagram, Dynamic and Static Signal to Noise Optimization, And Crossed Array Experiment.

Step 3: Tolerances Design.

This is the last step of Taguchi method. Some methods are applied in this step such as Quality Loss Function, Analysis Of Variance (ANOVA), And Design of Experiment.

b. On Line Quality Control

On Line Quality Control is an activity to directly observe and control quality for every step of production processes. This is very important to maintain low production cost and high product quality. Statistical process Control, Static Signal to Noise Ratio, Compensation, Loss Function are some method that commonly used for on line quality control.

2.3 Experimental Design

Experiment design is an experiment phase/activity design so that all information of the experiment running can be collected [5]. There are two types of design experiment, conventional and Taguchi. Compared to conventional approach, Taguchi method is preferred because it needs smaller number of experiment so that it can minimize time, cost, and energy.

Taguchi method, introduced by Genichi Taguchi, uses orthogonal array to determine minimum experiment number that can produce as much as possible information of factor that influence parameter. The most important of orthogonal array is in selection of level combination from input variables for each experiment [2]. Taguchi philosophy consists of three concepts, they are [6]:

1. Quality must be designed into the product and not only checking the product. The best quality can be reached by minimizing deviation of target.
2. Product must be designed so that robust from uncontrollable environmental factors
3. Quality cost must be measured based on deviation function from the target and loss must be measured for all system.

2.4 Signal to Noise Ratio (S/N Ratio)

S/N ratio is logarithm of quadratic loss function and used to evaluate quality a product. There are three S/N Ratio types, they are:

1. Smaller- the Better

Quality characteristic where by smaller value it gets, the better quality it has, however the biggest S/N ratio is used to determined optimum factor level [4]. S/N Ratio function of smaller- the better:

$$S/N\_STB = -10Log\left[1/n \sum_{i=n}^{n} yi^2 \right]$$

n= number of trial

yi= respon value of sample i

2. Larger the Better

The bigger value it gets, the better quality it has. The function is

$$S/N\_LTB = -Log\left[1/n \sum_{i=n}^{n} 1/yi^2 \right]$$

3. Nominal –the Better

Quality characteristic where by a nominal value (target) is determined. The closer value to the target, the better quality it has. The S/N ratio function is

$$\eta = 10\log\left[\frac{\mu^2}{\sigma^2}\right] \qquad \sigma^2 = \frac{\sum\left(y_i - \bar{y}\right)^2}{n-1}$$

2.5 Taguchi Multi Response

Taguchi approach is divided into two types, namely single response and multi response. Single response Taguchi only has one single response variable, so that the optimum combination is directly found. Multi responses Taguchi involve more than one response variable (minimum 2), and each response variable has different factor combination. To get optimum combination, it must do multi attribute analysis tools such as Multi Response Signal to Noise (MRSN) and *Technique for Order Preference by Similarity to Ideal Solution* (TOPSIS)[7].

2.6 Multi Response Signal to Noise (MRSN)

Three MRSN steps are:

1. Calculate quality loss for every trial. It depends on quality characteristics.

Bigger the better

$$L_{ij} = k\frac{1}{n_i}\sum_{k=1}^{n_i}\frac{1}{y^2_{ijk}}$$

Nominal the best

$$L_{ij} = k\frac{1}{n_i}\sum_{k=1}^{n_i}\left(y_{ijk} - m\right)^2$$

Smaller the best

$$L_{ij} = k\frac{1}{n_i}\sum_{k=1}^{n_i} y^2_{ijk}$$

Where :

L_{ij} = *quality loss* for response -i, trial -j

Y_{ijk} = data for response-i, trial -j, replication -k

n_i = replication response-i

k = Coefisien of *quality loss*

m = target Value

2. Determine MRSN Ratio

a. Determine the maximum Quality loss for each response

b. Normalization

$$C_{ij} = \frac{L_{ij}}{L_i}$$

Where: C_{ij} = *normalized quality loss* for response i, trial –j

L_{ij} = max $\left\{L_{i1}, L_{i2}, ..., L_{ij}\right\}$

ISSN 114-1284

c. Calculate *total normalized quality loss* (TNQL) every experiment :

$$TNQL_i = \sum_{i=1}^{m} w_i x C_{ij}$$

W= weight of normalization response-i

d. Calculate MRSN Ratio for every experiment

$$MRSN_j = -10\log(TNQL_j)$$

3. determine optimum level factor combination based on the bigest MRSN Ratio by:
   a. developing response table and response graph of MRSN
   b. determining control factor that has significant effect to MRSN
   c. determining optimum level of control factor based on the bigest MRSN
   d. confirming the experiment

3. EXPERIMENT DESIGN AND PLANNING

3.1 Experiment Planning

Experiment planning is an information provider phase to run experiment. Some steps in experiment phase are :

1. Selection of Poduct Quality Charateristics
   Quality charateristics of temple miniature are "good" when its shrinkage rate is low and its strength value is high.
2. Identification and selection factors that influence product quality charateristics. Five controlable factors and a noise factor influence the experiment. They are:
   a. Resin composition
      Level used is in between 55% and 66%. If resin composition is lower than 55%, the mixture is difficult to be mold because its viscosity is too high. In contrary, if composition is higher than 65%, the mixture is too watery.
      This will influence the thick and the strength of product.
   b. Cobalt Composition
      The possible level used is in between 0.3 % and 0.4 %. Mixture that contains cobalt composition that lower than 0.3 % will take longer time in drying process. This is in contrast to mixture that contains cobalt to much (more than 0.4%). It will be too fast.
   c. Catalist composition
      Catalist composition level is in between 0,4 % and 0,6 %. Mixture that contains catalist composition less than 0.4 % will take longer time in drying process. This is in contrast to mixture that contains catalist more than 0.6%
   d. Carbonate Calcium (Talk) Composition
      The level used is in between 33,3 % and 44%. The mixture will be too watery if it is less than 33,3% and it is incontrary if the talk composition is more than 44%
   e. Mixing Process
      It is between 5 minutes and 10 minutes.
   f. Room Temperature
      It is noise because this factor cannot be controlled.

3.2 Experiment Execution

To test the product, two measuremet are applied. They are product strength (kg/m^2) and shrinkage (%) measurement. The strength test was done in Concrete Laboratory FTSP UII. The shrinkage test is done by comparing product length and the molt. The measurement results are presented in Table 1 and Table 2.

Table 1: Temple miniature strength data (kg/cm^2)

						L4 OA (OUTER ARRAY)							
					F	1		1		2		2	
	L8 OA (INNER ARRAY)					Experiment Data							
	A	B	C	D	E								
	Column Number					Y1		Y2		Y3		Y4	
Trial	1	2	3	4	5								
1	1	1	1	1	1	99	112.5	111	125.5	111	110.5	126	168
2	1	1	2	2	2	112	126	124.5	126.5	182	126	126	140
3	1	2	1	2	2	140	139.5	140	140	139	140	153.5	140
4	1	2	2	1	1	140.5	153	140.5	149.5	155	156	158	168
5	2	1	1	1	2	140	126	139	124.5	125	125	140	113
6	2	1	2	2	1	167	125.5	167	112	140	139.5	120	125
7	2	2	1	2	1	140	149	127	126.5	168	142	140.5	140.5
8	2	2	2	1	2	154	155	168	115	181	114.5	195	142

Table 2: Temple miniature percentage shrinkage data (%)

						L4 OA (OUTER ARRAY)							
					F	1		1		2		2	
	L8 OA (INNER ARRAY)					Experiment Data							
	A	B	C	D	E								
	Column Number					Y1		Y2		Y3		Y4	
Trial	1	2	3	4	5								
1	1	1	1	1	1	3	2	2	3	2	3	3	3
2	1	1	2	2	2	5	5	4	5	3	4	4	5
3	1	2	1	2	2	2	2	2	1	2	3	2	2
4	1	2	2	1	1	2	3	2	3	4	2	4	4
5	2	1	1	1	2	3	3	3	3	3	4	3	4
6	2	1	2	2	1	6	6	6	6	5	6	6	6
7	2	2	1	2	1	2	4	4	5	4	4	5	5
8	2	2	2	1	2	3	3	4	4	3	4	3	3

4. RESULT AND DISCUSSION

4.1 Normality Test

Strength test data follow normal distribution because. χ^2_{cal} is 4.7111 less than χ^2_{table} (7,81472776) so do shrinkage test data. χ^2_{cal} is 4.8328 less than χ^2_{table} (5,99147636).

4.2 Homogeneity and Analysis of Variance (ANOVA)

Both data are homogenous. Strength test data is homogenous because χ^2_{cal} (3.726) less than χ^2_{table} (3,841). Shrinkage test data that are also homogenous because χ^2_{cal} (0.0529) less than χ^2_{table} (3,841).

All factors (A, B, C, D, and E) influence both strength and shrinkage based on ANOVA.

4.3 S/N Ratio Analysis

S/N Ratio of both strength and shrinkage are presented in Table 3. Effect factor for strength and % Shrinkage are presented in Table 4 and 5.

Table 3: Strength and % shrinkage mean and SNR

rial	Strength		% Shrinkage	
	Mean	SNR	Mean	SNR
	120.4375	59.7922	2.625	-8.5278
	132.875	60.0043	4.375	-12.9281
	141.5	60.1217	2	-6.2839
	152.5625	60.8785	3	-9.8900
	129.0625	60.6265	3.25	-10.3141
	137	60.9353	5.875	-15.3939
	141.6875	61.1457	4.125	-12.5225
	153.0625	60.8681	3.375	-10.6539

Table 4: Responses of factor effect e for strength

Level	Controlable Factor				
	A	B	C	D	E
Level 1	60.19	60.33	60.42	60.54	60.68
Level 2	60.89	60.75	60.67	60.55	60.40
Difference	0.69	0.41	0.	0.01	0.28
Rank	**1**	**2**	**4**	**5**	**3**

Table 5: Response of factor effect for % shrinkage

Level	Controlable Factor				
	A	B	C	D	E
Level 1	-9.40747	-11.7	-9.412	-9.846	-11.58
Level 2	-12.2210	-9.837	-12.21	-11.78	-10.0
Difference	2.81362	1.9534	2.8044	1.9356	1.5385
Rank	**1**	**3**	**2**	**4**	**5**

4.4 Determination of Factor Level with MRSN

MRSN is applied because optimal combination of strength (A2 B2 C2 D2 E1) is different from optimum combination of % shrinkage (A1 B2 C1 D1). MRSN Ratio is calculated by stating % shrinkage and strength weight 1/3 and 2/3. The MRSN ratios are performed in Table 6.

Table 6: Multi Response Signal to Noise Ratio (MRSN)

No	A	B	C	D	E	MRSN
1.	1	1	1	1	1	1.3408
2.	1	1	1	1	2	1.8575
3.	1	1	1	2	1	1.1266
4.	1	1	1	2	2	1.5607
5.	1	1	2	1	1	1.7567
6.	1	1	2	1	2	2.1135
7.	1	1	2	2	1	1.1777
8.	1	1	2	2	2	1.3862
9.	1	2	1	1	1	2.8824
10.	1	2	1	1	2	3.1263
11.	1	2	1	2	1	2.5519
12.	1	2	1	2	2	3.0585
13.	1	2	2	1	1	3.1743
14.	**1**	**2**	**2**	**1**	**2**	**3.3779**
15.	1	2	2	2	1	2.4975
16.	1	2	2	2	2	2.8942
17.	2	1	1	1	1	1.4077
18.	2	1	1	1	2	1.828
19.	2	1	1	2	1	0.8686
20.	2	1	1	2	2	1.2218
21.	2	1	2	1	1	1.306
22.	2	1	2	1	2	1.6274
23.	2	1	2	2	1	0.7321
24.	2	1	2	2	2	0.9974
25.	2	2	1	1	1	2.7315
26.	2	2	1	1	2	2.984
27.	2	2	1	2	1	2.0295
28.	2	2	1	2	2	2.511
29.	2	2	2	1	1	2.5431
30.	2	2	2	1	2	2.6825
31.	2	2	2	2	1	1.8474
32.	2	2	2	2	2	2.2074

Conclusion: the best combination based on MRSN is A1 B2 C2 D1 E2. It gives highest MRSN Ratio (3.3779).

4.5 Prediction test and T Test

Optimum combination based on MRSN (A1 B2 C2 D1 E2) has not been done in the previous experiment, so it needs prediction for the combination result. Regression method is applied to predict the result based on experiment performed. Shrinkage percentage are (2, 2, 2, 2, 3, 2, 2, 3) and the confirmation result is (2,1,3,1,1,3,2,2). S/N Ratio is – 6.15, this value is in confidence interval – 10.6899 < SNR < - 5.5019. This shows that SNR from experiment confirmation result is not significantly different from experiment prediction.

Strength prediction is (134, 152, 147, 139, 171, 131, 181, 159) and the experiment confirmation is (117, 123, 135, 132, 121, 169, 143, 155). SNR Value is 60.85. This value is in confidence interval (29.2634 < SNR < 91.5056). It means that prediction and confirmation result is not significantly different.

Based on T Test, there are not significantly different both strength and % shrinkage between prediction and confirmation experiment result. T_{cal} for shrinkage is 1.11, this is in confidence interval (-2.145 and 2.145). T_{cal} for strength is 1.67 this is also in confidence interval (2.145 and 2.145).

4.6 Cost Reduction and Quality Improvement

Cost reduction for cobalt per temple miniature is 25% x 1liter x Rp 250.000,-/liter)/2000 unit = Rp. 32.25. Catalyst cost reduction per unit is Rp. 9.99. Work force cost increase is Rp. 10.71/unit so total cost reduction per unit is Rp. 30.53.

Reduction of Shrinkage percentage average is 0.75 (initial shrinkage is 2.625 and optimum one is 1.875).
Strength percentage average increases from 120.43 kg/cm^2 to 136.87 kg/cm^2. It means optimum combination can increase 16.24 kg/cm^2 for strength.

CONCLUSION

1. Factors that influence the temple miniature are resin composition (A), cobalt composition (B), catalyst composition (C), talk composition (D), and mixing duration (E).
2. The optimal factor level combination is $A_1B_2C_2D_1E_2$ (55% resin composition, 0.3 % cobalt composition, 0.4 % catalyst composition, 44% talk composition and 10 minutes mixing duration). It can successfully improve quality and reduce cost.
3. Optimum parameter setting can reduce shrinkage to be 1.875 % and strength average can be improved to 136.875 kg/cm^2. This combination also reduces cost to Rp. 30.53/ product.

REFERENCES

[1] Vincent, G. *Total Quality Management.* Gramedia Pustaka Utama: Jakarta. 2001
[2] Peace, G. S. *Taguchi Methods.* Addison - Wesley Publishing Company, 1993
[3]Ross, P. J., *Taguchi Techniques For Quality Engineering*. McGraw-Hill, Inc., New York. 1988
[4] Belavendram, N. *Quality By Design*. Prentice Hall, Internasional. 1995.
[5] Sudjana , *Desain dan Analisis Eksperimen.* Penerbit Tarsito : Bandung, 1991.
[6] Montgomery. *Pengantar Pengendalian Kualitas*. UGM Press. Yogyakarta. 1998

[7] Tong, L. & Chao, T Su. Optimizing Multiresponse Problems in The Taguchi Methods by Fuzzy Multiple Atribute Decision Making. *Quality and Reability Engineering Internasional*, Vol 13, 25-34, 1997.

ISSN 114-1284

Optimum Routes Determination for Cylinder Gas Distribution Using Differential Evolution Algorithm

Arian Dhini, ST., MT[1], Kresentia Isabella Andinita[2]

[1]*Industrial Engineering Department*
Faculty of Engineering
University of Indonesia, Depok 16424
Tel : (021) 7270011 ext 51. Fax : (021) 7270077
E-mail : arian@ie.ui.ac.id

[2]*Industrial Engineering Department*
Faculty of Engineering
University of Indonesia, Depok 16424
Tel : (021) 7270011 ext 51. Fax : (021) 7270077
E-mail : kresentia_ti05@yahoo.com

ABSTRACT

The aim of this research is to obtain the optimal gas product's route distribution so that the distance can be reduced and the total distribution cost at the gas company can also be optimized efficiently. Routes optimization were achieved using Differential Evolution Algorithm. Differential Evolution is a population based and direct stochastic seacrh algorithm (minimizer or maximazer) with simple, yet powerful, and straightforward. The result from this research is the optimal product's route distribution based on the distance analysis, vehicle utilization, and delivery cost. The distance reduction of 351.96 km or 17.3% in a week is successfully obtained.

Keywords

Optimization, Vehicle Routing Problem, Differential Evolution Algorithm

1. INTRODUCTION

The companies all over the world are starting to realize that logistics had a significant impact to the total cost, and the decision of logistics is resulting to a different level of service to the customers. The definition of logistics itself, according to D.Lambert (1998), is a process of planning, implementing, and controlling the flow and the storage of goods, service and related information, effective and efficiently, from the starting location to the final destination in order to fill the customer needs. Moreover, the main objective of logistics management is to obtain a package of product or service at the right time, right place, and at the desired condition, by giving the largest contribution to the company. By achieving the proper logistics management, the work performance might be improved, and the effectiveness and the efficiency of the cost can also be obtained.

In order to reach the effectiveness and the efficiency in logistics cost, the optimization should be done in every aspects. One of them is by optimizing the distribution or the transportation. Transportation is a very important factor in distribution system because it has a big influence to customer satisfaction and the distribution cost. Transportation itself contributes 1/3 to 2/3 of the total distribution cost. The large sum of transportation cost contribution encouraged the companies to pay a special attention to this area. One of the major problems in distribution transportation is *Vehicle Routing Problem* (VRP). VRP is a design or a determination of a number of vehicle routes with a number of constraints faced, such as the vehicle must be started and ended in the depot, every customer is widespread geographically and only be served once by a vehicle, and the total demand brought will not surpass the vehicle capacity.

The distribution of gas is conducted based on the form, size of gas packaging and the amount of gas need of customers. Therefore, in distributing the product, the gas company is using two types of delivery, i.e. tank truck and cylinder gas transporter. In the cylinder gas product distribution, the company sends a number of cylinder gas to the destination as ordered, and picks up the empty cylinder gas to the depot to be refilled. This type of distribution is known as *delivery and pick-up service*, which is basically a vehicle serving a customer to send him a new product while at the same time taking the old product from that customer.

Therefore, in determining of when the delivery should be done best, and how to make a certain vehicle routing to reach a certain destination, the company has to make a delivery routing determination in daily basis. Those routes have been arranged based on the experience of the transportation division to the customer's location area and the tracks that have been passed through.

Therefore, an improvement in those problems is extremely necessary to be conducted in order to get fuel saving which is closely related to the distance taken by the vehicles, and the best way to do that is by doing the optimization.

There are various techniques applied for the routing optimization, and one of them is *Evolutionary Algorithms* (EA). EA is a optimization technique that using a strategy to move the variation of the parameters' vectors. In the application itself, EA is using the biological principles analogy such as selection, mutation, and combination. There are few algorithms that are categorized in this EA type, which are Genetic Algorithm, *Ant Colony*, *Particel Swarm*, and *Differential Evolution*. *Differential Evolution* (DE) algorithm is a new type of algorithm that is tough enough to be used in facing the problems with many constraints. Compared with the other EA algorithm in solving this case, DE is better in its simple type of structures, easy implementation, fast in reaching the objective, and quite tough. Therefore, the use of DE here is expected to be able to optimize the distribution problem, and in the other hand, still able to defend the service level to the customers.

2. VRP PICK-UP AND DELIVERY

2.1 Definition and Characteristics

VRP with Pick-up and Delivery (VRPPD) is one of the classic type of VRP in which a customer needs both delivery and pick-up service of the goods. In general, the purpose of VRPPD is to minimize cost of the system. Each service in a location covers delivery point and pick-up point, and a number of requests that must be met, at the same time, for any route, the vehicle cannot ignore the obstacles, such as vehicle capacity and distance. In short, there are some limitations that must be fulfilled:

- For each customer, delivery and pick-up can only be done once
- Not exceed vehicle capacity
- Delivery and pick-up in the same vehicle routes

VRPPD can be developed according to the problems faced by the case, when there are constraints such as time windows, then VRPPD developed into VRPPDTW (VRPPD with Time Windows), namely the form of the development of VRPPD and VRP with Time Windows (VRPTW).

Example of VRPPD case is in the soft drink industry. In this case, empty bottles must be returned to the factory to be used again, or at the grocery stores, pallet / container, where reusable pallets/containers are used for the transportation of merchandise. By using VRPPD, then there will be only one route, the route of delivery and pick-up simultaneously.

2.2 Mathematical Formulation

There are k vehicles in the depot 0, and stands for the set of customers to be visited, where n=V is the number of customers. The location of depot and customers are known. Each customer has a known delivery demand level and a known pick-up demand level, j=1,2,…,n. Delivery routes for vehicles are required to start and finish at the depot, so that all customer demands are satisfied and each customer is visited just by one vehicle.

Suppose there are k vehicles in the depot 0, dan V stands for the set of customers to be visited, where $n=|V|$ is the number of customers. Each customer has a known delivery demand level d_j pickup demand level p_j, where j = 1, 2, …, n. Delivery routes for vehicles are required to start and finish at the depot, so that all customer demands are satisfied and each customer is visited just by one vehicle. $V_0 = V \cup \{0\}$ is the set of clients plus depot (client 0); c_{ij} is the distance between i and j; and the capacity of each vehicle is Q. Decision variable is x_{ijk} = 1, if arc (i, j) belongs to the route operated by vehicle k, otherwise is 0. y_{ij} is the demand picked-up in clients routed up to node i and transported in arc (i, j); z_{ij} is the demand to be delivered to clients routed after node i and transported in arc (i, j).

The mathematical formulation of VRPPD is given by:

$$\min \sum_{k=1}^{k}\sum_{i=0}^{n}\sum_{j=0}^{n} c_{ij}x_{ij} \quad (1)$$

$$s.t. \sum_{i=0}^{n}\sum_{k=1}^{k} x_{ijk} = 1,\ j = 1,2,...,n \quad (2)$$

$$\sum_{i=0}^{n} x_{ijk} - \sum_{i=0}^{n} x_{jik} = 0, \quad j = 0,1,....n; k = 0,1,...,k \quad (3)$$

$$\sum_{j=1}^{n} x_{0jk} \le 1, k = 1,2,...,k \quad (4)$$

$$\sum_{i=0}^{n} y_{ji} + \sum_{i=0}^{n} y_{ij}, = p_j, \forall j \ne 0 \quad (5)$$

$$\sum_{i=0}^{n} z_{ij} - \sum_{i=0}^{n} z_{ji} = d_j, \forall \ne 0 \quad (6)$$

$$yij + zij \le Q\sum_{k=1}^{k} xijk, i, j = 0,1,...., n \quad (7)$$

$$\sum_{i=0}^{n}\sum_{j=0}^{n} d_{ij}x_{ijk} \le Lk = 0,1,2,...,k \quad (8)$$

$$x_{ijk} \in \{0,1\}, y_{ij} \ge 0, z_{ij} \ge 0, i, j = 0,1,...,n; \quad k = 0,1,...,k \quad (9)$$

The objective function seeks to minimize total distance traveled is shown in equation (1). Equation (2) to (9) is the limitations that should be noticed. Constraint (2) ensures that each customer will be only visited by exactly one vehicle, constraint (3) guarantees that the same vehicle arrives and departs from each client it serves. Restriction (4) defines that at most k vehicles are used. Restrictions (5) and (6) are flow equations for pick-up and delivery demands, respectively. Constraint (7) establishes that pick-up and delivery demands will only be transported using arcs included in the solution. Restriction (8) is the maximum distance limit, L is the upper limit on the total load transported by a vehicle in any given section of the route. Finally, constraint (9) is the decision variable.

3. DIFFERENTIAL EVOLUTION ALGORITHM

DE works by copying the theory of the evolution of biology. DE had several superiority compared with the optimization classic method, i.e. :

- Having population which is the solution candidates
- The method non-deterministic that produced solutions that were different although the model initially was not changed, because of working with used random sampling.
- Using elements from available solutions to create the new solution with the characteristics that were bequeathed from elements of its mother.

Similar to with other EA, DE used vectors that represent resolution candidates where its search technique was carried out at the same time on several solutions that were mentioned as the population.

In each generation, each individual of the resolution candidates will pass the process of the evaluation where these individuals will form the target vector and were counted by the function of its objective (or often was mentioned as fitness function). Moreover, these individuals will be done by the mutation process and crossover in order to be able to form the vector trial that was used to form the child population (the next generation's population). The next generation's population will be formed by comparing the objective of parent and child vectors (trial vectors) where the individual values with the best objective function will pass to the next generation. This process will be repeated until the termination's criteria fulfilled. In the process of finding the solution, DE will through the initialization (the determination of the control parameter, the initial population, and the evaluation of the function of the objective), mutation, crossover, selection, and termination.

3.1 Initialization

The initialization is the determination of the control parameter and the initial population (the 0 generation). The aim of the control parameter determination is to find the solution that could be accepted through several evaluations of the function and will have an impact on the performance of DE. The DE control parameter is the population size, mutation control parameter, and crossover control parameter.

The population size (Np) is the number of the population's channels in one generation (took form in the matrix column) that has the same value during solution searching process. The mutation control parameter (F) is the valuable control parameter of the positive original number that has functioned in controlling the population evolution level. The common effective F value is between 0,4 and 1. The crossover control parameter (Cr) is used to determine inheritance gene that is owned by the target and mutation vectors in order to form trial vector by comparing it with random numbers which are generated in the crossover process. This Cr value is between 0 and 1.

In this problem, the decisive variable or the number of dimensions was the number of visited customers, but especially for the outlet customers' case, it could be several outlet customers but in the same location, so it only visits one place. Therefore, for the outlet customers' case, the dimension size is the location of the delivery points. The number of delivery points is 63, so the outlet customer's population size is 126. In the meantime, for the industrial and the hospital customer, the number of delivery point is the same as the number of customers. So when the number of dimensions is 33, the population size is 66. The best mutation parameter (F) value is 0,4 and best crossover parameter (Cr) value is 0,5. Termination criteria are determined based on the number of maximum iteration which is 1000.

When determining the VRP initial population, each initial individual will represent the number of routes to serve all customers and the delivery points in each route. The initial population is appointed randomly. Every initial individual is elaborated by function:

Initial individual = lower limit + (upper limit – lower limit) x random number

In this process, the random numbers that was used is between 0 and 1. The lower and upper limit is -1 and 1. In this case, the parameter of the population size is twice the number of customers. It means if there are 33 customers, then the number of initial individuals is 66. Because the population consisted of 66 individuals and each individual consisted of 33 dimensions, then the initial population in this date is a 66 x 33 matrix.

The initial population was a random number between -1 to 1, so this initial population did not represent the

sequence of delivery points to each customer. Therefore, the random number must be translated into integer number so we can read the sequence of delivery points to each customer.

The objective function is to minimize the serving distance of the entire customer through determining the route and delivery sequences in this route with some constraints that have been mentioned at mathematical VRPPD model in the sub-chapter 2.2.

Each initial individual is evaluated by using the objective function above or by determining initial solution. The initial solution has a role as the target vector or parents' vector (the A Vector).

3.2 Mutation

The mutation process is intended to make a new individual called the mutant individual. Therefore, in order to create it, 3 random individuals should be picked from the starting population. Here is the equation to form the mutant individuals:

$$\text{Mutant Individual} = a + (b-c)* 0.4 \quad (10)$$

The number 0.4 is a mutation parameter (F) that has been determined at the earlier stage.

3.3 Crossover

The cross-over process is intended to create a new individual called the trial individual, so it will enrich the diversity of genes in a population that will enter the next generation. Parameter value or the individual dimensions of this part of the trial comes from the individual parameter target and some come from individual mutant, by considering the cross-operator move (Cr) and a random number. Cr value is set at initialization stage.

If the random number r (from 0 to 1) that is obtained is smaller or at least at the same value of CR, then the one who has the opportunity to be the i-th dimension value of the trial individual is the i-th dimension value of the mutant individual. Otherwise, then the i-th dimension value of the individual trial is the i-th dimension value of the starting individual. The visual representation is shown below:

$$u_{j,g} = u_{j,j,g} = \begin{cases} v_{j,j,g} & \text{if } (\text{rand}_j(0,1) \leq Cr \text{ or } j = j_{\text{rand}}) \\ x_{j,j,g} & \text{if } (\text{rand}_j(0,1) > Cr \text{ or } j = j_{\text{rand}}) \end{cases} \quad (11)$$

Each individual in trial population will be evaluated just as in the starting population. The individual with the least distance will enter the selection process next.

3.4 Selection

This process is the stage of determining the proper individual that deserves to be the member of the next generation, which is by comparing the target individual's objective function with that of the trial individual. In this case, the individual with the least distance will be chosen.

3.5 Termination

Termination occured when the process of searching optimal solution has been reached termination criteria. However, if the termination criteria has not been fulfilled, it will be established again with the new generation to repeat the previous steps from the beginning. Termination criterions are as follows:

- Maximum computation time
- Maximum iteration
- Reach the convergence (the value of the optimal objective function does not change)

In this research, maximum iteration is used as termination criterion. Stage 2 to stage 7 is a process for one time iteration. This process will keep repeating until the iteration number reaching 1000. The next program will select the individual with the least distance from the 1000 iteration that has been done.

4. VRPPD PROBLEM SOLVING FOR THE GAS PROVIDER COMPANY USING DIFFERENTIAL EVOLUTION

To write the DE algorithm along with the optimal solution searching, a programming language using *Visual Basic for Application* (VBA) Microsoft Excel 2007 is used. Through this program, the desired result is not only at the form of the solution of distance calculation using the DE algorithm, but it is also complied with the ability to integrate the customer database with the necessary data to do an optimization, such as the in-between customer distance matrix, amount of demand, vehicle capacity, vehicle velocity, and the time windows, in order to simplify the use of this application in scheduling and determining the optimal delivery routes in a shorter range of time. It is also supported by the situation in the company with the recent change in demand every day, whether it is from the demand or from the customer who asked for the delivery.

The creation of the this optimal distribution route using DE algorithm written in VBA Excel is based on the objective function which is to minimize the route distance, so that the desired output from this program will be in a form of a delivery routes sequence for each operating vehicles and the total distance of those routes.

This research is conducted in two distribution cases in the gas provider company, whereas the company has two types of customers which are outlet customers and industry & hospital customers. The transportation fleet that the company owned is around 5 vehicles, i.e. 2 pick-up cars to do delivery to the outlet customers, and 3 trucks to do delivery to the industry and hospital customers, to be more specific. The vehicle specification

can be seen on Table 1. The numbers of outlet customers that are served are 227 customers, widely spread

Table 1: Type and Number of Vehicles

No	Type of vehicles	Capacity (cylinders)	Number of vehicles
1	*Pick-Up*	40	2
2	Single Truck	60	2
3	Double Truck	90	1

throughout 63 locations, while the industry and hospital customers were spread out to 33 locations. The DE parameter used here is Np = 126 for the distribution route optimization for the outlet customers and Np = 66 for the distribution route optimization for the industry and hospital customers, F = 0.4 and CR = 0.5, with maximum number of iteration = 1000. The running of the program is conducted for the 5-days data request, which is from Monday, April 20th 2009 to Friday, April 24th 2009. Examples of outlet and industry & hospital customer data request are shown on Table 2 and 3.

Table 2: Outlet Customer Data Request Sample Friday, April 24th 2009

Delivery Destination	Delivery Demands	Pick-up Demands	Location	Total Delivery per location	Total Pick-up per location
MCK	2	2	AMGK	7	7
AMGK	7	7	MCK	2	2
PH-WB	6	6	WB	6	6
MC-DPL-ITDP	2	2	ITDP	23	23
A-ITDP	7	7	SCB	5	7
PH-ITDP	6	6	GRI	15	15
A-MD-ITDP	8	8	HLE	5	5
MC-MD-ITDP	2	2			
HRC-SCB	5	7			
BK-GRI	1	1			
BLT-GRI	14	14			
HLE	5	5			
			TOTAL	**63**	**65**

Table 3: Industry and Hospital Customer Data Request Sample (Friday, April 24th 2009)

Location	Total Delivery Demands	Total Pick-up Demands
PLMB	29	21
SM	15	24
RSBA	15	15
GSG	15	14
PMG	15	20
SLD	10	3
URMI	9	12
ALG	10	10
RSOM	5	2
RSEH	16	10
SM	10	9
MLC	10	11
TOTAL	**159**	**151**

While the new routes obtained from the running of the program is shown on Table 4 and 5.

Table 4: The Routing Sequence and the Total Distance after the Distribution Optimization for the Outlet Customers

Day	Vehicle	Route Delivery Sequence					Total Travelled distance (km)	Total Travelled Distance per day (km)
Monday, 20/04/2009	1	PUM	GNS	STD	ASEN	WTMD	41,57	94,94
		MDS	ITMD	JAY	UNT			
	2	RXM	MTA	KED	GG	DM	53,37	
		CIT						
Tuesday, 21/04/2009	1	HSHA	PLAZ	PAF	MTH	ITKN	63,61	128,40
		ITPH						
	2	PLM	EMP	MK	SM	GNS	64,79	
		TRW	TP					
Wednesday, 22/04/2009	1	CINM	CIM	POLB	AB	PLCPL	60,65	136,44
		DBF	PIM	CITS	PHCIP			
	2	BP	MOI	MAG	LPI	PHCP	75,79	
		ITCM	MKG					
Thursday, 23/04/2009	1	PLCIB	TMI	PGM	PLIB	BOS	203,43	257,55
		PHPAJ	SCB	SENY				
	2	PLGI	KM	PCIL	MC	HLE	54,12	
		GRI	AHC					
Friday	1	MCK	WB	ITDP	AMGK	SCB	85,82	111,01
4/24/09	2	HLE	GRI				25,18	

Table 5: The Routing Sequence and the Total Distance after the Distribution Optimization for the Industry and Hospital Customers

Day	Vehicle	Route Delivery Sequence								Total travelled distance (km)	Total travelled distance per day (km)
Monday, 20/04/2009	1	ALG	SLD	RSSA						26,68	111,19
	2	RSOM	PMG							31,70	
	3	RSHT	MMS	ALG	PLMB	HGC	RSBA			79,48	
Tuesday, 21/04/2009	1	PLMB	INC	HW						58,31	250,41
	2	PMG	URMI	LCI	GMW	ALG				54,26	
	3	BUT	RSOM	RSEH	RSSA	MMS	RSBA	TRI	RSHT	137,84	
Wednesday, 22/04/2009	1	MMS	GSG	SS	INTC	RST				56,43	252,74
	3	ALG	SLD	RSHO	HGC	PLMB	PMG			104,37	
Thursday, 23/04/2009	1	HGC	PMG							29,01	148,12
	2	INC	SS	HW	RSSA	RSHT	GMW			85,43	
	3	SPP	ALG	LCI						33,68	
Friday, 24/04/2009	1	MLC	SLD							26,19	191,28
	2	PLMB	GSG	RSBA						58,67	
	3	RSEH	RSOM	SM	URMI	ALG	PMG			106,42	

The totals distance comparison before and after the optimization done is shown on Table 6 and 7.

From the table 6 and 7, we can see that the optimization using the DE algorithm resulted a shorter distance compared to the current methods used by the company. It means that this algorithm has been successfully used to optimize the routes in order to minimize the total distance. The distance reduction is aligned with the distribution operational cost reduction or the fuel cost. With a fuel cost of IDR 900 per liter and fuel usage ratio of 1:5 for all the vehicles, then the distribution cost comparisons before and after the optimization are shown on Table 8 and 9, also in figure 1 and 2.

Table 6: The Routing Comparison Obtained from the Distribution Optimization for the Outlet Customers

Day/Date	Total Travelled Distance (km)	
	Current	After Optimization
Monday, 20 April 2009	109,84	94,94
Tuesday 21 April 2009	130,86	128,40
Wednesday 22 April 2009	149,85	136,44
Thursday 23 April 2009	291,80	257,55
Friday 24 April 2009	135,16	111,01
TOTAL	**817,51**	**728,33**

Table 7: The Routing Comparison obtained from the Distribution Optimization for the Industry Customers

Day/Date	Total Travelled Distance (km)	
	Current	After Optimization
Monday 20 April 2009	187,73	111,19
Tuesday 21 April 2009	269,75	250,41
Wednesday 22 April 2009	277,03	252,74
Thursday 23 April 2009	152,17	148,12
Friday 24 April 2009	329,84	191,28
TOTAL	**1216,52**	**953,73**

Table 8: The Distribution Cost Comparison Before and After the Optimization of the Distribution to the Outlet Customers

Day/Date	Distribution Cost	
	Current	After Optimization
Monday 20 April 2009	Rp98.856	Rp85.448
Tuesday 21 April 2009	Rp117.774	Rp115.556
Wednesday 22 April 2009	Rp134.865	Rp122.796
Thursday 23 April 2009	Rp262.620	Rp231.795
Friday 24 April 2009	Rp121.644	Rp99.905
TOTAL	Rp735.759	Rp655.500

Table 9: The Distribution Cost Comparison Before and After the Optimization of the Distribution to the Industry Customers

Day/Date	Distribution Cost	
	Current	After Optimization
Monday 20 April 2009	Rp168.957	Rp100.067
Tuesday 21 April 2009	Rp242.775	Rp225.368
Wednesday 22 April 2009	Rp249.327	Rp227.466
Thursday 23 April 2009	Rp136.953	Rp133.308
Friday 24 April 2009	Rp296.856	Rp172.152
TOTAL	**Rp1.094.868**	**Rp858.361**

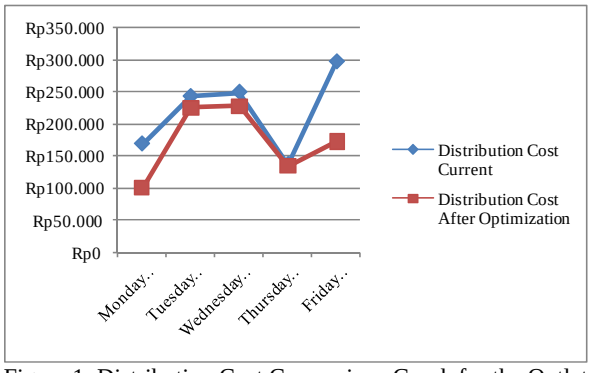

Figure 1: Distribution Cost Comparison Graph for the Outlet Customers

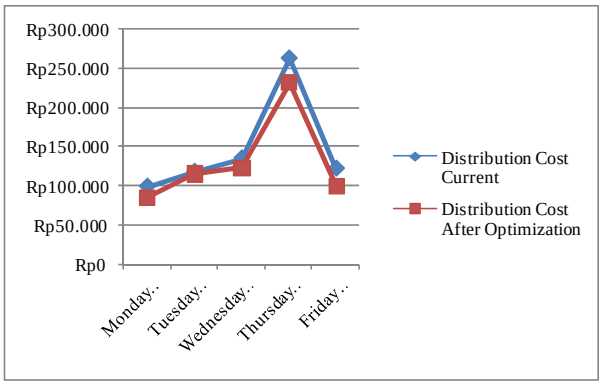

Figure 2: Distribution Cost Comparison Graph for the Industry and Hospital Customers

5. CONCLUSION

Based on the case study of the distribution route determination of the cylinder gas delivery in the gas provider company using the *Differential Evolution algorithm* and with the help of the VBA Excel programming, such conclusions may be reached as follow.

The daily route distribution determination using *Differential Evolution* algorithm has provided a new and better distribution route compared with the current methods used by the company. In the distribution of the outlet customers, the total distance reached for 5 days is 817.51 km with a distance reduction for 89.18 km or 10.9 % in percentage. Meanwhile, at the distribution for the industry and hospital customers, the distance reached for 5 days is 953.73 km with distance reduction by 262.79 km or 21.6% in percentage.

The distance reduction will directly affect the distribution cost spent. For the distribution to the outlet customers, the new distribution cost after it has been accumulated for one year is Rp.31.464.000,-, or in the other word the cost reduction in a year is Rp. 3.852.432,- or 10.9%. Meanwhile, the distribution cost for the industry and hospital customers is Rp. 41.201.350,-, or in other word, the cost reduction here is Rp.11.352.314,- or 21.6%. The total distribution cost that could be saved by the company for a year is Rp. 15.204.746,- or 20.92%.

REFERENCES

[1] Ballou, R.H. (2004). *Business logistics management* (5th ed). New Jersey: Prentice-Hall Inc.

[2] Berbane Dorronsoro Diaz, *What is VRP?*, 2004, <http://neo.lcc.uma.es>

[3] Brian Ratcliffe, *Economy and Efficiency in Transport and Distribution 2nd Edition*, London: Kogan Page, Ltd, 1987, p 69.

[4] Erbao, C., & Mingyong L. (2007). *An improved differential evolution algorithm for the vehicle routing problem with simultaneous delivery and pick-up service*. Third International Conference on Natural Computation.

[4] Ghiani G., Laporte G., & Musmanno R., *Introduction to Logistics Systems Planning and Control*, White Sussex: John Wiley & Sons, Ltd, 2004, p. 1.

[5] Onwubulo, C.G., & Davendra, D. (2008). *Differential evolution: A handbook for global-permutation based combinatorial optimization*. California: Springer.

[6] Price, K.V., Storn, M.R., & Lampinen, J.A. (2005). *Differential evolution: a practical approach to global optimization.* California: Springer.

[7] Rushton, A., Croucher, P., & Baker, P. (2006). *The handbook of logistics and distribution management* (3rd ed.). London: Kogan Page Ltd.

[8] Savelsbergh, M. W. P., & Sol, M. (1995, February). The general pickup and delivery problem. *Transportation Science*, 29, 17-29

[7] Toth, P., & Vigo, D. (2002). *The vehicle routing problem.* Philadelphia: Society for Industrial and Applied Mathemathics.

ISSN 114-1284

PROCESS IMPROVEMENT EFFORT OF SOFTWARE ENGINEERING IN BANK X THROUGH CAPABILITY MATURITY MODEL IMPLEMENTATION

Boy Nurtjahyo[1], Agus Sugiono[2]

[1]*Industrial Engineering Department*
Faculty of Engineering
University of Indonesia, Depok 16424
Tel: (021) 78888805
E-mail : Boy Nurtjahyo@ie.ui.ac.id
[2]*Industrial Engineering Department*
Faculty of Engineering
University of Indonesia, Depok 16424
Tel: (021) 78888805
E-mail : agus_industri2004@yahoo.com

ABSTRACT

Software engineering is urgently required by *Bank X to make its important business process faster and easier. In the other hand, Bank X's software engineering process sometimes gets some troubles. Those troubles are over budget, overtime, and inappropriate quality with the requirement. Therefore, process improvement effort is tried to be done through Capability Maturity Model (CMM) implementation as a software engineering standard process.CMM is implemented by measuring the maturity level of software engineering based on key process area of CMM repeatable level, then identifying the gap between CMM and Bank X's software engineering process, and formulizing the gap treatment to achieve repeatable level of maturity.*
From the measument process, we can know that the maturity level of its software engineering is 87% in CMM repeatable level. Meanwhile, from gap analysis, it is showed that 25% of CMM key practices in repeatable level have been partially implemented and 3% have not been impelemented. In order to handle those gaps and to improve software engineering process, some recommendations are formulated. The recommendations are training and orientation about key process areas CMM, measurement standard of developing activity status, configuration library procedure, SCM plan, automation testing tools implementation, and automation of software engineering procedure.

Keywords:

Capability, maturity model, maturity level, gap analysis, software engineering

1. Introduction

Nowadays, software engineering is urgently required by Bank X to make its important business process faster and easier. In the other hand, Bank X's software engineering process sometimes gets some troubles. Those troubles are over budget, overtime, and inappropriate quality with the requirement. The troubles can be caused by non transparency and consistency project management, inconsistency human resource management with the plan, inappropriate user requirement and documentation management.

To fix those problems is required improvement effort. One of the improvement efforts that can be establish is software process improvement through Capability Maturity Model (CMM) implementation. CMM was released by Software Engineering Institute. CMM is a set of best practices of software engineering process that divided into several Key Process Areas (KPAs). It will improve process maturity of Bank X's software engineering. If the maturity of software engineering increase, the system productivity and software quality will be better.

Based on this background, we can found that the main problem of this research is CMM implementation in Bank X's software engineering. This can be established through maturity level identification and quality improvement plan of software engineering based on gap analysis.

CMM is devided into 22 KPAs and take a long time to implement all of KPAs. Therefore, this reserch is tried to be done only in repeatable level that have 6 KPA, those are Software

Requirement Management, Software Project Planning, Software Project Tracking and Oversight, Software Subcontract Management, Software Quality Assurance, and Software Configuration Management.

Overall, this journal is about CMM implementation through maturity level measurement and gap analysis process in Bank X's software engineering in order to improve software process quality.

2. CAPABILITY MATURITY MODEL

In initial, Capability Maturity Model was developed to fulfill USA Defense Department need in selecting software vendor / supplier. Therefore, the Defense Department collaborates with Carnegie Mellon University establish Software Engineering Institute (SEI) for developing new model / standard in software process quality improvement.

Then the model was known as Capability Maturity Model, a model consist best practices of software engineering process that divided into several Key Process Areas (KPAs). Those KPAs can be looked at picture 1.

Picture 1. CMM *Key Process Areas* [2]

CMM is tried to be implemented step by step based on CMM level, start with initial level until optimizing level. The five levels in CMM cab be looked in the picture below.

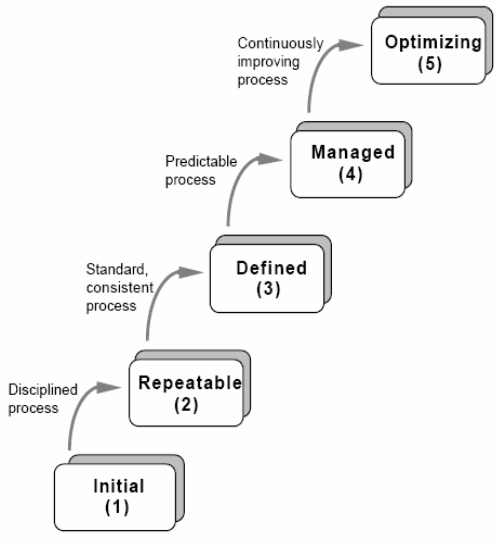

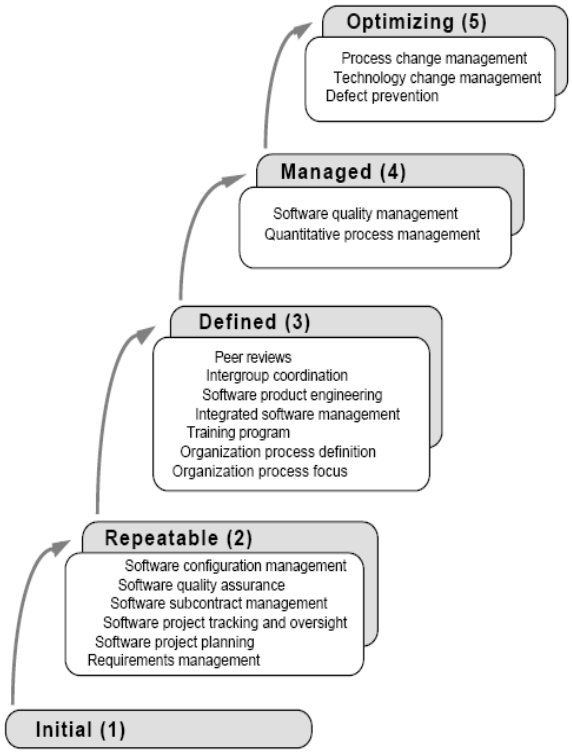

Picture 2. CMM Levels [5]

The key practices / best practices in CMM are activities that must be done and several procedures that must be had in software engineering process. These key practices in each KPA are divided into several group activities.

a. Commitment to perform, the activities to ensure stability and continuity process

b. Ability to perform, the activities group or requirement that must be had to implement good software engineering process

c. Activities performed, the procedures that needed to implement CMM key process area

d. Measurement & analysis, the needs to measure the process and analyze the result

e. Verifying Implementation, the steps to ensure activities run based on the process

3. METHOD

There are two steps that must be established to implement CMM. The first step is maturity level measurement and the second is gap analysis process to get gap treatment and

process improvement planning. Maturity level measurement process needs a good tool that gives a valid result.

To measure maturity level, Software Engineering Institute have published maturity questionnaire. In order to make easy the implementation, maturity questionnaire is developed and divided into 2 parts, process compliance interview and document review.

Process compliance interview was chosen and developed because through this process, the software engineering process in Bank X can be easily explored and confirmed.

The data that be gathered through this process are:

i. Applicability data each CMM key practice (6 KPAs CMM)

ii. Process compliance measurement of key practice (6 KPAs CMM)

The interview has closed questions and each question has 4 options: Yes, Partially, No, and Not Applicable with each weight: 1, 0.5, 0, and no weight. The amount of question is

Table 1. Question Competition of Interview

KPA	Amount of Question
SRM	12
SPP	25
SPTO	24
SSM	22
SQA	17
SCM	21
Total	**121**

To calculate the CMM compliance use the equation below

$$Q_n = \frac{(Fn+0.5Pn)}{(Fn+Pn+Nn)} \times 100\ \%$$

Legend:

Q : key practice mark

n : Number of Question

F : Total of "Yes" answer

P : Total of "Partially" answer

N : Total of " No" answer

Document review is the second step to get maturity level. The data that be gathered through this process are:

i. Document compliance measurement

ii. Documents gap based on CMM

The document review questionnaire has closed questions and each question has 4 options:

Table 2. The Answer Options for Document Review

Answer	weight	Document Status
E	1	*Evidence:* 1. Decided 2. Have a legal format 3. Implemented in all projects
F	0.8	*Formalized:* 1. Decided 2. Have a legal format 3. Implemented not in all projects
U	0.5	*Usable:* 1. Decided 2. Not have a legal format 3. Implemented not in all projects
N	0	*Not Available*

The amount of question is in the table 3.

Table 3. Question Competition of Interview

KPA	Amount of Question
SRM	9
SPP	20
SPTO	20
SSM	27
SQA	13
SCM	15
Total	**94**

To calculate the CMM document review use the equation below

$$Q_n = \frac{(En+0.8Fn+0.5Un)}{(En+Fn+Un+Nn)} \text{ X } 100\%$$

Legend:

Q : Key practice mark

n : Number of Question

E : Total of "E" answer

F : Total of "F" answer

U : Total of "U" answer

N : Total of "N" answer

4. RESULT AND ANALYSIS

From the interview process that explore 121 key practices applicability, there are 17 key practices that not applicable to be implemented in Bank X. It means only 86% key practices CMM from repeatable level can be implemented. Although the applicability is 86 %, the CMM implementation can not be troubled.

It means that the software engineering process in Bank X has good processes and compliance with almost key practice in CMM repeatable level. From data calculation and consolidation from interview and document review process, Bank X's maturity level is 87 % at repeatable level.

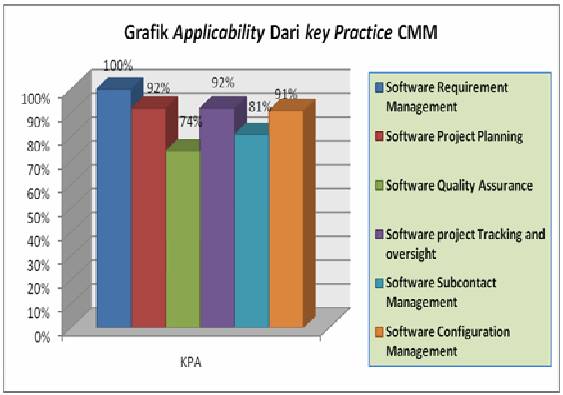

engineering that has 87 % of maturity level:

a. Bank X has software engineering policy that arrange development and maintenance of software

b. Have a good documentation in software development process

c. Good change management

d. Job of segregation has been defined very well

e. Risk in software development process always be identified

All those strengthen will keep software quality good and appropriate with the requirement standard. Good software quality is needed by Bank X because almost softwares that produced are used with national scope and critical in banking process. The maturity level for each KPA can be looked at picture 4.

In order to get CMM license in repeatable level, Bank X have to complete the CMM implementation, that is 13 % implementation. The highest priority to fulfill the implementation is Software Project Tracking and Oversight because have the lowest compliance with the CMM.

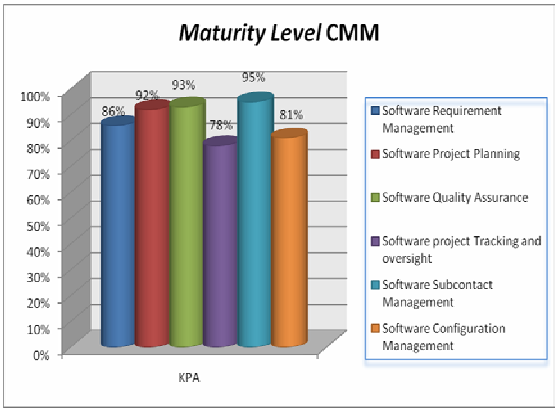

Picture 0. Calculation Result of Maturity Level

The result of maturity level measurement is also input for gap analysis process. Gap analysis process shows that 78 key practices have been implemented, 27 key practices partially have been implemented and 3 key practices not yet.

To find out root of problems why there are some key practice have partially and not been implemented, the fish bond diagram is used. The causes of problem are grouped into 3 categories. Those are human, method, and equipment. The root causes of problem are explained below:

a. Personnel Knowledge about technical aspect and management is less

b. Less of control in development policy implementation

c. Less of standard and procedure about KPA CMM

d. No measurement status from development activities

After get the causes root from the fishbod diagram, the next step is gap treatment formulation. The gap treatments are developed by analysing each gap and try to cover it.

These below are agp treatment plan to improve maturity level in Bank X's software development process

a. Training and orientation about CMM

- Requirement management

Give knowledge to make and arrange software engineering that needed to fulfill user's / customer's requirement.

- *Project management*

Give knowledge to personnel about creating a good planning in software project

- *Configuration management*

Give knowledge to personnel about goals, methods, and procedures in software configuration.

b. Measurement Standard

- Comparison between existing SQA activity and SQA planning

c. Status Measurement of software configuration management

d. Configuration library procedure

It needs a procedure for manage software configuration that cover configuration saving, using, and documenting.

e. Automation testing tool for software quality assurance

One of CMM implementation requirement is automation. The automation priority is in the software quality assurance activity, testing process.

f. Automation in software development procedure

With automation in software development procedure, documatation in developmenet process will be better managed and arranged

5. CONCLUTION

In overall, Bank X's software engineering almost complies with CMM. Based on maturity level measurement for CMM implementation in KPA: SRM, SPTO, SPP, SCM, SSM, & SQA, the maturity level is 87 %. To improve the maturity level, gap treatment planning are formulated, those are:

a. Training and orientation about CMM

a. Measurement Standard

b. Configuration library procedure

c. Automation testing tool for software quality assurance

d. Automation in software development procedure

Reference

[1] Dunaway, D. K., dan S. Masters. (2001). *CMM-Based Appraisal for Internal Process Improvement (CBA IPI), v1.2,* Pittsburgh, PA: Software Engineering Institute

[2] Mulafalija, Boris dan Harvey Strombert. (2003). *Systematic process improvement using ISO 9001:2000 and CMMI*. Boston, MA: Artech House Computing Library

[3] Mulafalija, Boris dan Harvey Strombert. (2002). Exploring CMMI-ISO 9001:2000 Synergy when developing a Process Improvement Strategy. Boston, MA: Artech House Computing Library

[4] Paulk, M. C., et al. (2001). *Capability Maturity Model for Software, Version 1.1,* Pittsburgh, PA: Software Engineering Institute

[5] Paulk, M. C., et al. (1993). *Key Practices of the Capability Maturity Model for Software, Version 1.1,* Pittsburgh, PA: Software Engineering Institute

[6] Zubrow, David, et.al. (1994). *Maturity Questionnaire,* Pittsburgh, PA: Software Engineering Institute

Confirming Relationship among Service Quality, Tourist's Satisfaction, and Behavioral Intention in Bandung Tourism Object

Budiarto Subroto[1], Kartika Akbaria[2], Achmad Jerry[3] , Safitry Tomarere[4], Ajeng Setianingrum[5]

[1]*Faculty of Industrial Technology*
Bandung Institute of Technology, Bandung 40132
Tel : (022) 250 8141. Fax : (022) 250 9336
E-mail : budiarto01@yahoo.com

[2]*Faculty of Industrial Technology*
Bandung Institute of Technology, Bandung 40132
Tel : +62 856 216 7776
E-mail : k.akbaria@gmail.com

[3]*Faculty of Industrial Technology*
Bandung Institute of Technology, Bandung 40132
Tel : +62 813 7887 6882
E-mail : achjer@yahoo.com

[4]*Faculty of Industrial Technology*
Bandung Institute of Technology, Bandung 40132
Tel : +62 815 625 2195
E-mail : tomare2_v3@yahoo.com

[5]*Faculty of Industrial Technology*
Bandung Institute of Technology, Bandung 40132
Tel : +62 817 652 6786
E-mail: hakutamanana@yahoo.com

ABSTRACT

Cole & Illum (2005) have researched about relationship among performance quality, experience quality, tourist's satisfaction, and behavioral intention. At the end, it was known that tourist's satisfaction became mediating variable between experience quality and behavioral intention, while performance quality affected behavioral intention indirectly through experience quality. This model was applied in festival research as the object. In service sector, service qualities play vital roles. A good service quality can emerge customer's behavioral intention.

This research will use Cole & Illum's model in different scope, which is applied in Bandung tourism destination. Bandung is chosen as the object research because it has diversity in tourism destination place such as artificial places, nature places, and historical building. Service quality is needed to enhance and preserve amount of the visitor for tourism's sustainability.

The research's objective is to study the relationship between behavioral intention and service quality in tourism destination place with mix tourism objects. Data is collected through questionnaire that will be distributed to several respondents. Structural equation modeling is used in confirming relationship between related variables in model measurement. The result is to confirm the continuity of tourism activity as implication of quality management in tourism destination place. Further practical implication will be discussed and be recommended to Bandung tourism stakeholders, especially local government and business' proprietor.

Keywords:
Service quality, Behavioral intention, Tourist's satisfaction, Tourism.

1. INTRODUCTION

In almost every country, tourism sector gives big contribution in increasing country's income and insensitive to economic crisis. There are several reasons which can be mentioned in order to improve management of tourism sector in Indonesia: 1)Indonesia has diversity of tourism destinations which are spreaded in every province; 2) prospect of tourism in Indonesia shows tendency which always increases every year; 3) contribution of oil and gas to country's income is become smaller; 4) tourism can enhance prosperity of community in Indonesia since they are involved in managing this sector. Tourism sector provides dominant job opportunity (take 10% of all job opportunity areas). In 2004, it was stated that 7.3 millions Indonesian worked as direct labors in this sector. While 5 millions Indonesian participated as indirect labors in similar sector (Santosa, 2004).

Although there were researches which proved that tourism sector could be superior sector in enhancing country's income, management of this sector was still low. Indonesia tourism hasn't grown significantly as tourism in

other country, such as Thailand, Malaysia, and Thailand (Rachbini, 2008). But the government always attempts to promote Indonesia tourism, both inside and abroad. Provinces which have superior tourism destination are Bali, West Java, East Java, Yogyakarta, and North Sumatra (BAPPEDA, 2005).

This study takes Bandung as the object. Nowadays, Bandung becomes show window for tourism sector in West Java since many tourists chose Bandung as their destination. Bandung has diversity in its tourism destinations, such as heritage, nature, artificial, and education destination. Base on statistic, number of tourists that visit Bandung shows significant incremental every year (BAPPEDA, 2005). Number of tourists' visit can be enhanced in two manners: 1) attracting tourist that has visited the tourism destination to revisit; 2) attracting potential tourist that hasn't visited the tourism destination. Tourist's intention to visit some destinations is affected by many factors. One factor that influences this intention is performance or service quality which is given by management team of tourism destination.

Hence, there should be an integrative cooperation among all tourism stakeholders in Bandung in developing and caring tourism destination. Through development of tourism destination, Bandung tourism sector is expected to give prosperity for local community and contributes externally in affecting development in other areas.

Objectives

The main objective in this study is to confirm Cole&Illum's model in selected tourism destination. It will be proven whether experience quality of the visitor affects behavioral intention directly or precise indirectly through tourist's satisfaction. Besides, this study is also intended to probe factors which conduct performance quality of management team in order to enhance behavioral intention of the visitor. Several reccomendations will be mentioned and can be used by tourism stakeholders, such as local government, management team of selected tourism destination, and business' proprietor.

2. CONCEPTUAL FRAMEWORK

Baker and Crompton (2000, p.788) defined tourists as 'an integral part of the service process, which is one of the characteristics that distinguishes services from products.' Because of this unique consumer, tourism has a different way to classify service quality and satisfaction. Cole & Illum (2005) classified service qualities and satisfaction at two levels, i.e. transaction level and global level. In this level, they divided in terms of performance quality and experience quality.

Many researchers studied performance quality in tourism service. Performance quality defined as a measurement of attribute level that can be controlled by the service's provider or tourism management (Cole & Illum 2005) According to this definition, performance quality can be measured by evaluating tourist's perception. (Baker & Crompton 2000). The service providers can control the attribute level such as the employee, the services or facilities that are provided by the tourism management.

On the other hand, experience quality is defined as 'those benefits or outcomes that people experience as a result of a trip or visit to a tourist attraction'. (Cole & Illum 2005, p.81). The other opinion said that experience quality shows the satisfaction of the tourists those refer to their emotional (Baker & Crompton 2000).

Performance quality can influence the experience quality of the tourist. Cole and Scott (2004, p.81) explain the 'relationship between performance quality and experience quality is intuitively straightforward'. The differences between performance quality and experience quality have been identified by Otto & Ritchie (1995, in Chen 2007, p.1131) by comparing them. The experience quality is more 'subjective to measure, evaluate tend to be holistic and focus evaluation for self (internal) and the scope is more general.' The psychological is more important than cognitive affecting to the tourist's opinion. Rather than experience quality, performance quality 'refers to service quality at attribute level, more objective to measure and the scope more specific because of the attribute.' (Otto & Ritchie, 1995, in Chen 2007, p.1131)

Lee et al (2007, p.404) said that visitor's satisfaction or tourist's satisfaction can 'increased through enhancing quality experiences by improving the quality of facilities and services.' And according to Chen (2007), between the satisfaction and service quality have a relationship on the variable that interchangeably. Previous study had indicated that service quality could influence the satisfaction of the tourists and also their behavior to intent some tourism's object (Baker & Crompton 2000, Cole et al 2002, Cole & Crompton 2003, Cole & Scott 2004, Cole & Illum 2006, Chen 2007).

Behavior intention refers to 'plans to visit the site again in the future' (Cole & Scott 2004). This behavior is an important key to the company or the service providers in tourism for a long term (Chen 2007). Behavior intention had been examined in many researches such as in wildlife refuge (Cole et al 2002), festival (Bake & Crompton 2000, Cole & Illum 2006, and Lee et al 2007), and zoo (Cole & Scott 2004, Tomas et al 2002). Model Cole and Illum (2006) is used in this research.

This research different with Cole and Scott (2004). They found that there were direct and indirect influence among the experience quality and overall satisfaction and behavior intention. But this research tries to examine direct relationship of experience quality to behavioral intention, then to see indirect relationship between experience quality to behavioral intention through overall satisfaction (Figure 1).

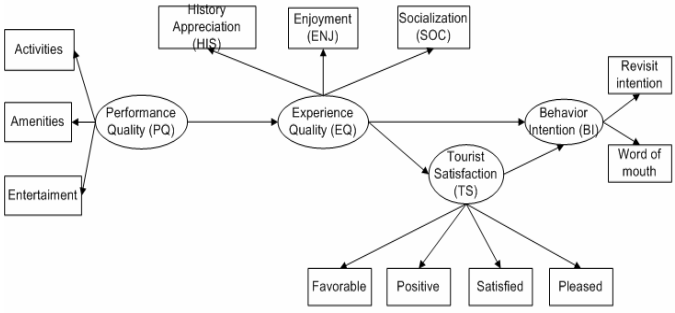

Figure 1
Model from Cole and Illum, 2006

3. RESEARCH METHODOLOGY

3.1. Study Area

Tourism destinations, which were selected to be research's objects, were decided after interviewing local government, tracing from BAPPEDA (2005) and related documents. Selected tourism destination must meet these requirements:

1. Taking location in Bandung.
2. Potential tourism destination to be developed. In other words, it must be tourism destination which hasn't been superior one.

Finally, two tourism destinations were chosen: THR. Ir. Djuanda (as representative of natural tourism object) and Asia Africa Museum (as representative of heritage object). These objects were potential ones to be developed in future.

3.2. Data Collection

Target population was visitors which fit these requirements:

1. Minimum age was 15 years. This minimum age was assumed to have adequate income or pocket money to visit researched tourism destination.
2. The visitor had ever come to selected tourism destination, maximum 5 years ago (2004).
3. The visitor must be Indonesian (domestic visitor).

This research used judgment sampling since respondent's profile was emerged.

Questionnaires were used to collect primary data. Initial questionnaires were first constructed in order to eliminate variables that would be used in main questionnaire. Thirty questionnaires for each selected tourism destination were distributed. By using SPSS 12.0, validity test and reliability test were done. From these tests, several variables were deleted. Chosen variables were kept to be used in main questionnaire. Finally, there were 54 main questions and 62 main questions respectively in questionnaire of Asia Africa Museum and THR. Ir. Djuanda.

Minimum sample size was decided by considering:

1. Amount of respondents in target population.
2. Amount of questions in questionnaire.

Since amount of respondents in target population couldn't be stated clearly, number of sample was decided by considering number of question in questionnaire. Greater number of respondents was better. Simamora (2004) stated that minimum sample size to be used in factor analysis was three to five times of number of questions. Thus, 343 questionnaires and 314 questionnaires, respectively, were distributed. For Asia Africa Museum, 221 questionnaires (rate of 64.43%) could be drawn back and be extracted. Whereas for THR. Ir. Djuanda, 257 questionnaires (rate of 81.84%) were gathered.

3.3. Operationalization of Constructs

Questions in main questionnaire were constructed by combining several items from other similar researches.

Initial questionnaire comprised of:

1. Part One Respondent's profile: age, gender, marital status, kind of work, living location, income per month, arrival frequency, and last arrival to selected tourism destination. Nominal scale was used in this part. Type of questions were closed questions. Output of this part was used in descriptive analysis of tourist's demography.
2. Part Two Variables identification, which consisted of 64 questions. In main questionnaire, there were only several questions used. Likert scale (from 1 to 5, strongly disagree to strongly agree) was used in this part. Output of this part will be used in confirmatory analysis.

3.4. Construct Measurement

Primary data from questionnaire's part two were classified in several factors by using factor analysis. After emerging those factors, overall model was constructed.

There are three constructed models:

1. Structural model, which stated relationship between latent variables (performance quality (PQ), experience quality (EQ), tourist's satisfaction (TS), and behavioral intention (BI)).
2. Measurement model, which stated relationship between latent variable and its factors.
3. Overall model, which showed all emerged relationships.

Testing of those models was done by using Lisrel 8.7. Yielded output will be analyzed in next step.

4. RESULTS

4.1. THR. Ir. Djuanda

From respondent's demography of THR Ir.Djuanda, it was showed that dominant respondent had these characteristic: interval age between 21-30 years old (42.02%), woman (57.20%), unmarried (71.21%), work as officer of private sector (41.25%), residing in North Bandung (41.25%), last arrival time is less than 6 months (37.74%), and arrival frequency is 1-2 times (54.86%). Data related to respondent's demography can be seen at Table 1.

Table 1. Respondent's demography of THR Ir. Djuanda

Gender		
Male	147	57.20%
Female	110	42.80%
Married Status		
Single	183	71.21%
Married	72	28.02%

Divorce	2	0.78%
Visiting Frequency		
1-2 times	141	54.86%
3-4 times	75	29.18%
more than 5 times	41	15.95%
Income		
1.000.000 and below	130	50.58%
1.000.000 - 3.000.000	91	35.41%
3.000.000 - 5.000.000	30	11.67%
5.000.000 and above	6	2.33%
Living		
North of Bandung	106	41.25%
East of Bandung	50	19.46%
South of Bandung	36	14.01%
West of Bandung	43	16.73%
Others	22	8.56%
Employment		
Government Employee	6	2.33%
Private Employee	106	41.25%
Entrepreneur	9	3.50%
Housewife	1	0.39%
Student	36	14.01%
College	95	36.96%
Others	4	1.56%
Last Visit		
6 months and below	97	37.74%
Last year	77	29.96%
A year and above	83	32.30%
Age		
20 years old and below	81	31.52%
21-30 years old	108	42.02%
31-40 years old	29	11.28%
40 years old and above	39	15.18%

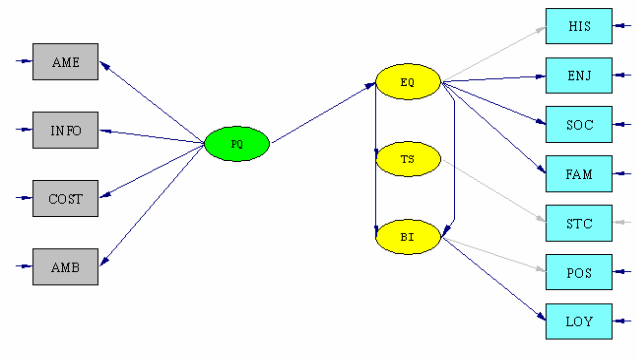

Figure 2. Conceptual Model for THR. Ir. Djuanda

From questionnaire part II, it was yielded that Alpha Cronbach of data was 0.992. Then, by using Spearman Correlation, it was showed that all data were valid in significance level = 0.01. SPSS 12.0 was used in completing these tests.

Figure 2 shows processed conceptual model by using LISREL 8.70. The result for the goodness-of-fit of model refers to Table 2. Commonly, the structure model is assessed by the χ^2 of the goodness-of-fit (Lee, 2009). The χ^2 goodness-of-fit has a function to compare between the 'adequacy of the theorized model's creation of a covariance matrix and estimated coefficients with the observed covariance matrix.' (Lee, 2009, p.228). McDonald and Ho (2002, in Lee, 2009, p.228) said that 'many researchers have divided the value of $\chi 2$ by degrees of freedom to accommodate large samples size.' But the ratio of the model could not determine the goodness-of-fit of the model (Anderson and Gerbing, 1982 in Lee,2009,p.228). Other indicators that can be used to assess model's goodness-of-fit are fit and alternate indices as showed in Table 2.

Table 2. GOF of structural model (THR Ir. Djuanda)

	Criteria	Initial	Revised
Chi-square			
$\chi 2$	p>0.05	338.29 (p < 0.00)	169.497 (p<0.00)
d.f	-	41	37
$\chi 2$/d.f	<5	8.2508	4.58101
Fit indicate			
GFI	>0.9	0.81	0.89
AGFI	>0.9	0.69	0.8
RFI	>0.9	0.62	0.81
NFI	>0.9	0.72	0.87
NNFI	>0.9	0.65	0.85
Alternative indicates:			
CFI	>0.95	0.73	0.9
RMSEA	<0.05	0.17	0.12
RMR	<0.05	0.2	0.08

The relationship among latent variable and its manifest is showed in Table 3. This data explain both initial and revised model. Improvement of standardized loading factor happened after model revised. Most of relationships among the latent variable with the manifest variables are significant except relationship between performance quality & amenities (0.02), and experience quality & socialization (0.1).

Table 3. Standardized Loading Factor and t-value

Construct & Indicators	Initial		Revised	
	SLF	t-value	SLF	t-value
Performance Quality (PQ)				
Amenities	0.02	0.38	0.03	0.48
Information	0.55	9.08	0.55	9.04
Cost sensitivity	0.86	16.15	0.85	15.96
Ambience	0.93	18.16	0.93	18.01
Experience Quality (EQ)				
History Appreciation	0.69	-	0.74	-
Enjoyment	0	0.05	0.14	2.22
Socialization	0.06	0.92	0.1	1.71
Family togetherness	0.24	3.35	0.44	5.36
Tourist Satisfaction (TS)				
Satisfied	1	-	1	-
Behavior Intention (BI)				
Say positive things	0.68	-	0.71	-
Loyalty	0.71		0.68	6.79

*) very significant,

Table 4 shows SLF and t-value of latent variables. From Table 4, it was known that the greatest effect was showed in path from EQ to TS. Besides, it was also known that effect from EQ to BI directly was better.

Table 4. Direct and Indirect effect Among Variables

Effect among variable	Effects			
	Direct	Indirect		TOTAL
		EQ	TS	
Performance Quality->Experience Quality	0.62			0.62
Performance Quality->Tourist Satisfaction		0.52		0.52
Performance Quality->Behavior Intention		0.34		0.34
Experience Quality -> Tourist Satisfaction	0.83			0.83
Experience Quality->Behavior Intention	0.55		-0.14	0.41
Tourist Satisfaction->Behavior Intention	0.17			0.17

4.2. Asia AfricaMuseum

From tourists' profile that have been visited Asia Africa Museum in Bandung, it was dominated by youth, students and colleges, living in East Bandung, and income less than IDR 1 million. Probably, this result was affected by distribution sampling that was centered to young respondent. According to visit frequency, most respondents have been visited 1-2 times and the last visit was 6 months and below. This result indicated their intention to revisit. Unfortunately, there was still no conclusion because there was no segregation between once and twice visit. Hence, it couldn't be concluded whether they had high intention to revisit or not. Completely, respondent's demography of Asia Africa Museum is showed in Table 5.

From questionnaire part II, it was yielded that Alpha Cronbach of data was 0.884. Then, by using Spearman Correlation, it was showed that all data were valid in significance level = 0.01. SPSS 12.0 was used in completing these tests.

Table 5. Respondent's demography of Asia Africa Museum

Gender		
Male	109	49.32%
Female	112	50.68%
Married Status		
Single	51	23.08%
Married	166	75.11%
Divorce	4	1.81%
Visiting Frequency		
1-2 times	182	82.35%
3-4 times	26	11.76%
more than 5 times	13	5.88%
Income (IDR)		
1.000.000 and below	150	67.87%
1.000.000 - 3.000.000	58	26.24%
3.000.000 - 5.000.000	12	5.43%
5.000.000 and above	1	0.45%
Living		
North of Bandung	50	22.62%
East of Bandung	62	28.05%
South of Bandung	36	16.29%
West of Bandung	29	13.12%
Others	44	19.91%
Employment		
Government Employee	39	17.65%
Private Employee	14	6.33%
Entrepreneur	7	3.17%
Housewife	4	1.81%
Student	57	25.79%
College	91	41.18%
Others	9	4.07%
Last Visit		
6 months and below	114	51.58%
Last year	36	16.29%
A year and above	71	32.13%
Age		
20 years old and below	118	53.39%
21-30 years old	55	24.89%
31-40 years old	16	7.24%
40 years old and above	32	14.48%
Not mentioned	1	0.45%

Factor analysis was done in order to probe number of factors that were used in confirmatory analysis by using LISREL 8.70. Results of rotated component matrix showed that there were 15 extracted factors which categorized each item as showed in Figure 3. Therefore, there were 15 manifest variables and 4 latent variables used as the inputs of LISREL. Factors of performance quality (PQ) are: facilities, activities, staffs, amenities, information, ambience, and emotional response. While factors for experience quality (EQ) are history appreciation, socialization, enjoyment, and cost. Tourist' satisfaction (TS) is constructed by two factors: pleased and satisfied. Behavioral intention is also constructed by two factors: say positive things and loyalty. Complete conceptual diagram for Asia Africa Museum is showed in Figure 3.

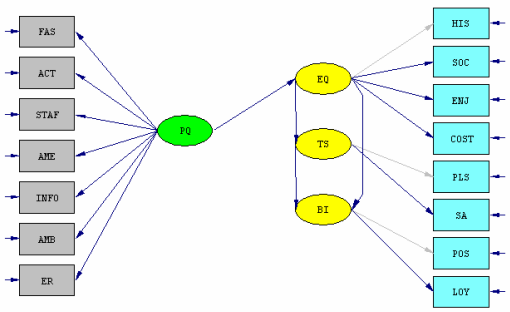

Figure 3. Conceptual Model for Asia Africa Museum

Revised model differed from initial one since there was alteration in setting error covariance of FAS (facilities) and

ACT (activities). Statistic data which was conducted by LISREL are showed below.

Table 6. GOF of structural model

	Criteria	Initial	Revised
Chi-square			
$\chi 2$	p>0.05	608.78 (p<0.00)	210.71 (p<0.00)
d.f	-	86	85
$\chi 2$/d.f	<5	7.07	2.48
Fit indicate			
GFI	>0.9	0.73	0.89
AGFI	>0.9	0.62	0.84
RFI	>0.9	0.70	0.88
NFI	>0.9	0.75	0.90
NNFI	>0.9	0.73	0.92
Alternative indicates:			
CFI	>0.95	0.78	0.94
RMSEA	<0.05	0.17	0.082
RMR	<0.05	0.18	0.11

From Table 6, it was showed that revised model met better fit than initial one.

Table 7. Standardized Loading Factor and t-value

Construct & Indicators	Initial		Revised	
	SLF	t-value	SLF	t-value
Performance Quality (PQ)				
Facilities	0.91	14.84	0.25	3.52
Activities	0.92	15.05	0.25	3.43
Staff	0.29	4.27	0.40	5.77
Amenities	0.23	3.26	0.46	6.77
Information	0.09	1.26	0.41	5.88
Ambience	0.20	2.92	0.71	11.28
Emotional response	0.28	4.06	0.86	14.59
Experience Quality (EQ)				
History Appreciation	0.87	-*	0.85	-*
Socialization	0.82	11.67	0.80	12.84
Enjoyment	-0.14	-1.93	-0.17	-2.44
Cost	0.51	7.30	0.51	7.60
Tourist's Satisfaction (TS)				
Pleased	0.39	-	0.38	-
Satisfied	0.92	4.25	0.95	4.22
Behavior Intention (BI)				
Say positive things	0.72	-*	0.72	-*
Loyalty	0.70	7.99	0.70	8.03

*) very significant,

From Table 7, it was showed that there were several differences in SLF and t-value between two models. Significant differences were among factors which constructed PQ and EQ. All factors which gave stronger effect to PQ in initial model became factors with weaker effect in revised model, and vice versa. Constructed factors in revised model for EQ showed weaker effect than initial one, although in insignificant value.

Table 8 showed SLF and t-value of latent variables. From this table, it was known that the greatest effect was showed in path from PQ to EQ. Besides, it was also known that effect from EQ to BI was better through TS.

Table 8. Direct and Indirect effect Among Variables

Effect among variable	Effects			
	Direct	Indirect		TOTAL
		EQ	TS	
Performance Quality->Experience Quality	0.85			0.85
Performance Quality->Tourist Satisfaction		0.56		0.56
Performance Quality->Behavior Intention			0.58	0.58
Experience Quality -> Tourist Satisfaction	0.66			0.66
Experience Quality->Behavior Intention	0.32		0.36	0.68
Tourist Satisfaction->Behavior Intention	0.55			0.55

5. DISCUSSION

5.1. THR. Ir. Djuanda

From the result, it is founded that performance quality has strong relation with ambience as the manifest variable. 'Ambience' refers to authenticity of place, individuality of place, and there is no similar tourism destination in Bandung. Result indicates that ambience has become superior factor of tourism and require to be preserved. Weak relation in performance quality is happened at amenities. 'Amenities' refer to supporting facilities that give visitor's freshness, such as availability of parking area, restroom, souvenir shop, staff which dress nattily and also friendly, variation of activities, and feel secure. This finding is enough occasions because amenities support visitor's freshness when reside in the tourism destination. Tourist's freshness will affect behavioral intention positively, shown with revisit behavior of the visitor. Base on respondent's demography, it is known that 58.76% visitors come from outside of North Bandung. Therefore, visitor's freshness becomes important factor to be notice. This factor will attract them to revisit although the duration journey, which usually becomes visitor's internal consideration, takes long time.

For experience quality, strong relation is happened at history as the manifest variable. 'History' refers to history's atmosphere which felt during at the tourism destination. While weak relation is happened at socialization. 'Socialization' refers to interaction between visitor and friend, family, and other visitors. THR Ir.Djuanda has a vast area which is useful for social activities like family vacation, school vacation or others social groups such as student group which explors the tunnels. Some respondents say that they choose THR Ir.Djuanda to do activity group because of the location is vast and the air is balmy. Respondent's demography shows that dominant respondent are in the age of 21-30 years old (42.02%) and unmarried (71.21%). This finding shows why THR Ir.Djuanda used for social activity. But the data showed that socialization gave weak relation. In fact, this tourism destination is usually used for social activity. Previous explanation, which describes about

amenities factor, states that freshness in tourism destination can also influence the visitor social interaction. Thus, both amenities and socialization need to be improved.

Pursuant to the last arrival of respondent, most respondents express that they just visit the tourism destination in the last 6 months. If last arrival data is related to the frequency of arrival, the result shows that most of them are new visitors who visit THR Ir.Djuanda once or twice. This finding needs to analyzed carefully since the result indicates that loyalty influences intention behavioral weakly. It means that arrival frequency (once or twice visit) may become indicator of low tourist's revisit to the tourism destination. Thus, developer has to notice and control performance quality because it is able to influence the tourist's behavioral intention.

From the relationship among latent variables, it can be seen that performance quality can affect the behavioral intention both directly and indirectly (Table 4). Indirect relationship between performance quality and behavioral intention doesn't show strong relationship. Although the relationship is not strong enough, but the influence of performance quality to behavioral intention needs to be considered. According to Cole and Illum (2005), performance quality is the factor that can be controlled by tourism management team. Significant relationship is happened between experience quality and tourist's satisfaction. Cole and Illum (2005) have already explained that in experience quality, mood of tourist has an important role to increase the tourist's satisfaction. Although experience quality could not be controlled by the tourism management team, but experience quality can be influenced by good performance quality.

Implication for THR. Ir. Djuanda management team is to keep the ambience of THR. Ir. Djuanda in order to preserve the authenticity of tourism destination. Besides , it is also recommended to improve the amenities by providing good facilities, such as restroom, parking area, variation of activities, etc. Other thing that should be noticed by management team is interaction of people which has been obtained in explanation about socialization variable. It means that improvement in amenities and socialization can influence the tourist's behavioral intention. especially to revisit to THR. Ir. Djuanda.

5.2. Asia Africa Museum

Acoording to statistic data which is showed in Table 8, it is founded that experience quality has greater effect to behavioral intention through tourist's satisfaction. In other words, for Asia Africa Museum, it can be concluded that indirect model is more suitable than direct model. It is because museum's visitor usually has high expectation to be served well when visit the museum. Performance quality has vital role in emerging tourist's satisfaction, especially in service from tour guide or staff. It will yield different emotional response when visitor is accompanied by tour guide. By receiving direct explanation from tour guide or museum's staff, it is possible to emerge higher visitor's sense of belonging to the history.

Besides, from Table 7 it is showed that variable 'positive' and 'loyalty' are similar in giving strong effect to behavioral-intention's construct. While for tourist's satisfaction, variable 'satisfied' gives stronger effect than variable 'pleased'. It can be interpreted that to enhance Behavioral Intention, satisfaction of the visitor should be increased.

For experience quality, variable 'history appreciation' and 'socialization' give stronger effect than other variables which construct similar latent variable. Variable 'cost' also gives positive effect, but weaker than other two variables. Whereas, variable 'enjoyment' gives negative effect to experience quality. If this finding is related with respondent's demography, it can be explained by respondent's age. Most of respondents are youth whose ages are under 20 years old. They usually come to Museum for academic task and their arrival isn't for get enjoyment or refreshing. There are also several respondents whose ages more than 40 years old. This type of respondents has tendency to visit museum with family. Their motive tends to introduce history of Indonesia to their children and not for enjoyment purpose.

For performance quality, variable 'emotional response' and 'ambience' give stronger effect than other variables. It can be interpreted that management team of Asia Africa Museum has given good performance quality which relates with these variables. Whereas, variable 'facilities' and 'activities' give similar effect which are the weakest of all. Other variables such as 'staff', 'amenities', and 'information' also show weak effect. According to data simulation, behavioral intention and its manifest variables will be higher if all factors which construct performance quality are also high.

Thus, there are several implications managerial for management team of Asia Africa Museum. Strong suggestion is preserving the authenticity of the place. If there will be some rehabilitations, it is not suggested to change the place significantly so that visitor still feel historic atmosphere.

Besides, other suggestion is availability of comfort facilities, include facility for handicapped person. Other facilities to be noticed are availability of parking area, restrooms, and restaurants which take place around the museum. For restaurant availability, management team of Asia Africa Museum can cooperate with business' proprietor around the museum. While, suggestions which relate with Museum's activities are availability of variation activities for visitor and promotion of museum.

It is also suggested to enhance performance quality which relates with amenities, staff, and information. Amenity refers to visitor's pleasure, such as cleanliness and layout arrangement. Staff refers to knowledge, hospitality, and availability of tour guide which also can speak other languages, especially English. Information refers to availability of information display, information centre, map, and catalogues.

6. CONCLUSION

It can be concluded that Cole&Illum's model can be applied in both heritage and nature tourism destination. Direct relationship from experience quality to behavioral intention is founded stronger in nature tourism destination. It implies higher visitor's behavioral intention can be achieved through higher experience quality. It isn't needed to notice tourist's satisfaction significantly.

Whereas, indirect relationship from experience to behavioral intention of the visitor is founded stronger in heritage tourism destination. It implies higher behavioral intention can be reached by enhancing experience quality through tourist's satisfaction.

Similar conclusion for nature and heritage tourism destination is higher performance quality can affect visitor's behavioral intention positively. It means that management team of those tourism destinations should notice their performance quality.

7. SUGGESTION

Several suggestions for further research are: 1) setting larger number of sample in order to get model comparation of behavioral intention for similar tourism destination. Besides, it has a purpose to state whether each museum and nature tourism destination has similar model. Therefore, model generalization of behavioral intention for each tourism destination can be yielded; 2) exploring respondent's demography and make segment categorization so that type of behavioral intention for each segment can be identified; 3) deeper analysis in profile segmentation can increase performance quality of management team at each tourism destination; 4) applying similar model for different tourism destination which haven't been discussed in this study. Therefore, there will be a complete model of Bandung tourism object which obtains about behavioral intention of the tourist.

ACKNOWLEDGMENT

Authors thank to management team of Asia Africa Museum, THR Ir. Djuanda, and Departement of Tourism for West Java.

REFERENCES

[1] BAPPEDA, "Master Plan of Local Tourism Development in West Java Province" (in Indonesia), *Rencana Induk Pengembangan Pariwisata Daerah Provinsi Jawa Barat*, 2005.

[2] B. Simamora, "Marketing Multivariate Analysis" (in Indonesia), *Analisis Multivariat Pemasaran*, Jakarta: PT.Gramedia Pustaka Utama, 2004.

[3] C.F Chen, "Experience Quality, Perceived Value, Satisfaction and Behavioral Intentions for Heritage Tourists", *Proceedings of the 13th Asia Pacific Management Conference*, Melbourne, Australia, p.1130-1136, 2007.

[4] D.Baker.J.L.Crompton, "Quality, Satisfaction and Behavioral Intention", *Annals of Tourism Research*, vol.27, no.3, pp.785-804, 2000.

[5] D.J. Rachbini, "Basic Weakness of Indonesia Tourism" (in Indonesia), *Kelemahan Mendasar Pariwisata Indonesia*, Jawa Pos *Online*, <http://g1s.org/blog/kelemahan-mendasar-pariwisata-indonesia-866/>, accesed on November 10, 2008.

[6] S.P. Santosa, "Investigating The Competitiveness of Indonesia Tourism" (in Indonesia), *Mengenali Daya Saing Pariwisata Indonesia*, http://kolom.pacific.net.id/ind/setyanto_p._santosa/artikel_setyanto_p._santosa/mengenali_daya_saing_pariwisata_indonesia.html, accesed on October 17, 2008.

[7] S.R Tomas, D.Scott, J.L.Crompton, "An investigation of the relationships between quality of service performance, benefit sought, satisfaction and future intention to visit among visitors to a zoo", *Managing Leisure*, vol.7, pp.239-250, 2002.

[8] S.T Cole, J.L.Crompton, V.L.Wilson, "An empirical investigation of the relationships between service quality, satisfaction and behavioral intentions among visitors to a wildlife refuge", *Journal of Leisure Research*, vol.34, no.1, pp.1-24, 2002.

[9] S.T Cole, S.F Illum, "Examining the mediating role of festival visitors' satisfaction in the relationship between service quality and behavioral intentions", *Journal of Vacation Marketing*, vol.12,no.2, 2006

[10] S.T. Lee, "A Structural model to examine how destination image, attitude and motivation affect the future behavior of tourist", *Leisure Science*, vol.31, pp.215-236, 2009

[11] S.Y. Lee, J.F.Petrick, J.L.Crompton, "The roles of quality and intermediary constructs in determining festival attendees' behavior intention", *Journal of Travel Research*, vol.54 no.4, pp.402-412, 2007.

ISSN 114-1284

Preventive Action for Quality Improvement of the VTL Lamp in the End Process Quality Control (Study Case at a Lamp Manufacturer)

Debora Anne Yang Aysia[1], Natalia Hartono[2], Thomas Harmani[3]

[1]*Faculty of Industrial Technology-Industrial Engineering Department*
Petra Christian University, Surabaya 60236
Tel: (031) 2983433 Fax: (031)8417658
debbie@peter.petra.ac.id

[2]*Faculty of Industrial Technology-Industrial Engineering Department*
Petra Christian University, Surabaya 60236
Tel: (031) 2983433 Fax: (031)8417658
natalia@peter.petra.ac.id

[2]*Faculty of Industrial Technology-Industrial Engineering Department*
Petra Christian University, Surabaya 60236
Tel: (031) 2983433 Fax: (031)8417658

ABSTRACT

Minor defect is a defect category that made to anticipate the types of potential defect. These preventive actions generate the increasing type and number of defect (there are more than 34 types of defect for minor defect and will continue to grow). Therefore, it's required a number of efforts to reduce the number of defect and to eliminate the types of defect.

MEDIC method is used to reduce the number of defect with high frequency of occurrence. We get 17 types of defect to be done, and then we identify the root causes that result 51 proposed solutions. From 51 solutions, 10 of them are implemented. As the result, the defect proportion of 11 from 17 defects are significantly reduced with α=5%.

The Deming Cycle (PDSA) method is used to eliminate the types of the defect with low frequency of occurrence from defect list. We get 14 types of defect to be eliminated. And then, for the trial period (11 days), we get 13 from 14 types of defect that will be proposed to be eliminated, because they have not emerged for the last 3 months and have passed the trial period.

Keywords

Preventive action, Minor defect, Occurrence's frequency, MEDIC, PDSA.

1. INTRODUCTION

"Quality is fitness for use" is a definition of quality by Joseph M. Juran. Quality must be maintained by a company in order to improve company's competitive advantage. Each company has to improve its product quality and process quality continually. There is no limitation for continuous quality improvement.

A company often focuses their quality improvement by doing a final inspection at the end of the production process. It seems too late, because the defective product will be detected at the end of the process, where all of the production's input has been used. This research focuses on the quality effort all along the production process, in order to prevent the defective product attain the end production process.

A lamp manufacturer, which produce VTL lamp, has four categories for their defect. They are as follow:

a. Critical safety defect, defect which is related to lamp user's safety.
b. Inoperative defect, defect which is related to the lamp reliability
c. Major defect, defect which influence customer's purchase interest.
d. Minor defect, defect which is tolerable but the company focuses on it, in order to maintain its product quality.

The focus of this research is on the minor defect because the number of minor defect is tending to increase. The objective of this research is to minimize several high frequency defect types and to eliminate several low frequency defect types from the minor defect list, at the end process quality control.

2. RESEARCH METHOD

This research follows MEDIC steps. The step can be seen at Figure 1. In the exploration and evaluation phase, the Deming Cycle is used to eliminate defect types with low frequency of occurrence. The application of Deming Cycle can be seen at Figure 2.

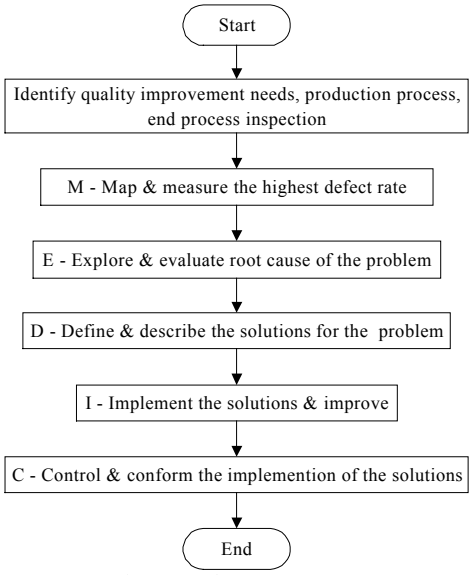

Figure 1: The MEDIC steps

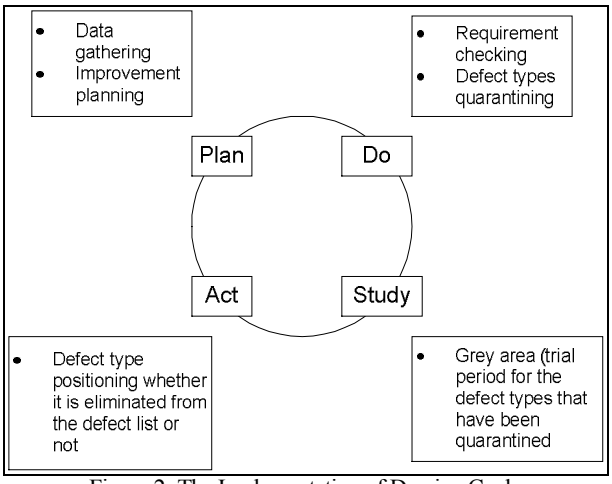

Figure 2: The Implementation of Deming Cycle

3. DATA ANALYSIS

3.1 Mapping and Measurement

The production division of the lamp manufacturer has eleven production processes to produce a VTL Lamp. They are as follow:

a. Washing and drying
b. Coating and drying
c. Oven sintering
d. Wiping and marking
e. Stem and mounting
f. Sealing
g. Pumping
h. Capping
i. Soldering
j. Flushing and testing
k. Packing

End process quality control is a quality control activity that is done at the end of production process (before packing). The objective is to inspect whether there is any defective VTL lamp or not, before the lamp is delivered to customer. The latest six month historical data from the end process quality control is used to find the highest minor defect rate. The data can be seen at Table 1.

Table 1: Historical data

Defect Type	Frequency
Foreign object	4
Mercury fleck	140
Swirling	108
Aslant cap	207
Cement waste	342
Knot 1	161
Dented cap	310
Unclear outer box's stamp	1
Unsticky tape	206
Loosen sleeve	113
Wrong packing date	5
Window	859
Powder off < 1 mm	65
Powder off 1-2 mm	63
Powder off > 2 mm	123
Dirty coating < 1 mm	90
Dirty coating 1-2 mm	30
Dirty coating > 2 mm	48
Pin hole	106
Rough coating	110
Stripe coating	98
Overflow 1/4 lamp's length	105
Air line glass	62
Defective glass	171
Fish eye > 10 mm	687
Fish eye < 10 mm	598
Blistered	230
Printed tape is sticky with the lamp	368
Long sleeve	72
Short sleeve	99
Clamp mark	58
Light stain	880
Motley	95
Glue stain	389
Wringkle	19
Aslant stel	59
No friction tape	11
Collide stel	16
Damaged sleeve	50
Damaged stel	2
High cap	31
Dirty tube	0
Blown	16
Bad sleeve	24
Folded seal	3
No coating	2
Thin coating	1
Glass stain	1
Sit high cap	1
Mire cap	4
Glass chips	1
Double sleeve	1
Flat lamp	1

Pareto Chart is built based on the data (see Figure 3). According to 80-20 rule, it can be seen from the chart that 80% defect types with high occurrence contains of 17 defect types. They are light stain, window, fish eye > 10 mm, fish eye < 10 mm, glue stain, printed tape is sticky with the lamp, cement waste, dented cap, blistered, aslant cap, unsticky tape, defective glass, knot 1, Mercury fleck, powder off > 2mm, loosen sleeve and rough coating. In the next step, these defect types will be analyzed, so they can be minimized in quantity.

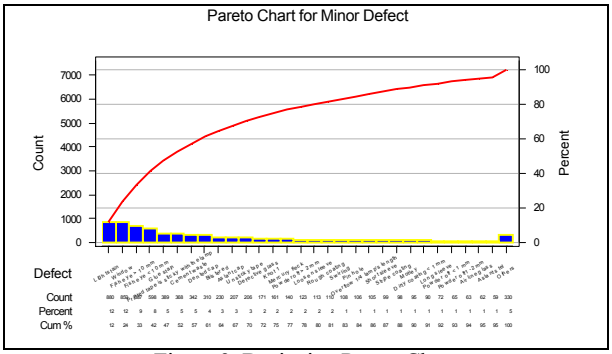

Figure 3: Beginning Pareto Chart

3.2 Exploration and Evaluation

3.2.1 Defect types with high frequency of occurrence

There are 17 defect types with high frequency of occurrence as mentioned before. In this phase, the root causes of all this defect types are explored using 5 WHY and Fault Tree Analysis (FTA). The objective of 5 Why is only to find the root causes of the problem, but the objective of FTA is not only to find the root causes of the problem, but also to find the relationship between the root causes. The example of 5 WHY and FTA for light stain can be seen at Table 2 and Figure 4.

Table 2: 5 WHY for light stain

No.	Problem	Why 1	Why 2	Why 3	Why 4	Why 5
1	Light Stain	Polluted suspension	Spray from cylinder air's oil	No cover at cylinder air's filter		
			Dew from cylinder air's oil			
		Unstable blast from drying blower	One or several butterflies are blocked	Saturated butterfly's filter at ducting		
			Unstable blast from segment 1-7	One or several butterflies are blocked by waste		
				Return pressure from segment 8-19		

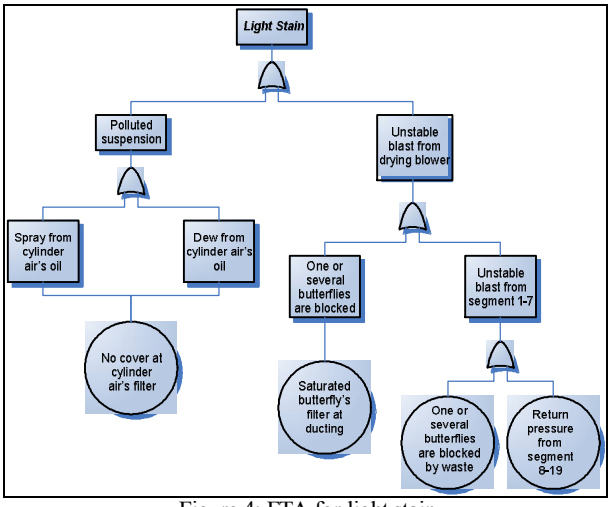

Figure 4: FTA for light stain

Totally, there are 49 root causes for the 17 defect types. The amount of root causes for each defect type can bee seen at Table 3.

Table 3: Number of root causes for each defect types

Defect Type	Number of Root Causes
Light stain	4
Window	5
Fish eye > 10 mm	2
Fish eye < 10 mm	
Glue stain	6
Printed tape is sticky with the lamp	7
Cement waste	3
Dented cap	4
Blistered	3
Aslant cap	2
Unsticky tape	2
Defective glass	1
Knot 1	1
Mercury fleck	1
Powder off > 2 mm	2
Loosen sleeve	5
Rough coating	1

3.2.2 Defect types with low frequency of occurrence

As mentioned before, Deming cycle is used to analyze defect type with low frequency of occurrence.

"Plan" phase has been done when the Pareto Chart was built. Some defect types with low frequency of occurrence can be seen from the chart.

In the "Do" phase, all of defect types are screened using four categories. They are as follow:

a. Process stability
   This requirement use Time Line Chart as a tool to examine the defect fluctuation and trend in the last three month, for defect types which have total number not more than 1 for the latest six month.
b. Customer requirement
   This requirement examine whether a defect type is included in the voice of customer or not.
c. Company requirement
   This requirement examine whether a defect type is included in company standard or not
d. IEC standard requirement
   This requirement examine whether a defect type is included in international lamp requirement or not.

As a result, there are 14 defect types that pass the screening. They are foreign object, unclear outer box's stamp, collide stel, damaged stel, dirty tube, folded seal, no coating, thin coating, glass stain, sit high cap, mire cap, glass chips, double sleeve, and flat lamp.

In the "Study" phase, 14 defect types enter the eleven days trial period, which is call grey area. If they can pass the trial period, which mean no defective item related with the defect types, then the defect types can be eliminated from the minor defect list. But if there is a defectives item related with them, they can not be eliminated from the defect list.

In the "Act" phase, the defect types' statue is determined, whether they can be eliminated from the minor defect list or not. The trial period result can be seen at Table 4. There are 13 defect types that pass the trial period, so they can be eliminated from the minor defect list. But there is only one defect type that fails to pass the trial period, which is unclear outer box's stamp. It can be seen that there are two unclear outer box's stamp in day 7.

Table 4: Trial period result

Defect Type	Day 1	Day 2	Day 3	Day 4	Day 5	Day 6	Day 7	Day 8	Day 9	Day 10	Day 11
Foreign object	0	0	0	0	0	0	0	0	0	0	0
Unclear outer box's stamp	0	0	0	0	0	0	2	0	0	0	0
Collide stel	0	0	0	0	0	0	0	0	0	0	0
Damaged stel	0	0	0	0	0	0	0	0	0	0	0
Dirty tube	0	0	0	0	0	0	0	0	0	0	0
Folded seal	0	0	0	0	0	0	0	0	0	0	0
No coating	0	0	0	0	0	0	0	0	0	0	0
Thin coating	0	0	0	0	0	0	0	0	0	0	0
Glass stain	0	0	0	0	0	0	0	0	0	0	0
Sit high cap	0	0	0	0	0	0	0	0	0	0	0
Mire cap	0	0	0	0	0	0	0	0	0	0	0
Glass chips	0	0	0	0	0	0	0	0	0	0	0
Double sleeve	0	0	0	0	0	0	0	0	0	0	0
Flat lamp	0	0	0	0	0	0	0	0	0	0	0

3.3 Definition and Description

As mentioned before, there are 49 root causes of 17 defect types. Through brainstorming, there are 51 proposed solutions; 10 of them will be implemented. They are as follow:

a. Modification of air cylinder sprayer filter.
   This solution prevents light stain, which is caused by suspension which is polluted by oil.
b. Additional cooling blower for tube which is come from oven sintering.
   This solution prevents window that is caused by tube which is not cool enough.
c. Additional automatic tool for suspension filling from offline to online,
   This solution prevents fish eye that is caused by bubble in the suspension which is flown from water base to production line.
d. Modification of glue needle.
   This solution prevent glue stain, that is caused by he position of the glue needle is change.
e. Modification of printed tape holding device.
   This solution prevent printed tape is sticky with the lamp, that is caused by the twisting position of printed tape.
f. Nozzle point modification by installing rubber seal.
   This solution prevents cement waste that come from turret cap filler.
g. Modification of cover tray.
   This solution prevents cement waste that is caused by dirty pin cap on the tray.
h. Additional upper holding device on the skater cap and turret meeting point.
   This solution prevents dented cap, which is caused by wide distance between skater cap and turret.
i. Glue viscosity study.
   This solution prevents unsticky tape that is caused by unfit dryness rate when the tape is assembled with the sleeve.
j. Socialization the new standard of suspension making process.
   This solution prevent powder off that is caused by less composition of material and prevent rough coating that is caused by less homogeneity of suspension.

3.4 Implementation and Improvement

The implementation has been done for a month at all line production. The result can be seen at Table 5. There is one defect type that the percentage after implementation is increased. It is loosening sleeve. After analyzing, it is known that supplier interface is needed to prevent this defect type. So it will become long term quality improvement for the company.

Pareto Chart after implementation can be seen at Figure 5. From the chart, it can be known that the defect types order is not the same with the beginning Pareto Chart. The highest defect type not light stains anymore, but window. Light stain is in the second order. In the third, the defect type not fish eye > 10 mm anymore, but change to cement waste, and so on.

Table 5: Implementation result

Defect Type	Before Implementation		After Implementation		Decreasing
	Number of cases	Percentage	Number of cases	Percentage	
Fleck merkuri	140	0.0201%	25	0.0134%	0.0067%
Aslant cap	207	0.0298%	19	0.0102%	0.0196%
Cement waste	342	0.0492%	70	0.0376%	0.0116%
Knot 1	161	0.0232%	12	0.0065%	0.0167%
Dented cap	310	0.0446%	49	0.0263%	0.0183%
Unsticky tape	206	0.0296%	45	0.0242%	0.0054%
Loosen sleeve	113	0.0163%	68	0.0366%	-0.0203%
Window	859	0.1236%	121	0.0651%	0.0585%
Powder off > 2 mm	123	0.0177%	21	0.0113%	0.0064%
Rough coating	110	0.0158%	24	0.0129%	0.0029%
Defective glass	171	0.0246%	10	0.0054%	0.0192%
Fish eye > 10 mm	687	0.0988%	66	0.0355%	0.0634%
Fish eye < 10 mm	598	0.0860%	68	0.0366%	0.0495%
Blistered	230	0.0331%	15	0.0081%	0.0250%
Printed tape is sticky with the lamp	368	0.0529%	40	0.0215%	0.0314%
Light stain	880	0.1266%	120	0.0645%	0.0621%
Glue stain	389	0.0560%	61	0.0328%	0.0232%
Total sample	695040		186000		

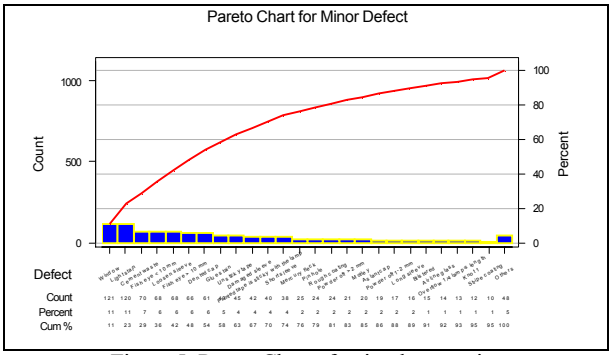

Figure 5: Pareto Chart after implementation

There is possibility that it is only order changing. A further analysis is needed. Two proportions test is done to find whether the percentage decreasing is significant or not ($\alpha = 0.05$). The result can be seen at Table 6. Among 17 defect types with high frequency of occurrence, there are 11 defect types which the percentage decreasing is significant. But the rest still not significant, include loosen sleeves which has a rising defect percentage after implementation. So, a continuous improvement is needed.

Table 6: Two proportions test

Defect Type	*P-Value*	Result
Light stain	0	Significant
Window	0	Significant
Fish eye > 10 mm	0	Significant
Fish eye < 10 mm	0	Significant
Glue stain	0	Significant
Printed tape is sticky with the lamp	0	Significant
Cement waste	0.096	Not significant
Dented cap	0.001	Significant
Blistered	0	Significant
Aslant cap	0	Significant
Unsticky tape	0.27	Not significant
Defective glass	0	Significant
Knot 1	0	Significant
Mercury fleck	0.065	Not significant
Powder off > 2 mm	0.052	Not significant
Loosen sleeve	1	Not significant
Rough coating	0.325	Not significant

4. CONCLUSION

There are 13 defect types with low frequency of occurrence that can be eliminated from the minor defect list, after the trial period. They are foreign object, collide stel, damaged stel, dirty tube, folded seal, no coating, thin coating, glass stain, sit high cap, mire cap, glass chips, double sleeve, and flat lamp.

There are 17 defect types with high frequency of occurrence that can be minimized. They are light stain, window, fish eye > 10 mm, fish eye < 10 mm, glue stain, printed tape is sticky with the lamp, cement waste, dented cap, blistered, aslant cap, unsticky tape, defective glass, knot 1, Mercury fleck, powder off > 2mm, loosen sleeve and rough coating. There are 51 proposed solutions, 10 of them are implemented. After implementation the defect types order at Pareto Chart is changed. Beside that, there are 11 defect types that decrease significantly.

REFERENCES

[1] Ariani, W. Dorothea, *Pengendalian Kualitas Statistik: Pendekatan Kuantitatif dalam Manajemen Kualitas*. Yogyakarta: Andi Offset, 2004.
[2] Dale, Barrie G., *Managing Quality* (2nd ed.). UK: Prentice Hall International, Ltd., 1994.
[3] Evans, J. R., and Dean, J. W., Jr. (2003). *Total Quality: Management, Organization and Strategy* (3rd ed.). USA: South-Western, 2003.
[4] Foster, S. T., *Managing Quality: An Integrative Approach* (2nd ed.). New Jersey: Pearson Education International, 2004.
[5] Garvin, D. A., *Managing quality: The Strategic and Competitive Edge*. New York: Macmillan, Inc., 1988.
[6] Groover, Mikell P., *Work Systems and the Methods, Measurement, and Management of Work*. New Jersey: Pearson Education International, 2007.
[7] Gryna, F. M., *Quality Planning & Analysis: From Product Development through Use* (4th ed.). New York: The McGraw-Hill Companies, Inc., 2001.
[8] Hunt, V. Daniel, *Managing for Quality: Integrating Quality and Business Strategy*. USA: V. Daniel Hunt Technology Research Corporation, 1993.
[9] Montgomery, Douglas C., *Introduction to Statistical Quality Control* (4th ed.). Singapore: John Wiley & Sons, Inc., 2001.
[10] Rampersad, Hubert K., *Managing Total Quality: Enhancing Personal and Company Value*. New York: The McGraw-Hill Companies, Inc. 2005

ISSN 114-1284

DEVELOPING INDUSTRIAL CLUSTER TROUGH ENTERPRISE ENGINEERING MODELLNG FRAMEWORK

(case study: metal industrial cluster's)

Dodi Permadi, Hilman Setiadi[1], T.M.A. Ari Samadhi[2]
[1]*Politeknik Pos Indonesia,Bandung,*
Jl. Sariasih No. 54 Bandung Telp.(022) 2009562 Fax(022) 2009568
permadi311@yahoo.com, hilmal_setiadi@yahoo.com
[2]*Departemen Teknik Industri, Institut Teknologi Bandung,*
Jl. Ganesha No. 10 Bandung Telp.(022) 2508141 Fax(022) 2514609
samadhi@mail.itb.ac.id

In a cluster, enterprises colaborate by means of information exchange and integrated into similar activities in order to achieve competitive advantage among its members and regional economic improvement (Bititci, 2004). Information exchanges and integrated activities can be conducted through interaction among the members (Boedisetio, 2004). Interaction can be described by modeling (Abdullah et. al; 2000). Modeling can map resource of knowledge, input-output, and flow of knowledge (Davenport and Prusak, 2000).

Enterprise engineering modeling framework is used as an alternative because of its better representative overview againts the whole organization (multi view) and representative tools (Presley, 1997). Presley has developed Holonic Enterprise Modelling Ontology (HEMO). This model/new schema is a schema for collaboration model in knowledge-based inter and intra-enterprise in industry cluster, process and configuration partner enterprise, followed by business rules, activity, resources, business process and organization.

This research will result as follows: 1) integrated of modeling framework and knowledge modeling, consisting of modelling method and tools which can be captured and created the knowledge, through modelling of cluster activities. 2) The cluster as holon and enterprise group consists of sub-holon in which makes interaction through the activities. 3) Process of capture and create conducted by mediator which facilitates tacit and explicit knowledge into domain knowledge.

Keyword: *HEMO methodology, knowledge, collaboration, industrial*

Introduction

The importance of an industry to grow make the selection process happens in that industry. Improvements in research and development (R&D) resources, product and service have to be done to make an industry able to follow the selection process in the enterprise. Impacts of the R&D are global innovations in that industry. Small and middle size industry cannot conduct R&D activities by them self as they have limited resources and technology. These limitations can be minimized by collaborating in industry cluster.

The collaboration process can be defined as a horizontal integration of supply chain characteristic, group planning and technology sharing between enterprises. The aim of this collaboration is to enable each enterprise to respond to the rapid change of product demand in the market as quickly as possible. Quick respond are a combination of each activities, knowledge and enterprise capability, so they can grow and develop rapidly. This idea should be transformed through knowledge and available capacities.

Presley, 1997, developed a model schema for integration multi-view model of an enterprise. This model/schema focuses on analysis of processes and configuration partner enterprise; include business rules, activity, resources, business process, and organization. This model schema known as the Holonic Enterprise Modeling Ontology (HEMO). The Process and configuration issues of this

enterprise are temporary and fixed nature of relationship and law to protect intellectual rights and core competency of each participant [10]. These issues have close relationship with the collaboration process characteristic in industry cluster.

This research follows systematically the HEMO methodology, where model developed is a new schema for model collaboration from interaction knowledge base inter and intra-enterprise on one industry cluster, through information flow development product (this research focused on metal product), and all that related to the working process. Model collaboration in this research includes exchange mechanism and knowledge web, relevant actor types, and collective learning in innovation.

The aim of this research is to make a new model schema based on the HEMO methodology for collaboration inters and intra enterprise in industry cluster.

1. Problem Solving Approach

Problem Solving approach in this research consists of two-step that identify basic activities in industry cluster and explorative study with collaboration mapping with HEMO approach, as illustrated in Figure 1

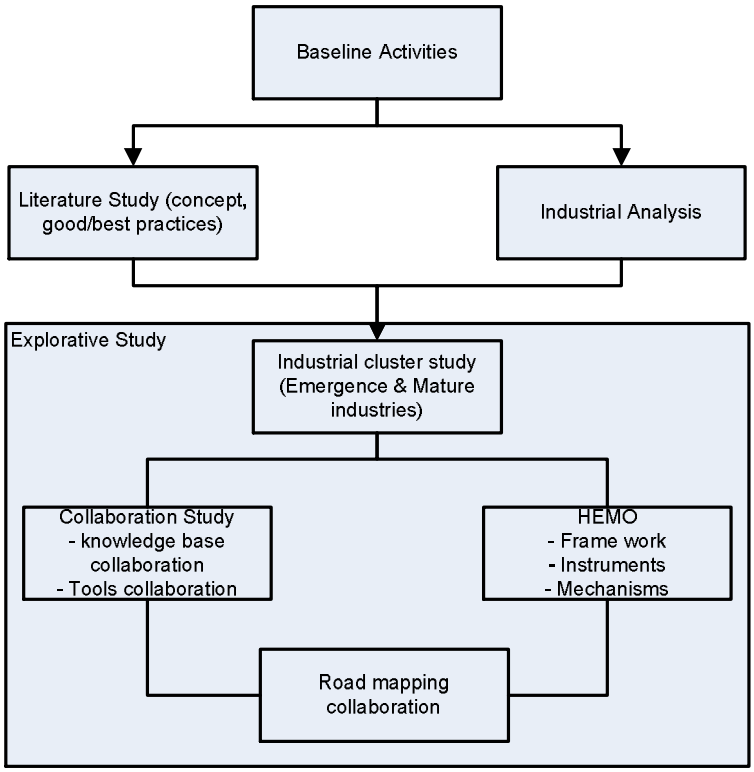

Figure 1. Problem Solving Frame work

Enterprise Modelling

Nowadays, enterprise modelling used in organization for predicting and estimating changes because of external factors.

Based on literature study [15] enterprise modelling is used:

- To facilitate understanding and communication
- To support management and to develop process
- To facilitate benchmarking
- To enable to communicate in enterprise engineering context (Bernus, 1995)
- For a mechanism at planning implementation level, namely strategic, tactics and operational.
- To fasten competition process (Wood, 1994)

Modelling Method

Recently, there are number of methods developed and implemented including IDEF-*Family* and mapping process that are always used in enterprise modelling. This section

explains the relationship between all methods used in this research, which are IDEF0, IDEF3 and IDEF5.

IDEF-*Family*

IDEF0 models is able to capture business activities but it is still not comfortable to be applied for one data base relation and IDEF1X which can accommodate that. Similarly, IDEF0 captures temporal information and limitation that can represent temporal relation between business activities (i.e. object in internal structure of those activities). In addition, that differentiation made strongest in IDEF0 [2].

InterDEF3 represents process, time interval and temporal relation, ideally illustration information about time and position; including capacity to illustration free information about participant in specified process [3].

Relationship between IDEF3 and IDEF5 is very clear. Schematic language IDEF5 is similar to IDEF1 and IDEF1X. The relationship between IDEF1/1X and IDEF5 analogically like IDEF0 and IDEF3. Information in model IDEF1/1X principally can be illustrated in elaboration language IDEF5. As it does not have better designs, the IDEF5 becomes impractical for planning database relational [4].

HEMO Methodology

Presley (1997) introduced holonic Enterprise Modelling Ontology (HEMO). This approach focuses on elements input, constraints, outputs and mechanism in business roles model, started with divinized existing model and information use for input on planning and business model using IDEF5, then it can be decomposed for each organization by available resources as an emphasis on model. Then output of activities in IDEF5 is applied as input for IDEF0 with output process template remodeling using IEF5. HEMO methodology is illustrated in Figure 2.

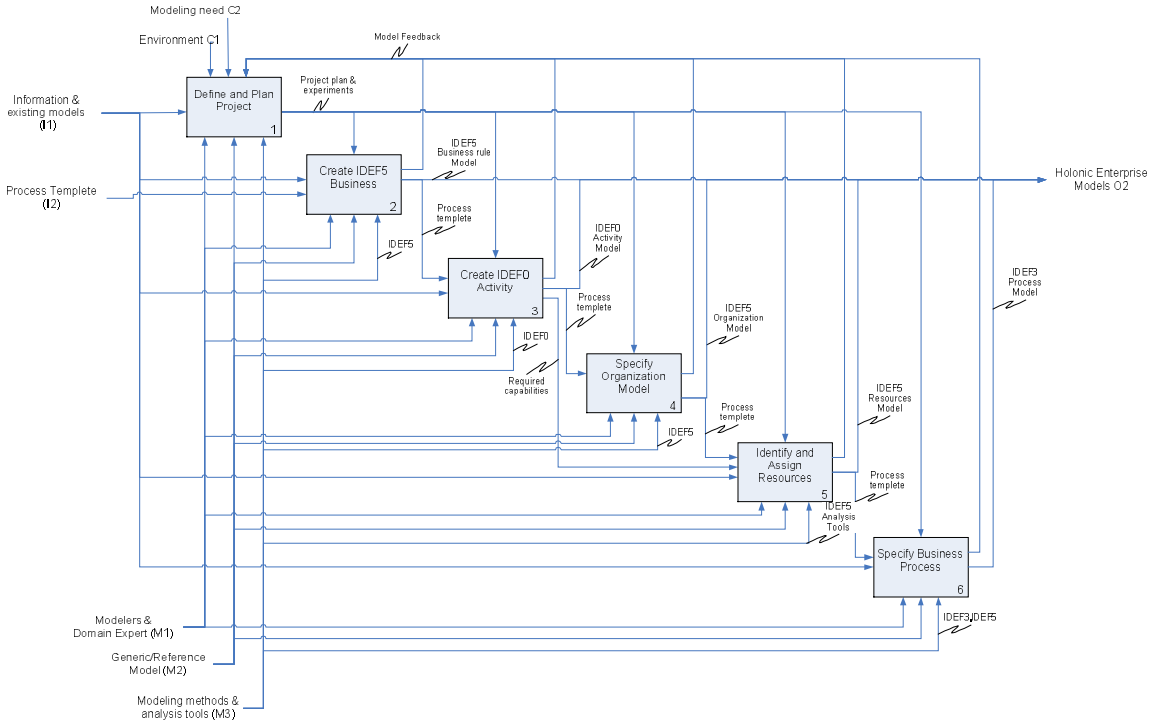

Figure 2. HEMO Methodology

From that model, HEMO methodology uses integration view from business rule model (IDEF5), activity model (IDEF0), organization model (IDEF5), resources model (IDEF5) and process model (IDEF3), as it can be seen on Figure 3.

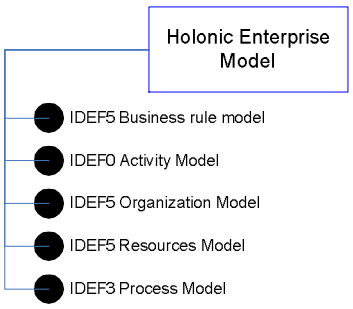

Figure 3. Elements of HEMO

Ontology (IICE,1994)

Word "ontology" has made a lot of contravention in discussion about AI. It has long history in philosophy, where it refers as a subject but it is still epistemology confusing, about knowledge and knowing.

In the contexts of knowledge sharing, ontology means as specification from a conceptualisation. Therefore, ontology means a description (like a formal specification of a program) of concepts and relationships that exist for one or community of agents. This definition consistent with the use of ontology as a set of definition concept but it is more general. Moreover, this definition has different sense of using word in philosophy.

Ontology usually resemblance with hierarchies of classes on taxonomy class, class definitions, and group of relations, but it cannot be limited with that kind of form. Ontology also cannot be limited by conservative definition where definition on traditional logic sense just to introduce terminology and not to add up knowledge in real world [5]. To elaborate a concept, it is important to mention axioms which have limited possibility interpretations on particular terms.

Ontology is a domain catalogue inside a set of details definitions or axioms, which limitation meaning from terms on catalogue completely which possible consistent interpretation from statements used on catalogue.

To make ontology minimum, three products should be made:

1. Catalogue of the terms
2. Capture the constraints that lead how those terms can be used to make descriptive statement about the domain.
3. Build a model that supported by a specific descriptive statement.

Motivation on using ontology:

1. Standardisation
2. Reusability

HOLON

Holon was introduced by Arthur Koestler (1989), as a basic unit for biology modeling and social system on his book, *The Ghost in the Machine*. This term, according to Koestler means, explaining every entity which definition as "a whole unto itself, and a part of other whole(s)." Holons as structure contains particular units, which is used independently but depends on other units. This structure is called as a Holarchy, which is temporal, combined from holons, which has a specified set of goals and temporal objectives. Strangest from a Holarchy is the ability to build multifarious, efficient resources system which fragile to internal and external disturbances and can be adapted with environment [10].

Holon and holarchy concepts can be applied to social structure like a company. A manufacture company can be considered as a Holon that concise of several set of Holon which represented several functions or engineering or organization of a company. For examples, consider manufacturing and engineering. Using control architecture, Automated Manufacturing Research Facility (AMRF), manufacture can be divided into five levels: facility, shop, cell, workstation equipment. The highest holon level determines the goal of the lowest level and coordinates the whole control. At the same time, the lowest level has specified autonomy on action and controlling. On virtual enterprise case, the virtual enterprise is the highest holon level, where every partner has beginning holon level.

Industry Cluster

Industry cluster consists of core industry element, unite industry, support industry, supplier, customer and supporting department, are skeleton of adaptation process in every industry in order to work together to make innovations and achieve competitive advantage [12].

Dynamic cluster is a model, which grows based on the combination of a company population and several companies, which grow faster. It constitutes a chain feedback effect that adds up on technology diversity from specified location. Dynamic cluster model is a cycle of the following components:

1. Cluster (enterprise specialization)

   Cluster connected with resources from productivity, value chain [10] refers to specialization for company supply and feedback such as the production factor. Specialisation build on cluster related to the process with objectives have a unique capability and competitive advantage.

2. Development enterprise (technology spin-off)

   This component generates a unique productive capability, raises technology differentiation, makes opportunities to develop a new product, and helps develop opportunities for other companies in specific location a special potential. Technology spin-off is defined on productive capabilities and interaction with market opportunities under urgent situations.

3. Technological Variation (industrial speciation)

   Represented new companies are needed to exploit of new product opportunities. In this process, they company made opportunities to have different specialization compared to other company.

4. Horizontal integration and re-integration (open system)

   Horizontal integration and reintegration are possible from different technology, which build collective knowledge or an "invisible college". In horizontal integration, speed and tough process build by combination from companies, or relationship explored from new opportunities.

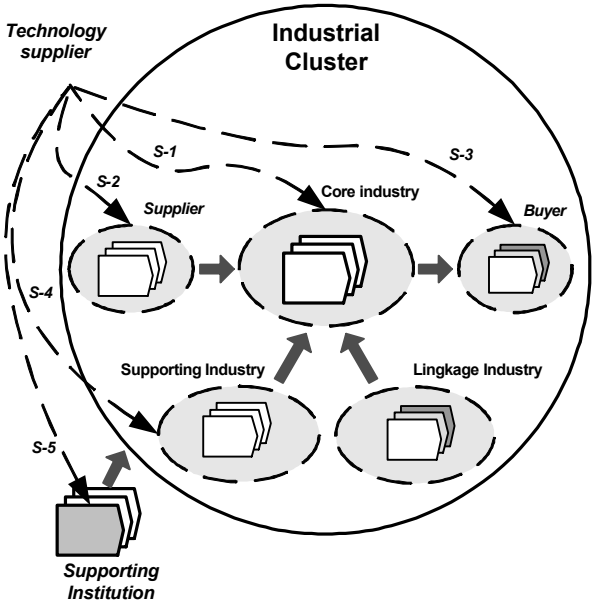

Figure 4. Interaction of Technology Supplier and Industrial Cluster
(Source: BBPT: 2004)

Collaboration Model

Collaboration is a process under knowledge, has the meaning that collaboration is process guided by knowledge (Simon, 1997). As process under knowledge, collaboration needs participants with knowledge on processing skill. Participants can be human, computer or hybrid of both human and computer (Holsapple and Joshi, 2002).

In the first stage, often need identification and analysis industry cluster as location that has coordination. Several quantitative tools often use to identify industry cluster based on detailed data (several digits) under SIC (*Standard Industrial Classification*), such as location-quotients, analysis input-output, growth-share matrix who develop by Boston Consulting Group, etc. [1]

This research will conduct collaboration process using HEMO methodology, which adds up on dynamic cluster concept as a formal media from cluster industry. HEMO methodology

[1] *Another source was discuss about this, ex http://www.hhh.umn.edu/centers/slp/ edweb/cluster.htm*

phase consists of conceptual stage and interaction inter and intra company.

Process Centred Enterprise Models as a basic HEMO modelling can be relevant to be used on cluster because activities which is explained on the process is the activities from company units, or units on group of companies on strategic alliance or virtual enterprise [10].

Data and Analysis

Cluster industry does not only reflect that product is important, but also explicitly reflect about the importance between subsystem elements process created value with subsystem element process other creation as one unity. If the attentions is just concentrated on products (usually dynamic and fragmented), it is difficult to expect to raise competitiveness significantly and able to assist effort (often sector and partial) [12].

Explorative study objectives are to find information from source actors (company, government and university) especially about potential support and obstacles on collaboration formation. This study consists of a comparison of multiple view architecture, which will be adopted to build new schema cluster (Table 1). The new schema adopts multiple views from HEMO (ARR [1]).

Table 1. Multiple View of Architecture [10]

Architecture	CIMOSA	Zahcman Framework (IDEF)	Stecher	Curtis	ARRI (HEMO)
Views	Function	Data	Entity	Functional	Activity
	Information	Process	Function or process	Behaviour	Process
	Resource	Network	Organization	Organizational (resource)	Organizational
	Organization	People	Location	Informational	Business Rule
		Time			Resource.
		Purpose			

Basic study is conducted based on the case study of metal industry cluster in Bandung. This study concentrates on automotives components. Collaboration area concise of business model on handling order process with area study as illustrated on Figure 5.

Based on requirement gathering, therefore building system can be suitable with that need; collaboration industry cluster expectantly can produce system, which is able to:

- Swiftly handling customer order process
- Swiftly capacity respond and production process ability on cluster
- Swiftly technology information flow on cluster

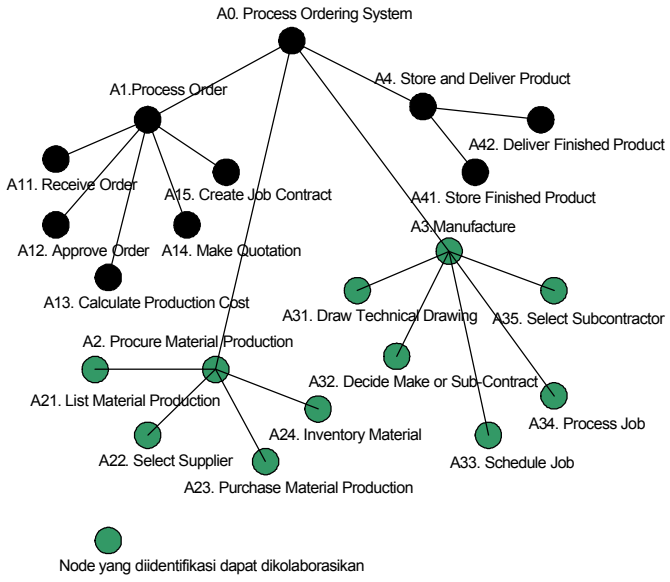

Figure 5. Process Order Diagram

ISSN 114-1284

With assumptions:

- Production is an external system and only gives information about production capacity and technology.
- Material purchase outer concern this system, therefore only give recommendation about supplier who has to be contact for complete production material basic from order and job specification, and also for job sub-contract.

Data Collection Methodologies

Killing (1993) explained that collaboration success based on complexity, which can be managed by actors. Three main factors that influence complexity are activities area, uncertainty of that activities, and collaboration skill.

Explorative studies focus on quarry of those factors from actors in each industry. Study will be done by interview (field survey) and restricted discussions. Sources of information are individual who has capacity as strategy decision making in organization and expert in their field.

Explorative Study

The goal of the explorative study is to make collaboration model by using interaction knowledge base inter and intra-enterprise on industry cluster, through information flow on develop product (in this research we focus on metal product), and related to its work process. Focus on developing activities, organization and resources on industry cluster. Collaboration models concise of exchange mechanism and knowledge networks, types of relevant actors, and collective learning in innovation.

The stages of this study are as follow:

- Identification of important elements for collaboration knowledge base formation, in particular area potential collaboration formation and collaboration mode.
- Find out sources of policies, in particular outline (issue and structure), instrument and mechanism.

Focus industry based on explorative study and input potential strategy complementary capability and need between actors, and indication good will to collaboration.

Business Model

Now companies on cluster have limited technology and production capacity, therefore if pull order happen, company executes subcontract process with similar company which has similar specification order. This has been already identified as collaboration process between those companies but only on going framework. Therefore, this research will modify collaboration process to become collaboration flow as seen on Figure 6. Focus on this problem is business process made by enterprise when they handle an order.

From two issues often appear problems like production process delay and shipping delay because of limited material source on warehouse and supplier. In this matter, will be changed on customer order handling by process adjustment on every activity selection process (companies that has ability basic on product on capacity and technology).

Then insert condition activities that involve cluster member on handling order because of limited technology and capacity on companies who receive order. This condition motorizes by companies, which receive order, and distributed to cluster member.

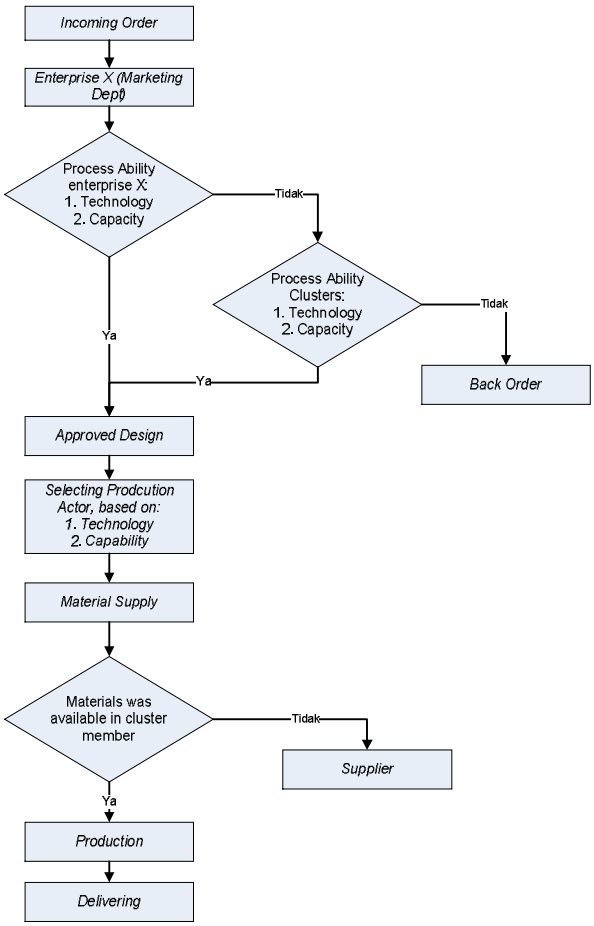

Figure 6. Order Handling Process Modelling

HEMO Multiple View adopted from ARRI with phase view as seen on figure 3. On new schema will be develop with basic consideration system order process on figure 4, which identification which area can be collaboration are manufacture and production, therefore this preliminary research can be made the new schema, therefore it needs verification and validation, as seen on figure 7.

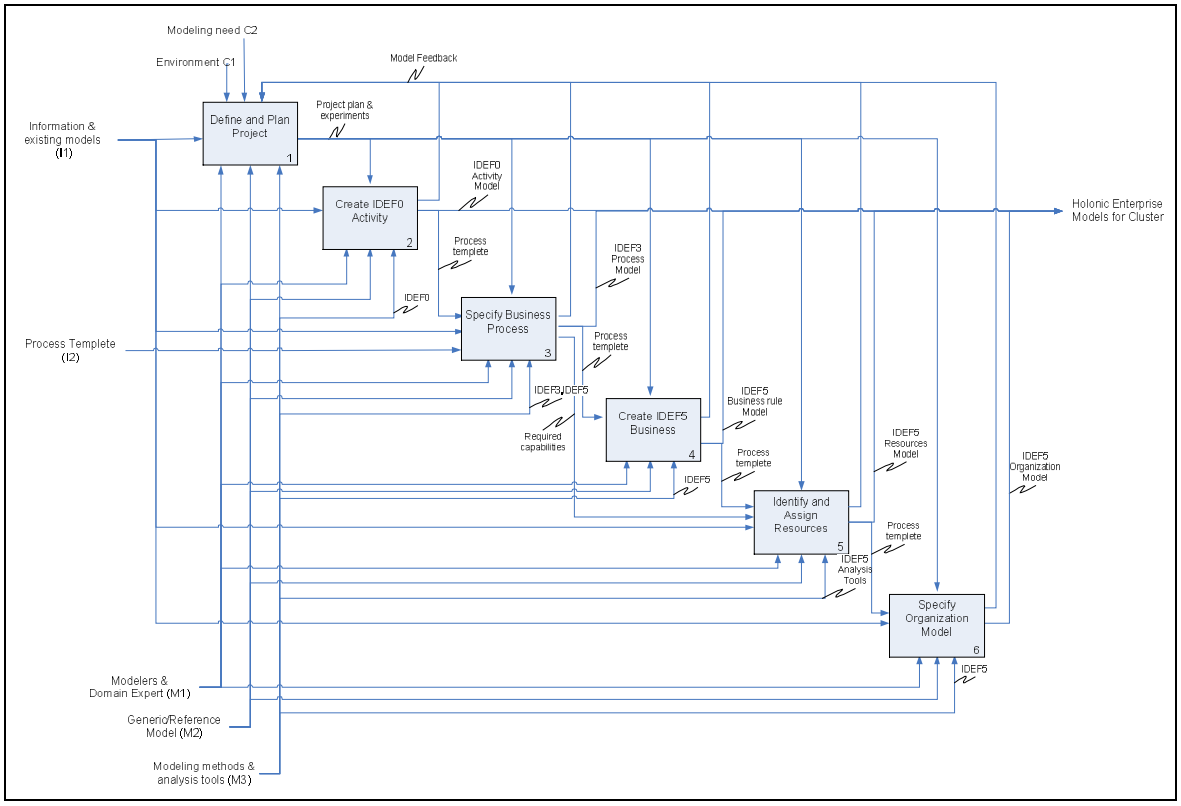

Figure 7. HEMO-Cluster Methodology

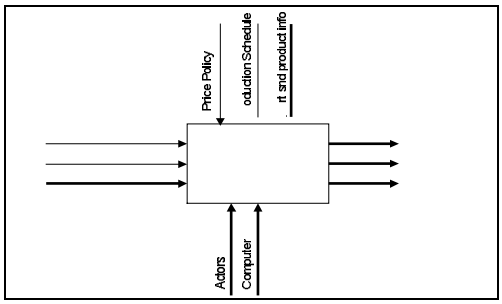

Figure 8. IDEF0 Model (A0-Order Handling)

This model using method from IDEF family such as IDEF0, IDEF3, to mapping order process handling as can be seen on the Figure 9

.

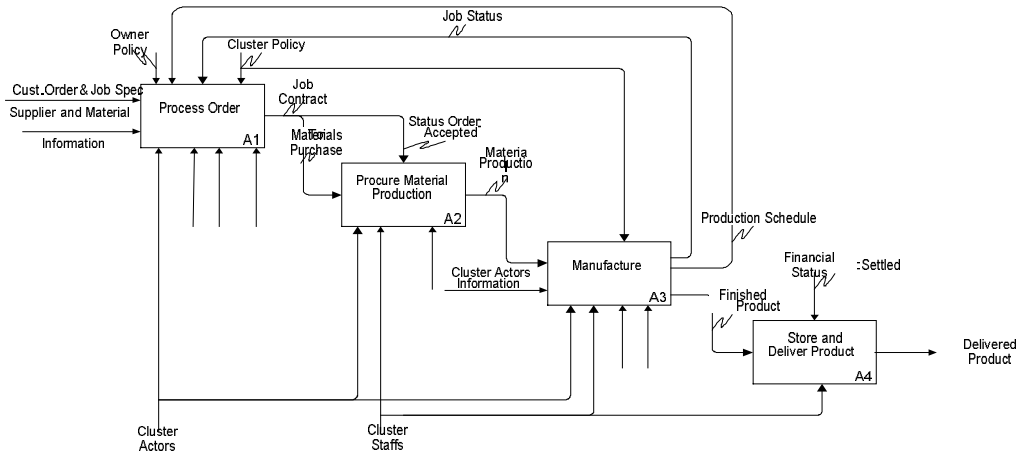

Figure 9. IDEF0 Model (A1-order Handling)

After concluding the modelling and decomposition process, output of the IDEF0 is reference as model on IDEF5, about process that becomes issue. Issue on this case is order process evaluated based on technology and capacity ability that reference for mapping organization on collaboration like the available resource. See Figure 10 and 11.

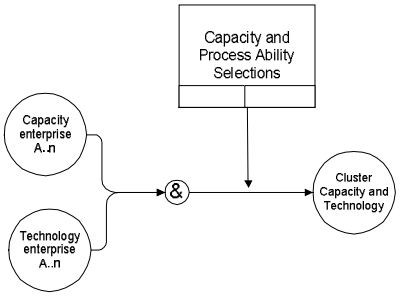

Figure 11. Resources Model IDEF5

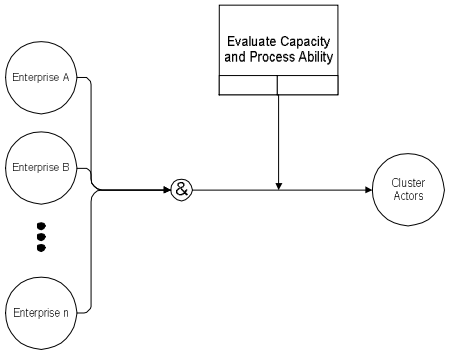

Figure 10. Organization Model IDEF5

IDEF5 model is used only until diagrammatic model, but not as elaborate language model. After organization model and available resource process, then decompositions based on capacity object and technology on IDEF5 model on IDEF3, with IDEF3 as Figure 12:

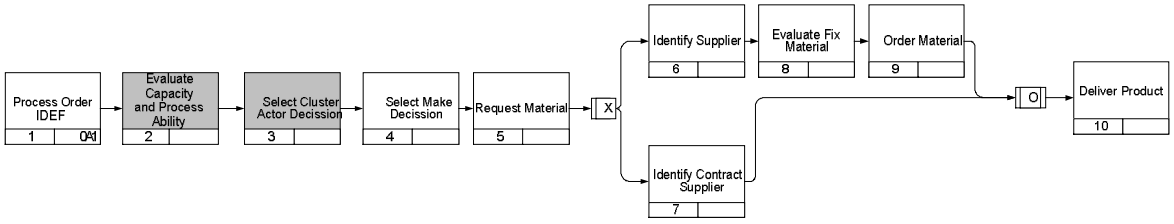

Figure 12. IDEF3 Order Process in Cluster

Analysis

On this paper, the schema is just on conceptual phase and it needs specific descriptions, but in overall, it can be compared as follow;

Table 2. HEMO and HEMO (Cluster)

	HEMO	HEMO (Cluster)
Focus	Process Centered	Process Centered
Design object	Activity	Activity
Model Scope	Business Rule	Activity
	Activity	Business Rule
	Organizational	Organizational
	Resource	Resource
	Process	Process

Based on characteristic of the industry cluster, several basic factors can be essential factors on the schema developed on collaboration process such as:

1. Activities area that has similar object, like metal industry cluster.
2. Unbalanced order in this case specification, involve ability of capacity and technology owned by companies on cluster.

On business model (Figure 6), input order handle by cluster actor has objectives as media on evaluated actor on cluster, which is able to fulfil order. Evaluation form and selection cluster actor based on:

1. Ability to fulfil specification (technology)
2. Production capacity

In this case, knowledge flow is accommodated by each actor on cluster by media information such as catalogue process, product and resources. This research decomposition have not particular complete about knowledge transformation process, as about media neither forms.

From this factor emerges value to collaboration through knowledge transformation on handling order process. Activities and process, through business process can be collaborated. They have several characteristic as follow:

1. Products that need expert skill and high precession.
2. Mass component products or specific product.
3. Products, which are made on small numbers and not fixed.
4. Products influenced by location and transportation cost.
5. Product, which has special design or the one, which has high innovation.
6. Operation flexibility and indirect low cost.

Conclusion and Suggestion

1. In particular, this schema concludes approach that possible for potential companies on cluster and scope can have significant result on process collaboration intra and inter companies especially involve:
   a. Captures process through activities model, process and limited resources on area cluster.
   b. Use of comparative advantages (particularly on flexible ability on handing order).
2. Using holon in this framework facilitate how people drawing knowledge, grouping and abridging knowledge transfer.
3. IDEF0 and IDEF3 is the tool for capturing knowledge from the actors, particularly on growing/nurturing technopreneurship on industry cluster.

Reference:

1. Automation & Robotics Research Institute (1991). *A Consensus Process Model for Small Manufacturers, an IDEF3 Model*, working paper, Automation & Robotics Research Institute, Fort Worth, TX.
2. *Draft Federal Information Processing Standards Publication 183, Integration Definition for Function Modeling* (IDEF0), 1993.
3. *Draft Federal Information Processing Standards Publication 183, Integration Definition for Function Modeling* (IDEF3), 1994.
4. *Draft Federal Information Processing Standards Publication 183, Integration Definition for Function Modeling* (IDEF5), 1995.
5. Enderton, H. (1972). *A Mathematical Introduction to Logic. New York*, Academic Press.
6. Holsapple CW, Joshi KD (2002). *Knowledge manipulation activities: Results of a Delphi study*. Information and Management 39(6): 477–490
7. Killing, J.P., 1983. *Strategies for Joint Ventures*. Praeger, New York.
8. Koestler, A. (1989). *The Ghost in the Machine*. London, Arkana Books.
9. N. Carbonara, *New models of inter-firm network within industrial district,* Proceedings of the RENT XIV Conference on Research in Entrepreneurship and Small Business, Prague, 2000.
10. Porter, M. (1998). "*Clusters and the new Economics of Competition"*, Harvard Business Review, Nov.-Dec. pp (77-90.)
11. Presley, A. R. (1997). *A Representation Method to Support Enterprise Engineering. Industrial and Manufacturing Systems Engineering*. Arlington, University of Texas at Arlington.
12. Richard J. Mayer, Ph.D et al, *Information Integration For Concurrent Engineering (Iice) Idef3 Process Description Capture Method Report*, 1995, di-*download* dari www.idef.com
13. Simonin, B. L. (1997). *The importance of collaborative know-how: An empirical test of the learning organization.* Academy of Management Journal, 40(5), 1150-1174.
14. Tatang, (2004). *Workshop Perkuatan Sistem Inovasi Daerah*, BPPT.
15. Whitman, L. E. and B. L. Huff (1997). *A Living Enterprise Model. The Sixth Industrial Engineering Research Conference*, Miami Beach, FL.
16. Zachman, J. A. (1987). *"A Framework for Information Systems Architecture." IBM Systems Journal* 26(3): 276-292.

Designing Integrated Terminal - Feasibility Study Of The Gedebage Integrated Terminal In Bandung

Ir. Dwi Novirani, MT[1], Ir.Tito Irianto, MT[2]

[1] *Faculty of Industrial Engineering*
National Institut of Technology
Jl. PHH. Mustofa No. 23, Bandung – 40124, Tilpon: (022) 7272215
Email:dwi_novirani@yahoo.com

[2] *Road Supervision Engineer*
Petrochina International Companies Indonesia, Jakarta 12940
E-mail : kabutrimbas@yahoo.com

ABSTRACT

A Passenger Terminal is a transportation facility as a station to controlling and managing the transportation mode, and moving the passenger between transportation modes. Integrated passenger terminal, a solution to provide travel efficiency, integrates all transportation modes such as train, bus, and/or connecting bus or train to airport.

Bandung city council has a plan to build an Integrated Passenger Terminal in Gedebage. The terminal will connect rail, road transportation modes, and commercial centers. A concept of the Integrated Terminal is to use the space effectively and efficiently as society activity centers. Space efficiency should consider the terminal planning by identifying the facility society needs to provide maximum services to the society.

Cost planning is an important aspect in building the infrastructure to provide space and the construction project. Therefore, the economy of the project should be analyzed in order to show feasibility of the project. It can be decided by analyzing the project feasibility indicators.

The feasibility analysis shows that the Gedebage Integrated Terminal is feasible to be built by the investors with investment 10% -70% of the total cost when the capital return is around 8-11 years with the concession for 30 years.

Keywords
Integrated Terminal, Feasibility Study.

.

1. INTRODUCTION

Nowadays intercity transportations are served by various transportation companies for variuos lines of transportation such as air, train and bus. Especially for busses, there are several large bus companies operate from Leuwipanjang Terminal to the west part of and Cicaheum Terminal to east part of. Both terminals are not convenient any longer for passengers. Those terminals create pollution, traffic jams, and cause travel time much longer. Because of these, ilegal terminals emerges as an alternative, for passengers and operators. Therefore, Bandung council planning to built an integrated terminal in devoloping of Gedebage areas.

2. METHODOLOGY

The analysis model for that being used are the Pre-design model analysis and financial analysis for Integrated Terminal Gedebage. Pre-design analysis model for Integrated Terminal Gedebage consider several parameters; forecast for growth of passengers, room space and capability of terminal facilities required.

To predict the size of activities in terminal and room space availability is very crucial (*Makridakis, Spyros, Steven C. Wheelwright, dan Victor E. Mc Gee,*. There are three steps in forecasting; determine model formulation, decide appropriate parameters, and model validation. These steps are needed to obtain the performance indicators of the terminal,

Room space required based on terminal activities and room facilities level needed, entry data based on peak-hours and other standard published by Dinas Lalu Lintas Angkutan dan Jalan (DLLAJ) and other references from Studi Kelayakan Terminal Regional Kotamadya Bandung, 1996 (PT. Citra Karya Utama) and *Apple, J.M. (1990)*

Room facilities needed depends on activities during the peak-hours, room requirement and length of time for every person on the facilities. Standard room space requirement per person on each facilities reference to a book published by architect Ernst Neufert as follows:

a. Rest room size =1,10 m^2.
b. First Aid room size =4,50 m^2.
c. Information room size =1,00 m^2.

d. Guard room size =1,05 m^2.
e. Prayer room size =2,0 m^2.
f. Restourant size =1,05 m2.
g. Waiting room size =1,50 m^2.
h. Departure Room size =1,00 m^2.
i. Arrival Room size =1,00 m^2.

Pre-design Financial analysis for Integrated Terminal Gedebage measured by the following feasibilities indicators level (*Newnan, Donald G)*:

(1) *Net Present Value* (NPV), is feasible if NPV for the project positive (NPV>0)
(2) *Internal Rate of Return* (IRR), if feasible if IRR for the project > *social opportunity cost* or *social interest rate*.
(3) *Benefit Cost Ratio* (BCR), is feasible if BCR for the project > one (BCR > 1,0).
(4) *Payback Period* (PP), is time required for Break Event Point (BEP).

3. DATA COLLECTION AND CUMPUTATION

Secondary datas used as input in research questionnaire arrange which it outputs are primary datas.
Secondary datas are collected interrelated with finance evaluation through pre-design integrated terminal Gedebage among other Bandung city general situation, Bandung Citizen and terminal as infrastructure.

The arise number of buses and passengers every month in Cicaheum and Leuwipanjang Terminals as shown in Table I and II:

Table I. Number of Buses and passenger in Cicaheum Terminal

Month	Year			
	2003		2004	
	Bus	Passenger	Bus	Passenger
January	11.789	130.257	11.548	118.608
February	12.002	132.589	10.982	111.606
March	12.983	95.515	12.755	133.538
April	14.134	140.474	13.007	147.389
Mei	14.302	147.763	13.017	136.154
Juni	14.481	139.982	13.666	141.622
Juli	14.856	167.629	14.949	182.178
August	13.915	153.687	14.915	137.801
September	9.688	109.569	12.470	124.050
Oktober	14.437	149.513	11.113	113.227
November	13.684	233.563	13.078	137.534
December	14.218	170.856	10.645	107.438
Total	160.489	1.771.397	152.145	1.591.145

Table I. Number of Buses and passenger in Cicaheum Terminal (continued)

Month	Year			
	2005		2006	
	Bus	Passenger	Bus	Passenger
January	15.539	139.300	15.539	139.300
February	14.308	123.637	14.308	123.637
March	13.982	108.439	13.982	108.439
April	14.778	122.264	14.778	122.264
Mei	13.748	104.212	13.748	104.212
Juni	14.269	114.288	14.269	114.288
Juli	14.674	126.490	14.674	126.490
August	15.197	115.209	15.197	115.209
September	13.689	103.191	13.689	103.191
Oktober	15.775	140.549	15.775	140.549
November	12.351	78.153	12.351	78.153
Desember	11.653	64.586	11.653	64.586
Total	169.963	1.340.318	169.963	1.340.318

Source: Terminal – Official Transportation Bandung city 2006

Table II. Number of Buses and passenger in Leuwi Panjang Terminal

Month	Year			
	2003		2004	
	Bus	Passenger	Bus	Passenger
January	17.379	483.117	16.141	435.112
February	16.158	445.284	15.148	420.260
March	13.641	539.694	14.954	376.644
April	17.415	491.559	14.868	364.678
Mei	18.702	534.499	15.394	400.632
Juni	13.294	514.430	15.103	393.661
Juli	18.472	542.665	16.540	512.291
August	15.274	426.045	16.383	504.654
September	15.122	421.980	15.667	525.424
Oktober	15.819	442.255	16.194	497.475
November	15.242	466.318	16.896	574.823
December	15.947	438.979	16.357	482.862
Total	192.465	5.746.825	189.645	5.488.516
Month	Year			
	2005		2006	
	Bus	Passenger	Bus	Passenger
January	17.290	537.630	17.290	537.630
February	14.867	480.364	14.867	480.364
March	15.925	536.943	15.925	536.943
April	15.047	458.824	15.047	458.824
Mei	16.764	524.168	16.764	524.168
Juni	16.384	500.149	16.384	500.149
Juli	18.615	603.470	18.615	603.470
August	17.735	548.553	17.735	548.553
September	17.916	509.904	17.916	509.904
Oktober	16.795	468.352	16.795	468.352
November	16.944	520.714	16.944	520.714
December	16.727	426.736	16.727	426.736
Total	201.009	6.115.807	201.009	6.115.807

Source: Terminal – official transportation Bandung city 2006

The secondary datas are from passenger Cicaheum and Luwipanjang Terminal. Its is used to forcast the maximum passengger in several time.
The forcasting model is Box-Jenkins thats mix model simple ARIMA(1,0,1)(0,0,1)^{12} with seasional factor. The result is constant (μ') = 5,6933526,autoregresif parameter AR1(Φ) = 0,95759947 moving average, parameter MA1 (θ) = 0,3284120 and seasonal moving average parameter SMA1 (Θ) = -0,5405997.

The calculation result of bus pessange growth is taken from the most number of passengger.in the length of forcasting time.
From spending time forecast 2007 – 2039, which is December 2031 with total passengers 493.574. Total Passengers per day 16.227

4. RESULT AND DISCUSION

Sample sizes by Slovin. Daily population taken based on the sum of average passengers per day at both Terminals (Leuwi Panjang and Cicaheum) plus safety factors 30% produce 23.025 samples with 10% error, so minimum sample has to be taken is 100 samples. To avoid data error, questioners spread out to 200 respondens. Returned questioners are 173.

The Terminal facilities for passengers is devided into main and minor facilities and from the primary entry from the questioners about their most preffered facilities. According to database and analysis, preffered facilties is similar to all facilities which are included inKEPMEN. Facilities are planned to be built in Terminal Terpadu Gedebage as shown in Table III.

Table III. Terminal Facilities

Main Facilities	Minor Facilities
o Embarkation Line for Public Transportation o Arrival Line for Public Transportation o Main Parking space, include rest area before departure o Main Building Office o Waiting room for passengers and relatives o Surveillance Tower o Tickets Box o Signs, Informations, Directions, Time-Schedule, Price-List,etc o Parking Area for Public, Family and Taxis	o Rest Room / toilets o Musholla o Kiosk / Canteen o Medical Room o Information o Public Phone o Luuggage Storage o Public Park

The size of integrated terminal gedebage is design according to the result of data calculation, which are primary and secondary datas. The component of primary datas are public faciliteis which must provided arround terminal. The size of room falilities in terminal are based on proximity of calculation number of maximum bus terminal user.
Pre-design of integrated terminal area are consist following things:

1. Arrival and departure terminal for passenggers
2. Commercial buildings
3. Train Station building
4. Work Shop building dan paper building
5. Parking areas

The design of commercial buildings have five floors, with total area 40.000 m2. The inside of facilities must accommodate customer needs which suitable with questionnaire distribution, so Commercial buildings will be usefull for people. The terminal integrated building for passenger design in two floors, which the first floor is arrival terminal and the second one is for departure.
The deferent of movement carakteristic between feeder, public transportation, also intercity transportation, so the three kind of vehicle movement must be separately.
The parking areas for intercity buses, interstate buses, east and west destination, also public transportation parking area must be separately.
Demand of room facilities in terminal based on calculation result whith assumption the shape of room is square, as shown in Table IV and V.

Table IV. Size (Square) of Departure Facilities Building

No	Facilities	Size (m^2)	Dimention (m)
1	Meeting Room / Wave Room	406	20,1 x 20,1
2	Passenger Waiting Room	236	15,4 x 15,4
3	Counter	150	12,2 x 12,3
4	Information Centre	135	11,6 x 11,6
5	Medical Centre	70	8,4 x 8,4
6	Security	50	7,0 x 7,0
7	Rest Room / Toilet	147	12,1 x 12,1
8	Restaurant	280	16,7 x 16,7
9	Prayer Room	100	10,0 x 10,0
Total Square Needed		1.574	

Source : Calculation Result 2006

Table V. Size (Square) of Arrival Facilities Building

No	Facilities	Size (m^2)	Dimention(m)
1	Meeting Room / Wave Room	98	9,9 x 9,9
2	Information Centre	44	6,6 x 6,6
3	Medical Centre	45	6,7 x 6,7
4	Security	16	4,0 x 4,0
5	Rest Room / Toilet	110	10,5 x 10,5
6	Restaurant	140	11,8 x 11,8
7	Prayer Room	100	10,0 x 10,0
Total Square Needed		553	

Source : Calculation Result 2006

Result obtained from the calculation with proper scenario as shown in Table VI below with Terminal Construction Cost

Rp. 79.645.259.426,, Comersial Building Construction Cost Rp. 482.455.204.704 for scenario 1 and Terminal Construction Cost Rp. 99.444.074.283. Comersial Building Construction Cost Rp. 602.931.505.880,- for scenario 2

Table VI. Scenario 1 and 2

Scenario 1.a :				
Investment Cost			Rp. 680.461.436.596	
Rent / Sell Commercial Building			Rp. 15.000.000	
Terminal anual revenue (Inc. Retribution)			Rp. 9.000.370.872	
Parameter	Bank Loan (%)			
	0	10	20	30
IRR (%)	11,84	11,38	10,93	10,49
NPV (billion)	-8.381	-32.370	-56.359	-80.349
PP (year)	10,18	10,61	11,05	11,59
BCR	3,06	2,87	2,70	2,55
Parameter	Bank Loan (%)			
	40	50	60	70
IRR (%)	10,05	9,62	9,21	8,79
NPV (billion)	-104.338	-128.327	-152.316	-176.306
PP (year)	12,10	12,51	12,93	13,33
BCR	2,42	2,30	2,19	2,09

Table VI. Scenario 1 and 2 (continued)

Scenario 1.b :				
Investment Cost			Rp. 680.461.436.596	
Rent / Sell Commercial Building			Rp. 20.000.000	
Terminal anual revenue (Inc. Retribution)			Rp. 9.000.370.872	
Parameter	Loan Factor (%)			
	0	10	20	30
IRR (%)	15,05	14,60	14,17	13,73
NPV (billion)	172.575	148.586	124.597	100.608
PP year	8,91	9,21	9,54	9,92
BCR	3,77	3,52	3,31	3,12
Parameter	Loan Factor (%)			
	40	50	60	70
IRR (%)	13,31	12,89	12,48	12,08
NPV (billion)	76.618	52.629	28.639	4.650
PP year	10,27	10,62	10,97	11,36
BCR	2,96	2,81	2,68	2,56

Table VI. Scenario 1 and 2 (continued)

Scenario 1.c :				
Investment Cost			Rp. 680.461.436.596	
Rent / Sell Commercial Building			Rp. 20.000.000	
Terminal anual revenue (Inc. Retribution)			Rp. 4.231.954.872	
Parameter	Loan Factor (%)			
	0	10	20	30
IRR (%)	14,67	14,23	13,78	13,35
NPV (billion)	148.580	124.591	100.602	76.612
PP (year)	8,91	9,21	9,54	9,92
BCR	3,77	3,52	3,31	3,12
Parameter	Loan Factor (%)			
	40	50	60	70
IRR (%)	12,92	12,50	12,08	11,67
NPV (billion)	52.623	28.634	4.644	19,345
PP (year)	10,27	10,62	10,97	11,36
BCR	2,96	2,81	2,68	2,56

Table VI. Scenario 1 and 2 (continued)

Scenario 2.a :				
Investment Cost			Rp. 850.199.295.747	
Rent / Sell Commercial Building			Rp. 15.000.000	
Terminal anual revenue (Inc. Retribution)			Rp. 9.000.370.872	
Parameter	Loan Factor (%)			
	0	10	20	30
IRR (%)	9,50	9,03	8,56	8,11
NPV (billion)	-150.441	-180.414	-210.388	-240.361
PP (year)	11,67	12,26	12,77	13,28
BCR	2,57	2,40	2,26	2,13
Parameter	Loan Factor (%)			
	40	50	60	70
IRR (%)	7,66	7,23	6,80	6,38
NPV (billion)	-270.335	-300.308	-330.281	-360.255
PP (year)	13,79	14,28	14,77	15,26
BCR	2,02	1,92	1,83	1,74

Table VI. Scenario 1 and 2 (continued)

Scenario 2.b :				
Investment Cost			Rp. 850.199.295.747	
Rent / Sell Commercial Building			Rp. 20.000.000	
Terminal anual revenue (Inc. Retribution)			Rp. 9.000.370.872	
Parameter	Loan Factor (%)			
	0	10	20	30
IRR (%)	12,47	12,02	11,57	11,13
NPV (billion)	30.682	1.062	-28.911	-58.885
PP (year)	9,87	10,28	10,69	11,12
BCR	3,34	3,12	2,92	2,75
Parameter	Loan Factor (%)			
	40	50	60	70
IRR (%)	10,69	10,27	9,85	9,44
NPV (billion)	-88.858	-118.831	-148.804	-178.778
PP (year)	11,61	12,08	12,47	12,87
BCR	2,60	2,47	2,35	2,24

Table VI. Scenario 1 and 2 (continued)

Scenario 2.c :				
Investment Cost	Rp. 850.199.295.747			
Rent / Sell Commercial Building	Rp. 20.000.000			
Terminal anual revenue (Inc. Retribution)	Rp. 4.231.954.872			
Parameter	Loan Factor (%)			
	0	10	20	30
IRR (%)	12,11	11,65	11,20	10,75
NPV (billion)	7.344	-22.628	-52.602	-82.575
PP (year)	10,01	10,42	10,85	11,32
BCR	3,18	2,96	2,78	2,62
Parameter	Loan Factor (%)			
	40	50	60	70
IRR (%)	10,31	9,88	9,46	9,04
NPV (billion)	-112.549	142.522	-172.496	-202.469
PP (year)	11,82	12,26	12,67	13,07
BCR	2,48	2,35	2,24	2,13

Result from observation above: Intergrated Terminal Gedebage is feasible observed from the financial analysis.

4. CONCLUSION

Based on the result, obtained in this research we have conclutions as follows:

1. Pre-design terminal, calculating project budget by public approach not by jobs, etc. Only focus on feasibility study of the investment
2. Forecasting high numbers of passengers movement create possibility to higher capacity so it need to be planned carefully in order to gain efficiency and effectively in operation.
3. Investment is not feasible if the selling price of commercial space Rp. 15.000.000/m^2.
4. Investment is feasible if the Municiple of Bandung funds the investment on land with interest rate at 12% / year, increase revenue 5%/year and increase operational and maintenance costs 5% / year with criteria as follows:
   a) Revenue on selling commersial buildings at Rp.20.000.000/m^2 plus annual revenue from retribution and other revenue such as display room, advertising boards, project budget based on price per unit published by P.U. Kota Bandung year 2006, investment is feasible if loan factors 10% - 70%. if project budget based on market price Kota Bandung year 2006, investment is feasible with maximun loan factors 10%.
   b) Loan factors impact toward NPV (Net Present Value) and payback Period, bigger loan factor longer payback period.
   Investment is still feasible altough revenue from retribution is excluded from the investment, if so price based on price per unit published by Pekerjaan Umum Kota Bandung at the price Rp. 20.000.000/m^2. for Commercial building.

REFERENCES

[1] Ati Widiati, A.U. Hadi, D.S. Riyadi, D.M. Arlianto, F. Moehtadi, Hamid, Muchdie, Kusrestuwardhani, N. Noviandi, S. Sewoyo, S. Prihawantoro, S.H. Mukti, S. Rudatin, S. Ary, Tukiyat, Warseno dan Yudi Widayanto (2001), *Manajemen Teknologi untuk Pengembangan Wilayah,* Penerbit Pusat Pengkajian Kebijakan Teknologi Pengembangan Wilayah, BPPT, Jakarta.

[2] Apple, J.M. (1990), *Tataletak Pabrik dan Pemindahan Bahan,* Penerbit ITB, Bandung

[3] Darmawan, Bargowo (1988), *Optimalisasi Terminal Angkutan Penumpang Antar Kota, Studi Kasus Kotamadya Palembang,* Tesis, Program Transportasi Fakultas Pascasarjana, Institut Teknologi Bandung.

[4] Departemen Perhubungan (1995), *Keputusan Menteri Pehubungan Tentang Terminal Angkutan Jalan Raya.*

. [5] *KBK Rekayasa Transportasi Jurusan Teknik Sipil Institut Teknologi Bandung & Lembaga Pengabdian Kepada Masyarakat (LPPM) – Institut Teknologi Bandung (1996),* Perencanaan Transportasi

[6] Morlok, Edward K. (1988), *Pengantar Teknik dan Perencanaan Transportasi,* Penerbit Erlangga, Jakarta.

[7] Makridakis, Spyros, Steven C. Wheelwright, dan Victor E. Mc Gee, *Metode dan Aplikasi Peramalan, Edisi Kedua, Jilid 1,* Penerbit, Binarupa Aksara, Jakarta

[8] Neufert, Ernst (1994), *Data Arsitek, Jilid 1 – 2,* Penerbit Erlangga, Jakarta

[9] Newnan, Donald G., *Engineering Economic Analysis Third Edition,* Penerbit Binarupa Aksara, Engineering Press, Inc, Jakarta

[10] Pemerintah Kota Bandung (2006), *Rencana Induk Kawasan (RIK) Gedebage,* Badan Perencana Pembangunan Daerah Kota Bandung.

[11] Pemerintah Kota Bandung (2004), *Rencana Tata Ruang Wilayah Kota Bandung 2013*, Badan Perencanaan Pembangunan Daerah Kota Bandung.

[12] Peraturan Pemerintah Nomor 43 Tahun 1993, *Tentang Tipe Terminal Angkutan Jalan Raya.*

[13] Singarimbun, Masri.& Sofian Effendi (1995), *Metodologi Penelitian Survai*, Penerbit, Pustaka LP3ES Indonesia, Jakarta.

[14] Sudar, Suherman (2002), *Studi Kebutuhan Fasilitas Penumpang di Terminal Bus Dalam Lokasi Terminal Intermoda Gedebage – Bandung,* Tesis Program Pascasarjana Magister Teknik Sipil, Universitas Katolik Parahyangan.

[15] Sudjana (1975), *Metoda Statistika*, Penerbit, Tarsito, Bandung.

[16] Sugiyono.(1999), *Statistika Untuk Penelitian*, Penerbit, Alfabeta, Bandung.

[17] Umar, Husein (1998), *Metode Penelitian untuk Skripsi dan Tesis Bisnis,* Penerbit Rajagrafindo Persada, Jakarta.

ISSN 114-1284

Performance Measurement Supply Chain By Using Method SCOR (*Supply Chain Operations Reference*) and AHP (*Analytical Hierarchy Process*) Case study in Furniture Industry Dheling Asri, Yogyakarta

Elisa Kusrini[1] Heri Furqon Sabana[2]

1) Majors Instructor Staff Industrial Engineering in University Islam Indonesia, Yogyakarta

2) Majors Student Industrial Engineering in University Islam Indonesia, Yogyakarta

ABSTRAK

Performance measurement can assist target of performance improvement to reach SCM excellence. Although some of empirical studies have done to measure performance SCM but there are no agreement of certain measurement method that used yet. Up to now, the currents performance measurement method which applied in SCM has significant difference in scopes and focuses. And it has different way to determine performance target. This research focused on design and measurement of performance in small industry. Supply chain performance measurement schemes use SCOR and AHP approach can used for knowing the performance of achievement company level in managing the supply chain. SCOR schemes gives common reference in assessment of factor and criteria, but the application adapted to supply chain field which will be evaluated.

Keywords *: Supply Chain Management, Performance Measurement, SCOR, AHP*

1. Introduction

Conventionally, measurement of performance defined as quantification process efficiency and effectiveness level of an activity into measurable value (Neely(1995),Lebas (1995)). At management of modern business, measurement of performance has broader and deeper meaning than to quantification and calculation. From management perspective, measurement of performance can provide feedback of information that very valuable for manager in monitoring performance of company improvement, to increase motivation, communications and diagnose of a problem (Rolstandas ,1995 ,Waggoner,1999 in Chan,2002). Performance measurement also applied to assess level of strategy effectiveness used in SCM and identified successfulness and opportunity in the future. Measurement of performance gives a real important contribution in decision making process in SCM especially in re- planning process purposes and corporate strategy then at re-engineering process.

Some of models to measure SCM performance have built by some researchers (Beamon,1999, Gunasekaran,2001,Bulinger,et all,2002,Chan,2002,Chan,2003). But measurement of performance conventionally

ISSN 114-1284

which only focused at financial aspect has weakness because focused at short term and profit orientation that in the end tends to reach local optimization, failed to support continous improvement and use one measurement dimensions only (Holmberg,2000,Kaplan and Norton,1992). Furthermore, measurement of performance in SCM also has many weaknesses that are inexistence of the relation of with corporate strategy, doesn't have any approach which balancing between financial and non financial, lack of system approach in SCM understanding where SCM must be viewed as unity of entity from overall member, loss or imprecisely measurement in SCM context. From mentioned above, measurement method of SCM performance is not able to use assist in SCM expansion yet. Effectiveness in Measurement Method of performance still in debate and requires exploration of research farther (Beamon,1999, Holmberg,2000,Ho and Newton,2002,Beamon,1998,Chan,2003,Chen and Labarni,2005).

Although some of empirical studies have done to measure SCM performance but there are no any agreement for using measurement method. Up to now, measurement methods of performance applied in SCM have significant difference in scope and focus. And there are have different way in determining the target of performance. Therefore require to make a framework measurement of performance merging performance scale to every member of supply chain. This research will focused at making of framework measurement of supply chain performance at small industry by taking case study at furniture company Dheling Asri Jogjakarta.

2. Purpose Of Research

Purpose this research is design and measures SCM performance at small industry and know action refinement.

3. Literature review

Research about performance measurement SCM has scope and different focus in significant (Ho and Newton, 2002). Beamon (1998) classification of performance measurement bases on qualitative based measures and quantitative based measures and emphasizes purpose of supply chain to reach level of high efficiency, level of customer service which is high and prosperity for effective response to environmental transformation in simultan. Further, Beamon (1999) submits measurement system focus at 3 purpose of strategic of the organization and proposes performance measurement from resources, output and flexibility for indicate level attainment in purpose organization.

Gunasekaran(2001) submits performance measurement method with emphasizing at balanced approach and categorizes performance measurement financial and non financial at level management strategic, tactical and operational and integrates this measurement with four activities interacting from a net-work supply chain (plan, source, production, delivery) with a purpose to service and satisfaction of consumer. Method balanced score card is measurement method internal performance of company that indicator financial integration and non financial. This approach aim to evaluate internal business out of four perspective that is financial perspective, customer perspective, internal business process perspective and learning and growth perspective (Kaplan and Norton,1992).

Supply chain council (2001) develops model to mention the supply chain operational reference (SCOR) for measure performance at all of business process involving in net-work supply chain. This model integrates three principal elements in management that is business process reengineering, benchmarking, and process measurement in passed function skeleton supply chain. Third the element has function as follow:

Business process reengineering in essence catch's complex process happened this

moment (as is) and definition desirous process (to be).

Benchmarking is activity to get operational performance data from Congener Company. Internal target then is appointment based on performance best in class obtained.

Measurement process functions to measure, controls, and repairs process supply chain

Business process in SCOR covers:

a. PLAN, that is process related to equilibrium between actual requests by what has been planned.

b. SOURCE, that is process related to purchasing of feedstock material to fulfill the request.

c. MAKE, that is process related to transformation process of feedstock becomes semi finished product and also product thus to fulfill the request.

d. DELIVER, that is process related to finished goods inventory, including in it about management of transportation, warehouse, all to fulfill consumer request.

e. RETURN, that is process related to return process of product because certain reason, for example because product unmatched to consumer request, and others.

From some things upper to be knowable that improvement of company performance through SCM has drawn interest from practitioner and researcher. Although some empirical studies has been done to measure performance SCM but has not there is an agreement for use measurement method. Till now measurement method of performance applied in SCM to have scope and different focus in significant. And also there is different way in determining target of performance. Therefore require to make a framework performance measurement of supply chain. In this research will be made framework measurement of supply chain applies approach of SCOR with load applies method Analytic Hierarchy Process (AHP).

3.2. Method Load and Normalization

To get performance value, a performance measurement must be able to show individual values every metric and also aggregate values at every level gauging hierarchy. Load at each factor is done with method Analytic Hierarchy Process (Saaty,1994), where every performance objective paired and done comparison of level of the importance.

Because every business process (factor) in method SCOR contains different weight with different parameter, therefore required equation process of parameter, that is way normalization. Here normalization plays a part enough important for the shake of reaching of finally value from performance gauging. At this measurement, every indicator weight converted to in certain value interval that is 0 to 100. Zero (0) interpreted bad, and one hundred (100) interpreted best. Trienekens and Hvolby (in I Nyoman Pujawan et al., 2002) applies model to do interpolation of performance measurement value as follows:

$$\frac{(S_i - S_{min})}{(S_{max} - S_{min})} x100$$

Where:

Si = Indicator value actual which successfully is reached

Smax = Attainment value of best performance from performance indicator

Smin = Attainment value of bad performance from performance indicator

4. Methodology Research

4.1 Research Object and Location of Research

Research Object is industry Mabel Bamboo Dheling Asri, which is goods producer from crafting of bamboo especially furniture having location in orchard Mlati, Sleman, yogjakarta.

4.2 Problem solving

Problem solving steps as follows:

Step 1.Research early stage is compile skeleton supply chain consisted of by party involving in levying, making and delivery of product so that product up to consumer hand.

Step 2.Second step is compile hierarchy in measurement of supply chain adapted for by company state of Dheling Asri.

Step 3.This phase is phase calculation performance value Supply chain based on measurement hierarchy of supply chain.

Step 4.This step is analyzing data and discussion.

Step 5.This step is conclusion and action of refinement.

5. Result Of Research and Discussion

Research is done in furniture company Dheling Asri Jogjakarta which active in bamboo industry, one of the product is table and chair. Bamboo furniture industry Dheling Asri has some distributors and also supplier which spread over in some regions in Yogyakarta, Surabaya, Magelang, Semarang and some other places. To get performance value supply chain to do through phases as follows.

Phase 1. Research early stage is compile skeleton supply chain consisted of by party involving in levying, making and delivery of product so that product up to consumer hand. Activity diagram of supply chain given in drawing 1.

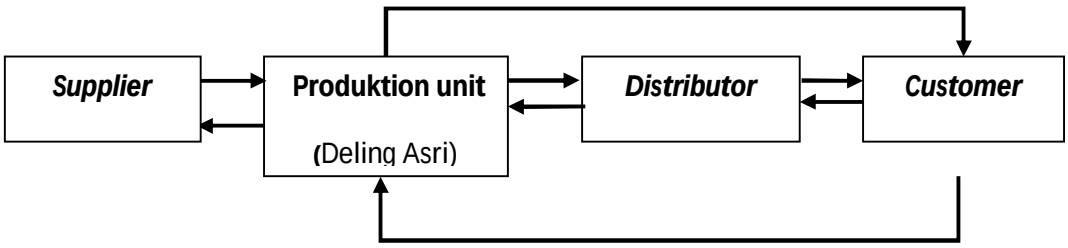

Drawing 1 . Activity Diagram Supply Chain

ISSN 114-1284

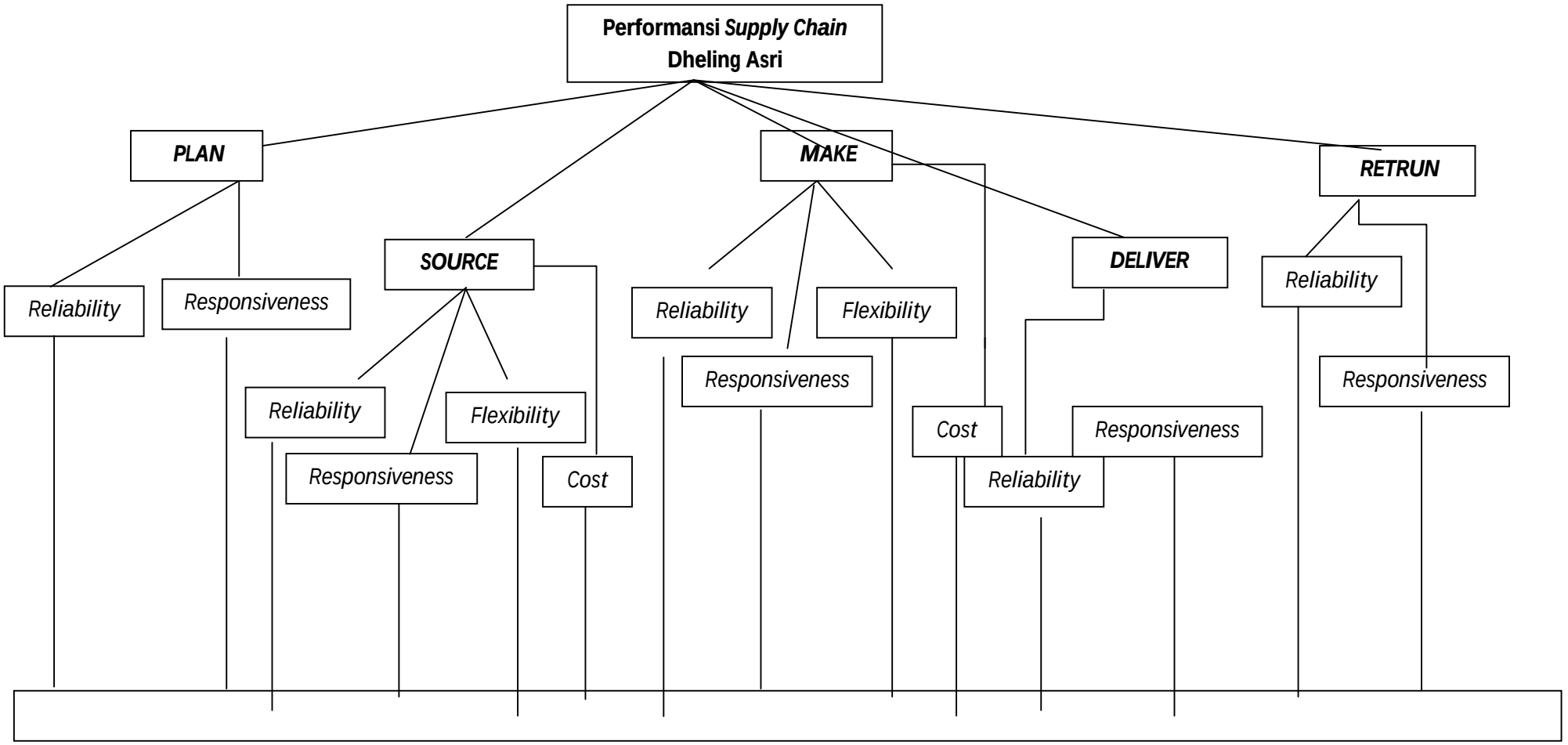

Drawing 2. Performance measurement Hierarchy supply chain Dheling Asri

Phase 2. Second phase is compile hierarchy in measurement of supply chain adapted for by company state of Dheling Asri. Hierarchy consisted of 3 level. Level 0 is performance value supply chain. Level 1 consisted of factors assessed in performance measurement supply chain. Factor entangled consisted of 5 factor that is plan, source, make, deliver, return (Levi,2000) Level 2 consisted of criterion criteria from each factor. There are four criteria applied that is: Reliability (relates to Reliability), Responsiveness (related to speed of response time all changes), Flexibility (relates to flexible in facing all changes) and Cost (relates to costs in supply chain). Level 3 consisted of is metric each criteria. Form of performance hierarchy supply chain in Dheling Asri given in drawing 2.

Phase 3. This phase is phase calculation performance value Supply chain based on measurement hierarchy of supply chain at drawing 2. Performance measurement value supply chain will be calculated based on formula (2)

Performance SC = $\sum$ (weight factor level1 x value factor level 1) ……(2)

Factor weight level 1 is calculated to apply method AHP. Whereas value factor level 1 is calculated based on formula (3).

Value factor level 1 = $\sum$ (load criteria at level 2 x value criteria at level 2)……..(3)

Load criteria at level 2 is calculated to applies method AHP. While assessing criteria at level 2 is calculated based on Formula (4)

Value criteria at level 2 = $\sum$ (load metrics x metric value)……(4)

Load each metrics is calculated based on proportion metrics to amounts metrics in every criteria. Value metrics got from direct measurement in company Dheling asri, where this value then is normalization applies formula (1).

Metric measurement at each criterion and factor in Dheling Asri, applies formula and measurement period as follows.

- . ***Plan***

Scope plan covers aspects and metrics-metrics like following:

1. *Forecast inaccuracy*

   - Definition : Percentage deviation of actual request with request result of forecasting.
   - Formula : $\frac{|\text{forecast of request - actual request}|}{\text{actual request}} \text{x1}$ 00% ……(5)
   - Measurement period: Once a month

2. *Inventory inaccuracy for finish product*

   - Definition: Percentage deviation from amount stocks product in warehouse (physical) with stock noted (documentation).
   - Formula: $\frac{|\text{amount of physical units - number of units is note}|}{\text{amount of units is note}}$ x100% ...(6)
   - Measurement period: Once a month

3. *Inventory level for finish product*

   - Definition : Average of stowage long in warehouse
   - Formula: $\frac{|\text{Average of inventory monthly}|}{\text{amount of average monthly request amounts}}$ x100% …….(7)
   - Measurement period: Once a month

4. *Number of trainee in PPC*

   - Definition : Average of employee amounts part of PPC which got

ISSN 114-1284

training about production planning in each time training.
- Measurement period: Once a year

B. *Responsiveness*

1. *Time to identify new product specifications*

- Definition : Time required to do new research and product development
- Measurement period: Every happened identification of new product

2. *Planning cycle time*

- Definition : Time required to compile production schedule
- Measurement period: Once a month

- ***Source***

Scope source include aspects and metrics like following:

A. *Reliability*

1. *Defect rate*

- Definition : Percentage of defect material unit amounts returned to by supplier
- Formula:

$$\frac{|\text{amount of defect units}|}{\text{amount of units sent}} x100\%$$

…….……. (8)
- Measurement period: Once a month

2. *Source fill rate*

- Definition : percentage of request amounts which able to be fulfilled supplier
- Measurement period: Once a month

3. *Incorrect quantity deliveries*

- Definition : Percentage of lacking of unit sent by supplier (imprecise of quantity) divided with entirety delivery total
- Formula :

$$\frac{|\text{amount of bambooes that is less}|}{\text{amount of bambooes order}} x100\%$$

…… (9)
- Measurement period: Once a month

4. *Fluctuation price frequency*

- Definition : How much happened increase price of bamboo material from supplier in one years
- Measurement period: Once a month

5. *Number of meeting with suppliers*

- Definition : Number of meetings with supplier to do evaluation
- Measurement period: Once a month

6. *Deviation wheat arrival schedule*

- Definition : Average deviation date of arrival bamboo cargo
- Measurement period: Once a month

B. *Responsiveness*

1. *Source lead time*

- Definition : Time from material order company to supplier up to company receives goods for the things first time
- Measurement period: Once a month

2. *Source Responsiveness*

- Definition : Time required by company to look for supplier substitution if first supplier cannot fulfill company request
- Measurement period: Each time happened seeking of supplier substitution

ISSN 114-1284

C. *Flexibility*

1. *Source Flexibility*

- Definition : Amount of supplier which able to be made as supplier substitution if first supplier cannot fulfill company request
- Measurement period: Each time happened seeking of supplier substitution

2. *Minimum Order Quantity*

- Definition: Amount of minimum quantities each time order which able to be fulfilled by supplier
- Measurement period: Once a month

D. *Cost*

1. *Cost For Order to Supplier*

- Definition : Amount of costs applied to order feedstock to supplier
- Measurement period: Each time happened ordering of feedstock supplier

- ***Make***

Scope make include aspects and metrics like following:

A. *Reliability*

1. *Yield*

- Definition : Comparison ratio between output is divided input (for chair)
- Formula : $\frac{|\text{Output chair}|}{\text{Input bamboo}} x100\%$ …….. (10)
- Measurement period: Once a month

2. *Packing failure rates*

- Definition : Amount of products failing process is divided with product total which ought to be yielded.
- Formula: $\frac{|\text{Amount of failing products}|}{\text{Amount of products which ought to be yielded}} x100\%$ (11)
- Measurement period: Once a month

3. *Sampling out of specification*

- Definition : Percentage of product unit amounts sampling, secretory from heavy specification limit
- Formula: $\frac{|\text{Amount of failing products}|}{\text{Amount of products which ought to be yielded}} x100\%$ …(12)
- Measurement period: Once a month

B. *Responsiveness*

1. *Make Item Responsiveness*

- Definition : Time required by company to fulfill request consumer in the event of order
- Measurement period: Each time happened ordering

C. *Flexibility*

1. *Make Item Flexibility*

- Definition : Amount of additions variation product item which able to be fulfilled company
- Measurement period: Each time happened addition variation item

D. *Cost*

1. *Cost for finish product*

ISSN 114-1284

- Definition: Amount of costs released for production process
- Measurement period: Once a month

- ***Deliver***

Scope deliver include aspects and metrics like following:

A. *Reliability*

1. *Fill rate*

- Definition : Percentage of goods unit which able to cover market request
- Measurement period: Once a month

2. *Stock out Probability*

- Definition: Probability the happening running out of stock
- Measurement period: Once a month

3. *Orders ready to pick by customer*

- Definition : Percentage of order frequency ready taken consumer is divided with entirety order frequency total
- Measurement period: Once a month

4. *Number of visit to customer*

- Definition : How many times company pays a visit to end customer to perform visit directly
- Measurement period: Once a month

B. *Responsiveness*

1. *Delivery deadline (in yogyakarta)*

- Definition: grace period given by company to consumer in Java to take goods in Deling Asri since Delivery Order is published.
- Measurement period: Once a month

2. *Delivery deadline (*outside *yogyakarta)*

- Definition: grace period given by company to consumer outside Java to take goods in Deling Asri since Delivery Order is published.
- Measurement period: Once a month

- ***Return***

Scope return includes aspects and metrics like following:

A. *Reliability*

1. *Customer complaint*

- Definition : Number of consumer complains to the side of company
- Measurement period: Once a month

2. *Return rate from Costumer*

- Definition : Percentage of return defect unit to company
- Formula : $\frac{\left|\text{Amount of units returned}\right|}{\text{Amount of units received}} x100\%$ ……(13)
- Measurement period: Once a month

B. *Responsiveness*

1. *Product replacement time*

- Definition : Time which can be fulfilled company to change product returned by consumer
- Measurement period: Once a month

From result of gauging and normalization is got metric value like presented in Table 1 until Table 14.

Table 1. Calculation of Terminal Value Plan-reliability

No	Metric	Score	weight	Score x weight
1	*Forecast inaccuracy*	45,88	25	11,47
2	*Inventory inaccuracy for finish product*	100	25	25
3	*Inventory level for finish product*	49,206	25	12,30
4	*Number of trainee in PPC*	40	25	10
			Total	58,77

Table 2. Calculation of Terminal Value Plan-Responsiveness

No	Metric	Score	weight	Score x weight
1	*Time to identify new product specifications*	66,67	50	33,335
2	*Planning cycle time*	100	50	50
			Total	83,335

Table 3. Calculation of Terminal Value *Source-Reliability*

No	Metric	Score	weight	Score x weight
1	*Defect rate*	100	16,67	16,67
2	*Source fill rate*	100	16,67	16,67
3	*Incorrect quantity deliveries*	100	16,67	16,67
4	*Fluctuation price frequency*	33,33	16,67	5,56
5	*Number of meeting with suppliers*	66,67	16,67	11,11
6	*Deviation wheat arrival schedule*	75	16,67	12,50
			Total	79,18

ISSN 114-1284

Table 4. Calculation of Terminal Value *Source-Responsiveness*

No	Metric	Score	weight	Score x weight
1	*Source lead time*	75	50	37,5
2	*Source Responsiveness*	100	50	50
			Total	87,5

Table 5. Calculation of Terminal Value *Source-Flexibility*

No	Metric	Score	weight	Score x weight
1	*Source Flexibility*	71,43	50	35,715
2	*Minimum Order Quantity*	75	50	37,5
			Total	73,215

Table 6. Calculation of Terminal Value *Source-Cost*

No	Metric	Score	weight	Score x weight
1	*Cost For finish product*	33,33	100	33,33
			Total	33.33

Table 7. Calculation of Terminal Value *Make-Reliability*

No	Metric	Score	weight	Score x weight
1	*Yield*	32	33,33	10,66
2	*Packing failure rates*	100	33,33	33,33
3	*Sampling out of specification*	100	33,33	33,33
			Total	77,33

Table 8. Calculation of Terminal Value *Make-Responsiveness*

No	Metric	Score	weight	Score x weight
1	*Make Item Responsiveness*	40	100	40
			Total	40

Table 9. Calculation of Terminal Value *Make-Flexibility*

No	Metric	Score	weight	Score x weight
1	*Make Item Flexibility*	75	100	75
			Total	75

Table 10. Calculation of Terminal Value *Make-Cost*

No	Metric	Score	weight	Score x weight
1	*Cost For Order to Supplier*	47,83	100	47,83
			Total	47,83

Table 11. Calculation of Terminal Value *Deliver-Reliability*

No	Metric	Score	weight	Score x weight
1	*Fill rate*	100	25	25
2	*Stock out Probability*	100	25	25
3	*Orders ready to pick by customer*	100	25	25
4	*Number of visit to customer*	100	25	25
			Total	100

Table 12. Calculation of Terminal Value *Deliver-Responsiveness*

No	Metric	Score	weight	Score x weight
1	*Delivery deadline (in yogyakarta)*	100	50	50
2	*Delivery deadline (outside yogyakarta)*	100	50	50
			Total	100

Table 13. Calculation of Terminal Value *Return-Reliability*

No	Metric	Score	weight	Score x weight
1	*Customer complaint*	100	50	50
2	*Return rate from Costumer*	100	50	50
			Total	100

Table 14. Calculation of Terminal Value *Return-Responsiveness*

No	Metric	Score	weight	Score x weight
1	*Product replacement time*	100	100	100
			Total	100

Value every factor is got by summing up value each criterion calculated applies formula (3) and formula (4). Result of value every factor presented in Table 15.

Table. 15 Calculations of Terminal Value Every Factor

		Terminal Value	weight	total	total factor
Plan	*Reliability*	58,77	0,889	52,24	61,50
	Responsiveness	83,34	0,111	9,259	
Source	*Reliability*	79,18	0,071	5,64	74,04
	Responsiveness	87,5	0,548	47,97	
	Flexibility	87,5	0,143	12,49	

	cost	33,33	0,237	7,92	
Make	*Reliability*	77,33	0,526	40,65	70,79
	Responsiveness	40	0,075	2,98	
	Flexibility	75	0,296	22,22	
	cost	47,83	0,103	4,95	
Deliver	*Reliability*	100	0,875	87,5	100
	Responsiveness	100	0,125	12,5	
Return	*Reliability*	100	0,875	87,5	100
	Responsiveness	100	0,125	12,5	

By Using Tables 15, countable assessed performance supply chain in company Deling Asri like given in Table 16.

Table 16. Calculation of Value Performance Supply Chain Dheling Asri

	Total Aspect	weight	Performance
Plan	61,501	0,136	8,36
Source	74,03	0,065	4,81
Make	70,79	0,26	18,41
Deliver	100	0,502	50,2
Return	100	0,0349	3,49
		Total	85,27

From calculation performance value supply chain it is known that company performance value Dheling Asri enough heights. Factor make and deliver has a real contribution significant to performance supply chain. From measurement of direct it is got that factor deliver and return has highest score, where this thing shows till now delivery of goods and the relation of company with very good consumer. Action of refinement can be done by paying attention to some metric having low relative score like presented in Table 17.

Tables. 17. Metric-metric with Low Score

Aspect	No	Metric	Score
Plan	1	*Forecast inaccuracy*	45,88
	2	*Inventory level for finish product*	49,2
	3	*Number of trainee in PPC*	40
Source	4	*Fluctuation price frequency*	33,33
Make	5	*Yield*	32
	6	*Make Item Responsiveness*	40

Some alternative refinement for example with repairing forecasting method applied, refinement quotation or better documentation for product and or product which have been sent by will to consider easy in doing gauging which will come, refinement planning of production schedule and inventory, improvement of skill employee, construction of the relation with supplier, controller quality of feedstock and employee productivity and cuts short manufacturing lead time.

6. Conclusion

Supply chain performance measurement schemes using SCOR and AHP approach can use to knowing attainment level of company performance in managing the supply chain. SCOR scheme gives common reference in assessment of factor and criterion, but for the application of adapted to supply chain area which will be evaluated. Refinement of supply chain can be start from metric with low score value by maintains performance metric with high score. Measurement of performance periodically will assist the company in performance evaluation.

BIBLIOGRAPHY

Beamon,B,M,.1998, supply chain design and analysis: models and methods International Journal of production economics, Vol 53 p. 281-294.

Beamon,B,M,.1999, Measuring supply chain performance. International Journal of Operation & Production management, Vol 19 p. 275-292.

Bulinger,H,.Kuhner,M,.Hoof,A,.2002, Analysing supply chain performance using a balanced measurement method, International Journal of production research,Vol 40, p 3533-3543

Chan,F.T.S, 2003, performance measurement in a supply chain, International Journal og adv manuf technology,Vol 21 p. 534-548.

Chopra,Suni land Meindel Peter,Supply Chain Management : Strategy, Planning, and operation, 2001 , New jersey prentice Hall,Inc.

Gunasekaran ,A.,Patel,C. and Tietiroglu,E.2001. Performance measures and metrics in a supply chain environment. International Journal of Operation & Production management, Vol 21 p.71-87

Ho,Danny and Newton,Edward (2002).Empirical research on supply chain management : a critical review and recommendations,IJPR, Vol 17 p. 4415-4430.

Neely,A.Mills,J.,Plats,K.,Gregory,M,.Richards,H,.1994.Realizing strategy through measurement. International Journal of Operation & Production management, Vol 14 p.140-152

Neely,Agregory and platts,K.1995,performance measurement system design : a literature review and research agenda, international Journal of operation and production managementm Vol 15,p 80-116.

Kaplan,R.S.,and Norton,D,P,.1992, The balanced Scorecard-Measures that drive performance (Harvard Business review).

Supply Chain council,2001,Supply chain Operation reference model,http://www.supply-chain.org.

I Nyoman Pujawan, (2005). *Supply Chain Management*. Guna Widya, Surabaya

I Nyoman Pujawan, A.A., Agustiya Novitayanti, Susanti., (2002), pengukuran kinerja supply chain : pengembangan kerangka dan setudi kasus. *Prosiding Seminar Nasional Teknik Industri dan Manajemen Produksi TIMP 2002*, 6-7 Agustus, Surabaya.

Levi, David Simchi, et. al, (2000). *Designing and Managing The Supply Chain: Concepts, Strategies, and Case Studies*. Singapore: Irwin Mc. Graw-Hill.

Saaty, T, L. (1994). *Pengambilan Keputusan Bagi Para Pemimpin : Proses Hierarki Analitik untuk Pengambialan Keputusan dalam Situasi yang Kompleks*, PT. Pustaka Binaman Pressindo, Jakarta.

ISSN 114-1284

Application of radial basis function neural network for tool wear condition monitoring using vibration signal.

J Emerson Raja[1], C K Loo[2], W S Lim[3], S Purushothaman[4]

[1]*Faculty of Engineering and Technology*
Multimedia University, Malaysia
Tel : 606 2523235. Fax 606 2316552
Email : emerson.raja@mmu.edu.my

[2]*Faculty of Information Science and Technology*
Multimedia University, Malaysia
Tel : 606 2523485. Fax 606 2318840
Email : ckloo@mmu.edu.my

[3]*Faculty of Engineering and Technology*
Multimedia University, Malaysia
Tel : 606 2523235. Fax 606 2316552
Email : wslim@mmu.edu.my

[4]*Faculty of Engineering and Technology*
Multimedia University, Malaysia
Tel : 606 2523235. Fax 606 2316552
Email : purushothaman@mmu.edu.my

ABSTRACT

Single point turning tool is an important mechanical component that is prone to premature failure. Hence it is mandatory to continuously monitor the status of the tool tip during continuous machining. In this research work an attempt is made to compare the performance of back propagation algorithm (BPA) and the Radial Basis Function (RBF) in tool wear detection. The vibration signals acquired using microphone of a new tool and worn out tool are used for this comparison study. The results show Radial Basis Function identifies the fault more accurately than the BPA.

Keywords: *Radial Basis Function, back propagation training algorithm, microphone, tool wear, fault identification, vibration.*

1. INTRODUCTION

Vibration monitoring of the machine during the machining operation is one of the important signal measuring procedure for detecting the status of the tool wear [1]. Vibration signals of good and damaged tool are used for analysis. The need for detection of status of the tool wear has warranted research and development of efficient fault diagnosis and prognosis. Many analysis include fuzzy logic, multivariate statistical analysis artificial neural network etc. Since neural network is a non-linear dynamic system and capable of mapping non-linear functions, it is widely applied in the field of pattern recognition and classification [2]. There are many types of neural networks, among them, the back propagation network, which is a kind of feed forward multilayer networks, is the most popular network used in engineering applications. Although many improved versions for BPA have been developed to increase the speed of training and to avoid trapping into local minima, their effectiveness of solving problems are not promising [3]. The determination of a suitable architecture for the BPA such as the number of neurons in the hidden layer, is difficult. The radial basis function (RBF) network offers a new and more effective method for training [4]. Since it can avoid complicated calculations, the time required for training can be much faster than that of the BPA. It has the ability of fast convergence and is able to fix centres in the hidden layer during training [5]. An optimized architecture for the RBF network can be obtained. In this paper both, RBF and BPA are used to detect the status of the tool wear from the vibration data. From the results it is clear that, RBF network is more suitable for tool wear detection from vibration data when compared to that of BPA.

2. ARTIFICIAL NEURAL NETWORK

An artificial neural network (ANN) is an abstract simulation of a real nervous system that contains a collection of neuron units, communicating with each other via axon connections. Such a model bears a strong resemblance to axons and dendrites in a nervous system. Due to this self-organizing and adaptive nature, the model offers potentially a new parallel processing paradigm [6]. This model could be more robust and user-friendly than the traditional approaches.

ANN can be viewed as computing elements, simulating the structure and function of the biological neural network. These networks are expected to solve the problems, in a manner which is different from conventional mapping [7]. Neural networks are used to mimic the operational details of the human brain in a computer. Neural networks are made of artificial 'neurons', which are actually simplified versions of the natural neurons that occur in the human brain. It is hoped, that it would be possible to replicate some of the desirable features of the human brain by constructing networks that consist of a large number of neurons. A neural architecture comprises massively parallel adaptive elements with interconnection networks, which are structured hierarchically.

Artificial neural networks are computing elements which are based on the structure and function of the biological neurons. These networks have nodes or neurons which are described by difference or differential equations. The nodes are interconnected layer-wise or intra-connected among themselves. Each node in the successive layer receives the inner product of synaptic weights with the outputs of the nodes in the previous layer. The inner product is called the activation value. The activation value is passed through a non-linear function. When the vectors are binary or bipolar, hard-limiting non-linearity is used. When the vectors are analog, a squashed function is used. Some of the squashed functions are sigmoid (0 to 1), tanh (-1 to +1), Gaussian, logarithmic and exponential. The BPA is a supervised training method which uses the error in the output layer of the network. The error is used to update the weights of the network so as to reach the minimum of the objective function which is defined to be the summation of averaged mean squared errors between the desired outputs and the network outputs [8, 9]. The convergence rate of BPA is much slower when compared to other neural network algorithm [10].

3. RADIAL BASIS FUNCTION

The concept of distance measure is used to associate the input and output pattern values. Radial Basis Functions (RBFs) are capable of producing approximations to an unknown function 'f' from a set of input data. The approximation is produced by passing an input point through a set of basis functions, each of which contains one of the RBF centres, multiplying the result of each function by a coefficient and then summing them linearly [11]. The data have been trained using radial basis functions. The RBF learns 27 patterns during training and testing. Table 1 gives training and testing steps by RBF.

4. PREPARING THE TEST DATA

Cepstrum analysis is an important sound processing algorithm that separates high frequency noise from low frequency information.

Steps involved in converting vibration data into training input for RBF and BPA are given below:

1. Acquire vibration data using PCB 130 series microphone
2. Remove zeros which does not give any information.
3. Apply linear predictive analysis.
4. Apply fast fourier transform.
5. Apply log for the output in step 4.
6. Apply inverse fast fast fourier transform.
7. Apply levinson Durban equation.
8. Repeat step 3 to step 7 for every 10 samples of the data and average all values to finally get only 10 values.
9. Label the averaged patterns using the corresponding vb values.
10. Repeat step 9 for 27 different turning conditions.

Table 1: Radial Basis function

Training RBF
Step 1: Apply Radial Basis Function.for the cepstrum values obtained from the collected vibration data No. of Input = 10 No. of Patterns = 27 No. of Centre = 4 Calculate RBF as RBF = exp (-X) Calculate Matrix as G = RBF $A = G^T * G$ Calculate $B = A^{-1}$ Calculate $E = B * G^T$ Step 2: Calculate the Final Weight F = E * D Step 3: Store the Final Weights in a File.
Testing
Step 1: Obtain cepstrum values from the vibrational data Step 2: Calculate RBF as. RBF = exp (-X) Step 3: Calculate. Value = F * RBF Step 4: Classify the value based on the stipulated threshold to decide the status of the tool wear.

5. EXPERIMENTAL SETUP FOR COLLECTING TOOL WEAR DATA

The experimental setup includes collection of sound from the turning machine in different turning conditions. The sound were collected using PCB 130 series of Array Microphones coupled with ICP sensor powered preamps and are thus referred to as ICP microphones. The 130 series provide an extremely cost effective method for large channel count sound pressure measurements. Figure 1 to 9 shows some of the sound files associated with different turning conditions. Table 2 shows the cepstrum values for the Figures 1 to 9. Out of 27 sound wave files only 9 wave files are shown as sample. Steps given in section 4 have been used to create the data in Table 2.

Table 1: Experimental data collection for A6061

S.No	Speed m/min	Feed rev/min	Depth of cut , mm	F_x N	F_y N	F_z, N	Flank wear V_b, mm	Sound wave file name
1	800	20	0.5	35	65	70	0.04	1.wav
2	800	20	1.0	40	65	75	0.15	2.wav
3	800	20	1.5	40	75	80	0.32	3.wav
4	800	30	0.5	50	75	90	0.16	4.wav
5	800	30	1.0	45	85	105	0.36	5.wav
6	800	30	1.5	60	90	110	0.05	6.wav
7	800	40	0.5	40	80	65	0.37	7.wav
8	800	40	1.0	45	80	70	0.05	8.wav
9	800	40	1.5	45	90	85	0.19	9.wav
10	1000	20	0.5	50	90	85	0.40	10.wav
11	1000	20	1.0	40	105	105	0.07	11.wav
12	1000	20	1.5	45	110	105	0.19	12.wav
13	1000	30	0.5	50	125	190	0.08	13.wav
14	1000	30	1.0	40	75	95	0.21	14.wav
15	1000	30	1.5	60	80	125	0.49	15.wav
16	1000	40	0.5	55	85	130	0.21	16.wav
17	1000	40	1.0	60	150	210	0.52	17.wav
18	1200	40	1.5	60	100	115	0.09	18.wav
19	1200	20	0.5	60	90	125	0.35	19.wav
20	1200	20	1.0	55	85	140	0.56	20.wav
21	1200	20	1.5	60	100	120	0.11	21.wav
22	1200	30	0.5	25	70	85	0.62	22.wav
23	1200	30	1.0	60	100	125	0.12	23.wav
24	1200	30	1.5	70	100	115	0.43	24.wav
25	1200	40	0.5	50	80	105	0.12	25.wav
26	1200	40	1.0	50	85	100	0.45	26.wav
27	1200	40	1.5	25	70	90	0.72	27.wav

Table 2 Ccepstrum values for the wave files given in the 9th column of table 1

Inputs for the ANN											
Ptn. No	1	2	3	4	5	6	7	8	9	10	
1	1.0000	-6.3950	-2.1934	2.7182	1.5176	1.4621	1.1132	3.0302	-1.8139	-7.9146	C I
2	1.0000	-14.930	0.7631	11.0424	1.7933	-7.4109	1.2374	10.4235	-1.1902	-15.4524	
3	1.0000	0.2196	-0.1980	-0.0545	0.3156	0.2388	-0.2458	-0.3038	0.1400	0.2242	
4	1.0000	-3.8591	-1.8633	2.2723	3.7506	-0.4554	-4.2168	-2.0770	2.1112	4.2532	
5	1.0000	4.9165	-0.3737	-3.8350	-0.1668	3.4701	1.0688	-2.4788	-0.4026	3.6174	
6	1.0000	0.2535	-0.5390	-0.7135	0.1204	0.4313	0.2522	0.0382	-0.2466	-0.0948	
7	1.0000	-4.3364	-1.7323	2.7347	2.5001	-1.0921	-2.4963	-0.5715	1.0389	0.8719	
8	1.0000	0.3099	-0.6044	-0.7800	-0.1365	0.4861	0.4648	0.1182	-0.1520	-0.1964	
9	1.0000	0.9157	-0.4377	-0.7827	0.2436	0.6203	-0.0417	-0.3803	-0.1386	0.3291	
..											
26											
27	1.0000	0.9157	-0.4377	-0.7827	0.2436	0.6203	-0.0417	-0.3803	-0.1386	0.3291	C II
C I (Class I) =0.1(Tool wear within the limit) C II (Class II) = 0.2 (tool worn out)											

6. RESULTS AND DISCUSSIONS.

The effects of number of centre (Table 3) in identifying normal and abnormal tool wear are shown in Figures 10 to 13.Table 3 gives the comparison performance of RBF and BPA.

7. CONCLUSIONS

Microphone has been used to record vibration sound during turning operation with normal condition and completely worn out tool. Sampling was done at 44khz. The data have been converted into cepstrum values to be used as inputs for RBF and BPA. The RBF with 3 centers is able to correctly identify tool which is about to reach

the non acceptable wear limit. However BPA does not show improvements in fault identification more than 70%. The future work can be focused on vibration data for many turning machines. and the suitability of RBF can be further analyzed.

Table 3: Performance of radial basis function centres

S.No	No. of centres	Percentage identification for averaged patterns in each category
1	1	0 %
2	2	25%
3	3	75%
4	4	100 %

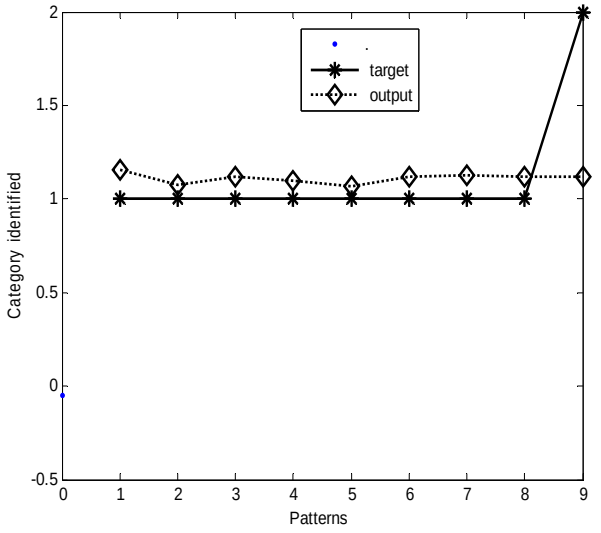

Figure 10: Performance of RBF when the centre is 1

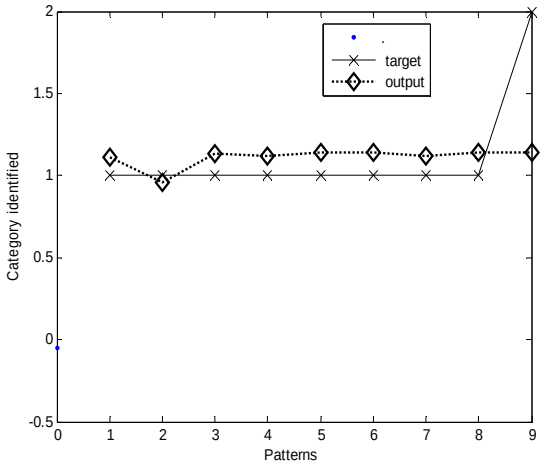

Figure 11: Performance of RBF when the centre is 2

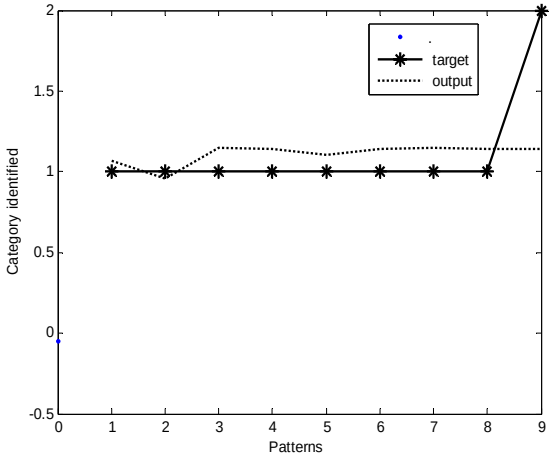

Figure 12: Performance of RBF when the centre is 3. It shows 100 % identification.

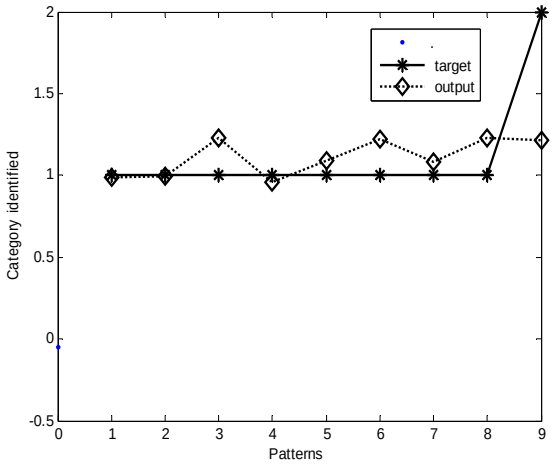

Figure. 13 : Performance of RBF when the centre is 4.

Table 3: Performance comparison of RBF and BPA

S.No	Algorithm	Topology of the network	Computation effort	Convergence rate	Number of iterations	Number of patterns used for testing	Number of patterns used for testing	Percentage identification
1	BPA	10 X 3 X 1	More	Does not converge below 0.00002344940511	4780	27	27	77 (21)
2	RBF	10 X 3 X 1	Less	Reaches the objective	1	27	27	100 (27)

Number in the paranthesis is the total number of patterns classified.
Total computational effort for BPA= np * number of iterations * number of arithmetic operations {(Forward computation in BPA) + Reverse computation in BPA}

Forward computational effort in BPA for one pattern	Reverse computational effort in BPA for one pattern
$2\sum_{i=1}^{l-1} n_{i+1}(n_i+1)$	$9n_L+7\sum_{i=1}^{L-1} n_i n_{i-1} + \sum_{i=L-1}^{2}(4n_i+5)n_{i-1}$

Total computational effort for RBF = 2*nc2 *np +inv(nc * nc)* np* nc2
nc is number of centers+1(bias)
np is number of training patterns
inv is inbuilt function inverse of a matrix
L is the total number of layers, which include input layer,
i is the layer number, and
n_i is the number of nodes in the i^{th} layer.

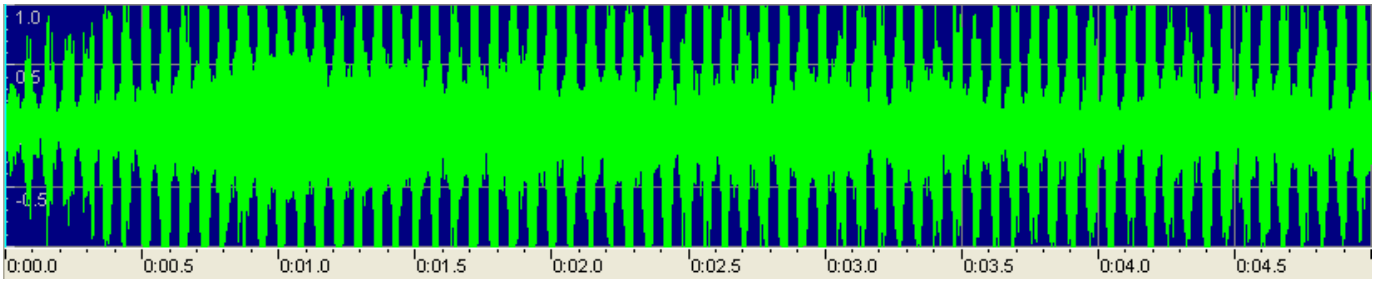

Figure 1 : 1.wav file signal (Refer Table 1 for turning condition)

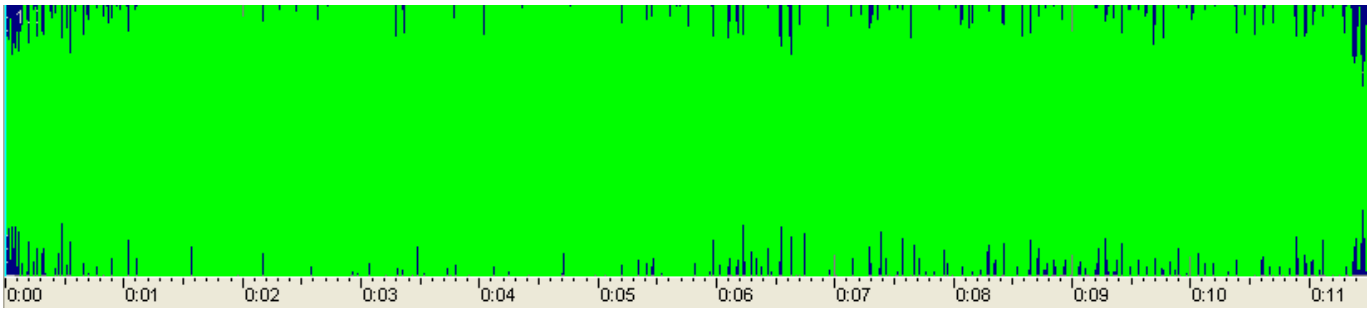

Figure 2 : 2.wav file signal (Refer Table 1 for turning condition)

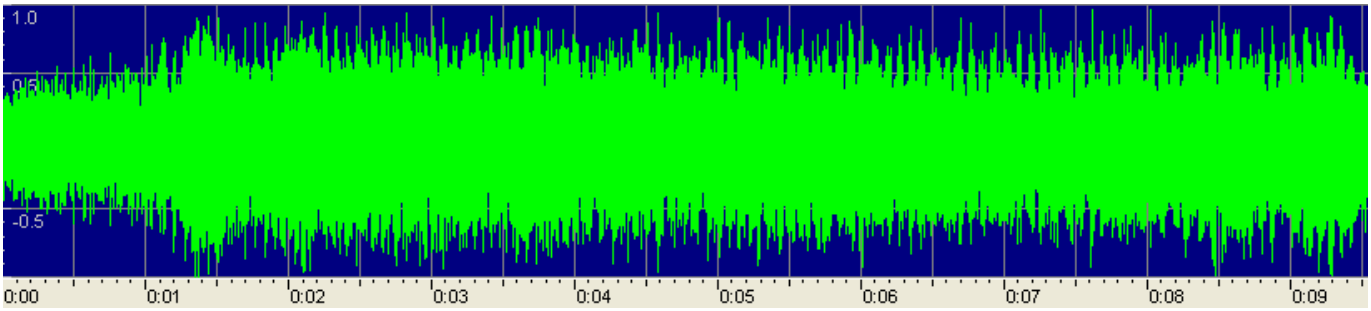

Figure 3 : 3.wav file signal (Refer Table 1 for turning condition)

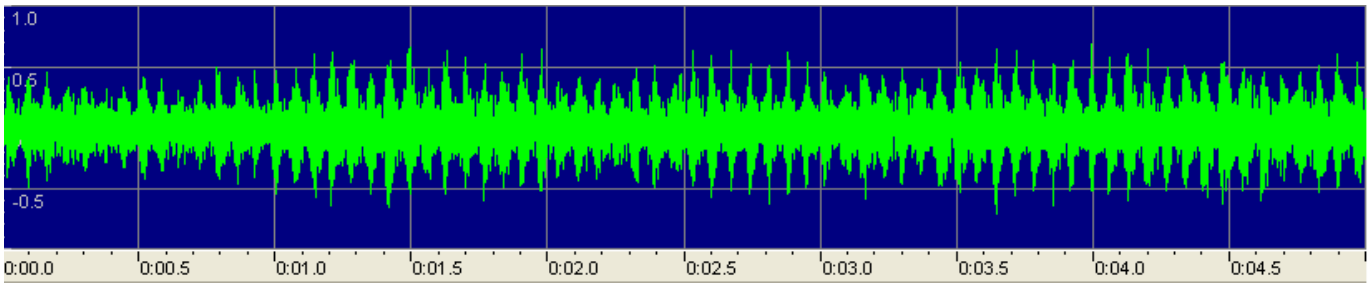

Figure 4 : 4.wav file signal (Refer Table 1 for turning condition)

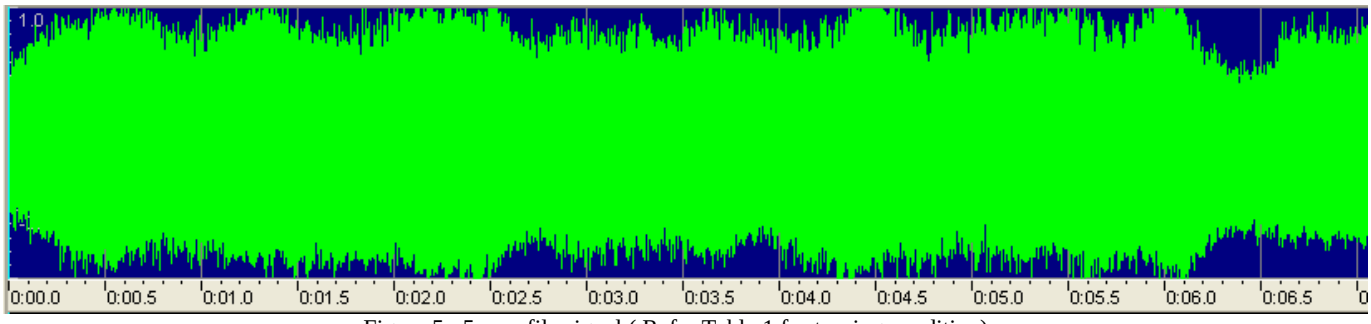

Figure 5 : 5.wav file signal (Refer Table 1 for turning condition)

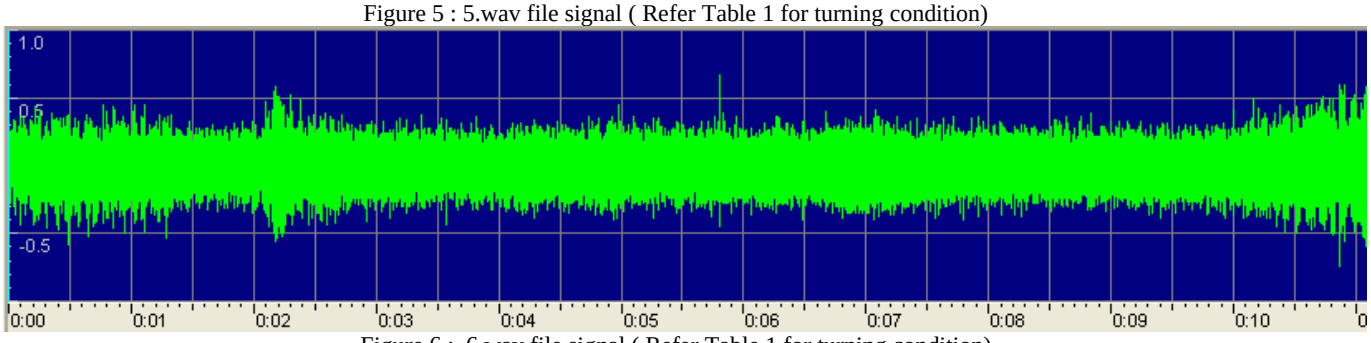

Figure 6 : 6.wav file signal (Refer Table 1 for turning condition)

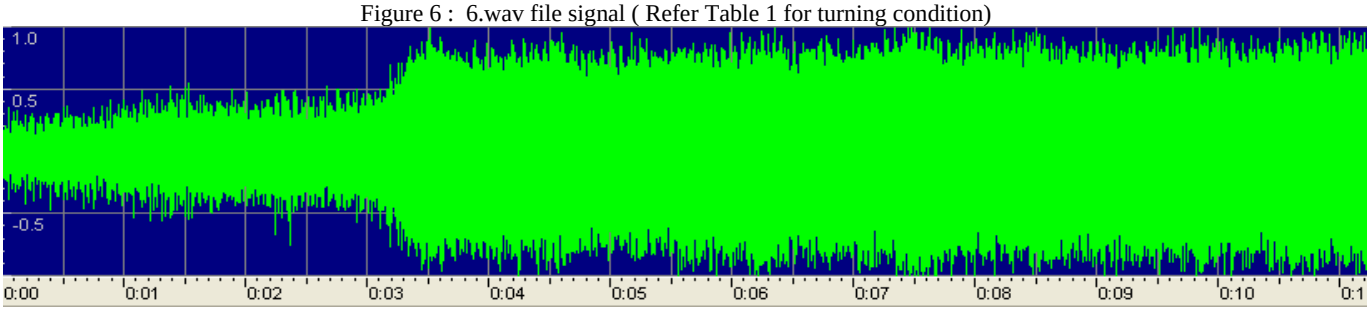

Figure 7 : 7.wav file signal (Refer Table 1 for turning condition)

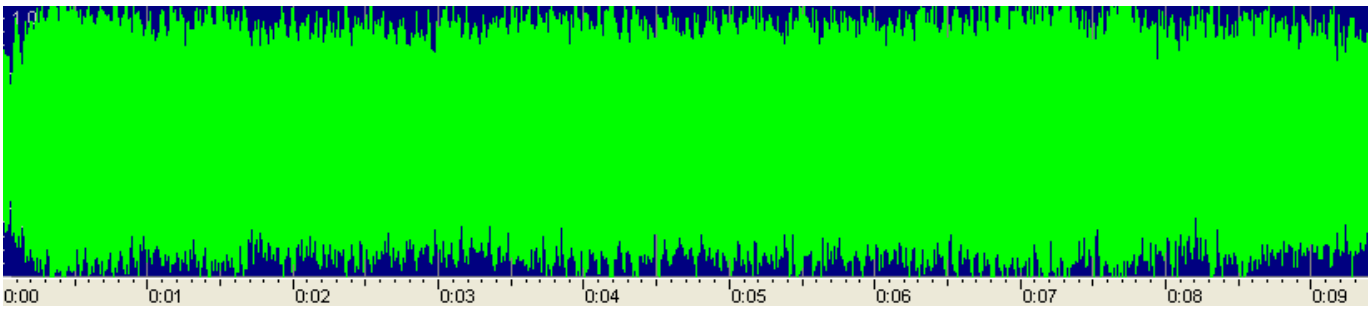

Figure 8 : 8.wav file signal (Refer Table 1 for turning condition)

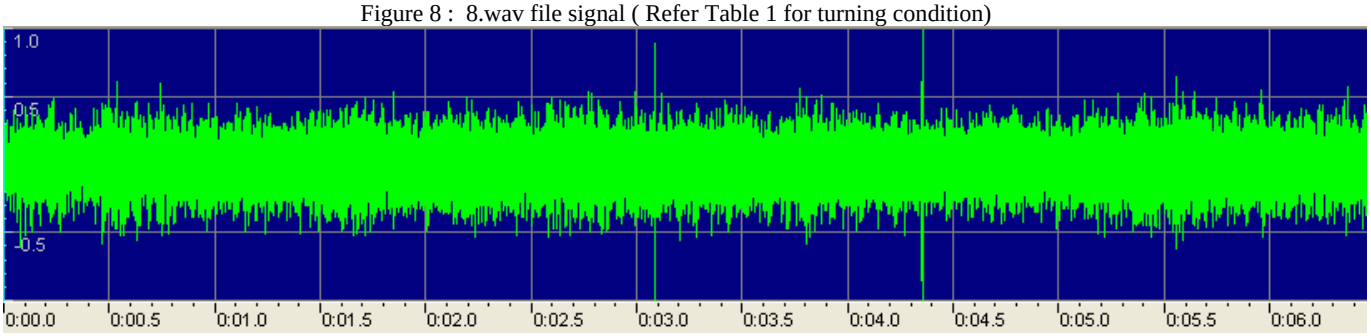

Figure 9 : 9.wav file signal (Refer Table 1 for turning condition)

REFERENCES

[1] Adman G Rehorn, Jin Jiang, Peter E Orban, State-of the art methods and results in tool conditioning monitoring: a review, International Journal of Advanced Manufacturing Technology (2005) 26: 693-710

[2] Sze-jung Wu, Nagi Gebraeel, Mark A. Lawley, and Yuehwern Yih, A Neural Network Integrated Decision Support System for Condition-Based Optimal Predictive Maintenance Policy, IEEE Transactions On Systems, Man, And Cybernetics—PART A: Systems And Humans, VOL. 37, NO. 2, March 2007.

[3] Lai Wuxing, Peter W. Tse, Zhang Guicai and Shi Tielin, Classification of gear faults using cumulants and the radial basis function network, Mechanical Systems and Signal Processing, Volume 18, Issue 2, March 2004, Pages 381-389

[4] Brezak, D., Udiljak, T., Majetic, D., Novakovic B., Kasac, J., Tool wear monitoring using radial basis function neural network, Neural Networks, 2004. Proceedings. 2004 IEEE International Joint Conference, : 25-29 July 2004, ISBN: 0-7803-8359-, INSPEC Accession Number: 8231208.

[5] P.Raviram, R.S.D.Wahidabanu and Purushothaman Srinivasan, Concurrency Control in CAD With KBMS Using Counter Propagation Neural Network, 2009 IEEE International Advance Computing Conference (IACC 2009)
Patiala, India, 6-7 March 2009.

[6] Nagi Z. Gebraeel and Mark A. Lawley, *Member*, A Neural Network Degradation Model for Computing and Updating Residual Life Distributions, IEEE Transactions ON Automation Science And Engineering, VOL. 5, NO. 1, January 2008.

[7] Jarmo Ilonen, Joni-Kristian Kamarainen, Tuomo Lindh, Jero Ahola, Heikki Kälviäinen, and Jarmo Partanen, Diagnosis Tool for Motor Condition Monitoring, IEEE Transactions On Industry Applications, VOL. 41, NO. 4, July/August 2005.

[8] S.Purushothaman, Y.G.Srinivasa, (1998), A procedure for training artificial neural network with the application of tool wear monitoring, International Journal of Production Research, Vol.36, No.3, PP.635-651.

[9] S.Purushothaman,Y.G.Srinivasa, (1994), A back-propagation algorithm applied to tool wear monitoring, International Journal of M/C Tools & Manufacturing, Vol 34, No.5, pp.625-631.

[10] S.Purushothaman, Tool Wear Monitoring Using Artificial Neural Network Based On Extended Kalman Filter Weight Updation With Transformed Input Patterns, Journal of Intelligent manufacturing, DOI: 10.1007/s10845-009-0249-y.

[11] S.Purushothaman, Sambasiva Rao Baragada, S. Ramakrishna, M.S.Rao, Polynomial Discriminant Radial Basis Function for Steganalysis, International Journal of Computer Science and Security, Korea, March 2009.

ISSN 114-1284

CUSTOMER LOYALTY MEASUREMENT MODEL FOR PREPAID CARD PRODUCTS FROM PROVIDER X IN BANDUNG

Endang Wiwiet K[1], Ferani Eva Z[2], R. Bahtiar Rahman H.[3], Yuli Sri A[4].

[1]*Student of Management and Industrial Engineering*
Faculty of Industrial Technology
Bandung Institute of Technology
Phone: (022) 2509164
Email: wiwit_31@yahoo.com

[2]*Student of Management and Industrial Engineering*
Faculty of Industrial Technology
Bandung Institute of Technology
Phone: (022) 2509164
Email: ve_zulvia@yahoo.co.id

[3]*Student of Management and Industrial Engineering*
Faculty of Industrial Technology
Bandung Institute of Technology
Phone: (022) 2509164
Email: bahtiar_hakim03@yahoo.com

[4]*Student of Management and Industrial Engineering*
Faculty of Industrial Technology
Bandung Institute of Technology
Phone: (022) 2509164
Email: yulisa_afrianti@yahoo.co.id

ABSTRACT

The increasing number of cellular provider companies causes customer disloyalty phenomena. This phenomena is a challenge for the cellular provider companies to defend and also to increase the number of their customers. The purpose of this paper is to identify factors that can influence customer loyalty and develop conceptual model of customer loyalty. This paper will focus on the loyalty of customers that have changed their number to other providers.

Based on literature studies, interviews and observations, loyalty model is influenced by the changing risk, product quality, promotional program, and environmental factors. Data is collected using a non probability sampling method, questionnaires and interviews. The concept of Structural Equation Modeling (SEM) is used as a basic model. Software LISREL 8.70 is used for the data processing. The results of the research are all of the factors can influence customer loyalty, with promotions and environmental factors being more dominant than the others.

Keywords:
Celullar provider, customer loyalty, SEM, LISREL.

1. INTRODUCTION

The rapid progress of communication technology today makes globalization (politics, social, economy and culture) spread all over the world. Indonesia as the biggest archipelago cannot resist this effect. Thousands of islands that spread from Sabang to Merauke are united because the residents can do the synergy works, this is possible because of the development of communication technology on cellular phone [10]. This technology development is very important because one percent progress in one area will increase economic development by three percent [14].

The appearance of so many cellular phone provider in Indonesia such as PT. Telekomunikasi Indonesia with the trade name Flexi, PT. Excelcomindo Pratama (XL) with trade name Bebas and Jempol, PT. Telkomsel with the trade name Hallo (postpaid), Simpati (prepaid) and AS (prepaid), PT. Indosat with the trade name Mentari and IM3, PT. Mobile-8 Telecom with the trade name Mobile-8, PT. Bakrie Telecom with the trade name Esia, Hutchison Charoen Pokphand Telecom with the trade name Three (3), makes the Indonesian communication business are very crowded.

In this tight competition, the companies need strong customer loyalty for survive, even if today many customers are only loyal to the price [9]. The Vice President of PT. Telkomsel of Java and Bali area. Agus Witjaksana said, "*Today, the cheap starter pack sales may increase the 13% growth rate on cellular phone industry. But the irony is the growth rate is threatened by the increase of churn rate that could reach 5%*". The same phenomena also happen on Indosat. According to the Indosat vice president cellular for east region Herry Moelyanto, one time use of the starter pack user occurs in about 11 % of their customer. He said, "*Churn rate percentage is never more than 6%, but since the Indosat customer number are increase, so does the churn rate*" [1].

The customer will be loyal as long as they gain financial benefit [7]. Besides that, about more than 100 million cellular phone users have more than one card [6]. This matter will definitely affect customer loyalty to the cellular provider, because the number of loyal customer will bring a significant effect to the company.

Base on the phenomenon, the paper is written to discover the factors that may affect customer loyalty and then create its conceptual model. Whole description on the paper is focused on customer who has changed their prepaid card from provider X in Bandung.

2. CUSTOMER LOYALTY

In the business context, customer loyalty as customer willingness to patron on one company for a long time and recommend their products to friend or other [3]. Customer loyalty is a deep commitment to repurchase a certain product or service consistently in the future, hard to accept other influence and difficult to change [8]. In this case, it is concluded that the loyal consumer cannot be defined from their purchase quantity, but from how often they repurchase and recommend other people to buy the product [5]. As Grifin (2003) in [3] said, that the loyal customers have these characteristics: repurchase regularly, buy from other variants of product or services from the same line, recommends product and shows consistency to the opponent products.

The final objective on successful companies is to create a relation with their customer and build strong loyalties [15]. To have loyal customers, the companies should understand at least four loyalty principles. They are customer value, customer characteristics, switching barrier, and customer satisfaction (Budi in [4]).

a. Customer value is about the customer perception from cost and benefit calculation result which will they obtain. If the customer perception of one provider has a bigger benefit than its cost, so it is called customer value.
b. Customer characteristics are regarded to the cultural background and customer experience that affect consumer characteristics.
c. Switching barrier is a barrier to prevent customer which move to other products.
d. Customer satisfaction explained that a satisfied customer is not really loyal but a loyal consumer is definitely satisfied.

According to the survey on Indonesian Customer Loyalty Index which was held by MARS and SWA [13], the five factors that create customer loyalty are:

a. Customer value is the customer perception which compares between the cost that they should take and the benefit.
b. Switching barrier are the difficulties or effort or cost that customer should take if they switch to other products.
c. Customer characteristics are the consumer character when using a product.
d. Customer satisfaction is the customer experience when using a contact with the product that they use.
e. Competitive environment is about the competition of different brands on one product.

The customer loyalty measurement is influenced by the four dimensions: word of mouth communication, purchase intention, price sensitivity and complaining behavior [15].

The factor that influence on customer loyalties, they are: the expense needed to switch to other products or services, the similar quality, quantity or services from the alternative products or services, the difference price risk from the switch of products or services and the changes of satisfaction level that can be obtained from a new brand compared to their old brand [2].

Based on the explanation above, the paper are uses: changing risk, product quality, promotional programs, and environmental factors for the research.

3. METHOD

This research is using secondary data (by interviews the provider X supervisor) and primary data (by questioner distribution, including the introduction and fixed questioners). From interviews and the introduction questioner distributions, we have found the dimensional identifications that can be used on customer loyalty measurement. The introduction questioners are distributed to 36 samples and the repaid results are used as construct variables on the fixed questioner. The Fix questioner is using Likert scale (1 to 5; where 1 = very disagree and 5 = very agree). This questioner is used to observe which factors that may affect customer loyalty, so the results can be applied to make the conceptual model.

Data is collected using a non probability sampling method (by accidental sampling). The samples are people who are on the survey location, and represent the sample criteria. The sample size is determined from the number of variance and covariance on observed variables [11]. Based on the explanation, so the sample size for the research is:

1. Required Data :
   - Observed variable: p = 18 item.
   - Variance and covariance on observed variables: p (p+1)/2 = 18 (18+1)/2 = 171.
     So, the numbers of data are 171.
2. Estimated parameters :
   - Regression coefficient (lambda = L): 18-4 = 14. Minus 4 because on the indicator standard, there is one L which set as 1 for standardization
   - Error variance (delta = d) = 18
   - Latent variable = 4
   - Variance and covariance : 4 (4+1) = 10
     So, the parameters are 14 + 18+ 10 = 42

From the calculation above, the minimal sample size for the research is:

Sample size = number of data – number of parameters
= 171-42 = 129

On data distribution, the research is using 273 samples. The populations are respondents who live in rural and city area in Bandung. They have used products from provider X, and are not using them anymore. The respondent consists of 131 males and 142 females with the distribution shows on Table 1 below.

Table 1: Sample distribution.

Segmentation	Frequency
Age	
<15 years old	2.93%
15-29 years old	79.12%
30-44 years old	16.21%
45-59 years old	1.83%
> 60 years old	0 .00 %
Level of education	
junior Hig sch	1.83%
Senior High Sch	60.07%
Diploma	12.09%
Bachelor	21.25%
Master	1.83%
others	2.93%
Income per month	
< Rp 500.000	27.63%
Rp 500.000 - Rp 999.999	26.85%
Rp 1.000.000 - Rp1.999.999	29.96%
Rp2.000.000 - Rp2.999.999	9.73%
>Rp 3.000.000	5.84%
Job	
Civil servant (PNS)	5.56%
Public Sector	0.74%
Private Sector	31.11%
Entrepreneur	12.59%
Collage Student	32.22%
others	17.78%
Term of Using	
< 1 year	3.30%
1-1.9 years	25.27%
2-2.9 years	26.47%
3-3.9 years	35.90%
>4 years	8.79%

4. IDENTIFICATION OF LOYALTY MEASUREMENT MODEL

Based on literature studies, interviews provider X and observations, it can be concluded that the customer loyalty measurement dimension (y) that will be used on the research are:

1. Changing risk.
   The dimension is a joint from two lovelock factors, they are: the amount of changing cost and changing risk. The factor are joint, because both of them are latent variable that can be explained by one observed variable, which is a variable that can be defined from several items, like: starter pack, cost to change phone number, phone tariff and SMS tariff. All of the item will create the different cost as a risk by changing providers. F1 dimension are measured by four observed variable:
   - Starter pack price (p1).
   - Expenses to confirm a new phone number (p2).
   - Phone tariff (p3).
   - SMS tariff (p4).

   H1: Changing risk has significant positive effects on customer loyalty at provider X.
2. The same quality with alternative products.
   The dimension is a provider quality measurement, and it can be divided into two groups, they are: network or signal quality and service quality. On the paper, services are means the customer service and operator assistances. Observed variables are:
   - Signal quality (p5).
   - Frequency of network trouble (p6).
   - Effort to contact the call centre (p7).
   - Customer service office location (p8).
   - Operator or customer service hospitality (p9).
   - Operator or customer service understanding to the customer problem (p10).
   - Understandable information which is given by the operator or customer service to solve customer problem (p11).
   - Operator or customer service speed, when solving the customer problem (p12).
   - Understandable instruction for user which written on starter pack (p13).

   Variable p7 to p13 are used to measure the quality of operator and customer service assistance. The variable can be determined, only from the customer who had contact operator or customer service. Therefore, the research is using two loyalty measurement models. One model involves operator and customer services assistance quality, and the other one is not.
   H2: The same quality with alternative products has significant positive effects on customer loyalty at provider X.
3. Promotional program.
   The dimension is used to measure the affect of promotional program to customers. The dimension is added because many providers offer the different kind of promotion to rises their sales rate. The dimension consists of several variables:
   - Media promotion (magazine, newspaper, radio, television, etc) (p14).
   - Program promotion (p15).
   - Condition and term applied (p16).
   - Promotional program frequency (p17).

   H3: Promotional program has significant positive effects on customer loyalty at provider X.
4. Environmental condition.
   Environmental condition is added on the research, since there is the different tariff when customers contact their family or friends at the same provider or the different one. This is can affect their tendency to choose the same provider with their family and friends.
   H4: Environmental condition has significant positive effects on customer loyalty at provider X.

Figure 1 and 2 below shows the measurement model on customer loyalty at provider X.

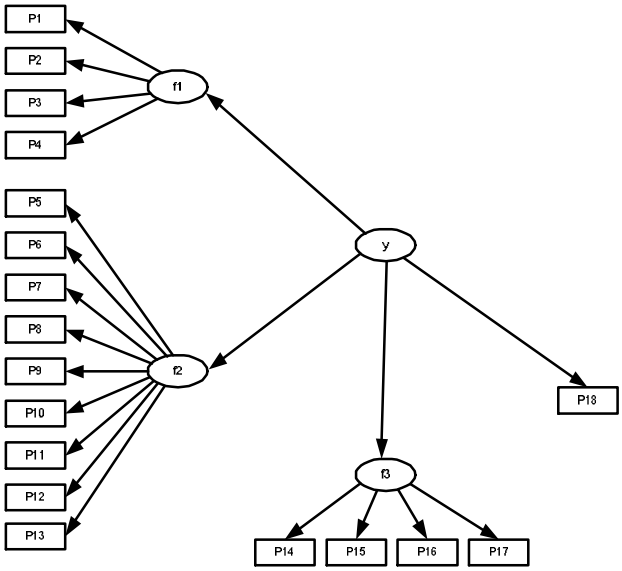

Figure 1: Measurement model on customer loyalty at provider X, by paying attention to the customer satisfaction factor on customer service and operator assistance.

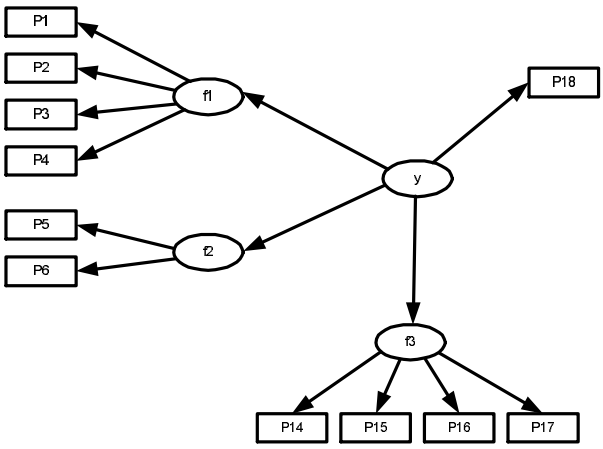

Figure 2: Measurement model on customer loyalty at provider X, without paying attention to the customer satisfaction factor on customer service and operator assistance.

5. RESULTS AND ANALYSIS

Data processing is done by using LISREL 8.70, and the analysis includes:

- Data fit test for the measurement models.
- Validity and reliability test for the measurement models.
- Hypothetical test analysis
- Customer segmentation analysis which includes: the influence of age, education, income and type of work to the dominant factors that may affect on customer loyalty.

5.1. Data Fit Test

Data fit measure for the measurement model are consists of three measures, they are: absolute-fit measures, incremental-fit measures, and parsimonious-fit measures also CN which represents the data fit size. Normal , p-value, GFI and RMSEA represents absolute-fit measures, NNFI represent incremental-fit measures and CFI represent parsimonious-fit measures. Table 2 shows the fit value size for model 1 and 2. Table 2 above indicates that the data has a good fit to the model.

Table 2: Parameter fit test for Model 1 and 2.

	absolute-fit measures				incremental -fit measures	parsimonious -fit measures	
	Normal	p-value	GFI	RMSEA	NNFI	CFI	CN
MODEL 1							
y	2.39	0.302	0.99	0.034	0.99	1	680.5
f1	1.67	0.43	1	0	1.01	1	954.72
f2	11.94	0.61	0.99	0	1	1	423.43
f3	1.14	0.57	1	0	1.02	1	1408.92
MODEL 2							
y	6.8	0.34	0.99	0.022	0.99	1	642.36
f1	1.39	0.24	1	0.038	0.99	1	1295.38
f3	3	0.22	0.99	0.043	0.99	1	863.27

5.2. Validity and Reliability Test

Model validity can be measured from the size of t-value and standard loading factor (SLF). Observed variable has a significant effect to the factor if t-value is greater than 1.96 [12]. Table 3 and 4 shows t-value and CR from the model 1 and 2. Construct reliability (CR) value indicates the reliability level from measurement model.

In Table 3 and 4 below can be shown that there is only one observed variable which not valid, it is P2. CR values for both model, are between 0.6 until 0.99. It means that the model has a good reliability level.

Table 3: Reliability and validity test for Model 1.

	t-value	SLF	residual	CR
Measurement model (f1)				
p1	3.36	0.25	0.94	
p2	1.74	0.13	0.98	
p3	13.09	0.81	0.34	
p4	18.65	1.00	1.00	0.60
Measurement model (f2)				
p5	8.10	0.58	0.66	
p6	5.26	0.40	0.84	
p7	9.47	0.67	0.55	
p8	5.26	0.40	0.84	
p9	13.61	0.86	0.26	
p10	14.49	0.90	0.18	
p11	11.46	0.77	0.40	
p12	9.27	0.65	0.57	
p13	11.54	0.78	0.39	0.89
Measurement model (f3)				
p14	6.78	0.54	0.71	
p15	9.37	0.74	0.48	
p16	11.35	0.88	0.23	
p17	5.00	0.40	0.84	0.74
Measurement model (y)				
f1	6.74	0.92	0.16	
f2	3.40	0.30	0.91	
f3	4.23	0.38	0.85	
p18	4.84	0.46	0.78	0.61

Table 4: Reliability and validity test for Model 2.

	t-value	LF	residual	CR
Measurement model (f1)				
p1	4.34	0.28	0.92	
p2	2.69	0.17	0.97	
p3	10.05	0.81	0.34	
p4	11.01	0.97	0.06	0.68
Measurement model (f2)				
p5	2.00	1.00	0.00	
p6	17.22	0.72	0.48	0.99
Measurement model (f3)				
p14	9.34	0.56	0.68	
p15	14.55	0.84	0.3	
p16	14.41	0.83	0.31	
p17	6.72	0.42	0.82	0.77
Measurement model (y)				
f1	23.27	1	0	
f2	5.92	0.35	0.48	
f3	6.02	0.35	0.88	
p18	3.76	0.23	0.95	0.62

5.3. Hypothetical Test Analysis

Based on the test above, it can be concluded that hypothetical H1, H2, H3 and H4 are proven. It indicates that t-value for the all latent variables are >1.96, which means that changing risk, product quality, promotional program, and environmental factors have significant positive effects on customer loyalty at provider X.

5.4. Customer Segmentation Analysis

One thing that can be used for making a product marketing strategy is to give more attention to the dominant factors which affects on the customer loyalty. By the data processing results, we may obtain the latent variable values from f1, f2, f3, and p18. Based on the latent score, it can be known that the most dominant factors which influence on customer loyalty are the environmental factor (54.6%) and promotional program (37.93%) (They are shown on figure 3).

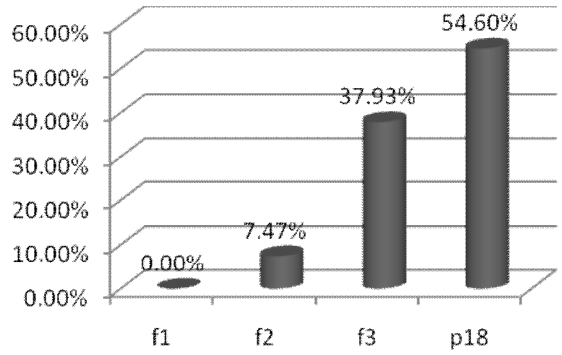

Figure 3: The influence of each factor on customer loyalty.

Environmental factor are affecting customer loyalty, because of the customer needs to contact their family or close relatives has a higher frequency compared to others. When the phone or SMS tariff across provider tends to be more expensive, this is of course raises the tendency of mobile phone users to select the same provider with their family or close relatives. The company also should give more attention to the promotional program. To increase the competitiveness, a provider must continue to innovate with their programs that offer promotion to attract more customers. For example, give cheap tariff promotions to customers who contact the phone numbers from other providers, of course with the terms and conditions that do not charge customers.

In this paper, the respondent is segmented into several groups based on the age, education, income and the type of their work, to see their influences to the dominant factors that may affect on customer loyalty. The segmentation result is shown in Figure 4.

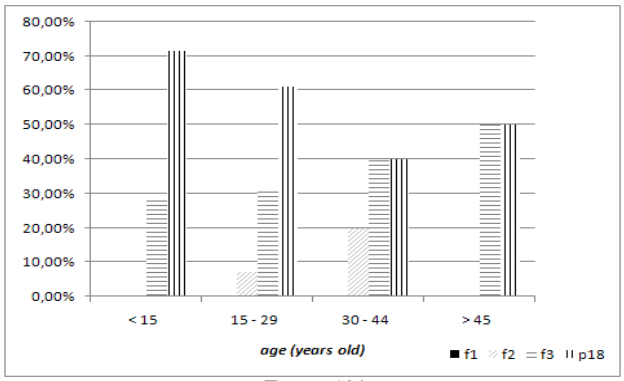

Figure 4(a)

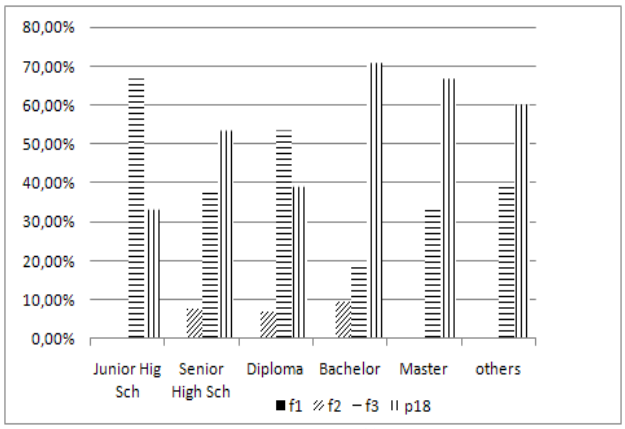

Figure 4(b)

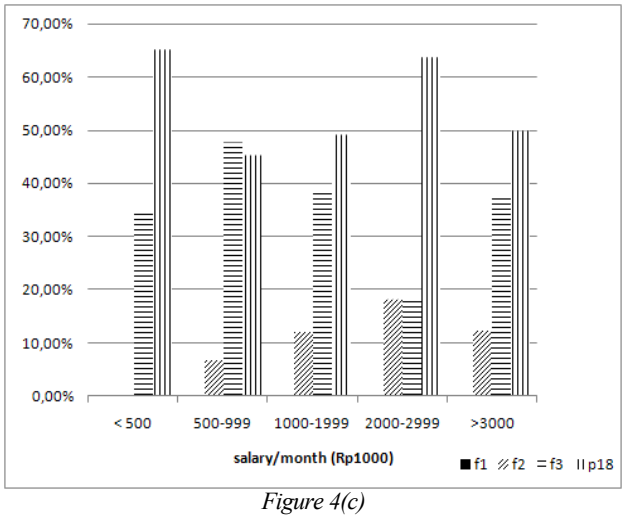

Figure 4(c)

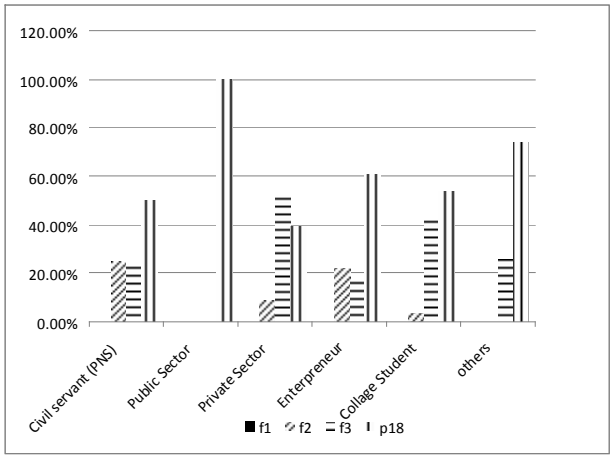

Figure 4(d)

Figure 4: The influence of each factor on customer loyalty, based on the segmentation of: (a) the age (b) level of education (c) income and (d) the type of work.

Figure 4 above shows that the most dominant factor which affect on customer loyalty for:

1. The age segment is environmental factor.
2. Level of education segment (for Junior High School and Diploma Program) is promotional program.
3. Income segment is environmental factor. But for the Rp2.000.000-Rp2.999.000 group, product quality and promotional program factors have the same influence on customer loyalty.
4. The type of work segment for work civil servants are product quality and promotional programs factors. Whereas for the private sector employee, promotional programs are more influence than the environmental factor.

From the segmentation results, it can be seen that the customer who 30-44 years old, working with civil servants or self-employed and have earnings above Rp2.000.000 give more attention to the product quality factor. So, it can be concluded that the customer whose profession involves associating with many people, also gives more attention to the signal and service quality factors to ensure reliable communication. Basically, quality is one of the key on customer loyalty towards the product.

6. CONCLUSION

Based on the previous discussion, it can be concluded that the customer loyalty are influenced by the changing risk, product quality, promotional program, and environmental factors. Overall, the factor provides a positive influence on customer loyalty for prepaid card products from provider X. The most dominant factor is environment by the 54.6%. It means that the customer tends to be more loyal if their close relatives or family using the same provider with them. So, the company may arrange the right marketing strategy by combine promotional program and environmental factors. For example: using the cheap tariff promotions to the customer who call to the different numbers even on different providers. For the next research is suggested to focus on marketing strategy for every customer segment based on their characteristic.

ACKNOWLEDGMENT

The author would like give acknowledge to Dr. Ir. Kadarsah Suryadi and the staff on Management and Industrial Engineering at Bandung Institute of Technology (ITB) for the suggestion that are useful for the improvement and progress of the research. Also to the provider X supervisor who had been interviewed, thank you for provide very useful information about customer loyalty of the prepaid card products.

REFERENCES

[1] Anonymous, '*Dilemma of Growth and Churn Rate' (*in Indonesia), *Dilema pertumbuhan vs nomor hangus*, was accessed 24 June 2009 from <http://www.bisnis.com>.

[2] C. Lovelock, *Service Marketing*, Second edition, New Jersey : Prentice-Hall Inc., 1991.

[3] C. Lovelock, W. Jochen, T.K. Hean, and L. Xiongwen, *Services marketing, people, technology, strategy. 2nd Edition*, Singapore : Pearson-Prentice Hall, 2005.

[4] D.H. Palupi, "The Champion Who Make Customer Loyalty On 2006" (in Indonesia), *Para Kampiun Pencetak Loyalitas Pelanggan* SWA, no. 06/XXII/23 March – 5 April, 2006.

[5] E. Japarianto, P. Laksmono, and A.N. Khomariyah, *'Analysis of Service Quality as Customer Loyalty Measurement at Surabaya Majapahit Hotel with The Rational Marketing as Intervening Variable'* (in Indonesia), *Analisa Kualitas Layanan Sebagai Pengukur Loyalitas Pelanggan Hotel Majapahit Surabaya Dengan Pemasaran Relasional Sebagai Variabel Intervening*, Journal of Hotel Management at Petra Christian University, vol 3, no.1, pp.34-42, 2007, was accessed 24 June 2009 from <http://www.petra.ac.id/~puslit/journals/dir.php?DepartmentID=HOT>.

[6] Hudzaifah, A. '*The Indonesian Customer Cellular Phone is The Six Biggest on World*' (in Indonesia), *Pelanggan Seluler Indonesia Terbesar Ke-6 di Dunia*, was accessed 31 March 2009 from <http://www.detiknet.com>.

[7] L.L. Berry, and A. Parasuraman, *Marketing Services: Competing Through Quality*, New York: The Free Press, 1991.

[8] L.R. Oliver, '*Whence Consumer Loyalty?*', The Journal of Marketing, Fundamental Issues and Directions for Marketing, American Marketing Association, Vol. 63, pp. 33-44, 1999, was accessed 26 June 2009 from <http://www.jstor.org/stable/1252099>.

[9] R.D. Meirina, '*The Influence of Customer Value on Customer Loyalty at Grapari Telkomsel Bandung*' (in Indonesia), *Pengaruh Customer Value Terhadap Loyalitas Pelanggan Simpati Di Grapari Telkomsel Bandung*, was accessed 24 June 2009 from <http://www.PENGARUH CUSTOMER VALUE TERHADAP LOYALITAS PELANGGAN simPATI di GraPARI TELKOMSEL BANDUNG _ INDOSKRIPSI.mht>.

[10] S. Budiharto, "Dilemma of The IT Convergence and Telecommunication In Indonesia" (in Indonesia), *Dilema Konvergensi IT dan Telekomunikasi di Indonesia*, was accessed 24 June 2009 from <http://www.Dilema Konvergensi IT dan Telekomunikasi di Indonesia _ HOKI _ Harian Online KabarIndonesia.mht>.

[11] S. Hatane, *Structural Equation Model with Lisrel 8.5* (in Indonesia), *Structural Equation Model dengan Liserel 8.5*, Surabaya : Science Management Team, Economic Faculty at Petra Christian University, 2003. S.

[12] Liao, and C. Wu, *'The Relationship Among Knowledge Management, Organizational Learning, and Organizational Performance'*. International Journal of Business and Management, Vol. 4(4), pp 64-76, 2009.

[13] Sudarmadi, '*Building The Customer Loyalty*' (inIndonesia), *Membangun Loyalitas Pelanggan*, was accessed 24 June 2009 from <http://www.swa.co.id/swamajalah/sajian(online).
[14] Teguh. '*USO for Telecommunication Generalization*' (in Indonesia), *USO Untuk Pemarataan Telekomunikasi.* was accessed 24 June 2009 from <http://www.SITUS RESMI PARTAI DEMOKRAT - USO Untuk Pemarataan Telekomunikasi.mht>.
[15] V.A. Zeithaml, L.L. Berry, and A. Parasuraman, '*The Behavioral Consequences of Service Quality*'. Journal of Marketing, (60), pp 31-46, 1996.

ISSN 114-1284

Economic Analysis of Mining Fleet Replacement Using Optimal Replacement Interval Method

Farizal [1] and Tri Heryanto [2]

Industrial Engineering Department, Faculty of Engineering
University of Indonesia, Depok 16424
Telp : (021) 78888805. Fax : (021) 78885656
E-mail : [a] farizal@ie.ui.ac.id, [b] tri_heryanto_tiui05@yahoo.com

ABSTRACT

Due to the increasing pressure to enhance production and reduce cost, asset management has become a top priority in the mining company. Equipment replacement problem become an important issue and should be optimized especially for fleet of dump trucks and excavators. Until now, a systematic approach for making replacement decision has not been applied to the industry so that the company does not know the most economical age of their equipments. Minimum life cycle cost namely optimal replacement age determination is crucial. In this study, the determination of optimal replacement age of the fleets is conducted based on optimal replacement interval method. The method uses costs per hour to determine the optimal replacement. From this study, a simple guideline to develop replacement strategy is obtained.

Keywords : *optimal replacement age, life cycle cost, cost per hour, optimal replacement interval methodology*

1. INTRODUCTION

Fierce competition coupled by the global economical crisis has forced every company to have a more competitive advantage than its competitors. Every company has to optimize their operational activities in order to reach the best operational performance level. A right decision making is also crucial in the investment decision because it involves a large sum of money. A decision that a company mostly facing is whether to replace the current asset, to continue using it after overhauling, or to replace the asset with the new ones.

Every asset used, whether to manufacture the goods, to transport them, or to provide services, should be replaced after a certain period of time. Replacement occurs when an asset fails and cannot be repaired, when the cost of keeping an asset operational is prohibitive, or when technology changes makes the asset inferior or obsolete [1]. The point on a replacement decision is to determine when the best time for an asset or equipment to better be replaced. The approach used for this replacement decision is usually depends on the economical optimization perspective that is an asset should be replaced at the minimal point of its life cycle cost [2].

In mining industry, asset management is crucial to determine whether the company will have more profit or the opposite. However, managing and maintaining of mining machinery, especially in underground applications, are a difficult task. In addition, the costs associated with running and maintaining a trackless fleet are significant. The costs increased resulting from older machines are not well understood or quantified, and hence accumulate a large proportion of hidden as well as direct costs. A number of reasons causes the problems, namely:

- The complex nature of the machines where numerous and various components exist and are interrelated
- The way and the type of information are recorded
- The nature of the mining cycle does not easily allow one to determine the impact of an unreliable machine.

2 THEORITICAL BASIS

2.1 Replacement Concepts

One of the biggest decisions in a company is deciding when an asset or equipment has to be replaced. As an optimization problem, the decision depends on expectations regarding how the existing and new equipment operating costs change over time and on expectations regarding future capital cost and salvages value [2]. The replacement itself is affected by few certain factors such as the decreasing performance of the equipment, the change in working environment, technology, and financial condition.

As the equipment aging, the operational costs (spare part cost, maintenance cost, and fuel cost) increases while at the same time its resale value decreases. At some moments, the operational cost will become extremely high that it will be profitable to replace that old equipment with the new one. In basic model of capital replacement, the economical age can be determined using the minimal equivalent cost flow of the equipment. The implicit assumption of this model is a machine will be replaced at the end of its economic life by a perpetual sequence of identical machines [5].

Basically, equipment's age can be divided into three, which are [6]:

- Physical life is the interval of time, typically measured in years or hours, between the purchase and the moment when the equipment ceases to operate.
- Useful life is the total time in which the equipment operates, continuously or intermittently.
- Economic life is the interval of time between the purchase and the point at which the equipment's total equivalent annual cost (EAC) curve reaches minimum.

Modern replacement theory is based on discounted cash flow. Discounting future transactions means that the value of money is changing with time. Based on this simple concept, all the costs and profit flows occur in different times should be converted into value at a time and then summed [7]. Replacement problem can be solved in a profit-maximizing or cost-minimizing framework. In a cost minimizing framework, minimum cost can be found with net present value method or the annual equivalent cost [5].

The EAC method is commonly applied to solve the replacement problem when the equipment economical age is determined based on the smallest EAC value [3]. Basically EAC comprises of two components; the capital cost (investment cost and the salvage value) and the operational cost of the equipment. In mining industry, there are some other components of cost that should also be considered. For instance cost that caused by the decreasing availability of the equipment [4]. This cost is also known as the availability cost.

2.2 Theory of Vehicle Replacement

Theory of vehicle replacement says that vehicles should be replaced when the sum of ownership and operating costs is at its lowest historical [8]. The total cost curve is different for every type of vehicles. This variability is caused by differences in the design and engineering of the vehicles, differences in operating environments, the quality of care the vehicle receives, and other factors. As a result, most organizations develop recommended replacement cycles for a class or type of vehicles, which will approximate the optimal replacement cycle for most of the units in that particular class. This is most often accomplished in an informal manner such as based on discussions with mechanics and drivers or a comparison of replacement cycles with peer organizations.

Some organizations, however, employ an empirical approach. This approach, known as life-cycle cost analysis (LCA), involves modeling the stream of costs associated with acquiring, maintaining, and disposing of vehicles over various replacement cycles, and then determining the cycle with the lowest cost [8]. To determine the minimum cost cycle, EAC of each cycle is calculated and compared. The EAC of a vehicle is a uniform dollar amount expressed in today's dollars that someone could pay to produce the net present value of a stream of future costs associated with owning and operating the asset.

2.3 Optimal Replacement Interval Method

The optimal replacement interval method uses cost per hour to determine the optimal replacement age. The method incorporates the fundamentals from the theory of vehicle replacement that uses the lifecycle costs analysis; meaning that the analysis is driven by the capital and the running cost parameters. On this method, moreover, the discounting factors multiplication and the future cash flow concept are applied just like in the equivalent annuity method. The steps to use the optimal replacement interval method are as followed (see Figure 1):

- Determine, by summing, the input parameters such as the operational cost, availability cost, and the capital cost for a certain period of time, for instance: each 1000 hour interval.
- Apply discounting factor in order to account for the risk and cost of money for future cash. Discounting factor is applied based on the annual utilization.
- Cumulate the costs to adjust fluctuating data. This cumulative cost represents the lifecycle cost of the equipment until that stage in its life.
- Divide the cumulative costs by the number of hours accumulated (1000, 2000, 3000, ...). The results are cost per hour, which represents the average cost over the life of the equipment.
- Compare with the alternate life options. The lowest cost per hour is the optimal replacement interval.

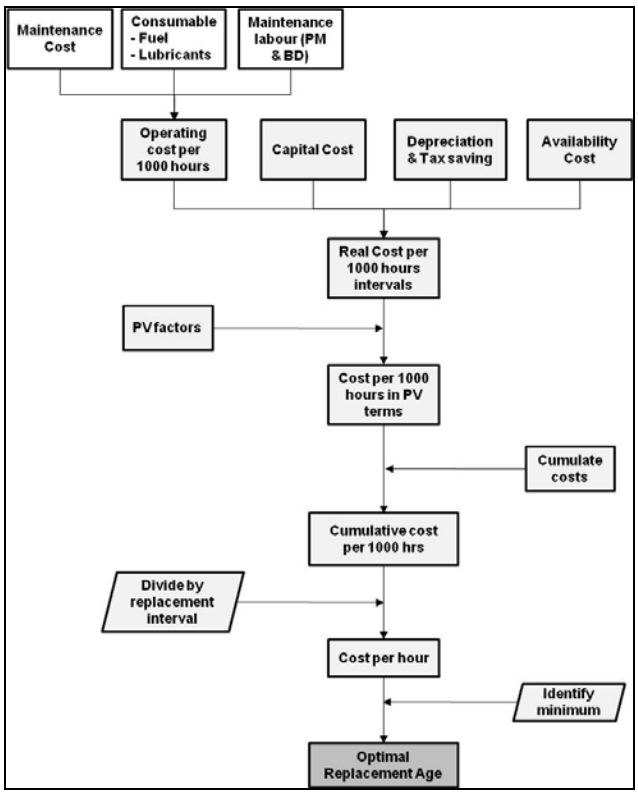

Figure 1: Optimal Replacement Interval Method

3. CASE STUDY

PT P is one of the biggest mining contractor companies in Indonesia that mines coal and gold. This company is often facing some complex replacement problems. Alas, no systematical approach applied there. The company just simply applies depreciation method. This raises doubts to the validity of the replacement strategy applied there. A more comprehensive and thorough method have to be implemented.

In this study case, the replacement age is calculated using the optimal replacement interval method developed by Sandvik Mining [4]. The method uses the cost per hour basis and it is developed based on the life cycle cost analysis concept, theory of vehicle replacement, cost per ton trends, and equivalent annuity. The input parameters are classed in the interval of 1000 hours. The availability cost is counted using two types of approaches, namely the productivity approach and the rental rate approach. Then, the replacement age obtained from these two approaches is compared.

This case is focused on Dump Truck type HD 7855 and the Excavator type PC 3000; both are the main production equipments for the company. The replacement age calculation is done to 8 units of dump truck and 2 units of excavator. The counting example can be seen in Table 2.

4. RESULTS and ANALYSIS

Of those 8 units of dump truck and 2 excavators, various results have been obtained. For each unit, two different replacement ages have been successfully obtained. The results are differentiated by availability cost value. The first age is obtained from the availability cost with the productivity approach, while the second age is obtained from the availability cost with rental rate approach. The best results are displayed on the table 1.

Table 1: Optimal Replacement Age (in hours)

Jenis Peralatan	Unit	Productivity	Rental Rate
Dump Truck	DT738	33000	33000
	DT741	30000	30000
	DT742	38000	38000
	DT746	38000	38000
	DT749	34000	38000
	DT750	39000	39000
	DT751	39000	39000
	DT752	34000	34000
Excavator	EX 705	30000	40000
	EX 707	27000	40000

The average replacement age for the dump truck is 35.625 hours using the productivity approach and 36.125 hours using rental rate approach. From the table above, it can be seen that the replacement age obtained with either productivity or rental rate approach are the same, except for unit DT 749.

For the excavator, the replacement age using the productivity and the rental rate approaches are different. The gap are due to the significant difference in availability cost value, after everything has been counted using the productivity and the rental rate approach. As seen from Figure 2, with the same downtime hours, the availability cost value obtained will be so much bigger if it is multiplied with the productivity. Using productivity approach, the value of availability cost has a large percentage at the cost per hour so that changes occur on the downtime hours will have a large impact on the replacement age.

To show how changing in cost per hour influences the age of the equipment, see the example followed. Figure 3 shows the moving of cost per hour of one the dump trucks. It shows clearly that at the interval of 1000 - 7000 hours, the cost per hour is still very high since at that time the capital cost is still highly dominated in a large number. After 15.000 hours, the cost per hour will get flatter that make it difficult to differentiate the value if it is seen only from the graph. This circumstance is due to decreasing in capital cost per hour traded off with the increasing in operational cost (the increment in cost per hour is extremely small). The availability cost percentage is started to show up and getting up, but the impact on the cost per hour is still very small. For the excavator, the availability cost percentage in cost per hour is bigger compared with that of the dump truck. The availability cost percentage also increases along with the increasing age. At the interval of 37.000 - 40.000 hours, the contribution of availability cost to cost per hour increases until it reaches the same level as the contribution of operational cost.

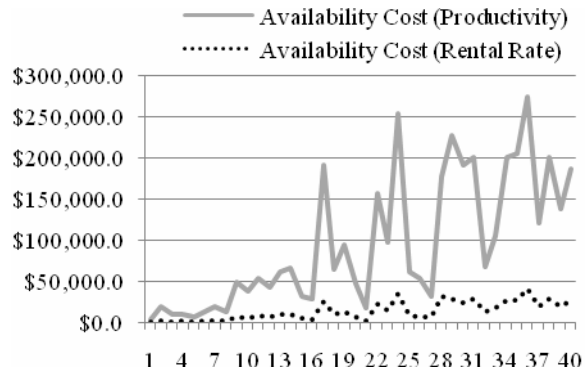

Figure 2: Excavator Availability Cost Comparison

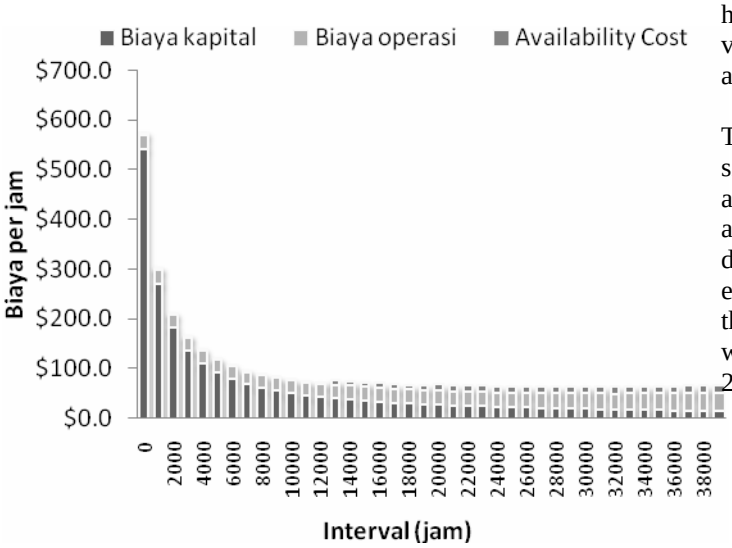

Figure 3: Cost per Hour

Next is to know the profit gained by applying the new strategy and the company's old replacement strategy. The comparison between the old replacement strategy and the new one, DT 752 is taken as example, is 40.000 hours to 34.000 hours. Figure 4 shows the cumulative cost for each replacement strategy. That cumulative cost is the total cost spent if the equipment is replaced every 40.000 hours and every 34.000 hours. This cumulative cost is simulated for long term, which is after the company has replaced the dump truck for few times. The total saving obtained by the company in a 40-year period is $894.225,9.

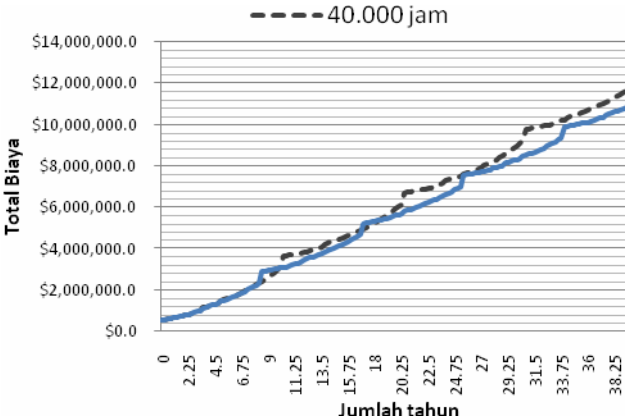

Figure 4: Cumulative Cost for Each Replacement Strategy

5. CONCLUSION

Based on the calculation, the optimal replacement age is 35.875 hours for the dump truck and 34.250 hours for the excavator. The availability cost that counted using two approaches namely the productivity and the rental rate gives different replacement age for the excavator. This happens because the excavator has a higher productivity value than the dump truck so that the availability cost affects the cost per hour.

The cost per hour of dump truck is affected so much by the size of the capital cost and the operational cost. The availability cost is around 40-50% for the operational cost and 20-45% for the capital cost. The replacement age depends so much on the changing of these two cost elements. While for the excavator, the availability cost and the operational cost is more dominating than the capital cost with a percentage of 38-40% for the operational cost and 27-36% for the availability cost.

Tabel 2 : Cost per Hour Calculation

Interval (Hours)	Operating Cost	Capital Cost	Availibility Cost		Depreciation	Tax	After-Tax		NPC		Cumulative		Cost Per Hour	
	Total	Total	Productivity	Rental Rate		Total	Productivity	Rental Rate	Productivity	Rental Rate	Productivity	Rental Rate	Productivity	Rental Rate
0	-	$540.000,0	-	-	-	-	$540.000,0	$540.000,0	$540.000,0	$540.000,0	$540.000,0	$540.000,0	-	-
1000	$44.575,0	-	$551,1	$240,6	$13.500,0	$12.776,5	$32.349,6	$32.039,1	$31.881,8	$31.575,8	$571.881,8	$571.575,8	$571,9	$571,6
2000	$39.690,7	-	$3.239,9	$1.546,7	$13.500,0	$11.702,0	$31.228,7	$29.535,4	$30.332,0	$28.687,3	$602.213,8	$600.263,1	$301,1	$300,1
3000	$39.443,4	-	$445,6	$199,3	$13.500,0	$11.647,6	$28.241,5	$27.995,2	$27.033,9	$26.798,1	$629.247,6	$627.061,2	$209,7	$209,0
4000	$39.954,3	-	$1.052,1	$571,9	$13.500,0	$11.760,0	$29.246,5	$28.766,3	$27.591,0	$27.138,0	$656.838,7	$654.199,2	$164,2	$163,5
5000	$41.808,6	-	$1.601,2	$870,2	$13.500,0	$12.167,9	$31.241,9	$30.510,9	$29.047,2	$28.367,6	$685.885,9	$682.566,9	$137,2	$136,5
6000	$39.487,4	-	$977,9	$510,1	$13.500,0	$11.657,2	$28.808,1	$28.340,3	$26.397,1	$25.968,4	$712.283,0	$708.535,3	$118,7	$118,1
7000	$35.661,7	-	$604,2	$292,8	$13.500,0	$10.815,6	$25.450,3	$25.138,9	$22.983,1	$22.701,9	$735.266,1	$731.237,1	$105,0	$104,5
8000	$33.549,5	-	$873,4	$422,1	$13.500,0	$10.350,9	$24.072,0	$23.620,7	$21.424,0	$21.022,3	$756.690,0	$752.259,4	$94,6	$94,0
9000	$34.989,7	-	$8.509,0	$4.663,3	$13.500,0	$10.667,7	$32.831,0	$28.985,3	$28.796,9	$25.423,7	$785.486,9	$777.683,2	$87,3	$86,4
10000	$44.565,1	-	$7.418,9	$4.033,7	$13.500,0	$12.774,3	$39.209,8	$35.824,5	$33.894,5	$30.968,1	$819.381,4	$808.651,3	$81,9	$80,9
11000	$41.051,2	-	$8.942,0	$5.859,4	$13.500,0	$12.001,3	$37.991,9	$34.909,3	$32.366,8	$29.740,6	$851.748,3	$838.391,9	$77,4	$76,2
12000	$42.998,2	-	$8.520,8	$5.716,4	$13.500,0	$12.429,6	$39.089,4	$36.285,0	$32.820,2	$30.465,6	$884.568,5	$868.857,5	$73,7	$72,4
13000	$43.683,8	-	$6.939,7	$4.356,7	$13.500,0	$12.580,4	$38.043,0	$35.460,1	$31.479,7	$29.342,4	$916.048,2	$898.199,9	$70,5	$69,1
14000	$90.823,6	-	$87.841,0	$56.263,7	$13.500,0	$22.951,2	$155.713,5	$124.136,1	$126.985,9	$101.234,3	$1.043.034,1	$999.434,2	$74,5	$71,4
15000	$49.966,3	-	$28.943,2	$16.334,0	$13.500,0	$13.962,6	$64.946,9	$52.337,7	$52.198,9	$42.064,7	$1.095.233,0	$1.041.498,9	$73,0	$69,4
16000	$51.911,7	-	$19.582,6	$11.311,9	$13.500,0	$14.390,6	$57.103,7	$48.833,0	$45.231,5	$38.680,3	$1.140.464,5	$1.080.179,2	$71,3	$67,5
17000	$52.636,8	-	$7.074,7	$3.809,6	$13.500,0	$14.550,1	$45.161,4	$41.896,3	$35.254,7	$32.705,9	$1.175.719,3	$1.112.885,0	$69,2	$65,5
18000	$45.678,3	-	$10.088,3	$6.113,7	$13.500,0	$13.019,2	$42.747,4	$38.772,8	$32.887,7	$29.829,9	$1.208.607,0	$1.142.714,9	$67,1	$63,5
19000	$45.352,7	-	$16.720,0	$9.713,0	$13.500,0	$12.947,6	$49.125,1	$42.118,1	$37.247,8	$31.934,9	$1.245.854,7	$1.174.649,8	$65,6	$61,8
20000	$54.429,1	-	$34.510,1	$19.419,1	$13.500,0	$14.944,4	$73.994,8	$58.903,8	$55.293,2	$44.016,3	$1.301.147,9	$1.218.666,1	$65,1	$60,9
21000	$83.598,7	-	$66.998,6	$36.865,3	$13.500,0	$21.361,7	$129.235,6	$99.102,3	$95.175,8	$72.984,0	$1.396.323,7	$1.291.650,2	$66,5	$61,5
22000	$52.760,6	-	$29.518,9	$16.226,8	$13.500,0	$14.577,3	$67.702,1	$54.410,0	$49.138,3	$39.490,9	$1.445.462,0	$1.331.141,0	$65,7	$60,5
23000	$52.896,1	-	$21.275,9	$13.354,8	$13.500,0	$14.607,1	$59.564,8	$51.643,8	$42.607,0	$36.941,0	$1.488.069,0	$1.368.082,1	$64,7	$59,5
24000	$57.584,6	-	$22.316,6	$13.066,6	$13.500,0	$15.638,6	$64.262,6	$55.012,6	$45.302,6	$38.781,7	$1.533.371,6	$1.406.863,7	$63,9	$58,6
25000	$59.482,8	-	$15.525,6	$10.887,0	$13.500,0	$16.056,2	$58.952,2	$54.313,6	$40.958,0	$37.735,2	$1.574.329,6	$1.444.599,0	$63,0	$57,8
26000	$97.154,0	-	$23.470,2	$13.366,1	$13.500,0	$24.343,9	$96.280,3	$86.176,3	$65.924,9	$59.006,5	$1.640.254,5	$1.503.605,4	$63,1	$57,8
27000	$67.049,4	-	$30.478,5	$19.436,5	$13.500,0	$17.720,9	$79.807,0	$68.765,0	$53.855,0	$46.403,7	$1.694.109,5	$1.550.009,2	$62,7	$57,4
28000	$69.158,1	-	$36.921,6	$22.605,7	$13.500,0	$18.184,8	$87.894,9	$73.579,0	$58.455,1	$48.934,2	$1.752.564,7	$1.598.943,4	$62,6	$57,1
29000	$60.427,2	-	$30.459,0	$18.202,8	$13.500,0	$16.264,0	$74.622,1	$62.366,0	$48.910,3	$40.877,1	$1.801.474,9	$1.639.820,5	$62,1	$56,5
30000	$125.651,4	-	$25.519,2	$15.860,9	$13.500,0	$30.613,3	$120.557,3	$110.899,0	$77.875,3	$71.636,4	$1.879.350,2	$1.711.456,9	$62,6	$57,0
31000	$91.157,8	-	$25.056,1	$14.322,7	$13.500,0	$23.024,7	$93.189,1	$82.455,8	$59.326,0	$52.492,9	$1.938.676,2	$1.763.949,8	$62,5	$56,9
32000	$92.556,3	-	$24.319,6	$15.493,6	$13.500,0	$23.332,4	$93.543,6	$84.717,5	$58.690,4	$53.152,8	$1.997.366,5	$1.817.102,6	$62,4	$56,8
33000	$57.014,9	-	$30.597,6	$17.884,0	$13.500,0	$15.513,3	$72.099,2	$59.385,7	$44.581,7	$36.720,5	$2.041.948,3	$1.853.823,1	$61,9	$56,2
34000	$161.573,7	-	$29.826,0	$18.845,4	$13.500,0	$38.516,2	$152.883,5	$141.903,0	$93.166,7	$86.475,2	$2.135.115,0	$1.940.298,3	$62,8	$57,1
35000	$133.020,7	-	$28.266,9	$17.787,6	$13.500,0	$32.234,6	$129.053,1	$118.573,7	$77.507,2	$71.213,5	$2.212.622,2	$2.011.511,7	$63,2	$57,5
36000	$131.887,0	-	$27.429,6	$16.611,2	$13.500,0	$31.985,1	$127.331,4	$116.513,0	$75.367,3	$68.963,9	$2.287.989,5	$2.080.475,6	$63,6	$57,8
37000	$69.565,5	-	$24.141,5	$15.906,4	$13.500,0	$18.274,4	$75.432,6	$67.197,5	$44.002,7	$39.198,9	$2.331.992,2	$2.119.674,5	$63,0	$57,3
38000	$195.230,6	-	$27.577,9	$16.329,7	$13.500,0	$45.920,7	$176.887,8	$165.639,6	$101.693,2	$95.226,6	$2.433.685,5	$2.214.901,1	$64,0	$58,3
39000	$184.591,8	-	$26.219,2	$17.210,1	$13.500,0	$43.580,2	$167.230,9	$158.221,7	$94.751,1	$89.646,6	$2.528.436,6	$2.304.547,7	$64,8	$59,1
40000	$105.139,5	-	$28.833,9	$17.610,4	$13.500,0	$26.100,7	$107.872,7	$96.649,2	$60.235,5	$53.968,4	$2.588.672,1	$2.358.516,2	$64,7	$59,0

REFERENCES

[1] Brown, Matt. (1991). *A Mean-Variance Serial Replacement Decision Model: The Independent Case*. Department of Industrial & Operations Engineering University of Michigan

[2] Dobs, Ian M. *Replacement Investment : Optimal Economic Life Under Uncertainty*. England : Department of Accounting and Finance

[3] Blank, L. and A. Tarquin. (1998). *Engineering Economy* (6th ed.). Singapore : WBC/McGraw Hill

[4] Nurock, D and Porteous, C. (2008). *Methodology to determine the optimal replacement age of mobile mining machine.* Third International Platinum Conference '*Platinum in Transformation'*. The Southern African Institute of Mining And Metallurgy

[5] Bethuyne, G. (1998). *Optimal Replacement Under Variable Intenstity Of Utilization And Technological Progress*. The Engineering Economist, 43(2), page 85-106

[6] Galisky, Ron and Ignacio Guzmán. (2008). *Optimal Replacement Intervals for Mining Equipment: A CRU Model To Improve Mining Equipment Management.* CRU Strategies

[7] E. Weiss et al. (2006). *Discounted Cash Flow (DCF) Assessment Method And Its Use In Assessment Of A Producer Company*. METABK 45 (1) 67-70

[8] *Survey of fleet best practices*, MercuryAssociates, March 2006

ISSN 114-1284

MODELING HUMAN RESOURCES INVESTMENT BASED ON HUMAN CAPITAL COMPETENCY

Fauzia Dianawati [1], Isti Surjandari [2], Nur Amalia Budhiarti[3]

Industrial Engineering Department, Faculty of Engineering, University of Indonesia
Kampus Baru UI, Depok 16424, Indonesia
Email : fauzia@ie.ui.ac.id[1] , surjandari.2@osu.edu[2] , NurAmalia.Budhiarti@id.abb.com[3]

Abstract

Employees are valuable investment in a company. However, they are somewhat assumed as expenses of the company. As part of the company resources, employees might be the biggest asset of a company, which is sometime neglected. This study attempts to determine the benefit produced by each employee based on human capital competency of a major electrical company in Indonesia. This is done by comparing the Return of Investment (ROI) for current condition and after using the human capital model. Sales, expenses and investment per month as employee's salary are used as factor or criteria to calculate the current ROI values. To modeling the human capital investment, pair wise comparison method is used to get the weight of each criteria of the human capital competency. The criteria were determined by doing benchmark with top management of the company. There are eleven criteria that may affect employee's performance. Afterward, the current ROI values are compared with that of the human capital model. Based on the human capital model, this study shows that almost 70% of the employees should receive higher benefit, while 30% should receive lower benefit compared with that of the current condition.

Keywords: *Human Capital, Competency, ROI*

1. INRODUCTION

Human Capital is one of new concept that has gained a tremendous amount of attention from both academic and practitioner communities. Human Capital is professional tool on Human Resources System which is used for strategy development in reporting, tracking, and organizational performance impact. Human Capital Concept considers anything that is done by employees will have effect to the company. Human Capital concept will give a significant effect if the company treat the employees not as a cost but as an investment. This study attempts to determine the benefit produced by each employee based on human capital competency of a major electrical company in Indonesia.

2. METHODS

Human Resources Management is a systems design in a formal organization to ensure that human is used as tools to achieve organization goal effectively and efficiently. Beforehand, human resources is defined as a process of recruitment and selection of prospectus employee. Once they become employees, then they will be trained and organized in accordance with the goals and the needs of the company. In its development, human resources were influenced by factors including: Law and Politics, Economic, and Cultural.

In some companies, human capital is used to find out talent, skills and knowledge of workers. Human capital is also concentrating on how the ability or capability can be developed and used to create productivity business performance goals and long-term strategy. Therefore, the measurement of human capital focused on the analysis development to measure and report the human capital management strategy with intervence whether the progress was in line with employee ability.

Human capital defined as "an approach to people management that treats it as a high-level strategic issue and seeks systematically to analyze, measure and evaluate how people policies and practices create value" [1]. Besides the knowledge and experience, this definition also includes dimensions of motivation and social interaction [1]. Qualitative and quantitative approaches can provide indications for the evaluation, assessment/evaluation, and control aspects of the human capital company.

Human Capital Management (HCM) focus on the acquisition, analysis, and reporting of data that directly inform strategy and value of the investment on the corporate level and Frontline Management [2]. HCM always focused on the purpose and objective measurement, not only measurement itself. Definition or other characteristics of HCM is they use metric approach, where employees seen as the asset and the emphasis on competitive advantage through strategy of investment of these assets, (i.e., with the retention and employee engagement, talent management, and learning and development programs).

There are four basic human capital management goals [2]:

1. The influence of human for the business and their contribution to shareholder value.
2. Shows that Human Resources practices can create added value in a period of time, such as Return on Investment (ROI).
3. Provide guidance for the future of human resource and business strategy.
4. Provide estimation and data that can used for planning and making strategy to improve effectiveness of a human organization.

The four fundamental objective of HCM are to [2]:

- Determine the impact of people on business and their contribution to shareholder value.
- Demonstrate that HR practice produce value for money in terms.
- Provide guidance for future HR and business strategy
- Provide diagnostic and predictive data that will inform strategies and practices designed to improve the effectiveness of people management in organization.

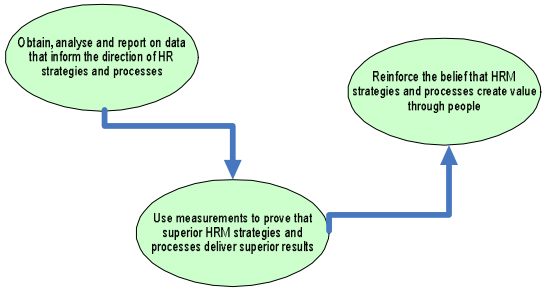

Figure 1: Specific Aims of HCM

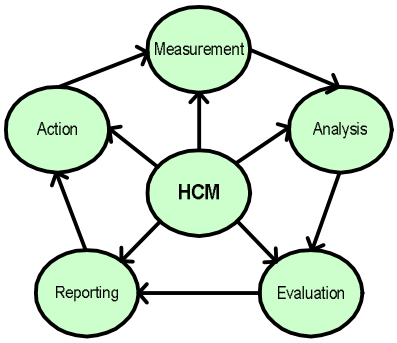

Figure 2: The Process of HCM (1)

Figure 3 and 4 below illustrate the HCM journey in which the key stages are measurement, reporting, drawing conclusion from data and action [1].

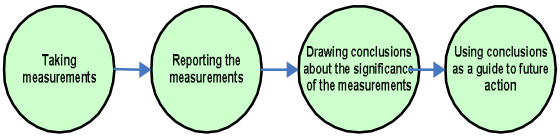

Figure 3: The Process of HCM (2)

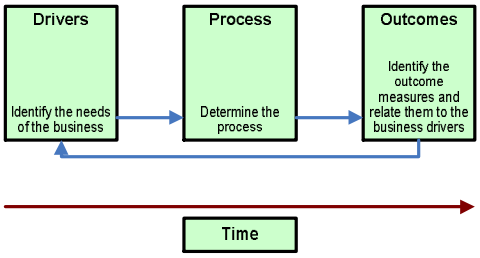

Picture 4: The Focus of HCM

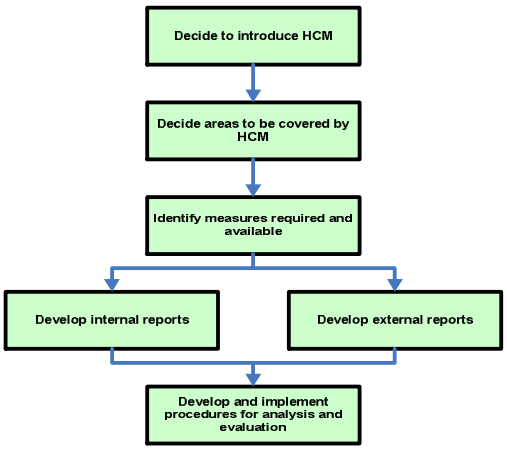

Figure 5: The Steps to Develop HCM

Pair wise comparison is a kind of divide-and-conquer relative order (ranking) of a group of items. This is often used as part of a process of assigning weights to criteria in design concept development. Using AHP in solving a decision problem involves four step [3] :

Step 1: Setting up the decision hierarchy by breaking down the decision problem into hierarchy of interrelated decision elements

Step 2: Colleting input data by paiwise comparisons of decision elements

Step 3: Using "Eigenvalue" Method to estimate the relative weights of decision elements

Step 4: Aggregating the relative weights of decision elements to arrive at a set of ratings for the decision alternative

Table 1: Pairwise Comparison Scale

Intensity of Importance	Definition
1	Equal importance of both elements
3	Weak importance of one element over another
5	Essential or strong importance of one element over another
7	Demonstrated importance of one element over another
9	Absolute importance of one element over another
2, 4, 6, 8	Intermediate values between two adjacent judgements

Results of pairwise comparison will processed to determine weight of each criteria.

$$MG = \sqrt[n]{\sum_{1=1}^{n} x_i} \quad (1)$$

where:
MG = *Geometric Mean*
X_i = Atribut i
n = total atribut

Normalization process is done by making the proportion Geometric mean. Formulation used in the process of normalization is

$$P_i = \frac{MGi}{\sum_{i=1}^{n} MGi} \quad (2)$$

where:
P_i = Proportion atribut– i.
MG_i = Geometric mean atribut - i.
N = Total atribut.

The weight of each alternative against the criteria specified with the formulation as follows:

$$V_i = \sum_{i=1}^{n} P_i x W_i \quad (3)$$

where:
P_i = Proportion atribut – i.
V_i = Weight atribut – i.
W_i = Wheight of Criteria – i.

In pairwise comparison, we have to check the consistency. For example, when in comparison A> B and B> C, then logically it should be A> C. Formula to measure the consistency in AHP can be written as follow:

$$CI = \frac{\lambda_{max}(n-1)}{n} \quad (4)$$

where:
λ_{max} = max eigen value
n = Matriks size.

$$CR = \frac{CI}{RI} \quad (5)$$

where:
CI = Consistency Index
RI = Ratio Index

Table 2: Index Ratio

N	1	2	3	4	5	6	7	8	9	10
RI	0	0	0.58	0.9	1.12	1.24	1.32	1.41	1.45	1.49

3. RESULT AND DISCUSSIONS

This analysis is done to one of Multinational Company in Electrical Solution for Utillity & Insdustry in Indonesia. Most of their employees were work as sales for their product. They have target to be as market leader in future.

Table 3: Turn Over 2007

Emp. Nr	Termination Date	Reason of Leaving	Year of Service
D0240	31-Jan-07	Move to another company	0.84
T0280	31-Jan-07	Terminated	17.93
T0333	31-Jan-07	Resigns based on personal reason	0.17
D0044	31-Mar-07	Move to another company who gives higher position and salary	11.05
D0239	30-Apr-07	Moves to another company who gives him more challenge	1.15
OS0012	30-Apr-07	Contract is expired	0.22
D0125	4-May-07	Terminated	4.95
T0216	31-May-07	Move to another company who gives higher position and salary	9.50
T0255	31-May-07	Move to another company who gives higher position and salary	7.14
T0329	26-Jun-07	Resigns based on personal reason	0.85
T0282	30-Jun-07	Resigns based on personal reason	15.76
D0120	31-Jul-07	Move to another company who gives higher position and salary	5.25
OS0007	31-Jul-07	Move to another company	0.54
D0133	14-Sep-07	Resigns based on personal reason	5.04
OS0023	19-Oct-07	Resigns based on personal reason	1.89
OS0001	22-Oct-07	Move to another company	0.89
T0338	31-Oct-07	Move to another company who gives higher position and salary	3.30
D0260	24-Nov-07	Move to another company	0.98
D0261	30-Nov-07	Move to another company	0.50
OS0011	30-Nov-07	Contract is expired	1.00
OS1010	30-Nov-07	Contract is expired	1.50
D0211	6-Dec-07	Resigns based on personal reason	3.39
D0125	12-Dec-07	Resigns based on personal reason	5.62
T0326	15-Dec-07	Move to another company who gives higher position and salary	5.63
D0235	31-Dec-07	Terminated	1.87
D0269	31-Dec-07	Terminated	0.08

As a trading company they depend on their employees to achieve their target. However, in 2007, the company faced the problem of high turn over. This problem has caused difficulty for the company in reaching the target.

In this case, the reason of employee resignation can be classified into 3 groups:

- Group 1 : *terminated (contract is expired)*
- Group 2 : *based on personal reason*
- Group 3 : *move to another company*

The ratio of employees to retirement can be calculated as below:

$$\overline{Ri} = \frac{\sum Xi}{N} \qquad (6)$$

where:

R = Ratio of retirement for Group i
Xi = Number of employees who submit a resignation group i
N = Number of employees who submit a resignation

R group 1 = $\frac{\sum Xi}{N}$
= 7/26
= 26,9%

R group 2 = $\frac{\sum Xi}{N}$
= 7/26
= 26,9%

R group 3 = $\frac{\sum Xi}{N}$
= 12/26
= 46.2%

From the analysis, it found that the reasons for employee to resign because most of them get a job other company. In other words, they are moving to other company hoping to get better reward. From twelve employees who moved to other company, six people or 50% of them clearly stated that they get a higher salary.

Below is salary data in 2007 for eleven employees who are salesperson.

1. A : USD 29,200 / year
2. B : USD 28,000 / year
3. C : USD 12,600 / year
4. D : USD 8,500 / year
5. E : USD 8,600 / year
6. F : USD 17,700 / year
7. G : USD 11,700 / year
8. H : USD 29,900 / year
9. I : USD 11,000 / year
10. J : USD 5,800 / year
11. K : USD 12,500 / year

Table 4 shows sales target of the eleven employees for 2007.

Table 4: Sales Target for 2007

Employee	Target 2007 (USD)	Achievement 2007
A	800,000	50%
B	20,000,000	80%
C	665,000	80%
D	1,000,000	80%
E	2,750,000	93,8%
F	15,000,000	74.0%
G	3,000,000	93.8%
H	3,000,000	93.8%
I	3,500,000	82.0%
J	Not assign yet	73.1%
K	2,750,000	73.1%

While the cost of the company issued in the form of facilities to the employees can be seen in Table 5.

Table 5: Facilites Obtained

Facilities	Manager	Staf
Jamsostek	4.89% x *gross salary*	4.89% x *gross salary*
Outpatient	Rp. 7,000,000 / year	Rp. 5,000,000year
Health Insurance	Rp. 4,100,000 / year	Rp. 2,580,000 / year
Car	Rp. 5,000,000 / month	Rp. 3,000,000 / month
THR	1 x *gross salary*	1 x *gross salary*

With the assumption of average gross margin of 20%, then the ROI can be calculated as:

$$ROI = \frac{Margin - Investment - Cost}{Investment - Cost} \qquad (7)$$

From data, 90% of employees get ROI > 1. It means that the employees give added value to the Company. However, the ROI is not absolute value; we still have to consider other factors of their performance. In this case, there are 10 other factors which affect sales performances, which are:

1. Education
2. Work Experience
3. Communication Skill
4. Product Knowledge
5. Initiative
6. Administrative Skill
7. Human relationship skill
8. Job description
9. Leadership
10. Thinking challence

By doing pairwise comparison, the weight of each criterion was found as follow:

Education = 1.59%
Work Experience = 10.99%
Communication Skill = 9.47%
Product Knowledge = 15.15%

Initiative = 6.37 %
Administrative Skill = 2.6%
Human relationship skill = 9.77%
Job description = 3.04%
Leadership = 7.17%
Thinking challenge = 10.7%
% Target Achievement = 23.16%

Therefore, the Human Capital Model can be written as follow:

$$Y = 1.59\% X_1 + 10.99\% X_2 + 9.47\% X_3 + 15.15\% X_4 + 6.37\% X_5 + 2.6\% X_6 + 9.77\% X_7 + 3.04\% X_8 + 7.17\% X_9 + 10.7\% X_{10} + 23.16\% X_{11}$$

4. CONCLUSIONS

From paiwise comparison result, it can be found the Human Capital Model. From the model, we can recalculate new ROI with assumption that maximum total cost and investment for each employee is 7.3% from total sales of each employee. By comparing the current ROI and the new ROI, we can see that 70% of the employees should have better benefit, and 30% of the employee have lower ROI compared with the model. Keep in mind that the investment which is calculated in the model is based on the maximum amount of investment, means that employees can get benefit and other costs but will not exceed that maximum amount, because the company has a policy that maximum amount of benefits for the employees is 7.3% of value sales.

REFERENCES

[1] Debbie Whitaker and Laura Wilson, *Human Capital Measurement: From Insight to Action.*. Organizational Development Journal. Chesterland. Fall 2007, 25, 3. ABI/INFORM Global. Pg. P59.

[1][2] Baron Angela & Armstrong, Michael., *Human Capital Mangement : Achieving Added Value Through People.* London & Philadelphia. Kogean Page

[2][3] Sri Mulyono *Teori Pengambilan Keputusan.* Lembaga Penerbit FEUI. Edisi Revisi. Jakarta. 1996.

Proceeding of the 11th International Conference on QiR (Quality in Research)
Faculty of Engineering, University of Indonesia, Depok, Indonesia, 3-6 August 2009
ISSN 114-1284

Production Plan for Wafer Stick Department Using Linear Programming

Gatot Yudoko[1], Isti R. Mirzanti[2]

[1] *School of Business and Management*
Bandung Institute of Technology, Bandung 40132
Tel : (022) 2531923 ext 219. Fax : (022) 2504249
E-mail : gatot@sbm.itb.ac.id

[2]*School of Business and Management*
Bandung Institute of Technology, Bandung 40132
Tel : (022) 2531923 ext 219. Fax : (022) 2504249

ABSTRACT

Wafer Stick Department of a company located in Bekasi, Indonesia, produces 18 kinds of cookies daily to serve both domestic and foreign markets. All these products had the same production processes, namely warehousing of raw materials, mixing, drying, and packing. This department had its own production plan and would like to know whether the existing plan was a good plan or not. The purpose of this paper is to propose linear programming as a technique that can be used to formulate daily production plan for the Wafer Stick Department. In this paper, we compare the maximum profit obtained by the linear programming to that of the existing plan. The comparison was based on a five week schedule.
Observations to the plant, especially at the Wafer Stick Department, interviews with the production planner of the Wafer Stick Department as well as the Marketing Department, and the collection of the required data were used to characterize parameters of the linear programming, namely profit contribution of each product, machine capacity, technological coefficients representing resource usage for producing each type of product in each machine, and other necessary requirements. We used WinQSB to solve our linear programming model which resulted in a feasible and optimal solution with a total profit for the five weeks 2.47 billion rupiahs and this is 0.73 billion rupiahs higher than the use of the existing production schedule.

Keywords: *production planning, linear programming, wafer stick*

1. INTRODUCTION

A cookie or biscuit producing company located in Bekasi, Indonesia, produces various kinds of cookies to meet both domestic and foreign markets. One of the departments responsible for the production was the Wafer Stick Department which produced 18 kinds of cookies. All products or cookies had the same production process, starting from warehousing of raw materials, mixing, drying, and packing. The drying process by oven was the major process in that production. The existing method used to schedule forecasted demands was based on historical production schedules. The Production Planner in the Wafer Stick Department would like to have an alternative schedule that could be used as comparison to the existing practice. Therefore, the objective of this paper is to propose the use of linear programming for scheduling in that department.
The production planning as shown in figure 1 began with demand forecasting by the Marketing Department. The forecasted demand would be given to production planner responsible for production planning and control (PPC). In this regard, the production planner would coordinate with warehousing concerning the available stock or inventory in the warehouse. The implementation of the production and material plan would be done by the production department. The finished goods would be kept in the warehouse.

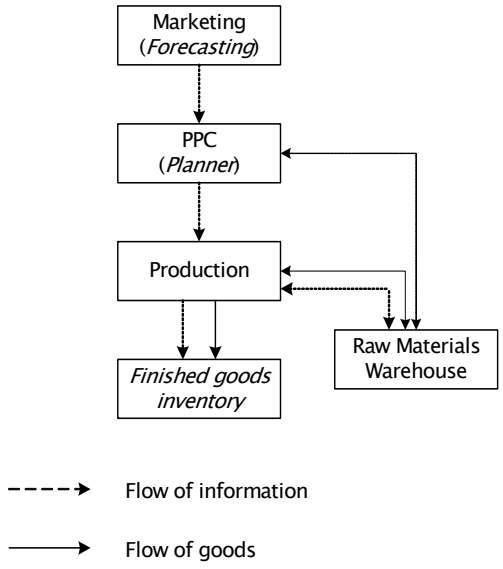

Figure 1. Production planning process

ISSN 114-1284

2. METHODOLOGY

We propose a linear programming model [2], consisting of decision variables, objective function, and constraints. We conducted direct observations to the plant, interviews with the Production Planner, and collected the required data from the Wafer Stick Department to characterize the linear programming model. In this paper, we only make the model for five weeks as agreed with the Production Planner.
The general form of the linear programming model would use the following notations: Z for total profit, X_{ij} for the number of product i to be produced in week j, d_i for demand of product i in one month, r_j for machine capacity in week j, a_j for maximum work-in-process (WIP) in week j, and b_{ij} for time required to make product i at week j (in minutes).

a. Objective function

The objective function was to maximize total profit (Z) by producing product i at week j (X_{ij}) with each product had its profit contribution of C_{ij}. In this regard, we consider 18 products (i = 1, 2, …, 18) being produced in five weeks (j = 1, 2, 3, 4, 5).

$$Z = \sum_{i=1}^{n}\sum_{j=1}^{m} C_{ij} X_{ij} \quad (1)$$

b. Constraints

* Machine capacity

$$\sum_{i=1}^{n} b_{ij} \sum_{i=1}^{n} X_{ij} \le r_j \quad (2)$$

* Forecasted demand from Marketing

$$\sum_{j=1}^{m} X_{ij} \le d_i \quad (3)$$

* *Secondary process*

$$\sum_{j=1}^{m} X_{ij} \le a_{ij} \quad (4)$$

* Non-negativity

$$X_{ij} \ge 0 \quad (5)$$

3. RESULTS

Based on our agreement with the Production Planner, we would use initials for all products. Table 1 shows profit per cart for each product.

Table 1. Profit for each product

Product initial	Size	Profit/cart (rupiahs)
X1	36 x 60 grams	6,340
X2	120 x 33 grams	8,500
X3	36 x 60 grams	6,500
X4	24 x 60 grams	6,340
X5	24 x 120 grams	4,500
X6	24 x 60 grams	6,000
X7	24 x 120 grams	6,200
X8	6 x 750 grams	15,500
X9	12 x 350 grams	10,800
X10	12 x 350 grams	5,800
X11	12 x 350 grams	16,800
X12	6 x 750 grams	16,800
X13	24 x 150 grams	11,200
X14	24 x 150 grams	9,200
X15	12 x 400 grams	4,100
X16	12 x 400 grams	1,100
X17	12 x 400 grams	12,900
X18	12 x 400 grams	20,500

Total forecasted demands for the overall five weeks provided by the Marketing Department are shown in Table 2. Times required to produce each cart of each product is shown in Table 3. Effective machine capacity for the five weeks is shown in Table 4.

Table 2. Forecasted demands

Product initial	Forecasted demand (carts)
X1	32,916
X2	21,608
X3	2,000
X4	23,972
X5	18,375
X6	550
X7	5,486
X8	7,050
X9	2,625
X10	1,470
X11	4,580
X12	3,790
X13	17,345
X14	6,300
X15	7,924
X16	53,848
X17	81,081
X18	5,940

Table 3. Production time

Product initial	Production time (minutes/cart)
X1	4.03
X2	4.87
X3	3.66
X4	4.03
X5	2.91
X6	4.03
X7	4.03
X8	3.66
X9	3.31
X10	2.91
X11	0.87
X12	0.87
X13	2.01
X14	1.34
X15	8.72
X16	9.26
X17	3.66
X18	4.03

Table 4. Machine capacity

Week	Effective capacity (minutes)
1	263,616
2	331,299
3	318,468
4	281,954
5	188,456

Data about the secondary process related to the capacity of work-in-process (WIP) of a particular product, namely product 16 (X_{16j}) is shown in Table 5. The capacity shown in that table represents a_{ij} in our linear programming model.

Table 5. Capacity of secondary process

Week	Capacity (carts)
1	12.897
2	21.569
3	16.087
4	14.359
5	11.797

Using WinQSB [1] we solve the linear programming (LP) model and the solution is summarized in Table 6. As shown in Table 7, this schedule is able to generate a total profit of 2.474 billion rupiahs. The company's production schedule is shown in Table 8 which generated a total profit of 1.737 billion rupiahs as shown in Table 9. Therefore, the company's schedule had 736.8 million rupiahs less than the proposed schedule using linear programming. This shows that linear programming could be used by the company to optimize its schedules in the future, provided that they would be willing to learn and use it.

Table 6. Proposed production schedule

Product	Week 1	Week 2	Week 3	Week 4	Week 5
X1			32,916		
X2			2,578	19,030	
X3		2,000			
X4		13,523			10,449
X5		18,375			
X6					550
X7					5,486
X8		7,050			
X9	2,625				
X10		1,470			
X11	4,580				
X12	3,790				
X13		17,345			
X14	6,300				
X15				6,458	1,466
X16		10,098	16,087	14,359	11,797
X17	65,356	15,725			
X18			5,940		

Table 7. Optimal profit using LP

Product	LP's schedule	Profit/ cart	Total profit
X1	32,916	6,340	208,687,440
X2	21,608	8,500	183,668,000
X3	2,000	6,500	13,000,000
X4	23,972	6,340	151,982,480
X5	18,375	4,500	82,687,500
X6	550	6,000	3,300,000
X7	5,486	6,200	34,013,200
X8	7,050	15,500	109,275,000
X9	2,625	10,800	28,350,000
X10	1,470	5,800	8,526,000
X11	4,580	16,800	76,944,000
X12	3,790	16,800	63,672,000
X13	17,345	11,200	194,264,000
X14	6,300	9,200	57,960,000
X15	7,924	4,100	32,488,400
X16	52,341	1,100	57,575,100
X17	81,081	12,900	1,045,944,900
X18	5,940	20,500	121,770,000
Total			2,474,108,020

Table 8. Company's production schedule

Product	Week 1	Week 2	Week 3	Week 4	Week 5
X1	7,520	10,191	15,184	4,880	
X2		5,457	1,786	7,802	4,173
X3			1,927		
X4	482	2,133	479	2,957	10,444
X5			1,276	690	
X6			35		
X7	2,227	357	2,555		
X8			1,675	4,590	
X9				289	1,906
X10	1,458		236	329	
X11	2,273	3,782	1,781	949	
X12	968				
X13	1,365	2,693	4,507	1,071	
X14	483	164		350	
X15			97	2,386	
X16	14,048	20,718	16,186	13,868	8,807
X17	12,956	11,804	8,993	7,943	8,482
X18	1,192				

Table 9. Total profit of existing schedule

Product	Company's schedule	Profit/ cart	Total profit
X1	37,775	6,340	239,493,500
X2	19,218	8,500	163,353,000
X3	1,927	6,500	12,525,500
X4	16,495	6,340	104,578,300
X5	1,966	4,500	8,847,000
X6	35	6,000	210,000
X7	5,139	6,200	31,861,800
X8	6,265	15,500	97,107,500
X9	2,195	10,800	23,706,000
X10	2,023	5,800	11,733,400
X11	8,785	16,800	147,588,000

Table 9. continued

Product	Company's schedule	Profit/ cart	Total profit
X12	968	16,800	16,262,400
X13	9,636	11,200	107,923,200
X14	997	9,200	9,172,400
X15	2,483	4,100	10,180,300
X16	73,627	1,100	80,989,700
X17	50,178	12,900	647,296,200
X18	1,192	20,500	24,436,000
Total			1,737,264,200

The use of the existing capacity through the existing production schedule is shown in Table 10 which shows total minutes used in each week. The use of the existing capacity through the use of LP production schedule is shown in Table 11.

The comparison of idle or unused capacity for each week by the company's production schedule to LP's schedule is shown in Table 10. It indicates that LP's schedule resulted in greater efficiency of machine capacity use.

Table 10. Comparison of idle machine capacity

Week	Company's schedule	LP's schedule
1	29,561	0
2	9,645	5
3	24,376	1
4	9,912	0
5	7,318	0
Total	80,632	6

4. DISCUSSION

The use of linear programming (LP) resulted in different product mix compared to the product mix of the schedule used by the company. The production planner could see and check that this alternative production schedule provided a higher total profit with less idle machine capacity. He/ she should be interested in using this model for future production scheduling in his/her department.

We were also interested in looking at the sensitivity analysis of the LP solution to see possible changes of certain parameters which do not change the optimal solution that had been obtained. In this regard, we took a look at the values of the decision variables or right-hand-side and machine capacity. From the WinQSB output, we can show the sensitivity of the decision variables indicating minimum and maximum values for each product. This is summarized in Table 11. The notation "M" indicates a very big number. Table 12 shows sensitivity of total machine capacity in each week.

Table 11. Sensitivity of values of decision variables (units)

Product	Minimum	Maximum
X1	29,744	36,032
X2	18,983	30,254
X3	0	27,550
X4	20,510	47,176
X5	13,581	50,510
X6	0	10,999
X7	2,024	15,935
X8	3,238	32,600
X9	0	30,876
X10	0	33,605
X11	0	112,065
X12	0	111,275
X13	10,404	63,868
X14	0	76,085
X15	6,458	12,753
X16	52,341	M
X17	77,269	106,630
X18	2,815	9,010

Table 12. Sensitivity of machine capacity (minutes)

Week	Minimum	Maximum
1	170,104	277,567
2	237,787	345,250
3	305,912	331,250
4	239,846	294,736
5	146,348	202,407

5. CONCLUSIONS

We conclude that linear programming (LP) could actually be used by the Production Planner to solve his/her scheduling task since it can help him/her to find the optimal schedule which would generate the maximum profit with respect to constraints. In addition, the optimal schedule would use existing resources, such as machine capacity, efficiently in which idle capacity would be minimized. We believe that through learning and exercises in mathematical formulation and the use of an optimization software, production planner would eventually get used to it. For large problem involving larger variables and constraints, we thought that a more powerful software than WinQSB would be needed.

REFERENCES

[1] J. A. Lawrence and B. A. Pasternak, "*Applied Management Science: A Computer-Integrated Approach for Decision Making*", New York: John Wiley & Sons, 1998.
[2] W. L. Winston, "*Operations Research: Applications and Algorithms*", Third Edition. Belmont, California: Duxbury Press, 1990.

Managing Soft Innovation Process under Uncertainty

Gembong Baskoro

Universitas Widya Kartika
Surabaya, Indonesia
email: gembong_baskoro@yahoo.com, gbaskoro@widyakartika.ac.id

ABSTRACT

It is not surprisingly for manufacturers to survive in the business they usually increase the market share of new products. This means manufacturers must increase the speed of innovation. Ideally, the innovation in the new products is done by manufacturers to compensate the previous product weaknesses related to classical business pressures. The classical business pressures are (1) Time, (2) Profitability, (3) Functionality, and (4) Quality/Reliability. In contrast, Baskoro indicated that new products delivered to the market may contain immature (1) Technology and/or (2) Production process [1]. Consequently, if a product is developed in immature Technology and/or Production process then the product potential of having hard reliability problems. Hard reliability problems or specification violation is a situation where a product is not able to meet the explicit technical product specifications. This paper argues that hard reliability problems closely related to hard innovation concept. However, Brombacher et al. indicated that these type of products, high-end consumer electronics, instead of having hard reliability problems they also suffer soft reliability problems [2]. Soft reliability problems or customer expectation deficiencies is a situation where, instead of meeting with the explicit product specifications, a customer explicitly complains about the lack of functionality of the product. This paper also argues that soft reliability problems closely related to soft innovation concept. If soft reliability problems appear in the product, customer will always dissatisfy with the product. Therefore, Baskoro argue that a strategy to secure customer satisfaction is to deliver a new product that having less (or free) soft reliability problems [1]. This can be done by managing the innovation process. For this reason the objective of this paper is to explore a method of soft innovation process that ensure a new product having less, if not free, soft reliability problems.

Keywords
Innovation, Hard Innovation, Soft Innovation, Hard reliability problems, Soft Reliability Problems

1. INTRODUCTION

It is not surprisingly that in today global market, in highly competitive business environment, only some companies can survive while others must leave from the playground because their products simply cannot compete. Among other reasons that make a product fails to survive in the market is due to "Product Reliability". Therefore, in order to survive in the business, companies must consider a number of potentially conflicting issues including but not limited to "Product Reliability" in their product development strategy [2]. It is familiar as the business pressures that contain the issues of Time, Profitability, Functionality, and Quality and Reliability.

- Time: does the product reach the market at the required moment in time?
- Profitability: is the difference between product cost and product sales price adequate?
- Functionality: is the product able to fulfill its intended function(s)?
- Quality and Reliability: does the product fulfill customer requirements at 'all' customers, not only at the moment of purchasing but also during operational life of the product?

However, Baskoro shows that although companies have understood the business pressure they are not secured yet in the business [1]. For example: to shorten Time-to-Market of their product in order to arrive in the market earlier. The expectation is that by arriving in the market earlier they have the privilege to dominate the market and dictate the market price. For this reason, companies can sometimes take risks to deliver a product to the market with less mature technology. Consequently, it is not surprise if this product may contain (reliability) problems and the problems can show up after real testing (use) by customers. In practice, there is reported an increasing number of complaints by customer, suspected by reliability problems, on specifically product performance. Sometimes the problems are unknown; there is no specific root causes related to the problems. On this situation, it is possible that the problems are caused either/both by (1) the product, and/or (2) the user. Many researches have tried to elaborate research on the product, and seldom on the

user. Therefore, this paper interests on dealing with (soft) reliability problems especially where problems are caused by extreme users.

2. RELIABILITY PROBLEM

Recently, manufacturers and/or customers should aware on product reliability instead of only product quality. For customers, on the one hand, reliability indicates that customers will get their right to at least replacement of the product when the product has problem during the warranty time. For manufacturers, on the other hand, reliability associates to the company reputation e.g. brand image especially if the problem on the product can cause injury and or damage. Therefore, problems occur in a product during warranty period are problems that related to product reliability. This is also known as "reliability problems".

Reliability problems can be categorized into (1) Hard reliability problems, and (2) Soft reliability problems [2].

1. Hard Reliability Problems (Specification Violation)
A situation when a product is not able to meet the explicit written technical product specifications.

2. Soft Reliability Problems (Customer Expectation Deficiencies)
A situation where, in spite of meeting with the written explicit product specifications, a customer will explicitly complains about the lack of functionality on the product.

The above classification of reliability problems is covered in the class of "non-inventive" reliability problems. However, there are also known the "inventive" reliability problems that are new both for manufacturers and users [1].

A problem in a product is recognized as an "inventive" problem if this problem is new and never seen before by the manufacturer. On the contrary, "non-inventive" problem is a problem that has been experienced before.

3. FACTS-FIGURES OF (SOFT) RELIABILITY PROBLEMS

Although reliability problems are identified during the use of the product, reasonably they are initiated during product development process. When the reliability problems occur and slip through the production process but do not reach the customer, the manufacturer has a chance to recall the products with reasonable cost consequences. However, if reliability problems occur after customers use the product, then the manufacturer will face several consequences. The consequences can be that the manufacturer risks customer dissatisfaction, legal warranty claims, and/or lawsuits. Usually, especially in Europe, if the reliability problems have potential consequences for customer safety, the manufacturer is urged by law to recall the product from the market (Directive 1999/34/EC). In real cases, if the problems can potentially create a bad reputation and damage the company image, then the company will take extreme actions by voluntarily recalling the product from the market and/or applying a product replacement program. In practice, this situation can happen to any company including but not limited to the established companies in the field. Baskoro showed several cases related to this situation that took place in Europe [1]. For example as reported by local news paper on August 2007 that a France branded car withdrew 80,000 cars from Germany and 10,500 cars from Denmark. In Indonesia several related cases have been publicly reported by customer in news paper related to reliability problems especially for consumer electronic products. For example on July 2007, a local news paper publishes a complaint from customer regarding reliability problems shortly after purchase of a Netherlands branded Hand Phone. On October 2007, the same news paper reported reliability problems (short product life) experienced by customer on a Finland branded Hand Phone.

These facts show that companies are willing to take extreme actions by voluntarily recalling the product from the market to protect the customer from being dissatisfied with the product and to secure potential business in the future. Mainly, the cost to settle the problems can be extremely high if manufacturers fail to prevent the problems earlier.

4. INNOVATION CONCEPT

There are many ways to distinguish the innovation concept. In general, Chesbrough classified innovation into a. Close Innovation and, b. Open Innovation [3]. This classification is based point of view on the influence of other to the innovation process. This method of classification enables to accelerate the process of innovation without spending too much cost. However, in practice this method especially open innovation requires open culture from the actors because they need to adapt and adopt something new from outside their organization. It simply not easy for organizations that still maintain a traditional culture and way of thinking on everything must be invented here.

4.1. Closed Innovation

It is a traditional concept of innovation where all (re)sources for the innovation process come within the organization. The close innovation, figure 1, is considered as old paradigm and tends to be ineffective for today business environment [3]. It is indicated by high investment spending to setup internal research and development division. However, in the past the concept of close

innovation has proved to deliver innovative products to customer. It was possible because time to market was not the main concern and the competition tends to be relatively small.

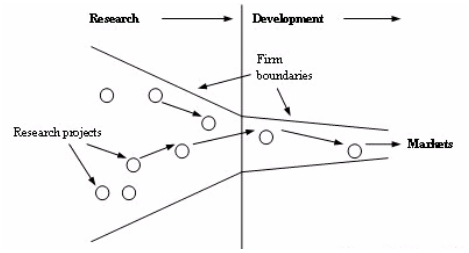

Figure 1. Close Innovation [Chesbrough 2003]

4.2. Open Innovation

The open innovation is a way of thinking that the process of innovation can be done not just by the company itself. There are two important things to be considered i.e. 1. Idea, and 2. Market. In this concept, the source and target of both idea and market is not limited to internal and or external sources. Open innovation, figure 2, can combine both internal and external ideas to advance the innovation [3]. Similarly, the result of innovation can be marketed to existing or new market opportunity even from outside company business channels. The main consideration is to efficiently and effectively generate value.

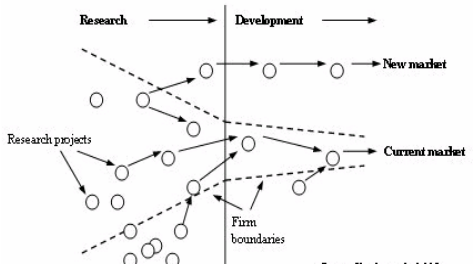

Figure 2. Open Innovation [Chesbrough 2003]

4.3. Hard Innovation

Hard innovation is an innovation process that focuses on the technology and functionality of a product. Hard innovation can be distinguished easily by the improvement or betterment made in a product. Hard innovation can be categorized into 1. Radical, and 2. Incremental Innovation. It is called radical if the innovation is totally changed the technology and or total replacement of the concept. Therefore it requires capability to do exploration of new technology. On the other hand, it is called incremental innovation if the innovation made is only partial. It is simply as step by step improvement on the product. Therefore, it is more or less the exploitation of the existing technology.

Hard innovation requires strong technology and resources capability. The sources can be within the organization (Close) or outside organization (open). Therefore, the capability to build up internal competence is a key success factor on hard innovation.

4.4. Soft Innovation

Soft innovation is an innovation focusing on the concept, system, procedure, etc. other than the hard factors. Therefore, investment requires in soft innovation is considered affordable. It can be done by any organizations so long they want to do it. The source of soft innovation may be come form outside organization (open) or within the organization (close).

5. DISCUSSION

The concept of Innovation therefore can be simplified into a matrix that consists of four quadrants as in Figure 3.

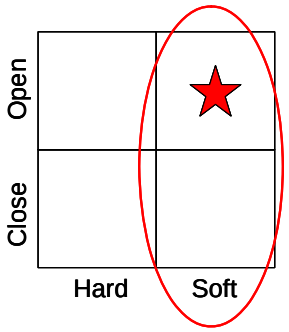

Figure 3. Matrix of Innovation

This diagram is a matrix that connects Open/Close Innovation versus Hard/Soft Innovation. It is shown from the matrix that a company can have innovation concept in between the quadrants. The star in figure 3 indicates that the innovation concept is soft and open innovation. This indicates that the innovation will be focused on the soft aspect and the idea can come within or from other organization. The matrix is considered acceptable for a company that has medium financial and resource strength but it has an ambition to go forward.

The reasoning of becoming a star is that an organization must keep moving regardless their capability to explore knowledge, either by performing radical or incremental innovation. Therefore, rather than making a lot of investment for building up the knowledge and its resources, the company can still go

forward with the innovation process on the soft side with limited resources.

This paper considers that in today uncertain economic downturn. Organization should consider seriously adopting the concept of soft and open innovation. The reason is that in the difficult situation, rather than seizing hard innovation process that will impact to the morale of organization, it is a better to keep the activity of the organization going on. One choice is that organization can focus to soft innovation process. However, to ensure the efficiency and effectiveness it is good to adopt idea and disseminate results outside organization by adopting open innovation concept.

REFERENCES

[1] Baskoro, G. (2006), "*The Design of an Accelerated Test Method to Indentify Reliability Problems During Early Phases of Product Development*", PhD Thesis, Technische Universiteit Eindhoven, Eindhoven, Nederland

[2] Brombacher, A.C.; Sander, P.C.; Sonnemans, P.J.M.; Rouvroye, J.L., "*Managing product reliability in business processes "under pressure*", Reliability Engineering & System Safety vol. 88, 2005, pp. 137-146

[3] Chesbrough, H. (2003), "*Open Innovation: the new imperative for creating and profiting from technology*", Harvard Business School Press

[4] Thomke, S.; von Hippel, E. (2002), "*Customers as Innovators: A new way to create value*", Harvard Business Review

[5] von Stamm, B. (2003), "*Managing Innovation Design and Creativity*", London Business School

ISSN 114-1284

ANALYSIS ON AUTOMOTIVE COMPONENTS INDUSTRY CAPABILITIES BY USING *SHINDAN SHI* MODEL AS AN EFFORT TO INCREASE THE SME_S PRODUCTIVITY

H a f i d[1]

[1]*Metal Industrial Industies Development Centre (MIDC), Ministry of Industry Indonesia*
Jl. Sangkuriang No. 12 Bandung 40135, Tel : (022) 2503171, Fax : (022) 2503978
Email : hafidochan@yahoo.com

ABSTRACT

This research is an analysis on automotive components industry capabilities by using Shindan Shi model as an effort to increase the SME_S productivity. The Shindan model adopted from Japan is a model which can be used to diagnose industries by using comprehensive management analysis to improve company performance. The variables of capabilities to be observed are : (1) 5S/5R/5K, (2) production quality, (3) accounting and book keeping, (4) human resource, and (5) organization management. The results of this research are expected to be able to contributed to the efforts of improving quality, productivity and competitiveness in global market of automotive industrial business. The results of this research carried out in Bandung area, in which involved 9 (nine) automotive components of SMEs, can define the following capability classifications : 1 company on class I (growth level), 5 companies on class II (potential level), and 3 companies on class III (autonomous level). By using the same method, the case study may also be implemented for other SMEs in other areas. For example of diagnosis in PT. W, with covers : (1) SWOT analysis, (2) increased CNC machine efficiency was more than 80%, (3) has decreased the average reject ratio of BCM KF 150 T Deluxe to be 5%, (3) 5S activities in machining center to be better. The results of this research are expected to be able to contributed to the efforts of improving quality, productivity and competitiveness in global market of automotive industrial business.

Keywords : *Shindan shi, automotive components, capabilities, SMEs, productivity*

1. INTRODUCTION

SMEs has an important and strategic role in national economy system, due to: (1) a very large number of business units (record about 3.4 millions), (2) absorbing many labors (in 2006 for 8.7 million people), (3) a relatively submissive creditor in cash return, (4) quite high SMEs endurance in confronting many fluctuations (monetary crisis in 1997). Thus, we may say that SMEs is economy spine with continuously proven contribution for more than 50% PDB.

Based on the SMEs study result in Indonesia conducted by Prof. Urata from Japan in 2000, he found 4 (four) SMEs's primary weaknesses, they are : (1) lack of production technology knowledge and quality control, (2) limited capability on marketing, (3) limited human resources for enhancing the quality of human resources, (4) lack of knowledge on financial accounting administration.

Now, in West Java there are approximately 200 automotive components industry needing supports in improving Quality (Q), Cost (C), Delivery time (D), Engineering (E), Management (M) and Technology (T). As efforts to strengthen Automotive Supporting Industries (ASI) in order to have competitiveness in global market, it is necessary to implement Shindan Shi system through "Accompaniment" and direct consulting in form of analysis and diagnosis of issues that SMEs confronts with.

This research methodology by using the method case study the implementation of model Shindan Shi system on selected automotive components industry in Bandung with identification purpose of : (1) SMEs's automotive component conditions and (2) gradual analysis of automotive components industry capability using Shindan Shi as efforts to increase SMEs productivity.

Whereas, expected benefits from this research are that it may be model program for development of automotive components industry in Bandung in particular and in general for SMEs in Indonesia to improve quality, productivity and companies' competitive excellence in global market.

2. METHODOLOGIES RESEARCH

The sequence of this research steps can be seen in Figure 1. And then do this : (1) the steps of solving problems in automotive components industry capabilities, (2) the steps of solving problems for the test of validity, reliabilities and sufficiency of data and (3) the steps of solving problems Shindan Shi model. For example the implementation of Shindan Shi model does at PT. W-21 that the representing one of the automotive component producer in Bandung.

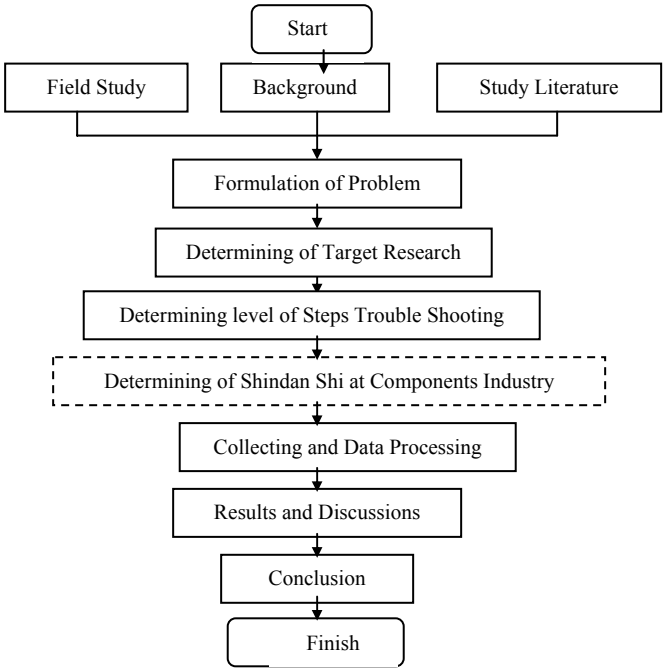

Figure 1. Flow chart of methodologies research

The methodologies research steps of automotive components industry capabilities shall be as follows :

1. Capabilities level :

   Which one to be criterion or parameter assessment of automotive components capabilities industry is show more clear at Table 1. For analysis quantitatively in this research is used by scale of Likert.

Table 1. Automotive components industry of SMEs parameter

No	Variable	Variable sub
1	5S/5R/5K	- Clearing up (X_1) - Tidying up (X_2) - Cleaning (X_3) - Standardizing (X_4) - Training and Discipline (X_5)
2	Production quality	- Reject ratio/NG (X_6)
3	Accounting and book keeping	- Book keeping (X_7) - Jurnal and ledger (X_8) - Balance Sheet and Income Statement (X_9) - NPWP (X_{10})
4	Human resources	- Total of labour (X_{11}) - Labour qualification (X_{12})
5	Organization Management	- Organization chart (X_{13}) - Vision and mission (X_{14}) - Vision mission implementation (X_{15}) - Corporate planning (X_{16})

2. The Parameter value

   a. 5S/5K/5R

      The Assessment 5S/5K/5R is classified to be 5 level with score that is as follows :

      5 = Very good, 4 = Good, 3 = Enough, 2 = Less, 1 = Very Less.

   b. Production quality

      For the assessment of production quality (Q) is used a reference based on rejection rate level that accepted by customer. Rejected level is calculated by calculate the average of total product (unit) that reject in specified period compared to the amount of product which is made in connection period. For the reject level (% NG) is divided to be 2 fields, that is : casting and machining/pressing. The Assessment of Production quality (Q) is classified to be 5 reject level (% NG) that is with the following score :

      - Level of reject casting : 5 = Very good (NG≤1), 4 = Good (1<NG≤3), 3 = Enough (3<NG≤5), 2 = Less(5<NG≤10), 1 = Very less (NG>10).
      - Reject machining/pressing Level : 5 = Very good (NG≤5), 4 = Good (5<NG≤10), 3 = Enough (10<NG≤20), 2 = Less (20<NG≤30), 1 = Very less (NG> 0).

   c. Accounting and book keeping

      The Assessment of Accounting and Bookkeeping (C) is relied on equipment from book keeping company of pertinent. Each equipment of book keeping get the following score :

      - Book keeping (cash, sale, etc.) score = 40
      - Journal and ledger score = 20
      - Financial statement score = 20
      - NPWP score = 20

      Based on the score, is arranged the furthermore assessment :

      5 = Very good (C ≥ 90), 4 = Good (75 ≤ C < 90), 3 = Enough (60 ≤ C < 75), 2 = Less (40 ≤ C < 60), 1 = Very less (C < 40).

   d. Human Resources

      The Labor which is concerned in business that calculated by average per month. From the result of the average conducted assessment base on to 2 (two) condition, that is : (a) Total of labor and (b) labor qualification. The Assessment of human resources to be 5 group level, that is with the following score :

      a. Total of labor :
         - 100 s/d 199 peoples score = 25
         - 50 s/d 99 peoples score = 20
         - 20 s/d 49 peoples score = 15
         - 10 s/d 19 peoples score = 10
         - 1 s/d 9 peoples score = 5

      b. Labor qualification (taken away from by highest value) :
         - Man power (S1) score = 25
         - Man power (So) score = 20
         - Man power experience score = 10
         - Man power not experience score = 5

      Based on the score, performed by furthermore

assessment as follows :
5 = Very good (D ≥ 150), 4 = Good (100 ≤ D < 150), 3 = Enough (50 ≤ D < 100), 2 = Less (10 ≤ D < 50), 1 = Very less (< 10).

e. Organization Management
The assessment of management organization is classified to be 5 levels that are as follows :
5 = Very good, 4 = Good, 3 = Enough, 2 = Less, 1 = Very less.

3. The Assessment of capabilities
The multiplication result weight with the parameter value is point per parameter. As quite high of point obtained to be high will also level of technical capabilities of components industry. More clear level of capabilities calculated by like shown at Table 2

Table 2. Parameter/Criterion Assessment

No	Parameter/ Criterion Assessment	Weight (%)	Value	Weight x Value
1	P1	B1	N1	B1 x N1
2	P2	B2	N2	B2 x N2
3	P3	B3	N3	B3 x N3
4	P4	B4	N4	B4 x N4
5	P5	B5	N5	B5 x N5
		ΣnB = 100%	ΣnN =	ΣPn =
		Final Value		

Notes : P = Point from at every criterion or parameter, B = Specified weight (%),
ΣnB = 100 %, N = Value every parameter, ΣPn = Showing level of capabilities technical from automotive components industry of pertinent

4. The Final Value
The Final value is multiplication between the score that to be got multiplied with each weight. Based on the final value, is known by level of automotive components capabilities pertinent, with the following rules : (a) Class I (Growth Level) : if the final value point (NA) obtained 20 – 40, (b) Class II (Potential Level) : if the final value point (NA) obtained 40 – 60, (c) Class III (Autonomous Level) : if the final value point (NA) obtained > 60 %.

3. RESULTS AND DISCUSSIONS

Based on address list data in Office on DINAS Industry and Commerce West Java Province in Bandung there are around 15 automotive components SMEs. And then, after checked direct through field visit survey to the companies, with rule of the following conditions : (a) Had business legality (SIUP/TDI/IUI/TDP and NPWP), (b) Had run at least 2 years, (c) Still performed production activity, (d) Had business organizations, (e) Had financial reports, (f) Were available to share necessary information and data proven by written statement.

From the result of observation and interview with the companies, 9 (nine) "selected" companies were determined with review criteria including : (a) high interest from their Owners/Directors to be Shindan Shi models and (b) good improvement (kaizen) themes to be followed up by Shindan.

Every companies with Shindan Shi programs will be decided which quantitative targets should be achieved in 6 months. In the end period the guidance and consulting for diagnosing achievement will be evaluated in a workshop attended by managements from companies with the programs.

3.1 Determining Level of SMEs Automotive Components

On the basis of evaluation from check list of questioner identify potency business and automotive components industry capabilities, then writer determine level classification of SMEs automotive components like shown at Table 7 (appendix 1).

3.2 Level of Automotive Components Capabilities of SMEs in Bandung

Based on primary data to obtained from result of field survey to 9 SMEs automotive components in Bandung. And then by using rules as elaborated at Determination level of SMEs automotive components (Table 7), finally will be obtained by SMEs automotive components capabilities to the each companies, like shown at Table 3.

Table 3. The Level Automotive Components Capabilities of SMEs in Bandung

Companies	Classification Value					Final Value	Level		
	5S/5R/5K	Production Quality	Accounting and Book Keeping	Human Resources	Organization Management		I (Growth)	II (Potential)	III (Autonomous)
W-21	3	3	5	3	3	66	-	-	III
W-22	3	2	5	3	3	61	-	-	III
W-23	2	2	5	3	3	53	-	II	-
W-24	2	1	5	3	3	48	-	II	-
W-25	1	1	2	2	1	25	I	-	-
W-26	1	3	2	3	3	41	-	II	-
W-27	2	1	5	3	3	48	-	II	-
W-28	2	2	5	3	3	53	-	II	-
W-29	3	3	5	3	3	66	-	-	III
Total results of classified companies capabilities							1	5	3

3.3 Analysis on Automotive Components Capabilities of SMEs In Bandung

3.3.1 Analysis of 5S Capabilities

1. Clearing up
   To dispose unnecessary materials from workplace, to create more work scope and more space to move, without blocked materials that not used.
2. Tidying up
   To manage matter storage, with purpose to : (a) identify if any violations, (b) facilitate to easily take matters, and (c) to accelerate restore matters.
3. Cleaning
   To keep everything clean in workplace, with purpose to : (a) create work place to keep clean and quite, (b) create work place to comfortable, (c) prevent work completeness so that do not quickly broken.
4. Standardizing
   To keep workplace clearing up, tidying up, and clening with purpose to: (a) prevent decreased environment conditions from 3S, (b) Maintain habit of 3S.
5. Training and Dicipline
   To accustom to following procedures properly and precisely, with purpose to : (a) Control "visual control" in workplace, (b) maintain care in workplace, (c) to prevent decreased condition 5S.

5S method is used to minimize waste in workplace. If employees do not follow 5S, it means that their ways are not good.

Writer have done activity identify companies to see the existing condition of work environment on SMEs automotive components in Bandung by using 5S check form. And then based on Table 4 we can know the value of capabilities 5S to the each companies shall be as follows : (a) 3 companies have value = 3 or Enough, (b) 4 companies have value = 2 or Less, (c) 2 companies have value = 1 or Very Less. From the result can be concluded that applying 5S is not applied in an optimal fashion yet by SMEs automotive components in Bandung.

3.3.2 Analysis On Capabilities Of Production Quality.

By seeing at the result of assessment capabilities of production quality from 9 SMEs automotive components, like shown at Table 4 we can know that value capabilities of production quality to the each companies shall be as follows : (a) 3 companies have value = 3 or Enough, (b) 3 companies have value = 2 or Less, and (c) 3 companies have value = 1 Very Less.

From the result we can conclude that produce of quality product by SMEs automotive components still lower or less. The mentioned can be caused for example by :

1. The technology process that is applied not exactly yet, because the equipments and machine that used is still limited. It's cause for example because limitation of capital owned.
2. The quality of human resources is less because of less education bases and is low ethos work so it causes to lower discipline activities.
3. The quality of raw material often do not standard, because raw material and assistant still depended by import. Other side of price often fluctuation. Nowadays, the selection of raw material becomes difficult to execute.

From low product quality, brings the impact to :

1. The product specification that is produced in limited variation, so that makes the limited marketing
2. The high reject ratio is affected to reworking or minimize repair so that cause the efficiency to be low because the expense to be increase, delivery time become late and the profit become decrease or even lose.

Because of that, SMEs automotive components earn more to development is needed steps, for example as follows :

1. Restructuring machine and production equipments : to support the increase of technology ability produce so the settlement and completion of factory by increment and replacement existing conventional to standard production equipments.
2. Implementation of Shindan Shi System from "Adjacently" and direct consultancy in the form of analysis and diagnosed problem that is faced by SMEs by Shindan Shi.

3.3.3 Analysis on Capabilities of Accounting and Book keeping

Based on Table 4 we can know that the value of accounting and book keeping capabilities from 9 SMEs automotive components shall be as follows : (a) 7 companies have value = 5 or Very Good, and (b) 2 companies have value = 2 or Less.

To both company that have the less value, so the effort that be able to be conducted is to improve the book keeping and financial report system. With applying of bookkeeping system, so the applying of logical advantage plan, sale plan, management plan etc can be executed. Besides also can control CGS (cost of goods sold) and budget control. With existence of production plan, can minimize change of production amount, so that can stabilize everyday production amount.

3.3.4 Analysis of Human Resource Capabilities

Based on Table 4 we can know the value of human resources capabilities from 9 SMEs automotive components shall be as follows : (a) 8 companies have value = 3 or Enough, and (b) 1 company have value = 2 or Less.

By seeing at Table 3, generally each every companies involved labor between 10 up to 99, labor qualification most have skills and not have back ground academic and expert labor.

Meanly the to labor in place have well-balanced skill

and way of activity which much the same to between company one with other company.

There is two labor faction running activity of the production in place, that is :

1. Class owning skill of production technique, for example : turner, worker of stamping, welder, molding worker
2. Class representing assistant in doing production process, for example : assistant of turner, ministrant worker of casting, ministrant welder and assistant of worker in other area.

Besides the mentioned above transfer of skill (to junior workers) can walk naturally, where more contagious skillful worker indirectly its skill to other labor which still not skillful yet and also which still have less job experience.

The Labor that exist in Class I (Growth Level) use the employees from the around company, both for blood is still a relation with owner of company and also with no blood relation.

Still lower labor productivity labor that exist in SMEs automotive component in Bandung, this matter can know from to the number of time which is castaway because the preparation of unfavorable job (time of dandori), but awareness about problem is very low. So that its high work productivity need the existence of increased skilled and knowledge of employees.

3.3.5 Analysis of Organization Management Capabilities

Based on the Table 4 can know the value of organization management capabilities from 9 SMEs automotive components shall be as follows : (a) 8 companies have to have value = 3 or Enough, (b) 1 company have value = 1 or Very Less.

From the result can be concluded that organizational management not yet goodness.

Therefore SMEs automotive components have good organizational management capabilities, so needed by the following the steps is : (a) company have to have organization chart complete with breakdown of task, authority and responsibility from each its shares, (b) company have to have mission and vision and also earn its it field, (c) company have to have planning, good that short term, middle term and long term.

3.4 The Implementation of Shindan System

PT. W-21 established in 1993, has been producing automotive components industry. produced product type of all kinds but product the core important is: (1) bracket compressor mounting (BCM), (2) exhaust manifold, and (3) spring bracket. The company in this time have labor about 140 peoples with earnings about Rp 4.5 billion/year (USD 500,000).

To know the condition of internal and external situation environment company of W-21 to analyse SWOT, like shown in Table 4.

Table 4. SWOT analysis of PT. W-21

Strength : 1. Has ISO 9001:2000 Certificate 2. Had financial statement 3. Having good relation with partnership 4. Average employees have productive age, active, energy and skilled.	Weakness : 1. It fails to enforce 5S activities to the fullest extent. 2. Low of CNC machine Efficiency for Mori Seiki and Topper 920 about 60% 3. BCM as the excellent product have the percentage of rejected the high was approximately 26%.
Opportunity : There is a good prospect for demand growth relating to domestic after markets and automotive OEM parts	Threaten : 1. Consumer claim of product quality which to high 2. Influenced by condition and situation of automotive industry 3. Company of a kind has more equipments and machine go forward.

3.4.1 Increased Of CNC Machine Efficiency

The problem arises on the decreased of CNC machine efficiency for Mori Seiki and Topper 920 in the line machining center was approximately 60 %. While expense of investment for the purchasing of the machine require big fund. Therefore company management and Shindan Shi target to increased efficiency 2007 becoming above 80 %. To decreased cost production carried out improvement : (1) decreased of machine stop time, (2) improving cycle time.

To improving it, hence factors causing of machine down time have to be immediately known in detail. From result of research in September 2007 known that trouble types (disturbance) at machine of Mori Seiki and of Topper 920 can be classified to become 6 (six) especial trouble type, that is like at Table 5. Then factors becoming cause of down time in October 2007 to December 2007 monitored and overcome.

Table 5. Down time machine of CNC in PT W

No	Disturbance	Mori Seiki		Topper 920	
		Per month (hour)	Presentation (%)	Per month (hour)	Presentation (%)
1	*M/C Trouble*	77	55	25	22
2	*Trial*	15	11	12	10
3	*Jig change*	*)11	8	**)40	34
4	*Tool change*	12	9	12	10
5	Material	-	-	4	3
6	Others	24	17	25	21
Total		139	100	118	100

Notes : *) 4 times only, **) 9 times only

Efforts to troubleshoot different down time troubles can be seen in Table 5, including : (1) jig changes include jig changing system, distributing lift-bolt to plat jig, jig compounding system, pallet address to jig drift, etc. (2) machine troubles include machine repair with agents, clamping system, etc. (3) others include chamfering process changes. The results of increased machine efficiency of Mori Seiki and of Topper 920 before and after repair can be seen in Table 6.

Table 6. The result of increased machine efficiency Mori Seiki and Topper 920

Type of Improvement	Mori Seiki		Topper 920	
	Before Improvement (hours)	After Improvement (hours)	Before Improvement (hours)	After Improvement (hours)
1. Jig change	38	23	50	37
2. M/C Trouble	40	18	18	0
3. Trial	19	15	14	15
4. Other	7	5	8	8
Total	104	61	90	60

By repairing jig change, machining center troubles, trial etc., as shown in Table 4. On January 2007 stop-machine time reduction in Mori Seiki machine and Topper 920 would be produced (from 104 hour become 61 hour) and Topper 920 (from 90 hour become 60 hour). Similarly in 1 time of jig change, the time may be decreased from 45 minutes to 30 minutes.

Based on increasing graph of efficiency result of Mori Seiki and Topper as shown in Figure 2, it is found that on September 2007 the bench mark is machine efficiency of Mori Seiki about 66% and Topper 920 about 74%. But after improvement by shindan team, the increasing result of efficiency of Mori Seiki machine was 81% and Topper 920 was 83%.

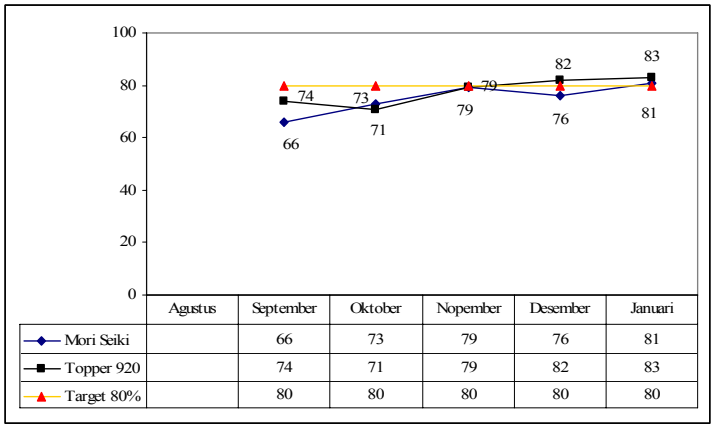

Figure 2. The result of machine efficiency of CNC : Mori Seki and of Topper 920

3.4.2 Increased of Product Quality

In Table 6, it is found that BCM KF 510 T deluxe products have highest reject ratio of 0.26% and damaged product size amounts 70 units. Therefore, top priority of quality control is directed to the product.

Target in 2007 was reject ratio not more than 0.10%. Repairing the quality of BCM KF 510 T deluxe product needs 5 recommendations, they are: (a) repairing documentation system, (b) identifying in-field process, (c) separation part NG from pallet, (d) counter measuring BCM KF 510 T deluxe products, and (e) repairing 50 items of work documents. The result of improved BCMKF 510 T deluxe product quality *deluxe* after improving becomes 5%.

Table 6. The results of production PT. W-21 (period of January to August 2007)

No	Components	Total of Production (Unit)	Total of Reject (Unit)	Reject (%)
1	BCM KF 510 T 2L	8.139	19	0,23
2	BCM KZ 2000	3.688	12	0,33
3	BCM KF 510 Deluxe	26.492	70	0,26
4	BCM KF Standard	4.124	8	0,19
5	Wagon R	3.683	42	1,14
6	BCM Baleno	3.105	16	0,52
7	BCM Tercel	4.500	9	0,20
8	BCM Expass X-479	1.629	7	0,43
9	BCM KZ 2D00	1.358	26	1,91
10	BCM Futura	6.580	21	0,32
11	Attachment	3.939	8	0,08
12	Proton Saga	1.624	4	0,25
13	Exh. Man 4JAI	10.450	24	0,23
14	Bracket ASM Powe	12.433	38	0,31
Total		91.744	Average reject	0,46

Based on the result graph of increased quality of BCM KF 510 T deluxe product (Figure 3), on September 2007 the bench mark is reject machining about 0.21%, after improvement 50 items of work documents (September 2007) and 57 items of work documents (January 2008). Reject machining results in 0.05% (December 2007) and 0.04% (January 2008).

To overcome of BCM KF 510 T deluxe products needs to find the causes. Figure 4 shows that the cause of highest damage is “slotting no good”. It is true because of : (1) used materials, (2) used equipments and machines, (3) employed methods, (4) operators, and (5) work place

environment. Therefore, in analyzing the cause and effect on to activity "slotting no good", factors above reruire to be paid attention. From analysis the cause and effect then we may find the ways to overcome it, so that it should eliminate or lower damages or improving activities from the occurring "slotting no good".

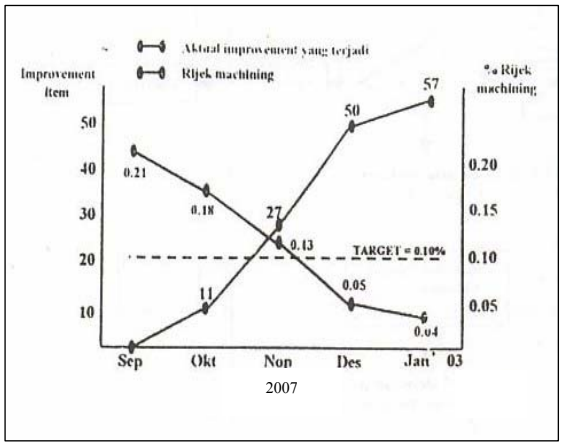

Fiqure 3. The result of increased quality of BCM KF 510 T Deluxe.

4. CONCLUSIONS

1. Based on the results of case study on 9 automotive components of SMEs selected in Bandung, can define the following capability classifications : (a) 1 company have value 25 to be classifications on class I (growth level), (b) 5 companies have value 53, 48, 41, 48, 53 to be classifications on class II (potential level), (c) 3 companies have value 66, 61, 66 to be classifications on class III (autonomous level).
2. Variables influencing automotive components SMEs capabilities posed at Table 1, known that its value capabilities is : (a) X_1, X_2, X_3, X_{10}, X_{11}, X_{12}, X_{14}, X_{15}, X_{16} have value = 3 (Enough), (b) X_4, X_5, X_6 have value = 2 (Less), (c) X_7, X_8, X_9 have value = 5 (Very Good), (d) X_{13} have value = 4 (Good).
3. The results of implemented Shindan System in PT. W-21, with cover : (a) SWOT Analysis, (b) increased CNC machine efficiency for Mori Seiki (from 66% to be 83%) and Topper 920 (from 74% to be 83%), (c) had decreased the average reject ratio of BCM 510 T deluxe from 26% to be 5%, (d) 5S in machining center workshop to be better.
4. By using the same method, the case study may also be implemented for other automotive components SMEs in other areas, like: Jakarta, Bogor, Sukabumi, Bekasi, Depok and Tangerang West Java and also for SMEs in Indonesia to increasing competitiveness in global market.

ACKNOWLEDGEMENT

The author would like to thank Mr. Korenori Takahashi, Mr. Yoshio Hirono and Mr. Fukaya as experts from Toyota Motor Cooperation Japan for her advice and suggestion during the research.

REFERENCES

[1] Ministry of Industry Indonesia, *"Guidance of Training and Education of Consultant Diagnose SMEs"*, DJIKM and of JICA Japan, Jakarta, 2006.
[2] Ministry of Industry Indonesia, *"Guidance of Forming and Management Of UPL Direct SMEs"*, DJIKM, Jakarta, 2007.
[3] Noor Nurdin, *"Consultant Diagnose IKM (Shindan Shi)"*, Directorate General Small and Medium Scale Industries (DJIKM) Ministry of Industry Indonesia, Jakarta, 2006.
[4] Hafid, *"Implementation Method of Kaizen In Order To Increase Quality, Productivity and 5S Automotive supporting Industries"*, Metal Industries Development Centre, Bandung, 2003.
[5] Ministry of Industry and Trade, *"Masterplan Development of SMEs 2002-2004, Book I : Public Strategy and policy Development of IKM"*, Jakarta, 2002.
[6] Hafid, *"Study Measurement Of Productivity Labour By Using Approach Of Analysis Ratio"*, Magazine Management & Entrepreneur, ISSN : 0302-9859, Institute of Management FE-UI, Jakarta, 1995.
[7] Imai Masaaki, "*Kaizen : The Key to Japan's Competitive Success"*, Random House, Inc, 1986.
[8] Jumingan, 2008, Analysis Financial Statement, Publisher of Bumi Aksara, Jakarta.
[9] Sugiono, *"Method Research Of Business"*, Publisher of Alpha Beta, Bandung, 2008.
[10] Toyota Astra Motor (TAM), *"Material of Training 5S"*, Human Resources Division, Jakarta, 2006.

Table 7. Determining level of SMEs automotive components

Value	Parameter / Criterion Assesment												
	5S (Score)	Production Quality (%)		Accounting and Book Keeping (Score)				Human Resources (Score)		Organization Management (Score)			
		Casting (NG)	Machining/ Press (NG)	Book Keeping	Journal & Ledger	Financial Report (Balance Sheet & Income Statement)	N P W P	Total of Labor	Labor Qualification	Organization Chart	Having Vision and Mission	Vision and Mission Implementation Have Employees	Having Plan (Short term, Long tern & Long term)
5	5S ≤ 5	NG ≤ 5	NG ≤ 1	C ≥ 90				D ≥ 150		E ≤ 5			
4	4 ≤ 5S ≤ 5	5 ≤ NG ≤ 10	1 ≤ NG ≤ 3	75 ≤ C < 90				100 ≤ D < 150		4 ≤ E ≤ 5			
3	3 ≤ 5S ≤ 4	10 ≤ NG ≤ 20	3 ≤ NG ≤ 5	60 ≤ C < 75				50 ≤ D ≤ 100		3 ≤ E ≤ 4			
2	2 ≤ 5S ≤ 3	20 ≤ NG ≤ 30	5 ≤ NG ≤ 10	40 ≤ C < 60				10 ≤ D < 50		2 ≤ E ≤ 3			
1	1 ≤ 5S ≤ 2	NG ≥ 30	NG ≥ 10	C < 40				< 10		1 ≤ E ≤ 2			
Weight (%)	40	25		15				10		10			

ISSN 114-1284

Mobile Phone Success Factors Identification

I. D. Widodo[1], Alva E. Tontowi[2], Subagyo[3], Sugiyanto[4]

[1]*Industrial Engineering Study Program, Islamic University of Indonesia, and*
Student of Mechanical and Industrial Engineering Department, University of Gadjah Mada
Email: Imamdjati@fti.uii.ac.id

[2,3]*Mechanical and Industrial Engineering Department*
University of Gadjah Mada, Yogyakarta, Indonesia
Email: menaet@ugm.ac.id[2]
Subagyo@ugm.ac.id[c]

[4]*Psychology Faculty*
University of Gadjah Mada, Yogyakarta, Indonesia
Email: Sugiyanto@ugm.ac.id

ABSTRACT

This article analyses some important factors that significantly contribute to the success of mobile phone, an example of a short life cycle product. Some variables are performed to represent the factors. Technical superiority is used to represent product quality, meanwhile, launching time, brand, and price represent marketing strategy factor. The analysis is classified based on its product segment.. The result shows that (1) there are different significant factors for each product segment. Brand is the only variable that positively significant correlates to product performance in all segments (2) price negatively correlates to product performance in low and medium end segments but it positively correlates to product performance for high-end product (3)technical superiority has significantly negative correlation to product performance for low end product. In medium and high end segment, technical superiority indirectly correlates to product performance. Technical superiority indirectly correlates to product performance through brand in medium end and through innovation in high end (4) launching timing has different effect to product performance for different segment. In low-end segment, time has significantly negative correlation to product performance. This is different to medium and high end products that tend to neutral. These indicate that life cycle of low-end product tends to be shorter than life cycle medium and high end product. (5) Innovation correlates to product performance for high-end product segment. It cannot be measured in low and medium end segment because of the same innovation value.

Keywords: *quality, brand, price, innovation, launching*

1. INTRODUCTION

In a review paper, Hart observed 'Recognition of the importance of new product development to corporate and economic prosperity, coupled with the high risk of failure in such endeavors, has triggered considerable research interest in the dynamics of new product development'[1]. NPD remains an important field of research since many companies were still not achieving the success rates that they and their governments desire [2]. Crawford identified that 35 % to 45 % of new products failed to compete in market [3]. Stevens and Burley even identified that the failure rate of new products was somewhere between 40 % and 75% [4]. Given the high costs associated with new product development, minimization of the high failure rate is a topic of considerable theoretical and managerial interest. Some significant causes of the failures were identified [5]. They were inadequate market analysis (24 %), product defect (16 %), lack of effective marketing effort, (14 %), and high cost (10%).

In contrast, there were also some researchers who tried to identify factors that influence new product success. Three most important factors were identified, they were: (1). Product advantage (2) Proficiency of pre-development activities. (3) Protocol [6]. Cooper identified 11 dimensions (from 77 observed independent variables) of product success [7]. They were product uniqueness/superiority, market knowledge and marketing proficiency, technical synergy/proficiency, market dynamics, market need (growth and size), price, marketing and managerial synergy, marketing competitiveness and customer satisfaction, newest to firm, strength of marketing communication and launch effort and source of idea/investment magnitude. Eight factors of two categories were the most frequently included factors in the studies reviewed and they were the ones for which integratable statistics were most consistently reported: (1) strategic factors-- product advantage, technological synergy, and marketing synergy, and (2) development process factors

proficiency of technological activities, proficiency of marketing activities, protocol, top management support/ skill, and proficiency of predevelopment activities [8].

Henard & Szymanski develop taxonomy of product success factors that consist of 4 main factors. They were product characteristics, firm strategies, firm process characteristics, and market characteristics [9]. By using meta analysis of 60 empirical studies, It also showed 8 important variables of product performance. They are product advantage, product innovativeness, marketing strategy, technological strategy, structured effort, market orientation, cross functional integration and competitive response intensity. Cooper & Kleinschimidt based on effect on profitability and impact, identified some critical factors which drived product success. Top four of them were high quality product process, new product strategy, adequate resources, R & D spending [10].

Based on the facts, a very important factor of product success/failure is customer knowledge though there are many factors influence product success or failure. Thus, this article will focus on analyzing some important factors that significantly contribute to the success of mobile phone, an example of a short life cycle product. Three important factors, namely product quality, marketing strategy and product innovation, are analyzed and compared.

2. PRODUCT DEVELOPMENT CONCEPT

Product design is a synthesis of technology and human needs into manufacturable products. Asimow defines engineering design as a purposeful activity directed toward the goal of fulfilling human needs, particularly those which can be met by the technological factors of our culture [11]. In practice, design means many things, ranging from styling to ergonomics to setting final product specifications. Product design and development has some variant of product development process. Ulrich and Eppinger claim there are fives variants [12]. Two of them are market-pull (affirm begin product development with market opportunity and then seek out whatever technologies are required to satisfy the market need), and technology push (begin with a new technology then find an appropriate market). Otto and Wood classify a design into original, adaptive, and variant design [13].

New product development projects comprise two main phases: pre-launch and post-launch. Learning about customer preferences (i.e., customer knowledge development) occurs in both phases but entails lower costs and lower strategic risk in the pre-launch phase. Ulrich and Eppinger also formulated pre-launch product phase in 5 phases: concept development, system level design, detailed design, testing & refinement and production ramp-up [12].

The term product performance is closely linked to product properties. Different definitions of performance are found in literature. According to the Oxford English Dictionary, performance is: “The accomplishment, execution, carrying out, working out of anything ordered or undertaken; the doing of any action or work; working, action (personal or mechanical); specification. The capabilities of a machine or device, now esp. those of a motor vehicle or aircraft measured under test and expressed in a specification also used attribute to designate a motor vehicle with very good performance”. Ulrich and Eppinger define product performance as: How well a product implements its intended functions. Typical product performance characteristics are speed, efficiency, life, accuracy, and noise [12]. Many of these given definitions imply that product performance is a measure of functional aspects of the product. When one talks about product performance he must also bring in properties such as form, durability, and so on. In the opinion of Hubka and Eder, the performance variables are related to three categories: *design properties* (e.g. function, form, tolerance, surface, materials, and dimensions), *internal properties* (e.g. strength, stiffness, hardness, elasticity, corrosion, resistance, etc.), and *external properties* (e.g. ergonomic, aesthetic, economy of operation, reliability, maintainability, and safety) [14]. The manufacturer is concerned with all three, but the customers are mainly concerned with the external product properties.

Stauffer and Kirby suggest that engineering design research should be increased in: (a) the connection between market, consumer and design information, (b) support launching products into the marketplace, and (c) equating product features with customer value to ensure a sustainable rate of return to small companies [15]. Launching timing is very important variable to product success [16, 17].

Brand value is very an important variable of company superiority. Brand equity is important variable for customers to buy a product [18, 19]. How product design (conceptualized as product aesthetics and function) interacts with brand strength to influence consumers’ product liking and quality evaluation is also important point to be discussed. Page and Herr stated that design and brand strength differentially impact liking and quality judgments [19]. In addition, judgments of liking and quality are found to be different in the way they are formed. Specifically, product *liking* appears to be readily formed through a process that integrates design information only; brand strength exhibits no significant influence. *Quality* judgments appear to take longer to process, and involve the integration of design and brand information.

3. METHODOLOGY

The mobile phones are classified into three class namely low-end, medium-end and high–end product based on their price. This research uses 38 samples (mobile phones models/types) that have very good sales performance report, consist of 17 low-end products, 10 medium-end products and 11 high-end products. . The product is classified as low end

ISSN 114-1284

product if its price is less than $ 150, meanwhile the high product has price more than $ 300. The medium product price is in between of the two classes. The data are collected from more than 200 mobile phone shops in Yogyakarta Indonesia in the period of January until September 2008.

Three factors, namely product quality, marketing strategy and product innovation, are analyzed. Some variables are involved in this analysis, they are launching date, technical specification, price, and brand value. Technical superiority is used to represent product quality, meanwhile, launching time, brand, and price represent marketing strategy factor. For each segment, some successful mobile phone series are analyzed to identify the important variables. Launching dates are used to determine both launching duration and innovation (with technical specification). Technical superiority values are determined by calculating the average of some technical specification such as screen resolution, data transfer speed, and features. Likert scoring is used to quantify the features rate. As same as technical superiority, innovation variable is generated based on modification of Booz-Allen & Hamilton [2]. The norm is presented in Table 1.

Table 1: Innovation Norm

Value	Description
5	New to the World Product
4	New Product line to the firm
3	Add to existing line
2	Improvement
1	Reposition

This research uses mobile phone brand value analysis done by SWA and MARS 2008 and % sales were taken from Yogyakarta Nokia Representative. Brand values were determined based on brand share, brand awareness, advertisement awareness, customer satisfaction, and gain index. They were analyzed from survey that involved 2648 respondents collected from 7 big cities of Indonesia [20]. In low and medium segment, innovation is not involved because of the similarity for all products.. Brand is not involved in high segment either.

4. RESULT AND DISCUSSION

Some variables are performed to represent the factors. Technical superiority is used to represent product quality, meanwhile, launching time, brand, and price represent marketing strategy factor. To identify the factors for product each segment, some successful mobile phone series of each product segment are analyzed. The correlation among variables is presented in Table 2.

The result shows that there are different significant factors for each product segment. Brand is the only variable that positively significant correlates to product performance in all segments. In high end segment, brand becomes an important variable because only one brand dominates market although the correlation value cannot be calculated. Besides, brand also correlates to other variables. In low end segment, brand negatively correlates with time from launching and technical superiority, though they are not significant. Brand has different effect to technical superiority in medium end segment. It significantly positively correlates with technical superiority. This is in line to Page and Herr finding that *Quality* judgments appear to take longer to process, and involve the integration of design and brand information [19].

Price negatively correlates to product performance in low and medium end segments but it positively correlates to product performance for high-end product. In low and medium segment, price is sensitive variable. In low end, it becomes variable that influence % sales through technical superiority that significantly negative correlation to product performance.

Technical superiority indirectly correlates to product performance through brand in medium end and through innovation in high end.

Launching timing has different effect to product performance for different segment. In low-end segment, time has significantly negative correlation to product performance. This is different to medium and high end product that tend to neutral (correlation coefficient is close to 0). These indicate that life cycle of low-end product tends to be shorter than life cycle medium and high end product.

Innovation correlates to product performance for high-end product segment. It cannot be measured in low and medium end segment because of the same innovation value.

Table 2: The performance comparative study among forecasting methods

	Price	Time From Launching	Tech. Superiority	Brand	Innovation	% Sales
Low-end Product(n=17)						
Price	1.000	.068	.840(**)	.001		-.289
Time From Launching	.068	1.000	.136	-.239		-.509(*)
Tech. Superiority	.840(**)	.136	1.000	-.393		-.599(*)
Brand	.001	-.239	-.393	1.000		.849(**)
% Sales	-.289	-.509(*)	-.599(*)	.849(**)		1.000
Medium-End (n=10)						
Price	1.000	-.445	.327	-.017		-.418
Time From Launching	-.445	1.000	-.142	-.065		-.055
Tech. Superiority	.327	-.142	1.000	.728(*)		.208
Brand	-.017	-.065	.728(*)	1.000		.701(*)
% Sales	-.418	-.055	.208	.701(*)		1.000
High-End(n=9)						
Price	1.000	.222	.561		.810(**)	.683(*)
Time From Launching	.222	1.000	.085		-.054	.053
Tech. Superiority	.561	.085	1.000		.794(*)	.036
Innovation	.810(**)	-.054	.794(*)		1.000	.574
% Sales	.683(*)	.053	.036		.574	1.000

Conclusion

1. There are different significant factors for each product segment. Brand is the only variable that positively significant correlates to product performance in all segments

2. For low end product, product performance correlates to time from launching, technical superiority and brand

3. Brand is the only significant variable to product performance for medium end product. Brand also significantly correlates to technical superiority.

4. In high end segment, product performance only correlated to price. Innovation correlates to price and technical superiority.

REFERENCES

[1] Fairlie-Clarke, T and Muller, M. An activity model of the product development process, *Journal Engineering Design*, VOL. 14, NO. 3, September, 247–272, 2003

[2] Cooper, R.G. dan Kleinschmidt, E.J. New product processes at leading industrial firms. *Industrial Marketing Management*, 10, 137–147, 1991

[3] Crawford, C. Marle, New Product failure rates: a reprise, *Research Management*, 30 (4), 20 – 24, 1987

[4] Stevens, G. A. dan Burley, J. Piloting the rocket of radical innovation, *Research Technology Management*, 46(2), 16–26, 2003

[5] Cooper, R. G., *Winning at New Products*, 3rd ed. Cambridge: Perseus Publishing, 2001, 22-25.

[6] Cooper, R. G. dan Kleinschmidt, E. 1987, *New products: what separate winner from loser?*, Journal of Product Innovation Management, 169-184, 1987

[7] Cooper, R. G., The dimensions of industrial new product success and failure. *Journal of Marketing*, 43, 93 – 103, 1999

[9] Henard, D. H. dan Szymanski, D. M. Why some products are more successful than others, *Journal of marketing Research*, 38, 362-375, 2001

[10] Cooper R. G. and Kleinschimidt Winning Businesses in product development: critical success factors, *Research Technology Management*, May-June, 52-66, 2007

[11] Asimow, M., *Introduction to Design*, Prentice Hall, Englewood Cliffs, New Jersey, USA, 1962

[12] Ulrich, K. dan Eppinger, *Product Design and Development*, McGraw Hill, Singapore, 1995

[13] Otto, K. N. and Wood, K. L. *Product Design: Technique in Reverse Engineering and New Product Development*, Prentice Hall, New Jersey, USA, 2001

[14] Osteras, T, Murthy, D. N., and Rausand, M. *Product Performance And Specification In New Product Development*, Journal of Engineering Design, Vol. 17, No. 2, 177–192, April 2006

[15] Sheldon, D. F. A Review on the Relevance Of Design Science In A Global Product Development Arena, *Journal of Engineering Design*, 15(6), 541–550, 2004

[16] Hultink, E. J. and Griffin, A. Industrial new product launch strategies and product development performance, *Journal of Product Innovation Management*, 14(4), 234-257, 1997

[17] Lee, Y. and O'Connor, G. C., The impact of communication strategy on launching new product: the moderating role of product innovativeness, *Journal of Product Innovation Management*, 20, 4-21, 2003

[18] Foxall, G. R. and James, V. K. The behavioral ecology of brand choice: how and what do customers maximize? *Psychology and Marketing*, 20(9), 811-836, 2003

[19] Page C. and Herr P. M. An Investigation of the Processes by Which Product Design and Brand Strength Interact to Determine Initial Affect and Quality Judgments, *Journal Of Consumer Psychology*, *12*(2), 133–147, 2003

[20] Suharjo, B. (2008) Metodologi best brand, *SWA*, XXIV (18), 40-60, 2008

The Prospect of Filtering Technology for Online Product Distribution

Vicky Laurencia Japhar[1], Ihan Martoyo[2]

[1]*Faculty of Industrial Technology*
Universitas Pelita Harapan, Lippo Karawaci, Tangerang 15811, Indonesia
E-mail : vicky_laurencia@yahoo.com

[2]*Faculty of Electrical Engineering*
Universitas Pelita Harapan, Lippo Karawaci, Tangerang 15811, Indonesia
UPH Graduate School Campus, Wisma Slipi, 2nd & 8th floor,
Jl. Let Jend. S. Parman Kav 12, Jakarta, 11480
E-mail : ihan_martoyo@uph.edu

ABSTRACT

Unlimited shelf in online store on internet allows much more variety of products to be offered to the customers than those can be offered by brick-and-mortar stores. This leads to the concept of Long Tail which argues that unlimited choice to customers can create unlimited demand and thus increases sales. However, as a consequence to the abundant choice available online, customer search-time to find the specific products they want definitely increases. Thus filtering mechanism is deemed to be increasingly important. In this paper, the value of pre-filter and post-filter process will be analyzed. In doing so, the long tail theory and case studies of some commercial and non-commercial websites are reviewed and analyzed. Each filtering mechanism appears to have a distinctive characteristic in the traditional brick-and-mortar and the Long Tail (online) business. We conclude that the pre-filter is indispensable for the success of the commercial online store because it provides the minimal quality control for the offered products. The post-filter that provides personalized offering, can be added as an additional commercial service.

Keywords
Long Tail, Pre-filtering, Post-filtering, Retailer, Commercial Value

1. INTRODUCTION

Ever since the emergence of the industrial revolution, consumers become more and more familiar with the existence of retailers. In Indonesia alone, there are various categories of retailers, starting from general retailers (e.g: Hypermart, Carrefour, Giant), electronic and appliances retailers (e.g: Electronic city, ACE Hardware) to hobby, books and music stores (e.g: Gramedia, Disc Tara). The word retailer itself refers to "a business that sells products and / or services to consumers for their personal or family use" [1]. It distributes products and creates values to consumers by [1]:

- Providing an assortment of products and services
- Breaking bulk
- Holding inventory
- Providing services

Providing a wide range of product assortments is costly to retailers because that means they need to provide more space for inventory while the main concern of the traditional retail stores is the space or capacity constraint. Shelf capacity constraint forces the retailers to only sell "popular products" that generate most sales and are favored by the mass market. Thus retailers limit the number of assortments and varieties of products sold on the shelf. They forego niche and obscure products that are not popular to the mass market but are still demanded by a very small number of customers. Prior to deciding on what to be displayed on the shelf, these retailers make predictions on which products are going to be popular, which brands to sell, what price range is acceptable to the customer, what level of quality of goods to be sold, local customer preferences and so on. These are some of the criteria used by the merchandisers to select and discriminate products to sell in order to maximize their sales.

Current innovation in technology has changed the way business is conducted. Internet has provided an alternative to the traditional retail product distribution. The minimum cost of adding the list of inventory on the internet attracts many retailers to branch out to the e-tailer or what is known as online retailer. Products ranging from highly demanded to obscure products, from the premium quality to the poor quality, from all over the world are available in the online market. Although much more variety and assortments of goods can now be found, consumers may find it harder to find the right product among the sea of junks. The customer search-time increases as the number of choice increases. Therefore, a filter is needed to screen the products available online.

This paper aims to analyze and evaluate the prospect and commercial value of the filtering process. That is, whether the filtering process has a distinctive selling point to make it saleable or whether it is something that can only be provided freely to the customers. To achieve this objective, first, the long tail theory will be reviewed. Then the value of filtering process, both pre-filter and post-filter, in brick-and-mortar and online retailers will be analyzed and discussed. Case studies of Amazon, Wikipedia, YouTube, Rhapsody and IEEE publications are also presented to point out the value of their filtering applications. Then conclusions will be drawn.

2. BRICK-AND-MORTAR VS. LONG TAIL

The Long Tail concept was coined by Chris Anderson in 2006 [2]. He built on the work by Brynjolfsson et. al, who observed that limited shelf space in conventional retail outlets constrains the type of products that can be discovered, evaluated, and easily purchased by consumers; while Internet customers have easy access to millions of products that they could not easily locate or purchase through brick-and-mortar retailers [3]. Brynjolfsson also provides empirical data for the Long Tail phenomenon. He claimed that the Internet purchases are more skewed toward obscure products, thus going further down the Long Tail online [4], [5].

The basic argument of the Long Tail phenomenon is depicted in Fig. 1. In Figure 1, the Short Head is the area prior to the first threshold line. The Short Head represents popular products that are mainly seen and displayed on the brick-and-mortar shelves. This Short Head is then followed by the Long Tail which underlines the fact that as retailers move to online market, more and more products can be offered to the customers. Anderson summarized the Long Tail phenomenon in these claims [2]:

In virtually all markets, there are far more niche goods than hits. The cost of reaching those niches is now falling dramatically due to digital distribution, powerful search technologies and critical mass of broadband penetration. Thus, in many markets, it is now possible to offer a massively expanded variety of products. Although none of the niche products sell in huge numbers, there are so many of them that collectively they can comprise a market rivaling the hits.

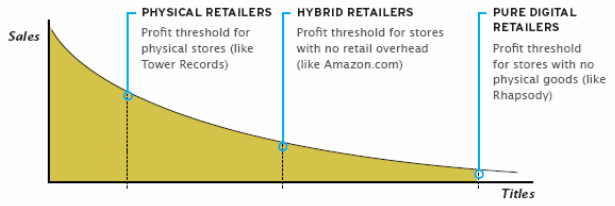

Figure 1: The Long Tail and its relation to the retailers [2]

Anderson argues that the Long Tail phenomenon is the new trend. However he is also confident that the brick-and-mortar retailers will remain to exist [2]. He writes *"Long tail markets tend to be a bit flatter than traditional markets, but they still have their share of blockbusters. For each way that we differ from one another, there are more ways that we're alike"*.

Therefore it is safe to assume that we will see the brick-and-mortar retailers to coexist with the Long Tail world of online distributors. The winners will be companies who know how to navigate through both worlds.

3. THE LONG TAIL DEBATE

In 2008, Anita Elberse wrote a seemingly refutation of the Long Tail theory [6]. She claimed that digital channels (online distributors) do not actually amplify the Long Tail phenomenon as is shown in Figure 2. On the contrary, it is still very much a Short Head world and the digital channel would only strengthen and amplify the hit products.

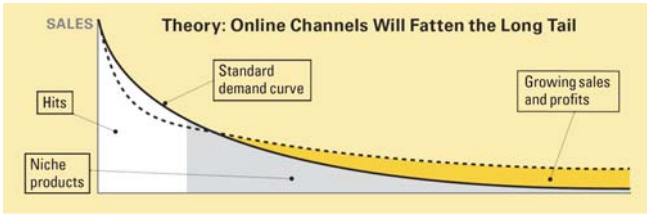

Figure 2: The Flattening of the Long Tail [6]

Elberse quoted the data from Rhapsody and Quickflix to back-up her claims. The data from Rhapsody (in 2006) showed the top 10% of titles accounted for 78% of all plays, and the top 1% of titles for 32% of all plays. "One percent of a million is still 10,000, when translated into album terms, equal to the entire music inventory of a typical Wal-Mart store" [6]. Elberse claimed that these data showed a clear high level of concentration. The same goes for the data from Quickflix. The top 10% of DVDs accounted for 48% of all rentals, and the top 1% for 18% of all rentals. In other words, some 150 titles (roughly the number of movies released annually to theaters by major Hollywood studios) accounted for nearly a fifth of all rentals. Elberse further argued that although the concentration of sales of Quickflix is not as strong as Rhapsody, it is still deemed substantial [6].

Elberse also observed the shopping carts of Quickflix video customers. She found that on average, 61% of these customers' rentals came from the highest decile, and another 13% from the second highest. Less than 1% of their choices came from the lowest decile – the most obscure titles [6]. For Elberse, these data are clear signs of concentration and there is no observable shift towards obscure products in online distributors.

There are interesting exchanges between Anderson and Elberse in the Harvard Business Blog [7], [8]. Anderson argues that the problem lies in the definition of the Head and the Tail. He pointed out that in Rhapsody, the 1% Head only represents 32% of all the plays. It means that the Tail represents 68%, thus the Tail is still showing its dominance. Likewise in Quickflix data, the top 10% only accounts for 48% of all rentals and the top 1% accounts for 18%. Therefore, Anderson argues that the different definitions of the Head and Tail will generate very different results [7].

Anderson also pointed out that the Long Tail has a fractal character [2]. It means that, if we zoom into the Long Tail curve, we always find another Long Tail structure. The Long Tail is made of many mini-tails, thus the big power-law curve of, say, "music", is really a superposition of all the little powerlaw curves formed by each musical genre. Therefore, the Short Head and the Long Tail are actually quite inseparable. The debate between Anderson and Elberse accentuates this fact. The Long-Tail-like curve can even be found in a typical supermarket, not necessarily an online distributor [9]. No wonder it becomes difficult to strictly define the exact boundary between the Head and the Tail.

Nevertheless, Anderson seems to be aware of the necessity of having the Short Head (popular products) in the Long Tail (obscure products) market. As many customers are not familiar to the long tail products and its quality, Short Head seems to be a must for an online distribution. The Short head becomes an entry point for customers to start their search of the products and to further explore down to the Long Tail. Here, post-filtering starts to play its role to screen the products and to give recommendation to customers who buy popular products. From this recommendation, customers are introduced to more obscure products and this eventually increases the sales of the e-tailer. The next section will discuss more about pre-filter and post-filter for brick-and-mortar and online market.

4. PRE-FILTER & POST-FILTER

Filtering denotes the process of making people find quality products. In the brick-and-mortar retails, filters come naturally because of the shelf space limitation. In the existing Short Head markets, where distribution is expensive and shelf space is at a premium, the supply side of the market has to be exceedingly discriminating in what it allows through [2]. Anderson calls this process pre-filtering, in which products are selected based on the prediction of their future popularity. The pre-filtering is performed by record label scouts, book editors, studio executives or department store buyers.

The Long Tail market is enabled by another kind of filtering. In the Long Tail paradigm, the maxim is to make everything available online, so pre-filtering seems, at the first sight, to be unnecessary. The function of the filter is shifting from being a gatekeeper to become an advisor [2]. Anderson uses the term post-filter. The post-filter amplifies, rather than predicts. It supplies demand to the goods which are already available, thus driving demand down the Tail. It functions in the form of peer or collaborative recommendations. This distinction of pre-filter and post-filter is summarized in Table 1. "Without the post-filter, the Long Tail risks just being noise", said Anderson [2].

Table 1: Pre-filters & post-filters differences [2]

Pre-Filters	Post-filters
Editors	Blogs
Record label scouts	Playlists
Studio executives	Reviews
Department store buyers	Customers
Marketers	Recommendations
Advertisers	Consumers

The post filtering itself takes form in various sophistication levels although they serve the same purpose as a guide or a screen to what to purchase. The simple form is the customer feedbacks written in words on blogs and reviews or simply customer ratings. By relying on customer rating, instead of having overflowing options of items with a very wide range of quality, the potential buyer or consumer can screen out their options to the best quality items only.

The more sophisticated post-filtering uses certain algorithms to provide recommendations to the potential buyers and consumers. Using a more advanced technology, these recommendation algorithms are commonly used on e-commerce websites such as Amazon [10]. Some of the commonly used techniques are traditional collaborative filtering and cluster method which provide a screening to the options based on similarity of a customer to another [10], [11]. Another post-filtering method is search based method, a search engine which filters the products based on keywords and certain criteria such as price, degree of quality and category. The latest one that is being used by Amazon is the Item-to-Item Collaborative filtering which allows customers to "filter their recommendations by product line and subject area, rate the recommended products, rate their previous purchases and see why items are recommended" [10].

The post-filtering mechanism, on the contrary, is not so dominant in the brick-and-mortar retailers. Many retailers do not display the popular and recommended products, although some have already done that. Gramedia book stores, for example, have a special section to display the best seller books, which provides a convenience to

customers who walk in to the store without knowing what to buy. The lack of post-filtering process in brick-and-mortar retailer may be due to the manual effort required to continually update the statistics and recommendations. Investment on technology to provide an access point for post-filtering mechanism can be done but needs further cost / benefit analysis.

5. THE PROSPECT OF FILTERING

As mentioned in Section 4, at the first sight, the pre-filter is not needed in the Long Tail market. Because the two maxims in the Long Tail market is: (1) Make everything available and (2) Help me find it [2]. However, when Amazon for example, delivers best seller books, the pre-filtering already exists as a part of the process. This goes also for blockbuster movies or top hits music, where the pre-filtering has been done by the record companies or the film studios.

Furthermore, from the discussion in the previous sections, it is also clear that the Short Head and the Long Tail will coexist and will be quite inseparable. Although the pre-filter is closely associated with the brick-and-mortar market and the post-filter is usually related to the Long Tail distributor; in reality, all cases involve a mix of the two types of filters. A predominantly Long Tail service will show a strong reliance on the post-filter strategy. This is displayed, for example, by YouTube and Wikipedia. However, common commercial online distributors will have a balanced mix of pre-filter and post-filter approach, for example, Amazon and Rhapsody. A peculiar example of online distribution, which shows more characteristics of a Short Head market is the IEEE journal publication.

5.1 YouTube and Wikipedia

YouTube and Wikipedia have different filtering mechanism from Amazon and Blockbuster movie online seller. YouTube, a Google subsidiary company, allows users to upload unlimited number of videos to the website which can be accessed by users for free. Pre-filtering process is impossible to be done as 20 hours of videos are uploaded every minute on website [12]. However, the post-filtering is very dominant. Users can rate the quality of the video and leave comments. The popular movies can be identified by looking at the number of viewers for each video.

Wikipedia, the collaborative online encyclopedia which aims to make all information available, is rather unique. It allows users with an account to log on and post anything on the website without pre-filtering. However, the post-filtering mechanism is also unique that other users can revise and update the previous post. Thus, the post-filtering mechanism enhances the quality of the posted information.

The similarity between the two groups is they make every thing, ranging from the popular products to obscure products, available online. The pre-filtering mechanism seems to be almost absent on these non-commercial websites. The enormous number of items being uploaded to the websites, such as in the Wikipedia case, make pre-filtering not cost justified. Therefore, such websites rely on customers to do the work "voluntarily" without a cost. A simple post-filtering mechanism, a search engine, is also provided to ease the work of finding a particular item among the huge amount of data. However, due to the absence of strong pre-filtering, the quality can diverse greatly.

Now, it is also misleading to think that Wikipedia performs absolutely no pre-filtering. One of the principle for posting in Wikipedia is "verifiability" [13]. Contributors should not submit original research. All materials must have been published by a reputable source. So, the focus is on verifiability, not truth. Editors are not responsible to determine the truthfulness of the quoted information, as long as the source is a reliable, peer-reviewed source. Thus this is a very weak version of pre-filtering. In YouTube, we can also find parts of commercial movies, which are mostly pre-filtered products. Therefore, although the pre-filters are very weak in YouTube and Wikipedia, they will not entirely disappear.

5.2 Amazon and Rhapsody

Amazon, online bookstore, music and video online stores, are for commercial purpose while Wikipedia and YouTube are for non-commercial purpose. The pre-filtering mechanism still exists on the e-commerce websites because that becomes one of their competitive advantages. When the potential buyers log on to the website, they already have the assurance to the quality of items sold on the website which later on increases the customer loyalty to continue the purchase from the websites.

Rhapsody, offering more than 5 million songs and thousands of artists, ensures that only master copy of songs are distributed in the site. In addition, Rhapsody also has editors which review new artists whose songs are uploaded to the site. Here, pre-filtering mechanism takes place to maintain the quality of songs distributed online. Amazon, which sells books online, ensures the quality of books sold by relying on the publishers.

Anderson also stressed the importance of pre-filtering for the commercial online distributors. The pre-filter delivers popular products (the Short Head), which serve as a point of entry for the customers. Anderson put it as follows [2]:
If you just have the products at the Head, you find that very quickly your customers want more and you cannot offer it. If you just have the products at the Tail, you find that

customers have no idea where to start. They are unable to get traction in the marketplace because everything you are offering is unfamiliar to them. The importance of offering the stuff at both the Head and the Tail is that you can start in the world that customers already know.

The post-filtering is clearly needed in the case of Amazon and Rhapsody. Reviews, collaborative recommendations and personalized offerings can really aid in navigating the Long Tail, thus enhancing the chance of finding the desired products.

5.3 IEEE Journal Papers

More peer-reviewed scientific journal papers are moving online, for example the IEEE publications. Online distribution makes accessing and searching for journal papers highly convenient. The IEEE conference and journal papers can be obtained fully online through http://ieeexplore.ieee.org.

However, despite the online nature of the distribution, the products in the IEEE site resemble the Short Head market more than the Long Tail characteristic of, for example, Wikipedia. The IEEE published papers are strongly peer-reviewed, maintaining the high quality of the papers. This represents a strong pre-filtering process. Post-filtering, on the other hand, is almost absent despite the easiness to deploy it in the online setting.

Although there are no collaborative recommendations in the IEEE journal site, the post-filtering is also not entirely absent. In this case, the post-filtering is embedded in the citations or references of the published papers. The IEEE Journal papers represent an online distribution which relies strongly on pre-filtering, with a weak post-filtering process.

5.4 The Commercial Value of Filters

From the discussed examples, it seems quite clear that the pre-filter is directly related to the commerciality of the products. Although the filtering process itself cannot be sold commercially, the cost is already included in the total cost of the products. The pre-filtering delivers popular products, hits music, blockbuster movies, or high quality journal papers. Therefore, the less commercial sites such as YouTube and Wikipedia do not rely on the pre-filtering as much as their commercial counterparts: Amazon and Rhapsody.

The post-filtering process arises because of the Long Tail phenomenon. It provides the ability to efficiently identify the desired product, while having everything available online. Whether the post-filtering process can be sold is debatable. Most of the current post-filtering process is provided freely, even in commercial sites such as Amazon. However, sophisticated and more effective post-filtering algorithms may provide added-value services that might be saleable.

6. CONCLUSIONS

The Long Tail theory and debate confirm that the Short Head and the Long Tail are actually inseparable. The pre-filter has already been an indispensable part of the brick-and-mortar retailers. It stays an important component of the distribution services, which aim at delivering quality products. In this sense, the pre-filter is closely related to the commercial value of the quality products distribution. It is understandable, for example that we pay quite a lot for the access to scientific peer-reviewed journal papers, while documents on Wikipedia are completely free. In Amazon and Rhapsody, pre-filtering is performed by editors and music editors. We pay for the high quality of products achieved through the pre-filtering.

The post-filtering is a new phenomenon triggered by the rise of the Long Tail market and the ease of digital technology. Because the Long Tail market makes all things virtually available, post-filtering in the form of product reviews, collaborative recommendations or personalized offerings must be provided for customers to efficiently find the desired products. Up to date, post-filtering is still a free-service. However, commercial value of post-filtering can perhaps be created if personalization according to customer taste is provided. It is also imaginable to have professionals, who review products, thus providing premium post-filtering services.

One interesting question regarding the Long Tail phenomenon is the effect of post-filtering to the movement of products between the Tail and the Head. Further research can be directed to measure the effectiveness of post-filtering mechanism in the long tail area, i.e., how fast can the quality products in the Tail be identified and move to the Head area. In addition, further study on a more advanced post-filtering algorithm for product offering personalization can also be conducted.

REFERENCES

[1] Levy & Weitz, *Retailing Management*, Mc-Graw-Hill, 2007.

[2] C. Anderson, *The Long Tail*, London: Random House Business Books, 2006.

[3] E. Brynjolfsson, Y. Hu and M.D. Smith, "Consumer Surplur in the Digital Economy", *Management Science*, vol. 49, no. 11, Nov. 2003.

[4] E. Brynjolfsson, Y. Hu, and D. Simester, "Goodbye Pareto Principle, Hello Long Tail: The Effect of Search Costs on the Concentration of Product Sales", downloadable from *Social Science Research Network*, http://papers.ssrn.com/, Jun. 2007.

[5] E. Brynjolfsson, Y. Hu, and M.D. Smith, "From Niches to Riches: The Anatomy of Long Tail", downloadable from *Social Science Research Network*, http://papers.ssrn.com/, Nov. 2007.
[6] A. Elberse, "Should You Invest in the Long Tail", *Harvard Business Review*, Jul – Aug, 2008.
[7] C. Anderson, "Debating the Long Tail, *Harvard Business Blog*, June 27, 2008. http://blogs.harvardbusiness.org/cs/2008/06/debating_the_long_tail.html
[8] A. Elberse, "The Long Tail Debate: A Response to Chris Anderson", *Harvard Business Blog*, July 2, 2008. http://conversationstarter.hbsp.com/2008/07/the_long_tail_debate_a_respons.html
[9] H. Sorensen, "Long Tail Media in the Store", *Journal of Advertising Research*, September 2008.
[10] G. Linden, Smith, B. and York, J.,"Amazon.com Recommendations", *IEEE Internet Computing*, IEEE Computer Society, Januari-February 2003.
[11] J. B. Schafer, J. A. Konstan and J. Riedl, "E-commerce recommendation applications", Data Mining and Knowledge Discovery, Kluwer Academic, 2001.
[12] Channel News Asia, "20 hours of video uploaded to YouTube every minute", last accessed: June 24th, 2009, from: http://www.channelnewsasia.com/stories/technologynews/view/430895/1.html
[13] S. Greenstein, "Wagging Wikipedia's Long Tail", *IEEE Micro*, IEEE Computer Society, March-April 2007.

EFFECT OF CONCUMER PERCEPTION TO CELLULAR PHONE DESIGN USING KANSEI ENGINEERING APPROACH

Insannul Kamil[1], Difana Meilani[2] and Ranti Mustika Putri[3]

[1,2,3]*Department of Industrial Engineering, Faculty of Engineering, Andalas University*
Kampus Limau Manis, Padang25163 – Indonesia
Email: sankamil@yahoo.com

ABSTRACT

In order to get outrival in the corporate world, company management should be oriented to market dynamics that is interaction between producer, consumer, and competitor. In order to make a reliable and high competitiveness product, the strategy is made an attempt on product development. Great number of cellular phone supply requires producer for meeting the consumer desires. One of the ways for the company to meet the consumer requirement is using Kansei Engineering methodology for esthetic aspect. Kansei Engineering is developed to involve a human's sense into a product development.

This research used questioner as the research instrument that is put down consumer expectation and perception toward cellular phone design through the Kansei's words. The research held in two kinds of treatments those are with and without touch of the cellular phone as the research object. After that, qualitative data collection was used to determine consumer's importance degree and significance difference test by use of software.

Resulting from the research has been done the analysis about consumer's importance degree and difference treatment that is significantly having an effect on Kansei's words. From the test result calculation, has been find out that consumer priority in cellular phone design's image in a row are easy to operate, durable, exclusive, modern, elegant, charming, impressive, interesting, strong, easy to keep, neat, masculine, striking, and dark. Research also found out that touch and no touch treatment of cellular phone produced two Kansei words having significantly difference on consumer appraisal. Those Kansei words are easy to operate and easy to keep.

Keywords: *Consumer Perception, Design, Cellular Phone and Kansei Engineering*

1. INTRODUCTION

Along with the development in the world of science and technology, industry is also experiencing a fairly rapid progress. Competition in the industry is also increasingly strict where each company makes a variety of design strategies in the planning, design manufacturing, and selling products in the market. Creating products that match the desired specifications of the consumers is very important. This is highly influential on the level of sales especially if the product is not the only one circulating in the market. In this case consumers have many opportunities to compare and select products that fit with their desire. With this market condition, strategy to win the competition is to provide products that can satisfy the needs and desires of consumers. To produce products that match market needs and desires, it is necessary to have knowledge about consumer behavior.

In order to get outrival in the corporate world, company management should be oriented to market dynamics that is interaction between producer, consumer, and competitor. In order to make a reliable and high competitiveness product, the strategy is made an attempt on product development. Product development process is a unity of activity needed to create a new concept to the market [Otto & Wood, 2001]. Product development is basically the company's efforts to create new products, improve, or modify old products, in order to meet market demands and consumer tastes [Yamit, 2000]. The criteria of product development process have a great opportunity because the companies are required to take advantage of opportunities in the development of products.

This study focuses on the cellular phone object. Great numbers of cellular phone supply require producers to satisfy the desire of consumer with a reliable and high competitiveness product. Consumer tastes for cellular phones that circulate in the market continue to shift. A sale of mobile devices is increasing rapidly over the cellular phone technology that increasingly sophisticated while the selling price decrease. IDC Indonesia's data indicate that the volume of sales of cellular phone in Indonesia during the quarter II/2008 increased very sharply, amounting to 74.9% compared with the quarter II/2007. This indicates the need for a cellular phone is getting higher. The cellular phone has also become a lifestyle and quite important in life at this time.

Design is also an important consideration in the consumer to purchase a cellular phone. Therefore, companies should also be able to respond the taste of the market cellular phone design. Design mobile phone is not only seen in terms of the design specifications but also involves the aspect of aesthetics.

One of the ways that companies can meet the needs of consumers in terms of aesthetics is to use a Kansei engineering method that was developed to involve feelings into product design. Kansei Engineering method was developed by Dr. Mitsuo Nagamishi in Japan and proven success in the design of Mazda cars in 1986 [Guerin, 2004]. Kansei can be defined as emotional or total effect obtained by someone's property, the environment, or situation by using the senses such as vision, hearing, or feeling [Nagamichi 2001, quoted from Schütte, 2005]. Kansei Engineering method can translate the feeling and impression of the product design process parameters. The most common way is through the measurement of Kansei

words. By using Kansei words as an indicator is ascertainable the desire and the perception of consumers towards the cellular phone design.
Based on the descriptions above is conducted research to determine consumer perceptions and willingness to design a cellular phone according to the feelings of consumer using Kansei Engineering.
Based on the background that has been described, the problems raised in this research is how consumers' desires and perceptions of mobile phone design is in accordance with the feelings and image using the method of Kansei Engineering.

2. RESEARCH METHODOLOGY

Research methodology chart is appeared in this following picture:

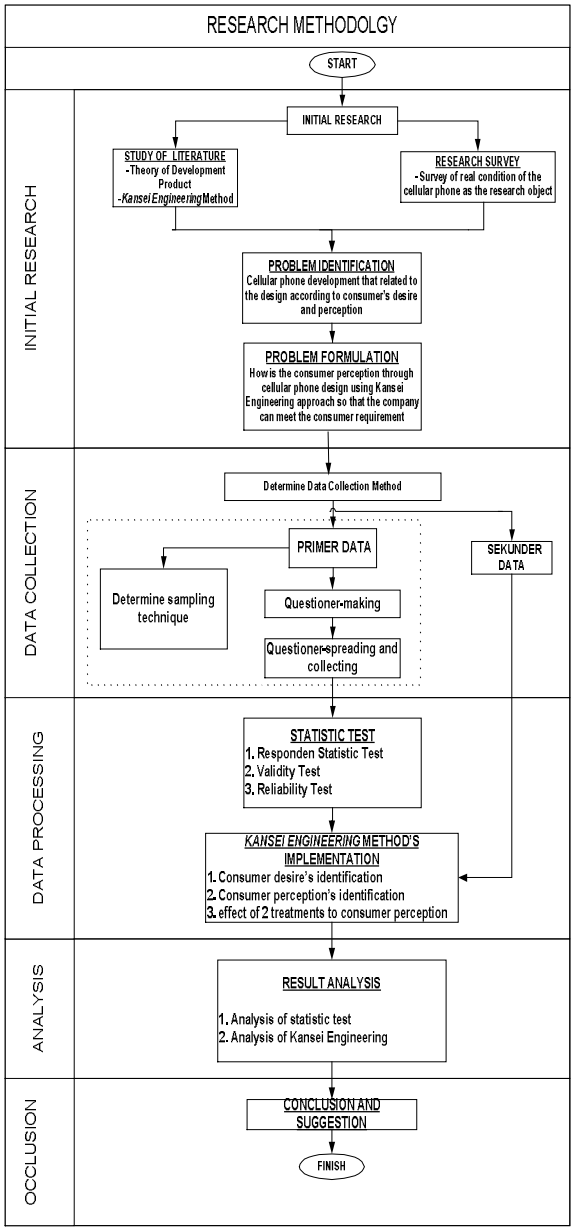

Figure 1: Research Methodology Chart

3. DATA COLLECTING AND PROCESSING

Kansei words used:

Table 1: Kansei words that is used in this research

No	Kansei words
1	Traditional
2	Modern
3	Antique
4	Strong
5	Rough
6	Soft
7	Clean
8	Durable
9	Wide
10	Safe
11	Easy to control
12	sweet
13	Cool
14	Neat
15	Dark
16	Exclusive
17	Fungtional
18	Aesthetics
19	Complex
20	Comfort
21	Relaxive
22	Simple
23	Solid
24	Smooth
25	Warm

the mobile phone as the objects of research is selected as many as five species. Election of five this mobile phones be done with the consideration of physical aspects of the mobile phone with a candybar type and size (dimensions and weight) is relatively the same.

Table 2: Cellular phone's specification

NO	JENIS HP	GENERAL		MEASUREMENT		DISPLAY		RING TONE	
		TYPE	NETWORK	DIMENSION	WEIGHT	TYPE	MEASUREMENT	TYPE	VIBRATION
1	NOKIA 1650	Candybar	GSM	104.2 x 43.8 x 17.8 mm	80 g	Color	65k	Polyphonic	Yes
2	NOKIA 1209	Candybar	GSM	102 x 44.1 x 17.5 mm	79 g	Color	65k	Polyphonic	Yes
3	SE J110i	Candybar	GSM	99 x 44x 17 mm	75 g	Color	65k	Polyphonic	Yes
4	SE R300	Candybar	GSM	101 x 46 x 12 mm	75 g	Color	65k	Polyphonic	Yes
5	SAMSUNG E200	Candybar	GSM	103 x 44.5 x 15.5 mm	79 g	Color	65k	Polyphonic	Yes

Furthermore, structured questionnaire that consists of two parts. The first section contains questions concerning consumer expectations of mobile phone design based on the kansei words. Whereas in the second section, containing questions about respondents' perceptions of several types of mobile phones. This category consists of 2 trials, which involve no touch and touch to engage the object of research.

1. Determine consumer's importance degree based on kansei words.
   Consumer's importance degree is the average value of the total value of respondents' answers to the points concerned.
   Total answers for grains 2 = 271
   Total respondents = 60
   consumer's importance degree = 271/60 = 4.52

Table 3: Recapitulation of consumer's importance degree

Kansei words	Consumer's Importance Degree
2 (Exclusive)	4,52
3 (Elegant)	4,20
4 (Modern)	4,35
5 (Strong)	4,08
6 (Easy to keep)	3,95
7 (Masculin)	3,85
9 (Interesting)	4,10
10 (Dark)	2,72
11 (Easy to operate)	4,67
13 (Durable)	4,67
14 (Impressive)	4,13
16 (Neat)	3,92
17 (Charming)	4,18
19 (Striking)	3,02

2. Determining influence of difference treatment that is significantly having an effect on consumer perception's value based on Kansei words. To know the significance of the different perceptions of kansei words through 2 treatments, with and without touch, is made a pair sample T test with significance milestone 0.05. T test is done for each kansei words and the type of cellular phone as the object of research.

   Example of calculation:
   Kansei word :exclusive
   Type :Nokia1650
   Hypothetical :
   H_0 = no difference in consumer perception of kansei words 2 through with and without touch treatment
   H_1 = there is a difference in consumer perception of kansei words 2 through with and without touch treatment

Calculation with the SPSS output:

Paired Samples Statistics

		Mean	N	Std. Deviation	Std. Error Mean
Pair 1	tanpa sentuhan	2,97	60	,780	,101
	dengan sentuhan	2,63	60	,663	,086

Paired Samples Test

		Paired Differences					t	df	ig. (2-tailed
		Mean	td. Deviatio	Std. Erro Mean	95% Confidence Interval of the Difference Lower	Upper			
Pair 1	tanpa sentuha dengan sentul	,333	,857	,111	,112	,555	3,013	59	,004

Decision : Because the value of P = 0004 < α then Ho is declined.
Conclusion : there are differences in consumer perception of the kansei word 2 through with and without touch treatment

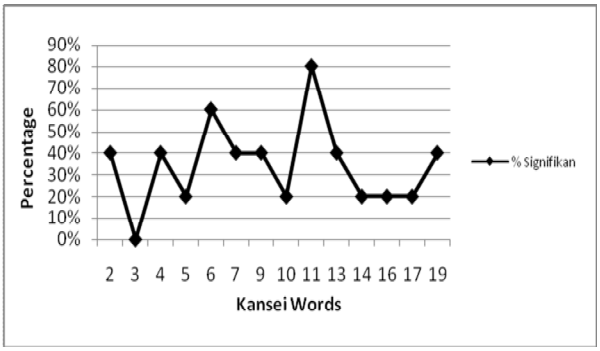

Figure 2: graphs of % Significant average from a pair Sample T Test through cellular phone design

4. RESULTS ANALYSIS

1. Analysis of consumer's importance degree Based on Kansei Words
   Based on the data processing that has done, it can be seen the most influential kansei words in determining the image of cellular phone design.

Table 4: Consumer's importance degree based on the Kansei Words

Kansei Words	Consumer's Importance Degree
11 (Easy to operate)	4,67
13 (durable)	4,67
2 (Exclusive)	4,52
4 (Modern)	4,35
3 (Elegant)	4,20
17 (Charming)	4,18
14 (Impressive)	4,13
9 (Interesting)	4,10
5 (Strong)	4,08
6 (Easy to keep)	3,95
16 (Neat)	3,92
7 (Masculin)	3,85
19 (Striking)	3,02
10 (Dark)	2,72

Based on the kansei words, product developers can provide best performance of the design of a cellular phone from the esthetic function. This design will make consumers like a product more from emotional aspect.

2. Analysis of 2 treatments of cellular phone that having significantly difference on consumer appraisal based on kansei words.
   Recapitulation shown that are 2 kansei words, which is easy to operate and easy to keep, that having % significantly more than 50%. This indicates that there is a difference of the consumer perception wirh different treatment for two of the kansei words. Two of the kansei of words that have a significant, that is easy to operate and easy to keep note that the assessment will change if given a two different treatment done in this research. This is because those words may not be considered to visualization only. While other Kansei-words are not to significantly alter the assessment because those are only need the senses of vision only. A large number of kansei words that tend to make significant influence in the treatment given, demanding the manufacturer of the cellular phone to make the design more eye-catching so that the resulting product has a reliability and high competitiveness.

5. CONCLUSION

1. From experiments carried out on the respondents with and without touch on the cellular phone, the two kansei words that have a significant difference in the results of the assessment that is easy to operate and easy to keep. This means that the respondents' assessment of kansei words are not enough only with the visualization, but also determined by the touch of the user.
2. Fourteen of the kansei word processed on the research, has been find out the consumer's importance degree that will reflect the consumer's desire of cellular phone design. consumer priority in cellular phone design's image in a row are easy to operate, durable, exclusive, modern, elegant, charming, impressive, interesting, strong, easy to keep, neat, masculine, striking, and dark.

6. SUGGESTIONS

1. Evaluating consumer perceptions by using the method of Quality Function Deployment (QFD), this can find out the needs of consumers in terms of performance, function, and quality of the mobile phone.
2. Perform data collection category by adding the sample to be taken such as income level, education level, and age.

REFERENCES

[1] Cohen, L. 1995. *Quality Function Deployment: How to Make QFD Work for You.* Massachusetts: Addison-Wesley Publishing Company.

[2] Grimsaeth, Kjetil. 2005. *Kansei-Engineering-Linking Emotions and Product Features*. Department of Product Design, Norwegian University of Science and Technology. www.ivt.ntnu.no/ipd/fag/PD9/2005/artikler/PD9%20Kansei%20Engineering%20K_Grimsaeth.pdf/15:29/18.08.2008.download.

[3] Kotler, P. 2000. *Marketing Management The Millenium Edition.* Prentice Hall International Edition.

[4] Lee, SeungHee et.al. 2002. *Pleasure with Products: Design based on Kansei*. Industrial Design Engineering, Delft University of Technology,Jaffalaan 9, 2628 BX Delft, The NetherlandsArt & Design Institute, University of Tsukuba.

[5] Nazir, Moh. 1988.*Metode Penelitian.* Jakarta: Ghalia Indonesia.

[6] Otto, Kevin and Wood, Kristin. 2001. *Product Design - Technique in Reverse Engineering and New Product Development*. New Jersey: Prentice Hall.

[7] Prawito, Kristan Teguh. 2008. *Implementasi Kansei Engineering dalam Perancangan Kursi Santai dengan Menggunakan Data Antropometri*. Jurusan Teknik Indsutri, Fakultas Teknik, Universitas Andalas.

[8] Schütte, Simon. 2002. *Designing Feelings into Products-Integrating Kansei Engineering Methodology in Product Development*. Quality and Human System Engineering, Department of Mechanical Engineering, Linköpings universitet SE-581 83 Linköping, Sweden. www.diva-portal.org/urn_nbn_se_liu_diva-2658-1_fulltext[1].pdf/14:39/18.08.2008/download.

[9] Schütte, Simon. 2005. *Engineering Emotional Values in Product Design -Kansei Engineering in Development.* Quality and Human System Engineering, Department of Mechanical Engineering, Linköpings universitet SE-581 83 Linköping, Sweden. www.diva-portal.org/urn_nbn_se_liu_diva-497-1_fulltext[1].pdf/15:01/18.08.2008/download.

[10] Singarimbun, M dan Sofian, E. 1989. *Metode Penelitian Survey Edisi Revisi.* Jakarta: LP3ES

[11] Sugiyono. 2001. *Metode Penelitian Bisnis Cetakan Ketiga. Bandung*: CV Alfabeta

[12] Ulrich, K.T dan Eppinger. 1995. *Product Design and Development*. Mc-Graw Hill International Edition.

[13] Umar, Husein. 2002. *Riset Pemasaran dan Perilaku Konsumen*. Jakarta: Gramedia.

[14] Walpole,R.E. 1995. *Ilmu Peluang dan Statistika untuk Insinyur dan Ilmuwan Edisi Ke-4.* Bandung: Penerbit ITB.

[15] Yamit, Z. 2000. Manajemen *Kualitas Produk dan Jasa. Yogyakarta*: Penerbit Ekonisia

ISSN 114-1284

IMPLEMENTATION OF KANSEI ENGINEERING METHOD INTO LAZY CHAIR DESIGN USING ANTHROPOMETRY DATA

Insannul Kamil[1], Bakri Bakar[2] and Teguh Prawito[3]
[1,2,3]*Department of Industrial Engineering, Faculty of Engineering, Andalas University*
Kampus Limau Manis Padang 25163 – Indonesia
Email: sankamil@yahoo.com

ABSTRACT

Competition in the corporate world now becomes tighter. Each company is doing many kinds of strategies in planning, design, production, and sale its product. With those strategies, the company expects that its product will be sold out in the market area.
Kansei Engineering is a method of product design from Japan. This method tries to bond between consumer desires to product specification design by translating consumer desires through Kansei words.
Research has been executed in Furniture Company, CV. "X" Padang. CV. "X" tried to develop the product market and Kansei Engineering was using to find the appropriate design. This research took lazy chair as the research object. Lazy chair should be set as people's ease because it is in direct correlation to the user.
Using of Kansei Engineering and combining it with ergonomic approach that is anthropometry in product design, will produce a design not only appropriate to consumer needs but also in an ergonomic manner.

Keywords: *Design, Lazy Chair, Kansei Engineering, and Anthropometry*

1. INTRODUCTION

Competition in the corporate world now becomes tighter. Each company is doing many kinds of strategies in planning, design, production, and sale its product. With those strategies, the company expects that its product will be sold out in the market area. Create a product that really appropriate to consumer's desire is very important. It will affect the number of product sold moreover if the product is not the only one circulating in the market. In this case consumers have many opportunities to compare and select products that fit with their desire.

Product development process is a unity of activity needed to create a new concept to the market (Otto & Wood, 2001). Ulrich and Eppinger (2001) explain that the development phase concept include identification of target market's needs, creation and evaluation of alternative product concept, and selection of the best product development concept. The criteria of product development process have a great opportunity because the companies are required to take advantage of opportunities in the development of products.
This study focuses on the lazy chair object. Lazy chair is a product that has been made by Furniture Company. This object has been chosen because lazy chair is directly correlated with the user. Consumers have different interest through a lazy chair. The company certainly has to pay an attention on the differences especially in production strategy. Market in concept strategy is a production based on consumer's suit.
In order to respond the changes of market's taste quickly was developed kansei engineering method to satisfy the desire of consumer. Kansei engineering method was developed by Dr. Mitsuo Nagamishi in Japan and proven success in the design of Mazda cars. The previous research that implements kansei engineering has done by Khoriyah and Nurwidiana (2006) with garden chair is the object. The purpose of their research predicted design element of garden chair that appropriate with the image of consumer. Now, in order to know the consumer's desire is also used kansei words as the indicator. In this research is also used an anthropometry data in design element to get save and comfort design.
Based on the descriptions above is conducted research to determine element design of lazy chair that properly with feeling and image by using kansei engineering, and an ergonomic design using anthropometry data.

2. RESEARCH METHODOLOGY

Research methodology chart is appeared in this following picture:

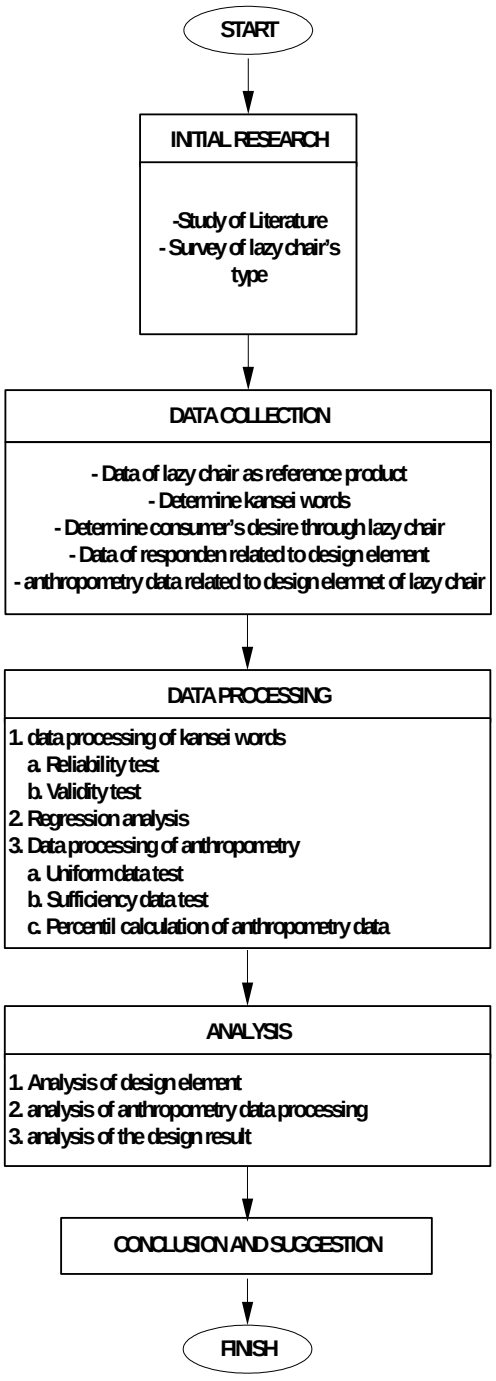

Figure 1: Research Methodology Chart

3. DATA COLLECTING AND PROCESSING

Table 1: Kansei words used in this research

No	Kansei words
1	Traditional
2	Modern
3	Antique
4	Strong
5	Rough
6	Soft
7	Clean
8	Durable
9	Wide
10	Safe
11	Easy to control
12	sweet
13	Cool
14	Neat
15	Dark
16	Exclusive
17	Fungtional
18	Aesthetics
19	Complex
20	Comfort
21	Relaxive
22	Simple
23	Solid
24	Smooth
25	Warm

Table 2: Category of element design

NO	ELEMENT DESIGN	AMOUNT OF CATEGORY
1	SITED SHAPE	8
2	BACK SHAPE	8
3	HAND PROP SHAPE	4
4	CHAIR'S LEG SHAPE	3
5	SHAKY'S BASE SHAPE	3

Figure 2: Picture of reference's lazy chair

Data processing has been done by doing the regression linear calculation. Regression testing is used to predict a variable (dependent variable) based on a variable or some other variable (independent variable) in a linear equation. In the regression analysis of this research is comprised of 2 types. The first regression explore the relationship between design elements, with the kansei word, which is the dependent variable is respondents's appraisal (likert scale) while independent variables is the result of the selection of design elements. The second regression that explore the relationship between the two categories of design elements with the kansei word, the dependent variable is the value of the respondents (likert scale) and the independent variable is the result of the election category of the design elements. In this regression used α = 0.05 or 5% error level. Regression analysis was conducted using the SPSS 15 software assistance.

Those who become the variables in the first regression is:

dependent variable (Y) is the value of the respondents (likert scale).

independent variable (X) is the result of the selection of design elements.

Those who become the variables in this second regression is:

dependent variable (Y) is the value of the respondents (likert scale).

independent variable (X) is the result of the election category design elements.

Example of calculation:

1. First regression

Model	R	R Square	Adjusted R Square	Std. Error of the Estimate	Durbin-Watson
1	.853(a)	.727	.659	.70711	2,700

Model		Sum of Squares	df	Mean Square	F	Sig.
1	Regression	5.333	1	5.333	10.667	.031(a)
	Residual	2.000	4	.500		
	Total	7.333	5			

Linear regression equation for word "traditional":

$Y_{traditional} = 12 + 4\ X_1 - X_2 - X_3 - 1{,}52\ X_5$

2. Second regression

Model	R	R Square	Adjusted R Square	Std. Error of the Estimate	Durbin-Watson
1	.830(a)	.688	.221	1.069	1.777

Model		Sum of Squares	df	Mean Square	F	Sig.
1	Regression	5.048	3	1.683	17.472	.043(a)
	Residual	2.286	2	1.143		
	Total	7.333	5			

Linear regression equation for word "traditional":

$Y_{traditional} = 16{,}857 - 0{,}429X_3 - 1{,}143\ X_4 + 1.571\ X_8$

4. RESULTS ANALYSIS

1. Analysis of element design selection
   From data processing of kansei engineering using linear regression, is procurable element design that affect the chair's image. There are 18 words that affect the element design.

2. Analysis of the design result
   The selection of element design produced some variations of lazy chair's design. Comparison between each design has done by 3D sketch using AutoCad software.

Figure 3: 3D sketch of currently lasy chair

Figure 4: 3D sketch of lazy chair's 1st alternative

Figure 5: 3D sketch of lazy chair's 2nd alternative

Figure 6: 3D sketch of lazy chair's 3rd alternative

5. CONCLUSION

1. From 25 kansei words there are 18 words that are affected by element design of lazy chair.

2. Producer can get some alternatives of product design by implementing kansei engineering.

6. SUGGESTIONS

1. Perform production planning process and economic analysis through the design result of lazy chair.

REFERENCES

[1] Arikunto, Suharsimi. 1997. *Prosedur Penelitian,Edisi revisi 5*. Jakarta: PT. Rineka Cipta

[2] Khoiriyah, Nuzulia dan Nurwidiana. 2006. *Implementasi Kansei Engineering dalam Perancangan Produk dengan Menggunakan Antropometri*. Laboratorium Analisis Perancangan Kerja, Jurusan Teknik Industri, Universitas Islam Sultan Agung.

[3] Grimsaeth, Kjetil. 2005. *Kansei-Engineering-Linking Emotions and Product Features*. Department of Product Design, Norwegian University of Science and Technology. www.ivt.ntnu.no/ipd/fag/PD9/2005/artikler/PD9%20Kansei%20Engineering%20K_Grimsaeth.pdf/16:13/01.03.2008.download.

[4] Nazir, Moh. 1988. *Metode Penelitian*. Jakarta: Ghalia Indonesia.

[5] Nurmianto, E. 1996. *Ergonomi-Konsep Dasar dan Aplikasinya, Edisi Pertama*. Jakarta: PT. Guna Widya.

[6] Otto, Kevin and Wood, Kristin. 2001. *Product Design - Technique in Reverse Engineering and New Product Development*. New Jersey: Prentice Hall.

[7] Supranto, J. 2001. *Statistik Teori dan Aplikasi, Edisi ke-VI*. Jakarta: PT. Rineka Cipta.

[8] Schütte, Simon. 2002. *Designing Feelings into Products-Integrating Kansei Engineering Methodology in Product Development*. Quality and Human System Engineering, Department of Mechanical Engineering, Linköpings universitet SE-581 83 Linköping, Sweden. www.diva-portal.org/urn_nbn_se_liu_diva-2658-1_fulltext[1].pdf/16:05/01.032008/download.

[9] Sutalaksana, I.Z. 1979. *Teknik Tata Cara Kerja, Edisi Pertama*. Jurusan Teknik Industri, Institut Teknologi Bandung.

[10] Ulrich, K.T dan Eppinger. 1995. *Product Design and Development*. Mc-Graw Hill International Edition.

[11] Umar, Husein. 2002. *Riset Pemasaran dan Perilaku Konsumen*. Jakarta: Gramedia.

[12] Wignjosoebroto, S. 2000. *Ergonomi, Studi Gerak dan Waktu: Teknik Analisis untuk Peningkatan Produktivitas Kerja, Edisi Pertama*. Surabaya: Guna Widya

WORKING TIME ARRANGEMENT EVALUATION BY WORK PERFORMANCE AND ENERGY EXPENDITURE FOR NORMAL AND FASTING CONDITION
(CASE STUDY:UNLOADING SEWING BAG OPERATOR, CEMENT BAG FACTORY PT "X")

Insannul Kamil[1], Lusi Susanti[2] and Windy Apriandy[3]

[1,2,3]Department of Industrial Engineering, Faculty of Engineering, Andalas University
Kampus Limau Manis Padang 25163 – Indonesia
[1]Email: sankamil@yahoo.com

ABSTRACT

Worker as human being have a limitation especially in work performance. This condition related to metabolism changing of body which is fatigue occurs in conducted working process. Fatigue can overcome by working time arrangement, which consist of work duration and resting time. Criterion that used in working time arrangement is working performance and energy expenditure. The objective of this study is to determine the extent of compliance with ergonomic principles in the relationship of working time arrangement in normal and fasting condition.

The working condition of unloading worker in cement bag factory is relocation each batch of sewing bag from belt conveyor to the destination place repetitively during 6 hour with standing position in normal and fast condition. Result of research is optimal productivity expressed by comparison of worker performance and consumption of energy. Optimal condition obtained if unloading worker do work activity with interval working duration every 4 hour totally 6 hour per day for normal condition, meanwhile in fasting condition every 2 hour totally 5 hour each day for optimal performance. While each interval working is given minimum resting time 30 minutes according to recommended interval working hour each condition.

Keywords
Working Condition, Working Performance, Energy Expenditure and Working Time

1. INTRODUCTION

Determining of company wisdom in scheme of work system has important influence to prosperity of operator. One of the aspect scheme of work system is relating to working time arrangement, for example; the duration someone can work in good productivity and healthy.

Arrangement in working time and resting time has contributed to organizational aspects which support company performance. Increasing in working time exceed ability, resulting degradation of productivity, incidence of fatigue, disease and also working accident. Research indicate that decreasing office hours from 8.75 hour/day become 8 office hours one day can improve work performance between 3% until 10 % [Tarwaka, 2004].

Base on result of interview with head and also human resources division of bag factory in PT. X, he said there is no research of in working time and resting time arrangement in normal and fasting condition. PT X is only use reference for working time and resting time arrangement based on company policy No.1120/ SED/ DESDM/ 07.2008. Working scheduling in this company pursuant to 2 division laboring working team by rotation during 7 day for shift A (08.00-15.00) and 6 day for shift B (15.00-22.00), commutation of each shift every one week. These policies also do in fasting condition (Ramadan Month) with tolerance reduction of resting time. It is based on company policy of No.113/PUM/ DESDM/ 08.2008.

The research is conducted by observation at unloading sewing bag operator work area. The working condition of unloading operator in cement bag factory is relocation each batch of sewing bag from belt conveyor to the destination place repetitively during 6 hour with standing position in normal and fast condition. this condition can be seen at Figure 1.1.

Figure 1. Work condition of *Unloading Operator*

2. LITERATURE STUDY

Quality human life base on (ILO) [Tarwaka, 2004] :

1. *work should respect the worker life's dan health.*
2. *work should leave the worker whit free time for rest and leisure.*

3. *work should enabel the worker to serve society and achive self-fulfillment by developing his personal capacities.*

3. RESEARCH METHODOLOGIES.

3.1. Phase Preparation.

Preparation step taken:

1. Introduction Research.
   Introduction Research is done for got information about condition of early from research object by interview and direct observation.

a. Interview
   Interview is done to know operator complaint when doing the job (unloading of sewing bag).

b. Observation.
   Observation is to know the condition of work activity at work station of unloading sewing bag operator in line 2 and characteristic work of fast and normal condition.

2. Literature Study.
   Literature study is reference research result and references related to in working time and resting time and also other related literature with this research.

3. Identify Problem.
   Observation with the working condition of unloading operator in cement bag factory is relocation each batch of sewing bag from belt conveyor to the destination place repetitively during 6 hour with standing position in normal and fast condition

4. Problem Formulation
   Strength of problem identifying result, hence becoming this research issue is How to arrange working and resting time base on work performance and energy expenditure for normal and fasting condition

5. Research boundary

- Object of research is unloading sewing bag workstation.
- Measurement criteria in this research are work performance and energy expenditure.
- Work performance is achievement measurement of unloading sewing bag process in certain time interval.
- Research is done in 1 shift each day (08.00 – 15.00) for normal and fasting condition every 30 minute interval of observing time.
- Time arrangement criteria are resting time and work duration for 1 shift.
- Research has been conducted at September 2008 for fasting condition and October 2008 for normal condition.
- Tools that use in this research is *Pulse Monitor* tipe PU-701 NSSG.
- This research just observing working time factor, another factor is assumed stabile and have no relationship.

6. Object of Research.

- Understanding relationship between work performance and energy expenditure for normal and fasting condition
- Analyze and arrange working time for normal and fasting condition.
- Analyze and arrange resting time for normal and fasting condition.

3.2. Collection and Processing Data

1. Data collecting
   Data required to this research shall be as follows:
   a. General Information about work system
   b. General Information about operator.
   c. Data about environment work
   d. Dimension physical data and method work station work now.
   e. Data of Anthropometry
   f. Heart pulse Measurement.
   g. Work Performance
2. Processing Data
   Data which have been collected was processed as according to requirement of research.
   a. Calculation of Anthropometry Data.
      Homogeneity test of Sample.
   b. Calculation of Energy expenditure.

3.3. Analysis.

3.3.1. Statistical Analysis.

Experiment 2 factor.
This experiment is used to investigate difference between energy expenditure and work performance in normal and fasting condition.

3.3.2. Result Analysis.

Result analysis will be studied result of data processing and also analyze obtained data curve. Pursuant to curve analysis will know optimize time of the working duration.

4. RESULT

4.1 Analysis Operator Election

Through homogeneous test to the operator, it is conclusion that there are no differences of ability (work performance) among operator.

Tables 1 *ANOVA for the operator election*

Source of Variation	SS	df	MS	F	F crit
Between Groups	1	3	0,333333333	0,012626	3,238872
Within Groups	316,8	16	26,4		
Total	317,8	19			

F_{table} :
Significance level 5 % ($\alpha = 0,05$)
$F_{(0,05;\ 5;\ 24)}$ in table = 3,238
F :
F = 0,012626

4.2 Analysis Experiment 2-Factor.

4.2.1 Experiment 2-Factor of Work Performance

This examination will be seen influence of some factor to work performance, the influences are:

- Operator and work performance relationship.
- Work condition and work performance relationship.
- Interaction between work condition and operator.

The conclusion of this examination:

1. There are not differences work performances among operator of unloading.
2. There is influence between work condition and work performance.
3. There is no influence of interaction between work condition and operator with work performance factor.

This strengthens the statement at the examination of ability for the election of operator. Equally, conclusions prove that ability of operator in work performance is same. The examination also obtained that working at normal condition give different work performance than in fasting condition.

Tables 2 *ANOVA experiment 2-Factor Work Performance.*

Source of Variation	JK	db	KT	F	F tabel
(A) Worker	4680,143	1	4680,143	0,233049	4,26
(B) Condition	250047	1	250047	12,45115	4,26
Interaksi	371,5714	1	371,5714	0,018502	4,26
Galat	481974	24	20082,24		
Total	737072,4	27			

4.2.2 Experiment 2-Factor of Energy Expenditure.

Tables 3 *ANOVA experiment 2-factor of Energy Expenditure*.

Source of Variation	JK	db	KT	F	F table
(A) Worker	0,037216	1	0,037216	0,002984	4,26
(B) Condition	1,793149	1	1,793149	0,143791	4,26
Interaksi	15,96735	1	15,96735	1,280407	4,26
Galat	299	24	12,47053		
Total	317,0904	27			

This examination will be seen influence of some factor to energy expenditure, the influences are

1. There is not differences work performance among operator of unloading.
2. There is no influence between work condition and work performance.
3. There is no influence of interaction between work condition and operator with work performance factor

5. DISCUSSION

5.1 Analysis of Working Time

5.1.1 Analysis of Working Duration

Analysis of working duration is done base on curve of energy expenditure and work performance. The curve showed there is change of performance (work performance) and physiological condition of body during period of work. It will be able to be conducted in working time arrangement. Assessment criterion the used are comparison between wok performance and energy expenditure in certain work duration.

Steps in analysis of work duration:

1. Analysis Curve of Energy Expenditure.

Curve show pattern which is same relative to the each work condition and operator. Values energy expenditure is increasing until at 11.00 am. After at 11.00, in the reality assess energy expenditure tend to downhill which represent response of operator peak burden activity cause exhaustion after operator stop over.

Figure 2 Representing alliance curve energy expenditure of operator 2 in both condition, it is show that value energy expenditure of operator 2 is more excessively in fasting condition rather than normal condition. Whereas operator 2, he has energy expenditure same relative in both condition seen at Figure 2.

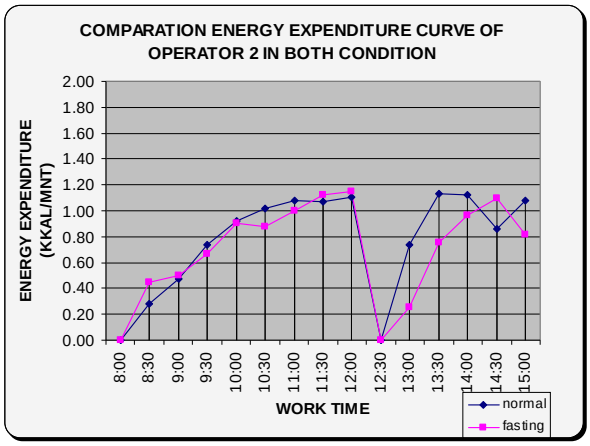

Figure 2. Curve energy expenditure of operator 1 in normal and fasting condition

2. Analysis Curve of Work Performance

Value work performance is found on curve represents work performance average value in time interval and same work condition. While statistically that is passing experiment 2-Factor work performances how there are no difference of work performance among operator and work condition.

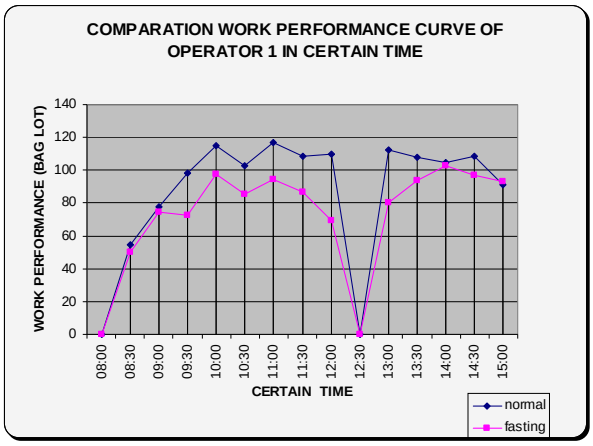

Figure 3. Curve work performance of operator 2 in both work condition.

Curve work performance show same fluctuation, but tend to happened degradation of work performance in fasting condition rather than in normal condition. Figure 3 is

representing work performance value of operator 2 in normal condition and fast. It is shown at curve that work performance value increasing until 10:30 am and have fluctuation during at 12:00 a.m. After at 11:00 operator work performance is tend to downhill until work activity rest. Similar after rest has experience of pattern which same to condition of working before rest.

3. Optimize work duration.

Seen at Figure 4 and 5 that is operator work performance early in working increasing till at 12:00 even there although there are work performance and energy expenditure fluctuations at 10:00 up to at 12:00 representing critical time or phase of operator. At time interval 10:00 - 12:00 many factor which possible influence operator, e.g others environmental factor and is psychological (it is not conducted measurement in this research).

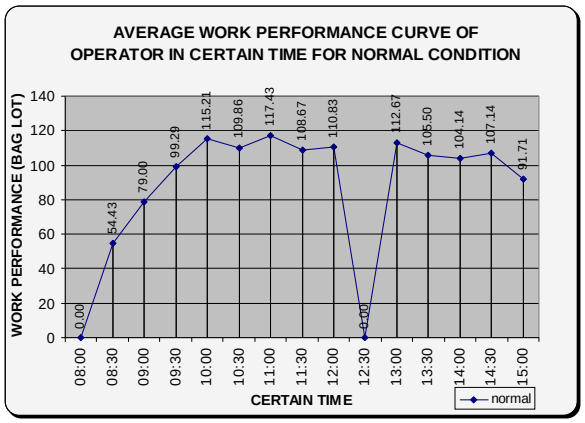

Figure 4 Curve of work performance in normal condition.

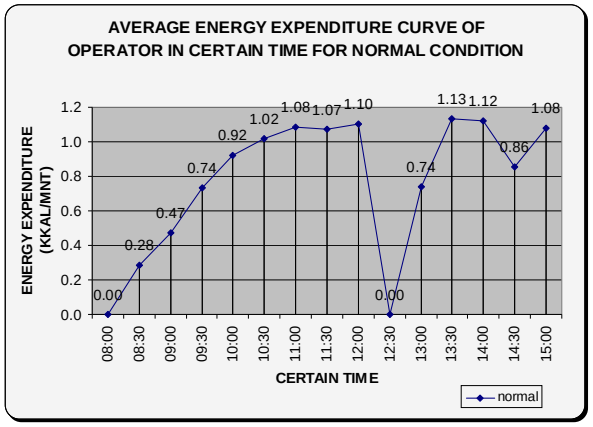

Figure 5. Curve of energy expenditure in normal condition.

Figure 6 is shown movement work performance operator of association of time. Therefore with Figure 6 seen clearly the condition of where natural operator fatigue is occur in time interval 10:00 up to 12:00, where curve tend to downhill. Degradation of curve at interval time of 10:00-12:00 supported also with make-up of value energy expenditure at the time (Figure 7). This matter indicate that at fasting condition after operator work average 2 hours represent critical time of operator to experience of fatigue marked with degradation of work performance and also the refreshing of energy expenditure. If this condition continue to take place will cause degradation of work productivity, degradation of quality work and also degradation of health of operator with the meaning loss of profit to company.

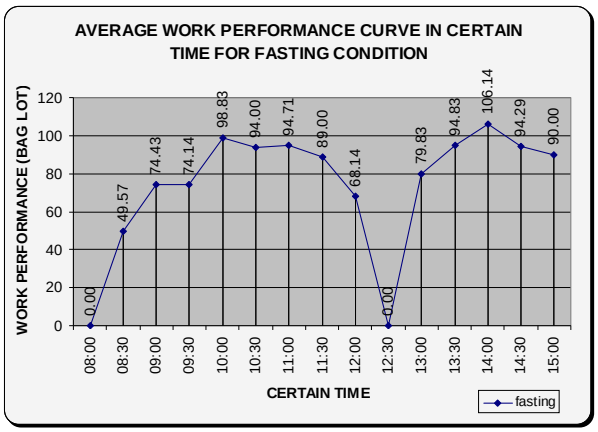

Figure 6 Work Performance curve in certain time in fasting condition

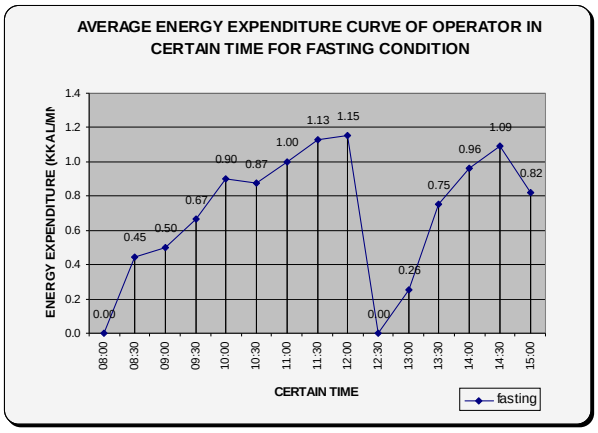

Figure 7 Energy expenditure curve operator in fasting condition

Figure 8 showing duration work during 4 hour give work performance per hour larger ones compared to work duration during 3 hour, 2 hour and 1 hour to both operators in normal condition. While in fasting condition working duration during 2 hour give best work performance compare energy expenditure per hour compared than work duration 1, 3 and 4 hours.

Furthermore, the comparison of work performance value and energy expenditure is show ability of operator to work performance 1 kkal. For example, the comparison of work performance versus energy expenditure of operator 1 for normal condition in work duration 2 hours is 102.655 lot /kkal. It is meaning with work duration 2 hour, operator 1 can produce 102.655 bag lot in 1 kkal.

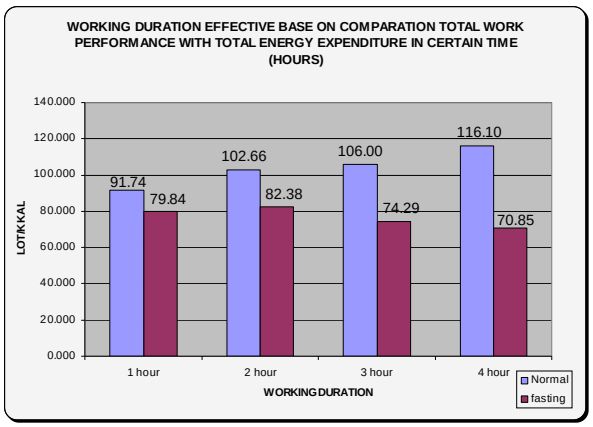

Figure 8 Curve determination of work duration

Pursuant to Figure 8 total comparison of work performance with energy expenditure obtained conclusion that optimal work duration in normal condition is 4 hours while at fasting condition is 2 hours.

5.2 Analysis Resting Time.

Result of research show, duration time for take a rest in 30 minute. This conclusion is obtained by seen the condition of pulse culminate at both the work condition which is same relative at heart rate 96.3 up to 96.4. So that equivalent required cure time both the work condition. Heart Pulse is recorded every 10 minute.

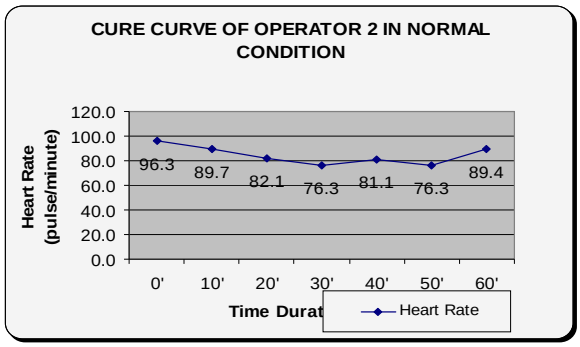

Figure 9 Curve cure of operator 2 in normal condition.

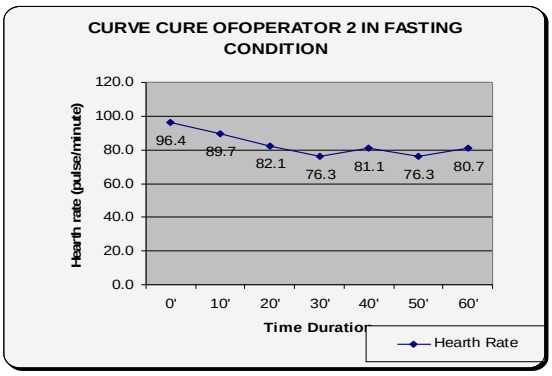

Figure 10 Curve cure of operator 2 in fasting condition.

While Figure 10 showing heart pulse operator 2 in fasting condition is 96.4 beat / minute. Heart pulse will return to refresh condition after 30 minute and relative constant until the operator starting his work.

All cure curves show that resting heart pulse of operator unloading sewing bag becoming to experience of degradation swiftly at first minute till the rest. The resting time duration of sewing bag operator normal in condition and fasting condition are same about 30 minute.

5.3 Working Time Arrangement

Hence in the working time suggestion got repetition each counted 3 times restating for the normal condition. Even more for the fasting condition is need be a change 5 times restating. Tables 4 and tables of 5 representing schedule work normal condition and fasting condition.

Tables 4 Schedule working time for normal condition.

Normal Condition		
Repetition	Work Duration	Note
1	08.00 - 12.00	Working Time
2	12.00 - 13.00	Resting Time
3	13.00 - 15.00	Working Time

Tables 5 Schedule working time for fasting condition

Fasting Condition		
Repetition	Work Duration	Note
1	08.00 - 10.00	Working Time
2	10.00 - 10.30	Resting Time
3	10.30 - 12.30	Working Time
4	12.30 - 13.30	Resting Time
5	13.30 - 15.00	Working Time

With existence of in working time arrangement pursuant to work performance criterion and energy expenditure, health and productivity level of operator will be more goodness.

5. CONCLUTION

Base on result of 2 factor experiment resulting about work performance and energy expenditure, there is a no different between operator, and also there is no influence work condition with energy expenditure .But it have different in influence of wok condition to work performance.

Optimal working and resting time duration;

Working Time Duration In Normal Condition: 4 hours

Working Time Duration In Fasting Condition: 2 hours

Resting Time Duration in Both Condition: 30 minutes.

REFERENCES

Anwar, Christin, *Analisis Pengaturan Waktu kerja Operator Hand Cliper Core Berdasarkan Kriteria Prestasi Kerja dan Konsumsi Energi*, Tugas Akhir, Jurusan Teknik Industri, Universitas Andalas, 2001.

Barnes, Ralph. M; *Motion and Time Study Design an Measurement of Work; Seventh Edition*; John Wiley & Sons Inc; New York, 1980.

Bedworth, David. D; Bailey James. E; *Integrated Production Control Systems*; John Wiley & Sons Inc; New York, 1987.

Christensen, Henne, et. al; *The Importance of The Work/Rest Pattern as A Risk Factor in Repetitif Monotonous Work* , Elsevier, 2000.

Coury, Helenice J.C.G; et al; *Influence Of Gender on Work-Related Musculoskeletal Disorders in Repetitif Tasks*, Elsevier, 2002.

Gaspersz, Vincent; *Metode Perancangan Percobaan*; Edisi pertama; Armico, Jakarta, 1990.

Grandjean, Etienne; *Fitting the Task to The Man*; Fourth Edition, Taylor & Francis, London, 1988.

Kroemer; Kroemer. Kroemer and Albert,*Ergonomics How to Design for Ease and Efficiency;* Second Edition; Prentice-hall, Inc, Upper Saddle River, New Jersey, 2001.

Mikkelsen, Aslaug; et al; *Working time Arragement and Safety for Offshore Worker in Nort Sea*; Pergamon Safety Science, 2004.

Nasution, Siti Rohana; *Penentuan Waktu Istirahat Guna Meningkatkan Kinerja Operator*. Seminar Nasional Ergonomi dengan tema Aplikasi Ergonomi dalam Industri, Yogyakarta, 2004

Nurmianto, Eko; *Ergonomi: Konsep Dasar dan Aplikasinya*; Edisi Pertama, PT. Guna Wydia; Jakarta, 1996.

Rusdjijati, Retno; *Penentuan Waktu Istirahat Pengemudi Bis Antar Kota Antar Propinsi (AKAP) Trayek Semarang-Yoyakarta Guna Menurunkan Tingkat Kecelakaan Kerja Dijalan Raya,* Seminar Nasional Ergonomi dengan tema Aplikasi Ergonomi dalam Industri, Yogyakarta, 2004.

Sanders, Mark S; McCormick, Ernest J; *Human Factors In Engineering and Design*.; Seventh Edition. MacGraw-Hill,Inc.1993.

Santiana, Made Anom; Yusuf, M; *Pengaturan Waktu Kerja Dapat Menurunkan Beban Kerja dan Keluhan Otot Skeletal Pada Pekerja Penyetrika Garmen "X" Didesa Kediri Kabupaten Tabanan*, Seminar Nasional Ergonomi dengan tema Aplikasi Ergonomi dalam Industri, Yogyakarta, 2004.

Sarjana, Putu; *Pemberian Istirahat Pendek Mengurangi Beban Kerja Gangguan Otot Skeletal dan Meningkatkan Produktivitas Pekerja Pengrajin Pintu Kuandi di Dusun Kederi Singapadu Sukawati Gianyar*, Seminar Nasional Ergonomi dengan tema Aplikasi Ergonomi dalam Industri, Yogyakarta, 2004.

Sutalaksana, I. Z.; *Teknik Tata Cara Kerja*, Edisi Pertama; Jurusan Teknik Industri, Institut Teknologi Bandung, Bandung, 1979.

Tarwaka; Bakri, Solichul HA; Lilik, Sudiajeng; *Ergonomi Untuk Keselamatan, Kesehatan Kerja dan Produktivitas*; Edisi Pertama, UNIBA Press, 2004.

Taylor, Francis; *Evaluation of Human Work Practical Ergonomics Methodology;* edited by Wilson, Jhon R, and Corlett, E. Nigel, Second Edition, Taylor & Francis, Ltd, 1999

Walpole, Ronald E.; *Pengantar Statistika*; Edisi Ketiga, Gramedia Pustaka Utama, Jakarta, 1990.

Wickens, Christopher D., Gordon, Sallie E., Liu, Yiyi; *An Introduction to Human Factor Engineering*, Addison Wesley, 1998.

Wignjosoebroto, S; *Ergonomi, Studi Gerak dan Waktu : Teknik Analisis untuk Peningkatan Produktivitas Kerja*; Edisi Pertama, Guna Wydia, Surabaya, 2000.

Wulanyani, Ni Made Swasti; *Pemberian Istirahat Pendek Aktif dan Lagu Pop Bali Menurunkan Keluhan Otot Skeletal dan Kebosanan serta Meningkatkan Produktivitas Pelinting Kertas Rokok*, Seminar Nasional Ergonomi dengan tema Aplikasi Ergonomi dalam Industri, Yogyakarta, 2004.

Analyzing Rural Potency of Lampung in Undertaking USO (Universal Service Obligation) Telecommunication Service by BTIP

Isti Surjandari[1], Amy Tambunan[2]

Industrial Engineering Department, Faculty of Engineering, University of Indonesia
Kampus UI, Depok 16424, Indonesia
E-mail : [1] surjandari.2@osu.edu , [2] amy_tambunan@yahoo.com

ABSTRACT

Rapid growth of telecommunication sector shows that nowadays information becomes a basic need. In order to realize telecommunication service to general public in Indonesia, the government builds minimal one telephone line (SST) in every village. This kind of program is known as USO (Universal Service Obligation). However, undertaking telecommunication service in rural area (Universal Service Obligation) in 2003 and 2004 has not served 43.000 villages by basic telephone service on the whole. Therefore, establishment of BTIP - organizer of rural telecommunication service which is supervised by Directorate General of Post and Telecommunication - signifies that government reverts to get prepared in implementing USO in order to realize development spreading throughout rural areas entirely. Different condition of villages will definitely influence the amount of cost services offered by operators to government. Also, in continuation of this program, developing aspect of rural potency is needed which could push flow of information exchange. Thus, analyzing rural potency is required. This study attempts to get classification of villages according to their potency and discovering selected village characteristics as indirect indicators toward call traffic by using Multivariate Analysis. It shows that business aspect gives a big contribution to utilization of telephone. The more advance level of business development indicates a higher level of need of information exchange. The results of this study will give some information for them who are in charge in USO. So, realization of following program planning will be involving some considerations which are expectedly going to attain effective and efficient result.

Keywords: *Rural Potency, Factor Analysis, Cluster Analysis, Universal Service Obligation*

1. INTRODUCTION

Rapid growth of telecommunication sector shows that nowadays information becomes a basic need which is necessary to be fulfilled because it gives a big contribution to the development of other sectors. It is reinforced by the result of ITU's (International Telecommunication Union) research declaring that 1% increasing of teledensity will support economic growth by 3% [1].

By definition, teledensity is a measurement indicating utilization of telecommunication facility in a country [2]. Teledensity is a ratio of telecommunication facility number to population in a country. In Indonesia, this number is not proper to be categorized into ideal. It can be seen from reality that Indonesia has just reached 6.7 million telephone connection units (SST) with 220 million of population number which means that only 3 SST is available for 100 inhabitants. In other word, teledensity is only 3% and 0.2% in rural area [3]. The fulfillment of information need can be carried out by every Indonesian people without exception, in other word, being able to attain spreading evenly information access, if telecommunication facilities already reach out entire area up to outlying districts, so that they are not in position of digital divide anymore.

Referring to the declaration of ITU, in order to realize telecommunication service to general public in Indonesia, the government, (i.e., Ministry of Communication and Informatics, Directorate General of Post and Telecommunication) builds minimal one telephone line (SST) in every village. This kind of program is known as USO (Universal Service Obligation) or KPU (Kewajiban Pelayanan Universal) which is organized by BTIP (Balai Telekomunikasi dan Informatika Pedesaan).

Undertaking USO by Indonesian governments had been taken place in 2003 through installation 3.010 telephone connection units in 3.010 villages and in 2004 through installation 2.620 telephone connection units in 2.341 villages. This number shows that 43.000 targeted villages have not been served by basic telephone service on the whole. Therefore, in doing the establishment of BTIP, the organizer of rural telecommunication service, which is supervised by Directorate General of Post and

Telecommunication, signifies that government reverts to get prepared in implementing USO in order to realize development spreading throughout rural areas entirely.

In preparing the following USO, BTIP strives to straighten former concepts of service providing. One of them is village categorizing which is aimed to arrange priority of installation based on rural potency. The different condition of villages will definitely influence the amount of cost services offered by operators to government. It becomes such an important thing concerning that government is expected to allocate operational fund wisely appropriate with the requirement. Furthermore, it is better that undertaking telecommunication service in rural area to be followed by monitoring of telephone utilization. It can be realized by tracing the average of phone call duration. The greater the phone call duration the more the frequency of information exchange. Therefore, in continuation of this program, aspect of rural potency pushing flow of information exchange needs to be developed which yields a high utilization of telephone.

For the purposes of this study, analysis will be done based on village characteristics in Lampung during period 2003-2004 and the following. It is because of the availability of call traffic (historical data) overwhelms only Lampung area as telecommunication service area of Sampoerna Telekomunikasi Indonesia. It refers to the objective of this study which is wrapping up information of rural potency. Hence, service characteristics given by operators in exertion of USO implementation will not be covered in this study. Thus, the main problem discussed in this study is analyzing rural potency of Lampung in undertaking USO by BTIP using multivariate statistics. This paper aims to achieve two objectives. The first objective is getting classification of villages according to their potency. And the second one is discovering village characteristics as indirect indicators of telecommunication facility utilization.

2. METHODS

Collected data is in the form of secondary data as BTIP's archives that is Rural Potency according to survey of BPS in the year 2005. This kind of data consists of village characteristics informing rural potency, the potency or capacity/power which enables to be developed within village autonomy area [5]. Characteristics selection is done refers to study of BTIP and also based on information acquired from literatures. Addition of characteristics is expected more encouraging in discovering other fundamental aspects needed to be considered. Besides adding characteristics, variable substitution is also executed. It is conducted not significantly different in meaning. In particular, that is done for the purpose of getting a more precise result.

This study also occupies historical data such a kind of call traffic of USO villages period 2003-2004 in Lampung (report of Sampoerna Telekomunikasi Indonesia) during 6 months in period of July-December 2005. It is not likely to collect data in period latter than that because the report just accommodates it concerning the policy of monitoring telecommunication facility assigned to operators prevails 1 year after facility establishment (2004).

This study involves population of villages of USO located in Lampung during period 2003-2004 and the following. It is conducted in order to gain information reflecting truly condition of Lampung. In fact, villages as the following WPUT (Telecommunication Universal Service Area) located in Lampung numbers ± 805 in amount, nevertheless based on the availability of data, only 789 villages are available to be observed. While, among 314 vilages of previous USO served by STI, there are only 303 of them feasible to be discussed by the same reason.

Data is processed by performing multivariate analysis. Multivariate analysis refers to all statistical methods that simultaneously analyze multiple measurements on each individual or object under investigation [6]. Conducting multivariate analysis is related to the requirement of measuring, explaining and predicting the degree of relationship between variates. Variate is a linear combination of variables along with their weights which are determined empirically. Multivariate analysis used in this study consists of factor analysis, cluster analysis and multiple regression analysis.

In case of arranging concepts, object which is going to be observed comprises candidate villages of next USO. Required techniques are factor analysis and cluster analysis. Factor analysis is a kind of statistical method whose primary purpose is to find interrelationship between variables which are independent with one another so that a number of original variables can be condensed into one or some sets of new factors. According to this study, this technique is aimed to make it easy in recognizing and understanding village characteristics as basis of rural potency assessment. That is summarizing 33 evaluating variables into some factors or underlying dimensions.

To complete the first objective, data processing is continued by implementing cluster analysis. Cluster analysis is a statistical procedure to classify objects based on identical characteristic they possess. It is organized with the aim of forming some clusters with respect to some characteristics implied. The case is classifying 789 villages into 4 clusters. Afterward, grading village is held by involving weight factors in determining rank. The biggest weight is assigned to factor which assumed as the most supporting aspect either in installation or maintenance of telecommunication facility later on.

The second objective is discovering rural potency as indirect indicators of telecommunication facility utilization together with their contribution toward telephone utilization level. This discussion is a kind of evaluation so that the objects observed are villages of previous USO located in Lampung during period 2003-2004. Multiple regression analysis is used to organize it.

3. RESULT AND DISCUSSIONS

There are 33 variables involved as indicators in assessing rural potency which can be seen in Table 1. Among 33 selected variables, there is one variables has no variance (zero variance) which means that the data has no value at all (null value). So observation is performed to the remaining variables (32 independent variables).

All of data processing is supported by SPSS 15.0. In order to be able to arrange potency factors of village teledensity which summarize selected variables, it is necessary to do proper test to these candidate variables. They are agreed to be processed. It can be seen from correlation test showed by 0, 672 of KMO value, Bartlett's Test of Sphericity value indicated by 2847.851 of Chi-Square value and Sig-value (0,000) < α = 0,05 (level of confidence chosen).

In factor analysis, number of factors to be formed is executed related to scree plot test, as can be seen in Figure 1. Based on the scree plot, with the aim of obtaining the best combination of 32 variables into factors, trial and error is carried out from 3 up to 5 in number of factors along with some rotating methods which are *varimax*, *quartimax*, *equamax*, *oblimin*, and *promax*. This procedure gave best arrangement as result of implementing varimax rotating factor method by 4 factors.

Table 1: Village Characteristics in Assessing Potency of USO Villages

Rural Potency			
Accessibility Aspect		**Affordability Aspect**	
Social Culture	**Accessibility**	**Social Economy**	**Basic Business Parameters**
Number of family	Number of terminal for four-wheel public vehicle	Percentage of agricultural household	Number of big industry
Number of state elementary school	Existence of post office	Number of Indonesia migrant workers (TKI)	Number of medium industry
Number of private elementary school	Existence of mobile post office	Number of market with non-permanent building	Number of small industry
Number of hospital	Geographical site of the village	Number of stall (warung)	Number of supermarket/minimarket/store
Number of clinic	Easiness to reach the village	Number of mini shop (toko kelontong)	Number of commercial banks
Number of public health centre (puskesmas)			Number of small financial institution (Bank perkreditan rakyat)
Number of midwives (bidan)			Number of village cooperative unit (KUD)
Number of public health sub-centre (posyandu)			Number of handicraft and small cooperative
Number of maternity clinic (polindes)			Number of saving and loan cooperative (koperasi simpan pinjam)
Density			Number of non-village cooperative unit (non-KUD)
Existence of mutual cooperation (gotong royong) in public facility construction			
Existence of main street lighting			
Number of household electricity users			

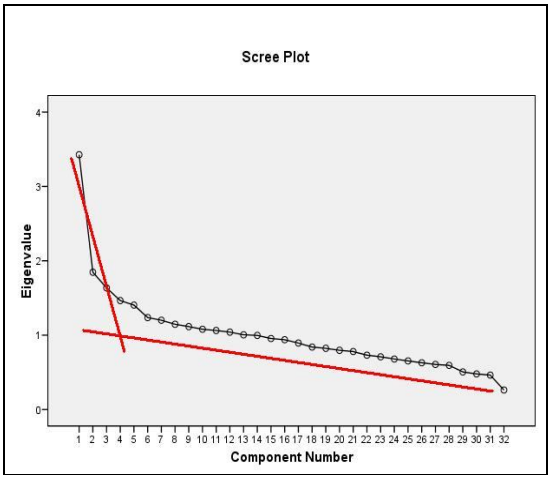

Figure 1: Scree Plot Factor Analysis

By applying rotating method, component rotated factor is produced which contains factor loading presenting correlation coefficients of variables in relation to factors. The highest loading identified membership for variables on any factors. Among 32 selected variables, 8 variables associate with factor 1, 11 variables associate with factor 2, 6 variables associate with factor 3 and 7 variables associate with factor 4. This allocating process developed 4 factors which are independent with one another. Subsequently, associating factors are labeled in accordance with information comprised. The arrangement of variables into factors accompanied by the name can be seen in Table 2.

Arrangement of rural characteristics (variables) into 4 factors is a little bit different from categorization generated by BTIP earlier. Rearrangement of variables is carried out with the aim of structuring factors statistically concerning with correlation among variables. Variables which grouped into one factor have a high correlation and they are influencing each other. Next, factor score is developed. Factor score, similar to original variables, is a value which blends grouped variables values (derived from factor analysis) consequently independent in nature as result (unrelated one another, no multicolinearity). Formulation of factor scores is useful as input in performing cluster analysis and multiple regression analysis.

By means of factors acquired, cluster analysis is executed. Number of cluster is four which is determined relates to treatment that would be held by BTIP and operators. Moreover, it allows comparing between output of research and study before. The result of cluster analysis can be seen in Table 3. The numbers show degree of rural potency of villages applied to factors acquired by description:

- Positive number indicates under average
- Negative number indicates above average

Table 2: Composition of Variables into 4 Factors

Factor	Factor Name	Variables
1	Characteristic and Facility of Basic Needs	Number of family, Number of state elementary school, Number of private elementary school, Number of public health sub-centre (posyandu), Number of stall (warung), Number of small shop (took kelontong), Existence of mutual cooperation (gotong royong) in public facility construction, Number of household electricity users
2	Economy and Health	Number of market with non-permanent building, Number of small financial institution (Bank Perkreditan Rakyat), Number of village cooperative unit, Number of handicraft and small cooperative, Number of saving and loan cooperative, Number of non-village cooperative unit, Number of Indonesian migrant workers (TKI), Number of hospital, Number of clinic, Number of public health centre (Puskesmas), Number of midwives.
3	Accessibility and Demography	Existence of mobile post office, Existence of main street lighting, Village geographical site, Easiness to reach the village, Density, Percentage of agricultural household
4	Business with its Supporting Facility	Existence of post office, Number of big industry, Number of medium industry, Number of small industry, Number of supermarket/minimarket/store, Number of maternity clinic, Number of terminal for four-wheel public vehicle

Table 3: Potency Value of Each Cluster Based on Factors Discovered

Factor	Cluster			
	1	2	3	4
Characteristic and Facility of Basic Need	0.1687550	-0.3654746	2.1639850	0.9351286
Economy and Health	2.3915211	-0.2118849	-1.1293309	-0.1807535
Accessibility and Demography	0.6416610	0.2191751	0.5324048	-0.8360114
Business with its Supporting facility	-0.3495429	0.0642848	9.5719679	-0.2155710

Clusters become references in accomplishing *grading* which is done by assigning weight in different number on each factor. Factor weight is settled refers to study of BTIP which can be seen in Table 4. Composition of villages resulted by cluster analysis is different with result of study before, which can be found out in Table 5. Afterward, cluster result in Table 4 might become some considerations in classifying villages; hence, on-hand fund would be allocated relevant to expenses required.

Table 4: Factor Weight

Factor	Factor Weight
Characteristic and Facility of Basic Need	10%
Economy and Health	45%
Accessibility and Demography	35%
Business with its Supporting Facility	10%
TOTAL	100%

Table 5: Comparison of Village Composition between BTIP's and This Study

Category of Village	Cluster based on BTIP	Cluster based on this study
Undeveloped village	155	190
Less developed village	490	533
Developed village	136	3
Highly developed village	8	63
TOTAL	789	789

Multiple regression analysis is constructed by involving all variables (33 village characteristics) along with call traffic. Backward is applied as approaching method in organizing this technique. Variables selection is made by eliminating variables that have less significant contribution. There are proposed variables which act as indirect indicators of villages toward telephone utilization, as can be seen in Table 6.

Table 6: Multiple Regression Result

Model	Unstandardized Coefficients (B)	P-Value
(constant)	-5.74429E-16	0.99999
Number of family	0.157617	0.00923
Number of maternity clinic	0.203566	0.00021
Density	-0.132288	0.01826
Percentage of agricultural household	0.101390	0.06436
Number of big industry	-0.136273	0.02023
Number of medium industry	0.178938	0.00095
Number of village cooperative unit	-0.153240	0.00475
Village geographical site	-0.150470	0.00617
Dependent variable: Zscore: Average of call traffic (6 months)		

By applying significance test toward each of regression coefficient at significance level of 5%, it is found that some variables influence telephone utilization significantly, they are: number of family, number of village giving birth house, density, number of big industry, number of medium industry, number of village unit cooperative and geographical site of village.

From this study, it is perceived that domination business aspect shows that it is so crucial to be considered in undertaking telecommunication infrastructure development. The advancement of business activity in a region indicates level of need of information exchange. According to this case, type of telecommunication service is definitely adjusted to the purpose of society's concern. Then, it concludes that region with a more advance business aspect is a more beneficial field to organizing business of telecommunication.

4. CONCLUSIONS

Based on the result, factors that summarize variables and become underlying aspect in assessing rural potency consist of: Characteristic and Facility of Basic Needs contains 8 variables, Economy and Health contains 11 variables, Accessibility and Civilization contains 6 variables and Business with Its Supporting Facility contains 7 variables. Afterward, according to these factors, villages are classified along with their grade, they are: immature village consists of 190 villages; semi mature village consists of 533 villages; mature village consists of 3 villages; and urbanized villages consists of 63 villages. In addition, there are 7 significant variables used as indirect indicator toward telephone utilization, they are: number of family, number of village giving birth house, density, number of big industry, number of medium industry, number of village unit cooperative and geographical site of village. It

concludes that business aspect gives a big contribution to utilization of telephone. The more advance level of business development indicates a higher level of need of information exchange. The results of this study will give some information for them who are in charge in USO. So, realization of following program planning will be involving some considerations which are expectedly going to attain effective and efficient result.

REFERENCES

[1] Abdul Salam Taba, "Harapan Pada Hari Telekomunikasi Sedunia", www.alumni.adsjakarta.or.id/articleattachment/articleastaba21.htm, 2005.

[2] Koperasi Telkomsel, "Baru 3% Pelanggan Telkomsel Manfaatkan", http://www.mykisel.com/index.php?menu=depan&action=detail&id=40&cat=2, 2005.

[3] Depkominfo cq. Ditjen Postel, "Kebijakan Penyediaan Sarana dan Prasarana Telekomunikasi Perdesaan KPU/USO", *Bahan presentasi Depkominfo cq. Ditjen Postel*, 2007, pp. 2.

[4] Eddy Satriya, "USO Telekomunikasi", *Majalah Bisnis Komputer*, No. 03, Maret 2004, pp. 3.

[5] Mastel, "BIM Untuk Kesejahteraan Masyarakat Perdesaan", http://www.mastel.or.id/id/?hlm=profil&show=tentangbim, 2008.

[6] Joseph F. Hair, JR., Rolph E. Anderson, Ronald L. Tatham, William C. Black, *Multivariate Data Analysis, Fifth Edition*, Prentice-Hall International, Inc, New York, 1998, pp. 6.

Improving Product Quality in Painting Production Line of Motorcyle Parts using Design of Experiments

Isti Surjandari[1] and Hanifa Dhina[2]

Industrial Engineering Department, Faculty of Engineering, University of ndonesia
Kampus Baru UI, Depok 16424, Indonesia
E-mail: [1] surjandari.2@osu.edu , [2] hanifa_dhina1@yahoo.com

ABSTRACT

Nowadays, quality is one of the key factors that have to be considered by a company to win a competition. Generally, quality is defined as meeting or exceeding customers' requirements. Quality is also become a major concern by PT Astra Otoparts Tbk, as one of the biggest producer of motorcycle parts in Indonesia. Data showed that defect rate is relatively high in some production lines, particularly in the painting process. The rejection number showed inefficiency in raw materials utilization because the rejected parts have to be replaced by producing new parts. In order to overcome this problem, an experiment is needed to analyze factors that affect the quality of painted parts in the painting production line. This study uses Design of Experiments (DOE), that is, the 2^k full factorial design method. DOE is a scientific method for identifying the critical parameters associated with a process and thereby determining the optimal settings for the process parameters for enhanced performance and quality. There are ten types of defect that are tested in this study, which are: orange peel, scratched, thin, dirt, oily, popping, dust, pervade, water dots, and painting melt. And there are four controllable factors used in the experiment, which are: conveyer speed, water spray pressure, hot water temperature, and degrease utilization. The results of this study show that controllable factors and their interactions are significantly affect the defect rate. There are five out of ten defect types which are statistically significant affected by the controllable factors in this experiment. Then, using response optimizer, this study finds the optimal setting for each of the controllable factors that might reduce the defect rate and improve the product quality.

***Keywords**: Design of Experiment, Full Factorial, Painting, Motorcycle Part*

1. INTRODUCTION

Recent economic condition in Indonesia indirectly affects transportation sector and its supporting industries. People now prefer to have transportation mode that support their mobility, such as a motorcycle. Motorcycle has more flexibility through the busy and crowded traffic conditions especially in the big cities such as Jakarta. It is also supported by its price, which is relatively achievable by most Indonesian people. This fact makes motorcycle sales in Indonesia increases every year.

Nowadays, PT Astra Otoparts Tbk (AOP) is the leading company in producing motorcycle parts in Indonesia. Its biggest customer is PT Astra Honda Motor (AHM), which is the leading company in producing motorcycles in Indonesia. In this case, AOP has to maintain and even increase its market share. In so doing, AOP has always give attention to quality improvement. Eventhough inspection and checking procedure take place in each production line, still defect may take place. Production lines which show relatively high rate in product defect are painting lines. In these lines, motorcycle parts, which were produced by the plastic injection section, are painted. Subsequently painted parts will be delivered to the assembling lines. There are three lines in this painting section, where the first two lines use hanging conveyor and the third line use manual conveyor. Figure 1 show parts which are painted in AOP.

Figure 1: Plastic Painted Parts in Motorcycle

Rejection rate in panting lines was 24.25% in Desember 2007, and increased to 30.20% in January 2008. It shows AOP has to bear high quality costs because the rejected parts have to be replaced by producing new parts. In this case, it becomes important for AOP to do quality improvements in the painting lines. The objective of this study is to investigate controllable factors that affect the defect product in painting lines using Design of

Experiments (DOE). Hence it can be determined the optimal setting of those factors in order to reduce rejection rate in the painting lines.

2. METHODS

For the purpose of this study, a 2^k *Full Factorial Design* will be used to improve product quality, which is plastic painted of motorcycle parts, in the second line of painting section. There are 10 types of defect that will be analyzed in this study, which are: orange peel, scratched, thin, dirt, oily, popping, dust, pervade, *water dots*, and paintings melt. Figure 1 shows percentage of each defect type in the second line.

Output of each experiments is the number of defect occurred for each of defect type, because there will be opportunity to have more than one type of defect occurred in the same part. The result will be converted into probability of success that is percentage of part without any defect type. Since the highest production rate in the painting lines is black colored parts (i.e., black is the preferred color by the consumen), but with the highest rejection rate, hence analysis will be focused on black color. Figure 3 shows rejection rate for each color.

Figure 4 shows flow process chart for painting in AOP. Basically, there 6 main processes in the painting line, which are: pre-treatment, air blow (1 and 2), dry and baking oven, setting room (1 and 2), under coat and top coat.

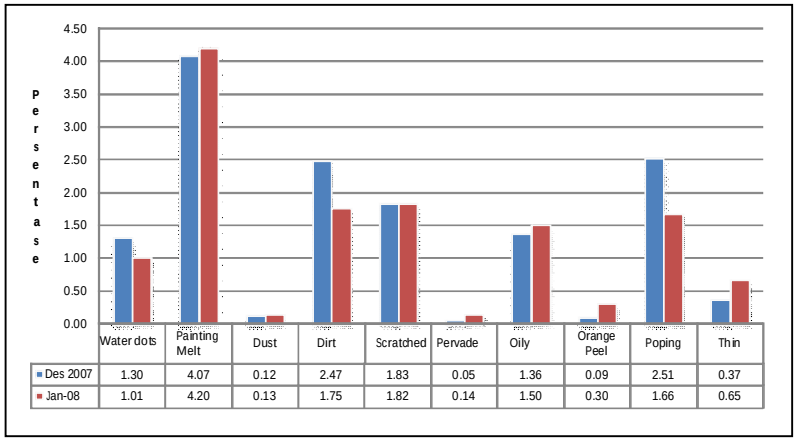

Figure 2: Percentage of each Defect Type in Line 2

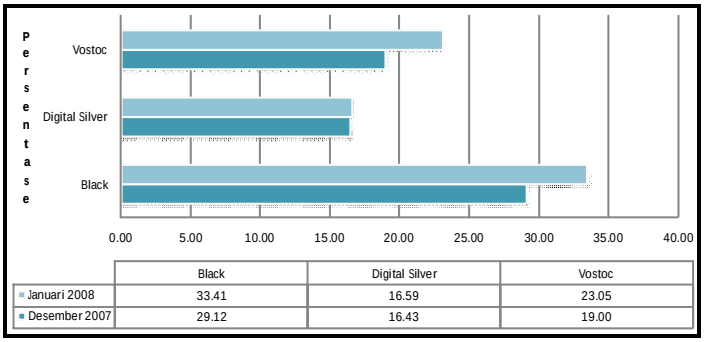

Figure 3: Rejection rate for each Color

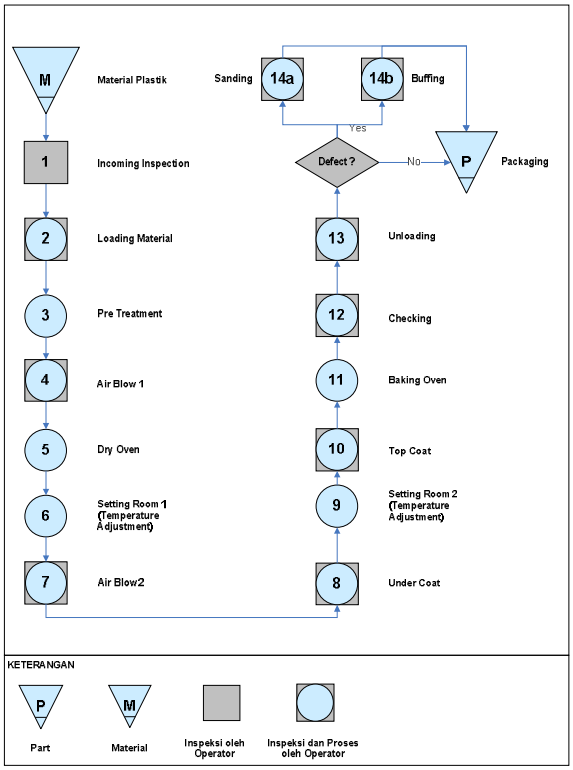

Figure 4: Flow process Chart of Painting Line

There are four controllable factors, each with two levels that will be analyzed in this experiment, which are:

1. *Conveyor speed:*
   A hanging conveyor is used in this line, where each plastic part will be loaded and hung on the conveyor. A hanger can load up to four big parts at once (e.g., rear wings and speedometer cover), and up to 12 small parts. There are 322 hangers in the second production line while 324 hangers remain in the first line. Cycle time for a material loaded until the final process is 1.5 hours. Each coloring process has different speed, depend on the color used. For the experiment, the speed for low level is 3.0 m/minute and for high level is 2.5 m/minute
2. *Water spray pressure:*
   Parts will be sprayed by water which comes out from nozzle surround the room. The range of water spray pressure is 0.6 psi to 0.8 psi. For the experiment, the water sprays pressure for low level is 0.6 psi and for the high level is 0.8 psi.
3. *Hot water temperature:*
   The hot water is required to demolish oil and grease left from the parts. The maximum temperature allowed to wash plastic materials is 60˚C. For the experiment, the hot water temperature for the low level is 52˚C and for the high level is 60˚C.
4. *Degrease utilization*
   Degrease is used in this process as detergent powder. It is used to demolish grease and oil left by compounding it with hot water in the first pump. For the experiment, the low level is not using degrease and the high level is using degrease.

The experiment will be run using two replications for each combination of the 2^k full factorial design, so the total number of experiments is 32 times. In order to minimize the effect of noise factors induced into the experiment, each trial condition was randomized. Randomization is aprocess of performing experimental trials in a random order, not that in which they are logically listed. The idea is to evenly distribute the effect of noise across the total number of experimental trials.The experimental design can be seen in Table 1, while Table 2 illustrate the results of the experimentfor scratched defect type. Since there are 5 defect types, each with its own experimental result, therefore, scratched type of defect will be used as an example for the discusion and analysis.

Table 1: Design using DOE Method

Replication No.	Without Degrease							
	Temperature 52°				Temperature 60°			
	2,5 m/mnt		3 m/mnt		2,5 m/mnt		3 m/mnt	
	0,6 psi	0,8 psi	0,6 psi	0,8 psi	0,6 psi	0,8 psi	0,6 psi	0,8 psi
1								
2								

Replication No.	With Degrease							
	Temperature 52°				Temperature 60°			
	2,5 m/mnt		3 m/mnt		2,5 m/mnt		3 m/mnt	
	0,6 psi	0,8 psi	0,6 psi	0,8 psi	0,6 psi	0,8 psi	0,6 psi	0,8 psi
1								
2								

Table 2: Experimental Results for Scratched Defect Type

StdOrder	RunOrder	CenterPt	Blocks	Speed konv.	Tekanan	Suhu	Degrease	Prob. Sukses
7	1	1	1	2.5	0.8	60	0	0.9
15	2	1	1	2.5	0.8	60	1	1
12	3	1	1	3	0.8	52	1	1
19	4	1	1	2.5	0.8	52	0	1
21	5	1	1	2.5	0.6	60	0	0.967
30	6	1	1	3	0.6	60	1	1
32	7	1	1	3	0.8	60	1	1
20	8	1	1	3	0.8	52	0	1
8	9	1	1	3	0.8	60	0	0.867
22	10	1	1	3	0.6	60	0	1
13	11	1	1	2.5	0.6	60	1	1
26	12	1	1	3	0.6	52	1	1
10	13	1	1	3	0.6	52	1	1
23	14	1	1	2.5	0.8	60	0	1
31	15	1	1	2.5	0.8	60	1	0.968
1	16	1	1	2.5	0.6	52	0	0.967
18	17	1	1	3	0.6	52	0	1
14	18	1	1	3	0.6	60	1	1
2	19	1	1	3	0.6	52	0	1
4	20	1	1	3	0.8	52	0	1
25	21	1	1	2.5	0.6	52	1	0.933
16	22	1	1	3	0.8	60	1	1
6	23	1	1	3	0.6	60	0	1
3	24	1	1	2.5	0.8	52	0	1
28	25	1	1	3	0.8	52	1	0.969
11	26	1	1	2.5	0.8	52	1	0.9
17	27	1	1	2.5	0.6	52	0	1
27	28	1	1	2.5	0.8	52	1	1
9	29	1	1	2.5	0.6	52	1	1
5	30	1	1	2.5	0.6	60	0	0.967
24	31	1	1	3	0.8	60	0	0.933
29	32	1	1	2.5	0.6	60	1	0.937

3. RESULT AND DISCUSSIONS

Table 3 shows the ANOVA result for scratched type of defect. It shows that no single factor in the experiment that affect scratched defect type. However, the two-way interaction between speed conveyor and degrease do have affect on the scratched defect type.

Table 3: Summary of Defect Type Significant Values

Factorial Fit: prob.sukses versus speed konv, tekanan, suhu, degrease

Estimated Effects and Coefficients for prob.sukses (coded units)

Term	Effect	Coef	SE Coef	T	P
Constant		0.97275	0.004464	217.93	0
speed konv	0.00725	0.003625	0.004464	0.81	0.429
tekanan	-0.0115	-0.00575	0.004464	-1.29	0.216
suhu	-0.00738	-0.00369	0.004464	-0.83	0.421
degrease	0.01275	0.006375	0.004464	1.43	0.172
speed konv*tekanan	-0.01175	-0.00588	0.004464	-1.32	0.207
speed konv*suhu	-0.00088	-0.00044	0.004464	-0.1	0.923
speed konv*degrease	0.02	0.01	0.004464	2.24	0.04
tekanan*suhu	-0.01238	-0.00619	0.004464	-1.39	0.185
tekanan*degrease	0.00825	0.004125	0.004464	0.92	0.369
suhu*degrease	0.018875	0.009438	0.004464	2.11	0.051
speed konv*tekanan*suhu	-0.01238	-0.00619	0.004464	-1.39	0.185
speed konv*tekanan*degrease	0.0075	0.00375	0.004464	0.84	0.413
speed konv*suhu*degrease	-0.00313	-0.00156	0.004464	-0.35	0.731
tekanan*suhu*degrease	0.024375	0.012187	0.004464	2.73	0.015
speed konv*tekanan*suhu*degrease	0.007875	0.003938	0.004464	0.88	0.391

S = 0.02525 R-Sq = 65.24% R-Sq(adj) = 32.65%

Analysis of Variance for prob.sukses (coded units)

Source	DF	Seq SS	Adj SS	Adj MS	F	P
Main Effects	4	0.003214	0.003214	0.000804	1.26	0.326
2-Way Interactions	6	0.00893	0.00893	0.001488	2.33	0.082
3-Way Interactions	4	0.006506	0.006506	0.001627	2.55	0.079
4-Way Interactions	1	0.000496	0.000496	0.000496	0.78	0.391
Residual Error	16	0.010201	0.010201	0.000638		
Pure Error	16	0.010201	0.010201	0.000638		
Total	31	0.029348				

Table 4 shows ANOVA result for the controllable factors which are statistically significant affecting defects with significance level of 5%. There are 5 defect types which are affected by factors in the experiment, which are: dirt, oily, water dots, and painting melt.

The purpose of using degrease is to remove dirt attached, and it is significantly affect defect. Its interaction with right temperature is also affecting defect. Conveyor speed is also significantly affecting defect, because as the the conveyor gets slower the more time for degrease with the right temperature to wash the parts. Possible causes for orange peel, thin, and dust are operator skills which are not adequate. While for poping, it may caused by poorly dried part which comes from the dry oven in the pre-treatment process, hence it creates bubble in the painting process.

Scratched might be caused by parts wich rub against each other from the same or different hanger. Also, when parts enter the pre treatment process, there is a possibility for each part to get scratched because it will be sprayed by high pressure water, so it can make the hanger unsteady and the parts may rub against each other. This is why conveyer speed and water pressure becomes statistically significant affecting the defect rate.

Table 3: Summary of Defect Type Significant Values

	Term	T	P-Value
Dirt	Degrease	4.25	0.001
	Temp * Degrease	-5.39	0
	Speed * Temp * Degrease	2.49	0.024
Scratched	Speed * Degrease	2.24	0.040
	Press * Temp * Degrease	2.73	0.015
Oily	Speed	67.01	0
	Press	-10.86	0
	Temp	75.26	0
	Degrease	76.85	0
	Speed * Temp	-68.92	0
	Speed * Degrease	-70.50	0
	Press * Temp	10.86	0
	Press * Degrease	9.28	0
	Temp * Degrease	-77.48	0
	Speed * Temp * Degrease	68.6	0
	Press * Temp * Degrease	-10.55	0
Water Dots	Speed * Press	2.21	0.042
	Temp * Degrease	2.33	0.033
Painting Melt	Speed	2.55	0.021
	Temp * Degrease	2.92	0.010
	Speed * Temp * Degrease	-2.4	0.029

Figure 5 shows the normal probability plot of the residual for scrathed type of defect. It shows that the data is normally distributed. The same results obtained from the other defect types.

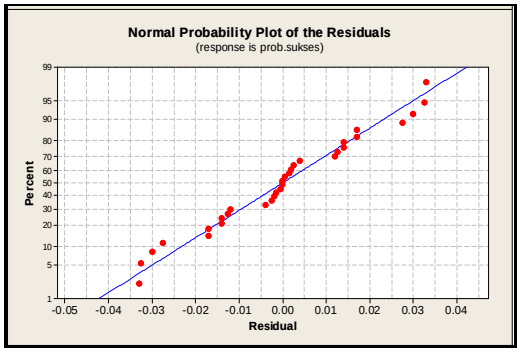

Figure 5: Normal Probability Plot for Scratched Type of Defect

After analyzing the defect causes, the next step is to find the optimal combination of factors in order to reduce the defect rate. Figure 6 sows the optimum combination for the controllable factors that is obtained using Response Optimizer. While Table 4 shows the interpretation of Responese Optimizer plot for scrathed type defect.

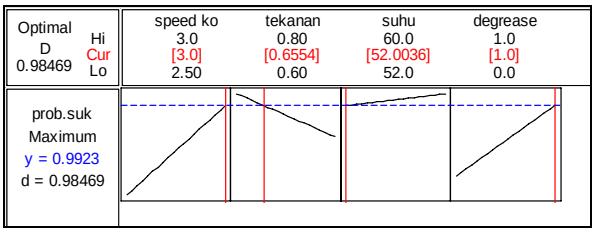

Figure 6: Response Optimizer for Scratched Type of Defect

Table 4: Response Optimizer Plot for Scratched Type of Defect

Setting	D-Value	conv. Speed	press	temp	degrease
Initial	0.98469	3	0.6554	52.0036	1
Optimal	0.98469	3	0.6554	52.0036	1

The response optimizer graph shows the best combination of controllable factors used to decrease the number of scratched part by using conveyor speed at high level (3 meter/minute), spray pressure at low level (0.6 psi), temperature at low level (52˚C), and using degrease.

Figure 7 shows the contour plot of interaction between Degrease and Speed Conveyor for the scratched type of defect.controllable factors used to reduce the other type of defect based on the Response Optimizer. It shows that the optimum setting of the controllable factors is generally the same to reduce all type of the defect types.

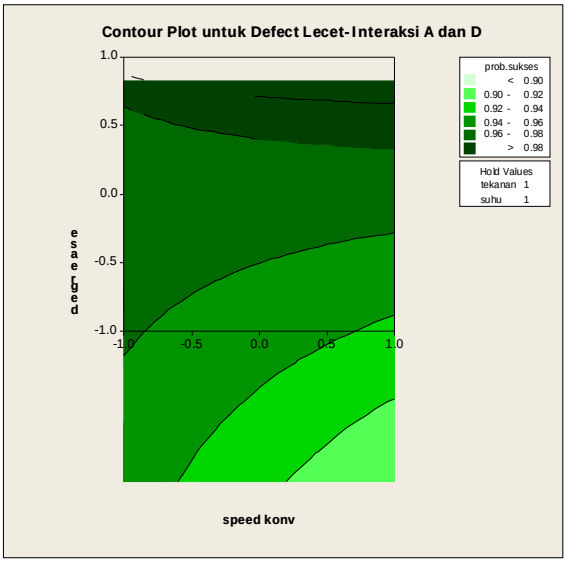

Figure 7: Contour Plot of Interaction between Degrease and Speed Coveyor for Scratched Type of Defect

Table 5 show the optimum combination of the

Table 5: Response Optimizer Combination

Defect Type	Conv. Speed		Pressure		Temperature		Degrease	
	2.5	3	0.6	0.8	52	60	Yes	No
Dirt		■		■	■		■	
Scratched		■	■		■		■	
Oily		■		■	■		■	
Water Dots		■		■		■	■	
Painting Melt		■		■	■		■	

CONCLUSIONS

The result of this study shows that there are 5 types of defect which are statistically significant affected by the controllable factors in the experiments. Those 5 defect types are scratched, dirt, oily, water dots, and painting melt. Each defect type is affected by different factors, and so they do for the interactions. Generally, the optimum combination of the controllable factors to decrease the defect rate is the almost same for each defect type.

REFERENCES

[1] Antony, Jiju, 1998, “Some key things industrial engineering should know about experimental design”, *Logistic Information Management*, Vol. 11, No.6.

[2] Antony, Jiju, 2001, “Improving the Manufacturing Process Quality Using Design of Experiments: a case study”, International *Journal of Operation & Production Management*, Vol.21, No.5/6.

[3] Antony, Jiju, et al., 2001, “Process Optimization Using Taguchi Method of Experimental Design”, *Work Study*, Vol.50, No.2.

[4] Berger, Paul D., dan Robert E. Murer, 2002. *Experimental Design with Applications in Management, Engineering, and Science.* Thompson, New York.

[5] Dean, Angela dan Daniel Voss, 1999, *Design and Analysis of Experiments*, springler-Verlag, New York.
[6] Ellekjaer, Marit Risberg, 1998, "The Use of Experimental Design in the Development in New Products", *International Journal of Quality Science*, Vol.3, No.3.
[7] Fryman, Mark A.,2002, *Quality and Process Improvement*, Delmar, New York
[8] Hosotani, Katsuya, 2003, *The QC Problem-Solving approach: Solving Workplace Problems the Japanese Way*, 3A Corporation, Tokyo.
[9] Antony, Jiju, Tzu-YaoChou, dan Sid Ghosh, 2003, "Training for Design of Experiment", *Work Study*, Vol.53, No.7.
[10] Montgomery, Douglas C., 2005, *Design and Analysis of Experiments*, John Wiley & Sons, New York.
[11] Rowlands, Hefin dan Jiju Antony, 2003, "Application of Design of Experiments to a Spot Welding Process", *Assembly Automation*, Vol.23, No.3.

ISSN 114-1284

Optimizing Injection Moulding Process for Plastics Recycled Material using Design of Experiment Approach

Iwan Halim Sahputra, Stefanie Alexandra

Industrial Engineering Department
Petra Christian University, Surabaya 60236
Tel : (031) 2983425. Fax : (031) 8417658
E-mail : iwanh@petra.ac.id

ABSTRACT

This paper reports a design of experiments approach to optimize the injection moulding processes using recycled plastic materials. Observation on a plastic manufacturing company was performed to find the factors that have significant effect on the injection moulding process and product. Barrel temperature, injection pressure, and clamping pressure were determined as the factors and their effect to the process was investigated. The experimental design method using 3k factorial design technique was formulated for the experiments. The experiments were performed on the injection moulding machine. From the ANOVA, main effect plot and interaction plot produced by Minitab software, a combination of barrel temperature, injection pressure, and clamping pressure was determined to be the optimum setting for the process. This result was implemented as the combination of the machine setting to produce 12 batches of products and the number of defect product was decreased.

Keywords
Injection molding, plastics recycled material, 3k factorial design method, design of experiment

1. INTRODUCTION

The world's annual consumption of polymer materials has increased from around 5 million tonnes in the 1950s to nearly 100 million tonnes today [1]. According to Seung-Soo and Seungdo, continuous accumulation of plastic wastes leads to serious problems all over the world [2]. The disposal of these materials also represents a significant loss of a potentially valuable, reusable material estimated by PlasticsEurope for 2005 at 11.6 million tones for Europe alone [3].

Although the recycling capacity for plastics has been progressively increased, but the fraction of plastics that end up in a landfill is still very significant [4]. As its consequence, there is great interest in finding the new possibilities to use post-consumer plastics to produce new product. For example, Sahputra investigated the mechanical properties of recycled PET/HDPE that can be used for an alternative material of new consumer product [5].

Polypropylene is one of the most popular polymers used for household product. In 2000, Polypropylene represented 23% of the polymer consumed in Western Europe [6]. In the world, its sales in tonnage is the third most important amongst polymers [7]. Therefore the production process using recycled Polypropylene is a challenge to be considered.

Injection moulding is one of the most common processing methods for polymer [8]. The major advantages of injection moulding process includes its versatility in moulding a wide range of products, the ease with which automation can be introduced, the possibility of high production rates and the manufacture of articles with close tolerance [9].

In the injection moulding process, polymers in the form of granules or powders are put into the barrel through a hopper. In the barrel, polymers are heated until they are completely melted. They are then pushed through a nozzle into a cold mould which is clamped closed. After the polymers are cooled and solidified, the product is ejected and the process cycle is repeated.

Operating parameter optimization is considered the main challenge for injection moulding process to produce household product from recycled Polypropylene. Design of Experiments (DOE) is an efficient problem solving quality improvement technique that can be used for various experimental investigations. For example Lu and Khim implemented this technique in the injection moulding of plastic optical lenses [10]. Statistical methods were employed in the experimental studies in order to systematically analyze the effect of various process parameters on the lens contour errors.

Operating injection moulding parameter optimization for recycled polypropylene is reported in this paper using DOE methods. The injection moulding process was selected for production of basket in the manufacturing company partner. The objective of the experiment is to determine the optimal injection moulding process parameter setting that minimizes the product defect.

2. EXPERIMENTAL PROCEDURE

2.1 Materials and machines

The raw material to be used for the experiments was polypropylene from post-consumer household products such as bin, pot, bucket, and basin. These waste products were put into the plastics grinding machine to be cut to size of eight to ten millimeter square. After cutting process, these materials were washed by plastics washing machine for fifteen minutes. After washing process, the materials were put into the drying oven for eight hours. The raw material after being processed can be seen in figure 1.

The experiments were performed on an Elite Machinery Systems Injection Moulding Machine provided by a plastic manufacturing partner. The machine was used to produce household basket as the sample product.

2.2 The DOE implementation

After a thorough investigation of the existing process, the factors that affect the defect of the produced basket were identified as follows:

- Barrel temperature (X1)
- Injection pressure (X2)
- Clamping pressure (X3)

A current injection moulding process was investigated to determine the level for each factor. The machine setting was:

- Barrel temperature between 275°C - 255°C - 150°C and 320°C - 255°C - 190°C
- Injection pressure between 150 kg/cm^2 and 250 kg/cm^2
- Clamping pressure between 125 kg/cm^2 and 175 kg/cm^2

The initial experiment was conducted to produce 22.869 baskets and the product defect obtained was 6.63%.

Three levels for each factor were selected as shown in the table 1. Characteristic of the selected response was lower the better because of the expected number of product defect was the lowest possible. The replication was performed twice therefore the number of run was 54. Every replication was performed on the two machines for four hours and the product defect data was obtained.

Table 1: Selected levels for the factors.

Factor	Level		
	1	0	-1
X1	320°C - 255°C - 190°C	295°C - 255°C - 170°C	275°C - 255°C - 150°C
X2	250 kg/cm^2	200 kg/cm^2	150 kg/cm^2
X3	175 kg/cm^2	150 kg/cm^2	125 kg/cm^2

3. RESULTS AND DISCUSSION

The number of product defect data obtained from the experiment is shown in the table 2. Analysis of variance (ANOVA) was used to investigate and model the relationship between the response variable (defect) and the independent variables (barrel temperature, injection pressure, and clamping pressure). The ANOVA was performed using Minitab software. The results are shown in the figure 2.

In the figure 2, it can be seen that all p-values are printed as 0.000. This means that all the actual p-values are less than 0.0005. Since all p-values are less than the chosen α-level of 0.05, it means the effects of three factors and their combinations on response are significant.

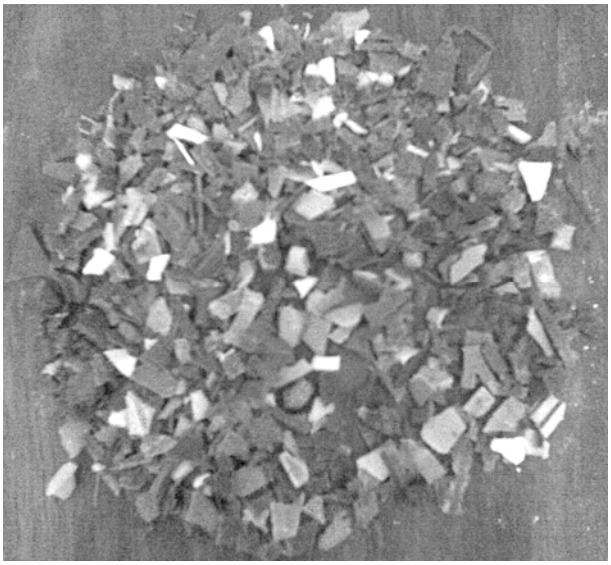

Figure 1. The recycled polypropylene

General Linear Model: Response versus X1, X2, X3

Factor	Type	Levels	Values
X1	fixed	3	-1 0 1
X2	fixed	3	-1 0 1
X3	fixed	3	-1 0 1

Analysis of Variance for Response, using Adjusted SS for Tests

Source	DF	Seq SS	Adj SS	Adj MS	F	P
X1	2	16631.01	16631.01	8315.50	5908.38	0.000
X2	2	1698.04	1698.04	849.02	603.25	0.000
X3	2	564.18	564.18	282.09	200.43	0.000
X1*X2	4	1142.35	1142.35	285.59	202.92	0.000
X1*X3	4	557.80	557.80	139.45	99.08	0.000
X2*X3	4	549.60	549.60	137.40	97.63	0.000
X1*X2*X3	8	439.84	439.84	54.98	39.06	0.000
Error	27	38.00	38.00	1.41		
Total	53	21620.81				

Figure 2. ANOVA results

Main Effects Plot was used to compare the changes in the level means to see which factors influence the response and to compare the relative strength of the effects. A main effect is present when different levels of a factor affect the response differently. Figure 3 shows the plot.

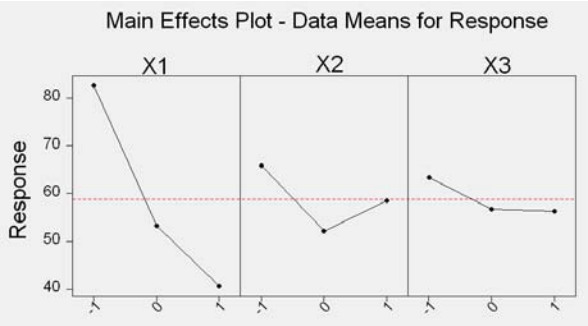

Figure 3. The Main Effect Plot

Table 2: The result of the experiments

RunOrder	X1	X2	X3	Response (unit)
1	1	1	1	50
2	0	-1	1	59
3	1	-1	1	43.5
4	1	0	0	33
5	0	0	0	60.5
6	-1	1	1	95
7	0	1	0	40
8	1	0	1	22
9	1	-1	0	48
10	-1	-1	0	76
11	1	0	-1	37
12	-1	0	-1	72
13	-1	1	-1	87
14	-1	-1	-1	93
15	-1	0	0	72.5
16	1	1	0	32.5
17	1	0	1	25
18	-1	0	0	71
19	-1	-1	-1	95
20	1	0	-1	37
21	1	0	0	34.5
22	0	1	1	37
23	0	0	1	36.5
24	-1	0	1	74
25	1	1	1	49
26	-1	1	0	85
27	0	1	1	38.5
28	-1	1	-1	87
29	0	0	1	39.5
30	1	-1	-1	53.5
31	0	-1	1	58.5
32	1	1	0	32
33	0	1	-1	55.5
34	0	-1	-1	70
35	0	0	-1	56
36	0	-1	0	62.5
37	-1	0	1	78
38	0	1	-1	55.5
39	0	-1	0	61.5
40	1	-1	0	49
41	-1	1	1	96
42	-1	1	0	85
43	1	-1	-1	54.5
44	0	-1	-1	71
45	1	-1	1	45
46	-1	0	-1	74
47	-1	-1	1	85
48	-1	-1	0	78
49	0	1	0	41
50	0	0	-1	56.5
51	1	1	-1	45
52	-1	-1	1	83
53	1	1	-1	42
54	0	0	0	60

From figure 3 we can see that all lines are not horizontal (parallel to the x-axis), therefore there are main effects present. The change in factor X1 (barrel temperature) shows the greatest magnitude of the difference on response as shown by its slope. This means that barrel temperature affect the product defect greater than injection pressure and clamping pressure.

Interaction plot was used to investigate the interaction between factors. An interaction occurs when the change in response from the one level of a factor to another level differs from the change in response at the same two levels of a second factor. That is, the effect of one factor is dependent upon a second factor. The plot is shown in the figure 3.

Figure 3 Interaction plot

From figure 3 it can be summarized as follows:

1. Row 1 panel shows level 1 (320°C - 255°C - 190°C) of factor X1 (barrel temperature) produced the least number of defect product
2. Row 2 panel shows level 0 (200 kg/cm^2) of factor X2 (injection pressure) produced the least number of defect product
3. Row 3 panel shows level 1 (175 kg/cm^2) of factor X3 (clamping pressure) produced the least number of defect product.

An experiment was conducted using the machine setting obtained from the DOE experiment result above. The machine setting was as follows:

- Barrel temperature : 320 ° C - 255 ° C - 190 ° C
- Injection pressure : 200 kg/cm^2
- Clamping pressure : 175 kg/cm^2

The experiment produced 12 batches of basket product. The total number product was 43.897 and the product defect was 1.2 %.

4. CONCLUSION

Experimental work using DOE method had been performed to find the optimum injection moulding process parameter setting. Three significant process parameters were investigated: barrel temperature, injection pressure and clamping pressure. An optimum setting for the three process parameters had been identified for producing basket products with minimum number of product defect.

REFERENCES

[1] F. Burat, A. Güney, M. Olgaç Kangal, Selective separation of virgin and post-consumer polymers (PET and PVC) by flotation method, Waste Management, vol. 29, pp. 1807–1813, 2009

[2] K. Seung-Soo, K. Seungdo, Pyrolysis characteristics of polystyrene and polypropylene in a stirred batch reactor. Chemical Engineering Journal, vol. 98, pp. 53– 60, 2004

[3] PlasticsEurope, Press Release 9 May 2007, Association of Plastics Manufacturers in Europe (AISBL), Brussels, Belgium, 2007

[4] European Environmental Agency, The European environment – State and outlook, European Environment Agency. Copenhagen K, Denmark, 2005

[5] I. H. Sahputra, Mechanical Properties of Recycled PET/HDPE Composite, The 9th International Conference on Quality in Research, Jakarta, Indonesia, 2006

[6] P. Brachet, L.T. Høydal, E.L. Hinrichsen, F. Melum, Modification of mechanical properties of recycled polypropylene from post-consumer containers, Waste Management, vol. 28, pp. 2456–2464, 2008

[7] S.M. Zebarjad, S.A. Sajjadi, M. Tahani, Modification of fracture toughness of isotactic polypropylene with a combination of EPR and CaCO3 particles. Journals of Materials Processing Technology, vol. 175 (1– 3), pp. 446–451, 2006

[8] A. Kumar, P.S. Ghoshdastidar, M.K. Muju, Computer Simulation of Transport Process During Injection Mold-Filling and Optimization of the Molding Conditions, Journal of Materials Processing Technology, vol 120, pp. 438-449, 2002

[9] R.J.Crawford, Plastics Engineering, 2nd edition, Pergamon Press, Oxford, 1989

[10] X.L. Lu and L.S. Khim, A Statistical Experimental Study of the Injection Moulding of Optical Lenses, Journal of Materials Processing Technology, vol. 113 (1-3), pp. 189-95, 2001

ISSN 114-1284

Relating Service Quality and Service Loyalty in Railway Transportation Provided by KA Parahyangan

Latifah Dieniyah MP[1], Ratih K Anggeraini [2]

[1]*Faculty of Science and Technology*
BINUS University, Jakarta 11480
Tel : (62-21) 5345830 Fax : (62-21) 5300244
E-mail : lputeri@binus.edu or latifahdmp@yahoo.com

[1]*Faculty of Engineering*
Pancasila University, Jakarta 12640
Tel : (62-21) 7864730 ext 30. Fax : (021) 7270128

ABSTRACT

As market mature and competition intensifies, firms are exploring ways to increase customer retention which has been shown to increase company profitability. One strategy to maintain customer retention is by improving determinant factors of service loyalty, that is service quality. This applied research in the marketing field is conducted to study determinant of customer loyalty using KA Parahyangan for Bandung-Jakarta trip. From 181 respondent, it is shown that service quality do have impacts on service loyalty with the pearson coefficient of 0.536 (p-value 0.000). Detailed refinement of correlation based on dimensionality perspective shown that every service quality dimension relate significantly to word-of-mouth communication dimension. Empathy dimension mainly determine the word-of-mouth communication, and this suggest the managerial of KA Parahyangan to improve the employee ability in treat customer as individual.

Keywords : *Service quality, service loyalty, railways services*

1. INTRODUCTION

Service quality has been the subject of considerable interest by both practitioners and researchers in recent years, spurred on by the original work of Parasuraman et. al. [10] An important reason for the interest in service quality by practitioners result from belief that this has a beneficial effect on bottom-line performance of the firm [3]. The concept of service quality and service loyalty are related to each other. Theoretically, the expectancy or disconfirmation paradigm can provide the grounding for this study, with service quality as an antecedent construct and service loyalty as an outcome variable. A better understanding of the effects of service quality and service loyalty can help academics in the development of a model of service marketing. It can also provide practitioners with indications as to where best devote marketing attention and scarce corporate resources [3]

This study seeks to contribute to the development of a conceptual framework that integrates service loyalty and service quality carried out among KA Parahyangan customer. As one of railway transportation, KA Parahyangan had ever been the first choice for Jakarta-Bandung roundtrip. After Cipularang freeway operated in 2005, significant number of railway customer are switch to other alternative because of the shorter travel time. In 2008, KA Parahyangan fare was reduce about 50% in order to maintain a large number of passenger. Based on that situation, it is needed to evaluate quality of transportation service provided by KA Parahyangan, and furthermore tested the hypothesis relationship of service quality and service loyalty.

2. LITERATURE REVIEW

2.1. Service Quality

Definition of service quality hold that this is the result of the comparison that customers make between their expectations about service and their perception of the way the service have been performed [10,11,12] According to Zeuthaml [14] service quality is often conceptualized as the comparison of service expectations with actual performance perceptions. On an operational level, research in service quality has been dominated by the SERVQUAL instrument, based on the so-called gap model. The central idea in this model is that service quality is a function of the difference scores or gaps between expectations and perceptions (P-E). It has been proposed that service quality is a multidimensional concept [10]. Five keys dimensions of service quality have been identified. *Reliability* is defined as the ability to deliver the promised service dependably and accurately. It is about keeping promises, furthermore, promises about delivery, pricing, complaint handling, etc. *Responsiveness* can be described as the willingness to help customers and provide prompt service. This dimension stresses service personel's attitude to be attentive to customer requests, questions and

complaints. *Assurance* is the dimension that focus on the ability to inspire trust and confidence. *Empathy* is the service aspect that stresses the treatment of customer as individuals. Finally, tangible is service dimension that focus on the elements that represent the service physically.

In spite of the widely use, SERVQUAL also been widely criticized. For instance, the validity and reliability of the difference between expectations and performance has been questioned and several authors have been suggested that perception scores alone offer a better indication of service quality [4]. An important advantage of SERVQUAL instrument is that it has been proven valid and reliable across a large range of service contexts. A considerably number of author have argued that service quality is an important determinant of service loyalty.

2.2 Service Loyalty

The conceptualization of service loyalty construct has evolved over the years. In the early days the focus of loyalty was brand loyalty with respect to tangible goods. Cunningham [6] defined brand loyalty simply as "the proportion of purchases of a household devoted to the brand it purchase more often". Loyalty was to broaden the spectrum of analysis by focusing on store as opposed to brand loyalty using the same measures he had use earlier for brands [7].

The behavioral and attitudinal aspects of loyalty are reflected in the conceptual definitions of brand loyalty offered by Jacoby and Chestnut [9] that brand loyalty was simply measured in term of outcome characteristics. Much of the work on loyalty in the 1970s and early 1980s has used this conceptualization. Dick and Basu [7] suggest an attitudinal theoretical framework that also envisages the loyalty construct as being composed of relative attitude and patronage behavior.

A further aspect of loyalty identified by other researchers in more recent years is cognitive loyalty. This is seen as a higher order dimension and involve the consumer's conscious decision-making process in the evaluation of alternative brands before a purchase is affected. Gremler and Brown [8] extend the concept of loyalty to intangible products, and their definition of service loyalty incorporates the three specific components of loyalty considered, namely : the purchase, attitude and cognition. Service loyalty is defined as the degree to which a customer exhibits repeat purchasing, behavior from a service provider, possesses a positive attitudinal disposition toward the provider, and considers using only this provider when a need for this service exists.

While loyalty is often included in service quality models as an outcome variable. Cronin & Taylor [4] measure service loyalty solely on repurchase intentions, while Boulding et al [2] operationalised repurchased intentions and willingness to recommend. As Zeithaml et al [14] argue, dimension of service loyalty, such as willingness to pay more and loyalty under increasing price. Singh [13] proposed customer evaluation following a negative service experience as a dimension of service loyalty also. Bloemer [2] studied the link between the individual dimensions of service quality and service loyalty.

3. RESEARCH METHODOLOGY

The questionnaire is used consisted of 37 items split between two instruments that 25 items measured service quality and 12 items measured service loyalty. Twenty five item measured service quality on the basis of perceived quality and consist of 6 items on Reliability, 4 items on Responsiveness, 5 items on Assurance, 5 items on Empathy and 5 items on Tangibles. Twelve items of service lotalty consists of 4 items for Word-of-Mouth-Communication, 2 items on Repurchase Intention, 3 items on Price sensitivity and 3 items on Complaining Behavior. Demographic variable were also collected. The research instrument consist of five-points scale. The questionnaire were pre-tested on a convenience sample of 30 passenger of KA Parahyangan. This pre-tested is aimed to verify the validity and reliability of questionnaire items. Tabel 1 and 2 shows the validity result and table 3 for reliability test

Table 1 : Validity Test for SQ Items

SQ Atribute	Item	Pearson Correlation	p-value	Description	
				Relationship	Validity
Reliability	V1	0.551	0.001	Moderate	VALID
	V2	0.664	0	Strong	VALID
	V3	0.607	0	Strong	VALID
	V4	0.444	0.007	Moderate	VALID
	V19	0.423	0.01	Moderate	VALID
	V25	0.58	0	Moderate	VALID
Responsiveness	V5	0.763	0	Strong	VALID
	V6	0.682	0	Strong	VALID
	V7	0.698	0	Strong	VALID
	V8	0.84	0	Very Strong	VALID
Assurance	V9	0.752	0	Strong	VALID
	V10	0.82	0	Very Strong	VALID
	V11	0.797	0	Strong	VALID
	V12	0.862	0	Very Strong	VALID
	V13	0.76	0	Strong	VALID
Empiaty	V14	0.745	0	Strong	VALID
	V15	0.413	0.012	Moderate	VALID
	V16	0.82	0	Very Strong	VALID
	V17	0.738	0	Strong	VALID
	V18	0.509	0.0002	Moderate	VALID
Tangible	V20	0.75	0	Strong	VALID
	V21	0.802	0	Very Strong	VALID
	V22	0.791	0	Strong	VALID
	V23	0.885	0	Very Strong	VALID
	V24	0.827	0	Very Strong	VALID

Based on the pilot sample, required number of sample is calculated. The highest standard deviation of 37 items was 0.817323, using 10% error and 90% confidence interval, expected number of sample is 180.76 ≈ 181.

Research data had been collected again aboard of KA Parahyangan until the number of sample requirement accomplished.

Table 2 : Validity Test for SL Items

SQ Atribute	Item	Pearson Correlation	p-value	Description	
				Relationship	Validity
WOM	A1	1	0	Very Strong	VALID
	A2	0.81	0	Very Strong	VALID
	A3	0.588	0	Moderate	VALID
	A4	0.417	0.011	Moderate	VALID
Repurchase Intention	A6	0.823	0	Very Strong	VALID
	A12	0.64	0	Strong	VALID
Price Sensitivity	A5	0.675	0	Strong	VALID
	A7	0.804	0	Very Strong	VALID
	A8	0.734	0	Strong	VALID
Complaining Behavior	A9	0.665	0	Strong	VALID
	A10	0.615	0	Strong	VALID
	A11	0.714	0	Strong	VALID

Table 3 : Reliability Test forSQ & SL Atrributes

Atribute	Cronbach's Alpha
Reliability	0.710
Responsiveness	0.798
Assurance	0.806
Empathy	0.757
Tangibles	0.808
WOM	0.895
Repurchase Intention	0.780
Price Sensitivity	0.785
Complaining Behavior	0.746

4. RESULT

Respondent were almost equally split between males (46.67 %) and female, 62.22% of respondent were in the range of 20 until 40 years old, and 64.99 % had completed tertiary level of education. Only 25.55% of respondent were student and the rest is working people. The most interesting demographic finding is only 8% of respondent were first time customer using KA Parahyangan, 62.22 % admitted for over than 5 times using KA Parayhangan. The reason why they choose to take KA Parahyangan was 51.66 % because of the lowest fare.

The relationship between service quality and service loyalty then investigated using person correlation. Moderate correlation between two research constructs indicated by pearson correlation of 0.536 (see Figure 1). The positive correlation shows that high perceived service quality will lead to loyalty to service provider [1].

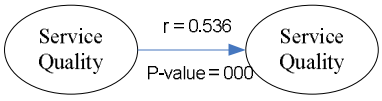

Figure 1 : Research finding of relationship between service quality and loyalty

Further testing of relationship between service quality and service loyalty construct in dimensional perspective is conducted. The valid relationship from all the five service quality dimensions only correlate to word-of-mouth communication dimension of service loyalty. No valid correlation coefficient that relate service quality dimension to the other service loyalty dimension (see Figure 2). Word-of-mouth communication is determined mainly by Empathy, service dimension aspect that stresses the treatment of customer as individuals. While high quality service had no effect on customer loyalty in using KA Parahyangan. Increasing fare, competitor lower price or negative experience may influence the customer to use the other alternative of Bandung-Jakarta transportation.

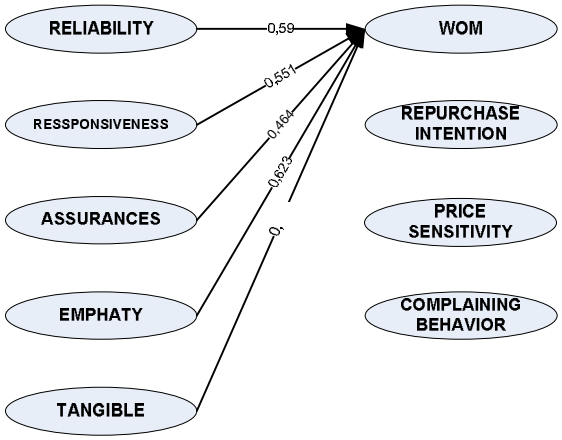

Figure 2 : Research finding of dimensional relationship between service quality and loyalty

The information on the service quality-service loyalty link on KA Parahyangan customer may provide actionable basis for improving performance through service quality. The managerial challenge of KA Parahyangan here is to train employees to give individualized attention to each customer and not treat them by the dozen [1]. Indices on service loyalty measured continuously over time may supplement measures of performance and signal changes in the value of customer assets.

Further research should be conducted to investigate determinant of the other service loyalty such as repurchase intention, price sensitivity and complaining behavior of KA Parahyangan customer.

REFERENCES

[1] Bloemer, Josee, "Linking perceived service quality and service loyalty : a multi-dimensional perspective", European Journal of Marketing, Vol 33 No 11/12, 1999, pp.1082-1106

[2] Boulding, W, Kalra A., Staelin R and Zeithaml V., " A dynamic process model of service quality : from expectations to behavioural intentions", Journal of Marketing Research, Vol. 30, February, 1993. pp. 7-27

[3] Caruana, Albert, "Service loyalty : the effects of service quality and the mediating role of customer satisfaction", European Journal of Marketing, Vol. 36, No. 7/8 2002, pp. 811-828

[4] Cronin, JJ and Taylor SA, "*Measuring service quality: a re-examination and extension*", Journal of Marketing, Vol 56, July, 1992, pp.55-68

[5] Cunningham RM, "Brand loyalty- what, where and how much", Harvard Business Review, Vol 39, November-December, 1956, pp.116-38

[6] Cunningham RM, "Customer loyalty to store and brand", Harvard Business Review, Vol 39, November-December, 1961, pp.127-37

[7] Dick, A.S. and Basu, K. "*Customer loyalty : toeard an integrated conceptual framework*", Journal of the Academy of Marketing Science, Vol.22 No. 2, 1994, pp. 99-113

[8] Greemler, DD. And Brown SW, " Service loyalty : its nature, importance and implications" in Edvardssoon, B, Brown SW., Johnston R and Scheuing EE, Proceedings American Marketing Association, 1996, pp. 171-80.

[9] Jacoby, J. and Chestnut, RW. "*Brand loyalty : Measurement and Management*", John Wiley New York, (1978)

[10}Parasuraman, A., Zeithaml, V.A. and Berry,L.L., " *A conceptual model of service quality and its implication for future research*", Journal of Marketing , Vol 49, April 1985, pp. 41-50

[11]Parasuraman, A., Zeithaml, V.A. and Berry,L.L., "*SERVQUAL : A multiple-item scale for measuring consumer perceptions of service quality*", Journal of Retailing , Vol 64, No. 1 Spring, 1988, pp. 12-40.

[12]Parasuraman, A., Zeithaml, V.A. and Berry,L.L., "*Alternative scales for measuring service quality : a comparative assessment based on psychometric and diagnostic criteria*", Journal of Retailing , Vol 70, No. 3 1994, pp. 201-30.

[13] Singh, J., "*Understanding the structure of onsumers' satisfaction evaluation of service deliveryr*", Journal of Academy of Marketing Science, Vol. 20.,1991, pp. 223-44

[14] Zeithaml, V.A., Berry,L.L. and Parasuraman A., "The behavioral consequences of service quality" Journal of Marketing, Vol.60 ,1996, pp.31-46.

5 PILLARS' SUSTAINABILITY TOWARDS CAPABLE QUALITY MANAGEMENT

Linda Herawati Gunawan[1], Lisa Mardiono[2]

Email: [1] linda@ubaya.ac.id,[2]lmardiono@ubaya.ac.id
Industrial Engineering Department
Engineering Faculty , University of Surabaya

ABSTRACT

Paradigm in Good Quality Management now becomes the soul in every enterprise which could be survived. In quality steps diagram, it's shown that towards good Total Quality Management should be start by 5S or 5 pillars culture as its basic. Many researches were done in applied 5S in an enterprises, nevertheless its sustainability always become the big questions. This research was done to get the data about involvement of each division in 5S application and its conjunction to Quality Management in large scope. Lack of involvement, understanding and awareness in Quality Management could affect on application of 5S itself. This research also using 5S checklist the capture how far the implementation of 5S in each enterprises, map its result to 5S radar and give recommendation needed. Main point in implementing 5S is how to keep it sustain. Each party should be realized their own role and responsibility.

Keywords: 5S sustainability, Quality Management, 5S radar

1. INTRODUCTION

Quality Management concept now becomes the main priority for each enterprise which needs to survive. One of the basic paradigms in creating good quality management is 5S. Applying 5S is not easy, because the succeed indicator is while 5 not only become a method, but it become company culture. Involvement of each part in the enterprise and good awareness of every personnel will be the key success of 5S implementation.
Practically, 5S is "behavior transformation" by doing neat arrangement and cleanliness of the workplace. Working place would reflect their employee treatment to the job, and this treatment would reflect their attitude and esteem to the job itself [1].
The purpose of this research is to find out what's the main cause of unsustainable 5S implementation and how to design the instrument to keep it sustain. Because sometime human factor who need/like to be controlled that make 5S hard to be a culture. Due to implementation of 5S, commonly nobody like to work in messy area, but he main problem is why 5S can not be sustain [1]. One of the case study is in garment industry which have applying 5S in the enterprise but can not be sustain because there's no control from the management. Messy workplace area, poor material coding, improper material stacking in the warehouse are some problems occur there. Furthermore 5S was applied in order to generate and maintain worker's spirit so that they can work more effective and efficient.

2. LITERATURE REVIEW

a. 5S method

5S is the name of a workplace organization methodology that uses a list of five Japanese words which, translated into English, start with the letter S. This list is a mnemonic for a methodology that is often incorrectly characterized as "standardized cleanup", however it is much more than cleanup. 5S is a philosophy and a way of organizing and managing the workspace and work flow with the intent to improve efficiency by eliminating waste, improving flow and reducing process unevenness.

5S is a method for organizing a workplace, especially a **shared** workplace (like a shop floor or an office space), and keeping it organized. It's sometimes referred to as a housekeeping methodology; however this characterization can be misleading, as workplace organization goes beyond housekeeping.

The key targets of 5S are workplace morale, safety and efficiency. The assertion of 5S is, by assigning everything a location, time is not wasted by looking for things. Additionally, it is quickly obvious when something is missing from its designated location. Advocates of 5S believe the benefits of this methodology come from deciding *what* should be kept, *where* it should be kept, and *how* it should be stored. This decision making process usually comes from a dialog about standardization which builds a clear understanding, between employees, of how

work should be done. It also instills ownership of the process in each employee.

In addition to the above, another key distinction between 5S and "standardized cleanup" is Seiton. Seiton is often misunderstood, perhaps due to efforts to translate into an English word beginning with "S" (such as "sort" or "straighten"). The key concept here is to order items or activities in a manner to promote work flow. For example, tools should be kept at the point of use, workers should not have to repetitively bend to access materials, flow paths can be altered to improve efficiency, etc.

The 5S's are :[2]

Phase 1 - **Seiri** (整理) Sorting: Going through all the tools, materials, etc., in the plant and work area and keeping only essential items. Everything else is stored or discarded.

Phase 2 - **Seiton** (整頓) Straighten or Set in Order: Focuses on efficiency. When we translate this to "Straighten or Set in Order", it sounds like more sorting or sweeping, but the intent is to arrange the tools, equipment and parts in a manner that promotes work flow. For example, tools and equipment should be kept where they will be used (i.e. straighten the flow path), and the process should be set in an order that maximizes efficiency. For every thing there should be place and every thing should be in its place. (Demarcation and labeling of place.)

Phase 3 - **Seisō** (清掃) Sweeping or Shining or Cleanliness: Systematic Cleaning or the need to keep the workplace clean as well as neat. At the end of each shift, the work area is cleaned up and everything is restored to its place. This makes it easy to know what goes where and have confidence that everything is where it should be. The key point is that maintaining cleanliness should be part of the daily work - not an occasional activity initiated when things get too messy.

Phase 4 - **Seiketsu** (清潔) Standardizing: Standardized work practices or operating in a consistent and standardized fashion. Everyone knows exactly what his or her responsibilities are to keep above 3S's.

Phase 5 - **Shitsuke** (躾) Sustaining the discipline: Refers to maintaining and reviewing standards. Once the previous 4S's have been established, they become the new way to operate. Maintain the focus on this new way of operating, and do not allow a gradual decline back to the old ways of operating. However, when an issue arises such as a suggested improvement, a new way of working, a new tool or a new output requirement, then a review of the first 4S's is appropriate.

A sixth phase, "Safety," is sometimes added. Purists, however, argue that adding it is unnecessary since following 5S correctly will result in a safe work environment. Often, however a poorly conceived and designed 5S process can result in increases in workplace hazard when employees attempt to maintain cleanliness at the expense of ensuring that safety standards are adequately followed.

There will have to be continuous education about maintaining standards. When there are changes that will affect the 5S program—such as new equipment, new products or new work rules—it is essential to make changes in the standards and provide training. Companies embracing 5S often use posters and signs as a way of educating employees and maintaining standards.

b. Eight Quality Management Principles:

Eight quality management principles come directly from TQM, there below are the definition [3]:

1. Customer focus - understanding customers' needs, striving to exceed their expectations. In term of ISO 9000:2000 [4], top management shall ensure that customer requirement are determined and are met with the aim of enhancing customer satisfaction. That definition note that customer complaints are common indicator to perceive.
2. Leadership - establishing direction, unity of purpose, and a supportive work environment. Top management should provide evidence of its commitment to the development and implementation of the quality management system and continually its effectiveness. Good leader will always concentrate in the employee, and act in democratic/autocratic depend on the situation.
3. Involvement of people - ensuring that all employees at all levels are able to fully use their abilities for the organization's benefit. Personnel performing work affecting product quality shall be competent on the basis appropriate education, training, skills and experience. As a core of the organization, employee should participate directly to support organization' advantage.
4. Process approach - recognizing that all work is done through processes, and managing them accordingly. This process contains with resources, asset, and all the supportive activities during the operational process.
5. System approach to management; expands on the previous principle in that achieving any objective requires a system of interrelated processes. In ISO terminology it called management review and management representative, that management have ensure the processes needed for the quality management system should be establish, implement and maintain.

6. Continual improvement; as a permanent organizational objective, recognizing and acting on the fact that no process is so good that further improvement is impossible. In Deming cycle, known by PDCA cycle (Plan, Do, Check, Action) [5]. One process that already taken being input to others process, and if does not meet the target then become feedback for further improvement.
7. Factual approach to decision making; acknowledging that sound decisions must be based on analysis of factual data and information, not on opinion or intuition. Management information system developed faster today, as it stand with information technology growing rapidly.
8. Mutually beneficial supplier relationships; to take advantage of the synergy that can be found in such relationships. Knowledge management that align with supply chain management give mutually benefit among the organization chain.

3. RESEARCH METHODOLOGY

Initial survey was done in some enterprises which have applied 5S. While implement the 5th S, usually it become stag. Because 5S not become a culture yet, looks like responsibility only for each worker. Literature review than was done to find out the effect of unsustainable 5S and how to improve it and the connection of 5S culture to Quality management. 5S audit by using checklist for each step than being design. This checklist being checked periodically to measure the improvement occurs. The pattern of these 5S audit (for each S) can be mapped in 5S radar. Each "S" axis from the 1st "S" to the 5th "S" than connected one another. The closer point to the tip of pentagon the better 5S implemented.

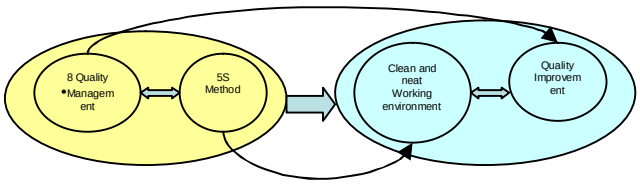

Figure 1: Integration of 5S method and 8 quality management principles to improve quality

4. RESULTS AND DISCUSSION

First of all, matrix of Quality Management and 5S is made to find the connection between 5S and eight quality management principles. The matrix as shown bellow:

Table 1: Matrix of 8Quality Management principles and 5S

No	8 Quality Mangement Principles	SEIRI	SEITON	SEISO
1	Customer Focus Organization	*Collect the customer's database *Collect the sales/purchase return items in different place *Collect the customer's complaints data	*Classified each purchase/sales return (based on type) *Keep good relation with customers	*Clean up the packaging/finished good area, so that customer will received the item in good and clear condition.
2	Leadership	*Separate all stuff that not really need for work (individual stuff) without any pressures *Inform the enterprise vision and mission and each worker should have the same vision toward goals achievement	*Good arrangement for all products and material *Creating good coding and filing in all area *evaluate the worker performance monthly *Periodically meeting to increase good communication	*Clean up all stationery and office inventory from dirt *cleanup schedule for every workplace area
3	Involvement of people	*Save the worker's database *unimportant stuff should be throw away	*clean up each workplace *put on the initial place (for the stuff being picked) *Classified stationery in one place	*Periodically clean up the working area
4	Process approach	*Give labels on all inventory * Collect the sales/purchase return items in different place	*Job description available for each worker *Try to make working process more efective	*Periodically clean up the working area
5	System approach to management	-	*Make sure that every inventory stack neatly, to make it easy to take *every workers do their job based on the job description	Have responsibility on their on working area (cleanliness)
6	Continual improvement	* Give training to all workers (routine)	*put on the initial place (for the stuff being	*Periodically clean up the working area

			picked)	
7	Factual approach to decision making	*Separate files based on function	*Classified files based on function	* clean up the working area from dirt, trash, dust and paper scrap
8	Mutually beneficial supplier relationships	*Save the supplier's database *do the filing if the supplier deliver reject items *Coding o all raw material	*Classified purchase invoice based on delivery time	* clean up the working area from dirt, trash, dust and paper scrap

Table 1: Matrix of 8Quality Management principles and 5S (continued)

No	8 Quality Management Principles	SEIKETSU	SHITSUKE
1	Customer Focus Organization	-	*Good response for each customer complaint *Communicate/inform all customer's complaints to the workers
2	Leadership	*Obey the rules and each punishment *Doing the first 3S without pressure *Supervising worker's performance	*Continuous audit every month by the supervisor *create discipline (reward and punishment) to create 5S habits and culture *Give responsibility and trust the worker
3	Involvement of people	*Spent 5 minutes daily(before and after work) to do the 3S before *Discuss every problem occur *Worker can give their opinion/suggestions	*Bottom up (always listen the worker's opinion) for enterprise development *Supervise the worker * Give responsibility and trust the worker
4	Process approach	*Periodically clean up the working area	*Evaluate worker's performance monthly (target achievement)
5	System approach to management	-	*Evaluate worker's performance monthly (target achievement) *Good communication between management and workers
6	Continual improvement	*Always check on the checklist	*Create habits to spent time 5 minutes daily to clean up working area *Give the rewards to the workers that achieve target. *Do continuous improvement to the product and process *Improvement on 5S
7	Factual approach to decision making	Hear the workers opinion based on facts	Find the accurate solutions
8	Mutually beneficial supplier relationships	-	*always check the quality of finished goods *Give inputs to supplier to improve their performance too

After mapping the 8 quality management principles to 5S, than form audit 5S is created as follow:
The point is 1 to 4 (1= Very poor/not appropriate; to 4= Very good/very appropriate)

Table2: Audit 5S' form (SEIRI)

			Point
			1 2 3 4
1	Drawer	There's no individual stuff	*Filled by the workers
2	Table	There's no paper document on the table	*Filled by the workers
3	Visual control	Needed stationery or files easily to get/reach	*Filled by the workers
4	Recycle standard	Recycle standard is applied (time, place)	*Filled by the workers
5	Filing cabinet	Every file is for routine activity (there is no other division file)	*Filled by the workers

Table 3: Audit 5S' form (SEITON)

			Point
			1 2 3 4
1	Labels for storage	Labels are clear, make easy it identify the stuff	*Filled by the workers
2	Label for stationery	Everything is easy to identify	*Filled by the workers
3	Ease of use	The storage is designed to make it easy to use	*Filled by the workers
4	Good arrangement on storage	Everything is put on its place	*Filled by the workers
5	Aisle	Every aisle looks clearly	*Filled by the workers

Table 4: Audit 5S' form (SEISO)

			Poin
			1 2 3 4
1	Floor	Clean and clear floor	*Filled by the workers

2	Dust and trash	Window, ceiling, table, filing cabinet and all drawers are clean	*Filled by the workers
3	Cleanliness responsibility	There are rotation and schedule to clean the workplace area	*Filled by the workers
4	Dust bin	Separated between dry and wet trash	*Filled by the workers
5	Clean habit	Swipe and mob as a routine	*Filled by the workers

Table 5: Audit 5S' form (SHITSUKE)

			Poin
			1 2 3 4
1	Ventilation	Clean air, not stinky, free of smoke cigarette etc)	*Filled by the workers
2	Lighting	The angle and luminance of the lamp or every lighting is suitable for the working area	*Filled by the workers
3	Environment	The environment is good (color, air, lamps, etc)	*Filled by the workers
4	Noise	There's no loud noise (the workers can concentrate)	
5	First 3S	System to maintain 3S is exist	*Filled by the workers

Table 6: Audit 5S' form (SHITSUKE)

			Point
			1 2 3 4
1	Inter personnel relationship	The environment is comfort, people greeting each other	*Filled by the workers
2	Entrance time, break time, end of time, meeting time	Everyone is on time	*Filled by the workers
3	Telephone ethics	Everyone can answer clearly, keep polite.	*Filled by the workers
4	Rules and obligation	Every rules are obey without any pressure	*Filled by the workers
5	Rewards and punishment	Transparent rewards and punishments applied	*Filled by the workers

For each form, the maximum point is 20 (the tip of pentagon). The closest to 20 point for each S, shows the better implementation of 5S in the enterprise. The radar curve showed in figure 1.

While the mappings of each S on the radar have not reach 20point, it shows that the implementation should be improved. It can be done by doing supervise tighter, or make the shorter periodic checking (eg. The previous checking in every 2 weeks become every week).
While it's reaching 20 point, it shows that implementation was done well. The next step is how to make it sustain.

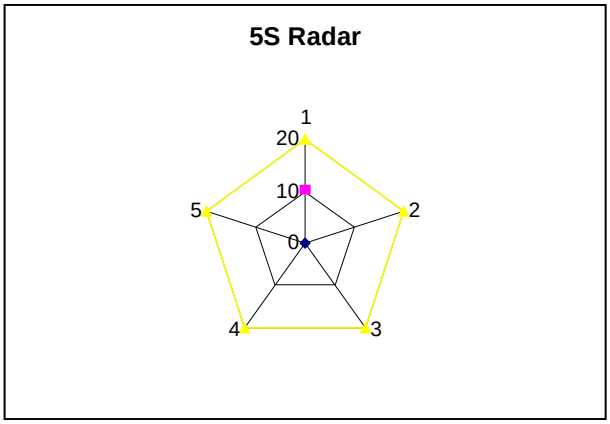

Figure 1 : 5S radar(1: Seiri point *;* 2: Seiton point *;* 3: Seiso point *;* 4 : Seiketsu point*;* 5 : Shitsuke point)

Due to the implementation in some enterprises, it's found that sometimes declared as very well sustained and sometimes declared as very badly sustained. This confirms that the sustainability of a process does not depend solely on the process itself, but is also very much related to the specific action which are carried out with an aim of making it sustainable. After identification, from the evaluation in which 5S application did not sustain as the expected before, it was found some factors which affect, illustrated on table 7.

Table 7. Identification factors from 5S application in tern of 8 Quality Management Principles

No	8 Quality Management Principles	Factors
1	Customer Focus Organization	• Employee feels unrelated directly to the customer
2	Leadership	• Lack of management's consistency and commitment • Involvement of top management • Implementation of 5S as a trial and error project (unserious preparing the goals)
3	Involvement of people	• Look down 5S role in productivity • Does not declare in job description • Less understanding the objective of 5S
4	Process approach	• Feel that implementing 5S increasing their workload • Lack of awareness in maintaining 5S
5	System approach to management	• Minimize of reward and punishment system • Lack of facility to support the implementation (shelf, cupboard, etc)
6	Continual improvement	• Lack of evaluation and controlling from the supervisor • Does not make 5S become routine activity
7	Factual approach to decision making	• Decrease on monitoring process (did not provide data

		on 5S appraisal) • Focus on qualitative measurement but not provide quantitative data • Subjective assessment (without any standards)
8	Mutually beneficial supplier relationships	• Does not align as quality culture

Based on the results above, to sustain an improvement process over time consists in grouping these factors into 3 categories which are:

1. Top Management awareness
2. Employee involvement
3. Facility

Category 1: Top Management Awareness

These indicate the intensity and willingness of the management in order to pursue 5S sustainability. In active participation from top management will affect the enterprise atmosphere. Top management should evaluate, whether the design and preparation of 5S implementation was poor from the first time. To reach top management awareness thus consist specific actions which must be asked:

1. How can the objective related to the improvement process be integrated into personal objectives of all employees?
2. How can the benefits obtained by the project and the future benefits be communicated
3. How can the entire hierarchy be involved in the continuity of the improvement process decided upon?
4. Which of the company value is the sustainability based on?

Category 2: Employee involvement

To reach good employee involvement thus consist in asking everyone a certain number of questions:

1. How can the procedure be simplified so that it can be applied naturally without any pressure?
2. How can the procedure be standardized so that it can be integrated into the company culture?
3. Which training courses must be organized in order to improve the personnel?
4. How can standard method and process be integrated into the development of new products?

Category 3: Facility

To define the specific actions to carry out on the facility, the following questions must be asked:

1. Which training course must be set up to train the operators to carry out the action?
2. Which type of assistance can be proposed to the operators to facilitate their execution of the action?
3. Which facilities needed to support the implementation?
4. How can the procedures in progress be simplified while yet sustaining the level of performance reached?

After try to answer these questions, hereby in table 8 the several generic actions which can be done to maintain the sustainability. It can be the design in a checklist, so that can be found which generic activities which have not applied.

Table 8. Generic actions in Maintaining 5S

No	Generic actions of sustainability	Yes	No
1	To make the objective of the sustainability, clear for all the personnel and try to help everyone work in this direction		
2	To clearly identify the project manager and to give him/her the means to be successful		
3	To set up the management of the project with objectives, indicators and piloting meetings at regular and frequent intervals		
4	To reveal the interest of the sustainability to show its correlation with a strategic objective		
5	To communicate these new values and to share them to all workers		
	To create a progress culture in which several improvement projects are implemented at the same time without competing with each other		
6	To control the negative actions of the people who would wish to slowdown the progress		
7	Not to change direction too early and too often. A new Manager must sustain continuity		
8	To plan regular reviews to validate that the marked values identified remain relevant		
9	To communicate on the project (internal newspaper, poster, etc)		
10	Involvement from the top management in the sustainability process		
11	Involvement of all hierarchy to designate the responsibilities		
12	Everyone must know which part of the sustainability his job belongs to		
13	Make sure that “experts” will be available throughout the sustainability phase in order to correct variation, to deepen and enrich the approach and always give further training		
14	To develop or invest in technical devices to simplify the tasks carried out by the personnel		
15	To set up the necessary training		
16	To develop the stuff and/or resources to support the implementation		
17	To standardize, to define coherent and specific missions		
18	To adapt the method to the company, to improve efficiency if required		
19	To Train the new recruits		
20	To systematically reposition the project within the total strategy of the company. How will this project enable to progress in company objective		

As long as these 20 variables done by the enterprises, sustainability can be reached constantly.

REFERENCES

[1] Maurice Pillet, Jean-Luc Maire, *How to sustain improvement at high level: Application in the field of statistical process control*, The TQM Journal, Vol. 20, Iss. 6, pp 570-587, 2008.

[2] Imai, Masaaki (1997). Gemba kaizen: a commonsense low-cost approach to management. New York: McGraw-Hill Professional. p. 64. ISBN 9780070314467.

[3] Goetch, D.L. & Davis, S.B., Introduction to Total Quality Management for Production, Processing, and Services, 5th.ed, Pearson Education International, 2007

[4] www.iso.org

[5] Hoyle, D, ISO 9000 Quality Systems Handbook, 4th.ed, Butterworth-Heinemann, 2001

ISSN 114-1284

Application of Ergonomics In PECS (Picture Exchange Communication System) Design For Autistic Children

Linda Herawati Gunawan[1], Goutama[2], Susanto[3]

Email: [1] linda@ubaya.ac.id,[2]goutama@ubaya.ac.id
Engineering Management Laboratory- Department of Industrial Engineering
Engineering Faculty , University of Surabaya

ABSTRACT

Nowadays, autism generally found among us. Autism spectrum disorders (ASD) might occur from childhood to adult. One serious problem which almost exist in all autism patients is communication problem. To overcome this problem, this research is being done to design communication tool using PECS' method. While doing the observation, it's found that the existing picture media is easily broken and sometimes the card is harmful for autistic children. It caused by the material (because they usually put it into their mouth) has no round tip for each card corner.

The purpose of this research is to design communication tool that's ergonomic for autistic children. The design process is using the theory of product design and development, which consist of some steps.

In identifying customer needs, it's found that they need communication tools which have these criteria: safe, the pictures should be clear enough and uneasily to be tore or broken, the pictures can represent the real object. While doing the prototype, the picture should be stuck on the both side of card, so that they can easily learn or understand the picture. These cards are categorized into some groups, such as: alphabeth, number, sports, musical equipment, flowers, animals, and much more.

From the implementation result to 10 therapists of autistic children, 100% therapist states that this tool can facilitate them in providing, use, and keeps picture in good condition. According to the therapists, this tool is safe and comfortable enough while used by the autistic children and they can learn more effective.

Keywords: PECS method, Autism Spectrum Disorders, Ergonomics tool, Product Design

1. INTRODUCTION

Autism Syndrome Disorders (ASD) might occur from childhood to adult. Nowadays, numbers of autistic children increase quiet significant. Government seems like don't really care about it and it cause high cost in their treatment. Less of people knowledge about autism is also contributing in this costly treatment. One serious problem which almost exist in all autism children is communication problem. PECS is found as an effective method to train autistic children to communicate using pictures as the media. Unfortunately, PECS method is not too familiar in Indonesia because less information about it. Recently, parents are also using picture card to communicate with their children, but from the survey, it's found that parents usually hard to find/prepare the pictures. Here are the problems occur: color of the picture is blur, picture's size (too small or even too large), unsafe card design, inappropriate picture with the meaning, broken easily(tear, wet, mess) and the most important is they don't know about PECS method.

2. LITERATURE REVIEW

Autism is development disorders which symptoms are deficiency in cognitive, language, behavior, communication and social interaction.[1]

a. Verbal and Non verbal communication disorders: deficiency in speaking and even can not talk; using word without knowing its meaning; using body language and only communicate in short time period; copycat what people say without knowing the meaning; monotonous intonation like robot; talking but not communicate; plain/no expression.
b. Social interaction disorders: no eye contact; look around while people call, many people think they're deaf; don't like being hugged; if they want something, they will pull other people arms (the nearest people) and ask them to do that for him/her; usually introvert; go away while people get close to them; no interaction with others.
c. Playing disorders: very monotonous playing, like turning balls or cars and watching the object steadily for a long time; have pacifier that can not be released from them; while they like a toy, they don't want another toys; don't like dolls, they like "uncommon" stuff like bottle, battery, rubber band, etc; have no reflect and don't have imagination while playing; can not pretend and copycat

what their friends do; usually watching their own fingers, moving object (fan), etc

d. Behavior disorders: hyperactive, moving around, run away with no destination; hurt themselves (hit their head to the wall, hit their head with their arms); petrifaction (no eye contact); anger easily without any reasons; very aggressive to other people (like to hit); hard to sleep, gastro intestinal disorders and metabolism.
e. Emotional disorders: laughing, crying and angry without any reasons; temper tantrum, especially while they didn't get something; lower empathy, while look at other children crying, they just hit the child.
f. Sensory perception disorders: very sensitive to an extra lighting, sound, touch, etc; bite, leak or smelling every stuff around them, shut their ears while hearing very loud noise; always crying while doing the hair wash, feel uncomfortable while wearing unusual fabric for their clothes.

PECS is one of non verbal communication method for the autistic children. It using pictures which can be made by drawing or take picture of the objects that will be communicate to them, such as brush, drink, eat, etc. PECS consist of 6 phases: physical exchange, spontaneity, picture classification, arrange a sentence, answer the questions and give spontaneous response.

ERGONOMICS

The aim of Ergonomics in this research is to increase comfortableness of autistic child in using communication tools and ease the parents to prepare the tools, so that the training can be more effective. [2]

To reach the purpose, theory about alphabet color and size need to be known as well. The colors of alphabet affect its ability to be read. Here are the combinations of alphabet and background color:

Table 1: Alphabet and background color combination

Level of easily reading	Color combination
Very good	Black alphabet with white background Black alphabet with yellow background
Good	Yellow alphabet with black background Dark blue alphabet with white background White alphabet with black background Green alphabet with white background
Enough	Red alphabet with white background Red alphabet with yellow background
Bad	Green alphabet with red background Red alphabet with green background Orange alphabet with black background Orange alphabet with white background
Very Bad	Black alphabet with blue background Yellow alphabet with white background

ANTHROPOMETRY

Antropometry comes from words "anthro" and "metrein" which mean human body dimension [2]. For anthropometry data, usually normal distribution is applied. In statistic, normal distribution is formulated from the mean and standard deviation of the existing data. Percentiles than can be calculated using probability table of normal distribution as follow:

Table 2: Normal distribution and percentile calculation

Percentile	Calculation
1st	Mean - 2.325.stdev
2.5th	Mean – 1.96.stdev
5th	Mean – 1.645.stdev
10th	Mean – 1.28.stdev
50th	Mean
90th	Mean + 1.28.stdev
95th	Mean + 1.645.stdev
97.5th	Mean + 1.96.stdev
99th	Mean + 2.325.stdev

PRODUCT DESIGN AND DEVELOPMENT

In designing the product, the steps as follows[3]: Identifying customer need, product specification, concept generation, concept selection, concept testing, prototyping.

3. RESEARCH METHODOLOGY

This research is start with identification on increasing numbers of autistic children and find out the using of PECS method. Questionnaire is given to 25 autistic children's parents, 25 usual parents. Respectively, it's given to 10 therapists in Terapi Bangun Bangsa (therapy centre for autistic children) and 10 teachers for autistic students in SDN Klampis Ngasem I/246 (Inclusive Primary School). Literature review than be done in this product design. For data collection, here are the data being collected: data about usual development and educational media for children, people knowledge about autism, ability and constraint of autistic children, weakness of existing PECS, needs for new PECS method, type of picture which suitable with autistic child, and anthropometry data. Using the product deign phases, ergonomics PECS communication tools were designed until creating the prototype and implementing the prototype, than analyze the results.

4. RESULTS AND DISCUSSION

From the questionnaire, we can get the customer need (therapists and parents) to design the new PECS. Here are the steps:

1. Existing PECS: Some weaknesses of the existing cards are uneasy to find appropriate picture to the need, size of the picture (too small) so that it has to be zoomed out while copy or sometimes too large so it has to be zoomed in, uneasy to understand, not suitable with characteristic of Indonesian people because there's no PECS in Indonesian, picture were taken from magazine or newspaper which too colorful so they can not focusing on the object, Picture's material is easily to be broken (from paper or laminated picture), for laminated picture, the corner is usually not round (it can hurt their arm), small size of the card (might be swallowed because their habit is biting objects), don't know how to use PECS correctly.
2. Here are the needs from the therapist:

    a. Therapist need pictures which can be represent what they want to say: represent every themes, autistic child can understand easily, almost the same with the real object.
    b. Therapist expected on suitable picture size: very ideal/clear while looking from the front side, easy to be grasped, bigger picture, so that easily to be recognized and remembered, the ideal size is 7x7 cm or 7x6 cm.
    c. Therapist advice on picture color: use the bright and clear color with good contrast, do not blur, large spectrum of color so that they can recognize so many color, it has to be in good contrast between picture and its background to reduce distraction (for example black and yellow, do not pink and red), for the first step, just using black and white, especially for alphabet and number.
    d. Therapist expected on the picture media that can be use for a long time: can be use repetitive at about one year usage, picture card not blur, and material for the card is not rigid (not from multiplex or wood)
    e. The tools should be safe: non toxic material, don't hurt the child while holding the card, don't make them worry (create sound), round tip for each corner, don't harm while it falling down.
    f. For the container: classification for each theme, neat, safe and simple, easily to be reached and carried by the child
    g. Can be used for many phases development: easy to understand, make them more independent, efficient and effective
    h. Description of the picture should be separated from the picture: to reduce their rigidity.

Table 3.Level of importance of each need

Criteria	Weight	Rank
1. Proper picture with the meaning	19.78%	1
2. Safe in use	12.50%	5
3. Picture's color	15.66%	3
4. Flexibility	11.55%	6
5. Picture's size	16.46%	2
6. Life long usage	9.02%	7
7. Easy to keep	15.03%	4

Knowing the weight and the rank of importance level, is needed, so it can be determine, which part of the design that become main priority (to fulfill the need), so that the new PECS design will meet the customer need.

Table 4. Need Metric for New PECS design

Need \ Metric	Picture with theme	Real object picture (almost the same)	Considering anthropometry data for the size	Cosntrast (color)	Picture's material	Layer's material	Design of picture's container
1. Proper picture with the meaning	*	*					
2. Safe in use					*	*	*
3. Picture's color				*			
4. Flexibility							
5. Picture's size			*				
6. Life long usage					*	*	*
7. Easy to keep							*

Table 4. Need Metric for New PECS design(continued)

Need \ Metric	Weight of picture	Types of printing ink	Can be use for many steps of development	Picture's design	Container's size	Weight of container
1. Proper picture with the meaning						
2. Safe in use	*	*		*		*
3. Picture's color		*				
4. Flexibility			*			
5. Picture's size						
6. Life long usage		*		*		
7. Easy to keep	*			*	*	*

Need-metric should be made to specify how to fulfill the need (metric). String mark (*) shows the correlation between need and the metric.

To accommodate therapists' need and overcome the weaknesses of the existing PECS, new design of PECS consider these criteria:

a. Picture are accommodate from CD Pics for PECS 2007 which should be adjusted (language and graphics) to Indonesian user. It will be divided into 20 categories: activity in the water, musical instruments, transportation, alphabet, number, prefix, human body, shape, weather, emotion, animals, verb, adjective, location, food and beverages, clothes, profession, vegetable and fruit, color, etc.
b. Material for the layer is made from Eva mate which is soft, untearable, flexible, water resistant light and thick (like a sponge), so that the autistic children feel comfort and safe while using it.
c. Picture being printed with clear and bright color
d. Picture being laminated by food grade plastic material, so that the picture not easily to be broken and avoid them from the ink on the picture
e. For the container, it consists of 9 picture cards for each sleeve, put them in the binder, which packed in a backpack. Each category is separated with partition.
f. The dimension for new PECS, using anthropometry data for 3-11 years autistic children and calculation of the font size and picture's description:

Table 5: Card design dimension.

Component	Body dimension and percentile	Calculation
Length and width	Hand's width; 5th percentile	Max. width = mean- (1.645 stdev) = 12.065-1.645*1.352 =9.84 cm Choosen: 7cm, as the input from therapist
Length of container	Length from shoulder to waist; 5th percentile	Max. length = mean- (1.645 stdev) = 36.9-1.645*1.308 =34.748 cm Choosen: 34 cm
Width of container	Width of the shoulder ; 5th percentile	Max. width = mean- (1.645 stdev) = 32.6-1.645*1.174 =30.669 cm Choosen: 30 cm
Width of backpack's webbing belt	Width of half shoulder (one shoulder only) ; 5th percentile	Max. width = mean- (1.645 stdev) = 11.10-1.645*0.615 =10.088 cm Choosen: 6 cm, as commonly backpack's webbing belt
Width between 2 webbing belts	Width of neck nucleus and width of the centre shoulder + webbing belt; 5th percentile	Minimum= 8cm Max. width = mean- (1.645 stdev) + 6cm = 21.5-(1.645*1.155) + 6 =25.6

PECS cards as shown below:

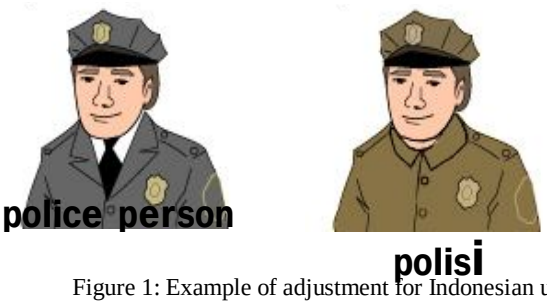

Figure 1: Example of adjustment for Indonesian user

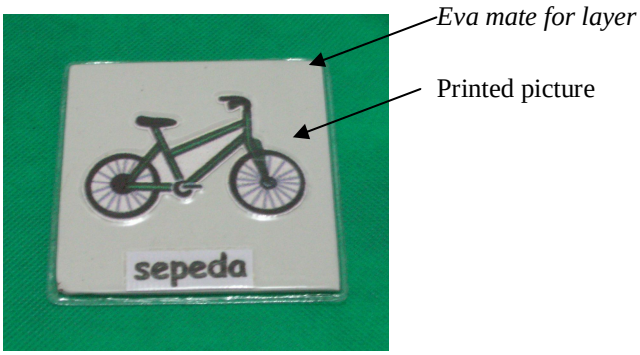

Figure 2: Example of PECS card (bicycle)

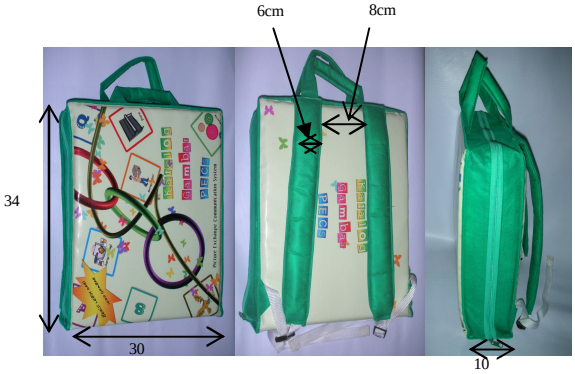

Figure 3: Backpack to pack the card and binder

For the font size, the specification as follow:

Tabel 6: Font size recommendation

Component	Theoretical	Accommodate

		(adjustment by considering therapist's input)
Height of alphabet	= Length of view (mm) /200 = 300mm / 200 = 1.5mm	Min = 0.5cm Max = 0.7cm
Width of alphabet	= 2/3 of height = 2/3 * 0.15cm =0.1cm	Min = 0.3cm Max = 0.5cm
Space between alphabet	= 1/5 of height = 1/5 * 0.15cm	Min = 1mm Max = 1.5mm
Space between word	= 2/3 of height = 2/3 * 0.15cm =0.1cm	Min = 0.3cm Max = 0.5cm

Product Testing/Implementation

Product testing was done to 10 therapist and 10 parents, they really satisfied with the new PECS. From the trial to the autistic children (15 children), with 10 repetition, it's found that there's reduction in picking up time (pick the card).

Existing (laminated card) = 5.61 second

New PECS (Eva Mate + printing) = 0.89 second

This improvement has good impact in their communication ways, so that they can communicate easily by picking up the card.

5. CONCLUSION

Here are the conclusions of this research:

1. Parents can do training at home and they don't need to worry in using the new PECS, because it's safe, comfort and life long.
2. PECS tool really helpful for parents, therapist and children to communicate
3. PECS catalogue increasing knowledge of the society about PECS

6. APPENDIX

Pervasive Developmental Disorder Screening Test (PDDST-II)

Give (v) mark to Yes or No answer which is appropriate

Table 7: Screening I (12-18 months toddler)

No	Variables	Yes	No
1	Do your baby often seems boring or unenthusiastic to their surrounding activity?		
2	Do your baby often doing something or playing with their toys repetitively in very long period (monotonous)?		
3	Do your baby often not turn their head while someone call out their name?		
4	Do your baby late to walk?		
5	Do your baby only play with one toy that he/she likes?		
6	Do your baby like to touch /felt a "weird" stuff? Like carpet, cotton, rough fabric		
7	Do you ever heard your friend or your family told that your child has disorder on their hearing senses?		
8	Do your baby often watching on their own fingers and play with their finger seriously?		
9	Do your baby can't say/express what they want, by using words or body language?		

Give (v) mark to Yes or No answer which is appropriate

Table 8: Screening II (18- 24 months toddler)

No	Variables	Yes	No
1	Do your baby unenthusiastic to learn how to talk?		
2	Do your baby has no fear to harmful stuff or animals?		
3	Do your baby hard to have eye contact with you?		
4	Do your baby like to running, but they don't like to play pick a boo?		
5	Do your baby ever seems like unenthusiastic to their toys?		
6	Do your baby avoid dolls or feathers toys?		
7	Do you baby doesn't like to play with dolls or feathers toys?		
8	Do your baby looks so impressed with the moving objects, like turn cars' wheel, look at the water flow, look at the moving fan?		
9	Do your baby often doesn't care whether you're around them or not?		
10	Do your baby moody (without any reasons)?		
11	Do your baby often hard to play with new toys? (rigid and dependent to one toy?		
12	Do your baby never use body language like waving hand, kiss your cheek?		
13	Do your baby often wave their hands up, down, front and to their body's side while they feel happy?		
14	Do your baby always crying while you left them go, but they don't care while you're coming/come back?		

This two screening can be use by all dear parents to check individually at home, whether their child is needed extra attention or not.
For each table screening:
If there are 3 or more on "YES" answer for the odd number of all the variables, maybe you need to check out whether they get autism or not (ask the expert).
If there are 3 or more on "YES" answer for the even number of all the variables, maybe you need to check out whether they get another disorder besides autism (ask the expert).

REFERENCES

[1]http://puterakembara.org/archives10/00000055.shtml, *Deteksi Dini dan Skrening Autis*, 16 Mei 2007.
[2] Wignjosoebroto, Sritomo., 2003, *Ergonomi, Studi gerak dan waktu*, PT. Guna Widya, Surabaya.
[3] Ulrich, Karl T., Eppinger, Steven D., 2001, *Product Design and Development*, Mc. Graw hill, Inc, International.

ISSN 114-1284

Usability Evaluation and Design Improvement on Electronic Device (Case Study: 6 in 1 Magic Jar)

Linda Herawati Gunawan[1], Utomo[2], Fransiska[3]

Email: [1]linda@ubaya.ac.id, [2]puspo@ubaya.ac.id
Engineering Management Laboratory- Department of Industrial Engineering
Engineering Faculty , University of Surabaya

ABSTRACT

Nowadays, Magic Jar was exists with many brands. Commonly, these brands have many similarities. Besides the strengths, there also found some weaknesses, such as the design, appearance, the way to operate the product, etc. Usability now becomes one of the considerations in deciding or choosing a product, especially electronic device. From the survey, it was found that many customers prefer to buy a multifunction product. On the other hand, they usually disable to use all of its function. In this research, benchmarking process was done in 4 brands: COSMOS type SRJ 351TS, MASPION type MRJ 2018, MIYAKO type MCM 706, DENPOO type DMJ 88A. The first analysis step is descriptive analysis to find out what's customer perception in those 4 brands. The second is quadrant analysis to find out the strengths and weaknesses of each brand. The third analysis is MANOVA to find out is there any gap between importance and satisfaction level among these 4 brands. After these three analyses, benchmarking was done then to decide what's should be adopted from the existing design and what should be redesigned.

Keywords: Usability, task analysis, quadrant analysis, MANOVA, Benchmarking,

1. INTRODUCTION

So many brand and function in Magic Jar which available now. From 2 in 1 (cook and warm only), 3 in 1 (cook, warm and porridge) and the latest technology is 6 in 1. Nowadays people prefer to buy 6 in 1 Magic Jar because they can use so many functions with reasonable price (not too much different with 2 in 1 or 3 in 1). Even it has 6 functions/features, there's still a problem. Commonly customers do not operate all of the functions with some reasons: can't use it (usually), not too need it, and not really sure with the results.
From the survey, it's found that sometimes they're not really understand about the function and they don't like to read the manual book, because it's too complicated (also the language). In this research four brands will be benchmarked to find the strengths and weaknesses of each brand. These four brands have the same features (6 in 1 Magic Jar), which types are: COSMOS SRJ35ITS, MASPION MRJ2018, MIYAKO MCM706 and DENPOO DMJ 88A.
The benchmark results will become the basic for recommended design (especially the control button) at the outer part of the Magic Jar and how to design the manual book which consists of "easy steps".

2. LITERATURE REVIEW

a. Usability of consumer electronic products
Usability of the product recently become important factor, so that the customer feels that the price is comparable with the function, quality and service [1]. Usability means the assessment of easiness usage of an object by anyone to reach a goal or specific job. At the beginning, usability concept is to measure how ease and efficient for a customer while doing a job (in HCI area) [2]. Nowadays usability is also use in measuring the effectiveness of consumer electronic products which have different indicator in HCI. On subjective aspect, image and impression has the same value with objective aspect.
The main reason why consumer product usability is different from HCI:

1. Electronic product is different from software product
2. In designing the control button (shape and color) should consider that it can give the good perception how to operate it
3. Using electronic product is not the same with using/operate software

Usability of electronic products consist of 2 aspect : performance and image/impression.
In performance aspect, there are three groups of indicators which have these dimensions: Perception/cognition (the dimensions are directness, explicitness, modelessness, observability, responsiveness, and simplicity); Learning/memorization (the dimensions are consistency,familiarity, informativeness, learnability, memorability, predictability); Control/action (the dimensions are accessibility, adaptability, controllability, effectiveness, efficiency, error prevention, flexibility, helpfulness, multithreading, recoverability, task conformance.
In Image/impression aspect, there also three groups of indicators which have these dimensions: Basic sense (the dimensions are shape, color, brightness, texture, translucency, balance, heaviness, volume); Description of image (the dimensions are metaphoric design image, elegance, granularity, harmoniousness, luxuriousness, magnificence, neatness, rigidity, salience, dynamicity); Evaluative feeling (the dimensions are acceptability, comfort, convenience, reliability, attractiveness, preference, satisfaction).

b. Quadrant Analysis

Main priority (IV)	Maintain performance (I)
Attribute to Improve (III)	Overacting (II)

Axis : Satisfaction level
Ordinate: Importance level
Quadrant analysis is use to find the strength and weakness of the products or services. It is mapped on satisfaction level and importance level. There four quadrant being created:

c. MANOVA
It's use to measure the difference between mean of group respondents. MANOVE is use to analyze total variation which consist of many factors that's affect in one or more variables.

d. Theory of benchmarking
Benchmarking is product assessment to the competitor, of which steps are:

1. Identify the subject being benchmarked
2. Identify the competitors
3. Define the gap
4. Create the development
5. Adjust the benchmark measurement

3. RESEARCH METHODOLOGY

Survey being done to get the strengths and weaknesses of each brand. Aims of the research are: benchmark in four brands, doing the usability testing, new design of 6 in 1 magic jar (especially on its appearance), button and manual book.
Data being collected are: questionnaires to find out respondents complaints while using 6 in 1 Magic Jar, usability testing (how fast in operating 1 task), sequences steps of each function/feature. From these data, than MANOVA, quadrant analysis and benchmarking done respectively.
The last step is designing new concept of Magic Jar, with unique push button and appearance.

4. RESULTS AND DISCUSSION

From the questionnaires results, description analysis was done:

1. Women are the dominant user
2. They choose 6 in 1 because the price is almost the same with 2 in 1 and 3 in 1
3. At the first time they use it, they don't read manual book (just trial and error) in pushing the button and predicts its function
4. Respondents said that the availability of manual book is preferable as long as it's easy to understand (language and flowchart)

Here by the strengths and weakness of each brand:

1. COSMOS
   Strength: easy and comfort to be used
   Weakness: manual book is difficult to understand; not really satisfied having Cosmos; takes time to understand how to use it for the very first time; steps of operation is difficult to remember and complicated.
2. MASPION
   Strength: easy to operate; simple, uncomplicated
   Weakness: manual book is difficult to understand; takes time to understand how to use it for the very first time; manual book consist of so many text

without picture; commonly they don't really satisfied in using Maspion

3. MIYAKO
   Strength: easy and comfort to be used
   Weakness: manual book is difficult to understand; takes time to understand how to use it for the very first time
4. DENPOO
   Strength: simple, uncomplicated
   Weakness: manual book is difficult to understand; takes time to understand how to use it for the very first time; the color is not suitable (not so good)

MANOVA results as shown below:

Table1: Level of satisfaction of 4 brands

No	Variables	Sig. Value	Result	Addition
1	Appearance of Magic Jar: simple, uncomplicated	0.005	Difference exist	Highest score: Denpoo
2	Appearance of manual book:simple, uncomplicated	0.027	Difference exist	Highest score: Denpoo
3	Steps to operate: not complicated	0.167	No difference	The same for all brands (medium)
4	Times need to use it for the first time	0.000	Difference exist	Highest score: Miyako
5	Steps to operate : easy to remember	0.173	No difference	The same for all brands (medium)
6	Easy to operate	0.009	Difference exist	Highest score: Miyako
7	Accurate in attaining goals (each task)	0.197	No difference	The same for all brands (medium)
8	Task can be done effective and efficient	0.200	No difference	The same for all brands (medium)
9	Ability to reduce error	0.051	No difference	The same for all brands (medium)
10	User reaction to improve from error/mistake	0.000	Difference exist	Highest score: Miyako
11	The shape of the Magic Jar	0.011	Difference exist	Highest score: Cosmos
12	The color is suitable and looks good	0.000	Difference exist	Highest score: Cosmos
13	Composition looks balance	0.187	No difference	The same for all brands (high)
14	Magic jar look clean, neat and well organized	0.231	No difference	The same for all brands (medium)
15	Simple manual book	0.891	No difference	The same for all brands (medium)
16	Easy and comfort with the magic jar	0.055	No difference	The same for all brands (medium)
17	Customer feels satisfied with the magic jar	0.005	Difference exist	Highest score: Miyako
18	Customer feels satisfied with the manual book	0.841	No difference	The same for all brands (medium)

Benchmark analysis according to quadrant analysis:

Table 2: Benchmark of 4 brands based on quadrant analysis

No	Variable	COSMOS	MASPION
1	Appearance of Magic Jar: simple, uncomplicated	Attribute to improve	Main-tain perfor mance
2	Appearance of manual book:simple, uncomplicated	Main priority	Main priority
3	Steps to operate: not complicated	Main priority	Main priority
4	Times need to use it for the first time	Main priority	Main priority
5	Steps to operate : easy to remember	Main priority	Main priority
6	Easy to operate	Main priority	Main-tain perfor mance
7	Accurate in attaining goals (each task)	Overacting	Main priority
8	Task can be done effective and efficient	Attribute to improve	Overac ting
9	Ability to reduce error	Attribute to improve	Attribu te to improv e
10	User reaction to improve from error/mistake	Attribute to improve	Overac ting
11	The shape of the Magic Jar	Overacting	Overac ting
12	The color is suitable and looks good	Overacting	Overac ting
13	Composition looks balance	Overacting	Maintai n perfor mance
14	Magic jar look clean, neat and well organized	Overacting	Overac ting
15	Simple manual book	Attribute to	Main

		improve	priority
16	Easy and comfort with the magic jar	Maintain performance	Main priority
17	Customer feels satisfied with the magic jar	Main priority	Main priority
18	Customer feels satisfied with the manual book	Main priority	Main priority

Table 2: Benchmark of 4 brands based on quadrant analysis (continued)

No	Variable	MIYAKO	DENPOO	Decision
1	Appearance of Magic Jar: simple, uncomplicated	Maintain performance	Maintain performance	Adopted
2	Appearance of manual book:simple, uncomplicated	Main priority	Overacting	Improved
3	Steps to operate: not complicated	Main priority	Attribute to improve	Improved
4	Times need to use it for the first time	Overacting	Maintain performance	Adopted
5	Steps to operate : easy to remember	Maintain performance	Maintain performance	Adopted
6	Easy to operate	Main priority	Maintain performance	Adopted
7	Accurate in attaining goals (each task)	Overacting	Attribute to improve	Improved
8	Task can be done effective and efficient	Overacting	Maintain performance	Adopted
9	Ability to reduce error	Overacting	Main priority	Improved
10	User reaction to improve from error/mistake	Overacting	Attribute to improve	Improved
11	The shape of the Magic Jar	Overacting	Overacting	Improved
12	The color is suitable and looks good	Attribute to improve	Main priority	Improved
13	Composition looks balance	Overacting	Over acting	Adopted
14	Magic jar look	Main	Maint	Adopted
	clean, neat and well organized	priority	ain performance	
15	Simple manual book	Over acting	Attribute to improve	Improved
16	Easy and comfort with the magic jar	Maintain performance	Maintain performance	Adopted
17	Customer feels satisfied with the magic jar	Maintain performance	Main priority	Adopted
18	Customer feels satisfied with the manual book	Main priority	Main priority	Improved

From the quadrant analysis, it's found that 9 variables need to improved, and the others should be maintain (customers feels satisfied enough). How to determine adopted variable, if there's 1 brand that result on "maintain performance", and the brand being adopted its feature.

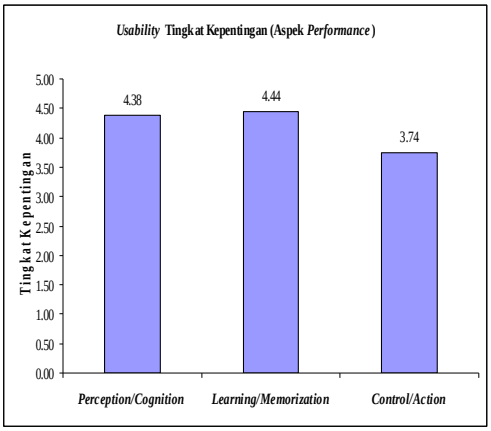

Figure 1. Level of importance (usability-performance)

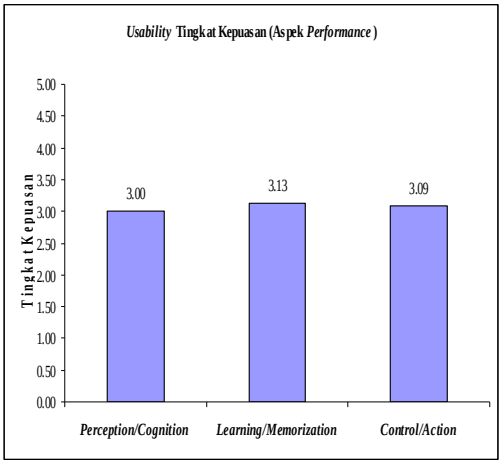

Figure 2. Level of satisfaction (usability performance)

Refers to figure 1 and 2, it's shown that there's gap between customer expectation and customer need. The top two needs are Learning and Perception, but they don't really satisfied on the existing products.

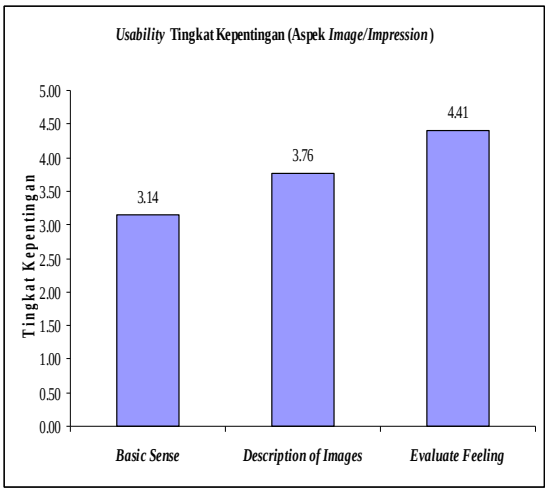

Figure 3. Level of importance (image/impression aspect)

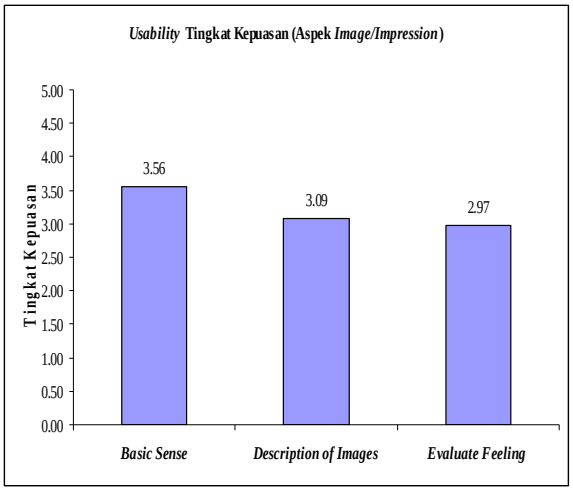

Figure 4. Level of satisfaction (image/impression aspect)

Refers to figure 3 and 4, it's shown that gap is also occur between customer expectation and customer need. The top two needs are Description of images and Evaluate feeling, but they don't really satisfied on the existing products.

Improvement than applied in the new design as follow:

1.Appearance of manual book: simple, uncomplicated, is improved by designing a systematic manual book, using more picture and chart.
2. Steps to operate: not complicated, is improved by designing "one touch button" system (push 1 button only to define what function need to be done)
3. Accurate in attaining goals (each task). By designing one touch button, make it accurate for each operation/feature.
4. Ability to reduce error, is improved by creating cancel button to cancel the process
5. User reaction to improve from error/mistake: in every feature/function process, there's a display so that the user can detect error faster than before (if the display didn't match with the condition that needed/set)
6. The shape of the Magic Jar, new design is ellipse, looks like tube
7. The color is suitable and looks good, simple but elegant, using millennium color, that being surveyed as the symbolized of technology.
8. Simple manual book: giving sketch of the product and each detail component
9. Customer feels satisfied with the manual book: systematic manual book with picture/figure to make it clear.

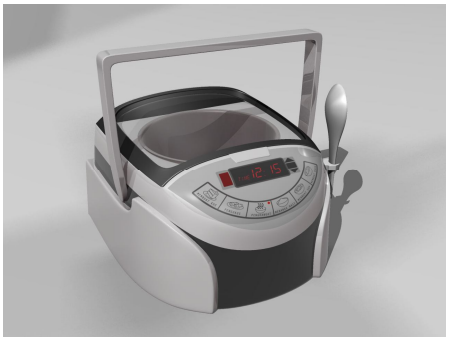

Figure 5. New Design- Magic Cooker

Figure 6. Top view – Transparent top cover

Figure 7. Display of each function

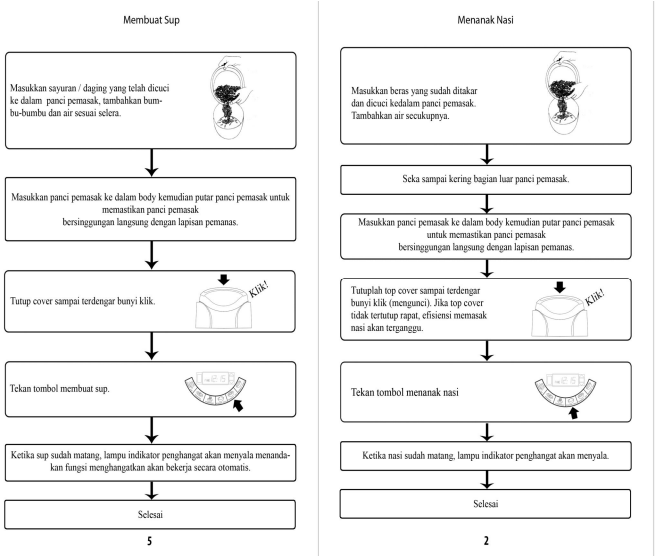

Figure 8. Design of systematic manual book

Feature of 6 in 1 Magic cooker:

1. Millenium theme, shows on color and its shape
2. Simple, elegant and look balance
3. Timer, to define processing time
4. Cancel button is applied
5. One touch button is applied
6. Easy button consist of picture that shows it function, and fulfill with lighting
7. Transparent top casing, to check the condition of the food being cooked
8. Handle is designed to make it easy to lift or move.

After the design being applied in paper prototype, than usability testing was done to 10 users. Each function was tested (using existing Magic Jar and new design). Time process being calculated to check is the new design more effective than the old ones. And the results as follow:

Table 3: Usability testing of all brands

Process	COS MOS	MASPION	MIYAKO
Cooking rice	15.13	16.11	9.26
Warm	12.38	12.93	7.95
Steam	11.41	11.25	7.92
Cooking soup	12.47	11.91	7.41
Cooking porridge	10.88	10.76	7.57
Making Cakes	10.54	11.16	6.05

Table 3: Usability testing of all brands(continued)

Process	DENPOO	Mean Four brands	MAGIC COOKER
Cooking rice	11.05	12.89	5.51
Warm	6.17	9.86	3.71
Steam	8.28	9.72	4.11
Cooking soup	7.51	9.83	4.90
Cooking porridge	8.81	9.51	4.10
Making Cakes	6.80	8.64	3.55

Based on the result above, it's found that the new design, MAGIC COOKER, is better than the other brands. The user can use all the function easily and effective.

5. CONCLUSION

From this research, can be conclude that mew design of MAGIC COOKER has a simple design, not complicated, with futuristic shape and color. And one touch button system with description process in Indonesia plus icon of the function, make the user more satisfied.
New design of manual book consist of flowchart of each function to make easy to understand, and give more picture.

REFERENCES

[1] Sung H, Han. Hwan Yun, Myung. Kwkh, Jiyoung. Sang W, Hong. 2000. *Usability of Consumer Electronic Product*. Departement of Industrial Enggineering Pohang University of Science and Technology. San 31, Hyoja, Pohang, 790-784
[2] ._____. *What is theDifference Between Usability Engineering and Usabilitu Testing? (online),available:* http://www.usability.gov/basics/

APPLICATION OF MULTIFACTOR PRODUCTIVITY MEASUREMENT MODEL IN SERVICE INDUSTRY (CASE STUDY: HOUSE OF SAMPOERNA CAFÉ)

Lisa Mardiono[1], Benny Lianto[2], Novi Indriyati[3]
Industrial Engineering Department – University of Surabaya
Tel: (031) 2981392 Fax: (031) 2981376
Jl. Raya Kalirungkut, Surabaya, 60292, Indonesia
Email: lmardiono@ubaya.ac.id[1]

Abstract

The importance of productivity management in the service industries is widely accepted. Multifactor Productivity Measurement Model determines the total productivity into key terminal parameters (KTPs) and subkey terminal parameters (SKTPs). KTPs divided into static indicators and dynamic indicators, while as SKTPs are development indicators. To concise the assessment, this research integrate Multifactor with Multi Level Objective Matrix (MULOMAX) framework, Pairwise Comparison to estimate the weight of indicator, Radar Curve, and Ishikawa analysis to develop the problem solution. The application of this integrated model implemented in House of Sampoerna Café, one of the popular boutique café in Surabaya. Begin with the deployment of vision, mission and strategy that breakdown into Key Result Areas (KRAs), the indicators have been clustered in Static, Dynamic and Development indicators, in the organization functions (division) that are kitchen, steward, service, bar, cashier, public area, and purchasing in internal café.

Keywords:
multifactor productivity, indicator, Café

1. INTRODUCTION

Majority of service organizations still use production surrogates such as, number of customers served output, and time consumed to serve customers as input. The intangible nature of service adds to the complexity of measurement, requiring a multi-dimensional analysis [1]. Few organizations appear to have systematic processes in place to ensure that their performance measurement systems continue to reflect their environment and strategies [2]. Most services are provided through facilities and it has been suggested that the measurement of facilities should relate to the core business objectives such as customer satisfaction [3]. Multifactor productivity measurement model is one of service performance measurement model that infuse this complexity with the terminology of static, dynamic and development indicators through the data identification. However, this model lack of structure in how to arrange all indicators to be a link structure and tend to perform in partial measure. Regarding to this weakness, this research combine Multifactor with Mulomax method that have hierarchy structure to relate all indicators to be one measurement. The case study has been carried out in House of Sampoerna Café in Surabaya.

2. LITERATURE REVIEW

This research classify studies into two themes of model as follows

2.1 Multifactor Productivity Measurement Model for Service Organization

Sahay [1] has developed this model based on productivity indices of the multifactor key terminal parameters (KTPs) and sub key terminal parameters (SKTPs). KTPs act as output of the organization. These parameters have further been segregated into static parameters and dynamic parameters. Static parameters are those criteria measure which captures the performance of organization is making use of its resources. Dynamic parameters are those criteria measures which identify different activities which impose immediate cost on the organization bestow results sometimes in future. Productivity index for KTPs is the sum of productivity indices of static indicators and dynamic indicators. The productivity indices for static and dynamic indicators depends on actual and target productivity factor values and the weight age of the corresponding factors.

Subkey terminal parameters (SKTPs) are basically development factors which create a strong knowledge and database for the organization's internal usages to improve its efficiency and productivity, and if needed could also be used by other agencies as intellectual property created by the organization. Development indicators divided into four indicators that are business development index, vendor development index, research & development index, and standardization index.
Total productivity index (TPI) for a service organization may be computed as follows:

$$TPI = PI_{KTP} + PI_{SKT}$$

$$PI_{KTP} = PI_{SI} + PI_{DI}$$

ISSN 114-1284

$$PI_{SI} = \frac{\sum_{i=1}^{n} W_i . P_{SIi}}{P_{STi}}$$

$$PI_{DI} = \frac{\sum_{j=n+1}^{m} W_j . P_{DIj}}{P_{DITj}}$$

$$PI_{SKT} = \sum_{k=m+1}^{0} W_k . P_{SKTk}$$

$$TPI = PI_{SI} + PI_{DI} + PI_{SKT}$$

$$= \frac{\sum_{i=1}^{n} W_i . P_{SIi}}{P_{STi}} + \frac{\sum_{j=n+1}^{m} W_j . P_{DIj}}{P_{DITj}} + \sum_{k=m+1}^{0} W_k . P_{SKTk}$$

where:

TPI = Total productivity index
PI_{KTP} = Productivity index of key terminal parameters
PI_{SKT} = Productivity index of sub-key terminal parameters
PI_{SI} = Productivity index of static indicators
P_{SIi} = Productivity factor values for static indicators of key terminal parameters
P_{SITi} = Target values of productivity indicators for static indicators of key terminal
PI_{DI} = Productivity index of dynamic indicators
P_{DIj} = Productivity factor values for dynamic indicators of key terminal parameters
P_{DITj} = Target values of productivity indicators for dynamic indicators of key terminal
P_{SKTk} = Productivity index of sub-key terminal parameters $W_i + Wj + W_k = 1$
Wi = Weighted attached to static indicators of key terminal parameters
W_j = Weighted attached to dynamic indicators of key terminal parameters
W_k = Weighted attached to sub-key terminal parameters

A participative methodology has been adopted for measurement of multifactor productivity that includes:

1) analysis of corporate mission, objectives and functions of the organization
2) study of various departments/sections and find out goals and key result areas (KRAs)
3) design multifactor productivity model
4) select relevant productivity indices
5) calculate productivity indices and validate results
6) develop action plan for implementation and monitoring of the model

2.2 Multi Objective Matrix (Mulomax)

Mulomax is the performance measurement model developed from original Objective Matrix (Omax). In this research Mulomax used to fill the disability of Multifactor productivity in indicators structure arrangement [4]. Due to many functions/departments in organization which obtained many criteria to become indicator measures, Mulomax approach can facilitate the hierarchy of KRAs among the functions and cluster those in terminal parameters of Multifactor productivity. In figure 1 describe the structure of Multifactor productivity using Mulomax.

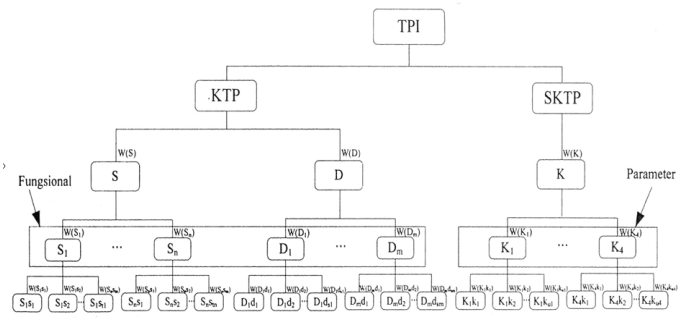

Figure 1. Multifactor Productivity Measurement Model for Service Organization in Mulomax Structure

where:

KTP = key terminal parameter value
SKTP = sub-key terminal parameter value
S = static indicators value
D = dynamic indicator value
K = development indicators value
W(S) = weight of static indicators
W(D) = weight of dynamic indicators
W(K) = weight of development indicators
$W(S_x)$ = weight of x-function in static indicators, x = 1,2……n
$W(D_y)$ = weight of y-function in dynamic indicators, y = 1,2……n
$W(K_z)$ = weight of z-function in dynamic indicators, z = 1,2……n
$W(S_nS_{xn})$ = weight of x_n- criteria in static indicators
$W(D_md_{ym})$ = weight of y_m criteria in m-function in dynamic indicators
$W(K_ud_{zu})$ = weight of z_u criteria in u-function in development indicators
S_x = value of x-function in static indicators
D_y = value of y-function in dynamic indicators
$S_n s_{y_n}$ = score of x_n criteria in n-function in static indicators
x_n = $1 \ldots t_n$ → t_n = sum of criteria in n-function
$D_m d_{y_m}$ = score of y_m criteria in m-fucntion in dynamic indicators
y_m = $1 \ldots s_m$ → s_m = sum of criteria in m-function

ISSN 114-1284

3. RESULTS AND DISCUSSION

The discussion below will show the modify Multifactor with Mulomax, and for the research object, the measurement in House of Sampoerna Café as the case study also included.

3.1 Productivity Indicators Determination

KRAs determination deploy from the Café vision, mission, and goals. The Café has 7 functions, those are kitchen, steward, service, bar, cashier, public area, and purchasing functions. Based on the analysis of the KRAs and singularities of the organization, KTPs and SKTPs are selected. Table 1 denotes the KRAs in the each function, which are occurs productivity indicators with static, dynamic and development terminal parameters.

Table 1. Productivity Indicators for KTPs and SKTPs

Key terminal parameters		
Static indicators		**Productivity indicators**
Function	Kitchen	Full-time cook staff attendance (A)
		The rate of energy consumed (B)
		The percentage of spoiled foodstuff (C)
	Steward	Steward staff attendance (D)
		The number of broken/stolen equipment (E)
	Service	Service staff attendance (F)
		VIP room utilization (G)
		Function Hall utilization (H)
	Bar	Full-time bartender staff attendance (I)
		Machine utilization (J)
	Cashier	Cashier staff attendance (K)
	Public Area	Public area staff attendance (L)
	Purchasing	Purchasing staff attendance (M)
Dynamic indicators		**Productivity indicators**
Function	Kitchen	The rate of income on food sales (N)
		The number of complaint in food (O)
		The achievement rate of Chef-special menu promotion (P)
	Bar	The rate of income on beverage sales (Q)
		The number of complaint in beverage (R)
		The achievement rate of Bar-recommended menu promotion (S)
	Service	The number of complaint in server service (T)
		Sales growth revenue (U)
	Cashier	The number of complaint in cashier service (V)
		The amount rate of cash payment (W)

Sub-key terminal parameters		
Development indicators	**Criteria**	**Productivity indicators**
Business development index	To measure Café capability in building capability in market through technology development	The rate of accomplishment on Wi-Fi service for free of charge (X)
Vendor development index	To measure Café capability in building capability in market through business development	The degree of cooperativeness with food & beverage supplier (Y)
		The degree of cooperativeness with Travel Agent (Z)
		The market enhancement rate of advertisement (A1)
		The market enhancement rate of discount promotion (The degree of cooperativeness with Bank's credit card) (B1)
Research & development index	To measure Café capability in building capability in market through research and development	The achievement rate of 'happy hour' program (C1)
		The achievement rate of Live Music program (D1)
Standardization index	To measure Café capability in building capability in market through standardization process	The rate of accomplishment on sstandard of service development (E1)

3.2 The measurement method

Since Mulomax adapted from OMAX, therefore the measurement of key terminal parameter indicators use 0 to 10 degree of level to represent score in order to show the achievement value. Level 0 means the degree of the worst acquisition, level 3 means the degree of standard, and level 10 means the degree of the best achievement that organization ever acquire. Thus, the value for levels between 0, 3, and 10, obtained through interpolation calculation. For sub-key terminal parameter, the indicators assessment value started in range point 1 to 4 with score 4 for very good till score 1 for very poor. Subsequently, justification to Mulomax score (0 to 10) are needed to compose same measurement result with KTPs.

The weight of indicators and functions utilize Pairwise Comparison, adapted from Analytical Hierarchy Process [5]. This method selected due to similarity hierarchy structure like Multifactor model, and has consistency testing as its strength. Table 2 depicts the aggregate value of weight in each indicators and functions.

3.3 Productivity Evaluation

Based on the above indicators and data availability, the measurement operated for every indicator in every function in term of terminal parameters. This section divided into 4 part, evaluation in static indicators, evaluation in dynamic indicators, evaluation in development indicators, and for the final result is overall evaluation.

Table 2. Aggregate Weight

Name	Weight (%)
Static Indicators	26,05
Kitchen Function	14,29
Indicator A	58,89
Indicator B	15,93
Indicator C	25,19
Steward Function	14,29
Indicator D	83,33
Indicator E	16,67
Service Function	14,29
Indicator F	58,89
Indicator G	25,19
Indicator H	15,93
Bar Function	14,29
Indicator I	80,36
Indicator J	13,39
Cashier Function	14,29
Indicator K	100
Public Area Function	14,29
Indicator L	100
Purchasing Function	14,29
Indicator M	100
B. Dynamic Indicators	63,33
Kitchen Function	25
Indicator N	59,07
Indicator O	7,55
Indicator P	33,38
Bar Function	25
Indicator Q	59,07
Indicator R	7,55
Indicator S	33,38
Service Function	25
Indicator T	12,5
Indicator U	87,5
Cashier Function	25
Indicator V	33,33
Indicator W	66,67
C. Development Indicators	10,62
Bussines Develop Index	9,48
Indicator X	100
Vendor Development Index	36,69
Indicator Y	32,14
Indicator Z	32,14
Indicator A1	32,14
Indicator B1	3,57
Research & Development Index	13,57
Indicator C1	12.5
Indicator D1	87,5
Standarisation Index	40,26
Indicator E1	100

1. Static indicators

Static indicator is productivity measurement criteria to find degree of accomplishment of resources efficiency. Therefore the assessment does in each productivity indicator and each function. However, because of many measurements actionable, in this paper only showed one indicators which is 'Full-time cook staff attendance' in table 3. All the productivity indicators in static indicators outlined as radar curve in figure 2.

Table 3. Degree of achievement of Full-time cook staff attendance

Period	Actual working hour	Standard working hour	Ratio	Score	Percentage of ratio deviation
1	320,3	350	0,9151	3	-
2	307,78	350	0,8794	0	-0,0391
3	330,5	350	0,9443	5	0,0738
4	320,9	350	0,9169	3	-0,0290
5	329,28	350	0,9408	5	0,0261
6	325,94	350	0,9313	4	-0,0101
7	330,06	350	0,9430	5	0,0126
8	336,33	350	0,9609	6	0,0190
9	330,58	350	0,9445	5	-0,0171
10	332,33	350	0,9495	5	0,0053
11	328,92	350	0,9398	5	-0,0103
12	321,79	350	0,9194	3	-0,0217

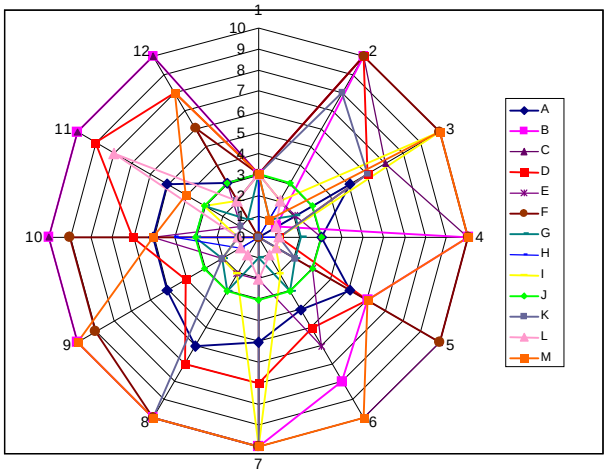

Figure 2. Radar Curve for Static Indicators

Regarding to percentage of ratio deviation and radar curve, it seen that all the indicators in static indicator have different score, and none get the highest score in all period.

Now, the evaluation continued for the function that related with static indicators. With same reason, only one function from 7 functions will be describe, 'kitchen' function in table 4 and productivity value in figure 3 for all of the functions.

Table 4. Productivity value of Kitchen function

Period	Value	Percentage of value deviation
1	0,4287	-
2	0,5876	0,37053

3	0,6955	0,183633
4	0,8401	0,207845
5	0,9173	0,091959
6	0,8787	-0,04211
7	1,0084	0,147585
8	1,0925	0,083455
9	1,0084	-0,07703
10	1,0084	0
11	1,0084	0
12	0,8401	-0,16691

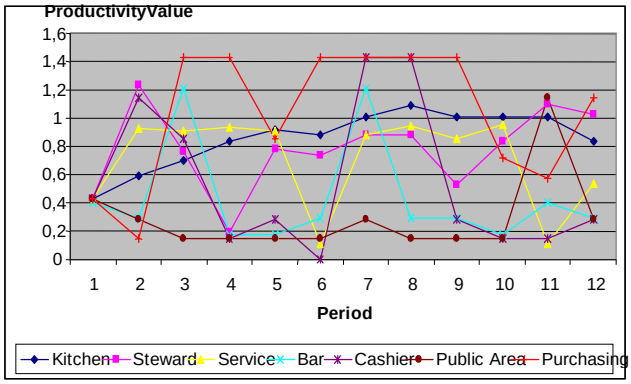

Figure 3. Productivity value for all function in static indicators

The calculation to get value is:

Value = weight of kitchen function x $\sum_{i=1}^{n}$(weight of *i* indicator x score of *i* indicator)

2. Dynamic indicators

Dynamic indicator is productivity measurement criteria to find degree of utilization of resources effectiveness. Similar with static indicators, the measurement run in productivity indicators and the functions. Figure 4 shows radar curve among indicators and productivity value in figure 5 for all of the functions.

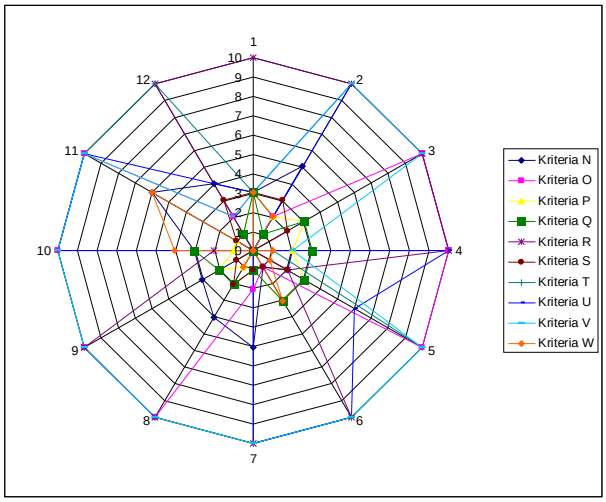

Figure 4. Radar Curve for Dynamic Indicators

The weight of dynamic indicator is higher than static and development indicator. For further development the weight proportion can be change based on the business plan. There are some criteria that have been used to arrive at the weightages, such as:

- Organization business strategy
- Degree of alignment with organization objectives
- Contribution analysis by improvement of individual factors
- Needs and scope for improvement. Customer and others stakeholder rewuirement
- Characteristics and degree of variability of factors
- Sensitivity analysis ot TPI with provisional weightages

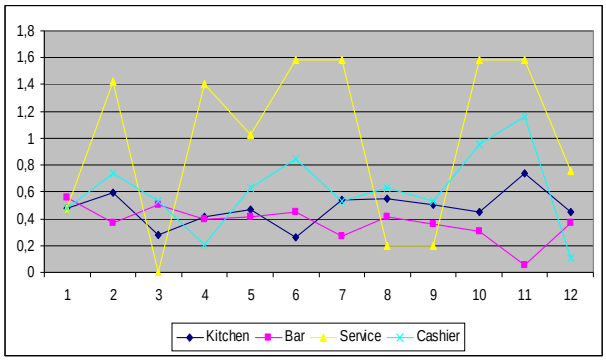

Figure 5. Productivity value for all function in dynamic indicators

3. Development indicators

Development indicator is productivity measurement criteria to find degree of enhancement of business development. The productivity index of SKTPs depends on business development, vendor development, R&D, and standardization. The depth of coverage of these parameters are measured based on the specific achievement with strong support from top level management. Here in table 5 shown score of productivity indicators in this area, and productivity value of SKTPs parameter in table 6.

Table 5. Productivity indicators of development indicators

Productivity indicators	Score
The rate of accomplishment on Wi-Fi service for free of charge	7
The degree of cooperativeness with food & beverage supplier	10
The degree of cooperativeness with Travel Agent	10
The market enhancement rate of advertisement	3
The market enhancement rate of discount promotion (The degree of cooperativeness with Bank's credit card)	0
The achievement rate of 'happy hour' program	0
The achievement rate of Live Music program	10
The rate of accomplishment on sstandard of service devevelopment	10

Table 6. Productivity value of sub-key terminal parameter

Parameter	Weight	Value
Business development index	0,0948	0,6636

Vendor development index	0,3669	2,7122
Research & development index	0,1357	1,1874
Standarisation index	0,4026	4,0260
		8,5892

4. Final result

The final result is total measurement for House of Sampoerna Café. Summary for measurement in KTPs (static & dynamic) and SKPTs (development) listed in table 7.

Table 7. Productivity value in key terminal parameter and sub-key terminal parameter

Period	Static indicators	Dynamic indicators	Development indicators
1	0,7748	1,9835	0,9122
2	1,2004	3,1325	0,9122
3	1,5646	1,3116	0,9122
4	1,0039	2,4286	0,9122
5	1,0616	2,5376	0,9122
6	0,9336	3,1445	0,9122
7	1,8539	2,9212	0,9122
8	1,6180	1,7899	0,9122
9	1,1799	1,5908	0,9122

We can see that dynamic indicators reach higher value compared with two others indicators. It makes for total productivity (TP) value, KTPs more dominant than SKTPs. However, important factor we have to consider is that these assessments include degree of weight which could dynamic indicator as though as the biggest contribution in TP value. In fact, perhaps the original score of dynamic indicators, insides of the degree of weight included, lack of difference with two others indicators. Therefore, this might be weakness of Multifactor measurement, with the intention of how large degree of weight given.

Table 8. Productivity value of House of Sampoerna Café

Period	Value	Percentage of value deviation
1	3,6705	-
2	5,2451	0,4289
3	3,7884	-0,2777
4	4,3447	0,1468
5	4,5114	0,0384
6	4,9903	0,1061
7	5,6873	0,1397
8	4,3201	-0,2404
9	3,6829	-0,1475
10	5,2371	0,422
11	5,6075	0,0707
12	3,7402	-0,333

Café achieve the highest value in period 7 and the lowest in period 1. However, all of the period's value reaches above borderline (score 3) that means Café performance is good enough. For further improvement, this research uses Ishikawa Diagram to identify the possible factors influence that could be improved in order to increase the performance value.

4. CONCLUSION

This paper has outlined a Multifactor productivity measurement model to measure in service organization, which represented by House of Sampoerna Café. The basic objective of productivity measurement is to establish the potential for improvement and make people accountable for the state of productivity. The case study has shown how different factors of static, dynamic and development parameters can be taken into account to calculate the total productivity of the organization. Although, the weakness of this model is rely on the subjectivity on degree of weight, it is important to highlight that the characteristic of the services itself are very subjective to measure, and the acknowledgement that benchmarking should not be the only performance mechanism within an organization overall system [6].

Though the Multifactor productivity is good for the organization, this gives opportunity to identify area for further development. The difficulty in kind of research is to identify productivity area in order to obtain accurate indicator measures. The productivity indicators calculations are carried out for key result areas, thus expecting the responsibility from management officer.

5. REFERENCES

[1] Sahay, B.S., *Multifactor Productivity Measurement Model for Service Organization*, International Journal of Productivity and Performance Management, Vol.54 No.1, pp.7-22, 2004

[2] Fitzsimmons, James, *Service Management: Operations, Strategy and Information Technology*, 3rd.ed, McGraw Hill, New York, 2001

[3] Tucker, M. & Smith, A., *User Perceptions in Workplace Productivity and Strategic Facilities Management Delivery*, Facilities, Vol.26 No.5/6, pp.196-212, 2008

[4] Lianto, Benny & Aryo, Denny, *Analisis Sistem dan Pengembangan Model Pengukuran Produktivitas pada Sektor Industri Jasa*, Staff Research Grant, TPSDP, University of Surabaya, 2005

[5] Saaty, T.L., *Multicriteria Decision Making, The Analytical Hierarchy Process*, University of Pittsburgh, USA, 1998

[6] Pitt, Michael & Tucker, Matthew, *Performance Measurement in Facilities Management: Driving Innovation?*, Journal of Property Management, Vol.26 No.4, pp. 241-254, 2008

ISSN 114-1284

DEVELOPING MODEL OF PERFORMANCE MEASUREMENT IN SOCIAL ORGANIZATION

Lisa Mardiono
Industrial Engineering Department – University of Surabaya
Tel: (031) 2981392 Fax: (031) 2981376
Jl. Raya Kalirungkut, Surabaya, 60292, Indonesia
Email: lmardiono@ubaya.ac.id

Abstract

Social organization is the enterprise that priorities the organization as the enterprising entity rather than the individual entrepreneur. Social organization owned by the private or not for profit sectors. As a consequence of the emphasis on the organization versus the individual entrepreneur, the performance measurement systems have potentially overemphasized the role of the stakeholder, versus creating a mechanism for looking at financial performance. This paper presents a knowledge-based framework for designing the performance of NPO using a model based on Malcolm Baldrige National Quality Award (MBNQA) criteria and Social Enterprise Balanced Scorecard (SEBC) approach. The purpose is capturing both the benefits and consequences of those models by integrating their perspectives and categories into a comprehensive model. Using this comprehensive model, hopefully social organization could easily deploy their strategies into indicator criteria and measure its in order to encourage social organization get best achievement.

Keywords:
Social organization, SEBC, MBNQA

1. INTRODUCTION

Social organizations provide important contribution services throughout the world [1]. Social organization, which the other statement called Non Profit Organization (NPO), are today commonly operating in a highly competitive environment that is characterized by increasing demand of services from the community, growing competition for contracts with the public and for-profit sector, as we also called Profit Organization [2]. The trigger of this growth was social movement increase that concern from many level in society [3]. This exponential growth also happened in Indonesia as developing countries. A lot of corporate social responsibility program rise in order to facing social problem. The World Bank defines NPOs as 'private organizations that pursue activities to relieve suffering, promote the interests of the poor, protect the environment, provide basic social services or undertake community development' [1]. This significant development more complex recently because of many factors, such as quality program demand, number of program and its variation that suitable with community requirement, more service expanded interrelation with public and business organization, and many more. Social organization management should organize more professional, modern, accomplish by strategic management, thus competitive advantage could be achieve and reach high performance value [4, 5].

1.1 Need for Performance Measurement

The important point in professional organization arrangement is performance measurement. The fact, however, many performance measurement method had been developed to profit organization and less for social organization. Why these NPOs need specific performance measurement model? One of the principal differences between NPO and profit organization is that they have different reasons for their existence. In oversimplified terms, it might be said that the ultimate objective of a commercial organization is to realize net profits for its owners through the provision of some product or performance of some services wanted by other people, whereas the ultimate objectives of a NPO is to meet some socially desirable need of the community. The basic different that arises is that as there is no profit motive in the NPO sector, and thus no single indicator of performance comparable to business enterprise is bottom-line. It may be stated that the best indicators of the performance of NPO are generally not measurable in currency terms, though currency is the language of financial reporting. That indicates that is more difficult to measure performance in NPO than in profit organization.

The performance measurement models that implemented nowadays mostly adopted from performance measurement models used from profit organization [1,3,6,7]. *Balanced Scorecard* (BSC) which admitted as powerful strategic management tool, is model applied frequently in this decade [8]. BSC also influences social organization in many researches [9,10,11]. Nevertheless, Somers [12] modify BCS model into *Social Entreprise Balance Scorecard* (SEBC) that amended in fill the gap in NPO performance measurement model.
The reason is even though BSC is popular performance framework but it has inadequacy. Kaplan and Norton in their book, BSC for NPO [13], discuss the difficulty to rely intangible asset on organization strategy, which only capture in learning and growth perspective. Integration of Social Enterprise Balance Scorecard (modeled closely to

BSC for NPO specification) with Malcolm Baldrige National Quality Award (MBNQA) try to develop a unified framework for translating the award requirements into a set of objectives and measures to achieve the ultimate results. Hope, both models with strengthens and weakness can create a synergy model suitable with NPO characteristics.

2. NON PROFIT ORGANIZATION

Social organization is enterprise structure which social mission to achieve. Similar terminology states Non Profit Organization (NPO) or Not-for-profit organization. Social organization has many definitions depend on the willingness we see. World Bank in their definition above notes the humanity point of view. Other states that social organizations have a form an intermediate structure between the market (private/for-profit sector) and government (public sector) [1]. However, goes on to argue that focusing on the differences seems to widen the divide between the two sectors and, that it is far more beneficial to focus on the similarities. Table 1 describes the diverse between NPO and profit organization [14].

Tabel 1.. Differences between Profit Organisation and Non Profit Organisation

No.	Profit Organisation	Non Profit Organisation
1	Focus on bottom line	Focus on social good
2	Aim to create shareholder value	Aim to provide a service to those in need
3	Rely on hired managers to run their operations	Rely on volunteers
4	Sources of revenue come from sales of their goods and services	Sources of revenue rely on donation and government funding

Future economic success of social organizations depend not only the quality of its social and economic activities, but also on communicating their performance to the multiple and diverse stakeholders. The Performance Prism developed by Cranefield School of Management (formerly at University of Cambridge) states that the focus of any organization whether for profit or non-profit should be on stakeholder satisfaction and stakeholder contribution. It should find relevant answers to five basic questions in order to assess its performance objectively:

1. *Stakeholder satisfaction* – who are the key stakeholders and what do they want and need?
2. *Strategies* – what strategies do we have to put in place to satisfy the wants and needs of these key stakeholders?
3. *Processes* – what critical processes do we require if we are to execute these strategies?
4. *Capabilities* – what capabilities do we need to operate and enhance these processes?
5. *Stakeholder contribution* – what contributions do we require from our stakeholders if we are to maintain and develop these capabilities?

From these 5 questions chain, we can summarize what social organization need to measure its performance, is a model that:

- Concentrate in organization strategic planning and the key result areas that delpoy from vision and mission.
- Implicate stakeholder in organization internal activities
- To measure capability not only from *tangible asset* but also *intangible asset*
- Focus on *critical success factors* balanced in term of their weight and for further improvement

3. MALCOLM BALDRIGE NATIONAL QUALITY AWARD for NON PROFIT ORGANIZATION

Since its inception in the US Congress in 1987 to promote quality awareness towards performance excellence, the Malcolm Baldrige National Quality Award (MBNQA) is now been accepted widely as a standard for performance excellence. From 1987 to present, MBNQA had been changed many times to ensure the continued growth im competitiveness. The MBNQA has 2 objectives, (1) To aware performance excellence as an increasingly important element in competitiveness, (2) To share information of successful performance strategies and the benefits derived from using thes strategies [15].

The award eligibility organization categories into:

- Manufacturing businesses
- Service businesses
- Small businesses
- Education organizations
- Health care organizations
- Non profit organizations

The system perspective of non profit organizations has same with manufacturing businesses, therefore they has identical criteria framework also. The Baldrige Award framework as describes in figure 1 shows the relationship between those criteria.

To explain the relationship among the categories, as we can see in figure 1, there are 7 categories that composed of the six categories in the center and one category in the foundation. Leadership (category 1), Strategic Planning (category 2), and Customer Focus (category 3) represent the leadership triad. These categories are placed together to emphasize the importance of a leadership focus on strategy and customers. Workforces Focus (category 5), Process Management (category 6), and Business Results (category 7) represent the results triad. The organization's workforce and key process accomplish the work of the organization that yields the overall performance results. The horizontal arrow in the center of the framework links the leadership triad to the results triad, a linkage critical to organizational success. Furthermore, the arrow indicates the central relationship between Leadership and Results. The two-headed arrows indicate the importance of feedback in an effective performance management system. Measurement, Analysis, and Knowledge Management (category 4) serve as a foundation for the performance management system.

This category is critical to the effective management of organization and to a fact-based, knowledge driven system for improving performance and competitiveness.

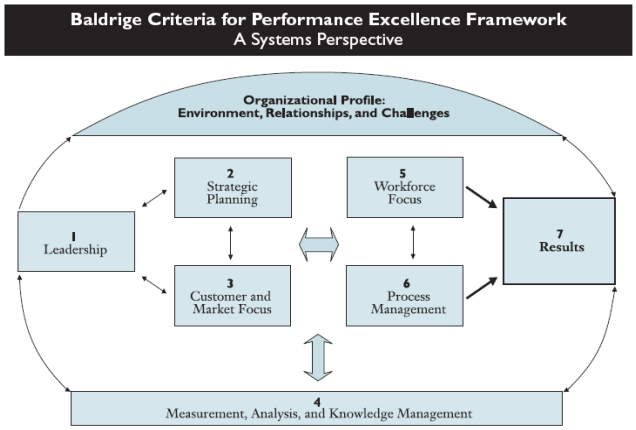

Figure 1. MBNQA framework

In term of Total Quality Management (TQM), one of the major obstacles to empirical investigations of quality in organizations has been the difficulty id defining precisely what quality is. Although is has been many variety of attributes as core aspects of organizational quality, those are not comprehensive due to point out the tremendous diversity of dimensions, attributes, and definitions that are discussions of quality [16]. Therefore, when MBNQA created, there is some examination of this model framework to accomplish that significant step forward. As illustrated in figure 2, the categories are structured in driver, system and outcomes classification.

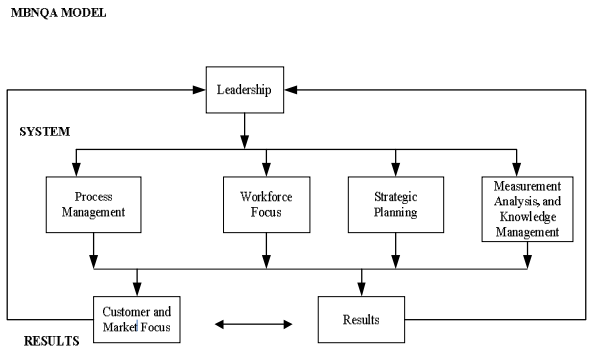

Figure 2. Classification of MBNQA framework

The Leadership category is classified as a *driver* of quality. Four categories - strategic planning, measurement analysis and knowledge management, workforce focus, and process management – are classified as *systems*. Two categories are assumed to be desirable *outcomes*, namely, customer and market focus, and results. This framework specifies that the driver of quality has both direct and indirect impact on outcomes and that the systems mediate the driver as well as has direct impact on the quality outcomes.

4. SOCIAL ENTERPRISE BALANCED SCORECARD MODEL

Social Enterprise Balanced Scorecard was created by Somers in 2005 when he done his research in UK social organization [12]. Inspired from Kaplan original BSC framework to NPOs which is illustrated in figure 3 [17], there were three changes adjusted: an additional layer was added in which social goals are articulated above the financial perspective. The financial perspective was broadened to focus on sustainability, and the customer perspective was widened to capture a larger number of stakeholder groups.

Figure 3. Balanced Scorecard for Non Profit Organization

In SEBC framework showed in figure 4, social enterprises begin by stating their social goals as desired outcomes, and then move into perspectives. In the financial sustainability perspectives, each bubble represents an objective. The stakeholder perspective is the advantageous from this model. Pearce [18] state stakeholder definition is those people or groups who are either affected by or who can affect the activities of an organization. Thus in SEBC model, the customer perspective has to consider as more stakeholders as well as the organization's wider impact. Since social organization is a response for greater community and employee involvement in, and ownership of, it is important for managers to be able to distinguish between those who pay for a service, those who use them, those who benefit from the intervention in the long term, and those who consume it (donors, grant funders, employees, and the wider community), as these are not always the same. The arrows illustrate cause and effect chain from the strategy map.

In Financial Sustainability perspective, the main focus is not increasing productivity for financial gain from product sales revenue, but to increasing productivity for social gain. For instance, a company produces soap. In term of achieving good earnings, profit organization will plan attraction promotion, boost their capacity, and manage the production schedule accurately, in order to estimate manufacture forecast and profit margin for further improvement. In social organization, however, the

objective mainstream is how healthiness impact to community. Do the effluent soap have negative effect for environment? Or do the soap ingredients or other product knowledge written in soap package to show transparent information to consumer. Then, to the employee itself, do they provide work safety policy tightly.

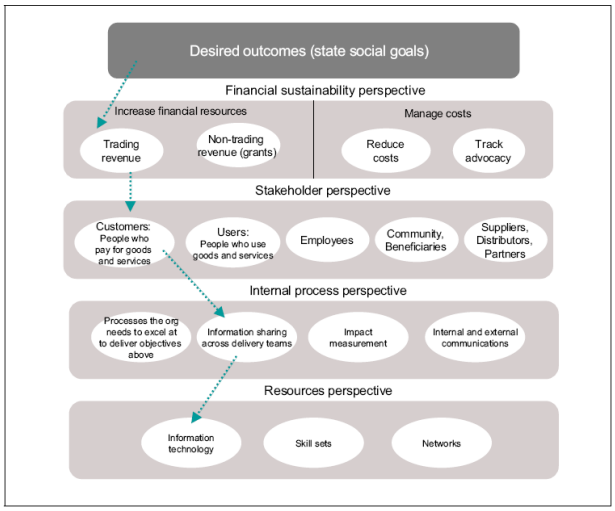

Figure 4. Social Enterprise Balanced Scorecard Model

The next perspective is internal process that has similarity with original BSC concept. The important point to note is that there are not only one stakeholder here, like shareholder in profit organization, but various stakeholders in social organization could make various impact to the process. The process need to attend communication relationship and information management in internal and external stakeholders. Regarding to this necessity, the resources perspective as the support for the internal process allocate and evaluation all of the resources required for the social organization operational.

5. LINK SEBC AND MBNQA

Chua [19] stated the framework for evaluating performance using BSC and Singapore Quality Award (SQA). Even though their model inspiring this research, however, it have never been tested empirically if the platform also alignmnet in social organization. The lack of how key performance indicators emphaized and how its measured also being limitation of their model. This paper has desirable objectives to bring to light how the MBNQA can be further leveraged upon with strategic tool like SEBC to capture the effect on financial performance due to the perceived impact of quality improvement activities. Through the model design by using MBNQA classification, the SEBC perspective took place in contribute the assessment in scorecard method.

While MBNQA regrouped into driver, systems, and results, thus the SEBC taking their four perspectives and incorporate them into another set of framework. Now, the integrated framework consist of (1) *driver* - MBNQA leadership and strategic planning categories, integrate with SEBC resources perspective (2) *systems* - MBNQA workforce focus, process management, measurement analysis and knowledge management categories, put together with SEBC financial and internal business perspectives, (3) *results* - MBNQA customer and market focus and results, integrate with SEBC stakeholder perspective. This groups listed in table 2 and framework illustrated in figure 5.

Table 2. Integration Model Group

Classification	MBNQA (category)	SEBC (perspective)	Key Result Area
Driver	• Leadership • Strategic Planning	Resources	• Leadership • Strategic Development • Strategic Deployment • Asset Management • Network & IT
System	• Workforce Focus • Process Management • Measurement, Analysis, and Knowledge Management	• Financial • Internal Business	• Funding & Expense Management • Employee (volunteer) availability • Information & Comunication • Operational Process • Audit, Monitoring & Evaluation • Knowledge Management
Result	• Customer and Market Focus • Results	Stakeholder	• Stakeholder requirement & expectation • Stakeholder Willingness • Community advantage • Relationship (customer, supplier, partner) • Society Need

5.1 Driver

Driver explains in how the management defines the organization goals, create the value, target, policy and drive those to excellent business performance and customer delight. The important point to note is that 'customer' here meaning person who serve and take advantage from organization with/out paying. In other word, customers in social organization do not have contributed to profit organization at all. This is seriously to understand because of the priorities of social organization determine in how best to achieve social outcomes than revenue outcomes. Therefore, in *driver*, leadership category focuses on how leaders' action guide and sustain the organization. For

social organizations that rely on volunteers to accomplish their work, responses to communication also should consider the efforts to communicate with and engage the volunteer workforce. As it stands, network and asset management from resources perspective, supported by information technology, become encompasses input to develop the strategy and corrective feedback for the next improvement.

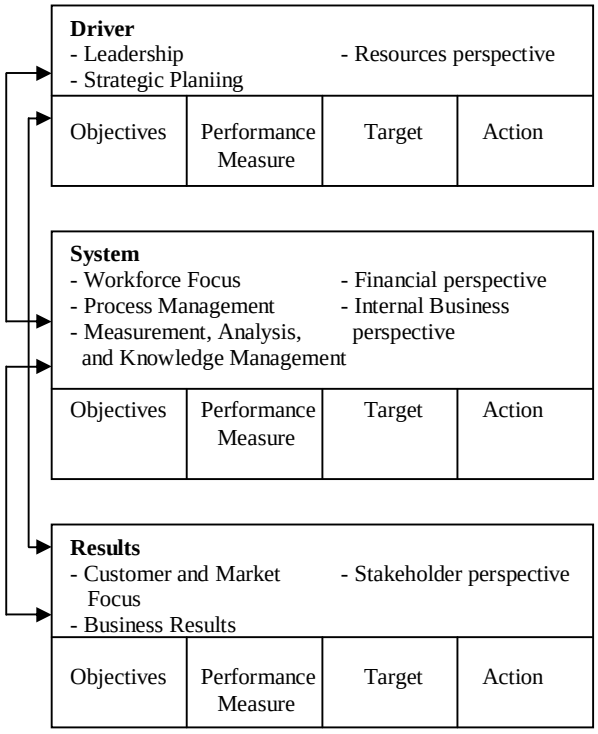

Figure 5. Integrate Framework of MBNQA and SEBC

5.2 System

In term of input process output, system is the process itself. System consists of well-plan activities that define systematically in order to fulfill the stakeholder requirement and perform the evaluation indeed. Due to driver value chain, system builds with most of MBNQA categories and couple perspectives of SEBC included cash flow. Financial perspective usually stated in top line of enhancement. This is main different between original BSC and SEBC. Stakeholder satisfaction is more essential than earnings collection. The ultimate objectives in social organization rely on social value added. However, this does not mean that financial is not important. Social activities needs money in run their operation, for communication, training, transportation, food, and other necessity. In order to ensure social mission focus, the categories and perspectives should be linked and oriented towards its social bottom line.

By this point of view, workforce in social organization term, are not limited in employees, who get salary from their work, but also volunteers. Therefore, workforce productivity can not measure only by the ratio of earning, thus feeling of social service willingness is the main motivation of this volunteers. This issue also make why social organization workforce measurement are more complex than commercial organization. This not only talked about how many working hour spend, or how much income the organization could have as the profit, but also social emotion that rely on the volunteers. That, perhaps, be the reason why social organization management lack of discipline and authority in managing their employees. Knowledge management could also assist in continuous improvement by addressing 'know how, know why, know what, know who, and know where'. Knowing these will help to streamline the organization's internal processes.

5.3 Results

Results discuss in how leadership and system emphasized the stakeholder performance, market and business. In term of customer, social organization states stakeholder as customer, supplier, donors, government, and widely community, and specially the client itself. Product offerings should consider all the important characteristics of products and services and their performance throughout their full life cycle and the full consumption chain. The focus should be on features that affect stakeholder preference and expectation. This feature makes differentiate between profit organizations that compete offering with other organizations, and socially improving impact in social organization. The results of performance measurement are not only useful in gaining additional funds but can also be used in the programs run by social organization, such as changing program design or operations, planning future programs, promoting the program to potential clients and improving outreach and public relations.

5.4 Measurement Deployment Model

To complete the integrate model measurement, it is necessary to construct the scorecard and the cause-effect relationship among the key performance indicator deployed from the MBNQA and SEBC items. As it stands in table 3 is the example scorecard for *driver* classification. The *system* and *results* classification can framed with the same deployment like *driver*.

Table 3. Scorecard for Driver

	Items	KPI	Objective	Target	Weight	Score Range	Score
DRIVER	Senior Leadership (D1)	K1	O1	T1	0.58	K1 ≥ T1 x1≤K1≤x2 K1 ≤ x3	3 2 1
	Governance & Societal Responsibilities (D2)	K2	O2	T2	0.42	K2 ≥ T2 x4≤K2≤x5 K2 ≤ x6	3 2 1
	Strategic Development (D3)	K3	O3	T3	0.47	K3 ≥ T3 x7≤K3≤x8 K3 ≤ x9	3 2 1
	Strategic Deployment (D4)	K4	O4	T4	0.53	K4 ≥ T4 x10≤K4≤x11 K4 ≤ x12	3 2 1
	Resources (D5)	K5	O5	T5	0.25	K5 ≥ T5 x13≤K5≤x14 K5 ≤ x15	3 2 1

where:

$D_i, i = 1,....n$ is items subsection from Driver

D1 and D2 items from MBNQA Leadership
D3 and D4 items from MBNQA Strategic Planning
D5 item from SEBC Resources perpective

$T_i, i = 1,....n$ is ultimate target to achieve of the KPI

$K_i, i = 1,....n$ is key performance indicator deployed from the items

$O_i, i = 1,....n$ is objective determined from the KPI

$x_i, i = 1,....n$ is score range for KPI

Score divided into three section, whereas (score) 3 when K_i achieve the target, and others two when it not meet the target.

Weight quotition differentiate between MBNQA items and SEBC items. As SEBC is modified model from original BSC, the weight from each perspective establish from the management priority. In this integrated model, we use equal degree of weight for 4 perspectives which is 0.25 each. For further application it can be change depend on the importance concern.

Degree of weight for MBNQA items adopted from the MBNQA point values. From MBNQA 2009 [15] point values have already stated for each categories and items. This MBNQA point values listed in table 4.

Table 4. Degree of Weight for MBNQA Items

Classification	Category	Point	• Item	Point	Weight
1. *Driver*	*Leadership*	120	• Senior Leadership	70	0.58
			• Governance and Societal Responsibilities	50	0.42
	Strategic Planning	85	• Strategic Development	40	0.47
			• Strategic Deployment	45	0.53
2. System	*Workforces Focus*	85	• Workforce Engagement	40	0.47
			• Workforce Environment	45	0.53
	Measurement, Analysis, and Knowledge Management	90	• Measurement, Analysis, and Improvement of Organizational Performance	45	0.5
			• Management of Information, Knowledge, and Information Technology	45	0.5
	Process Management	85	• Work Systems	35	0.41
			• Work Processes	50	0.59
3. Result	*Customer Focus*	85	• Customer Engagement	40	0.47
			• Voice of the Customer	45	0.53
	Results	450	• Product Outcomes	100	0.225
			• Customer-Focused Outcomes	70	0.155
			• Financial and Market Outcomes	70	0.155
			• Workforce-Focused Outcomes	70	0.155
			• Process Effectiveness Outcomes	70	0.155
			• Leadership Outcomes	70	0.155
Total		1000		1000	

The cause-effect relationship describes in figure 6 show the connection among the classification (driver, system, results) and their items. These relations indicate input direction through the indicators in order to support affect performance within the process. Performance measures with both lagging and leading, are then linked to strategic identified in organization mission, which align with the vision of the organization.

6. MODEL IMPLICATION

The measurement told the results of activities already taken. If any indicators can not meet the target determined, then some action to improve should be needed. This similar with the Deming quality cycle – PDCA (Plan, Do, Check, Action), that remind us the quality journey is always like a wheel in escalation way to consistently do continuous improvement. There are some implications of the integrate model that need some consideration, for instance:

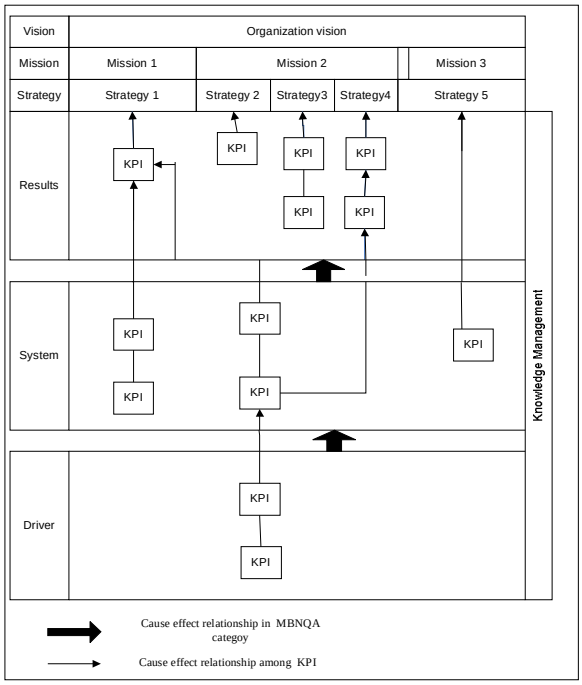

Figure 6. Cause Effect Relationship

- Strategy and performance measurement should focus on what output and outcomes of the organization intends to achieve, not what programs and initiatives are being implemented.
- Stakeholder, especially recipients, are more critical than other perspective
- Management of social organization should rely the policy on socially motif than commercial motif
- The organization should focus its limited resources on a limited set of objectives and constituents.
- Key performance indicators generate from MBNQA should consider in effectiveness results. As excellent model that cover up all aspect in the organization, MBNQA has widely attributes to assess, and lack of effective goals.
- In subsequence, key performance indicators generate from SEBC should concentrate in efficiency results. As excellent reporting tool with a discrete set of level indicators, provides management with a quick, comprehensive of organizational performance [3]. For this purpose, there is awareness that SEBC focusing in effectively more than its efficiency.

As a conclusion, measuring success in social organizations need three important lessons to learn, which are: measuring depend on the objectives, keep measures simple and easy to communicate, and stay focus on social line. This MBNQA and SEBC integrate model hopefully can give another measurement model in NPO that in today world changing, need humanity balance than just gaining more revenue.

7. REFERENCES

[1] Singh, CA.Jyoti & Mirchandani, Pooja, *Performance Measurements For Not-For Profit Organisations*, The Chartered Accountant, 2006

[2] Kong, Eric, *The strategic Importance of Intellectual Capital in The Non Profit Sector*, Journal of Intellectual Capital Vol.8 Iss.4 pg.721, 2007

[3] Clarkson, Paul & Challis, David, *Performance Measurement in Social Care: A Comparison of Efficiency Measurement Methods*, Personal Social Services Research Unit (PSSRU), Faculty of Medical and Human Sciences, University of Manchester, UK, 2006

[4] Salamon et al, *Excerpted from Global Civil Society: Dimensions of the Nonprofit Sector*, Johns Hopkins Center for Civil Society Studies, 1999

[5] Wilderom et al, *High Quality Management of Private Nonprofit Organizations*, International Journal of Public Sector Management, Vol. 9 No. 7 pp. 60-71, 1996

[6] Cutt, James, *Performance Measurement in Non Profit Organisations: Integration and Focus Within Comprehensiveness*, Asian Journal of Public Administration, Vol.20 No.1 pp.3-29, 1997

[7] Wu, Cheng Ru, et al, *FAHP Sensitivity Analysis For Measurement Nonprofit Organizational Performance*, Department of Finance, Yuanpei University, Taiwan, 2006

[8] Neely, Andy, *Perspectives of Performance: The Performance Prism", The Evolution of Business Performance Measurement Systems*, Research Project sponsored by EPSRC under grant number GR/K88637, 2002

[9] Wu, SI & Hung, JM, *A Performance Evaluation Model of CRM on Nonprofit Organizations*, journal Total Quality Management & Business excellent, 2008

[10] Niven, Paul R., *Balanced Scorecard: Step-by-Step for Government and Non-Profit Agencies*, John Wiley, 2003

[11] Zimmerman, Joel, *Using a Balanced Scorecard in a Nonprofit Organization*, Creative Direct Response, Inc., 2004

[12] Somers, Ali.B, *Shaping The Balanced Scorecard for use in UK Social Enterprises*, Social Enterprise London, 2005

[13] Kaplan, R.S. & Norton, D.P., *Strategy Maps: Converting Intangible Assets into Tangible Outcomes*, Harvard Business Review, Vol.82, 2004

[14] Yeung, AK. & Connel, J., *The application of Niven's Balanced Scorecard in a Not-for-Profit Organization in Hongkong*, Journal of Asia Business Studies, 2006

[15] www.baldrige.nist.gov

[16] Winn, BA. & Cameron, KS., *An Examination of The Malcolm Baldrige National Quality Framework*, Research in Higher Education, Vol.39 No.5, 1998

[17] www.balancedscorecard.org

[18] Pearce, John, *Social Enterprise in Anytown*, London: Calouste Gulbenkian Foundation, 2003

[19] Chua, CC. & Goh, M., *Framework for Evaluating Performance and Quality Improvement in Hospitals*, Managing Service Quality, Vol.12 No.1 pp. 54-66, 2002

Proceeding of the 11th International Conference on QiR (Quality in Research)
Faculty of Engineering, University of Indonesia, Depok, Indonesia, 3-6 August 2009
ISSN 114-1284

Application of Response Surface Method in Optimizing Process Parameters in Drilling Process with Modification Tools

Mahros Darsin[a)], Yuni Hermawan[b)], Ainnur Rohman[c)]

[a)] *Faculty of Engineering*
the University of Jember, Jember 68111
Tel: (0331) 484977 ext 102. Fax (0331)484977
E-mail: mahros.azzahra@yahoo.co.id

[b)] *Faculty of Engineering*
The University of Jember, Jember 68111
Tel: (0331) 410243 Fax (0331)410243
E-mail: yuni_kaka@yahoo.co.id

[a)] *Faculty of Engineering*
The University of Jember, Jember 68111
Tel: (0331) 410243 Fax (0331)410243
E-mail: jayadies@yahoo.com

ABSTRACT

In drilling process with standard twist drill usually roundness is deviate, because of single feed rate. To get desired roundness it needs advanced drilling. Another way to reduce processes step is modification of tool. In this method edge of $2k_r$ is reduced by cutting the ends. In this way, in one step of drilling there are two different feed rates. This research is focused on influence drilling parameters, i.e. cutting speed (V), feed rate (f) and depth of cut (a), on roundness of hole resulted of modified twist drilling tool. Each chosen parameters is varied 3 levels. Research developed using materials of ST 41 steel with dimension of h = 1 cm, d = 25.4 mm amount of 30 specimens. Ends of twist drill were cut from normal/standard half of k_{r1} (59°) to be 45° and length of lips is 0.2 x D. Variable response is value of roundness (MLA). Variation and combination of each parameters according Box-Behnken design experiment of Response Surface Method. Mathematical model roundness respond of a hole resulted from drilling for constant nominal relief edge (α) is $T=K/(V^m f^n \alpha^\gamma)$, where T is roundness respond. Logarithmic model is $\ln T = \ln K - m \ln V - n \ln f - \gamma \ln a$. Square regression of the model for roundness of standard tool is $\hat{Y}_{MLA} = 87.692 + 10 X_1 + 7.5 X_2 - 5 X_3 + 11.538 X_2^2 + 6.538 X_3^2$. Where X_1 is cutting time, X_2 is feed rate and X_3 is depth of cut. The developed model then tested by many tests. By the method it is found that the optimum V =15.000, f = 0.125 and a = 8.500 with roundness value is 83.2692 and desirability 0.91673. Where as for modified tool, the optimum predicted roundness is 64.7388 with desirability degree of 0.93526 when V = 15.0000, f = 0.1250 and a = 8.4832.

Keywords
Optimization, drill, roundness, RSM

1. INTRODUCTION

In order to develop an adequate relationship surface finish and the cutting parameters (such as cutting speed, depth of cut, feed, etc), a large number of tests are needed, requiring a separate set of tests for each combinations of cutting parameters. This increases the total number of tests and as a result the experimentation cost also increases. As a group of mathematical and statistical techniques, response surface methodology (RSM) is useful for modeling the relationship between the input parameters and output responses. RSM could save cost and time by reducing number of experiments required.

In assessing machinability, some researchers have tried to employ response surface methodology to design their experimentations, and to establish the models. Alauddin *et al* [1], Ginta et al [2], and Mansour *et al* [5] applied response surface methodology to optimize the surface finish in milling. Manurung used RSM for optimizing transesterification of biodiesel processing [5]. Oktem *et al* used response surface methodology with a developed genetic algorithm (GA) in the optimization of cutting conditions for surface roughness [9]. Sharif *et al* used factorial design coupled with response surface methodology in developing the surface roughness model in relation to the primary machining variables such as cutting speed, feed, and radial rake angle [10]. In short, relative smaller number of designed experiments is required by applied the method to generate much useful information.

The main objective of this work is to find-out optimum roundness in drilling of ST 41 using modified tool. Roundness will be established based on cutting speed, feed rate and depth of cut. Box-Behnken with k = 3 used to design the experimentations. Minitab version 14 program will be used to analyze the data and to develop the models [3]. The adequacy of the model was tested at 95% confidence level.

2. BASIC THEORY

Element of Machining. There are five basic elements in maching i.e cutting speed (v) in m/minute, feeding speed (f) in mm/rot, depth of cut (a) in mm, cutting time (t_c) in min., rate of metal removal (z) in cm^3/min.

Twist drill is a cutting tool used for making holes in solid materials. It basically consist of two partas; the body cutting edges and shank which is used for holding purposes. This has two cutting edges and two opposite spiral flutes cut into its surface as shown figure 1.

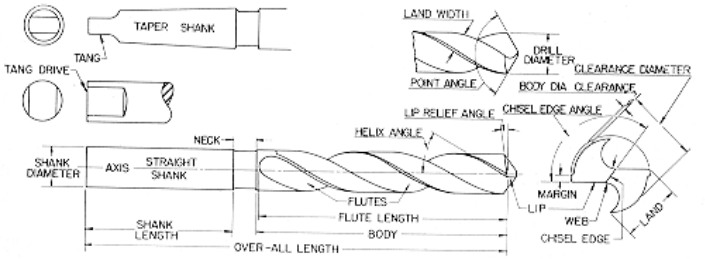

Figure 1—Illustrations of Terms applying to Twist Drills.

Modified Tool. Modification of tool end has been developed to reduce deviation in drilling by standard tool. One method to modify is by changing angle of $2k_r$ become two stages. In effect it will reduce value of unroundness, because tool not only to drill but also to bore. For ST 41 material optimum of $2k_r$ edge 118^0 [8]. End of tool is grinded up to k_{r1} half of end normal tool 59° and length of side k_{r1} 3/5 from normal tool. Therefore edge of $k_{r2} < k_{r1}$ i.e. 45° and lengrh of side is k_{r2}

3. EXPERIMENTAL METHOD

Research developed using materials of ST 41 steel with dimension of h = 1 cm, d = 25.4 mm amount of 30 specimens. Where as, diameter of twist drill used is 13 mm, 15 mm and 17 mm. Ends of twist drill were cut from normal/standard half of k_{r1} (59°) to be 45° and length of lips is 0.2 x D as shown in the following figure.

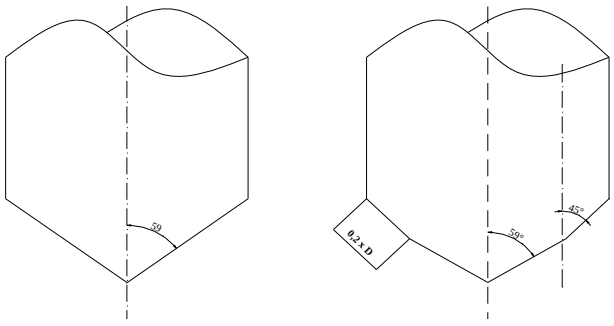

Figure 2. Comparison between standard and modified tool

Three process variables are chosen with three level of each one. Each level coded as lower level (-1), middle level (0) and upper level (+1).

Table1: Variation of parameters

Factor	Lower Level	Middle Level	Upper Level
Code	-1	0	1
cutting speed /v (X_1) in m/min.	15	17	20
feed rate /f (X_2) in mm/rot	0.125	0.200	0.315
depth of cut /a (X_3) in mm	6.5	7.5	8.5

Variable response is value of roundness (MLA). Those values are according to recommended ones for drilling with HSS tools and also number of feed available on the machine. Variation and combination of each parameters according Box-Behnken design experiment of Response Surface Method.

Table 2: Design experiment of Box- Behnken with k-3

No	X_1	X_2	X_3
1	-1	-1	0
2	1	-1	0
3	-1	1	0
4	1	1	0
5	-1	0	-1
6	1	0	-1
7	-1	0	1
8	1	0	1
9	0	-1	-1
10	0	1	-1
11	0	-1	1
12	0	1	1
13	0	0	0
14	0	0	0
15	0	0	0

Mathematical model roundness respond of a hole (T) resulted from drilling for constant nominal relief edge (α) is

$$T=K/(V^m f^n \alpha^\gamma) \quad \text{.....(1)}$$

where K, m, n, γ are constants.
Logarithmic model is

$$\ln T = \ln K - m \ln V - n \ln f - \gamma \ln a \quad \text{.....(2)}$$

Linier mode of the above equation (2) become:

$$\eta = \beta_0 + \beta_1 X_1 + \beta_2 X_2 + \beta_3 X_3 \quad \text{.....(3)}$$

Second order equation for mathematics modeling is developed from equation 3 is:

$$Y = b_0 + b_1 X_1 + b_2 X_2 + b_3 X_3 + b_{11} X_1^2 + b_{22} X_2^2 + b_{33} X_3^2 + b_{12} X_1 X_2 + b_{13} X_1 X_3 + b_{23} X_2 X_3 \quad \text{.....(4)}$$

with: X_i = independent variable, i = 1, 2, 3... k
b_0 = constant
b_i = coefficient of model parameter, i = 1, 2, 3... k

4. EXPERIMENTAL RESULTS AND DISCUSSION

Results of experiments are shown in table 3 for standard tool and modified tool. From the data of table 3 then developed mathematical model for estimated coefficients using Minitab 14 program. Regression model for the model results the estimated coefficients as shown at table 4.

Table 3: Data of parameters and roundness

No	V (mm/min)	F (mm/rot)	a (mm)	MLA STD*) (μm)	MLA Modif**) (μm)
1	15	0,125	7,5	80	60
2	20	0,125	7,5	100	70
3	15	0,315	7,5	100	80
4	20	0,315	7,5	120	100
5	15	0,200	6,5	90	90
6	20	0,200	6,5	110	100
7	15	0,200	8,5	80	70
8	20	0,200	8,5	100	90
9	17	0,125	6,5	100	80
10	17	0,315	6,5	120	100
11	17	0,125	8,5	100	80
12	17	0,315	8,5	100	90
13	17	0,200	7,5	90	80
14	17	0,200	7,5	90	80
15	17	0,200	7,5	80	70

*) STD: Standard tool
**)Modif: Modified tool

Table 4 Estimated Regression Coefficients for Roundness

Term	Coef	SE Coef	T	P
Constant	87.692	2.412	36.354	0.000
v	10.000	1.775	5.633	0.000
f	7.500	1.775	4.225	0.002
a	-5.000	1.775	-2.816	0.020
f*f	11.538	2.605	4.429	0.002
a*a	6.538	2.605	2.510	0.033
S = 5.021	R-Sq = 90.1%		R-Sq(adj) = 84.6%	

Square regression of the model for roundness of standard tool is $\hat{Y}_{MLA} = 87.692 + 10\ X_1 + 7.5\ X_2 - 5\ X_3 + 11.538\ X_2^2 + 6.538\ X_3^2$. Where X_1 is cutting time, X_2 is feed rate and X_3 is depth of cut.

The developed model then tested by lack of fit test. Analysis of variance (Table 5) shows that P-value lack of fit is 0.704, greater than $\alpha = 0.05$. It means that there is no lack of fit in the model or the model is suitable.

Table 5 Analysis of Variance for Roundness

Source	DF	Seq SS	Adj SS	Adj MS	F	P
Regression	5	2066.41	2066.41	413.282	16.39	0.000
Linear	3	1450.00	1450.00	483.333	19.17	0.000
Square	2	616.41	616.41	308.205	12.22	0.003
Residual Error	9	226.92	226.92	25.214		
Lack-of-Fit	7	160.26	160.26	22.894	0.69	0.704
Pure Error	2	66.67	66.67	33.333		
Total	14	6.79209				

P-value for linear is 0.000 and for square 0.003; both are less than $\alpha = 0.05$. It means that all variable parameters X_1, X_2, and X_3 contribute significantly to the model (Iriawan, 2006). Determination coefficient (R^2) is 90.1 %, it means that response can be declared by regression model resulted. Residual test shows that chart of residual versus the fitted values for standard and modification tool are randomly distributed and do not form certain pattern. It means the identical assumption for roundness is fulfilled.

Three residual tests are also carried out i.e. identical test, independent test and normal distribution test. Chart of residual versus the fitted values for cycle time (Figure 3) is randomly distributed and do not form certain pattern. It means the identical assumption for cycle time is fulfilled.

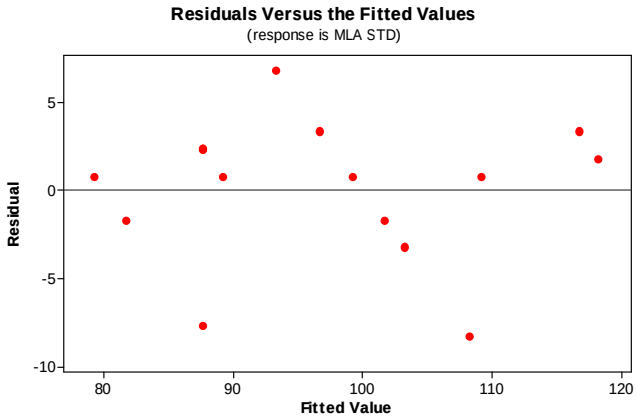

Figure 3. Residual versus the fitted values for response is roundness in standard tool

Normal distribution test (figure 4) ensures that line is plotted from left lower to right upper corner. It means the data is normal distributed.

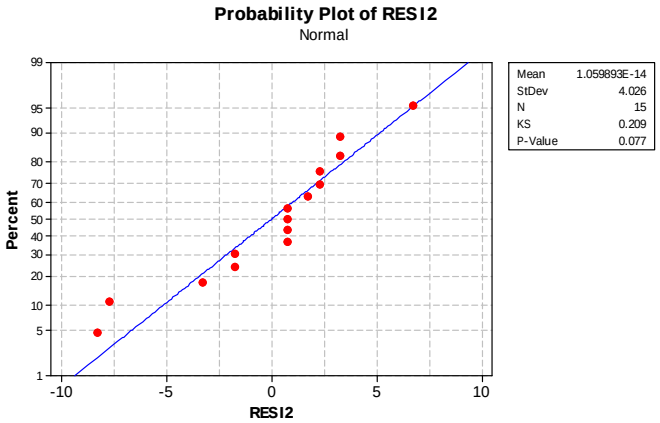

Figure 4. Probability Plot of Residual for normal distribution

Optimization of cycle time is searched by Response Surface Method using Minitab 14 version. Desirability function used for respond is The Smaller is Better, which means minimum value is desired. By the method it is found that the optimum v =15.000, f = 0.125 and a = 8.500 with roundness value is MLA STD = 83.2692 and desirability 0.91673.

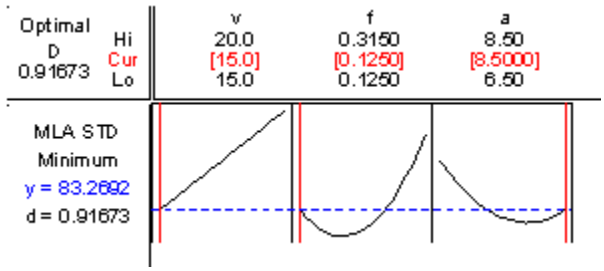

The same procedure was developed for modified tool which resulted Square regression of the model for roundness $\hat{Y}_{Modif\_MLA} = 77{,}143 + 7{,}5\ X_1 + 10\ X_2 - 5\ X_3 + 10.357\ X_3^2$. The developed model result in optimum predicted roundness of 64.7388 with desirability degree of 0.93526 when v = 15.0000, f = 0.1250 and a = 8.4832.

5. CONCLUSION

According to calculation using Minitab 14th version, variables influence cycle time in order are cutting speed, feeding rate, and depth of cut. By individual, the most influencing process variable onto roundness is cutting speed.

The optimum of roundness for normal tool is 83.2692 is achieved when cutting speed 15.000, feeding rate 0.125 and depth of cut is 8.500 with desirability 0.91673.

ACKNOWLEDGMENT

We would like to thanks to PT BBI Surabaya for their helpfulness during measuring session in the factory.

REFERENCES

1. Alauddin, M., El Baradie, M.A., Hashmi, M.S.J.. 1996. "Optimization of surface finish in end milling Inconel 718", Journal of Material Process and Technology 56, pp. 54 – 65.
2. Ginta, T.L., Amin, A.K.M.N., Karim, A.N.M., Lajis, M.A. 2008. Tool Life Prediction by Response Surface Methodology for End Milling Titanium Alloy Ti–6Al–4V Using PCD Inserts. Proceeding of the 2008 International Joint Conference in Engineering IJSE2008, Jakarta, Indonesia
3. Irawan, N. 2006. Mengolah Data Statistik dengan Mudah Menggunakan Minitab 14. Yogyakarta: Andi Yogyakarta.
4. Mansour, H., Abdalla, 2002. "Surface roughness model for end milling: a semi-free cutting carbon casehardening steel (EN32) in dry condition," Journal of Materials Processing Technology 124, pp. 183 – 191.
5. Manurung, R., 2008. "Application of Response Surface Methodology To Optimize Transesterification Process in Palm Biodiesel Production". Proceeding of the 2008 International Joint Conference in Engineering IJSE2008, August 4-5, Jakarta, Indonesia
6. Montgomery, D. C. 1997. "Design and Analysis of Experiments". 5th edition. New York: John Wiley & Sons.
7. Oktem, H. Erzurumlu, T. Kurtaran, H., 2005. "Application of response surface methodology in the optimization of cutting conditions for surface roughness," Journal of Material Processing and Technology 170, pp. 11 – 16.
8. Rochim, T. 1993. *"Teori dan Teknologi Proses Pemesinan"*. Jakarta : Higher Education Development Support Project
9. Sudjana. 1994. "Desain dan Analisis Eksperimen". Edisi III. Bandung: Tarsito.
10. Sharif,S., Mohruni, A.S., Noordin, M.Y., Vencatesh, V.C., 2006. "Optimization of surface roughness prediction model in end milling titanium alloy (Ti-6Al-4V)", Proceeding of ICOMAST, pp. 55 – 59.

Optimization of Cycle Time by Response Surface Method in Manufacturing Chamomile 120 ml Bottle Using Blow Molding Process

Mahros Darsin[1)], Yuni Hermawan[2)], Tatag Kristiyantoro[3)]

[1)] *Faculty of Engineering*

the University of Jember, Jember 68111
Tel: (0331) 484977 ext 102. Fax (0331)484977
E-mail: mahros.azzahra@yahoo.co.id

[2)] *Faculty of Engineering*
The University of Jember, Jember 68111
Tel: (0331) 410243 Fax (0331)410243
E-mail: yuni_kaka@yahoo.co.id

[3)] *Faculty of Engineering*
The University of Jember, Jember 68111
Tel: (0331) 410243 Fax (0331)410243
E-mail: tattag@gmail.com

ABSTRACT

Chamomile is a package which is applied for cosmetic. In industry this package is being processed by blow molding. The project aim is to optimize time for processing the package. There are many parameters that influence cycle time during production; in this project only three of them were varied, i.e. blowing pressure (X_1), blowing time(X_2) and stopping time(X_3). Three level of each parameter are X_1 (0.1, 0.55, and 1.0 second), X_2(10.5, 11.5 and 12.5 second) and X_3 (4, 5 and 6 bar). Combination of among levels is based on Box Behnken design of Response Surface Method. Each combination is replicated 5 times and then averaged. The data then is processed by using Minitab version 14th. Square regression of the model for cycle time is $\hat{Y}_{CT} = 21{,}1300 - 0{,}0912\ X_1 + 0{,}2000\ X_2 + 0{,}6313\ X_3 + 0{,}6100\ X_1^2 + 0{,}6975\ X_2^2 - 0{,}1000\ X_1 X_2 - 0{,}1725\ X_1 X_3 + 0{,}1100\ X_2 X_3$. Optimization of cycle time is searched by Response Surface Method and it is found that the optimum of cycle time is 20.5 seconds. The optimum condition is achieved when stopping time is 0.1 second, blowing time 11.35 second and blowing pressure 5.1 bars.

Keywords

Optimization, packaging, RSM, blow molding, cycle time

1. INTRODUCTION

Processing time influences quality and quantity of product. The less processing time the more quantity but not must the more in quality. Chamomile is a plastic bottle applied for cosmetic product. At the moment, production of the bottle is not optimum yet, from target of 20.000 products per shift its only reach 9.870 for cycle time of 26 seconds and 5.000 for 23 seconds. There are many parameters that influence cycle time during production blowing pressure, blowing time and stopping time, temperature, and dry cycle; in this project only first three of them were varied. Choosing of these three parameters is in accordance with fish bone diagram. Stopping time is time need for stopping in order to open and close the mold. Blowing time is time need for blow and fills the mold cavity. If blowing pressure is less that its requirement product will not well performed but if it too high product will explode. The research aim is to find out the optimum cycle time by varying those three parameters. Optimization is carried out using response surface method. In this research we do not explore chemical content of plastic materials.

2. BASIC THEORY

2.1 Chamomile manufacturing

Chamomile 120 ml is manufactured in a blow molding machine through several steps as detailed below:

a. Preparation of materials; the bottle is made of High Density Polyetilene (HDPE) granules, a thermoplastics which have melting time of 177 – 260°C (A. Brent Strong, 2000). HDPE used is combination 50% new and the rest is after used one.
b. Processing; the mixed granules feed into a machine hooper then fed through an opening in the injection cylinder onto the surface of a rotating screw drive which carries them towards the mold. The rotation of the screw (at continuous speed of 26 rpm) forces the granules against the heated walls of cylinder, causing them to melt due to the heat of compression, friction, and the hot walls of the cylinder. When sufficient plastic materials is melted at the mold end

of the screw, the screw stops and by a plunger like motion ejects a "shot" of melted plastic (parison) through a die head and then places between the jaws of a mold. The mold is closed to pinch off the ends of the cylinder, and compressed air is blown in, forcing the plastic against the walls of the mold. In chamomile forming it no need of colorants because HDPE color has same color as final product.

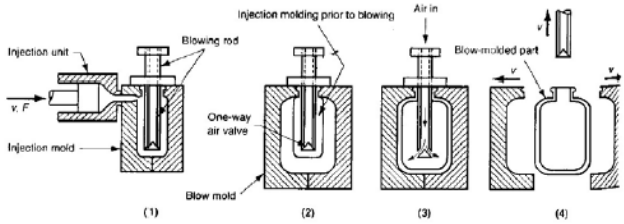

Figure 1. Blow molding; from parison to product

c. Last process is printing and labeling to the blown product

2.2 Cycle Time

Production cycle time is time needed for the machine to finish one product. In blow molding, one cycle is rotation of mold starts from opening the mold, followed by feeding of parison. Parison, then trapped by mold and blow pin come into the mold then controlled air compressed. Blow pin then taken out and follows by cooling. The last steps are opening the mold and ejecting. The process is return to the first step for next parison. One cycle time of chamomile processing is shown in figure 2.

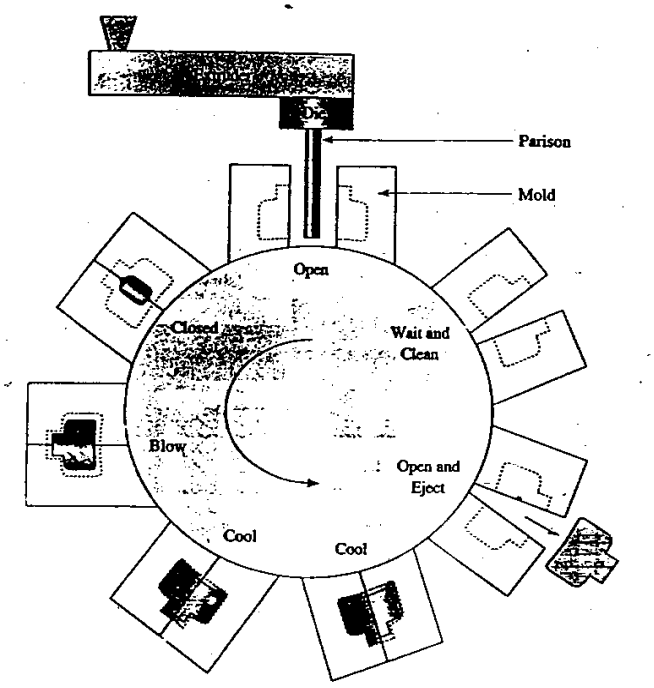

Figure 2. One cycle time for blow molding

3. EXPERIMENTAL METHOD

The project was carried out in a plastic manufacturing factory on Pandaan, East Java using blow molding Ekei Linier 4/8. The plastic material used is HDPE (*High Density Polyethylene*) which have specification: melting temperature 300 °C; specific mass 0,941-0,965 g/cm^3; crystalline degree 85-95 %; tensile strength 245-335 kgf/cm^2; elongation 100-25 %; impact strength 17-13 Kgf.cm/cm^2.

Three process variables are chosen with three level of each one. Each level coded as lower level (-1), middle level (0) and upper level (+1). For blowing pressure (coded as X_1) the level chosen are 4, 5 and 6 bars. Blowing time (X_2) is varied as 10.5, 11.5, and 12.5 seconds. Last process variable, stopping time (X_3), leveled as 0.1, 0.55 and 1.0 seconds. The experiment is developed according to Box Behnken for Response Surface Method as shown at table 1.

Table 1: Design experiment of Box- Behnken with k-3

No	X_1	X_2	X_3
1	-1	-1	0
2	1	-1	0
3	-1	1	0
4	1	1	0
5	-1	0	-1
6	1	0	-1
7	-1	0	1
8	1	0	1
9	0	-1	-1
10	0	1	-1
11	0	-1	1
12	0	1	1
13	0	0	0
14	0	0	0
15	0	0	0

Second order equation for mathematics modeling is developed from equation 1.

$$Y = b_0 + b_1 X_1 + b_2 X_2 + b_3 X_3 + b_{11} X_1^2 + b_{22} X_2^2 + b_{33} X_3^2 + b_{12} X_1 X_2 + b_{13} X_1 X_3 + b_{23} X_2 X_3 \quad (1)$$

With: X_i = independent variable, i = 1, 2, 3... k
b_0 = constant
b_i = coefficient of model parameter, i = 1, 2, 3... k

4. EXPERIMENTAL RESULTS AND DISCUSSION

A result of experiments is shown in table 2.

Table 2: Data resulted from *experiments*

No.	Parameter			*Cycle Time* (second)
	Blowing Pressure **(bar)**	***Blowing Time*** **(second)**	***Stop Time*** **(second)**	
1	4	10,5	0,55	22.22
2	6	10,5	0,55	22.33
3	4	12,5	0,55	22.77
4	6	12,5	0,55	22.48
5	4	11,5	0,1	21.08
6	6	11,5	0,1	21.15
7	4	11,5	1,0	22.65
8	6	11,5	1,0	22.03
9	5	10,5	0,1	21.05
10	5	12,5	0,1	21.28
11	5	11,5	1,0	22.13
12	5	12,5	1,0	22.80
13	5	11,5	0,55	21.19
14	5	11,5	0,55	21.15
15	5	11,5	0,55	21.10

From the data of table 2 then developed mathematical model for estimated coefficients using Minitab 14 program. Regression model for the model results the estimated coefficients as shown at table 3.

Table 3 Estimated Regression Coefficients for Cycle Time

Term	Coef	SE Coef	T	P
Constant	21.1300	0.03492	605.141	0.000
BP	-0.0912	0.02570	-3.551	0.012
BT	0.2000	0.02570	7.783	0.000
ST	0.6313	0.02570	24.564	0.000
BP*BP	0.6100	0.03772	16.174	0.000
BT*BT	0.6975	0.03772	18.494	0.000
BP*BT	-0.1000	0.03634	-2.752	0.033
BP*ST	-0.1725	0.03634	-4.746	0.003
BT*ST	0.1100	0.03634	3.027	0.023
S = 0.07269	R-Sq = 99.5%		R-Sq(adj) = 98.9%	

From equation (1) we develop equation model according to table 2 and we find:

$$\hat{Y}_{CT} = 21{,}1300 - 0{,}0912\ X_1 + 0{,}2000\ X_2 + 0{,}6313\ X_3 + 0{,}6100\ X_1^2 + 0{,}6975\ X_2^2 - 0{,}1000\ X_1 X_2 - 0{,}1725\ X_1 X_3 + 0{,}1100\ X_2 X_3 \quad (2)$$

The developed model then tested by lack of fit test. In this test, first hypotheses (H_0= there is no lack of fit) is refused if P-value is less than α and vice versa. In this experiment α is 5%. Analysis of variance, as shown at table 4, shows that *P-value lack of fit* is 0.241, greater than α = 0.05. It means that there is no *lack of fit* in the model or the model is suitable.

Table 4 Analysis of Variance for Cycle Time

Source	DF	Seq SS	Adj SS	Adj MS	F	P
Regression	8	6.76039	6.76039	0.84505	159.95	0.000
Linear	3	3.57443	3.57443	1.19148	225.52	0.000
Square	2	2.97854	2.97854	1.48927	281.88	0.000
Interaction	3	0.20742	0.20742	0.06914	13.09	0.005
Residual Error	6	0.03170	0.03170	0.00528		
Lack-of-Fit	4	0.02763	0.02763	0.00691	3.40	0.240
Pure Error	2	0.00407	0.00407	0.00203		
Total	14	6.79209				

It also clear stated from table 4 that, P-value for linear and square is 0.000; both are less than α = 0.05. It means that all variable parameters X_1, X_2, and X_3 contribute significantly to the model (Iriawan, 2006).

From table 3 we can see the determination coefficient (R^2) is 99.5% (nearly 1), it means that response can be declared by regression model resulted.

Three residual tests are also carried out i.e. identical test, independent test and normal distribution test. Chart of residual versus the fitted values for cycle time (Figure 3) is randomly distributed and do not form certain pattern. It means the identical assumption for cycle time is fulfilled.

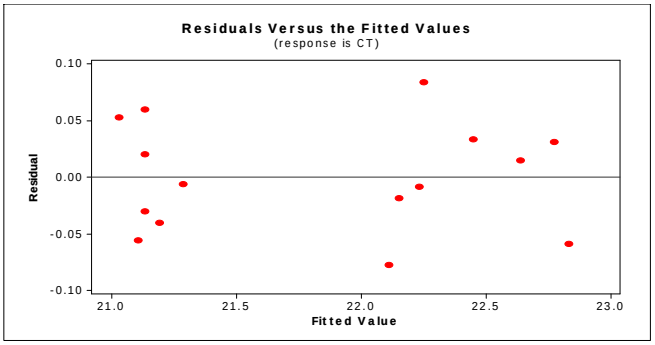

Figure 3. Residual versus the fitted values for response is cycle time

Independent test was carried out to ensure that observations have been done randomly or between observations there is no correlation (independent). *Auto Correlation Function* (ACF) plot (figure 4) shows that correlation values are in the interval of $\pm \frac{2}{\sqrt{n}}$ which means independency assumption is fulfilled.

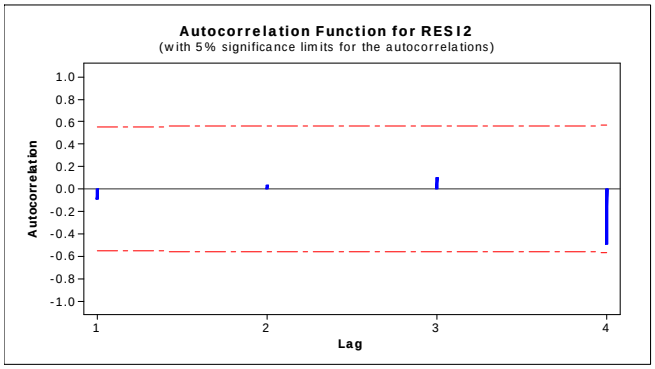

Figure 4. Autocorrelation Function for cycle time

Last test is normal distribution test. As shows at figure 5 that all plot distributed closed a straight line. It means that residual is normally distributed (figure 5).

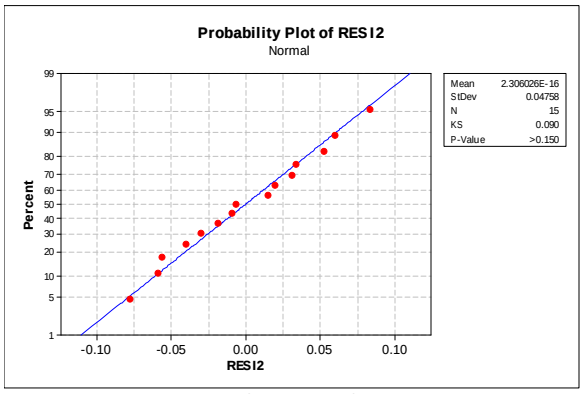

Figure 5. Probability Plot of Residual for normal distribution

Optimization of cycle time is searched by Response Surface Method using Minitab 14th version. The suitable method for this case is The Smaller is better which means minimum value is desired between values of 19 $\leq \hat{Y}_{CT} \leq$ 23 according to cycle time standard from the factory. By the method it is found that the optimum of cycle time is 19.20 seconds. The optimum condition is achieved when stopping is 0.1 second, blowing time 11.35 second and blowing pressure 5.1 bars with degree of desirability of 80.01%.

A graph of surface plot blowing pressure, blowing time and stopping time onto cycle time is shown at figure 6.

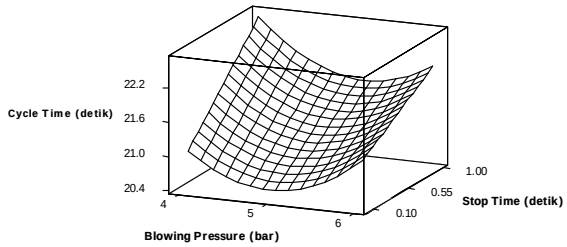

Figure 6. Surface Plot Blowing Pressure and *Stopping Time* onto *Cycle Time* at *Blowing Time* 11.5 seconds

5. CONCLUSION

According to calculation using Minitab 14th version, variables influence cycle time in order are blowing pressure, blowing time, and stop time. By individual, the most influencing process variable onto cycle time is stopping time.
The optimum of cycle time is 19.20 seconds is achieved when stopping is 0.1 second, blowing time 11.35 second and blowing pressure 5.1 bars with degree of desirability of 80.01%

ACKNOWLEDGMENT

We would like to thanks to PT Berlina plastic for their permission to do research in the factory.

REFERENCES

[1] Amrillah, Rodhy. 2006. *Penentuan Setting Parameter pada Proses Blow Molding dengan Metode Response Surface*. Surabaya: Jurusan Teknik Mesin Institut Teknologi Sepuluh Nopember [17 Maret 2008].
[2] Irawan, Nur. 2006. *Mengolah Data Statistik dengan Mudah Menggunakan Minitab 14*. Yogyakarta: Andi Yogyakarta.
[3] Montgomery, Douglas. C. 1997. *Design and Analysis of Experiments*. 5th edition. New York: John Wiley & Sons.
[4] PT. Berlina Tbk. 2007. *Diktat Design Mould Blow.* Pasuruan: PT. Berlina Tbk
[5] Setyawan, Nawang. 2008. *Penentuan Setting Parameter pada Proses Blow Molding Mesin AUTOMA PLUS AT2DS*. Surabaya: Jurusan Teknik Mesin Institut Teknologi Sepuluh Nopember.
[6] Strong, A. Brent. 2000. *Plastics Materials and Processing Second Edition*. New Jersey: Pearson Education.
[7] Sudjana. 1994. *Desain dan Analisis Eksperimen.* Edisi III. Bandung: Tarsito.
[8] Surdia T, Saito S. 2000. *Pengetahuan Bahan Teknik*. Jakarta: Pradnya Paramita.
[9] Tjitro, Soejono., Marwanto Henry. *Optimasi Waktu Siklus Pembuatan Kursi Dengan Proses injection Moulding*. http://www.google.co.id/optimasi_waktu_siklus/user_files/91019/Soejono_Jurnal%20Poros06.doc [17 Maret 2008].

COMPARISON BETWEEN CRITICAL CHAIN AND CRITICAL PATH METHOD IN TELECOMMUNICATION TOWER CONSTRUCTION PROJECT MANAGEMENT

M. Dachyar[1], Utomo Dhanu Saputra[2]

[1]*Industrial Engineering Department, Faculty of Engineering*
University of Indonesia, Depok 16424
Tel : Tel : (021) 78888805 Fax (021) 78885656
E-mail : mdachyar@yahoo.com

[2]*Industrial Engineering Department, Faculty of Engineering*
University of Indonesia, Depok 16424
Tel : (021) (021) 78888805 Fax (021) 78885656
E-mail : utomo_dhanu_ti04@yahoo.com

Abstract

The purpose of this research is looking for appropriate method in Telecommunication Tower Construction Project Management by doing comparison between critical chain and critical path method.
Researching in project time management of telecommunication tower construction which researcher made two scheduling, critical chain and critical path, base on Project Management Body of Knowledge and compare the result with triple constraint factor and general factor as comparator factors.
The result of this research are total of duration of critical chain method is 197,75 days and total of duration critical path method is 207 days. Conclusion of comparison is critical chain method is better in scope, time and output factors whereas critical path method is better in input and process factors.

Keywords: *Project time management, critical path method, critical chain method, telecommunication tower construction.*

1. Introduction

Telecommunication industry in Indonesia growth rapidly at this term, it make telecommunication provider especially in cellular race to get market share by improve their service. One of the way to improve their service is enlarge the coverage area by add BTS tower in the blind spot area of signal. This phenomena also make demand of BTS tower increase, but if this phenomena are not supported by good project time management it will effect project delay. It come because their have limitation especially in resource and time.
Project time management is needed to solve delay problem in tower construction project and to improve project quality that are combination of triple constraint factors[1]. Expancement of project management knowledge is very fast, so at this time this knowledge is not only use in construction industry but it used widely in other industry like telecommunication industry.
Waktu, biaya, dan ruang lingkup merupakan tiga faktor dalam *triple constraint*, dimana untuk mendapatkan kualiatas proyek maka harus didapatkan titik optimum diantara tiga hambatan tersebut. Untuk itu diperlukan suatu metode penjadwalan yang baik yang dapat mengatasi masalah keterlambatan proyek tersebut. Maka dibuatlah penelitian dalam rangka menentukan metode terbaik dalam proyek pembangunan menara telekomunikasi yaitu memperbandingkan dua metode penjadwalan yakni *critical chain* dengan *critical path*. Perbandingan 2 metode penjadwalan ini pernah dilakukan tetapi dalam ruang lingkup yang masih terlalu besar yaitu karakteristik metode, dimana dihasilkan bahwa penurunan durasi proyek mencapai 25% atau lebih, memastikan proyek berjalan tepat waktu, dan tanpa adanya penambahan sumber daya[2]. Selain itu terdapat penelitian yang menyimpulkan bahwa metode *critical chain* dapat digunakan sebagai dasar penjadwalan dimana terdapat ketidakpastian dari segi durasi[3]. Ataupula terdapat penelitian yang melihat apakah metode *critical chain* merupakan metode baru atau hanya bentuk pengemasan baru dari metode *critical path*[4]. Untuk itu penelitian ini berfokus pada perbandingan antara dua metode pada bidang industry telekomunikasi, yaitu pada manajemen proyek pembangunan menara telekomunikasi.

Time, cost, and scope are three factors in triple constraint, so in getting good project quality we have to find optimum point among triple those factors. For the reason it need a good scheduling method to prevent project delay. This research was made to find best method in telecommunication tower construction project by compare two scheduling method there are critical chain and critical path method. Comparison between critical chain and critical path method have been made but the comparison only in wide scope and only touched the characteristic of method. Base on previous research result, using critical chain method scheduling will make reductions of 25% or more on project duration, ensure that each project finishes on time, and complete more project without adding

resources [2]. Another research show critical chain method can be use as scheduling baseline in uncertainty in project duration [3]. Previous research observed critical chain to answer the question, "is it a new method or only current method in new packaging?" [4]. There is no research that compare critical chain and critical path method deeply because of that this research is focusing in comparison between critical chain and critical path method on telecommunication industry especially in telecommunication tower construction project management.

2. Theory

Two methods that is compared have different characteristic on each project. It is very important to choose appropriate method on each project.

2.2 Critical Chain Method

Critical chain method was developed and publicized by Goldratt (1997). Critical chain method is an extension of Theory of Constraint (TOC) designed specially for project environment[5].
Critical chain method is scheduling method to protect the entire project from delays, caused by uncertainty and task duration variation, by inserting buffer in the end of the critical chain path of the project. Critical chain path is defined as a longest chain of dependent task and also consider about resources availability of each task. Critical chain method relocate safety time on each task and put it on the end critical chain path as project buffer, ideally it size 50% duration of critical chain path [6].

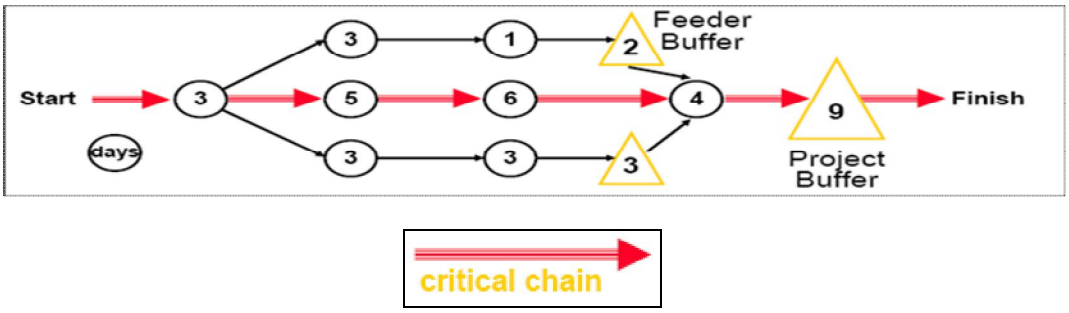

Picture 1. Critical Chain Network Illustration

There are 9 approaches on using critical chain method that are different with another scheduling method:

1. Estimating
2. Buffer
3. Student Syndrome& Parkinson's Law
4. Bad Multitasking
5. Early finishes
6. Backward Scheduling and As Late As Possible (ALAP) Scheduling
7. Relay Race Approach
8. Buffer management
9. Resource allocation

2.2 Critical Path Method

Critical path method in the first time was develop by DuPont in 1957, that used to handled project management of maintenance chemical plants. Critical Path Method is a procedure for using network analysis to identify those tasks which are on the critical path or mathematically based algorithm for scheduling a set of project activities.

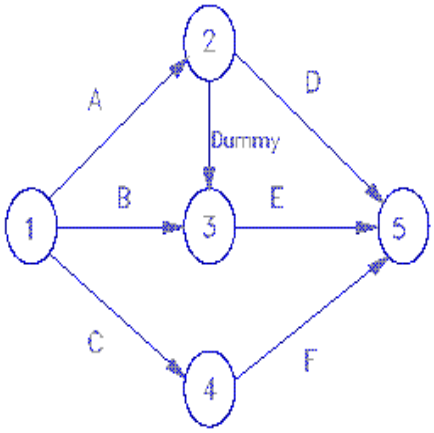

Picture 2. Critical Path Method Network Illustration

In this method we can use two kinds technique to reduce project duration. First, fast tracking technique that make two task run parallel. Second, crashing the critical path that reduce duration by add resources of the task.

3. Methodology

In comparing two method, first we have to make scheduling with those methods and evaluate projects of telecommunication tower construction during June up to December 2007 that are 549 projects base on two methods. Methodology that used in make scheduling are base on project time management in project management body of knowledge. That are have six step in make scheduling [7]:

1. Activity Definition: identifying the specific schedule activities that need to be performed to produced to produce the various project deliverables.
2. Activity Sequencing: identifying and documenting dependencies among schedule activities
3. Activity resources estimating: estimating the type and quantities of resources required to perform each schedule activity.
4. Activity duration estimating: estimating the number of work periods that will be needed to complete individual schedule activity.
5. Schedule development: analyzing activity sequences, duration, resource requirement, and schedule constraint to create the project schedule.
6. Schedule control: controlling changes to the project schedule.

Methodology in evaluate project is looking for differences between actual project duration and schedule duration. Measurement in duration differences use two techniques, Time slip and Schedule Performance Index (SPI). Time Slip is technique to find differences between actual project duration and plan duration of the task in the project.

Time Slip = actual duration – Plan duration (1)

SPI is a technique to calculate comparison ratio between plan duration and actual duration of the task in the project. The best ratio of this technique is 1.

$$SPI = \frac{Plan\ Duration}{Actual\ Duration} \quad (2)$$

After get the result of scheduling and evaluation project base on two methods then next step is compare the result with triple constraint factor and general factor as comparator factor.

4. The Result

4.1 Scheduling Result

Scheduling that used critical chain method have total duration about 197,75 days. And there are 141 activities that included 14 feeding buffer activities and 1 project buffer activity. Schedule baseline and network diagram of this method will be show bellow.

Table 1. Schedule Baseline of Critical Chain Method

Schedule Baseline		
No	**Aktivitas**	Critical Chain
1	PO	-
2	PO - RFC	26
3	RFC - Konstruksi	6
4	Konstruksi - RFI	73
5	RFI - BAUF	18
6	BAUF - BAPS	28
7	BAPS - On Air	3

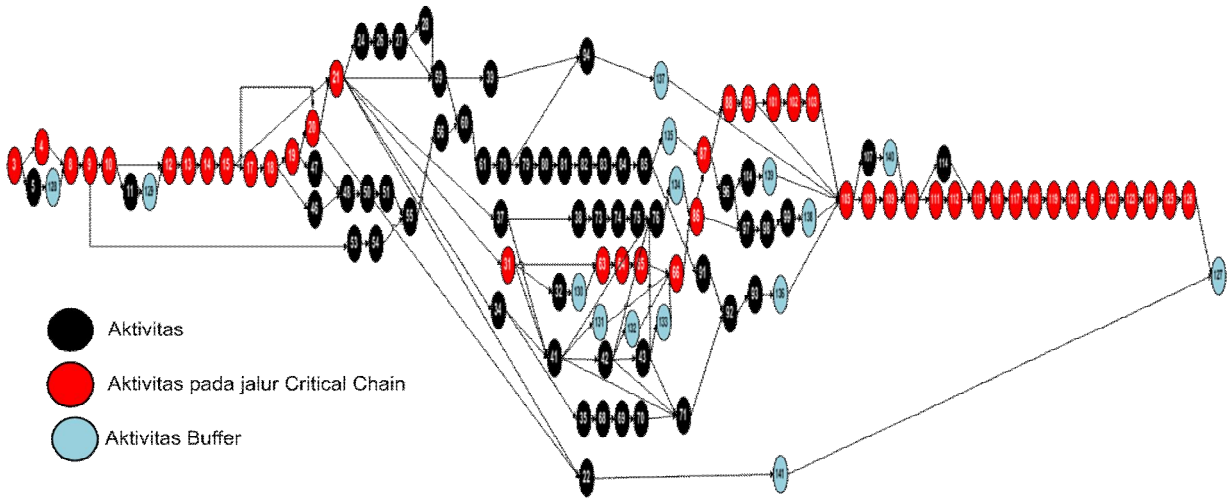

Picture 3. Network Diagram of critical Chain Method

4.2 Evaluation Project Result

Result of evaluation project that used critical chain method approach are: average differences between scheduling duration and duration of company target is 8,33 days; average percentage of project that finished on time is 44,7%; average time slip of each step is 18,1 days; and average SPI ratio of each step is 0,9.
Result of evaluation project that used critical path method approach are: average differences between scheduling duration and duration of company target is 16,67 days; average percentage of project that finished on time is 55,2%; average time slip of each step is 21,2 days; and average SPI ratio of each step is 1,17.

4.4 Research Result

Triple constraint factor and general factor used in comparison two methods as comparator factors. Triple constraint factor consist of three factors that are scope, time, and cost. Whereas general factors consist of three factors that are input, process, and output. Result of comparison two method in each factor are:

- Scope Factor

Critical chain method have total duration of schedule baseline up to 154 days, and average differences between scheduling duration and duration of company target in this method is 8,33 days. Whereas critical path method have total duration of schedule baseline up to 204 days and average differences between scheduling duration and duration of company target in this method is 16,67 days.

- Time Factor

Critical chain method have total duration up to 197,75 days; average percentage of project that finished on time on this method is 44,7%; average time slip of each step is 18,1 days; and average SPI ratio of each step is 0,9. Whereas Critical path method have total duration up to 207 days; average percentage of project that finished on time on this method is 55,2%; average time slip of each step is 21,2 days; and average SPI ratio of each step is 1,17.

- Cost Factor

There is no different between using critical chain or critical path method on cost factor because project contract is not base on duration project.

- Input Factor

Critical chain method need complex input because it need data of optimist duration estimation and need software that uncommon use in company. Whereas critical path method need simple input that is most likely duration estimation and this method can use common software to help in scheduling.

- Process Factor

Critical chain method have long process because it have to calculate buffer duration. Whereas critical path method don't have to calculate buffer duration because the process complete up to get critical path duration so this method have sorter process.

- Output Factor

Critical chain method have buffer management in the result. It is an added value that make process control easier. Critical path method doesn't have any added value in the result.

5. Conclusion

The result of this research is critical chain method scheduling have shorter total duration than critical path method scheduling. Total duration of critical chain method is 197,75 days whereas total duration of critical path method is 207 days.
Base on comparator factor that used, the conclusion are critical chain method is better in scope, time, and output factors. Whereas critical path method is better in input and process factors. There is no different between critical chain and critical path method in cost factor.
Conclusion of this research are critical chain method is better than critical path on project of telecommunication tower construction because this method have sorter total duration and have more number strength factor on triple constraint and general factors.

References

[1]. Project Management Institute, *A Guide to the Project Management Body of Knowledge 3rd edition*, Project Management Institute, 2004, p.8.
[2]. Kendall Gerald.I, *Critical Chain and Critical Path – What's the Difference?*, tocinternational, p.11.
[3]. T. Raz, R. Barnes, D. Dvir, A Critical Look at Critical Chain Project Management, *Project Management Journal*, ABI/INFORM Global, 2003, p.24-31.
[4]. T.G. Lechler, B. Romen, E.A. Stohr, *Critical chain: A New Project Management Paradigm or Old Wine in New Bottle?*, Engineering Management Journal, Dec 2005, Vol 17, no.4, P.45.

[5] A. Kalton, H. Robinson, R. Richards, *Enhanced Critical Chain Project Management via Advanced Planning & Scheduling Technology*, PMICOS 2007 Annual Conference, p.1.

[6]. H. Kerzner, *Project Management: A Systems Approach to Planning, Scheduling, and Kontrolling, Eighth Edition*, John Wiley & Sons, Canada, 2003. *Chapter* 22.3.

[7]. Project Management Institute, *A Guide to the Project Management Body of Knowledge 3rd edition*, Project Management Institute, 2004, p.123.

ISSN 114-1284

Measurement of Service Quality Telecommunication Tower Provider Industry by Using SERVQUAL Method and Quality Function Deployment

M. Dachyar[1] and Fony Carolina[2]

[1]*Industrial Engineering Department, Faculty of Engineering*
University of Indonesia, Depok 16424
Tel : Tel : (021) 78888805 Fax (021) 78885656
E-mail : mdachyar@yahoo.com

[2]*Industrial Engineering Department, Faculty of Engineering*
University of Indonesia, Depok 16424
Tel : (021) (021) 78888805 Fax (021) 78885656
E-mail : fonycarolina_ti03@yahoo.com

Abstract

Telecommunication holds a significant role as an information provider. Cellular phone customer themselves, with the CAGR of 26.7% will gradually increase into 122.1 million in 2010. The telecommunication tower provider company will take part in developing BTS (Base Transceiver Station) tower to all telecommunication provider service (cellular operator).
SERVQUAL method is used to identification customer's need and service succeeded by the company. Quality Function Deployment (QFD) method is used to arrange a new strategy for giving the best service to the customer. Data which writer got is from the questionnaire of all cellular operator managers.
Found that operator cellular's expectation only reached 67.41% with the effort that have been done by the tower provider company. Therefore, the service element priority (technical response) that ought to be done by the company is increasing coordination between cellular operator and tower provider.

Keywords: Quality Service, SERVQUAL, QFD

1. Introduction

Business globalization and international competition is assisted by improving technology, for instance in telecommunication industry. Telecommunication holds a significant role as an information provider. Improving Technology that support communication, makes information transmission become faster so that would make as though constrict [1]. Communication is a must because every human being always needs interaction and new information.

The more and more demand of telecommunication these days, the number of customer growth rate Cumulative Annual Growth Rate (CAGR) in all telecommunication business sectors in Indonesia keep increasing up to 20% per annual. This is including telecommunication service cellular based, fixed phone, internet, and wide type access. Cellular phone customers themselves with CAGR of 26.7% will gradually increase into 122.1 million in 2010. In the end of 2007, customer is forecasted reaching 78.5 million from 66.5 million in last year. Besides, fixed phone's customer either cable or noncable will gradually increase into 31.2 million in 2010 with 20.1% CAGR, as though in the end of 2007, customer is forecasted reaching 16.2 million from 14 million in last year.

Customer's wanted and need become important successful key. There are something that customer seek, something that makes them want to pay more, keep loyal on one brand or company, and which can make them recommended for others. Therefore, customers begin to selective in choosing operator. Thus, cellular phone operators must have the ability to fulfill customer's need. Even less competition in telecommunication becomes harder. With all of economical offer, cellular phone operators must increase good signal for their customer.

Telecommunication tower provider company is an organization which activity are building and lending BTS (Base Transceiver

Station) to all telecommunication tower provider services (cellular operator). The more tighten competition makes them have to increase customer satisfaction and create customer loyalty. How satisfy the cellular operator, BTS tenant, while using the service? This is a basic important question. So much complain about the efficiency of telecommunication tower provider company in receiving problems from their tower's user and the service speed they give. They need continuous quality service improvement, so that, the company still keep going and produce profit.

SERVQUAL is a method for measuring service quality based on five service quality dimension (Tangible, Reliability, Responsiveness, Assurance, and Empathy) by analyzing the gap caused of inappropriate between expectation and customers perceived.

The reason of hard competition, company should do loyalty program in order to keep holding out. Service development is one of the efforts which company does to give the best service for their customer. QFD (Quality Function Deployment) method can be used to measure how far the company has fulfilled the customer's need and it can be a basic in preparing new strategy for the company to fulfill the customer's need.

QFD is an important part of process development product and service whereas consist of human investment such as people who activate and information as the activator [2]. It needs tough cooperation in determining what customer's need and translating into design and specification of structured service that is produced to fulfill customer's need through service development.

2. Research Method

2.1. Measurement of Service Quality

A company should always introduce service culture as continuous improvement [3]. According to Cronin and Taylor, a manager has to understand certain aspect of good quality service. Furthermore, these aspects will become main company's power in competition with their competitors. In order to understand direct effect that is produced from each service they give ought to measure and compare the quality performance. Besides, it purposes to give illustration company's successfulness in satisfying their customers.

Many methods to do the measurement customer satisfaction, there are applying complain system and customer's suggestions kind of suggestion box, hotline, e-mail, etc. Another way, ghost shopper, is a method by asking someone to pretend as a shopper, and then he/she has to report anything that has judged satisfied and unsatisfied. Next method is organizing customer survey by means of questionnaire or interview. Knowing customer satisfaction could be done by analyzing missing customer to get information about their reason and cause.

2.2. SERVQUAL

Parasuraman et al. (1985), develop SERVQUAL instrument to measure service quality that customer's got according to gap model. SERVQUAL method is based on assumption that customer comparing performance service of relevant attributes with ideal/ perfect standard for each service attribute. If the performance suitable or above standard, so that perceive all of service quality will be positive as in the other hand. In other words, this method analyze gap between 2 main variables, that is expected service and perceive service.

Measurement of service quality in SERVQUAL method is based on scale items created to measure expected and perceives customer, and also the gap between in five dimension of service quality. Those five main dimensions spell out into two attributes detail for expected variable and perception variable which are arranged based on likert scale statements, from 1 (very unimportant) until 7 (very important) and 1 (very disagree) until 7 (very agree). Service quality evaluation by using SERVQUAL method include the difference calculation between result which given from the customer for each statements according to expectation and perception. Measurement of every service quality dimensions is using sum scale whereas respondent was asked to give the percentage for those dimensions, so that sum of all reaches 100 %. This main objective is to give a result of accuracy service quality.

2.3. Quality Function Deployment (QFD)

QFD is firstly developed in the end of 1960 in Japan by Yoji Akao [4]. Yoji Akao defined

QFD as a method and technique that used to develop quality design which its aim to satisfy the customer and translate what customer's need in design target and main service quality assurance to be used to production process [5].
QFD is listing voice of customer (VOC) or customer requirement into final product for assuring customer satisfaction. QFD has some objectives such as decrease the product developments cycle time and at once increase product quality along with deliver product which is cheaper. More objective of QFD is increasing company's target market. And of course product or service resulted pass trough QFD process is customer's want and appropriate with their needs.
Main tools in arranging QFD is HOQ (House of Quality). HOQ is matrix which fuses customer's need and the process that company should do in order to fulfill them. There are three phase of service based QFD process, such as [6]:

1. *Service planning*.
2. *Element planning*.
3. *Operations planning*.

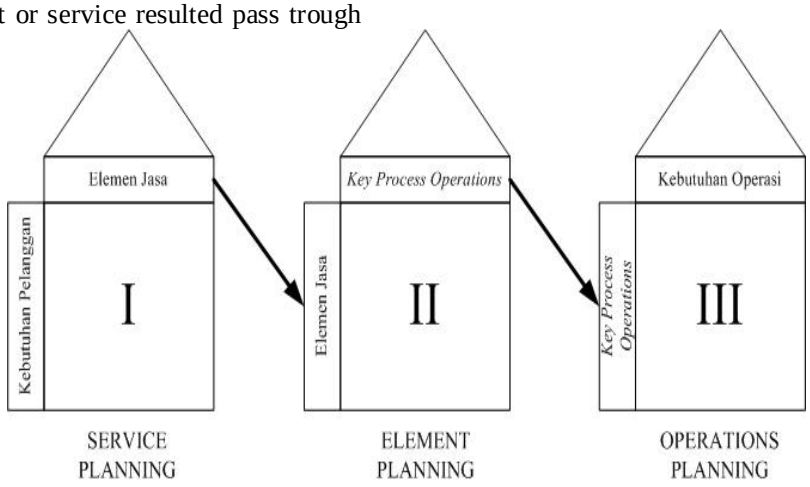

Figure 1.
Quality Function Deployment Process (Source: H. Brian Hwarng dan Cythia Teo, 2001, pg. 202)

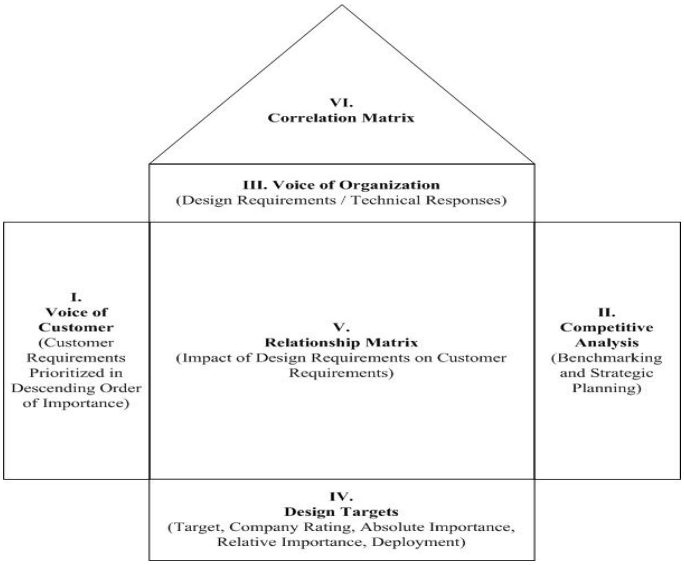

Figure 2.
House of Quality Structure (Source: S. Bruce Han, et. al., 2001, pg. 798)

3. **Result and Discussion**

3.1.Defining of Customer's need

Customer's need is an item that should analyze to create the research. These items are spelling out from 5 service quality dimensions which are used in SERVQUAL method. In this phase, will be indentified the research items which reflect the operator cellular's expectation in their tower provider's service by spreading the questionnaire. The questionnaire divided into three sections, such as:

1. First section
   There are two kind of this section, first for measuring customer's expectation and other for measuring customer's perception. There are 19 questions. Respondent is asked to give the appraisal about the expectation and perception by using likert scale.

2. Second section
   This section includes five statements which describe five dimensions of SERVQUAL. The objective of this measurement is measuring the expectation score of all dimensions by using sum scale. Respondent is asked to give the appraisal of each statement with the total of all is 100.

3. Third section
   The last section is some kind of giving critical opinion and suggestions from all cellular operator to their tower providers. Respondent feels free to write down anything about the service they got from their tower provider. Therefore, this last section would help writer to arrange the Quality Function Deployment (QFD).

This table below is showing the result of service quality calculation from all 5 dimensions.

3.2. Quality Function Deployment (QFD)Service element matrix is an element which is used to fulfill customer requirement by the company. In arranging this service matrix, writer had interviewed and consulted the one of Tower Provider Telecommunication Maintenance Manager.
After getting the item of customer's need and service elements to fulfill voice of

customer (VOC) or customer requirement, next step is making the service planning matrix. The making of service planning matrix include; Relationship between customer's need and service element, correlation between every service element, improvement direction of service element, and last is the calculation result of weighted service element.

Table 1.
Service Quality of 5 dimensions

No	Dimension	Expectation	Perception	SERVQUAL Score	Importance Score	Weighted SERVQUAL Score	Actual SERVQUAL Score
1	Tangible	4,27	3,15	1,12	0,175	-0,1960	73,77%
2	Reliability	4,77	3,05	1,72	0,210	-0,3612	63,94%
3	Responsiveness	4,76	3,14	1,62	0,240	-0,3888	65,97%
4	Assurance	4,63	3,20	1,43	0,170	-0,2431	69,11%
5	Empathy	4,76	3,06	1,70	0,205	-0,3485	64,29%

Table 2.
The Calculation Result of Weighted Service Element

Service Element		Absolute Importance	Relative Importance	Priority
TECHNIQUE	Routine preventive maintenance	43,2	1,58%	22
	Maintenance recapitulation	42,3	1,55%	25
	Repair recapitulation	42,3	1,55%	24
	Routine inspection to location	157,8	5,78%	5
	Good materials supplying	43,2	1,58%	21

	Good tools supplying	37,8	1,38%	26
	Good logistic system	55,8	2,04%	17
	Automatic recovery	43,2	1,58%	23
	Check list book	122,4	4,48%	8
	Log Book	86,4	3,16%	14
	Reward system	37,6	1,38%	27
COMPLAIN SERVICE	Quick respond	141,6	5,18%	6
	Follow up complain	127,8	4,68%	7
	Report system flow	99,6	3,65%	12
RECRUITMENT & TRAINING	Training program	89,5	3,28%	13
	Recruitment test for operator	84,6	3,10%	16
	Interpersonal skill	28,2	1,03%	28
OPERATOR	Operator identity system	110,4	4,04%	9
	Rotation operator system	14,7	0,54%	30
	Expert operator	171,9	6,29%	4
SITE ENTERING	Simple rule	44,1	1,61%	19
	Operator allocation	100,8	3,69%	10
	Total of operator	100,5	3,68%	11
COMMUNICATION	24 hours day call center	172,8	6,33%	3
	Evaluation / periodically report	86,4	3,16%	15
	Coordination between operator cellular and tower provider	341,1	12,49%	1
	PIC contact number is being cleared	186,3	6,82%	2
	Reconciliation of citizens	44,1	1,61%	20
SERVICE LEVEL AGREEMENT	Service Level Agreement (SLA) detail	27,9	1,02%	29
	Service Level Agreement (SLA) comprehension	46,9	1,72%	18

3. Summary

Refers to the objective of this research, to know the gap caused of inappropriate between expectation and customers perceived, writer could sum up that there is no reached expectation. Furthermore, based on telecommunication tower provider service quality development by using Quality Function Deployment (QFD), determined some service element priorities that company should do in order to decrease the service gap:

1. Coordination between operator cellular and tower provider : 12.49%
2. PIC (Person in Charge) contact number is being cleared : 6,82%
3. 24 Hours day call center : 6.33%
4. Expert operator : 6.29%
5. Routine inspection : 5.78%
6. Quick respond : 5.18%
7. Follow up complain : 4.68%

Reference

1. Krishnamurthy Sriramesh, "The Dire Need for Multiculturalism in Public Relations Education: An Asian Perspective", in *Journal of Communication Management,* Vol.7, No.1, ABI/INFORM Global, 2002, p.54.
2. Mark A. Voderembse dan T. S. Raghhunathan, *Op.Cit.*, p.255.
3. Martin A. O'Neill, et. al., "Diving Into Service Quality-The Dive Tour Operator Service"2000, in *Managing Service Quality*, vol.10, no.3, p.13.
4. S. Bruce Han, et. al., "A conceptual QFD planning model", in *International Journal of Quality & Reliability Management*, Vol.18, No. 8, 2001, p.797.
5. K.F. Pun et.al, "A QFD/hoshin approach for service quality deployment: a case study", in *Managing Service Quality*, Vol.10, No.3, 2000, p.157.
6. H. Brian Hwarng dan Cynthia Teo, "Translating *Customer*'s *Voice*s into Operations Requirements: A QFD Application in Higher Educations", in *International Journal of Quality & Reliability Management*, Vol.18, No.2, 2001, p. 20

A case study on using SPC tools to improve manufacturing quality of empty hard gelatin capsules:

Omar Bataineh[1], Abdullah Al-dwairi[2]

[1]*Department of Industrial Engineering*
Jordan University of Science and Technology, Irbid, Jordan
Tel : (962) 27201000 ext. 22464
E-mail : omarmdb@just.edu.jo

[2]*Department of Industrial Engineering*
Jordan University of Science and Technology, Irbid, Jordan
Tel : (962) 27201000 ext. 22548
E-mail : dwairy@just.edu.jo

ABSTRACT

Quality control and improvement at the process level is a vital activity for the achievement of quality in products and services of organizations. This paper employs SPC (statistical process control) tools such as control charts and process capability ratio for quality improvement. The control charts employed are $\overline{X}$ *, s and the Exponentially Weighted Moving Average (EWMA). The process capability ratio employed is the centered process capability ratio (*C_{pm}*). These tools have been implemented to the manufacturing process of empty hard gelatin capsules as a case study. This implementation has led to an expected reduction in the number of defective capsules by 29% relative to the stage before implementation.*

Keywords: *SPC; control charts; capability assessment; EWMA; quality control*

1. INTRODUCTION

The implementation of SPC tools, mainly control charts and capability assessment, can significantly facilitate quality improvement through the reduction of process variability and shifts in process mean [1]. Application of these tools for quality improvement of manufacturing processes is widely popular in the literature [2-7]. Following the first control charts that were developed by Shewart in the 1930s, more types of control charts have been developed to deal with different situations that arise in practice [8]. In the last three decades, many studies have been devoted to new concepts such as adaptive and more economical control charts [9-11], control chart's pattern recognition [12], and design optimization of control charts [13].

However, these concepts have led to considerable complexity for applying the new control charts and were less desirable compared to traditional ones which are still the most widely used today. In this work, a practical implementation of a set of selected SPC tools, namely $\overline{X}$, s and the Exponentially Weighted Moving Average (EWMA) control charts combined with the centered process capability ratio (C_{pm}) is presented in the case of manufacturing process of empty hard gelatin capsules.

2. CASE STUDY

As a case study, SPC tools have been applied to the manufacturing process of *empty hard gelatin capsules* produced by the Arab Center for Pharmaceutical and Chemical (ACPC) Industries Co., Amman, Jordan. The product is used by many drug companies to sell their drug powders in the form of capsules. A capsule is composed of two pieces that are differently colored and joined together, as shown in Figure 1. The longer piece is usually called the *body* and the shorter one is called the *cap*. Because the two pieces are manufactured in the same manner, only manufacturing of the body is considered. Thereafter, the word *capsule* is used interchangeably with the word *body*.

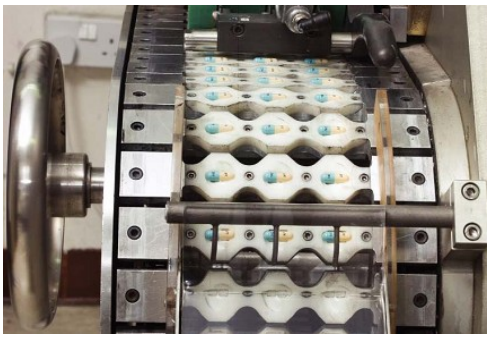

Figure 1: Finished capsules are composed of two pieces: body and cap

The first stage in the manufacturing of capsules is to immerse a set of steel pins in a pool of liquid gelatin, as shown in Figure 2. Then, capsules are formed on the pins due to adhesion between liquid gelatin and steel pins. Factors such as temperature of steel pins, immersion time and gelatin concentration and temperature have an effect on the characteristics of the final capsules in terms of weight, thickness, length, and surface defects. After the capsules are formed on the pins, the pins are steadily moved through a drying chamber under controlled conditions of temperature and humidity. This gives the capsules the required rigidity before they are stripped off the pins. The capsules are finally cut to size. However, due to factors such as thermal shrinkage and behavior of the cutting mechanism capsules are not always within specifications.

Figure 2: Formation of capsules after immersing steel pins in a pool of liquid gelatin

A number of defects may appear on a capsule such as uncut body, wrinkles, air bubbles …etc. However, the capsule's body length is considered the most important quality characteristic. Thus, it is selected in this study for quality control and monitoring. The standard size of the capsule's body length is 20.60 mm with lower and upper specification limits of 20.20 mm and 21.00 mm, respectively.

4. SPC IMPLEMENTATION AND RESULTS

In implementing SPC tools, twenty samples (each consisting of thirty observations of body length) were collected to construct $\overline{X}$ and *s* control charts. The charts were setup with the aid of Minitab® and shown in Figure 3. It can be seen in this figure that an out-of-control point exists on the $\overline{X}$ chart. Thus an *alarm* was issued confirming the process is out-of-control. After brainstorming by the quality management team and conducting CEA analysis, it was possible to identify one potential assignable cause which rendered the capsule manufacturing process out-of-control. This was the sudden change in the relative humidity of the facility atmosphere. After implementing a better monitoring policy and control of room humidity, a new set of samples was collected and used to reconstruct the $\overline{X}$ and *s* control charts. No out-of-control point was detected on the new charts.

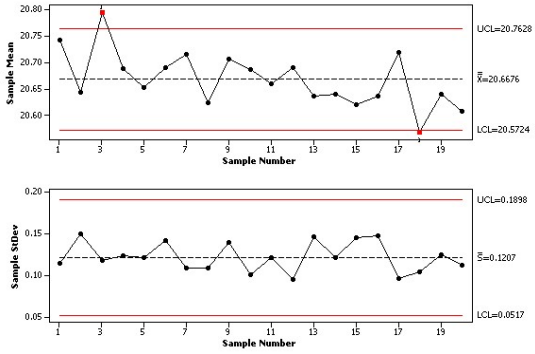

Figure 3: $\overline{X}$ and *s* control charts at the beginning of implementation of the three-phase scheme

The last set of samples was re-used to construct the *EWMA* control chart, as shown in Figure 4. As can be seen in this figure, an out-of-control point exists on the third sample. Therefore, other potential causes were further examined and focus was turned onto the repetitive screw adjustment in the cutting mechanism. After redesigning the cutting mechanism to eliminate the need to adjust the screw, the same procedure in Phase I was repeated and no alarms had occurred. Additionally, more *EWMA* control charts were constructed on weekly basis but no alarms had occurred. This continued for 17 weeks, which is the preset time, where the process capability was assessed.

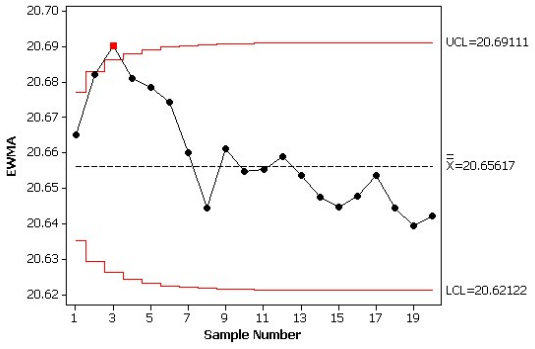

Figure 4: *EWMA* control chart after Phase I was completed

Figures 5 and 6 show process capability output at the beginning of implementation and after 17 weeks of implementation. It can be seen in Figure 5 that the process mean is initially off-target (sample mean = 20.6676 mm) with

C_{pm} value of 0.91. This corresponds to an expected number of 5219 capsules with body length out of specifications per million. Figure 6 shows that the process mean is closer to target (sample mean = 20.612 mm) with C_{pm} value of 0.97. This corresponds to an expected number of 3700 capsules with body length out of specifications per million. Therefore, an expected 29% reduction in the number of capsules that will not meet specifications due to improper body length can be achieved through the implementation of the SPC tools used in this study.

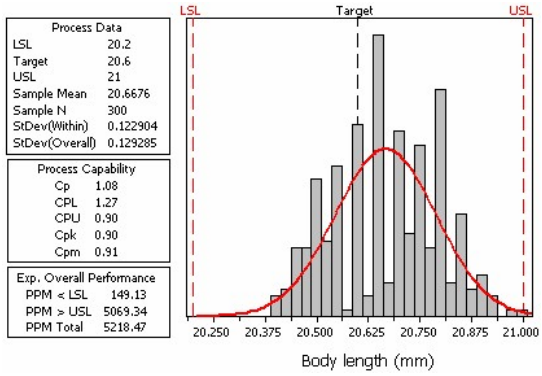

Figure 5: Process capability output at the start of implementation of the three-phase scheme

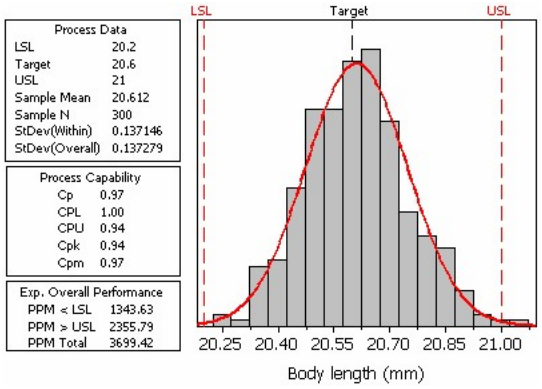

Figure 6: Process capability output after 17 weeks of implementation of the three-phase scheme

5. CONCLUSIONS

In this work, a set of SPC tools was applied to the manufacturing process of empty hard gelatin capsules as a case study. It can be concluded from the case study that by applying the proposed tools it was possible to:

1. Detect short term changes in process mean that resulted from variations in the relative humidity of the facility atmosphere and the repetitive screw adjustment in the cutting mechanism.
2. Detect gradual changes that occurred slowly over time due to poor lubrication of the cutting mechanism.
3. Assess process capability based on periodic basis, i.e. when $i = i^*$.

REFERENCES

[1] D. C. Montgomery, *Introduction to Statistical Quality Control*. Hoboken, NJ: John Wiley & Sons, Inc., 2005, Chapter 1.

[2] G. Lanza, J. Fleischer, and M. Schlipf, "Statistical process and measurement control for micro production," *Microsyst Technol*, vol. 14, pp. 1227–1232, 2008.

[3] H. Sohn, J.A. Czarnecki, and C.R. Farrar, "Structural health monitoring using statistical process control," *Journal of Structural Engineering*, pp. 1356–1363, 2000.

[4] A.R. Motorcu, and A. Gullu, "Statistical process control in machining, a case study for machine tool capability and process capability," *Materials and Design*, vol. 27, pp. 364–372, 2006.

[5] S.H. Chenb, C.C. Yanga, W.T. Lina, and T.M. Yeh, "Performance evaluation for introducing statistical process control to the liquid crystal display industry," *Int. J. Production Economics*, vol. 111, pp. 80–92, 2008.

[6] S.S. Leu and Y.C. Lin, "Project performance evaluation based on statistical process control techniques," *Journal of Construction Engineering and Management*, vol. 134, no. 10, pp. 813–819, 2008.

[7] J. Cao, Y.S. Wong, and K.S. Lee, "Application of statistical process control in injection mould manufacturing," *International Journal of Computer Integrated Manufacturing*, vol. 20, no. 5, pp. 436–451, 2007.

[8] S. Chakraborti, S.W. Human, and M.A. Graham, "Phase I statistical process control charts: an overview and some results," *Quality Engineering*, vol. 21, no. 1, pp. 52–62, 2009.

[9] S. Panagiotidou and G. Nenes, "An economically designed, integrated quality and maintenance model using an adaptive Shewhart chart," *Reliability Engineering and System Safety*, vol. 94, pp. 732–741, 2009.

[10] Y.C. Lin, and C.Y. Chou, "Adaptive $\overline{X}$ control charts with sampling at fixed times," *Qual. Reliab. Engng. Int.*, vol. 21, pp. 163–175, 2005.

[11] D.A. Serel, "Economic design of EWMA control charts based on loss function," *Mathematical and Computer Modelling*, vol. 49, pp. 745–759, 2009.

[12] Z. Wu, M. Xie and Y. Tian, "Optimization design of the $\overline{X}$ & S charts for monitoring process capability," *Journal of Manufacturing Systems*, vol. 2, no. 2, pp. 83–92, 2002.

[13] A. Hassan, M.S. Baksh, A.M. Shaharoun, and H. Jamaluddin, "Improved SPC chart pattern recognition using statistical features," *INT. J. PROD. RES.*, vol. 41, no. 7, pp. 1587–1603, 2003.

ISSN 114-1284

Analysing And Improving Implementation of FIFO System at Warehouse

Rahmat Nurcahyo[1], Akhyar P Siddiq[2]

[1]*Industrial Engineering Department Faculty of Engineering*
University of Indonesia, Depok 16424
Tel : (021) 78888805
E-mail :rahmat@eng.ui.ac.id

[2]*Industrial Engineering Department Faculty of Engineering*
University of Indonesia, Depok 16424
Tel : (021) 78888805
E-mail : akhyarps@indosat.net.id

ABSTRACT

Common objective of a warehouse is to minimize cost and maximize service to internal and external customers. The purpose of the research is to attain a new system that would resolve the First In First Out (FIFO) system in the Finished Product Store (FPS) warehouse. Analysis of historical data comes out with a new solution designed for the system, that is a periodic arrangement of items in FPS. Forecasting technique is used to determine a review period for rearrangement of goods placement in FPS. It also adapts some important material handling principles in a warehouse. One consideration used is the popularity of the product. Based on this concept, identical products are placed in zones, in order that each zone consist of one or just two brand of flour products.
Some advantage expected to be gain by the enhancement of this storage and retrieval strategy is an improvement of FIFO system, also the ease of storage, retrieval, and identification of items which further would increase the FPS throughput.

Keywords

First In First Out (FIFO) system, warehouse

BACKGROUND

Warehouse must be able to meet customer demand with minimum cost. To be able to run effective and efficient operation of the warehouse, there are several factors to be considered, such as the availability of facilities and resources, production capacity, human resources, recording and documentation system, the market situation, and the distribution system.

This research was conduted at PT SRR, which produce finished product in the form of wheat flour with different kinds of variations. Products characteristics are:

- Wheat flour is frailty when stored too long.
- Finished product storage (FPS) is a temporary storage, before being distributed to the stock point or taken by the customer. The deadline is considered critical and product specification (best use of the product) for the storage of wheat flour is one month, starting from wheat flour is produced to finish in the hands of customers.
- If the time limit is exceeded, then the risk of being contaminated is greater due to the attack of head lice to the flour.
- Given the distribution chain wheat flour long enough, the storage in the FPS should be made with a certain time limit.
- Services provided to customers should consider the product quality, accuracy and the amount of time. In connection with this case, the storage of goods in the warehouse also prioritized the aspects of it.

PROBLEM DEFINITION

Based on the results of a Quality Audit, condition associated with the current FPS situation are:

- The problems appear after the system and procedures of FPS at this time cannot guarantee the success implementation of First In First Out (FIFO). FIFO cannot be run due to many factors, namely facilities, labor or based on direct loading instructions from management to the truck. One quite clear thing is the current system and procedure cannot trace the previously wheat flour used to enter FPS.
- Without the guarantee of FIFO implementation there is no certainty that storage time does not exceed the maximum time limit, ranging from flour handling time, including receiving, storage, and delivery at FPS or others stock point outside FPS. This will impact the increased risk of damage to wheat flour.

The increased risk of damage to wheat flour due to the failure of FIFO system at FPS and damage to wheat flour is related to the complaint of the buyer. A large number of customer complaints which are related to the quality of products, proving that it is time for PT SRR to evaluate the system of warehousing.

OBJECTIVES

Objectives of the research is to improve the system and procedures of FPS, such as:

- To generate a system and procedures that can guarantee the movement of goods in the FPS based on the implementation of the FIFO.
- To ensure information for the FPS, stock point, distributors and users about the date that is best use of the product.

PROBLEM LIMITATION

The problem is limited to the design of systems and procedures of the new FPS. The issues related to distribution and marketing must be solved first so that systems and procedures can be done well. In addition, the design of systematization storage procedure is made for the fixed production capacity, namely 35,000 wheat bags per day, without any additional production capacity.

RESEARCH METHODOLOGY

The steps of research methodology are:

1. The assessment of current FPS system and procedure
   The current system must be understood first before implementing the corrective action. By doing the assessment, the shortage, the system scope, problems and obstacles that are in it can be identified more clearly. The assessment also covers the facilities and manpower. The data collecting is done through interviews, direct observation and from primary and secondary data.
2. Making the plan of a new FPS system
   The making of this plan is done in the scope of the system, so that the collected data is not out of the determined scope, and the problem solving can be more focused.
3. Evaluation of the new FPS system
   Making the plan of a new system is not free from obstacles such as the cost, time, manpower, facilities and other resources, so that before the plan needs to be running, it needs a more mature consideration.
4. A good implementation procedure is required for the designed system to run well

The research was conducted based on consideration of stock location and order taking.

Stock Location

Stock location or warehouse layout in the storage area are related to the location where the goods are placed in a warehouse. Factors that need to be considered in the storage area design procedure are:

1. The commodity

Commodities are considered as factor that affecting the location and space needs, including:

a. Similarity
In general, materials are grouped in classes. Material has relevance (similarity) to one another.

b. Popularity
Level of turnover is another factor in choosing the location. For example, the goods with high level of turnover are placed at the front, and the lower turnover ones in the more remote locations.

c. Size
The consideration here is not only the size of unit, but also in the number of overall size.

d. Characteristic
Characteristics of the stored material should also be considered, such as:

- Dangerous commodity
- Frailty commodity
- High value commodity
- Short-lived commodity

2. The Space

Factors associated with the space are important to determine where the commodity can be stored. These factors are:

a. Space size (volume)
b. Nature of the location (a match with a certain type of goods)
c. Location-related with other relevant activities.
d. Availability when needed
e. Characteristics of the building, such as the capacity load of the floor, door (number, location, and size), loading facility, distance (pole field, size and number) and , limit height of stack
f. Area required for the function and activity of service
g. Space required for the gang.

There are two basic systems to assign a particular location with the placement of stock items: fixed location and floating location. Both systems are used with attention to the factors above.

The Order Taking and Collection

Once the order is received, the listed goods in the order must be taken from the warehouse, collected and prepared to be sent. All this activity requires labor and goods movement. This work should be arranged well in order to give desired service to the customer.

ISSN 114-1284

There are some systems that can be used to manage the work as follows :

1. Area system

Order taker walks around to select items that are in order, such as those who shop in supermarkets. The goods are then taken to the delivery area. This order has been collected by itself when the order taker is finished doing its work. This system is usually used in a small warehouse with fixed location.

2. Zone system

The warehouse is divided into zones, and the order taker is only working on their own zone. Orders are divided into zones, each order taker selects goods in the zone and takes them to the collection area where orders are assembled to be sent.

3. Multi-order system

This system is similar to the zone system. The difference is this system does not only deal with one order, but a number of orders are collected and the goods are divided by their zone.

DATA COLLECTION AND ANALYSIS

In general, the assessment of FPS is good, but it is still found areas for improvement, they are :

- Material handling that requires tow people, working with frequently hands, repetitive, and short distance.
- Difficulties in stock control

This difficulty occurs when the control is done visually to monitor whether any damage on packaging.

- Lack of Space

More clearly, the analysis of this case will be discussed in the utilization analysis. Lack of space occurs when the FPS wants to be improved its functionality into the wheat flour aging area.

- Unused overhead space

Overhead is a region at up of the range of people. In the current conditions, the overhead area, especially in the middle of the FPS is still very minimal use. The main cause why the overhead space not being used is the limitation of palette capacity. Based on interviews, the addition of stacked palette has been tried but the lower palette is not capable of holding the load. The effect of unused the overhead space is low utilization of FPS.

- Difficult access to take the goods

Orientation of good storage in the FPS is horizontal not vertical (non-accumulation). This results in a lot of wheat flour which is difficult to access, both to be controlled or to be taken. If the condition of FPS is full plus the use of additional los, the access of goods becomes more difficult because more additional los in the main street or alley for forklifts.

- Customer complaint

Customer of FPS is the buyer who wants to take the ordered wheat flour. The current customer complaint is particularly about the availability of goods in FPS so that they have to wait long enough in the PT. SRR until their order can be taken.

- Too Narrow Gang

Gang in the FPS is not planned layout. Layout are preferred to increase the storage capacity so that there are some narrow alleys. Especially when the additional los is used, the movement area will be more narrow.

- Stacking

Stacking is the accumulation attached to the wall. This causes problems of access, control, and taking.

- Low level of in and out flow material is stored in the front; High level of in and out flow material is stored behind; Material with the same level of in and out flow is stored in the same place. This is because the selection of storage (los) is based only on the currently empty los at that time. There is no consideration based on the frequency of movement of each type of wheat flour.
- Limited building hampering the storage method

The limited building can be observed through the dimensions of the FPS building that is different among the front, middle and back.

- Not planned material handling method

Theoretically, FPS should have a schedule of materials handling as well as the production division has a production schedule. With the schedule, the utilization of equipment, manpower and space will be able to be maximized.

Queue of truck

Gate Office (GO) is the entry gate for customers who want to take the ordered wheat flour. GO service is begun when the trucks arriving at the location of the factory until the truck leaving the factory. Last days, it is indicated that the truck queue is quite long, since they arrive to leave the factory.

The comparison of the total service time data, the loading time data with the queuing time data indicates the contrast difference, even the unit that is used is very different namely minute and day. This indicates a quite serious problem and must be handled to reduce losses, both losses in the PT. SRR and in the transportation.

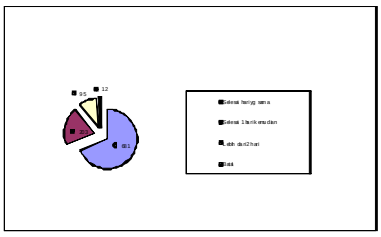

Figure 1: Queuing Time of trucks at Gate Office

ISSN 114-1284

Utilization of FPS

Utilization of storage space illustrates the comparison between the available volume of storage space (in cubic meters) with the available volume of room for storage (in cubic meters).

To calculate the available volume of warehouse space (Nett) then the number of cubic meters of warehouse space is subtracted from the part of the room that can not be used for storage, such as pole / column, space for movement, space and facilities. The available volume of FPS is 14,070.50 (max) and 12849.60 (normal) in cubic meters.

Volume of space that currently used for storage is calculated by counting the number of los and the stack. Los is the term currently used to describe the distribution of warehouse to be some place that can be filled with some palettes. There are various sizes of los namely los that can load 1 palette up to 9 palettes. In addition, there is also a temporary los that is only used when the warehouse full.

The current volume room used for storage in normal conditions is 2,862.09 (cubic meters). Based on the available volume of warehouse space and the volume of space that is currently used for storage, the utilization of FPS in normal conditions is 22.27%. Meanwhile, based on data storage, the utilization of FPS space in February was 18.42%.

Customer Complaints

Customer complaint data for 1 year was 44 complaints. This complaint data are grouped into 5 groups, namely: Expiration, contents do not match. After processed the product becomes worse, the stock and the number of deliveries, and quality (color, wad, wet). Based on this complaint, the largest number of complaints is about the results of processing wheat flour at PT. SRR which is considered less good finished products.

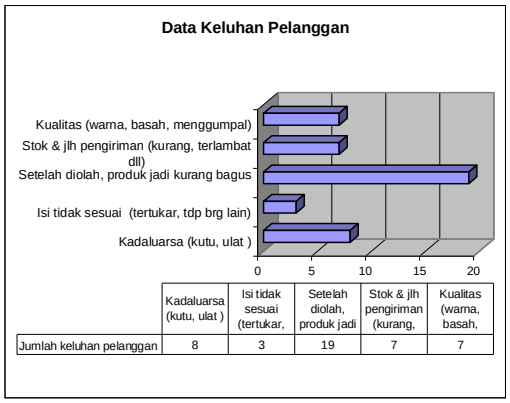

Figure 2: Number of Customers Complaints Data

From 44 customer complaints, it needs to identify the possibility of not running FIFO system. Identification is done by utilizing the existing product code on each bag. Product code consists of 5 digits. The first digit indicates the production month (A = January, B = February, and so on). Second and third digits indicate the date (01 to 31). Fourth digits indicate carousel (4 units have carousel). Last digits indicate the bin (A = bin 1, B = bin 2, etc). This identification product code show the date of production. Date of production then is compared with the date the complaint submitted by the buyer / user to obtain the time interval. Assuming the best time since the wheat flour from the date of production to 2 weeks is used mostly, and the transportation time from PT SRR to the location (e.g. food industry) is 7 days old, the complaint may be a possibility due to the nor running of FIFO system

ALTERNATIVE SOLUTION AND EVALUATION

Through analysis of various indicators of issues, then the main cause of not running FPS system is the difficulties in storage.
When examined further, it appears that this difficulty is influenced by the following conditions:

- Small size of FPS
  Small size of FPS limits the amount of products stored in there. In other words, the capacity becomes limited. The great number of demand makes the production to result a more output, while FPS is only able to accommodate as many as the production capacity of 2 days, namely 70,000 units sack of wheat.
- Low utilization of FPS
  With the limited storage capacity as described above, the space used for storage capacity is far below the available space.
- Not arranged storage and layout
  This can be identified from check sheet made by observing the FPS area directly. Products stored in the FPS are only based on the availability of empty los, and not considering the principles of material handling.

PERIODICAL GOODS STORAGE SYSTEMATIZATION

The effective and efficient alternative to implement is by storing the goods periodically. This alternative does not require great costs, simply perform the review of certain period to determine the amount of los allocation to specific products. Thus, FPS is able to provide more services to more popular products.

The proposal of this alternative is to assume that proportionality amount of wheat stored in the FPS is not arranged yet optimally according to the frequency and number of orders. So far, the popular products are

ISSN 114-1284

sometimes not able to be stored in the FPX, if the FPS is full. Under this circumstance, the direct loading is executed.

Determination Review Period

To set the storage periodically, the first note is how many times the storage systematization at FPS will be reviewed and changed in a year. The periodic time is determined in accordance with the fluctuation of pattern, so that FPS is still able to handle the fluctuation of demand under the period of observation.

The observation of storage systematization can be done more often when there are symptoms that the level of demand between products is fluctuation from time to time. However, the frequent changes of systematization way will be fussed over and not efficient. Therefore, the storage systematization should be done more frequently, that is to anticipate demand, but the period should be also long enough so that it is not too difficult to make changes in how the storage is.

In general, the steps undertaken to determine the frequency and period of time to change how the storage of goods in the FPS is as follows:

1. To make demand forecasting for each product and for some period of time.
2. To calculate the forecast error.
3. To specify the periodic time for observation according to the smallest error.

Creating Demand forecasting

Requests are evaluated by using fulfilled Delivery Order (delivered DO) data, as in table 1. From the table, it can be seen that the highest demanded product is NM and followed by BB. Evaluation based on the delivered DO with the reason the fulfilled DO is actual demand.

Forecasting is done by three methods, namely Moving Average method, Single Exponential Smoothing, and Double Exponential Smoothing. The calculation of forecasting was made with the help of MINITAB software.

Tabel 1: Delivered DO

MONTHS	WHEAT FLOUR (BAGS)							TOTAL
	TE	BB	PM	NB	NM	NE	IRD	
Jan	51,048	154,990	53,925	0	0	0	0	**259,963**
Feb	85,815	172,900	55,530	0	0	0	0	**314,245**
Mar	80,360	137,845	36,745	6,500	0	0	0	**261,450**
Apr	52,795	112,715	33,050	5,925	32,310	0	55,850	**292,645**
May	97,330	132,530	35,980	12,125	208,380	0	96,150	**582,495**
Jun	63,210	161,530	32,800	24,750	296,110	0	78,585	**656,985**
Jul	94,310	170,145	36,050	13,600	340,540	0	89,597	**744,242**
Aug	108,495	137,150	21,862	300,950	280,895	0	85,500	**934,852**
Sep	117,238	114,123	33,025	30,100	327,522	0	72,200	**694,208**
Oct	98,715	143,690	33,500	72,250	276,408	50	76,580	**701,193**
Nov	116,030	169,017	34,768	93,230	460,550	0	78,500	**952,095**
Dec	69,298	82,515	14,168	34,800	253,297	0	43,778	**497,856**
	1,034,644	**1,689,150**	**421,403**	**594,230**	**2,476,012**	**50**	**676,740**	**6,892,229**

In forecasting method with Single Exponential Smoothing (SES) and Double Exponential Smoothing (DES), the weight used is the result of the calculation done by MINITAB to find the smallest value of the error (Square Error).

The time period tested in the forecasting is the multiplication factor 12, without using 2, that is 3, 4 and 6. So, an alternative way to observe it can be done every 3, 4 or 6 months. Time-periodic 2 months is not included because 2 months is considered too fast to do changes of storage at FPS.

Forecasting is done by using the actual data for the calculated period. Then, forecasting is done for some future period of time in accordance with the currently tested period. For example, a review conducted for 4 months, forecasting is done for 4 months in the future using the data from the previous 4 months.

Forecasting is done for each type of wheat flour produced by PT SRR for a year, so with a certain periodic time, it is known how many times the review should be conducted during the year.

Calculation of the error value of forecasting

The forecasting error is simply the diversion of forecast value to actual value. The small value of the error then the better the forecasting is done.

The best periodic time is chosen based on the smallest forecasting error for each of the tested periodic time. The forecasting error for a tested periodic time is compared with each type of wheat. The used type of error is Mean Absolute Deviation (MAD), Mean Absolute Percentage (MAP) and Mean Square Deviation (MSD).

Types of error that become main priority is MAD and is followed by MAP. MAD shows the average of the amount of wheat that are less or more than the actual amount of wheat required. MAP shows the average percentage of the diversion of wheat amount from the actual demanded wheat.

The chosen periodic time is especially focused for the popular products, the highest demanded products. It needs to pay attention to two products that have the highest demand, they are NM and BB. Table 2 and Table 3 respectively show the error value of the NM and BB forecasting, for each methods, and for each periodic time.

Tabel 2: Forecasting Error for NM product

Periodic Time	MA			SES			DES		
	MAD	MAP	MSE	MAD	MAP	MSE	MAD	MAP	MSE
3	231,340.3	85.12	6.34E+10	103,148.5	46.14	1.85E+10	95,903.6	43.19	1.41E+10
4	259,981.5	85.38	7.23E+10	160,305.2	53.83	3.79E+10	144,121.3	52.19	2.71E+10
6	314,985.3	97.36	1.04E+11	**59,239.7**	**15.54**	**7.58E+09**	101,063.0	36.41	1.80E+10

Tabel 3: Forecasting Error for BB product

Periodic Time	MA			SES			DES		
	MAD	MAP	MSE	MAD	MAP	MSE	MAD	MAP	MSE
3	24,314.3	20.93	9.12E+08	24,624.9	21.69	9.09E+08	34,583.2	27.10	1.77E+09
4	23,920.3	21.21	9.31E+08	**23,487.8**	**20.82**	**8.81E+08**	29,979.1	20.97	1.22E+09
6	25,420.0	23.23	1.03E+09	26,047.0	23.96	1.07E+09	65,527.0	59.69	5.99E+09

Determining The Review Period

The review period or periodic time is determined based on the smallest error value of forecasting without considering the forecasting method used.

The choosing of the smallest error value is prioritized by considering the value of MAD first. MAD values in the table above shows the average amount of wheat flour that deviates from the actual required amount of wheat flour. This is the amount for a month. The second priority is to consider the value of MAP. MAP values in the table above shows the average percentage of wheat flour that deviates from the actual required amount of wheat flour. The percentage is derived from the deviation in the amount of wheat a month. Thus, for this case the value of MAD can be interpreted more easily.

The table 2 indicates that the minimum value for the MAD for the type of wheat NM occurs when forecasting is done for the period of 6 months, i.e. 59,240 units. With this value, it is estimated that FPS can meet with the lack or excess of NM production approximately 59,240 units per month. So it is MSE value which reaches the minimum value 15.54% for the same periodic time, i.e. 6 months. This MAP values can be interpreted that the FPS may be excess or shortage of stock of 15.54% of the NM quantity demanded.

Because the demand for wheat NM is greater than the BB, the priority can be given to more wheat flour NM periodically so that the time chosen to make the observation room is 6 months.

Demand patterns and forecasting for product NM are shown in the table 4. Forecasting is done in the diagram is the Single Exponential Smoothing (SES) method for the period of 6 months.

Table 3: Product NM 6 months period forecast with Single Exponential Smoothing

Month	Forecast	Actual	Error	ABSOLUTE ERROR	Square of Error	Percentage of Error
Jul	269295	340540	71245	71245	5.076E+09	0.209
Aug	269295	280895	11600	11600	1.346E+08	0.041
Sep	269295	327522	58227	58227	3.390E+09	0.178
Oct	269295	276408	7113	7113	5.059E+07	0.026
Nov	269295	460550	191255	191255	3.658E+10	0.415
Dec	269295	253297	-15998	15998	2.559E+08	0.063

Making Procedure Storage Systematization

After the periodic time to perform storage review has been determined, that is 6 months, then the storage systematization procedure can be carried out every 6 months.

To be able to make the storage systematization, FPS (warehouse) is divided into three parts according to the Pareto principle, namely:

- Zone A, the front room of FPS that can be used to store the most high-frequency (high popularity) wheat flour.
- Zone B, the deeper room of FPS that is used to store for the lower frequency (the medium popularity) wheat flour.
- Zone C is the behind space of FPS that is used to store the most low frequency (low popularity) wheat flour.

To determine the capacity of zone A, B and C, it needs to observe the order frequency for each type of wheat, and the amount ordered. The frequency of ordered wheat determines whether a type of wheat are placed in Zone A, Zone B or Zone C. The quantity of order determines the capacity of each zone by considering the minimum stock.

Based on the Pareto principle, the product grouping used is a small part of high frequency order and a huge part of low frequency order.

In this way, products are grouped based on ABC classification. ABC classification of Pareto settles that:

- Class A is item with cumulative percentage 10% - 55%.
- Class B is item with cumulative percentage 56% - 90%.
- Class C is item with cumulative percentage 91% - 100%.

The steps of classification are as follows.

- The order frequency of each product is calculated in total.
- The ordered product is arranged by the order frequency.
- Create the percentage calculation of cumulative frequency.
- The classification is done based on ABC classification of Pareto.

Table 4: Order Frequency

Type	Frequency	Cumulative Frequency	Cumulative Percentage
NM	517	517	44.23%
BB	284	801	68.52%
TE	201	1002	85.71%
NB	121	1123	96.07%
PM	46	1169	100.00%

Table 6: The amount of ordered wheat

Type	Amount of order (unit)	Percentage
NM	2.476.012	39.84%
BB	1.689.150	27.18%
TE	1.034.644	16.65%
NB	594.230	9.56%
PM	421.403	6.78%
TOTAL	6.215.439	100.00%

Table 6 shows the order quantity for each type of wheat. NM ranks first with a percentage of 44.23%, so that items classified as group A. BB and PB belong to group B, while NB and PM are group C.

The size of the zones A, B and C are determined from the percentage of ordered wheat quantity.

- Zone A consists of wheat NM, with percentage of 39.84%. So that the capacity for the zone A :
  Zone capacity = 39.84% x 62,100 units
  = 24,740.64 units
- Zone B consists of wheat BB and TE, with percentage of 43.83%. Capacity for the zone B :
  Zone capacity = 43.83% x 62,100 units
  = 27,218.43 units

- Zone C consists of wheat NB and PB, with total percentage of 16.34%. Capacity for the zone C :
  Zone capacity =16.34% x 62,100 units
  = 10,147.14 units

Table 7: The Calculation of Capacity for Each Los

Los No.	Capacity (unit)	Cumulative Capacity (unit)	Los No.	Capacity (unit)	Cumulative Capacity (unit)
1	1620	1620	26	1620	41220
2	1620	3240	27	1620	42840
3	1620	4860	28	900	43740
4	1620	6480	29	900	44640
5	1620	8100	30	900	45540
6	1620	9720	31	900	46440
7	1620	11340	32	900	47340
8	1620	12960	33	900	48240
9	1620	14580	34	900	49140
10	1620	16200	35	900	50040
11	1620	17820	36	900	50940
12	1620	19440	37	900	51840
13	1620	21060	38	900	52740
14	1620	22680	39	540	53280
15	1620	24300	40	540	53820
16	720	25020	41	360	54180
17	1620	26640	42	720	54900
18	1620	28260	43	900	55800
19	1620	29880	44	900	56700
20	1620	31500	45	900	57600
21	1620	33120	46	900	58500
22	1620	34740	47	900	59400
23	1620	36360	48	900	60300
24	1620	37980	49	900	61200
25	1620	39600	50	900	62100

By observing Table 7, the boundaries of Zone A are los 1 to los 16 (total capacity of 25,020 units). The limit of Zone B is from los 17 until los 38 (total capacity of 27,720 units). Then, the remaining los, they are los 39 to los 50 are allocated as Zone C (total capacity of 9360 units). Recapitulation zone capacity can be seen in table 8.

The los allocation also must consider the minimum quantity to be saved for each product in each period. The quantity of stored product is determined based on the daily maximum demand occurred in the previous period (last six months).

If the minimum quantity of wheat excesses the zone capacity, then the zone capacity needs to be adjusted by taking one or more los to the nearest zone, so that the zone capacity can anticipate the minimum requirement.

The mechanism of the storage systematization is prepared to be additional procedures from the existing procedures of FPS.

Table 8: Recapitulation of Calculation for the Capacity of Los

Zone	Los No.	Capacity	Percentage
A	Los 1 - Los 16	25.020	40.29%
B	Los 17 - Los 38	27.720	44.64%
C	Los 39 - Los 50	9.360	15.07%
Total		62.100	100.00%

CONCLUSION

There are some conclusions derived from this research:

1. The main cause of not running FIFO system at PT SRR is the difficulty of wheat flour storage.
2. The storage difficulty is caused by a lot of factors, they are the limitations of FPS, such as :
   a. Capacity of FPS, which is only able to accommodate 70,000 bag (2 days of production)
   b. The low utilization, which is only 22.27% in normal condition.
3. The most efficient alternative in terms of time and money to solve problems and improve the system FIFO is making periodical storage systematization, which is written in the form of operational procedure.
4. The storage systematization is done periodically based on the popularity of the product, so that the high frequency wheat is placed on the front and the low frequency one is placed on the back of the FPS.
5. Based on the forecasting by using Single Exponential Smoothing method and historical data, the periodic time to conduct storage systematization is every 6 months.
6. To prevent the occurrence of the expired product delivery, the wheat bags are labeled with the date that is the best use of products.

REFERENCES

Adam, Everett, 1992, *Production And Operation Management :Concept, Model And Behavior*, Fifth Edition, Prentice-Hall, New York.

Apple, J.M, 1972, *Material Handling Systems Design*, Ronald Press, New York.

Arnold, Tony, 1997, *Introduction to Material Management*, Prentice-Hall, New York.

Heizer and Render, 2008, *Operations Management*, Ninth edition, Pearson International.

Robbins and Coulter, 2004, *Management*, Prentice Hall.

Voehl, Frank, 1995, *ISO 9000 An Implementation Guide for Small to Mid-Sized Businesses*, St. Lucie Press, Singapore.

ISSN 114-1284

The Blue Ocean Strategy Model and Its Application in Transportation Industry: A Case Study of Private Autobus Company

Ronald Sukwadi [1,2], Ching-Chow Yang[2], Trifenaus P. Hidayat[1], Hotma A. Hutahaean[1]

[1]*Department of Industrial Engineering*
Atma Jaya Catholic University, Jakarta 12930, Indonesia
Tel : (021) 5708826 ext 3132
E-mail : trifenaus.hidayat@atmajaya.ac.id

[2]*Department of Industrial and Systems Engineering*
Chung Yuan Christian University, Chung Li 32023, Taiwan, R.O.C.
Tel :886-3-2654405. Fax : 886-3-2654499
E-mail : chinchow@cycu.edu.tw

ABSTRACT

There is no doubt that land transportation is the most dominant transportation mode compared to another transportation ways such as air and marine transportations in Java. This is shown that the most number of passengers and mails are using land transportations. As the transportation companies, there are many problems found and the one of those is the competition among companies which have the same route and market segmentation. The competition among bus companies becomes tighter and bloody, in other words, those companies are in the Red Ocean. The Porter's Five Forces Models and SWOT Analysis were used to identify the situation of Red Ocean. To escape from the Red Ocean, the company should be able to take some strategies, such as technological innovation, the innovation in services and the mix of them, so the newly and different innovation could be reached. Initial strategy canvas would be made based on result of the questionnaires. Finally, using the four action framework proposed by Kim and Mauborgne, the company will determine which factors that should be eliminated, reduced, raised and invented to create the innovative idea of the Blue Ocean Strategy.

Keywords

Porter's Five Forces Model, SWOT Analysis, Red Ocean, Strategic Canvas, Four Action Framework.

1. INTRODUCTION

Transportation has a major impact in the socio economic life of the country, transporting people and cargo, and connecting among islands, as a means to promote regional economic development, as a means to support other sectors, to increase and equalize people prosperity, to increase national industry competitiveness. It is indeed, national integration and unity, and poverty alleviation depends on good transport links [1].

Land transport is one of the important transport means to boost economic activities. There is no doubt that land transportation is the most dominant transportation mode compared to other transportation modes such as air and marine transportations in Java. This is shown that most of the passengers and mails are using land transportations [2]. Based on Ministry of Transportation Directorate General of Land Transportation data, the land transport is dominant mode with an estimate share of about 92 percent of total freight transport in tons, and about 84 percent passenger movements [3]. The acceleration of development activities will in turn need land transport improvement to make smooth mobility of passengers and goods from one place to another.

However, currently most land transportation modes in Indonesia do not show an efficient and sustainable service performance. This fact is indicated by many complaints from the passengers and the delivered goods [1]. The competition among bus companies becomes tighter and bloody, in other words, those companies are in the situation of Red Ocean [4]. The Porter's Five Forces Models and SWOT Analysis were used to identify the situation of Red Ocean. The potential value created with a new service provided by a bus company is given by the difference between its benefit, in the view of the customers, and the price that customers pay to the company. To what extent this potential value can be exploited as a market opportunity depends on the company's success in obtaining a competitive advantage over other autobus companies (competitors) in the transportation industry. In order to acquire a competitive advantage, a company must outperform its rivals in value creation [5].

Kim and Mauborgne [4] offer an innovative concept to strategy development. At the core of their approach is the

ISSN 114-1284

realization that it is much more valuable for firms to focus their strategy on finding or creating new, uncontested market space (a 'blue ocean') than to compete against incumbent firms on existing markets ('bloody oceans'). The main instrument for finding blue oceans is a 'strategy canvas,' a visual depiction of strategies as value curves allowing the comparison and differentiation of industries and competitors. Within this framework the Blue Ocean Strategy (BOS) can then be derived as the optimal choice of innovative strategy formulation. Therefore, the aims of this research are:

1. to identify the competition status among bus companies using the Porter's Five Forces Models and SWOT Analysis
2. to design Blue Ocean Strategy using strategy canvas and the four action framework.
3. to formulate some innovative strategies based on Blue Ocean Strategy result.

2. METHODOLOGY

2.1 Blue Ocean Strategy Methodology

The methodology developed here is based on the Blue Ocean Strategy model proposed by Kim and Mauborgne [4]. A methodology that will be utilized for developing an innovative strategy for an autobus company is shown in Figure 1. The methodology is categorized into three main phases. The first phase involves identifying current competition condition in autobus industry. This phase will include The Porter's Five Forces Models and SWOT Analysis that will be analyzed for describing the situation. The second phase is a Blue Ocean Strategy Design. It involves Strategy Canvas and Four Actions Framework. The purpose of strategy canvas is to visualize value curves allowing the comparison and differentiation of industries and competitors and by using the four strategic actions framework, the company will determine which factors that should be deleted, decreased, raised and invented to create the innovative idea. The last phase involves developing an innovative strategy based on the Blue Ocean Strategy.

Figure 1: Blue Ocean Strategy Methodology

2.2 Sampling

The questionnaire asked the respondents for their profile details, their customer satisfaction of existing attributes, and the expectation of those attributes and their future usage intentions for different bus. A survey amongst bus passengers was conducted and 100 responses were obtained. The objects of autobus were PO.X and its close competitors. The survey was conducted at several bus stations and bus agents in Jakarta. The purposive sampling technique was used to collect the responses. An attempt was made to see that there was diversity in the type of respondents that covered business executives, businessmen, academics, etc.

3. RESULT

3.1 Identifying the Competition Condition

Force factors that affect the conditions of competition need to be identified. Concept Five Forces analysis

introduced by Michael E. Porter helps the company to understand the competitive environment. It uses five forces which determine the competitive intensity and therefore attractiveness of an autobus market [6].

Beside that, the SWOT analysis is used to provide information that is helpful in matching the company's resources and capabilities to the competitive autobus industry's environment. As such, it is instrumental in strategy formulation and selection [7]. Figure 2 and Figure 3 in Appendixes show respectively the Five Forces Competitive Strategy analysis in autobus industry and how a SWOT analysis for autobus industry.

3.2 Blue Ocean Strategy Design

The main instrument for finding blue oceans is a 'strategy canvas'. It depicts strategies as value curves allowing the comparison and differentiation of a form and competitors based on customer satisfaction attributes from questionnaire's result. Figure 4 shows the initial strategy canvas for PO.X and its competitors.

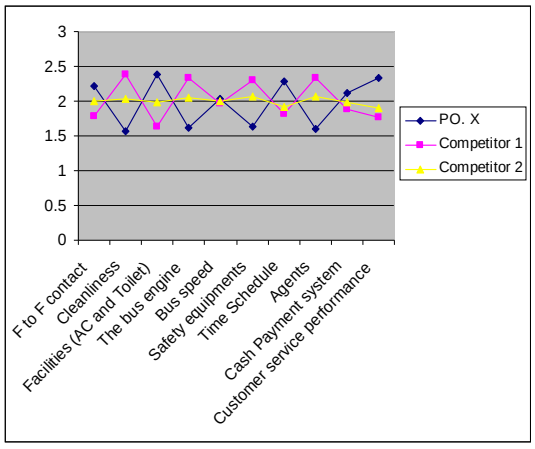

Figure 4: Initial Strategy Canvas

The strategic attributes that the industry competes on and invests in are displayed on the horizontal axis in Figure 4. The vertical axis shows the offering level buyers receive for each strategy attribute. Thus, strategic attributes can be viewed as attributes of the products or services being offered. Competitors are judged on the level of their offerings to the customer in each attribute and may be sorted into strategic groups, which are defined by equal or similar offering levels in each strategy factor. The result is a set of value curves for competing strategic groups in an autobus industry.

After describing the initial strategy canvas, the company will determine which factors that should be deleted, decreased, increased and created using four actions framework (Table 1).

Table 1: Four Actions Framework

Eliminated	Raised
Face to face contact	Cleanliness
Time Schedule	Facilities (AC and Toilet)
Agents	Safety equipments
	Customer service performance
Reduced	**Created**
Cash Payment system	On line payment system
Bus speed	New supporting facilities
	Kinship situation

Kim and Mauborgne [4], therefore, suggest to shift the market focus to alternative customers, who place less weight on the competitive strategy factors under consideration, while valuing other (new) attributes more strongly. As a consequence, some attributes can be reduced or eliminated altogether for strategy factors of lower importance, while relevant attributes can be expanded and new ones created. In Figure 5, future strategy canvas for PO.X illustrates the contrast to the two dominating strategic groups.

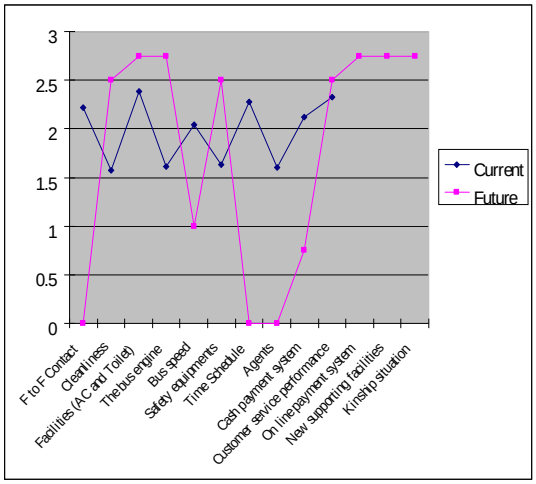

Figure 5: Future Canvas Strategy of PO.X

3.3 Creating Innovative Strategies

Then, the blue ocean idea will be formulated into two innovative strategies. They are marketing and product design strategies. The current company marketing strategies will be changed after the idea of Blue Ocean Strategy. Therefore, PO.X also need to focus or change their market target and do repositioning. Table 2 and Table 3 show the marketing strategy differences before and after the blue ocean idea.

Table 2: New Segmenting, Targeting and Positioning

STP	Current Strategy	Blue Ocean Strategy
Segmentation	Low, middle, high-middle segment	Low, middle, high-middle, and high segment
Targeting	Low and middle class group	High class group (business executives, businessmen, company)
Positioning	Public bus	Create new market as family bus

Table 3: New Marketing Mix (7P)

7P	Current Strategy	Blue Ocean Strategy
Product	Economy and executive bus	Super executive family bus
Promotion	Banners, Sponsorship	Radio advertising, newspaper, and internet
Price	Based on government policy	Depend on given facilities
Place	Convenience agents	On line order and payment
People	No attention	Training
Process	No attention	Has a new division to handle the process
Physical Evidence	No attention	More attention

Besides new marketing strategy, the company's product design approach must be linked to the Blue Ocean Strategy. The visualization of family bus is considered by the autobus industry.

4. DISCUSSION

The metaphor of red and blue oceans describes the market universe. Red oceans here are all autobus companies in existence today—the known market space. In the red oceans, autobus industry boundaries are defined and accepted, and the competitive rules of the game are known. SWOT Analysis and Porter's Five Forces Model were used to identify that situation [7]. Using SWOT analysis, PO.X can audit itself and its environment. It is the first stage of planning and helps PO.X to focus on key issues. Based on the SWOT results, the company should manage its internal and external factors. For internal factors, the company should enhance its strengths such as competitive price and good driver and should improve its weakness by updating the website. For external factors, the company should catch the opportunities up such as development of technology and niche market. Beside that, the company also should pay attention on the economic situation and the competitors.

While, Five Forces Analysis helps the company to understand a competitive environment. It has similarities with SWOT analysis, but tends to focus on the autobus business rather than a single product or range of products [6]. Five forces analysis looks at five key areas namely the threat of entry, the power of buyers, the power of suppliers, the threat of substitutes, and competitive rivalry [8]. Here, PO.X tries to outperform their rivals to grab a greater share of product or service demand. As the market space gets crowded, prospects for profits and growth are reduced. Products become commodities or niche, and cutthroat competition turns the red ocean situation.

Blue oceans, in contrast, denote the unknown market space in autobus industries not in existence today, untainted by competition. In blue oceans, demand is created rather than fought over. There is ample opportunity for growth that is both profitable and rapid. In blue oceans, competition is irrelevant because the rules of the game are waiting to be set [4], [9].

The initial strategy canvas is made as an elegant qualitative and didactic tool for understanding and explaining the strategic deviation of high performers from traditional market incumbents in creating value. Here, in the autobus industry, based on questionnaires result, it has been identified 10 critical factors influenced passenger satisfaction. They are face to face contact, cleanliness, facilities, bus engine, bus speed, safety, time schedule, agents, and cash payment system and customer service performance. However, it is easy to argue that a PO.X strategy must have been 'better' than those of its competitors, knowing that the company turned out to be successful.

To reconstruct customer value elements in crafting a future strategy canvas, we use the Four Actions Framework. As shown in Figure 5, to break the trade-off between differentiation and low cost and to create a new value curve, there are four key questions to challenge an industry's strategic logic and business model [4]:

1. Which of the factors that the industry takes for granted should be *eliminated*?
2. Which factors should be *reduced* that do not unsatisfy customers?
3. Which factors should be *raised well above* the industry's standard?
4. Which factors should be *created* that the industry has never offered?

Based on the result, there are some factors must be eliminated (face to face contact, time schedule, and agents), reduced (cash payment system and bus speed), raised (cleanliness, facilities, safety equipments, and customer service performance), and created (on line payment system, new supporting facilities and kinship situation).

After that, PO.X should change the current marketing strategy to gain niche market whenever it can attract new potential customers and make competitive forces with its rivals irrelevant. The company should do re-segmenting, re-targeting and re-positioning to reach its niche market. The focus of this marketing strategy is to make sure that products and services meet customer needs within that market and

developing long-term and profitable relationships with those customers [8].

To achieve this, PO.X will need to create an innovative strategy that can respond to changes in customer perceptions and demand because it can help company find new, uncontested market space that company successfully target. The visualization of this innovative strategy is a family bus concept. The family bus has 'rooms' and equipments like living at the home (see Figure 6). Finally, new segmentation, targeting, positioning, marketing mix, and bus design are needed in order to support this Blue Ocean Strategy implementation.

5. CONCLUSION

This research uses Blue Ocean Strategy model that proposed by Kim and Mauborgne to escape from bloody Red Ocean and to understand the demands of customers. The results not only can be used to identify the attributes of service elements, it also can suggest the attributes that should be deleted, decreased, increased and invented to create the innovative idea in blue ocean. This result is beneficial for PO.X management to formulate their strategy when they devote significant portion of their organizational resources to them

Despite the limitations resulted from the context of data collection and the sample, the research provides some valuable findings for PO.X management by identifying critical attributes as customer voices. It also contributes to future development of Blue Ocean Strategy model for other industries.

REFERENCES

[1] Rochma, Malia, "Prospek sektor transportasi di Indonesia," *Economic Review*, no. 211, March 2008.
[2] http://www.bismania.org
[3] http://www.hubdat.web.id.
[4] Kim, W. Chan and Renee Mauborgne, *Blue ocean strategy*, Jakarta : Serambi Ilmu Semesta, 2006.
[5] Purba, Humiras Hardi, *Strategi bersaing : teknik menganalisa industri dan pesaing*, Jakarta : Erlangga, 2008.
[6] Porter, M. E., *Inovasi nilai pelanggan dalam perencanaan dan pengembangan produk*, Jakarta : Graha Ilmu, 1995.
[7] Rangkuti, Freddy, *Analisis SWOT teknik membedah kasus bisnis*, Jakarta : PT Gramedia Pustaka Utama, 1998.
[8] David Besanko, David Dranove, Mark Shanley, and Scott Schaefer, *Economics of strategy*, 4th edition, NJ: J. Wiley & Sons, Hoboken, 2007.
[9] David, Fred R, *Manajemen strategis*, Jakarta : Salemba Empat, 2006.
[10] Isnaini, Arif, *Integrated marketing strategy 13P*, Jakarta : NTP Press, 2006
[11] Umar, Husein, *Metodologi penelitian aplikasi dalam pemasaran*, Jakarta : PT Gramedia Pustaka Utama, 1997.

APPENDIXES

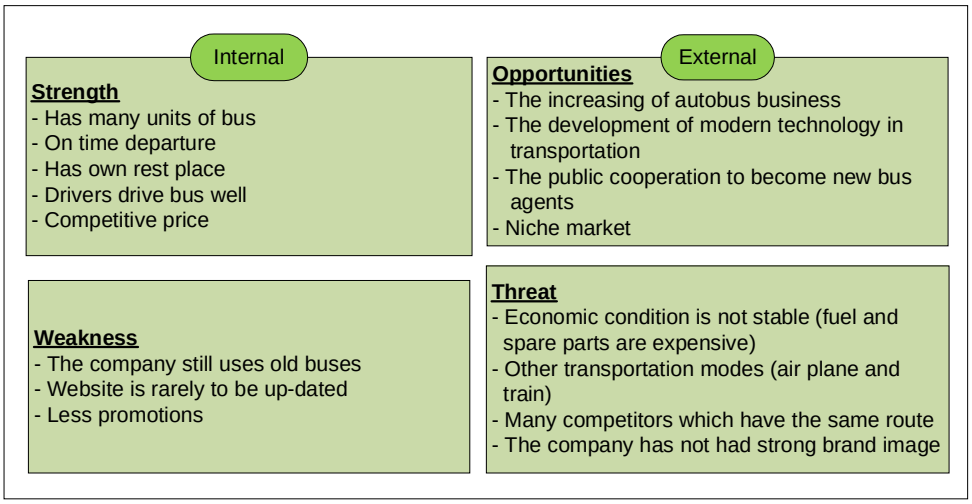

Figure 2: SWOT Analysis

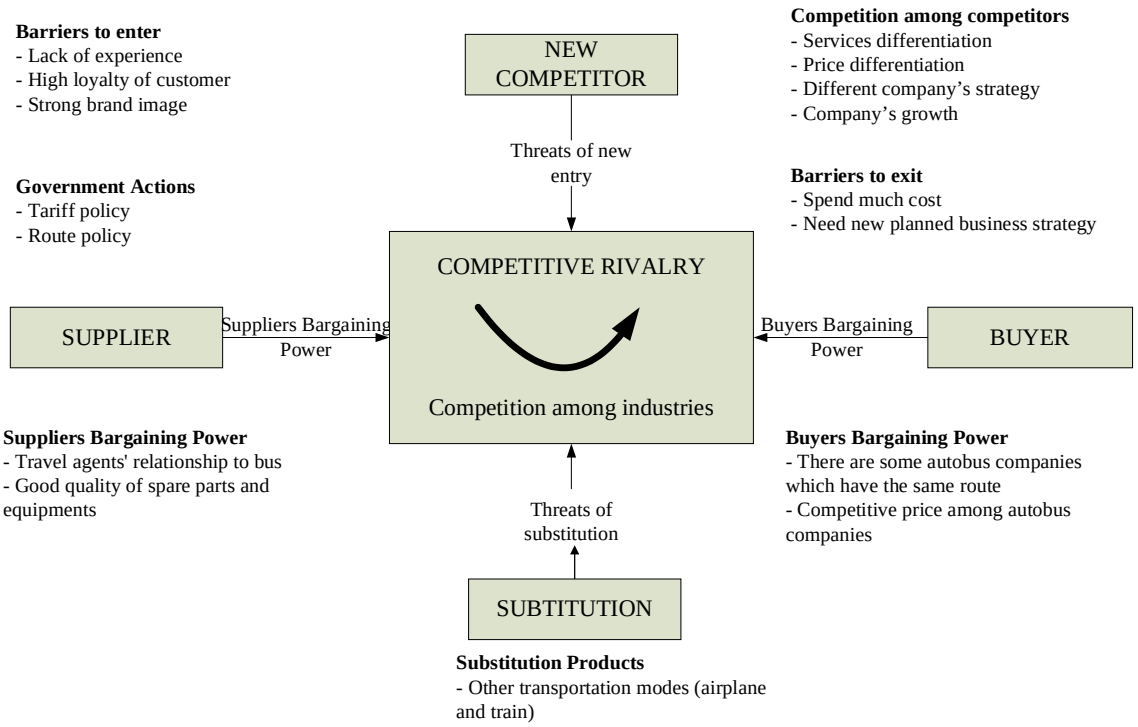

Figure 3: Porter's Five Forces

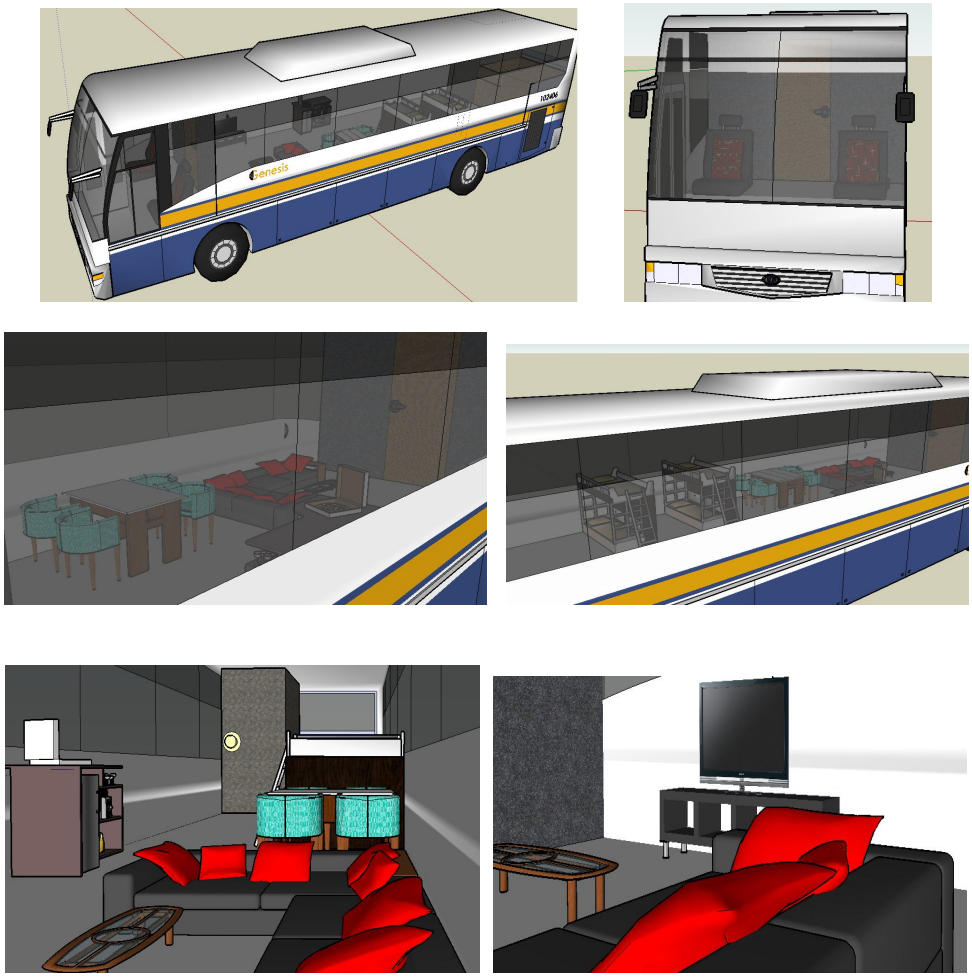

Figure 6 : Bus Design Visualization (Family Bus)

ISSN 114-1284

A SIMULATION TECHNIQUE WITH APPROXIMATION PROCEDURE ON A SIMULTANEOUS EQUATIONS MODEL

Sri Bintang Pamungkas

Industrial Engineering Department, Faculty of Engineering
University of Indonesia, Depok 16424
Tel : (021) 78888805 Fax (021) 78885656
E-mail : sribintang p@yahoo.com

ABSTRACT

In his book, Operation Research, An Introduction (second edition; 1976), Hamdy A. Taha differentiated three kinds of models, a mathematical model, a simulation model and a heuristic model. Those three models in fact could be integrated in a way to solve a model of a real system under our investigation, either it is in engineering or non-engineering fields.
This paper is to show the integration of those three models through a simple mathematical manipulation; that is, by distinguishing endogenous and exogenous variables which contain in a system of simultaneous equations. The simultaneous equations represent a mathematical model of the system; the simulation proceeds by fixing the exogenous (or independent) variables of the equations with certain figures or quantity representing various possible events; and the heuristic approach is used to develop improved solutions to the system of equations until it reaches a set of convergence or unique solution.
The technique can be used in many fields of concentration, including engineering, economics, business, industry and social. That is, as long as a system of equations can be constructed to represent the model. A computer may help us to solve a complex model.

Keywords: *Simulation, heuristic, model*

Three types of models for a system has been mentioned by Hamdy Taha, in his book on operation research (Taha, 1978), which are mathematical model, simulation model and heuristic model. In a system under our observation, either in engineering or non-engineering field, such as economics and business, the three building models can be integrated in one, and solve the problem inside the model to reach a unique solution.

Mathematical Model of Simultaneous Equations

The mathematical model which will be discussed here is a simultaneous system of equations. The general format of system of equations can be written as follows:

F1(X) = **F**1[x1, x2, x3, ……, xn]
F2(X) = **F**2[x1, x2, x3, ……, xn]
:
:
Fn(X) = **F**n{x1, x2, x3, ……, xn]

Which is a system of equations with n number of equations [F1, F2, F3, …., Fn], and n number of variables [x1, x2, x3, …., xn], that is (nxn) simultaneous equations. The system of equations describes the behavior of the real world system under our observation. Each of the equations can be either linear or non-linear. The system of equations can be solved simultaneously to reach a unique solution for [x1, x2, x3, …., xn], therefore it can be written also in a new form as follows:

x1 = **G**1[x1, x2, x3, ……, xn]
x2 = **G**2[x1, x2, x3, ..…., xn]
:
:
xn = **G**n[x1, x2, x3, …..., xn]

A unique solution can still be reached, eventhough there are more than n number of variables, if and only if the value of each extra variables, say the **P**s and **E**s variables, are known. Involving these variables, then the above system of equations can be written as follows:
x1 = **G**1[x1, x2, x3, ……, xn], **P**1, **E**1
x2 = **G**2[x1, x2, x3,……., xn], **P**2, **E**2
:
:
xn = **G**n[x1, x2, x3, ……., xn], **P**n, **E**n

Here, the **X**(x1, x2, x3, ……., xn) variables are called endogenous or dependent variables, which value of each is determined simultaneously by the system; while the **P**n(p1, p2, p3, ……, pk) and the **E**n(e1, e2, e3, …., el) variables are called exogenous or independent variables, which value of each is known before hand.
In a system that we observed, the **P** variables are policy-variables, which value are under our control; and the **E** variables are external-variables which value are out-of our control.

ISSN 114-1284

Simulation Model

The above mathematical model is derived from the real world system under our observation. Each equation that constructs the model can be in many forms: (1) a causal relationship among variables, a relation which frequently subjective or depend on the objective of the observer or the modeler; (2) a specific equation, which depend on the behavior of the system or part of the system, such as physical equation; (3) a parametric relation, which includes some ratios, specific working factors, or coefficients resulted from observations or experiments, including a mathematical equality; and (4) a statistical or econometric relationship, if the factors or the coefficients involved are resulted from a statistical data processing.

Functionally, the relationship among variables can be technical, behavioral, legal, arithmetical, or just an identity. The overall relationships among variables, therefore, is more subjective in character, which depends on the way the observer designs the model, even though the objectivity of the model is still maintained within the whole system. Because of this subjectivity of the relationships, the model is categorized as a simulation model.

Besides, the word "simulation" is used to describe "the process to achieve a number of solutions from model". That is, to see how the model responds from a number of assumed changes, either the changes on the value of the exogenous variables, or the changes on the parameters involved in the model which are is considered significant.

A simulation model to find solution on the endogenous variables **X** which depend on or due to changes on the value of the exogenous variables **P** and **E**, can be shown in Figure-1 below:

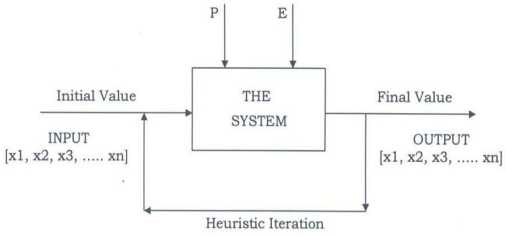

Figure-1: A process to find solution in a simulation model

The choice of value of the exogenous variables **P** and **E** will influence the final results on the value of the endogenous variables **X**[x1, x2, x3, ……, xn]. As long as the number of equations in the system of the model and the number of the endogenous variables are the same, that is (nxn), then a set of unique solution of **X** will always be reached. Any changes in the value of the exogenous variables **P** and **E** will always reach another set of unique solution. Simulation is the agenda to set values of **P** and **E**, each time to get a set of values of **X**.

Heuristic Model

A heuristic model is a model of a system which its solution needs a heuristic process, that is through trial & error, or through *approximation* procedure. Therefore, a heuristic model refers to the way it solves the model system.

Here, the writer uses a numerical method (*Burden and Faires, 1985*) as an approximation way to solve simultaneous equations. Figure-1 also describes the way the general numerical method works. A set of initial values of the endogenous variables **X** are assumed, say [0,0,0,…….,0], which values are feed-in as input into the system (the exogenous variables of **P**s and **E**s, with their values, are inclusive in the system.) The first round of output resulted from the system, which are new values of the endogenous variables **X**, is then feed-in again as second round input into the system. This process is repeated again and again until the final output, that is the unique solution to the simultaneous equations, converges to certain values of **X**.

In this paper the Gauss-Seidel technique is chosen. This technique can be used for linear and non-linear system of equations. Besides of some weaknesses, the Gauss-Seidel technique is relatively easy and brings a fast solution. Another numerical technique is the successive approximation which is also easy, but is not as fast as the Gauss-Seidel technique. Newton technique, on the other hand, is able to cover-up the weaknesses of the Gauss-Seidel technique, but the use of differentials and matrices in its initial procedures for solution are quite complex, especially for a large scale model.

The main weakness of the Gauss-Seidel technique is the possibility of no solution, due to output divergence. A unique solution can only be reached if the output from a step of iteration to the next converges. The ordering of the equations, and the degree of normalizing the values of each variable in each equation within the system are greatly influence the process of solution: it can be fast or slow; it may converge or diverge (no solution). After normalization, there is no certain rule for reordering the set of equations when the solution diverges, except a trial and error procedure (*Challen and Hagger, 1983*).

Using the Gauss-Seidel technique, the above system of equations can be written in an iterative way (with *superscript*-k) as follows:

$x1^{k+1} = \mathbf{G}1[x1^{k}, \; x2^{k}, \; x3^{k}, \ldots\ldots, xn^{k}], \mathbf{P}1, \mathbf{E}1$
$x2^{k+1} = \mathbf{G}2[x1^{k+1}, \; x2^{k}, \; x3^{k}, \ldots\ldots, xn^{k}], \mathbf{P}2, \mathbf{E}2$
$x3^{k+1} = \mathbf{G}3[x1^{k+1}, \; x2^{k+1}, \; x3^{k}, \ldots\ldots, xn^{k}], \mathbf{P}3, \mathbf{E}3$
:
:
$Xn^{k+1} = \mathbf{G}n[x1^{k+1}, x2^{k+1}, \; x3^{k+1}, \ldots.., xn^{k}], \mathbf{P}n, \mathbf{E}n$

where k indicates the number of iteration from k=0 to k=M (M is *stopping device*) which is the final iteration that converges to the *unique solution*.

ISSN 114-1284

Example of Cases

1. Linear System of Equations

An example of a linear system of equations (*Burden and Faires*, 1985, p. 428) is as follows:

$$\begin{aligned} 10x1 - x2 + 2x3 &= 6 \\ -x1 + 11x2 - x3 + 3x4 &= 25 \\ 2x1 - x2 + 10x3 - x4 &= -11 \\ 3x2 - x3 + 8x4 &= 15 \end{aligned}$$

X[x1, x2, x3, x4] is a set of endogenous variables which values are to be found; while the number in the right hand side [6, 25, -11, 15], are the value of the exogenous variables of **P** and **E**.

With the use of Gauss-Seidel technique the above system of equations is changed into the following:

$$\begin{aligned} x1^{k+1} &= 1/10\, x2^{k} - 2/10\, x3^{k} + 6/10 \\ x2_{k+1} &= 1/11\, x1^{k+1} + 1/11\, x3^{k} + 3/11x4 + 25/11 \\ x3^{k+1} &= -2/10\, x1^{k+1} + 1/10\, x2^{k+1} + 1/10\, x4 - 11/10 \\ x4^{k+1} &= -3/8\, x2^{k+1} + 1/8\, x3^{k+1} + 15/8 \end{aligned}$$

The results of the heuristic iteration are as follows:

	k=0	k=1	k=2	k=3	k=4	k=5
$x1^k$	0.0000	0.6000	1.0300	1.0065	1.0009	1.0001
$x2^k$	0.0000	2.3272	2.0370	2.0036	2.0003	2.0000
$x3^k$	0.0000	-0.9873	-1.0140	-1.0025	-1.0003	-1.0000
$x4^k$	0.0000	0.8789	0.9844	0.9983	0.9999	1.0000

By using a set of initial values of **X**[0, 0, 0, 0], the final result as the unique solution is reached at **X**[1, 2, -1, 1] at k=M=5. Some simulation agenda using different values of **P** and **E** will result at different values of unique solution.

2. Non-Linear System of Equations

Another example is shown for a non-linear system of equations (*Burden and Faires*, 1985, pp. 493-494):

$3x1 - \cos(x2x3) - \frac{1}{2} = 0$

$x1^2 - 81(x2 + 0.1)^2 + \sin x3 + 1.06 = 0$

$e^{-x1x2} + 20x3 + \frac{(10 - 3)}{3} = 0$

With the same procedures, by using initial values of **X**[0.1, 0.1, -0.1], a unique solution of **X**[0.50000000, 0.10000000, -0.52359877] is reached:

	k=0	k=1	k=2	k=3	k=4
$x1^k$	0.10000000	0.49998333	0.49997747	0.50000000	0.50000000
$x2^k$	0.10000000	0.02222979	0.00002815	0.00000004	0.00000000
$x3^k$	-0.10000000	-0.52304613	-0.52359807	-0.52359877	-0.52359877

3. Actual Cases

Some examples of actual cases in engineering field, economics, business and industry are presented in the appendix.

APPENDIX

1. Case in Structural Engineering: *Truss*

The equilibrium of forces in horizontal (H) and vertical (V) direction at joints (1), (2) and (3) of a simple truss like the one below (*Chapra and Canale*, pp. 258-259) produces a system of six equations with six unknowns of endogenous variables and three exogenous variables:

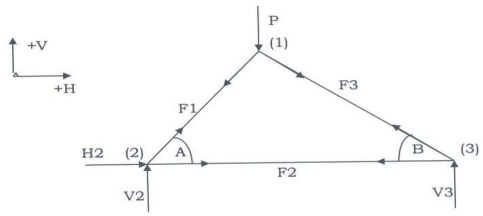

$$\begin{aligned} -F1\cos A + F3\cos B &= 0 \\ -F1\sin A - F3\sin B &= P \\ F1\cos A + F2 + H2 &= 0 \\ F1\sin A + V2 &= 0 \\ -F2 - F3\cos B &= 0 \\ F3\sin B + V3 &= 0 \end{aligned}$$

By giving values to exogenous variables A, B and P, the system of equations determines a unique solution of the endogenous variables of **X**[F1, F2, F3, H2, V2, V3]. Different values of the exogenous variables will produce different unique solution.

By the help of a computer, complicated trusses and frames with different values of exogenous variables can always be simulated quite easily to reach unique solution for each case.

2. Case in Mechanical Engineering: Machine Element

This is a design of a machine element, such as key (*Shigley, 1977, pp.265-266*), with length p, height t and width b, which transmits a rotation from a shaft. The shaft with D in diameter rotates with an angular velocity of N revolution per minute (rpm) and with a transmission power of HP (horsepower). The key material is a steel of UNS G-10350 (*yield strength*, Sy = 65 kpsi). The design of a key produces a system of equations of the following:

Torque : T = 63000 (HP/N)
Tangential Force : F = T/(D/2)
Shear Stress : Ssy = f (F/b.p)
Tension Stress : Sy = f (2F/t.p)
Stress Ratio : Ssy = r.Sy

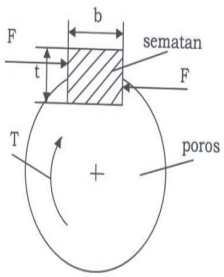

From the above five equations there are eleven variables in total, six of them are endogenous variables. To reach a unique solution for the six endogenous variables, the dimension of the key [p; b; and t], the diameter of the shaft D, the torque T and tangential force F, the value of one of these six endogenous variables must be known or fixed as an exogenous variable. There were two options: whether the diameter D of the shaft was given a certain value; or D had to be determined as an unknown variable, then b and t could be assumed equal, such as b=t or a square key.

Other variables, which are N (rpm) and HP (horsepower); and f, Sy and Ssy, are exogenous variables which values are fixed or given. A simulation can be done for different values of exogenous variables.

3. Case in Economics: a *Macro-Economics Model*

A simple macro-economics model is proposed like the one below (*Dornbusch and Fischer, 1981, pp. 21*). Based on the model a system of equations is derived as follows (Pamungkas, 2005):

(1) National income identity: $Y = C + I + X + G$

where:

Consumption function: $C = Co + 0.6(Y - T)$

Tax level: $T = To + 0.3Y$

Investment function: $I = Io + 0.14Y - 5r - 0.35E$

Net-export function: $X = Xo - 0.1Y + 0.4E - 250p$

(2) Aggregate Supply Equation: $Y = Yo + w(W/p)Y + k(K/E)$

where: w = real wage coefficient

k = technology coefficient

(3) Money market Equation: $r = 0.0015Y - 0.1(M/p)$

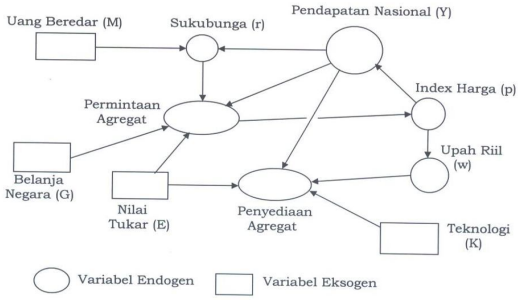

From those three equations a unique solution can be found for the three endogenous variables, which are national income Y, interest rate r (in percent) and the price index p. The value of the exogenous variables, such as government expenditure G, money supply M, exchange rate E (in Rupiah/Dollar), nominal wage W, and technology level K (a dummy variable which values are scaled between 1 and 100), including all autonomous factor (with *subscript* "o") and other coefficient (w, k) are all known. A simulation can be done to know the response of the system for different values of exogenous variables, especially the affect of different policies on G and M, or different values of external shocks such as E.

To bring the model more complete, that is to find the to number of labor employment N in the economy some more equations must be added, like production function Y = F(N, K), and demand function of labor W = F (N, p).

Many large scale economics model have been developed with many equations and variables including one by the writer (Pamungkas, 1984)

4. Case in Mathematical Programming: Input-Output

This is an example of an MP (mathematical programming) problem *(Pfaffenberger and Walker,* 1976, pp. 121-122):

Max: $Y = P'X$

St: $(I - A)X > G$: number of production output in industry

$Ao'x < Lo$: number of labor in industry

$X > 0$: non-negativity

Where **X**[x1, x2, …., xn] is output in industry 1, 2, ….N; **P**[p1, p2, …., pn] is price vector of *output in* industry 1, 2, …., N; and Y is national product (*Gross National Product*).

Matrix **A** represents input-output coefficients in industry, where (aij) showed a part of output in industry (i) which is used as input to produce output in industry (j); and **G**[G1, G2, …., Gn] is the government demand for each output; therefore $Ax + G < X$.

Where as Ao is the number of labor employed in each industry; and Lo is the number of labor in each country.

The above LP formulation is based on Leontief model on industrial data (NxN) which example is shown below, for N = 3:

By adding **S**[s1, s2, s3] as the number of unsold output (*inventory*), and **U**[u1, u2, u3] as the number of unemployed labor, the inequality in the above LP system can be changed into an equality of system of equations:

$$\begin{vmatrix} a11 & a12 & a13 \\ a21 & a22 & a23 \\ a31 & a32 & a33 \end{vmatrix} \begin{vmatrix} x1 \\ x2 \\ x3 \end{vmatrix} + \begin{vmatrix} s1 \\ s2 \\ s3 \end{vmatrix} = \begin{vmatrix} G1 \\ G2 \\ G3 \end{vmatrix}$$

and

$$[ao1 \quad ao2 \quad ao3] \begin{vmatrix} x1 \\ x2 \\ x3 \end{vmatrix} + \begin{vmatrix} u1 \\ u2 \\ u3 \end{vmatrix} = Lo$$

By considering the residuals of **S**[s1, s2, s3] and **U**[u1, u2, u3] as exogenous variables which values are known, and with the value of **G**[G1, G2, G3] and Lo are also known, the system of equations which originally is an LP type model with inequalities, now can be solved to find **X**[x1, x2, x3], by using a numerical technique in solving simultaneous system of equations

Notes:

(1) The above example problem is a typical MP problem (can be linear or non-linear) which solution is more complicated, because of optimality and inequality terms.

(2) It can be noticed, that the number of equations is greater than the number of endogenous variables; this frequently happens in an MP model. In that case, to find the optimum objective function, another step of solution procedure must be established; that is to search the optimum solution from a number of possible unique solutions.

(3) In general, the value of residuals **S**[s1, s2, s3] and **U**[u1, u2, u3] (or slack variables) are unknown, therefore the values must be found using a trial and error procedure such as a heuristic model.

READINGS:

Burden, Richard L. and J. Douglas Faires.1985. Numerical Analysis. Boston: Prindle, Weber & Schmidt
Challen, DW. And AJ. Hagger.1983. Macroeconometric Systems Construction,
Validation and Application. London: Macmillan Press
Chapra, Steven C. and Raymond P. Canale. 1985. Numerical Methods for Engineers,
with Personal Computers Application. New York: McGraw-Hill
Dornbusch, Rudiger and Stanley Fischer. 1981. Macro-Economics. New York:
McGraw-Hill
Pfaffenberger, Roger C. and David A. Walker. 1976. Mathematical Programming
for Economics and Business. Ames: Iowa State University Press
Pamungkas, Sri-Bintang. 1984. A Medium-Term Dynamic Simulation of the Indonesian Economy, disertasi, Philosophy Doctor. Ames: Iowa State
University
Pamungkas, Sri-Bintang. 1990. Modul Kuliah Teknik Numerik. Jakarta: Universitas Indonesia
Pamungkas, Sri-Bintang. 2002. Modul Kuliah Ekonomi-Makro. Jakarta: Universitas Indonesia
Shigley, Joseph E. 1977. Mechanical Engineering Design. New York: McGraw- Hill
Taha, Hamdy A. 1976. Operations Research, An Introduction. New York: Macmillan
Publication

Design Jig of Fitting Sliding Door Roller for Increasing Productivity (Case Study : Product X)

Sri Lisa Susanty [1], Ekaterina Setyawati [1], Sulistyo Agustinus[2]

1.Lecture of Industrial Engineering Department , Sahid University Jakarta
Jln Prof.Dr Soepomo no.84.Tebet, Jakarta Selatan
Telp (021)8312813-15 ext 504, Fax (021) 8354763
Email: sls_lisa@yahoo.com, eka_ptpp02@yahoo.com

2. Student of Industrial Engineering Department , Sahid University Jakarta
Jln Prof.Dr Soepomo no.84.Tebet, Jakarta Selatan
Telp (021)8312813-15 ext 504, Fax (021) 8354763

ABSTRACT

Increasing of commercial cars demand in Indonesia, car producers compete in making commercial car with bigger capacity, more comfortable, more efficiency and globally acknowledged quality as well as reasonable price for Indonesian market as consequenes there is sliding door technology. One of the advantage sliding door is to provide wider space and more compactible. The manufacturing process of the sliding door is very crucial in car assembly. Until now, the fitting of roller is still conducted manually and pure performance or not good (NG) products are still resulted. The defecst are produced by the length unstandarize an, the highest level of the unsymetri door. This is to encourage PT Y to design a new tool (jig) to improve the product in line with the highest standard. In this paper, a new developing of the jig is proposed, while the manufacturing cost is main concern for the economic analysis .

Methodology of he research is based on the design scheme of a product design using Ullrich start, data collection and analysis in PT Y. To get the detail and the right design of the product, the consumer need identification, product specification, design concept, selection concept, testing concept, architecture concept, industrial design, manufacturing process design, economic analysis and product development to calculate the optimum cost by choosing the most efficient material.

Based on the whole steps, it is found that there are two alternative concepts of jig. Concept A is to using manual tools that consists of two mains supporting tools and the concept B is to operating semiautomatic tools by pneumatic force and consist of one main tool. Based on the data analysis, the reults show that the concept B of jig design has the more optimum and efficient to assembly process door roller fitting, reducing NG product to become zero and increasing of the cycle time.

Keywords : *NG Sliding Door, Design Jig, Zero Defect*

1. INTRODUCTION

Increasing of commercial cars demand in Indonesia, car producers compete in making commercial car with bigger capacity, more comfortable, more efficiency and globally acknowledged quality as well as reasonable price for Indonesian market as consequenes there is sliding door technology. One of the advantage sliding door is to provide wider space and more compactible. The manufacturing process of the sliding door is very crucial in car assembly. Until now, the fitting of roller is still conducted manually and pure performance or not good (NG) products are still resulted. The defecst are produced by the length unstandarize an, the highest level of the unsymetri door. This is to encourage PT Y to design a new tool (jig) to improve the product in line with the highest standard. In this paper, a new developing of the jig is proposed, while the manufacturing cost is main concern for the economic analysis. Some of research about jig and fitting design have been proposed such as: jig for fitting locks to door by Wilson, 1999; A jig for removable fitment along the edge of a door which provides a suitable combination of guides and stops to allow the location and operation of suitable cutting tools such as drill or router. A frame unit for tensioning a printing screen and a jig for fitting of print screen to remove the printing screen has been proposed by Keith, 2005. A frame unit for tensioning a printing screen, the frame unit comprises a frame including at least one of frame member, and at least one frame member comprise a supporting frame element.

2. SYSTEM MODEL

2.1. The Customer Need Identification

The customer need identification is used to evaluate the need of customers and effectively communicate to the developer team. The next step, the Matrix Design Requirements of Metric Tool is created as shown in Figure 1.

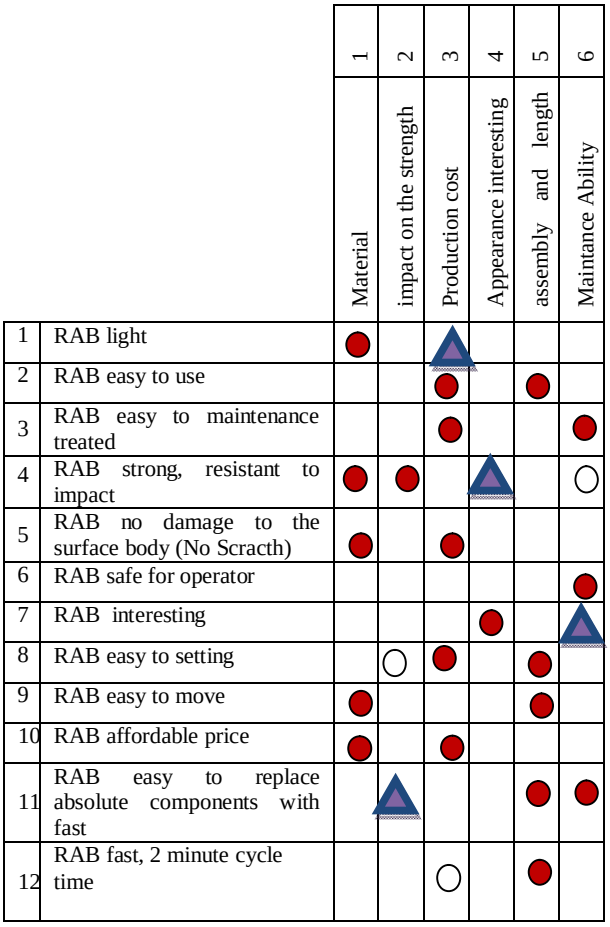

Figure 1. Matrix Design Requirements of Metric Tool

2.2. Product Specifications

The product specification of the design of the sliding door roller is shown in the attachement file 2 of this paper.

2.3. Concept of Product Design

The concept of product design is provided into two concepts, they are: the concept A is namely as two-way manual with the tool) and the concept of B is namely as a semi-automatic pneumatic booster and consists of a tool. The concept A proposed a way for clamping either manually, or setting screw, that consists of two tools to make the center of roller and the lower roller. The advantages of this concept ara: simple, faster to develop, nad the price is cheaper. The weakness of the design are: too heavy (weight of 1 jig around 3 kg. If one day the car should be up 100, the operator must lift the 2 x 100 = 200 times so that the total load is 200 kg x 3 = 600 kg, difficult operation, all manual clamping, the possibility of wound / lacerated body door is very high. The concept B is is propsoed with semi-automatic, manual positioning for the roller, and for the automatic clamping, positioning pins using wind energy (penumatic) that 1 unit consists of a tool with two functions for the lower roller and roller center at the same time. The advantages of this concept are easy to use, fast, accurate results, light, setting only once. The weaknessof this concept are : expensive, and takes longer time for manufacturing process.

3. METHODOLOGY OF RESEARCH

Methodology of research is based on the scheme of a product design using Ullrich start where a research, data collection and analysis is proposed in PT Y. To get the detail and the right design of the product, the customer need identification, product specification, design concept, selection concept, testing concept, architecture concept, industrial design, manufacturing process design, economic analysis and product development to calculate the optimum cost by choosing the most efficient material.

4. RESULTS

4.1. Screening of the Concept

Results from the screening of two concept are shown in Table 1.

Table 1. Screening of the Concept

Selection criteria	Concept	
	Concept A	Consept B
	Full Manual	Semi Automatic
Functional		
Light weight tool	-	+
Cycle time of rapid and permanent	-	+
Accurate	-	+
Comfort		
Bound on the rail	-	+
Comfort in the placement tool	-	+
Comfort in the use of	-	+
Ergonomic		
It takes less energy to setting up	-	+
Clamping/unclamping one movement	-	+
Ease of use	-	+
Resistance		
Long life	-	+
Other		
Cost	+	-
Manufacturing process	+	-
Ease to carry	0	0

Amount (+)		2	10
Amount (-)		10	2
Amount (0)		1	1
Net Value		-8	8
Ranking		2	1
	Continue?	Tidak	Ya

From Table 1. we can see that the concept B is better than the concept of A, where value of + in the concept B is much more than the concept A.

4.2. The Assessment Concept

The assessment concept of jig of fitting sliding door roller is shown in Table 2.

Table 2. The Concept of Assessment

Selection criteria	Weight	Concept			
		Concept A		Consept B	
		Rating	Value	Rating	Value
Ease of handling	5%	2	0.10	3	0.15
Ease of use	25%	3	0.75	5	1.25
Accuracy results	25%	3	0.75	5	1.25
Resistance	25%	2	0.50	4	1.00
Easy to make	10%	5	0.75	3	0.30
Price	5%	5	0.25	2	0.10
Ease to carry	5%	5	0.25	3	0.15
	Total value	3.10		4.20	
	Ranking	2		1	
	Continue?	No		Yes	

4.3 Testing and Design Concept

Testing of both concept, especially in product design jig of fitting sliding door roller, is to ensure that customer needs have been fulfilled by the product concept. Testing of this concept is only proposed to the product development team, to make photos and graphics (rendering) and the simulation of 3-dimensional images obtained from Catia. Testing of the concept of product design is proposed for the structure analysis using software.

4.4. Industrial Design

Product design jig of fitting sliding door roller is to have a high esthetic value. This product is designed to install a roller in accordance with the standards applicable to quickly and optimally. Assessment of the level of interest of the design industry for jig is shown in Table 3.

Table 3. Interest Level Industrial Design

Needs	Level Interest Low-Midle-High	Rank Description
Ergonomic		
Ease of use	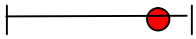	Production capacity of 150 units per day, it becomes very important
Convenience Care	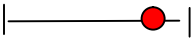	Need a little care
Updates the user interaction	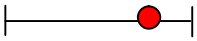	There is a different pneumatic control equipment, in general, with many of the electric control.
Security	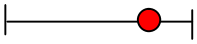	Importance so that security does not bind clamp
Esthetics		
Product differentiation	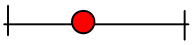	The tool is only available in Indonesia
Prestige of ownership		Plans become more bergensi using this tool
Team motivation	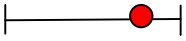	Kaizen tool to make operator creative

4.5. Design for Manufacturing

Design for manufacturing proposed for a variety of machinery and assembly. A suitable technique is proposed to know how to design manufacture mapping using the process operation. This mapping provides a description more carefully about the flow pattern. Detail of product figure is attached in the attachement file 1. And the product component is shown in the attcahement file 3. For simulation and design of slidding door is shown in the attachement file 4 and 5. Table 4 is the total cost of manufacturing jig.

Table 4. Cost Manufakturing

Cost Manufacturing		
1	Component-Component	
	a. Standar	
	Pneumatic	12,000,000
	Screw	500,000
	THK Linear Block	4,050,000
	Spring balancer	9,600,000
	Magnet	150,000

	b. Custom Made	
	1. Frame	
	Material : Aluminium	10,000,000
	Machining	3,000,000
	Jig	1,000,000
	2. Jig parts	
	Material : S45C	12,500,000
	Machining	6,250,000
	Jig	3,000,000
	Material : SS400	5,000,000
	Machining	1,500,000
	Jig	450,000
	Material : MC Nylon	2,000,000
	Machining	750,000
	Jig	0
	3. Rail	
	Material : SS400	7,500,000
	Machining	1,750,000
	Jig	1,000,000
2	Assembly	
	a. Frame	
	Manhour (2 H x 2O)	240,000
	Jig	
	b. Jig Parts	
	Manhour (2 H x 3O)	360,000
	Jig	108,000
	c. Pneumatik	
	Manhour (3 H x 2O)	360,000
	Jig	108,000
	d. Rail	
	Manhour (3 H x 6O)	2,160,000
	Jig	648,000
	e. Total	
	Manhour (2H x 4O)	480,000
	Jig	144,000
		86,608,000
3	Overhead	
	a. Support (10%)	8,660,800
	b. Alocation indirect (5%)	4,330,400
	TOTAL	99,599,200

4. CONCLUSIONS

Selection of concept B is based on the total assessment amounted to 4.20 points that compared to the concept A 3:10 points B with semi-automatic, which is a combination of pneumatic system. The concept B has several advantages as follows: a. Precision, because the position of roller always in right position with the locating pins and clamping using Pneumatic cylinder, b. Quickly, using this tool, the cicle time is increase to 2 minutes for a single assembly, c. Easy operation, one of things that are important for equipment operators is more simple, more tractable, and d. Although the relative price but the benefits are much helpful in the long term.

Materials that used is aluminum and because the light has a high aesthetic value with the total cost to make the tool manufacturing of sliding door roller fitting for the concept B is Rp. 99,599,200

5. REFERENCES

[1] K. T. Ulrich, and S. D. Eppinger, *Product Design Development*, 2nd Edition, New York: McGraw Hill. 2000.
[2] N. Cross , *Engineering Design Methods: Strategies for Product Design*, Second Edition, New York: John Wiley & Sons, 1994.
[3] A. R. Eide, *Introduction to Engineering Design & Problem Solving*, Int Edition, New York: McGraw Hill, 2003.
[4] J. G. Bralla, *Design for Excelence*, Int Edition, New York: McGraw Hill, 2096.
[5] M. D. Rosenav, *The PDMA Handbook of New Product Development*, New York: John Wiley & Sons, 1996.
[6] J. R. Lindbeck John R. and R. M. Wygant. *Product Design and Manufacturing*. New York: Prentice-Hall International, Inc. 2008.
[7] Wilson. Garry and Adrian. Jig for Fitting to Door. Wilson & Young 225 Lawrence Street Alexandria, 1999
[8] Keith. and Mc.Murray.A frame unit for tensioning a printing screen and a jig for fitting a print screen to removing printing screen. Fry Heath & Spence LLP, The Gables, Massetts Road, Horley, Surrey , 2005

ISSN 114-1284

Attachement 1. Jig of Fitting Sliding Door Roller for Concept B

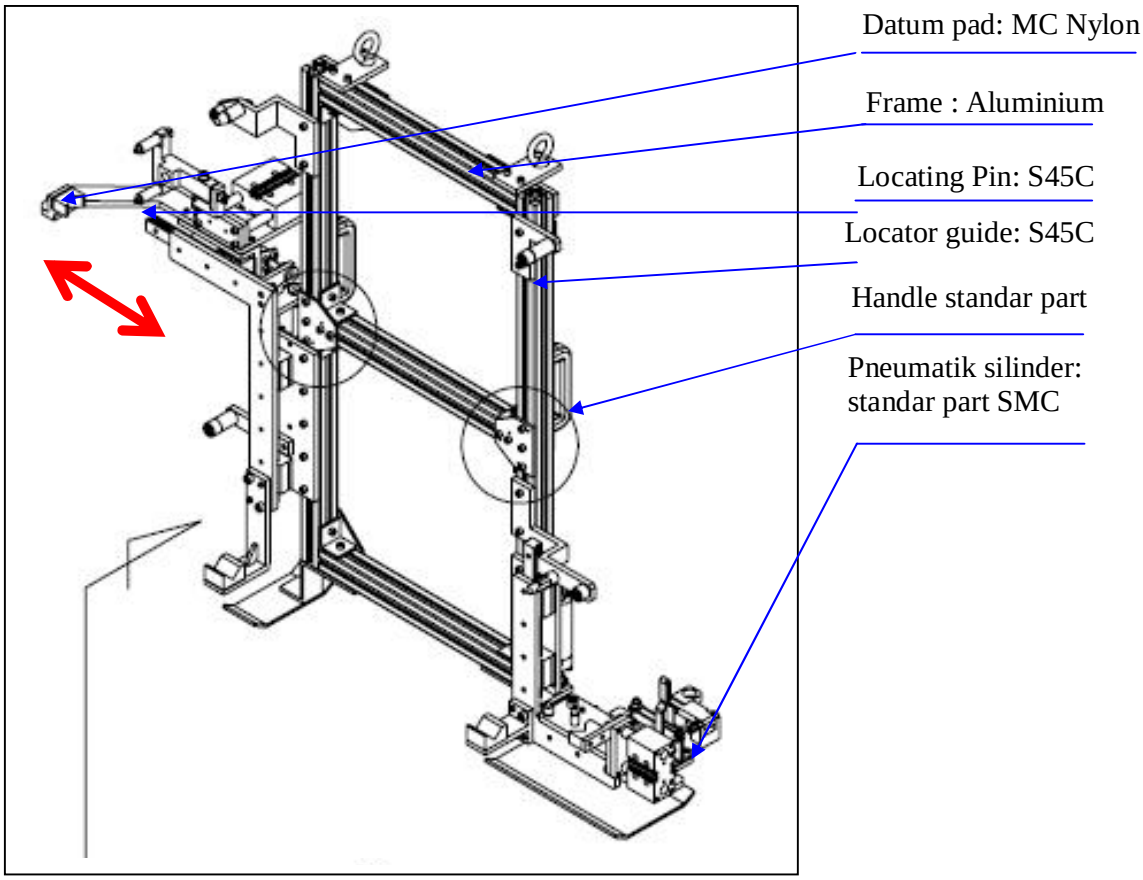

Attachement 2. Target Specification for Concept B

Item		Unit	Concept B
Dimention dan Weight	Tool dimention	mm	1200x750x550
	Tool weight	kg	60
Lain lain	*Cycle Time*	Second	2
	Sumber Tekanan Udara	Mpa	0.6
Locating Elements	Diamond Pin Locator	Pcs	4
	Round Pin Locator	Pcs	4
Clamping Element	Togle clamp	Pcs	Tidak
	Grip Clamp	Pcs	Tidak
	Silinder Pneumatik	pcs	3
	Magnet	Pcs	2
Setting Elements	Shim 0,5 mm	Pcs	15
	Shim 1 mm	Pcs	9
	Shim 2 mm	Pcs	6
Price	Million	Rp	99.599.200

Attachement 3. Component-compenent for asembly

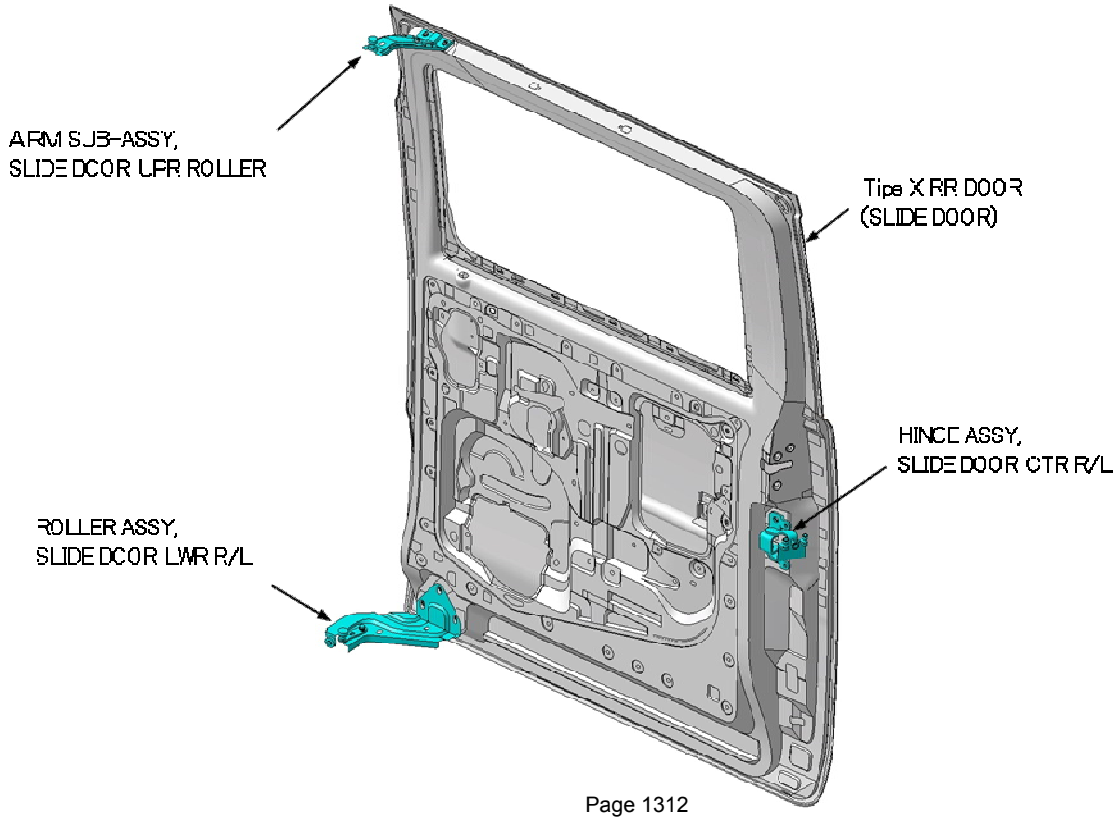

Attachement 4. Layout Asembly

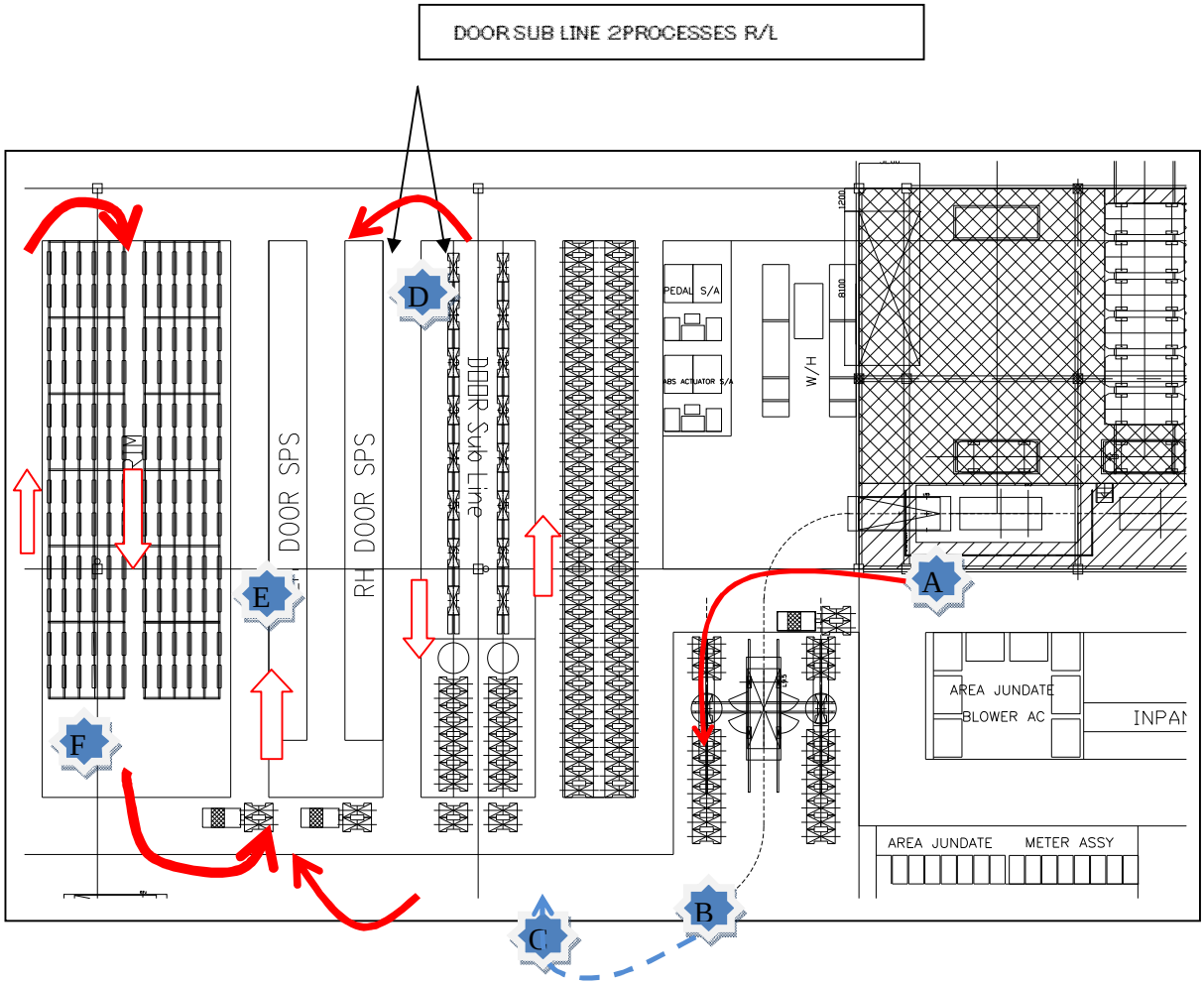

Attachement 5. Simulation Asembly Jig of Fitting Sliding Door Roller

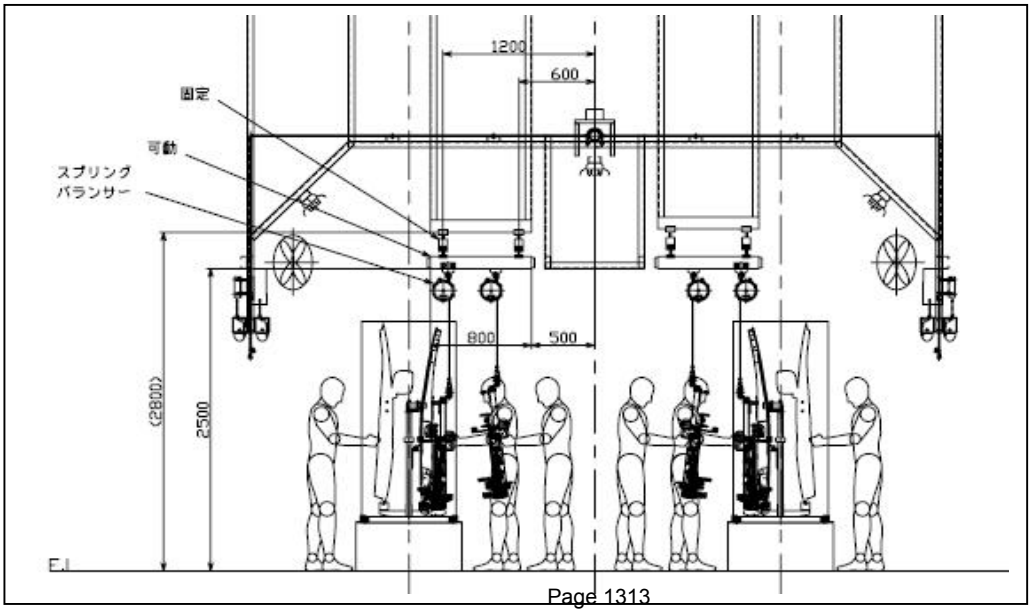

ISSN 114-1284

Taguchi Method for Optimizing the Cycle Time of the Bending and Cutting Compacts

Sri Yulis M. Amin[1], Mahfuzah Abd Salam[2]

[1]*Faculty of Mechanical and Manufacturing Engineering*
University of Tun Hussein Onn Malaysia, Johore 86400
Tel: (07) 4537000 ext 7717. Fax: (07) 4536080
E-mail : yulis@uthm.edu.my

[2]*Faculty of Mechanical and Manufacturing Engineering*
University of Tun Hussein Onn Malaysia, Johore 86400
E-mail : cd060082@siswa.uthm.edu.my

ABSTRACT

Making improvements in products or in processes can be one of the most challenging tasks confronting an organization. One of the semi-finished products manufactured at Fujitsu Component Malaysia Sdn. Bhd (Batu Pahat, Johore) is made by bending and cutting operation at the slow speed hydraulic press machine. It has a standard cycle time 2.5 second per piece and monthly usage is 400k pieces per month. The company wants to eliminate waste by optimizing the cycle time without compromising towards product quality. This research's objective is to identify causes of defects associated with bending and cutting processes at each phases of operations. A detail of methodologies is offered through which an identification of defects and effective solutions for their removal could be done. This research also wants to show how the parameters of the problem could be established and how Design of Experiments (DOE) technique could be applied to achieve the stated objectives by using the Taguchi method and results at 18 test runs. A detailed ten-phase methodology is offered through which an identification of defects and effective solutions for their removal could be done. MINITAB software is used to analyze the data and result. Analysis of Variance (ANOVA), factor interaction and other method is used. The results of the initial experiments are subjected to a verification procedure to determine their viability and accuracy. As a result of this experiment, the company enables to make the changes need to reduce the cycle time requiring producing products and thus, increase productivity while maintaining high quality standards. The expected result from this project is the cycle time for the bending and cutting operation can be reducing by at least 20%. This will lead to cost reduction and increase profit.

Keywords
Design of Experiment (DOE), Taguchi Method, Analysis of Variance (ANOVA), Cycle time, Bending.

1. INTRODUCTION

Fabrication of strip metal for miniaturized components by progressive metal stamping is receiving greater attention because of the rapid growth in demand for such components in electronic and microelectronics industry. With a short cycle time, the high volume of production could lead to cost reduction while maintaining the high quality of the product. The combination of bending and cutting by progressive stamping with a single stroke is made possible by the aid of precision stamping machine. One of the semi-finished products manufactured at Fujitsu Component Malaysia Sdn. Bhd is made by bending and cutting operation at the slow speed hydraulic press machine. It has a standard cycle time 2.5 second per piece and monthly usage is 400k pieces per month. It was considered as a slight loss to the company as if they could reduce the cycle time and managed to increase their profit.

To eliminate this problem, in this study, the optimum level for parameters in the bending and cutting operation will be determined for the best yield of minimum time. Time is considered as an important factor that affects the productivity, hence affecting the profit as well as the production cost. To achieve the objective, Design of Experiment (DOE) approach will be implemented whereby it is a powerful technique used to study the effect of several process parameters affecting the response or quality characteristic of a process or product (Montgomery, 2005). Various parameters as assumed to be significant to the process are press holding time, press descending time, press variable tonnage, and the spring force of machine. However, all these parameters will be sort out according to their level of significance through screening test at the preliminary level of this study.

There are several previous researches that have been conducted research regarding the quality of bending and cutting parts by using DOE approach. Mkaddem and Bahloul (2007) used Response Surface Methodology (RSM) to

investigate the behaviors of automotive safety parts that obtained by successive sequences of blanking and bending. The results showed that the significant parameters are die radius and clearance while the responses are bending load and damage response. On the other hand, Mkaddem and Saidane (2007) also used RSM technique in their research to investigate the springback on bending part using wiping-die bending process. The parameters recognized are stroke, clearance, die radius, anisotropy and bobbing. Using Taguchi method, Dowlatshahi (2003) studied the cycle time reduction for injection molding process for five factors considering injection pressure, injection velocity, cure time, mould temperature, material melt temperature and percentage of regrind. Because the number of factors was more than four, Taguchi method is more practical in order to reduce cost, time and number of experiment.

2. EXPERIMENTAL PROCEDURES

The powder used in this study was phosphor bronze strip (PBS), a copper alloy that has good electrical conductivity and high fatigue strength. This alloy typically contains up to 16% of tin (Sn) to strengthen the alloy and 35% phosphorous to reduce the electrical conductivity dramatically.

For this study, the PBS used is F4-C5191R-1/2H with thickness of 0.2 mm and 21 mm width. The chemical composition by weight is shown in Table 1:

Table 1: Chemical composition by weight

Chemical Composition	Weight (%)
Cu + Sn +P	99.5
Sn	5.55 – 7.0
P	0.03 – 0.35
Cu	balance

Then, the alloy was tempered to ½ H (Hardness) grade between 150 Hz to 250 Hz before undergoing machining process through Japan Automatic Machine (JAM) bending and cutting machine model HYP505H. The main specification of the machine is listed in Table 2:

Table 2: Main specification of JAM Machine Model HYP505H

Press capacity (kN)	24.5 – 49
Stroke length (mm)	*30 – 150*
Ram approaching speed (mm/sec)	350
Ram pressure speed (mm/sec)	39
Press range (MPa)	3.9 – 7.7
Shank hole diameter (mm x mm)	25 x 60
Power	3 phases AC 200V 10A
Motor (kW)	1.5

In order to evaluate the process parameters's influence, holding time, descending time and press variable tonnage were varied at three levels according to Table 3:

Table 3: Description of factors and levels

Factors	Level 1	Level 2	Level 3
A: Holding time (s)	1.35	1.40	1.45
B: Descending time (s)	0.35	0.40	0.45
C: Press variable tonnage (MPa)	5.0	5.5	6.0

3. RESULTS AND DISCUSSION

This section discusses about preliminary experimental result to evaluate these factors' affect on the cycle time. Table 4 illustrates the data obtained after 9 run of experiments:

Table 4: Data for preliminary result

Run of Experiment	Factors			Response			
	A	B	C	Cycle Time (s)			
				Sample 1	Sample 2	Sample 3	Average
1	1,35	0,35	5,0	1,86	1,89	1,85	**1,87**
2	1,35	0,40	5,5	2,04	2,09	2,05	**2,06**
3	1,35	0,45	6,0	2,28	2,26	2,23	**2,26**
4	1,40	0,35	5,5	1,81	1,84	1,83	**1,83**
5	1,40	0,40	6,0	2,05	2,04	2,03	**2,04**
6	1,40	0,45	5,0	2,26	2,24	2,25	**2,25**
7	1,45	0,35	6,0	1,88	1,85	1,86	**1,86**
8	1,45	0,40	5,0	2,06	2,09	2,10	**2,08**
9	1,45	0,45	5,5	2,15	2,17	2,18	**2,17**

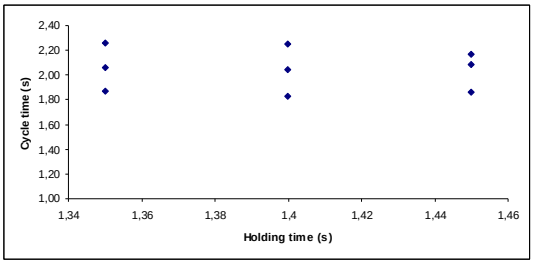

Figure 1: Cycle time as a function of holding time

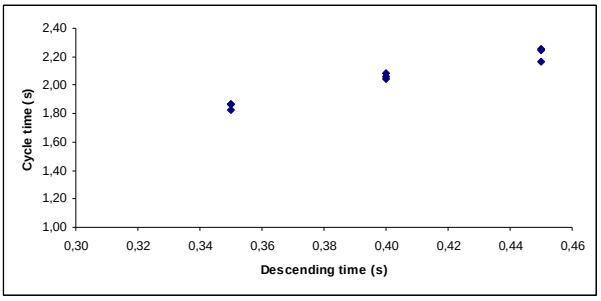

Figure 2: Cycle time as a function of descending time

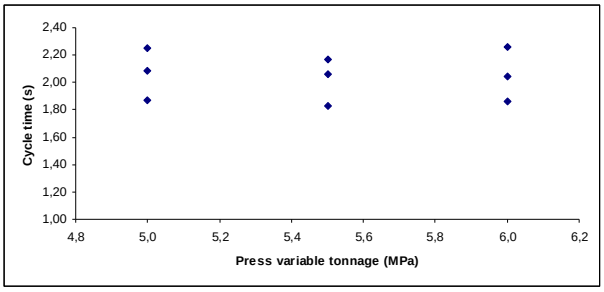

Figure 3: Cycle time as a function of press variable tonnage

Figure 1 until Figure 3 illustrate the interaction between the response function, i.e cycle time to the various factors, holding time, descending time and press variable tonnage. In general, the result shows that the holding time and press variable tonnage (Figure 1 and 3) give low impact to the cycle time, whereby the pattern data is about the same, with very low decrement or incremental. However, as shown in Figure 2, the compact's cycle time is proportional to the descending time. This has its significant because press descending time is period taken by upper die to rise up after the press holding stage that will affect the cycle time at the post processing level.

3.1 Analysis of Variance

One way analysis of variance (ANOVA) was conducted in order to see the level of significance for each factor to the response, i.e cycle time before being optimized by using Design of Experiment method. Significant level, α was obtained through F-test towards variance ratio of the factor. Critical F value is symbolized as F_{α,ϕ_1,ϕ_2} with α is significant level, ϕ_1 as factor's degree of freedom and ϕ_2 as degree of freedom for error. For example, for critical F value with significant level α of 0.01, it was written as $F_{0.01}$. It shows that it is 1% significant or ranking at 99% confidence level.

Table 5: ANOVA for holding time affect towards cycle time

Source	Degree of freedom (DF)	Sum of squares (SS)	Mean square (MS)	F value	P value
A: holding time	2	0.0013	0.0006	0.02	0.983
Error	6	0.2151	0.0359		
Total	8	0.2164			
S = 0.1754		R = 0.5%		R^2=0.0%	

Table 6: ANOVA for descending time affect towards cycle time

Source	Degree of freedom (DF)	Sum of squares (SS)	Mean square (MS)	F value	P value
B: descending time	2	0.2098	0.105	96.37	0.00
Error	6	0.00653	0.0011		
Total	8	0.2164			
S = 0.033		R =96.98%		R^2=95.97%	

Table 7: ANOVA for press variable tonnage affect towards cycle time

Source	Degree of freedom (DF)	Sum of squares (SS)	Mean square (MS)	F value	P value
C: press variable tonnage	2	0.0035	0.0017	0.05	0.953
Error	6	0.2129	0.0355		
Total	8	0.2165			
S = 0.1884		R =1.6%		R^2=0.0%	

Table 5 until Table 7 shows the ANOVA table for each factor towards the performance of cycle time. It can be concluded that, only factor B: descending time has a strong significance as the P value is less than 0.5 and has the highest F value among all, which is 96.37. The higher the F-value, the more likely the relationship is real. In addition, the R^2 value is the coefficient of multiple determinations and it measures how much the real model validates with existed model. In this case, since the R^2 value for factor B: descending time is almost full (95.97%), subsequently it strengthen the fact that only this factor (descending time) has significant factor towards the performance of cycle time in this project. While the other two factors (holding time and press variable tonnage) could be considered as unimportant factor due to their ANOVA table, as well as the similar graph's pattern for the preliminary result. These both factors should be eliminate and replace with any other factor that can be statistically significant through DOE method.

4. CONCLUSIONS

From the experiment carried out, it was concluded that, the significant factor for press bending and cutting operation was only press descending time and suitable in controlling the operation's cycle time. The results shows the holding time and press variable tonnage factors were less significant to the cycle time and should be considered for being eliminated. Thus, the objective for this preliminary study has been achieved, whereby we apply DOE in the early stage of experiment, to find out the most important variables that affect the performance measure, i.e the cycle time for the stamped part.

ACKNOWLEDGMENT

The author would like to express her token of appreciation to University of Tun Hussein Onn Malaysia for the research short term grant.

REFERENCES

[1] Dowlatshashi, S. (2004). "An application of Design of Experiments for Optimization of Plastic Injection Molding Processes'. Journal of Manufacturing Technology Management. Vol. 15. No. 6. pp. 445-454.

[2] Montgomery, D. C. (2005). "Design and Analysis of Experiment". 6th ed. New York. John Wiley.

[3] Mkaddem, A. & Bahloul, R. (2007). "Experimental and Numerical Optimisation of the Sheet Products Geometry Using response Surface Methodology". Journal of Materials Processing Technology. Vol 189. pp. 441-449

[4] Mkaddem, A. & Saidane, D. (2007). "Experimental Approach and RSM Procedure on the Examination of Springback in Wiping-die Bending Processes". Journal of Materials Processing Technology. Vol. 189(1-3). pp. 325-333

Quality Improvement Using Model-Based and Integrated Process Improvement (MIPI) Methodology

T. Yuri Zagloel[1], M. Dachyar[2] and Febi Nur Arfiyanto[3]

University of Indonesia, Depok 16424
Tel: (021) 7270011 ext 51. Fax: (021) 7270077
E-mail: yuri@ie.ui.ac.id [1] mdachyar@ie.ui.ac.id [2] febi1802@yahoo.com [3]

ABSTRACT

Industry environment is not just to meet customer requirement, but also to run their business effectively and efficiently in order to face the global competition. Although there are many methods have been developed, practitioner still finds difficulties when implement the methods. MIPI (Model-based and Integrated Process Improvement) by Sola Adesola and Tim Baines showed a holistic, structured and procedural guidance for improving business processes.

MIPI is developed by reviewing and analysing current methodologies and selecting a few frameworks against key performance indicators.. By using MIPI methodology, industry not only can identify non value added activities in their processes but also can align with organization vision and mision. Hence, practitioners can have structured steps which are consistent and efficient when improving business process.

Case study taken on hatchery produced Days Old Chicks (DOC) which identify business needs and problem areas using pareto chart shows that small and weak DOC is the highest rank (39%). As-Is Process Mapping also conducted to capture current business process architecture. Using Cause and Effect Diagram and Failure Mode and Effect Analysis (FMEA) organization can identify that improper heater control in hatchery machine is the main problem (Risk Priority Number : 36). Action plan created in to a matrix as road map for process improvement plan.

Key words *: MIPI, Seven Procedural Steps, Performance Indicator, Quality Improvement and FMEA*

1. INTRODUCTION

Growing and competitive industries creating high quality product or services as a compulsory requirement. While in the other side, company also requires to effectively and efficient in order to face dynamic business changes.
In order to survive in such environment, reviewing, evaluating and develop plans for improving business process performance is a must thing to do. These activities called *Business Process Improvement (BPI)*.

Business Process Improvement (BPI) can be recognizing as an organized and planned business activity improvement methodology.
Business Process Improvement is a structural approach to analyze and continuously improve company activity by focusing on waste elimination and bureaucratic.
Under big BPI umbrella there are three common strategy and activity adopted by organization: *Continuous Process Improvement (CPI), Business Process Re-Engineering (BPR)* and *Business Process Benchmarking*. Although there are many method of BPI has been developed, practitioner still found difficulties when implement the methods. MIPI *(Model-based and Integrated Process Improvement)*, a BPI method created by Sola Adesola and Tim Baines as a result from doctorate research showed a holistic, structured and procedural guidance for improving business processes.
Research conducted resulting on identifying company's criteria and target to improve its business process performance.

2. RESEARCH METHODOLOGY

Model-Based and Integrated Process Improvement (MIPI) methodology is a Business Process Improvement (BPI) methodology from a research program by Sola Adesola and Tim Baines on Cranfield University, 2005.
MIPI is a generic model of BPI consists of seven procedural steps as guidance for action and decision. MIPI methodology can be use for improvement process and engineering process initiative. This methodology describe "what" to do and "how" to make it happen. The structure for this methodology contains a hierarchical structure includes: *aim, actions, people involved, outcome/exit, checklists, hints and tips, and relevant tolls and techniques*
Model-Based and Integrated Process Improvement (MIPI) was developed from literature and discussion from practitioners. This methodology has been tested in two steps. First, a single case study was carried out which the researcher participated to nurse the newly formed BPI methodology through assessment. The second step by conducting case studies without direct involvement from researcher. Detail of BPI steps is shown in Table 1 below.

Tabel 1: BPI steps and techniques

	Step	Step Description	Techniques
1	Understand business needs	Develop vision and strategic objectives Perform competitor analysis Develop organizational model Evaluate current practices, prioritize objectives Scope change Establish measurable targets Develop process objectives and asses readiness Obtain approval and initial project resource Benchmark the process	Organization model SWOT analysis Force field analysis Readiness assessment Stakeholder analysis Process prioritization matrix Pareto analysis Process performance table
2	Understand the process	Identify the business process architecture Scope and define the process Capture and model AS IS process information Model the process	Xpat process IDEFO Walkthrough Process flowchart ABC Cause and effect analysis
3	Model and analyze the process	Verify and validate the model Measure the existing process performance Analyze the business process	Value added analysis
4	Redesign process	Benchmark the process Identify performance criteria for re-design process Identify focus of re-design activity Model and validate new TO BE process model Identify IT requirements Estimate performance of re-designed process	Benchmarking Creative silent workshop Brainstorming
5	Implement new process	Plan the implementation Obtain implementation approval Review change management plan Communicate the change Technological development Make new process operational Train staff Roll-out changes	
6	Assess new process and methodology	Conduct process deployment and performance data reflections Revise organizational approach	Action plan Evaluation measurement report Customer measurement survey
7	Review new process	Develop strategic view of the business Set process targets and performance Develop a plan to meet targets Implement	Process improvement matrix

3. RESULT

Data collection gathers by conducting interview and company documents. Data collected are:

- company vision & mission, strategy and organization structure;
- performance indicator;
- process flow;
- production capacity & location;
- product specification & quality;
- technology;
- resources & infrastructure;
- others.

Understand Business Needs

From data collection and interview with it was observed that company want to improve customer satisfaction and improving existing process performance. Process Improvement Team (PIT) consists of representative from each department also created to conduct business process improvement.

Understand the Processes

Deep understanding of business goals is very important in business process improvement program. Many efforts will be useless and program will not appropriately execute if improvement program not align with organization goals. This research continues by understanding existing processes after knowing company needs. Understanding processes is conducted by mapping existing process, method used was IDEF0 (*Integrated Computer Aided Manufacturing Definition),* one of modeling tools being use in business process improvement activity. IDEF0 format consist of diagram describing process or system. Using box connected by arrow line to show direction. Process, function or activity represent by boxes inside diagram while arrow line connected to box represent specific data such as object, information or data required or produced by a specific activity. Type of arrow line used in IDEF0:

(1) *Input*: class of arrow that express IDEF0 input. Input arrows are associated with the left side of an IDEF0 box. This arrow describe object or information which cab use as activity.
(2) *Output*: the class of arrows that express IDEF0 output, i.e.: the data or object produced by a function. Output arrows are associated with the right side of an IDEF0 box.
(3) *Control*: the class of arrows that express IDEF0 Control, i.e.: condition required to produce correct output. Data or objects modeled as controls may be transformed by the function, creating output. Control arrows are associated with the top side of an IDEF0 box.
(4) *Mechanism*: the class of arrow that express IDEF0 mechanism, i.e.: the mean used to perform a function; includes the special case of Call Arrow. Mechanism arrowa are associated with the bottom side of an IDEF0 box.

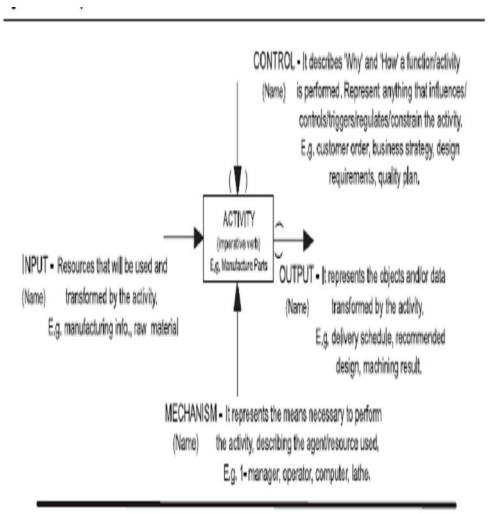

Figure 1. IDEF0 diagram

Below are IDEF0 diagrams for hatchery process PT. X:

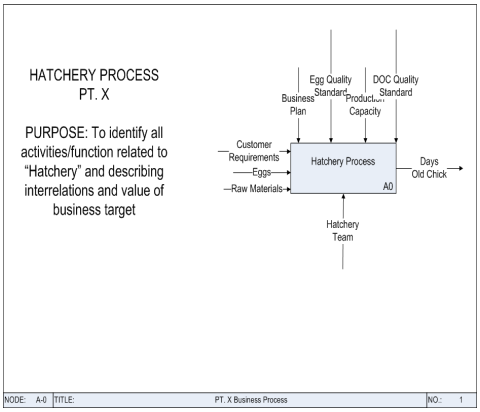

Figure 2. *Top Level Diagram* PT.X

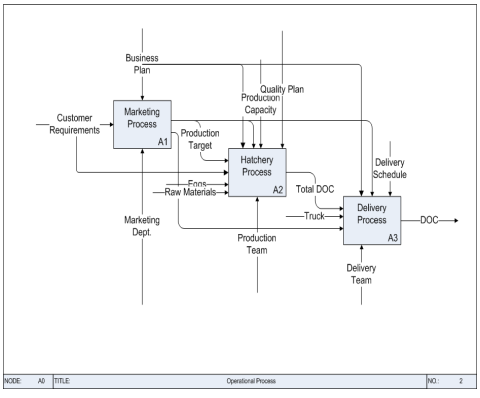

Figure 3. *Child Diagram* Operational Activity PT.X

Problem Area Identification

From brainstorming result, PIT team will focus on customer complaint. PIT team using Pareto Chart to identify the most frequent causes of customer complaint. From diagram created showed that the major problem was *small and week DOC (days of chicks).*

From Pareto Chart result, PIT team continue the research by develop a cause and effect diagram to identify root cause from small and weak DOC problem. Through discussion and brainstorming, PIT team develop probability from each nonconformance. Below is the cause and effect diagram from small and weak DOC (Figure 5). As the result from the diagram, PIT team can identify type of problems and each causes (Table 2.)

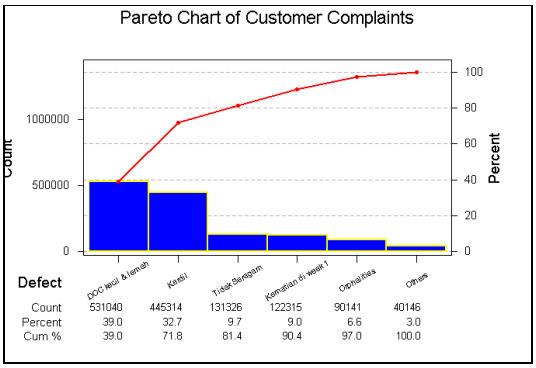

Figure 4. Pareto Chart of Customer Complaint

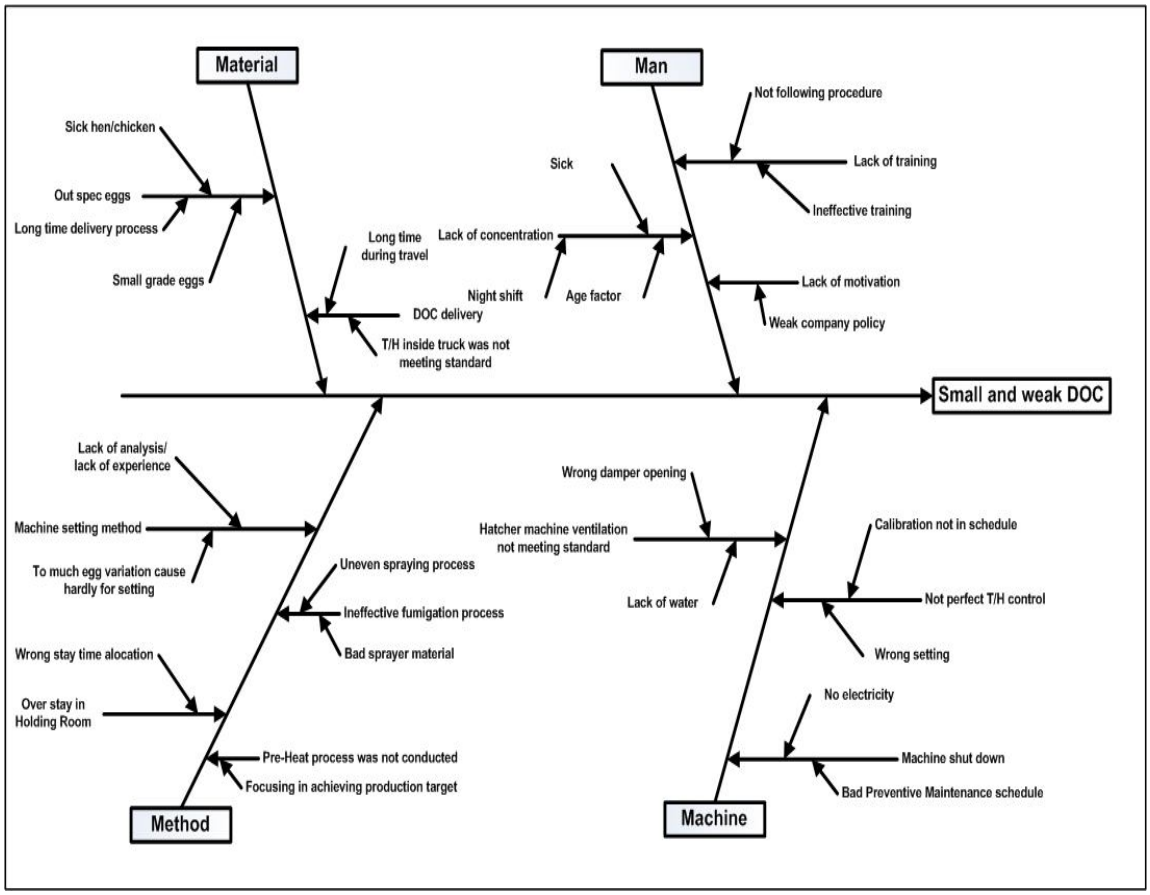

Figure 5. Cause and Effect Diagram from Small and Weak DOC

Factor		Problems	Causes
Man	1	Not following procedure	Employee doing their job as their own experience
Method	2	Pre-Heat process was not conducted	Focusing to achieve production target
	3	Over stay in Holding Room	Wrong placement
Material	4	Hen/Chicken not in god health	Lack of control of farm sanitation
	5	Over time during travel	Traffic Jam
	6	T/H inside truck was not meet standard	Limited truck with good standard T/H
	7	Small grade eggs	Limited of good quantity eggs from supplier
Machine	8	T/H control not meet standard (too cold of to hot)	Inappropriate setting, calibration not conducted as per schedule
	9	Machine shutdown	No electricity

Table 2. List of Problem Causes – Small and Week DOC

Analysis and Corrective Action Plan

During this step, FMEA or *Failure Mode and Effect Analysis* is as an improvement tool used to make prioritation of each failure mode from *Small and Weak DOC*. *Severity*, *Occurrence* and *Detection* criteria are created to identify the highest risk of failure modes and prepare the corrective action. Several failure modes with the highest risk selected as action plan.

In this research, action plans selected is detailed into matrix called *Process Improvement Matrix (PIM)*. PIM is a tool created to monitor the progress of process improvement activities. Each action plan are clearly described its progress using rating and Color Coding. Three Color Coding (Red/Yellow/Green) is use to describe its status againt deadline target.

Detail of process improvement matrix from *Small and Weak DOC* problem can be found in below table:

Process Improvement Matrix for Small and Weak DOC			Hatchery Manager	OA/OSHE Manager	Spv Preshabal	Spv Preshabal Mtenh	Spv Holding Room	Analis	Customer Care (Marketing)
Rank	Potential Failure Mode	Action Plan							
1	Wrong setting (to cool or to hot)	Prepare biweekly calibration schedule for each equipment	0	0	0		0	0	0
		- Identify and re-register all measuring equipment	N/A	N/A	N/A	r	N/A	N/A	N/A
		- Equipment historical data collection	N/A	N/A	N/A	r	N/A	N/A	N/A
		- Send calibrator master to National Calibration Body (external)	N/A	N/A	N/A	r	N/A	N/A	N/A
		- Conduct verification to calibrating tools againts calibrator master	N/A	N/A	N/A	r	N/A	N/A	N/A
2	Sick chicken	Additional sanitationitem in IQC checklist form	0			0	0	0	0
		- Revise IQC Checklist Form	N/A	r	r	N/A	N/A	N/A	N/A
3	Machine problem/shutdown	Prepare ATC (automatic transfer current) easily changing electrical resources from PLN to generator or vice versa.	0	0	0		0	0	0
		- Calculate total electricity consumption and compare to existing electricity capacity	N/A	N/A	N/A	r	N/A	N/A	N/A
		- Identify generator capacity	N/A	N/A	N/A	r	N/A	N/A	N/A
		- Installation of ATC (Automatic Transfer Current)	N/A	N/A	N/A	r	N/A	N/A	N/A
		- Trial test ATC (Automatic Transfer Current)	N/A	N/A	N/A	r	N/A	N/A	N/A
4	T/H inside truck not meet with standard	Prepare standard recommendation for ideal truck condition	0	0		0	0	0	
		- Give recommendation and checklist	N/A	N/A	r	N/A	N/A	N/A	r
5	Over stay in Holding Room	Tag must be sign and controlled by supervisor	0	0		0	0	0	0
		- Tag must be sign and controlled by supervisor	N/A	N/A	r	N/A	N/A	N/A	N/A
6	Pre-Heat process was not conducted	Create transfer form to ensure that no step is skipped	0	0		0	0	0	0
		- Create transfer form to ensure that no step is skipped	N/A	N/A	r	N/A	N/A	N/A	N/A
7	Long time delivery process	Marketing & SCM Dept. conducting mapping area study	0	0	0	0	0	0	
		- Review location and capacity from each supplier	N/A	N/A	N/A	N/A	N/A	N/A	r
8	Small grade eggs	Using grader machine. Create guidance to evaluate supplier performance	0	0	0		0	0	0
		- Procure grader machine	N/A	N/A	N/A	r	N/A	N/A	N/A
		- Install and conduct trial	N/A	N/A	N/A	r	N/A	N/A	N/A
		- Training and handover to production team	N/A	N/A	N/A	r	N/A	N/A	N/A
9	Not following procedure	Display work instruction and checklist in every process	0			0	0	0	0
		- Review existing work instruction againts actual process and guidance	N/A	r	r	N/A	N/A	N/A	N/A
		- Validate work instruction	N/A	r	r	N/A	N/A	N/A	N/A

Table 3. Process Improvement Matrix of Small and Weak DOC

4. CONCLUSIONS

From the business process improvement research using Model-Based and Integrated Process Improvement, criteria's and target shall executed by company has been identified. Several quality improvement plans created to ensure company to meet with the business needs. *"Small and Weak DOC"* was identify as the highest customer complaint and by using cause and effect diagram several causes has been identified, i.e.: *wrong setting; sick chicken; machine problem; temperature and humidity not meet with standard; over stay in holding room; pre-heat process was not conducted; long time delivery process; small grade eggs; not following procedure*. As per Risk Priority Number from FMEA, it was observed that the *"Wrong Setting"* has the highest RPN. To easily monitor the progress of action plan taken, the Process Improvement Matrix is being used.

REFERENCES

[1] Sola Adesola and Tim Baines (2005). Developing and evaluating a methodology for business process improvement. Business Process Management Journal, Vol. 11 No. 1. pp. 37-46
[2] K.T. Lee and K.B. Chuah (2001). A SUPER methodology for business process improvement. International Journal of Operations & Production Management. Vol. 21 No. 5/6, pp. 687-706
[3] Barry Povey (1998). The development of a best practice business process improvement methodology. Benchmarking for Quality Management & Technology.Vol. 5 No. 1. pp. 27-44
[4] Kettinger, W., Teng, J. and Guha, S (1997). Business Process Change: a study of methodologies, techniques, and tools - Appendices MISQ Archivist.
[5] Nancy R. Tague (2005). The Quality Tool Box – Second Edition. ASQ Quality Press.
[6] Harrington, H.J. (1991). Business Process Improvement – The Breakthrough Strategy for Total Quality, Productivity and Competitiveness, McGraw-Hill, New York, NY
[7] Bjorn Andersen (1999). Business Process Improvement Toolbox. ASQ Quality Press
[8] Tinnila, M. (1995). Strategic perspectives to business process redesign. Business Process Reengineering & Management Journal, Vol. 1 No.1, pp. 44-50.
[9] CEI/IEC 60812:2006, Analysis techniques for system reliability – Procedure for failure mode and effects analysis (FMEA),
[10] Chandrasa Sedyalaksana (2006). Introduction to Failure Mode and Effect Analysis. Indonesia Production Operations Management Society.

Analysis of Base-Stock Level and Cost in Uncertainty Demand

Tanti Octavia[1], Felecia[2], Grace Natalia[3]

[1]*Faculty of Industrial Technology*
Petra Charistian University, Surabaya
Tel : (031) 2983430. Fax : (031)
E-mail : tanti@peter.petra.ac.id

[2]*Faculty of Industrial Technology*
Petra Charistian University, Surabaya
Tel : (031) 2983431. Fax : (031)
E-mail : felecia@peter.petra.ac.id

ABSTRACT

Uncertain demand of garment products has become an obstacle in determining the amount of supply. Inventory management itself has an error perspective that the higher the uncertainty of demand, the larger the amount of supply required. There is also an error assumption in the usage of normal distribution for high uncertain demand where in it does not necessarily fit. Both of those perspectives have caused higher risk of lost.

This paper will conduct an analysis on characteristic of demands and inventory cost which might potentially influence the determination of base-stock level, but still considering maximum profit. Three types of approximations which will be utilized to determine a product's base-stock level are normal approximation, lognormal approximation, and maximal approximation.

It is found that distribution of a product's demand does not have any impact on the selection of the best approximation. The best approximation selection to be used in determining base-stock level is influenced by salvage price which is determined and stockout cost. On the other hand, level of uncertainty demand does not give any impact towards the selection of the best interpretation in condition where salvage price or stockout cost is ignored, or salvage price equal to unit cost.

Keywords

Base-stock level, Coefficient of variation, Inventory

1. INTRODUCTION

Inventory is one of the most important elements for production activity. Inventory itself sometimes depend to demand, which has different degree of uncertainty. One of industry with high degree of demand uncertainty is garment industry and this effect the level of inventory it has to keep. Inventory level can be shortage or spoilage without taking accounts the demand, and this will reduce potentials profits.

Inventory management sometimes has incorrect perception about demand and inventory level, the higher the demand uncertainty requires higher inventory level. On the other hand inventory management often used normal distribution assumption to describe demand uncertainty, which is not always true. Both perceptions create higher risk of lost for company. These are the reason this research is conducted to analyze effect of demand characteristic and inventory cost to determine level of inventory by considering maximum profit.

2. SINGLE ORDER PROBLEM

Single order problem is known with newsboy problem or Christmas tree problem. A product is a single problem product when it has demand that happened during specific time interval. Example of these products are perishable goods like newspaper and fresh product like fruits and vegetables.

Single order product has demand pattern with limited selling or usage period, because it has only has one change to order in the beginning of period. There is no second chance to order. This inventory has to fulfill customer demand for that period of time, because at the end of period the product will be not be valuable to sell anymore.

The amounts of product ordered effects company profitability. When demands overcome inventory level, this will caused loss of opportunity to gain profit. When demands below inventory level available this will cause overstock. There are three alternative for overstock products: being disposed because it parish or obsolete, sold at lower price or kept for the next season. Every alternative required cost.

3. COST MINIMATION

High coefficient of variation (cυ) become major issue for product with short lifetime. Demand assumed as non-negative random variable with mean (μ) and variance ($\sigma 2$). It is also assumed zero inventory level at the beginning of period.

Expected profit for order level $y > 0$ unit, can be calculated with equation:

$$\pi(y) = (p-c)\mu - G(y) \quad (1)$$

$$G(y) = h\,E(y-D)^{+} + b\,E(D-y)^{+} \quad (2)$$

Where:

p = product price per unit
c = buying cost per unit
s = salvage price per unit
g = ill-will cost
b = p-c+g = stockout cost
h = c-s = holding cost

The problem face by newsboy problem is how to minimized G(y) which is stock out cost (b) and holding cost (h). The condition where base–stock level do not equal product demand, G(y) has limited minimizer y*. Newsvendor problem often considered as cost minimizing problem, and analysis stopped when y* is found. Expected profit could be negative when Newsboy cost G(y*) is higher than profit.

There are three way to minimized cost (Gallego, Katircioglu, & Ramachandran, 2007) :

a. Normal approximation

Normal approximation caused y* to be linier for σ, this can be calculated using equation:

$$y^* = \mu + \sigma z_{\beta} \quad (3)$$

$$\pi(y^*) = (p-c)\mu - (h+b)\sigma\phi(z_{\beta}) \quad (4)$$

where $z\beta = \Phi^{-1}(\beta)$

b. Maximal approximation

Maximal approximation minimizes cost for worst non-negative distribution using mean and variance. Base-stock level can be calculated with equation:

$$y^* = \mu + \frac{1}{2}\sigma\left(\sqrt{\frac{b}{h}} - \sqrt{\frac{h}{b}}\right) \quad (5)$$

When $c\upsilon < \sqrt{\frac{b}{h}}$, profit is calculated using this equation:

$$\pi(y^*) = (p-c)\mu - \sigma\sqrt{hb} \quad (6)$$

When $c\upsilon > \sqrt{\frac{b}{h}}$, the result will be optimized if ordering not below maximal approximation.

c. Lognormal approximation

Random variable D which has lognormal distribution has mean parameter (v) and standard deviation (τ). When ln (D) has normal distribution it has mean parameter (μ) and standard deviation (σ>0)

Demand expectation for lognormal distribution known as $E(D^n) = \exp(n\mu + n^2\sigma^2/2)$. With parameters $v = \exp(\mu + \frac{\sigma^2}{2})$ and $\tau^2 = v^2\left(\exp(\sigma^2) - 1\right)$.

Parameters for lognormal distribution are:

$$\mu = \ln v - \ln\sqrt{1+cv^2} \quad \sigma = \sqrt{\ln(1+cv^2)}\,.$$

Base stock level for lognormal distribution can be calculated through this equation:

$$y^* = \exp(\mu + \sigma z_{\beta}) \quad (7)$$

while profit can be calculated through this equation:

$$\pi(y^*) = (p-c)v - (h+b)v\Phi(\sigma - z_{\beta}) + hv \quad (8)$$

4. RESEARCH METHOD

The research begin with data collection from fashion product case study. The data needed are product demand, purchase cost per unit, selling cost per unit, and salvage price from 8 different fashion product. These products grouped besed on its lifetime into: short lifetime (less than 1 year) and long lifetime (more then 1 year).

Product demand data is fitted to know its aproximation distribution and parameters. The goal is to find data coevicient of variation (cv), which shows level of demand uncertainty. The next steps is to calculate base-stock level and profit of the product using normal, lognormal and maximal approximation. These information used to do sensitivity analysis for cv, salvage price, and stockout cost.

Profit sensitivity analysis for cv fluctuation is done by changing mean and standard deviation consecutively. While salvage price sensitivity analysis is done by increasing it for every 10% of buying price. Stockout cost sensitivity analysis is done by changing stockout cost. Profit sensitivity analysis to salvage price changing also done by using few possibility of stockout cost and cv. Sensitivity

analysis for profit to stockout cost is done by using few possibility of cv and salvage price.

Those sensitivity analysis used to determined which is the best distribution approximation to overcome changes in cv, salvage price and stockout cost.

5. DISCUSSION

A case study in a fashion small enterprise is applied. The parameters and cost component of each item can be seen in the table 1 and table 2, respectively, as follows:

Table 1. The Distribution Parameter and CV of each Item

No	Item	The best approximation (% Purchase Price)		
		Normal	Maximal	Lognormal
1	X1	$90.03 \le s < 99.37$	$99.37 \le s \le c$	$0 \le s < 90.03$
2	X2	$96.43 \le s < 99.69$	$99.69 \le s \le c$	$0 \le s < 96.43$
3	X3	$94.55 \le s < 99.64$	$99.64 \le s \le c$	$0 \le s < 94.55$
4	X4	$96.72 \le s < 99.72$	$99.72 \le s \le c$	$0 \le s < 96.72$
5	X5	$96.06 \le s < 99.74$	$99.74 \le s \le c$	$0 \le s < 96.06$
6	X6	$96.28 \le s < 99.77$	$99.77 \le s \le c$	$0 \le s < 96.28$
7	X7	$97.79 \le s < 99.78$	$99.78 \le s \le c$	$0 \le s < 97.79$
8	X8	$96.47 \le s < 99.66$	$99.66 \le s \le c$	$0 \le s < 96.47$

Based on data above we calculate base-stock level and profit each item using three approximations. The best approximation of each item can be seen in table 3.

Table 2. Cost Component of each Item

No	Item	*Base -Stock Level* (Unit)	Profit (Rupiah)	The best approximation
1	X1	58.9	560,197	Lognormal
2	X2	14.7	537,735	Lognormal
3	X3	18.890	220,188	Lognormal
4	X4	3,972.8	1,239,270	Maximal
5	X5	2,217.1	271,316	Maximal
6	X6	1,565.1	183,680	Maximal
7	X7	1,007.3	406,308	Maximal
8	X8	980.68	360,223	Maximal

We can see demand distribution does not affect the best approximation to determine base-stock level each item. For example, X7 fits with a 3-parameter lognormal and has maximal as the best approximation. Therefore, we attempt to observe the effect of CV, salvage price and stockout cost to the best approximation.

Table 3. Base-Stock Level, Maximum Profit, and the best approximation each Item

No	Item	Distribution	Mean	Std.dev	CV
1	X1	3 parameter-Lognormal	16.1977	34.6701	2.140
2	X2	3 parameter -Lognormal	5.1301	5.5452	1.081
3	X3	3 parameter -Lognormal	4.9682	14.5770	2.934
4	X4	3 parameter -Weibull	41.5711	45.3952	1.092
5	X5	3 parameter - Lognormal	11.0291	27.9054	2.530
6	X6	3 parameter –Lognormal	8.3019	20.7582	2.500
7	X7	3 parameter -Lognormal	11.6657	10.6442	0.912
8	X8	3 parameter -Lognormal	12.0720	11.1849	0.927

Table 4. The Range of Salvage Price Related to Purchase Price

No	Item	p	c	S	b	h
1	X1	55	35	0.00	20	35
2	X2	135	105	0.00	30	105
3	X3	80	60	0.00	20	60
4	X4	145	115	114.99	30	≈ 0
5	X5	135	110	109.99	25	≈ 0
6	X6	127	105	104.99	22	≈ 0
7	X7	210	175	174.99	35	≈ 0
8	X8	125	95	94.99	30	≈ 0

Table 4 presents the maximum salvage price of each item for each approximation ; i.e., the maximum salvage price for item X1 for maximal approximation is purchase price. On the other hand, if the actual salvage price of X1 is less than it, the best approximation of base stock level is maximal. Moreover, if actual salvage price is greater than purchase price, item X1 should not be ordered.

The sensitivity analysis is also applied to several conditions of each item. It shows that if stockout is not ignored then salvage price, CV and stockout cost affects to the normal and lognormal approximation. Moreover, Lognormal approximation is the best approximation in determining base stock level when stockout cost or salvage price is ignored.The result also indicates that maximal approximation is affected by CV. These can be seen in appendix 1 and appendix 2. It is plausible since the result of maximal approximation never gives a loss.

7. CONCLUSION

Salvage price and stockout cost are key factors affect the best approximation to determine base stock level. Furthermore, a demand distribution does not affect the best approximation. Lognormal approximation is the best approximation in determining base stock level when stockout cost or salvage price is ignored. Maximal

approximation is only affected by CV. It is hoped that sensitivity analysis can assist practitioners and provides a basis for future research on allocation of fashion orders.

REFERENCES

[1] D. J. Beebe Gallego, Guillermo., Katircioglu, Kaan., and Ramachandran, Bala. "Inventory management under highly uncertain demand". *Operations Research Letters*, 35, 281 – 289, 2007.

[2] Tersine, Richard. J. (1994). *Principles of inventory and materials management*. (4th ed). New Jersey: Prentice-Hall International.

[3] *Wikipedia*. Coefficient of variation. Retrieved Agustus 5, 2008 from http://en.wikipedia.org/wiki/Coefficient_of_variation.

[4] *Wolfram mathworld*. (n.d.). Continuous distributions. Retrieved Agustus 4, 2008 from http://mathworld.wolfram.com/topics/ContinuousDistributions.html

Appendix 1

	b = 0	b = 10% c		b = 20% c		b = 30% c		b = 40% c		b = 50% c		b = 60% c		b = 70% c		b = 80% c		b = 90% c		b = c	
cv	s_1	s_1	S_2	S_1	S_2	S_1	S_2	s_1	S_2	s_1	s_2	s_1	S_2	s_1	s_2	s_1	s_2	s_1	s_2	s_1	s_2
0.1		99.46		98.92		98.38		97.84		97.30		96.76		96.22		95.68		95.13		94.59	
0.2		99.44		98.87		98.30		97.73		97.16		96.59		96.02		95.45		94.88		94.31	
0.3		99.39		98.78		98.16		97.55		96.93		96.32		95.70		95.04		94.48		93.86	
0.4		99.33		98.66		97.98		97.31		96.63		95.96		95.28		94.61		93.93		93.26	
0.5		99.26		98.51		97.76		97.02		96.27		95.52		94.78		94.03		93.28		92.54	
0.6		99.18		98.35		97.52		96.69		95.87		95.04		94.21		93.38		92.55		91.73	
0.7		99.09		98.18		97.26		96.35		95.43		94.52		93.60		92.69		91.77		90.86	
0.8		99.00		98.00		97.21		95.99		94.98		93.98		92.97		91.97		90.96		89.96	
0.9		98.91		97.82		96.72		95.63		94.53		93.44		92.34		91.25		90.16		89.06	
1.0		98.82		97.64		96.46		95.28		94.09		92.91		91.73		90.55		89.36		89.30	
1.1		98.74		97.47		96.21		94.94		93.67		92.41		91.14		89.88		88.61		87.34	
1.2		98.66		97.31		95.97		94.62		93.28		91.93		90.59		89.24		87.90		86.55	
1.3		98.59		97.17		95.75		94.33		92.92		91.50		90.08		88.66		87.24		85.82	
1.4		98.52		97.04		95.55		94.07		92.58		91.10		89.61		88.13		86.65		85.16	
1.5	100.00	98.46	99.89	96.92	99.78	95.38	99.67	93.83	99.56	92.29	99.45	90.75	99.34	89.20	99.23	87.66	99.12	86.12	99.01	84.57	98.90
1.6		98.41		96.82		95.22		93.63		92.03		90.44		88.84		87.25		85.65		84.06	
1.7		98.37		96.73		95.09		93.45		91.81		90.17		88.53		86.90		85.26		83.62	
1.8		98.33		96.65		94.98		93.30		91.63		89.95		88.28		86.60		84.93		83.25	
1.9		98.30		96.36		94.89		93.19		91.48		89.78		88.08		86.37		84.67		82.96	
2.0		98.28		96.55		94.83		93.10		91.38		89.65		87.92		86.19		84.47		82.74	
2.1		98.26		96.52		94.78		93.04		91.30		89.56		87.82		86.08		84.33		82.59	
2.2		98.26		96.51		94.76		93.01		91.26		89.51		87.63		86.01		84.26		82.51	
2.3		98.25		96.50		94.75		93.00		91.25		89.49		87.74		85.99		84.24		82.49	
2.4		98.26		96.51		94.76		93.01		91.27		89.52		87.77		86.02		84.27		82.53	
2.5		98.27		96.53		94.79		93.05		91.31		89.58		87.84		86.10		84.36		82.62	
2.6		98.28		96.56		94.83		93.11		91.39		89.66		87.94		86.22		84.49		82.77	
2.7		98.30		96.60		94.89		93.19		91.48		89.78		88.08		86.37		84.67		82.97	
2.8		98.33		96.65		94.97		93.29		91.61		89.93		88.25		86.59		84.89		83.21	
2.9		98.35		96.70		95.05		93.40		91.75		90.10		88.45		86.80		85.15		83.50	
3.0		98.39		96.77		95.15		93.53		91.92		90.30		88.68		87.06		85.44		83.83	

Lognormal: $0 \leq$ *salvage price* $< s_1$ Normal: $s_1 \leq$ *salvage price* $< s$ Maximal: $s_2 \leq$ *salvage price* $\leq c$

Appendix 2

	s = 0	s = 10% c		s = 20% c		s = 30% c		s = 40% c		s = 50% c		s = 60% c		s = 70% c		s = 80% c		s = 90% c		s = c
cv	b_1	b_1	b_2	B_1	B_2	b_1	b_2	b_1	b_2	b_1	b_2	b_1	b_2	B_1	B_2	b_1	b_2	b_1	b_2	B_2
0.1		16.627		14.780		12.932		11.085		9.238		7.390		5.543		3.695		1.848		
0.2		15.813		14.327		12.479		10.632		8.784		7.028		5.271		3.514		1.757		
0.3		14.650		13.462		11.614		9.767		8.139		6.512		4.884		3.256		1.628		
0.4		13.344		11.862		10.379		8.896		7.414		5.931		4.448		2.966		1.483		
0.5		12.054		10.715		9.375		8.036		6.697		5.358		4.018		2.679		1.340		
0.6		10.872		9.664		8.456		7.248		6.040		4.832		3.624		2.416		1.208		
0.7		9.841		8.747		7.653		6.560		5.467		4.374		3.280		2.187		1.094		
0.8		8.962		7.966		6.970		5.975		4.979		3.983		2.988		1.992		0.996		
0.9		8.226		7.312		6.398		5.484		4.570		3.656		2.742		1.828		0.914		
1.0		7.615		6.769		5.923		5.077		4.231		3.385		2.539		1.693		0.847		
1.1		7.109		6.319		5.530		4.740		3.950		3.160		2.370		1.580		0.790		
1.2		6.692		5.948		5.205		4.461		3.718		2.974		2.231		1.488		0.744		
1.3		6.348		5.643		4.937		4.232		3.527		2.821		2.116		1.411		0.706		
1.4		6.065		5.391		4.717		4.043		3.370		2.696		2.022		1.348		0.674		
1.5	∞	5.833	81.401	5.185	72.356	4.537	63.313	3.889	54.267	3.241	45.223	2.593	36.178	1.945	27.134	1.297	18.089	0.649	9.045	0
1.6		5.645		5.018		4.463		3.764		3.136		2.509		1.882		1.255		0.628		
1.7		5.494		4.883		4.273		3.663		3.052		2.442		1.832		1.221		0.611		
1.8		5.374		4.777		4.180		3.584		2.986		2.389		1.792		1.195		0.598		
1.9		5.282		4.696		4.109		3.522		2.935		2.348		1.761		1.174		0.587		
2.0		5.215		4.636		4.056		3.477		2.898		2.318		1.739		1.159		0.580		
2.1		5.170		4.596		4.021		3.447		2.873		2.298		1.724		1.149		0.575		
2.2		5.145		4.574		4.002		3.431		2.859		2.287		1.715		1.144		0.572		
2.3		5.139		4.568		3.997		3.426		2.855		2.284		1.713		1.142		0.571		
2.4		5.151		4.578		4.006		3.434		2.862		2.289		1.717		1.145		0.573		
2.5		5.111		4.603		4.028		3.453		2.877		2.302		1.727		1.151		0.576		
2.6		5.223		4.643		4.063		3.482		2.902		2.322		1.741		1.161		0.581		
2.7		5.284		4.697		4.110		3.523		2.936		2.349		1.762		1.175		0.588		
2.8		5.361		4.765		4.170		3.574		2.979		2.383		1.787		1.192		0.596		
2.9		5.454		4.848		4.242		3.636		3.030		2.424		1.818		1.212		0.606		
3		5.565		4.947		4.328		3.710		3.092		2.474		1.855		1.237		0.619		

Lognormal: $0 \leq$ *stockout* cost $< b_1$ Normal: $b_1 \leq$ *stockout* cost $< b_2$ Maximal: $b_2 \leq$ *stockout* cost $\leq \infty$

ISSN 114-1284

DESIGN OF RELIABILITY MODELS IN REPAIRABLE SYSTEM TO DETERMINE OPTIMUM TIME TO OVERHAUL ENGINE OF DUMP TRUCK: A CASE STUDY ON RELIABILITY ANALYSIS OF DUMP TRUCK IN COAL MINING

Yadrifil [1], Novianti Dian Pratiwiningtyas [2]

[1]*Industrial Engineering Department, Faculty of Engineering*
University of Indonesia, Depok 16424
Tel : (021) 78888805. Fax : (021) 78885656
E-mail : yadrifil@ie.ui.ac.id

[2]*Industrial Engineering Department, Faculty of Engineering*
University of Indonesia, Depok 16424
Tel : (021) 78888805. Fax : (021) 78885656
E-mail : vit_bcool3724rb@yahoo.com

Abstract

Repairable system in engine operations is a complex system that has interval between failure where the failure does not follow equal distribution. Engine's condition as a repairable system has worn-out by time which the impact is on reducing the performance and increasing the cost. The impact is a critical problem especially in the operating of dump truck fleet in mining. It is difficult to estimate the time of engine overhaul because there is no guidance from the company to determine when the engine needs to be overhauled economically. Therefore, it is highly needed to design a model that is able to determine optimum overhaul time of engine dump truck.
In this design, Non Homogeneous Poisson Process (NHPP) model is used as initial estimate failure intensity method that can describe reducing of engine performance. If this model is not appropriate then the General Renewal Process (GRP) model is used. Result of choosing model combined with average maintenance and overhaul cost are used to determine optimum overhaul engine.
The following are the research results GRP model is the best model for repairable systems than NHPP model based on LKV value that is more positive.

Key words: *Repairable System, Reliability Analysis, Non Homogeneous Poisson Process, General Renewal Process, optimum overhaul.*

1. Introduction

Consumers' expectations toward product's and system's ability with their own functions are usually always high and even higher. The ability of product and system is called as reliability. While the expectation of consumers becomes higher, the chance for product to fulfill the expectation is decreasing. That fact has created a gap. For the gap to disappear, measuring and reliability boost toward the product and system are needed.

The objective of reliability can be understood through the phenomenon of estimation failure, reliability prediction, and optimization. Reliability is one of the characteristic that is important in defining the quality of product or system for manufacture and also consumer.

In running the major activity, coal mining company uses two main equipments which are loader and dump truck. Knowing how important these two equipments

are in the mining activity, it is vital to pay attention on their capability in the application. Failure on engine as a main component of a mining system can cause failure to the whole system.

System is a group of subsystem, assembling, or components that is assembled to achieve a particular function. Beside repairable system, there is also non-repairable system. That difference creates the need of different approach in analysis method in the closing stage. In this writing, analysis with stochastic process model is done because of the complexity of repairable system. Some warranty analysis on non-repairable system can use distributed analysis method which is mainly using weibull analysis. In the other hand, for repairable system, distributed analysis is not valid because it has the characteristic that makes the system cannot set off for new condition after it is fixed. Generally, the interval between failures of non-complex system is not equally distributed. When we do the cross-check on distribution, there is

ISSN 114-1284

assumption that an event is statistically independent and identically distributed (s.i.i.d.). The repairable system does not stick to that s.i.i.d. pattern.

After being fixed, commonly system can operate just like the original condition without having any improvement (as bad as old). That can occur in a complex system where replacement of a component does not give significant change in the reliability system. If we use the distributed analysis method, then we do not have to determine when the system needs to be overhauled. Distributed analysis is not the methodology to analyze repairable system because time between failures does not stick to the s.i.i.d (statistically independent and identically distributed). Therefore, we have to choose the analysis using stochastic process model like Homogeneous Poisson process (HPP), Non Homogeneous Poisson Process (NHPP), or General Renewal Process (GRP).

Engine condition as repairable system will be having worn-out through the time and it will cause performance declining and increasing cost. This is a serious problem, especially in designating the time of engine overhaul in PAMA on operating dump trucks. Considering the difficulty in estimating the time of engine overhaul that is caused by the unavailability of guideline from the company about determining when an engine needs to be overhauled economically, then it is necessary to design a model that can determine the optimum overhaul time of engine dump truck.

2. Methods

One of the considerations in decreasing the cost of maintenance for repairable system is by designing the overhaul policy that can decrease the total cost of system. However, the overhaul policy can be implemented only if $\beta > 1$. If $\beta < 1$, then there is no need to apply the overhaul policy because that condition is a sign of no wear out phase. If there is an assumption that there is lower value for system overhaul than continuing the repair, then we should know the time of overhaul that can reduce the total cost by considering the repair cost and the cost of overhaul.

In the calculation of optimum overhaul point, there are some input data such as C1, C2, C3, λ, and β. Parameter λ and β can be determined by using reliability model. Reliability model that is used in this research is stochastic point process model. This model is chosen because the system that is investigated is repairable system. In this repairable system, record of failures does not tag along the pattern of s.i.i.d. (statistically independent and identically distributed). This matches the assumption in stochastic point process model which does not go along the s.i.i.d. pattern. Non homogeneous Poisson process with Power Law model is used as the method in creating the hypothesis of failure intensity that can illustrate the reduction in engine performance. If that model is not suitable, then GRP model is used to illustrate the engine performance reduction. The result of the model combined with the maintenance cost will be used to determine the optimum time to overhaul engine.

In the calculation of optimum overhaul point, there are some input data such as C1, C2, C3, λ, and β. C1 is the average repair cost (unscheduled), C2 is overhaul cost, and C3 is average scheduled maintenance cost. Scheduled maintenance is done in certain period of time with S as time interval that has been determined. In addition, N1 is the amount of failure in [0,t] and N2 is the amount of changing in [0,t]. If $\beta > 1$, then average lowest cost when machine is overhauled happen when instantaneous maintenance cost is equal to the average system cost.

The formula of optimum overhaul point can be explained throughout these following sequences:
Total of system cost when overhaul or replacement is:

$$TSC(T) = C_1 E(N(T)) - C_1 - C_3 \frac{T}{S} \quad (1)$$

Therefore, the average cost becomes:

$$C(T) = \frac{C_1 E(N(T)) + C_2 + C_3 \frac{T}{S}}{T} \quad (2)$$

Instantaneous maintenance cost at T as time is:

$$IMC(T) = C_1 \lambda \beta T^{\beta-1} + \frac{C_3}{S} \quad (3)$$

According to the equations above, the optimum time to overhaul (T0) is:

$$C_1 \lambda \beta T_0^{\beta-1} + \frac{C_3}{S} = \frac{C_1 E(N(T)) + C_2 + C_3 \frac{T}{S}}{T} = \frac{C_1 \lambda T_0^{\beta} + C_2 + C_3 \frac{T_0}{S}}{T_0} \quad (4)$$

Then, the equation becomes:

$$T_0 = \left[\frac{C_2}{\lambda(\beta - 1) C_1} \right]^{1/\beta} \quad (5)$$

Based on the formula processing above, scheduled maintenance cost does not affect the equation of optimum time to overhaul (T0). Therefore, in this research, the data that is used as model is unscheduled maintenance data.

Data calculation based on failure truncated means that a data can be called as the last data if it is the time of last failure, not the time that is last examined. In doing this model, we use two softwares which are RGA 6 for Power Law model and Weibull++ 7 for GRP model.
In this case, the data that is tested is repairable at fielded systems and the model that is available in RGA 6 is Power

Law model, therefore the test is done using cramér-von mises method.

After doing statistical test with cramér-von mises method, it appears that not all system is suitable with Power Law model. For that reason, another model that can explain system reliability is needed. Based on the literature, the research is continued using GRP model that is built with Power Law model. The difference of these two models is on the level of restoration factor (RF). In Power Law model, the value of RF is 0 which means that repair does not cause change in system and only bring the system back to the original operation condition which is ordinary or we can also say that the condition is as bad as old. In the other hand, GRP model the value of restoration factor is 0<RF<1 which means that restoration makes the condition of system is between as good as new and as bad as old.

In the formulating of this model, we can see the general outline of how input and output of the research just like the diagram below

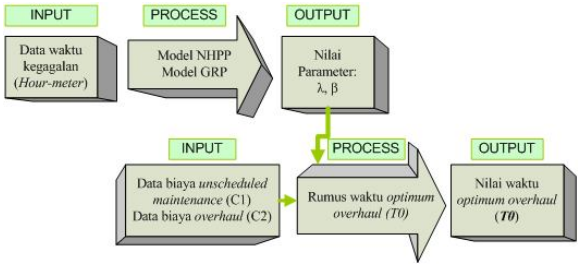

Figure 1. IPO (Input-Process-Output) Diagram

WO data processing generates parameter C1 as unscheduled maintenance and C2 as overhaul cost. The formulating of model generates parameter λ and β. The result of the formulation added with the result of WO data processing will become the input for the T0 formula just like in equation (5).

3. Results and Discussion

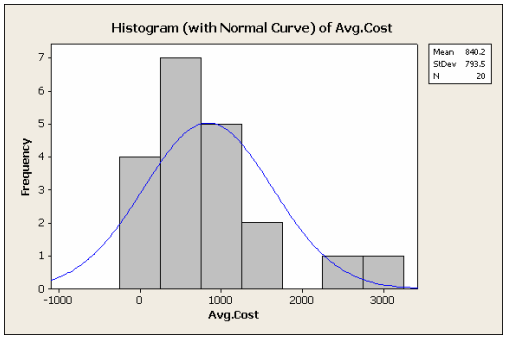

Figure 2. Average Maintenance Cost
(Source: Minitab)

Data of descriptive statistic shows that sample has average cost $ 840.2227258 with standard deviation of $ 793. Minimum cost is $ 39 and maximum cost is $ 3228, so data has range of 3189. Skewness value is 1.87 which means that the gradient is positive and most likely to the right. The gradient indicates that most of average maintenance cost is distributed on right area which means that the cost is relatively high.

3.1. NHPP Power Law Model

This assumption is used in the initial of the process because this model is already used commonly. Beside that, if there is any restoration on certain component in a system, usually the restoration does not change the system into something new, but only restore the operation condition to the original condition. In this model, the level of restoration factor (RF) is equal to 0, or the value of q in the model is equal to 1 where there is relation of RF = 1-q.

The objective in this model is to get the parameter β, λ, and LKV value. There is no LKV value in the result of RGA 6, so we still have to process it again using Weibull++7 with GRP 2-parameter model where the value of q is entered 1. Thus, NHPP Power Law in RGA 6 has similarity with the GRP 2-parameter model in Weibull++7.

From the figure below, can be seen how the pattern of time between failures is, whether it is packed or not at certain time. If each system has its own pattern, the failure that happens is independent and not statistically identical. Furthermore, this system does not tag along the pattern of s.i.i.d (statistically independent and identically distributed). For that reason, the assumption of using certain distribution is not suitable to analyze the repaired system.

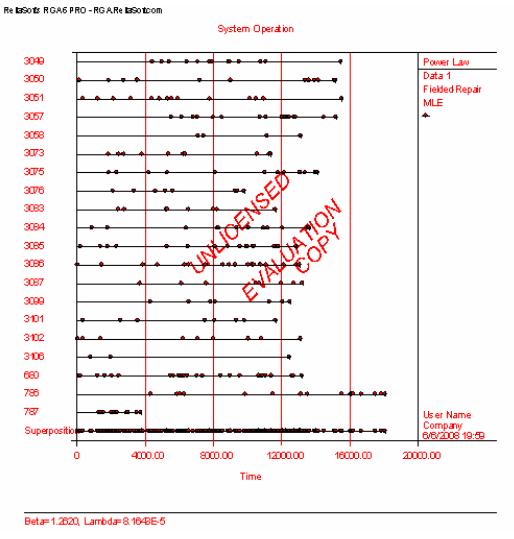

Figure 3. Failure Plotting
(Source: Software RGA 6)

Table 1. Result of Power Law Model

Jenis DT	DT3049	DT3050	DT3051	DT3057	DT3058	DT3073	DT3075
N	13	14	15	19	4	10	16
Beta	1.491096	1.076587	0.852329	2.613351	2.977711	1.272771	2.179155
Lambda	7.35E-06	0.000441	0.004012	2.24E-10	2.18E-12	6.88E-05	1.45E-08
Intensitas [u(t)]	0.001252	0.000993	0.000822	0.003267	0.000907	0.001119	0.002471
Overhaul Cost ($)	55000	55000	55000	55000	55000	55000	55000
Maintenance Cost($)	353.9069	166.95	629.5847	468.3516	39.025	823.423	1714.705
To Overhaul	131701	3101324	#NUM!	25409.12	74842.15	140390.9	18004.72
Jenis DT	DT3076	DT3083	DT3084	DT3085	DT3086	DT3087	DT3099
N	8	8	12	17	22	8	8
Beta	1.726228	1.363899	1.553065	1.226555	1.04495	2.520103	2.92168
Lambda	1.03E-06	2.28E-05	4.54E-06	0.000155	0.0011	3.28E-10	8.58E-12
Intensitas [u(t)]	0.001408	0.000937	0.001366	0.00162	0.00176	0.001524	0.00187
Overhaul Cost ($)	55000	55000	55000	55000	55000	55000	55000
Maintenance Cost($)	1011.053	820.0088	590.8508	866.6947	867.3595	413.8488	3228.239
To Overhaul	35843.79	116150	74725.03	126391.7	700307.4	34171.91	12946.41
Jenis DT	DT3101	DT3102	DT3106	DT680	DT786	DT787	
N	10	9	3	31	17	11	
Beta	0.827461	0.663323	0.657843	1.144236	2.397329	2.005157	
Lambda	0.004316	0.0167	0.006066	0.000598	1.06E-09	7.51E-07	
Intensitas [u(t)]	0.00071	0.000455	0.000158	0.002689	0.002255	0.005887	
Overhaul Cost ($)	55000	55000	55000	55000	55000	55000	
Maintenance Cost($)	1314.096	2337.374	314.7333	196.1674	411.2906	236.7927	
To Overhaul	#NUM!	#NUM!	#NUM!	490929.1	37157.7	17106.73	

From the table above, can be concluded that the value of T0 is inversely proportional with the value of β and cost (C1), and it is also indirectly connected with the amount of failure. The higher β and λ value, then there will be higher intensity value [u(t)]. The increasing failure intensity is causing faster speed sign of engine system in having failure and lower time between failures. Therefore, by knowing the existence of this intensity function, we can take the wise policy in implementing when the engine should be overhauled economically. According to the table above, instead of optimum time to overhaul (T0), there is only an information said "#NUM!" which means that the system is still in growth phase (baby mortality) because $\beta < 1$ so there is no importance to calculate T0 while the system is not in wear out phase yet.

Next, statistical test with cramér-von mises is done for model's suitability test. Go with the preliminary assumption which says that we are using Power Law model, then the most suitable test in this case is cramér-von mises.

There is null hypothesis to test if the data is suitable with Power Law model. The assumption of the null hypothesis is:

H0: Power Law is accepted

H1: Power Law is not accepted

The result of statistical test by cramér-von mises has two possibilities which are failed or passed. If the result is passed, then we accept H0 which means that Power Law model is suitable with the data in this case. Then, if the result is failed, it means the other way. According to the experiment, 13 out of 20 dump trucks are passed.

3.2. GRP I Model

If we assume that partially reparation will renew the system and it is not an as-bad-as-old condition after reparation, then Power Law model does not become the most suitable model in order to analyze the system.

Table 2. Result of GRP I Model

Jenis DT	DT3076	DT3083	DT3084	DT3085	DT3086	DT3087	DT3099
N	8	8	12	17	22	8	8
Beta	1.77287	1.363899	1.553065	1.439289	0.771441	2.688086	3.029724
T^ beta	11931954	351320.3	2641702	822089.8	1497.125	1.2E+11	2.58E+12
Lambda	9.55E-07	2.28E-05	4.54E-06	3.63E-05	0.00815	3.28E-10	8.58E-12
LKV	-63.8074	-65.9158	-95.4252	-129.091	-161.543	-63.541	-63.0755
q	0.522282	1	1	0.170923	0.000608	0.279562	0.524604
Overhaul Cost ($)	55000	55000	55000	55000	55000	55000	55000
Maintenance Cost($)	1011.053	820.0088	590.8508	866.6947	867.3595	413.8488	3228.239
To Overhaul	27397.25	116042.6	74751.8	38502.29	#NUM!	17123.37	9070.112
Jenis DT	DT3049	DT3050	DT3051	DT3057	DT3058	DT3073	DT3075
N	13	14	15	19	4	10	16
Beta	1.491096	0.698802	0.852329	2.613351	3.039559	1.272771	2.263716
T^ beta	1767802	835.0266	3738.796	8.48E+10	3.29E+12	145359.8	2.47E+09
Lambda	7.35E-06	0.00899	0.00401	2.24E-10	2.18E-12	6.88E-05	1.45E-08
LKV	-104.16	-110.407	-118.954	-139.483	-34.497	-80.0997	-120.342
q	1	0.000401	1	1	0.644925	1	0.462158
Overhaul Cost ($)	55000	55000	55000	55000	55000	55000	55000
Maintenance Cost($)	353.9069	166.95	629.5847	468.3516	39.025	823.423	1714.705
To Overhaul	131746.2	#NUM!	#NUM!	25409.83	58988.5	140382.6	12110.92
Jenis DT	DT3101	DT3102	DT3106	DT680	DT786	DT787	
N	10	9	3	31	17	11	
Beta	0.698737	0.663323	0.657843	0.735874	2.457924	2.005157	
T^ beta	694.1866	538.9124	494.5736	1076.483	2.91E+10	14648636	
Lambda	0.00883	0.0167	0.00607	0.0134	1.06E-09	7.51E-07	
LKV	-80.0474	-73.6884	-27.6912	-216.091	-130.36	-73.0002	
q	0.0144	1	1	0.00007	0.626429	1	
Overhaul Cost ($)	55000	55000	55000	55000	55000	55000	
Maintenance Cost($)	1314.096	2337.374	314.7333	196.1674	411.2906	236.7927	
To Overhaul	#NUM!	#NUM!	#NUM!	#NUM!	28168.26	17105.86	

Therefore, we can use General Renewal Process (GRP) Model instead. Kijima developed the imperfect repair (GRP) model by using the thinking of real aging process on repairable system. In Kijima I (GRP I) model, can be said that n repair can only vanish the coming damage only while in period between (n-1) and n failure. This data processing is done by using Parametric Reliability Growth Analysis (Parametric RGA) with GRP model that is built based on Power Law function.

Deviation of T0 value with standard overhaul time is not as big as the previous model. The three who have highest T0 value in the previous model are now having no T0 in this model because they all have $\beta < 1$. Biggest deviation is suffered by DT 3073 with T0 = $ 140,382 supported with β = 1.2727 which is the lowest β value compared with the system that has $\beta > 1$. In GRP I model, average β value is 1.603443 and average optimum time to overhaul (T0) is 53,599.97.

3.3. GRP II Model

In Kijima I model, it is said that n repair can only vanish the coming damage only while in period between (n-1) and n failure. In fact, on practice, n repair does not only depend on (n-1) repair, but also can depend on all of the repairs before. We assume that reparation can vanish all damage accumulation on n failure. That statement is developed become Kijima II or GRP II model.

Conceptually, this model is not significantly different with

GRP I model where the q, which is degree of n repair, has the value of $0 \leq q \leq 1$. In GRP II model, the analysis that is used is also using Maximum Likelihood Estimate (MLE).

Biggest deviation is suffered by DT 3085 with T0 = $ 126,261 supported with $\beta = 1.2265$ which is the lowest β value compared with the system that has $\beta > 1$. In GRP II model, average β value is 1.625463 and average optimum time to overhaul (T0) is 40,798.89.

Table 3. Result of GRP II Model

	DT3049	DT3050	DT3051	DT3057	DT3058	DT3073	DT3075
N	13	14	15	19	4	10	16
Beta	1.763235	0.657714	0.852329	2.646788	3.083116	1.641418	2.179155
T^ beta	24414604	562.2261	3738.796	1.17E+11	4.98E+12	4546724	1.1E+09
Lambda	8.45E-07	0.0127	0.00401	2.24E-10	2.18E-12	3.85E-06	1.45E-08
LKV GRP 2	-103.624	-110.263	-118.954	-139.119	-33.9406	-79.6842	-120.711
q GRP2	0.865697	0.023	1	0.972928	0.662783	0.634575	1
Overhaul Cost ($)	55000	55000	55000	55000	55000	55000	55000
Maintenance Cost($)	353.9069	166.95	629.5847	468.3516	39.025	823.423	1714.705
To Overhaul	56720.34	#NUM!	#NUM!	22181.25	50163.78	33719.2	18006.43

	DT3076	DT3083	DT3084	DT3085	DT3086	DT3087	DT3099
N	8	8	12	17	22	8	8
Beta	1.726228	1.808916	1.553065	1.226555	0.531828	2.57205	2.955729
T^ beta	7771967	22655245	2641702	109816.3	154.5293	3.99E+10	1.29E+12
Lambda	1.03E-06	8.81E-07	4.54E-06	0.000155	0.0717	3.28E-10	8.58E-12
LKV GRP 2	-63.8918	-64.8478	-95.4252	-129.37	-160.033	-64.5136	-63.4517
q GRP2	1	0.510886	1	1	0.434977	0.872824	0.933694
Overhaul Cost ($)	55000	55000	55000	55000	55000	55000	55000
Avg. Maintenance Cost($)	1011.053	820.0088	590.8508	866.6947	867.3595	413.8488	3228.239
To Overhaul	35830.49	25584.7	74751.8	126261.4	#NUM!	27328.11	11538.4

	DT3101	DT3102	DT3106	DT680	DT786	DT787
N	10	9	3	31	17	11
Beta	0.773745	0.662785	0.657843	0.744144	2.397329	2.075284
T^ beta	1401.209	536.1748	494.5736	1164.341	1.6E+10	26086007
Lambda	0.00467	0.0168	0.00607	0.012671	1.06E-09	8.61E-07
LKV GRP 2	-80.1257	-73.6884	-27.6912	-216.127	-130.516	-72.2895
q GRP2	0.00124	1	1	0.000233	1	0.817935
Overhaul Cost ($)	55000	55000	55000	55000	55000	55000
Avg. Maintenance Cost($)	1314.096	2337.374	314.7333	196.1674	411.2906	236.7927
To Overhaul	#NUM!	#NUM!	#NUM!	#NUM!	37146.91	11152.78

3.4. The Chosen Model

To decide which model is the best, then we need a standard of comparison indicator from all models. LKV value is the indicator to show how good a model is to suit our data. The more positive the LKV, the better that model is. This value is used in comparing some best models.

The LKV is only available in Weibull ++7, for that reason, we use the Parametric Reliability Growth Analysis with parameter-2. This parameter-2 indicates the output of a model is only two which are β and λ value. And for the parameter (1-RF), it is already set in the start point by filling the q value according to our assumption. Model with parameter-2 is arranged with q = 1 so we get the LKV for NHPP Power Law model. By setting the q = 1, it means that we have assumed an as-bad-as-old condition to the system. All of the GRP value parameter-2 with q = 1 has β and λ value that equal to the Power Law model from RGA 6.

On table below, the average $\beta > 1$, which is 1.6510253, so generally, the system is having deterioration and analysis of optimum time to overhaul is needed to be done to be able to reduce the cost. B value is around $0.5318284 \leq \beta \leq 3.0831163$ and λ value is around $2.18E\text{-}12 \leq \lambda \leq 0.0717$. From data, there are 7 dump trucks that is still in growth phase (baby mortality) with $\beta < 1$. For that reason, we do not have to do the analysis of optimum time to overhaul. From the chosen model, there are 4 kinds of dump truck that has q equal to 1; it means that on the system the all three models are already suitable. Based on the experiment, the model that is the most chosen is GRP model.

Table 4. Parameter of The Chosen Model

CHOICE MODEL				
Choice Model	LKV	Beta	Lambda	q
GRP II	-103.62	1.7632	8.45E-07	0.8657
GRP II	-110.26	0.6577	1.27E-02	0.02
Semua	-118.95	0.8523	0.004	1
GRP II	-139.12	2.6468	2.24E-10	0.9729
GRP II	-33.941	3.0831	2.18E-12	0.6628
GRP II	-79.684	1.6414	3.85E-06	0.6346
GRP I	-120.34	2.2637	1.45E-08	0.4622
GRP I	-63.807	1.7729	9.55E-07	0.5223
GRP II	-64.848	1.8089	8.81E-07	0.5109
Semua	-95.425	1.5531	4.54E-06	1
GRP I	-129.09	1.4393	3.63E-05	0.1709
GRP II	-160.03	0.5318	7.17E-02	0.435
GRP I	-63.541	2.6881	3.28E-10	0.2796
GRP I	-63.075	3.0297	8.58E-12	0.5246
GRP I	-80.047	0.6987	8.83E-03	0.01
Semua	-73.688	0.663	0.0168	1
Semua	-27.691	0.6578	0.0061	1
GRP I	-216.09	0.7359	1.34E-02	7.0E-05
GRP I	-130.36	2.4579	1.06E-09	0.6264
GRP II	-72.289	2.0753	8.61E-07	0.8179

4. Conclusions

Power Law model that is used as reliability model for the system of engine dump truck HD 785-5 at mining operation in PAMA is not suitable for all system that is examined. That based on the test result using cramér-von mises (CVM) which shows that not all are success, in detail, from 20 dump trucks that is examined, 7 dump trucks turn out to be failed.

Because of the test toward NHPP model of two available models is not suitable for all dump trucks, so the alternative model will be more suitable. That means that the suitable model is GRP. Furthermore, GRP model is the best for repairable system based on the most positive value of LKV

Calculation of GRP model generates the value of parameter β and λ. β value is around $0.5318284 \leq \beta \leq 3.0831163$, while λ value is around $2.18E\text{-}12 \leq \lambda \leq 0.0717$. By having average β value > 1, which is 1.6510253, means that, generally, the system is enduring the wear out phase.

Entirely, the value of optimum time to overhaul (T0) for each dump truck is:

1. DT 3049 = 56720 hmr
2. DT 3057 = 22181 hmr
3. DT 3058 = 50164 hmr
4. DT 3073 = 33719 hmr
5. DT 3075 = 12110 hmr
6. DT 3076 = 27397 hmr
7. DT 3083 = 25584 hmr
8. DT 3084 = 74703 hmr
9. DT 3085 = 38502 hmr
10. DT 3087 = 17123 hmr
11. DT 3099 = 9070 hmr
12. DT 786 = 28168 hmr
13. DT 787 = 11152 hmr

Therefore, the average for engine to be overhauled economically is 31,277 hour meter. In the other hand, 7 other dump trucks, the value of T0 cannot be calculated yet because it only has $\beta < 1$.

5. Reference

[1] Billinton, Roy & Ronald N. (1987). Reliability Evaluation of Engineering Systems. New York: Plenum Press.

[2] Crow, Larry H. (1975). Reliability Analysis for Complex, Repairable Systems. Technical Report No.138, US Army Material Systems Analysis Activity, Aberdeen Proving Ground, Maryland.

[3] Crow, Larry H. (2008). Practical Methods for Analyzing the Reliability of Repairable Systems. Maret 10, 2008. Reliability HotWire Magazine, issue 64.http://www.reliasoft.com/newsletter/v5i1/ repairable.htm

[4] Kijima, M. & Sumita, N. (1986). A useful generalization of renewal theory counting process governed by non-negative Markovian increments. Journal of Applied Probability, 23, 71-88.

[5] Kijima, M. (1989). Some results for repairable systems with general repair. Journal of Applied Probability, 20, 851-859.

[6] Lewis, E.E. (1987). Introduction To Reliability Engineering. New York: John Wiley & Sons.

[7] Mettas, A. & Wenbiao Z. (2004). Modeling and Analysis of Complex Repairable Systems, Technique Report, Reliasoft Corporation: Annual Reliability and Maintabilility Symposium.

[8] Mettas, A. & Wenbiao Z. (2005). *Modelling and Analysis of Repairable Systems with General Repair*. ReliaSoft Corporation: Annual Reliability and Maintanability Symposium.

[9] Rao, S.S. (1992). *Reliability-Based Design.* New York: Mc Graw Hill.

[10] ReliaSoft Corporation. (2005). *Software Training Guide Reliasoft's RGA 6*. USA

[11]ReliaSoft Corporation. (2008). *Avoiding a Common Mistake in the Analysis of Repairable Systems*. Maret 10, 2008. Reliability Edge, Volume 7, Issue 1, Tucson, AZ. http://www.reliasoft.com/ newsletter/v7i1/ index.htm

[12] Rigdon, Steven & Asit P. Basu. (2000). *Statistical Methods for the Reliability of Repairable Systems*. New York: John Wiley & Sons, Inc.

[13]Veber, B., M.Nagode & M. Fajdiga. (2007). *Generalized renewal process for repairable systems based on finite Weibull mixture*. Mei 9,2008. Reliability Engineering and System Safety 93 (2008) 1461-1472. http://www.sciencedirect.com/

[14] Yanez, M. et al. (2002). *Generalized renewal process for analysis of repairable systems with limited failure experience*. Mei 9,2008. Reliability Engineering and System Safety 77 (2002) 167-180. http://www.sciencedirect.com/

[15] Novianti Dian Pratiwiningtyas. (2008). *Skripsi Sarjana*. Departemen Teknik Industri, Fakultas Teknik Universitas Indonesia.

ISSN 114-1284

FAILURE RISK ANALYSIS ON CORE NETWORK OF GPRS EQUIPMENT USING FMEA & FTA METHOD AND SIMULATION SCENARIOS OF TREATMENT COST ALLOCATION

Yadrifil[1], Anisa Fithrasari[b]

[a]*Industrial Engineering Department, Faculty of Engineering*
University of Indonesia, Depok 16424
Tel : (021) 78888805 Fax 78885656
E-mail : yadrifil@ie.ui.ac.id

[b]*Industrial Engineering Department, Faculty of Engineering*
University of Indonesia, Depok 16424
Tel : (021) 78888805 Fax 78885656
E-mail : anisafithrasari@yahoo.com

Abstract

Due to increasing of technology development, telecommunication corporate must provide more efficient data services on higher traffic data, and also introduce new services. GPRS can be a solution to achieve that things. Now application of GPRS technology is more developing and give a lot of advantages for user. That's why corporate telecommunication use GPRS to increase their value added services. But, there is potential failure risk on GPRS equipment, so risk analysis need to be done. Objectives of risk analysis in this research are to get idea of risk treatment action on GPRS equipment and scenario of treatment cost allocation. By using FMEA method, be able to have critical risk which will be further analysed using FTA to have basic event from those critical risk. And also by using OptQuest-Crystal Ball simulation can have optimal treatment cost allocation.

Keywords *: GPRS, risk analysis, FMEA, FTA, OptQuest-Crystal Ball simulation.*

1. Introduction

GPRS is a technology that can be used by GSM operators for providing data services on higher traffic data with low price to attrack market. For GSM operators, GPRS is a key to compete in market development especially in internet services. Rapid development in mobile communication motivate GSM operators for increasing kind of services to get higher revenue and create customer's loyalty. GPRS can be a solution to achieve more efficient data services on higher traffic data and also introduce new services. The point is, GPRS can create relation phase faster, still connect permanently, use faster data speed, dan only pay every transferred bit. The reason is clear, market tendency is away from technology that increase price.

Now, GPRS is also a corporate solution. GPRS can give solution for banking corporate in cost efficiency. Banking corporate can get more efficient bandwith lease by using GPRS for providing link service in ATM machine. GPRS can also make *Electronic Data Capture* (EDC) more flexible to use. EDC technology usually use in hypermarket and taxi company.

GPRS also use in Blackberry application. Blackberry can really support businessman in doing their job. So, by using GPRS corporate can have a lot of benefit.

GSM operators that use GPRS for increasing value added services must give attention to GPRS equipment. Maintenance of GPRS equipment is a must to have good performance. So, every potential failure can be avoided or eliminated and company goals can be achieved. The principle is to get customer loyalty and also have more customer because of excellent service.

For achieving excellent services, maintenance division must determine *Key Performance Indicator* (KPI). In this research, company determine 2 point of KPI, which is Attach Success Rate and PDP Context Success Rate. Attach Success Rate refer to success of having signal and PDP Context Success Rate refer to success of internet connection. The common problem is signaling and connection failure. Company can have loss revenue and give unsatisfaction to their customer because of those problem. Beside 2 factors of KPI, company also give attention in Attack Security because Attack Security can make fraud in GPRS system.

Every problem either ever happen or not is a potential risk. That's why, risk analysis is need to be done for identifying, measuring, and then making response

strategy. Risk management is a process to identify, assess risk, and then develop strategy to manage risks. By those background, I make this research which have title 'Failure Risk Analysis on Core Network of GPRS Equipment using FMEA & FTA method and Scenario of Treatment Cost Allocation'.

2. Methods

This research only review risks in operational and maintenance activity of GPRS equipment. Expert team that involve in this research are Network Service O&M Center General Manager, VAS Celullar Team Leader, and VAS Cellular Engineer which have more than 5 years experience.

Research method refer to standardization of FMEA step.

- Risk event identification
  To identify risk, previously we need to collect data. Data collection is done by collecting historical data of GPRS system failure, searching literature data, and then making *Cause Failure Mode Effect* (CFME) diagram, so risks can be identified and listed.
- Determine occurrence, severity, and detection rating
  Determination of occurrence, severity, and detection rating is done by expert brainstorming which is supported by literature data.
- Assess occurrence, severity, and detection of every risks
  Assessment of occurrence, severity, and detection is done by filling quesioner
- Calculate *Risk Priority Number* (RPN) and determine critical risks
  This step is done by calculating questioner result
- Analyze risks and develop risk response planning
  Fault Tree Analysis (FTA) is a tool that is used in this step. By FTA, can get root cause of critical risk so we can have idea of treatment action. Based on treatment cost that is need to do those treatment actions, so in this research also create scenario of treatment cost allocation for having optimal value by using OptQuest-Crystal Ball simulation. To run the simulation, it is need loss revenue data and treatment cost data which are get from historical data, expert judgment, and data analysis.

3. Result and Discussion

3.1 Risk Identification

Risk identification is the important step in risk management before doing next step. Risk identification involve risk determination which may be influence performance of GPRS equipment. The goal of this step is to know risk earlier so we can decrease or eliminate the impact.

After knowing every failure and potential failure which are get from expert brainstorming, historical problem, and literature, then Cause Failure Mode Effect (CFME) diagram is made. The result of CFME can make FMEA easier in identification, failure mode, and root cause. CFME diagram can be seen in picture 1.

3.2 Determination of Occurrence, Severity, and Detection Rating

In FMEA step, after having risk item, the next step is detemination of occurrence, severity, and detection rating. That determination will effect of having risk priority.

Rating determination is done by expert brainstorming in accordance with company condition. Occurrence rating is a quantification from level risk probability. The used scale is 1 - 5, which is value 1 refer to low probability and value 5 refer to high probability, that rating can be seen at table 1.

Severity rating is a quantification from level of impact from the risk. The used scale is 1 – 5, which is value 1 refer to no effect from risk and value 5 refer to fully system failure as impact from risk. That rating can be seen at table 2.

Detection rating is a quantification from level of risk detection. Detection fucntion is for knowing whether risk can be detected before the failure is happen and also knowing whether current detection is effective enough. The used scale is 1 -5, which is higher value showing that level of control getting lower of quality/effectiveness. That rating can be seen at table 3.

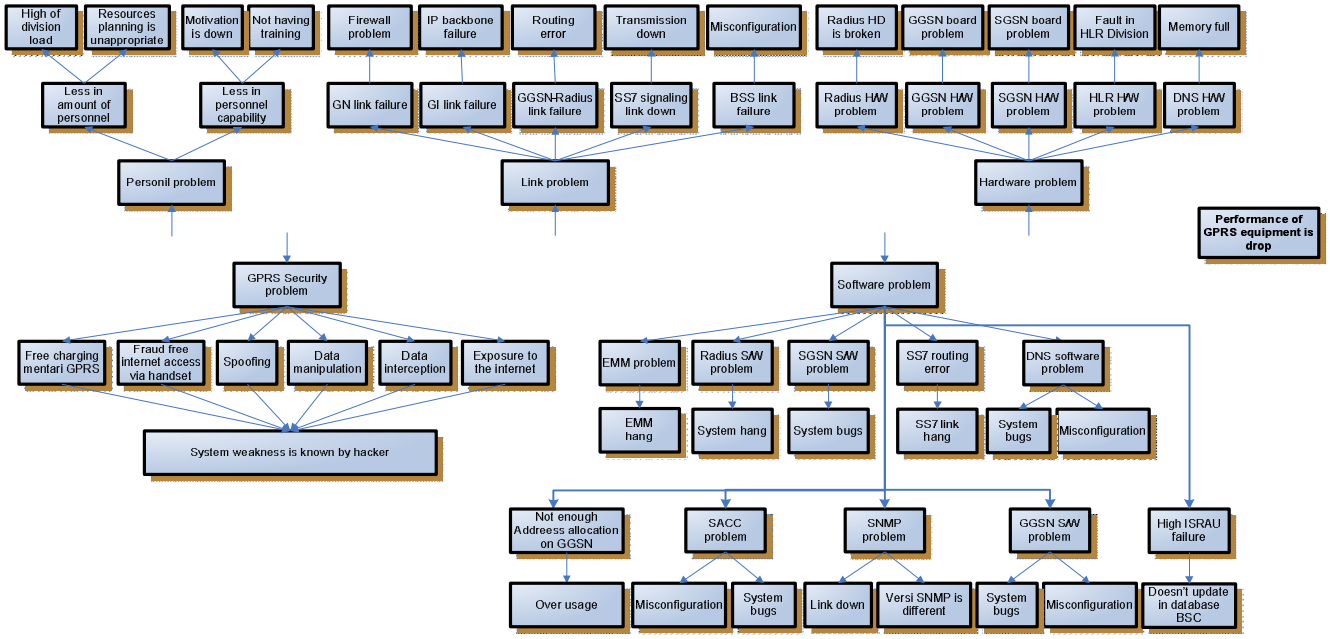

Figure 1: ***Cause Failure Mode Effect Analysis*** **(CFME) Diagram**

Table 1 Occurence Rating

Scale	Risk Probability	Note
5	Very high : can not be avoid	Risk probability per year : 81 - 100
4	High : repetitive	Risk probability per year : 61 - 80
3	Moderate	Risk probability per year : 41 - 60
2	Low : seldom	Risk probability per year : 21 - 40
1	Very low	Risk probability per year : 0 - 20

Table 2 Severity Rating

Scale	Risk Impact	Note
5	Emergency	Fully system failure, it cause loss of charging data
4	Critical	System error, the risk give impact to revenue management system
3	Major	The risk give impact only on certain work area not on entire system
2	Minor	Have minor effect to product function, but not give impact to service and data traffic
1	Warning	Does not give impact neither to service nor system

Table 3 Detection Rating

Scale	Risk Detection	Note
5	Very low	Detection method / alert system is not available
4	Low	Current detection method is not effective enough to detect the risk on time
3	Moderate	Current detection method is less effective, so it needs more time to detect the risk
2	High	Current detection method is effective enough to detect the risk
1	Very high	Current detection method is very effective to detect the risk real time

3.3 Assessment of Occurrence, Severity, Detection for Every Risk and Calcution of Risk Priority Number (RPN)

After risk is identified, the next step is determination of occurrence, severity, and detection value for every risk. This step is done by filling quesioner through expert brainstorming. The value of occurrence, severity, and detection for every risk can be seen at table 5.

Calculation of RPN is important point in FMEA because from that we can have risk priority for further analyze. RPN can be calculate by this formula :

RPN = *Occurrence * Severity * Detection* (1)

Table 4 Occurrence, Severity, Detection and RPN Value for Every Risks

Risk ID	Risk on Core Network of GPRS Equipment	*O*	*S*	*D*	RPN
1	SGSN Hardware Problem	1	4	3	12
2	HLR Hardware Problem	1	4	3	12
3	SGSN Software Problem	1	3	3	9
4	SS7 signaling link down	3	4	3	36
5	BSS link failure	3	3	3	27
6	SS7 routing error	3	3	4	36
7	GGSN Hardware Problem	1	4	4	16
8	Radius hardware problem	1	4	5	20
9	GGSN Software problem	3	4	4	48
10	Radius sofware problem	2	4	5	40
11	GGSN-radius link failure	4	5	5	100
12	High ISRAU failure	2	3	4	24
13	Not enough address allocation on GGSN	2	3	3	18
14	EMM problem	5	5	5	125
15	SACC problem	1	4	5	20
16	DNS hardware problem	2	4	3	24
17	DNS software problem	4	4	5	80
18	GN link failure	1	4	4	16
19	GI link problem	4	4	4	64
20	Free charging mentari GPRS	1	5	5	25
21	Fraud free internet access via handset	1	5	5	25
22	Spoofing	1	5	5	25
23	Data manipulation	1	5	5	25
24	Data interception/unauthorized access to confidential data	1	5	5	25
25	Exposure to the internet	1	5	5	25
26	SNMP problem	2	1	2	4
27	Jumlah personil kurang	2	3	5	30
28	Kapabilitas personil kurang	2	3	5	30

After having RPN value for every risk, the next step is determine the critical risks. That critical risks will be further analyzed as first step of treatment action for having good performance of GPRS equipment. Risk is categorized as critical risk if having RPN value higher than critical value. RPN critical value is determined from average of RPN value from entire risks.

$$Nilai\ Kritis\ RPN = \frac{Total\ RPN}{Jumlah\ Risiko} = \frac{986}{31} = 31{,}81$$

According to RPN critical value and based on expert agreement, there are 8 critical risks, which those risks have RPN value more than 31,81. Those critical risks are:

- EMM Problem, RPN = 125
- GGSN-Radius Link Failure, RPN = 100
- DNS Software Problem, RPN = 80
- GI Link Problem, RPN = 64
- GGSN Software Problem, RPN = 48
- Radius Software Problem, RPN = 40
- SS7 Signaling Link Down, RPN = 36
- SS7 Routing Error, RPN = 36

3.4 Risk Analysis

Risk analysis is started by making fishbone diagram. Fishbone diagram is a tool for seeking root cause which is classified in 5M & 1E (Man/Personnel, Method, Machine, Material, Measurement, and Environment). Based on quesioner result, there are 3 classification, method, personnel, and equipment. Fishbone diagram is further developed by making Fault Tree Analysis (FTA). The result of FTA is having basic event of top event (critical risk).

FTA is a graphical model which is consist of many fault combination parallel and sequence that may cause failure event as top event. In this research, critical risk is determined as top event. Finally, we can get basic event which is root cause of top event, so the right action can be made for handling critical risk. After knowing the right treatment actions, then will appear treatment cost of those actions. Here is example of fault tree analysis for EMM problem.

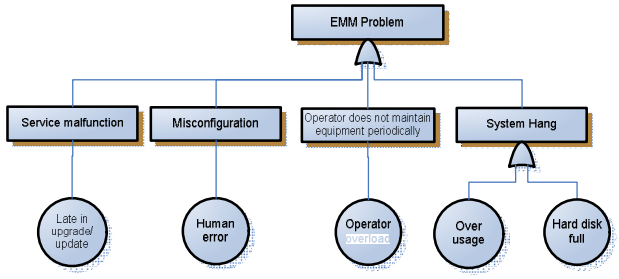

Figure 2: FTA of EMM Problem

After making FTA, then determine Cut Set from that FTA for knowing basic event of critical risk.

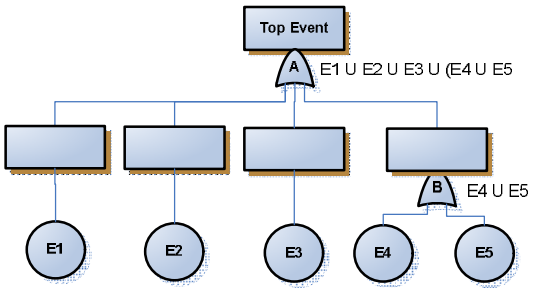

Figure 3: CutSet of EMM Problem

Cut set of this fault tree: E1 U E2 U E3 U (E4 U E5). It means if event 1 or 2 or 3 or 4 or 5 is happen will cause the top event.

- Top Event : EMM Problem
- Basic event 1 : Late on update/upgrade software
- Basic event 2 : Human error
- Basic event 3 : Operator overload
- Basic event 4 : Over usage
- Basic event 5 : Harddisk full

After knowing basic event of every critical risks, then appear treatment action. Treatment action is done by risk mitigation in 2 ways which are mitigate the risk probability and mitigate the impact from risk. Risk impact mitigation is done by doing remedy action. Remedy action is first action from operator when risk is happen. For having effective remedy action, based on data analysis and evaluation the suggestion are :

- Make automatic monitoring system for every equipment in GPRS infrastructure
- Make standardization of problem solving action
- Manage historical problem

If operator still can not solve the problem then it is escalated to the vendor (Risk Transfer).

To mitigate the risk probability, based on the result of FTA, the suggestion for entire critical risks are :

- Provide more operator for handling operator overload problem
- Give training for every person in charge in current problem
- Upgrade harddisk
- Ask vendor commitment not to late for upgrading equipment information
- Doing periodic maintenance for hardware and changing broken part immediately
- Coordinate with other division about IP routing, transmission, hardware HLR, and router internet gateway problem

3.5 Optimization of Treatment Cost Allocation using OptQuest Simulation

OptQuest is one of function in Crystal Ball. OptQuest can be used for determine cost allocation which give optimal benefit. There are many terms in OptQuest :

- *Risk cost/loss revenue* : appearance of cost / loss revenue when risk is happen.
- *Risk coverage* : risk cost / loss revenue that can be covered with given treatment cost allocation.
- *Decision* : variable for knowing how much fund allocation for any risk, the value is 1 if the risk is given fund allocation.
- *Advantage*: (risk coverage – treatment cost)*decision

For run the simulation, it needs data of loss revenue and treatment cost. For getting loss revenue, critical risks is classified in 3 groups. EMM problem refer to loss revenue historical data which is captured on GGSN equipment-duration based; DNS software problem, GI link failure, GGSN software problem, dan radius software problem refer to loss revenue historical data which is captured on GGSN equipment-volume based; SS7 signaling link down and SS7 routing error based on expert judgment. According to data collection, here are data of loss revenue for every critical risks.

- EMM problem (normal distribution) :
  - Mean : Rp 214.870.286
  - Standard deviation : 43856839
- DNS software problem, GI link failure, GGSN software problem, and radius software problem (normal distribution) :
  - Mean : Rp 345.108.000
  - Standard deviation : 87460770
- SS7 signaling link down and SS7 routing error (uniform distribution) :
  - Maximum : Rp 360.000.000
  - Minimum : Rp 12.000.000

Treatment cost is got from cost of treatment action which is resulted from FTA. Total treatment cost for entire critical risks is Rp505.000.000, and the detail are :

- EMM Problem : Rp 130.000.000
- DNS Software Problem : Rp 20.000.000
- GI Link Failure : Rp 20.000.000
- GGSN Software Problem : Rp 130.000.000
- Radius Software Problem : Rp 55.000.000
- SS7 Routing Error : Rp 50.000.000
- SS7 Signaling Link Down : Rp 100.000.000
- GGSN-Radius Link Failure :
  Fund allocation for GGSN-Radius link failure does not run in this simulation because that problem is connected with GGSN software problem and radius software problem are handled, which if those problems are handled then automatically GGSN-Radius link failure will solve.

Before running the simulation, it is need to determine assumption, decision, and forecast variable. Assumption variable is uncertainty values which have

certain distribution. In this model, risk cost/loss revenue is as assumption variable. Decision variable is fund allocation that is given for treat risk. And forecast variable is a cell that contain formula which is connected with assumption cell and decision cell, that is value of total advantage that is want to maximized.

Constraint in this simulation is treatment cost allocation ≤ budget. It is assumed that company provide 4 conditions of budgeting, which are ≤ 25%, ≤ 50%, ≤ 75%, and 100% from total treatment cost.

The next step is running the OptQuest simulation. Simulation is done for every condition. Every simulation is fun for 1000 trial. The simulation gives different result for every condition.

Table 7 The Result of Treatment Cost Allocation using OptQuest Simulation

Critical Risk	Condition of Budget Availability			
	≤ 25% from total treatment cost	≤ 50% from total treatment cost	≤ 75% from total treatment cost	100% from total treatment cost
EMM problem	Rp 0	Rp 0	Rp 4.704.900	Rp 130.000.000
DNS software problem	Rp 20.000.000	Rp 20.000.000	Rp 20.000.000	Rp 20.000.000
GI link problem	Rp 20.000.000	Rp 20.000.000	Rp 20.000.000	Rp 20.000.000
GGSN software problem	Rp 0	Rp 107.580.000	Rp 130.000.000	Rp 130.000.000
Radius software problem	Rp 53.657.000	Rp 55.000.000	Rp 55.000.000	Rp 55.000.000
SS7 signaling link down	Rp.0	Rp 0	Rp 99.481.000	Rp 100.000.000
SS7 routing error	Rp 32.593.000	Rp 49.727.000	Rp 50.000.000	Rp 50.000.000
	Rp126,250,000	**Rp252,307,000**	**Rp378,749,900**	**Rp505,000,000**

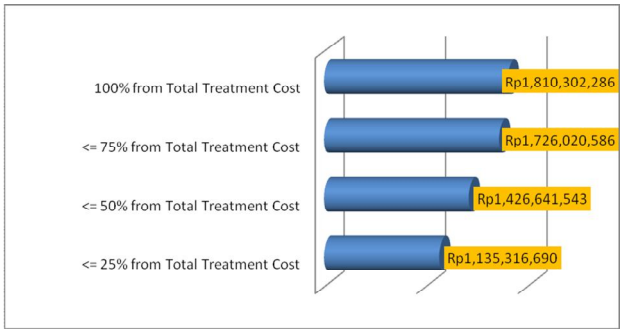

Figure 4: Total Advantage on Every Condition of Budget Availibility

Based on simulation result, it is shown that in higher fund allocation will give higher total advantage, it can be seen at picture 4.

Here are the result of cost allocation for every condition using OptQuest simulation.

- In condition ≤ 25% from total treatment cost, GI link problem and DNS software problem have full fund. Maximum total advantage is Rp. 1.135.316.690.
- In condition ≤ 50% from total treatment cost, GI link problem, DNS software problem, and radius software problem have full fund. Maximum total advantage is Rp. 1.426.641.543.
- In condition ≤ 75% from total treatment cost, GI link problem, DNS software problem, GGSN software problem, radius software problem, and SS7 routing error have full fund. Maximum total advantage is Rp. 1.726.020.586.
- In condition 100% from total treatment cost, entire critical risks have full fund. Total advantage is Rp. 1.810.302.286.

4. Conclusion

- There are 8 critical risks from 28 identified risks. The critical risks are EMM problem, GGSN-Radius link problem, DNS software problem, GI link problem, GGSN software problem, Radius software problem, SS7 signaling link down, and SS7 routing error.
- Every critical risk will have different treatment action. Treament action is done by 2 methods, which are risk mitigation and risk transfer.
- The result of cost allocation using OptQuest simulation can be seen in analysis data. Higher cost allocation that is given to treat critical risks it will give higher maximum total advantage.

5. Reference

Carbone, T & Tippett, D. (2004). Project Risk Management Using the Project Risk FMEA. *Engineering Management Journal*. Vol 16, No.4. hal 31.

Crystal Ball® 7.2.2 User Manual.

Harold Kerzner,(20060. *Project Management, A System Approach to Planning, Scheduling, and Controlling 9th ed.* John Wiley & Sons, Inc.

Information Risk Management. *GPRS/3G Services : Security*. O2 White Paper.

Project Management Institute. (2000) .*A Guide to The Project Management Body of Knowledge : PMBOK Guide.* Pennsylvania : Project Management Institute, Inc.

ISSN 114-1284

Six Sigma e-tools: An Overview of Knowledge Management Application for Improvement Activities in Hospitality Industry

Yudha Satya Perdana

Six Sigma & Operational Excellence
Sheraton Media Hotel & Tower 10720
Tel : (021) 6363001 ext 4020
E-mail : Yudha.satya@sheraton.com

ABSTRACT

In a competing market environment, improvement has been critical for company to survive. Six Sigma has been developed into a practical management system for continuous business improvement. Many company both manufacturing and services; have reported on their successive work with Six Sigma programs. In 2001, Starwood became the first hospitality company to embrace Six Sigma and began to develop a knowledge management system. Six Sigma e-Tools Knowledge Management System (SSeKMS) was initiated as an integrated systematic approach in managing all of information assets, including database, documents, as well as expertise and experience for improvement initiatives (Six Sigma Project) held by 1,081 hotel chains world wide. SSeKMS provides step-by-step templates and information about six sigma. SSeKMS enables each hotel property to identify improvement opportunities, develops innovative customer focused solutions, track the bottom-line result and transfer those innovations rapidly. This paper aims to give an overview of knowledge Management System implementation which supports the successive of Six Sigma adoption in hospitality industry

Keywords
Six Sigma, Knowledge Management, Hospitality, improvement

1. INTRODUCTION

In recent days the consumers is no longer in the passive market where goods or services are offered at the exact face value. Today consumers are more educated, and they demand more. The developments of recent technology have support them in providing information about market and its competition. This has initiated new and radical changes in the business world. Manufacturer or service provider has to fully respond to customer expectation and deal with societal, cultural, and technical challenges.

Many organizations see process improvement can help improve organizational process effectiveness, they see process improvement as the generic medicine that will solve all internal and external problems, improve the bottom line and win the competition.

However, many organizations still do not understand how process improvement can help them. They know process improvement is good, they learn tools and methodology and try to implement it, but the result is not essential for their company. The reason many organizations do not achieve sustainable progress is not result of lack of hard work or dedication. On the contrary most of the people involved with improvement activities have put in countless hours and effort to make them work. Here are some reasons of failure of process improvement implementation in company [1]:

1. **Lack of understanding on the level of maturity.** Process improvement initiative generally has experienced only modest success because organization fails to address culture or defining level of maturity. Too often, organizations decide to jump into process improvement without assessing current levels of understanding and the collective level of maturity in relation to process improvement. Support and recognition of the need for change from leadership team are critical before beginning a process improvement. Without the

support, resources will not be provided, roadblock will be established, and well intentioned effort will fail. In *Leading Cha*nge, John P Kotter reminds the need for leadership team to acknowledge that change is needed and leadership team willingness to take on change. The relationship of management and leadership is captured on figures below [2]

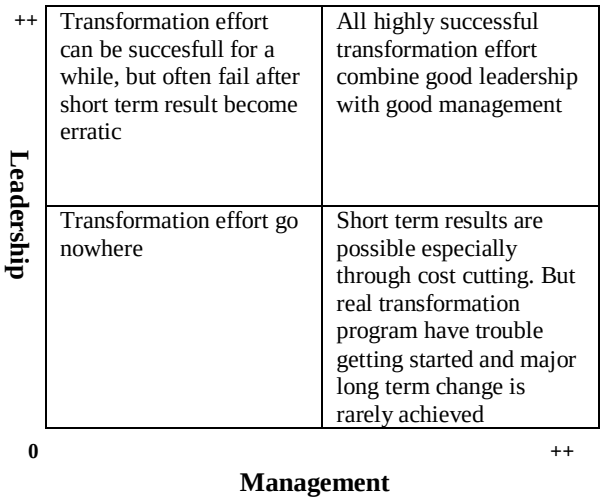

Figure 1: The relationship between leadership and management

The important of defining organization level of maturity that is well known to everyone in every aspect of the operation is a prerequisite for process improvement initiative. And it won't occur unless it is enabled by leadership commitment in an environment of innovation [3]

2. **Process improvement not link to the strategic plan and the criteria for success not establish.** Any successful process improvement implementation must be linked to organization's strategic plan. Strategic plans state organizational direction in a mission and vision statement with associated goals and objectives which then be measured. To ensure the goals and objectives were being met, criteria for success (CSF) need to be established and easily tracked.
3. **Inappropriate resource allocation.** Many organizations recognize the benefit of process improvement but they are unwilling to allocate the needed resources to make it happen.
4. **Lack of Training and Communication.** To implement a successful process improvement, employee must shift the way they think and work. Training is the critical initial step needed to initiate cultural change. Permanent shift in organization culture must involve all employees, and each employee must have at least a basic knowledge of what is expected and how the change will be accomplished. Beside training, communication also needed to create awareness. The difficult part of any process improvement program is the implementation and institutionalization of a solution. If people not engaged, the process improvement program doesn't become institutionalized, and then it could be the cost of poor communication [4]
5. **Lack of Coordination throughout the organization.** Organizations often fail to coordinate process improvement effort across and within organization. One section of the organization may improvement effort locally without any communication with leadership team, this result in sub optimization of process improvement. An effort to include every organization under one umbrella to ensure all employees speak with same language and the entire organization focuses on process improvement as part of its culture. People get enthusiastic when improvement process are well planned and executed
6. **Lack of Data Management.** Good improvement process generally starts with solid data collection and analysis [4] This involve all type of data such as measurement process, customer feedback, or service parameter which will aggregated, summarized, and presented in an integrated manner to become information. Weak data management will lead to failure of process improvement initiative.

ISSN 114-1284

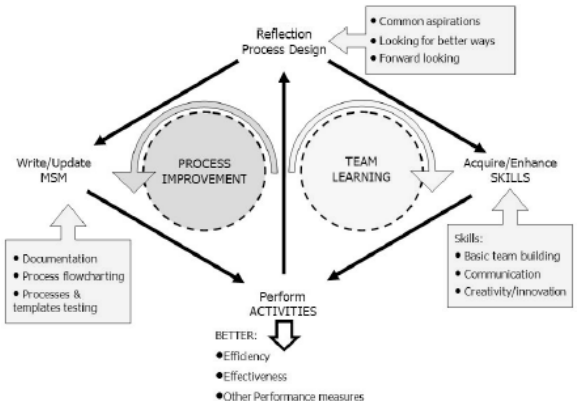

Figure 2: Embedding Learning in Process Improvement activities [5]

Process Improvement programs are seen as the desire to commit to learning in order to avoid making the same mistakes over and over again. "Learning organizations" are the result. It offers the following definition: "A learning organization is an organization skilled at creating, acquiring, and transferring knowledge, and at modifying its behavior to reflect new knowledge and insights" [6]. Knowledge can lead to competitive advantage and that knowledge-creating companies are those that will succeed in fast changing market conditions [7]. Drucker (1994) defines it in a very similar manner by saying that "knowledge has become the key economic resource and the dominant, if not the only, source of comparative advantage". Their main goal is "making personal knowledge available to others"

Process improvement and learning organization can achieve its full potential if only when people, culture, process, and system come together with the right tools, methodology, management, and technology.

2. SIX SIGMA AND KNOWLEDGE MANAGEMENT

Knowledge management and Six Sigma share a notable distinction in a corporate universe full of change initiatives and improvement philosophies. These two approaches have been integrated into regular operations at leading companies to guide and maintain the learning cultures within organizations [8]

2.1 Value of Six Sigma

Six Sigma provides set of tools, proven methodology, and management system to boost profitability, increase market share and improve customer satisfaction. As a result of those, Six Sigma eventually increases the company's competitiveness.

2.1.1 Six Sigma as a metric, methodology, and Management System

Six Sigma as a metric is represents how well a process is performing and how often a defect is likely to occur. It is labeled by sigma (6) as unit of measurement that designates the distribution or spread about the mean (average) of a process improvement. Six Sigma is the standard of excellent at only 3.4 defects per million opportunities.
Six Sigma methodology is described as DMAIC [9]

- **Define,** select the appropriate responses to be addressed
- **Measure,** gathering data to measure the response variable
- **Analyze** identify the root causes of defect, defectives, or significant measurement deviation whether in or out of specifications
- **Improve** reduce variability or eliminate the causes
- **Control,** with desired improvement in place, monitor the process to sustain the improvement

At the highest level, Six Sigma has been developed into a practical management system for continuous improvement that focuses management and the organization or four key areas [10]

- Understanding and managing customer requirement
- Aligning key processes to achieve those requirement
- Utilizing rigorous data analysis to understand and minimize variation in key processes
- Driving rapid and sustainable improvement to the business process

2.1. 2 Six Sigma Organization Structure

Prior to deployment, during deployment, and transition to the organization, there are critical role and responsibilities that ensure Six Sigma methodologies become ingrained in the business.

Understanding the roles and responsibilities for each activities will leads to effective deployment [11]:

- **Executives,** create the vision for the Six Sigma initiative and create an environment within the organization that will promote the use of Six Sigma methodology and tools
- **Project Champion,** Leads in project identification, prioritization, and defining the project scope. Select and mentors Black Belt also removes barriers and align resource
- **Master Black Belt,** assist champion and process owner. Trains, coaches, and mentors Black Belt and Green Belts in order to able to apply the methodology and tools
- **Black Belt,** assist in identifying project opportunities and refining project details and scope.
- **Process owner,** takes ownership of the project when it is complete, and responsible for maintaining the project's gain.
- **Green Belt,** works small scope projects, typically in his/her respective work area.

2.2 Knowledge Management

Knowledge management provides strategy of putting tacit and explicit knowledge into action by creating context, an infrastructure, and learning cycles that enable people to find and use the collective knowledge of the enterprises

2.2.1 Knowledge Definition

Knowledge is defined as "understanding gained through experience or study." It is "know-how" or a familiarity with how to do something that enables a person to perform a specialized task. It may also be an accumulation of facts, procedural rules, or heuristics. These elements are defined as follows:

- A fact is a statement of some element of truth about a subject matter or a domain.
- A procedural rule is a rule that describes a sequence of relations relative to the main.
- A heuristic is a rule of thumb based on years of experience

In his study of Smart Business, Botkin (1999) suggests six top attributes of knowledge products and services:

- **Learn**. The more you use them, the smarter they get and the smarter you get, too.
- **Improve with use**. These products and services are enhanced rather than depleted when used, and they grow up instead of being used up.
- **Anticipate**. Knowing what you want, they recommend what you might want next.
- **Interactive**. There is two-way communication between you and them.
- **Remember**. They record and recall past actions to develop a profile.
- **Customize**. They offer unique configuration to your individual specifications in real time at no additional cost

Knowledge also can be considered as the integration of human perceptive processes from data into information that helps them to draw meaningful conclusions

Figure 3: Wisdom, Knowledge, Information, Data

2.2.2 Type of Knowledge

Two different kinds of knowledge need to be distinguished from each other. External (or formal) knowledge that can be easily shared and is often well documented; its transfer is possible in an impersonal way, e.g. through written instruction [12]. Tacit (or informal) knowledge on the other hand is much more difficult to articulate;

it is very personal, context specific and transferred mainly through social interactions [8].

Table 1: The Four models of knowledge

	Tacit Knowledge	to Explicit Knowledge
Tacit Knowledge from	Socialization (sharing experiences with others)	Externalization (writing down tacit knowledge)
Explicit Knowledge	Internalization (embodying, i.e. „learning by doing")	Combination (systemizing it into a knowledge system)

The above model describes the contents of knowledge and applies to a learning organization where tacit knowledge is nurtured and converted into explicit knowledge and then back into tacit knowledge [13]

2.2.3 Knowledge-based Organization

Knowledge management helps organization reduce both time and costs by reusing existing knowledge and also enhance facilitate generating newer knowledge by using existing knowledge as a base [14]. Chase International Survey (1997) stated that knowledge management benefits are:

- Improving organization ability for decision making (89%)
- Improving response time to customer (82%)
- Improving work and process efficiency (73%)
- Improving ability to innovate (73%)
- Improving productivity of services (73%)

But, most of organization knowledge lies on employee brains (tacit).

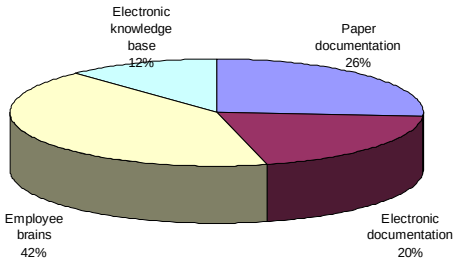

Figure 4: Repositories of Corporate Knowledge Resources [15]

In bringing knowledge management into organization, it needs to establish system that help organization to be better at creating, finding, acquiring, organizing, storing, accessing, sharing and using the knowledge and creating new knowledge as well.

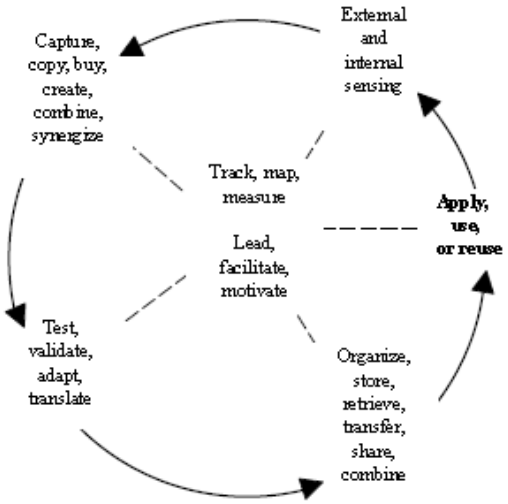

Figure 5: Knowledge Management Cycle [16]

The level of successfulness of knowledge management system is depending on the designing a mix of appropriate skills, relevant information, support systems (technology), and relational context which can produce better results

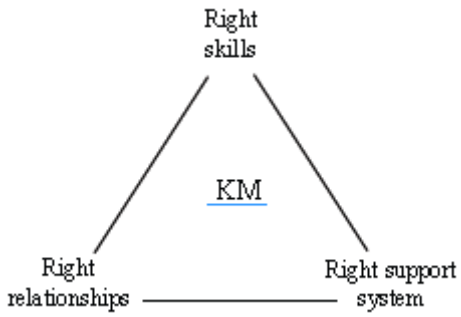

Figure 6: Effective KM requires Skills, System, and Relationship

The ideal knowledge organization is where people exchange knowledge across the functional areas of the business by using technology and established processes. People exchange ideas and knowledge for policy formulation and strategy. Knowledge is also internalized and adopted within the culture of the organization. All knowledge workers (people) are in an environment where they can freely exchange and produce knowledge assets by using various technologies.

3. SIX SIGMA IPLEMENTATION IN STARWOOD HOTEL & RESORTS

Starwood is the world's largest hotel and leisure. Starwood brand include: St. Regis, Sheraton, Luxury Collection, Le Meridien, W, Aloft, Element, Bliss, Westin, and Four Points. In 1990s Starwood began with a culture of creativity by introducing Starwood Improvement System (SIS) and Starwood Care Experience (SCE) before introducing the management tool.

In 2001, Starwood became the first hospitality company to embrace Six Sigma, an internationally recognized approach that enables associates to develop innovative customer focused solutions and transfer those innovations rapidly across an organization. Starwood developed a top-down give and take process for setting priorities and optimizing change investment. The objectives and process included [17]:

- Provide high level direction to local unit managers on high priority areas for improvement
- Allow local autonomy with localized guideline. The leadership team of each hotel responsible for developing its own list of priority projects (depending on the specific strength and weakness of the local operation
- Maintain high level review and control of the overall portfolio.

3.1 Six Sigma Organization Structure

In order to exceed its very audacious goals, Starwood has built a robust infrastructure. We have three defined roles at Starwood, each with a set of defined responsibilities:

- **Black Belts**: A full-time position that sits on a hotel's Executive Committee, a Black Belt works on projects that address Black Belts lead teams to gather voice of the customer, remove root causes and pilot solutions. Starwood employs approximately 150 Black Belts worldwide
- **Green Belts**: A part-time role, Green Belts transfer into their hotels the solutions that Black Belts create. Using project warehouse to access data, SOPs and dashboards, Green Belts can implement solutions from any hotel across the globe into their hotels. Starwood has developed over 2,700 Green Belts.
- **Master Black Belts**: MBBs are project portfolio managers who are deployed regionally. 53 MBBs worldwide drive a series of "creation" and "transfer" projects throughout operations.

Every Six Sigma project represents an integrated effort between the field and Six Sigma resources. Starwood has seven divisions: Asia Pacific, Latin America, North America, Europe & Middle East (EAME), SVO, Franchise, and Corporate. Each division's Six Sigma organization reports to divisional leadership and is aligned with the division's goals and priorities. Members of the divisional, regional and property leadership teams take on a variety of roles, including Sponsor, Process Owner and Team Member, in all stages of each Six Sigma project from proposal to completion.

Figure 7: Starwood Six Sigma Organization Structure

3.2 Six Sigma Deployment

Global, divisional, regional and property Six Sigma Councils meet throughout the year to determine priority initiatives, drive best practice transfers and ultimately determine which projects should become required for an area or group of properties. Six Sigma projects fall into three categories:

- **DMAIC projects** seek to uncover opportunities and root causes and make existing processes more efficient and effective. The acronym DMAIC refers to the five stages in the Six Sigma project process: Define, Measure, Analyze, Improve and Control.
- **Quick Hits** are small projects that can be quickly implemented, generally lasting 3 to 4 weeks, which typically can be completed within the boundaries of a single function or department. Quick Hit projects follow the general DMAIC methodology, but are not subject to as many "tollgate" reviews. They contain some Voice of Customer research and must involve a change in the process

Transfer Projects are Six Sigma projects (whether DMAIC project or a Quick Hit) which is can be implemented in many properties.

Each of property is responsible for researching solutions that may apply to face their problems. The benefits of project transfer are significant. The effort and resources in reinventing the wheel can be reduced or eliminated by learn to other properties and adopt the best practices. Project transfer can be divided into two: Required best practice and Optional best practice.

Figure 8: Six Sigma Project Type

To become a required best practice, a project should have characteristic as follow:

- Deliver a higher return on investment than other Six Sigma projects. The investment is the time and effort a team spends finding a solution and implementing it successfully. The return is the increase in guest and/or associate satisfaction produced by the solution, the revenue generated, and the cost savings.
- Easy to transfer to other properties, and should not require a dedicated black belt while implementing it because the project initiator has provides step by step and guideline how to implement it
- The best practices is adopting the way project being executed and learn from other company's experience, so the implementation of best practice could be fast and the benefit could be realized immediately.

To nominate, select and assign some of Best Practice projects the property, area, and division councils work together

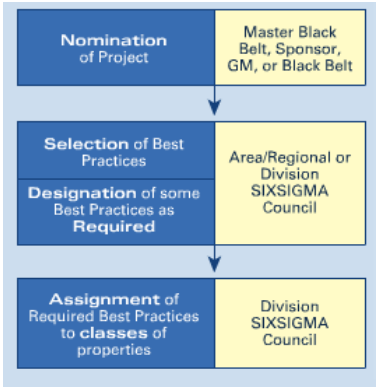

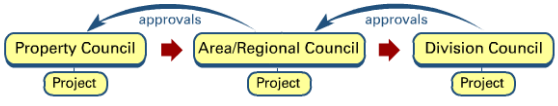

Figure 9: Approval Sequence for Best Practice

4. SIX SIGMA E-TOOL KNOWLEDGE MANAGEMENT SYSTEM

To retain knowledge and expertise in a whole 1,081 hotel chain world wide has been a challenge for Starwood. Knowledge and expertise are essential asset in order to maintain excellent work, process improvement, and continue being an industry leader. In 2002, with the advance of information technology, Starwood initiated Six Sigma e-Tool Knowledge Management System to speed up the learning process and projects transferability.

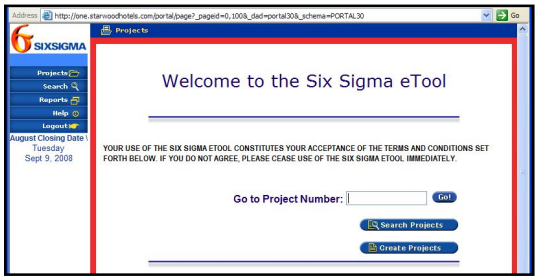

Figure 10: Six Sigma e-Tool Web Layout

4.1 The Knowledge Management Implementation

The Six Sigma e-Tool application is a web-enabled, global repository of Six Sigma projects. By integrating the document management system and database, The Six Sigma e-Tool enables project and financial tracking and senior leadership reporting.

4.1.1 Six Sigma e-Tool for Project Reporting and Tracking

Six Sigma e-Tool is a robust warehousing capability houses project information from the initial through the completed project. The format of the Six Sigma reports and document are standardized and regulated for projects progress and tracking.

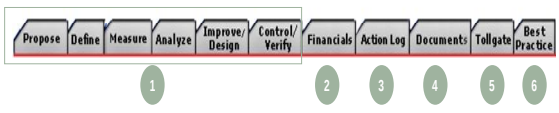

Figure 11: Six Sigma E-Tool's Report Element

Table 2: The Six Sigma e-Tool Element Description

Item	Name	Description
1	Six Sigma Process Phases	Each Tab is represents one phase of the Six Sigma process. Only a successful tollgate will advance the project to the next phase. Once a tollgate is complete, Users can only view information in past phases. Users cannot edit or add documents to past phases of a project.
2	Financials	Tab that allows View only details of project financials. Financials are only updated within the Financials subpage located within a Project Phase.
3	Action Log	Discussion Space for project participants to place comments/ issues regarding the project.
4	Documents Tab	Documents tab allows users to review all documents attached to project. Users can also attach new documents from this tab.
5	Tollgate Tab	View tollgate status. MBB access this page to approve, cancel, reject or place tollgates On Hold.
6	Best Practice	Only Active when the project is a Nominated, Optional or Required Best Practice.

Depending on type of project there are up to 8 phases within a project:

- A DMAIC project has eight phase
- A Quick project has five phase
- Project transfer (which known as i-DMAIC project) has four phase

Within a Phase, a project will also have a project status. Each phase within a project has more than one project status as defined in the table below.

When a project has been submitted for a tollgate review, the eTool adds a "-t" next to the project status to indicate the project is awaiting tollgate. When in tollgate review status, all items within the project are locked from editing/modification.

In most cases, only the MBB can tollgate a project to another phase

Table 3: e-Tool Project Status for each Project Phase

Project Type	Propose	Define	Measure	Analyze	Improve A	Improve B	Control	Complete
DMAIC	x	x	x	x	x	x	x	x
Quick Hit	x	x					x	x
iDMAIC	x		x		x		x	x

4.1.2 Six Sigma e-Tool for Financial Reporting and Tracking

Six Sigma e-Tool provides financial report for leadership council. The benefit from projects can be tracked and validated. Financial benefit for Quick Hit is recorded for 12 months; DMAIC and i-DMAIC are recorded for 18 months. In the e-Tool, financial benefit is categorized into 3 types:

- **Type 1**: Financial benefits that can be directly tied to the P&L. More specifically, there must be a quantifiable cause and effect relationship between the project deliverable and the reduction or increase in one or more general ledger accounts during a specified period. This will include revenue generating, cost reduction and cost avoidance projects
- **Type 2**: Benefits that have a financial impact but cannot be tied to the P&L during a specified period. The majority of type 2 project benefits will be realized in projects involving future focused revenue processes; for example, group room conversions from tentative to definite vs. using actualized bookings. Type 2 financial benefits will require RVP/AMD/Area Director, MBB and Regional Controller approval before the project is tollgated to Control for baseline and financial benefit calculations because of the added complexity of not knowing exactly when the benefits will show up on the P&L
- **Type 3**: Benefits including defect reductions, cycle time improvements, non-value added hours reduced (where we saved time in doing a certain task, but redirected that time spent to another, more valuable task, so we did not actually save payroll dollars), GSI (customer satisfaction index), ASI (Employee satisfaction), LRA improvements (Brand standard), conversion ratios, sigma levels, etc

Financials benefits are presented in the following format on the e-Tool:

- Incremental revenue, difference in revenue attributable to the process change. The calculation of incremental revenue should involving flow through % to EBITDA
- Cost reduction or expense reduction
- Non capital expense of implementing. startup costs related to the project, examples would include costs associated with mailing customer questionnaires or the purchase of equipment to small to qualify as capital
- Impact on working capital, this refers to movement in accounts payable, accounts receivable and inventory
- Non working capital investment. An item of cost for the project that is recorded against the balance sheet in an asset account other than working capital - a long-term asset, such as property, plant or equipment

For case study, below is the benefit figure of Asia Pacific division from 2002 up to YTD June 2009:

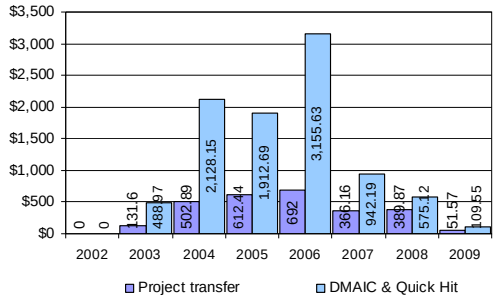

Figure 12: Six Sigma AP Division Type-1 Figure (number in thousands dollars)

The figure shows that more than US$ 12 millions have been generated by AP Division through DMAIC and Quick Hit (US$ 9.3 millions) and project transfer (US$ 2.7 millions)

4.1.3 Six Sigma e-Tool for Sharing Knowledge

As explained previously, the implementation of Six Sigma e-Tool knowledge management system is to speed up process learning. Different with DMAIC and Quick Hit project which starts with problem or opportunity and focuses on developing and implementing a solution, a project transfer (i-DMAIC) stars with a known solution and focuses on implementing that solution to address a problem that property has in common with the exporting property

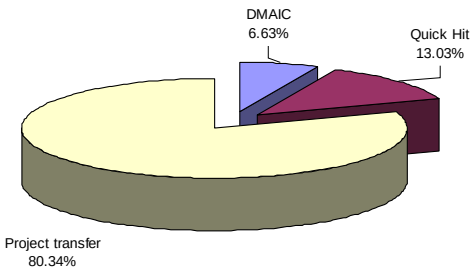

Figure 13: Proportion of Project Type in Starwood

In total, Starwood has generated 29,677 projects since 2001, where 80.34% is project transfer.

All Starwood Associates can access, view and search for projects in e-Tool. All Six Sigma Community members have the ability to view projects, create projects, edit projects, view reports and edit financials. Black Belts can only tollgate iDMAIC (Transfer) projects for the Propose, Measure and Control Phases only. And the Master Black Belts have the ability to Tollgate all projects

Table 4: the roles and rights for users of the e-Tool

Six Sigma Role	eTool Project Role	eTool Project Rights						
						Tollgate Ability		
		View	Create / Edit	View Reports	Edit Financials	DMAIC	(i) DMAIC	QUICK HIT
Green Belt	Proposed By	√	√	√	√			
	Project Leader/GB	√	√	√	√			
Black Belt	Proposed By	√	√	√	√			
	Project Leader/GB	√	√	√	√			
	Black Belt	√	√	√	√		P, M, C Phases Only	
Master Black Belt	Proposed By	√	√	√	√			
	Project Leader/GB	√	√	√	√			
	Master Black Belt	√	√	√	√	√	√	√
Financial Controller	Proposed By	√	√	√	√			
	Project Leader/GB	√	√	√	√			
	Controller	√	√	√	√			

5. CONCLUSION

Six Sigma is a proven management system for process improvement. On the other hand, Knowledge Management (KM) is a modern approach that deals with the greatest capital of organization. Six Sigma achievements are also based on proper knowledge and its flow. As a systematic approach to managing knowledge and process improvement activities with the aid of an information system in Starwood, Six Sigma e-Tool knowledge management system has been strongly emphasized and promoted throughout hotel chain. It has played important role in support growth, profitability and powerful tool to speed up organization learning process to become market leader.

REFERENCES

[1] leo Spackman, "Change That Stick", Quality Progress Volume 42/Number 4, 2009, pp. 23-28
[2] John P. Kotter, *Leading Change*, Harvard Business School Press, 1994, pp. 51-52.
[3] Robert P. Warda, "*Know Thyself*", Quality Progress Volume 24/Number 4, 2009, pp. 31-36.
[4] John E, West, "*Small Change, Big Payoff*" Quality progress Volume 24/Number 4, 2009, pp. 46-52.
[5] Serafin D. Talisayon, Jasmin Suministrado, Deanna Dolor, "*team learning and learning-oriented Manualization: experiences of the Malampaya multipartite monitoring team*", Asian Productivity Organization, 2008, pp.159
[6] D. A. Garvin, "*Building a Learning Organization*" *Harvard Business Review*, 71 (4), 1993, pp.78-92
[7] I. Nonaka, "*The Knowledge Creating Company*" Harvard Business Review, 69(6), 1991, pp. 96-104
[8] Paige Levitt, " *Knowledge Management and Six Sigma: Exploring the Potential of Two Powerful Disciplines*", APQC (www.scribd.com) , 2006
[9] Quality Council of Indiana, "*The Certified Six Sigma Black Belt Primer*", QCI, 2007, pp. II.1 – II.59
[10] Thomas Mc. Carty, Lorraine Daniels, Michael Bremer, Praveen Gupta, "*The Six Sigma Black Belt Handbook*", Motorola University – Mc. Graw Hill Companies Inc., 2005, pp. 3-6
[11] Paul Sheely, Daniel Navarro, Robert Silvers, Victoria Keyes, Deb Dixon, Bob Page, et all, "*The Black Belt Memory Jogger*" GOAL/QPC and Six Sigma Academy, 2002, pp 8-10
[12] K. Korth, "*Re-establishing the Importance of the Learning Organization*", Insight, 11, 2007, pp.12
[13] I. Nonaka, H. Takeuchi, "*The Knowledge Creating Company: How Japanese Companies Create the Dynamics of Innovation*", Oxford University Press, New York, NY, 2005
[14] E. Ofek, M. Salvary, "*Leveraging the Customer Base: Creating Competitive Advantage through Knowledge Management*", Management Science, 47, p. 1441-1456

[15] Lendy Widayana, *"Knowledge Management: Meningkatkan Daya Saing Bisnis"*, Bayu Media, 2005, pp. 15
[16] Serafin D. Talisayon, *"Knowledge Management in Asia: Experiences and Lessons"*, Asian Productivity Organization, 2008, pp. 5
[17] Peter S. Pande *"The Six Sigma Leader"*, Mc. Graw Hill, 2007, pp. 50-51

Design of Program Book by Pijar Suciati © FTUI

NOTHING BUT ASSURANCE

TIKI®

DOMESTIC & INTERNATIONAL COURIER SERVICE

Customer Service Hotline

Phone : (021) 3151617, 31922309 Fax : (021) 31907901

csr@tiki-online.com

www.tiki-online.com